

Marc® 2014.2

User's Guide

Corporate

MSC Software Corporation
4675 MacArthur Court, Suite 900
Newport Beach, CA 92660
Telephone: (714) 540-8900
Toll Free Number: 1 855 672 7638
Email: americas.contact@mscsoftware.com

Japan

MSC Software Japan Ltd.
Shinjuku First West 8F
23-7 Nishi Shinjuku
1-Chome, Shinjuku-Ku
Tokyo 160-0023, JAPAN
Telephone: (81) (3)-6911-1200
Email: MSCJ.Market@mscsoftware.com

Europe, Middle East, Africa

MSC Software GmbH
Am Moosfeld 13
81829 Munich, Germany
Telephone: (49) 89 431 98 70
Email: europe@mscsoftware.com

Asia-Pacific

MSC Software (S) Pte. Ltd.
100 Beach Road
#16-05 Shaw Tower
Singapore 189702
Telephone: 65-6272-0082
Email: APAC.Contact@mscsoftware.com

Worldwide Web

www.mscsoftware.com

User Documentation: Copyright © 2015 MSC Software Corporation. All Rights Reserved.

This document, and the software described in it, are furnished under license and may be used or copied only in accordance with the terms of such license. Any reproduction or distribution of this document, in whole or in part, without the prior written authorization of MSC Software Corporation is strictly prohibited.

MSC Software Corporation reserves the right to make changes in specifications and other information contained in this document without prior notice. The concepts, methods, and examples presented in this document are for illustrative and educational purposes only and are not intended to be exhaustive or to apply to any particular engineering problem or design. THIS DOCUMENT IS PROVIDED ON AN "AS-IS" BASIS AND ALL EXPRESS AND IMPLIED CONDITIONS, REPRESENTATIONS AND WARRANTIES, INCLUDING ANY IMPLIED WARRANTY OF MERCHANTABILITY OR FITNESS FOR A PARTICULAR PURPOSE, ARE DISCLAIMED, EXCEPT TO THE EXTENT THAT SUCH DISCLAIMERS ARE HELD TO BE LEGALLY INVALID.

MSC Software logo, MSC, MSC., MD Nastran, Adams, Dytran, Marc, Mentat, and Patran are trademarks or registered trademarks of MSC Software Corporation or its subsidiaries in the United States and/or other countries.

NASTRAN is a registered trademark of NASA. Python is a trademark of the Python Software Foundation. LS-DYNA is a trademark of Livermore Software Technology Corporation. Unigraphics, Parasolid and I-DEAS are registered trademarks of Siemens Product Lifecycle Management, Inc. All other trademarks are the property of their respective owners.

This software may contain certain third-party software that is protected by copyright and licensed from MSC Software suppliers. Additional terms and conditions and/or notices may apply for certain third party software. Such additional third party software terms and conditions and/or notices may be set forth in documentation and/or at <http://web.mscsoftware.com/thirdpartysoftware> (or successor website designated by MSC from time to time).

METIS is copyrighted by the regents of the University of Minnesota. HP MPI is developed by Hewlett-Packard Development Company, L.P. MS MPI is developed by Microsoft Corporation. PCGLSS 7.0, Copyright © 1992-2014 Computational Applications and System Integration Inc. All rights reserved.

Use, duplication, or disclosure by the U.S. Government is subject to restrictions as set forth in FAR 12.212 (Commercial Computer Software) and DFARS 227.7202 (Commercial Computer Software and Commercial Computer Software Documentation), as applicable.

Contents

Marc User's Guide

Preface

Organization of this Manual	48
Part 1	48
Part 2	48
Part 3	49
Documentation Conventions	49

Section 1: Introduction

1 Introduction

Introducing Mentat	54
Brief Look at the Finite Element Analysis Process	54
Some Mentat Hints and Shortcuts	55
Mechanics of Mentat	56
Marc/Mentat Window Layout	57
How Mentat Communicates with You	58
How This Manual Communicates with You	58
How You Communicate with Mentat	61
Model Navigator	65
Menu Structure	75
Model Length Unit	95
List Specification	114
Identifiers	120
Menu Customization	121
Comprehensive Sample Session	122
Background Information	166
Mesh Generation	166
Boundary Conditions, Initial Conditions, and Links	177
Material and Geometric Properties	178
Contact	180

Loadcases and Jobs	181
Results Interpretation	182
Getting Started	183
Starting the Mentat Program	184
Procedure Files	185
Stopping the Mentat Program	186
Recommended Starting Chapters	187
Following a Sample Session	188
A Simple Example	198
Background Information	199
Overview of Steps	200
Detailed Session Description	200
Input Files	215
Answers to Frequently Asked Questions	216
Consistent Units	216
Evaluation of Stresses in Finite Elements	217
Shear Strains used in Marc	217
Extrapolation/Averaging Tips in Mentat	218
Stress Coordinate Systems	220
Composite Shells	222
Material Axis Definition	226
Gauss Point Results	228
Selective Results to the Post File	228
Continuum and Generalized Stresses	229
Result Types	233
Appendix A: Shape Function Interpolation	272
Implication: The Evaluation of Element Displacements	275
Implication: Linear Versus Quadratic Elements?	275
Implication: Nodal Temperature Loading With Temperature Dependent Materials	277
Implication: Element Thickness Interpolation	278
Appendix B: Finite Element Equilibrium	280
Implication: Smoothed or Unsmoothed Stress Contours?	281
Implication: Limitations of the Averaging Scheme	283
Appendix C: Coordinate Transformation	285
Appendix D: Principal Stresses (Plane Stress)	285
Appendix E: Python Example (Max Stress Results)	286
Appendix F: Python Example (Displacements at Nodes)	290

Section 2: Recent Features

2.1 New-style Table Input

Summary of Reinforced Cylinder	296
Post Buckling Analysis of a Reinforced Shell with Nonuniform Load	297
List of User Subroutines	310
Input Files	316
Summary of Can Analysis	317
Can Analysis	318
Input Files	337

2.2 Thermo-Mechanical Analysis of Cylinder Head Joint with Quadratic Contact

Summary	340
Simulation of a Cylinder Head Joint	342
Mesh	342
Geometric Properties	342
Material Properties	343
Modeling Tools	352
Contact	358
Initial Conditions	359
Boundary Conditions	360
Load Steps and Job Parameters	361
Save Model and Run Job	364
View Results	364
Input Files	370

2.3 RBE3 (General Rigid Body Link)

Chapter Overview	372
Soft and Rigid Connections	372
Mesh Generation	373
Geometric Properties	376

Material Properties	377
Contact	378
Links	379
Boundary Conditions	380
Loadcases	381
Submit Job and Run the Simulation	381
Results	382
Input Files	384

2.4 Arc Welding Process Simulation

Chapter Overview	386
Welding Process Simulation of Cylinder-Plate Joint	386
Procedure File	387
Mesh Generation	388
Geometric Properties	388
Material Properties	389
Weld Path Setup	390
Weld Filler Setup	392
Contact Body Setup	393
Initial/Boundary Conditions	394
Loadcase Definition	398
Job Parameters	399
Results and Discussion	401
Input Files	404

2.5 FEM Simulation of NC Machining and PRE STATE

Chapter Overview	406
Example 1: Pocket Cutting	407
Input data	407
Initial Geometry and Stresses	408
Local Mesh Adaptivity Definition	416
Visualization of Results	419
Verification of Material Removal	423
Example 2: Thin Frame Cutting	424
Input Data	424
Initial Stress and Local Adaptive Remeshing Definition	425

Loadcases and Machining Job Definition	426
FEA Results	428
Example 3: Imported Initial Stresses	432
Overview	432
Import with Text Data File	432
Import with PRE STATE Feature	437
Input Files	442

2.6 Parallelized Local Adaptive Meshing

Chapter Overview	444
Simulation	444
Input Files	447
Animation	447

2.7 Magnetostatic Elements

Chapter Overview	450
Magnetostatic Field Around a Coil	450
Mesh Generation	450
Material Properties	452
Inserts	452
Boundary Conditions	453
Loadcases and Job Parameters	455
Save Model, Run Job, and View Results	456
Input Files	458

2.8 Coupled Electrostatic Structural Analysis of a Capacitor

Chapter Overview	460
Capacitor Loaded with Charge	460
Mesh Generation	460
Material Properties	461

Contact	463
Boundary Conditions	465
Mesh Adaptivity	467
Loadcases and Job Parameters	468
Save Model, Run Job, and View Results	471
Input Files	474

2.9 3-D Contact and Friction Analysis using Quadratic Elements

Chapter Overview	476
Sliding Mechanism	477
Model Generation	477
Material Properties	480
Contact	482
Boundary Conditions	485
Loadcases	487
Jobs	488
Results	490
Input Files	493

2.10 Pin to Seal Contact with Various Friction Models

Chapter Overview	496
Problem Description	496
Friction Modeling	497
Results	499
Input Files	500

2.11 Analysis of a Manhole with Structural Zooming

Chapter Overview	502
Background Information	502
Global Analysis	502

Local Model and Analysis	503
Conclusion	509
Input Files	509

2.12 Radiation Analysis

Chapter Overview	512
Background Information	512
Description	512
Idealization	512
Full Disclosure	512
Overview of Steps	513
Detailed Session Description	514
Input Files	541

2.13 Application of BC on Geometry with Remeshing

Geometry and Finite Element Mesh	544
Overview of Steps	544
Detailed Session Description	545
Input Files	558

2.14 Glass Forming of a Bottle with Global Remeshing

Chapter Overview	560
Idealization	560
Analysis with Remeshing	561
Overview of Steps	562
Detailed Session Description	562
Conclusion	575
References	577
Input Files	577

2.15 Marc – Adams MNF Interface

Chapter Overview	580
Generation of an MNF for HDD HSA Suspension Arm	580
Problem Description	580
HSA Suspension Arm Model	581
Local Model and Analysis	582
Input Files	587

2.16 Analysis of Stiffened Plate Using Beam and Shell Offsets

Chapter Overview	590
Analysis of Beam Reinforced Shell Structure using Offsets	590
Procedure File	592
Mesh Generation	592
Geometric Properties	592
Material Properties	595
Boundary Conditions	595
Loadcase Definition	596
Job Parameters	596
Results and Discussion	596
Input Files	598

2.17 3-D Tetrahedral Remeshing with Boundary Conditions

Chapter Overview	600
Simulation Examples	600
Pressure on a Rubber Cylinder	600
Metal Compression with Prescribed Displacements	602
Rubber Ring Seal with Pressure Testing after Compression	603
Tube Hydro-forming	605
Rubber Seal Insertion	606
Rubber Seal and Steel Interaction	607
Glass Forming	609
Rubber Bars with Prescribed Displacement on Curves	610

Rubber Seal Insertion	611
Model Generation	611
Input Files	620

2.18 Induction Heating of a Tube

Chapter Overview	622
Heating of a Tube	622
Mesh Generation	622
Material Properties	624
Radiation	627
Initial Conditions and Boundary Conditions	627
Loadcases and Job Parameters	629
Save Model, Run Job, and View Results	631
References	633
Input Files	634

2.19 Magnetostatics with Tables

Chapter Overview	636
Nonlinear Analysis of an Electromagnet Using Tables	636
Reading the Model and Adding Material Properties	636
Boundary Conditions	641
Loadcases and Job Parameters	642
Save Model, Run Job, and View Results	643
Input Files	644

2.20 Delamination and Crack Propagation

Summary	646
Model Review	647
Results	651
Input Files	653

2.21 Progressive Failure Analysis of Lap Joint

Summary	656
Model Review	657
Results	658
Modeling Tips	660
Input Files	661

2.22 Sheet Metal Forming With Solid Shell Elements

Summary	664
Model Review	665
Results	667
Input Files	668

2.23 Plastic Limit Load Analysis of a Simple Frame Structure

Summary	670
Detailed Marc Input Description	671
Detailed Mentat Session Description	673
Results	674
Modeling Tips	675
Input Files	675

2.24 Directional Heat Flux on a Sphere from a Distance Source

Summary	678
Model Review	679
Results	683
Input Files	685

2.25 Deep Drawing of A Sheet With Global Remeshing

Summary	688
Model Review	689
Results	691
Modeling Tips	692
Input Files	692

2.26 Artery Under Pressure

Summary	694
Material Modeling	695
Job Parameters	697
Results	697
Modeling Tips	699
References	699
Input Files	700

2.27 Modeling Riveted Joint with Bushing, CFAST, or CWELD

Summary	702
Model Review	703
Results	711
Modeling Tips	713
Input Files	713

2.28 Performance and Memory Tuning

Summary	716
Domain Decomposition Method (DDM)	717

Assembly Parallelization using SMP	721
ELSTO	721
Parallel Solver Decomposition	722
Fast Integrated Composite Shells	728
Combined Multi Frontal Sparse and Iterative Solver	730
Input Files	731

2.29 Implicit Viscoplastic Creep Analysis of Solder

Summary	734
Introduction	735
Flow Equation	735
Requested Solutions	736
Modeling Details	736
Element Modeling	737
Material Modeling	737
Loading and Boundary Conditions	739
Solution Procedure	741
Result and Plots	744
Conclusion	746
Input Files	746
Video	746

2.30 Crack Propagation Capability in Shells

Summary	748
Introduction	749
Requested Solution	749
Modeling Details	749

Geometric Properties	749
Material Properties	750
Crack Modeling	750
Loading and Boundary Conditions	751
Solution Procedure	753
Results	753
Input Files	754

2.31 Segment-to-Segment with Friction

Summary	756
Introduction	757
Available Contact Options	757
Requested Solutions	757
Modeling Details	757
Element Modeling	758
Material Modeling	758
Friction Modeling	759
Loading Conditions	760
Contact	760
Solution Procedure	761
Results	763
Input Files	763

2.32 Directionally Dependent Friction

Summary	766
Introduction	767
Requested Solutions	767

Modeling Details	767
Element Modeling	768
Material Modeling	769
Loading and Boundary Conditions	772
Contact	775
Solution Procedure	776
Result and Plots	777
Input Files	781
Video	781

2.33 Improved Accuracy with Remeshing of Herrmann Elements

Summary	784
Introduction	785
Simulation of Elastomeric Seal	785
Mesh	785
Material Properties	785
Contact Body Definitions	786
Contact Table	787
Mesh Adaptivity	788
Boundary Conditions	788
Solution Procedure	790
Results	791
Input Files	791
Video	792

2.34 3-D Crack Propagation at Material Interface

Summary	794
Modeling Details	795
Delamination	795
VCCT	797
Cohesive Model	798
Crack Initiation	799
Solution Procedure	800
Results	801
VCCT	802
Cohesive	804
Crack Initiation	805
Input Files	807

2.35 Fatigue Crack Propagation in a Lug with Multiple Cracks

Summary	810
Modeling Details	811
VCCT	812
Crack Initiation	813
Loading and Solution Procedure	814
Remeshing	814
Results	815
Crack Path	816
Cycle Count	817
Input Files	819

2.36 3-D Fatigue Crack Propagation: Corner Cracks at a Hole

Summary	822
Modeling Details	823
VCCT	823
Crack Initiation	824

Loading and Solution Procedure	824
Remeshing	825
Results	825
Shape of the Crack Fronts	825
Cycle Count	827
Input Files	827

2.37 CAD Import and Automatic Meshing

Summary	830
Import of the CAD Model	831
Defeaturing the Model	833
Meshing the Model	836
Conclusions	842
Input Files	842

Section 3: Mechanical Analysis

3.1 Solid Modeling and Automatic Meshing

Chapter Overview	846
Background Information	846
Overview of Steps	847
Detailed Session Description	847
Tetrahedral Meshing on Solids	862
About HexMesh	865
Advantages of HexMesh	865
Advantages of Hexahedral Elements	865
Activating the HexMesh Feature	866
About the HexMesh Menu in Mentat	866
About the Input for HexMesh	867
Key Steps in the Meshing Process	868

Using HexMesh Parameters and Commands	869
Specifying Element Size	869
Specifying Edge Sensitivity	869
How the Value of Edge Sensitivity Affects the Edge Detection Process	870
Specifying Gap	871
How the Value of Gap affects the Mesh	871
Specifying the Number of Shakes	872
Using the Runs Parameter	873
Using the Coarsening Parameter	873
How the Level of Coarsening affects the Elements	873
Using the Allow Wedges Parameter	874
About the Coons Patches Parameter	875
Using the Detect Edges Command	876
Selecting Edges	876
Deselecting Edges	876
Checklist for the HexMesh Command	877
Applying the HexMesh Command	877
About the Meshing Tools	877
Rectifying an Unsuccessful Hexmeshing Operation	878
Using HexMesh – Example	878
About the Example	878
Example Overview	879
Running the Procedure File	879
Preparing the Model for Surface Meshing	879
Applying the Delaunay Tri-Mesh	881
Preparing the Input List for HexMesh	882
Applying HexMesh	883
Input Files	884

3.2 Manhole

Chapter Overview	886
Background Information	886
Description	886
Idealization	887
Requirements for a Successful Analysis	888
Full Disclosure	888
Overview of Steps	900
Detailed Session Description	900

Conclusion	925
Input Files	926

3.3 Contact Modeling of Pin Connection Joints using Higher-Order Elements

Chapter Overview	928
Pin Connection	929
Boundary Conditions	931
Material Properties	933
Contact Bodies and Contact Tables	934
Loadcases	937
Jobs	939
Input Files	943

3.4 Beam Contact Analysis of an Overhead Power Wire of a Train

Chapter Overview	946
Pantograph of a Train Touching the Overhead Power Wire	946
Boundary Conditions	948
Initial Conditions	950
Links	950
Material Properties	952
Geometry Properties	952
Contact	954
Loadcases	955
Job Parameters	957
Save Model, Run Job, and View Results	959
Input Files	962

3.5 Gas Filled Cavities

Chapter Overview	964
Simulation of an Airspring	964
Problem Description	964
Axisymmetric Analysis	965
Input Files	978

3.6 Tube Flaring

Chapter Overview	980
Background Information	980
Idealization	980
Requirements for a Successful Analysis	981
Full Disclosure	981
Overview of Steps	981
Detailed Session Description	982
Conclusion	1003
Input Files	1004

3.7 Punch

Chapter Overview	1006
Background Information	1006
Idealization	1006
Requirements for a Successful Analysis	1007
Full Disclosure	1007
Overview of Steps	1009
Detailed Session Description	1009
Input Files	1027

3.8 Torque Controlled dies with Twist Transfer

Chapter Overview	1030
Belt and Pulley Assembly	1030
Preprocessing	1030
Results	1036
Input Files	1041

3.9 Break Forming

Summary	1044
Detailed Session Description of Break Forming	1046
Run Job and View Results	1052
Discussion	1056
Input Files	1057
Animation	1059

3.10 Hertz Contact Problem

Summary	1062
Run Jobs and View Results	1068
FEA versus Theoretical Solutions	1069
Input Files	1070

3.11 Anisotropic Sheet Drawing using Reduced Integration Shell Elements

Chapter Overview	1072
Simulation of Earing for Sheet Forming with Planar Anisotropy	1073
Boundary Conditions	1074
Material Properties	1075
Geometric Properties	1082

Contact	1082
Load Steps and Job Parameters	1085
Save Model, Run Job, and View Results	1087
Advanced Topic: Drawbead Modeling using Nonlinear Spring	1089
Links	1089
Boundary Conditions	1092
Save Model, Run Job, and View Results	1093
Input Files	1094
References	1095

3.12 Chaboche Model

Chapter Overview	1098
Blade on a Fan of a Turbine Engine	1098
Mesh Generation	1098
Boundary Conditions	1101
Initial Conditions	1104
Material Properties	1104
Geometric Properties	1106
Contact	1106
Loadcases and Job Parameters	1108
Save Model, Run Job, and View Results	1109
Input Files	1112

3.13 Modeling of a Shape Memory Alloy Orthodontic Archwire

Chapter Overview	1114
Simulation of an Archwire with Shape Memory Alloy Models	1114
Boundary Conditions	1115
Initial Conditions	1118
Material Properties	1118
Load Steps and Job Parameters	1124
Save Model, Run Job, and View Results	1127
Save Model, Run Job, and View Results	1131
Input Files	1132
References	1132

3.14 Implicit Creep Analysis of Solder Connection between Microprocessor and PCB

Chapter Overview	1134
Microprocessor Soldered to a PCB	1134
Mesh Generation	1134
Boundary Conditions	1138
Initial Conditions	1141
Material Properties	1141
Contact	1145
Loadcases and Job Parameters	1147
Save Model, Run Job, and View Results	1150
Input Files	1152
References	1152

3.15 Continuum Composite Elements

Chapter Overview	1154
Background Information	1154
Analysis	1155
Model Generation	1155
Boundary Conditions and Loads	1156
Material Properties	1157
Composite Layer Property Definition	1159
Composite Layer Orientation Definition	1160
Define Job Parameters, Save Model, and Run Job	1162
View Results	1163
Comparison	1164
Input Files	1164

3.16 Super Plastic Forming (SPF)

Summary	1166
SPF Modeling	1168
Preprocessing	1168
Analysis	1181
Results	1182

Discussion	1185
SPF with Adaptive Remeshing	1185
Results	1187
Discussion of Adaptive Meshing	1189
Input Files	1190

3.17 Gaskets

Chapter Overview	1192
Simulation of a Cylinder Head Joint	1193
Mesh Generation	1193
Tyings and Servo Links	1194
Boundary Conditions	1199
Initial Conditions	1202
Material Properties	1202
Geometric Properties	1209
Contact	1209
Load Steps and Job Parameters	1211
Save Model, Run Job, and View Results	1215
Input Files	1220

3.18 Cantilever Beam

Summary	1222
Detailed Session Description of Cantilever Beam	1224
Add Plasticity to Cantilever Beam	1229
Run Job and View Results	1232
Input Files	1234

3.19 Creep of a Tube

Summary	1236
Detailed Session Description of Oval Tube	1238

Run Job and View Results	1242
What can improve the results?	1244
Results	1247
Input Files	1252

3.20 Tensile Specimen

Summary	1254
Detailed Description Session	1255
Tensile Specimen Analysis	1255
Overlay Technique	1258
Advancing Front Technique	1259
Mapped Meshing Technique	1259
Run Job and View Results	1262
Tensile Specimen Uniform Gage Section	1268
Tensile Specimen Composite Material	1271
Modeling Tips	1273
Input Files	1277

3.21 Rubber Elements and Material Models

Summary	1280
Lower-order Triangular Rubber Elements	1281
Using Quadrilateral Elements	1281
Results	1291
Using Triangular Elements	1292
Run Job and View Results	1293
Tube with Friction	1296
Cavity Pressure	1298
Buckling of an Elastomeric Arch	1302
Overview	1302
Run Job and View Results	1307
Comparison of Curve Fitting of Different Rubber Models	1310
Mooney	1313
Arruda-Boyce	1315
Input Files	1317

3.22 Modeling of General Rigid Body Links using RBE2/ RBE3

Chapter Overview	1320
Cylindrical Shell	1320
Mesh Generation	1320
Boundary Conditions	1322
Transformation	1324
Links	1324
Material Properties	1324
Geometric Properties	1325
Loadcases and Job Parameters	1326
Save Job, and Run the Simulation	1327
Results	1328
Input Files	1329

3.23 Cyclic Symmetry

Chapter Overview	1332
Pure Torsion	1333
Mechanical Analysis of Friction Clutch	1336
Coupled Analysis of Friction Clutch	1339
Input Files	1344

3.24 Axisymmetric to 3-D Analysis

Chapter Overview	1346
Simulation of a Rubber Bushing	1346
Description of Problem	1346
Axisymmetric Analysis	1347
3-D Analysis	1354
Automobile Tire Modeling with Rebar Elements	1359
Description of Problem	1359
Axisymmetric Analysis	1360
3-D Analysis	1361

Analysis of a Rubber Cylinder using Remeshing	1366
Description of Problem	1366
Axisymmetric Analysis	1366
3-D Analysis	1368
Input Files	1374

3.25 Interference Fit

Summary	1376
Run Job and View Results	1381
Input Files	1383

3.26 3-D Remeshing with Tetrahedral Elements

Chapter Overview	1386
Why Remeshing with Tetrahedral Elements?	1386
Tetrahedral Element Type 157	1386
Tetrahedral Remeshing Criteria	1388
Tetrahedral Remeshing Controls and Meshing Parameters	1389
Tetrahedral Remeshing Tests	1391
Elastomeric Seal Simulation	1398
Model Generation	1400
Material Properties	1401
Contact Definitions	1402
Mesh Adaptivity	1405
Loadcases	1406
Jobs and Run Analysis	1407
Results	1409
Input Files	1410

3.27 Rubber Remeshing and Radial Expansion of Rigid Surfaces

Chapter Overview	1412
Model Highlights	1412
Results Highlights	1416
Modeling Tips	1417
Input Files	1417

3.28 Automatic Remeshing/ Rezoning

Chapter Overview	1420
Elastomeric Seal Simulation	1421
Analysis	1422
Tape Peeling Simulation	1431
Analysis	1432
Input Files	1445

3.29 Multibody Contact and Remeshing

Chapter Overview	1448
Squeezing of a Rubber Body	1448
Background information	1448
Input Files	1468

3.30 Container

Chapter Overview	1470
Background Information	1470
Description	1470
Idealization	1471
Requirements for a Successful Analysis	1472
Full Disclosure	1472
Overview of Steps	1473

Detailed Session Description	1473
Conclusion	1501
Input Files	1501

3.31 Analyses of a Tire

Steady State Rolling Analysis	1504
Simulation of a Tire	1504
Run Job and View Results	1517
More Results on Contact Friction Stresses	1520
Tire Bead Analysis	1523
Overview	1523
Background Information	1523
Analysis	1524
Overview of Steps	1525
Detailed Session Description	1525
Conclusion	1548
Input Files	1548

3.32 Transmission Tower

Chapter Overview	1550
Background Information	1550
Tower Description	1550
Idealization	1551
Requirements for a Successful Analysis	1551
Full Disclosure	1551
Overview of Steps	1552
Detailed Session Description	1552
Conclusion	1600
Input Files	1600

3.33 Bracket

Chapter Overview	1602
Background Information	1602
Description	1602
Idealization	1602
Requirements for a Successful Analysis	1602
Full Disclosure	1603
Overview of Steps	1604
Detailed Session Description of the Linear Static Case	1604
Conclusion	1624
Dynamic Modal Shape Analysis	1625
Overview of Steps	1625
Detailed Session Description of the Modal Shape Analysis	1625
Dynamic Transient Analysis	1629
Overview of Steps	1629
Detailed Session Description of Dynamic Transient Analysis	1629
Conclusion	1636
Pressure Table	1636
Input Files	1637

3.34 Single Step Houbolt Dynamic Operator

Chapter Overview	1640
Impact of a Ball on a Plate	1640
Background Information	1640
Eigenvalue Analysis	1640
Transient Analysis	1651
Input Files	1660

3.35 Dynamic Analyses of a Cantilever Beam

Summary	1662
Modal Analysis1663	
Overview	1663
Modal Analysis1664	
Harmonic Analysis1666	
Overview	1666
Harmonic Analysis and Results	1666
Transient Analysis1669	
Overview	1669
Analysis and Results	1669
Damping Analysis	1671
Over Hanging Beam Analysis	1673
Input Files	1677

3.36 Plastic Spur Gear Pair Failure

Summary	1680
Gear Geometry	1681
Material Modeling	1682
Contact	1682
Failure Criteria	1683
Model Review	1685
Experimental Test Machine	1687
Results & Conclusions	1688
Modeling Tips	1689
Input Files	1690
References	1690
Animation	1690

3.37 Girkmann Verification Problem

Summary	1694
Detailed Description	1695
Results	1697
Modeling Tips	1699
Input Files	1704

3.38 Interference Fit Demonstration with All Five Available Methods

Summary	1706
Requested Solutions	1707
Modeling Details	1707
Element Modeling	1709
Material Modeling	1709
Interference Fit modeling	1709
Loading and Boundary Conditions	1716
Contact	1717
Solution Procedure	1718
Result and Plots	1718
Input Files	1731

3.39 Segment-to-Segment Contact of Stiffened Panel and Beams

Summary	1734
Requested Solutions	1735
Modeling Details	1735
Element Modeling	1737
Material Modeling	1738
Loading Conditions	1738

Contact	1739
Setup of Contact Body and Table	1739
Setup of Geometric Properties for Contact	1742
Setup of Job Options for Contact	1743
Result and Plots	1744
Input Files	1747

3.40 Frequency Response Analysis of a Flexible Bushing

Summary	1750
Bushing and Model Geometry	1752
Material Modeling	1753
Loads, Boundary Conditions, and Constraints	1755
Loadcase and Job Definition	1757
Results and Conclusions	1758
Modeling Tips	1761
Input Files	1761

Section 4: Heat Transfer Analysis

4.1 Thermal Contact Analysis of a Pipe

Chapter Overview	1766
Pipe in a House	1766
Mesh Generation	1766
Boundary Conditions	1767
Initial Conditions	1768
Material Properties	1769
Contact	1770
Loadcases and Job Parameters	1771
Save Model, Run Job, and View Results	1773
Input Files	1778

4.2 Dynamics with Friction Heating

Summary	1780
Friction Heat Analysis	1782
Run Jobs and View Results.....	1789
Input Files	1793

4.3 Radiation with Viewfactors

Summary	1796
Detailed Session Description	1798
Run Job and View Results.....	1802
Input Files	1804

4.4 Cooling Fin Analyses

Summary	1806
Steady State	1807
Background Information	1807
Overview of Steps.....	1808
Detailed Session Description	1808
Transient	1817
Detailed Session Description with Fin.	1817
Detailed Session Description without Fin	1820
Input Files	1823

Section 5: Coupled Analysis

5.1 Coupled Structural – Acoustic Analysis

Chapter Overview	1828
Two Spherical Rooms Separated by a Membrane.	1828
Background Information	1828

Harmonic Analysis with Stress-free Membrane	1829
Harmonic Analysis with Pre-stressed Membrane	1838
Input Files	1841

5.2 Coupled Electrical-Thermal-Mechanical Analysis of a Micro Actuator

Chapter Overview	1844
Simulation of a Microelectrothermal Actuator	1844
Problem Description	1844
Actuator Model 1845	
Run Job and View Results	1851
Input Files	1853

5.3 Coupled Transient Cooling Fin

Summary	1856
Detailed Session Description	1857
Run Jobs and View Results	1858
Input Files	1860

5.4 Temperature Dependent Orthotropic Thermal Strains

Chapter Overview	1862
Detailed Session Description	1863
Run Jobs and View Results	1866
Thermal Expansion Data Reduction	1868
References	1871

5.5 Tube Welding using Induction Heating

Summary	1874
Introduction.....	1875
Preparations for Creating the Coil	1877
Material Properties	1879
Contact	1879
Creation of the Coil and Circuit.....	1882
Boundary Conditions	1884
Loadcase and Jobs.....	1885
Creating the Surrounding Air Mesh	1886
Results and Discussion	1889
Input Files	1894

Section 6: Miscellaneous Analysis

6.1 Magnetostatics: Analysis of a Transformer

Chapter Overview	1898
3-D Analysis of a Transformer.....	1898
Mesh Generation	1899
Boundary Conditions	1903
Material Properties	1906
Loadcases and Job Parameters.....	1906
Save Model, Run Job, and View Results	1907
Input Files	1910

6.2 Fracture Mechanics Analysis with the J-integral

Chapter Overview	1912
Specimen with an Elliptic Crack	1912

Background Information	1912
Modeling Strategies	1913
Mesh Generation	1914
Crack Definitions	1922
Material Properties	1924
Contact Definitions	1925
Run Job and View Results	1931
Input Files	1933

6.3 FEM Simulation of NC Machining Process

Chapter Overview	1936
Input Data	1936
Model Generation	1937
Mesh Generation	1937
Residual Stresses	1938
Procedure Files	1939
Machining Process Simulation	1940
Loadcase1 (<i>cut the top part of the workpiece</i>)	1941
Loadcase2 (<i>release the bottom boundary condition and apply to the top face</i>) 1942	
Loadcase3 (<i>cut the pocket from the lower face part</i>)	1943
Loadcase4 (<i>final release – springback</i>)	1944
Job Definition	1945
Visualization of Results	1946
Input Files	1951

6.4 Piezoelectric Analysis of an Ultrasonic Motor

Chapter Overview	1954
Eigenvalue Analysis of the Stator of an Ultrasonic Motor	1954
Mesh Generation	1956
Boundary Conditions	1957
Loadcases and Job Parameters	1965
Save Model, Run Job, and View results	1966

Harmonic Analysis of the Stator of an Ultrasonic Motor	1967
Boundary Conditions	1967
Loadcases and Job Parameters	1968
Save Model, Run Job, and View Results	1969
Transient Analysis of the Stator of an Ultrasonic Motor	1973
Loadcases and Job Parameters	1974
Save Model, Run Job, and View Results	1975
Input Files	1977
Reference	1977

6.5 Analysis Performance Improvements

Chapter Overview	1980
Speed and Memory Improvements	1980
Case 1: Rigid-Deformable Body Contact	1980
Case 2: Deformable-Deformable Contact	1981
Case 3: Model with Solid and Shell Elements	1982
Conclusion	1985
Input Files	1985

6.6 Robustness of Automatic Load Stepping Schemes

Chapter Overview	1988
Usage of the Auto Step Feature	1988
Input Files	1998

6.7 Marc Running in Network Parallel Mode

Run CONTACT WITH DDM	2000
Run CONTACT WITH DDM on a Network	2000
UNIX	2000
Windows	2001
Input Files	2006

6.8 Convergence Automation and Energy Calculations

Chapter Overview	2008
Convergence Automation	2008
AUTO SWITCH Option	2009
Energy Calculation	2015
Usage of the Energy Values	2016
Input Files	2025

6.9 Capacitors

Chapter Overview	2028
Capacitance Computation in Symmetric Multiconductor Systems ..	2029
Mesh Generation	2030
Element and Node Set Selection	2030
Material Properties	2034
Contact	2035
Boundary Conditions	2037
Loadcase and Job Parameters	2037
Save Model, Run Job and View Results	2041
Results and Discussion	2045
Input Files	2046
Reference	2046

6.10 Inductance Between Two Long Conductors

Summary	2048
Inductance Computation in Two Infinitely Long Rectangular Conductors	2050
Mesh Generation	2051
Element Selection as Sets	2052
Material Properties	2054
Contact	2055
Modeling Tools	2056
Boundary Conditions	2058
Loadcase and Job Parameters	2060
Save Model, Run Job, and View results	2064

Results and Discussion	2068
Input Files	2068
Reference	2069

6.11 Lamination Loss in Magnetostatic-Thermal coupling

Summary	2072
Lamination Loss Computation and ohmic Winding Loss in a ‘C’ Core Cylindrical Inductor	2073
Mesh Generation	2077
Material Properties	2080
Contact	2083
Modeling Tools	2084
Initial and Boundary Conditions	2085
Table	2087
Loadcase and Job Parameters	2088
Save Model, Run Job, and View Results	2091
Results and Discussion	2095
Input Files	2096

6.12 Magnetic Levitation of a Ferromagnetic Sphere

Summary	2098
Magnetic Levitation of a Ferromagnetic Sphere	2099
Mesh Generation	2099
Material Properties	2100
Boundary Conditions	2101
Modeling Tools and Contact	2102
Links	2104
Loadcases and Job Parameters	2104
Save Model, Run Job, and View Results	2107
Results and Discussion	2108
Input Files	2109
References	2109

6.13 Compression of Workpiece by Punch

Summary	2112
Requested Solutions	2113
Modeling Details	2113
Element Modeling	2114
Material Modeling	2114
Contact	2114
Adaptive Remeshing	2115
Result and Plots	2116
Input Files	2121

Section 7: Mentat Features and Enhancements

7.1 Past Enhancements in Marc and Mentat

Chapter Overview	2126
Preprocessing Enhancements	2126
New Attach Concept	2126
Boundary Conditions on Geometric Entities	2132
Combined Mesh Generation Commands	2133
Change Class	2135
Improved Links Handling	2136
Patran Tetrahedral Mesher	2138
New Select Methods	2140
New Domain Decomposition Methods	2143
Multi-Dimensional Tables	2144
User-defined Text Input	2152
64-bit Version of Mentat	2153
Python	2153
Postprocessing Enhancements	2154
MPEG and AVI Animations	2154
Creating a Movie	2156
Postprocessing in 3-D	2156
Input Files	2158
Animation	2159

7.2 Importing a Model

Chapter Overview	2162
Background Information	2162
Description	2162
Overview of Steps	2162
Detailed Session Description	2162
Input Files	2176

7.3 HyperMesh® Results Interface

Chapter Overview	2178
About Postprocessing of Results	2178
Interfacing Analysis and Postprocessing	2178
Data Written into the HyperMesh Results File	2178
About Preprocessing	2179
Mentat Preprocessing for HyperMesh	2179
Important Data Preparation Considerations Regarding Eigenmodes	2186
Relation to other Types of Results Files	2186
Postprocessing using HyperMesh	2188

7.4 Translators

Chapter Overview	2200
Mentat Writers	2200
dxfout:	2200
stlout:	2200
vdaout:	2200
vrmlout:	2200
Mentat Readers	2201
c-mold:	2201
stl:	2203
acis:	2203
dxs:	2203
ideas:	2204

nastran:	2204
patran:	2205

7.5 Sweep Nodes on Outlines

Chapter Overview	2208
Background Information	2208
Overview Steps	2208
Detailed Session Description	2208
Input Files	2212

7.6 Transition Parameter for Meshing

Chapter Overview	2214
Background Information	2214
Overview Steps	2214
Detailed Session Description	2214
Input Files	2218

7.7 Mentat Features 2001 and 2003

Chapter Overview	2220
2001 Features	2220
Optimized Element Graphics Generation	2220
Optimized Entity Recoloring	2220
Post Reader Optimization	2220
Flowline Plotting	2221
Particle Tracking	2222
PostScript Thin Lines Option	2223
Curve Direction	2224
New Viewing Capability	2225
2003 Features	2227
User Defined Variable Names	2227
Status File Information	2228
DCOM Server Support for Windows NT	2228

User-defined NUMERIC Format	2229
Previous and Last Increment Buttons	2230
Input Files	2230

7.8 Generalized XY Plotter

Chapter Overview	2232
Background Information	2232
Overview Steps.	2232
Detailed Session Description	2232
Input Files	2237

7.9 Beam Diagrams Example

Chapter Overview	2240
Background Information	2240
Overview of Steps.	2240
Detailed Session Description	2241
Input Files	2248

Preface

- Organization of this Manual 48
- Documentation Conventions 49

Organization of this Manual

This manual introduces the first-time user to the Mentat program. The User's Guide covers the basics of the program and helps the novice user in becoming comfortable with Mentat through a number of examples.

The manual is divided into several parts

- a basic introduction
- sample problems
- an archive of past new features highlighted during each release of the product.

Part 1

Section 1 – Introduction

The first section introduces the basics of the program and provides information that helps user interaction with Mentat. It also consists of a *sample session* that provides the user with hands-on experience with the functionality of the Mentat program:

Introduction	provides information on the basic steps of the finite element analysis cycle and on how Mentat is used as a tool to accomplish these steps.
Mechanics of Mentat	describes the user interface aspects of the program
Background Information	expands on the common features of Mentat and describes some of the underlying philosophies of the program.
Getting Started	introduces you to Mentat with a simple example of how to create a finite element model.
A Simple Example	introduces you to use Mentat and Marc to perform a complete linear elastic analysis of a rectangular strip with a hole subjected to tensile loading. Both the preprocessing, analysis, and postprocessing steps will be demonstrated.

Section 2 – Recent Features

This consists of examples of recent features for Marc and Mentat.

Part 2

Section 3 – Sample Session

This section demonstrates how to set up the basic requirements for a linear elastic stress analysis.

Part 3

Section 4 – Example Features 2000 - 2003

Section 4 consists of prior releases of the new feature examples for Mentat versions 2000 through 2010.

Documentation Conventions

Listed below are some font and syntax conventions that are used to make the information in this manual easier to understand:

- Cross-references (links) are highlighted in [Blue](#).
- Names of buttons that appear on the Mentat screen are UPPER CASE in the Arial font.
- Literal user input and program prompts are in `courier` font.
- Names of processors are indicated in **BOLD UPPER CASE**.
- A carriage return keystroke is indicated by <CR>.
- The left mouse button is indicated by <ML>.
- The middle mouse button is indicated by <MM>.
- The right mouse button is indicated by <MR>.
- The mouse cursor is indicated by <↑>.
- A filename implies a concatenation of pathname and filename. The pathname may be omitted if the filename is in your current directory.

Section 1: Introduction

1 Introduction

- Introducing Mentat 54
- Some Mentat Hints and Shortcuts 55
- Mechanics of Mentat 56
- Comprehensive Sample Session 122
- Background Information 166
- Getting Started 183
- A Simple Example 198
- Input Files 215
- Answers to Frequently Asked Questions 216
- Appendix A: Shape Function Interpolation 272
- Appendix B: Finite Element Equilibrium 280
- Appendix C: Coordinate Transformation 285
- Appendix D: Principal Stresses (Plane Stress) 285
- Appendix E: Python Example (Max Stress Results) 286
- Appendix F: Python Example (Displacements at Nodes) 290

Introducing Mentat

Welcome to Mentat – a graphical user interface program that allows you to execute a finite element analysis process from start to finish.

Brief Look at the Finite Element Analysis Process

In order to enhance your understanding of Mentat, we will review the finite element analysis cycle before introducing the mechanics of the program. The finite element analysis cycle involves five distinct steps as is shown in [Figure 1.1-1](#). This process may be traversed more than once for a particular design; that is, if the results do not meet the design criteria, you can return to either the conceptualization (Step 1) or modeling (Step 2) phase to redefine or modify the process.

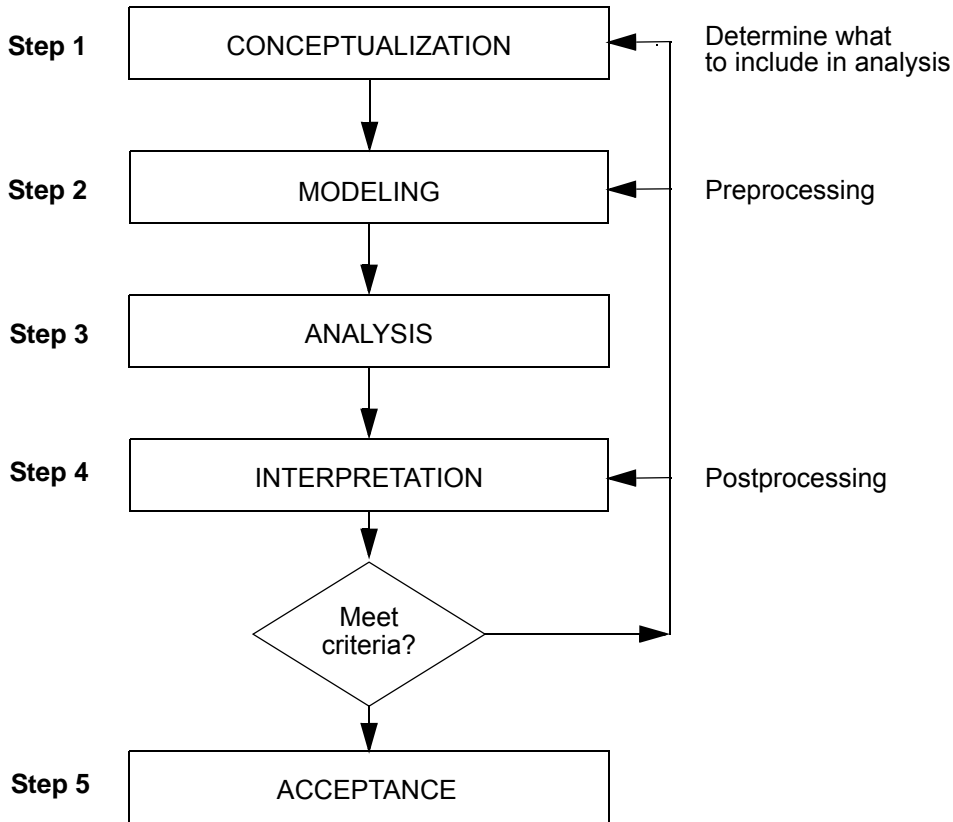


Figure 1.1-1 The Analysis Cycle

The five distinct steps of the finite element analysis cycle provide the foundation for this guide. In order to improve your productivity, this guide has been designed to focus your attention on two steps of the finite element analysis cycle: Step 2: the model generation phase, and Step 4: results interpretation phase.






Typical engineering problems are used in this guide as a vehicle to demonstrate the key features of Mentat. Steps 2 and 4 of the analysis cycle, modeling and results interpretation, were the pacing parameters for the selection of the example problems. The engineering problems were further selected to meet two criteria:

1. to introduce you to the intricacies of generating a model in a variety of ways,
2. to demonstrate a diversity of analysis types so that you become familiar with as many of the different capabilities of Mentat as possible. The analysis will be performed with the general purpose finite element program Marc. Within the graphical user interface, the complete input requirements can be specified.

The dimensionality of each object prescribes the technique used to generate a model and display the results. Accordingly, the finite element models have been grouped by dimensionality and, in many cases, the complexity of the model corresponds to dimensionality. From this you could conclude that once you know how to solve three-dimensional problems, you also know how to solve one-dimensional problems. However, the unique features of one-dimensional objects require that we cover examples of that particular topology. For example, it is difficult to contour a quantity on line elements. With this in mind, the geometry and analysis types, such as heat transfer, statics, or dynamics, have been selected to minimize duplicity in this guide.

The material covered in this tutorial is very basic and should be easy to access and understanding for the first time user. Once you have worked through the sample sessions in [Comprehensive Sample Session](#), you should feel comfortable enough to do a complete analysis simply by extrapolating from what you have learned from the example problems.

Some Mentat Hints and Shortcuts

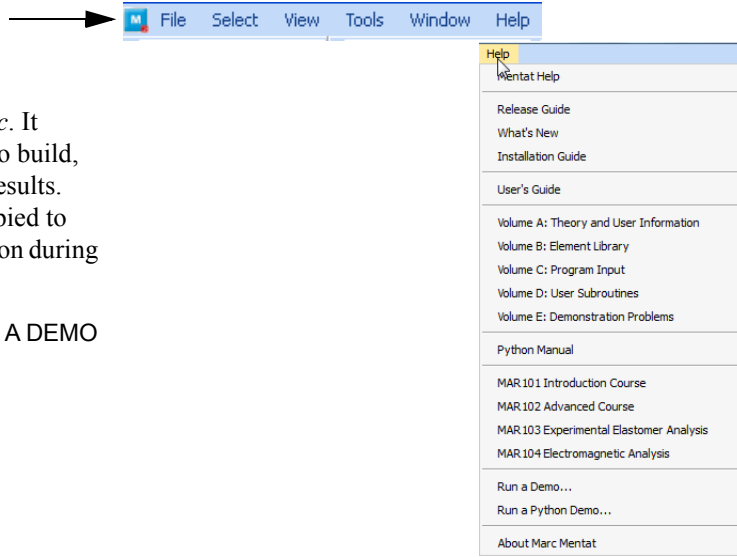
1. Enter Mentat to begin, Quit to stop
2. Mouse in Graphics: Left to pick, Right to accept pick
3. Mouse in Menu: Left to pick another menu or function, Middle (or F1) for help, Right to return to previous menu. <CR> means keyboard return.
4. Save your work frequently. Go to FILES and select SAVE AS and specify a file name. This will save the current Mentat database to disk. Use SAVE  from then on.
5. Dialog region at the lower left of screen displays current activity and prompts for input. Check this region frequently to see if input is required.
6. Dynamic Viewing   can be used to position the model in the graphics area. When activated, the mouse buttons, Left translates the model, Right zooms in/out, Middle rotates in 3-D. Use RESET VIEW  and FILL  to return to original view. Be sure to turn off DYNAMIC VIEW before picking in the graphics area.
7. CTRL P/N recall previous/next commands entered.
8. All of the workshop problems have Mentat procedure and data files. They are located in a `marc.ug` directory under Mentat's main directory. The directory/file structure looks like:

`~mentat/examples/marc.ug/s3/c3.9/` for Section 3, Chapter 3.9.

Furthermore, you can click on the filename listed in the input files table to download the files via the web.

Where, say in directory `/marc_ug/s3/c3.9`, there is a procedure file called `s4.proc`. It automatically runs Mentat to build, run Marc, and process the results. These directories can be copied to your local disk area to work on during the workshop.

Check out the HELP & RUN A DEMO menus.



Mechanics of Mentat

Before you get started with Mentat, you need to know how to communicate with the program. The goal of this section is to give you an overview of how Mentat works and to provide you with the basic information to interact comfortably with the program. Upon completion of this, you should have a clearer understanding of the following areas:

- The basic window layout
- How Mentat communicates with you
- How you communicate with Mentat
- The menu system

Marc/Mentat Window Layout

The starting point for all communication with Mentat is the window shown below that appears at the start of the program.

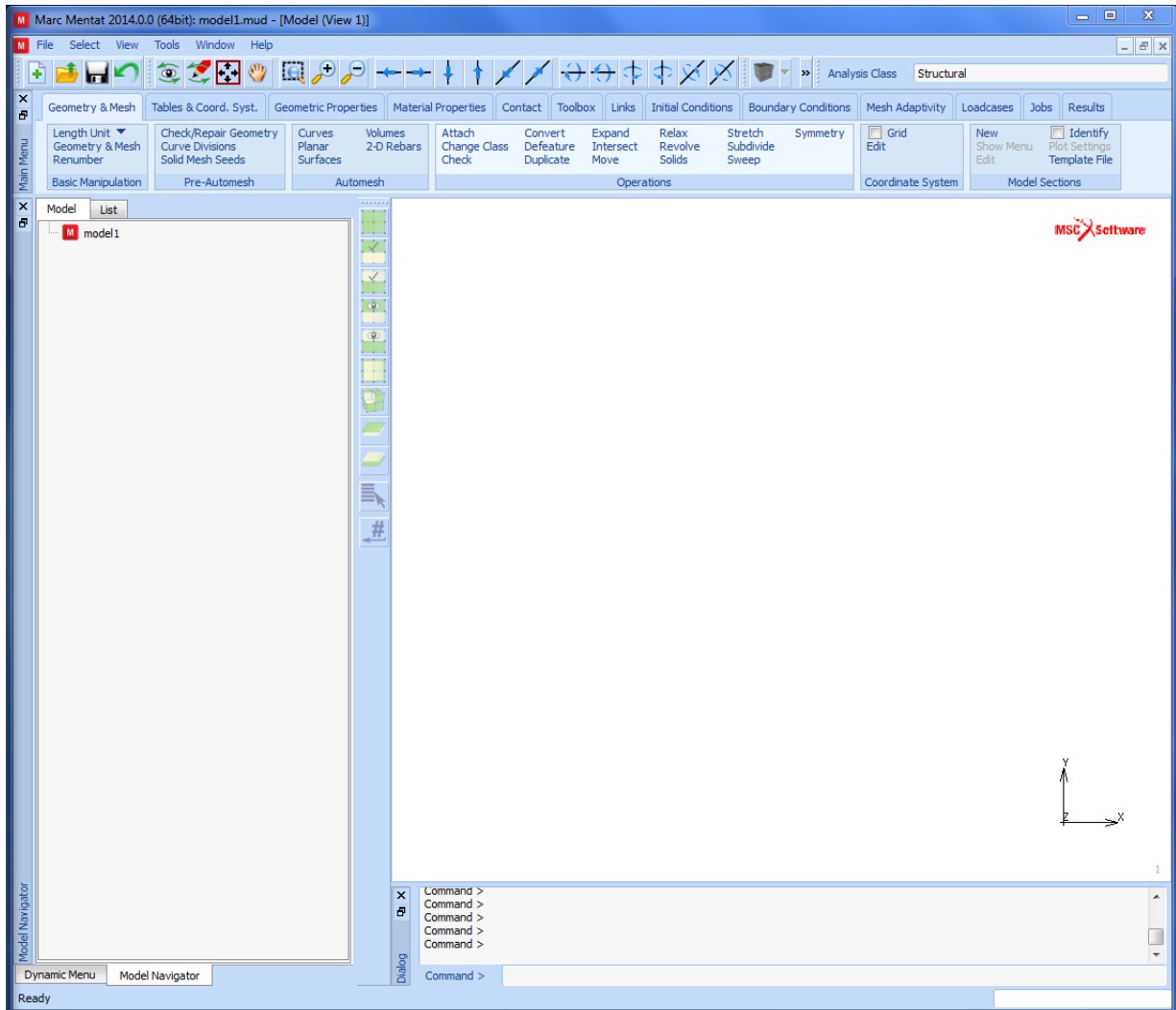


Figure 1.1-2 Basic Mentat Window

The Mentat Window is divided into three major areas:

Graphics area is used to display the current state of the database. When you start Mentat, the graphics area is blank to indicate that the database is empty.

Menu area	is reserved to show the selectable menu-items and is divided into two submenus, Static always present and contains items that are applicable and selectable at all times Dynamic contents of the dynamic menu area change as the menu items are selected.
Dialogue area	is a scrollable area of about five visible lines where all program prompts, warnings, and responses appear, and where the user can input data or commands. Status Area within the dialogue area and reserved to communicate the state of the program to the user. Either <i>working</i> or <i>ready</i> appears in the status area to reflect the current state of the program. For intensive operations, an additional progress widget will appear.

How Mentat Communicates with You

Mentat communicates with you via prompts and messages and other visual queues. Mentat's prompts urge you to take action through the input of data or commands. These prompts have three types of trailing punctuation marks to indicate the required type of input:

- : enter numeric data, e.g., .283/384;
- > enter a character string, typically a command, file name or set name;
- ? enter a YES or NO answer.

If you misspell a keyword or enter an incorrect response, Mentat warns you through a message posted in the dialogue area. Mentat does not require that you complete every action you initiate. For example, if you are prompted for a filename, and you change your mind, entering a <CR> instead of typing in the filename tells Mentat to abort the action. If the program is waiting for a list of items to operate on, and instead you enter a command that also requires a list of items or any additional data, Mentat ignores your original request and process the command. If the command you enter does *not* request additional data, you are returned to the original data request from before the interrupt.

The program assumes at all times that you want to repeat the previous operation on a new set of items and prompts you for a new list to operate on. This process repeats itself until you indicate otherwise by entering a new command or a <CR>.

How This Manual Communicates with You

Mentat menus suggest the next step or steps to complete for the simulation; commonly the menus are abstracted into a button name sequence leaving room for more meaningful figures. For example, to save the current model in Mentat, the button sequence:

MAIN MENU	(panel title)
FILES	(pulldown)
SAVE AS spf	(button that launches a file browser)
<CR> or Cancel	(submenu button)

is used to represent the actual menus as shown in [Figure 1.1-2](#) where clicking on FILES in the static menu (1) brings up the FILE I/O menu. Clicking on the button SAVE AS (2), brings up the SAVE AS FILE file browser, and it is implied that you enter the file name, spf, (3) and accept the entry by clicking the OK button (4). Placing the mouse in the menu area and clicking the right mouse button will RETURN (5) you to your previous menu (**MAIN MENU**). This button sequence has colored the buttons as they appear in the menus and a few introductory chapters use the colored button names whereas others use black fonts assuming you have understood how the button sequence represents the menus. In summary, green buttons take you to another menu, where as blue (cyan) buttons perform an action.

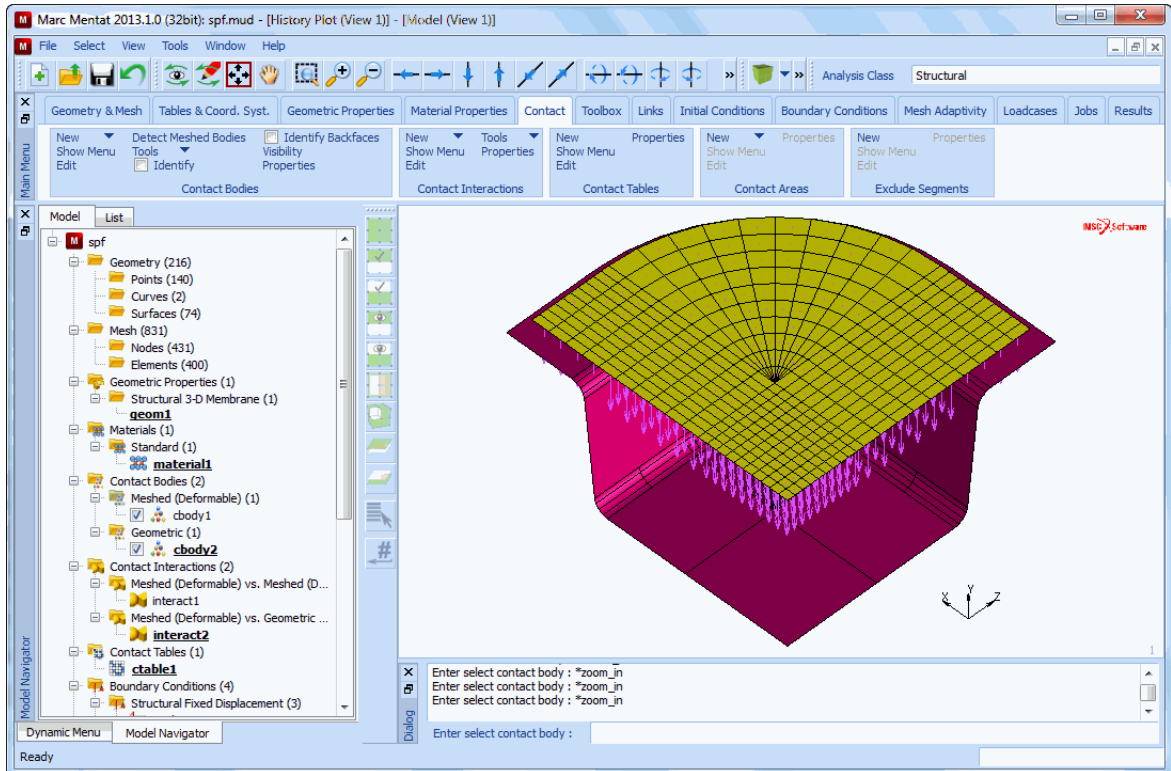


Figure 1.1-3 Screen View when using Model Navigator Mode

Note: The menus in the current version of Mentat do not exactly agree with what is given in this manual. The manual is only updated when the menus are substantially different.

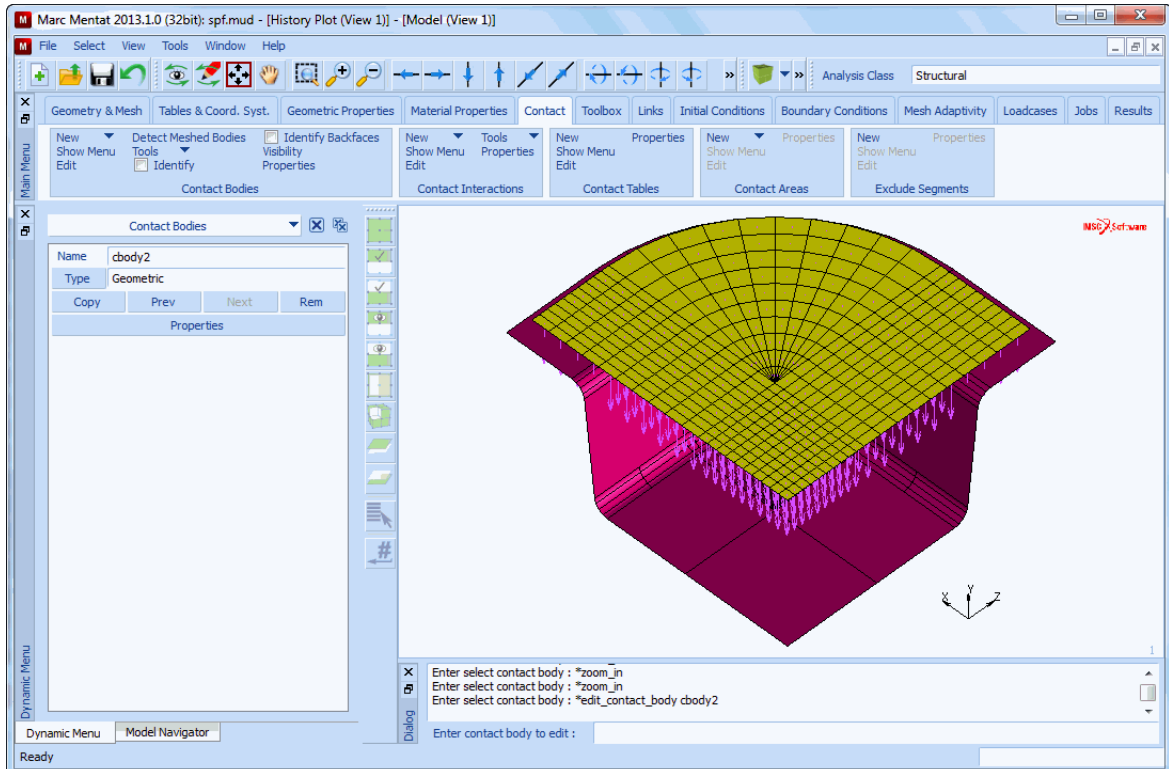


Figure 1.1-4 Screen View when using Dynamic Menu Mode

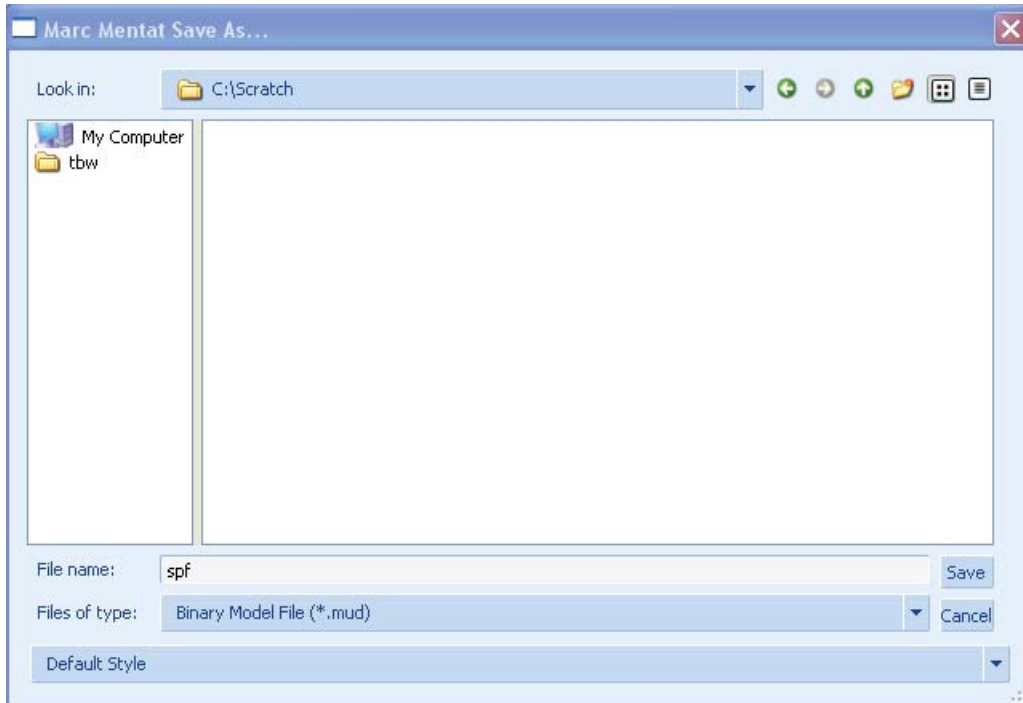


Figure 1.1-5 Mentat Menu

How You Communicate with Mentat

All interaction with Mentat is done through the mouse, keyboard, or a combination of both. This section first discusses the usage of the mouse, followed by a discussion on how to use the keyboard as a means to enter commands and data.

The Mouse

The mouse is used to select items from the menu area or to point at items in the graphics area. It is important to make a distinction between using the mouse in the menu area versus the graphics area because the three mouse buttons have very different functions in each area. [Figure 1.1-6](#) shows a graphical representation of the mouse, mouse buttons, and corresponding cursor.

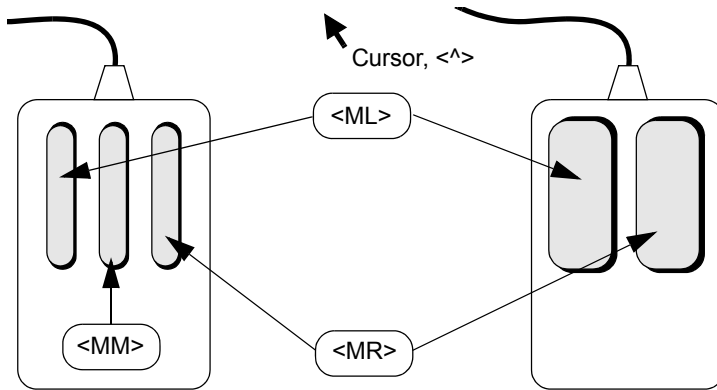


Figure 1.1-6 The Mouse, Mouse Buttons, and Corresponding Cursor

The left button is represented by <ML>, the middle button by <MM>, and the right button by <MR>. For a two button mouse <MM> = <ML> + <MR> depressed at the same time. *Click* refers to a quick single depress-release action.

Using the Mouse to Select a Menu Item

To select a menu item with the mouse, move the <↑> over the item that you want to select and click the <ML>. To return to the previous menu, move the <↑> over the menu area, and click the <MR>. Alternatively, you can click on the RETURN button in the menu area using <ML>. Clicking on the MAIN button takes you to the main menu.

On-line Help

Using the Classic version of Mentat, each menu item has a help panel with a short description and explanation of the function of that menu item. To activate the help feature, position the <↑> over the menu item on which you require help, followed by a click of the <MM>. The help panel disappears the moment you select another menu item. You may also use the F1 function key to activate the HELP feature.

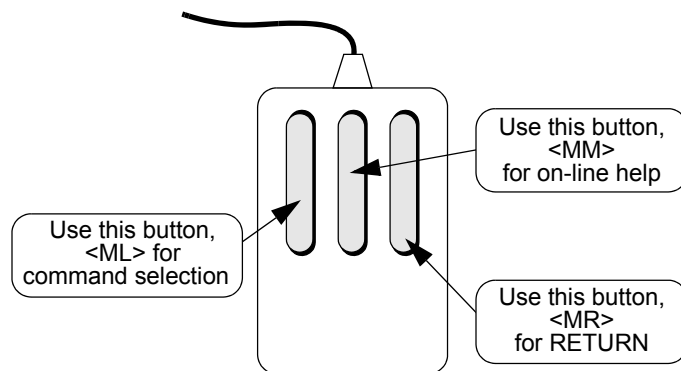


Figure 1.1-7 Using the Mouse in the Menu Area

Using the Mouse to Point

The mouse is used in two ways to operate in the graphics area: to point to or pick existing items, or to point to or pick the location of yet to be created items.

1. To pick, the mouse is used by moving the <↑> over the item to be identified followed by a click of the <ML>. Henceforth called by *clicking on an item*. You can undo that action by clicking the <MM> anywhere in the graphics area. At times, you will need to identify more than a single item. A list of items must be terminated by a click of the <MR> with the <↑> positioned anywhere in the graphics area. Alternatively, you can click on the END LIST button in the menu area using <ML>.
2. To locate a position in Mentat, it is possible to define a grid that is positioned in space and where the grid consists of points that can be pointed to. If you click in the vicinity of a grid point, the coordinates of the item that you created are snapped to that grid point. In addition, you can also pick an existing node, point, or surface-grid-point to specify a location.

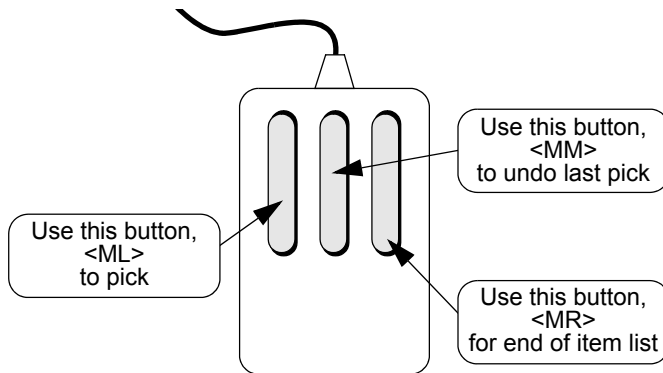
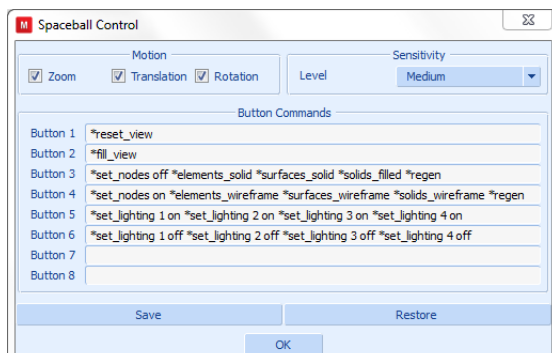


Figure 1.1-8 Using the Mouse in the Graphics Area

Spaceball

A spaceball is a programmable device that can be used to manipulate the model view and permit the user to define shortcuts. The programming of the shortcuts is done using the Spaceball Control Menu. One simply defines the Mentat commands associated with the different buttons shown in the Spaceball Control menu referenced by the VIEW pull-down.



Keyboard Input

Not all data can be entered through the mouse; numerical and literal data *must* be entered via the keyboard. The program mode prescribes the specific requirements for proper entry of each type of data. The program can be in data mode or in command/literal data mode and is described under the following two headings.

Numerical Data

You must use the keyboard for numerical data entry. The program interprets the data entry according to the context in which it is used. If the program expects a real number and you enter an integer, Mentat automatically converts the number to its floating point value. Conversely, if a floating point format number is entered where an integer is expected, the program converts the real number to an integer.

Scientific notation for real numbers is allowed in the following formats:

```
.12345e01  
.12345e01  
-0.12345e-01
```

The interpreter does not allow imbedded blanks in the format. Whenever the program encounters an illegal format, the message `bad float!` appears in the dialogue area. The prompt for numerical data is a colon (:).

Literal Data

Literal data is used for file, set, and macro names. A literal data string may *not* be abbreviated. Commands as introduced in the beginning are considered string data (as opposed to literal string data) and *can* be abbreviated as long as the character string is unique within the Mentat command library. For example, `*add_elements` cannot be abbreviated to `*add` because of the other commands that start with the same characters such as `*add_nodes` and `*add_curves`. The program checks the input for validity against the internal library of valid responses. For example, if you enter an ambiguous or misspelled command, Mentat responds by listing all the valid entries that start with the same first letter of the command. The prompt for literal data is a greater-than symbol (>).

If the program is in data mode which is identified by the `:` prompt, you must enter a command preceded by an asterisk (*) to instruct the program that you are entering a command.

For example: Enter node (1): `*add_nodes`

If you enter a command without the asterisk when the program is in data mode, Mentat responds with an error message in the dialogue area.

The asterisk *can* be omitted when the program is in command or literal data mode which is indicated by the greater-than symbol (>).

For example: Command > `add_nodes`

Editing the Input Line

The experienced user can enter a sequence of commands or requests in a single 160-column input line. Note that anything typed beyond the input line limit is lost! Use <CR> to avoid this. You must use a blank space to separate entries when you are entering multiple responses on a single input line. All entries in the buffer are processed sequentially.

Mentat maintains a history of lines that are entered and offers limited recall and editing capabilities for the command line. The arrow keys \wedge and \vee on the keyboard can be used to scroll up and down in the dialogue area to make these lines visible. Use CTRL-p (that is, hold down the CTRL key and press the p key) to recall a previously entered input line. Repeat the CTRL-p sequence to recall as many lines as you need. Use CTRL-n to move to the next line in the history of command lines. (*p* and *n* stand for *previous* and *next*, respectively, in these control sequences.)

Edit functions for the current line are: backspace for character delete and CTRL-u for line delete. The left and right arrow keys are used to position the cursor at the desired location to overwrite or insert characters. The TAB key is used as a toggle to switch from insert to overwrite mode and vice versa. For example, if you type `*view_viewpont 0.0p 0.0 1.0`, the program responds with the message `unknown command` in the dialogue area. To correct the entry, recall the line using CTRL-p, use the left arrow key to move the cursor to the letter *n* of `view_viewpont`, press the TAB key, type `i`, and press <CR> to enter the line. The command will now be `*view_viewpoint`.

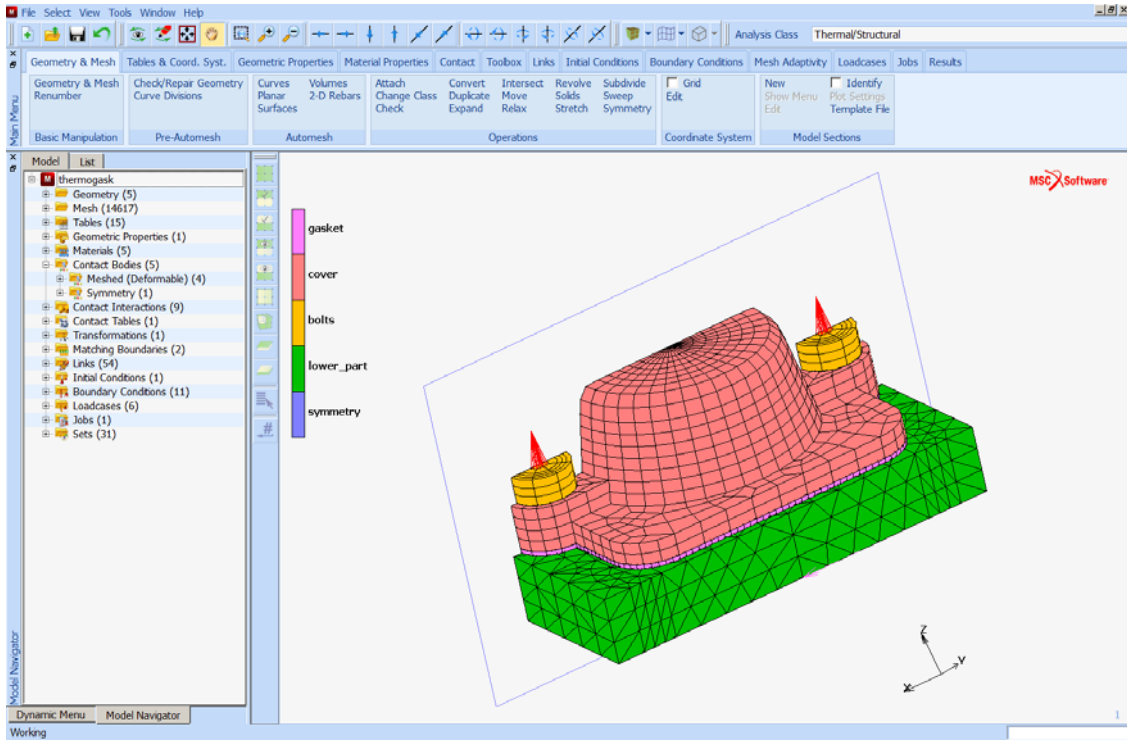
Model Navigator

The Model Navigator in Mentat provides the user the option to easily investigate the contents of a model. It allows the user to quickly view the contents and to determine the completeness of the model. The Model Navigator not only effectively provides a tree representation of the model, it also allows one to quickly move to different menus. All menus, which can be accessed from within the Main Menu, can also be accessed from within the Model Navigator.

The Main Menu and the Dynamic Menu are not required anymore, though in some cases (especially when working with the Geometry & Mesh and Results tabs), it can be easier to access menus from within the Main Menu. Note that there are startup options to hide the Main Menu, the Dynamic Menu, and the Dialog Area (`-hide_main_menu`, `-hide_dynamic_menu` and `-hide_dialog`). Hiding the Main Menu and the Dialog Area increases the size of the Graphics Area (hiding and unhiding can also be done any time Mentat is running, by using the Right Mouse Button (RMB) when the cursor is positioned on the Menu Bar at the top of the Mentat window, respectively, below the List Specification Toolbar or the Results Navigation Toolbar).

The Model Navigator is illustrated using same model as shown in Chapter 2.2, *Thermo-Mechanical Analysis of Cylinder Head Joint with Quadratic Contact*. The images are created with a hidden Dialog Area.

Upon running the procedure file in Chapter 2.2, the model shown below is obtained. The finite elements are plotted in solid mode and Contact Bodies are identified. The Model Navigator is shown in the (default) Model view, as opposed to the List view, which will be briefly discussed later on.

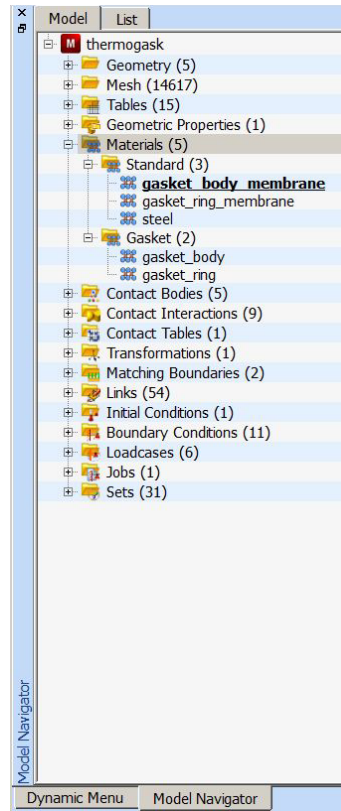
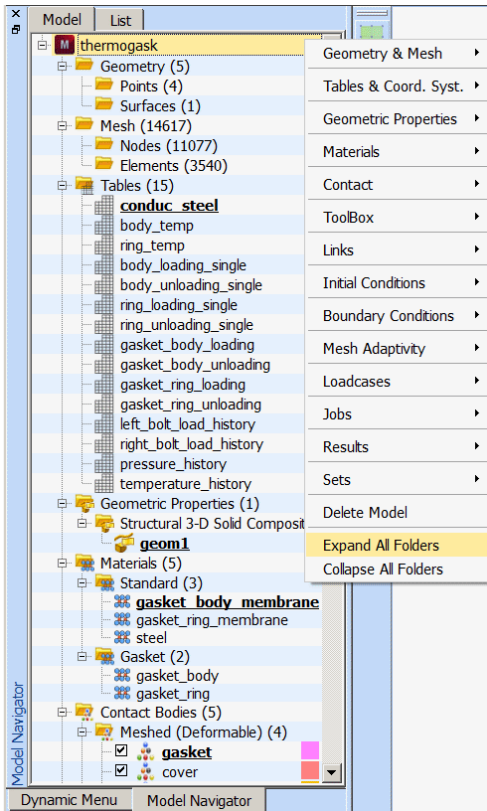


At the top of the navigator, the name of the model is displayed. Then, from the top to the bottom, the model entries are shown, starting with the Geometry and Mesh data.

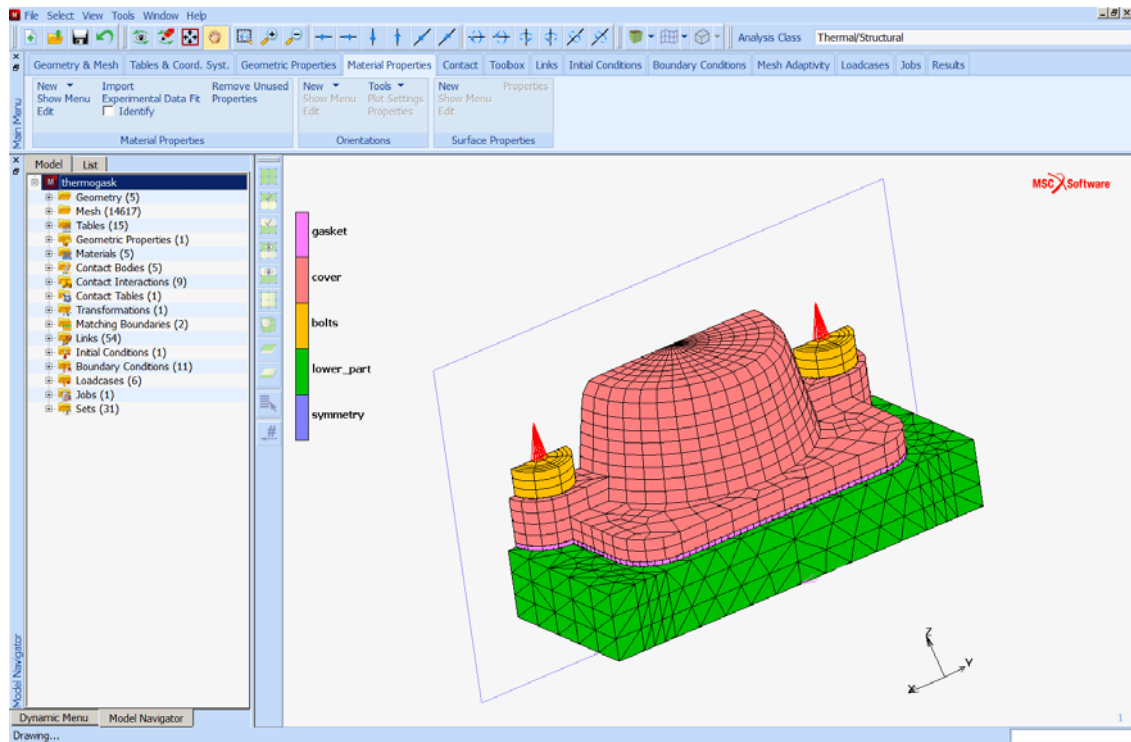
There are several options to expand and collapse the different folders of the Model Browser:

- Open the RMB menu when the cursor is positioned on the top item (name of the model), the top bar (showing the Model and List tabs) of the Model Navigator, or below the last entry in the free area of the Model Navigator, and select Expand All Folders or Collapse All Folders;
- Open the RMB menu when the cursor is positioned on a folder and select the Expand Folder option;
- Click on the [-] / [+] icons to expand and collapse an individual folder.

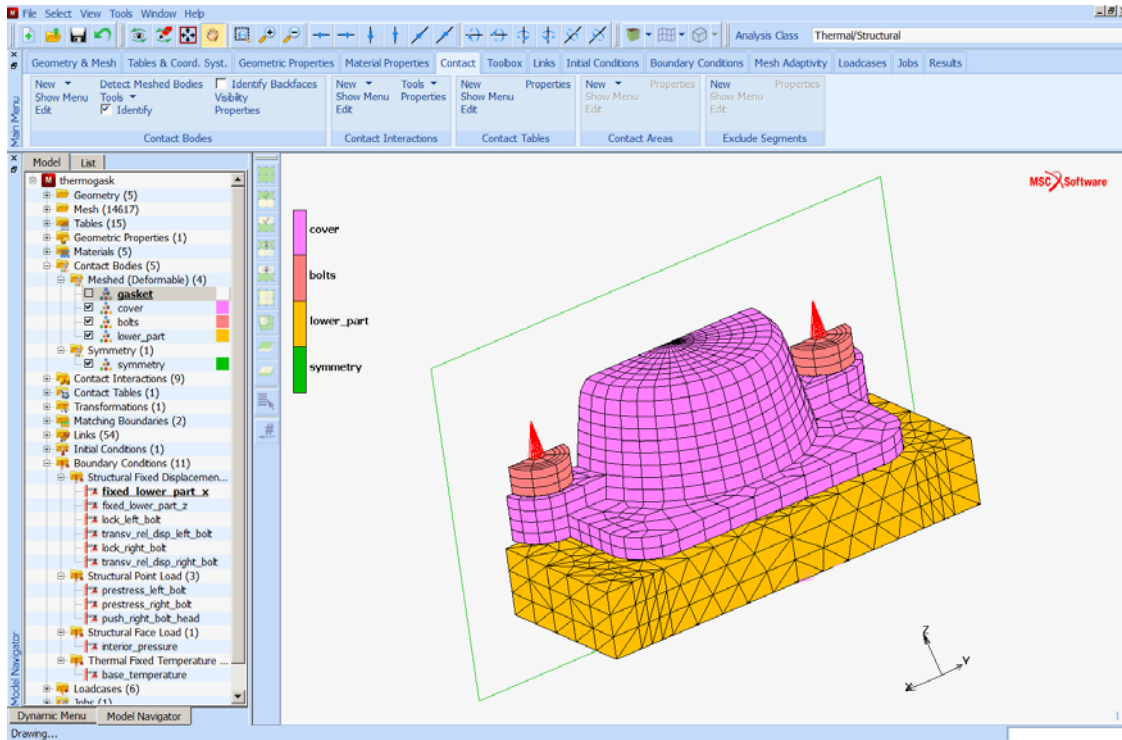
The figure below shows the effect of the various options. On the left, all folders have been expanded, where on the right only the Materials folder has been expanded.



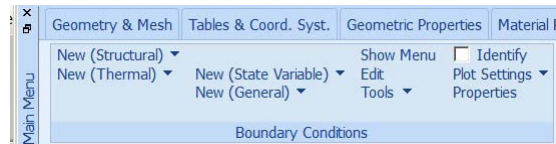
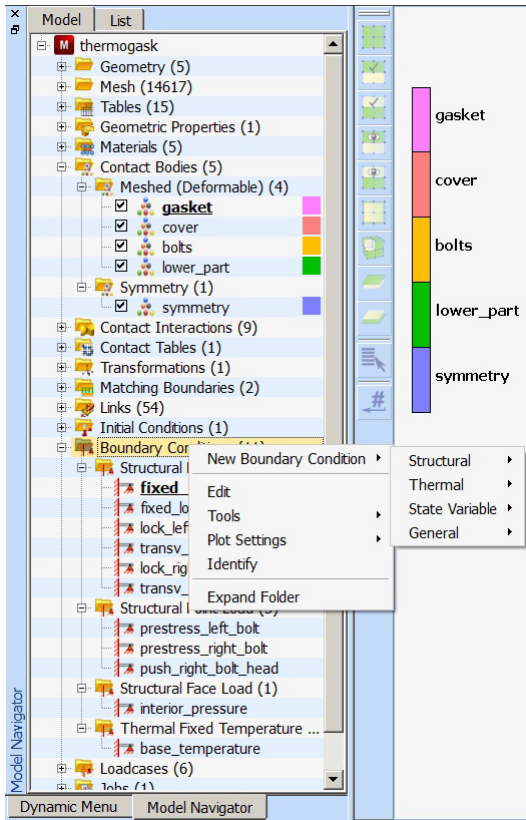
If one closes all of the sub-folders, one sees the following view:



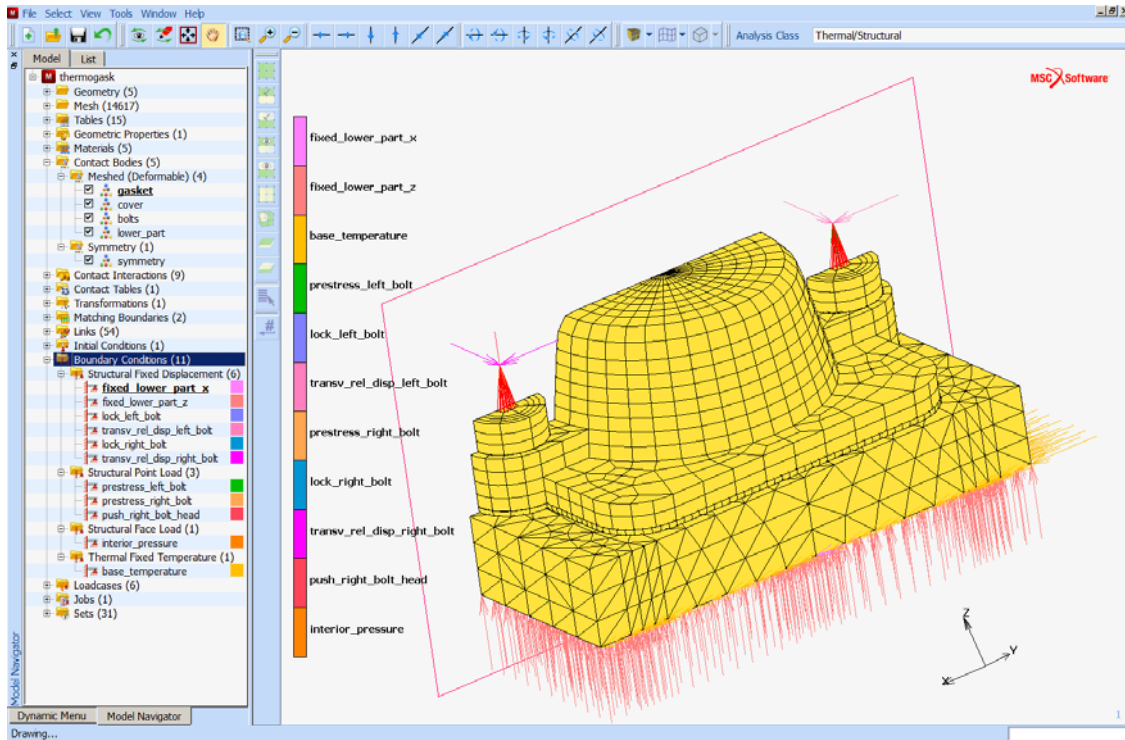
Opening up the Contact Bodies folder, one can see that the colors in the navigator match those in the identification legend. Note that the navigator facilitates the use of picking. By clicking the check box in front of an individual contact body, the display of this body can be easily switched on or off. In the figure below, the check box of contact body *gasket* is inactive and this body is not displayed in the graphics area.



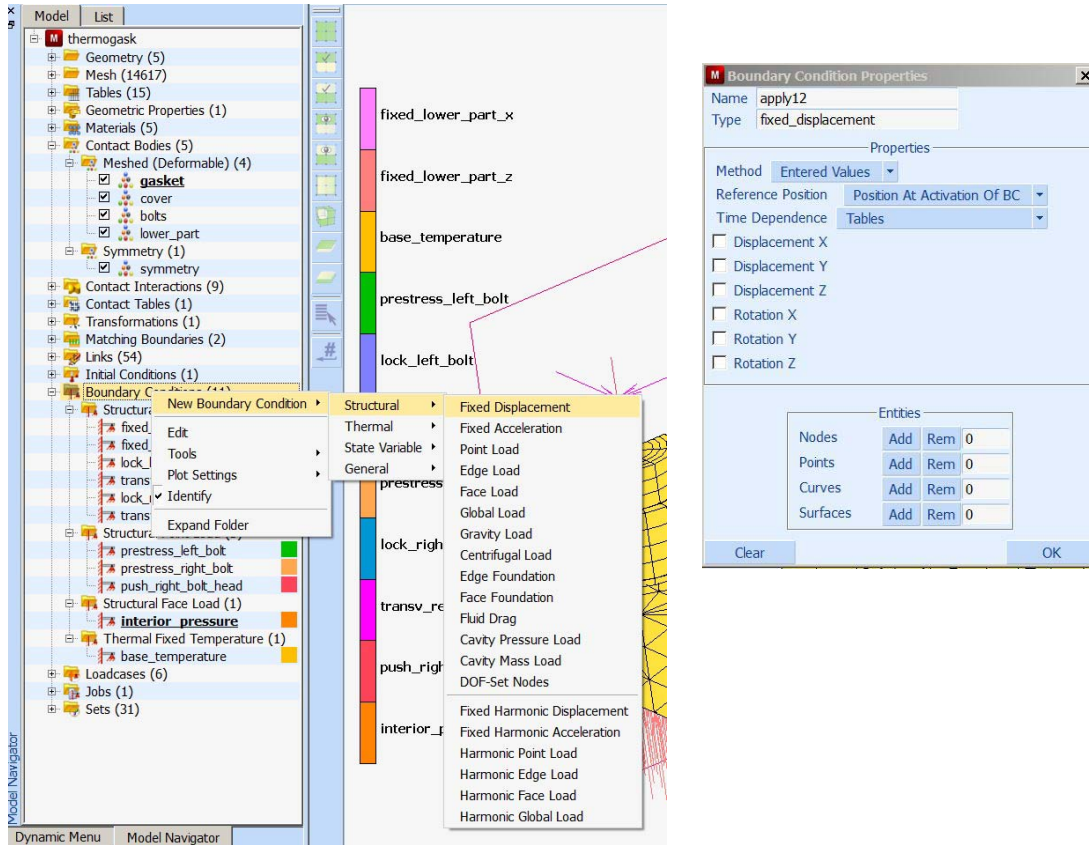
In a similar manner, if one opens the Boundary Conditions folder and use the RMB, one sees the following menu. Here one can clearly see the correspondence with the Boundary Conditions tab in the Main Menu. One can add a New Boundary Condition, Edit an existing boundary condition, merge duplicate or remove all boundary conditions (using the Tools menu), define Plot Settings, switch the identification of boundary conditions on and off, and expand the Boundary Conditions folder.



By selecting Identify, one then sees (note that the Main Menu has been hidden):

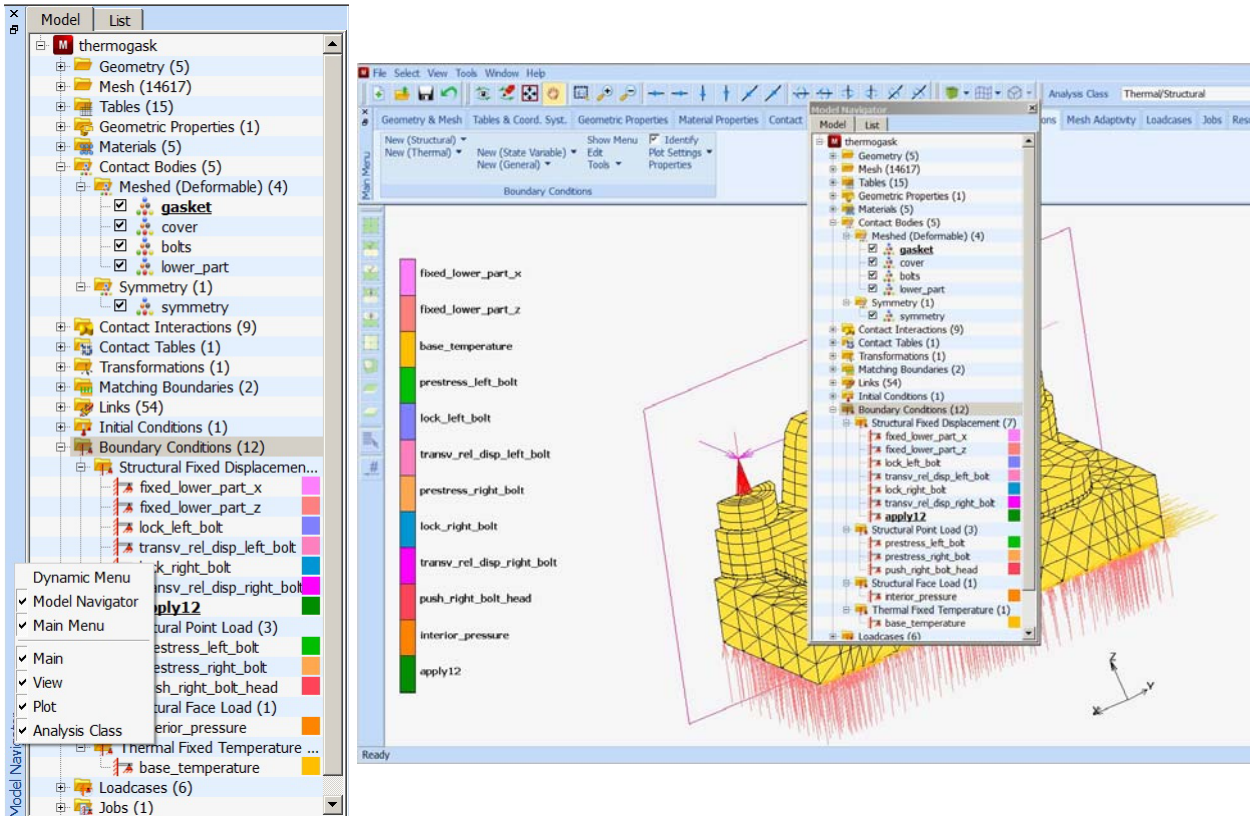


If one selects New Boundary Condition, then one can use the Model Browser to navigate through the menu system. The following figure shows how a structural boundary condition can be added. The pop-up menu where the data has to be entered also has an area where the entities have to be defined to which the boundary condition will be applied.



When double clicking the left mouse button (LMB) over an entity, one will be placed into the appropriate menu to edit that particular entity.

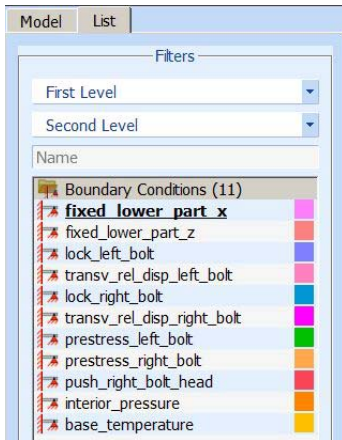
If one completely hides the Dynamic Menu, then better use of one's monitor display area may be achieved by undocking the Model Browser. The following figure shows how the Dynamic Menu can be hidden (using the RMB in the left bar of the Dynamic Menu) and the Model Navigator is undocked (by double clicking or dragging using the LMB in the left bar of the Model Navigator). This way it can be arbitrarily positioned by the user.



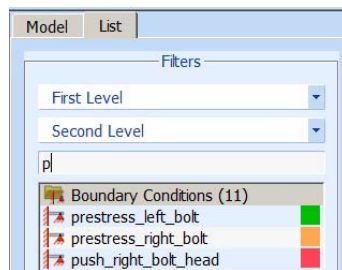
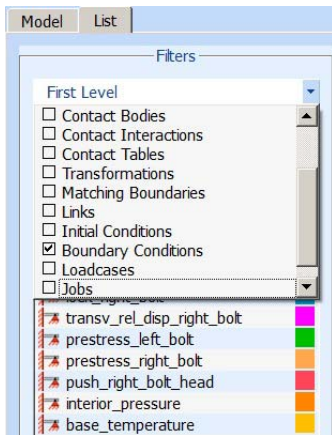
The Model Browser has two views: the Model and List view:



If one switches to the List view, one has additional tools to filter what is shown in the Model Navigator. Continuing to work in the Boundary Condition menus, one obtains:



The First Level filter allows selecting main folders of the Model Navigator. In the current example, only the Boundary Conditions folder is selected. The Second Level filter allows selecting sub-folders, while the Name filter allows selecting entities based on the starting character(s) of the entity. The following figure shows the First Level filter, and the use of the Name filter where only Boundary Conditions with a name starting with the character “p” are listed.

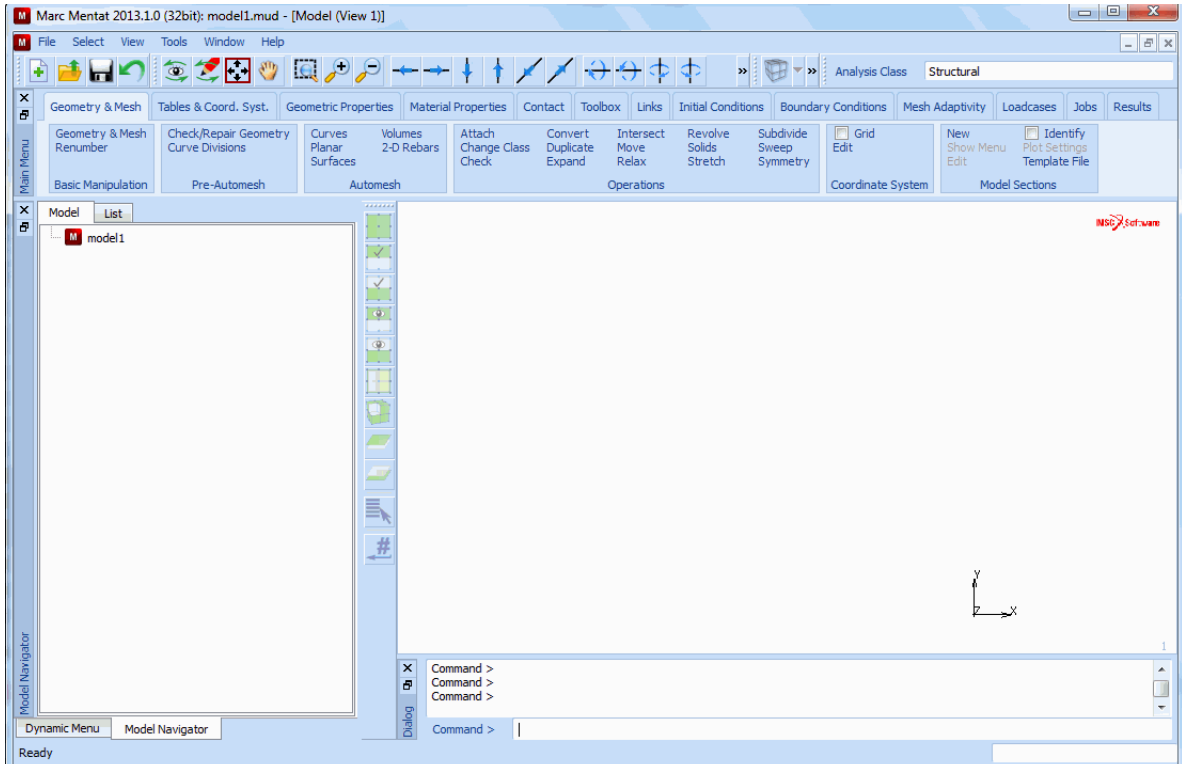


When executing a procedure file which causes a huge number of model navigator entities to be created, one may see a slow down of the program. This can be avoided by editing the procedure file and adding the command `*model_navigator_update off` at the top of the procedure file, which causes the program to not update the model navigator. This command can also be set via the menu system by either using by using Tools → Procedures... → Update Model Navigator On/Off or using Tools → Program Settings... → Model Navigator Update On/Off.

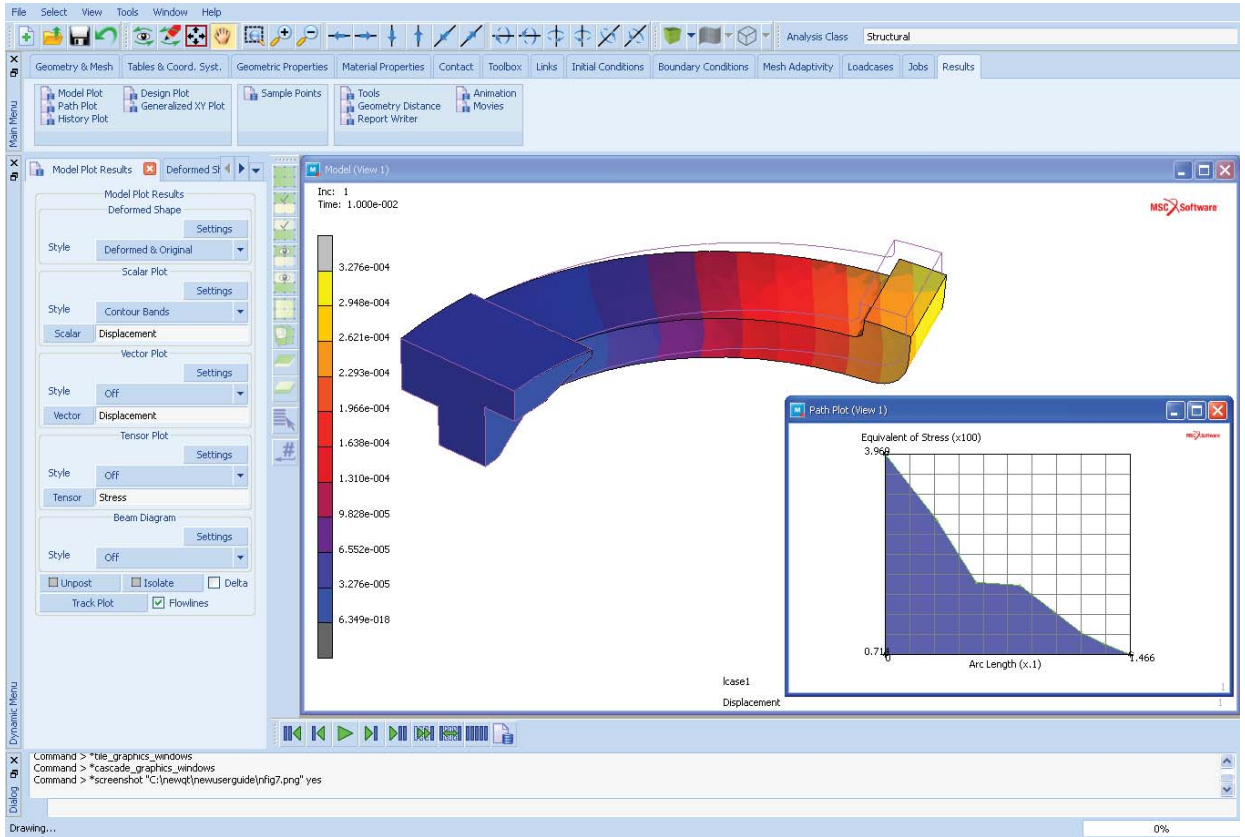
Menu Structure


This section focuses on the menu system as a means to communicate with Mentat. The first subsection discusses the structure of menus that constitute the program. The second subsection analyzes the components of each menu.

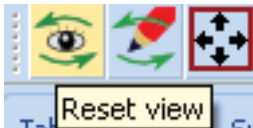
Upon starting Mentat, one will see the following menu.



The display is divided into several areas that will be reviewed here.




Mentat is driven by icons such as: . If the main menu is not hidden by any other menu, then hovering the mouse over the icon will result in a short description of the icon, such as:



Menu Bar


The first layer is the Menu bar which consists of seven Icons:

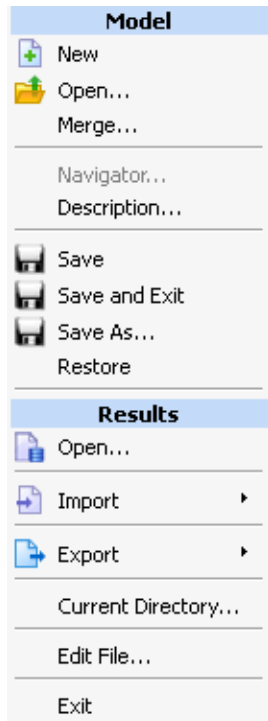


-  - Program Icon – activates Pull-down

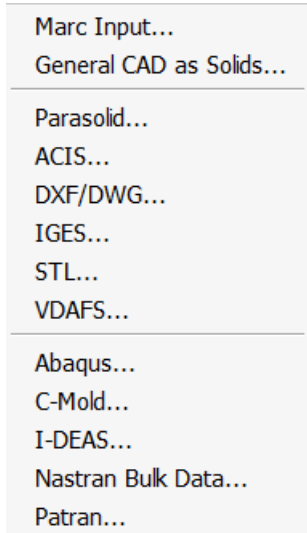
-  Restore
- Move
- Size
-  Minimize
-  Maximize

X Close **Alt+F4**

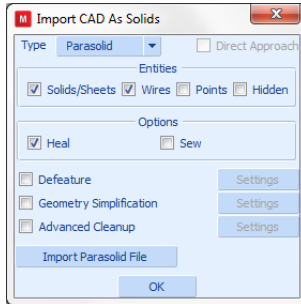
-  **File** Icon – activates Pull-down to control the setting of the home directories, opening and closing files, and saving the data base model. The Import and Export pull-downs are critical for interoperability with other systems.



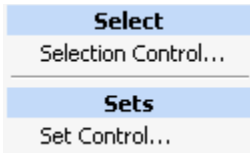
In particular, the **Import Button** activates a pull-down that allows the import of CAD models and other finite element models into the system. After specifying the type, the file browser will be activated.

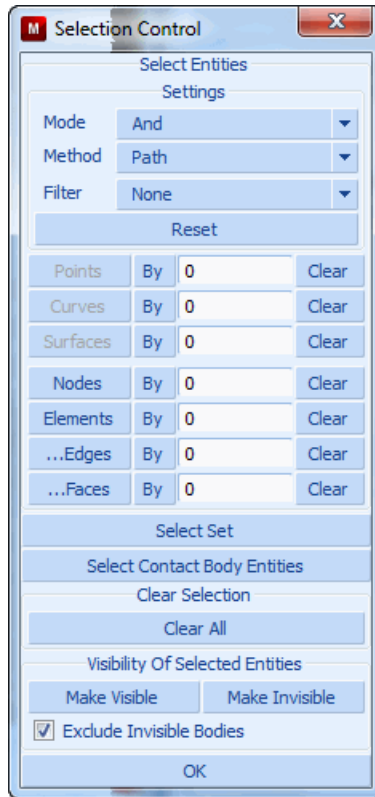


The Import CAD as solid activates the following menu.

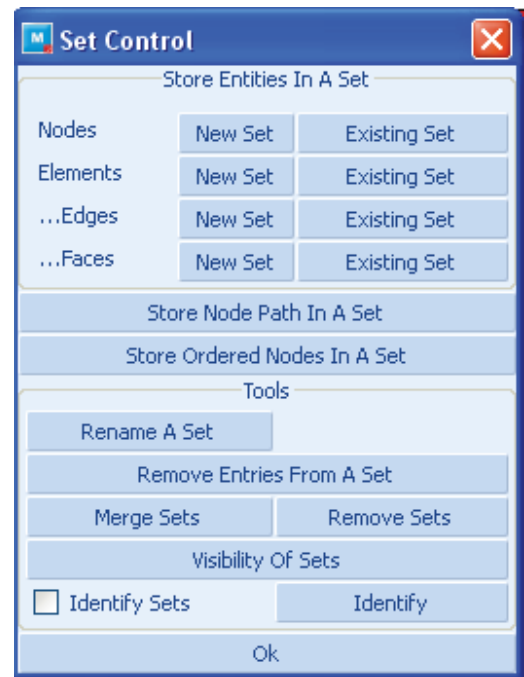


- **Select** - The Select Icon activated menus that allow the user to gather a subset of the model to be either put into a set, control the model being viewed or used in a subsequent command. The Menus are similar to the previous release, but slightly reorganized.





Selects a Group of Entities

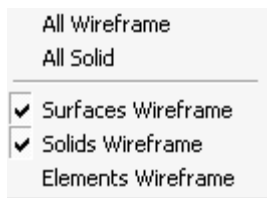


Creates and Manipulates Sets

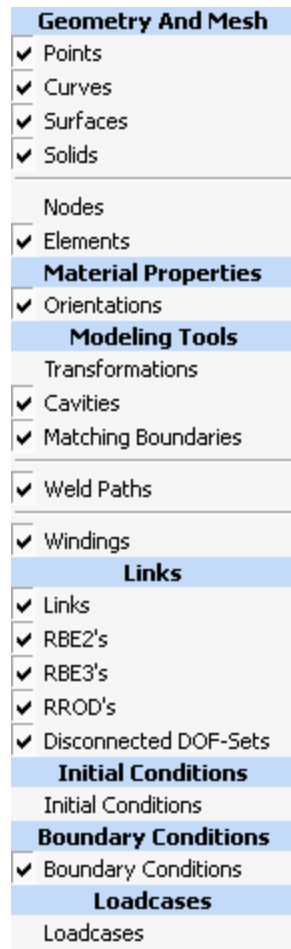
Note that the Selection Control and Set Control menus are floating menus and it is often advantageous to have both of them open at the same time. In fact, it is often useful to have the Selection Control menu open throughout the session.

- **View** - The View Icon activates multiple pull-downs and pop-up menus to control what is displayed in the graphics area. Initially, the following pop-up is seen.
 - Lead View Pull-down - activates a series of menus



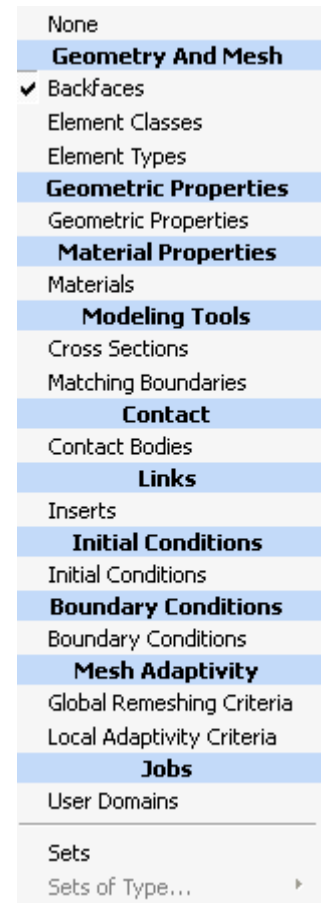


Wireframe vs. Solid



Model Entity Type

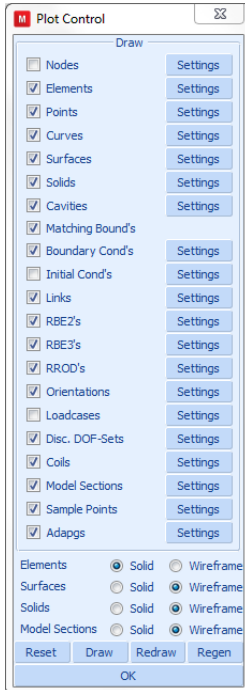
Selects which type of entities will be displayed



Identify

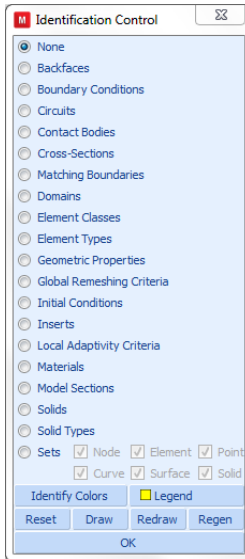
Selects which entity type will be used for displaying groups

- The Plot Setting and Visibility menus - floating menus and it is often useful to have the Plot Setting menu open throughout the session.

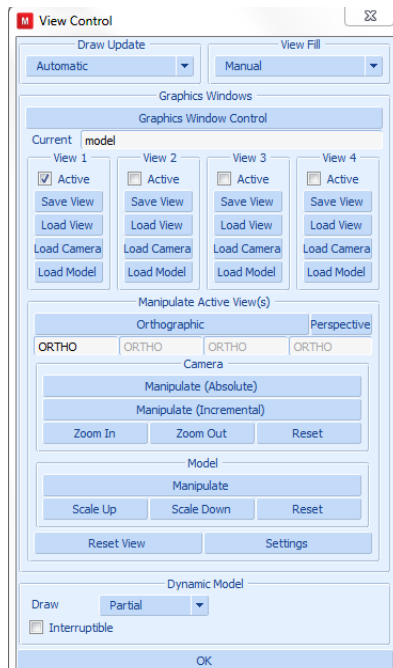


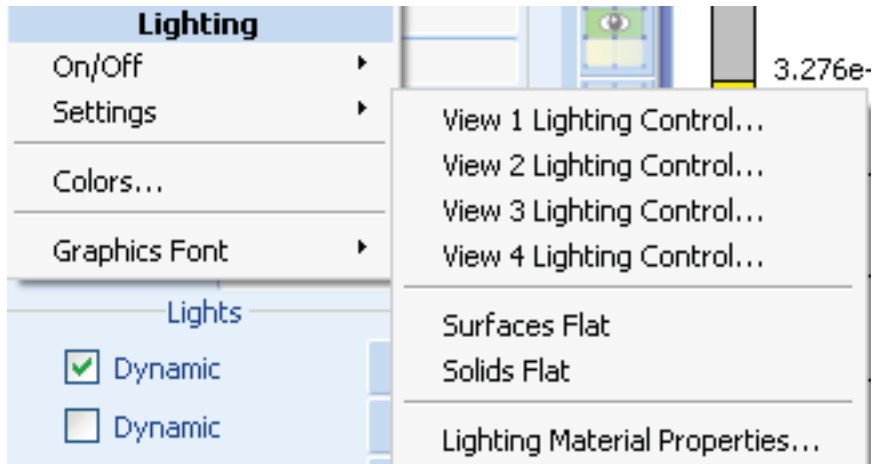
- Identify Menu

Selects which entity type will be used to control the displayed groups.

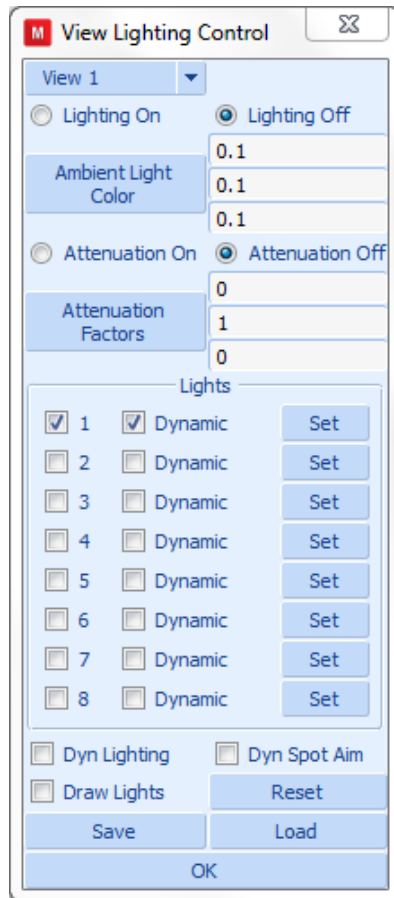


- Viewing Menu - Controls the viewing orientation and rate at which the display will be updated.



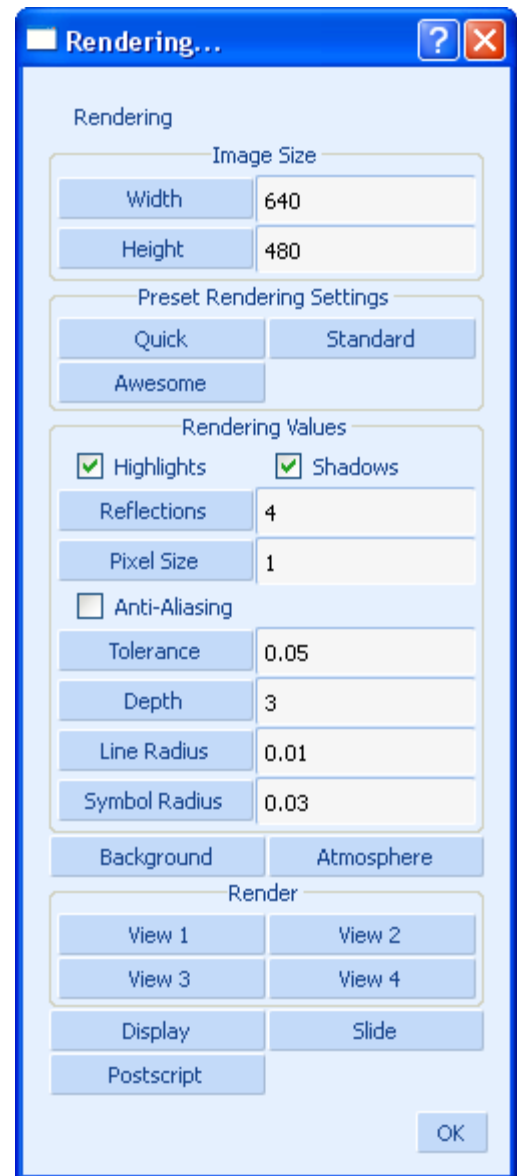


Activate Light Source Shading



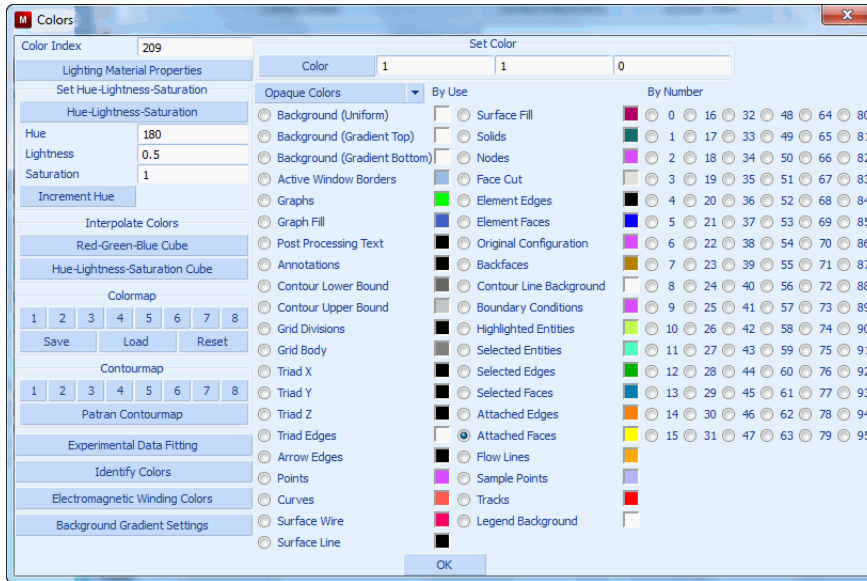
Light Setting

Controls the image of the model when light source shading is used.

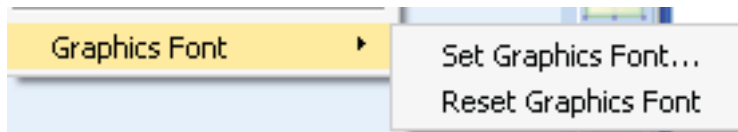


Rendering

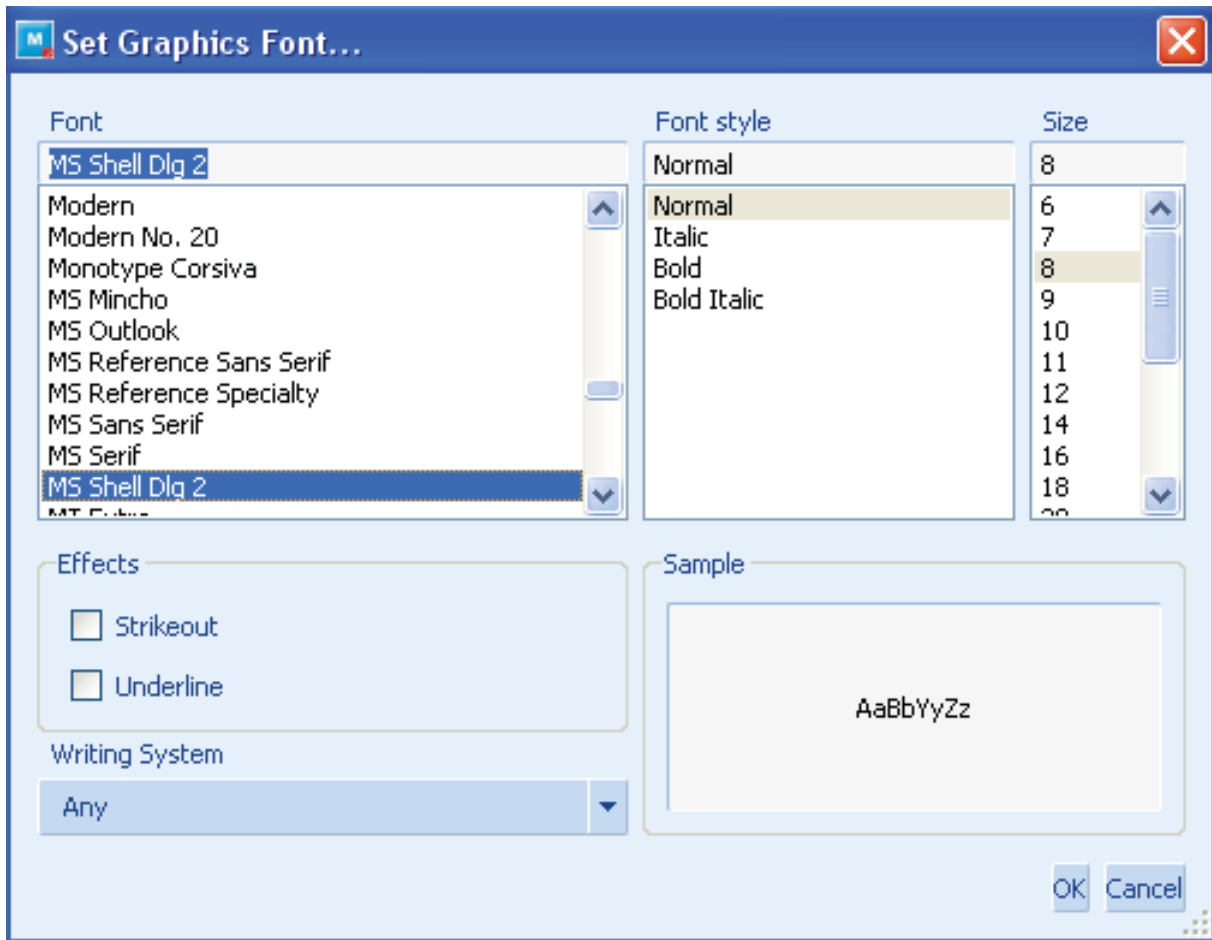
Controls the image of the model when photo-realistic rendering is used.



Define Colors used in Display



Define or Reset Graphic Font



Graphic Font Selection

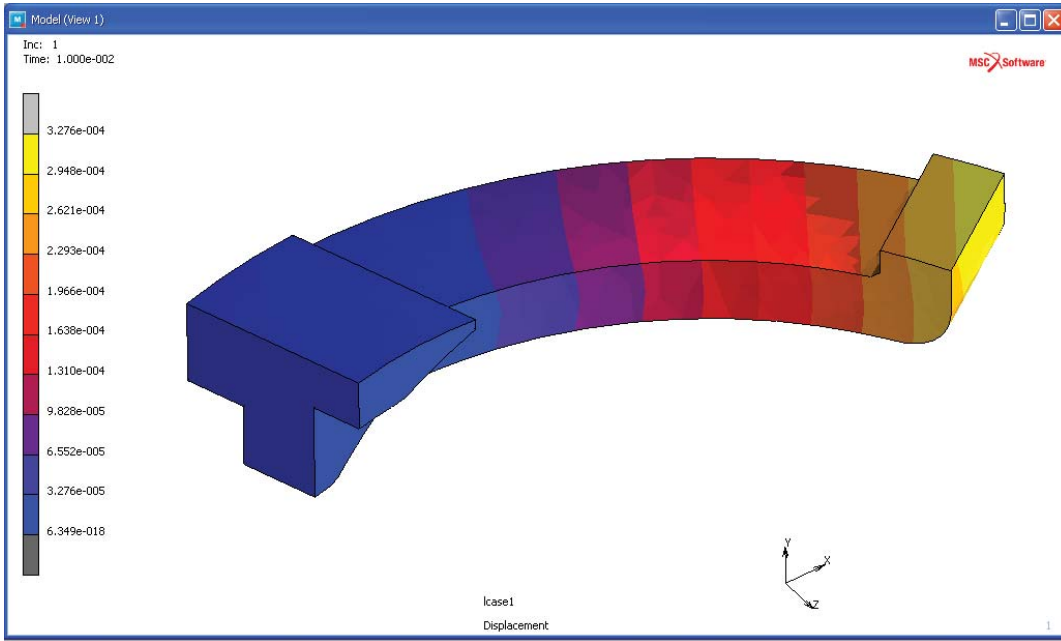


Image using Default Graphic Font

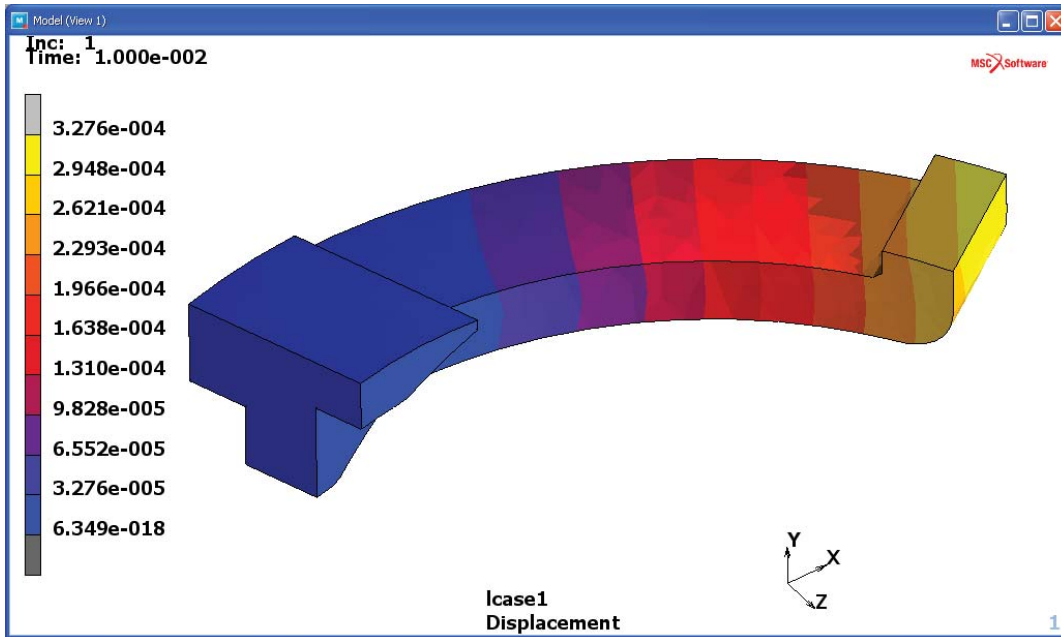
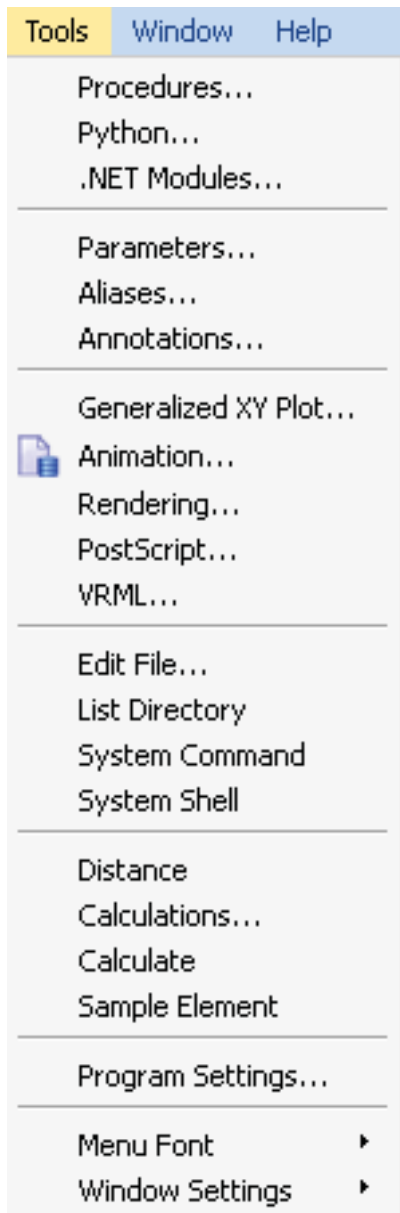
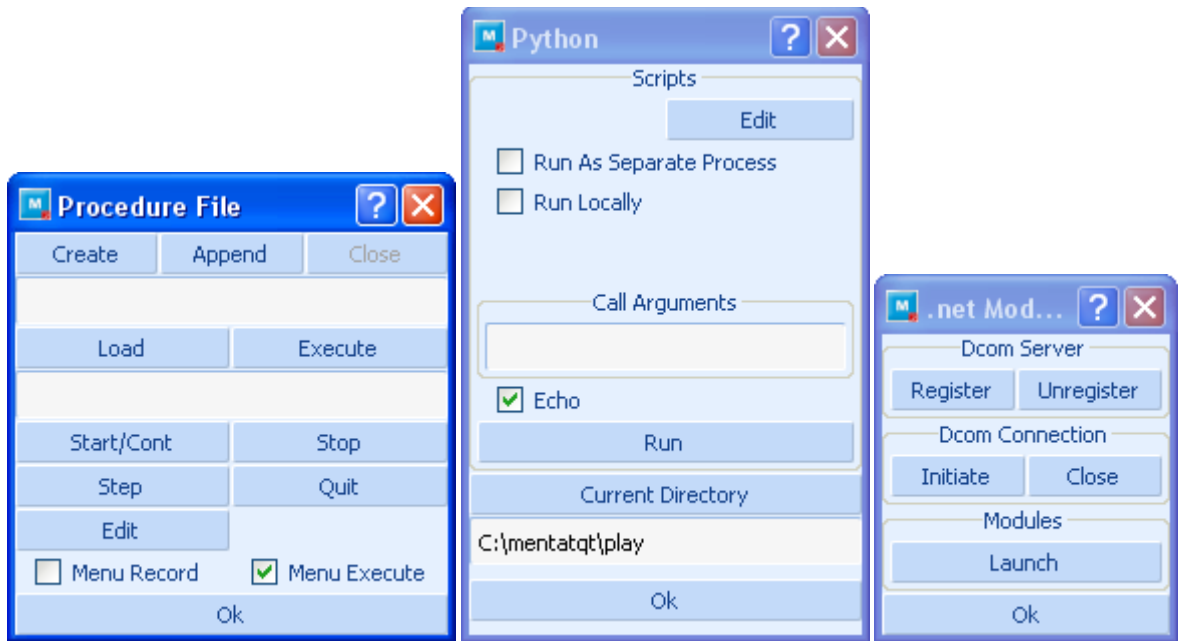


Image using Size 14 Bold Graphic Font

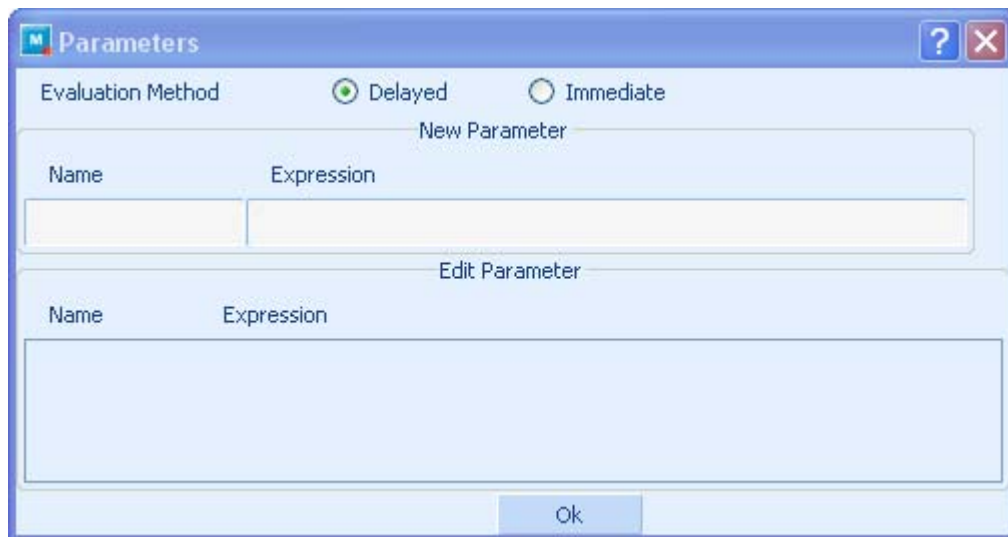
- **Tools** - The Tools Icon is used to allow the user to select utilities that may be used to assist in creating the model. The following pull-down is activated.



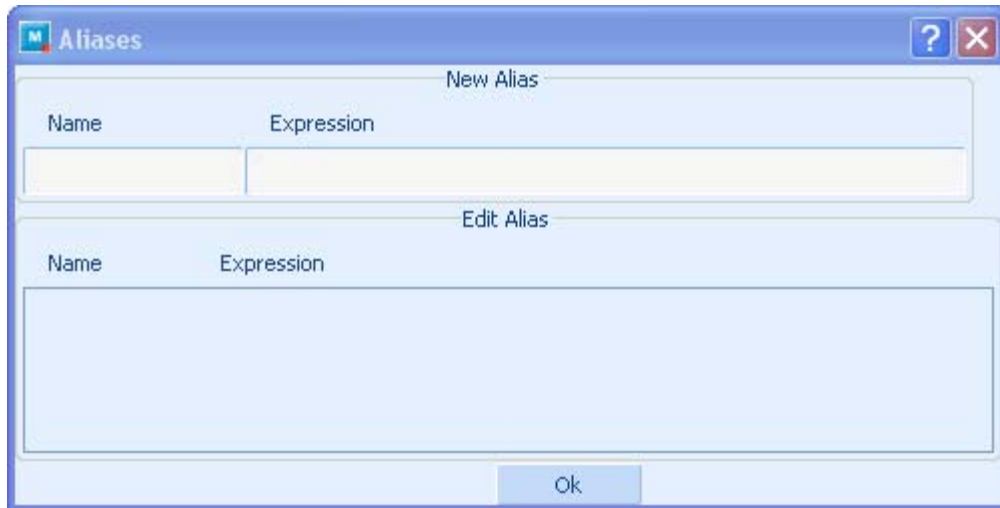


Controls the creation and playback of procedure files

Controls Python



Allows the user to define Parameters that will be used later or repetitively in the session. If the expression contains other parameters, one has the choice of evaluating the value of the parameter now or when it is used.



Allows the user to rename a command within Mentat

Generalized XY Plot

Get Curves From

History Plot	Path Plot
Design Plot	Table
Exper. Data Fit	Table List

Curve Operations

Shift	Scale	Rotate	Swap
Name	Copy	Remove	Function

Clear Curves

Show Model ▼ Legend

Filled Curves ▼ Show Ids 1

Limits

	Fit
Xmin	0
Xmax	1
Ymin	0
Ymax	1
Xstep	10
Ystep	10

Label

Title	X-Axis	Y-Axis	Reset
-------	--------	--------	-------

Clipboard Copy To

Read	Write	Export
------	-------	--------

Allows user to combine multiple X-Y type plots

Animation

Create

Base File Name	animation
Index	100
Single Frame	Increments
Mode	Harmonics
Attributes	

Play

Play Stop

Resume Interrupt

Show Model ▼ Plot Settings

All Begin To End

Begin	100
End	100
Current	100
Pause	0

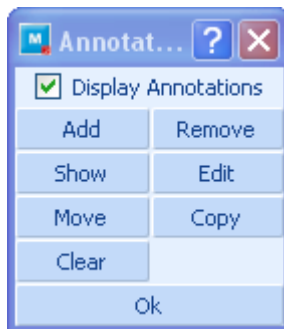
Forward ▼ Single Play ▼

Make Movie Play Movie

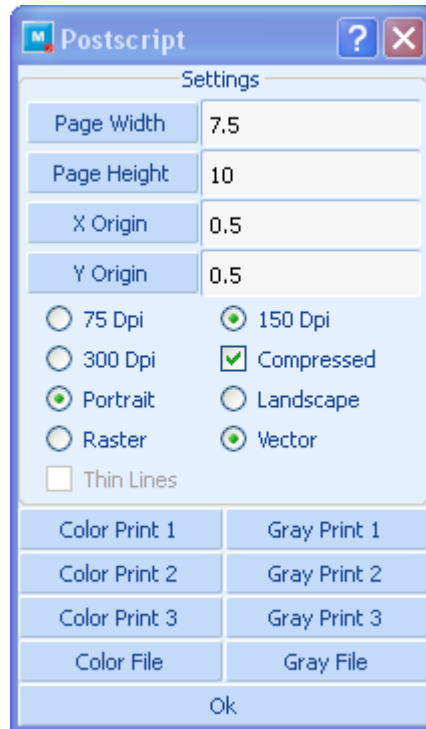
Clean Files

Gif/Mpeg/Avi Movies

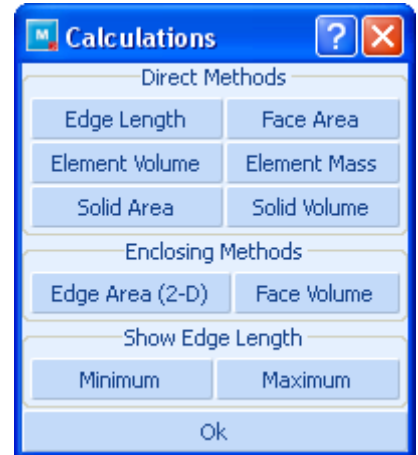
Controls the creation of movies



Allows user to add annotations to the image

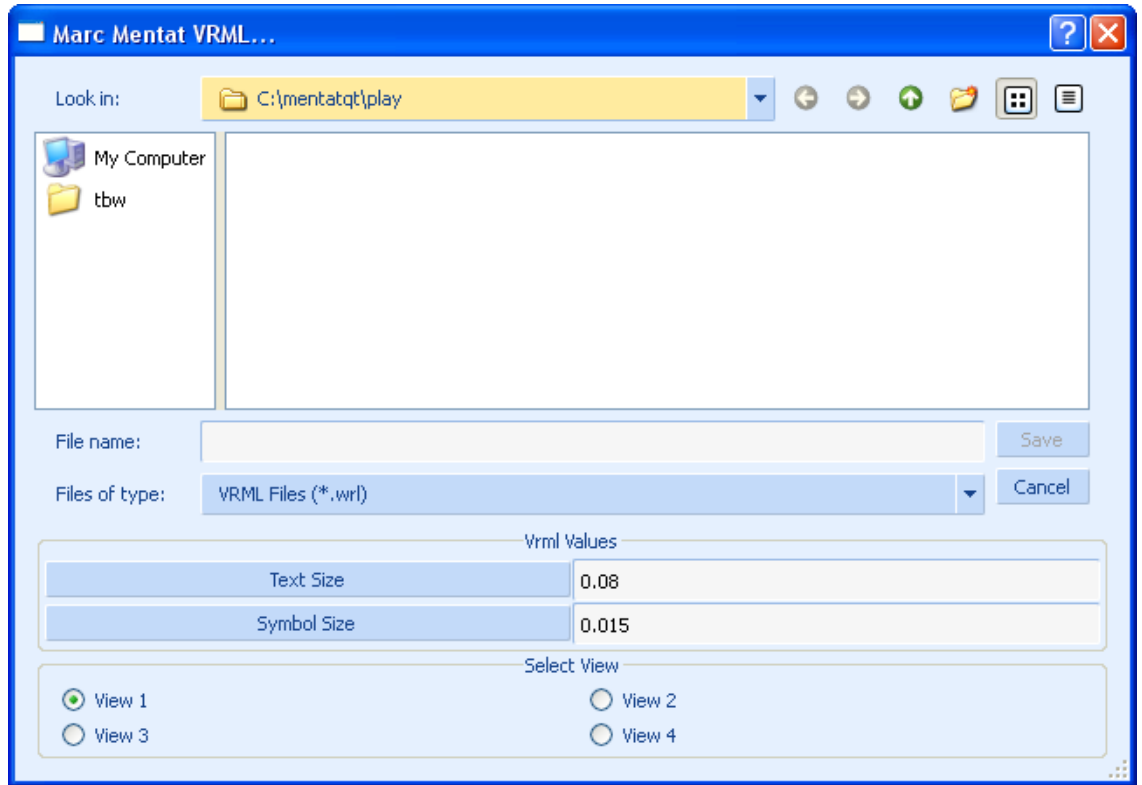


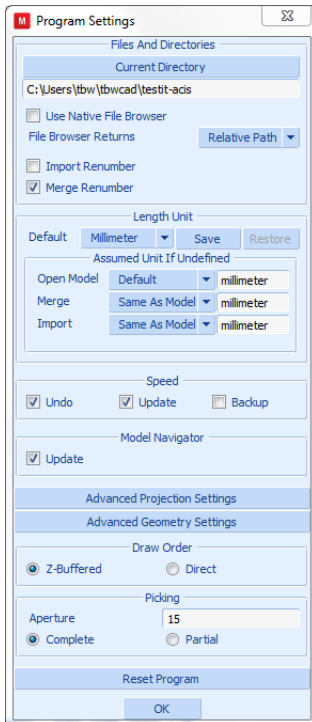
Controls the use of a postscript display



Allows the user to obtain geometric parameters or subregions of the model

- VRML - Controls the creation of VRML files.





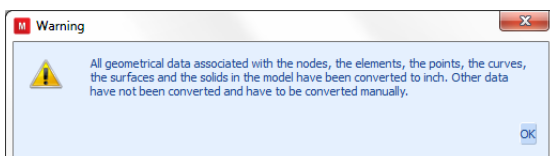
Controls Drawing Process, Picking Process, and Save Undo Process

Model Length Unit

The Length Unit option sets the unit of length for the current model. The coordinates of the nodes and points, as well as all other geometrical data, are stored in the model in this length unit and are written to the Marc input file also in the unit when the job is submitted (i.e., no unit conversion is performed). The unit of length is stored in the model file (.mu_d or .mf_d) if the model is saved in the default style.

The Length Unit should preferably be set once when a new model is created. The default unit for new models is in millimeters.

If the length unit of a model is changed (i.e., from millimeter to meter), then all geometrical data associated with the geometry and the mesh in the model are converted to the new length unit. All other data in the model, such as material properties, geometric properties, boundary conditions, contact data, etc., is not converted to the new unit and has to be changed manually.



More specifically, only the following data is converted.

- Coordinated of nodes, points, and solid vertices
- Curve divisions applied to the curves (target length, minimum and maximum lengths, and the L1 and L2 lengths for biased seed points)
- Target lengths of solid mesh seeds

Models Created by Mentat Versions Prior to 2014

For models created by Mentat prior to 2014, the length unit is not known. These models have been created in a particular unit system, but this information has not been saved in the model file. If such a model is opened in the 2014 Mentat version, then the unit of length in which the model has been created must be specified. By default, the length unit is set to the default unit (millimeter). However, if the model has been created in a different unit system, then the appropriate length unit for the file can be set in the Tools → Program Settings menu. This must be done prior to opening the model file. Note that this is a one time operation. If the model is subsequently saved in the default style, then the unit of length is saved in that model file as well.

Import

CAD models are converted upon import from the length unit in which they have been created to the model length unit. This applies to the following options in the File → Import menu:

- Import of Parasolid, ACIS, and IGES models via the respective Parasolid, ACIS, and IGES options
- Import of general CAD models as solids via the General CAD as Solids option

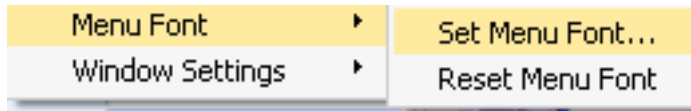
The length unit of files imported via one of the other import options File → Import menu is not known. If such a file is imported, then it is assumed that the file is defined in the same length unit as the current model. If this is not the case, then the appropriate length unit for the file can be selected in the Tools → Program Settings menu. This must be done prior to importing the file. The data in the file is then converted to length unit of the current model upon import.

Merge

If the model file created by Mentat 2014 or newer is merged into the current model via the File → Merge option and the length unit of the model file differs from the length unit of the current model, then all geometrical data from the model file associated with the geometry and the mesh are converted to the length unit of the current model before adding the model to the current model. All other data in the model, such as material properties, geometric properties, boundary conditions, or contact data are not converted.

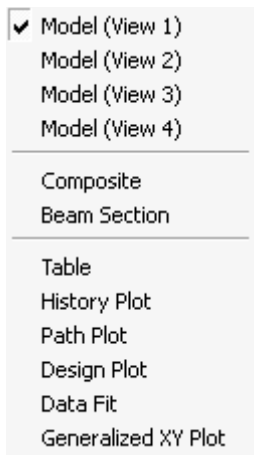
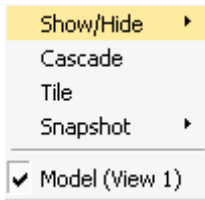
As the unit of length is not known for models created by Mentat versions prior to 2014. If such a model is merged into the current model, then it is assumed that the model is defined in the same unit of length as the current model. If this is not the case, then the appropriate length unit can be selected in the Tools → Program Settings menu. This must be done prior to merging the file. All geometrical data from the model file associated with the geometry and the mesh are then converted to the length unit of the current model before adding the model to the current model.

By turning off UNDO, one can improve performance but user error cannot be reversed.



Controls Fonts in the Menu

- **Window** - This Icon is used to control the layout of the graphic windows. This initiates the following pull-down.



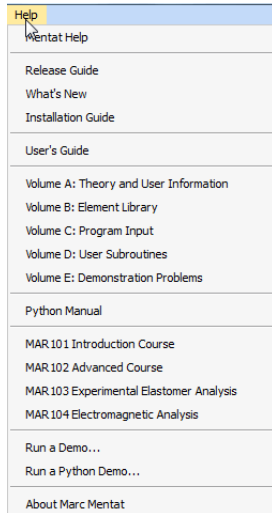
Show/Hide controls which model representation is going to be displayed



Allows the quick creation of window captures

Note the types of plots to be displayed will be dependent on what has been previously requested.

- **Help** - This icon initiates the Marc documentation set. The following menu appears to allow you to select the particular manual.



In the new version of Mentat, clicking Mentat Help activates a HTML based help system. This help system can be downloaded separately containing the latest information about the Mentat produce.

In the Classic version, text help files will be displayed.

Manual	Description
<i>Release Guide</i>	Summarizes the New Capabilities of the Release
<i>What's New</i>	PDF that shows images of problems that can be solved in the current release
<i>Installation Guide</i>	Instructions of how to install and customize the software
<i>Users Guide</i>	Describes Usage of Program through Mentat
<i>Volume A: Theory and User Information</i>	Theoretical review of the mechanics available in Marc
<i>Volume B: Element Library</i>	Description of the different element types.
<i>Volume C: Program Input</i>	Description of the Marc input format
<i>Volume D: User Subroutine</i>	Templates for the user subroutines
<i>Volume E: Demonstration Problems</i>	Example of techniques used for engineering analysis
<i>Python Manual</i>	Describes the Mentat API
<i>MAR 101 Introduction Course</i>	Introductory Class Material
<i>MAR 102 Advanced Course</i>	Advanced Class Material
<i>MAR 103 Experimental Elastomer Analysis</i>	Class notes for elastomer material testing and parameter identification
<i>MAR 104 Electromagnetic Analysis</i>	Class notes for electrostatic, magnetostatic, electromagnetic, Piezo electric, and Joule heating.






About Marc Mentat will provide the customer identifier required to obtain customer support.



Tool Bar

The TOOL BAR contains the following icons. Moving your cursor over the icon, results in a short definition its function.

Icon	Description
	Deletes the current model and clears the database
	Open a new directory
	Save current data base
	Undo – Mentat has only one level of undo
	Reset View
	Regenerate graphics area
	Expand or contract image to fill the graphics area
	Activate / Deactivate the interactive model manipulation
	Zoom in on a region identified by a polygon
	Zoom in (+) ; Zoom out (-)

Icon	Description
	Translate in +x, -x, +y, -y, +z, -z directions respectively
	Rotate about +x, -x, +y, -y, +z, -z axis
	Switch between wireframe element and solid display of elements
	Switch between wireframe element and solid display of surfaces
	Switch between wireframe element and solid display of solids

Tabs

The Tabs are the major control to the Mentat functionality. One can move from one tab to another tab at any time as long as a locked pop-up is not displayed

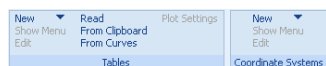


The tab that is currently selected is a slightly lower color. Once the tab is selected, one or more panels appears in the “Main Menu Area”

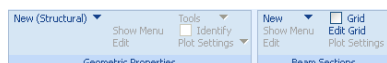
Geometry & Mesh



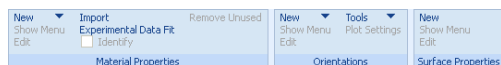
Tables and Coordinate Systems



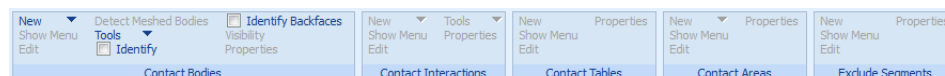
Geometric Properties



Material Properties



Contact



Toolbox



Links



Initial Conditions



Boundary Conditions



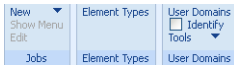
Mesh Adaptivity



Loadcases



Jobs



Results



Side Bar

The Side Bar has two sets of icons, the first are short-cuts to control the selecting of entities. The second are used for controlling the positioning of the post file. These icons can be repositioned around the graphics window.

Selection control



The menu on the left is what appears when the user actually needs to select a list of entities. If this is not currently required, then the menu is deactivated and has the appearance of the figure on the right.

Post File control



When the post file is open for postprocessing, the post file control menu will appear.

Windows Controls

The Mentat product uses standard window control which allows you to resize the main menu. One can also resize the display image. The pop-up menus come in either two forms – floating/undockable and floating/dockable.

In the floating/undockable style, such as the Identify Menu shown above, the menu can be repositioned anywhere on the screen and will remain open until it is closed using the OK command. Any other command may be executed before this pop-up is closed.

In the floating/dockable menu as shown below, the Plasticity Property menu can be repositioned anywhere, but only the commands in the Plasticity Property menu can be executed. The command in the parent Structural Properties pop-up cannot be executed and the parent menu cannot be moved until the child pop-up is closed. This restriction applies to all parent windows including the Main window. To execute any of these commands, the child must be closed using the OK button.

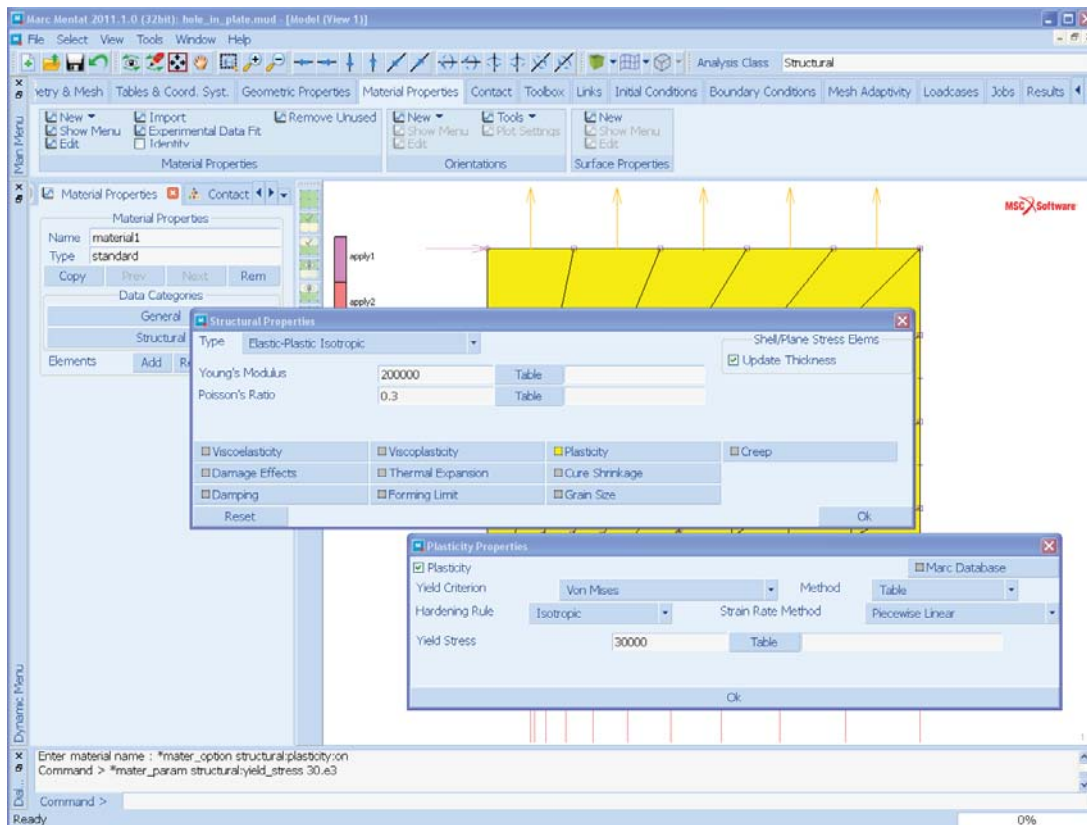


Figure 1.1-9 Main Window with Structural Properties Pop-up and Child Plasticity Properties Pop-up.

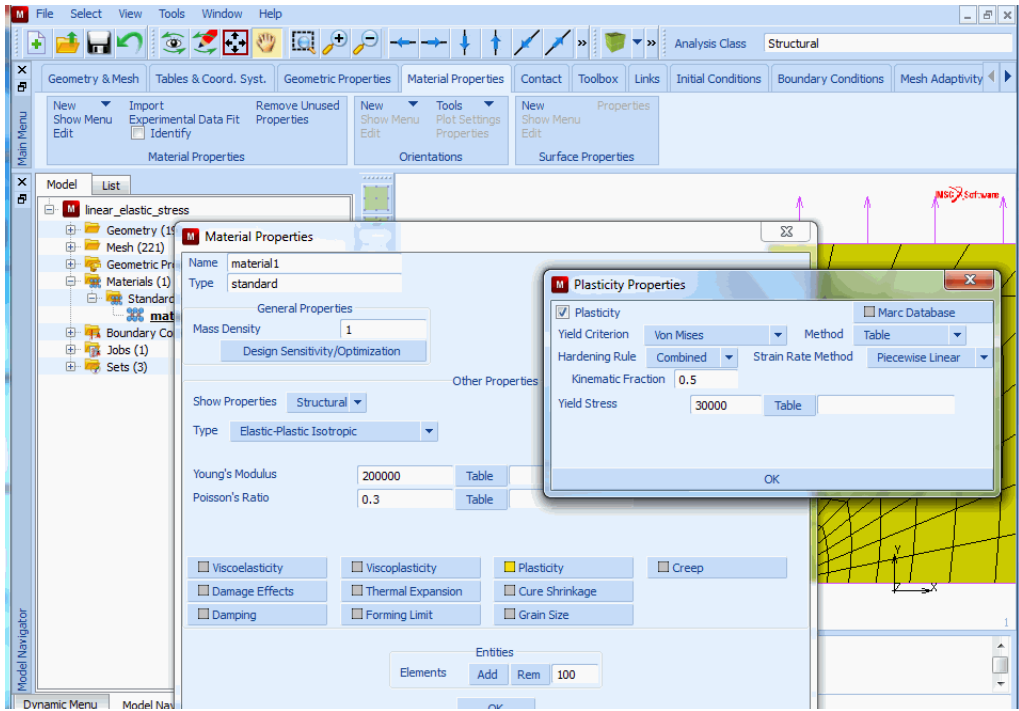
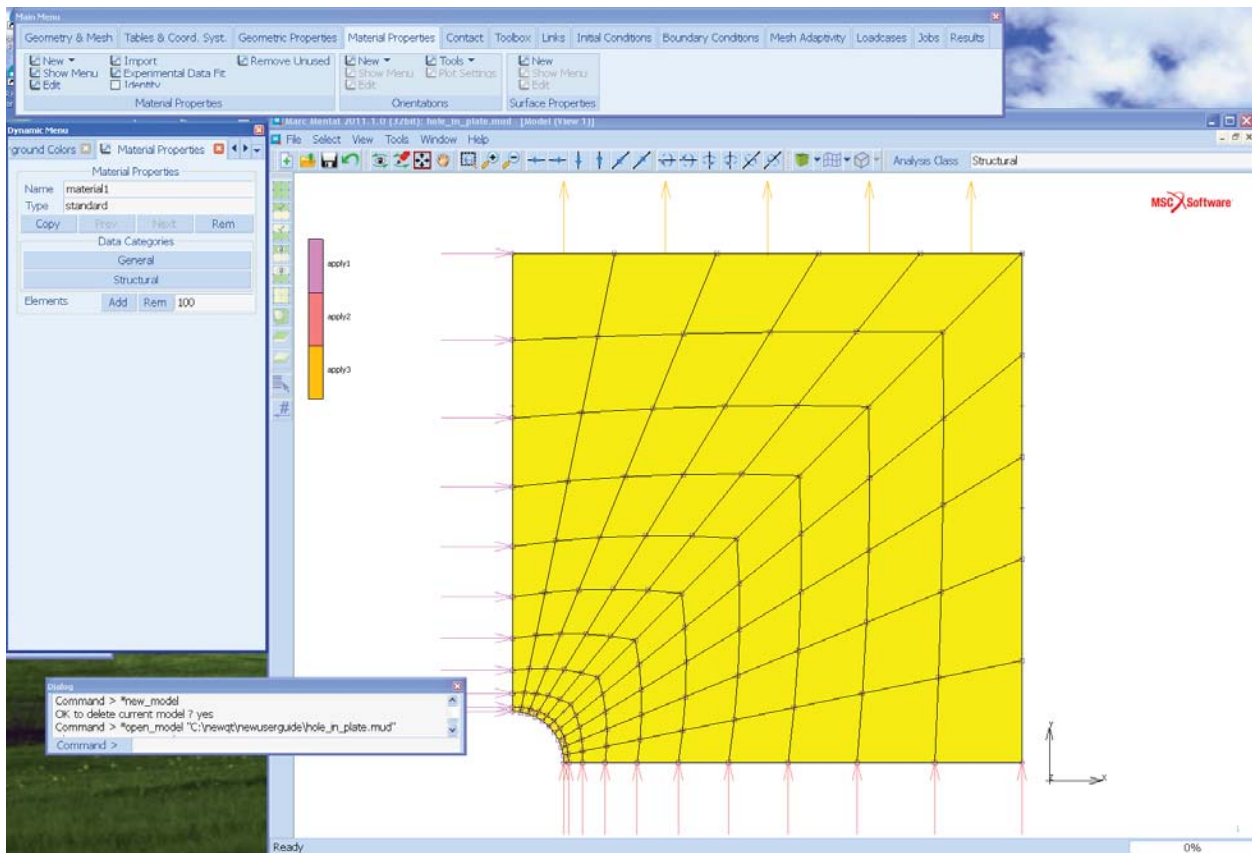




Figure 1.1-10 Repositioning Child Pop-up, Parent Pop-up cannot be Repositioned

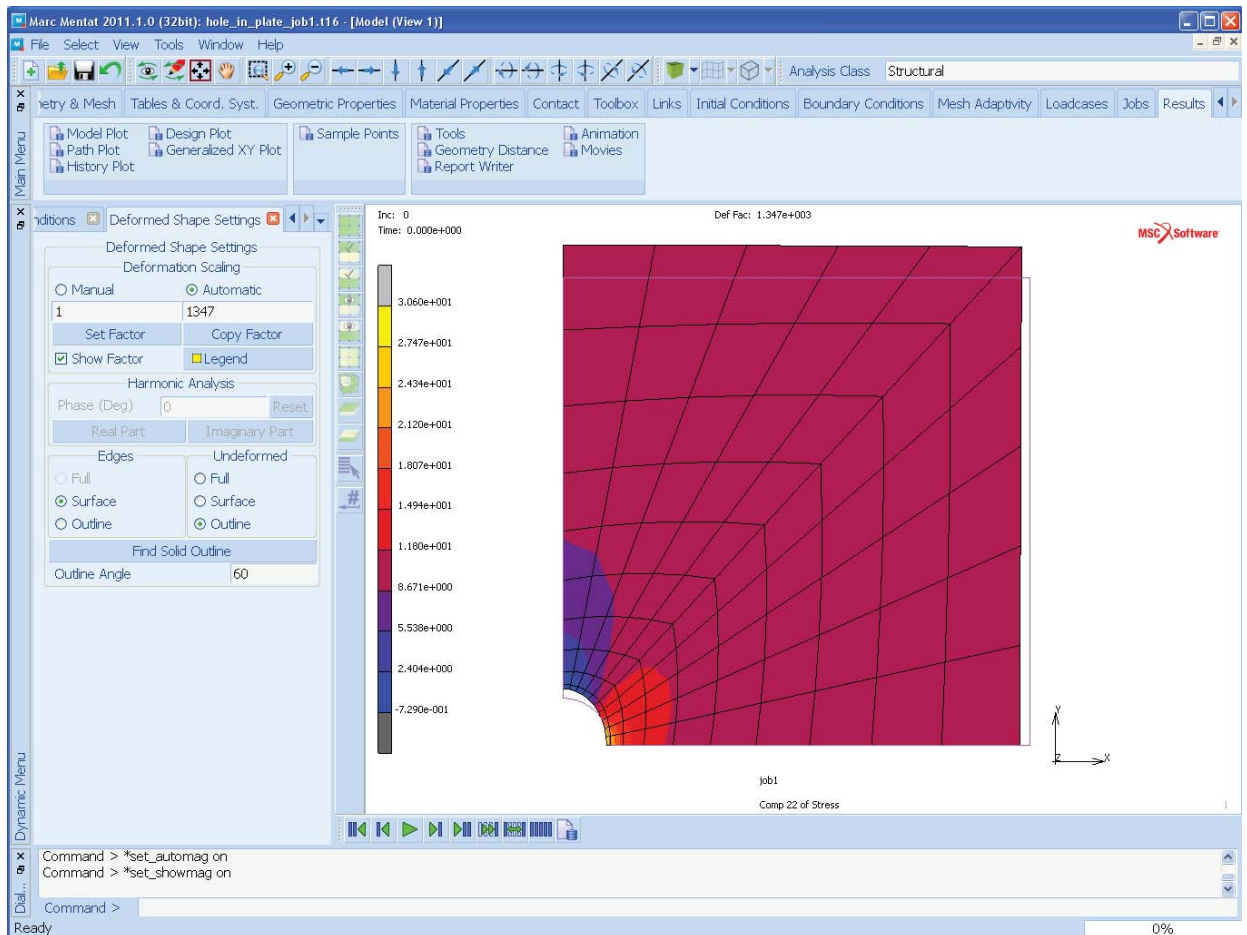
The Main, Dynamic and Dialog Menus may also be undocked from the Graphics Area. This is often useful for two-terminal type displays. In this case, these menus can be shifted to the second monitor, allowing a larger graphical display region for the model.



To achieve this click on the Window Icon  associated with these menus. To rejoin these menu to the full image double click on the menu header **Dynamic Menu** 

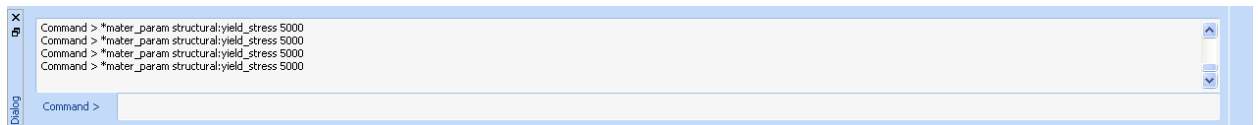
Drag and Drop

The icons in the tool bar can be customized using drag and drop. Click on the little dots with the left mouse button and move the icons. This allows you to customize the behavior of the interface.



The post file control icons have been moved to bottom.

The user can see all the commands that the program is generating in the Dialog menu.

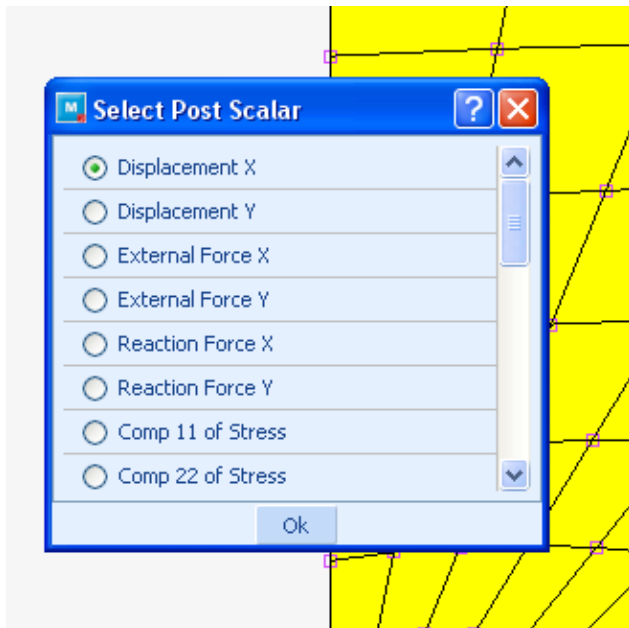


These commands are also put into a file called `Mentat.proc` that is started when the user invokes the program. They are also put into the Procedure File for later use if a procedure file has been created. Note that the user can scroll in the Dialog area. Additional use of the dialog area is discussed later.

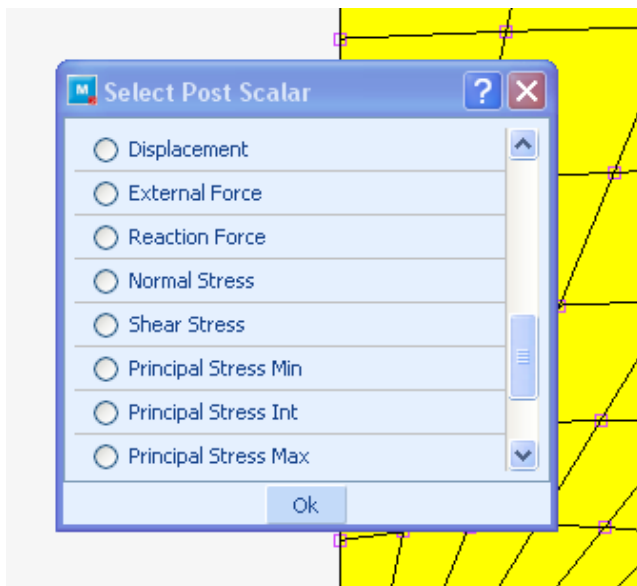
The command line area can be used to manually enter commands or literal strings such as Set Names or Boundary Condition Names or Numerical Data such as the Young's modulus.

Scrollable Widgets.

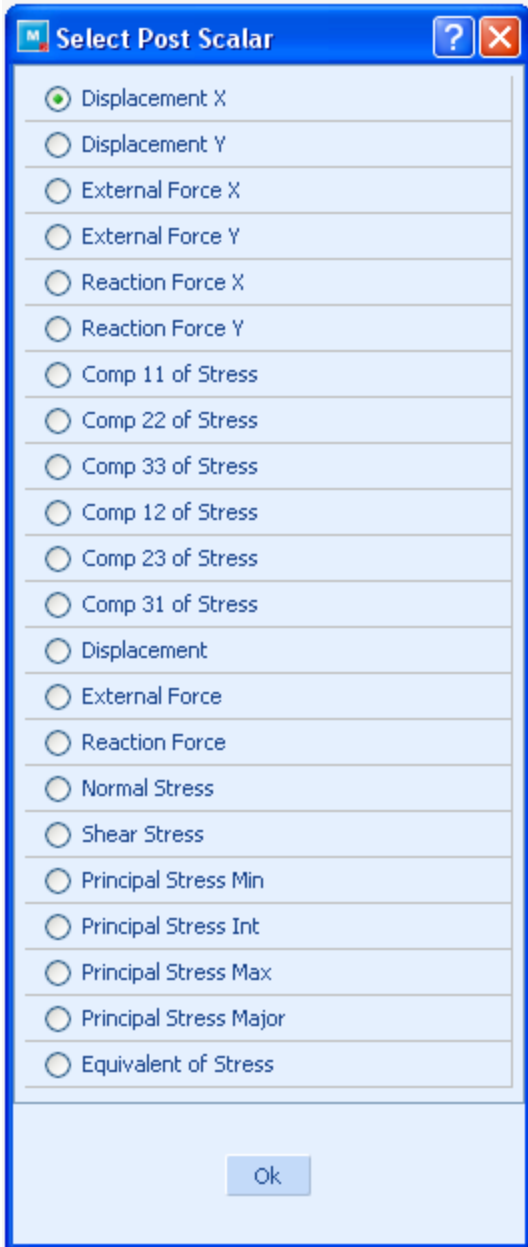
Mentat makes significant use of scrollable widgets such as when selecting the scalar value to be displayed.



One can either use the scroll bar to control



Or one can expand the scroll menu or do both.



If all items are visible, then the scroller disappears.

Menu System

The kernel of the Mentat program consists of a set of processors in a parallel configuration that operate on the data base. The data base is the most compact, yet complete, description of the current state of the model you are analyzing. Typical examples of processors are **SUBDIVIDE** and **PATH PLOT**.

Every processor may depend on a number of parameters that influence the process. The combined number of processors and parameters in Mentat is too large to show in one menu. To help you in the scheduling of tasks, we have structured menus around the processors that lead you through the steps from top down. [Figure 1.1-11](#) shows you the organization of the main menu that appears when you start Mentat and how it corresponds to the main tasks of the analysis cycle depicted in [Figure 1.1-1](#).

For your convenience, the menu items have been grouped in panels by the four main tasks: preprocessing, analysis, postprocessing, and configuration. The menu items and subtasks on each of these panels represent yet another group of corresponding tasks. It is important to realize that most of the menus for the global tasks do not contain processors; these menus are for navigation purposes only and are not part of the kernel of the program.

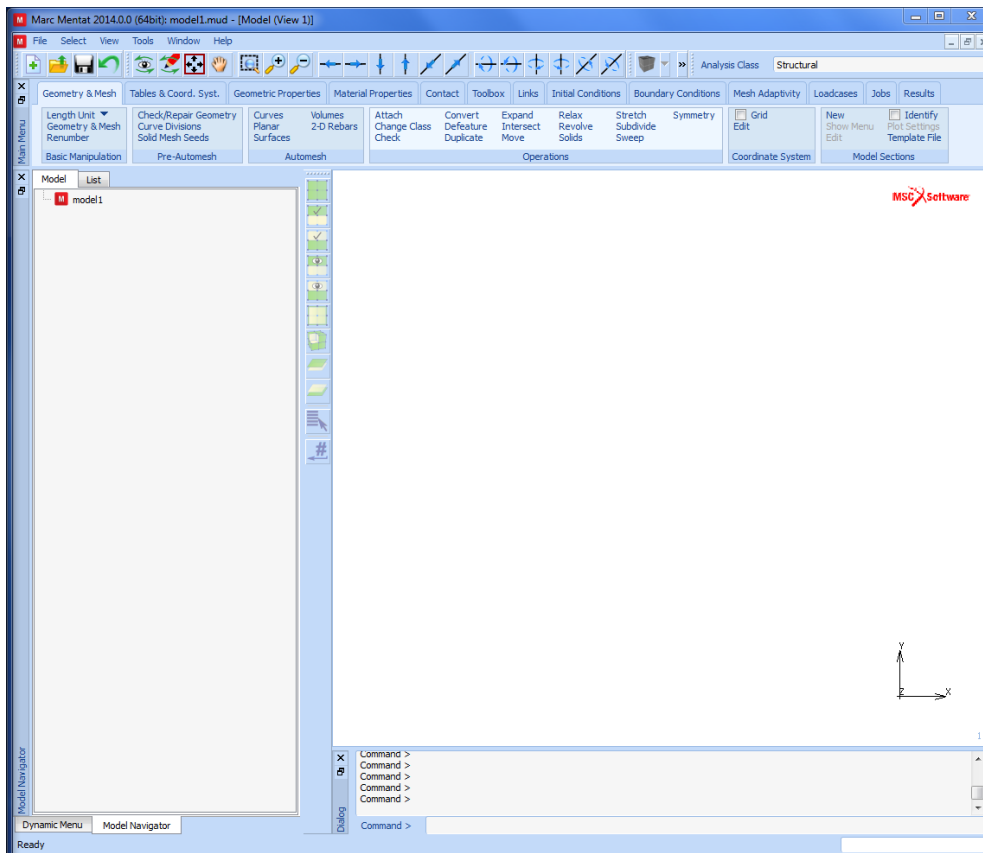


Figure 1.1-11 Organization of Main Menu

A task and corresponding subtask is selected by clicking on a menu item of that menu. After the (sub)task is accomplished, it is necessary to traverse the menus in the opposite direction. There are two ways to do this:

1. Click on the RETURN or MAIN menu items in the static menu area.
RETURN takes you to the previous menu and MAIN takes you to the main menu.
2. Move the <↑> over the menu area and click the <MR>. The result of this sequence is equivalent to clicking on the RETURN menu item.

Menu Components

This section describes the anatomy or different components of the Mentat menu and the meaning of each component.

Understanding the definition of components will help you to use the menu system in a proficient manner. We have already mentioned that the menu items are grouped into panels or submenus by task and related subtasks. Each menu has a title that describes its task.

Positioned on the panel are flat and raised rectangles. The raised rectangles in the released state suggest a light shining directly from above. The task is printed on the raised rectangle and is selectable by clicking on it with the <ML>. Flat rectangles are not selectable; they convey the setting of parameters. The program does not respond to clicking the <ML> or <MM> on the flat rectangles.

Mentat contains five types of raised rectangles. Throughout the remainder of this document, the term **button** is used for a raised rectangle. Below is a list of the different types of buttons and their functions.

Cycle Button

A cycle button is used to set a parameter to a value when there is a choice of three or more alternatives. The parameter is set to the value that is currently displayed on the button. Clicking on this button changes the displayed value to the next consecutive value in the list of alternatives. If the list is exhausted, the process starts over again with the first alternative. This button is identified by a ▽ symbol. Note that the symbol is indicative of the unidirectional way the list of alternatives is traversed.

Toggle Button

A special type of cycle button is the toggle button where the number of alternatives is limited to two. It is a switch that denotes a state of *on* or *off*; a button is *depressed* to flag on or active, and *released* (or *raised*) to flag that the listed parameter is off or inactive. This button is identified by a ◐ symbol.

Tabular Button

A tabular button represents a combination of a parameter button and a flat rectangle. They show one or more numerical or alpha-numerical values that are associated with the parameter represented by the button. Clicking on this button type usually implies that you have to enter data through the keyboard, which is then displayed in the rectangular fields after the keyboard input is completed.

Tabular buttons may contain a large number of numerical data fields. There are instances where the tabular buttons pop-up over the graphics area. If this is the case, you need to confirm that all entries have been completed by clicking on the OK button. Before returning to regular menu selection, you can clear all entries by clicking on the RESET button which usually appears in the lower left-hand side of the panel. The pop-up table then disappears from the graphics area

and the original graphics area is restored. Typical examples of these compounded tabular buttons can be found in the boundary conditions and material properties menus.

ACTIVATE/DEACTIVATE

A button that changes the behavior of the program that looks like a square. When not activated, it looks like . When activated, it looks like .

One-Only Button Group

The alternative values of cycle buttons are also represented as individual toggles under a one-only button group. In a cycle, only one value can be selected; hence if a button in a one-only group of buttons is depressed, another is released. The one-only button sequence is identified by an symbol that is picked resulting in .

As a typical example of a menu, the Coordinate System panel of the Mesh Generation menu as shown in [Figure 1.1-12](#) will be discussed. These buttons are also summarized in [Figure 1.1-16](#).



Figure 1.1-12 Coordinate System Panel

The GRID button is a toggle; it can be switched *on* or *off*. The default position for this button is the raised or released state which means that the grid is off. Clicking it will turn the grid *on* and leave the button in a depressed state.

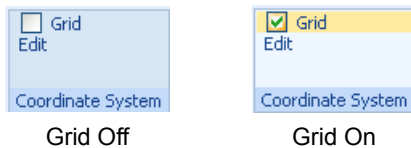


Figure 1.1-13 Released and Depressed States of a Toggle Button

The button next to it displays RECTANGULAR and has the symbol which implies one only. In this example, the button is an adjective to grid and specifies the type of grid to be used.

Figure 1.1-14 gives you examples of tabular buttons that are found in the SET submenu.

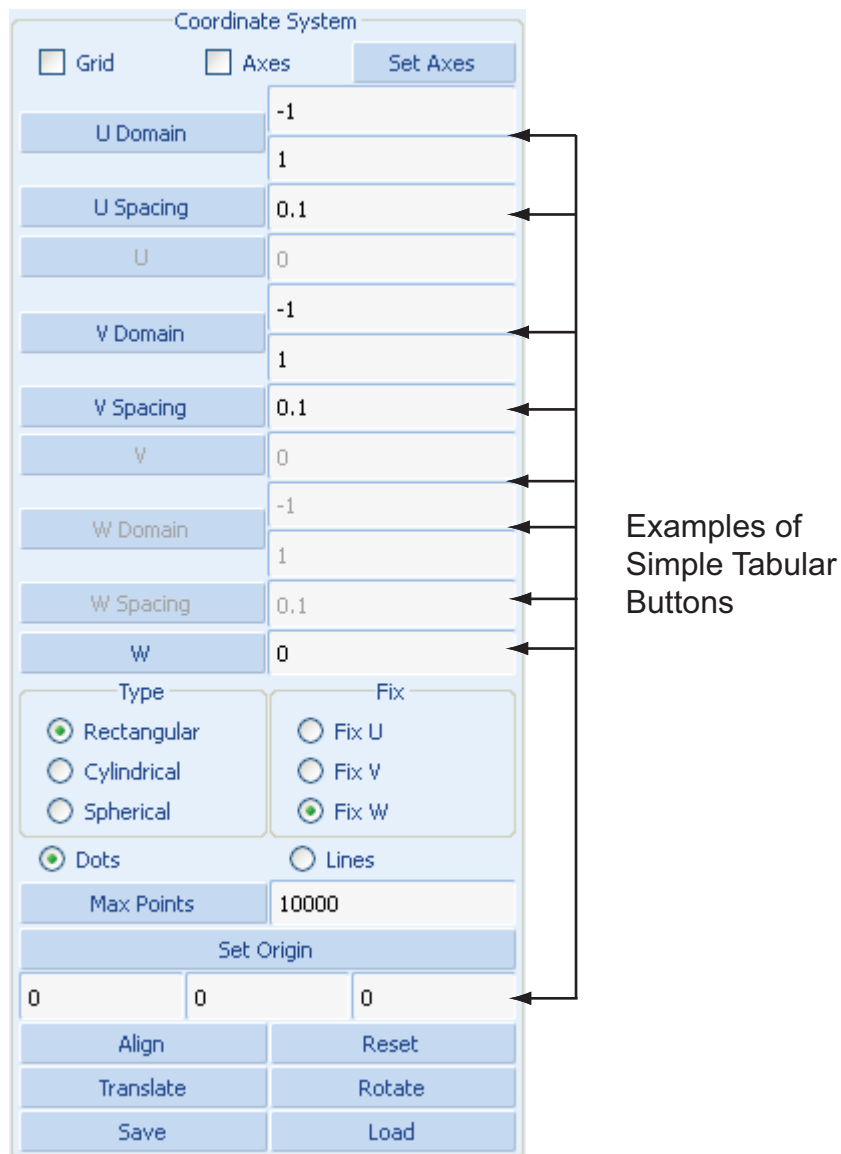


Figure 1.1-14 Example of Simple Tabular Buttons

The [Figure 1.1-15](#) summarizes the different types of buttons found in the Mentat menu.

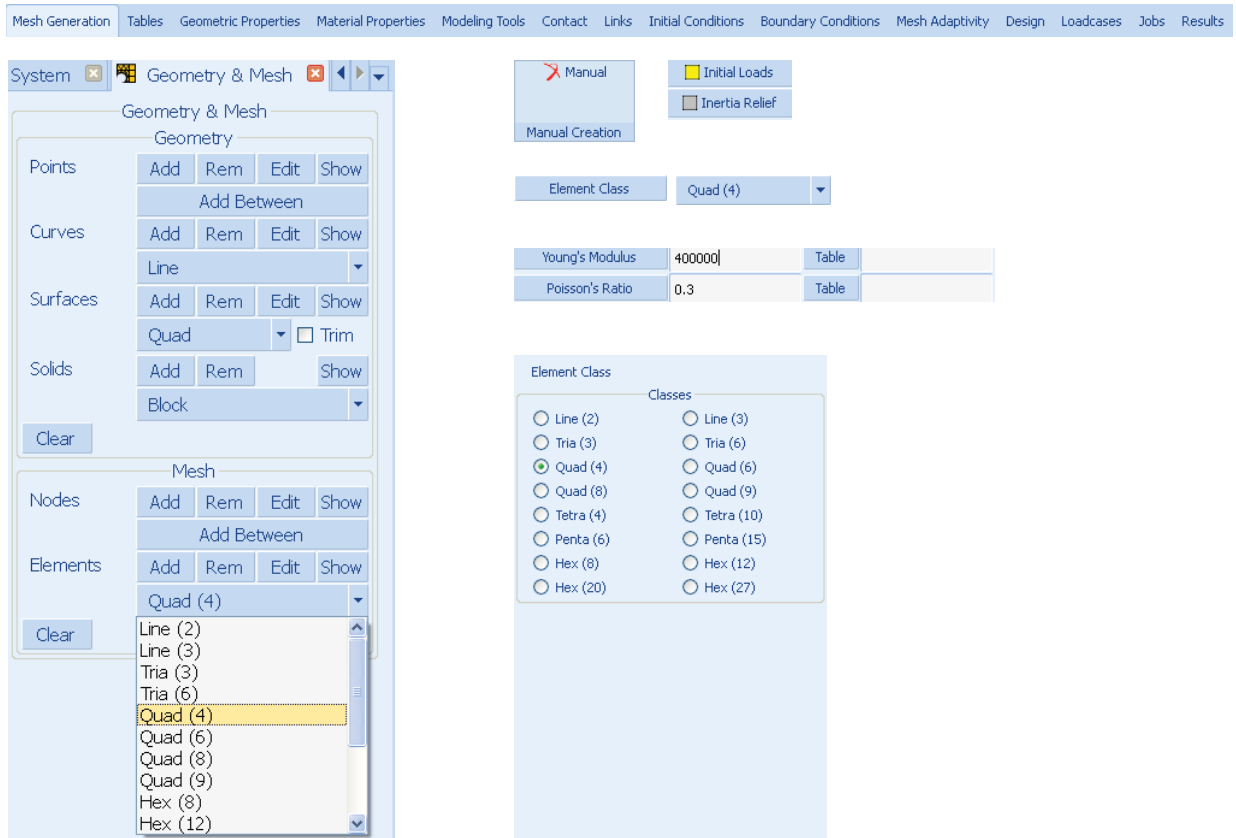


Figure 1.1-15 Summary of Mentat Menu Buttons

List Specification

[How This Manual Communicates with You](#) discussed the difference between menu buttons that are used to navigate through the menus and buttons that represent processors. Processors generally require two types of data:

- Parameters associated with the process
- A list of items to operate on.

If the list to operate on consists of only one item, you can use the mouse to point to that item on the graphics screen (see [Using the Mouse to Point](#)). If the list of items contains twenty items, pointing to each item individually becomes a cumbersome task; if the list contains a hundred items, pointing becomes an impossible task. This section concentrates on the capabilities in Mentat to specify a list of items.

The Mentat program recognizes the following items:

- Points
- Curves

- Surfaces
- Solids
- Vertices of solids
- Edges of solids
- Faces of solids
- Nodes
- Elements
- Edges of elements
- Faces of elements.

A simple example of how to generate a list follows. You can then extrapolate from what you have learned in this section to do more intricate examples. Assume you want to subdivide an existing element that is already displayed in the graphics area of the Mentat window. The processor to use is **SUBDIVIDE**, and it operates on elements only.

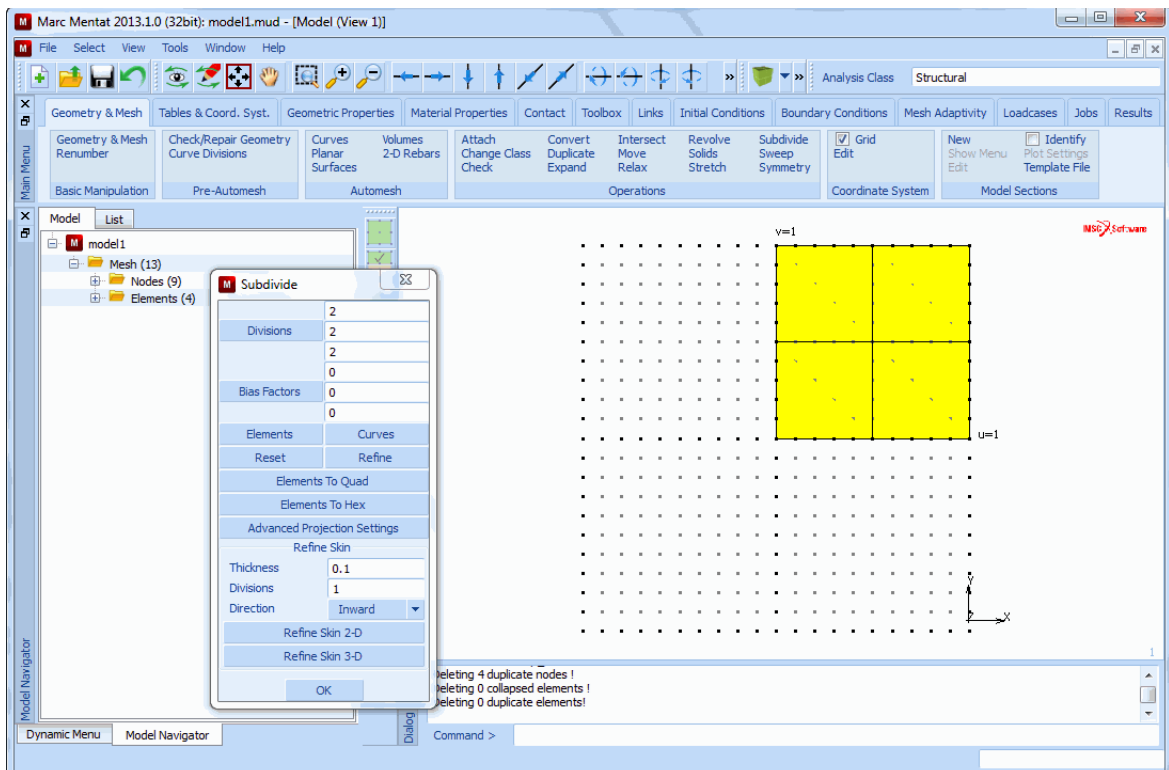



Figure 1.1-16 Locating the SUBDIVIDE Processor in the Mesh Generation Menu

After you activate the **SUBDIVIDE** processor and click on the **ELEMENTS** button in the subdivide submenu, the following program prompt appears in the dialogue area:

```
Enter subdivide element list:
```

Chances are that you don't know the element number (nor should you care at this point). For this reason, answering this question by typing a number in the dialogue area may be possible but is not necessarily a viable option. Instead, move the mouse over the graphics area and use the <ML> to click on the center of the element. You have now entered the first element in the list. The program keeps prompting you for more elements; if this is the only one you want to subdivide, you must let the program know that this is the end of the list. This can be done in one of three ways:

1. Press the **END LIST** button in the menu area, 
2. Type a '#' sign in the dialogue area, or
3. Click <MR> with <↑> anywhere over the graphics area.

The most convenient way of ending the list is of course to click <MR> since the <↑> is most likely already over the graphics area and saves you a keystroke from the keyboard.

Using a Box to Specify a List

Suppose the number of subdivisions was set to 20 by 20, creating 400 elements. Assume you want to enter the left 200 elements in a list by creating a rectangle to fence in those elements. Position the <↑> at one of the corners of the box. Depress the <ML> and move the <↑> to the opposite corner of the box you want to create. The rectangle that appears tells you exactly which elements are included in the box. Once you have reached the desired position, release <ML> (see [Figure 1.1-17](#)). For Every element that is *completely* inside the box is included in the list specification.

There are times when you may need the guidance of cross hairs to help you determine what is to be included in your selection. To activate the cross hairs, press the **SHIFT** key while moving the <↑> in the graphics area.

Note: You can relax the completely inside constraint mentioned previously by using the **PARTIAL** button on the picking panel under **DEVICE**.

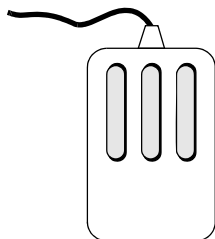
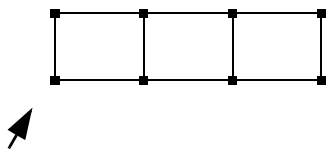
Using a Polygon to Specify a List (CTRL Key + <ML>)

An alternative to using the box pick for list specification is to use a polygon around the elements ([Figure 1.1-18](#)) that you want to include in the list. As with the box pick method, only those elements that are completely inside the polygon are entered into the list. To use the polygon pick, move the <↑> to the first corner point of the polygon. Click <ML> while holding down the **CTRL** key on the keyboard. Move to the next vertex of the polygon and click <ML> again, continue to hold the **CTRL** key down. Repeat this process until a closed loop is formed. The last point needs to be in the vicinity of the starting point and must be clicked on to end the selection. A variation on this polygon pick is the **lasso pick** This is done by holding down the **CTRL** key and the <ML> down simultaneously while slowly moving the mouse, until the elements to be selected are surrounded by the lasso ([Figure 1.1-19](#)). With either approach, a final click on <ML> is required at the position near the beginning of the polygon or lasso.

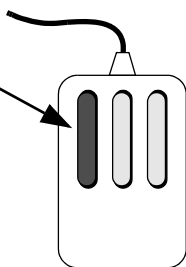
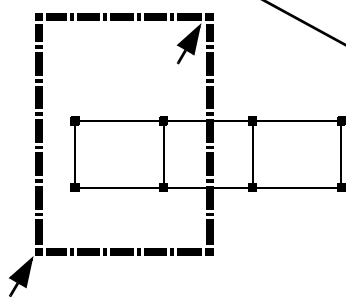
Note: The **PARTIAL** and **COMPLETE** buttons mentioned under the **VIEW > DEVICE** menu Pick Method also apply to the Polygon Pick Method.

Table 1.1-1 at the end of this chapter summarizes the mouse selection options in both the graphics and menu areas.

Step 1: Position the cursor



Step 2: Hold down the <ML> and drag the cursor to the desired position



Step 3: Release the <ML> button

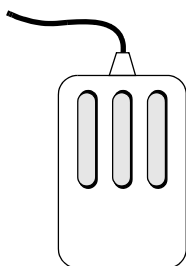
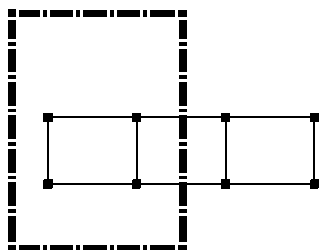


Figure 1.1-17 Selecting an Element Using the Box Pick Method

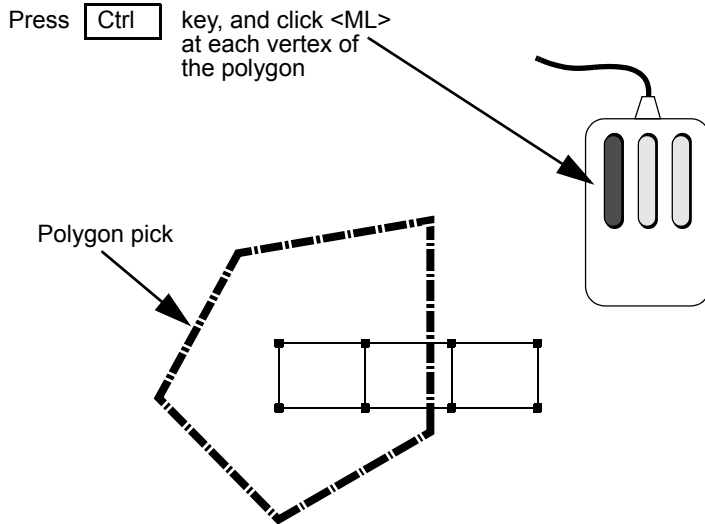


Figure 1.1-18 Selecting an Element Using the Polygon Pick Method

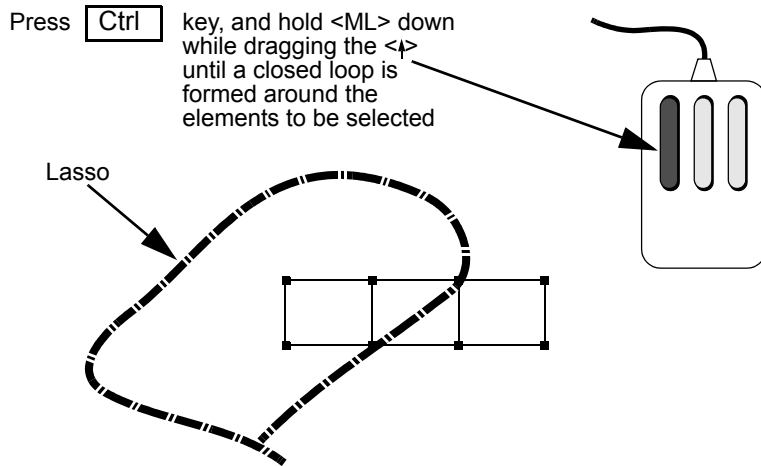


Figure 1.1-19 Selecting an Element Using the Lasso Pick Method

LIST Buttons

For your ease of use, we have preprogrammed some of the more common list options and assigned them buttons which are located in the lower left-hand side of the static menu.

The LIST buttons are:

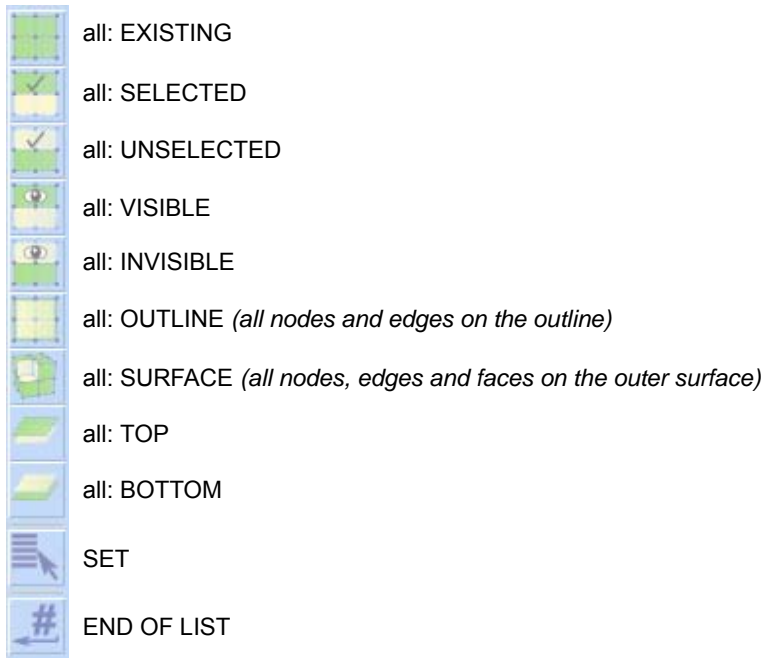


Figure 1.1-20 Location of LIST Buttons

All: EXISTING

Perhaps the most used list button is all EXISTING. It specifies all existing elements, nodes, curves, points, or surfaces (whichever is applicable), to be operated on by the processor that requested the list.

The contents of the selected/unselected, visible/invisible list are determined by the two operators: SELECT and VISIBLE. The meaning of each and their connection is explained in the next paragraphs.

All: SELECTED/UNSELECTED

The SELECT operator is a very powerful way to separate specific items from others. The methods by which items are selected range from a single item to a path of nodes, a box of items, or all items on a plane, and are connected by Boolean operators such as *and*, *except*, *invert*, and *intersect*. An example of this syntax is:

(use) single [items] and (a) box (of) [items] except single [items]

where the words *use*, *a*, *of*, and *item* are implied because they do not appear as buttons. A powerful feature of the **SELECT** processor is the ability to name a group of items, and refer to them by that name in list specifications. The STORE command facilitates this process.

All: VISIBLE/INVISIBLE

Sometimes the model may be so complex that it takes an unacceptably long time to update the graphics screen every time the database changes. It is advantageous to focus on the items that you are working on. By activating and

deactivating items from the display list, you can minimize the items that are displayed. Note that activating or deactivating does not imply that they are removed from the database.

The **VIEW>VISIBILITY** processor facilitates this activation and deactivation process by using the **VISIBLE** and **INVISIBLE** commands.

Tables 1.1-1 and 1.1-2 summarize the functions of the three-mouse buttons in the graphics and menu areas.

Table 1.1-1 Mouse Button Functions in Graphics Area

	<ML>	<MM>	<MR>
	single pick or box pick	unpick	end of list
SHIFT	single pick or box pick with cross hairs	unpick	end of list
CTRL	polygon pick or lasso pick	unpick	end of list

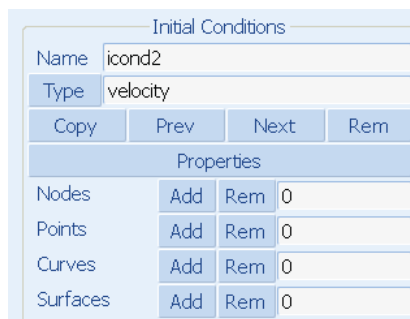
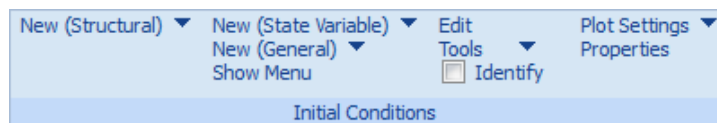
Table 1.1-2 Mouse Button Functions in Menu Area

	<ML>	<MM>	<MR>
	command selection	on-line help	return

Identifiers

In many applications, an identifier is associated with a group of data. These applications include material properties, link properties, geometric properties, boundary conditions, initial conditions, tables, transformations, beam sections, loadcases, and jobs. The identifier can be any name, if none is given a default name is given. These ID names are then referenced in other commands. The use of IDs is detailed below.

When using many of the menus, the following buttons appear.



Creates a new entry in the list of applications and makes it the current application.



Removes the current application ID and the associated data.

Name

Allows you to provide a name to the current application.

Copy

Creates a new entry in the list of applications by copying the current application ID; the new entry becomes the current application.

Prev Next

Allows you to position to either the previous or next item.

Type

Displays a list of the IDs and allows you to select a particular ID. The selected ID becomes the current one.

Menu Customization

You may customize the menu system of Mentat to suit your special requirements.

The menus in Mentat are defined by the files in the *mentatvers\menus* directory. There are two sets of files in that directory: files with extension *.ms* and three files with extension *.xml*. The **.ms* files define the menus for Mentat Classic and the menus in the Dynamic Menu and the popup menus in the new Mentat. The **.xml* files are used to define the contents of the menu bar at the top (*menubar.xml*) with the File, Select, etc menus, the tool bars (*toolbars.xml*) and the main menu ribbon (*main.xml*). The **.xml* files are not used by Mentat Classic.

The **.ms* file in the menus directory are compiled into a binary menu file, called *main.msb*. This file is located in the *mentatvers\menus\win32* (for 32-bit Windows) or *mentatvers\menus\win64* (for 64-bit Windows). If a binary menu file exists, then Mentat will use it and will not read the **.ms* files. So, if you change the **.ms* files, then you have to recompile the binary menu file, as follows:

```
mentatvers\bin\mentat -compile main.msb
```

and the copy the file to the appropriate menus folder. Alternatively, you can force Mentat to use the **.ms* files and ignore the binary menu file, by starting it as follows:

```
mentatvers\bin\mentat -mf main.ms -ra
```

However, start up is slower in this way.

If you make only make changes to the **.xml* files, you don't have to recompile the binary menu file. You only have to restart Mentat.

If you are going to make changes to the existing menus, then it makes sense to create a folder, *C:\mymenus* say, in which you put your modified menu files, instead of changing the files in the Mentat installation. You can tell Mentat to look in the *C:\mymenus* folder for menu files, using the `-mp` option, as follows:

```
mentatvers\bin\mentat -mp C:\mymenus
```

When Mentat looks for a menu file, the *C:\mymenus* searched first, so any modified files in that folder will be used instead of the original files in the Mentat installation. This applies to both the `*.ms` and `*.xml` files. You can even put your own binary menu file `main.msb` in that directory.

The only documents that we have on customization of the Mentat menus are included in the directory `...\Marc\vers.0.0\doc_install\doc\menu` of the installation (you have to install the documentation separately). The files are called:

```
MenuGuide.html
MenuSpec.html
MenuCompile.html
```

These documents have not been updated recently, but the main concepts are still valid. However, they only discuss structure `*.ms` files.

There is no documentation on the `*.xml` files for the new Mentat yet. However, the structure of these files is straightforward. For example, `menubar.xml` defines the menu bar of the new Mentat as a list of `<menu>` items. Each `<menu>` corresponds to a pulldown menu in the menubar (File, Select, View, Tools, and Help). A `<menu>` consists of a number of menu items which show up if you open the pulldown menu. There are several types of menu items:

- `<label>` Defines a label item (text)
- `<exec>` Defines a menu item that executes a command (or a string of commands)
- `<file>` Defines a file browser
- `<popmenu>` Defines a menu item that opens a popmenu which must be defined in a `*.ms` file

Menus can be nested. A `<menu>` inside another `<menu>` defines a submenu.

Mentat Classic

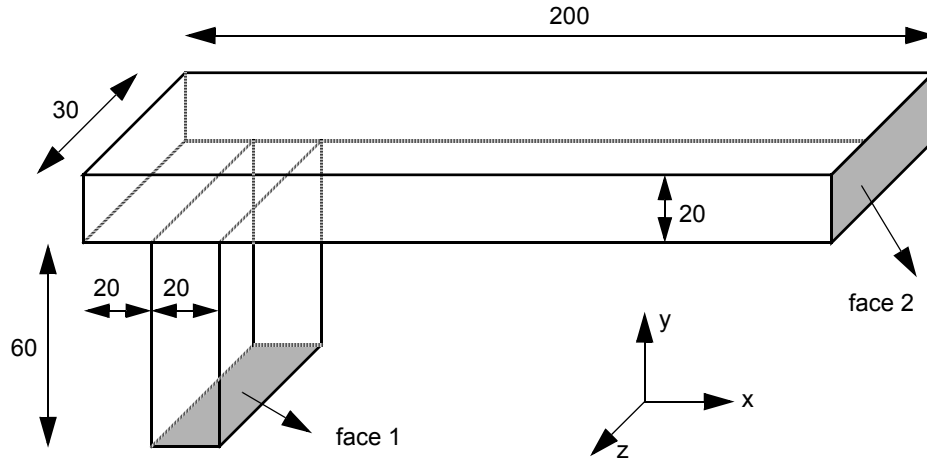
The SHORTCUTS menu button in the lower left-hand corner provides some useful shortcuts; however, these can be changed to be any list of quickly accessible commands. See the *Mentat Menu Customization Guide* under the Mentat directory of `doc/menu/MenuGuide.html`. You may open a menu file for editing by moving the cursor over a displayed menu and pressing the F2 function key.

Comprehensive Sample Session

In this hands-on session, you will create a simple 3-D mesh and add all appropriate boundary conditions, material properties, etc. You will run the analysis and view the results.

Note: The example sessions in this manual are based upon Mentat over the last few releases. The commands shown provide an indication of what you should do to create models and perform analysis. Some on the syntax of the commands may have changed in this release.

A linear elastic analysis of the following 3-D structure will be performed:



- **Boundary conditions:**

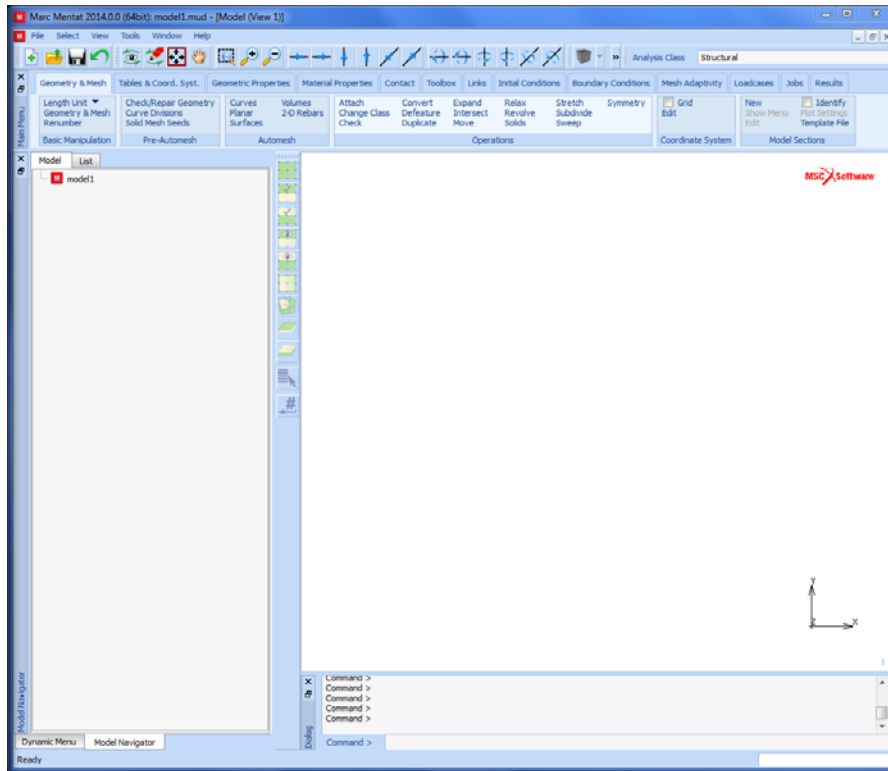
- face 1: clamped
- face 2: loaded by a uniformly distributed shear load (force per unit area), magnitude 40, direction

$$\begin{bmatrix} 0 & 1 & -1 \end{bmatrix}^T$$

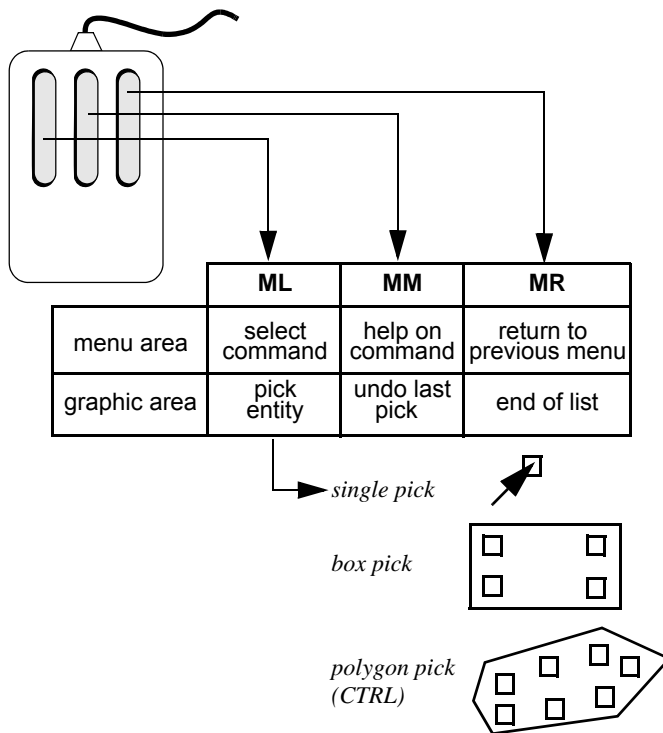
- **Material properties:**

- Young's modulus $E = 4 \times 10^5$
- Poisson's ratio $\nu = 0.3$

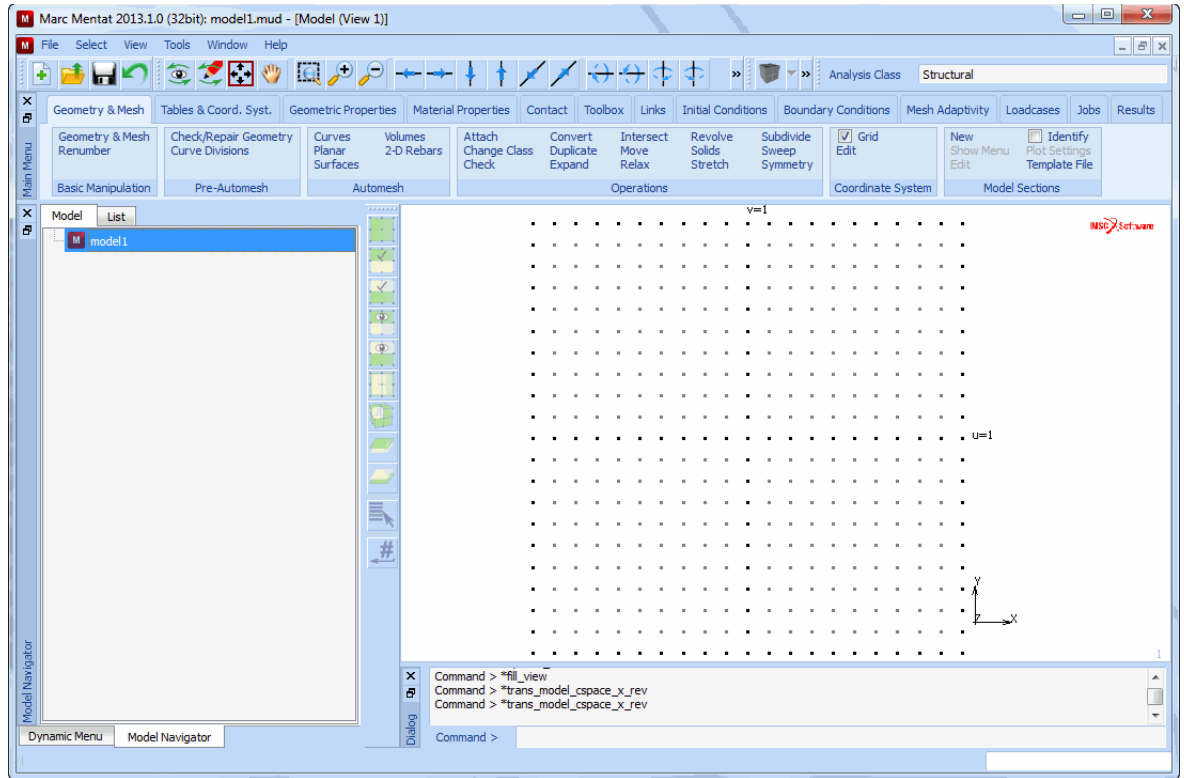
- **Start up window Mentat:**



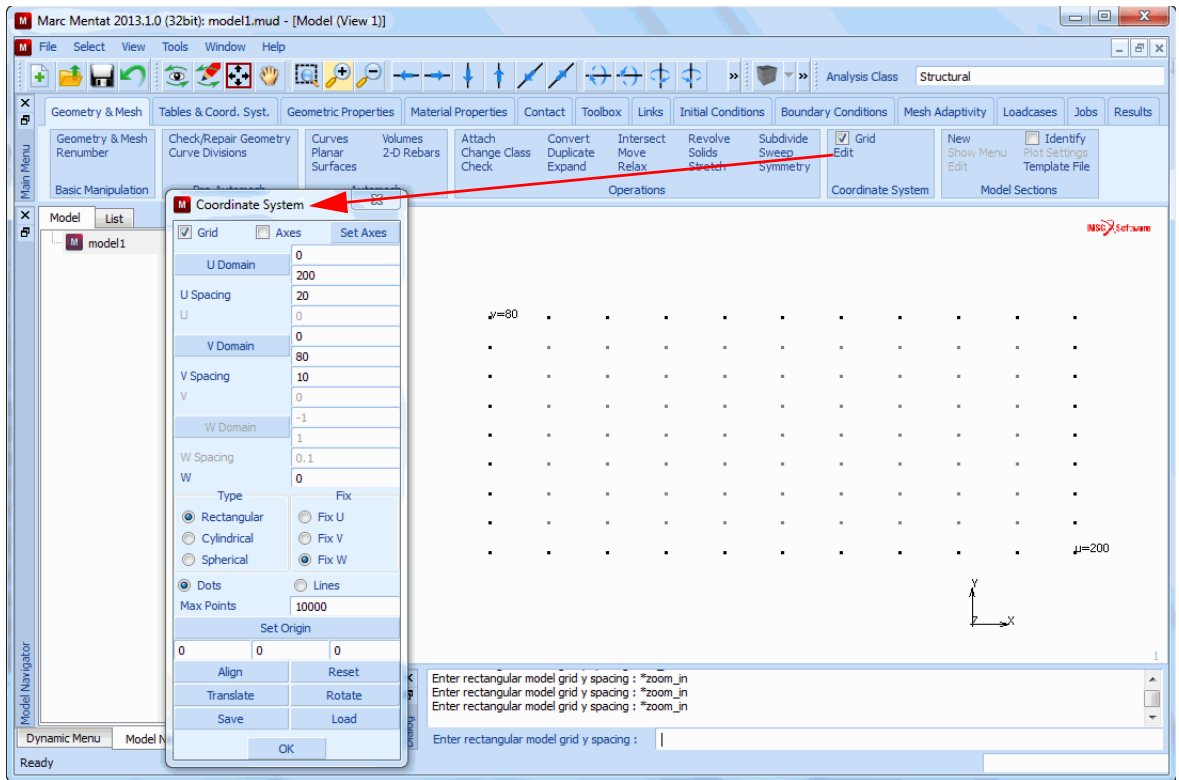
• Mouse buttons



- Mesh generation: top menu, default grid on



- **Mesh generation (continued): set and display grid for easy input of coordinates and fill view**



SET: COORDINATE SYSTEM

GRID ON

U DOMAIN

0 200

U SPACING

20

V DOMAIN

0 80

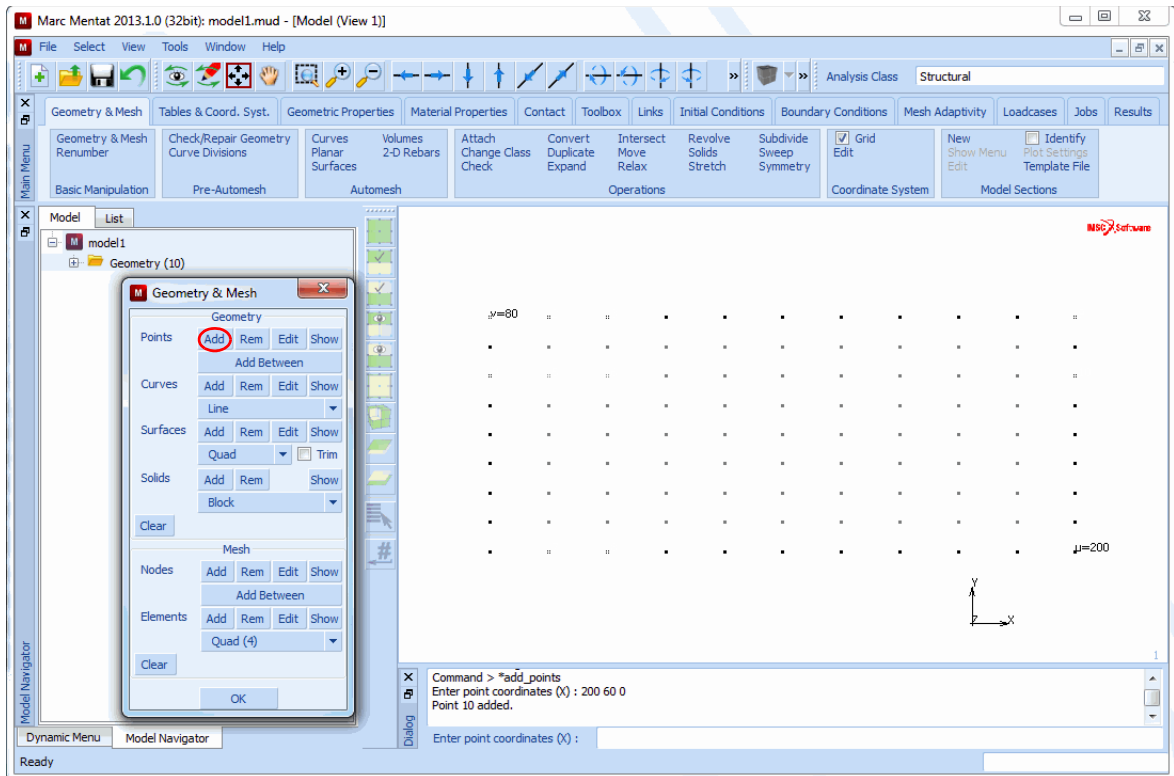
V SPACING

10

FILL

RETURN

- **Mesh generation (continued): create points (geometric entities), switch off grid and fill view**

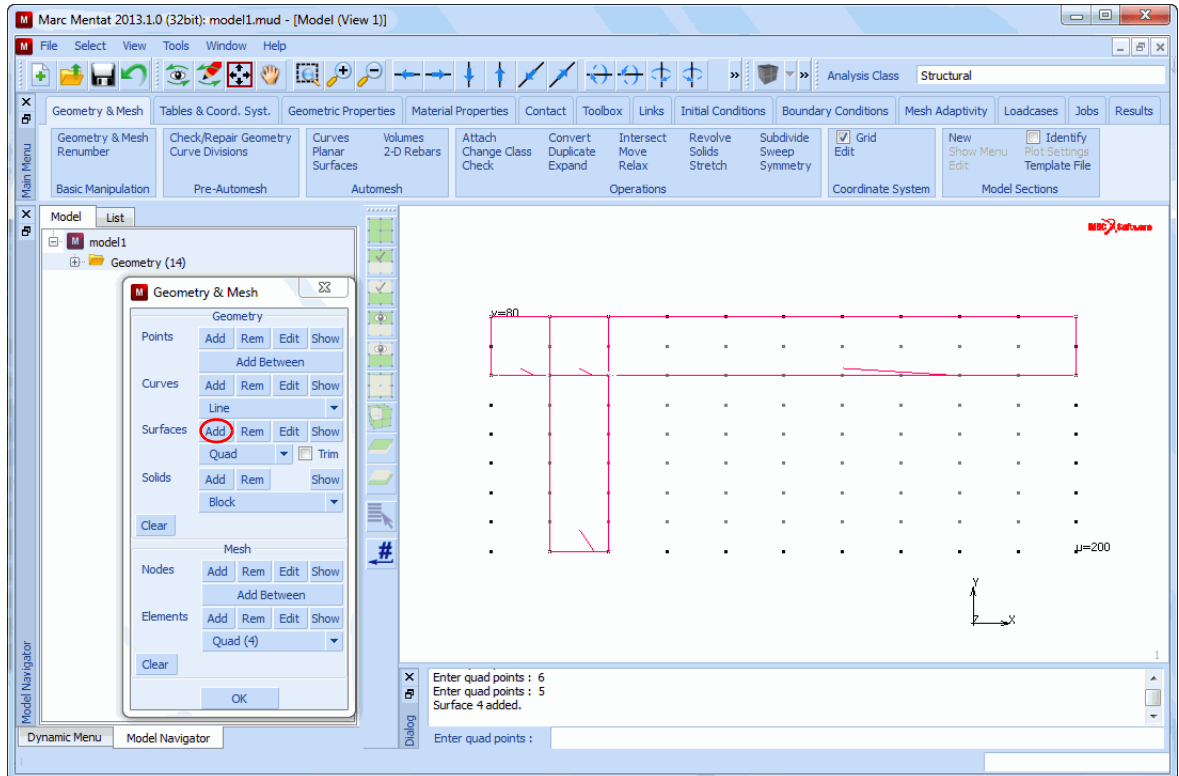


PTS: ADD (Add the following points with mouse clicks)

- (0,80,0)
- (20,80,0)
- (40,80,0)
- (0,60,0)
- (20,60,0)
- (40,60,0)
- (20,0,0)
- (40,0,0)
- (200,80,0)
- (200,60,0)

FILL

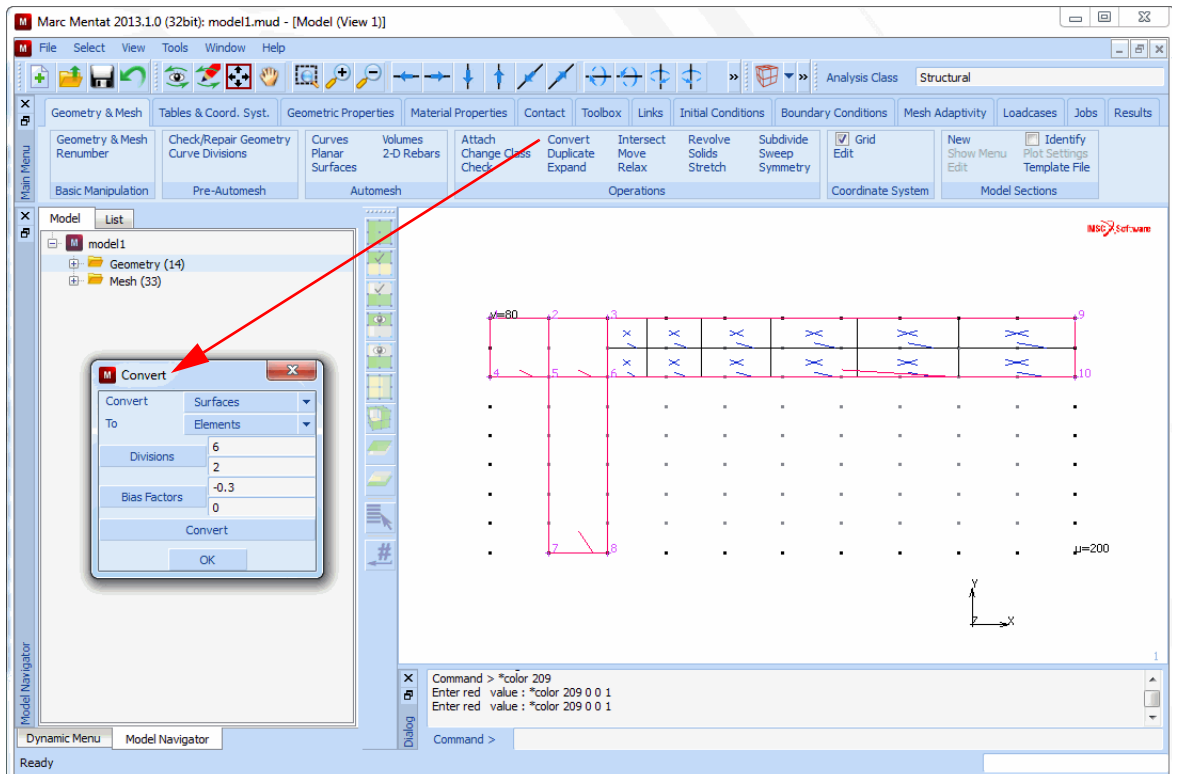
- Mesh generation (continued): create quad surfaces (geometric entities)



SRFS: ADD

Pick corner points for quad surfaces with mouse clicks to obtain four surfaces as shown. A half-arrowhead is used to indicate the first side of the surface.

- Mesh generation (continued): convert surfaces to elements (mesh entities)



CONVERT

DIVISIONS

6 2

BIAS FACTORS

-0.3 0

SURFACES TO ELEMENTS

DIVISIONS

2 2

BIAS FACTORS

0 0

SURFACES TO ELEMENTS

DIVISIONS

2 3

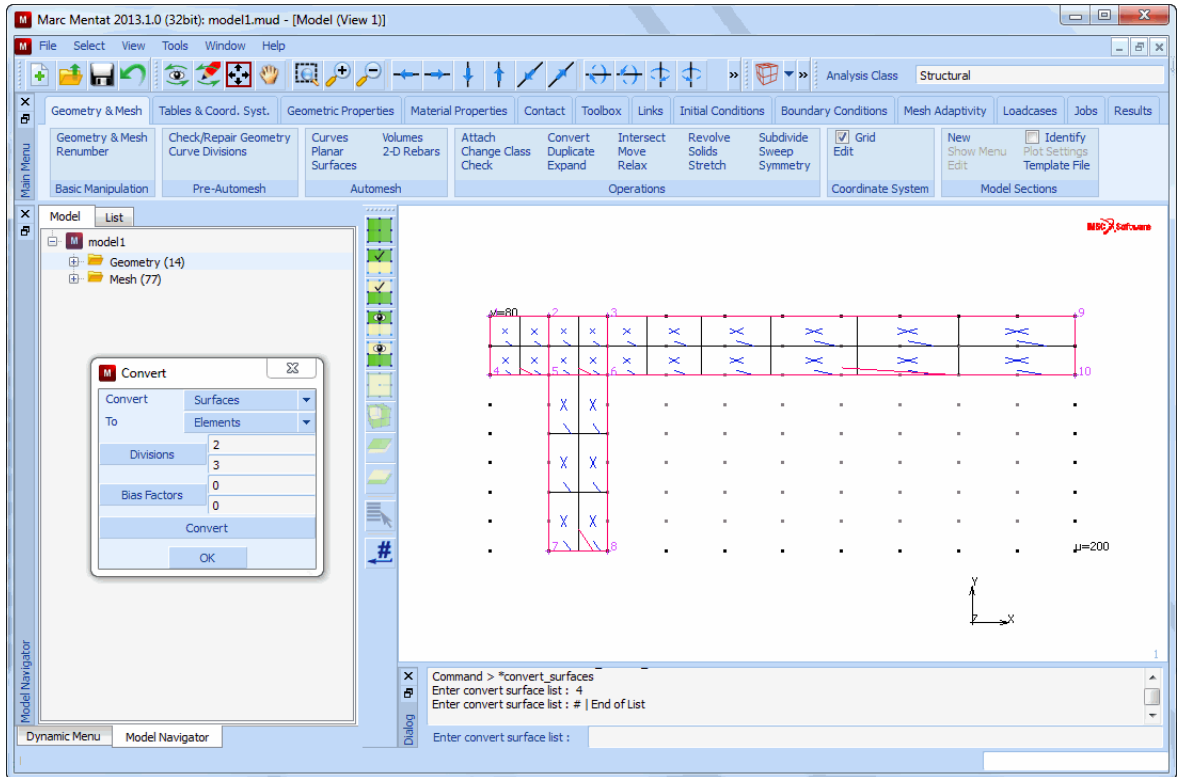
SURFACES TO ELEMENTS

(pick the rightmost surface)

(pick the two small surfaces)

(pick the lower surface)

- Mesh generation (continued): modify sweep tolerance and use sweep option to merge coincident nodes



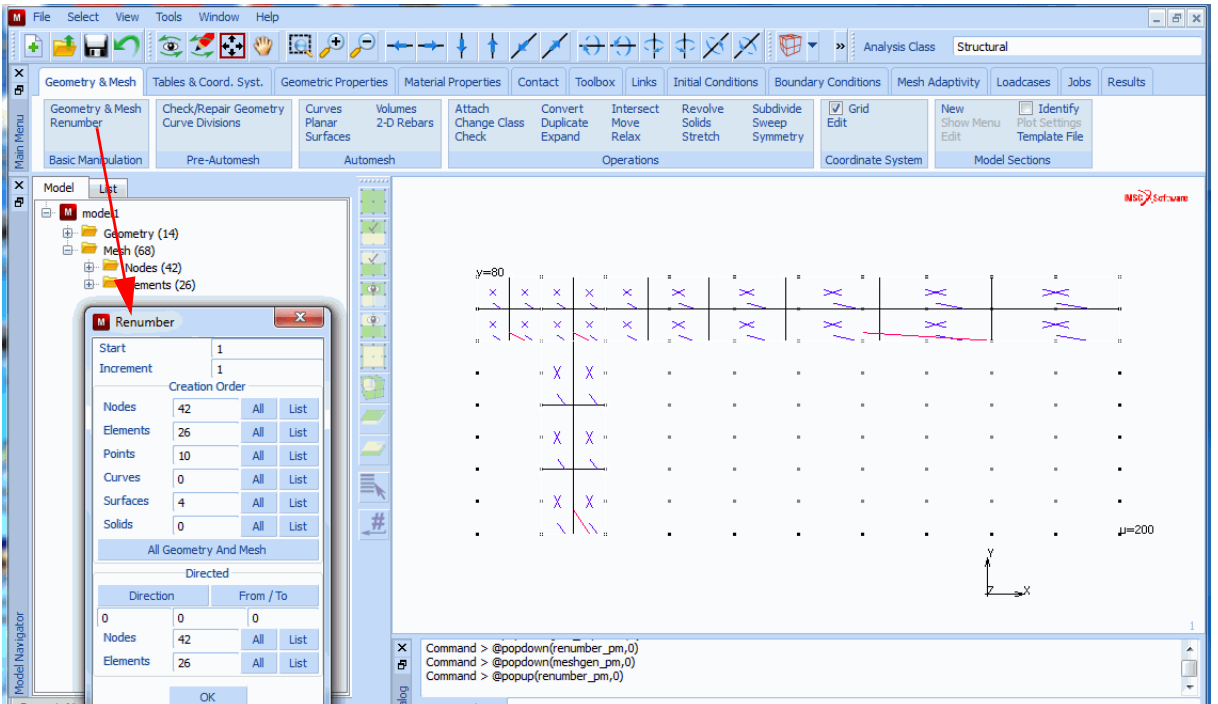
SWEEP

TOLERANCE

0.001

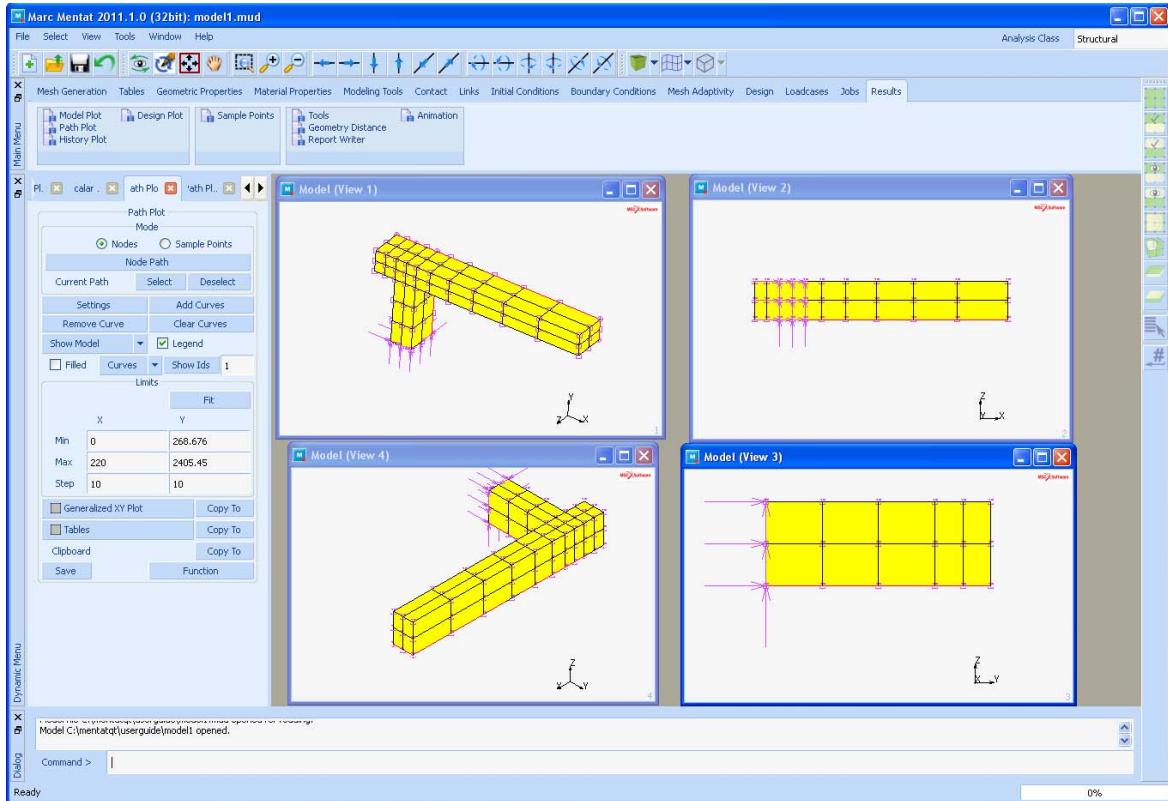
ALL

- Mesh generation (continued): use renumber option to obtain consecutive numbering



RENUMBER
ALL

- Mesh generation (continued): use expand option to expand the mesh in z-direction



EXPAND

TRANSLATIONS

0 0 15

REPETITIONS

2

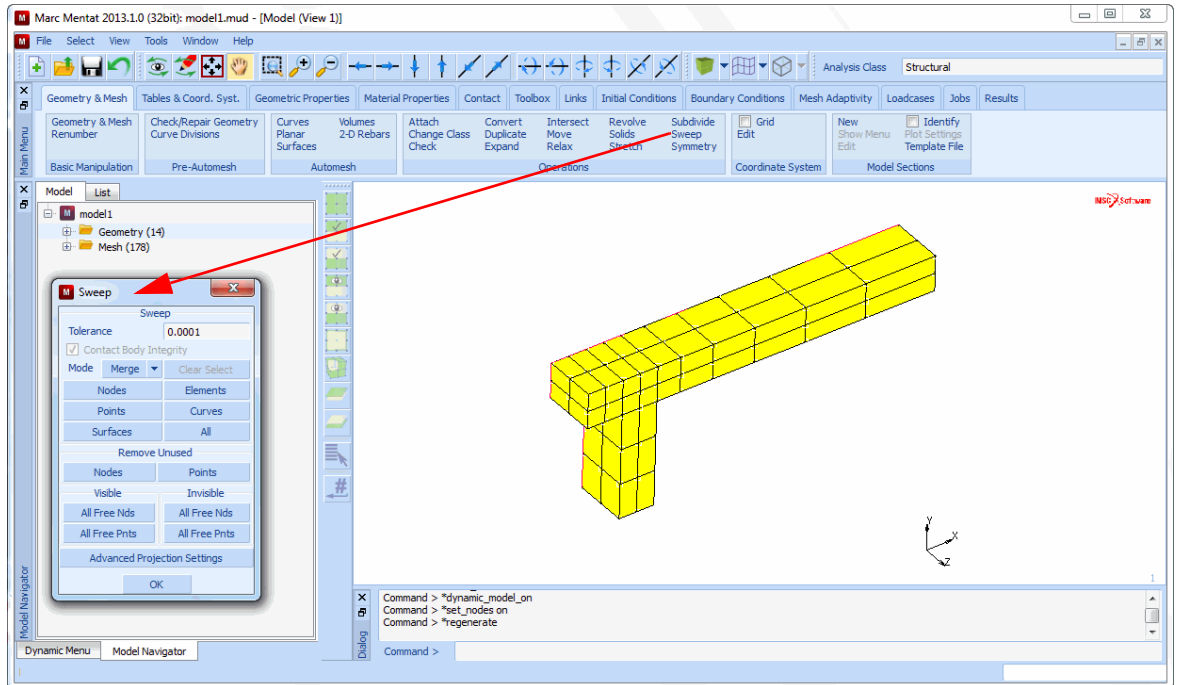
MODE: REMOVE

ELEMENTS

ALL: EXISTING

(no action required, this is the default)

- Mesh generation (continued): remove unused nodes and repeat renumber command



SWEEP

REMOVE UNUSED: NODES

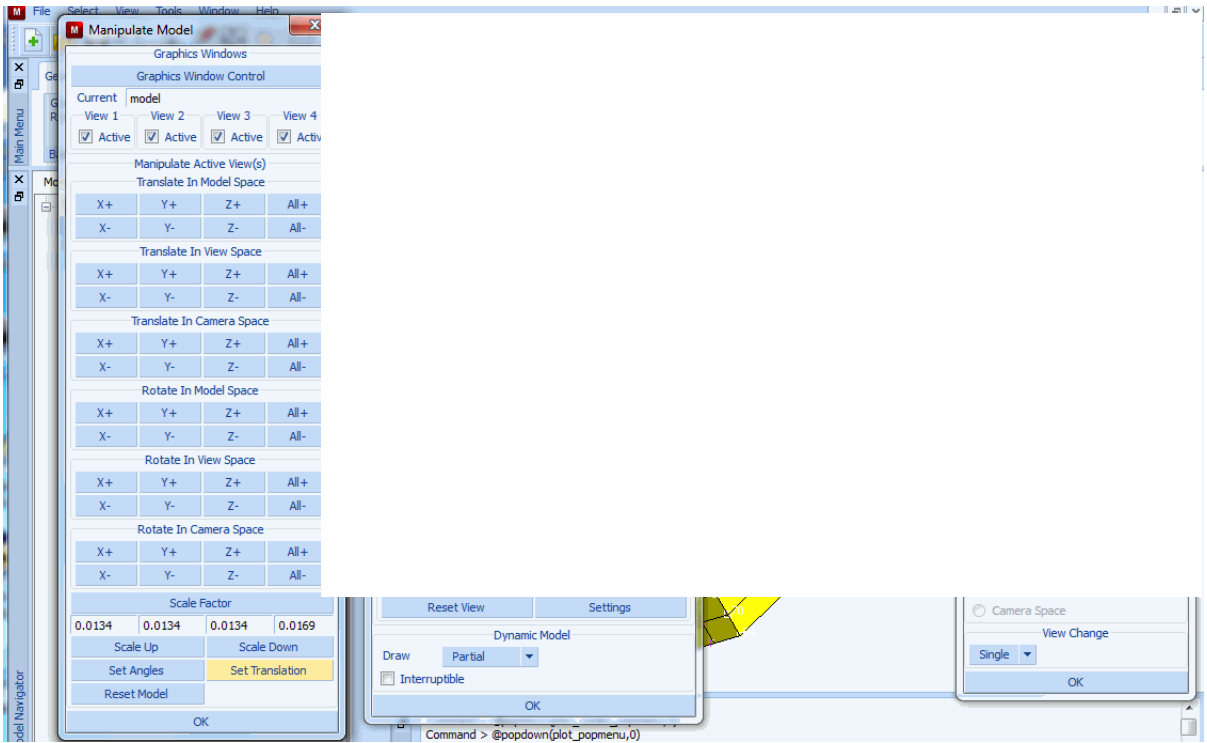
ALL

RETURN

RENUMBER

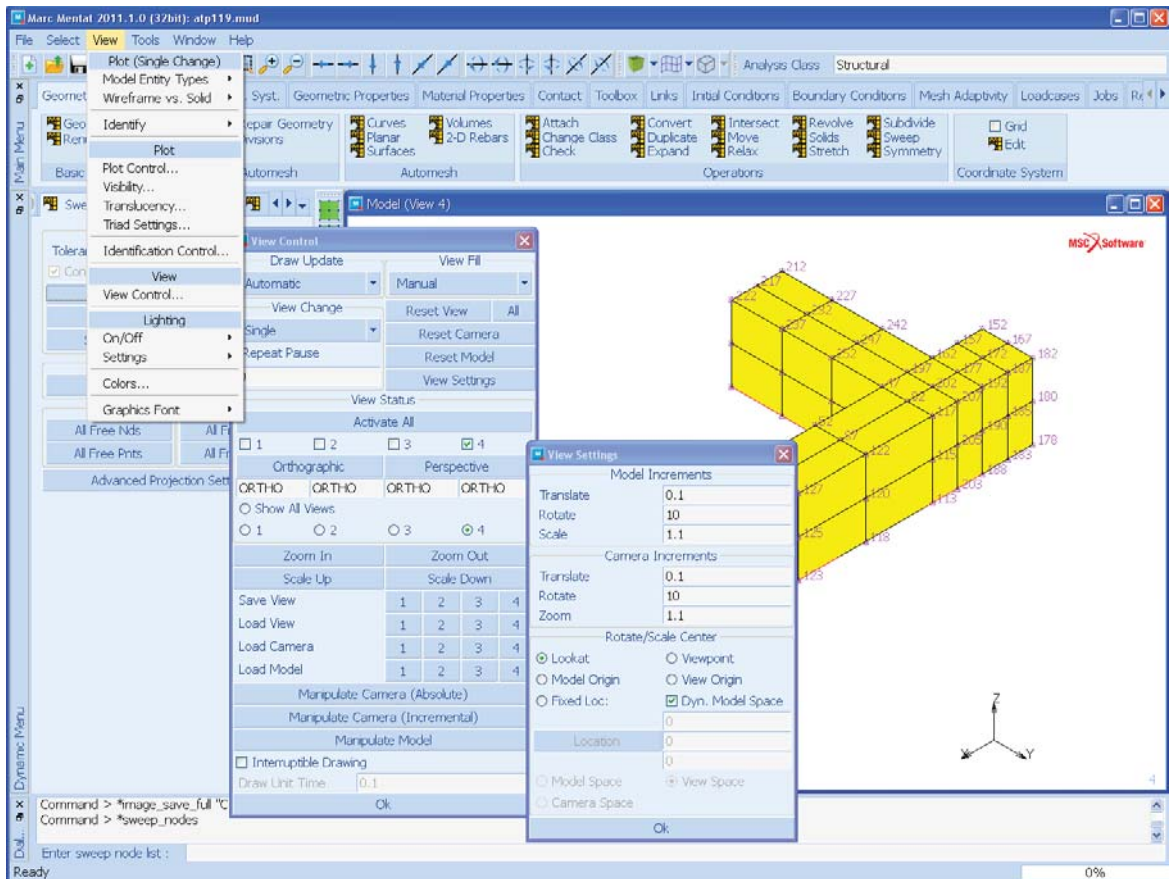
ALL

- Mesh generation (continued): show view 4 and fill view



VIEW
SHOW VIEW
4
FILL

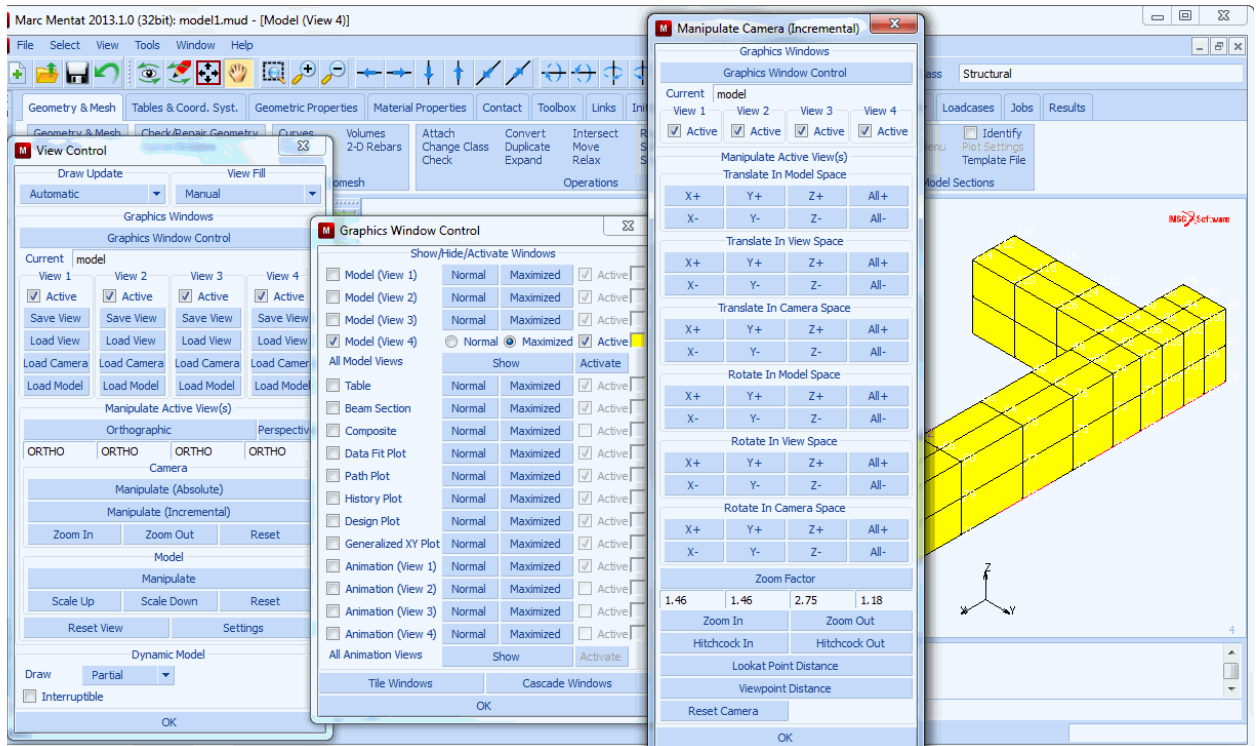
- Mesh generation (continued): define increment of rotation for the model



VIEW SETTINGS

MODEL INCREMENTS: ROTATE

- **Mesh generation (continued): rotate model in positive direction around model x- and y-axis and fill view**



MANIPULATE MODEL

ROTATE IN MODEL SPACE:

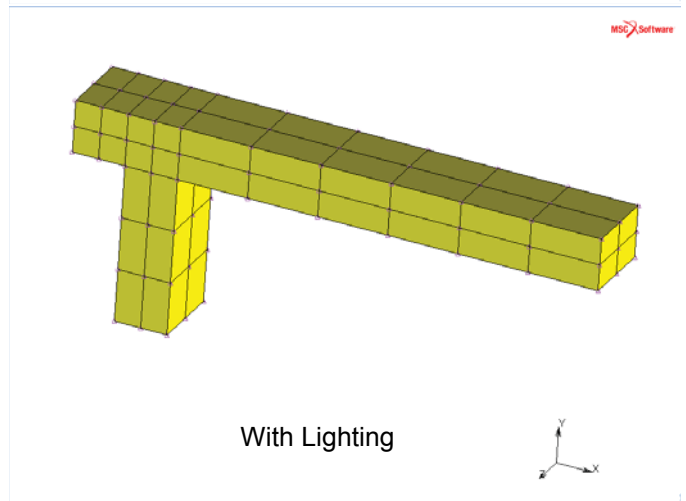
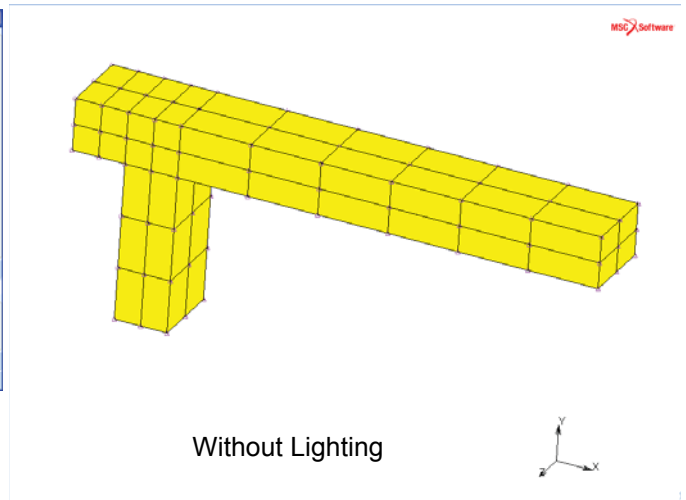
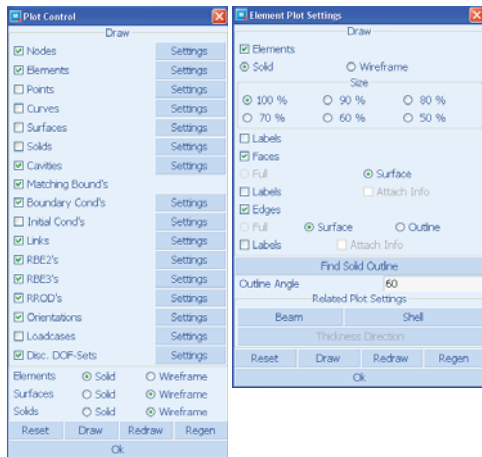
X+

ROTATE IN MODEL SPACE

Y+

FILL

- Mesh generation (continued): plot elements in solid mode, switch off plotting geometric entities



VIEW

DRAW SETTING

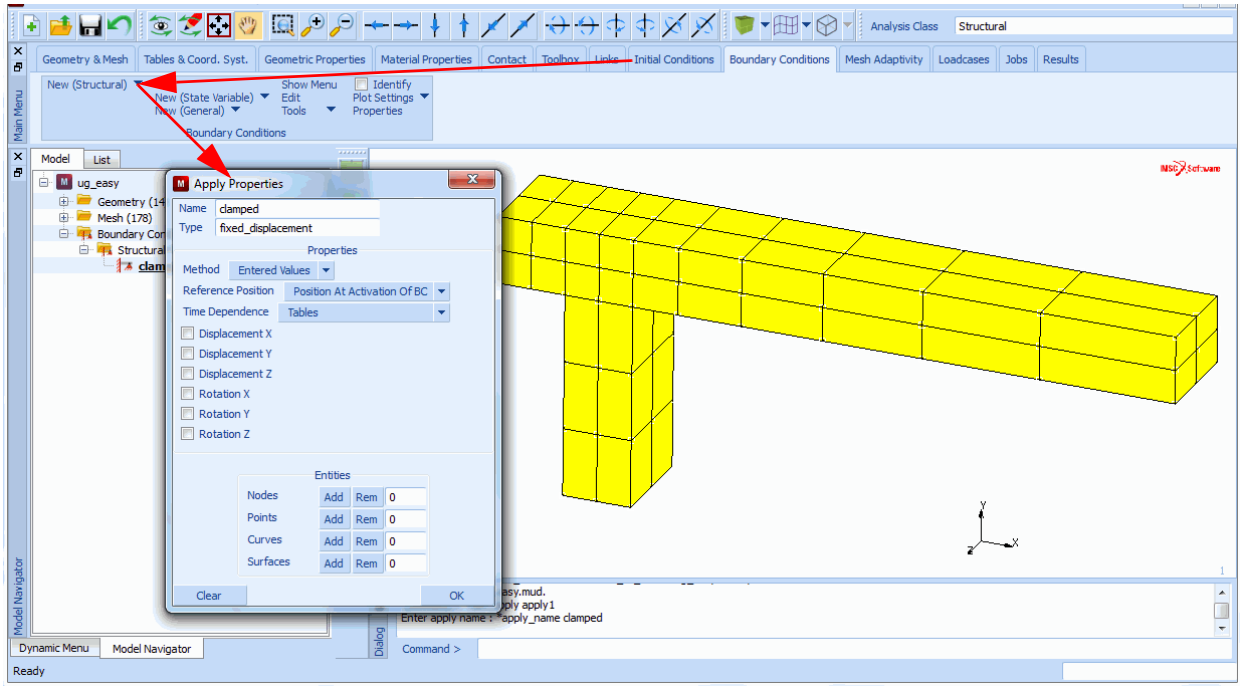
turn off **POINTS** and **SURFACES**

ELEMENTS: SOLID

REDRAW

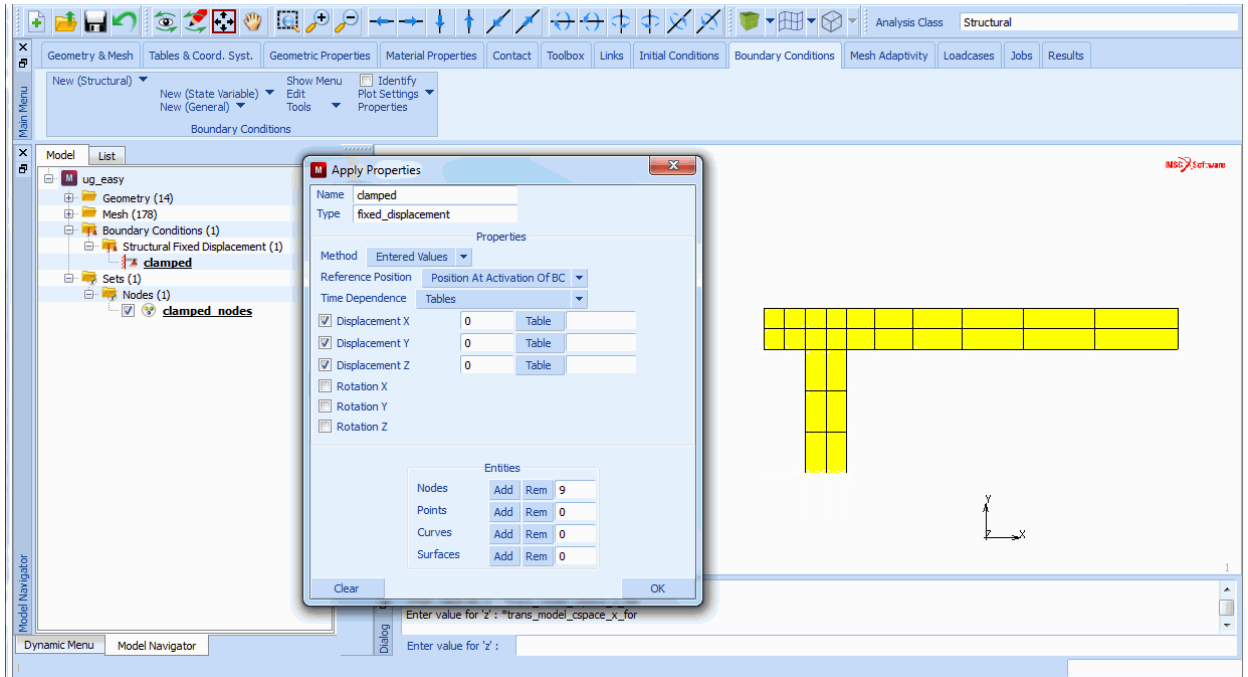
OK

- **Boundary conditions: top menu**



BOUNDARY CONDITIONS
MECHANICAL

- **Boundary conditions (continued): switch to view 1 and select appropriate nodes**



VIEW

SHOW VIEW

1

FILL

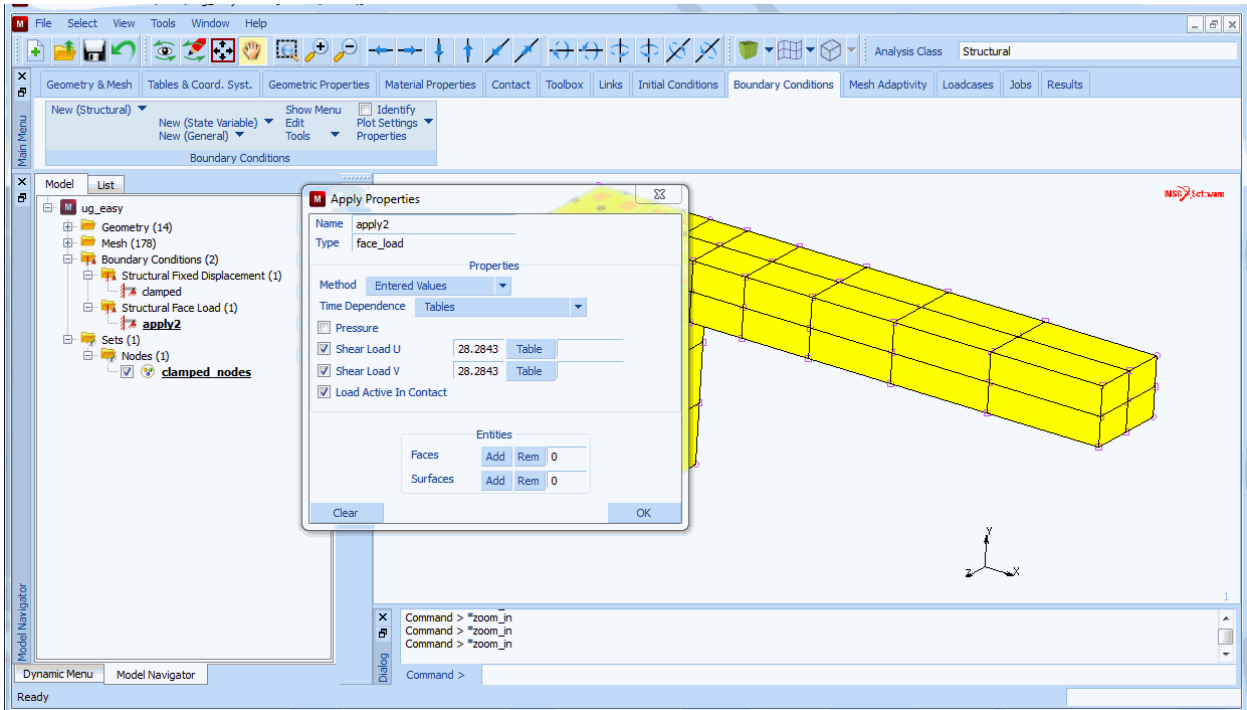
OK

NODES: ADD

END LIST

*(add as shown by the box pick method)
(for end list use button or use right mouse
click in graphics area)*

- **Boundary conditions (continued): switch to view 4, define mechanical boundary conditions, face loads**



VIEW

SHOW VIEW

4

OK

NEW

NAME shear

FACE LOAD

U SHEAR

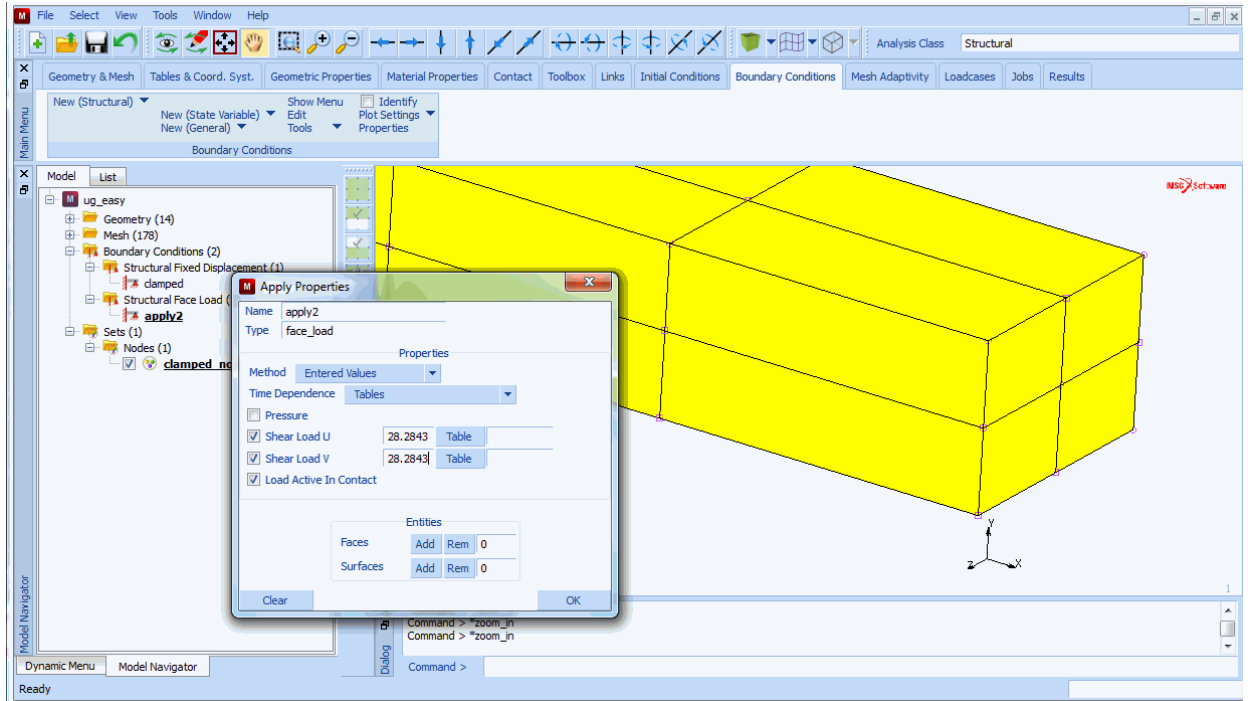
28.2843

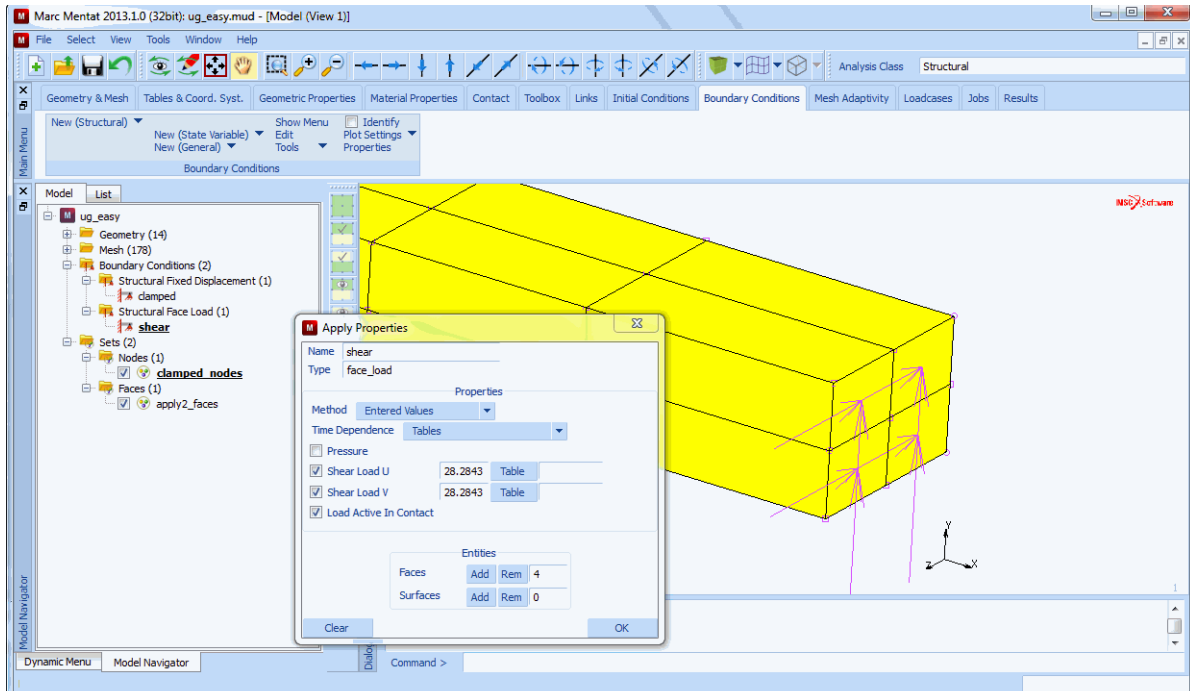
V SHEAR

28.2843

OK

- **Boundary conditions (continued): zoom in locally and select appropriate element faces**

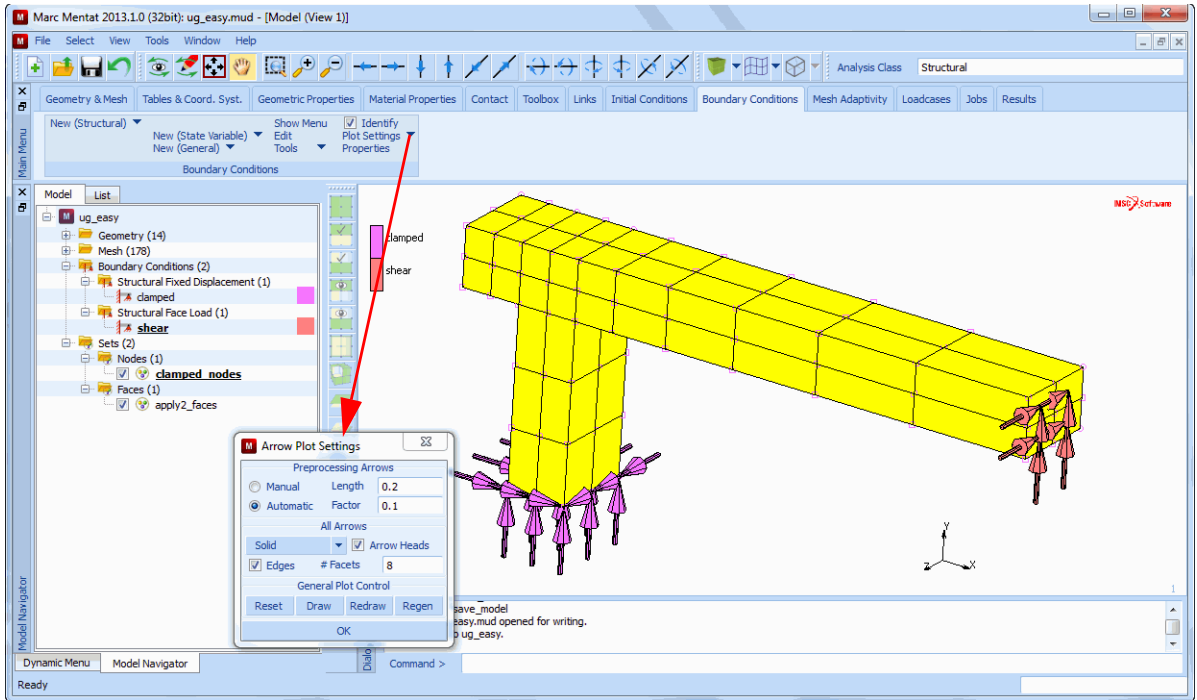




ZOOM BOX
FACES: ADD
END LIST

*(zoom in on the right end of structure)
(add appropriate element faces with mouse)*

- **Boundary conditions (continued): overview of boundary conditions**



ID BOUNDARY CONDITIONS (on)

FILL

ARROW PLOT SETTINGS

SOLID (on)

DRAW

OK

SAVE

- Material properties: top menu

Standard
Composite
Mixture
Rebar
Interface/Cohesive
Gasket
PSHELL

Material Properties			
Name	material1		
Type	standard		
Copy	Prev	Next	Rem
Data Categories			
General			
Structural			
Elements	Add	Rem	0

MATERIAL PROPERTIES

MATERIAL PROPERTIES

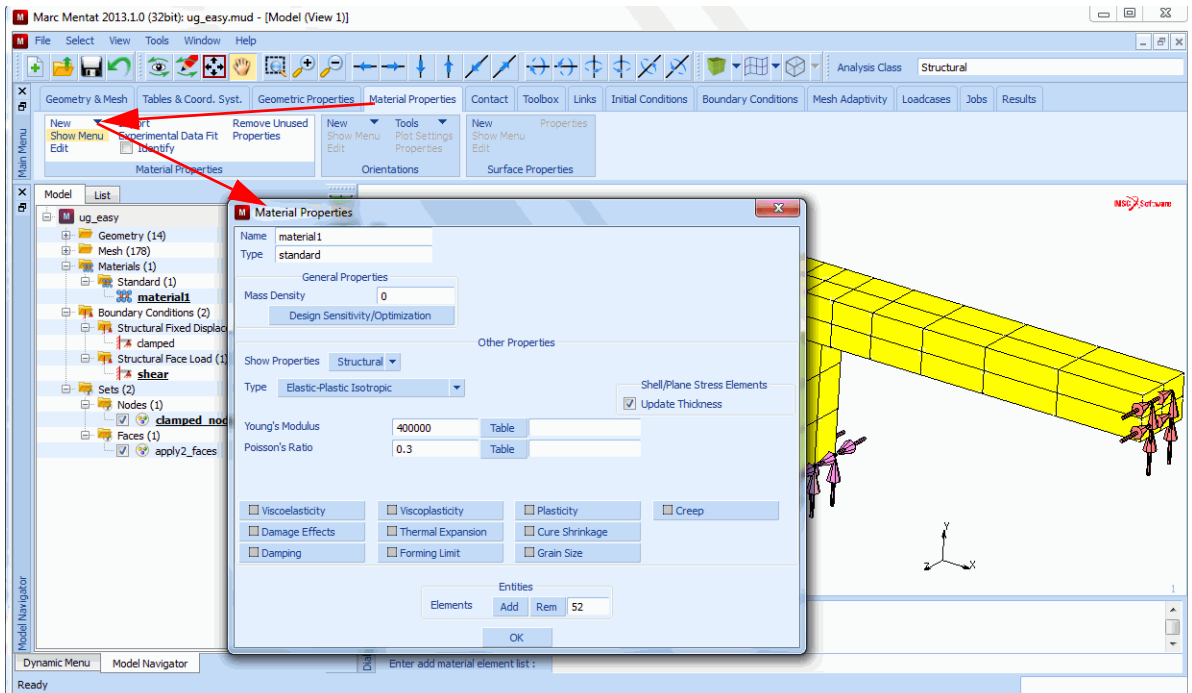
NEW

STANDARD

NAME

linear_elastic

- **Material properties (continued): mechanical material type, isotropic properties, apply to all elements**



STRUCTURAL

YOUNG'S MODULUS = 400000

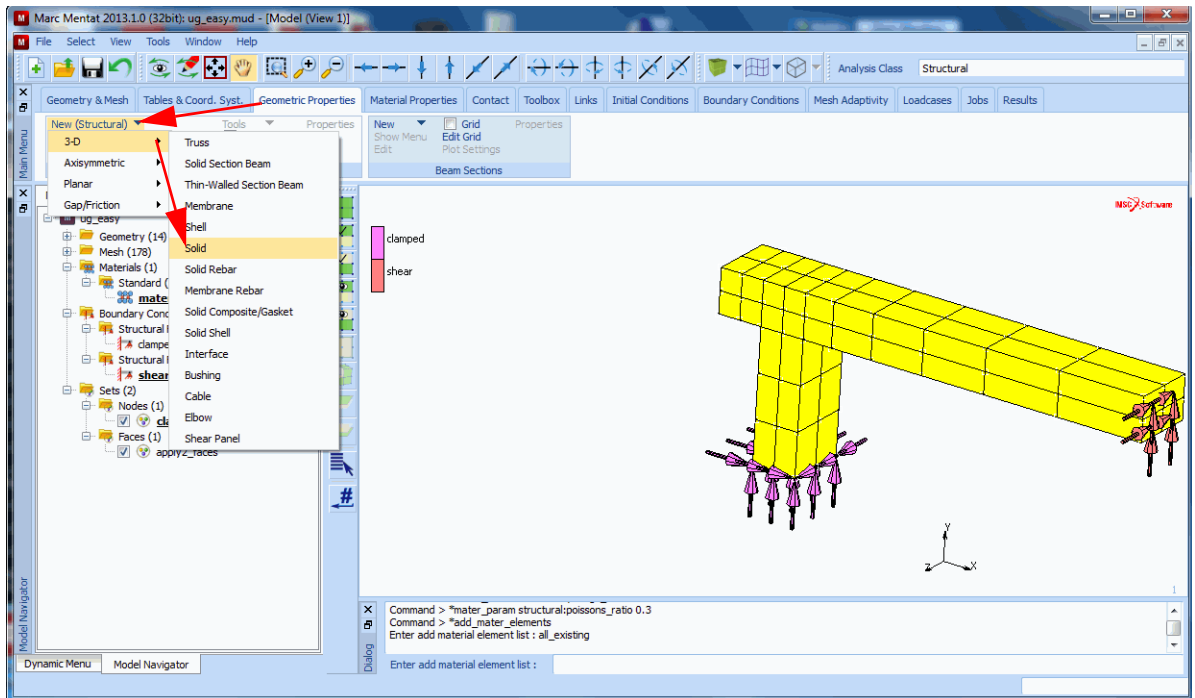
POISSON'S RATIO = 0.3

OK

ELEMENTS: ADD

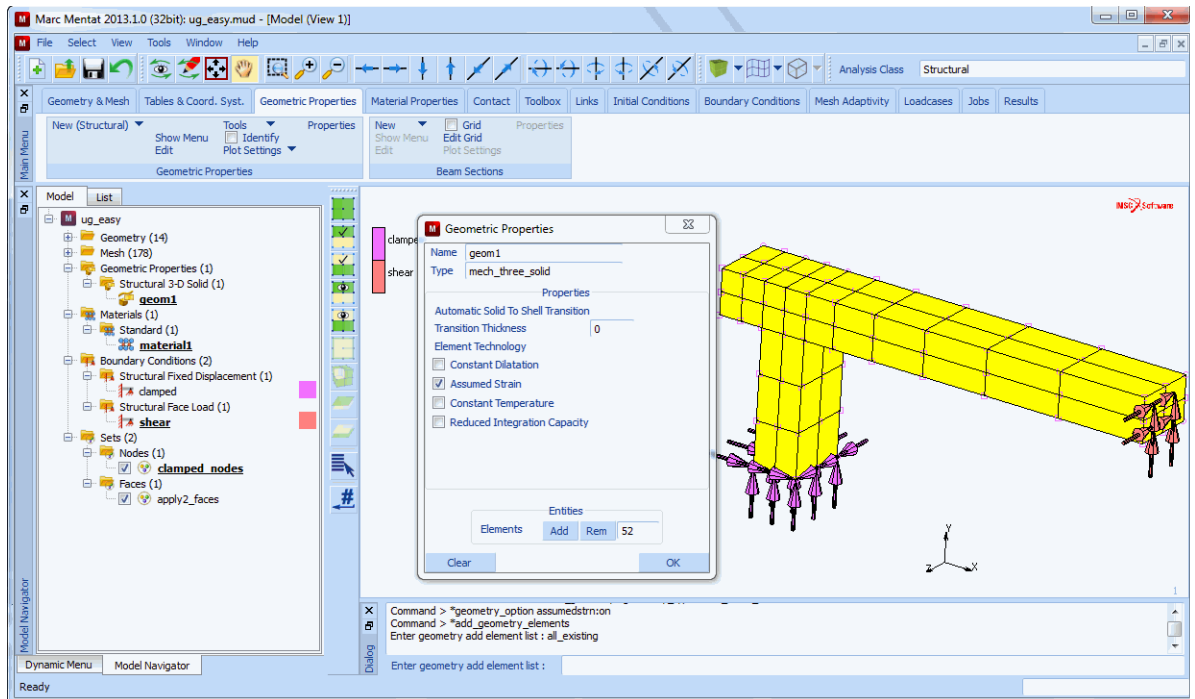
ALL: EXISTING

• Geometric properties: top menu



GEOMETRIC PROPERTIES

- **Geometric properties (continued): select assumed strain formulation for all existing elements to improve bending behavior**



NEW
NAME

assumed_strain

3-D
SOLID

ASSUMED STRAIN
OK

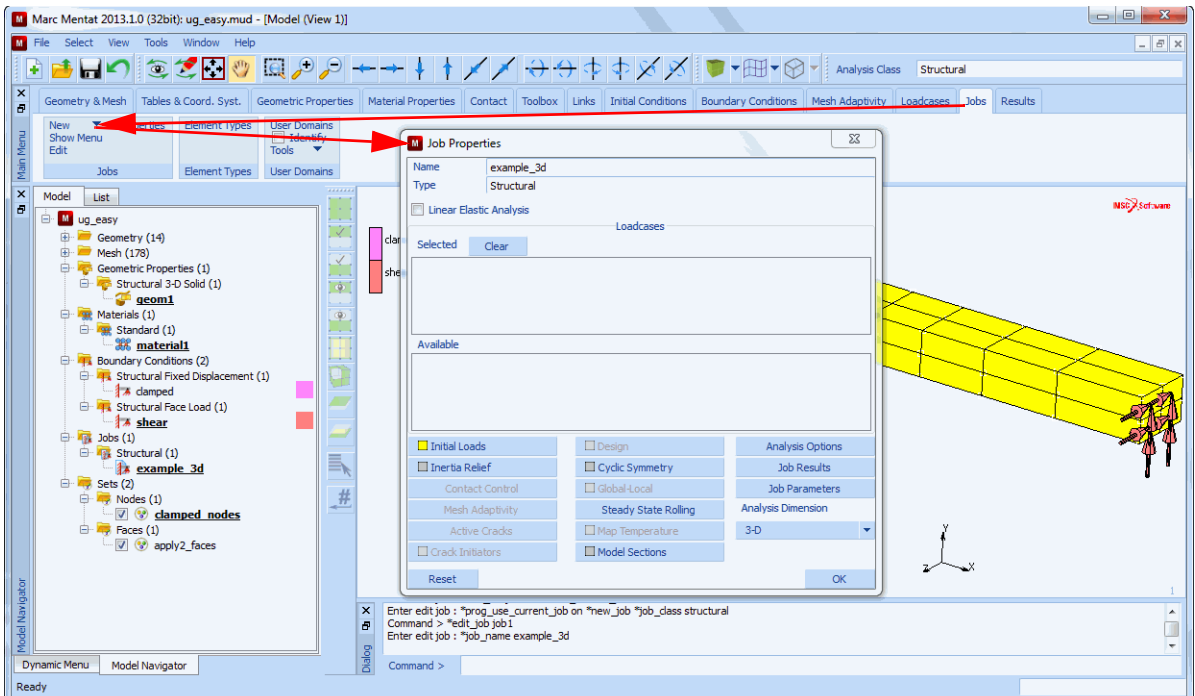
ELEMENTS

ADD

ALL: EXISTING

(on)

- Jobs: define mechanical analysis; for a single linear analysis no loadcases are necessary and the default analysis options can be used



JOBS

NEW (TYPE)

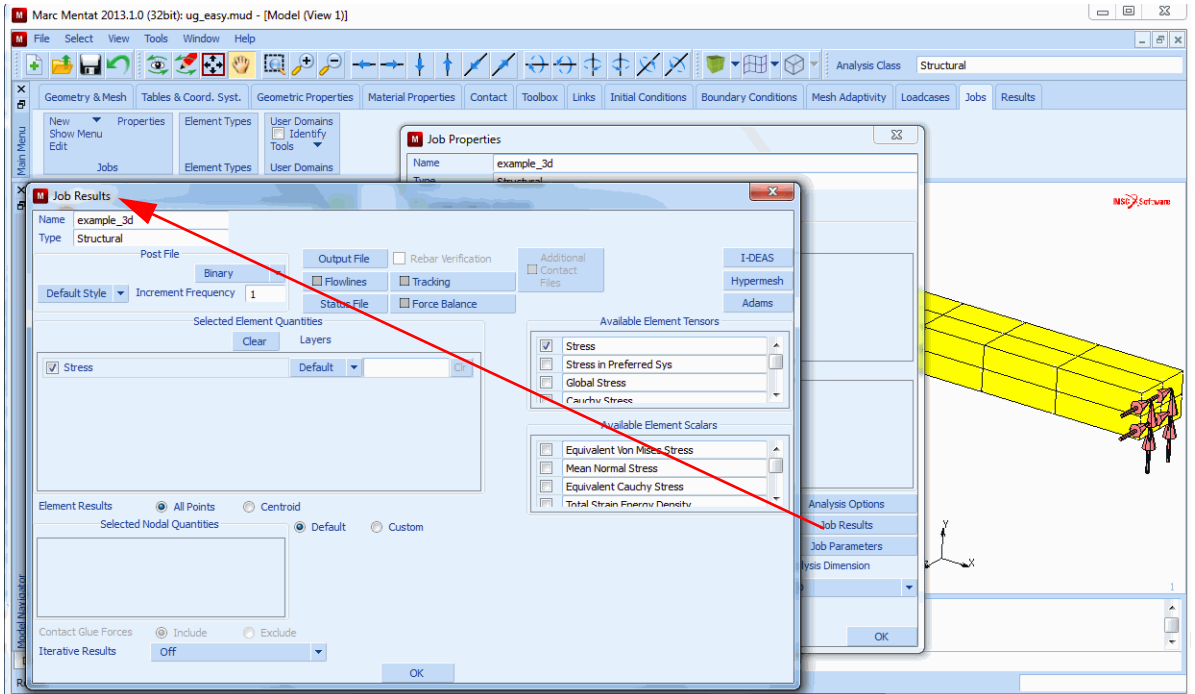
MECHANICAL

NAME

example_3d

PROPERTIES

- **Jobs (continued): select post file quantities**



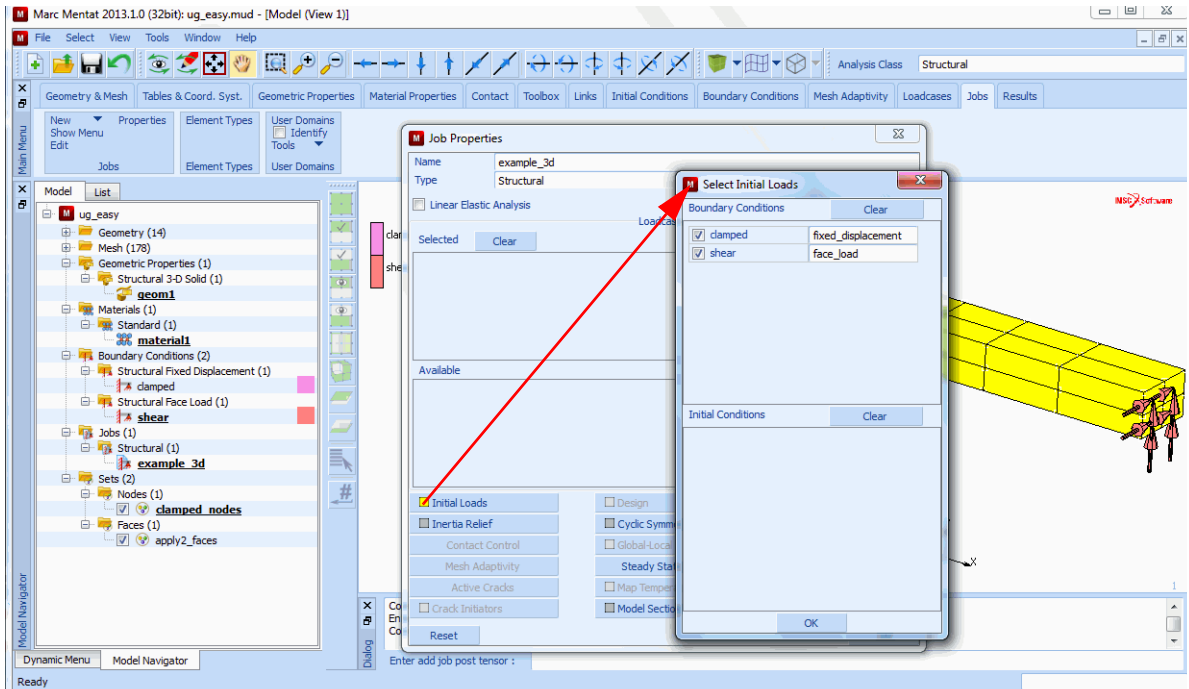
JOB RESULTS

AVAILABLE ELEMENT TENSORS

Stress

OK

- Jobs (continued): check if boundary conditions are selected as initial loads



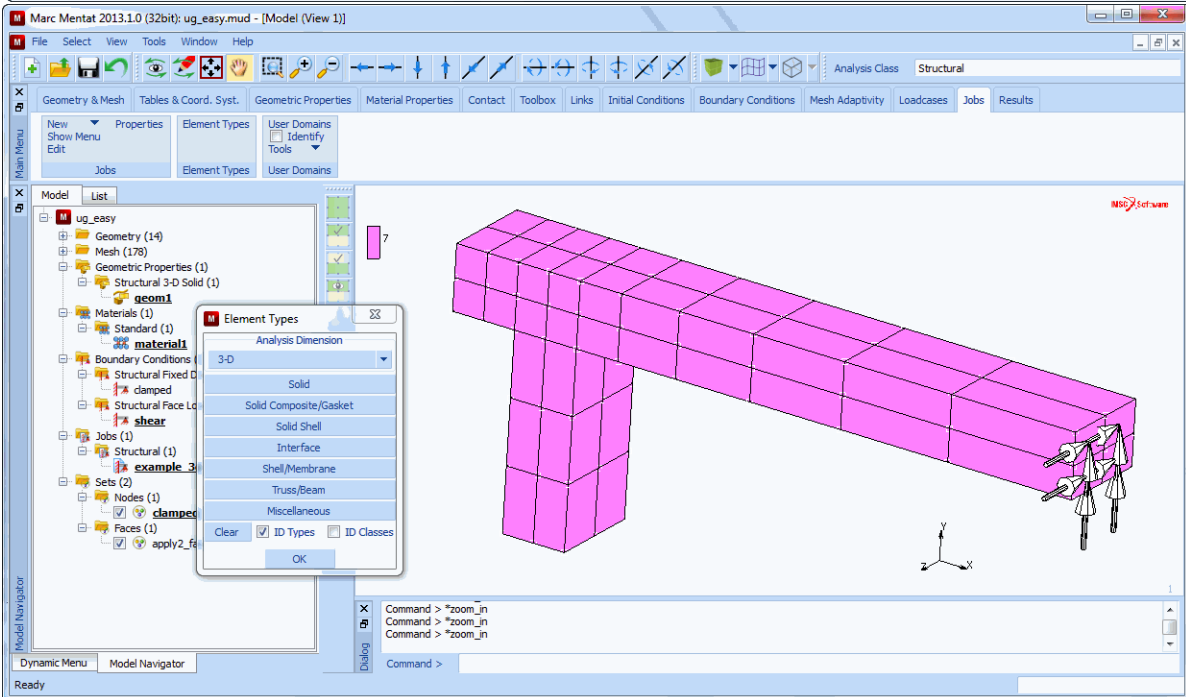
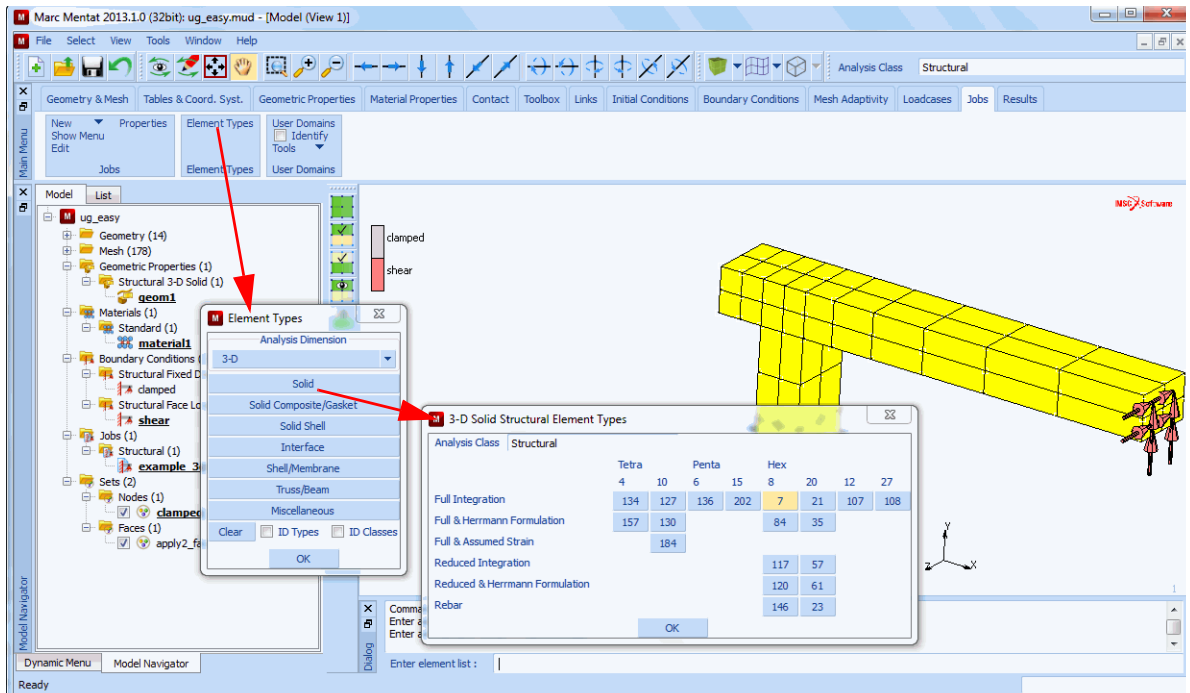
INITIAL LOADS

OK

OK

(check to see if they are on)

- Jobs (continued): select mechanical 3-D solid element type 7, save model



ELEMENT TYPES

ANALYSIS DIMENSION

3-D

(select element type 7)

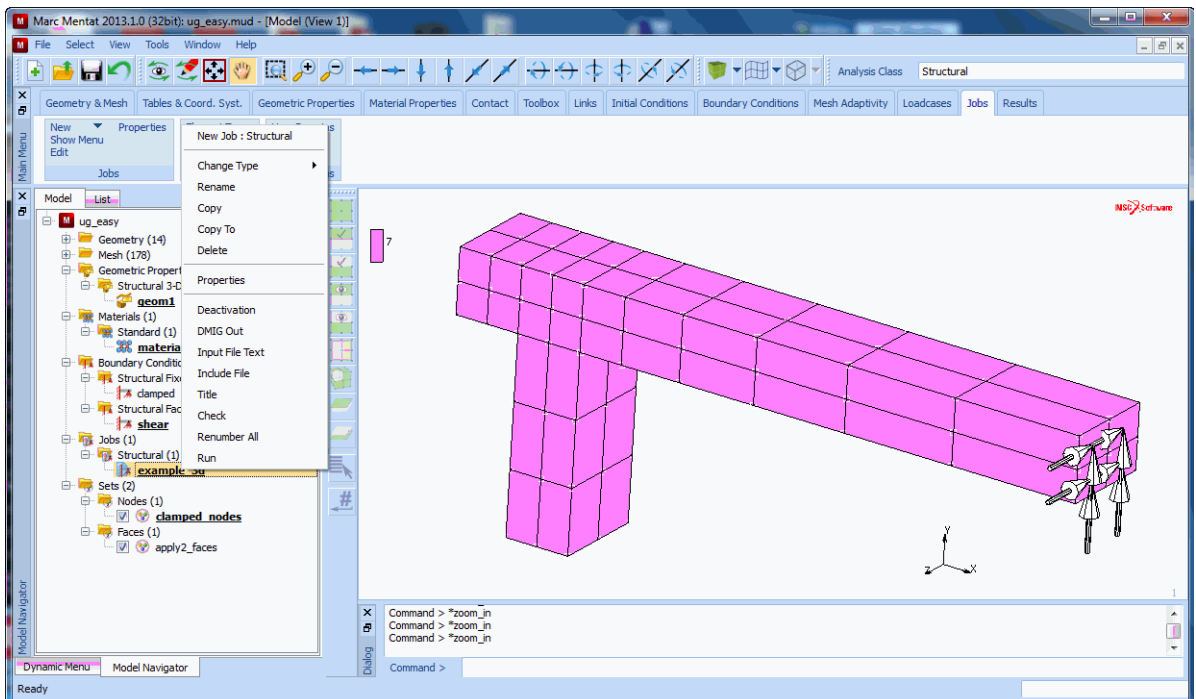
OK

ALL: EXISTING

SAVE

OK

- **Jobs (continued): save Mentat database and submit job model11_example_3d**



RUN

STYLE

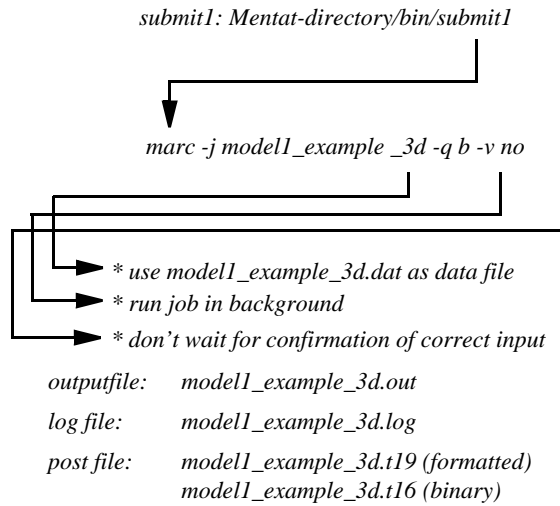
OLD

SUBMIT 1

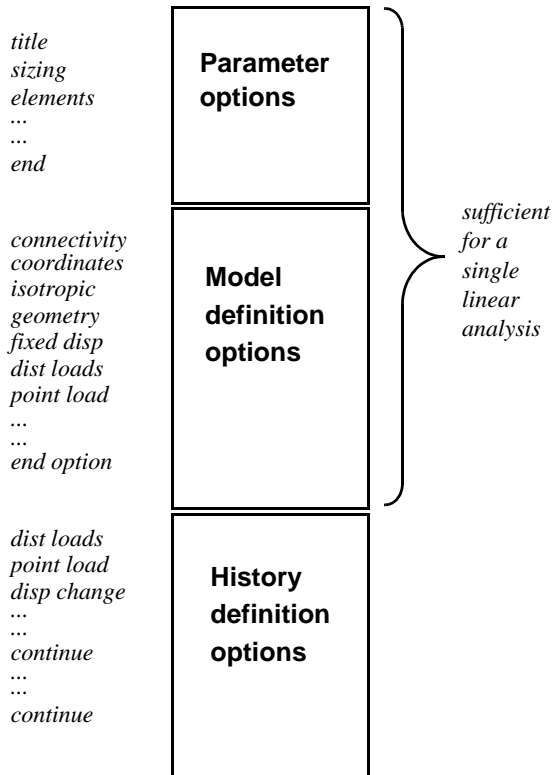
(old style of table input)

(look for EXIT NUMBER 3004)

- **Submitting a job:**



- **Marc data file:**



- **Jobs (continued): use monitor to observe current status**

The screenshot shows the 'Run Job' dialog box with the following details:

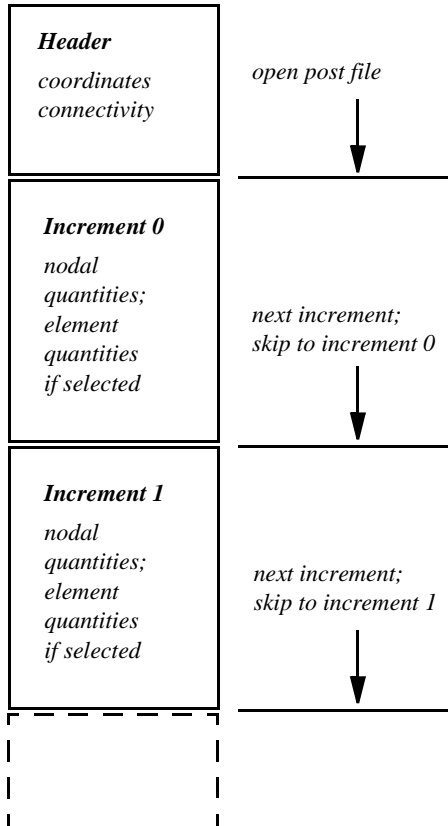
- User Subroutine File:** (empty)
- Parallellization:** (unchecked)
- No DDM:** (checked)
- 1 Solver Process:** (selected)
- Title:** (empty)
- Style:** (empty)
- Old:** (dropdown menu)
- Save Model:** (button)
- Submit (1):** (button)
- Advanced Job Submission:** (button)
- Update:** (button)
- Monitor:** (button)
- Kill:** (button)
- Status:** Complete
- Current Increment (cycle):** 0 (1)
- Singularity Ratio:** 0.0019793
- Convergence Ratio:** 0
- Analysis Time:** 0
- Wall Time:** 1
- Total:** (summary section)
- Cycles:** 1
- Cut Backs:** 0
- Separations:** 0
- Remeshes:** 0
- Exit Number:** 3004
- Exit Message:** (empty)
- Edit:** (button)
- Output File:** (button)
- Log File:** (button)
- Status File:** (button)
- Any File:** (button)
- Open Post File (results Menu):** (button)
- Reset:** (button)
- Ok:** (button)

MONITOR

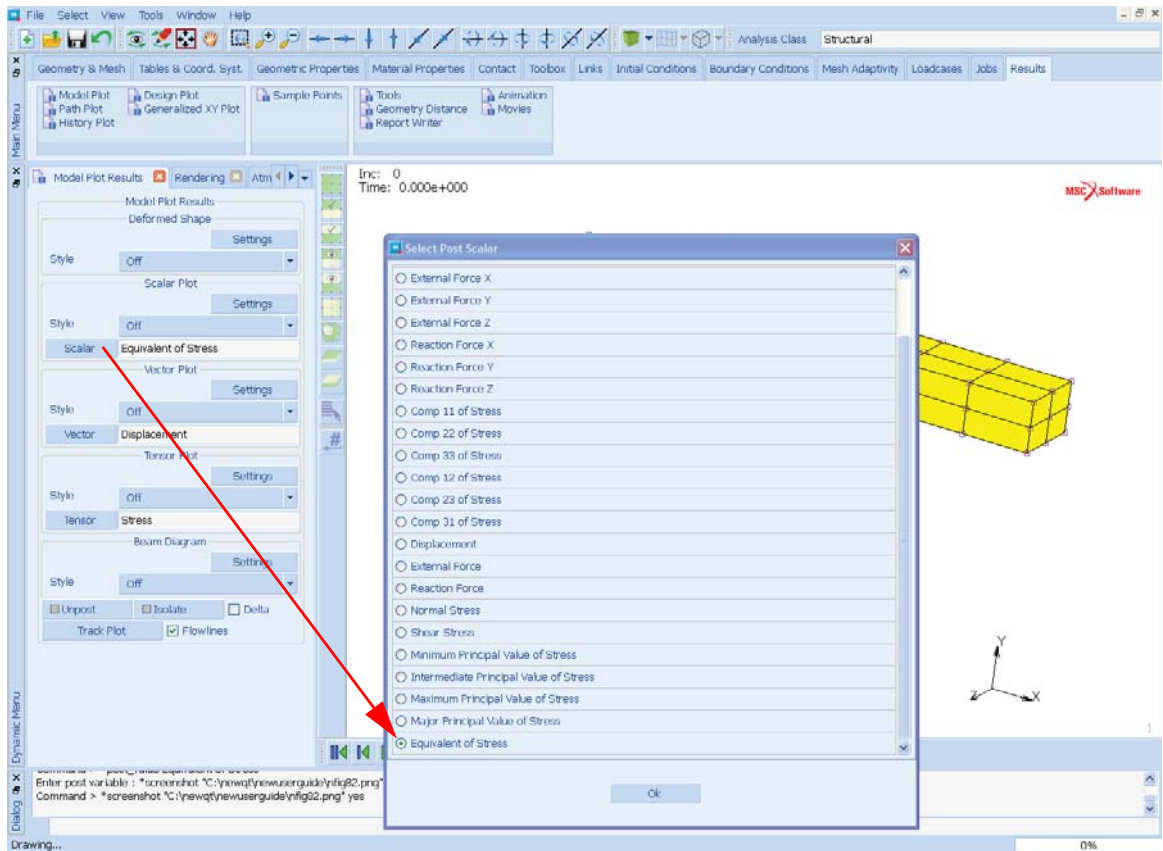
OPEN POST FILE (RESULTS MENU)

(opens default post file and goes to results menu)

- **Marc post file:**



- **Postprocessing (continued): skip to increment 0 and select equivalent von Mises stress to be displayed**

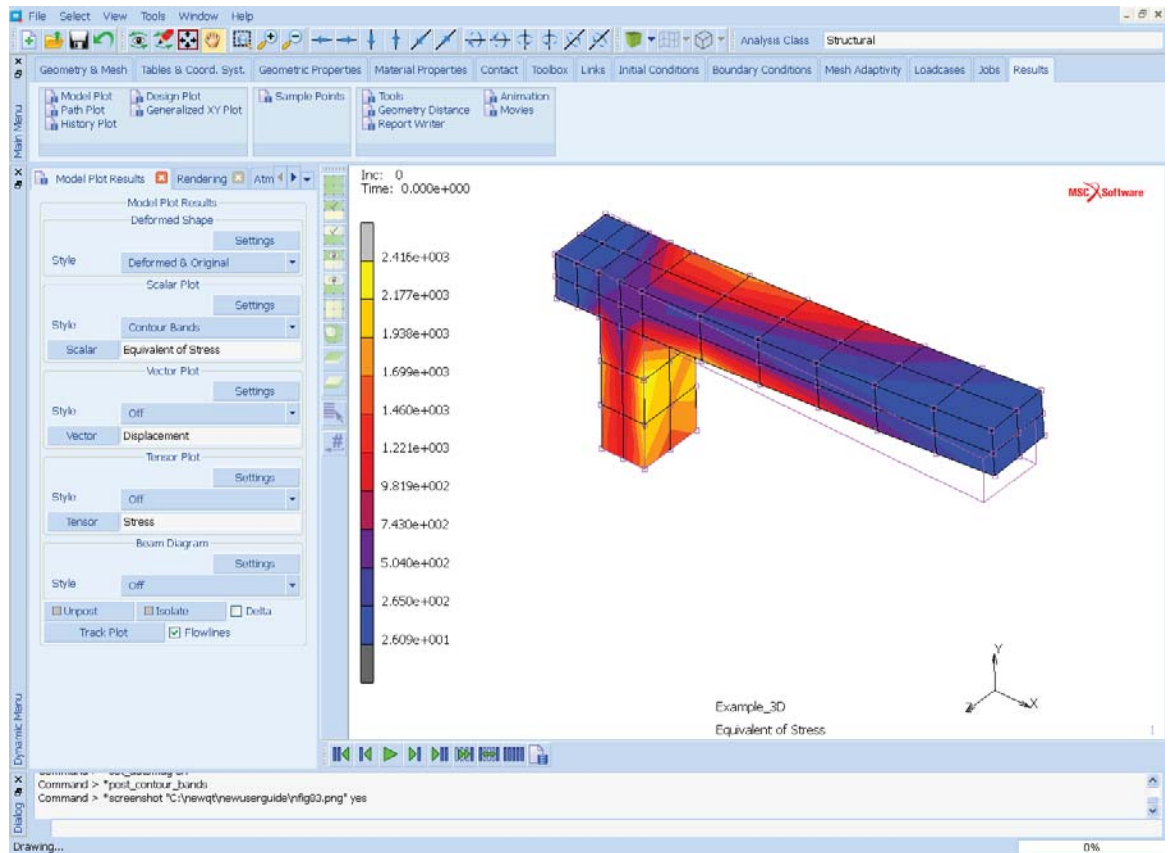


SCALAR

EQUIVALENT OF STRESS

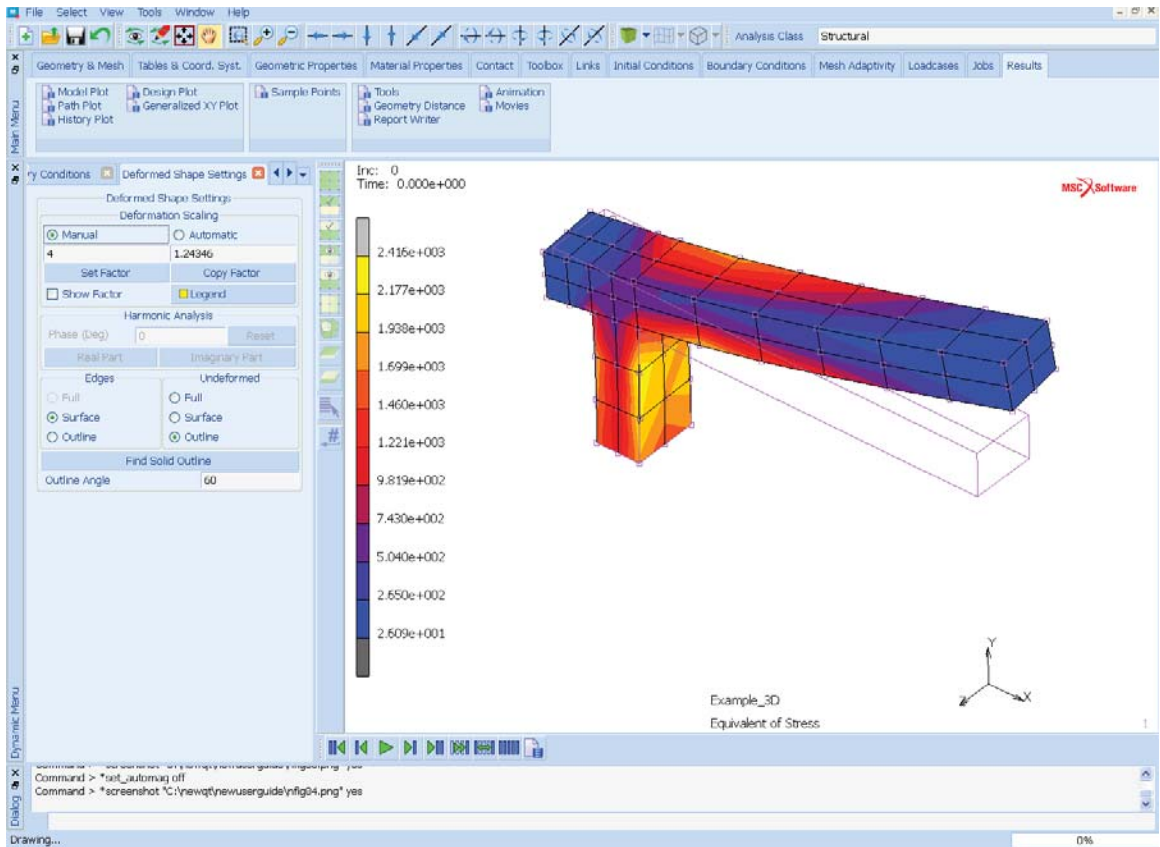
OK

- **Postprocessing (continued): plot deformed and undeformed structure for increment 0 using contour bands**



**DEFORMED AND ORIGINAL
CONTOUR BANDS**

- **Postprocessing (continued): deformed shape settings. You may magnify the displacements.**



DEFORMED SHAPE: SETTINGS

MANUAL FACTOR

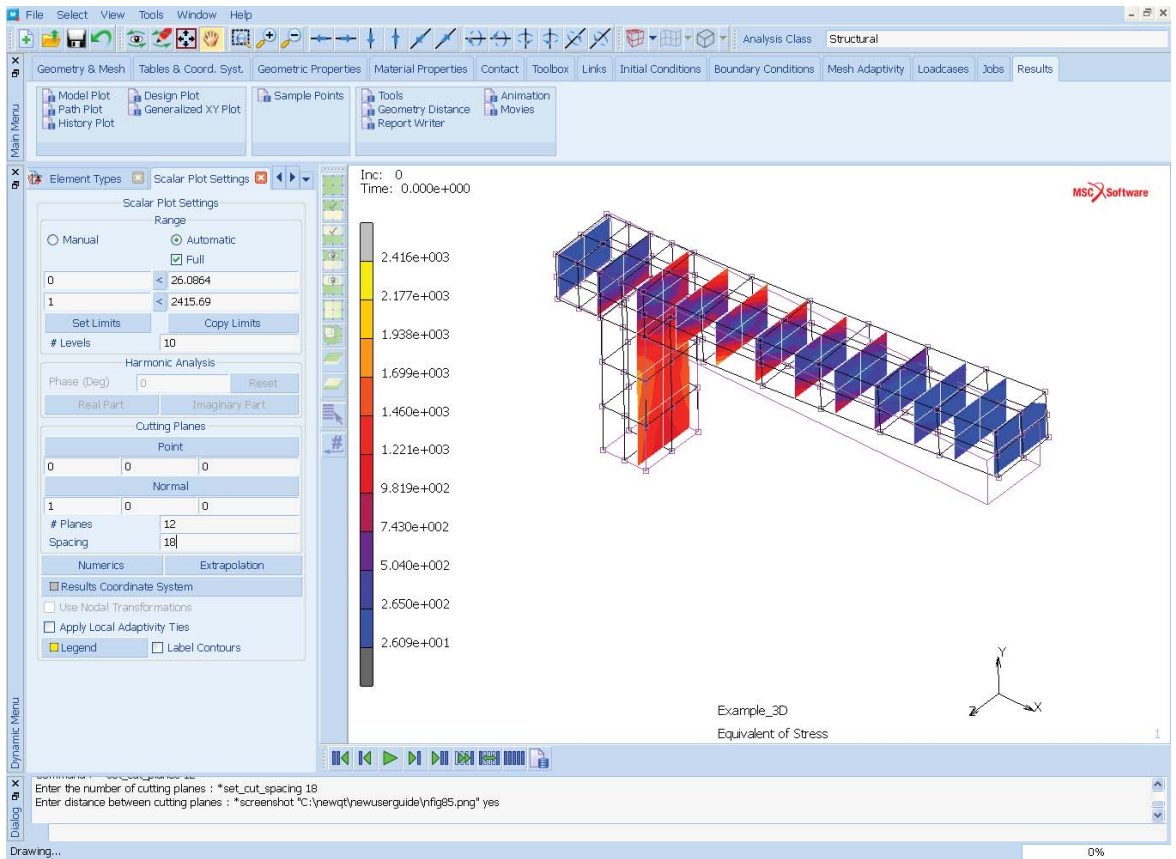
4

MANUAL FACTOR

1

RETURN

- **Postprocessing (continued): define plotting style settings for cutting planes**



SCALAR PLOT: SETTINGS

POINT

00 00

NORMAL

1 0 0

PLANES

12

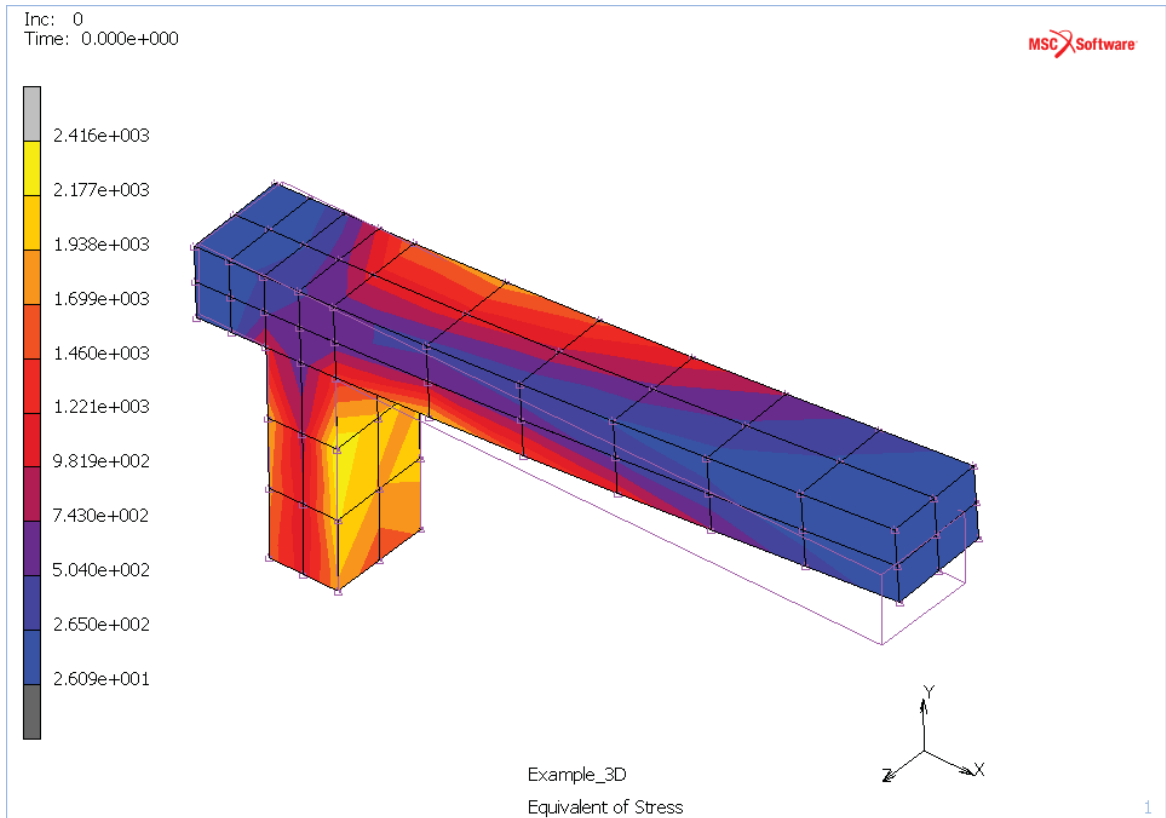
SPACING

18

CUTTING PLANES

SCALAR PLOT: SETTINGS

- **Postprocessing (continued): switch back to contour bands plotting and define a node path for a path plot**



CONTOUR BANDS

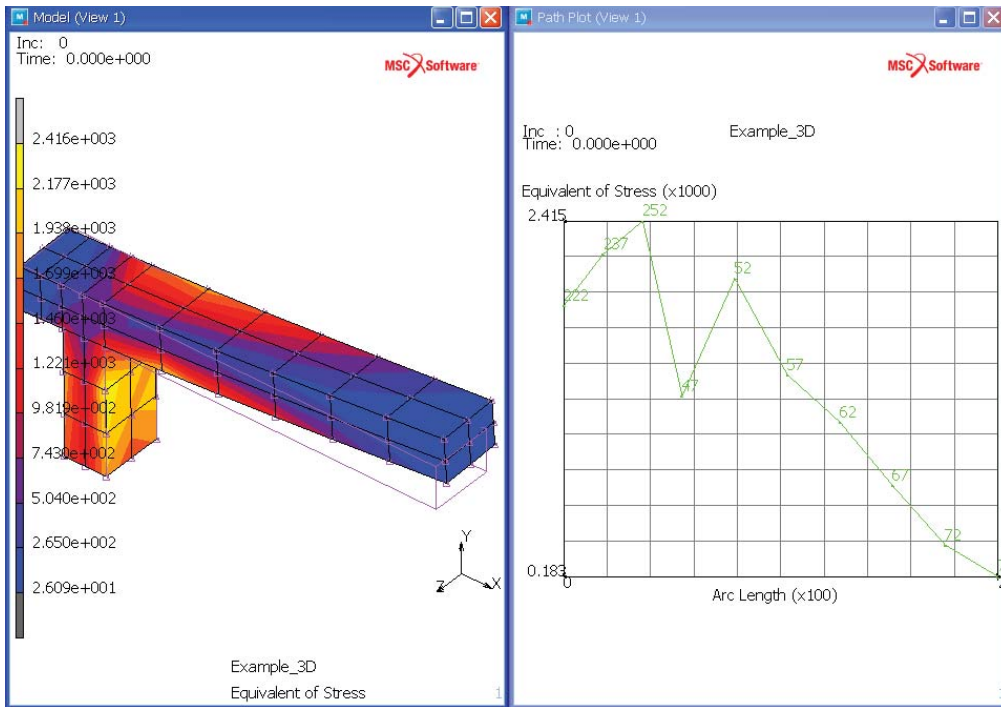
PATH PLOT

NODE PATH

END LIST

(pick the nodes shown to define the path - N1, N2, N3)

- Postprocessing (continued): add path plot curve and scale the plot axes



ADD CURVES

ADD CURVE

ARC LENGTH

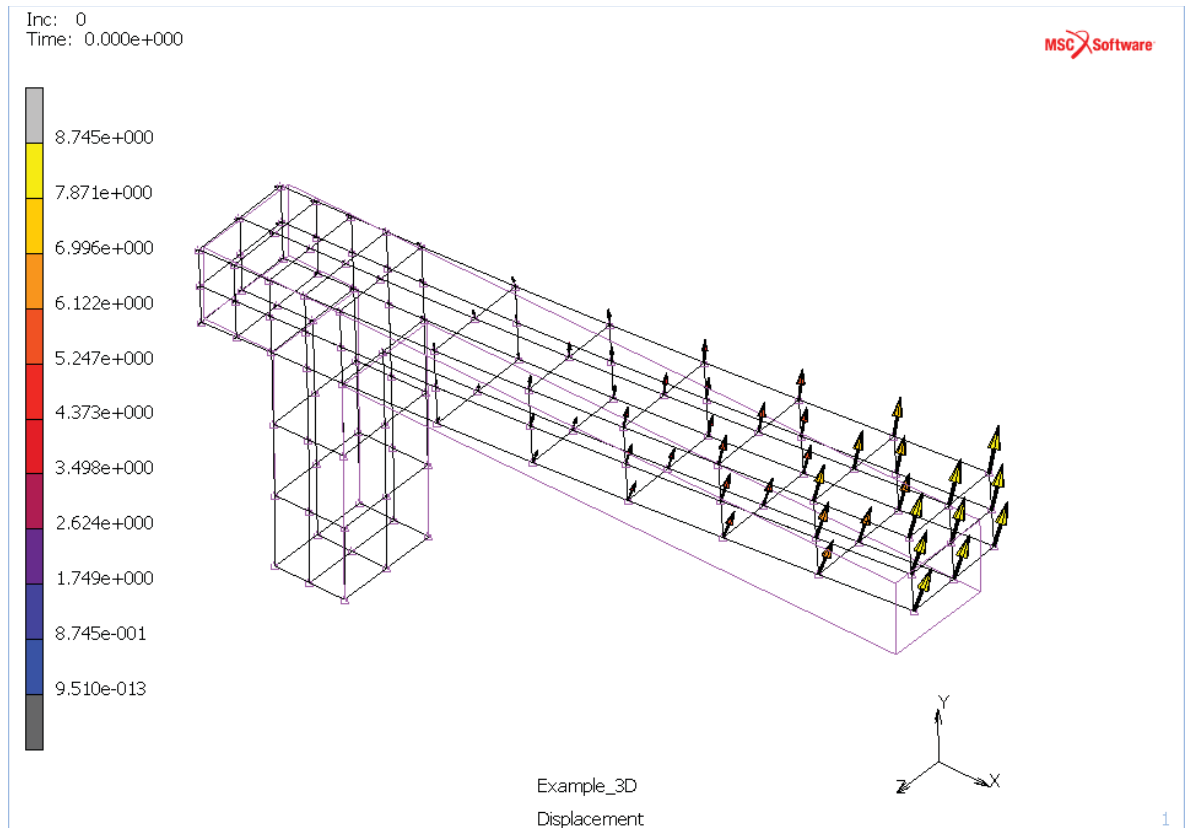
EQUIVALENT OF STRESS

FIT

(X variable)

(Scroll Down to Y variable)

- **Postprocessing (continued): vector plot of displacements**



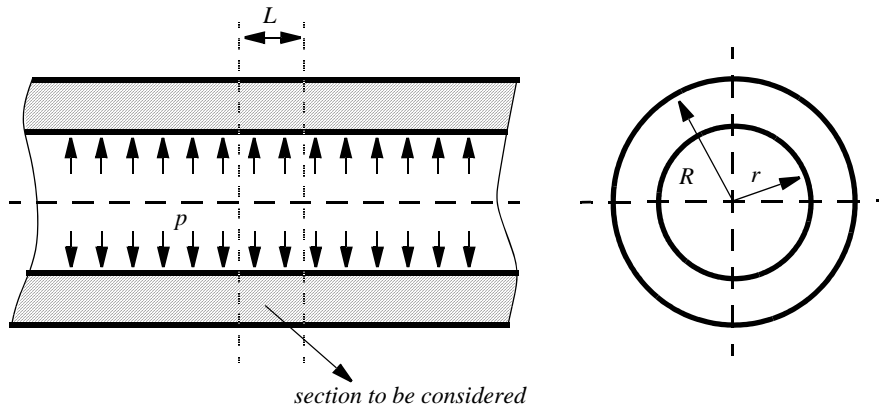
MORE

VECTOR PLOT: ON

- **Workshop tasks:**

- **Perform the discussed 3-D analysis and store the Mentat commands** in a procedure file, which can be created in the TOOLS Menu Bar
- Analyze the same 3-D structure, but now subjected to a distributed shear load with a magnitude 40 and a direction of $[0 \ -1 \ 0]^T$ (bending load)
- Analyze the structure subjected to the bending load using 4-node plane strain elements (select Marc element type 11) and compare the results with the 3-D solution

- **Additional workshop: linear elastic analysis of an infinitely long pressurized thick-walled cylinder**



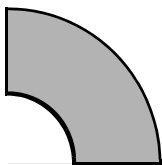
- Dimensions: $L = 4$, $r = 5$, $R = 12$
- Apply fixed displacements in axial direction
- Internal pressure: $p = 15$
- Material: $E = 2.1 \times 10^5$, $\nu = 0.3$
- **Workshop tasks:**

Determine the radial stress as a function of the radial coordinate using:

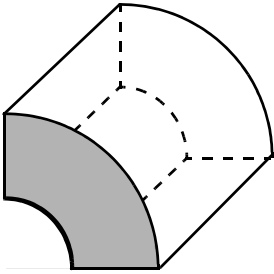
A: axisymmetric element 10:



B: plane strain element 11 (model one quarter of the cross section):

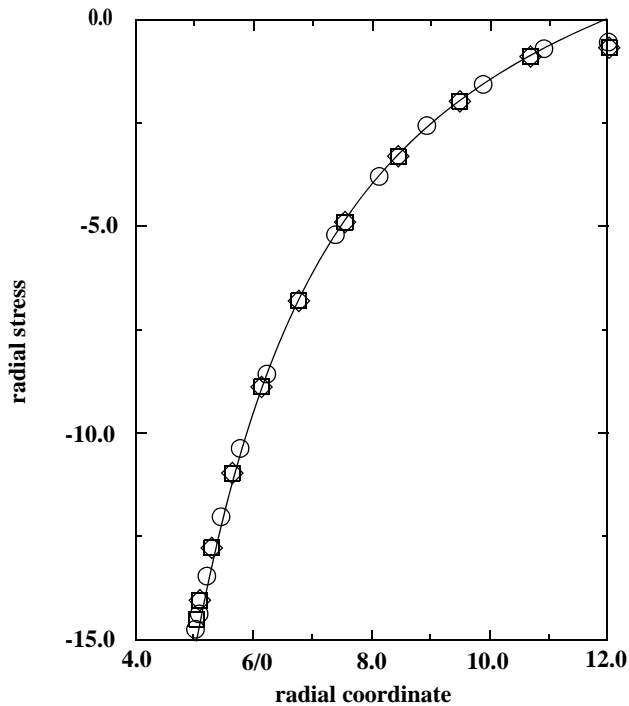


C: brick element 7 (model one quarter of the section to be considered):



Apply the correct boundary conditions and compare the results.

Infinitely long pressurized thick-walled cylinder



- Analytical solution
- 10 axisymmetric elements; radial bias -0.5
- 80 plane strain element; radial bias -0.5
- ◇ 80 brick elements; radial bias -0.5

Background Information

The purpose of this section is to give you an overview of the most common Mentat features. These features recur throughout the sample sessions in the last part of this guide. For example, all sample sessions contain a mesh generation step.

You may find it helpful to use the information in this section as you work through the example problems. The order in which the common Mentat features are described in this section is based on the preprocessing, analysis, and postprocessing sequence of the finite element analysis process.

The key features discussed in this chapter are listed below.

- Mesh generation
 - mesh entities
 - geometric entities
 - direct meshing technique
 - geometric meshing technique
- Boundary conditions, initial conditions and links
- Material and geometric properties
- Contact
- Loadcases and jobs
- Results interpretation

Mesh Generation

The preprocessing task is considered a significant part of the finite element analysis process. In fact, at times it may be the most complex and time consuming part of the entire job. For this reason it is important that you use the conceptualization phase as indicated in [Figure 1.1-1](#) to determine in advance what the objective of your analysis is and what answers you are seeking since both factors strongly influence the choice of your model.

Mentat distinguishes two techniques to build a mesh. The first is the **direct** or manual approach where you generate finite elements from bottom up. The second is the **geometric** approach where the model is first generated using *geometric entities* followed by a conversion step in which these entities are converted to finite elements. The two techniques are by no means mutually exclusive and often the best results are obtained by alternating between the two.

The following guidelines will simplify the task of generating a mesh using either one of the available methods.

Plan your model

Plan your model carefully and take the time to formulate a strategy. This will save you time and resources.

Look for symmetry and duplication

Many structures exhibit some form of symmetry. Look for the simplest component of your model. Also look for duplicates (or close duplicates) of another portion, and use the **SYMMETRY** or **DUPLICATE** processor.

Select a unit system

The Length Unit option sets the unit of length for the current model. The coordinates of the nodes and points, as well as all other geometrical data, are stored in the model in this length unit and are written to the Marc input file also in the unit when the job is submitted (i.e., no unit conversion is performed). The unit of length is stored in the model file (.mud or .mfd) if the model is saved in the default style.

The Length Unit should preferably be set once when a new model is created. The default unit for new models is in millimeters, but this can be changed in the Tools → Program Settings menu. The latter also provides an option to save the default unit for future Mentat sessions.

If the length unit of a model is changed (i.e., from millimeter to meter), then all geometrical data associated with the geometry and the mesh in the model are converted to the new length unit. All other data in the model, such as material properties, geometric properties, boundary conditions, contact data, etc., is not converted to the new unit and has to be changed manually. More specifically, only the following data is converted.

- Coordinated of nodes, points, and solid vertices
- Curve divisions applied to the curves (target length, minimum and maximum lengths, and the L1 and L2 lengths for biased seed points)
- Target lengths of solid mesh seeds

Select a logical origin

The lower-left corner of your model or drawing is not necessarily the best location for the origin. Take some time to examine the model for an origin that makes the creation process easier. For example, if a model is symmetrical about a hole in a plate, consider placing the origin at the center of the hole. You may change the location of the origin within the same session while generating your model.

Choose a logical coordinate system

The default coordinate system in Mentat is rectangular Cartesian. A cylindrical or spherical coordinate system may be more suitable for a particular model.

Create 1-D and 2-D before 3-D

For many structures, often the best mesh generation strategy is to create first a 1-D and/or 2-D mesh and to drag it into a 3-D mesh using the **EXPAND** processor.

Mesh Entities

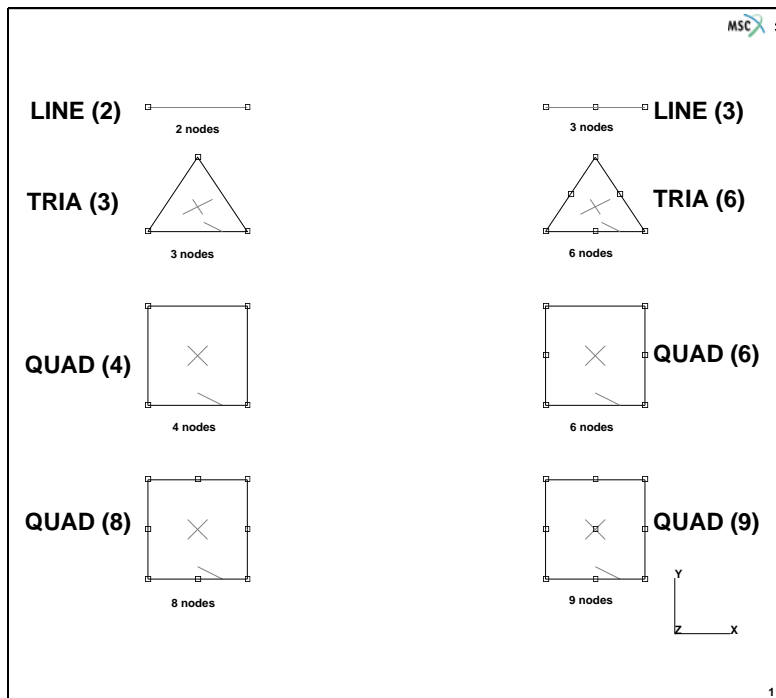


Figure 1.1-17 Element Classes

Two types of mesh entities can be distinguished: nodes and elements.

Nodes

Nodes are characterized by three coordinates and symbolized by a \square on the screen. When nodes are attached to a geometric entity, the symbol \circ is used instead.

Elements

Elements consist of element edges and element faces and are defined by a sequence of nodes. The number of edges, faces and nodes depend on the element class. Mentat employs a wide variety of element classes which are identified in [Figure 1.1-17](#) and [Figure 1.1-18](#). The **CHANGE CLASS** processor allows you to change the class of existing elements. The **CLEAR MESH** button in the **MESH GENERATION>MANUAL** menu enables you to remove all mesh entities from the database. When elements are drawn in wireframe mode, the faces are indicated with a cross and the first edge is indicated with a half-arrowhead.

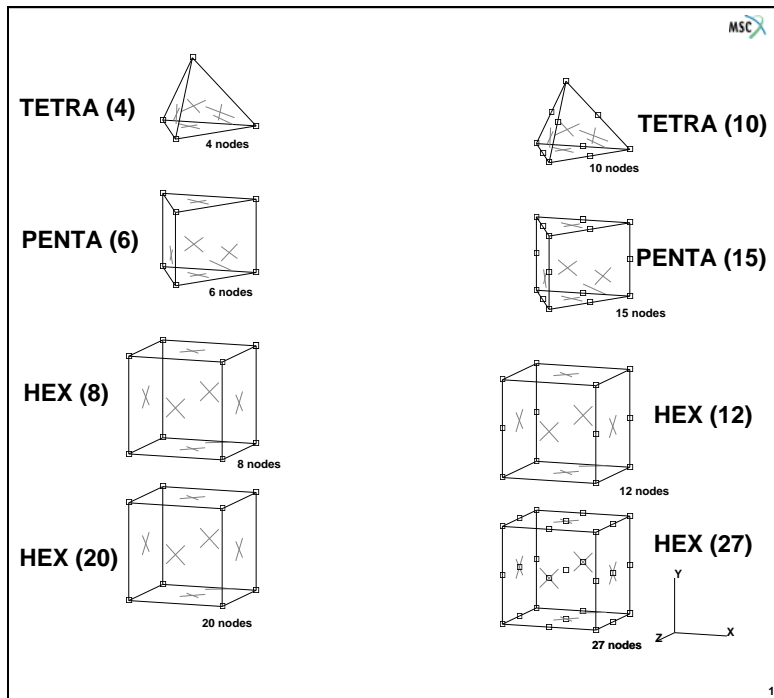


Figure 1.1-18 Element Classes

During the mesh generation phase, it is not required to make a decision on the element type to be used. Only the element class is important at this stage. For instance, planar elements can be used to model a planar or an axisymmetric structure. In the phase of the analysis type definition, it has to be decided if the element is axisymmetric, plane stress or plane strain.

Geometric Entities

The building blocks of the geometric mesh technique are points, curves, surfaces, and solids.

Points

Points are characterized by three coordinates and symbolized by a '+' on the screen.

Curves

The following curve types can be used to define curves: line, polyline, tangent, arc, fillet, circle, cubic spline, interpolate, Bezier curve, NURB curve, composite curve, and sampled.

The line curve is a straight line segment between two points, the polyline is a concatenation of linear line segments through a series of points. The tangent is a straight line tangent to an existing curve. The arc curve is part of a circle and five methods are available to specify this circle segment. The fillet curve creates an arc between two curves. The circle curve is a complete circle and can be specified in two ways. The cubic spline and the interpolate curve pass

through a series of points (a curve fitting technique). The Bezier curve and NURB curve can be used to define more general curves. The composite curve enables joining several previously defined curves.

Surfaces

Currently, Mentat recognizes the following surface types which can be specified directly: quad, ruled surface, driven surface, cylinder, Bezier surface, NURB surface, sphere, swept surface, interpolate, coons, skin surface, and sampled.

The *quad* surface is the most simple surface definition as it is defined by 4 (non-collinear) points. The *cylinder* surface is a cone which is defined by the coordinates of two points on the axis and two radii. The *sphere* surface is defined by the center and the radius. The *ruled* surface is spanned by a family of straight lines between two curves. Both the *driven* and the *swept* surface are generated by dragging a curve along another curve. The *interpolate*, *Bezier* and *NURB* surfaces are logical extensions of the interpolate, Bezier and NURB curves. The *coons* surface is created from a closed boundary consisting of four curves. The *skin* surface is created through a list of curves.

You can also generate axisymmetric surfaces by revolving a curve about the local y-axis using the **REVOLVE** processor.

In addition, the CAD interfaces allow Mentat to read in trimmed surfaces.

When you display a curve or surface, you often see a crude representation of that entity on your screen. We emphasize the word *representation* here. By default, the resolution of a curve is set to 10. The curve is represented by 10 straight line segments. For small curves, this may be sufficient to give the impression of a smooth curve. For larger curves, however, 10 subdivisions may not be sufficient. You can change the resolution by increasing the number of divisions in the DIVISIONS submenu of the continued part of the NEW>PLOT SETTING>SETTINGS menu. Be aware that increased resolution requires more time for the program to draw the curve.

Solids

A solid is a volume which is bounded by a number of faces. Solid faces are bounded by edges and solid edges are bounded by solid vertices. Mentat offers five basic solid types: block, cylinder, sphere, torus, and prism.

The *block* entity is a rectangular block which is defined by the coordinates of a corner point and three dimensions. The *cylinder* entity is a solid cone which is defined by two points on the axis of revolution and two radii. The *sphere* is defined by the center point and the radius and the *torus* is defined by the coordinates of the center and the two radii. The *prism* is defined by two axis points, a radius, and the number or prism faces.

The basic solids can be manipulated through the **SOLIDS** processor. First a series of boolean operations such as UNITE, SUBTRACT, and INTERSECT can be used to modify the basic solid entities. In addition, the BLEND and CHAMFER operations exist to make smooth transitions between various faces.

Geometric entities can be converted to other geometric entities using the **CONVERT** or **SOLIDS** processor. This allows the following conversions:

curve	polyline curve
curve	interpolated curve
surface	polyquad surface

surface	interpolated surface
solid vertex	point
solid edge	curve
solid face	trimmed surface
trimmed surface	solid face

The CLEAR GEOM button in the mesh generation menu allows you to remove all geometric entities from the database.

The Direct Meshing Technique

Elements are used as the basic building blocks to generate a coarse mesh that can be refined later using the tools provided by Mentat specifically for this purpose. This approach is particularly suitable for a domain with a simple geometry. The direct meshing technique is not based on an algorithm but consists of the enumeration, by you, of the most coarse mesh that still represents the desired geometry. Use the ADD button of the element and node panels in the mesh generation menu to define the building blocks.

Once you have generated a coarse model (Figure 1.1-19), you can refine it (locally) to the desired level using the **SUBDIVIDE** processor. You can expand the model to a higher dimension using the **EXPAND** processors. The **DUPLICATE**, **SYMMETRY**, and **MOVE** processors allow scaling, translation, rotation, and duplication of part of the model. The **RELAX** and **STRETCH** processors are available to relocate nodal points based on a given element connectivity. Removal of duplicate nodes or elements is achieved through the **SWEEP** processor and renumbering of the mesh can be performed with the RENUMBER option. CHECK allows specific checks on the correct definition of the mesh.

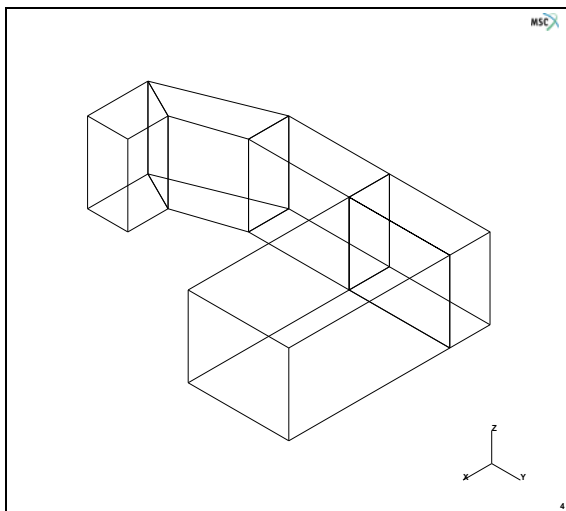


Figure 1.1-19 Example of a Coarse Mesh

The direct mesh generation process in Mentat is a three step procedure:

- Step 1 Generate nearly correct coordinates and fully correct connectivity. Subdivide and refine the initially specified elements where necessary.
- Step 2 Modify the boundary nodes for exact boundary coordinates.
- Step 3 Redistribute the internal coordinates to create reasonably shaped or relaxed elements.

The Geometric Meshing Technique

The basic building blocks for this technique are geometric entities rather than mesh entities. The geometric entities available in Mentat are points, curves, surfaces, and solids. They may be converted to mesh entities after you have completed the geometric model. This approach is more complex than the direct meshing technique as it involves the extra layer of geometric entities. However, the advantage of the geometric meshing technique is that increased complexity is offset by increased flexibility in generating geometries of complex shape. It is important to differentiate mesh entities from geometric entities; for example, a two-noded line element is not the same as a line curve, and a node is not the same as a point.

Convert

To change the geometric model to a finite element mesh, you may *convert* the geometric entities to finite elements. For instance, curves can be converted into line elements and surfaces into quadrilateral elements. The following conversions are possible:

point	node
curve	line elements
surface	quadrilateral elements

The **ATTACH** processor is a very powerful tool to put nodes on a curve or surface. Please note that after a **CONVERT** operation, the resulting nodes have been attached to the geometric entity.

Automesh

Mentat contains as optional products automatic mesh generators which generate finite element meshes on solids, on trimmed surfaces, and within curves in a plane.

Typically, three steps can be considered.

1. Clean up and repair of the curves (coming from a CAD tool)
2. Set the curve divisions which basically controls the mesh density
3. Automatic generation of the mesh

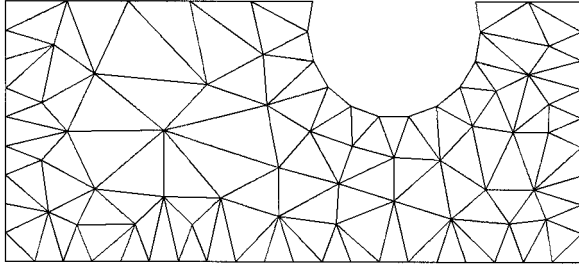
Three classes can be distinguished for the automatic meshers:

1. 2-D PLANAR MESHING
2. SURFACE MESHING
3. SOLID MESHING

Both the 2-D Planar and the Surface meshing have several alternatives for creation of a mesh. All meshers with exception of the **OVERLAY** mesher use the seed points defined in the **CURVE DIVISIONS** menu.

The **OVERLAY** processor allows you to describe the geometry by its boundary instead of a surface. This can be applied either to a planar structure or a trimmed surface. You may use any curve type available in Mentat to specify the boundary. (This also implies that a combination of curve types is permitted.)

The **TRI MESH!** mesh generator creates triangular elements, on a trimmed surface or within curves in a plane. Either the Delaunay technique or the Advancing Front technique can be used.



Triangular Mesh

The **QUAD MESH!** mesh generator creates quadrilateral elements on the faces of a solid, on a trimmed surface, or within curves in a plane based on an Advancing Front technique.

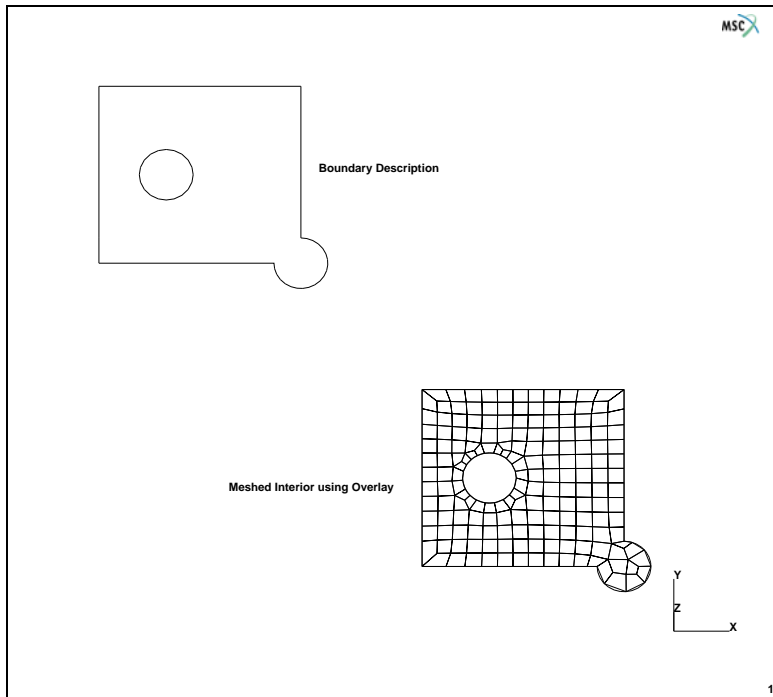
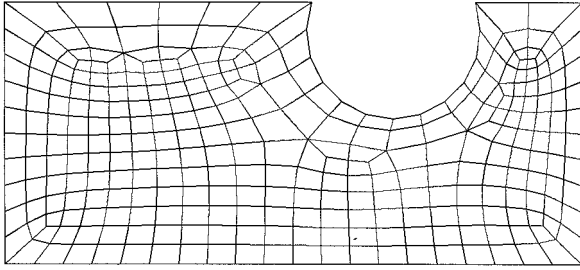


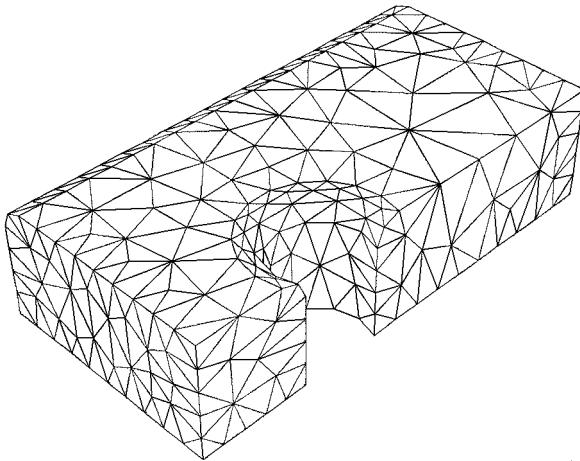
Figure 1.1-20 Overlay Mesh



Quadrilateral Mesh

In addition, mixed triangular and quad elements can be generated using the Advancing Front technique.

The two solid meshers use the surface mesh created with the above mentioned meshers as input. The TET MESH! mesh generator creates tetrahedral elements in a solid volume or within a volume bounded by triangular elements. The HEXMESH! generator creates hexahedral solid elements in a volume spanned by the surface mesher.



Tetrahedral Mesh

What Constitutes a Good Mesh?

Unfortunately, this question can only be answered a posteriori. Only when the analysis is complete, and a convergence study conducted, is it possible to quantify the answer to this question. A priori qualifications, although often necessary, are generally not sufficient.

Elements have ideal shapes when there is little or no error in the numerical computation of individual stiffness matrices. It would be convenient if triangles were always equilateral, quadrilaterals always squares, and hexahedra always cubes. However, it is almost impossible to model complex systems with a mesh of ideally shaped elements. Therefore, it is advisable to match the mesh density to stress gradients and deformation patterns which imply that elements vary in size, have unequal side lengths, and are warped or tapered.

With the above in mind, the remainder of this section concentrates on a few guidelines you can use to determine the quality of a mesh. These guidelines are aspect ratio, distortions, and transitioning.

Aspect Ratio

The element aspect ratio is the quotient between the longest and the shortest element dimensions. This ratio is by definition greater than or equal to one. If the aspect ratio is 1, the element is considered to be ideal with respect to this measure. Acceptable ranges for the aspect ratio are element and problem dependent, but a rule of thumb is:

$AR \leq 3$ for linear elements

$AR \leq 10$ for quadratic elements.

Elements with higher-order displacement functions and higher-order numerical quadrature for a given displacement function are less sensitive to large aspect ratios than linear elements. Elements in regions of material nonlinearities are more sensitive to changes in the aspect ratio than those in linear regions. If a problem has a deflection or stress gradient dominant in a single direction, elements may have relatively large (10) aspect ratios, provided that the shortest element dimension is in the direction of the maximum gradient.

Distortions

Skewing of elements and their out-of-plane warping are important considerations. Skewness is defined as the variation of element vertex angles from 90° for quadrilaterals and from 60° for triangles. Warping occurs when all the nodes of three-dimensional plates or shells do not lie on the same plane, or when the nodes on a single face of a solid deviate from a single plane.

Transitioning

Two types of transitioning exist. The first type is the change in element density in the direction of the stress gradient. The greatest refinement is then in the region with the highest gradient. A good tool to apply to this type of transitioning is biased subdivision.

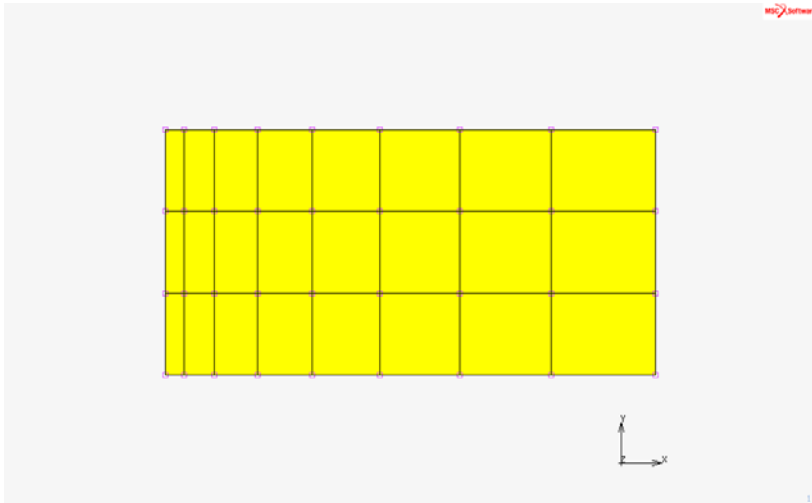


Figure 1.1-21 A Biased Mesh, Bias = -0.4 in X-direction

The second type is transverse transitioning, which is used between element patterns with different densities across a transverse plane.

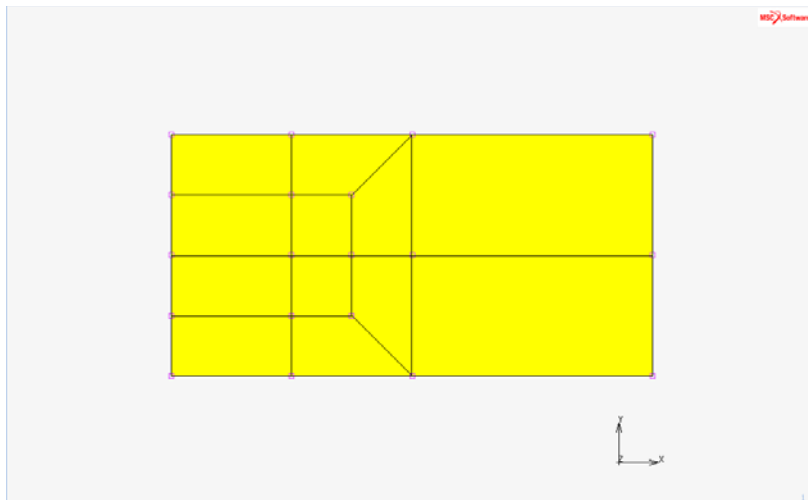


Figure 1.1-22 A Transition Mesh

If a model requires transverse transition regions, they should only be used in low-stress gradient regions, never near regions of maximum stress, deflection, or other regions of interest. The REFINE option in Mentat allows you to create a transition region.

Note: Within the framework of the CONTACT option, Marc and Mentat allow the automatic connection of two different parts which do not have common nodal points. Thus, various parts in the structure can be modelled with different mesh densities without the need for transition regions.

Boundary Conditions, Initial Conditions, and Links

The **BOUNDARY CONDITIONS** processor is used to define the boundary conditions applied to the model in order to perform the analysis.

Mentat distinguishes the following groups of boundary conditions based upon the Analysis Class:

- Structural
- Thermal
- Joule
- Acoustic
- Bearing
- Electrostatic
- Magnetostatic
- Magnetodynamic

Depending on the analysis class, boundary conditions must be taken from one of these groups. An exception to this rule is the coupled analysis, for which both mechanical and thermal boundary conditions may be defined. The following boundary condition types can be found in the Mechanical submenu:

- Fixed displacement
- Fixed acceleration
- Point load
- Edge load
- Face load
- Global load
- Gravity load
- Centrifugal load
- Fluid drag
- Edge foundation
- Face foundation
- Cavity pressure load
- Cavity mass load
- Degree of freedom - set nodes
- State variable

- Nodal temperature
- Release nodes

The specifications of the boundary conditions and associated parameters, along with the location, are grouped in one menu. The application of boundary conditions can best be thought of as an answer to the question: “Apply *what*, *where*, and *when*”.

Every *what* requires a list specification for *where* and possibly *when*. It will be clear that fixed displacements are applied to nodes as are point loads. Edge loads are applied to edges of elements, while face loads to faces of elements, etc. For specification of the *where* part we refer back to the beginning of Chapter 2 on [List Specification](#). If nodes have been attached to a curve or surface, it is also possible to apply the boundary conditions to the curve or surface. The associated nodes, element edges or element faces will inherit this boundary condition.

An important consideration of the *when* part is that one is defining potential boundary conditions, based upon a unique boundary conditions id. The boundary conditions are not applied in an analysis, unless they are selected in the **LOADCASE** processor, and the loadcase is selected in the **JOBS** processor or unless they are selected as INITIAL LOADS in the **JOBS** processor. Note that boundary conditions can also be specified as a function of time through the TABLE option.

Note: It is important to apply the correct number of boundary conditions. Too many causes the system of equations to become over constrained; too few causes a rigid body mode.

In addition to the boundary conditions, often a set of initial conditions can be present. Examples of these are the initial velocity in a dynamic analysis, and the initial temperature in a heat transfer analysis. The initial conditions can be defined in the **INITIAL CONDITIONS** processor.

Similar to boundary conditions, one defines here only potential initial conditions. They become active only if they are selected as INITIAL LOADS in the **JOBS** processor.

For specific analyses, it can be required to set up constraint equations between various components of the boundary conditions. Also springs can be present between two nodes. The **LINKS** processor allows the definition of constraint equations and links or dashpots. (Note that springs are not associated with element behavior.)

Material and Geometric Properties

Virtually all of the required material data for an analysis with Marc may be entered through Mentat. The program recognizes the following material data:

- Elastic-Plastic Isotropic
- Elastic-Plastic Orthotropic
- Elastic-Plastic Anisotropic
- Rigid Plastic
- Hypoelastic
- Mooney
- Ogden

- Gent
- Arruda-Boyce
- Marlow
- Bergstrom-Boyce
- Anisotropic Hyperelastic
- Foam
- NLELAST
- Shape Memory
- Composite
- Gasket
- Soil
- Powder
- Heat transfer
- Joule heating
- Acoustic
- Bearing
- Electrostatic
- Magnetostatic
- Magnetodynamic

Note that for a coupled analysis the heat transfer material type must be combined with one of the mechanical material types.

In [List Specification](#), it explains how to apply material data to elements. The **MATERIAL PROPERTIES** processor in the main menu facilitates the application of material constants and functions to elements.

Both in the Orthotropic and the Anisotropic material type, direction dependent material constants have to be defined. These material properties are usually defined in a local material axis system. The **ORIENTATION** processor allows specification of the material axis system. In addition, the **COMPOSITE** processor is available to define layered shell structures with different (direction dependent) properties and thicknesses.

Truss, beam, plane stress, plane strain, axisymmetric, membrane, plate, and shell elements are based on theories that are limiting cases of the general continuum theory. Shell theory, for instance, requires the shell element to have a thickness. This thickness (although strictly speaking a part of the geometry) does not enter into the mesh generation phase. This data is entered through the **GEOMETRIC PROPERTIES** processor. Other element types have similar properties such as area for truss elements and moments of inertia and local axis systems for beam elements.

For some element types, special options may be flagged in order to get more accurate results. For instance, the classical 4-node plane strain element is known to give a too stiff behavior if the element is subjected to bending. By selecting the assumed strain formulation, the element type is modified into a description with improved bending behavior. If,

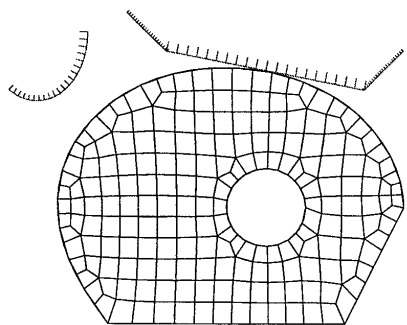
for the same element, the material behavior is nearly incompressible, the constant dilatation formulation has to also be selected. These special options are also defined in the **GEOMETRIC PROPERTIES** processor.

Furthermore, the data for the Marc gap/friction elements can be entered here.

Contact

The automatic contact analysis is a very powerful capability in the Marc program. The boundary nodes and segments for a given set of elements are determined, and when the analysis requires it, the boundary conditions to be applied are automatically adapted. Mentat supports this analysis capability completely. It allows definition of both deformable and rigid bodies, friction and thermal contact.

A deformable contact body is defined by a list of elements. A rigid contact body is defined by curves for 2-D applications and surfaces for 3-D applications.



The **CONTACT** processor in the **MAIN** menu allows the definition of the following tasks:

- CONTACT BODIES:** defining the contact bodies, the properties of the contact body and allowing a graphical verification if the bodies are defined correctly.
- CONTACT TABLES:** defining for which bodies contact will be checked, local friction coefficients, local separation forces, and heat transfer coefficients. Also here it can be specified that the so-called glued contact will occur, which implies automatic coupling of different parts.
- CONTACT AREAS:** defining for which subset of the nodes in a contact body contact will be checked.

Note that similar to Boundary and Initial Conditions, both the **CONTACT TABLES** and **CONTACT AREAS** only define potential different applications of these options. They are only applied if they are selected in the **LOADCASE** or the **JOBS** processor.

Loadcases and Jobs

Linear finite element analysis is characterized by a force-displacement relationship that only contains linear terms. The system of equations always produces a unique solution. In contrast, nonlinear analysis does not guarantee a unique solution. In fact, there may be multiple solutions or no solution at all. The task of providing analysis directives (i.e., controls by which the program will come to a solution) is far from simple. Solving nonlinear equations is an incremental and iterative process.

A linear static mechanical analysis with a known external load can be performed in one step. If nonlinearities are expected, it may be necessary to apply the load in increments and let each load increment iterate to the equilibrium state, within a specified tolerance, using a particular iteration scheme such as Newton-Raphson. Also the complete load history might consider of a number of load vectors, each applied at a specific time in the load history. Each (set of) loads to be applied in a specific time period can be considered as a loadcase. A job is then the subsequent performance of various loadcases. In this way, the complete loading history can be defined. Note that a loadcase is not necessarily identical to a load step. A loadcase may consist of 10 load steps to reach the total load of the loadcase. In a loadcase, multiple boundary condition IDs can be present.

A dynamic transient analysis of a beam structure with pre-load P1 and dynamic load P2 using the modal superposition technique consists of the following loadcases:

- Loadcase 1: Apply pre-load P1.
- Loadcase 2: Perform eigenfrequency analysis based on pre-stressed structure
- Loadcase 3: Perform transient analysis using superposition of eigen modes. The load P2 is defined as a function of time through the TABLE option. Each loadcase can have different control values for the iterative processes used.

Depending on the analysis type (e.g. mechanical, heat transfer), the **LOADCASE** processor on the analysis panel of the main menu allows you to specify the following:

Load incrementation i.e selecting the boundary conditions, the number of steps, automatic versus fixed stepping, and the controls for this loadcase.

The **JOBS** processor is used to control the overall flow of the analysis process. This includes the analysis class, the selection of the loadcases, the analysis options, the results which are required, the initial loads, contact control, and other parameters. Also the element type specification, the check on integrity of the job, and the actual submitting of the job is done in this processor.

Typically, the finite element analysis produces an enormous volume of numerical data. Before you submit the job for analysis, use the **JOB RESULTS** processor to control which variables are to appear in the results file beyond the default parameters associated with the analysis type.

Before you submit the job, it is advisable to perform an integrity verification to check for inconsistencies in geometrical and material properties. The program automatically verifies the determinant of the Jacobian for all elements in the mesh. Errors found during this process are reported and corrective action should be taken before the job is submitted.

Once the data is verified by the program and passes the validity test, the job may be submitted. The SUBMIT button initiates the job in the background and leaves the terminal free to do other tasks. Use the UPDATE or MONITOR button to monitor the progress of the job during execution.

Results Interpretation

Once you have completed the analysis, you need to analyze the results and verify the criteria for acceptance. For each increment, the requested results are stored in a sequential file. Use the following three basic steps to gain access to the results.

- Step 1 Open the results file.
- Step 2 Select the desired information.
- Step 3 Select an appropriate display technique and display the results.

The **RESULTS** processor on the postprocessing panel gives you access to the various plot options available in Mentat.

As we have already mentioned, a typical nonlinear finite element analysis consists of several steps called *increments*. The results for an increment can be accessed through the OPEN, NEXT, or SKIP sequence of commands. OPEN accesses the file and opens it for reading. The results file name is a concatenation of the job name and the suffix *.t19* or *.t16*. NEXT forwards the file pointer to the next increment. The results data for the increment that was read by the NEXT command is available for processing.

The solution of the finite element analysis involves a geometrical discretization of the object and, if applicable, a temporal discretization. The geometrical discretization is obtained by creating the finite element mesh that consists primarily of nodes and elements. The results (depending on their nature) are supplied at either the nodes or the integration points of the elements. We make the distinction by referring to one as *data at nodes*, and the other as *data from elements at integration points*.

Data at nodes is a vector where the number of degrees of freedom of the quantity indicates the number of components in the vector. Data from elements at integration points is either scalar, vector, or tensor data.

The data from elements at integration points are not in a form that can be used directly in a graphics program. Data from elements at integration points is extrapolated to the nodes thus creating *data at nodes from elements*. The values at the nodes are calculated by a linear extrapolation of the average centroidal value and the integration point closest to the node.

A node may be shared by several elements. Each element contributes a potentially different value to that shared node. The values are summed and averaged by the number of contributing elements.

If a node is shared by elements of different materials, the averaging process may not be appropriate. To prevent the program from averaging values, use the ISOLATE option.

Scalar Plots

Scalar data may be represented graphically by means of contour bands, contour lines, symbols, numerics, iso-surfaces, cutting planes, beam contours, or beam values. A legend to the left of the drawing shows the correspondence between

the colors used and the numeric interval they represent. *Contour plots* are lines or bands of equal value drawn over the elements. This display technique is applicable to two-dimensional elements, such as shells and plates, or to faces of three-dimensional elements, such as bricks. The three-dimensional counterpart to contour plot is the *iso-surfaces* plot, where the surfaces of constant value are displayed.

Vector Plots

Vector data may be represented graphically by arrows that are displayed at the nodes.

Tensor Plots

Tensor data may be represented graphically by arrows that are displayed at the centroid of the elements.

Deformed Shape Plots

The deformations found in a mechanical analysis can be shown in what is known to Mentat as a *deformed shape plot*. The mesh is deformed by an amount that is proportional to the actual displacement at the node.

Beam Diagrams

Display a shear diagram or a moment diagram for beam structures is with this option.

Path Plots

Path plots are snapshots created by freezing time or an increment. The variables for the abscissa and ordinate are selected from the list of available variable names. For path plots, the position where the quantity is evaluated is the most likely candidate for the abscissa.

History Plots

As the name indicates, history plots capture phenomena over time or increments. The abscissa variable is very likely to be time or an increment number. As Mentat keeps only one increment of data in memory, it is necessary to collect data by scanning over the range of increments or time that is of interest before the history can be displayed.

Getting Started

This section describes the routine interactions with Mentat listed below.

- Starting Mentat,
- Using the PROCEDURE option,
- Stopping a Mentat session,
- Recommended Starting Chapters.

This section concludes with a simple example to acquaint you with the program. It is best to focus on the overall session and not to dwell on the details. Once you have mastered the basic steps described in this chapter, you should feel comfortable enough with Mentat to venture on to the sample sessions in the remaining of this manual.

Starting the Mentat Program

Before you start the Mentat program. . .

1. You will need an account so you can use Mentat on your system.
2. If you don't know how to invoke Mentat, ask a current Mentat user or call MSC Software customer support. Although the starting command is system dependent, it most likely is `mentat`. On machines supporting OpenGL graphics, one would type: `mentat -ogl`.
3. The Mentat program is based on X-Windows™; you must start the program in a window environment.

Assuming you are already logged in on your computer, type `mentat` at the prompt of your operating system. Provided your version has been installed correctly, once Mentat is loaded into memory, the program should start by opening a window on your X-terminal. This displays the basic Mentat screen which consists of a main menu, a blank graphics, and a dialogue area. [Figure 1.1-23](#) shows you the initial Mentat display.

If the Mentat script does not invoke the program or does not invoke it correctly, ask your system administrator or call your nearest MSC Software office for support. Our telephone numbers are on the back cover of this manual.

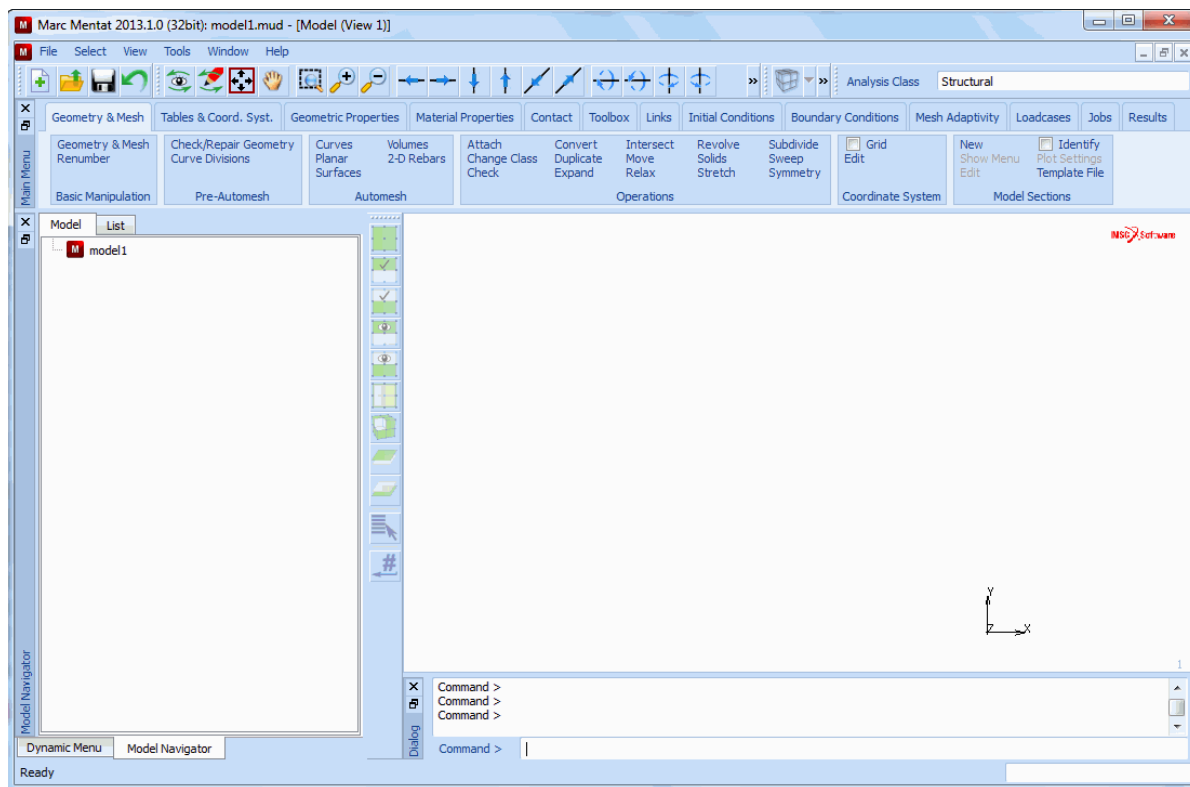


Figure 1.1-23 Initial Mentat Display

Procedure Files

A procedure file is a record of all commands issued during a session and is useful for the tasks listed below.

- Protecting your work.
- Performing repetitive operations.
- Doing parametric design.
- Demonstrating your work.
- Reporting errors.

The PROCEDURES command has two modes of operation:

1. Record mode: creates a new procedure file or appends an existing procedure file
2. Playback mode: partial or complete execution of a procedure file

In both modes of operation, a choice can be made if the procedure file should reflect the changes in the menus. If the MENU RECORD button is activated, all changes in the menu are recorded while creating procedure files. If the MENU EXECUTE button is activated and if a procedure file is used in which the menu changes have been recorded, the menus modify while playing back the procedure file. Upon clicking on any of the CREATE, APPEND, LOAD, or EXECUTE buttons, a file browser appears. The FILTER block indicates the file extensions for the file type being used in the current application (here *a.proc* extension). Either click an existing file in the FILES block, or type a new file name in the SELECTION blocks followed by an OK.

In playback mode, the LOAD button followed by the STEP mode allows stepwise playback of the procedure file. (Observe that the Mentat Procedure Control window can be moved to any position of the screen). START/CONT will start the execution of the procedure file until the STOP button is clicked.

All sessions listed in Section II through IV of this manual are procedure files that are included on the Mentat installation CD in the *examples/marc_ug* directory.

You can play these sessions back by executing the procedure file using the following button sequence:

```

UTILS                                     (located at the bottom of the static menu)
PROCEDURES
LOAD                                       (located on the PROCEDURE window)
    path/filename
OK
STEP or START/CONT

```

Remember to use <ML> to click on a button. After you click on the LOAD button, enter the file name of the procedure file you want to execute. Once you have done this STEP, observe the changes as the information stored in the procedure file is executed. START/CONT automatically continues until either the STOP button is activated or until in the procedure file the **stop_procedure* command is present. Continue with the remaining information with either STEP or START/CONT.

An excellent way to learn more about the program is to make changes to the procedure file or to mimic it and to try to predict the results.

On the previous page, you were introduced to the concept of a **button sequence diagram**. A button sequence diagram is a way of prescribing a sequence of mouse clicks and corresponding data entry. An indent indicates a new menu. Aligned options indicate they are available from the same menu. A button sequence diagram starts at the main menu and works its way to the desired option. Buttons in the static menu do not require you to start with the **main** menu. The button sequence diagram is used frequently throughout the remainder of this chapter and in the sample sessions.

If there is any ambiguity as to which button you must click on, the button will be preceded by the specific panel or menu title. For example, if elems ADD appears in a button sequence, the idea is to click on the ADD button next to “elems” rather than nodes or curves on a particular panel. Another example is all: EXIST. which indicates that you should click on the EXIST. button of the “all:” panel.

If you are not at the main level before you execute the button sequence diagram, you can click on the <MR> with <↑> anywhere over the menu area until you reach the main menu. You can also click on the MAIN button in the lower left hand corner of the menu area to return immediately to the main menu.

The initial state of the program prescribes, wherever possible, a default for every setting. These settings are chosen because they are applicable to most cases. For example, the default number of divisions for SUBDIVIDE is set to 2, 2, 2. You can return to this default state at any time during the execution of the program by clicking on the RESET PROGRAM button. Use the following button sequence from the TOOLS tab:

PROGRAM SETTINGS

RESET PROGRAM

When you create a procedure file, you are only recording commands that are issued from the time the procedure was started. The procedure file does not contain information on the state, or settings of the program at the time it was started.

Stopping the Mentat Program

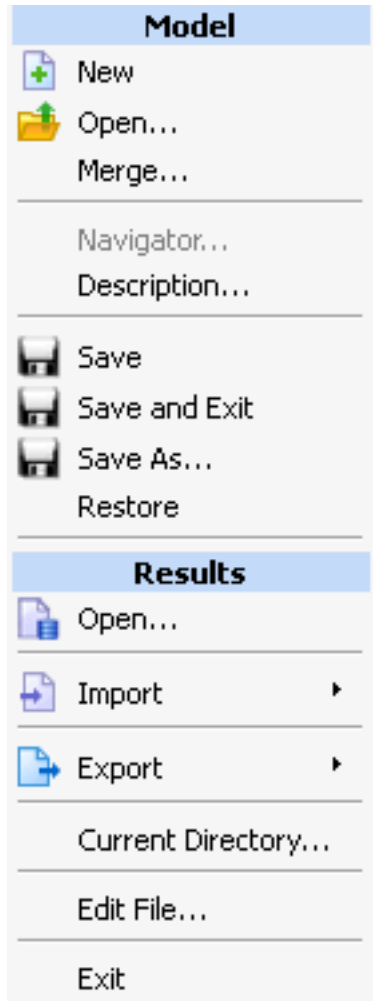
Always make sure to save your work before you stop the Mentat program. Use the SAVE button to write a copy of the database in Mentat format. The SAVE button is located in the static menu directly under the graphics area. This way you are assured all data is saved. Using other formats such as the Marc format does not guarantee all information is saved.

Normal Stop

Use the EXIT button located on the FILE pop-up to end a Mentat session. Be sure you save your model before exiting the program. Alternatively, you can type `*quit` in the dialogue area followed by a `y` for yes at the `Exit program?` prompt at any time during a session.

Emergency Stop

An emergency stop can be made at any time by using CTRL-C (that is, hold down the CTRL key and press C) from the parent window. Typing CTRL-C in the dialogue area does not stop the program. A host-induced stop usually does not offer you much of an option as you lose some or all of the data in memory.



Recommended Starting Chapters

The subsequent chapters in this User's Guide perform a variety of simulations with varying levels of difficulty; if you are just starting with Mentat, the table below recommends some of the simpler starting problems keeping the model complexity to a minimum while covering the basic functionality of Mentat. You might consider taking these chapters

in the order below since the later ones assume you have gained confidence with changing views, turning node displays off, or rotating the model and the button sequences to perform simple manipulations are omitted.

Analysis Type	User Guide Chapter Problems: Recommended Starting Chapters
Static	Chapter 3.20: Tensile Specimen
Static	Chapter 3.18: Cantilever Beam
Static	Chapter 3.21: Rubber Elements and Material Models
Static	Chapter 3.9: Break Forming
Static	Chapter 3.16: Super Plastic Forming (SPF)
Static	Chapter 3.19: Creep of a Tube
Static	Chapter 3.25: Interference Fit
Static	Chapter 3.10: Hertz Contact Problem
Heat Transfer	Chapter 4.4: Cooling Fin Analyses
Coupled Thermal Mechanical	Chapter 5.3: Coupled Transient Cooling Fin
Coupled Thermal Mechanical	Chapter 4.2: Dynamics with Friction Heating
Heat Transfer	Chapter 4.3: Radiation with Viewfactors
Dynamics	Chapter 3.35: Dynamic Analyses of a Cantilever Beam

Following a Sample Session

At this point, you may begin duplicating the first sample session on your computer. Do not try to understand everything at once; all concepts are explained as you progress through the subsequent chapters. For now, concentrate only on becoming comfortable with the Mentat user interface.

The structure you are going to model has the dimensions shown in [Figure 1.1-24](#).



Figure 1.1-24 Dimensions of Structure to be Modeled

The first step is to type `mentat`. The MSC logo appears on your screen and is immediately replaced with a window that displays the main menu.

Use the <ML> to click on the MESH GENERATION tab.

The next step is to establish an input grid to help you specify the nodes of your model. Click on the EDIT button of the COORDINATE SYSTEM panel. The dynamic portion of the menu is replaced by the set coordinate system menu where the grid settings are located. In [Mechanics of Mentat](#), we mentioned that the “GRID” button was a toggle button that can be switched *on* or *off*. Click on the GRID button to turn the grid *on*.

The object you want to model has maximum dimensions 8 x 6 units. Click on the U DOMAIN button and use the keyboard to enter 0 10 to set the grid size in x-direction.

The updated coordinate system menu with the numerals 0 and 10 appearing in the flat fields next to the U DOMAIN button will appear.

The spacing between the grid points does not need to be finer than 1 unit since all the corner points are at integer distances from the origin.

Click the U SPACING button and type in 1. The program updates the menu accordingly as is shown in. Repeat the steps for the V DOMAIN and V SPACING to set the values in y-direction.

Click on the FILL button to scale the picture to fit the screen. The FILL button is located in the Tool Bar directly under the graphics area.

The window will appear as shown in [Figure 1.1-25](#).

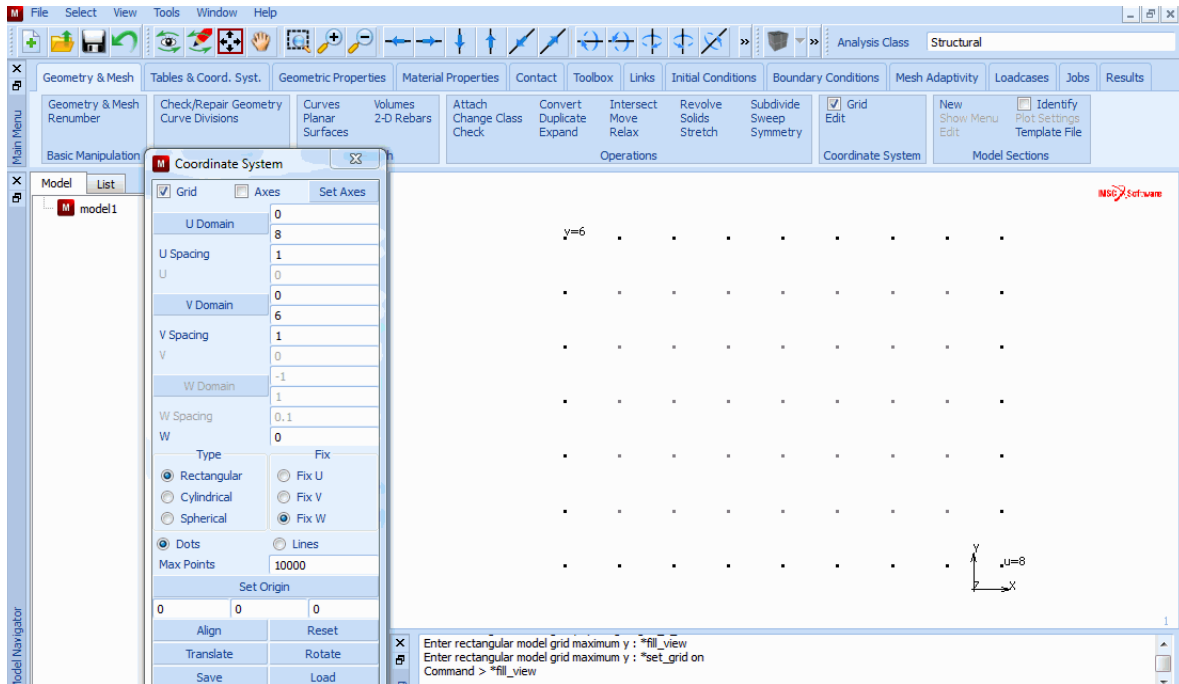


Figure 1.1-25 Scaling the Picture

Below follows a button sequence diagram of the steps required to set the coordinate system that we discussed in the previous pages. A comparison of this button sequence to a detailed step description shows you that the button sequence step format is condensed and easy to follow.

MESH GENERATION

Grid Activate

Edit

U DOMAIN

0 10

U SPACING

1

V DOMAIN

0 10

V SPACING

1

FILL

To help you keep track of the elements and nodes that you are going to create, you must label them. Click on the Fix View Draw Setting pull down to control the plots.

The VIEW DRAW Setting panel determines whether or not an entity is drawn. With the LABEL panel, it can be indicated if the entity will be labeled. Click on the NODES button of the LABEL panel. The NODES button is a toggle button; as long as it is depressed, every node you create is labeled by its respective node number.

Similarly, click on the ELEMENTS button of the LABEL panel. The ELEMENTS button is also a toggle and stays depressed indicating that every element you create is labeled by the corresponding element number.

Turn Off Faces

Return to the mesh generation menu by clicking on the RETURN button located in the bottom left corner of the menu area or by clicking <MR> with the <↑> over the menu area.

To enter an element, click on the ADD button of the ELEM panel. The default element class is QUAD(4), a 4-noded quadrilateral, which is the element type you are going to use for your model.

The program prompts you to enter four nodes. Look for the prompt in the dialogue area.

Pick the grid point at the origin of the u-v system shown on the screen for the first node of a quadrilateral element. Click the <ML> with the <↑> close to that grid point. The program confirms the location of the first node with a small square at the grid point and the node number 1 in the graphics area. The entry is confirmed in the dialogue area with `node(0,0,0)` at the `Enter element node (1) :` prompt.

To create Node 2, repeat the steps for Node 1 six units, or grid points, to the right of the first node.

Repeat this for Node 3 at a location two units above Node 2.

Finally, pick a location two units above Node 1 for the fourth node.

The program draws the entire element. It includes a cross at the center of the element and a half-arrowhead on the first side of the element in the direction of the connectivity. The cross in the middle of the element is the *handle* of the face of the element; in 2-D, the face is the element itself. If you need to pick this element, click the <↑> in the center of the element.

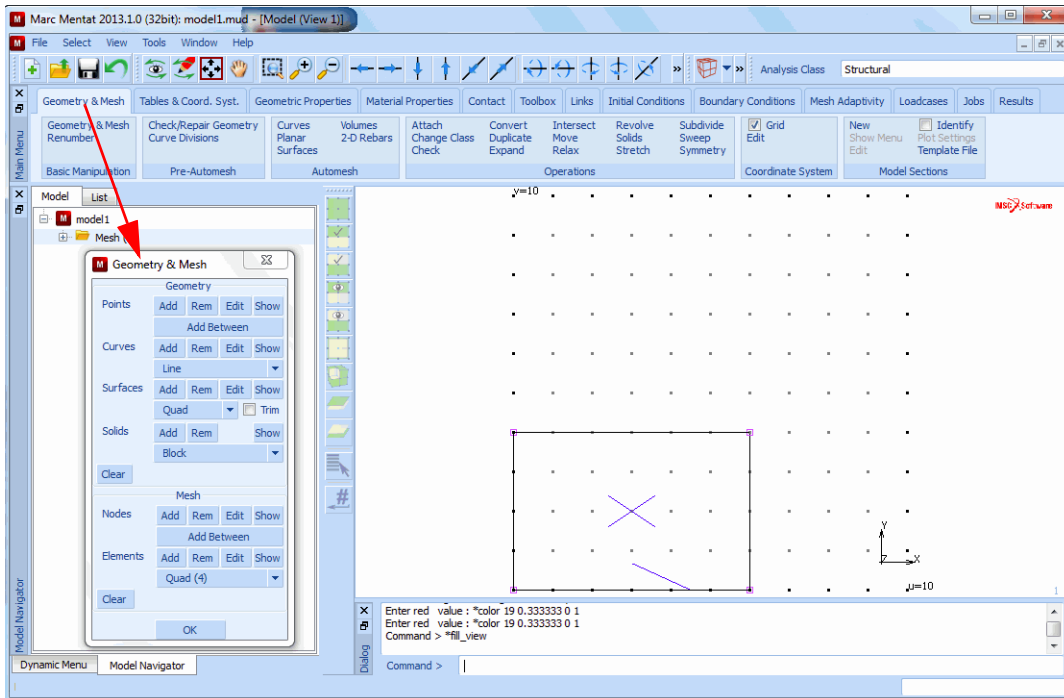


Figure 1.1-26 Element 1 Completed

You do not need to click on the ADD button on the ELEMS panel again to enter a second element. As discussed in [How Mentat Communicates with You](#), until you explicitly instruct it otherwise, the program assumes you want to continue the previous action: in this case, adding elements.

Pick Node 2 of Element 1 for the first node of the second element. You will see this node light up on your screen.

The second node of Element 2 is positioned two units to the right of the first node. Again, the program confirms this by drawing a square and the node number, Node 5, at that location.

The third node is positioned four units above Node 5. Click the <ML> on that particular grid point to create Node 6.

Pick the last node of Element 2 so that it coincides with the third node of Element 1. The program confirms this pick by highlighting the existing node. The connectivity for this element is complete and is confirmed by the display of the entire element.

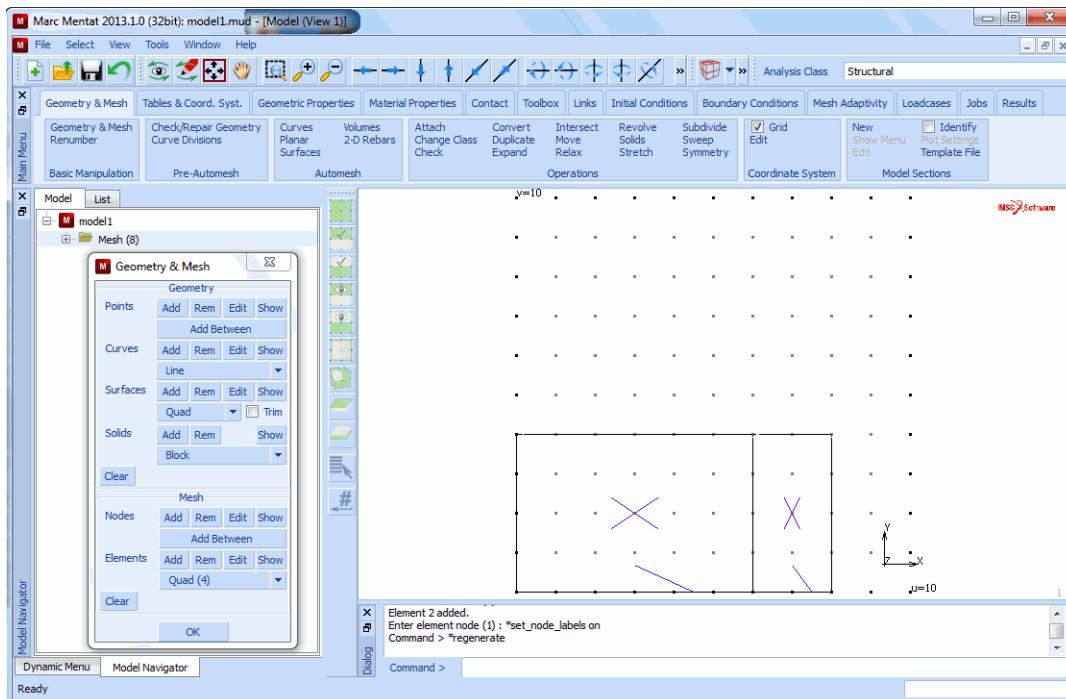


Figure 1.1-27 Element 2 Completed

Add the third element by repeating the same sequence of steps. Pick Node 1 of Element 3 to coincide with Node 4 of Element 1.

To create the second node of Element 3, pick Node 3 of Element 1 which also coincides with Node 3 of Element 2. Once again, the node will light up to confirm it has been picked.

The third node of Element 3 is positioned above the second node (Node 3). Use <ML> to pick this node by clicking on the grid point that is two units above the previous one.

Complete the element by picking a grid point two units above the first node of this element (Figure 1.1-28).

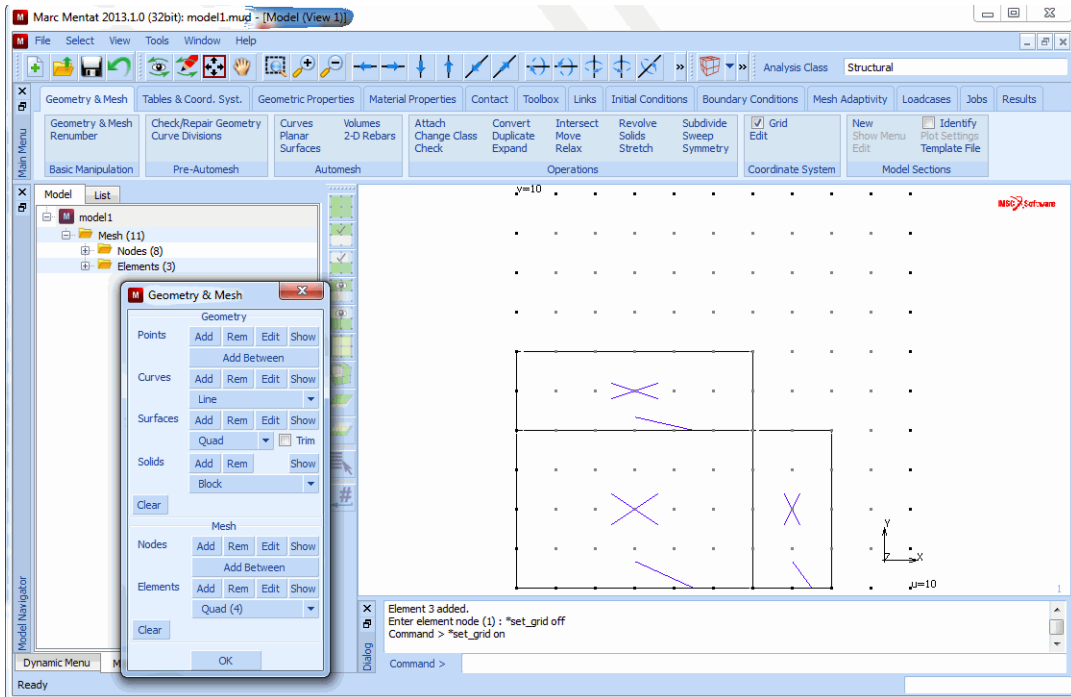


Figure 1.1-28 Element 3 Completed

Turn the grid off by clicking on the GRID button located on the Tool bar (Figure 1.1-29). The toggle returns to the default released state.

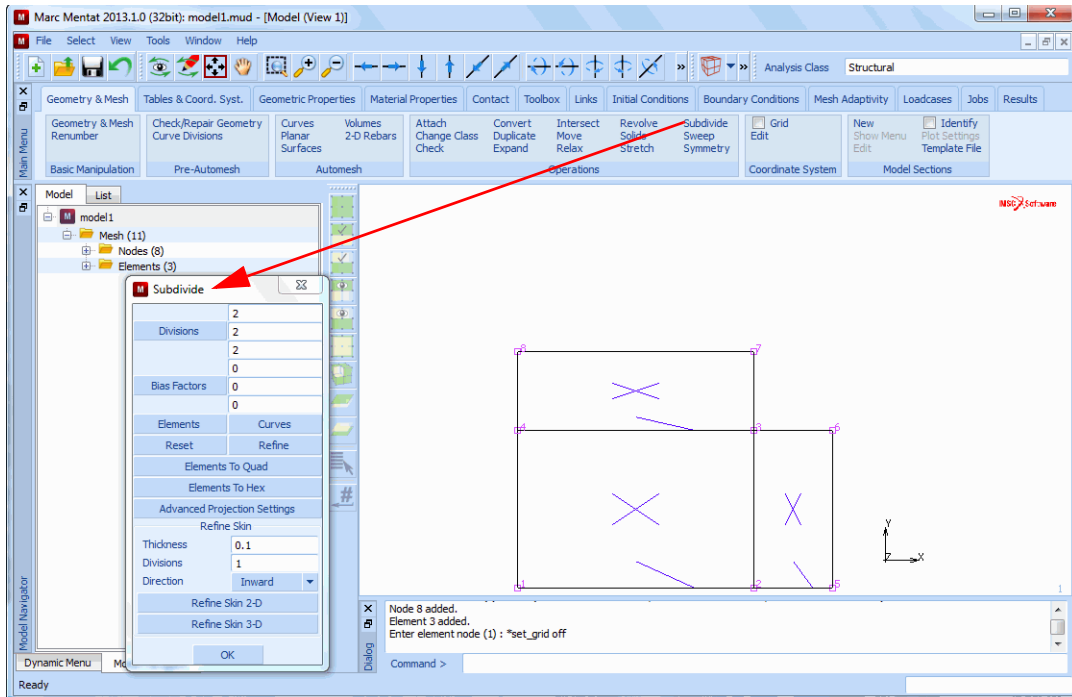


Figure 1.1-30 Activating the Subdivide Processor

Use the <ML> to click on the handle of each element to indicate that you want to subdivide it. Each element that you click on will light up.

Once you have picked every element on the screen, click the <MR> with <↑> anywhere over the graphics area to indicate an *end of list* to the program. Alternatively, you can click on the END LIST (#) button icon. All elements are now subdivided. Instead of picking all the individual elements, you can click on the all: EXIST. button to subdivide all elements.

Notice the double nodes at the corners of the original elements. The SWEEP processor eliminates duplicate nodes.

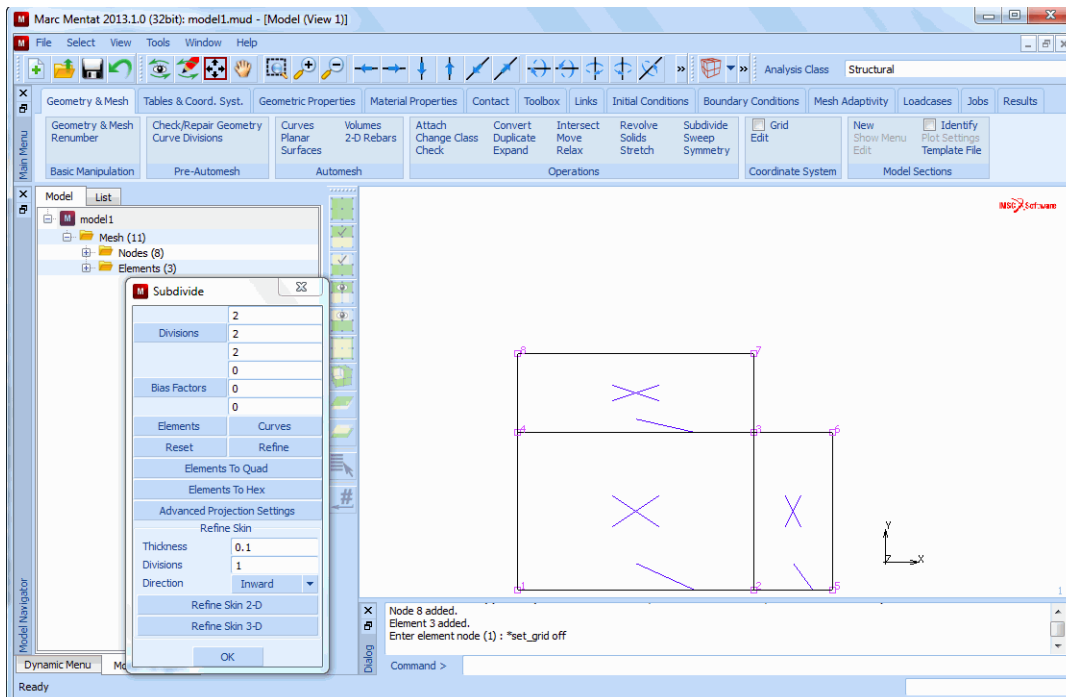


Figure 1.1-31 After Elements were Subdivided

Note that there are 35 nodes, some of which are duplicate nodes. Click on the **NODES** button on the **SWEEP** panel to eliminate the duplicate nodes. Use the default value 0.0001, for the tolerance.

The program prompts you for the list of nodes to sweep with the following string:

Enter sweep node list:

Click on the **all: EXIST.** icon to indicate that you want to sweep all nodes (Figure 1.1-32). The program removes the duplicate nodes and displays the mesh with only 21 nodes remaining.

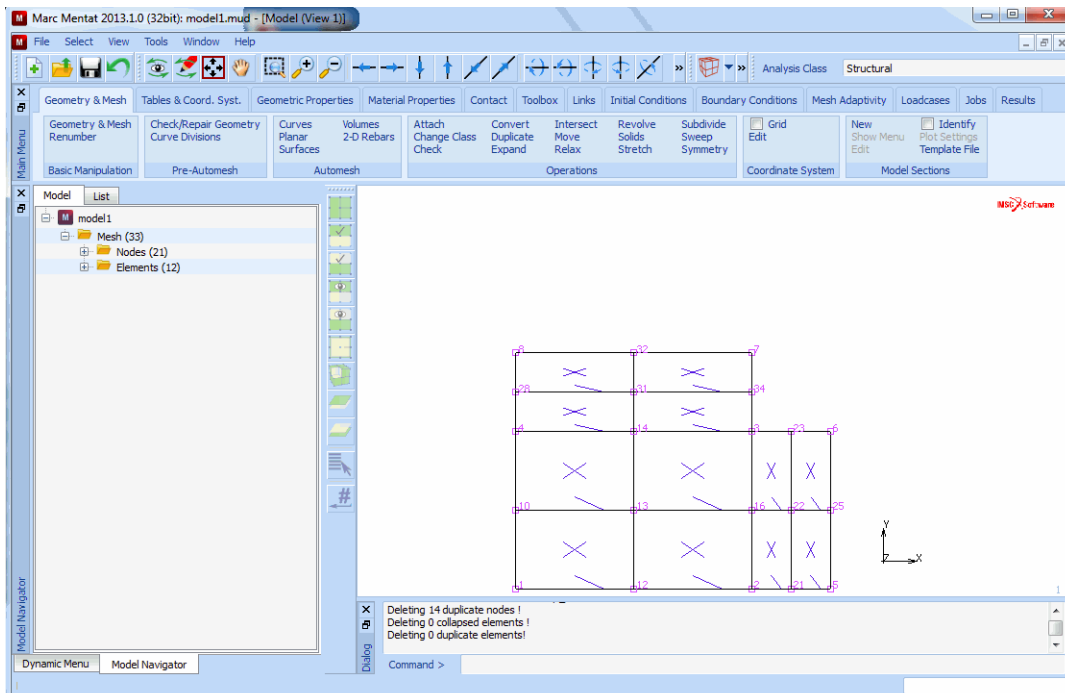


Figure 1.1-32 Identifying the Nodes to Sweep

Save the mesh by clicking on the SAVE icon. The mesh is saved in Mentat format in a binary file called *model1.mud*. If *model1.mud* already exists on the disk, the numeral in the file name is automatically incremented by one, and the file name is thus called *model2.mud*.

Stop the session with the following button sequence:

FILE
EXIT

You should now feel comfortable interacting with Mentat. We encourage you to practice with the example detailed in this chapter, and to build on the experience you gained through this session.

A Simple Example

In this section, it will be demonstrated how to set up the basic requirements for a linear elastic stress analysis. For this purpose, a flat square plate with a circular hole subjected to a tensile load will be analyzed. It is generally known that a stress concentration exists around the hole. Both the deformed structure and the stress distribution need to be determined. The goal of the analysis is to demonstrate:

- a simple mesh generation technique, using the geometric meshing approach

- how to apply boundary conditions
- how to set material properties
- how to set geometric properties
- selecting quantities to be calculated in the analysis for subsequent postprocessing
- how to submit a job using the Marc finite element program
- how to generate deformed structure plots, contour plots, and path plots

Background Information

A square plate with dimensions 20×20 mm and a thickness of 1 mm contains a circular hole with radius 1 mm at the center of the plate. The material behavior is assumed to be linear elastic with Young's modulus $E = 200000 \text{ N/mm}^2$ and Poisson's ratio $\nu = 0.3$. A tensile load with magnitude $p = 10 \text{ N/mm}^2$ will be applied both at the top and the bottom of the plate.

Calculate the deformed structure and determine the yy -component of stress along the cross-section near the hole.

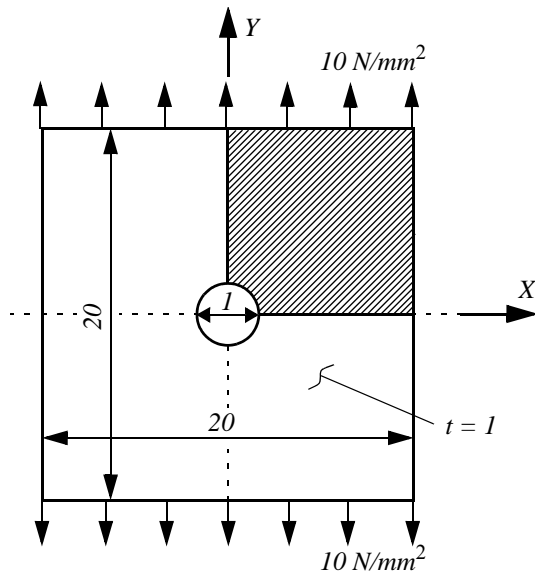


Figure 1.1-33 Plate with a Hole Subjected to Tension

Due to the symmetry of the problem, it is sufficient to analyze only a quarter of the problem. At the line $x = 0$ and $y = 0$ symmetry boundary conditions have to be applied.

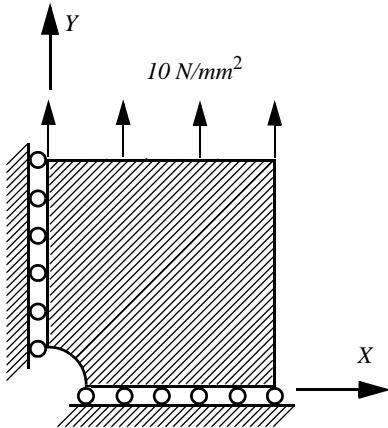


Figure 1.1-34 Quarter of the Plate with Symmetry Conditions and Tensile Load

Overview of Steps

Step 1: **Mesh generation**

Step 2: **Boundary conditions**

Step 3: **Material behavior**

Step 4: **Geometric properties**

Step 5: **Job definition**

Step 6: **Postprocessing**

Detailed Session Description

Step 1: Mesh generation

The applied approach for generating the model is to use the geometrical technique to specify the boundary curves and the surface spanned by these curves. Subsequently, the surface will be converted into finite elements.

As in the sample session in [Following a Sample Session](#), the first step for building the mesh is to establish an input grid. Click on the MESH GENERATION tab.

Next click on the SET button to access the coordinate system menu where the grid settings are located. Use the following button sequence to set the horizontal and vertical grid spacing to 1 and both the horizontal and vertical grid dimensions to 10.

MAIN MENU

MESH GENERATION

SET**U DOMAIN**

0 10

U SPACING

1

V DOMAIN

0 10

V SPACING

1

GRID ON*(on)***FILL**

Two geometrical entities are used to describe the boundary contour. First, set the curve type to a circular arc and define the arc segment.

MAIN MENU**MESH GENERATION****CURVE TYPE****CENTER/POINT/POINT****RETURN****CRVS ADD***(pick the following points from the grid)*

0 0 0

(center point)

1 0 0

(starting point)

0 1 0

(ending point)

In the graphics window, a circular arc will now be visible. Change the curve type subsequently to a polyline.

MESH GENERATION**CURVE TYPE****POLY LINE****RETURN****CRVS ADD***(pick the following points from the grid)*

point(10,0,0)

(or type in POINT(x,y,z))

point(10,10,0)

point(0,10,0)

END LIST (#)
FILL

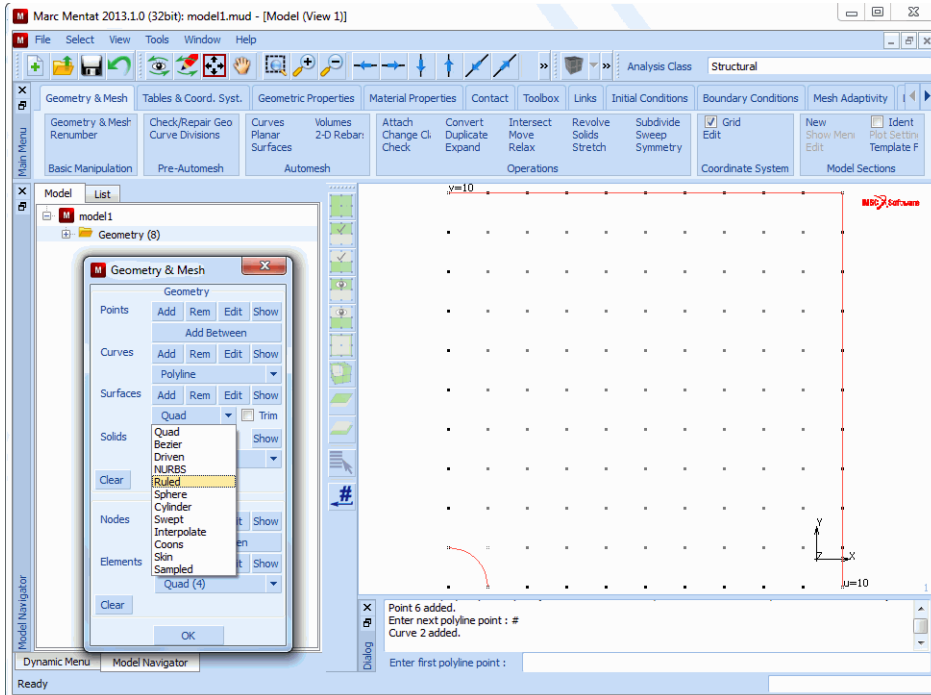


Figure 1.1-35 Boundary Curves of Quarter of the Plate

The two basic curves will now be used to describe a ruled surface. Set the surface type to ruled and specify the both curves.

MESH GENERATION

SURFACE TYPE

RULED

RETURN

SRFS ADD

- 1
- 2

(pick the arc)
(pick the polyline)

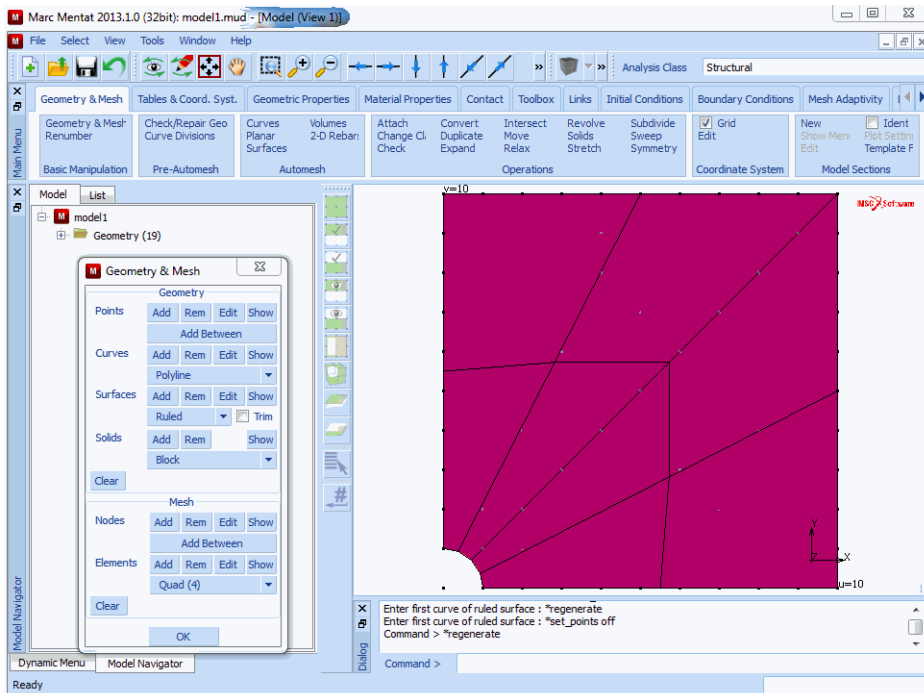


Figure 1.1-36 Surface Definition

With the **CONVERT** processor, the surface are converted to finite elements. In the **CONVERT** menu, it can be observed that by default the mesh division are set to 10 by 10 elements. The **BIAS FACTORS** will be used to ensure that the mesh is more refined in the direction of the hole. The first surface direction is along the arc; the second surface direction runs from the arc to the polyline. A negative bias factor will be specified here, indicating that the refinement must be near the hole. Now convert the surface to a finite element mesh.

MESH GENERATION

CONVERT

BIAS FACTORS

0 -0.5

SURFACES TO ELEMENTS

1

(pick the surface)

END LIST (#)

DEACTIVATE GRID

(off)

FILL

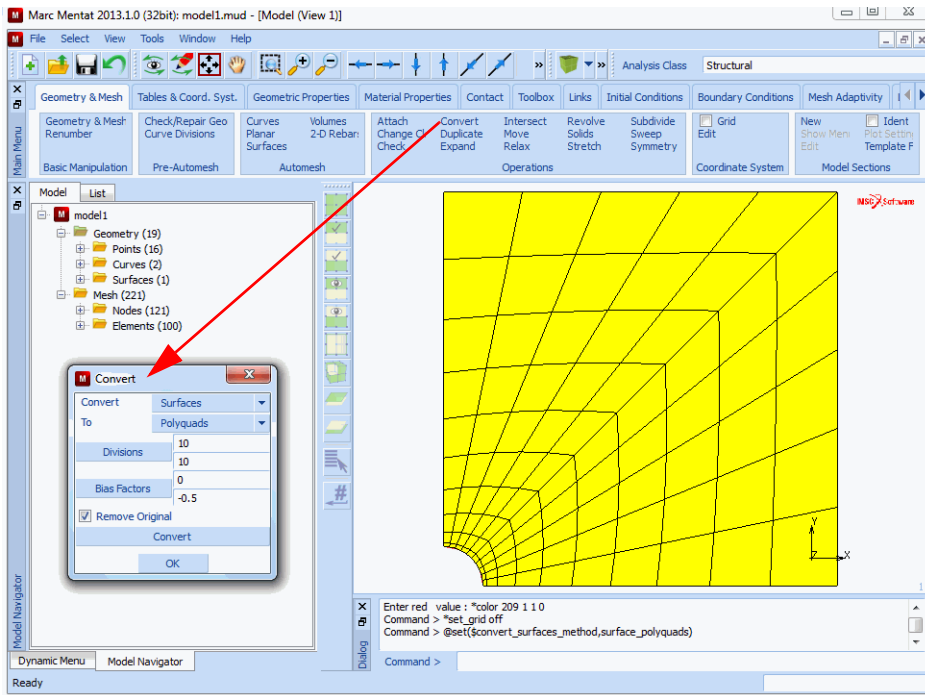


Figure 1.1-37 Generated Element Mesh

The arrows near the element edges indicate that the elements are numbered clockwise. Marc requires that planar elements are numbered counter-clockwise. The numbering can be changed using the UPSIDE DOWN and FLIP ELEMENTS options in the CHECK menu.

While checking, all elements with incorrect numbering are put in the temporary selection buffer, which is graphically shown by a change of color. Therefore, the list of elements that need to be flipped can easily be specified using the ALL: SELECTED icon. Repeating the check will show that no upside-down elements are found anymore so that the temporary selection buffer will be empty again.

MESH GENERATION

CHECK

UPSIDE DOWN

(this will automatically select "upside down" elements)

FLIP ELEMENTS

ALL: SELECTED

UPSIDE DOWN

(no elements should be selected - they have all been fixed)

Step 2: Boundary conditions

The symmetry conditions can be applied using the following button sequence:

BOUNDARY CONDITIONS

MECHANICAL

FIXED DISPLACEMENT

DISPLACEMENT X

(on)

OK

NODES ADD

(box pick the nodes on the line $x=0$)

END LIST (#)

NEW

FIXED DISPLACEMENT

DISPLACEMENT Y

(on)

OK

NODES ADD

(box pick the nodes on the line $y=0$)

END LIST (#)

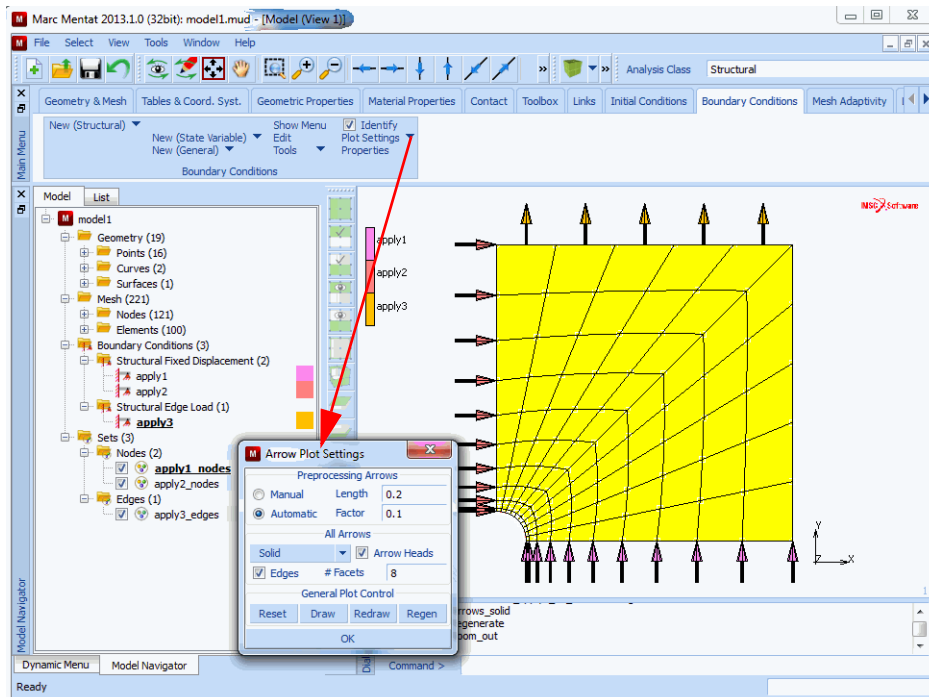


Figure 1.1-38 Applied Boundary Conditions at the Lines $x=0$ and $y=0$

The applied loading is a tensile edge load with magnitude 10. Mentat allows to prescribe a distributed pressure on element edges. The following button sequence will give the prescribed loading.

BOUNDARY CONDITIONS

MECHANICAL

NEW

EDGE LOAD

PRESSURE

-10

(specify pressure)

OK

EDGES ADD

(box pick the edges on the line $y = 10$)

END LIST (#)

A graphical verification of the applied edge loading is now obtained.

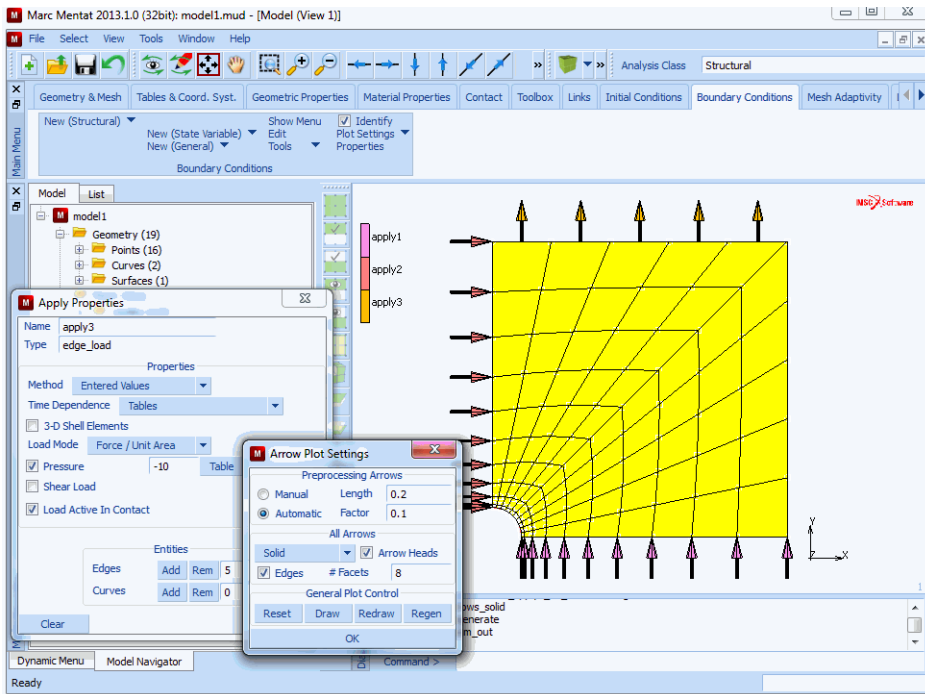


Figure 1.1-39 Boundary Conditions and Edge Loading

Step 3: Material behavior

The material behavior is identical for all elements. Elastic behavior with Young's modulus and Poisson's ratio must be specified for this material. The following button sequence fulfills the requested task. Note that after entering the Young's modulus, Mentat automatically requests for the Poisson's ratio, which can subsequently be entered. After entering this value, the mass density is requested. By entering a <CR>, this sequence may be stopped.

After specifying the list of elements, the material description is complete.

MAIN MENU

MATERIAL PROPERTIES

MATERIAL PROPERTIES

NEW

STANDARD

STRUCTURAL

YOUNG'S MODULUS 200000 .

POISSON'S RATION 0.3

OK

ELEMENTS ADD

ALL: EXIST.

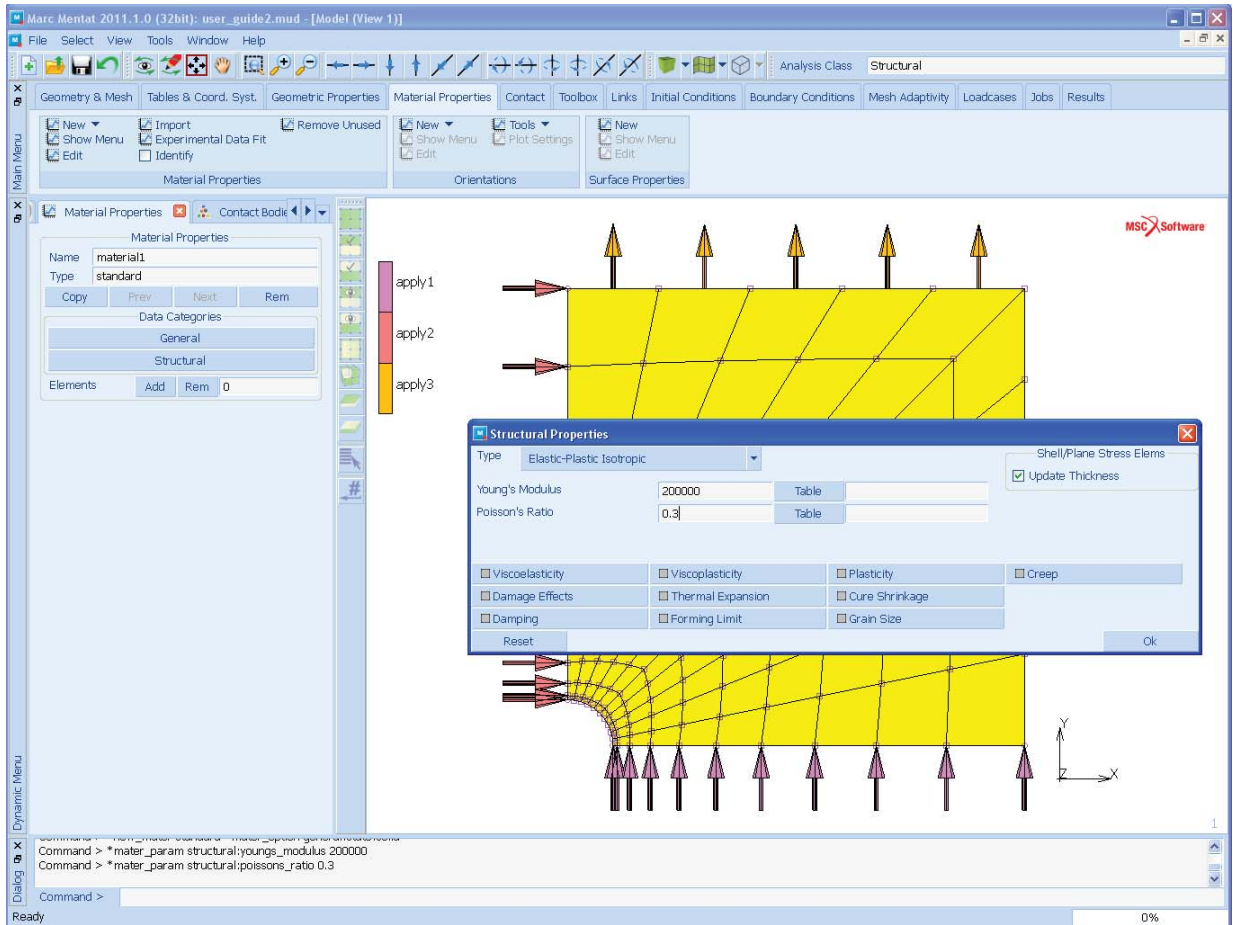


Figure 1.1-40 Material Properties

Step 4: Geometric properties

Many elements require geometrical properties such as cross-sectional areas for beams and thickness for plate and shell elements. For this plane stress analysis, the thickness must be specified for all elements.

GEOMETRIC PROPERTIES

PLANAR

PLANE STRESS

THICKNESS

1

OK

ELEMENTS ADD

ALL: EXIST.

Step 5: Job definition

All ingredients for a linear elastic static analysis are now created. No incremental steps are required nor does the loading consist of various load vectors. Therefore, entering the LOADCASES menu is not necessary.

In the JOBS menu, first set the analysis class to MECHANICAL, indicating that a stress analysis will be performed. In the pop-up menu first select JOB RESULTS. Here, the analyst has to specify which element quantities have to be written to the post file. For simplicity, the full stress tensor is selected. Alternatively, all requested components of the stress tensor can be selected. (Note that the stress tensor writes 6 components to the post file; three of them are zero for a plane stress element).

In the INITIAL LOADS menu, it can be verified if all boundary conditions (symmetry conditions and edge load) are active as initial loads. The initial loading is the complete loading for a linear elastic analysis. Loading histories or different loading steps require the use of the LOADCASE option. The INITIAL LOADS screen must contain the following below:

JOBS

NEW

NEW JOB: MECHANICAL

PROPERTIES

JOB RESULTS

AVAILABLE ELEMENT TENSORS

Stress

(select stress)

OK

INITIAL LOADS

OK *(twice)*

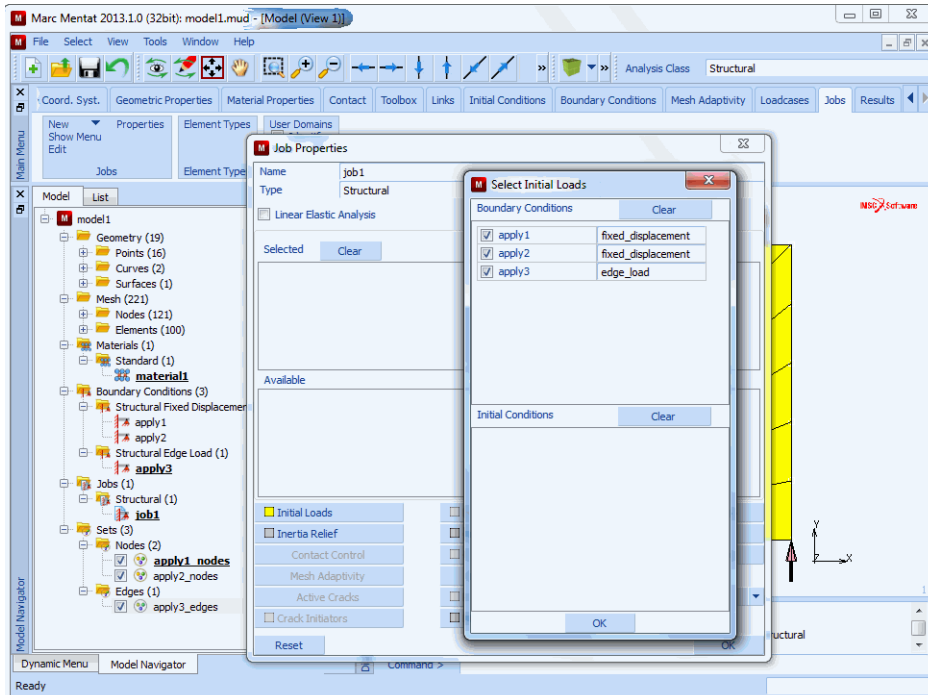


Figure 1.1-41 Initial Loads

Next, the element type will be set. In this analysis, the 4-noded plane stress element type 3 with full integration will be used for all elements.

JOBS

ELEMENT TYPES

ANALYSIS CLASS

USE CURRENT JOB ON (MECHANICAL), OK

ANALYSIS DIMENSION

PLANAR

SOLID

3

OK

ALL: EXIST.

(full integration, QUAD(4))

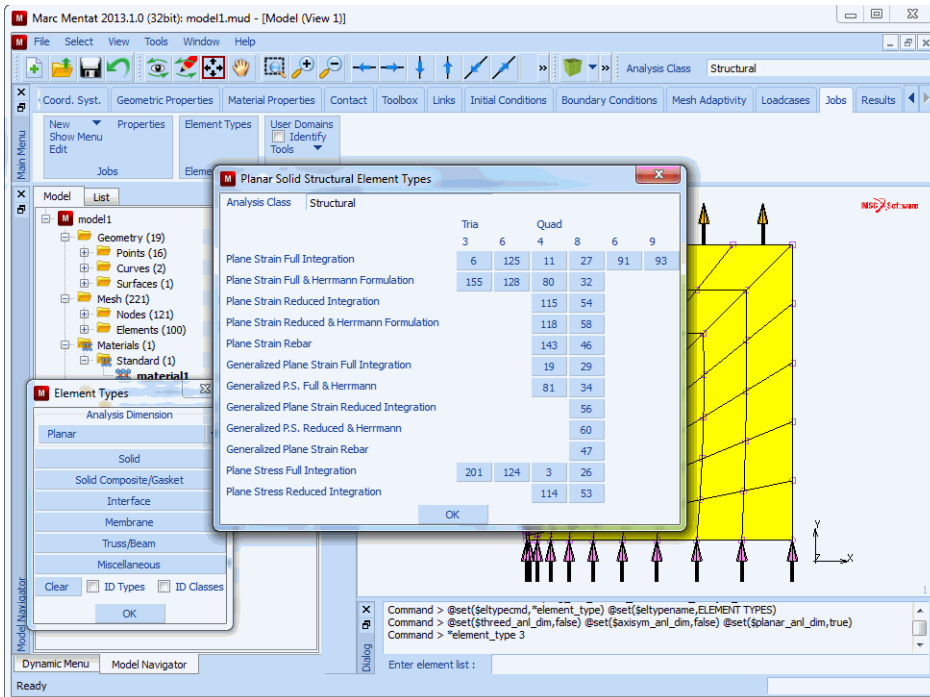


Figure 1.1-42 Selecting the Element Type

The job is now ready for submission. The RUN command controls the submission of the job. One of the SUBMIT commands starts the analysis, and with the MONITOR option, the current status of the job can be observed.

JOBS

RUN

SAVE MODEL

SUBMIT (1)

(this will automaticall monitor the job)

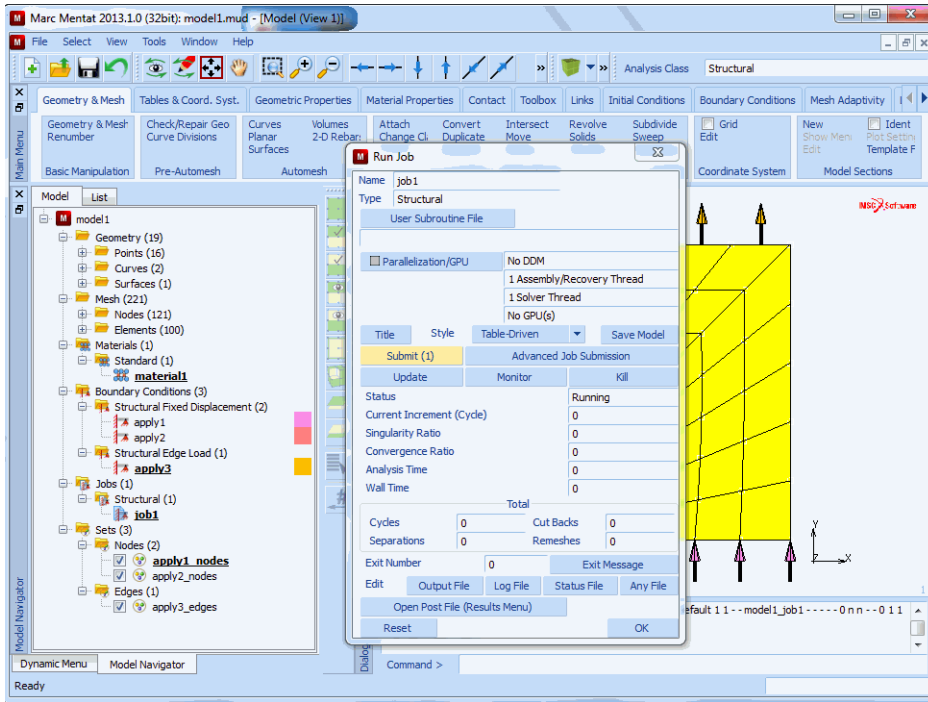


Figure 1.1-43 Screen After Job Completion

Step 6: Postprocessing

Once the job is complete, we are able to do postprocessing. The postprocessing tasks are performed on the Marc post file which does not contain all the information from the Mentat database. Therefore, it is always recommended to save the database before doing any postprocessing.

The Marc post file contains an analysis header (containing the mesh topology information) and the results of the various increments. Therefore, NEXT INC must be used after opening the post file to view the results of the first increment (usually increment 0). Clicking the DEF & ORIG button only does not seem to show any deformation on the screen. The magnitude of the displacement is simply too small for any visual effect. (By default the displacement will be added with multiplication factor 1 to the original coordinates to get the deformed structure). Automatic scaling will show the requested deformed structure.

- FILE
- OPEN DEFAULT
- RESULTS
- MODEL PLOT
- DEFORMED SHAPE
- STYLE: DEFORMED & ORIGINAL
- FILL

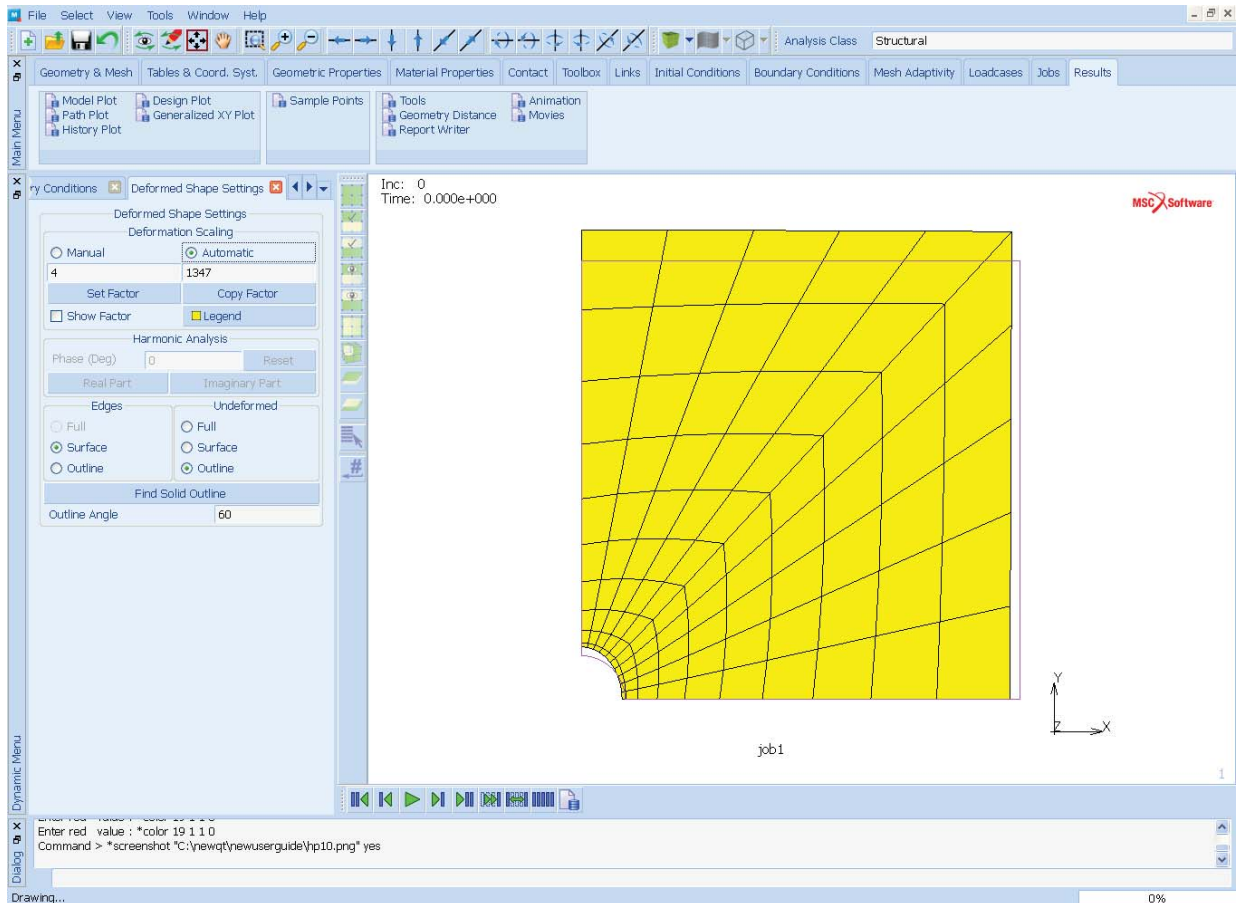


Figure 1.1-44 Deformed Structure Plot

Contour plots of stress or displacement components can be made with the continuous contours or the contour bands option. First, the quantity to be contoured has to be selected followed by clicking the CONTOUR BANDS option.

RESULTS

SCALAR

Comp 22 of Stress

OK

CONTOUR BANDS

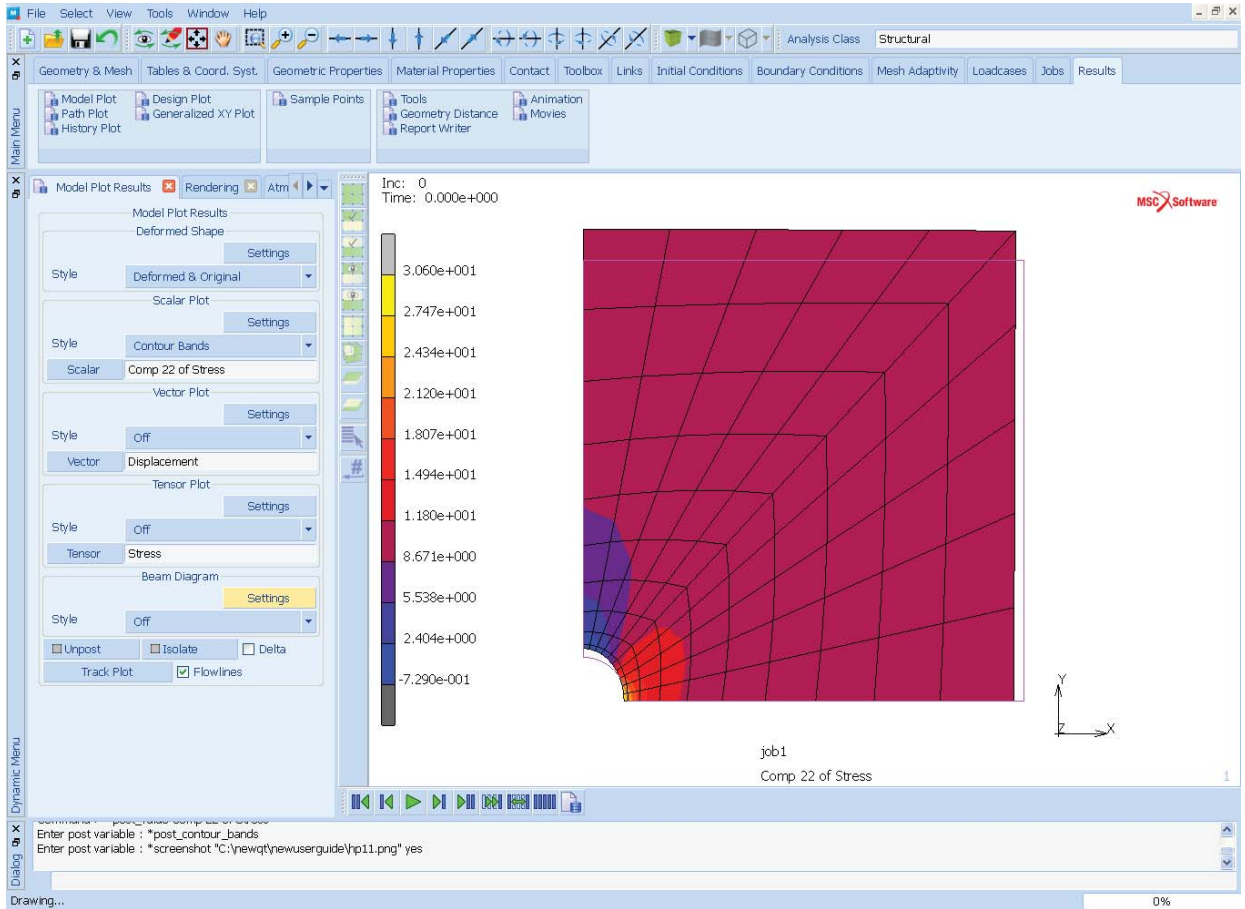


Figure 1.1-45 Contour Plot of yy Component of Stress

A plot of the yy component of stress along the cross-section near the hole can be obtained with the PATH PLOT option. First, a node path has to be selected (followed by an end list) and then the curve to be plotted can be specified. With the SHOW MODEL option, the screen can be changed to display the model again.

RESULTS

PATH PLOT

NODE PATH

END LIST (#)

ADD CURVES

ADD CURVE

Arc Length

Comp 22 of Stress

FIT

(pick the first and last node at the line y = 0)

SHOW PATH PLOT SHOW MODEL

(select *SHOW MODEL* to return to model view)

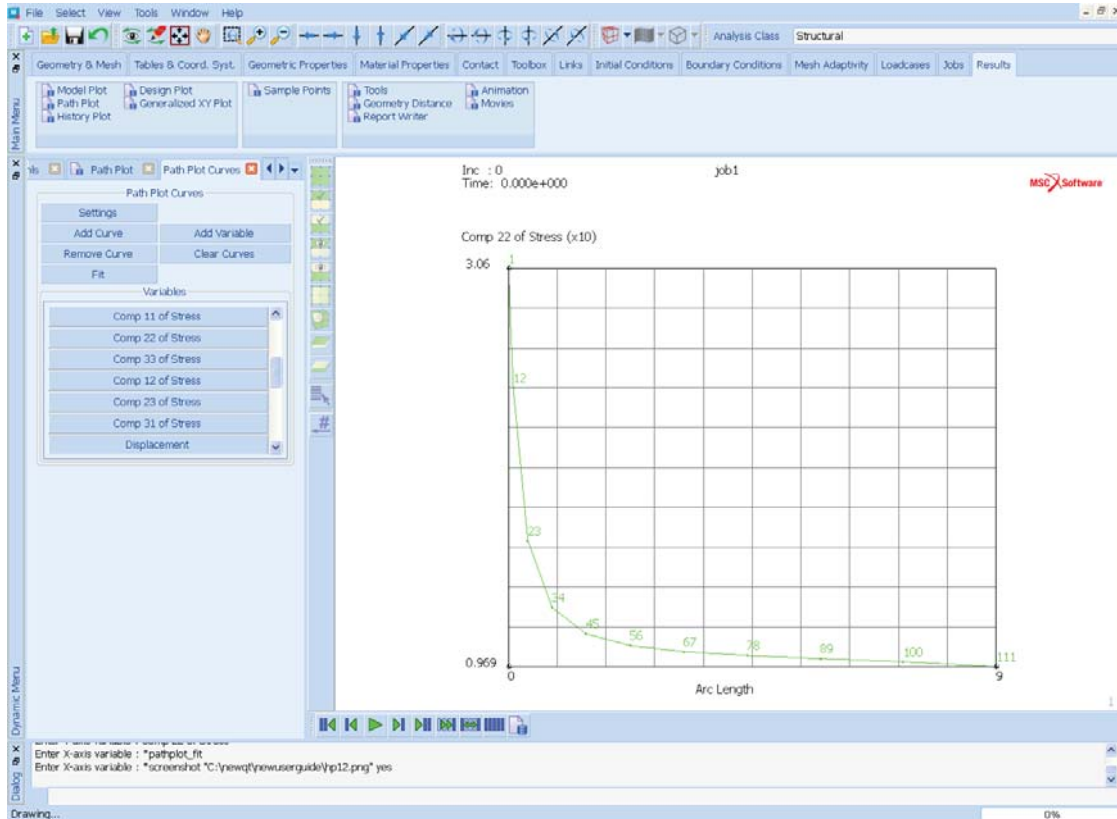


Figure 1.1-46 Path Plot

The results show that the plate has been analyzed correctly. Around the hole, a stress concentration factor of about three is present and the deformed structure plot shows an to be expected deformation field.

Close the post file and leave Mentat.

Input Files

The file `~/mentat/examples/marc Ug/s1/c1.1/linear_elastic_stress.proc` is on your delivery media or it can be downloaded by your web browser by clicking the link (file name) as follows:

File	Description
linear_elastic_stress.proc	Mentat procedure file to run the above example

Answers to Frequently Asked Questions

This section is an ongoing collection of answers to frequently asked questions that relate to the output of results from Marc and Mentat. A general description of some of the derived results available for each element is given in *Marc Volume A: Theory And User Information* under the heading "Element Information". The specific results available for each element are indicated in the *Marc Volume B: Element Library* under the heading Output of Stresses and Output Of Strains. Details on obtaining specific results in the output file are available in the section entitled "Selective Printout" in *Marc Volume A: Theory And User Information*. Further information of beams and bars may be found in Chapter 4 of the *Marc Volume A: Theory And User Information*.

[Appendix A: Shape Function Interpolation](#) presents a simplified description of the definition and use of shape functions in finite element analysis, as well as some important implications of their use.

[Appendix B: Finite Element Equilibrium](#) discusses issues such as averaging and unaveraging of element stresses in more detail.

[Appendix C: Coordinate Transformation](#)) presents the equations necessary to transform stresses for the plane stress case.

[Appendix D: Principal Stresses \(Plane Stress\)](#) presents the equations necessary to evaluate principal stresses from component stresses.

[Appendix E: Python Example \(Max Stress Results\)](#) gives an example of extracting the maximum stress found using a Python script.

[Appendix F: Python Example \(Displacements at Nodes\)](#) gives an example of extracting nodal displacements using a Python script.

Consistent Units

- MARC is unit independent and any system of units may be used. It is essential, however, that all data input quantities are specified using a consistent unit system. For example, if N, m, and kg are used, then the model dimensions must be specified in meters, the elastic modulus in N/m^2 and density as kg/m^3 . With respect to the output of results - if N, m, kg have been used in the data input, the results will provide stresses in N/m^2 , forces and reaction in N, displacements in m etc.
- Rotations are output in radians. This includes angular velocity and acceleration results.
- The units of temperature being used in an analysis are dependent on what is specified in Jobs> Heat Transfer> Job Parameters> Units & Constants.... The default is Celsius.
- When choosing a set of units, an appropriate system should be used to avoid problems with numerical round-off. For instance using the unit of meters to model a component that is only a fraction of a millimeter in overall size would require that the distance between element nodes would be of the order of $1\text{e-}6$. Similarly, the use of Mega-Tonnes would be preferable when analysing a massive civil engineering structure compared to kg.

- Using a dimensionally “consistent” set of units is essential in dynamic analyses to obtain meaningful results. For a static analysis without any body force loading (using density), the requirement for consistency is relaxed. In general, if units are chosen for mass (m), length (l) and time (t), the measure used for force must dimensionally correspond with $F = m a = ml/t^2$.
- The standard SI unit system is normally recommended; i.e., Newton, Metres, Kilograms. This complies by definition with the equation $F=Ma$ ($N = kg\ m/s^2$) and is termed a consistent set of units. If both sides are divided by 1000, a further set of consistent units becomes apparent as ($kN = Tonnes\ m/s^2$). Similarly, multiplying both sides gives ($N = T\ mm/s^2$).
- Any consistent system can be used; for example:
 - N, Millimetres, Tonnes
 - KN, Metres, Tonnes
 - MN, Metres, kTonnes
 - Dyne, Gram, Centimetre
 - Poundal, Pound, Feet

An example of nonstandard sets of units would be (kN, Millimetres, Tonnes), (N, Millimetres, kg).

Evaluation of Stresses in Finite Elements

In a finite element analysis, the stresses are evaluated at positions in each element called “Gauss” points. These points are usually not located at the element nodes but some distance into the element. These points are used to numerically integrate system matrices like stiffness, mass, surface and volumetric loads. See the section entitled “Marc Element Classifications” in *Marc Volume B: Element Library* for details on the exact positions of these points for each element class). Gauss point values are the most accurate results from a finite element analysis.

For general ease of use, however, nodal results are required and in order to obtain them it is necessary to “**extrapolate**” the Gauss point stresses to the nodes. This is performed by using the “*assumed element displacement (shape) functions*”. These shape functions are one of the basic building blocks of the finite element method and vary for each element type. In the general case, there are linear and quadratic shape functions. The former is typically used for corner-noded elements (e.g., 4-node quadrilaterals, 8-node bricks) and are often called “linear” or “lower order” elements. The latter is used for midside noded elements (e.g., 8-node quadrilaterals or 20-node bricks) and often termed “quadratic” or “higher order” elements. For the elements in Marc, see the section entitled “Marc Element Classifications” in *Marc Volume B: Element Library* for details on the shape functions used for individual element classes. See [Appendix A: Shape Function Interpolation](#) for a brief explanation of both shape functions and extrapolation.

Shear Strains used in Marc

Marc uses full tensor components for the stress matrices when all components are available (e.g. continuum elements) - except for the shear strains, where Marc uses a modified definition of shear strain namely $\gamma_{xy} = \epsilon_{xt} + \epsilon_{yx}$, instead of the actual tensor components ϵ_{xy} . Since the strain tensor is symmetric, then $\gamma_{xy} = 2\epsilon_{xy}$. This nontensor form

comes from the equation $\sigma_{xy} = G\gamma_{xy}$ where G is the shear modulus of the material. Herein, we shall refer to γ_{xy} as the shear angle. Shear angles are used through out Marc and are always given in the user subroutines.

Stress and strain measures must be considered when displacements become large, for example strain measures used in:

- Large Displacement → Green Lagrange
- Updated Lagrangian → Logarithmic
- Nothing → Engineering

To obtain a correct energy evaluation using the standard $1/2\sigma\varepsilon$ equation (area under the stress-strain curve), it is necessary to multiply the correct stress and strain matrices together, otherwise they are not energy-conjugate and will not give the correct result. The tensor stress and strain matrices are not energy-conjugate in this regard. The incremental energy is evaluated as:

$$\text{sum}_i \{ \text{sig}(i) * \text{deps}(i) + \text{dsig}(i) * \text{deps}(i) \}$$

where sig is the beginning increment stress, dsig is the incremental stress and deps is the incremental strain. i ranges from 1 to the number of stress/strain components.

Extrapolation/Averaging Tips in Mentat

There are three element extrapolation methods in Mentat (RESULTS> SCALAR PLOT SETTINGS> EXTRAPOLATION) where:

- *Linear* - the average of the integration point values is calculated and placed at the centroid. Then Mentat performs a linear extrapolation of the values from the centroid through the integration point to the nodes.
- *Translate* - the values at the integration points are simply copied to the nearest nodes. If there are fewer integration points than nodes, Mentat averages the values of neighbouring integration points. When combined with the Isolate feature (RESULTS>ISOLATE) to isolate just one element, this enables you to see the exact integration point values produced by Mentat in history plots. No extrapolation is used.
- *Average* - Mentat computes the average of all the values at the integration points and assigns an equal value to all the nodes. No extrapolation is used.

The accuracy of the extrapolation procedure is dependent on both the presence of a reasonably uniform stress field and the type of shape function used in the element chosen. For instance, a high stress gradient across an element would be more likely to extrapolate incorrectly; particularly if a linear shape function element is being used. Thus, although equilibrium conditions will always be met, the stress distribution can be wholly inaccurate for an insufficiently refined mesh.

In a typical analysis, each node point will be connected to more than one element and, hence, an averaging process is required to obtain a single value of stress at this node (simply adding all the component stresses and dividing by the number of components) - this is the output obtained in Mentat when choosing “nodal averaging = on” in SCALAR PLOT> SETTINGS> EXTRAPOLATION. Setting “nodal averaging = off” will not perform this process. See [Appendix B: Finite Element Equilibrium](#) for a more detailed description of the nodal averaging process.

In areas of interest where stresses will be used as input to the design process, a contour plot of averaged nodal stress should very similar to one using unaveraged nodal results (a smooth transition across element boundaries). This would indicate that the stress distribution in the structure is being simulated sufficiently accurately. For other sections of the model which are not of interest, a coarser mesh would normally be used and a comparison in these areas would typically give significantly different contour plots - the unaveraged contours appearing more like a patchwork quilt. The difference in contour values at the element boundaries indicating either that the mesh is too coarse or the element type insufficient to simulate the stress variation adequately.

- To turn on/off nodal averaging, select RESULTS> SCALAR PLOT SETTINGS> EXTRAPOLATION
- NUMERICS in Mentat always displays nodal averaged values, unless the ISOLATE feature is used (RESULTS> ISOLATE)
- The maximum and minimum values on the legend for a NUMERICS plot are obtained by looping over all the nodes. This means that values at nodes that do not belong to any element (contact control nodes, for example) do influence the min/max for NUMERICS plots

Contact control nodes can be excluded from the nodes that are being considered in the NUMERICS plot by using

```
RESULTS> POST NODES REM
```

...the list of nodes to remove can be generated easily:

```
SELECT
  SELECT BY
    NODES BY ELEMENTS
  ALL: EXIST.
  POST NODES REM
  ALL: UNSELEC.
```

- The maximum and minimum values on the legend for a CONTOUR PLOT are obtained by looping over all the nodes of each element. This means that values at nodes that do not belong to any element (contact control nodes, for example) do not influence the min/max for CONTOUR plots.
- If all values in a CONTOUR plot are identical (say equal to v), the automatic range is set to $(v, 1.01*v)$.
- Nodal averaging in Mentat is independent of what is currently visible on the screen. This means that when contouring selected parts of a structure, the elements that have been removed from the active list will still make a contribution to the averaging process. Depending on the relative size of the stress contributions from the elements that are missing, the contours around the edge could have changed significantly if this was not the case.
- To suppress averaging for specific elements select RESULTS> SCALAR PLOT SETTINGS> EXTRAPOLATION> ISOLATE ELEMENTS. This means that when contouring selected parts of a structure, the elements that have been removed from the active list will no longer make a contribution to the averaging process. Depending on the relative size of the stress contributions that are now missing, the contours around the edge could change significantly.

- Nodal averaging of element results to the **output file** is carried out using a weighted averaging scheme based on the angle spanned at a node of an element. This should not have an effect for a perfectly regular mesh.
- The CONTOUR CENT method in Mentat (RESULTS) is a further way to obtain contour plots. Specifying this command sets the results plotting style to element centroid contours. The element centroid value is determined by the extrapolation method being used. If it is set to linear, the Gauss point stresses are extrapolated to the centroid, averaged and displayed. If it is set to translate, the Gauss point values are directly averaged and then displayed.
- Both Mentat and Patran use the same Mentat libraries (when the attach option is used) to extract results. This means that a comparison of extrapolated results will be identical. When reading results from a post (t16) file using the Import option, then Patran will use its own libraries and a slightly different algorithm to extrapolate the Gauss point results.
- It can look like gravity and volumetric loads are applying a moment on the mid-side nodes of shell elements 49 and 72. This is a post processing issue, since Mentat uses the average of the corner node values for the midside node results - not only for displacements, but also for forces. When running the analysis without no print, the midside nodes of elements 49 and 72 have zero external forces

Stress Coordinate Systems

- Search for “Material Preferred Direction” or “Material Property (Element) Coordinate Systems in Marc” in *Marc Volume C: Program Input* for further details of the coordinate systems available in Marc.
- Every element type in Marc has a default orientation (that is, a default coordinate system or reference axis) within which element stress-strain calculations take place. There are three coordinate systems used by Marc:

1. Global Coordinate System

For 2-D or 3-D solid continuum and composite solid elements the coordinate system is aligned, by default, with the global XYZ coordinate system. This is not normally a problem for isotropic materials since every direction is then a principal direction. For orthotropic materials, however, the material principal coordinates are seldom aligned with the global coordinates. For this reason the Orientation command is used to define a “preferred” or “material” coordinate system.

2. Local (or Marc) Coordinate System

For truss, beam, and shell elements, “local” element dependent coordinate systems are used by default. For example, for shell element 72, the local coordinates are the (v^1, v^2, v^3) surface coordinates, where v^1 is defined by the first edge direction (node 1 \rightarrow 2). v^3 is in the normal shell surface direction. (v^1, v^2, v^3) correspond to the local $\sigma_x, \sigma_y, \sigma_z$ result directions. As in continuum problems, the Orientation command may be used to define a preferred coordinate system if required.

3. User-defined (or Preferred/Material) Coordinate System

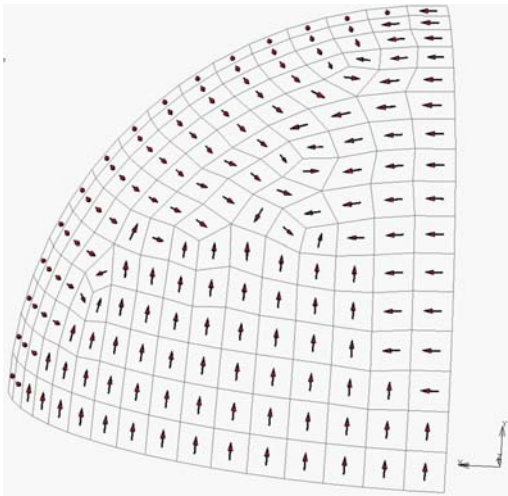
If the stress/strain results are required in coordinate axes that cannot be achieved through the Global or Local systems, then the user-defined Preferred or Material coordinate system should be used. This coordinate system is usually organized such that it coincides with the material principal axes and is defined through the Orientation command on an element basis. This is especially important for non-isotropic materials

(orthotropic, anisotropic, nlelast, or composite materials). Thus, the Orientation command determines the relationship between the material or element coordinate system and the global coordinate system (or the 0° ply angle direction, if composite). Essentially, the Orientation command defines the axis system into which the stress and strain results will be transformed. For isotropic materials, this could be carried out as a postprocessing calculation using SCALAR PLOT> SETTINGS> RESULTS COORDINATE SYSTEM (in Mentat). For orthotropic materials assigned to a regular, quadrilateral mesh, this would also be the case. For orthotropic materials assigned to non-regular shell meshes (quadrilateral or triangular), the orientation of the 0° ply will not be consistent, and require the Orientation command to be used.

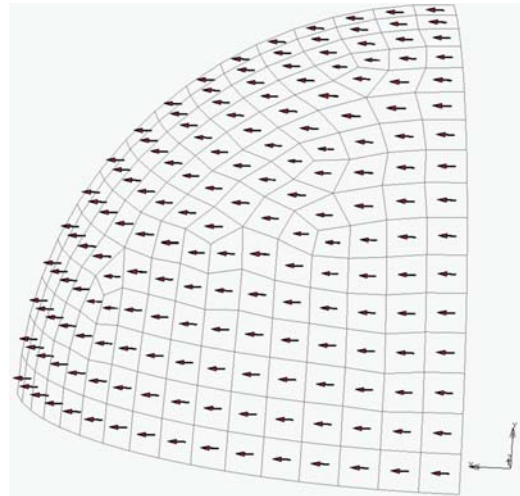
Consider the following examples, in which a 2-D and 3-D mesh is shown together with arrows defining the element x-axis direction:

Figure 1.1-47 panels 1 and 2 show a 3-D shell mesh, in which the default coordinate axes are, respectively the local system (as defined by the first edge direction) and the global system; panels 3 and 4 show a 2-D solid mesh, in which the default coordinate axes are, respectively the local system (as defined by the first edge direction) and the global system.

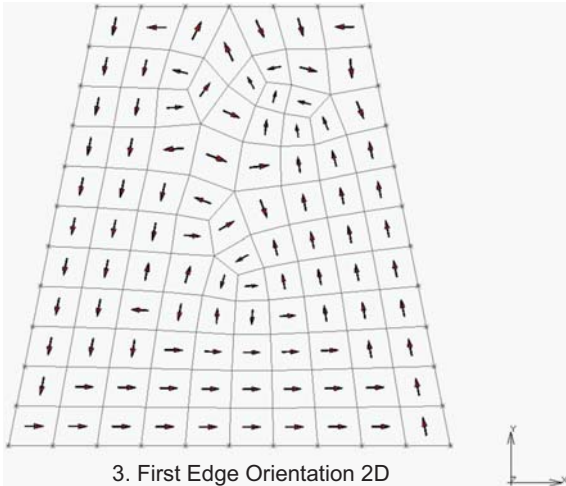
- One of the main issues to consider for both isotropic and orthotropic materials is the difficulties in interpreting results if a local element axis is used and the local element axes are not aligned consistently. In Figure 1.1-47 panels 1 and 3, a σ_x in one element is in a different direction to the σ_x of an adjacent element in many cases. The remedy is to define a preferred system for all elements. Contouring using global result values will not be affected by the local axis definitions and, hence, quadrilateral and triangular elements may be mixed without difficulty, as shown in panel 4. However, in the case panel 2 in which the shell surface is curved, the stresses will be difficult to interpret since the chosen stress component “intersects” the element plane. In such cases direction independent stress measures such as principal or von Mises would be easier to interpret. In addition, for thin shell elements where the stress output does not include out of plane stress terms (σ_{yz}, σ_{zx}), Marc will transform the stress state for panel 2 from the default local stress state to a global state which, for an arbitrarily positioned element in space, will give the appearance of through-thickness shear.



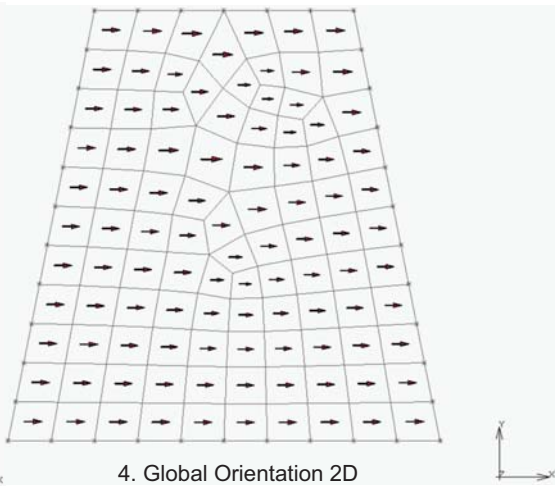
1. First Edge Orientation 3D



2. Global Orientation 3D



3. First Edge Orientation 2D



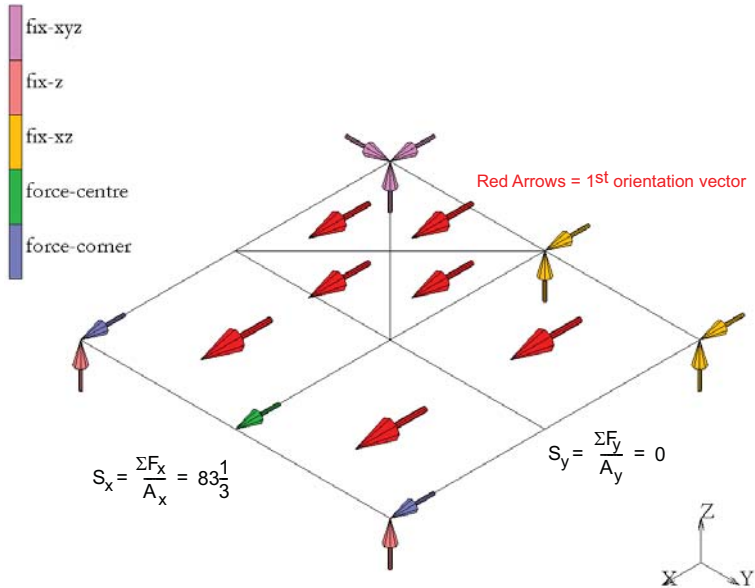
4. Global Orientation 2D

Figure 1.1-47 Local (First Edge) and Global Orientations for 3D and 2D Elements

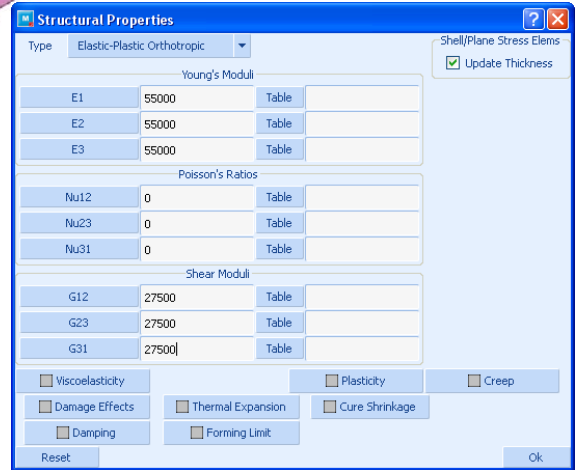
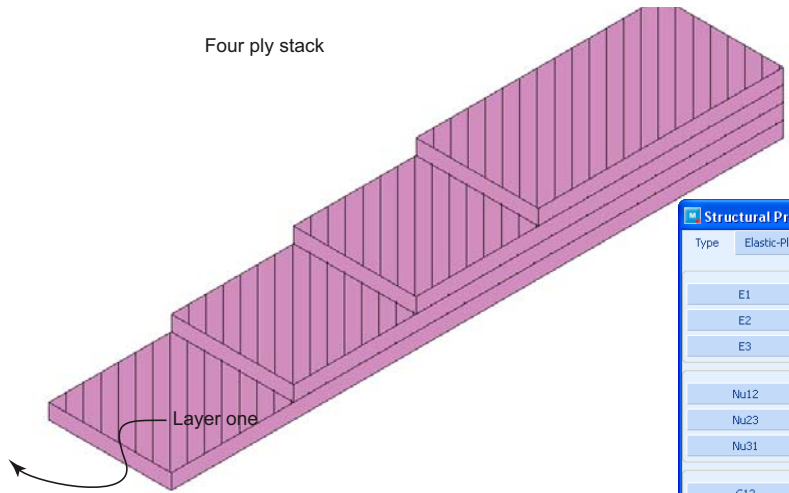
Composite Shells

In composite shells, the orientation of the materials in each shell layer can vary from layer to layer. In this case, the Orientation command is used to locate the 0° ply angle direction in the shell element surface. If the Orientation command is omitted, the 0° ply angle direction coincides with the v^1 axis. For each layer, additional ply angle offsets from this 0° ply angle direction are given in the COMPOSITE command. This allows the arbitrary orientation of a composite layup in shells with local coordinates. Consider a four element composite shell model in which a

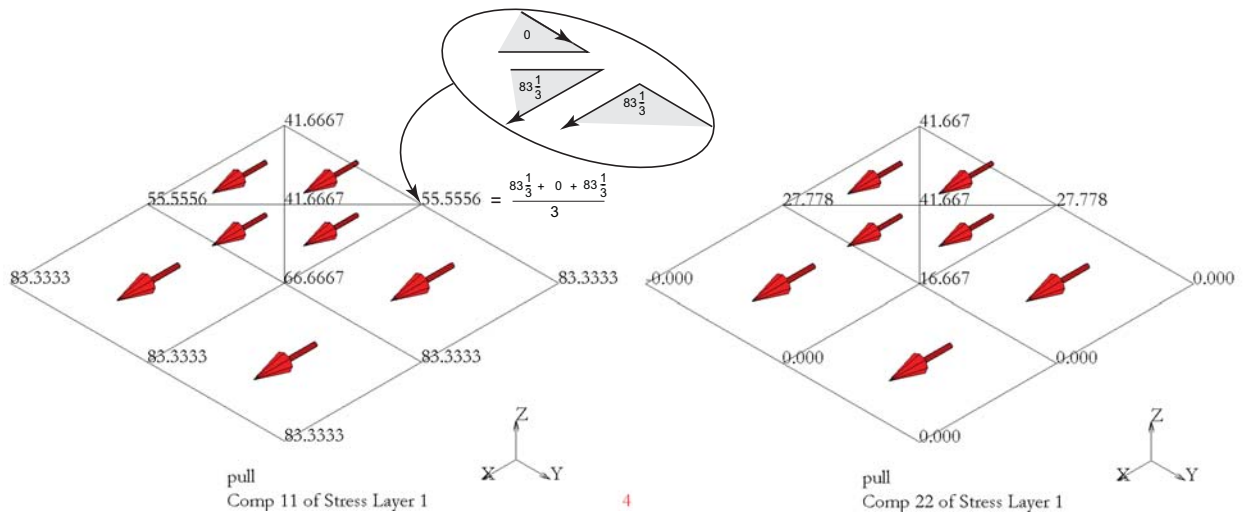
uniform in-plane force load is applied to one end. One of the elements has been split into four triangles. The boundary conditions are minimal to allow free movement. The red arrows show the direction of the first Orientation vector that has been assigned – the preferred x-axis:



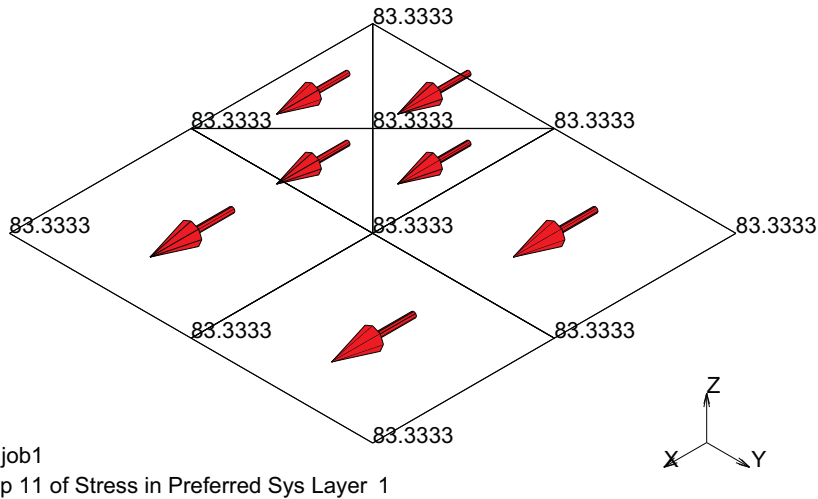
The material used is a four-ply layup of a single orthotropic material with an angle to the preferred x-axis of 45° for each ply, where layer one is at the bottom of the stack shown below and the material properties for each ply are shown on the right.



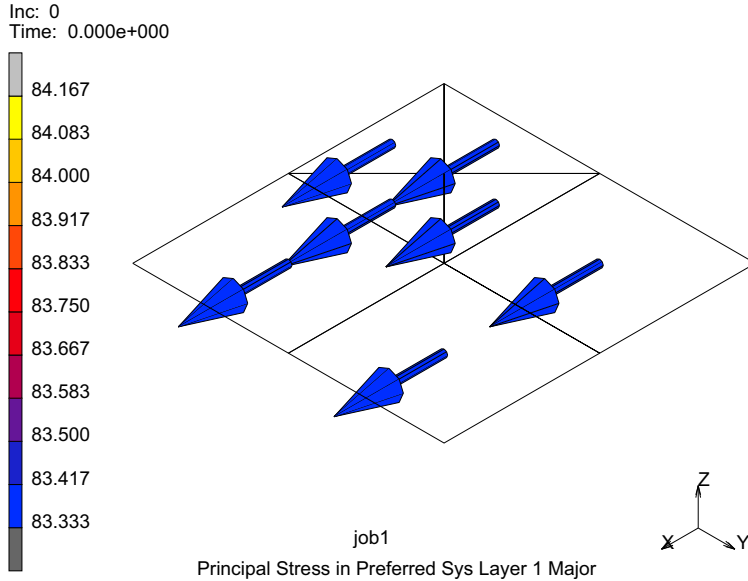
Clearly, this represents an isotropic material and will simplify the discussion of the results to the uniaxial case. Plotting the numerical results for the non-preferred stresses in layer one presents a nonuniform picture because of mixing of components since shells use element dependent coordinate systems, namely:



Whereas, if the preferred directions are used, the nodal averaging proceeds correctly by adding components in the correct directions as shown below.



As shown below, the principal values of the preferred stress components are drawn in the principal direction.



- See the sections entitled “Output of Strains” or “Output of Stresses” in the *Marc Volume B: Element Library* to determine the default element orientation axis for specific elements.

- All results quantities can be transformed in Mentat using the RESULTS> SCALAR PLOT> SETTINGS> RESULTS COORDINATE SYSTEM. See [Appendix C: Coordinate Transformation](#) for an example of Plane Stress transformation.

The preferred coordinate system of an element can be requested by selecting the element quantities 1st Element Orientation Vector, 2nd Element Orientation Vector, and Ply Angle in the JOB RESULTS menu. The latter should be selected for all layers of interest.

If the element orientation vectors and the ply angle are available on the post file, then Mentat will display the preferred coordinate system as an orientation in postprocessing.

The stress in preferred system is now transformed to the global system and the principal directions are displayed correctly. Furthermore, if the preferred system information is not available on the post file, then the user will not be able to plot the principal stresses in preferred system anymore as they will be wrong.

A similar problem exists for the regular stress tensor for shell elements. This tensor is defined in the local coordinate system of the element (which may be different from the preferred system). At this point, Marc does not output the directions of this coordinate system to the post file, so Mentat cannot compute the principal directions correctly for these elements. The principal direction will still be displayed incorrectly.

Material Axis Definition

- In the presence of either orthotropic or anisotropic material behaviour, the material axes may be defined accordingly. In general this transformation is termed “orientation”
- “Orientation” is different from “Transformation” (found in BOUNDARY CONDITIONS> TRANSFORMS). The latter permits the transformation of individual nodal degrees of freedom from the global direction to a local direction through an orthogonal transformation that facilitates the application of boundary conditions and the tying together of shell and solid elements.

Transformations are assumed to be orthogonal. Once you invoke a transformation on a node, you must input all loads and kinematic conditions for the node in the transformed system. Nodal output is in the transformed system. This option is invoked using the TRANSFORMATION option. The UTRANSFORM option allows transformations to be entered via the UTRANS user subroutine to change; for example, the transformation with each increment. When you invoke this option, the nodal output is in both the local and the global system. Note that, when a node of a deformable body contacts a deformable body, a multipoint constraint (called tying) is automatically imposed. These can produce conflicts with any other nodal transformations and is not recommended. A preferred method to apply transformations in this case would be to use a rigid line or surface.

- See the ORIENTATION option in *Marc Volume C: Program Input* for further details on the data file syntax to orientate the material axes.
- Various user specified orientations may be specified from within Mentat using MATERIAL PROPERTIES >ORIENTATIONS.
- With the ORIENTATION option, it is possible to specify the orientation of the material axes of symmetry (or the 0-ply angle line, if composite) in one of five different ways:

1. A specific angle offset from an element edge (in Mentat: edge12, edge23, edge34, edge31, edge41) Edge types for 2-D continuum and shell elements. The direction vector along the specified edge is projected onto the surface tangent plane (x-y plane if continuum, V1-V2 plane if shell) at each integration point. The first preferred direction is given by a rotation about the surface normal (z axis if continuum, V3 axis if shell) equal to the orientation angle. The third preferred direction is given by the surface normal, and the second preferred direction is given by the cross product of the third and first directions.
2. A specific angle offset from the line created by two intersecting planes (in Mentat: xy plane, zx plane, yz plane). Global intersecting plane types for 2-D elements. The specified global coordinate plane is intersected with the surface tangent plane. The first preferred direction is given by a rotation about the surface normal from this intersection equal to the orientation angle. The third preferred direction is given by the surface normal, and the second preferred direction is given by the cross product of the third and first directions.
3. A specific angle offset from the line created by two intersecting planes (in Mentat: xu plane, yu plane, zu plane, uu plane). User-defined intersecting plane types for 2-D elements. For types xu, yu, and zu plane, the plane determined by the coordinate direction and a user-defined vector is intersected with the surface tangent plane. For type uu plane, the plane determined by two user-defined vectors is intersected with the surface tangent plane. The first preferred direction is given by a rotation about the surface normal from this intersection equal to the orientation angle. The third preferred direction is given by the surface normal, and the second preferred direction is given by the cross product of the third and first directions
4. A particular coordinate system specified by user-supplied unit vectors (in Mentat: 3d_aniso) 3-D type for 3-D elements. The first and second preferred directions are as given by the user. The third preferred direction is given by the cross product of the first and second directions.
5. Direct specification of a local coordinate system. This is consistent with the CP identification number on the MD Nastran GRID Bulk Data Entry. The coordinate systems are similar to the MD Nastran CORD1R, CORD1C, CORD1S, CORD2R, CORD2C, and CORD2S options. Note that the data entered here should not be changed upon restart (COORDINATE SYSTEM)
6. For hexahedral elements, a local element system defined by element nodal connectivity may be used. This system can be rotated around the three local axes. The first preferred direction joins the centroids of faces 4-1-5-8 and 3-2-6-7. A second vector joins faces 1-2-6-5 and 4-3-7-8. The third preferred direction is given by the cross product of the first preferred direction and this vector. This system is then rotated around the three local axes by the three given angles (3D LOCAL)
7. One or more NURBS curves may be used to define the preferred system. These curves must be defined with the CURVES model definition option and only the NURBS variant is allowed. Using the centroid of the element, the closest point on any of the given curves is found. The first preferred direction is given by the tangent vector at this point. For 2-D elements, the second preferred direction is given by the cross product of the global z direction and the first preferred direction. For 3-D elements, this option is only supported for solid shell elements and solid composite elements. The third preferred direction is given by the thickness direction and the second preferred direction by the cross product between the third and first preferred direction. The first preferred direction is recalculated as the cross product between the second and third preferred directions to insure that we have an orthogonal system (CURVES).
8. As specified by the ORIENT user subroutine (in Mentat: Usub Orient), the UORIENT user subroutine type for all types of elements. Marc will call UORIENT to obtain the transformation matrix between global coordinates (for continuum elements) or local coordinates (for beams, plates, or shells)

In addition to the preceding orientation options, the following facilities are available in Mentat:

1. **Align:** This command sets the type of the current orientation to `3d_aniso` and determines the user-defined vectors from the three specified points representing a cartesian coordinate system. This command should only be used for orientations that are applied to 3-D elements
2. **Rotate:** This command rotates the current orientation by the specified rotations and should only be used for orientations of type `3d_aniso`
3. **Local:** This command creates a separate orientation of type `3d_aniso` for each of the specified elements and determines the user-defined vectors from the two specified points representing the axis of a local coordinate system. The resulting orientations are initialised to be aligned with the local coordinate system of each element, and then rotated about the local X, Y, and Z axes by the given angles. The specified elements should be 3-D elements.
4. **Cylindrical:** This command creates a separate orientation of type `3d_aniso` for each of the specified elements and determines the user-defined vectors from the two specified points representing the axis of a cylindrical coordinate system. The specified elements should be 3-D elements.

Gauss Point Results

- To obtain Gauss point results in Mentat, select the TRANSLATE extrapolation method and switch off nodal averaging. When combined with the Isolate feature (RESULTS>ISOLATE) to isolate just one element, this enables the exact integration point values to be displayed by MARC in history plots.
- User subroutines such as PLOTV and ELEVAR can also be used to provide such results.
- Selecting JOBS> JOB RESULTS> OUTPUT FILE> Full Element and Node Print in Mentat will give Gauss point element results directly to the output file.
- PRINT ELEM can be used to obtain a selective set of elements.
- Temperature results using post codes 9/180 (elements) are given at integration points. It is possible to select Gauss point results from Patran also.
- By default, if the `t16` file is attached, the standard extrapolation to the nodes as done by Mentat is available. If on the translation parameter form Gauss points are requested, then on attachment, the gauss point results are accessed. Unfortunately, the limitation in Patran is that you can't swap back and forth between these without detaching and re-attaching the results.

Selective Results to the Post File

- In an analysis with large models, the post (`results/t16/t19`) file often becomes large, involves significant I/O and utilizes a large amount of disk space. Post file version 13 has been implemented in Marc to reduce the size of the post file. The default remains as version 12. This allows Patran to be able to read the default post file. To select the version 13 post file format in Mentat:

```
Jobs> Job Results> POST FILE = 2006 Style
```

- To select the version 13 post file format directly in the Marc data file, specify “13” in the 11th field of the 2nd data block of the POST option. A zero in this field will give the default version 12 format post file. Note that only those elements or nodes selected will be available/visible when post processing, and care should be taken to ensure all entities of interest are selected

Using version 13 provides the following benefits:

- The option to select a subset of elements, contact bodies and nodes for output to the post file via additional options *select element*, *select body* and *select node* on the POST option. For example, the user can select only the exterior elements of contact bodies to be on the post file. It would also be possible to change the elements, nodes, and postcodes for each loadcase independently.
- If the post files are used as input for further analysis such as in jobs with PRE STATE, INITIAL STATE, AXITO3D, and GLOBAL LOCAL options, the full model must be present in the post file. In Mentat, this may be specified using both LOADCASE> LOADCASE RESULTS and JOB> JOB RESULTS.
- The version 13 format of the post file is different from earlier versions since the element variables are stored based on the element types. In version 12 and earlier, the maximum number of integration points is used for all elements, and postcodes are applied to all element types. In version 13, the true number of integration points for that element type is used. Post codes with layers apply only to layered elements and postcodes for beams apply only to beam elements. This leads to significant post file size reduction if there are mixed element types, postcodes with layers and postcodes for beams in the analysis

The reduction of post file size depends on the element types and postcodes in the analysis. In one example using 2400 brick elements and 200 shell elements, stress tensors of two layers are requested for the post file. In version 12, post file size is 56 Mbytes. In version 13, it reduces to 36 Mbytes. If only exterior elements of the contact bodies are selected, the post file size further reduces to 21 Mbytes.

Continuum and Generalized Stresses

There are two main types of stress output for elements in Marc:

Continuum Stresses

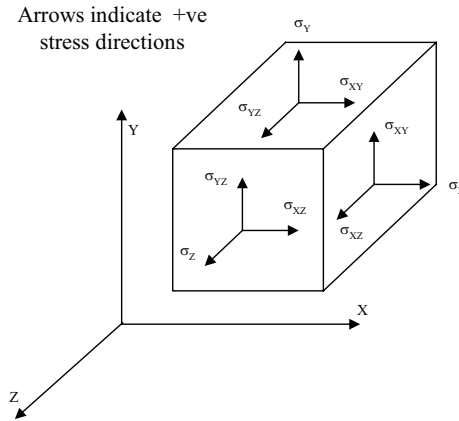
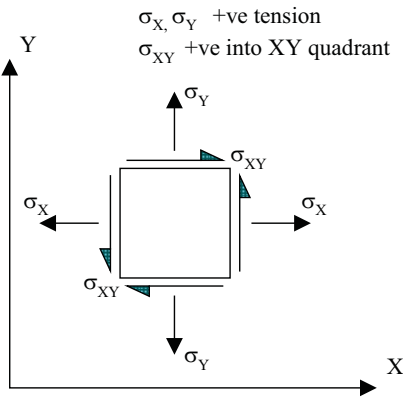
Also known as “physical stresses” in Marc, these are named after the stress definitions used in classical continuum mechanics theory and are defined in the usual manner as force per unit area and are denoted by the following symbol types

$$\sigma_x, \sigma_y, \sigma_z, \sigma_{xy}, \sigma_{yz}, \sigma_{zx}$$

$$\sigma_x, \sigma_y, \sigma_z, \tau_{xy}, \tau_{yz}, \tau_{zx}$$

$$S_x, S_y, S_z, S_{xy}, S_{yz}, S_{zx}$$

The first subscript for the shear stress component stresses represents the face on which the stress acts, the second is the normal direction of this face. Hence, the stress σ_{xy} is acting on the x-face in the global y-direction. The Marc definition is given as follows:



- Normal Stress values:

$$\sigma_{xy} = \sigma_x$$

$$\sigma_{yy} = \sigma_y$$

$$\sigma_{zz} = \sigma_z$$

- The shear stress in two perpendicular cutting directions at a point have the same value, i.e.

$$\sigma_{xy} = \sigma_{yx}$$

$$\sigma_{xz} = \sigma_{zx}$$

$$\sigma_{yz} = \sigma_{zy}$$

- The stress tensor σ_{ij} comprises the 6 independent stress values from 3 perpendicular cutting planes at a point

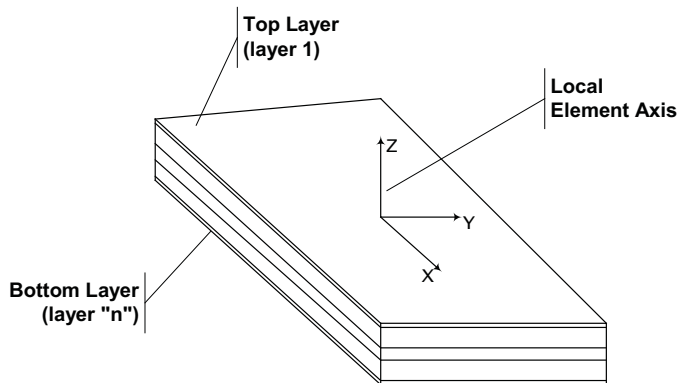
and describes the stress behavior completely: $\sigma_{ij} = \begin{bmatrix} \sigma_{xx} & \sigma_{xy} & \sigma_{xz} \\ \sigma_{yx} & \sigma_{yy} & \sigma_{yz} \\ \sigma_{zx} & \sigma_{zy} & \sigma_{zz} \end{bmatrix}$ where $\sigma_{ij} = \sigma_{ji}$.

- Further to the in-plane Gauss point evaluation, shell elements also evaluate stresses at a number of points through their thickness. This is carried out in order to obtain bending and membrane effects as a result of increasing distance from the neutral axis. These through-thickness stress evaluation points evaluate what are commonly termed “surface”, “layer” or “fibre” stress results.
- Numerical integration through the shell thickness is performed using Simpson’s rule for homogeneous shells and the trapezoidal rule for a composite shell. The number of equally spaced integration points (layers) can be defined for homogeneous shells via the data file SHELL SECT parameter or using JOBS> JOB PARAMETERS> # SHELL/BEAM LAYERS in Mentat. For nonhomogeneous materials, the number of layers is

defined through the COMPOSITE data file parameter. For homogeneous material, the number of layers must be odd. Seven points are enough for simple plasticity or creep analysis. Eleven points are enough for complex plasticity or creep (for example, thermal plasticity). For linear material behavior, three points are sufficient. The default is 11 points

- For shell and beam elements, the layers at which stress results are required may be specified in JOBS> JOB RESULTS> SELECTED ELEMENT QUANTITIES> LAYERS. The options from within Mentat are:
 1. All: This command activates all element layers for a selected post tensor. Values for this tensor will be written at all layers.
 2. Out & Mid: This command activates the outer and middle element layers (top, middle, and bottom) for a selected post tensor.
 3. List: User specified layer numbers at which the selected post tensor should be output
 4. Default: This sets the default layer for the selected post tensor - which, for shells, is the mid-plane (see the Mentat User Guide command `post_tensor_default_layer`). Furthermore, the results will be generalised stress/strain measures.

Shell Layer Convention: The layer number convention is such that layer one lies on the side of the positive normal to the shell, and the last layer is on the side of the negative normal. The normal to the element is based upon both the coordinates of the nodal positions and upon the connectivity of the element:



- The local element directions are defined from the element numbering with the local X-axis defined from the first element node to the second. The element numbering can be obtained from the output file or from the MESH GENERATION> ELEMENT> SHOW command (it will print the element node numbering to the Mentat command window). The local Y-axis is at right angles in the plane of the element surface and the local Z-axis is the normal direction according to the right hand rule.
- The orientation of the local z-axis can be displayed by using MESH GENERATION > CHECK > ID BACKFACES. This presents a contoured display indicating the orientation of this element normal. If both the surfaces and their underlying elements are displayed, the surface contours will be visualised – hence turn of the surface display (PLOT> SURFACES...) to see the element orientation.

- Back/Outside refers to the bottom surface, Front/Inside refers to the top surface and Front refers to the top surface. The top surface corresponds to layer 1 (most positive normal direction). The bottom surface to layer n (most negative normal direction). The middle layer for a seven layer shell will be layer 4, whilst for a five layer shell, layer 3. For Nastran shell elements, the bottom surface is layer 1.
- Middle surface stresses represent membrane action only. For Example top and bottom surface stresses additionally include the effects of bending stress.
- If you have a mixture of elements on a shell that may not have been created at the same time, then there is a possibility that some local z-directions will point in opposite directions. In this case, use the MESH GENERATION > CHECK > ALIGN SHELLS (pick the reference element and Mentat will make all adjoining elements to have the same outward normal by changing the node orientation) to get them all pointing in the same direction. Aligning shells does not align the in-plane x/y-axes. Aligning shells does not take account of visible groups and will always work on all the analysis elements.
- This choice is not available if the shell bifurcates, but it is possible subsequently to ‘flip elements’ for groups that may be wanted in different directions. The flip element command works by spinning the element through 180° about a line parallel to the element node 1-2 line that passes through the element centroid.
- With composite elements, the layer numbering follows the same rules; however, the stress recovery points are at midlayer. If a uniform material is represented as a composite material, the surface stresses will not be recovered.

For plate elements, not having the additional membrane stress terms, this layered approach is not necessary and continuum stress output is computed at the neutral axis only - giving a single set of stresses.

Generalised Stresses

- Generalised stresses are also known as “average membrane” stresses and are available for shell elements. They are dimensionally defined as a stress. They are not to be confused with “stress resultant” output, defined as force or moment per unit width
- Generalised stresses are obtained at each Gauss point by integrating the shell “layer” continuum stresses over the thickness of the shell. In the same way, generalised strain are their work-conjugate counterparts and examples include curvature and rotation
- More information on how the generalised stresses and strains are evaluated can be obtained from the “Shell Elements” section of *Marc Volume A: Theory And User Information* (search for “Element Information”). The equation given for the generalised stress is:

$$\sigma_G = \int_{-t/2}^{t/2} \sigma dy$$

- Where σ_G is the generalised stress and dy corresponds to the through-thickness direction. To see what this means a little more clearly:

$$\sigma_G = \int_{-t/2}^{t/2} \sigma dy \approx \frac{1}{t} \sum_i \left(\frac{f_i}{l t_i} \right) t_i$$

- Where σ_1, t_1 , and f_1 are the stress, thickness and force associated with layer 1. l is the shell width. The quantity $\frac{f_i}{l}$ is the force per unit width for the layer i .
- Generalised stresses and strains are only available from the Marc output file.

Result Types

Search for “Element Post Codes” and “Nodal Post Codes” in *Marc Volume C: Program Input* for details of the element/node-based results available from a Marc analysis.

Stress (post code 311)

- Element-based results.
- If an updated Lagrangian analysis is being carried out, then this will be the Cauchy stress. If a total Lagrangian analysis, this will be the 2nd Piola-Kirchhoff stress. See later section on Updated and Total Lagrangian solutions.
- Post Codes 11-16 give generalised stress quantities if no layer number is specified for a shell analysis. In this case, the Mentat display can be confusing, because Mentat still uses comp11, comp22 etc. If a layer number is given, these are physical layer quantities (i.e. local continuum stresses).

This stress measure may be local or global, depending on the element type. For shells and beams, it will be based on the local element coordinate system whilst for continuum it will be global.

Cauchy Stress (post code 341)

- Element-based result. Also known as the “true” stress.
- The stress is thus given in terms of current area and current deformed geometry (force per unit deformed area). As a result, it is the most naturally understood stress measure, that is, it most naturally describes the material response.
- If a total Lagrangian analysis is being carried out, then this will be evaluated accurately from the 2nd Piola-Kirchhoff stresses used by preference in a total Lagrangian analysis. See later section on Updated and Total Lagrangian solutions.
- This stress measure may be local or global, depending on the element type. For shells and beams, it will usually be based on the local element coordinate system whilst for continuum it will be global.
- Its corresponding True/Log strain measure is also available using post code 681.

Stress in Preferred System (post code 391)

- Element-based result.
- Components of stress in the user “preferred” coordinate system defined by the ORIENTATION option (MATERIAL> ORIENTATIONS in Mentat). This is a material characteristic and may be modified on this basis throughout the mesh.
- If an Updated Lagrangian analysis is being carried out, then this will be the Cauchy stress. If a Total Lagrangian analysis, this will be the 2nd Piola-Kirchhoff stress. See later section on Updated and Total Lagrangian solutions.
- If no ORIENTATIONS are defined, the stress measure may then be local or global, depending on the element type. For shells and beams, it will be based on the local element coordinate system; while for continuum, it will be global.

Note: When the LARGE STRAIN parameter is used, Cauchy stress in the Preferred system is automatically shown in the Post File for all cases for post code 391 - i.e., for both Total Lagrangian and Updated Lagrangian.

Global Stress (411)

- Element-based result.
- Stresses in global (X,Y,Z) directions.
- If an Updated Lagrangian analysis is being carried out, then this will be the Cauchy stress. If a Total Lagrangian analysis, this will be the 2nd Piola-Kirchhoff stress. See later section on Updated and Total Lagrangian solutions.
- For post codes 411 (and 421, 431, 441), global quantities for shell elements are reported for as many layers as requested and the same layer numbering system is used as for regular shell quantities. Layer 1 is the top surface; layer 2 is the next surface, etc.
- Useful measure for shells that are not regularly aligned – particularly in the case of triangular elements.
- See “Interpretation of results” for issues regarding shell global stresses.

Default Stress

- Element-based result.
- Stresses in the element directions (i.e. for shells their local directions and global directions for continuum elements).

Tresca Intensity

- Element-based result.
- This is defined in Chapter 12 of *Marc Volume A: Theory And User Information* and is the maximum shear stress obtained from Mohr's circle. There is no post code for this quantity and is not available in the post file at present. The PLOTV user subroutine would be needed to obtain this quantity in the post file. It is evaluated and printed to the output file when stresses are requested.

- If an Updated Lagrangian analysis is being carried out, then this will be based on the Cauchy stress. If a Total Lagrangian analysis, it will be based on the 2nd Piola-Kirchhoff stress. See later section on Updated and Total Lagrangian solutions.

Normal Stress

- Element-based result.
- At the outer surface of the structure the normal stress can be evaluated from the stress tensor using the normal vector to the surface ($\sigma_{ij} * n_j$).
- If an Updated Lagrangian analysis is being carried out, then this will be based on the Cauchy stress. If a Total Lagrangian analysis, it will be based on the 2nd Piola-Kirchhoff stress. See later section on Updated and Total Lagrangian solutions.

Shear Stress

- Element-based result.
- At the outer surface of the structure the shear stress can be evaluated from the stress tensor using the tangential vector to the surface ($\sigma_{ij} * t_j$).
- If an Updated Lagrangian analysis is being carried out, then this will be based on the Cauchy stress. If a Total Lagrangian analysis, it will be based on the 2nd Piola-Kirchhoff stress. See later section on Updated and Total Lagrangian solutions.

Normal Total Strain

- Element-based result.
- At the outer surface of the structure the normal strain can be evaluated from the strain tensor using the normal vector to the surface ($\epsilon_{ij} * n_j$).
- If an Updated Lagrangian analysis is being carried out, then this will be based on the log (true) strain. If a Total Lagrangian analysis, it will be based on the Green-Lagrange strain. See later section on Updated and Total Lagrangian solutions.

Shear Total Strain

- Element-based result.
- At the outer surface of the structure the shear strain can be evaluated from the strain tensor using the tangential vector to the surface ($\epsilon_{ij} * t_j$).
- If an Updated Lagrangian analysis is being carried out, then this will be based on the log (true) strain. If a Total Lagrangian analysis, it will be based on the Green-Lagrange strain. See later section on Updated and Total Lagrangian solutions.

Mean Normal Intensity

- Element-based result.
- This is defined in Chapter 12 of *Marc Volume A: Theory And User Information* and is otherwise known as “mean normal stress”. It is the trace of the stress tensor divided by three (i.e. the hydrostatic pressure part of the stress).
- If an Updated Lagrangian analysis is being carried out, then this will be based on the Cauchy stress. If a Total Lagrangian analysis, it will be based on the 2nd Piola-Kirchhoff stress. See later section on Updated and Total Lagrangian solutions.

Equivalent Mises Stress/Equivalent von Mises stress (post code 17)

- Element-based result.
- This and other related issues are discussed in a separate technical note “Equivalent Stresses”.
- This is alternatively called the “von mises intensity” and corresponds to the “mises intensity” obtained in the output file. It is described in the section entitled “Element Information” in *Marc Volume A: Theory And User Information*.
- The “equivalent von Mises” stress is evaluated in Marc during the solution and passed to Mentat as Gauss point results, where the values are linearly extrapolated to the nodes and then averaged (usually). This extrapolation can result in negative values and is a sign of poor mesh quality in that area.
- Mentat also provides an “equivalent stress” measure. This uses the same equations as for post code 17, but is computed directly from the stress tensor during post processing by extrapolating the Gauss point stress tensor, averaging to obtain a nodal value and then evaluating the equivalent stress in the usual manner. Small differences may be seen between this measure and postcode 17 in some circumstances...the difference is broadly that the equivalent von Mises stress (postcode 17) is a derived-extrapolated result whilst the “equivalent stress” is an extrapolated-derived result.
- The differences should be minimal when the “translate” extrapolation method is used, as expected.

Equivalent Stress/yield (post code 59)

- Element-based result.
- The initial yield stress is used, not the current. The values will be in the range 0-1 for un-yielded material and greater than 1 for yielded material. For temperature dependency (where so is normally specified as unity, this will give the equivalent stress).
- If an Updated Lagrangian analysis is being carried out, then this will be based on the Cauchy stress. If a Total Lagrangian analysis, it will be based on the 2nd Piola-Kirchhoff stress. See later section on Updated and Total Lagrangian solutions.

Equivalent Stress/yield at Current Temperature (post code 59)

- Element-based result.
- The initial yield stress is used, not the current. In this case, account is taken of the temperature dependency. The values will be in the range 0-1 for un-yielded material and greater than 1 for yielded material.

- If an Updated Lagrangian analysis is being carried out, then this will be based on the Cauchy stress. If a Total Lagrangian analysis, it will be based on the 2nd Piola-Kirchhoff stress. See later section on Updated and Total Lagrangian solutions.

Effective Plastic Strain

- Element-based result.
- There are two ways of using the equivalent (von Mises) plastic strain.
 - a. “Total” Equivalent Plastic Strain (post code 7): The integral of equivalent plastic strain rate
 - b. “Current” Equivalent Plastic Strain (post code 27)

Both are evaluated using the same equation ($d\varepsilon^P = SQRT(2/3) * (d\varepsilon_{ij}^P:d\varepsilon_{ij}^P)^{1/2}$).

- a. represents the integration of the incremental equivalent plastic strain values of the analysis time period. This is what the plasticity routines use since plasticity is, by definition, a history-dependent process as seen in the incremental nature of the numerical flow rules. This measure may increase (or remain constant) throughout the analysis. It will not decrease. Broadly, it captures the maximum value of the von Mises plastic strain measure provided by the continuously changing combination of the direct plastic strain components at each increment.
- b. is the equivalent value of the plastic strain tensor at a particular increment. This may increase or decrease over the analysis - especially so in the case of cyclic loading. The reason for this is due to the negative cross-terms in the equation. It is hard to think of a useful application for this result quantity. Note that the plastic strain components themselves will not decrease - only the scalar result from this von Mises equation. Nastran does not output this measure.

For example:

$$TEPS_t = TEPS_{t-1} + d(TEPS)$$

$$EPS = EPS_t$$

where $TEPS$ is the “total equivalent plastic strain” and EPS , the “equivalent plastic strain”. Also, $d(TEPS) = d(EPS)$, the incremental equivalent plastic strain.

As $d(TEPS)$ is always positive, $TEPS$ will always increase and never reduce, whilst EPS can increase and decrease. If a simple bar tension and compression test is carried out, $TEPS$ will be seen to go from 0 to 1 and then to 2, whilst EPS goes from 0 to 1 and back to 0. $TEPS$ measures the accumulated total plastic deformation regardless if it is in compression or tension.

- In general it can be said that the “current” measure will never rise above the “total” measure.
- The effective plastic strain output from Nastran is a “total” quantity. It is an accumulative scalar that accounts for the plastic flow during the analysis. Thus, to compare the “current” scalar result of the von Mises strain equation using total strain components with that from the “accumulated” von Mises strain equation with plastic components is not appropriate.

- An additional point is that when evaluating the Total Equivalent Strain (using the total strain components), the use of the “current” plastic strain components means that the result is some sort of combination of the elastic and the “current” plastic strains, i.e. not the total plastic strains - hence the plastic strain component being used in this evaluation will necessarily be less than the Total Equivalent Plastic Strain that is evaluated separately. The difference can be significant.
- It should also be born in mind that the summation of the “current” equivalent plastic strain and the elastic equivalent strain will rarely (and even then, coincidentally) equal the total equivalent strain, simply because it is not a strain in the usual sense and the additive assumption made does not apply. The summation only applies to the direct strain components:

$$\varepsilon_{elastic(i)} + \varepsilon_{plastic(i)} + \varepsilon_{creep(i)} + \varepsilon_{damage(i)} = \varepsilon_{total(i)}$$

- Apart from the von Mises strain measure being an unusual one to use in general, it is not recommended to use the total effective strain measure to interpret structural response when both plastic and elastic strains are present. These measures need to be investigated separately.
- The easiest way to get plastic strain tensor components for elements from Marc is to select Full Element & Node Print in the JOBS> JOB RESULTS > OUTPUT FILE menu of Mentat. This will print the information to the output file. If the output needs to be minimised, then the PRINT CHOICE command may be manually added to the data file to specify only those elements for which plastic strain results are required. NUMERICS can also be used in Mentat to obtain the plastic strain component values individually - note that the shear strains in Marc are engineering values and not tensor values.

Principal Stress

- Element-based result.
- The principal stresses associated with either the generalised stress or continuum stresses are available for output. The axis system will be the same as that discussed above.
- If an Updated Lagrangian analysis is being carried out, then this will be based on the Cauchy stress. If a Total Lagrangian analysis, it will be based on the 2nd Piola-Kirchhoff stress. See later section on Updated and Total Lagrangian solutions.
- Principal stresses ($\sigma_{min}, \sigma_{max}, \sigma_{int}$) are assumed to act along planes in which shear stress is zero and are computed using the standard equations developed from the Mohr's circle stress diagram. The minimum and maximum principal stresses are always orthogonal and are used frequently for problems involving crack progression.
- Principal stresses are not stored in the post file, but are calculated directly from the stress tensor in Mentat. This means that they are not calculated in the element loops during the incremental solution (unless locally required for one or two of the material models). Principal stresses are seen in the output because they have been requested specifically - and they are calculated in a separate loop during the writing of the output file.
- The principal values are calculated from the physical components. Marc/Mentat solve the eigenvalue problem for the principal values using the Jacobi transformation method. Note that this is an iterative procedure and may give slightly different results from those obtained by solving the cubic equation exactly.
- Mentat uses an extrapolate-derive approach to evaluate the Principal nodal stress in Mentat.

- There are four Principal results quantities available in Mentat:

1. Principal Stress Min
2. Principal Stress Int
3. Principal Stress Max
4. Principal Stress Major

The first three are based on both the sign and the magnitude of this derived quantity – that is, the minimum principal stress will be the most negative value obtained and the maximum will be the most positive obtained. The principal major stress is simply the maximum value obtained without taking the sign into account

- Principal directions in Mentat

From a stress tensor, Mentat computes principal values and these can be displayed as a triad (with their directions) as a tensor plot. At present, that is all that is available, that is, it is not possible to obtain the principal angles from Mentat or the Marc output file.

The principal stress directions need not be tangential to the plane of the element. This is the case for thin shell elements, but not for thick shells. Due to the presence of the xz and yz stress components, the principal directions may have a component normal to the plane of the element.

- There are certain circumstances when the maximum principal stress value is not the same as the major principal stress value. If you consider a node where the following principal stresses exists:

Node 1: $P_{max} = 5.0$ $P_{int} = -2.0$ $P_{min} = -9.0$

Then maximum principal will be 5.0, while the principal major will show -9.0 (the largest numerical modulus value).

- The maximum principal shear stress may be important if the shear strength of a material is significantly lower than the direct strength. “Luders” bands, for instance, are shear lines along which failure can occur and are typically seen when the yield stress is just attained.

At present Mentat does not evaluate the maximum shear stress or strain. It is necessary to write a user subroutine or a python script (`py_post` module) to evaluate the maximum principal shear values if required.

Damage:

- Damage post code 80.

This is actually a damage indicator for Cockroft-Latham, Oyane, Principal stress and one defined in `UDAMAGE_INDICATOR.F`.

- For Lemaitre damage criterion, use 178 (Damage factor) or 179 (relative damage).

Thermal/Temperature / Flux:

- Common result post codes are as follows:

Post Code	Element Results	Notes
9	Total temperature	For heat transfer, this is used for all heat transfer elements. Known in Mentat (pre/post processing), as “Temperature (Integration Point)”. Available for use with structural analyses to check that any temperatures have been applied correctly.
10	Increment of temperature	Available for use with both thermal and structural analyses to check that any temperatures have been applied correctly
180	Total temperature	Available for use with thermal/coupled only
371	Thermal strain tensor	Known in Mentat as the “Thermal strain” element tensor. Available for use with structural analyses (not sensible for thermal analyses)
181-183	Components of temperature gradient T	Available for use with thermal / coupled only
184-186	Components of flux	Available for use with thermal / coupled only Provides heat flux per unit area
Nodal Results		
14	Temperature	Available for use with thermal / coupled only
15	External Heat Flux	Available for use with thermal / coupled only External Heat Flux is a total nodal value
16	Reaction Heat Flux	Thermal / coupled only Reaction Heat Flux is a total nodal value

- When using shells in heat transfer, it is important to enter a code for each layer in chronological order if post file is to be correctly read by the INITIAL STATE or CHANGE STATE options.
- It is not recommended to use nodal temperatures obtained by extrapolating the Gauss point temperatures (postcodes 9/180) when post processing in Mentat.

This is because such nodal temperatures will have firstly been interpolated back to the Gauss point locations to obtain the derived temperatures and then a further extrapolation will have been carried out to obtain the nodal values.

It is far better to use the **nodal** temperatures from the solution directly (post code 14)

For the same reason, it is not reasonable to compare the nodal temperatures from the output file to the nodal temperatures obtained in the post file by extrapolating the Gauss point results to the nodes.

Any differences will be less significant as the mesh is refined and the temperature gradient across an element is reduced.

- An example of the data file syntax follows that saves nodal displacements (1) and temperatures (14) as well as the global element stress tensor (411):

```
POST
  2, 16, 17, 0, 0, 19, 20, 0, 1, 0, 0, 0, 1,
  411,
  9,
NODAL, 1
NODAL, 14
```

- The Marc “q” that is found in *Marc Volume A: Theory And User Information* is total flux (Q) per unit area and is consistent with the generally accepted definition.

Energies

- The undocumented Marc data command:

```
POST, , 5
```

permits all energy variables to be written to the post file – although this is the default anyway.

- *Marc User’s Guide*, Chapter 6.8 demonstrates the use of the energy results

- The following energies are available:

a. Total strain energy density

Available (total or group-based) in OUT via PRINT ELEM/VMAS, and POST via postcode 48 or Global Variables.

Total over the whole model is always in the output file.

b. Elastic strain energy density

Available (total or group-based) in OUT via PRINT ELEM/VMAS and POST via postcode 58 or Global Variables.

Total over the whole model is always in the output file.

c. Plastic strain energy density

Available (total or group-based) in OUT via PRINT ELEM/VMAS and POST via postcode 68 or Global Variables.

Total over the whole model is always in the output file (where applicable).

d. Creep strain energy

Available (total only) in POST via Global Variables.

Total over the whole model is always in the output file (where applicable).

e. Work done by applied force or displacement

Available (total only) in POST via Global Variables. Not available on an element or group basis (not sensible).

Total over the whole model is always in the output file.

f. Work done by frictional forces

Available (total only) in POST via Global Variables. Not available on an element or group basis (not sensible).

Total over the whole model is always in the output file.

g. Work done by contact forces

Available (total only) in POST via Global Variables.

Total over the whole model is always in the output file.

h. Kinetic energy (dynamic analyses)

Available (total only) in POST via Global Variables. Not available for groups since element mass matrices would need to be recomputed – costly.

Total over the whole model is always in the output file (where applicable).

Defining dummy contact bodies for the elements of interest would cause Marc to provide contact body velocities as a global output. Getting kinematic energies from these would then be possible (mass is available on a contact body basis).

i. Damping energy (dynamic analyses)

Available (total only) in POST via Global Variables. Not available for groups since element damping matrices would need to be recomputed – costly.

Total over the whole model is always in the output file (where applicable).

j. Thermal energy (thermal analyses)

Available (total only) in POST via Global Variables.

Total over the whole model is always in the output file (where applicable).

- Damping Energy

Damping energy and total work done by friction forces can have negative values

Damping energy is calculated for mass dampers

The way to view the energy balance is dependent on the analysis type

For analysis with dynamics, the energy is balanced between the change of kinetic energy and the work done by external forces, excluding the energies dissipated by plastic/creep strain and dampers

Energy loss might be observed for dynamic analysis because of numerical dissipation

- Energy Balance

$$SE + CSE + KE - DE = WE + KE_{initial} \quad (1-1)$$

The total work done by external forces should be viewed as:

$$WE = WC + WA + WF \quad (1-2)$$

For static analysis, the energy balance can be calculated by Equation 1-3.

$$WE = SE + CSE + ES + EF \quad (1-3)$$

From Equations (2) and (3), the energy balance can be calculated by Equati1-4

$$WC + WA + WF - ES - EF = SE + CSE \tag{1-4}$$

where:

Total Strain Energy	<i>SE</i>
Total Elastic Strain Energy	<i>ESE</i>
Total Plastic Strain Energy	<i>PSE</i>
Total Creep Strain Energy	<i>CSE</i>
Thermal Energy	<i>ME</i> (Available for heat transfer or coupled stress/thermal analysis)
Total Kinetic Energy	<i>KE</i>
Initial Kinetic Energy	<i>KE_{initial}</i>
Total Energy Dissipated By Dampers	<i>DE</i>
Total Energy Contributed By Springs	<i>ES</i>
Total Energy Contributed By Foundations	<i>EF</i>
Total Work By All External Forces	<i>WE</i>
within which various contributions are also calculated as:	
Total Work By Contact Forces	<i>WC</i>
Total Work By Applied Forces	<i>WA</i>
Total Work By Friction Forces	<i>WF</i>

- The strain energy (*SE*) output from Marc is obtained from:

$$\sigma * \varepsilon * V$$

where σ and ε are the stress and strain at the integration point. V is the element volume. This integration is numerically “exact” for both fully and reduced integration elements – but the constant stress fields associated with the single integration points of reduced integration elements will have the expected tendency to produce less accurate stress and, therefore, strain energy results. For a coarse mesh, this lack of accuracy gets more profound.

This means that the Work Done (*WD*) value is much better than the *SE* value, in particular when the mesh is coarse, since the stiffness and internal forces of a reduced integration element do vary across the element and, hence the energy evaluation can be more accurate

A finer reduced integration mesh will improve the SE value and brings it closer to the WD value. Using full integration also improves the SE values, even for a coarse mesh (more integration points in the element) and the agreement of SE and WD is good for coarse and fine meshes

- Re: Differences between ‘total strain energy’ and the area under the load-deflection curve

This may be noticed when carrying out a crack growth analysis in which the area under the load-deflection curve is being evaluated using a user subroutine. The difference is related to an initial hydrostatic pressure load being applied since this means that work was being done against the pressure field as the crack grew. If this work is calculated from the volume change of the model when the crack is introduced and subtracted from the strain energy reduction, the results for the energy release rate will be consistent the force-deflection curve.

There may still be a very small difference in the absolute values of the energy, which will be attributable to approximations in the numerical integration

Confusion can arise because when calculating the STRAIN energy release rate, since this is only accurate if no work is done against external forces. This is usually achieved by preventing movement of the model boundaries.

- Re: Negative or positive contact work quantities

The work done by external contact forces usually means the work done “to” deformable bodies. So, if a deformable body receives work from an external or contact/friction force, the work contributed to this body will be positive. However, if the deformable body does work to the environment, e.g. other bodies contacting it, the work contributed to this deformable body will be negative.

Especially in the case of friction, the sign of frictional work is merely determined by the friction force and relative motion between the contact bodies.

Assume that a body is moving on a contact surface and let $F1$ denote the frictional force, $V1$ the velocity of the deformable body and $V2$ the velocity of the contact body. Based on our method for work calculation, the total work done by the friction force will be $Wf = |F1| * V1 * sign(F1)$.

Please note that at this moment $F1$ will take the sign determined according to the relative velocity of the two contact bodies, say, $V2 - V1$, That is:

$$Wf = |F1| * sign(V2 - V1)$$

From the equation above, we will know that if $sign(V2 - V1)$ is positive, Wf will be positive. Otherwise, Wf will be negative. Here, it is assumed that the coordinate system is defined so that $V1$ is positive.

- In Marc, the values are accumulated from increment to increment, so it is therefore possible to observe such phenomena that the total frictional work may go from positive to negative or maybe the opposite
- Because of the incremental accumulation required in a nonlinear analysis, the energy results are, to some degree, dependent on the number of steps of applied loading. The extent of this variation will depend on the degree and type of nonlinearity in the system.

Herrmann Variable (Nodal post code 40):

- This is only available via ELEVAR and PLOTV user subroutines for linear elements
- It is available in the post file for quadratic elements however
- The additional Herrmann degree of freedom is:

$$\begin{aligned} & \sigma_{kk}/E \text{ (mean pressure variable for Herrmann)} \\ & -p \text{ (negative hydrostatic pressure for Mooney, Ogden, or Soil)} \\ & (\varepsilon_{xx} + \varepsilon_{yy} + \varepsilon_{zz})/(1 - 2\nu) \end{aligned}$$

Reaction Forces (Nodal post codes 5 and 6)

- Reaction forces may also be obtained in the output file by selecting a “Full Element & Node Print” (Summary only gives max/min values). The nodal results obtained are reactions at fixed boundary conditions and residual load correction values elsewhere. The residual load correction is the difference between the internal forces and the externally applied loads and its magnitude is controlled by the residual convergence criterion mainly. In theory, the residual load correction values should be zero. In practice they should simply be negligible compared to the reactions. The component and resultant reaction values can be made available in Mentat.
- Total reaction forces can be obtained most easily by using rigid bodies and then viewing the results for the rigid body directly.
- To find the total force acting along a section: The easiest way to do this is via the PATH PLOT facility in Mentat. In this way, the beginning and end nodes are specified between along the section of interest. It is then possible to specify a variable to evaluate over this specified length. If σ_X is specified (for example), a graph of the variation of σ_X along this length is plotted (this can also be done in Patran). Note that the NODE PATH should be selected in the order in which the nodal values are expected in the graph.
- In Mentat, this variation can be readily converted to a table (CONVERT > TABLE) - where there is also an integration tool. Simply click on Integrate and the final graph point that is calculated represents the area under the curve.
- If you do not have much experience of Mentat then, for a third party application like Excel, MathCAD, etc. would be able to do similar.
- Note that the free body facility found in Patran under the Nastran preference is only for Nastran use. It uses forces that are evaluated during the Nastran solution.
- Shell elements print stress and strain to the post file – but can give forces and moments to the output file if requested..

Electric Current (Nodal post code 88)

- In an electric analysis, the results “Electric Current (I)” and “Current Density (J)” can be confused. Mentat displays the Current Density (J).
- Here is an example of a 3-D solid bar:

$$\begin{aligned} & L=20, \quad l=2, \quad h=0.1, \quad \text{Resistivity} = 1.7e-7, \quad U=5 \\ & R = \text{Rho} * L / S \end{aligned}$$

$$U = R * I \text{ and}$$
$$I = J * S = [U / (Rho * L)] * S$$

Giving

$$J = 1.47e6 \text{ and } I = 2.94e5$$

- The electric current as mentioned above (Ohmic) is a global quantity and cannot be used in a fem analysis. The same is true for applied nodal currents, these are also different from the Ohmic current.
- The same issue exists in magnetodynamic analyses. This would be an enhancement, although this is not straightforward, since this current is the summation of the integration point current densities divided by the local areas, in which the direction of the current and the normal of the area needs to be taken into account.

Composite Layer Results

- If there are different numbers of layers across the composite materials used, it is possible to still get the top, middle and bottom layer results easily:
 - Layer = 1 will be the first (or top) layer if no global IDs are specified.
 - Layer = 15,000 will give the first (or top) layer if global layer IDs are used and ID=1 is not the top layer.
 - Layer = 5,000 will give the midsurface layer results based upon $(1 + \text{number of layers})/2$.
 - Exact for an odd number of layers.
 - Close for an even number of layers.
 - Layer = 10,000 will give the last (or bottom) layer.

Composite Failure Indices

- Element-based result.
- Search for “Failure Index” in *Marc Volume A: Theory And User Information* for details on the failure models available.
- It is only possible to specify a maximum of three of the available failure models in any analysis.
- There are 13 failure indices available as post codes (91 to 103) for use in the post file. The meaning of these post codes is determined by the failure models specified – and the order in which they are specified. From the theory manual it can be seen that the number of failure indices varies between the failure modes as follows:

Maximum stress	(6 failure indices)
Maximum strain	(6 failure indices)
Tsai-Wu	(1 failure index)
Hoffman	(1 failure index)
Hill	(1 failure index)

This means that the maximum number of failure indices possible would be if the maximum stress, maximum strain and one of the other single term models were used together – creating 13 failure indices. In the case of this example, the first 6 terms would be related to the maximum stress model, terms 7-12 with the maximum strain and the last term to the single term model. There are also post codes for the corresponding Strength Ratios available, where Strength Ratio = Margin of safety + 1.

- F (in the failure criteria definitions of the theory manual) is the failure index that is the result from these material models. If it is equal to or greater than unity failure has occurred. The mathematical form (from the Maximum Stress Criterion) of $[\sigma_1/X_t]/F$ is not an uncommon form to state a failure criterion, but actually means $F = \sigma_1/X_t$ where X_t is the maximum allowable stress in the 1-direction in tension and σ_1 is the actual stress calculated in the 1-direction from the analysis.
- The use of the user failure model would require that the user post codes be used and specified separately in PLOTV.

Iterative Post File Result

- Post file results for a contact analysis are available for individual iterations within an increment. The following information can be displayed if a number is put in the 12th field of the POST option:

Number	Information
1	displacements
2	displacements + reaction forces
3	displacements + reaction forces + contact information

- The Mentat commands to activate and deactivate this feature are:


```
*job_option post_trial:on
*job_option post_trial:off
```
- This can generate a large post file.

Effect of Updated or Total Lagrangian Solution

- For all “stress” quantities (apart from the “Cauchy” stresses), the stress that is output is dependent on the type of analysis solution undertaken, namely, whether Updated or Total Lagrangian has been used. Total Lagrangian is naturally formulated in terms of Green-Lagrange strains and second Piola Kirchhoff stress and is based on the initial element geometry. Updated Lagrangian is naturally formulated in terms of Cauchy stress and logarithmic strain since the current configuration is the reference configuration.
- For example, stress components such as “Stress”, “Stress in preferred system”, “Global stress”, “Shear stress” etc. will be based on Cauchy stress for Updated Lagrangian solutions and 2nd Piola-Kirchhoff stress for Total Lagrangian.

- The 2nd Piola-Kirchhoff stress is given in terms of the initial area and current deformed geometry (transformed current force per unit undeformed area) and is work conjugate to the Green-Lagrange strain measure. For small strain, the 2nd Piola-Kirchhoff stress can be interpreted as the Cauchy stress related to (local) axes that rotate with the material. Without additional knowledge concerning the deformations, these stresses are difficult to interpret. 2P-K stresses are not uncommonly transformed into Cauchy stress to give a “true” stress of use to engineers. Marc supports this transformation and “Cauchy Stress” may be selected within a total Lagrangian solution.
- All stress and strain measures will produce the same response as the small strains engineering stress/strain.
- To tell whether an updated analysis is being used or not, the following notes may help:
 1. If none of LARGE DISP, UPDATE, or FINITE are used, Marc uses and prints Engineering stress and strain measures.
 2. Using only the LARGE DISP parameter, Marc uses the Total Lagrangian method. The program uses and prints 2nd Piola-Kirchhoff stress and Green-Lagrange strain.
 3. With the combination of LARGE DISP and UPDATE, Marc uses the Updated Lagrangian method. The program uses and prints Cauchy stresses and true strains.
 4. The combination of LARGE DISP, UPDATE, and FINITE (with constant dilatation also invoked), results in a complete large strain plasticity formulation using the Updated Lagrange procedure. The program uses and prints Cauchy stresses and true strains.
 5. The use of PLASTICITY (option 3) is equivalent to the above combination and also results in a complete large strain plasticity formulation using the Updated Lagrange procedure. The program uses Cauchy stress and rotation neutralized strains (in Marc’s case, the Jaumann rate of stress is used – see *Marc Volume A: Theory And User Information* for more information).
 6. The use of PLASTICITY (option 5) results in a complete large strain plasticity formulation in a mixed framework using the Updated Lagrange method. The results are given in Cauchy stress and logarithmic strains.
 7. The use of PLASTICITY (option 1) results in a large displacement, small strain formulation using the Total Lagrange scheme. The results are given in 2nd Piola-Kirchhoff stress and Green-Lagrange strains.
 8. Large strain rubber elasticity can be modelled in either Total Lagrange (ELASTICITY, option 1) or Updated Lagrange (ELASTICITY, option 2). The former uses 2nd Piola-Kirchhoff stress with Green-Lagrange strains, the latter, Cauchy stress with Logarithmic strain (Mooney or Ogden). Note that a Total Lagrangian solution is also performed if Elasticity> Small Strain is selected in Mentat (hence, Green-Lagrange and 2nd P-K stresses).

where:

- LARGE DISP corresponds to JOBS> ANALYSIS OPTIONS> LARGE DISPLACEMENT.
- FINITE does not have a direct correspondence.
- UPDATE corresponds to JOBS> ANALYSIS OPTIONS> ADVANCED> Updated Lagrangian in Mentat.
- PLASTICITY (option 1) corresponds to JOBS> ANALYSIS OPTIONS> PLASTICITY PROCEDURE> Small Strain.

- PLASTICITY (option 3) corresponds to JOBS> ANALYSIS OPTIONS> PLASTICITY PROCEDURE> Large Strain Additive.
- PLASTICITY (option 5) corresponds to JOBS> ANALYSIS OPTIONS> PLASTICITY PROCEDURE> Large Strain Multiplicative.
- ELASTICITY (option 1) corresponds to JOBS> ANALYSIS OPTIONS> RUBBER ELASTICITY PROCEDURE> Large Strain – Total Lagrange.
- ELASTICITY (option 2) corresponds to JOBS> ANALYSIS OPTIONS> RUBBER ELASTICITY PROCEDURE> Large Strain – Updated Lagrange.

Selective Results to the Output (.out) File

- For details on results output to the .OUT file, search for “Selective Printout” in *Marc Volume A: Theory And User Information*.
- To obtain stress and strain results in the output file, select Full Element & Node Print in the JOBS> JOB RESULTS > OUTPUT FILE menu of Mentat.

This prints the information to the output file. Selecting this option removes the “No Print” command from the data file.

- This also includes temperature results (where appropriate) at nodal locations. In this case, temperatures are obtained directly from the solution as the primary unknown and are the most accurate values
- The following types of result are then available for a continuum element (mechanical analysis)....

```

      tresca      mises      mean      principal values      physical components
intensity intensity normal minimum intermediate maximum      1      2      3      4      5      6
element      2 point 1 integration pt. coordinate=      0.254E-01      0.431E-03      0.431E-03
Cauchy      3.309E+05      3.309E+05      1.103E+05-7.990E+00-7.990E+00      3.309E+05      3.309E+05-7.990E+00-7.990E+00-5.738E-05-1.092E-05-5.741E-05
Logstn      2.687E+00      1.792E+00      9.452E-05-8.957E-01-8.957E-01      1.792E+00      1.792E+00-8.957E-01-8.957E-01-4.020E-10-1.881E-11-4.022E-10
plas.st      2.475E+00      1.650E+00-1.850E-16-8.250E-01-8.250E-01      1.650E+00      1.650E+00-8.250E-01-8.250E-01-3.283E-10-4.775E-12-3.284E-10

```

where

- “Element” is the element number. In the example above, this is 2.
- “Point” is the Gauss point number for the following section of results. In the example, this is 1.
- “Integration pt. Coordinate” is, as implied, the coordinates of the current Gauss point.
- For more information on “Tresca intensity”, “Mises intensity”, “Mean normal intensity” and “Principal values” search for “tresca intensity” in *Marc Volume A: Theory And User Information*.
- The individual stress and strain components are given in six columns under the heading “Physical Components”. The correspondence of the column number with the actual stress/strain values is given at the top of the output file in a section that looks similar to:

```

key to stress, strain and displacement output
      element type7
8-node isoparametric brick
stresses and strains in global directions
1=xx
2=yy
3=zz
4=xy
5=yz

```

$$6 = xz$$

f. In the example above, for each of the columns 1,2,3... the Cauchy stress (cauchy), the true strain (Logstrn) and the plastic strain (plas.st) components are given.

- In the same way as above, the following types of result are available for shell elements (mechanical analysis)....

element section	thickness =	25 point 2 intensity	mises intensity	mean normal intensity	principal values			physical components					6		
					minimum	intermediate	maximum	1	2	3	4	5			
average membrane								0.677E+00	0.842E+00	-0.677E+00					
PK2str	9.999E+00	9.999E+00	3.333E+00	-2.747E-04	3.690E-04	9.999E+00	9.999E+00	9.435E-05	-8.699E-05	-3.184E-04	4.284E-04				
moment	1.666E-02	1.662E-02	5.507E-03	-6.889E-05	0.000E+00	1.659E-02	1.659E-02	-6.842E-05	8.878E-05	2.647E-22	0.000E+00				
Grnstch	9.999E-05	1.155E-04	0.000E+00	0.000E+00	0.000E+00	9.999E-05	9.999E-05	9.435E-10	-1.740E-09	-6.368E-09	8.567E-09				
curvatr	1.999E-04	2.294E-04	0.000E+00	-8.267E-07	0.000E+00	1.991E-04	1.991E-04	-8.210E-07	2.131E-06	0.000E+00	0.000E+00				
layer 1															
PK2str	1.100E+01	1.100E+01	3.663E+00	-4.038E-03	2.512E-05	1.099E+01	1.099E+01	-4.011E-03	5.240E-03	-3.184E-04	4.284E-04				
Cauchy	1.100E+01	1.100E+01	3.664E+00	-4.038E-03	2.512E-05	1.100E+01	1.100E+01	-4.011E-03	5.240E-03	-3.184E-04	4.284E-04				
Grnstn	2.198E-04	1.269E-04	0.000E+00	-1.099E-04	-4.013E-08	1.099E-04	1.099E-04	-4.011E-08	1.048E-07	-6.368E-09	8.567E-09				
layer 2...															

where

- “Section thickness” is the shell thickness.
 - The values under the heading “average membrane” are based on the “generalised stresses”.
 - The values under the headings “Layer 1”, “Layer 2”, etc are based on the layer continuum stresses in the local shell element directions.
- There is a SUMMARY command in the Marc data file which prints a summary of the results obtained in the analysis.

This option prints the maximum and minimum quantities in tabular form. The table is designed for direct placement into reports. The increment frequency of summary information and the file unit to which the information is written can be controlled from within Mentat using JOBS> ...> JOB RESULTS> OUTPUT FILE> SUMMARY. Note that in the summary output the incremental and total displacements are given, but any prescribed displacement boundary conditions are filtered out to give the “real” maximum and minimum displacements.

- “Selective” nodal and element output to the .OUT file can be obtained using the PRINT NODE and PRINT ELEMENT commands. This option allows you to choose which elements, and what quantities associated with an element are to be printed.

The results can only be printed on an individual node/Gauss point basis – not as a total for the specified elements/nodes. For total quantities over a group of elements, see PRINT VMASS.

PRINT NODE supports the following results:

- INCR: Incremental displacement or potentials
- TOTA: Total displacement or potentials
- VELO: Velocity
- ACCE: Acceleration
- LOAD: Total applied load
- REAC: Reaction / Residual force
- TEMP: Temperature

FLUX: Flux (only available if the HEAT, 0, 0,2 parameter is used)
MODE: Eigenvector (modal or buckle)
STRESS: Average generalized stresses at nodes
VOLT: Voltage (Joule analysis)
PRES: Pressure (bearing analysis)
COOR: Coordinates (for rezoning)
INER: Inertia relief load (for inertia relief analysis)
ALL: All relevant quantities

PRINT ELEMENT supports the following results:

STRAIN: Total strain
STRESS: Total stress
PLASTIC: Plastic strain
CREEP: Creep, swelling and viscoelastic strain
THERMAL: Thermal strain
ENERGY: Strain energy densities:
 Total strain energy
 Incremental total strain energy
 Total elastic strain energy
 Incremental elastic strain energy
 Plastic strain energy
 Incremental plastic strain energy
CRACK: Cracking strain
CAUCHY: Cauchy stress
STATE: State variables
PREFER: Stresses in preferred system
ELECTRIC: Electric field and electric flux
MAGNETIC: Magnetic field and magnetic flux
CURRENT: Current
ALL: All of the above

An example follows that prints nodal displacements and temperatures for all nodes as well as the stress tensor only for element 1. It should be placed before the POST command:

```
print node
```

```

      1      1
tota temp
1 to 1890
print element
      1      1
stress
1 to 1
1

```

Here is an example of the data file commands needed to obtain the energies for two sets of elements (1-10, 20-30) at GPs 1-4:

```

print elem
2,1
energy
1,2,3,4,5,6,7,8,9,10
1,2,3,4

energy
20,21,22,23,24,25,26,27,28,29,30
1,2,3,4

```

- Spring forces have an independent control for their output via the PRINT SPRING command.

One can also visualize spring forces when one end is fixed via reactions.

Spring forces are written to the post file as well, and can be visualized from the Global Variables list when graphing results.

Another way of obtaining spring forces visually is to use bush elements instead of springs. The results are then obtainable through the Beam Axial Force variable on the post file.

- “Selective” mass, costs, volume, 2nd moment of inertia about origin and energy (strain and plastic) results may be output to the .OUT file using the PRINT VMASS command.

Options are provided to print:

- a. Total quantities for each group of elements and the quantities for each element in the group or
- b. Total quantities for each group of elements (or element SETS) only.

The following will print the summed values only for the two sets of elements (1-10, 11-21):

```

print vmass
2,1,
1 to 10
11 to 21

```

In order to have correct mass computations, mass density for each element must be entered through the ISOTROPIC/ORTHOTROPIC option.

In order to have the correct cost, the cost per unit mass or the cost per unit volume must be defined through the ISOTROPIC/ORTHOTROPIC option.

Note that volumes and masses for some special elements (for example, gap element, semi-infinite element, etc.) are not computed. Similarly, the lumped mass initial conditions are not included. These quantities can be written on either standard output file unit 6, or a specified unit.

Currently, creep, kinetic, damping and thermal energies are not available for output on a group basis.

- The Marc PRINT CHOICE command permits the selection of how much of the element and nodal information is to be printed, for example, group of elements, group of nodes, which shell/beam layers, which integration points etc. Mentat does not support this. An example to print results at the five layers of each of the four integration points for three shell element sets is as follows:

```
print choice
3,0,4,5,1
2649,2650,3090,3090,3154,3154
1,2,3,4
1,2,3,4,5
```

- Mentat supports these model definition options: PRINT ELEMENT, PRINT NODE, PRINT SPRING, PRINT VMASS, PRINT CONTACT, ELEM SORT, and NODE SORT via:

```
JOBS> PROPERTIES> JOB RESULTS> OUTPUT FILE
```

In addition, support has been added for the history definition options: PRINT ELEMENT, PRINT NODE, PRINT SPRING, PRINT VMASS, PRINT CONTACT, ELEM SORT, and NODE SORT via:

```
LOADCASES> Loadcase Results
```

The old job option “noprint” is no longer used

The case of job option “noprint=off” is now covered by “result_element_output”, “full” and “result_node_output”, “full”

Compatibility in reading of old model files has been achieved. Compatibility in writing to old model files remains to be done. Old procedure files that set the “noprint” job option can be made compatible by adding the line:

```
*prog_option compatibility:prog_version:ment2010
```

- It is also possible to make use of the IMPD and ELEVAR user subroutines to process and print the required results. This would give the most flexibility if experience in Fortran is available. There is a simple example of the use of these subroutines in *Marc Volume D: User Subroutines and Special Routines*.
- Error Estimates

This can be requested for printing to the Marc output file in Mentat via JOBS> MECHANICAL> JOB RESULTS> OUTPUT FILE> STRESS DISCONTINUITY/GEOMETRIC DISTORTION. The corresponding command in the Marc data input file is `Error Estimate`.

There are two measures available:

- The stress discontinuity between elements in which Marc calculates a nodal stress based upon the extrapolated integration point values. These nodal values are compared between adjacent elements and reported.
- The geometric distortion in the model in which the aspect ratios and warpage of the elements are monitored - subsequent increments indicating how much these ratios change.

More details are given in *Marc Volume A: Theory And User Information* under the heading `Error Estimates`. The output obtained in the output file is as follows:

```
worst current aspect ratio is 2.044 at element 391
worst current warpage ratio is 1.252 at element 1
largest change in aspect ratio is 1.250 at element 21
largest change in warpage ratio is 1.252 at element 1
largest normalized stress jump is 3.661E+03 at node 371 component 5 mean value is 9.11E-7
largest stress jump is 5.773E-01 at node 22 component 2 mean value is -8.399E-01
```

The term “warpage” used here actually means the ratio of the largest and the smallest diagonal in quad/hex elements. This would not have any significant meaning for triangles/tets. The aspect ratio used is, as usual, related to the largest and smallest element edge lengths.

The evaluation of the stress error measure is moderately expensive. The evaluation of the geometric error measure is very inexpensive.

The ERROR ESTIMATE option can be used for either linear or nonlinear analysis.

The ADAPTIVE option can be used to ensure that a specified level of accuracy is achieved. The elastic analysis is repeated with a new mesh until the level of accuracy requested. This is detailed further in *Marc Volume A: Theory And User Information* under the heading “Adaptive Meshing”.

- Sort node and element quantities by magnitude

This is invoked using the NODE SORT or ELEMENT SORT commands and allows results to be sorted, with the output given in report format. NODE SORT allows either an ascending or descending sort order. In addition, either real numeric value or absolute value can be used. A range can also be given over which to sort

This option is in effect until a NO ELEM SORT or NO NODE SORT command is encountered

The element sort codes (through which ordering is controlled) are as follows:

Code	Description	Code	Description
1	First stress	28	Fourth plastic strain
2	Second stress	29	Fifth plastic strain
3	Third stress	30	Sixth plastic strain
4	Fourth stress	31	Equivalent plastic strain
5	Fifth stress	32	Mean plastic strain
6	Sixth stress	33	Tresca plastic strain
7	Equivalent stress	34	First principal plastic strain
8	Mean stress	35	Second principal plastic strain
9	Tresca stress	36	Third principal plastic strain
10	First principal stress	37	First creep strain
11	Second principal stress	38	Second creep strain
12	Third principal stress	39	Third creep strain
13	First strain	40	Fourth creep strain
14	Second strain	41	Fifth creep strain
15	Third strain	42	Sixth creep strain
16	Fourth strain	43	Equivalent creep strain
17	Fifth strain	44	Mean creep strain
18	Sixth strain	45	Tresca creep strain
19	Equivalent strain	46	First principal creep strain
20	Mean strain	47	Second principal creep strain

Code	Description	Code	Description
21	Tresca strain	48	Third principal creep strain
22	First principal strain	49	Temperature
23	Second principal strain	61	Voltage
24	Third principal strain	73	First gradient
25	First plastic strain	74	Second gradient
26	Second plastic strain	75	Third gradient
27	Third plastic strain		

Similar codes are available for NODE SORT (see *Marc Volume C: Program Input*).

Nodal Force Output for Continuum Elements

- It is possible to obtain a node point force balance similar to Nastran, using the GRID FORCE data command. This option controls the output of the contribution to the nodal force at either an element level or a nodal level. This is useful when constructing a free body diagram of part of the structure. The grid force balance is with respect to the global coordinate system.

On an element level, the grid force balance is based upon:

- Internal forces
- Distributed Loads
- Foundation Forces
- Reaction Force

On a nodal basis, it is much more complete and includes:

- Internal Forces Distributed + Point Forces
- Foundation Forces Spring Forces
- Contact Normal Forces Contact Friction Forces
- Tying/MPC Forces Inertia Forces
- Damping Forces DMIG Forces
- Reaction Force
- Using nodal stress and an associated area is not recommended because of its inherent inaccuracy.

Eigenvalue Output File Results

- The following three results are provided:
 - a. Frequency: The magnitude of the frequency of vibration for each mode. The relationships between the eigenvalue, λ , circular frequency, ω , and frequency, f , are

$$\omega = 2\pi f \quad \lambda = \omega^2 \quad \lambda = (2\pi f)^2 \quad f = \lambda^{1/2}/2\pi$$

- b. (th)trans*m*th: This represents $\phi^T M \phi$ (the diagonal modal/generalised mass) as described in the finite element equations given in *Marc Volume A: Theory And User Information*. The magnitude is equal to unity when mass normalisation has been requested.

Generalised mass or stiffness do not have any helpful physical meaning. They are mathematical concepts that enable the use of the “real” stiffness (K) and mass (M) of a component in the modal domain. Unlike static analyses, the modal domain is frequency dependent, so that the effective values of the generalized stiffness and mass will change according to the frequency of excitation. That is why there are terms like $\phi^T M \phi$ and $\phi^T K \phi$ - the ϕ corresponds to the natural frequency shapes of the structure - these are used to “factor” the static M and K .

The value of the generalized mass can be made any value simply by choosing a different normalization method. Moreover, the relative size of the modal mass between modes do not have any significance – a low value of modal mass in mode A and a high value in mode B cannot be interpreted to imply that mode A is unimportant with respect to mode B or that more of the structural mass is associated with mode B. The modal mass is given so that an analyst can perform subsequent modal response calculations.

Generalized mass is most often used to normalize the eigenvector results so that, together with the modal stiffness, they can be later used in a post-eigensolution analysis such as a harmonic/forced frequency response. Again, this normalization with mass is a mathematical requirement.

What you can say is that the ratio of the modal stiffness (i) to modal mass (i) is the eigenvalue (i). Alternatively, it can be seen as an indication of the amount of mass participating in a particular mode compared to the mass participating in rigid body motion – but this is only for an individual mode.

- c. (th)trans*k*th/w*w: This represents $\phi^T K \phi / \omega^2$ (the diagonal modal/generalised stiffness, divided by the eigenvalue) as described in the finite element equations given in *Marc Volume A: Theory And User Information*. Similar to the modal mass, this has no particular significance. The ratio of the modal stiffness to the modal mass is always the eigenvalue however. For mass normalization, the modal stiffness becomes the eigenvalue.

What are of use are the participation and mass participation factors. But these are only available from a frequency response calculation where there is some form of frequency dependent loading input to compare with the actual response of the structure.

Output from Contact Analyses

- Detailed contact information to the output file:

When the debug printout PRINT parameter is used in a contact analysis (value of 5 or 8), it produces information on when any node on the boundary comes into contact or separates from any surface. It also produces information on whether a contact node is fixed to a surface or is free to slide along it. For example:

```

node      101 of body      1 is touching body      2 segment      24
the retained nodes are      59      5
the normal vector is      0.00000      -1.00000

contact body      =      1
number of nodes in contact      =      0

contact body      =      2
number of nodes in contact      =      5
total friction force change      =      0.43415E+00
current total friction force      =      0.43415E+00
current total normal force      =      0.10007E+03
friction convergence ratio      =      0.10000E+01

maximum friction force change      =      0.20546E+00
current maximum friction force      =      0.20546E+00

```

In addition to the information printed with IDEV = 5, when IDEV = 8 is entered (IDEV is an internal variable name), the incremental displacement and the reaction forces for those nodes in contact with rigid surfaces are printed in a local coordinate system.

incremental displacements in transformed system
nodes in contact: tangential,normal

```

node      incremental displacements
1      1.914E-21      1.388E-17
32      9.715E-17      1.388E-17

```

reaction forces/residuals at transformed shell nodes in transformed system

```

node      residuals and reactions
1      -2.474E+00      -4.127E+00
32      -4.036E+00      -5.458E+00

```

PRINT, 5 can also be specified from Mentat via Jobs> Mechanical> Job Results> Output File> Contact.

- PRINT CONTACT:

Controls the printing of the contact summary information at the end of each increment in a more granular manner. Previously, when NO PRINT was specified, this suppressed the contact summary.

This option ensures that the summary of contact information for each body is printed to the output file even if the NO PRINT option is activated.

NO PRINT CONTACT: This option deactivates the output of the summary of contact information.

- Selecting CONTACT NORMAL FORCE X/Y when a post file is loaded in Mentat will give the contact forces directly. The forces are given in global directions. To have these forces rotated into normal and shear components automatically, select the CONTACT NORMAL FORCE and CONTACT SHEAR FORCE results variables.

- For analytical contact, the force direction will have been evaluated according the spline directions at each node. For discrete contact, the force direction will be an average of all the element face directions attached to each node in question.
- The global contact forces may also be obtained in the output file via JOBS> MECHANICAL> JOB RESULTS> OUTPUT FILE> Full Element & Node Print. The amount of result data output may be controlled via the data file - this is not possible using Mentat at present.
- Contact Status (node post code 38):

Marc allows you to select the contact status as a post file variable...

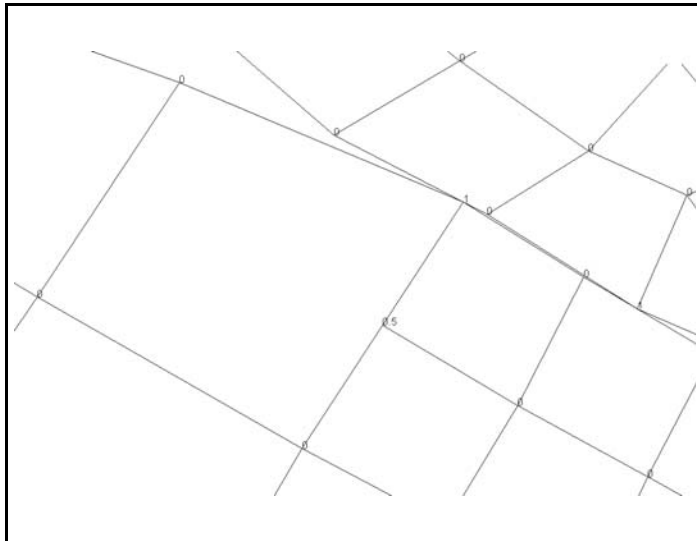
A value of 0 means that a node is not in contact.

A value of 0.5 means the node is in near thermal contact.

A value of 1 means that a node is in contact.

A value of 2 means the node is on a cyclic symmetry boundary.

The image below shows a contact status values of 0.5 on one node that is part of an adaptively split element that is not in contact – but should be zero. This is a known feature of Mentat in conjunction with local adaptive meshing. For refinement tying it will average the values at the corner nodes. This works in the majority of the time, but is not appropriate for discrete quantities such as contact status.



- Contact Touched Body (node post code 39):
 - a. The “contact touched body” nodal result will give the body number of the contact body being contacted by the node. In fact, it is an array of length three; thus, it can include up to two or three bodies (depending on whether the problem is 2-D or 3-D) if a node is touching more than one.
 - b. If all entries of the array are zero, it means the node is not touching any contact body.

- Contact Stress:
 - a. “Contact Normal Stress” (nodal post code 34) is the underlying element stress tensor components transformed normal to the surface.
 - b. “Contact Friction Stress” (nodal post code 36) is computed in a similar way and can be interpreted as the friction generated shear stress.

Contact stresses for quadratic elements (with true quadratic contact) are derived from the extrapolated element integration point stresses (rotated normal and tangential to the element surface at the contact location points) and are less accurate than the contact forces. For linear elements (or quadratic elements and linearised contact), the contact stress is derived from the contact force divided by the area. The contact forces are obtained directly from the FE solution at the same time as the reactions and displacements. The contact forces are the most accurate. Contact forces are available in the output file (choose Full Element & Node Print from Mentat). It is not possible to obtain contact stresses directly in the output file however – these are evaluated during post-processing only. You can only control this via the nodal post code 34 (= Contact Normal Stress) - but this writes the information to the post file only. PLDUMP could be used to extract this information from the post file, or a suitable user subroutine during the analysis if this suits better (using ELMVAR).

Note that for contacting nodes, we know if there is friction or not, so then the friction stress vector can be set to zero. But for nodes of contacting segments, we don't know if they are involved in friction (or glue) so, there, the friction stress is always calculated as the extrapolated/averaged nodal shear stress.

- Only contacting nodes are given a value for the result CONTACT STATUS. Contacted nodes have a value of zero.
- Nodes that are in contact, but are considered to have “slid off” do not get marked as in contact in the CONTACT STATUS.
- Global results variables are available for all contact bodies (“body variables”) when in History Plot. These are:
 - POS X/Y/Z <body name>: The displacement of the contact body in the component X/Y/Z directions. This is not available for deformable bodies.
 - POS <body name>: The resultant displacement of the contact body. This is not available for deformable bodies.
 - Angle POS <body name>: The rotation (radians) of the contact body. This is not available for deformable bodies.
 - VEL X/Y/Z <body name>: The velocity of the contact body in the component X/Y/Z directions.
 - VEL <body name>: The resultant velocity of the contact body.
 - Angle VEL <body name>: The rotational velocity (radians/second) of the contact body.
 - FORCE X/Y/Z: <body name>: The force on the contact body in the component X/Y/Z directions. Based on the contact forces created during the solution.
 - FORCE <body name>: The resultant force on the contact body. Based on the contact forces created during the solution.
 - MOMENT X/Y/Z: <body name>: The moment on the contact body in the component X/Y/Z directions. Based on the contact forces created during the solution. This would not be available for a deformable body based on continuum elements.

- Contact Area

The contact normal stress on the post file depends on whether or not we have quadratic elements and true quadratic contact. For linear elements (or quadratic elements and linearised contact), we get the force divided by the area. For quadratic elements (and true quadratic contact), we get the extrapolated stresses.

For linear elements, therefore, it is possible to use the fact that the contact stress results are based on the contact force divided by the contact area around the node. Marc uses shape functions to get this area, so simply extract the contact force and contact stress, divide one by the other to leave a fairly accurate contact area. This could be automated with a Python script if using Mentat or PCL if using Patran.

For quadratic elements, it would be possible to edit a Marc routine to print the contact area (oarea) – but this is only called for stress-based extrapolation.

Iterative Solver Output

- The iterative sparse solver prints out its measure of convergence every 50 iterations. Three numbers are listed. They are all related to the convergence behaviour of the solver. They are not at all related to the global convergence control from the (say) displacement and residual criteria.

- Conceptually, one sequence of iterations would correspond to a single N-R solution. As for the three numbers, they signify checks on different quantities, to make sure satisfaction on all fronts, they are as follows:

Term 1 checks on the Euclidean norm of the residual force vector vs. the norm of the right-hand side.

Term 2 checks on the relative change in the maximum displacement component vs. the maximum value in the updated solution vector.

Term 3 checks on the maximum residual force component vs. the maximum value in the right-hand side.

Interpretation of Results

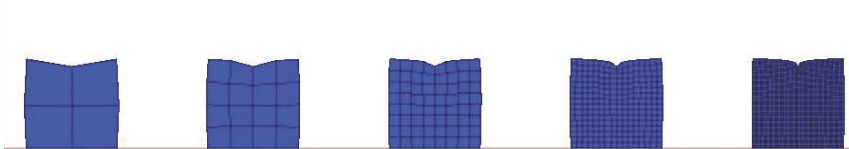
- Search for “Results Interpretation” in the *Marc User's Guide* for general information.
- A negative stress is generally taken as compressive, positive as tensile.
- Bending moment distributions from the use of lower-order shell elements can predict nonzero values at a “pinned” boundary where, theoretically, no moment should exist. This is normally due to the fact that a parabolic moment distribution has been developed in the solution, while these elements can only sustain a constant or linear moment distribution. In this case, the moment distribution will be increasingly better approximated as the mesh is refined. Note, however, that the values of the bending moment at the boundary will normally be significantly smaller than the maximum values obtained.
- When performing simple tests on a shell or plate element, it should be noted that the M_x and M_y results are coupled through the Poisson's ratio material parameter (standard shell and plate theory). Hence, this value may need setting to zero to establish correlation with simpler theories. The effect of this coupling may be seen if the deformation is exaggerated - in which case there will be either hogging or sagging across the width (depending on the orientation of the load).
- All plate elements suffer a theoretical singularity in the vicinity of the support around an obtuse skew angle. This limitation is documented in various academic papers. This may be mostly overcome through the use of the thick shell elements. Also the effect of the singularity can be minimised by thickening the plates locally.

- Isolating groups of planar surfaces from a model containing a mixture of planar and curves shells will permit the use of averaged contour plotting without any averaging errors. Generally, however, unaveraged results should be displayed since large stress gradients can be revealed which might otherwise have been hidden by the averaging process.
- Averaged or unaveraged stress results may be used when contouring global variables since averaging will occur on a global basis, independent of the local axis or orientation of the shell surface.
- Contouring using local values will be affected by the local axis definitions and, hence, quadrilateral and triangular elements may not be mixed without difficulty. This is because the element local axes may not be aligned in the same direction for all elements. The use of unaveraged output is recommended, particularly for any non-planar shell geometries such as curves and intersections. In the case of shell elements in which a shell surface is curved or intersecting geometries are present, an averaged contour plot will not be correct at the lines of intersection since averaging for each node will be performed over different planes. In such cases, direction independent stress measures such as principal or von Mises may be easiest to interpret.

Stress Concentrations

- Stress concentrations are an “expected” behavior of a finite element to a localised stress discontinuity. The more you refine the mesh, the higher the stress will get, until the element dimensions become too small for the computer to handle due to precision problems.
- Point loads and point boundary conditions will always give this effect (as will sudden changes in geometry or material properties).
- Such behavior is particularly a problem in material nonlinearity, since these can give local failure and cause no end of problems with convergence.

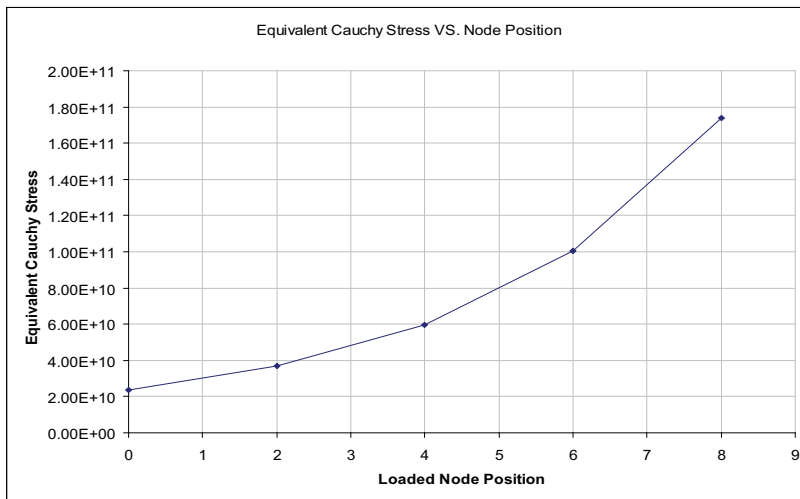
One way of explaining this is in terms of degrees of freedom (see the figure below). It is a series of square blocks – each with double the mesh density and each having exactly the same loading conditions, that is, glued to the rigid body at the bottom and a point displacement in the y-direction only at the top centre. It is clear from the coarse mesh that there are simply not enough degrees of freedoms present in the loaded area to adequately capture the deformation required. As the refinement increases, so the localised deformation that would be expected is achieved. In other words, the coarser mesh behaves in a “stiffer” manner than the refined mesh – another common trait with the finite elements.



- The problem is partly due to the numerical model not replicating what is happening in reality. In real life, there are very few times when a “point load” is actually applied. It is almost always distributed (albeit over a small area). Even if it is a very localized load in real life, if the results of interest are in that area, a sufficiently refined mesh is required over which a distributed load can be applied. This will make a lot of difference to the stresses.

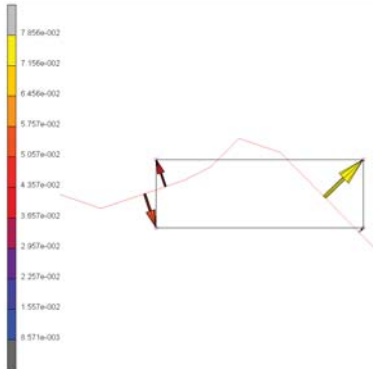
- This problem is the one that people dealing with fracture have to deal with. The stresses near a point of fracture rise in an exponential manner. Various ways are used to get a better distribution of stress at this point. One of them is via the “crack tip” elements.
- If the results near the point load/boundary condition are not of interest, then it is quite acceptable to ignore those high stresses - as long as there have been checks made that determine that there is nothing “real” happening that may be of consequence. In a nonlinear analysis with slack convergence criteria thresholds, it is common to see stress concentrations in unexpected locations. These are eliminated by an appropriate choice of convergence threshold values.

The graph below shows the increase in equivalent stress underneath the loaded nodes as the mesh density increases for the meshes above:



Mentat Results (General)

- To show the value of a single node:
`RESULTS> TOOLS> SHOW NODE`
 ...and then click on the node in question – or type the node number into the dialog box as requested.
- Display the values of multiple nodes:
`RESULTS> POST NODES|REMOVE – SELECT ALL EXISTING`
 Since all nodes have been added by default, to view specific nodes use the REM button first to remove the nodes that are not to be displayed.
`RESULTS> POST NODES| ADD – SELECT NODES REQUIRED`
- To evaluate the distance of nodes from geometric entities such as curves and surfaces, use:
`RESULTS> GEOMETRY DISTANCE>`
 The results of this computation are made available as scalar and vector plots. Controls are available to control the accuracy and cost of the computation:



- Mentat has the capability to reflect your results from a 3-D section (say) into a full 3-D structure by simply carrying out a symmetry copy (in mesh generation) after plotting the results.

Alternatively:

- a. Write a PLDUMP application that would produce the full 360° post file from the current one.
 - b. Write a PLDUMP application that would produce an axisymmetric elements post file and then use AXITO3D.
 - c. Redo the analysis with axisymmetric elements and then use AXITO3D.
- To more clearly visualise the difference between results of different increments, the following option may be of use:

```
RESULTS>DELTA
```

This command toggles the difference results plotting feature, which, when turned on, plots the difference between the current increment with the previously plotted increment.

Keyboard command:

```
*set_post_delta <on/off>
```

- Mass and Volume Results:

In Mentat under UTILS, there are commands that calculate the ELEMENT MASS or ELEMENT VOLUME. The quantities will be the current values if an updated Lagrangian solution has been specified.

In Marc, the PRINT VMASS command (Model Definition section) evaluates element volumes, masses, costs, strain energies, and second moment of inertia about origin. See separate section on VMASS.

- Flowline Plotting:

- a. Flowlines are computed by Marc and displayed in Mentat to visualise how material flows during an analysis. They are to be used in conjunction with global remeshing, since the mesh is not “attached” to the material in this case.

Typically, the original mesh is used below to form the flowlines. Marc then evaluates the location of the original mesh at each increment. This can then be superimposed in post-processing onto the deformed/remeshed mesh to indicate material flow. In large displacement analyses, it is not possible to superimpose the original, undeformed mesh.

- b. This is invoked using the FLOW LINE command in the Marc data file or via Mentat:

```
JOBS> JOB RESULTS> FLOWLINES> BODY
```

This will turn on the calculations of the flowlines that are attached to the material/

- c. The flowlines are automatically plotted until turned off. Controls are available for selecting which flowline edges are plotted, and whether or not to restrict them to the model outline or surface. Use the following button sequence to get to the FLOWLINES submenu to change the plot controls:

```
RESULTS> FLOWLINES
```

- d. A little more detail is given in the *Marc User's Guide* (search for “Flowline Plotting”).
- e. Changing the options in the FLOWLINE form of Mentat requires the DRAW button to be clicked to activate the changes.

- Particle Plotting:

- a. This facility displays position of a particle as a function of time by means of a curve. The color of the curve indicates the value of the equivalent stress of a particle as a function of time. The particles must be identified during preprocessing by means of a node set. This button is located in:

```
RESULTS> PARTICLE TRACKING
```

- b. A little more detail is given in the *Marc User's Guide* (search for “Particle Tracking”).

- Generalized XY Plotter:

An example of the use of this Mentat facility can be found by searching for “Generalised XY Plotter” in the *Marc User's Guide*.”.

- Rezoning:

- a. There is a capability in the ‘Post’ part of Mentat called ‘Rezone’. It can be found in RESULTS> TOOLS> REZONE MESH. It adds the current displacements of each node to its original coordinates to enable a new mesh to be created from the current results increment that has been selected.

In addition, the post file is closed and all post plotting is turned off. The model existing before the post file is opened, is replaced by the model from the post file.

To use it, go to the time step that has the necessary displacement vector, and with the deformed shape switched off, run the rezone option (do it once only). If the displacements are large, you will see the change in shape happening. Then SAVE AS another Mentat file.

If the deformed shape is left on, the displacement will be doubled and the results will, therefore, look rather odd. It won't make any difference to the actual mesh created.

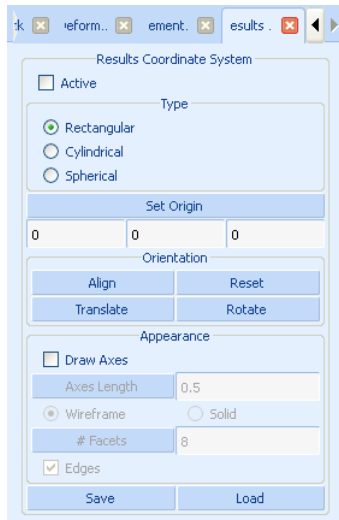
- b. It is possible to obtain the deformed mesh in this way, and then to export it as geometry (IGS format, for example). This is most easily done by defining the structure with one or more contact bodies, and specifying that these bodies are defined using an analytic definition (`CONTACT> CONTACT BODIES> DEFORMABLE> ANALYTICAL`). Assuming that analytic surface output has been requested (`JOBS> MECHANICAL> JOB RESULTS> CONTACT MODEL FILES`), then it is a simple case of reading in the analytic surface definition file corresponding to the increment required (e.g., `filename_job1_spline_2.mfd` for increment 2), and then exporting via `FILES> EXPORT`.
- c. If the spline information is not available for some reason, then it is possible to convert the element faces to surfaces and then export these surfaces.

To do this mesh “skinning”:

- Display the solid mesh in minimum edges (outline) and faces (Surface). This is in the `PLOT> ELEMENTS > SETTINGS` menu.
 - Then convert faces to elements (`GEOMETRY> CONVERT`) by picking all the faces in the view using a “box pick” after `REGEN` to make sure that the display is refreshed completely so you get them all.
 - Select by class `hex8` and delete `ALL SELECTED`. Remove unused nodes.
- Reducing the post file size:
 - a. The `pst_reader` program in the Marc bin directory can be used to remove increments from a post file.
 - b. Alternatively, the default behaviour of the `PLDUMP` program can do the same.
 - c. Using post file version 13 provides significant savings in file size by grouping element types together.
 - Transforming Nodal Results
 - a. Commands are available to control the coordinate system used to decompose tensors and vectors into scalar components for scalar plotting. Normally tensors and vectors are decomposed in a rectangular coordinate system aligned with the global axes.

Alternatively, the user may desire to decompose the tensors and vectors in another coordinate system, such as a cylindrical one, not aligned with the global axes, and having a different origin.
 - b. To create and activate a local coordinate system for post processing:

```
RESULTS> SCALAR PLOT SETTINGS> RESULTS COORDINATE SYSTEM
```
 - c. The easiest way to create the coordinate system is using `Align`. In this way, one can select three existing nodes or points. For example, pressing `Align` and then points (1), (2), (3) in order will create a local coordinate system as shown.



- d. The effect of the current local coordinate system may be switched on or off using the Active button.
- e. Transformations or coordinate systems are not stored in the post file, and must be created as needed.
- f. Commonly used coordinate systems may be stored using the Save button and restored using the Load button.

Python Scripting

- The Mentat scripting language, Python, may be used very effectively to extract the required results directly from a post file. There are a number of references to the Python API that are available:
 - *Python Reference Manual* (in `..\examples\python\tutorial\python_ref.pdf`): This document describes the functions available to Python scripts that use the PyMentat or PyPost interface modules.
 - *Python 1.5 Documentation* (in `..\Python\Doc\index.html`): Contains Tutorial, Library reference, Language Reference, Extending and Embedding (tutorial for C/C++ programmers) and Python/C API (reference for C/C++ programmers).
 - *Tutorial and Reference Manual* (in `..\examples\python\tutorial\python_manual.pdf`): Introduces the user to the Python modules through examples. The examples cover the basics of the modules and display some typical uses of creating and processing a model at various stages.
 - A recommended Python programming manual would be *Programming Python* by Mark Lutz or *Learning Python* by Mark Lutz and David Ascher.
 - Visit the Python web site at <http://www.python.org>.
- An example of extracting scalar results and contact body information is given at the end of this document in [Appendix E: Python Example \(Max Stress Results\)](#).
- An example of extracting nodal displacement results is given at the end of this document in [Appendix F: Python Example \(Displacements at Nodes\)](#).

Saving Results Directly From Mentat

- A Report Writer is available in RESULTS> REPORT WRITER.
- There is an undocumented Mentat command, `*post_dump`, which one typed manually – specifying an external file and a list of nodes. Mentat then writes the results, line per line, as the node number followed by the value of the actual plotted variable (as defined in the SCALAR PLOT menu) for the list of nodes. An example procedure file to demonstrate this is as follows:

```

*post_contour_bands
*post_value total strain energy
density
*post_skip_to 10

*post_dump
results.txt
yes
1
all_existing
#

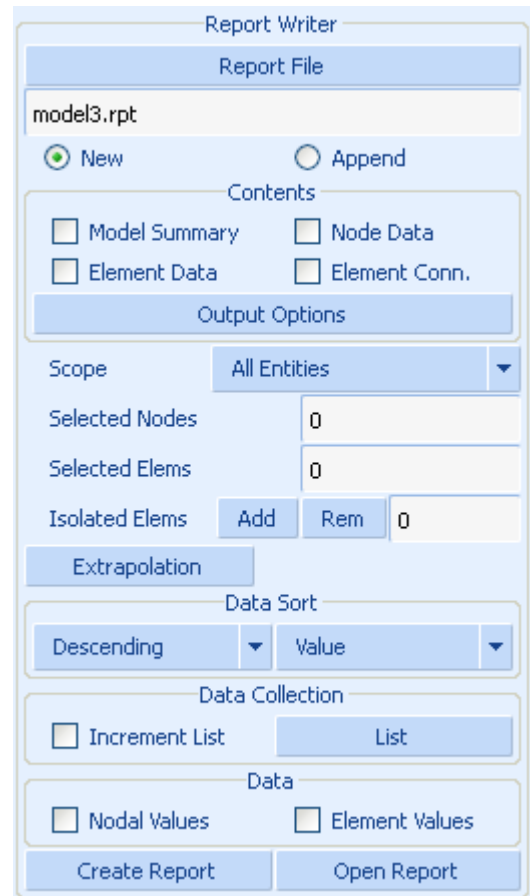
```

The results are listed in value order and not node order. Mentat will always display and `post_dump` by averaging across all elements (including those that are not visible).

- The general remedy to this provided in Mentat is to ISOLATE (RESULTS> ISOLATE) the elements on the screen. In this way, you define over which elements the averaging will occur. So, no matter what is selected on the screen, the results for the isolated elements will not change.
- Unfortunately, the `*post_dump` does not handle the isolate command properly. It seems to take the nodal isolated value from the associated element, and not the element you have isolated. This means that you should always use contours in the Mentat display when using `*post_dump`.

With averaging on, the legend in Mentat will show the same max and min values whether NUMERICS or CONTOUR is chosen. With averaging off, the legend in Mentat will show different max and min values when NUMERICS or CONTOUR is chosen. The reason is that NUMERICS will always average (unless isolate is used), whereas CONTOUR BAND does not. What you see on the screen should be the same as what you find in the `post_dump` files, but there will be differences depending on whether you have contours or numerics turned on in the display.

- It is possible to copy certain results (tabular data) to the Windows NT clipboard only. This is available for results produced using PATH PLOT, HISTORY PLOT, TABLES, or GENERALIZED XY PLOT.
- This data can then be pasted into a Word or Excel document.
- For non-NT platforms it is possible to save results directly to a specified file when using PATH PLOT and HISTORY PLOT.



Visualizing Analytic Contact Surfaces

1. Create a file named `file.proc` text file (for example) with the following commands:

```
*reset_view
*view_model_angles
-45 45 45
*dynamic_model_on
*fill_view
*set_lighting 1 on
*set_light 1 4 on
*surfaces_solid
*set_surface_lines off
*redraw
```

2. Double click on the `mfd` file (that Marc has created containing the spline information) to open up Mentat with the file loaded (or FILE> OPEN from Mentat directly).
3. Bottom Menu Bar: UTILS> PROCEDURES> LOAD>,select the proc file (from 1 above) - then press START/CONT.

Press OK when done.

4. Each of the contact body surface definitions has a group: UTILS> SELECT> SELECT SET.

Pick the sets you want, and then press MAKE VISIBLE.

To get all back, just press CLEAR SELECT, and then MAKE INVISIBLE.

With the DYN. MODEL lit up, one can pan (left mouse), rotate (middle mouse) or zoom (right mouse) RESET VIEW, followed by FILL brings everything back in the display.

Making Movies

- The quick method to dynamically animate the results is via RESULTS> MONITOR (preceded by a Rewind). This is for a “live” view and does not save the animation.

Once the mouse is used to move/rotate the model, the Monitor will stop and the Monitor button pressed again to restart it “animating”. The Animation form is found in RESULTS> ANIMATION.

- This is used to create movies and save them as a file for presentations.
- It is possible to create MPEG, AVI and GIF movies.
- From the Help menu you can access the New Features and in the section entitled “MPEG and AVI Animations”.
- An example of the use of animation from a nonlinear load incrementation analysis can be found in the “Tube Flaring”, “Container” or “Tire” examples herein.
- See the “Transmission Tower” example for an example of the use of animation with modal analysis types.

The recommended method is the GIF movie. These are good quality, and can be embedded into presentations (not linked, and needing to copy the avi / mpeg with the presentation).

- GIF MOVIE shares many of the settings with the MPEG/AVI movie generation commands. It will use the values displayed under INCREMENT SETTINGS, FIRST (movie_first_increment), LAST (movie_last_increment), STEP (movie_step_increment), VIEW (movie_view), and DELAY (animation_pause).
- The view will be that specified in the VIEW display and must be the current view.

The screenshot shows the 'Animation' dialog box with the following details:

- Animation** (Title)
- Create** (Section)

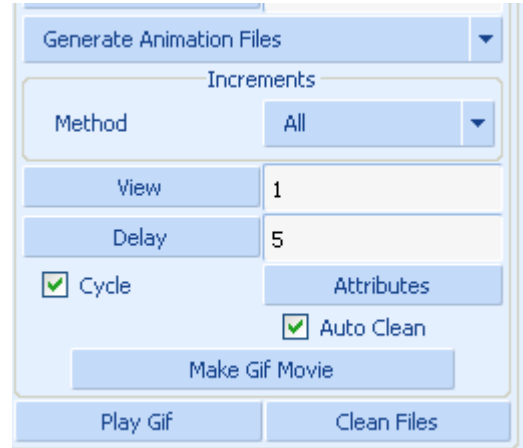
 - Base File Name: C:\marcpf2011\run_time
 - Index: 100
 - Single Frame: Increments
 - Mode: Harmonics
 - Attributes (button)

- Play** (Section)

 - Play (radio button, unselected)
 - Stop (radio button, selected)
 - Resume (button)
 - Interrupt (button)
 - Show Model (dropdown menu)
 - Plot Settings (button)
 - All (radio button, selected)
 - Begin To End (radio button, unselected)
 - Begin: 100
 - End: 100
 - Current: 100
 - Pause: 0
 - Forward (dropdown menu)
 - Single Play (dropdown menu)
 - Make Movie (button)
 - Play Movie (button)
 - Clean Files (button)
 - Gif/Mpeg/Avi Movies (button)

- The GIF animation is generated in a three step process:
 1. The animation files are automatically generated when the “Make Gif Movie” is pressed.
 2. Once the animation files are created, the animation is played and screen images are captured into a sequence of .gif files. These files are required for the GIF animation file encoder.
 3. The sequence of .gif files will be read and written to the GIF animation file in the current working directory.

Mentat grabs the screen image from the graphics window. This means that they have to be visible and not obscured in any way for the images to be saved properly. Mentat must also be pointing to an active display without the screen saver on.



- Note that this command will remove all animation display list files and .gif files that begin with the base file name (*animation_name) before it starts unless the GENERATE ANIMATION FILES option (movie_gen_files command) has been turned off.
- One can interrupt the process of making the GIF animation file by pressing the Escape key, however, you will be returned to the animation play mode. In this case, you will need to run the show_model command in the ANIMATION menu to display the model again.
- If the movie is not being created correctly, check that the OpenGL version of Mentat is being used (see the title bar of Mentat, it should have “(OpenGL) in it - and not GDI).

Creating AVI Animations

- Mentat stores AVI animations as a series of RGB files. There is a utility (normally in ...\\mentat\\bin\\marc_movie.exe) on the PC to convert these multiple files to a single AVI formatted file. This can subsequently be imported to a Power Point presentation. Working on PC machines you may use this program directly to create animation files.

SGI machines have a similar utility program called Media Convert or movieconvert - there is no such utility on other unix platforms. If a PC machine is available, then the PC marc_movie application may be obtained from MSC to convert the series of RGB files created on a unix machine to a PC format AVI file.

The steps to use the PC-based marc_movie application are as follows:

- a. Create the RGB files on the unix system. This done by creating the on-screen animation as usual (RESULTS> ANIMATION...). The files created from creating the animation do not have the extension RGB and are simply display lists – basically binary snapshots of the screen that are only readable by Mentat. To generate RGB images that can be manipulated to create individual images or an AVI animation, it is necessary to select MAKE MOVIE. This will take the animation images previously created and produce the appropriate RGB images. Selecting Make Movie will ask Enter View to Create Movie From – this refers to the current view that is active, either 1, 2, 3, or 4, as selected from the View button.
- b. FTP the *.RGB files to the PC (if running Marc on a Unix box).

- c. Run `marc.movie.exe`. On FILE> OPEN, select all the files that are required to be part of the animation. On FILE> SAVE AS... save the animation in avi format.

Note: The numbering of the RGB files is critical to showing the proper sequence. This is due to a quirk in how Windows saves and displays file names. If there are less than 10 RGB files, they should be numbered ...01.rgb, ...02.rgb, > ...09.rgb.

- d. In Powerpoint, use the Insert option to attach this file to the desired slide
- Before creating the movie files, it is suggested that changes are made to the colormap. This is done under VISUALIZATION> COLORS. Either use colormap 2 or change the colour sliders as:
 - a. BACKGROUND to white.
 - b. TEXT & WINDOW BORDERS to black.
 - c. EDGES to black.
 - d. POSTPROCESSING TEXT to black.
 - e. ANNOTATIONS to black.
- A proc file can be used to save this configuration for later use.

Assembling RGB files for Animation

- To create an animation from a series of RGB display files:
 - a. Assemble the RGB files into a directory together.
 - b. Find the program `Marc_Movie.exe` - normally in `..\mentat\bin`. Then double click on it and run it.
 - c. In `Marc_Movie`, do FILES>OPEN>... and browse to the directory containing the RGB files, select them all at the same time (holding down the control key) and press Open
- Press the play button on the right-hand side of the `Marc_Movie` screen. File save as will save the animation as an AVI file. The best compression scheme for the is Microsoft 1.

Appendix A: Shape Function Interpolation

Displacement shape or interpolation functions are a central feature of the displacement-based finite element method. They primarily characterise the assumptions regarding the variation of displacements within each element. Because of their relationship with displacements, the variation of both strains and stresses is also consequently defined.

The basic assumption of the finite element method is that the subdivision of a complex physical structure into the assembly of a number of simple “elements” will approximate the behaviour of the structure. Because of this subdivision, each finite element need not attempt to simulate the complex behaviour of the whole structure but, rather, assumes a relatively simple displacement variation so that the sum of the individual finite element responses approximates the response of the whole structure.

Shape functions are polynomial expressions. Any order of polynomial can theoretically be used but, in general, linear and quadratic variations are most common. It is from the order of the shape function polynomial that the terms linear and quadratic elements originate.

A consequence of these assumed displacement variations enables the finite element method to be able to solve the equilibrium equations at discrete points, thus transforming a continuous “physical” system (having infinite degree of freedom) into something manageable for numerical procedures.

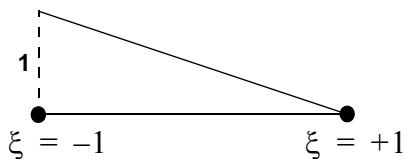
Typically, Marc uses Lagrangian shape functions which provide $C(0)$ continuity between elements (primary variables only, and not their derivatives, are continuous across element boundaries). Shape functions are defined in terms of the natural coordinate system (ξ) for line elements (bars, beams), (ξ, η) for surface elements (shells, plates, plane membranes,) and (ξ, η, ζ) for volume elements (solids).

For many two-noded line elements a linear variation is assumed as follows:

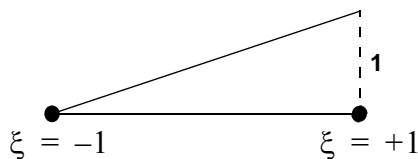
$$N_1 = \frac{1}{2}(1 - \xi)$$

$$N_2 = \frac{1}{2}(1 + \xi)$$

where N_1 and N_2 are the shape functions at nodes 1 and 2 of the element respectively (the order being dependent on the element node numbering). Diagrammatically, their variation is as follows:

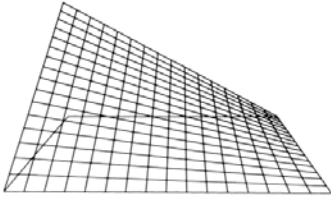


Variation of N_1



Variation of N_2

Linear variations are also used on four-noded surface elements as follows:



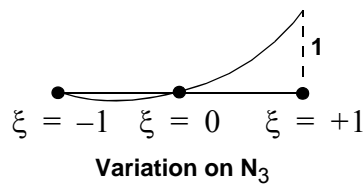
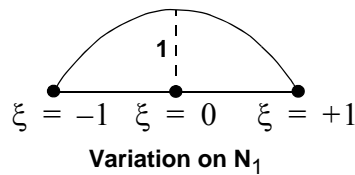
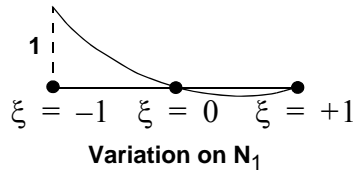
Three-noded line elements typically assume a quadratic variation as follows:

$$N_1 = \frac{\xi}{2}(\xi - 1)$$

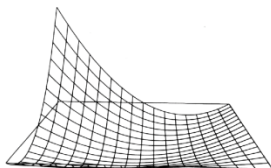
$$N_2 = (1 + \xi)(1 - \xi)$$

$$N_3 = \frac{\xi}{2}(\xi + 1)$$

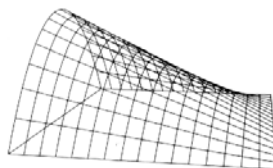
where N_1 , N_2 , and N_3 are the shape functions at nodes 1, 2 and 3 of the element respectively. Diagrammatically, their variation is as follows:



Quadratic variations are also used on eight-noded surface elements. The following diagrams show the variations of the shape functions at both corner and midside nodes.



Corner Nodes



Midside Nodes

Shape functions need to have the following characteristics:

$$N_i(\xi_j, \eta_j, \zeta_j) = 1 \text{ (for } i = j \text{)}$$

- This means that the value of each shape function evaluated at its nodal position must be unity. For example,

$$N_1(\xi = -1) = \frac{\xi}{2}(\xi - 1) = 1$$

$$N_2(\xi = 0) = (1 + \xi)(1 - \xi) = 1$$

$$N_3(\xi = 1) = \frac{\xi}{2}(\xi + 1) = 1$$

$$N_i(\xi_j, \eta_j) = 0 \text{ (for } i \neq j \text{)}$$

- Requires that the values of each shape function, evaluated at the other nodes must be zero. That is,

$$N_1(\xi = 0) = \frac{\xi}{2}(\xi - 1) = 0$$

$$N_1(\xi = 1) = \frac{\xi}{2}(\xi - 1) = 0$$

$$\sum_i N_i(\xi, \eta) = 1$$

- The sum of all the shape functions, evaluated at any point must be unity. That is

$$N_1(\xi = 1/2) = \frac{\xi}{2}(\xi - 1) = -\frac{1}{8}$$

$$N_2(\xi = 1/2) = (1 + \xi)(1 - \xi) = \frac{6}{8}$$

$$N_3(\xi = 1/2) = \frac{\xi}{2}(\xi + 1) = \frac{3}{8}$$

Furthermore, to ensure that a finite element converges to the correct result, certain requirements need to be satisfied by the shape functions, as follows

- The displacement function should be such that it does not permit straining of an element to occur when the nodal displacements are caused by rigid body displacement. This is self evident, since an unsupported structure in space will be subject to no restraining forces.
- The displacement function should be of such a form that if nodal displacements produce a constant strain condition, such constant strain will be obtained. This is essential since a significant mesh refinement will cause near-constant strain conditions to occur in elements and they must be able to handle this condition correctly.

- The displacement function should ensure that the strains at the interface between elements are finite (even though indeterminate). By this, the element boundaries will have no “gaps” appear between them and, hence, will show a continuous mesh.

The following sections deal with some of the more frequently encountered practical implications that are related to the use of shape functions.

Implication: The Evaluation of Element Displacements

The isoparametric element formulation assumes that

$$\{u\} = [N]\{d\}$$

where $\{u\}$ are the displacements at any point within an element and $\{d\}$ are the displacements at the nodes of an element.

This equation relates the displacements at any point within an element to the nodal displacements according to the element shape function $[N]$. Therefore, the displacement at any point (ξ) in a two-noded line element can be obtained from the nodal values using the following equation

$$u(\xi) = N_1(\xi)d_1 + N_2(\xi)d_2 = \frac{1}{2}(1 - \xi)d_1 + \frac{1}{2}(1 + \xi)d_2$$

If this element is fully fixed at one end ($d_1 = 0$) and sustains a displacement of 2 at the other end ($d_2 = 2$), the displacement at the centre of this element ($\xi=0$) would be given thus

$$u(0) = \frac{1}{2}(0) + \frac{1}{2}(2) = 1$$

i.e., half the end displacement as expected.

The same can be done with any quantity that varies across an element, for example, coordinates, strain, stress, and thickness.

Implication: Linear Versus Quadratic Elements?

Consider a 3-noded element that uses a quadratic shape function variation of the form

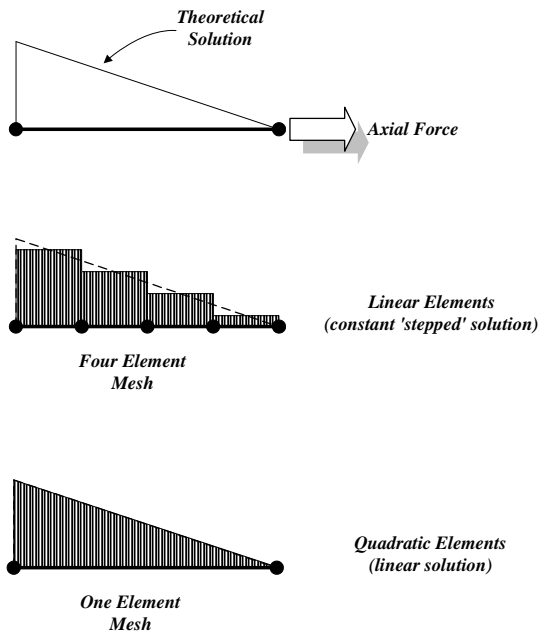
$$[N] = \left[\frac{\xi^2 - \xi}{2} \quad 1 - \xi^2 \quad \frac{\xi^2 + \xi}{2} \right]$$

The quadratic terms in ξ thus giving a corresponding quadratic variation of displacement over the element. The strain variation can be defined as

$$\varepsilon_x = [B]\{d\} = \frac{d\xi}{dx} \left[\xi - \frac{1}{2} \quad -2\xi \quad \xi + \frac{1}{2} \right] \{d\} = \frac{1}{J} \left[\xi - \frac{1}{2} \quad -2\xi \quad \xi + \frac{1}{2} \right] \{d\}$$

where $[B]$ is that strain-displacement matrix and $\{d\}$ are the three element axial displacements. It can be seen from the ξ terms that the strain is now a linear variation – as will be the stress variation. In a similar manner, for a linear element, the strain and stress variation will be constant.

This has a direct bearing on the type of element to be chosen for an analysis. For instance, consider a bar element under the action of a constant uniformly distributed load along the length of the element. The resulting axial force variation will be theoretically linear as in the topmost picture of the following diagram.



If this bar is modeled using linear elements (i.e., linear terms in the shape function), the axial force will be approximated by a constant, “stepped” response in each element, since the shape function derivatives only contain constant terms. A quadratic element (i.e., quadratic terms in the shape function) will, however, support a linear response and provide the correct answer directly, since the shape function derivatives contain linear terms. Thus, the exact solution can be obtained with a relatively small number of elements (or even with one element only) if the actual strain field can be matched by the shape functions of the element that is being used. In the above example, the shape function derivative terms did indeed match the linear strain of the actual analysis.

A frequent observation when inspecting force output at a simply supported section of a structure is to find (unexpectedly) non-zero values. Depending on the degree of mesh refinement, these values can be significant compared to the peak values. The reason is directly related to the above discussion. For example, if the force distribution is at least quadratic in form and linear elements are used (typically supporting a constant force distribution), a stepped response will be seen – hence the nonzero values – these constant values represent an average

of the force distribution and, if summed across the structure would be found to be equilibrium. The use of quadratic elements will improve the situation, but even these will not be able to match third order or higher force distributions without a measure of mesh refinement performed.

In spite of this sort of discrepancy, it should be noted that, during the solution stage, the equilibrium equation is used ($\{f\} = [K]\{d\}$) to ensure that the product of the stiffness matrix and the computed displacements exactly balances the externally applied forces. This means that, unless there are pertinent warnings or errors output during the solution, static equilibrium will have been fully achieved. Moreover, the derived quantities of strain and stress will also be found to be in equilibrium – but not necessarily according to an expected distribution as noted in preceding paragraphs.

Similar difficulties can be observed when attempting to compare the reactions at a location in a structure with the element force output at the same location. The explanation in most cases is, again, related to the order of shape function that has been used to formulate the element.

The remedies are to either increase the number of linear elements used (and reduce the size of the “step change” between each element) or change to quadratic elements (to more closely match the actual variation). The specific element notes section in *Marc Volume B: Element Library* will typically give details on the variation of force that is supported by each element.

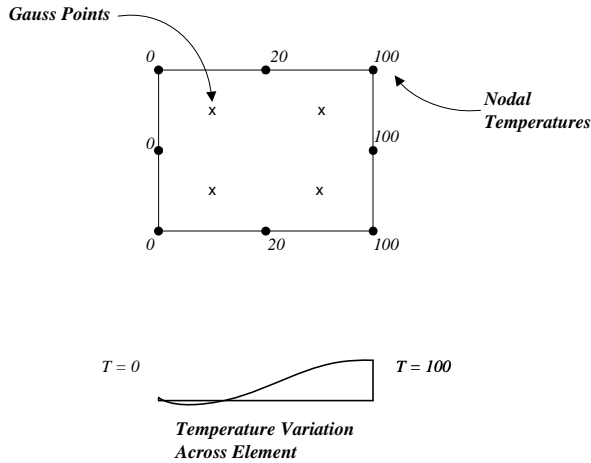
Apart from the consideration of element selection related to the order of shape function, quadratic elements would be recommended in the presence of high degrees of plastic strain since they are less susceptible to “locking”. Linear elements, however, would be recommended when the stress distributions anticipated are constant or linear. Such elements are computationally cheaper and, in such circumstances, render the use of higher order elements unnecessary.

Implication: Nodal Temperature Loading With Temperature Dependent Materials

Although the temperature loading is defined at element nodes, it is actually used by Marc at a Gauss point level. The nodal temperature loading is interpolated from the nodes to the Gauss points using the element shape functions.

The presence of significant temperature loading distributions over higher order elements can cause negative temperature loading to be applied at the Gauss points – even though the applied temperature field is entirely positive in magnitude. Such negative temperatures can be unexpectedly out of the user-specified temperature dependent material property table.

As an example, consider the situation described in the first of the following diagrams. The temperature loading is applied at the nodes as shown.



As a result of the quadratic displacement assumption used in higher order elements, the interpolation to the Gauss points yields the variation of temperature across the length of the element as shown.

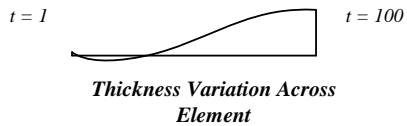
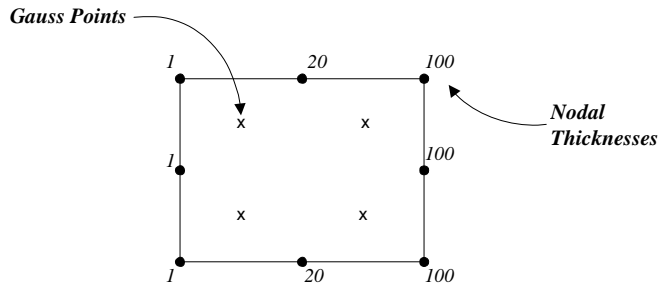
This variation will ensure that the applied temperature loading is applied correctly to the structure, but for the Gauss points nearest to the zero temperature specification this may not be so.

For most cases the negative value is insignificant compared to the temperature loading specified and the variation in the temperature dependency of the material properties. Mesh refinement in the area of the greatest temperature variations is the most appropriate remedy.

Implication: Element Thickness Interpolation

Although the thickness for an element is defined at element nodes, it is actually used by Marc at a Gauss point level. The thickness is interpolated from the nodes to the Gauss points using the element shape functions.

For a constant thickness element, the interpolation will always produce the same constant value at the Gauss points. For a varying thickness over an element, the actual thickness used will not be that specified at the nodes, but rather an interpolated value. See the top diagram below.

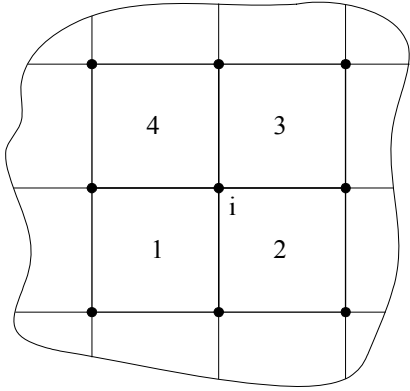


When using the quadratic displacement assumption used in higher order elements, the interpolation to the Gauss points yields the variation of thickness across the element as shown in the second picture (above). The effect of a significant variation of thickness over a single element may, thus, cause a zero or negative thickness value at a Gauss point.

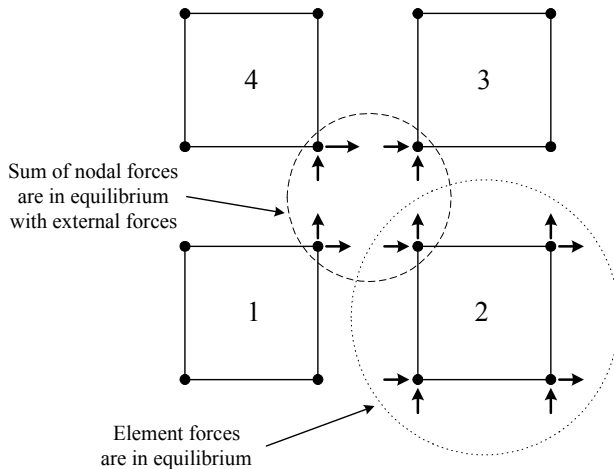
The remedy is to check that the thickness variation applied to the specified element is applied correctly. If so, then the mesh should be refined to reduce the severity of the thickness variation over the element.

Appendix B: Finite Element Equilibrium

In terms of finite element equilibrium, there are two important properties that are always satisfied by the finite element solution using either a coarse or a fine mesh. To describe these properties consider the following portion of a mesh under the application of an arbitrary force, the four elements (1,2,3,4) share the same node (i).



The following diagram, representing an exploded view of these four elements, shows the forces obtained at the nodal position (i) and those on element (2).



The two properties may now be defined as

- Nodal point equilibrium: At any node, the sum of the internal element point forces is in equilibrium with any external loads that are applied to the node. The internal forces include the effects due to body forces, surface tractions, initial stresses, concentrated loads, inertia and damping forces, and reactions. Thus, for an externally non-loaded node in a linear static analysis, such a summation will be zero.
- Element equilibrium: Each element is in equilibrium under its internal forces

Nonlinear analyses may produce out-of-balance residual forces at a node, depending on the degree of convergence obtained during the solution. For a well-converged solution, however, these are insignificant. See nonlinear iterative strategy for more information.

Although nodal and element equilibrium is achieved as described above, in a general finite element analysis, differential equilibrium (e.g. stress equilibrium) is not necessarily achieved at all points of the continuum considered – most notably at the shared boundaries of elements. The reason is as follows...

In the displacement-based finite element method, a C^0 continuous approximation for the displacements is assumed within each element. This means that the displacements at any point in a mesh will be continuous and ensures that no gaps appear between elements. The element stresses are calculated using derivatives of the displacement, which means that they will not necessarily be continuous and give rise to inter-element discontinuities or “jumps” in stress between adjacent elements. This is particularly the case for coarse element meshes. The discontinuities at adjacent element boundaries are reduced with mesh refinement and the rate at which mesh refinement reduces such discontinuities is determined by the order of the elements in the mesh – higher order elements converging faster than low order.

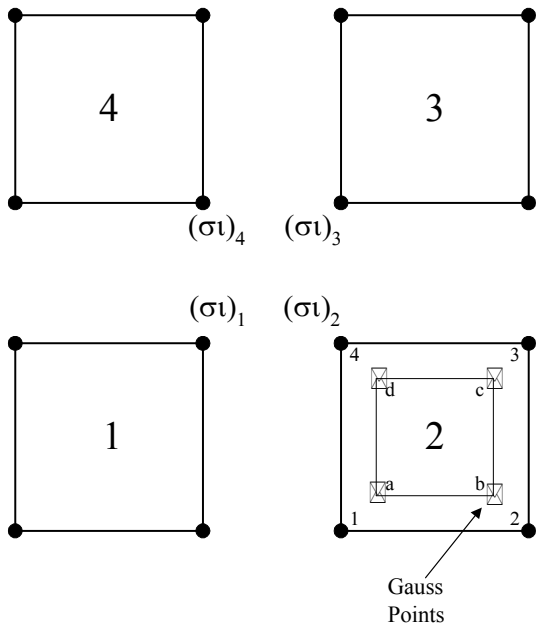
For the same reasons that element stresses are not continuous across element boundaries, the element stresses at the surface of a finite element model are, in general, not in equilibrium with the external applied tractions. Again, this effect is minimised with mesh refinement.

Experience has shown that the most accurate locations for stress output are the Gauss points. Nodal points, which are the most accessible, are actually the worst output location for stresses. Reasons have been given above, but include the fact that shape functions tend to behave badly at element extremities and it is reasonable to expect that the shape function derivatives (i.e. strains/stresses) sampled in the interior of the element would be more accurate than those sampled at the periphery of the element.

This evokes the question of how to obtain accurate stress results from a finite element model?

Implication: Smoothed or Unsmoothed Stress Contours?

One method for obtaining reasonable nodal stress output is by extrapolating the “exact” stresses at Gauss points to the nodal positions using the element shape functions. Consider the following diagram, representing the same exploded view of the four elements shown earlier.



For element 2, the nodal stresses at nodes (1,2,3,4) are obtained by

- Defining a fictitious element (shown by the dashed lines) with nodes at the element Gauss points (a,b,c,d)
- Extrapolating the Gauss point stresses to the nodal points of the real element (1,2,3,4) using the displacement shape functions of the fictitious element, i.e.

$$\sigma_i = \sum_{I=1}^N N_I(\xi_i, \eta_i) \sigma_I$$

where N is the number of Gauss points, and subscripts i and I denote nodal and Gauss point values, respectively.

The accuracy of the extrapolation procedure is dependent on both the presence of a reasonably uniform stress field and the type of shape function used in the element chosen. For instance, a high stress gradient across an element would be more likely to extrapolate incorrectly, particularly if a linear shape function element is being used.

This procedure is carried out for the other elements and the nodal stresses at the common node (i) are obtained as $(\sigma_i)_1$, $(\sigma_i)_2$, etc. As pointed out above, these stresses are not usually equal and a single “averaged” or “smoothed” nodal stress value is obtained using

$$\sigma_i = \frac{(\sigma_i)_1 + (\sigma_i)_2 + (\sigma_i)_3 + (\sigma_i)_4}{4}$$

When this procedure is carried out for all nodes in an element assembly, the ensuing averaged stress values provide a reasonable approximation to a continuous stress field. This is a straightforward and economic solution and works well on the whole. See later for more details on the circumstances that smoothing should not be used. This is the default method used in Mentat when smoothed results are selected in the contour layer properties. If smoothed results are not selected then the extrapolation procedure is still performed, but the averaging process is omitted.

Note that, for shell elements, the local Gauss point stresses and strains are transformed to global stresses and strains before extrapolation to the nodes. The mean global stresses are then transformed to the local shell system at the nodal point before evaluation of the nodal stress resultants.

Other methods are available, based on a least squares fit over the integration point stress values of the elements. The least squares procedure might be applied over the patches of adjacent elements or even globally over a whole mesh. However, if the domain over which the least squares fit is applied involves many stress points, the solution will be expensive and, in addition, a large error in one part of the domain may affect rather strongly the least squares prediction in the other parts.

In general, it is recommended to display unsmoothed stress contours at an early point during the processing of results. In this way, severe stress discontinuities between elements will be apparent and the possible requirement of mesh refinement and/or the use of higher order elements may be considered.

In areas of interest where the stress results will be used in the design process, smoothed contours would ideally be similar to unsmoothed contours. The inference from this being that a smooth stress transition across the element boundaries indicates that the stress distribution in the structure is being simulated sufficiently accurately. For sections of the model that are not of interest, a coarser mesh would normally be used and such a comparison in these areas would typically give significantly different contours - smoothed contours appearing more like a patchwork quilt!

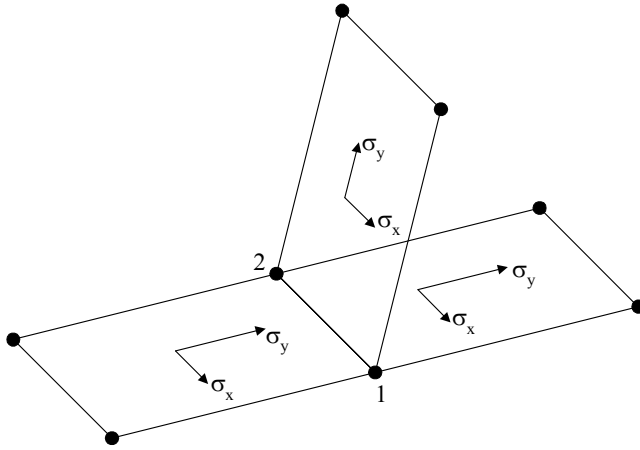
The nodal averaging technique is sufficiently robust that such stress values will tend to be pretty much those that would be obtained at the same location with mesh refinement – as long as the element mesh is reasonably uniform.

At all times, it is imperative to remember that the finite element method is an approximate numerical technique (albeit a good one) and that smoothed stress results can give good results but need careful attention.

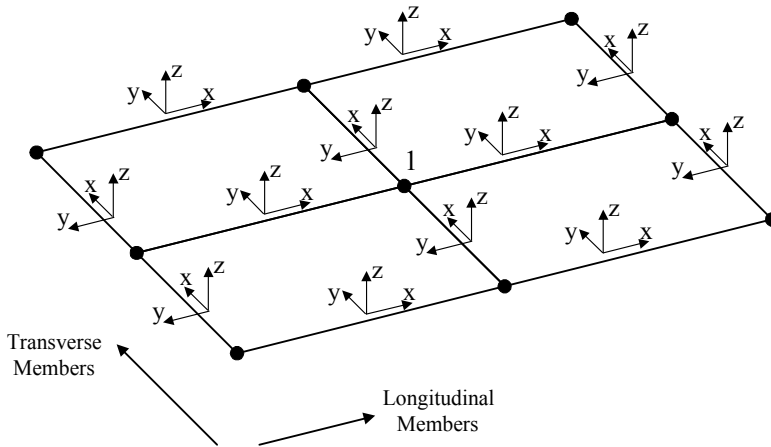
Implication: Limitations of the Averaging Scheme

In addition to taking no account of the size of the adjacent elements, the averaging method must not be used:

- At mesh locations in which geometric or material properties change
- For local or global stress output for shell elements that are nonplanar



- Interconnecting BEAM elements. It is necessary to extract results for longitudinal members and transverse members separately.



Consider the situation in which M_x results have been selected for display, and both transverse and longitudinal members are active. The averaged value displayed at the central node number (1) will be comprised of the local M_x values from the two longitudinal and two transverse members that connect to this node. It must be noted that the M_x values are local to the elements (as shown in the diagram), so that the M_x values for the longitudinal members act at 90° to the M_x results in the transverse members. This means that the averaged values will be meaningless since the M_x results from the longitudinal members will be averaged with the M_x values of the transverse members that are acting in a completely different direction.

Appendix C: Coordinate Transformation

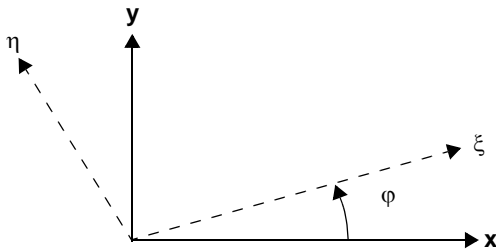
The stress transformation equations for plane stress are as follows

$$\sigma_x = 1/2(\sigma_x + \sigma_y) + 1/2(\sigma_x - \sigma_y)\cos 2\varphi + \tau_{xy}\sin 2\varphi$$

$$\sigma_\eta = 1/2(\sigma_x + \sigma_y) - 1/2(\sigma_x - \sigma_y)\cos 2\varphi + \tau_{xy}\sin 2\varphi$$

$$\tau_{\eta\xi} = -1/2(\sigma_x - \sigma_y)\sin 2\varphi + \tau_{xy}\cos 2\varphi$$

φ is the angle between the x and the rotated ξ -axis:



Appendix D: Principal Stresses (Plane Stress)

The principal stresses are the maximum values of normal stresses under the condition:

$$d\sigma_x/d\varphi = 0$$

and

$$d\sigma_\eta/d\varphi = 0$$

and φ , η , and ξ are defined in the diagram in [Appendix C: Coordinate Transformation](#):

Giving, for the plane stress condition (using the transformation equations from [Appendix C: Coordinate Transformation](#)):

$$-(\sigma_x - \sigma_y)\sin(2\varphi) + 2\tau_{xy}\cos(2\varphi) = 0$$

And leading to

$$\tan(2\varphi^*) = \tan[2(\varphi^* + \pi/2)] = [2\tau_{xy}]/[\sigma_x - \sigma_y]$$

where φ^* and $(\varphi^* + \pi/2)$ are two perpendicular cutting directions, called Principal Directions.

Appendix E: Python Example (Max Stress Results)

```
# -----
# Purpose:
#   PyPost example
#   Find the max nodal scalar values
#
# Usage:
#   python <file>.py
#
# Dependencies
#   Uses PyPost methods:
#     node_scalars
#     node_scalar_labels
#     moveto
#
# Notes
#   index = node/element number
#   id     = internal node/element index number (pointer)
#   Scalar stress/strain results values are:
#   Comp 11 of Cauchy Stress
#   Comp 22 of Cauchy Stress
#   Comp 33 of Cauchy Stress
#   Comp 12 of Cauchy Stress
#   Comp 23 of Cauchy Stress
#   Comp 31 of Cauchy Stress
#
#   Comp 11 of Total Strain
#   Comp 22 of Total Strain
#   Comp 33 of Total Strain
#   Comp 12 of Total Strain
#   Comp 23 of Total Strain
#   Comp 31 of Total Strain
#
#   Equivalent Cauchy Stress
#   Total Strain Energy Density
#
# -----
from py_post import *
import sys

# specify the post file to read
def main(fname):

# open post file and define as object
    p = post_open(fname)

# select loadcase of interest - don't forget that increment 0 is counted. this means
# that the last increment for a 10 increment analysis will be increment number 11
    p.moveto(11)

#-----initialisation
# ..arrays
    element_list = []
    celements    = []
    max_scalars  = []
    max_nodes    = []
    total_volume = []
# ..variables
    stress_threshold = 1100
#-----extract global variables
# ..number of increments in post file
    nincrements = p.increments()
# ..number of contact bodies
    n_contact_bodies = p.cbodies()
    print 'number of contact bodies = ', n_contact_bodies
# ..time at this increment
    inc_time = p.time
# ..increment number
    inc_number = p.increment
# ..extrapolation method
    p.extrapolation('translate')
    print 'Extrapolation method is ', p.extrapolate

#-----loop over the contact bodies
    for i in range(0, n_contact_bodies):
# contact body id number
```

```

        cid = p.cbody(i).id
# contact type
        ctype = p.cbody(i).type
# contact body type
        cbodytype = p.cbody(i).bodytype
# number of elements in contact body
        cnelements = p.cbody(i).nelements
# element id list for contact body
        celements = p.cbody(i).elements
# contact body name
        cname = p.cbody_name(i)
# contact body volume
        cvolume = p.cbody_volume(i)
# print contact information
        print ' contact body id: ', cid
        print ' body name           = ', cname
        print ' body volume         = ', cvolume
        print ' body type           = ', ctype
        print ' contact body type    = ', cbodytype
        print ' elements in contact body = ', cnelements
        print ' increment time       = ', inc_time
        print ' increment number      = ', inc_number

#-----loop over the elements in each contact body
        for j in range(0, cnelements):
# extract element number
            element_number = celements[j]
# extract element id
            element_id = p.element_sequence(element_number)
# print element number/id
            print ' element id: ', element_id
            print ' element number ', element_number
# extract number of nodes on this element
            nnodes = p.element(element_id).len
# extract number of element scalars available
            nelement_scalars = p.element_scalars(element_id)
            print ' number of element scalars: ', nelement_scalars
            print ' number of nodes: ', nnodes, ' ', p.element(j).items
# initialise current element volume
            element_volume = 0
#-----loop over the scalars to find the current element volume
            for k in range(0, nelement_scalars):
# extract the element scalars data label
                scalar_label = p.element_scalar_label(k)
# look for volume of this element
                if (scalar_label == 'Current Volume'):
# extract the element volume data (nodal-based)
                    tlist = p.element_scalar(element_id, k)
# extract the number of bits of information in the scalar
                    length_scalar = len(tlist)
# print the scalar label
                    print ' scalar: ', scalar_label, ' (size: ',length_scalar,')'

#-----loop over the nodal volume data
                for m in range(0, length_scalar):
# ...extract next scalar component
                    scalar_data = tlist[m].value
# ...print the scalar values
                    print ' ',scalar_data
# check for a specific scalar result for further processing
                    element_volume = element_volume + scalar_data
# store the total volume for each element here for later use
                    total_volume.append(element_volume)
# print the total volume for this element
                    print ' total volume: ',total_volume[j]

#-----loop over the contact bodies again for the stress/strain results
        for ii in range(0, n_contact_bodies):
# contact body id number
            cid = p.cbody(ii).id
# number of elements in contact body
            cnelements = p.cbody(ii).nelements
# element id list for contact body
            celements = p.cbody(ii).elements

#-----loop over the elements in each contact body

```

```

        for jj in range(0, cnelements):
# extract element number
        element_number = celements[jj]
# extract element id
        element_id = p.element_sequence(element_number)
# print element number/id
        print ' element id:      ', element_id
        print ' element number ', element_number
# extract number of nodes on this element
        nnodes = p.element(element_id).len
# extract number of element scalars available
        nelement_scalars = p.element_scalars(element_id)

#-----loop over the number of element scalars
        for nn in range(0, nelement_scalars):
#         print ' element number ', element_number
# extract the element scalars data label
            scalar_label = p.element_scalar_label(nn)
# extract the element scalars data
            tlist = p.element_scalar(element_id, nn)
# extract the number of bits of information in the scalar
            length_scalar = len(tlist)
# print the scalar label
            print ' scalar: ', scalar_label, ' (size: ',length_scalar,')'

            iloop_counter = 0
#-----loop over the data within the scalar
            for ip in range(0, length_scalar):
#             ..extract next scalar component
                scalar_data = tlist[ip].value
#             ..print the scalar values
                print ' ',scalar_data

# check for a specific scalar result for further processing
            if (scalar_label == 'Comp 11 of Cauchy Stress'):
                if (iloop_counter == 0):
                    print ' scalar data: ', scalar_data
                    if (abs(scalar_data) > stress_threshold):
                        print ' scalar: ', scalar_label, ' (size: ',length_scalar,')'
                        print 'element ', element_number, 'exceeded threshold ',scalar_data,' volume ', total_volume[jj]

# set the loop counter since we are searching for the FIRST occurrence of a stress above the threshold value
                iloop_counter = 1

        return 1

if __name__ == '__main__':
    main("python_result_extract_3d_job1.t16")

#     element_list.sort()
#     print element_list()
#     print '----- '

```

The results from this script will look as follows

```

number of contact bodies = 2
Extrapolation method is translate
contact body id: 1
body name           = rubber
body volume         = 0.0499988384545
body type           = 0
contact body type   = 2
elements in contact body = 8
increment time      = 1.0
increment number    = 10
contact body id: 2
body name           = metal
body volume         = 0.0400002449751
body type           = 0

```



```
contact body type          = 2
elements in contact body = 8
increment time             = 1.0
increment number           = 10
element 17 exceeded threshold -1189.01721191 volume 0.00624981324654
element 18 exceeded threshold -1173.24584961 volume 0.00624981324654
element 19 exceeded threshold -1105.20239258 volume 0.00624981324654
element 21 exceeded threshold -1179.69567871 volume 0.00624981324654
element 22 exceeded threshold -1199.10046387 volume 0.00624981324654
element 23 exceeded threshold -1118.07836914 volume 0.00624981324654
element 26 exceeded threshold -1592.05969238 volume 0.00624981324654
element 28 exceeded threshold -1529.88928223 volume 0.00624981324654
element 29 exceeded threshold -1208.35742188 volume 0.00624981324654
element 30 exceeded threshold -2732.16430664 volume 0.00624981324654
element 31 exceeded threshold -1222.24694824 volume 0.00624981324654
element 32 exceeded threshold -2766.19677734 volume 0.00624981324654
```

Appendix F: Python Example (Displacements at Nodes)

```

#-----
#!/usr/bin/env python
#*description
#   PyPost example to find the time history of a specified node
#
#*usage
# to obtain all the results from this script:
#   python node_loop.py filename.t16 1
#
# to obtain only the results ids without scanning the post file fully:
#   python node_loop.py filename.t16 0
#
# The results are in columns:
#   inc number - time - dispX - dispy - dispz - rotx - roty - rotz
#
#-----
from py_post import *
import sys

#-----extract command line parameters
#   ...post file name (without t16 extension)
mno   = str(sys.argv[1])
#
#   ...flag to indicate whether full scan or
#   just post file summary required
mns_only = int(sys.argv[2])

def main(fname):
    try:
#       open post file
        p = post_open(fname)
#       vectors for user node numbers
        nodes = []
#       set pointer to first loadstep
        p.moveto(1)
#       extract number of nodal scalars available in
#       the post file
        mns = p.node_scalars()

#-----User Defined Variables Start:
#       number of nodes for which results are needed
        mnodes = 2
#       node numbers of interest
        nodes.append(18)
        nodes.append(15)

#-----User Defined Variables End:

        print " "
        print " "
        print " Found", mns, "Node Scalars in POST file",fname

```



```
        k = k + 1
#           increment nodal loop counter
        kk = kk + 1

except AttributeError:
    print ""
    print " Post File is not accessible: ", fname
    return

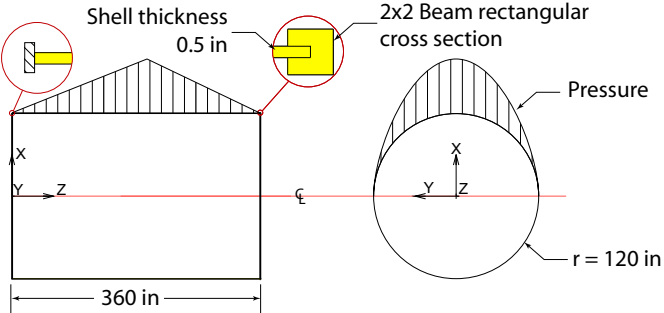
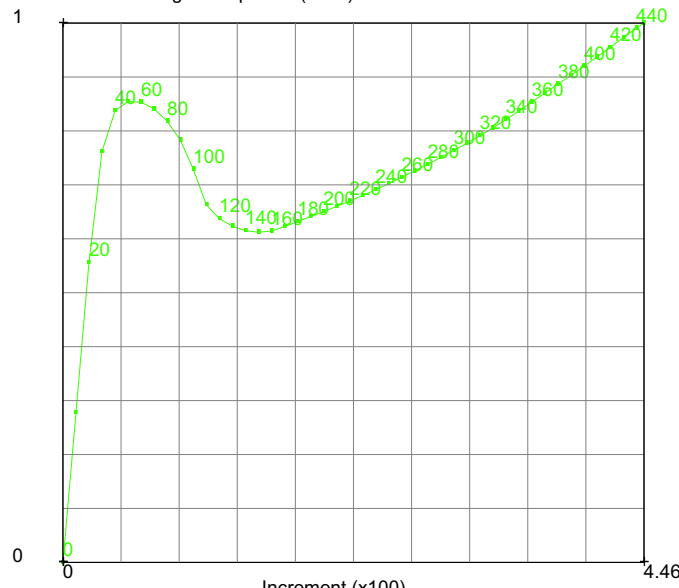
if __name__ == '__main__':
    main(mno)
```

Section 2: Recent Features

2.1 New-style Table Input

- Summary of Reinforced Cylinder 296
- Post Buckling Analysis of a Reinforced Shell with Nonuniform Load 297
- Input Files 316
- Summary of Can Analysis 317
- Can Analysis 318
- Input Files 337

Summary of Reinforced Cylinder

Title	Post buckling analysis of a reinforced cylinder with nonuniform load																																																
Problem features	New style of table input for pressure load and user subroutine for post																																																
Geometry	 <p>Shell thickness 0.5 in</p> <p>2x2 Beam rectangular cross section</p> <p>Pressure</p> <p>$r = 120$ in</p> <p>360 in</p>																																																
Material properties	$E = 30 \times 10^6$ Psi, $\nu = 0.3$																																																
Analysis type	Static with Riks-Ramm arc-length load stepping method																																																
Boundary conditions	Clamped at $z = 0$ with external pressure of $30 * \cos(\theta) * \left(1 - \left \frac{Z - 180}{180}\right \right)$																																																
Element type	Brick element type 75 and 98																																																
FE results	<p>Pressure history as cylindrical shell buckles</p> <p>Buckling of Reinforced Shell with Nonuniform Load</p> <p>Loadcase Percentage Completion (x100)</p>  <table border="1"> <caption>Data points from the buckling pressure history graph</caption> <thead> <tr> <th>Increment (x100)</th> <th>Loadcase Percentage Completion (x100)</th> </tr> </thead> <tbody> <tr><td>0</td><td>0</td></tr> <tr><td>0.2</td><td>20</td></tr> <tr><td>0.4</td><td>40</td></tr> <tr><td>0.6</td><td>60</td></tr> <tr><td>0.8</td><td>80</td></tr> <tr><td>1.0</td><td>100</td></tr> <tr><td>1.2</td><td>120</td></tr> <tr><td>1.4</td><td>140</td></tr> <tr><td>1.6</td><td>160</td></tr> <tr><td>1.8</td><td>180</td></tr> <tr><td>2.0</td><td>200</td></tr> <tr><td>2.2</td><td>220</td></tr> <tr><td>2.4</td><td>240</td></tr> <tr><td>2.6</td><td>260</td></tr> <tr><td>2.8</td><td>280</td></tr> <tr><td>3.0</td><td>300</td></tr> <tr><td>3.2</td><td>320</td></tr> <tr><td>3.4</td><td>340</td></tr> <tr><td>3.6</td><td>360</td></tr> <tr><td>3.8</td><td>380</td></tr> <tr><td>4.0</td><td>400</td></tr> <tr><td>4.2</td><td>420</td></tr> <tr><td>4.46</td><td>440</td></tr> </tbody> </table>	Increment (x100)	Loadcase Percentage Completion (x100)	0	0	0.2	20	0.4	40	0.6	60	0.8	80	1.0	100	1.2	120	1.4	140	1.6	160	1.8	180	2.0	200	2.2	220	2.4	240	2.6	260	2.8	280	3.0	300	3.2	320	3.4	340	3.6	360	3.8	380	4.0	400	4.2	420	4.46	440
Increment (x100)	Loadcase Percentage Completion (x100)																																																
0	0																																																
0.2	20																																																
0.4	40																																																
0.6	60																																																
0.8	80																																																
1.0	100																																																
1.2	120																																																
1.4	140																																																
1.6	160																																																
1.8	180																																																
2.0	200																																																
2.2	220																																																
2.4	240																																																
2.6	260																																																
2.8	280																																																
3.0	300																																																
3.2	320																																																
3.4	340																																																
3.6	360																																																
3.8	380																																																
4.0	400																																																
4.2	420																																																
4.46	440																																																

Post Buckling Analysis of a Reinforced Shell with Nonuniform Load

This problem demonstrates the use of applying a nonuniform load by defining an equation to prescribe the pressure. The load is placed on the geometric surface. The thin shell is reinforced with beam elements at the top. The Riks-Ramm arc-length method is used to control the applied load.

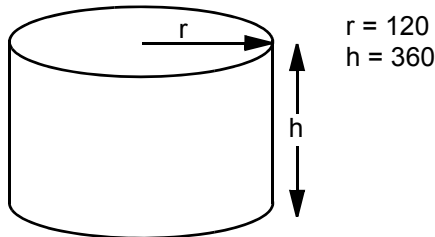


Figure 2.1-1 Geometry of Tank

The cylindrical shell as shown in [Figure 2.1-1](#) has a diameter of 20 feet = 240 inches, and a height of 30 feet = 360 inches. The shell thickness is 0.5 inch. The material is steel with Young's modulus = 30×10^6 psi, and Poisson's ratio = 0.3. The steel beams have a square solid section with a 2 inch width, where the shell is at the midsection of the beam. The pressure magnitude has a cosine like distribution with a bilinear axial variation. The magnitude may be expressed as

$$30 * \cos(\theta) \cdot \left(1 - \left|\frac{Z - 180}{180}\right|\right)$$

This distributed load is applied on only half of the surface. This problem also demonstrates the use of user subroutine *plotv*.

The following steps are used to perform the analysis:

- Step 1: Create Model**
- Step 2: Define Geometrical Properties for the Shells and Beams**
- Step 3: Define Material Properties**
- Step 4: Attach element edges to curves**
- Step 5: Apply Boundary Conditions**
- Step 6: Create loadcase**
- Step 7: Write user subroutine**
- Step 8: Create Job and submit model**
- Step 9: Review results**

Step 1: Create Model

The cylindrical model (Figure 2.1-2) will be created first by creating two ruled surfaces representing each half of the cylinder and converting these to elements. Two surfaces are used as opposed to the conventional single surface, because the load is to be applied on only half of the surface. The curves on the top are then converted to beam elements.

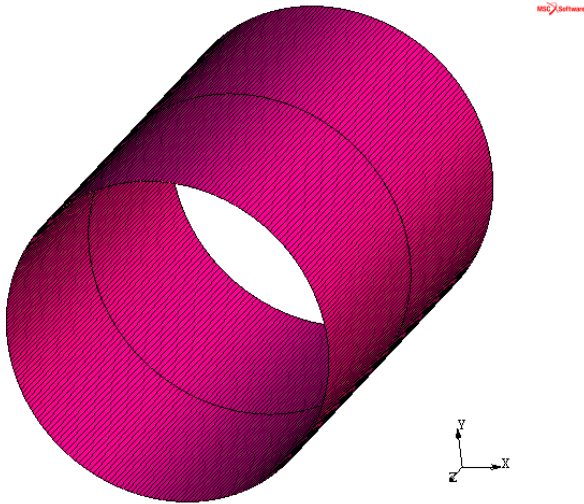


Figure 2.1-2 Definition of Cylinder Geometry

FILES

SAVE AS

reinforced

(create model file reinforced)

OK

RETURN

MESH GENERATION

COORDINATE SYSTEM

SET

(create grid)

U DOMAIN

-120 120

U SPACING

10

V DOMAIN

-120 120

V SPACING

10

```

GRID (on)
FILL
RETURN
CURVE TYPE (create curves used to make ruled surface)
  ARCS
    CENTER/RADIUS/ANGLE/ANGLE
  RETURN
  CRVS ADD
    0 0 0 120
    -90 90
    0 0 0 120
    90 -90
  PLOT
    CURVES SETTINGS
    PREDEFINED SETTINGS
      HIGH
    DRAW
      DIRECTION (on)
    REGEN
  RETURN
  SURFACES SETTING
    HIGH
    REGEN
  RETURN (twice)
  DUPLICATE
  TRANSLATIONS
    0 0 360
  CURVES
    1 2
    # END LIST
  RETURN
  SURFACE TYPE (create surfaces)
    SURFACES
      RULED
    TRIM (on)
      TRIM NEW SURFACE

```

RETURN

SRFS ADD

1 3

SRFS ADD

2 4

CONVERT

(convert surfaces to elements)

DIVISIONS

18 30

*(as 18 divisions are used for each shell,
the shell elements will be 10° wide.*

The result is shown in [Figure 2.1-3](#))

GEOMETRY/MESH

SURFACES TO ELEMENTS

1 2

END LIST

RETURN

SWEEP

SWEEP

ALL

RETURN

COORDINATE SYSTEM

GRID

(off)

CONVERT

(convert curves to line elements)

GEOMETRY/MESH

CURVES TO ELEMENTS

3 4

END LIST

RETURN

SWEEP:

ALL

RETURN

RENUMBER

ALL

RETURN

MAIN

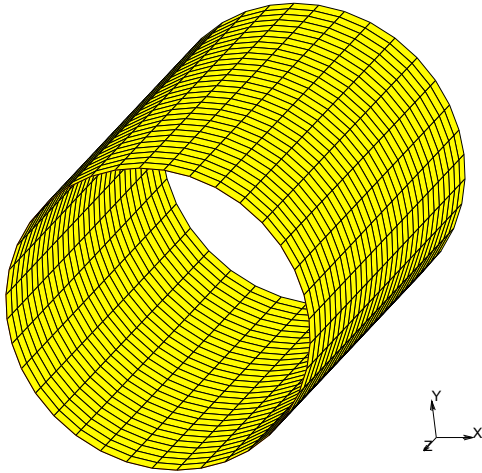


Figure 2.1-3 Mesh Converted from Surface and Automatically Attached (shown as yellow)

Step 2: Define Geometrical Properties for the Shells and Beams

The shell thickness, the beam cross section and orientation are defined. The thickness is applied to the geometric surface. The beam is located at the top of the shell.

MAIN MENU

PREPROCESSING

GEOMETRIC PROPERTIES

STRUCTURAL ELEMENTS

3-D

GEOMETRIC PROPERTY TYPE

SHELL

STRUCTURAL 3-D SHELL PROPERTIES

THICKNESS

0.5

OK

SURFACES ADD

1 2

END LIST

RETURN

GEOMETRIC PROPERTIES

NEW

STRUCTURAL ELEMENTS

3-D

GEOMETRIC PROPERTY TYPE

SOLID SECTION BEAM

STRUCTURAL 3-D SHELL PROPERTIES

CROSS SECTION

PROPERTIES

ENTERED

AREA

4

Ixx

1.33333

Iyy

1.33333

VECTOR DEFINING LOCAL ZX-PLANE

Z

1

OK

SELECT

CLEAR SELECT

SELECT BY

ELEMENTS BY

CLASS

LINE (2)

OK

RETURN

MAKE VISIBLE

RETURN

ELEMENTS ADD

ALL: VISIB.

RETURN

PLOT SETTINGS

BEAM

BEAM ORIENTATION

(associate beam elements with the geometry)

*(display beam element orientation
as shown in Figure 2.1-4)*

DRAW LOCAL AXES (on)
REDRAW
RETURN
MAIN MENU
PREPROCESSING
MESH GENERATION
SELECT
ELEMENTS
ALL: EXIST.
MAKE VISIBLE
PLOT
ELEMENT (display shell orientation and thickness)
SETTINGS
RELATED PLOT SETTING
SHELL
PLOT EXPANDED (on)
DEFAULT THICKNESS
0.5
REDRAW
MAIN

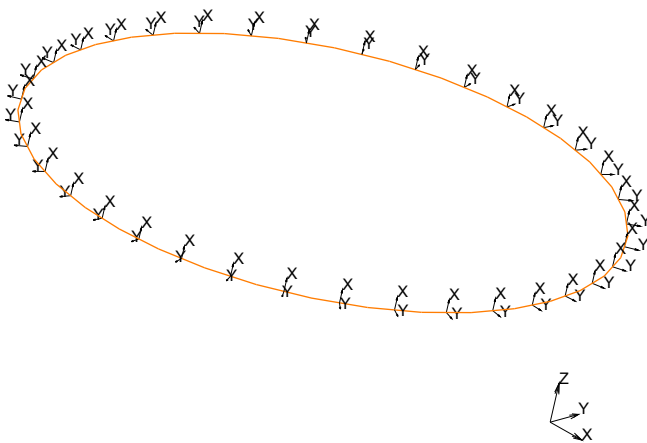


Figure 2.1-4 Orientation of Reinforcement Beams at Top of Shell

Step 3: Define Material Properties

Both the shell and the beams are made of standard steel, and will remain elastic.

```
MAIN MENU
PREPROCESSING
  MATERIAL PROPERTIES
    MATERIAL PROPERTIES
      NEW
        NEW MATERIAL
          STANDARD
            STRUCTURAL
              STRUCTURAL PROPERTIES
                YOUNG'S MODULUS
                  30e6
                POISSON'S RATIO
                  0.3
              OK
            ELEMENTS ADD
              ALL: EXIST.
```

Step 4: Attach element edges to curves

The CONVERT option attached the shell elements to the surface and attached the beam elements to the curve. To facilitate the application of boundary conditions, it is also useful to attach the edges of the shell elements to the curve. This will be demonstrated in this step.

```
MAIN MENU
PREPROCESSING
  MESH GENERATION
    ATTACH
      EDGES -> CURVE
        3
      EDGES -> CURVE
        4
      EDGES -> CURVE
        1
      EDGES -> CURVE
        2
  MAIN
```


Step 5: Apply Boundary Conditions

This problem has two boundary conditions: the base of the shell is clamped, and a nonuniform pressure is applied. The displacement boundary condition is applied to the curves at the base. The pressure is applied on a surface by giving a reference value of 30 psi and referencing a table. This table defines a mathematical equation. Then for each element attached to the surface, it will, for each integration point, determine the integration point coordinates and evaluate the table. Later in this analysis, we will activate the FOLLOWER FORCE option. When applying distributed load type boundary conditions to curves or surfaces, it is important to indicate if the load is to the top or bottom part of the surface. The SELECT option is used to filter the surface.

MAIN MENU**PREPROCESSING****BOUNDARY CONDITIONS****STRUCTURAL****NAME**

fixed_base

*(clamped boundary condition)***BOUNDARY CONDITION TYPE****FIXED DISPLACEMENT**

X, Y, Z, RX, RY

OK

CURVES ADD

1 2

END LIST

RETURN**DRAW BOUNDARY COND ON MESH****NEW****NAME**

pressure

*(pressure boundary condition)***STRUCTURAL****FACE LOAD**

30

(enter the reference value)

OK

SELECT*(select the top side of surface 1)***FILTER**

TOP

RETURN

CLEAR SELECT**SURFACES**

1

END LIST

RETURN

SURFACES ADD

ALL SELEC.

(associate the selected surface
with this boundary condition)

The pressure load is to look like a cosine function multiplied by a bilinear function, such that the load is maximum at $Z=180$ and linearly decreases as one approaches the edge. A working sketch for defining the load is shown in Figure 2.1-5.

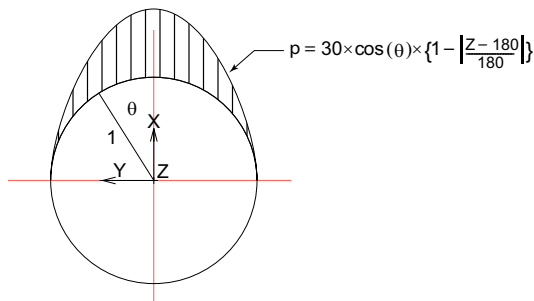


Figure 2.1-5 Definition of Function

$$\cos \theta = x/l = x/\sqrt{x^2 + y^2}$$

Note that initially this is x/r , but as deformation occurs, this would no longer be true.

As the independent variables are given in the order of 1=x, 2=y, 3=z, when entering the equation, the variable names are replaced with the generic names v_1, v_2, v_3 . The equation used is then:

$$(v1/\text{sqrt}(v1 * v1 + v2 * v2)) * (1 - (\text{abs}(v3 - 180)/180))$$

TABLES

NEW

3 INDEPENDENT VARIABLES (toggle)

INDEPENDENT VARIABLE V1

TYPE

X0_coordinate

OK

MAX

120

VARIABLES

MORE

LABEL

X0_coordinate

PREVIOUS**INDEPENDENT VARIABLE V2****TYPE**

Y0_coordinate

MIN

-120

MAX

120

VARIABLES**MORE****LABEL**

Y0_coordinate

PREVIOUS**INDEPENDENT VARIABLE 3****TYPE**

Z0_coordinate

MIN

0

MAX

360

MORE**LABEL**

Z0_coordinate

PREVIOUS**FORMULA***(define function with a formula)***ENTER**
$$(v1/\sqrt{v1 * v1 + v2 * v2}) * (1 - \text{abs}(v3 - 180)/180)$$
FIX V3

5

*(evaluate the table at the 5th value of V3 which is located at z=180 or midway up the cylinder)*Use **DYN. MODEL** to rotate model*(the Mentat evaluated table is shown in Figure 2.1-6)***NAME**

load_factor

toggle **SHOW TABLE** to **SHOW MODEL****RETURN**

FACE LOAD
TABLE
load_factor
OK
MAIN

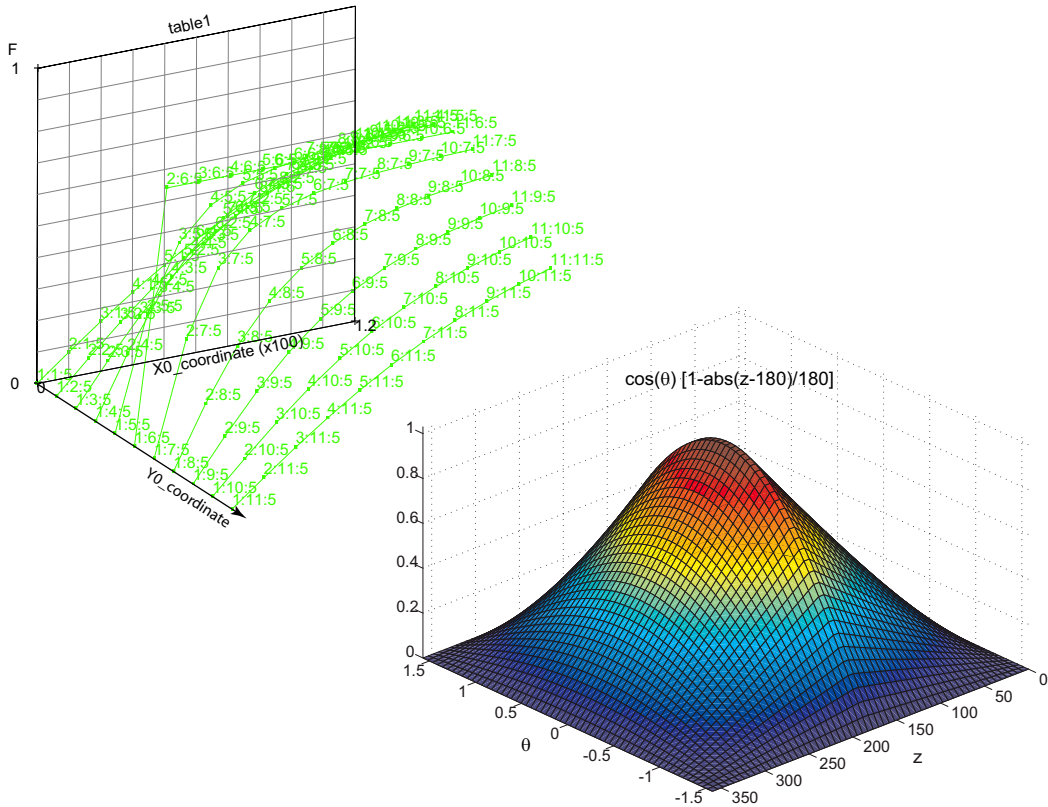


Figure 2.1-6 Table Describing Load Evaluated at Z=180, X-direction along Axis, Y-direction is Out-of Plane. Complete surface, $p = p(\theta, z)$, at lower right.

Note: When evaluating the function, Mentat indicates numerical errors because it evaluates the function at $v_1=0, v_2=0$, which results in a divide by zero. In the analysis program, the function is evaluated at the element integration points which are not at this position.

Step 6: Create loadcase

This demonstration problem contains one loadcase. It is anticipated that this thin shell will buckle, so the Arc Length procedure is invoked (Figure 2.1-7).

For more information about continuation methods in buckling analyses, see *Marc Volume A: Theory and User Information*. In most analyses of this type, it would be necessary to adjust the convergence tolerances. In this simulation, this was not required.

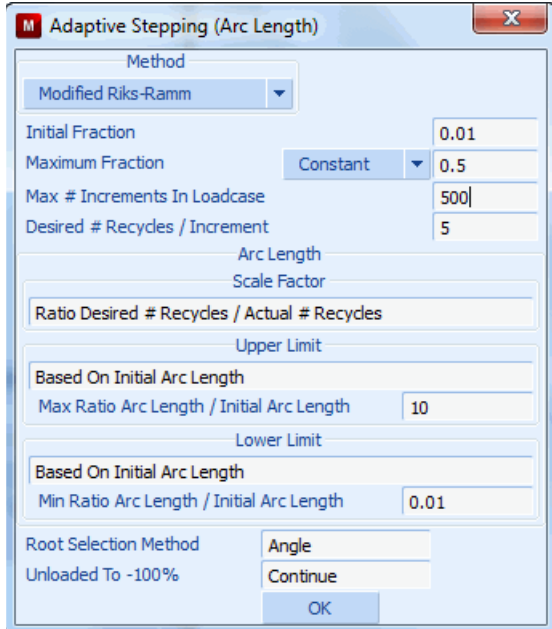


Figure 2.1-7 Loadcase Menu

MAIN MENU

ANALYSIS

LOADCASES

ANALYSIS CLASS

STRUCTURAL

NEW

STATIC

PROPERTIES

ADAPTIVE

ARC LENGTH

PARAMETERS

MAX # INCREMENTS IN LOADCASE

OK (twice)

MAIN MENU**Step 7:** Write user subroutine

In this problem, it is worthwhile displaying the actual applied pressure on the surface of the element associated with the applied boundary condition. Marc, by default, places the total equivalent nodal load associated with all boundary conditions on the post file. This may be displayed as a contour or a vector plot.

Here, additionally, we would like to see the pressure which is based upon the reference magnitude, the evaluation of the equation, and the fraction of the load applied. As this is not normally available, PLOTV user subroutine is invoked based upon a user defined post code. This subroutine will be called for every element of the model. As the load is only applied on the shell elements when $X > 0$, ignore all other elements.

There are five steps to achieve this:

1. Begin with a skeleton *plotv.f* routine obtained from the /user subdirectory or from *Marc Volume D: User Subroutines and Special Routines*.
2. Identify elements of interest.
3. Obtain the integration point coordinates and store them in the appropriate place.
4. Evaluate the function and scale with the a reference value.
5. Scale with the fraction of the load applied in this loadcase.

Subroutine *tabva2* may be used to obtain the current value of a table or equation by the user. It is documented in *Marc Volume D: User Subroutines and Special Routines*. Here, the key parameters are:

refval – the reference value; here 30 psi
prxyz – the calculated pressure
idtab – the table ID; here 1.

List of User Subroutines

```
subroutine plotv(v,s,sp,etot,eplas,ecreep,t,m,nn,layer,ndix,
* nshearx,jpltcd)
c* * * * *
c
c   select a variable contour plotting (user subroutine).
c
c   v           variable
c   s (idss)    stress array
c   sp          stresses in preferred direction
c   etot        total strain (generalized)
c   eplas       total plastic strain
c   ecreep      total creep strain
c   t           current temperature
c   m(1)        user element number
```

```

c      m(2)          internal element number
c      nn           integration point number
c      layer        layer number
c      ndi (3)      number of direct stress components
c      nshear (3)   number of shear stress components
c
c* * * * *
include '../common/implicit.cmn'
      dimension s(*),etot(*),eplas(*),ecreep(*),sp(*),m(2)
      include '../common/elmcom.cmn'
      include '../common/ctable.cmn'
      include '../common/array4.cmn'
      include '../common/heat.cmn'
      include '../common/space.cmn'
      include '../common/autoin.cmn'
      jcrxpt=icrxpt+lofr+(nn-1)*ncrdel
c
c      obtain coordinates of integration point
c      for distributed load on shell face, integration point location
c      is the same as element stiffness integration point location
c      if x-coordinate is less than zero, skip as load was only applied
c      to half of cylinder
c
      xyz0(1)=varselem(jcrxpt)
      if(xyz0(1).gt.0.0.and.ndix.ge.2) then
        xyz0(2)=varselem(jcrxpt+1)
        xyz0(3)=varselem(jcrxpt+2)
c
c      refval is reference value of applied pressure
c      idtab is the table id
c      prxyz is the value of the table/function after evaluation
c      the original coordinates in xyz0 are passed into the
c      evaluator via common/ctable/
c
      refval=100.0
      idtab=1
      call tabva2(refval,prxyz,idtab,0,1)
      else
        prxyz=0.0
      endif
c
c      scale by the total percentage of load applied (autacc)
c
      v=prxyz*autacc
c
      return
      end

```

Step 8: Create Job and submit model

The job will be created and submitted for analysis. A large displacement elastic analysis will be performed. In this model, the four-node shell element, type 75 and the two-node elastic beam element, type 52 will be used. These are default element types.

The output to be written to the post file is selected, and the inclusion of the user subroutine is invoked.

MAIN MENU

ANALYSIS

JOBS

NEW

STRUCTURAL

PROPERTIES

AVAILABLE

Select **lcase1**

INITIAL LOADS

pressure

(deactivate pressure from the initial conditions)

OK

ANALYSIS OPTIONS

FOLLOWER FORCE (toggle)

(invoke follower force)

LARGE STRAIN

OK

JOB RESULTS

AVAILABLE ELEMENT SCALARS

Equivalent Von Mises Stress

(select post variable)

LAYERS

toggle **DEFAULT** to **OUT & MID**

AVAILABLE ELEMENT SCALARS

User Defined Var #1

(select post variable change label

Rename it **pressure**

of user-defined post variable)

POST FILE

FREQUENCY

2

OK

OK

RUN

USER SUBROUTINE FILE

shellcos_buckle.f

(select user subroutine)

COMPILE / SAVE

STYLE

TABLE-DRIVEN (toggle)

(invoke table driven input)

ADVANCED JOB SUBMISSION

WRITE INPUT FILE

EDIT INPUT FILE

OK

SUBMIT

MONITOR

Note: This analysis will run for 2 - 10 minutes depending upon the computer.

Step 9: Review results

In this type of analysis, it is interesting to examine how the load increased such that it reached the final magnitude. This is dependent on the accuracy requirements and in this model the buckling phenomena. The other areas of interest are the applied distributed load and the deformations.

MAIN MENU**POSTPROCESSING****RESULTS****OPEN**

reinforced_job1.t16

PLOT

NODES

(off)

POINTS

(off)

SURFACES

*(off)***ELEMENT SETTINGS**

SOLID

RETURN (twice)**HISTORY PLOT****COLLECT DATA**

ALL INCS

SHOW IDS

2

ADD CURVES

GLOBAL

Increment

Loadcase Percent Completion

FIT
RETURN

(This is shown in Figure 2.1-8)

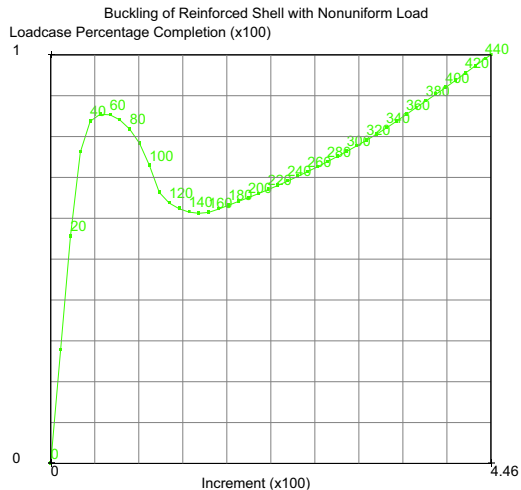


Figure 2.1-8 Loadcase Percentage Completion versus Increment Number

SHOW MODEL

RETURN

RESET VIEW

FILL

rotate model

LAST

RETURN

CONTOUR BANDS

SCALAR

pressure

DEF ON (toggle)

(examine pressure on deformed configuration,
see Figure 2.1-9)

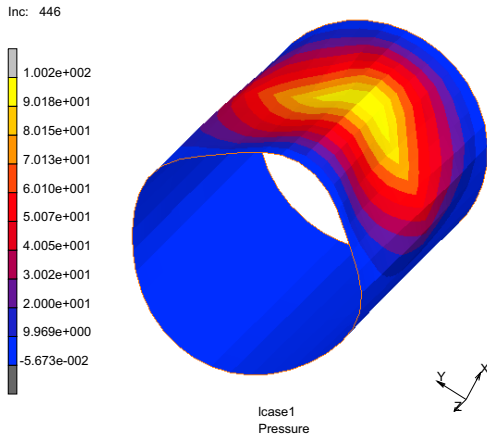


Figure 2.1-9 Applied Pressure on Deformed Structure

You can observe that the load has a cosine-like distribution along the circumference and increases, then decreases along the height. The maximum value is at (0,0,180).

SCALAR

Equivalent Von Mises Stress Top Layer

OK

SCALAR PLOT

SETTINGS

SET LIMITS

0 2.E5

MANUAL

RETURN

REWIND

MONITOR

The final stress on the deformed shell is shown in [Figure 2.1-10](#).

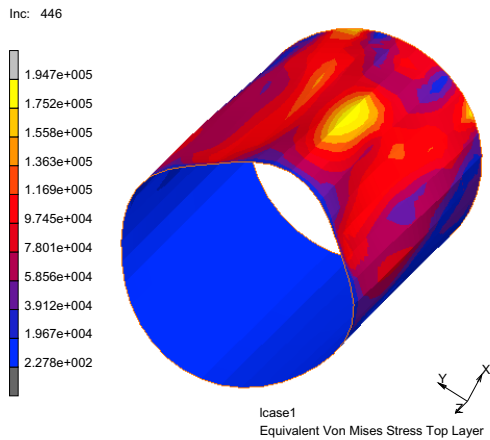


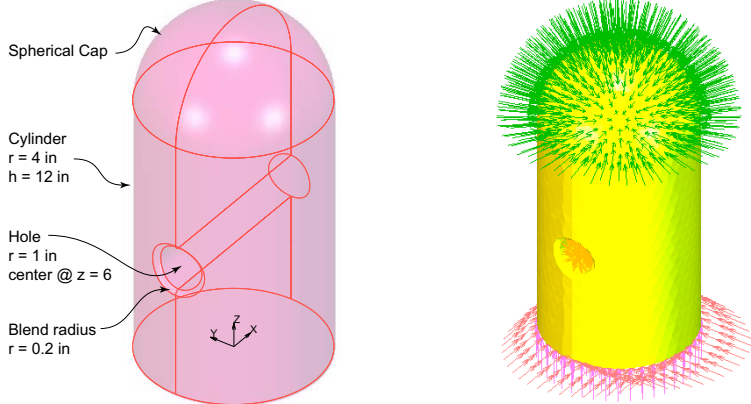
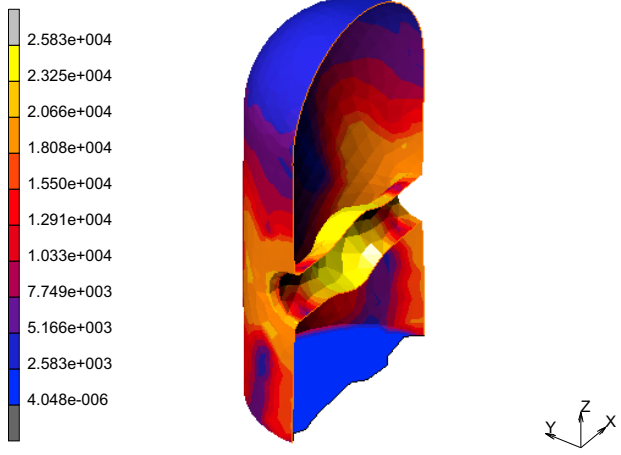
Figure 2.1-10 Equivalent Stress on Deformed Structure

Input Files

The files below are on your [delivery media](#) or they can be downloaded by your web browser by clicking the links (file names) below.

File	Description
reinforced.proc	Mentat procedure file to run the above example
shellcos_buckle.f	Associated user subroutine

Summary of Can Analysis

Title	Capped Cylindrical Shell
Problem features	New style of table input for material properties and boundary conditions
Geometry	 <p>Spherical Cap</p> <p>Cylinder $r = 4$ in $h = 12$ in</p> <p>Hole $r = 1$ in center @ $z = 6$</p> <p>Blend radius $r = 0.2$ in</p>
Material properties	$E = 10 \times 10^6$ Psi, $\nu = 0.3$, with workhardening
Analysis type	Static with variable load stepping
Boundary conditions	Fixed at $z = 0$ with pressure in hole and on dome
Element type	Brick element type 138
FE results	<p>Stress contours at end of load history</p> <p>Inc: 61 Time: 1.000e+000</p>  <p>2.583e+004 2.325e+004 2.066e+004 1.808e+004 1.550e+004 1.291e+004 1.033e+004 7.749e+003 5.166e+003 2.583e+003 4.048e-006</p> <p>Icase1 Equivalent Von Mises Stress Top Layer</p>

Can Analysis

This problem demonstrates the use of tables for material properties and boundary conditions. Additionally, the boundary conditions are applied on surfaces created from a solid model. The geometry is shown in [Figure 2.1-11](#).

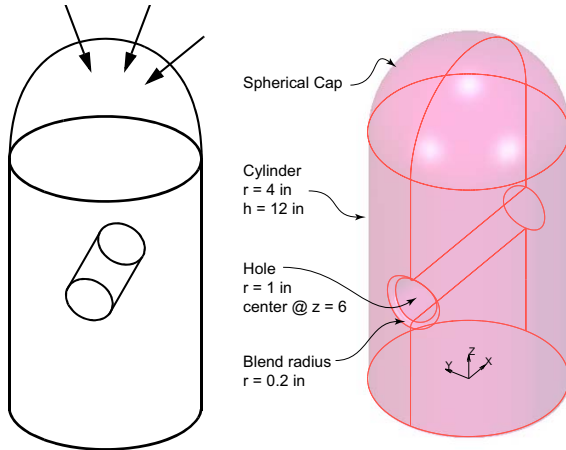


Figure 2.1-11 Creating the Geometric Model

The hollow cylinder is 12 inches high and has a radius of 4 inches. A cylindrical slot is located 6 inches from the bottom and has a radius of 1 inch. The simulation can be performed by exercising the following steps.

Overview of Steps

Step 1: Create the geometric model

Step 2: Define shell thickness

Step 3: Define Material Properties

Step 4: Apply Boundary Conditions

Step 5: Create Loadcase

Step 6: Job creation

Step 7: Evaluate Results

Step 1: Create the geometric model

The model consists of a cylindrical shell with a hemispherical dome and a cylindrical slot. One side of the cylindrical slot is blended into the larger cylinder. The creation of the finite element model involves three substeps.

- A. Form solid model
- B. Convert solid faces into surfaces
- C. Use the automatic Delaunay mesher to create the mesh.

It should be noted that since the automatic mesh generator is used, the faces of the elements are automatically attached to the surfaces. Additionally, element edges are attached to the curves.

FILES**SAVE AS**

table_bc_shell

OK**RETURN****MESH GENERATION****SOLID TYPE****CYLINDER****RETURN****SOLIDS ADD***(create cylinder)*

0 0 0

0 0 12

4 4

FILL**SOLID TYPE****SPHERE****RETURN****SOLIDS ADD***(create sphere)*

0 0 12

4

COORDINATE SYSTEM**SOLIDS****BOOLEANS****UNITE**

1 2

END LIST**PLOT****SOLIDS****SOLID****DRAW****MAIN****CONFIGURATION****VISUALIZATION**

```
LIGHTING (on)
VIEW1 (on)
RETURN
RETURN
MESH GENERATION
SOLID TYPE
CYLINDER
RETURN
SOLIDS ADD
-6 0 6
6 0 6
1 1
COORDINATE SYSTEM
SOLIDS (create slot by subtracting cylinder from solid)
BOOLEANS
SUBTRACT
1 2 #
MISCELLANEOUS
SPLIT FACES
ALL: EXIST.
BLEND
RADIUS
0.2
CHAMFER
ROLLING (turn on rolling blend)
EDGE
1:19
RETURN
```

The result is shown in [Figure 2.1-12](#).



Figure 2.1-12 Solid Representation of Can

```

CONVERT
  FACES TO SURFACES
ALL: EXIST.
PLOT
  POINTS
  SOLIDS
  SURFACES
    SETTING
    SOLID
  RETURN
  IDENTIFY
    
```

(off)

(off)

*(For application of boundary conditions
 and for mesh generation, it is important
 that the surface orientation is consistent.)*

```

BACKFACES
DRAW
    
```

(the orientation is shown in Figure 2.1-13)

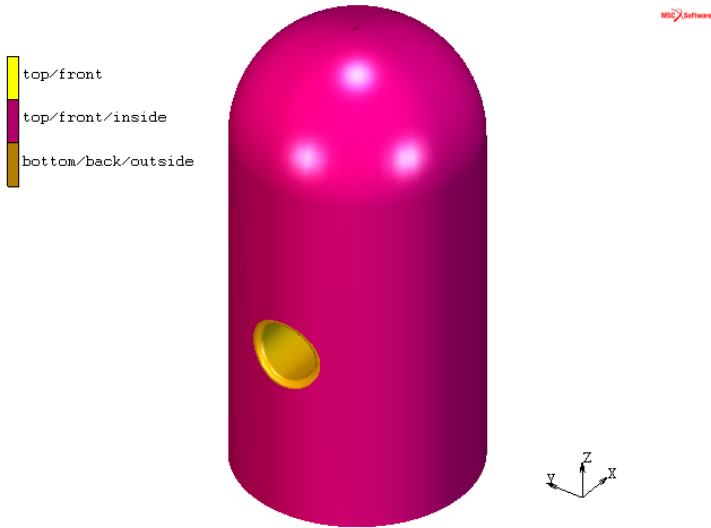


Figure 2.1-13 Orientation of Surfaces before Slot is Flipped

```
MAIN MENU
PREPROCESSING
  MESH GENERATION
    CHECK
      FLIP SURFACES
        1 7 #
      FILL
    RETURN
    SWEEP
  ALL
  RETURN
  AUTOMESH
  PRELIMINARY
    CURVE DIVISIONS
      FIXED AVG LENGTH
        AVG LENGTH
          0.6
      APPLY CURVE DIVISION
    ALL: EXIST.
  TOOLSS
    MATCH CURVE DIVISIONS
      0.1
```

*(make sure all surfaces have
a consistent orientation)*

ALL: EXIST.
 RETURN
 CHOOSE
 SURFACE MESHING
 TRIANGLES (DELAUNAY)
 SURFACE TRI MESH!
 ALL: EXIST.

(create finite element mesh on the surface)

(the finite element mesh is show in Figure 2.1-14)

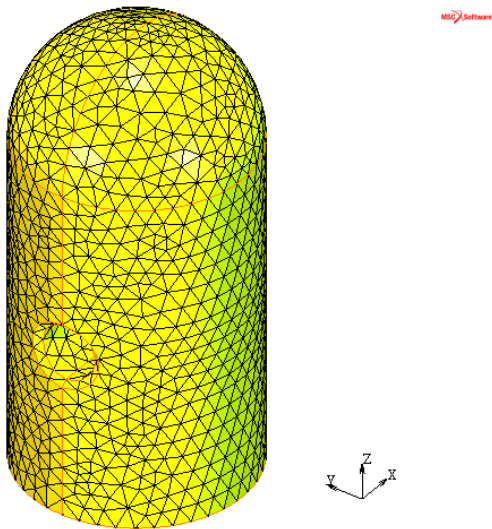


Figure 2.1-14 Finite Element Mesh Created with Delaunay Mesh Generator

PLOT
 SURFACES
 ELEMENTS
 SETTING
 EDGES
 OUTLINE
 DRAW
 RETURN
 RETURN
 RETURN

(off)

(this allows one to check for gaps in the model, see Figure 2.1-15)

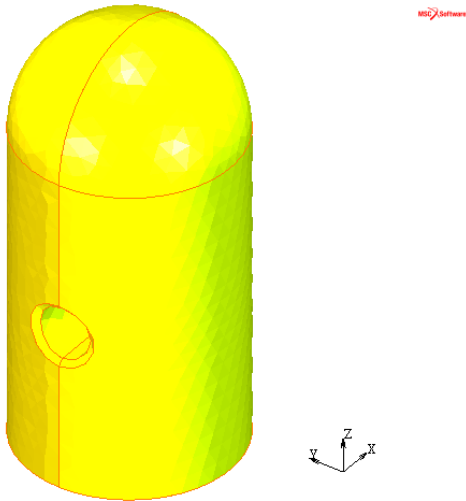


Figure 2.1-15 Finite Element Mesh - Elements in Outline Mode to Verify No Gaps in Model

```
SWEEP
  TOLERANCE
    0.1
  SWEEP
    NODES
  ALL: EXIST.
  PLOT
    NODES (off)
    CURVES (off)
    DRAW
  RETURN
RETURN
AUTOMESH
  CURVE DIVISIONS
  CLEAR CURVE DIVISION
  ALL: EXIST.
  RETURN
MAIN
```

Step 2: Define shell thickness

The shell has a thickness of 0.1 applied to all elements.

```
GEOMETRIC PROPERTIES
  STRUCTURAL ELEMENTS
    3-D
      SHELL
        THICKNESS
          0.1
        OK
      ELEMENTS ADD
      ALL EXIST.
    MAIN
```

Step 3: Define Material Properties

The shell is made up of steel. It is anticipated that the stress will exceed the yield stress. The workhardening data is entered as a table.

```
MATERIAL PROPERTIES
  MATERIAL PROPERTIES
    TABLES
      NEW
        1 INDEPENDENT VARIABLE
        NAME
          workhardening
        TYPE
          eq_plastic_strain
        FUNCTION VALUE F
          MIN
            20000
          MAX
            30000
        ADD
          0 20000
          0.1 23000
          0.3 25000
          0.6 26000
          1.0 27000
```

MORE

INDEPENT VARIALBE V1

LABEL

Equivalent Plastic Strain

FUNCTION VALUE F

LABEL

Flow Stress

(the flow stress table is shown in [Figure 2.1-16](#))

RETURN

SHOW MODEL (toggle)

RETURN

NEW

STANDARD

STRUCTURAL

YOUNG'S MODULUS

1.e7

POISSON'S RATIO

0.3

PLASTICITY

YIELD STRESS

1.0

TABLE

workhardening

OK (twice)

ELEMENTS ADD

ALL: EXIST.

MAIN

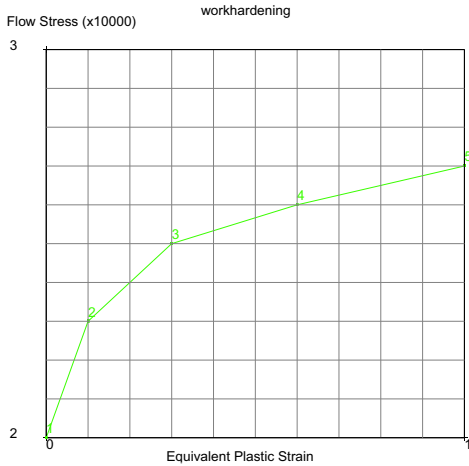


Figure 2.1-16 Flow Stress Table

Step 4: Apply Boundary Conditions

The *Can* has three boundary conditions:

1. The Can is constrained by prescribing a fixed displacements in the z-direction to the bottom surface and clamping the curve at the bottom edge.
2. Applying a nonuniform load to the surface representing the circular slot.
3. Apply a uniform pressure to the spherical cap.

The nonuniform load is applied by defining a bilinear equation, where the independent variables are the time and the x-coordinate position. The load on the dome is ramped up as a function of time.

BOUNDARY CONDITIONS

STRUCTURAL

NAME

no_axial

(axial constraint on surface)

FIXED DISPLACEMENT

DISPLACEMENT Z

0

OK

SURFACES ADD

4 #

(BOTTOM SURFACE)

RETURN

DRAW BOUNDARY CONDS ON MESH

NEW

(clamp condition on curve)

STRUCTURAL

FIXED DISPLACEMENT

DISPLACEMENT X

DISPLACEMENT Y

ROTATION X

ROTATION Y

OK

CURVES ADD

19 21 22 27 #

NEW

NAME

press_in_hole

(pressure in slot)

TABLES

NEW

2 INDEPENDENT VARIABLES

INDEPENDENT VARIABLE V1

TYPE

x0_coordinate

MIN

-4

MAX

4

FUNCTION VALUE F

MAX

4

INDEPENDENT VARIABLE V2

TYPE

time

FORMULA

ENTER

$(4 - \text{abs}(v1)) * v2$

MORE

FUNCTION VALUE F

LABEL

time

INDEPENDENT VARIABLE V1


```

    LABEL
      x-coordinate
    PREVIOUS
    SHOW IDS
      0
    RETURN
    FACE LOAD
    PRESSURE
      800
    TABLE
      table2
    OK
    SURFACES ADD
      1 7 #
    
```

(this function is shown in Figure 2.1-17)

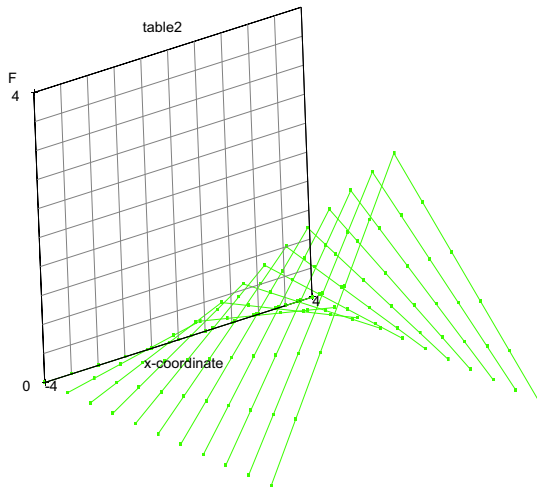


Figure 2.1-17 Table Describing Pressure in Slot

```

    NEW
    NAME
      domeload
    TABLES
    NEW
    INDEPENDENT VARIABLES V1
    
```

(uniform pressure on dome)

```

NAME
    ramp
TYPE
    time
ADD
    0 0
    1 1
RETURN
FACE LOAD
    PRESSURE
        200
    TABLE
        ramp
OK
SURFACES
    2 6 #

```

MAIN

(all of the boundary conditions applied on the geometry are shown in Figure 2.1-18)

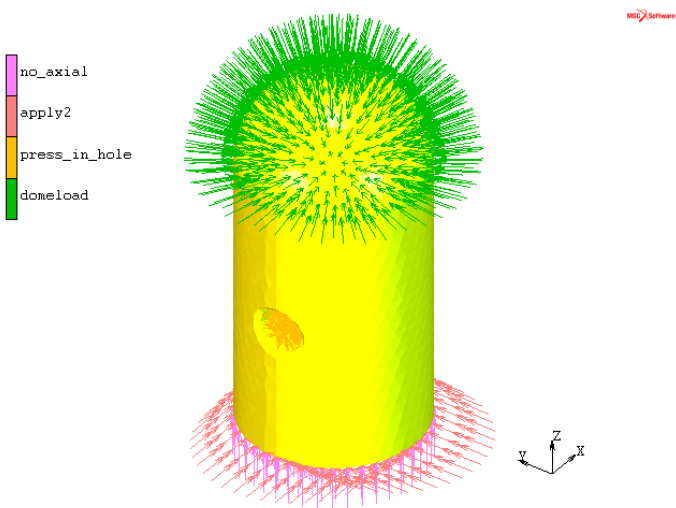


Figure 2.1-18 All Boundary Conditions Shown

Step 5: Create Loadcase

The three boundary conditions are combined into a single loadcase. The adaptive time stepping procedure is used. Because the shell is thin and subjected to an external pressure on the dome, the nonpositive definite flag is activated. All other parameters are default.

```

MAIN MENU
ANALYSIS
  LOADCASES
  ANALYSIS CLASS
    STRUCTURAL
    NEW
    STATIC
  PROPERTIES
    MULTI-CRITERIA
    SOLUTION CONTROL
    NON-POSITIVE DEFINITE
  OK (twice)
MAIN

```

Step 6: Job creation

It is anticipated that the plastic strains may be large in the slot, so the LARGE STRAIN (plastic) option is invoked. Furthermore, the FOLLOWER FORCE option is activated so the pressure load is always based upon the current geometry. The equivalent stress and plastic strains are written to the post file for the outside and middle layer. Using Mentat, the default number of layers is five, so output is obtained for layers 1, 3, and 5. The three-node thin shell element is used in this analysis.

```

MAIN MENU
ANALYSIS
  JOBS
    NEW
    STRUCTURAL
    PROPERTIES
      lcase1 (add loadcase)
        ANALYSIS OPTIONS
          LARGE STRAIN
          FOLLOWER FORCE (toggle)
        OK
    JOB RESULTS
    AVAILABLE ELEMENT SCALARS
      Equivalent Von Mises Stress
    LAYERS
      OUT & MID (toggle)

```

AVAILABLE ELEMENT SCALARS

Total Equivalent Plastic Strain

LAYERS

OUT & MID (toggle)

OK

OK

TITLE

Boundary Conditions on Geometric Entities Driven by Table and Equation

ELEMENT TYPES

STRUCTURAL

3-D SHELL/MEMBRANE

138

OK

ALL: EXIST.

RETURN

RUN

ADVANCED JOB SUBMISSION

WRITE INPUT FILE

EDIT INPUT FILE

OK

SUBMIT

MONITOR

OK

Step 7: Evaluate Results

The objective of the simulation is to examine the plastic strains, the deformations, and the stress in the vicinity of the slot. The satisfaction of the flow stress curve are also verified. Finally, the effectiveness of the adaptive time stepping procedure is examined.

MAIN MENU

POSTPROCESsing

RESULTS

OPEN

table_bc_shell_job1.t16

OK

PLOT

ELEMENTS (on)
 CURVES (off)
 NODES (off)
 POINTS (off)
 SURFACES (off)
 ELEMENTS **SETTING**
 OUTLINE
 FILL
 DRAW

MAIN

CONFIGURATION

VISUALIZATION

LIGHTING (on)
 VIEW 1 (on)

MAIN MENU

POSTPROCESSING

RESULTS

LAST

CONTOUR BANDS

SCALAR

Total Equivalent Plastic Strain Top Layer

OK

SELECT

METHOD

USER BOX

RETURN

ELEMENTS

-10 10
 -0.002 10
 -100 1000

MAKE VISIBLE

RETURN

rotate model using **DYN. MODEL**

DEF ONLY

The equivalent plastic strain is shown in [Figure 2.1-19](#).

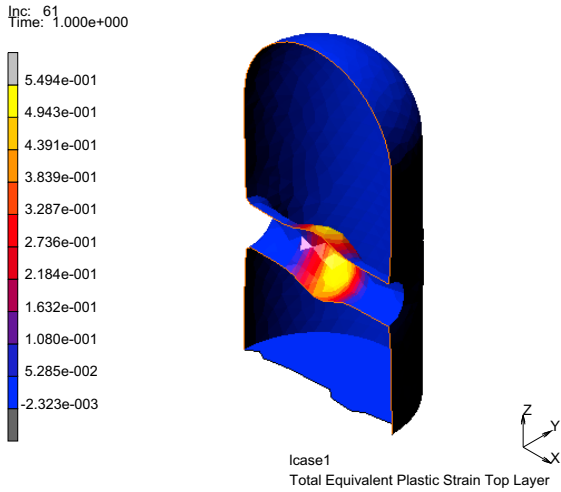


Figure 2.1-19 Equivalent Plastic Strain in Slot

SCALAR
Equivalent Von Mises Stress Top Layer
OK
SELECT
METHOD
SINGLE
RETURN
ELEMENTS
ALL: EXIST.
MAKE VISIBLE
RETURN
PLOT
ELEMENTS SETTINGS
OUTLINE
DRAW
RETURN
RETURN

The equivalent stress is shown in [Figure 2.1-20](#).

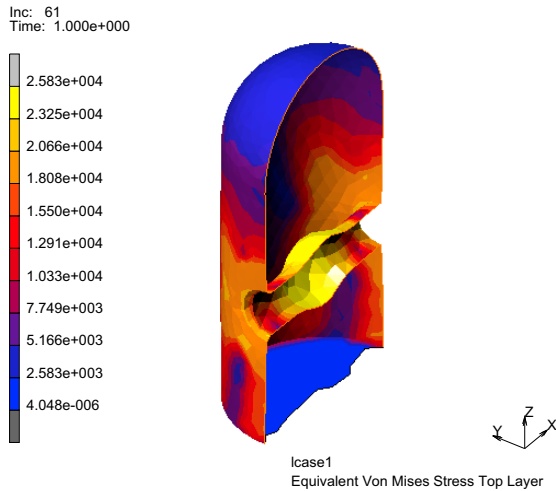


Figure 2.1-20 Equivalent Stress

You can observe that large plastic strain occurs. In examining node 569 located in the center of the slot, the tracking of the yield stress is compared with the defined flow stress. This is shown in [Figure 2.1-21](#).

HISTORY PLOT

SET LOCATIONS

n: 569

(or whatever node is at center of slot)

#

ALL INCS

SHOW IDS

5

LIMITS

MAX X

1

MIN Y

20000

MAX Y

30000

ADD CURVES

ALL LOCATIONS

Total Equivalent Plastic Strain Top Layer

Equivalent von Mises Stress Top Layer

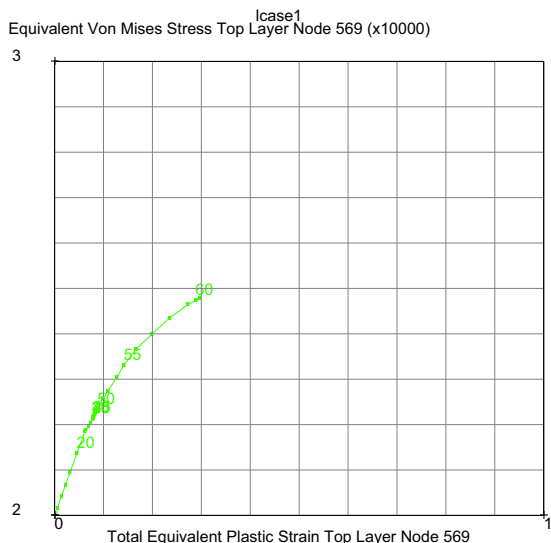


Figure 2.1-21 Stress-Strain Behavior at Node 569

You can observe that the behavior follows the stress-strain law that was defined in Figure 2.1-16. At increment 23, this node unloads elastically, and a few increments later, it reloads.

The next step is to examine the application of the load, this can be done by displaying the history of the time.

- CLEAR CURVES
- RETURN
- ADD CURVES
 - GLOBAL
 - INCREMENT
 - TIME
 - FIT

The result is shown in Figure 2.1-22. The user observes that from increment 20 to 45, there is only a slight increase in the time.

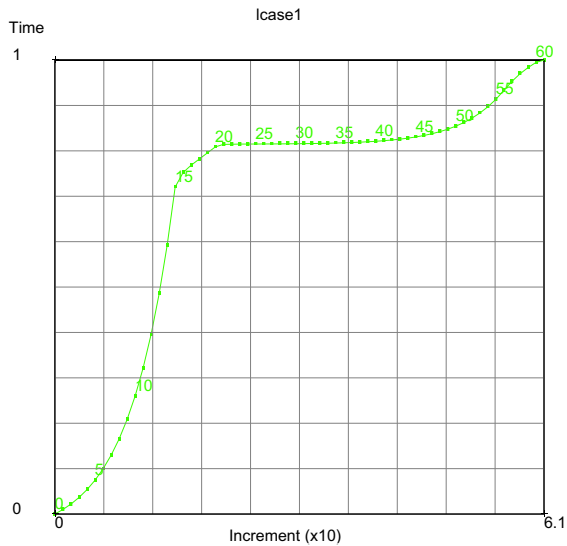


Figure 2.1-22 Time versus Increment Number

Input Files

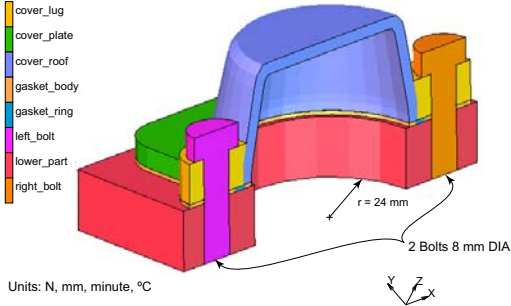
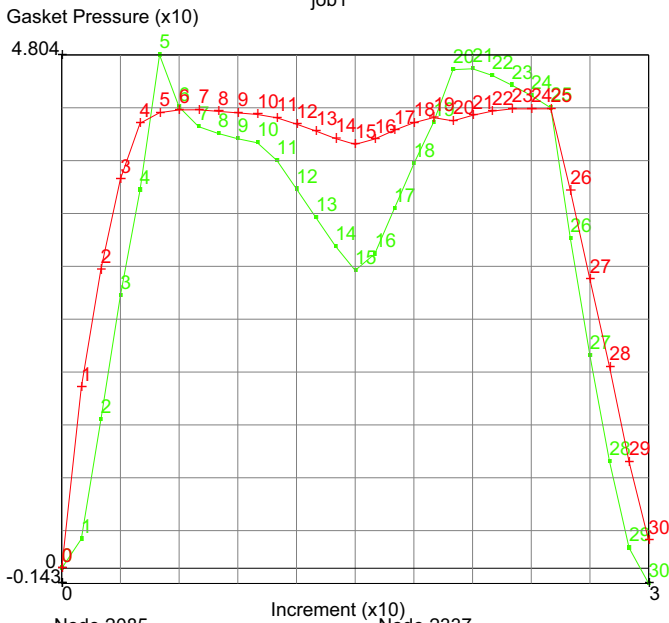
The files below are on your [delivery media](#) or they can be downloaded by your web browser by clicking the links (file names) below.

File	Description
can.proc	Mentat procedure file to run the above example

2.2 Thermo-Mechanical Analysis of Cylinder Head Joint with Quadratic Contact

- Summary 340
- Simulation of a Cylinder Head Joint 342
- Input Files 370

Summary

Title	Thermo-mechanical analysis of a cylinder head																																																																																																
Problem features	Automated mesh splitting for bolt modeling																																																																																																
Geometry	 <p>Legend:</p> <ul style="list-style-type: none"> cover_lug cover_plate cover_roof gasket_body gasket_ring left_bolt lower_part right_bolt <p>Annotations: $r = 24 \text{ mm}$, 2 Bolts 8 mm DIA</p> <p>Units: N, mm, minute, °C</p>																																																																																																
Material properties	Steel and Gasket Material from Chapter 3.17																																																																																																
Analysis type	Thermo-mechanical coupled																																																																																																
Boundary conditions	Fixed block, Bolted head, Pressure head, Temperature history																																																																																																
Element type	Parabolic element types 57, 127, and linear composite brick, 149																																																																																																
FE results	<p>Gasket pressure history</p> <p>job1</p>  <p>Y-axis: Gasket Pressure (x10)</p> <p>X-axis: Increment (x10)</p> <p>Legend:</p> <ul style="list-style-type: none"> Node 2085 (Green line with dots) Node 2337 (Red line with crosses) <table border="1"> <caption>Approximate data points from the Gasket Pressure History graph</caption> <thead> <tr> <th>Increment (x10)</th> <th>Node 2085 Pressure (x10)</th> <th>Node 2337 Pressure (x10)</th> </tr> </thead> <tbody> <tr><td>0</td><td>0</td><td>0</td></tr> <tr><td>1</td><td>0.1</td><td>0.2</td></tr> <tr><td>2</td><td>0.5</td><td>1.0</td></tr> <tr><td>3</td><td>1.5</td><td>2.0</td></tr> <tr><td>4</td><td>3.0</td><td>3.5</td></tr> <tr><td>5</td><td>4.8</td><td>4.0</td></tr> <tr><td>6</td><td>4.5</td><td>4.0</td></tr> <tr><td>7</td><td>4.0</td><td>4.0</td></tr> <tr><td>8</td><td>3.5</td><td>4.0</td></tr> <tr><td>9</td><td>3.0</td><td>4.0</td></tr> <tr><td>10</td><td>2.5</td><td>4.0</td></tr> <tr><td>11</td><td>2.0</td><td>4.0</td></tr> <tr><td>12</td><td>1.5</td><td>4.0</td></tr> <tr><td>13</td><td>1.0</td><td>4.0</td></tr> <tr><td>14</td><td>0.5</td><td>4.0</td></tr> <tr><td>15</td><td>0.0</td><td>4.0</td></tr> <tr><td>16</td><td>0.5</td><td>4.0</td></tr> <tr><td>17</td><td>1.5</td><td>4.0</td></tr> <tr><td>18</td><td>2.5</td><td>4.0</td></tr> <tr><td>19</td><td>3.5</td><td>4.0</td></tr> <tr><td>20</td><td>4.5</td><td>4.0</td></tr> <tr><td>21</td><td>4.8</td><td>4.0</td></tr> <tr><td>22</td><td>4.5</td><td>4.0</td></tr> <tr><td>23</td><td>4.0</td><td>4.0</td></tr> <tr><td>24</td><td>3.5</td><td>4.0</td></tr> <tr><td>25</td><td>3.0</td><td>4.0</td></tr> <tr><td>26</td><td>2.0</td><td>3.5</td></tr> <tr><td>27</td><td>1.0</td><td>2.5</td></tr> <tr><td>28</td><td>0.5</td><td>1.5</td></tr> <tr><td>29</td><td>0.1</td><td>0.5</td></tr> <tr><td>30</td><td>0</td><td>0</td></tr> </tbody> </table>	Increment (x10)	Node 2085 Pressure (x10)	Node 2337 Pressure (x10)	0	0	0	1	0.1	0.2	2	0.5	1.0	3	1.5	2.0	4	3.0	3.5	5	4.8	4.0	6	4.5	4.0	7	4.0	4.0	8	3.5	4.0	9	3.0	4.0	10	2.5	4.0	11	2.0	4.0	12	1.5	4.0	13	1.0	4.0	14	0.5	4.0	15	0.0	4.0	16	0.5	4.0	17	1.5	4.0	18	2.5	4.0	19	3.5	4.0	20	4.5	4.0	21	4.8	4.0	22	4.5	4.0	23	4.0	4.0	24	3.5	4.0	25	3.0	4.0	26	2.0	3.5	27	1.0	2.5	28	0.5	1.5	29	0.1	0.5	30	0	0
Increment (x10)	Node 2085 Pressure (x10)	Node 2337 Pressure (x10)																																																																																															
0	0	0																																																																																															
1	0.1	0.2																																																																																															
2	0.5	1.0																																																																																															
3	1.5	2.0																																																																																															
4	3.0	3.5																																																																																															
5	4.8	4.0																																																																																															
6	4.5	4.0																																																																																															
7	4.0	4.0																																																																																															
8	3.5	4.0																																																																																															
9	3.0	4.0																																																																																															
10	2.5	4.0																																																																																															
11	2.0	4.0																																																																																															
12	1.5	4.0																																																																																															
13	1.0	4.0																																																																																															
14	0.5	4.0																																																																																															
15	0.0	4.0																																																																																															
16	0.5	4.0																																																																																															
17	1.5	4.0																																																																																															
18	2.5	4.0																																																																																															
19	3.5	4.0																																																																																															
20	4.5	4.0																																																																																															
21	4.8	4.0																																																																																															
22	4.5	4.0																																																																																															
23	4.0	4.0																																																																																															
24	3.5	4.0																																																																																															
25	3.0	4.0																																																																																															
26	2.0	3.5																																																																																															
27	1.0	2.5																																																																																															
28	0.5	1.5																																																																																															
29	0.1	0.5																																																																																															
30	0	0																																																																																															

This chapter introduces a number of new features in Marc and Mentat in the area of engine modeling:

- A new tying type called *overclosure tying*, for prestressing structures like bolts and rivets. The new tying combines and generalizes the tying and servo link that have traditionally been used in Marc for this purpose (see, for example, Chapter 3.17 of this *Marc User's Guide*) and can be used in combination with the automatic contact algorithm.
- New tools for automated mesh splitting and tying generation in Mentat, that allow fast and easy set up of bolt models.
- Improvements made to the automatic contact algorithm in the way user-coordinate transformations are treated. It is now possible to define coordinate transformation for nodes that come in contact.
- The possibility to run a job in parallel using a single input file without the need for a preprocessor to generate the domains and split the model data into input files for each domain.
- Improvements made to Mentat in terms of visualization of the local directions of coordinate transformations defined at the nodes and of the thickness direction of gaskets and composite solid elements.

For this purpose, a described analysis of a cylinder head joint in Chapter 3.17 of this *Marc User's Guide* is suitably modified. In brief, the modifications involve the following:

change to the shape of the cylinder head cover
 change from linear elements to quadratic elements for some components of the cylinder head joint
 change from mechanical analysis to thermo-mechanically coupled analysis
 incorporation of temperature dependence for gasket properties
 addition of thermal loading
 incorporation of the new way of modeling bolt preload.

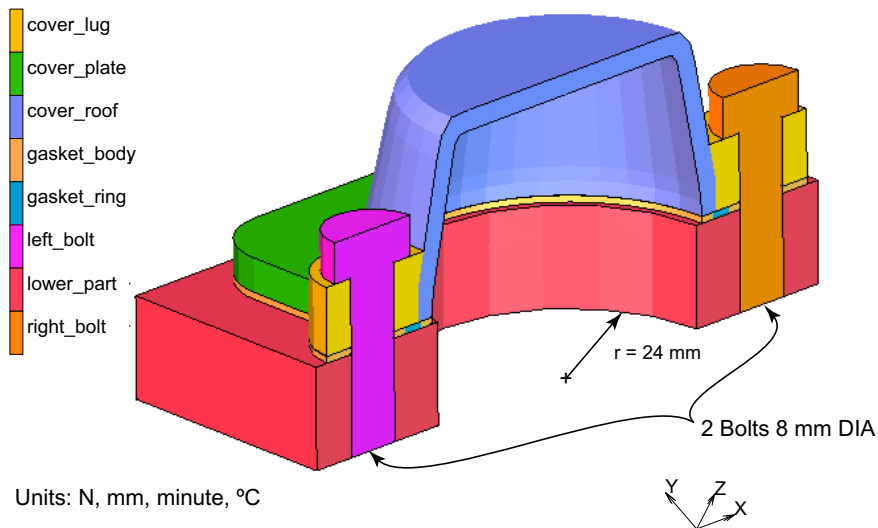


Figure 2.2-1 Finite Element Mesh of the Cylinder Head Joint

Simulation of a Cylinder Head Joint

The model consists of the cylinder head cover and a small portion of the lower part of the cylinder head (see [Figure 2.2-1](#)). Both the cover and the lower part are made of steel. A thin gasket layer seals the joint between the cover and the lower part. The joint is fastened by two steel bolts.

The assembly is loaded in six stages. In the first two stages, the fastening of the joint is simulated by applying a pretension of 12 kN to each of the bolts. After the bolts have been loaded, the three-stage thermo-mechanical loading cycle starts. First, the base of the assembly is heated to 200°C, while an interior pressure of 1.2 MPa is simultaneously applied to the cover and the lower part of the assembly. Next, the base is cooled down to -20°C, while retaining the interior pressure. In the fifth stage, the pressure is removed and the temperature of the base is increased again to room temperature of 20°C. The final loadcase of the analysis consists of disassembling the joint by loosening the bolts.

Mesh

The finite element mesh used in this chapter is somewhat different from that used in [Chapter 3.17](#). The changes are highlighted here:

- The shape of the engine head cover has been cosmetically changed from a spherical to a cylindrical shape and meshed with 20-noded hexahedral elements.
- To demonstrate the use of the new overclosure tyings in combination with the automatic contact algorithm, the radius of the lugs has been reduced such that the bolts fit exactly into the lugs.
- The bolts are meshed with 20-noded hexahedral elements.
- The lower part of the assembly has been meshed with 10-noded tetrahedral elements.
- To demonstrate the use of coordinate transformations for prestressing the bolts and to show that transformations can be used on nodes that come into contact, the entire model has been rotated about -30° around the global x -axis.

The base model obtained after meshing of the different components is available in *thermogask_mesh.mud*. Suitable element sets like `gasket`, `cover`, `bolts`, `lower_part` have already been identified in this file. A procedure file that then reads in this file and incorporates the other changes mentioned below is available in *thermogask.proc*. The user is also referred to the comments in the procedure file for more details.

Geometric Properties

The gasket used in this example is modeled as a flat sheet with a thickness of one millimeter and consists of two regions with different material properties: the body and the ring (see [Figure 2.2-2](#)). For the gasket material, the behavior in the thickness direction, the transverse shear behavior, and the membrane behavior are fully uncoupled. The thickness direction of the gasket elements must be specified by means of a geometric property of type 3-D SOLID COMPOSITE/GASKET. The finite element mesh of the gasket has been created in such a way that for all elements in the gasket, the thickness direction is given by the direction from FACE 4 (1-2-3-4) to FACE 5 (5-6-7-8). In this model, the two sides of the gasket actually have different orientations. This is not significant here because a gasket element has only one layer (integration point) through the thickness. If the model was composed of composite brick elements with multiple layers, this would be important.

Mentat has introduced the possibility to visualize the thickness direction of solid composite and gasket elements via the SOLID COMP./GASKET PLOT SETTINGS menu. The latter can be accessed both from the various GEOMETRIC PROPERTIES menus and from the PLOT-> ELEMENT SETTINGS menu. If switched on, an arrow is drawn that points from the bottom face of the solid composite or gasket element to the top face of the element. Note that visualization of the thickness direction is available only if the elements are drawn in wireframe mode. The picture on the right-hand side of Figure 2.2-2 depicts the thickness directions for some of the gasket elements in the present model.

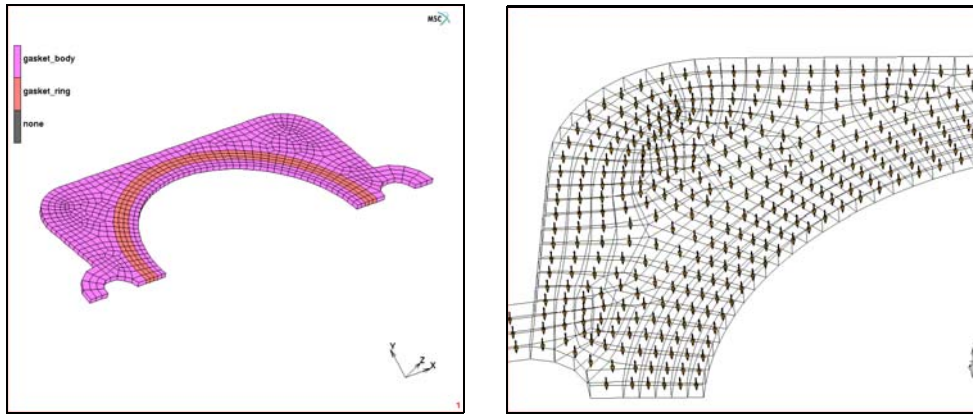


Figure 2.2-2 The Finite Element Mesh of the Gasket and Thickness Direction of the Gasket Elements

Note: The arrows indicating the thickness direction point from the bottom face to the top face of the elements.

Material Properties

Details for temperature independent gasket properties are available in Chapter 3.17. The incorporation of thermal dependence in the gasket behavior is emphasized in this section.

As already mentioned in the preceding section, for the gasket material, the behavior in the thickness direction, the transverse shear behavior, and the membrane behavior are fully uncoupled. The transverse shear and membrane behavior are linear elastic, characterized by a transverse shear modulus and the in-plane Young's modulus and Poisson's ratio, respectively. In the thickness direction, the behavior in tension is also linear elastic and is governed by a tensile modulus, defined as a pressure per unit length. All the moduli used to characterize the in-plane membrane, transverse shear, and tensile behavior can be varied with temperature using single variate tables.

Thickness Direction Gasket Properties

For elastic-plastic compressive behavior in the thickness direction, the user specifies the loading path, the yield pressure above which plastic deformation develops and up to ten unloading paths. Mandatory pressure-closure relationships can be directly input for specifying the loading and unloading paths. Additionally, optional pressure-temperature relationships can be simultaneously input for these paths. Pressure varying as a function of both closure distance and temperature is input using the Multi-Variate table capability in Mentat. A table varying as a function of temperature can be specified for the yield stress. While specifying the loading path, unloading paths, and yield pressure as a function of temperature, care should be exercised that the yield pressure at a particular temperature

should intersect the loading curve at that temperature, and that the unloading curve at a particular temperature should intersect the loading curve at that temperature.

The structural element types that are used to model the mechanical aspects of the gasket material are 149 (3-D solid), 151 (plane strain) and 152 (axisymmetric). The associated heat transfer element types that are used to model thermal aspects of the gasket material are 175 (3-D solid), 177 (planar) and 178 (axisymmetric). The heat transfer properties of the gasket are specified through the mass density, isotropic thermal conductivity and specific heat which can also be varied with temperature.

As mentioned earlier, the gasket used in this example is modeled as a flat sheet with a thickness of one millimeter and consists of two regions with different material properties, the body and the ring (see [Figure 2.2-2](#)). For both regions, the data of the loading path and one unloading path are created using Multi-Variate Tables in Mentat. The variation of the data with temperature is assumed in a simple form. The temperature is considered to vary between -20°C and 200°C. For the ring portion of the gasket, the pressure reduces by 10% over this temperature range, while for the body portion of the gasket, the pressure reduces by 20%.

The creation of a typical multi-variate table for the pressure-closure-temperature relationship is described. The table consists of two independent variables and one dependent variable. The two independent variables are closure distance and temperature, respectively; while the dependent variable (referred to as function in Mentat) is pressure. The closure distance varies from 0.0 to 0.175, the temperature varies from -20°C to 200°C. It is further assumed that the pressure values reduce by 10% over this temperature range. The creation of such a multi-variate table can be handled using one of two available procedures.

The first procedure is to create two single-variate tables and then use the MULTIPLY TABLE option in Mentat to create a third multi-variate table. Note that this procedure is only feasible when $F(V1,V2)$ can be written as $F(V1,V2) = G(V1)H(V2)$. The single-variate tables, $G(V1)$ and $H(V2)$, can be created by reading in an existing file or by adding data points or by entering a formula.

```

FILES
  OPEN
    thermogask_mesh.mud
  SAVE AS
    new
  OK
MAIN
MATERIAL PROPERTIES
  MATERIAL PROPERTIES
    TABLES
      NEW
        1 INDEPENDENT VARIABLE
      TYPE
        temperature
    ADD
  
```



```

-20 1.0
200 0.9
FIT
NAME
    body_temp
READ
    RAW
        ch02_body_loading.raw
    OK
TYPE
    gasket_closure_distance
MULTIPLY TABLE
    body_temp
NAME
    gasket_body_loading

```

The table `gasket_body_loading` is a two variate table obtained by multiplying the current table which has `gasket_closure_distance` as its independent variable with `body_temp` which has temperature as its independent variable.

The second procedure is to create the two-variate table directly. This procedure is more general than the first procedure since it allows values of the independent variables $V1$, $V2$ and the corresponding function values $F(V1,V2)$ to be entered directly. This is accessed by clicking on the **ADD ALL POINTS** button in Mentat and answering a number of questions at the command prompt. These questions pertain to the number of data points for $V1$, number of data points for $V2$, the numerical values of $V1$, the numerical values of $V2$, and finally the values of $F(V1,V2)$.

```

NEW
    2 INDEPENDENT VARIABLES
INDEPENDENT VARIABLE V1
    TYPE
        gasket_closure_distance
INDEPENDENT VARIABLE V2
    TYPE
        temperature
ADD ALL POINTS
    7
    2
    0.0 0.027 0.054 0.081 0.108 0.135 0.175

```

```
-20.0 200.0  
0.0 2.08 8.32 18.72 33.28 52.0 56.0  
0.0 1.872 7.488 16.848 29.952 46.8 50.4  
FIT  
NAME  
gasket_body_loading
```

Note that if any errors are made while entering the data during the second procedure, there is no chance to immediately correct it. The best technique is to continue entering the rest of the requested information and correct the function values afterwards using the EDIT command.

The above commands illustrate how the 2-variate table `gasket_body_loading` can be created in Mentat. In a similar manner, other 2-variate tables `gasket_body_unloading`, `gasket_ring_loading`, `gasket_ring_unloading` are created.

In certain situations, data may only be available over a limited range of values. In those situations, for independent variable values that are beyond the data provided, the user can instruct the program if the function values in the table should be extrapolated or kept constant when creating a table with Mentat, the default is that extrapolation will be performed. For example, if the gasket pressure needs to be obtained via extrapolation for temperature values not given in the table, this would be set up as:

```
TABLES  
EDIT  
gasket_body_loading  
MORE  
INDEPENDENT VARIABLE V2  
EXTRAPOLATE  
RETURN  
READ  
ch02_gasket_body_unloading  
TYPE  
gasket_closure_distance  
NAME  
ch02_gasket_body_unloading  
READ  
ring_loading  
TYPE  
gasket_closure_distance  
NAME
```

```

    ring_loading
READ
    ring_unloading
TYPE
    gasket_closure_distance
NAME
    ring_unloading
RETURN

```

Temperature dependent yield pressure, tensile modulus, and transverse shear modulus for the body and ring regions are specified through appropriate single variate tables, `body_temp` and `ring_temp`, respectively. For the body, these moduli are reduced by 10% over the temperature range of (-20°C, 200°C), and for the ring, they are reduced by 20%.

Membrane/Thermal Gasket Properties

For mechanical membrane properties and thermal properties, the GASKET material refers to an existing isotropic material. Temperature dependence of these properties can also be specified through appropriate tables for the isotropic material.

In the present example, no temperature dependence of the membrane/thermal properties is considered. The mechanical properties are taken to be the same as those in Chapter 3.17. For the thermal properties, the gasket is intended to behave as an insulator and the properties assumed herein are consistent with those for a hard type of rubber. The units for the thermal quantities are consistent with those for the mechanical quantities: N for force, mm for length, minute for time, and °C for temperature.

```

ANALYSIS CLASS
  COUPLED
    NEW
    STANDARD
    STRUCTURAL
      YOUNG'S MODULUS
        120 (N/mm2)
      THERMAL EXP. (twice)
        ALPHA
          5e-5 (1/°C)
        OK
      OK
    THERMAL
      K
        6.5378

```

SPECIFIC HEAT

9.79056E12

MASS DENSITY THERMAL

VALUE

1.15689E-13

OK

NAME

gasket_body_membrane

NEW

STANDARD

STRUCTURAL

YOUNG'S MODULUS

100

THERMAL EXP. (twice)

ALPHA

1e-4

OK

OK

THERMAL

K

6.5378

SPECIFIC HEAT

9.79056E12

MASS DENSITY THERMAL

VALUE

1.15689E-13

OK

NAME

gasket_ring_membrane

Gasket Material Specification

After defining appropriate tables for the through thickness behavior and defining an isotropic material for the membrane/thermal behavior, all this information is jointly specified for the body and ring regions of the gasket as follows:

```
NEW GASKET
STRUCTURAL
  YIELD PRESSURE
    52
  TABLE
    body_temp
  TENSILE MODULUS
    72
  TABLE
    body_temp
  INITIAL GAP
    1/11
  LOADING PATH TABLE
    gasket_body_loading
  UNLOADING PATHS TABLE 1
    gasket_body_unloading
  TRANSVERSE SHEAR BEHAVIOR MODULUS
    40
  TABLE
    body_temp
  OK
  GENERAL
  BASE MATERIAL
    gasket_body_membrane
  OK
  ELEMENTS ADD
  SET
    gasket_body
  OK
  NAME
    gasket_body
NEW GASKET
```

```

STRUCTURAL
  YIELD PRESSURE
    42
  TABLE
    body_temp
  TENSILE MODULUS
    64
  TABLE
    body_temp
  LOADING PATH TABLE
    ring_loading
  UNLOADING PATHS TABLE
    ring_unloading
  TRANSVERSE SHEAR BEHAVIOR MODULUS
    35
  TABLE
    body_temp
  OK
  GENERAL
  BASE MATERIAL
    gasket_ring_membrane
  OK
  ELEMENTS ADD
  SET
    gasket_ring
  NAME
    gasket_ring

```

Material Specification for Other Components

The cylinder head cover, the lower part, and the bolts are all made of steel. No temperature dependence is considered for the mechanical quantities. For thermal properties, the thermal conductivity is varied with temperature. A table `cond_steel` is specified for the steel with the following values: (-20,830), (0,830), (100,965), (200,1053) where the first value represents the temperature and the second value represents the thermal conductivity.

```

NEW
STANDARD
STRUCTURAL

```

YOUNG'S MODULUS

2.1e5

(N/mm^2)

POISSON'S RATIO

0.3

THERMAL EXP. (twice)

ALPHA

1.5e-5

($1/^\circ C$)

OK

OK

THERMAL

K

1

SPECIFIC HEAT

1.65686E+12

MASS DENSITY THERMAL

VALUE

2.17139E-12

OK

ELEMENTS ADD

SET

cover

lower_part

bolts

NAME

steel

MAIN

Modeling Tools

Transformations

As mentioned before, compared to the model from Chapter 3.17, the present model is rotated about -30° around the global x -axis. To make sure that boundary conditions are applied correctly, a local coordinate system is defined by creating a transformation. The orientation of the local coordinate system is obtained by rotating the global coordinate system about -30° around the global x -axis:

```
MODELING TOOLS
  TRANSFORMATIONS
    NEW
    ROTATE
      -30 0 0
    SELECT
      SELECT SETS
        bolts
        lower_part
      OK
    SELECT BY
      NODES BY
        ELEMENTS
      ALL: SELECTED
    RETURN
  RETURN
  NODES ADD
    ALL:SELECTED
```

The local z -direction of this coordinate system thus coincides with the axial direction of the bolts and the local x -direction with the global x -direction. Several nodes, including all nodes at the base of the lower part and the bolts are added to this transformation, so that boundary conditions applied to these nodes will act in the local x -, y - and z -directions.

Transformations are allowed for any nodes including the ones coming in contact.

Mentat has introduced the possibility to visualize the local coordinate directions of the coordinate systems at the nodes via the TRANSFORMATION PLOT SETTINGS menu. The latter can be accessed both from the TRANSFORMATIONS menu and from the PLOT-> NODE SETTINGS menu. If transformations are drawn, the local coordinate systems are indicated by three arrows, pointing from the node in the direction of the local x -, y - and z -axis. To distinguish the directions, the local x -direction is indicated by a red arrow, the local y -direction by a green arrow and the local z -direction by a blue arrow. Plotting of each of these arrows can be controlled individually by the FIRST, SECOND,

and THIRD DIRECTION buttons in the TRANSFORMATION PLOT SETTINGS menu. Note that transformation are displayed only if the nodes are drawn. Figure 2.2-3 depicts the local coordinate systems of the nodes at the base of the lower part of the model.

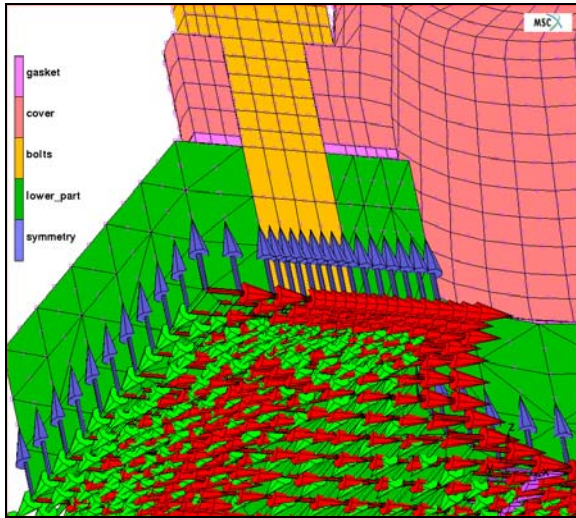


Figure 2.2-3 The Local Coordinate Systems of the Nodes at the Base of the Lower Part Defined by the Transformation

Matching Boundaries and Overclosure Tyings – Bolt Modeling

As mentioned earlier, in the first two stages of the analysis, the fastening of the joint is simulated by applying pretension loads of 12 kN to each of the bolts. In the first stage, the left bolt (see Figure 2.2-1) is pretensioned while the right bolt is locked, and in the second stage, the right bolt is loaded while the length of the left bolt is fixed. During the subsequent three-stage thermo-mechanical loading cycle, the bolts will be locked and in the final stage of the analysis, the joint will be disassembled by loosening the bolts.

The pretension force in the bolt is simulated using the standard TYING option existing in Marc. The basic idea is that the finite element mesh of the bolt is split across the shaft of the bolt in two disjoint parts with congruent meshes at the split and that corresponding nodes on both sides of the split are connected to each other and to a special node, called the *control node* of the bolt, by multi-point constraints (see Figure 2.2-4). The latter are used to create an overlap between the two parts of the bolt in the axial direction and in this way introduce a tensile stress in the bolt.

In Chapter 3.17, the finite element meshes of the bolts are split up into a top and a bottom part during the mesh generation process. A combination of tyings of type 203 (to prevent relative tangential motion of the two parts) and servo links is used to pretension the bolts. The servo links are chosen in such a way that a pretension force can be applied to the bolt simply by applying a POINT LOAD boundary condition to the control node of the bolt. Alternatively, the bolt can be tightened, locked or loosened by applying a FIXED DISPLACEMENT boundary condition to the control node.

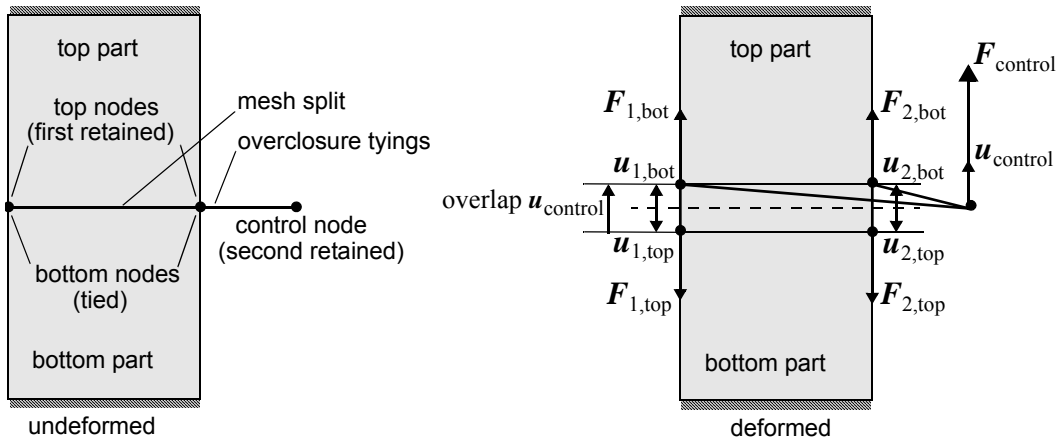


Figure 2.2-4 Pre-stressing a Structure by Creating an Overlap Between the Top and the Bottom Part using Overclosure Tyings

Mentat provides tools for automatically splitting a continuous finite element mesh along a list of edges (in 2-D) or faces (in 3-D). The new boundaries on both sides of the split, that are created in this process, are stored pair-wise along with the rest of the model in the *mud* or *mfd* file. This so-called *matching boundary information* can subsequently be used to automatically generate tyings, servo links, or springs between the corresponding nodes on both sides of the split. This greatly speeds up the modeling process, as no special measures have to be taken during the meshing phase. A bolt can simply be modeled by a continuous finite element mesh that is subsequently split up in two parts which are then connected by multi-point constraints.

In addition, a new tying type that combines and generalizes the tying type 203 and the servo link used in Chapter 3.17. The new type (69) is called *overclosure tying* and has one tied node and two retained nodes. Like the servo links, overclosure tyings should be applied in such a way that the tied node and the first retained node of the tyings are the corresponding nodes at the split. The second retained node of the tyings should be a fixed external node which is shared by all tyings of a bolt. This node is also called the *control node* of the tying, since it can be used to control the size of the gap or overlap between the parts:

1. The displacement of the control node in a particular direction is equal to the size of the gap or overlap in that direction; and
2. The force on the control node is equal to the sum of the forces on the tied nodes of all overclosure tyings which share that control node. It is equal (but with opposite sign) to the sum of the forces on the first retained nodes of the overclosure tyings.

The tying is functionally equivalent to n servo links of the form used in Chapter 3.17, on the n displacement and rotational degrees of freedom of the nodes of the bolt and the control node. The important differences with the approach of Chapter 3.17 are:

1. The overclosure tying always acts on the displacement and rotation components in the **global** coordinate system, while the tying type 203 and the servo link act on the components in the **local** coordinate systems of the nodes (if a coordinate transformation has been defined); and

2. The control node of an overclosure tying has the same displacement and rotational degrees of freedom as the nodes of the bolt, while the control node in Chapter 3.17 has only one degree of freedom.

The latter implies that sufficient boundary conditions have to be applied to the control node of overclosure tyings to suppress any rigid body modes.

The advantages of the new tying type over the servo link approach are twofold. First of all, only a single tying needs to be created between corresponding nodes on both sides of the split instead of a tying **and** a servo link. Secondly, the bolt can be loaded in any direction or combination of directions by applying FIXED DISPLACEMENT or POINT LOAD boundary conditions to the control node in the appropriate directions. If the loading is not parallel to one of the global coordinate directions (for example, because the bolt is not aligned with one of the global axes, as in the present model), a coordinate transformation can be defined at the control node, such that one of the local directions coincides with the loading direction. By contrast, the bolts of Chapter 3.17 can be loaded in one direction only and coordinate transformations are needed on all nodes of the split to ensure that the pretension is applied in the correct direction.

In nonmechanical passes of a coupled analysis (e.g., in the heat transfer pass of a thermo-mechanical analysis), the overclosure tying reduces to tying type 100 between the tied and the first retained node, thus ensuring continuity of the primary field variable (e.g., temperature) cross the split.

Overclosure tyings can be used in combination with the automatic contact algorithm; that is, nodes at the surface of the same contact body can be connected by overclosure tyings. Since constraints imposed by contact can potentially conflict with the constraint imposed by the tying, the tied nodes of these tyings cannot come into contact, so the contact status of the tied nodes is always 0. However, this will not lead to penetration of these nodes, as they are fully tied to the retained nodes via the tying. For more details about the overclosure tyings, please refer to Chapter 9 in *Marc Volume A: Theory and User Information*.

Assuming that a continuous finite element mesh has been created, the general procedure for pretensioning a bolt is as follows:

1. Create a new pair of matching boundaries of the appropriate dimension (1-D for meshes consisting of beam, truss, or axisymmetric shell elements; 2-D for meshes consisting of 2-D solid and 3-D shell elements; 3-D for meshes consisting of 3-D solid elements) and split the finite element mesh of the bolt in two parts using one of the automatic mesh splitting methods.
2. Use the matching boundary information to connect each pair of corresponding nodes on the matching boundaries to each other and to a common control node, using the MATCHING BOUNDARY NODAL TIES submenu of the MATCHING BOUNDARIES menu.
3. Apply POINT LOAD and/or FIXED DISPLACEMENT boundary conditions to the control node of the overclosure tyings to apply the pretension force to the bolt or to prescribe the tightening (change) of the bolt.

In the present example, two 3-D matching boundaries are created (one for each bolt) and the PLANE method is employed to automatically split the meshes of the bolts across the shaft (please refer to the Mentat online help of the MATCHING BOUNDARIES menu for the other available methods). The latter splits the mesh along a list of faces by disconnecting the elements on one side of a plane from the elements on the other side. The plane is defined by a normal vector and a node. In this case, the normal vector to the plane is the axial direction of the bolts or the local z-direction of the previously defined transformation. The normal vector can be supplied either by providing its components with respect to the global coordinate system or by clicking two nodes on the axis of the bolt using the FROM/TO method.

In this case, the former method is employed, and the `dsin` and `dcos` functions (which return, respectively, the sine and cosine of an angle specified in degrees) are used to specify the global y- and z-components of the vector:

MODELING TOOLS

MATCHING BOUNDARIES

NEW

3-D (3-D SOLID)

AUTOMATIC MESH SPLITTING METHOD: PLANE

NORMAL

0 `dsin(30)` `dcos(30)`

SPLIT MESH

9916

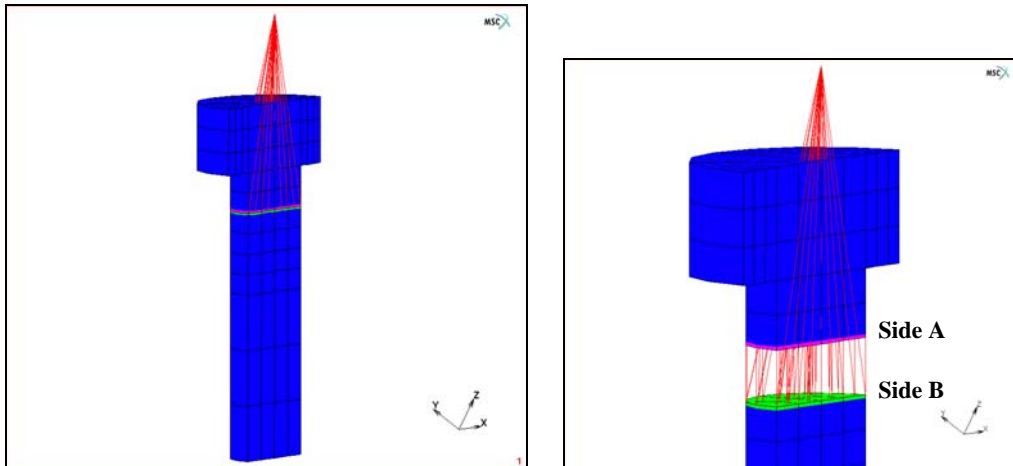


Figure 2.2-5 Bolts Split up into a Top and Bottom Parts with Matching Boundaries Connected by Overclosure Tyings

The matching boundary information generated by the mesh splitting process is displayed graphically by drawing the faces at the boundaries thicker than usual and using different colors to distinguish the faces on the side of the positive normal to the plane, referred to as “side A”, from those on the opposite side of the plane, “side B” (see [Figure 2.2-5](#)). By default, the faces on side A are drawn in magenta and the faces on side B in green.

The matching boundary information is used to connect corresponding nodes on both boundaries to each other and to a common control node by overclosure tyings using the **MATCHING BOUNDARY NODAL TIES** menu. The **ADD NODE** submenu is employed to create the control node and to add it to the previously created transformation, so that the local z-direction of the control node coincides with the axial direction of the bolt:

```
NODAL TIES CREATE
  ADD NODE
    ADD
      -36.05 40*d sin(30) 40*d cos(30)
    TRANSFORMATIONS
      NODES ADD
        11049
      RETURN
    RETURN
```

The overclosure tyings are created by selecting the new node as the second retained of the tyings to be generated and clicking the CREATE TIES button:

```
RETAINED: NODE 2
  NODE
    11049
  CREATE TIES
```

This generates for each pair of corresponding nodes on the matching boundaries a separate tying (see [Figure 2.2-5](#)). The way in which these tyings are created can be controlled by the user. The default settings (the tied node in each tying is the node on side B, the first retained node is the corresponding node on side A, and the second node is a fixed external node) are such that a force applied to the control node in the direction of the positive normal to the plane used to create the split results in an overlap of the two parts in that direction, and hence, in a tensile stress in the bolt in that direction.

Contact

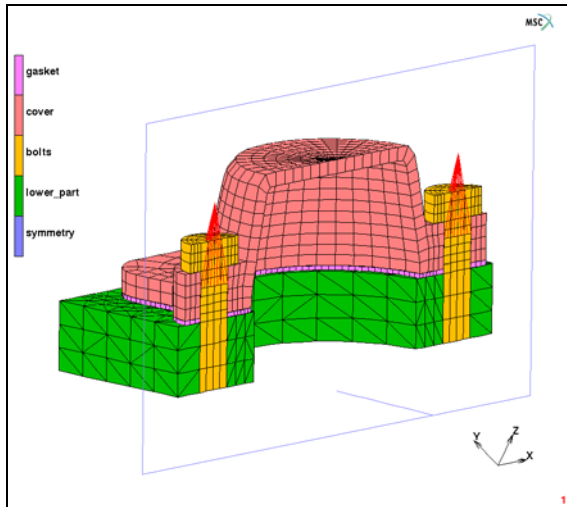


Figure 2.2-6 Contact Body Definition for Joint Assembly

The automatic contact algorithm is used to describe the contact between the gasket and the metal parts of the joint and between the bolts and the cylinder head cover. Moreover, a contact symmetry surface is used to take symmetry conditions into account.

The definition of the various contact bodies is shown in [Figure 2.2-6](#). The first contact body consists of the HEX8 gasket elements. The second contact body consists of the HEX20 cover elements. The third contact body consists of the HEX20 bolt elements. Note that some nodes on the surface of this body are connected by overclosure tyings and recall from the preceding section that this is allowed. The fourth contact body consists of the TET10 lower part elements. The last contact body is the symmetry plane. Note that the nodes at the base of the bolts and the lower part have a local coordinate system defined by the transformation. Some of these nodes will be in contact with the symmetry plane or (for the nodes of the bolt) with the lower part.

The gasket is glued to the cover and lower part and is not allowed to separate. Normal touching contact is used between the gasket and the bolts and between the cover and bolts. Glued contact is used between the bolts and lower part. Also, a contact heat transfer coefficient of 10 N/mm/min/°C is used for any metal-metal contact and a contact heat transfer coefficient of 0.5 N/mm/min/°C is used for any gasket-metal contact. A CONTACT TABLE is created to activate these options.

```

CONTACT
  CONTACT TABLES
    NEW
  PROPERTIES
    1 2
    CONTACT TYPE: GLUE
  
```

```

THERMAL PROPERTIES
  CONTACT HEAT TRANSFER COEFFICIENT
    0.5
13
  CONTACT TYPE: TOUCHING
  CONTACT HEAT TRANSFER COEFFICIENT
    0.5
14
  CONTACT TYPE: GLUE
  CONTACT HEAT TRANSFER COEFFICIENT
    0.5
15
  CONTACT TYPE: TOUCHING
23
  CONTACT TYPE: TOUCHING
  CONTACT HEAT TRANSFER COEFFICIENT
    10.0
25
  CONTACT TYPE: TOUCHING
34
  CONTACT TYPE: GLUE
  CONTACT HEAT TRANSFER COEFFICIENT
    10.0
35
  CONTACT TYPE: TOUCHING
45
  CONTACT TYPE: TOUCHING

```

Initial Conditions

The temperature of the model is initialized to 20°C (room-temperature) by means of a TEMPERATURE initial condition.

```

INITIAL CONDITIONS
  THERMAL
    NEW
    TEMPERATURE

```

```
CONTINUUM ELEMENTS TEMPERATURE                                (yellow light comes on)
    20
    OK
    NODES ADD
    ALL: EXIST.
    NAME
    initial_temperature
```

Boundary Conditions

The boundary conditions applied in this model are similar to those applied in Chapter 3.17. The main difference is in the time variation of the loading. Since the current analysis is modeled as a transient thermal coupled with a static mechanical analysis, time is a physical quantity and any time variations for the loading need to be physically based. Time is expressed in *minutes* in the current analysis.

Recall that the control nodes of the bolts have the same degrees of freedom (three) as the nodes of the bolt. The displacements of the control nodes in the local z-direction of these nodes (the axial direction of the bolts) are equal to the amount of overlap between the top and bottom parts of the bolts in this direction, and hence equal to amount of tightening of the bolts. The displacements in the local x- and y-direction represent the relative tangential motion of the two parts. Throughout the analysis, the latter is suppressed by applying FIXED DISPLACEMENT boundary conditions to the control nodes, of which the second and third degree of freedom are fixed to 0 mm.

Two POINT LOAD boundary conditions are used to load the bolts with a pretension of 12 kN. The time duration for each of these pretensioning events is taken as 1 minute. Since only half of the bolts is taken into account in the model, half of the pretension load is applied to the control nodes of the bolts. The loads are applied to the third degree of freedom of the control nodes. Tables are used to define the loading history of both bolts.

In the first loadcase, when the left bolt is preloaded, the right bolt is unlocked and unloaded and can, therefore, freely shorten or lengthen. As this may introduce a rigid body mode of the top part of the bolt, the latter is pushed onto the cover by applying a small force of 1 N in the axial direction of the bolt. This force is removed again in the second loadcase when the right bolt is preloaded. In that loadcase, the left bolt remains locked. Locking of the left bolt in this loadcase and of both bolts in the subsequent thermo-mechanical loading cycle is simulated by applying FIXED DISPLACEMENT boundary conditions to the control nodes, of which the third degree of freedom is fixed to 0 mm in the loading cycle. The loosening of the bolts in the final loadcase of the analysis is simulated by gradually releasing the forces on the control nodes in the local z-direction of these nodes.

In the three-stage thermo-mechanical loading cycle that follows the prestressing of the bolts, the cylinder head joint is subjected to a combination of mechanical and thermal loads. The mechanical loading consists of a pressure of 1.2 MPa applied to the interior of the cylinder head cover and the lower part over a period of 5 minutes, retained for 25 minutes and then gradually removed over another 5 minutes. The TABLE that defines the history of the pressure is of type time and is defined by the points (0,0), (2,0), (7,1), (32,1), (37,0) and (38,0).

The thermal part of the loading cycle consists of an increase of the temperature at the base of the assembly to 200°C over 5 minutes, a decrease to -20°C over 25 minutes and again an increase back to room temperature (20°C) over 5 minutes. This is achieved by applying a FIXED TEMPERATURE boundary condition to all nodes at the base of the

model, setting the TEMPERATURE (TOP) to 1 and employing a TABLE to a table of type time defined by the points (0,20), (2,20), (7,200), (32,-20), (37,20) and (38,20).

Finally, to suppress rigid body motions, the displacements in the local z -direction of all nodes at the bottom of the lower part of the cylinder head assembly are suppressed as well as the displacements in the local x -direction of the nodes at the bottom of the lower part that lie in the local yz -plane. The applied loads are depicted in Figure 2.2-7.

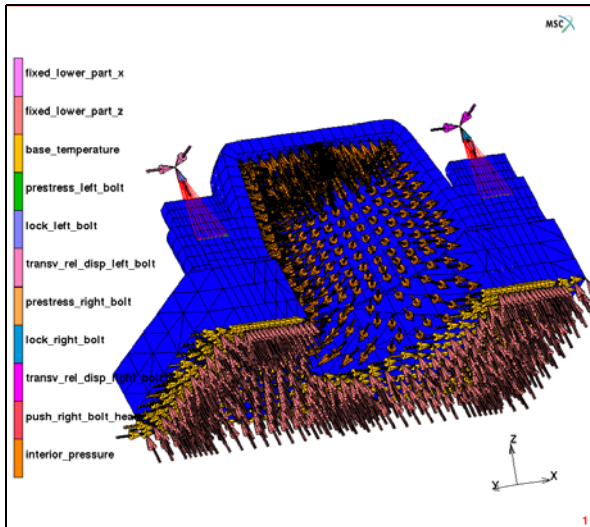


Figure 2.2-7 Boundary Conditions applied to the Cylinder Head Joint

Load Steps and Job Parameters

The job consists of six loadcases. The user is referred to Chapter 3.17 for details on the boundary conditions applied in each loadcase. All the loadcases are run as quasi-static thermo-mechanically coupled analyses using five increments each. For the loadcases in which there are temperature changes, a temperature error in estimate of 50°C is used. This improves the accuracy of the temperature dependent material property estimation by allowing the solution to iterate if the difference between the calculated temperature and estimated temperature is greater than 50°C. The setup for a typical loadcase is shown below:

```
LOADCASES
  COUPLED
  NEW
  QUASI-STATIC
  LOADS
    deactivate:
      prestress_left_bolt
      prestress_right_bolt
```

```

        push_right_bolt
    OK
CONTACT
    CONTACT TABLE
        ctable1
CONVERGENCE TESTING
    MAX ERROR IN TEMPERATURE ESTIMATE
        50
TOTAL LOADCASE TIME
    5
STEPPING PROCEDURE
FIXED
PARAMETERS
    # STEPS
        5
    OK
    OK
NAME
    loading

```

The analysis is set up as a coupled analysis in the JOBS menu and all six loadcases are preformed in sequence. The quadratic segments in contact bodies `cover`, `lower_part`, and `bolts` can be treated in one of two ways:

- GENUINE wherein midside nodes are independently checked for contact, separation, penetration, etc.;
- LINEARIZED wherein midside nodes of a face are tied to the corresponding corner nodes of that face.

GENUINE is the default scheme – this requires that the separation checking be based on stresses rather than forces. Furthermore, the separation checking for quadratic contact should be based on nodal stresses obtained by extrapolating from integration point stresses rather than those obtained as the ratio of an effective force to effective area. Control of these buttons are available under **ADVANCED CONTACT CONTROL** in the JOBS menu in Mentat. It should be noted that when Mentat detects quadratic elements in contact bodies, the GENUINE scheme and separation checking based on extrapolated stresses is automatically set. The button sequence shown here for these advanced contact options is mainly for instructive purposes.

```

JOBS
NEW
    TYPE
        COUPLED

```

PROPERTIES

CONTACT CONTROL

INITIAL CONTACT

CONTACT TABLE

```
ctable1
```

ADVANCED CONTACT CONTROL

DEFORMABLE-DEFORMABLE METHOD

```
SINGLE-SIDED
```

QUADRATIC SEGMENTS

```
GENUINE
```

SEPARATION CRITERION

```
STRESS
```

```
DERIVATION
```

```
EXTRAPOLATION
```

Under the ANALYSIS OPTIONS menu, the LARGE DISPLACEMENT option is selected. In addition to Equivalent Von Mises Stress (Marc post code 17), Gasket Pressure (Marc post code 241), Gasket Closure (Marc post code 242), and Plastic Gasket Closure (Marc post code 243), you can also choose Temperature (Integration Point) (Marc post code 180).

For the lower part of the assembly, element type 127 (TET10 element) is used. For the cover and the bolts, element type 57 (reduced integration HEX20 element). For the gasket, element type 149 is selected.

ELEMENT TYPES

ANALYSIS TYPE

```
COUPLED
```

ANALYSIS DIMENSION

```
3-D
```

SOLID

```
57
```

```
cover
```

```
127
```

```
lower_part
```

```
57
```

```
bolts
```

```
OK
```

SOLID COMPOSITE/GASKET

```
149
```

```
gasket  
OK
```

Save Model and Run Job

```
FILE  
  SAVE AS  
    thermogask.mud  
  OK  
  RETURN (twice)
```

Write out the Marc input file `thermogask_job1.dat` and run the job in serial mode, using the **SUBMIT 1** button in the **RUN** menu:

```
JOBS  
  RUN  
    SUBMIT 1  
    MONITOR  
    OK  
  RETURN  
MAIN
```

To run the job in parallel mode using the domain decomposition method, previous Marc versions required that the model was decomposed into domains using the **DOMAIN DECOMPOSITION** menu in Mentat. In that case, Mentat would split the model data into input files for each domain. While this is still possible, Marc can also run the job in parallel using the same single input file that was created for the serial run. In that case, the domain decomposition is done internally within Marc. The input file is read on one processor, decomposed into domains, and the domain data is passed to the other processors.

To run the job in single input file parallel mode, use the `-nprocs` option to specify the number of domains:

```
path/tools/run_marc -jid thermogask_job1 -nprocs 2
```

View Results

```
RESULTS  
  OPEN DEFAULT
```

To monitor the temperature distribution on the assembly, make a contour plot of the temperature, set the range, and the legend, and monitor the results.

```
PLOT
  DRAW
    switch off NODES
  RETURN
SCALAR PLOT SETTINGS
  RANGE
    MANUAL
    SET LIMITS
      -20
      200
  # LEVELS
    22
  LEGEND
    FORMAT: INTEGER
    RETURN
  RETURN
SCALAR
  Temperature
CONTOUR BANDS
MONITOR
```

Figure 2.2-8 shows a contour plot of the temperature distribution at the end of the third loadcase when the joint has been fastened, the temperature at the base of the assembly has been increased to 200°C and the interior pressure has been applied. Due to the insulating properties of the gasket, the heat transmitted to the cover through the gasket is quite small.

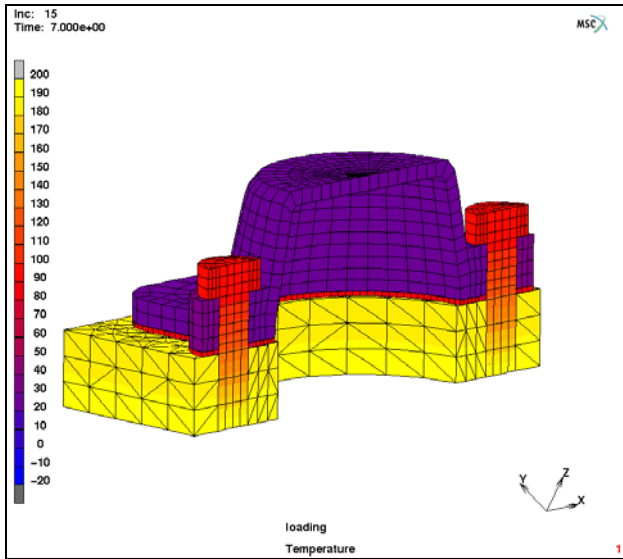


Figure 2.2-8 Contour Plot of the Nodal Temperatures at the End of the Third Loadcase

Figure 2.2-9 shows a contour plot of the temperature distribution at the end of the fourth loadcase when the joint is still fastened and the temperature at the base of the assembly has been decreased to -20°C .

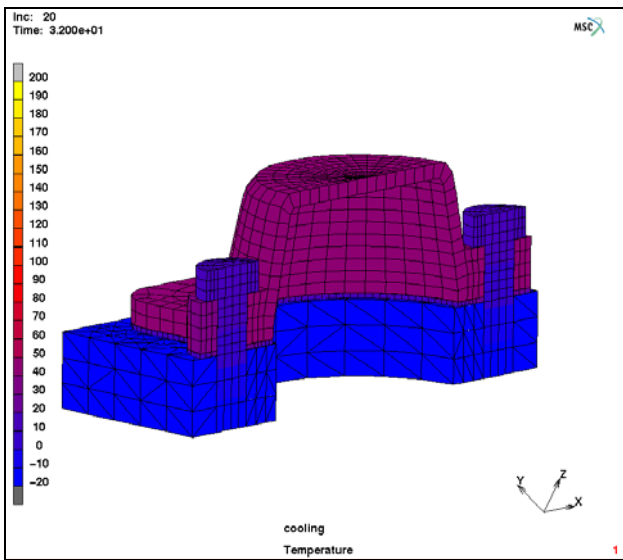


Figure 2.2-9 Contour Plot of the Nodal Temperatures at the End of the Fourth Loadcase

In order to assess the thermo-mechanical effects on the gasket response, variations of the gasket pressures at nodal points in the gasket body and ring, where the plastic gasket closure is a maximum, are computed and displayed in Figure 2.2-10.

RESULTS

SCALAR PLOT SETTINGS

HISTORY PLOT

SET NODES

2085 2337 #

COLLECT DATA

0 30 1

NODES/VARIABLES

ADD VARIABLE

Increment

Gasket Pressure

FIT

RETURN

As the gasket is heated, the gasket pressure drops in accordance with the compression data that has been provided, and that upon cooling, the pressure increases back to the previous level. Also, as expected, the pressure drop-off and subsequent increase is more pronounced in the gasket body than in the gasket ring.

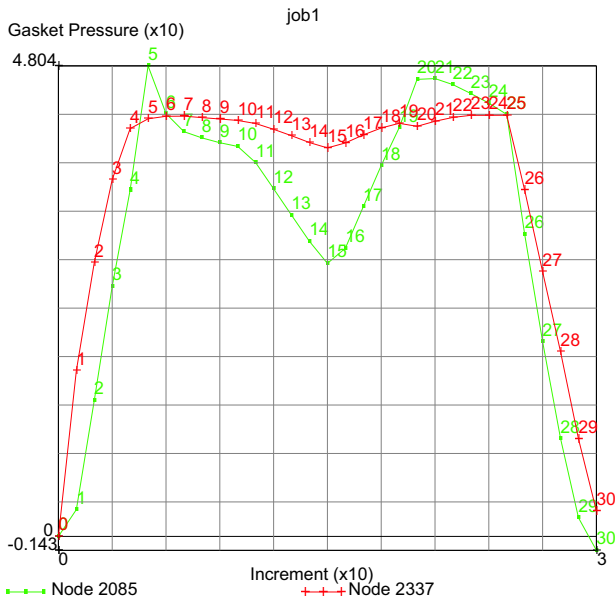


Figure 2.2-10 Variation of the Gasket Pressure with Increment Number in Body and Ring

Finally, in [Figure 2.2-11](#) and [Figure 2.2-12](#), the time variation of the bolt forces is depicted. [Figure 2.2-11](#) shows the bolt forces in the axial (pretension) direction of the bolts. In the loadcase in which the bolts are prestressed, these forces

are given by the external forces on the control nodes in the local coordinate system of these nodes. This is also the case in the final loadcase when the bolt forces are released. In the loadcases where the bolts are locked, the bolt forces are given by the reaction forces on the control nodes in the local coordinate system of the nodes.

```
RESULTS
  SCALAR PLOT SETTINGS
    USE NODAL TRANSFORMATIONS
    RETURN
  HISTORY PLOT
    SET NODES
      11049 11977 #
    COLLECT DATA
      0 30 1
    NODES/VARIABLES
      ADD VARIABLE
        Time
        Reaction Force Z
      ADD VARIABLE
        Time
        External Force Z
    FIT
    RETURN
```

Figure 2.2-12 shows the bolt forces in the x-direction of the model. This is basically the total shear force on the matching boundaries in that direction. In the three-stage thermo-mechanical cycle, both bolts are sheared in outward directions pointing away from the center of the cover due to the applied internal pressure of the cover.

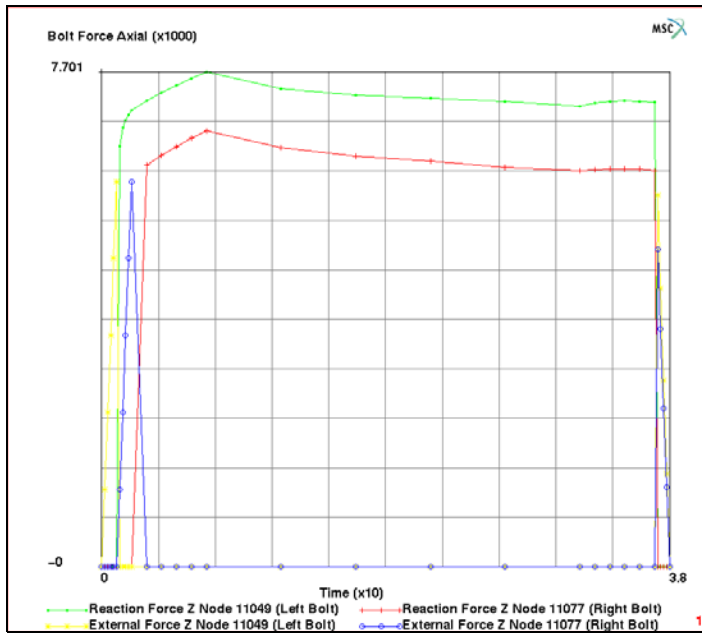


Figure 2.2-11 History Plot of the Bolt Forces in the Axial Direction

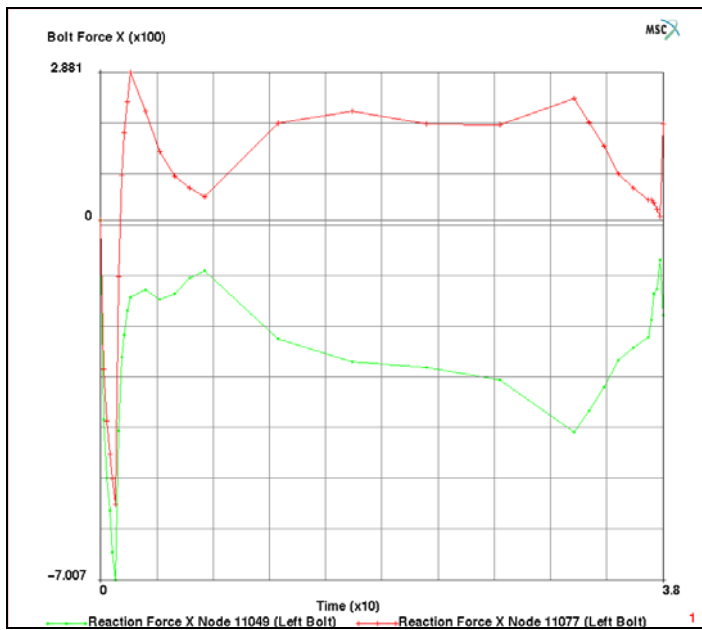


Figure 2.2-12 History Plot of the Bolt Force in the X-direction

Input Files

The files below are on your [delivery media](#) or they can be downloaded by your web browser by clicking the links (file names) below.

File	Description
thermogask.proc	Mentat procedure file to run the above example
thermogask_mesh.mud	Original geometry read by procedure file
ch02_body_loading.raw	Gasket material curve read by procedure file
ch02_ring_loading.raw	Gasket material curve read by procedure file
ch02_body_unloading.raw	Gasket material curve read by procedure file
ch02_ring_unloading.raw	Gasket material curve read by procedure file

2.3 RBE3 (General Rigid Body Link)

- Chapter Overview 372
- Soft and Rigid Connections 372
- Submit Job and Run the Simulation 381
- Input Files 384

Chapter Overview

This chapter describes the use of RBE2 and RBE3 in Marc. In this example, RBE2 is used to simulate really rigid connection while RBE3 is used to simulate soft connection. Rigid connection means that the displacement of nodes is under controlled while soft connection means that the distribution of forces is under controlled.

Soft and Rigid Connections

A rectangular tube with a stopper is loaded on one end and partially fixed on the other end as shown in [Figure 2.3-1](#). The cross section of the tube is $100 \times 50 \text{ mm}^2$. The thickness is 5 mm. The length is 1000 mm.

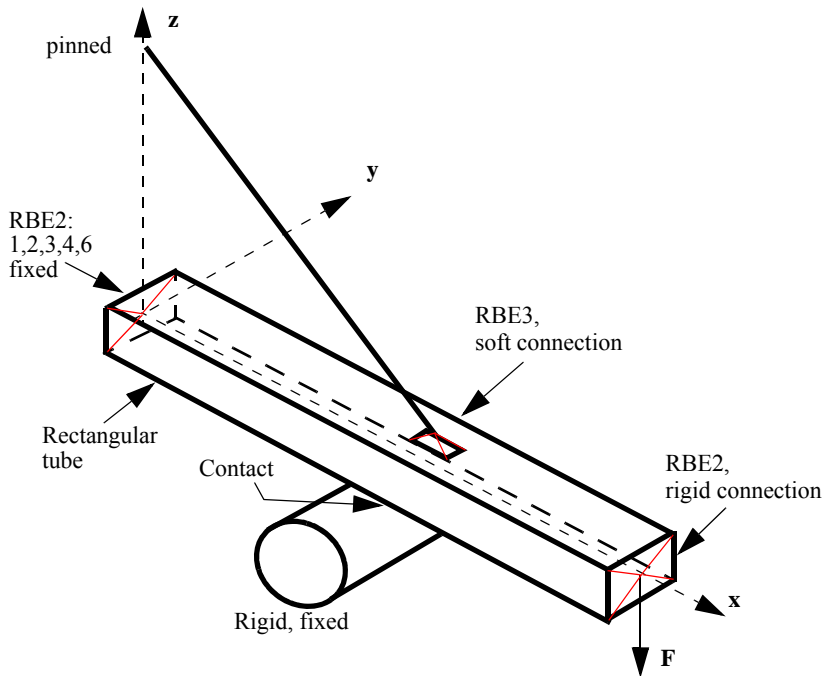


Figure 2.3-1 Schematic Model

The size of the connection pad is about $40 \times 40 \text{ mm}^2$. The connection between the rod and the tube is assumed to be soft and is about 50 mm above it. The supported (pinned) end of the rod is located at 500 mm above the tube. The simulation of the soft connection is done using RBE3. In this case, the displacement of the tube along the connection pad is free while the force distribution is controlled using the simple RBE3 formulation. Another possibility is using rigid RBE2 connection which could result in an over stiff simulation. The end sections of the tube are assumed to be rigid. They are simulated using RBE2.

A concentrated load is applied on one end of the tube and the other one is fixed on all degrees of freedom except the rotation about y-axis. Initially there is a gap of 20 mm between the tube and the cylindrical stopper. The finite element model is shown in [Figure 2.3-2](#).

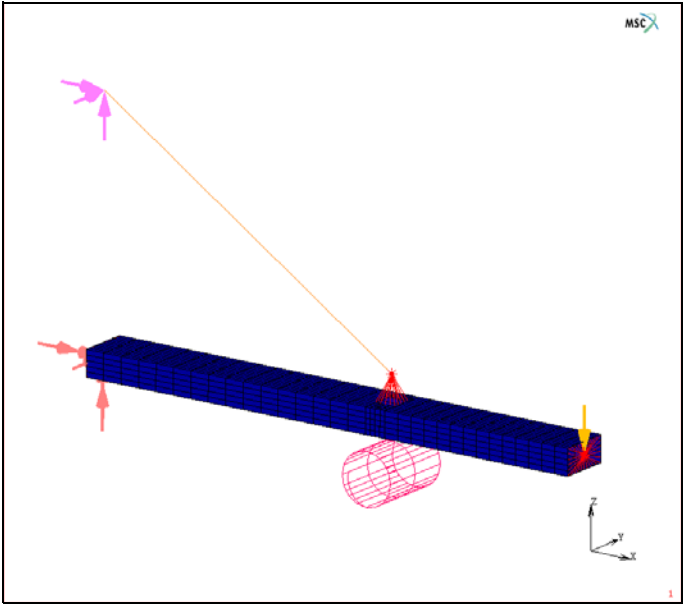


Figure 2.3-2 Finite Element Model

Mesh Generation

The final mesh can be seen in [Figure 2.3-2](#). One extra (reference) node is also created to define RBE3's.

```

MESH GENERATION
PTS ADD
    0 0 0
    580 0 0
    580 50 0
    0 50 0
    620 0 0
    1000 0 0
    1000 50 0
    620 50 0
DUPLICATE
TRANSLATIONS
    0 0 50
POINTS
EXIST.
```

SRFS
ADD

1 2 3 4
2 5 8 3
5 6 7 8
4 3 11 12
3 8 16 11
8 7 15 16
9 10 11 12
10 13 16 11
13 14 15 16

CONVERT

DIVISIONS

16 5

SURFACES TO ELEMENTS

1 4 7 #

DIVISIONS

4 5

SURFACES TO ELEMENTS

2 5 8 #

DIVISIONS

14 5

SURFACES TO ELEMENTS

3 6 9 #

RETURN

SWEEP

SWEEP

NODES

EXIST.

ELEMENTS

EXIST.

REMOVE UNUSED

NODES

RETURN

ELEMS

REM

```
      281 282 258 284 285 286 287 288 #  
SWEEP  
  REMOVE UNUSED  
    NODES  
  RETURN  
SYMMETRY  
  SYMMETRY PLANE  
    NORMAL  
      0 1 0  
  SYMMETRY  
    EXIST.  
  RETURN  
SWEEP  
  SWEEP  
    NODES  
      EXIST.  
    ELEMENTS  
      EXIST.  
  REMOVE UNUSED  
    NODES  
  RETURN  
NODES  
  ADD  
    0 0 25  
  1000 0 25  
    600 0 100  
    0 0 500  
ELEMENT CLASS  
  LINE(2)  
  RETURN  
ELEMS  
  ADD  
    1223  
    1222  
  RETURN
```

```
SURFACE TYPE
  CYLINDER
  RETURN
SURFACES
  ADD
    600 -75 -70
    600 -75 -70
    50
    50
MAIN
```

Geometric Properties

The thickness of the plate is 5 mm. The area of the rod is 4 mm².

```
GEOMETRIC PROPERTIES
  NEW
    3-D
      SHELL
        THICKNESS
          5
        OK
      ELEMENTS ADD
        SELECT ALL QUAD ELEMENTS
    NEW
      TRUSS
        AREA
          4
        OK
      ELEMENTS ADD
        SELECT LINE(2) ELEMENTS
    MAIN
```


Material Properties

The material for the tube is elastoplastic with 73000 MPa Young's modulus. The Yield stress is 340 MPa and 400 MPa at 0 and 0.15 equivalent plastic strain. The Young's modulus for the rod is 210000 MPa. The Yield stress is 550 MPa and 600 MPa at 0 and 0.15 equivalent plastic strain.

MATERIAL PROPERTIES

NEW

ISOTROPIC

YOUNG'S MODULUS

72E+3

POISSON RATIO

0.3

ELASTIC-PLASTIC

INITIAL YIELD STRESS

1

OK

OK

TABLES

NEW

TYPES:

eq_plastic_strain

DATA POINTS

ADD

0 340 0.15 400

COPY

DATA POINTS

EDIT

1

0 550

2

0.15 600

RETURN

SHOW MODEL

ELEMENTS

ADD

SELECT ALL QUAD ELEMENTS

```
ISOTROPIC
  ELASTIC-PLASTIC
    TABLES
      table1
    OK (twice)
NEW
  ISOTROPIC
    YOUNG'S MODULUS
      210E+3
    POISSON'S RATIO
      0.3
    ELASTIC-PLASTIC
      INITIAL YIELD STRESS
        1
      TABLES
        table2
      OK (twice)
ELEMENTS
  ADD
    SELECT LINE(2) ELEMENTS
MAIN
```

Contact

Define a contact between the tube and the rigid cylinder.

```
CONTACT BODIES
  DEFORMABLE
    OK
  ELEMENTS
    ADD
      select all quad elements
NEW
  RIGID
    SURFACES
      ADD
```

19 #

MAIN

Links

One RBE3 and two RBE2's are defined. The RBE3 is used to create soft connection between the rod and the connection pad on the tube. A RBE2 on one end of the tube is defined to allow simple application of revolute support while the other RBE2 is created where the applied point load is applied.

LINKS

RBE3'S

REFERENCE NODE

NODE

1222 *(node at end of truss)*

DOF

1 2 3 4 5 6 # *(all DOF selected)*

CONNECTED NODES

DOF

1 2 3 # *(only displacement DOF)*

COEFF.

1.0

ADD

903 984 985 986 987 986 221 238 255 37 *(nodes on pad)*

379 380 381 376 371 983 #

RETURN

RBE2'S

RETAINED (REFERENCE)

NODE

1221 *(node at center of box beam)*

TIED NODES

NODE

ADD

SELECT ALL NODES OF THE TUBE AT X=1000

DOF

1 2 3 *(only displacement dof)*

NEW

RETAINED (REFERENCE)

```
      NODE
      1152
TIED NODES
      NODE
      ADD
      SELECT ALL NODES OF THE TUBE AT X=0
      DOF
      1 2 3 4 5 6 (all dof)
MAIN
```

Boundary Conditions

All degrees of freedom on the edges of the tube are fixed except the rotation about the y-axis. The end rod is simply supported. Concentrated load F_z of -22.6 kN is applied at the other end of tube.

```
BOUNDARY CONDITIONS
MECHANICAL
  FIXED DISPLACEMENT
    ALL DISPLACEMENT DOF'S SELECTED
    OK
  NODES ADD
    1223 #
  NEW
    FIXED DISPLACEMENT
      ALL DOF'S SELECTED EXCEPT ROTATION Y
      OK
    NODES ADD
      1220 #
  NEW
    POINT LOAD
      FORCE Z= -22600
      OK
    NODES ADD
      1221 #
MAIN
```

Loadcases

One loadcase is defined. The convergence testing is done using residuals and displacements with the relative tolerance of 0.01 for both of them. An automated load step with default setting is used.

```
LOADCASES
  MECHANICAL
    STATIC
      CONVERGENCE TESTING
        RESIDUALS AND DISPLACEMENTS
          RELATIVE FORCE TOLERANCE
            0.01
          RELATIVE DISPLACEMENT TOLERANCE
            0.01
        OK
      ADAPTIVE: MULTI CRITERIA
        OK
    MAIN
```

Submit Job and Run the Simulation

The line(2) element must be assigned as element type 9 (truss). The simulation is run with LARGE DISPLACEMENT option. Extra output for tying forces is request for postprocessing.

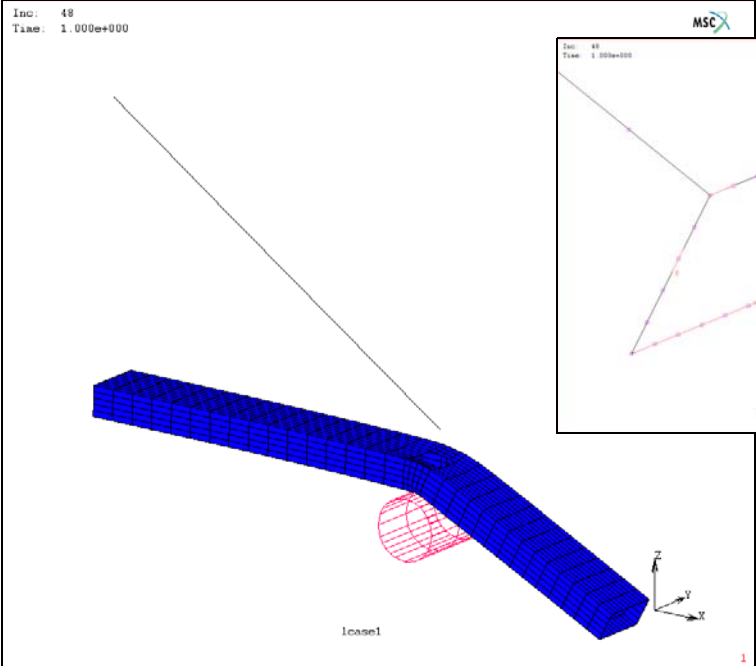
```
JOBS
  NEW
  MECHANICAL
    lcase1
    INITIAL CONDITIONS
      unselect apply3
      OK
    ANALYSIS OPTION
      select LARGE DISPLACEMENT
      select UPDATED LAGRANGE PROCEDURE
      OK
    OK
  JOB RESULTS
    SELECTED NODAL QUANTITIES
```

```
CUSTOM
  DISPLACEMENT
  TYING FORCE
  OK
OK
ELEMENT TYPES
  MECHANICAL
    3-D TRUSS/BEAM
      choose element type 9
      select all line(2) elements
    RETURN
  RETURN
RUN
SUBMIT
```

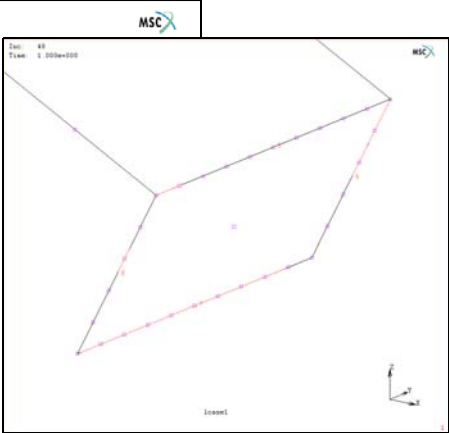
Results

The deformed configuration at the end of the simulation is shown in [Figure 2.3-3\(a\)](#). As expected, the deformation of the end tube remains rigid [Figure 2.3-3\(b\)](#). The deformation of the tube along the connection does not remain rigid. It can deform freely as seen in [Figure 2.3-3\(c\)](#). The tying force distribution follows the simple RBE3 formulation as shown in [Figure 2.3-3\(d\)](#).

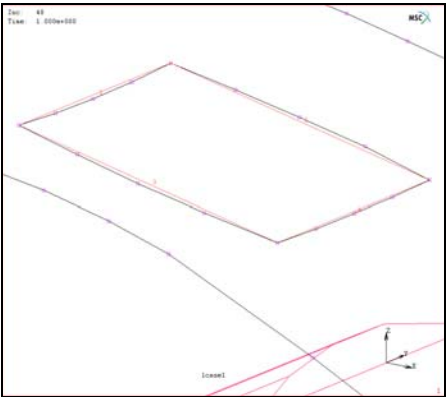
(a) Deformed configuration



(b) Rigid end form



(c) Deformed connection pad



(d) Tying force distribution

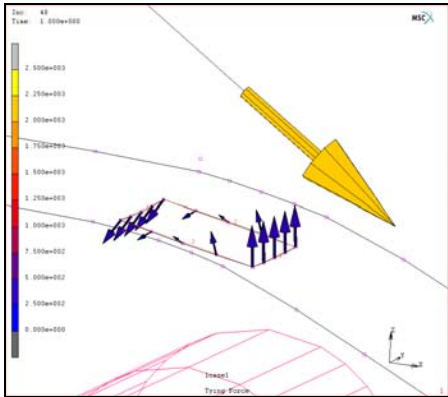


Figure 2.3-3 Results of the Analysis

Input Files

The files below are on your [delivery media](#) or they can be downloaded by your web browser by clicking the links (file names) below.

File	Description
rbe3.proc	Mentat procedure file to run the above example
rbe3.mud	Associated model file
rbe3.dat	Associated Marc input file

2.4 Arc Welding Process Simulation

- Chapter Overview 386
- Welding Process Simulation of Cylinder-Plate Joint 386
- Input Files 404

Chapter Overview

In many manufacturing processes, smaller components are joined together by a variety of joining techniques to form the main structure. Welding is one such commonly used joining technique. An undesirable side-effect of welding is the generation of residual stresses and deformations in the component and the quality of the weld has a substantial impact on the fatigue life of the structure. These resultant deformations may render the component unsuitable for further use. Also, the residual stresses form the input for subsequent manufacturing or structural processes.

This chapter demonstrates the various features available in Marc to simulate the welding process. For this purpose, the simulation of the welding of a cover plate to a cylinder is described in depth. The objective is to demonstrate the various options available to simulate the weld thermal loading, weld motion, filler element treatment and time stepping. In order to keep the problem small and run within a reasonable time interval, the mesh used is somewhat coarse, reduced integration elements are used and the time stepping thermal tolerances are rather loose.

Welding Process Simulation of Cylinder-Plate Joint

A solid cylinder with a number of holes machined through it is joined to a thin cover plate. The joining is achieved through two short fillet welds placed at the junction of the cylinder and two flanges of the cover plate. The objective of the welding simulation is to study the temperatures generated during the welding process and investigate the residual stresses in the component after welding. The finite element mesh of the cylinder-plate joint is shown in [Figure 2.4-1](#).

Only half the model is considered herein. Though the four welds (2 on each half) are placed sequentially and the whole model should be considered for a full description of the welding effects, in order to understand the local stresses and deformations effects introduced by each weld, only the half-model is considered here.

The solid cylinder of radius 100 mm is modeled using hexahedral elements. The cover plate of radius 125 mm and flanges are modeled using shell elements. Weld filler 1 is modeled using shell elements and weld filler 2 is modeled using solid elements. The various components are identified in [Figure 2.4-1](#). The thermal loading comprises of the heat input from the welds which increases the temperatures at the joints to about 1200°C.

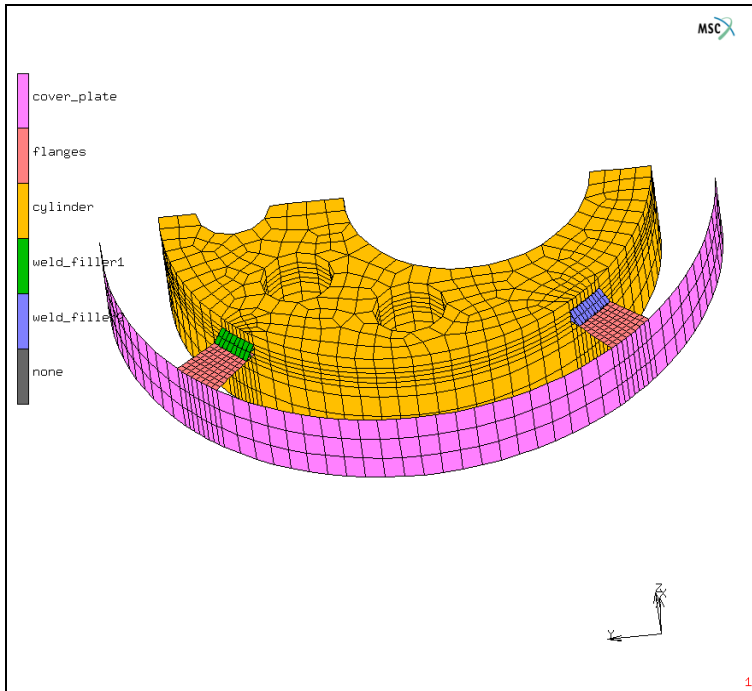


Figure 2.4-1 Finite Element Mesh of Cylinder-Plate Joint

Procedure File

The analysis has been completely set up using Mentat. The procedure file to demonstrate the example is called *weld.proc* under *path/examples/marc_ug/s2/c2.4*.

To run the procedure file and build the model from start to finish, the following button sequence can be executed in Mentat:

```
UTILS
  PROCEDURES
    EXECUTE
      weld.proc
```

If one wishes to understand each and every command in the procedure file, the procedure file can be sequentially executed through the following button sequence:

```
UTILS
  PROCEDURES
    LOAD
```

```
weld.proc  
STEP
```

Every STEP click executes the next command in the procedure file and simultaneously shows the associated menu and button click. When the model is being dynamically rotated or translated, due to the large number of rotations/translations, it is highly advisable to run through those portions quickly by clicking on START/CONT to execute the commands continuously and clicking on STOP when the model motion is completed.

Mesh Generation

The generation of the finite element mesh is not discussed in detail here. Instead, the reader is referred to the procedure file and the comments in that file. A finer mesh is used for the flanges, weld fillers, and for the cylinder in the vicinity of the welds. It is important to use a fine mesh in the vicinity of the weld in order to capture the thermal gradients accurately.

For the set of parameters used in the present example, the resulting finite element mesh is depicted in [Figure 2.4-1](#). All dimensions are in mms. There are a total of 2480 elements and 3314 nodes.

Geometric Properties

The thickness of the cover plate wall and flanges are specified as 1 mm and 2 mm, respectively. The CONSTANT TEMPERATURE option is specified for the solid elements (both the solid cylinder and the second weld filler elements) as follows:

```
GEOMETRIC PROPERTIES  
  MECHANICAL ELEMENTS  
    3-D  
      SOLID  
        CONSTANT TEMPERATURE
```

It is recommended in general literature that when first-order full integration elements are used for the thermal part of the welding analysis, second-order elements should be used for the corresponding mechanical analysis. This allows accurate capture of stresses due to linear thermal strains. The CONSTANT TEMPERATURE option allows the use of first-order elements for both the thermal and mechanical passes without inducing artificial stresses due to linear thermal strains. Note that for the reduced integration elements used herein with just one integration point, the CONSTANT TEMPERATURE option is not really needed.

As previously mentioned, the first weld filler is modeled with shell elements while the second weld filler is modeled with solid elements. The cross-sectional area for each weld is 12.5 mm². The equivalent thickness of the shell weld filler is obtained by:

(Perimeter length of shell weld filler cross-section) x (Equivalent Thickness) = 12.5.
This results in a value of 0.801 mm for the shell thickness of the first weld filler.

Note that as the thickness value is provided, the shell elements are plotted in expanded mode. The menu to control this expanded plotting mode can be accessed as follows:

```
PLOT
  ELEMENTS
    SETTINGS
      RELATED PLOT SETTINGS
        SHELL
          PLOT EXPANDED
            REGEN
```

Material Properties

The material database in Mentat is used to define the temperature dependent material properties of the cylinder-cover structure and the weld fillers. It is assumed that both the cylinder-cover plate and the fillers are made of steel material. Based on the assumed composition of the materials, the cylinder, cover-plate and flanges are given the properties of 100Cr6 and the weld fillers are given the properties of 41Cr4. The material database is accessed as follows:

```
MATERIAL PROPERTIES
  READ
    100Cr6
```

Note that the units for the material properties in this database are:

Length (milli meter), Mass (mega gram), Time (second), and Temperature (centigrade).

It is important to ensure that other provided data like dimensions, temperature boundary conditions, etc. are in consistent units.

Note also that, when the material database is used, the temperature dependence of mechanical properties like Young's modulus, Poisson's ratio, Coefficient of thermal expansion and of thermal properties like Specific heat, Conductivity is read in through tables. The X-axis of these tables (Temperature) extends from about -100°C to 1500°C . It is important to note that if the temperatures in the problem were expected to exceed these limits, the provided data should be extended. Also, the provided tabular data can be modified/extended; e.g., the thermal conductivity can be increased significantly for high enough temperatures to model stirring effect in molten metal. These extensions are not made in the present study. Also, latent heat of solidification is not considered here. It can be easily incorporated if desired by modifying the specific heat or by using the LATENT HEAT option in Marc. It should also be noted that solid-solid phase transformation capability are not considered in this example. The T-T-T parameter and TIME-TEMP option are available in Marc for defining solid-solid phase transformations. It should, however, be noted that these options are not supported by the GUI and that the data requirements for these options are significant.

Finally, note that the yield stress and its dependence on plastic strain, strain rate, and temperature is not directly provided in the GUI. This is accessed from the AF_FLOWMAT directory at run-time. The '*.out' file produced by Marc at run-time indicates the name of the file being accessed for the flow stress data.

Weld Path Setup

Two weld paths are setup here, one for each weld source. Prior to setting up weld path 1, two poly-line curves are defined at the root and throat of the first weld filler, as shown in [Figure 2.4-2](#).

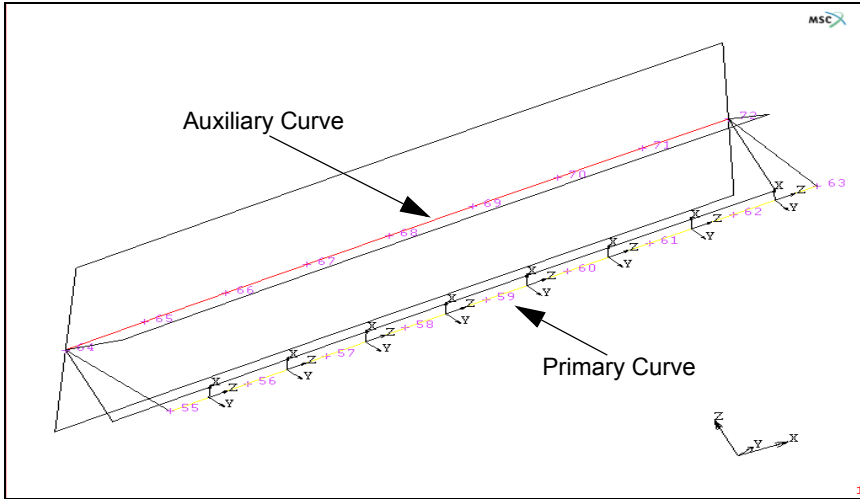


Figure 2.4-2 Weld Path Definition using Poly-Line Curves

Note that both curves should have the same number of points and the direction in which the curves are defined should be the same. Also, the order in which the points are clicked is important. The first weld path is then defined in Mentat as follows:

```
MODELING TOOLS
WELD PATHS
  PATH INPUT METHOD
    CURVES
      CURVES ADD
        pick primary curve
    ORIENTATION INPUT METHOD
      CURVES
        CURVES ADD
          pick auxiliary curve
  ANGLE
    180
```

As the weld path is created, the local X-Y-Z axes of the weld path are shown in Mentat. The Z-axis is along the weld motion direction, the Y-axis indicates the orientation direction of the weld arc, and the X-axis indicates the width

direction of the weld. The DRAW WELD PATHS option allows the path to be shown as a yellow line with the associated local weld directions indicated on the path. The ANGLE value of 180° allows the weld orientation direction to be reversed.

Prior to setting up weld path 2, an auxiliary node is defined at the center of the model at 0,0,-10. This node is used to define the orientation of the weld arc. Note that the number of auxiliary nodes can either be 1 (as in this model) or equal to the number of primary nodes defining the weld path. Once again, the order in which the nodes are clicked is important.

The second weld path is then defined using nodes as follows:

```
MODELING TOOLS
WELD PATHS
  PATH INPUT METHOD
    NODES
  NODES ADD
    pick Primary line of nodes
  ORIENTATION INPUT METHOD
    NODES
  NODES ADD
    pick Auxiliary node
  ANGLE
    45
```

The ANGLE value of 45° allows the weld orientation direction to be rotated about the weld path direction, as shown in Figure 2.4-3. The ARC INTERPOLATION option is turned on for this path.

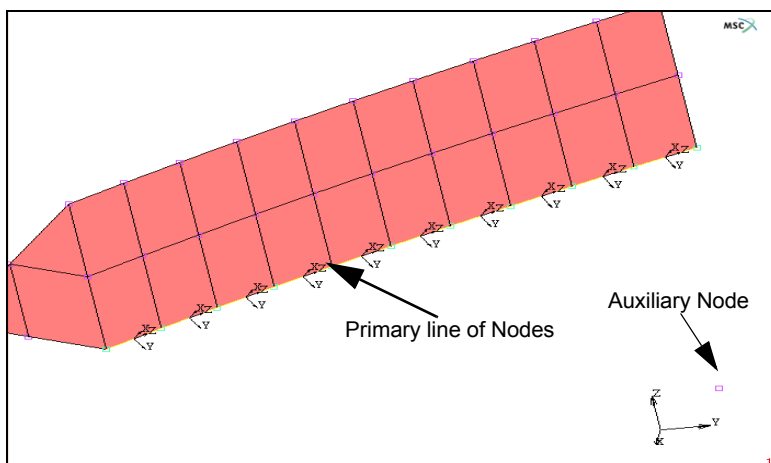


Figure 2.4-3 Weld Path Definition using Nodes

Weld Filler Setup

Three optional features can be defined for any weld filler:

- **Melting Point Temperature** – if this is set, the weld filler is introduced in the model at this temperature. If not set, the usual approach is to heat up the filler through direct weld flux boundary conditions.
- **Filler Bounding Box** – if the default is used, weld dimensions set on the WELD FLUX option are used to define the filler bounding box in order to identify when filler elements are active in the model. If the default is not used, the bounding box dimensions in the local X, Y, +Z and -Z directions are set here.
- **Initial Status** – can be set as either Deactivated (usual option) or Quiet. The deactivated option should be used when large motions are not expected in the model and large deformations are not expected in the vicinity of the filler elements. If these conditions are not satisfied, the quiet option could be used. The quiet option requires an appropriate property scaling factor to be set (default is 1e-5). It should be noted that the quiet option is susceptible to ill-conditioning, and the property scale factor may have to be massaged in order to avoid problems.

Two weld fillers are set up in the current model.

Weld Filler 1

The first weld filler, comprising of shell elements, is set up without a melting point temperature. Weld flux boundary conditions, described later in the [Initial/Boundary Conditions](#) section, is used to heat up the weld filler directly. The filler bounding box dimensions are set here. In the X- (width) and Y- (depth) directions, coarser dimensions (10 mm) are used in order to ensure that the entire cross-section of the filler element set is activated simultaneously. In the Z- (length) direction, the filler bounding box values correspond to the physical filler length that participates in the weld pool. This is set to 5 mm. The initial status is set to deactivated.

MODELING TOOLS

WELD FILLERS

FILLER BOUNDING BOX DEFAULT

X 10

Y 10

+Z 5

-Z 5

INITIAL STATUS

DEACTIVATED

ELEMENTS ADD

Add elements belonging to weld filler 1

Weld Filler 2

The second weld filler, comprising of solid elements, is set up with a melting point temperature of 1200°C. The temperature ramp time is left as 0, which implies that the temperature is introduced instantaneously. Default filler

bounding box values are to be used which implies that the bounding box dimensions are equal to: 1.5 times the weld width in the X-direction (15 mm), 2 times the weld width in the Y-direction (20 mm), the weld forward length in the +Z-direction (2 mm) and the weld rear length in the -Z-direction (8 mm). Note again that in the local X- and Y-directions, the bounding box dimensions can be loosely set to larger values in order to ensure that the entire solid cross-section is activated simultaneously; whereas, in the Z-direction, the bounding box dimension is tightly coupled with the associated weld pool dimensions. The initial status of the solid weld filler is also set to deactivated.

MODELING TOOLS

WELD FILLERS

MELT POINT TEMP

1200

INITIAL STATUS

DEACTIVATED

ELEMENTS ADD

Add elements belonging to weld filler 2

Contact Body Setup

The weld fillers can be linked to the other components in the model either through homogeneous meshing or through contact bodies. In the current model, the mesh for weld filler 1 (shell) is continuous with the flange and cylinder meshes.

Weld filler 2 (solid) is defined as a contact body. The flange in the vicinity of weld filler 2 (shell) and the cylinder (solid) are also defined as contact bodies. The contact body setup is shown in [Figure 2.4-4](#).

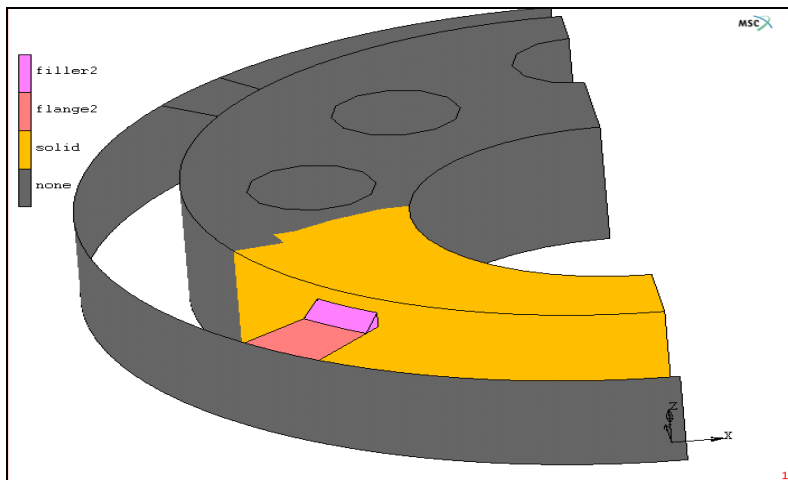


Figure 2.4-4 Contact Body Definition for Weld Filler 2

A contact table is then set up between the three contact bodies. Weld Filler 2 is glued to the flange and to the solid. The flange is allowed to touch the solid. A heat transfer coefficient of $100 \text{ N/mm}^2/\text{sec}/^\circ\text{C}$ is used between the bodies. Note that the units used for the heat transfer coefficient should be consistent with the other dimensions and properties used in the model.

Initial/Boundary Conditions

All the nodes in the model are set to an initial temperature of 30°C . Due to the presence of shell elements with linear temperature through-thickness variation, both the top and bottom temperature values are set to 30°C .

The solid cylinder and shell cover plate are fixed in the X-direction along the centerline. The fixtures holding the system are modeled by fixing the base of the solid cylinder and shell cover plate in the X-, Y-, and Z-directions.

A face film boundary condition is applied to all the exposed faces of the cylinder, flanges and cover plate. The sink temperature is set to 30°C and the film coefficient is taken as $0.02 \text{ N/mm}^2/\text{sec}/^\circ\text{C}$. For the shell elements, the film boundary conditions are applied to both the top and bottom faces. The face film boundary condition is not applied to the flange and cylinder faces that are covered by the weld fillers.

The weld fluxes applied to the solid cylinder and the weld fillers are described in detail here.

Weld Flux Associated with Weld Filler 2

This is a volume weld flux that is applied to the elements in the vicinity of weld filler 2. No power is provided since the heat input is to come from the molten filler elements. The dimensions are specified as width = 10 mm, depth = 0 mm, forward length = 2 mm and rear length = 8 mm. Note that since the provided flux has zero magnitude, the width, forward length, and rear length are only used here to define the filler box dimensions. The Initial Weld Position is taken as default (internally set to the first point of the weld path). The velocity is set to 2 mm/sec. Weld path 2 is chosen for the weld path and weld filler 2 is used for the weld filler. The button clicks for setting up weld flux 2 are as follows:

BOUNDARY CONDITIONS

THERMAL

VOLUME WELD FLUX

FLUX

DIMENSIONS

WIDTH

10

DEPTH

0

FORWARD LENGTH

2

REAR LENGTH

8

MOTION PARAMETERS

VELOCITY

2

WELD PATH

weldpath2

WELD FILLER

weldfill2

ELEMENTS ADD

Pick a few elements in the vicinity of weld filler 1

Since the flux is 0 and all the heat input in this boundary condition is from the molten filler, it is not very critical to identify which elements receive the flux. Note, however, that it is important to apply this boundary condition to at least one element so that it gets written out to the input file.

Weld Fluxes associated with Weld Filler 1

Two weld fluxes (weld flux 3 and weld flux 1) are applied to weld filler 1 and to the elements in the vicinity of this weld filler, respectively. While it is certainly convenient to apply the temperature of the weld filler directly as shown for weld flux 2, the objective of these two boundary conditions is to demonstrate the use of actual weld fluxes to heat up the weld filler and the surrounding elements. It is assumed that the total heat input from the weld torch can be divided up into the heat input going to the weld filler (weld flux 3) and the heat input going to the surrounding material (weld flux 1). The total heat input from the weld torch is taken as $1.5e6$ Nmm/sec (about 1.4 BTU/hour). 66% of this heat ($1E6$) is assumed to be directly taken by the solid cylinder and 33% ($5E5$) is assumed to be taken by the weld filler. Furthermore, it is assumed that weld flux 1 should have a double ellipsoidal variation over the cylinder while weld flux 3 should be nearly uniform over the weld filler.

Weld Flux 1: A conventional double ellipsoidal volume weld flux (weld flux 1) with appropriate dimensions is set up for the solid cylinder as follows:

BOUNDARY CONDITIONS

THERMAL

VOLUME WELD FLUX

FLUX

MAGNITUDE

POWER

1e6

EFFICIENCY

0.7

DIMENSIONS

WIDTH

```

4
DEPTH
2
FORWARD LENGTH
2
REAR LENGTH
8
MOTION PARAMETERS
VELOCITY
2
WELD PATH
weldpath1
ELEMENTS ADD
Pick all the solid elements that can potentially
receive the heat input

```

Weld Flux 3: A disk shaped face weld flux (weld flux 3) is set up for weld filler 1. The path followed by the weld flux is identical to weldpath1 with the exception that it is offset from the given path by 3.53 mm in the local negative Y-direction.

Since the stipulation is that the weld filler should receive uniform heat, additional modifications to the standard disc model in Marc are necessary. The Gaussian expression for the heat source is given by the expression below:

$$q(x, y, z) = \frac{3Q}{\pi r^2} \exp\left(\frac{-3x^2}{r^2}\right) \exp\left(\frac{-3z^2}{r^2}\right)$$

In order to heat the weld filler uniformly, it is necessary that the exponential functions in the above expression have a value of about 1 for representative x and z values of the weld filler. This can only be achieved by assuming a very large radius (r = 30 mm) for the face weld flux. When such a large value is used for r, for values of x and z in the range of 3 to 5 mm (note that this range corresponds to the width of the actual weld filler elements), q(x,y,z) is nearly uniform. This non-physical assumption for the weld radius, however, requires two additional parameters to be flagged for the face weld flux.

The first parameter is the scale factor s. Note that the integral of the face weld flux over the surface of the weld filler should still equal Q. So, the scale factor s is given by:

$$s \frac{3Q}{\pi 900} \int_{-3.53}^{3.53} \exp\left(\frac{-3x^2}{900}\right) dx \int_{-5}^5 \exp\left(\frac{-3z^2}{900}\right) dz = Q$$

By assuming the exponential terms to be nearly unity, integrating over the entire cross section and taking into account both top and bottom faces for the weld flux, s can be given by:

$$s = \frac{900\pi}{3} \times \frac{1}{(5 + 7.5\sqrt{2})} \times \frac{1}{10} \times \frac{1}{2}$$

x - term
z term
top and bottom faces

This yields a value of $s = 3.019$. Due to the approximations involved in the integral, s is set to 3.25 in the current model.

The second parameter is the maximum weld distance. This refers to the maximum distance beyond which weld flux is not considered. It can be left undefined if physical values are used for the weld dimensions. However, since $r = 30$ mm is not a physical dimension, the maximum distance within which nonzero flux values are to be considered needs to be set. In the current example, the maximum weld distance is set to 5 mm, which implies that for integration points that are located more than 5 mm from the weld origin, the weld flux is taken as 0. This is particularly important to restrict the number of filler elements participating in the weld pool in the z direction.

The face weld flux for weld filler 1 is then set up as follows:

BOUNDARY CONDITIONS

THERMAL

FACE WELD FLUX

FLUX

MAGNITUDE

POWER

5e5

EFFICIENCY

0.7

SCALE FACTOR

3.25

DIMENSIONS

SURFACE RADIUS

30

MAXIMUM DISTANCE

5

MOTION PARAMETERS

VELOCITY

2

WELD PATH

weldpath1

OFFSET-Y

```
weldpath1
FACES ADD
Pick the top and bottom faces of weld filler 1
```

Loadcase Definition

Two thermo-mechanically coupled loadcases are used to conduct the welding analysis. Loadcase 1 is used to simulate the weld at filler 1 and loadcase 2 is used to simulate the weld at filler 2. Adaptive Stepping (AUTO STEP) is used for loadcase 1 while fixed stepping (TRANSIENT NON AUTO) is used for loadcase 2.

Loadcase 1

The weld fluxes associated with weld filler 1 (weld flux 1 and weld flux 3) are applied in this loadcase. Weld flux 2 is deselected. The maximum error in temperature estimate is set to 30°C. This is an important quantity to specify and ensure that the thermal analysis is conducted with converged temperature dependent material properties. The total loadcase time is set to 10 seconds. The ADAPTIVE STEPPING - MULTI-CRITERIA stepping procedure is used. All defaults are used for the time stepping. A temperature user criterion is specified with an allowable temperature increment of 200°C. This supersedes the default temperature criterion of 20°C. The appropriate button clicks to set up the loadcase are as follows:

```
LOADCASES
  COUPLED
    QUASI-STATIC
      LOADS
        deselect weld_flux2
      CONTACT
        select ctable1
      CONVERGENCE TESTING
        MAX ERROR IN TEMPERATURE ESTIMATE
          30
      TOTAL LOADCASE TIME
        10
      STEPPING PROCEDURE
        ADAPTVE MULTI-CRITERIA
          USER-DEFINED CRITERIA
            TEMPERATURE INCREMENT PARAMETERS
              200
          PROCEED WHEN NOT SATISFIED
```

Loadcase 2

The weld fluxes associated with weld filler 2 (weld flux 2) are applied in this loadcase. Weld flux 1 and Weld flux 3 are deselected. The maximum error in temperature estimate is set to 30°C. This tolerance is specially important to specify for fixed stepping loadcases since no other checks on allowable temperature change are made in the case of fixed stepping. The total loadcase time is set to 10 seconds. The FIXED STEPPING procedure is used with a total of 50 increments (0.2 seconds per increment). The appropriate button clicks to set up the loadcase are as follows:

```
LOADCASES
  COUPLED
    QUASI-STATIC
      LOADS
        deselect weld_flux1 and weld_flux3 and
        select weld_flux2
      CONTACT
        select ctable1
      CONVERGENCE TESTING
        MAX ERROR IN TEMPERATURE ESTIMATE
          30
      TOTAL LOADCASE TIME
        10
      STEPPING PROCEDURE
        FIXED
          PARAMETERS
            # STEPS
              50
```

Job Parameters

A coupled job is set up and the defined loadcases are selected. The shell contact is simplified by only checking on the top surface and ignoring the thickness. This is necessary since the model has been built by putting weld filler 2 on the flange midsurface. The bias factor is taken as 0.95.

The LARGE STRAIN procedure is chosen. LUMPED MASS AND CAPACITY option is flagged. This is an important option to use for welding problems since it reduces thermal oscillations induced by the sudden thermal shocks in the system. The layer von Mises stress, equivalent plastic strain, and temperatures are requested. Additional print-out in the ‘*.out’ file for contact and welding are requested as follows:

```
JOBS
  COUPLED
```

JOB RESULTS
OUTPUT FILE
CONTACT
WELDING

A restart file at the end of every loadcase can be requested as follows:

JOBS
COUPLED
JOB PARAMETERS
RESTART
<> WRITE
INCREMENT FREQUENCY
500000

The large increment frequency allows Marc to only write out the restart file at the end of every loadcase (assuming that the loadcase takes fewer than 500000 increments).

Results and Discussion

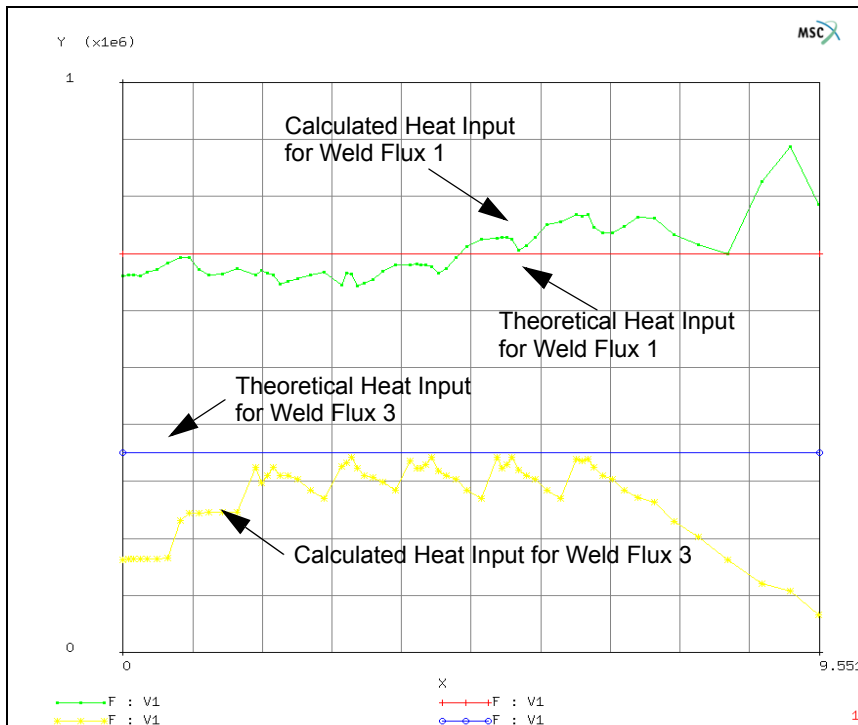


Figure 2.4-5 Comparison of Theoretical and Calculated Heat Input for Volume Weld Flux and Face Weld Flux at Filler 1

A good accuracy check is to compare the theoretical and calculated heat inputs for the weld fluxes. Assuming that the entire heat input acts on the structure, the theoretical heat input for the weld fluxes are given by $H = \eta Q$. The calculated heat input is obtained in the '*.out' file by requesting the additional print-out for welding.

The theoretical heat input for weld flux 1 (volume weld flux) is $7e5$ N mm/sec. This is based on the assumption that the entire double ellipsoid is acting on the solid.

Since the heat input is oriented at 45° to the surface, this is not strictly valid in the current case. It is still seen that the calculated heat input is relatively close to the theoretical value.

The theoretical heat input for weld flux 3 (face weld flux) is $3.5e5$ Nmm/sec. The calculated heat input is seen to be reduced at the beginning and at the end. This is because only half of the Gaussian distribution is captured by the weld filler elements at the beginning and end. For intermediate stages, it is seen that the calculated heat input has a wavy pattern. This wavy pattern coincides with the activation of the filler elements. With a finer filler element mesh, the waviness would reduce. For the purposes of the current demonstration, it is deemed that the accuracy of the calculated heat input is sufficient. The weld flux parameters and/or the mesh size can be adjusted to make the correspondence between the calculated and theoretical heat inputs closer. Tables as a function of time could be employed to improve the comparison especially at the beginning and end stages.

The von Mises Stress (Layer 1) and Temperature profile (Top) at the end of loadcase 1 (after laying weld filler 1) is shown in Figure 2.4-6 and Figure 2.4-7 respectively. It is seen that the highest temperatures are close to 1200°C and the highest residual stresses are in the solid cylinder elements close to the weld filler.

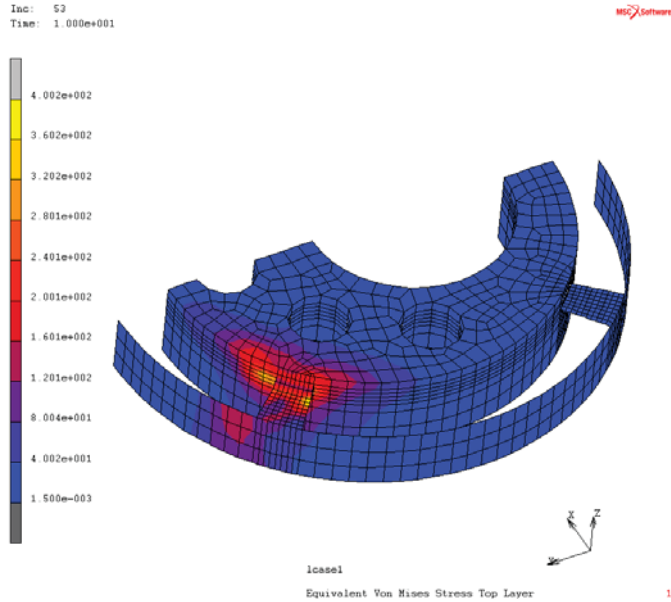


Figure 2.4-6 von Mises Stress Contours at the End of Loadcase 1

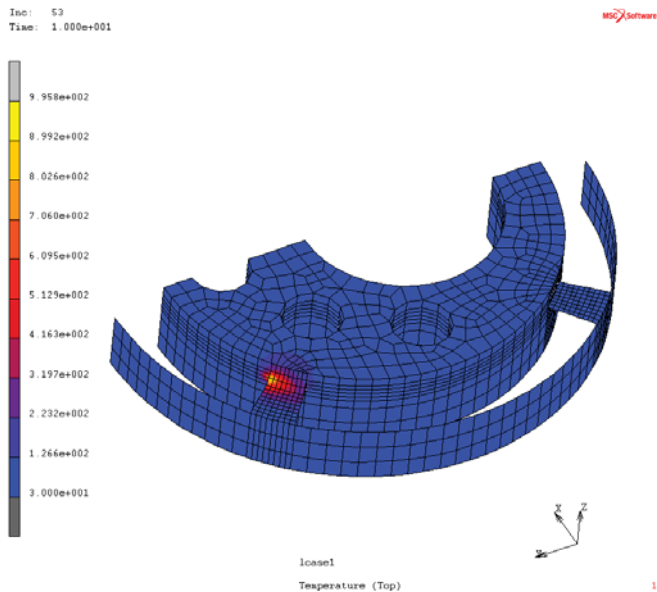


Figure 2.4-7 Temperature Profile at the End of Loadcase 1

The von Mises Stress (Layer 1) and Temperature profile at the end of loadcase 2 (after laying of both weld filler 1 and weld filler 2) are shown in Figure 2.4-8 and Figure 2.4-9 respectively. It is seen that the largest temperature of 1200°C is at the right end of the filler and portions of the filler that have moved out of the weld pool are significantly cooler. The residual stresses are significant in the flange, shell wall and solid regions.

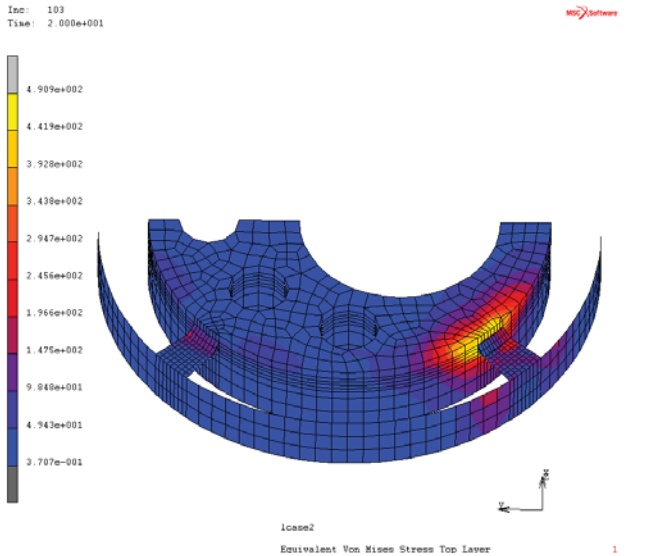


Figure 2.4-8 von Mises Stress Contours at the End of Loadcase 2

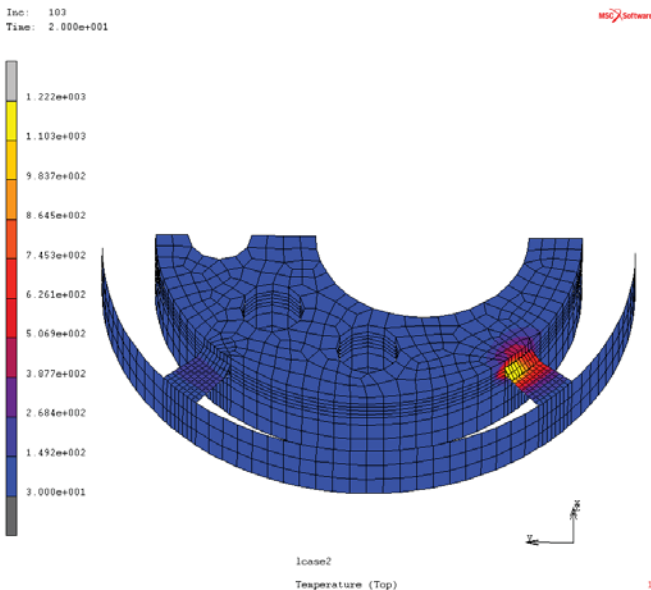


Figure 2.4-9 Temperature Profile at End of Loadcase 2

Input Files

The files below are on your [delivery media](#) or they can be downloaded by your web browser by clicking the links (file names) below.

File	Description
weld.proc	Mentat procedure file to run the above example
weld.mud	Associated model file
weld.dat	Associated Marc input file

2.5 FEM Simulation of NC Machining and PRE STATE

- Chapter Overview 406
- Example 1: Pocket Cutting 407
- Example 2: Thin Frame Cutting 424
- Example 3: Imported Initial Stresses 432
- Import with PRE STATE Feature 437
- Input Files 442

Chapter Overview

In manufacturing industry, NC machining is a material removal process that is widely used to produce a part with the desired geometry. After removal of the machined material, re-establishment of equilibrium within the remaining part of the structure causes some distortion due to the relief of the residual stresses in the removed materials. The deformation caused by this process usually depends on the residual stress level and its distribution inside the part. It also depends on the final geometry of the part after machining. For a part with final geometry that includes thin wall or large plate structures, the deformation can be so large that it causes severe distortions of the shape. The highly distorted part may no longer be able to serve its designated functionality. Such types of failures result in high scrap rates and increased manufacturing costs.

Finite element procedure is a powerful tool to analyze the potential distortion caused by the deformation during the machining process. With the FEM results, it is then possible for engineers to predict the potential failures and reduce overall manufacture costs.

The following features in Marc have been developed in order to enable Marc to conduct the automatic simulation of NC machining processes:

1. Interface between Marc and CAD/NC data that describes the cutter shape and cutter path;
2. Detection of FE mesh-cutter intersection;
3. Automatic deactivation of elements that are cut;
4. Visualization of the machining process during postprocessing of FEA results.
5. The support of CYCLE statement has been expanded from CYCLE/DRILL only to CYCLE/(DRILL, DEEP, TAP, BORE, and CBORE).
6. More efficient and accurate cutter-mesh intersection detection has been implemented.
7. Loadcase time synchronization is now allowed so that time-dependent contact and user boundary conditions can be used in conjunction with machining.
8. Cutter visualization is allowed during postprocessing of simulation results.
9. Local adaptive remeshing feature is added for NC machining analysis. For NC machining simulation purpose, this feature has been further enhanced so that multi-level element splitting, regular and irregular adaptive remeshing are possible.
 - a. Multi-level splitting of an element: This allows an element to be subdivided into the maximum allowed subdivision levels within one incremental step.
 - b. Regular adaptive remeshing: Elements that are partially intersected will be subdivided at each increment. Note that this can cause mesh size and computational time to increase significantly.
 - c. Irregular adaptive remeshing: Elements that are partially intersected are not subdivided during the first coarse stage of machining. These elements are subdivided during a second fine stage of machining, wherein all the splitting is conducted in the last increment of the loadcase. This two-stage remeshing process can save significantly on the computational time and memory usage.

10. Automated residual stress import: Based on the source of residual stresses, Marc can accept stress input data from Marc result data files obtained from previous numerical analyses or residual stress data saved in text format data file from experimental analyses.

Three methods have been made available in Marc to import residual stresses into the model prior to machining:

- a. **Pre State:** This method directly transfers data from a previously obtained Marc post file into the new Marc Machining model.
- b. **Text data file:** By this method, Marc reads in the residual stress data stored in a text format data file. The stress data are automatically mapped into the FE model by Marc.
- c. **Table format:** User can define the residual stresses as tables defined in space.

The cutter path data are stored in either APT source or CL data format. The APT source is the NC data output by CAD software CATIA. The CL data is the cutter location data provided by APT compilers.

This chapter describes the usage of the enhanced capability in the Marc program for simulation of NC machining (material removing) processes. Three examples are chosen to demonstrate the utilization of the major new features:

Example 1: Pocket Cutting

Example 2: Thin Frame Cutting

Example 3: Imported Initial Stresses

For each example, Mentat procedures show how to enclose this functionality into the machining process simulation by defining the Marc models together with the NC data in either APT source or the CL data is described in a step-by-step manner.

Example 1: Pocket Cutting

Input data

The input data required for the simulation of machining process with Marc including both sides of CAD interface that defines the NC machining process and Marc which defines the input for finite element analysis. They are summarized as following:

- NC data to define the cutter geometry and cutter path for the machining process. (*.apt* or *.ccl* files). For details of the format of the *apt* or *ccl* files, please refer to *Marc Volume A: Theory and User Information Manual* and the references listed there.

Notes:) 1) In the current version, circular motion is required to transform into point-to-point motion type when output by CAD NC software. In addition, the TRACUT and COPY statements are necessary to be explicitly interpreted into cutter motion statements. Major statement CYCLE is supported in combination with DRILL minor statement for the definition of drilling motion type.

2) The flipping over of a part during the course of machining process is supported by converting the flip over of the part into the rotation of cutter axis. MLTAXS statement is used to define the rotation of cutter axis.

- Marc input data includes the file names for cutter path definition and finite element model definition for the workpiece. The workpiece can be also imported from an IGES data which is written by CAD software.
- Initial stress data before the cutting process started. In the current example, the initial stress is the course of distortion after cutting. For this particular example, the initial stresses are provided in a 2-D model. We just converted 2-D data into our 3-D model using corresponding adjustments regarding unit and dimension definitions.

Initial Geometry and Stresses

The FE model is created by preprocessing capability of Mentat. The purpose of preprocessing is to generate the model and input data for Marc to analyze the metal cutting process. After the enhancements added in the current version, it allows the user to specify the file name of cutter path data.

The geometry of the part before cutting is shown in [Figure 2.5-1](#). The initial part is a block with size of length by width by thickness = 28x14x4.5 (inches). The residual stresses are predefined in the model already, and is defined in Mentat shown in [Figure 2.5-2](#).

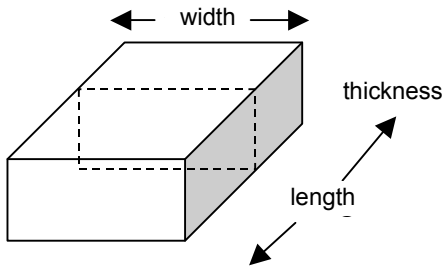


Figure 2.5-1 Initial Part Geometry

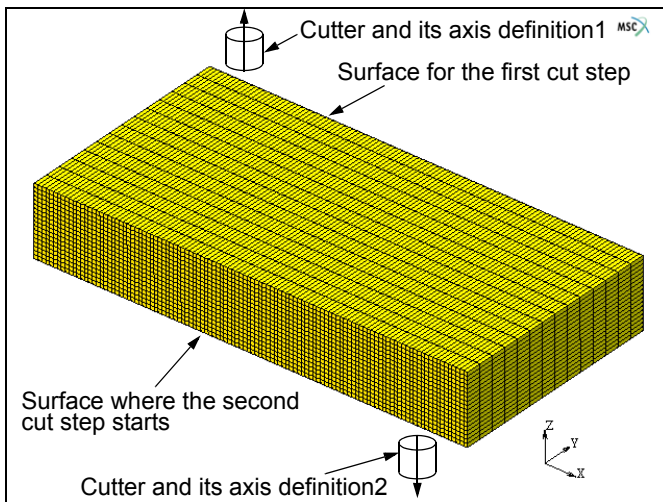


Figure 2.5-2 Definition of Cutting Processes

The cutting process includes two cut steps:

- The first step is to cut 2 inches off the upper surface as shown in [Figure 2.5-2](#). The cutting depth of each cutting step is defined by the cutter path data file *m2q0090s1.ccl*.
- The second step is to cut two pockets over the lower surface of the part after the first cut step is done. The cutter path for this step is defined by the cutter path data file *m2q0090s2.ccl*. The *ccl* files are created based on the APT sources generated by the CAD software CATIA.

Between the first and second step, the part is supposed to be flipped over, so that the cutter axis is unchanged in the second cut step. However, for the convenience of FE model definition and analysis, the flipping over of the part is equivalently simulated by the rotation of the cutter. Therefore, the second cut is conducted by rotating the cutter into the opposite direction, as shown in [Figure 2.5-2](#).

See below the step-by-step commands to execute the procedure to define the boundary conditions and loadcases in order to conduct the cutting processes sequentially and automatically.

Here, we will create the model by reading a predefined model file. This assumes that the users are familiar with the model generation. The model file to be read in is *ex_r01.mud*. The cutter path files are defined and saved in the current working directory. First, we will read in this mud file using the procedure file: *mc_nfg.proc*. As show in [Figure 2.5-3](#), after clicking on the command LOAD, and selecting the file name: *mc_nfg.proc*, then click command START/CONT, the file *ex_r01* is read into Mentat. The sequence is recorded as (after Mentat is started):

```
UTILS
  PROCEDURES
    LOAD
      mc_nfg.proc
    OK
  START/CONT
```

Up to now, the initial model file *ex_r01.mud* has been read in. The next step is to work on this model by defining boundary conditions and loadcases before submitting the job. So, we click the START/CONT button again.

```
START/CONT
```

Totally, 28224 brick elements and 32205 nodes are defined in the model. [Figure 2.5-3](#) shows the model and its initial stresses.

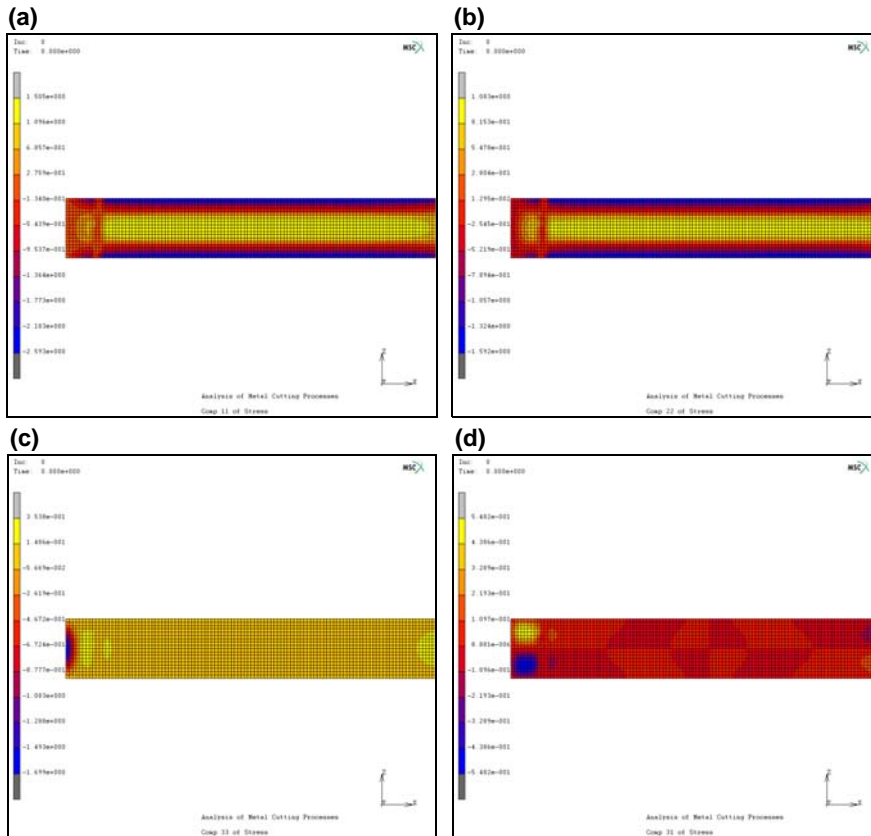


Figure 2.5-3 Model with Initial Stresses before Machining (a) σ_x , (b) σ_y , (c) σ_z , (d) σ_{xz} , $\sigma_{zy} = \sigma_{xy} = 0$

By now, the model is in and all the elements have been applied to *initial stress*. The initial stress information was provided by the company. What we did is to convert 2-D data into our 3-D model using the corresponding adjustments regarding unit and dimension definitions. Isotropic material property parameters are used, which are defined: E (Young's Modules) = 1000, Poisson's ratio = 0.3.

Next step of model definition is to define boundary conditions and loadcases. This procedure is very long and recorded in procedure file: *machining_rcd*. By loading this procedure file and click on START/CONT, Mentat will complete all the tasks automatically. For better understanding, the user may use the STEP button to conduct the procedure step-by-step. In this *Marc User's Guide*, we only selectively demonstrate the key steps that are needed to generate the input data for the metal cutting analysis.

There are a total of four loadcases defined in this model. They are:

1. **Cut the top part of the workpiece.** The cut file used here is *m2q0090s1.ccl*.
2. **Release the bottom boundary condition and apply to the upper face.** This loadcase is the one to flip over the part by switching the boundary conditions from bottom to the newly generated top surface.

3. **Cut the pocket from the lower face.** This loadcase is the one used to cut the pocket on the lower side of the part. The cut file used here is *m2q0090s2.ccl*.
4. **Final release (springback).** This loadcase is to finally release all the boundary conditions, except those required to clear the rigid body motion of the part.

The total sets of boundary conditions defined by this procedure are:

- `Fix_bottom`: This set fixes the x-y-z displacement of all the nodes at the bottom surface. It is used in loadcase 1.
- `Fix_middle`: This set fixes the x-y-z displacement of all the nodes at the top surface of the part after the first cut. It is used in loadcases 2 and 3.
- `Fix_xyz`: This set fixes the x-y-z displacement of node 2266.
- `Fix_x`: This set fixes the x displacement of node 9.
- `Fix_y`: This set fixes the y displacement of node 32065.
- `Fix_z`: This set fixes the z displacement of node 32058. Boundary Condition sets 3 to 6 are used in the loadcase 4.

The Mentat commands to define all the loadcases are shown as below:

Loadcase1 (*Cut the top part of the workpiece*):

```

MAIN
  LOADCASES
    NEW
    NAME
      cutface1
    MECHANICAL
    STATIC
    LOAD
      fixbottom: (to the B.C. for the loadcase)
    CONVERGENCE (defining convergence criteria)
    RESIDUAL
      AUTO SWITCH
        Relative Force Tolerance
          0.01
        OK
    CONSTANT TIME STEP
    STEPS
      10
    OK
  
```

AUTO TIME STEP CUT BACK (OFF)
OK
DEACTIVATION / NC MACHINING (enter the parameters)
NC MACHINING
FILE
m2q0090s1.ccl (name cutter path definition)
LAST INCREMENT (select remeshing method)
(take defaults for other parameters)
RETURN
TITLE
cut the top part of the workpiece

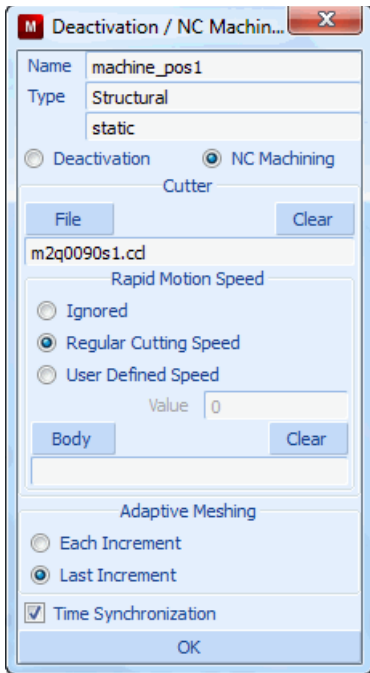


Figure 2.5-4 Definition of First Cutting Loadcase

Now, as shown in [Figure 2.5-4](#), the first loadcase has been defined. Next step is to define the loadcase to flip over the part after the first cut step is completed.

Loadcase2 (Release the bottom boundary condition and apply to the top face):

```
MAIN
LOADCASES
  NEW
  NAME
    release_bot
  MECHANICAL
  STATIC
  LOAD
    fixbottom (OFF to free B.C. for the loadcase 1)
    fixmidface (apply B.C. on middle surface)
  CONVERGENCE (defining convergence criteria)
  RESIDUAL
  AUTO SWITCH
    Relative Force Tolerance
      0.01
      OK
  CONSTANT TIME STEP
  STEPS
    10
    OK
  AUTO TIME STEP CUT BACK (OFF)
  OK
  MANUAL (for Inactive Elements)
  TITLE
    Release the bottom B.C. and apply to the top face
  OK
```

Now, the second loadcase has been defined. Next step is to define the loadcase to cut the pockets over the other side of part. The procedure is recorded as following:

Loadcase3 (cut the pocket from the lower face part):

```
MAIN
LOADCASES
  NEW
  NAME
    cut pocket
```

```
MECHANICAL
STATIC
LOAD
    fixbottom (to apply B.C.)
CONVERGENCE (defining convergence criteria)
RESIDUAL
    AUTO SWITCH
        Relative Force Tolerance
            0.01
            OK
CONSTANT TIME STEP
    STEPS
        10
        OK
    AUTO TIME STEP CUT BACK (OFF)
    OK
DEACTIVATION / NC MACHINING (enter parameters)
    NC MACHINING
        FILE
            m2q0090s2.ccl
            (name cutter path definition)
    LAST INCREMENT (select remeshing method)
(take defaults for other parameters)
    RETURN
    TITLE
        cut the pocket from the lower face part
    OK
```

When the second cutting step is finished, we need to do the analysis of springback. This process requires Marc to free all the restraints except those that are needed to prevent rigid body motion. So, we define the minimum boundary condition for this loadcase (only 6 DOF's are fixed for the whole model). The procedure is recorded as following:

Loadcase4 *(Final release (springback)):*

```
MAIN
LOADCASES
NEW
```

NAME
 final_release_bc

MECHANICAL

STATIC

 LOAD

fixmidface *(free B.C.)*

fix_xyz *(fix x, y and z)*

fix_x *(fix x)*

fix_y *(fix y)*

fix_z *(fix z)*

CONVERGENCE *(defining convergence criteria)*

RESIDUAL

 AUTO SWITCH

 Relative Force Tolerance

 0.01

 OK

 CONSTANT TIME STEP

 STEPS

 2

 OK

 AUTO TIME STEP CUT BACK *(OFF)*

 OK

 MANUAL *(for Inactive Elements)*

 TITLE

final release (spring back)

 OK

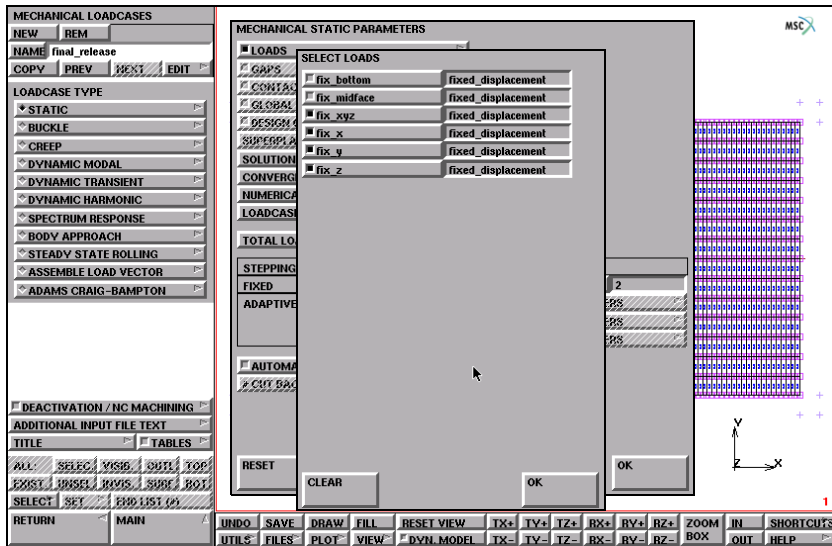


Figure 2.5-5 Definition of Final Springback Analysis

Local Mesh Adaptivity Definition

After the loadcases are defined, it is necessary to define the Marc job. The following procedure records the job definition with this model.

First, it is necessary to define the parameters for local adaptive remesh:

MAIN

MESH ADAPTIVITY

LOCAL ADAPTIVITY CRITERIA

MORE

ELEMENT WITHIN CUTTER PATH

MAX # LEVELS

1

OK

ADD

EXIST

(choose all existing elements)

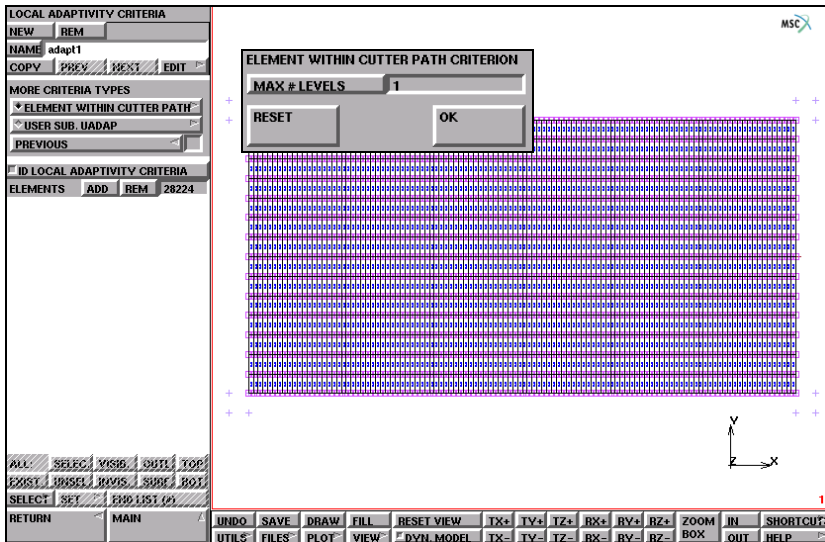


Figure 2.5-6 Definition of Parameters for Local Adaptive Remeshing

Before job definition, we define the element type for this analysis by:

```

MAIN
  JOB
    ELEMENT TYPES
      MECHANICAL
        3-D Solid
        select 7
      OK
    EXIST (choose all existing element)
    
```

Then the job definition is done with the following procedure.

```

MAIN
  JOB
    NEW
    NAME
      metal_cut
    MECHANICAL
      Select loadcases 1, 2, 3, and 4 sequentially
      (Applying loadcases)
    
```

- INITIAL LOADS *(click OFF all the b.c.)*
- INITIAL CONDITIONS *(check if they are all on)*
- ANLYSIS OPTIONS *(use defaults for this)*
- MESH ADAPTIVITY *(use defaults for this, [Figure 2.5-7](#))*
- OK
- JOB RESULTS *(select the results that are interested)*
- CENTROID *(reduce the post file size by clicking this button)*
- OK
- JOB PARAMETER
- SOLVER *(choose correct solver)*
- ITERATIVE SPARSE
- INCOMPLETE CHOLESKI
- OPTIMIZATION
- OK
- (Iterative solver is used to reduce memory requirement and total computation time)*
- OK
- OK

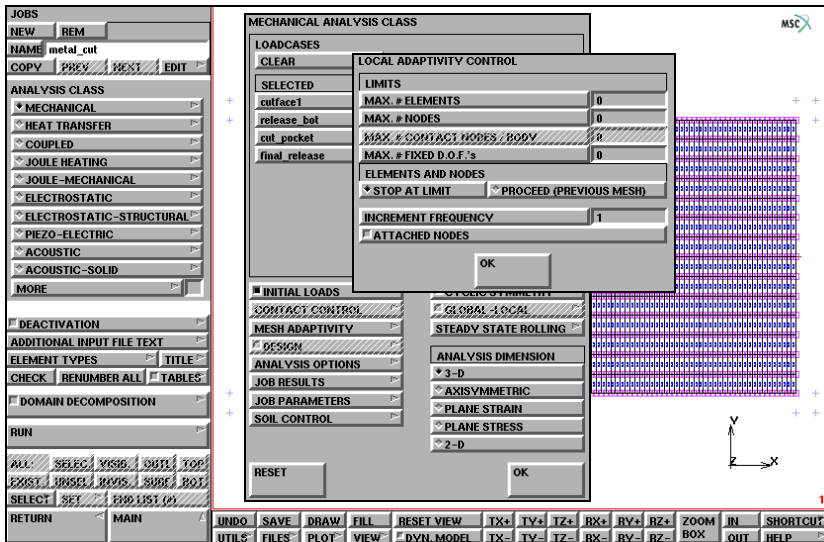


Figure 2.5-7 Definition of Machining with Mesh Adaptivity

After the job is defined, to run the job and see the results, it is necessary to do following:

```
MAIN
  JOB
    RUN
      SUBMIT (1)
      OK
MAIN
  RESULTS
  OPEN DEFAULT
  DEF ONLY
  CONTOUR BAND
  SCALAR
    Total Displacement
    OK
  FILL
  DYN. MODEL
  MONITOR
```

Up to now, the FE analysis of machining (namely, metal cutting) process has started. By clicking the MONITOR button, Mentat instantly shows the progress of the calculation.

Visualization of Results

Enhancements have been made for better visualization of the results of Metal Cutting analysis. Particularly, the elements being cut off from the part are not displayed in Mentat, so that only the remaining part of the FE model is displayed for postprocessing purposes.

To check the results, we first need to check whether the cutter paths have been followed exactly. Secondly, we need to check the deformations and stresses left in the remaining part. By analyzing the deformation/displacement results, we can see the effect of residual stress and machining process to the geometry of the final part.

As shown in [Figure 2.5-11](#), we see that the cutter path has been processed properly during the FE analysis. The part displayed strong deformation after springback, as shown in [Figure 2.5-11](#). The maximum displacement of the part is about 20 times larger after springback (from 0.0005688 increases to 0.01055 in.). [Figure 2.5-12](#) shows the deformation pattern after machining process with the residual stress provided.

For places with corner of small radius, a fine mesh is required in order to have better resolution of the part shape after machining. [Figure 2.5-13](#) shows the finer mesh after local adaptive remeshing at one of the corner areas.

In [Figure 2.5-8](#), the model displays the results after each loadcases, respectively.

1. Cut upper face

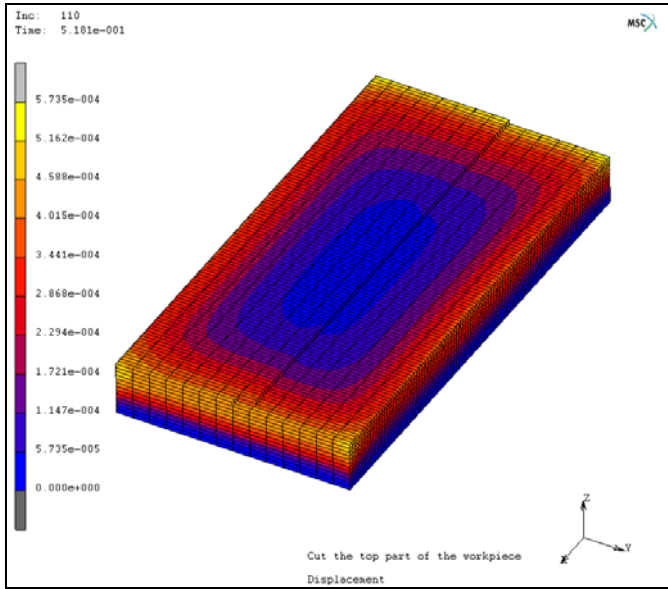


Figure 2.5-8 Machining of the Upper Surface

2. Flipping over (switch boundary conditions)

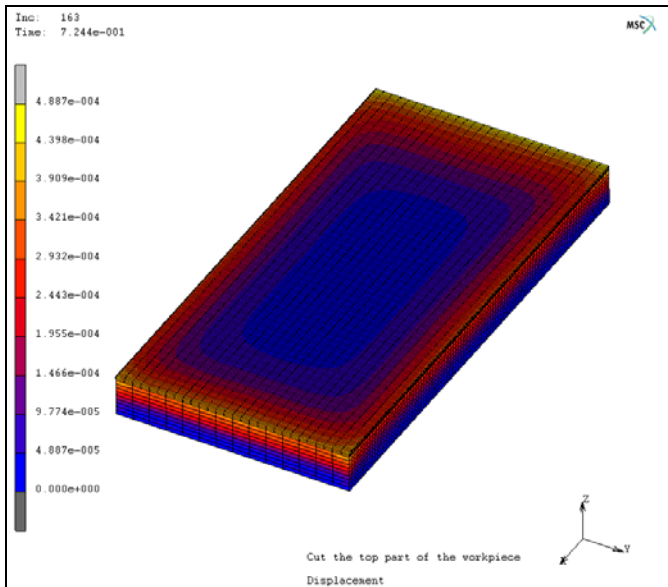


Figure 2.5-9 Flip over the Part after First Cutting Process

3. Cut pockets

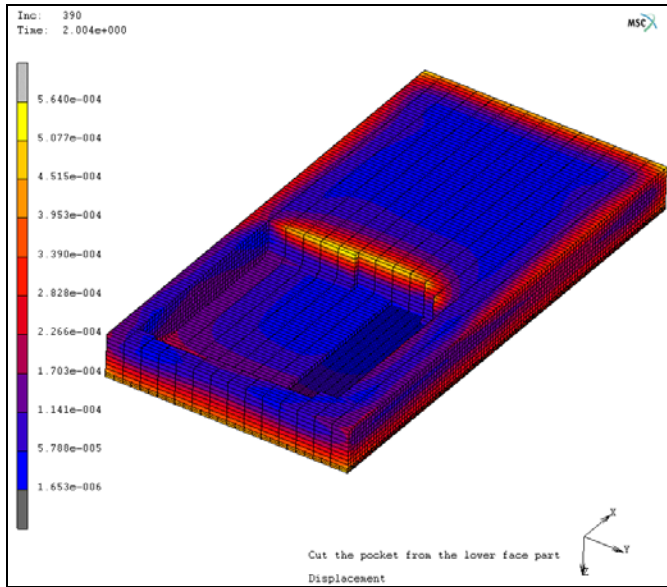


Figure 2.5-10 Process of Pocket Cutting

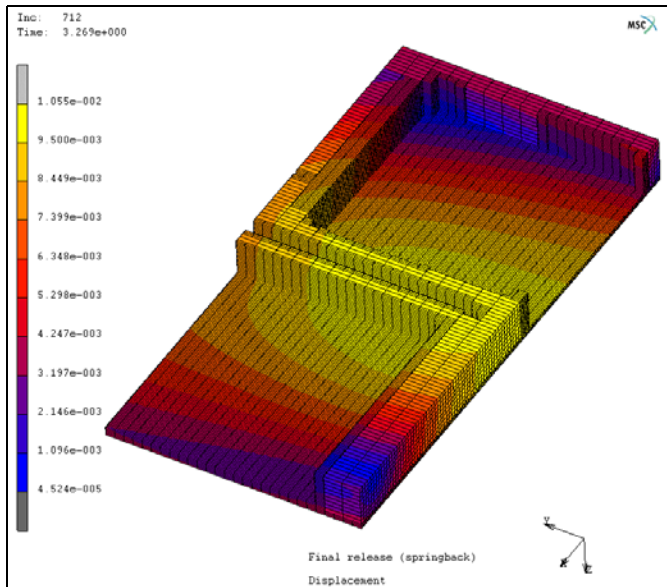


Figure 2.5-11 Geometry after Pocket Cutting

4. Final release (springback)

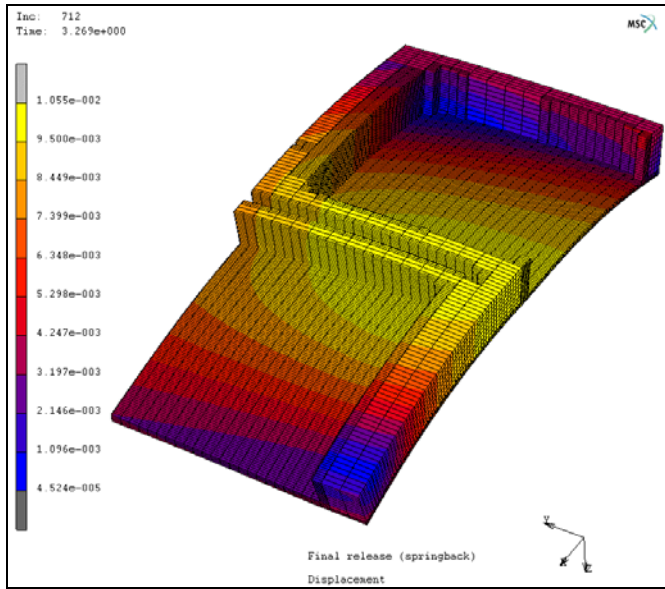


Figure 2.5-12 Final Geometry and Deformation after Springback (with scaling)

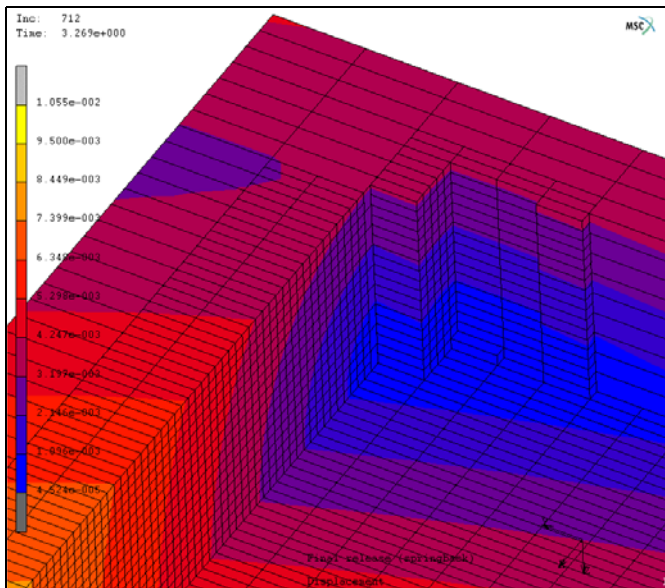


Figure 2.5-13 Visualization of Mesh after Adaptive Remeshing

Verification of Material Removal

Material removal during machining causes a redistribution of residual stresses that change the dimensions of the final part. An experimental verification of this machining behavior is included as a 1.5 inch thick stock aluminum beam that is bent to a prescribed radius. A 2.5 inch slot is cut through 75% of its thickness. The displacements of the ten gage points shown in Figure 2.5-14 are measured before and after the machining process.

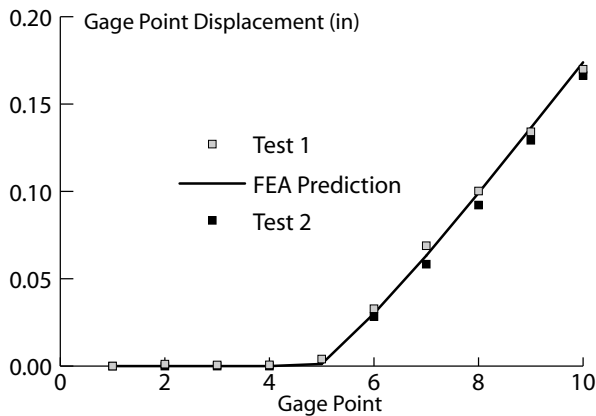
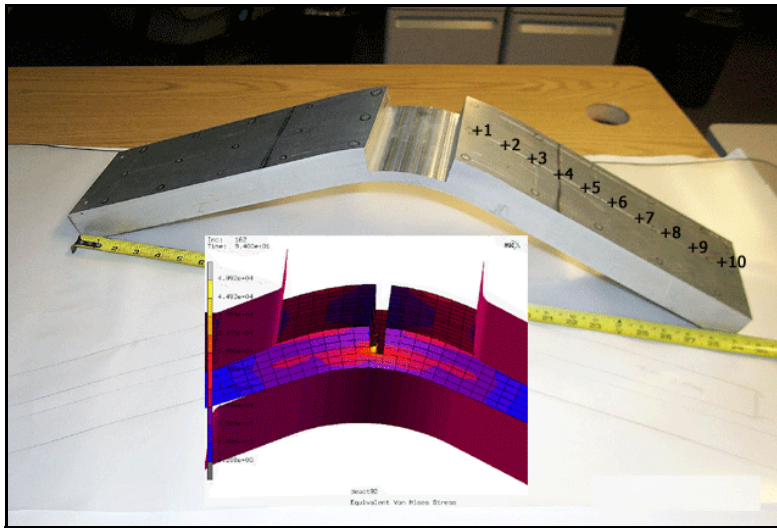


Figure 2.5-14 Machining Simulation and Test of Aluminum Beam: Experimental Versus Simulation Deflection of the Ten Gage Points

Example 2: Thin Frame Cutting

Input Data

The purpose of this example is to compare the local adaptive remeshing methods for NC machining analysis. One method is the regular adaptive remeshing, which the adaptive remeshing is conducted progressively with the cutter motion. The other method is the irregular adaptive remeshing which the adaptive remeshing is conducted at the end of the cutting loadcase after the cutting path is completed.

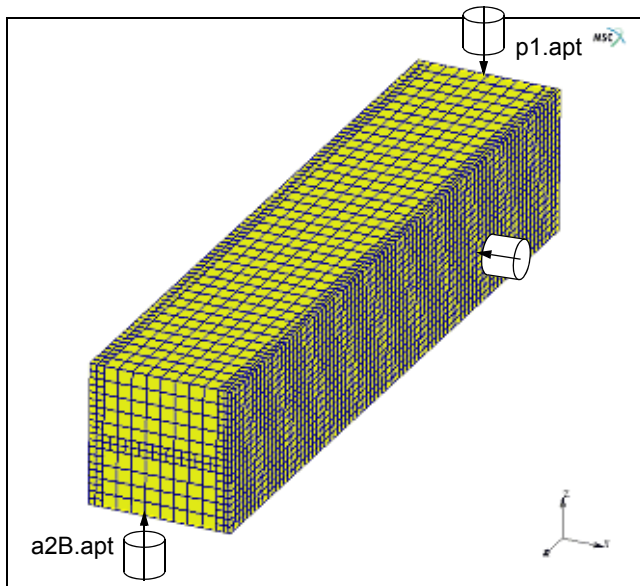


Figure 2.5-15 Initial Geometry of the Workpiece

The input data available for this example is summarized as:

- **NC data:** APT format data is used for this example. There are three cutting passes (each pass has its own APT file). They are: *p1.aprt*, *a2B.aprt*, and *b3A.aprt*. The three cutting paths are illustrated in [Figure 2.5-15](#).
- **Initial Marc model:** For this example, it is imported from the *.mud* file which includes the finite element model definition for the workpiece and the file names for cutter path definition. The workpiece is a slab with dimensions of 3.9x3.9x20. Totally, 13440 brick elements and 18135 nodes are defined in the model.
- **Initial stress data before the cutting process started:** For this particular example, the initial stresses are set by the user with constant value of $s_{xx}=10000$, $\sigma_{yy} = \sigma_{zz} = \sigma_{zx} = \sigma_{xy} = \sigma_{yz}=0$.

As the Marc model has been predefined, it is assumed that the user is already familiar with model definition procedures for material properties and boundary condition, etc. So, we have set a procedure file to read in the predefined model and continue from there to define the corresponding loadcases and job parameters to run the machining analysis of this cutting example.

This is done by reading in the procedure file: *example2.proc*. As shown in [Figure 2.5-3](#), after clicking the LOAD button, and selecting the file name *example2.proc*, then click command START/CONT. The sequence is shown as (after Mentat is started):

```
UTILS
  PROCEDURES
    LOAD
      example2.proc
    OK
```

Up to now, by clicking on START/CONT button, the procedure file is executed. First, the initial model file *machining_mp1_cm_r1.mud* is read in, initial stress is defined, then job parameters and loadcases are set. Finally, the job is submitted and the visualization of results are started. The Mentat command is:

```
START/CONT
```

Initial Stress and Local Adaptive Remeshing Definition

First, the initial stress is defined by (see [Figure 2.5-16](#)).

```
MAIN
  INITIAL CONDITIONS
    NEW
  MECHANICAL
    STRESS
      Click on the 1st component of stress
      Enter value: 10000
    OK
  ADD
  EXIST (choose all existing elements)
```

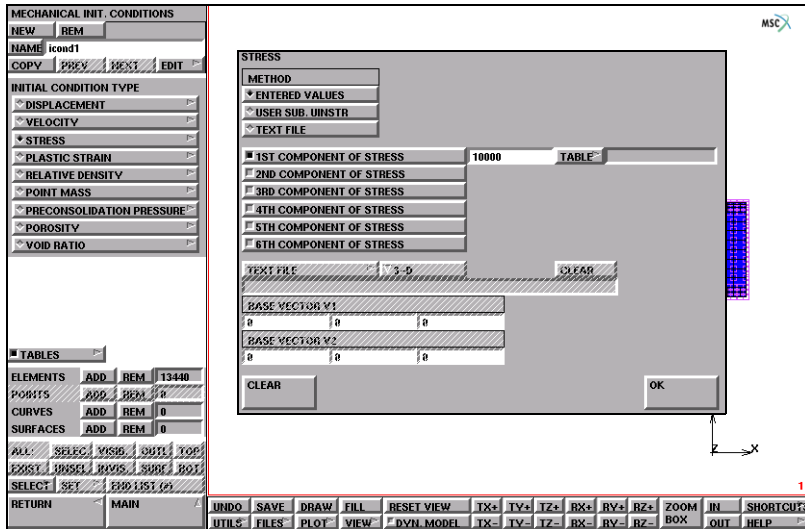


Figure 2.5-16 Definition of Initial Stress

Then, it is necessary to define the parameters for local adaptive remesh. This is done in a similar way as shown in Figure 2.5-6 as:

```

MAIN
  MESH ADAPTIVITY
    LOCAL ADAPTIVITY CRITERIA
      MORE
        (ELEMENT WITHIN CUTTER PATH)
        MAX # LEVELS
          1
        OK
      ADD
      EXIST
  
```

(choose all existing elements)

Loadcases and Machining Job Definition

There are a total of six loadcases defined in this model. They are:

1. **The first cutting path defined by APT file:** *p1.apt*. In this loadcase, boundary condition set *m_clamp* is applied.
2. **Release pos1:** To remove the current *m_clamp* boundary condition set and apply the release boundary condition set of *m_clamp*.

3. **The second cutting path defined by APT file:** *a2B.apt*. In this loadcase, boundary condition set `m_clamp` is re-applied.
4. **Release pos2:** To remove the current `m_clamp` boundary condition set and apply the release boundary condition set `m_clamp`.
5. **The third cutting path defined by APT file:** *b2A.apt*. Similarly, boundary condition set `m_clamp` is applied in this loadcase.
6. **Net Release:** In this loadcase, both boundary condition sets: `m_clamp` and `release` are applied. So, this workpiece is not totally freed from the clamps.

In the Mentat procedure file, the parameter definition of all the machining (metal cutting) loadcases has been recorded. However, due to the similarity, only the first one is shown below:

Loadcase1 (*Cut path of p1.apt*):

```
MAIN
  LOADCASES
    EDIT
      machine_pos1
    OK
  DEACTIVATION / NC MACHINING                                     (enter parameters)
    NC MACHINING
      FILE
        p1.apt                                                    (name cutter path definition)
    LAST INCREMENT                                              (select remeshing method)
                                                                (take defaults for other parameters)
  RETURN
```

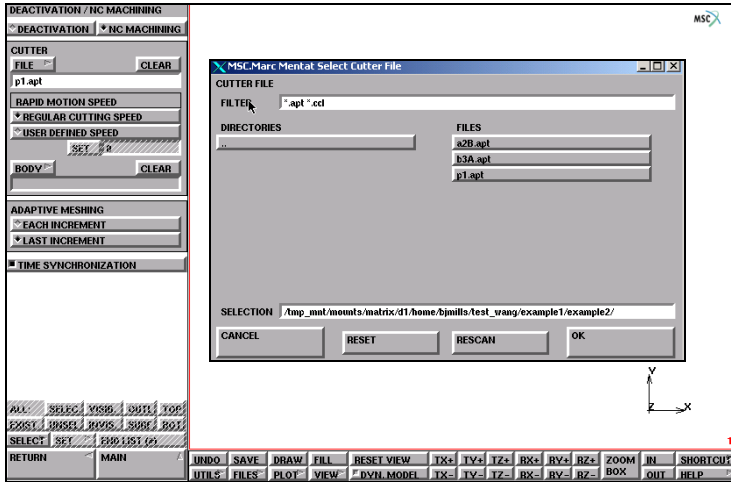


Figure 2.5-17 Definition of the First Case for Cutting Path: p1.apr

Similarly, the loadcases for the other two cut paths (*a2B.apr* and *b2A.apr*) can be defined.

FEA Results

This analysis uses the local adaptive remeshing at each cutting loadcase. The adaptive remeshing is only conducted at the last increment of each loadcase. [Figure 2.5-18](#) shows the intermediate stage of the first cut path. In [Figure 2.5-18](#), the original mesh is still present for the first cutting path until the last increment is completed ([Figure 2.5-19](#)). After three cutting paths, the workpiece and deformation are displayed in [Figure 2.5-21](#), respectively.

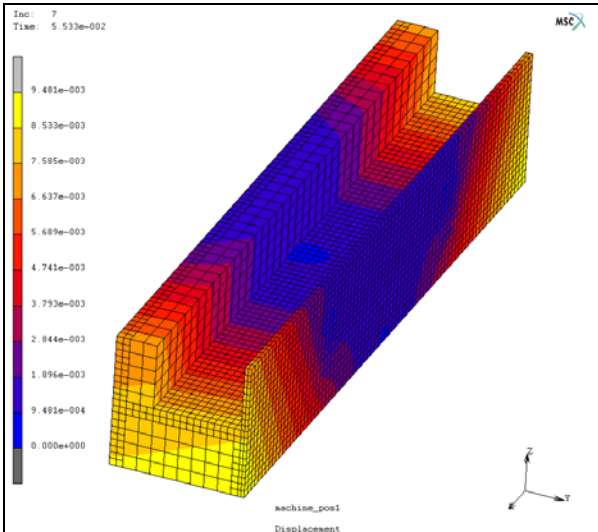


Figure 2.5-18 Intermediate Stage of the First Cutting Path

1. The workpiece after cutting path, *p1.apr*:

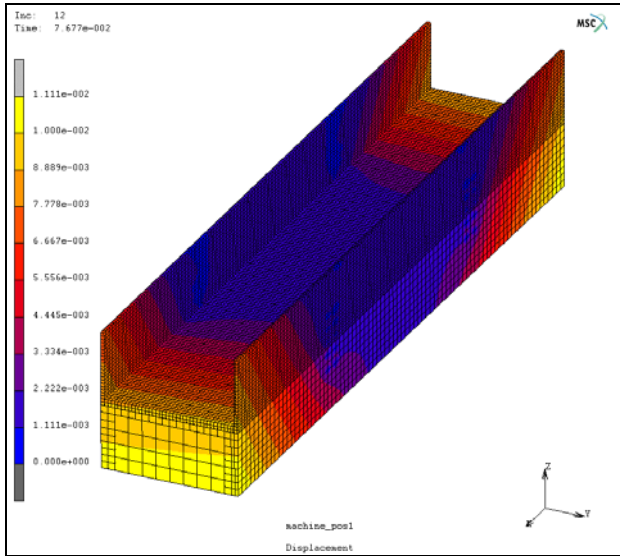


Figure 2.5-19 Workpiece after First Cutting Path

2. The workpiece after cutting path, *a2B.apr*:

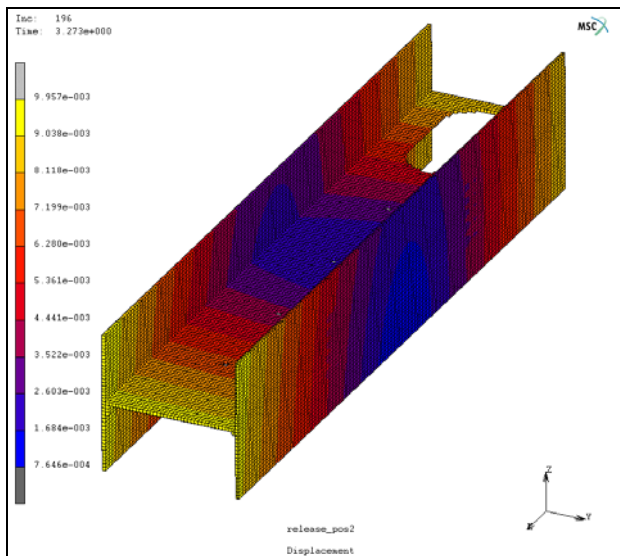


Figure 2.5-20 Workpiece after the Second Cutting Path

3. The workpiece after cutting path, *b2A.apr*:

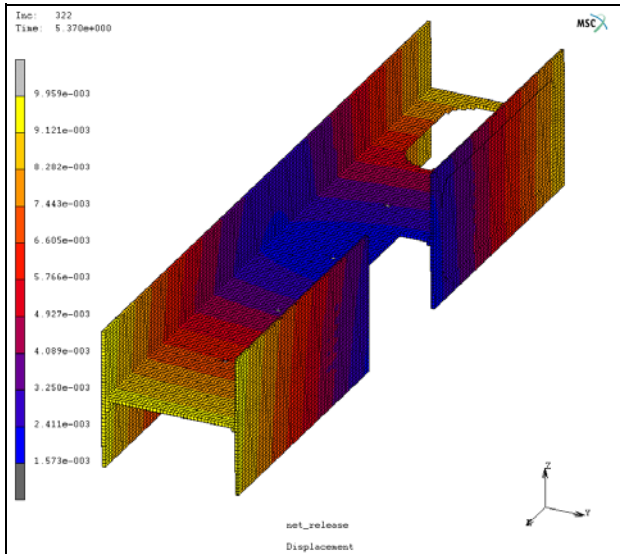


Figure 2.5-21 Workpiece after the Third Cutting Path

For comparison purpose, the regular adaptive remeshing method is also used to conduct the analysis. User can achieve this by selecting the EACH INCREMENT button when defining the adaptive remeshing method for the machining loadcases. In this way, the adaptive remeshing is performed instantly at each increment if an element is found partially intersected by the cutter path. As shown in Figure 2.5-22, some elements are already subdivided at the intermediate stage of the first cutting path because of the intersection with the cutter. Comparing to the previous analysis with adaptive remeshing only at the final increment of the loadcase, additional new elements and nodes are generated due to the adaptive remeshing. Correspondingly, more CPU time and larger memory capacity are required.

Table 2.5-1 compares the general information of the two analysis. It can be seen that the analysis with instant adaptive remeshing at each increment whenever any element needs to be subdivided causes the model to become extremely large. Therefore, an increase in computer memory and CPU time are needed to complete the analysis. However, as shown in Figure 2.5-23, the results are not significantly different as compared with the results shown in Figure 2.5-21.

For this example, using the irregular method for adaptive remeshing can significantly reduce the maximum number of elements and nodes generated during the remeshing process with nearly the same accuracy.

Table 2.5-1 Comparison of the Two Adaptive Remeshing Methods for Machining Analysis

Adaptive Remeshing Method	Total Number Increments	Max. # Nodes	Max. # Elements	Memory (MB)	Total CPU Time (sec)
Regular (Each increment)	362	105280	91200	1154	34429
Irregular (Last increment)	326	65892	51200	693	20688

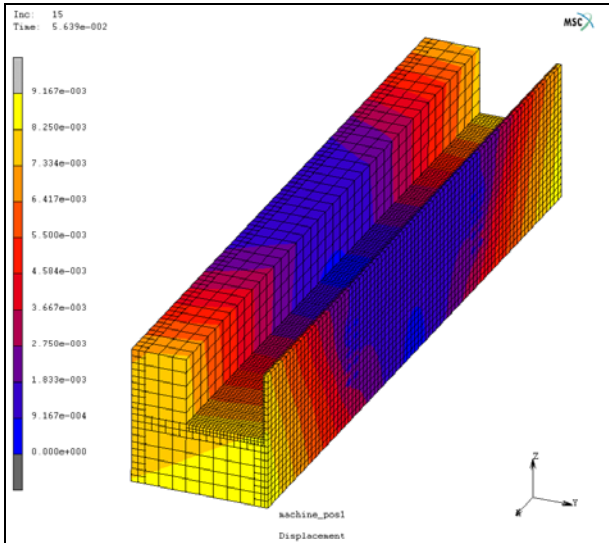


Figure 2.5-22 Intermediate Stage of the First Cutting Path with Instant Adaptive Remeshing

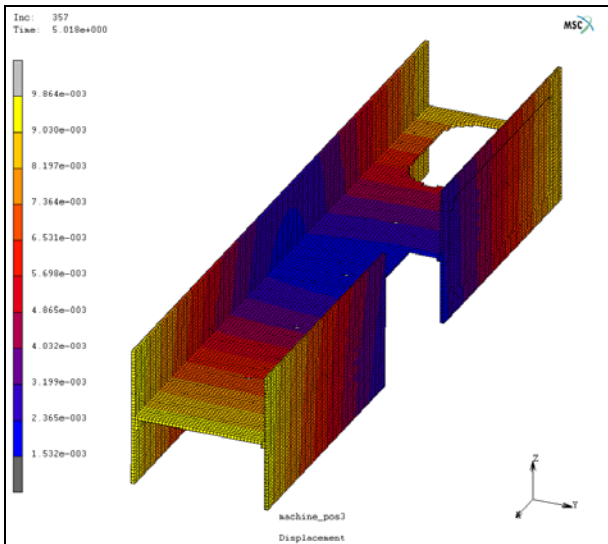


Figure 2.5-23 Workpiece after Final Cutting Path with Instant Adaptive Remeshing

Example 3: Imported Initial Stresses

Overview

As mentioned before, the existing three possible approaches for the user to import the initial stresses are: **Pre State**, **Text Data File**, and **Table Input**. This section demonstrates usages of the Text Data File and the Pre-State approach for the import of the initial stress into the FE Model for machining analysis.

Import with Text Data File

Input Data

The text data file stores the initial stress data of the workpiece of the machining process. These data, generated either by analytical or experimental methods, are saved in a text file in the format as described in *Appendix B* of the *Marc Volume A: Theory and User Information Manual*.

The initial model is a block as shown in [Figure 2.5-24](#). The red-lined surface is the tool surface created in the model for the visualization of cutter motion. One side of the block is fixed during the cutting process (see the arrows).

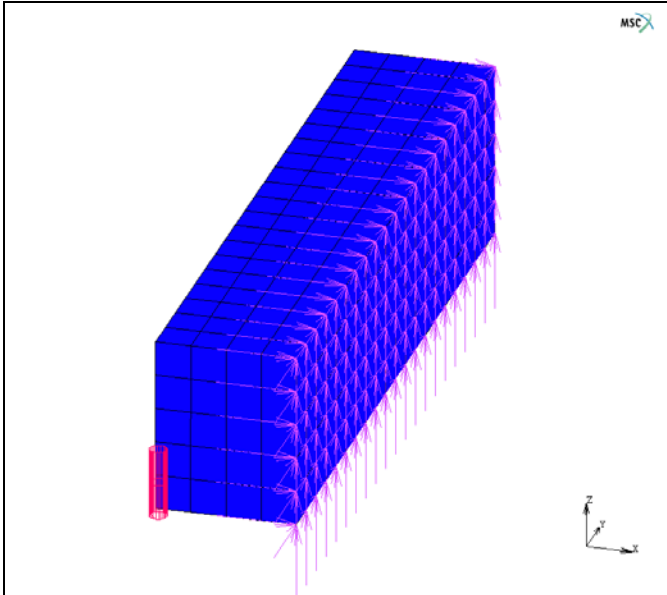


Figure 2.5-24 Initial Geometry of the Workpiece

Model and Loadcase Definition

The whole procedure of running this example has been recorded in procedure file: *example3a.proc*. The user can follow that file to reproduce the input deck and visualize the results. To run this procedure file within Mentat, the user only needs to follow the commands as shown below:

```
UTILS
  PROCEDURES
  LOAD
    example3a.proc
  OK
START/CONT
```

In order to make it easier to understand how to define a text data as initial stress and to define the tool surface as the cutter so that the cutter motion can be visualized, two extra procedures are shown below, respectively:

Use the command procedure below to define the initial stress data file (Figure 2.5-25):

```
MAIN
  INITIAL CONDITIONS
  NEW
  MECHANICAL
  STRESS
  TEXT FILE
    Initialstressn
  OK
  3-D
  Click on each areas to define each components of
  the two base vectors required for this analysis
  1
  0
  0
  0
  1
  0
  OK
  ADD
  EXIST (choose all existing elements)
```

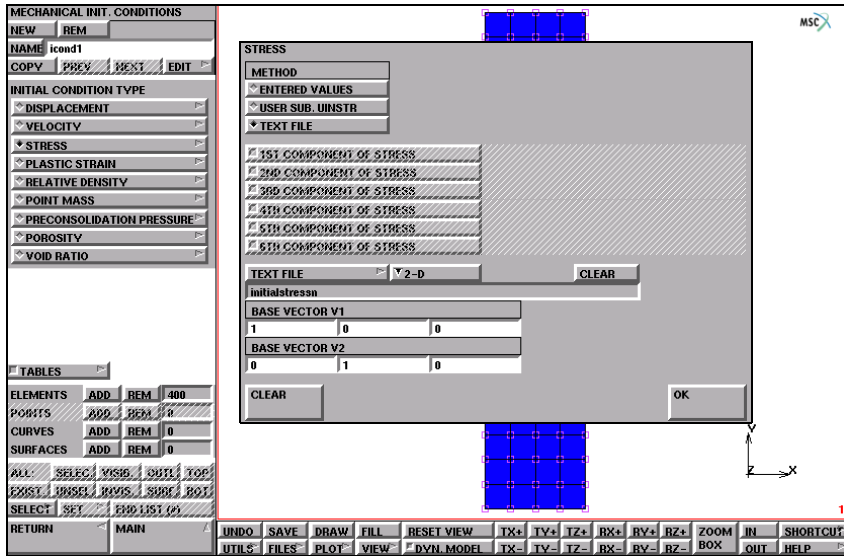


Figure 2.5-25 Definition of Text Data File for Initial Stress

Below is the Mentat command procedure to define the tool surface to represent the cutter in the model (Figure 2.5-26). Note that this tool surface must be located at position (0,0,0) before the first cutting process starts.

```

MAIN
  LOADCASES
    NEW
    NAME
      lcase1
  MECHANICAL
  STATIC
  ...
  OK
  DEACTIVATION / NC MACHINING (enter parameters)
  NC MACHINING
  FILE
    extru-test.aprt
  BODY (select contact surface as cutter)
    cbody2 (see Figure 2.5-26)
  RETURN
  
```

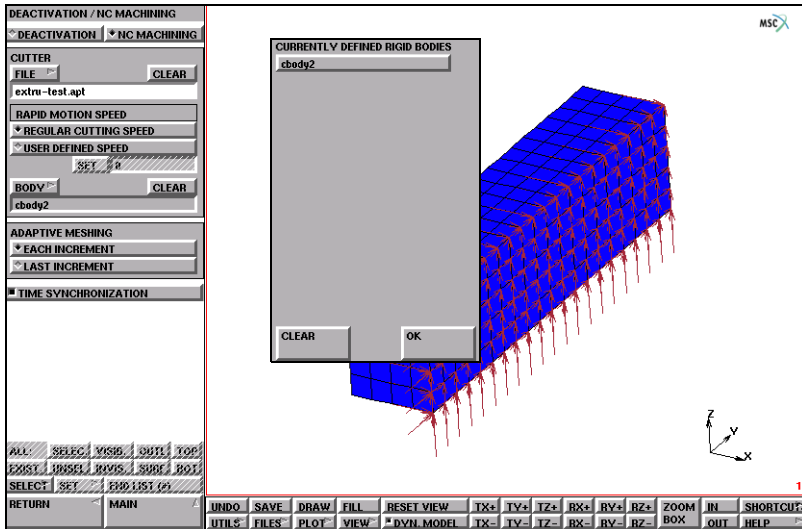


Figure 2.5-26 Definition of the Tool Surface to represent the Cutter

Job Definition

In this example, the contact tool surface has been defined as the cutter surface, so it is necessary to prevent this tool surface from contact detection. Therefore, as contact table: *ctable1* has been created. As shown in Figure 2.5-27, it can be seen that the contact surface: *cbody2*, is deactivated for contact detection. In addition, the local adaptive remeshing is also adopted with maximum of one level splitting for each element.

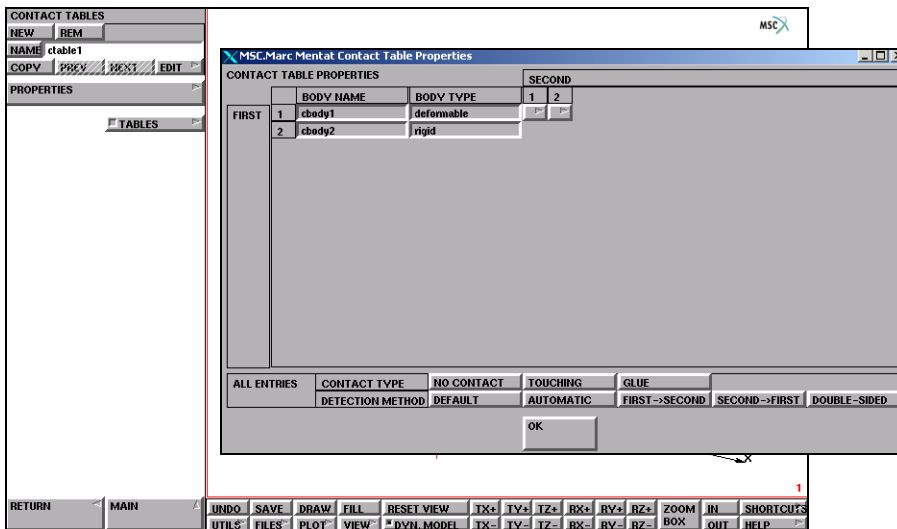


Figure 2.5-27 Contact Table to prevent the Cutter Surface from Real Contact

Visualization of Results

Figure 2.5-28 shows the initial stress at increment zero. The stress values displayed in the FE model are those transferred from the text data file: *initialstressn*. This puts the cutter position at an intermediate stage of the cutting process (Figure 2.5-29).

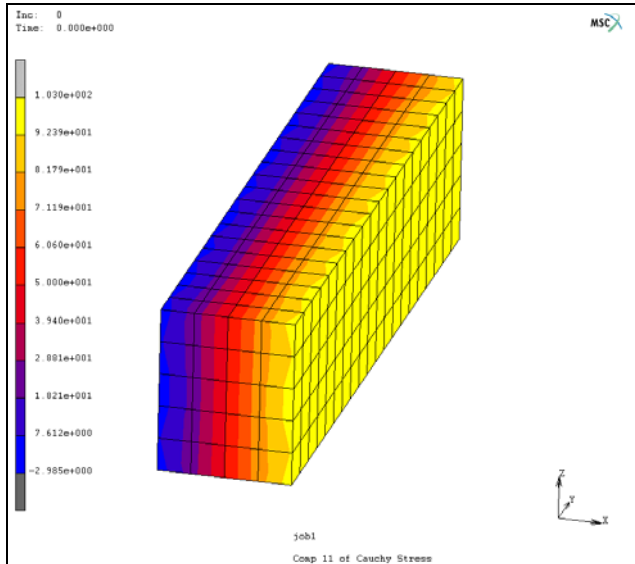


Figure 2.5-28 Initial Stress at Increment Zero

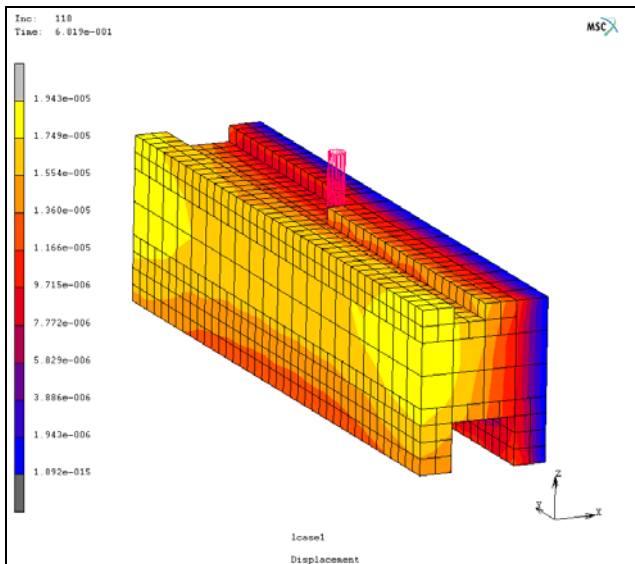


Figure 2.5-29 Cutter Position in the Machining Process

Import with PRE STATE Feature

PRE STATE is a feature that enables users to transfer result data from a previous Marc analysis to a new Marc analysis as an initial state. This feature also allows users to expand a 2-D model of a plane strain or axisymmetric application to a 3-D model, transferring the history data automatically from 2-D to 3-D as the initial conditions. In this sense, AXITO3D (from axisymmetric 2-D to 3-D) feature supported in earlier releases is now a special case of PRE STATE. This feature also allows users to select contact bodies that are needed in the new analysis.

The following example shows its application with NC machining simulation. To use this feature, users will simulate the process leading to the NC machining. After the pre-state values are obtained, the deformed workpiece needs to be merged into the new model in order to start the new analysis. The examples described here shows how to use this feature. The two procedures are described, respectively, for the pre-analysis and final machining analysis.

It is necessary to notice that the pre-state feature is generally available in Marc, not limited to machining analysis. For more information about this feature, refer to *Marc Volume A: Theory and User Information* and *Marc Volume C: Program Input*.

Input Data

The initial model is a block (Figure 2.5-24), which is the same one as used in the example below (Figure 2.5-30). The only difference is that there is no pre-defined initial stress. The boundary conditions are applied in order to pre-deform the body before the machining process started. The boundary condition set *compress* is to compress the workpiece from the right side. The boundary condition set *tension* is to pull some nodes on the front end of the workpiece. The boundary condition set *appy1* is to fix the all nodes on the left side.

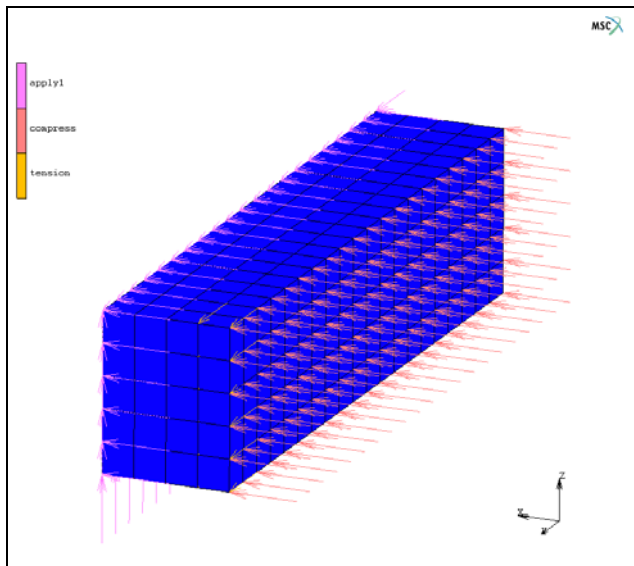


Figure 2.5-30 Workpiece and Boundary Conditions

The first step is to run the analysis using *3dcut1.mfd*. This provides the initial conditions and the deformed mesh for the NC machining simulation. When the analysis is completed, read in the result file. Assuming the NC machining simulation starts at the end of the previous analysis, users need to scan to the last increment. Apply REZONE MESH to extract the mesh configuration at the end of the analysis. This mesh will be used in the NC machining simulation. The following steps are used to extract the deformed mesh in Mentat:

Step 1: read in *3dcut1_job1.t16*

Step 2: scan to the last increment

Step 3: apply REZONE MESH

Step 4: save the mesh in a model file: *test_1.mfd*.

In the new model file, *3dcut2.mfd*, users can replace the mesh using MERGE with *test_1.mfd*.

Pre-deformed FE Mesh

There are two methods to define the mesh for the FEA model after the pre-deformation:

1. To import the post data into Mentat and take the last deformed workpiece as the initial geometry of the new FE model. The advantage of this method is that the user can take into account the pre-deformed geometry of the workpiece during the model design stage.
2. To use the original (undeformed) body and additionally select total displacement as one of the pre-state variables that needs import into the new model during the FE analysis by Marc. This method is simple and easy to use, providing there is no global remeshing or any mesh changes in the previous analysis.

For the demonstration purpose, the first method is used in this example. The whole procedure run of this example has been recorded in procedure file: *example3b.proc*. The user can follow that file to reproduce the input deck and visualize the results. To run this procedure file within Mentat, follow the commands as shown below:

```

UTILS
  PROCEDURES
    LOAD
      example3b.proc
    OK
  START/CONT

```

Within procedure file: *example3b.proc*, the deformed mesh is automatically merged into the new model for machining analysis. The command procedure is recorded as below:

```

MAIN
  RESULTS
  OPEN
    3dcut1_job1.t16
  OK

```

```
DEF ONLY
LAST
TOOLS
    REZONE MESH
MAIN
FILES
SAVE AS
    test.1.mfd
    OK
MAIN
```

The new model is created at the end of the above procedure. The user can either generate a new model from *test_1.mfd* or merge it into the model file *3dcut2.mfd* by replacing the FE mesh in *3dcut2.mfd* with *test_1.mfd*.

Import of the Pre-State Results

Using the following procedure below completes the definition of the pre-state results (Figure 2.5-31):

```
MAIN
    INITIAL CONDITIONS
        NEW
        MECHANICAL
            PREVIOUS ANALYSIS STATE
                STRESS
                STRAIN
                PLASTIC STRAIN
                TOTAL EQUIVALENT PLASTIC STRAIN
            POST FILE
                3dcut1_job1.t16
            OK
        INCREMENT
        LAST
        SELECT BODY
            cbody1 (defaults)
        OK
    OK
```

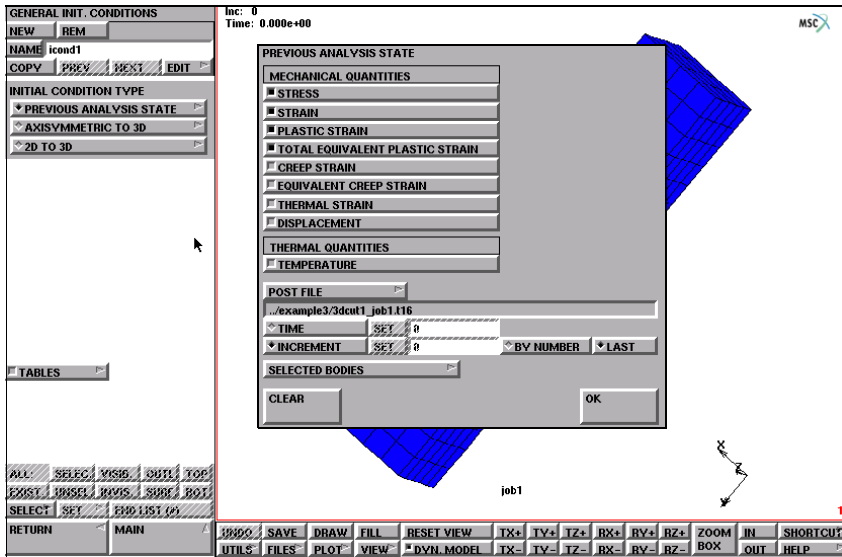


Figure 2.5-31 Definition of the Pre-State Option for Initial Conditions

Job and Loadcase Definition

Now, we can see that the initial condition is automatically activated when the job is created, as shown in Figure 2.5-32:

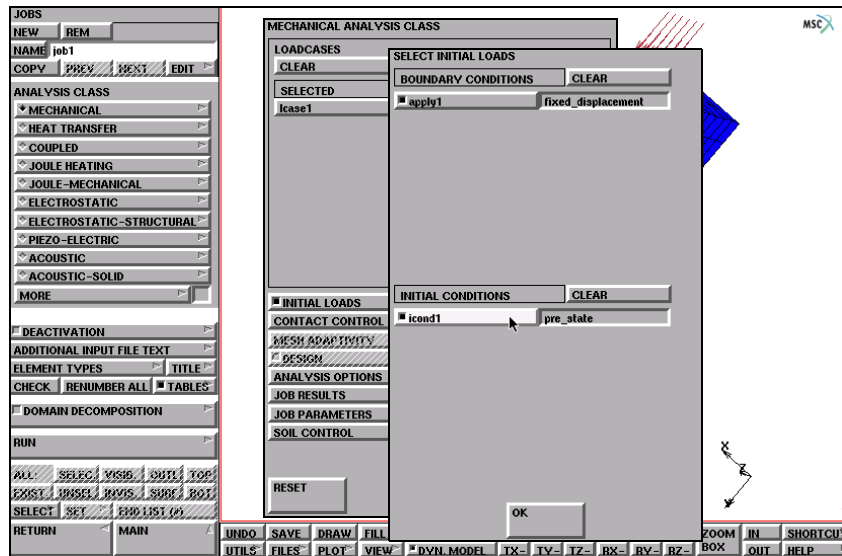


Figure 2.5-32 Job Definition with PRE-STATE Initial Conditions

Visualization of Results

In confirming that the initial stress set by the Pre-State feature had successfully transferred the initial data into the new model, you can compare the stress data at the last increment in the previous analysis of the stress data at increment zero in the current analysis (Figure 2.5-33). The final stress and displacement after machining are shown in Figure 2.5-34.

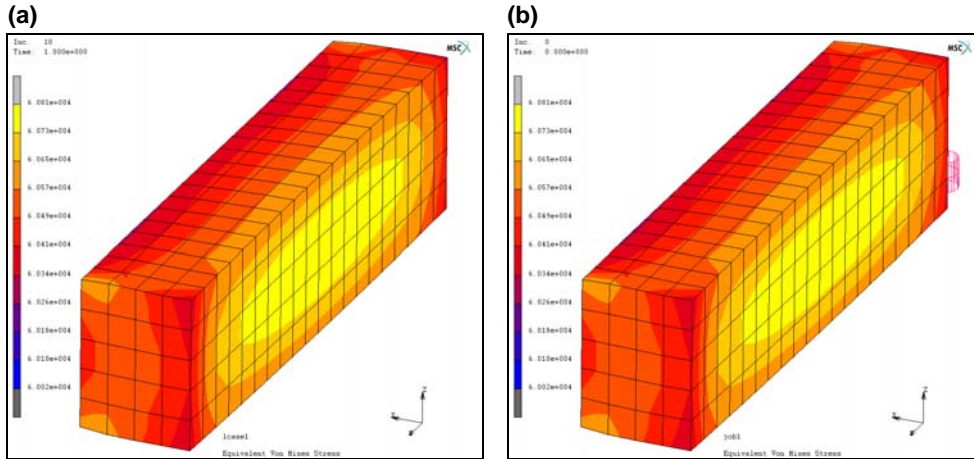


Figure 2.5-33 Stress Data before (a) and after (b) Transferred by Pre-State Feature

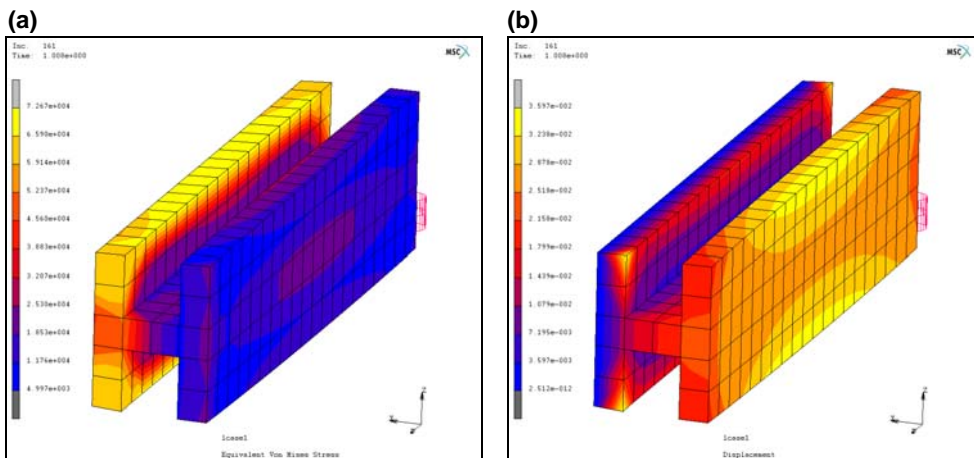


Figure 2.5-34 The Equivalent Stress (a) and Displacement (b) after Machining

Input Files

To run the examples, to type in the commands or execute the following procedure files:

```
Example1: %MENTATDIR%/mentat -pr mc_nfg.proc
Example2: %MENTATDIR%/mentat -pr example2.proc
Example3: %MENTATDIR%/mentat -pr example3a.proc
          %MENTATDIR%/mentat -pr example3b.proc
```

The files below are on your [delivery media](#) or they can be downloaded by your web browser by clicking the links (file names) below.

File	Description
3dcut1.mfd	deformed mesh for the NC machining simulation
3dcut2.apt	cutter path data
3dcut2.mfd	new model file
a2B.apt	cutter path data
b3A.apt	cutter path data
ex_prestate.mfd	model file to define pre-stress
ex_r01.mud	predefined model file
example2.proc	procedure file to run example 2
example3a.mfd	predefined model file called by example3a.proc
example3a.proc	procedure file to run example 3a
example3b.proc	procedure file to run example 3b
extru-test.apt	cutter path data
initialstressn	text file of initial stresses
m2q0090s1.ccl	cutter path data file
m2q0090s2.ccl	cutter path data file
machining.proc	post processes results from machining_mp1_cm_r1.mud
machining_mp1_cm_r1.mud	model file used in example 2
machining_rcd	procedure file that applies loads and BCs
mc_nfg.proc	procedure file to run example 1
p1.apt	cutter path data
prestate.proc	procedure file to load prestress & visualize
prestate_table.proc	procedure file to postprocess 3dcut1.mfd

2.6 Parallelized Local Adaptive Meshing

- Chapter Overview 444
- Simulation 444
- Input Files 447
- Animation 447

Chapter Overview

The sample session described in this chapter demonstrates the process of bending a tube around a mandrel. The simulation will use local adaptive meshing with parallel processing using a single input file. Local adaptive meshing will add elements and thus improve the accuracy of the simulation. In prior versions, parallel processing was not available for local adaptive meshing. Furthermore, parallel processing also needed each domain to be written to a separate input file. These limitations have been removed as demonstrated herein.

The goal of the analysis is to demonstrate:

- Local adaptive meshing with parallel processing
- The use of a single input file

Simulation

A metal tube will be bent ninety degrees around a mandrel as shown in [Figure 2.6-1](#). The local adaptivity criterion is based upon relative equivalent plastic strain with a threshold value of 0.75 and two levels of subdivision. [Figure 2.6-2](#) shows a close up of the total equivalent plastic strain contours in the final position.

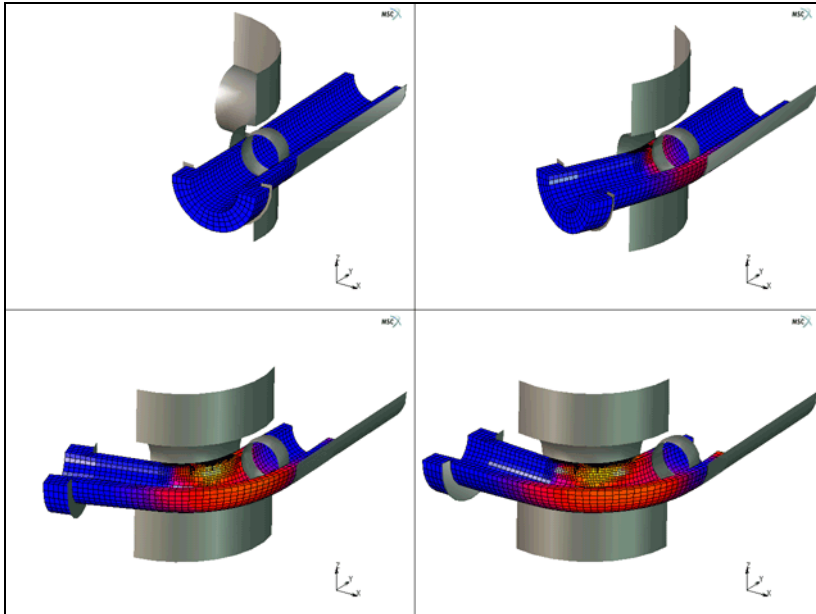


Figure 2.6-1 Metal Tube Bent Around Mandrel

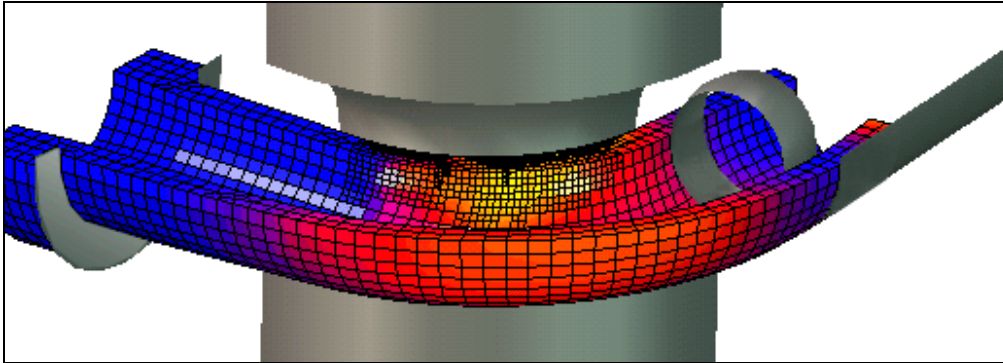


Figure 2.6-2 Metal Tube in Final Position (Plastic Strain Contours)

The simulation uses symmetry and only half of the tube is modeled. Poisson's ratio is 0.3; Young's modulus is 200,000 Mpa with initial yield of 200 Mpa with work hardening. To run the simulation in parallel using the single input file mode, simply submit the single input file, say `tubebend_job1.dat` with the following procedure:

Procedure: run single input file in parallel using 4 processors

```
../path/tools/run_marc -j tubebend_job1 -v n -b n -nps 4
```

where the option `-nps 4` indicates the number of processors, 4, in the single input mode. Running the job in parallel will produce $n+1$ post files that can be read into Mentat individually or consolidated by choosing the root post file.

Figure 2.6-3 identifies the 4 domains that were automatically chosen. In this case, the number of elements in each domain vary because of the adaptive meshing during the analysis. Originally each domain had only 576 elements, however, at the end of the analysis there are 576, 1563, 3383 and 688 elements in domains 1, 2, 3, and 4, respectively as depicted in Table 2.6-1. For this implementation, the domains are fixed and elements are not re-balanced among the domains.

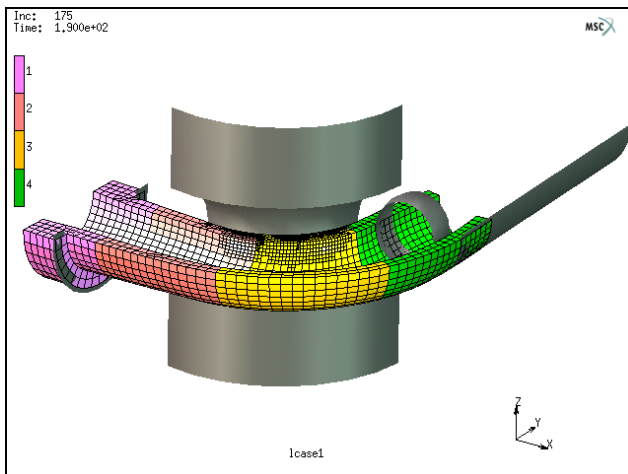


Figure 2.6-3 Automatically Generated Domains

Table 2.6-1 Comparison of Results for Parallel and Adaptive Meshing

Compare Parallel and Local Adaptive Meshing	Local Adaptive Meshing		No Adaptive Meshing	
	4 CPU	1 CPU	4 CPU	1 CPU
	Single File		Single File	
Mwords	45.6	44.5	11.9	13.2
Normalized Time	0.63	1.0	0.55	1.0
Increments	100	100	100	100
# Recycles	1173	1166	1374	1374
Max Plastic Strain	0.6198	0.6499	0.4845	0.4846
# Elements	6210	7616	2304	2304
Domain 1	576	NA	576	NA
Domain 2	1563	NA	576	NA
Domain 3	3383	NA	576	NA
Domain 4	688	NA	576	NA
Speedup	1.6	NA	1.8	NA
% Change Max Plastic Strain	21.8%	25.4%	0.0%	Baseline

Table 2.6-1 compares four different runs of the same simulation. The baseline is a case with no adaptive meshing using one CPU to run 100 increments with 2304 elements. The maximum total equivalent plastic strain at the last increment is 0.4846.

Adding parallel processing with four processors shows a speedup factor of 1.8 with no change in the maximum total equivalent plastic strain at the last increment. Adding more elements using local adaptive meshing increases the maximum total equivalent plastic strain at the last increment by about 25%. Clearly the more elements used in the simulation will capture the solution better. Furthermore, since local adaptive meshing is now available with parallel processing, this more accurate solution can be obtained quicker. In this example the speedup for local adaptive meshing was 1.6 but the total number of elements generated differed running parallel. This is because neighboring elements in different domains that require subdivision with local adaptive meshing are not allowed in the parallel version at this time. Therefore the parallel version tends to add fewer elements than the single model simulation. In this release, new domains are not created after local adaptive refinement occurs.

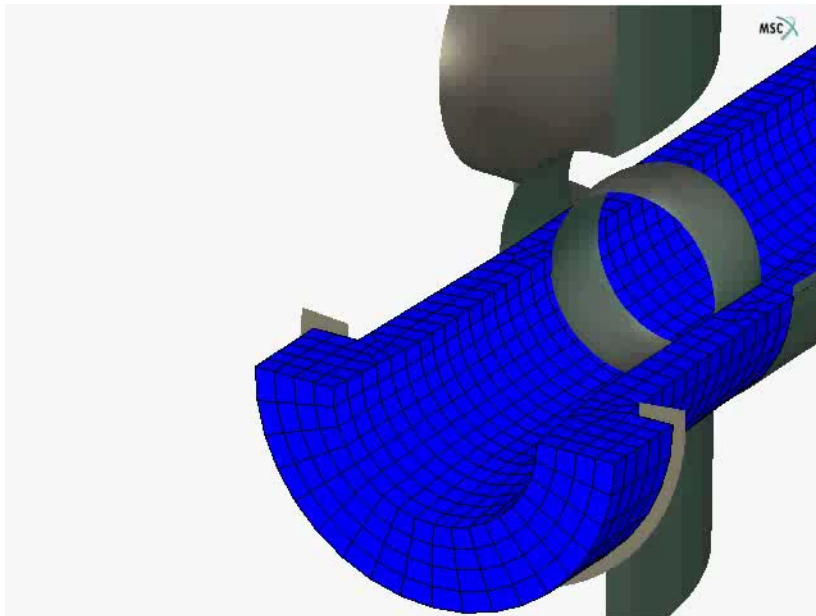
Input Files

The files below are on your [delivery media](#) or they can be downloaded by your web browser by clicking the links (file names) below.

File	Description
tubebend.proc	Mentat procedure file to run the above example
tubebend.mud	Associated model file

Animation

Click on the figure below to play the animation (ESC to stop).



2.7 Magnetostatic Elements

- Chapter Overview 450
- Magnetostatic Field Around a Coil 450
- Input Files 458

Chapter Overview

This chapter describes the use of three magnetostatic elements in Marc. These elements are 4-node and 10-node tetrahedral elements, and a 2-node line element. With the tetrahedral elements, it is possible to use automatic meshers which will facilitate meshing of complex structures. The purpose of the line element is to define an external loading; the current in a wire. This element does not have material or geometric properties. The line element can be either placed on element edges of the solid elements or embedded in these solid elements. The direction of the current is in the direction of the line elements, following the connectivity.

Magnetostatic Field Around a Coil

This example demonstrates the use of the 10-node magnetostatic tetrahedral element with the use of the magnetostatic line element in Marc. The function of the latter is to simplify defining a current as an external loading. A one wire coil in air is analyzed. The results will be compared with an analytical solution using the Biot-Savart law. A schematic view of the model is shown in [Figure 2.7-1](#).

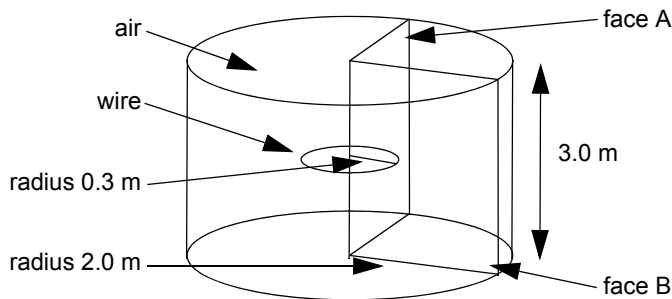


Figure 2.7-1 Schematic View of the Coil with Surrounding Air

Mesh Generation

The mesh is generated previously, and can be seen in [Figure 2.7-2](#). The mesh is refined around the location where the coil will be to better capture the gradient of the magnetic field near the coil. Due to symmetry, only a quarter of a cylinder is modeled. A curve with a radius of 0.3 m is added in the center of the densely meshed area. This curve is then converted to line elements. The number of line elements should match the density of the solid elements, so that the size of the line elements is at least the same as the average edge length of the solid elements.

```
FILE
  NEW
  RESET PROGRAM
  OPEN
    mesh_mag.mfd
  OK
```

```
RETURN
MESH GENERATION
  CURVE TYPE
    CENTER/RADIUS/ANGLE/ANGLE
    RETURN
  CRVS ADD
    0 0 0
    0.3
    0
    90
  MOVE
    ROTATION ANGLES (DEGREES)
      0 -90 0
    CURVES
      1 #
    RETURN
  CONVERT
    DIVISIONS
      24 1
    CURVES TO ELEMENTS
      1 #
    SELECT
      SELECT BY
        CLASS
          line(2)
        OK
      RETURN
    RETURN
  RETURN
```

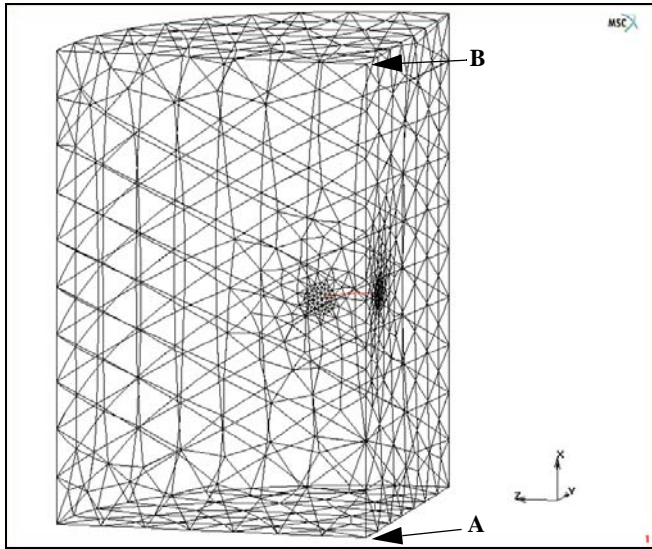


Figure 2.7-2 Finite Element Mesh

Material Properties

The permeability of the air surrounding the coil is 1.2566×10^{-6} H/m. The line elements which form the coil do not need material properties since they are only used to define the loading.

MATERIAL PROPERTIES

NAME

air

MANETOSTATIC

PERMEABILITY

1.2566e-6

OK

ELEMENTS ADD

ALL UNSELECT

RETURN

Inserts

To transfer the current from the line elements to the solid elements, the INSERT option is used. The line elements are inserted in the solid elements where the solid elements are the host elements, and the line elements the embedded

entities. Marc automatically ties the degrees of freedom of the nodes to be inserted to the corresponding degrees of freedom of the nodes of the host elements.

```
LINKS
  INSERTS
    HOST ELEMENTS ADD
    ALL UNSELECT
    EMBEDDED ENTITIES ADD
    ALL SELECT
    RETURN
  RETURN
```

Boundary Conditions

Symmetry conditions are applied on the two rectangular faces of the quarter section (face A and B in [Figure 2.7-1](#)) in such a way, that the potential is forced to be perpendicular to the surface of the rectangular faces. A current of -0.5 A is prescribed to the line elements.

```
BOUNDARY CONDITIONS
  MAGNETOSTATIC
    NAME
      fix_xy
    FIXED POTENTIAL (3-D)
      POTENTIAL X
      POTENTIAL Y
      OK
    SELECT
      CLEAR SELECT
      METHOD
        BOX
      RETURN
    NODES
      -10 10
      -10 10
      -10 0.001
    RETURN
  NODES ADD
  ALL SELECT
```

```
NEW
NAME
    fix_xz
FIXED POTENTIAL (3-D)
    POTENTIAL X
    POTENTIAL Z
    OK
SELECT
    CLEAR SELECT
    NODES
        -10 10
        -10 0.001
        -10 10
    RETURN
NODES ADD
ALL SELECT
NEW
NAME
    load
WIRE CURRENT (define current in wire)
    CURRENT
        -0.5
    OK
SELECT
    CLEAR SELECT
    SELECT SET
        insert_embed_elements
    OK
    RETURN
ELEMENTS ADD
ALL SELECT
RETURN
RETURN
```

Loadcases and Job Parameters

A steady state analysis is performed. [Figure 2.7-3](#) shows the element type menu, where in 3-D SOLID element type 182 is selected for the 10 node tetrahedral elements, and in 3-D WIRE element type 183 is selected for the line elements.

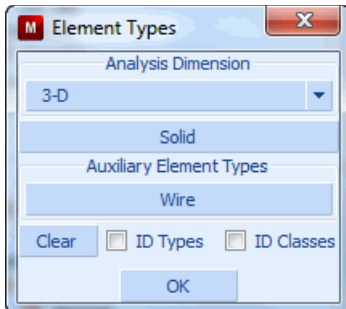


Figure 2.7-3 Element Types Menu

```
LOADCASES
  MAGNETOSTATIC
    STEADY STATE
      OK
      RETURN (twice)
JOBS
  ELEMENT TYPES
    MAGNETOSTATIC
      3-D WIRE
        183
        OK
      ALL SELECT
      3-D SOLID
        182
        OK
      ALL UNSELECT
      RETURN (twice)
  MORE
  MAGNETOSTATIC
    lcase1
  INITIAL LOADS
    fix_xy
```

```
    fix_xz
    load
    OK
JOB RESULTS
    1st Comp of Magnetic Induction
    2nd Comp of Magnetic Induction
    3rd Comp of Magnetic Induction
    1st Comp of Magnetic Field Intensity
    2nd Comp of Magnetic Field Intensity
    3rd Comp of Magnetic Field Intensity
    OK (twice)
```

Save Model, Run Job, and View Results

After saving the model, the job is submitted and the resulting post file is opened.

```
FILE
    SAVE AS
        coil.mud
    OK
    RETURN
RUN
SUBMIT(1)
MAIN
RESULTS
    OPEN DEFAULT
    NEXT
    PATH PLOT
        NODE PATH
            9266 9268 #
    VARIABLES
        ADD CURVE
        Arc Length
        1st Component of Magnetic Induction
    FIT
```


Figure 2.7-4 shows the contour plot of the 1st component of the magnetic induction. A subsection of the elements just below the coil including the line elements of the coil is plotted here. The magnetic induction in the plane of the coil should be perpendicular to this plane, and changing sign going from the inside to the outside of the coil.

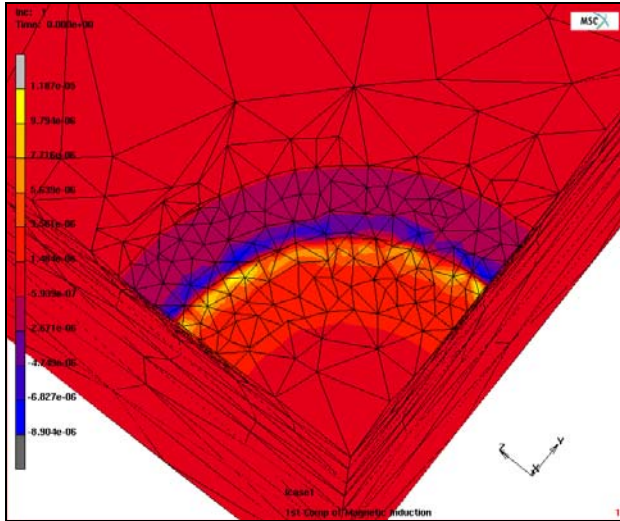


Figure 2.7-4 Contour Plot of the 1st Component of the Magnetic Induction

An analytical solution for the magnetic field of this example can be obtained using the Biot-Savart law. The magnetic induction along the line going through the center axis of the coil is given by,

$$B_{\text{axis}} = \frac{1}{2} \mu \frac{r^2 I}{(r^2 + l^2)^{3/2}}$$

with,

B_{axis} – magnetic induction along the axis of the coil

μ – magnetic permeability

r – radius of the coil

l – position on the axis through the coil

I – current

The axis of the coil is shown in Figure 2.7-2, indicated by the arrows. Figure 2.7-5 shows a path plot of the magnetic induction along the path going from A to B (see Figure 2.7-2). The analytical solution is also shown in this figure. The result corresponds very well with the analytical solution.

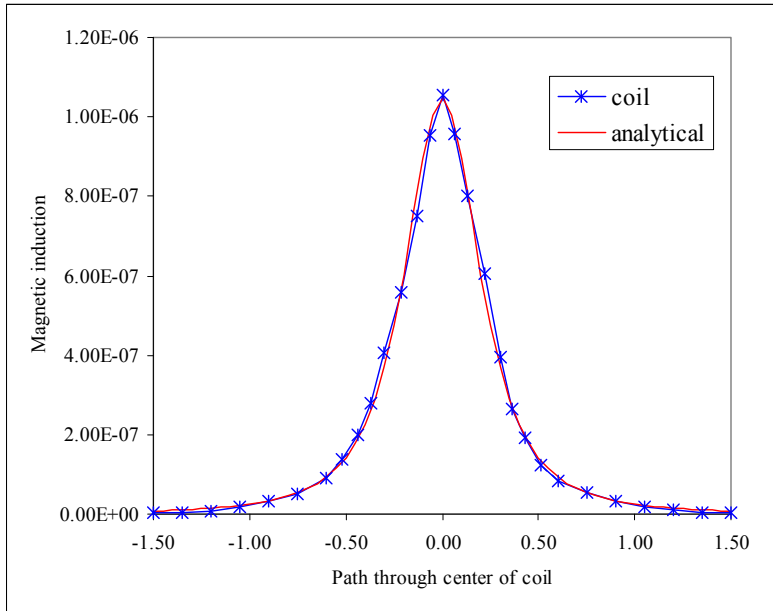


Figure 2.7-5 Magnetic Induction along the Axis of the Coil Compared with the Analytical Solution

Input Files

The files below are on your [delivery media](#) or they can be downloaded by your web browser by clicking the links (file names) below.

File	Description
coil.proc	Mentat procedure file to run the above example
mesh_mag.mfd	Associated model file

2.8 Coupled Electrostatic Structural Analysis of a Capacitor

- Chapter Overview 460
- Capacitor Loaded with Charge 460
- Input Files 474

Chapter Overview

This chapter describes the use of coupled electrostatic structural analysis in Marc. In this analysis type, the Coulomb force, the force between charged bodies, links the electrostatic part to the structural part, and the deformation influences the electrostatic field. This is a weak coupling where, in the first pass, the electrostatic field is computed and the corresponding Coulomb forces are calculated. In the next pass, the structural response is evaluated, such that the Coulomb forces are treated as additional external forces. In a subsequent increment, the deformed state is used in the calculation of the electrostatic field. Since the electrostatic solution is a steady state solution, a time dependent problem will be solved as quasi-static during the electrostatic phase of the solution.

Capacitor Loaded with Charge

Two parallel plates form a capacitor, that contains a charge (see Figure 2.8-1). One plate is fixed and electrically grounded, while the other plate is attached to a spring. Boundary conditions are chosen so that the plate connected to the spring can only move perpendicular to the fixed plate. Then, when this plate is loaded with charge, it will move towards the fixed plate. The charge is chosen as the applied load instead of potential since with increasing charge at a certain moment the potential will decrease as shown later in the results.

Since the two plates are circular, an axisymmetric analysis will be performed. Air, both between the two plates and outside the plates, is taken into account to get a good representation of the electrostatic field. The air is only active in the electrostatic pass. The position of the nodes of the air region “contacting” the plates is updated based on the displacements of the plates. In order to avoid getting badly shaped elements due to the motion of the free plate, a region of air surrounding the plates is periodically remeshed.

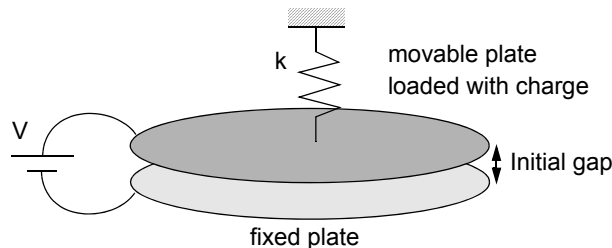


Figure 2.8-1 Schematic Representation of the Capacitor

Mesh Generation

A previously defined mesh is read in as an *mfd* file. A curve is added along the x-axis, which is needed as a boundary for remeshing. Then the mesh is split around the plates, so that only the inner part of the air surrounding the plates can be remeshed. This way the mesh on the outside stays coarse, while the mesh directly surrounding the plates will be sufficiently refined to capture the gradient in the electric field. Splitting the mesh is done using **MATCHING BOUNDARIES** in **MODELING TOOLS**. This tool splits a mesh and creates matching boundaries. The latter information is not needed in this analysis. The radius of the two plates is 10 mm, the thickness 1 mm, the initial gap is 0.4 mm, and the radius of the air modeled around the plates is 50 mm.

```
FILE
  NEW
  RESET PROGRAM
  OPEN
    capmesh.mfd
  OK
  RETURN
MESH GENERATION
  CRVS ADD
    -0.05 0 0
    0.05 0 0
  RESET VIEW
  RETURN
MODELING TOOLS
  MATCHING BOUNDARIES
    NEW
      2-D (SOLID, 3-D SHELL)
    SELECT
      METHOD
        BOX
      RETURN
    ELEMENTS
      -0.00407 0.00407
      -1 0.0136
      -1 1
    RETURN
  SPLIT MESH
  ALL SELECT
  SELECT
    CLEAR SELECT
    RETURN (three times)
```

Material Properties

The plates are made of copper with a Young's modulus of 124 GPa and a Poisson's ratio of 0.3. The permittivity is 0.001 F/m. The air surrounding the plates will only be active in the electrostatic pass, so no mechanical properties are needed. The permittivity is 8.854 pF/m.

MATERIAL PROPERTIES

NAME

*(define structural and electrical
properties of conductor)*

conductor

ISOTROPIC

YOUNG'S MODULUS

124e9

POISSON'S RATIO

0.3

O

K

ELECTROSTATIC

PERMITTIVITY

0.001

OK

SELECT

METHOD

FLOOD

RETURN

ELEMENTS

3 103 #

RETURN

ELEMENTS ADD

ALL SELECT

NEW

(define electrical properties of air)

NAME

air

ELECTROSTATIC

PERMITTIVITY

8.854e-12

OK

SELECT

CLEAR SELECT

ELEMENTS

731 734 #

RETURN

ELEMENTS ADD

```

ALL SELECT
SELECT
    CLEAR SELECT
    RETURN (twice)

```

Contact

The Coulomb force is calculated at the interface of contact bodies. It is important that contact bodies are connected in the right direction. In general, an insulator is touching a conductor; so for this example, air should be touching the plates. When a body is only active in the electrostatic pass (the air), it must be a so-called Meshed (Fluid) body (see [Figure 2.8-2](#)). Then, in the CONTACT TABLE section, such a body cannot be touched by a DEFORMABLE body, thus facilitating the required connection

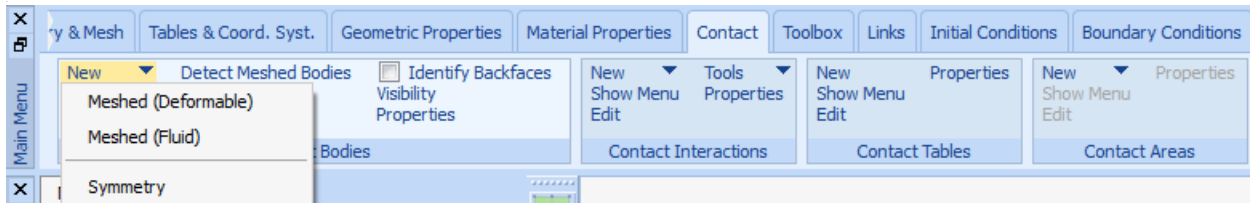


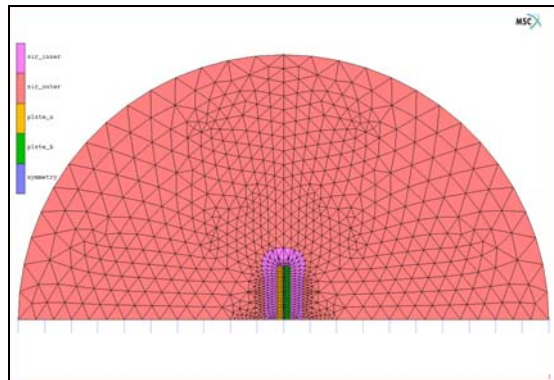
Figure 2.8-2 Contact Bodies Menu

```

CONTACT
    CONTACT BODIES
        NAME
            plate_a
        DEFORMABLE
            OK
        SELECT
            ELEMENTS
                103 #
            RETURN
        ELEMENTS ADD
        ALL SELECT
        NEW
        NAME
            plate_b
        DEFORMABLE
            OK

```

```
SELECT
  CLEAR SELECT
  ELEMENTS
    3 #
  RETURN
ELEMENTS ADD
ALL SELECT
NEW
NAME
  air_inner
ZERO STIFFNESS
  OK
SELECT
  CLEAR SELECT
  ELEMENTS
    731 #
  RETURN
ELEMENTS ADD
ALL SELECT
NEW
NAME
  air_outer
ZERO STIFFNESS
  OK
SELECT
  CLEAR SELECT
  ELEMENTS
    734 #
  RETURN
ELEMENTS ADD
ALL SELECT
NEW
NAME
  symmetry
SYMMETRY
  OK
```




```
CURVES ADD
  1 #
RETURN
CONTACT TABLES
NEW
PROPERTIES
  1 2
    CONTACT TYPE: GLUE
    OK
  1 3
    CONTACT TYPE: GLUE
    OK
  1 4
    CONTACT TYPE: GLUE
    OK
  1 5
    CONTACT TYPE: GLUE
    OK
  OK
RETURN (twice)
```

Boundary Conditions

A spring with a spring constant of 50 N/m is attached to the moving plate to balance the Coulomb force. The moving plate (left, or top plate in [Figure 2.8-1](#)), is loaded with an in-time linear increasing charge, which reaches 20°C after one second. This should result in a continuous increase of the Coulomb force, so that the plates move toward each other. If a linear increasing potential was applied to the moving plate, the system would, at a certain point, become unstable, and the plates would collapse. The right plate is fixed, and the potential is set to 0 volts.

```
LINKS
  SPRINGS/DASHPOTS
    NEW
    PROPERTIES
      STIFFNESS SET
        50
      OK
    BEGIN NODE
```

```
      1
    DOF
      1
    END NODE
      103
    DOF
      1
    RETURN (twice)
BOUNDARY CONDITIONS
NAME
  fix
MECHANICAL
  FIXED DISPLACEMENT
    DISPLACEMENT X
      0
    OK
  NODES ADD
    1 4 #
  RETURN
NEW
NAME
  pot_0
ELECTROSTATIC
  FIXED POTENTIAL
    POTENTIAL (TOP)
      0
  NODES ADD
    4
  OK
  RETURN
NEW
NAME
  fix_y
MECHANICAL
  FIXED DISPLACEMENT
    DISPLACEMENT Y
```

```
0
OK
NODES ADD
  1 4 104 #
RETURN
NEW
NAME
  load
ELECTROSTATIC
  TABLES
    NEW
      1 INDEPENDENT VARIABLE
    TYPE
      time
    ADD
      0 0
      1 1
    RETURN
  POINT CHARGE
    CHARGE(TOP)
      2e-8
    TABLE
      table1
  NODES ADD
    104
  OK
  RETURN (twice)
```

Mesh Adaptivity

The mesh surrounding the two plates is remeshed every five increments to accommodate the deformation of the air when one plate moves towards the other plate. A triangular mesh is created using the Delaunay method, where the target element edge length is 0.4 mm.

```
MESH ADAPTIVITY
  GLOBAL REMESHING CRITERIA
    DELAUNAY TRIA
```

```

INCREMENT
FREQUENCY
    5
ELEMENT EDGE LENGTH SET
    0.0004
OK
REMESH BODY
    air_inner
RETURN (twice)
    
```

Loadcases and Job Parameters

A quasi-static analysis is performed. MULTI-CRITERIA load stepping method (AUTO STEP in *Marc Volume C: Program Input*) is used to control the time step. The time step control is based on a maximum displacement per increment of 3 μm in the x-direction. The axisymmetric mechanical element 10 is selected for the elements of the plates, and the axisymmetric electrostatic element 38 is selected for the elements of the air. In performing coupled electrostatic-structural analysis, two procedures are available for calculation electrical forces. The first method (default) is based upon the nodal charges and is applicable if the bodies are close to one another. The second method is based upon the electrical field and is more accurate when the bodies are further apart. The default procedure is used here, but in the menu used to select the procedure is shown in [Figure 2.8-3](#).

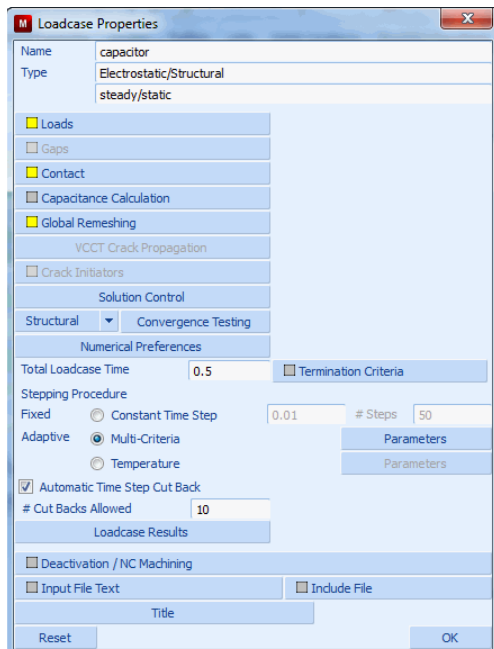


Figure 2.8-3 Electrostatic-Structural Analysis Options Menu

```
LOADCASES
  ELECTROSTATIC-STRUCTURAL
    NAME
      capacitor
    QUASI-STATIC
      CONTACT
        CONTACT TABLE
          ctable1
        OK
      GLOBAL REMESHING
        adapg1
        OK
      MULTI-CRITERIA
      PARAMETERS
        USER DEFINED
          DISPLACEMENT INCREMENT
          PARAMETERS
            DISPLACEMENT INC ALLOWED
              1
              3e-6
            OK
          OK
        OK
      RETURN
    RETURN
  JOBS
    NAME
      capacitor
    ELEMENT TYPES
      SELECT
        CLEAR SELECT
        SELECT CONTACT BODY ENTITIES
          plate_a
          plate_b
        OK
```

```
      RETURN
ELECTROSTATIC-STRUCTURAL
      ELECTROSTATIC-STRUCTURAL ELEMENT TYPES:
          AXISYM SOLID
              10
          OK
      ALL SELECT
      ELECTROSTATIC ELEMENT TYPES:
          AXISYM SOLID
              38
          OK
      ALL UNSELECT
      RETURN (twice)
ELECTROSTATIC-STRUCTURAL
    capacitor
  INITIAL LOADS
    fix
    pot_0
    fix_y
    load
    OK
  CONTACT CONTROL
    INITIAL CONTACT
      CONTACT TABLE
        ctable1
      OK
    OK
  ANALYSIS OPTIONS
    LARGE DISPLACEMENT
    OK
  JOB RESULTS
    1st Comp of Electric Field Intensity
    2nd Comp of Electric Field Intensity
    1st Comp of Electric Displacement
    2nd Comp of Electric Displacement
  SELECTED NODAL QUANTITIES:
```

```
CUSTOM
Electric Potential
External Charge
Reaction Charge
Displacement
Reaction Force
Coulomb Force
Contact Status
OK (twice)
```

Save Model, Run Job, and View Results

After saving the model, the job is submitted and the resulting post file is opened.

```
FILE
  SAVE AS
    capacitor.mud
  OK
  RETURN
RUN
  SUBMIT(1)
MAIN
RESULTS
  OPEN DEFAULT
  HISTORY PLOT
  SET NODES
    104
  COLLECT GLOBAL DATA
  NODES/VARIABLES
    ADD VARIABLE
    Electric Potential
    Displacement X
  FIT
  RETURN
SHOW IDS
  O
```

YMAX

0.0004

Figure 2.8-4 shows the contour plot of the x-component of the electric field intensity. You can observe that this field is constant between the two plates, except at the top (outer radius) of the two plates.

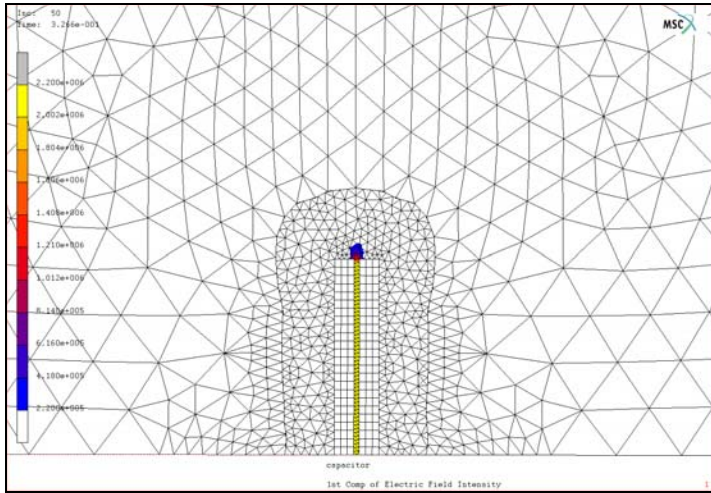


Figure 2.8-4 Contour Plot of the X-Component of the Electric Field Intensity

The electrical potential in the vicinity of the capacitor is shown in Figure 2.8-5.

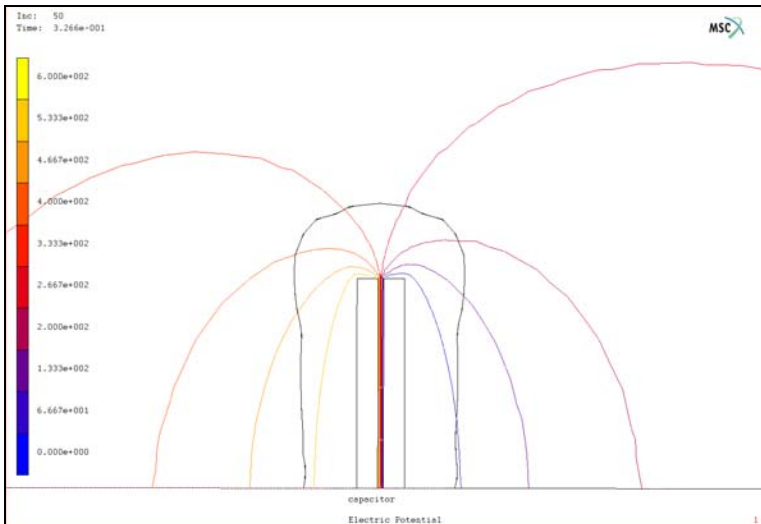


Figure 2.8-5 Electrical Potential

The following equation for the potential as a function of the gap opening, can be derived for the ideal situation where the electric field intensity is constant between the plates:

$$V = \sqrt{\frac{2k}{\epsilon_0 A} g^2 (g_0 - g)}$$

With the potential, V , the spring constant, k , the permittivity, ϵ_0 , the area of the plate, A , the gap opening, g , and the initial gap opening, g_0 . Note that $g_0 - g$ is the gap closing displacement computed by Marc. In Figure 2.8-6, the result is compared with the analytical solution where the gap closing displacement is plotted as a function of the electrostatic potential.

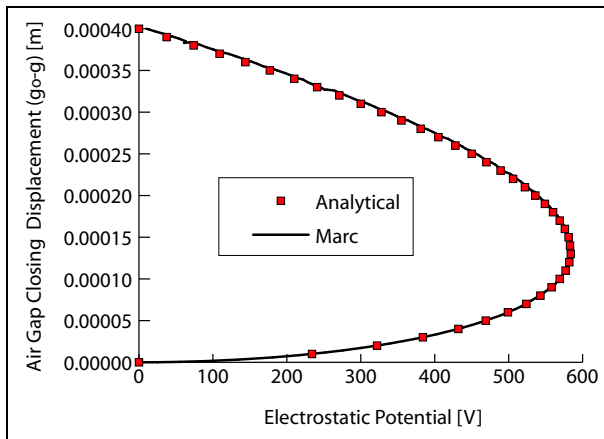


Figure 2.8-6 Potential as a Function of Gap Opening

Also, note that a maximum of the potential is reached when $g_0 - g = \frac{1}{3}g_0$, or when the current gap opening is $\frac{2}{3}$ of the initial gap. If the loading was prescribed with an increasing potential, the plates would become unstable at this point and collapse. Figure 2.8-7 gives a close up look of the remeshed area of the air at the top of the plates during different stages of the analysis.

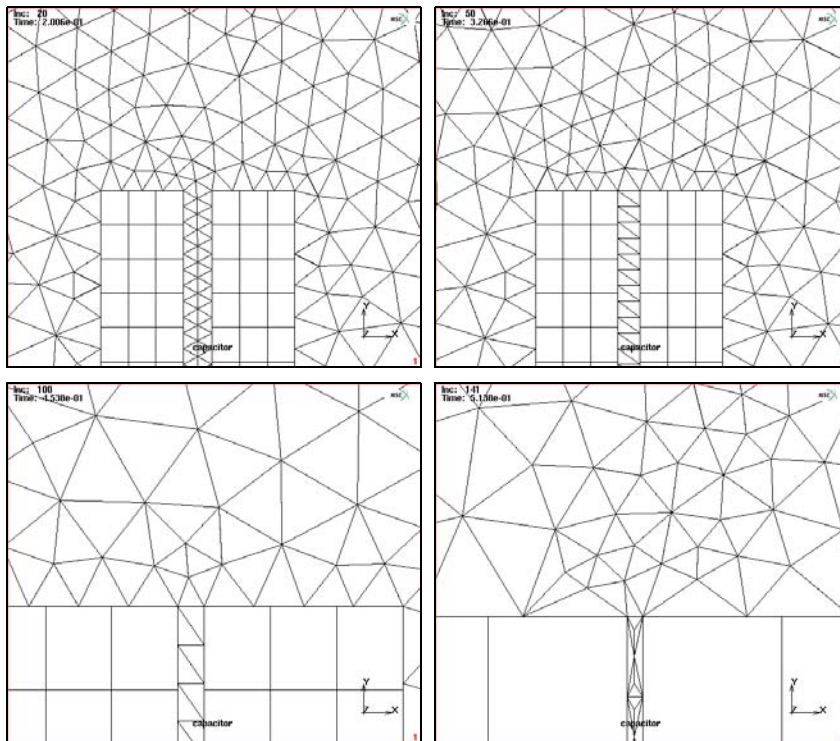


Figure 2.8-7 Result of Remeshing at Different Steps (increment 20, 50, 100, and 141) in the Analysis

Note: The figures are zoomed in at the top of the plates.

Input Files

The files below are on your [delivery media](#) or they can be downloaded by your web browser by clicking the links (file names) below.

File	Description
capacitor.proc	Mentat procedure file to run the above example
cap_mesh.mfd	Associated model file

2.9 3-D Contact and Friction Analysis using Quadratic Elements

- Chapter Overview 476
- Sliding Mechanism 477
- Input Files 493

Chapter Overview

Various new options have been added to further enhance the capabilities to analyze contact problems. In this chapter, attention will be mainly paid to the following items:

- Bilinear friction model;
- Table input to define a velocity dependent friction coefficient;
- Automatic optimization of contact constraint equations;
- Postprocessing contact stresses.

The friction model uses a bilinear approximation of the theoretical stick-slip step function as shown in [Figure 2.9-1](#). The slip threshold parameter is, by default, determined by the program based on the average element edge length of the elements defining the deformable contact bodies. A second parameter of the model is the friction force convergence ratio, which is used to compare the length of the friction force vector of the current iteration with the previous iteration. The default value of this parameter is 0.05. Both default values of the parameters have been designed to produce accurate results in a wide range of applications. If needed, they can be modified by the user.

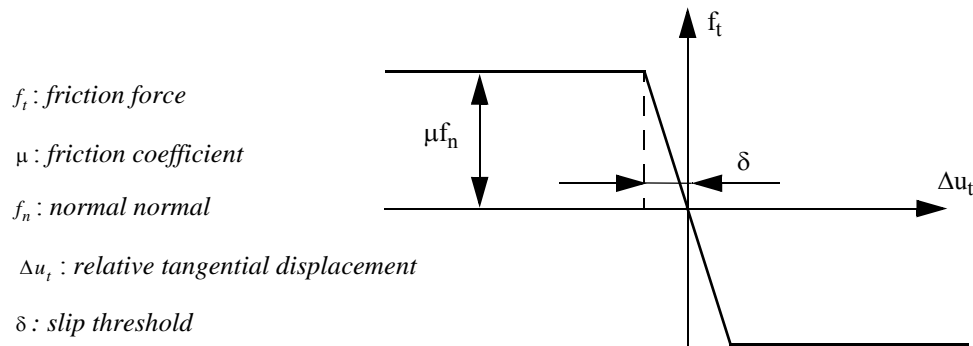


Figure 2.9-1 Bilinear Friction Model

In order to get more flexibility in defining e.g., boundary conditions, material properties, etc. as a function of various independent variables, like position, time, equivalent plastic strain, etc. The table input has been introduced. In this chapter, use is made of tables to define boundary conditions as a function of time, but also a friction coefficient as a function of the relative sliding velocity between contact bodies. Notice that the latter would not have been possible in earlier versions of Marc without user subroutines.

In Marc, deformable contact problems are traditionally solved using multipoint constraint equations. For certain problems, the accuracy of the solution strongly depends on the order in which the constraint equations have been defined. New logic has been added to automatically optimize the constraint equations. The procedure is based on first defining all possible constraint equations using true double-sided contact and then, taking into account the average stiffness of the contact bodies involved and the size of the element segments in the areas of contact, reducing this to a set of optimal constraint equations.

The units used herein are Force [N], Length [mm], and Time [sec].

Sliding Mechanism

A sliding mechanism, as shown in Figure 2.9-2, is analyzed. A square block with flattened edges can slide in a U-shaped section which, at its ends, is mounted on two support blocks. The square block has a circular hole in which a rigid cylinder is inserted. The block is loaded via the cylinder by a vertical force in the global y -direction $F_y = -300$ and prescribed displacements in global x - and z -direction of $u_x = 25 \sin(2\pi t)$ and $u_z = 0.05(\sin(\pi t))^2$, in which t denotes the time. The material behavior of the square block is described using a Neo-Hookean material model defined through the MOONEY property menu with $C_{01} = 100$, while the material behavior of the U-shaped section and the supports is isotropic and linear. Young's modulus and Poisson's ratio of the section are $E = 5.0 \times 10^4$ and $\nu = 0.3$, and of the supports $E = 2.2 \times 10^5$ and $\nu = 0.28$. Frictional contact between the block and the section is assumed based on Coulomb's friction law with a velocity dependent friction coefficient $\mu = 0.03 + 0.07e^{-0.01v}$, in which v is the relative sliding velocity. For all components, except the cylinder, 10-node tetrahedral elements with full integration (Marc element type 127) will be used.

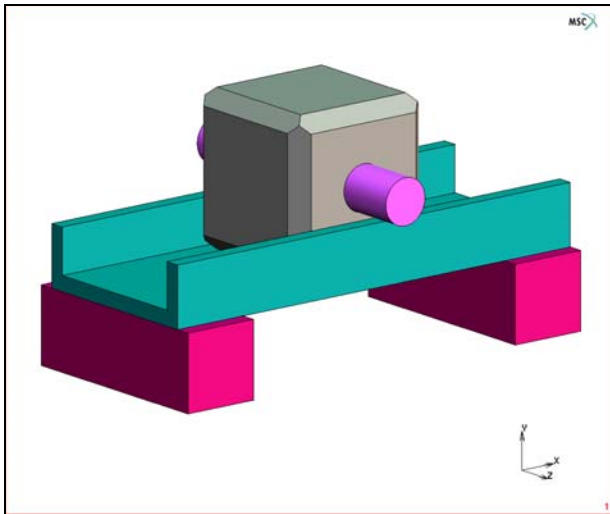


Figure 2.9-2 Solid Model of the Sliding Mechanism

Model Generation

First, the Mentat database is cleaned, the view point is set and a colormap with a white background is selected. Then the finite element model is set up by subsequently merging the various components of the structure, which have been stored in individual files, called *support.mfd*, *section.mfd*, *block.mfd*, and *cylinder.mfd*. The first three files contain a solid model of the component as well as a finite element mesh obtained by automatic mesh generation. The last file contains a solid model and the surfaces obtained by conversion of the solid faces into surfaces. After reading the models, element and node sets are generated, which makes it easy later on to assign material properties, define contact bodies, and assign boundary conditions. Finally, an extra node above the block is added, which will be used as the

control node for the rigid cylinder to apply the force and prescribed displacements. The finite element model is shown in [Figure 2.9-3](#).

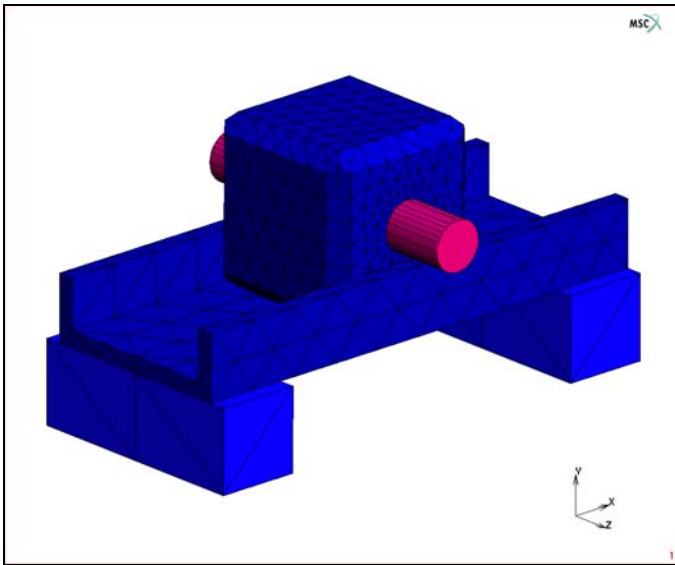


Figure 2.9-3 Finite Element Model

FILES

NEW

OK

RESET PROGRAM

RESET VIEW

VIEW

SHOW VIEW 1

RY+

RY+

RY+

RY+

RX+

MAIN

VISUALIZATION

COLORS

COLORMAP 2

MAIN

FILES

MERGE

support.mfd

OK

MERGE

section.mfd

OK

MERGE

block.mfd

OK

MERGE

cylinder.mfd

OK

FILL

PLOT

POINTS

(off)

CURVES

(off)

SOLIDS

(off)

ELEMENTS SOLID

SURFACES SOLID

MAIN

MESH GENERATION

SELECT

METHOD

FLOOD

RETURN

ELEMENTS

8 20

(click a node of each of the support blocks)

ELEMENTS STORE

support

OK

ALL: SELECTED

ELEMENTS CLR

ELEMENTS

223

(click a node of the section)

```
ELEMENTS STORE
  section
  OK
ALL: SELECTED
ELEMENTS CLR
ELEMENTS
  1458
ELEMENTS STORE
  block
  OK
ALL: SELECTED
ELEMENTS CLR
METHOD
  SINGLE
  RETURN
NODES
  5 8 11 12 13 14 64 65 66 74 84 85 86 87 89
  17 20 23 24 25 26 94 95 96 104 114 115 116
  117 119
END LIST (#)
NODES STORE
  support_bottom
  OK
ALL:SELECTED
NODES CLR
RETURN
NODES ADD
  25 60 25
MAIN
```

(click a node of the block)

(nodes at the bottom of the support)

Material Properties

The definition of the material properties is straightforward. One Mooney and two isotropic materials are defined and assigned to the corresponding element sets.

```
MATERIAL PROPERTIES
  NEW
```



```

NAME
    Support_material
ISOTROPIC
    YOUNG'S MODULUS
        2.2e5
    POISSON'S RATIO
        0.28
    OK
ELEMENTS ADD
SET
    support
    OK
NEW
NAME
    Section_material
ISOTROPIC
    YOUNG'S MODULUS
        5e5
    POISSON'S RATIO
        0.3
    OK
ELEMENTS ADD
SET
    section
    OK
NEW
NAME
    Block_material
MORE
MOONEY
    C10
        100
    OK
ELEMENTS ADD
SET
    block

```

OK
 MAIN

Contact

Three deformable contact bodies and one rigid contact body are defined in the following order: first the support, next the U-shaped section, then the block, and finally the rigid cylinder. The bodies are called *Support*, *Section*, *Block*, and *Cylinder*, respectively. Contact body Cylinder will be a load-controlled rigid body with the previously defined free node as the control node. A contact table is defined to enter the different contact conditions between the bodies. Glued contact is used between the bodies Block and Cylinder and the bodies Section and Support. Frictional contact is used between the bodies Block and Section. The velocity dependent friction coefficient is defined using a table of type velocity, as shown in [Figure 2.9-4](#).

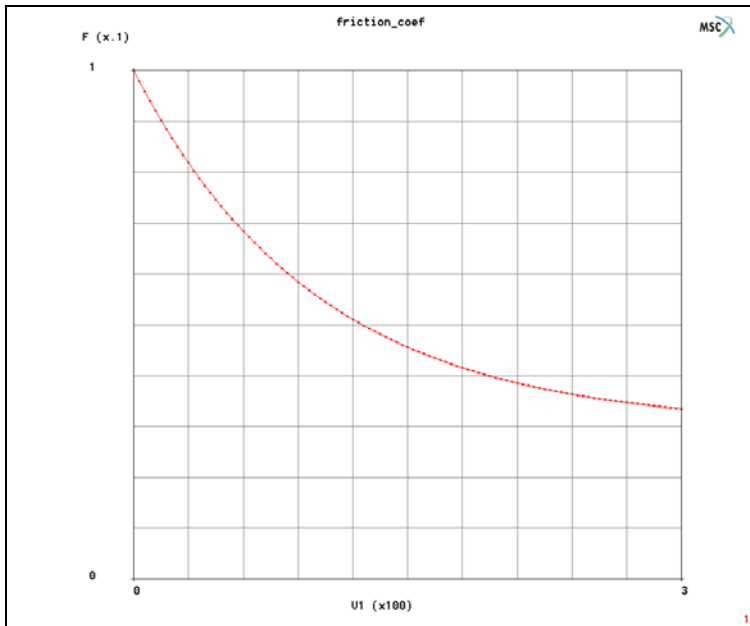


Figure 2.9-4 Table Defining Velocity Dependent Friction Coefficient

In order to illustrate the effect of the new contact constraint optimization procedure, a user-defined detection order for one set of contact bodies (Block and Section) is used together with the global optimization procedure for the other set (Section and Support). In such cases, a nondefault order defined via a contact table takes precedence over the global procedure.

CONTACT
 CONTACT BODIES
 NEW

```
NAME
  Support
DEFORMABLE
  OK
ELEMENTS ADD
SET
  support
  OK
NEW
NAME
  Section
DEFORMABLE
  OK
ELEMENTS ADD
SET
  section
  OK
NEW
NAME
  Block
DEFORMABLE
  OK
ELEMENTS ADD
SET
  block
  OK
NEW
NAME
  Cylinder
RIGID
  LOAD
  OK
CONTROL NODE
  5374
SURFACES ADD
  54 55 56 57
```

END LIST (#)
RETURN
CONTACT TABLES
TABLES
NEW
1 INDEPENDENT VARIABLE
NAME
friction_coef
TYPE
velocity
OK
FORMULA
ENTER
 $0.03+0.07*\exp(-0.01*v1)$
MAX (INDEPENDENT VARIABLE V1)
300
STEPS (INDEPENDENT VARIABLE V1)
100
REEVALUATE
FIT
RETURN

NEW

PROPERTIES

1 2

CONTACT TYPE: GLUE
PROJECT STRESS-FREE

(click entry 1-2)

(on)

2 3

CONTACT TYPE: TOUCHING
FRICTION COEFFICIENT

(click entry 2-3)

1

TABLE

friction_coef

OK

3 4

CONTACT TYPE: GLUE
PROJECT STRESS-FREE

(click entry 1-4)

(on)

OK (twice)

MAIN

Boundary Conditions

The following boundary conditions have to be defined: fixing the bottom of the support blocks, prescribing the motion of the cylinder in global x- and z-direction, and applying the force in global y-direction on the cylinder. Since contact body Cylinder is a load-controlled rigid body, the prescribed motion and force is assigned to its control node.

BOUNDARY CONDITIONS

TABLES

NEW

1 INDEPENDENT VARIABLE

NAME

motion-x

TYPE

time

OK

FORMULA

ENTER

$25 * \sin(2 * \pi * v1)$

STEPS (INDEPENDENT VARIABLE V1)

100

REEVALUATE

FIT

NEW

1 INDEPENDENT VARIABLE

NAME

motion-z

TYPE

time

OK

FORMULA

ENTER

$0.05 * \sin(\pi * v1)^2$

STEPS (INDEPENDENT VARIABLE V1)

100

```
    REEVALUATE
    FIT
    RETURN
NEW
NAME
    fix-support
MECHANICAL
    FIXED DISPLACEMENT
        DISPLACEMENT X (0)
        DISPLACEMENT Y (0)
        DISPLACEMENT Z (0)
    OK
    NODES ADD
    SET
        support_bottom
    OK
    RETURN
NEW
NAME
    motion
    FIXED DISPLACEMENT
        DISPLACEMENT X
            1
        TABLE
            motion-x
            OK
        DISPLACEMENT Z
            1
        TABLE
            motion-z
            OK (twice)
    NODES ADD
        5374
    END LIST (#)
    RETURN
NEW
```

```

NAME
  force-y
MECHANICAL
  POINT LOAD
    FORCE Y
      -300
    OK
  NODES ADD
    5374
  END LIST (#)
  RETURN
MAIN

```

Loadcases

A mechanical static loadcase is defined, in which the previously defined contact table and boundary conditions are selected (note that the boundary conditions are automatically selected if they have been defined before defining the current loadcase). The total loadcase time is 1 (which is also the default loadcase time), so that the block gets one complete cyclic motion in the global x-direction. A fixed stepping procedure is chosen with 100 steps and the default control settings for the Newton-Raphson iteration process are used.

```

LOADCASES
  NEW
  MECHANICAL
    STATIC
      CONTACT
        CONTACT TABLE
          ctable1
          OK (twice)
      # STEPS
        100
      OK
    TITLE
      Sliding Mechanism
      OK
  MAIN

```

Jobs

A mechanical job is defined in which the previously defined loadcase is selected. The available contact table is also used for initial contact. The friction type is switched to the bilinear Coulomb model with default parameters (see [Figure 2.9-5](#)). The newly introduced procedure to optimize the contact constraint equations is activated, while the other contact parameters are left default. The updated Lagrange procedure for rubber is selected, which allows the use of regular displacement-based elements instead of Herrmann elements with additional pressure degrees of freedom. As post file variables, the Cauchy stress tensor is selected as an element tensor, while the displacements, external forces, reaction forces, contact normal stress, contact normal force, contact friction stress, contact friction force, and contact status are selected as nodal quantities. The element type for all finite elements is set to 127, the 10-node tetrahedral element with full integration. Before submitting the job, the new style table input is activated. This causes the Marc data file to be written in a format which allows all tables to be used directly by Marc in equation format.

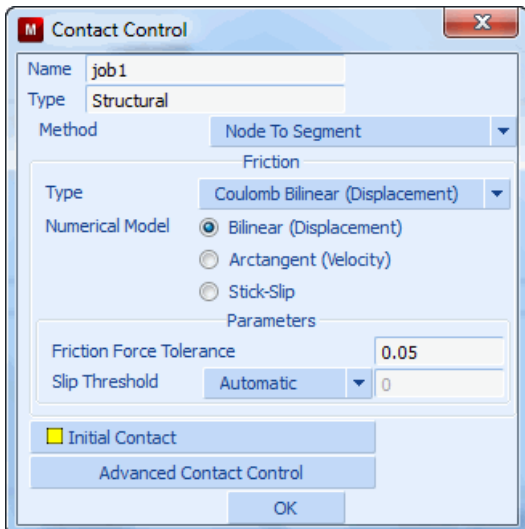


Figure 2.9-5 Contact Control: Friction Model and Parameters

JOBS

MECHANICAL

lcase1

CONTACT CONTROL

FRICITION TYPE: COULOMB BILINEAR (DISPLACEMENT)

(pull-down menu)

INITIAL CONTACT

ctable1

OK

ADVANCED CONTACT CONTROL

OPTIMIZE CONTACT CONSTRAINT EQUATIONS

OK(twice)

ANALYSIS OPTIONS

LARGE STRAIN

(roller button)

OK

JOB RESULTS

Cauchy Stress

(on)

CUSTOM

Displacement

(on)

External Force

(on)

Reaction Force

(on)

Contact Normal Stress

(on)

Contact Normal Force

(on)

Contact Friction Stress

(on)

Contact Friction Force

(on)

Contact Status

(on)

OK

OK

ELEMENT TYPES

MECHANICAL

3-D SOLID

127

OK

ALL: EXISTING

RETURN

RETURN

TITLE

Sliding Mechanism

OK

RUN

NEW-STYLE TABLES

(on)

SUBMIT 1

MONITOR

OK

MAIN

Results

In [Figure 2.9-6](#), the initial contact status of the nodes of contact body Section is given. Clearly, the nodes of body Section are contacting body Support, which is a result of the procedure to optimize the contact constraint equations.

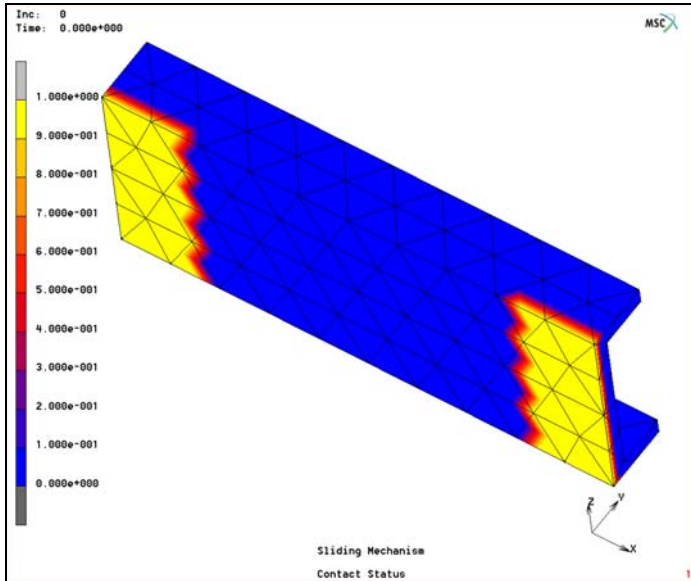


Figure 2.9-6 Initial Contact Status of the Nodes of Contact Body Section

[Figure 2.9-7](#) shows the contact normal stress on the deformable bodies for increment one. Both the contacting nodes and the nodes corresponding to contacted segments can be seen to have nonzero values. The distribution is not exactly symmetric, since the block already has some displacement in the global x -direction.

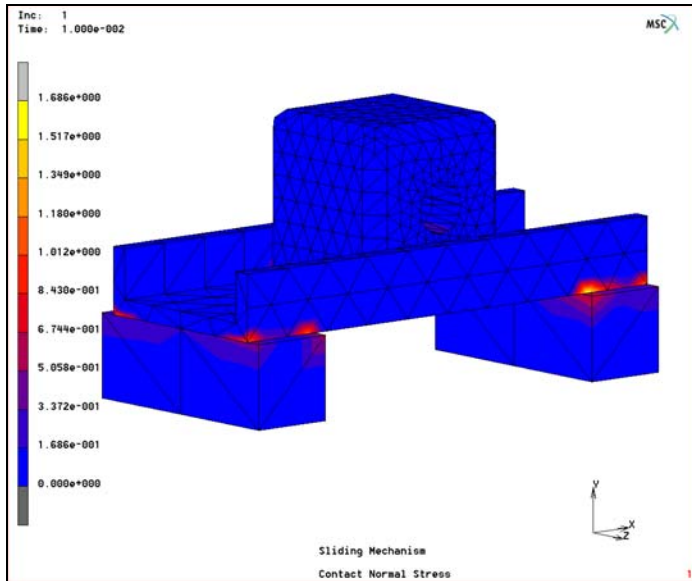


Figure 2.9-7 Contact Normal Stress for Increment 1

Finally, [Figure 2.9-8](#) contains a history plot of the x-component of the total force on the cylinder. The nonlinear response is partly due to the prescribed motion of the cylinder in the z -direction, but mostly due to the velocity dependent friction coefficient, which causes more friction at lower sliding velocities. Notice that due to the motion in the z -direction, the magnitude of the x-component of the total force can be larger than the maximum friction coefficient times the applied load in the y -direction.

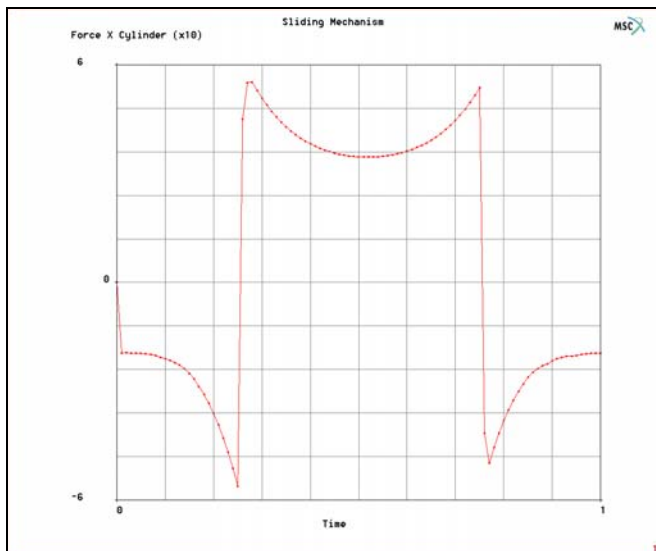


Figure 2.9-8 Total X-force on Contact Body Cylinder as a Function of Time

RESULTS

OPEN DEFAULT

DEF ONLY

SCALAR

Contact Status

OK

CONTOUR BANDS

SELECT

CONTACT BODY ENTITIES

Section

OK

MAKE VISIBLE

RETURN

NEXT

SELECT

CONTACT BODY ENTITIES

Support

Section

Block

Cylinder

OK

MAKE VISIBLE

RETURN

SCALAR

Contact Normal Stress

OK

MONITOR

HISTORY PLOT

COLLECT GLOBAL DATA

NODES/VARIABLES

ADD GLOBAL CRV

Time

Force X Cylinder

Fit

Input Files

The files below are on your [delivery media](#) or they can be downloaded by your web browser by clicking the links (file names) below.

File	Description
friction.proc	Mentat procedure file to run the above example
block.mfd	Associated model file
cylinder.mfd	Associated model file
section.mfd	Associated model file
support.mfd	Associated model file

2.10 Pin to Seal Contact with Various Friction Models

- Chapter Overview 496
- Problem Description 496
- Friction Modeling 497
- Results 499
- Input Files 500

Chapter Overview

The sample session described in this chapter demonstrates various friction models of a rigid pin being inserted into and extracted from a rubber seal. The simulation will use all of the available friction models to discuss their benefits. In any simulation with friction, it is always best to start with the no friction case first whenever possible. This allows for an understanding of how friction impacts the simulation which is generally not intuitive.

The goal of the chapter is to demonstrate:

- The basic insertion/extraction process with and without friction
- Demonstrate the benefits of the new Bilinear friction model by comparing to the Arc Tangent and Stick Slip Coulomb friction models.

Problem Description

The model is shown in [Figure 2.10-1](#) where the axisymmetric rubber seal is modeled with a Neo-Hookean material with $C_{10} = 50\text{N/cm}^2$.

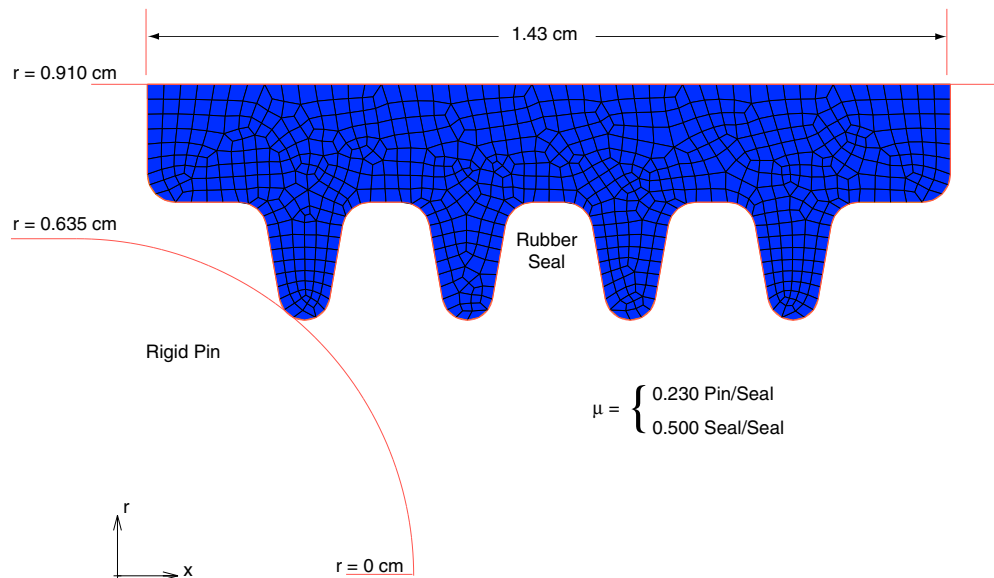


Figure 2.10-1 Rigid Pin Inserted into and Extracted from Rubber Seal

The pin is inserted into and extracted from the seal for five cases: no friction, bilinear, arc tangent (two different sliding velocities), and the stick-slip Coulomb friction models. The coefficient of friction between the pin and seal is 0.230; whereas, the coefficient of friction between the seal to seal contact is 0.500. The seal-to-seal contact is created as the rubber fingers bend and touch the surrounding rubber material.

Friction Modeling

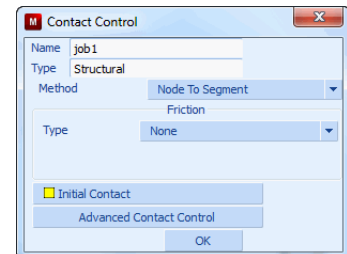
The preexisting models are shown in Table 2.10-1 with the various Coulomb friction types used. By default, contact defaults to the frictionless case, and as mentioned before, this is the first place to start if physically possible.

Table 2.10-1 Preexisting Models and Coulomb Friction Type Used

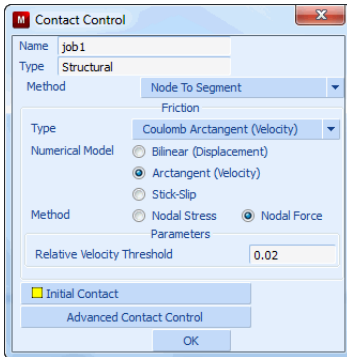
Mentat Model File	Coulomb Friction Type Used
sealinsert_nf.mud	No Friction Case
sealinsert_arctanv1.mud	Arc Tangent with default sliding velocity
sealinsert_arctanv2.mud	Arc Tangent with correct sliding velocity
sealinsert_bilinear.mud	Bilinear with default settings
sealinsert_stickslip.mud	Stick Slip with default settings

Procedure: to run above models:

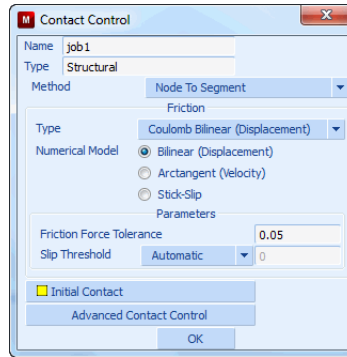
- FILE
- OPEN
 - sealinsert_nf.mud *(open model file)*
- OK
- MAIN
- JOBS
- MECHANICAL
- CONTACT CONTROL
- FRICTION TYPE
 - none
 - OK (twice)
- RUN
- SUBMIT



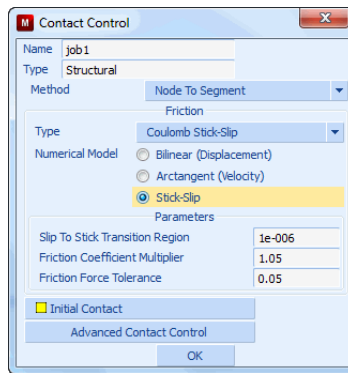
A similar procedure is used for the remaining files. While running the other files, check the friction type selection for the various models as shown in Figure 2.10-2.



Arc Tangent Control Parameters



Bilinear Control Parameters



Stick Slip Control Parameters

Figure 2.10-2 Control Parameters for Coulomb Friction Types

When selecting a friction type, it is easy to forget to set the various parameters unique to each type. For the *Arc Tangent* type, the sliding velocity is defaulted to unity which in most cases is not correct. The *bilinear* and *stick-slip* model parameters default to usable values for most of the cases. Hence, when using the Arc Tangent type, you must pay particular attention to the value of the sliding velocity. In general the sliding velocity is about 1% to 10% of the characteristic sliding velocity as based upon the physics. Even a static contact problem uses time to control the position of the rigid bodies and the sliding velocity must be selected correctly. In our suite of models, there are two different Arc Tangent types with the default and correct value of the sliding velocity.

As mentioned, the new Bilinear and existing Stick-Slip friction model parameters do not need to be changed, and as such, are easier to use correctly. Also, intuitively, one expects that the simulation run times increase from no friction, arc tangent, bilinear, and stick-slip friction types which is shown in this demonstration.

Results

Figure 2.10-3 plots the insertion and extraction force history for the five models.

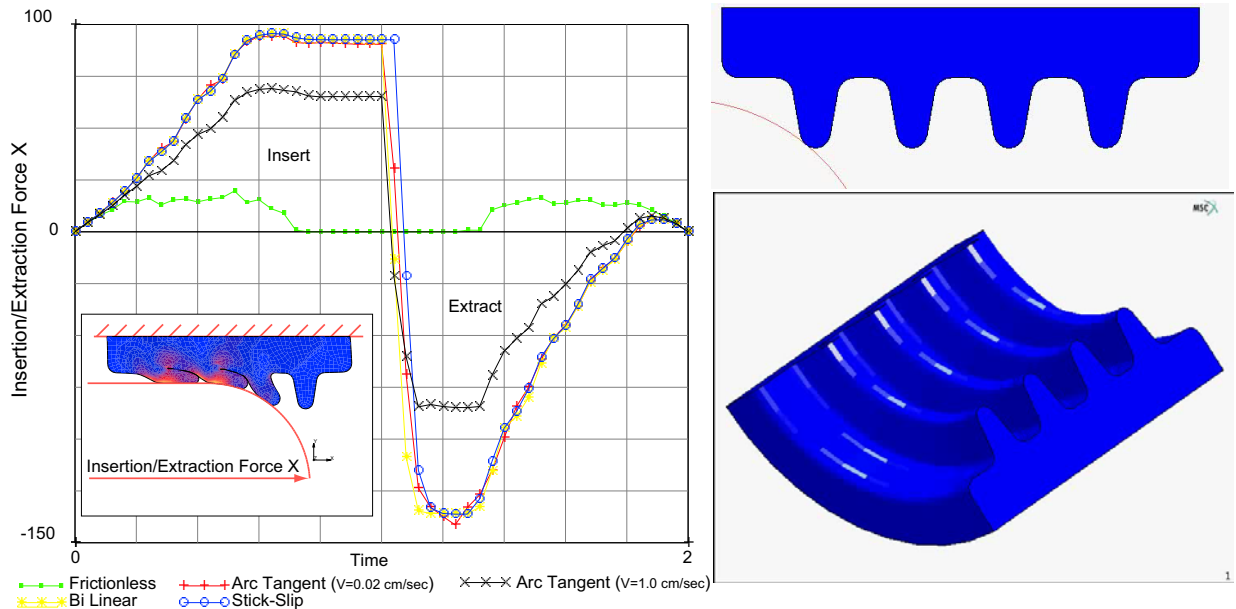


Figure 2.10-3 Insertion and Extraction Force History All Models (click right figures to play animation ESC to stop)

The frictionless case, as expected, has the lowest insertion and extraction force whose peak value is around 9 N. Adding friction dramatically increases the peak insertion force to about 100N, and the extraction force minimum peak is about -145 N. All three friction types produce nearly the same force history as long as the sliding velocity of the Arc Tangent type is properly set. The proper sliding velocity for this case is determined by the velocity of the pin during the insertion which gives a value of 0.020 cm/sec. Note what happens when the default sliding velocity is used, the effectiveness of the friction is dramatically diminished, and is incorrect.

Comparing run times that are shown in Table 2.10-2 for the various cases helps understand the benefits. Of course, the frictionless case requires the least amount of run time, followed by the Arc Tangent, then Bilinear, and the Stick-Slip model last. As designed, the Bilinear takes a bit more time but has the benefit of realistic default parameters that do not underestimate the friction forces like the Arc Tangent friction type.

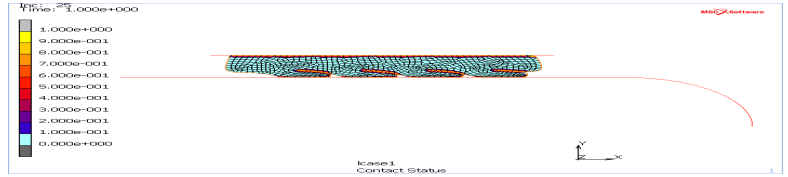
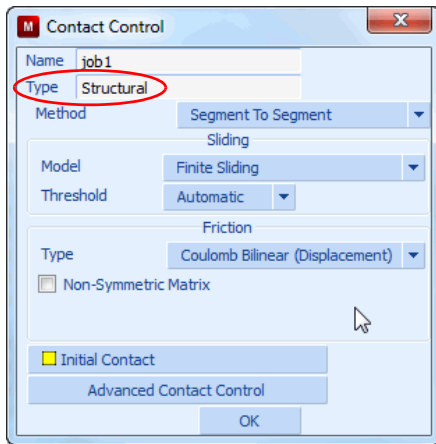
Table 2.10-2 Run Times of Coulomb Friction Type Used

Coulomb Friction Type Used	Normalized Run Times
No Friction Case	1
Arc Tangent with default sliding velocity	.90
Arc Tangent with correct sliding velocity	1.45

Table 2.10-2 Run Times of Coulomb Friction Type Used

Coulomb Friction Type Used	Normalized Run Times
Bilinear with default settings	1.15
Stick Slip with default settings	3.20

As an alternative, one can perform this analysis with the segment-to-segment friction approach. This method is advantageous in that it does a better job for self-contact that occurs in this model. This is activated using the Jobs Contact Control menu shown below. The resultant contact status is also shown.



Contact Status based upon Segment-to-segment Contact

Input Files

The files below are on your [delivery media](#) or they can be downloaded by your web browser by clicking the links (file names) below.

File	Description
sealinsert.proc	Mentat procedure file to run the above example
sealinsert_arctanv1.mud	Associated model file
sealinsert_arctanv2.mud	Associated model file
sealinsert_bilinear.mud	Associated model file
sealinsert_nf.mud	Associated model file
sealinsert_stickslip.mud	Associated model file

2.11 Analysis of a Manhole with Structural Zooming

- Chapter Overview 502
- Background Information 502
- Global Analysis 502
- Local Model and Analysis 503
- Conclusion 509
- Input Files 509

Chapter Overview

This chapter demonstrates the Marc structural zooming capability.

The chapter starts with a brief description of the background information. The model for analysis involves one cylinder joined to another cylinder of a larger radius. A local model with a finer finite element mesh, focusing on the joint of two cylinders and its vicinity, is then generated. Based on the global results, an analysis of the local model is performed to achieve a refined evaluation of the stress concentration around the cylinder joint.

Background Information

The problem used to demonstrate structural zooming capability in this chapter is the same as the one described in Chapter 3.2 in this manual. Also, refer to this chapter for detailed description on model geometry, materials, boundary conditions/loads, and mesh generation.

In Chapter 3.2, the problem is considered linear. The total value of loads are applied at increment 0. In order to demonstrate the use of structural zooming in a nonlinear analysis, the problem is slightly modified to have the loads applied in 10 equal increments. The large strain nonlinear behavior is modeled using updated Lagrangian, additive plasticity method.

Furthermore, shell thickness in the global model has to be written into post file for a structural zooming analysis involving shell elements in the global model.

Global Analysis

The global model *manhole.mud* is generated in Chapter 3.2 of this manual. The modifications regarding nonlinear analysis and shell thickness, mentioned in [Background Information](#), are taken into account in *manhole.mud*.

The steps in this section includes:

- Open the established model *manhole.mud*
- Run global model
- View stress distribution

FILES

OPEN

manhole.mud

OK

FILL

MAIN

```

JOBS
  RUN
    SUBMIT (1)
    MONITOR
    OPEN POST FILE (RESULTS)
  DEF & ORI
  CONTOUR BAND
  SCALAR
    Equivalent Von Mises Stress
  OK
  MONITOR
  
```

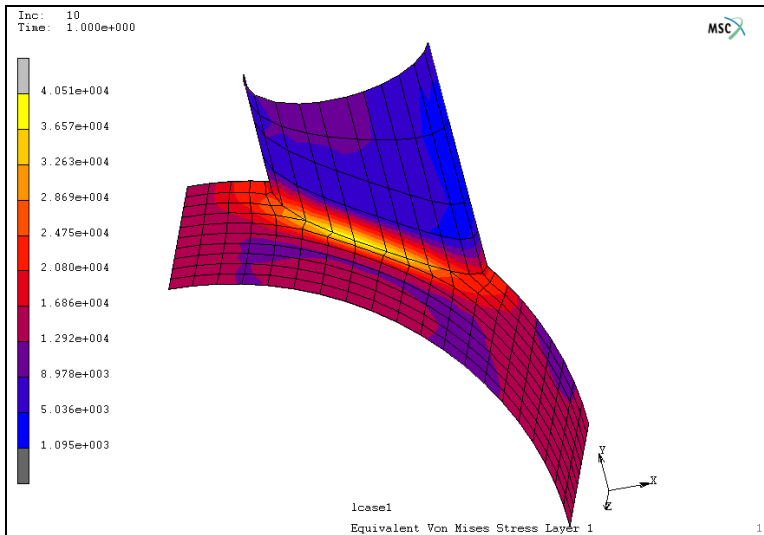


Figure 2.11-1 Distribution of Equivalent Stress, Obtained from Global Analysis

Local Model and Analysis

This section will include the following three steps:

- Step 1: Build a local model with a refined mesh**
- Step 2: Modify boundary conditions and apply GLOBAL-LOCAL boundary conditions**
- Step 3: Save model, run model, and view results**

Step 1: Build a local model with a refined mesh

To build a local model with a refined mesh, the elements out of the considered local area must be deleted first.

CLOSE

MAIN

MESH GENERATION

ELEMS: REM

```

449 450 451 452 453 454 455 456 457 458 459 460 461 462 463
464 465 466 467 468 201 202 203 204 205 221 222 223 224 225
241 242 243 244 245 261 262 263 264 265 281 282 283 284 285
301 302 303 304 305 321 322 323 324 325 341 342 343 344 345
346 347 348 349 350 351 352 353 354 355 356 357 358 359 360
366 367 368 369 370 371 372 373 374 375 376 377 378 379 380
386 387 388 389 390 391 392 393 394 395 361 362 363 364 365
381 382 383 384 385 469 470 471 472 396 397 398 399 400 220
240 260 280 300 320 340

```

END LIST (#)

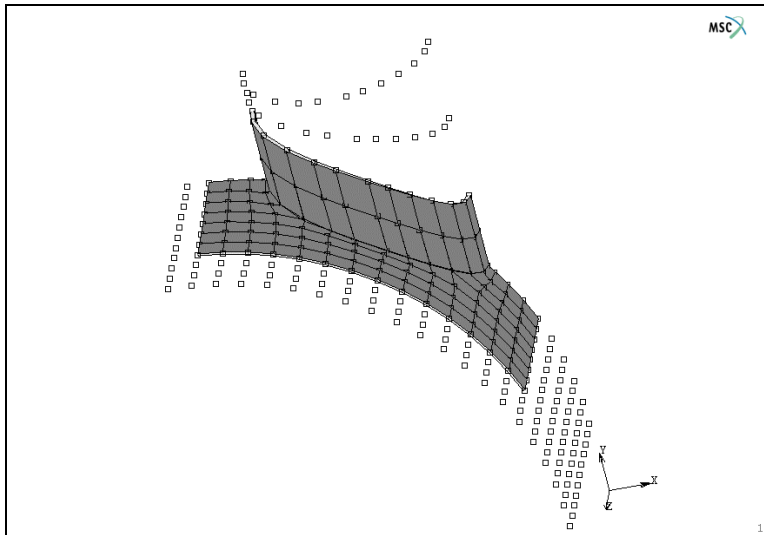


Figure 2.11-2 Delete Elements NOT in Considered Local Area

The mesh is then refined using the Mentat SUBDIVIDE option. One element becomes four by default because the subdivision in each direction is 2. After cleaning up the model by removing unused node and by sweeping all elements and nodes, the local mesh is established.


```
SUBDIVIDE
  ELEMENTS
  ALL: EXIST
  RETURN
SWEEP
  REMOVE UNUSED: NODES
  ALL
```

Step 2: Modify boundary conditions and apply GLOBAL-LOCAL boundary conditions

All boundary conditions existing in the global model are still available for the local model. However, due to the mesh refinement, new nodes are added. The relevant boundary conditions for these newly added nodes must be specified.

```
MAIN
BOUNDARY CONDITIONS
  MECHANICAL
    NODES: ADD
      598 601 604 610 613 619 622 628 631 634 637 640 646 649
      655 658 664 667 1318 1319 1327 1328 1342 1343 1351 1352
    END LIST (#)
  RETURN
```

To establish a link between the global model and the local model, a list of connecting nodes must be defined. The kinematic boundary conditions of these nodes are automatically calculated by Marc program, based on the results obtained from global analysis. We refer to the definition of the connecting nodes as the specification of GLOBAL-LOCAL boundary conditions.

```
NEW
GENERAL
  GLOBAL-LOCAL
    CONNECT NODES TO GLOBAL MODEL
    POST FILE
      manhole_job1.t16
    OK
  NODES: ADD
    598 599 600 671 672 743 744 815 816 941 942 1067 1068
    1193 1194 667 668 669 740 1197 1200 1206 1209 1215 1218
    1224 1227 1233 1236 1242 1245 1251 1254 1260 1263 741 812
```

813 938 939 1064 1065 1190 1191 1316 1317 1269 1272 1278
1281 1287 1290 1296 1299 1305 1308 1314 1345 1348 1351
1381 1384 1417 1420 1528 1438 1441 1456 1459 1474 1477
1492 1495 1510 1513 1405 1402 1366 1369 1327 1330 1333

END LIST (#)

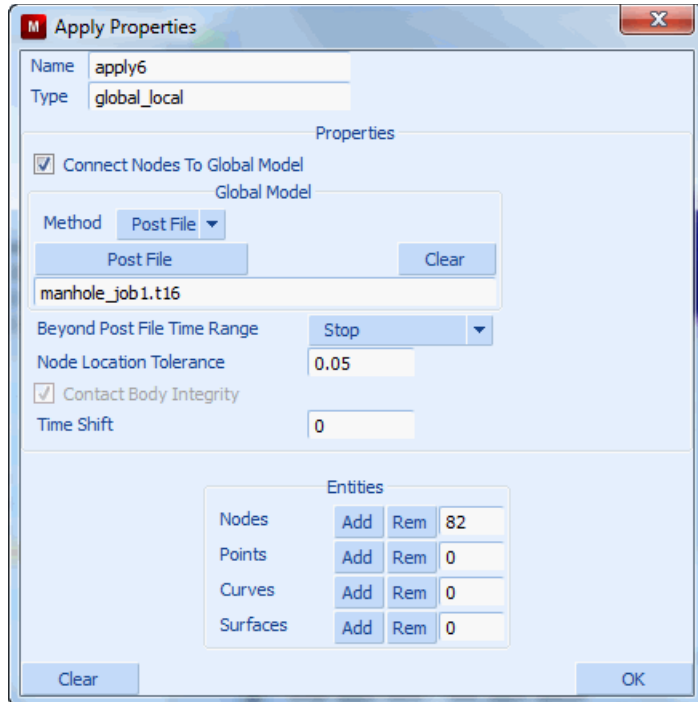


Figure 2.11-3 Define GLOBAL-LOCAL Boundary Conditions

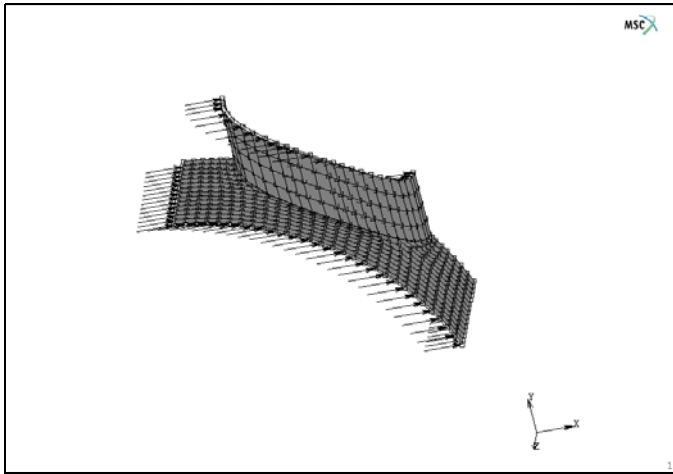


Figure 2.11-4 Connecting Nodes with GLOBAL-LOCAL Boundary Conditions

GLOBAL-LOCAL boundary conditions must be activated under the JOBS.

```
MAIN
JOBS
  MECHANICAL
    GLOBAL-LOCAL
      GLOBAL-LOCAL BOUNDARY CONDITIONS
        apply6
        OK (three times)
```

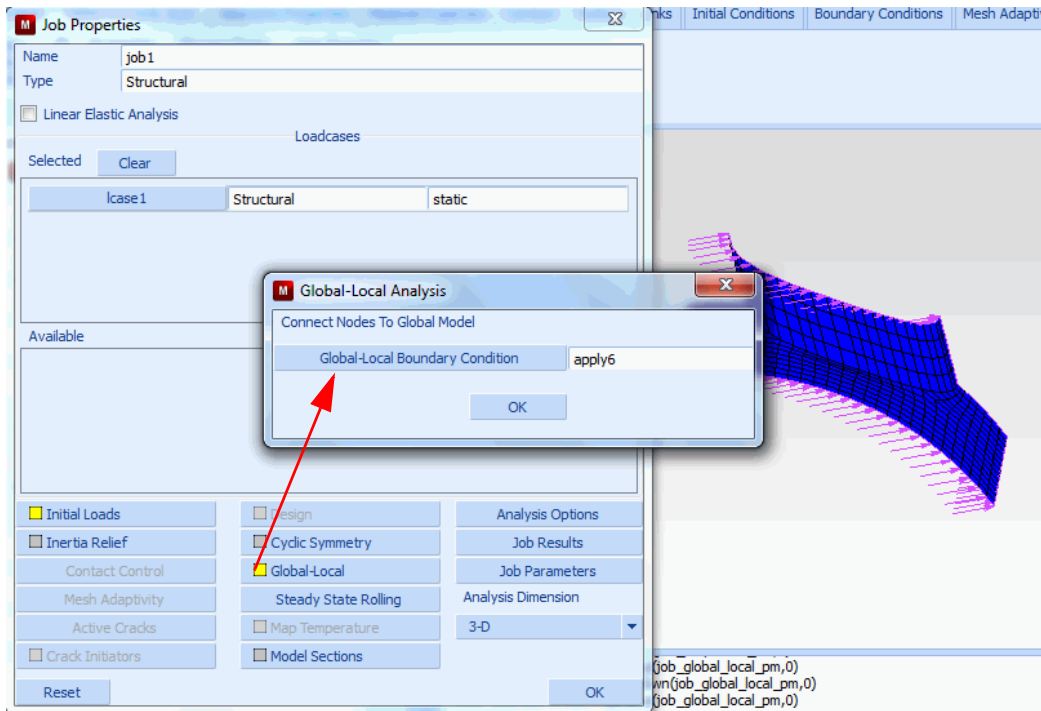


Figure 2.11-5 Activate GLOBAL-LOCAL Boundary Conditions

Step 3: Save model, run model, and view results

The local model has been fully established so far. To avoid over-writing the global model and the global results, the local model must be saved with a different file name. Use the following button to save model, run local analysis, and to view results.

FILES

SAVE AS

manhole_shell.mud

OK

MAIN

JOBS

RUN

SUBMIT (1)

MONITOR

OPEN POST FILE (RESULTS)

DEF & ORI

CONTOUR BAND

SCALAR
 Equivalent Von Mises Stress
 OK
 MONITOR

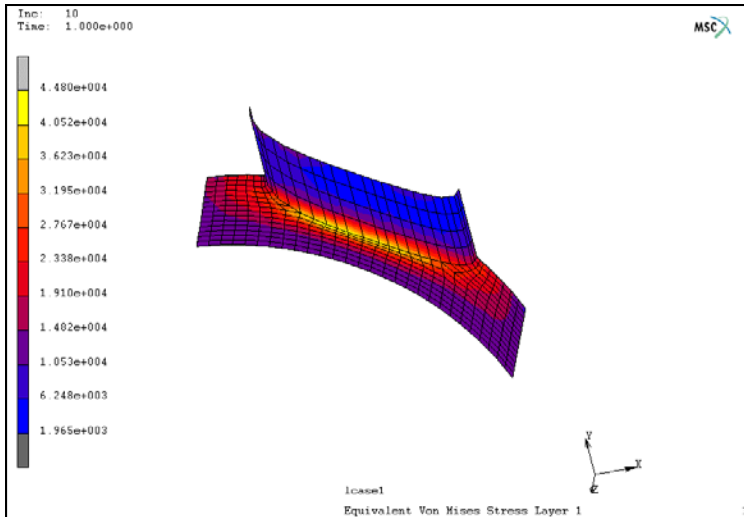


Figure 2.11-6 Distribution of Equivalent Stress, Obtained from Local Analysis

Conclusion

The maximum equivalent stress obtained from the local analysis is $4.48e4$, which is about 10% higher than the stress from global analysis. In comparison of [Figure 2.11-1](#) and [Figure 2.11-6](#), a sharper stress concentration is observed in the local analysis, representing a better evaluation of stress gradient.

Using the structural-zooming technique, it is also possible to model the local intersection of the cylinders with brick elements that use the global results from a global shell model.

Input Files

The files below are on your [delivery media](#) or they can be downloaded by your web browser by clicking the links (file names) below.

File	Description
manhole_shell.proc	Mentat procedure file to run the above example
manhole.mud	Associated model file

2.12 Radiation Analysis

- Chapter Overview 512
- Background Information 512
- Detailed Session Description 514
- Input Files 541

Chapter Overview

This chapter demonstrates how to perform a heat transfer simulation that incorporates both conduction and radiation. An analysis of a pressure vessel will be performed using both axisymmetric and three-dimensional techniques. This chapter will also demonstrate:

- The pixel based semi-hemi-cube method for calculating viewfactors.
- Application of boundary conditions on geometric entities.
- Usage of tables to define temperature dependent boundary conditions.

Background Information

Description

This session demonstrates the analysis of a large vessel that is subjected to a heat flux. The heat is transmitted both by conduction through the vessel material and by radiation. Radiation is an inherently nonlinear phenomena.

Additionally, the material properties of the vessel are dependent on the temperature. The axisymmetric analysis will be performed both with and without the radiation included to show the significance. Finally, a three-dimensional analysis will also be performed using symmetry conditions.

A 2-D representation of the vessel is shown below (Figure 2.12-1). It consists of a cylindrical section of length of 30 m and outer radius of 3 m. Each end is closed with a spherical cap. The thickness is 0.3 m. The bottom of the vessel is subjected to a constant flux.



Figure 2.12-1 Pressure Vessel

Idealization

The model has rotational symmetry and is first modeled using axisymmetric elements. The 3-D model is performed to demonstrate the use of symmetry surfaces and to show some novel modeling techniques.

Full Disclosure

The pressure vessel is modeled with both four-node axisymmetric quadrilateral and eight-node brick elements. Both the geometric and the finite element will be constructed. The temperature dependent thermal conductivity and specified heat are shown in Figure 2.12-2. The density is 7800 kg/m^3 . The emissivity is 0.75 on the interior surface and 0.2 on the exterior surface. In order to clearly show the effect of radiation, the specific heat is chosen to be low.

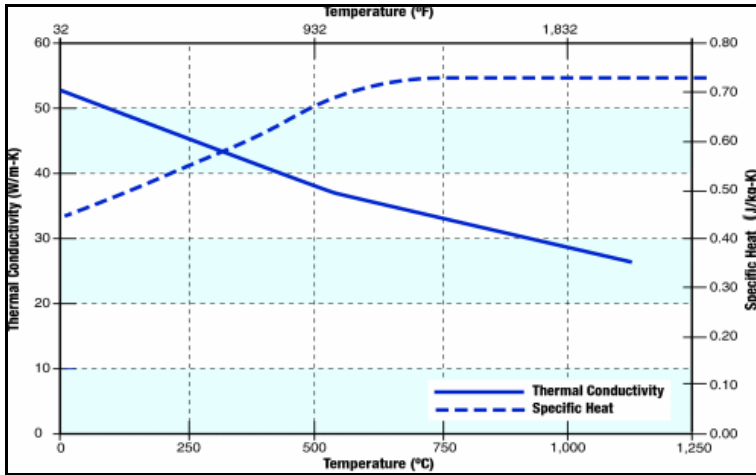


Figure 2.12-2 Thermal Properties at Elevated Temperatures

The internal applied flux is 1000 W/m^2 .

Overview of Steps

- Step 1: Create Axisymmetric Geometry, Finite Element Mesh, and Associate the Two Together
- Step 2: Apply Material Properties
- Step 3: Define Geometry of Radiating Cavity
- Step 4: Define Initial Conditions and Boundary Conditions
- Step 5: Define Emissivity on Cavity Surface
- Step 6: Define the Loadcases
- Step 7: Define the Jobs and Submit
- Step 8: Review the Results
- Step 9: Convert Axisymmetric Geometry and Mesh to 3-D
- Step 10: Convert the Remainder of the Model, including Adding Symmetry Surfaces
- Step 11: Create Planes to be Used for Symmetry Surfaces
- Step 12: Loadcase Creation and Job Creation
- Step 13: Review Results

Detailed Session Description

Step 1: Create Axisymmetric Geometry, Finite Element Mesh, and Associate the Two Together

The geometric model is created first by creating a grid and generating a series of straight lines and circular arcs. The circular arcs are created using the center, radius, beginning and ending angle technique.

```

MAIN
  MESH GENERATION
    SET
      U DOMAIN
        0 36
      U SPACING
        1
      V DOMAIN
        0 3
      V SPACING
        1
    GRID
    RETURN
  FILL
    CURVE TYPE CENTER/RADIUS/ANGLE/ANGLE
    ADD CURVE
      33.0 0.0 0.0 3    0 90
      33.0 0.0 0.0 2.7  0 90
      3.0  0.0 0.0 3.0 90 180
      3.0  0.0 0.0 2.7 90 180
    CURVE TYPE LINE
    ADD CURVE
      3 7
      6 10
      9 12
      4 1
    CHECK
      FLIP CURVES
        2 4 6 #
  
```

The result is shown in [Figure 2.12-3](#).

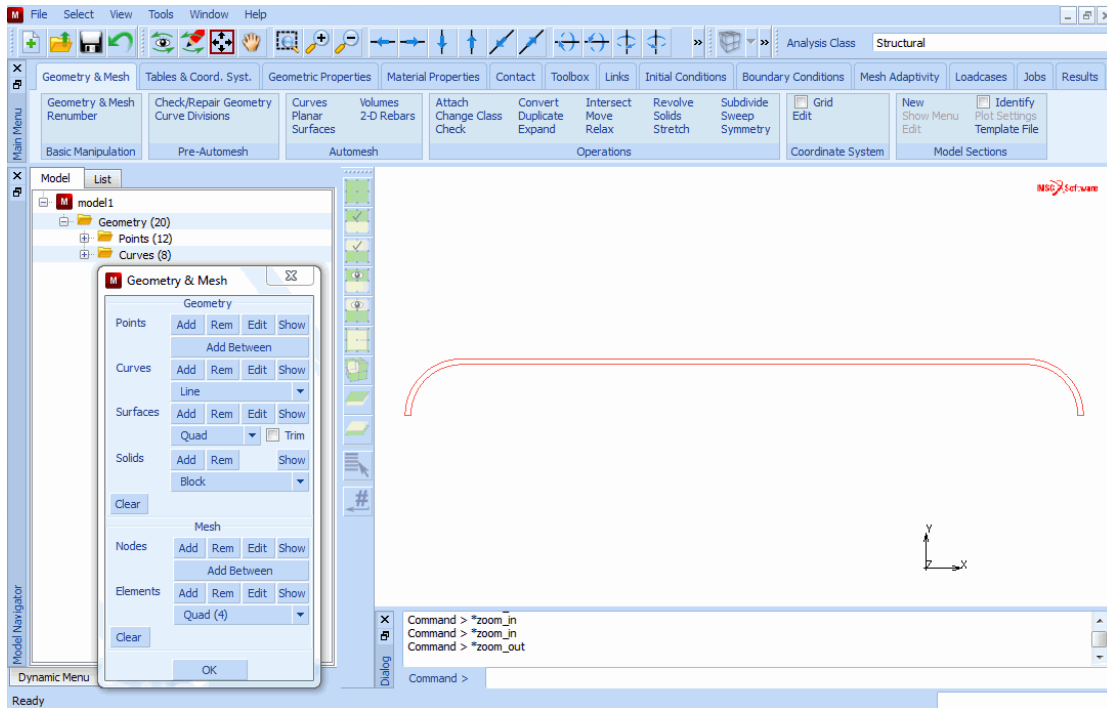


Figure 2.12-3 Geometric Representation of Vessel, Composed of Curves

The finite element mesh is then created by using a combination of local coordinate systems, creating three elements and subdividing them, then attaching the edges to the curves.

```

SET
  ORIGIN
    3 0 0
  CYLINDRICAL
    U DIVISION
      0 4
  RETURN
  ADD ELEMENT
    node (2.7, 90, 0)
    node (3.0, 90, 0)
    node (3.0, 180, 0)
    node (2.7, 180, 0)
  SUBDIVIDE
    2 9 1
  
```

```

ELEMENT 1 #
RETURN
SET
ORIGIN
      33 0 0
RETURN
ADD ELEMENT
      node ( 27,  0,  0)
      node ( 30,  0,  0)
      node ( 30,  90,  0)
      node ( 27,  90,  0)
SUBDIVIDE
ELEMENT 20 #
RETURN

```

(is shown in Figure 2.12-4)

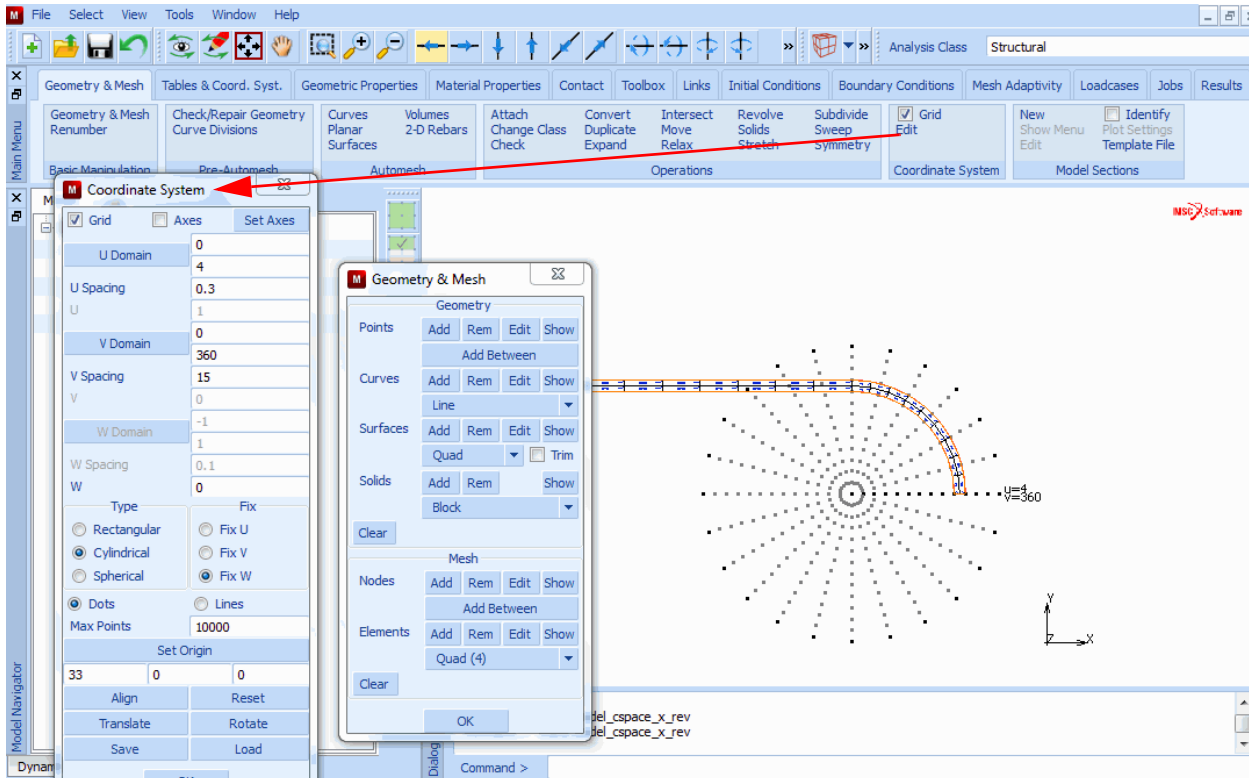


Figure 2.12-4 Finite Element Model

ADD ELEMENT

38 37 2 1

ATTACH

EDGES - CURVE

4	<i>(inner left curve)</i>
2:3 3:3 ... 10:3 #	<i>(inner left edges)</i>
3	<i>(outer left curve)</i>
11:3 12:1 ... 19:1 #	<i>(outer left edges)</i>
7	<i>(left small flat curve)</i>
19:2 10:2 #	<i>(left small flat edges)</i>
2	<i>(inner right curve)</i>
21:3 22:3 ... 29:3 #	<i>(inner right edges)</i>
1	<i>(outer right curve)</i>
30:1 31:1 ... 38.1 #	<i>(outer right edges)</i>
8	<i>(right small flat curve)</i>
21:0 30:0 #	<i>(right small flat edges)</i>
6	<i>(inner large flat curve)</i>
39:3 #	<i>(inner large flat edges)</i>
5	<i>(outer large flat curve)</i>
39:1 #	<i>(outer large flat edges)</i>

RETURN

SUBDIVIDE

DIVISIONS

2 3 1

ELEMENTS

39 #

RETURN

The result is shown in [Figure 2.12-5](#).

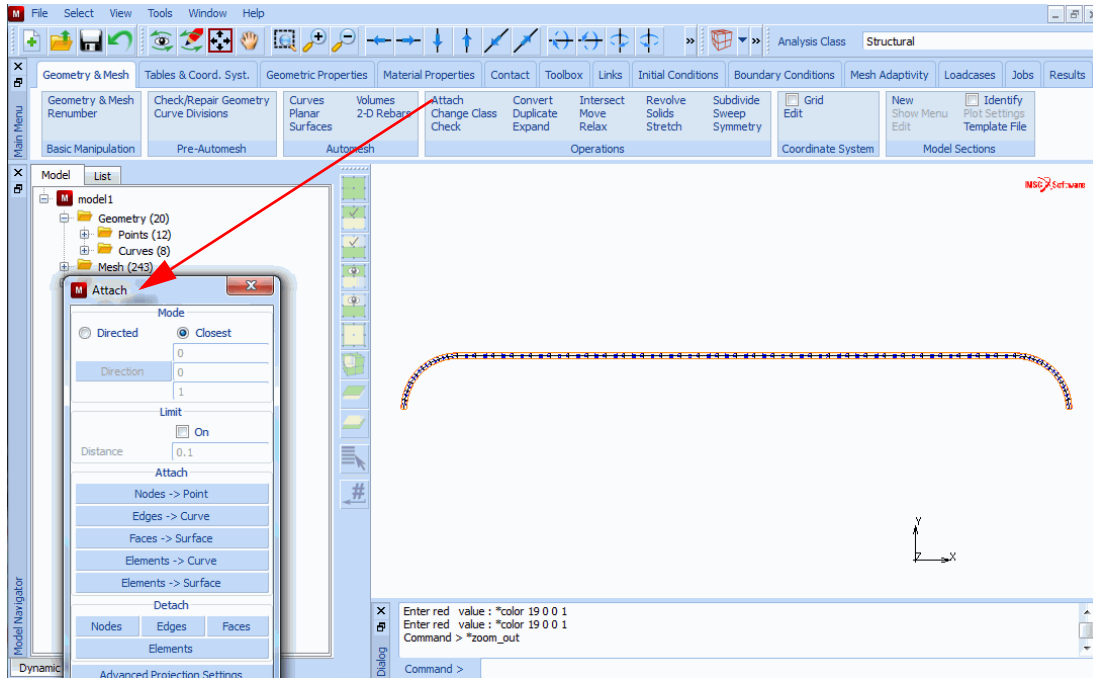


Figure 2.12-5 Finite Element Model with Edges of Elements Attached to Curves

Step 2: Apply Material Properties

The thermal material properties are defined by first entering the temperature dependent tables, then associating them with a material and finally associating this with all of the elements. Commands associated with labeling of the tables are omitted here for brevity (they are included in the procedure file).

Note: By default in Mentat, if the independent variable is outside of the range, entered the table that will be extrapolated. To change this, select the MORE button and turn off extrapolation.

The analysis program obtains the values of the thermal conductivity and specific heat at each integration point by evaluating the table and multiplying it by the reference value which is one. The surface emissivity will be defined in a separate stage.

The temperature dependent data provided in Figure 2.12-2 is given with respect to degrees Celsius, this will be shifted here to degrees Kelvin.

MATERIAL PROPERTIES

TABLE

NEW

INDEPENDENT VARIABLE

TYPE

TEMPERATURE

```
ADD
    273  52
    773  38
    1273 28
FIT
NAME
    thermal_conductivity
RETURN
TABLE
NEW
    1 INDEPENDENT VARIABLE
TYPE
    TEMPERATURE
ADD
    273  .43
    873  .70
    1523 .73
FIT
NAME
    specific_heat
RETURN
```

The temperature dependent properties are shown in [Figure 2.12-6](#) and [Figure 2.12-7](#)

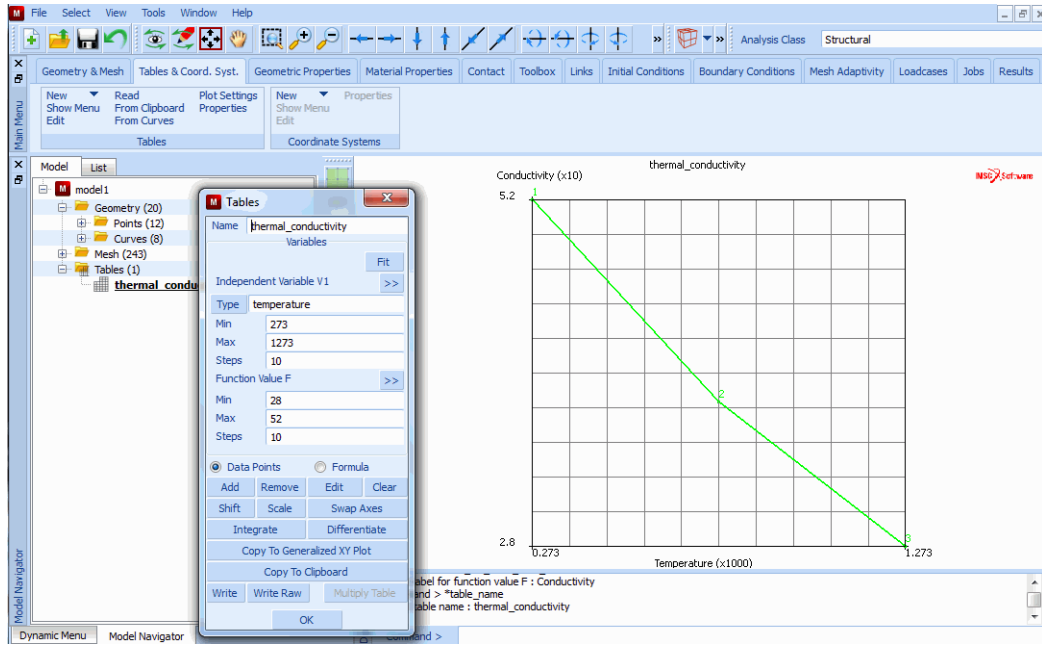


Figure 2.12-6 Definition of Temperature Dependent Conductivity with Table

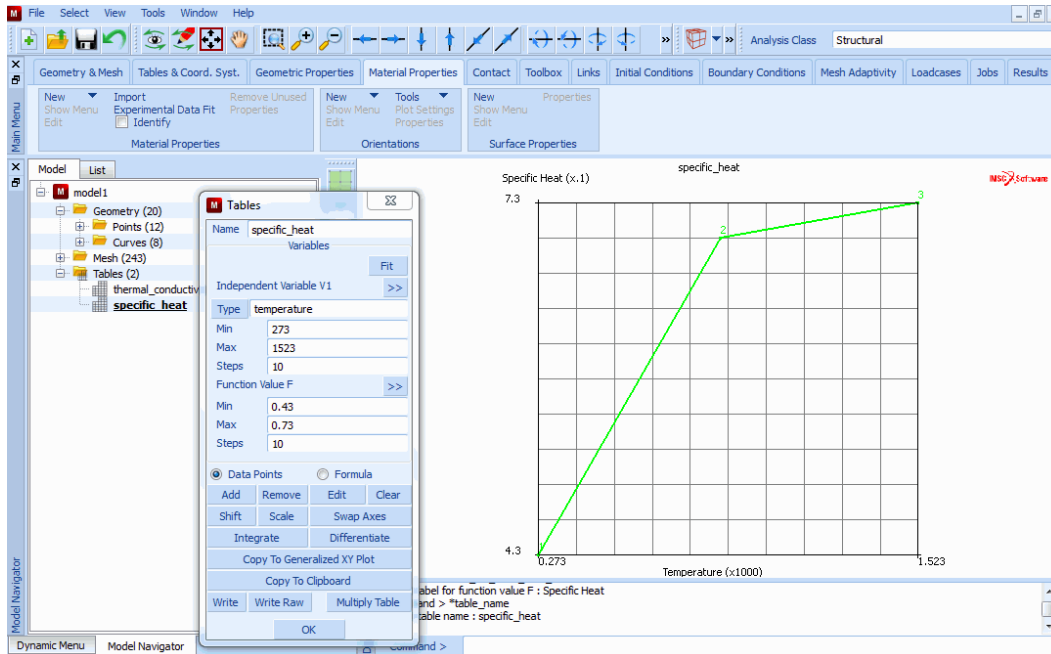


Figure 2.12-7 Definition of Temperature Dependent Specific Heat with Table

HEAT TRANSFER

CONDUCTIVITY TABLE

thermal_conductivity

SPECIFIC HEAT

1.0

SPECIFIC HEAT TABLE

specific_heat

MASS DENSITY

7800

OK

ADD

ALL:EXIST

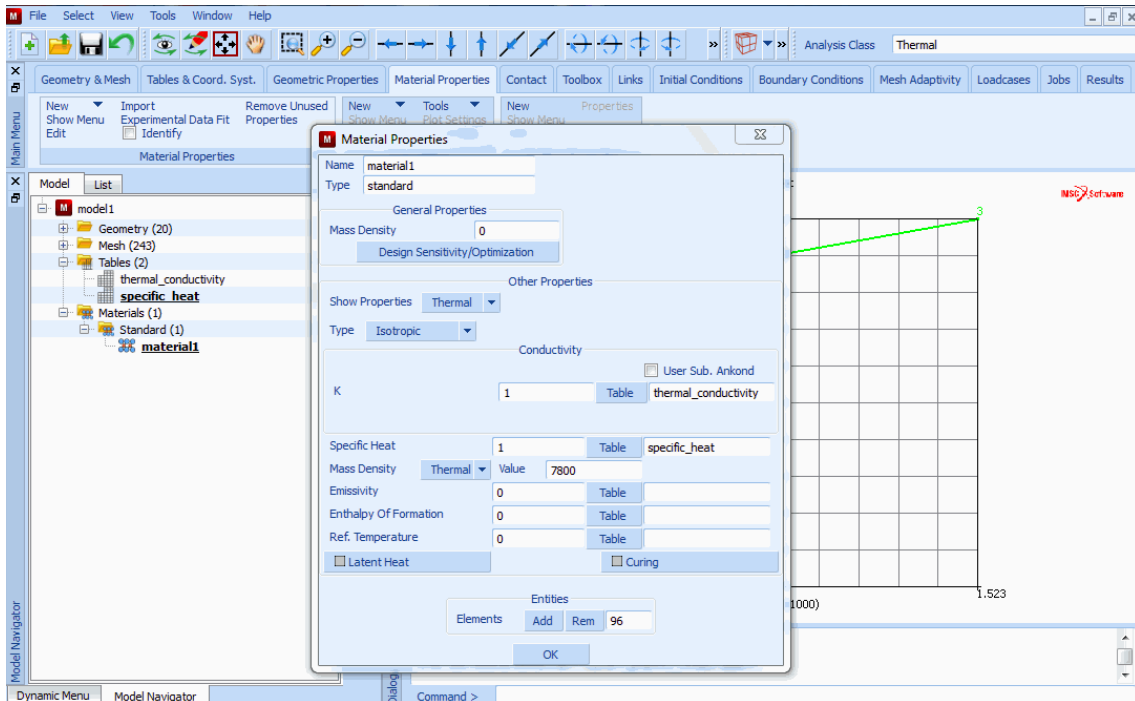


Figure 2.12-8 Association of Tables with Material Properties and Elements

Step 3: Define Geometry of Radiating Cavity

In this analysis, the radiating cavity is the closed region of the vessel. It is defined by entering the three curves that were constructed earlier. As it is an axisymmetric structure, there is no reason to enter a symmetry surface/curve at

$r = 0$. As the cavity is closed, there is no need to define the environment temperature that internal heat can escape through a control node.

MAIN

MODELING TOOLS

CAVITIES

DIMENSION:2-D

ADD CURVES

2 4 6

ENDLIST

MAIN

In this model, the cavities are defined by curves. This facilitates the use of radiation with either local or global adaptive meshing. Its continuum elements are used; the orientation of the curves is not important; this is not the case when shell elements are used. The menu is shown in [Figure 2.12-9](#).

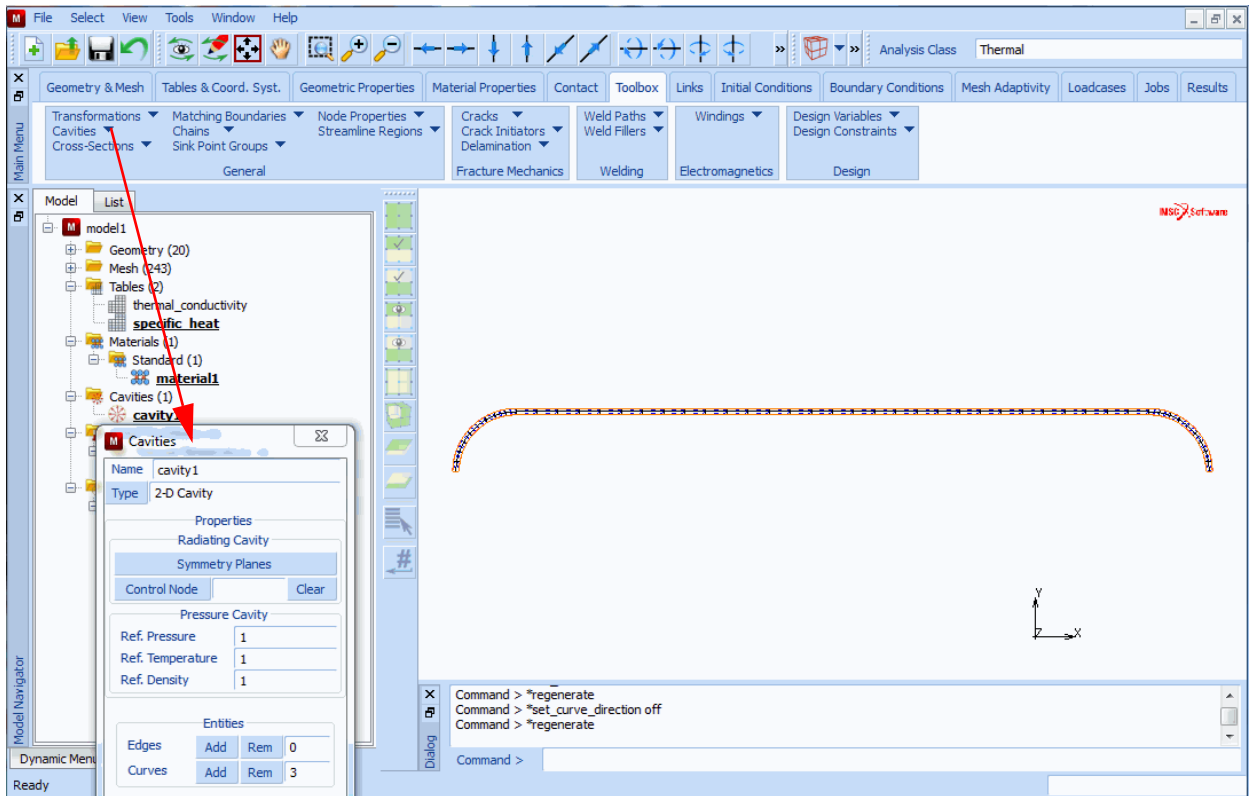


Figure 2.12-9 Definition of Cavities

Step 4: Define Initial Conditions and Boundary Conditions

The initial conditions of 293°K are entered for all nodes as shown in [Figure 2.12-10](#). Note that in radiation analysis, the flux associated with radiation is calculated in absolute units.

The user should either define temperatures in absolute units, or specify the offset temperature between user units and absolute.

Three boundary conditions are defined, though they are not all used for each analysis. This includes:

1. A flux (as shown in [Figure 2.12-11](#)) of 1000 W/m² is applied on the inside surface of one of the hemispherical caps. This represents the heating device that is present in a reacting vessel.
2. Internal radiation is applied as shown in [Figure 2.12-12](#). This is based upon the cavity that is as defined in the previous step.
3. Radiation to the environment occurs on from the external surfaces as shown in [Figure 2.12-13](#). As none of the external faces can see each other, a viewfactor calculation is not required. The emissivity on the external surfaces is 0.2, and the environment temperature is 293K.

INITIAL CONDITIONS

THERMAL

TEMPERATURE

TEMPERATURE

293

OK

NODE:ADD

ALL:EXIST

MAIN

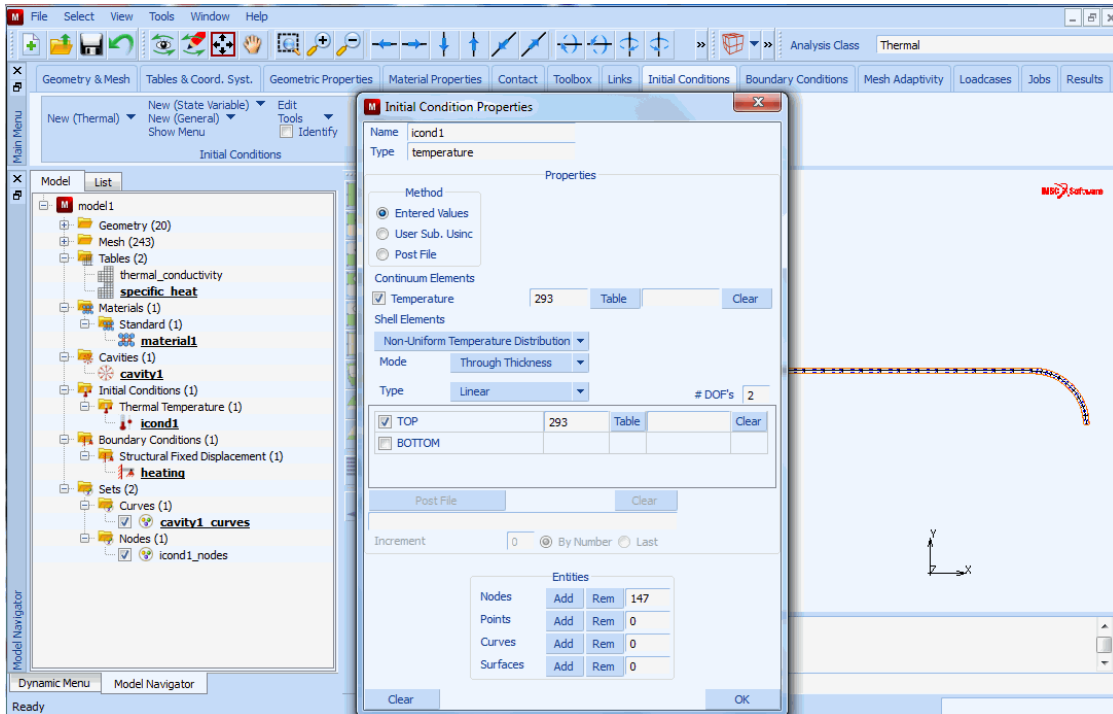


Figure 2.12-10 Definition of Initial Temperature

BOUNDARY CONDITIONS

THERMAL

(define internal heating)

NAME

heating

EDGE FLUX

FLUX

1000

OK

CURVES:ADD

4

NEW

NAME

internal rad

(define internal radiation)

CAVITY RADIATION

RADIATION

CLOSED

CALCULATE

WRITE TO POST FILE

OK

CAVITIES:ADD

cavity1

OK

NEW

NAME

external rad

(define external radiation)

EDGE FILE

SINK TEMPERATURE

293

EMISSIVITY

0.2

OK

CURVES:ADD

3 5 1

RETURN

ID BOUNDARY CONDITIONS

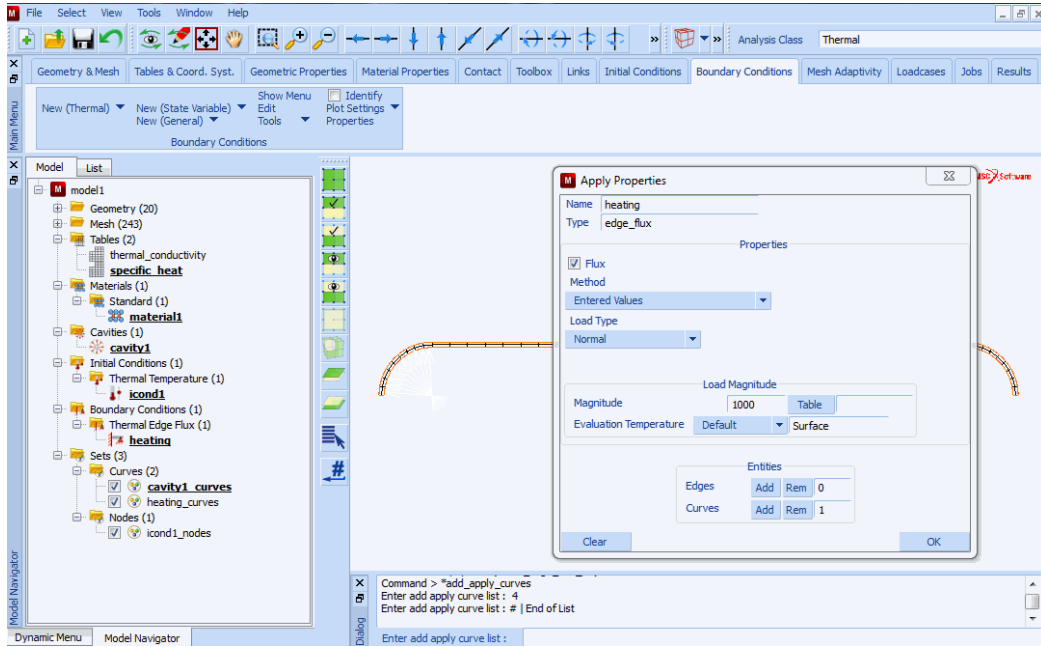


Figure 2.12-11 Thermal Flux on Surface

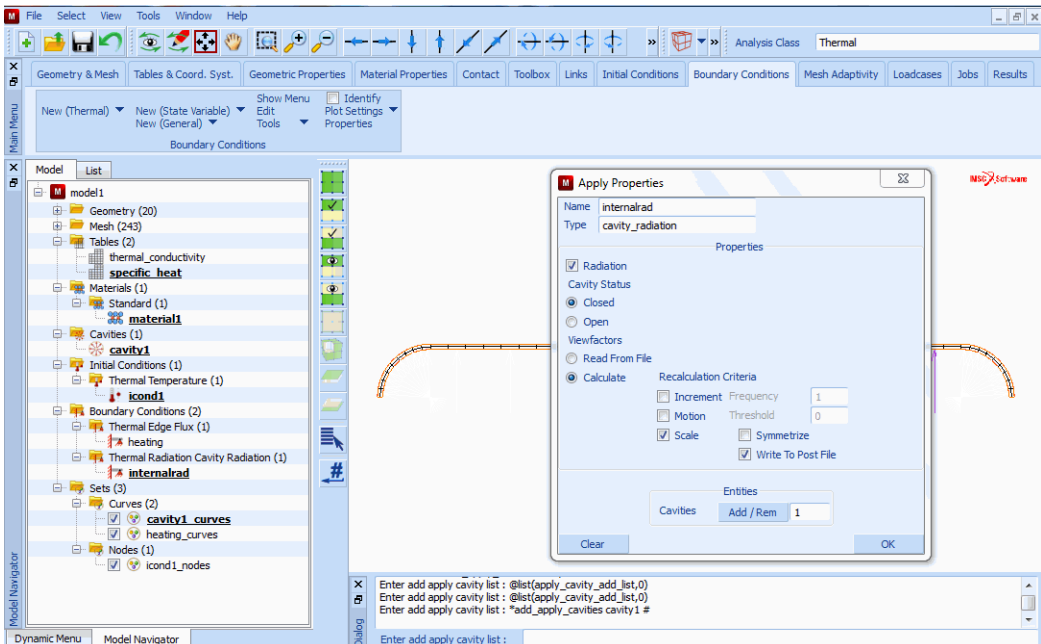


Figure 2.12-12 Radiation Cavity Boundary Condition

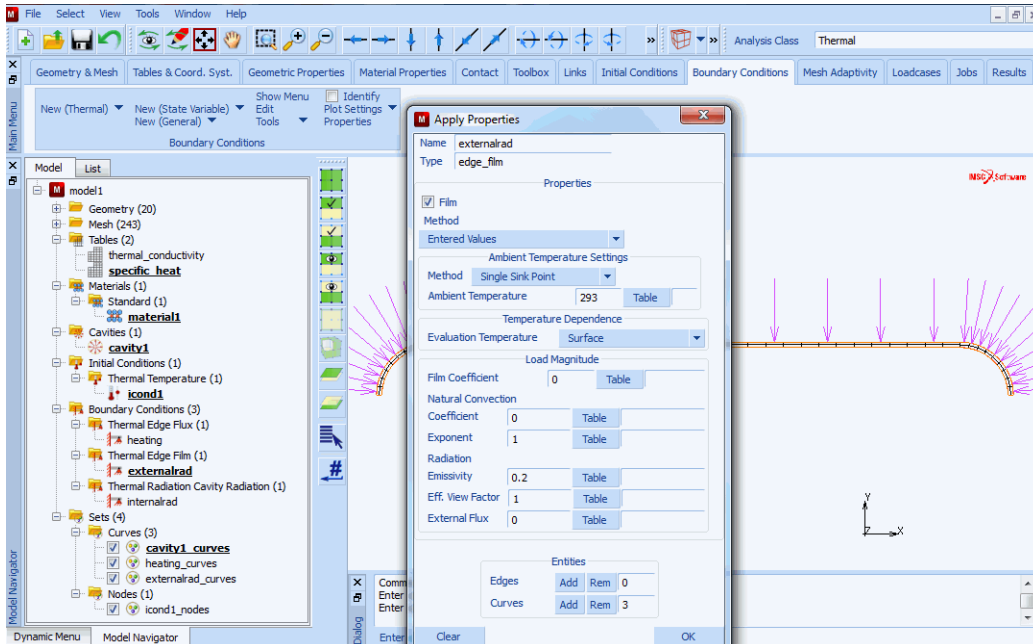


Figure 2.12-13 External Radiation to the Environment

Step 5: Define Emissivity on Cavity Surface

The emissivity associated with a radiating cavity may either be applied as material data applied to the elements or as a surface property applied to an edge or face. The latter (surface property) is the preferred method. It permits different emissivities to be applied to the same model or element to reflect surface coatings, polish and/or wear. In this problem, the emissivity on the internal region is constant, but substantially higher than the emissivity on the outside surface. This reflects the degradation of the surface due to the chemical and thermal reactions in the tank.

MAIN

MATERIAL PROPERTIES

SURFACE PROPERTIES

RADIATION PROPERTIES

COEFFICIENT

0.75

OK

CURVES:ADD

4 6 2

MAIN

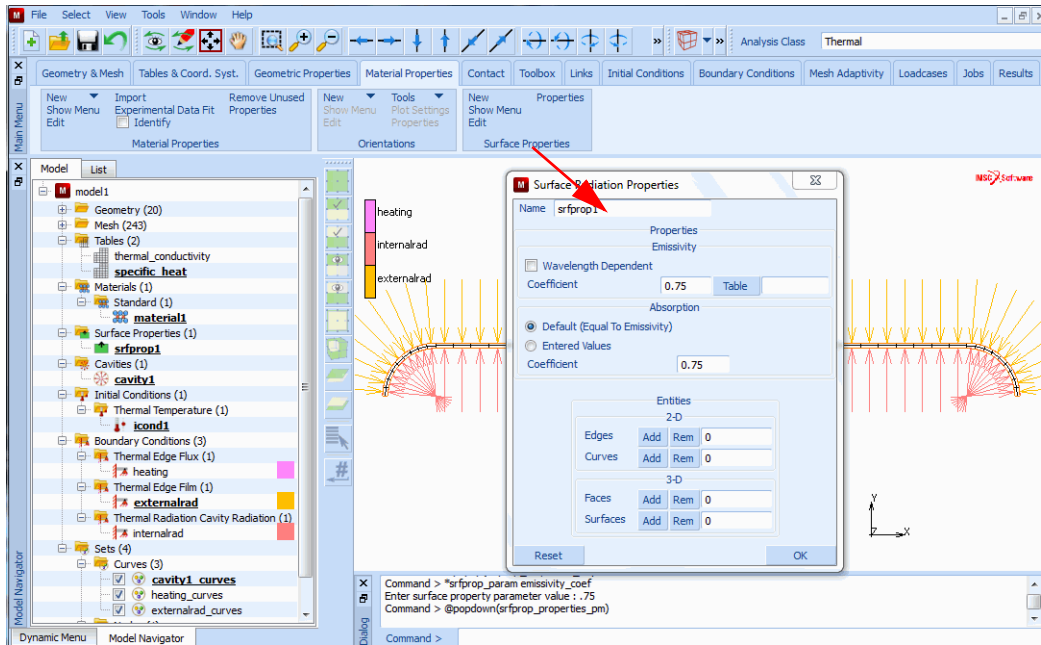


Figure 2.12-14 Surface Emissivity for Radiating Cavity

Step 6: Define the Loadcases

In this problem, three loadcases are defined and they are activated in three jobs. In all three cases, a period of 300 seconds are analyzed using the adaptive time stepping procedure. The initial time step is 0.1 sec. The first loadcase has only the heater boundary condition; the second loadcase – the heater and the internal radiation, and the third loadcase – has all three boundary conditions.

This procedure allows the user to associate multiple analyses with the same model file. Because of the highly nonlinear nature of radiation, a tight tolerance of 10° is placed on the maximum error in the temperature estimate. This insures an accurate analysis.

LOADCASES

(create 1st loadcase)

HEAT TRANSFER

TRANSIENT

LOADS

internal rad

(deactivate)

external rad

(deactivate)

OK

CONVERGENCE TESTING

MAX ERROR IN TEMPERATURE ESTIMATE

OK
ADAPTIVE:TEMPERATURE
PARAMETERS
 INITIAL TIME STEP
 0.1
 MAX # INCREMENTS
 500

OK
TOTAL LOADCASE TIME
 300

OK
COPY *(create 2nd loadcase using 1st as a base)*

TRANSIENT
 LOADS
 internal rad *(activate boundary condition)*

 O
 K
COPY *(create 3rd loadcase using 2nd as a base)*

 LOADS
 external rad *(activate boundary condition)*
 OK

MAIN

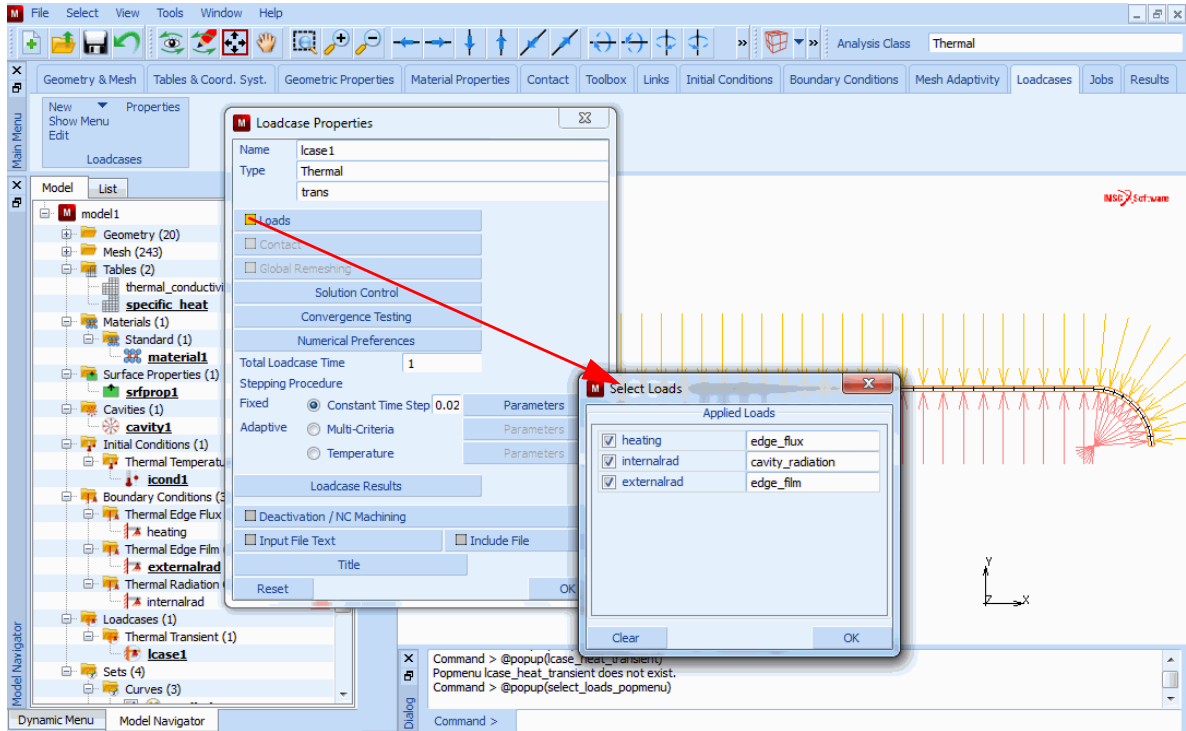


Figure 2.12-15 Loadcase 3 with all Three Boundary Conditions Activated

Step 7: Define the Jobs and Submit

In this step, parameters associated with the heat transfer analysis are set. Many default values are used, but they are reviewed here to indicate other possibilities. Three jobs are created, each with a single loadcase and subsequently submitted for analysis. The results are compared in a later step.

JOBS

(create the 1st job)

```

RENUMBER ALL
TITLE
    AXISYMMETRIC HEATING OF VESSEL
HEAT TRANSFER
LOADCASE SELECT LCASE1
ANALYSIS DIMENSION: AXISYMMETRIC
ANALYSIS OPTIONS
    LUMPED CAPACITANCE
    RADIATION
OK
    
```

Note: Defaults are considered adequate for analysis

```
JOB PARAMETERS
  UNITS AND CONSTANTS
    TEMPERATURE IN KELVIN
    OK (thrice)
COPY (create the 2nd job)
  HEAT TRANSFER
    CLEAR
    LOADCASE SELECT LCASE2
    OK
  RUN
  SUBMIT
  OK
COPY (create the 3rd job)
  HEAT TRANSFER
    CLEAR
    LOADCASE SELECT LCASE3
    OK
  RUN
  SUBMIT
```

There are several considerations when performing a radiation analysis.

First, the user should be careful in choosing the units and indicate the units to the program. Here all units are in Kelvin, so under the JOB-> HEAT TRANSFER-> JOB PARAMETERS-> UNITS AND CONSTANTS menu, this needs to be defined. Associated with radiation analysis is the Stefan Boltzmann constant. It must be given in consistent units. If frequency dependent emissivity is defined, then it is also necessary to define Planck's 2nd constant and the speed of radiation (light) in a vacuum.

The speed must be given in a unit that is consistent with the wavelength unit used to define the emissivity.

Second, the viewfactor calculation is approximate; the accuracy is dependent upon user entered parameters. When the Monte Carlo procedure is used (see BOUNDARY CONDITIONS-> THERMAL-> COMPUTE RADIATION VIEWFACTOR), the accuracy is controlled by the number of rays randomly emitted.

In the Pixel Based Semi-Hemi-cube method used in this example, the accuracy is based upon the number of pixels used. This is controlled on via the JOBS-> HEAT TRANSFER-> ANALYSIS OPTION-> RADIATION menu (shown in [Figure 2.12-17](#)).

Here, 500 is entered (default), which is the number of pixels between (0-1). The actual calculation goes from (-1 to 1) in both a local x- and y-direction, so the actual number of pixels is $(2 \times 500)^2 = 1$ million.

For axisymmetric models, the viewfactors are actually calculated in 3-D and then reassociated with the 2-D edge. The **AXISYMMETRIC # DIVISIONS** button controls the accuracy in this calculation.

Finally, the viewfactors may be neglected by the analysis program or treated explicitly. If the viewfactor is below the **USE VIEWFACTOR** control, it is ignored. If the viewfactor is greater than this value but less than the **TREAT VIEWFACTOR IMPLICITLY** button, the radiation flux associated with this viewfactor is treated explicitly. This may result in more iterations, but reduces the size of the stiffness matrix.

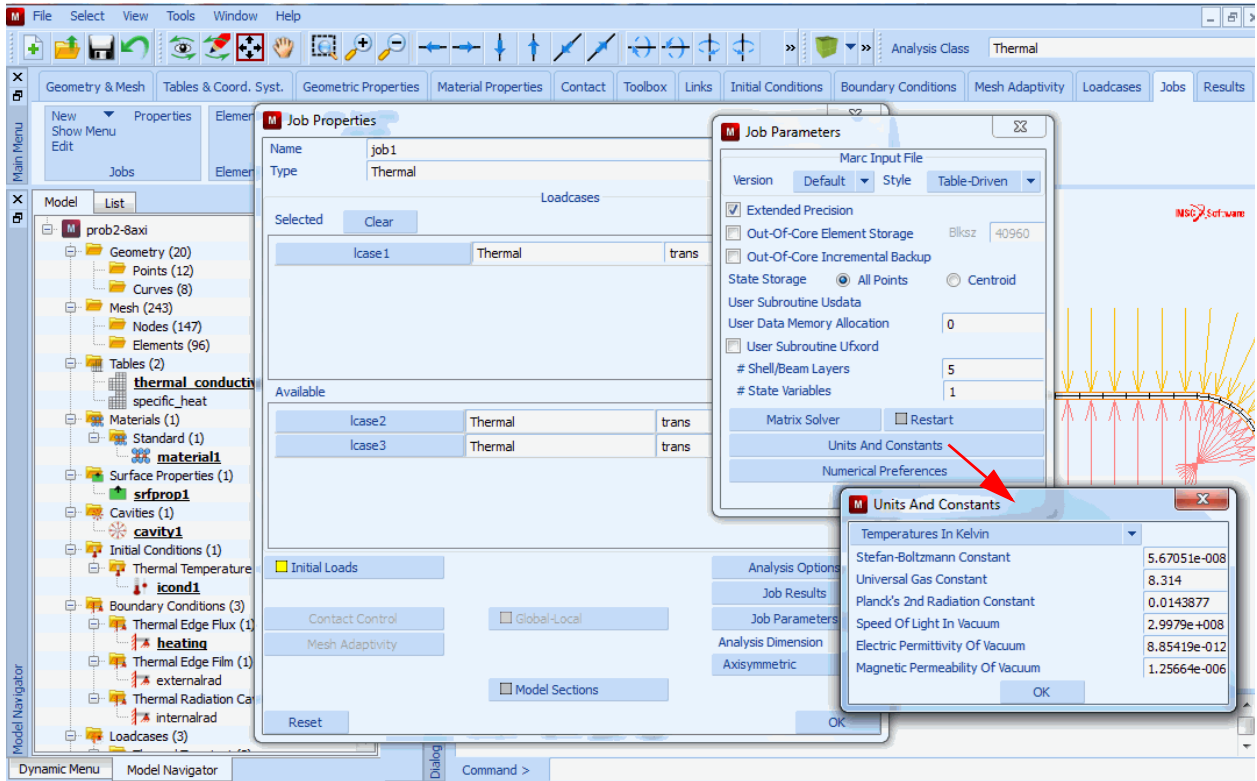


Figure 2.12-16 Heat Transfer Units and Constants Menu

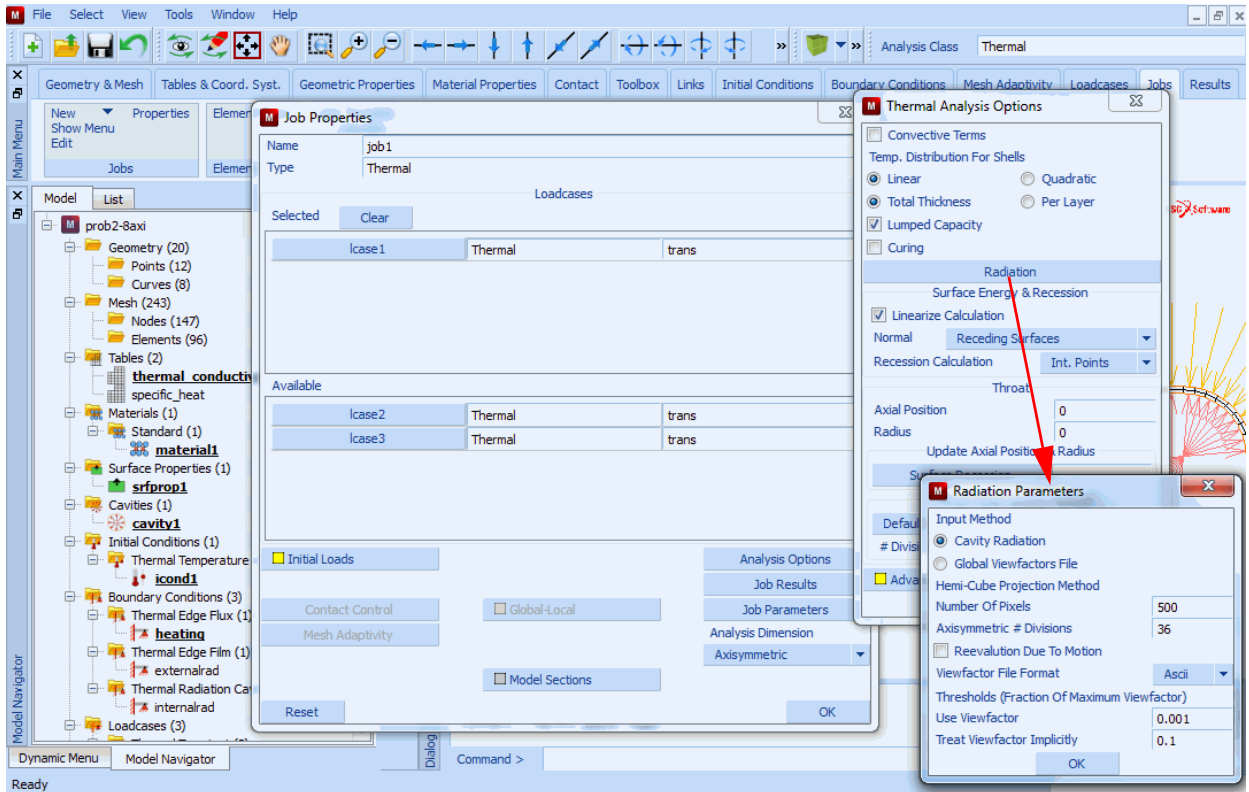


Figure 2.12-17 Radiation Parameter Settings

Step 8: Review the Results

A contour plot and the time history plot of selective nodes are examined for the three runs. The transient behavior of the three jobs is compared.

It is assumed that the post file associated with the job to be examined has already been opened using the RESULTS->OPEN command or the OPEN DEFAULT COMMAND.

FILL VIEW

LAST

CONTOUR BANDS

HISTORY PLOT

SET NODES

1 4 7 40 80

COLLECT DATA

NODES/VARIABLES

ADD VARIABLE
Time
Temperature
FIT

Observing the results.

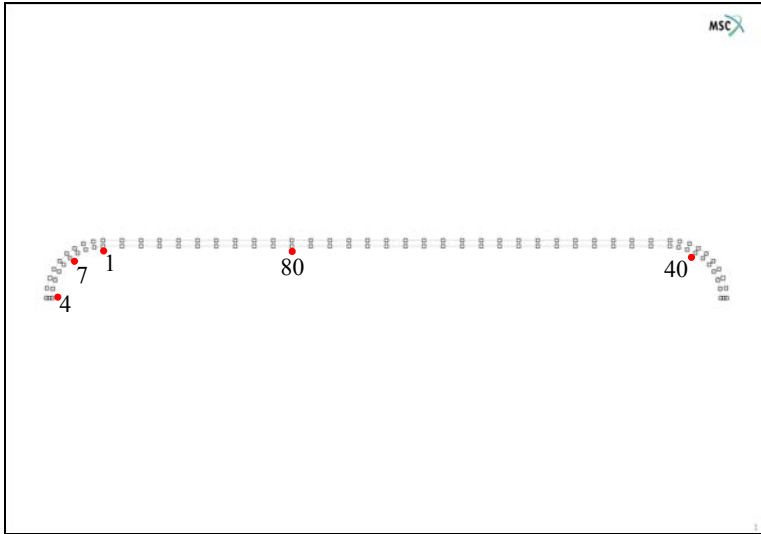


Figure 2.12-18 Location of Nodes being Tracked

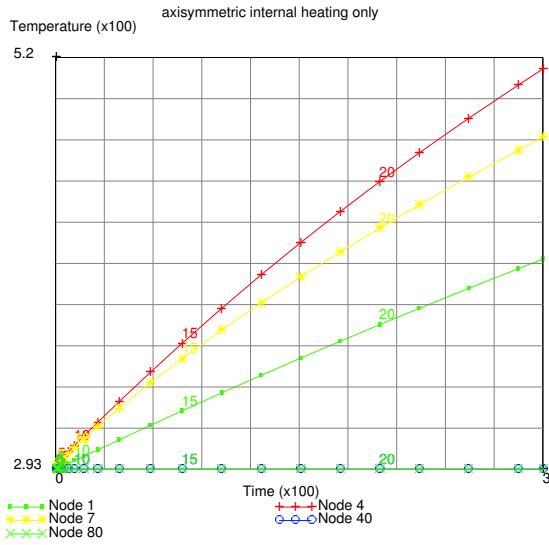


Figure 2.12-19 Transient Response for Job1 – Heating Only

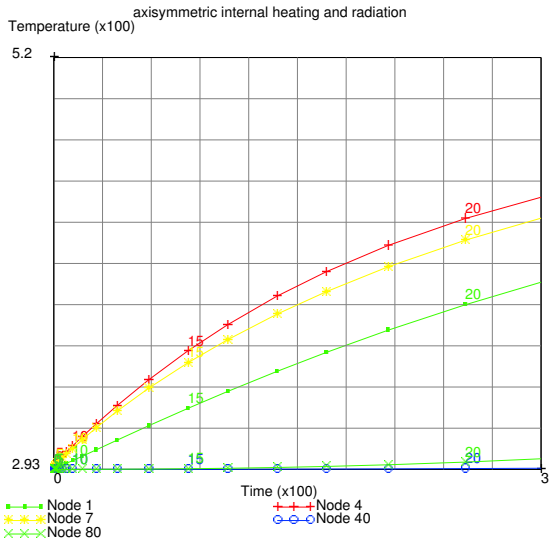


Figure 2.12-20 Transient Response for Job2 – Heating and Internal Radiation

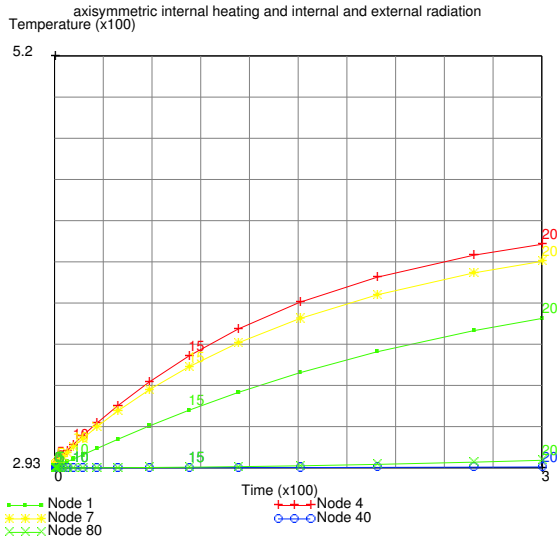


Figure 2.12-21 Transient Response for Job3 – Heating, Internal and External Radiation

In observing that radiation is not included in job1, the left side of the vessel gets the hottest. When internal radiation is included (job2), some of the heat radiates to the opposite side, and hence, the maximum temperature is lower. When both internal and external radiation is included, the vessel temperature is the lowest as expected.

When examining the output of job2 or job3 after the message start of increment 1, you can see the following information regarding the calculation of the viewfactors.

```

s t a r t   o f   i n c r e m e n t   1
calculating viewfactor for cavity      1
allocated      8688 words of memory due to radiation viewfactors

view factors read in from .vfs file
cavity number      :      1
number of faces    :      48
number of pixels used :      500

number of factors   :      2304

minimum viewfactor : 0.0000164
maximum viewfactor  : 0.1723900
    
```

maximum connectivity in stiffness matrix is 32 at node 75

maximum half-bandwidth is 146 between nodes 2 and 147

The user observes that the number of radiating faces is 48 which is equal to the number of elements on the inside; this indicates that applying the cavity onto the geometry was successful. Then you can observe that there are 2304 calculated viewfactors, as this is an axisymmetric problem, the maximum possible is $48 \times 48 = 2304$. Hence, all possible

viewfactors have been found. Then one observes that the minimum viewfactor is 0.0000164 and the maximum is 0.17239, or the minimum is 0.009% of the maximum. Based upon the default thresholds, some of the viewfactors are treated explicitly and some are neglected. Even so, the inclusion of the radiation viewfactors significantly increases the size of the stiffness matrix, as the number of profile entries increases from 581 in job1 to 1233 in job2 and job3.

Step 9: Convert Axisymmetric Geometry and Mesh to 3-D

In this step, the axisymmetric model is expanded into a quarter section of a 3-D model, and the boundary conditions are updated from 2-D to 3-D. The combined expand option is used to expand the mesh, geometry, and simultaneously attach the 3-D finite element mesh to the surfaces. When using the combined expand, it expands all entities activated. Here, nodes and points are turned off so unnecessary lines and 2-node elements are not created.

The nodal initial conditions are automatically expanded. The distributed boundary conditions are copied over, but need to be updated.

MESH GENERATION

EXPAND

ROTATION ANGLE

10 0 0

REPETITIONS

9

COMBINED

NODES

(deactivate nodes)

POINTS

(deactivate points)

RETURN

SWEEP

ALL

RETURN

RENUMBER

ALL

RETURN

Step 10: Convert the Remainder of the Model, including Adding Symmetry Surfaces

BOUNDARY CONDITIONS

THERMAL

FACE FLUX

(change boundary condition "heating"

from edge flux to face flux)

OK

SURFACE ADD

28 29 30 31 32 33 34 35 36

NEXT

CAVITY RADIATION

(review radiating cavity boundary condition)

OK

NEXT

FACE FILM

*(change boundary condition "external rad"
from edge film to edge flux)*

OK

SURFACE ADD

1 2 3 4 5 6 7 8 9
19 20 21 22 23 24 25 26 27
37 38 39 40 41 42 43 44 45

Step 11: Create Planes to be Used for Symmetry Surfaces

With the steps below, create two planes that will be used as symmetry surfaces for the viewfactor calculation. This is shown in [Figure 2.12-22](#).

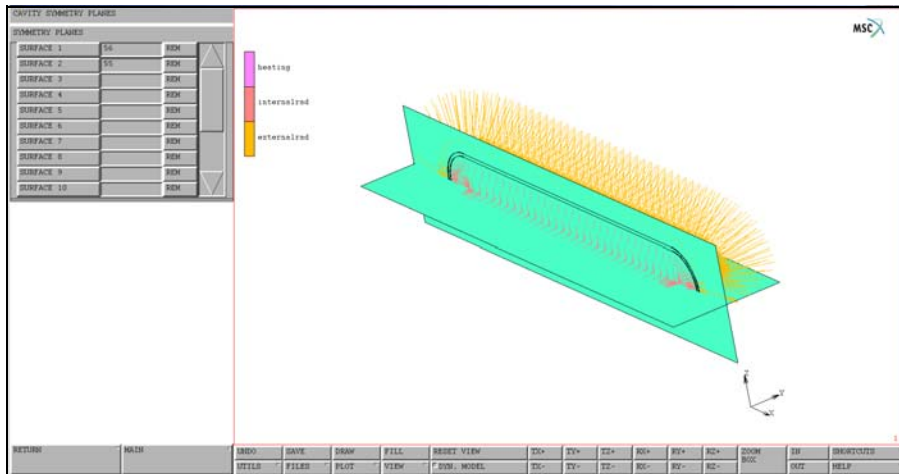


Figure 2.12-22 3-D Model with Symmetry Surfaces

MESH GENERATION

SET

U DOMAIN

-4 40

U SPACING

5

V DOMAIN

```

-5 5
V SPACING
GRID
RETURN
SRF ADD
-5 -5 0
40 -5 5
40 5 0
-5 5 0
SET
FIX V
W DOMAIN
-5 5
W SPACING
1
SRF ADD
-5 -5 -5
40 0 -5
40 0 5
-5 0 5
GRID
MAIN
MODELING TOOL
CAVITIES
SYMMETRY PLANE
SURFACE 1
56
SURFACE 2
55
MAIN

```

(turn off grid)

Step 12: Loadcase Creation and Job Creation

As this model is based upon the previously created axisymmetric model, the loadcases (1,2,3) and Jobs (1,2,3) are already created. The first loadcase is reviewed, and then the 3rd job (which has the internal heating, internal radiation, and external radiation) is submitted.

```
LOADCASE
  HEAT TRANSFER
    TRANSIENT
      LOADS
MAIN
JOBS
  NEXT
  NEXT
  TITLE
    3-d radiation analysis with symmetry
  OK
  SAVE
    prob_2_8_3d
  HEAT TRANSFER
    3-D
  OK
RUN
  ADVANCED JOB SUBMISSION
    WRITE INPUT FILE
    EDIT INPUT FILE
  OK
  SUBMIT
```

Step 13: Review Results

The post file is opened and the last increment is examined as shown in [Figure 2.12-23](#). As expected, an axisymmetric distribution of the temperatures is obtained. A time history plot is made of the node (4) at center of the hemisphere, see [Figure 2.12-24](#). It is almost identical to the behavior shown in [Figure 2.12-21](#).

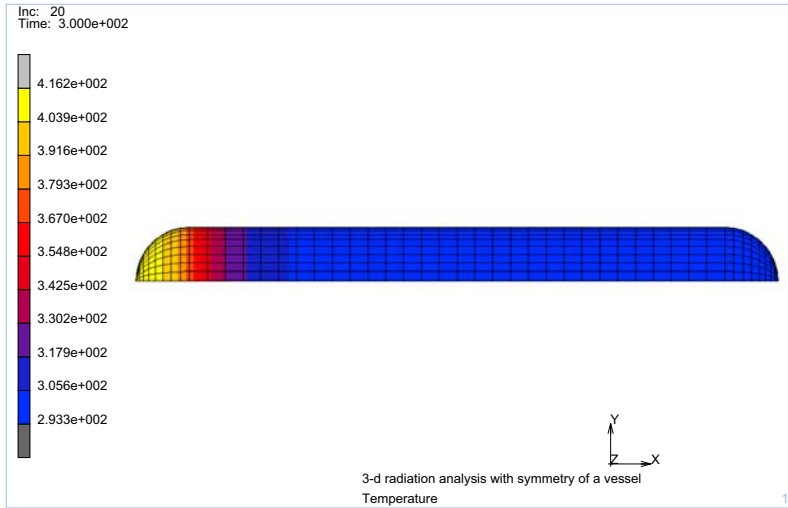


Figure 2.12-23 Contour Plot of Temperatures

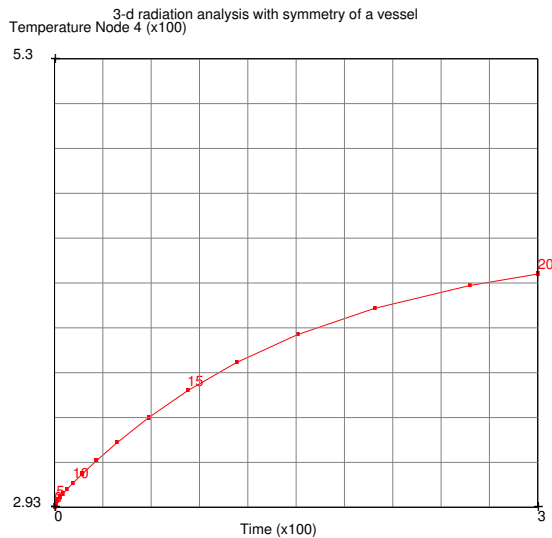


Figure 2.12-24 Transient Response for 3-D Heating, Internal and External Radiation

Input Files

The files below are on your [delivery media](#) or they can be downloaded by your web browser by clicking the links (file names) below.

File	Description
<code>3drad.proc</code>	Mentat procedure file to run the above (3-D) example
<code>3drad_post.proc</code>	Mentat procedure file to post process the above (3-D) example
<code>axirad_solid.proc</code>	Mentat procedure file to run the above (axisymmetric) example
<code>axirad_solid_post.proc</code>	Mentat procedure file to post process the above (axisymmetric) example
<code>prob2-8axi.mud</code>	Associated model file (axisymmetric model)
<code>prob2_8_3d.mud</code>	Associated model file (3-D model)

2.13 Application of BC on Geometry with Remeshing

- Geometry and Finite Element Mesh 544
- Detailed Session Description 545
- Input Files 558

Geometry and Finite Element Mesh

This chapter provides a simple example of the large deformation, large strain of a rubber component subjected to distributed loads such that remeshing is required. The boundary conditions are applied to geometric entities (points and curves).

The finite element nodes and edges are attached to these geometries and after automatic remeshing occurs, the new finite element mesh is reassociated to the geometry to insure that the boundary conditions are correctly applied. The model is shown in [Figure 2.13-1](#).

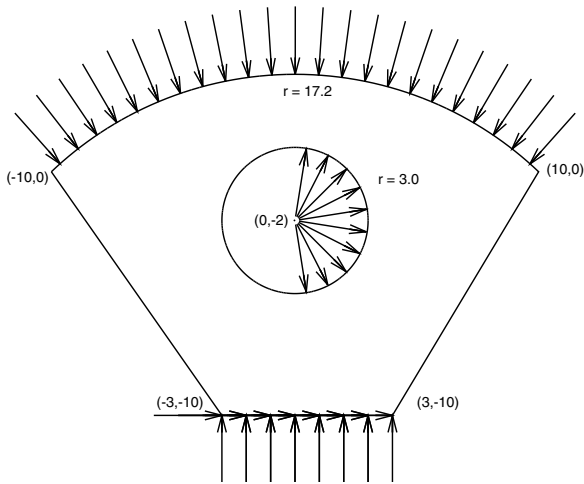


Figure 2.13-1 Geometry (All units are in cm)

Overview of Steps

- Step 1: [Create Geometry and Finite Element Mesh](#)
- Step 2: [Defining the Material Properties](#)
- Step 3: [Add All Elements to Contact Body](#)
- Step 4: [Apply Boundary Conditions](#)
- Step 5: [Define Criteria for Global Adaptive Remeshing](#)
- Step 6: [Define Loadcase](#)
- Step 7: [Create Job and Submit](#)
- Step 8: [Review Results](#)

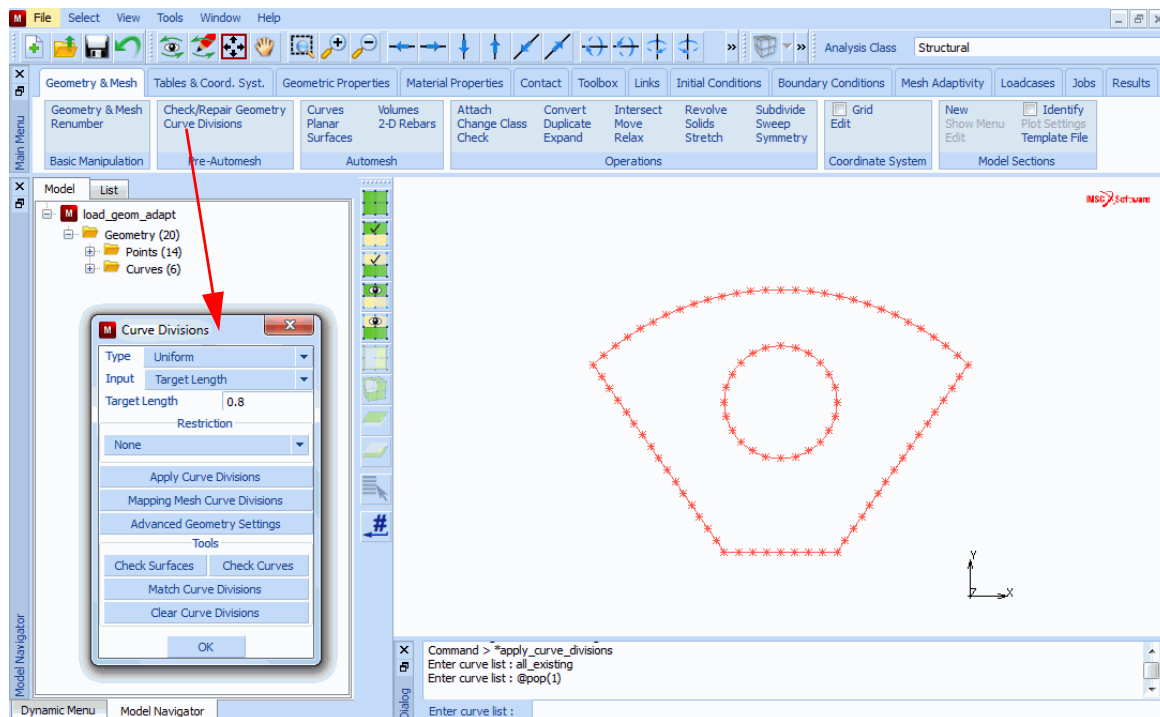


Figure 2.13-2 Applying Seed Points to Curves before Meshing

2D PLANAR MESHING
QUADRILATERALS (ADV FRNT)
QUAD MESH
ENTER CURVES LISTING
ALL EXISTING
MAIN

The resulting mesh is shown in [Figure 2.13-3](#).

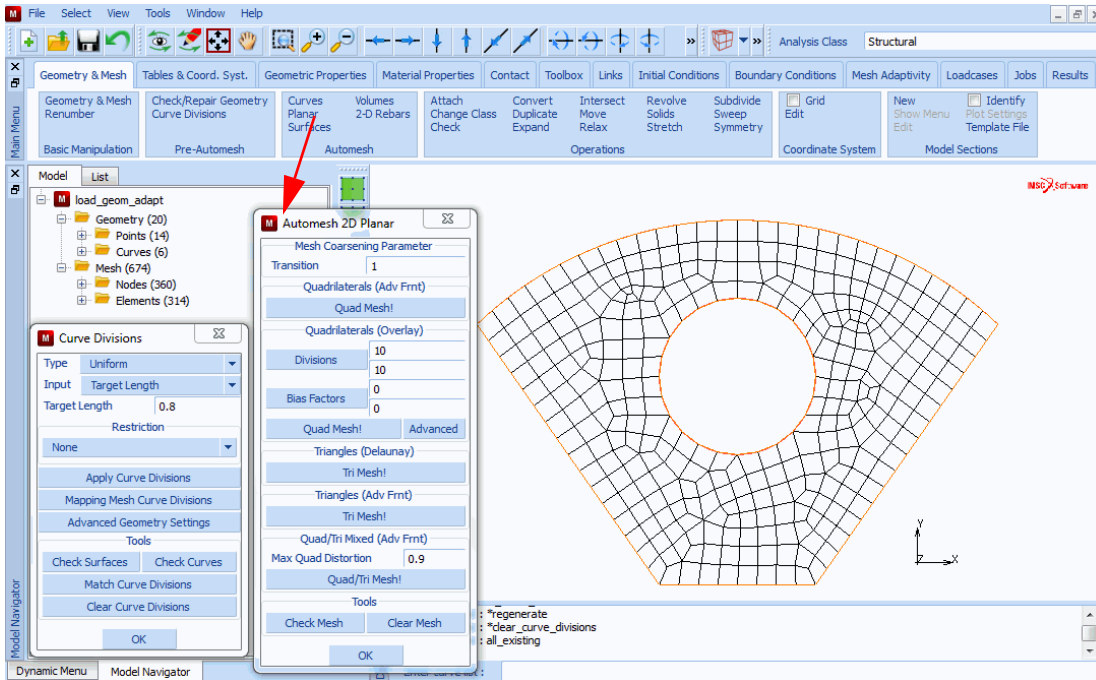


Figure 2.13-3 Finite Element Mesh

Edges that are in red indicate that they are attached to curves. Nodes that are shown as circles are attached to the points.

Step 2: Defining the Material Properties

The rubber piece is modeled using the Mooney-Rivlin model, with the properties:

$$c_{10} = 20.3 \text{ N/cm}^2$$

$$c_{01} = 5.8 \text{ N/cm}^2$$

The material properties are constant.

MATERIAL PROPERTIES

MORE

MOONEY

$$c_{10} = 20.3$$

$$c_{01} = 5.8$$

OK

ELEMENTS ADD

ALL EXISTING

MAIN

Step 3: Add All Elements to Contact Body

The global adaptive remeshing procedure is based upon contact bodies. While in this simulation, the load is not large enough to cause the hole to close upon itself, all of the elements are put into a single contact body.

```
CONTACT
  CONTACT BODIES
    NEW
    DEFORMABLE
    OK
  ELEMENTS ADD
    ALL EXIST
MAIN
```

Step 4: Apply Boundary Conditions

The problem has three boundary conditions: the base is fully constrained, the top arc has a pressure applied, and half of the circle has a load applied to it. In all cases, the boundary condition is applied to a curve. Because the boundary conditions are applied to a curve as opposed to finite element edges, after remeshing occurs, the boundary conditions are automatically applied correctly. The pressure loads are linearly ramped up over a loadcase of one second to their reference value of 12N/cm² by using a table.

```
APPLY
  NAME (apply pressure on top arc)
    pressure_on_top
  MECHANICAL
    TABLE (create ramp function)
    NEW
      1 independent variable
    TYPE
      time
    NAME
      ramp
  ADD
    0 0
    1 1
  MORE
  LABEL
    time
```

LABEL
 Scale Factor
 SHOW MODEL
 RETURN
 EDGE LOAD
 pressure 12
 OK

(the ramp function is shown is Figure 2.13-4)

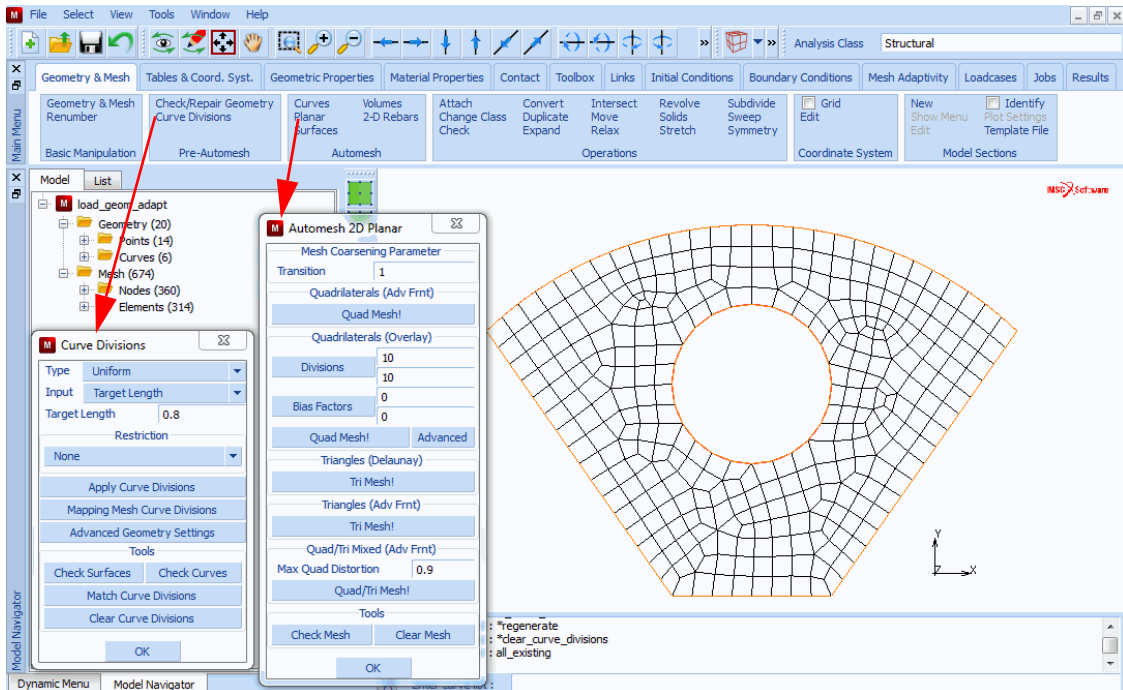


Figure 2.13-4 Ramp Function used to Apply Pressure

CURVES ADD
 4 #
 NEW
 NAME
 pressure_in_hole
 EDGE LOADS
 PRESSURE
 12

(apply pressure to half of hole)

TABLE
 ramp
 OK (twice)
 CURVES ADD
 5 #
 NEW
 NAME
 fixed_bottom
 FIXED DISPLACEMENT
 DISPLACEMENT X
 DISPLACEMENT Y
 OK
 CURVES ADD
 2 #
 RETURN
 ID BOUNDARY CONDITIONS
 DRAW BOUNDARY CONDITIONS ON MESH
 MAIN

(fully constrain base)

(see Figure 2.13-5)

(see Figure 2.13-6)

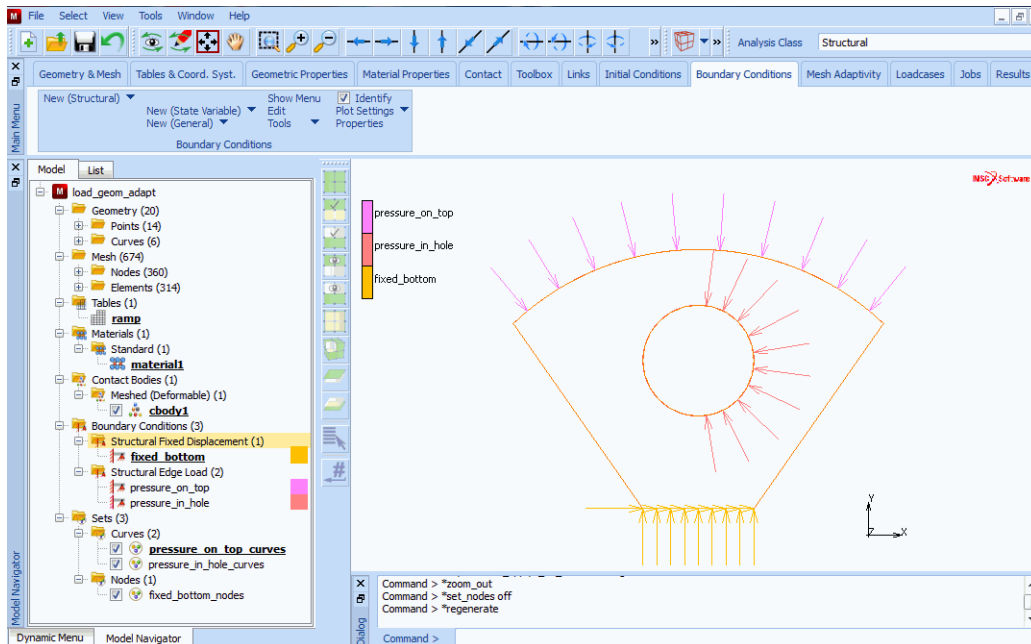


Figure 2.13-5 Boundary Conditions on Geometric Entities

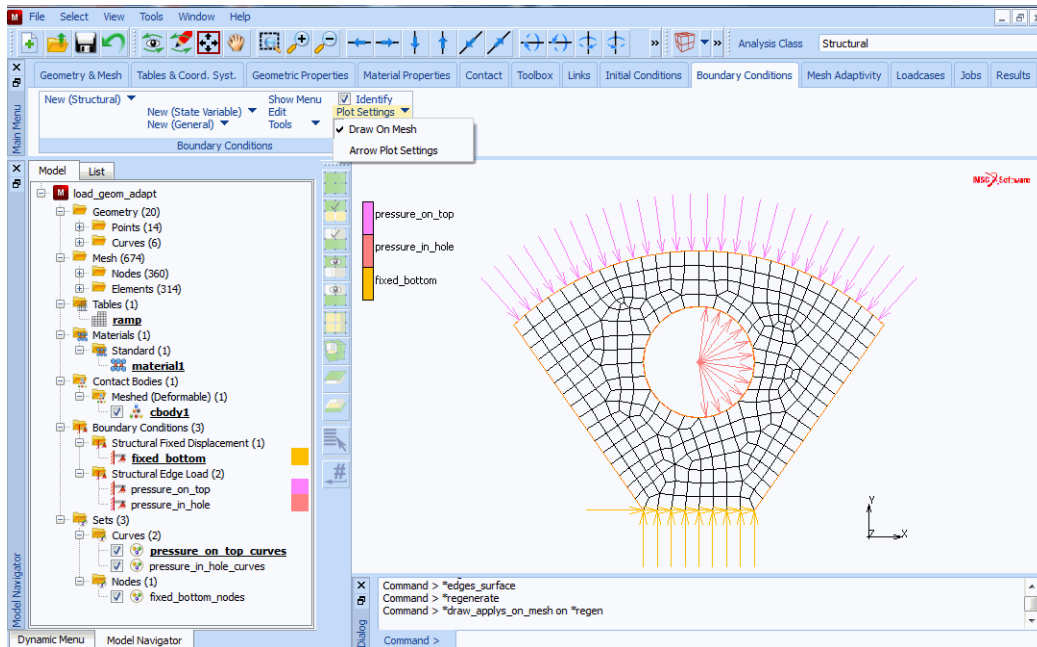


Figure 2.13-6 Boundary Conditions on Finite Element Entities

Step 5: Define Criteria for Global Adaptive Remeshing

In this simulation, because of the large deformation and in particular shear, the finite element mesh may become highly distorted. To insure an accurate analysis, the adaptive meshing procedure is invoked. The user needs to indicate when or why remeshing should occur, parameters controlling the new mesh, and the region to which this will be applied. In this simulation, remeshing may be due to element distortion, change in strain, or increment frequency. While the initial mesh used a target seed distance of 1.0, here the new mesh is based upon a target distance of 0.8. Both the initial mesh and all remeshing uses the advancing front quadrilateral automatic mesher. The finite element edge is automatically reattached to the curves.

- MESH ADAPTIVITY
 - GLOBAL REMESHING ADAPTIVITY
 - ADVANCING FRONT QUAD
 - ADVANCED
 - STRAIN CHANGE
 - ELEMENT DISTORTION
 - OK
 - INCREMENT
 - FREQUENCY

ELEMENT EDGE LENGTH

0.8

OK

REMESH BODY

cbody 1

OK

ID GLOBAL REMESHING CRITERIA

The global adaptive meshing menu is shown in [Figure 2.13-7](#).

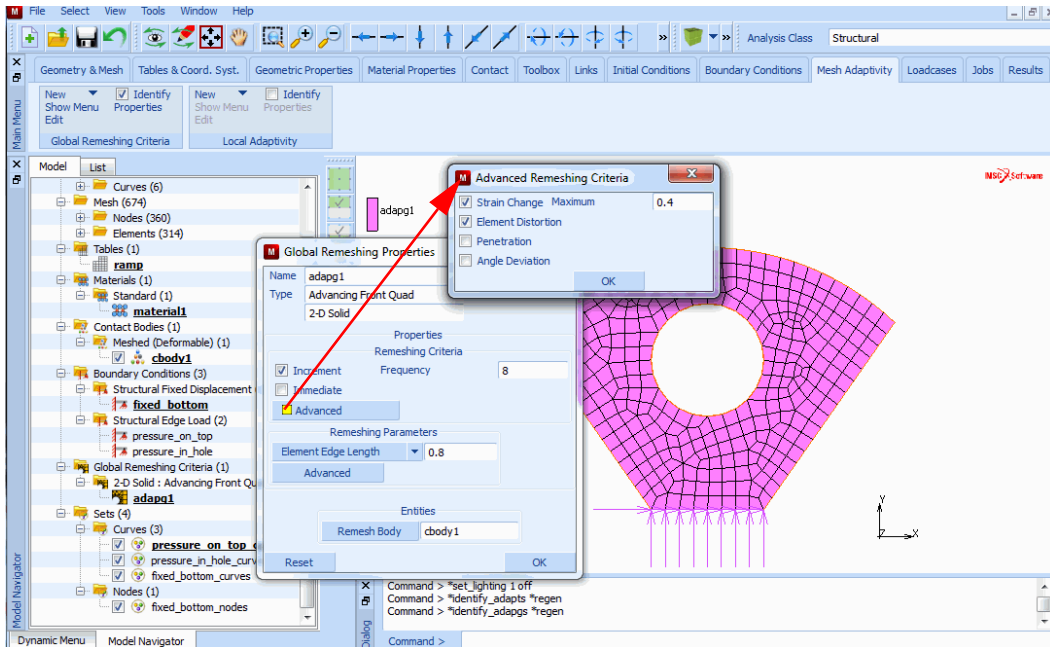


Figure 2.13-7 Global Adaptive Meshing Menu

Step 6: Define Loadcase

A single loadcase of duration one second is analyzed using a fixed time step procedure. Because of the nonlinearities involved and potential buckling of the rubber part, a tight convergence criteria is requested.

LOADCASES

MECHANICAL

STATIC

GLOBAL REMESHING

adapg

(activate global remeshing)


```
OK
SOLUTION CONTROL
MAX # RECYCLES
    30
Contribution of Initial Stress to Stiffness:Deviatoric Stress
OK
CONVERGENCE TESTING
    RESIDUALS AND DISPLACEMENTS
    RELATIVE FORCE TOLERANCE
        0.01
    RELATIVE DISPLACEMENT TOLERANCE
        0.01
OK
CONSTANT TIME STEP
# STEPS
    20
OK
```

Step 7: Create Job and Submit

The output to be placed on the post file is selected and upper bounds are specified. The large strain -updated Lagrange procedure is used for this rubber analysis. Follower Force is activated, but using the deformation at the beginning of the increment. This is not as accurate, but may lead to less iterations. Note that the default element type 11, a conventional four-node element, is used in this analysis. The table driven input is activated; this insures that both the geometric and finite element data is written to the input file, and that the boundary conditions and material data use the new input format.

```
JOBS
    TITLE
        Adaptive Meshing of Rubber part with Pressure on Curves
    MECHANICAL
        lcase1
        MESH ADAPTIVITY
            MAX # ELEMENTS
                1000
            MAX # NODES
                1000
    OK
```

```
ANALYSIS OPTIONS
  FOLLOW FORCE (Begin Inc)
  LARGE STRAIN-UPDATED LANGRANGE
OK
OUTPUT RESULTS
  Equivalent Von Mises Stress
  Total Strain Energy
OK
RETURN
RUN
  NEW-STYLE TABLE (activate table driven input)
  ADVANCED JOB SUBMISSION
    WRITE INPUT FILE
    EDIT INPUT FILE
  OK
  SUBMIT
  MONITOR
```

Step 8: Review Results

The objective of this problem is to see that the boundary conditions are correctly applied after remeshing occurs in the model. The post file is opened and a SCAN is performed, from this, the user observes that initially there are 217 elements in the model. This is increased to 341 in increment 9 and finally to 345 in increment 17. The post file is positioned to the last increment, and then the deformed mesh is examined ([Figure 2.13-8](#)).

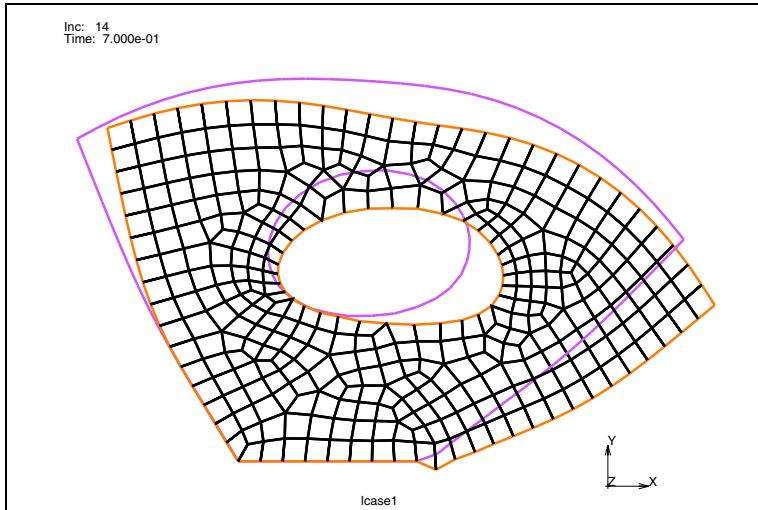


Figure 2.13-8 Deformed Part

From the red outline, it is clear that the edges are attached to curves as desired. Points, curves, and surfaces are placed on the post file in their original configuration. Hence, by comparing the final mesh to the original curves, we can observe the total deformation. The externally applied forces are shown in Figure 2.13-9; you can see that all of the edges attached to the top arc contribute to the force, as well as, the edges on the right side of the hole.

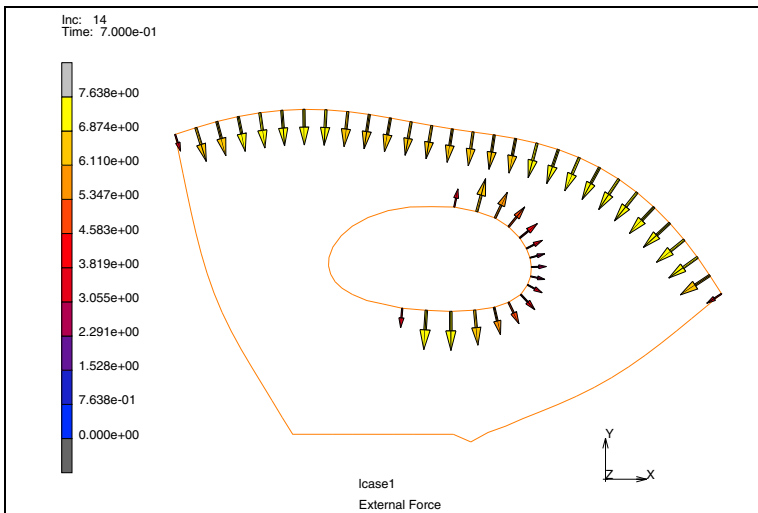


Figure 2.13-9 Externally Applied Force on Remeshed Curves

Finally, Figure 2.13-10 and Figure 2.13-11 show the elastic strain energy and the equivalent von Mises stress, respectively. Note that a large portion of the energy is at the base, where the nearly singular stress field exists and the material folds over.

RESULTS

OPEN

load_geom_adapt_job1.t16

OK

PLOT

ELEMENT SETTING

FACES

(off)

RETURN

POINTS

(off)

NODES

(off)

CURVES SETTING

HIGH

RETURN

RETURN

SCAN

20

(skip to increment 20)

DEF ONLY

PLOT

CURVES

(off)

ELEMENT SETTING

OUTLINE

RETURN

MORE

VECTOR PLOT

(on)

VECTORS

External Force

OK

CONTOUR BANDS

SCALAR

Total Strain Energy Density

SCALAR SETTING

EXTRAPOLATION

TRANSLATE

RETURN

SET LIMITS

0 16

LEVELS
8
MANUAL
RETURN
SCALAR
Equivalent Von Mises Stress
SCALAR SETTING
SET LIMITS
0 80

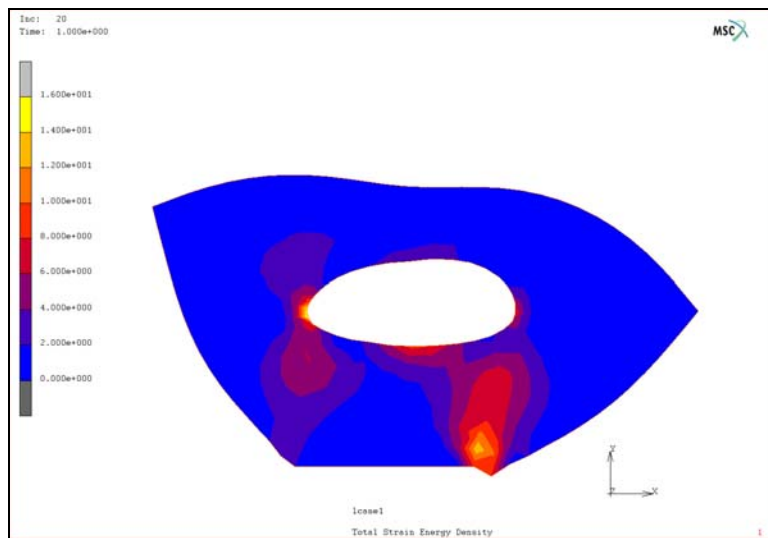


Figure 2.13-10 Strain Energy Density

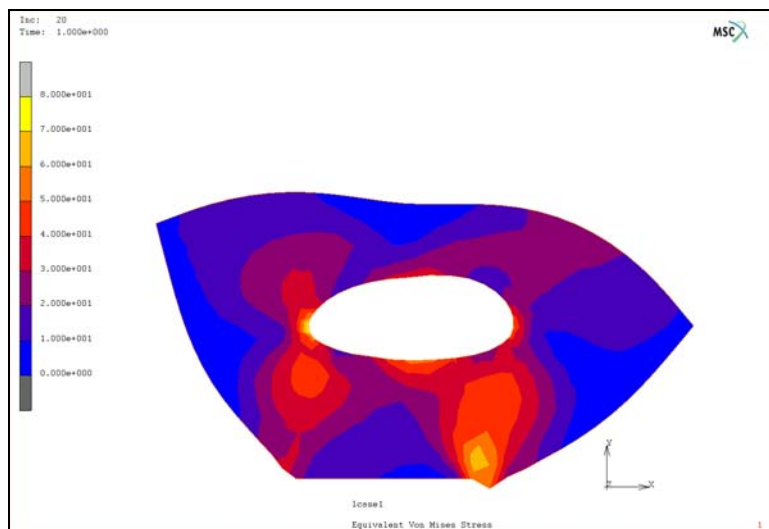


Figure 2.13-11 Equivalent Stress

Input Files

The files below are on your [delivery media](#) or they can be downloaded by your web browser by clicking the links (file names) below.

File	Description
adapt.proc	Mentat procedure file to run the above example
adapt_post.proc	Mentat procedure file to run the above example
sector.igs	IGES input file for geometry

2.14 Glass Forming of a Bottle with Global Remeshing

- Chapter Overview 560
- Detailed Session Description 562
- Conclusion 575
- Input Files 577

Chapter Overview

This example demonstrates a glass forming simulation of a bottle (Figure 2.14-1). The bottle is blow-formed. The purpose of the simulation is to assist in the design forming process, mold shape, and the glass gob to ensure a successful end product.

The capability of global remeshing together with pressure loading and fixed displacement boundary conditions is presented. Thermal and mechanical coupled analysis is required. The glass material is modeled by a user subroutine, although, Marc's Narayanaswamy model for glass could also be used. The bottle thickness, stress, and temperature distribution can be predicted in the simulation.

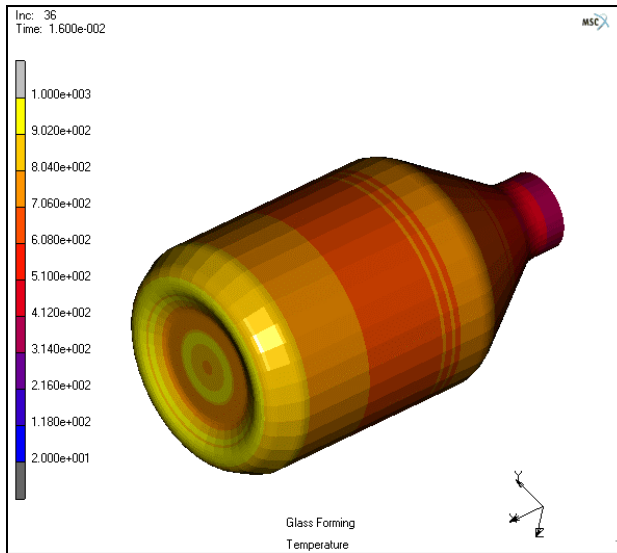


Figure 2.14-1 Bottle Glass Forming

Idealization

A glass gob is shown in Figure 2.14-2. A rigid axisymmetric mold is assumed in the analysis. Initial temperature of the glass is at 1000C. The mold temperature and the environment sink temperature are both at 20C. A pressure loading is applied to the glass inner surface to model the blow forming process. A rigid-viscoplastic material model are adopted for the analysis.

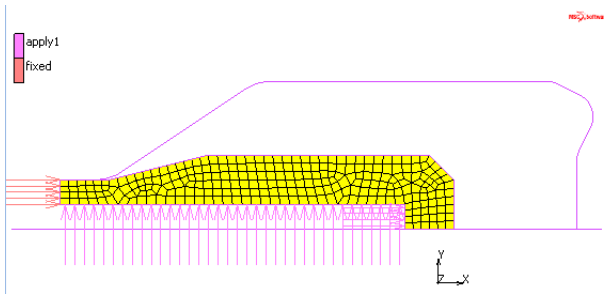


Figure 2.14-2 Initial Model Setup

Element type 10 of 4-node quadrilateral is adopted for the glass gob with 265 elements in the initial mesh. For thermal-mechanical coupled analysis, the element type 40 is used by default for to be Newtonian fluid with a viscosity that is temperature dependent. This can be modeled as a rigid-visco-plastic material in Marc and through a URPFLO user subroutine. The flow stress function can be described as follows [Reference 1]:

$$\sigma_y = 3 \dot{\epsilon} \cdot 10^{-2.58 + \frac{4332}{T+25}}$$

where T is the temperature in °C. The viscosity unit is in Poises. A Poises= 0.1 Newton.second/m². Therefore, the stress shown above is converted to SI (mm) unit with

$$\sigma_y = 3 \dot{\epsilon} \cdot 10^{-2.58 + \frac{4332}{T+25}} \cdot 10^{-7}$$

To avoid problems with artificially high strain rates, an upper bound to the flow stress is also provided.

The thermal properties are listed in the following:

- Conductivity = 40 N/sec/C
- Specific Heat = 0.5 mm²/sec²/C
- Mass Density = 1.0 Mg/mm³

The contact bodies are shown in Figure 2.14-2. The pressure loading applied on the surface has the magnitude of 0.0016N/mm² from 0 to 0.016 seconds. The bottle is formed in 0.016 seconds and followed by 1 second of cooling time. A fixed displacement in X is applied to the top of the glass gob.

No friction is assumed. The convection coefficient between the workpiece and the mold is 40 (N/sec/C/mm) and the convection coefficient to the environment is 0.04 (N/sec/C/mm).

Analysis with Remeshing

Because of large deformation, a global remeshing is activated whenever there is an element distortion. After remeshing, the boundary conditions applied to the elements will be transferred to the new mesh as well as those history data.

The following controls are utilized in the global remeshing:

- Advancing front quad mesher to generate the mesh
- Number of Elements: 500
- Curvature control division: 36

The target number of elements is used to generate the new mesh of about the same number of elements. The remeshing is activated when any one of the following criteria is met:

- Every 5 increments
- Element distortion

The new style table input format is required for the global remeshing to work with the boundary conditions. In the new input format, boundary conditions are defined in sets and applied later to different loadcases with the set names. In this example, set information is utilized in the remeshing to replace boundary conditions with the new mesh.

Overview of Steps

Step 1: [Read in Predefined Mold Geometry and the Mesh for the Glass Gob](#)

Step 2: [Define Material Properties](#)

Step 3: [Define Contact Bodies](#)

Step 4: [Define Initial Conditions](#)

Step 5: [Assign Boundary Conditions](#)

Step 6: [Define Global Remeshing Controls](#)

Step 7: [Define Loadcase](#)

Step 8: [Define Analysis Controls and Run Job](#)

Step 9: [View Simulation Results](#)

Detailed Session Description

Step 1: Read in Predefined Mold Geometry and the Mesh for the Glass Gob

In order to save time, the mold geometry and the mesh are read in from a Mentat database file: *glass_bottle_geometry.mfd* and save it as *mytest.mfd*. Users need to copy this file to the working directory. The following steps read in the geometry and mesh:

```
FILES
OPEN
    select: glass_bottle_geometry.mfd
```

```

OK
SAVE AS
  mytest

```

Step 2: Define Material Properties

The material type is defined as rigid plastic and a URPFLO user subroutine is used. This subroutine is created in a FORTRAN file called *glass_bottle_material.f*. Users need to copy this file into the working directory.

```

MAIN
  MATERIAL PROPERTIES
    ISOTROPIC
      RIGID-PLASTIC
        METHOD
          urpflo
    INITIAL YIELD STRESS
      1
      OK (twice)

```

The user subroutine file is provided in JOBS menu.

Heat Transfer material properties are defined under the HEAT TRANSFER menu.

```

HEAT TRANSFER
  CONDUCTIVITY
    40
  SPECIFIC HEAT
    0.5
  MASS DENSITY
    1
  OK
  elements: ADD
  all: EXISTING

```

(assign the material properties to all elements)

Step 3: Define Contact Bodies

The gob is defined as a deformable body and the mold as a rigid body.

```

MAIN
  CONTACT

```

CONTACT BODIES

NEW

NAME

glass

Contact body type

DEFORMABLE

MECHANICAL PROPERTIES

select THERMAL PROPERTIES

heat transfer to env

HEAT TRANS. COE

0.04

SINK TEMPERATURE

20

heat transfer due to contact

CONTACT HEAT TRANSFER COEF.

40

OK

Define and assign the contact properties to all the elements:

elements: ADD

all: EXISTING

NEW

NAME:

mold

RIGID

MECHANICAL PROPERTIES

THERMAL PROPERTIES

(select thermal properties)

TEMPERATURE

20

heat transfer due to contact:

CONTACT HEAT TRANSFER COE.

40

OK

Define and assign the contact properties to the mold.

curves: ADD

select the curve representing the mold <MR>

NEW

NAME

sym

SYMMETRY

OK

curves:ADD

select the symmetry curve <MR>

Use ID CONTACT to show all defined contact bodies and the orientation of the rigid and symmetric bodies (Figure 2.14-3).

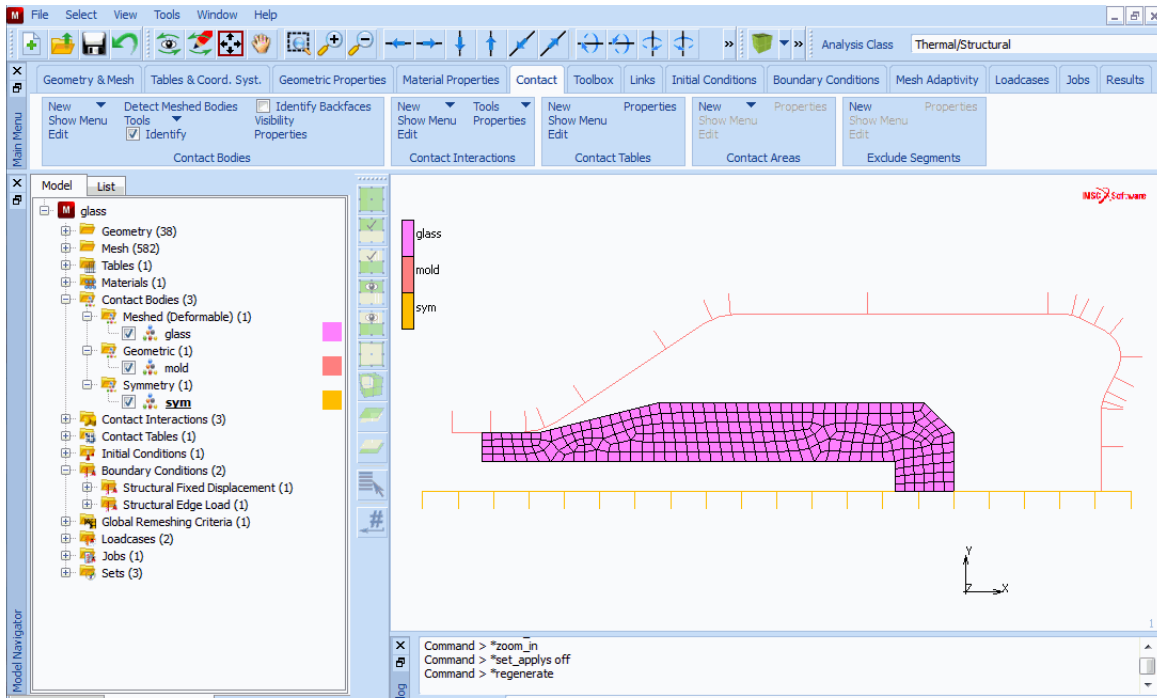


Figure 2.14-3 Defined Contact Bodies

Step 4: Define Initial Conditions

The initial temperature of the glass gob needs to be defined.

MAIN

INITIAL CONDITIONS

```
THEMAL
  TEMPERATURE
    TEMPERATURE (top)
      1000
    OK
  nodes: ADD
  all: EXISTING
```

Step 5: Assign Boundary Conditions

We need to define pressure the glass blowing and a fixed boundary condition to fix the top of the bottle.

```
MAIN
  BOUNDARY CONDITIONS
    NEW
    NAME
      pressure
    MECHANICAL
      EDGE LOAD
      PRESSURE
        1
    OK
```

A table function is defined for the pressure.

```
TABLES
  NEW
    select 1 INDEPENDENT VARIABLE
  NAME
    pressure
  type
    TIME
  ADD
    0      0
    0.016 0.0016
    5      0.0016
  FIT
  RETURN
```

EDGE LOAD

TABLE

pressure

(select table)

OK

edges: ADD

select all internal element edges <MR>

Now for the fixed displacement condition:

NEW

NAME

fixed

FIXED DISPLACEMENT

DISPLACEMENT X

(select fixed in X direction)

OK

nodes: ADD

select nodes on the top of the gob <MR>

Use ID BOUNDARY CONDS to show defined boundary conditions ([Figure 2.14-4](#)).

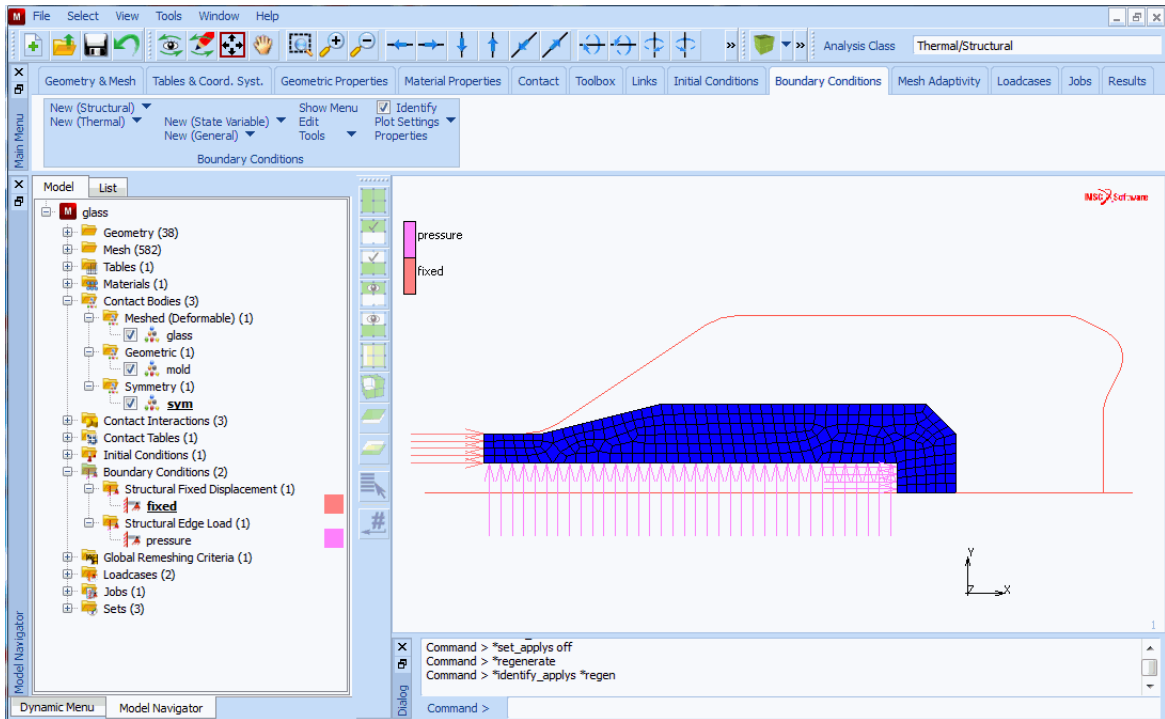


Figure 2.14-4 Defined Boundary Conditions

Step 6: Define Global Remeshing Controls

MAIN

MESH ADAPTIVITY

GLOBAL REMESHING CRITERIA

ADVANCING FRONT QUAD

INCREMENT FEQUENCE

5

ADVANCED

ELEMENT DISTORTION

O

K

elements SET

500

(enter target number of elements)

OK

REMESH BODY

glass

(select contact body for remeshing)

Step 7: Define Loadcase

Define two loadcases here; the first one for the blowing and the second one for the cooling. For rigid-plastic model, using only the tensile contribution of initial stress to the stiffness matrix is a better control to avoid divergence.

```

MAIN
  LOADCASES
    COUPLED
      QUASI-STATIC (first loadcase)
        GLOBAL REMESHING
          adapg1 (select remeshing)
          OK
        TOTAL LOADCASE TIME
          0.016
      MULTI-CRITIA
        INITIAL FRACTION
          0.1
        DESIRED # REC. SET: 10
        DEFAULT CRIT.
          MAX TEMP.:
            100
          OK
        OK
      SOLUTION CONTROL
        MAX # RECYCLES
          20
        contribution to stiffness:
          TENSILE STRESS
          OK
      CONVERGENCE TESTING
        RESIDUALS OR DISPLACE.
        RELATIVE DISP. TOL
          0.01
          OK (twice)
    NEW (second loadcase)
      QUASI-STATIC
        TOTALL LOADCASE TIME
  
```

```
1.0
MULTI-CRITIA
  INITIAL FRACTION.:
    0.1
  DESIRED # REC. SET
    10
    OK
  DEFAULT CRIT.
    MAX TEMP.
    100
    OK
  OK
SOLUTION CONTROL
  MAX # RECYCLES:
    20
  contribution to stiffness:
    TENSILE STRESS
    OK
CONVERGENCE TESTING
  RESIDUALS OR DISPLACE
  RELATIVE DISP. TOL
    0.01
    OK (twice)
```

Step 8: Define Analysis Controls and Run Job

The two loadcases are activated in the coupled thermal-mechanical analysis. the FOLLOWER FORCE option is activated because of the large deformation in the forming of the bottle. The equivalent plastic strains are written to the post file for later display. The file which contains the URPFOL user subroutine is identified. When the job is submitted, this routine will be compiled and linked to standard Marc.

```
MAIN
  JOBS
    COUPLED
      available: lcase1 and lcase2 (select loadcases)
  INITIAL CONDITIONS
    select all conditions
    AXISYMMETRIC
```

ANALYSIS OPTIONS
 FOLLOWER FORCE
 LARGE STRAIN
 LARGE STRAIN
 OK

(on)

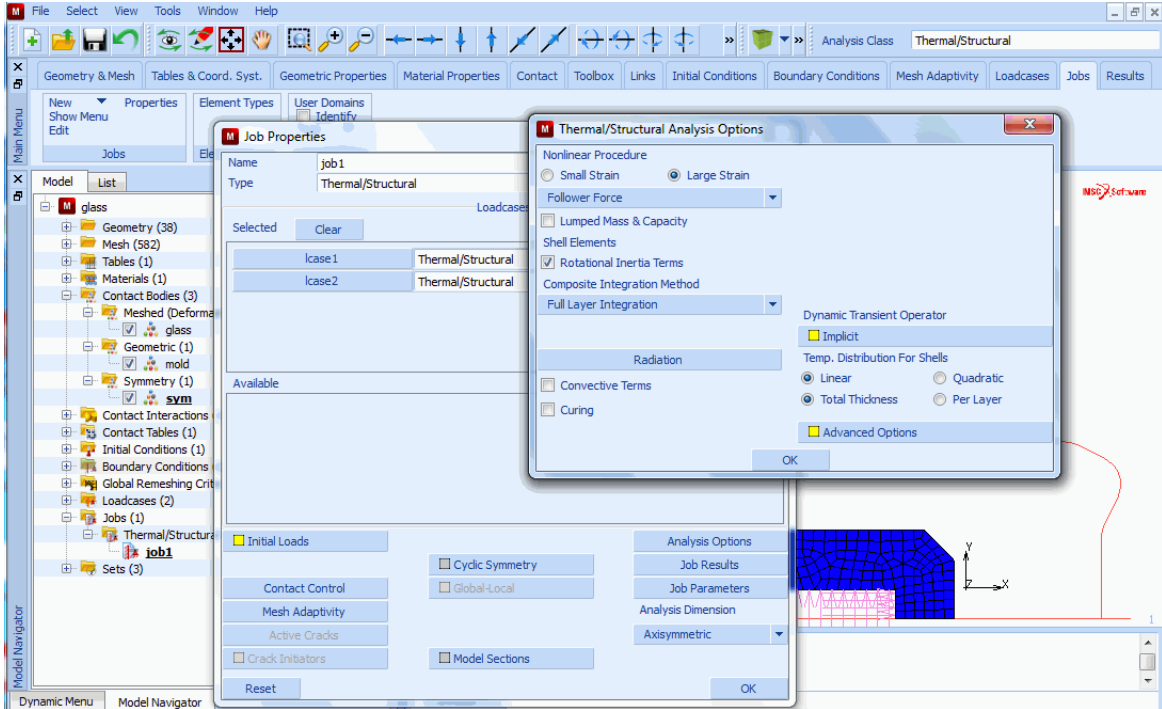


Figure 2.14-5 Defined Analysis Options

Select extra result output:

JOB RESULTS

select: TOTAL EQU. PLASTIC STRAIN

OK (twice)

SAVE

(save the model)

RUN

NEW-STYLE TABLE

(on)

USER SUBROUTINE FILE

glass_bottle_material.f

(select the filename)

SUBMIT (1)
MONITOR

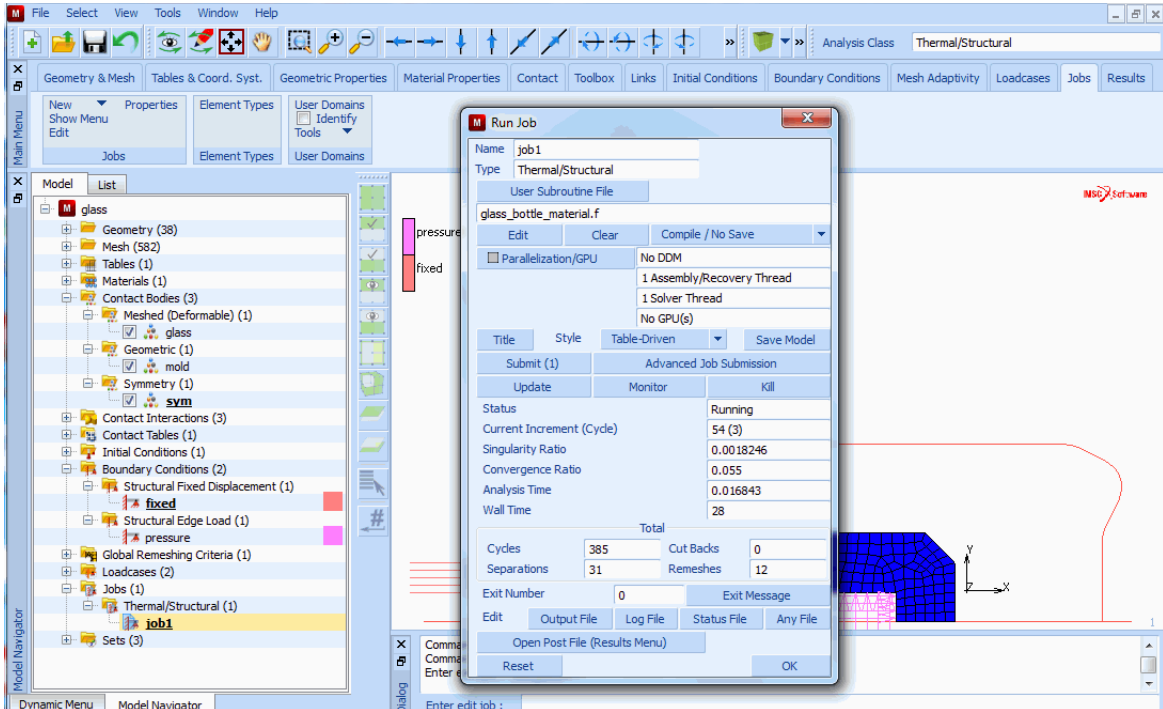


Figure 2.14-6 The RUN JOB Screen

Step 9: View Simulation Results

To view vector plot of the external forces applied to the glass:

MAIN

RESULTS

OPEN DEFAULT

DEF ONLY

deformed shape SETTINGS

edges

OUTLINE

(display outline only)

SCAN

20

(select increment 20)

OK

MORE

vector

EXTERNAL FORCE

(select)

vector plot:

ON

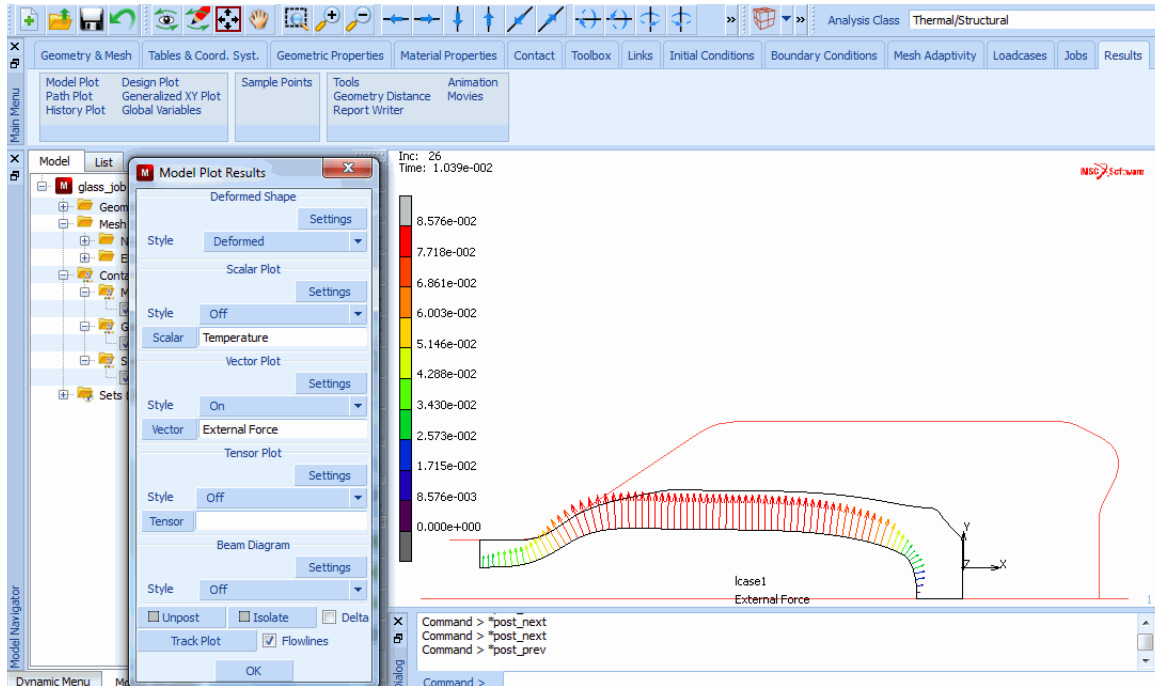


Figure 2.14-7 External Force Vector Plot

To view temperature contour at the end of forming before cooling:

MAIN

RESULTS

SCALAR

TEMPERATURE

(select)

scalar plot:

CONTOUR BAND

SCAN

35

(select the step at time=0.016)

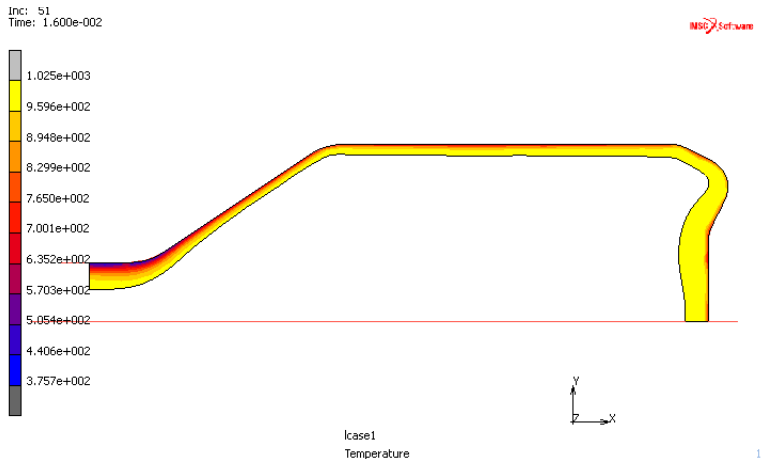


Figure 2.14-8 Temperature after Forming

Similarly, the temperature at the end of cooling can be viewed in [Figure 2.14-9](#).

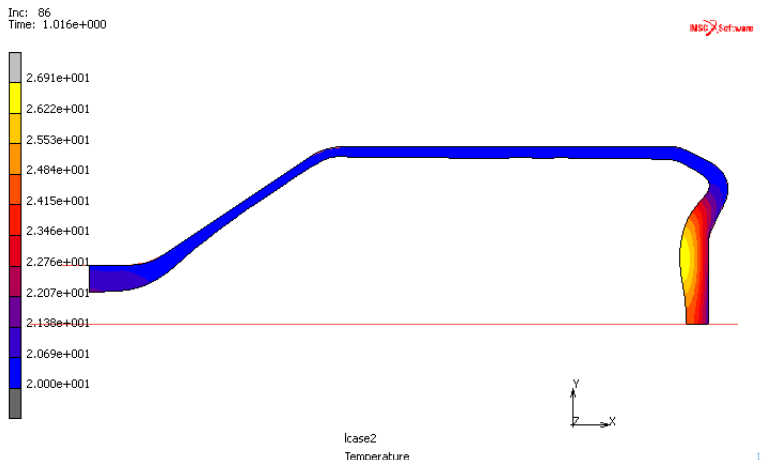


Figure 2.14-9 Temperature after Cooling

Also, by selecting the total equivalent plastic strain, we can see the plastic deformation in [Figure 2.14-10](#).

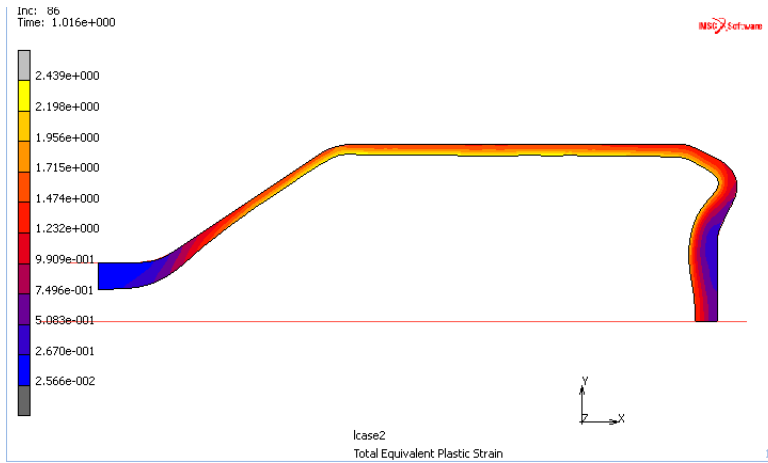


Figure 2.14-10 Plastic Strain Contour

Conclusion

The external force in [Figure 2.14-7](#) shows that the pressure loading is applied correctly after remeshing. The temperature contours in [Figure 2.14-8](#) and [Figure 2.14-9](#) show temperature changes after forming and cooling stages. The bottle wall thickness can also be viewed in these figures.

The simulation can be utilized for gob shape and process design so that an optimal bottle thickness can be formed.

For example, by blowing the glass 10 times slower, the thickness of the bottle will vary dramatically as cooling effect on the wall that touches the mold first makes material harder to flow. This comparison can be seen in [Figure 2.14-11](#).

If the mold temperature is at 500C, this also affects the wall thickness. The upper part of bottle wall is easier to flow and becomes much thinner than the mold that is at 20C. Comparison can be seen in [Figure 2.14-12](#).

The total force required to form the bottle can be seen in [Figure 2.14-13](#).

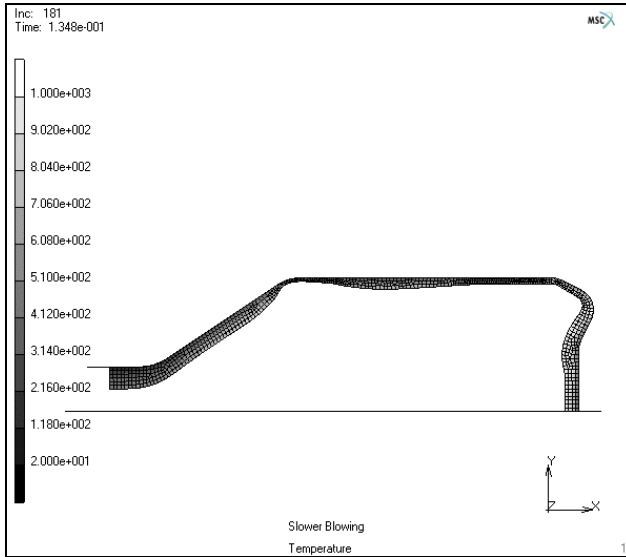


Figure 2.14-11 Different Thickness by Blowing 10 Times Slower

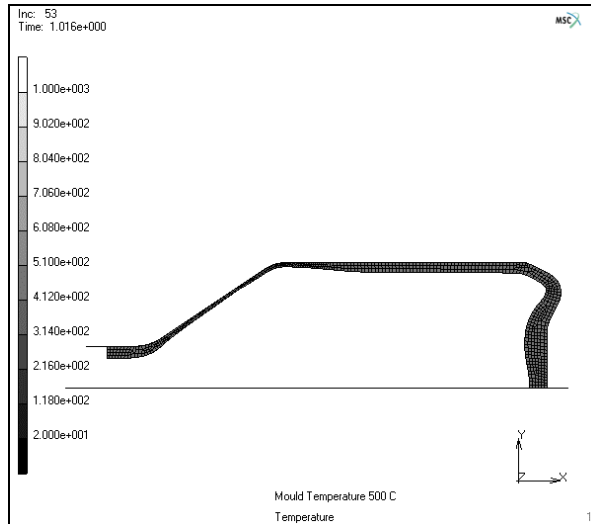


Figure 2.14-12 Different Thickness with Mold at 500C

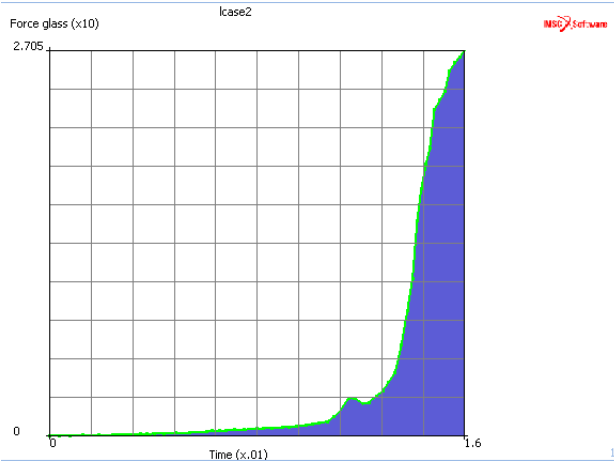


Figure 2.14-13 Blowing Force History

References

1. J.M.A.Cesar de Sa, “Numerical modeling of glass forming processes”, Eng.Comput., 1986, Vol.3, December.

Input Files

The files below are on your [delivery media](#) or they can be downloaded by your web browser by clicking the links (file names) below.

File	Description
glass_forming.proc	Mentat procedure file to run the above example
glass_bottle_geometry.mfd	Associated model file
glass_bottle_material.f	User subroutine

2.15 Marc – Adams MNF Interface

- Chapter Overview 580
- Generation of an MNF for HDD HSA Suspension Arm 580
- Local Model and Analysis 582
- Input Files 587

Chapter Overview

This chapter demonstrates the generation of a Modal Neutral File (MNF) for the Marc-Adams interface. Adams/Flex allows flexible components to be included into Adams models through MNFs that represent the flexible components. Marc- is capable of generating MNFs that can be integrated into the Adams model. Generating an MNF from Marc- is based on performing the most general method of component mode synthesis techniques, namely the Craig-Bampton method. Craig-Bampton analysis of a Hard Disk Drive (HDD) Head Stack Assembly (HSA) suspension arm is used as an example in this chapter. The HSA arm MNF is later uploaded into an Adams HDD model.

Generation of an MNF for HDD HSA Suspension Arm

Problem Description

A hard disk drive is a complex electromechanical device that employs many technologies. It mainly consists of a printed circuit board to communicate with the computer motherboard, a stack of disks (the storage media), a spindle motor to rotate the disks, a stack of recording heads, a suspension arm to carry the head stack, an actuator to move the head stack assembly to the target data tracks, all contained within a sealed enclosure as shown in [Figure 2.15-1](#).

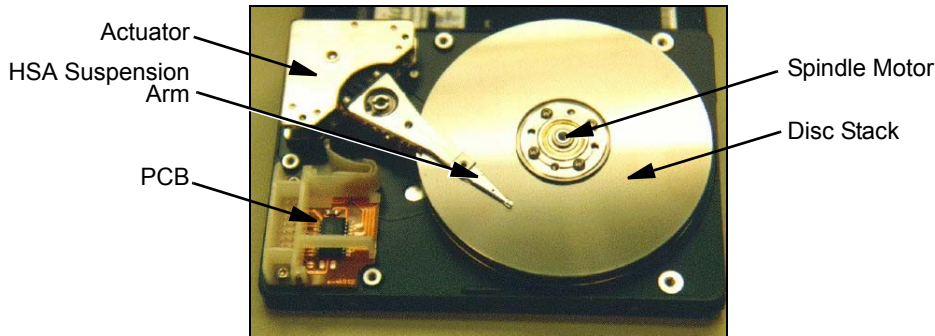


Figure 2.15-1 HDD Main Components

HDD usually contain more than one disk in a stacked assembly. Data is written onto each disk surface (top and bottom) by a separate recording head, so an HDD with five disks will normally have ten separate recording heads. Recording heads are miniature electromagnets that are bonded to a metal suspension gimbal, which is a small arm that holds the head in position above or beneath a disk. Sets of gimbals stacked together for installation in a disk drive are called a head-stack assembly (HSA).

When the disks spin up to operating speed, air flows at high speeds causing the recording heads to fly over the surface of the disks. Heads are said to be riding on an “air bearing”. The separation between the recording heads and the disks during operation, known as the flying height, is one of the important design parameters that controls the performance and durability of an HDD. The flying height in present-day HDD is in the range of 0.2 - 0.8 micro inches (or 5 - 20 nanometers) and is getting lower as technology progresses. In order to increase the recording density, it is necessary to decrease the flying height so that the signal to noise ratio obtained from the read element is within an acceptable range. Thus, zero spacing is preferred. However, zero spacing or contact recording would lead to higher friction and

wear at the head-disk interface, hence degrading the performance of the HDD. Ideally, the designed flying height should be maintained during operation. In reality, partial contact between the head and disk may occur. Also, vibration and shock become more of a concern. Among the controlling factors over the interactions between the head and the disk during flying are the suspension arm and disk geometries, materials, and tolerances used in the industry. Due to reasons outlined above, it is important to study the vibration characteristics of the HSA suspension arm. In this example, we are interested in the dynamics of the HSA suspension arm shown in [Figure 2.15-2](#). This HSA arm supports ten recording heads.

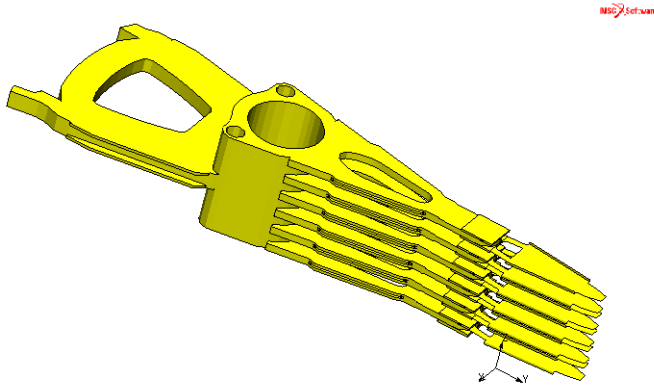


Figure 2.15-2 HSA Suspension Arm Geometry

HSA Suspension Arm Model

The finite element model for HSA suspension arm is shown in [Figure 2.15-3](#). It consists of 8534 brick and shell elements (element types 7 and 75). The model file `hdd_hsa_arm.mfd` contains the geometry and finite element model. In the following, we complete the model by adding the necessary boundary conditions and loadcases to perform the Craig-Bampton analysis and generate the MNF. The Craig-Bampton analysis consists of computing two sets of mode shapes: the constraint modes and the fixed-boundary normal modes.

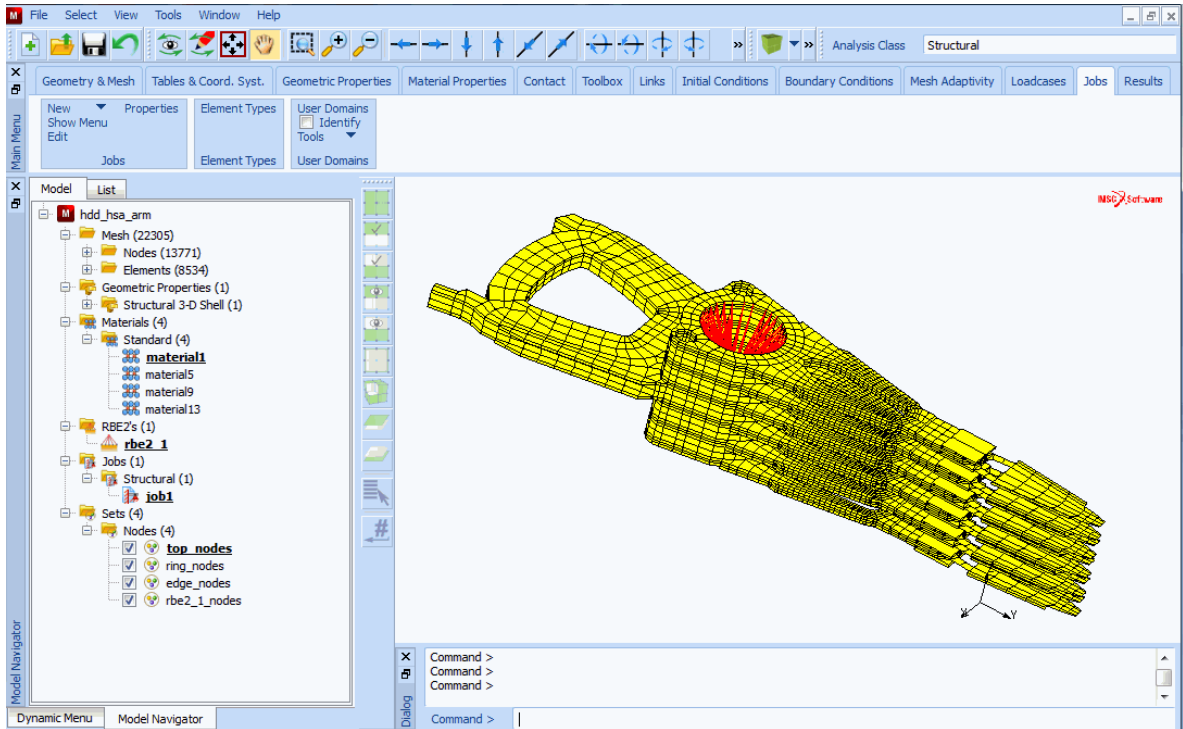


Figure 2.15-3 HSA Suspension Arm Model

Local Model and Analysis

To open the model:

FILES

OPEN

hdd_hsa_arm.mfd

OK

After opening the model and examining it, the first step in performing the Craig-Bampton analysis is to define the boundary or attachment degrees of freedom that will connect the arm to the rest of the Adams HDD model. The boundary degrees of freedom are used to compute the constraint modes as the static shapes obtained by giving each boundary degree of freedom a unit displacement while holding all other boundary degrees of freedom fixed.

The axis of the actuator that drives the arm is at the centerline of the cylindrical hole of the arm. To ease the attachment of the arm when the MNF is uploaded into the Adams HDD model, an extra node is defined in the finite element model at the center of the cylindrical hole and an RBE2 is used to couple all the nodes within the cylindrical surface to the node at the center. The six degrees of freedom of this node are used as boundary degrees of freedom.

The air bearing and contact between the heads and the disks can be represented in the Adams model by springs acting in the z-direction normal to the planes of the arm leaves. Thus, the z degree of freedom of ten nodes at the location of the ten heads on the arm are also used as boundary degrees of freedom.

In Mentat, the boundary degrees of freedom can be defined in the CRAIG-BAMPTON NODES menu, shown in Figure 2.15-4, under the MECHANICAL BOUNDARY CONDITIONS menu. After defining the boundary degrees of freedom, the next step is to create an Adams CRAIG-BAMPTON loadcase and make sure that the CRAIG-BAMPTON NODES boundary conditions are selected in this loadcase. In Mentat, the Adams CRAIG-BAMPTON loadcase, shown in Figure 2.15-5, is located under the MECHANICAL LOADCASES menu. The number of fixed-boundary normal modes requested is specified in this loadcase menu. In this example, 20 modes should be enough to prevent mode truncation.

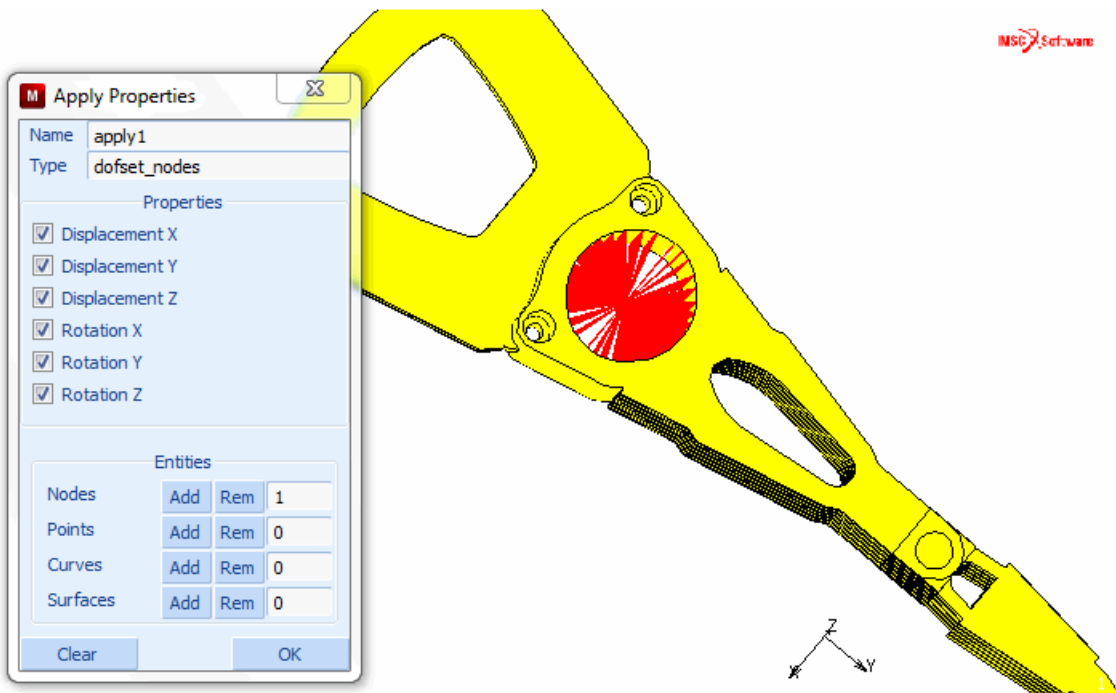


Figure 2.15-4 CRAIG-BAMPTON NODES Menu

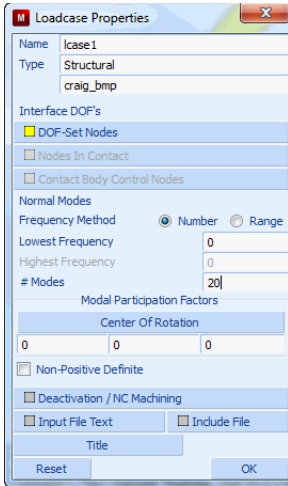


Figure 2.15-5 Adams CRAIG-BAMPTON Loadcase Menu

The next step is to select the Adams CRAIG-BAMPTON loadcase in the JOBS menu. We should also choose the LUMPED MASS option from the ANALYSIS OPTIONS. From the Adams JOB RESULTS menu, shown in Figure 2.15-6, we can pick whether or not stress and/or strain modes should be computed. In the same menu, we should indicate the units used to create the model. In this example, slug, pound-force, inch, and second are used.

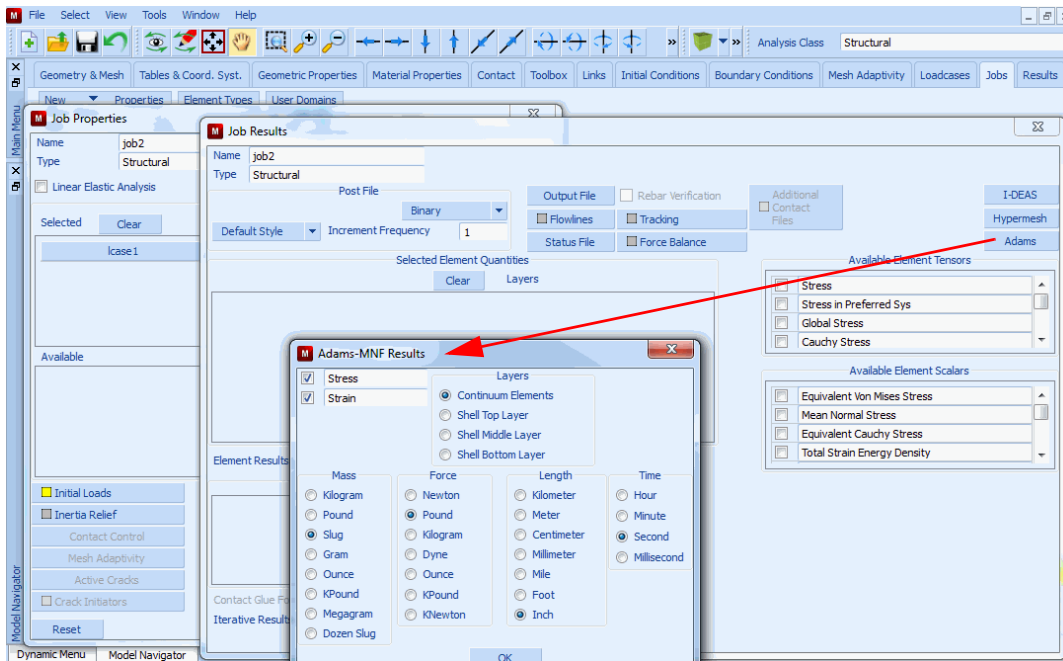


Figure 2.15-6 Adams JOB RESULTS Menu

Follow the steps described below to complete the model definition:

```

MAIN
  BOUNDARY CONDITIONS
    NEW
      MECHANICAL
        MORE
          CRAIG-BAMPTON NODES
            DISPLACEMNT X
            DISPLACEMNT Y
            DISPLACEMNT Z
            ROTATION X
            ROTATION Y
            ROTATION Z
            OK
          NODES
            ADD
              13771 #
        NEW
          CRAIG-BAMPTON NODES
            DISPLACEMNT Z
            OK
          NODES
            ADD
              13012 13055 13120 13121 13212
              13213 13305 13306 13397 13398 #
    MAIN
      LOADCASES
        MECHANICAL
          Adams CRAIG-BAMPTON
            # MODES
              20
            OK
    MAIN
      JOBS
        MECHANICAL
    
```

```
lcase1
ANALYSIS OPTIONS
  LUMPED MASS
  OK
JOB RESULTS
  Adams
    STRESS
    STRAIN
    SLUG
    POUND
    INCH
    OK (three times)
FILES
  SAVE
  AS
    hdd_hsa_arm_mnf.mfd
  OK
To run the job:
MAIN
  JOBS
    RUN
      RESET
      SUBMIT (1)
      MONITOR
      OK
```

Successful job completion and generation of the MNF is indicated by Exit Number 3018. The post file could be opened in Mentat to check the Craig-Bampton mode shapes. The MNF `hdd_hsa_arm_mnf_job1.mnf` is created in the job directory. The MNF can now be uploaded into Adams HDD models to represent the flexible HSA suspension arm.

[Figure 2.15-7](#) and [Figure 2.15-8](#) show the results of an Adams simulation in which the generated MNF is used. Flying height design and parametric studies can be performed in the Adams simulation.

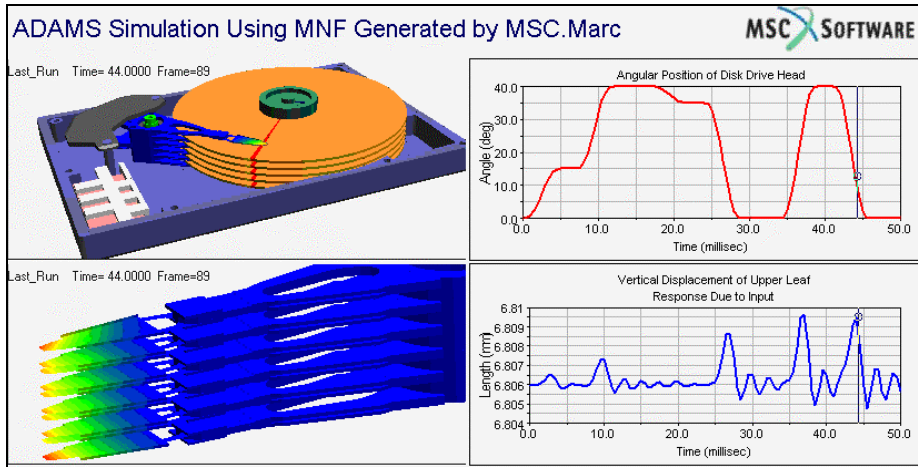


Figure 2.15-7 Adams Results for the Vertical Displacement for the Arm's Upper-leaf due to an Input

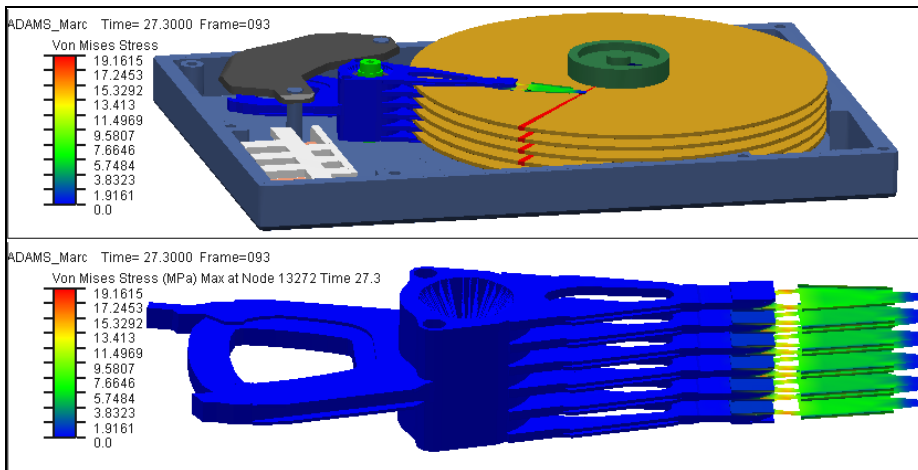


Figure 2.15-8 Adams Results for the Stress Distribution in the HSA Arm

Input Files

The files below are on your [delivery media](#) or they can be downloaded by your web browser by clicking the links (file names) below.

File	Description
hdd_hsa_arm.proc	Mentat procedure file to run the above example
hdd_hsa_arm.mud	Associated model file

2.16 Analysis of Stiffened Plate Using Beam and Shell Offsets

- Chapter Overview 590
- Analysis of Beam Reinforced Shell Structure using Offsets 590
- Input Files 598

Chapter Overview

In many finite element analyses using beams and shells, it is common to model the beams and shells at a geometric location that is different from the actual physical location. Such cases are common when shells or beams of varying thicknesses are adjacent to each other and the top/bottom shell surfaces or beam flanges are to be aligned with each other. It is convenient to model all the shell nodes at the midsurface of one of the shells or the beam nodes at the neutral axis of one of the beams. The alignment of the top shell surfaces or beam flanges is then achieved by providing a suitable shell or beam offset to the elements. Another common instance is when beams are used as stiffeners for shells. It is most convenient to model the beam elements at the mid-surface of the shell and sharing the shell nodal connectivity. The fact that the beam is actually offset by half the plate thickness and half the height of the beam section is achieved by providing a suitable beam offset.

There are two methods by which beam/shell offsets can be modeled in Marc:

- The first method is to place the beams and shells at the actual offset position and then tie the nodes of these elements back to the original position through manually defined RBE2 links. While this method is quite accurate, it is quite cumbersome for large models. Furthermore, if the offset elements have to contact other bodies, it is not possible since all degrees of freedom of the offset element nodes are already tied through the RBE2 links.
- The second method is to use the in-built beam/shell offset capability in Marc. This chapter demonstrates the various features available in Marc to analyze beam/shell structures with in-built beam/shell offsets. The RBE2 approach is only used to compare the accuracy of the solution obtained using in-built beam/shell offsets and the emphasis in this chapter is placed on describing the setup and solution using the actual in-built beam/shell offset capabilities of Marc. The `.dat` files for the beam-shell offset approach (`e3x43a.dat`) and for the RBE2 approach (`e3x43b.dat`) are also in the demo directory.

Analysis of Beam Reinforced Shell Structure using Offsets

An overhanging flat shell that is reinforced by beams is subjected to a top face load. The plate has a variable thickness along the length and the top surfaces of the thick and thin shells are aligned at the same level. The top portion of the reinforcement beam cross-sections are welded to the bottom surface of the thicker plate. In the geometric model, all the elements are modeled at the midsurface of the thicker shell. Suitable beam/shell offsets need to be provided to account for the difference between the geometric model and the physical model.

The finite element mesh of the beam-plate structure is shown in [Figure 2.16-1](#) and [Figure 2.16-2](#). The physical model with the beams and shells at their actual offset locations is displayed in [Figure 2.16-1](#). This model can be used with RBE2 links set up between the offset beams and the shell. The geometric model where the beams are at the shell midsurface and in-built beam/shell offsets are used, see [Figure 2.16-2](#). The beams and shells with a solid cross-section in the figures clearly indicate where they are modeled in the two cases.

The plate is of length 6000 mm and width 4000 mm. The plate has a variable thickness along the length (70 mm over the first 4000 mm and 35 mm over the remaining 2000 mm). The top surfaces of the thick and thin shells are aligned at the same level. One reinforcement beam (beam 1 in [Figure 2.16-1](#)) with a cross-sectional radius of 100 mm and thickness of 25 mm is placed along the plate width at the point where the plate thickness transition occurs. Two other

reinforcement beams (beam 2 and beam 3 in Figure 2.16-1), each with a cross-sectional radius of 125 mm and thickness of 40 mm, are placed along the length on either side of the plate. The top portion of the beam cross-sections are welded to the bottom surface of the plate.

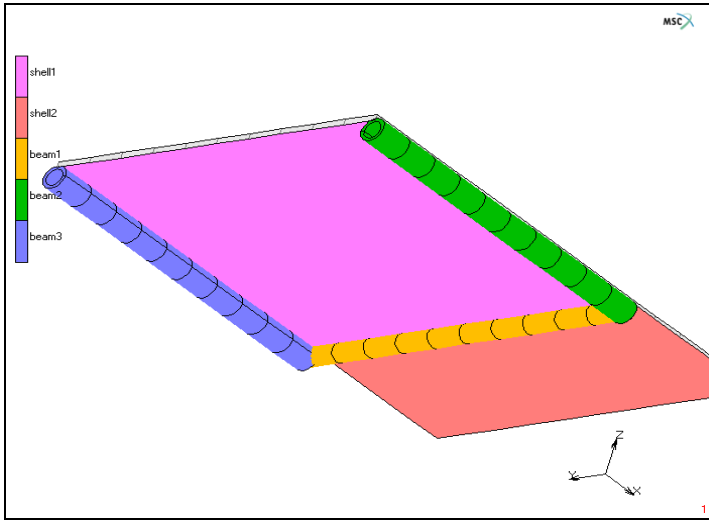


Figure 2.16-1 Finite Element Mesh showing Physical Beam-shell Model

Note: The beam-shell offsets are modeled here using RBE2 links

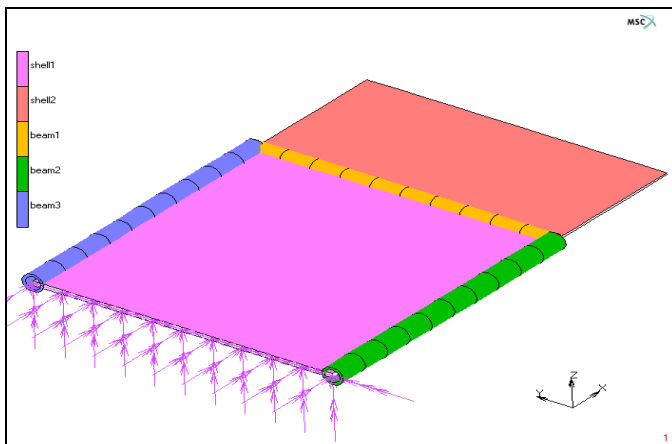


Figure 2.16-2 Finite Element Mesh showing Geometric Beam-shell Model

Note: The beam-shell offsets are modeled using the in-built offset features of Marc.

Procedure File

The analysis has been completely set up from Mentat. The procedure file to demonstrate the example is called *bmslloffset.proc* under `path/examples/marc Ug/s2/c2.16`.

To run the procedure file and build the model from start to finish, the following button sequence can be executed in Mentat:

```
UTILS
  PROCEDURES
    EXECUTE
      bmslloffset.proc
```

Mesh Generation

The generation of the finite element mesh is not discussed in detail here. Instead, refer to the procedure file and the comments in that file. Element type 75 is used for the shells and element type 14 is used for the beams. All shell and beam elements are modeled at the midsurface of the thicker shell. All dimensions are in milli meters. There is a total of 180 elements and 176 nodes.

Geometric Properties

The shell thickness is specified as 70 mm over the first 4000 mm of the length and as 35 mm over the next 2000 mm of the length. For the thinner shell, an offset of 17.5 mm ($\text{offset} = (t1 - t2)/2$ where $t1$ is the thickness of the thicker shell and $t2$ is the thickness of the thinner shell) is specified in order to allow the top shell surface to be aligned with that of the thicker shell.

```
GEOMETRIC PROPERTIES
  MECHANICAL ELEMENTS
    3-D
      SHELL
        THICKNESS
          35
        [] USE OFFSETS
          OFFSET
            17.5
```

For beam 1, the beam radius is specified as 100 mm and the thickness as 25 mm. An offset of -135 mm ($\text{offset} = (t1/2 + r1)$ where $t1$ is the thickness of the thicker shell and $r1$ is the radius of beam 1) is specified in the global Z-direction in order to allow the apex of the beam cross-section to be aligned with the bottom surface of the shell.


```

GEOMETRIC PROPERTIES
  MECHANICAL ELEMENTS
    3-D
      GENERAL BEAM
        THICKNESS
          25
        RADIUS
          100
        VECTOR DEFINING LOCAL X AXIS
          X
            1
        BEAM-SHELL OFFSETS >
          [] USE OFFSETS
          OFFSET VECTOR AT NODE 1
            V GLOBAL
              Z
                -135
            COPY 1 TO 2

```

For beam 2, the beam radius is specified as 125 mm and the thickness as 40 mm. The LOCAL(SHELL) option is used to specify the offset. In this case, only the offset magnitude is specified and the offset vector is along the normal to the associated shell element at the node. Since the shell normal is in the global Z-direction, an offset magnitude of -160 mm ($\text{offset} = (t_1/2 + r_2)$ where t_1 is the thickness of the thicker shell and r_2 is the radius of beam 2) is specified in order to allow the apex of the beam cross-section to be aligned with the bottom surface of the shell.

```

GEOMETRIC PROPERTIES
  MECHANICAL ELEMENTS
    3-D
      GENERAL BEAM
        THICKNESS
          40
        RADIUS
          125
        VECTOR DEFINING LOCAL X AXIS
          Y
            1
        BEAM-SHELL OFFSETS >

```

```

[] USE OFFSETS
OFFSET VECTOR AT NODE 1
V LOCAL(SHELL)
X
    -160
COPY 1 TO 2
  
```

For beam 3, the beam radius is specified as 125 mm and the thickness as 40 mm. The LOCAL(BEAM) option is used to specify the offset. In this case, the offset vector is along the local beam coordinate system. The local Z axis is along the beam (from node 1 to node 2), the local X axis is defined by the user on the same menu and the local Y axis is defined by the cross-product of Z and X. Since the local Z axis of beam 3 is (-1,0,0) and the local X axis is defined as (0,-1,0), the local Y axis of the beam comes out as (0,0,1). An offset of -160 mm (offset = $t_1/2 + r_3$) where t_1 is the thickness of the thicker shell and r_3 is the radius of beam 3) is specified along the local Y axis in order to allow the apex of the beam cross-section to be aligned with the bottom surface of the shell.

GEOMETRIC PROPERTIES

MECHANICAL ELEMENTS

3-D

GENERAL BEAM

THICKNESS

40

RADIUS

125

VECTOR DEFINING LOCAL X AXIS

Y

-1

BEAM-SHELL OFFSETS >

```

[] USE OFFSETS
OFFSET VECTOR AT NODE 1
V LOCAL(BEAM)
Y
    -160
COPY 1 TO 2
  
```

Note that the data entered for local X axis on the menu has a close bearing on the local beam coordinate system and, in turn, on the offset vector components specified using the LOCAL(BEAM) option. A visual check for the correctness of the local beam coordinate system can be obtained as follows:

GEOMETRIC PROPERTIES
PLOT SETTINGS
BEAM >
BEAM ORIENTATION
DRAW X-Y AXES

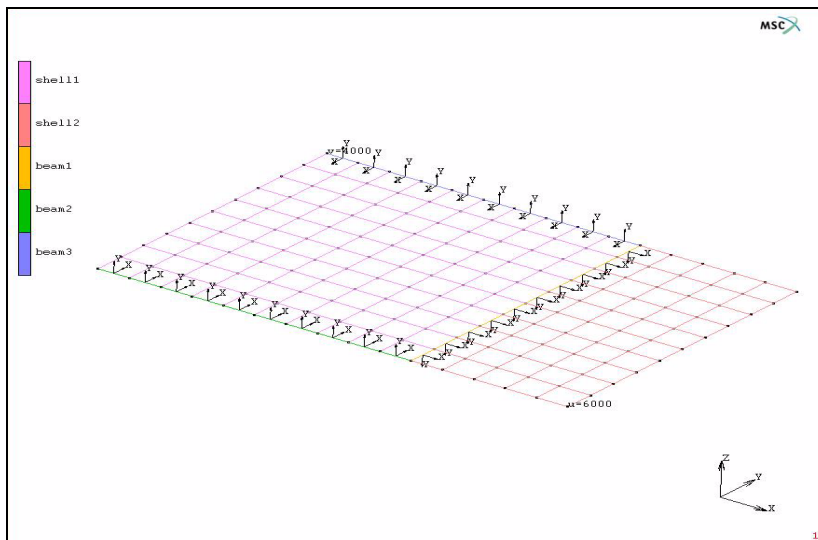


Figure 2.16-3 Orientation of Beams

Material Properties

Isotropic, elastic-perfectly plastic material properties are defined for all elements in the model. Young's modulus is defined as $2.1e4 \text{ N/mm}^2$, Poisson's ratio as 0.3 and initial yield stress as 40 N/mm^2 .

Boundary Conditions

The nodes at the left edge of the thicker shell are fixed in all translations and rotations. The top surface of the shell is subjected to a face load of $7.5e-3 \text{ N/mm}^2$.

BOUNDARY CONDITIONS

MECHANICAL

FACE LOAD

PRESSURE

7.5e-3

FACES ADD

ALL:

TOP

Loadcase Definition

A mechanical loadcase is defined to conduct the analysis. Adaptive Stepping MULTI-CRITERIA (Auto Step) is used for the time stepping. Convergence testing is done on both residuals and displacements with tolerance of 0.01.

Job Parameters

The LARGE STRAIN procedure is chosen. Select the FOLLOWER FORCE parameter in order to allow the pressure load follow the geometry. The layer von Mises stress and equivalent plastic strain are requested. Use 5 layers for the shell element. Note that for the beam element, 16 layers are used by default for the circular cross-section. Layer results are requested at layers 1,3,5 (outer,midbottom layers of shell), 1,9 (layers at beam neutral axis), and 5,13 (layers at extreme fibers of beam).

Results and Discussion

The variation of the Z component of the displacement with time is plotted in [Figure 2.16-4](#). The results obtained from the in-built offset formulation at the center of the free edge of the thinner shell are compared with the corresponding RBE2 solution at the same location. The results are nearly identical to each other. It should be noted that for the offset solution, only the displacements at the original user-specified location are available on the post file.

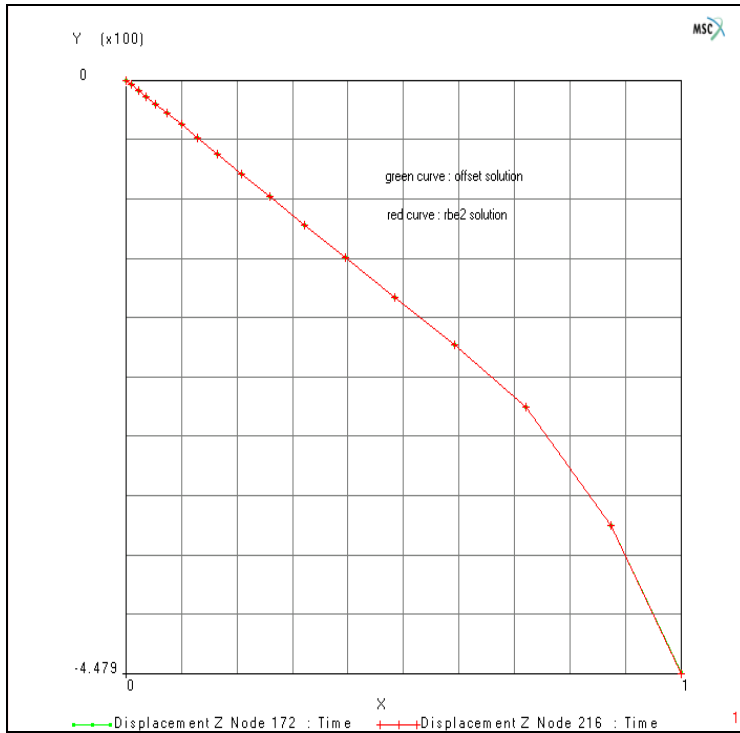


Figure 2.16-4 Displacement Z Variation with Time at Center of Free Edge of Shell

The layer 1 equivalent von Mises stress contours obtained for the offset solution are plotted in [Figure 2.16-5](#). It should be noted that while calculating elemental quantities like strains, stresses, and associated nodal quantities like reaction forces, elements, and nodes are taken in the actual physical location by applying appropriate offset values. It should also be noted that the contour bands shown in the figure are based on the translated values at the element integration points and with nodal averaging turned off. This avoids smearing of the quantities between shells and beams at common nodal locations. Results obtained from the RBE2 solution are identical and are not shown here.

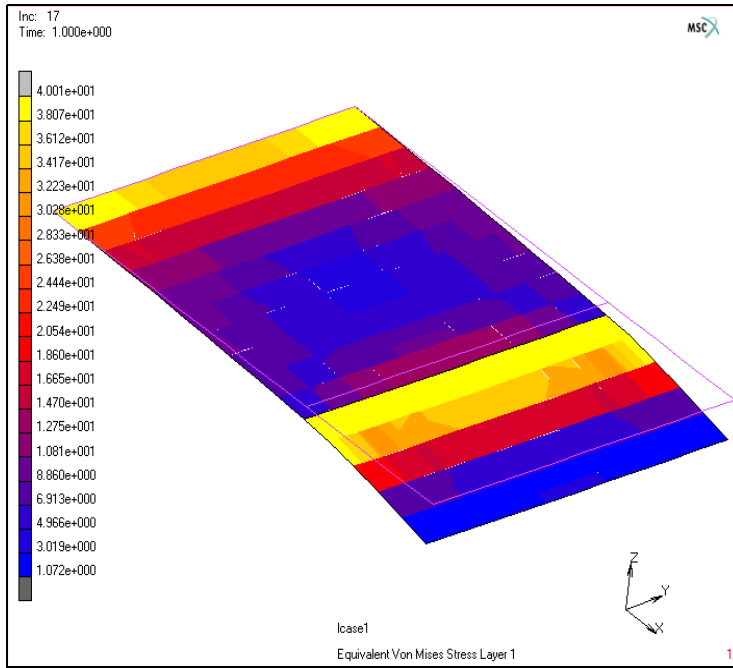


Figure 2.16-5 Deformed Configuration and Equivalent Stress Contours for In-Built Beam/Shell Offset Model

Input Files

The files below are on your [delivery media](#) or they can be downloaded by your web browser by clicking the links (file names) below.

File	Description
bmslloffset.proc	Mentat procedure file to run the above example

2.17 3-D Tetrahedral Remeshing with Boundary Conditions

- Chapter Overview 600
- Simulation Examples 600
- Rubber Seal Insertion 611
- Input Files 620

Chapter Overview

This chapter demonstrates the capability for a user to assign boundary conditions to a remeshing body in 3-D. Remeshing with boundary condition is available in 2-D and 3-D.

The boundary conditions can be applied to nodes or element faces. They can also be applied to geometry entities such as points, surfaces or curves (limited to curves with prescribed nodal displacements and temperatures) providing the geometry entities are attached to the mesh. The following boundary conditions are tested in the development:

- point loads
- nodal displacement/temperature/flux
- face distributed load/flux
- multiple remeshing bodies and boundary conditions
- boundary conditions in thermal-mechanical coupled analysis
- curves with fixed displacements

The following are the limitations to this feature:

- maximum two boundary conditions can be assigned to the same element face
- maximum 99 surfaces can be used in geometry attachment
- boundary conditions can only be assigned to the boundary, not to the interior of the remeshing body
- element types are restricted to 157 and 134 tetrahedral elements
- table style input format is required

Simulation Examples

By allowing boundary conditions to be used in a remeshing body, it creates many possibilities in simulations. The following applications demonstrate some of these possibilities.

Pressure on a Rubber Cylinder

This example shows a pressure applied to a circular area on the top of a rubber cylinder. As the pressure increases, the rubber deforms to such an extent that remeshing is necessary. As the result, the pressure boundary condition is transferred to the new mesh and the simulation continues.

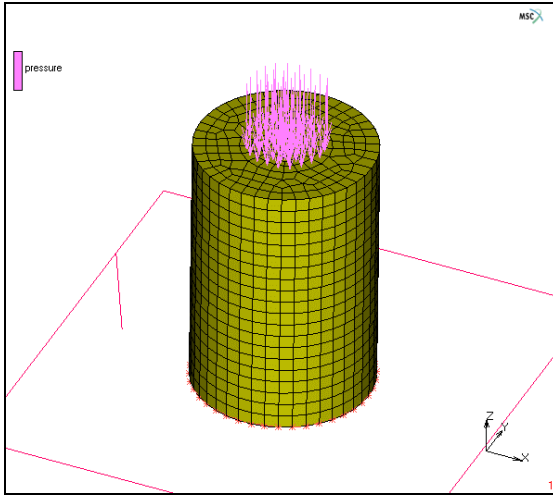


Figure 2.17-1 Pressure Boundary Condition

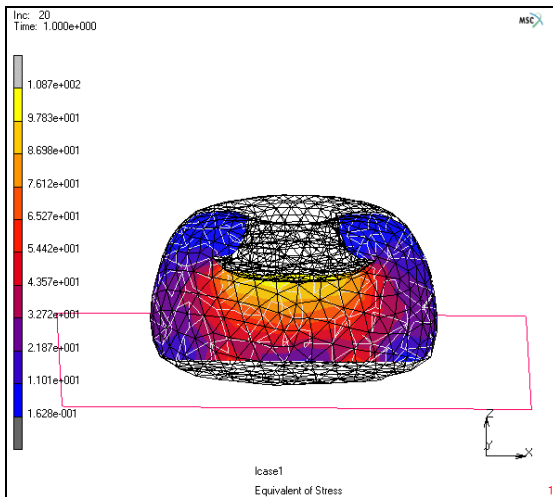


Figure 2.17-2 Effective Stress Display on a Cutting Plane

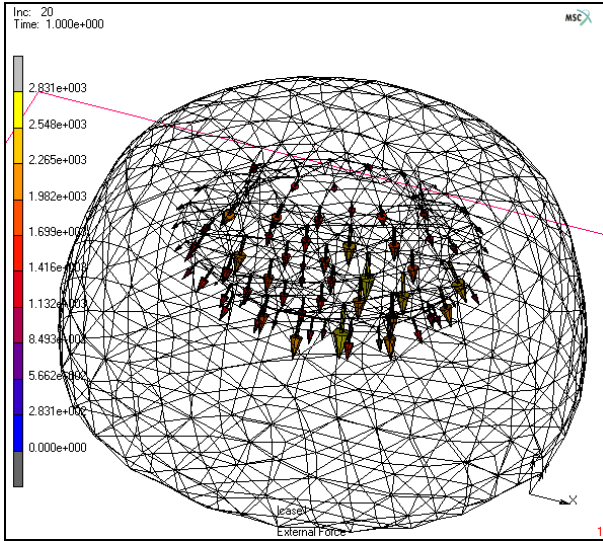


Figure 2.17-3 Pressure showing here as an External Force Vector after Remeshing

Metal Compression with Prescribed Displacements

Metal compression is normally simulated with rigid die and punch. In this example, simple prescribed nodal displacements and temperatures are used to demonstrate the capability of remeshing with boundary conditions in a thermal-mechanical coupled analysis. This example shows multiple boundary conditions assigned to the same element faces.

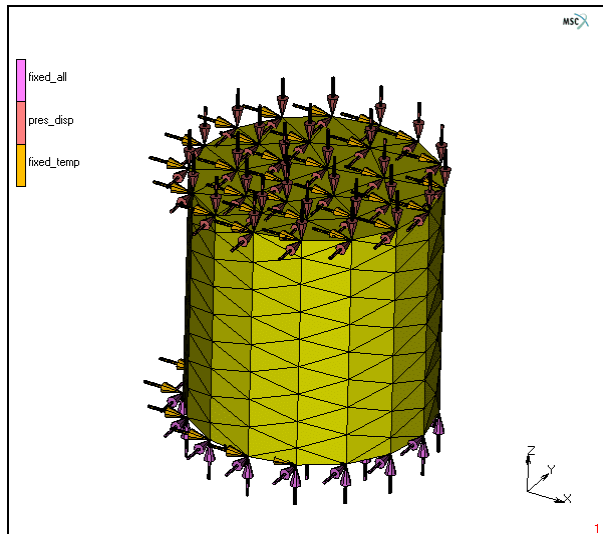


Figure 2.17-4 Prescribed Nodal Displacement and Temperature at 20°

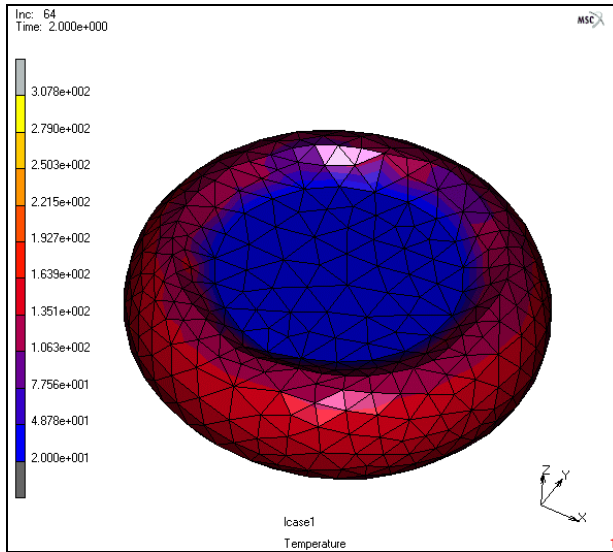


Figure 2.17-5 Temperature Distribution at the End of Simulation

Rubber Ring Seal with Pressure Testing after Compression

A section of rubber ring is compressed and then pressured on one side to test possible leakage. This example shows applications of geometry attachment with pressure boundary conditions and suppression of pressure on element faces that are in contact. The geometry attachment is applied to an area that will have pressure after compression and is transferred to new mesh after remeshing. When pressure is applied to this geometry, only element faces that are not in contact are subjected to this pressure. In the following figures, the geometry attachment is shown in red color.

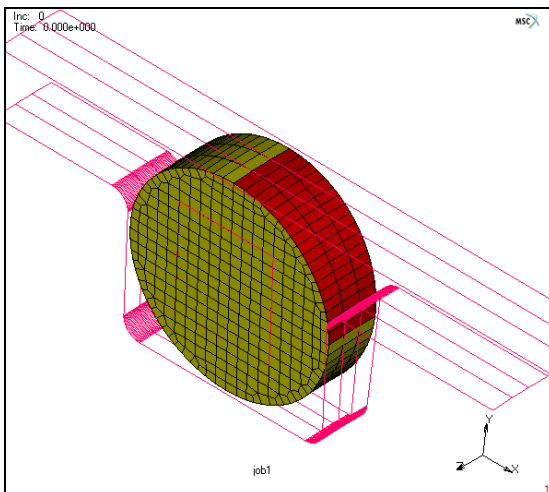


Figure 2.17-6 Pressure is Pre-Applied to the Attached Surface

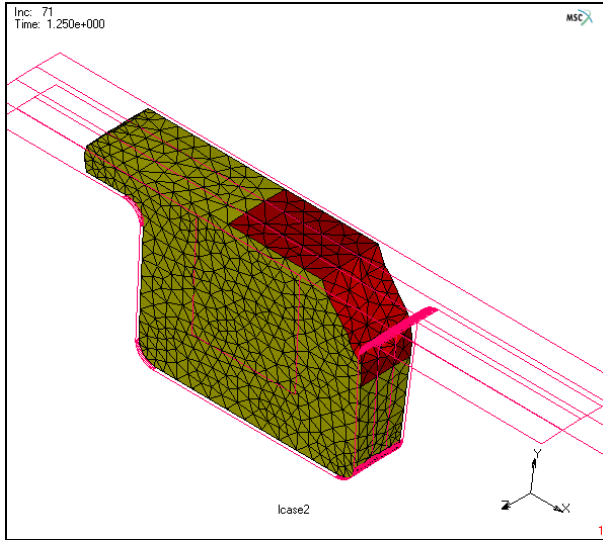


Figure 2.17-7 Geometry Attachment is Transferred to the New Mesh correctly

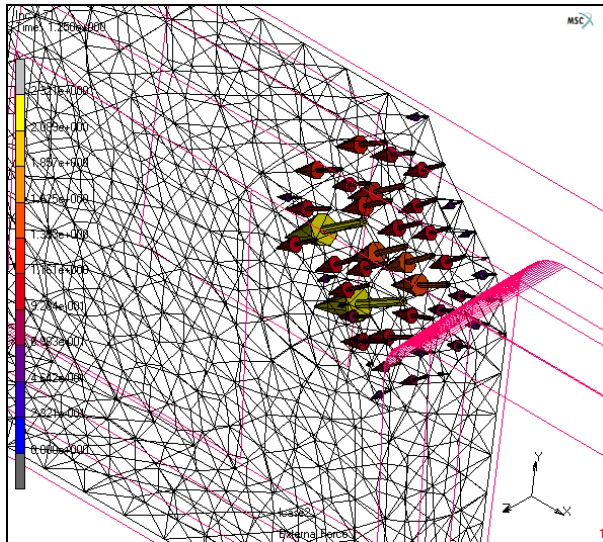


Figure 2.17-8 Pressure is Applied Automatically to the Element Faces that are not in Contact

Tube Hydro-forming

Hot hydro-forming with thick tubes requires remeshing. The tube is subjected to an internal pressure on the inner surface, a fixed nodal displacement on both ends, and a symmetry boundary condition on the symmetry surfaces. Thermal-mechanical coupled analysis is assumed with initial temperature at 1000°C and 500°C in the rigid die.

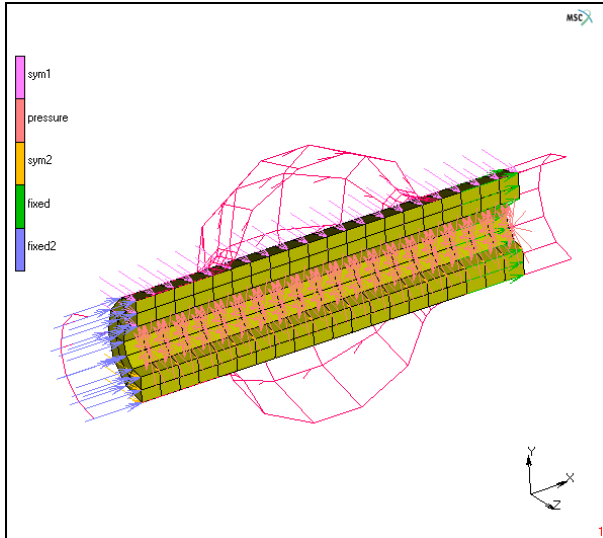


Figure 2.17-9 Boundary Conditions

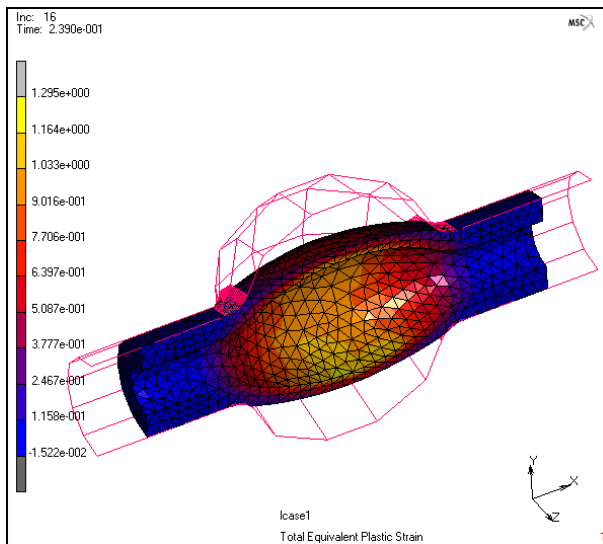


Figure 2.17-10 Total Equivalent Plastic Strain at an Intermediate Stage

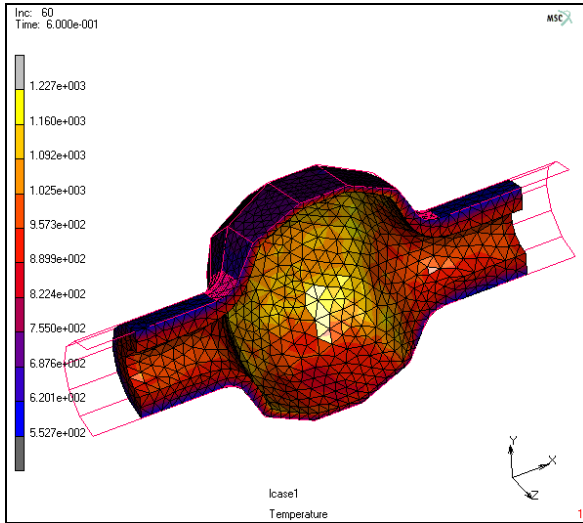


Figure 2.17-11 Temperature Distribution at the Final Stage

Rubber Seal Insertion

In using boundary conditions, we can avoid having to use rigid contact surfaces to apply symmetry conditions on a remeshing body. This well-shown rubber seal example is simulated now without symmetry surfaces and a rigid surface to push the rubber seal.

Geometry attachment with prescribed displacement is used to push the rubber seal. This example is demonstrated in detail later in the *Marc User's Guide*.

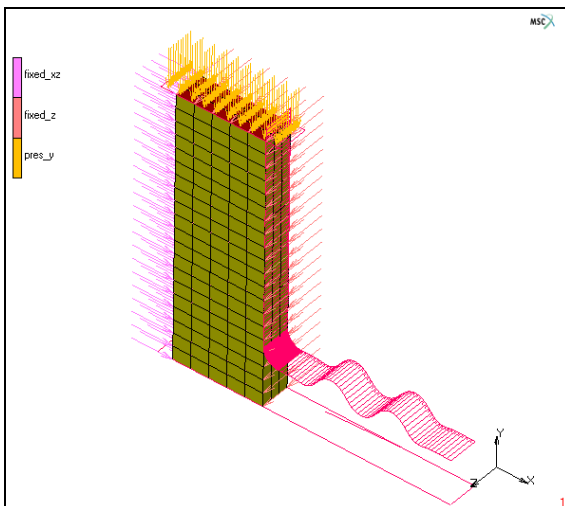


Figure 2.17-12 Boundary Conditions

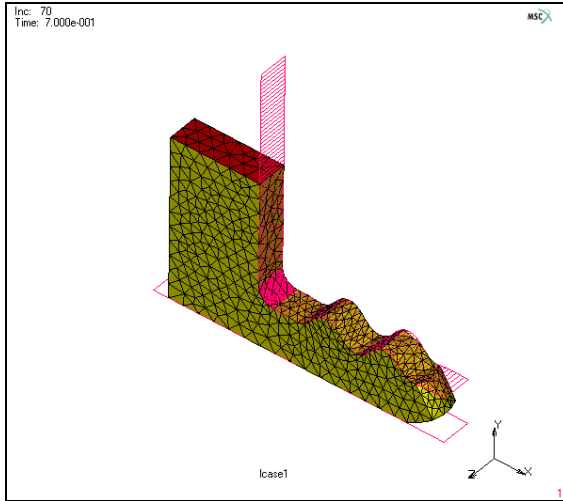


Figure 2.17-13 Final Deformation showing Geometry Attachment in Red

Rubber Seal and Steel Interaction

This example demonstrates multiple deformable bodies in contact and the remeshing with pressure boundary conditions. The rubber between a steel plate and a steel tube is under pressure and pushed against the steel tube. This causes large deformation in the rubber, so the remeshing is required.

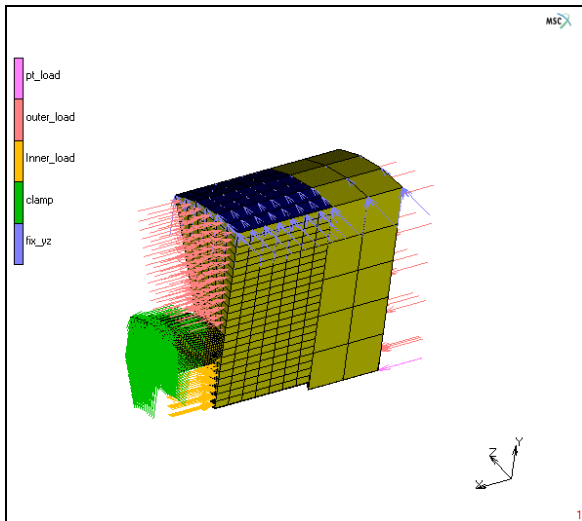


Figure 2.17-14 Boundary Conditions

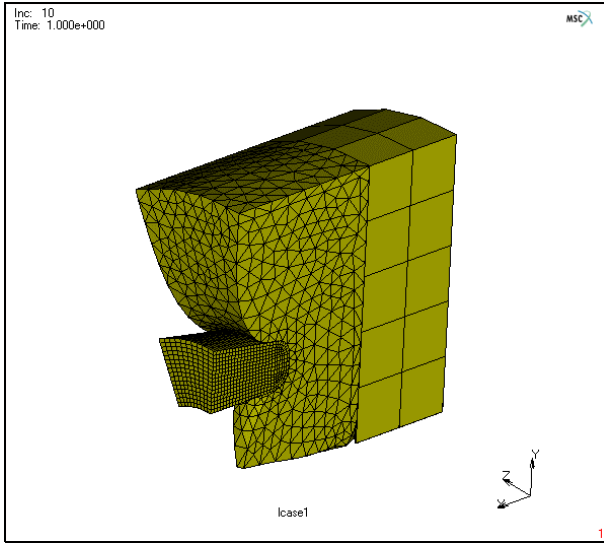


Figure 2.17-15 End of Deformation

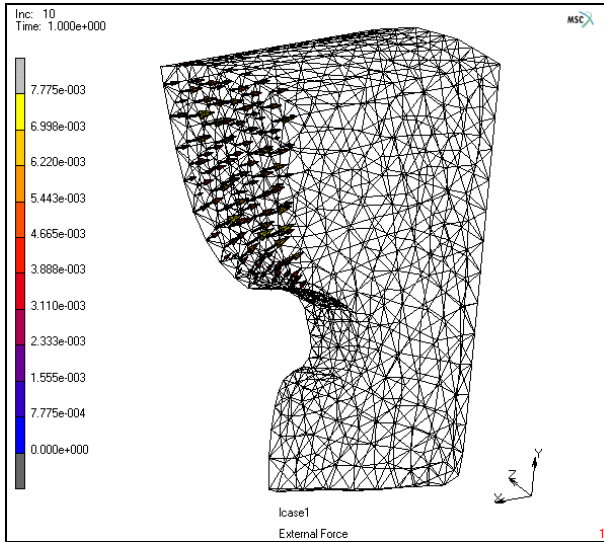


Figure 2.17-16 Pressure showing as External Force Vectors after Remeshing

Glass Forming

Glass forming is another type of application. With the internal pressure, this example is simulating a blow forming process of a glass container. Thermal-mechanical coupled analysis with rigid-plastic material model is assumed.

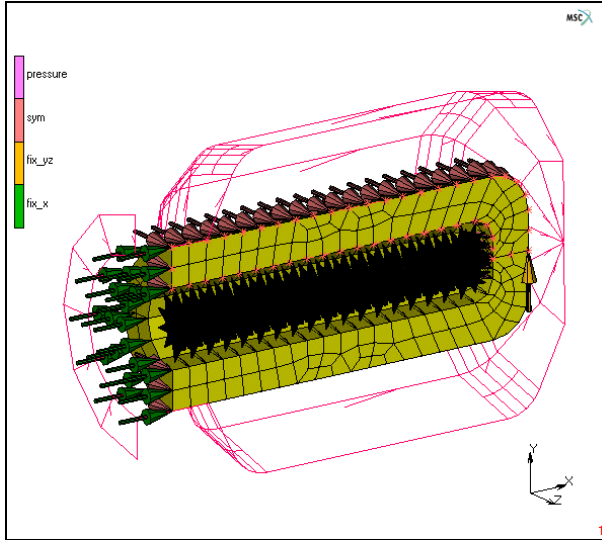


Figure 2.17-17 Boundary Conditions

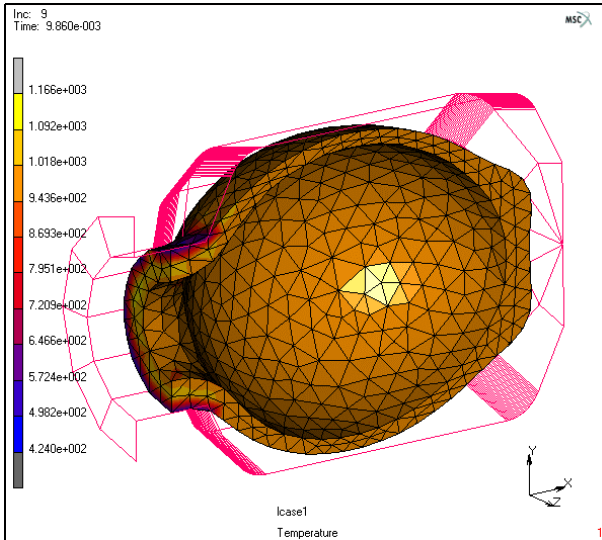


Figure 2.17-18 Temperature Distribution at an Intermediate Stage

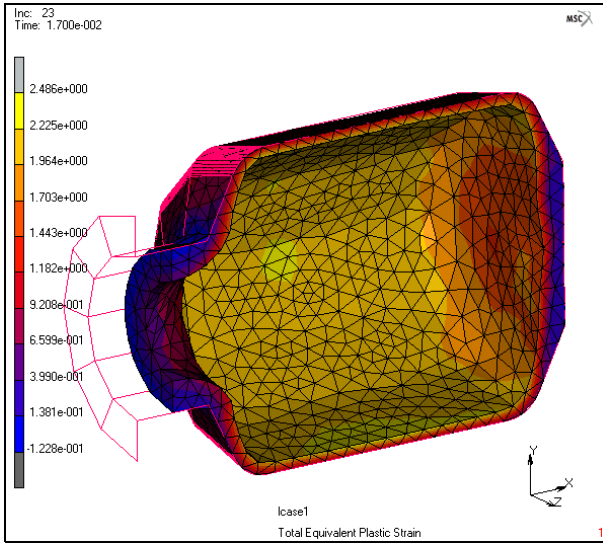


Figure 2.17-19 Final Deformation

Rubber Bars with Prescribed Displacement on Curves

This example demonstrates curve attachments to a 3-D rubber bar. A prescribed displacement boundary condition is applied to the curves. These curves are attached to some element edges. Shown in the following pictures are curve attachments before and after the remeshing in the red color.

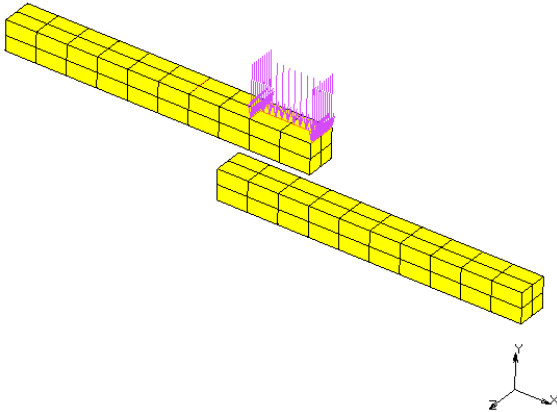


Figure 2.17-20 Boundary Condition applied to Curves with Attachment

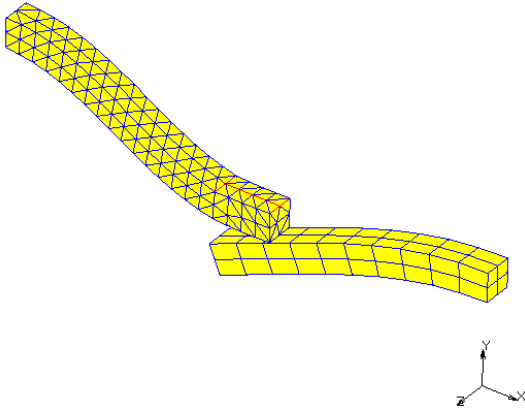


Figure 2.17-21 Curve Attachments after Remeshing and Deformation

Rubber Seal Insertion

A rubber seal with a rectangular cross section ($1.8 \times 1.2 \text{ cm}^2$) is compressed laterally by a prescribed displacement boundary condition. Because of the symmetry, only a half of the seal is considered. With a thickness of 0.2 cm, the model is setup as a 3-D problem. Assuming this is a long rubber seal in the thickness direction, additional two symmetry surfaces are used. The three symmetric surfaces are constrained with boundary conditions applying to the nodes and the moving surface is simulated by an attached surface with a prescribed displacement.

The rubber seal is modeled using Mooney constitutive model. The material parameters are given as $C1=8\text{N/cm}^2$ and $C2=2\text{N/cm}^2$. The bulk modulus is 10000N/cm^2 .

The analysis starts with a hexahedral mesh. After immediate remeshing, the hexahedral element is converted into tetrahedral elements. In the rest of the analysis, the remeshing/rezoning is done based on the strain change check to prevent severe element distortion. An adaptive meshing based on the surface curvature is used to generate smaller elements near the curved areas. It allows the analysis to capture the geometry changes correctly in those areas without creating excessive number of the elements to slow down the analysis. Element type 157 is used in the analysis within the updated Lagrangian framework.

Model Generation

We will start with a pre-defined model file and concentrate on the applications of the new features. A model file `initial_setup.mfd` is read as follows:

```
FILE
  OPEN
    Open file
      initial_setup.mfd
  OK
```

In the model file, most of the basic information is already provided. We will concentrate on the following:

1. Attach a surface to element face
2. Boundary conditions
3. Global remeshing criteria
4. Loadcase
5. Job submission
6. Results

First of all, reset some plot controls so that we have a better view of the model (Figure 2.17-22).

PLOT

NODES

(click to unselect)

POINTS

(click to unselect)

ELEMENTS

SOLID

(click to select)

DRAW

DYN.MODEL

(set dynamic modeling on and rotate model to a better position)

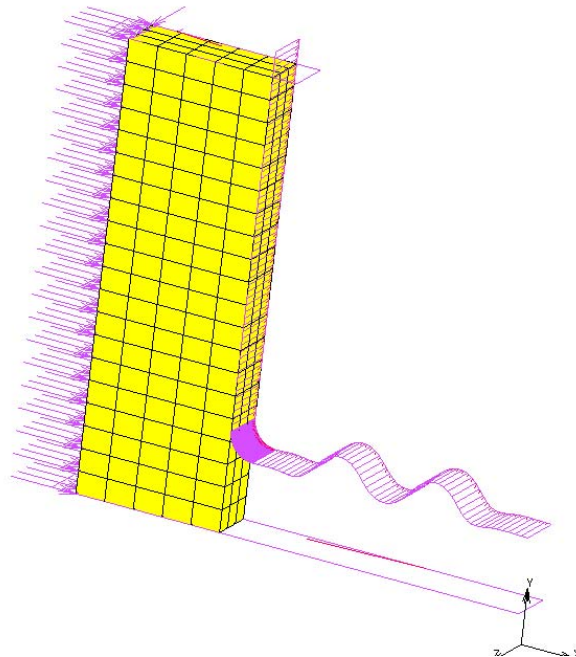
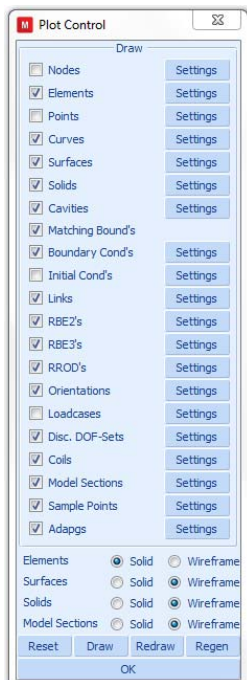


Figure 2.17-22 Initial Model Setup

Attach a Surface to Element Faces

In order to demonstrate boundary conditions assigned to a geometry surface, we need to attach this surface to some element faces. Here is how:

MAIN
 MESH GENERATION
 ATTACH
 FACE
 SURFACE

Select surface on top (you have to deselect DYN MODEL first)

Select all element faces on the top

END LIST (#)

You can see the attached element faces change the color to dark blue. If you prefer, you can change this color to red (Figure 2.17-23):

MAIN
 VISUALIZATION
 COLORS
 ATTACHED FACES
 OK

(change it to red)

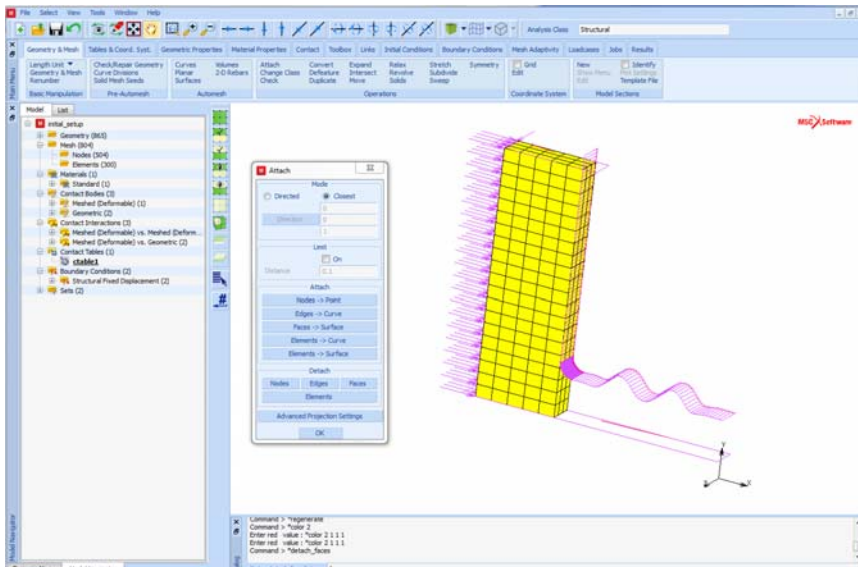


Figure 2.17-23 Surface Attachment

Boundary Conditions

The symmetry boundary conditions are set up by applying the proper constraints to the nodes on the surfaces. These boundary conditions are already done in the initial model. Now, we are going to add a prescribed nodal displacement condition to the attached surface that pushes the rubber seal:

```
MAIN
  BOUNDARY CONDITIONS
    MECHANICAL
      NEW
        NAME
          pres_y (enter a new name)
```

Define a time table for the prescribed displacement:

```
TABLE
  NEW
    1 INDEPENDENT VARIABLE
  TYPE
    time
  ADD
    0 0 (enter point 1)
    1 1 (enter point 2)
  SHOW TABLE
  SHOW MODEL (back to the model view)
  RETURN
```

Define prescribed displacement:

```
FIXED DISPLACEMENT
  DISPLACEMENT Y
    -1 (enter -1)
  TABLE
    table1- (select time table)
  OK
```

Assign it to the attached surface:

SURFACES

ADD

END LIST (#)

(select the surface)

If you show all boundary conditions now,

RETURN

ID BOUNDARY CONDS

You should have the view similar to [Figure 2.17-24](#).

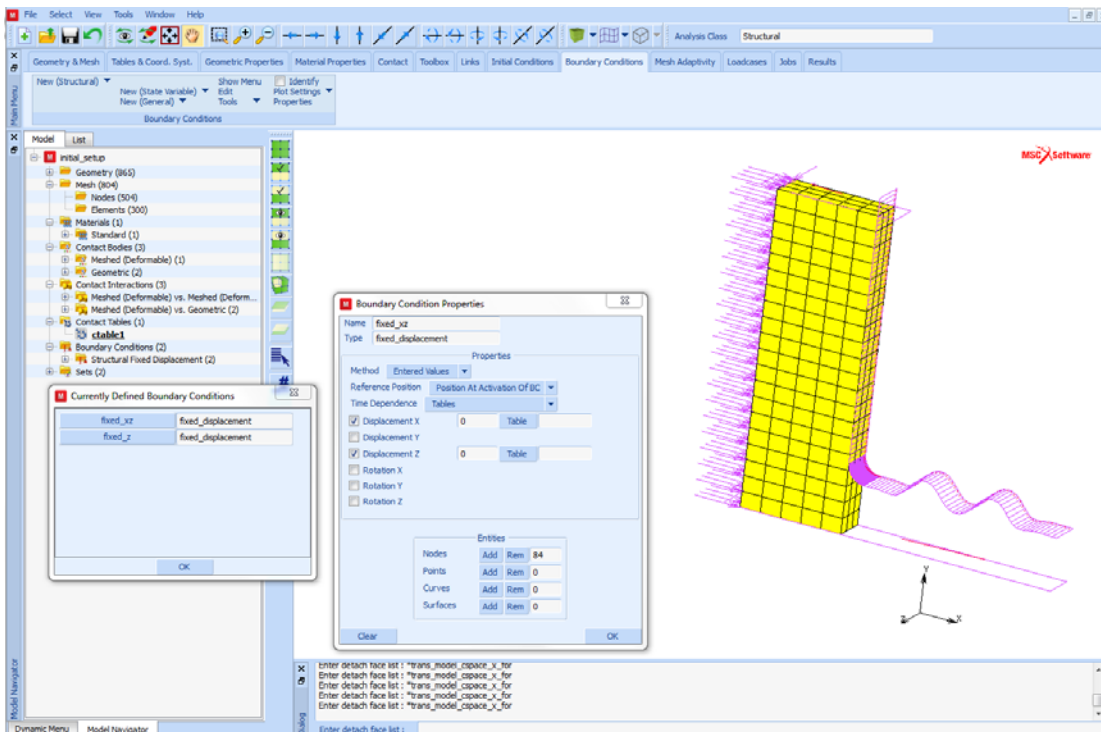


Figure 2.17-24 Boundary Conditions

Global Remeshing Criteria

We need to define global remeshing list criteria so that the initial hexahedral mesh is converted to tetrahedral mesh and remeshing is done whenever the strain change level is reached.

MAIN

MESH ADAPTIVITY

GLOBAL REMESHING CRITERIA

PATRAN TETRA

IMMEDIATE

(on)

ADVANCED

STRAIN CHANGE

0.4

OK

#ELEMENTS

SET

1000

ADVANCED

CURVATURE CONTROL

10

CHANGE ELEMENT TYPE

157

OK

OK

REMESH BODY

rubber

(select rubber)

Loadcase

Define a loadcase to push the rubber seal.

MAIN

MECHANICAL

STATIC

LOADS

(select all boundary conditions)

GLOBAL REMESHING

(select remeshing criterion)

SOLUTION CONTROL

MAX # RECYCLES

20

MIN # RECYCLES

2

Contribution of initial stress


```
TENSILE STRESS
OK
CONVERGENCE
  RESIDUALS OR DISPLACEMENTS
  RELATIVE FORCE TOLERANCE
    0.1
  RELATIVE DISPLACEMENT TOLER.
    0.01
OK
TOTAL LOADCASE TIME
  0.5
CONSTANT TIME STEP
  0.01
  #STEPS
    50
OK
```

Job Submission

It is important to select NEW STYLE TABLE format for this analysis.

```
MAIN
  MECHANICAL
    Lcase1 (select load case 1)
    INITIAL LOAD (select all boundary conditions)
    ANALYSIS OPTIONS
      LARGE STRAIN
      OK
    JOB RESULTS
      Select Cauchy stress for element output
      OK
    OK
  RUN
    NEW-STYLE TABLES - (select new format)
    SUBMIT(1) (run job)
```

Results

Results can be viewed and compared with others using the contact bodies.

MAIN

RESULTS

OPEN DEFAULT

DEF ONLY -

(show deformed shape)

First, we can check if all boundary conditions are transferred to the new mesh after each remeshing step.

Figure 2.17-25 shows the tetrahedral mesh after immediate remeshing and Figure 2.17-26 shows the mesh at the final step. You can see that boundary conditions are transferred correctly after about nine remeshing steps.

Note: The attached element faces are shown in red.

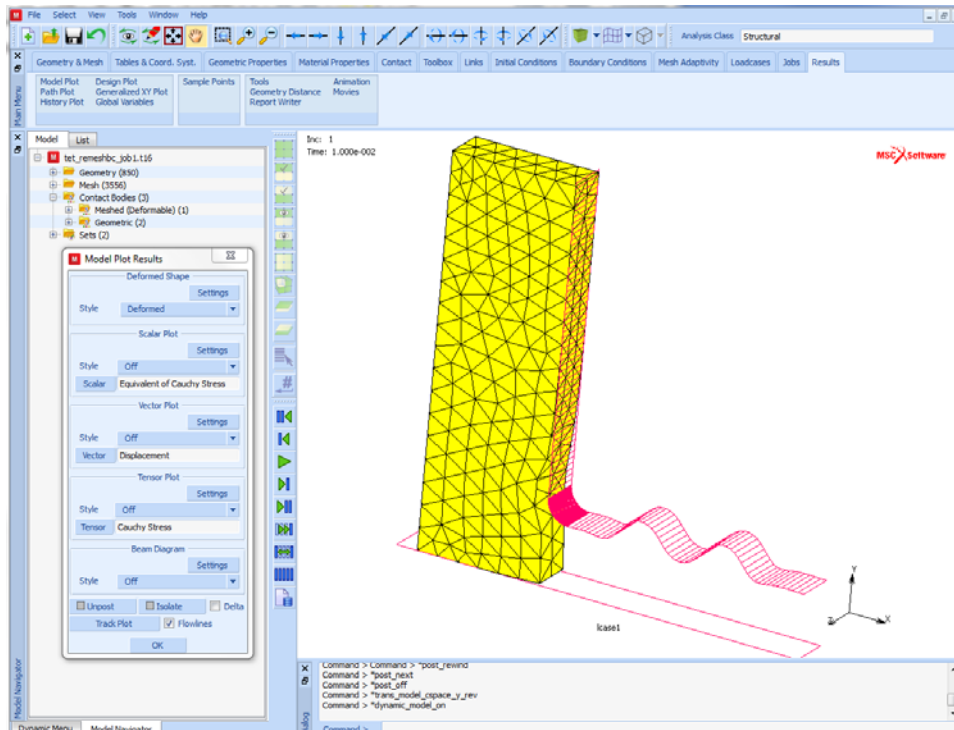


Figure 2.17-25 After Converting to Tetrahedral Mesh in the First Remeshing

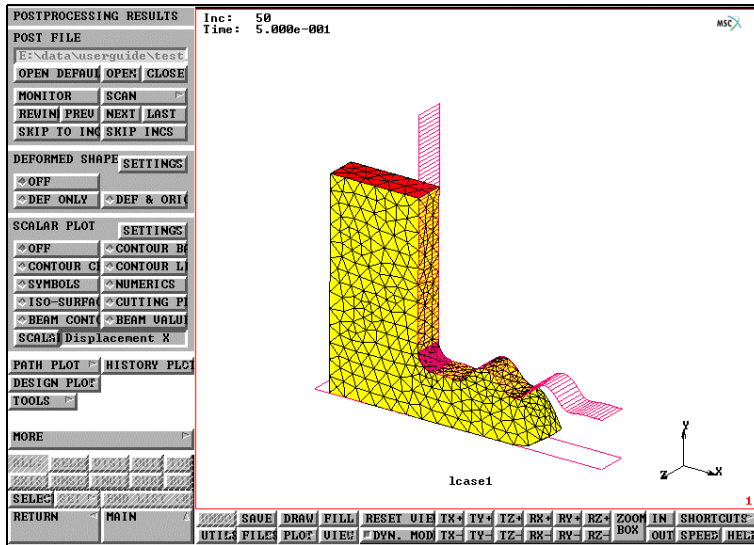


Figure 2.17-26 Mesh at the Last Increment

The Cauchy equivalent stress can be seen in [Figure 2.17-27](#) and [Figure 2.17-28](#).

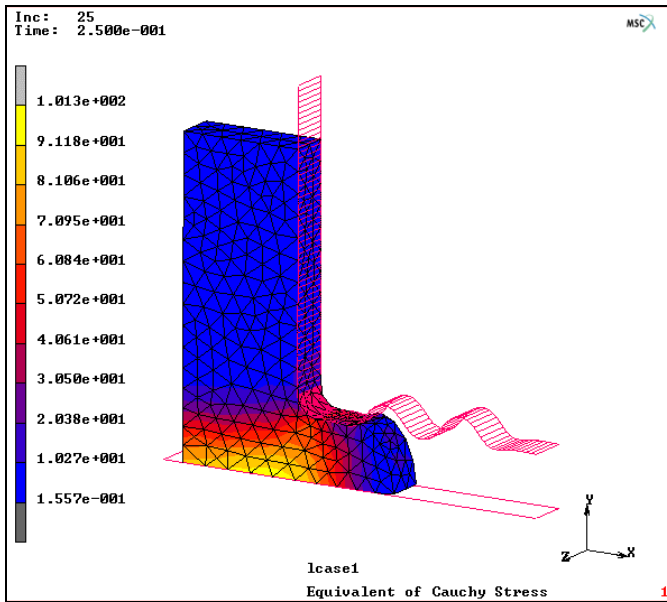


Figure 2.17-27 Equivalent Cauchy Stress at Increment 25

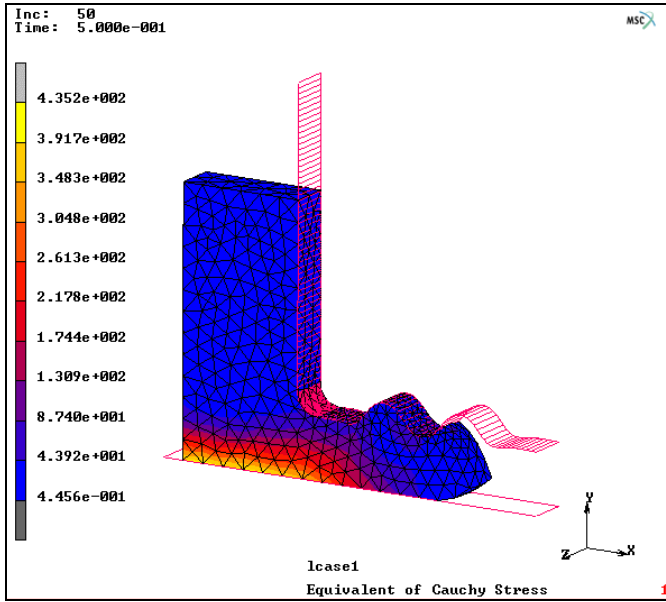


Figure 2.17-28 Equivalent Cauchy Stress at Increment 50

Input Files

The files below are on your [delivery media](#) or they can be downloaded by your web browser by clicking the links (file names) below.

File	Description
tet_remeshbc.proc	Mentat procedure file to run the above example
initial_setup.mfd	Associated model file

2.18 Induction Heating of a Tube

- Chapter Overview 622
- Heating of a Tube 622
- Input Files 634

Chapter Overview

This chapter describes the use of coupled magnetodynamic-thermal analysis in Marc. With this coupling, procedure induction heating type analyses can be performed. The implementation in Marc follows a staggered approach. First, a harmonic magnetodynamic analysis is performed followed by a thermal analysis. The harmonic magnetodynamic field generates induction currents in the workpiece. From these induced currents a heat flux is computed, which is then used in the thermal analysis. The thermal analysis can be either a time dependent, or a steady state solution.

Heating of a Tube

In this example, an iron tube is heated by six coils. The upper part of the workpiece is placed inside the coils. [Figure 2.18-1](#) shows the model where axisymmetry is considered around the x-axis. A complete description of this example can be found in [\[Reference 1\]](#).

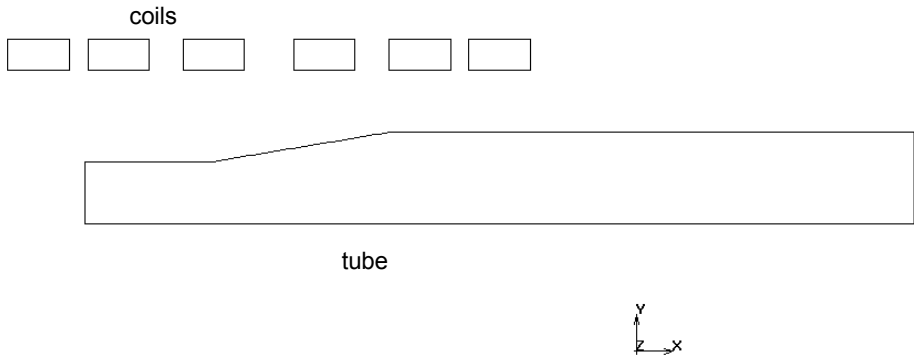


Figure 2.18-1 Axisymmetric Representation of the Tube Surrounded by Coils

Mesh Generation

The geometry was generated previously, and is read in as an *mfd* file. The model contains the tube and the coils. Sufficient space around the tube and coils is meshed to capture the magnetodynamic field correctly. The mesh of the tube coils and air directly surrounding it is refined. The surrounding air is meshed more coarsely in order to increase computational efficiency. The curves in the geometry already have divisions assigned to them.

```
FILE
  NEW
    OK
  RESET PROGRAM
  OPEN
    tube_geom.mfd
  OK
```

```
RETURN
MESH GENERATION
  AUTO MESH
    2D PLANAR MESHING
      QUADRILATERALS (ADV FRNT): QUAD MESH
        1 to 11 #
      QUADRILATERALS (ADV FRNT): QUAD MESH
        12 to 35 #
    SELECT
      ELEMENTS
        1 to 2080 #
      ELEMENTS: STORE
        tube
      OK
      ALL: SELECTED
      CLEAR SELECT
      ELEMENTS
        2081 to 2320 #
      ELEMENTS: STORE
        coils
      OK
      ALL: SELECTED
      RETURN
      QUADRILATERALS (ADV FRNT): QUAD MESH
        1 to 9 12 to 35 37 to 40 46 47 #
      MESH COARSENING PARAMETER: TRANSITION
        0.9
      QUADRILATERALS (ADV FRNT): QUAD MESH
        38 to 45 #
      RETURN (twice)
  SWEEP
    SWEEP: ALL
    REMOVE UNUSED: NODES
    RETURN (twice)
```

Material Properties

The tube is made of a non-ferromagnetic stainless steel X5CrNi 18/9 (1.4301). Temperature dependent material properties for this steel were taken from [Reference 1], which are permeability $\mu = \mu_0 = 1.25 \times 10^{-6} \text{ Hm}^{-1}$, permittivity $\varepsilon = 1 \text{ Fm}^{-1}$, electrical conductivity $\sigma(T) = \frac{1}{a + b \cdot T - c \cdot T^2 + d \cdot T^3} \Omega^{-1}\text{m}^{-1}$, with $a = 4.9659 \times 10^{-7}$, $b = 8.4121 \times 10^{-10}$, $c = 3.7246 \times 10^{-13}$, and $d = 6.196 \times 10^{-17}$.

Then the thermal conductivity $\lambda(T) = 100(0.11215 + 1.4087 \times 10^{-4}) \text{ Wm}^{-1}\text{K}^{-1}$, the mass density $\rho = 7900$, and the specific heat $C(T) = 1000(0.3562 + 0.988 \times 10^{-4}) \text{ Jkg}^{-1}\text{K}^{-1}$.

For the surrounding air permeability $\mu = \mu_0 = 1.25 \times 10^{-6} \text{ Hm}^{-1}$, permittivity $\varepsilon = 8.854 \times 10^{-12} \text{ Fm}^{-1}$, and electrical conductivity $\sigma = 0 \text{ } \Omega^{-1}\text{m}^{-1}$. The thermal conductivity $\lambda = 0.024 \text{ Wm}^{-1}\text{K}^{-1}$, mass density $\rho = 1.3$, and the specific heat $C = 1000 \text{ Jkg}^{-1}\text{K}^{-1}$. For the coil, the same material properties as air are taken. An emissivity of 0.4 is taken for the tube.

MATERIAL PROPERTIES

MATERIAL PROPERTIES

NAME

air

HEAT TRANSFER

CONDUCTIVITY

0.024

SPECIFIC HEAT

1000

MASS DENSITY

1.3

OK

MORE

MAGNETODYNAMIC

PERMEABILITY

1.25e-6

PERMITTIVITY

8.854e-12

OK

PREVIOUS

ELEMENTS ADD


```
ALL EXISTING
NEW
NAME
    steel
TABLES
NEW
    1 INDEPENDENT VARIABLE
NAME
    tcond
TYPE
    temperature
INDEPENDENT VARIABLE V1: MAX
    1000
FORMULA
ENTER
    100e0*(0.11215+1.4087e-4*v1)
VARIABLES: FIT
NEW
    1 INDEPENDENT VARIABLE
NAME
    htcap
TYPE
    temperature
INDEPENDENT VARIABLE V1: MAX
    1000
FORMULA
ENTER
    1e3*(3.562e-1+0.988e-4*v1)
VARIABLES: FIT
NEW
    1 INDEPENDENT VARIABLE
NAME
    sigma
TYPE
    temperature
INDEPENDENT VARIABLE V1: MAX
```

```
1000
FORMULA
ENTER
1./(4.9659e-7+8.4121e-10*v1-3.7246e-13*v1^2+6.196e-17*v1^3)
VARIABLES: FIT
RETURN
HEAT TRANSFER
CONDUCTIVITY
1
CONDUCTIVITY: TABLE
tcond
SPECIFIC HEAT
1
SPECIFIC HEAT: TABLE
htcap
MASS DENSITY
7900
EMISSIVITY
0.4
OK
MORE
MAGNETODYNAMIC
PERMEABILITY
1.25e-6
PERMITTIVITY
1
CONDUCTIVITY
1
CONDUCTIVITY: TABLE
sigma
OK
ELEMENTS ADD
ALL: SET
tube
OK
RETURN (twice)
```

Radiation

In this example, heat loss due to radiation is also taken into account. This is activated in Marc by defining an open cavity. In Mentat, the cavity is defined in MODELING TOOLS, and activated in BOUNDARY CONDITIONS.

```
MODELING TOOLS
  CAVITIES
    NEW
    CURVES: ADD
      1 TO 9 #
    RETURN (twice)
```

Initial Conditions and Boundary Conditions

The initial temperature of all the nodes in the model, and the sink temperature of the radiating cavity are set to 20°C. At the outer boundary, the magnetic potential and the electric potential are set to zero. In [Reference 2], a total current of 1293 A flows in each coil. This is a net or effective current in a coil and can be represented as a coil current density in the following way. The cross-sectional area of each of the coils is $A = 5 \times 10^{-5} m^2$. Then the magnitude of the current density is,

$$J = \frac{1293}{5 \times 10^{-5}} = 2.586 \times 10^7 Am^{-2}.$$

In the axisymmetric model, this current points in the z-direction. It is also possible to apply a point current to all the nodes of the coils. The magnitude of the point current for each node is then

$$I = \frac{1293}{n}$$

where n is the total number of nodes in any of the coils.

```
INITIAL CONDITIONS
  THERMAL
    TEMPERATURE
      TEMPERATURE (TOP)
        20
      OK
    NODES: ADD
    ALL: EXIST
    RETURN (twice)
BOUNDARY CONDITIONS
  NAME
```

```
fix_A
MAGNETODYNAMIC
HARMONIC BC's
  FIX MAGNETIC POTENTIAL
    POTENTIAL X
    POTENTIAL Y
    POTENTIAL Z
    OK
  CURVES: ADD
    43 44 45 #
  NEW
  NAME
    load
  VOLUME CURRENT
    CURRENT Z
    2.586e7
    OK
  ELEMENTS: ADD
  ALL: SET
    coils
    OK
  NEW
  NAME
    fix_E
  FIX ELECTRIC POTENTIAL
    POTENTIAL
    OK
  CURVES: ADD
    43 44 45 #
  RETURN (twice)
NEW
NAME
  radiation
THERMAL
  CAVITY RADIATION
  RADIATION
```

```
CAVITY STATUS: OPEN
SINK TEMPERATURE
    20
VIEWFACTORS: CALCULATE
OK
CAVITIES: ADD
    cavity1
OK
RETURN (twice)
```

Loadcases and Job Parameters

A transient analysis is performed with a fixed time step. The loading consists of two stages, in the first 25 seconds the workpiece is heated, and in the second 10 seconds a temperature relaxation takes place without heating. The time step used is 0.5 seconds, and the excitation frequency is 10 kHz. The axisymmetric magnetodynamic element 112 is selected for all the elements.

```
LOADCASES
MAGNETODYNAMIC-THERMAL
NAME
    heating
TRANSIENT
FREQUENCY
    10000
TOTAL LOADCASE TIME
    25
OK
COPY
NAME
    relaxation
TRANSIENT
LOADS
    load (deselect)
    O
    K
FREQUENCY
    0
```

TOTAL LOADCASE TIME

10

PARAMETERS

STEPS

20

OK (twice)

RETURN (twice)

JOBS

NAME

induction

ELEMENT TYPES

MAGNETODYNAMIC-THERMAL

AXISYM

112

OK

ALL: EXIST

RETURN (twice)

MOR

E

MAGNETODYNAMIC-THERMAL

heating

relaxation

INITIAL LOADS

icond1

OK

JOB RESULTS

1st Real Component Magnetic Induction

2nd Real Component Magnetic Induction

3rd Real Component Magnetic Induction

1st Imag Component Magnetic Induction

2nd Imag Component Magnetic Induction

3rd Imag Component Magnetic Induction

1st Real Comp Current Density

2nd Real Comp Current Density

3rd Real Comp Current Density

1st Imag Comp Current Density

2nd Imag Comp Current Density
3rd Imag Comp Current Density
Temperature
Generated Heat
Electric Current
OK (twice)

Save Model, Run Job, and View Results

After saving the model, the job is submitted and the resulting post file is opened.

```
FILE
  SAVE AS
    tube.mud
  OK
  RETURN
RUN
  NEW-STYLE TABLES
  SUBMIT(1)
  OK
  RETURN
RESULTS
  OPEN DEFAULT
  HISTORY PLOT
  SET NODES
    221 161 #
  COLLECT GLOBAL DATA
  NODES/VARIABLES
  ADD VARIABLE
  Time
  Temperature
  FIT
  RETURN
  SHOW IDS
  0
  YMAX
```

1200
YSTEP
6

Figure 2.18-2 shows the contour plot of the temperature at the end of the heating period, and at the end of the relaxation period. In [Reference 2] at two points, the temperature is measured during the analysis. One point is located at 0.005 m from the tip of the tube, and the other point is located at 0.035 m from the tip of the tube. Figure 2.18-4 shows a history plot of the temperatures of these two points, where a comparison is made with the measured data taken from [Reference 2].

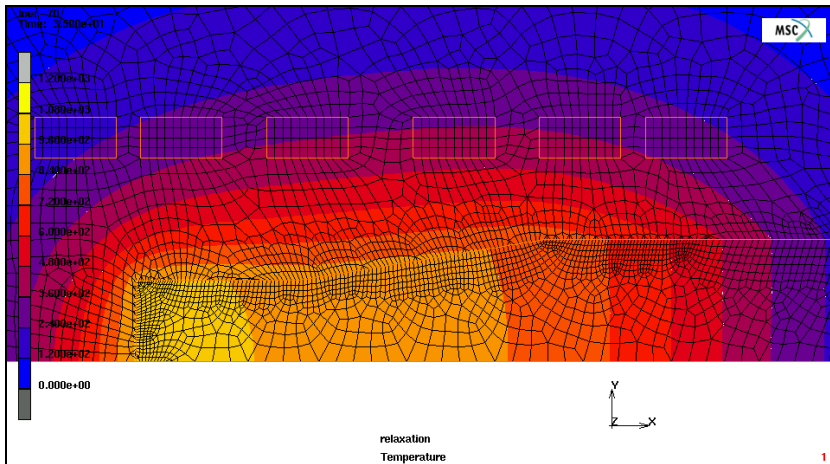
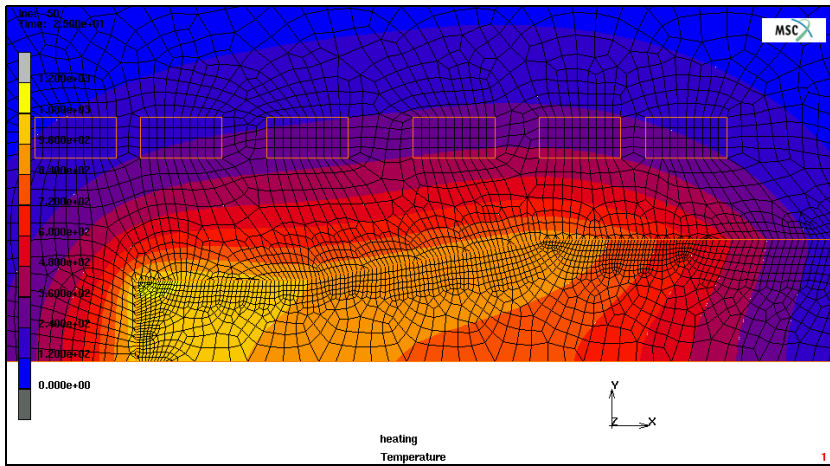


Figure 2.18-2 Contour Plot of the Temperature at the End of the Heating Period, and After the Relaxation Period

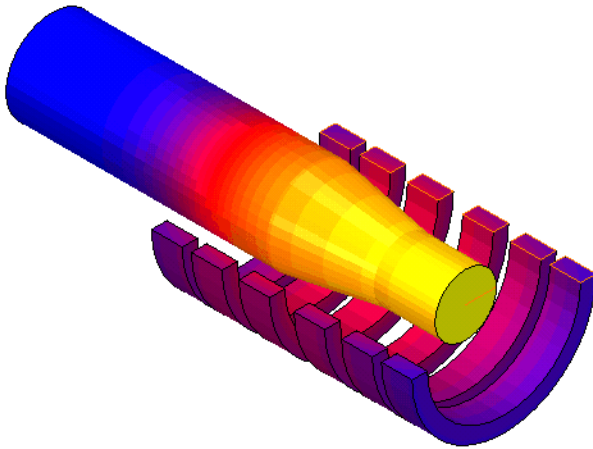


Figure 2.18-3 Contour Plot of the Temperature at the End of the Heating Period Expanded about the Axis of Revolution - Elements Representing the Air are not Drawn,

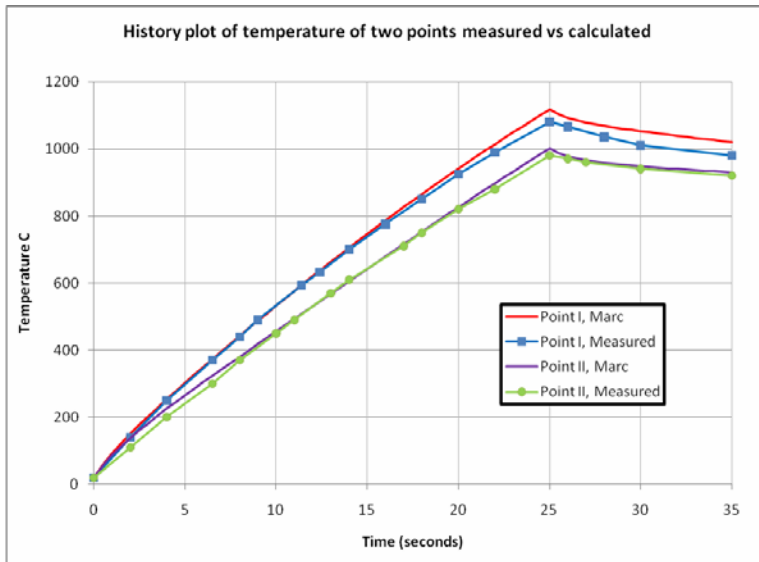


Figure 2.18-4 History Plot of the Temperature at Two Nodes on the Workpiece

References

1. C. Chaboudez, S. Clain, R. Glardon, J. Rappaz, M Swierkosz, and R. Touzani, “Numerical Modelling of Induction Heating of Long Workpieces”, IEEE Trans. Magn., Vol 30, 5026-5037, 1994

2. C. Chaboudez, S. Clain, R. Glardon, D.Mari, J. Rappaz, and M Swierkosz, "Numerical Modeling of Induction Heating of Axisymmetric Geometries", IEEE Trans. Magn., Vol 33, 739-745, 1997

Input Files

The files below are on your [delivery media](#) or they can be downloaded by your web browser by clicking the links (file names) below.

File	Description
tube_heating.proc	Mentat procedure file to run the above example.
tube_heating_post.proc	Mentat procedure file to create Figure 2.18-3 from the post file. This file also contains information on how to create an animation.
view	File containing view settings used by tube_heating_post.proc .
expand.proc	Mentat procedure file used in the post procedure option and called by tube_heating_post.proc . This procedure file created the 3-D representation and is executed at each increment.
tube_geom.mfd	Associated model file.

2.19 Magnetostatics with Tables

- Chapter Overview 636
- Nonlinear Analysis of an Electromagnet Using Tables 636
- Input Files 644

Chapter Overview

This chapter describes the use of tables in a magnetostatic analysis. With this option, a magnetization curve (B-H relation) can be entered in different ways. It is set through the ISOTROPIC or ORTHOTROPIC material option, which contains either the permeability, the inverse permeability, the H-B relation, or the B-H relation. For the H-B relation and the B-H relation, a table has to be given, where for the H-B relation B and B-H relation H is the independent variable. A magnetization can also be prescribed using the permeability or inverse permeability, where a table has to be given which depends on either B, or H. A table can be either a set of data points, or a function. The different ways of defining a magnetization curve will be illustrated in this example. The magnetic field of an electromagnet is computed, where magnetization curves are used for the material inside of the magnet.

Nonlinear Analysis of an Electromagnet Using Tables

In this example, an electromagnet is modeled. This is a planar analysis. [Figure 2.19-1](#) shows the model and its dimensions.

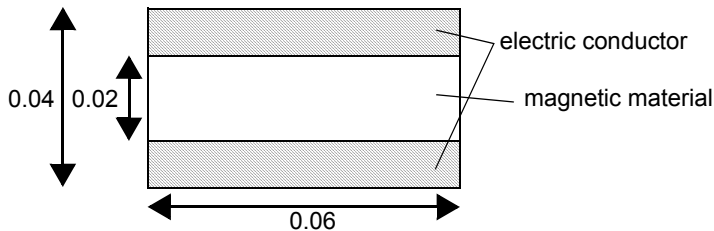


Figure 2.19-1 View of the Electromagnet (Dimensions in m)

The material properties of the material inside the conductors follows magnetization curves, which are prescribed with tables. In this example, a number of ways on how this can be done will be demonstrated. A quarter section of [Figure 2.19-1](#) is modeled using proper boundary conditions to take care of the symmetry.

Reading the Model and Adding Material Properties

The mesh was generated previously, and is read in as an *mfd* file. The magnetization relation for the material inside the electromagnet is defined using the ORTHOTROPIC model definition option with tables. The following equations are used for the magnetization

$$H_x = B_x^5 + 150 \cdot B_x,$$

$$H_y = |B_y| \cdot B_y + 1.5 \cdot B_y,$$

for part of the elements,

$$\mu_x(B_x) = \frac{B_x}{H_x} = \frac{B_x}{B_x^5 + 150 \cdot B_x} = \frac{1}{B_x^4 + 150}$$

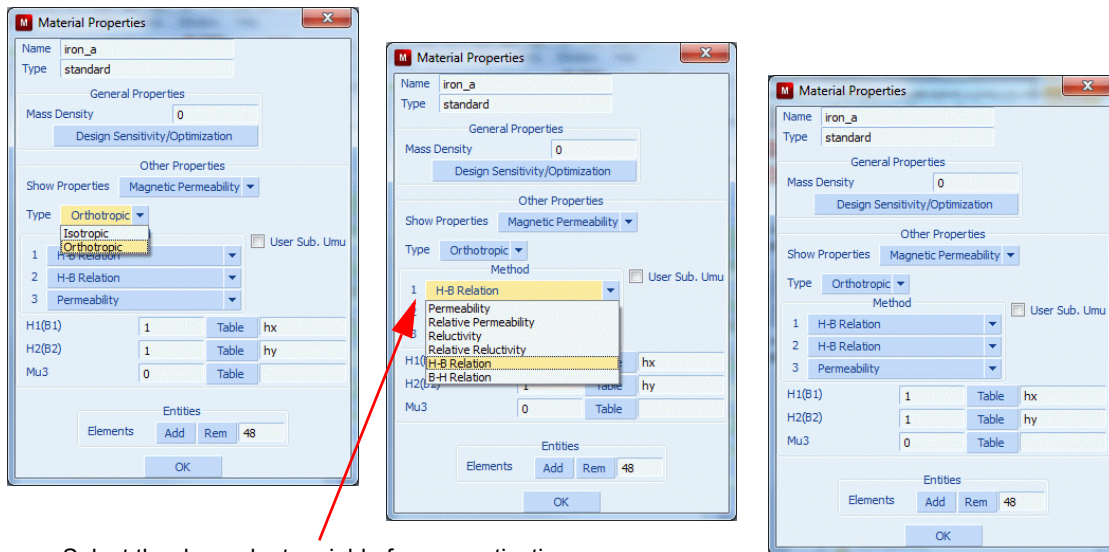
$$\mu_y(B_y) = \frac{B_y}{H_y} = \frac{B_y}{|B_y| \cdot B_y + 1.5 \cdot B_y} = \frac{1}{|B_y| + 1.5},$$

for another part of the elements, and

$$\frac{1}{\mu_x}(B_x) = B_x^4 + 150,$$

$$\frac{1}{\mu_y}(B_y) = |B_y| + 1.5.$$

for the remaining elements inside the conductors. In these equations, B is the independent variable. The permeability for the electric conductor and the air $\mu = 1.2566 \times 10^{-6} \text{ Hm}^{-1}$. Figure 2.19-2 shows the menu for selecting the different magnetization methods.



Select the dependent variable for magnetization

Figure 2.19-2 New Menu Layout for Magnetostatic Material Properties

```

FILE
  RESET PROGRAM
  OPEN
    e1mag.mfd
  OK
  RETURN
    
```

MATERIAL PROPERTIES

MATERIAL PROPERTIES

NAME

air

MORE

MAGNETOSTATIC

PERMEABILITY

1.2566E-6

OK

ELEMENTS ADD

ALL EXISTING

TABLES

NEW

1 INDEPENDENT VARIABLE

NAME

hx

TYPE

magnetic induction

FORMULA

ENTER

$v1^5 + 150.0 * v1$

NEW

1 INDEPENDENT VARIABLE

NAME

hy

TYPE

magnetic induction

FORMULA

ENTER

$abs(v1) * v1 + 1.5 * v1$

NEW

1 INDEPENDENT VARIABLE

NAME

mu_Bx

TYPE

magnetic induction

FORMULA

ENTER

$1.0/(v1^4+150.0)$

NEW

1 INDEPENDENT VARIABLE

NAME

mu_By

TYPE

magnetic induction

FORMULA

ENTER

$1.0/(abs(v1)+1.5)$

NEW

1 INDEPENDENT VARIABLE

NAME

invmu_Bx

TYPE

magnetic induction

FORMULA

ENTER

$v1^4+150.0$

NEW

1 INDEPENDENT VARIABLE

NAME

invmu_By

TYPE

magnetic induction

FORMULA

ENTER

$abs(v1)+1.5$

RETURN

NEW

NAME

iron_a

MAGNETOSTATIC

ORTHOTROPIC

MAGNETIZATION 11 : MAGNETIC FIELD INTENSITY

11 TABLE

hx

MAGNETIZATION 22 : MAGNETIC FIELD INTENSITY

22 TABLE

hy

OK

ELEMENTS ADD

541 to 588

NEW

NAME

iron_b

MAGNETOSTATIC

ORTHOTROPIC

MAGNETIZATION 11 : PERMEABILITY

11 TABLE

mu_Bx

MAGNETIZATION 22 : PERMEABILITY

22 TABLE

mu_By

OK

ELEMENTS ADD

589 to 684

NEW

NAME

iron_C

MAGNETOSTATIC

ORTHOTROPIC

MAGNETIZATION 11 : INVERSE PERMEABILITY

11 TABLE

invmu_Bx


```
MAGNETIZATION 22 : INVERSE PERMEABILITY
22 TABLE
    invmu_By
OK
ELEMENTS ADD
    685 to 732
RETURN (twice)
```

Boundary Conditions

The potential is set to zero on the outer boundary of the model, and along the x-axis to support the inverse symmetry. The potential is left free along the y-axis. The current density in the electric conductor is $2.5 \times 10^8 \text{ Am}^{-2}$.

```
BOUNDARY CONDITIONS
NAME
    current
MAGNETISTATIC
VOLUME CURRENT
    CURRENT
        2.5e8
    OK
ELEMENTS ADD
    733 to 924
NEW
NAME
    fix
FIXED POTENTIAL
    POTENTIAL
    OK
NODES ADD
    274 to 286 561 to 572 12 325 338 351 1 364 377 390 403 429
    442 455 468 481 494 507 520 533 546 559 1725 1779 1 to 13 636
    645 654 663 672 681 690 699 708 717 726 735 288 to 299 #
RETURN (twice)
```

Loadcases and Job Parameters

A steady state analysis is performed, the relative convergence tolerance is set to 1e-4.

LOADCASES

MAGNETOSTATIC

STEADY STATE

CONVERGENCE TESTING

RELATIVE CURRENT TOLERANCE

1e-4

OK (twice)

RETURN (twice)

JOBS

ELEMENT TYPES

MAGNETOSTATIC

PLANAR

39

OK

ALL : EXIST

RETURN (twice)

MORE

MAGNETOSTATIC

lcase1

JOB RESULTS

1st Comp Magnetic Induction

2nd Comp Magnetic Induction

3rd Comp Magnetic Induction

1st Comp Magnetic Field Intensity

2nd Comp Magnetic Field Intensity

3rd Comp Magnetic Field Intensity

OK (twice)

Save Model, Run Job, and View Results

New style tables is selected so that the tables describing the magnetization is used. After saving the model, the job is submitted and the resulting post file is opened. [Figure 2.19-3](#) shows the contour plot of the first component of the magnetic induction. Note that the different magnetization curves used here should all give the same results; so, in this example, the magnetization curves used for the elements can be interchanged, and the computed magnetic induction will be the same. Only small differences can occur due to the different ways the magnetization curves are handled.

```
FILE
  SAVE AS
    electromagnet.mfd
  OK
  RETURN
RUN
  NEW-STYLE TABLES
  SUBMIT(1)
  OK
  RETURN
RESULTS
  OPEN DEFAULT
  NEXT
  CONTOUR BANDS
  SCALAR
    1st Comp Magnetic Induction
  OK
```

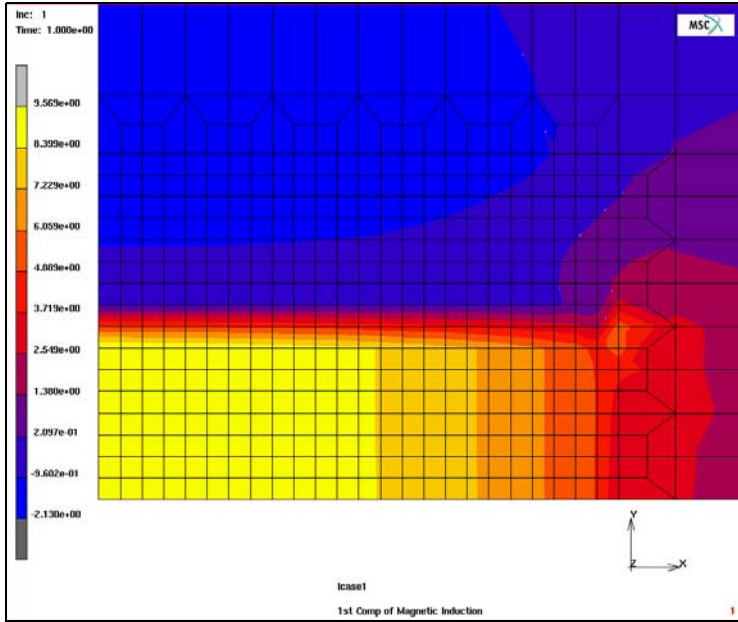


Figure 2.19-3 Contour Plot of the First Component of the Magnetic Induction

Input Files

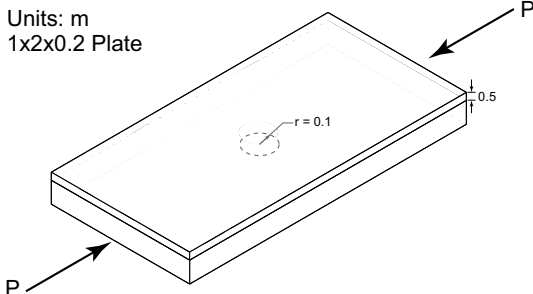
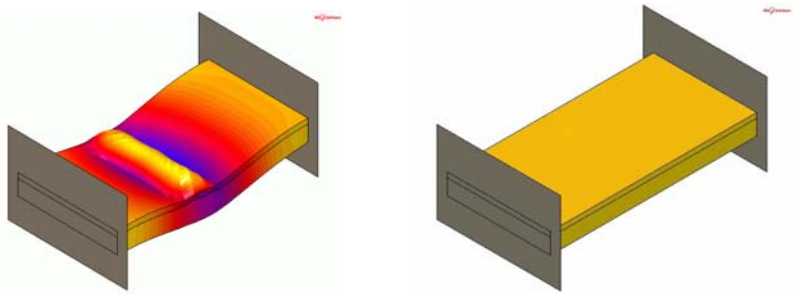
The files below are on your [delivery media](#) or they can be downloaded by your web browser by clicking the links (file names) below.

File	Description
elmag.proc	Mentat procedure file to run the above example
elmag.mfd	Associated model file
elmag.vw	View used by procedure file

2.20 Delamination and Crack Propagation

- Summary 646
- Model Review 647
- Results 651
- Input Files 653

Summary

Title	Delamination Crack Propagation
Problem features	<ul style="list-style-type: none"> • Composite ply delamination. • Crack propagation using Virtual Crack Closure Technique (VCCT) and cohesive zone model
Geometry	<p>Units: m 1x2x0.2 Plate</p> 
Material properties	<p>Composite layup: [0 45 90 -45 0] Orthotropic material: $E_1 = 100\text{ GPa}$ $E_2 = E_3 = 50\text{ GPa}$ $G_{12} = G_{31} = 7\text{ GPa}$ $G_{23} = 8\text{ GPa}$ $\nu_{12} = \nu_{31} = 0.3$ $\nu_{23} = 0.4$ VCCT: $G_c = 5 \times 10^6\text{ N/m}$ Cohesive: $G_c = 7 \times 10^5\text{ N/m}$ $\nu_c = 0.001\text{ m}$</p>
Analysis type	Quasi-static analysis
Boundary conditions	Clamped ends
Applied loads	Compression of the clamped ends, fixed displacement of 0.1
Element type	Solid composite element type 149. Cohesive element 188
Contact properties	Glued contact, deact glue
FE results	<ol style="list-style-type: none"> 1. Plot of updated crack front after growth 2. Plot of damage zone after growth  <p style="text-align: right;">Click to play animation (ESC to stop)</p>

The delamination in a thick composite structure is studied. Two approaches are used: crack propagation by Virtual Crack Closure Technique, VCCT, and damage evolution with a cohesive zone model using interface elements. The composite has four layers, and there is an initial defect between layers 3 and 4. The structure is loaded in compression causing buckling of the part at the initial defect. The defect is then allowed to grow using VCCT for the first example and using a cohesive zone model for the second. The bottom part of the structure is modeled with three-layered solid element with a single element through the thickness. The top part has a single layer and also one element through the thickness.

The VCCT model defines the initial defect by means of the DEACT GLUE option. The nodes at the defect should do regular contact (to avoid penetration). By identifying them as part of a DEACT GLUE region, we tell the program to let them do regular contact even though they are part of a glued interface.

In the cohesive zone model, the top and bottom parts do not touch each other directly. A layer of interface elements is placed between the two parts. These elements have the same topology as standard eight-noded bricks. Here, they have zero thickness in order to model the infinitely thin region between the composite parts. The top part of the composite is glued to the top part of the interface elements and the bottom part of the composite to the bottom part of the interface elements.

In the VCCT case, the two parts are rigidly connected until crack growth occurs. With the interface elements, there is an elastic layer between the parts.

The two different methods are not expected to give the same results. Although both methods can be used for studying this type of problem, they use quite different approaches. With VCCT, the parts have a perfect bonding until crack growth occurs. The user enters a crack growth resistance (G_c) to indicate when the crack should grow. The cohesive zone model uses an elastic layer in the interface. This also influences the deformation of the structure before any damage occurs. The cohesive energy (also denoted as G_c) that is input for the cohesive material law is related to the crack growth resistance in the VCCT case in that both have to do with the energy required to split up material. The way this quantity is used, though, is different in the two approaches and, for this chapter, different values are used for the VCCT case and the cohesive zone case.

Model Review

The Mentat model for the VCCT variant is available in the file `delam_vcct.mfd`. [Figure 2.20-1](#) shows the model with the different contact bodies identified. The top part has a finer mesh in order to accurately describe the defect region and allow the crack to grow.

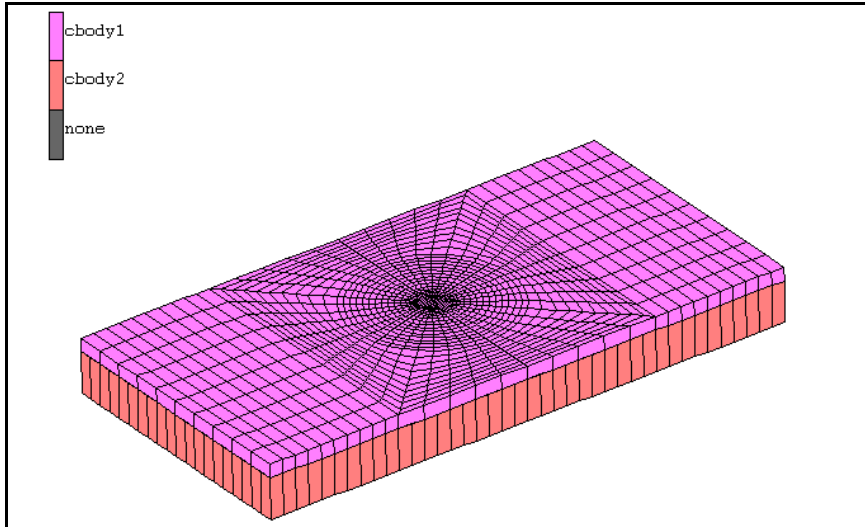


Figure 2.20-1 Model for VCCT Calculation

In [Figure 2.20-2](#), we show the bottom side of the top part, with the DEACT GLUE region and the crack front.

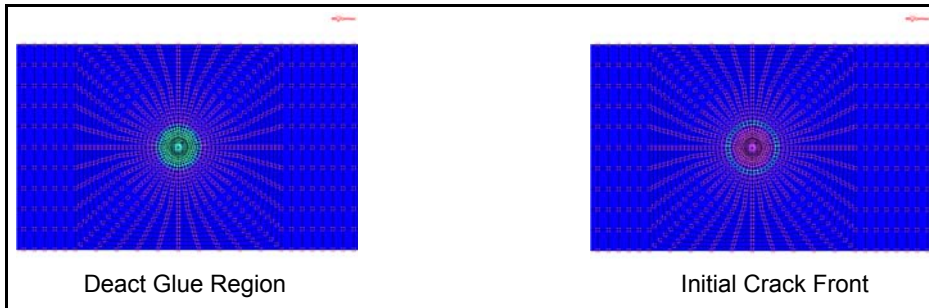


Figure 2.20-2 Deact Glue Region and Initial Crack Front

The DEACT GLUE setting can be found in Mentat under the menu CONTACT -> CONTACT AREAS and the option to use is GLUE DEACTIVATION. The setting for the crack is in MODELING TOOLS -> CRACKS. Here, we select the application to be VCCT, and we fill out the settings for the crack propagation in the CRACK PROPAGATION menu (see [Figure 2.20-3](#)). We make sure to set direct growth, release constraints, and enter the crack growth resistance for when crack growth should occur.

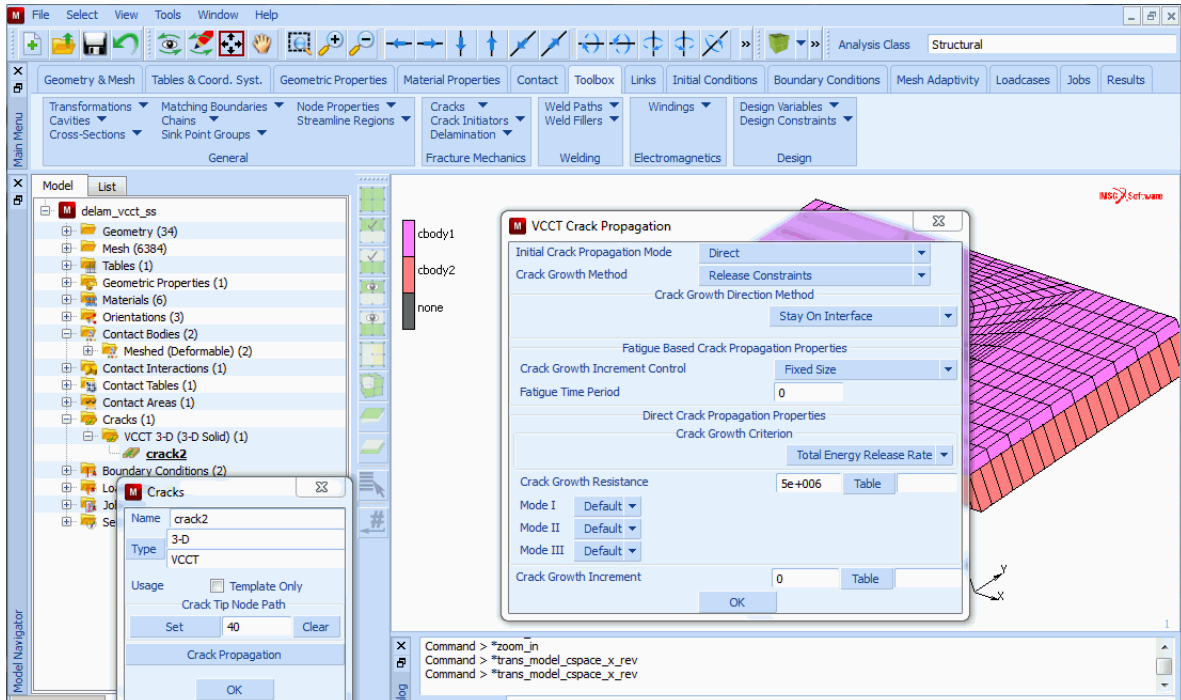


Figure 2.20-3 Mentat Menu for Crack Propagation Settings

The model for the cohesive zone variant is shown in [Figure 2.20-4](#). The top part is using the same mesh as the interface element part. Although this is, strictly speaking, not necessary for the contact glue part, we still need a fine mesh for the deformation of the defect region. It also allows a fair comparison with the VCCT case. From the figure, it is also clear how the initial defect is modeled: as a hole in the part with interface elements.

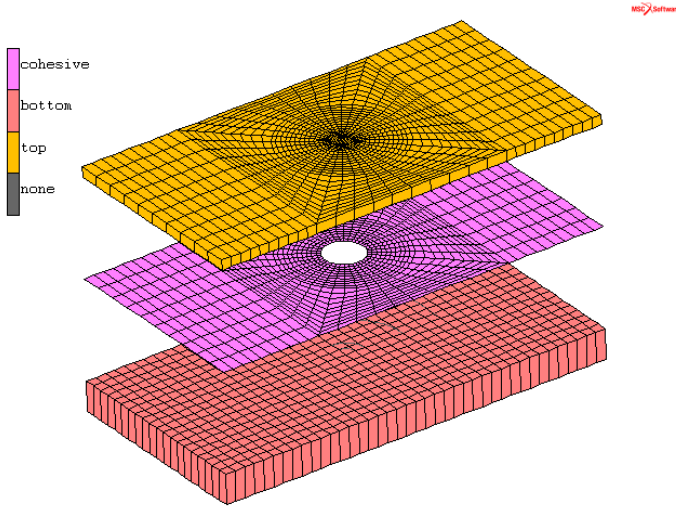


Figure 2.20-4 Exploded View of Cohesive Zone Model

The material properties for the cohesive zone model are given in the menu shown in Figure 2.20-5.

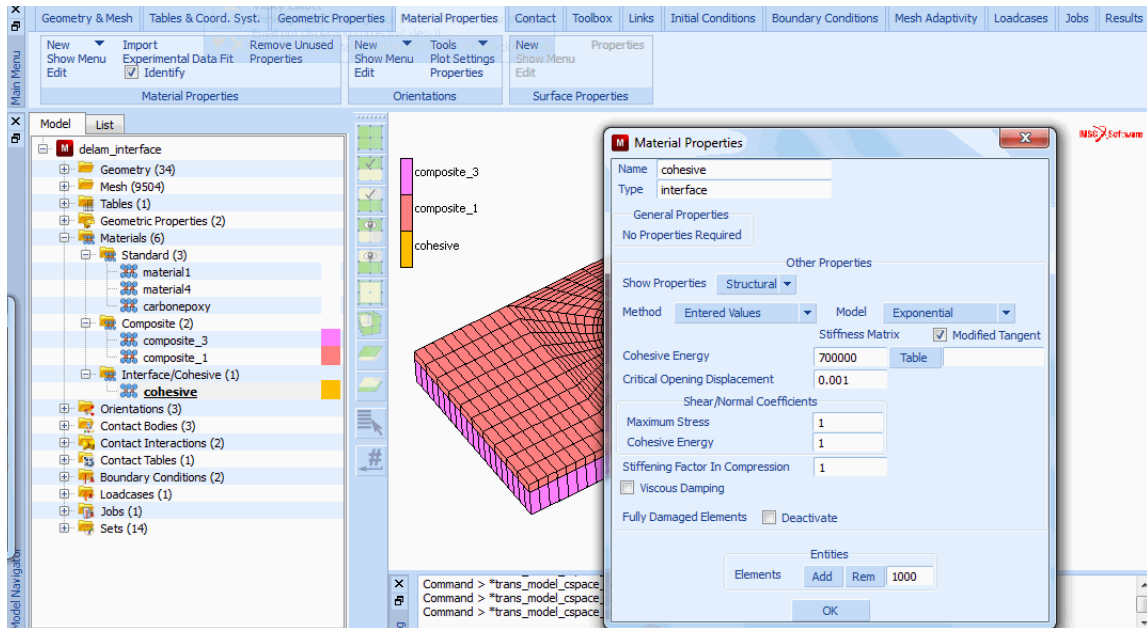


Figure 2.20-5 Mentat Menu for Cohesive Zone Model

Both models use the same settings for the load stepping: 20 fixed steps with a maximum of 20 cycles. The convergence tolerance is set to 0.01. Defaults are used for other control settings.

Results

Figure 2.20-6 shows the deformed shape for the two models. The plate bends down and the region with the defect buckles. The VCCT and cohesive variants show a little difference in how much the defect grows. This, of course, changes with the selected values for VCCT and the cohesive material.

Figure 2.20-7 shows how much the crack has grown in the VCCT case. The arrows show the x-coordinate of the local crack tip system for each crack tip. It starts out as a circular crack, and the crack front is allowed to grow nonuniformly. The VCCT evaluation and crack growth stops as soon as the crack reaches an outer boundary. Note that no specification is needed about the sequence of the crack nodes as it grows; this is automatically determined by the program. The user only provides the initial crack front and an interface along which the crack can grow. It is important to give a reasonable regular mesh in order to get accurate results.

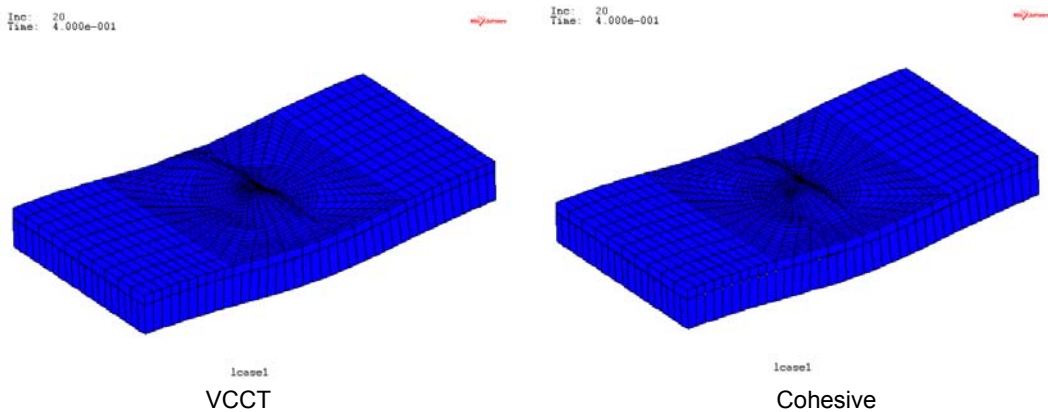


Figure 2.20-6 Overall Deformed Shape

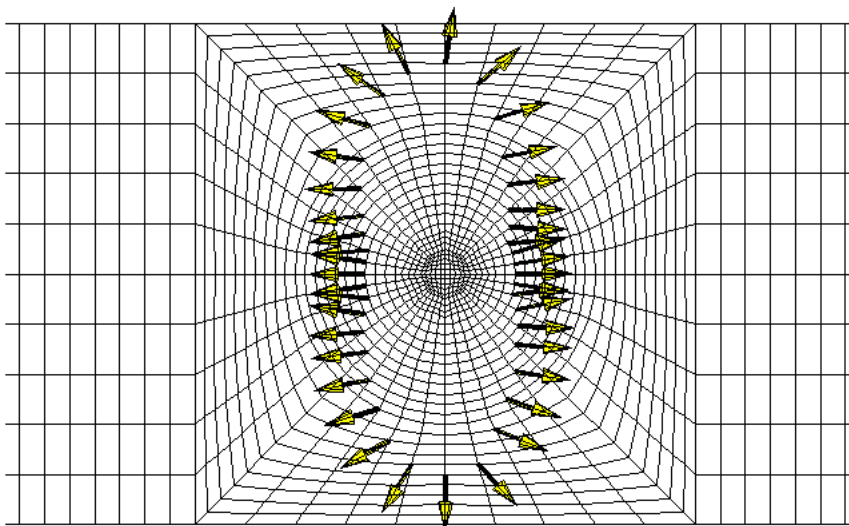


Figure 2.20-7 Crack Front at Final Load (Arrows show X-coordinate of Crack Tip System)

The damaged zone for the cohesive zone model is shown in Figure 2.20-8. The yellow portion in the middle indicates where full damage occurs. The damage occurs in the interface elements, and there is no sharp crack front as in the VCCT case. Here, we have larger freedom in designing the mesh.

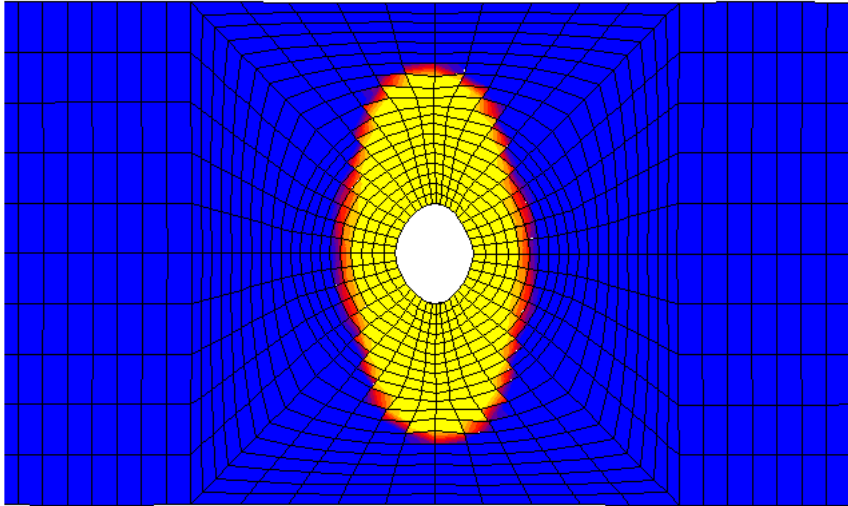
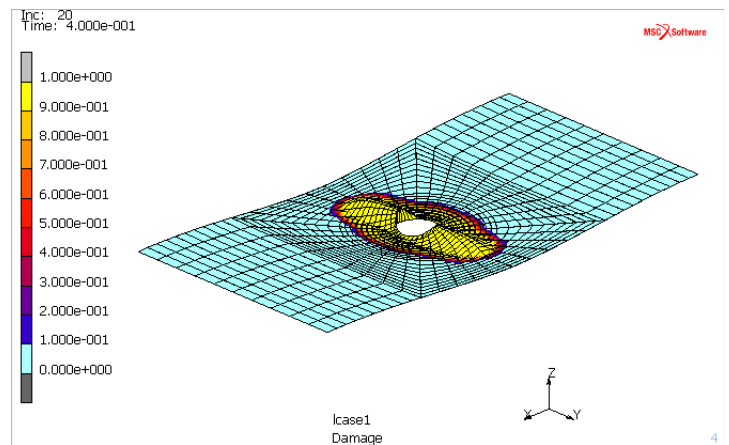
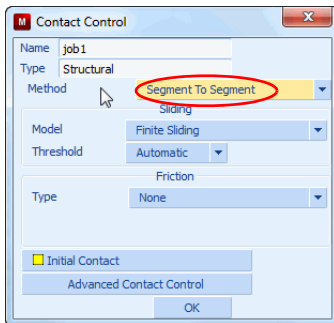


Figure 2.20-8 Extent of Damage Zone for Interface Elements at Final Load

As an alternative one can use the segment-to-segment contact method with this model. In this case, double-sided contact is used. This capability is activated using the Job Contact Control menu as shown below. The resultant damage on the deformed geometry is also shown.



Damage based upon Segment-to-segment Contact Method

Input Files

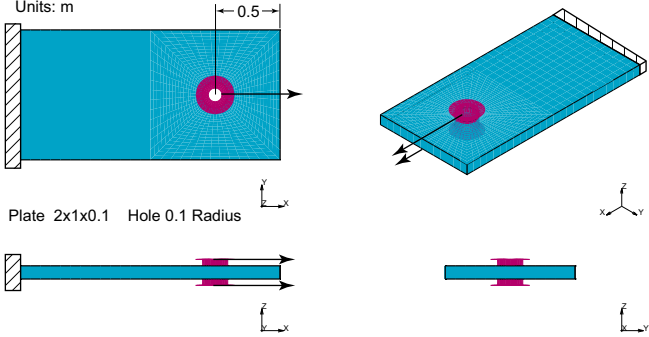
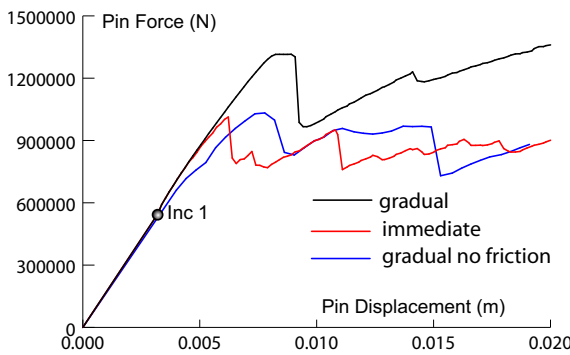
The files below are on your [delivery media](#) or they can be downloaded by your web browser by clicking the links (file names) below.

File	Description
delam_vcct.proc	Mentat procedure file to run the above example
delam_interface.proc	Mentat procedure file to run the above example
delam_vcct.mfd	Associated model file
delam_interface.mfd	Associated model file
delam_vcct_job1.dat	Associated model file
delam_interface_job1.dat	Associated model file

2.21 Progressive Failure Analysis of Lap Joint

- Summary 656
- Model Review 657
- Results 658
- Modeling Tips 660
- Input Files 661

Summary

Title	Progressive Failure Analysis of Lap Joint
Problem features	<ul style="list-style-type: none"> • Progressive failure analysis • Composite material
Geometry	 <p>Units: m</p> <p>Hole 0.1 Radius</p> <p>Plate 2x1x0.1</p>
Material properties	<p>Composite layup: 5 layers of equal thickness [0 45 90 -45 0]</p> <p>Orthotropic material: $E_1 = 100\text{ GPa}$ $E_2 = E_3 = 50\text{ GPa}$</p> <p>$G_{12} = G_{31} = 7\text{ GPa}$ $G_{23} = 8\text{ GPa}$ $\nu_{12} = \nu_{31} = 0.3$ $\nu_{23} = 0.4$</p> <p>See Figure 2.21-2 for Failure Data.</p>
Analysis type	Quasi-static analysis
Boundary conditions	Clamped end, rigid body contact
Applied loads	Forced motion of rigid body
Element type	Layered solid shell
Contact properties	Rigid body contact, bilinear friction, $\mu = 0.3$
FE results	<ol style="list-style-type: none"> 1. Plot of damage zone 2. Force–displacement curves 

This chapter studies progressive failure of a lap joint. A composite plate has a hole with a bolt in it, where the bolt is modeled as a rigid body. One end of the plate is clamped, and the rigid pin has a forced motion associated with it. This simulates a symmetric lap joint with a pin which is much stiffer than the composite plate.

The composite material can suffer damage due to excessive loading. The Puck failure criterion is used to indicate failure. The progressive failure option is used for degrading the material properties as failure occurs. The Puck method is used here since it allows separate degradation due to fiber and matrix failure. The matrix material of the composite is weaker than the fiber. When failure occurs in the matrix in a certain layer, the structure can still carry a substantial load due to the undamaged fibers in other layers.

Two of the supported options for degrading the material properties are studied in this chapter: the gradual and immediate reduction methods with selective degradation. In the gradual method, after damage has occurred, the material is assumed to also sustain loading. The stiffness is reduced only so much that the largest failure index stays below 1.0. With immediate stiffness reduction variant, the material stiffness is set to the minimum value as soon as damage is indicated. This corresponds to a brittle behavior of the material.

Model Review

The base model is available in the Mentat database `pinplate.mfd`. The model used is shown in [Figure 2.21-1](#). The figure also shows the material orientation.

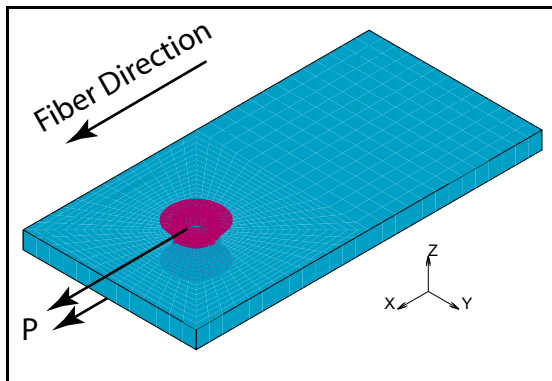


Figure 2.21-1 Model used for PFA analysis

The settings for the progressive failure are done in the menus as shown in [Figure 2.21-2](#). There we see that we have chosen the GRADUAL SELECTIVE option for progressive failure, and it also shows the material parameters used for the Puck failure criterion. We define all four failure envelope slopes since we are using solid elements. For plane stress shells, we only specify the first two and let the program calculate the others. We use the defaults for the residual stiffness factor and the options for stiffness reduction. The latter are used if we want to control in more detail how the different moduli are degraded. We also have the option of using the UPROGFAIL user subroutine for specifying the reduction factors, but it is not used here.

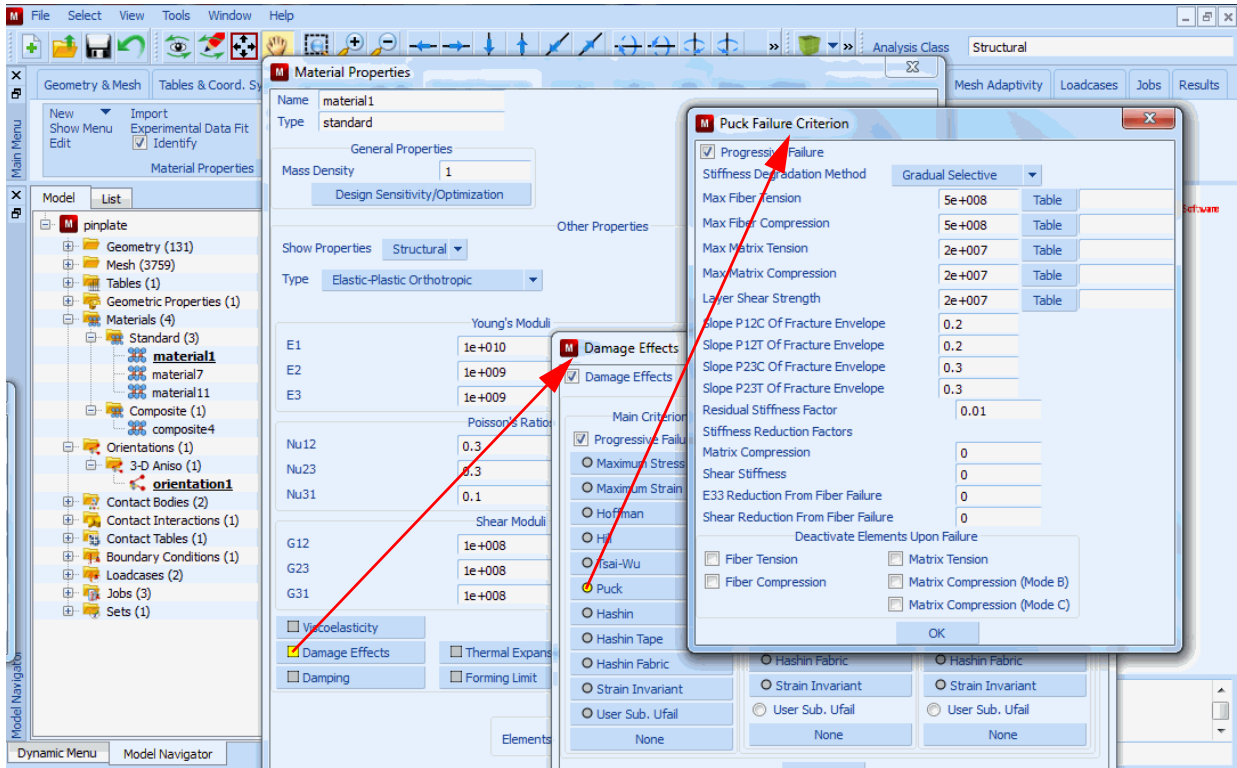


Figure 2.21-2 Menus for the Progressive Failure Settings

The analysis is done in two load cases. The first load case does one increment up to a load level which is close to where the first failure occurs. The second load case has 100 increments, and the step size is small in order to properly capture the damage of the material.

Results

Figure 2.21-3 shows a plot of the third failure index for the fourth layer at the end of the first load case. This failure index corresponds to matrix tension. This is the largest failure index and it indicates where the first failure will occur, as can also be seen in Figure 2.21-4. This layer is in the -45° direction. With increasing load, there is more failure. Figure 2.21-5 shows the failure in the mid (90°) layer. The failure in this layer starts out in front of the pin and spreads out with increasing load. At some point, there is a drastic stiffness reduction in the structure as several elements fail at the same time. The force-displacement curve for the rigid body is shown in Figure 2.21-6. Here, we clearly see the sudden drop in structural stiffness but that the structure can continue to carry load. We see that the failed elements tend to bulge up along the rigid pin.

Figure 2.21-6 illustrates the case of using the immediate stiffness degradation method. The sudden drop in structural stiffness comes much earlier as compared with the gradual degradation. This shows the brittle effect of this method. The structure can still continue to carry an increased load since there are layers with intact fibers.

Figure 2.21-6 also illustrates the effect of friction on the example. The gradual stiffness reduction option is used, and here we clearly see the effect of friction. Without friction, the failure is more localized to the compressed part of the structure next to the pin, and the largest load is substantially lower. The maximum load is closer to the case with immediate stiffness reduction.

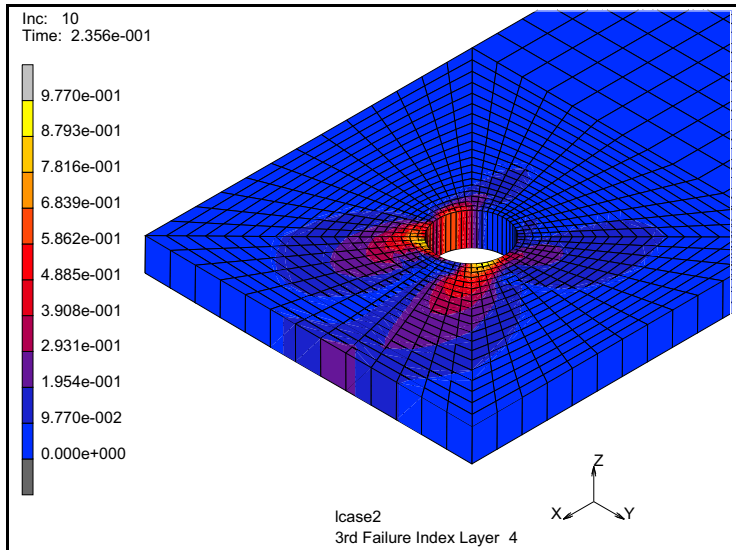


Figure 2.21-3 Largest Failure Index Before Failure Occurs

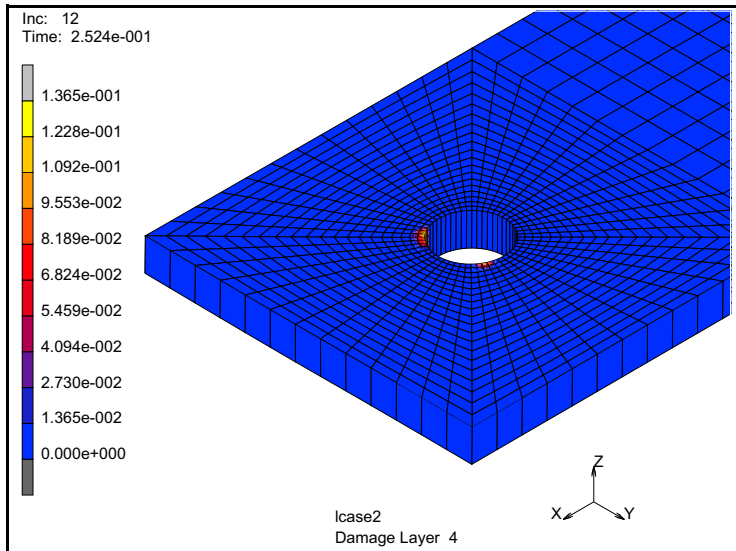


Figure 2.21-4 First Occurrence of Failure

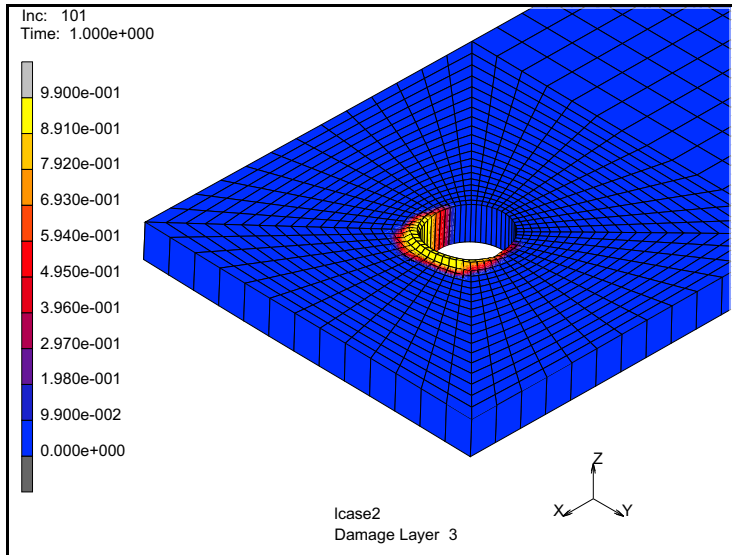


Figure 2.21-5 Damage in Mid-layer at Final Load

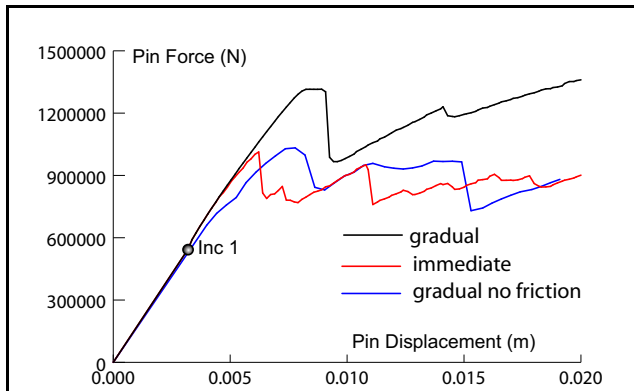


Figure 2.21-6 Pin Force versus Pin Displacement for all Three Cases

Modeling Tips

When a lot of damage takes place, it is often difficult to obtain convergence. If unstable growth of the damage zone occurs, it may even not be possible to obtain a solution for a certain load level. It is important to allow for more recycles than one would normally do in a geometrically nonlinear analysis.

Using automatic time stepping with damping may stabilize the solution. This should be used with care, since too much damping easily destroy the real solution.

The elements that suffer severe damage tend to cause convergence problems as they have a low stiffness. This can be avoided by using the deactivation option. Elements that have full failure in all integration points can be deactivated, and this can be chosen for selected failure modes.

Input Files

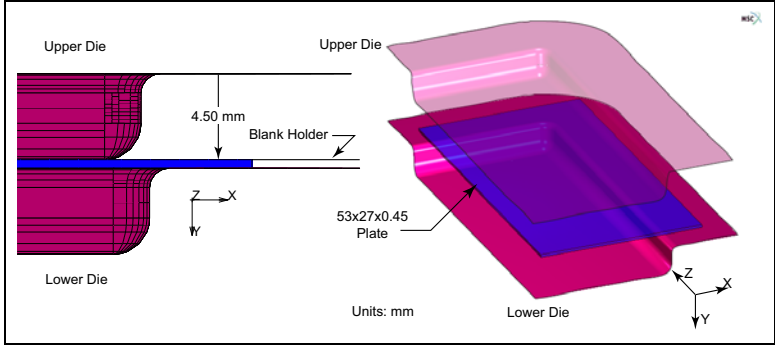
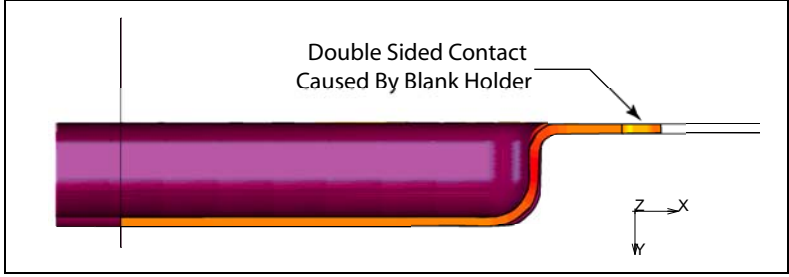
The files below are on your [delivery media](#) or they can be downloaded by your web browser by clicking the links (file names) below.

File	Description
pinplate_immediate.proc	Mentat procedure file to run the above example
pinplate_gradual.proc	Mentat procedure file to run the above example
pinplate.mfd	Associated model file
pinplate_immediate.dat	Associated Marc file
pinplate_gradual.dat	Associated Marc file

2.22 Sheet Metal Forming With Solid Shell Elements

- Summary 664
- Model Review 665
- Results 667
- Input Files 668

Summary

Title	Sheet Metal Forming With Solid Shell Elements
Problem features	<ul style="list-style-type: none"> • Solid shell elements facilitate blank holders, shell elements cannot. • Mentat reading the Marc input file history definition.
Geometry	 <p>The diagram illustrates the geometry of a sheet metal forming process. It shows an upper die and a lower die forming a rectangular plate. A blank holder is positioned to hold the plate against the dies. The plate dimensions are 53x27x0.45 mm. A coordinate system with X, Y, and Z axes is provided. The units are in millimeters.</p>
Material properties	$E_{\text{cylinder}} = 210 \times 10^9 \text{ Pa}$, $\nu = 0.3$, $\frac{d\sigma}{d\varepsilon_p} = 6.5 \times 10^7 \text{ Pa}$
Analysis type	Quasi-static analysis
Boundary conditions	Symmetric displacement constraints along two symmetry planes.
Applied loads	Upper die is displaced 4.5 mm in the y-direction.
Element type	Solid shell element type 185. Compare to stacked bricks type 7.
Contact properties	Coefficient of friction $\mu = 0.0$ and $\mu = 0.3$
FE results	<ol style="list-style-type: none"> 1. Contour plot of plate thickness, equivalent plastic strain 2. History plot of die load versus stroke  <p>The diagram shows a cross-section of the plate and blank holder. The blank holder is shown in contact with both sides of the plate, labeled as 'Double Sided Contact Caused By Blank Holder'. A coordinate system with X, Y, and Z axes is shown.</p>

Higher formability and accuracy for sheet metal forming can be achieved by using blank holders and varying the holder force during the forming process. Unfortunately, shell elements cannot sustain double-sided contact where the shell is approached by the dies from both sides. Solid elements can sustain double-sided contact but require stacking in the thickness direction in order to improve bending characteristics. The stacked bricks generate many degrees of freedom and requires computer times from days to weeks instead of hours. The solid-shell element, type 185, is specially formulated to overcome this situation by simulating a shell type element while facilitating double-sided contact.

Model Review

The mesh building of a similar structure can be found in Chapter 3.16, similar steps are not repeated here other than mention that the flat plate is made of solid shells, element type 185 instead of the 3-D membrane elements used in Chapter 3.16. The solid-shell element designed for plate or shell type geometry (where the thickness, t , is much smaller than the in-plane length, L) begins to lose accuracy when the element's aspect ratio (t/L) drops below $1/100$. Another feature of element type 185 is that it defines the thickness direction as normal to the first face created by the first four nodes in the elements connectivity (Figure 2.22-3), and the thickness of the element can be contour plotted.

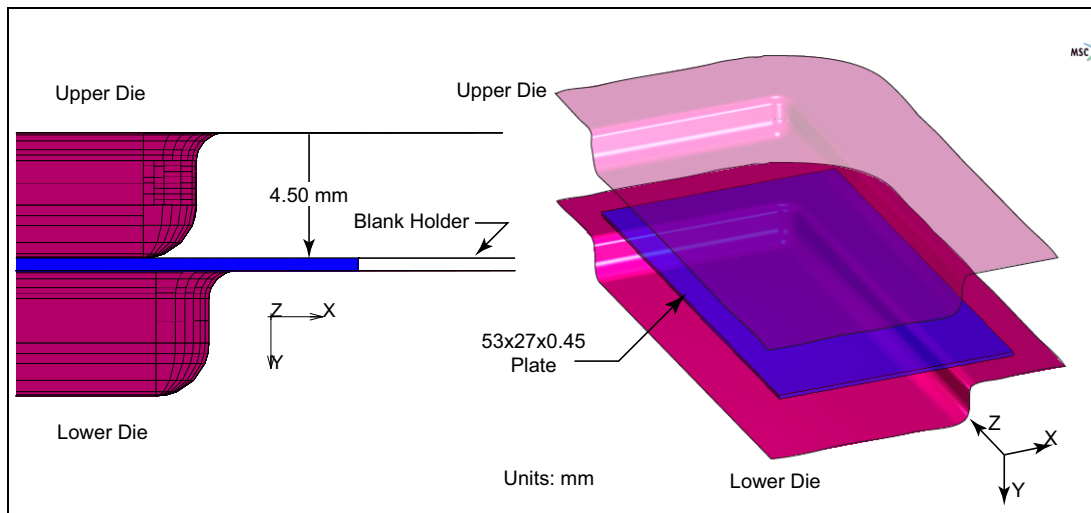


Figure 2.22-1 Sheet and Die Geometry

Let's suppose this model has already been built and exists as a Marc input file named `sheetform.dat`, and then read this file into Mentat. Unlike previous versions of Mentat, the history definition of the model is obtained. The model is saved, and the job is submitted as shown below.

```
FILES
MARC INPUT FILE READ
  sheetform.dat
OK
SAVE AS
```

sheetform
OK
MAIN

You can review the model in Mentat or preview the assembly in [Figure 2.22-2](#).

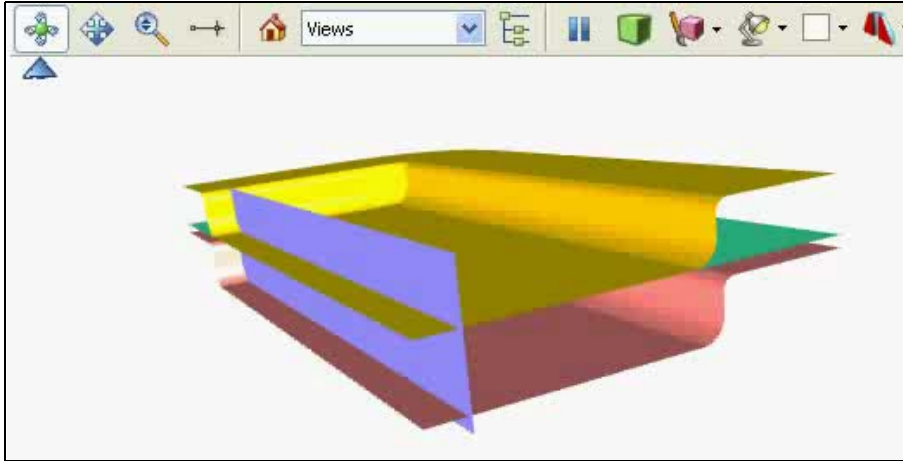


Figure 2.22-2 3D Assembly View - Click Above to Activate 3-D (ESC to stop)

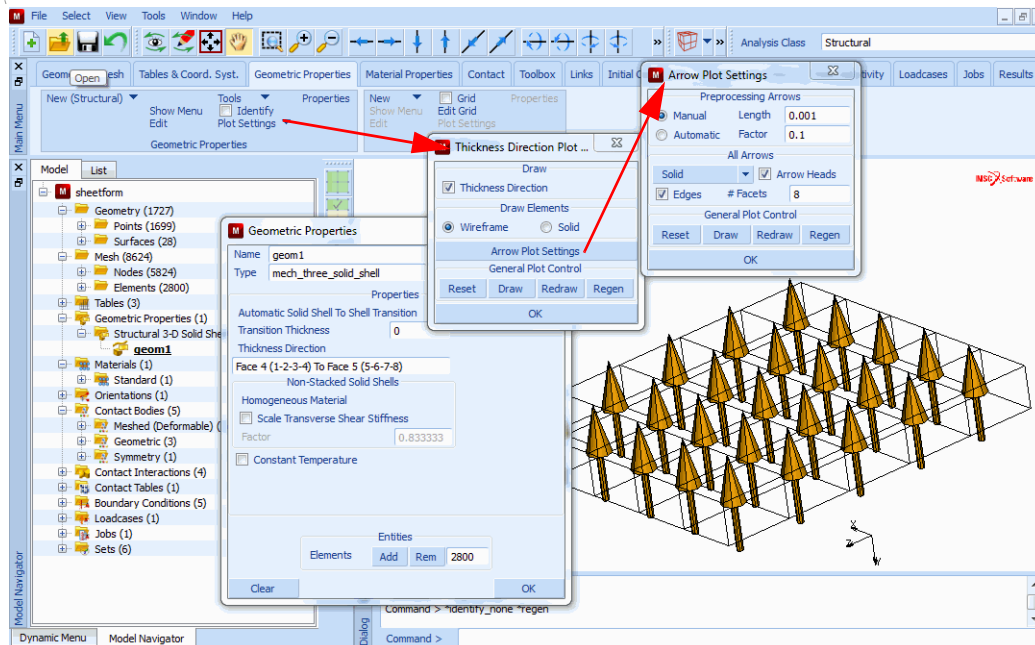


Figure 2.22-3 Visualization of Thickness Orientation for Solid-Shell Elements

Now the job can be submitted, and as the results become available they can be viewed by opening the post file as:

```
JOBS
  RUN
    SUBMIT

  OPEN POST FILE (RESULTS MENU)
```

and we begin examining the results.

Results

The model read from disk already had friction selected. The no friction case is a new job that simply turns off the friction. Comparing the frictionless and friction results, we see that the friction case gives a substantially thinner sheet, particularly in the corner as shown in [Figure 2.22-4](#).

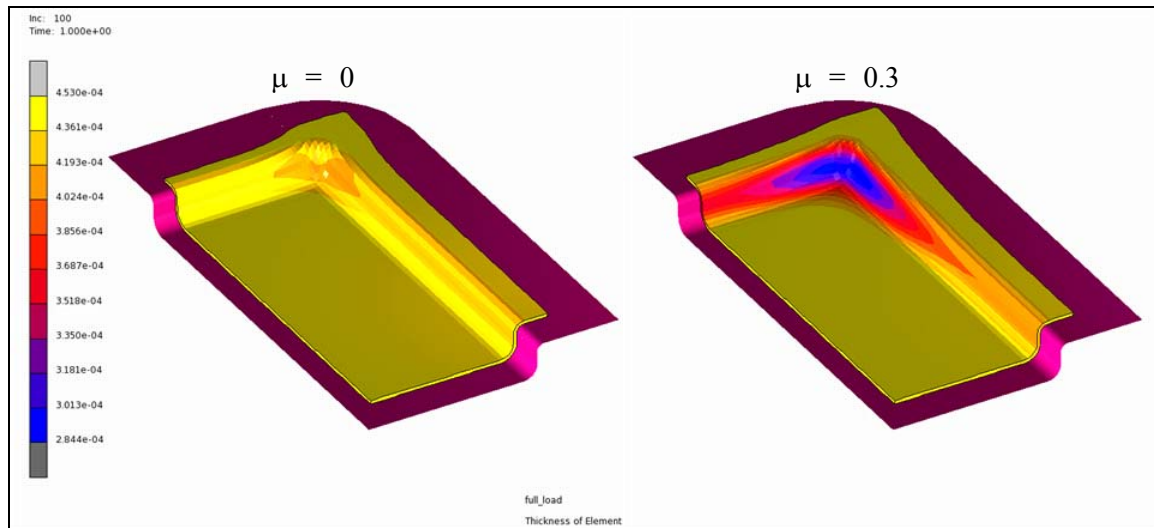


Figure 2.22-4 Thickness Contours With and Without Friction

Upon closer examination of the two jobs using the path plot for a section from point A (Node 5290) to B (Node 5330) in [Figure 2.22-5](#), the friction drops the thickness from 0.45 mm to 0.28 mm, whereas there is only a small drop in thickness for the frictionless case to 0.40 mm.

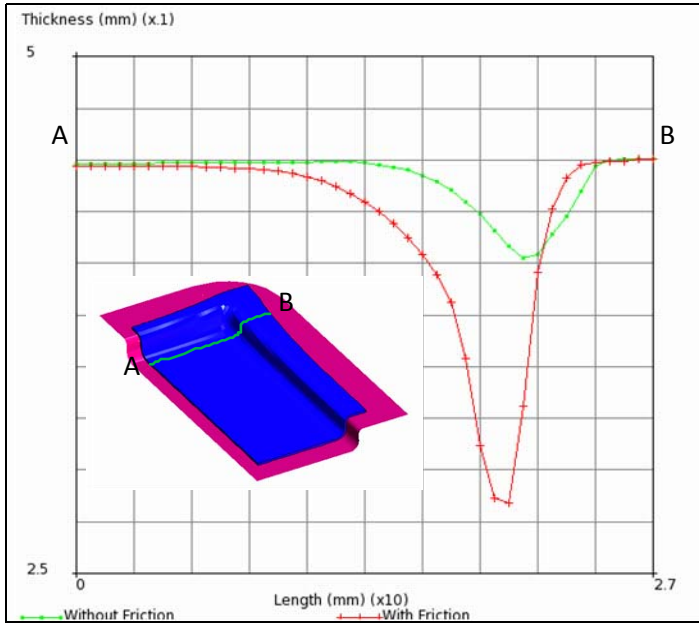


Figure 2.22-5 Thickness Profile

Input Files

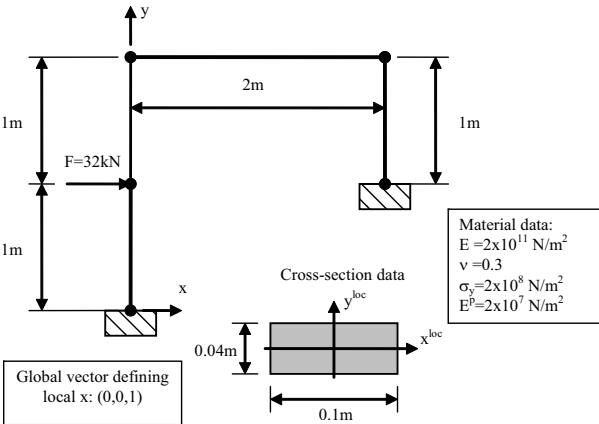
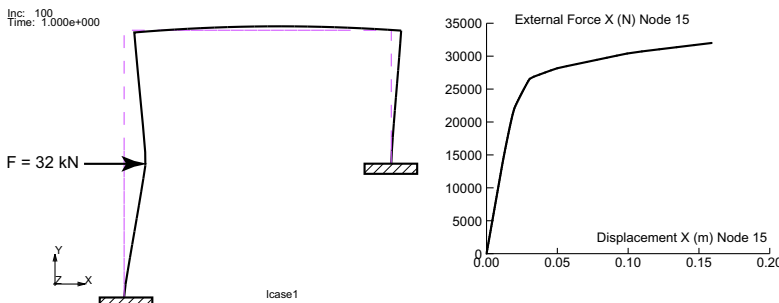
The files below are on your delivery media or they can be downloaded by your web browser by clicking the links (file names) below.

File	Description
sheetform.proc	Mentat procedure file to run the above example
sheetform.mud	Associated model file
sheetform.dat	Associated Marc file

2.23 Plastic Limit Load Analysis of a Simple Frame Structure

- Summary 670
- Detailed Marc Input Description 671
- Detailed Mentat Session Description 673
- Results 674
- Modeling Tips 675
- Input Files 675

Summary

Title	Plastic Limit Load Analysis of a Simple Frame Structure
Problem features	Beam element type 52 is used with a rectangular cross-section that can account for plastic deformation through the section by performing numerical integration of the nonlinear material behavior across the cross section.
Geometry	 <p>Material data: $E = 2 \times 10^{11} \text{ N/m}^2$ $\nu = 0.3$ $\sigma_y = 2 \times 10^8 \text{ N/m}^2$ $E^p = 2 \times 10^7 \text{ N/m}^2$</p> <p>Global vector defining local x: (0,0,1)</p> <p>Cross-section data: 0.04m 0.1m</p>
Material properties	$E = 200 \text{ GPa}$, $\nu = 0.3$, Initial yield strength, $\sigma_y = 200 \text{ MPa}$, $d\sigma/d\epsilon_p = 20 \text{ Mpa}$
Analysis type	Nonlinear static analysis
Boundary conditions	Fully clamped in the two supports
Applied loads	Apply a load of 32 kN in x-direction half way the 2m high vertical member
Element type	Beam element type 52
Cross-section properties	Rectangular cross-section, 0.1 m x 0.04 m, using a 5x5 Simpson numerical integration rule
FE results	<p>Deformed frame structure and force displacement response of the loaded point</p>  <p>Inc: 100 Time: 1.000e+000</p> <p>$F = 32 \text{ kN}$</p> <p>External Force X (N) Node 15</p> <p>Displacement X (m) Node 15</p> <p>case1</p>

The simple frame structure in the [Summary](#) is loaded by a horizontal load of 32 kN with its associated geometry, cross-section properties and material data. The material is elastic-plastic with a small isotropic work hardening slope in the plastic range. The maximum load of 32 kN is close to the plastic limit load of the structure. The material data relevant in this analysis are: Young's modulus, Poisson's ratio, initial yield strength, and the plastic work hardening slope.

Detailed Marc Input Description

This section describes the Marc input file where tables are used in the old input format. The input file is: `limit_load_old_job1.dat`.

The beam element type used in this analysis is type 52, and it is used with numerical integration over its cross section. The `LARGE STRAIN` parameter has been activated, since it is anticipated that when the cross section turns fully plastic in some locations, the deflections of the frame may become larger than acceptable in a geometrically linear analysis. The cross-section properties are defined in the `BEAM SECT` parameter and its definition is shown in the block below.

```
beam sect
rectangle
0,-2.0,0.1,0.04
...
...
last
```

Beam Sect Parameter Definition

The line following the `beam sect` keyword defines the title of this section. The line following the title specifies the type of section and its dimensions. The first field is zero, meaning a standard section is used. The second field specifies the section type is rectangular. The third and fourth fields specify the dimensions of the rectangle. Then follow two blank lines (represented by the two dotted lines). The first blank line means that the default 5 x 5 Simpson rule is used for the cross-section integration and that numerical integration is used throughout the analysis. This is important, because the cross section will first develop plasticity in its outer fibers and the plastic zone will gradually grow inward. The next blank line has no meaning in this analysis. The `BEAM SECT` parameter definition is concluded with the keyword `last`.

The material data is defined through the `ISOTROPIC` and `WORK HARD` options and is listed in the block below.

```
isotropic
...
1,von mises,isotropic
2e11,0.3,1.0,0.0,2.0e8
4 to 53
work hard,data
2,0,1,
2.0e8,0.0
2.2e8,1.0
```

Material Definition

The ISOTROPIC option defines a material with `id=1` using the von Mises yield surface and isotropic hardening. Its data line defines the elastic material properties and the initial yield stress. The WORK HARD option defines the plastic hardening data. It defines two yield limits: one at zero plastic deformation and one at a plastic strain value of 1.

The GEOMETRY option input assigns the cross-section properties to all the elements. In this case, it refers to the first (and only) section defined in the BEAM SECT parameter by entering a zero in the 1st field and the beam section number in the 2nd field. Through the 4th, 5th, and 6th fields, it specifies a vector in the global coordinate system that defines the local x-direction of the cross section. The input is listed in the block below.

```
geometry
...
0.0,1.0,0.0,0.0,0.0,1.0
4 to 53
```

Geometry Definition

The two nodes in the supports (nodes 1 and 4) are fully clamped. These boundary conditions are defined through the FIXED DISP and the input is listed in the block below.

```
fixed disp
...
0.0,0.0,0.0,0.0,0.0,0.0
1,2,3,4,5,6
1,4
```

Boundary Conditions at Frame Supports

The POST option defines the element quantities that are desired for further postprocessing. The element quantities requested in this case are the equivalent von Mises stress (code 17) in layers 3, 8, 13, 18, and 23. These represent the integration points at $x=0$ and $y=-0.02$, $y=-0.01$, $y=0.0$, $y=0.01$ and $y=0.02$, respectively, in the cross section which can be verified from the BEAM SECT output written to the analysis output (.out) file. Post code 265 is the generalized bending moment about the local x-axis of the cross section. The POST option input is listed in the block below.

```
post
6,
17,3
17,8
17,13
17,18
17,23
265,0
```

Output Quantities Requested for Postprocessing

The END OPTION input concludes the model definition. All input following this line is part of the history input. The total load of 32 kN is subdivided into 100 equal steps and is defined through the AUTO LOAD, TIME STEP, and POINT LOAD options in the history input. The load definition input is listed in the block below.

```
auto load
100,0,10
```



```
time step
0.01,
point load
...
3.2e2,
15
continue
Load history applied to the frame structure
```

Detailed Mentat Session Description

This section describes the Mentat menus that are used to define a solid cross section that employs numerical integration and, thus, can account for nonlinear material behavior. The complete input for the frame model, including the cross-section definition described here, can be generated in Mentat by running the procedure file:

```
limit_load_new.proc.
```

Beam cross-sections are defined in the GEOMETRIC PROPERTIES main menu. Beam element types 52 and 98 are three-dimensional beam elements; therefore we enter the 3-D submenu as shown in [Figure 2.23-1](#). For 3-D beam elements, we have the choice between solid cross-sections or thin-walled cross-sections. For element types 52 or 98, we enter the SOLID SECTION BEAM menu. We can set the desired type through the ELEMENT TYPES menu. The PROPERTIES switch determines if the properties are CALCULATED by numerical integration or if they are ENTERED directly. Here, we choose CALCULATED, because we need to account for plastic deformations in the cross section. In the SHAPE menu, we can toggle through a number of standard cross-section geometries. We choose RECTANGULAR for our purpose and define the dimensions of the rectangle through the DIMENSION A (=0.1) and the DIMENSION B (=0.04) inputs. The MATERIAL BEHAVIOR in the section is set to GENERAL to allow for plastic deformations. It can also be set to LINEAR ELASTIC ONLY, in which case the cross-section properties like area A and moments of area I_{xx} and I_{yy} are computed by numerical integration prior to the start of the analysis (i.e., pre-integrated) and no further numerical integration over the cross section is carried out during the analysis. The section uses the default integration scheme which for a rectangular section is a 5x5 Simpson scheme. Finally, the three components of the VECTOR DEFINING LOCAL ZX-PLANE are entered which define the orientation of the cross section in space. In this example, it is expedient to use a vector pointing in global z-direction for all beam elements in the model.

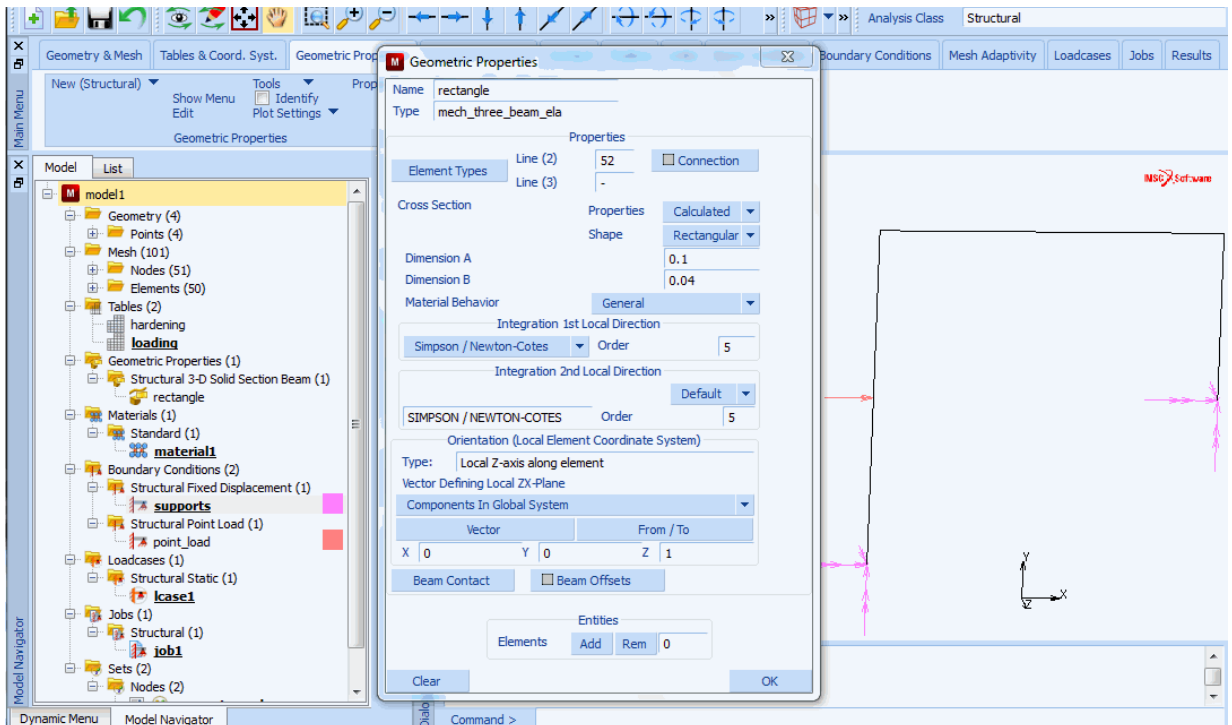


Figure 2.23-1 Creating a Solid Rectangular Cross-section Definition

Results

The results of the analysis are shown in Figure 2.23-2. It displays the deformed frame after application of the full load and the force-displacement curve of the external load versus the displacement of the loaded point. Initially, the behavior of the frame is elastic. At a certain stage, some locations develop plasticity and the stiffness is reduced. At a later stage, some locations completely turn plastic. At this stage, the load carrying capacity of the frame is almost exhausted. The maximum horizontal displacement of the loaded point is 0.159 m.

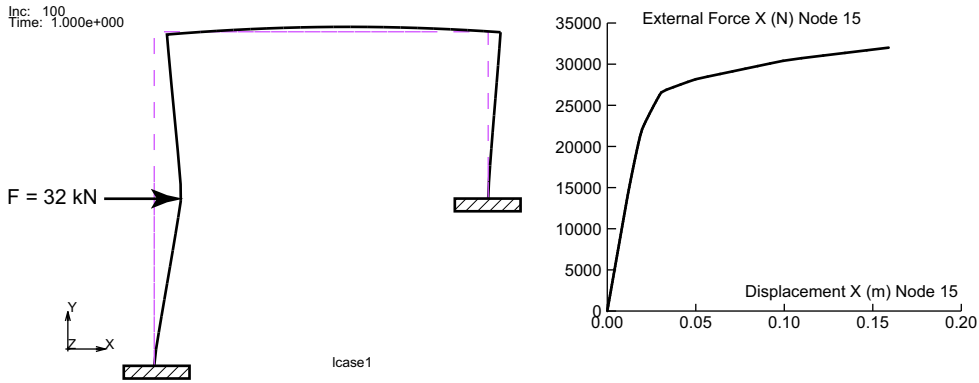


Figure 2.23-2 Deformed Frame Structure and Force Displacement Response of the Loaded Point

Modeling Tips

If the material behavior is linear elastic only, pre-integrated sections can be used to save storage and analysis time. In this case, the section properties like area and moments of area are computed only once prior to the analysis by numerical integration. During the analysis, no numerical section integration is carried out and the beam behaves as if its section properties were entered directly in the input. The solid section beam formulation that allows for numerical cross-section integration to account for the nonlinear material behavior is also available for element type 98.

Input Files

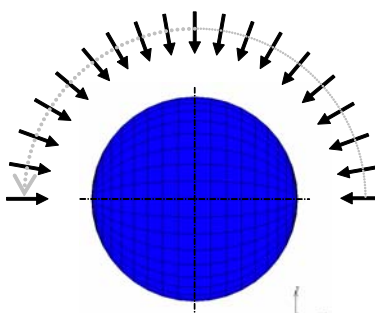
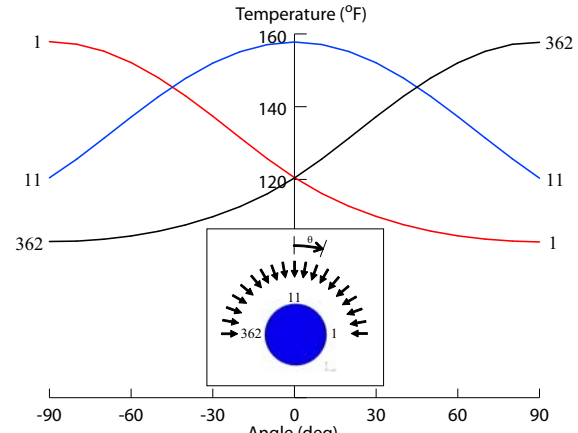
The files below are on your [delivery media](#) or they can be downloaded by your web browser by clicking the links (file names) below.

File	Description
limit_load.proc	Mentat procedure file to run the above example using the new style table input format.
limit_load_old_job1.dat	Associated Marc file using the old style table input format.

2.24 Directional Heat Flux on a Sphere from a Distance Source

- Summary 678
- Model Review 679
- Results 683
- Input Files 685

Summary

Title	Directional heat flux on a sphere from a distance source
Problem features	<ul style="list-style-type: none"> • Directional heat flux • Heat transfer membrane elements • Radiation boundary condition
Geometry	<ul style="list-style-type: none"> • Sphere radius = 1.0 ft • Membrane thickness = 0.01 ft  <p>The diagram shows a blue sphere with a grid pattern. A semi-circle of arrows points towards the sphere from the top, representing directional heat flux. A coordinate system with x and y axes is shown at the bottom right of the sphere.</p>
Material properties	<ul style="list-style-type: none"> • Thermal conductivity = 204.0 BTU/hr ft² • Emissivity = Absorption = 1.0
Analysis type	Steady state heat transfer analysis at a series of angles of incidence for the directional heat flux
Boundary conditions	Radiation to the environment, $T_{\infty} = 60^{\circ}\text{F}$
Applied loads	Directional heat flux magnitude = 300.0 BTU/hr ft ²
Element type	4 node heat transfer membrane elements type 198
Contact properties	None
FE results	<p>Temperature variation with directional heat flux angle of incidence</p>  <p>The graph plots Temperature (°F) on the y-axis (ranging from 120 to 160) against Angle (deg) on the x-axis (ranging from -90 to 90). Three curves are shown: a red curve (labeled 1 at both ends), a blue curve (labeled 11 at both ends), and a black curve (labeled 362 at both ends). The red curve peaks at 160°F at 0 degrees. The blue curve peaks at 120°F at 0 degrees. The black curve peaks at 120°F at 0 degrees. An inset diagram shows the sphere with arrows and labels 1, 11, and 362 corresponding to the curves.</p>

This chapter demonstrates the use of the directional heat flux thermal loading. Heat flux from a distant source can be treated in a directional sense with the QVECT model definition input option. The flux is applied on a spherical shell modeled using heat transfer membrane elements. For illustrative purposes, the angle of incidence of the directional heat flux is varied to create a plot for the temperature versus the angle of incidence. A simple radiation boundary condition to space represents the loss mechanism and keeps the sphere in a state of radiative equilibrium.

Model Review

A model for the sphere is available in the file `directional_heat_flux.mfd` shown in [Figure 2.24-1](#). The table driven input style must be used for directional heat flux thermal loading. The spherical shell is modeled using 720 heat transfer membrane elements type 198. The membrane thickness is 0.01 ft. The initial temperature of all the nodes in the model is equal to the environment temperature = 60 °F. The thermal conductivity of the material is 204.0 BTU/hr ft °F. The surface emissivity and absorption are both equal to 1.0.

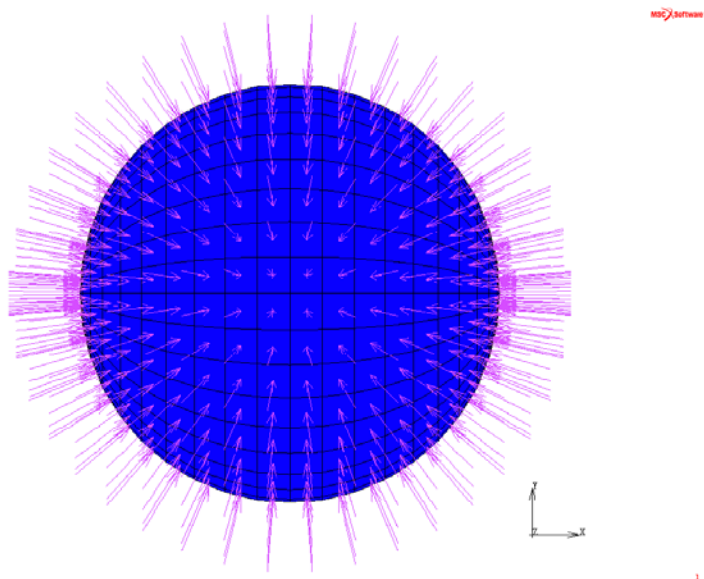


Figure 2.24-1 Model for a Sphere with Directional Heat Flux.

The directional heat flux is defined with the QVECT model definition option. The directional heat flux settings can be found in Mentat menus under BOUNDARY CONDITIONS -> THERMAL -> HEAT FLUX as shown in [Figure 2.24-2](#). The LOAD TYPE should be set to DIRECTED. The magnitude of the heat flux is 300.0 BTU/hr ft².

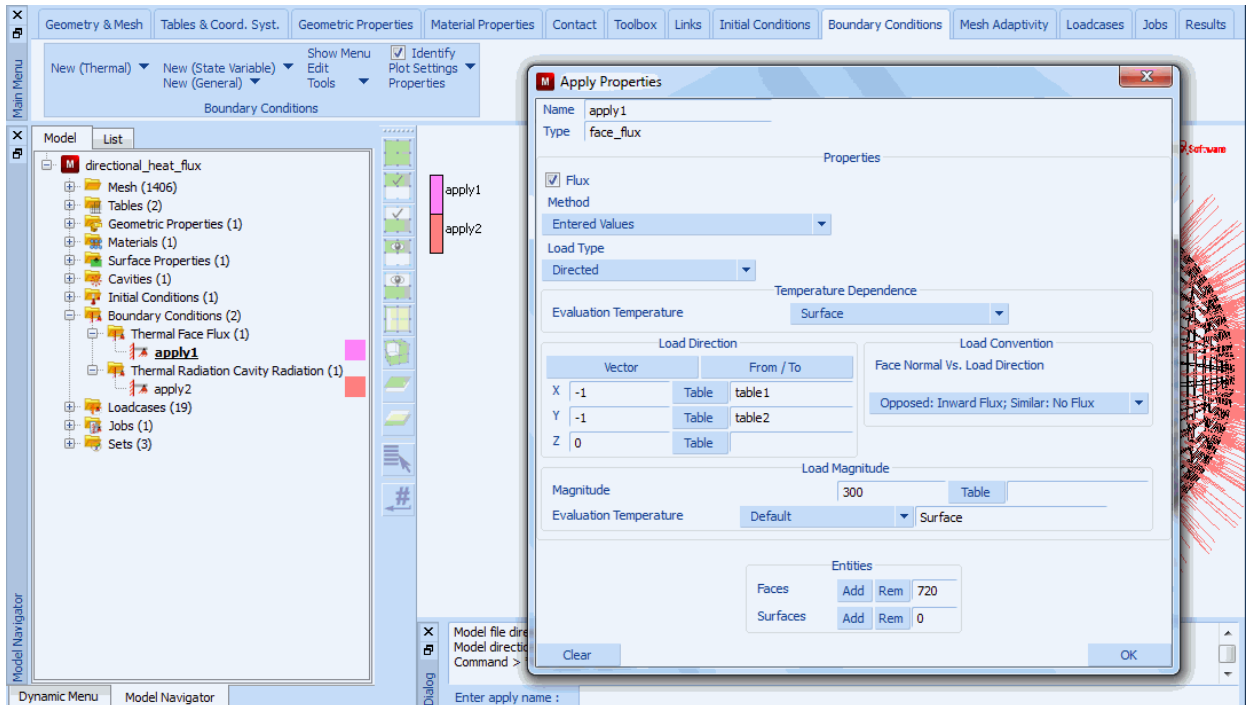


Figure 2.24-2 Mentat Menu for Directional Heat Flux

The angle of incidence of the heat flux is to be varied through 180° . The vector is initially pointing in the negative x-direction and rotates counterclockwise via 10° increments to be finally aligned with the positive x-axis. Nineteen steady state load cases are used to vary the angle of incidence which is measured with respect to the positive y-axis. The direction cosines of the heat flux vector are varied through formula-type tables. The expressions for the x and y components of the direction cosines are

$$\sin\left(\left(90 - 10 \cdot (v1 - 1)\right) \cdot \frac{\pi}{180.00}\right) \text{ and } \cos\left(\left(90 - 10 \cdot (v1 - 1)\right) \cdot \frac{\pi}{180.0}\right),$$

respectively, where $v1$ is the increment number. The table entries in Mentat are shown in [Figure 2.24-3](#).

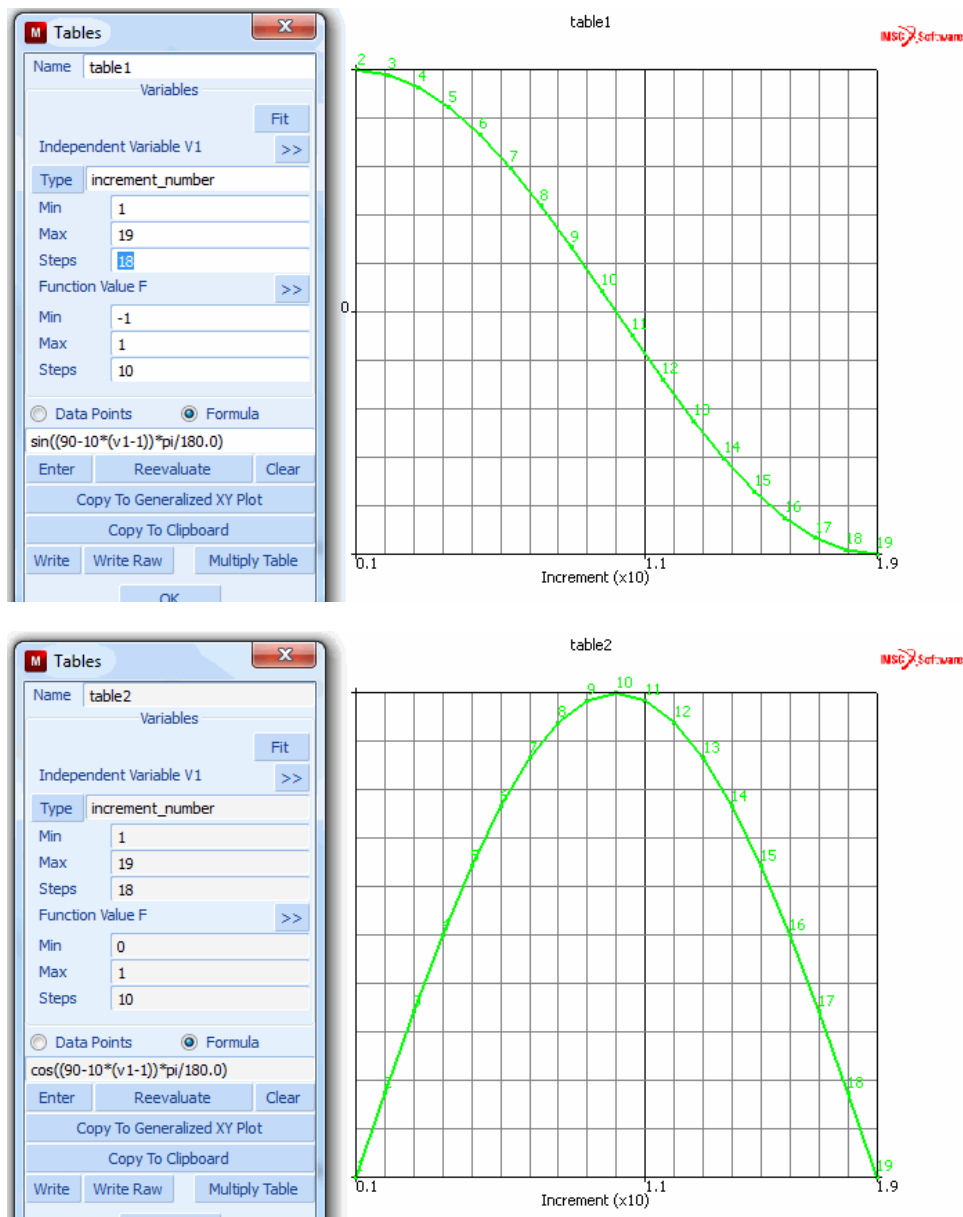


Figure 2.24-3 Formula-type Tables used to change the Heat Flux Angle of Incidence

The second boundary condition controls the radiation back to the environment. A radiating cavity is defined and the environment temperature is set to 60°F. Mentat menu for the cavity radiation is shown in Figure 2.24-4.

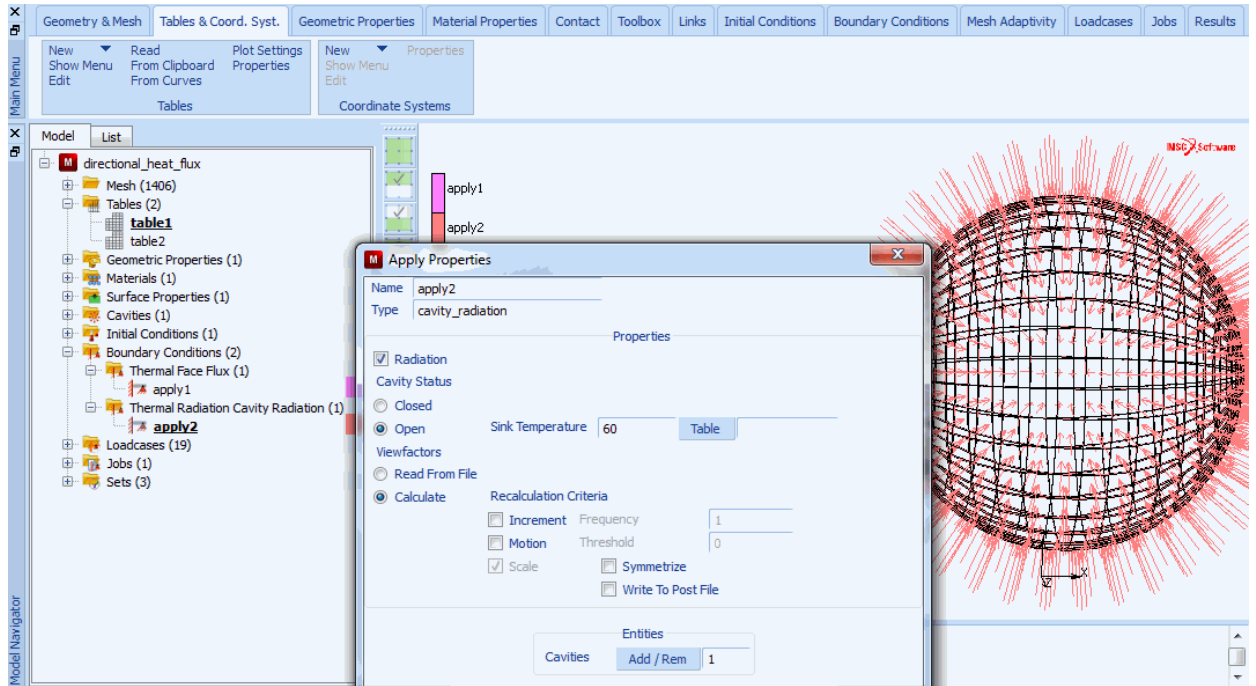


Figure 2.24-4 Radiation Boundary Condition

The convergence tolerance for each loadcase is set such that recycling occurs if the difference between the temperature calculated and estimated is greater than 1°F as shown in Figure 2.24-5. Because the English unit system is used, it is necessary to define the absolute temperature to be 459.67 and the Stefan-Boltzmann constant to be 1.714×10^{-9} Btu/hr ft^2R^4 .

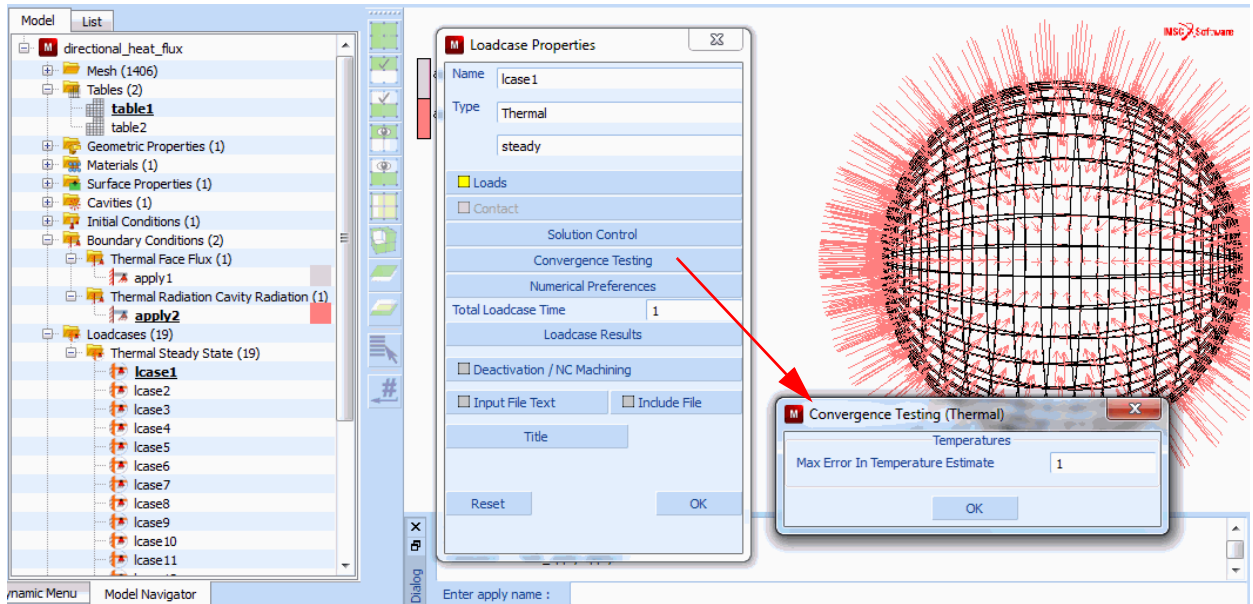


Figure 2.24-5 Steady State Heat Transfer Loadcase with Convergence Testing

Results

Steady state temperatures at three nodes on the surface of the sphere versus angle of incidence are shown in the history plot of [Figure 2.24-6](#). The same results are given in [Table 2.24-1](#) versus angle of incidence of the directional heat flux.

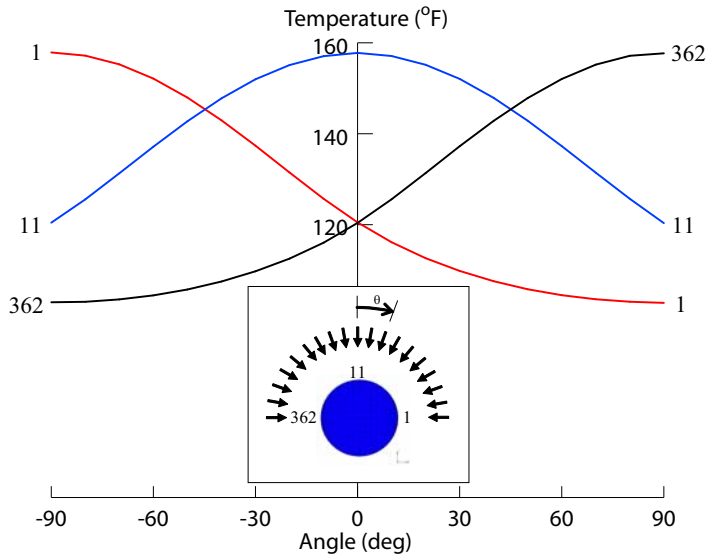


Figure 2.24-6 Temperature versus Increment Number.

Table 2.24-1 Temperature versus Angle of Incidence of Directional Heat Flux .

Increment #	Angle of Incidence θ (deg)	Node 1 (°F)	Node 11 (°F)	Node 362 (°F)
1	90	157.687	120.347	102.805
2	80	157.144	125.691	103.053
3	70	155.197	131.437	103.597
4	60	152.041	137.274	104.493
5	50	147.851	142.86	105.799
6	40	142.84	147.885	107.566
7	30	137.25	152.067	109.832
8	20	131.351	155.163	112.629
9	10	125.586	157.095	116.138
10	0	120.387	157.778	120.505
11	-10	116.029	157.06	125.709
12	-20	112.535	155.102	131.481
13	-30	109.751	151.98	137.378
14	-40	107.497	147.776	142.959
15	-50	105.744	142.738	147.957
16	-60	104.453	137.146	152.128
17	-70	103.57	131.307	155.258

Table 2.24-1 Temperature versus Angle of Incidence of Directional Heat Flux (continued).

Increment #	Angle of Incidence θ (deg)	Node 1 (°F)	Node 11 (°F)	Node 362 (°F)
18	-80	103.041	125.565	157.176
19	-90	102.938	120.442	157.878

Input Files

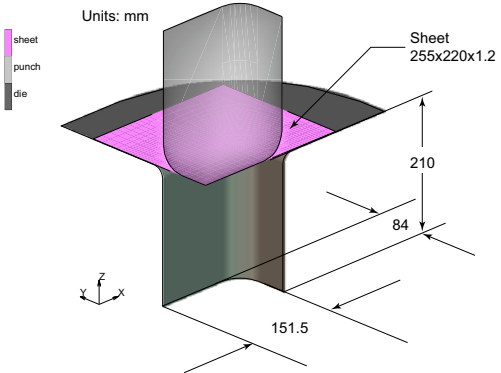
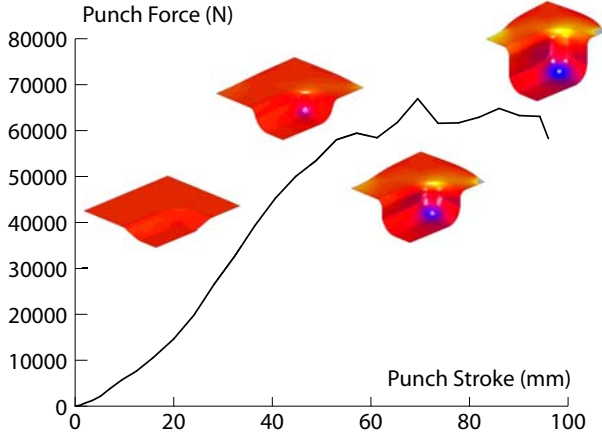
The files below are on your [delivery media](#) or they can be downloaded by your web browser by clicking the links (file names) below.

File	Description
directional_heat_flux.proc	Mentat procedure file to run the above example
directional_heat_flux.mfd	Associated model file
directional_heat_flux.dat	Associated Marc file

2.25 Deep Drawing of A Sheet With Global Remeshing

- Summary 688
- Model Review 689
- Results 691
- Modeling Tips 692
- Input Files 692

Summary

Title	Deep Drawing of A Sheet With Global Remeshing
Problem features	<ul style="list-style-type: none"> • A punch and die form a deep box with friction • The sheet is remeshed when either one of two criteria is met
Geometry	 <p>Units: mm</p> <p>Sheet 255x220x1.2</p> <p>210</p> <p>84</p> <p>151.5</p> <p>Legend: sheet (purple), punch (grey), die (dark grey)</p>
Material properties	$E = 210 \text{ GPa}$, $\nu = 0.3$, Initial yield strength, $\sigma_Y = 188.66 \text{ MPa}$
Analysis type	Quasi-static analysis
Boundary conditions	Symmetric displacement constraints are applied through symmetric contact surfaces.
Applied loads	The punch is pushed opposite to Z-direction a stroke of 96 mm
Element type	Shell element type 75 with full integration with 7 layers
Contact Properties	Coefficient of friction $\mu = 0.4$
FE results	<p>1 Contour plot of plate thickness, equivalent plastic strains</p> <p>2 History plot of die load versus stroke</p> 

Severe deformation often occurs in sheet metal forming processes. When applying the technique of finite element analysis to such processes, the shell elements deformed so severely that the FE analysis is not able to continue with the distorted mesh. This is because the distorted elements are unable to provide stable solution due to the extremely small singularity ratio of the equation system or negative Jacobian. Besides, during sheet forming processes, the contact condition between die surfaces and blank sheet changes so fast, the old mesh easily penetrates into die surfaces without remeshing. Therefore, remeshing is necessary in order to obtain accurate results.

This chapter describes the usage of the new extension of the 3-D remeshing technique of Marc to the shell elements. In the current release of Marc, the shell remeshing is activated by adding the REZONE parameter and ADAPT GLOBAL model and history definition options into the input data file. The 3-D surface meshers (quadrilateral/triangular elements) are used to generate new shell elements. This is applicable to both quadrilateral and triangular shell type elements.

Model Review

The sheet plate is initially subdivided as 636 4-node shell elements for the finite element analysis. Element type 75 (thick shell element with full integration) is chosen for the analysis. The initial geometry of die surfaces and blank sheet are shown in the [Summary](#). Two criteria are used to control the frequency of mesh rezoning for the finite element model. They are the number of increment and the amount of strain change. For example, if the incremental frequency for remeshing is set as 5, then new mesh will be regenerated after every 5 incremental steps. To set the criteria of strain change as 0.3, the new mesh will be created if the strain change reaches 0.3. In this example, these two criteria are combined to control the regeneration of new meshes in order to properly control the frequency of remeshing. The mesh size of the new meshes can be controlled by setting the element edge length or setting the upper bound of maximum number of elements allowed for the new mesh. Here, it is given the value of 3000. In this case, the mesh size will be determined automatically by the 3D surface mesher. As shown below, the global adaptive remeshing is defined by the ADAPT GLOBAL option, the mesher 19 is entered for quadrilateral shell mesher. For triangular shell element, mesher 12 is needed. The two criteria for remeshing are defined as criterion 1(to generate new mesh after every 5 incremental steps) and criterion 5 (which stands for strain change).

```
ADAPT GLOBAL
      1          0          0
     19         1          1          0          2          0          0
      1          5 0.000000000000000+0 0.000000000000000+0
      5          0 3.000000000000000-1 0.000000000000000+0
0.000000000000000+0 0.000000000000000+0 1.000000000000000+2
6.000000000000000+1 1.500000000000000+0
```

The analysis takes 32 steps in total, within which remeshing is conducted after increment step 5, 10, 20, 23, 25, 26, 27, 28, 29, 30, 31. Initially, the remeshing becomes necessary due to criterion of increment frequency, like increments 5, 10, 15, 20, and 25.

When the deformation becomes large, the remeshing is more often triggered by strain changes, such as the steps 23, 26, 27, 28, 29, 30, and 31. The final mesh and die surface are shown in [Figure 2.25-1](#).

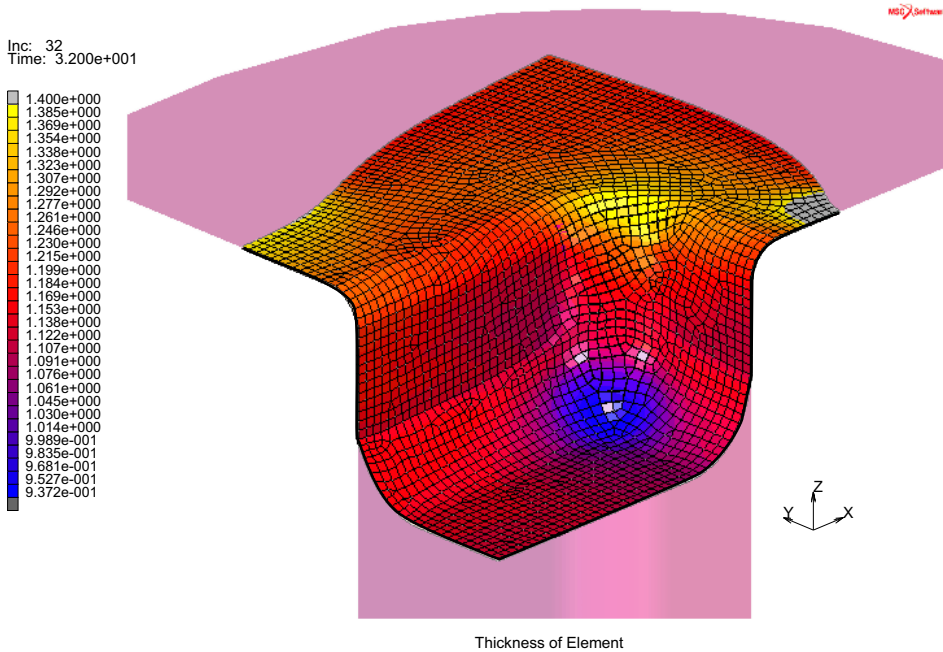


Figure 2.25-1 Sheet and Die Geometry at the Final Stage of Deep Drawing

Let's suppose this model has already been built and exists as a Marc input file named `ug_shlremesh.dat`, and then read this file into Mentat. Unlike previous versions of Mentat, the history definition of the model is obtained. The model is saved, and the job is submitted as shown below.

```

FILES
  MARC INPUT FILE READ
    ug_shlremesh.dat
  OK
  SAVE AS
    ug_shlremesh.dat
  OK
  MAIN
JOBS
  RUN
  SUBMIT

```

As the results become available, they can be viewed by opening the post file as:

OPEN POST FILE (RESULTS MENU)

And we begin examining the results.

Results

The model read from disk already set the option of global adaptive remeshing. Once the job is run, we just need to see the results and check how the remeshing is conducted during the analysis. Figure 2.25-2 (a) and (b) shows the equivalent stress at increment 5 and 32, respectively. The number of elements has increased from 636 at increment 5 to 2866 at increment 32.

The thickness contour of the part after the deep drawing is shown in the Figure 2.25-3 (a). Upon closer examination of the two jobs using remeshing and without using remeshing, the thickness contour with remeshing shows less thinning at the punch corner area than the job without using remeshing (see Figure 2.25-3 (b)).

Time: 3.200e+001

Equivalent of Global Stress Layer 1

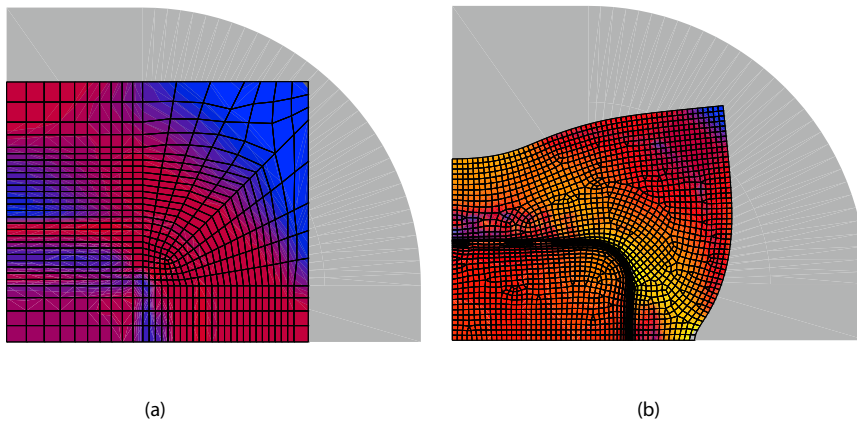


Figure 2.25-2 Equivalent Stress at Increment 5 (a) and 32 (b)

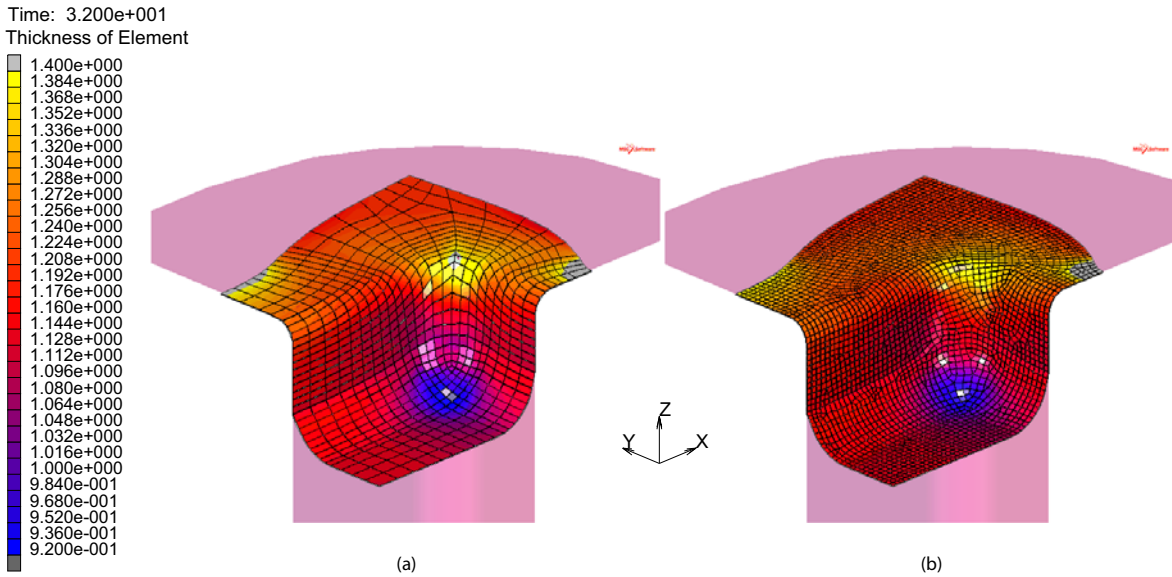


Figure 2.25-3 Thickness Distributions With Remeshing (a) and Without Remeshing (b)

Modeling Tips

In the current release, three criteria are available for both quadrilateral and triangular shell remeshing which include: increment frequency, strain change, and penetration. Additionally, when using triangular elements, curvature-based criteria is also supported.

The sheet was glued to the die to simulate a binder since shell elements were used and cannot support double-sided contact.

Input Files

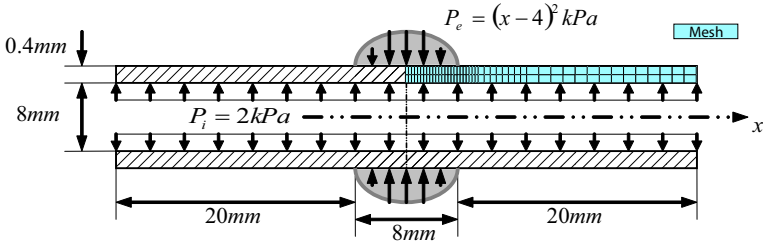
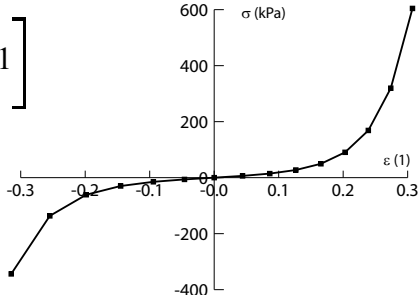
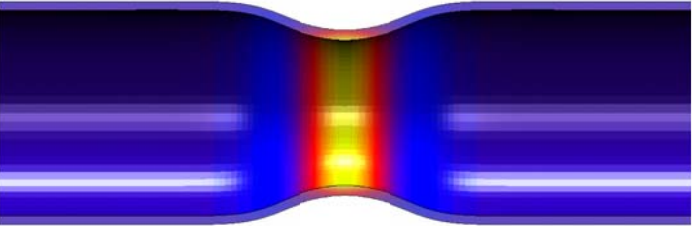
The files below are on your [delivery media](#) or they can be downloaded by your web browser by clicking the links (file names) below.

File	Description
ug_shlremesh.proc	Mentat procedure file to run the above example
ug_shlremesh.dat	Associated Marc file
ug_shlremeshn.dat	Associated Marc file - no remeshing

2.26 Artery Under Pressure

- Summary 694
- Material Modeling 695
- Results 697
- Modeling Tips 699
- Input Files 700
- References 699

Summary

Title	Artery Under Pressure
Problem features	<ul style="list-style-type: none"> • NLELAST option to model nonlinear elastic material • UELASTOMER user subroutine to define same material
Geometry	
Material properties	<ul style="list-style-type: none"> • NLELAST option uses experimental data • UELASTOMER user subroutine uses data fit to Fung's Model as; $W = \frac{a}{b} \left[e^{\frac{b}{2}(I_1 - 3)} - 1 \right]$ <p> $a = 44.25 \text{ kPa}$ $b = 16.73$ </p> 
Analysis type	Quasi-static analysis
Boundary conditions	Symmetric displacement constraints are applied at the left end of the model. Axial displacements at right end of the tube are fixed.
Applied loads	The internal and external pressures are shown above.
Element type	4-node axisymmetric element type 10 with a fine gradient at the center.
FE results	<ol style="list-style-type: none"> 1 Stress versus strain plots for both models 2 Radial displacement plots during loading for both models 3 Deformed model with the distribution of equivalent stresses 

This chapter is to demonstrate the use of the UELASTOMER user subroutine and the NLELAST option to model nonlinear elastic behaviors of soft tissue materials.

Material Modeling

Soft tissue materials exhibit a highly nonlinear behavior. Fung's (Fung, 1967) model is one of the most commonly used models for such materials. Fung's material model assumes the strain energy density can be expressed as an exponential

of the first strain invariant, namely, $W = \frac{a}{b} \left[e^{\frac{b}{2}(I_1-3)} - 1 \right]$ where the material constants a and b are from (Mofrad, 2003).

With the help of the user subroutine, this model can be implemented with a few lines of code. The new code in uelastomer.f will look like the following:

```

subroutine uelastomer(iflag,m,nn,matus,be,x1,x2,x3,detft,
    $                enerd,w1,w2,w3,w11,w22,w33,w12,w23,w31,
    $                dudj,du2dj,dt,dtdl,iarray,array)
#ifdef _IMPLICITNONE
    implicit none
#else
    implicit logical (a-z)
#endif
c    ** Start of generated type statements **
    real*8 array, be, detft, dt, dtdl, du2dj, dudj, enerd
    integer iarray, iflag, m, matus, nn
    real*8 w1, w11, w12, w2, w22, w23, w3, w31, w33, x1, x2, x3
    real*8 aa,bb,ccc
c    ** End of generated type statements **
    dimension m(2),be(6),dt(*),dtdl(*),iarray(*),array(*),matus(2)
c    implement Fung's model for bio-materials
c    W = a/b * { exp[0.5*b*(I_1-3)] - 1 }
c    define material parameters
    aa=44.25
    bb=16.73
    ccc=exp(0.5d0*bb*(x1-3.d0))
c    w1 is the derivative of the strain energy with respect to
c    the first invariant
    w1=0.5*aa*ccc
c    w11 is the second derivative of the strain energy with
c    respect to the first invariant
    w11=0.25*aa*bb*ccc
    enerd=aa/bb*(ccc-1)
    return
end

```

To activate the user subroutine, simply click MATERIAL PROPERTIES -> MOONEY in Mentat and define a list of elements associated and submit the user subroutine with the run.

The NLELAST option provides an even simpler way to simulate nonlinear elastic materials. In such a case, the experimentally obtained data can be used directly as the material input in a table. The effort of curve fitting to get the material parameters is no longer needed.

To define NLELAST:

MAIN

MATERIAL PROPERTIES

MATERIAL PROPERTIES

HYPOELASTIC

SIMPLIFIED NONLINEAR ELASTIC

Choose stress model

Define the table for effective stress-strain curve (tab_mod_nlelast)

Define the Poisson's ratio (0.49)

OK

The effective stress versus strain material data for the soft tissue contained in the table `tab_mod_nlelast` selected in [Figure 2.26-1](#) is plotted [Figure 2.26-2](#) connected by dashed lines.

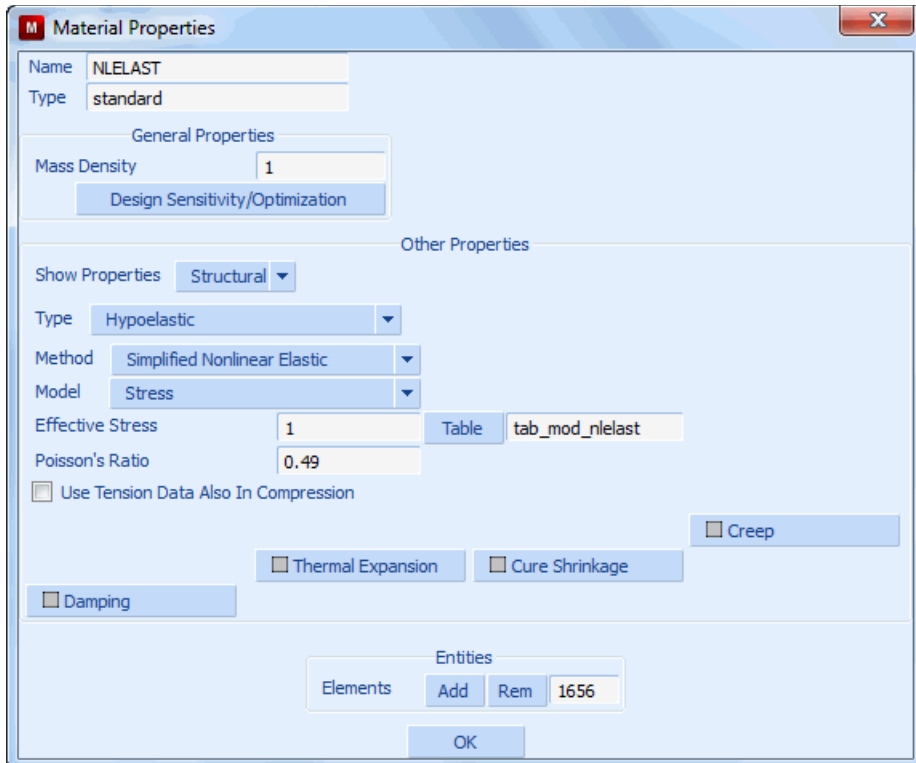


Figure 2.26-1 Define NLELAST

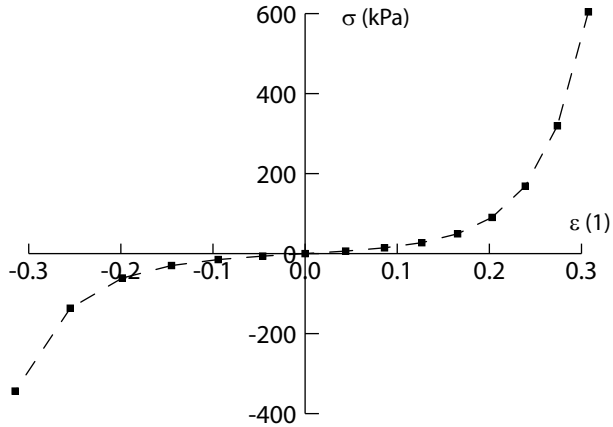


Figure 2.26-2 Plot of Soft Tissue Material Stress - Strain Behavior

Job Parameters

For the Mooney/uelastomer model, large strains are automatically activated. For the NLELAST model, it needs to be activated using JOB -> ANALYSIS OPTIONS -> LARGE STRAIN

Results

The cross plots of the maximum equivalent stress versus the maximum equivalent strain, occurring on the inner surface at the center of the artery, are illustrated in [Figure 2.26-3](#). It can be observed that the results from both models are very close up to the level of 25% strain. Fung's model is smooth because of its analytical description, whereas NLELAST is piece-wise linear between experimental data points shown in [Figure 2.26-2](#). The maximum stresses reached at full loading are 155 kPa and 154 kPa for Fung's model and NLELAST, respectively. The stress difference between the two material models is smaller than the strain difference. This is reasonable because it is a load-controlled problem.

The history plots of the change of tube radius at the center and the end of the tube are shown in [Figure 2.26-4](#). It can be observed that the results from both models are very close. It is particularly true when the strain is less than 5%.

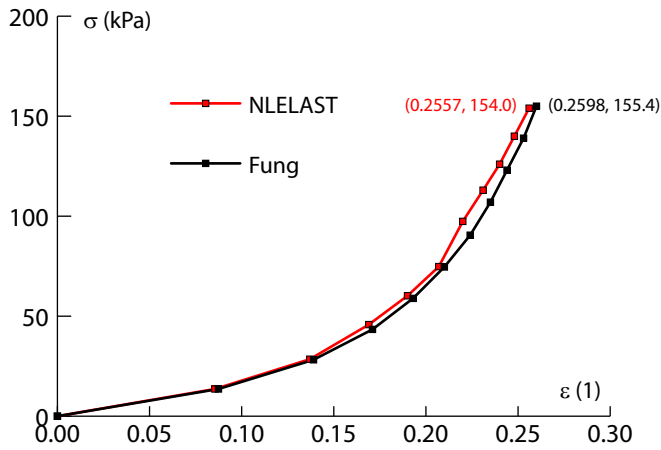


Figure 2.26-3 Stress versus Strain at Node 1

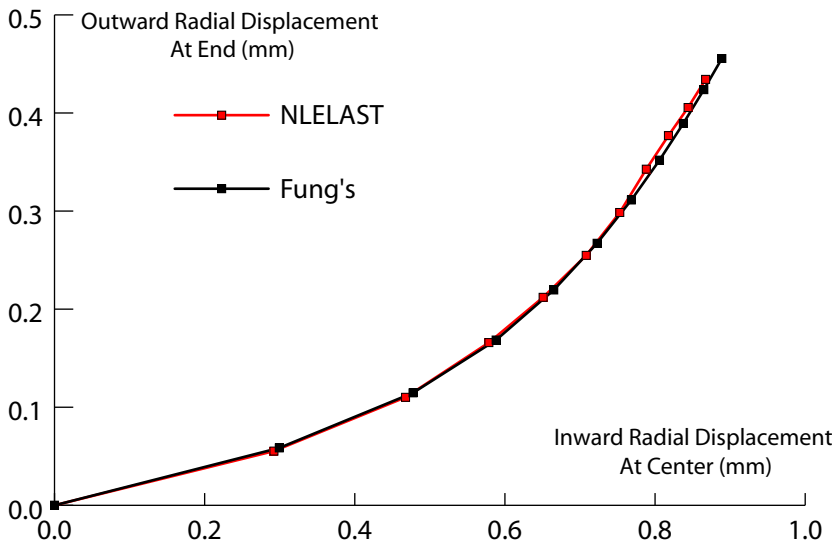


Figure 2.26-4 Radial Displacements at End versus at Center

Figure 2.26-5 shows the deformed model with the distribution of equivalent stresses, obtained using Fung's material model.

Inc: 10
Time: 1.000e+000

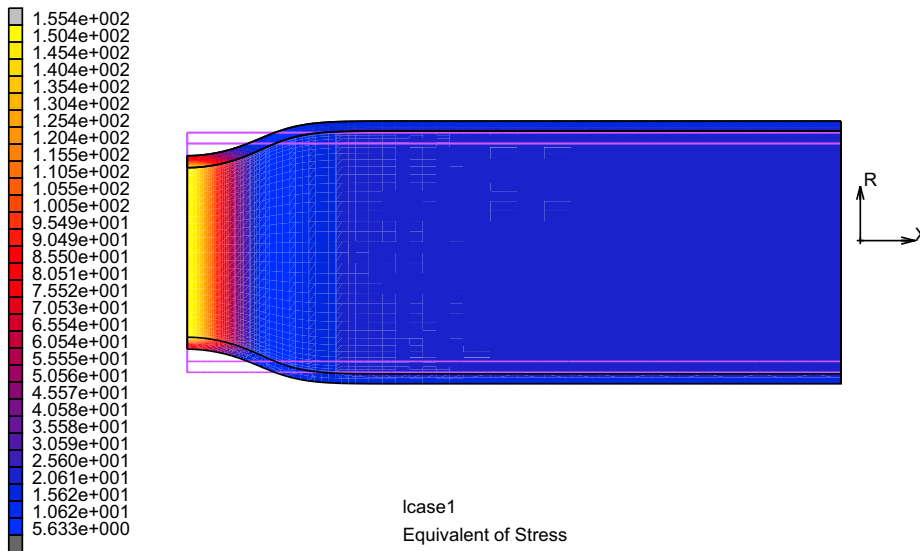


Figure 2.26-5 Equivalent Stress Contours on Deformed Artery

Modeling Tips

- A relatively large bulk modulus is required to enforce incompressibility of the materials in defining Fung's model using the UELASTOMER user subroutine. This can be done under the MOONEY option.
- Because the deformation is large and the updated Lagrange formulation is used in the analysis, the stress-strain curve must refer to the true (Cauchy) stress and true (logarithmic) strain.

References

1. Fung, Y. C. (1967) Elasticity of soft tissues in simple elongation. *Am. J. Physiol.* **28**, 1532-1544.
2. Mofrad, (2003) et al. *Computers and Structures* **81**(2003) 715–726

Input Files

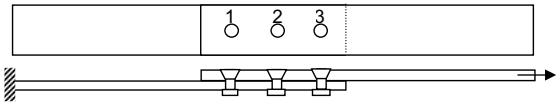
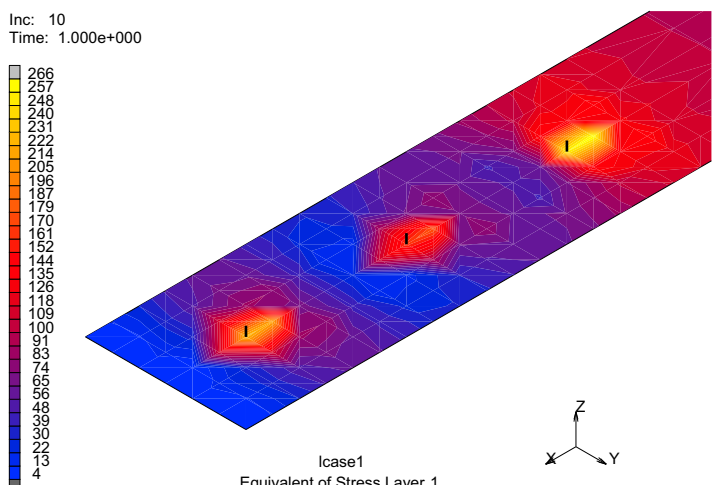
The files below are on your [delivery media](#) or they can be downloaded by your web browser by clicking the links (file names) below.

File	Description
tube_nlelast.proc	Mentat procedure file to run the above example
tube_uelastomer.proc	Mentat procedure file to run the above example
tube.mud	Mentat model file for geometry
tube_nlelast.dat	Marc input file using NLELAST
tube_uelastomer.dat	Marc input file using the UELASTOMER user subroutine
uelastomer.f	User subroutine to define Fung's model

2.27 Modeling Riveted Joint with Bushing, CFAST, or CWELD

- Summary 702
- Model Review 703
- Results 711
- Modeling Tips 713
- Input Files 713

Summary

Title	Modeling Riveted Joint with Bushing, CFAST or CWELD
Problem features	<ul style="list-style-type: none"> Using empirical formulation to characterize the rivet. Using the so-called point-wise and patch-wise connection.
Geometry	<p>The joint has 3 rows of rivets in the loading direction. For analysis purpose only a slice (one rivet-pitch wide) of the joint is analyzed with a proper symmetric boundary condition along the edges of the plates.</p> <p>Units: mm plate length = 160 rivet diameter = 4 plate overlap = 60 rivet pitch = 20 plate thickness = 1.2</p> 
Material properties	$E = 60000 \text{ MPa}$, $\nu = 0.3$
Analysis type	Quasi-static with geometrical non-linear analysis
Boundary conditions	Clamped on the left side of the joint. Symmetric displacement constraints along two symmetry lines.
Applied loads	Axial load of 2400 N in the x-direction is applied on the right side of the joint.
Element type	Shell element type 75 and bushing element type 195 or beam element type 98.
FE results	<ol style="list-style-type: none"> Deformed plot and Contour plot of equivalent stress Load transfer through the rivets  <p>Inc: 10 Time: 1.000e+000</p> <p>Icase1 Equivalent of Stress Layer 1</p>

This example demonstrates modeling and analysis of a lap joint. Two plates are joined using riveted connection. The rivet is modeled with bushing element since its flexibility is determined empirically. The bushing elements are connected with the plates using the so-called point-wise and patch-wise connection. The first way requires that the nodes of the plates that need to be connected must be predefined, since these nodes must belong both to the bushing element and the plates. Thus, it puts a limitation on how the plates should be meshed. Moreover, this type of connection creates a nearly stress singularity in the plate around the rivet position.

The second way, patch-wise connection, is demonstrated using the CFAST model definition option. This method does not require that the bushing nodes have to be congruent with the nodes of the plate. Internally, CFAST creates a bushing element and a set of tying that connect the bushing nodes with a set of nodes (this set of nodes form patches) of the plates. This type of connection does not have a singularity as it does for point-wise connection.

For the patch-wise connection, another model using CWELD/PWELD model definition option is setup to simulate the rivet connection. Internally, CWELD creates a beam element and a set of tying that connect the beam nodes with a set of nodes (this set of nodes form patches) of the plates. In this case, the stiffness of the rivet is derived using the standard formulation of beam element by giving the geometry and the material properties of the rivet.

Model Review

The plates will be meshed using standard finite elements. The rivets will be modeled using bushing element in which their flexibility/stiffness is calculated using an empirical or simple formula. The shear flexibility (see Vlieger, H., Broek, D., “Residual Strength of Cracked Stiffened Panels, Built-up Sheet Structure”, Fracture Mechanics of Aircraft Structure, AGARD-AG-176, NATO, London, 1974) is calculated as follows:

$$C_s = \frac{1}{E_{rv}d} \left[5 + 0.8 \left(\frac{E_{rv}d}{E_{pl}t_{pl}} + \frac{E_{rv}d}{E_{pu}t_{pu}} \right) \right] = 4.3 \times 10^{-5} \frac{\text{mm}}{\text{N}}$$

The axial rivet stiffness is calculated using a simple formula:

$$K_a = \frac{AE}{L(= 2.4 \text{ mm})} = 314159 \frac{\text{N}}{\text{mm}}$$

The rotational stiffness' are assumed to be zero. For model with point-wise connection, small torsion stiffness is added to avoid system matrix singularity.

The geometry of the model is quite simple. Here are the steps that should be followed:

- Step 1:** Create the finite element mesh for the lower plate. There should be nodes at the location of the rivets.
- Step 2:** Create the finite element mesh for the upper plate. There should be nodes at the location of the rivet.
- Step 3:** Define GEOMETRY and MATERIAL for both plates

For point-wise connection with bushing element

- Step 4:** Create bushing elements that connect nodes of the upper plate with the lower plate
- Step 5:** Create PBUSH

For patch-wise connection with CFAST/PFAST or CWELD/PWELD

Step 6: Create POINTS at the location of the rivets

For CFAST/PFAST

Step 7: Create CFAST and PFAST

For CWELD/PWELD

Step 8: Create CWLED and PWELD

Step 9: Create boundary conditions and loading,. then create load case

Step 10: Submit the jobs

Step 11: Postprocessing the results

Step 1 to Step 3 is ending up with the creation of the mesh for the plates as shown in [Figure 2.27-1](#). Please run the procedure file, step by step, until the MATERIAL definition

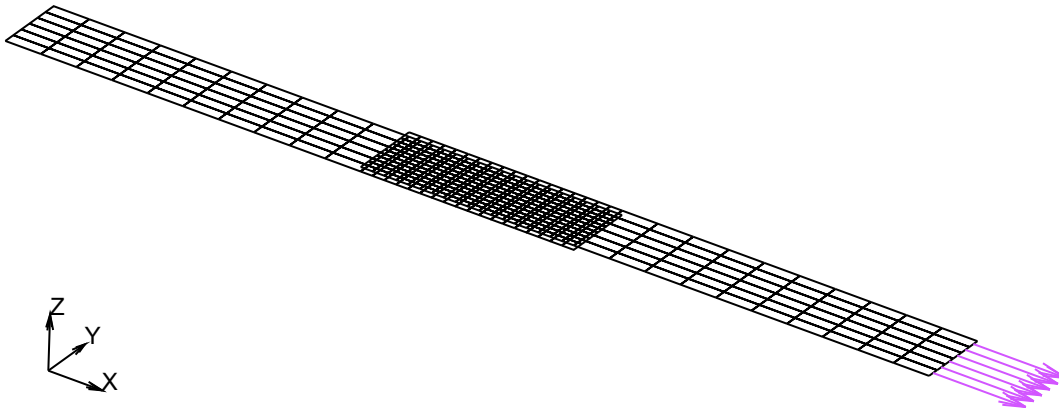


Figure 2.27-1 Finite Element Meshes for the Plates

For point-wise connection: using bushing element

Step 12: Create bushing elements that connect nodes of the lower and upper plates at the rivet location. The created bushing elements are shown in [Figure 2.27-2](#).

MAIN

MESH GENERATION

ELEMENT CLASS: LINE (2)

ELEMS: ADD

83

216

97

230
 111
 244

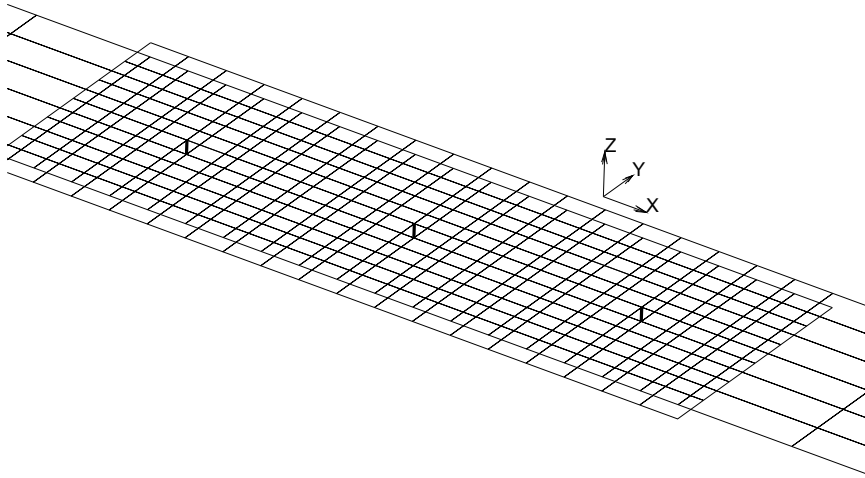


Figure 2.27-2 Created Bushing Elements that Connect Lower- and Upper-plate

Step 13: Creating PBUSSH by stepping through the following menus and filling in the requested value for stiffness properties as shown in Figure 2.27-3. And then assign this property for all bushing element created in Step 4.

MAIN

GEOMETRIC PROPERTIES

MECHANICAL ELEMETS: 3-D

BUSHING (please note: CONNECTION toggle must be OFF)

STIFFNESS/DAMPING PROP.: VALUES

VALUE X = 3.14159e5

VALUE Y = 2.3226e4

VALUE Z = 2.3226e4

VALUE RX = 100.

VECTOR

0

1

0

OK
ELEMENTS: ADD
All bushing elements

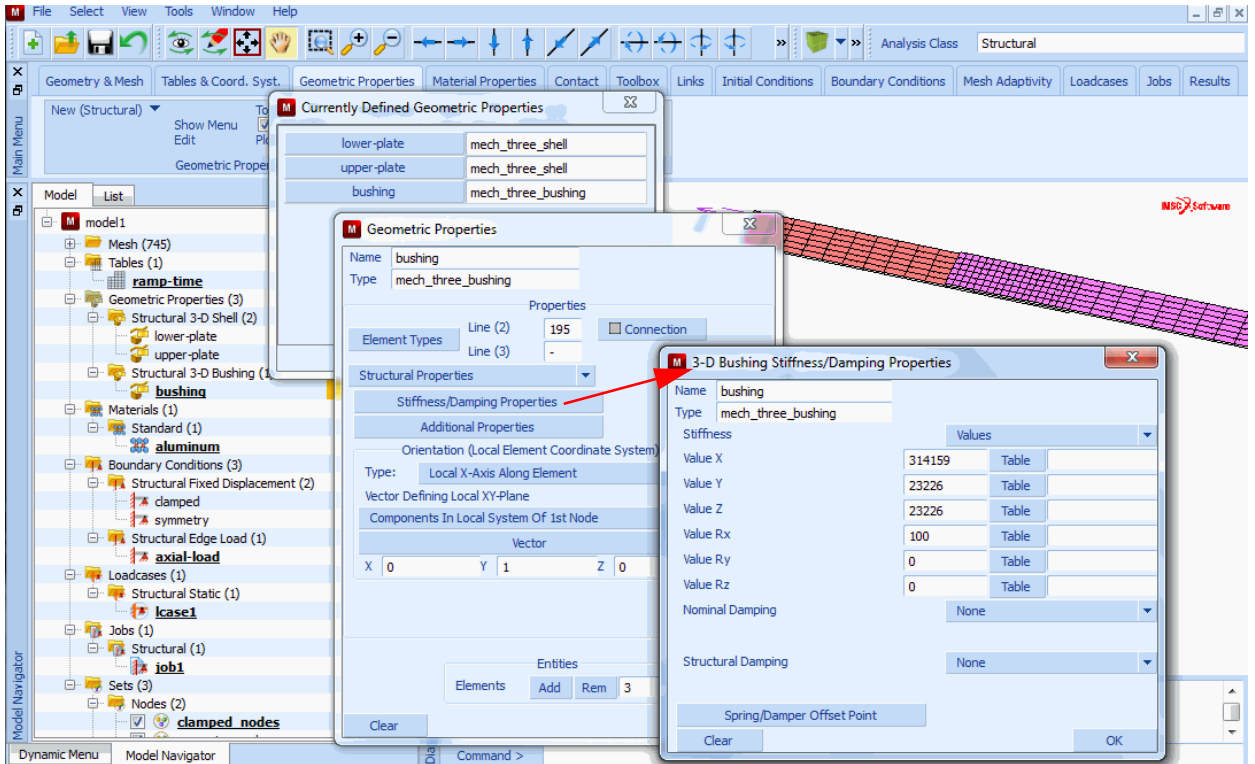


Figure 2.27-3 Menus of PBUSH for Stiffness Input

For patch-wise connection: using CFAST/PFAST or CWELD/PWELD

Step 14: Create POINTS at the location of the rivets

MAIN

MESH GENERATION

PTS: ADD

110 10 2.4

130 10 2.4

150 10 2.4

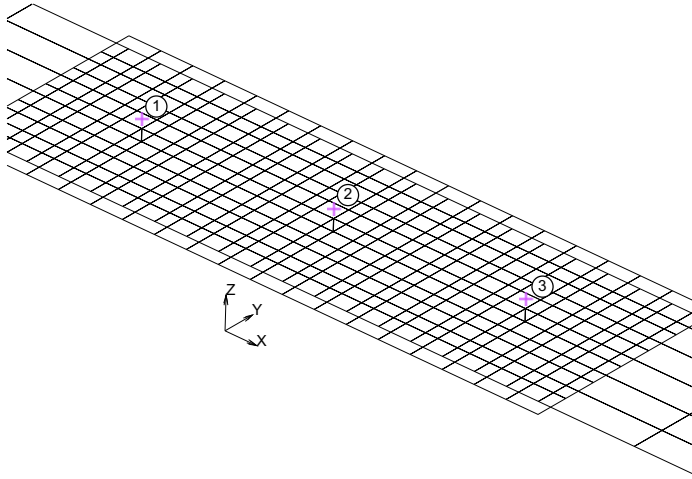


Figure 2.27-4 Created POINTS at the Location of the Rivets

Step 15: Creating CFAST and PFAST

MAIN

LINKS

CONNECTIONS

NEW

NAME: rivets

TYPE: FASTENER

CREATE AND SET

DIAMETER: 4

CREATE AND SET (please note: CONNECTION toggle must be ON)

STIFFNESS/DAMPING PROP.: VALUES

VALUE X = 3.14159e5

VALUE Y = 2.3226e4

VALUE Z = 2.3226e4

OK

2ND DIRECTION OF COORDINATE SYSTEM

COORDINATE SYSTEM: Global

OK

METHOD AND LOCATIONS

MASTER PATCH: FROM PATCH SET

ELEMENT END NODES: GENERATED

PROJ. POINT'S: POINT
LOCATIONS: ADD

1 2 3 #

PATCH SETS

A: FACES: ADD

All faces belong to the lower plate

B: FACES: ADD

All faces belong to the upper plate

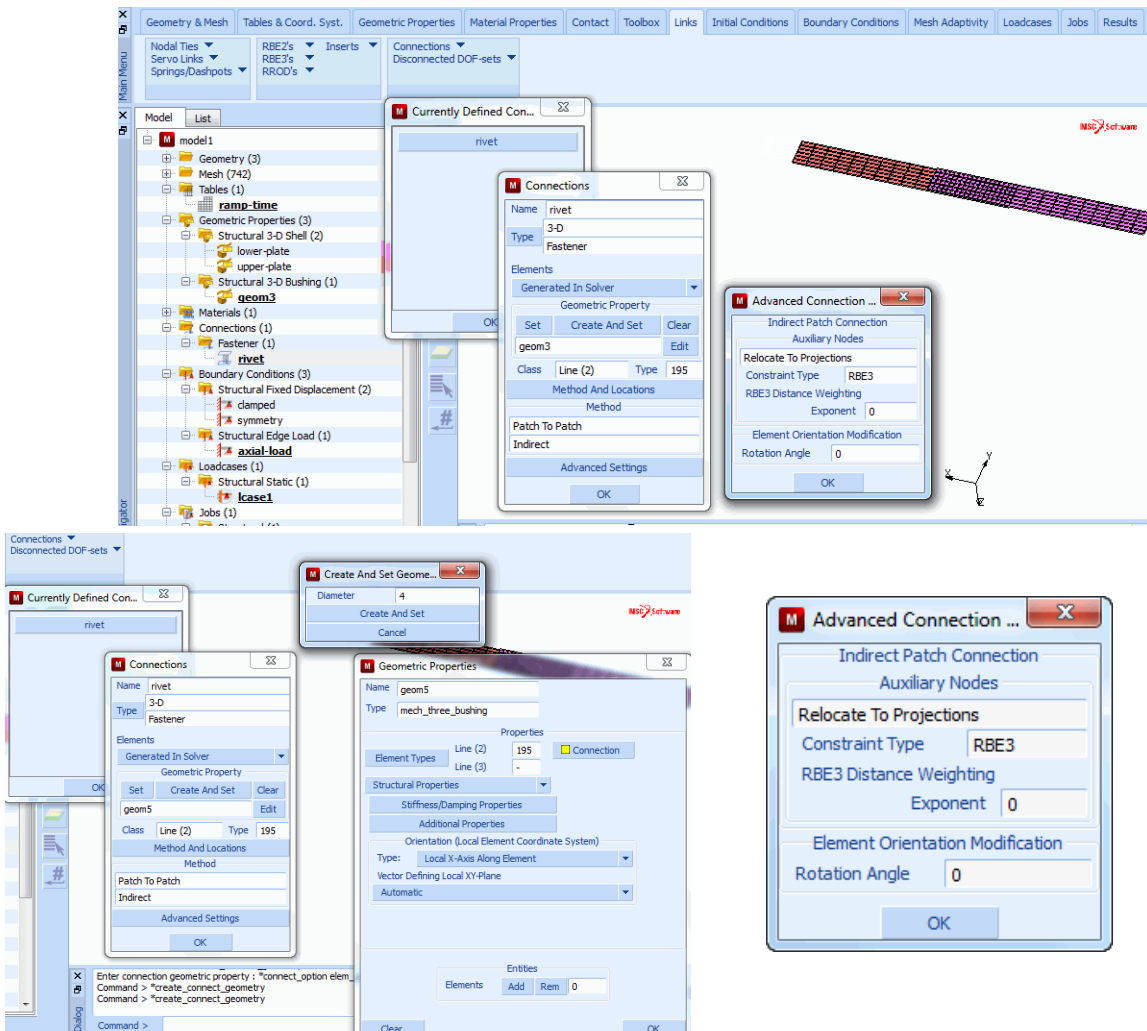


Figure 2.27-5 Menus to Create PFAST

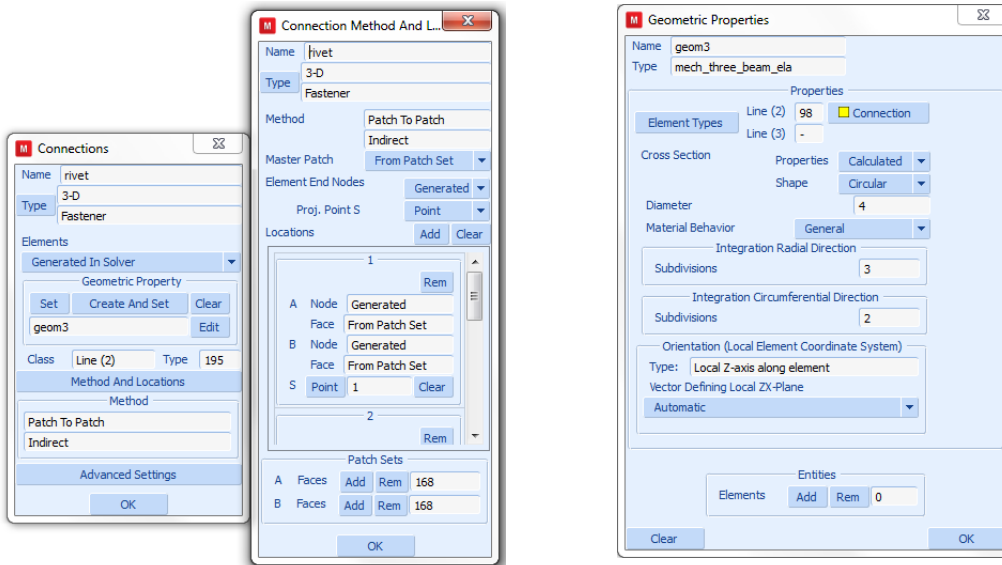


Figure 2.27-6 Menus to Create CFAST

Step 16: Creating CWELD and PWELD

MAIN

LINKS

CONNECTIONS

NEW

NAME: rivets

TYPE: WELD

CREATE AND SET

DIAMETER: 4

MATERIAL: aluminum

CREATE AND SET

VECTOR DEFINING LOCAL ZX-PLANE

COMPONENT IN GLOBAL SYSTEM

VECTOR

0 1 0

OK

METHOD AND LOCATIONS

METHOD: PATCH TO PATCH

MASTER PATCH: FROM PATCH SET

ELEMENT END NODES: GENERATED

PROJ. POINT'S: POINT

LOCATIONS: ADD

1 2 3 #

PATCH SETS

A: FACES: ADD

All faces belong to the lower plate

B: FACES: ADD

All faces belong to the upper plate

The remaining three steps are creating boundary condition and loading, running the analysis, and postprocessing the results.

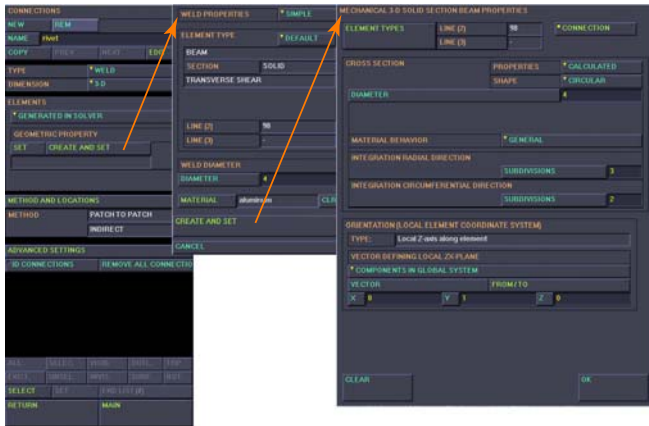


Figure 2.27-7 Menus to Create PWELD

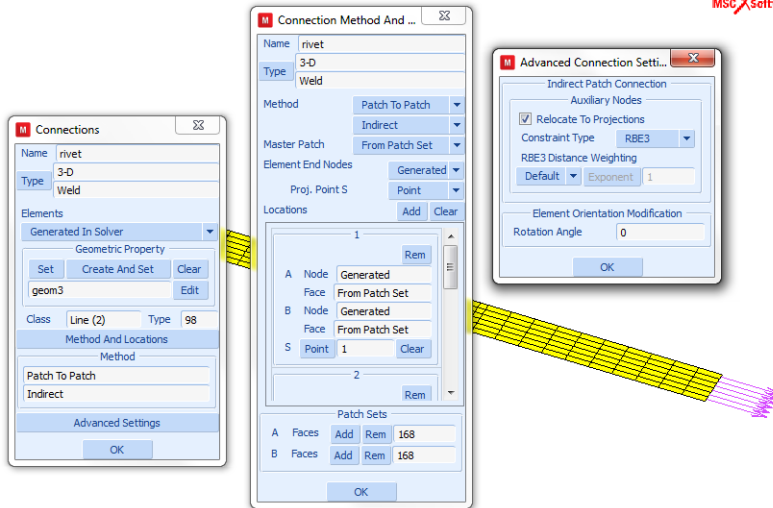


Figure 2.27-8 Menus to Create CWELD

Results

The deformed plot and the contour of the von Mises stresses of the lower plate for model with bushing, CFAST, and CWELD are shown in Figure 2.27-9, Figure 2.27-10, and Figure 2.27-11, respectively. Comparing the stress contour of the model with bushing and CFAST, as expected, the point-wise connection shows a greater stress concentration around the first rivet.

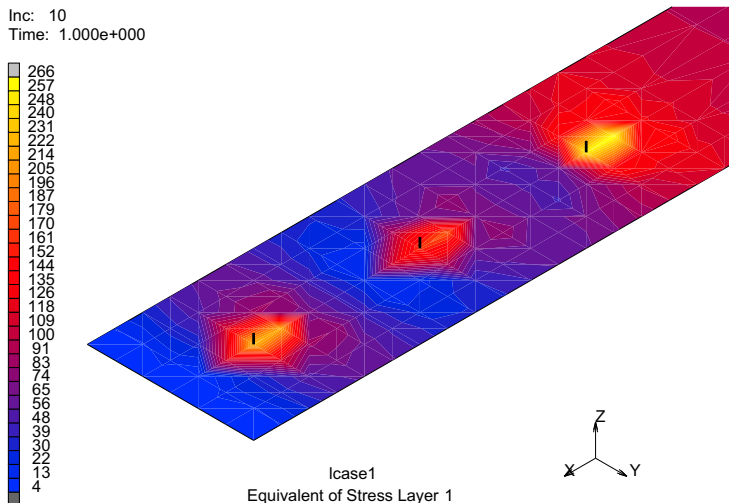


Figure 2.27-9 Deformed Plot and Stress Contour of the Lower-plate for Model with Bushing/PBUSH

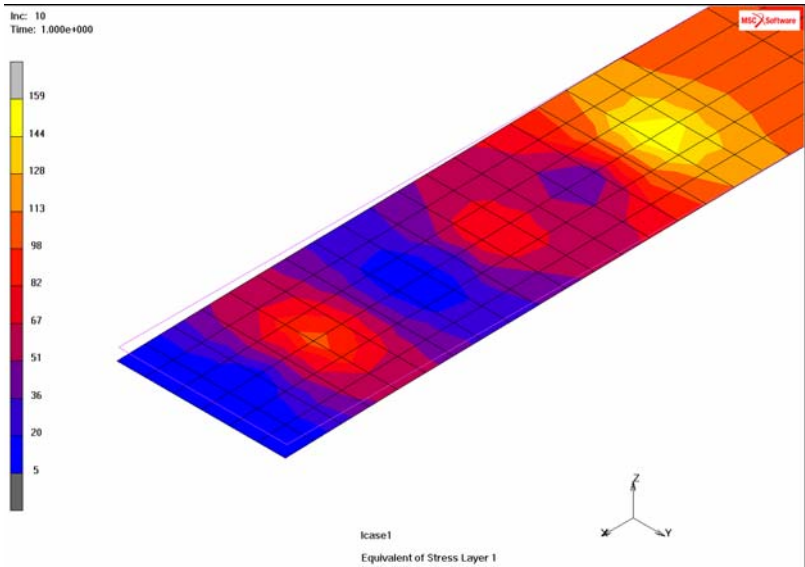


Figure 2.27-10 Deformed Plot and Stress Contour of the Lower-plate for Model with CFAST/PFAST

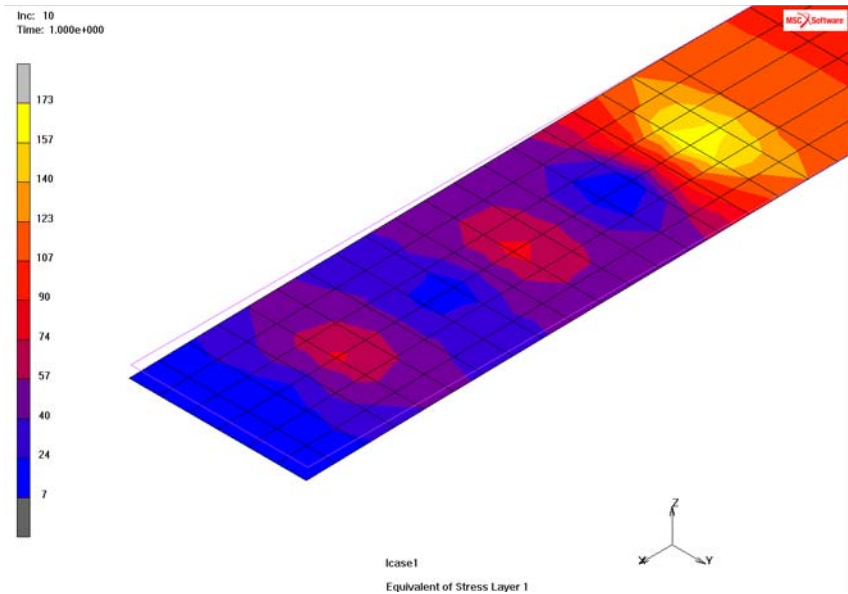


Figure 2.27-11 Deformed Plot and Stress Contour of the Lower-plate for Model with CWELD/PWELD

The load transfer through the rivets using all types of connection is shown in the following table. The load transfer through the first and third rivets for model with PBUSH are slightly less than that of the model with CFAST. This is obviously due to singularity condition which causes the effective stiffness of the rivet for the model with bushing elements is less than that of the model with CFAST.

	$F_{\text{Rivet-1 (N)}}$	$F_{\text{Rivet-2 (N)}}$	$F_{\text{Rivet-3 (N)}}$
Point-wise (CBUSH/PBUSH)	825	745	825
Patch-wise (CFAST/PFAST)	843	711	843
Patch-wise (CWELD/PWELD)	923	553	923

The load transfer through the first and third rivets using CWELD/PWELD is much greater than that of using CFAST/PFAST. This indicates that the stiffness of beam, given the geometry and material of the rivet, is much greater than that given by the empirical formula.

Modeling Tips

For geometrically complicated structures, modeling rivet joint with point-wise connection using bushing elements will be a laborious task since it will need meshes with hard points at the rivet location. Moreover, this type of connection will create singularity at the point of connection. CFAST and CWELD eliminate these drawbacks. For rivet connection, CFAST has more flexibility to define the mechanical properties of the rivet, normally defined by using empirical formula, compared to that with CWELD.

As extra exercises, please try the following variation of the analysis:

- Using scaled beam stiffness with CWELD/PWELD to meet the value given by the empirical formula
- Using noncongruent meshes with CFAST/PFAST or CWELD/PWELD

Input Files

The files below are on your [delivery media](#) or they can be downloaded by your web browser by clicking the links (file names) below.

File	Description
lapjoint_cbush.proc	Mentat Procedure File for point-wise connection
lapjoint_cfast.proc	Mentat Procedure File for patch-wise connection with CFAST
lapjoint_cweld.proc	Mentat Procedure File for patch-wise connection with CWELD
lapjoint_cbush.dat	Associated Marc file
lapjoint_cfast.dat	Associated Marc file
lapjoint_cweld.dat	Associated Marc file

2.28 Performance and Memory Tuning

- Summary 716
- Fast Integrated Composite Shells 728
- Combined Multi Frontal Sparse and Iterative Solver 730
- Input Files 731

Summary

Title	Performance and Memory Tuning
Solver Performance	<ul style="list-style-type: none"> • Domain Decomposition • Parallel Element Assembly • Use of ELSTO • Parallel Solver Technology • Iterative Solver • Fast integration schema for elastic composite shells • Combined multi frontal sparse and iterative solver • Storage of element data
Speed improvements for the presented models	<p>Fast integrated composite shells</p> <ul style="list-style-type: none"> • No thermal effects: speedup of 4 • With thermal effects: speedup of 2 <p>Combined multi frontal sparse and iterative solver</p> <ul style="list-style-type: none"> • Speedup of 1.8 and 5
Memory improvements for the presented models	<p>Fast integrated composite shells</p> <ul style="list-style-type: none"> • Memory reduction factor of 2 <p>Storage of element data</p> <ul style="list-style-type: none"> • Memory reduction factor ranging from 0 to 2 to 13

Finite elements is now applied to very large models, which were intractable just a short while ago. This is motivated by the desire to solve complete assemblies as opposed to single parts and the desire for greater accuracy. Engineers have the tendency to increase the size of the model as the hardware resources increase; hence, there still is a need to run jobs in an efficient manner to improve productivity.

There are multiple considerations for very large models, memory requirements, and wall time. There are two major computational aspects of the numerical analysis processes: the forming of the stiffness matrices and the solution of the linear equations.

There are several things that control the resources for forming the stiffness matrix, including:

1. The number of elements.
2. The number of integration points/layers in the element.
3. The complexity of the stress-strain matrix.

There are several methods for minimizing the costs associated with element assembly.

The most obvious is to reduce the number of elements, so the challenge would be to reduce the number of elements while maintain the same level of accuracy in the solution. This may be achievable by using adaptive meshing which is demonstrated in Chapters 2.6, 3.16, and 6.13 of this manual.

For composite shell elements, different methods for integration through the thickness are available when elastic material is used; this improves both speed and memory. A combined multi-frontal sparse and iterative solver is available where the decomposition of the direct solver is used as a preconditioner for the iterative solver; this can improve speed for mildly nonlinear problems.

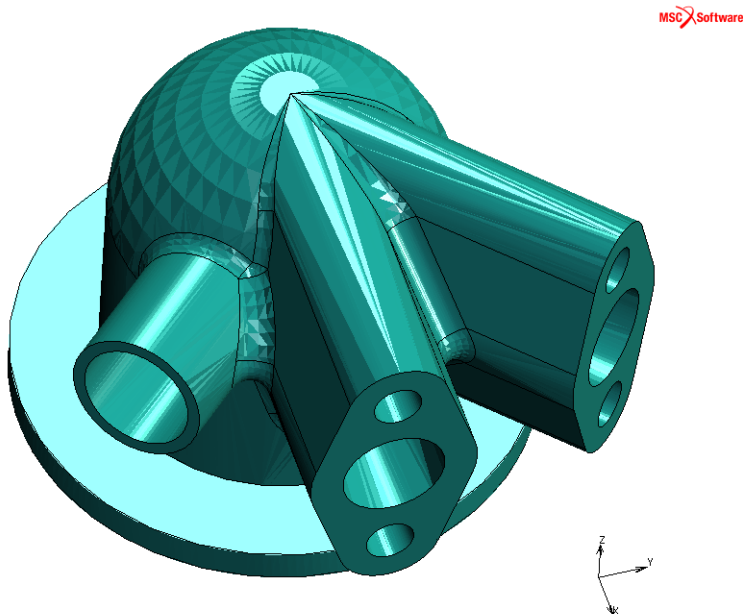
Domain Decomposition Method (DDM)

This is a procedure to remove the wall time by using parallelization. This method can be used in either a Shared Memory Parallel (SMP) or a Distributed Memory Parallel (DMP) environment. Using DDM is very effective for reducing the wall time for large models. For more information on Domain Decomposition, see *Marc Volume A: Theory and User Information*, Chapter 12. A key aspect of DDM is the solution process which will be brought up later. One can either create the domains within Mentat or let Marc create the domains.

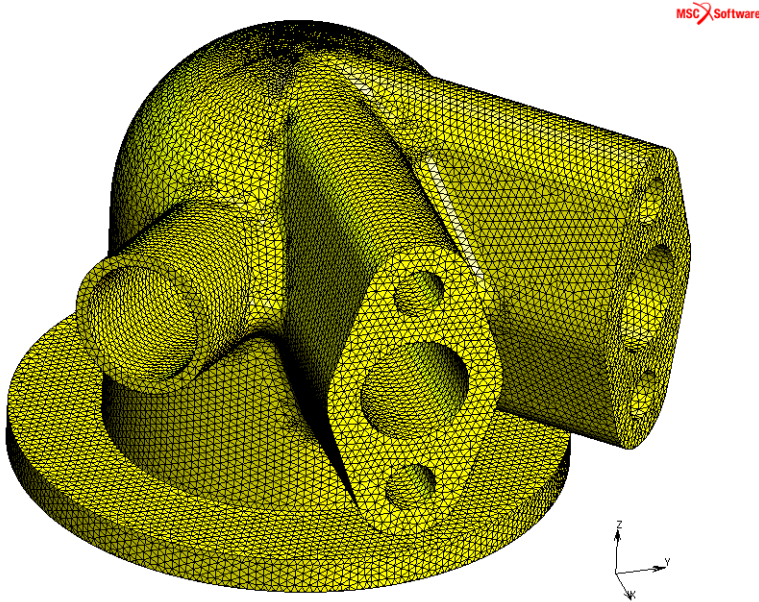
The advantages of defining the domains in Mentat is that you can see the domains before doing the numerically intensive process. It also saves time in the input phase of the analysis and is also necessary if global adaptive meshing is going to be used in any body.

The advantages of defining the domains in Marc is that the user needs to maintain one input file.

Beginning with a housing that is imported as an ACIS solid shown in the figure.



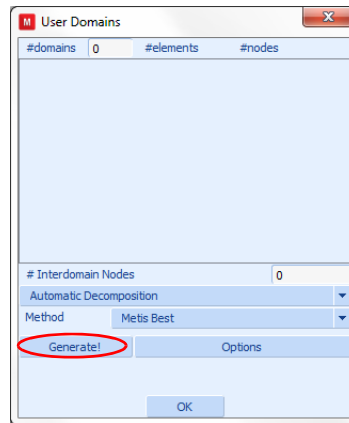
One can create a mesh using the volume mesher as shown below. The mesh contains 419,152 elements and 87,575 nodes.



The menus to create the domains are as follows.



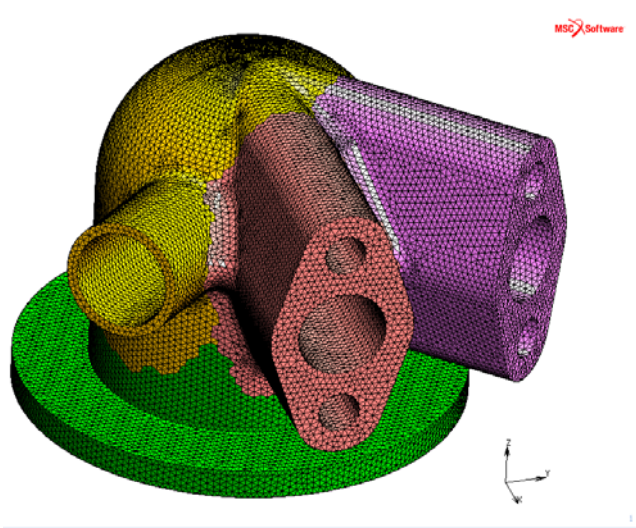
Define Domains Manually



Automatic Creation of Domains

When using the manual procedure, one needs to identify the number of domains and the elements in each domain. When using the automatic method, one simply needs to enter the number of domains. Note that there are several methods to decompose the model, but usually the default Metis Best is adequate. If one is using the DDM procedure with the iterative solution method between the domains, one would want to minimize the # Interdomain Nodes.

If one uses the automatic creation of the domains, one obtains:



One also gets the information about domains.

#domains	#elements	#nodes
1	109744	21786
2	109370	21824
3	97658	23016
4	102380	22376

Interdomain Nodes: 1408

Automatic Decomposition: [dropdown]

Method: Metis Best [dropdown]

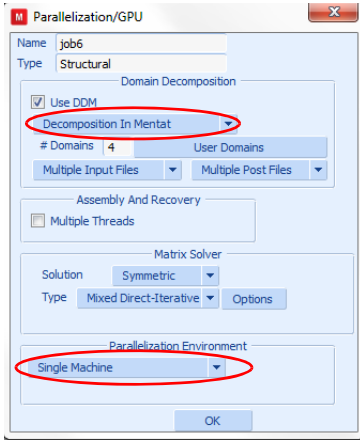
Generate! Options

OK

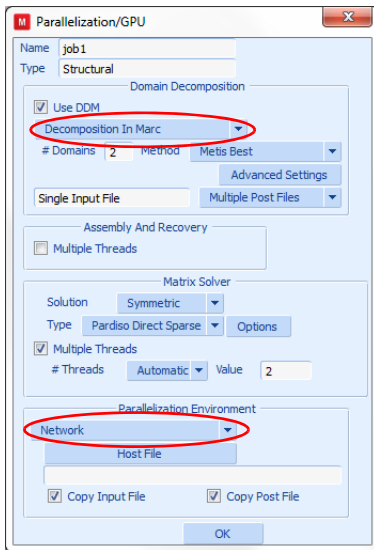
There are two modes when using Domain Decomposition for solving the system. In the first method, the stiffness matrix of each domain is decomposed to the inter-domain nodes, and then an iterative solver is used between the domains. This is the method used when the multi-frontal solver is used. It is effective when the system is well conditioned. It results in a lower use of memory and often faster calculations because a total stiffness matrix is not formed or decomposed.

In the second method, the stiffness matrix of each domain is formed, and then globally formed on a master process. The solution of the global stiffness matrix is then done using the parallel equation solver. This method produces the same result as if the job ran in serial mode. There is no iterative process, but this method uses more memory.

The DDM method is activated using the following menus that are activated through the Run menu



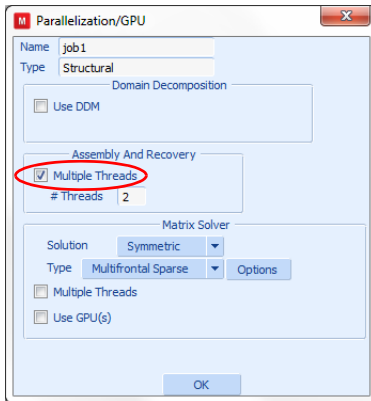
This menu appears when the domains are created using Mentat. Also, the parallel processing is done using SMP.



Here, Marc is being used to create the domains. Also, the Network – DMP method is requested. One would need to use the Host File model browser to define the host file that would identify the computers that are to be used in the analysis. For more details on the Host File, see the *Marc User's Guide*, Chapter 6.7.

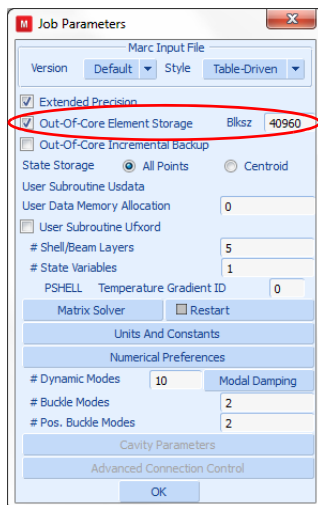
Assembly Parallelization using SMP

An alternate method for reducing stiffness matrix time is by using the SMP procedure. This is easy to use, and is very effective for all models. It takes advantage of the multi-core chips that are found on all modern computers. It is recommended that one uses all of the cores except one or two that are necessary for the operating system. This is activated by using the following menu.



ELSTO

The final issue associated with element data is the potentially large amount of data required for storing element quantities. A significant amount of memory can be saved by activating the ELSTO parameter on the following menu.



The Marc output file when ELSTO is not used.

```
flag for element storage (ielsto) 0
element data in core

memory usage per element group
group # elements nelsto MByte words
1 419152 294 470 123230688
-----
total 419152 470 123230688
```

The Marc file output when ELSTO is used is

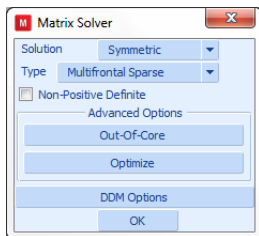
```
flag for element storage (ielsto) 1
element data out-of-core
record size 40960
info per element group
group # elements nelsto # records # elements per record
1 419152 294 1508 278
-----
total 419152 1508

approximate size of elsto scratch file (MB bytes):
471 494141440
```

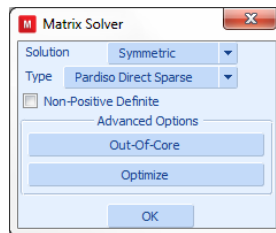
One can observe that the using ELSTO, the 470 Mbytes of element data will be written to disk. Because of buffering, it requires 471 Mbytes. One should note that activating this option increases the I/O time hence the wall time, but this is not too significant. This is especially true for machines that have Solid State Disks (SSD) as opposed to mechanical disks.

Parallel Solver Decomposition

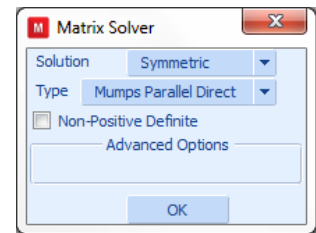
The DDM capability is not available for all Marc capabilities, so as an alternative one can use the parallel direct solvers. There are three options (the multi-frontal, Pardiso solver, or MUMPS solver) which are activated using the menus below. The first two are designed for SMP, while the MUMPS solver is designed for DMP.



Multifrontal Solver

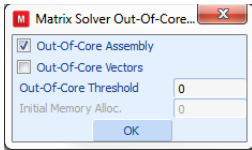


Pardiso Solver

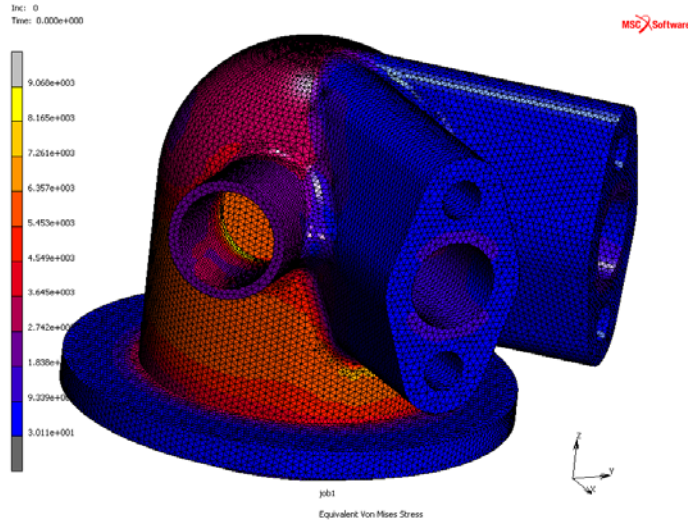
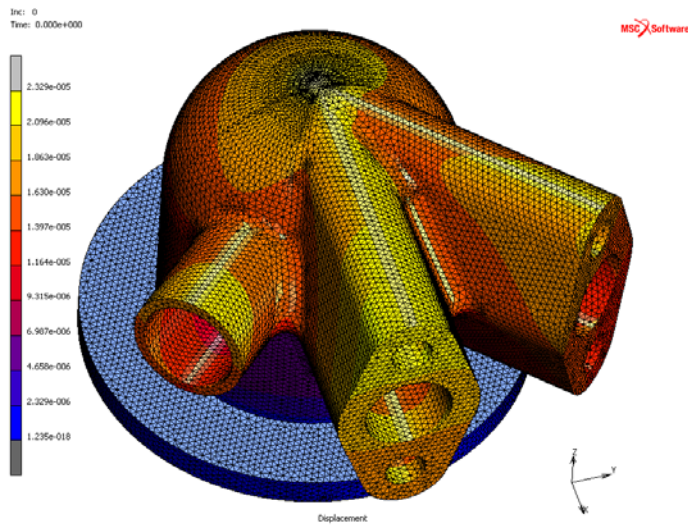


MUMPS Solver

One can also control whether the stiffness matrix and the decomposed stiffness can be stored out-of-core. This allows for larger models to be solved with fewer resources. This is activated using the following menu.



To demonstrate the performance, the model was run under a variety of circumstances. The bottom was fixed and internal pressure in the major cavity and the major tubes. The resultant displacement and stresses in the linear analysis are shown in the following figure.



The performance numbers achieved when using the conventional 4-node tetrahedral element (type 134) and the advanced 5-node Herrmann element (type 157).

4-node Tetrahedral Element

Cores	Assembly Recovery	% Reduction	Scaling	Recovery	% Reduction	Scaling	Solver	% Reduction	Scaling
1	3.7	0	1.00	2.62	0	1.00	15.01	0	1.00
2	2	46	1.85	1.52	42	1.72	9.24	38	1.62
4	1.2	68	3.08	0.9	66	2.91	6.65	56	2.26
6	0.95	74	3.89	0.66	75	3.97	6.65	56	2.26

5-node Tetrahedral Element

Cores	Assembly Recovery	% Reduction	Scaling	Recovery	% Reduction	Scaling	Solver	% Reduction	Scaling
1	11.74	0	1	7.28	0	1	38.76	0	1
2	6.69	43	1.754858	4.17	43	1.745803	23.37	40	1.658537
4	3.98	66	2.949749	2.45	66	2.971429	17.67	54	2.193548
6	3.11	74	3.77492	1.91	74	3.811518	17.66	54	2.19479

The analysis was also performed using higher order elements. Note, that while one might be tempted to use the Change Class option to convert the lower-order tetrahedral elements into higher-order tetrahedral elements, this is not a good idea. The reason is that if one has curved regions, especially concave regions (such as around holes), it is likely to get distorted/inside-out elements. The better technique is to go back to the initial CAD geometry and create a new higher-order mesh.

When this was done, the number of elements was 419,475, and the number of nodes was 1,050,073.

If one examines either the bottom of the output or the bottom of the log file, one would observe the following:

```

memory usage:                MByte      words  % of total
within general memory:
element stiffness matrices:   109      28678534    0.6
solver: first part           1233     323171184    6.8
overall allocation initial allocation  0         4    0.0
other:                       3       840760    0.0
allocated separately:
solver 11                    16189    4243753216   89.3
nodal vectors:              375     98373302    2.1
defined sets:               0       115784    0.0
transformations:           10     2522392    0.1
kinematic boundary conditions: 2       551828    0.0
points, curves and surfaces: 0         86    0.0
mem_none:                   102     26822106    0.6
element storage:            74     19388892    0.4
material properties:        0       2968    0.0
executable and common blocks: 27     7000000    0.1
miscellaneous                0         212    0.0
-----
total:                       18124    4751221268
general memory allocated:    1345     352690482
general memory used:        1345     352690478
peak memory usage:          18789    4925295814

timing information:          wall time    cpu time
total time for input:       35.33       35.27
total time for stiffness assembly: 17.50       17.35
total time for stress recovery: 28.83       14.66
total time for matrix solution: 1101.22     822.00
total time for output:      11.06       10.51
total time for miscellaneous: 2.79        2.25
-----
total time:                  1196.73     902.04

```

These analyses were performed on a lap-top machine with 16GB of main memo; so, effectively, part of the job was run out-of-core. This could also have been seen in the following messages:

```

estimated minimum memory required for in-core matrix solution
using PARDISO solver is      16648 MBytes.

```

```

estimated minimum memory required for out-of-core matrix solution
using PARDISO solver is      3278 MBytes.

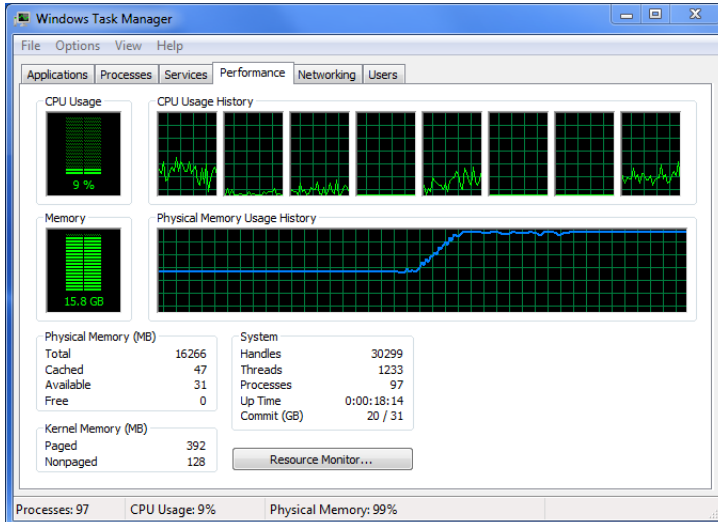
```

```

start of matrix solution
wall time =      112.00

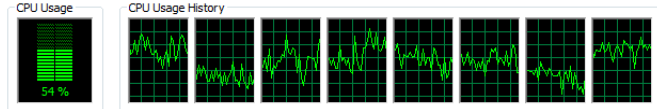
```

In fact, if one would have used the Windows Task Manager, one would have observed:



which indicates that all of the memory is in use.

During certain phases, the task manager would have shown the following indicating that all the cores were engaged and over 50% of all 8 cores were being used.



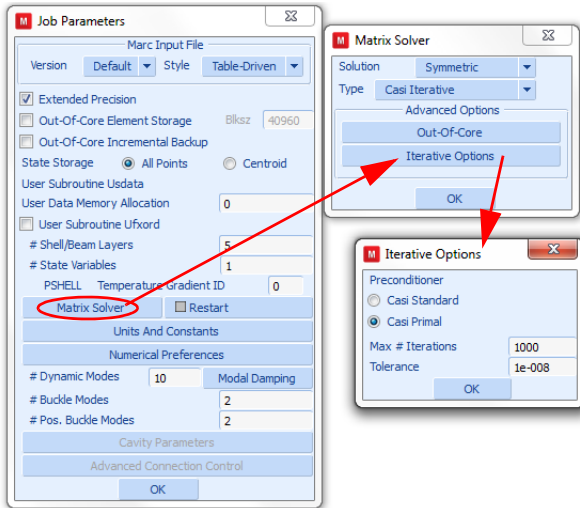
The simulation was also run with parallel assembly and solution, and from the output one would have observed:

timing information:	wall time	cpu time
total time for input:	35.30	35.24
total time for stiffness assembly:	4.74	27.50
total time for stress recovery:	16.30	57.21
total time for matrix solution:	441.92	1098.76
total time for output:	11.87	11.11
total time for miscellaneous:	3.18	2.39

total time:	513.32	1232.21

One can see that even though the job is running out-of-core, there is still a reduction in wall time of a factor of two for the complete simulation.

In fact, this problem is conditionally well behaved and, hence, suitable for the CASI iterative solver. The iterative solver is also advantageous because it does not form a global stiffness matrix or a decomposed stiffness matrix. One can activate this solver using the following menus.



The performance, shown as follows, is much better.

memory usage:	MByte	words	% of total
within general memory:			
element stiffness matrices:	101	26576258	1.9
solver: first part	963	252393316	18.3
other:	3	841760	0.1
allocated separately:			
solver 9	1197	313891113	22.8
nodal vectors:	370	97112106	7.0
defined sets:	0	115784	0.0
transformations:	10	2522392	0.2
kinematic boundary conditions:	2	551828	0.0
points, curves and surfaces:	0	86	0.0
mem_none:	1884	493829258	35.8
element storage:	1600	419475976	30.4
material properties:	0	2968	0.0
element coloring resident:	3	839150	0.1
element coloring peak:	18	4617198	0.3
multi-threading scratch array:	0	144	0.0
executable and common blocks:	27	7000000	0.5

total:	5256	1377893497	
general memory allocated:	162	42552374	
general memory used:	1067	279811334	
peak memory usage:	5285	1385460685	
timing information:	wall time	cpu time	
total time for input:	33.60	33.60	
total time for stiffness assembly:	4.79	26.55	
total time for stress recovery:	2.23	13.24	
total time for matrix solution:	63.79	65.16	
total time for output:	9.70	10.87	
total time for miscellaneous:	2.08	2.07	
total time:	116.19	151.51	

One observes that the memory requirement is substantially less for the analysis. As this is an ideal model, the time required for the solution time is close to seven times faster than using the parallel direct solver.

Fast Integrated Composite Shells

The fast integration option leads to significant speed improvements for composite shell structures with a large number of layers. The improvements occur due to a different method of integration through the thickness. The layers need to have elastic material properties, either ISOTROPIC, ORTHOTROPIC, or ANISOTROPIC. When large displacements occur the Total Lagrange (LARGE DISP) formulation should be used. The method can be set globally on the SHELL SECT parameter and locally for each group of elements with the COMPOSITE option. Three integration methods are available:

- FULL Original method, can be used with all the material models
- FAST NO THERMAL Integration method for elastic material without temperature effects
- FAST THERMAL Integration method for elastic material with temperature effects

The method can be selected in Mentat for composite materials as follows (see also [Figure 2.28-1](#))

- MATERIAL PROPERTIES
- MATERIAL PROPERTIES
- LAYERED MATERIALS
- NEW COMPOSITE
- INTEGRATION METHOD: DEFAULT

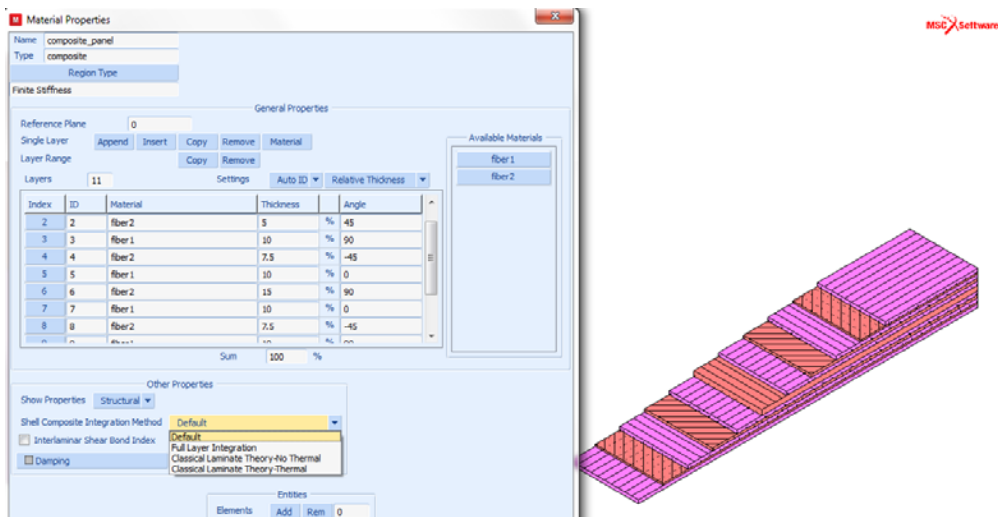


Figure 2.28-1 Define Integration Method

Analyzed is a plate supported by a rigid and deformed by another rigid, see [Figure 2.28-2](#). The plate has 30 layers, consisting of two different materials, and consists of 7168 elements. Both a structural and a coupled thermal-structural analysis is performed to compare the different integration methods.

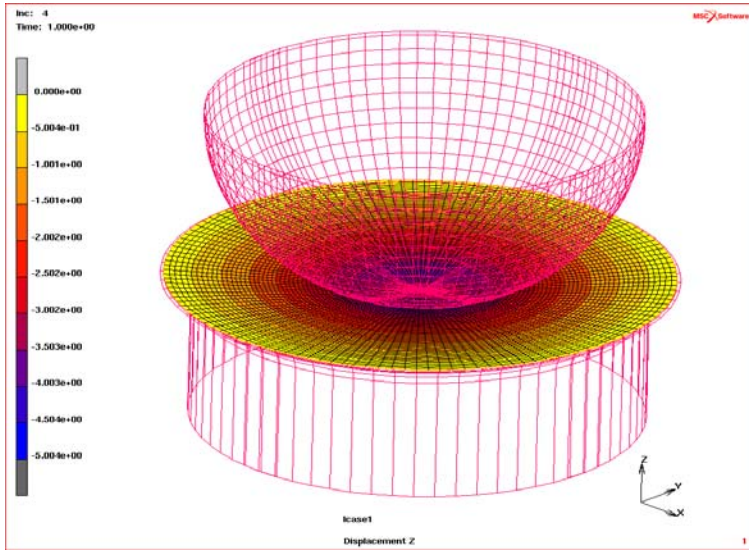


Figure 2.28-2 Analyzed Plate Showing Deformation

[Table 2.28-1](#) shows the results of the speed and memory improvements of the different examples.

Table 2.28-1 Speed and Memory Improvements for Fast Integrated Composite Shells

	Structural		Coupled Thermal Structural	
	Full	Fast no thermal	Full	Fast thermal
Normalized CPU time (s)				
Total	1	0.27	1.31	0.67
Assembly	0.39	0.06	0.48	0.19
Stress Recovery	0.44	0.03	0.57	0.20
Memory (Mb)				
Total	692	236	728	386
Incremental backup	222	20	186	113
Element storage	283	29	354	185

Combined Multi Frontal Sparse and Iterative Solver

This procedure can reduce the total solver time significantly for nonlinear analyses. This is reached by using the decomposition obtained from the multi-frontal sparse solver as a preconditioner for the iterative solver. The first solution is obtained with the multi-frontal sparse solver, and then in the next cycles or increments, the decomposition is used as the preconditioner for the iterative solver. This is done until the iterative solver needs too many cycles to find a solution, or when it fails to find a solution. Then, the solution is again obtained with the multi-frontal sparse solver so that a new decomposition is available for the iterative solver for upcoming cycles and/or increments. If, repeatedly, no solution is found by the iterative solver, this procedure is switched off, and only the multi-frontal sparse solver is used. This procedure is useful for mildly nonlinear problems. In Mentat, this solver can be set as follows

```
JOBS
  MECHANICAL (or other analysis class)
    JOB PARAMETERS
      SOLVER
        MIXED DIRECT-ITERATIVE
```

The number of iteration can be controlled by

```
SERIAL ITERATIVE
  MAX # ITERATION
    40
```

Note that the number of iteration for the iterative solver should be low. The time needed for this amount of iterations should be much less than the time needed for the multi-frontal sparse solver to find a solution. Marc has some logic to come up with a number based on wall times. It will reduce the maximum number when it is too large. Note that since the estimation from Marc is based on wall time, it can change when the analysis is repeated.

As an example, a rectangular block of elastic-plastic material and a rubber top layer is analyzed. A rigid cylinder is pressed into this block, and in the second loading stage, this cylinder is rolled. Large plastic deformation is anticipated in this analysis. The rubber is analyzed with a Mooney material model and Hermann elements since these elements can handle the incompressibility of the Mooney Material better. The elastic-plastic material is modeled with normal brick elements. [Figure 2.28-3](#) shows deformation and the total plastic strain of the rectangular block at the end of the analysis.

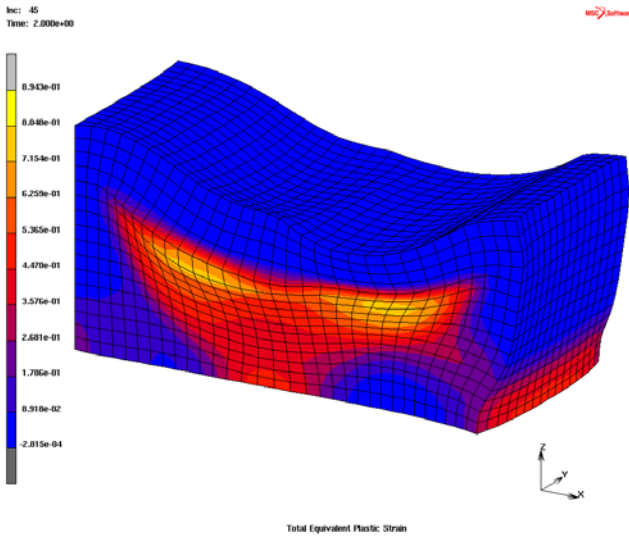


Figure 2.28-3 Contourplot of the Plastic Strain of the Deformed block

This model consists of 8192 elements and needs about 400 Mbytes of memory during the analysis. The total analysis time is 3981 seconds for the multi-frontal sparse solver versus 2236 seconds for the combined method. This is a speedup of 1.8. Comparing only the solver times the speedup is even 2.7. Note that no solution is found when only the iterative solver is used. A few increments of this example are repeated for an ever finer meshed model, where each element was subdivided into 8 new elements. This model consists of 65536 brick elements and needs about 3.9 Gbytes of memory during the analysis. For this example, the total analysis time is 36467 seconds for the multi frontal sparse solver versus 7276 seconds for the combined method. This is a speedup of 5. Comparing only the solver times the speedup is 7.

Input Files

The files below are on your [delivery media](#) or they can be downloaded by your web browser by clicking the links (file names) below.

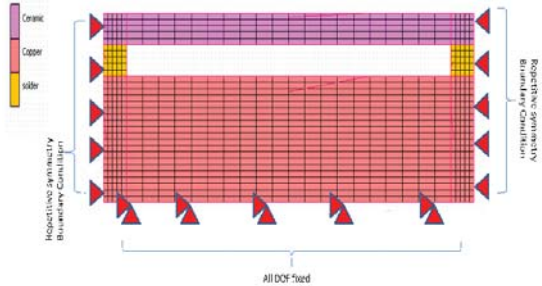
File	Description
For Fast Composite Shell Integration	
composite_plate.proc	Mentat Procedure File
composite_plate.mud	Associated Mentat model file
composite_plate.dat	Associated Marc file
For Fast Composite Shell Integration, Coupled Analysis	
composite_plate_cpl.proc	Mentat Procedure File
composite_plate_cpl.mud	Associated Mentat model file

File	Description
For Fast Composite Shell Integration	
<code>composite_plate_cpl.dat</code>	Associated Marc file
For Mixed Solver	
<code>block_rolling.proc</code>	Mentat Procedure File
<code>block_rolling.mud</code>	Associated Mentat model file
<code>block_rolling.dat</code>	Associated Marc file
For Element Storage Example	
<code>disk_drive_head_tet.proc</code>	Mentat Procedure File with tetrahedral elements
<code>disk_drive_head_tet.mud</code>	Associated Mentat model file with tetrahedral elements
<code>disk_drive_head_tet.dat</code>	Associated Marc file with tetrahedral elements
<code>disk_drive_head.proc</code>	Mentat Procedure File
<code>disk_drive_head.mud</code>	Associated Mentat model file
<code>disk_drive_head.dat</code>	Associated Marc file with 3 layers
<code>disk_drive_head_11layer.dat</code>	Associated Marc file with 11 layers

2.29 Implicit Viscoplastic Creep Analysis of Solder

- Summary 734
- Introduction 735
- Flow Equation 735
- Requested Solutions 736
- Modeling Details 736
- Loading and Boundary Conditions 739
- Solution Procedure 741
- Result and Plots 744
- Conclusion 746
- Input Files 746
- Video 746

Summary

Title	Implicit Viscoplastic Creep Analysis of Solder
Features	Viscoplasticity Anand solder material model.
FE Mesh	
Material properties	<p>Material for</p> <p>Copper Block: $E = 1.30e6\text{Mpa}$; $\nu = 0.344$; $\text{Alpha} = 1.78e-5$</p> <p>Ceramic Block: $E = 3.75e5\text{Mpa}$; $\nu = 0.22$; $\text{Alpha} = 5.36e-6$</p> <p>Temperature dependent material properties are used for solder.</p>
Analysis characteristics	Nonlinear Elastoplastic Creep Analysis
Boundary conditions and Applied loads	<ol style="list-style-type: none"> 1. Copper Block is fixed in all degrees of freedom at the bottom. 2. Repetitive Symmetric boundary conditions are applied at the edges. 3. Cyclic Thermal loads applied on model with temperature ranging from 0°C to 125°C. 4. Sinusoidal structural displacement is applied on two middle nodes of the ceramic block varying from 0.5 to -0.5mm.
Element type	<ul style="list-style-type: none"> • 2-D 4-noded isoparametric, plain strain elements. (Element 11)
FE results	<ol style="list-style-type: none"> 1. Total Equivalent Creep Strain. 2. Equivalent Creep Strain.

Introduction

Thermal cycling causes thermo-mechanical deformations in electronic assemblies, which results in damage of solder connections. Accurate prediction of stresses in the solder connections is a critical step in design for reliability of interconnected parts which requires a well defined material model for solder. The Anand Solder model is used to model solders response to loading in the electronics industry.

The Anand Solder material model is implemented under Viscoplastic Material Model in Marc/Mentat. The model is implemented using a semi implicit (implicit in deformation resistance and stress, explicit in temperature) approach, and a backward Euler time integration scheme is adopted for solving the set of constitutive viscoplastic equations.

Note: The viscoplastic creep solder model needs a creep load case from the outset. It will not work in case a static load case is followed by a creep load case.

Flow Equation

Anand Solder material model uses a single scalar internal variable, s , which denotes the averaged isotropic resistance to macroscopic plastic flow offered by the underlying isotropic strengthening mechanisms such as dislocation density, solid solution strengthening, subgrain, and grain size effects, etc. The deformation resistance s is consequently proportional to the equivalent stress. The flow equations and the evolution equations are give below:

Flow Equation:

$$\frac{d\varepsilon_p}{dt} = A \left[\sinh\left(\frac{\xi\sigma}{s}\right) \right]^m \exp\left(-\frac{Q}{kT}\right)$$

where

s	Single internal variable representing deformation resistance s_0
A	Pre-exponential factor
ξ	Multiplier of stress
m	Strain rate sensitivity of stress
Q/k	Activation Energy/Boltzmann's Constant

where the evolution equation is expressed as:

Evolution Equations:

$$\frac{ds}{dt} = \left\{ h_0 |B|^a \frac{B}{|B|} \right\} \frac{d\varepsilon_p}{dt}$$

$$B = 1 - \frac{s}{s^*}$$

$$s^* = \hat{s} \left[\frac{1}{A} \frac{d\varepsilon_p}{dt} \exp\left(\frac{Q}{kT}\right) \right]^{-n}$$

where

h_0	Hardening constant
\hat{s}	Deformation resistance saturation coefficient
n	Strain rate sensitivity of saturation
a	Strain rate sensitivity of hardening

s^* represents the saturation value of s associated with a set of given temperatures and strain rates. Thus the Anand Solder model has nine material parameters: A , Q , ξ , m , h_0 , \hat{s} , n , a , where s_0 is the initial value of the deformation resistance needed to determine the evolution of the deformation resistance.

Requested Solutions

Numerical analysis is performed to find Equivalent Creep Strain and Total Equivalent Creep Strain values in the solder material.

Note: The equivalent Plastic strain in case of the Solder model can be visualized by plotting of the equivalent Creep strain.

Modeling Details

The analysis model assembly is made of ceramic and copper blocks bonded together at the ends and center by a eutectic tin-lead solder and is subjected to cyclic thermal and structural loads. A 2D Plain strain modeling is done by creating points, surfaces and then by creating mesh from surfaces using “convert surface to mesh” option in Mentat.

The bottom of the PCB is fixed in all directions ($u_x, u_y=0$) and the edges are subjected to repetitive symmetry boundary conditions ($u_x=0$). Material properties and thermal loading are applied shown above.

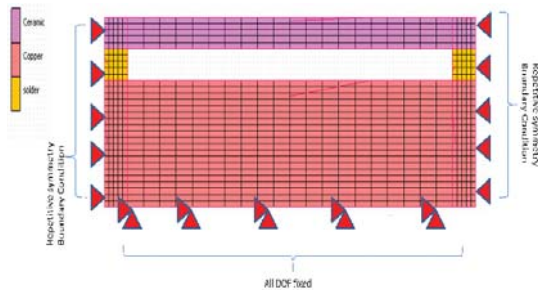


Figure 2.29-1 Finite Element Model of the Structure

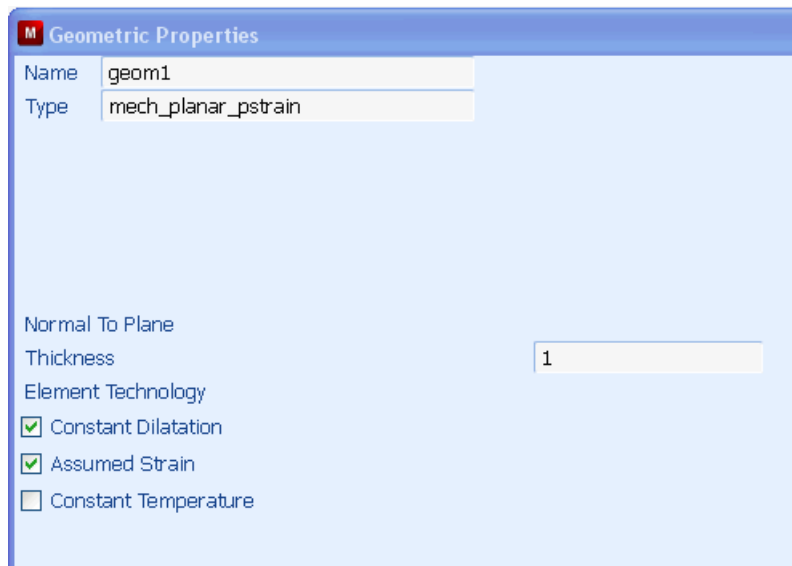
Element Modeling

The 4-noded plane strain elements (Element 11) have been used to mesh the model. The assumed strain option and constant dilatation have been flagged on using geometry option.

Constant dilatational option is used for element 11 to avoid volumetric locking of elements.

Assumed Strain Formulation is used for element 11 for improved results; especially in bending as it better captures the linear variation in shear strain.

For more information on these options, please refer *Marc Volume A: Theory and User Information*.



Material Modeling

Elastic Plastic Isotropic material with viscoplasticity and is selected for Solder material. Method used is Anand Solder with secant approximation material tangent. Temperature dependent material properties (Young's Modulus, Poissons ratio and coefficient of thermal expansion) are used for solder material and are defined using [Tables](#).

For copper and ceramic blocks, Elastic Plastic isotropic material without Viscoplasticity option is used.

To Create Tables in Mentat use the following steps.

Table and Co-ordinate Systems >>New

Select the Independent Variable Type >>Time (for loads) or Temp (Material Properties)

To Create Material Properties in Mentat use the following steps.

Material properties>>New>>Standard>>Structural>>Viscoplasticity.

Anand Solder>> Secant Approximation.

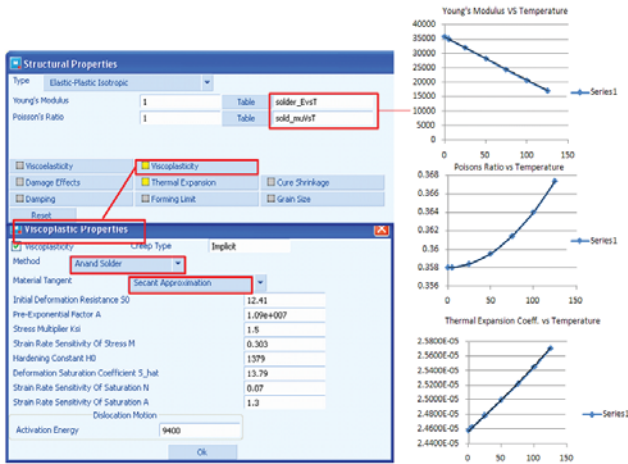
Select the appropriate tables in the Structural Properties widget.

Table 2.29-1 Constants used for Anand Solder Model

Anand Solder Constants in Mentat	Parameter	Value	Units
C1	Single internal variable (s0) representing deformation resistance	12.41	Stress
C2	pre-exponential factor (A)	400000 0	1/time
C3	the multiplier of stress (1.5	Dimensionless
C4	strain rate sensitivity of stress (m)	0.303	Dimensionless
C5	hardening constant (h0)	1379	Stress
C6	deformation resistance saturation coefficient (s)	13.79	Stress
C7	strain rate sensitivity of saturation (n)	0.07	Dimensionless
C8	strain rate sensitivity of hardening (a)	1.3	Dimensionless
	Activation Energy / Boltzmann's Constant	9400	Energy/Volume

Table 2.29-2 Temperature Dependent Material Properties used for Solder

Temperature (°C)	Young's Modulus (Mpa)	ν (Poisson's Ratio)	Thermal Expansion Coefficient (°C)
0.00E+00	3.56E+04	3.58E-01	2.46E-05
5.00E+00	3.49E+04	3.58E-01	2.46E-05
2.50E+01	3.19E+04	3.58E-01	2.48E-05
5.00E+01	2.82E+04	3.60E-01	2.50E-05
7.50E+01	2.44E+04	3.61E-01	2.52E-05
1.00E+02	2.07E+04	3.64E-01	2.55E-05
1.25E+02	1.70E+04	3.67E-01	2.57E-05



Defining Temperature Dependent Material Properties in Mentat

Loading and Boundary Conditions

Figure 2.29-1 shows the loading and boundary conditions applied on the finite element model of the assembly. The total duration of analysis is 120 seconds and the both the thermal and structural loads are applied as varying with respect to time with the help of tables.

To **Create Tables** in Mentat use the following steps.

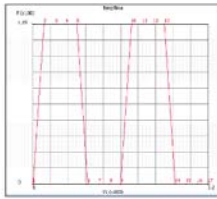
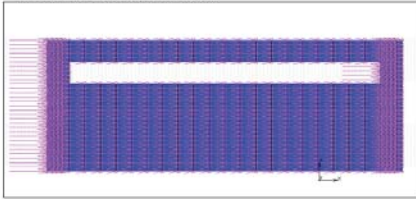
Table and Coordinate Systems>New

Select the **Independent Variable Type>Time** (for loads) or **Temp** (for Material Properties) plotted in X-axis of Graph.

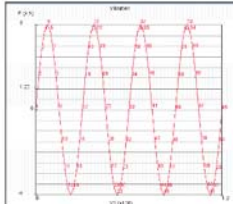
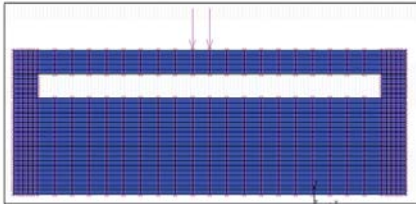
Use data points option to add points or use formula to create the dependent variable plotted in Y-axis of Graph.

Thermal and Structural Loads

Thermal Load Applied (on all nodes)

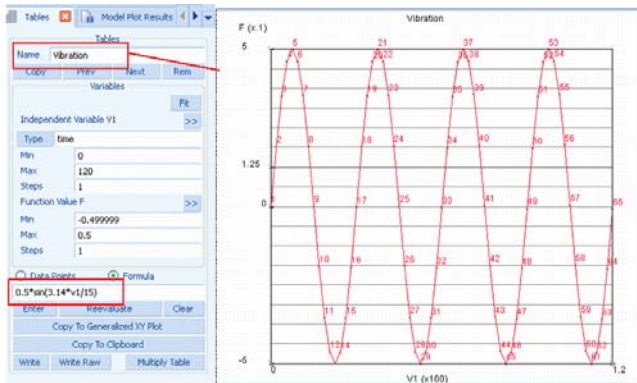


Structural /Vibrational Load Applied (on ceramic block) = $0.5 * \sin(3.14 * v1 / 15)$

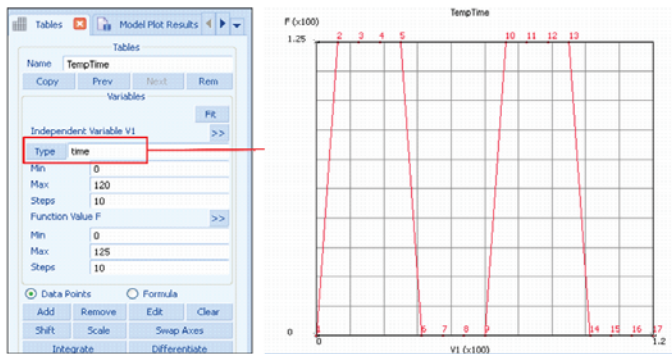


Total Solution Time = 120 Sec

Thermal and Structural Loads Applied



Creating Tables for Sinusoidal Structural Loading using Formula Option



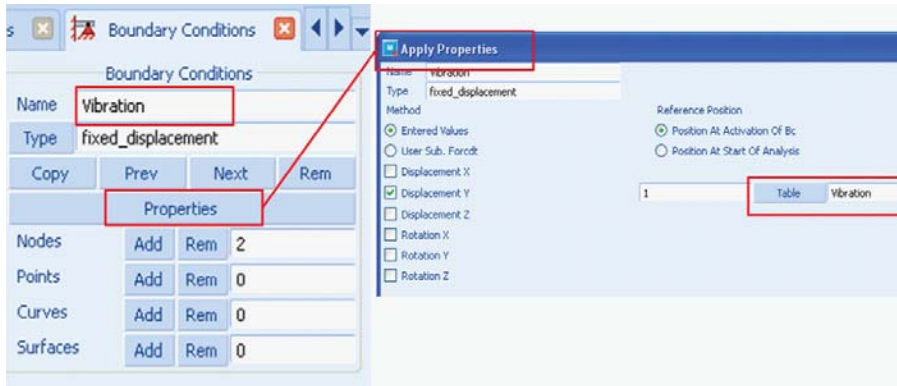
Creating Tables for Thermal Loading with Datapoints

To Create Boundary Conditions in Mentat use the following steps

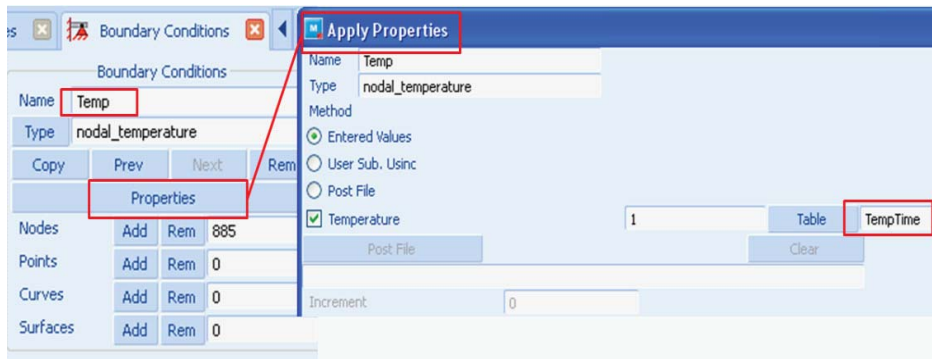
Boundary Conditions>New>Type>Structural>Fixed Displacement

Boundary Conditions>New>Type>State Variable>Nodal Temperature

Select the appropriate tables in the Apply Properties widget.



Creating and Applying Structural Loads by using Tables



Creating and Applying Thermal Loads by using Tables

Solution Procedure

The problem is analyzed in Marc with an implicit creep procedure.

Control parameters for the nonlinear solution scheme are described through the CONTROL option and AUTO STEP option. This can be done using Mentat by the following steps

To create a new Creep loadcase in Mentat use the following steps

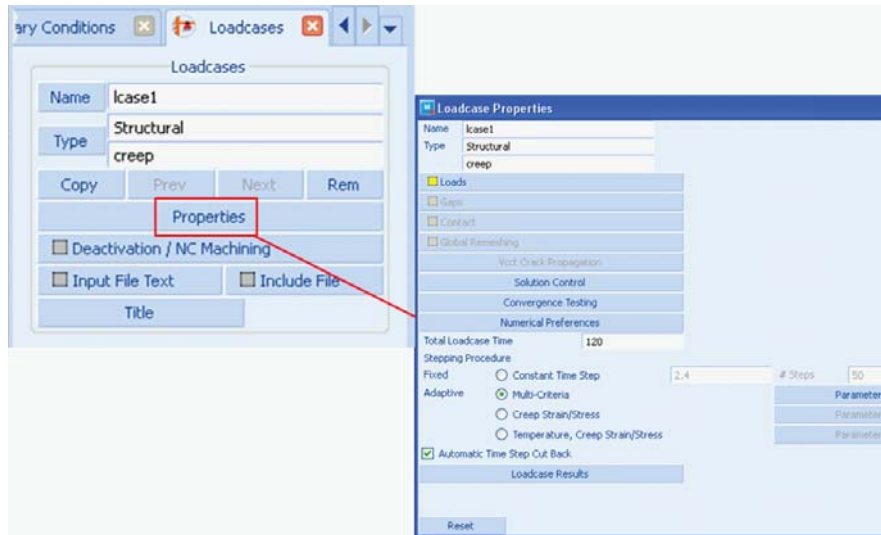
Loadcase>New>Creep

To create the Autostep option in Mentat use the following steps

Loadcases>Properties>Multicriteria

To Create the Control option in Mentat use the following steps

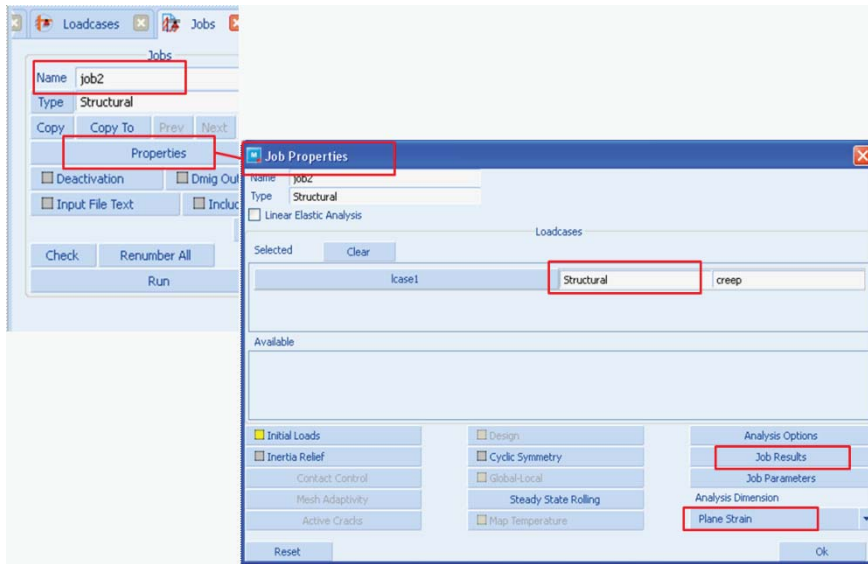
Loadcases>Properties>Solution Control



Creating Creep Load Case

To set up a Job in Mentat use the following steps

JobsNew >Properties>Select Required Load case (under Available)



Selecting Required Load Case

Select the required results, Submit and post processing in Mentat can be done using

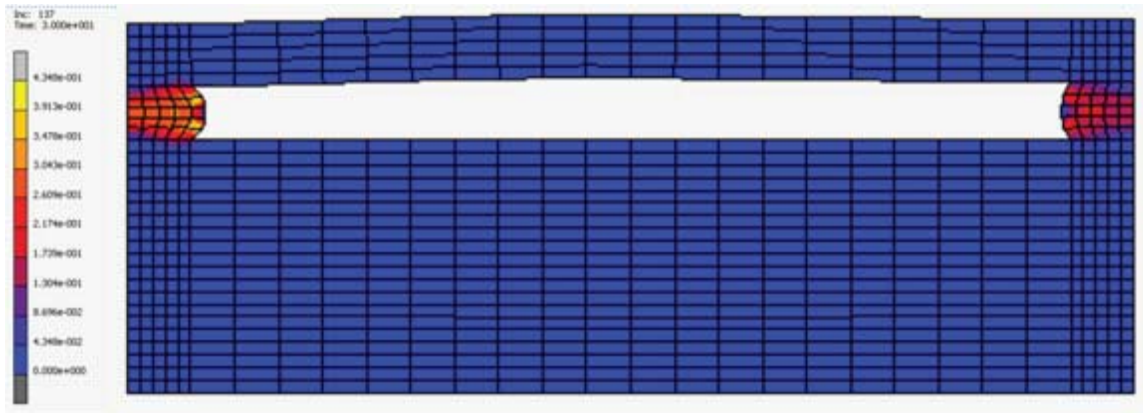
Jobs>New >Properties>Job Results tab

Set the Analysis Definition as plane strain.

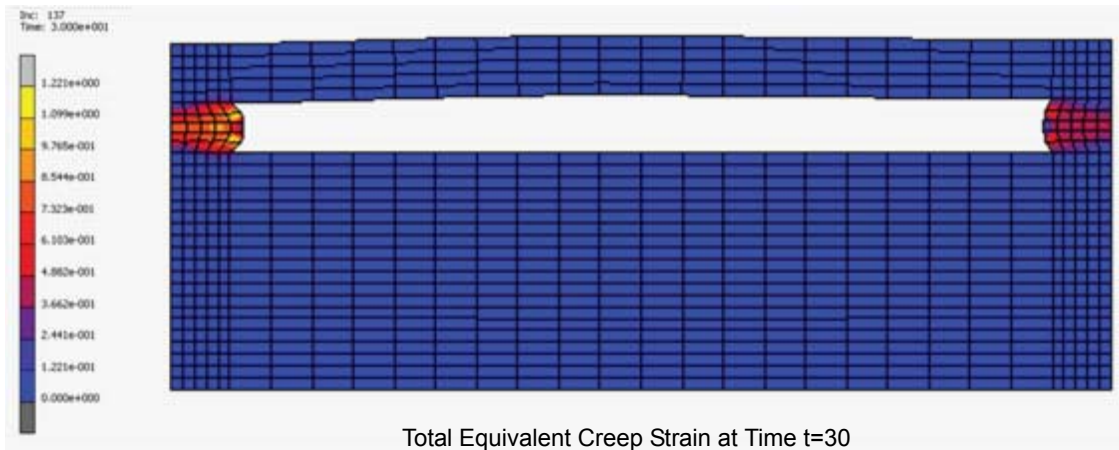
Jobs>Run>Submit(1)

Jobs>Run>Open Post File

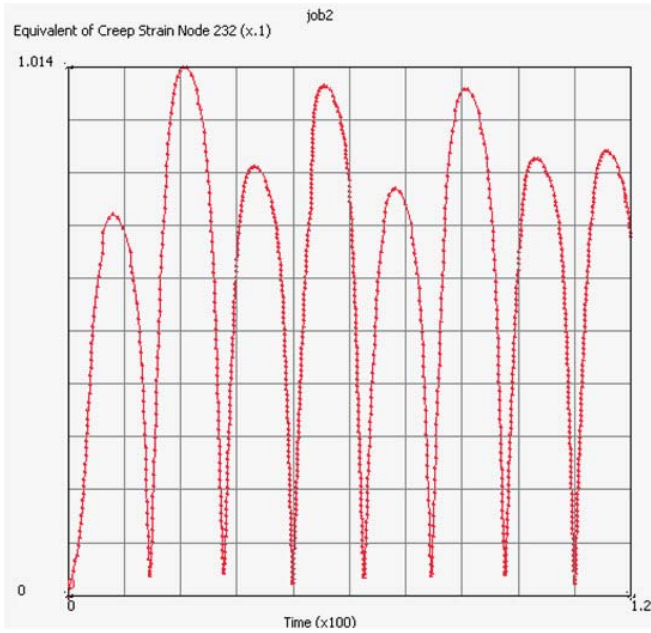
Result and Plots



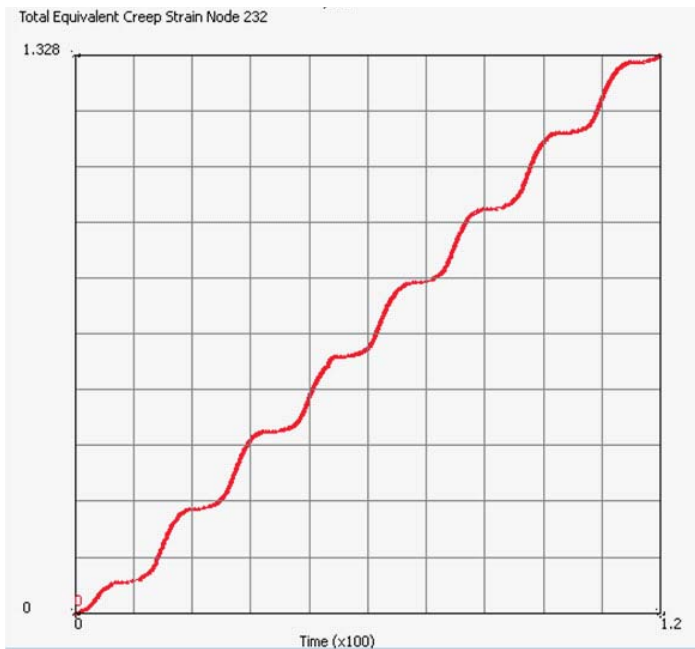
Equivalent Creep Strain at Time t=30



Total Equivalent Creep Strain at Time t=30



Result Plot of Equivalent Creep Strain at Node = 232 (on Solder)



Result Plot of Total Equivalent Creep Strain at Node = 232 (on Solder)

Conclusion

From the graph of the results it is recognized that the creep strain is influenced more by the structural loading as compared to thermal loads.

Input Files

The files below are on your [delivery media](#) or they can be downloaded by your web browser by clicking the links (file names) below.

File	Description
SOLDER_TEST_pstrain.mud	Mentat model for creep analysis of solder.
create_points1.proc	Procedure files to generate points
mentat-sur-creat1.proc	Procedure files to generate surface
mentat-meshdone1.proc	Procedure files to generate mesh

Video

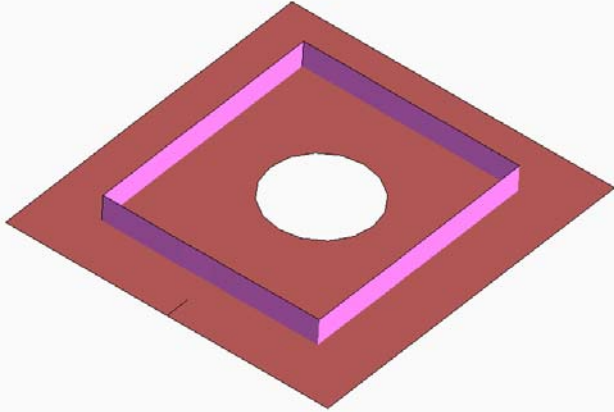
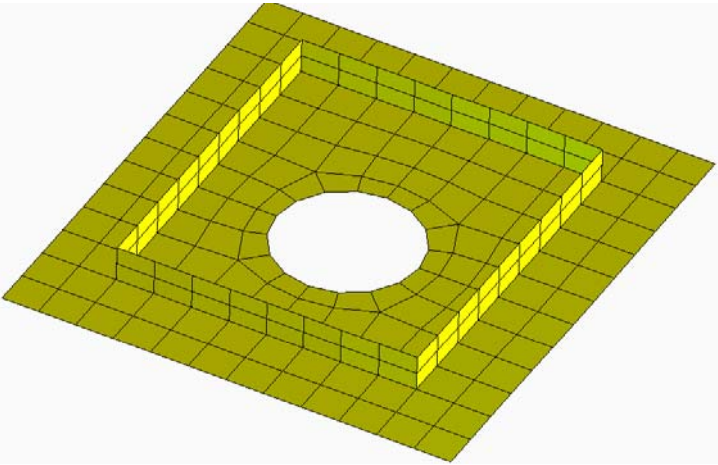
Click on the link below to view a streaming video of this problem.

File	Description
ch02-29.swf	Video for implicit viscoplastic creep analysis of solder.

2.30 Crack Propagation Capability in Shells

- Summary 748
- Introduction 749
- Requested Solution 749
- Modeling Details 749
- Geometric Properties 749
- Material Properties 750
- Crack Modeling 750
- Loading and Boundary Conditions 751
- Solution Procedure 753
- Results 753
- Input Files 754

Summary

Title	Crack propagation capability in shells
Features	Shell crack growth
Geometric Model with Crack	
FE Mesh	
Material properties	Isotropic material with, $E = 2 \times 10^{11} \text{ N/mm}^2$; $\nu = 0.3$
Analysis characteristics	Nonlinear static analysis with crack propagation
Boundary conditions and Applied loads	One end of the plate is completely fixed. The opposite side is forced to remain straight and given a prescribed vertical displacement of 0.1. This load is varied cyclically during a time period of 10
Element type	4-noded quad shell element type 75 is used
FE results	VCCT energy release

Introduction

Marc has a number of capabilities for crack propagation, including growth along predefined paths and growth in general directions. The current example will illustrate crack propagation in a shell structure with a stiffener. A crack starts in the skin of the structure and bifurcates when it reaches the stiffener.

The crack grows in a user specified direction using the method to cut through the mesh. Hence, the growth occurs independently of the mesh.

Requested Solution

The change in the mesh as a result of the growing crack. In particular, a crack should be introduced in the stiffener.

Modeling Details

As shown in [Figure 2.30-1](#), the model comprises of a plate with a stiffener. There is also a hole at the center of plate. The stiffener shares the nodes with the plate, and no shell offset is used in this example.

The plate is fixed on one end and, on the other end, a cyclic fatigue load is applied as a varying prescribed displacement of amplitude 0.1. The fatigue cycle consists of a loading and an unloading and the crack will grow after each fatigue cycle.

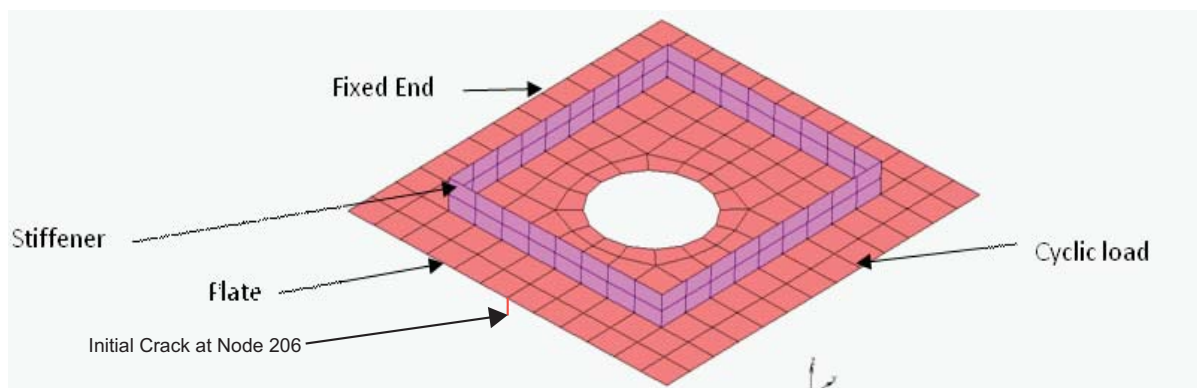


Figure 2.30-1 Plate with Stiffener

Geometric Properties

Four-noded quad shell elements are used for both plate and stiffener. A shell thickness of 0.01 is defined in the geometric properties of the elements as shown in [Figure 2.30-2](#).

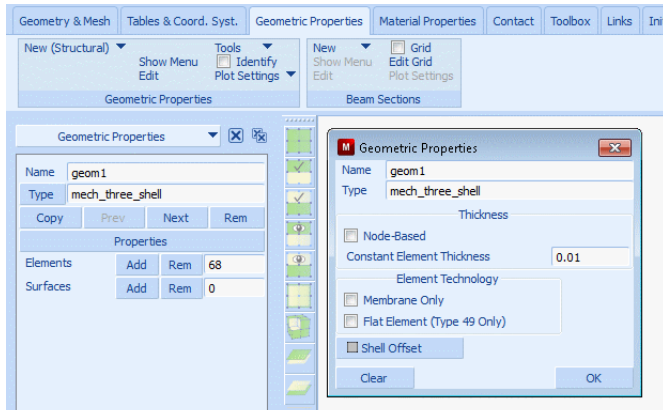


Figure 2.30-2 Geometric Properties of Elements

Material Properties

Linear isotropic material properties are defined as shown in Figure 2.30-3.

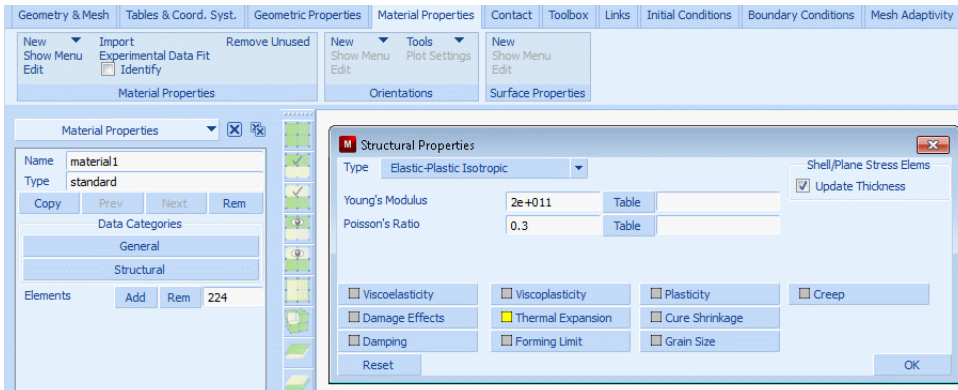


Figure 2.30-3 Linear Isotropic Material Properties

Crack Modeling

The crack is modeled using the VCCT technique as shown in Figure 2.30-4.

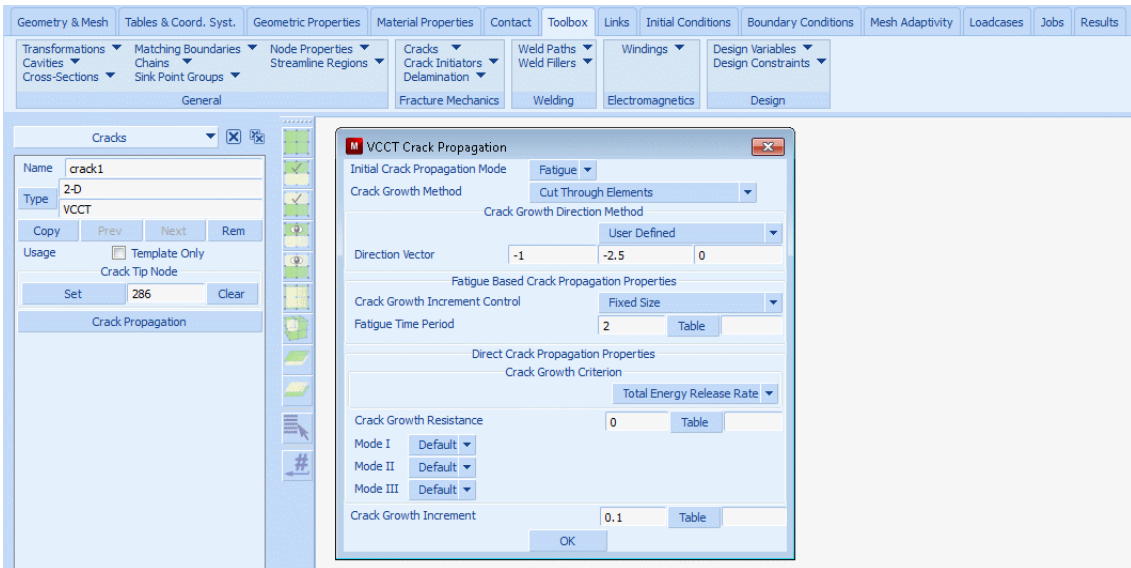


Figure 2.30-4 Crack Modeled with VCCT

Fatigue mode is selected as the crack propagation mode. The Fatigue Time Period is set to 2, and is selected to be consistent with the time period of the loading. The fatigue cycle consists of a loading and unloading of the structure, and this is repeated five times.

The Crack Growth Method is set to use the option Cut Through Elements. With this option the mesh around the crack tip is modified in order to grow the crack and in order to improve accuracy. Only the mesh in the vicinity of the crack is affected by this mesh modification.

The crack is given a prescribed growth direction of $(-1, -2.5, 0)$ and a prescribed growth increment of 0.1. Each time the end of the fatigue load cycle is reached, the crack will grow according to this specification.

As the crack reaches the stiffener it will branch into two cracks. One which continues in the plate and one which grows in the stiffener, perpendicular to the plate. The new crack in the stiffener will inherit the properties from the first crack. One exception is the growth direction. This direction would not be meaningful in the stiffener. Marc uses the maximum hoop stress criterion for crack growth for branched cracks if the original cracks uses a user defined direction.

Loading and Boundary Conditions

One end of plate is completely constrained as shown in [Figure 2.30-5](#).

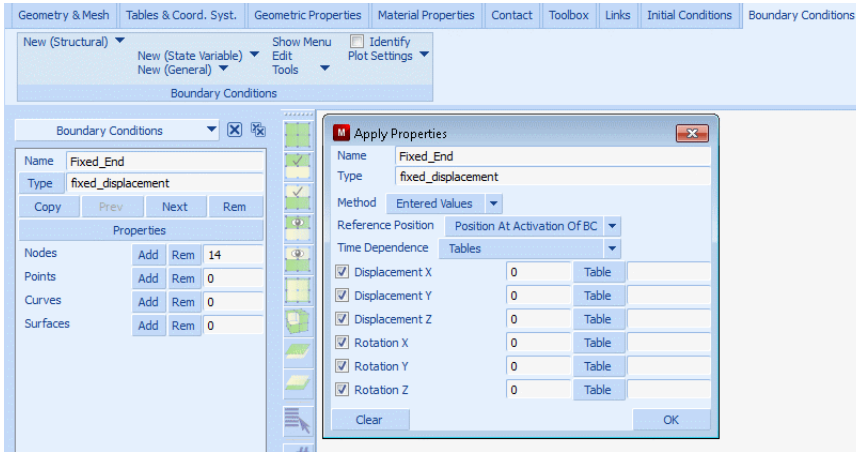


Figure 2.30-5 Loading and Boundary Conditions

On the other side, a load with an amplitude of 0.01 is applied as shown in Figure 2.30-6.

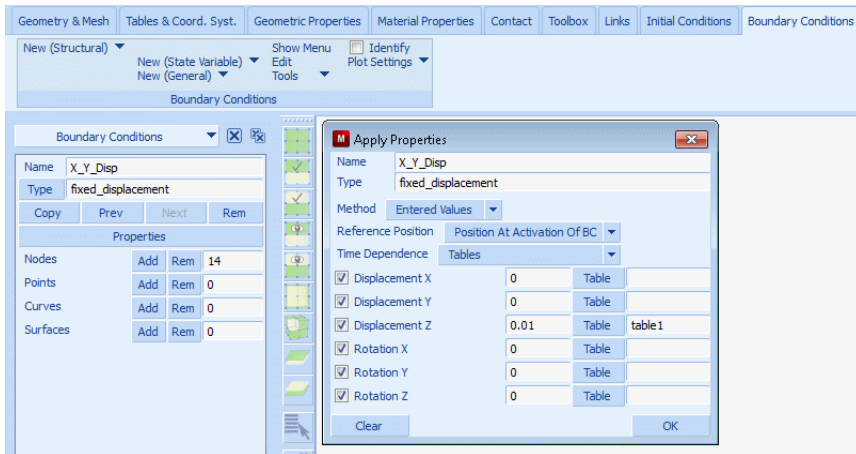


Figure 2.30-6 Cyclic Load

The following table is used for applying the cyclic load.

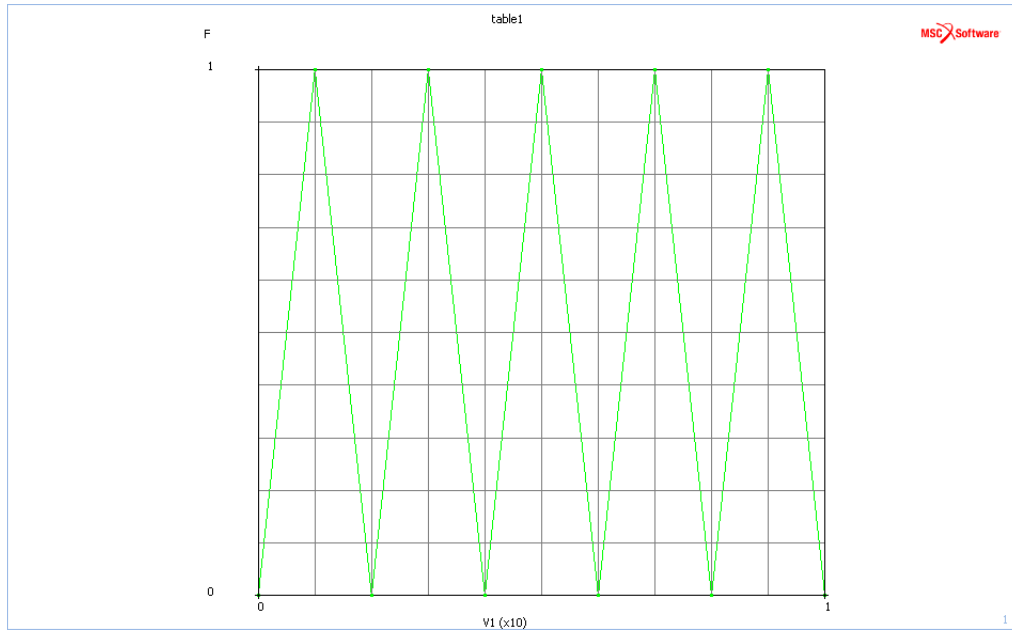


Figure 2.30-7 Cyclic Load Graph

Solution Procedure

The problem is solved using fixed time stepping with a total of 20 increments.

This is a non-linear analysis so the large strain option is turned on.

Results

Figure 2.30-8 shows the results at increment 18. This is at final crack length with the full load. The crack bifurcated into the stiffener, where the new crack has grown through it. The crack passes close to the inner hole, and the mesh is adjusted so as to improve the accuracy of the solution.

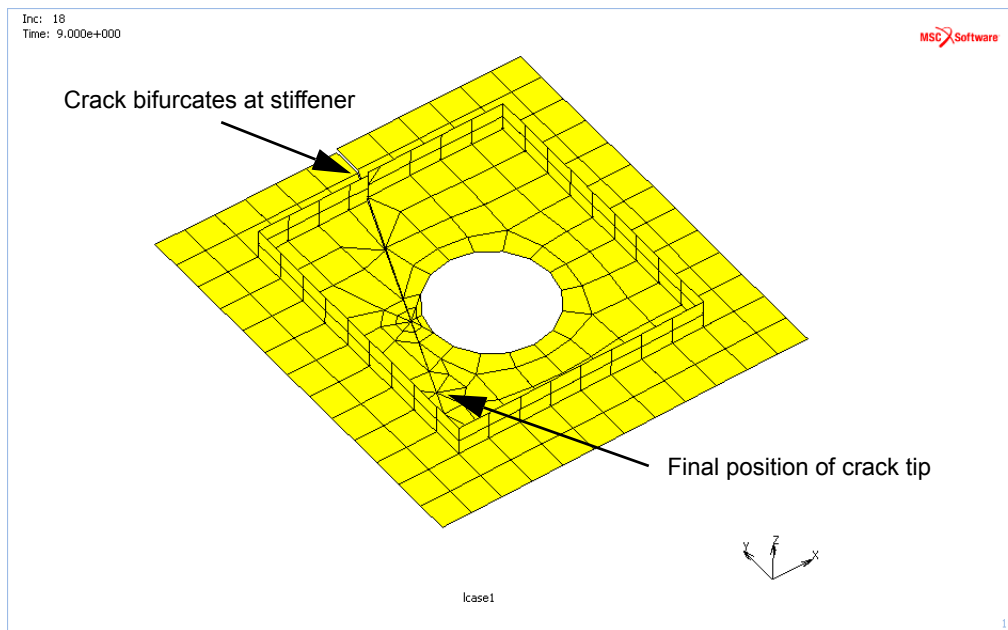


Figure 2.30-8 VCCT Energy Release Results

Input Files

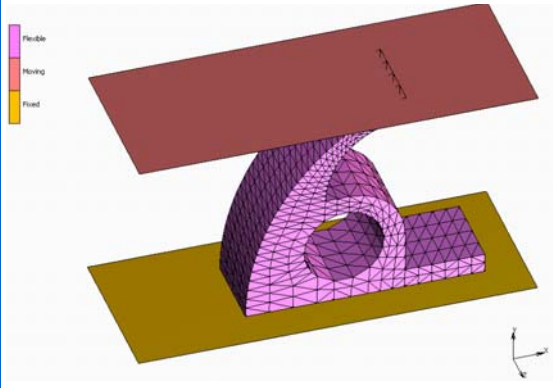
The files below are on your [delivery media](#) or they can be downloaded by your web browser by clicking the links (file names) below.

File	Description
UG_2D_Crack.mud	Mentat model for crack propagation in shells
UG_2D_Crack_job1.dat	Marc input file for crack propagation in shells

2.31 Segment-to-Segment with Friction

- Summary 756
- Introduction 757
- Available Contact Options 757
- Requested Solutions 757
- Modeling Details 757
- Contact 760
- Solution Procedure 761
- Results 763
- Input Files 763

Summary

Title	Segment-to-Segment with Friction
Features	Contact, Friction, Segment-to-Segment versus Node-to-Segment algorithm
FE Mesh	
Material properties	Material for deformable body Neo-Hookean material model with $C_{10} = 100$
Analysis characteristics	Nonlinear static analysis
Boundary conditions and Applied loads	Moving: Rigid body is moved downward by 200 mm in -Y direction All the loads have been applied to the moving rigid body by activating the position controlled method when creating the contact body
Element type	3-D 4-noded Tetrahedral Herrmann elements (Marc element type 157)
Contact properties	<ol style="list-style-type: none"> 1. Deformable body has self-contact 2. Moving rigid body is glued to the deformable body 3. Fixed rigid body is glued to the deformable body Bilinear Coulomb friction has been activated Coefficient of friction=0.1 (used for deformable body only)
FE results	Comparison of contact status and body force between node-to-segment and segment-to-segment

Introduction

The segment-to-segment contact algorithm has been introduced to better analyze models which suffer from limitations inherent in the node-to-segment algorithm. A typical example of such a limitation is the optimal set up of multi-point constraint equations, especially for large deflection problems involving self-contact. In Marc 2014, a new set of default parameters has been introduced to improve the robustness of the segment-to-segment algorithm and to reduce the computational time required to run a contact analysis.

Available Contact Options

The segment-to-segment algorithm is applicable for:

- rigid-to-deformable contact
- deformable-to-deformable contact
- 2-D and 3-D linear and quadratic solid elements
- 2-D and 3-D linear and quadratic shell elements
- 2-D and 3-D beam elements
- small and finite sliding contact
- Coulomb and shear friction

Unlike the node-to-segment algorithm, it does not use the master-slave concept. This simplifies the set up of model, in particular if areas with different mesh densities will come into contact.

Requested Solutions

A numerical analysis will be performed to compare the contact status and the contact body force between the node-to-segment and the segment-to-segment algorithm.

Modeling Details

The model shown in [Figure 2.31-1](#) is a structure consisting of one deformable body and two rigid bodies. Both rigid bodies are glued to the deformable body. The load on the deformable body is applied by moving the top rigid body over a distance of 200 mm in the negative Y direction. To this end, this rigid body is defined as a position controlled body.

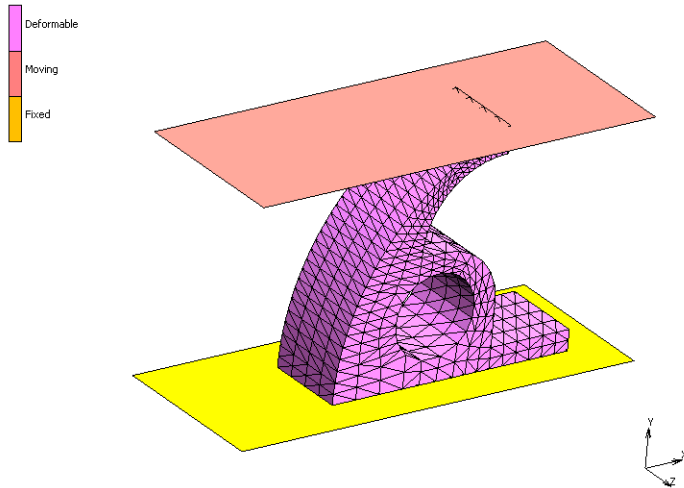


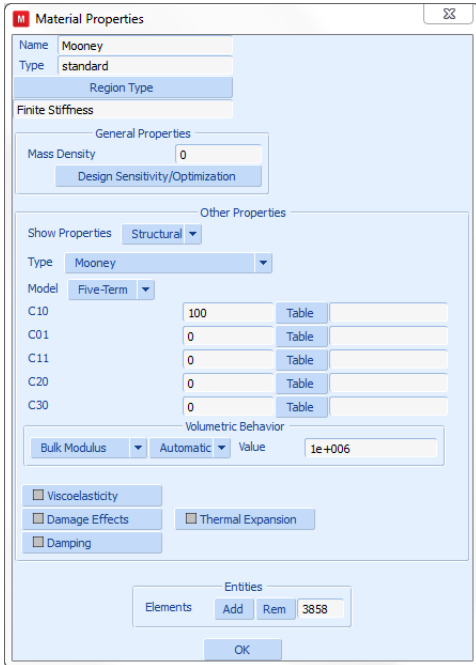
Figure 2.31-1 Finite Element Model of the Structure

Element Modeling

Four-noded tetrahedral Herrmann elements (Element 157) are used for the elements defining the deformable body. These elements do not suffer from volume locking, which is important to describe e.g. (nearly) incompressible rubber materials.

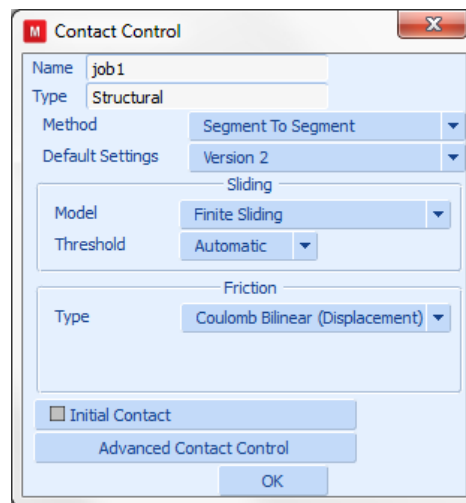
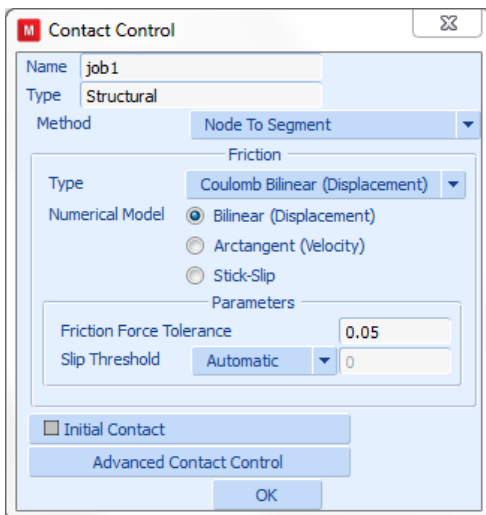
Material Modeling

A Neo-Hookean material model is defined through the Mooney material properties and is assigned to all the elements of the deformable body.



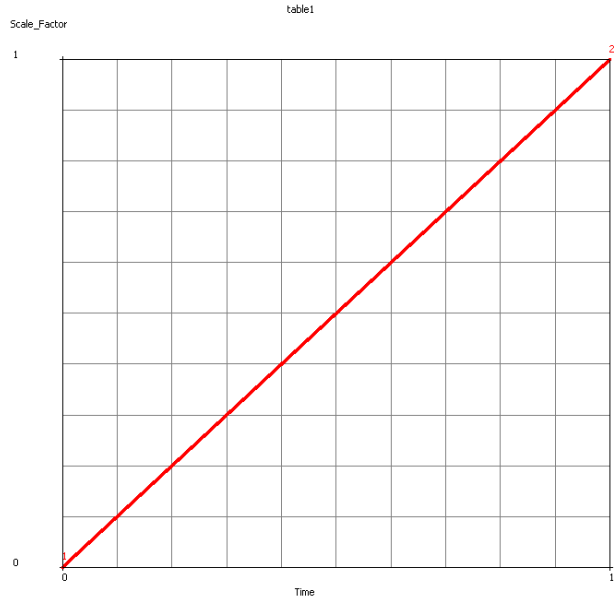
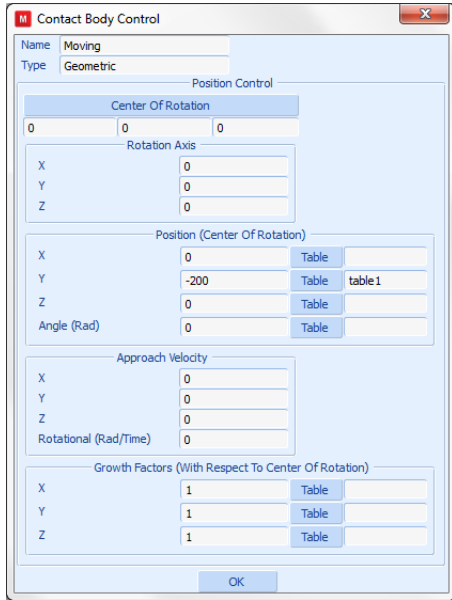
Friction Modeling

Two different friction types are available: one is the bilinear Coulomb model and the other the bilinear shear model. The bilinear Coulomb friction will be activated for both the node-to-segment and segment-to-segment analysis.



Loading Conditions

As shown in [Figure 2.31-1](#), the moving rigid body is coming down by 200 mm in the negative Y direction. All the loading on to the deformable is applied via this rigid body movement. The position of the rigid body is defined as a function of time as shown below.

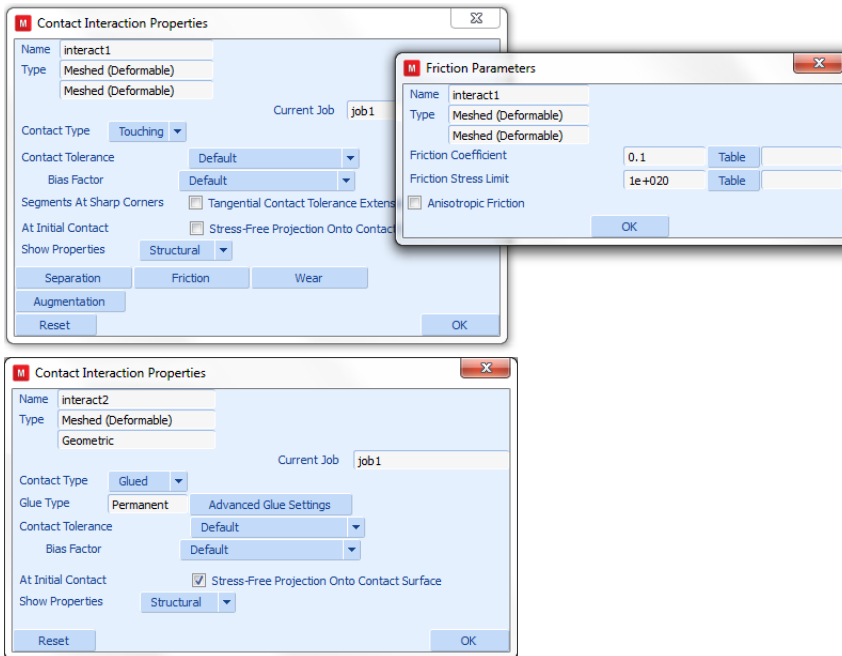


Contact

The following contact conditions will be defined:

- Self-contact for the deformable body with a coefficient of friction set to 0.1;
- Moving rigid body is glued to the deformable body;
- Fixed rigid body is glued to the deformable body.

The friction and glue conditions have to be defined as *Contact Interactions*, which can be assigned to contact body pairs via a *Contact Table*. Entering the coefficient of friction is done in the menu for a *Meshed (Deformable) vs. Meshed (Deformable)* Contact Interaction, where the glue condition is entered in the menu for a *Meshed (Deformable) vs. Geometric* Contact Interaction, as shown below.



Solution Procedure

The problem is analyzed using both the node-to-segment and the segment-to-segment contact algorithm, with adaptive time stepping.

Since there is potentially a lot of self-contact and no contact areas have been defined, the Job option *Optimize Contact Constraints* is activated for the node-to-segment algorithm. In this way, the contact algorithm tries to find an optimal set of constraint equations to minimize penetration in the areas of self-contact (or, in general, in the areas of deformable-deformable contact).

The analysis with the segment-to-segment algorithm is based on the *Version 2 Default Settings*, which is also defined as a Job option. One of the features of this set of defaults is the pressure dependent tangential stiffness for friction, which typically provides improved performance compared to using a fixed value of the tangential stiffness. Augmentation in the normal direction is activated to reduce possible penetration based on the default penalty stiffness.

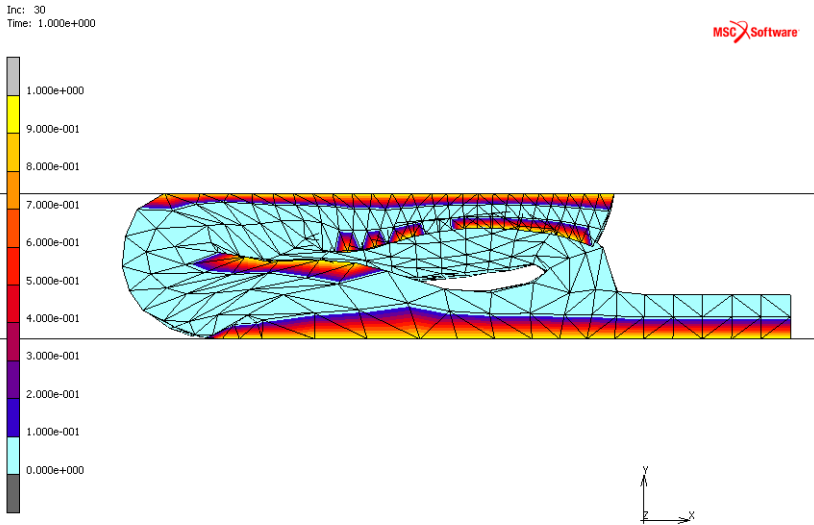


Figure 2.31-2 Contact Status of Deformable Body in the final configuration (Node-to-Segment Contact Analysis)

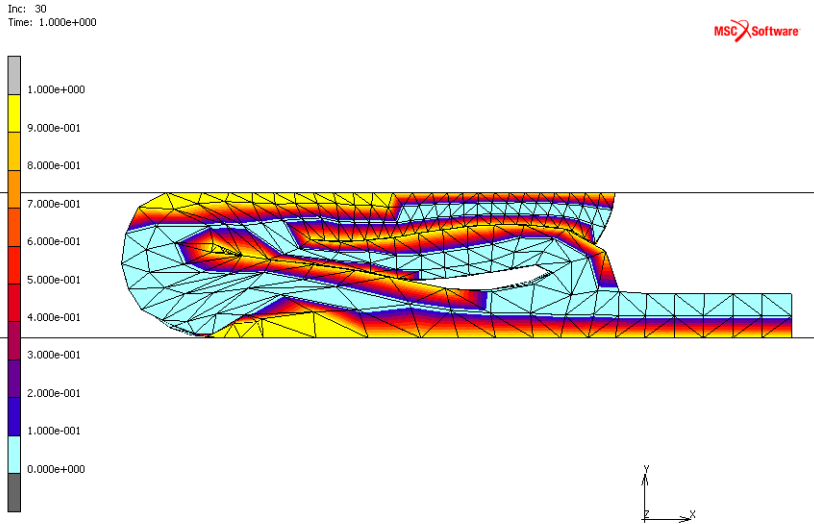


Figure 2.31-3 Contact Status of Deformable Body in the Final Configuration (Segment-to-Segment Contact Analysis)

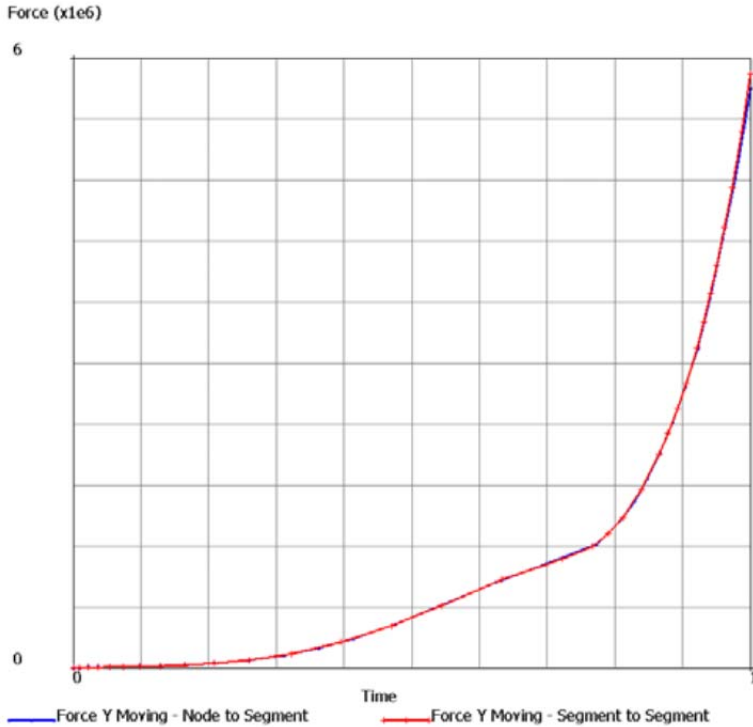


Figure 2.31-4 Contact Body Force Y for the Node-to-Segment and Segment-to-Segment Solution

Results

The contact status plots for these two models are given in Figures 2.31-2 and 2.31-3. As can be seen, there clearly is some penetration in the node-to-segment solution, which is inherent in the node-to-segment algorithm, given the loading conditions and the mesh density of the deformable contact body. The segment-to-segment algorithm does not suffer from this drawback. In Figure 2.31-4, the total Body Force in Y direction on the moving rigid body is given. Despite the fact that self-contact is not accurately described, the maximum predicted force by the node-to-segment algorithm matches that of the segment-to-segment algorithm relatively closely; it only is slightly smaller.

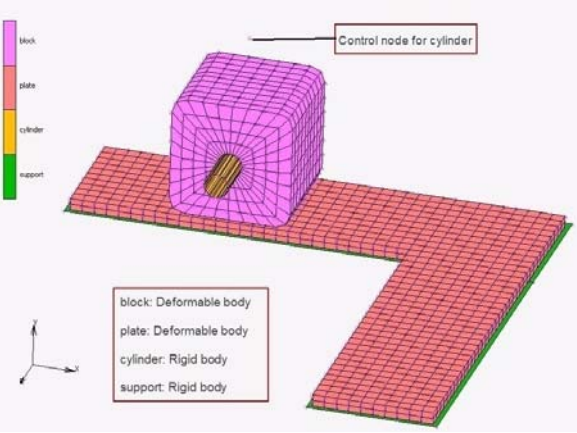
Input Files

File	Description
nod2seg_fric.mud	Mentat model for node-to-segment contact
nod2seg_fric_job1.dat	Marc input file for node-to-segment contact
seg2seg_fric.mud	Mentat model for segment-to-segment contact
seg2seg_fric_job1.dat	Marc input file for segment-to-segment contact

2.32 Directionally Dependent Friction

- Summary 766
- Introduction 767
- Requested Solutions 767
- Modeling Details 767
- Loading and Boundary Conditions 772
- Contact 775
- Solution Procedure 776
- Result and Plots 777
- Input Files 781
- Video 781

Summary

Title	Directionally Dependent Friction
Features	Anisotropic Friction
FE Mesh	 <p>The diagram shows a 3D finite element mesh of a mechanical assembly. A purple cube (block) sits on a red L-shaped plate (plate), which is supported by a green base (support). A yellow cylinder (cylinder) is positioned between the block and the plate. A legend in the bottom left identifies the components: block: Deformable body, plate: Deformable body, cylinder: Rigid body, support: Rigid body. A label 'Control node for cylinder' points to a specific node on the cylinder. A 3D coordinate system is shown in the bottom left.</p>
Material properties	<p>Material for deformable bodies, plate and block</p> <p>Plate: $E = 50000 \text{ N/mm}^2$; $\nu = 0.3$</p> <p>Block: Neo-Hookean material model defined through the Mooney property menu with $C_{10} = 100$</p>
Analysis characteristics	Nonlinear static analysis
Boundary conditions and Applied loads	<ol style="list-style-type: none"> Block is moving forward using rigid cylinder by 100 mm in +X and +Z direction respectively and then moving back by 100 mm in -Z and -X direction respectively. Block is subjected to -100N force in -Y direction using rigid cylinder when moving forward and then -200N force in same direction while moving back to original position. <p>All the loads have been applied to rigid body cylinder with load control option activated.</p>
Element type	3D- 8 noded hexahedron (Elem 7) elements.
Contact properties	<ol style="list-style-type: none"> block is glued to cylinder block is touching plate plate is glued to support. <p>Anisotropic friction has been activated for contact pair block-plate. Coefficient of friction=0.1 and 0.01 have been applied using local coordinate system whose X and Y axes is parallel to global X and Z axes respectively.</p>
FE results	<ol style="list-style-type: none"> Body force on Cylinder vs. time plot. Validate Isotropic friction formula

Introduction

For certain applications such as pipe lying, dragging of chains, Bowden cable (cable in tube) the frictional behavior is dependent on the direction. The effective coefficient of friction may be less in the direction along the cable or pipe and greater in the perpendicular direction. In general there can be many applications where the coefficient of friction differs significantly in two orthogonal directions.

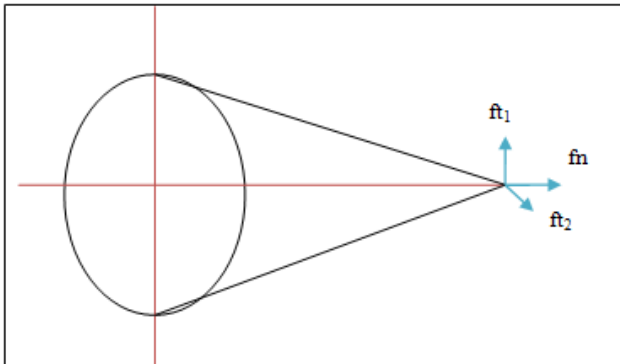
Orthotropic friction law can be expressed in mathematical and graphical forms as below.

$$\left[\left(\frac{f_{i1}}{\mu_1} \right)^2 + \left(\frac{f_{i2}}{\mu_2} \right)^2 \right]^{1/2} \leq f_n$$

μ_1 and μ_2 Friction coefficients in first and second slip direction

f_{i1} and f_{i2} Frictional forces in first and second slip direction

f_n Normal force acting on touching node



Requested Solutions

A numerical analysis will be performed to find body force, frictional force in first and second slip direction and normal force.

Modeling Details

The model shown in [Figure 2.32-1](#) is a structure having a deformable block moving on a deformable plate which is resting over a rigid support. Vertical load 100N is applied to the block and then the block is displaced over the plate by 100 mm in +X direction and +Z direction respectively. After completion of this motion, the vertical force is increased to 200 N and the block is moved in the reverse path so to reach the original position. All the loading on the block have been applied via a rigid cylinder using the load controlled motion where a control node is define to apply load and displacement to the cylinder which is blued to the block.

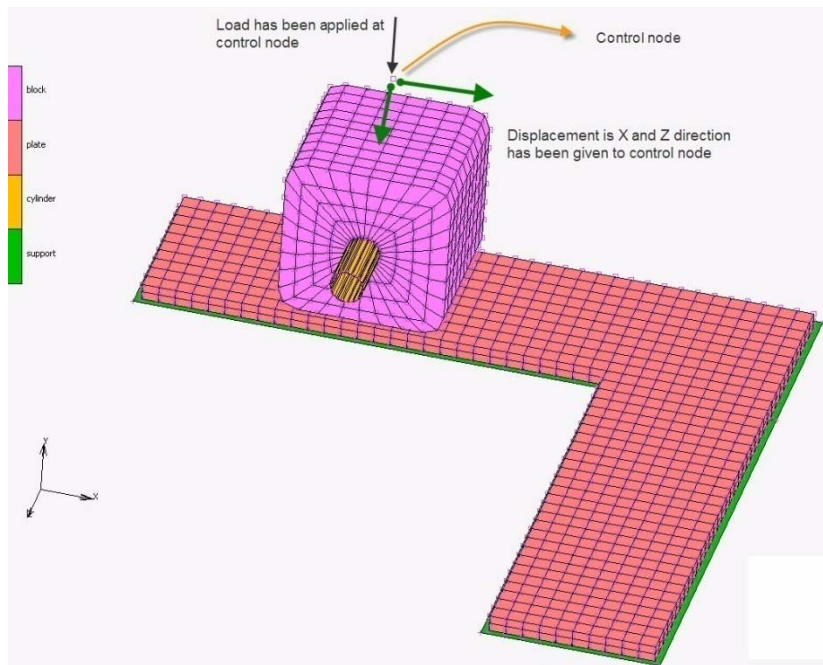
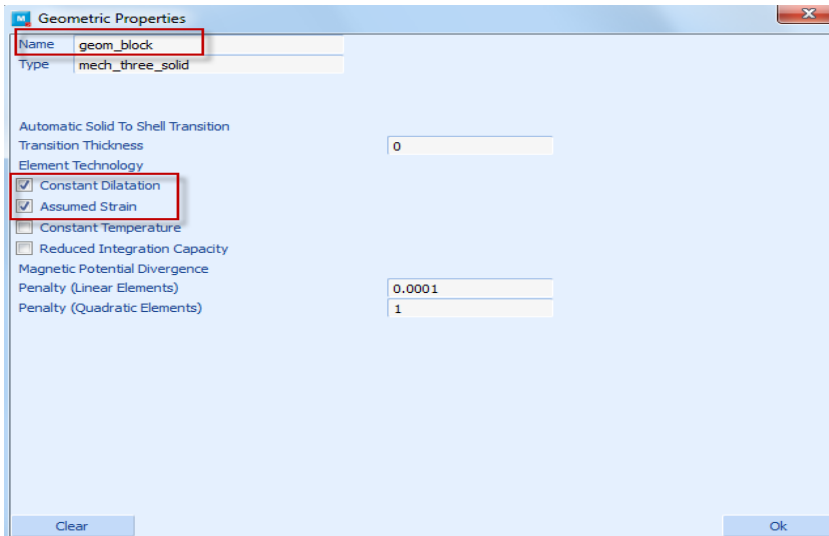


Figure 2.32-1 FE model of the structure

Element Modeling

Eight-noded hexahedral elements (Element 7) have been used for both the block and plate. Support and cylinder are modeled using surfaces. For plate, assumed strain option and for block, both the assumed strain and constant dilatation have been flagged using the geometry option.



Material Modeling

The plate is a linear isotropic material. The block is considered a Neo-Hookean material model defined through the Mooney menu.

Anisotropic Friction Modeling

For the anisotropic friction model, one has to both define two coefficients of friction and also the orientation.

There are five ways to define orientations for the anisotropic friction.

1. Coordinate System
2. Curve
3. 1-D Element direction
4. Sharp edge direction
5. User subroutine

In this exercise, orientation for the anisotropic friction has been defined using "Coordinate System" method. One local coordinate system (crdsyst1) has been created such that X and Y axes is parallel to the global X and Z axes respectively. Coefficient of friction=0.1 and 0.01 have been applied in 1st slip and 2nd slip direction.

Geometry & Mesh Tables & Coord. Syst. Geometric Properties Material Properties

Coordinate Systems

Coordinate Systems

Name: crdsyst1

Type: rectangular

Copy Prev Next Rem

System

X, Y, Z

Positions

A	Origin
B	$X=0, Y=0, Z>0$
C	$X>0, Y=0$

Method

Coordinates

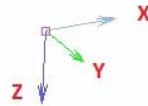
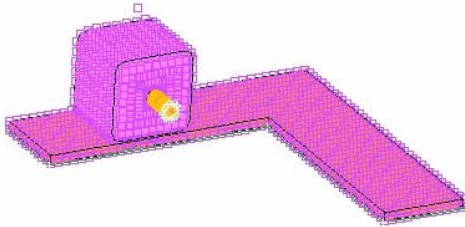
Coordinates

Reference Coordinate System

Global

Type: Rectangular

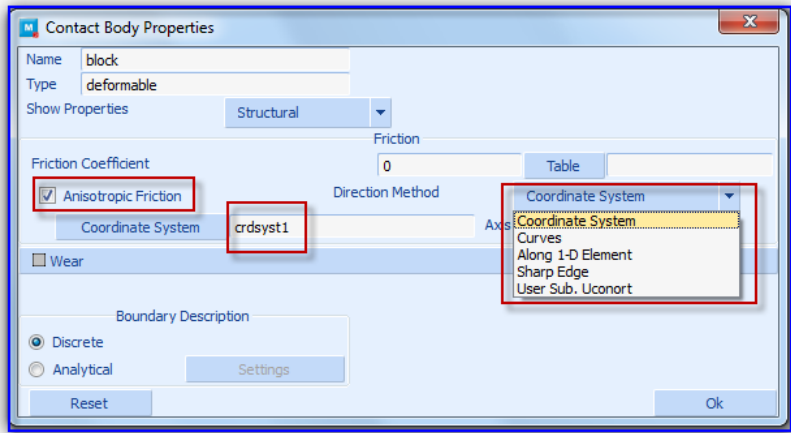
	X	Y	Z
A	0	0	0
B	0	-1	0
C	1	0	0



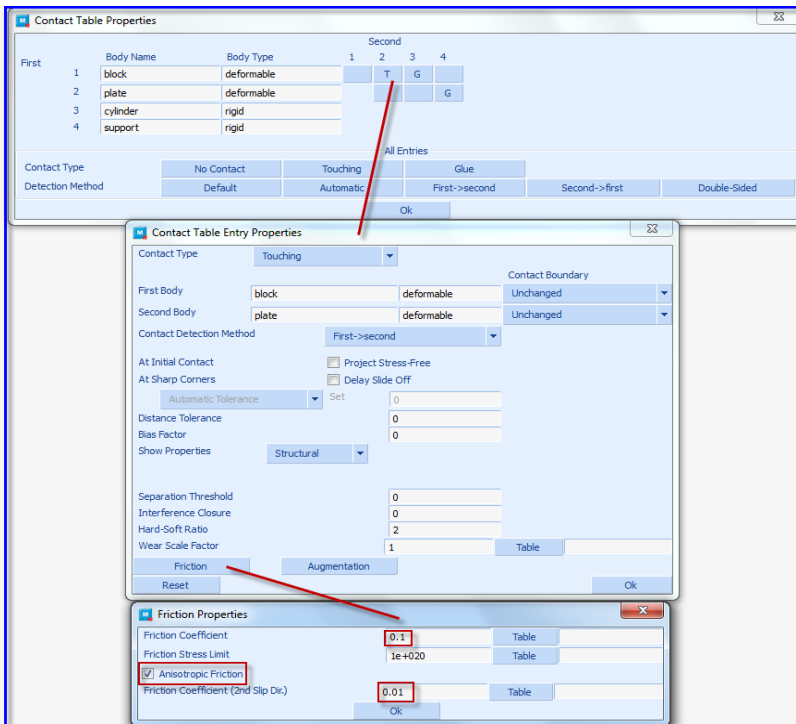
Local coordinate system



Global coordinate system



Activating the **Anisotropic Friction** model and prescribing the local orientation system.



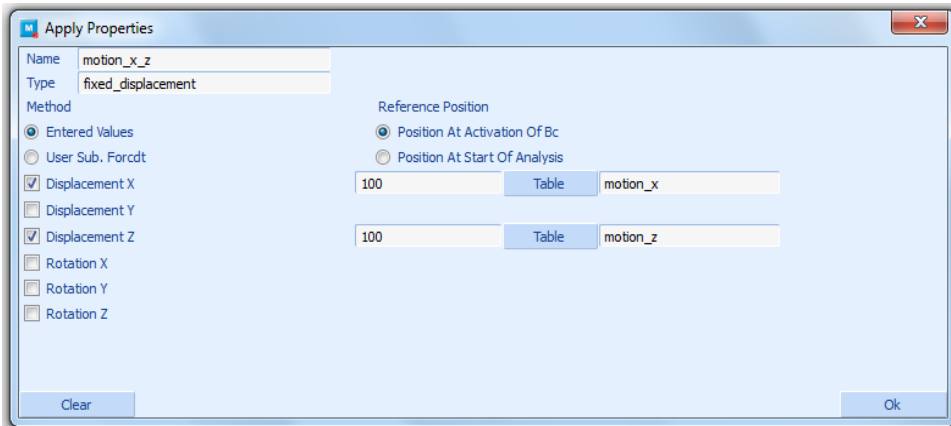
Defining the two coefficients of friction on the **Contact Table Entry Properties** menu.

Loading and Boundary Conditions

Figure 2.32-1 shows the loading and boundary conditions applied on the finite element model of the solid structure. Analysis is done in four load cases as explained below.

- Loadcase-1 (motion+X)** Vertical load of 100N is instaneously applied and displacement in +X direction is ramped to 100 mm
- Loadcase-2 (motion+Z)** Vertical is held constant at 100N and displacement in +Z direction is ramped to 100 mm.
- Loadcase-3 (motion-Z)** Additional vertical load of 100N is instaneously applied and displacement in -Z direction is ramped to 100 mm
- Loadcase-4 (motion-X)** Vertical load is held constant at 200N and displacement in -X direction is ramped to 100 mm

Load and displacement have been applied via Table



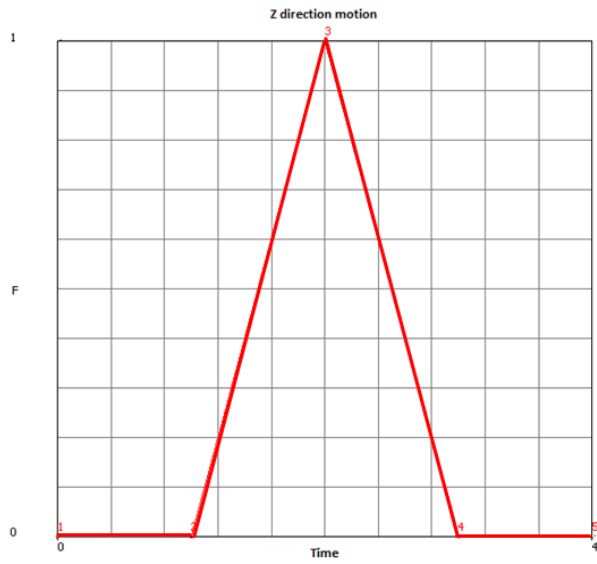


Table for Displacement in X Direction

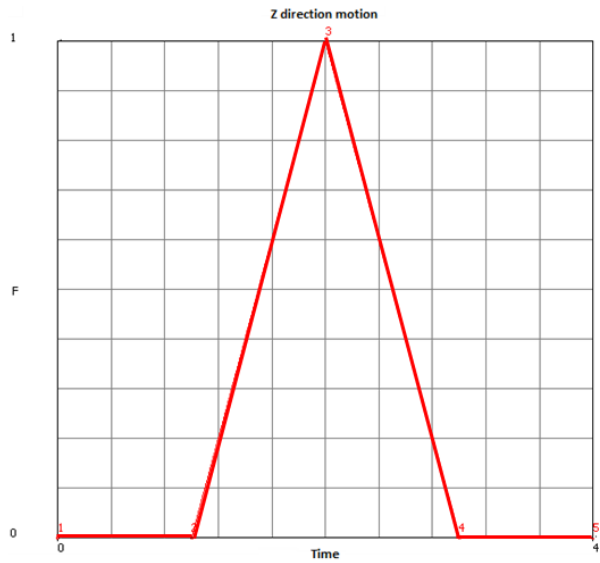


Table for Displacement in Z Direction

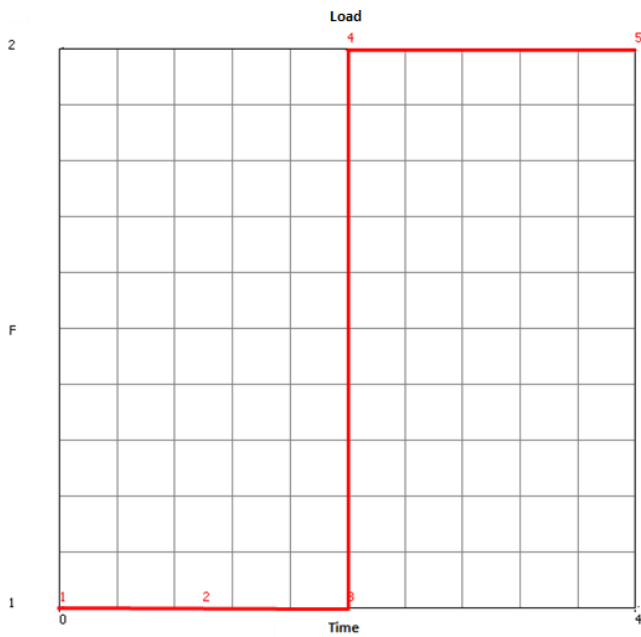
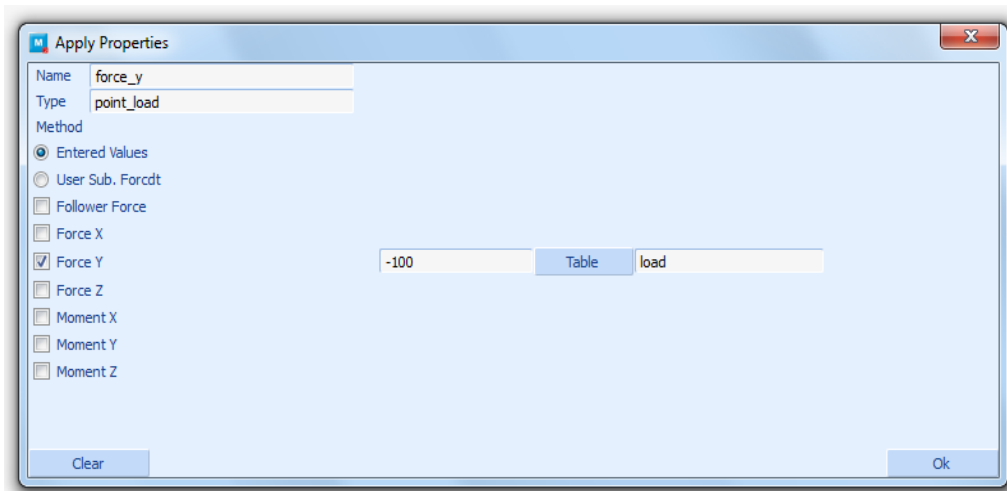


Table for Applying the Point Load in -Y direction

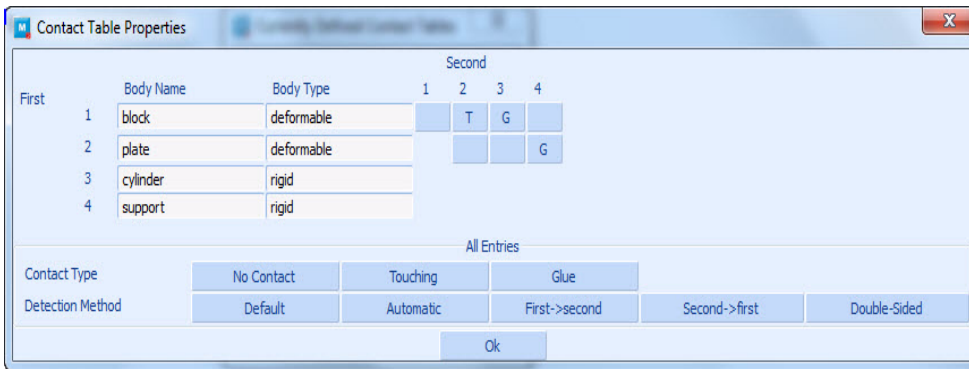
Contact

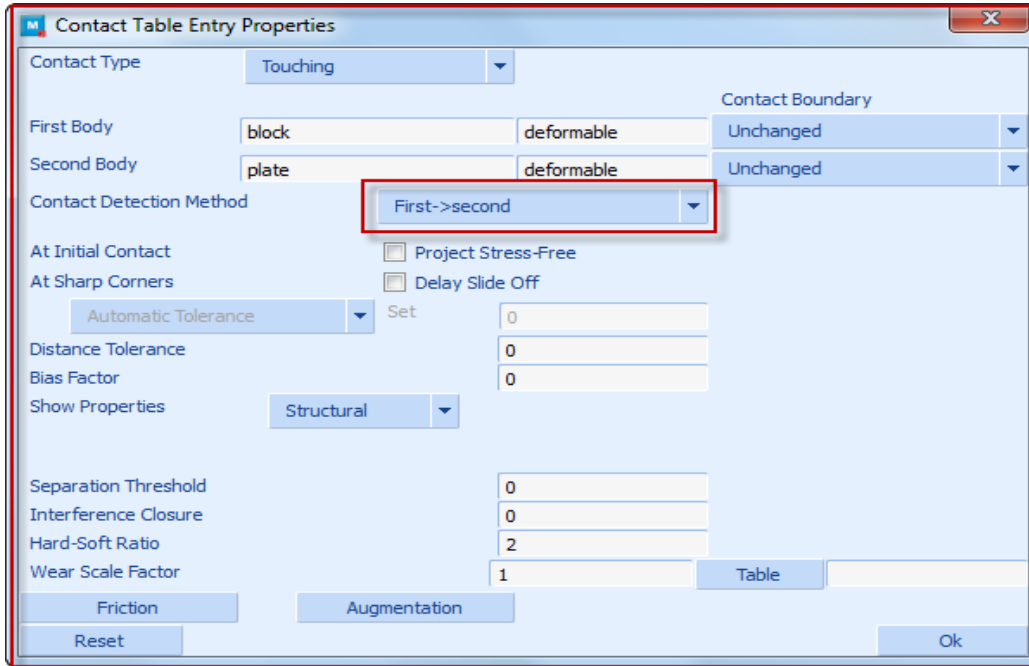
In total, four contact bodies are used. Block and plate are deformable contact body while cylinder and support are rigid body. There are three contact pair defined.

- 1: block is touching plate

For this contact pair, contact detection method chosen is "first to second" to ensure that block acts as slave body and contact status on the its base, first slip direction vector and second slip direction vector can be seen during post - processing.

- 2: block is glued to cylinder
- 3: plate is glued to support.

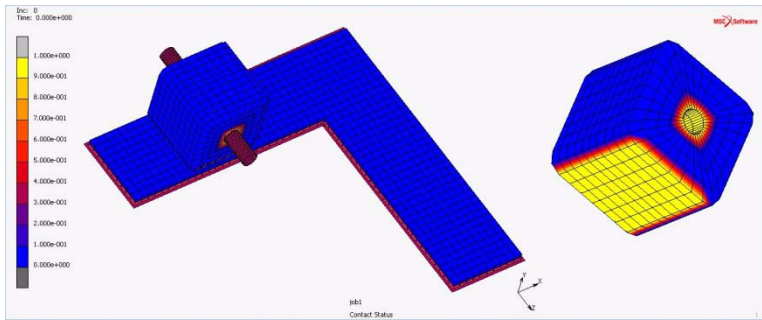




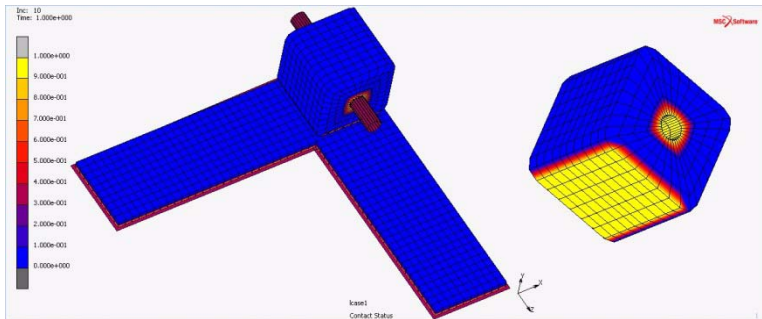
Solution Procedure

The problem is analyzed in Marc which is an implicit nonlinear solution procedure. Control parameters for the nonlinear solution scheme are described through the **Loadcase.Convergence** control. Four load cases are created using a fixed time stepping procedure, where the time period of each load case is one second and ten increments are taken per load case.

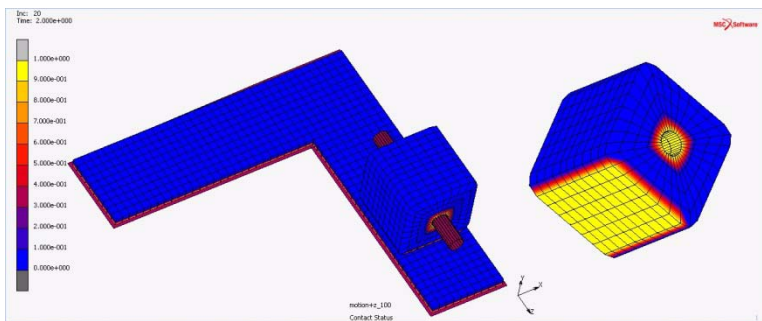
Result and Plots



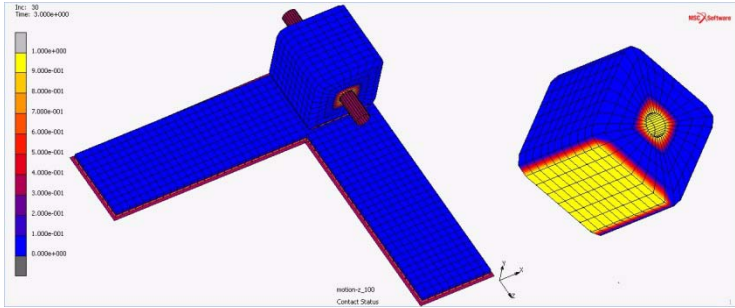
Position of Block and Contact Status at Base of the Block at time $t=0.0$



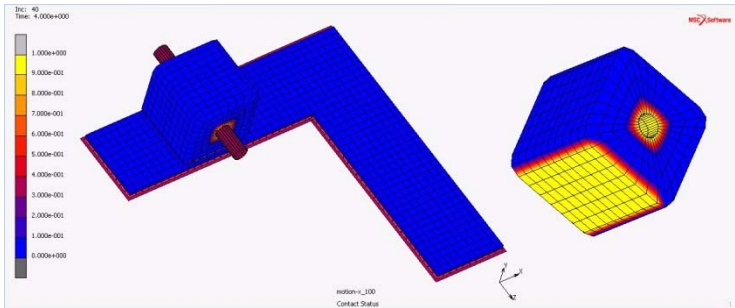
Position of Block and Contact Status at Base of the Block at time $t=1.0$



Position of Block and Contact Status at Base of the Block at time $t=2.0$



Position of Block and Contact Status at Base of the Block at time t=3.0



Position of Block and Contact Status at Base of the Block at time t=4.0

Calculation of the force on the block and so on cylinder:

During the 1st loadcase block in moving in +X direction

Force required to move the block would be $\mu_1 * \text{Reaction force (R1)} = 0.1 * 100 = 10 \text{ N}$

Here, R1 is the vertical point load applied on the block = 100 N

During the 2nd loadcase block in moving in +Z direction

Force required to move the would be $\mu_2 * R1 = 0.01 * 100 = 1 \text{ N}$

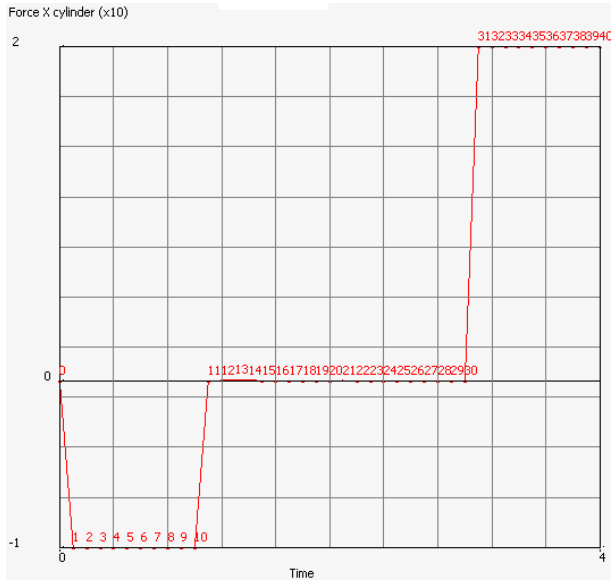
During the 3rd loadcase block in moving in -Z direction

Force required to move the would be $\mu_2 * R2 = 0.01 * 200 = 2 \text{ N}$

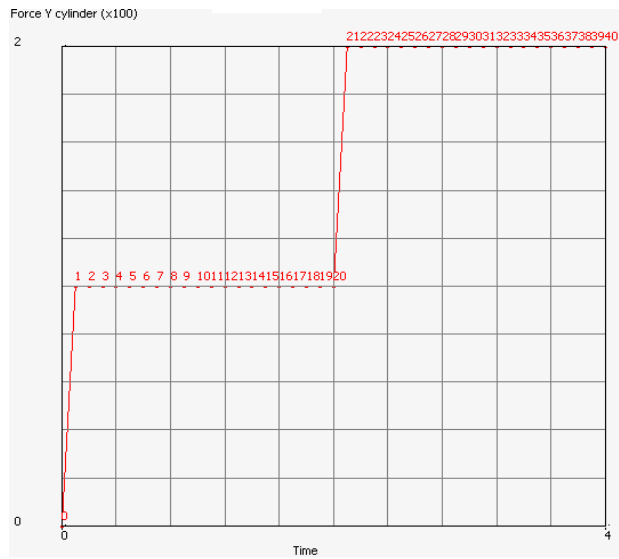
Here, R2 is the vertical point load applied on the block = 200 N

During the 4th loadcase block in moving in -X direction

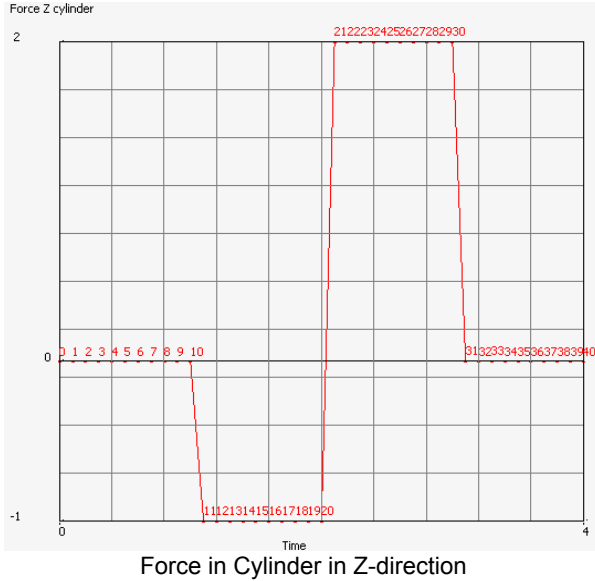
Force required to move the would be $\mu_1 * \text{Reaction force (R2)} = 0.1 * 200 = 20 \text{ N}$



Force in Cylinder in X-direction



Force in Cylinder in Y-direction



Checking the result with anisotropic friction formula

The formula for anisotropic friction $\left[\left(\frac{f_{t1}}{\mu_1} \right)^2 + \left(\frac{f_{t2}}{\mu_2} \right)^2 \right]^{1/2} \leq f_n$

$\mu_1 = 0.1$, $\mu_2 = 0.01$

At node number 3969 (end of 3rd load case)

Contact Frictional force local X (f_{t1}) = 4.01E-05N

Contact Frictional force local Y (f_{t2}) = 0.03729

Contact Normal force (f_n) =RHS= 3.72956

LHS of the anisotropic formula= 3.729

LHS \leq RHS

Hence, anisotropic friction formula is satisfied

At node number 3765 (end of 4th load case)

Contact Frictional force local X (f_{t1}) = 0.40085

Contact Frictional force local Y (f_{t2}) = 0.0000000197

Contact Normal force (f_n) =RHS= 4.0085

LHS of the anisotropic formula= 4.0085

LHS \leq RHS

Hence, anisotropic friction formula is satisfied

Input Files

The files below are on your delivery media or they can be downloaded by your web browser by clicking the links (file names) below.

File	Description
dir_fric.mud	Mentat model for direction dependent friction
dir_fric.dat	Marc input file for direction dependent friction
reference_dir_fric.mud	Reference file used in end-to-end video demonstration

Video

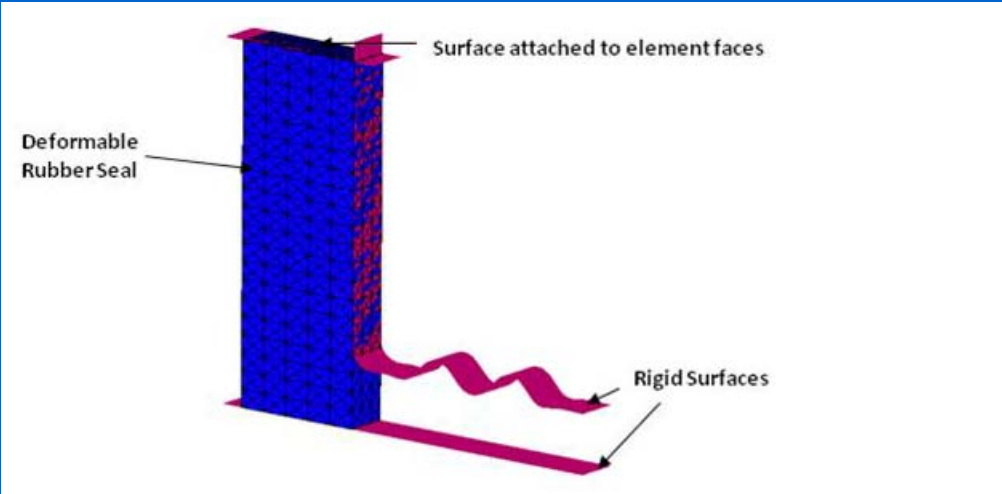
Click on the link below to view a streaming video of this problem.

File	Description
ch02-32.swf	Video for directionally dependent friction.

2.33 Improved Accuracy with Remeshing of Herrmann Elements

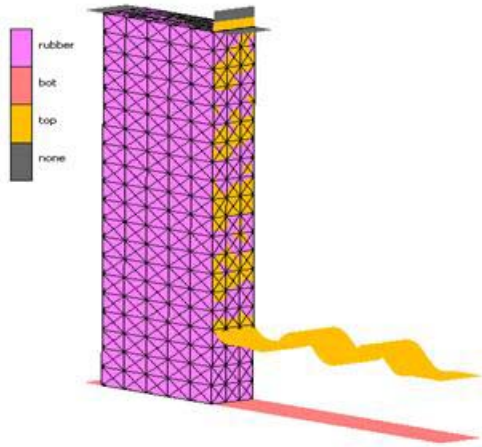
- Summary 784
- Introduction 785
- Simulation of Elastomeric Seal 785
- Mesh 785
- Material Properties 785
- Contact Body Definitions 786
- Contact Table 787
- Mesh Adaptivity 788
- Boundary Conditions 788
- Solution Procedure 790
- Results 791
- Input Files 791
- Video 792

Summary

Title	Improved accuracy with remeshing of Herrmann elements
Problem Features	The chapter demonstrates the improved accuracy such as more accurate results and improved convergence associated with remeshing of Herrmann integration elements 155, 156 and 157.
Model	
Material Properties	The deformable rubber seal is modeled with Mooney constitutive model. The material parameters are given as $C1=8\text{N/cm}^2$ and $C2=2\text{N/cm}^2$. The bulk modulus is 10000N/cm^2 .
Boundary Conditions	The vertical faces of rubber seal block are constrained by applying suitable boundary conditions to restrict the lateral movement of seal during deformation. The fixed displacement of one ramped over time period of one is applied in negative Y-direction on the surface which is attached to the top elements faces of rubber seal.
Analysis Type	Static analysis with hyperelastic material behavior
Element Type	Low-order Tet4 elements with Herrmann integration
FE Results	History plot of body force & its comparison with that of older version of Marc

Introduction

The chapter demonstrates the improved accuracy with associated with remeshing of Herrmann integration elements. Marc has the capability to perform the remeshing/rezoning automatically with the GLOBAL ADAPT option. However, difficulties had been observed in the Marc remeshing analysis using elements 155, 156, and 157. Those difficulties were inaccurate results and failure in achieving convergence immediately after remeshing/rezoning. With the new implementations, these difficulties have been overcome.



Simulation of Elastomeric Seal

Model consists of rubber seal is squeezed between top and bottom rigid plates by applying a pressure on the surface which is attached to the top element faces of rubber seal block. Suitable boundary conditions are applied on the vertical faces of rubber seal to restrict the lateral movement of seal during deformation.

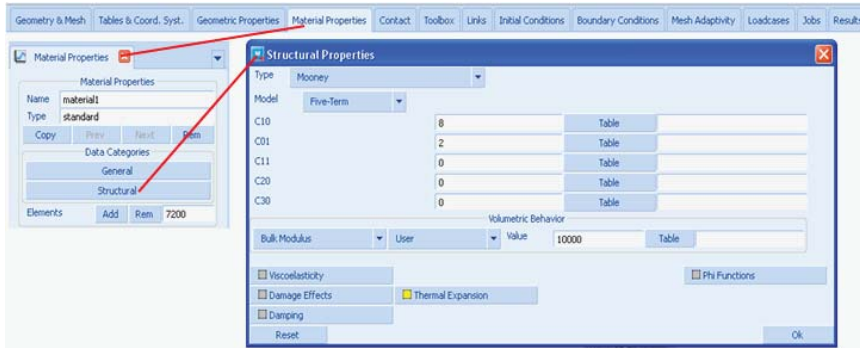
Mesh

The rubber seal is meshed with Tet4 elements with Herrmann integration of type element 157.

Material Properties

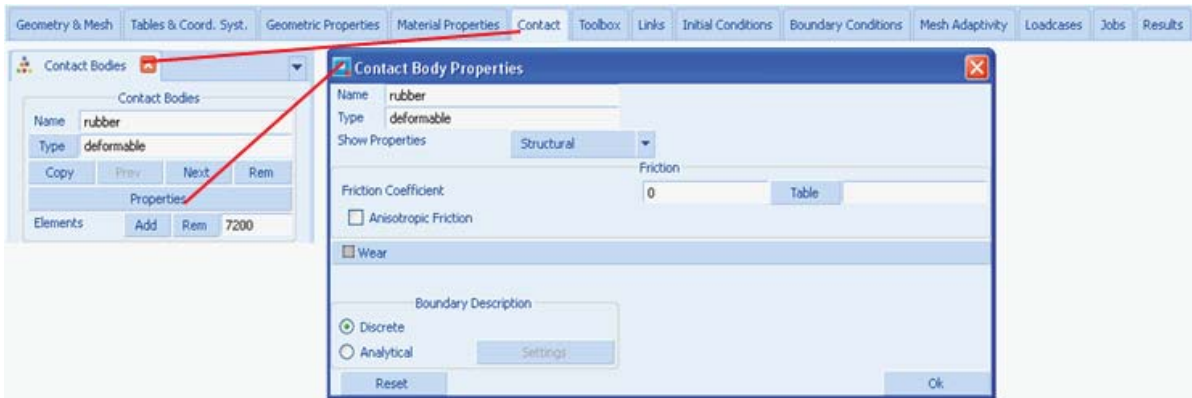
The rubber seal is modeled with Mooney constitutive model. The material parameters are given as $C1=8\text{N/cm}^2$ and $C2=2\text{N/cm}^2$. The bulk modulus is 10000N/cm^2 .

The material properties in Mentat are entered in the following figure.

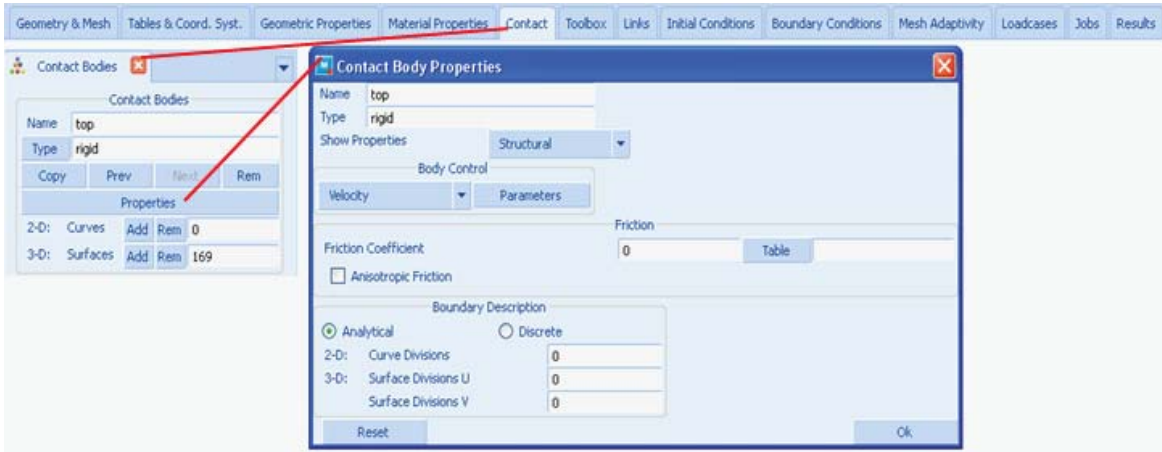


Contact Body Definitions

The rubber seal is defined as “deformable body” by adding the elements to the selection as shown in the following figure.

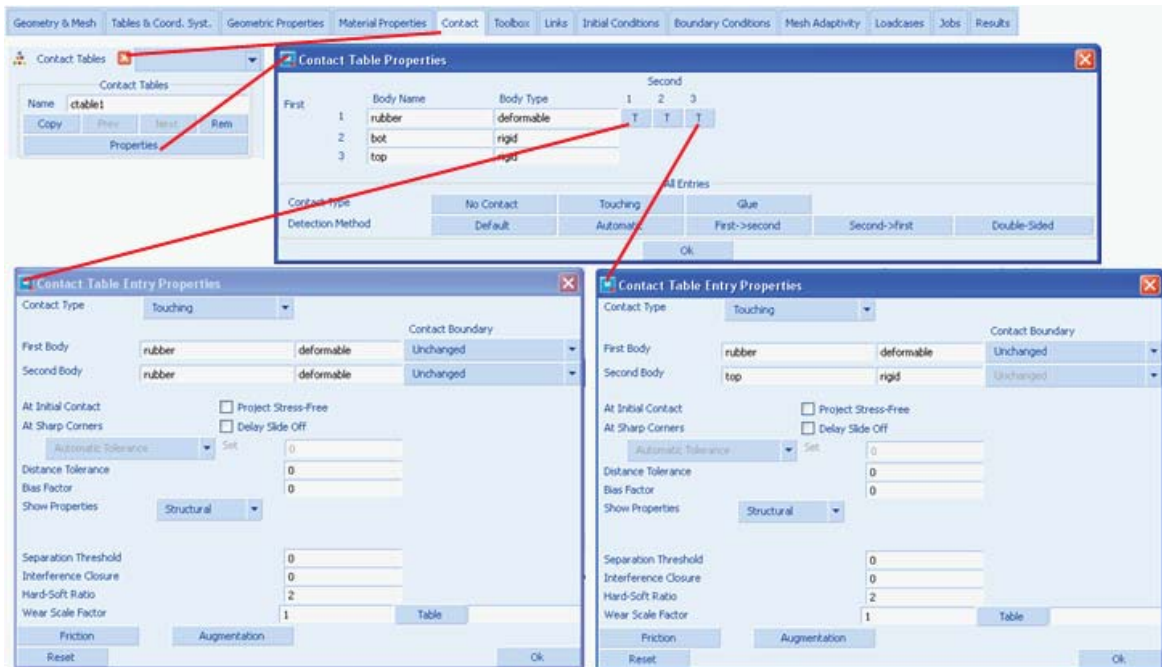


The two surfaces (top & bottom) are defined as rigid surfaces by adding the surfaces to the selection as shown in the following figure.



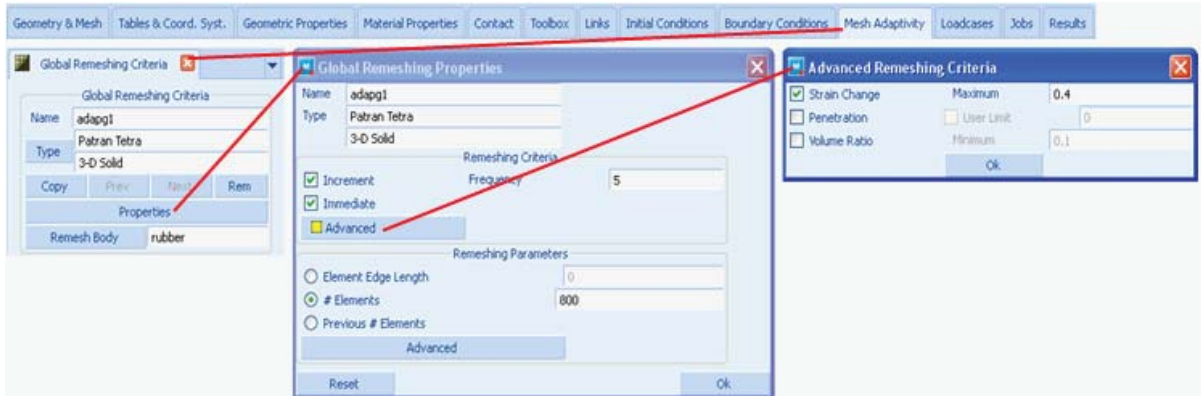
Contact Table

The contact relationship between the bodies is defined via contact table. The deformable rubber seal is defined to be in touching contact with two other rigid bodies as well as with itself.



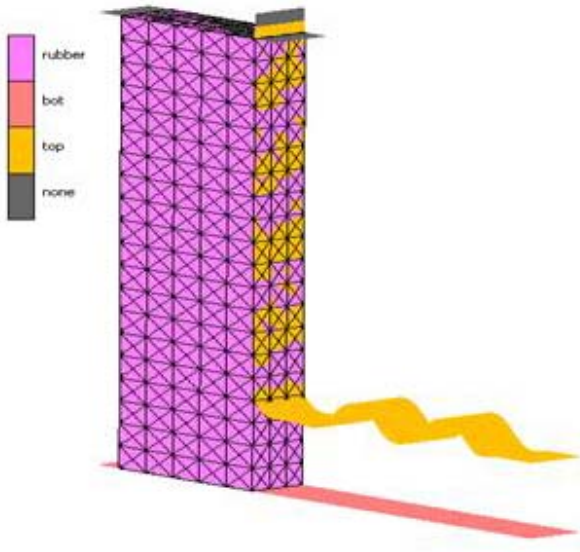
Mesh Adaptivity

“Patran Tetra” type mesh adaptivity was defined by adding deformable body “rubber” to the selection. Remeshing frequency of five increments with immediate is defined in remeshing criteria. Maximum strain change of 0.4 is defined as advanced remeshing criterion. 800 numbers of elements are defined as remeshing parameters.

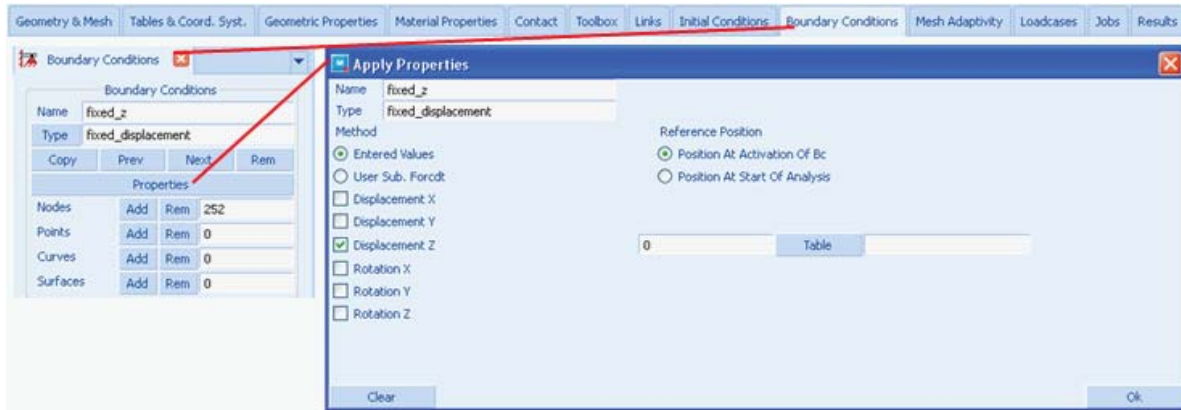
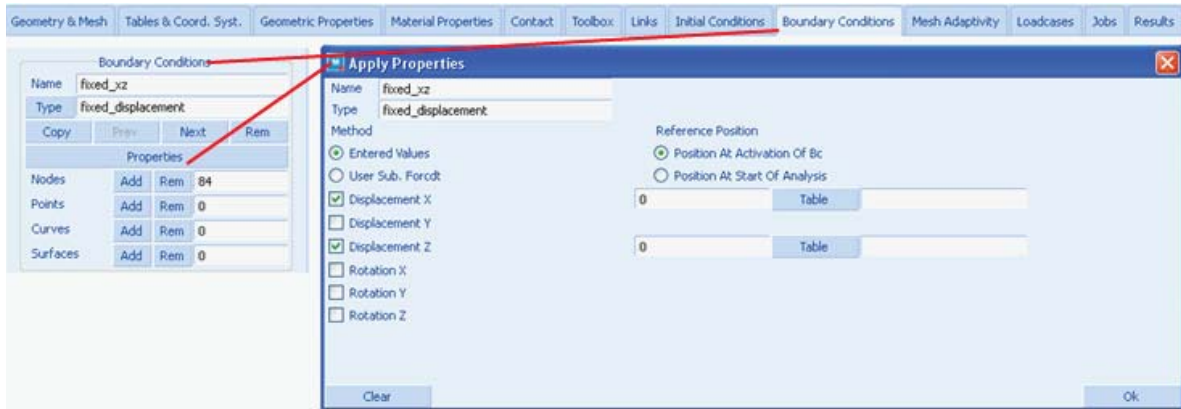


Boundary Conditions

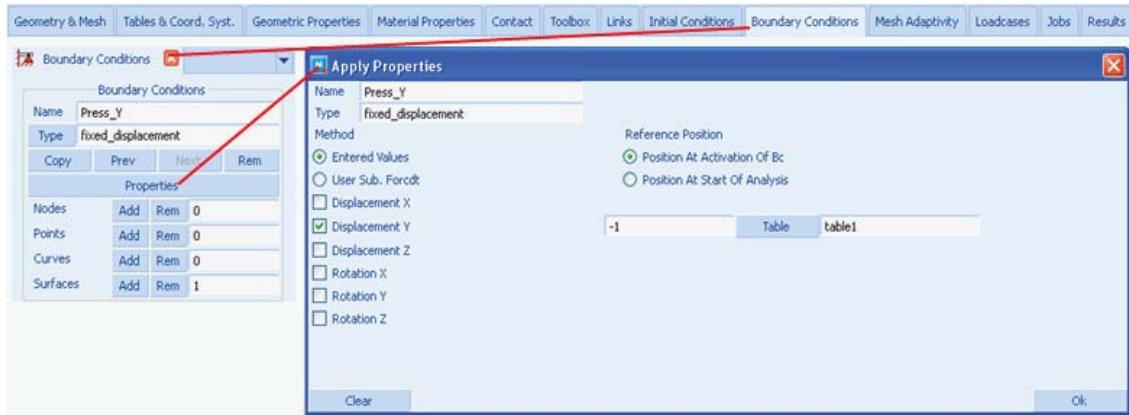
The different boundary conditions applied on the model are as shown in the following figure



The vertical face which is on the opposite side of the “top” rigid body is constrained in X and Z direction. The other two larger vertical surfaces of rubber seal block are constrained in Z-direction.

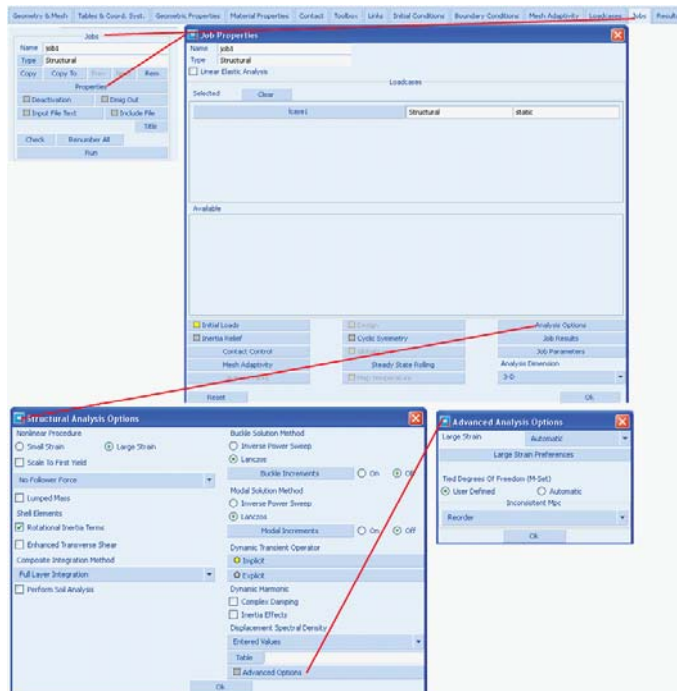


The enforced displacement one in ramped over time period of one is applied in negative Y-direction on the surface which is attached to the element faces at the top of rubber block seal.



Solution Procedure

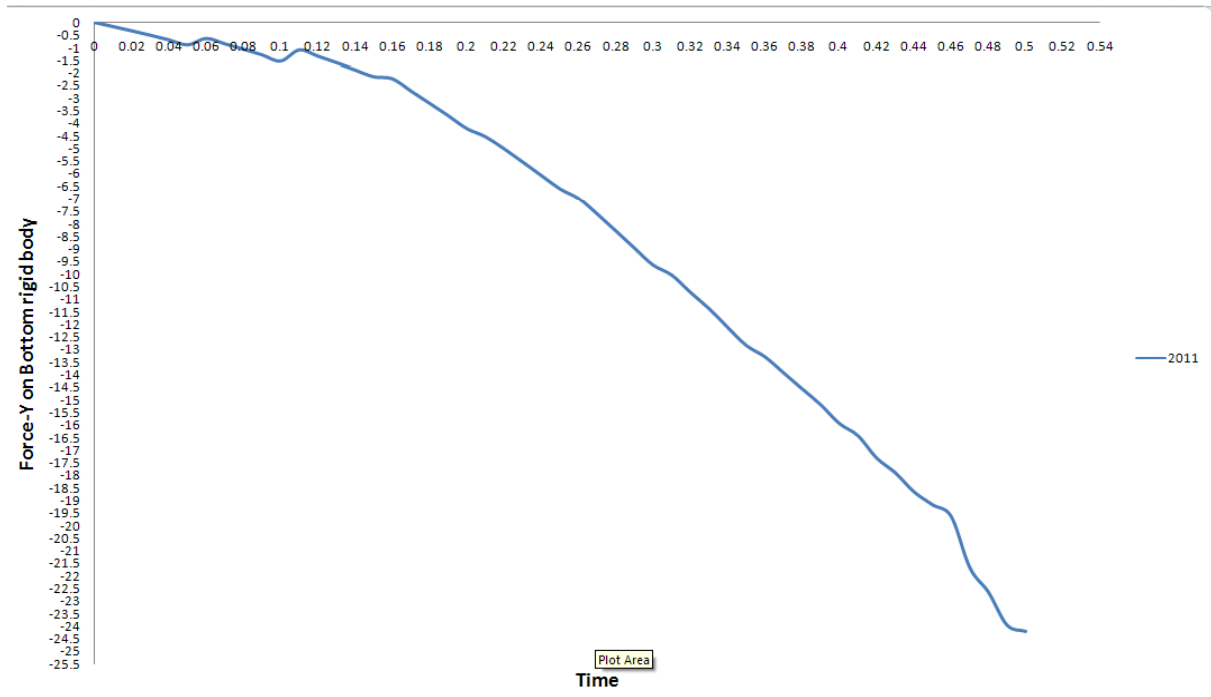
Problem is solved with fixed-time stepping criterion 50 steps over time period of 0.5. The large strain option is turned on in **Jobs** menu. For large strain analysis procedure, the “automatic” option is selected as shown in the following figure.



The “automatic” option of large strain analysis procedure writes out the LARGE STRAIN, 4 parameter in the input deck. With the LARGE STRAIN, 4 parameter for each element and material combination, the optimal choice of formulator flags is automatically determined by the program. In this case, with the combination of element 157 with Mooney material model, Marc uses updated Lagrangian procedure with multiplicative decomposition ($F_e F_p$).

Results

The history plot of body force in Y direction on “bottom” rigid body is plotted against time in the figure below.



Input Files

The files below are on your [delivery media](#) or they can be downloaded by your web browser by clicking the links (file names) below.

File	Description
Herrmann_Remesh_2011.mud	Mentat model for remeshing with Herrmann elements
Herrmann_Remesh_2011_job1.dat	Marc input file for remeshing with Herrmann elements

Video

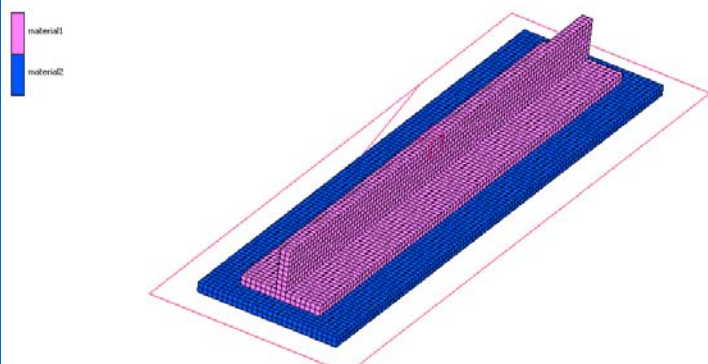
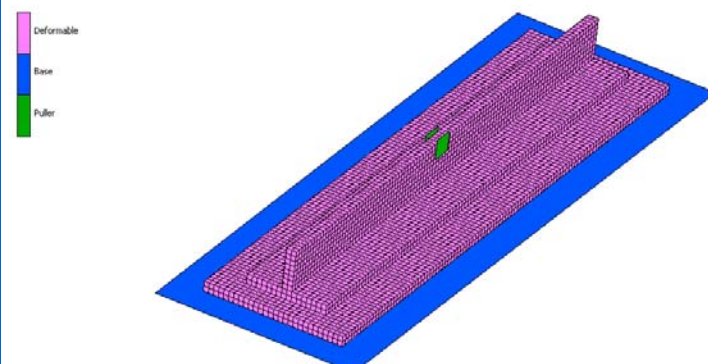
Click on the link below to view a streaming video of this problem.

File	Description
ch02-33.swf	Video for improved accuracy with remeshing of Herrmann elements.

2.34 3-D Crack Propagation at Material Interface

- Summary 794
- Modeling Details 795
- Solution Procedure 800
- Results 801
- Input Files 807

Summary

Title	3-D crack propagation at material interface
Problem Features	New 3-D crack features such as crack initiation, enhanced Delamination option, cohesive material and crack growth along element faces.
Model	
Material properties	<p>Linear elastic material: $E = 2 \times 10^{11} N/m^2$; $\nu = 0.3$</p> <p>The model has two materials with the same properties</p>
Analysis characteristics	Nonlinear static analysis
Boundary conditions and Applied loads	<p>The deformable body is glued to the contact bodies Base and Puller. The Base is fixed and Puller is given a vertical displacement of 0.1.</p> 
Element type	8-noded hexahedron elements (element type 7).
FE results	<ol style="list-style-type: none"> 1. Results of crack growth. 2. Results with cohesive elements.

This example illustrates some features related to the simulation of failure at a material interface. The model is constructed so that a failure will be initiated at the material interface, and the failed zone will be enlarged at the interface.

The failure is first initiated using the **Delamination** feature, where a stress criterion determines when and where a failure will occur. After the initial failure, two methods will be used for modeling further growth of the failed region:

1. Crack propagation using VCCT
2. Growth using the cohesive zone model

Secondly, an initial crack is introduced using the **Crack Init** feature. A set of element faces are used for defining the location of the crack. The crack will then grow using VCCT based crack propagation.

It should be noted that the current example does not attempt to model a real structure with real material properties. It is only used for illustrating the procedures available in Marc.

Modeling Details

The model with dimensions is shown in [Figure 2.34-1](#). The model consists of three bodies: the mesh and two rigid bodies (the puller and the base). Note that, initially, there are no duplicate nodes between the T-stiffener and the bottom plate. The puller is positioned centrally along the length.

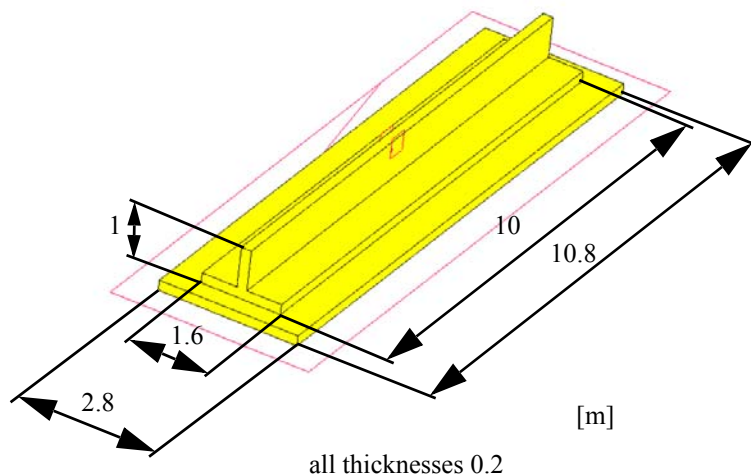


Figure 2.34-1 The Model

Delamination

The **Delamination** option is used for determining when and where the failure occurs, and to determine what should happen after the initial failure.

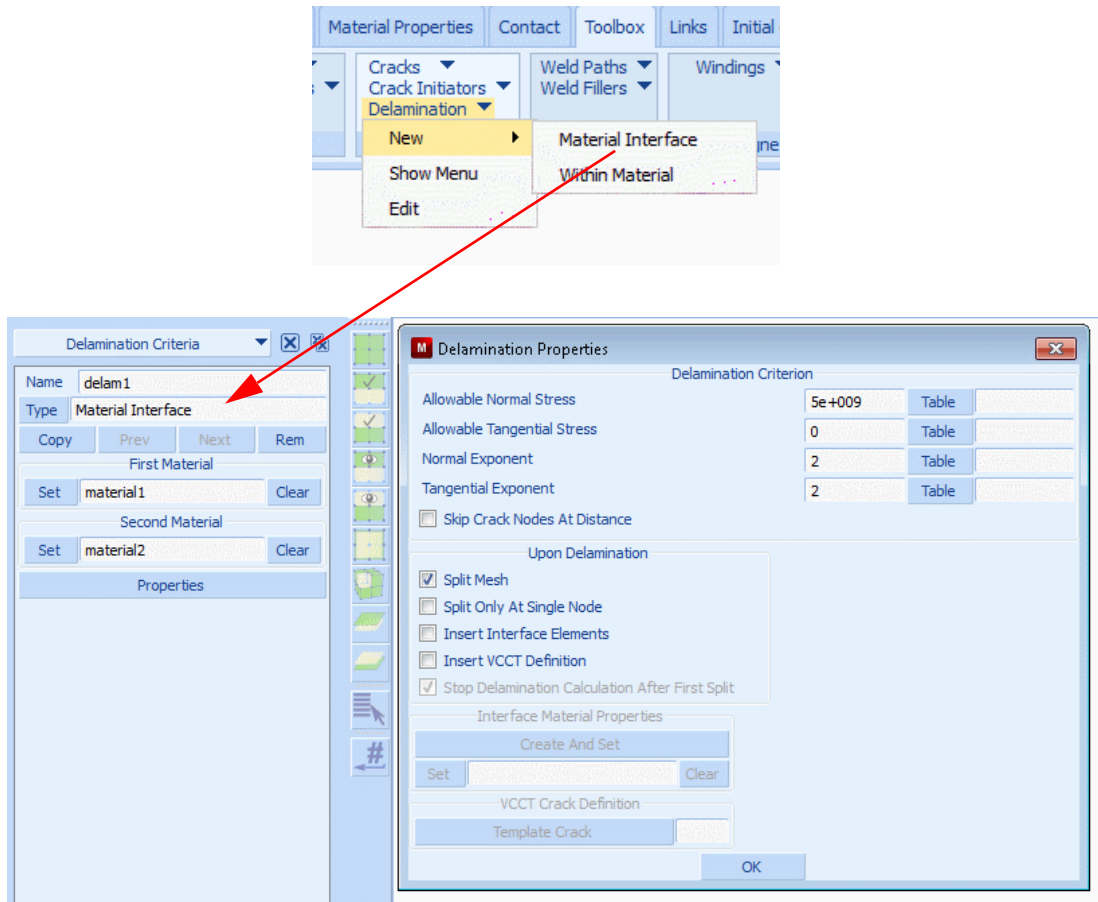


Figure 2.34-2 Mentat Menu for Creating the Delamination

The failure criterion is expressed as

$$\left(\frac{\sigma_n}{S_n}\right)^m + \left(\frac{\sigma_t}{S_t}\right)^n = 1$$

where σ_n is the stress normal to the material interface and σ_t the sum of the stresses tangential to the interface. The normal stresses only contribute in tension.

We see in the picture that S_n is set to 5×10^9 . The factor for the tangential stresses is left at zero which means that this part is not active.

The options under Upon Delamination determine what should happen after failure. **Split Mesh** is active. If this is not set, Marc will only provide the value of the failure criterion for post processing with the post quantity Delamination Index.

Two variants will be used in this example:

1. Insert VCCT Definition
A template VCCT crack definition is provided, which is used for the inserted cracks
2. Insert Interface Elements
The material properties for the inserted interface elements are provided

VCCT

Figure 2.34-3 shows how the VCCT template crack is created. The tick box **Template Only** defines that it is a template and that the crack front has no initial nodes associated with it. The program determines the crack front nodes based upon the delamination. Defining it as a template allows it to be selected in the **Delamination** menu.

The type of crack propagation here is direct propagation along the material interface. We start out with a connected mesh which is split up by the **Delamination** option, so the crack growth method **Split Element Edges/Faces** is the appropriate one to use here. **Stay On Interface** ensures that only element faces that are located on the material interface are considered when the crack is growing.

The crack growth criterion chosen is the simplest: **Total Energy Release Rate**. A crack front node will grow when $G \geq G_c$ where G_c is the crack growth resistance, here set to 4×10^7 .

After the split occurs, the delamination criterion is turned off. Once the crack is created, we want the crack growth criterion to determine when the crack should grow and not the stress criterion in the **Delamination** option.

Each time growth is detected for a crack front node, the crack is extended and the increment iterations are continued. This continues until convergence is obtained and no more crack growth is detected. The **Crack Growth Increment** in the menu below determines how much the crack should grow when growth is detected. In general, this distance should not be too large, since then we may grow the crack too far for the current load. It should also not be too small, since this would require many iterations to find the final crack length at the current load. With remeshing based growth this could also lead to a large number of elements in the model. Since we here release element faces, the smallest amount we can release is a single element. In this example we leave the value at zero, which means that the program should release one element face each time growth is detected. If a value would be provided then the program will release as many faces as needed in order to honor the given length.

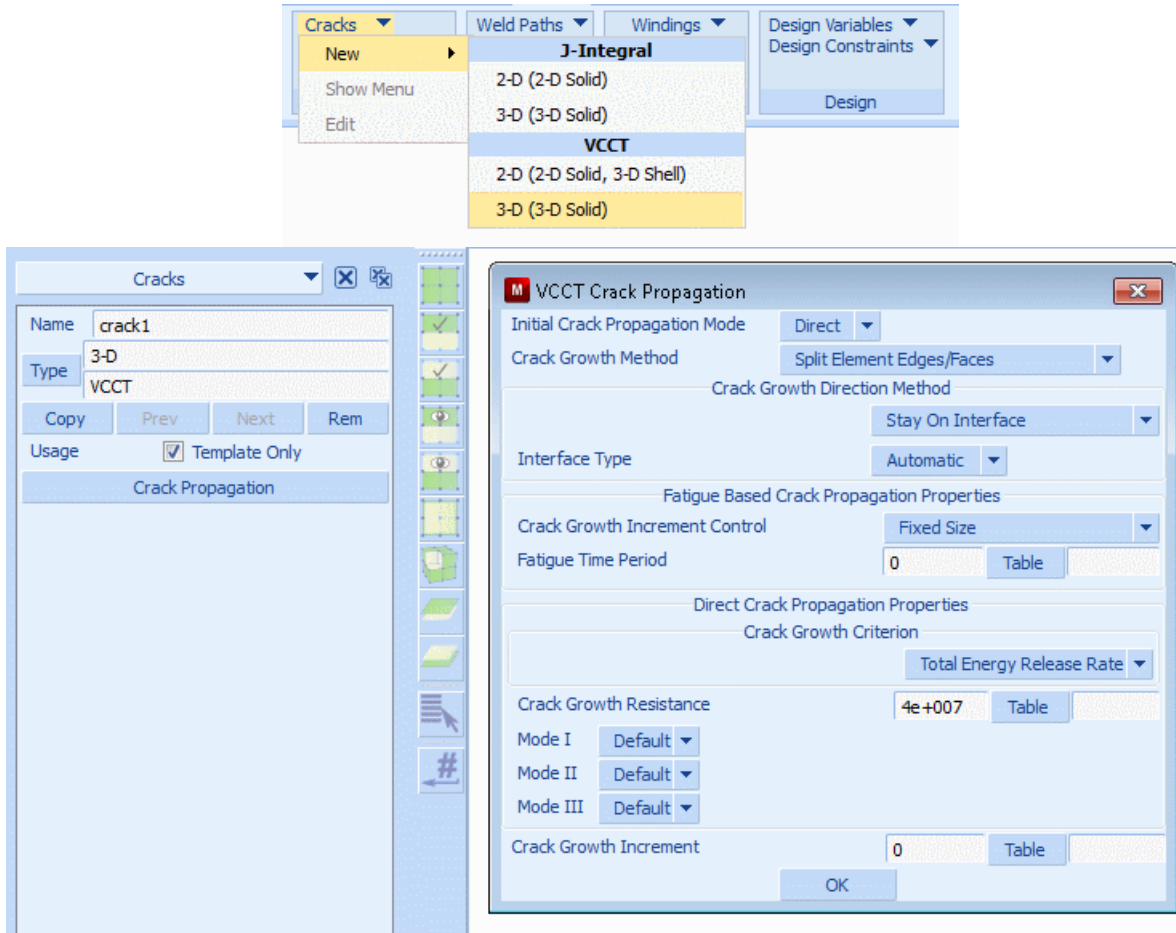


Figure 2.34-3 Mentat Menu Showing VCCT Settings

Cohesive Model

When the option to insert interface elements is used, we need to define the cohesive material properties. In [Figure 2.34-4](#), we see the steps to create the cohesive material from the **Delamination** menu. It is also possible to create the material in the **Materials** menu and refer to it with the **Set** button.

When the material data has been entered, a new material is generated and is associated with the current **Delamination** definition. Note that we have activated **Deactivate** and **Exclude From Post File** for fully damaged elements.

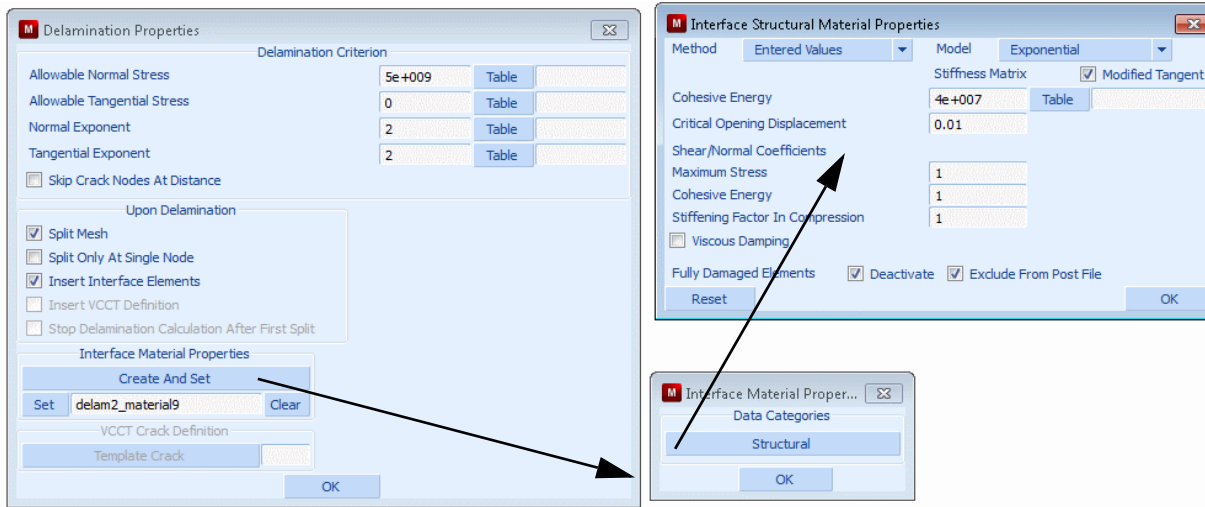


Figure 2.34-4 Mentat Menus for Creating Cohesive Properties

Crack Initiation

In this variant of the example, we will create the crack explicitly, without the use of the **Delamination** option. This is done by means of a so-called **Crack Initiator** as shown in Figure 2.34-5. It shows the location of the **Crack Initiator** menu under the **Toolbox** menu.

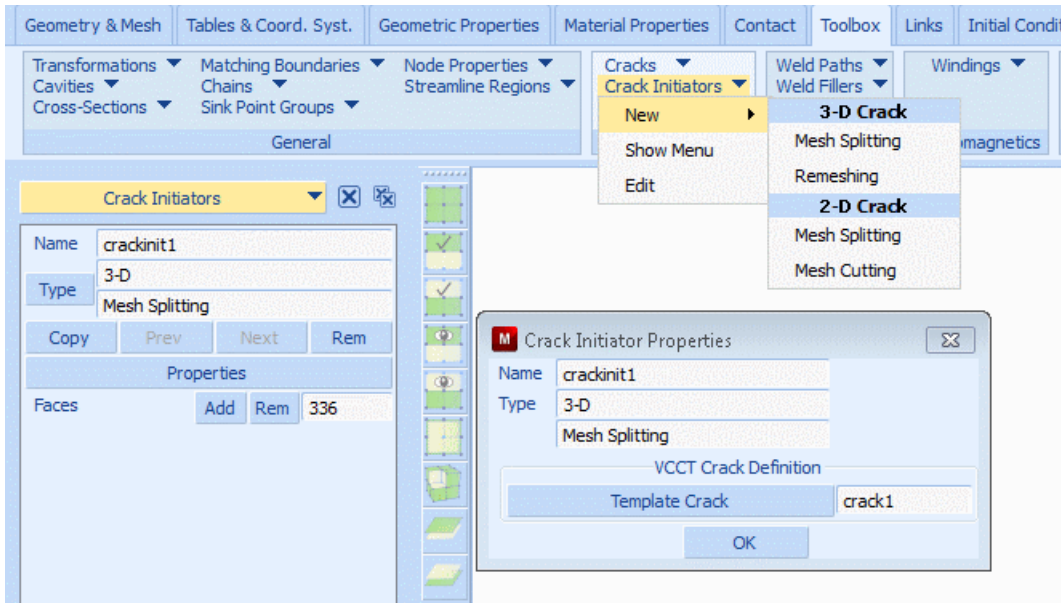


Figure 2.34-5 Mentat Menus for Crack Initiator

The location of crack initiation is defined by selecting the faces of elements as shown in [Figure 2.34-6](#). Some elements of the T-stiffener at the center are not shown. These elements have been placed in a set called “Center” to simplify postprocessing. The blue area is the set of element faces used as a crack initiator. The area selected is somewhat larger than needed. This is fine, since Marc will only use the faces which are internal to the structure and split up the mesh there. As we will see in the results section below, this input will give two crack fronts along the boundary of the crack initiator.

The crack crack1 is the template VCCT crack that was previously defined as shown in [Figure 2.34-3](#).

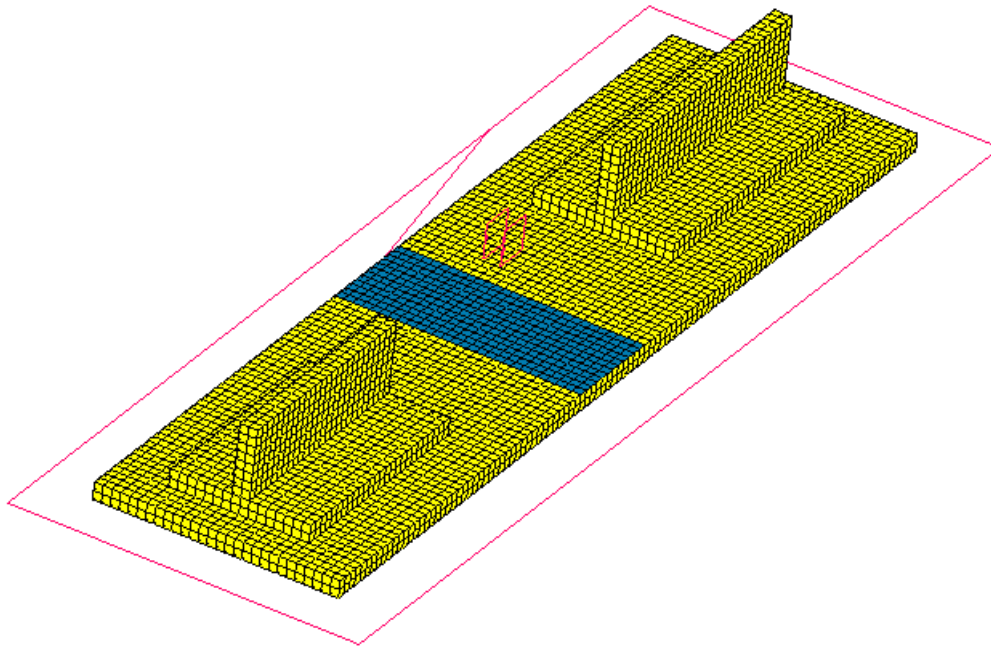


Figure 2.34-6 Element Faces for Crack Initiation

Solution Procedure

Each variant of the problem is solved using fixed time stepping in ten increments. This is sufficient for this simple case. The amount of crack growth in each increment is relatively small. In general, the time step needs to be tuned so that it matches the growth behavior and the convergence properties of the model. For more complicated cases it is often advantageous to use adaptive load stepping. The program will then automatically adjust the time step based upon convergence and other controls.

The **Crack Initiator** needs to be selected in the load case where it should be activated as shown in [Figure 2.34-7](#).

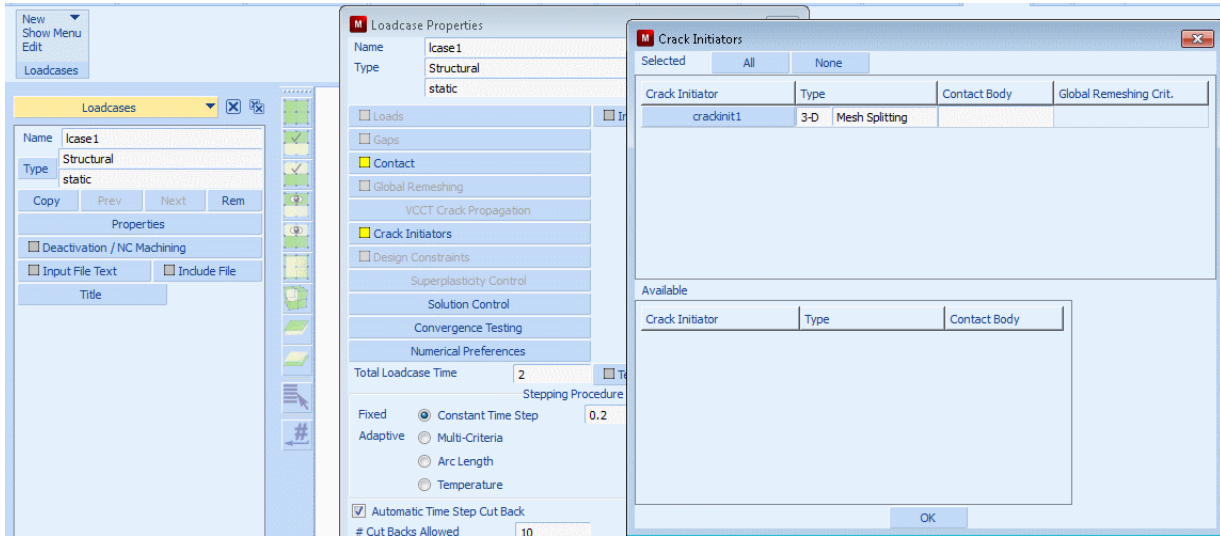


Figure 2.34-7 Load Case Settings for Crack Initiator

Results

Figure 2.34-8 shows the results for the **Delamination Index** (value of the failure index) right before failure occurs. Element set “center” has been taken out in the picture in order to show the results. The failure index shows a maximum under the load as expected.

In the following sections we show results for the two cases of post failure behavior: VCCT and Cohesive.

Inc: 2
Time: 4.000e-001

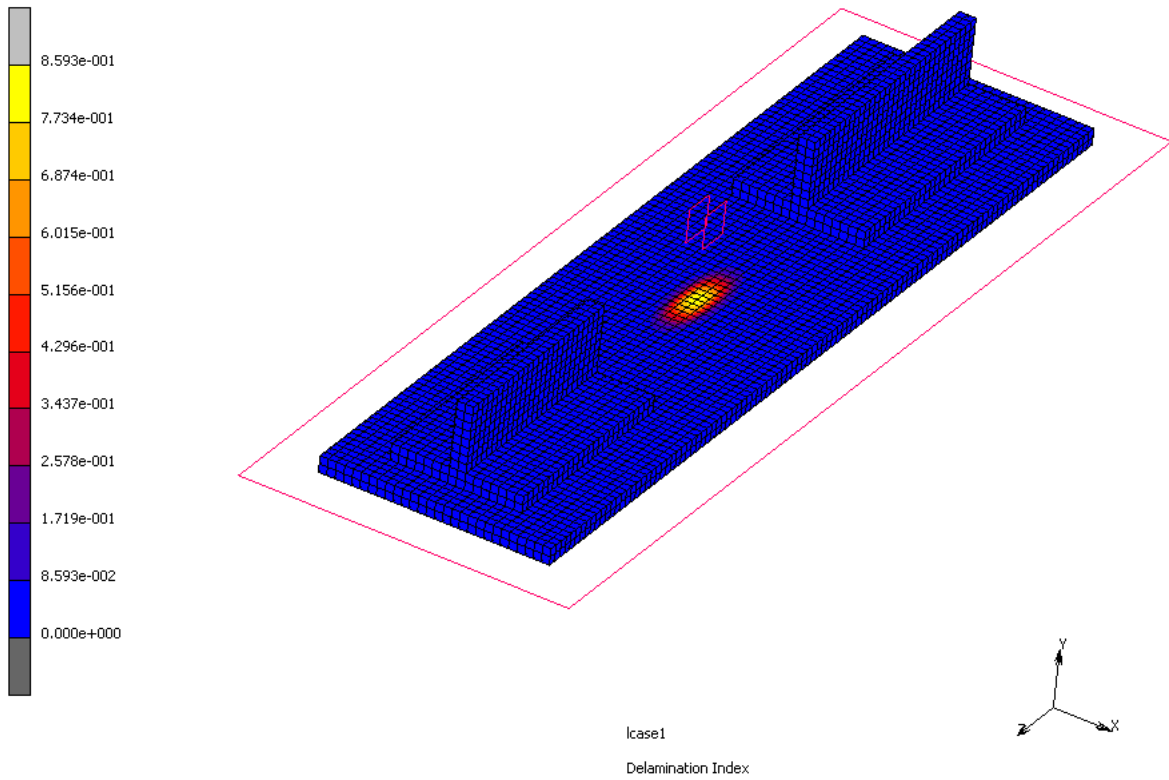


Figure 2.34-8 Delamination Results

VCCT

First, we have the results from using **Delamination** together with VCCT. [Figure 2.34-9](#) shows the crack which is first initiated when failure occurs in increment 3. It is a wire frame outline plot with a vector plot of Crack System Local X. In the settings for vector plot, the arrows are set to solid for better visualization. The failed region does not reach the boundary so a single closed crack front is created.

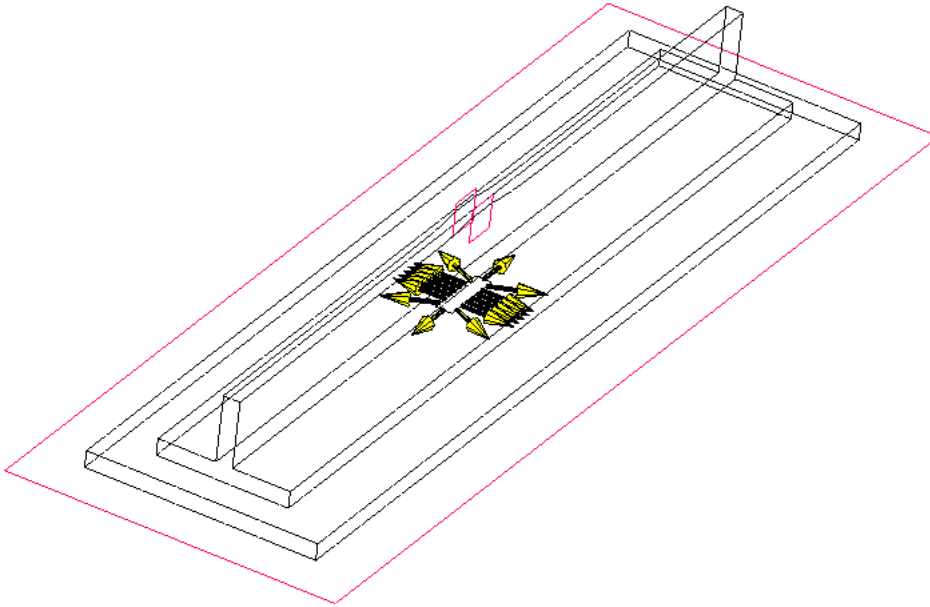


Figure 2.34-9 Initial Crack for VCCT

As the load is increased, the crack will grow. Remember, we have set the growth to only occur along the material interface. In [Figure 2.34-10](#), we see the final crack front at the final load.

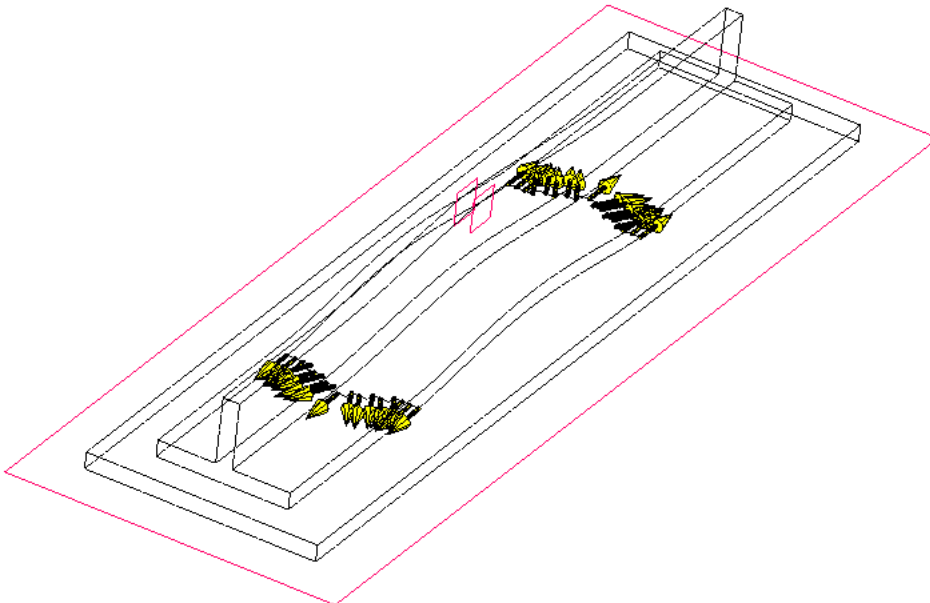


Figure 2.34-10 Solution at Final Load

Cohesive

Here, we show the results using a plot of element types. Element 7 is the standard brick element and 188 is the corresponding 8-noded interface element. When the first failure occurs, we get a region of inserted interface elements in the center of the model.

Inc: 3
Time: 6.000e-001

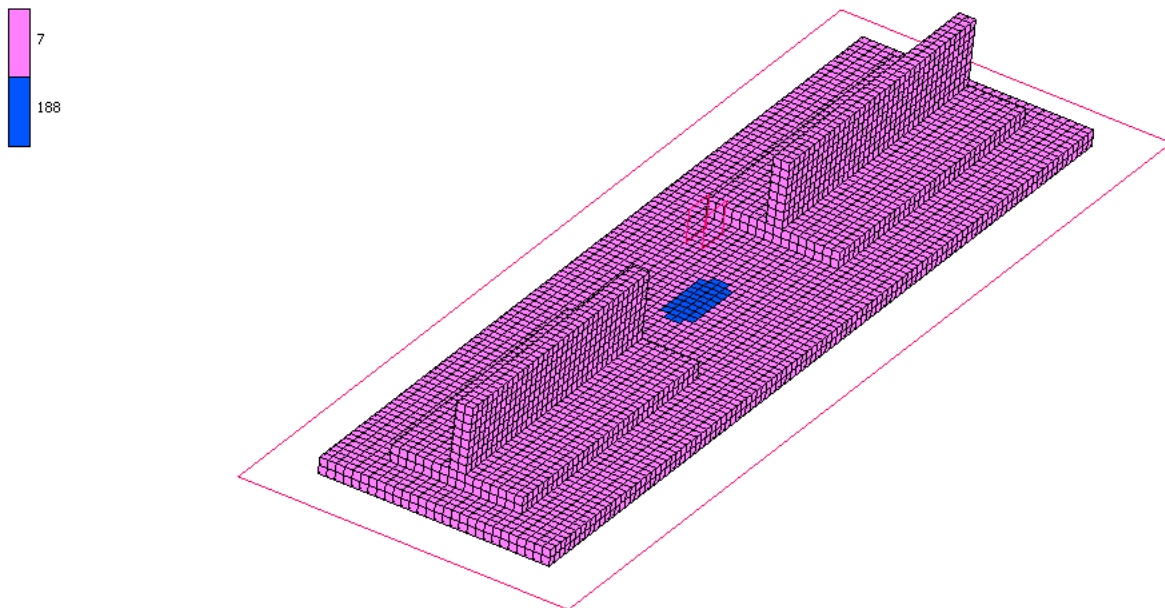


Figure 2.34-11 Element Types for Cohesive Case

Similarly to the crack growth case, we get an increasing failed zone which is for this case filled with interface elements. The size of the zone at the final load is shown in [Figure 2.34-12](#). Here, we also see that some elements in the middle have been deactivated, since they reached full damage.

The failed zone is clearly smaller than what we obtained for VCCT. No attempt has here been made to tune the material parameters in order to make the solutions match. Although they use a similar approach, the results are not expected to be the same. In the VCCT case, the new faces due to crack growth are free; while in the cohesive case, they are still constrained until full damage is reached.

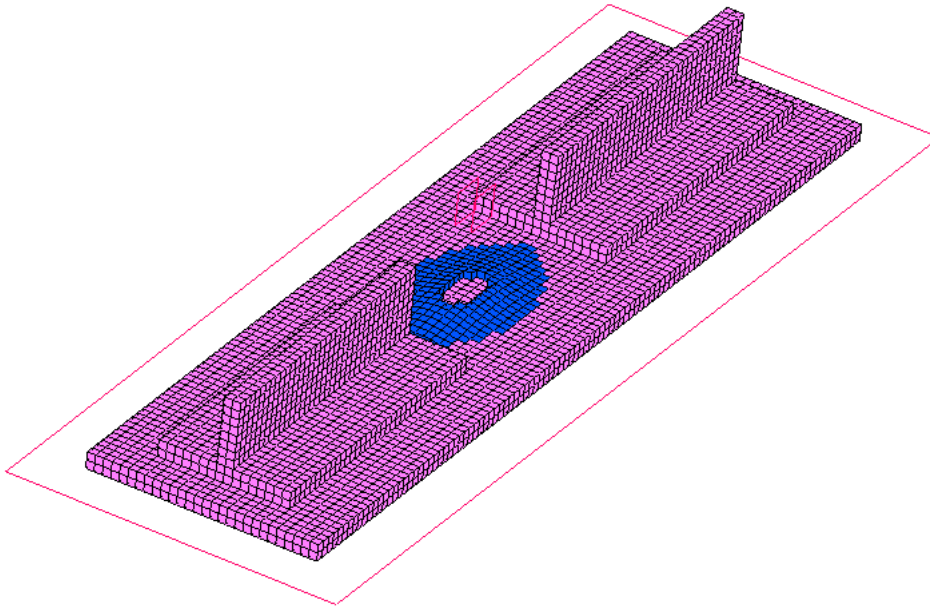


Figure 2.34-12 Extent of Damage Zone at Full Load

Crack Initiation

Finally, we have the case of manual crack initiation. The crack initiator is shown in [Figure 2.34-6](#) above. This leads to two crack fronts as shown in [Figure 2.34-13](#).

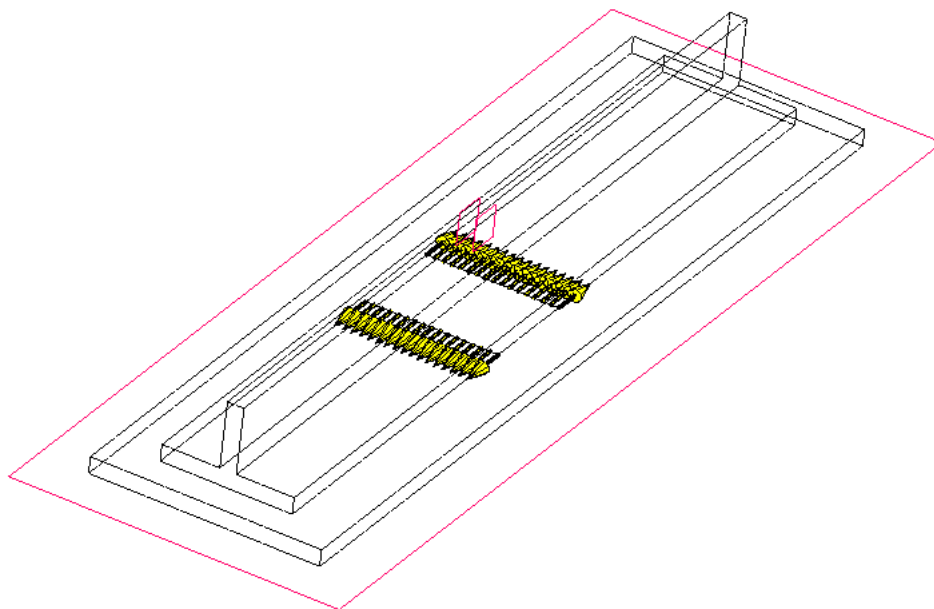


Figure 2.34-13 Crack Fronts After Crack Initiation with Set of Element Faces

With the same load as in the previous cases, we get the final configuration as shown in [Figure 2.34-14](#). Note that the results are the same as for the case of Delamination with insertion of VCCT crack in [Figure 2.34-10](#).

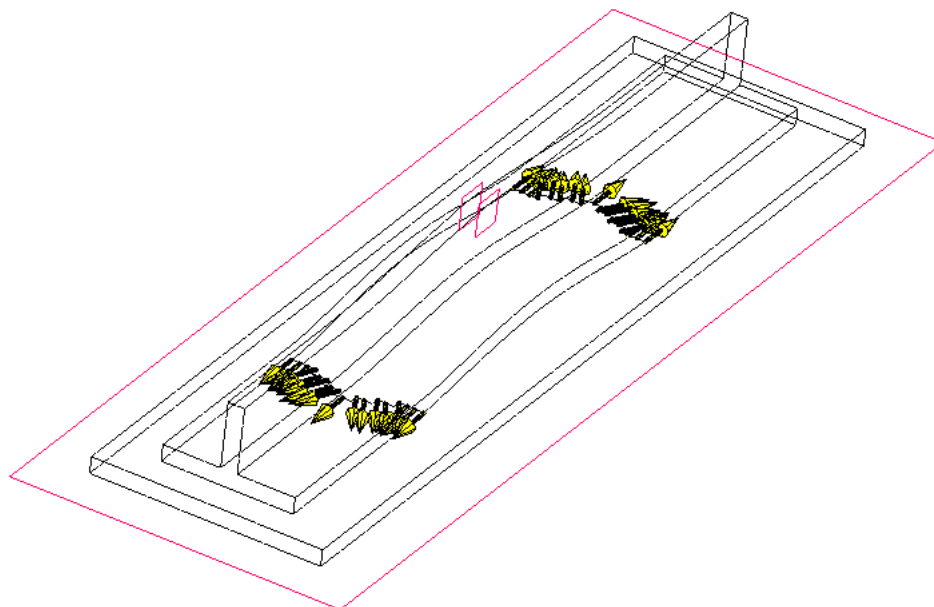


Figure 2.34-14 Crack Fronts at Final Load

Input Files

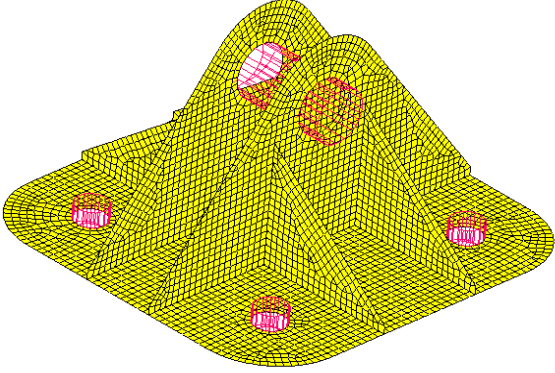
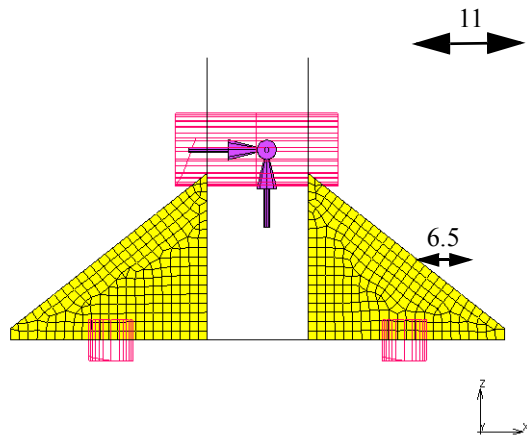
The files below are on your [delivery media](#) or they can be downloaded by your web browser by clicking the links (file names) below.

File	Description
crackgrowth_delam_vcct.mud	Model file for VCCT case
crackgrowth_delam_cohesive.mud	Model file for cohesive case
crackgrowth_crackinit.mud	Model file for crack initiation case

2.35 Fatigue Crack Propagation in a Lug with Multiple Cracks

- Summary 810
- Modeling Details 811
- Loading and Solution Procedure 814
- Results 815
- Input Files 819

Summary

Title	Fatigue crack propagation in a lug with multiple cracks.
Problem Features	New fatigue procedure with high cycle fatigue count and growth of multiple cracks.
Model	 <p>A 3D finite element model of a lug, rendered in yellow. The model shows a complex, multi-faceted structure with several cracks highlighted in red. The cracks are distributed across the top and side surfaces of the lug.</p>
Material properties	Linear elastic material: $E = 2 \times 10^5$ MPa; $\nu = 0.3$
Analysis characteristics	Nonlinear static analysis
Boundary conditions and Applied loads	<p>There are four fixed rigid bodies to which the base plate is glued. They represent fastening bolts. A fifth rigid body represents a cylindrical pin, on which a load is applied. This load is located on the center line of the pin, shifted towards one side as shown in the picture below. The pin is fixed in the x direction, and has a prescribed displacement with magnitude 0.01 mm in the y direction and 0.03 mm in the z direction.</p>  <p>A 2D cross-sectional view of the lug, rendered in yellow. The model shows a central cylindrical pin (purple) and four fastening bolts (pink) at the base. A load is applied to the pin, indicated by a purple arrow pointing downwards. The distance from the center of the pin to the center of the left bolt is labeled as 11. The distance from the center of the pin to the center of the right bolt is labeled as 6.5. A coordinate system is shown at the bottom right, with the z-axis pointing upwards and the x-axis pointing to the right.</p>
Element type	4-noded shell elements (element type 75).
FE results	<ol style="list-style-type: none"> 1. Results of crack growth (crack path). 2. Results of cycle count.

This example illustrates the modelling of high cycle fatigue in a structure with two cracks. Since the loading is unsymmetric, the cracks will grow at different rates.

Starting out with a small crack at each of the holes at the pin, the cracks will grow, and we obtain the paths the cracks will take due to the loading. Using Paris' law, we also estimate the number of cycles it would take for the cracks to reach the boundary.

Modeling Details

One crack of initial length of 3 mm are positioned on each of the flanges as shown in [Figure 2.35-1](#). The vertical position is the same as the center line of the pin. They are modeled using the CRACK INIT option using mesh cutting. A straight line is used for each of the cracks.

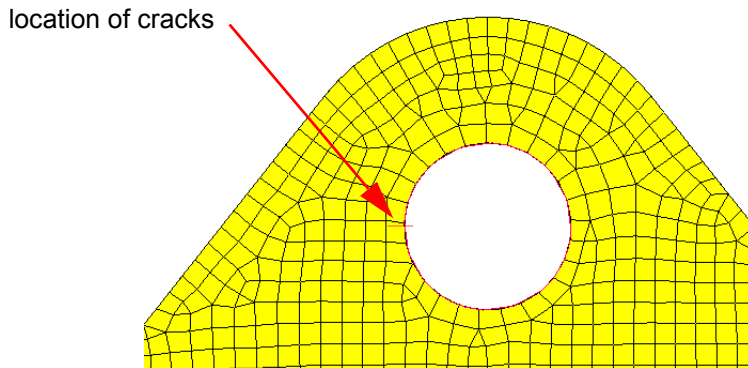


Figure 2.35-1 Position of Initial Cracks

We use three deformable contact bodies. The reason for using three bodies is that we will use remeshing, and remeshing currently does not support intersecting shells. Hence, each flange is a separate body and they are glued to the rest of the structure. The base plate and the stiffeners (body “plateandstiff”) are glued to the bolts and the flanges are glued to the base plate and stiffeners. Regular sliding contact is used between the flanges and the pin.

The pin is a load controlled rigid body. The control node has the prescribed displacements (shown above) and the auxiliary node for the rotations has suppressed rotation around the axis of the pin while the other rotations are free.

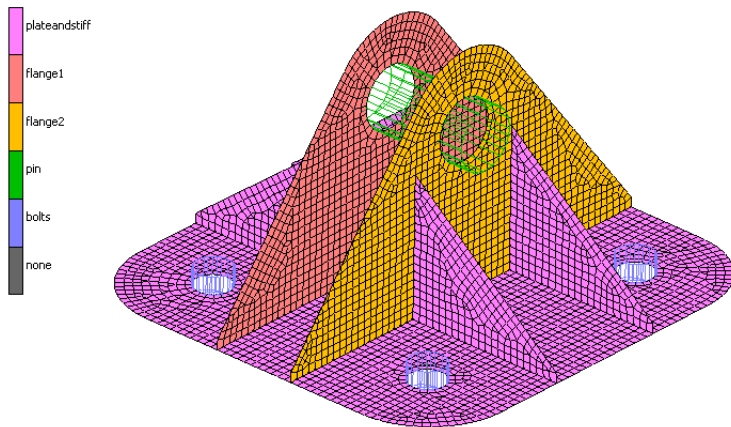


Figure 2.35-2 Contact Bodies

VCCT

Figure 2.35-3 shows the VCCT settings. We use a template crack since the cracks will be created using Crack Initiation. We perform a crack growth calculation using Remeshing. We want to calculate the crack paths so we use the Maximum Hoop Stress criterion for the crack growth method.

The Fixed With Scaling option allows us to scale the crack growth rates between the two cracks and to make a High Cycle Fatigue Calculation. We will be using Paris' law for the fatigue cycle count, and the parameters used are shown in the figure.

The Crack Growth Scale Method defines how the growth increments between cracks (and along crack fronts for 3-D cracks) should be scaled. Here, we select it to use the fatigue law, so it is consistent with the cycle count. Consistent here means that the cycle count for both cracks will be the similar, since we scale the growth increments according to Paris' law.

The Fatigue Time Period is set to 1, and this will be taken into account when defining the table for the load variation. The Crack Growth Increment is set to 0.5 mm. The distance from a crack to the boundary is about 6 mm, so we would expect the fastest growing crack to reach the boundary in about 12 loading cycles.

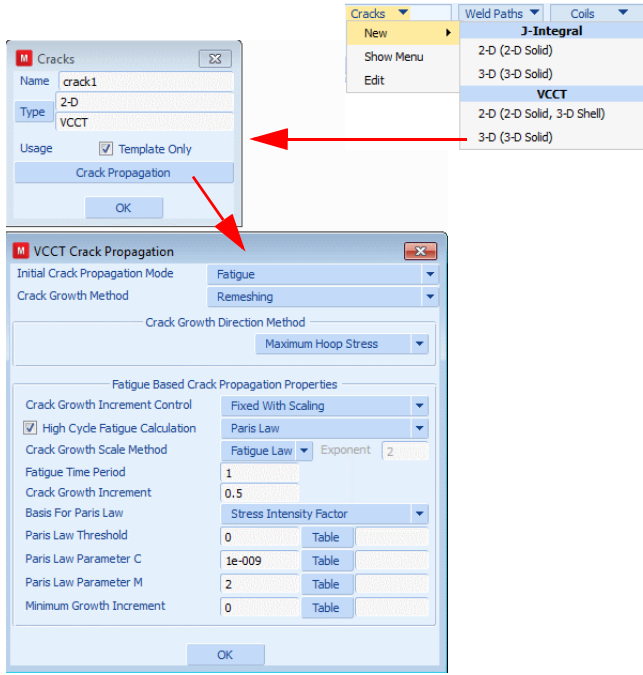


Figure 2.35-3 Mentat Menu Showing VCCT Settings

Crack Initiation

Figure 2.35-4 shows the menu used for defining the crack initiator. The cracks are 2-D crack in shells (through cracks), and we identify the two curves used to define the cracks. We refer to the template crack that was defined above.

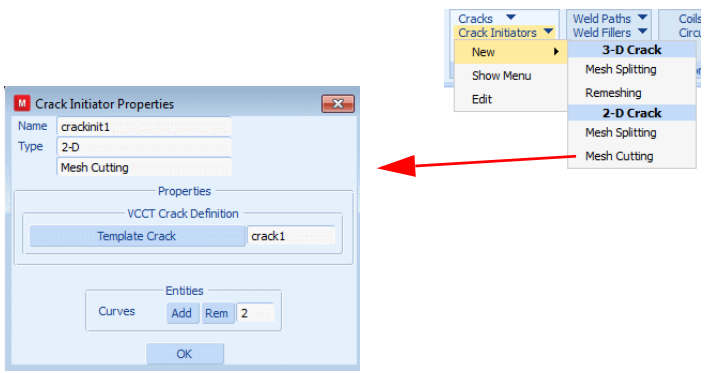


Figure 2.35-4 Mentat Menu for the Crack Initiator

Loading and Solution Procedure

The loading consists of prescribed displacements on the control node of the pin. There is a pre-load followed by a cyclic variation of the load. In order to model this, we use two load cases: one for the pre-load and one for the cyclic variation. Figure 2.35-5 shows the table variation of the load. The pre-load is done for a time of 0.5, shown in green. The cyclic part, shown in red, is modeled through an equation:

$$F = \frac{1}{4} \left(1 + \sin \left(2\pi v_1 + \frac{\pi}{2} \right) \right) + \frac{1}{2}$$

The fixed time step used in the second load case is 0.5, so the use of an equation is not necessary since we only make use of the peak points. One might as well have ramped the load up and down. The equation is, however, convenient since it is easy to enter and valid for infinite time.

Some comments on the load table. We want the time period of the cyclic load to be 1 since this is what we defined for the fatigue time period. We do not want to reach the end of a fatigue cycle during the pre-load. Hence, it is set smaller than the fatigue time period. The starting point of a fatigue period is always reset at the start of a load case.

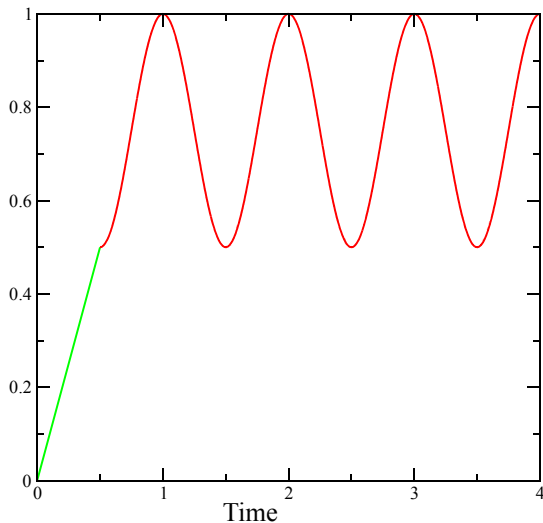


Figure 2.35-5 Table for load variation

The crack initiation is done in the first load case, which consists of a single increment.

Remeshing

The settings for remeshing parameters are shown in Figure 2.35-6. We use the Full mesh density control so we can control the mesh density variation in detail. The default control is a target edge length of 1. This is close to the element in the initial mesh. Then we use a distance control using the distance to all cracks in the model. Since we use crack initiation, we cannot pick individual cracks. The region within a radius of 3 will be affected by this density control. Near the crack, we use a rather fine mesh of 0.075. This value should take the chosen growth increment of 0.5 into

account. We have not set a minimum growth increment (remember, the growth increment of one crack will be scaled), so the smallest growth increment that may occur is 1/10 of the growth increment. This means that we might get crack growth as small as 0.05 per increment. If this would happen then we should probably decrease the target edge length near the crack. The target edge length at the radius of influence is here set to 0.2. This is done in order to avoid a too abrupt change in the mesh density. The mesh generator will make a smooth transition zone if the same edge length is used in the whole refined region, but this will make the transition even smoother.

The remeshing is only active in the second load case. We use the Immediate remeshing option so we get a fine mesh in the first fatigue cycle.

We use two identical remeshing controls, one for each contact body with a crack.

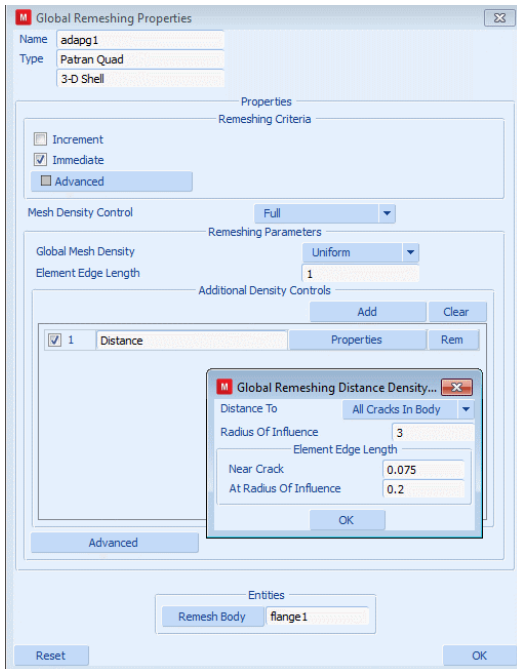
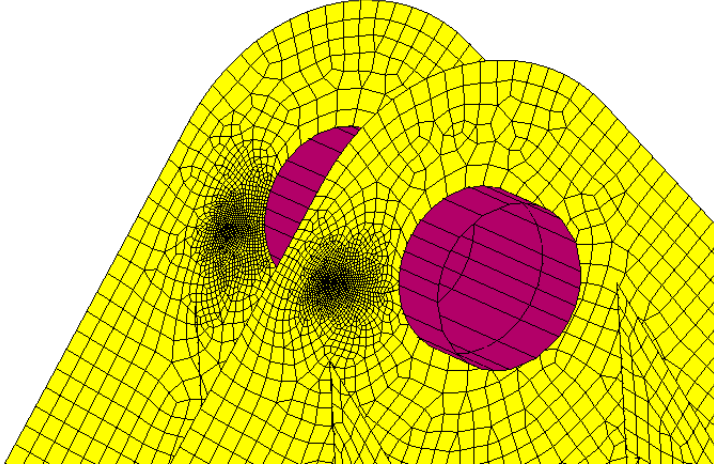


Figure 2.35-6 Remeshing Settings

Results

Figure 2.35-7 shows the results at increment 15. Here we can see the mesh, which is focused around the two cracks. The bottom graphic shows an outline plot, and there we can clearly see that one crack grows faster. This crack is the one which is closest to the applied load.

Inc: 15
Time: 7.500e+000



Inc: 15
Time: 7.500e+000

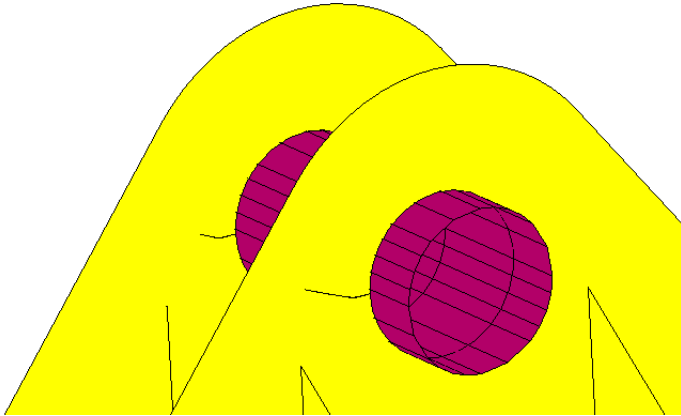


Figure 2.35-7 Crack Growth Results

Crack Path

The path the cracks will take is one of the things we want to obtain from the analysis. [Figure 2.35-8](#) shows this path when one crack has grown through the section. The crack starts out horizontally and directly aligns itself perpendicular to the applied load. The arrow shown in the picture is the reaction force at the node where the prescribed displacement is applied.

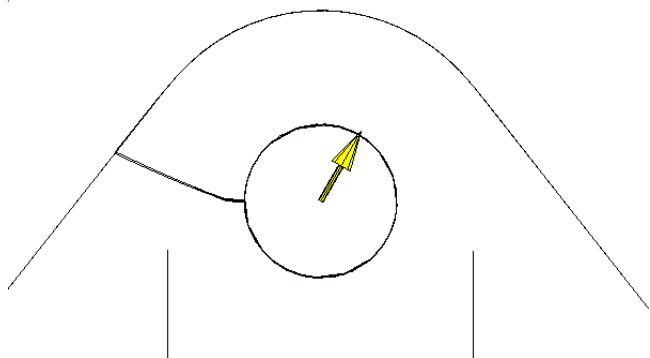


Figure 2.35-8 Crack Path

Cycle Count

The main objective of the analysis is to estimate the number of cycles it takes for a crack to reach the boundary.

The results for the cycle count can be found as Global Variables in postprocessing and more detailed information is provided in the output file.

The crack reaches the boundary at increment 30. [Figure 2.35-9](#) shows on the left-hand side the cycle count at increment 31. This is what we have for the **Cracking Variables**. These results are for the so-called leading crack. This is the crack which currently has the highest growth rate. One does not see the individual cracks since the crack initiation is used with a template crack. In order to see an individual crack for the global variables, they need to be explicitly defined in the model. The right-hand side of the figure shows a time history plot of the cycle count up to increment 31.

The estimated number of cycles to failure is thus 383,128.



Figure 2.35-9 Results for Cycle Count

The output file contains more detailed information, as shown in Figure 2.35-10. It mentions that one has reached the end of the fatigue load sequence. The “accumulated number of fatigue cycles” is the number of fatigue cycles done so far. Increment 1 was the pre-load, and one does two increments per fatigue cycle so here at increment 17 one has done 8 cycles. It says that the leading crack is `initcrack_2` (crack initiation assigns names for each crack automatically). To see which one it is, one can look at the VCCT results at the end of the previous increment. Then, it writes information about the cycle count. When doing the cycle count, one can assume a linear variation of ΔK from the previous and current fatigue cycle. For this fatigue cycle, one observes that it goes from about 126 to 131, leading to a contribution of 30203 cycles to a total of 310,370 cycles. This was for the leading crack, and for the other crack, one has a smaller ΔK but also a smaller Δa (due to the scaling) so one ends up with almost the same cycle count. Finally, one observes the accumulated crack growth for each crack. This is the value one sees as “VCCT, length, lead crack” for the global variable in postprocessing.

```

e n d   o f   i n c r e m e n t      19
binary post data at increment      19.  subincrement      0.  on file 16
wall time =          156.00

end of fatigue load sequence for crack initcrack_2
accumulated number of fatigue cycles      9

the leading crack is initcrack_2

performing fatigue cycle count
starting delta k
ending   delta k
      1.2613E+02  1.3124E+02

fatigue cycle calculation for crack initcrack_2
number of cycles calculated for the current period      30203
total accumulated number of cycles      310370

end of fatigue load sequence for crack initcrack_3
accumulated number of fatigue cycles      9

performing fatigue cycle count
starting delta k
ending   delta k
      6.8816E+01  6.8554E+01

fatigue cycle calculation for crack initcrack_3
number of cycles calculated for the current period      28916
total accumulated number of cycles      299985

remeshing body      2 due to crack growth

accumulated crack growth, initcrack_3  1.7379E+00

remeshing body      3 due to crack growth

accumulated crack growth, initcrack_2  4.5000E+00

```

Figure 2.35-10 Output for Fatigue Results

After increment 31, when the first crack has reached the boundary, the other crack continues to grow. Now the structure is much more flexible, and since one used a prescribed displacement, one gets lower stress intensity factors. Hence, the cycle count goes up a lot, and the final cycle count is 43,923,128.

Input Files

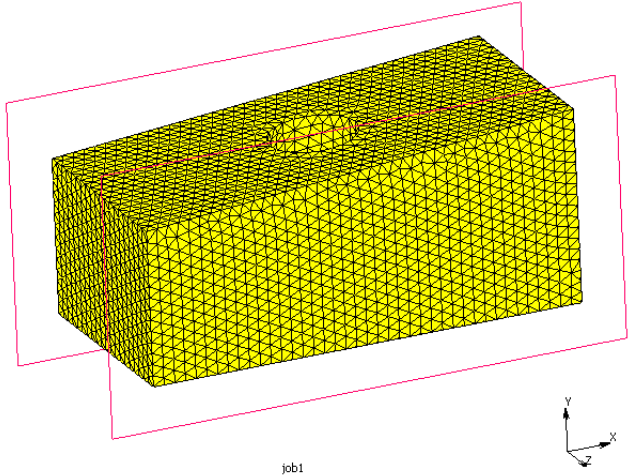
The file below is on your [delivery media](#), or it can be downloaded by your web browser by clicking the link (file name) below.

File	Description
lug_shell.mud	Model file

2.36 3-D Fatigue Crack Propagation: Corner Cracks at a Hole

- Summary 822
- Modeling Details 823
- Loading and Solution Procedure 824
- Results 825
- Input Files 827

Summary

Title	3-D fatigue crack propagation of cracks at a hole.
Problem Features	New fatigue procedure with high cycle fatigue count in a 3-D structure
Model	
Material properties	Linear elastic material: $E = 2 \times 10^5$; $\nu = 0.3$
Analysis characteristics	Nonlinear static analysis
Element type	4-noded tetrahedral elements (element type 134).
FE results	<ol style="list-style-type: none"> 1. Results of crack growth (shape of crack fronts). 2. Results of cycle count.

This example illustrates the modelling of high cycle fatigue in a 3-D structure. Two circular cracks are located at the corner of the hole. The shapes of the crack fronts will change during the analysis. We will also have the effect that the cracks will grow at different rates. We use remeshing based crack growth, and the cracks are closed when the remeshing takes place. Hence, we here also illustrate remeshing during self contact.

Modeling Details

A tapered block has a through hole of radius 0.2. [Figure 2.36-1](#) shows the solid model and also the surfaces used. Two cracks will be added at the corner of the hole. They are modeled with crack initiation using disk shaped faceted surfaces. The larger one has a radius of 0.1 and the smaller 0.05.

One rigid body is fixed in space, and the other is a load controlled body which will move in the z direction with prescribed displacement. All other motion of this body is suppressed.

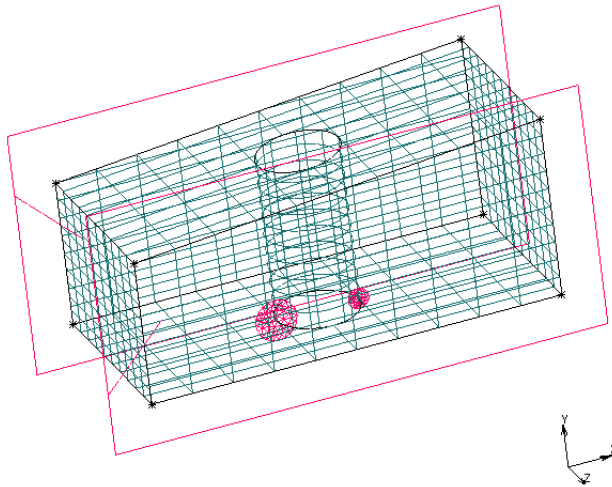


Figure 2.36-1 Solid Model with Cracks and Rigid Bodies

VCCT

[Figure 2.36-2](#) shows the VCCT settings. We use a template crack since the cracks will be created using Crack Initiation. We use a crack growth calculation using Remeshing. In this example, we are not interested in finding if the cracks will change shape due to mixed mode, we primarily want to find the shape of the crack front. Hence, we use the crack growth direction method Mode I and Normal. Using a normal of $(0,0,1)$ makes the cracks stay in the x-y plane.

The Fixed With Scaling option allows us to scale the crack growth rates along the fronts and between the cracks and to make a High Cycle Fatigue Calculation. We will be using Paris' law for the fatigue cycle count, and the parameters used are shown in the figure.

The Crack Growth Scale Method defines how the growth increments between cracks and along crack fronts should be scaled. Here, we select it to use the fatigue law.

The Fatigue Time Period is set to 1, and this will be taken into account when defining the table for the load variation. The Crack Growth Increment is set to 0.8. This value may be somewhat large, but since this is a demonstration example we want to avoid that it takes a long time to run.

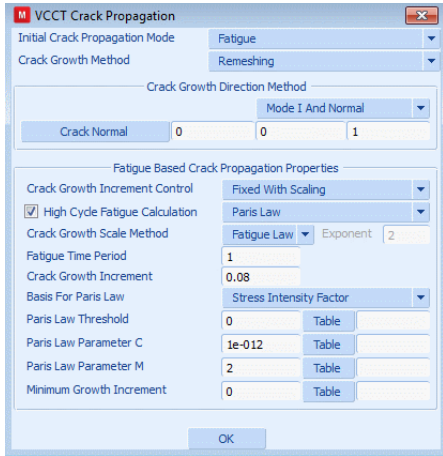


Figure 2.36-2 Mentat Menu Showing VCCT Settings

Crack Initiation

A single Crack Initiator is defined using remeshing. It refers to the previously defined template crack and indicates that the cracks should be initiated in the deformable contact body. Both the faceted surfaces are selected for the crack initiator.

Loading and Solution Procedure

The loading consists of a prescribed displacement of the control node of the load controlled rigid body. There is loading and unloading using a single increment for each part. The load variation is for convenience modelled through an equation:

$$F = \frac{1}{2} \left(1 + \sin \left(2\pi v_1 - \frac{\pi}{2} \right) \right)$$

The convergence tolerance in the load case setting uses a residual tolerance of 1%. We also use a minimum reaction force cutoff of 0.001. This is done in order to avoid unnecessary recycles during unloading when the reaction forces and residual forces are almost zero. The value of 0.001 is chosen as a small fraction of the reaction forces obtained during loading (which are of the order of 5000).

We use 20 increments with a time step of 0.5. Hence, we will reach the end of the fatigue cycle every second increment, when the structure has unloaded. There is no expected self contact penetration since we do not compress the structure,

only unload. We still use self contact in the contact table definition. This is to demonstrate that the self contact remeshing works, even if small overlaps would occur.

Remeshing

We use the Full mesh density control for remeshing so we can control the mesh density variation in detail. The initial mesh is uniform, but here we want a varying mesh density. The default control is a target edge length of 0.1, which should be fine enough away from the hole. In order to preserve the shape of the hole, we use a cylindrical region around the hole with a target edge length of 0.05. Finally, within a distance of 0.2 from any crack, we use a target edge length of 0.02.

Results

Figure 2.36-3 shows the mesh after crack initiation. We see that the mesh is properly refined around the cracks and that there is a reasonable mesh density transition to the rest of the structure.

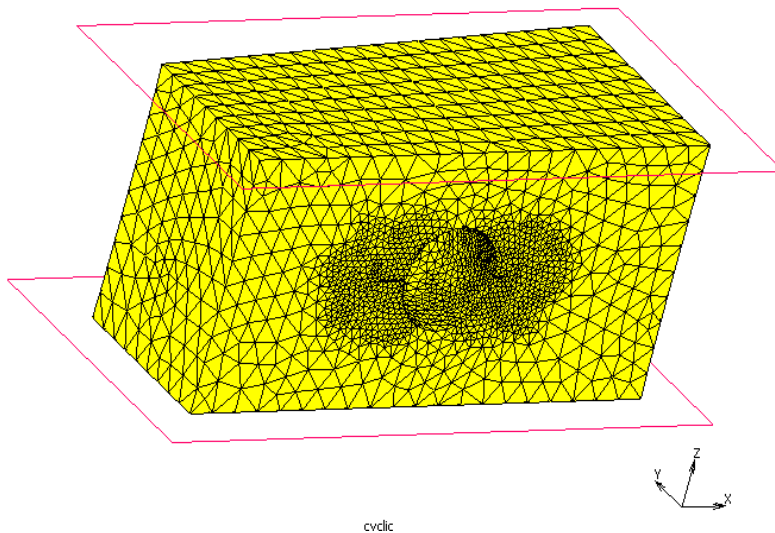


Figure 2.36-3 Mesh After Crack Initiation

Shape of the Crack Fronts

One of the primary targets of the analysis was to find the shape of the crack fronts after growth. One would expect that the cracks grow faster through the thickness of the plate. Figure 2.36-4 shows a sequence of results at different increments. With an outline plot in wire frame mode, it is easy to see the shape of the crack fronts. We clearly see that the cracks grow faster through the thickness than radially from the hole.

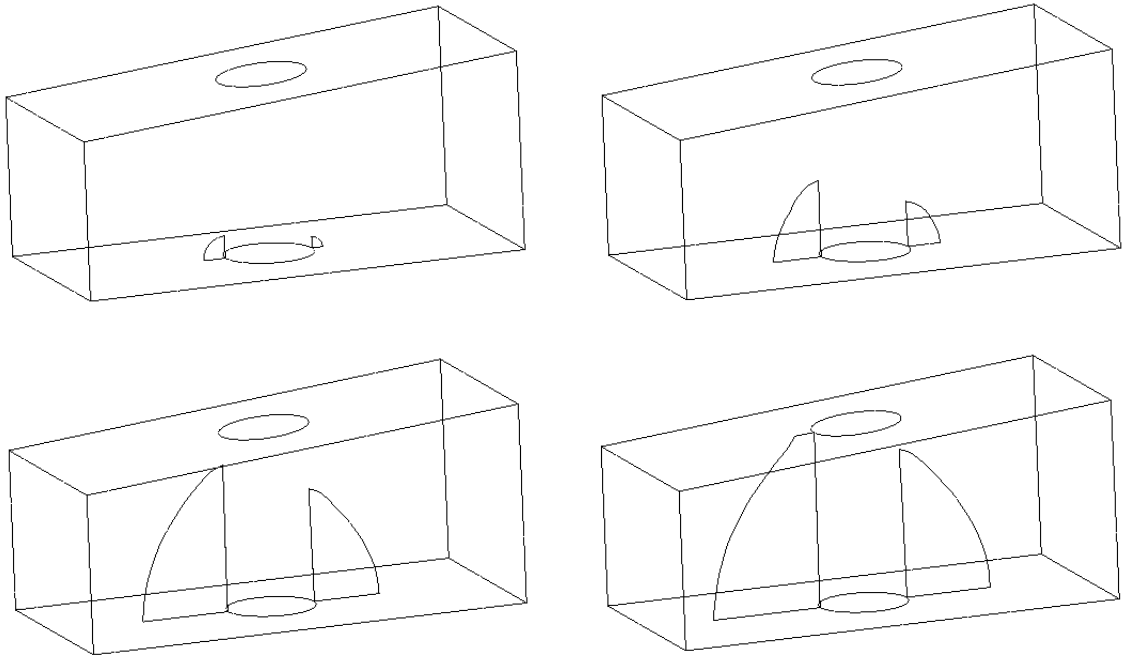


Figure 2.36-4 Crack Front Shapes

In Figure 2.36-5, we show a plot of the accumulated crack growth using a Symbols plot in outline mode. This shows how far each crack front node has grown. This clearly shows the variation of growth distance along the fronts and also that the crack on the left-hand side, which initially had the larger crack, grows faster.

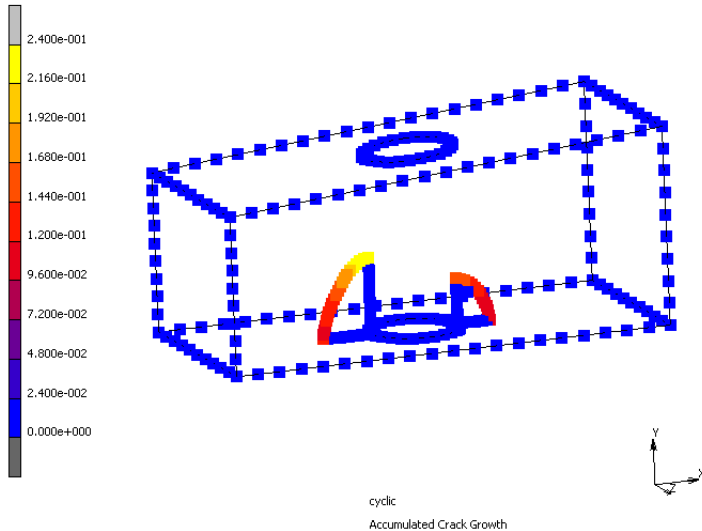


Figure 2.36-5 Plot of Accumulated Crack Growth

Cycle Count

This analysis also includes a high cycle fatigue count using Paris' law. The results for the cycle count can be found as Global Variables in postprocessing and also more detailed information in the output file.

The analysis is run for 20 increments, and increment 20 is when the first crack grows through the thickness. [Figure 2.36-6](#) shows the cycle count at increment 20. Here, we find the result that the number of cycles it takes to grow a crack through the thickness is 35,843.

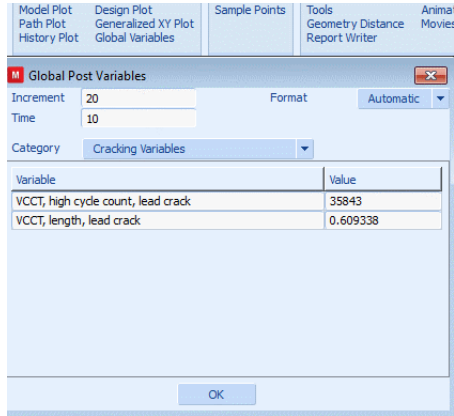


Figure 2.36-6 Results for Cycle Count

Input Files

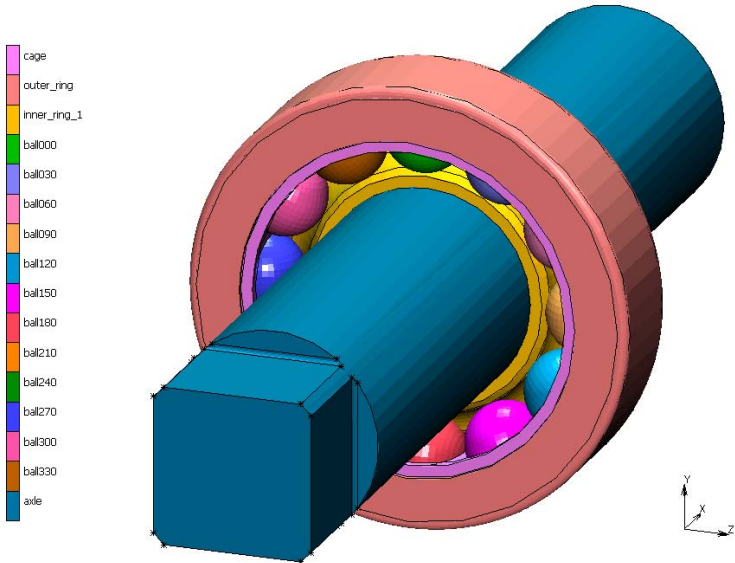
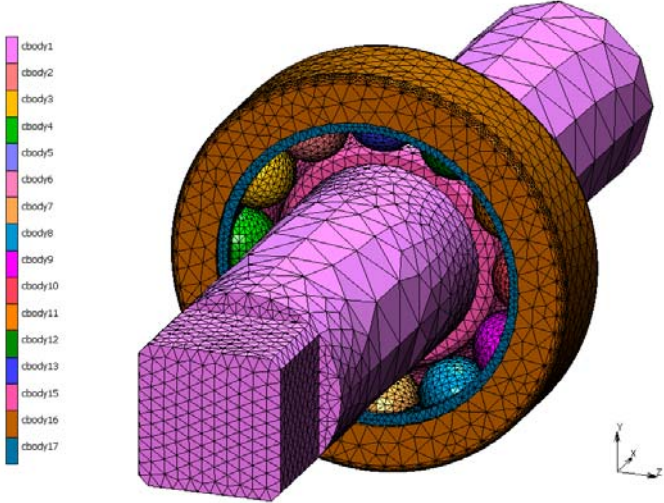
The file below is on your [delivery media](#), or it can be downloaded by your web browser by clicking the link (file name) below.

File	Description
holecrack.mud	Model file

2.37 CAD Import and Automatic Meshing

- Summary 830
- Import of the CAD Model 831
- Defeaturing the Model 833
- Meshing the Model 836
- Conclusions 842
- Input Files 842

Summary

Title	CAD Import and Automatic Meshing
Problem features	Import of CAD models and automatic meshing of these models
Geometry	 <p>MSC Software</p>
Finite Element Mesh	 <p>MSC Software</p>

This example demonstrates the process of importing CAD models and automatic meshing of these models in Mentat. A Parasolid model of a ball bearing is imported and meshed with tetrahedral elements. The different options to control the mesh density in the various parts of the model are discussed. Tools to simplify the geometry by removing features, such as holes, fillets, and chamfers, are demonstrated as well.

Import of the CAD Model

Mentat provides a number of options to import CAD models into the system:

- Parasolid models can be imported via the File → Import → Parasolid option
- ACIS models can be imported via the File → Import → ACIS option
- All major CAD formats, including ACIS, Catia, Inventor, Parasolid, Pro/Engineer, SolidWorks and Unigraphics, can be imported via the File → Import → General CAD As Solids option

All three options import the full CAD geometry of the model into the system, in the form of a number of solid bodies (volumes), sheet bodies (surfaces), and wire bodies (curves). The third option not only imports the CAD model, but also provides tools to clean up the geometry and automatically remove features upon import. The feature removal is based on size criteria and works fully automatically without user intervention. For example, options are available to automatically remove all holes with a radius within a given range from the model upon import. Note that a separate Defeature is also available to remove features *after* import of the bodies. This menu can also be used on bodies imported from a Parasolid or ACIS model via one of the first two options. The Defeature menu will be discussed in the next section.

The Parasolid model of the ball bearing is imported via the File → Import → Parasolid option:

```
File → Import → Parasolid  
bearing.x_t
```

The model consists of 17 solid bodies:

- The outer ring of the bearing
- Two inner rings, one on each side of the bearing
- 12 Rolling balls
- A cage which keeps the balls in place
- An axle on which the bearing is mounted

After import, the solid bodies that have been imported from the Parasolid model are listed in the Solids folder of the model tree on the left hand side of the main Mentat window (see [Figure 2.37-1](#)). Each body in the tree has a check box to toggle the display of the body on the graphics windows.

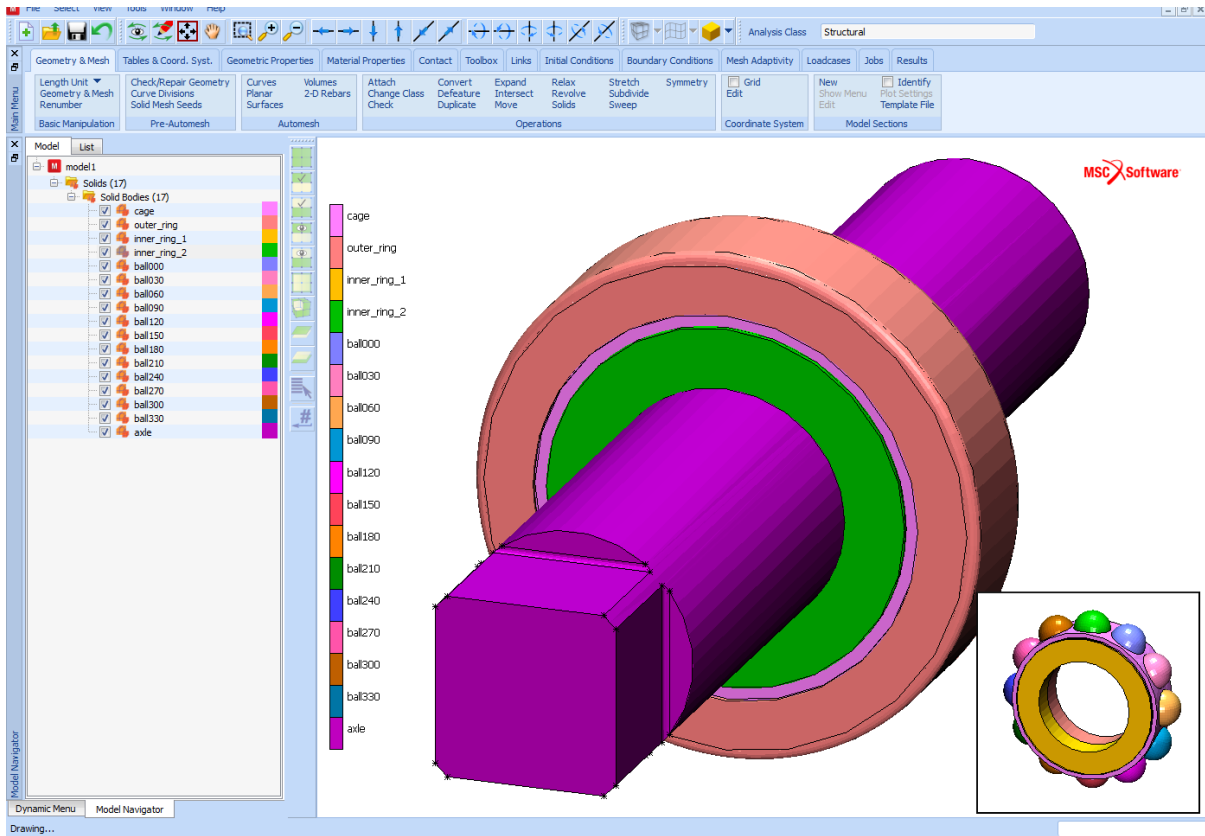


Figure 2.37-1 Bearing Model

By default, all bodies are displayed in the same color. To identify the different parts of the model, the Identify Solids option is used:

View → Identify → Solids

The latter displays each body in a different color. The colors assigned to the bodies are listed both in the model tree and in the legend on the graphics window. The identify option can also be found in the context menu of the Solids folder in the model tree, which can be accessed with a right mouse button click on the folder.

Solid, sheet and wire bodies are displayed on the graphics window by approximating the edges of the solid by a series of line segments and by approximating the faces of the solid by a number of facets (in solid mode). The View → Plot Control → Solids Settings menu contains two parameters that control the quality of these approximations. The Chordal Tolerance is the maximum distance allowed between the line segments and the actual shape of the edge. The Planar Tolerance is the maximum distance allowed between the facets and the actual shape of the face. Both tolerances have the dimension of a length and depend, to some extent, on the size of the model. In general, smaller tolerances yield a more accurate rendering of the bodies.

The default Planar Tolerance is too large to properly render the rolling balls of the bearing, the radius of which is 1.75 mm. The tolerance is set to 0.01 mm to improve the quality of the rendering:

```
View → Plot Control
      Solids Settings
          Planar Tol.
              0.01
          Regenerate
```

The resulting model is depicted in [Figure 2.37-1](#).

Defeaturing the Model

Defeaturing is the process of removing or modifying features such as holes, fillet and chamfers. When meshing a body, it can be useful to remove features which are not critical for the finite element solution first, in order to reduce the number elements that will be created when the bodies are meshed (see the next section). Furthermore, in design of experiments, one might like to make small modifications to the geometry (for example, change the size of a hole) and study the effects that these modifications have on the stress distribution in the model.

As mentioned in the preceding section, the File → Import → General CAD As Solids option offers tools to automatically remove features from a model upon import based on size criteria. In addition, a separate Defeature menu is available on the Geometry & Mesh tab of the main menu to remove and modify features after the bodies have been imported from the CAD model. The tools in the Defeature menu are generally preferred over the automatic feature removal during import, since they provide more control over which features are removed from the model. Furthermore, the menu offers tools to modify features (like changing the size of holes). The Defeature menu is depicted in [Figure 2.37-2](#).

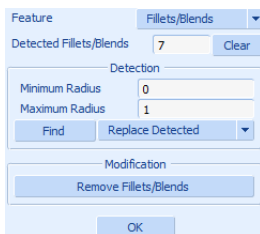


Figure 2.37-2 Defeature Menu

The following types of features are recognized:

- Holes and pockets
- Fillets and blends
- Chamfers
- Small surfaces
- Small bodies

Features are searched for using a size criterion. Fillets, for example, are searched for on the size of the radius. The Find button in the Detection box searches for fillets in a list of bodies whose radii lie within the range defined by the

Minimum Radius and the Maximum Radius. The bodies can be entered in the usual way, by picking them graphically from the graphics windows, using either the single pick, the box, polygon pick methods, or by using the `all_existing`, `all_visble`, `all_selected`, etc. wildcards.

To find the fillets in the bearing model, a radius range of 0-1 mm is used. Fillets are searched for in all bodies:

```

Geometry & Mesh
  Operations
    Defeature
      Feature
        Fillets/Blends
          Minimum Radius
            0.0
          Maximum radius
            1.0
      Find
        all_existing
  
```

Features that have been found are listed the Defeature folder of the model tree and are named after the body in which they appear (see [Figure 2.37-3](#)). In addition, the faces of the solid that define the feature are selected and are displayed in the standard color for selected faces. Each feature in the model tree has a context menu that can be accessed via a right mouse button click on the item. The context menu has three options:

- The Delete option deletes the features from the solid and repairs the remaining geometry
- The Highlight option highlights the feature and can be used to quickly locate it in the model
- The Clear option removes the item from the Defeature folder without changing the model

As can be seen in the model tree shown in [Figure 2.37-3](#), seven fillets exist in the bearing model with a radius between 0 mm and 1 mm. Three fillets are located on the outer ring (two on the outer surface and one inside). The other four fillets are located on the axle. The latter are removed from the model. There are two ways to remove these features. Each feature can be removed individually using the Delete option in the context menu in the model tree or, alternatively, the Remove button in the Defeature menu can be used to remove features in bulk. The latter removes a list of features which can be picked graphically from the graphics window, using the single pick and box or polygon pick methods. The latter is used to remove the fillets from the axle:

```

Geometry & Mesh
  Operations
    Defeature
      Feature
        Fillets/Blends
          Remove Fillets/Blends
            axle:fillet1 axle:fillet2 axle:fillet3 axle:fillet4
            # | End of List
  
```

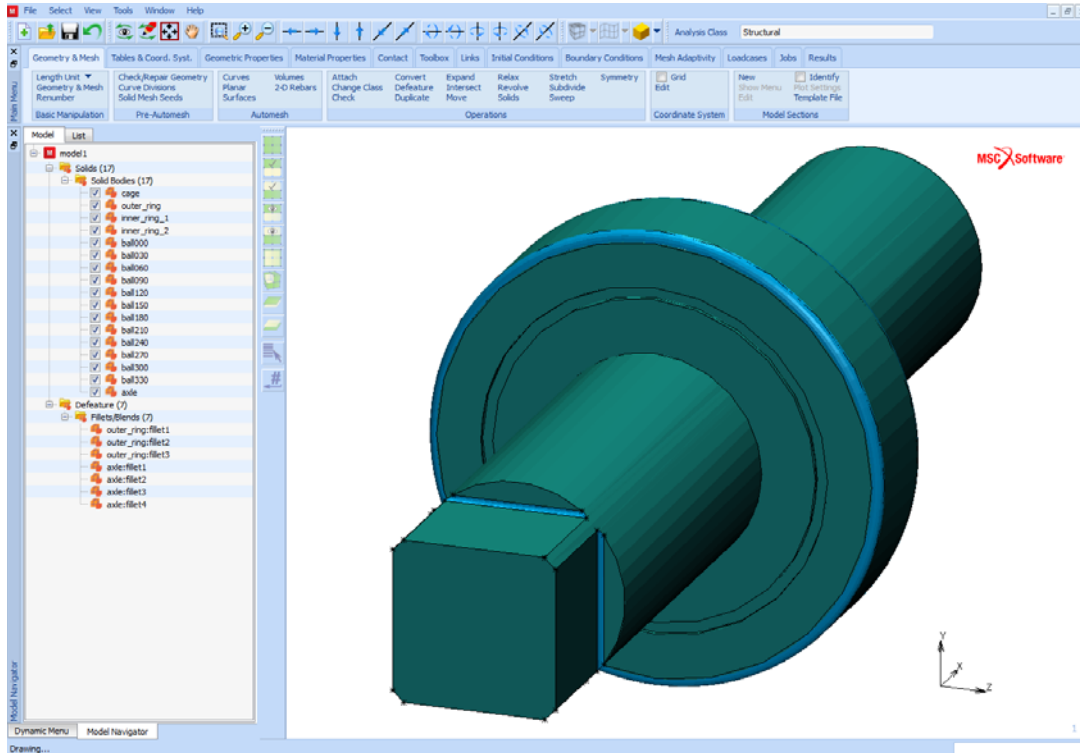


Figure 2.37-3 Fillets Detected in the Bearing Model

The resulting model is depicted in Figure 2.37-4. As can be seen from this figure, the fillets have indeed been removed from the axle.

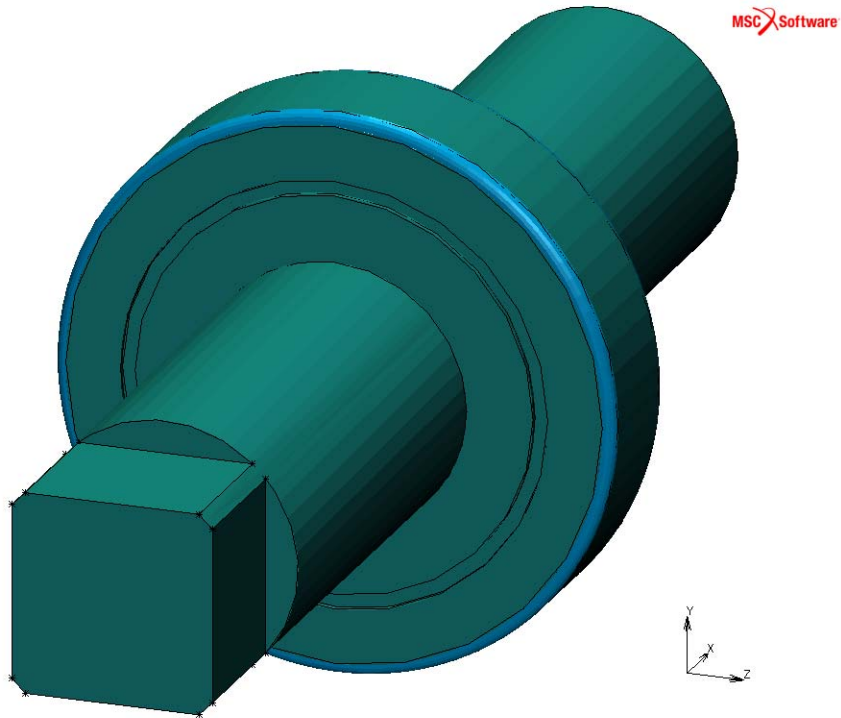


Figure 2.37-4 Bearing Model After Fillets Have Been Removed

Meshing the Model

The solid, sheet and wire bodies imported from CAD models via the options discussed in [Import of the CAD Model](#) can be meshed directly via the Automesh Volumes, Automesh Surfaces, and Automesh Curves menus, respectively (see [Figure 2.37-5](#)):

- Solid bodies can be meshed with tetrahedral elements
- Sheet bodies can be meshed either with triangular elements or with (predominantly) quadrilateral elements
- Wire bodies can be meshed with line elements

All body types can be meshed with either linear or quadratic elements.

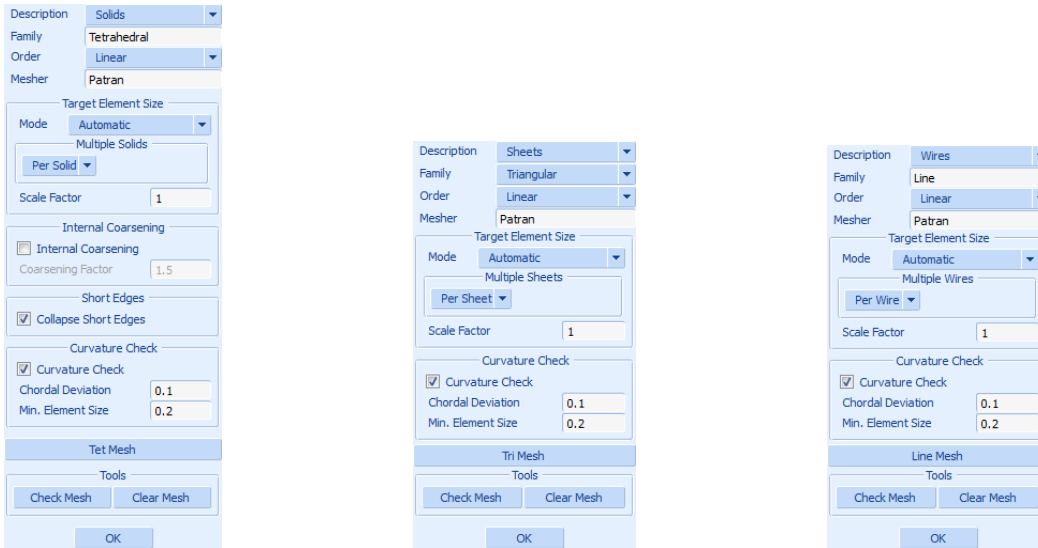


Figure 2.37-5 Automesh Volumes, Automesh Surfaces and Automesh Curves Menus

To mesh the bodies, the Description option at the top of the menus must be set to the appropriate type (Solids, Sheets or Wires) and the type of elements to mesh the bodies with must be selected via the Family and Order options. In addition, a Target Element Size must be specified for each body that is meshed. The latter defines the size of the elements that will be created in the body.

The Target Element Size box in the meshing menus (see Figure 2.37-6) provides a number of options to set the target element size. If the Mode option is set to Automatic (the default), then the program computes for each body that is meshed in a meshing operation, automatically a target element size from its volume and area. If only one body is meshed in the meshing operation, then that body is simply meshed using this size, but if multiple bodies are meshed simultaneously in the meshing operation, then there are two options:

1. Each body is meshed using the target element size computed for that body; or
2. Each body is meshed using the *same* (global) target element size, which is derived from the individual target element sizes of the bodies.

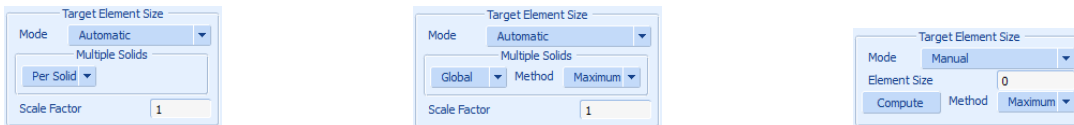


Figure 2.37-6 Automatic/Per Solid, Automatic/Global and Manual Methods to Define the Target Element Size

The first option is the default. The second option can be activated by changing the Per Solid (or Per Sheet, or Per Wire) option to Global. In that case, the Method to derive the global target element size from the individual target element sizes of the bodies can be selected:

- The Minimum method takes the smallest of the target element sizes of the bodies.
- The Maximum method takes the largest of the target element sizes of the bodies.
- The Average method takes the average of the target element sizes of the bodies.
- The Median method takes the median of the target element sizes of the bodies (the size in the middle, if the target element sizes of the bodies are sorted from small to large).

The Scale Factor is a multiplication factor on the target element sizes (both per body and globally) and can be used to scale the automatically computed target sizes if the latter yield a mesh which is either too fine or too coarse.

If the Mode is set to Manual, then the target element size must be set manually in the Element Size field. In this case, the target element size is a global size; i.e., all bodies which are meshed simultaneously in a meshing operation are meshed using the same the target element size. The Compute button computes a target element size for a list of bodies using the same algorithm and the same options as the Automatic/Global option and sets the Element Size to this value. It can be used to obtain an estimate for the target element size, which can then be adjusted before the bodies are actually meshed.

In addition to the target element size, there are a number of other options that affect finite element meshes of the bodies:

- If multiple bodies are meshed simultaneously in one meshing operation and if the surfaces of two bodies (partially) coincide, then these (parts of the) surfaces are meshed using the *same* element size. The element size used is the smallest of the two element sizes of the surfaces. The resulting meshes on these surfaces are not congruent, but have a similar density. This can be very useful for certain classes of (small sliding) contact problems, to get an accurate description the contact conditions between the bodies.
- The Internal Coarsening option (for solid bodies only) coarsens the mesh in the interior of the body.
- The Curvature Check option creates smaller elements in regions of high curvature, in order to better capture the curvature of the surface. The Chordal Deviation is the maximum distance allowed between an element edge and the actual surface, relative to length of that edge. Smaller values yield smaller elements in regions of high curvature and a more accurate description of the actual surface of the body.
- Mesh seeds can be defined on the faces, the edges or the vertices of the body to locally control the mesh density on these entities. Two types of mesh seeds are available:
 - Mesh seeds of type # Divisions can be defined on an edge of a body to specify the number of element edges that must be created on that edge.
 - Mesh seeds of type Target Length can be defined on a face, an edge or a vertex of the solid to specify the size of the elements that must be created on that entity (or in the vicinity of that entity).

Mesh seeds can be defined in the Solid Mesh Seeds menu on the Geometry & Mesh tab of the main menu (see [Figure 2.37-7](#)).

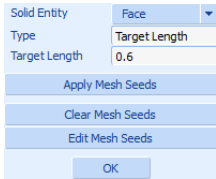


Figure 2.37-7 Solid Mesh Seeds Menu

The Tet Mesh, Tri Mesh, and Line Mesh buttons in the respective Automesh menus mesh a list of bodies of the appropriate type. The bodies can be entered in the usual way, either by picking them graphically from the graphics windows or via the `all_existing`, `all_visible`, `all_selected`, etc. wildcards.

Figure 2.37-8 shows the finite element mesh obtained by meshing all bodies in one meshing operation using the default settings (i.e., each body is meshed using a dedicated target element size computed for the body and the Curvature Check is switched on). The Detect Meshed Bodies command is used after the mesh has been created to automatically create contact bodies from the different parts of the model:

```
Geometry & Mesh
  Automesh
    Volumes
      Tet Mesh
        all_existing
Contact
  Contact Bodies
    Detect Meshed Bodies
    Identify
```

For visualization purposes, one of the inner rings has been made invisible in Figure 2.37-8. A number of things can be observed from this figure:

1. For each body, the element size is adapted to the body size.
2. The mesh of the axle is finer in the region where the bearing is located. This is due to the fact that the inner rings fit exactly on the axle and that the bodies are meshed in the same meshing operation. The smaller element size of the rings is reflected in the mesh of the axle.
3. Smaller elements are created for the fillets on the outer ring to better capture the curvature of the fillets.

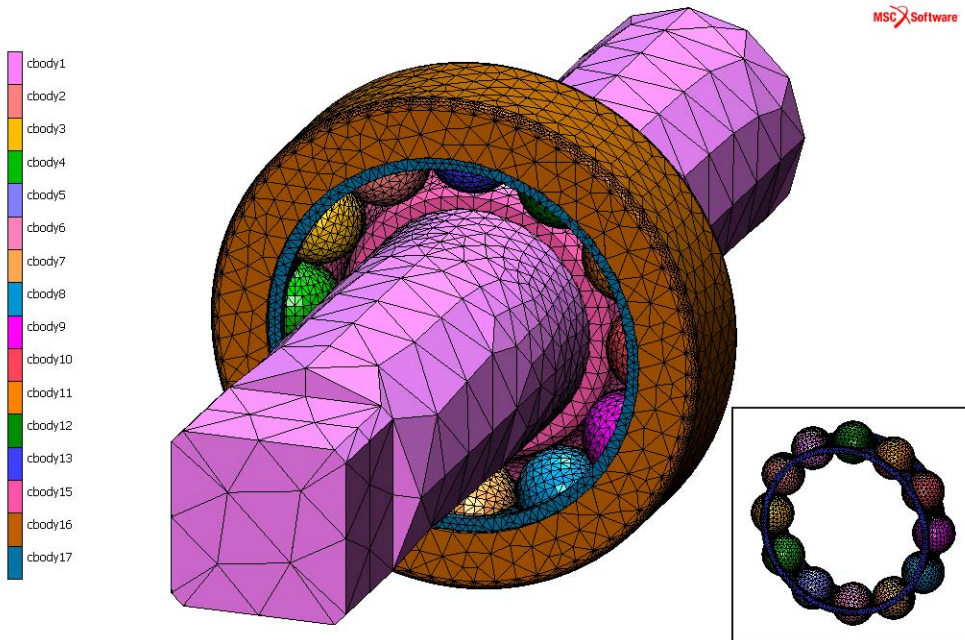


Figure 2.37-8 Finite Element Mesh Obtained with Default Settings

In contrast, [Figure 2.37-9](#) shows two finite element meshes created by meshing all bodies in one meshing operation, but now using the Automatic/Global target element size option with the Maximum method:

```

Geometry & Mesh
  Automesh
    Volumes
      Multiple Solids
        Global
      Tetmesh
        all_existing
  Contact
    Contact Bodies
      Detect Meshed Bodies
      Identify
  
```

In that case, all bodies are meshed using the target element size computed for the largest body (the axle). The picture on the left shows the finite element mesh obtained with the Curvature Check option switched on. The picture on the right shows the mesh obtained with the Curvature Check option switched off. Clearly, if the Curvature Check option is off, then all bodies are meshed with elements of approximately the same size (the element size is only limited by the size of the body, such as in the thickness direction of the cage). Also, the finite element meshes of the balls are clearly too coarse. The Curvature Check option greatly improves the quality of the mesh for all bodies in the model.

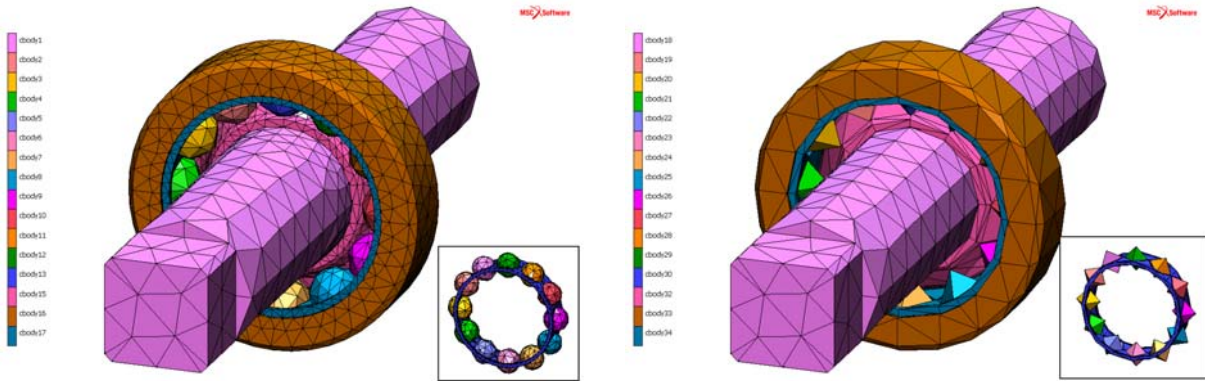


Figure 2.37-9 Finite Element Meshes Obtained with the Automatic/Global Target Element Size Method

Note that also in this case, the element size of the inner rings is reflected in the mesh of the axle. If the Curvature Check option is on, then smaller elements are created in the inner rings to capture the curvature correctly and this is reflected in the mesh of the axle. If the Curvature Check is off, then the element sizes in the inner rings and in the axle are virtually the same and the effect is negligible.

Finally, [Figure 2.37-10](#) shows the effect of mesh seeds. On the flat faces of the axle, mesh seeds are defined with a Target Length of 0.6 mm:

```

Geometry & Mesh
  Pre-Automesh
    Solid Mesh Seeds
      Solid Entity
        Face
          Target Length
            0.6
    Apply Mesh Seeds
      axle:1 axle:3 axle:5 axle:7 axle:9
      # | End of List
  
```

The mesh seeds are visualized by line segments with small dots on each end. The length of the line segment (i.e., the distance between the dots) is equal to the Target Length of the mesh seed. For faces, two such line segments are displayed in the center of the face along the parametric directions (see the picture on the left). The picture on the right shows the resulting finite element mesh. All bodies have again been meshed in a single meshing operation and default settings have been used. The effect of the mesh seeds is apparent. Compared with the mesh in [Figure 2.37-8](#), the flat faces have been meshed with much smaller elements, while the rest of the mesh is the same.

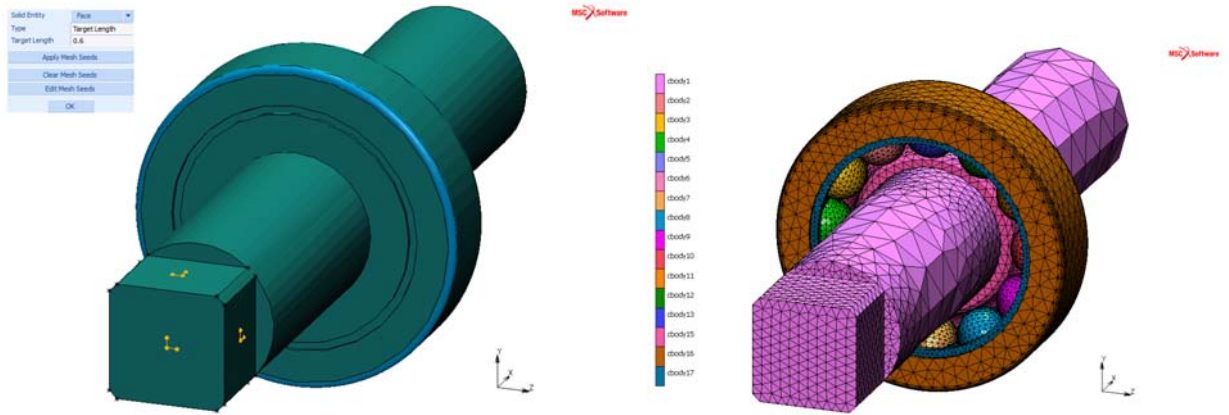


Figure 2.37-10 Finite Element Mesh Obtained with Default Settings and Mesh Seeds on the Flat Faces of the Axle

Conclusions

A number of options are available to import CAD models in Mentat. All major CAD formats are supported. The models are imported in form of a number of solid, sheet, or wire bodies. Options are available to remove or modify features, such as holes, fillets, and chamfers, either automatically upon import, or after the model has been imported. The bodies that have been imported from the CAD models can be meshed directly. Several options are available to control the mesh density, including different ways to set the target elements size and mesh seeds to locally control the mesh density on a face, an edge, or a vertex of a body.

Input Files

The file below is on your [delivery media](#), or it can be downloaded by your web browser by clicking the link (file name) below.

File	Description
bearing.x_t	Parasolid model of the ball bearing
bearing.proc	Mentat procedure file to run the above example

Section 3: Mechanical Analysis

3.1 Solid Modeling and Automatic Meshing

- Chapter Overview 846
- Background Information 846
- Detailed Session Description 847
- About HexMesh 865
- Using HexMesh Parameters and Commands 869
- Using HexMesh – Example 878
- Input Files 884

Chapter Overview

The sample session described in this chapter demonstrates the process of solid modeling and automatic meshing. A simple bolt structure is modeled. The goal of the analysis is to demonstrate:

- Solid modeling, entering simple building blocks.
- Using Boolean operations and blending techniques to complete the solid model.
- Use of symmetry to reduce the solid model.
- Convert solid faces into surfaces and use of automatic surface meshers.
- Use of the automatic tetrahedral mesh generator to generate the mesh.
- Use of the symmetry and duplicate options to complete the model.

Background Information

This example demonstrates how to generate an element mesh for a simple bolt structure as shown in [Figure 3.1-1](#).

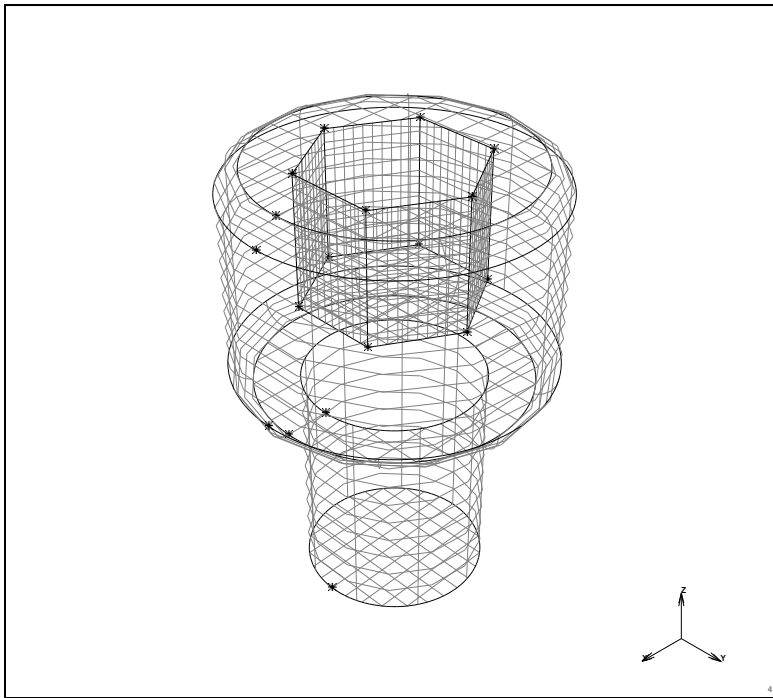


Figure 3.1-1 Simple Bolt Structure

As can be seen from this figure, the model globally consists of three simple geometrical components: two cylinders with different radii and a 6-sided prism. A solid model of the structure can be created using two Boolean operations. Two cylinders must be united and from the resulting solid a prism must be subtracted.

After these operations, a complex solid is obtained. Some of the edges of this solid must be given a specific curvature. This is achieved with the BLEND operator.

Before using the mesh generators however, the solid model is reduced. The model is symmetrical with respect to a segment of 30° . By subtracting two solid blocks from the solid model, the 30° segment is obtained.

Solid meshes are generated with a three step approach. First the faces of a solid are converted to surfaces. These surfaces are used to generate a surface mesh. This surface mesh is used to create a solid mesh.

After specifying an average edge length for all edges of the solid, the segment is automatically meshed, creating tetrahedral elements. The resulting mesh subsequently expands to a mesh for the complete bolt by use of the SYMMETRY and DUPLICATE processors.

Overview of Steps

Step 1: Input of Basic Solids

Step 2: Refining the Solid Model

Step 3: Reducing the Solid Model to the Smallest Segment with Symmetry

Step 4: Surface Meshing on the Reduced Solid Model

Step 5: Meshing of the Solid Model Based on the Generated Surface Mesh

Step 6: Use of Symmetry and Duplication Operations to Complete the Mesh

Detailed Session Description

Step 1: Input of Basic Solids

The approach used in generating the solid model is to start with three simple building blocks. The building blocks are two cylinders and one prism.

MAIN

MESH GENERATION

SOLID TYPE

CYLINDER

RETURN

solids ADD

0 0 0

(solid cylinder origin coordinates)

0 0 1

(solid cylinder axis coordinates)

0.4 0.4

(solid cylinder radii)

0 0 1

(solid cylinder origin coordinates)

0 0 2
0.7 0.7

(solid cylinder axis coordinates)

(solid cylinder radii)

VIEW

activate 4

(on)

activate 1

(off)

PERSPECTIVE

show 4

FILL

RETURN

In the above VIEW process, view 4 has been activated and set to a perspective projection. View 1 has been deactivated to prevent switching on perspective plotting for this view.

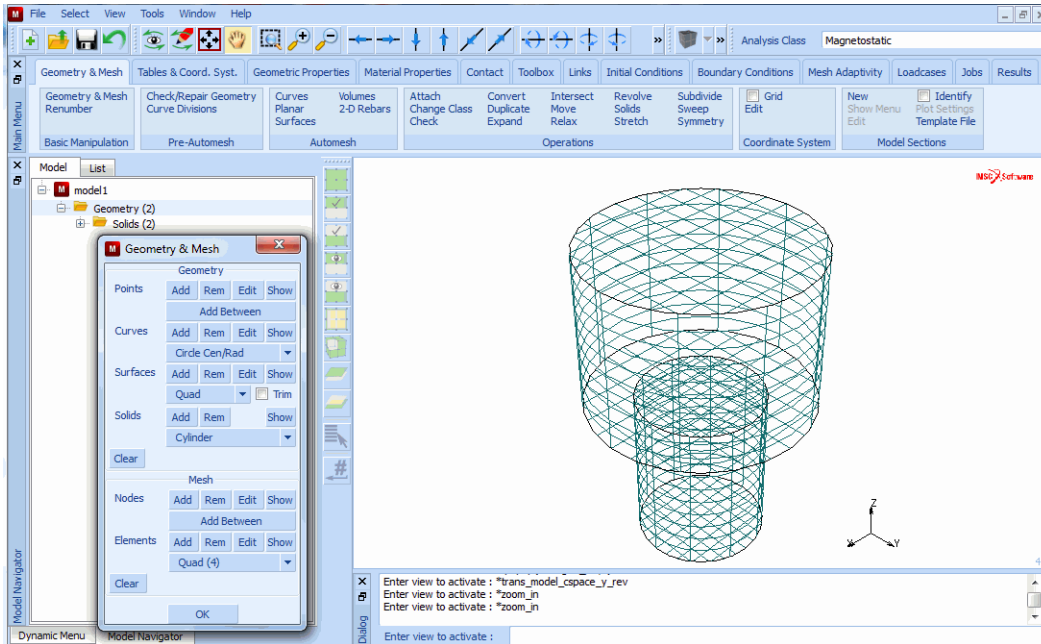


Figure 3.1-2 Two Cylindrical Solids

The two basic cylinders will now be united.

MAIN

MESH GENERATION

SOLIDS

UNITE

1 2
END LIST (#)
RETURN

(Pick solid 1 and 2)

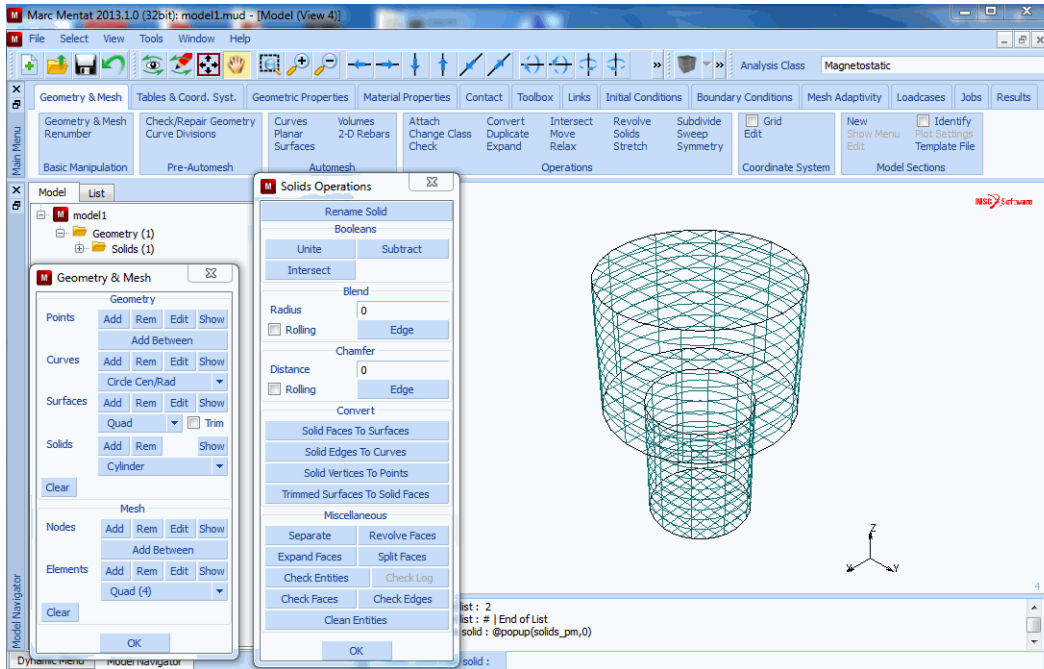


Figure 3.1-3 Result of UNITE Operation

Next, the prism is defined and subtracted from the current solid.

MAIN

MESH GENERATION

SOLID TYPE

PRISM

RETURN

solids ADD

0 0 1.4

(solid prism base coordinates)

0 0 2.1

(solid prism axis coordinates)

0.4

(solid prism radius)

6

(number of solid prism faces)

SOLIDS

SUBTRACT

1 2

(Pick solids)

END LIST (#)

The basic solid model is now completed and the result is shown in Figure 3.1-4. Note that at this stage only one solid exists. The basic building blocks are no longer present in the database after the Boolean operations.

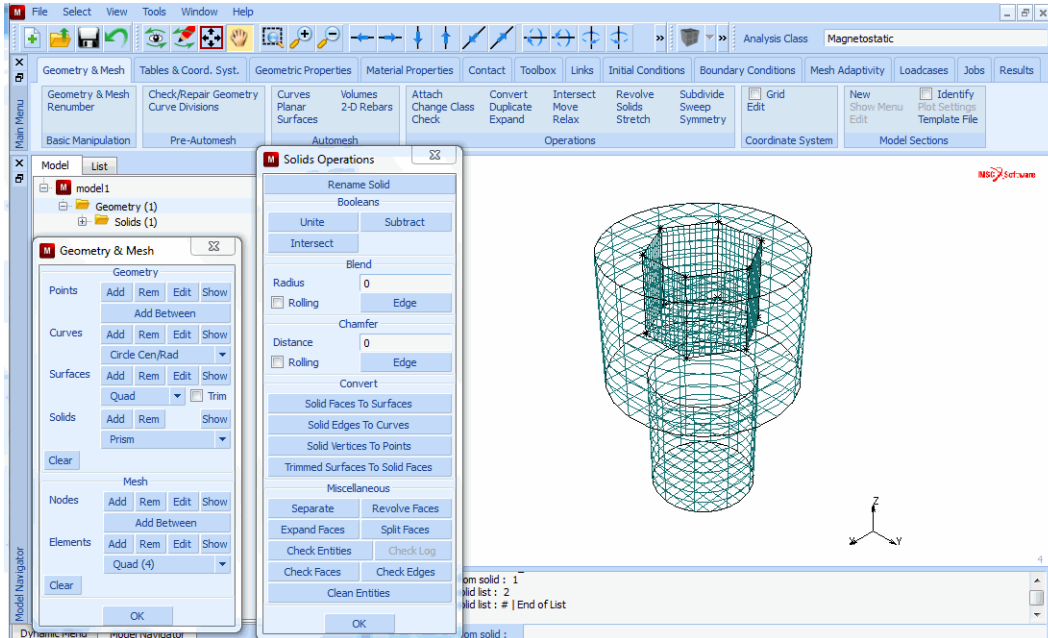


Figure 3.1-4 Result of SUBTRACT Operation

Step 2: Refining the Solid Model

In this step, two blending operations are applied to the outer edges of top cylinder of the basic solid model. The blending process consists of specifying a radius and indicating to which solid edge the blending operation is applied. Before performing the blending operations, the solid edges is labeled. This is not strictly necessary for the process, since all edges are graphically picked. For describing the process, however, it is useful to indicate the edge labels.

Note that after each blending operation the edge numbering changes.

MAIN

MESH GENERATION

PLOT

solid SETTINGS

edges LABELS

REGEN

(on)

RETURN
 SOLIDS
 blend RADIUS
 0.1
 blend EDGE
 1:12

(Pick the solid edge)

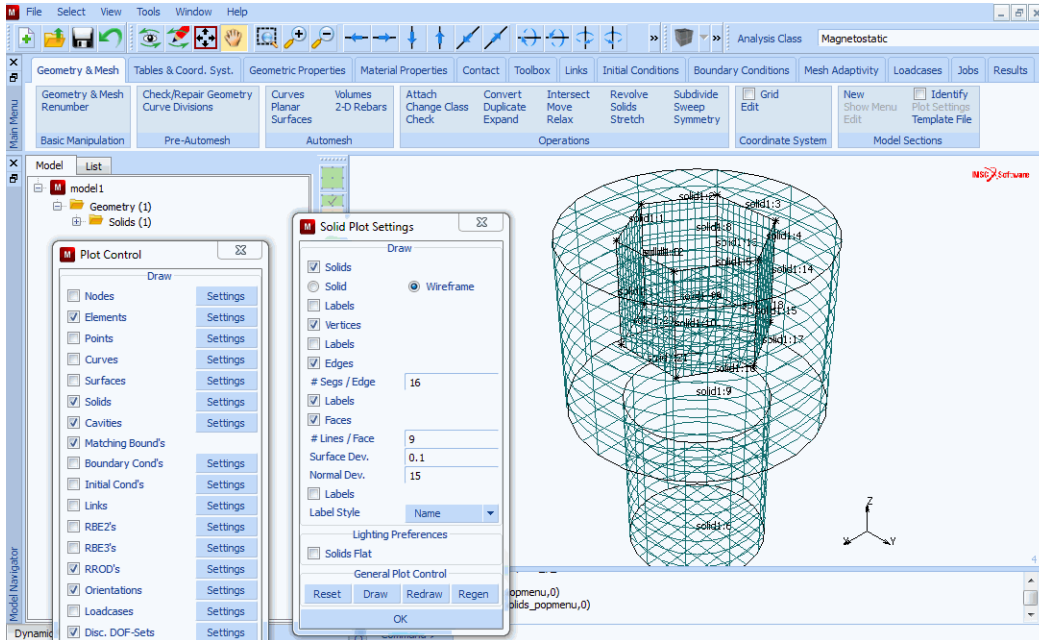


Figure 3.1-5 Activating the Labeling of Solid Edges

The result after the first blending is shown in Figure 3.1-6. The second edge will now be blended and the labelling of the solid edges will be switched off.

MAIN
 MESH GENERATION
 SOLIDS
 blend EDGE
 1:20
 PLOT
 solids SETTINGS
 edges LABELS

(off)

REGEN
RETURN (twice)

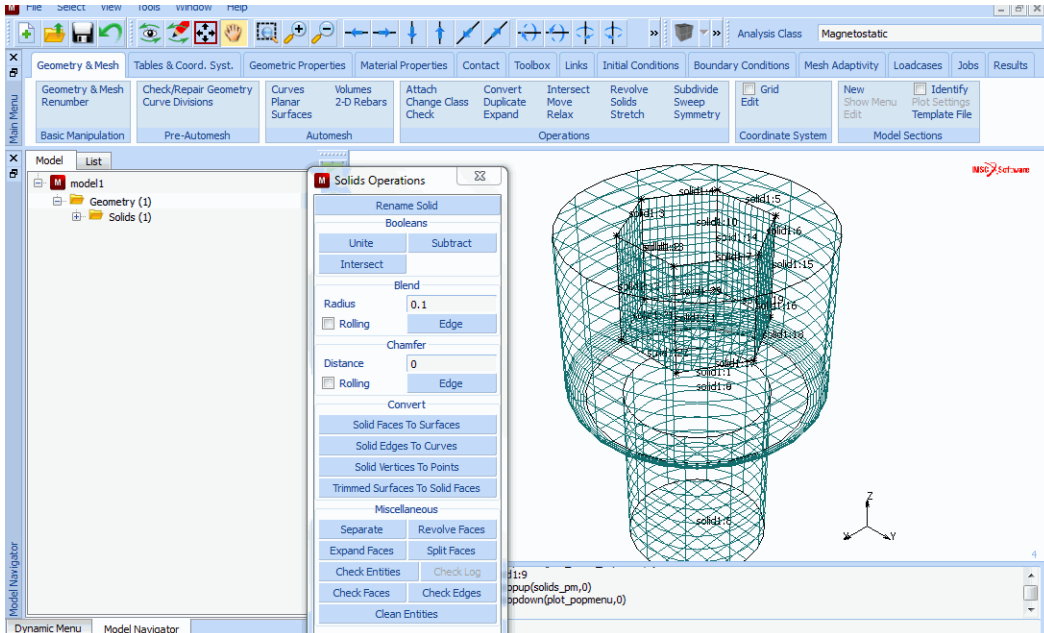


Figure 3.1-6 First Edge Blended

The solid modeling phase is completed as shown in Figure 3.1-7.

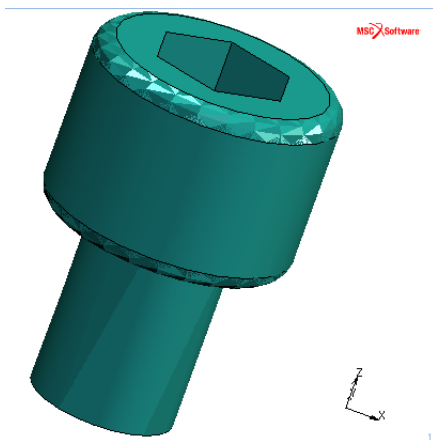


Figure 3.1-7 Completed Solid Model

Step 3: Reducing the Solid Model to the Smallest Segment with Symmetry

By looking at the model, we can observe that the solid model has certain symmetry planes. Since the complete model (360°) has a prism with six edges, the model can be considered as a duplication of six segments.

Furthermore, this 60° segment is symmetric. Thus, a 30° segment is the smallest section for which a mesh is required. In this step, the solid model is reduced to a 30° segment. This is achieved by adding two solid blocks and subtracting them from the solid model.

MAIN

MESH
 GENERATION

VIEW

show 1

FILL

RETURN

SOLID TYPE

BLOCK

RETURN

solids ADD

-1 0 -1

2 2 4

(solid block origin coordinates)

(solid block X, Y, and Z dimensions)

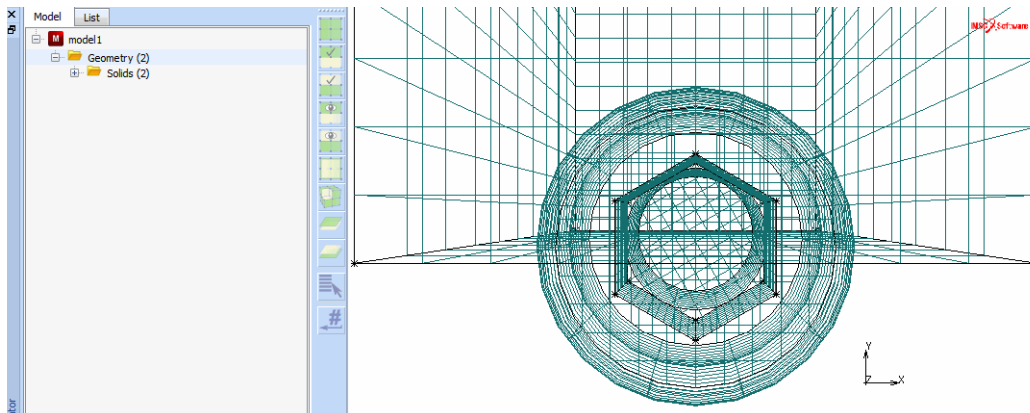


Figure 3.1-8 First Solid Block Added

The second block is duplicated from the first one.

MAIN

MESH GENERATION

DUPLICATE

ROTATION ANGLES

0 0 150

(duplicate rotations in X, Y, and Z)

SOLIDS

2

(Pick the solid block)

END LIST (#)

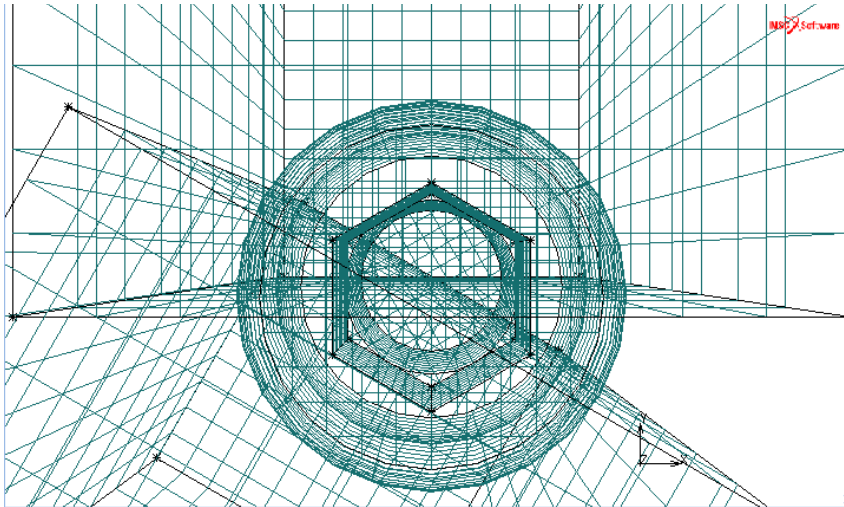


Figure 3.1-9 Duplicating the Solid Block

Finally, solid 3 and solid 2 is subtracted from body 1.

MAIN

MESH GENERATION

SOLIDS

SUBTRACT

1

(Pick solid to subtract from)

2

(Pick solid to be subtracted)

3

(Pick solid to be subtracted)

END LIST (#)

FILL

VIEW

show 4
 RETURN
 FILL

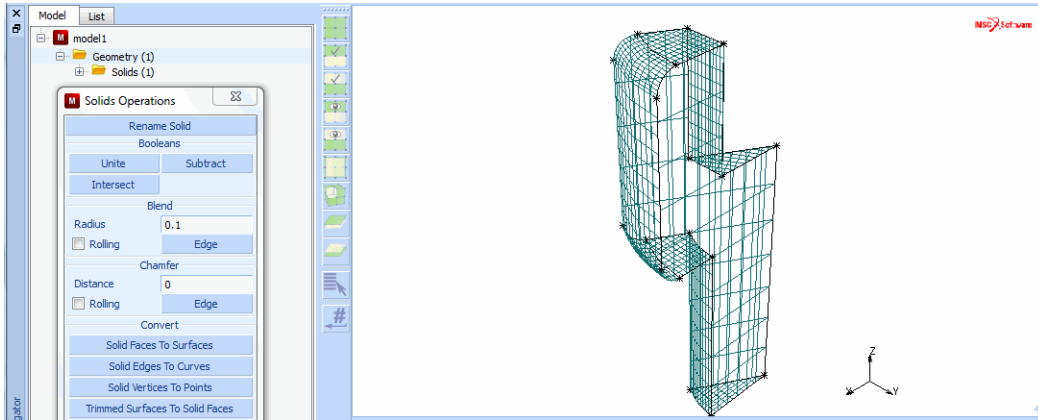


Figure 3.1-10 Completed Solid Segment

Step 4: Surface Meshing on the Reduced Solid Model

In this step, the surface of the reduced model is automatically meshed using one of the automatic surface meshers. First all faces of the solids are converted into surfaces; then plotting of surfaces and points is switched off.

MAIN

MESH GENERATION

SOLIDS

convert SOLID FACES TO SURFACES

all: EXIST.

PLOT

draw SOLIDS

(off)

draw POINTS

(off)

REGEN

RETURN (twice)

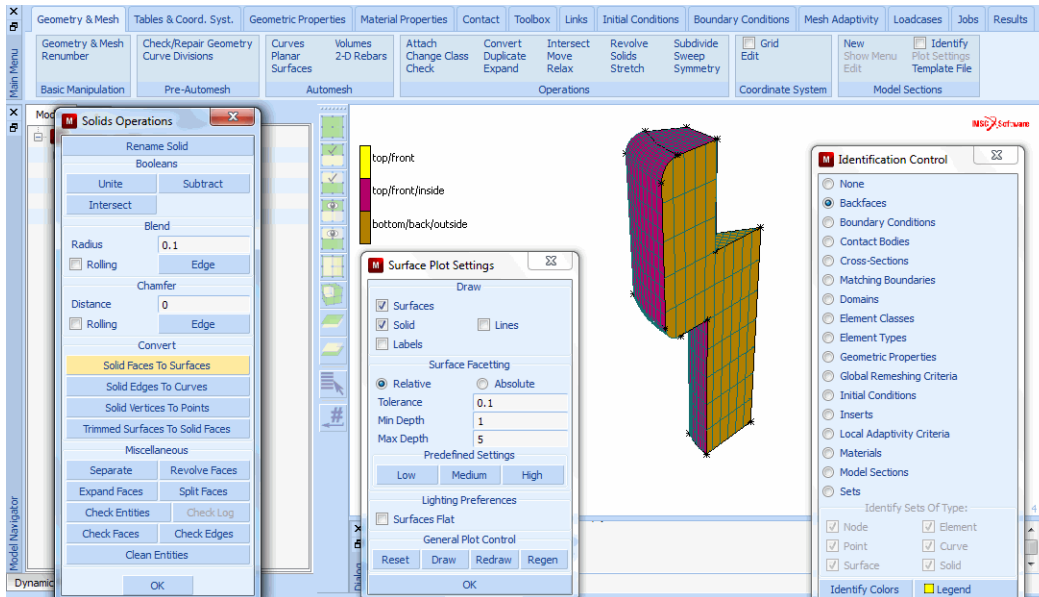


Figure 3.1-11 Convert Solids to Surfaces

Next, a target element edge length is specified by using the curve division command.

Here, for all curves, an average element edge length of 0.1 is used. In order to ensure that elements generated for specific surface match, the curve divisions along particular curves is matched.

MAIN

MESH GENERATION

AUTOMESH

CURVE DIVISIONS

AVG LENGTH

0.1

(enter length for curve divisions)

APPLY CURVE DIVISIONS

all: EXIST

(for all curves)

MATCH CURVE DIVISIONS

0.005

(enter tolerance for vertex points)

all: EXIST.

(for all curves)

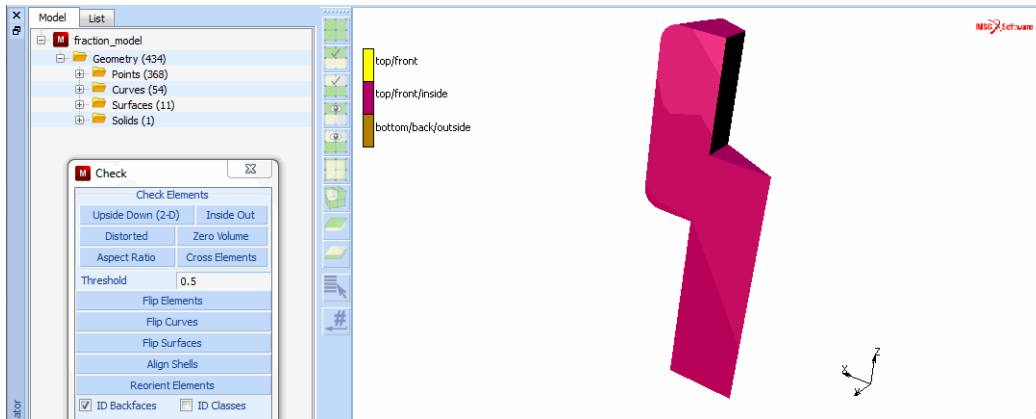


Figure 3.1-12 Check Elements

In Figure 3.1-13, the resulting *seed points* are shown.

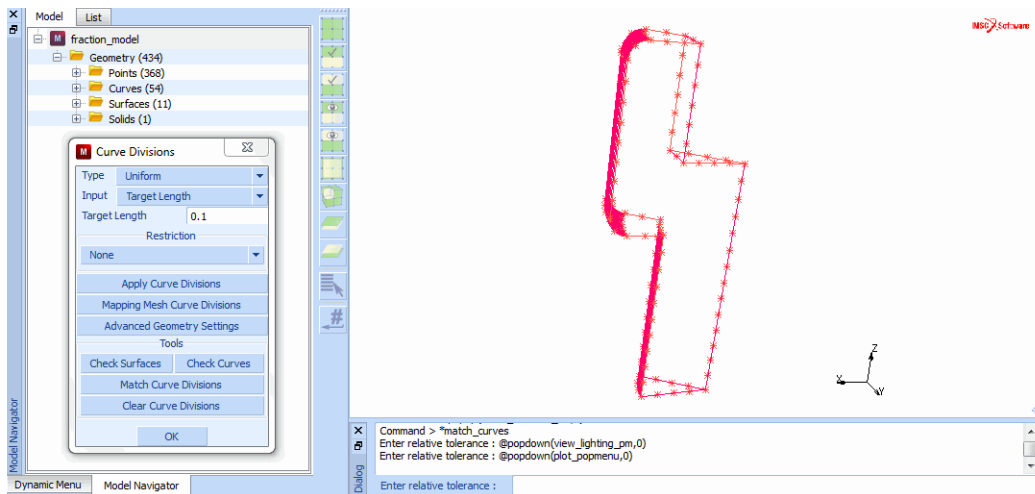


Figure 3.1-13 Seed Points for Automatic Meshing

Next, the automatic surface mesh generator is used to generate a surface mesh. After the mesh generation, the drawing of the nodes is switched off for easier verification of the generated elements (the elements are drawn in solid mode instead of wireframe mode).

MAIN

MESH GENERATION

AUTOMESH

SURFACE MESHING

triangles (delauany) SURFACE TRI MESH!

all: EXIST (for all surfaces)

PLOT

draw NODES (off)

draw SURFACES (off)

draw CURVES (off)

elements SOLID

REGEN

RETURN

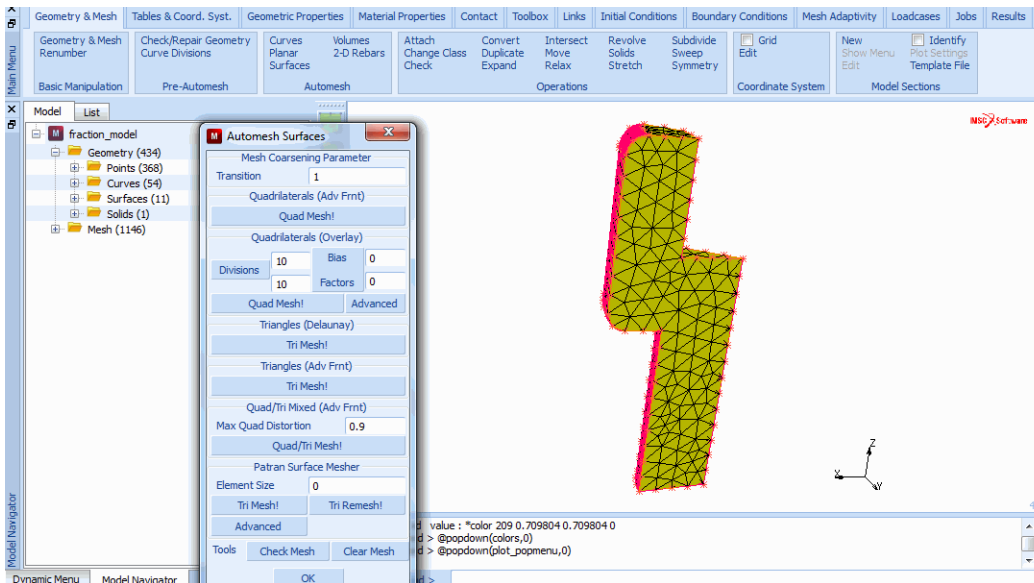


Figure 3.1-14 Completed Surface Mesh for the Segment

Note that for each surface, a surface mesh has been created. Due to the use of match curve divisions, it is ensured that nodes along the curves are close to each other. However, there are still duplicate nodes at these points.

Step 5: Meshing of the Solid Model Based on the Generated Surface Mesh

The results of the surface mesh generator can be used as input for the solid mesh generators. It is required that a closed surface is present. Duplicate nodes present to the use of the surface mesher for each surface are removed with the SWEEP processor. This can be verified by plotting the outline edges only for the structure.

MAIN

MESH GENERATION

PLOT

elements SETTINGS

OUTLINE
RETURN (twice)
SWEEP
TOLERANCE
.0001
NODES
all: EXIST
RETURN
PLOT
elements SETTINGS
REGEN
RETURN (twice)

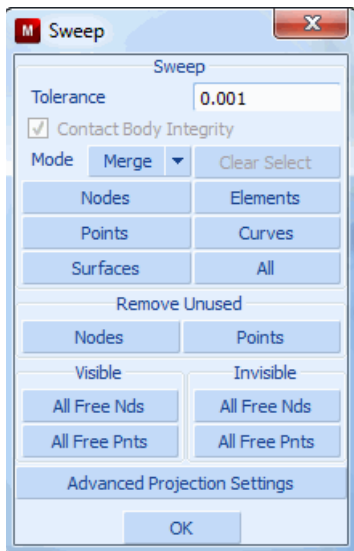


Figure 3.1-15 Sweep Menu

Subsequently, it is specified that the automatic tetrahedral mesher is used for all triangular elements generated in the previous step.

MAIN
MESH GENERATION
AUTOMESH
SOLID MESHING

tetrahedra TET MESH!

all: EXIST

(list of triangular elements)

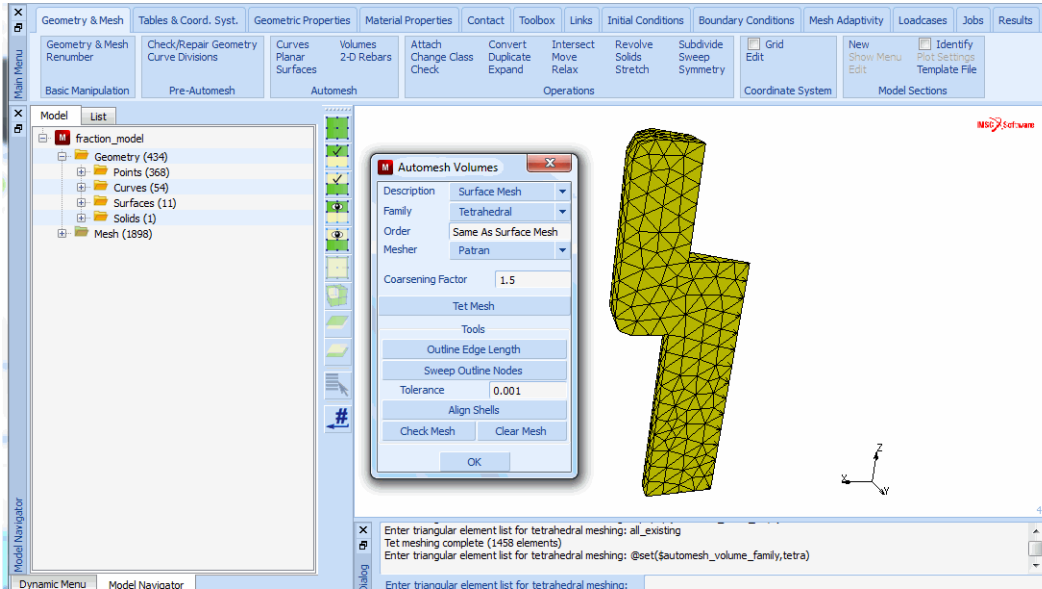


Figure 3.1-16 Completed Tetrahedral Mesh

Step 6: Use of Symmetry and Duplication Operations to Complete the Mesh

The mesh for the solid segment has been generated automatically. As discussed before, the complete model consists of six identical parts each with a symmetry plane. First, the SYMMETRY processor is used to generate a 60° segment. Note that a formula is used to enter the symmetry plane normal.

MAIN

MESH GENERATION

SYMMETRY

NORMAL

$\sin(30*\pi/180)$

$\cos(30*\pi/180)$

0

ELEMENTS

all: EXIST.

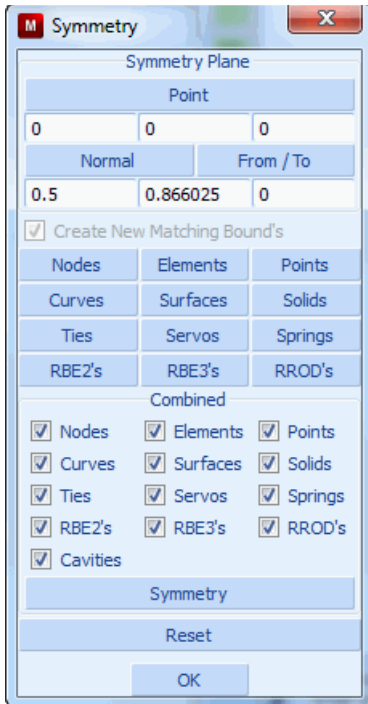


Figure 3.1-17 Symmetry Menu

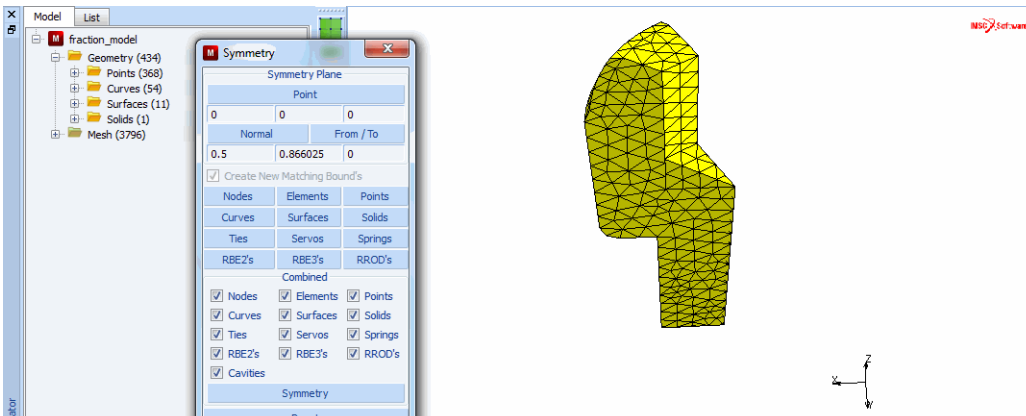


Figure 3.1-18 Mesh after use of the SYMMETRY Operator

The generated 60° segment is now duplicated five times to generate the complete model.

MAIN

MESH GENERATION

DUPLICATE

ROTATION ANGLES

0 0 60

REPETITIONS

5

ELEMENTS

all: EXIST.

FILL

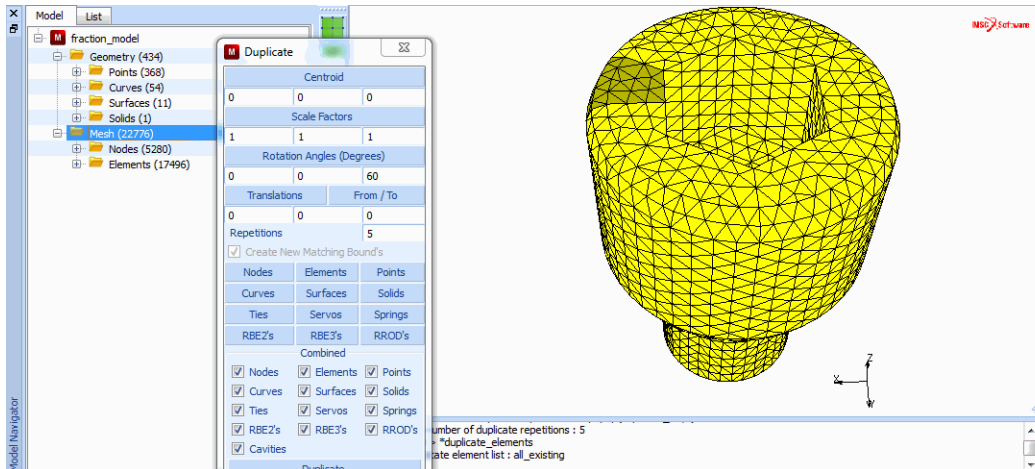


Figure 3.1-19 Element Mesh after the DUPLICATE Process

Both the SYMMETRY and the DUPLICATE processor generate new elements but do not check if duplicate nodes are created which have to be removed in order to make the connection between the different parts. This removal of duplicate nodes is achieved with the SWEEP process using the tolerance of 0.001.

The mesh for the bolt structure is now completed. The model is saved in a Mentat model file.

MAIN

MESH GENERATION

SWEEP

sweep NODES

all: EXIST.

SAVE

Tetrahedral Meshing on Solids

TBW to provide text

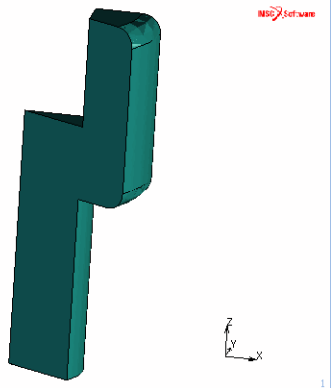


Figure 3.1-20 Parasolid Model of Sector

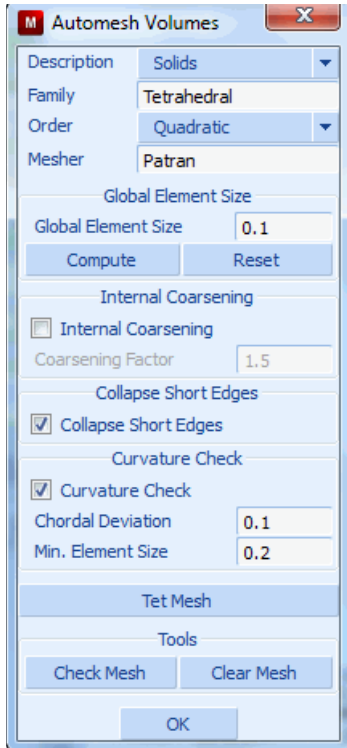


Figure 3.1-21 Meshing on Solids Menu

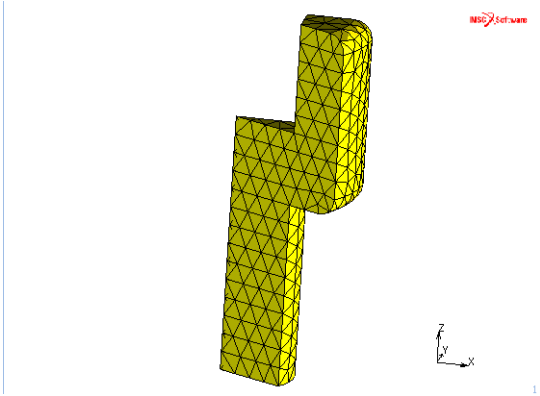


Figure 3.1-22 Generated Mesh of Sector

About HexMesh

Advantages of HexMesh

HexMesh generates a hexahedral mesh automatically from your CAD geometry enabling you to move rapidly from a CAD model to a finite element model of even the most complex shapes.

A model generated with HexMesh allows you to perform linear and nonlinear finite element analyses and to achieve the kind of quality results associated with finite element models composed of hex elements.

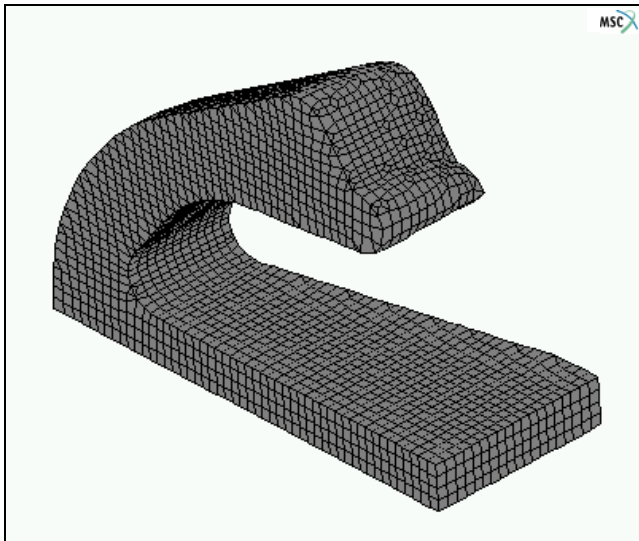


Figure 3.1-23 Hexahedral Elements Generated by HexMesh

Advantages of Hexahedral Elements

A mesh with hexahedral elements is generally more accurate and requires fewer elements than meshes that contain tetrahedral elements. For complex geometries, hexahedral meshes are easier to visualize and edit than tetrahedral meshes.

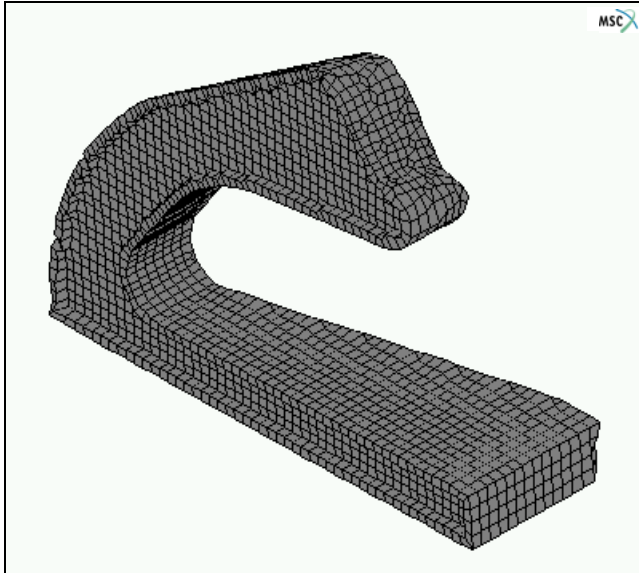


Figure 3.1-24 Interior of Model Meshed with HexMesh

Activating the HexMesh Feature

HexMesh is an add-on feature. If you purchased HexMesh with your original purchase or license renewal, your license file includes the feature line, HEXMESH which activates HexMesh.

If you wish to purchase HexMesh for an existing license, contact your local MSC Software office. You will receive an additional feature line for your license file from els.admin@mscsoftware.com.

About the HexMesh Menu in Mentat

Use the HexMesh menu in Mentat to define the parameters and apply the commands for the HexMesh. To display the HexMesh menu, choose MESH GENERATION-> AUTOMESH-> SOLID MESHING.

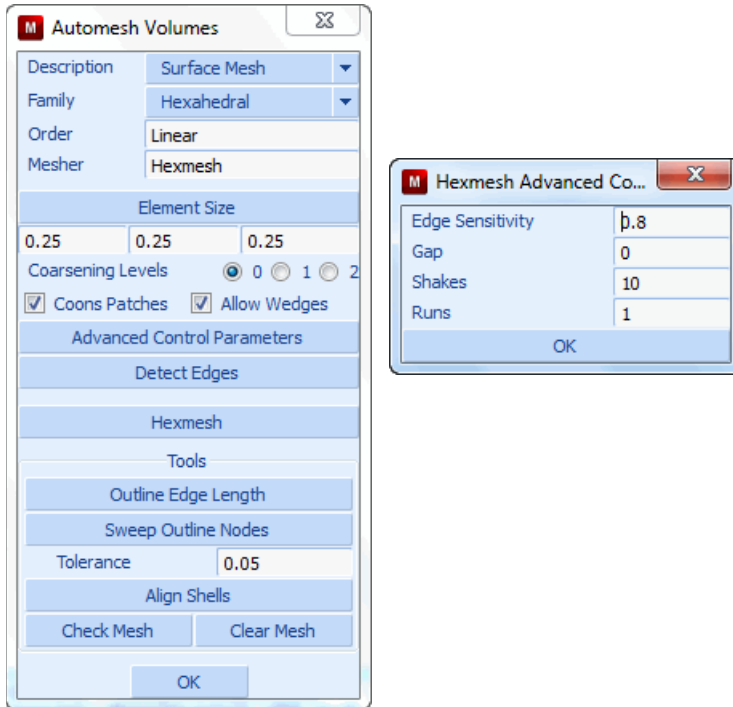


Figure 3.1-25 Automesh Solids Menu

About the Input for HexMesh

The HexMesh takes a description of a surface that is based on 3- or 4-node elements and performs an edge detection and a hexahedral mesh generation on that surface.

Before you apply the HexMesh, you should create a surface mesh of the volume to be meshed. This volume should be totally enclosed with no free edges or ‘torn seams’. The surface mesh serves as a bounding surface of the volume to be meshed.

Key Steps in the Meshing Process

Here are the key steps in the meshing process:

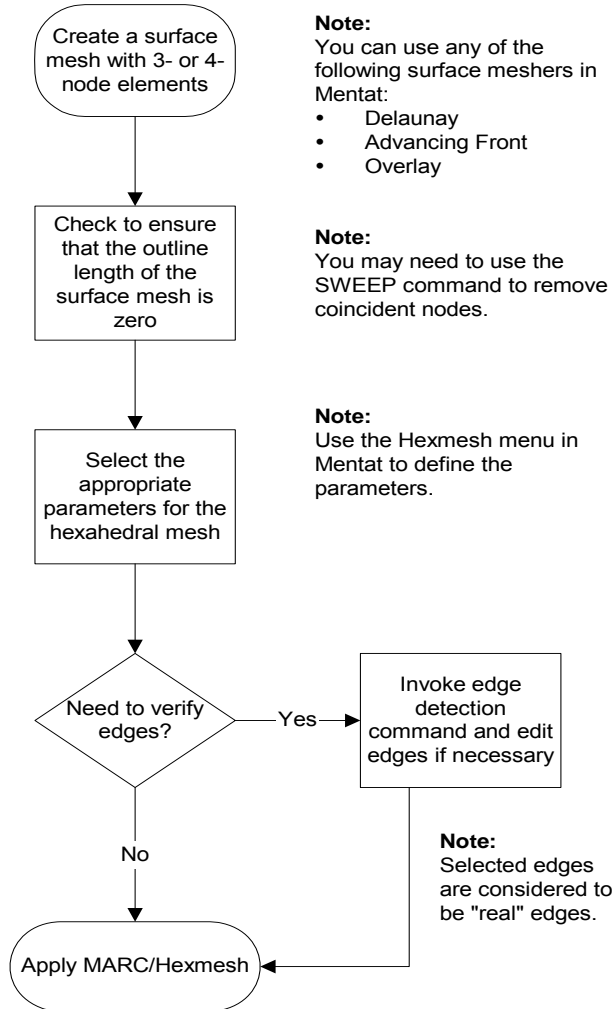


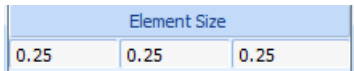
Figure 3.1-26 Key Steps in Meshing Process

You can regulate the accuracy and speed of the hexmeshing operations by specifying the different parameters and applying the HexMesh commands in Mentat.

Using HexMesh Parameters and Commands

Specifying Element Size

Use the Element Size parameter to specify the sizes of hexahedral elements generated in the x-, y-, and z-directions. The default element sizes for the x-, y-, and z-directions are 0.1.



Mesh Generation-> Automesh-> Solid Meshing

Figure 3.1-27 Element Size Parameter

The size of the element determines the number of resulting hexahedral elements. The following table demonstrates how element size affects the meshing process:

If you specify...	then...
smaller elements,	the quality of the mesh is better. However, since there are more elements, the meshing process is slower. Also, if you specify too small an element size, the meshing grid may become too large and the mesher may fail.
a large element size (in comparison to the object size),	meshing might fail.

To set the element size:

1. Click ELEMENT SIZE.
2. Type the element sizes in the x, y, and z-directions. You must specify an element greater than zero.
3. Press Enter.

Specifying Edge Sensitivity

Use the Edge Sensitivity parameter to specify when, in the edge detection process, the shared edge between two input elements represents a “real” edge. The mesher uses these real edges to maintain the geometric representation of the model.



Mesh Generation-> Automesh-> Solid Meshing

Figure 3.1-28 Edge Sensitivity Parameter

A higher value of edge sensitivity makes the HexMesh more sensitive during the edge detection process. The default value of edge sensitivity is 0.5. The range of values is $0 \leq x \leq 1$.

How the Value of Edge Sensitivity Affects the Edge Detection Process

The following illustrations show how the value of edge sensitivity affects the edge detection process:

Edge sensitivity = 0:

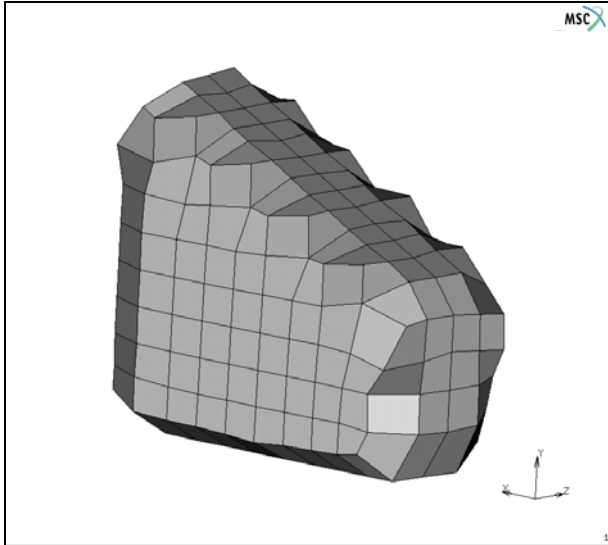


Figure 3.1-29 Edge Detection Process with Fewer Edges Detected

Edge sensitivity = 1:

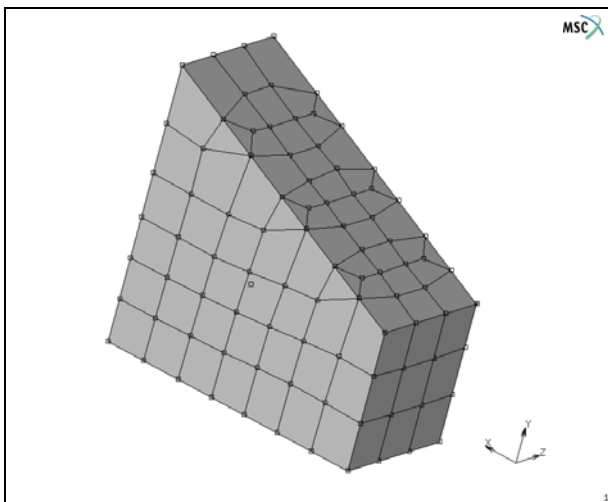


Figure 3.1-30 Edge Detection Process with More Edges Detected

To specify edge sensitivity:

1. Click EDGE SENSITIVITY and type in a value.
2. Press Enter.

Specifying Gap

Use the Gap parameter to specify the size of the gap that is initially left between the inner hexahedral elements and the surface during mesh generation.

After the mesher creates the overlay grid, it removes elements that are either close to or outside the surface mesh depending on the value of the gap that you specify. The mesher then meshes the gap area.

The range of values for the Gap parameter is -1 to 1. Negative values result in a smaller gap and can even result in mesh penetration.

To set the value of the Gap parameter:

1. Click GAP and type in a value.
2. Press Enter.

How the Value of Gap affects the Mesh

Figures 3.1-31, 3.1-32, and 3.1-33 demonstrate how the value of gap affects the mesh.

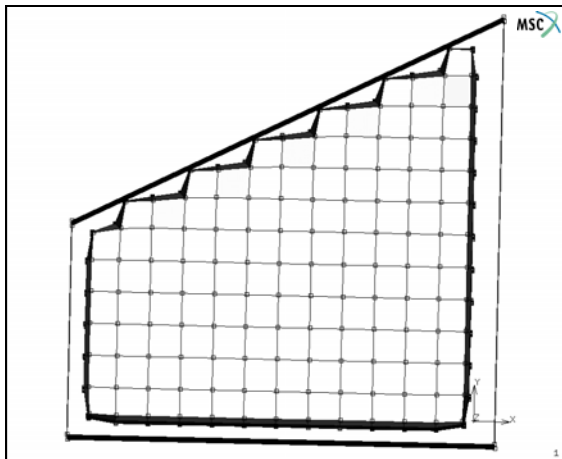


Figure 3.1-31 Gap Set to -0.3

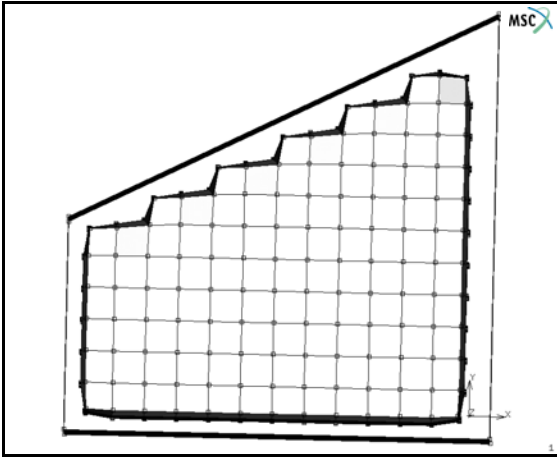


Figure 3.1-32 Gap Set to 0

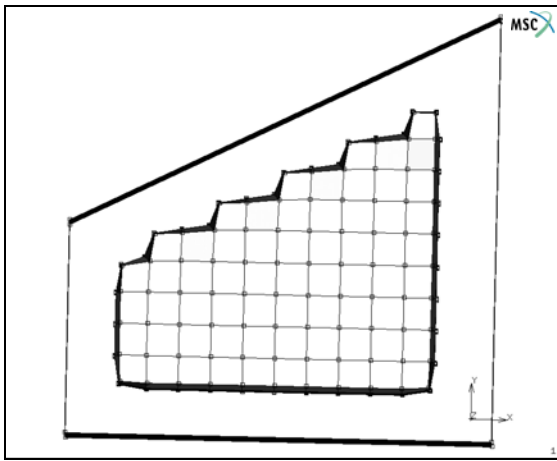


Figure 3.1-33 Gap Set to 1

Specifying the Number of Shakes

Shaking is a process of global mesh enhancement where the nodes tend to move to places of less potential energy. This has a relaxing effect on the nodes and often results in a better mesh quality.

Higher values of the Shakes parameter take up greater computing resources. Here are some guidelines for setting the values of the Shakes parameter for test and final meshes:

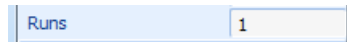
Situation	Suggested Value
Test mesh	10
Final mesh	100

To specify the number of shakes:

1. Click SHAKES and type in a value.
2. Press Enter.

Using the Runs Parameter

If the HexMesh does not produce a valid mesh, it can automatically run again with a smaller element size. Using the Runs parameter, you can specify the maximum number of reruns performed by the HexMesh.



Mesh Generation-> Automesh-> Solid Meshing

Figure 3.1-34 Runs Parameter

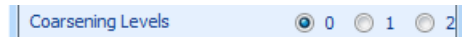
To specify the number of runs:

1. Click RUNS and type in a value.
2. Press Enter.

To prevent reruns, type in the value, 1.

Using the Coarsening Parameter

Use the Coarsening parameter to specify a difference in size between the elements in the interior and the elements in the surface. This may reduce the overall number of elements generated.



Mesh Generation-> Automesh-> Solid Meshing

Figure 3.1-35 Coarsening Parameter

You can specify one of three levels of coarsening - 0,1, or 2. A value, 0, indicates that there is no coarsening. A value, 2, specifies that the elements in the interior can be up to four times larger on each side than the elements on the surface.

To specify a level of coarsening, click on the radio button next to the level.

How the Level of Coarsening affects the Elements

The following illustrations represent two different levels of coarsening.

Coarsening set to 0:

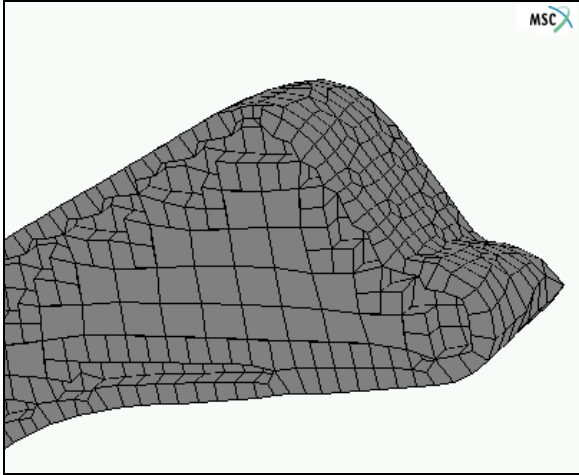


Figure 3.1-36 Interior Elements of the Model are Uniform

Coarsening set to 2:

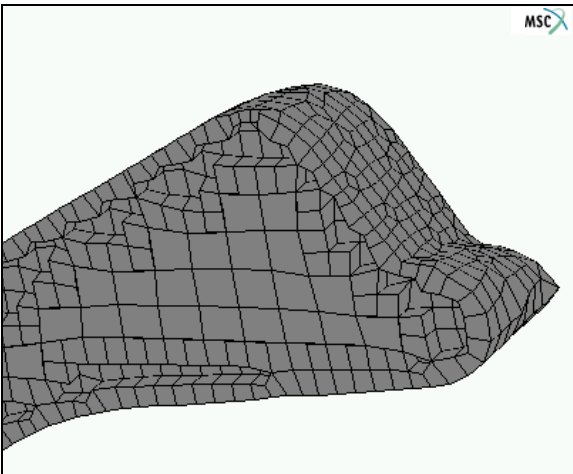


Figure 3.1-37 Interior Elements are larger than the Elements on the Surface

Using the Allow Wedges Parameter

Use the Allow Wedges parameter to create wedge elements if an edge crosses the diagonal of a face of the hexahedral element. This improves the quality of the resulting mesh.

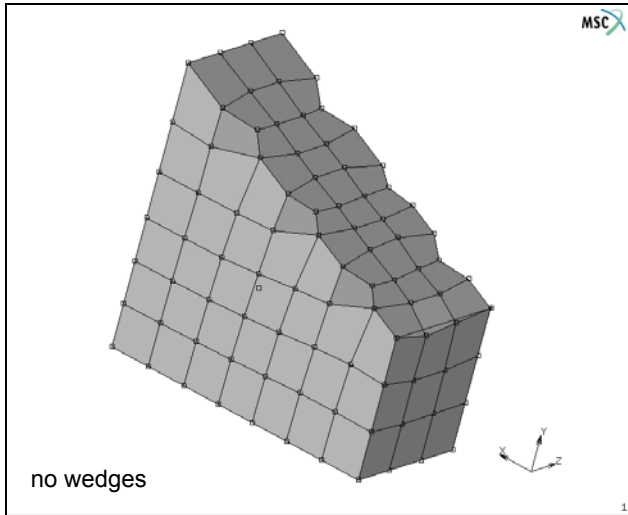


Figure 3.1-38 Allow Wedges Parameter OFF

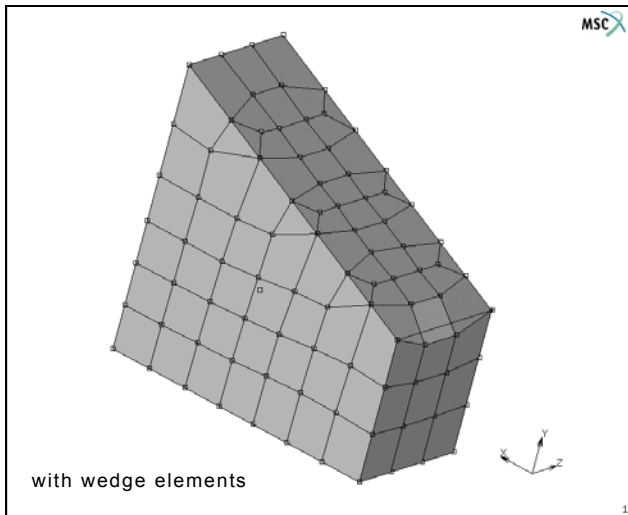


Figure 3.1-39 Allow Wedges Parameter ON

About the Coons Patches Parameter

Use the Coons Patches parameter to reduce the loss of volume while meshing regions with curved surfaces. This results in a smoother representation of the input surfaces and a better approximation of the input geometry. However, this parameter consumes greater CPU resources.

The default setting for the Coons Patches parameter is OFF.

Using the Detect Edges Command

Use the Detect Edges command to automatically select geometric edges from an input list of triangular and quadrilateral elements that enclose the volume to be meshed. These detected edges help define the input geometry for the HexMesh.

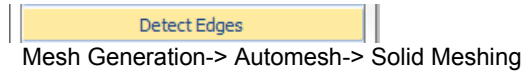


Figure 3.1-40 Detect Edges Command

The elements in the input list should be oriented with their tops facing outward and there must not be any free edges or holes in the list.

To apply the Detect Edges command:

1. Click EDGE SENSITIVITY and specify a value other than 0.
2. Click DETECT EDGES and enter a list of triangular or quadrilateral elements.
3. Press Enter.

When you apply the Detect Edges command, the detected element edges are automatically included in the list of selected edges. However, you can modify this list by selecting (or deselecting) edges before applying the HexMesh command.

Selecting Edges

To select edges:

1. Choose Mesh Generation-> Select.
2. Choose the select mode, AND.
3. Enter a list of edges.
4. Press Enter.

Any element edges that you select using the Detect Edges command are considered to be real edges.

To remove these edges, clear them from the selection list using the Select menu options in Mentat (see Deselecting Edges).

Deselecting Edges

To deselect edges:

1. Choose Mesh Generation-> Select.
2. Choose the select mode, EXCEPT.

3. Enter a list of edges.
4. Press Enter.

Checklist for the HexMesh Command

Before you apply the HexMesh command you should ensure that:

- the input list of triangular and quadrilateral elements enclose the volume to be meshed.
- there are no free edges or holes in the input list.
- the elements are oriented with their tops facing outward
- the length assigned to the element edges does not exceed the thickness of geometry to be meshed (a good rule-of-thumb is: edge length = 1/3 thickness of the smallest section)

Applying the HexMesh Command

To apply the HexMesh command:

1. Click HEXMESH



Mesh Generation-> Automesh-> Solid Meshing

Figure 3.1-41 HexMesh Command

2. Specify a list of triangular and quadrilateral elements.
3. Press Enter.

About the Meshing Tools

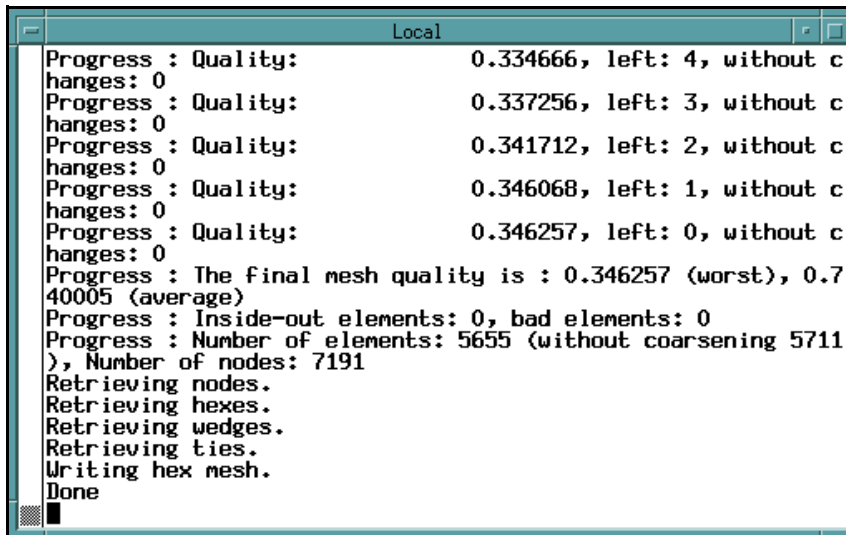
The following table describes the operations supported by meshing tools available for the hexmesher:

Tool	Operation
Outline Edge Length	Computes the outline edge length. A value, 0, signifies that there are: <ul style="list-style-type: none"> • no free edges • all elements have the same orientation
Sweep Outline Nodes	Removes coincident nodes on the outline.
Tolerance	Specify tolerance for sweeping operation.
Align Shells	Make all the surface elements to have same orientation.
Check Mesh	Checks mesh for distorted, upside-down, or inside-out elements. Reverses the orientation of elements, curves, and surfaces.
Clear Mesh	Removes the entire mesh leaving the geometry intact.

Rectifying an Unsuccessful Hexmeshing Operation

If your hexmeshing operation is unsuccessful, here are some measures that you can take before running the operation again:

- In the static menu area, click UNDO to return to the input mesh.
- Check the detected edges and edit them if necessary (see [Using the Detect Edges Command](#)).
- Select a gap parameter value other than 0 (see [Specifying Gap](#)).
- Specify a different element size (see [Specifying Element Size](#)).
- Modify the input list.
- Check the Mentat shell window for any status, warning, and error messages:



```
Local
Progress : Quality:      0.334666, left: 4, without c
changes: 0
Progress : Quality:      0.337256, left: 3, without c
changes: 0
Progress : Quality:      0.341712, left: 2, without c
changes: 0
Progress : Quality:      0.346068, left: 1, without c
changes: 0
Progress : Quality:      0.346257, left: 0, without c
changes: 0
Progress : The final mesh quality is : 0.346257 (worst), 0.7
40005 (average)
Progress : Inside-out elements: 0, bad elements: 0
Progress : Number of elements: 5655 (without coarsening 5711
), Number of nodes: 7191
Retrieving nodes.
Retrieving hexes.
Retrieving wedges.
Retrieving ties.
Writing hex mesh.
Done
```

Figure 3.1-42 Mentat Shell Window

Using HexMesh – Example

About the Example

The meshing example in this chapter demonstrates the steps in meshing a solid model with HexMesh. The example is a procedure file, *hexmesh.proc*, and uses the model, *hexmesh.mfd*.

The procedure file and the model are located in the Mentat directory, *examples/marc_ug*.

Example Overview

The key stages in this example are:

- **Stage 1:** Running the Procedure File.
- **Stage 2:** Prepare the Input Model for Surface-Meshing using the Delaunay Surface Tri-Mesh.
- **Stage 3:** Applying the Delaunay Tri-Mesh
- **Stage 4:** Prepare the Input List for HexMesh using the HexMesh Parameters
- **Stage 5:** Applying HexMesh

Running the Procedure File

To run the procedure file, *hexmesh.proc*:

1. Choose UTILS-> PROCEDURES.
2. In the Mentat Procedure Control window, click LOAD.
3. In the Mentat Procedure Files window, locate the file, *hexmesh.proc*, in the directory, *examples/marc Ug*.
4. Click OK. The procedure file appears in the Mentat Procedure Control window.
5. Use one of the following options to run the procedure file:
 - To run the procedure file without interruptions, click START/CONT.
 - To run the procedure file step by step, click STEP.

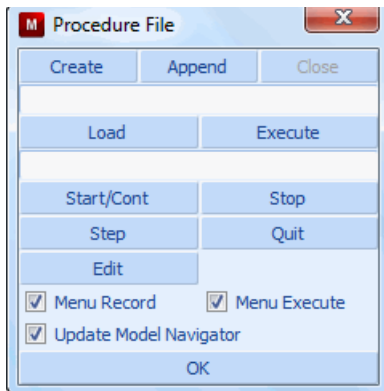


Figure 3.1-43 Procedure File Menu

Preparing the Model for Surface Meshing

To prepare the model for surface-meshing using the Delaunay surface tri-mesh:

1. Click FILL to make the entire model visible.

2. Click DRAW and turn the drawing of nodes and points to OFF.
3. Choose VIEW-> VIEW STATUS-> SHOW VIEW 4.

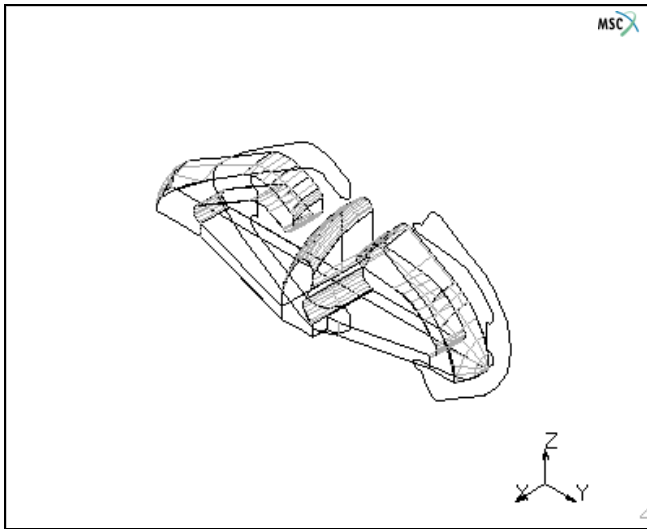


Figure 3.1-44 Displaying View 4

4. Click MESH GENERATION-> AUTOMESH-> REMOVE FREE CURVES to remove curves not attached to the surface.
5. Click BREAK CURVES and specify:
 - a vertex tolerance (0.5)
 - a list of curves (all existing)
6. Clean the surface geometry by specifying the following tolerance settings:
 - minimum tolerance (.01)
 - surface parametric space tolerance (.01)
7. Click CLEAN SURFACE LOOPS and specify a list of surfaces (all existing).
8. Click CHECK SURFACES and specify a list of surfaces (all existing).
9. Choose AUTOMESH-> CURVE DIVISIONS-> TYPE.
10. Specify a curve division with fixed average length (1).
11. Click APPLY CURVE DIVISIONS and specify a list of curves (all existing).
12. Click MATCH CURVES and specify:
 - a vertex tolerance (.05)
 - a list of curves (all existing)

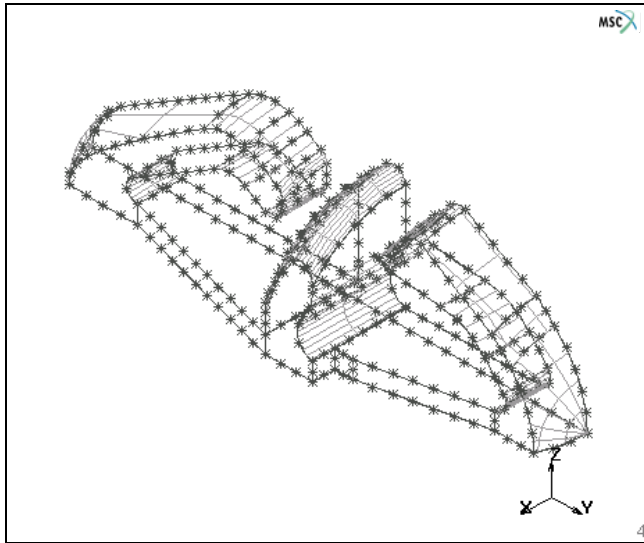


Figure 3.1-45 Displaying Matched Curves

Applying the Delaunay Tri-Mesh

To apply the Delaunay tri-mesh to the model:

1. Choose Surface MESHING-> SURFACE TRI MESH.
2. Specify a list of curves (all existing).

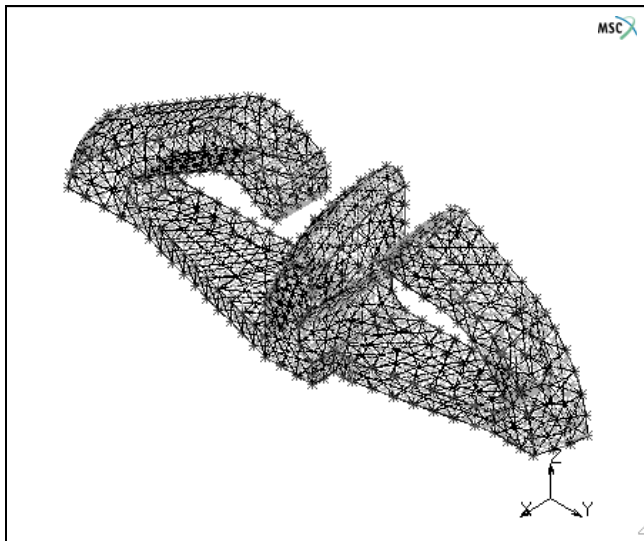


Figure 3.1-46 Surface Tri-mesh Applied

Preparing the Input List for HexMesh

To prepare the input list for HexMesh:

1. Sweep any extra nodes by specifying:
 - a sweep tolerance (.05)
 - a list of nodes to sweep (all existing)
2. Click PLOT and change the following plot settings to view the mesh more clearly:
 - Set the drawing of curves and surfaces to OFF.
 - In the Elements areas, click SOLID to display the element faces in solid color.
3. Click REDRAW to redraw the model with the new settings.
4. Choose MAIN-> MESH GENERATION-> AUTOMESH-> SOLID MESHING.
5. In the Hexmesh area, CLICK EDGE SENSITIVITY and specify a value (.5).
6. Click DETECT EDGES to identify the geometric edges in the triangular elements and specify a list of edges (all existing).
7. Choose MAIN-> VISUALIZATION-> COLORS-> SELECT EDGES.
8. Change the selected edge color by specifying a colormap number (23 1 0.6 0).
9. Choose MAIN-> MESH GENERATION-> AUTOMESH-> SOLID MESHING.
10. Click EDGE SENSITIVITY and specify a higher edge sensitivity (.6).
11. Click DETECT EDGES again and specify a list of edges (all existing).
12. Click EDGE SENSITIVITY and set the edge sensitivity even higher (.7) to detect more edges.
13. Specify a list of edges (all existing).
14. Zoom in on the model and pick a few more edges.
15. Click FILL VIEW to make the entire model visible.
16. Rotate the model, zoom in, and pick a few more edges.
17. Rotate the model again to ensure that you picked all the edges.
18. Click RESET VIEW to reset the view to its original state.
19. Click FILL VIEW to make the entire model visible again.

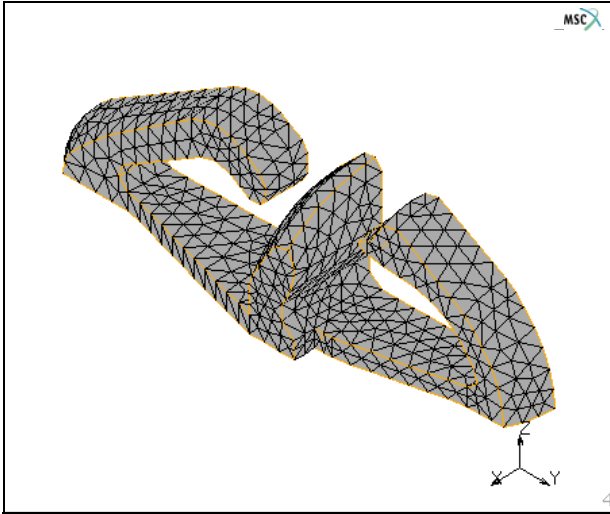


Figure 3.1-47 Edges Picked

Applying HexMesh

To apply HexMesh:

1. Choose MAIN-> AUTOMESH-> SOLID MESHING.
2. In the HexMesh area, click ELEMENT SIZE and specify the element sizes in x, y, and z-directions (.25, .25, .25).
3. Click HEXMESH! and specify a list of edges (all existing).

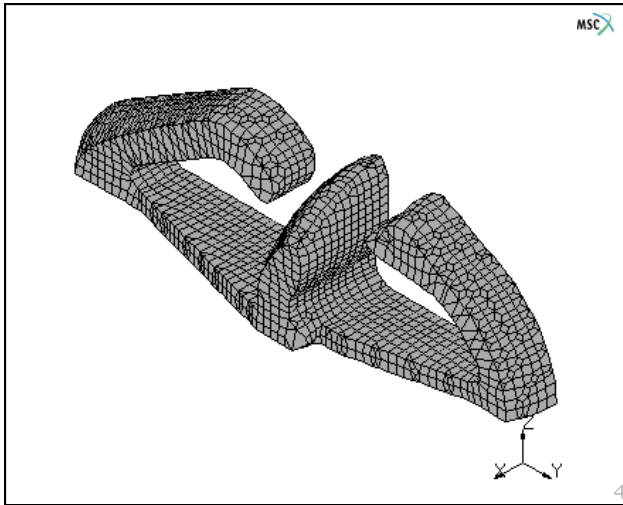


Figure 3.1-48 HexMesh Applied

Input Files

The files below are on your [delivery media](#) or they can be downloaded by your web browser by clicking the links (file names) below.

File	Description
solid_modeling_auto_meshing.proc	Mentat procedure file to run the above example
hexmesh.proc	Mentat procedure file to run the above example
hexmesh.mfd	Associated model file

3.2 Manhole

- Chapter Overview 886
- Background Information 886
- Detailed Session Description 900
- Conclusion 925
- Input Files 926

Chapter Overview

This chapter demonstrates the analysis of a region where one cylinder penetrates another cylinder of a larger radius and where the structure is loaded by an internal pressure. The radius thickness ratio of the structure warrants the use of shell theory instead of a full three-dimensional analysis using hexahedral elements.

The objective of this chapter is to highlight the following three Mentat capabilities.

- Generation of a cylinder-cylinder intersection.
- Application of face loads.
- Display of results in a contour plot.

Background Information

Description

In this session, you analyze a cylindrical pressure vessel penetrated by an off-centered manhole. The diameter of the vessel is 168 inches and the plate thickness is 0.54 inches. The manhole has a diameter of 48 inches and a plate thickness of 1.0 inches. The dimensions of the structure are shown in [Figure 3.2-1](#).

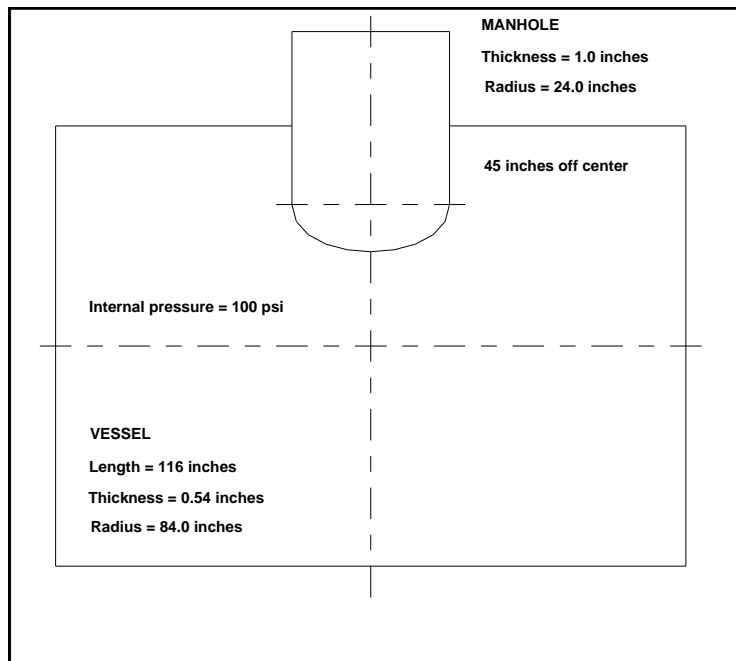


Figure 3.2-1 Vessel Dimensions

The manhole is positioned 45 inches from the center line as indicated by [Figure 3.2-2](#).

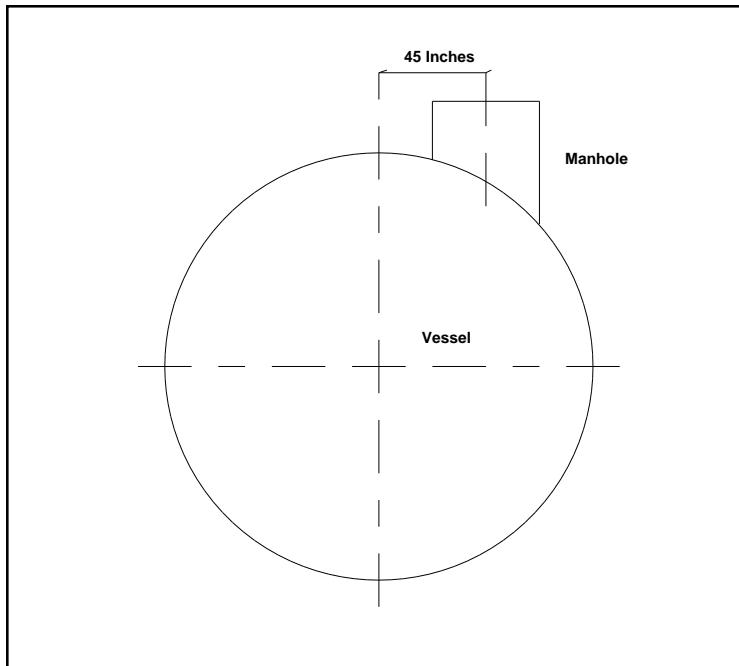


Figure 3.2-2 Side View of Vessel

Idealization

Only a portion of the vessel needs to be modeled due to symmetry and to the way arched structures respond to localized loads. The thickness/radius ratio is small enough that it allows you to use the shell approximation instead of a full three-dimensional analysis. As the focus of this analysis is on the response in the vicinity of the penetration, the mesh can be limited to the portion of the structure shown in [Figure 3.2-3](#).

It can be theoretically proven that for a material with a Poisson's ratio of 0.3, when measured at a distance $2.5\sqrt{rt}$ removed from the edge, the influence of the penetration is reduced to 4% of the value at the edge. Here r is the radius and t the thickness. For this particular case, the decay distance is 16.84 inches.

Therefore, the boundary conditions can be applied at the shell edge without affecting the stresses at the vessel-manhole intersection. Due to symmetry, it is sufficient to analyze half the vessel section shown in [Figure 3.2-3](#).

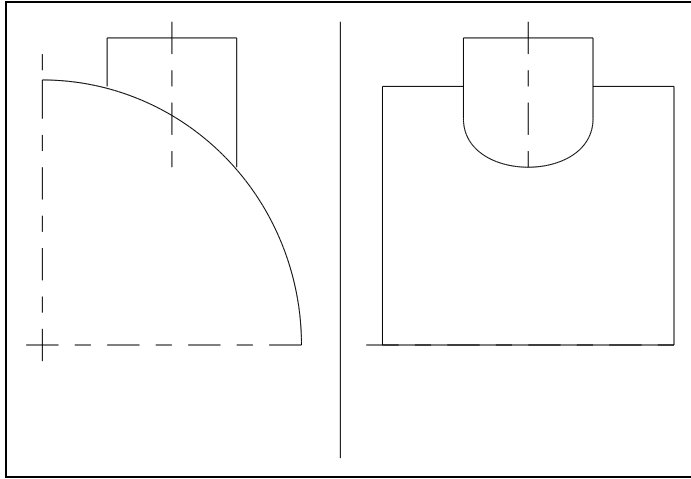


Figure 3.2-3 Section to be Analyzed

Requirements for a Successful Analysis

The analysis is considered successful if the localized stresses are known at the intersection of the two cylinders. The decay distance of 16.84 inches is assumed to be valid, and therefore, the stresses at the edge of the analyzed structure should be less than 4% of the peak value.

Full Disclosure

- **Analysis Type**
Linear static.
- **Element Type**
Marc Element Type 75, four-noded shell element.
- **Material Properties**
Steel
Young's Modulus = 30e6 psi
Poisson's Ratio = 0.3

The creation of the model will be constructed in three ways to demonstrate different procedures to create the finite element mesh.

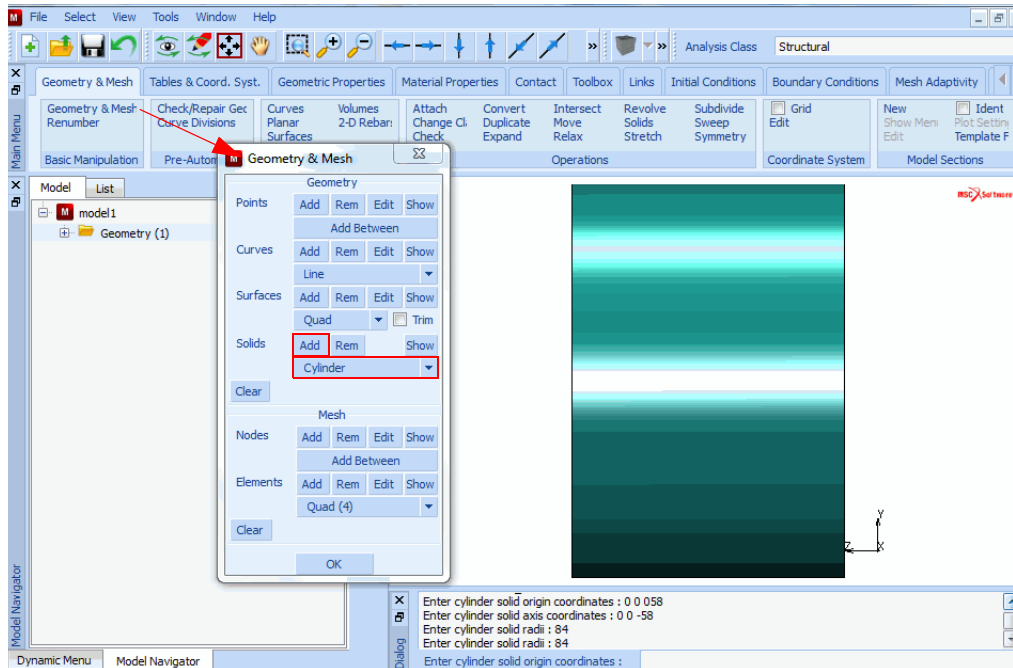
These three methods can be summarized as follows.

1. A solid geometry is created, then meshed with tetrahedral elements, then skinned and finally the tetrahedral elements are thrown away.
2. A solid geometry is created, then converted to surfaces and then meshed with quadrilateral elements.

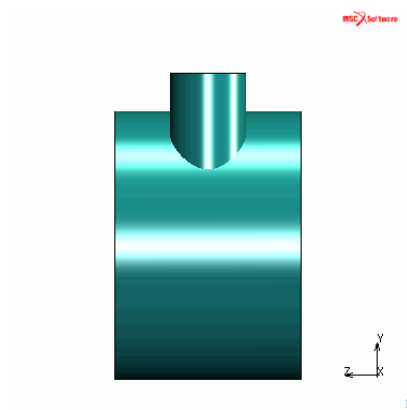
3. A manual procedure is used find the intersection between two mapped quadrilateral meshes. Only this procedure demonstrates the application of material properties, load, and boundary conditions.

In the first and second method, the complete geometry is meshed, while in the last method symmetry is accounted for to reduce the mesh size.

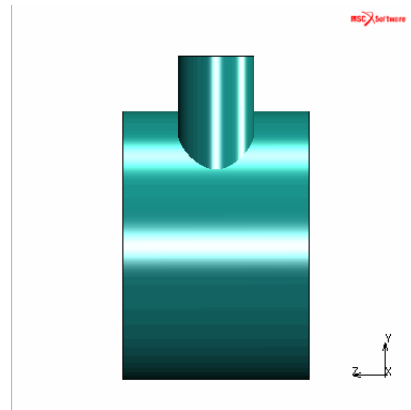
In both the first and second method, the same procedure is used to create the solid model. Effectively, the main pipe is created as a solid with an axis from $(0,0,-58)$ to $(0,0+58)$ and radius of 84. First, the solid type cylinder is selected and then added to the model.



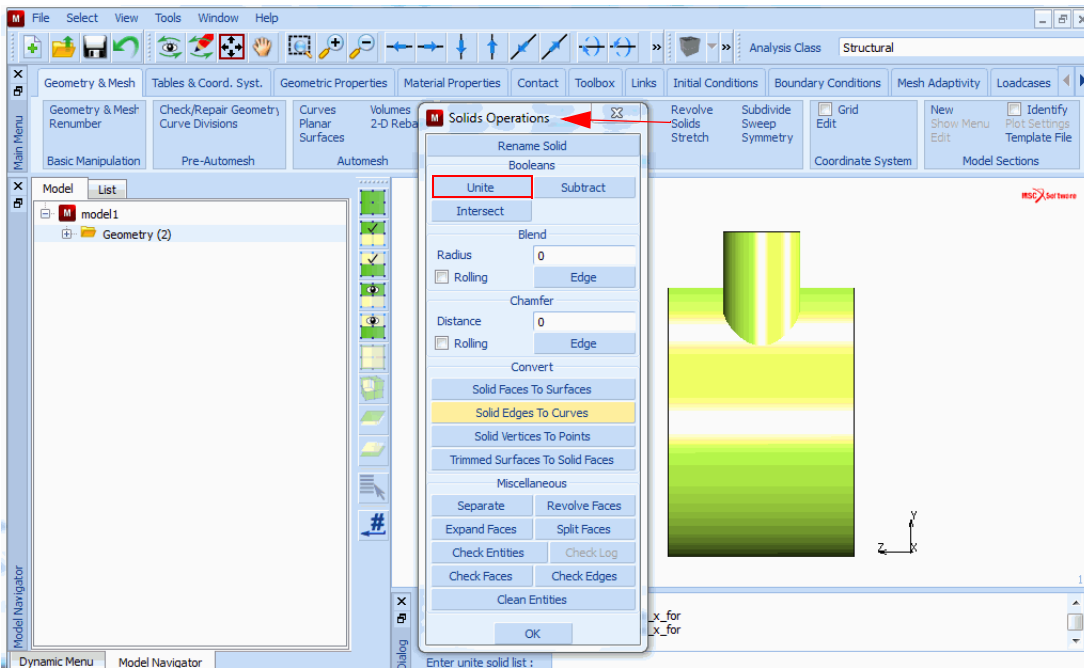
A second cylinder is added with an axis from $(45,0,108)$ to $(45,0,0)$ and a radius of 24. The second cylinder is considered to be too short, so a Move – Scale operation is performed to lengthen the cylinder. These two solid cylinders are then combined using a Boolean Unite operation from the Solid menu. One should note that this will effectively determine the intersection between these cylinders. Using solid geometry is very useful because it would be very easy to fillet the intersection.



Joined Second Cylinder

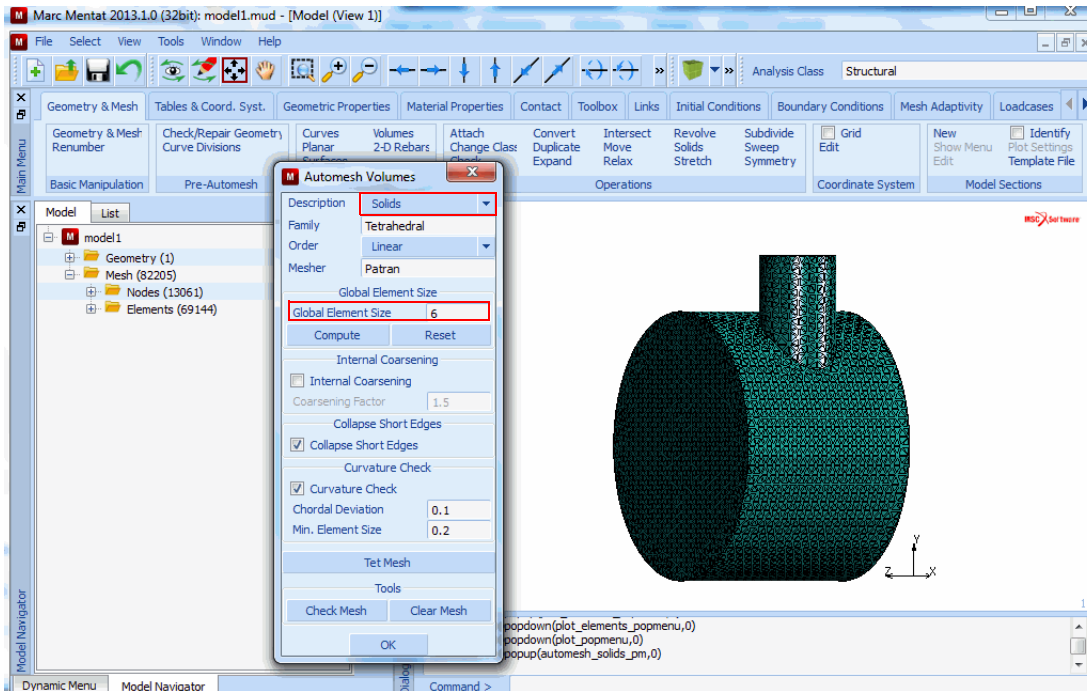


Stretched Cylinder after Scale



Unite Operation

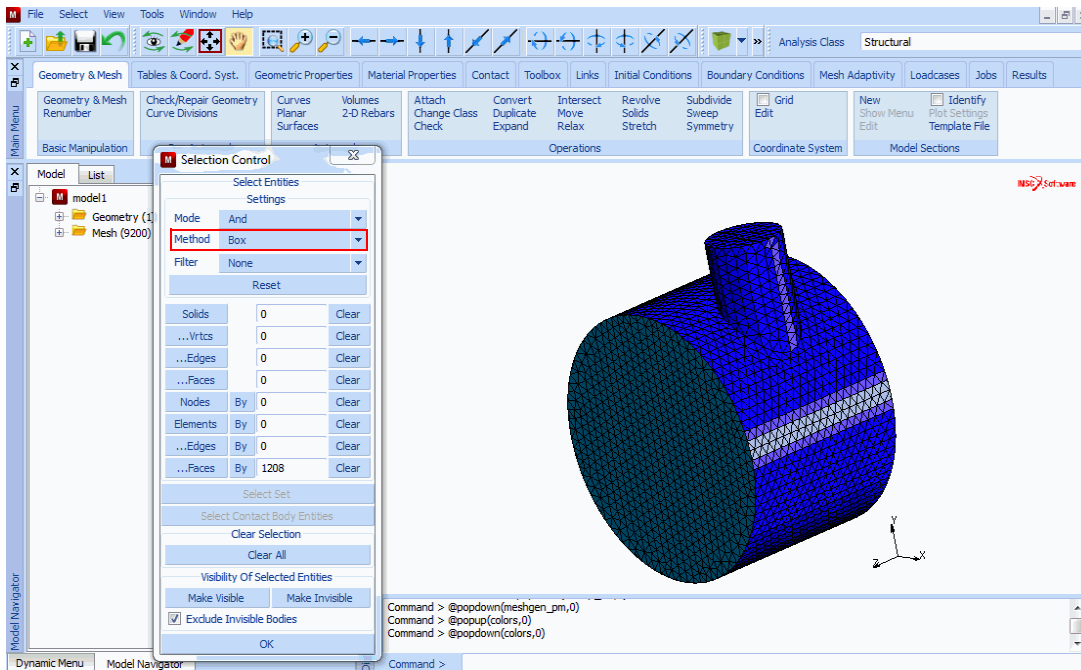
At this point, we have the combined solid. We will now focus on the first meshing procedure. A tetrahedral mesh is generated based upon the solid model.



Tetrahedral Finite Element Mesh based upon Solid

The next step is to select the exterior faces and convert them into triangular elements. The Surface Filter is used to select only the exterior faces.

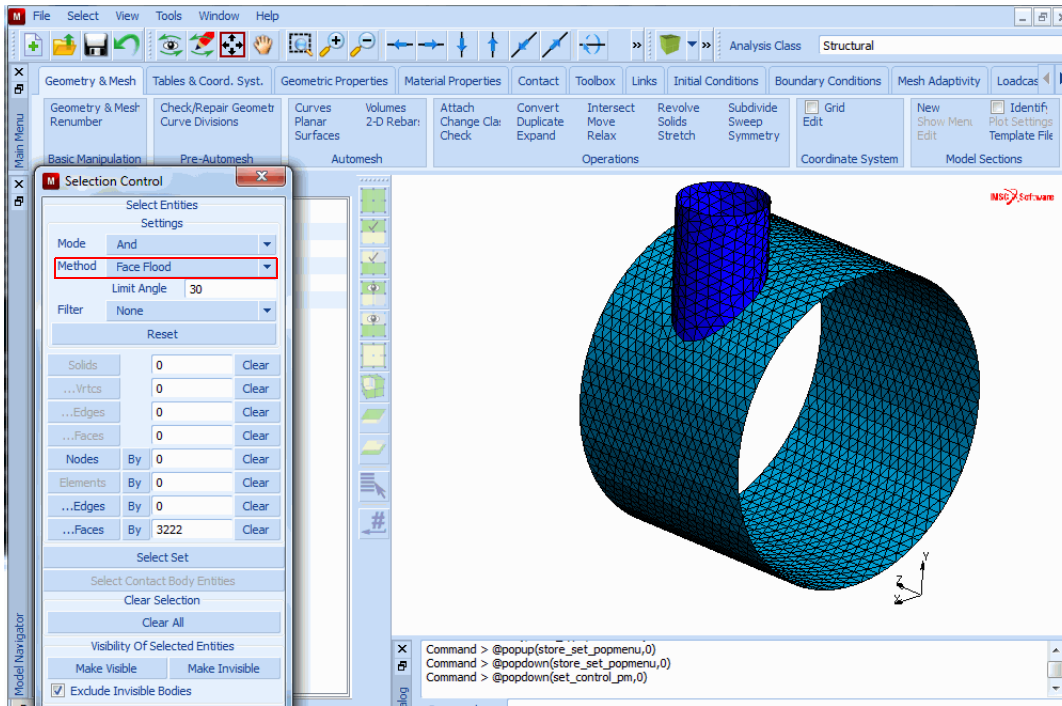
The solid tetrahedral elements are then selected by class and deleted. The unused nodes are eliminated, and the model is renumbered.



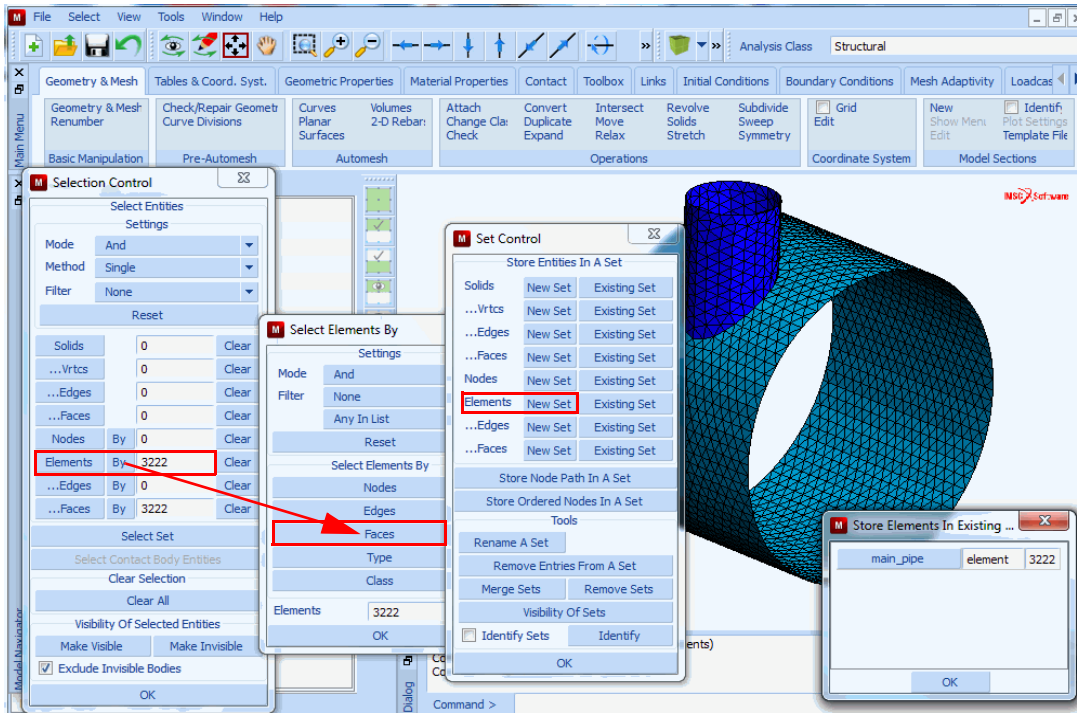
Use Box Method to select Elements

The next operation is to select elements on the end-caps of the cylinders using the box method and deleting these elements.

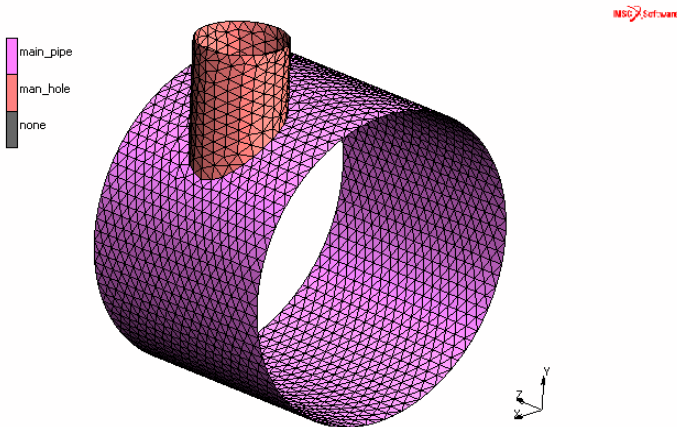
The Select option is used to select the faces on the main pipe using the face flood method.



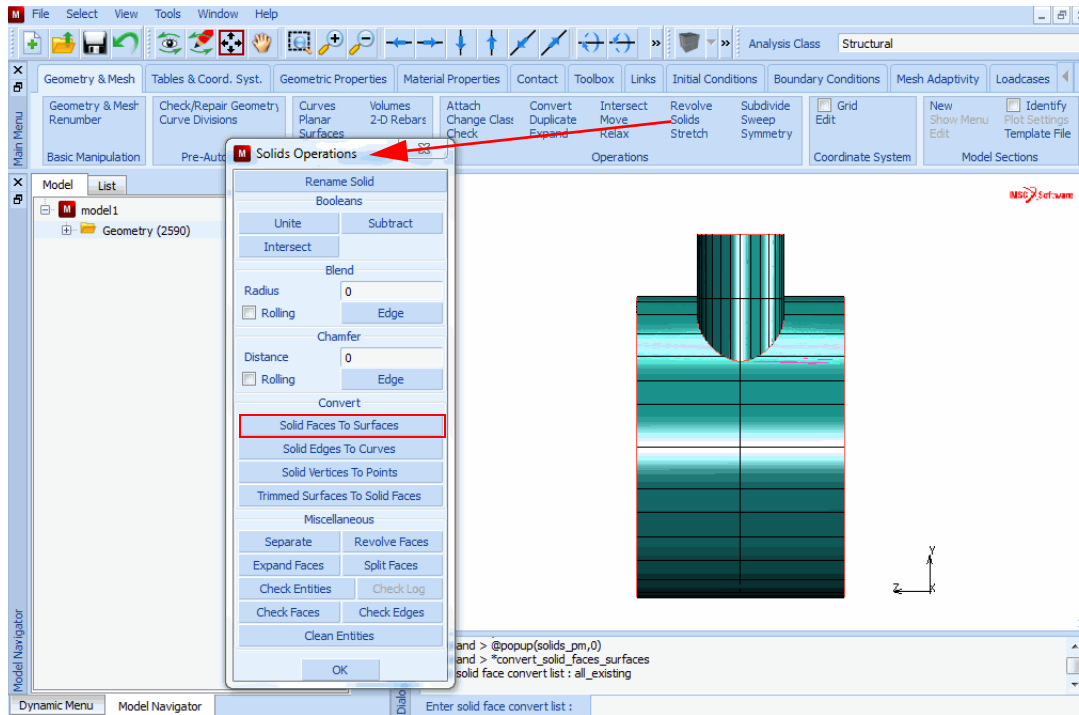
The Select option is used again to select elements on the main pipe and manhole pipe and put each one of these groups of elements into a set.



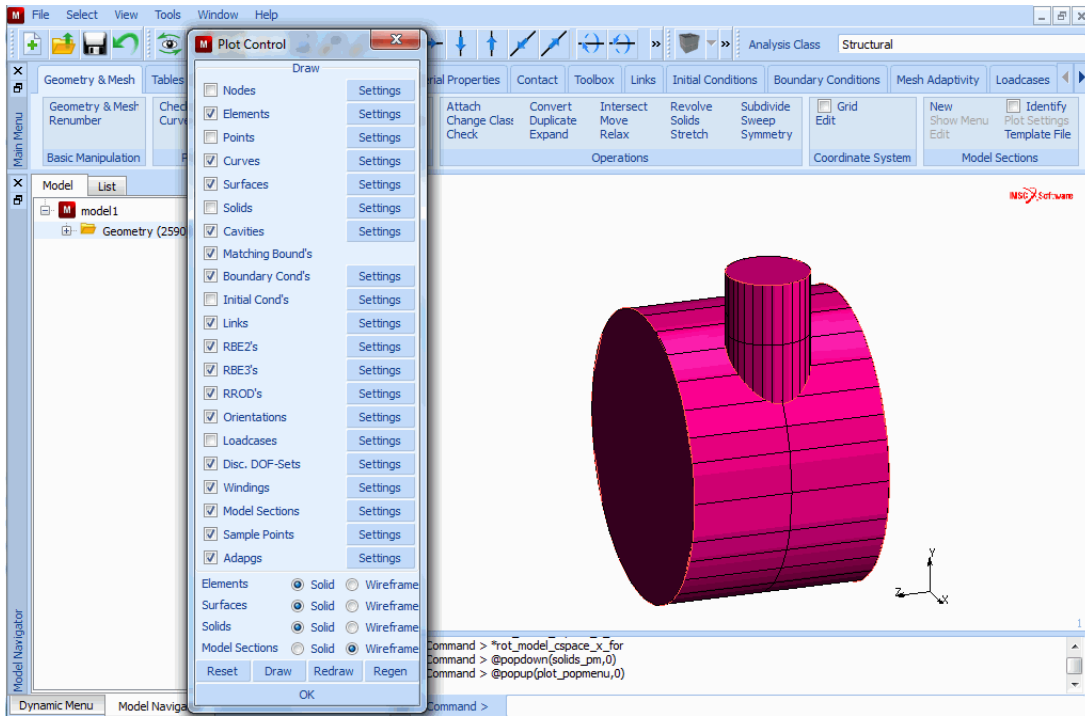
The result is the final model.



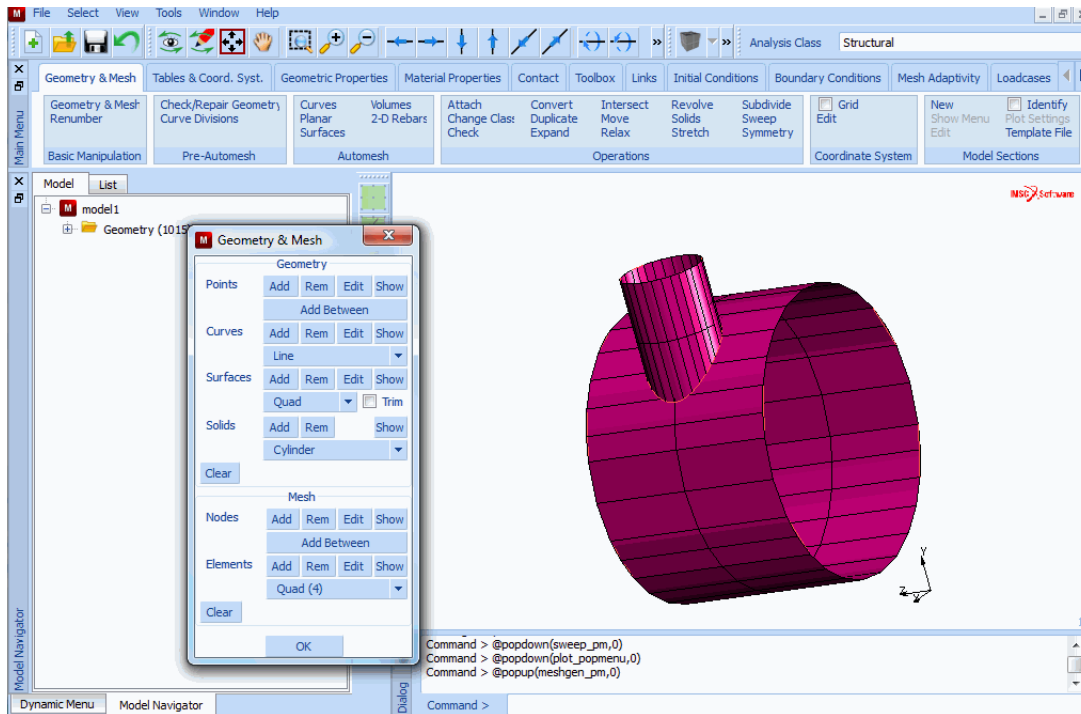
Now going back to the solid, method two will be used to generate a quadrilateral mesh. The faces of the solids will be first converted to NURB surfaces as shown below.



The solids are turned off so one can see the NURB surfaces.



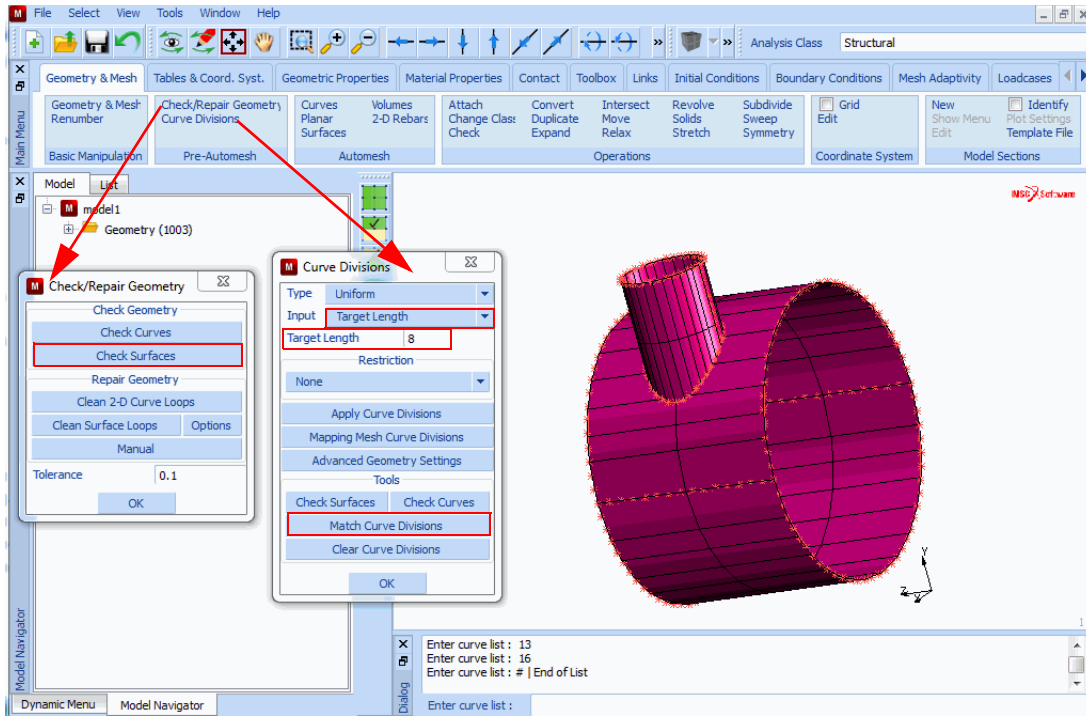
The end cap surfaces are then selected and removed.



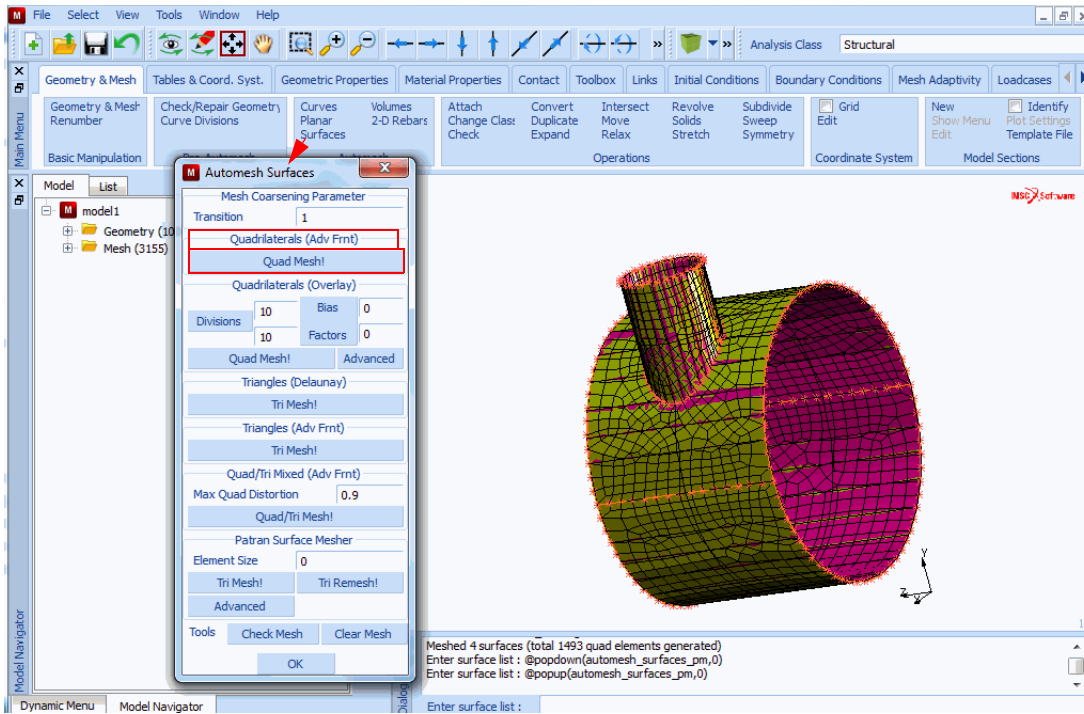
Remaining Surfaces

The surface model is cleaned up by eliminating duplicate curves and surfaces. Seed points are applied on the curves.

The target element size is five for the intersection curves and the manhole tube. The target element size is eight for the curves in the main pipe.

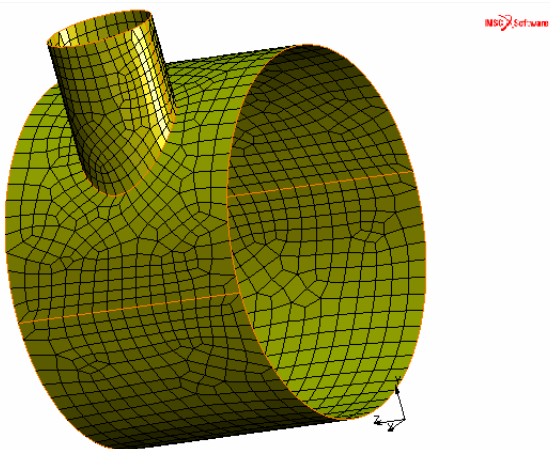


The seed points on the curves are matched and the quadrilateral mesh is created.



The surfaces are made invisible leaving the resultant finite element mesh. Note that the elements match along the intersection.

The model should be swept and renumbered.



Overview of Steps

- Step 1:** Create two cylindrical surfaces: one for the vessel and one for the manhole.
- Step 2:** Convert the surface of the vessel into a finite element mesh.
- Step 3:** Remove the elements in the vicinity of the manhole, creating a hole in the surface of the vessel.
- Step 4:** Attach the nodes of the circumference of the hole to the intersection of the vessel and the manhole surfaces.
- Step 5:** Redistribute the nodes on the perimeter of the hole.
- Step 6:** Add line elements to the circumference of the circular hole.
- Step 7:** Drag the line into shell elements thus creating the manhole.
- Step 8:** Attach the rim of the manhole to a flat surface.
- Step 9:** Subdivide the top row of elements of the manhole to improve the element aspect ratio of these elements.
- Step 10:** Sweep the entire mesh to remove duplicate nodes.
- Step 11:** Apply boundary conditions.
- Step 12:** Apply material properties.
- Step 13:** Apply geometrical properties.
- Step 14:** Submit the analysis.
- Step 15:** Postprocessing: contour the equivalent von Mises stress on the structure.

Detailed Session Description

As mentioned in earlier sample sessions, the first step is to establish a coordinate system. It seems natural to orient the z-axis of the global coordinate system in the direction of the axial axis of the vessel.

Step 1: Create two cylindrical surfaces: one for the vessel and one for the manhole.

Choose an origin that lies in the plane of the end cap of the vessel. This way the x-y axes of the global coordinate system span a plane that coincides with the plane of the end cap. [Idealization](#) mentions the need to model only a quarter section in circumferential direction. It is in this quarter section of the hull of the vessel that the manhole is modeled.

Make use of the ruled surface to create the quarter section of the vessel. The two curves necessary for ruled surfaces are arcs of equal radius extending 90° at a z-coordinate of 0 and 116, respectively. Click on the following button sequence to use the Center/Radius/begin Angle/end Angle arc type (CRAA) and to enter the data for the two curves.

MAIN

MESH GENERATION

```

CURVE TYPE
  CENTER/RADIUS/ANGLE/ANGLE
  RETURN
crvs ADD
  0 0 0 (Center point)
  84 (Radius)
  0 (Beginning angle)
  90 (Ending angle)
  0 0 116 (Center point)
  84 (Radius)
  0 (Beginning angle)
  90 (Ending angle)
PLOT
  curves SETTINGS
    LABEL (on)
    RETURN
  REGEN
  FILL

```

To make the two arcs visible, you need to deviate from the default viewpoint of 0 0 1. There are two ways to do this: you can change the view (and the viewpoint) by clicking the appropriate view number on the view menu, or you can rotate the picture by an increment of 45° about the y-axis.

Use the latter method and set the rotate increment in the VIEW menu using the following button sequence:

```

MAIN
  VIEW
    VIEW SETTINGS
      model increments ROTATE
        45
      RETURN
    RY+ (in the static menu next to RX+)
  FILL

```

Now that both curves can be distinguished, add the surface by first specifying the surface type:

```

MAIN
  MESH GENERATION

```

SURFACE TYPE

RULED

RETURN

srfs ADD

1

(Pick first curve)

2

(Pick second curve)

To pick the two previously defined curves, use the <ML> with the <↑> in the vicinity of the curve. The program displays the surface. Similar to the button sequence outlined above, set the surface type to CYLINDER to add the surface of the manhole. The surface of the manhole is only used here to determine the intersecting curve; it is not used as a primitive entity to be converted to elements.

MAIN

MESH GENERATION

SURFACE TYPE

CYLINDER

RETURN

srfs ADD

45 40 58

(1st point on the axis of the cylinder)

45 120 58

(2nd point on the axis of the cylinder)

24 24

(Radii at 1st and 2nd point)

The basic geometry of the model is now complete. Rotate the picture about the y-axis over -45° . Switch off the drawing of points and display four views of the model. Fill the graphic area for all views after activating them.

MAIN

RY-

(in the static menu next to RX -)

PLOT

draw POINTS

(off)

RETURN

VIEW

SHOW ALL VIEWS

ACTIVATE ALL

FILL

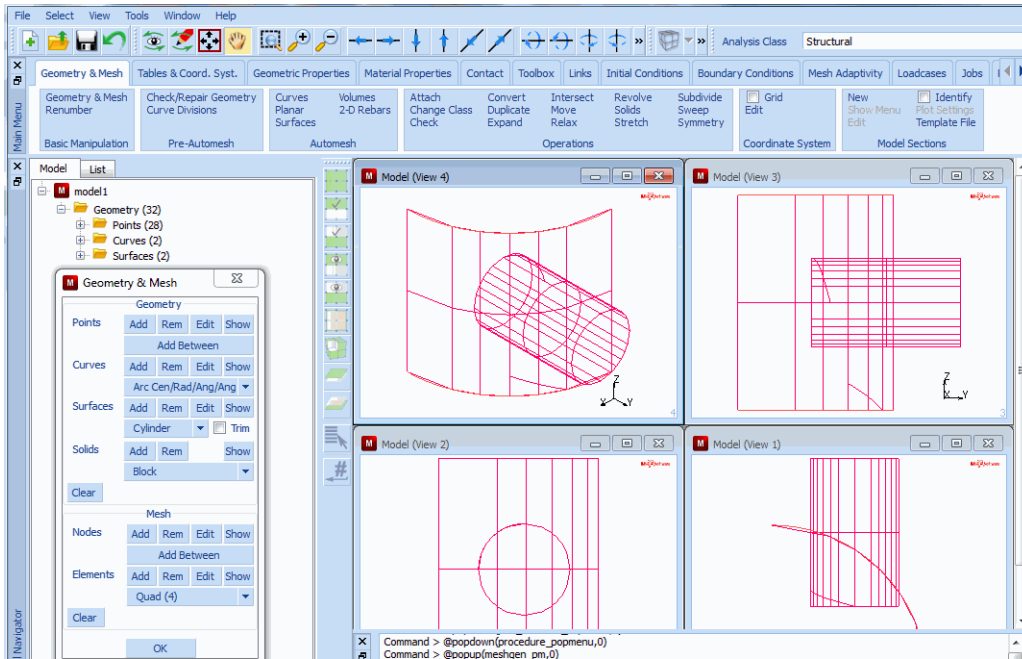


Figure 3.2-4 Four Views of Completed Model Geometry

Step 2: Convert the surface of the vessel into a finite element mesh.

Use the CONVERT processor to convert the surface of the vessel to finite elements. Click on the following button sequence to create a mesh of 20x20 elements on the quarter cylinder surface.

```

MAIN
  MESH GENERATION
    CONVERT
      DIVISIONS
        20 20
      SURFACES TO ELEMENTS
        1
      END LIST (#)
  
```

(Pick the ruled surface)

To get a better overview of the model, change the view option to 2 and deactivate the face identification option to clarify the picture. Display curves and surfaces using a high accuracy. Figure 3.2-5 illustrates where the manhole cylinder penetrates the surface of the vessel.

```

PLOT
  elements SETTINGS
  
```

FACES
RETURN
curves SETTINGS
HIGH
RETURN
surfaces SETTINGS
predefined settings HIGH
RETURN
REGEN
VIEW
show 2
RETURN

(off)

(Below SHOW ALL VIEWS)

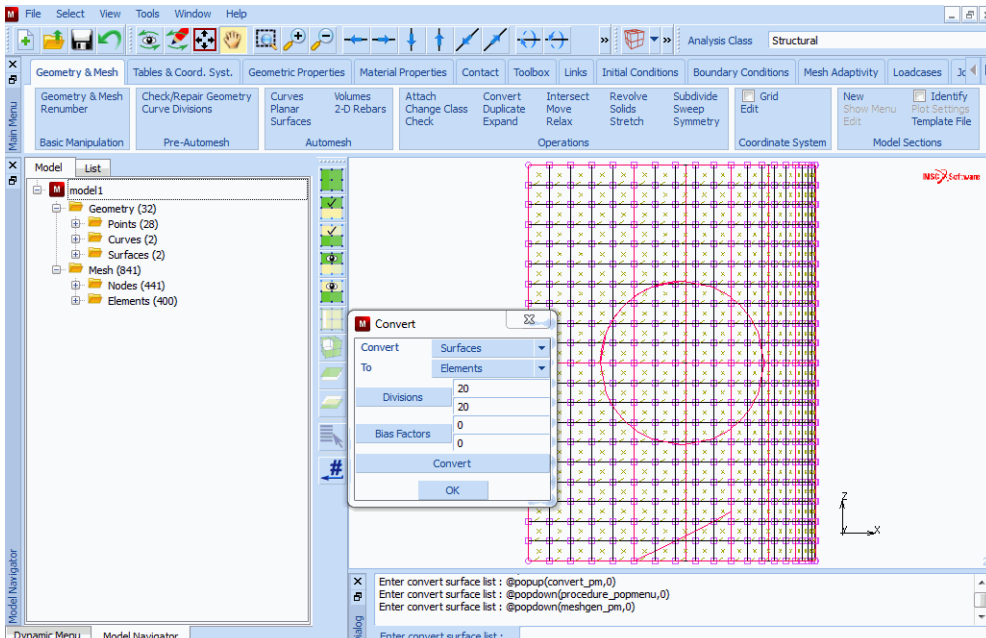


Figure 3.2-5 Elements Generated on Vessel Surface

Step 3: Remove the elements in the vicinity of the manhole, creating a hole in the surface of the vessel.

Remove a group of 6x6 elements from the vessel surface that occupy the hole caused by the penetrating manhole. Next, all unused nodes must be removed.

MAIN
MESH GENERATION

elems REM

(Box pick the elements)

END LIST (#)

SWEEP

remove unused NODES

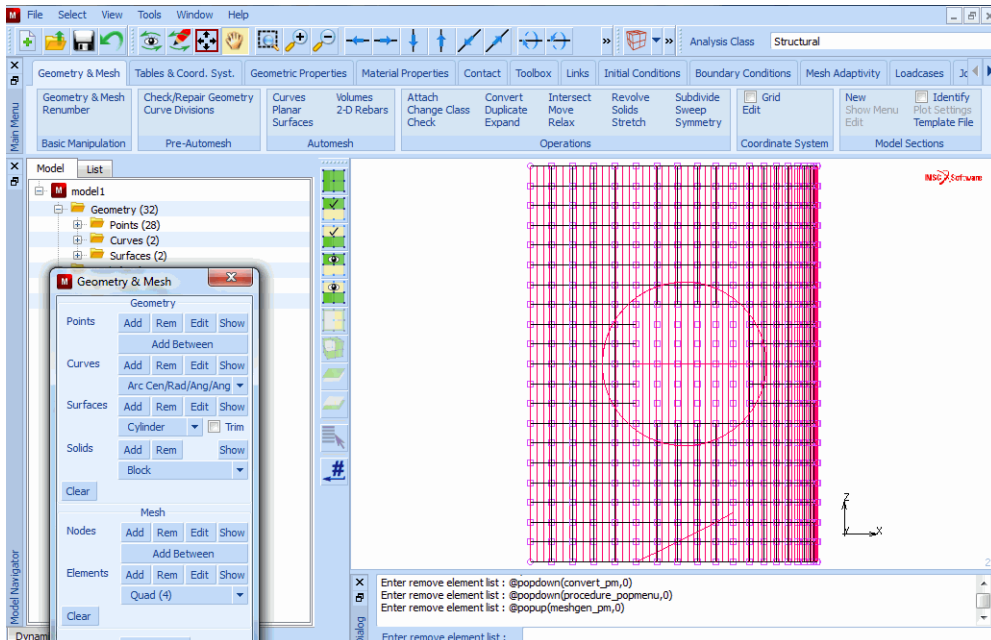


Figure 3.2-6 Vessel with Elements Removed

Step 4: Attach the nodes of the circumference of the hole to the intersection of the vessel and the manhole surfaces.

The surface of the vessel now has a square hole. The nodes on the perimeter of the square hole must now be attached to the intersection of the vessel and manhole surfaces which is done using the following button sequence:

MAIN

MESH GENERATION

MOVE

MOVE TO GEOMETRIC ENTITIES

move nodes INTERSECT

2

(Pick the manhole surface)

1

(Pick the vessel surface)

(Box pick the nodes on the perimeter of the hole)

END LIST (#)

Relax the nodes while keeping the outline of the mesh fixed, using the button sequence given below. The resulting mesh is shown in [Figure 3.2-7](#).

MAIN
MESH GENERATION
RELAX
NODES
all: EXIST.

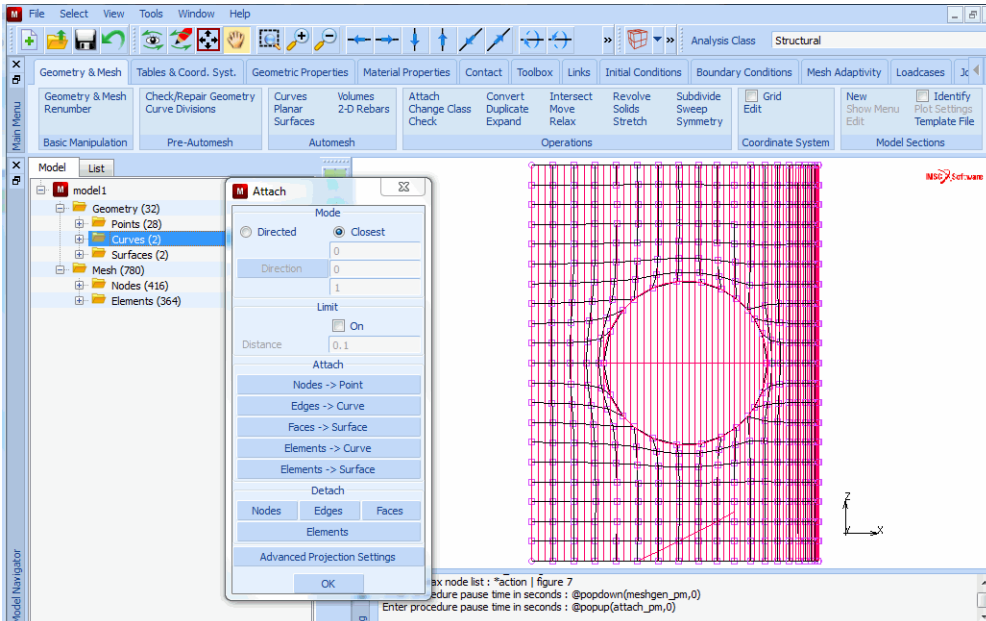


Figure 3.2-7 Peripheral Nodes Attached to Cylinder

Step 5: Redistribute the nodes on the perimeter of the hole.

[Figure 3.2-7](#) clearly indicates that the mesh pattern around the hole is not optimal. The primary cause of this is the irregular node distribution around the hole. In order to redistribute the nodes, you must **STRETCH** the nodes in groups so that the nodes are evenly distributed as indicated in [Figure 3.2-8](#).

The following button sequence is used to stretch the nodes:

MAIN
MESH GENERATION
STRETCH
NODES

161

(Pick the last node of the stretch node path)

END LIST (#)

Repeat this operation for the other nodes on the perimeter of the hole as indicated in Figure 3.2-8.

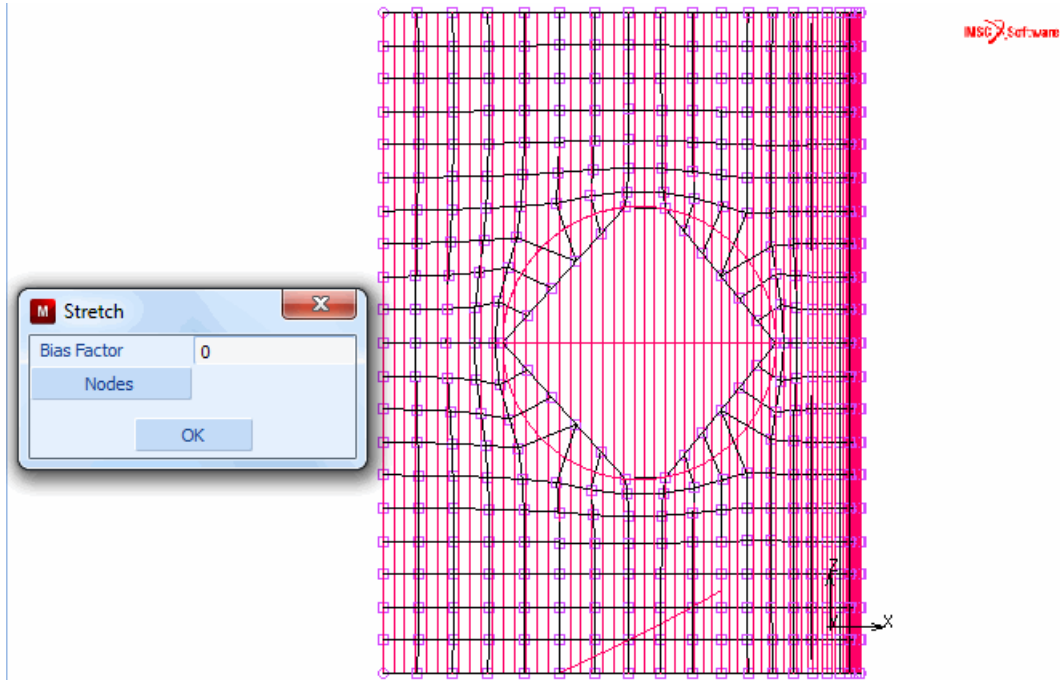


Figure 3.2-8 Evenly Distributed Nodes

It is obvious from the picture, the stretch operation no longer preserves the requirement that the perimeter of the hole is on the intersection of the two main surfaces.

To re-attach the nodes, use a directed attach method which guarantees that the nodes are moved to the intersection along a specified direction. The following button sequence demonstrates the steps required to apply the directed attach method.

MAIN

MESH GENERATION

MOVE

MOVE TO GEOMETRIC ENTITIES

move nodes INTERSECT

2

(Pick the surface)

1

(Pick the surface)

247 268 289 288
END LIST (#)

(Pick the nodes)

Repeat this process for all four sides that have been stretched using a different direction for each side. The result of the first attach operation is shown in [Figure 3.2-9](#).

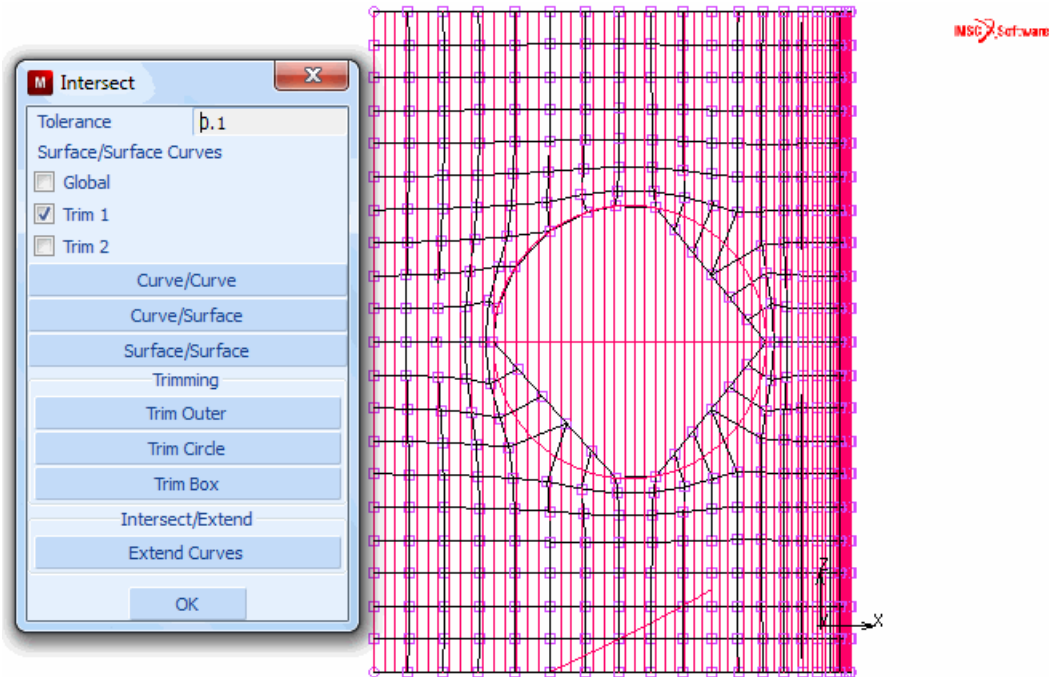


Figure 3.2-9 Using the Directed Attach Method to Re-Attach the Nodes

As noted before, it is sufficient to create only half of the model shown in [Figure 3.2-10](#) due to symmetry. The reason for generating the entire model is that the nodes on the boundary of a mesh remain at their location during relax operation and only interior nodes are moved. Had we generated only half the model, the nodes on the line of symmetry (in the XY plane) would have required a manual redistribution.

MAIN

MESH GENERATION

elems REM

(Box pick all elements below the symmetry line)

END LIST (#)

SWEEP

remove unused NODES

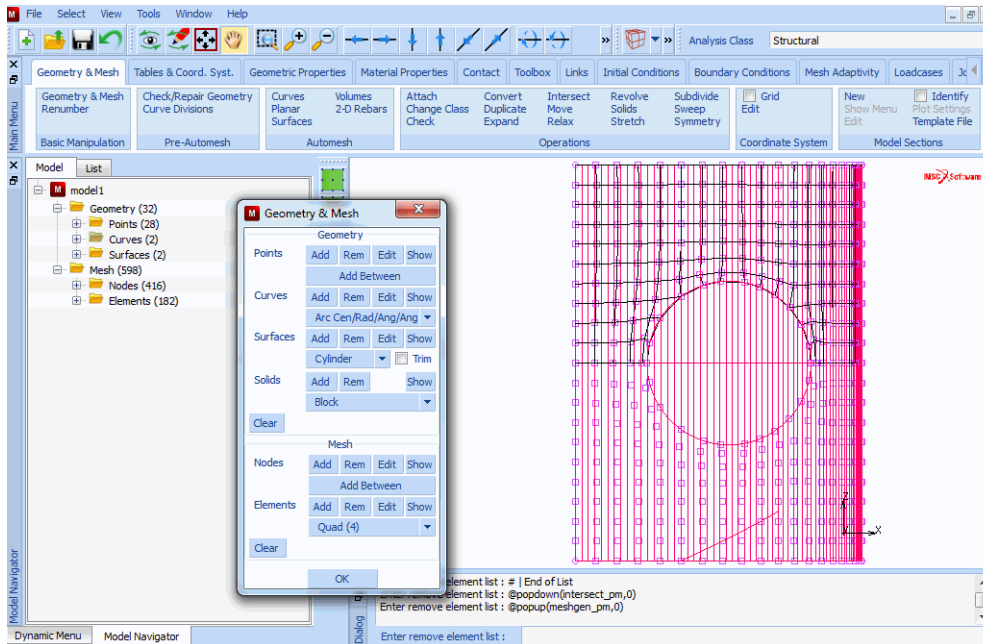


Figure 3.2-10 Removing Unused Nodes

Step 6: Add line elements to the circumference of the circular hole.

There are several ways to create the manhole. The user is to follow the same steps used for the vessel. The cylindrical surface is first converted to elements. The bottom edge of the manhole elements is then attached to the intersecting line of the vessel and manhole surface. Instead, you use a different approach that involves the use of line elements. The edge of the existing hole in the vessel is *plated* with line elements that serve as the generating elements in an expand operation. Use the following button sequence to create line elements to the exposed side of the quadrilateral elements:

MAIN
MESH GENERATION
CONVERT
EDGES TO ELEMENTS
(Pick the edges at the perimeter of the hole)
END LIST (#)

Use the following button sequence to select and store the line elements generated by this operation into a set name for later reference.

MAIN
MESH GENERATION

```
SELECT
  SELECT BY
    elements by CLASS
      LINE(2)
      OK
      RETURN
  elements STORE
    sticks
    all: SELECT.
  CLEAR SELECT
```

The EXPAND processor drags line elements into shell elements and shell elements into volume elements, effectively increasing the dimensionality of the element type by one. Use the EXPAND operation to drag the line elements equidistantly over 10 inches for three layers. The rim of the manhole created in this manner has the same shape as the intersection line of the two cylinders.

Step 7: Drag the line into shell elements thus creating the manhole.

Use the following button sequence to perform the expand operation.

```
MAIN
  VIEW
    SHOW ALL VIEWS
    RETURN
  MESH GENERATION
    EXPAND
      TRANSLATIONS
        0 10 0
      REPETITIONS
        3
      ELEMENTS
        sticks
```

Use the SWEEP processor and click on NODES from the SWEEP panel to eliminate the duplicate nodes created by the expand operation. Click on the all: EXIST. button of the static menu to indicate that you want to rid the entire mesh of duplicate nodes. You can verify the elimination of the nodes by only drawing the outline of the mesh.

```
MAIN
  MESH GENERATION
```

SWEEP

sweep NODES

all: EXIST.

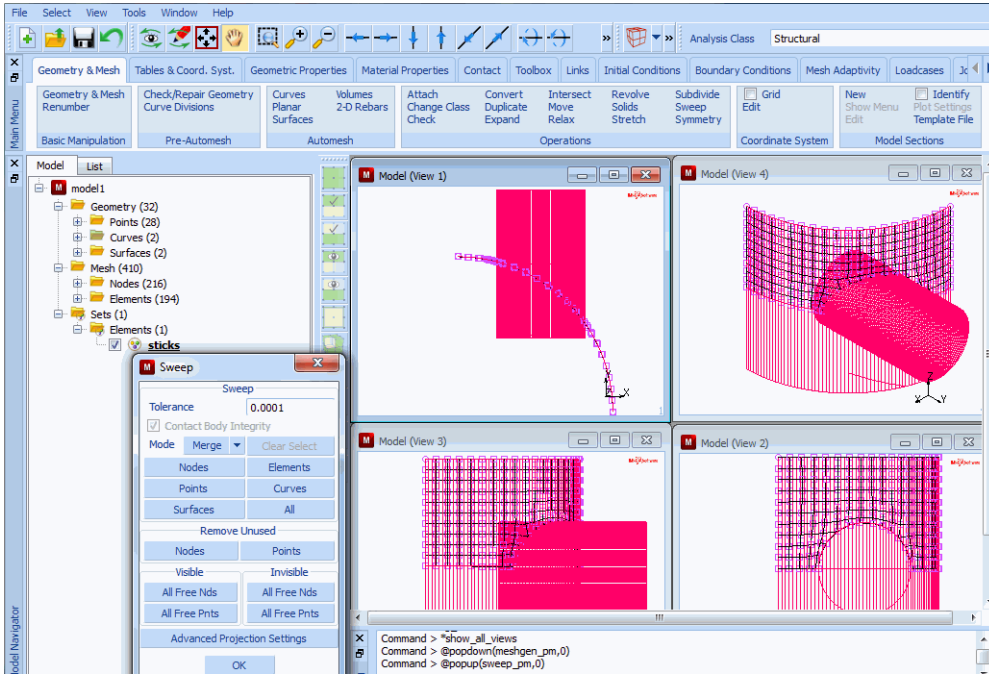


Figure 3.2-11 Manhole with Nearly Correct Coordinates

Step 8: Attach the rim of the manhole to a flat surface.

Attach the doubly curved rim of the manhole to a patch. To create the patch, select QUAD as the current surface type. Use the coordinates given below to add the patch in a local coordinate system. Create the local coordinate system by rotating 90° about the global x-axis and translating it 112 inches in the global y-direction.

MAIN

MESH GENERATION

SURFACE TYPE

QUAD

grid ON

RETURN

coordinate system SET

U DOMAIN

-100 100

(on)

```
U SPACING
  10
V DOMAIN
  -100 100
V SPACING
  10
grid ON                                     (on)
ROTATE
  90 0 0
TRANSLATE
  0 112 0
RETURN
PLOT
  draw POINTS                               (on)
  RETURN
pts ADD
  -10 0 0
  100 0 0
  100 100 0
  -10 100 0
FILL
srfs ADD
  29 30 31 32                             (pick the four points generated above)
GRID                                         (off)
FILL
```

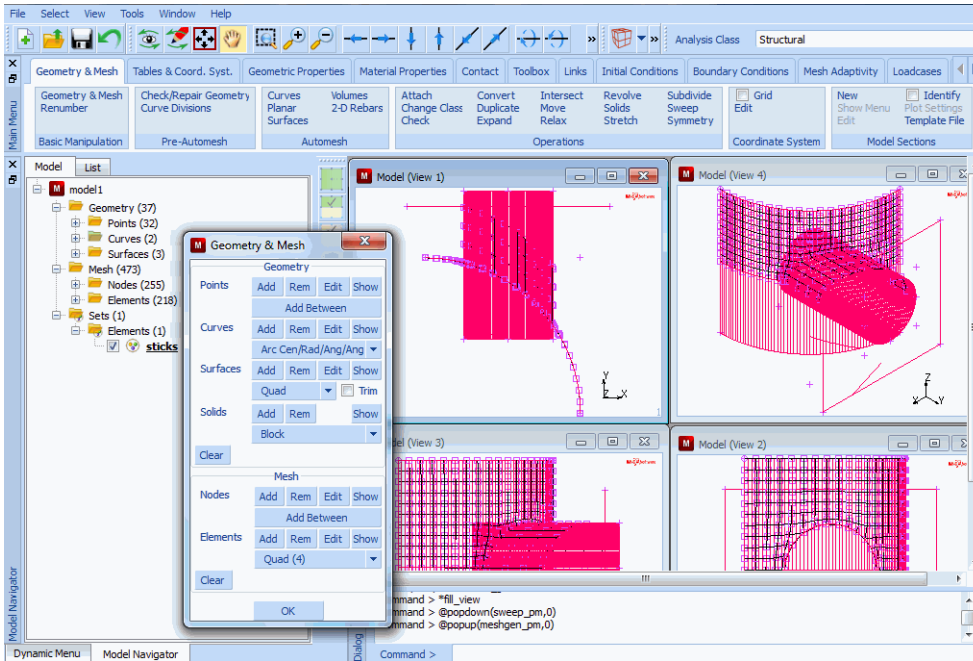



Figure 3.2-12 Creating the Patch

The nodes on the cut-off boundary of the manhole need to be moved to the intersection of the two surfaces. Use the following button sequence to move the nodes:

MAIN

MESH GENERATION

MOVE

MOVE TO GEOMETRIC ENTITIES

move nodes INTERSECT

2

(Pick the cylinder)

3

(Pick the quad)

(Use the Polygon Pick Method to pick the nodes from view 1)

The results of the move operation are shown in [Figure 3.2-13](#).

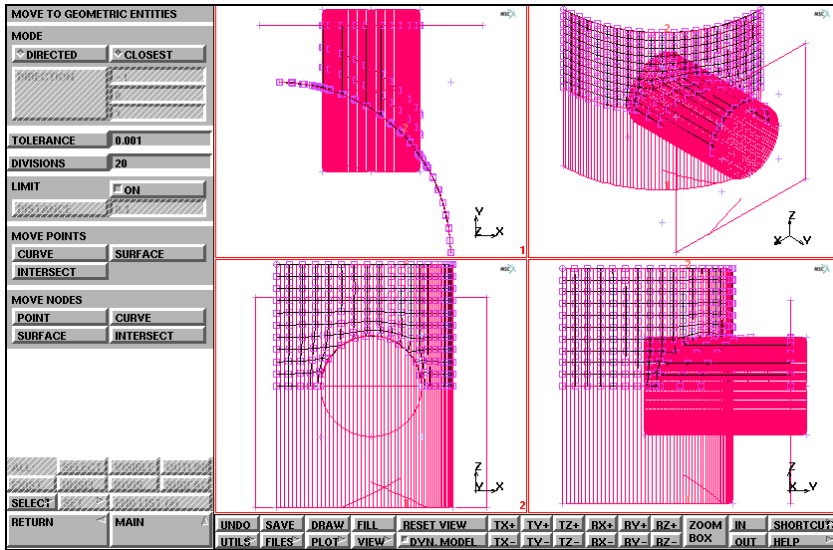


Figure 3.2-13 Moved Nodes to Patch

Step 9: Subdivide the top row of elements of the manhole to improve the element aspect ratio of these elements. Subdivide the top row of elements in the second direction of connectivity to improve the aspect ratio. Once again, it is most convenient to use the Polygon Pick Method to select the elements.

MAIN

MESH GENERATION

SUBDIVIDE

DIVISIONS

1 2 1

ELEMENTS

END LIST (#)

(Pick the top row of elements)

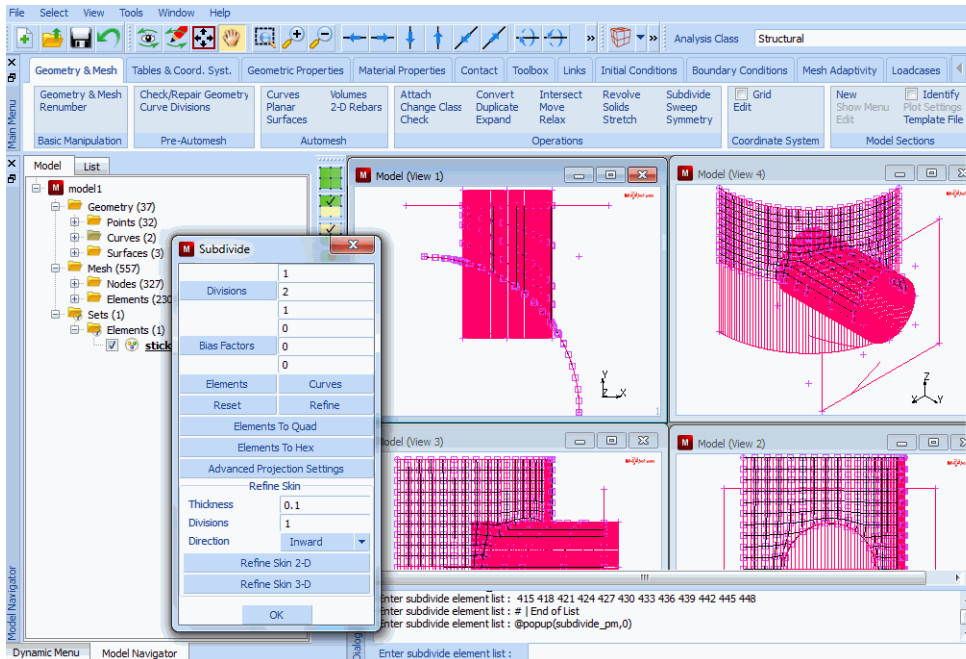


Figure 3.2-14 Improved Aspect Ratio for Top Row Elements

Step 10: Sweep the entire mesh to remove duplicate nodes.

Sweep the mesh to eliminate duplicate nodes after each operation that generates elements.

MAIN

MESH GENERATION

SWEEP

NODES

all: EXIST.

You have now completed the topological part of the mesh. For subsequent tasks, it is no longer required to use the geometric entities points, curves, and surfaces, and therefore, the plotting of these items is switched off.

PLOT

draw POINTS (off)

draw CURVES (off)

draw SURFACES (off)

REGEN

FILL

Step 11: Apply boundary conditions.

There are two types of symmetry conditions across the edge that cut the vessel and manhole in half:

1. Zero displacement in z-direction,
2. Zero local rotations along the edge.

The first boundary condition (1) is expressed in global coordinates. To apply the second boundary condition, it is necessary to apply a transformation to the nodes of the vessel such that the boundary conditions can be expressed as a function of the global degrees of freedom. Use the following button sequence to create the transformations.

```

MAIN
  BOUNDARY CONDITIONS
    MECHANICAL
      VIEW
        show 2
      RETURN
    TRANSFORMS
      CYLINDRICAL
        0 0 0
        0 0 100
                                          (center line)
                                          (Pick the nodes along the curved and straight edges
                                          of the vessel; not those of the manhole)
      END LIST (#)

```

The boundary conditions (1) and (2) mentioned on the previous page are then applied through the following button sequence:

```

MAIN
  BOUNDARY CONDITIONS
    MECHANICAL
      FIXED DISPLACEMENT
        DISPLACEMENT Z
        ROTATION Y
      OK
    nodes ADD
                                          (Pick the nodes along the symmetry
                                          plane of the vessel and manhole)
      END LIST (#)
    VIEW

```

show 4
 RETURN
 FILL

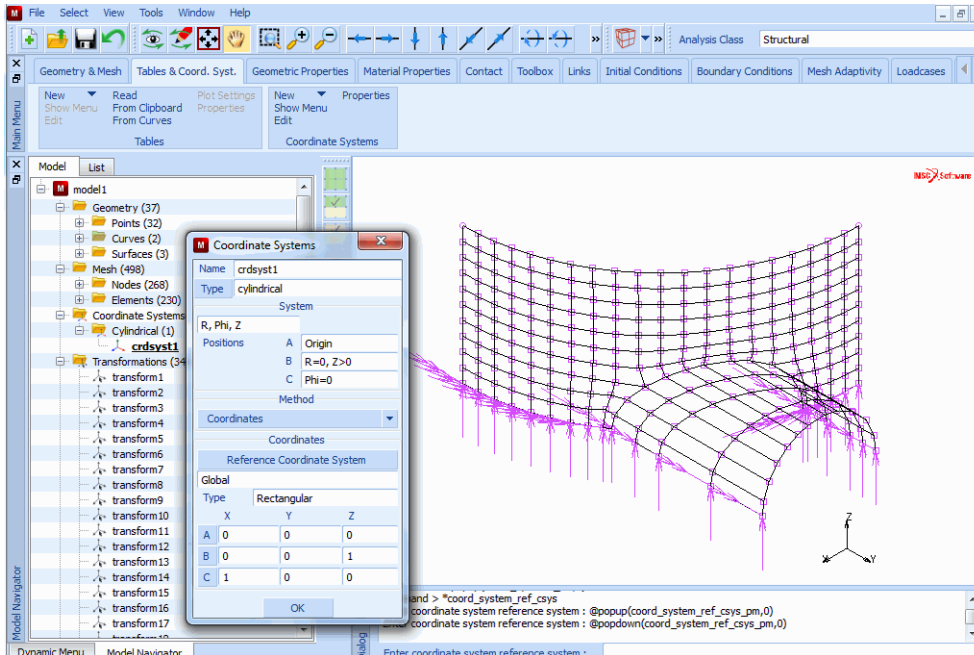


Figure 3.2-15 Boundary Conditions Applied

The other curved edge of the vessel has an edge load applied in the direction of the center line.

MAIN

BOUNDARY CONDITIONS

MECHANICAL

NEW

EDGE LOAD

PRESSURE

-4200

OK

edges ADD

*(Pick the edges on the curved side
of the vessel)*

END LIST (#)

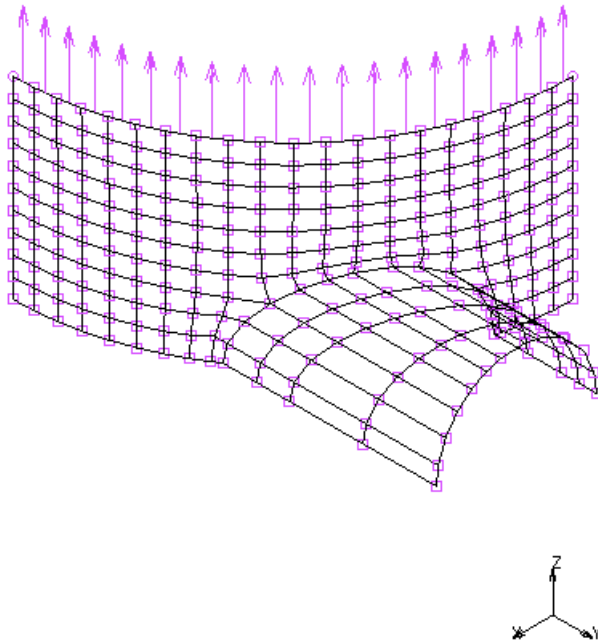


Figure 3.2-16 Edge Loads Applied in Direction of Center Line

The vessel is under internal pressure which is applied through the following button sequence:

```
MAIN
  BOUNDARY CONDITIONS
    MECHANICAL
      NEW
      FACE LOAD
        PRESSURE
          -100.0
        OK
      faces ADD
        all: EXIST.
```

Note: The definition of a positive pressure is one that is directed towards the face of the element.

Figure 3.2-17 shows that the pressure on the manhole is applied as an external pressure. Two methods can be used to correct the direction in which the load is applied: either the sign of the applied pressure load for the manhole elements is changed or the direction of the connectivity of the elements of the manhole is changed.

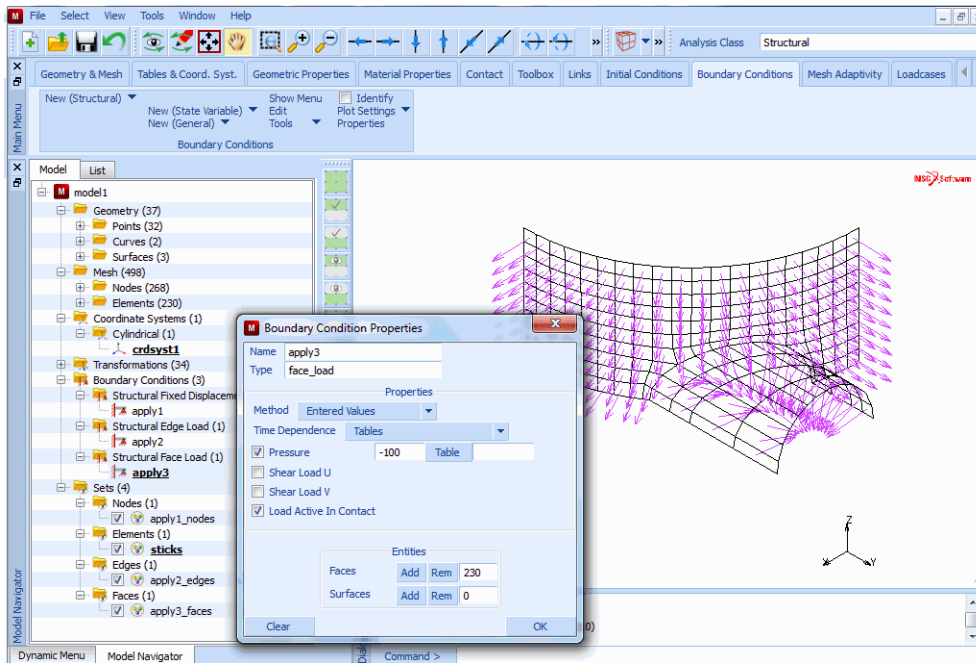


Figure 3.2-17 Internal Pressure Applied

The latter method used in the container sample session described in Chapter 3.30 is also used in this session and invoked with the following button sequence:

MAIN

MESH GENERATION

CHECK

VIEW

show 2

RETURN

FLIP ELEMENTS

END LIST (#)

VIEW

show 4

RETURN

(Use the Polygon Pick Method to select the elements of the manhole)

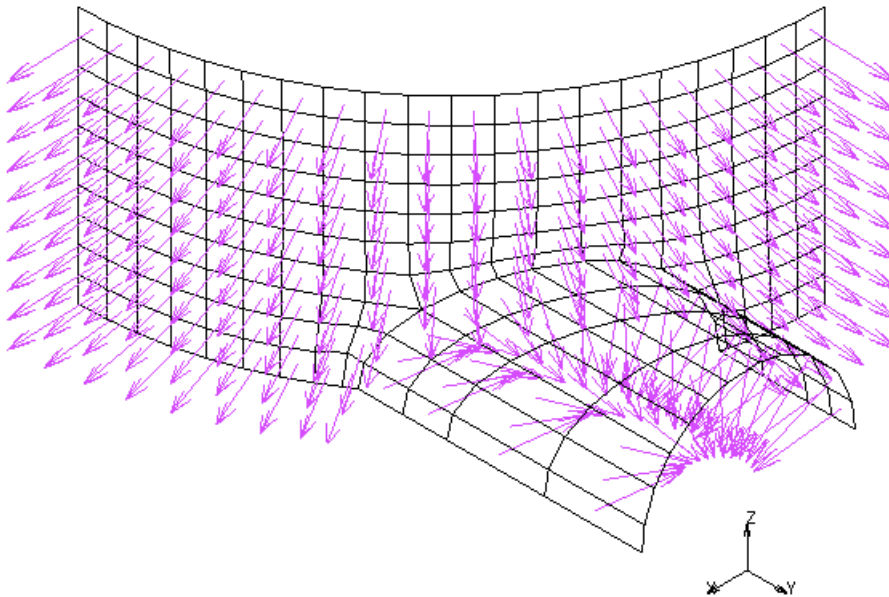


Figure 3.2-18 Corrected Load Direction

The following two types of symmetry conditions exist along the straight edges of the vessel: displacement in tangential direction is zero, rotation in axial direction is zero.

Due to the previously defined transformations, these boundary conditions can be applied using the following button sequence:

```
MAIN
  BOUNDARY CONDITIONS
    MECHANICAL
      NEW
      FIXED DISPLACEMENT
        DISPLACEMENT Y (on)
        ROTATION Z (on)
      OK
    nodes ADD
  END LIST (#)
```

(Pick the nodes on the straight edges of the vessel)

MSC Software

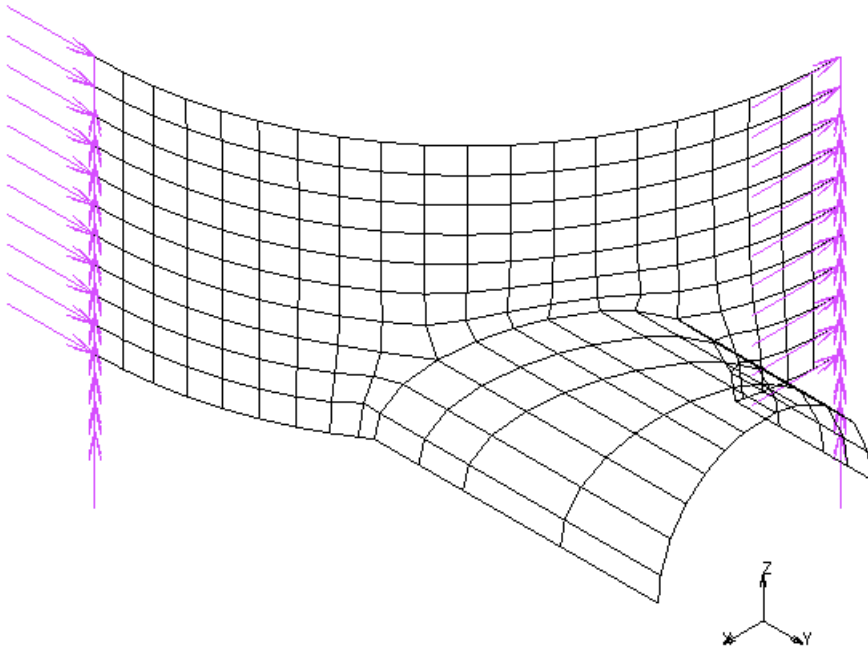


Figure 3.2-19 Boundary Conditions Applied to Vessel Edges

Finally, an edge load is applied to the top perimeter of the manhole.

```
MAIN
  BOUNDARY CONDITIONS
    MECHANICAL
      NEW
      VIEW
        show 1
      RETURN
    EDGE LOAD
      PRESSURE
        -1200
      OK
    edges ADD

    END LIST (#)
  VIEW
```

(Pick the edges at the top rim of the manhole)

show 4
RETURN

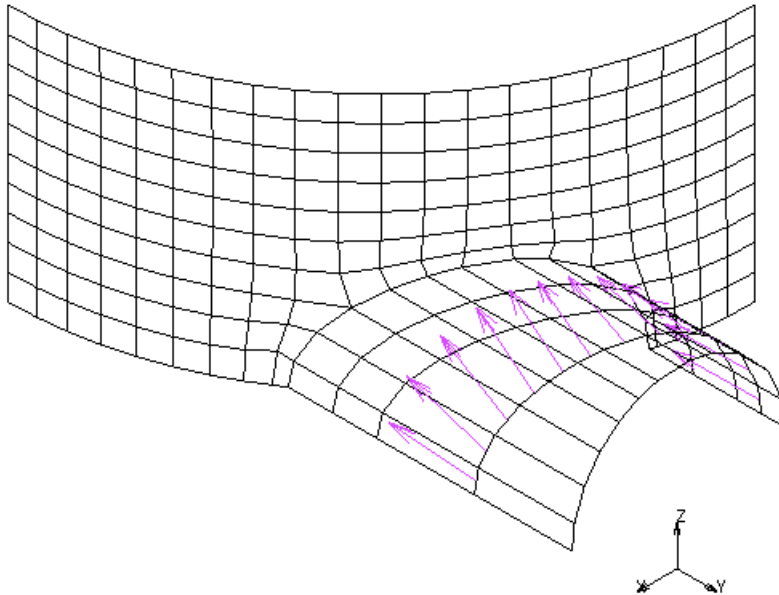


Figure 3.2-20 Edge Load Applied to Top Rim of Manhole

Step 12: Apply material properties.

The material properties for both the vessel and the manhole are specified in [Material Properties](#). Use the following button sequence to apply steel properties to the two structures.

MAIN

MATERIAL PROPERTIES

ISOTROPIC

YOUNG'S MODULUS

30.0e6

POISSON'S RATIO

0.3

OK

elements ADD

all: EXIST.

Step 13: Apply geometrical properties.

The manhole is manufactured out of a steel plate with a thickness of 1 inch. The thickness of the vessel is 0.54 inches. Click on the GEOMETRIC PROPERTIES button of the main menu and go to the “mechanical elements 3-D” submenu. Enter the SHELL pop-up menu, click on the THICKNESS button and type in 0.54. To confirm the correctness, click on the OK button. Assign the thickness to the elements of the vessel only. Repeat this process for the manhole using the following button sequence:

```
MAIN
  GEOMETRIC PROPERTIES
    mechanical elements 3-D
      SHELL
        THICKNESS
          .54
        O
        K
      VIEW
        show 2
      RETURN
    elements ADD
                                          (Pick the elements of the manhole)
  END LIST (#)
```

Confirm the correctness of the thickness application using the ID GEOMETRIES button.

You have now completed the modeling process, Step 2 of the Analysis Cycle. Continue with the preparatory steps for the finite element analysis.

As this is a linear static analysis, you do not need to create a loadcase. The INITIAL LOADS option in the JOBS menu is used to specify the loading pattern.

Step 14: Submit the analysis.

Use the following button sequence to define the Marc element type, to verify that the appropriate initial loads have been activated, to specify the desired result variables, and to submit the job.

```
MAIN
  JOBS
    ELEMENT TYPES
      MECHANICAL
        3-D MEMBRANE/SHELL
          75
```

```
      OK
    all: EXIST.
    RETURN
  RETURN
MECHANICAL
  JOB RESULTS
    available element tensors
      Stress
      layers: OUT & MID
    scalars
      Equivalent Von Mises Stress
      layers: OUT & MID
      OK
  INITIAL LOADS
    OK
  JOB PARAMETERS
    #SHELL/BEAM LAYERS
      3
    OK (twice)
SAVE
RUN
  SUBMIT 1
  MONITOR
```

Step 15: Postprocessing: contour the equivalent von Mises stress on the structure.

The screen is updated periodically to report the progress of the job. If the job has been successfully completed, the exit message on the panel will be 3004.

To display the results of the analysis for interpretation, use the following button sequence:

```
MAIN
  RESULTS
    OPEN DEFAULT
    NEXT
    PLOT
      draw NODES
    RETURN
```

(off)

SCALAR
Equivalent von Mises Stress Layer 1
OK
CONTOUR BANDS
DEF & ORIG
FILL

Figure 3.2-21 shows the resulting model contoured with von Mises stresses.

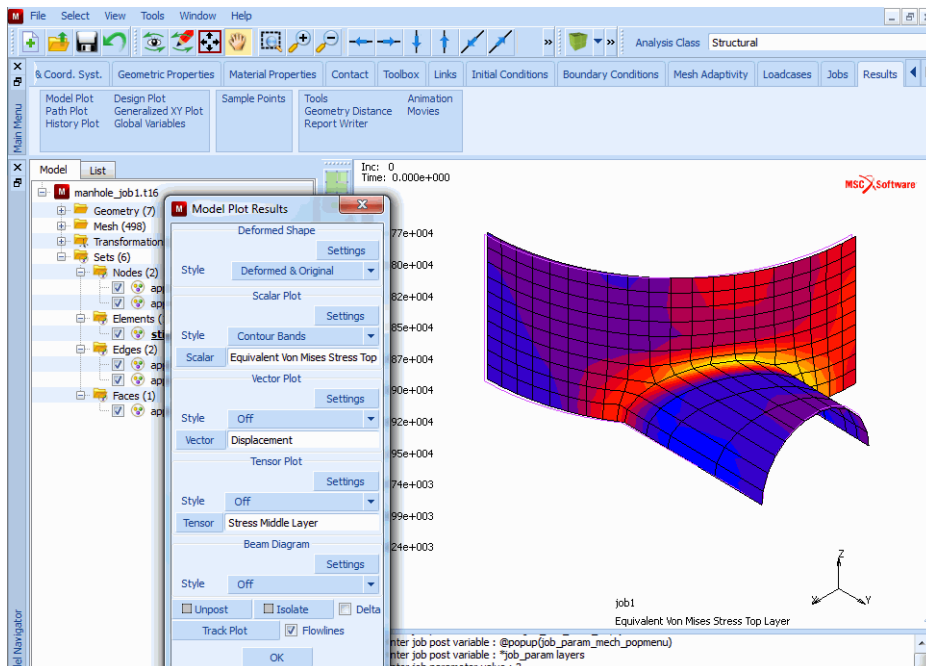


Figure 3.2-21 Model with von Mises Stress Contours

Conclusion

Due to reproduction constraints, Figure 3.2-21 does not give you a clear representation of the actual resulting stress distribution that appears in the graphics area on your screen. The results indicate that, due to the penetration of the manhole into the vessel, the localized stress concentrations occur near the intersection.

Input Files

The files below are on your [delivery media](#) or they can be downloaded by your web browser by clicking the links (file names) below.

File	Description
manhole.proc	Mentat procedure file to run the above example

3.3 Contact Modeling of Pin Connection Joints using Higher-Order Elements

- Chapter Overview 928
- Pin Connection 929
- Input Files 943

Chapter Overview

This chapter is intended to show the Marc capability of modeling contact using quadratic elements. You have a choice as to whether the boundaries are to be linearized or genuine quadratic contact is to be used. Quadratic contact takes into account the curved geometry and shape functions of such elements. This implies that both the corner and mid-side nodes may come into contact. In case of deformable contact, searching for contact is done with respect to curved elements and the multi-point constraint equations to enforce the contact conditions are based on the complete quadratic displacement field.

Due to the nature of equivalent nodal forces following from a uniformly distributed pressure, the separation behavior is based on nodal stresses and not the nodal forces. These stresses are based on extrapolated and averaged integration point values.

Contact with quadratic elements is demonstrated using a pin connection. A number of pin connections is used to mount a thick polymer insulation layer on a perforated steel plate (see [Figure 3.3-1](#)). Plastic “bolts” with grooves are positioned in the holes of the insulation layer and the steel plate. They are pressed into the insulation layer, so that the steel pins can be moved into the grooves. The bolt heads and the pins hold the insulation layer fixed to the steel plate.

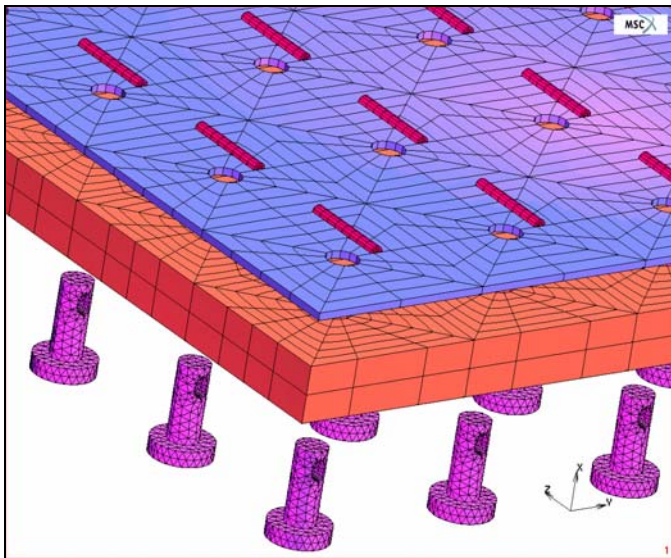


Figure 3.3-1 Perforated Steel Plate with Insulation Layer

Assuming symmetry conditions, the analysis is carried out using half a bolt and pin and corresponding parts of the steel plate and insulation layer. In total, eight contact bodies will be used: four deformable bodies (bolt, pin, insulation layer, and steel plate) and four rigid bodies (all symmetry planes).

The analysis consists of two loadcases. During the first loadcase, the bolt is inserted into the insulation layer by prescribed displacements. The pin is initially modeled to be in contact with the bolt, but contact between the pin and the steel plate is not allowed. Preventing separation between the bolt and the pin yields a small gap between the pin and the steel plate at the end of the first loadcase. During the second loadcase, the displacement constraint in axial

direction on the bolt is removed and the pin comes into contact with the steel plate, thus causing the insulation layer to be fixed to the steel plate. Friction between the various contact bodies is neglected.

The material behavior of all materials is assumed to be linear elastic with the following Young's moduli and Poisson's ratios:

$$E_{\text{steel plate}} = E_{\text{pin}} = 2100 \text{ N/cm}^2, \nu_{\text{steel plate}} = \nu_{\text{pin}} = 0.3;$$

$$E_{\text{bolt}} = 20 \text{ N/cm}^2, \nu_{\text{bolt}} = 0.28;$$

$$E_{\text{insulation}} = 0.7 \text{ N/cm}^2, \nu_{\text{insulation}} = 0.2.$$

The analysis is geometrically nonlinear, but materially linear. The finite elements used are 10-node tetrahedral elements for the bolt and the pin and 20-node hexahedral elements for the other parts.

Pin Connection

The analysis of the pin connection is done using the standard steps: define finite element mesh and geometric entities (symmetry planes), apply boundary conditions, assign material properties, define contact bodies and contact tables, define loadcases and collect them in a job with the proper job settings. After running the analysis, some postprocessing is performed.

Finite Element Mesh and Geometric Entities

The finite element mesh and geometric entities are available in an Mentat model file, called *pin_fe_model.mfd*. After resetting, the program defaults activating view 1, and this file is opened. The various parts of the model are stored in element sets called `bolt`, `pin`, `insulation`, and `steel_plate`, where the elements are selected using the select method flood. In order to easily apply displacement boundary conditions on the bolt, the nodes on the top of the bolt head are stored in a set called `bolt_top_nodes`; they are selected using the select method box.

```
FILES
  NEW
    OK
  RESET PROGRAM
  VIEW
    SHOW VIEW 1
    RESET VIEW
    RETURN
  OPEN
    pin_fe_model.mfd
    OK
  FILL
```

```
MAIN
MESH GENERATION
SELECT
  METHOD
    FLOOD
    RETURN
  ELEMENTS
    3861
  STORE
    bolt
    OK
  ALL SELECTED
  CLEAR SELECT
  ELEMENTS
    1066
  STORE
    pin
    OK
  ALL SELECTED
  CLEAR SELECT
  ELEMENTS
    119
  STORE
    insulation
    OK
  ALL SELECTED
  CLEAR SELECT
  ELEMENTS
    690
  STORE
    steel_plate
    OK
  ALL SELECTED
  CLEAR SELECT
  METHOD
    BOX
```

```

RETURN
NODES
  -0.01 0.01 (define range in x-direction)
  -2 2 (define range in y-direction)
  -2 2 (define range in z-direction)
STORE
  bolt_top_nodes
OK
ALL SELECTED
CLEAR SELECT
METHOD
  SINGLE
  RETURN
MAIN

```

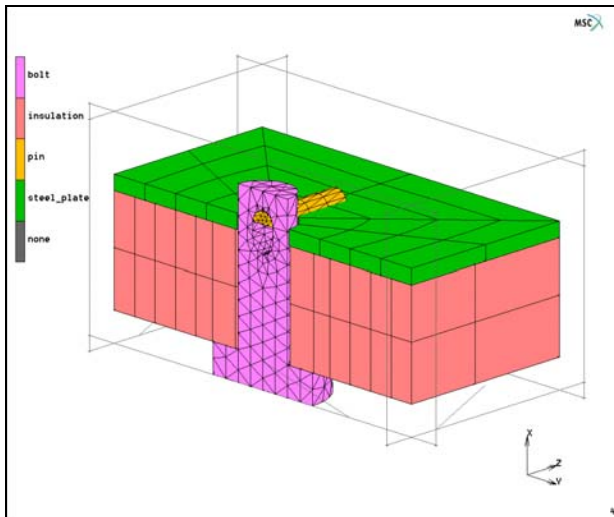


Figure 3.3-2 Finite Element Model Used

Boundary Conditions

As mentioned before, the analysis is carried out using two loadcases. During the first loadcase, the bolt is inserted into the insulation layer by prescribing the displacement component in global x-direction as a function of time for the nodes on the top of the bolt head. Moreover, the displacement in global y-direction of one of these nodes is suppressed to

prevent a rigid body motion of the bolt. Two nodes at the end face the pin are constrained similarly. For the assembly, the displacement component in global x-direction of two corner nodes of the steel plate is also suppressed.

BOUNDARY CONDITIONS

MECHANICAL

TABLES

NEW

1 INDEPENDENT VARIABLE

NAME

displacement_time

TYPE

time

ADD

0 0

1 1

RETURN

NEW

NAME

press_bolt

FIXED DISPLACEMENT

DISPLACEMENT X

0.7

TABLE

displacement_time

OK

NODES ADD

bolt_top_nodes

END LIST (#)

NEW

NAME

suppress_rigid_body_motion

FIXED DISPLACEMENT

DISPLACEMENT Y

NODES ADD

3557

4297

4056

```

END LIST (#)
NEW
NAME
    hold_steel_plate
FIXED DISPLACEMENT
    DISPLACEMENT X
NODES ADD
    664 670
END LIST (#)
MAIN

```

An overview of the boundary conditions is shown in [Figure 3.3-3](#).

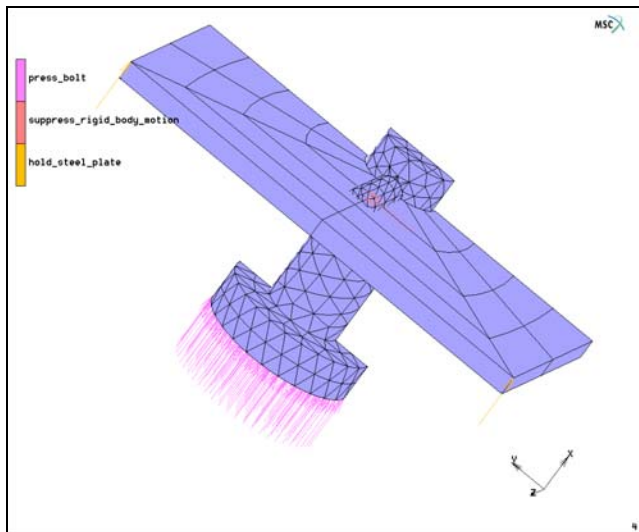


Figure 3.3-3 Overview of Applied Boundary Conditions

Material Properties

The elastic material properties of the bolt, pin, insulation layer, and steel plate are easily entered using the previously introduced element sets.

```

MATERIAL PROPERTIES
NEW
NAME
    steel

```

```
ISOTROPIC
  YOUNG'S MODULUS
    2100
  POISSON'S RATIO
    0.3
  OK
ELEMENTS ADD
  steel_plate
  pin
NEW
NAME
  bolt
ISOTROPIC
  YOUNG'S MODULUS
    20
  POISSON'S RATIO
    0.28
  O
  K
ELEMENTS ADD
  bolt
NEW
NAME
  insulation
ISOTROPIC
  YOUNG'S MODULUS
    0.7
  POISSON'S RATIO
    0.2
  OK
ELEMENTS ADD
  insulation
MAIN
```

Contact Bodies and Contact Tables

The contact body definition for quadratic elements is similar to that for linear elements. The main difference occurs in the definition of separation, where either relative or absolute testing on stresses has to be selected. Although this is done in the JOBS menu, it is necessary to recognize at this stage the method that is chosen, since separation threshold

values are entered within the contact tables. It obviously makes a difference if this threshold value is interpreted as a stress (absolute testing) or as a percentage (relative testing).

Four deformable contact bodies and four symmetry planes are defined. Different contact tables are needed to easily move the pin together with the bolt during the first loadcase by avoiding contact between the pin and the steel plate. During this first loadcase, separation between the pin and the bolt is not allowed by defining a large separation threshold. Then, during the second loadcase, contact between the pin and the steel plate is allowed, and the separation behavior between all bodies is based on realistic values: 10 percent of the maximum contact normal stress in the corresponding contact body. Since the insulation layer is significantly softer than the bolt, it is numerically preferable that nodes of the insulation layer contacts the bolt. This is achieved by setting the contact detection method from the second to the first body for this body combination. To maintain contact at the boundary of the bolt head, the delayed slide off option is invoked.

```

CONTACT
  CONTACT BODIES
    NEW
    NAME
      bolt
    DEFORMABLE
      OK
    ELEMENTS ADD
      bolt
  NEW
  NAME
    pin
  DEFORMABLE
    OK
  ELEMENTS ADD
    pin
  (repeat for deformable contact bodies insulation and steel_plate)
  NEW
  NAME
    symmetry_1
  SYMMETRY
    OK
  SURFACES ADD
    1
  END LIST (#)
  NEW

```

```
NAME
  symmetry_2
SYMMETRY
  OK
SURFACES ADD
  2
END LIST (#)
(repeat for symmetry bodies symmetry_3 and symmetry_4)
RETURN
CONTACT TABLES
NEW
NAME
  table_press_bolt
PROPERTIES
  1 2
    CONTACT TYPE: TOUCHING
    PROJECT STRESS-FREE
    SEPARATION THRESHOLD
      1e30
  1 3
    CONTACT TYPE: TOUCHING
    CONTACT DETECTION METHOD: SECOND ->FIRST
    PROJECT STRESS-FREE
    DELAY SLIDE OFF
  1 5
    CONTACT TYPE: TOUCHING
    PROJECT STRESS-FREE
  1 6
    CONTACT TYPE: TOUCHING
    PROJECT STRESS-FREE
  1 7
    CONTACT TYPE: TOUCHING
    PROJECT STRESS-FREE
  1 8
    CONTACT TYPE: TOUCHING
    PROJECT STRESS-FREE
```


(repeat for body combinations 2-6, 3-4, 3-5, 3-6, 3-7, 3-8, 4-5, 4-6, 4-7, 4-8)

OK

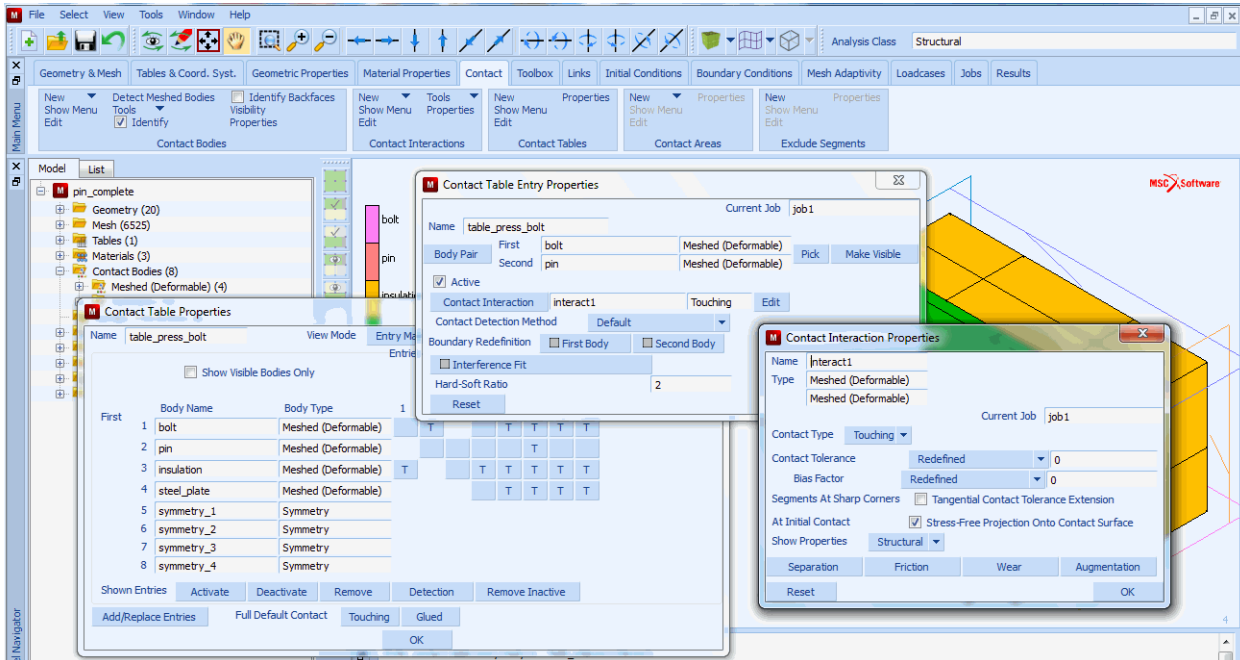


Figure 3.3-4 Settings of First Contact Table

COPY

NAME

table_depress_bolt

PROPERTIES

1 2

CONTACT TYPE: TOUCHING

SEPARATION THRESHOLD

0.1

2 4

CONTACT TYPE: TOUCHING

OK

Loadcases

The analysis is performed using two mechanical static loadcases, both with a loadcase time of one. The first is carried out in two *equally* sized steps, the second in one step. During the first loadcase, all boundary conditions are active and contact table `table_press_bolt` is selected. During the second loadcase, boundary condition `press_bolt` is deactivated and contact table `table_depress_bolt` is selected. The control settings are left default for the first

loadcase, while relative displacement checking with a tolerance of 0.05 is selected for the second loadcase, since the maximum reaction force drops due to removal of boundary conditions.

```
LOADCASES
  NEW
  NAME
    press_bolt
  MECHANICAL
  STATIC
  CONTACT
  CONTACT TABLE
    table_press_bolt
  OK
  # OF STEPS
    5
  OK
  NEW
  NAME
    depress_bolt
  STATIC
  LOADS
    press_bolt (deselect)
  CONTACT
  CONTACT TABLE
    table_depress_bolt
  OK
  CONVERGENCE TESTING
  DISPLACEMENTS
  RELATIVE DISPLACEMENT TOLERANCE
    0.05
  OK
  # OF STEPS
    1
  OK
  MAIN
  RETURN
```

Jobs

A mechanical job is created in which the two previously defined load cases are selected. The analysis is geometrically nonlinear, so the large displacement option is selected. During increment 0, the first contact table is selected to avoid wrong contact detection between the pin and the steel plate and to get stress-free initial contact. The contact tolerance and the bias factor are set to 0.005 and 0.9, respectively. In this way, a small contact tolerance due to the small elements in the bolt is avoided, while the outside contact tolerance remains small due to the bias factor. The separation method is set to relative stress-based, using the default tolerance of 0.1, and single-sided contact is activated. Notice, that the quadratic segment button “genuine” is turned on, indicating true quadratic contact. In addition to the default nodal post file variables, the equivalent von Mises stress is selected as an element variable. The element types used are 127 (10-node tetrahedral) for the bolt and 21 (20-node hexahedral) for the pin, insulation, and steel plate. After saving the model, the job is submitted for analysis.

```

JOBS
  MECHANICAL
    press_bolt (select)
    depress_bolt (select)
  CONTACT CONTROL
    ADVANCED CONTACT CONTROL
      RELATIVE SEPARATION STRESS
      OK
    OK
  ANALYSIS OPTIONS
    LARGE DISPLACEMENT
    OK
  JOB RESULTS
    EQUIVALENT VON MISES STRESS
    CENTROID
    OK
  ELEMENT TYPES
    MECHANICAL
      3-D SOLID
        127
      bolt
        127
      pin
        21
      insulation
        21

```

```
        steel_plate
      OK
    RETURN (twice)
  FILES
  SAVE AS
    pin_complete
  OK
  RETURN
  RUN
  SUBMIT 1
  OK
  MAIN
```

Results

After running the job, the post file is opened and some characteristic results are examined. [Figure 3.3-5](#) shows the deformations at the end of the first loadcase. Clearly, there is a gap between the pin and the steel plate. [Figure 3.3-6](#) shows the deformation at the end of the second loadcase and illustrates how contact between the pin and the steel plate is established. Finally, [Figure 3.3-7](#) shows the stress concentrations around the bolt-pin and pin-plate contact areas.

```
RESULTS
  OPEN DEFAULT
  DEF ONLY
  SCALAR
    Contact Status
  OK
  NEXT
  NEXT
  NEXT
  SCALAR
    Equivalent Von Mises Stress
  OK
```

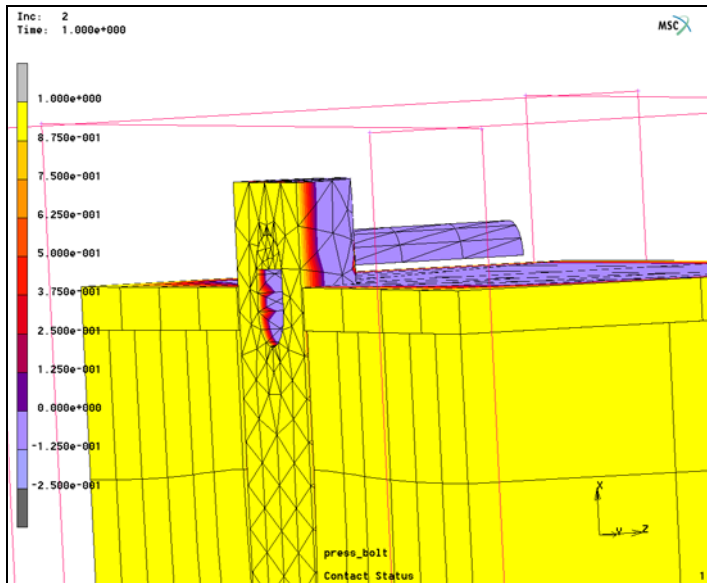


Figure 3.3-5 Contact Status and Deformations at End of First Loadcase

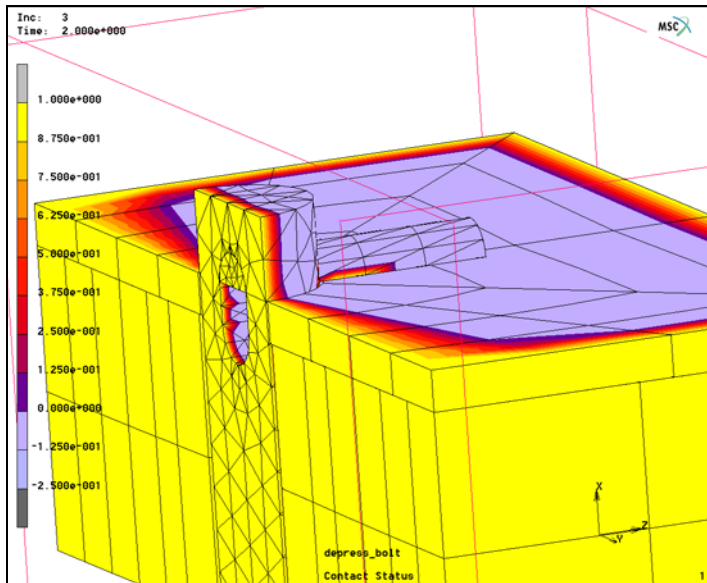


Figure 3.3-6 Contact Status and Deformations at End of Second Loadcase

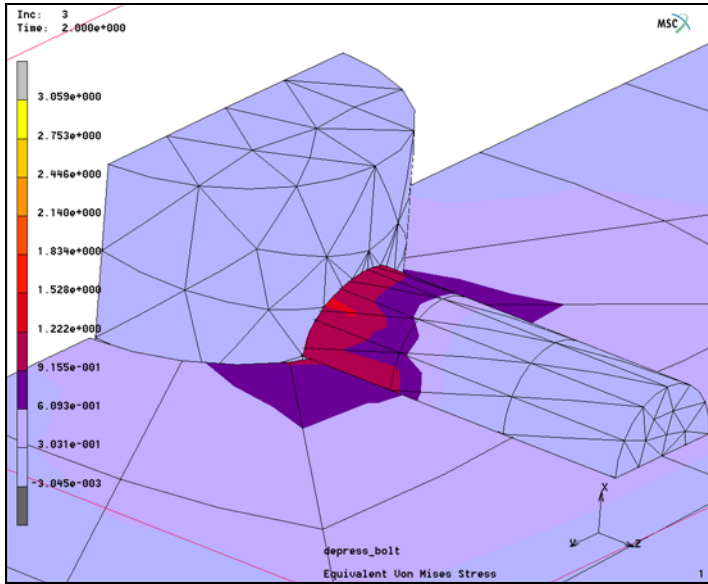
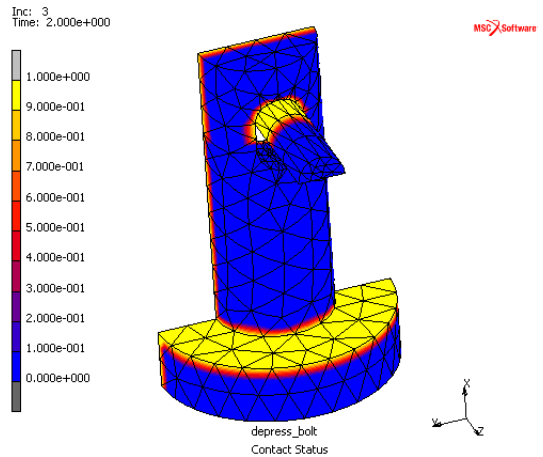
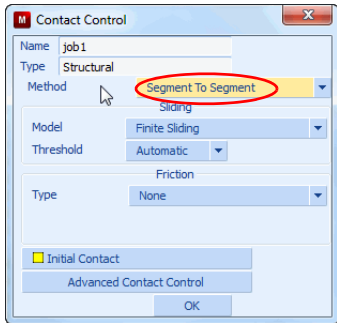


Figure 3.3-7 Equivalent von Mises Stress Around Bolt-pin and Pin-plate Contact Areas

As an alternative, one can use the segment-to-segment contact method with this model. In this case, double-sided contact is used. This capability is activated using the Job Contact Control menu as shown below. The contact status on the bolt and pin is also shown.



Contact Status using Segment-to-segment Contact

Input Files

The files below are on your [delivery media](#) or they can be downloaded by your web browser by clicking the links (file names) below.

File	Description
higher_order.proc	Mentat procedure file to run the above example
pin_fe_model.mfd	Associated model file

3.4 Beam Contact Analysis of an Overhead Power Wire of a Train

- Chapter Overview 946
- Pantograph of a Train Touching the Overhead Power Wire 946
- Input Files 962

Chapter Overview

This chapter demonstrates the beam-to-beam contact feature of Marc. The options required for a beam-to-beam contact analysis are discussed in detail. The capability is illustrated by the analysis of a pantograph of a train that touches the overhead wire to extract electrical power, while the train moves with a velocity of 40 m/s, or 144 km/h.

Pantograph of a Train Touching the Overhead Power Wire

The model consists of the pantograph of a train and the overhead power wire (see [Figure 3.4-1](#))

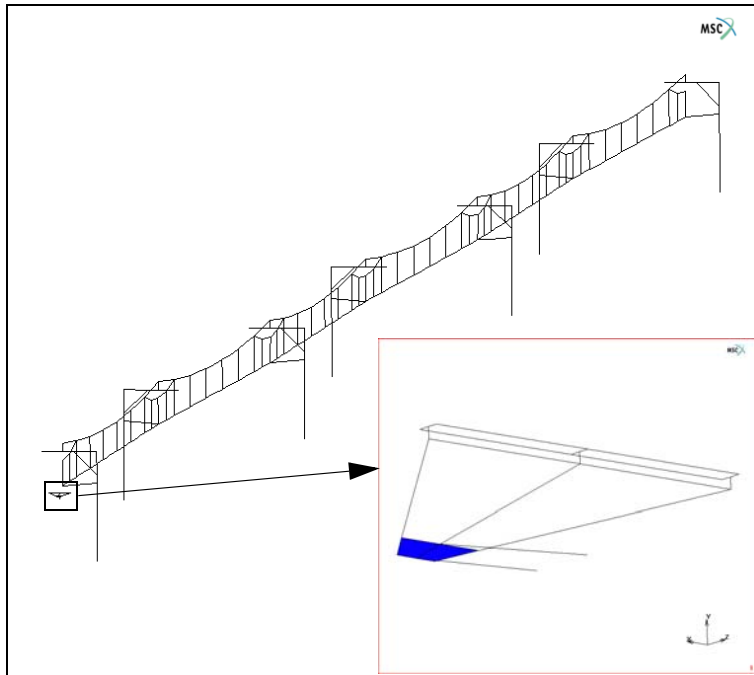


Figure 3.4-1 Model of the Pantograph and the Overhead Wire

The wire is located 5.5 m above the railway tracks and is suspended from a system of catenary wires and vertical droppers, that are fastened to seven mast poles (see [Figure 3.4-2](#)). Stabilizers restrict the horizontal movement of the wire. They are connected to the mast poles by pin joints. The masts are 70 m apart, resulting in a total track length of 420 m, and are positioned in such a way that the overhead power wire follows a zig-zag pattern between the masts with a maximum horizontal deflection of 60 cm. This ensures that any damage of the pantograph, that may occur due to friction with the power wire, is spread out over a large portion of the pantograph head.

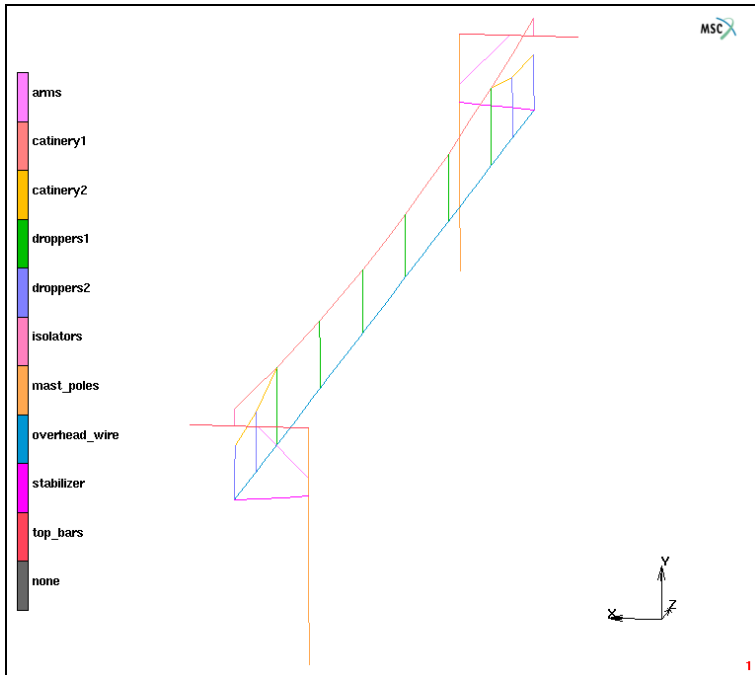


Figure 3.4-2 The Different Components of the Overhead Wire and the Mast Poles

The pantograph is a mechanism that consists of three parts: the lower frame and the thrust, the main frame, and the head (see [Figure 3.4-3](#)). The latter contains the horizontal bars that are pushed upwards to the overhead power wire to extract electrical power. The three parts are connected by hinges and nonlinear springs. The hinges allow only relative rotation of the connected parts around the global x-axis, while the nonlinear rotational springs add a certain amount of stiffness to this relative rotation. The pantograph head is pushed upwards by moving the end point B of the thrust in the negative z-direction, towards end point A of the lower frame. Once the head is in its final position, the hinges are locked. This is simulated by specifying the stiffness of the springs as a function of time: the stiffness is zero when the head is pushed upwards and is set to a large value once the head is its final position.

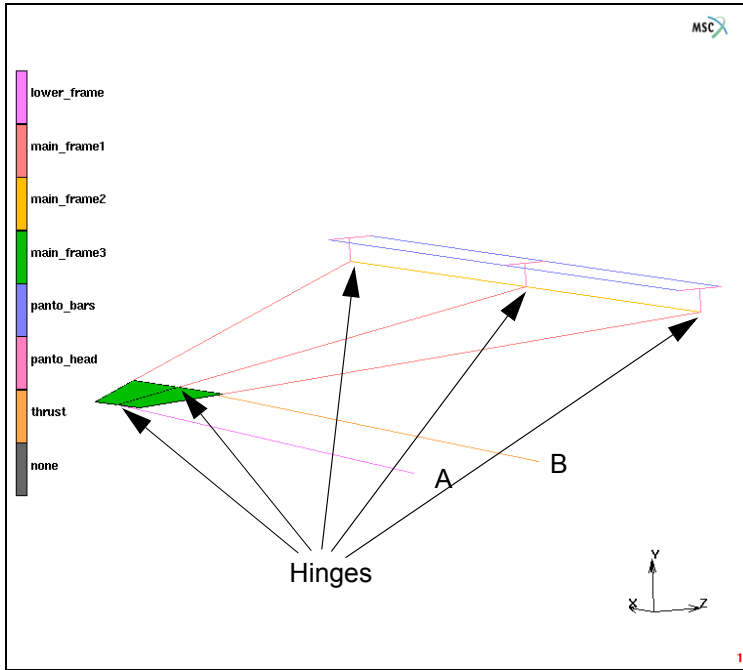


Figure 3.4-3 The Pantograph Example

Boundary Conditions

The analysis consists of three loadcases. In the first loadcase, a static pre-tension force of 30 kN is applied to the overhead power wire and the catenary wires. Simultaneously, a gravity load is applied to all elements in the model. In this stage, six of the seven mast poles are allowed to move freely in the z-direction while the other degrees of freedom are suppressed. The resulting boundary conditions on the overhead wire (except for the gravity load) are depicted in [Figure 3.4-4](#).

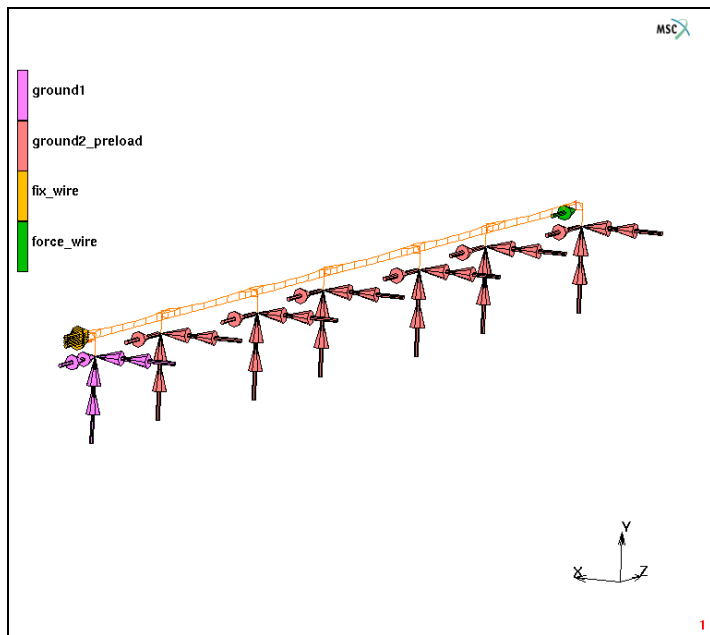


Figure 3.4-4 The Boundary Conditions (except the gravity load) on the Overhead Wire during the Static Preloading of the Wire

In the second stage of the analysis, the pantograph head is moved up towards the overhead wire. This is achieved by moving the end node (B) of the thrust in the negative z-direction, towards the end node of the lower frame (A). The displacements of the latter are suppressed in this loadcase. The rotation of the pantograph head and its displacement in the z-direction are suppressed by the boundary condition `fix_panto_head` (see Figure 3.4-5). The loads on the overhead wire are retained and the mast poles are all fixed to the ground.

In the final loadcase, the motion of the pantograph is prescribed: the nodes A and B are moved 400 m in the positive z-direction. The rotation of the pantograph head is no longer suppressed and the loads on the overhead wire are the same as in the second loadcase.

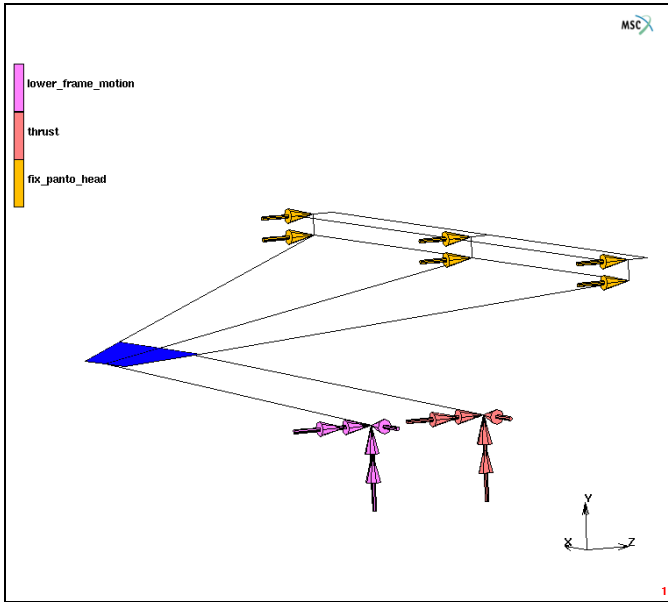


Figure 3.4-5 The Boundary Conditions (except the gravity load) on the Pantograph

Initial Conditions

The initial velocity of the all the nodes of the pantograph is set to 40 m/s.

Links

The stabilizers that restrict the horizontal movement of the overhead power wire are connected to the mast poles by means of beam pin joints (tying type 52). The hinges between the lower frame and the main frame, and between the main frame and the head of the pantograph consist of tying types 103 and 506, to suppress all relative displacements and the relative rotations about the y- and the z-axis. The stiffness of the nonlinear spring that acts on the relative rotation about the x-axis of the connected parts (the fourth degree of freedom) is defined as a function of time by means of a table: in the first two loadcases (0-2s), the stiffness is 0 Nm and in the last loadcase (2-12s), the stiffness is 1000000 Nm. The table is subsequently selected in the MECHANICAL PROPERTIES menu of the spring (see [Figure 3.4-6](#)).

```
LINKS
  SPRINGS/DASHPOTS
    TABLES
      NEW
        1 INDEPENDENT VARIABLE
          NAME
```

```

        spring_stiffness
    TYPE
        time
    ADD
        0 0
        1 0
        2 0
        2.001 1
        12 1
    FIT
    RETURN
NEW
PROPERTIES
    STIFFNESS
    SET
        1e6
    TABLE
        spring_stiffness
    OK
BEGIN NODE
    542
DOF 4
END NODE
    517
DOF 4
RETURN (twice)

```

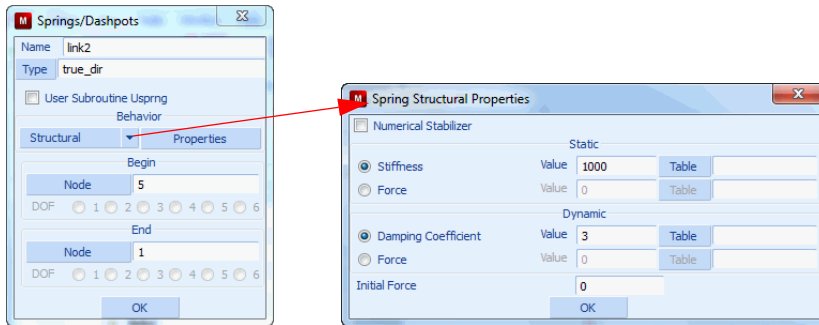


Figure 3.4-6 The SPRINGS/DASHPOTS Menu

Material Properties

The overhead wire, the catenary wire, and the vertical droppers are made of copper and the mast poles and the pantograph are composed of steel. Young's moduli of these materials are 120 GPa and 210 GPa, respectively, Poisson's ratios are given by 0.33 and 0.3, and the mass densities are equal to 8900 kg/m^3 and 7850 kg/m^3 . No material nonlinearities are taken into account in this example.

Geometry Properties

The beam-to-beam contact option assumes that the beam elements are cylinders with a circular cross-section. The radius of these cylinders, the *contact radius*, must be entered via the GEOMETRIC PROPERTIES menu (see [Figure 3.4-7](#)), along with the other parameters that define the actual shape of the cross-section for the stiffness computation of the beam elements. The contact radius is used for the detection of contact and in the multi-point constraint when contact is found. It must be defined for all beam elements that belong to a contact body. Furthermore, the contact radius must be the same for all elements in a contact body.

In the present example, the elements of the overhead wire and the horizontal bars of the head of the pantograph are part of a contact body (see below). Consequently, the contact radius must be defined for these elements.

GEOMETRIC PROPERTIES

3-D

NEW

NAME

overhead_wire

ELASTIC BEAM

AREA

$\text{pi} * 0.006 * 0.006$

Ixx

$\text{pi} * 0.006 * 0.006 * 0.006 * 0.006 / 4$


```

lyy
  pi*0.006*0.006*0.006*0.006/4
VECTOR DEFINING LOCAL X-AXIS
  1 0 0
CONTACT RADIUS
  0.006
OK
ELEMENTS ADD
SET
  overhead_wire
OK
NEW
NAME
  panto_bars
ELASTIC BEAM
AREA
  pi*0.01*0.01
Ixx
  pi*0.01*0.01*0.01*0.01/4
Iyy
  pi*0.01*0.01*0.01*0.01/4
VECTOR DEFINING LOCAL X-AXIS
  0 0 1
CONTACT RADIUS
  0.01
OK
ELEMENTS ADD
SET
  panto_bars
OK

```

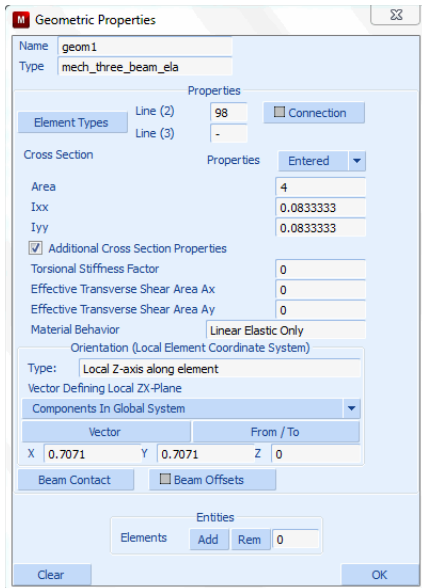


Figure 3.4-7 The GEOMETRIC PROPERTIES Menu for 3-D Elastic Beams

Contact

The first contact body consists of the beam elements of the overhead power wire. The second contact body contains the beam elements that constitute the horizontal bars of the pantograph head. Coulomb friction is taken into account in the analysis and the friction coefficients are set to 0.2 for both bodies.

CONTACT

CONTACT BODIES

NEW

overhead_wire

NAME

DEFORMABLE

FRICITION COEFFICIENT

0.2

OK

ELEMENTS ADD

overhead_wire

NEW

NAME

pantograph

```

DEFORMABLE
  FRICTION COEFFICIENT
    0.2
  OK
ELEMENTS
  panto_bars

```

Loadcases

As mentioned before, the analysis consists of three loadcases. In the first loadcase, the overhead wire and the catenary wires are loaded by the static preload, while, simultaneously, the gravity load is applied to all elements in the model. The `ground2_preload` boundary condition is chosen over the `ground2` boundary condition to allow six of the seven mast poles to move freely in the *z*-direction. The total loadcase time is 1 second and the loading is applied incrementally in 20 increments.

```

LOADCASES
  MECHANICAL
    NEW
    NAME
      preload
  STATIC
    LOADS
      ground2 (deactivate)
      OK
    CONVERGENCE TESTING
      DISPLACEMENTS
      OK
    # STEPS
      20
    OK

```

In the second stage of the analysis, the pantograph head is pushed upwards until it touches the overhead power wire. In this static loadcase, all mast poles are fixed to the ground (using the `ground2` boundary condition). The total loadcase time is again one second and the loading is applied incrementally in 20 increments.

```

NEW
NAME
  thrust

```

```

STATIC
LOADS
    ground2_preload (deactivate)
    OK
CONVERGENCE TESTING
DISPLACEMENTS
    OK
# STEPS
    20
    OK
    
```

The final loadcase of the analysis simulates the motion of the train. In this dynamic transient loadcase, the rotation of the pantograph head is no longer suppressed and the train moves with a constant velocity of 40 m/s in the positive z-direction. The total loadcase time is 10 seconds, so that the total displacement of the train is 400 m. The displacement is prescribed in 160 increments.

Note that in a dynamic contact analysis, where the single-step Houbolt dynamic operator is used (this is the default operator and is also employed in this example), nodes and also beam elements that are found in contact are not projected onto the surface unless the DYNAMIC CONTACT PROJECTION FACTOR in the NUMERICAL PREFERENCES menu is set to a nonzero value. The reason is that a nonzero projection factor may introduce undesired (artificial) inertia effects in the analysis.

A zero projection factor can lead to a gradual increase of the amount of penetration (even though the elements are in contact). In the case of beam elements, the amount of penetration may even grow to such an extent that the elements move through each other and separate. This can happen if the relative rotation of the beam elements is large, as illustrated in Figure 3.4-8.

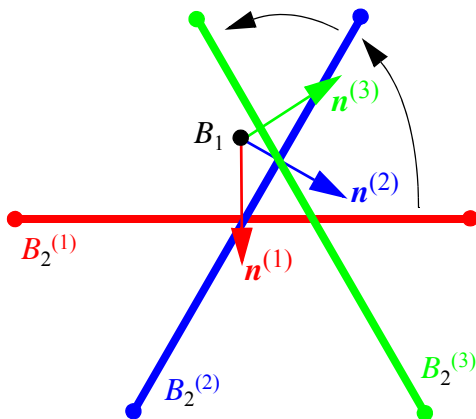


Figure 3.4-8 Penetration due to Zero Dynamic Contact Projection Factor

In this figure, the beam elements B_1 (oriented in the direction perpendicular to the plane) and B_2 are in contact and B_2 rotates around its current point in contact. Since the latter is continuously updated and since the multi-point constraint that suppresses the relative motion of the beams, acts in the direction of the current normal vector \mathbf{n} , the distance between the beam elements decreases gradually. If the dynamic contact projection factor is set to a nonzero value, a displacement correction is included in the multi-point constraint that ensures that the distance between the beam elements remains constant. In this example, the projection factor is set to 1.

```

NEW
NAME
    motion
DYNAMIC TRANSIENT
LOADS
    ground2_preload (deactivate)
    fix_panto_top (deactivate)
OK
CONVERGENCE TESTING
DISPLACEMENTS
    OK
NUMERICAL PREFERENCES
    DYNAMIC CONTACT PROJECTION FACTOR
        1
    OK
TOTAL LOADCASE TIME
    10
# STEPS
    160
    OK
RETURN (twice)

```

Job Parameters

The Coulomb friction model is selected in the CONTACT CONTROL menu and the relative sliding velocity is set to 1. Note that friction between beam elements is always based on nodal forces.

Beam-to-beam contact is activated in the ADVANCED CONTACT CONTROL menu (see [Figure 3.4-9](#)). Note that beam-to-beam contact automatically activates penetration checking per iteration and that separation is always based on nodal forces.

The LARGE DISPLACEMENT option, the UPDATED LAGRANGE PROCEDURE, and the LARGE ROTATION BEAM option are used. The latter improves the large rotation behavior of the beam elements.

Element type 98, a 2-node straight beam element including transverse shear effects, is automatically set for all beam elements in the model. Element type 75, a 4-node thick shell element, is used for the two shell elements of the main frame of the pantograph.

JOBS

NEW

MECHANICAL

preload

thrust

motion

INITIAL LOADS

ground2 (deactivate)

OK

CONTACT CONTROL

FRICTION TYPE

COULOMB

RELATIVE SLIDING VELOCITY

1

ADVANCED CONTACT CONTROL

BEAM TO BEAM CONTACT

ON

OK (twice)

ANALYSIS OPTIONS

LARGE DISPLACEMENTS

ADVANCED OPTIONS

UPDATED LAGRANGE PROCEDURE

LARGE ROTATION BEAM

OK (twice)

JOB RESULTS

1st Comp of Stress

2nd Comp of Stress

3rd Comp of Stress

4th Comp of Stress

OK (twice)

3-D MEMBRANE/SHELL

75

OK

ALL EXIST
RETURN (twice)

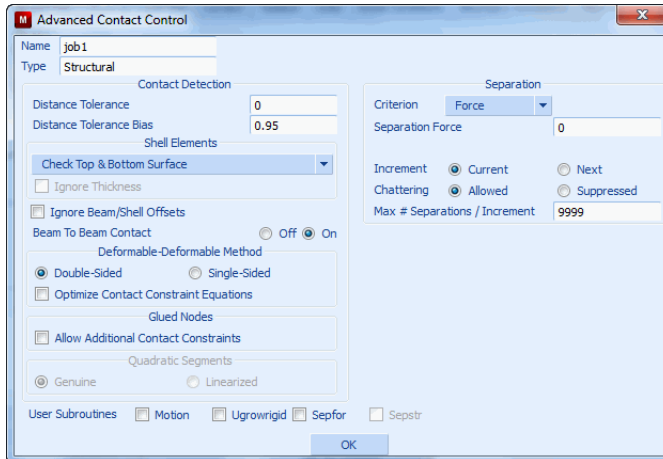


Figure 3.4-9 The ADVANCED CONTACT CONTROL Menu

Save Model, Run Job, and View Results

After saving the model, the job is submitted and the post file is opened.

```
FILE
  SAVE AS
    train.mud
  OK
  RETURN
RUN
  SUBMIT(1)
  OPEN POST FILE (RESULTS MENU)
```

Figure 3.4-10 shows the contact status of the nodes at increment 200, when the train is halfway down the track. Note that if two beam elements are in contact, the contact status of all four nodes involved in the contact is set to 1. Inspection of the contact status during the motion of the train reveals that from increment 334 through 337, due to friction and dynamic effects, contact between the pantograph and the overhead wire is lost.

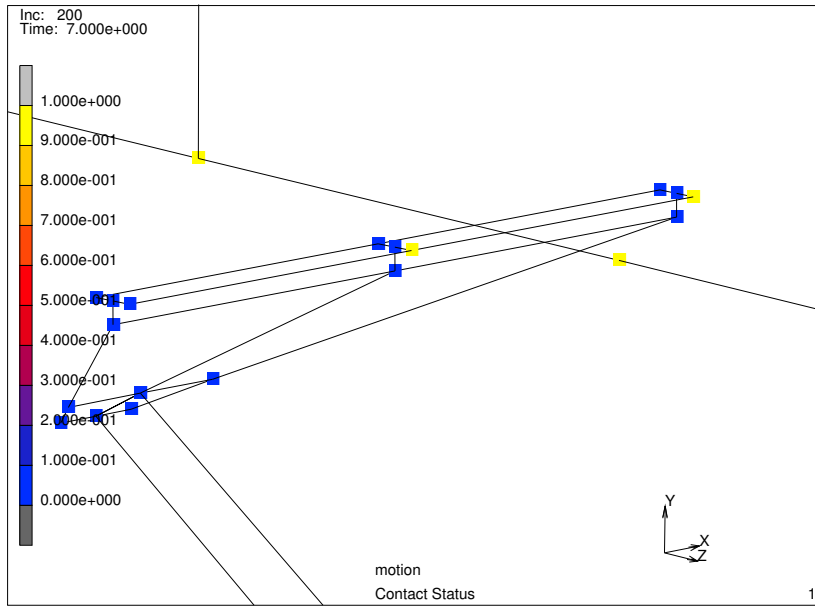


Figure 3.4-10 Contact Status at Increment 200

In [Figure 3.4-11](#), the friction forces on the nodes (again at increment 200), due to the contact between the pantograph and the overhead wire are depicted and [Figure 3.4-12](#) displays the velocity distribution of the overhead wire. Finally, the vertical displacement (in the y-direction) of the overhead wire at three positions (beginning, halfway and end) are plotted as a function of time in [Figure 3.4-13](#).

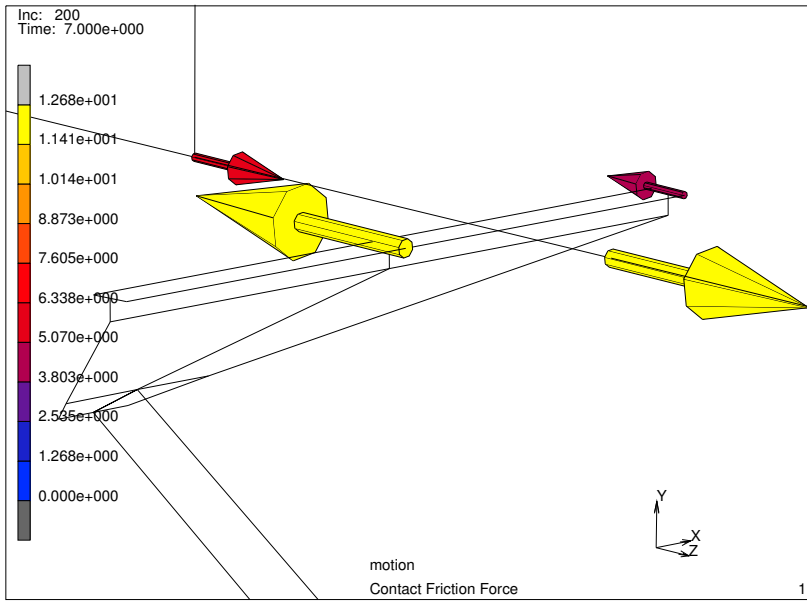


Figure 3.4-11 Friction Force at Increment 200

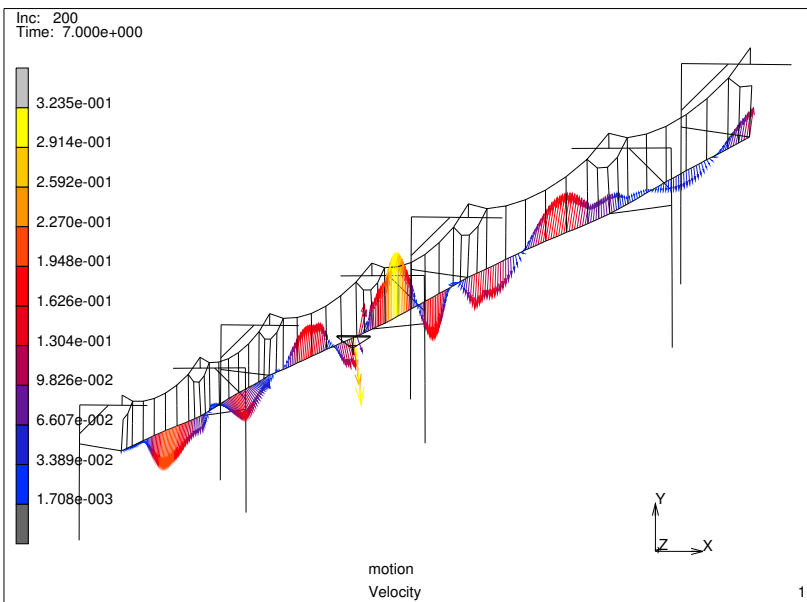


Figure 3.4-12 Velocity of the Overhead Wire at Increment 200

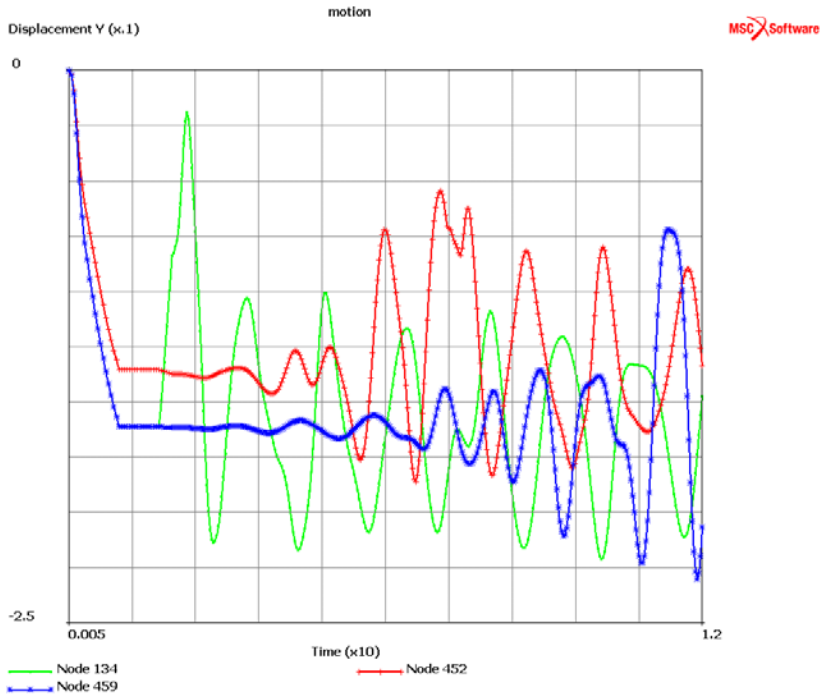





Figure 3.4-13 Displacement in the Y-direction of the Overhead Wire at the beginning of the Track

Note that the track shows node 134,  (green) curve, halfway down the track node 452,  (red) curve, and at the end of the track node 459,  (blue) curve as a function of time.

Input Files

The files below are on your [delivery media](#) or they can be downloaded by your web browser by clicking the links (file names) below.

File	Description
train.proc	Mentat procedure file to run the above example

3.5 Gas Filled Cavities

- Chapter Overview 964
- Simulation of an Airspring 964
- Input Files 978

Chapter Overview

This chapter demonstrates the modeling of gas filled cavities. The cavity option allows the automatic update of the cavity pressure as the cavity volume change. The application of this functionality can be found in several places: airsprings, athletic shoes with pneumatic soles, as well as lungs, etc. The simulation of an airspring is used as an example in this chapter. The example also employs the AXITO3D capability for automatic transfer of axisymmetric data to 3-D.

Simulation of an Airspring

Problem Description

Airsprings are flexible containers that inflate by compressed air and can be used as pneumatic actuators or vibration isolators. Depending on the inflation pressure, airsprings can provide variable amounts of loads and strokes. Airsprings are known for being versatile, robust and easy to maintain. The airspring model discussed in this example is constructed from cord-reinforced rubber clamped by metal beads.

The airspring is loaded in three stages: first clamping and inflation, followed by axial compression, and finally axial expansion with lateral deflection. The first two loading stages can be performed using an axisymmetric analysis. The axisymmetric model is then expanded into a 3-D model where the final loading step can be executed.

Figure 3.5-1 shows a 3-D schematic of the airspring. The airspring is initially cylindrical in shape with a length and diameter of 200 and 95 mm, respectively. The wall thickness is 1.7 mm. The airspring material is taken to be a rubber matrix with two layers of positively and negatively oriented skew rebars. The rubber is modeled using the Mooney constitutive model with $C_{10} = 3$ MPa and $C_{01} = 1$ MPa. The rebars are made of steel with $E = 210.0$ GPa and $\nu = 0.3$ with a cross-sectional area of 10^{-6} mm² and $\pm 45^\circ$ orientations.

The air inside the cavity of the airspring has a reference density of 1.0 kg/m³ at a reference pressure of 0.1 MPa and a reference temperature of 300°K and is assumed to follow the ideal gas law.

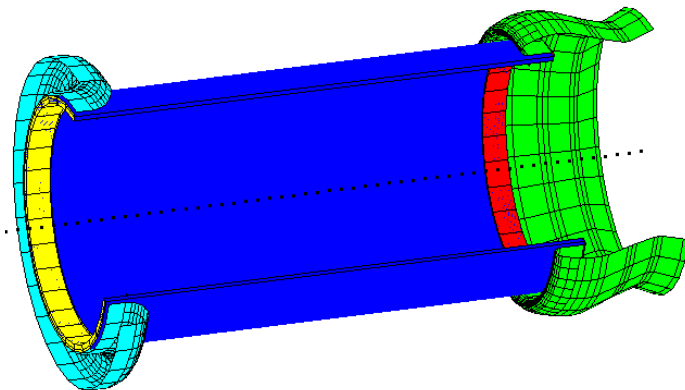


Figure 3.5-1 Schematic of the Airspring

Axisymmetric Analysis

An axisymmetric model for the airspring is shown in [Figure 3.5-2](#). The model is constructed of 100 4-noded axisymmetric rubber elements (element type 10) and 100 rebar elements (element type 144) sharing the same nodes. The airspring is first clamped and pressurized to 1.5 MPa. It is then subjected to an axial displacement of 150 mm by the left clamps. The loading is thus divided into two loadcases. The model file `airspring_axi.mfd` contains the complete model for the problem except for the cavity definition and the associated pressure load.

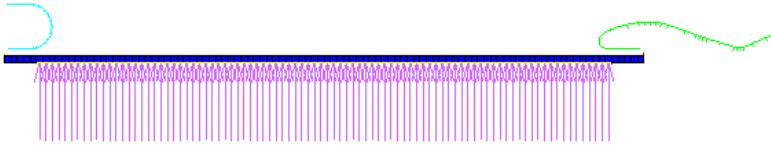


Figure 3.5-2 Axisymmetric Model of the Airspring

To define the cavity, the user needs to select the rubber element edges forming the cavity. The user can select these edges by first making only the rubber elements (element type 10) visible, then interactively selecting the edges shown in [Figure 3.5-2](#). For convenience, the cavity edges (edges 6:1 to 95:1) have already been selected and stored into a set named `cavity_edge_list` in `airspring_axi.mfd`. To open the model:

```
FILES
  OPEN
    airspring_axi.mfd
  OK
```

After opening the model and examining it, follow the steps described below to define the cavity and apply the cavity pressure load:

```
MAIN
  MODELING TOOLS
    CAVITIES
      NEW
        EDGES
          ADD
            ALL
              SET
                cavity_edge_list
              OK
    PARAMETERS
```

REF. PRESSURE
1.0E5
REF. TEMPERATURE
300.0
REF. DENSITY
1.0

MAIN

BOUNDARY CONDITIONS

NEW

MECHANICAL

MORE

CAVITY MASS LOAD

MASS

CLOSED CAVITY

OK

CAVITIES

ADD

ALL

EXISTING

NEW

CAVITY PRESSURE LOAD

PRESSURE

1.5E6

TABLE

table2

OK

CAVITIES

ADD

ALL

EXISTING

MAIN

LOADCASES

MECHANICAL

STATIC

LOADS

apply2

OK (twice)

```

NEXT
STATIC
    LOADS
        apply1
        OK (twice)
MAIN
    JOBS
        MECHANICAL
            INITIAL LOADS
                apply1
                OK
FILES
    SAVE AS
        airspring_axi_wcav.mfd
        OK
    
```

Figure 3.5-3 through Figure 3.5-5 show the CAVITIES menu, the CAVITY MASS LOAD menu, and the CAVITY PRESSURE LOAD menu.

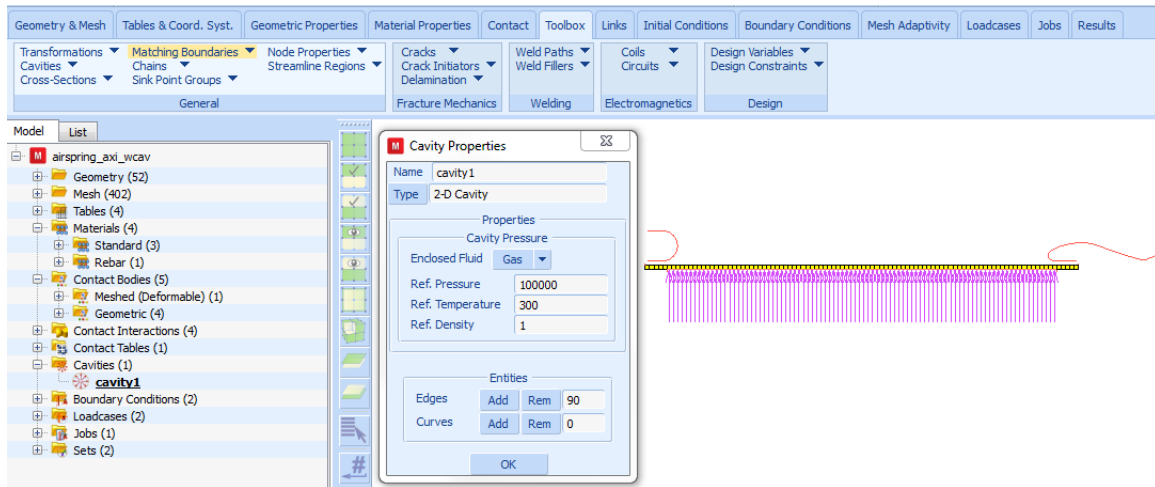


Figure 3.5-3 Cavities Menu

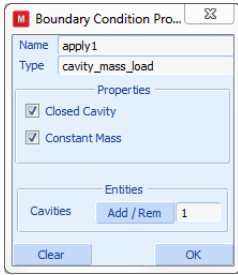


Figure 3.5-4 Cavity Mass Load Menu

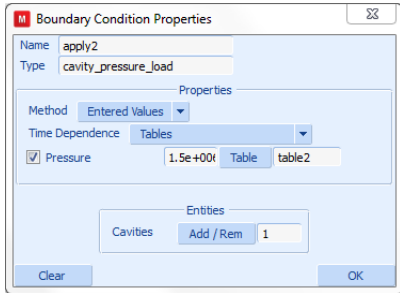


Figure 3.5-5 Cavity Pressure Load Menu

To run the job:

```
MAIN
  JOBS
    RUN
      RESET
      SUBMIT (1)
      MONITOR
      OK
  MAIN
  RESULTS
    OPEN DEFAULT
    DEF & ORIG
    MONITOR
    HISTORY PLOT
      COLLECT GLOBAL DATA
      NODES/VARIABLES
      ADD GLOBAL CRV
```



```

GLOBAL VARIABLES
  Time
  Pressure Cavity 1
FIT
REMOVE CURVE
CLEAR CURVES
ADD GLOBAL CRV
  GLOBAL VARIABLES
    Volume Cavity 1
    Pressure Cavity 1
  FIT
RETURN (twice)
CLOSE
  
```

The final deformed shape is shown in [Figure 3.5-6](#). [Figure 3.5-7](#) (a) and (b) show the variation of cavity pressure with time and with cavity volume, respectively.



Figure 3.5-6 Deformed Shape of the Axisymmetric Airspring Model

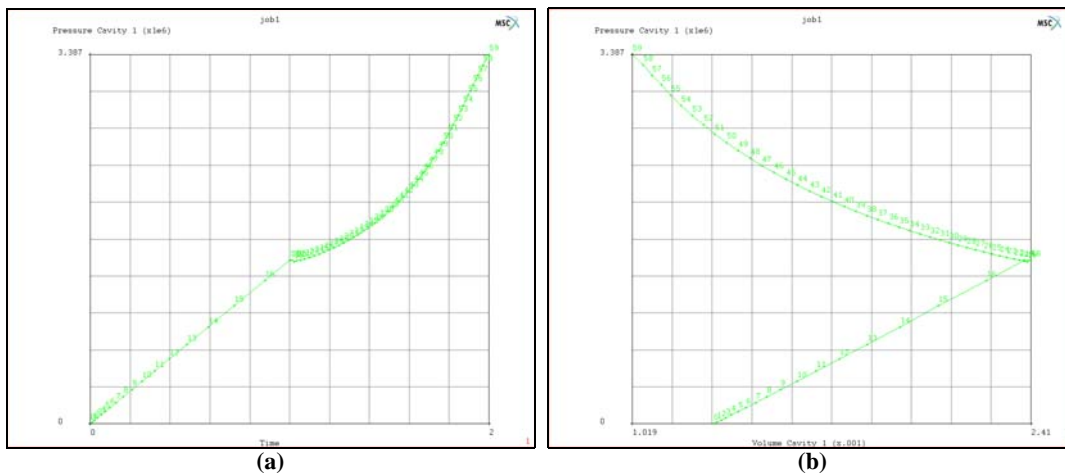


Figure 3.5-7 (a) Cavity Pressure vs. Time (b) Cavity Pressure vs. Volume

After reviewing the axisymmetric results and closing the post file, the next step is to transfer the axisymmetric model into 3-D where the axial expansion with lateral deflection can be applied. The AXITO3D option is used to perform the transfer. Before expanding the model into 3-D, the rigid contact bodies must first be moved to their final position at the end of the axisymmetric analysis.

```
MAIN
  MESH GENERATION
    MOVE
      TRANSLATIONS Y
        0.002
      CURVES
        1 3 4 6 7 8 #
      RESET
      TRANSLATIONS X
        0.15
      CURVES
        1 2 6 8 9 10 #
```

Follow the steps below to expand the axisymmetric model into 3-D.

```
MAIN
  MESH GENERATION
    EXPAND
      AXISYMMETRIC MODEL TO 3D
        ANGLE
          12
        REPETITIONS
          30
        TIME
          SET
            2
      EXPAND MODEL
MAIN
  INITIAL CONDITIONS
    MECHANICAL
      AXISYMMETRIC TO 3D
      POST FILE
        airspring_axi_wcav_job1.t16
      OK (twice)
```

Notice that during the model expansion to 3-D, the 2-D cavity has been automatically expanded into a 3-D one as indicated by the cavities menu in [Figure 3.5-8](#). Also notice that a new table, `table2.5`, has been created based on `table2` and has been used to apply the cavity pressure load. Contact bodies 2 and 3 are now moved and deflected using load control. A control node and an auxiliary node must first be defined.

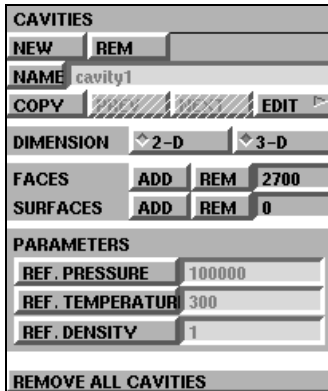


Figure 3.5-8 Cavity Menu after AXITO3D Expansion

```

MAIN
  MESH GENERATION
    NODES
      ADD
        0.15 -0.07 0.0
      ADD
        0.16 -0.07 0.0
  
```

This creates nodes 6061 and 6062. Contact bodies 2 and 3 are now switched to load control and associated with nodes 6061 and 6062 as control and auxiliary nodes. Contact body 4 position is fixed.

```

MAIN
  CONTACT
    CONTACT BODIES
      NEXT
      RIGID
        BODY CONTROL
          LOAD
            PARAMETERS
              ROTATION AXIS
                Z
  
```

```
                OK (twice)
LOAD CONTROL
  CONTROL NODE
    6061
  AUX. NODE
    6062
NEXT
RIGID
  BODY CONTROL
    LOAD
    PARAMETERS
    ROTATION AXIS
      Z
      1
    OK (twice)
LOAD CONTROL
  CONTROL NODE
    6061
  AUX. NODE
    6062
NEXT
RIGID
  BODY CONTROL
    POSITION
    PARAMETERS
    POSITION
      Y
      0
    TABLE
      CLEAR
    OK (twice)
```

Figure 3.5-9 shows the load control menu of bodies 2 and 3. The next step is to apply the displacements and rotations to the control and auxiliary nodes, respectively. This is accomplished on two loadcases: axial expansion followed by combined axial expansion and lateral deflection.

LOAD CONTROL		
CONTROL NOD	6061	CLEAR
AUX. NODE	6062	CLEAR
CENTER OF ROTATION		
0.15	-0.07	0

Figure 3.5-9 Load Control Menu for Contact Bodies 2 and 3

```

MAIN
  BOUNDARY CONDITIONS
    NEW
      MECHANICAL
        FIXED DISPLACEMENT
          DISPLACEMENT X
            -0.075
          TABLE
            table3
          DISPLACEMENT Y
            -0.01
          TABLE
            table1
          DISPLACEMENT Z
            0.0
        OK
      NODES
        ADD
          6061 #
    NEW
      FIXED DISPLACEMENT
        DISPLACEMENT X
          0.0
        DISPLACEMENT Y
          0.0
        DISPLACEMENT Z
          0.1
  
```

```
TABLE
  table1
OK
NODES
  ADD
    6062 #
```

The final step is to set up the loadcases and job parameters before submitting the job.

```
MAIN
  LOADCASES
    PREV
    MECHANICAL
      STATIC
        LOADS
          apply1 (add)
          apply2 (remove)
          apply3 (add)
          apply4 (add)
        OK
      CONSTANT TIME STEP
      # STEPS
        10
      OK
    NEXT
    STATIC
      LOADS
        apply3 (add)
        apply4 (add)
      OK
    CONSTANT TIME STEP
    # STEPS
      20
    OK
```

MAIN

JOBS

MECHANICAL

ANALYSIS DIMENSION

3-D

INITIAL LOADS

apply1 (remove)

apply2 (add)

apply3 (add)

apply4 (add)

icond1 (add)

OK (twice)

FILES

SAVE AS

airspring_axito3d_wcav.mfd

OK

MAIN

JOBS

RUN

RESET

SUBMIT (1)

MONITOR

OK

MAIN

RESULTS

OPEN DEFAULT

DEF ONLY

MONITOR

HISTORY PLOT

COLLECT GLOBAL DATA

NODES/VARIABLES

ADD GLOBAL CRV

GLOBAL VARIABLES

Time

Pressure Cavity 1

FIT

```
REMOVE CURVE
CLEAR CURVES
ADD GLOBAL CRV
  GLOBAL VARIABLES
    Volume Cavity 1
    Pressure Cavity 1
  FIT
RETURN (twice)
CLOSE
```

Figure 3.5-10 (a) and (b) shows the initial and final configurations of the airspring for the 3-D analysis.

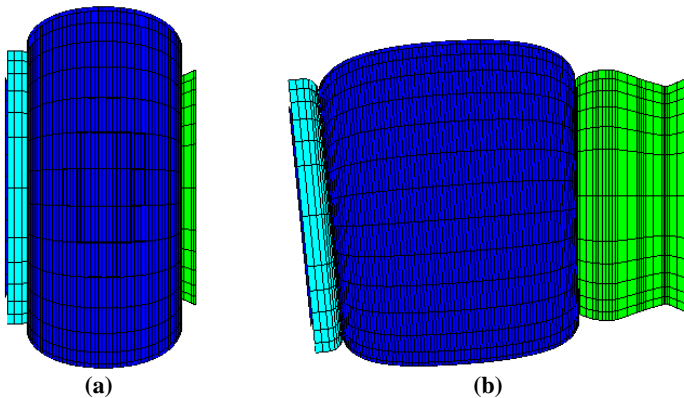


Figure 3.5-10 (a) Initial 3-D Configuration (b) Final 3-D Configuration

The loads applied to the control and auxiliary nodes as well as the number of fixed time steps used were selected such that the total solution time is reasonably small. For more expansion and deflection of the airspring, one can use the following:

- `table4` instead of `table3` for the x-displacement of node 6061
- `-0.05 m` for the y-displacement of node 6061
- `0.4 radians` for the rotation applied to node 6062
- `50 time steps` for loadcase 1
- `80 time steps` for loadcase 2

The final shape of the 3-D airspring using the above loading parameters is displayed in Figure 3.5-11. Figure 3.5-12 (a) and (b) shows the variation of cavity pressure with time and with cavity volume, respectively.

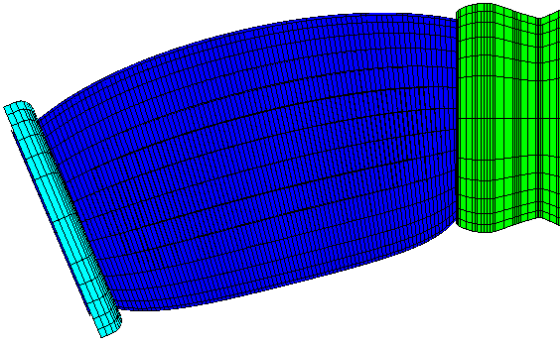


Figure 3.5-11 Final Configuration for 3-D Analysis at Higher Loads

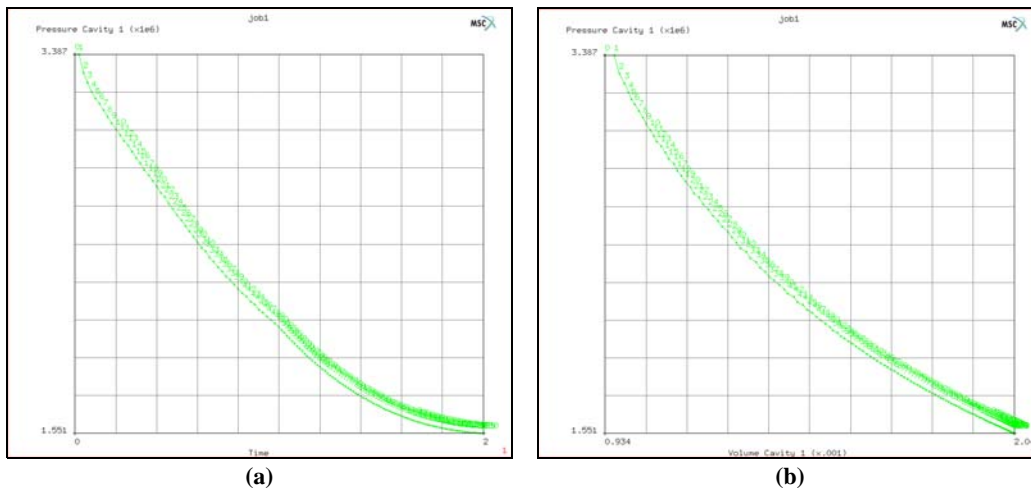


Figure 3.5-12 (a) Cavity Pressure vs. Time (b) Cavity Pressure vs. Volume

Figure 3.5-13 combines the curve in Figure 3.5-12 (a) for the 3-D analysis with that of Figure 3.5-7 (a) for the axisymmetric analysis and compares the combined curve with the case where the cavity option is not used. The comparison clearly shows the effect of using the cavity option on the airspring internal pressure and demonstrates its significance.

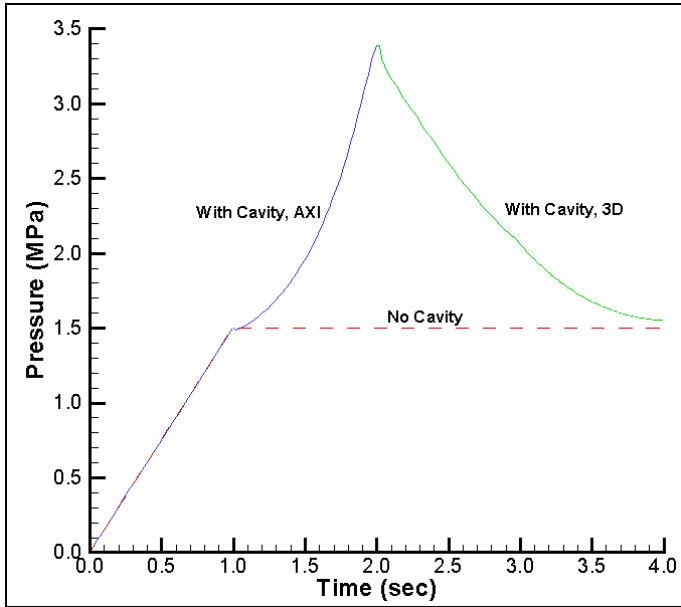


Figure 3.5-13 Cavity Pressure vs. Time with and without Cavity Option

Input Files

The files below are on your [delivery media](#) or they can be downloaded by your web browser by clicking the links (file names) below.

File	Description
airspring.proc	Mentat procedure file to run the above example
airspring_axi.mfd	Associated model file

3.6 Tube Flaring

- Chapter Overview 980
- Background Information 980
- Detailed Session Description 982
- Conclusion 1003
- Input Files 1004

Chapter Overview

The sample session described in this chapter analyzes the process of flaring. A cone-shaped flaring tool is pushed into a cylindrical tube to permanently increase the diameter of the tube end. Both the steel tube and flaring tool are modeled as deformable contact bodies. The goal of the quasi-static analysis described in this chapter is threefold:

- to determine whether the final shape of the tube meets the objective of the analysis
- to study whether residual stresses are present in the steel tube and flaring tool
- to determine the magnitude of the residual stresses (if present)

Background Information

This session demonstrates the analysis of a contact problem involving two deformable contact bodies, multiple materials, kinematic constraints and loads. The nonlinear nature of the problem along with the irreversible characteristics make it impossible to determine in advance the load required to drive the tool into the tube. As a result, multiple runs through the analysis cycle are necessary to determine the maximum load required to meet the objective of the analysis.

The diameter of the tube is 8 inches, the thickness is 0.3 inches and the length is 8 inches. The flaring tool is modeled as a hollow cone with an apex angle of 30° , a wall thickness of 0.6 inches, and a length sufficient to model the process.

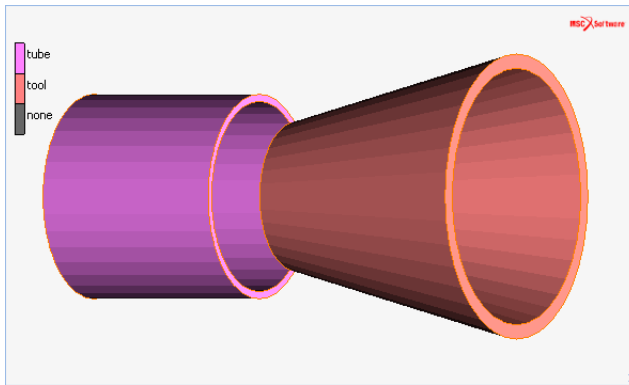


Figure 3.6-1 Cylindrical Tube and Flaring Tool

Idealization

The loading and geometry of the structure are symmetrical about the center line of the cylindrical tube. Due to the nature of the analysis, you are only required to analyze an axisymmetric model of the structure. If the appropriate boundary condition is prescribed, the tube is prevented from moving in the axial direction but is free to move in a radial direction at one end. A load is applied to the rim of the flaring tool to push it into the free end of the pipe.

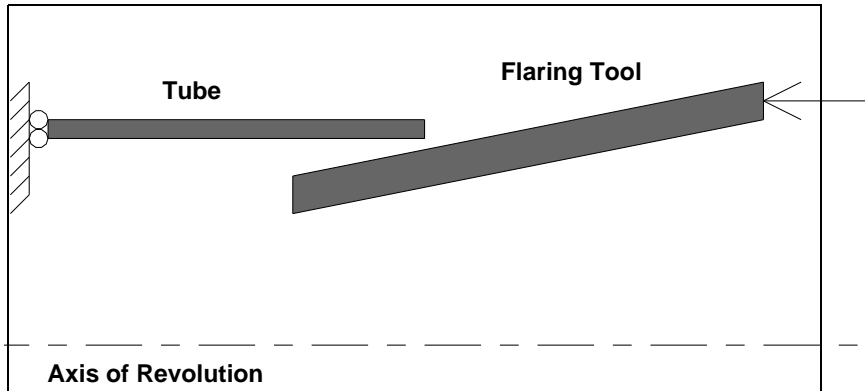


Figure 3.6-2 Axisymmetric Model of Tube and Flaring Tool

Requirements for a Successful Analysis

The analysis is considered successful when the flaring tool expands the tube diameter by 10%. You can plot the tool load versus the radial displacement at the tube end for several load increments to adjust the maximum load and repeat the analysis cycle until you reach the objective.

Full Disclosure

The steel tube is modeled by four-noded axisymmetric elements with a Young's Modulus of 30.0e6 psi and a Poisson's Ratio of 0.3. It is assumed that the tube material with an initial yield stress of 3.6e4 psi will not harden during the process. The tube diameter is 8.0 inches, and the thickness is 0.3 inches.

The flaring tool is modeled as a hollow cone with an apex angle of 30 degrees and a thickness of twice that of the tube with a suitable length to model the working area. The flaring tool is modeled as a case hardened steel object with a Young's Modulus of 40.0e6 psi, a Poisson's ratio of 0.3, an initial yield stress of 6.0e4 psi. The larger diameter end of the flaring tool is loaded to drive the smaller end of the flaring tool into the steel tube.

Overview of Steps

- Step 1:** Create a model of two patches and convert to finite elements. Apply kinematic constraints to the tube and add a low stiffness spring to avoid rigid body motions of the tool.
- Step 2:** Apply material properties to the tube and flaring tool.
- Step 3:** Create contact bodies.
- Step 4:** Apply edge loads to the larger diameter end of the tool to push it into the steel tube and create a loadcase.
- Step 5:** Create a job and activate appropriate large strain plasticity procedure.

Step 6: [Submit the job.](#)

Step 7: [Postprocess the results by looking at the deformed structure and a history plot of the tip deflection of the tube.](#)

Detailed Session Description

Step 1: Create a model of two patches and convert to finite elements. Apply kinematic constraints to the tube and add a low stiffness spring to avoid rigid body motions of the tool.

The approach used in this session to generate the model is the geometric meshing technique which involves converting geometric entities to finite elements. Refer to [Mesh Generation](#) in Chapter 1 for a detailed discussion on mesh generation techniques.

As in the sample session described in [Getting Started](#) in Chapter 1, the first step for building a finite element mesh is to establish an input grid. Click on the MESH GENERATION button of the main menu.

Next click on the SET button to access the coordinate system menu where the grid settings are located. Use the following button sequence to set a grid in the u domain between 0 and 8 with spacing 1 and in the v domain between 0 and 5 with spacing 1.

```
MAIN
  MESH GENERATION
    SET
      U DOMAIN
        0 8
      U SPACING
        1
      V DOMAIN
        0 5
      V SPACING
        0.5
      GRID (on)
      RETURN
    FILL
```

The geometric entity used in this session is a patch. The surface type used to enter a patch is a QUAD which is the default setting for surface types. Use the following button sequence to define the first patch:

```
MAIN
  MESH GENERATION
```

```
PLOT
  label POINTS
  RETURN
srf ADD
  point(0,4,0)
  point(8,4,0)
  point(8,4.5,0)
  point(0,4.5,0)
```

(on)
(Pick the following corner points from the grid)

These points are the four corners of the first patch defined as the cross-section of the cylindrical tube. Next, move the top two points of the patch to their exact location.

```
MAIN
  MESH GENERATION
    MOVE
      TRANSLATIONS
        0 -0.2 0
      POINTS
        3 4
      END LIST (#)
```

(Pick top 2 points)

The next step is to define a second patch for the cross-section of the flaring tool. Due to the conical shape of tool, it is best to use the cylindrical coordinate system to enter a set of points for the cone angle of 15° from the horizontal axis.

```
MAIN
  MESH GENERATION
    RECTANGULAR
    pts ADD
      5 15 0
      16 15 0
    GRID
    FILL
```

(to switch to CYLINDRICAL)
(to switch off the grid)

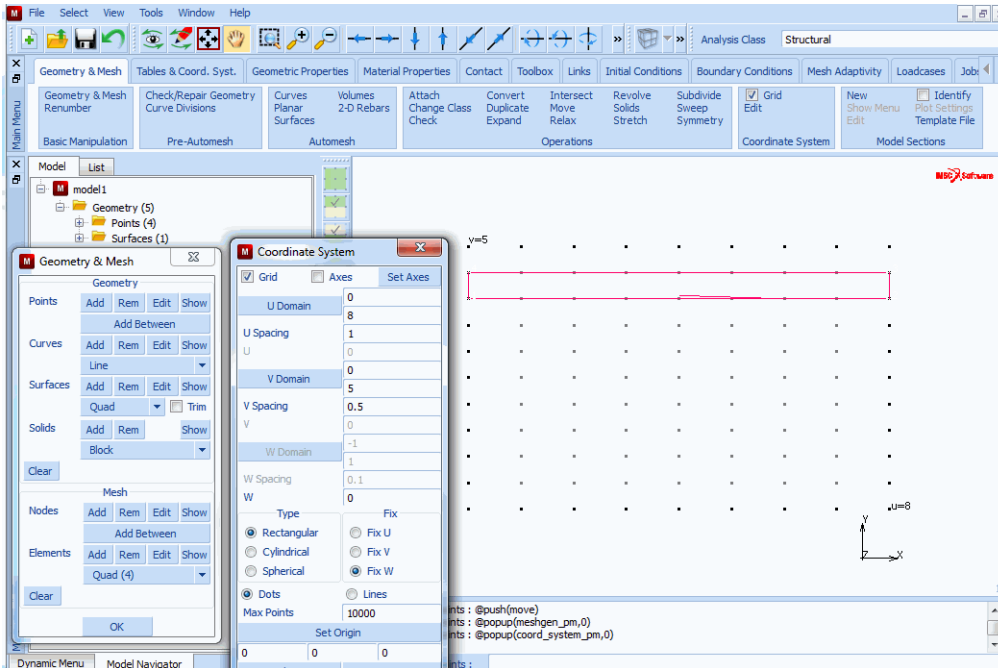


Figure 3.6-3 First Patch (Cross Section of Cylindrical Tube)

Before duplicating the newly generated points, it is important to realize that all operations are done in the local coordinate system. For now, simply change the coordinate system back to rectangular. This can be done by clicking on the CYLINDRICAL button twice.

Duplicate the just entered points and translate them 0.6 in the y-direction using the following button sequence to form the upper-corners of the flaring tool.

MAIN

MESH GENERATION

CYLINDRICAL

(to switch to SPHERICAL)

SPHERICAL

(to switch to RECTANGULAR)

DUPLICATE

TRANSLATIONS

0 0.6 0

POINTS

5 6

(Pick the two points generated above)

END LIST (#)

The four points for the second patch have now been defined. Use the `srf`s ADD command to enter the second patch.

MAIN

MESH GENERATION

`srf`s ADD

5 6 8 7

(Pick points in counter-clockwise direction)

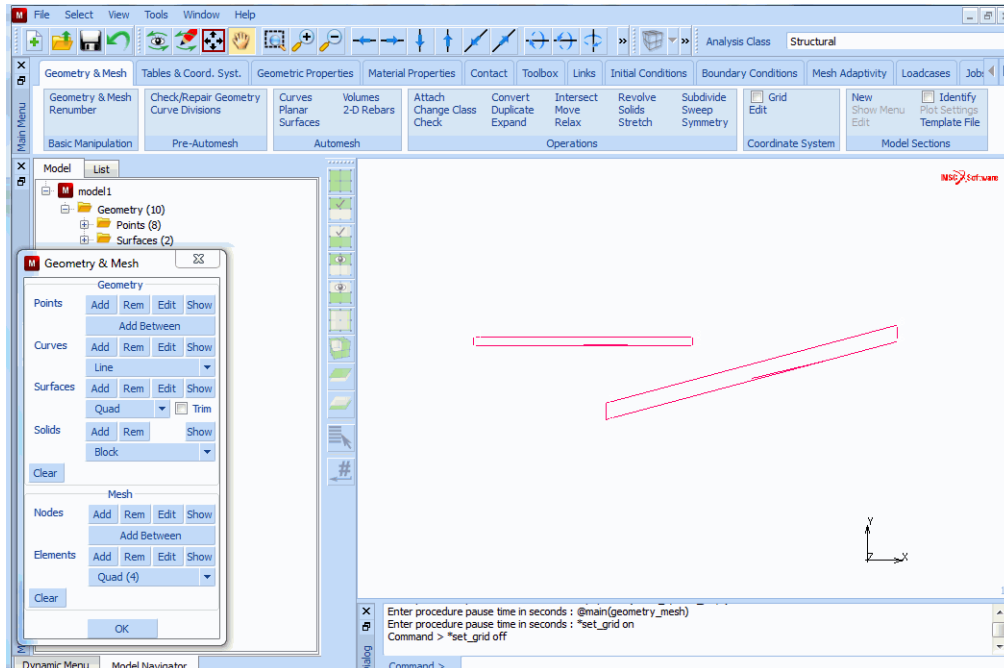


Figure 3.6-4 Second Patch (Cross Section of Flaring Tool)

Use the following button sequence to translate the second patch until it almost meets the cylindrical tube.

MAIN

MESH GENERATION

MOVE

TRANSLATIONS

0 1.25 0

SURFACES

2

(Pick the surface to move)

END LIST (#)

The two patches that outline the cylindrical tube and conical flaring tool respectively are shown in [Figure 3.6-5](#).

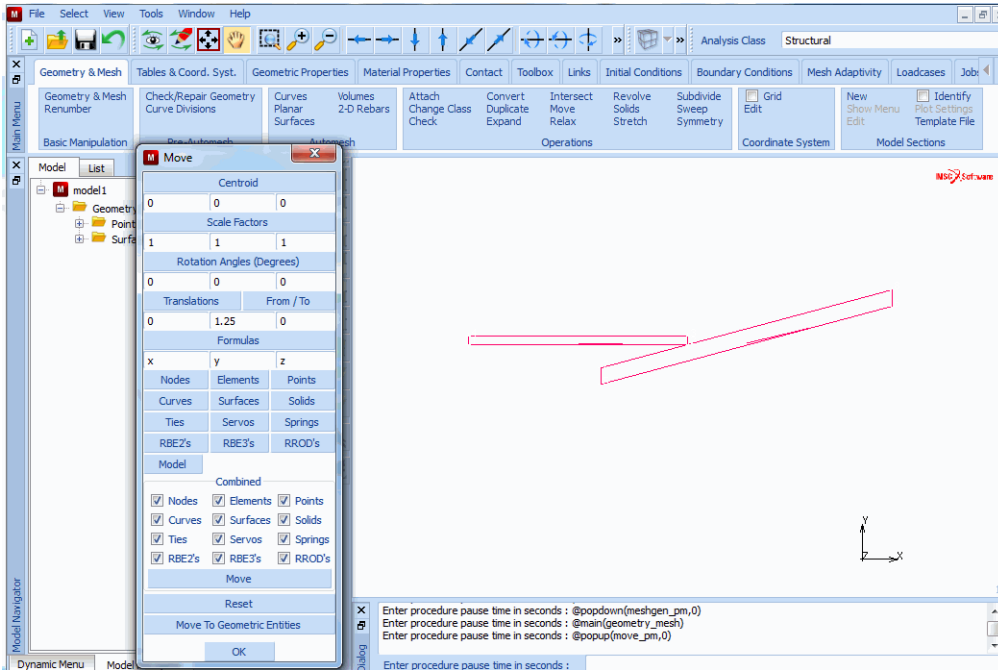


Figure 3.6-5 Tube and Flaring Tool Patches Defined

The two patches are converted to elements. The number of subdivisions is set to 8 x 3 for the cylindrical tube and to 14 x 6 for the conical flaring tool. Use the following button sequence to convert the two patches.

MAIN

MESH GENERATION

CONVERT

DIVISIONS

8 3

SURFACES TO ELEMENTS

1

(Pick the surface to convert)

END LIST (#)

DIVISIONS

14 6

SURFACES TO ELEMENTS

2

(Pick the surface to convert)

END LIST (#)

PLOT

draw POINTS

(off)

label POINTS

(off)

draw SURFACES

(off)

REGEN
RETURN

In this sample session, the CONVERT option is used instead of the AUTOMESH option. Although both options would create a finite element mesh, the CONVERT processor allows for better control of the element distribution.

Figure 3.6-6 shows the results of the conversion process.

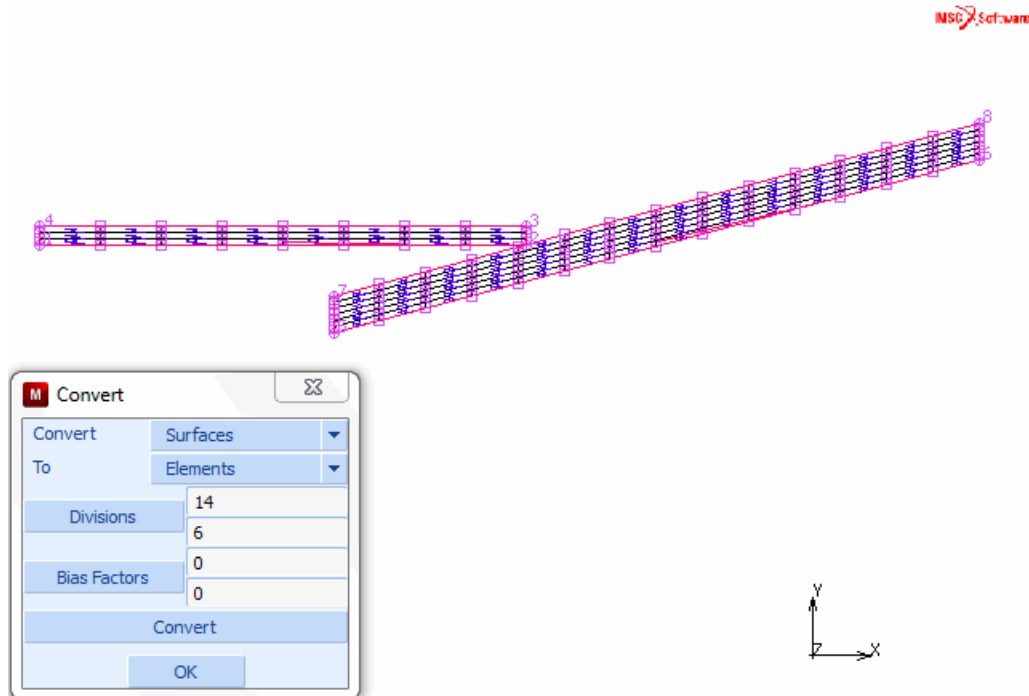


Figure 3.6-6 Tube and Flaring Tool Patches Converted

Once you have converted the two patches to elements, you can assign a Marc element type to the elements. Although Mentat assigns a default type to elements, based on the dimensionality of the problem, it is advised to explicitly set the element type. The element type selected for this analysis is Marc element type 10, a four-noded axisymmetric quadrilateral element. Use the following button sequence to select this element type for all existing elements (pick from row FULL INTEGRATION and column QUAD(4)).

MAIN

JOBS

ELEMENT TYPES

mechanical elements AXISYMMETRIC SOLID

10

(FULL INTEGRATION / QUAD(4))

OK
all: EXIST.

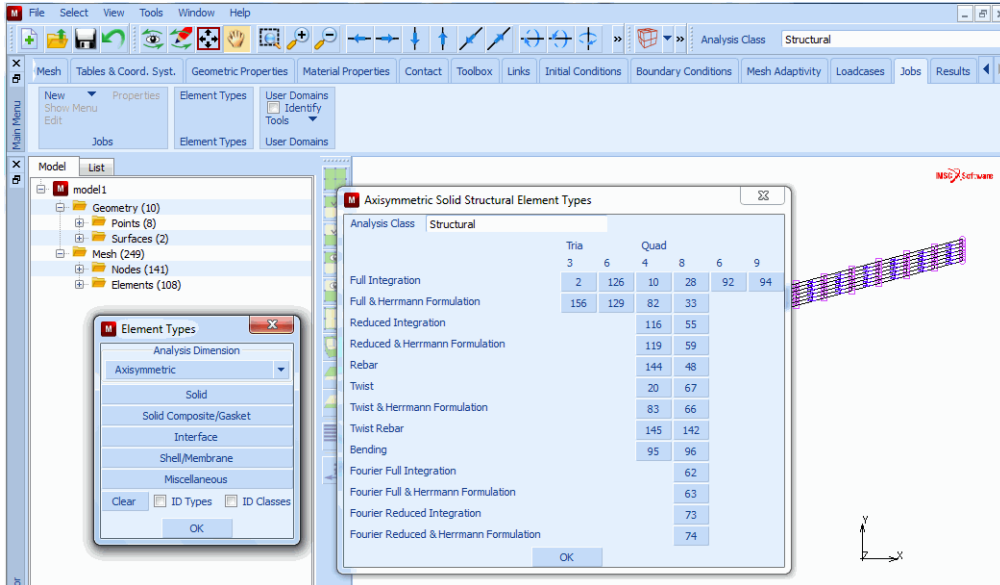


Figure 3.6-7 Select Marc Element Type

The displacement degree of freedom in the x-direction for the nodes at the far left end of the cylindrical tube is fixed.

MAIN

BOUNDARY CONDITIONS

MECHANICAL

FIXED DISPLACEMENT

DISPLACEMENT X

(on)

OK

nodes ADD

1 10 19 28

(Pick left row of nodes)

END LIST (#)

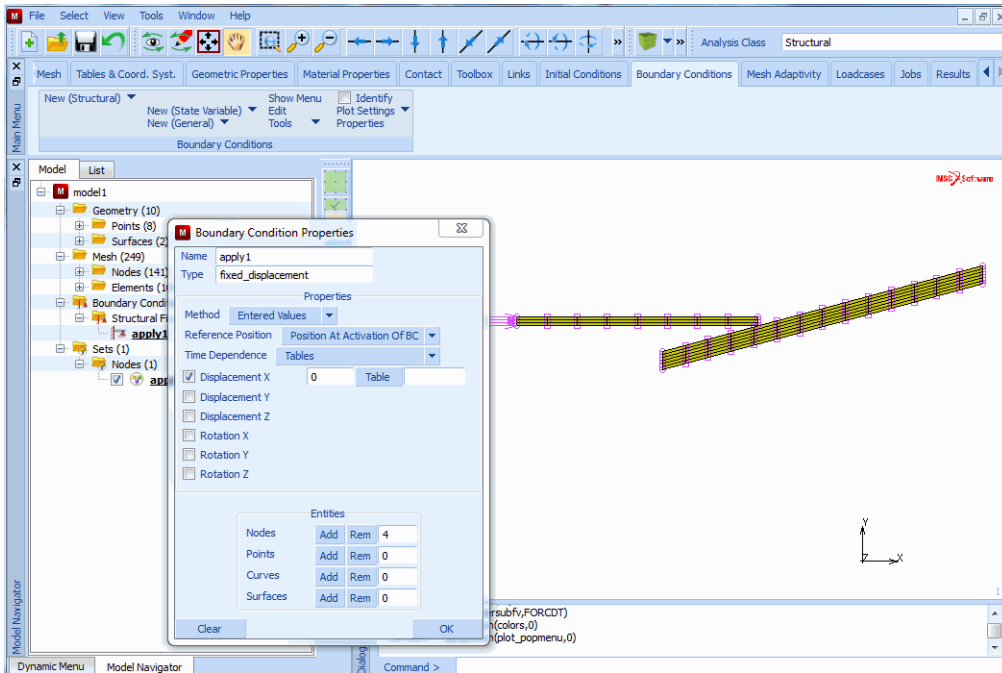


Figure 3.6-8 Fixed Nodes of Cylindrical Tube in X-Direction

The deformable tool will be loaded by a pressure load. If there is no contact between tube and tool, a rigid body mode is present. This rigid body mode can be removed by entering a weak spring between tube and tool. Enter a spring by using the following button sequence below:

MAIN

LINKS

SPRING/DASHPOT

ZOOM BOX

(create a zoom box by moving <↑>
while keeping <ML> depressed)

STIFFNESS

10.0e3

NODE 1

131

DOF 1

1

NODE 2

9

DOF 2

1

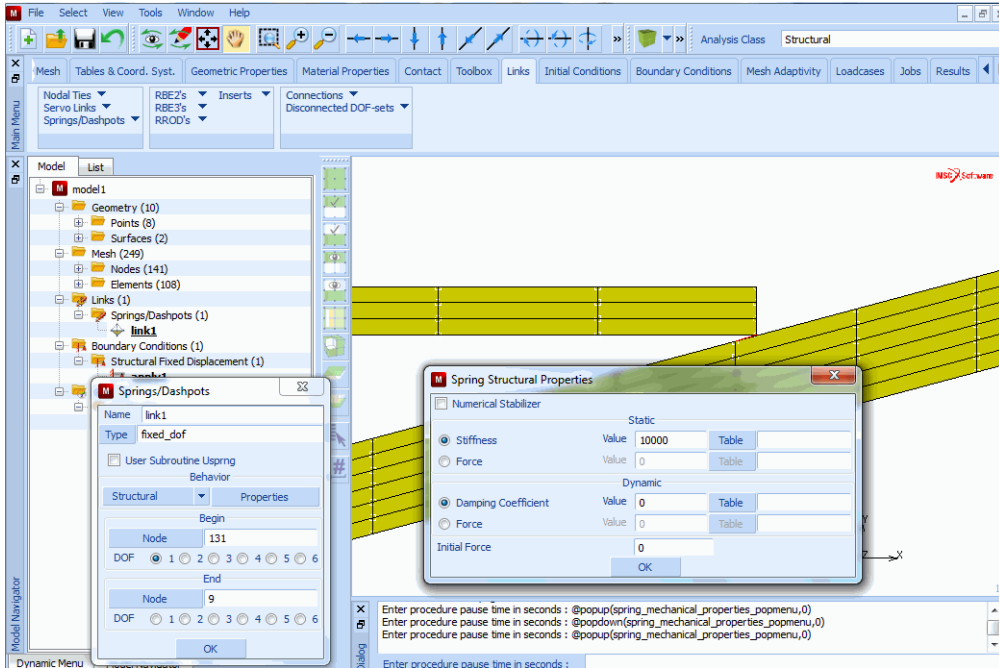


Figure 3.6-9 Specifying the Spring Between the Deformable Bodies

Step 2: Apply material properties to the tube and flaring tool.

Apply material properties to both the tube and flaring tool. The properties for the tube are different from those of the flaring tool. Use the following button sequence to assign the material to all elements of the tube.

MAIN

FILL

MATERIAL PROPERTIES

ISOTROPIC

YOUNG'S MODULUS

30.0e6

POISSON'S RATIO

0.3

PLASTICITY

INITIAL YIELD STRESS

3.6e4

OK (twice)
 elements ADD
 END LIST (#)
 ID MATERIALS

*(use the Box Pick Method to
 select all tube elements)*

(on)

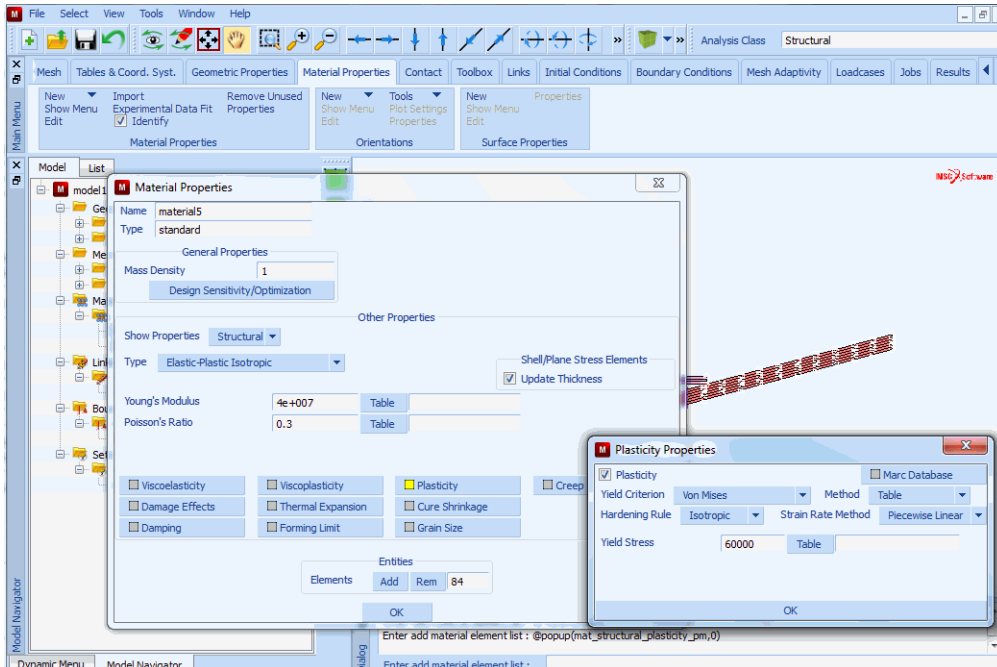


Figure 3.6-10 Material Properties Applied to all Tube Elements

Apply the material properties for all elements of the flaring tool using the following button sequence.

MAIN
 MATERIAL PROPERTIES
 NEW
 ISOTROPIC
 YOUNG'S MODULUS
 40.0e6
 POISSON'S RATIO
 0.3
 PLASTICITY
 INITIAL YIELD STRESS

```
6.0e4
OK (twice)
elements ADD
END LIST (#)
```

(Use the Polygon Pick Method to
select all tool elements)

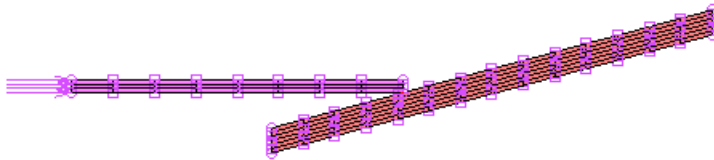
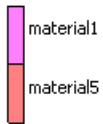


Figure 3.6-11 Material Properties Applied to all Elements

Step 3: Create contact bodies.

Identify the two contact bodies by storing the elements of each deformable body in a set using the following button sequence:

```
MAIN
CONTACT
CONTACT BODIES
NAME
tube
DEFORMABLE
OK
elements ADD
```

(Use the Box Pick Method to

select all tube elements)

END LIST (#)

NEW

NAME

tool

DEFORMABLE

OK

elements ADD

(Use the Polygon Pick Method to
 select all tool elements)

END LIST (#)

The easiest way to identify the contact bodies is to request the program to draw the bodies in different colors.

MAIN

CONTACT

CONTACT BODIES

ID CONTACT

(on)

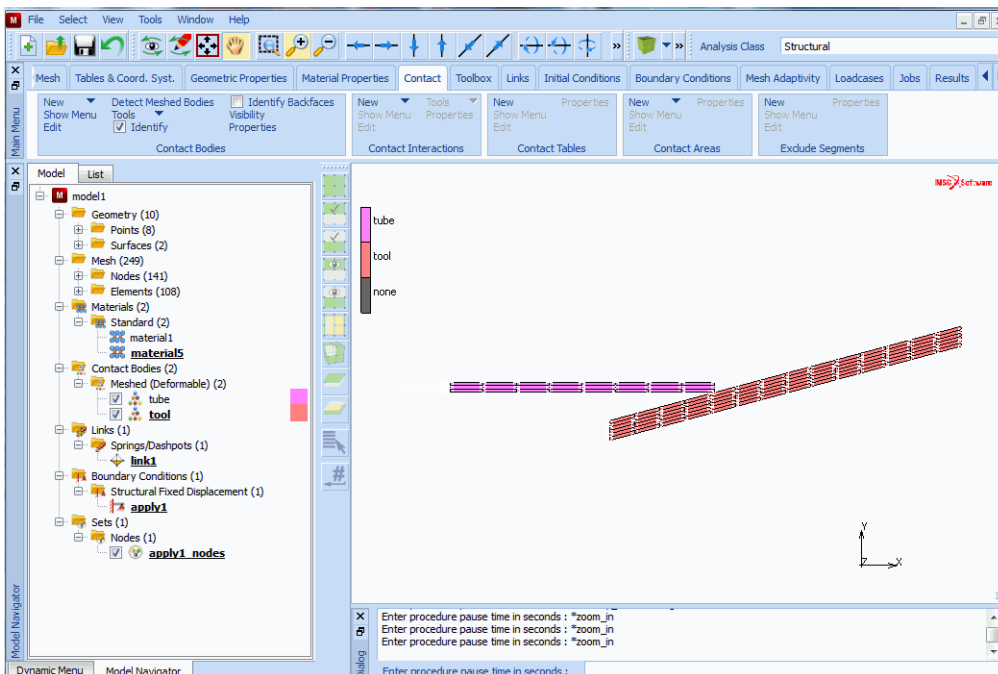


Figure 3.6-12 Identifying the Tube and Flaring Tool by Color

Although maybe not apparent in [Figure 3.6-12](#), the color of the tube is different from the flaring tool and is indicated in the key that appears in the upper left-hand corner of the graphics area. Click on ID CONTACT once again to switch off the PLOT IDENTIFY mode.

```
MAIN
  CONTACT
    CONTACT BODIES
      ID CONTACT (off)
```

Step 4: Apply edge loads to the larger diameter end of the tool to push it into the steel tube and create a loadcase.

The following button sequence defines a table to specify the loading of the flaring tool. [Figure 3.6-13](#) gives a graphical representation of the flaring tool being loaded.

```
MAIN
  BOUNDARY CONDITIONS
    MECHANICAL
      TABLES
        NEW
          1 INDEPENDENT VARIABLE
        NAME
          loading
        TYPE
          time (Select OK button only if type time was typed in)
        OK
        independent variable v1: MAX
          87
        independent variable v1: STEPS
          87
        function value f: MAX
          2400
        ADD
          0 0
          9 900
          39 2400
          8 0
        FILLED
```

SHOW TABLE
 SHOW MODEL

(Select **SHOW MODEL** from list)

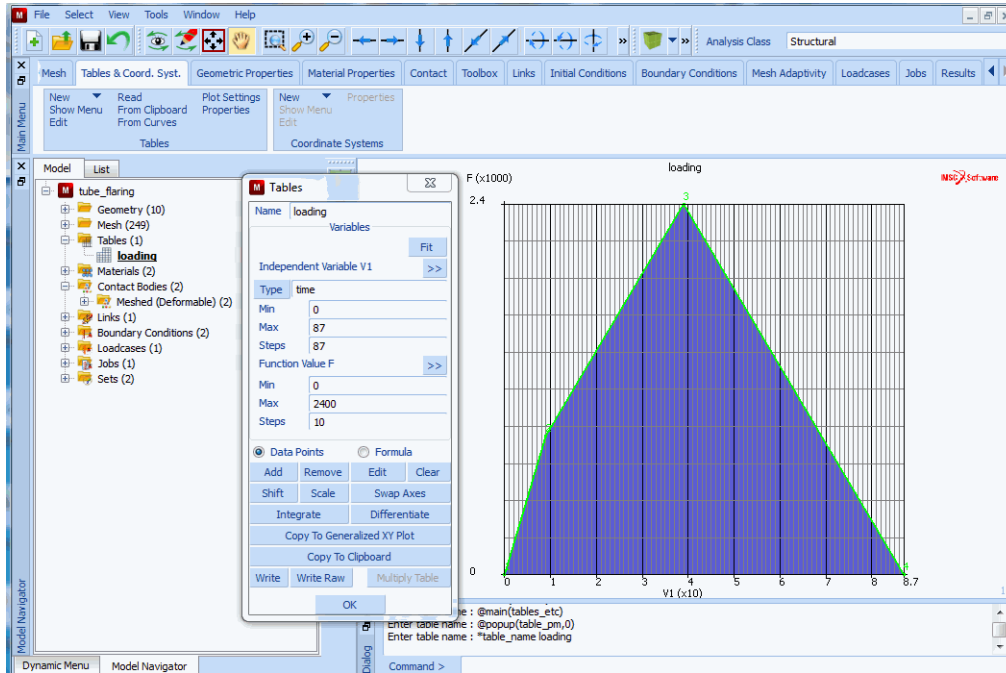


Figure 3.6-13 Loading of Flaring Tool

Apply the load to all edges at the far right end of the flaring tool.

MAIN

BOUNDARY CONDITIONS

MECHANICAL

NEW

EDGE LOAD

pressure TABLE

loading

OK (twice)

edges ADD

38:1 52:1 66:1 80:1 94:1 108:1

END LIST (#)

(Pick edges)

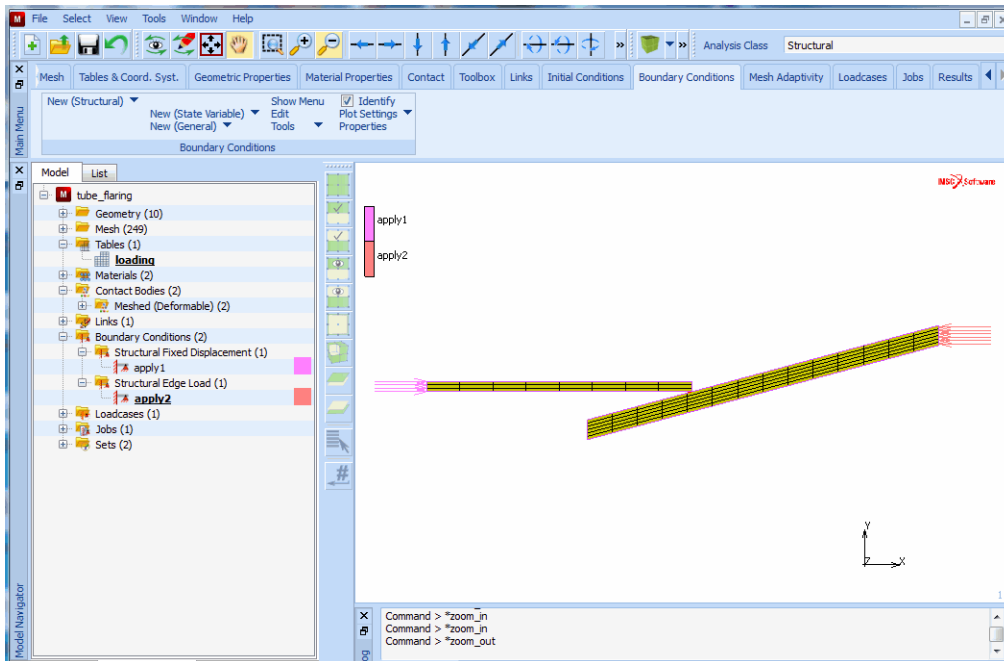


Figure 3.6-14 Loading Applied to Far Right End of Flaring Tool

The following button sequence creates a loadcase with the default name *lcase1*.

MAIN

LOADCASES

mechanical STATIC

LOADS

(select all loads - done by default)

OK

TOTAL LOADCASE TIME

87

STEPS

87

OK

Step 5: Create a job and activate appropriate large strain plasticity procedure.

Once you have defined the loadcase, activate the constant dilatation procedure for all elements to avoid numerical problems due to the incompressible plasticity and activate the large strain plasticity procedure based on the mean normal plasticity solution procedure.

Step 6: Submit the job.

Select the result to be written on the post file, switch to axisymmetric analysis, and submit the job.

```
MAIN
  JOBS
    MECHANICAL
      loadcases available
        lcase1
    ANALYSIS OPTIONS
      ADVANCED OPTIONS
        CONSTANT DILATATION (on)
        OK
        plasticity procedure SMALL STRAIN
                                          (Switch to large-strain additive procedure)
      OK
    JOB RESULTS
      available element tensors
        Stress
        Plastic Strain
      available element scalars
        Equivalent Von Mises Stress
        Total Equivalent Plastic Strain
      OK
    AXISYMMETRIC
      OK
  SAVE
  RUN
    SUBMIT 1
    MONITOR
```

Step 7: Postprocess the results by looking at the deformed structure and a history plot of the tip deflection of the tube.

The final phase of the analysis cycle (shown in [Figure 1.1-1](#) of *Introduction*) is postprocessing. Postprocessing involves viewing and evaluating the results of an analysis.

In order to evaluate analysis results with Mentat, you must have a post file which consists of analysis results from the finite element analysis program Marc.

A typical postprocessing session may consist of the following steps:

- Reading the post file created by submitting the job

- Creating a history or path plot of the model
- Displaying a plot of the model at specific increments
- Viewing different levels of stress types on the model

The results of the flaring process analysis have been saved in a post file. Use the following button sequence to open the file:

MAIN
RESULTS
OPEN DEFAULT
FILL

Zoom in on the area of contact for better access of the node that represents the tip deflection of the tube. The resulting close-up of the contact area shown in [Figure 3.6-15](#) should now appear in the graphics area.

MAIN
RESULTS
ZOOM BOX

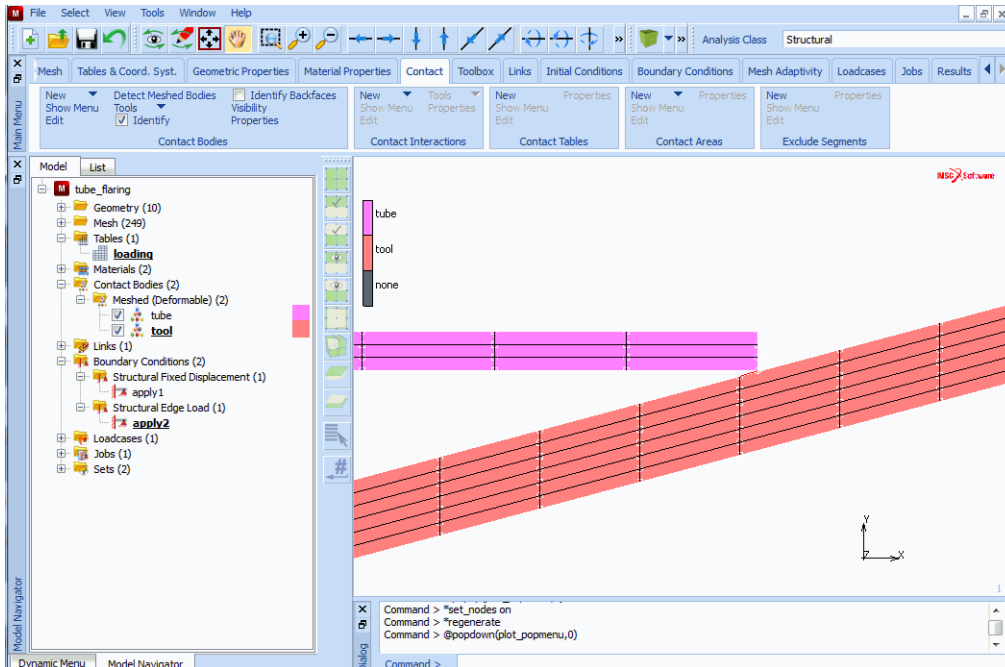


Figure 3.6-15 Close up of Contact Area

The objective of the analysis, stated in [Requirements for a Successful Analysis](#), requires a plot that demonstrates the tip displacement versus the load. Since the loading pattern is given in [Figure 3.6-13](#), a displacement versus the increment plot can also be used. The tip displacement in y-direction on the inner diameter of the tube is collected and displayed using the HISTORY PLOT option.

```
MAIN
  RESULTS
    HISTORY PLOT
      SET NODES
        9
      END LIST (#)
    COLLECT DATA
      0 100 1
```

The 0 is the first history increment, 100 the last history increment, and 1 is the increment step size. The program reads the increments indicated by the message `Collected increment (number)` in the dialogue area.

Once all the data for a plot has been collected, it can be displayed in a diagram where the increment number is the x-axis variable and the displacement in the y-direction is the y-axis variable. The FIT option allows you to view the history plot in the graphics area. Use the following button sequence to display the graph:

```
NODES/VARIABLES
  ADD 1-NODE CURVE
    9 (from the NODES panel)
    Increment (from the GLOBAL VARIABLES panel)
    Displacement Y (from the VARIABLES AT NODES panel)
  FIT
```

Recall the objective of our analysis: to expand the tube diameter by 10%. The Y-axis variable, displacement y, has to reach a value of 0.4 in the unloaded configuration to meet the objective.

Click on the YMAX button and enter 0.5. Set the following plot settings to label the history graph.

```
MAIN
  RESULTS
    HISTORY PLOT
      SHOW IDS
        10
      XSTEP
        20
```

```
YSTEP
    20
YMAX
    0.5
FILL
SHOW TABLE
SHOW MODEL      (Switch to SHOW MODEL to view the model)
```

The maximum value for y-displacement is obtained in increment 39. After this increment, the flaring tool is unloaded. The overshoot is necessary to obtain a 10% permanent diameter increase in the load-free state.

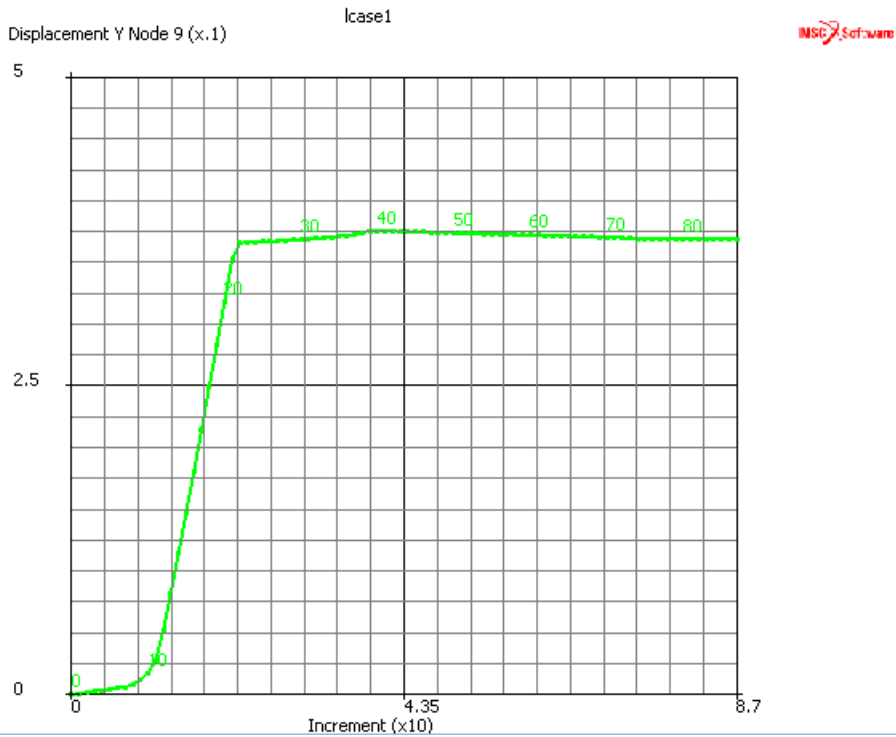


Figure 3.6-16 History Plot of Node 9 over 87 Increments

To better understand the process, it is helpful to look at an animation of the deformation of the tip of the tube. Return to the postprocessing results panel and click on the DEF & ORIG button to view both the original and the deformed structure. At this point, drawing the nodes and the internal edges of the mesh is no longer necessary.

Use the following button sequence to change the plot settings so that only the outline edges of the model are displayed.


```
MAIN
  PLOT
    elements SETTINGS
      OUTLINE (on)
      FACES (off)
      RETURN
    draw NODES (off)
  REGEN
  FILL
```

Once the nodes and element faces of the interior mesh have been suppressed, leaving only an outline of the two structures, you get a much clearer picture of the extent of the deformation that has taken place.

For animation purposes, the data that is processed needs to be condensed. The data is automatically condensed and written to disk for each frame of animation. Once this process has been completed, the frames can be traversed when shown in playback mode. Use the following button sequence to condense the data and activate the playback.

```
MAIN
  RESULTS
    REWIND
    NEXT
    DEF & ORIG
    MORE
    ANIMATION
      create INCREMENTS
      100 1
      FILL
      PLAY
      SHOW MODEL (To display the model)
```

The 100 increments is a user-defined upper limit of the number of frames that are to be created for the animation. The numeral 1 on the same line represents the interval at which to create a frame. In this case, each increment is defined to be a frame. The SHOW MODEL command is selected to switch from the *animation view* back to the *model view*.

The von Mises stresses induced by the flaring process on the model can be viewed using the following button sequence:

```
MAIN
  RESULTS
```

SKIP TO INC
39
SCALAR
Equivalent von Mises Stress
OK
CONTOUR BANDS

The resulting model shown in [Figure 3.6-17](#) clearly indicates that the von Mises stress is concentrated in two areas: the tip of deflection, where the tube made contact with the tool, and in the area where the tube is deformed.

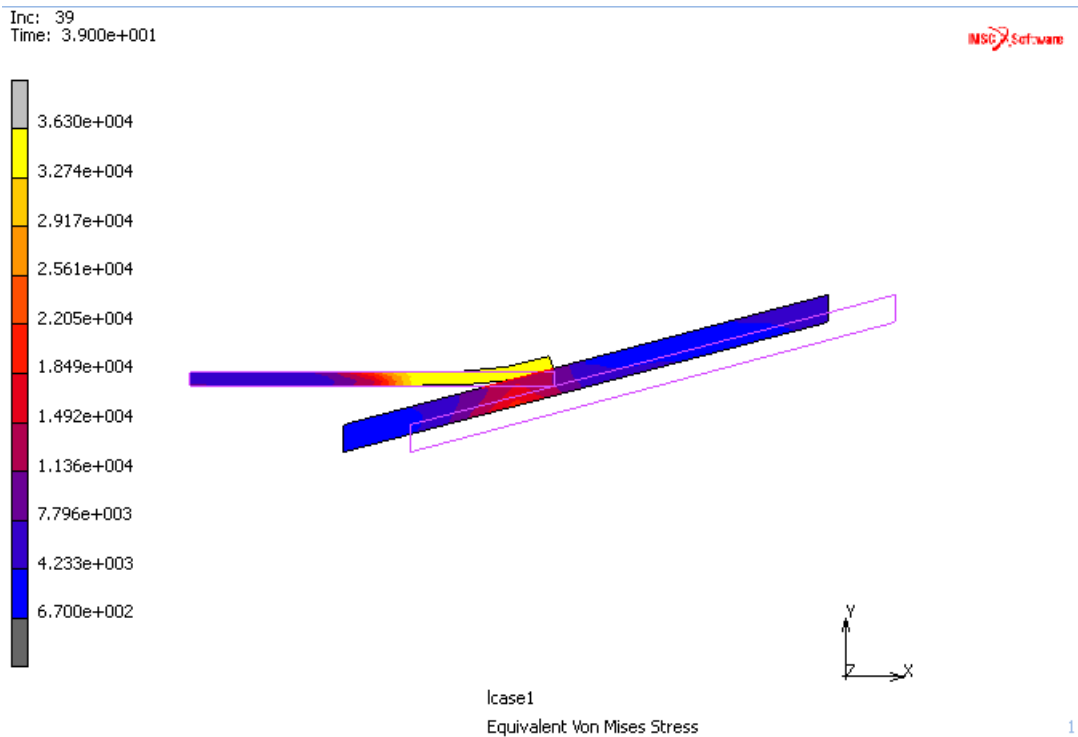


Figure 3.6-17 Plot of Original & Deformed Tube showing von Mises Stresses at Increment 39

Next, you can check the model for the plastic strain. Since you have already specified the increment and have contour bands selected, you only need to click on SCALAR and Total Equivalent Plastic Strain from the pop-up menu to check for permanent deformation. The resulting model, shown in [Figure 3.6-18](#), indicates where plastic strain is found.

Inc: 39
Time: 3.900e+001

MSC Software

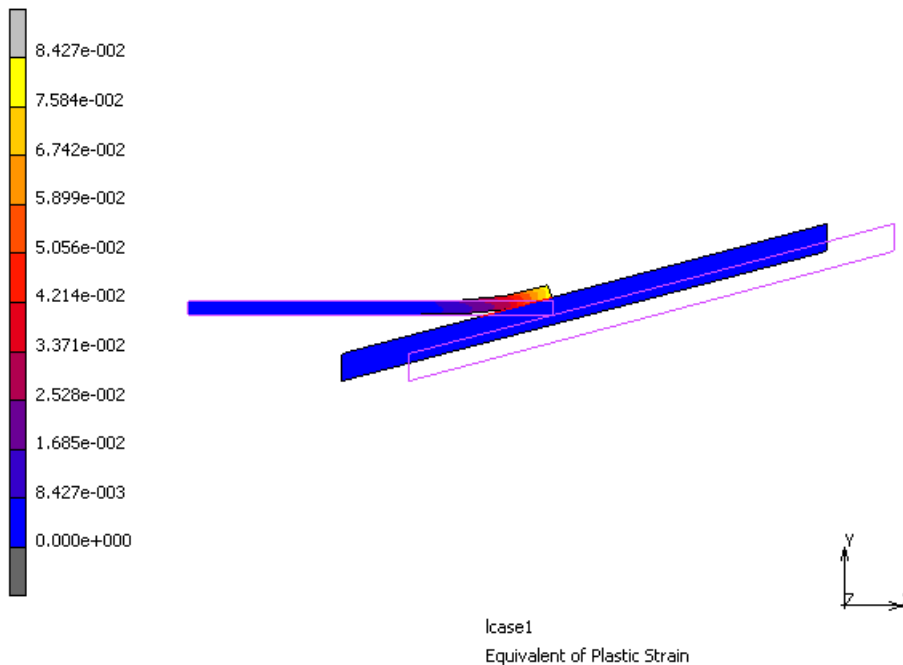


Figure 3.6-18 Plot of Original & Deformed Tube showing Plastic Strain at Increment 39

If you are interested in viewing the von Mises stresses over the course of 87 increments, make sure you have CONTOUR BANDS selected under the SCALAR PLOT panel, and von Mises as scalar quantity, prior to animating the model using the button sequence shown before.

Conclusion

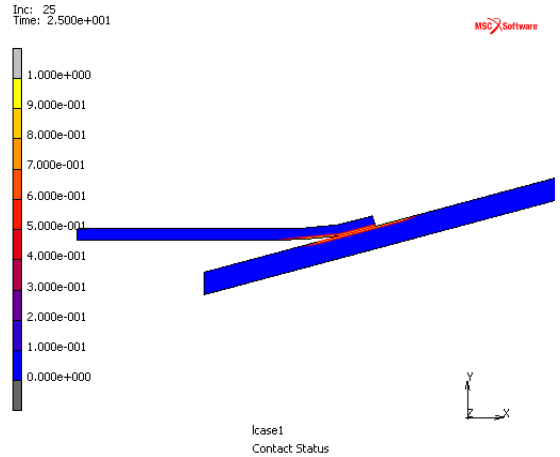
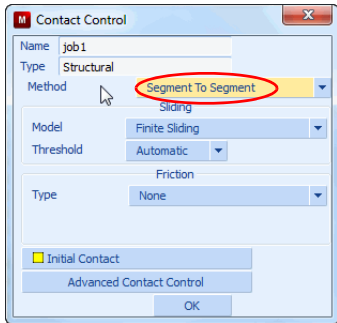
As mentioned in the chapter overview, the goal of the analysis described in this sample session was threefold.

1. To determine whether the final shape of the tube meets the objective of the analysis.
2. To determine whether residual stresses are present in the steel tube and flaring tool.
3. If residual stresses are present, to determine what are the residual stresses.

The results of the analysis demonstrate that the goals of the analysis have been met.

1. You have seen that the flaring tool expands the diameter of the tube by 10%.
2. Residual stresses are present in the steel tube; however, there are not any noticeable stresses in the flaring tool.
3. [Figure 3.6-18](#) shows the equivalent plastic strain just before the tool is released.

As an alternative, one can use the segment-to-segment contact method with this model. In this case, double-sided contact is used. This capability is activated using the Job Contact Control menu as shown below. The contact status on the tube and tool is also shown. Notice the contact status is shown on both bodies.



Contact Status using Segment-to-segment Contact

Input Files

The files below are on your [delivery media](#) or they can be downloaded by your web browser by clicking the links (file names) below.

File	Description
tube_flaring.proc	Mentat procedure file to run the above example

3.7 Punch

- Chapter Overview 1006
- Background Information 1006
- Detailed Session Description 1009
- Input Files 1027

Chapter Overview

The sample session described in this chapter analyzes the process of punching. A tool with a rigid dimple is pushed into a circular plate. The object of this process is to produce a circular plate with spherical indentation. The goal of the static analysis described in this chapter is to determine the residual stresses and plastic strains in the workpiece after the operation.

Background Information

This problem demonstrates the preparation of a contact analysis involving multiple rigid bodies (the tool) and a deformable body (the workpiece). The top of the tool is a sphere blended in with a flat rigid plate. The workpiece is supported such that radial displacements are constrained at the outer diameter while axial displacements are constrained at the node positioned at the corner of the outer diameter and the backing plate. The bottom part of the tool is a flat backing plate with a hole at the same location as the dimple of the top part of the tool. The plate of the tool supports the entire workpiece, except for the region of the hole.

Idealization

Because of the axisymmetric nature of the geometry and the loading, this process can be idealized to an axisymmetric model. The edge of the workpiece is clamped which prevents rigid body motion of the workpiece. The backing plate that backs the workpiece is modeled as a rigid body and remains in place during the analysis. The punch is modeled as a rigid body and moves during the analysis towards the static backing plate, while indenting the workpiece.

The tool is stopped when the flat surfaces of both parts of the tool are in full contact with the workpiece. This occurs when the total displacement of the punch is 0.1488 inches, which is reached in 0.4 seconds. Hence, the velocity of the top part of the tool (i.e. punch) is 0.372 inch per second. The friction between tool and workpiece is assumed to be negligible and is therefore not taken into consideration in this analysis.

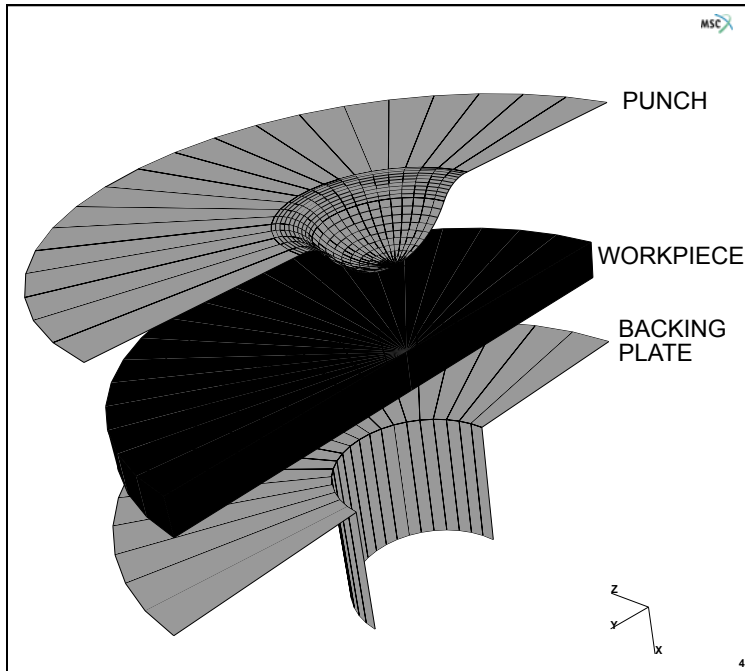


Figure 3.7-1 Punch, Workpiece, and Backing Plate

Requirements for a Successful Analysis

The analysis is considered successful when the punch becomes flush with the workpiece and is released afterwards to determine the residual stresses.

Full Disclosure

The workpiece is constructed out of steel with a Young's Modulus of 30.0e6 psi and a Poisson's Ratio of 0.3. It has a yield stress of 39,000 psi. The material exhibits workhardening. The workpiece has a radius of 0.7874 inches and a thickness of 0.117 inches.

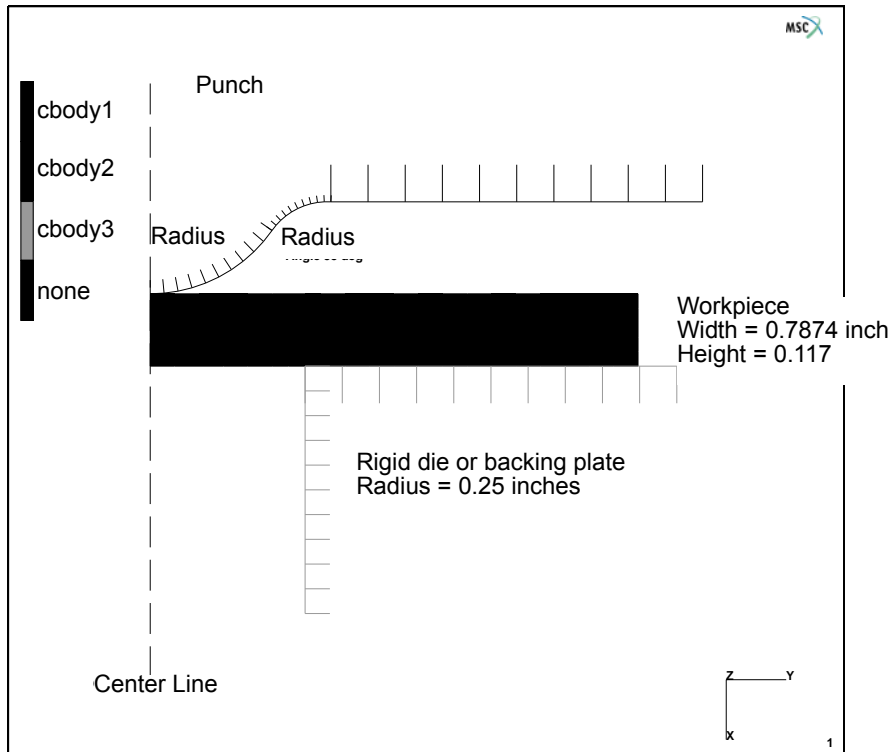


Figure 3.7-2 Dimensions of Punch, Workpiece, and Backing Plate

The punch is a sphere of radius 0.24 with a fillet of radius 0.109 that brings it tangent to a horizontal piece. It will move over a total distance of 0.1488 inches in a period of 0.4 seconds. The backing plate has a cylindrical hole of radius 0.25 inches into which the workpiece is forced. Both punch and backing plate are considered to be rigid during the analysis.

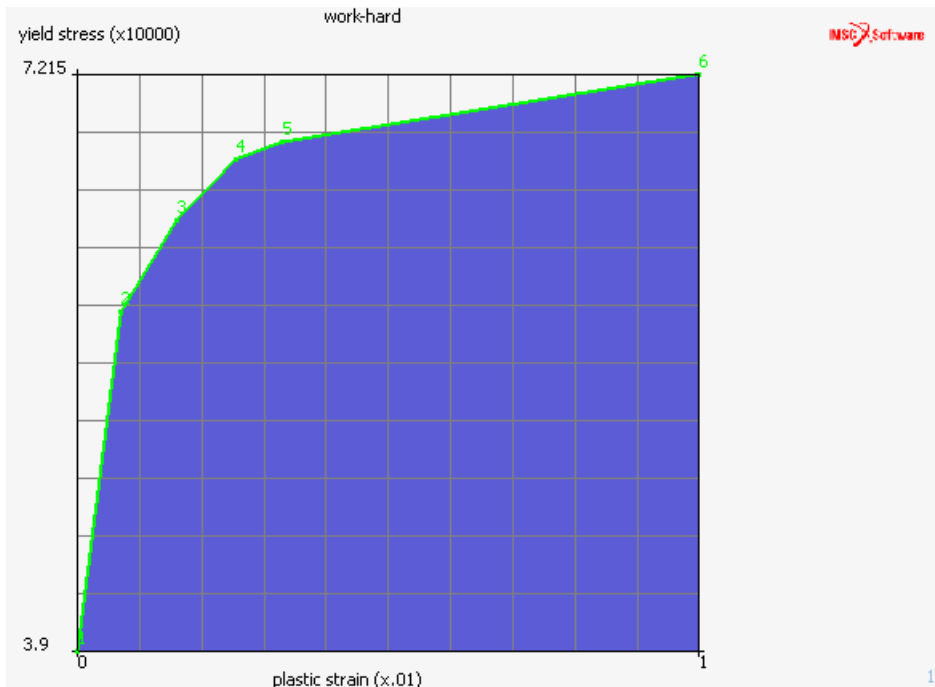


Figure 3.7-3 The Workhardening Curve for the Workpiece Material

Overview of Steps

- Step 1:** Create a model of a rectangular patch and convert it to finite elements.
- Step 2:** Create the curves required for the punch & backing plate.
- Step 3:** Apply the required fixed displacements to the rim of the workpiece. Apply the material data.
- Step 4:** Identify the contact bodies and create the table that defines the motion of the rigid die, representing the punch.
- Step 5:** Define the incremental steps and convergence testing parameters.
- Step 6:** Activate the large strain parameters and submit the job.
- Step 7:** Postprocess the results by displaying the deformed structure and the residual stresses and strains.

Detailed Session Description

Step 1: Create a model of a rectangular patch and convert it to finite elements.

The approach used in this session to generate the model is the geometric meshing technique.

The first step is to create the workpiece. The recommended method is to create a point and expand it to a line curve, followed by expanding this curve to a quad surface. Use the following button sequence to create the first point.

```
MAIN
  MESH GENERATION
    pts ADD
      0.24 0 0
```

Next, expand the point using a translation of 0.117 inches in the x-direction and then expand the resulting curve using a translation of 0.7874 in the y-direction. Use the following button sequence to create the quad surface.

```
MAIN
  MESH GENERATION
    EXPAND
      TRANSLATIONS
        0.117 0 0
      POINTS
        all: EXIST.
      TRANSLATIONS
        0 0.7874 0
      CURVES
        all: EXIST.
      FILL
```

The next step is to convert the geometric entities to finite elements. This is done using the CONVERT processor. Five divisions will be used through the thickness and 20 along the radius. Use the following button sequence to mesh the surface.

```
MAIN
  MESH GENERATION
    CONVERT
      DIVISIONS
        5 20
      SURFACES TO ELEMENTS
        all: EXIST.
      PLOT
        draw SURFACES (on)
      REGEN
      RETURN
```

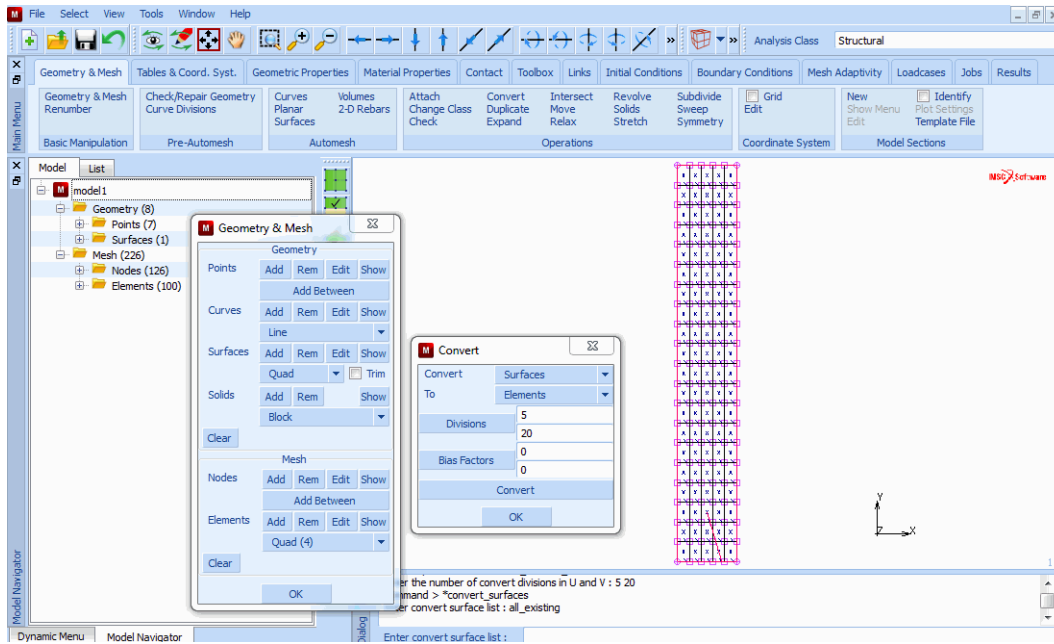


Figure 3.7-4 Result of the Convert Command

An important portion of the analysis requires that a sharp corner will be developed at the lip of the cylinder. To do this, the mesh must be refined in that area. The user will need to zoom in on that area. The nodes near the radius of 0.25 will be moved to exactly that location. The y-coordinates of these nodes can be determined by the SHOW command on the NODES panel. The move operation is done using the following button sequence:

```

MAIN
MESH GENERATION
coordinate system SET
V DOMAIN
0 .25
V SPACING
.25
GRID
RETURN
MOVE
FORMULAS
x
0.25
z
NODES
37 38 39 40 41 42
END LIST (#)
RETURN
    
```

(on)

(Box pick the 8th row of nodes)

The next step is to subdivide the sixth row of elements. Use the following button sequence to subdivide the elements.

```

MAIN
  MESH GENERATION
    SUBDIVIDE
      DIVISIONS
        1 2 1
      ELEMENTS
        26 27 28 29 30
      END LIST (#)
  
```

(Box pick the 7th row of elements)

After subdividing, it is usually necessary to remove all the duplicate nodes. It is also advisable to renumber the elements because there is a gap in the numbering from the subdivide operation. This can be done with the following button sequence.

```

MAIN
  MESH GENERATION
    SWEEP
      sweep NODES
        all: EXIST.
      RETURN
    RENUMBER
      ALL
  
```

Step 2: Create the curves required for the punch & backing plate.

The next step is to create the dies. The dies will be represented by geometric entities. These entities are a combination of curves.

For the punch, the first step is to put a point at the center of the sphere. Then use that point to create an arc. It is easier to have a rigid body almost touching the deformable body. That is why the center point will be created by duplicating the top center point of the workpiece at a distance equal to the sphere radius. The following button sequence will create the center point and arc.

```

MAIN
  MESH GENERATION
    DUPLICATE
      TRANSLATIONS
        -0.24 0 0
      POINTS
        1
      END LIST (#)
    RETURN
  CURVE TYPE
    CENTER/RADIUS/ANGLE/ANGLE
    RETURN
  crvs ADD
    0 0 0
    0.24
    0 55
  
```

(Pick the lower left point)

(Pick the point just created (Center))

(Radius)

(Beginning angle, ending angle)

The next curve must be tangent to the one just created. Therefore, the curve type must be changed to arc type tangent/radius/angle before creating the curve. The radius of the arc is 0.109 inches and the angle will be a negative 55°. The negative sign makes the arc go clockwise. The following button sequence will create the arc.

```

MAIN
MESH GENERATION
CURVE TYPE
TANGENT/RADIUS/ANGLE
RETURN
crvs ADD
11
0.109
-55
    
```

*(Pick the end point of the arc just created (Tangent point))
 (Radius)
 (Angle)*

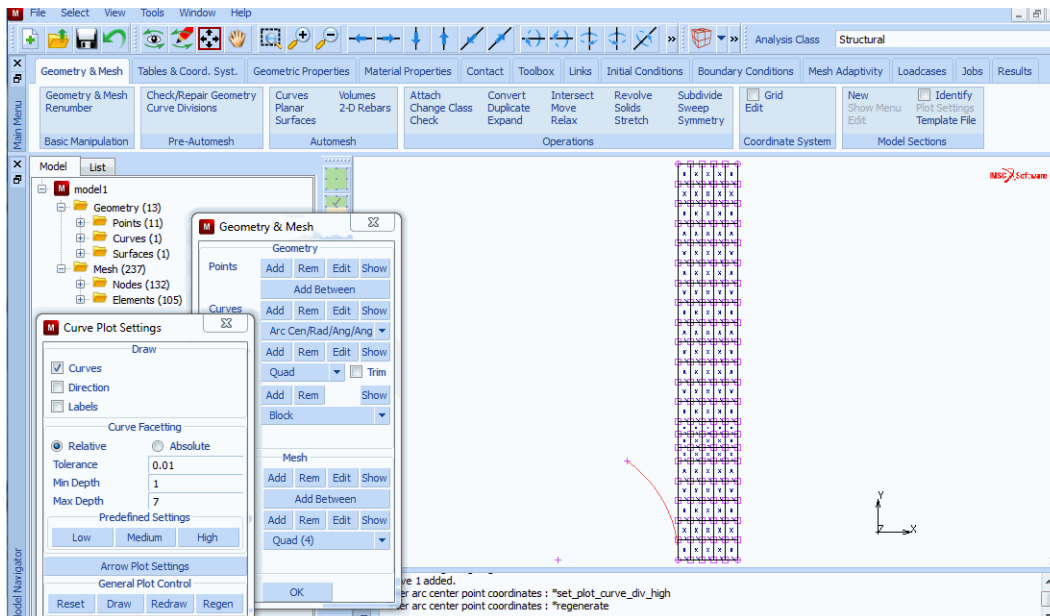


Figure 3.7-5 The Spherical Part for the Punch

The next step is to finish the rigid body. There is one line required to finish the punch. This is a horizontal line tangent to the second arc. The following button sequence will create the line.

```

MAIN
MESH GENERATION
EXPAND
TRANSLATIONS
0 0.6 0
POINTS
14
END LIST (#)
FILL
    
```

(Pick the end point of the last arc)

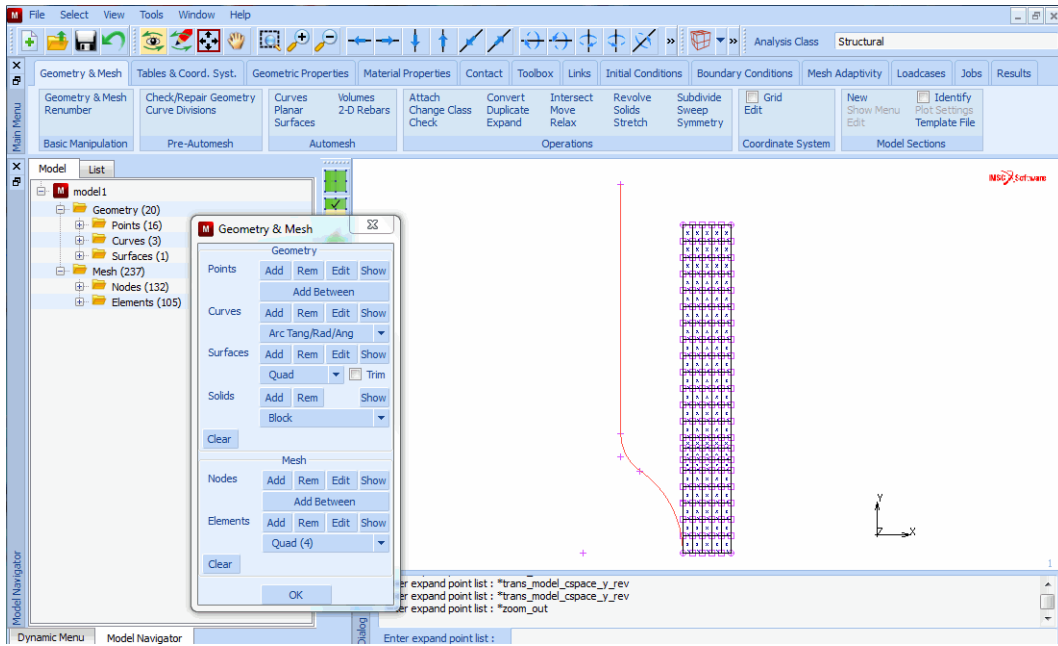


Figure 3.7-6 The Geometry of the Punch

The next step is to create the backing plate. First, a point will be added at the bottom of the workpiece at a y location of 0.25. It will then be expanded in the x and y-direction creating the two lines required for the rigid body. The following button sequence will generate these curves.

MAIN

MESH GENERATION

pts ADD

0.357 0.25 0

EXPAND

POINTS

16

END LIST (#)

TRANSLATIONS

0.4 0 0

POINTS

16

END LIST (#)

FILL

(Pick the point just created)

(Pick the corner point)

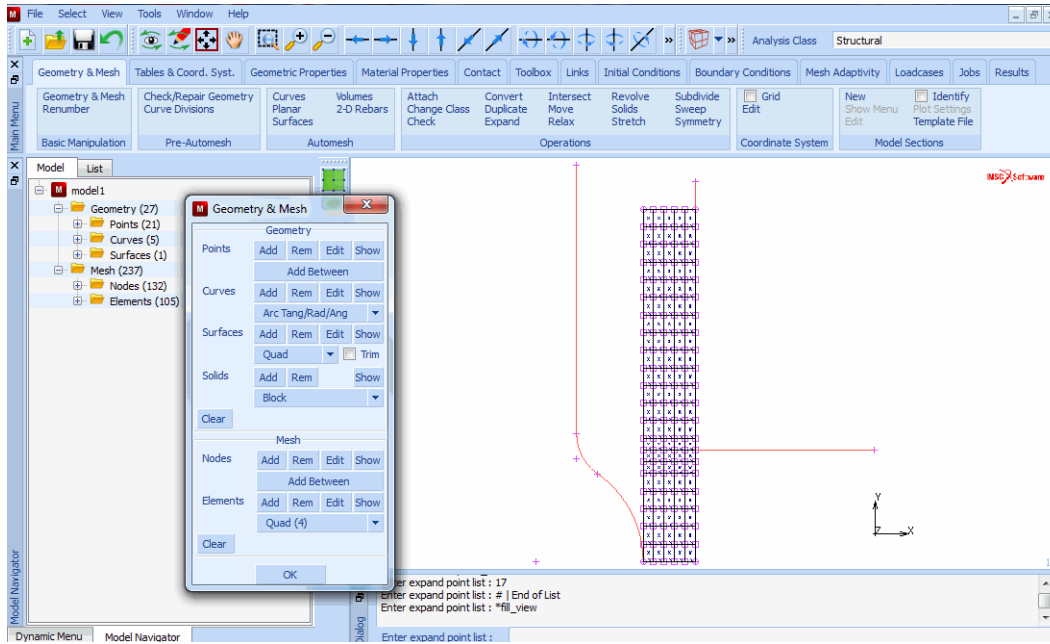


Figure 3.7-7 Punch, Workpiece, and Backing Plate

Step 3: Apply the required fixed displacements to the rim of the workpiece. Apply the material data.

The first step is to create a table with the stress versus plastic strain table. The following button sequence creates the table.

```

MAIN
MATERIAL PROPERTIES
TABLES
NEW
1 INDEPENDENT VARIABLE
TYPE
eq_plastic_strain
OK (Select OK button only if type eq_plastic_strain was typed in)
ADD
0 39000
0.7e-3 58500
1.6e-3 63765
2.55e-3 67265
3.3e-3 68250
10e-3 72150
FIT
NAME
work-hard
MORE
independent variable v1: LABEL

```

```

        plastic strain
    function value f: LABEL
        yield stress
    RETURN
    FILLED
    SHOW TABLE
    SHOW MODEL
    
```

(select *SHOW MODEL* to go back to model view)

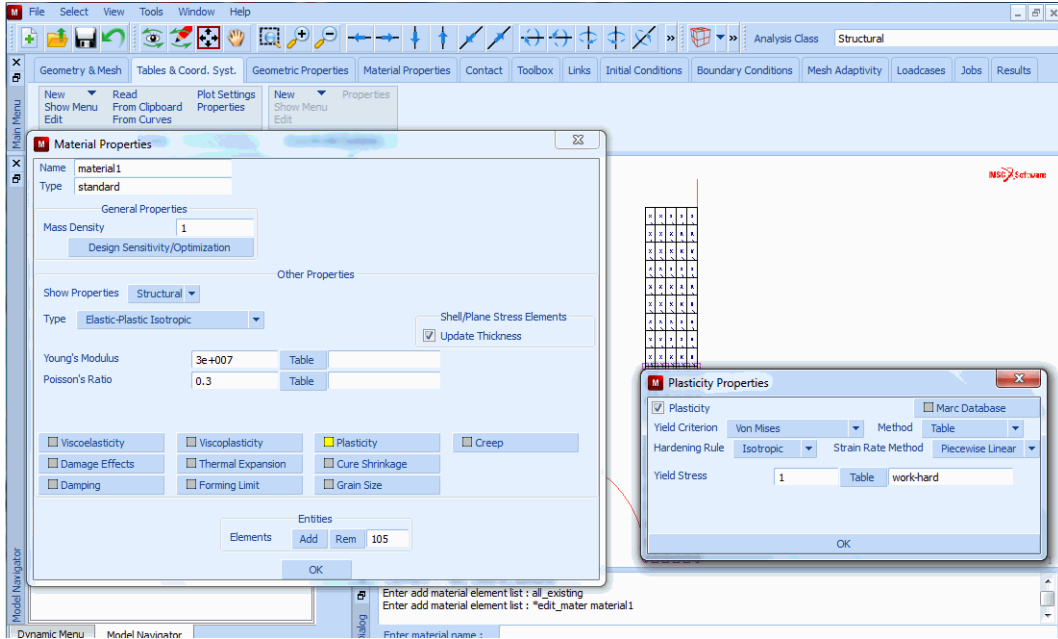


Figure 3.7-8 Plasticity Properties

The next step is to input the material properties and assign them to the elements. The table must be assigned to the yield stress value to include the workhardening. The following button sequence will assign the material properties.

```

MAIN
MATERIAL PROPERTIES
ISOTROPIC
YOUNG'S MODULUS
    30.0e6
POISSON'S RATIO
    0.3
PLASTICITY
    ELASATIC-PLASTIC
        INITIAL YIELD STRESS
            1
        initial yield stress TABLE
            work-hard
        OK (twice)
elements ADD
    
```


all: EXIST.

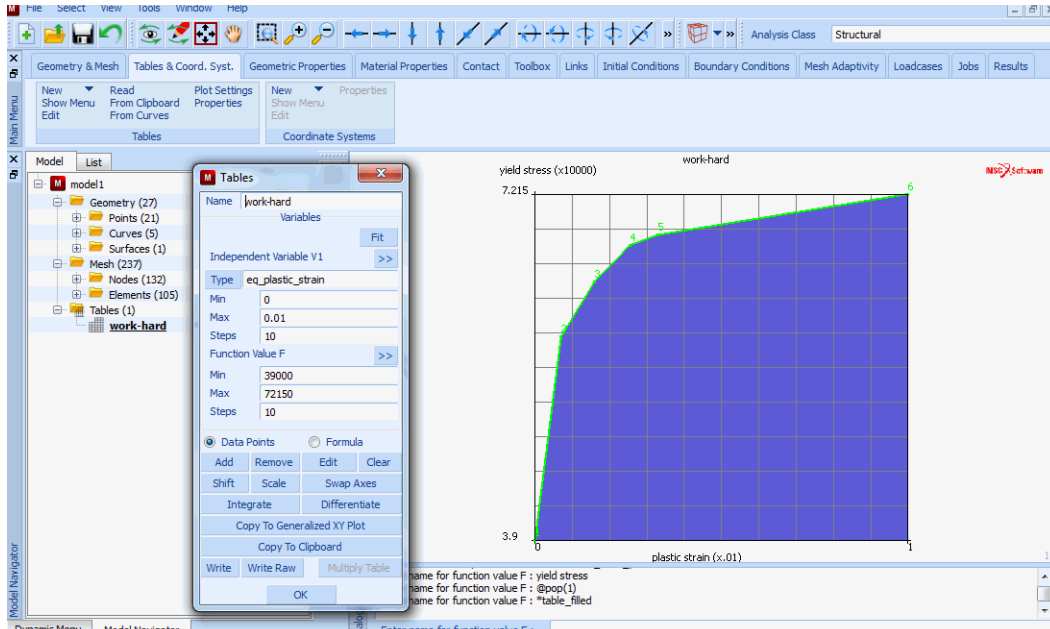


Figure 3.7-9 Workhardening Curve

The next step is to clamp the end of the workpiece. The model is axisymmetric and therefore, has only two degrees of freedom at each node. The first set of boundary conditions will clamp the node on the top right in both axial and radial direction. The second set of boundary conditions will constrain the radial motion of both the nodes on the axis of symmetry and the nodes on the outer radius of the workpiece.

MAIN

BOUNDARY CONDITIONS

MECHANICAL

FIXED DISPLACEMENT

DISPLACEMENT X

(on)

DISPLACEMENT Y

(on)

OK

nodes ADD

1 2 6

(Pick the node at the top right point)

END LIST (#)

NEW

FIXED DISPLACEMENT

DISPLACEMENT Y

(on)

OK

nodes ADD

(Pick the bottom edge nodes)

(Pick the top edge nodes)

END LIST (#)

Step 4: Identify the contact bodies and create the table that defines the motion of the rigid die, representing the punch.

This step assigns the elements and curves to the correct contact bodies. Rigid bodies must always follow all deformable bodies. The following button sequence will assign all the elements to deformable body 1.

```
MAIN
  CONTACT
    CONTACT BODIES
      DEFORMABLE
        NAME
          workpiece
      elements ADD
        all: EXIST.
```

The next step is to assign the curves to rigid bodies. By default, analytical curves will be used for rigid bodies composed of curved entities. Therefore, no manual interference is required to specify the number of subdivisions used to discretize the curves.

The following button sequence will create the 2 rigid bodies.

```
MAIN
  CONTACT
    CONTACT BODIES
      NEW
        NAME
          punch
      crvs ADD
        1 2 3 (Pick curves of punch)
      END LIST (#)
      NEW
        NAME
          back
      crvs ADD
        5 4 (Pick curves of backing plate)
      END LIST (#)
```

At this point, it is advisable to check the correctness of the definition direction of the curves used in the rigid bodies.

```
MAIN
  CONTACT
    CONTACT BODIES
      PLOT
        elements SOLID
      REGEN
      RETURN
      ID CONTACT (on)
```

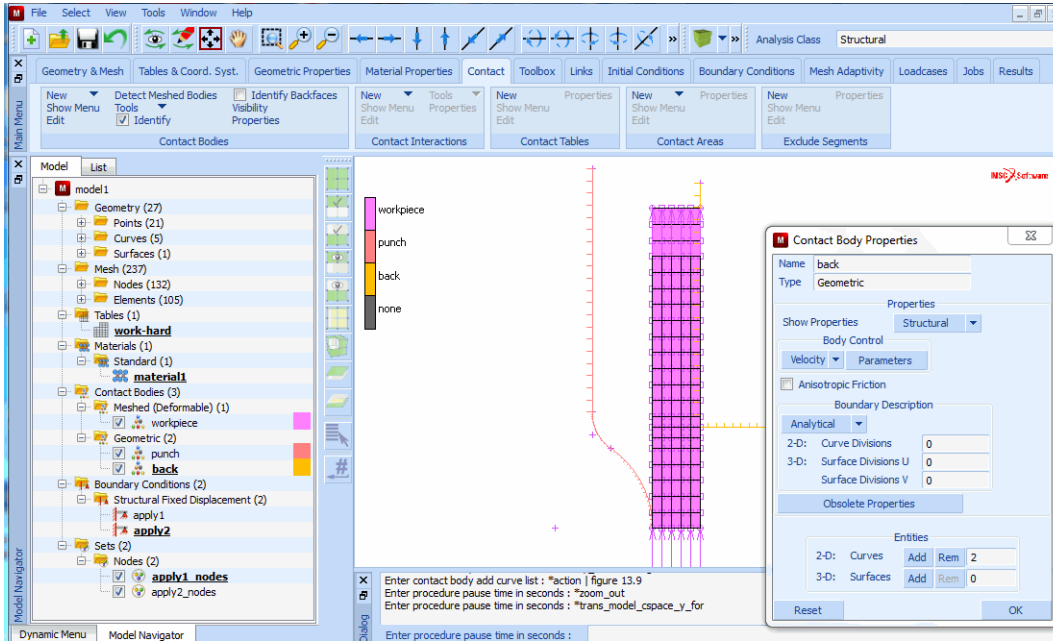


Figure 3.7-10 Incorrect Definition Direction of Curves in Back-Plate

The ID CONTACT button will show the rigid bodies and their direction. If either of the curves is defined such that the rigid body is on the same side as the deformable body, the curve can be flipped by using the FLIP CURVES button.

MAIN

CONTACT

CONTACT BODIES

FLIP CURVES

4

END LIST (#)

ID CONTACT

(Pick curve)

(off)

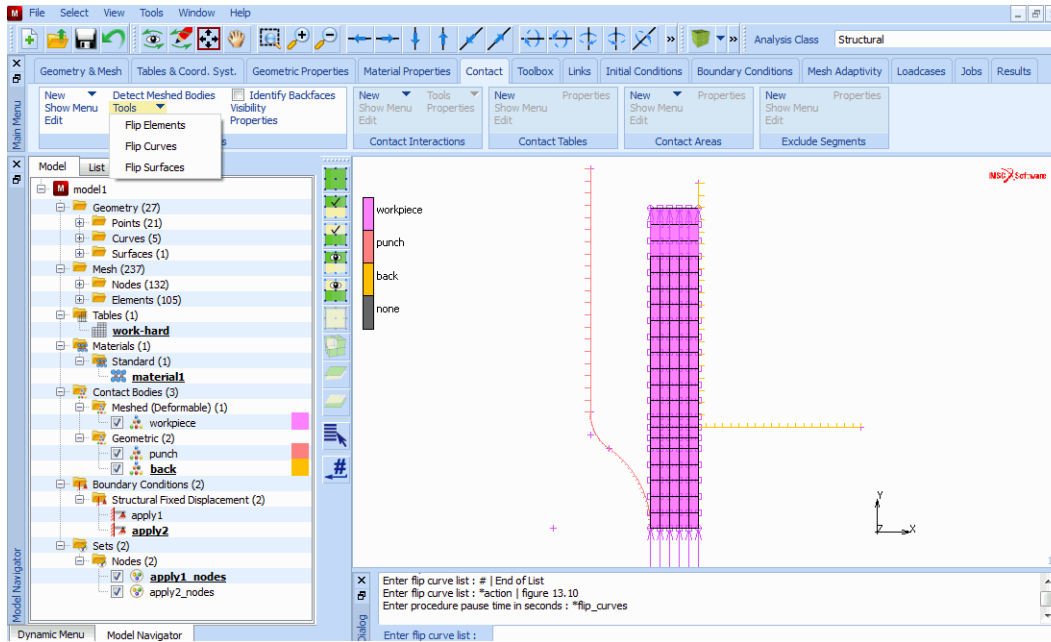


Figure 3.7-11 Corrected Definition

The punch will move during the analysis. To define the motion, a table of time versus velocity must be defined. The axial distance of the straight section of the punch and the workpiece is 0.1488 inches. This value can be determined with the DISTANCE command on the second page of the UTILITIES menu (use MORE).

As stated before, this gap will be closed in 0.4 seconds. As soon as the horizontal part of the punch touches the workpiece, the motion will be reversed and the release option will be switched on. In order to accomplish separation within this single increment, the punch will be withdrawn at high velocity.

The following button sequence will define the table.

```

MAIN
CONTACT
CONTACT BODIES
TABLES
NEW
1 INDEPENDENT VARIABLE
NAME
punch_motion
TYPE
time
OK (Select OK button only if type time was typed in)
ADD
0 0.1488/0.4 (0.1488/0.4 = velocity)
0.4 0.1488/0.4
0.4 -10*0.1488/0.4 (-10*velocity)
    
```

0.5 -10*0.1488/0.4
 FIT
 SHOW TABLE
 SHOW MODEL *(Select SHOW MODEL to go back to model view)*

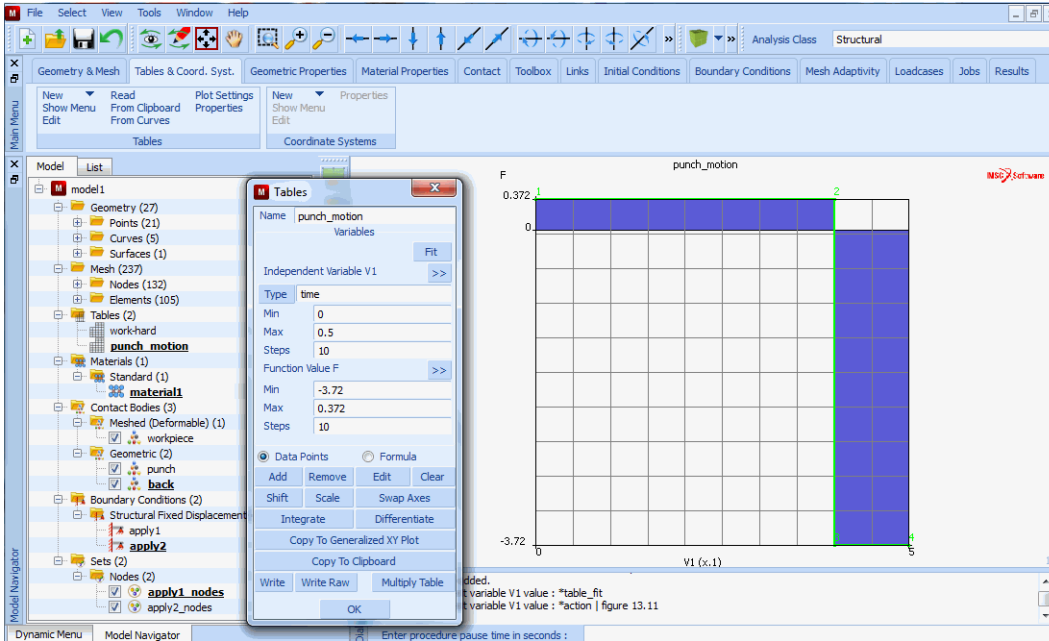


Figure 3.7-12 Velocity as a Function of Time

The following button sequence will assign the table to the punch motion (please notice that the current and therefore active body is body 3, the backing plate!).

MAIN
 CONTACT
 CONTACT BODIES
 body control velocity PARAMETERS *(to activate body 2)*
 CONTACT BODY PROPERTIES
 velocity X
 1
 velocity x TABLE
 punch_motion
 OK (twice)

Step 5: Define the incremental steps and convergence testing parameters.

The loadcases describe the first and second part of the loading history and the loads used during those parts. The following button sequence will create the loadcases.

MAIN
 LOADCASES
 NAME

```
    indent
mechanical STATIC
  LOADS
    OK
  TOTAL LOADCASE TIME
    0.4
  # STEPS
    100
  SOLUTION CONTROL
    MAX # RECYCLES
      20
    OK
  OK
NEW
NAME
  release
mechanical STATIC
  LOADS
    OK
  TOTAL LOADCASE TIME
    0.1
  # STEPS
    1
  SOLUTION CONTROL
    MAX # RECYCLES
      20
    OK
CONTACT
  CONTACT RELEASES
    SELECT
      punch
    OK
```

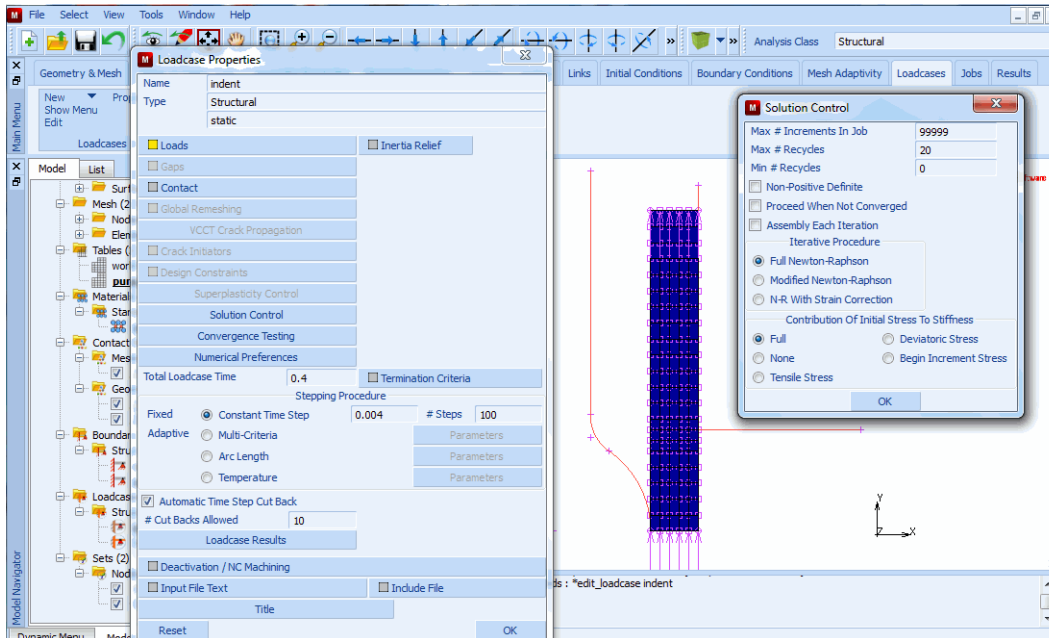


Figure 3.7-13 Specify Loadcase for Indentation

Step 6: Activate the large strain parameters and submit the job.

The final preprocessing step is to create the job and submit it to run in the background. The job menu defines the special analysis options, the results saved, and other global parameters. This is also where the loadcases can be selected in the desired order. The following button sequence below will create the job and submit it.

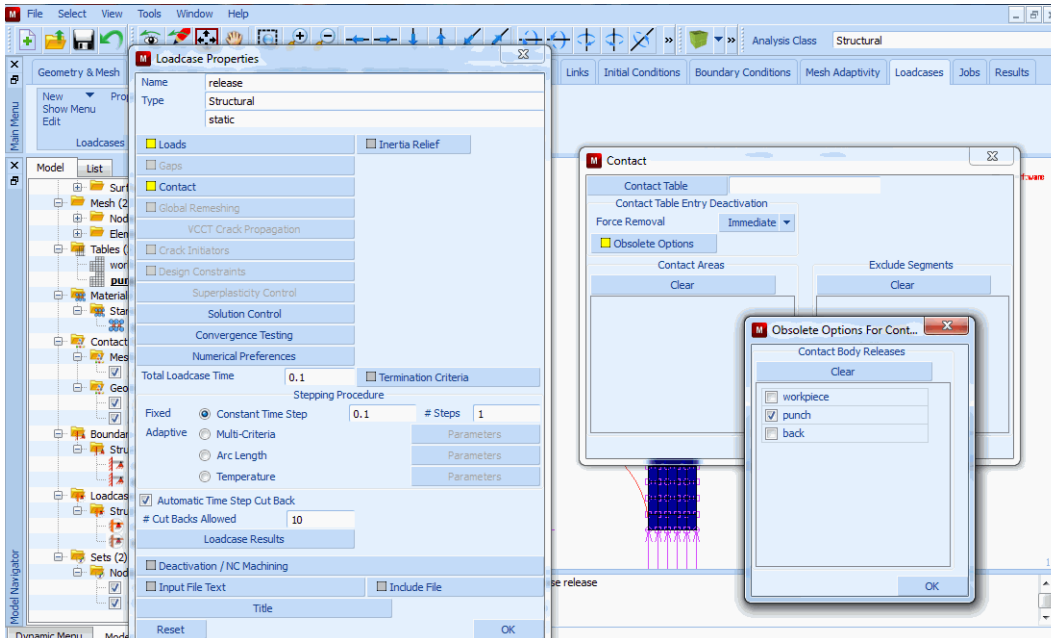


Figure 3.7-14 Specify Release of Contact Body

MAIN

JOBS

MECHANICAL

available loadcases

indent

release

ANALYSIS OPTIONS

ADVANCED OPTIONS

CONSTANT DILATATION

OK

plasticity procedure SMALL STRAIN

(Switch to large strain additive procedure)

JOB RESULTS

available element tensors

Stress

available element scalars

Equivalent Von Mises Stress

Total Equivalent Plastic Strain

OK

AXISYMMETRIC

(This makes sure that the default element type 10 is used)

OK

SAVE

RUN

SUBMIT 1

MONITOR

The MONITOR option will continually update the log and return the program control to the user when the analysis is complete. If the user wishes, there is a monitor capability in the RESULTS menu which will allow the user to watch the deformations and stresses during the analysis.

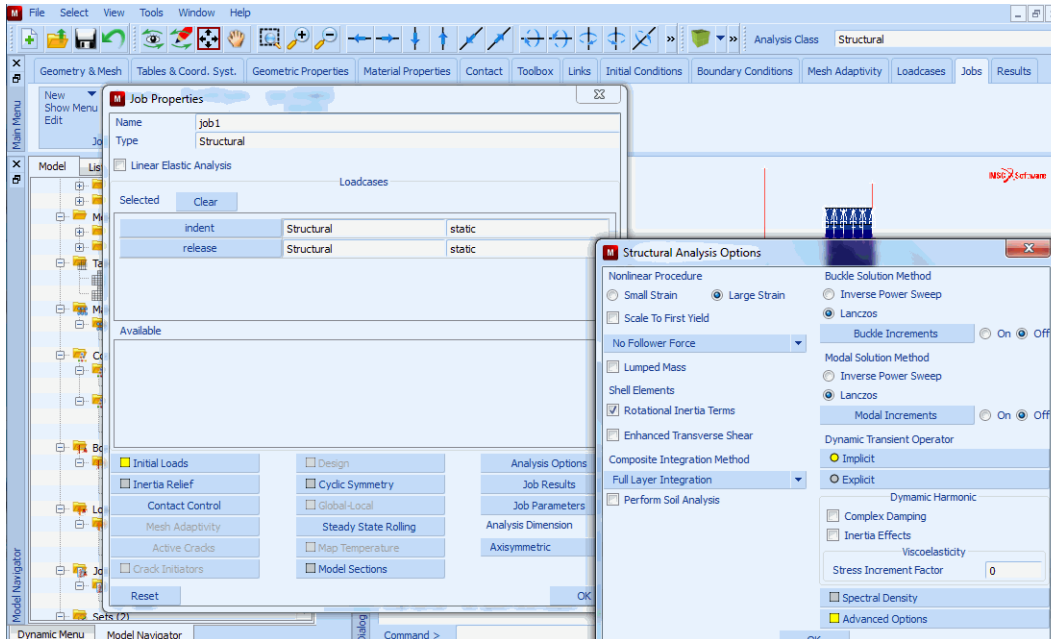


Figure 3.7-15 Select Job Options

Step 7: Postprocess the results by displaying the deformed structure and the residual stresses and strains.

The analysis requires the final deformed shape and the stresses at that time. The following button sequence will present the results.

```

MAIN
  RESULTS
    OPEN DEFAULT
    FILL
    PLOT
      draw NODES
      elements SETTINGS
      draw OUTLINE
    RETURN
  RETURN
DEF & ORIG
SCALAR
  Equivalent Von Mises Stress
  OK
CONTOUR BANDS
  
```

(off)

MONITOR

The deformed shape shows that the 90 degree lip is well developed. It also shows the final stresses after the punch operation. The last increment (101) shows the residual stresses after the punch has been withdrawn.

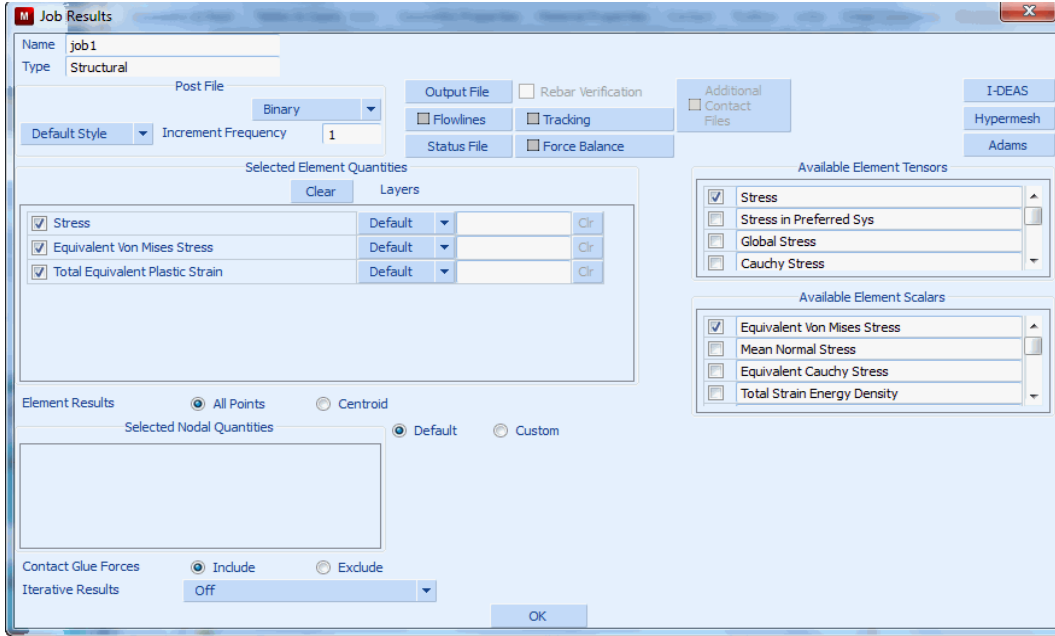


Figure 3.7-16 Select Quantities to be Written on Post Tape

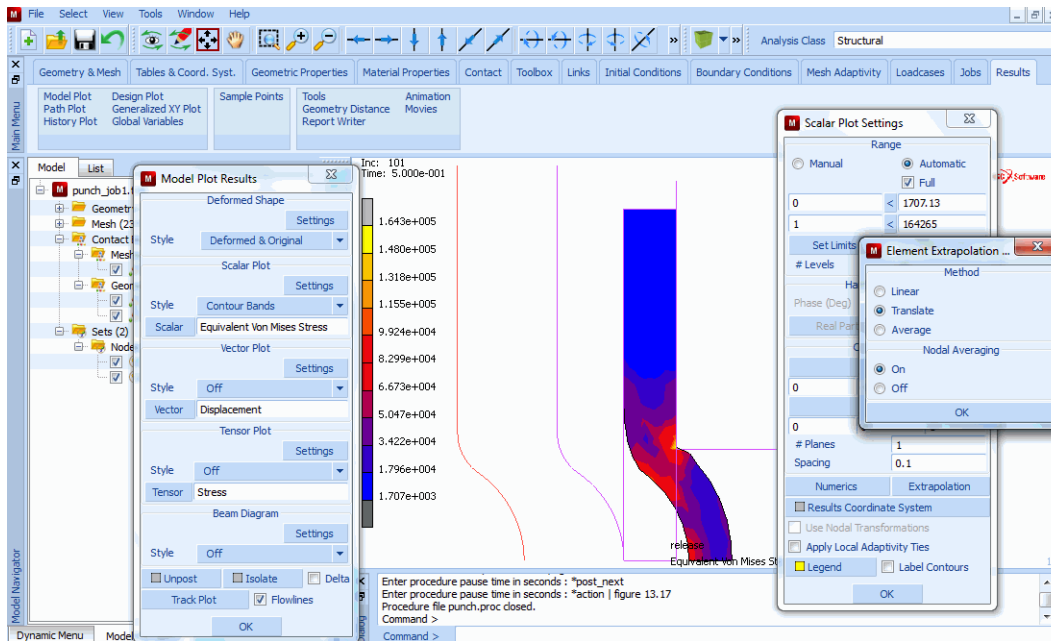


Figure 3.7-17 Deformations and Stresses after Springback

Input Files

The files below are on your [delivery media](#) or they can be downloaded by your web browser by clicking the links (file names) below.

File	Description
punch.proc	Mentat procedure file to run the above example

3.8 Torque Controlled dies with Twist Transfer

- Chapter Overview 1030
- Belt and Pulley Assembly 1030
- Preprocessing 1030
- Results 1036
- Input Files 1041

Chapter Overview

Belt and Pulley Assembly

Rotational motion (twist) is prescribed on a rigid drive pulley. This twist is transferred to another rigid pulley driven by an elastic belt. The belt is stretched between the two rigid pulleys as shown in Figure 3.8-1. The drive pulley on the right has a constant rotational velocity about its center, whereas the driven pulley on the left rotates about its center constrained by a torsional spring. The rotational velocity of the driven pulley is unknown and depends upon the stiffness of the torsional spring and friction. Friction between the belt and pulleys transfers power from the drive to the driven pulley. As the driven pulley rotates, the spring torque continues to increase until it overcomes the friction between the pulley and belt. Then the left pulley begins to slip transmitting a constant torque. A small nub on the outer portion of the belt helps visualize the belt rotation. Units are MNewtons, meters, seconds, and radians.

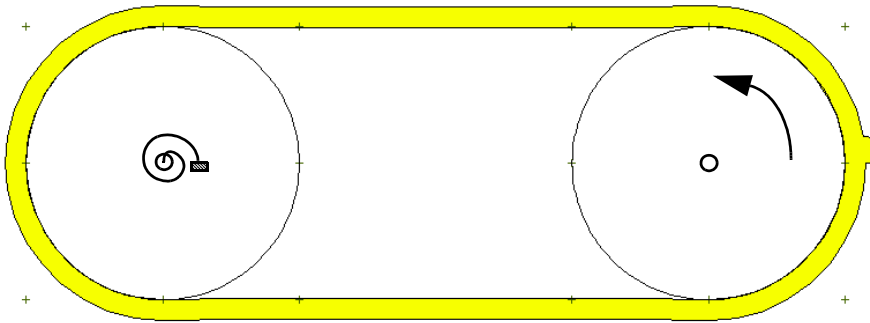


Figure 3.8-1 Belt and Pulleys

Preprocessing

Let's tour the existing model file by opening it in Mentat.

FILES

OPEN ch23

RETURN

CONTACT

CONTACT BODIES

ID CONTACT

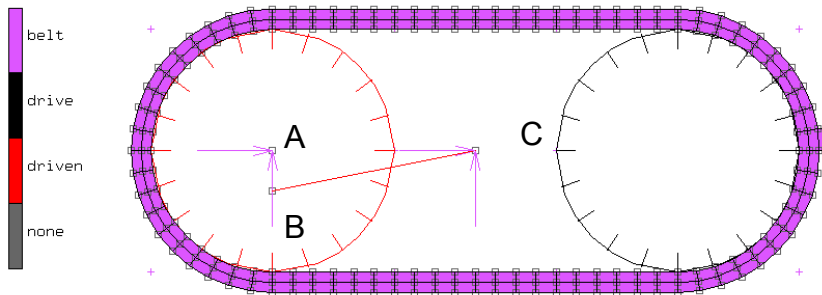


Figure 3.8-2 Existing Model

Nodes A and B above are associated with the driven pulley. Node A is called the control node which controls the location of the center of rotation and the translational degrees of freedom (DOF) that may be applied to this rigid body.

Note: Node B is called the auxiliary node and it controls the rotational DOF that may be applied to this rigid body. The auxiliary node is special because it has either one DOF (as in this problem) or three DOF's in 3-D. Either rotations or moments can be prescribed on the auxiliary node.

In 2-D, the first DOF is rotation about the Z-axis, whereas in 3-D, DOF 1,2,3 are rotations about the X-, Y-, and Z-axis, respectively. Note the link (spring) that grounds the Z-moment of auxiliary node B to ground, node C. Select the driven contact body and look at the control information shown in [Figure 3.8-3](#).

The belt is a deformable body containing all of the elements. The drive contact body is the curve on the right and is a velocity controlled rigid body as shown in [Figure 3.8-4](#).

The tables translate the drive to the right pre-tensioning the belt and then begin rotating counter clockwise. The coefficient of friction of 0.5 is entered by using contact table.

The boundary condition is shown in [Figure 3.8-2](#) where the control node of the driven pulley is pinned along with node C that is used to ground a torsional spring to the auxiliary node B. [Figure 3.8-5](#) shows the link used to ground the torsional spring with a spring constant of 0.002 [kN-m/radian].

The belt is a Mooney material with $C_{10} = 1$ MPa. There are two loadcases, the first translates the drive pulley to the right pre-tensioning the belt. The second loadcase begins rotating the drive pulley.

In JOBS, the loadcases are chosen, element type 118 is selected, and the friction type is selected as shown in [Figure 3.8-6](#). The relative sliding velocity is set to 0.01 or 30 times slower than the tangential velocity of the drive pulley as per the guide lines using this friction model as outlined in *Marc Volume A: Theory and User Information*. This value of the relative sliding velocity will insure adequate friction resistance without causing numerical convergence problems with friction.

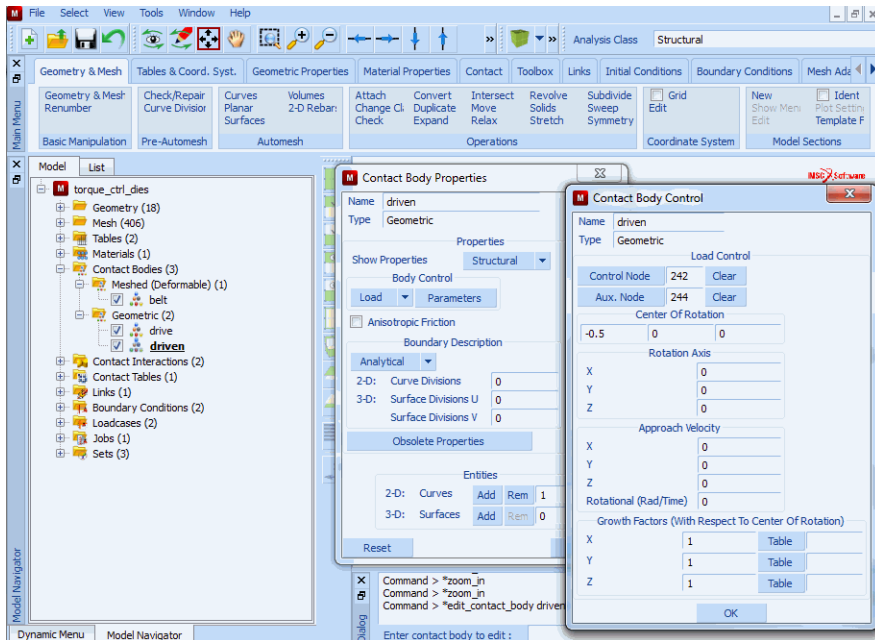


Figure 3.8-3 Details of Rigid Body-Driven, Control, and Auxiliary Nodes

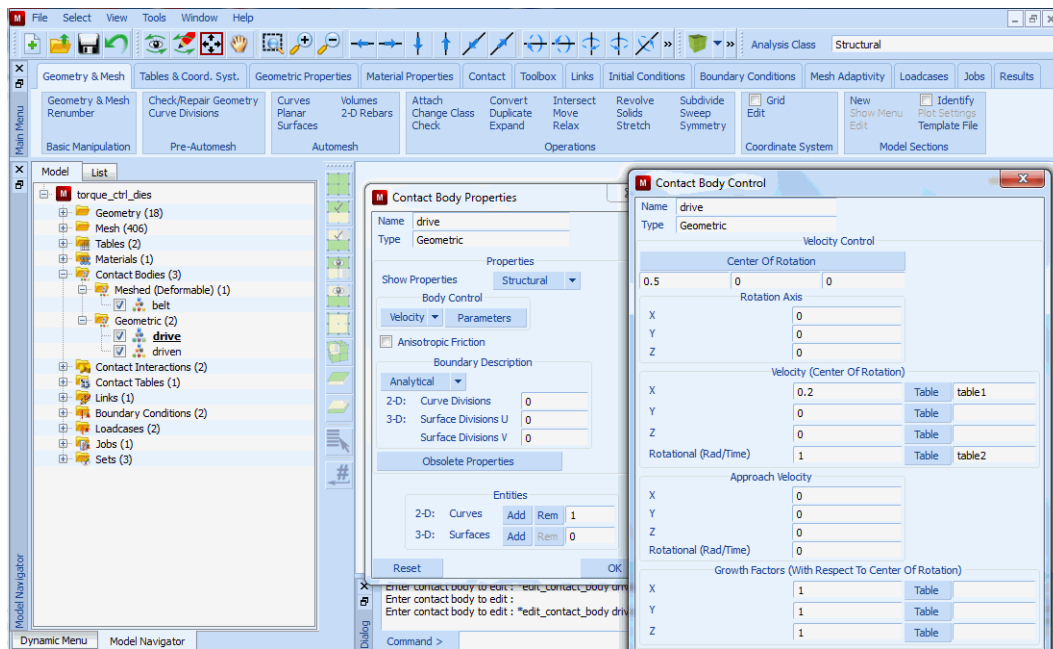


Figure 3.8-4 Details of Rigid Body-Drive

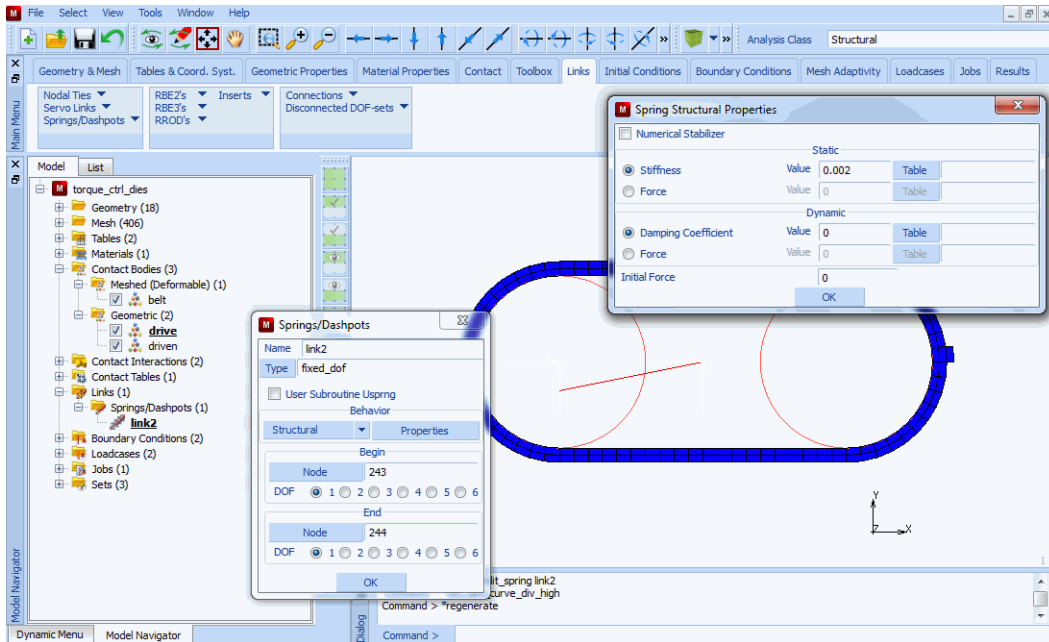


Figure 3.8-5 Link (Torsional Spring) from Driven Pulley to Ground

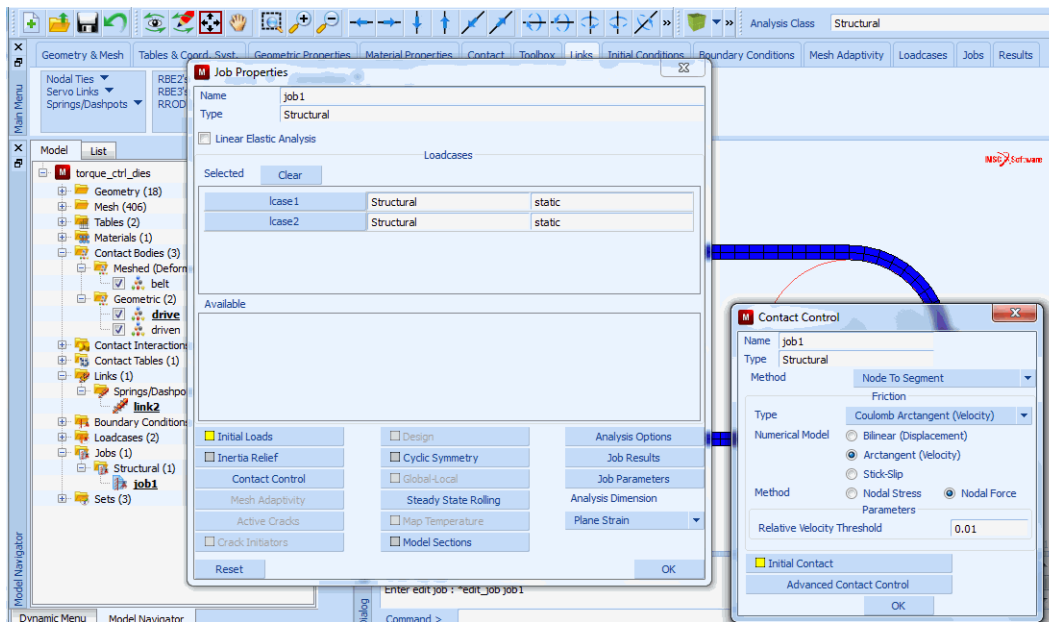


Figure 3.8-6 Select Friction Type

In JOB RESULTS, custom nodal quantities are requested (Figure 3.8-7). They include the normal and tangential (friction) contact force, along with a user-defined nodal vector that is the vector sum of the normal and tangential contact force. The UPSTNO user subroutine is used to add this combined contact nodal vector to the post file.

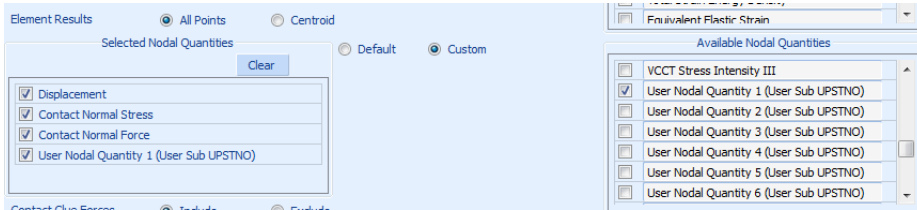


Figure 3.8-7 Select Custom Nodal Quantities

This vector will be the sum of the normal and friction components of the belt contact forces. It is in a file called *ch23.f* and is listed below:

```

subroutine upstno(nqcode,nodeid,verno,nqncomp,nqtype,
*              nqaver,nqcomptype,nqdatatype,
*              nqcompname)
implicit real*8 (a-h,o-z)
dimension verno(*)
character*24 nqcompname(*)

c
c input:  nqcode      user nodal post code , e.g. -1
c        nodeid      node id
c        nqcompname  not used (future expansion)
c
c output: verno()    nodal values
c          real/imag verno(      1: nqncomp) real
c                  verno(nqncomp+1:2*nqncomp) imag
c          magn/phas verno(      1: nqncomp) magn
c                  verno(nqncomp+1:2*nqncomp) phas
c
c        nqncomp     number of values in verno
c        nqtype      0 = scalar
c                  1 = vector
c        nqaver      only for DDM 0 = sum over domains
c                  1 = average over domains
c        nqcomptype  0 = global coordinate system (x,y,z)
c                  1 = shell (top,bottom,middle)
c                  2 = order (1,2,3)
c        nqdatatype  0 = default
c                  1 = modal
c                  2 = buckle
c                  3 = harmonic real
c                  4 = harmonic real/imaginary
c                  5 = harmonic magnitude/phase
c
c to obtain nodal values to be used in this subroutine from
c the marc data base the general subroutine NODVAR is available:

```

```
c
c call nodvar(icod,nodeid,verno,nqncomp,nqdatatype)
c
c output: verno
c         nqncomp
c         nqdatatype
c
c input:  nodeid
c         icod
c         0='Coordinates           '
c         1='Displacement           '
c         2='Rotation               '
c         3='External Force         '
c         4='External Moment        '
c         5='Reaction Force         '
c         6='Reaction Moment        '
c         7='Fluid Velocity         '
c         8='Fluid Pressure         '
c         9='External Fluid Force   '
c         10='Reaction Fluid Force  '
c         11='Sound Pressure        '
c         12='External Sound Source '
c         13='Reaction Sound Source '
c         14='Temperature           '
c         15='External Heat Flux    '
c         16='Reaction Heat Flux    '
c         17='Electric Potential    '
c         18='External Electric Charge '
c         19='Reaction Electric Charge '
c         20='Magnetic Potential    '
c         21='External Electric Current '
c         22='Reaction Electric Current '
c         23='Pore Pressure         '
c         24='External Mass Flux    '
c         25='Reaction Mass Flux    '
c         26='Bearing Pressure      '
c         27='Bearing Force         '
c         28='Velocity              '
c         29='Rotational Velocity   '
c         30='Acceleration          '
c         31='Rotational Acceleration '
c         32='Modal Mass            '
c         33='Rotational Modal Mass '
c         34='Contact Normal Stress '
c         35='Contact Normal Force  '
c         36='Contact Friction Stress '
c         37='Contact Friction Force '
c         38='Contact Status        '
c         39='Contact Touched Body '

```

```

c          40='Herrmann Variable          '
c
c          dimension valno1(3),valno2(3)
c
c          if (nqcode.eq.-1) then
c... pick up contact normal force
c          call nodvar(35,nodeid,valno1,nqncomp,nqdatatype)
c... pick up contact friction force
c          call nodvar(37,nodeid,valno2,nqncomp,nqdatatype)
c... add normal and friction force
c          valno(1)=valno1(1)+valno2(1)
c          valno(2)=valno1(2)+valno2(2)
c... indicate that valno represents a vector
c          nqtype=1
c          end if
c... only use nodes on belt, zero otherwise
c          if(nodeid.ge.242.and.nodeid.le.244) then
c            valno(1)=0.0d0
c            valno(2)=0.0d0
c          end if
c
c          return
c          end
  
```

The job is then submitted including the user subroutine above.

Results

Open the post file and skip to increment 50 which is the end of the pre-tensioning and contour plot equivalent Cauchy stress as shown in [Figure 3.8-8](#).

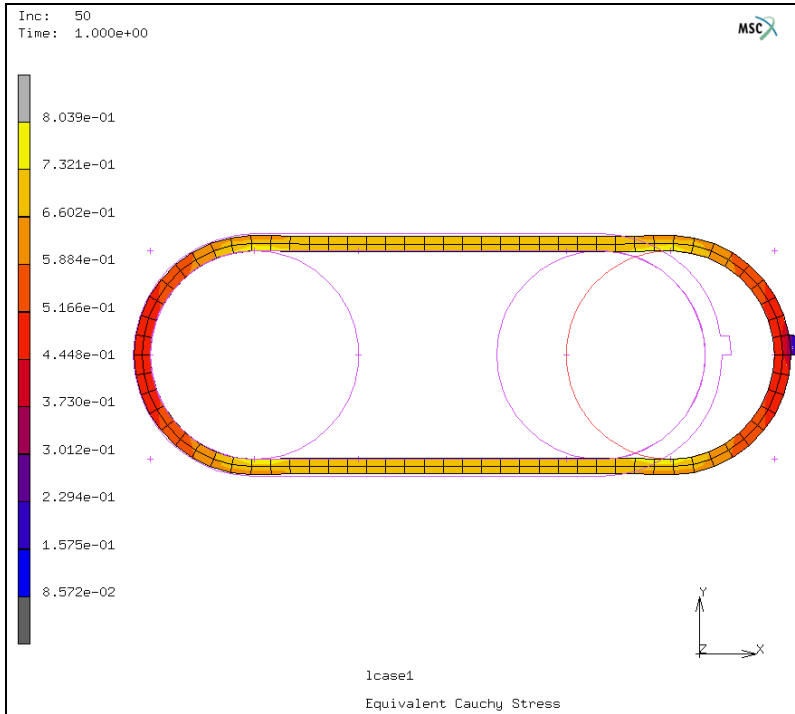


Figure 3.8-8 Pre-tensioning the Belt

Between the pulleys, the tensile stress is about 0.80 MPa and is very uniform.

Skip to increment 203, and plot component 11 of the Cauchy stress. The belt has revolved half way around the pulley assembly and the nub is on the left. The difference in belt tension between the upper and lower parts is due to friction.

The coefficient of friction can be computed from the belt tension as: $\mu = \frac{1}{\pi} \ln \left(\frac{\sigma_{11}^b}{\sigma_{11}^t} \right) = 0.51$

Of course this is very close to the actual value used, hence the ratio of the above stresses are correct, and friction is correctly simulated.

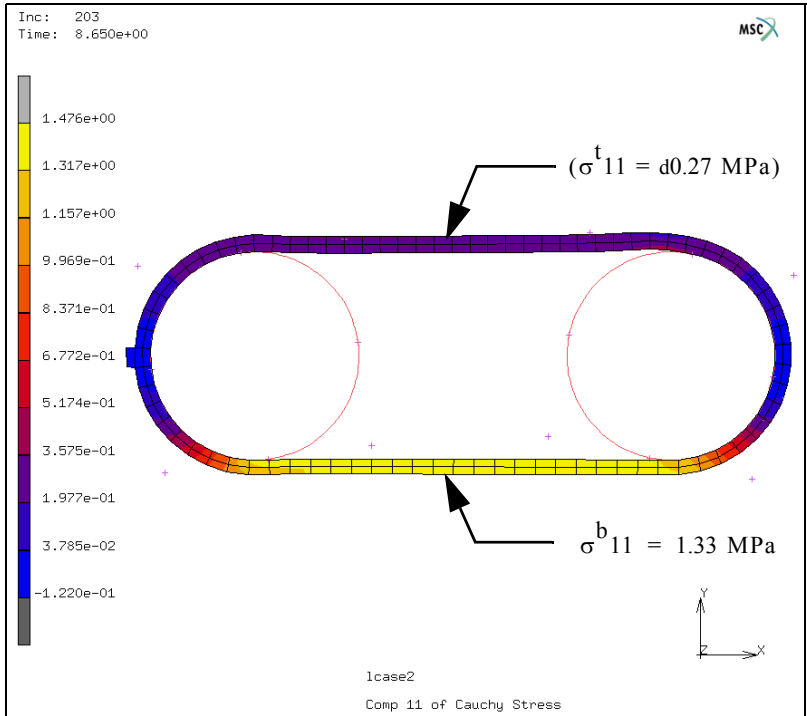


Figure 3.8-9 Belt Stresses and Friction

Figure 3.8-10 plots the contact forces on the belt, from the user subroutine. The presence of the friction shifts the contact force vector off normal by an angle θ , where $\tan \theta = \mu$. Since the coefficient of friction is 0.5, this angle is about 27° .

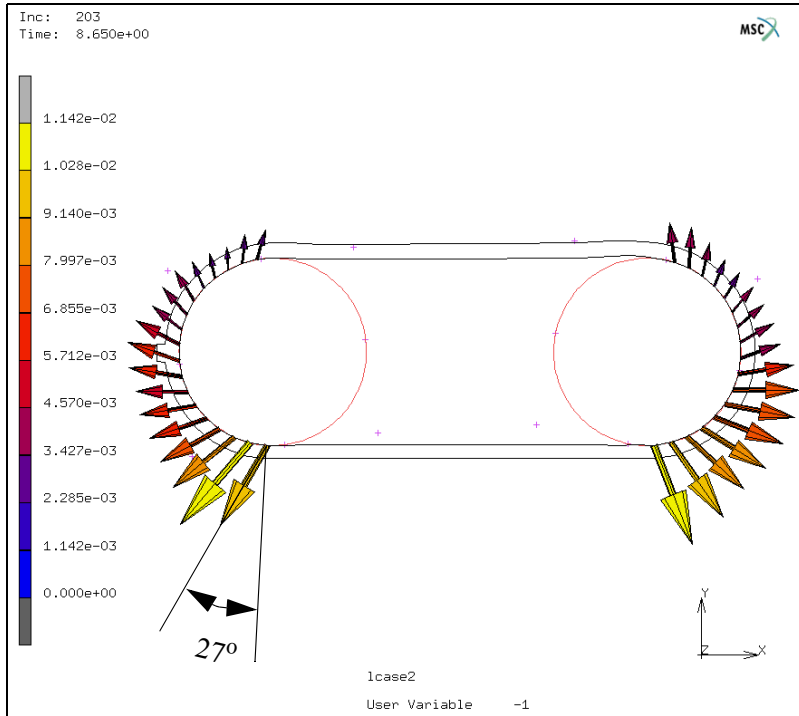


Figure 3.8-10 Contact Forces on Belt

Figure 3.8-11 is a history plot of the pulley's velocity. The driven pulley initially rotates quickly; however, because of the load induced by the torsional spring, it quickly slows down and oscillates slightly.

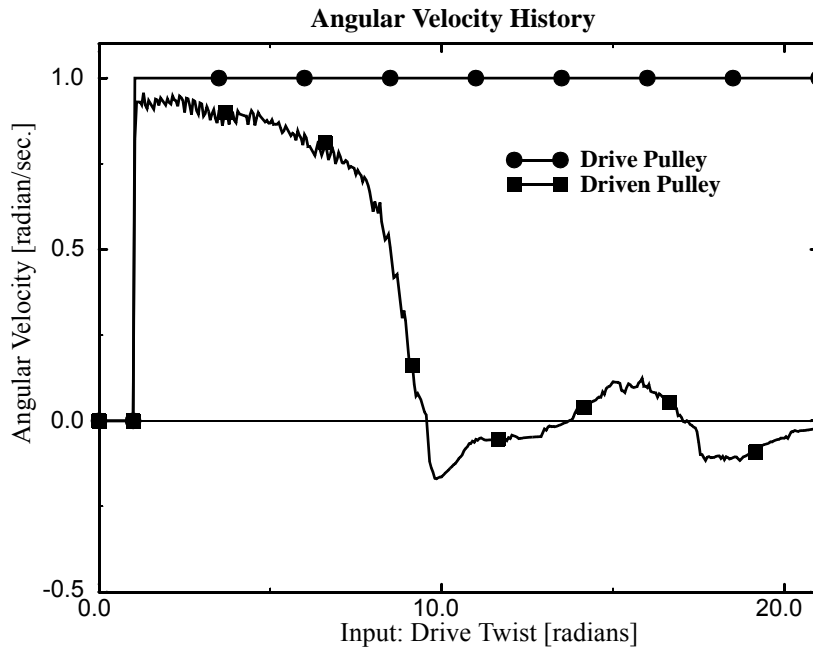


Figure 3.8-11 Angular Velocity of Pulleys

This oscillation occurs when the driven pulley slips and then sticks again.

Clearly the driven pulley's angular velocity magnitude and oscillation frequency is a function of the friction and the torsional spring stiffness. The torsional spring is used here to represent a load to the system. Remember that this is only a statics problem and that inertial effects of the system can be important during start/stop transients as well as high angular velocities. Although a dynamic simulation would be interesting, it is beyond the intent of this demonstration. This simulation represents a steady quasi-static condition and time is only used to move the drive pulley.

Figure 3.8-12 is a history plot of the input twist versus the output twist for various torsional spring constants. Clearly as the load (torsional spring stiffness, κ) increases, the output twist drops. For $\kappa = 0.020$, the driven pulley rotates less. Finally, if there was no load ($\kappa = 0$), the driven pulley would be free wheeling and this quasi-static problem would become singular.

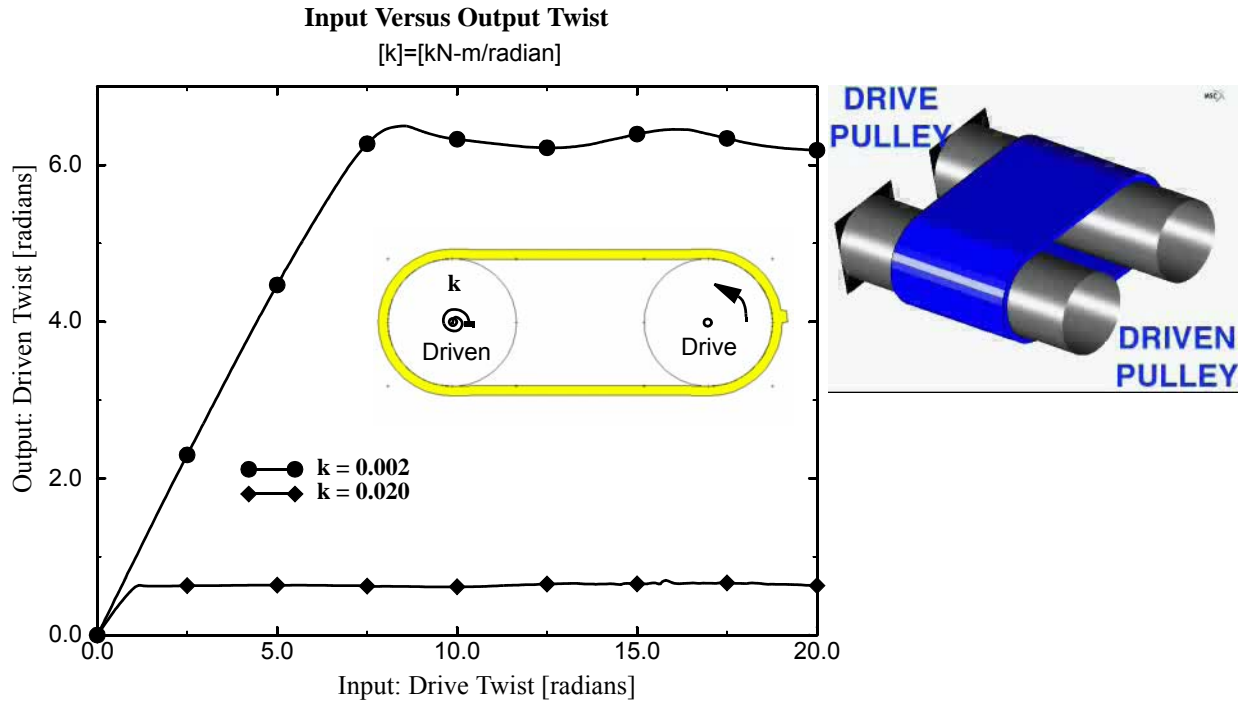


Figure 3.8-12 Output Versus Input Twist of Pulleys (click right figure for animation, ESC to stop)

Using load controlled rigid surfaces one can apply a torque to the pulleys. This is better than using velocity controlled rigid surfaces because the angular velocity of the driven pulley is initially unknown.

Input Files

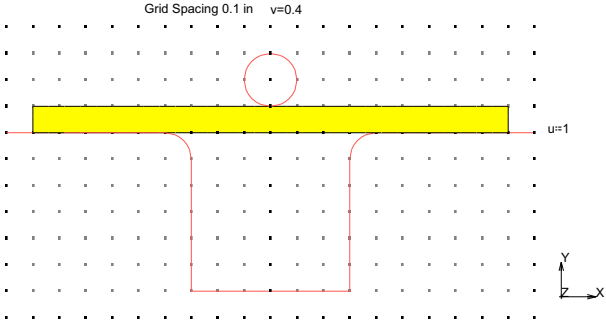
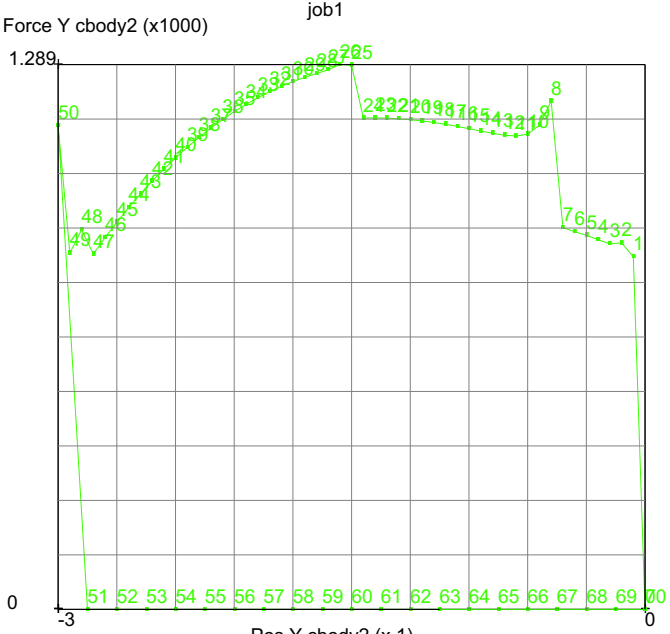
The files below are on your [delivery media](#) or they can be downloaded by your web browser by clicking the links (file names) below.

File	Description
torque_ctrl_dies.mfd	Mentat model file of above example
torque_ctrl_dies.f	Mentat model file of above example

3.9 Break Forming

- Summary 1044
- Detailed Session Description of Break Forming 1046
- Run Job and View Results 1052
- Discussion 1056
- Input Files 1057
- Animation 1059

Summary

Title	Break forming of a metal bracket																																												
Problem features	Contact and metal forming - click here for interactive preview																																												
Geometry																																													
Material properties	$E = 30 \times 10^6$ Psi, $\nu = 0.3$, $\sigma = 5 \times 10^4 (1 + \epsilon_p^{0.6})$																																												
Analysis type	Static with elastic plastic material behavior																																												
Boundary conditions	$U_x = 0$ at center nodes, cylindrical rigid body bends metal sheet																																												
Element type	Plane strain element type 11																																												
FE results	<p>Punch load verses stroke</p>  <table border="1"> <caption>Data points from the Force vs Stroke graph</caption> <thead> <tr> <th>Pos Y cbody2 (x.1)</th> <th>Force Y cbody2 (x1000)</th> </tr> </thead> <tbody> <tr><td>50</td><td>50</td></tr> <tr><td>51</td><td>48</td></tr> <tr><td>52</td><td>45</td></tr> <tr><td>53</td><td>44</td></tr> <tr><td>54</td><td>46</td></tr> <tr><td>55</td><td>48</td></tr> <tr><td>56</td><td>50</td></tr> <tr><td>57</td><td>52</td></tr> <tr><td>58</td><td>54</td></tr> <tr><td>59</td><td>56</td></tr> <tr><td>60</td><td>58</td></tr> <tr><td>61</td><td>60</td></tr> <tr><td>62</td><td>62</td></tr> <tr><td>63</td><td>64</td></tr> <tr><td>64</td><td>66</td></tr> <tr><td>65</td><td>68</td></tr> <tr><td>66</td><td>70</td></tr> <tr><td>67</td><td>765</td></tr> <tr><td>68</td><td>750</td></tr> <tr><td>69</td><td>735</td></tr> <tr><td>70</td><td>432</td></tr> </tbody> </table>	Pos Y cbody2 (x.1)	Force Y cbody2 (x1000)	50	50	51	48	52	45	53	44	54	46	55	48	56	50	57	52	58	54	59	56	60	58	61	60	62	62	63	64	64	66	65	68	66	70	67	765	68	750	69	735	70	432
Pos Y cbody2 (x.1)	Force Y cbody2 (x1000)																																												
50	50																																												
51	48																																												
52	45																																												
53	44																																												
54	46																																												
55	48																																												
56	50																																												
57	52																																												
58	54																																												
59	56																																												
60	58																																												
61	60																																												
62	62																																												
63	64																																												
64	66																																												
65	68																																												
66	70																																												
67	765																																												
68	750																																												
69	735																																												
70	432																																												

A flat sheet is formed into an angled bracket by punching it through a hole in a table using the contact option.

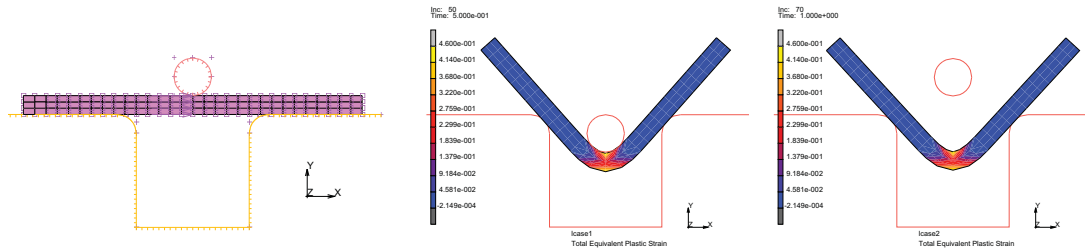


Figure 3.9-1 Punching Examples

The cylindrical punch drives the sheet down into the hole of the table to a total stroke of 0.3". The punch then returns to its original position. The material is elastic plastic with workhardening.

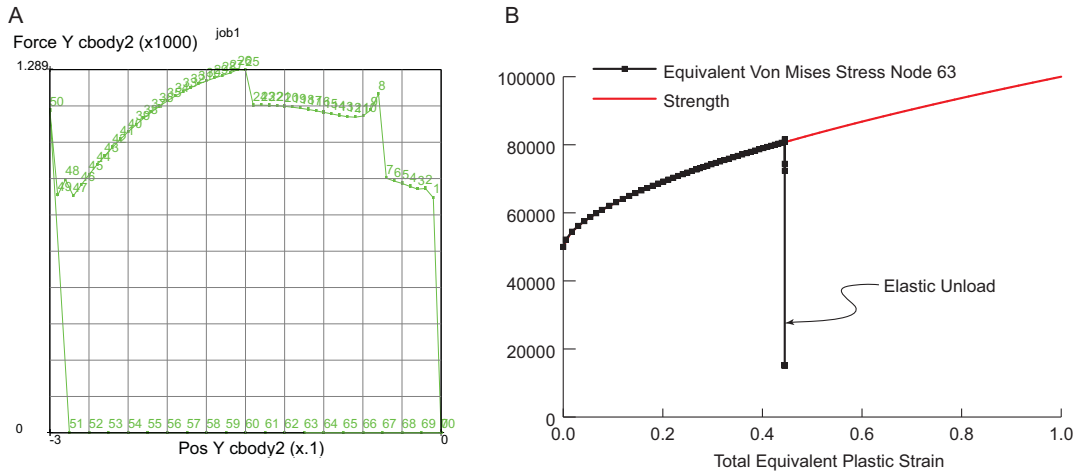


Figure 3.9-2 (A) Vertical Punch Load versus Stroke (B) Stress versus Plastic Strain

At the bottom of the stroke, the total plastic strain is nearly 45%. The vertical punch force is plotted versus its vertical position. This force rises quickly, hardens though about half of the stroke, then softens near the end of the stroke. Upon lifting the punch, the punch force drops rapidly and the sheet has very little springback.

The stress-plastic strain response of a point in the sheet under the punch is plotted and shown to overlay the material data. This workshop problem exemplifies how every point in the sheet must follow the material's constitutive behavior as well as being in equilibrium throughout the deformation. The vertical line in the history plot to the right is the elastic unloading of this point in the sheet.

This is a break forming problem where a punch indents a sheet over a table to make an bracket. The problem geometry is shown below:

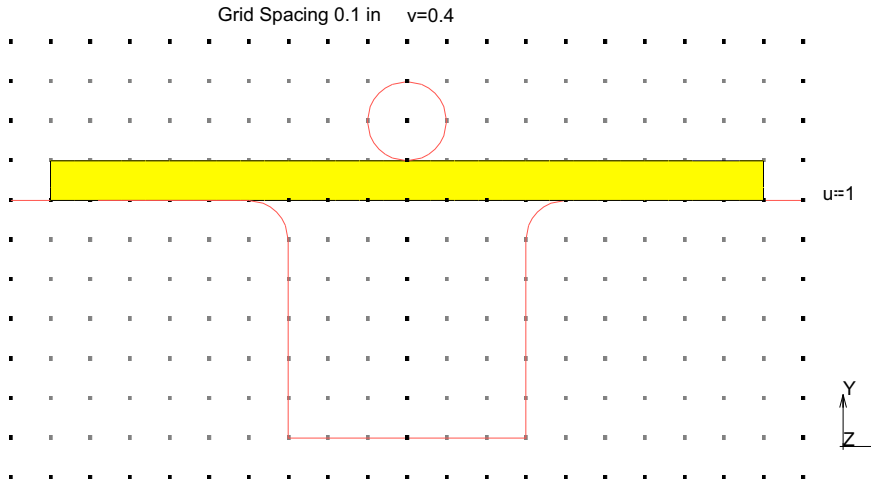


Figure 3.9-3 Break Forming Geometry Problem

Detailed Session Description of Break Forming

MESH GENERATION

COORDINATE SYSTEM SET: GRID ON

V DOMAIN

- .7 .4

FILL

RETURN

CURVES ADD

POINT (1,0,0), POINT(.3,0,0)

POINT(.3,0,0), POINT(.3,-.6,0)

POINT(.3,-.6,0), POINT(-.3,-.6,0)

POINT(-.3,-.6,0), POINT(-.3,0,0)

POINT(-.3,0,0), POINT(-1,0,0)

CURVE TYPE

FILLET

RETURN

CURVES ADD

radius

0.1

radius

(pick indicated points on grid)

(right horizontal curve, right vertical curve)

(left vertical curve, left horizontal curve)

```
0.1
CURVE TYPE
  CIRCLES: CENTER/RADIUS
  RETURN
CURVES ADD
  0 .2 0
  .1
ELEMENTS ADD
  NODE (-.9,0,0), NODE(.9,0,0)
  NODE(.9,.1,0), NODE(-.9,.1,0)
SUBDIVIDE
  DIVISIONS
    30, 3, 1
  ELEMENTS
    ALL:EXISTING
  RETURN
SWEEP
  ALL
  RETURN
RENUMBER
  ALL
  RETURN
COORDINATE SYS: SET GRID OFF
  RETURN (twice)
BOUNDARY CONDITIONS
  MECHANICAL
    FIXED DISP
    X=0
    OK
  NODES:ADD
  MAIN
MATERIAL PROPERTIES
  MATERIAL PROPERTIES
  NEW
  STANDARD
  STRUCTURAL
```

(pick points on grid)

(pick nodes along x=0,)

```

E = 3E7
ν = .3
OK
ELEMENTS ADD
ALL: EXISTING
TABLES
NEW
1 IND. VARIABLE
TABLE TYPE
    
```

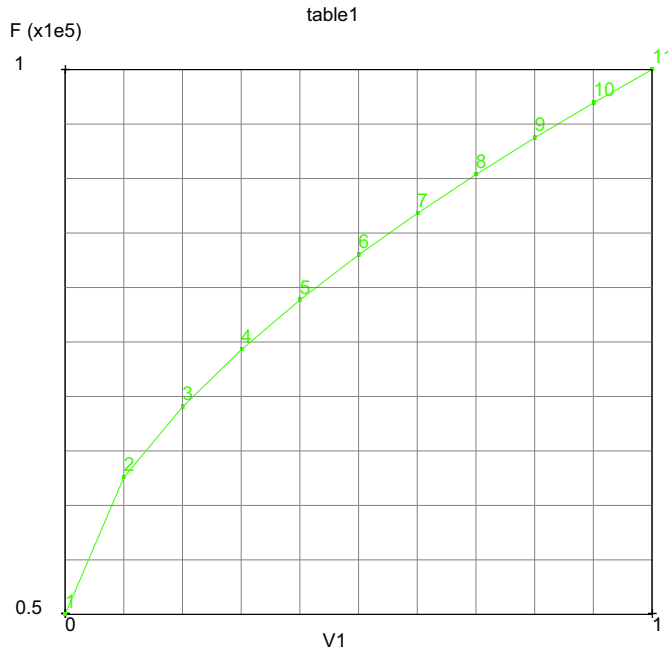


Figure 3.9-4 Flow Stress

```

eq_plastic_strain
OK
FORMULA
ENTER
5E4*(1+V1^.6)
FIT
    
```

The equation describing the flow stress is $\sigma_y = 5 \times 10^4 (1 + \bar{\epsilon}_p)^{.6}$


```

NEW
  1 IND. VARIABLE
  TABLE TYPE time
  OK
ADD POINT
  0, 0, .5, -.3, 1, 0
  FIT
  SHOW MODEL
RETURN
  
```

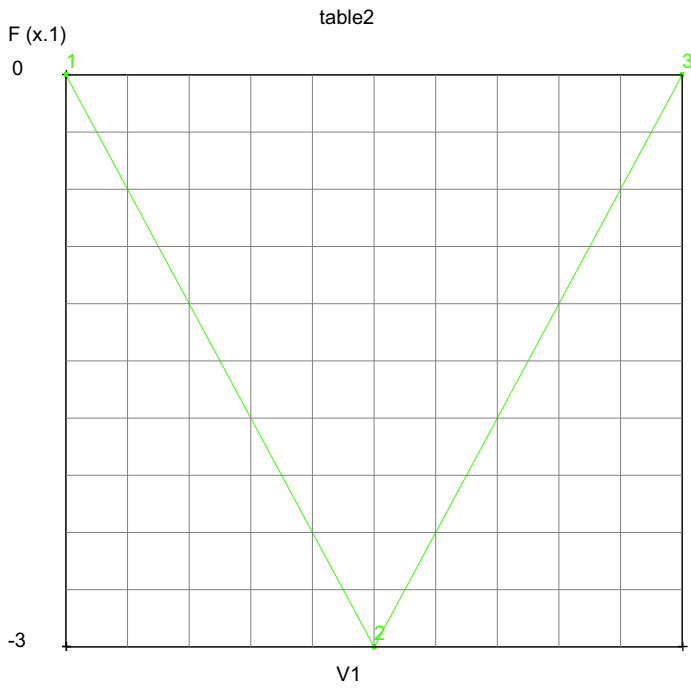


Figure 3.9-5 Punch Position

```

STRUCTURAL
  PLASTICITY (twice)
    INITIAL YIELD STRESS
      1
    TABLE1
      table1 (eq_plastic_strain)
  
```

```
      OK (twice),
MAIN
CONTACT
CONTACT BODIES
  DEFORMABLE
  OK
  ELEMENTS ADD
  ALL:EXISTING
NEW
RIGID
  POSITION PARAMS
    Y=1
  TABLE
    table2 (time),
    OK (twice)
  CURVE ADD
  END LIST
ID CONTACT
NEW
  CONTACT BODY TYPE RIGID
  OK
  CURVES ADD
  END LIST
MAIN
```

(pick cylinder)

(pick all remaining curves)

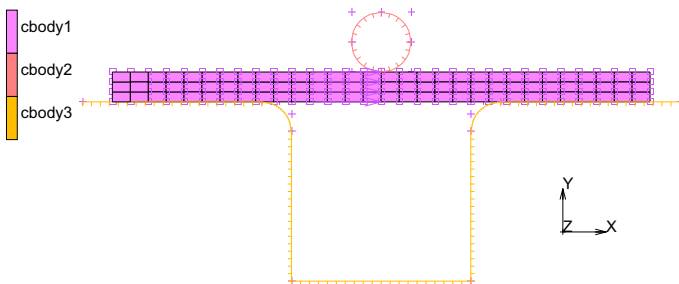


Figure 3.9-6 Identify Contact Bodies

```
LOADCASES
  MECHANICAL
    STATIC
    LOADCASE TIME
      .5
    # OF STEPS
      50
    CONVERGENCE TESTING
      DISPLACEMENTS
      RELATIVE DISPLACEMENT TOLERANCE
        0.001
    OK (twice)
    COPY
    STATIC
      LOADCASE TIME
        .5
      # OF STEPS
        20
    OK
  MAIN
JOBS
NEW
  MECHANICAL
    PROPERTIES
      ANALYSIS OPTIONS
      LARGE STRAIN
      OK
    lcase1
    lcase2
    ANALYSIS DIMENSION: PLANE STRAIN
  JOB RESULTS
    EQUIVALENT VON MISES STRESS
    TOTAL EQUIVALENT PLASTIC STRAIN
    OK
```

CONTACT
CONTROL

ADVANCED CONTACT CONTROL

SEPARATION FORCE

.1

OK

OK (thrice)

SAVE

Run Job and View Results

RUN

SUBMIT

MONITOR

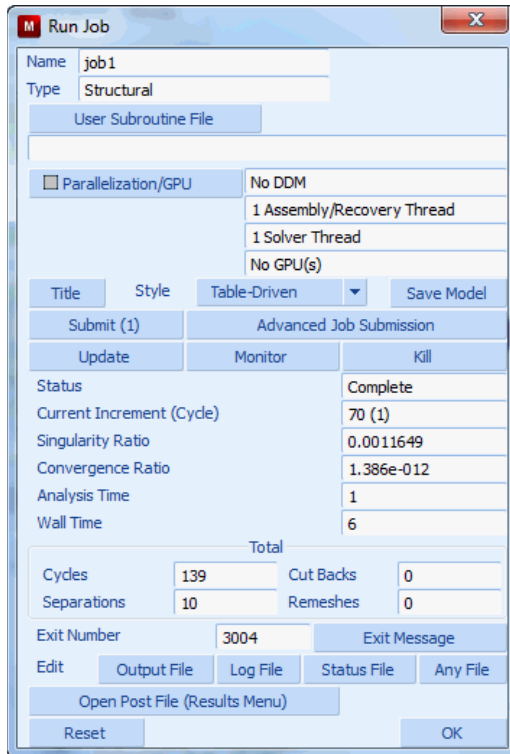


Figure 3.9-7 Run Job Menu

OPEN POST FILE (RESUTLS MENU)
DEF ONLY
SCALAR
TOTAL EQUIVALENT PLASTIC STRAIN
CONTOUR BANDS
SKIP TO INCREMENT 50

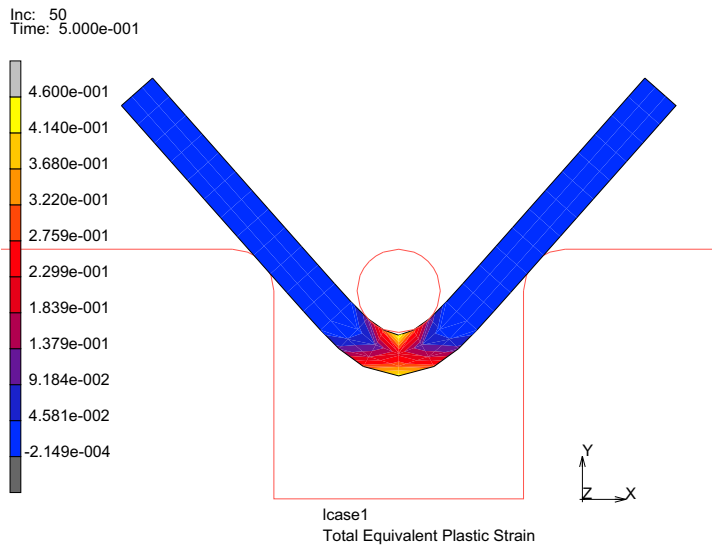


Figure 3.9-8 Plastic Strain Plot at Increment 50

RESULTS
SKIP TO INCREMENT 70

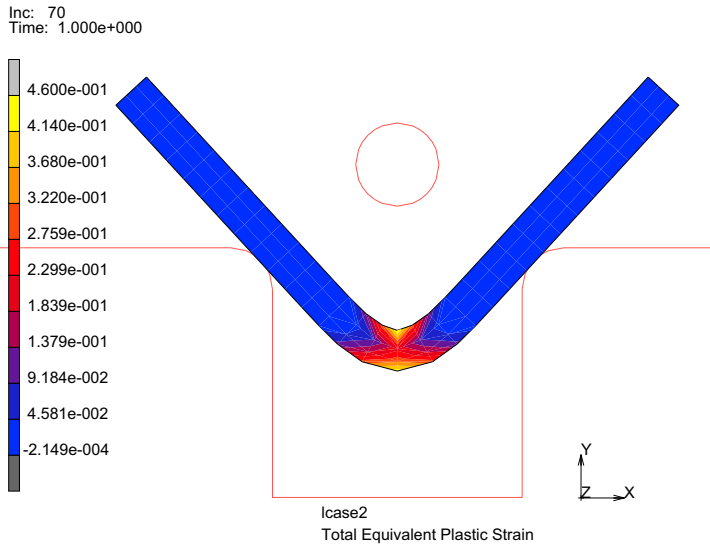


Figure 3.9-9 Plastic Strain Plot at Increment 70

RESULTS

HISTORY PLOT

SET LOCATIONS

n:63 #

ALL INCS

ADD CURVES

GLOBAL

Pos Y cbody2

Force Y cbody2

FIT

(pick bottom middle node n:63)

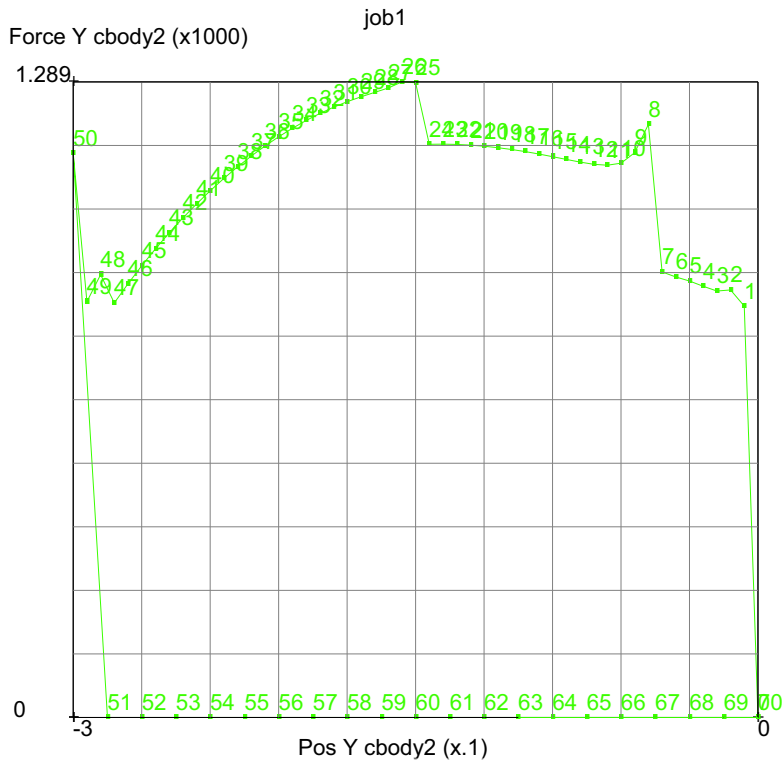


Figure 3.9-10 History Plot of Punch Force versus Stroke

RESULTS

HISTORY PLOT

CLEAR CURVES

ALL INCS

ADD CURVES

ALL LOCATIONS

Total Equivalent Plastic Strain

Equivalent Von Mises Stress

FIT

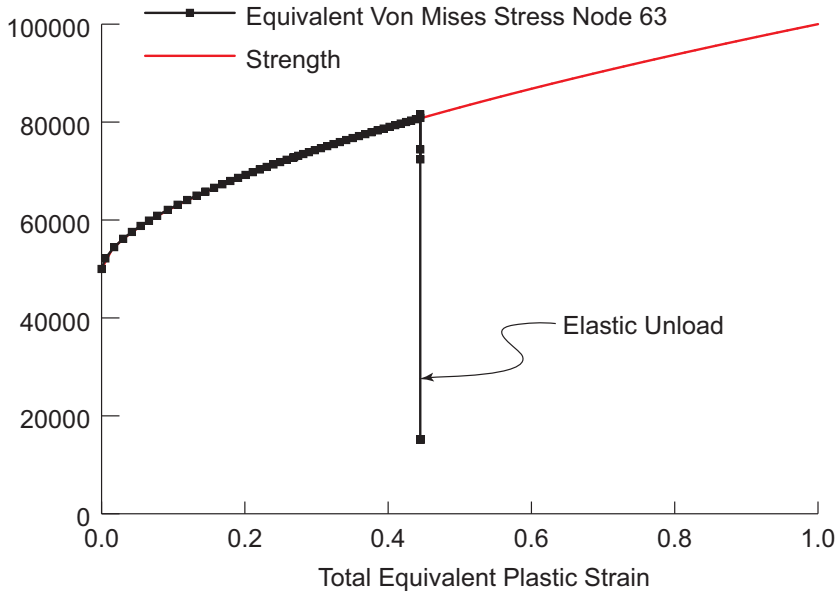


Figure 3.9-11 Stress versus Plastic Strain Node 63

Discussion

Since the sheet completely wraps around the rigid cylinder at the end of the bending, we can estimate the strain assuming that the sheet completely surrounds the cylinder, and by knowing the strain, the stress can also be estimated as shown in Figure 3.9-12.

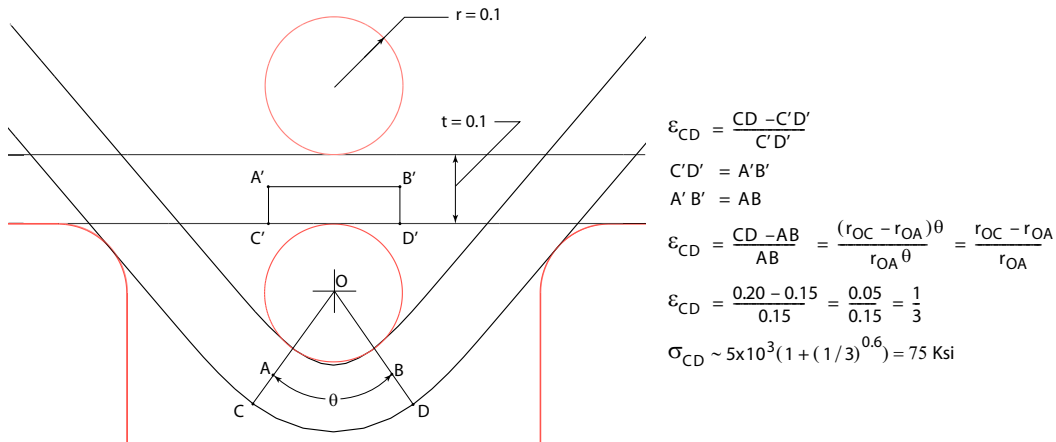


Figure 3.9-12 Estimating the Bending Strain and Stress in the Center of the Sheet

With the stresses estimated, we can assume that a fully plastic hinge forms in the center of the sheet and estimate the punch load as shown in Figure 3.9-13.

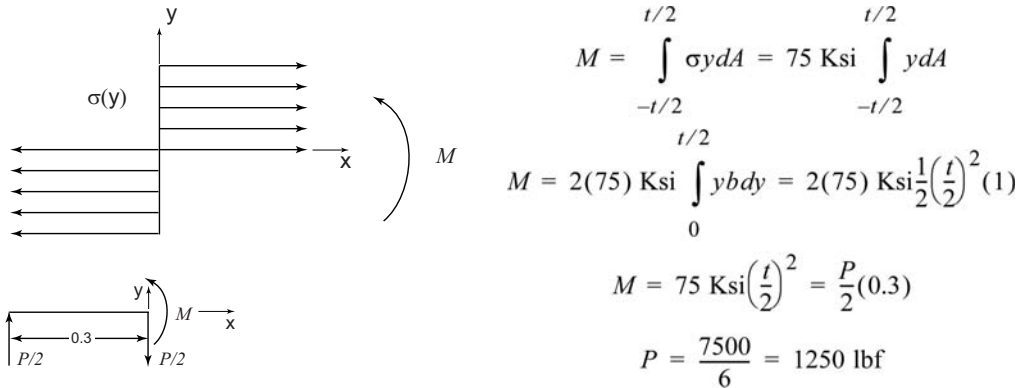


Figure 3.9-13 Estimating the bending moment and maximum punch load

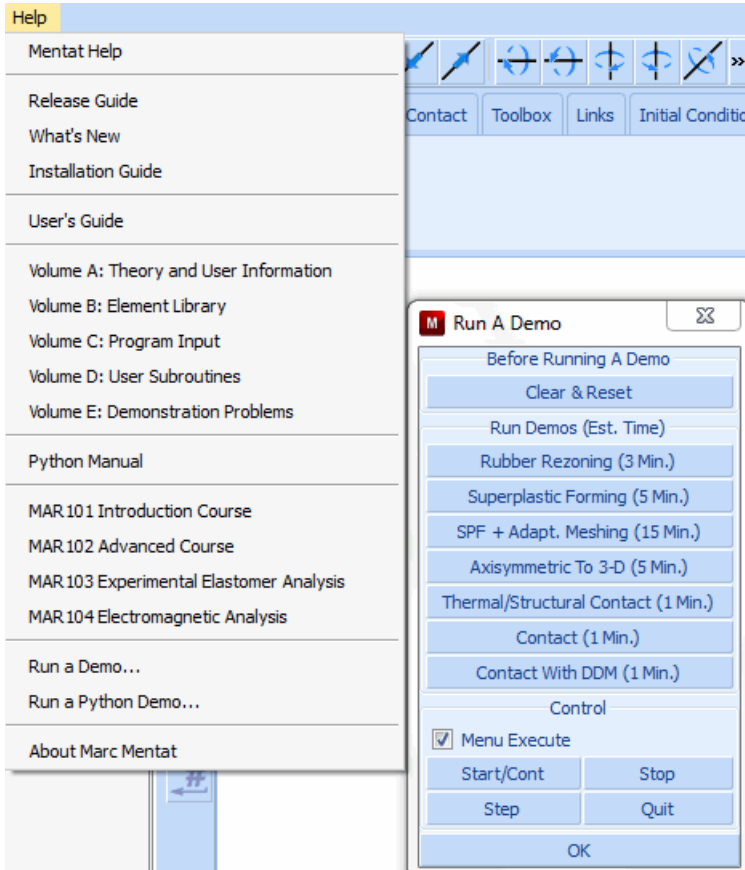
The estimate for the maximum punch load, 1250 lbf, is very close to that found by the analysis as shown in Figure 3.9-10 of 1289 lbf. Finally, although the final angle after spring back appears close to 90° , its actual value is 84° , and the punch stroke should be slightly reduced to form a right angle after springback.

Input Files

The files below are on your [delivery media](#) or they can be downloaded by your web browser by clicking the links (file names) below.

File	Description
s4.proc	Mentat procedure file to run the above example

Also, this problem can automatically be run from the HELP menu under DEMONSTRATIONS > RUN A DEMO PROBLEM > CONTACT as shown below.

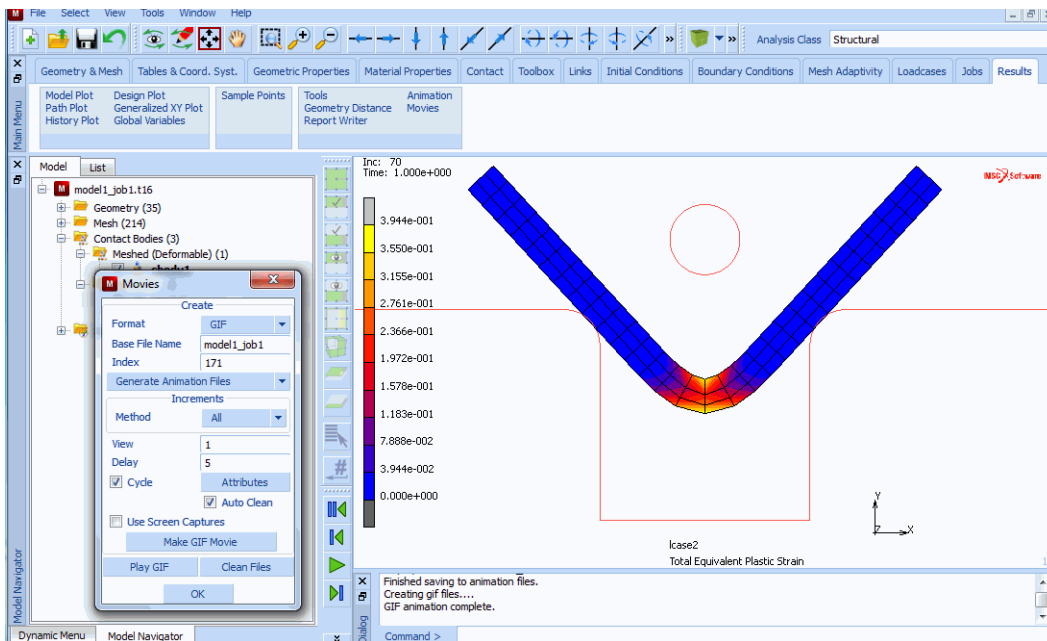


Animation

Click on the figure below to activate the video; it lasts about 10 minutes and explains how the steps above are done. Once the video is activated, a right click of the mouse will open the menu shown at the right; you can switch to various screen sizes or stop the video by disabling the content.

Close Floating Window
Full Screen Multimedia

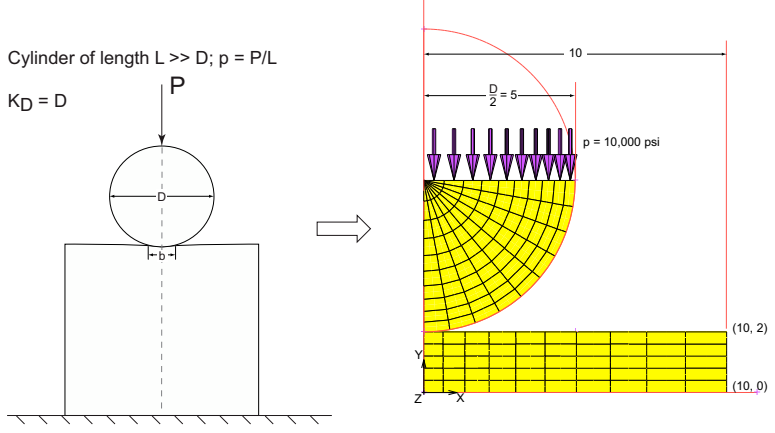
Properties...
Disable Content



3.10 Hertz Contact Problem

- Summary 1062
- Run Jobs and View Results 1068
- FEA versus Theoretical Solutions 1069
- Input Files 1070

Summary

Title	Hertz contact problem									
Problem features	Steel cylinder contacting an aluminum block									
Geometry	<p>Cylinder of length $L \gg D$; $p = P/L$ $K_D = D$</p> 									
Material properties	$E = 30 \times 10^6$ Psi, $\nu = 0.3$ for steel and $E = 10 \times 10^6$ Psi, $\nu = 0.33$ for Al									
Analysis type	Static with elastic material behavior									
Boundary conditions	Symmetry with point load pushing cylinder into block									
Element type	Linear and parabolic plane strain quads									
FE results	<p>Comparison to theory</p> <p>$Max \ \sigma[ksi]\$ Theory versus FEA</p> <table border="1" data-bbox="388 1124 1043 1256"> <thead> <tr> <th>Theory</th> <th>Linear Elements</th> <th>Quadratic Elements</th> </tr> </thead> <tbody> <tr> <td>230.9</td> <td>181.6</td> <td>225.3</td> </tr> <tr> <td>Error (%)</td> <td>-21.4</td> <td>-2.4</td> </tr> </tbody> </table>	Theory	Linear Elements	Quadratic Elements	230.9	181.6	225.3	Error (%)	-21.4	-2.4
Theory	Linear Elements	Quadratic Elements								
230.9	181.6	225.3								
Error (%)	-21.4	-2.4								

In this example problem, a steel cylinder with a radius of 5” is pressed against a 2” deep aluminum base. A small strain elastic analysis is performed, so the only nonlinearity introduced is due to contact. A comparison between using linear and quadratic elements is shown. The problem is similar to the Hertz contact problem in Timoshenko and Goodier, *Theory of Elasticity*, 1951.

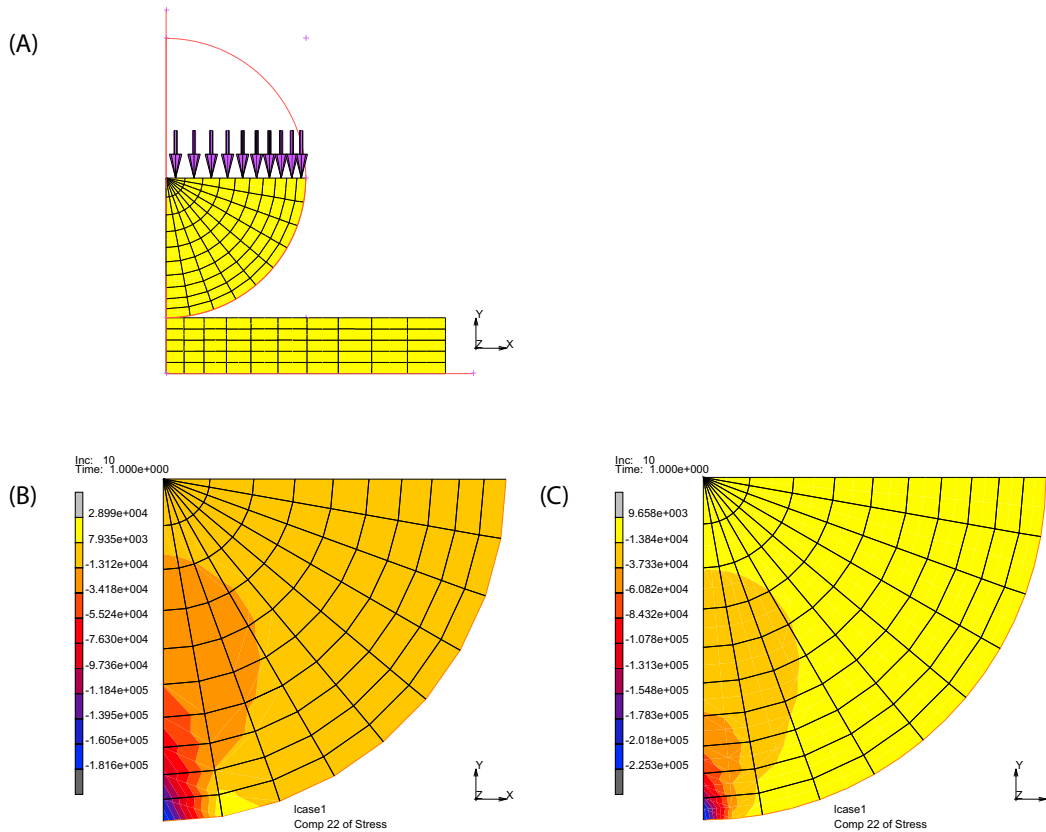


Figure 3.10-1 (A) Finite Element Mesh (B) σ_{yy} using Linear Element (C) σ_{yy} using Quadratic Elements

In this problem, you will modify an existing model and add quadratic elements with contact. The steel material properties have an elastic modulus of 30E6 and a Poisson’s ratio of 0.30 and the aluminum properties have an elastic modulus of 10E6 and a Poisson’s ratio of 0.33. The cylinder and base plate are pressed together with a load of 100,000 lbf or 10,000 psi applied across the diameter of the hemisphere.

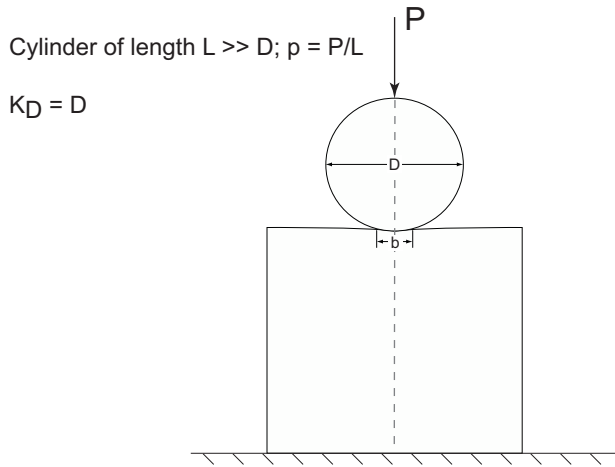


Figure 3.10-2 Cylinder and Base Pressed Together

```
FILES
  OPEN
    hertzbase.mud
  OK
  MAIN
CONTACT
  CONTACT BODIES
  ID CONTACT
  MAIN
```

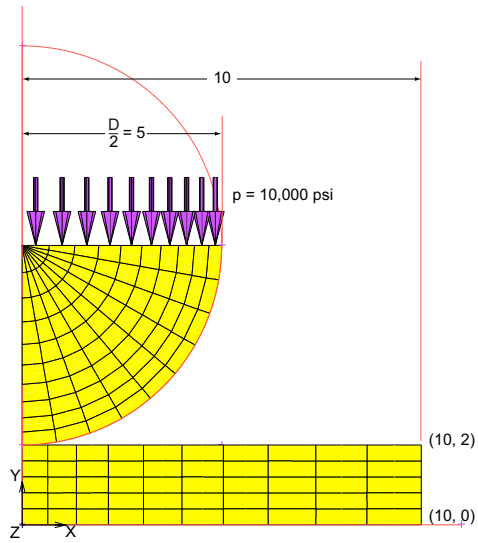



Figure 3.10-3 Hertz Base Analysis

JOBS

RUN

SUBMIT(1)

MONITOR

OK

OPEN POST FILE (RESULTS MENU)

DEF ONLY

SCALAR

Comp 22 of Stress

OK

CONTOUR BANDS

LAST

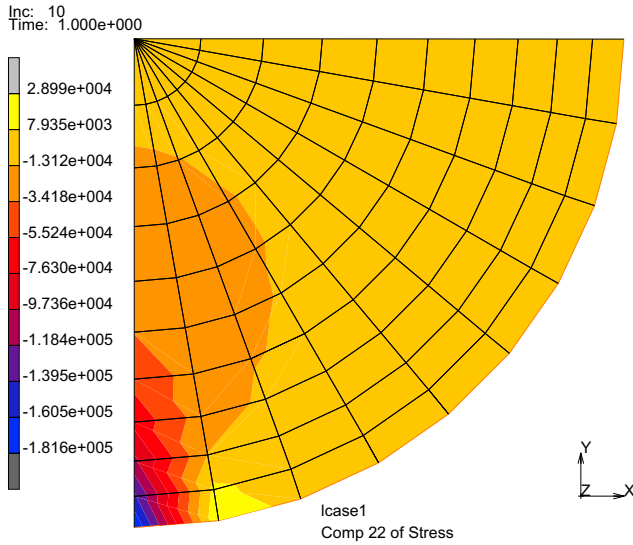


Figure 3.10-4 Hertz Base at Comp 22 of Stress (using Lower-order Elements)

Here, we see that the peak stress using linear elements is around 141 Ksi in compression. We suspect that this is low due to the fact that linear elements cannot capture stress concentration as well as quadratic elements. Therefore, we will change the element type and rerun the problem.

```
CLOSE
FILES
  SAVE AS
    hertzbasequad.mud
  MAIN
```

First, we move the aluminum sheet down one inch, attach edges to the arc, change element types, sweep, and move the aluminum sheet back to its original position.

```
MESH GENERATION
  MOVE
  TRANSLATIONS
    0 -1 0
  ELEMENTS
    a1
  END LIST
  SELECT
```

(select the aluminum elements)

METHOD = PATH
 OK
 EDGES
 END LIST
 OK (twice)

(pick nodes N1, N2, N3)

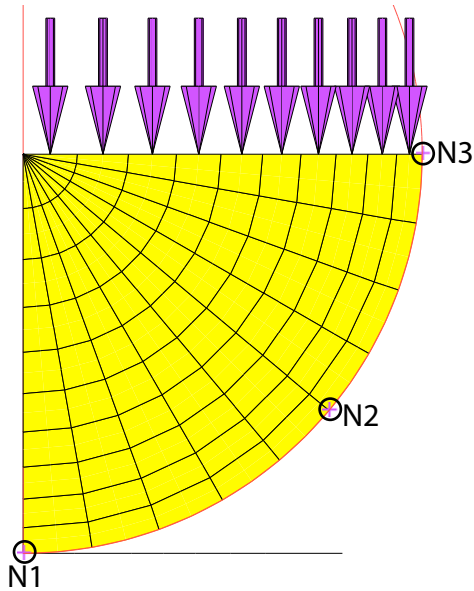


Figure 3.10-5 Steel Cylinder Nodes N1, N2, and N3

ATTACH
 EDGES -> CURVE\
 ALL: SELECTED EDGES
 RETURN
 CHANGE CLASS
 QUAD(8)
 ELEMENTS
 ALL: EXISTING
 RETURN
 SWEEP
 ALL
 RETURN
 RENUMBER

(select circular arc)

ALL
RETURN
MOVE
TRANSLATIONS
0 1 0
ELEMENTS
END LIST
MAIN

(select aluminum elements)

Run Jobs and View Results

JOBS
ELEMENT TYPES
ANALYSIS DIMENSION
SOLID
27
OK
ALL: EXISTING
RETURN
PROPERTIES
CONTACT CONTROL
ADVANCED CONTACT CONTROL
QUAD. SEGMENTS GENUINE,
OK (thrice)
SAVE
RUN
SUBMIT(1)
MONITOR,
OK
OPEN POST FILE (RESULTS MENU)
LAST
DEF ONLY
SCALAR
CONTOUR BANDS
SELECT

(Comp 22 of Stress)

SELECT CONTACT BODY ENTITIES
(steel)
OK
MAKE VISIBLE
FILL

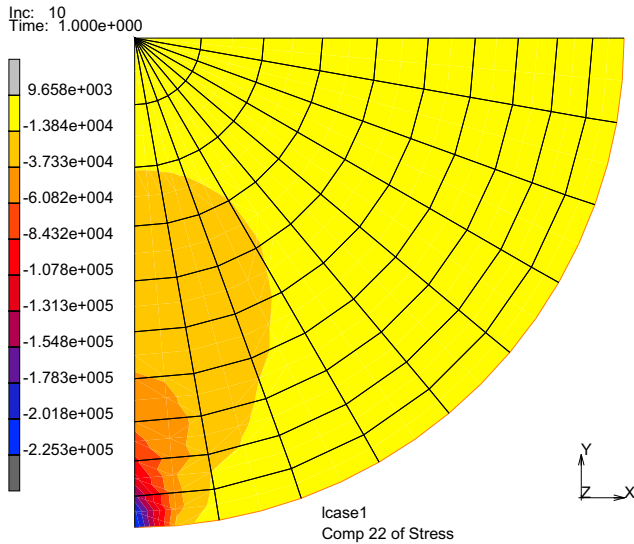


Figure 3.10-6 Results in Steel Cylinder (using Higher-order Elements)

FEA versus Theoretical Solutions

From the 6th Edition of Roark's Formulas for Stress and Strain (by Warren C. Young, 1989, pg 651), we can derive the contact patch, b , and the maximum compressive stress, $Max \sigma$.

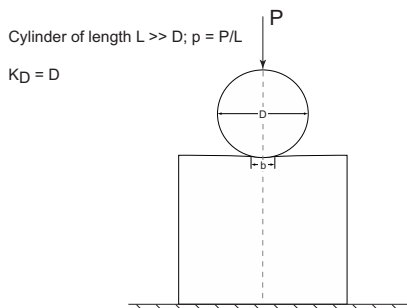


Figure 3.10-7 Steel Cylinder in Contact with Aluminium Base

The contact width for model depicted is given by $b = 1.60 \sqrt{p K_D C_E}$. Where $C_E = \frac{1 - \nu_1^2}{E_1} + \frac{1 - \nu_2^2}{E_2}$, and the contact area for the half model becomes, $\frac{b}{2} = 0.80 \sqrt{p K_D C_E} = 0.276$.

The maximum stress becomes $Max \sigma = 0.798 \sqrt{\frac{p}{K_D C_E}} = 230.9 Ksi$.

Table 2.10-1 $Max \|\sigma [ksi]\|$ Theory versus FEA

Theory	Linear Elements	Quadratic Elements
230.9	181.6	225.3
Error (%)	-21.4	-2.4

Input Files

The files below are on your [delivery media](#) or they can be downloaded by your web browser by clicking the links (file names) below.

File	Description
s8.proc	Mentat procedure file to run the above example
hertzbase.mud	Mentat model file read by above procedure file

3.11 Anisotropic Sheet Drawing using Reduced Integration Shell Elements

- Chapter Overview 1072
- Simulation of Earing for Sheet Forming with Planar Anisotropy 1073
- Boundary Conditions 1074
- Advanced Topic: Drawbead Modeling using Nonlinear Spring 1089
- Input Files 1094
- References 1095

Chapter Overview

In many manufacturing area such as packing, automotive, aerospace, and electronics industries, the control of sheet metal forming processes has become a key factor to reduce the development time and the final cost of products. In general, sheet metal forming is analyzed on the basis of stretching, drawing, bending, or various combinations of these basic modes of deformation, which, from the viewpoint of mechanics, involve nonlinearity resulting from geometry, material, and contact aspects. Numerical simulations of sheet forming processes need to account for those nonlinearities. The following aspects warrant special attention:

1. Geometric Nonlinearity:

In order to describe the nonlinear geometric behavior, especially shells, three basic approaches can be identified: degenerated shell elements, classical shell elements, and more recently, enhanced strain formulation. The need for large-scale computations together with complex algorithms for geometrical and material nonlinear applications motivated finite element researchers to develop elements that are simple and efficient. Various significant research has been carried out to develop reduced integration shell element based on the degenerated shell approach. A one point quadrature shell has been developed in Marc based on the work of Cardoso, [Reference 1](#). This is a four-node, thick-shell element with global displacements and rotations as degrees of freedom. Bilinear interpolation is used for the coordinates, displacements and the rotations. This shell introduced the MITC4 shell geometry with the ANS (Assumed Natural Strain) method in conjunction with the physical stabilization scheme to construct an element with reduced integration, which is free of any artificial correction for warping. This procedure improves the accuracy of one point quadrature shell element without sacrificing the computational speed and permits large nonlinear behavior. The nodal fiber coordinate system at each node is update by a step-by-step procedure in order to consider the warping of the element. A rigid-body projection matrix is applied to extract out rigid-body motion so the element can undergo large rotations.

2. Material Nonlinearity:

The nonlinear plastic behavior must account for the anisotropy exhibited by sheet metals. During cold working, anisotropic properties change due to the material microstructure evolution. The assumption that the change of anisotropic properties during plastic deformation is small and negligible when compared to the anisotropy induced by rolling has been widely adopted in the analysis of sheet metal forming. The appropriate anisotropic yield functions for sheet metal forming simulations is important to obtain a reliable material response. Barlat, [Reference 2](#) proposed a general criterion for planar anisotropy that is particularly suitable for aluminum alloy sheets. This criterion has been shown to be consistent with polycrystal-based yield surfaces, which often exhibit small radii of curvature near uniaxial and balanced biaxial tension stress states. An advantage of this criterion is that its formulation is relatively simple as compared with the formulation for polycrystalline modeling and, therefore, it can be easily incorporated into finite element (FE) codes for the analysis of metal forming problems. Mentat provides the automatic calculation of the anisotropic coefficients directly from experimental data.

3. Drawbead Modeling:

To form complex shaped surface, drawbeads are used to insure the accuracy of the final shape, and also to prevent fracture and cracks. Extreme caution has to be placed in installing drawbeads, especially in the case of an aluminum plate that has low flexibility. The design of drawbeads are determined based on the result of try-out, which causes forming tool design to be rather difficult. Therefore, there is the need for the development of a logical numerical method, for understanding the quantitative effect of the drawbeads at the stage of die design. In Marc, a simple drawbead model based on nonlinear spring concepts has been developed. The nonlinear drawbead force with displacement is applied to the nodes located on the blank edges.

4. Forming Limit Analysis:

Forming Limit Diagrams (FLD) are used extensively during tool design for the manufacturing of sheet metal parts. It is also used for trouble shooting during regular shop floor production. It is observed that FLD is strongly dependent on the basic mechanical properties of sheet metal like the work hardening exponent, initial sheet thickness, and the strain rate sensitivity. In addition, it is found that strain paths have significant influence on the limit strains that develop during sheet metal forming. In Marc, the combined method accommodating localized necking and diffused necking with Keeler's experimental work (IDDRG, 1976) was adopted to predict FLD.

The cup drawing example presented here was designed to demonstrate four features: One-point integration shell element, Barlat's yield function, drawbead modeling with nonlinear springs, and FLD. The tool geometry and material data was taken from NUMISHEET 2002 benchmark, [Reference 3](#). But, process conditions are slightly different from the original data.

Simulation of Earing for Sheet Forming with Planar Anisotropy

The cup drawing test simulation with circular punch and blank is one of most popular tests to verify the planar anisotropic behavior through the prediction of the earing profile. In the cylindrical cup drawing test, the material undergoes compressive deformation in the flange area due to the circumferential contraction. Some stretching occurs also in the radial direction of a cup. This test was simulated for a 6111-T4 aluminum alloy sheet based on the new one-point shell element and Barlat's yield function. Also, FLD prediction and drawbead modeling with nonlinear spring were investigated. Assuming isotropic hardening, the yield function coefficients are kept constant during the simulation. The schematic view of the cup drawing process analyzed are shown in [Figure 3.11-1](#).

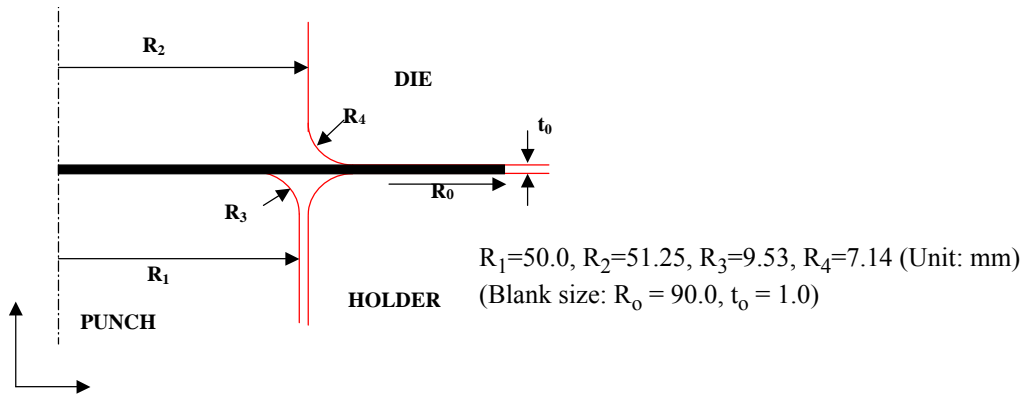


Figure 3.11-1 Tool for Cylindrical Cup Drawing

Only a quarter section of the cup was analyzed in the light of the orthotropic symmetry. The generation of mesh using Mentat is straightforward, so it is not discussed here. The generated mesh was stored in `sheet_mesh.mud`.

Boundary Conditions

The symmetric boundary conditions were imposed for the corresponding symmetric nodes using two boundary node sets: (1) x-displacement y and z rotations are zero for the nodes located in $y=0$ and (2) y-displacement x and z rotations are zero for the nodes located in $x=0$.

BOUNDARY CONDITIONS

NEW

MECHANICAL

FIXED DISPLACEMENT

DISPLACEMENT X

0

ROTATION Y

0

ROTATION Z

0

OK

NODES ADD

2 39 57 75 93 111 129 147 165 183 201

219 237 255 273 291 309 327 345 363 381

END LIST

```

NEW
MECHANICAL
  FIXED DISPLACEMENT
    DISPLACEMENT Y
      0
    ROTATION X
      0
    ROTATION Z
      0
  OK
  NODES ADD
    2 3 4 5 6 7 8 9 10 11 12
    13 14 15 16 17 18 19 20 21 1
  END LIST
  
```

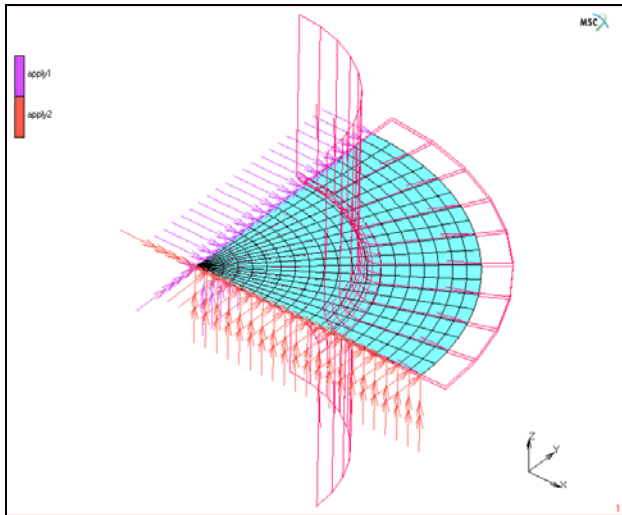


Figure 3.11-2 Boundary Condition ID

Material Properties

Two tables are provided to characterize stress vs. strain behavior and to control the motion of rigid surface (punch). The stress-strain law for 6111-T4 aluminum alloy sheet is given as follows:

$$\bar{\sigma} = 429.8 - 237.7 * \exp(-8.504 \bar{\epsilon}_p)$$

Voce-hardening curve is used to fit the saturation behavior of the aluminum alloy.

MATERIAL PROPERTIES

TABLES

NEW

NEW TABLE

1 INDEPENDENT VARIABLE

TYPE

eq_plastic_strain

FORMULA

$428.8 - 237.7 * \exp(-8.504 * v1)$

FIT

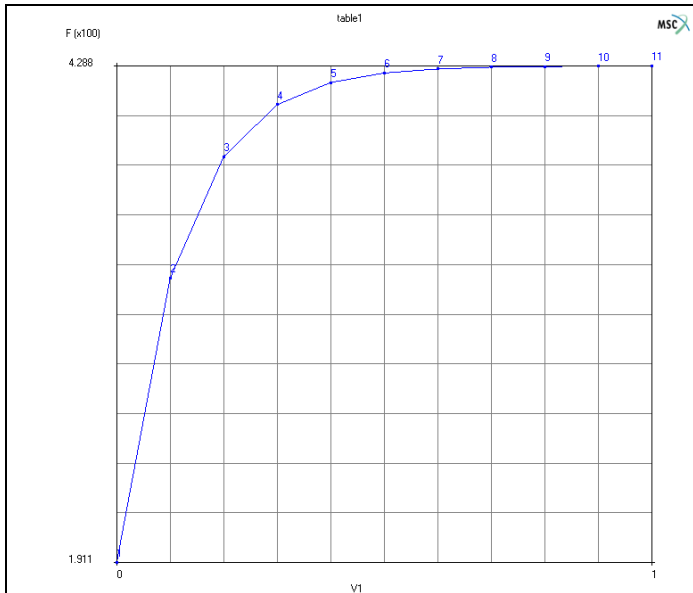


Figure 3.11-3 Generated Table for Stress-Strain Curve

A second table representing a ramp function for control of rigid-body (especially for punch) is generated by simply adding few points.

TABLES

NEW

NEW TABLE

1 INDEPENDENT VARIABLE

```

TYPE
      time
ADD
      0 0
      1 1
FIT
    
```

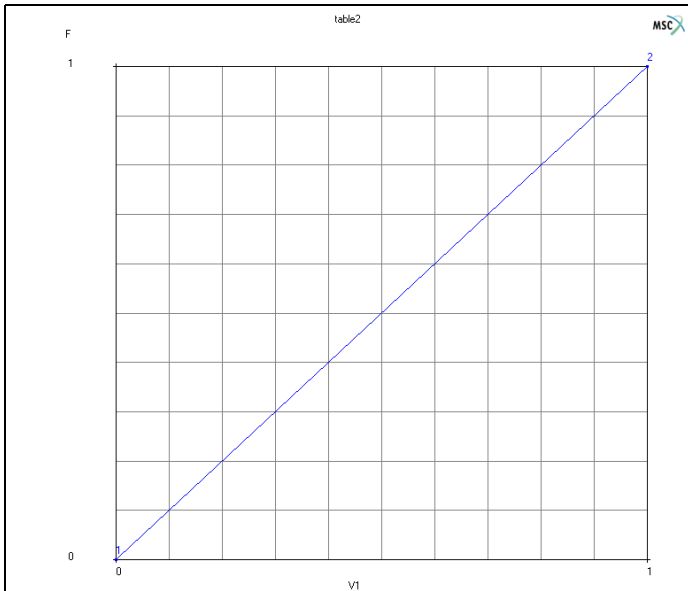


Figure 3.11-4 Generated Table for Rigid-Body Control

The material for all elements is treated as an elasto-plastic properties with Young's modulus of 70 Gpa, Poisson's ratio of 0.3, and the initial yield stress of 192.1. Anisotropic material data for Barlat's yield functions is taken from Numisheet 2002 benchmark:

Anisotropic material data for Barlat's (1991) yield criterion

Yield stresses: $Y_0 = 192.1, Y_{45}=187.4, Y_{90}=181.2, Y_b=191.4$
 (Ratio: $Y_{45}/Y_0 = 0.9755, Y_{90}/Y_0 = 0.9432, Y_b/Y_0 = 0.9963$)

Exponent: $m=8$

Marc calculates Barlat's anisotropic coefficients ($C_1, C_2, C_3, C_4, C_5, C_6$) directly from raw experimental data (initial yield stresses along 0,45,90, biaxial directions) by solving a nonlinear equation. If Barlat's anisotropic coefficients are already known, then the calculation is not necessary and direct input of the coefficients is also allowed in Mentat. If the biaxial yield stress (Y_b) is not available, Y_b/Y_0 could be assumed to be 1. The material coefficients, $C_{i=1-6}$,

represent anisotropic properties. When $C_{i=1-6}=1$, the material is isotropic and Barlat's (1991) yield function reduces to the Tresca yield condition for $m = 1$ or ∞ , and the von Mises yield criterion for $m = 2$ or 4. The exponent “m” is mainly associated with the crystal structure of the material. A higher “m” value has the effect of decreasing the radius of curvature of rounded vertices near the uniaxial and balanced biaxial tension ranges of the yield surface, in agreement with polycrystal models. Values of $m = 8$ for FCC materials (e.g. aluminum) and $m = 6$ for BCC materials (e.g. steel) are recommended.

The yield surface has been proven to be convex for $m \geq 1$. Figure 3.11-5 shows the yield surfaces obtained from von Mises, Hill, and Barlat's yield functions for an aluminum alloy.

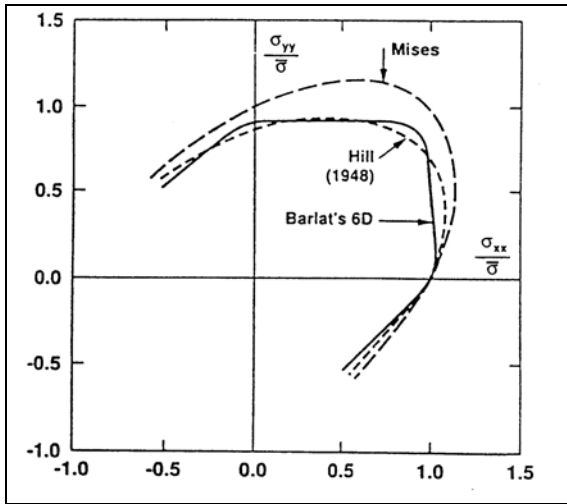


Figure 3.11-5 Comparison of Yield Surfaces Obtained from von Mises, Hill, and Barlat's Yield Functions

The ORIENTATION option is required to assign the initial rolling and transverse direction for all elements. In the simulation, rolling direction vector is (1,0,0) and transverse direction is (0,1,0).

FLD Prediction

In order to accommodate failure prediction in the analysis results, the FLD_0 value as shown in Figure 3.11-6 need to be inserted. The FLD_0 value increases with the strain-hardening exponent, n , and the strain-rate exponent, m .

According to large amount of experiments, the real FLD curves are also affected by the thickness of the sheet metal. This phenomenon is referred as thickness effect and it is characterized as thickness coefficient t_c . Experiments tended to express this relationship by Keeler:

$$FLD_0 = Q \cdot (0.233 + t_c \cdot T)$$

where $Q = n/0.21$, if n is less than 0.21 otherwise $Q = 1.0$. T is the thickness of the sheet metal. The thickness coefficient, t_c is the set as 3.59 if the unit used to define the thickness is 'Inch'. If unit of 'mm' is used, t_c is the set as 0.141. For this material, the effective value of n is 0.226.

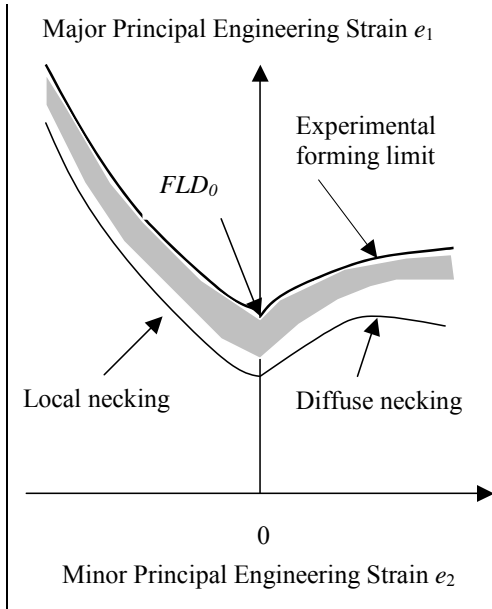


Figure 3.11-6 Forming Limit Diagram

MATERIAL PROPERTIES

NEW

ISOTROPIC

YOUNG'S MODULUS

70000

POISSON'S RATIO

0.3

ELASTO-PLASTIC

YIELD SURFACE

BARLAT

INITIAL YIELD STRESS

1

TABLE

table1

EXPERIMENTAL DATA INPUT

EXPERIMENTAL DATA

M

Y45/Y0

0.9755

Y90/Y0

0.9432

YB/Y0

0.9963

COMPUTE

COMPUTED DATA

APPLY

OK (twice)

FORMING LIMIT

PREDICTED

STRAIN HARDENING EXP.

0.226

THICKNESS COEFFICIENT

0.141

OK (twice)

ORIENTATIONS

NEW

ZX PLANE

ELEMENTS ADD

ALL EXIST

RETURN

ELEMENTS ADD

ALL EXIST

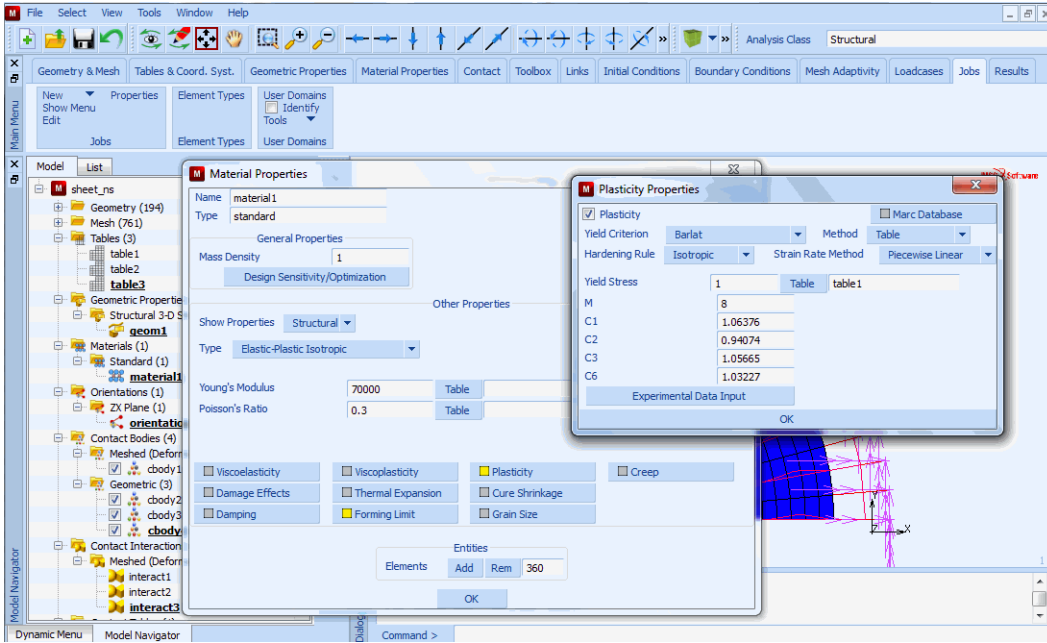


Figure 3.11-7 Calculation of Barlat's Anisotropic Coefficients

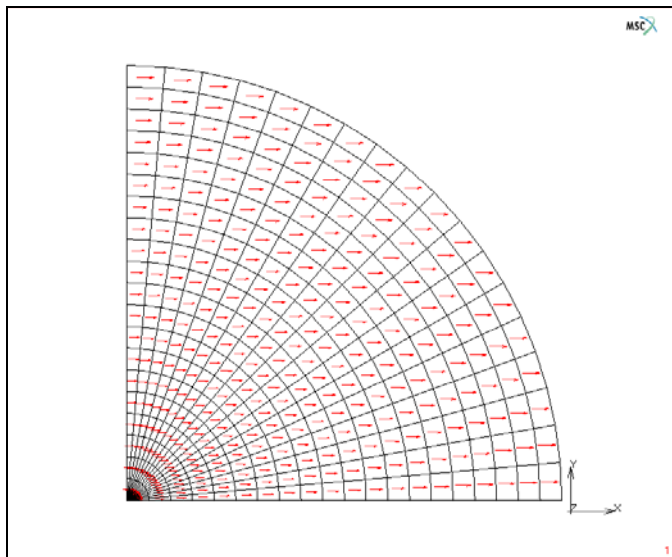


Figure 3.11-8 Orientation Arrow for Rolling Direction

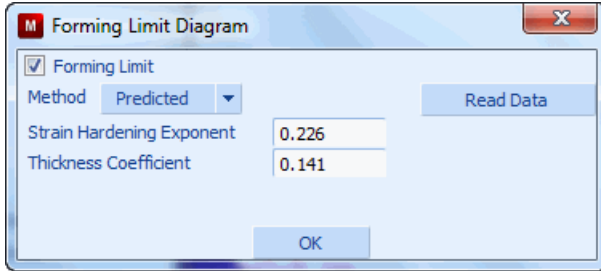


Figure 3.11-9 FLD (Forming Limit Diagram) Input

Geometric Properties

The sheet thickness is 1 mm and shell elements are also used for the analysis

GEOMETRIC PROPERTIES

NEW

3D

SHELL

THICKNESS

1

FLAT ELEMENT

OK

ELEMENTS ADD

ALL EXIST

Contact

The first body is the deformable workpiece; the second, the third, and the fourth are respectively the rigid punch, rigid die, and rigid holder defined with analytical surfaces. Friction coefficient was taken as 0.05. The second body (punch) is moved up to 40 mm with fixed displacement boundary condition using `table2` in CONTACT BODY option. The gap between die and blankholder is uniform.

CONTACT

CONTACT BODIES

NEW

DEFORMABLE

FRICITION COEFFICIENT

0.05

OK

```

ELEMENTS ADD
ALL EXIST
NEW
RIGID
    POSITION
    PARAMETERS
        POSITION (CENTER OF POSITION)
            Z
                40
            OK
        TABLE
            table2
        OK
    FRICTION COEFFICIENT
        0.05
    ANALYTICAL
    OK
SURFACES ADD
    1 2 3 4 5 6 7 8 9 10 11 12 13 14 15
    16 17 18 19 20 21 22 23 24 25 26 27
END LIST
NEW
RIGID
    VELOCITY
    FRICTION COEFFICIENT
        0.05
    ANALYTICAL
    OK
SURFACES ADD
    28 29 30 31 32 33 34 35 36 37 38 39 40 41 42
    43 44 45 46 47 48 49 50 51 52 53 54
END LIST
NEW
RIGID
    VELOCITY
    FRICTION COEFFICIENT

```

```
0.05
ANALYTICAL
OK
SURFACES ADD
56 57 58 59 60 61 62 63
END LIST
RETURN
CONTACT TABLE
NEW
PROPERTIES
  cbody1 cbody2
    CONTACT TYPE
      TOUCHING
    DISTANCE TOLERANCE
      0.1
    SEPARATION THRESHOLD
      10.0
    OK
  cbody1 cbody3
    CONTACT TYPE
      TOUCHING
    DISTANCE TOLERANCE
      0.1
    SEPARATION THRESHOLD
      10.0
    OK
  cbody1 cbody4
    CONTACT TYPE
      TOUCHING
    DISTANCE TOLERANCE
      0.1
    SEPARATION THRESHOLD
      10.0
    OK (twice)
```

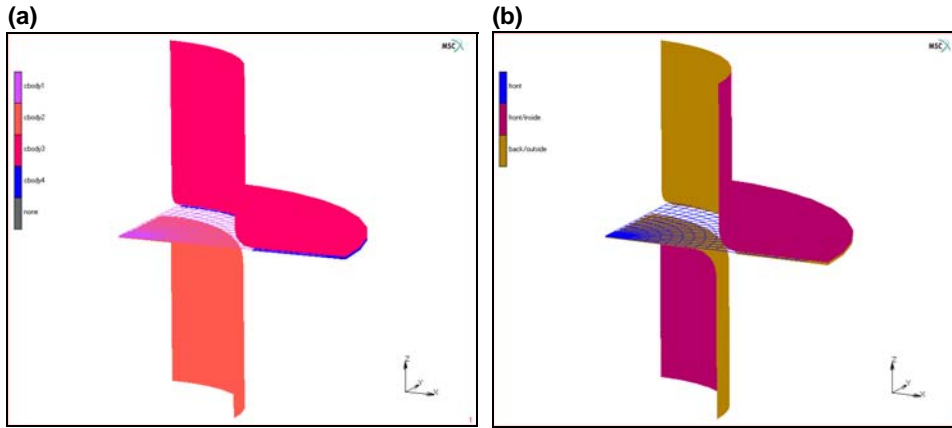


Figure 3.11-10 Contact ID: (a) ID Contact (b) ID Backface

Load Steps and Job Parameters

A total of 100 fixed steps are used for the entire analysis with a convergence displacement norm of 0.1.

```

LOADCASES
  MECHANICAL
    NEW
    STATIC
      CONTACT
        CONTACT TABLE
          ctable1
        OK
      CONVERGENCE TESTING
        RELATIVE
        DISPLACEMENTS
        RELATIVE DISPLACEMENT TOLERANCE
          0.1
        OK
      STEPPING PROCEDURE
        CONSTANT TIME STEP
        # STEP
          100
        OK
    
```

The analysis is a normal mechanical analysis with one loadcase. COULOMB FOR ROLLING option is selected with a bias factor of 0.9. New post variable Forming Limit Parameter is selected in this example, besides the Equivalent Von Mises Stress and Equivalent Plastic Strain. The ADDITIVE DECOMPOSITION option must be chosen for plasticity procedure when the anisotropic yield function is used.

JOBS

NEW

MECHANICAL

LOADCASES

activate:

lcase1

CONTACT CONTROL

FRICITION TYPE

COULOMB FOR ROLLING

INITIAL CONTACT

CONTACT TABLE

ctable1

OK

ADVANCED CONTACT CONTROL

DISTANCE TOLERANCE

0.1

DISTANCE TOLERANCE BIAS

0.9

SEPARATION FORCE

10

OK (twice)

ANALYSIS OPTIONS

PLASTICITY PROCEDURE

LARGE STRAIN ADDITIVE

OK

JOB RESULTS

AVAILABLE ELEMENT SCALARS

Equivalent Von Mises Stress

Total Equivalent Plastic Strain

Forming Limit Parameter

Major Engineering Strain

Minor Engineering Strain
OK (twice)

For the analysis of the cup-drawing, newly developed one-point quadrature shell element of 140 is being used.

ELEMENT TYPES
MECHANICAL
3-D MEMBRANE SHELL
140
OK
ALL: EXIST

Save Model, Run Job, and View Results

FILE
SAVE AS
sheet.mud
OK
RETURN
RUN
SUBMIT 1
MONITOR
OK
MAIN
RESULTS
OPEN
sheet.t16
OK
DEF & ORIG
CONTOUR BAND
SCALAR
Equivalent Von Mises Stress
OK
MONITOR
SCALAR
Forming Limit Parameter

OK
MONITOR
SCALAR
Equivalent Plastic Strain
OK

MONITOR

Figure 3.11-11 shows the top view of deformed configurations based on simulation and experiment. The experimental cup shape measured from Numisheet 2002 benchmark is used for the comparison. It is shown that both results are compatible. Figure 3.11-12 shows FLD parameter and equivalent plastic strain. Forming Limit Parameter covers the range of 0 to 1, where “0.0” means no strain and “1.0” means failure.

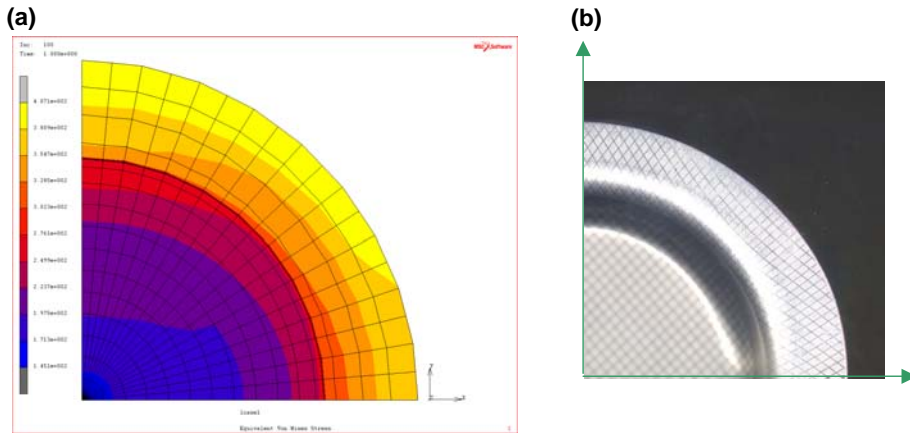


Figure 3.11-11 Top View for Deformed Shape at the Punch Stroke of 40 mm: (a) Simulation (b) Experiment

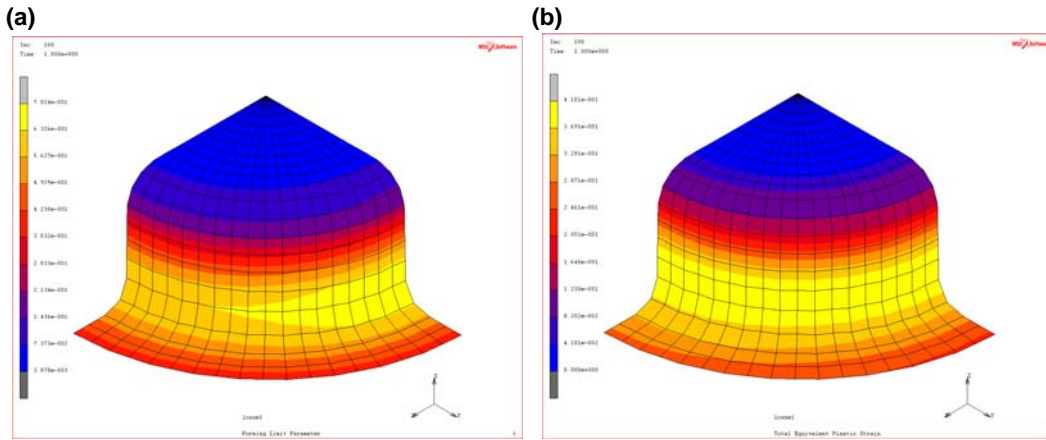


Figure 3.11-12 Deformed Configuration at the Punch Stroke of 40 mm:
 (a) Forming Limit Parameter (b) Equivalent Plastic Strain

Advanced Topic: Drawbead Modeling using Nonlinear Spring

Nonlinear springs in Marc is designed for multiple purposes. Nonlinear springs can be specified using either *spring stiffness* or *spring force*. Spring stiffness method is usually used for heat transfer coefficients for thermal springs, electrical conductivity for electrical springs. While, spring force method can be used for flux for thermal springs, current for electrical springs and drawbead model in sheet metal forming, etc. When nonlinear spring force option is employed, the use of a table as a function of displacement is required, the spring stiffness based on the table gradient is then internally calculated.

In order to utilize a simple drawbead model based on nonlinear spring concepts, the nonlinear drawbead force with displacement is applied to the nodes located on the blank edges. For the implementation, force vs. displacement table, LINKS and boundary condition need to be added.

Links

For the spring force-displacement table, analytical formula using $500 * \tanh(x)$ was used.

```

TABLES
  NEW
  TYPE
    displacement
  FORMULA
    500*tanh(v1)
  FIT
    
```

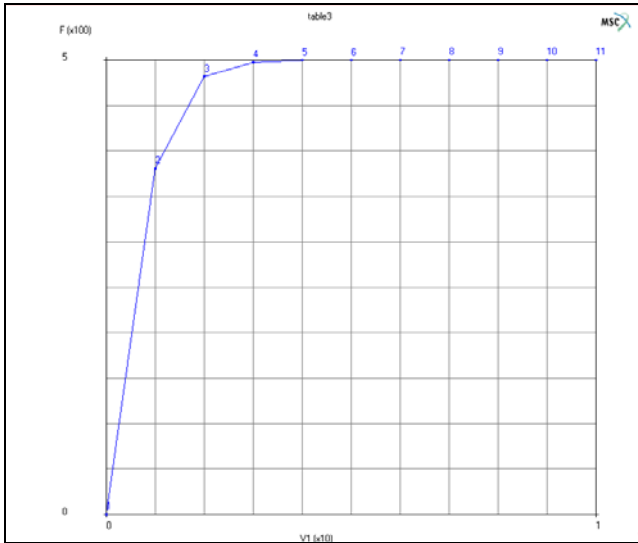


Figure 3.11-13 Generated Table for Nonlinear Spring Behavior (Force vs. Displacement)

For the creation for nonlinear springs, the N TO N SPRING option is used to generate 19 springs combined with table3 (force vs. displacement).

LINKS

SPRINGS/DASHPOTS

N TO N SPRINGS

TYPE

TRUE DIRECTION

BEHAVIOR

PROPERTIES

FORCE

SET

1

TABLE

table3

OK

ADD SPRINGS

(Enter n to n spring/dashpots begin node path)

364 365 366 367 368 369 370 371 372 373

374 375 376 377 378 379 380 381 1

END LIST

(Enter n to n spring/dashpots begin node path)

383 384 385 386 387 388 389 390 391 392
 393 394 395 396 397 398 399 400 401

END LIST

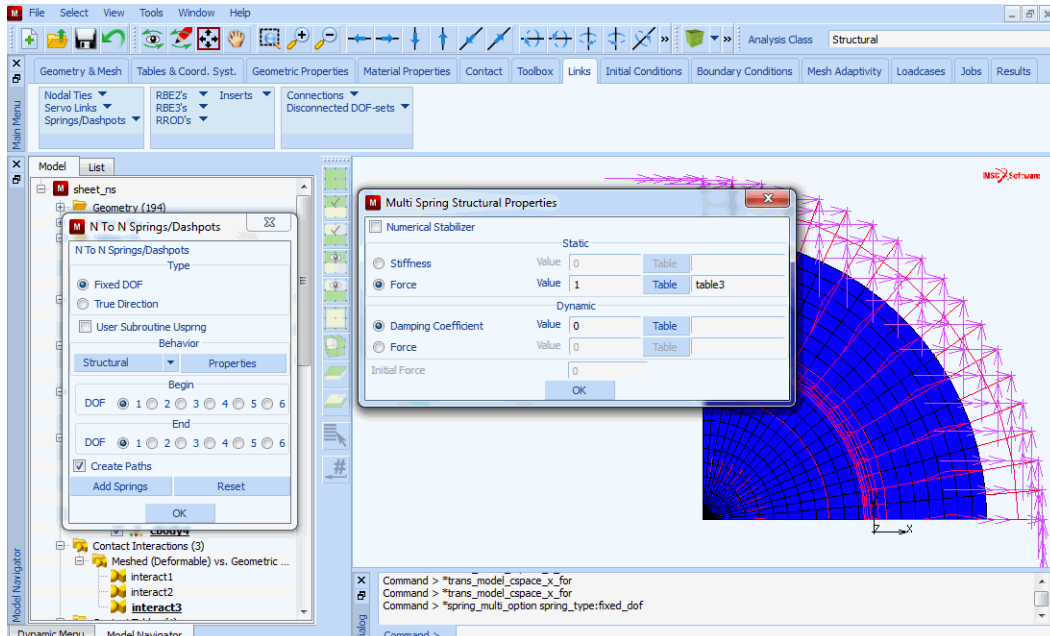


Figure 3.11-14 Nonlinear Springs based on Spring Force Method

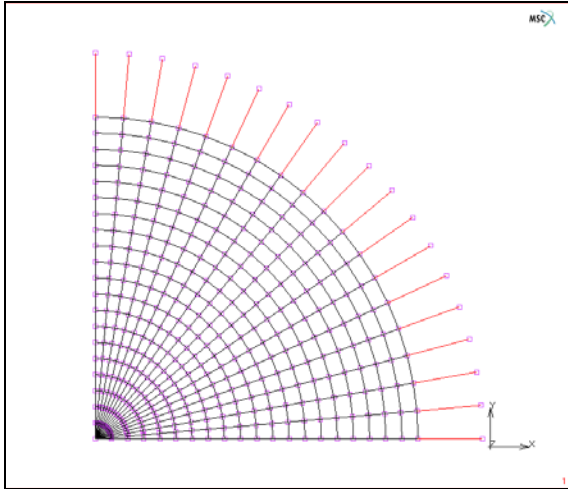


Figure 3.11-15 Generated Nonlinear Springs

Boundary Conditions

The spring nodes, which are not connected with sheet metal must be constrained in all directions.

BOUNDARY CONDITIONS

NEW

MECHANICAL

FIXED DISPLACEMENT

DISPLACEMENT X

0

DISPLACEMENT Y

0

DISPLACEMENT Z

0

ROTATION X

0

ROTATION Y

0

ROTATION Z

0

OK

NODES ADD

```

383 384 385 386 387 388 389 390 391 392 393
394 395 396 397 398 399 400 401
END LIST

```

Save Model, Run Job, and View Results

```

FILE
  SAVE AS
    sheet_ns.mud
  OK
  RETURN
RUN
  SUBMIT 1
  MONITOR
  OK
MAIN
RESULTS
  OPEN
    sheet.t16
  OK
  DEF & ORIG
  CONTOUR BAND
  SCALAR
    Equivalent Von Mises Stress
  OK
  MONITOR
  SCALAR
    Forming Limit Parameter
  OK
  MONITOR
  SCALAR
    Equivalent Plastic Strain
  OK
  MONITOR

```

Figure 3.11-16 shows the top views for the deformed configuration. As shown in the figure, the use of nonlinear springs as drawbead constrains the flow of sheet metal into die cavity. Hence, less draw-in is observed compared to the results based on the simulation without nonlinear springs. Also, Figure 3.11-17 shows Forming Limit Parameter and Equivalent Plastic Strain contours. Compared with Figure 3.11-12 (simulation without nonlinear spring), the levels of Forming Limit Parameter and Equivalent Plastic Strain are larger due to more plastic deformation.

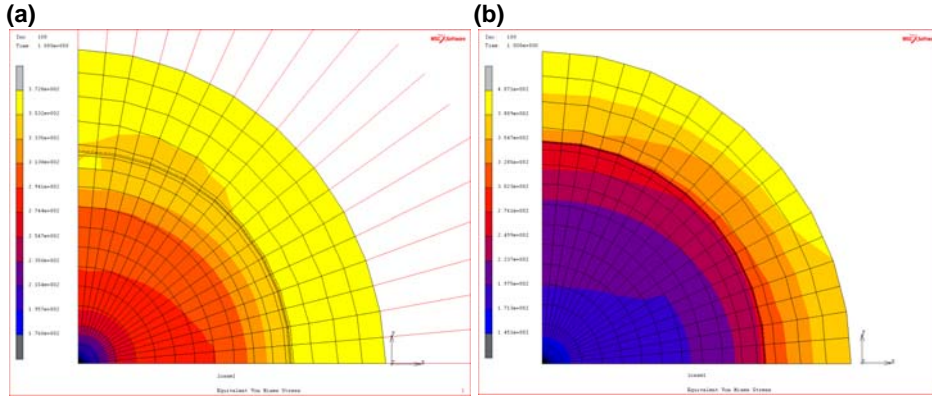


Figure 3.11-16 Top View for Deformed Shape at the Punch Stroke of 40 mm:
(a) with Nonlinear Springs (b) without Nonlinear Springs

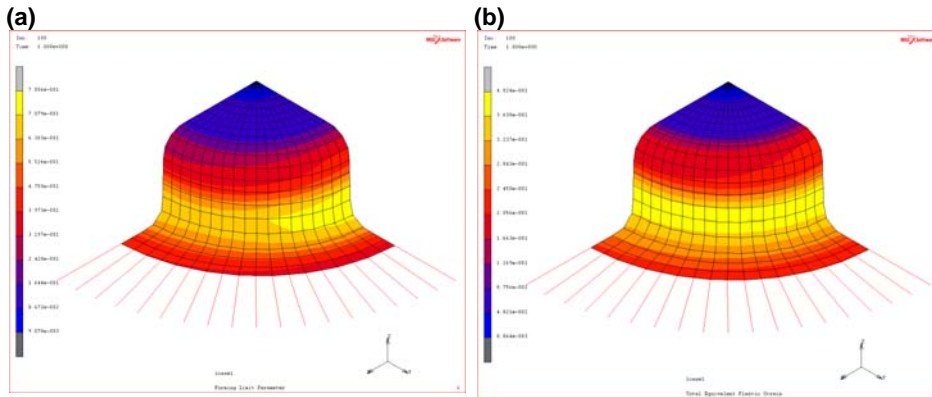


Figure 3.11-17 Deformed Configurations at the Punch Stroke of 40 mm with Nonlinear Springs:
(a) Forming Limit Parameter (b) Equivalent Plastic Strain

Input Files

The files below are on your [delivery media](#) or they can be downloaded by your web browser by clicking the links (file names) below.

File	Description
<code>sheetforming_nolink.proc</code>	Mentat procedure file to run the above example
<code>sheetforming_link.proc</code>	Mentat procedure file to run the above example
<code>sheet_mesh.mud</code>	Mentat model file read by above procedure files

References

1. Cordosa, R.P.R., Yoon, J.W., Gracio, J.J., Barlat, F.I., and Cesar de Sa, J.M.A., Development of a one point quadrature shell element for nonlinear applications with contact and anisotropy, *Comput. Methods Appl. Mech. Engrg.*, 191, 5177-5206 (2002).
2. Barlat, F., Lege, D.J., and Brem, J.C., A six-component yield function for anisotropic metals, *Int. J. Plasticity*, 7, 693-712 (1991).
3. Yang, O.Y., Oh, S.I., Huh, H., and Kim, Y.H., *Proceedings of NUMISHEET 2002*, Oct. 21-25, Seju Island, Korea (2002).

3.12 Chaboche Model

- Chapter Overview 1098
- Blade on a Fan of a Turbine Engine 1098
- Input Files 1112

Chapter Overview

This chapter describes the use of the Chaboche hardening feature in Marc. This option describes the plastic response under cyclic loading. In this chapter, a blade of a fan from a turbine engine is simulated under thermal loading. A coupled analysis is performed where different cyclic variation in temperature is prescribed at the tip and at the root of the blade. This time dependent temperature results in a nonsymmetric strain-controlled cyclic loading of the blade.

Blade on a Fan of a Turbine Engine

This example describes a blade on a fan of a turbine engine. The blade is modeled as a wing shaped body mounted on a surface (Figure 3.12-1). In this model, the mounting is done with contact using the glue option. The interest is in analyzing this blade under cyclic loading at short term high output stages on the turbine engine. The Chaboche model is used to represent the plastic deformation. The focus is on the plastic behavior and not on the complex hot air flow around the blade. The blade is cooled internally and we assume that the part where the blade is mounted gets much warmer than the tip of the blade. This temperature difference is applied as the loading.

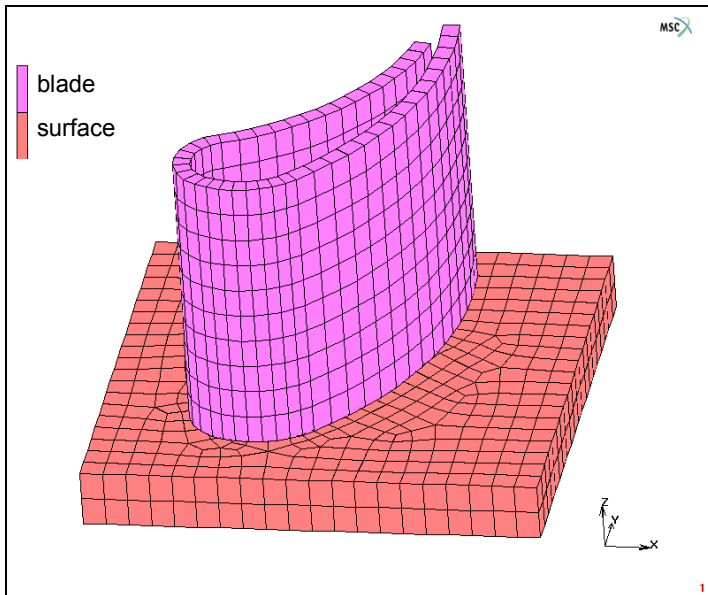


Figure 3.12-1 Model of the Blade

Mesh Generation

The mesh generation starts from an existing model file containing the geometry. The curves in this geometry are converted into the blade and the surface on which it is mounted. This is performed by using a combination of the CONVERT curve to element, EXPAND SHELL, EXPAND ELEMENT, and the advancing front AUTOMESH commands. The span of the blade is 0.05 m and the chord length is about 0.07 m.

```
FILE
  NEW
  RESET PROGRAM
  OPEN
    blade_geom.mfd
  OK
  SAVE AS
    blade.mud
  RETURN
MESH GENERATION
  ELEMENT CLASS
    LINE(2)
  RETURN
  CONVERT
    DIVISIONS
      15 1
    CURVES TO ELEMENTS
      1 4 #
    DIVISIONS
      8 1
    CURVES TO ELEMENTS
      2 3 #
  RETURN
  EXPAND
    SHELL/LINE ELEMENTS EXPAND
      THICKNESS
        0.003
      LINE ELEMENTS
      ALL EXIST
      RETURN (twice)
  SWEEP
    ALL
  RETURN
  EXPAND
    TRANSLATIONS
      0 0 0.005
```

```
REPETITIONS
  10
EXPAND ELEMENTS
ALL EXIST
RETURN
AUTOMESH
  CURVE DIVISIONS
    AVG LENGTH
      0.004
    APPLY CURVE DIVISIONS
      5 6 7 8 9 10 #
    RETURN
  2D PLANAR MESHING
    QUADRILATERALS (ADV FRNT):QUAD MESH!
      5 6 7 8 9 10 #
    RETURN (twice)
EXPAND
  TRANSLATIONS
    0 0 -0.005
  REPETITIONS
    2
  SELECT
    METHOD
      BOX
    RETURN
  ELEMENTS
    -10 10
    -10 10
    -1E-6 1E-6
  RETURN
EXPAND ELEMENTS
ALL SELECT
RETURN
SWEEP
  REMOVE UNUSED:NODES
  RETURN (twice)
```

Boundary Conditions

Temperature is prescribed at the tip and root of the blade. At the tip, the temperature increases from 300K to 800K in 50 seconds, and then decreases to 300K in 50 seconds. At the root, the temperature increases from 300K to 1300K in 50 seconds, and then decreases to 300K in 50 seconds. This temperature change is repeated five times. Displacement boundary conditions are applied to remove rigid body modes, and the z-displacement is 0 at the root of the blade.

```
BOUNDARY CONDITIONS
```

```
THERMAL
```

```
TABLES
```

```
NEW
```

```
1 INDEPENDENT VARIABLE
```

```
TYPE
```

```
time
```

```
ADD
```

```
0 300
```

```
50 1300
```

```
100 300
```

```
150 1300
```

```
200 300
```

```
250 1300
```

```
300 300
```

```
350 1300
```

```
400 300
```

```
450 1300
```

```
500 300
```

```
FIT
```

```
NEW
```

```
1 INDEPENDENT VARIABLE
```

```
TYPE
```

```
time
```

```
ADD
```

```
0 300
```

```
50 800
```

```
100 300
```

```
150 800
```

```
200 300
```

250 800
300 300
350 800
400 300
450 800
500 300

FIT

RETURN

FIXED TEMPERATURE

TEMPERATURE(TOP)

TABLE

table1

OK

SELECT

CLEAR SELECT

NODES

-10 10

-10 10

-0.01-1e-6 -0.01+1e-6

RETURN

NODES ADD

ALL SELECT

NEW

FIXED TEMPERATURE

TEMPERATURE(TOP)

TABLE

table2

OK

SELECT

CLEAR SELECT

NODES

-10 10

-10 10

0.05-1e-6 0.05+1e-6

RETURN

NODES ADD

```
ALL SELECT
RETURN
NEW
MECHANICAL
  FIXED DISPLACEMENT
    DISPLACEMENT X
    DISPLACEMENT Y
    DISPLACEMENT Z
  OK
  NODES ADD
    2813 #
  NEW
  FIXED DISPLACEMENT
    DISPLACEMENT X
    DISPLACEMENT Z
  OK
  NODES ADD
    3113 #
  NEW
  FIXED DISPLACEMENT
    DISPLACEMENT Z
  OK
  SELECT
    CLEAR SELECT
    NODES
      -10 10
      -10 10
      -0.01-1e-6 -0.01+1e-6
    RETURN
  NODES ADD
  ALL SELECT
  SELECT
    CLEAR SELECT
    RETURN (thrice)
```

Initial Conditions

The initial temperature of the blade is 300K.

```
INITIAL CONDITIONS
  THERMAL
    TEMPERATURE
      TEMPERATURE(TOP)
        300
      OK
    NODES ADD
    ALL EXIST
    RETURN (twice)
```

Material Properties

The blade is made from steel, where the Young's modulus is 210 GPa, the Poisson's ratio 0.3, the Thermal Expansion Coefficient is $1.8e-5K^{-1}$, the Conductivity is 80 W/m/K, and the Mass Density is $7800 kg/m^3$. The Specific Heat is taken to be 0 to simulate fast cooling due to the internally open structure of the blade. The initial Yield stress is 100 MPa, and the nonlinear kinematic hardening coefficients C and γ are taken 100 GPa and 2000 respectively. [Figure 3.12-2](#) shows the Mentat menu to add the Chaboche properties.

```
MATERIAL PROPERTIES
  ISOTROPIC
    YOUNG'S MODULUS
      2.1e11
    POISSON'S RATIO
      0.3
    MASS DENSITY
      7800
    THERMAL EXP.
      COEFFICIENT
        15e-6
      OK
    ELASTIC-PLASTIC
      METHOD
        CHABOCHE
```


INITIAL YIELD STRESS
 1e7
 COEFFICIENT C
 1e11
 COEFFICIENT GAMMA
 1000
 OK (twice)
 HEAT TRANSFER
 CONDUCTIVITY
 80
 MASS DENSITY
 78
 00
 OK
 ELEMENTS ADD
 ALL EXIST
 RETURN

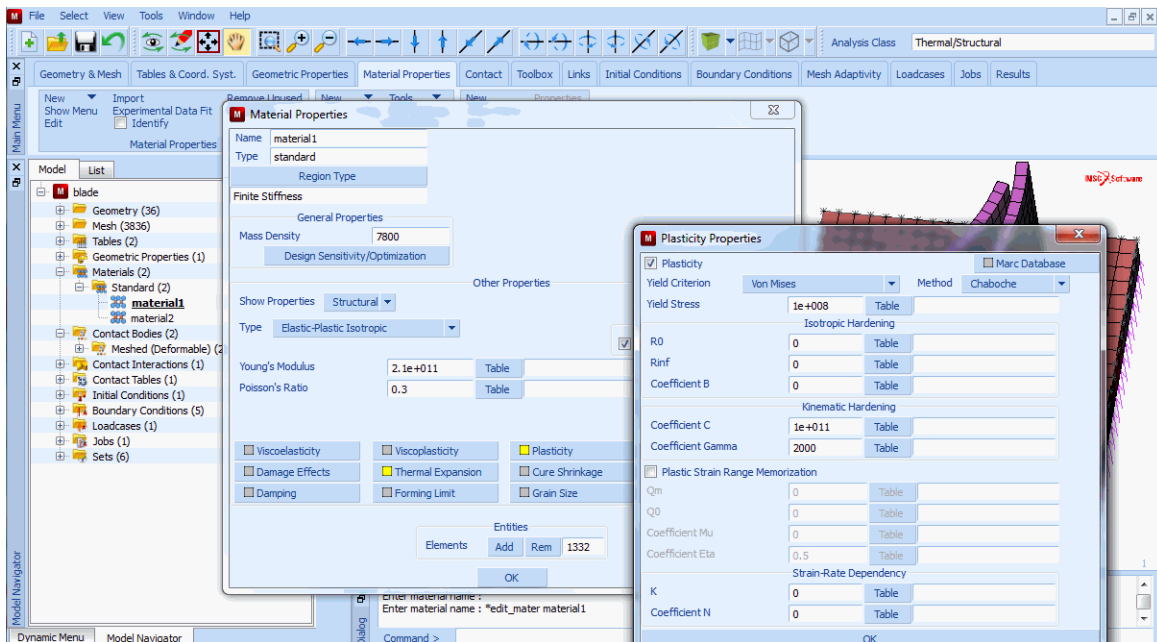
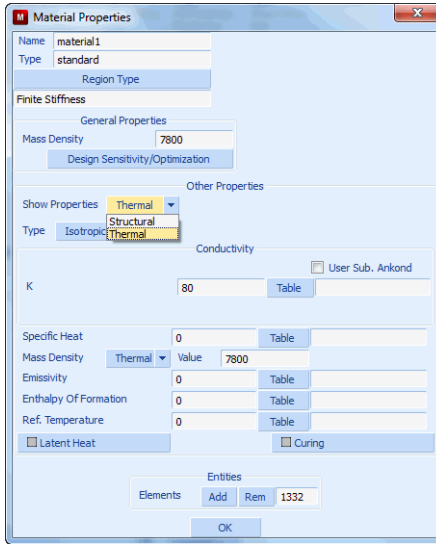


Figure 3.12-2 Chaboche Properties Menu



Geometric Properties

The CONSTANT TEMPERATURE option is selected for all the elements. A constant temperature is then computed throughout the element. This improves the stress calculation in the elements.

GEOMETRIC PROPERTIES
MECHANICAL ELEMENTS 3-D
SOLID
CONSTANT TEMPERATURE
OK
ELEMENTS ADD
ALL EXIST
RETURN (twice)

Contact

The blade and the underlying surface are taken as separate contact bodies. The glue option is used for the interface where contact bodies touch each other. The contact heat transfer coefficient for this interface is set to 1 MW/m^2 .

CONTACT
CONTACT BODIES
DEFORMABLE
OK

```
SELECT
  CLEAR SELECT
  ELEMENTS
    -10 10
    -10 10
    -1e-6 10
  RETURN
ELEMENTS ADD
ALL SELECT
NEW
DEFORMABLE
  OK
SELECT
  CLEAR SELECT
  ELEMENTS
    -10 10
    -10 10
    -10 1e-6
  RETURN
ELEMENTS ADD
ALL SELECT
RETURN
CONTACT TABLES
  NEW
  PROPERTIES
    1 2
    CONTACT TYPE: GLUE
    THERMAL PROPERTIES
    CONTACT HEAT TRANSFER COEFFICIENT
      1e6
    OK (twice)
  RETURN (twice)
```

Loadcases and Job Parameters

A coupled thermal mechanical analysis are performed. The analysis is performed in 80 increments of a constant time step, where the total analysis time in 500 seconds. The multifrontal sparse solver is used in this analysis.

LOADCASES

COUPLED

QUASI-STATIC

CONTACT

CONTACT TABLE

ctable1

OK

TOTAL LOADCASE TIME

500

PARAMETERS

STEPS

80

OK (twice)

RETURN (twice)

JOBS

ELEMENT TYPES

COUPLED

3-D SOLID

7

OK

ALL EXIST

RETURN (twice)

COUPLED

lcase1

CONTACT CONTROL

INITIAL CONTACT

CONTACT TABLE

ctable1

OK (twice)

ANALYSIS OPTIONS

PLASTICITY PROCEDURE: LARGE STRAIN ADDITIVE

```
        OK (twice)
JOB RESULTS
  Stress
  Total Strain
  Elastic Strain
  Plastic Strain
  Total Equivalent Plastic Strain
  OK
JOB PARAMETERS
  SOLVER
    MULTIFRONTAL SPARSE
  OK
```

The LARGE STRAIN ADDITIVE formulation is selected.

Save Model, Run Job, and View Results

After saving the model, the job is submitted and the resulting post file is opened.

```
FILES
  SAVE AS
    blade.mud
  RETURN
RUN
  SUBMIT(1)
  OPEN POST FILE (RESULTS MENU)
  HISTORY PLOT
    SET NODES
      308 #
    COLLECT GLOBAL DATA
    NODES/VARIABLES
      ADD VARIABLE
        Comp 33 of Total Strain
        Comp 33 of Stress
      FIT
    RETURN
```

SHOW IDS

0

Figure 3.12-3 shows the equivalent stress in the blade at the maximum temperature difference.

As mentioned in the *Volume A: Theory and User Information* manual, one of the material phenomenon that can be simulated by Chaboche hardening rule is mean-stress-relaxation. This happens when the material is subject to nonsymmetric strain-controlled cyclic loading.

Figure 3.12-4 shows the time history of component 33 of the total strain at Node 308 (It is on the outside of the blade close to the surface). There are five cycles and they are nonsymmetric with regard to the zero axis (Please notice that the strain is a combination of thermal and mechanical ones). Therefore, the associated stress strain curve shows mean-stress-relaxation phenomenon as shown in Figure 3.12-5. A large number of cycles is necessary to reach the stabilized one or this model since the plastic strain per cycle is relatively small.

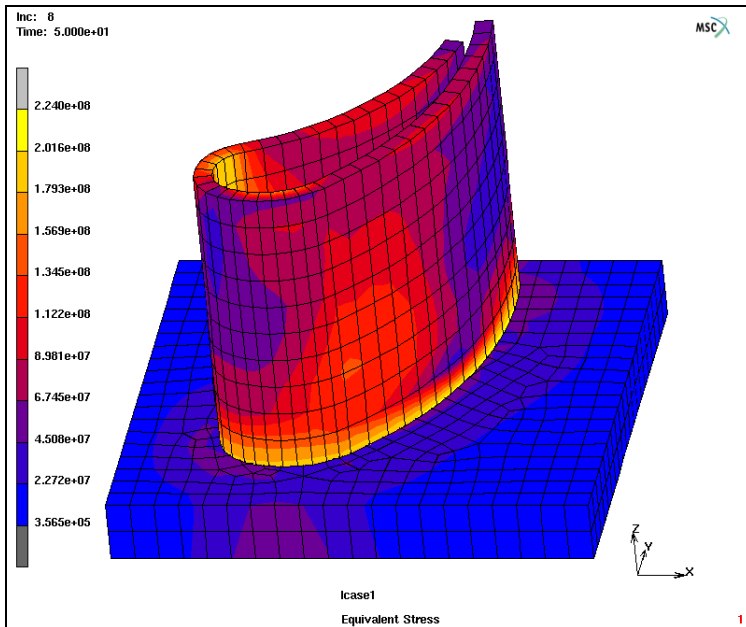


Figure 3.12-3 Equivalent Stress at the First Occurrence of the Maximum Temperature Difference

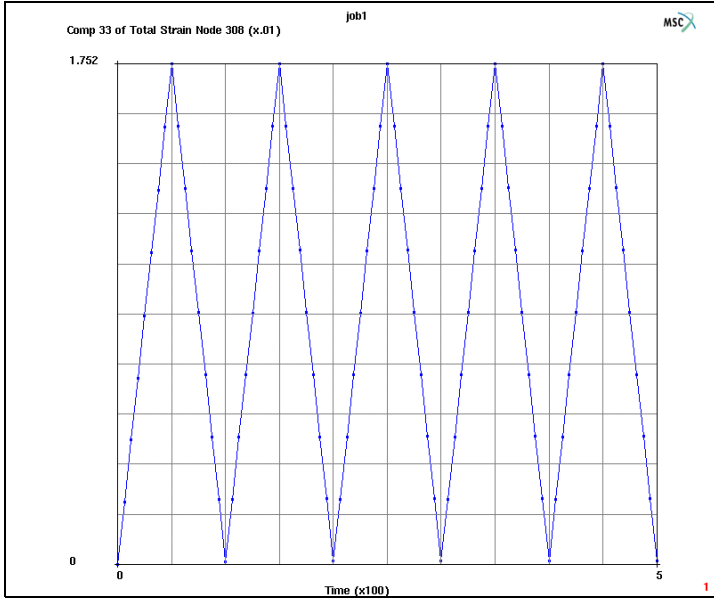


Figure 3.12-4 Time History Plot of Component 33 of the Total Strain

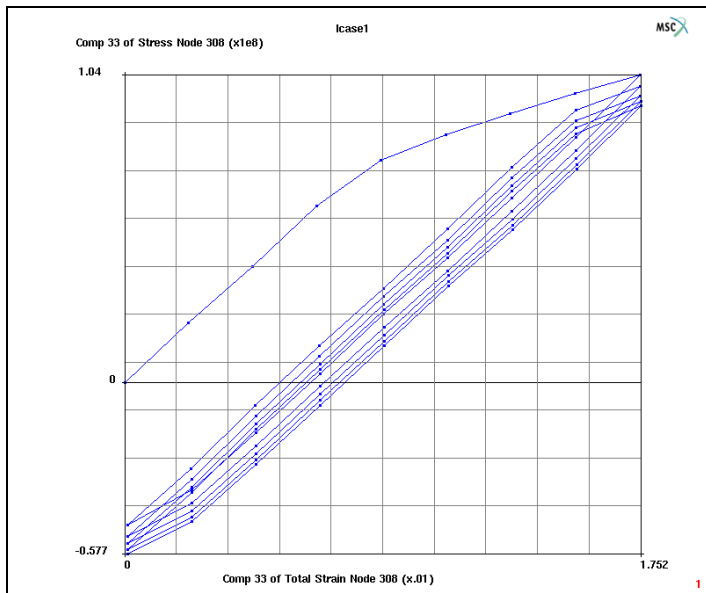


Figure 3.12-5 History Plot of Component 33 of the Total Strain versus Component 33 of the Stress

Input Files

The files below are on your [delivery media](#) or they can be downloaded by your web browser by clicking the links (file names) below.

File	Description
blade.proc	Mentat procedure file to run the above example
blade_geom.mfd	Mentat model file read by above procedure file

3.13 Modeling of a Shape Memory Alloy Orthodontic Archwire

- Chapter Overview 1114
- Simulation of an Archwire with Shape Memory Alloy Models 1114
- Input Files 1132
- References 1132

Chapter Overview

Shape-memory properties for nickel (Ni) titanium (Ti) alloy were discovered in the 1960s, at the Naval Ordnance Laboratory (NOL); hence, the acronym NiTi-NOL or Nitinol, which is commonly used when referred to Ni-Ti based shape-memory alloys. Since 1970, Ni-Ti has been widely investigated due to its frequent use in applications and today it is probably the shape-memory materials most frequently used in commercial applications. The amount of thermally activated recoverable memory strain and the size of the hysteresis loop strongly depend on alloy composition, thermo-mechanical processing, testing direction and deformation mode (that is, if the material is in simple tension, simple compression or shear). For the full austenite–martensite phase transformation, the recoverable memory strain is of the order of 8%, while the hysteresis width is typically of 30-50°C. For uniaxial states of stress and in the usual range of applications, the stress-temperature regions in which the phase transformation may occur are delimited with good approximation by straight lines with slopes ranging from 2.5 Mpa/°C to over 15 Mpa/°C.

Experimental evidence shows that:

1. Phase transformations do not exhibit pressure dependence in the case of long-aged Ni-Ti; for short-aged Ni-Ti the R-phase transition is unaffected by pressure, while the martensitic transformation is pressure dependent
2. Phase transformation are insensitive to temperature rates and to stress rates.

The SMA underlying micro-mechanics is quite complex. Moreover, due to the increasing sophistication of SMA-based devices, there is a growing need for effective computational tools able to support the design process. Two shape memory models based on the Auricchio [Reference 1] mechanical model and the Saeedvafa and Asaro [Reference 2] thermo-mechanical model have been implemented in Marc and are reviewed with an Archwire example.

Simulation of an Archwire with Shape Memory Alloy Models

In order to show how to use two shape memory alloy models available in Marc, we consider the simulation of an orthodontic archwire, (Figure 3.13-1). The dimensions are taken from Auricchio (Int. J. Plasticity, 2001) and they are reported in Table 2.13-1 for the entire segment indicated in Figure 3.13-1. Moreover, we assume that the archwire is made out of a wire with rectangular 0.635 x 0.432 mm cross section.

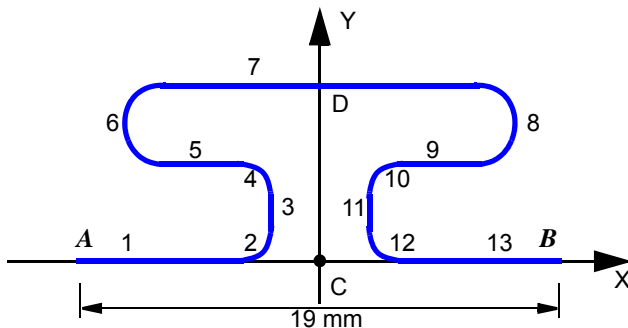


Figure 3.13-1 Orthodontic Archwire: Geometry Data

Table 2.13-1 Orthodontic Archwire: Details on the Geometry

Segment Number	Segment Type	Length (mm)	Angle (°)	Radius (mm)
1	Straight	7.5	–	–
2	Circular	–	90	1
3	Straight	2.0	–	–
4	Circular	–	90	1
5	Straight	2.5	–	–
6	Circular	–	180	1
7	Straight	9.0	–	–
8	Circular	–	180	1
9	Straight	2.5	–	–
10	Circular	–	90	1
11	Straight	2.0	–	–
12	Circular	–	90	1
13	Straight	7.5	–	–

The right half of geometry was modeled considering symmetry. The generation of mesh using Mentat is straightforward. So, it is not discussed here. The generated mesh was stored in `sma_mesh.mud`.

Boundary Conditions

The boundary conditions are set to reproduce displacement control during loading and unloading. Fixed boundary condition is applied to the symmetric nodes. Another set of boundary condition is applied to the right edge nodes to impose the displacement control in x-direction by inserting `table1`. The movement in the z-direction is also constrained for the nodes.

```
BOUNDARY CONDITIONS
NEW
MECHANICAL
    FIXED DISPLACEMENT
        DISPLACEMENT X
            0
        DISPLACEMENT Y
            0
```

```
DISPLACEMENT Z
  0
ROTATION X
  0
ROTATION Y
  0
ROTATION Z
  0
OK
NODES ADD
  11 12 13 14 251 252 253 254
END LIST
NEW
TABLES
  NEW
    NEW TABLE
    1 INDEPENDENT VARIABLE
    TYPE
      time
  ADD
    0 0
    1 1
    2 0
    10 0
  SHOW MODEL
    MECHANICAL
    FIXED DISPLACEMENT
      DISPLACEMENT X
        5
      TABLE
        table1
      DISPLACEMENT Z
        0
      ROTATION X
        0
```

```
ROTATION Y
    0
OK
OK
NODES ADD
    185 212 213 214 425 452 453 454
END LIST
```

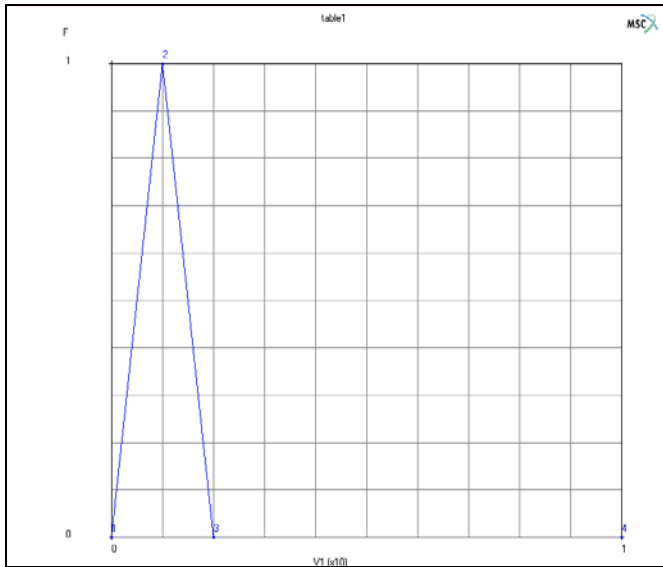


Figure 3.13-2 Generated Table for Displacement Control

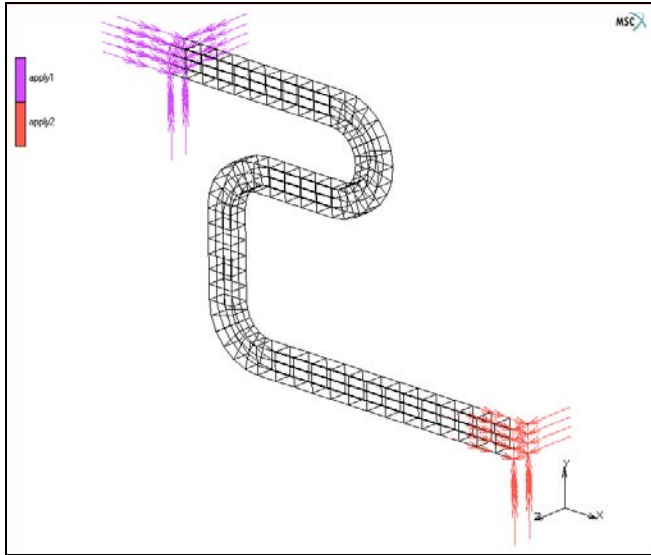


Figure 3.13-3 Boundary Condition ID

Initial Conditions

The option is only active for thermo-mechanical shape memory alloy. The temperature was initialized to 19°C (room temperature) by means of a STATE VARIABLE initial condition.

INITIAL CONDITIONS

NEW

MECHANICAL

STATE VARIABLE

STATE VARIABLE

19

OK

ELEMENTS ADD

ALL EXIST

Material Properties

Material property data for mechanical model and thermo-mechanical model are completely different. Here is the summary for both data.

1. Mechanical Shape Memory Model

<i>Values with stress dimension</i>					
<i>E</i>	σ_s^{AS+}	σ_f^{AS+}	σ_s^{SA+}	σ_s^{SA+}	σ_s^{AS-}
<i>Mpa</i>					
5×10^4	500	500	300	300	700

Other parameters used:

$$\nu = 0.3, \varepsilon_L = 0.007, \alpha = 0.12.$$

In the above summary, superscript “+” and “-” mean tensile and compression properties, respectively. Also, subscript “s” and “f” mean starting and finishing points, respectively. In addition, superscript “AS” means austenite-to-martensite transformation and “SA” means martensite-to-austenite transformation. Then, the meaning of the symbols are summarized as follows:

- σ_s^{AS+} : Starting tensile stress in austenite-to-martensite transformation
- σ_f^{AS+} : Finishing tensile stress in austenite-to-martensite transformation
- σ_s^{SA+} : Starting tensile stress in martensite-to-austenite transformation
- σ_f^{SA+} : Finishing tensile stress in martensite-to-austenite transformation
- σ_s^{AS-} : Starting compressive stress in austenite-to-martensite transformation

Noting that, given σ_s^{AS+} and σ_s^{AS-} , the parameter α , which is measured from the difference between the response in tension and compression, can be obtained as follows:

$$\alpha = \frac{\sqrt{2}}{\sqrt{3}} \frac{\sigma_s^{AS-} - \sigma_s^{AS+}}{\sigma_s^{AS-} + \sigma_s^{AS+}} = 0.12$$

When the compression test data is not available, α is usually set to be zero. It means that tensile and compressive responses are the same. ε_L is a scalar parameter representing the maximum deformation obtainable only by detwinning of the multiple-variant martensite. Classical value for ε_L is in the range 0.0 to 0.10. In this example, it was set to 0.007.

MATERIAL PROPERTIES

NEW

MORE

SHAPE MEMORY ALLOY

MECHANICAL (AURICCHIO'S) MODEL

YOUNG'S MODULUS

50000

POISSON'S RATIO

0.3

sigAS_s

500

sigAS_f

500

sigSA_s

300

sigSA_f

300

alpha (0.0 - 1.0)

0.12

espL (0.0 - 0.10)

0.007

OK (twice)

ELEMENTS ADD

ALL EXIST

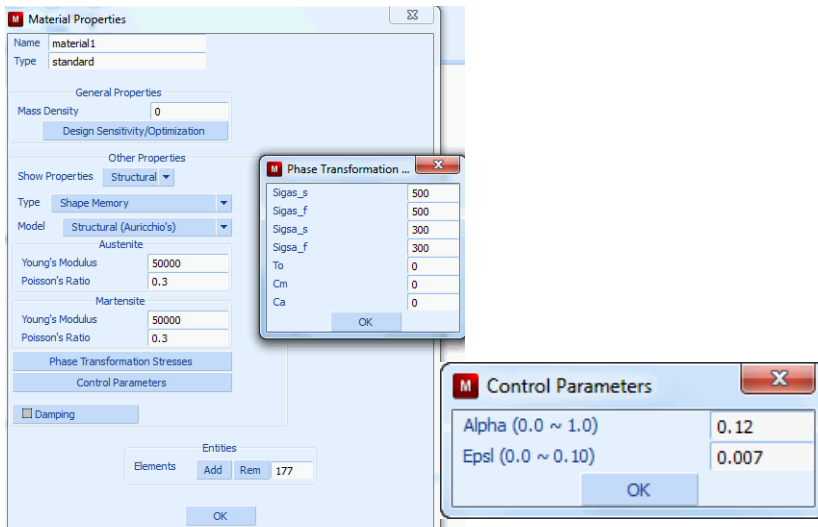


Figure 3.13-4 Material Properties Menu in Mechanical Shape Memory Model

2. Thermo-Mechanical Shape Memory Model

Austenite properties

Young's modulus (E): 50000 Mpa, Poisson's ratio (ν): 0.33, Thermal expansion coefficient (α) = 1.0e-5, Equivalent tensile yield stress: 10000 Mpa

Martensite properties

Young's modulus (E): 50000 Mpa, Poisson's ratio (ν): 0.33, Thermal expansion coefficient (α) = 1.0e-5, Equivalent tensile yield stress: 10000 Mpa

Austenite to Martensite

Martensite start temperature in stress-free condition (M_s^0): -45°C, Martensite finish temperature in stress-free condition M_f^0 : -90°C, Slope of the stress-dependence of martensite start-finish temperatures (C_m): 6.6666

Martensite to Austenite

Austenite start temperature in stress-free condition (A_s^0): 5°C, Austenite finish temperature in stress-free condition (A_f^0): 20°C, Slope of the stress-dependence of austenite start-finish temperatures (C_a): 8.6667

Transformation strains

Deviatoric part of transformation strain (ϵ_{eq}^T): 0.0

Volumetric part of the transformation strain (ϵ_v^T): 0.0

Twinning stress (σ_{eff}^g): 100 Mpa

Coefficients of g function

$$g\left(\frac{\sigma_{eq}}{g_o}\right) = 1 - \exp\left[g_a\left(\frac{\sigma_{eq}}{g_o}\right)^{g_b} + g_c\left(\frac{\sigma_{eq}}{g_o}\right)^{g_d} + g_e\left(\frac{\sigma_{eq}}{g_o}\right)^{g_f}\right]$$

$$g_a = -4, g_b = 2, g_c = 0.0, g_d = 2.75, g_e = 0.0, g_f = 3.0$$

$$g_o = 1000.0, g_{max} = 1.0, g_{max}^g = 1.0+e20$$

So, the chosen "g" function is $g\left(\frac{\sigma_{eq}}{1000}\right) = 1 - \exp\left[-4\left(\frac{\sigma_{eq}}{1000}\right)^2\right]$.

MATERIAL PROPERTIES

NEW

MORE

SHAPE MEMORY ALLOYS

THERMO-MECHANICAL MODEL

AUSTENITE PROPERTIES

YOUNG'S MODULUS

50000

POISSON'S RATIO

0.3

MASS DENSITY

1

THERMAL EXP. COEF.

1e-5

INITIAL YIELD STRESS

10000

OK

MARTENSITE PROPERTIES

YOUNG'S MODULUS

50000

POISSON'S RATIO

0.3

MASS DENSITY

1

THERMAL EXP. COEF.

1e-5

INITIAL YIELD STRESS

10000

OK

AUSTENITE TO MARTENSITE

MARTENSITE START TEMPERATURE

-45

MARTENSITE FINISH TEMPERATURE

-90

SLOPE

6.6667

OK

MARTENSITE TO AUSTENITE

AUSTENITE START TEMPERATURE

5

AUSTENITE FINISH TEMPERATURE

20

```

SLOPE
    8.6667
OK
TRANSFORMATION STRAINS
    DEVIATORIC TRANS. STRAIN
        0
    VOLUMETRIC TRANS. STRAIN
        0
    TWINNING STRESS
        100
    g-A
        -4
    g-B
        2
    g-C
        0
    g-D
        2.75
    g-E
        0
    g-F
        3
    g-0
        1000
    g-max
        1
    STRESS AT g-max
        1e+020
    OK (thrice)
ELEMENTS ADD
ALL EXIST

```

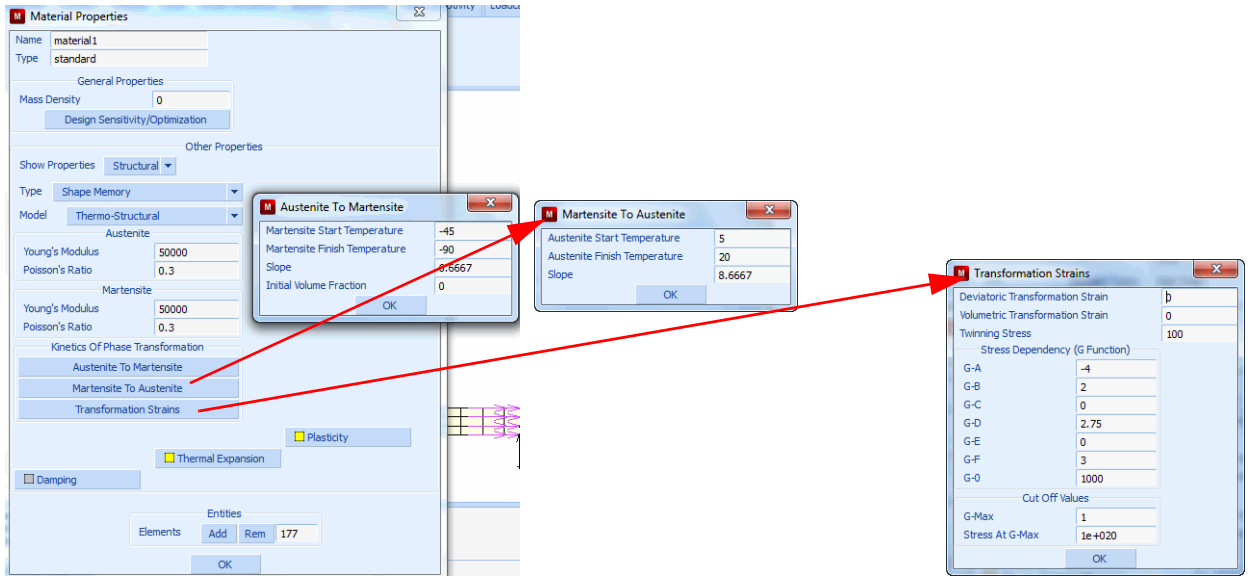


Figure 3.13-5 Material Properties in Thermo-mechanical Shape Memory Model

Load Steps and Job Parameters

The job consists of two mechanical loadcases. The loading histories is given as follows:

Time (s)	Displ (mm)
0	0.0
1	5.0
2	0.0

Total 200 fixed steps are used for the entire analysis with residual norm of 0.1. Each loadcase consists of 100 steps.

```

LOADCASES
NEW
  MECHANICAL
    STATIC
      SOLUTION CONTROL
        MAX # RECYCLES
          20
        OK
      STEPPING PROCEDURE
  
```

```

CONSTANT TIME STEP
# STEP
    100
OK
NEW
STATIC
SOLUTION CONTROL
    MAX # RECYCLES
        20
    OK
STEPPING PROCEDURE
CONSTANT TIME STEP
# STEP
    100
OK

```

The analysis is a normal mechanical analysis in which all two loadcases are performed in sequence. INITIAL LOADS is only active for thermo-mechanical shape memory alloy in order to set initial temperature. Also, when mechanical shape memory alloy is used, LARGE STRAIN MULTIPLICATIVE option is activated in the PLASTICITY PROCEDURE. If user choose other options, Marc changes the option internally to LARGE STRAIN MULTICATIVE option. New scalar quantity for Volume Fraction of Martensite was selected in this example, as well as Equivalent von Mises Stress.

1. Mechanical Shape Memory Alloy

```

JOBS
    NEW
    MECHANICAL
        LOADCASES
            activate:
                lcase1
                lcase2
        ANALYSIS OPTIONS
            LARGE DISPLACEMENT
            PLASTICITY PROCEDURE
                LARGE STRAIN MULTIPLICATIVE
            OK
        JOB RESULTS
            AVAILABLE ELEMENT SCALARS

```

Equivalent Von Mises Stress
Volume Fraction of Martensite
ELEMENT RESULTS
CENTROID
OK (twice)

2. Thermo-mechanical Shape Memory Alloy

JOBS
NEW
MECHANICAL
LOADCASES
activate:
lcase1
lcase2
INITIAL LOADS
INITIAL CONDITIONS
activate:
icond1 state_variable
OK
ANALYSIS OPTIONS
LARGE DISPLACEMENT
JOB RESULTS
AVAILABLE ELEMENT SCALARS
Equivalent Von Mises Stress
Volume Fraction of Martensite
ELEMENT RESULTS
CENTROID
OK (twice)

For the analysis of the Archwire model, element type 7 is being used. Mechanical shape memory model only supports 3-D, plane strain, and axisymmetric continuum elements.

ELEMENT TYPES
MECHANICAL
3-D SOLID

```
OK
ALL:EXIST
RETURN
```

Save Model, Run Job, and View Results

1. Mechanical Shape Memory Alloy

```
FILE
  SAVE AS
    sma_m.mud
  OK
  RETURN
RUN
  SUBMIT 1
  MONITOR
  OK
MAIN
RESULTS
  OPEN
    sma_m.t16
  OK
  DEF & ORIG
  CONTOUR BAND
  SCALAR
    Volume Fraction of Martensite
  OK
  MONITOR
  SCALAR
    Equivalent Von Mises Stress
  OK
  MONITOR
```

2. Thermo-mechanical Shape Memory Alloy

```
FILE
  SAVE AS
    sma_tm1.mud
```

```
      OK
    RETURN
  RUN
    SUBMIT 1
    MONITOR
    OK
  MAIN
RESULTS
  OPEN
    sma_tm1.t16
  OK
  DEF & ORIG
  CONTOUR BAND
  SCALAR
    Volume Fraction of Martensite
  OK
  MONITOR
  SCALAR
    Equivalent Von Mises Stress
  OK
  MONITOR
```

For two shape memory model, the contours for Volume Fraction of Martensite were compared in [Figure 3.13-6](#) and [Figure 3.13-7](#) and the contours for Equivalent Von Mises Stress were compared in [Figure 3.13-8](#) and [Figure 3.13-9](#) at the step of 100 and 200, respectively. For thermo-mechanical shape memory alloy, initial temperature were set to 19°C in INITIAL CONDITIONS. As shown in the figures, in both models, two scalar properties reach to maximum at the maximum displacement and come back close to zero at the last step. Both models predicts superelasticity behavior (shape memory effect) well.

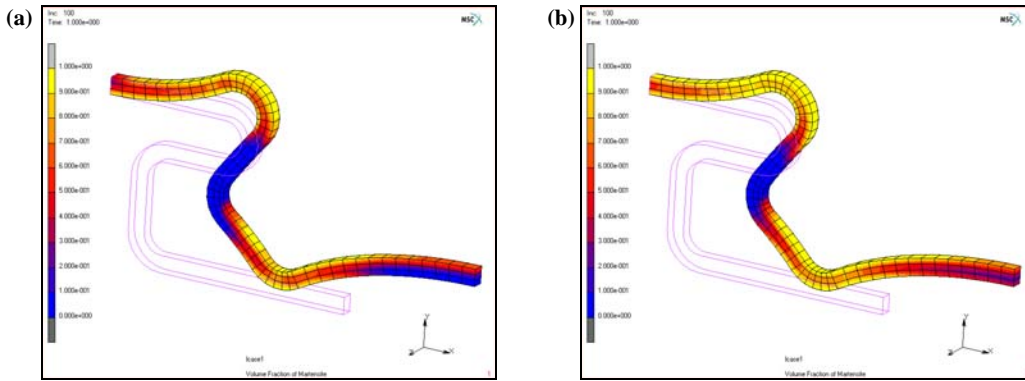


Figure 3.13-6 Volume Fraction of Martensite at the Maximum Displacement:
 (a) Mechanical Model (b) Thermo-mechanical Model

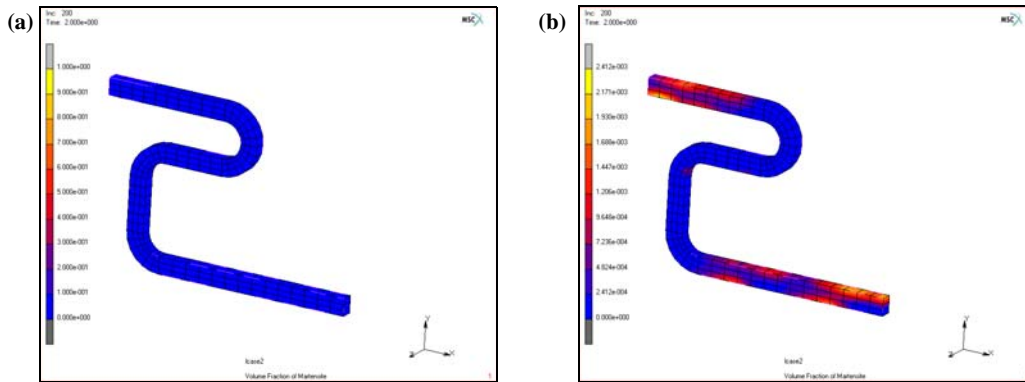


Figure 3.13-7 Volume Fraction of Martensite at the Last Step:
 (a) Mechanical Model (b) Thermo-mechanical Model

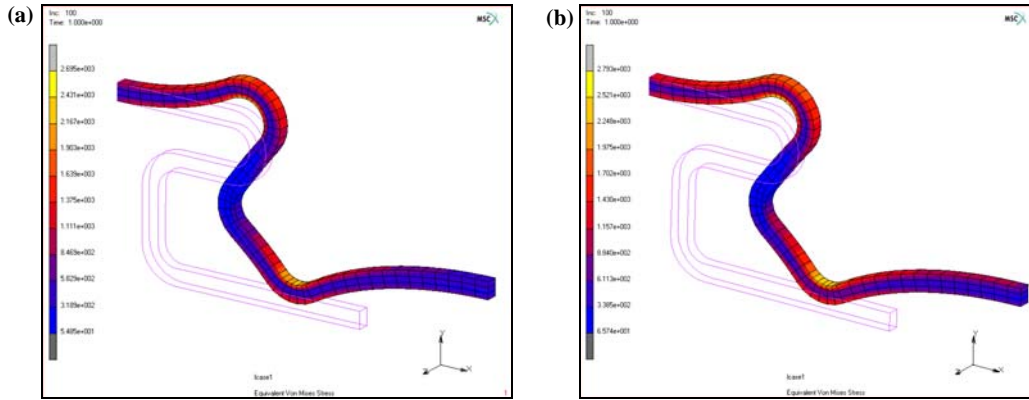


Figure 3.13-8 Equivalent Von Mises Stress at the Maximum Displacement:
 (a) Mechanical Model (b) Thermo-mechanical Model

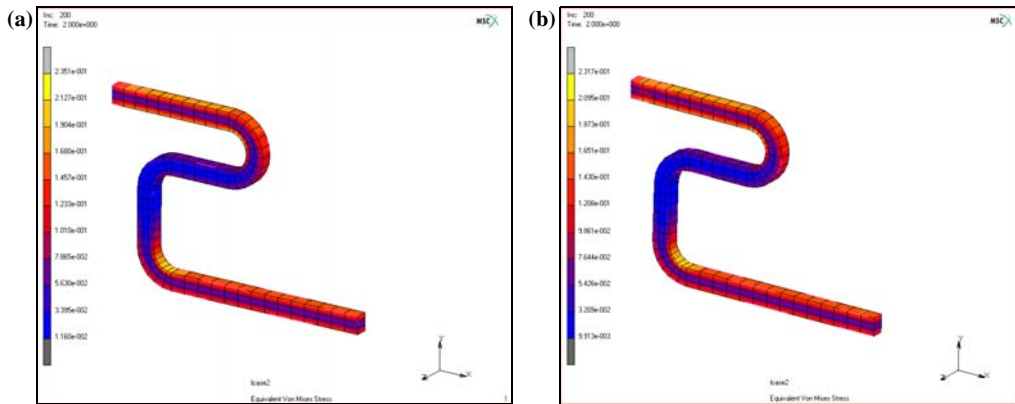


Figure 3.13-9 Equivalent Von Mises Stress at the Last Step:
 (a) Mechanical Model (b) Thermo-mechanical Model

In order to show the different behavior according to initial temperature for thermo-mechanical shape memory model, additional simulation was performed with initial temperature of 5°C.

INITIAL CONDITIONS
 NEW
 MECHANICAL
 STATE VARIABLE
 STATE VARIABLE
 5
 OK

```
ELEMENTS ADD  
ALL:EXIST
```

Save Model, Run Job, and View Results

```
FILE  
  SAVE AS  
    sma_tm2.mud  
  OK  
  RETURN  
RUN  
  SUBMIT 1  
  MONITOR  
  OK  
MAIN  
RESULTS  
  OPEN  
    sma_tm2.t16  
  OK  
  DEF & ORIG  
  CONTOUR BAND  
  SCALAR  
    Volume Fraction of Martensite  
  OK  
  MONITOR  
  SCALAR  
    Equivalent Von Mises Stress  
  OK  
  MONITOR
```

As shown in [Figure 3.13-10](#), Volume Fraction of Martensite is not decreased for the simulation of thermo-mechanical model under the temperature of 5°C even at the last step.

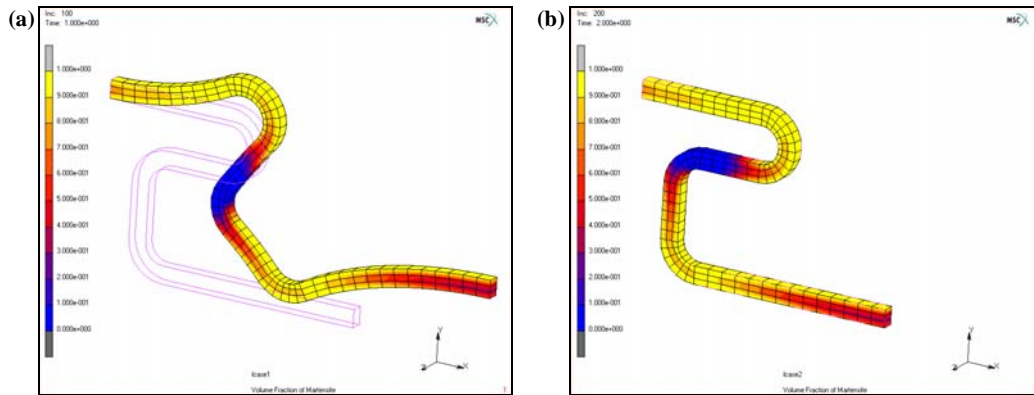


Figure 3.13-10 Volume Fraction of Martensite for Thermo-mechanical Shape Memory Alloy under the Temperature of 5°C: (a) step =100 (b) step = 200

Input Files

The files below are on your [delivery media](#) or they can be downloaded by your web browser by clicking the links (file names) below.

File	Description
sma_mech.proc	Mentat procedure file to run the above example
sma_mesh.mud	Mentat model file read by above procedure file

References

1. Auricchio, F., A robust integration-algorithm for a finite-strain shape-memory-alloy superelastic model, *Int. J. Plasticity*, 17, 971-990 (2001).
2. Saeedvafa, M. and Asaro, R.J., Los Alamos Report, LA-UR-95-482 (1995).

3.14 Implicit Creep Analysis of Solder Connection between Microprocessor and PCB

- Chapter Overview 1134
- Microprocessor Soldered to a PCB 1134
- Input Files 1152
- References 1152

Chapter Overview

This chapter describes the use of the implicit creep feature in Marc. The available options to simulate power law creep in conjunction with von Mises plasticity are described in detail. The example chosen for this purpose is a Microprocessor-solder-PCB assembly that is subjected to both electrical and thermal loads.

Microprocessor Soldered to a PCB

This example describes a ceramic ball grid array (CBGA), a ceramic substrate package. This is one of the ways ICs are packaged in the electronic industry. In a CBGA, the die is glued to a ceramic. This ceramic is soldered with small solder balls to the PCB (printed circuit board), where the solder balls represent the electric contacts. The stress free temperature is 443 K (170°C), so the chip needs to be cooled down to room temperature before it can be used.

Figure 3.14-1 shows the CBGA, where the different components can be seen.

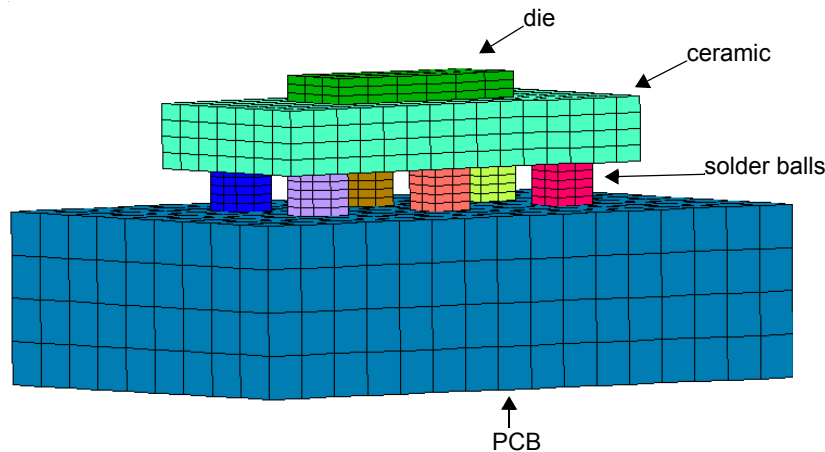


Figure 3.14-1 Model of the CBGA Showing the Different Contact Bodies

Mesh Generation

The mesh is generated by first making the solder balls, these are represented as cuboids. Two rows of three balls are generated. Then the ceramic is generated, the die, and finally the PCB. Note that all parts are generated away from each other. This is done to prevent components from being joined when the model is swept to remove double nodes. After sweeping, the parts are brought into contact.

MESH GENERATION

NODES ADD

0.002 0.001 0

0.004 0.001 0

0.004 0.003 0

```

0.002 0.003 0
ELEMENTS ADD
  1 2 3 4
DUPLICATE
  TRANSLATIONS
    0.007 0 0
  REPETITIONS
    2
  ELEMENTS
  ALL EXIST
  TRANSLATIONS
    0 0.006 0
  REPETITIONS
    1
  ELEMENTS
  ALL EXIST
  RETURN
EXPAND
  TRANSLATION
    0 0 0.002
  REPETITIONS
    1
  ELEMENTS
  ALL EXIST
  RETURN
ADD NODES
  0.00 0.00 0.003
  0.02 0.00 0.003
  0.02 0.01 0.003
  0.00 0.01 0.003
ADD ELEMENTS
  97 98 99 100
EXPAND
  TRANSLATIONS
    0 0 0.003

```

REPETITIONS

1

ELEMENTS

13 #

RETURN

ADD NODES

0.005 0.003 0.007

0.015 0.003 0.007

0.015 0.007 0.007

0.005 0.007 0.007

ADD ELEMENTS

113 114 115 116

EXPAND

TRANSLATIONS

0 0 0.0012

REPETITIONS

1

ELEMENTS

15 #

RETURN

ADD NODES

-0.005 -0.005 -0.01

0.025 -0.005 -0.01

0.025 0.015 -0.01

-0.005 0.015 -0.01

ADD ELEMENTS

129 130 131 132

EXPAND

TRANSLATIONS

0 0 0.008

REPETITIONS

1

ELEMENTS

17 #

RETURN


```

SELECT
  ELEMENTS
    18 #
  STORE
    pcb
  ALL SELECT
  CLEAR SELECT

```

Other parts of the model are stored in sets in the same way. Then the elements are subdivided.

```

  RETURN
SUBDIVIDE
  DIVISIONS
    16 9 4
  ELEMENTS
    18 #
  DIVISIONS
    2 2 5
  ELEMENTS
    7 8 9 10 11 12 #
  DIVISIONS
    15 7 4
  ELEMENTS
    14 #
  DIVISIONS
    6 3 3
  ELEMENTS
    16 #
  RETURN
SWEEP
  ALL
  RETURN
RENUMBER
  ALL
  RETURN

```

```
MOVE
  SELECT
    SELECT SET
      pcb
    OK
  RETURN
TRANSLATIONS
  0 0 0.002
ELEMENTS
  ALL SELECT
SELECT
  CLEAR SELECT
```

The other sets are moved towards each other in a similar way.

```
RETURN (twice)
```

Boundary Conditions

Displacement boundary conditions are applied to prevent the rigid body modes, and the potential is set to 0 V for a node on each solder ball, the ceramic, and the PCB. A temperature drop to 298 K (25°C) is prescribed at the bottom of the PCB, and a potential difference of 10 V is applied across the die.

```
BOUNDARY CONDITIONS
MECHANICAL
  NAME
    fix
  FIXED DISPLACEMENT
    DISPLACEMENT X
    DISPLACEMENT Y
    DISPLACEMENT Z
  OK
NODES ADD
  67 #
NEW
NAME
  fix_xz
```

```

FIXED DISPLACEMENT
  DISPLACEMENT X
  DISPLACEMENT Z
  OK
NODES ADD
  66 #
NEW
NAME
  fix_z
FIXED DISPLACEMENT
  DISPLACEMENT Z
  OK
NODES ADD
  68 #
RETURN
JOULE
TABLES
NEW
  1 INDEPENDENT VARIABLE
TYPE
  time
NAME
  temp
  ADD
    0 443
    100 298
    3E4 298
  FIT
  RETURN
NEW
NAME
  temp
FIXED TEMPERATURE
  TEMPERATURE
    1

```

```
TABLE
  temp
OK
SELECT
  METHOD
  BOX
  RETURN
NODES
  -10 10
  -10 10
  -8e-3-1e-6 -8e-3+1e-6
RETURN
NODES ADD
ALL SELECT
NEW
NAME
  pot_0
FIXED VOLTAGE
  VOLTAGE
  OK
SELECT
  CLEAR SELECT
  NODES
    0.015-1e-6 0.015+1e-6
    -10 10
    -10 10
  RETURN
NODES ADD
ALL SELECT
NODES ADD
  66 8 20 7 19 2 14 50 #
SELECT
  METHOD
  SINGLE
  RETURN
  CLEAR SELECT
```

```

RETURN
NEW
NAME
    pot_10
FIXED VOLTAGE
    VOLTAGE
        10
    OK
NODES ADD
    1831 1827 1828 1832 #
RETURN (twice)

```

Initial Conditions

The initial temperature for the whole model is set to 443 K (170°C).

```

INITIAL CONDITIONS
THERMAL
    TEMPERATURE
        TEMPERATURE (TOP)
            443
    OK
NODES ADD
ALL EXIST
RETURN (twice)

```

Material Properties

The material properties used are listed in the following two tables. The ceramic, the die, and the PCB are taken to be elastic. Solder A consists of Sn63/Pb37, which are the layers of the solder balls touching the ceramic and the PCB, and solder B consists of Sn10/Pb90, which is the middle part of the solder balls.

	Solder A	Solder B	Ceramic
Young's modulus (GPa)	30.2	30.2	300
Poisson's ratio	0.4	0.4	0.23
Thermal Expansion Coefficient (K^{-1})	24×10^{-6}	27.8×10^{-6}	6.7×10^{-6}
Conductivity (W/m/K)	50.6	35.5	16.5

	Solder A	Solder B	Ceramic
Resistivity (Ωm)	1×10^6	1×10^6	1×10^6
Specific Heat (J/kg/K)	200	130	1050
Mass Density (kg/m^3)	9000	11000	2000

	Die	Die part	PCB
Young's modulus (GPa)	162	162	18.2
Poisson's ratio	0.28	0.28	0.25
Thermal Expansion Coefficient (K^{-1})	23×10^{-6}	23×10^{-6}	15×10^{-6}
Conductivity (W/m/K)	120	120	5
Resistivity (Ωm)	600	0.25	1×10^6
Specific Heat (J/kg/K)	700	700	820
Mass Density (kg/m^3)	2330	2330	2000

Creep and plasticity properties are used for both solder A and solder B. A perfectly-plastic behavior with no strain hardening and no temperature dependence has been assumed. Yield stress of 49.2 GPa is specified [Reference 1 and Reference 2]. The creep properties that are available for 60%Sn-40%Pb in Reference 1 are used herein for both solder A and solder B. The creep behavior used herein is an approximation of Garofalo's hyperbolic sine law used for relating steady-state creep rate to stress and temperature. The sine law taken from Reference 1 and Reference 3 is shown below:

$$\dot{\epsilon}^c = C_1 \left(\frac{G}{T}\right) \left[\sinh\left(\alpha \frac{\bar{\sigma}}{G}\right) \right]^n \exp\left(-\frac{Q}{kT}\right)$$

where $C_1 = 16.7 \times 10^{-6} \text{ (K/sec)/(N/m}^2\text{)}$; T = temperature in Kelvin; G = temperature dependent shear modulus = $(28388 - 56 T)10^6 \text{ (N/m}^2\text{)}$; $\alpha = 866$; $n = 3.3$; Q - activation energy for creep deformation process = .548 eV; and $k = 8.617 \times 10^{-5}$ (Boltzmann's constant).

It should be noted that the default implicit creep capability in Marc allows the creep strain rate to be expressed in terms of power law expressions of stress, temperature, creep strain, and time.

$$\dot{\epsilon}^c = A \bar{\sigma}^m \bullet (\bar{\epsilon}^c)^n \bullet T^p \bullet (qt^{q-1})$$

Figure 3.14-2 shows the Mentat menu to add the implicit creep properties.

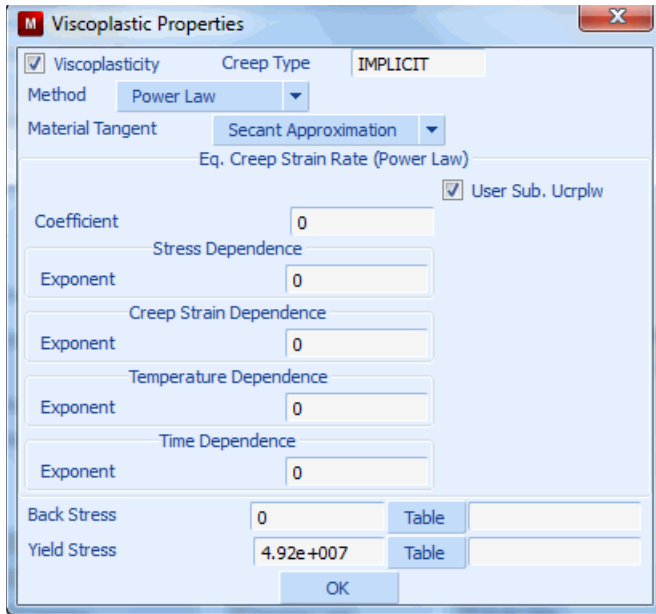


Figure 3.14-2 Creep Properties Menu

Use can be made of the UCRPLW user subroutine to specify more complex relationships for the creep strain rate.

$$\dot{\bar{\epsilon}}^c = A \cdot \bar{\sigma}^m \cdot g(\bar{\epsilon}^c) \cdot h(T) \cdot \frac{dk(t)}{dt}.$$

In the current example, the temperature dependence in the Garofalo law is treated exactly while the hyperbolic sine function for stress is reduced to a power function using a one-term Taylor series expansion. UCRPLW.F is written below:

```

SUBROUTINE UCRPLW(CPA,CFT,CFE,CFTI,CFSTRE,CPTIM,TIMINC,
*
*           EQCP,DT,DTD1,MDUM,NN,KC,MAT)
C* * * * *
C   user routine to define implicit creep law
C   input:
C   cptim  time at beginning of increment
C   timinc  time increment
C   eqcp   creep strain at beginning of increment
C   dt     temperature at beginning of increment
C   dtd1   incremental temperature
C   mdum(1) user element number
C   mdum(2) elsto element number
C   nn     integration point number
C   kc     layer number
C   mat    material number
C   output:
C   cpa    creep constant

```

```

C      cft      temperature factor
C      cfe      creep strain factor
C      cfti     time factor
C      cfstre   stress exponent
C      where:
C      creep strain rate = cpa*cft*cfe*cfti*(stress**cfstre)
C* * * * *

```

```

IMPLICIT REAL*8 (A-H,O-Z)
DIMENSION MDUM(*)
DTEND=DT+DTDLE
CFTI=1.D0
CFE=1.D0
CFSTRE=3.3D0
C1=16.7D-6
ALP=866.D0
G=(28388.D6-56.D6*DTEND)
CPA=C1*(ALP/G)**CFSTRE
Q=0.548D0
AK=8.617D-5
CFT=DEXP(-Q/AK/DTEND)*G/DTEND
RETURN
END

```

MATERIAL PROPERTIES

NAME

solder_A

ISOTROPIC

YOUNG'S MODULUS

3.02e10

POISSON'S RATIO

0.4

MASS DENSITY

9000

THERMAL EXP

THERMAL EXP COEF

2.4e-5

OK

CREEP

YIELD STRESS

4.92e7

USER SUB. UCRPLW

OK (twice)


```

Joule HEATING
CONDUCTIVITY
    50.6
RESISTIVITY
    1e6
SPECIFIC HEAT
    200
MASS DENSITY
    9000
OK
ELEMENTS
    577 582 587 592 597 602 607 612 617 622 627 632 637 642 647
    652 657 662 667 672 677 682 687 692 581 586 591 596 601 606
    611 616 621 626 631 636 641 646 651 656 661 666 671 676 681
    686 691 696 #
    
```

The material properties for the other components are added in a similar way where, for the elastic components, the creep section is omitted.

```

RETURN
    
```

Contact

The solder balls, the ceramic, the die, and the PCB are taken as separate contact bodies. The glue option is used for each interface where contact bodies touch each other, and the contact heat transfer coefficient is set to 100 W/m^2 for these interfaces.

```

CONTACT
CONTACT BODIES
DEFORMABLE
    OK
ELEMENTS
    577 to 596 #
NEW
DEFORMABLE
    OK
ELEMENTS
    597 to 616 #
    
```

The other solder balls are added as contact bodies in a similar way.

```
NEW
DEFORMABLE
  OK
SELECT
  CLEAR SELECT
  SELECT SET
    ceramic
    OK
  RETURN
ELEMENTS
ALL SELECT
```

The other components are selected as contact bodies in a similar way.

```
RETURN
CONTACT TABLES
  NEW
  PROPERTIES
    1 7
      CONTACT TYPE: GLUE
      THERMAL PROPERTIES
      CONTACT HEAT TRANSFER COEFFICIENT
        100
    2 7
      CONTACT TYPE: GLUE
      CONTACT HEAT TRANSFER COEFFICIENT
        100
```

In this contact table, the same properties are also set for the following combinations: 3 7, 4 7, 5 7, 6 7, 1 9, 2 9, 3 9, 4 9, 5 9, 6 9, 7 8.

```
    OK (twice)
  RETURN (twice)
```

Loadcases and Job Parameters

A coupled Joule-mechanical creep analysis will be performed. The loading is divided in three stages. In the first loadcase, the temperature is decreased from 170°C to 25°C at the bottom of the PCB over a period of 100 seconds. Only plasticity is allowed for the solder balls during this period. In the second loadcase, the temperature is maintained at 25°C and the solder balls are allowed to creep over a period of 10000 seconds. In the third loadcase, an electric potential of 10 V is applied across the die for 10000 seconds. The generated heat due to the induced electric currents causes a temperature increase in the assembly. The fixed time-stepping scheme TRANSIENT NON AUTO is used for loadcase 1. An adaptive time-stepping scheme based on MULTI-CRITERIA is used for loadcases 2 and 3. It should be noted that the thermal loading in loadcase 1 is linearly ramped over 10 increments, whereas, the electrical loading in loadcases 3 is instantaneously applied.

Fixed Stepping (TRANSIENT NON AUTO in *Volume C: Program Input*) uses the time step specified by the user. Any specified tolerance for allowable temperature change is ignored. The thermal solution is recycled till the tolerance for temperature error in estimate (if nonzero) is satisfied.

MULTI-CRITERIA (AUTO STEP in *Volume C: Program Input*) controls the time step based on the convergence characteristics of the thermal and mechanical passes of the loadcases. For the thermal pass, the time step control is based on the actual temperature change compared to a user-specified tolerance on temperature change (default is 20°). If the temperature change in any increment exceeds the allowed value, the time step is reduced, and the electrical and thermal passes are repeated with a smaller time step. For the mechanical pass, by default, the time step control is based on the number of recycles used to reach convergence compared to a desired number of recycles (default is 3). If the number of recycles in the mechanical pass exceeds the number of desired recycles, the time step of the increment is cut back, and the electrical, thermal and mechanical passes are repeated. In addition to these numerical criteria, if deemed necessary, one can choose to add user-specified or automatic physical criteria to control the time stepping. In the latter case, the algorithm also keeps track of the changes in the specified physical quantity and cuts back as soon as the change exceeds allowed tolerances. In the current example, an allowed temperature change of 100 K is specified. Also, the initial time step for loadcase 2 is specified as 0.001 of 10000 = 10 seconds. This matches the time step used in the first loadcase. At transition stages where loading changes, it is advisable to use smaller time steps in order to capture the creep more accurately. Alternately, physical criteria based on creep strain changes can be used. These are not used in the current example.

```

LOADCASES
  JOULE-MECHANICAL
    TRANSIENT
      LOADS
        pot_10
      OK
    CONTACT
      CONTACT TABLE
        ctable1

```

CONVERGENCE TESTING

MAX. ERROR IN TEMPERATURE ESTIMATE

5

OK

TOTAL LOADCASE TIME

100

CONSTANT TIME STEP

PARAMETERS

STEPS

10

OK (twice)

CREEP

LOADS

pot_10

OK

CONTACT

CONTACT TABLE

ctable1

CONVERGENCE TESTING

MAX. TEMPERATURE CHANGE ALLOWED

100

OK

TOTAL LOADCASE TIME

10000

MULTI-CRITERIA

PARAMETERS

INITIAL FRACTION OF LOADCASE TIME

0.001

OK

COPY

CREEP

LOADS

temp

pot_10

OK (twice)

RETURN (twice)

The implicit creep analysis option needs to be set from the JOBS menu. Also, three choices are provided as to what kind of tangent matrix is to be formed. The first is using an elastic tangent, which requires more iterations, but can be computationally efficient because re-assembly might not be required. The second is a secant (approximate) tangent that gives the best behavior for general viscoplastic models. The third is an algorithmic tangent that provides the best behavior for small strain power law creep. When implicit creep is specified in conjunction with plasticity, the elastic tangent option is not available.

JOBS

ELEMENT
TYPES

 JOULE-MECHANICAL

 3-D SOLID

 7

 OK

 ALL EXIST

 RETURN (twice)

JOULE-MECHANICAL

 lcase1

 lcase2

 lcase3

CONTACT CONTROL

 INITIAL CONTACT

 CONTACT TABLE

 ctable1

 OK (twice)

ANALYSIS OPTIONS

 CREEP TYPE & PROCEDURE: IMPLICIT MAXWELL

 CREEP TYPE & PROCEDURE: SECANT TANGENT

JOB RESULTS

 Stress

 Plastic Strain

 Creep Strain

 Equivalent Von Mises Stress

 Total Equivalent Plastic Strain

 Total Equivalent Creep strain

 1st Comp of Heat Flux

 2nd Comp of Heat Flux



 3rd Comp of Heat Flux

- Electric Current
- Generated Heat
- Displacement
- Temperature
- Electric Potential
- External Heat flux
- External Electric Current
- Reaction Force
- Reaction heat Flux
- Reaction Electric Current
- Contact Normal Stress
- Contact Normal Force
- Contact Friction Stress
- Contact Friction Force
- Contact Status
- Contact Touched Body
- OK (twice)

Save Model, Run Job, and View Results

After saving the model, and selecting the user subroutine *ucrplw.f*, the job is submitted.

```
FILE
  SAVE AS
    die.mud
  OK
RETURN
RUN
  USER SUBROUTINE FILE
    ucrplw.f
  SUBMIT(1)
```

[Figure 3.14-3](#) shows the plastic strain in the solder balls. The plastic deformation occurs in the first few increments of the analysis, when the temperature change is the highest. [Figure 3.14-4](#) shows the equivalent creep strain as a function of time for a node on two solder balls. The  (blue) curve is from a node from a solder ball at the outside of the grid and the  (red) curve is from a node from a solder ball at the center of the grid. [Figure 3.14-5](#) shows the temperature as a function of time for a node at the top of the die and a node at the bottom of the PCB.

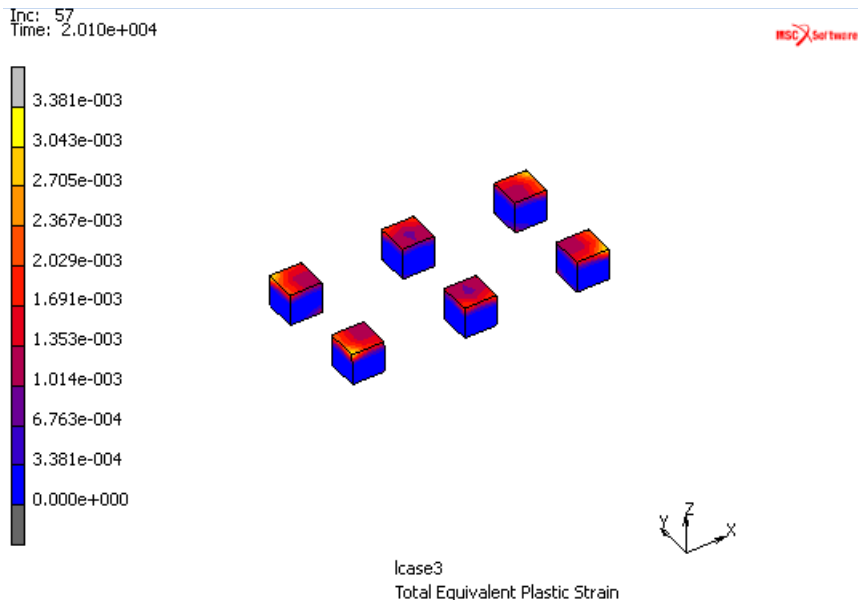


Figure 3.14-3 Equivalent Plastic Strain in the Solder Balls

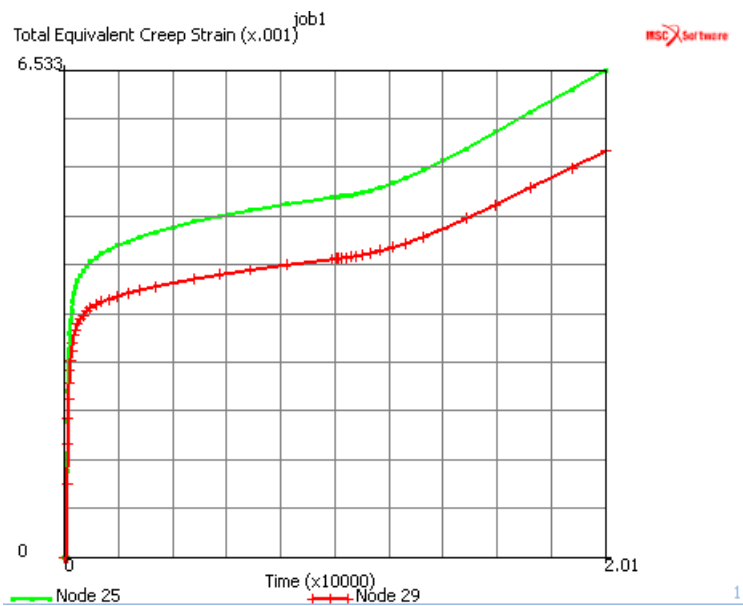


Figure 3.14-4 Equivalent Creep Strain as a Function of Time for a Node on two Solder Balls

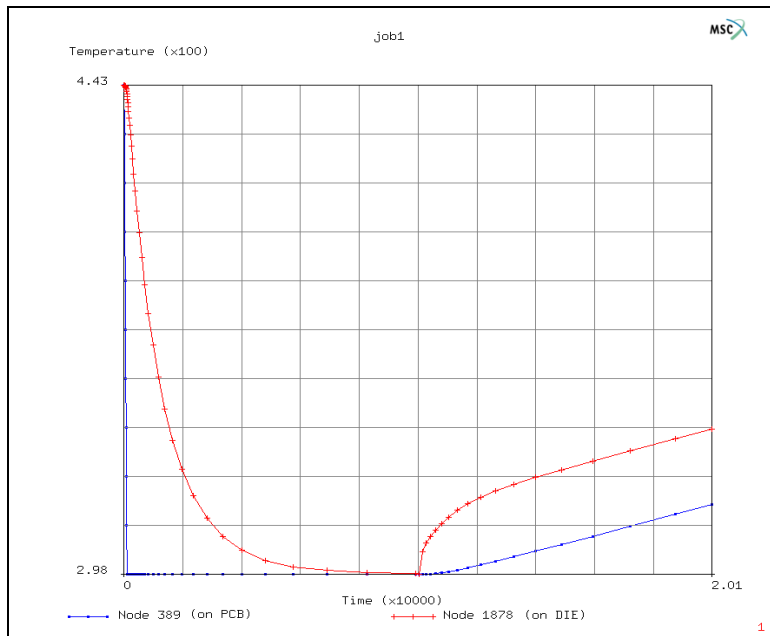


Figure 3.14-5 Temperature as a Function of Time for two Nodes, one at the Top of the Die and one at the Bottom of the PCB

Input Files

The files below are on your [delivery media](#) or they can be downloaded by your web browser by clicking the links (file names) below.

File	Description
die.proc	Mentat procedure file to run the above example
ucrplw.f	User subroutine

References

1. H.L.J. Pang, C.W. Seetoh, *Elasto-Plastic Creep Analysis of Ceramic BGA Solder Joints Subjected to Temperature Cycling Loading*, Proceedings, The 17th MARC Users' Meeting, 1997, pp.183 - 194
2. H.U. Akay, Y. Tong, N. Paydar, *Thermal fatigue analysis of a SMT solder joint using non-linear FEM approach*, The Int. Journal of Microcircuits and Electronics Packaging, Vol. 16, No. 2, pp. 79-88, 1993.
3. R. Darveaux and K. Banerji, *Constitutive relations for tin-based solder joints*, IEEE Transactions on Components, Hybrids, and Manufacturing Technology, Vol. 15, No. 6, pp. 1013-1024, 1992

3.15 Continuum Composite Elements

- Chapter Overview 1154
- Background Information 1154
- Analysis 1155
- Input Files 1164

Chapter Overview

This chapter demonstrates the use of the continuum elements. Compared to the composite shell elements, the continuum composite elements are often advantageous especially in the cases that the use of continuum elements are unavoidable to achieve an accurate solution. For example, if the nonlinear deformation behavior is not negligible through the thickness because of either material and/or geometrical nonlinearity, a discretization along thickness direction is required.

A thick composite cylinder subjected to an inner pressure is considered. The detailed description of the analysis procedure is presented using Mentat GUI. Steps on defining material properties for each composite layer and defining layer orientations will be highlighted.

Background Information

An infinitely long thick cylinder with an interior radius of 60 mm and an exterior radius of 140 mm is subjected to the inner pressure of 50 N/mm². The cylinder consists eight layers with equal thickness. From interior to exterior, the material layers are numbered from 1 to 8. The orthotropic material properties for layers 1, 3, 5, and 7 are given as

$$E_{11} = 250000 \text{ N/mm}^2, E_{22} = E_{33} = 10000 \text{ N/mm}^2,$$

$$\nu_{12} = \nu_{31} = 0.01, \nu_{23} = 0.25,$$

$$G_{12} = G_{23} = 5000 \text{ N/mm}^2, G_{31} = 2000 \text{ N/mm}^2.$$

The orthotropic material properties for layers 2, 4, 6, and 8 are given as

$$E_{11} = E_{22} = 10000 \text{ N/mm}^2, E_{33} = 250000 \text{ N/mm}^2,$$

$$\nu_{12} = \nu_{31} = 0.25, \nu_{23} = 0.01,$$

$$G_{12} = 2000 \text{ N/mm}^2, G_{23} = G_{31} = 5000 \text{ N/mm}^2.$$

The material orientations are based on global coordinate system; i.e., axial, radial, and circumferential directions, respectively.

See [Figure 3.15-1](#) for the cross-section geometry of the cylinder and the loading configuration.

Element type 154 (8-node, isoparametric, axisymmetric continuum composite element) is used in the analysis.

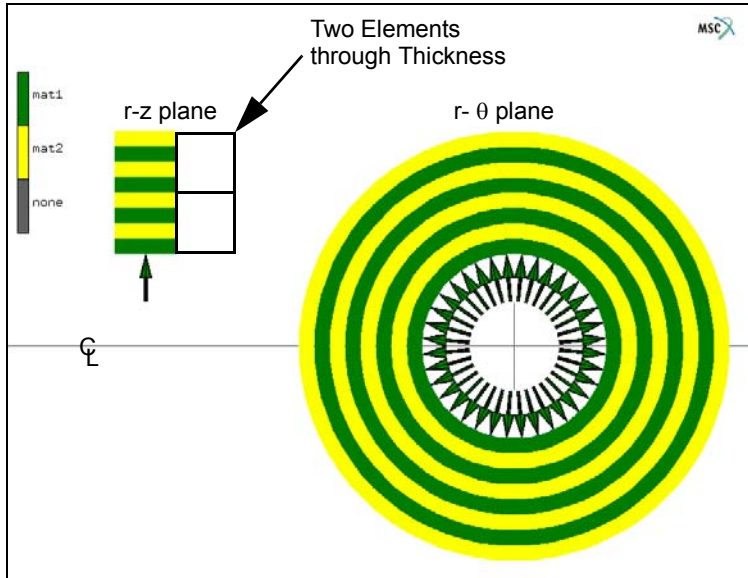


Figure 3.15-1 Cross-Section Geometry and Loading of a Thick Composite Cylinder

The cylinder is modeled with only four axisymmetric elements in the r - z plane, with two elements spanning the thickness of the cylinder. Since the cylinder's thickness spans eight layers of two orthotropic materials, each element spans four layers of two orthotropic materials each. Prior to this feature, each layer would have been modeled with a single element, hence requiring more elements. With the composite continuum element, we may span several layers of different materials.

Analysis

Model Generation

There are two elements along the radial (thickness) direction; i.e., each element contains four material layers.

MESH GENERATION

nodes ADD

0 140 0

0 60 0

80 60 0

80 140 0

FILL

elems ADD

1 2 3 4

SUBDIVIDE

DIVISIONS

2 2 1

ELEMENTS

all: EXIST.

RETURN

CHANGE CLASS

QUAD (8)

ELEMENTS

all: EXIST.

RETURN

SWEEP

ALL

RETURN

RENUMBER

ALL

RETURN

MAIN

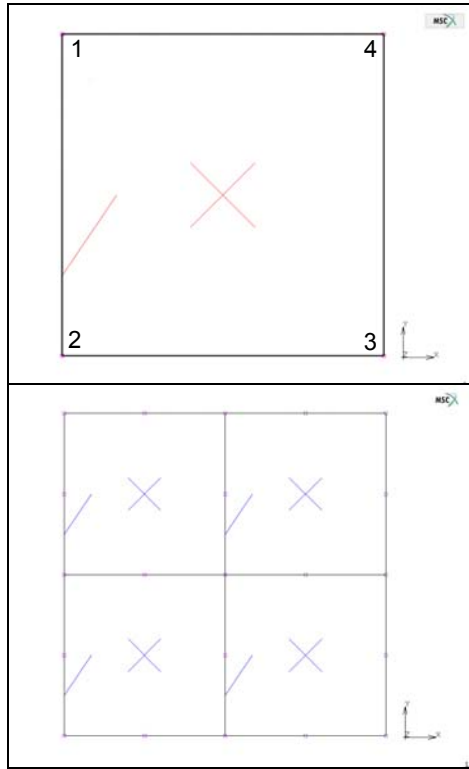


Figure 3.15-2 FE-Mesh

Boundary Conditions and Loads

BOUNDARY CONDITIONS

MECHANICAL

FIXED DISPLACEMENT

DISPLACEMENT X

OK

nodes ADD

```
(boxes A)
END LIST (#)
NEW
EDGE LOAD
PRESSURE
50
OK
edges ADD
(box B)
END LIST (#)
MAIN
```

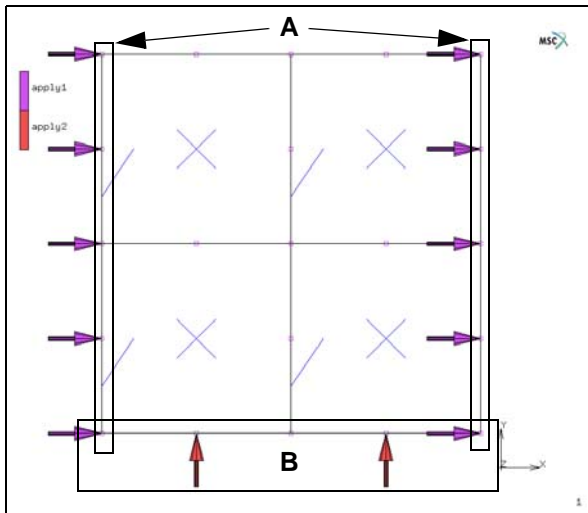


Figure 3.15-3 Mesh for the Thick Composite Cylinder

Material Properties

Define two sets of orthotropic materials, but no elements associated with material sets are given. This is defined afterwards.

MATERIAL PROPERTIES

NAME mat1

ORTHOTROPIC

(fill out form to right)

1e4

1e4

25e4

.25

.01

.25

2e3

5e3

5e3

OK

mat1

The screenshot shows the 'Material Properties' dialog box for material 'mat1'. The 'Type' is set to 'Elastic-Plastic Orthotropic'. The 'Young's Moduli' table has values 10000 for E1 and E2, and 250000 for E3. The 'Poisson's Ratios' table has values 0.25 for Nu12 and Nu31, and 0.01 for Nu23. The 'Shear Moduli' table has values 2000 for G12, 5000 for G23, and 5000 for G31. The 'Update Thickness' checkbox is checked. The 'Entities' section shows 0 elements.

Young's Moduli		
E1	10000	Table
E2	10000	Table
E3	250000	Table

Poisson's Ratios		
Nu12	0.25	Table
Nu23	0.01	Table
Nu31	0.25	Table

Shear Moduli		
G12	2000	Table
G23	5000	Table
G31	5000	Table

Figure 3.15-4 (Mat1) Orthotropic Materials

NEW
 NAME mat2
 ORTHOTROPIC
 (fill out form to right)
 25e4
 1e4
 1e4
 .01
 .25
 .01
 5e3
 5e3
 2e3
 OK

mat2

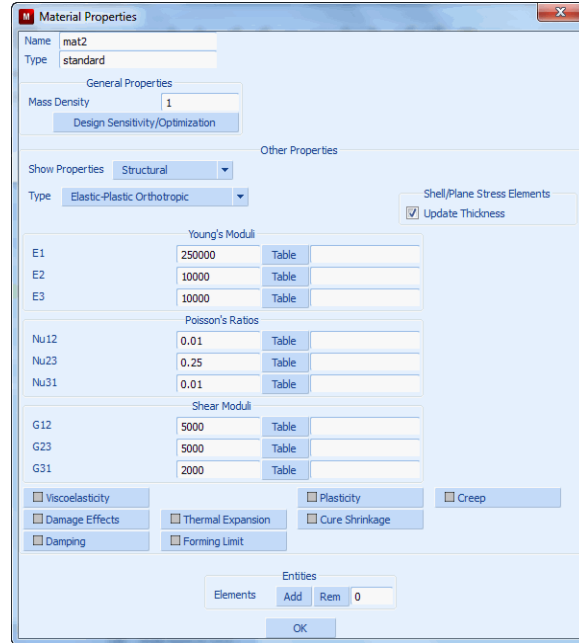


Figure 3.15-5 (Mat2) Orthotropic Materials

Composite Layer Property Definition

Definition of composite layer properties is a key step in performing an analysis with continuum composite elements. This includes the number of layers within the elements, the material set associated with each layer, the percentage of the layer thickness respect to the total element thickness, and the elements using this set of definition.

LAYERED MATERIALS
 NEW COMPOSITE
 ADD LAYER
 1
 mat1
 THICKNESS
 25
 ADD LAYER
 2
 mat2
 THICKNESS

25
ADD LAYER
3
mat1
THICKNESS
25
ADD LAYER
4
mat2
THICKNESS
25
OK
NAME
comp1
elements ADD
all: EXIST.
MAIN

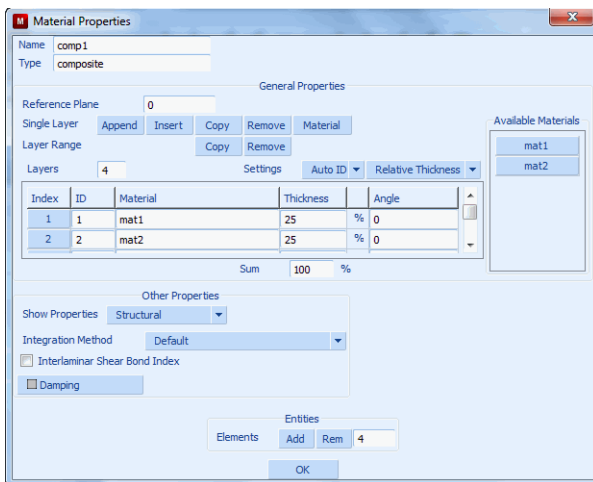


Figure 3.15-6 Define Composite Material

Composite Layer Orientation Definition

The composite layer orientation is defined using geometric properties. In our problem, the layers are similar to element edge 3 defined by node 4 to node 1.

GEOMETRIC PROPERTIES

AXISYMMETRIC

SOLID COMPOSITE

thickness direction

EDGE 3 (1-4)

OK

elements ADD

all: EXIST.

MAIN

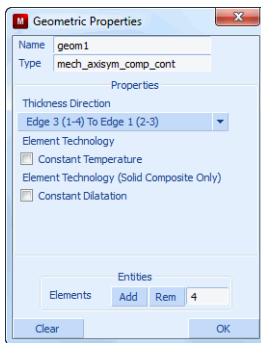


Figure 3.15-7 Solid Composite Menu

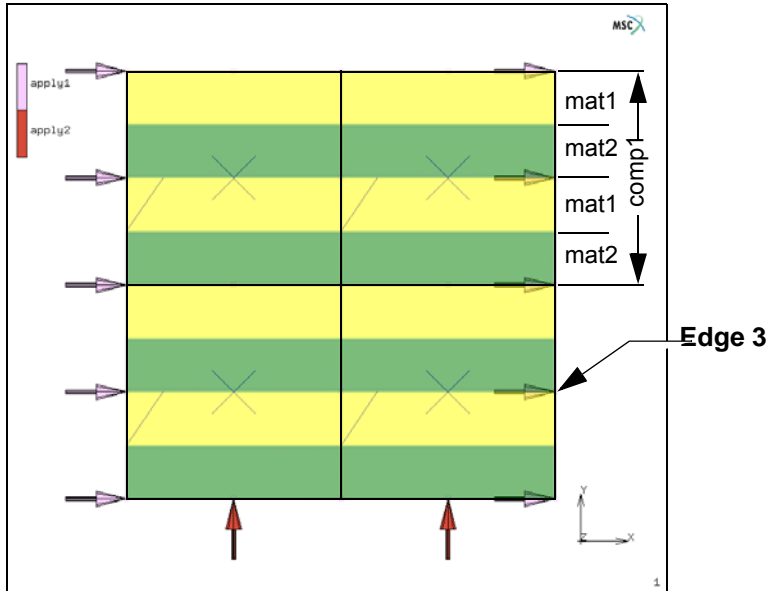


Figure 3.15-8 Definition of Composite Layer Orientations

Define Job Parameters, Save Model, and Run Job

Element type 154 is used. This element type is one of the special designed continuum composite elements. Stresses are written into the post file.

```

JOBS
  MECHANICAL
    OK
  ELEMENT TYPES
    MECHANICAL
      AXISYM
        154
      OK
    all: EXIST.
    RETURN (twice)
  MECHANICAL
    JOB RESULTS
      available element tensors
        Stress
        OK (twice)
  
```

RUN
SUBMIT 1
MONITOR
OK
SAVE

View Results

MAIN
RESULTS
OPEN DEFAULT
NUMERICS
SCALAR
Displacement Y
OK
OUT (zoom out)

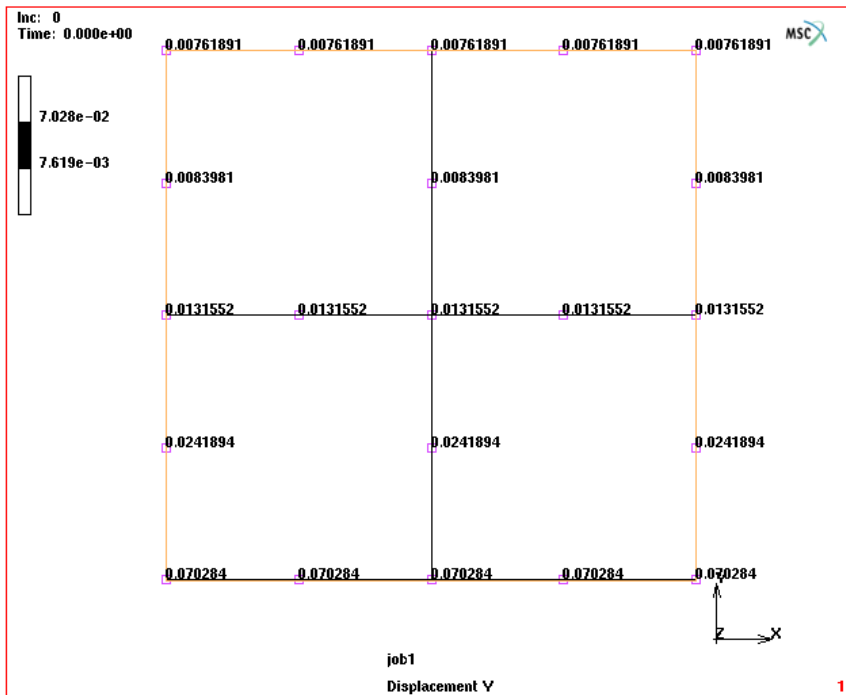


Figure 3.15-9 Radial Displacements of Thick Composite Cylinder

Comparison

The analytical solution for this thick cylinder problem is available (see S.G. Lekhnitskii, Anisotropic Plates, 1968). The radial displacements of the interior and the exterior surfaces of the thick cylinder are $7.20e-2$ and $7.38e-3$, respectively. These results are in good agreement with our finite element solutions which are $7.03e-2$ and $7.62e-3$, respectively. Considering the relatively coarse mesh, the results are encouraging.

For the purpose of comparison, an analysis based on the same mesh but low-order elements (Element type 152) is also performed. The radial displacements of the interior and the exterior surfaces of the thick cylinder are $5.84e-2$ and $4.18e-3$, respectively. Obviously, if the low-order elements are used, a finer mesh is needed to achieve reasonably good results.

You may wish to run Mentat procedure files that are in the `examples/new_features` subdirectory under Mentat. The procedure file `c17.proc` builds, runs, and postprocesses this simulation.

Input Files

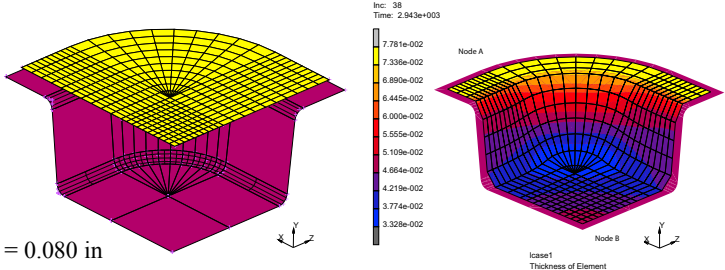
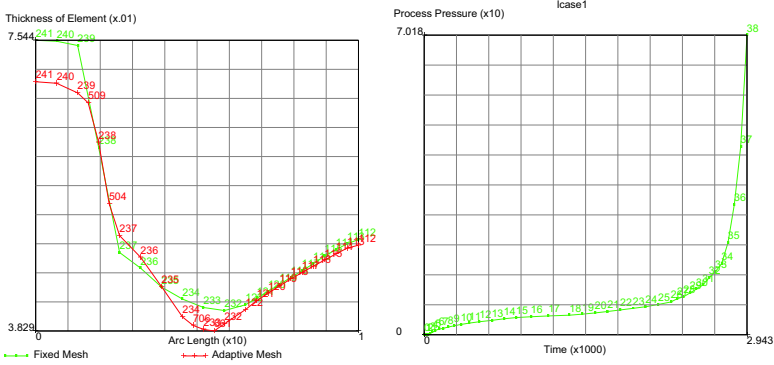
The files below are on your [delivery media](#) or they can be downloaded by your web browser by clicking the links (file names) below.

File	Description
continuum_composite_elem.proc	Mentat procedure file to run the above problem

3.16 Super Plastic Forming (SPF)

- Summary 1166
- SPF Modeling 1168
- Discussion 1185
- SPF with Adaptive Remeshing 1185
- Discussion of Adaptive Meshing 1189
- Input Files 1190

Summary

Title	Superplastic forming
Problem features	Flat sheet formed into a die by pressure
Geometry	 <p>$t = 0.080 \text{ in}$</p> <p>Inc: 38 Time: 2.943e+003</p> <p>7.781e-02 7.336e-02 6.890e-02 6.445e-02 6.000e-02 5.555e-02 5.109e-02 4.664e-02 4.219e-02 3.774e-02 3.328e-02</p> <p>Node A</p> <p>Node B</p> <p>lcase1 Thickness of Element</p>
Material properties	Rigid plastic flow
Analysis type	Static
Boundary conditions	Edges fixed with pressure adjusted to maintain proper strain rate
Element type	Membrane elements with local mesh adaptivity
FE results	<p>Edge thickness profiles and pressure history</p>  <p>Thickness of Element (x.01)</p> <p>7.544 241 240 239 238 504 237 236 235 234 233 232 231 230 229 228 227 226 225 224 223 222 221 220 219 218 217 216 215 214 213 212</p> <p>3.828 0 1</p> <p>Arc Length (x10)</p> <p>Fixed Mesh Adaptive Mesh</p> <p>Process Pressure (x10)</p> <p>7.018 38 37 36 35 34 33 32 31 30 29 28 27 26 25 24 23 22 21 20 19 18 17 16 15 14 13 12 11 10 9 8 7 6 5 4 3 2 1</p> <p>0 2.943</p> <p>Time (x1000)</p>

A flat sheet is formed into a rigid die by pressure. The die is three-dimensional and represents a corner of a pan. This fine-grained material is assumed to be a rigid-plastic material with no elasticity and the flow stress is only a function of the strain rate.

As the sheet contacts the die, friction causes the thickness of the sheet to vary. In addition the pressure must be adjusted to keep this strain rate sensitive material within a certain target range. This is necessary to maintain the proper flow of the super plastic material. Prediction of thinning of the sheet is very important since the sheet may become too thin for its application.

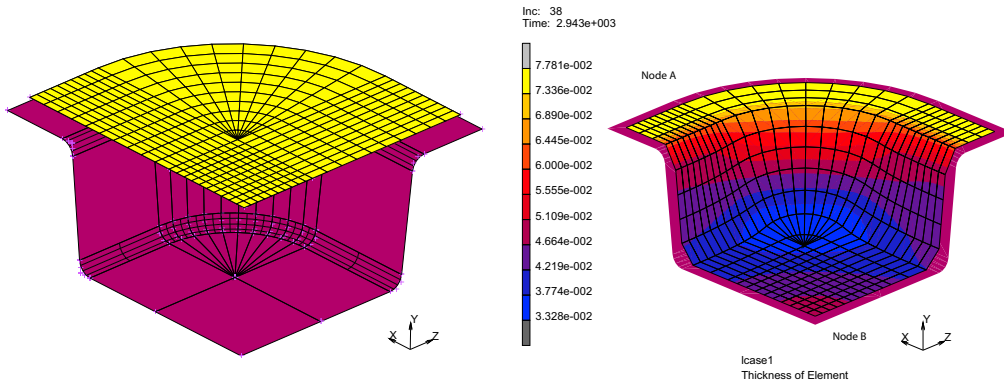
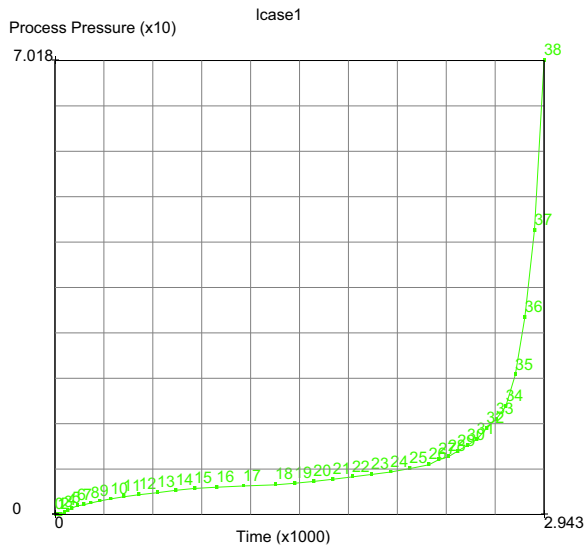


Figure 3.16-1 Sheet Before and After Forming

The SPF Pressure control in Loadcase (see graphic below) is used to automatically adjust the pressure on the sheet to keep within the target strain rate. Furthermore, the maximum pressure is limited by the capacity of the rig used to form the sheet. Units used are inches, pounds, and seconds.



SPF Modeling

This problem does a Super Plastic Forming of a corner using the Super Plastic Forming loading scheme that keeps adjusting the applied pressure to maintain an average target strain rate in the material.

```
FILES
SAVE AS spf
RETURN
```

Preprocessing

Model Generation consists of making the die and sheet. Building the die first, we begin in Mentat with a curve:

```
MESH GENERATION
coordinate system SET
  GRID (on)
  U DOMAIN
    -7 7
  U SPACING
    .5
  V DOMAIN
    0 5
  V SPACING
    .5
  FILL
  RETURN
crvs: ADD
  point( 7.0, 4.5, 0.0)
  point( 4.0, 4.5, 0.0)
  point( 4.0, 4.5, 0.0)
  point( 3.5, 0.0, 0.0)
  point( 3.5, 0.0, 0.0)
  point( 0.0, 0.0, 0.0)
  point( 0.0, 0.0, 0.0)
  point(-4.0, 0.0, 0.0)
```

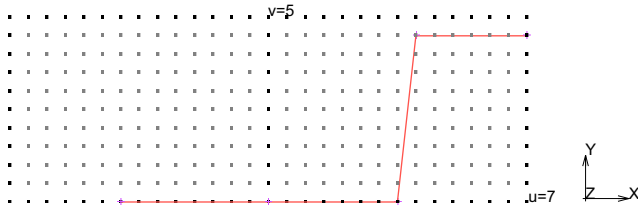



Figure 3.16-2 Start with Rough Layout

CURVE TYPE

FILLET

RETURN

crvs: ADD

1

2

.5

8

3

.5

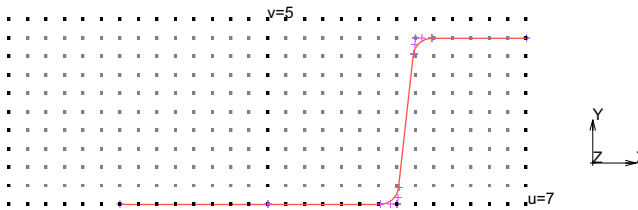


Figure 3.16-3 Trim Lines with Fillets

VIEW

SHOW VIEW 2

FILL

RETURN

EXPAND

SHIFT

TRANSLATIONS

0 0 3.5

CURVES

all: EXIST.

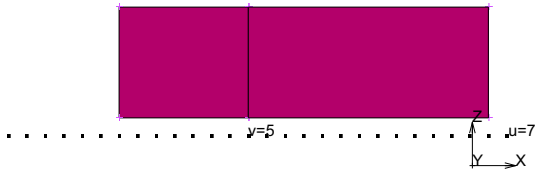


Figure 3.16-4 Build Surface from Trimmed Curves

RESET
SHIFT
CENTRIOD
0 0 3.5
ROTATIONS
0 -90/10 0
REPETITIONS
10
CURVES
pick curves shown
FILL

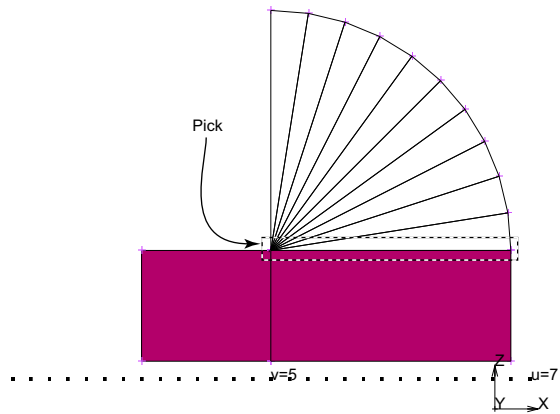


Figure 3.16-5 Continue Building Surface

RESET
SHIFT
CENTROID
0 0 3.5
TRANSLATIONS

```

-4.0 0 0
REPETITIONS
1
CURVES
END LIST (#)
RETURN
CURVES REMOVE
ALL:EXISTING

```

(pick curves shown)

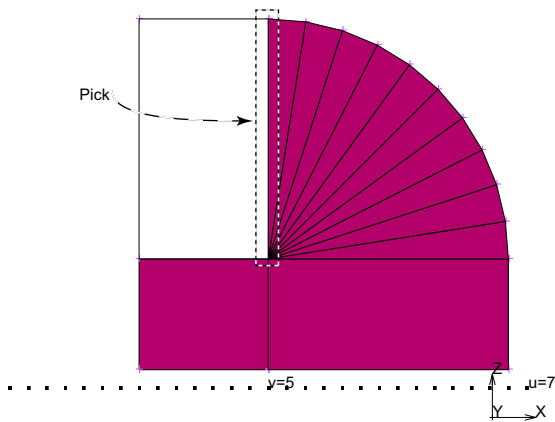


Figure 3.16-6 Finish Die Surface

Now, we add nodes that will contain the mesh.

```

SELECT
SURFACES
ALL:EXISTING
MAKE INVISIBLE
RETURN
CURVE TYPE
LINE
RETURN
VIEW 1, RETURN

```

crvs: ADD

```

point(-3.5, 5.0, 0.5)
point( 0.0, 5.0, 0.5)
point( 0.0, 5.0, 0.5)
point( 6.5, 5.0, 0.5)

```

(type in coordinates as shown)



Figure 3.16-7 Add More Lines to Make Mesh

```
EXPAND
  RESET
  SHIFT
  TRANSLATIONS
    0 0 3.0
  CURVES
  all: EXIST.
```

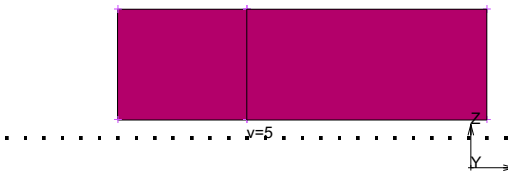


Figure 3.16-8 Expand Lines to make Mesh Surface

```
RESET
SHIFT
CENTRIOD
  0 0 3.5
ROTATIONS
  0 -90/10 0
REPETITIONS
  10
CURVES
```

(pick curve shown)

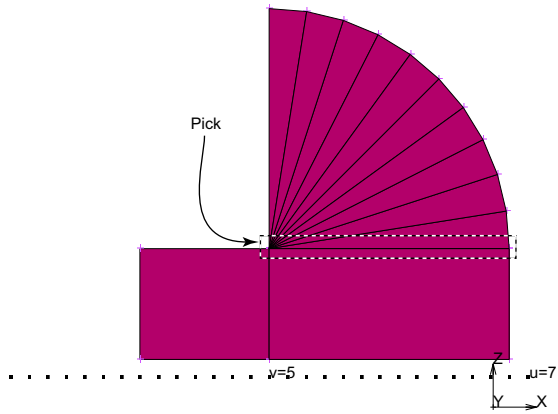


Figure 3.16-9 Continue Building Mesh Surface

```

RESET
SHIFT
TRANSLATIONS
  -3.5 0 0
REPETITIONS
  1
CURVES
END LIST (#)
RETURN

```

(pick curve shown)

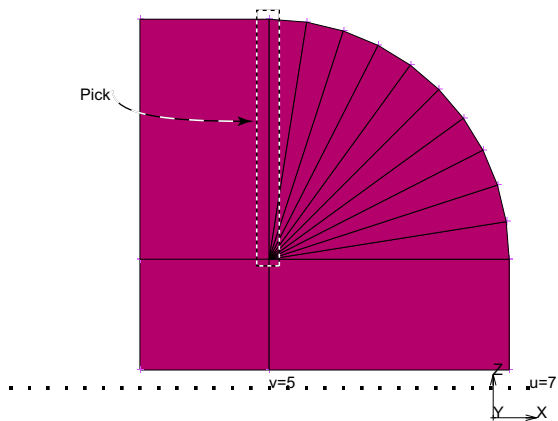


Figure 3.16-10 Finish Building Mesh Surface

```
CONVERT
DIVISIONS
  10 1
SURFACES TO ELEMENTS
```

(pick those shown)

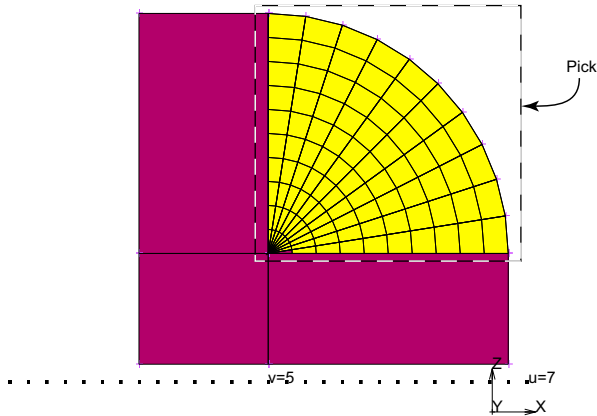


Figure 3.16-11 Convert Sector Surfaces to Elements

```
DIVISIONS
  10 10
SURFACES TO ELEMENTS
END LIST (#)
RETURN
SWEEP
ALL
RETURN
RENUMBER
ALL
RETURN (twice)
```

(pick remaining rectangular surfaces)

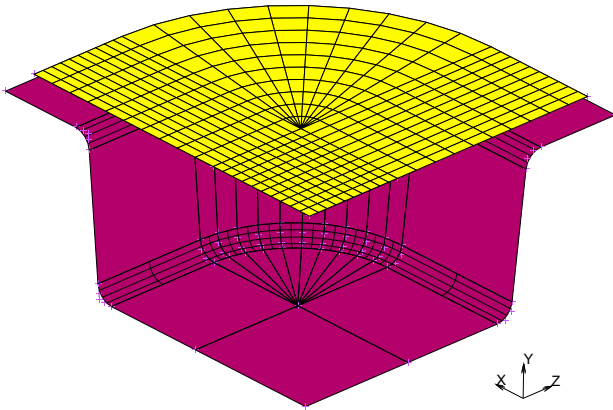


Figure 3.16-12 Final Mesh

BOUNDARY CONDITIONS

MECHANICAL

SELECT

ELEMENTS

all: EXIST.

MAKE VISIBLE

RETURN

FIXED DISPLACEMENT

FIX X,Y,Z = 0

OK

SELECT

METHOD PATH

NODES

END LIST (#)

RETURN

nodes: ADD

all: SELECTED

(pick 1st middle and last node of outer path)

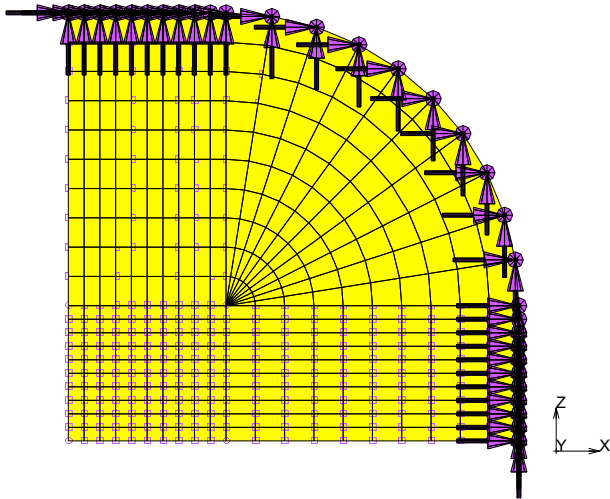


Figure 3.16-13 Fix Displacements on Outer Binding

NEW

FIX X = 0, OK

nodes: ADD

(along x=0)

END LIST (#)

NEW

FIX Z = 0

nodes: ADD

(along z=0)

END LIST (#)

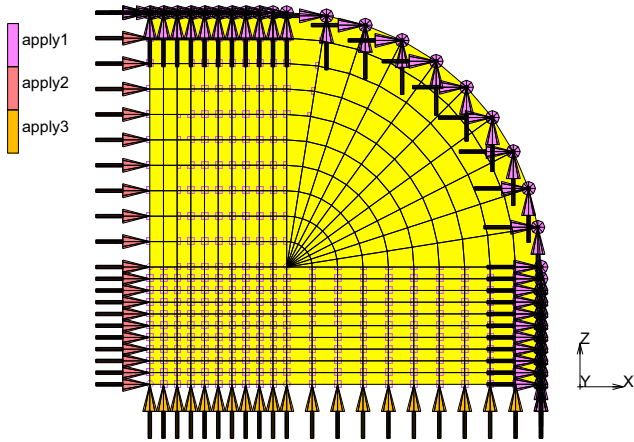


Figure 3.16-14 Fix Symmetry Displacements

NEW
 FACE LOAD
 SUPERPLASTICITY CONTROL
 ON PRESSURE NEGATIVE
 OK
 FACES ADD
 ALL EXISTING

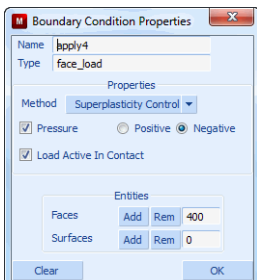


Figure 3.16-15 Turn on SPF Pressure Control

MAIN
 MATERIAL PROPERTIES (twice)
 NEW
 STANDARD
 STRUCTURAL
 TYPE: RIGID-PLASTIC
 PLASTICITY
 METHOD: POWER LAW

(fill out as shown in [Figure 3.16-16](#))

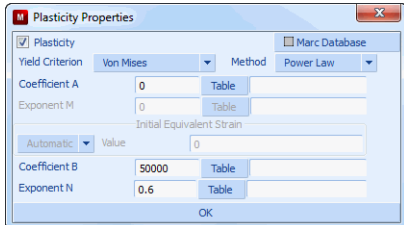


Figure 3.16-16 Enter SPF Material Behavior

```
OK (twice)
ELEMENTS ADD: ALL EXISTING
MAIN
GEOMETRIC PROPERTIES
3-D
MEMBRANE
THICKNESS
    .080
OK
ELEMENTS ADD
all: EXIST.
SELECT
MAKE INVISIBLE
MAIN

CONTACT
CONTACT BODIES
NEW
NAME
    workpiece
DEFORMABLE
FRICITION COEFFICIENT
    .3
OK
elements ADD
All: EXIST.
NEW
NAME
```

```

die
RIGID
VELOCITY PARAMETERS
  APPROACH VELOCITY Y
    .01
  OK
  FRICTION COEFFICIENT
    .3
  OK
surfaces: ADD
  END LIST (#)
ID BACKFACES
FLIP SURFACES
  all: EXIST.
MAIN
  
```

(pick surfaces forming die)

(flip die surfaces until gold color will touch the workpiece)

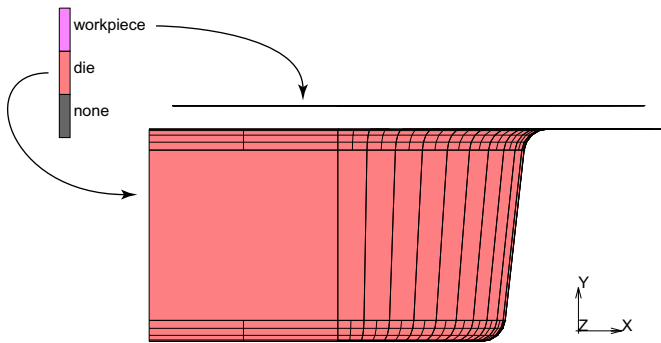


Figure 3.16-17 Define Contact Bodies

```

LOADCASES
MECHANICAL
  STATIC
  TOTAL LOADCASE TIME
    3000
  stepping procedure
  MULTI-CRITERIA
  PARAMETERS
  INITIAL FRACTION
    1e-4
  
```

```
MAXIMUM FRACTION
  5e-3
OK
CONVERGENCE TESTING
RELATIVE/ABSOLUTE
RESIDUALS AND DISPLACEMENTS
  RELATIVE FORCE TOLERANCE = 0.01
  MAXIMUM REACTION FORCE CUTOFF
    6
  MAXIMUM ABSOLUTE RESIDUAL FORCE
    6
  RELATIVE DISPLACEMENT TOLERANCE = 0.05
  MINIMUM DISPLACEMENT CUTOFF
    5e-5
  MAXIMUM ABSOLUTE DISPLACEMENT
    5e-5
OK
SUPERPLASTICITY CONTROL
pressure
  MINIMUM
    .001
  MAXIMUM
    300
  TARGET STRAIN RATE METHOD
    2e-4
  TARGET STRAIN RATE METHOD
  CONSTANT
  PRE_STRESS
    50
  # INCREMENTS
    5
```

(on)
(on)

(filled out as shown in [Figure 3.16-18](#))

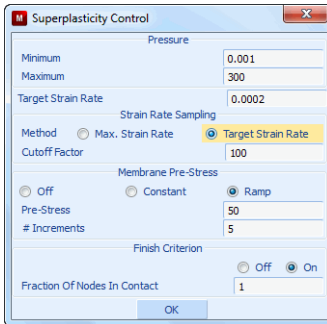


Figure 3.16-18 Define Loadcase with SPF Parameters

OK (twice)
 MAIN

Analysis

Here, we set up the problem to run with Coulomb frictions using membrane elements. Later, we will run the problem with adaptive meshing.

JOBS

NEW (MECHANICAL)

PROPERTIES

lcase1

ANALYSIS OPTIONS

LARGE STRAIN

(on)

FOLLOWER FORCE

(on)

OK

JOB RESULTS

available element scalars

Equivalent Plastic Strain Rate

Thickness of Element

OK

CONTACT CONTROL

ADVANCED CONTACT CONTROL

COULOMB

BILINEAR

OK (twice)

ELEMENT TYPES, MECHANICAL

3-D MEMBRANE/SHELL

18

(Quad 4)

OK

all: EXIST.

RETURN (twice)

SAVE

RUN

STYLE: OLD

SUBMIT1

MONITOR

OK

MAIN

Results

RESULTS

OPEN DEFAULT

NEXT

DEF ONLY

CONTOUR BAND

SCALAR

Thickness of Element

LAST

(Last Increment)

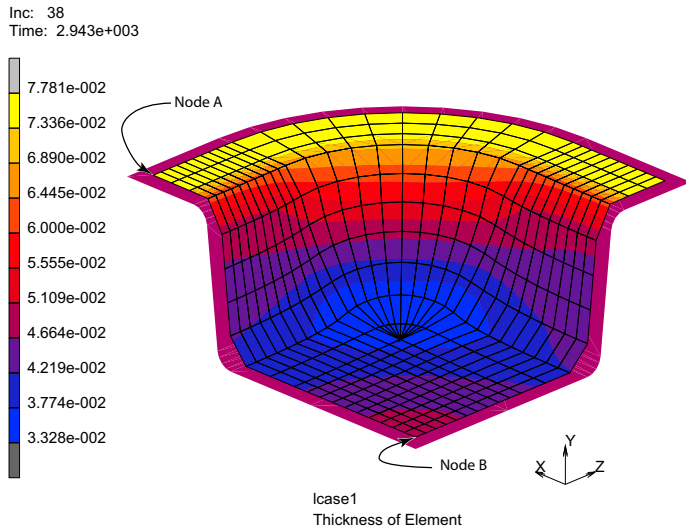


Figure 3.16-19 Thickness Contours

```

PATH PLOT
SET NODES
    (Node A) (Node B)
END LIST (#)
ADD CURVES
    ADD CURVE
        Arc Length
        Thickness
FIT
RETURN
generalized xy plot: COPY TO
    
```

(Send to XY plotter)

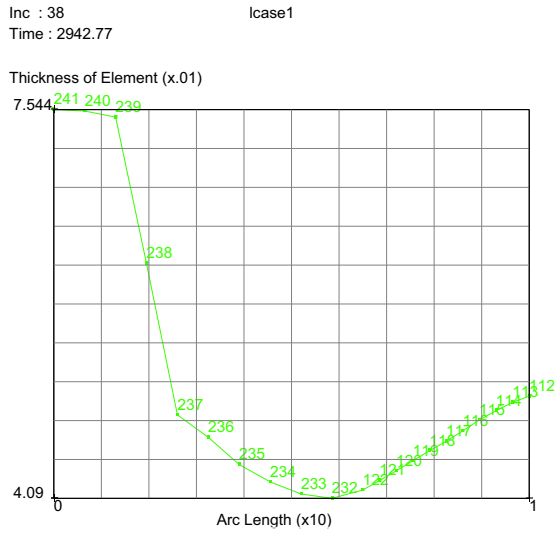


Figure 3.16-20 Thickness Profile along Edge

RESULTS

HISTORY PLOT

ALL INCS

ADD CURVES

GLOBAL

Time

Process Pressure

FIT

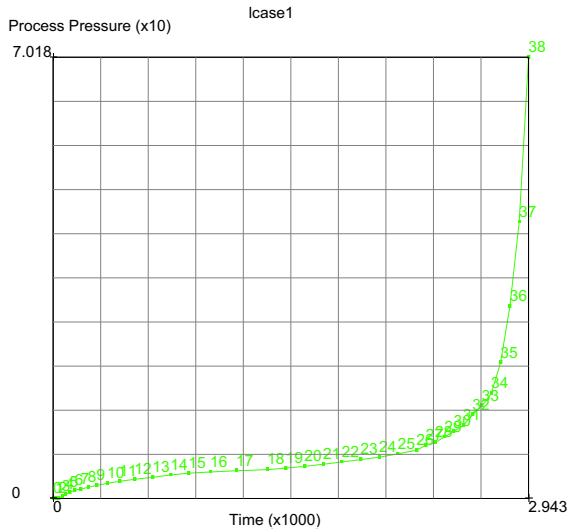


Figure 3.16-21 Pressure Schedule

Discussion

From [Figure 3.16-19](#), we see a minimum thickness of about 0.034 which is 2.3 fold decrease in the original sheet thickness of 0.080. The path in [Figure 3.16-20](#) shows how rapidly the thickness reduces from the binder to the center of the sheet. [Figure 3.16-21](#) shows how the pressure is automatically adjusted to keep the average strain rate in the sheet at the target strain rate specified in [Figure 3.16-18](#). Also the procedure stops when 100% of the nodes come into contact with the die at a time before the allotted 3000 seconds.

You will find it very instructive to turn off the friction (JOBS>PROPERTIES>CONAT CONTROL>FRICTION TYPE: NONE). Then, compare the thickness profile with [Figure 3.16-19](#) to see how much friction thins the sheet. Many times the thinning (thanks to friction) is too severe and another forming technique may be necessary.

As the mesh forms over the die the original element size may be too large to capture local surface details properly. Now that the SPF simulation is running, we can use the adaptive remeshing with local refinement to increase the number of elements where they can improve this situation.

SPF with Adaptive Remeshing

Preprocessing consists starting with our original model and adding adaptive remeshing and running a new model. Starting from Mentat, let's open our previous model and save as a new model.

FILES

- OPEN spf
- SAVE AS

```
spE_adapt  
OK  
RETURN  
ADAPTIVE REMESHING  
LOCAL ADAPTIVITY CRITERIA  
  NODES IN CONTACT  
  MAX # LEVELS = 2  
  OK  
  ELEMENTS ADD  
END LIST  
ID LOCAL ADAPTIVITY CRITERIA
```

(pick elements shown in [Figure 3.16-22](#))

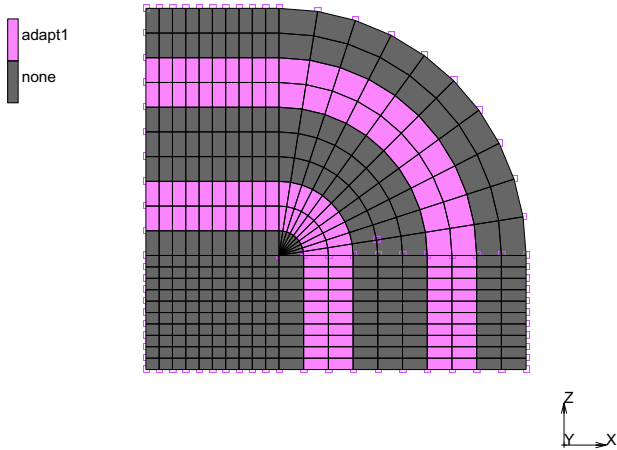


Figure 3.16-22 Elements Selected for Local Refinement

```
MAIN  
JOBS
```

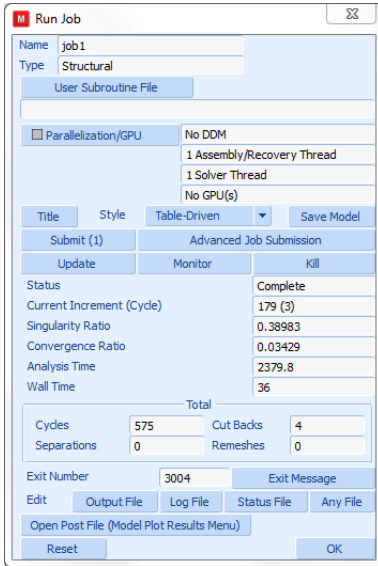


Figure 3.16-23 Status of Job

RUN
 SAVE MODEL
 SUBMIT1
 MONITOR
 OK
 MAIN

Results

RESULTS
 OPEN DEFAULT
 NEXT
 DEF ONLY
 CONTOUR BAND
 SCALAR
 Contact Status
 LAST

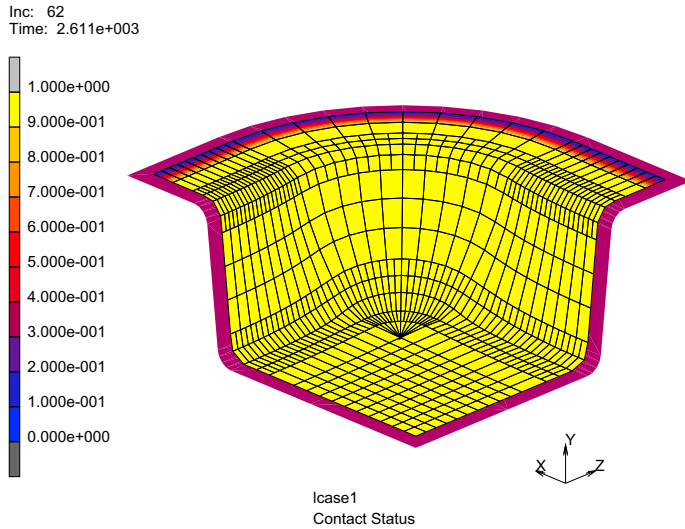


Figure 3.16-24 Contact Status (1 = touching, 0 = not touching)

SCALAR
Thickness of Element

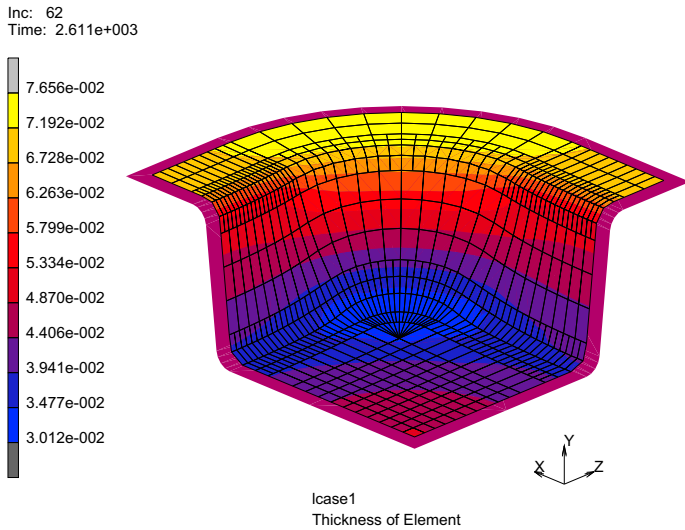


Figure 3.16-25 Adapted Thickness Contours

PATH PLOT
NODE PATH

```
(Node A) (Node B)
END LIST
ADD CURVES
  ADD CURVE
    Arc Length
    Thickness Of Element
  RETURN
FIT
generalized xy plotter: COPY TO
FIT
```

(Send to XY plotter)

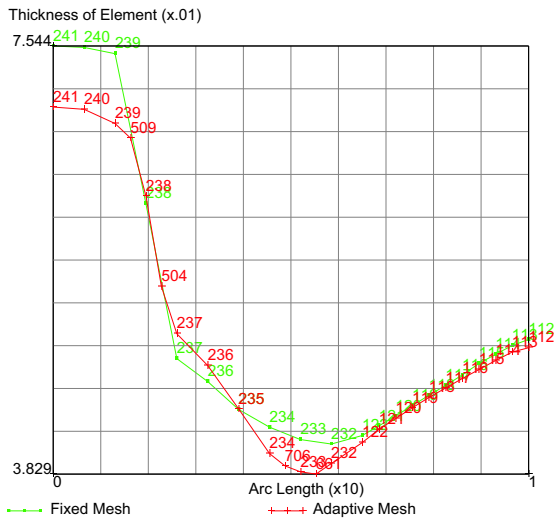


Figure 3.16-26 Thickness Profile along Edge (with and without Adaptive Meshing)

Discussion of Adaptive Meshing

From Figure 3.16-24 that all of the nodes touching the binder have a contact status of 1. Note that with more elements in the die corners that the minimum thickness is a bit lower than the coarse mesh as shown in Figure 3.16-25. Using the adaptive remeshing with local refinement to increase the number of elements has given a better fit to the die.

Figure 3.16-26 uses the Generalize XY plotter to compare results between these two runs. The original mesh had 400 elements and the final adapted mesh has 760 elements. More elements can easily be added by changing the remeshing criteria to continue to improve the results.

Input Files

The files below are on your [delivery media](#) or they can be downloaded by your web browser by clicking the links (file names) below.

File	Description
super_plastic_forming.proc	Mentat procedure file to run the above example
super_plastic_forming_b_help.proc	Mentat procedure file to run the above example with adaptive meshing

Also, this problem can automatically be run from the HELP menu under DEMONSTRATIONS > RUN A DEMO PROBLEM > SUPERPLASTIC FORMIN and SPF + ADAPT. MESHING.

3.17 Gaskets

- Chapter Overview 1192
- Simulation of a Cylinder Head Joint 1193
- Input Files 1220

Chapter Overview

Engine gaskets are used to seal joints between the metal parts of the engine to prevent steam or gas from escaping. They are complex (often multi-layer) components, usually rather thin and typically made of several different materials of varying thickness. The gaskets are carefully designed to have a specific behavior in the thickness direction. This is to ensure that the joints remain sealed when the metal parts are loaded by thermal and mechanical loads. The through-thickness behavior, usually expressed as a relation between the pressure on the gasket and the closure distance of the gasket, is highly nonlinear, often involves large plastic deformations, and is difficult to capture with a standard material model. The alternative, modeling the gasket in detail by taking every individual material into account in the finite element model of the engine, is not feasible as it requires a large number of elements, making the model unacceptably large. The GASKET material model addresses these problems by allowing gaskets to be modeled with only one element through the thickness, while the experimentally or analytically determined complex pressure-closure relationship in that direction can be used directly as input for the material model.

This chapter introduces the GASKET material. For this purpose, a cylinder head joint subjected to a combination of mechanical and thermal loadings will be analyzed. The mechanical loading consists of sequentially fastening the bolts of the joint, followed by application of an internal pressure to the cylinder head. The fastening of the bolts is simulated by introducing a pre-tension force in the bolts. This is achieved by splitting up the finite element mesh of the bolts in two parts and connecting them by using the standard options, TYING and SERVO LINK. The thermal loading involves uniformly heating the joint, cooling it down, and bringing it back to room temperature.

The procedure file to demonstrate this example is called `gasket .proc` under `path/examples/marc Ug/s3/c3.17`.

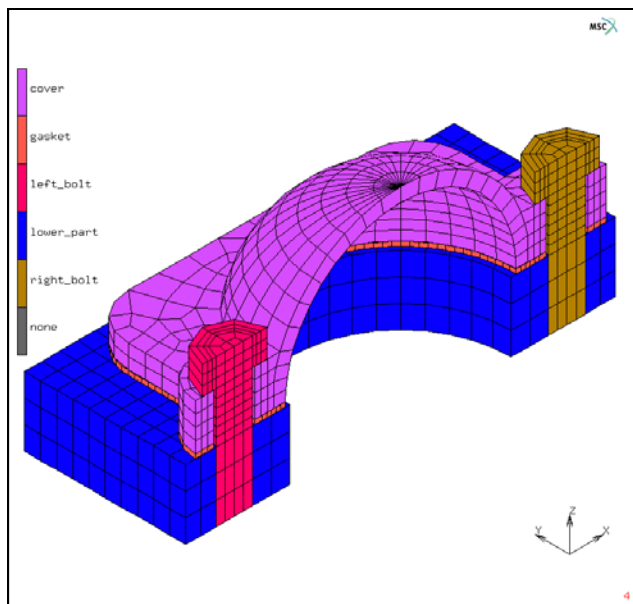


Figure 3.17-1 Finite Element Mesh of the Cylinder Head Joint

Simulation of a Cylinder Head Joint

The model consists of the cylinder head cover and a small portion of the lower part of the cylinder head (see [Figure 3.17-1](#)). Both the cover and the lower part are made of steel. A thin gasket layer seals the joint between the cover and the lower part. The joint is fastened by two steel bolts.

The assembly is loaded in six stages. In the first two stages, the fastening of the joint is simulated by applying a pre-tension of 12000 N to each of the bolts. After the bolts have been loaded, the three-stage thermo-mechanical loading cycle starts. First, the assembly is heated uniformly to 180°C, while simultaneously an interior pressure of 1.2 MPa is applied to the cover and the lower part of the assembly. Next, the joint is cooled down uniformly to -10°C, while retaining the interior pressure. In the fifth stage, the pressure is removed and the temperature is increased again to room temperature. The final loadcase of the analysis consists of disassembling the joint by loosening the bolts.



Figure 3.17-2 PARAMETERS Menu

Note: The PARAMETERS menu and the parameters describes the finite element mesh of the cylinder head joint. The values of the parameters are in millimeters.

Mesh Generation

Since the assembly and the applied loads are symmetric with respect to the zx -plane (see [Figure 3.17-1](#)), only one half of the assembly is taken into account in the model, while symmetry conditions are imposed by means of a contact symmetry plane.

The model is setup in a fully parametric fashion, allowing different, but similarly shaped models to be created by modifying the parameters. The parameters are defined in the UTILS-> PARAMETERS menu. [Figure 3.17-2](#) displays the menu and lists the parameters that govern the dimensions of the different components of the model, as well as their respective values. The PARAMETERS menu offers two methods of defining or modifying parameters. If the EVALUATION METHOD is DELAYED (the default), the parameter becomes an abbreviation for the expression that is assigned to it. If the EVALUATION METHOD is IMMEDIATE, the expression is evaluated first and its value is being assigned to the parameter. The difference becomes apparent when the expression contains other parameters or calls to numerical functions that return information about the model. The value of a parameter defined using the delayed evaluation method is the value of the expression assigned to it at the time the parameter is being used. By contrast, the value of a parameter defined using the immediate evaluation method is the value of the expression at the time of the definition of the parameter.

The generation of the parametric finite element mesh will not be discussed in detail here. Instead, the reader is referred to the procedure file that belongs to this chapter and the comments in that file. For the set of parameters used in the present example, the resulting finite element mesh is depicted in [Figure 3.17-1](#).

Tyings and Servo Links

As mentioned earlier, in the first two stages of the analysis, the fastening of the joint is simulated by applying pre-tension loads of 12000 N to each of the bolts. In the first stage, the left bolt (see [Figure 3.17-1](#)) is pre-tensioned while the right bolt is locked and in second stage the right bolt is loaded while the length of the left bolt is fixed. During the subsequent three-stage thermo-mechanical loading cycle, the bolts are locked and in the final stage of the analysis, the joint is disassembled by loosening the bolts.

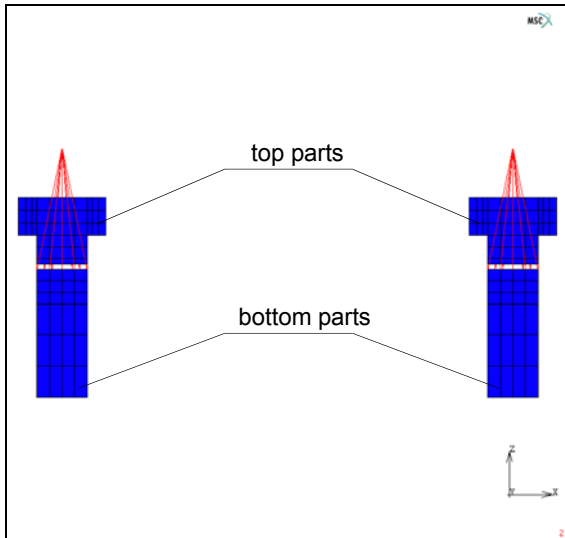


Figure 3.17-3 Bolts split up into a Top and Bottom Parts connected by Tyings and Servo Links

The pre-tension force in the bolt is simulated using standard options existing in Marc, namely, TYING and SERVO LINK. During the mesh generation process, the finite element meshes of the bolts have been split up into a top and a

bottom part as depicted in [Figure 3.17-3](#). Corresponding nodes on both sides of the cut are now connected to each other and to a special node, called the *control node* of the bolt, by means of a set of tyings (to prevent relative tangential motion of the two parts) and servo links. As is shown below, the servo links can be chosen in such a way that a pre-tension force can be applied to the bolt simply by applying a POINT LOAD boundary condition to the control node of the bolt. Alternatively, the bolt can be tightened, locked, or loosened by applying a FIXED DISPLACEMENT boundary condition to the control node.

Note: Please note that the small gap between the top and bottom parts shown in [Figure 3.17-3](#) is purely for visualization purposes and to allow easy selection of the nodes on both sides of the gap. The gap is closed by moving down the nodes of the top part just above the gap in the negative z-direction after the links have been created, although the duplicate nodes remain.

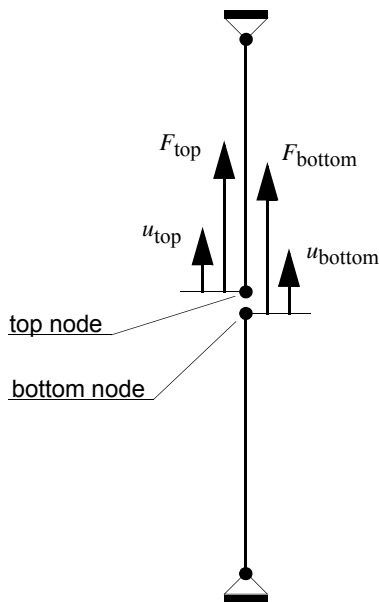


Figure 3.17-4 Applying Pre-tension to a Truss Modeled by Two Truss Elements

Consider a truss that is clamped at both ends and that is divided into two truss elements, as show in [Figure 3.17-4](#). The elements are not connected to each other; at the center of the truss, two distinct nodes exist, called the *top node* and *bottom node*. Let

$$\mathbf{u} = [u_{top} \ u_{bottom}]^T \quad \text{and} \quad \mathbf{F} = [F_{top} \ F_{bottom}]^T \quad (3.17-1)$$

be the vectors with, respectively, the displacements of these two nodes in the axial direction of the truss and the corresponding forces. The required continuity of the displacement field in the truss can be ensured by stating that both displacements are equal. Denoting this common displacement value by u^* , the continuity of the displacement field is expressed by the constraint equation,

$$\mathbf{u} = \mathbf{T}u^*, \quad (3.17-2)$$

in which $\mathbf{T} = [1 \ 1]^T$. One of the properties of a constraint equation is the fact that the work done by the constraint is zero. If F^* is the force that is work conjugate to u^* , the zero-work principle can be stated as follows,

$$F^* u^* = \mathbf{F}^T \mathbf{u} . \tag{3.17-3}$$

Substitution of equation (3.17-2) into equation (3.17-3) and requiring that the result is valid for arbitrary values of u^* , yield the following expression for the force F^* ,

$$F^* = \mathbf{F}^T \mathbf{T} = \begin{bmatrix} F_{\text{top}} & F_{\text{bottom}} \end{bmatrix} \begin{bmatrix} 1 \\ 1 \end{bmatrix} = F_{\text{top}} + F_{\text{bottom}} . \tag{3.17-4}$$

Due to the zero-work principle, the displacement constraint equation (3.17-2) is equivalent to the force constraint equation (3.17-4).

At this point, it is important to realize that the pre-tension force in the truss is nothing but the force on the bottom node F_{bottom} (or minus that on the top node). Prescribing that force basically amounts to stating that,

$$F_{\text{bottom}} = F_{\text{pre-tension}} . \tag{3.17-5}$$

The latter relation can be viewed as an additional constraint expressed in terms of forces. Introducing a new force vector \mathbf{F}_{new} given by,

$$\mathbf{F}_{\text{new}} = \begin{bmatrix} F^* & F_{\text{pre-tension}} \end{bmatrix}^T , \tag{3.17-6}$$

allows both force constraints (equations (3.17-4) and (3.17-5)) to be combined into the matrix equation

$$\mathbf{F}_{\text{new}} = \mathbf{T}_{\text{new}} \mathbf{F} , \quad \text{with} \quad \mathbf{T}_{\text{new}} = \begin{bmatrix} 1 & 1 \\ 0 & 1 \end{bmatrix} . \tag{3.17-7}$$

To find the equivalent displacement variant of equation (3.17-7), the zero-work principle is again applied. Let $u_{\text{pre-tension}}$ be the degree of freedom that is work conjugate to the pre-tension force and define,

$$\mathbf{u}_{\text{new}} = \begin{bmatrix} u^* & u_{\text{pre-tension}} \end{bmatrix}^T . \tag{3.17-8}$$

The zero-work principle now reads,

$$\mathbf{F}^T \mathbf{u} = \mathbf{F}_{\text{new}}^T \mathbf{u}_{\text{new}} = \mathbf{F}^T \mathbf{T}_{\text{new}}^T \mathbf{u}_{\text{new}} , \tag{3.17-9}$$

in which equation (3.17-7) is used. Since equation (3.17-9) must hold for all force vectors \mathbf{F} , it finally follows that

$$\mathbf{u} = \mathbf{T}_{\text{new}}^T \mathbf{u}_{\text{new}} \tag{3.17-10}$$

or,

$$\begin{bmatrix} u_{\text{top}} \\ u_{\text{bottom}} \end{bmatrix} = \begin{bmatrix} 1 & 0 \\ 1 & 1 \end{bmatrix} \begin{bmatrix} u^* \\ u_{\text{pre-tension}} \end{bmatrix} . \tag{3.17-11}$$

From the first row of equation (3.17-11), it follows that $u_{\text{top}} = u^*$. Substitution of this relation into the equation given by the second row then yields

$$u_{\text{bottom}} = u_{\text{top}} + u_{\text{pre-tension}} \quad (3.17-12)$$

The latter equation is the desired servo link. It is the displacement equivalent of equation (3.17-5) and relates the displacements of the top and bottom nodes to the “pre-tension displacement”. Rewriting equation (3.17-12) as,

$$u_{\text{pre-tension}} = u_{\text{bottom}} - u_{\text{top}} \quad (3.17-13)$$

shows that the “pre-tension displacement” can be interpreted as the shortening of the truss.

A pre-tension force can thus be applied to the truss by creating one additional node and by tying the displacement of the bottom node to that of the top node and of the additional node using the servo link equation (3.17-12). Then, by virtue of equation (3.17-5), if a POINT LOAD is applied to the additional node, a pre-tension force of that amount is introduced in the truss. Conversely, if a FIXED DISPLACEMENT boundary condition is applied to the additional node, the shortening of the truss is prescribed.

Since the pre-tension forces and the shortening of the bolts must be controlled separately, two additional nodes (one for each bolt) are introduced in the present example. For each bolt, the nodes of the bottom part just below the cut (the node set `bolt_bottom_nodes`) are tied to the corresponding nodes of the top part just above the cut (the node set `bolt_top_nodes`) and the control node of the bolt. The servo links are defined between the first degrees of freedom of the nodes. A local coordinate system is defined in the `bolt_bottom_nodes` and the `bolt_top_nodes` such that the local x -axis coincides with the global z -direction (the axial direction of the bolts). Since servo links and nodal ties always act on local degrees of freedom, the servo links between the `bolt_bottom_nodes` and the `bolt_top_nodes` act in the global z -direction (a local coordinate system allows the servo link to act in any desired direction and not just in one of the global directions). In addition to the servo links, the `bolt_bottom_nodes` are tied to the `bolt_top_nodes` using tying type 203 (second and third degree of freedom, or global y - and x -directions) to prevent relative tangential motion between the top and the bottom part.

Multiple servo links and nodal ties are most easily created using the ADD SERVOS command in the N TO N SERVO LINKS menu, respectively the ADD TIES command in the N TO N NODAL TIES menu. Since these commands require an equal number of nodes to be entered for each term in the constraint, the nodes of `bolt_top_nodes` set are duplicated first and the copies are put in a set called `bolt_control_nodes` (and removed from the `bolt_top_nodes` set). After the servo links have been created, the `bolt_control_nodes` for each bolt are merged into a single node using a sweep operation. The button sequence for creating the servo links, the nodal ties and the local coordinate system reads:

```
LINKS
  SERVO LINKS
    N TO N SERVO LINKS
      TIED DOF
        1
      RETAINED # TERMS
        2
```

TERM 1 DOF

1

TERM 1 COEF.

1.0

TERM 2 DOF

1

TERM 2 COEF.

1.0

CREATE PATHS

(off)

ADD SERVOS

bolt_bottom_nodes

bolt_top_nodes

bolt_control_nodes

RETURN (thrice)

LINKS

NODAL TIES

N TO N NODAL TIES

TYING TYPE

203

OK

CREATE PATHS

(off)

ADD TIES

bolt_bottom_nodes

bolt_top_nodes

RETURN (thrice)

MESH GENERATION

SWEEP

SWEEP_NODES

bolt_control_nodes

RETURN (twice)

BOUNDARY CONDITIONS

MECHANICAL

TRANSFORMS

NEW

```
ROTATE
    0 -90 0
ADD NODES
    bolt_bottom_nodes
    bolt_top_nodes
RETURN (thrice)
```

Boundary Conditions

To load the bolts with a pre-tension of 12000 N, two POINT LOAD boundary conditions are created. Since only half of the bolts is taken into account in the model, half of the pre-tension load is applied to the control nodes of the bolts. The locking of the bolts in the subsequent thermo-mechanical loading cycle and the loosening in the final loadcase of the analysis is simulated by applying FIXED DISPLACEMENT boundary conditions to the control nodes. The first degree of freedom is fixed to 0 mm in the loading cycle and decreased to -0.2 mm in the final loadcase, to prescribe an elongation of 0.2 mm. Tables are being used to control the loading history of these boundary conditions. For the left bolt, the button sequence is given by:

```
BOUNDARY CONDITIONS
MECHANICAL
TABLES
    NEW
    TABLE TYPE
        time
    ADD POINT
        0 0
        1 1
        6 1
    NAME
        left_bolt_load_history
    NEW
    TABLE TYPE
        time
    ADD POINT
        0 0
        5 0
        6 1
    NAME
        left_bolt_lock_history
```

```
        RETURN
    NEW
    POINT LOAD
        X FORCE
            6000
        TABLE
            left_bolt_load_history
    OK
    NODES ADD
        4104
    END LIST
    NAME
        prestress_left_bolt
    NEW
    FIXED DISPLACEMENT
        X DISPLACE
            -0.2
        TABLE
            left_bolt_lock_history
    OK
    NODES ADD
        4104
    END LIST
    NAME
        lock_unlock_left_bolt
```

For the right bolt, a similar sequence is used, except that the table that defines the history of the POINT LOAD is slightly different. Since the second bolt is loaded in the second loadcase, the table defined by the points (0,0), (1,0), (2,1) and (6,1).

In three-stage thermo-mechanical loading cycle that follows the prestressing of the bolts, the cylinder head joint is subjected to a combination of mechanical and thermal loads. The mechanical loading consists of a pressure of 1.2 MPa applied to the interior of the cylinder head cover and the lower part. The pressure is applied in the first stage of the loading cycle and removed in the third stage, using a FACE LOAD boundary condition in which the PRESSURE is set to 1.2 MPa. The TABLE that defines the history of the pressure is of type time and is defined by the points (0,0), (2,0), (3,1), (4,1), (5,0) and (6,0). The pressure is applied to the element faces at the interior boundary of the cover and the lower part using the FACES ADD button. These faces may be picked by clicking each of them using the left mouse button. However, this is cumbersome. Therefore, during the mesh generation process, the nodes at the interior

boundary have been stored in a set called `interior_nodes`. Using this node set, the faces are selected easily by means of the SELECT FACES BY NODES operation,

```
SELECT
  SELECT BY
    ALL IN LIST
      FACES BY NODES
        SET
          interior_nodes
        RETURN (twice)
```

and subsequently added to the boundary condition using the ALL: SELECT. button.

The thermal part of the loading cycle consists of a uniform increase of the temperature to 180°C in the first stage, a uniform decrease to -10°C in the second stage and again a uniform increase back to room temperature (20°C) in the third stage of the loading cycle. This is achieved by applying a NODAL TEMPERATURE boundary condition to all nodes in the model, setting the TEMPERATURE to 1 and employing a TABLE to a table of type time defined by the points (0,20), (2,20), (3,180), (4,-10), (5,20) and (6,20).

Finally, to suppress rigid body motions, the displacements in the z-direction of all nodes at the bottom of the lower-part of the cylinder head assembly are suppressed as well as the displacements in the x-direction of the nodes at the bottom of the lower-part that lie in the yz-plane. The applied mechanical loads are depicted in [Figure 3.17-1](#).

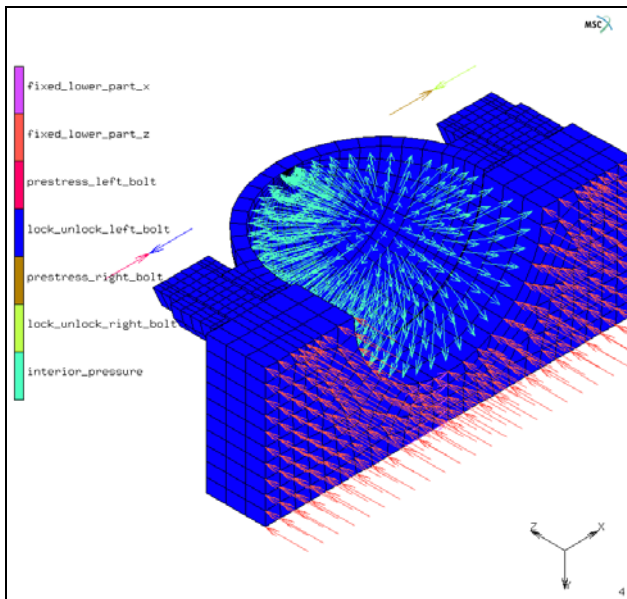


Figure 3.17-1 Mechanical Boundary Conditions applied to the Cylinder Head Joint

Note: The thermal loading consists of a NODAL TEMPERATURE boundary condition applied to all nodes of the model and is not drawn here.

Initial Conditions

The temperature of the model is initialized to 20°C (room-temperature) by means of a NODAL TEMPERATURE initial condition.

```
INITIAL CONDITIONS
MECHANICAL
NEW
NODAL TEMPERATURE
ON
TEMPERATURE
    20
OK
NODES ADD
ALL: EXIST.
NAME
    initial_temperature
```

Material Properties

The new GASKET material allows gaskets to be modeled with only one element through the thickness, while the analytically or experimentally determined complex pressure-closure relationship can be used directly as input for the material model. The behavior in the thickness direction, the transverse shear behavior, and the membrane behavior are fully uncoupled in the model. The transverse shear and membrane behavior are linear elastic, characterized by a transverse shear modulus and the in-plane Young's modulus and Poisson's ratio, respectively. In the thickness direction, the behavior in tension is also linear elastic and is governed by a tensile modulus, defined as a pressure per unit length.

In compression, two types of gasket behavior can be simulated: *fully elastic* and *elastic-plastic*. For the fully elastic model, the user only supplies the loading path in the form of a (nonlinear) relation between the pressure on the gasket and the closure distance of the gasket.

In the elastic-plastic model, the user specifies the loading path, the yield pressure above which plastic deformation develops and up to ten unloading paths. The loading and unloading paths must be supplied as (nonlinear) relations between the pressure on the gasket and the closure distance of the gasket. The unloading paths define the elastic unloading behavior at different amounts of plastic deformation. If the gasket unloads at an amount of plastic deformation for which no unloading path has been given, the unloading path is constructed automatically by interpolation between the two nearest user supplied paths. The elastic-plastic model allows for large plastic deformations.

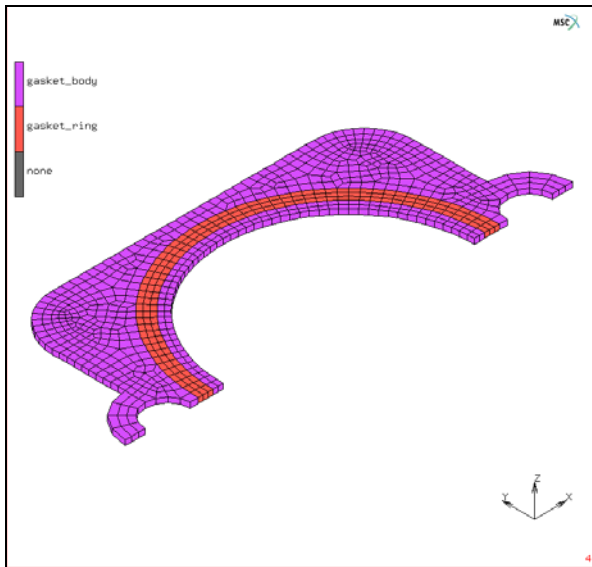


Figure 3.17-2 The Finite Element Mesh of Gasket

Since the thickness of a gasket can vary considerably throughout the gasket, an initial gap may be set for the gasket material to account for the fact that the gasket is actually thinner than the finite elements used to model it. As long as the closure distance is smaller than the initial gap, no pressure is built up in the gasket. The gasket can then be modeled as a flat sheet of uniform thickness and the initial gap parameter can be set for those regions where the gasket is thinner than the mesh.

The gasket material must be used with the gasket element types 149 (3-D solid), 151 (plane strain) or 152 (axisymmetric). Note that these elements currently have no associated heat-transfer element, so gaskets cannot be used in coupled thermo-mechanical analyses. However, the material can exhibit isotropic thermal expansion, characterized by a single thermal expansion coefficient.

The gasket used in this example is modeled as a flat sheet with a thickness of one millimeter and consists of two regions with different material properties (see [Figure 3.17-2](#)). For both regions, the data of the loading path and one unloading path are stored in four two-column data files. The first column in these files contains the closure distances, the second column the corresponding pressures. These data are used as input for the gasket material model by creating four tables of type `gasket_closure` and reading in the files.

MATERIAL PROPERTIES

TABLES

READ

RAW

body_loading.raw

OK

```
TABLE TYPE
    gasket_closure
NAME
    gasket_body_loading
READ
    RAW
    ch31_body_unloading.raw
    OK
TABLE TYPE
    gasket_closure
NAME
    gasket_body_unloading
READ
    RAW
    ring_loading.raw
    OK
TABLE TYPE
    gasket_closure
NAME
    gasket_ring_loading
READ
    RAW
    ring_unloading.raw
    OK
TABLE TYPE
    gasket_closure
NAME
    gasket_ring_unloading
```

The loading and unloading paths of the gasket materials can be displayed in one graph using the Generalized XY Plotter. The GET PLOTS FROM TABLE operation copies the data from every table in the model to the plotter, including the data from the load history tables of the boundary conditions. The latter are subsequently being removed from the XY plotter. The resulting picture is depicted in [Figure 3.17-3](#).

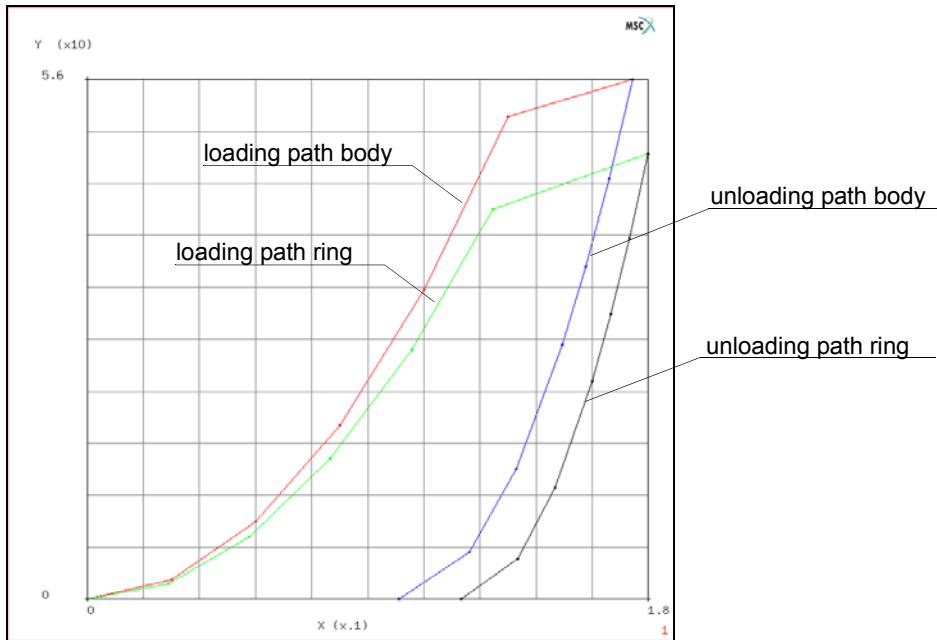


Figure 3.17-3 The Loading and Unloading Paths of the Gasket in the two Regions

UTILS

GENERALIZED XY PLOT

GET PLOTS FROM

TABLE

FIT

REMOVE

1 1 1 1 1 1

FIT

RETURN (twice)

The definition of the membrane properties and the thermal expansion coefficient of the gasket is separated from the definition of the properties in the thickness direction and the transverse shear behavior. For the former, the GASKET material refers to an existing isotropic material. Multiple gasket materials can refer to the same isotropic material for their membrane properties and thermal expansion. However, in the present example, the membrane stiffness of the body of gasket is 120 MPa and its thermal expansion coefficient is 5×10^{-5} per °C, while for the ring the membrane modulus is 100 MPa and the thermal expansion coefficient is 1×10^{-4} per °C. Poisson's ratio is 0 for both regions. Therefore, two isotropic materials are created with the membrane properties and thermal expansion coefficient of the two gasket regions.

```
MATERIAL PROPERTIES
  NEW
  ISOTROPIC
    YOUNG'S MODULUS
      120
    THERMAL EXP.
      THERMAL EXP. COEF.
        5e-5
      OK (twice)
  NAME
    gasket_body_membrane
  NEW
  ISOTROPIC
    YOUNG'S MODULUS
      100
    THERMAL EXP.
      THERMAL EXP. COEF.
        1e-4
      OK (twice)
  NAME
    gasket_ring_membrane
```

The behavior in the thickness direction and the transverse shear behavior of the gasket is defined by creating a new GASKET material and supplying the yield pressure, the tensile modulus, the initial gap parameter (if necessary), the tables of the loading and unloading paths and the transverse shear modulus in the GASKET MATERIAL PROPERTIES menu as depicted in [Figure 3.17-4](#). In this menu, also the isotropic material for membrane behavior has to be selected.

In the example, the thickness of the gasket ring is 10% larger than the thickness of the body of the gasket. Since the gasket is modeled as a flat sheet of uniform thickness, the INITIAL GAP is used for the body of the gasket to take this into account.

The yield pressure of the body of the gasket is 52 MPa, its tensile modulus is 72 MPa/mm, and the transverse shear modulus is 40 MPa. For the ring, the yield pressure is 42 MPa, the tensile modulus is 64 MPa/mm and the transverse shear modulus is 35 MPa.

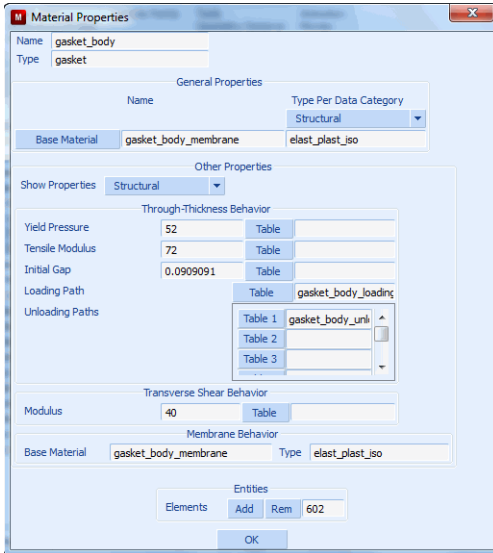


Figure 3.17-4 The GASKET MATERIAL PROPERTIES Menu

```

NEW GASKET
  YIELD PRESSURE
    52
  TENSILE MODULUS
    72
  INITIAL GAP
    1/11
  LOADING PATH TABLE
    gasket_body_loading
  UNLOADING PATHS TABLE 1
    gasket_body_unloading
  TRANSVERSE SHEAR BEHAVIOR MODULUS
    40
  MEMBRANE BEHAVIOR MATERIAL
    gasket_body_membrane
  OK
ELEMENTS ADD
  SET
    gasket_body
  OK

```

```
NAME
    gasket_body
NEW GASKET
    YIELD PRESSURE
        42
    TENSILE MODULUS
        64
    LOADING PATH TABLE
        gasket_ring_loading
    UNLOADING PATHS TABLE 1
        gasket_ring_unloading
    TRANSVERSE SHEAR BEHAVIOR MODULUS
        35
    MEMBRANE BEHAVIOR MATERIAL
        gasket_ring_membrane
    O
    K
ELEMENTS ADD
    SET
        gasket_ring
    OK
NAME
    gasket_ring
RETURN
```

The cylinder head cover, the lower part and the bolts are all made of steel. Young's modulus is 2.1×10^5 , Poisson's ratio 0.3, and thermal expansion coefficient 1.5×10^{-5} .

```
MATERIAL PROPERTIES
NEW
ISOTROPIC
    YOUNG'S MODULUS
        2.1e5
    POISSON'S RATIO
        0.3
    THERMAL EXP.
```



```
THERMAL EXP. COEF.  
    1.5e-5  
OK (twice)  
ELEMENTS ADD  
SET  
    cover  
    lower_part  
    bolts  
OK  
NAME  
    steel
```

Geometric Properties

The thickness direction of the gasket elements has to be specified by means of a geometric property of type 3-D SOLID COMPOSITE/GASKET. The finite element mesh of the gasket is created in such a way that for all elements in the gasket, the thickness direction is given by direction from FACE 4 (1-2-3-4) to FACE 5 (5-6-7-8).

```
GEOMETRIC PROPERTIES  
3-D  
NEW  
SOLID COMPOSITE/GASKET  
    THICKNESS DIRECTION  
        FACE 4 (1-2-3-4) TO FACE 5 (5-6-7-8)  
    OK  
ELEMENTS ADD  
SET  
    gasket  
    OK  
NAME  
    thickness_direction
```

Contact

The automatic contact algorithm is used to describe the contact between the gasket and the metal parts of the joint and between the bolts and the cylinder head cover. Moreover, a contact symmetry surface is used to take symmetry conditions into account.

Since the finite element mesh of the gasket is finer than the meshes of the metal parts, the best results are obtained if the gasket touches the latter. Therefore, the first contact body consists of the gasket elements. The second contact body consists of the lower part and the bolts and the third is the cover. The last contact body is the symmetry plane.

```
CONTACT
  CONTACT BODIES
    NEW
    DEFORMABLE
      OK
    ELEMENTS ADD
      gasket
    NAME
      gasket
    NEW
    DEFORMABLE
      OK
    ELEMENTS ADD
      lower_part
      bolts
    NAME
      lower_part

    NEW
    DEFORMABLE
      OK
    ELEMENTS ADD
      cover
    NAME
      cover
    NEW
    SYMMETRY
      OK
    SURFACES ADD
      1
    END LIST
    NAME
      symmetry_plane
```

The gasket is glued to the metal parts and is not allowed to separate. Normal touching contact is used between the cover and the bolts. To activate GLUE contact for the gaskets, a CONTACT TABLE is created.

```
CONTACT
  CONTACT TABLES
    NEW
    PROPERTIES
      1 2
        CONTACT TYPE: GLUE
      1 3
        CONTACT TYPE: GLUE
      1 4
        CONTACT TYPE: TOUCHING
      2 3
        CONTACT TYPE: TOUCHING
      2 4
        CONTACT TYPE: TOUCHING
      3 4
        CONTACT TYPE: TOUCHING
```

Load Steps and Job Parameters

The job consists of six loadcases, each with a total loadcase time of one second. The first two loadcases, `prestress_left_bolt` and `prestress_right_bolt`, are dedicated to the prestressing of the bolts. In the `prestress_left_bolt` loadcase, the left bolt is pre-tensioned while the right bolt remains locked. Of the two boundary conditions applied to the control node of the left bolt, `prestress_left_bolt` and `lock_unlock_left_bolt`, only the POINT LOAD `prestress_left_bolt` is active in this loadcase. The FIXED DISPLACEMENT `lock_unlock_left_bolt` is deactivated. Conversely, of the two boundary conditions applied to the control node of the right bolt, `lock_unlock_right_bolt` and `prestress_right_bolt`, only the FIXED DISPLACEMENT `lock_unlock_right_bolt` is active and the POINT LOAD `prestress_right_bolt` is deactivated. The fixed stepping procedure is employed in this loadcase using ten increments.

```
LOADCASES
  MECHANICAL
    NEW
    STATIC
    LOADS
      deactivate:
        lock_unlock_left_bolt
```

```
        prestress_right_bolt
    OK
    STEPPING PROCEDURE
    CONSTANT TIME STEP
    # STEPS
        10
    OK
    NAME
        prestress_left_bolt
```

The `prestress_right_bolt` loadcase is identical to the `prestress_left_bolt` loadcase, except that the `lock_unlock_left_bolt` and `prestress_right_bolt` boundary conditions are active, while `prestress_left_bolt` and `lock_unlock_right_bolt` are deactivated.

In the next three loadcases, `loading`, `cooling` and `unloading`, the thermo-mechanical loading cycle is simulated and in the final loadcase, `disassemble`, the joint is disassembled. Since the bolts are locked (in the `loading` cycle) or loosened (in the `disassemble` loadcase), only the `FIXED DISPLACEMENT` boundary conditions on the control nodes of the bolts are active. The `POINT LOADS` are deactivated. The fixed stepping procedure is also employed for these four loadcases, now using five increments per loadcase. The button sequence for the `loading` loadcase reads:

```
    NEW
    STATIC
    LOADS
        deactivate:
            prestress_left_bolt
            prestress_right_bolt
    OK
    STEPPING PROCEDURE
    CONSTANT TIME STEP
    # STEPS
        5
    OK
    NAME
        loading
```

The remaining three loadcases are similar.

The analysis is a normal mechanical analysis in which all six loadcases are preformed in sequence. The `lock_unlock_left_bolt` and `prestress_right_bolt` initial loads are deactivated to make sure that the active

initial loads match those of the first loadcase. The contact table is activated and the LARGE DISPLACEMENT option and the ASSUMED STRAIN formulation are selected. The latter is used to improve the bending behavior of the lower order solid elements.

Three new scalar quantities are available for postprocessing the gaskets: Gasket Pressure (Marc post code 241), Gasket Closure (Marc post code 242), and Plastic Gasket Closure (Marc post code 243). All three are selected in this example, as well as, the Equivalent Von Mises Stress (see [Figure 3.17-5](#)).

```
JOBS
  NEW
  MECHANICAL
  LOADCASES
    activate:
      prestress_left_bolt
      prestress_right_bolt
      loading
      cooling
      unloading
      disassemble
  INITIAL LOADS
    deactivate lock_unlock_left_bolt
    deactivate prestress_right_bolt
  OK
```

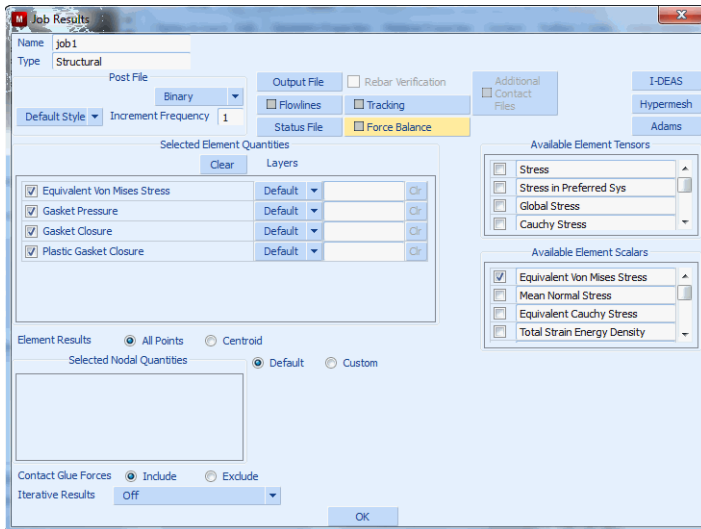


Figure 3.17-5 JOB RESULTS Menu and the Selected Quantities for Postprocessing

CONTACT CONTROL

INITIAL CONTACT

CONTACT TABLE

ctable1

OK (twice)

ANALYSIS OPTIONS

LARGE DISPLACEMENT

ADVANCED OPTIONS

ASSUMED STRAIN

OK (twice)

JOB RESULTS

AVAILABLE ELEMENT SCALARS

Equivalent Von Mises Stress

Gasket Pressure

Gasket Closure

Plastic Gasket Closure

OK (twice)

For the metal parts of the model, element type 7 is being used. For the gasket, element type 149 is selected.

```
ELEMENT TYPES
  MECHANICAL
    3-D SOLID
      7
      SET
      cover
      7
      SET
      lower_part
      7
      SET
      bolts
      149
      SET
      gasket
      OK
```

Save Model, Run Job, and View Results

```
FILE
  SAVE AS
    gasket.mud
  OK
  RETURN
JOBS
  RUN
  SUBMIT 1
  MONITOR
  OK
  RETURN
RESULTS
  OPEN DEFAULT
```

To monitor the pressure distribution on the gasket throughout the analysis, select the gasket elements and make them visible. Switch of drawing of the nodes and isolate the gasket ring elements. Make a contour plot of the gasket pressure, set the range and the legend, and monitor the results:

```
SELECT
  SELECT SET
    gasket
  MAKE VISIBLE
  RETURN
PLOT
  DRAW
    switch off NODES
  RETURN
MORE
  ISOLATE ELEMENTS
  SET
    gasket_ring
  OK
  RETURN
SCALAR PLOT SETTINGS
  RANGE
    MANUAL
  LIMITS
    -2
    56
  # LEVELS
    29
  LEGEND
    INTEGER
    RETURN (twice)
SCALAR
  Gasket Pressure
CONTOUR BANDS
MONITOR
```

Figure 3.17-6 shows a contour plot of the gasket pressure distribution at the end of the third loadcase when the joint has been fastened, the temperature has been increased to 180°C and the interior pressure has been applied. In Figure 3.17-7, the plastic gasket closure distribution at the end of the analysis is depicted. It can be observed from both pictures that, due to the asymmetric fastening sequence of the bolts, the plastic deformation of the gasket is also slightly asymmetric.

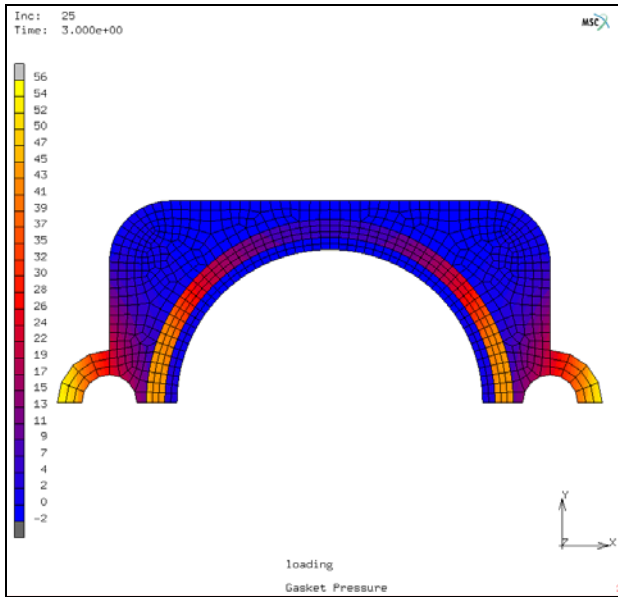


Figure 3.17-6 Contour Plot of the Gasket Pressure at the end of the Third Loadcase

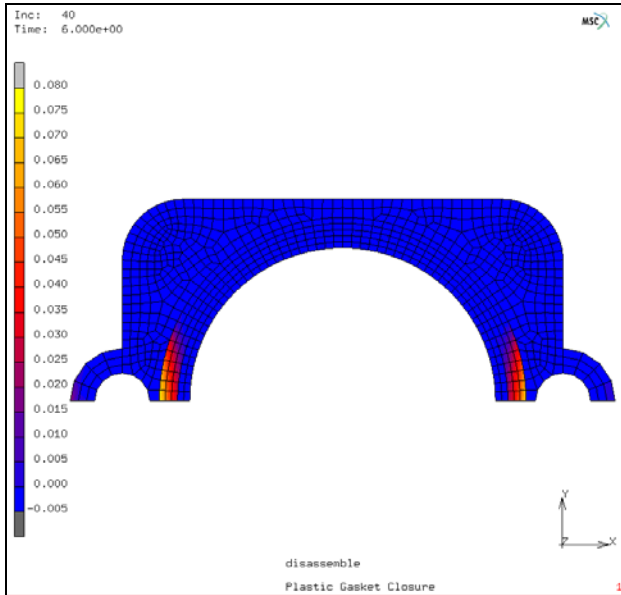


Figure 3.17-7 Contour Plot of the Plastic Gasket Closure at the end of the Analysis

In order to compare the response of the gasket ring with the loading and unloading paths that were read in from the data files, select the nodes where the plastic gasket closure assumes its maximum, create a history plot of the gasket pressure versus the gasket closure of those nodes and copy the plot to the generalized XY plotter for comparison.

```
RESULTS
  TOOLS
    SELECT BY EXTREMES
    NODES MAXIMUM
    RETURN
  HISTORY PLOT
    SET NODES
      ALL: SELECT.
    COLLECT DATA
      0 40 1
    NODES/VARIABLES
      ADD VARIABLE
        Gasket Closure
        Gasket Pressure
      RETURN
    > XY
  UTILS
    GENERALIZED XY PLOT
      FIT
```

The resulting plot is displayed in [Figure 3.17-8](#). It shows that when the gasket is being loaded, the response of the ring closely follows the loading path and that upon unloading, the unloading path is interpolated between the loading path and the supplied unloading path.

Finally, in [Figure 3.17-9](#), the forces on the bolts are depicted and in [Figure 3.17-10](#), the deformed shape of the cover at the end of the thermo-mechanical loading cycle is shown. In the latter picture, the displacements are enlarge by a factor of 25.

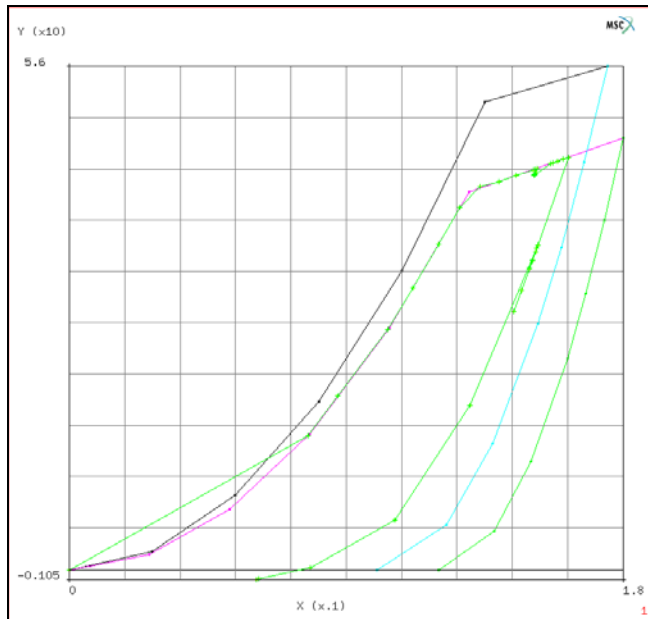


Figure 3.17-8 Pressure-closure History of the Gasket Ring at the Nodes where the Plastic Closure assumes its Maximum

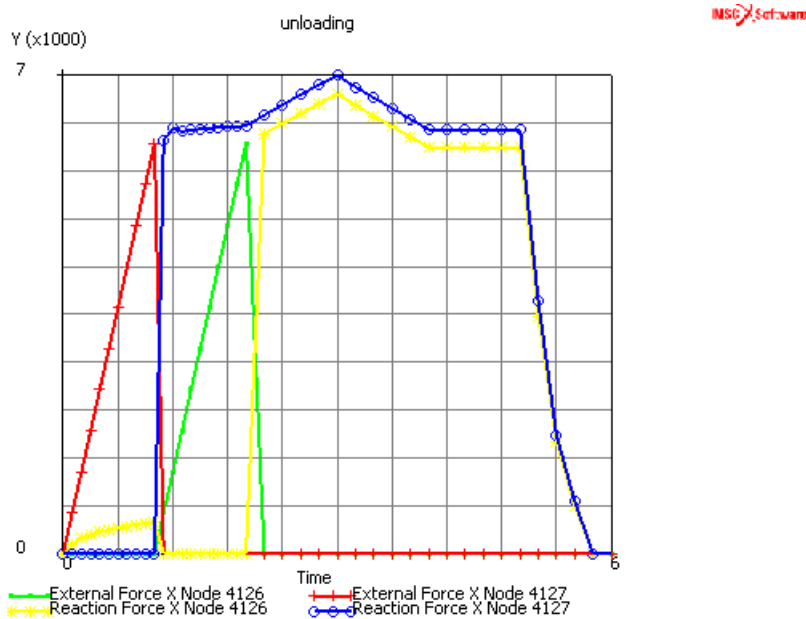


Figure 3.17-9 History Plot of the Bolt Forces

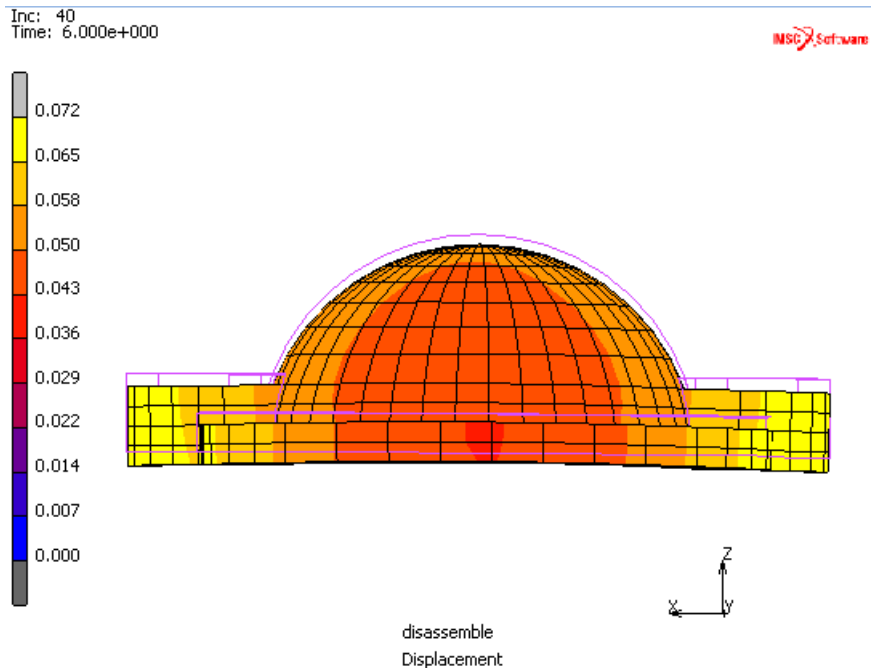


Figure 3.17-10 Deformation of the Cover (enlarged 25 times) at the end of the Thermo-mechanical Loading Cycle

Input Files

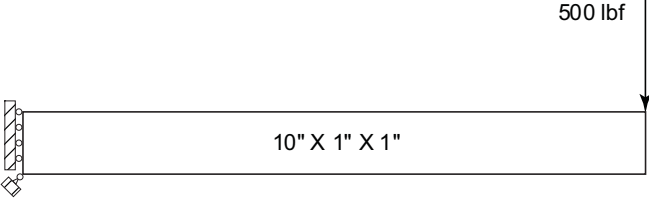
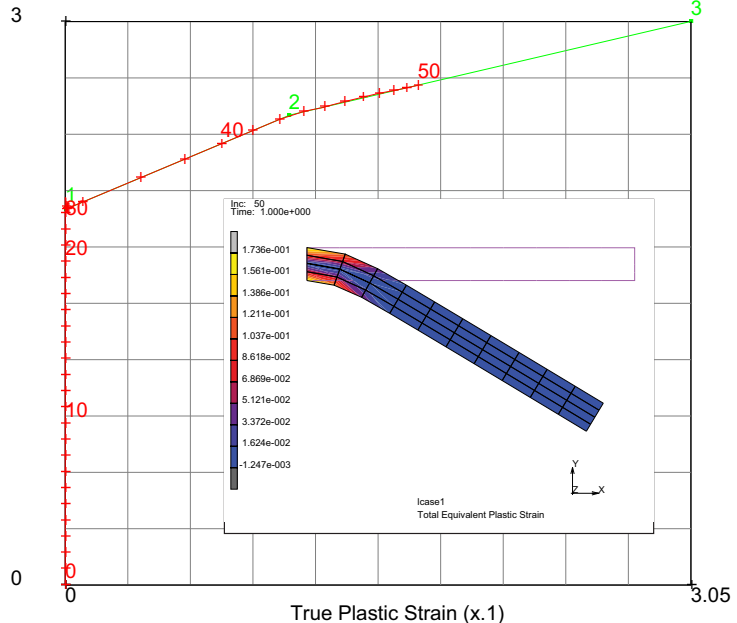
The files below are on your [delivery media](#) or they can be downloaded by your web browser by clicking the links (file names) below.

File	Description
gasket.proc	Mentat procedure file to run the above example
gasket_csect.proc	Mentat procedure file to run the above example
body_loading.raw	Mentat procedure file to run the above example
body_unloading.raw	Mentat procedure file to run the above example
ring_loading.raw	Mentat procedure file to run the above example
ring_unloading.raw	Mentat procedure file to run the above example

3.18 Cantilever Beam

- Summary 1222
- Detailed Session Description of Cantilever Beam 1224
- Add Plasticity to Cantilever Beam 1229
- Run Job and View Results 1232
- Input Files 1234

Summary

Title	Cantilever Beam
Problem features	Elastic-plastic solution of a cantilever beam with a tip load
Geometry	
Material properties	$E = 10 \times 10^6$ Psi, $\nu = 0.3$, $\rho = 0.283/386$ lbf s ² /in ⁴ and workhardening
Analysis type	Static with elastic-plastic material behavior
Boundary conditions	Left end fixed, right end point load
Element type	Plane stress element type 3
FE results	<p>Tracking of stress versus plastic strain behavior</p> <p>Y (x10000) —+— Strength +--+ Equivalent Von Mises Stress Node 4</p>  <p>True Plastic Strain (x.1)</p>

This example session describes the simulation of loading a cantilever beam with a tip load. This model will be used later in Chapter 3.35 for dynamics and will be saved.

The linear elastic solution is found. The bending stresses and tip displacements are then compared to theory.

The material properties are changed to include plasticity with workhardening.

The beam is then loaded with a larger load of 1500 pounds in 50 equal load steps. We will see how every integration point must track the material's constitutive relation.

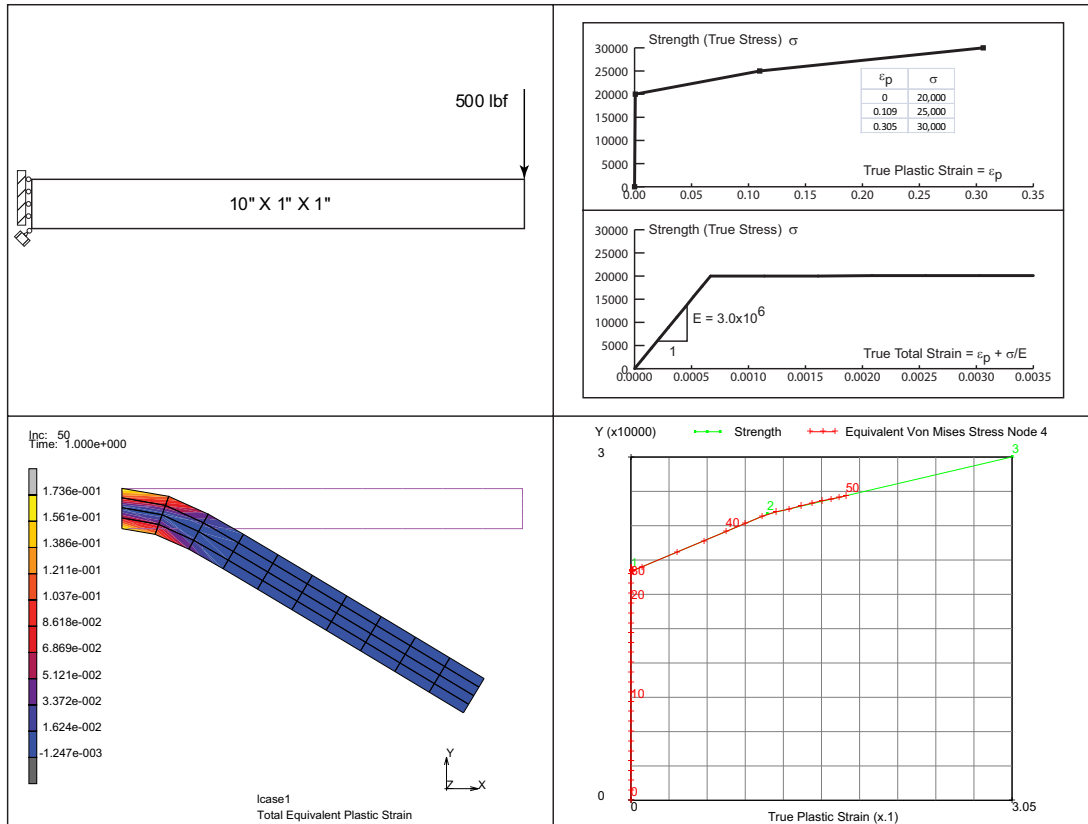


Figure 3.18-1 Cantilever Beam Problem Description

Detailed Session Description of Cantilever Beam

Here is an example of a cantilever beam below. Later, we will look at its dynamic behavior and the model created here will be used later.

```
FILES
  NEW
  OK
SAVE AS
  beam1
MAIN
```

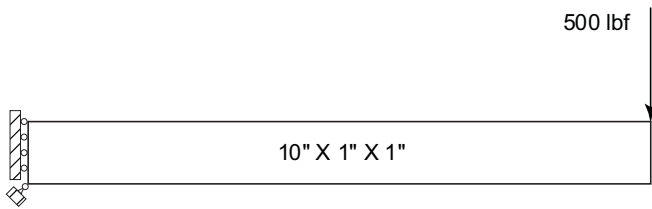


Figure 3.18-2 Cantilever and Beam Descriptions

```
MESH GENERATION
  NODE ADD
    0 0 0
    10 0 0
    10 1 0
    0 1 0
  FILL
ELEMENT ADD                                     (Pick above nodes in CCW)
SUBDIVIDE
  DIVISIONS
    10 4 1
  ELEMENTS
  ALL: EXISTING
  RETURN
SWEEP
  ALL & RETURN
RENUMBER
  ALL & RETURN
MAIN
```

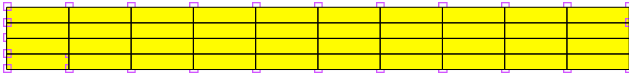



Figure 3.18-3 Cantilever Beam Mesh

BOUNDARY CONDITIONS

MECHANICAL

FIXED DISPLACEMENT

ON X DISPLACEMENT

OK

NODES ADD

Select all nodes on left edge

END LIST

NEW

FIXED DISPLACEMENT

ON Y DISPLACEMENT

OK

NODES ADD

Select bottom node on left edge

END LIST

NEW

POINT LOAD

ON Y FORCE -500

OK

NODES ADD

Select top right node

END LIST

RETURN

ID BOUNDARY CONDITIONS

MAIN

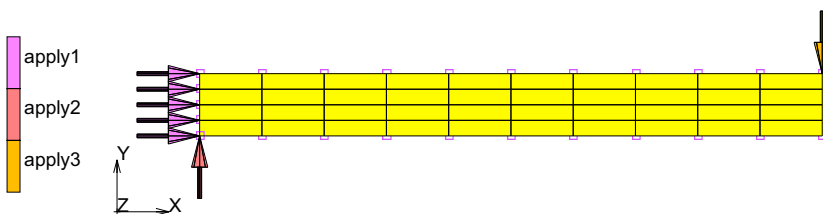


Figure 3.18-4 Loads and Boundary Conditions

MATERIAL PROPERTIES (twice)

NEW

STANDARD

STRUCTURAL

$E = 3E7$

$\nu = .3$, OK

GENERAL

$\rho = .283/386$, OK

ELEMENTS ADD

ALL: EXISTING

MAIN

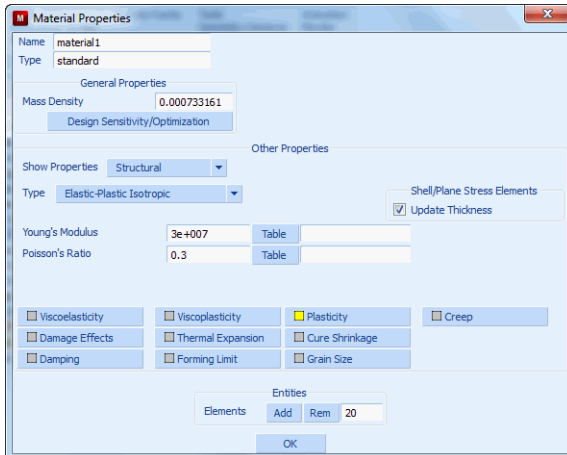


Figure 3.18-5 Material Properties: Isotropic Properties

GEOMETRIC PROP.

PLANAR

PLANE STRESS

THICKNESS = 1

ASSUMED STRAIN

OK

ELEMENTS ADD

ALL: EXISTING, MAIN

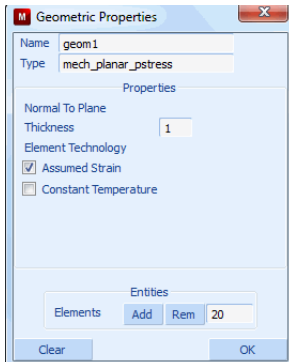


Figure 3.18-6 Flag Assumed Strain Formulation

JOBS
NEW
 MECHANICAL
 PROPERTIES
 PLANE STRESS
 JOB RESULTS
 TENSORS STRESS
 OK (twice)
SAVE
RUN
SUBMIT1
MONITOR
OK
OPEN POST FILE (RESULTS MENU)
 SCALAR
 COMP 11 OF STRESS
 CONTOUR BANDS

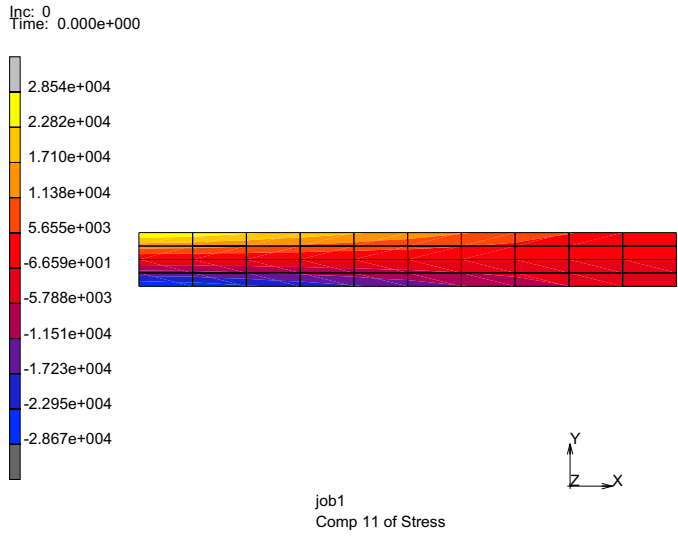


Figure 3.18-7 Bending Stress Contours

SCALAR
DISPLACEMENT Y
OK

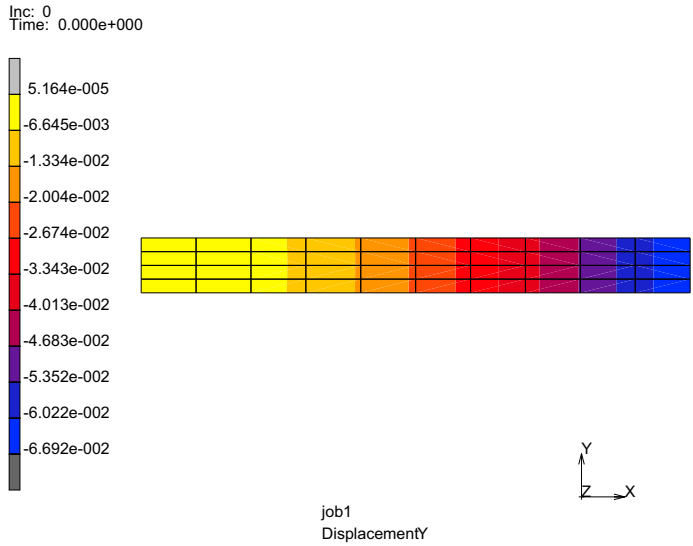


Figure 3.18-8 Y-Displacement Contours

- Complete Modeling: Check Load

- Peak Bending Stress +/- 29Ksi, Max Disp 6.7e-2.
- How does this compare to beam theory?
- What can improve the results?

Add Plasticity to Cantilever Beam

Here is a cantilever beam. Let's convert it to an elastic-plastic model and increase the load.

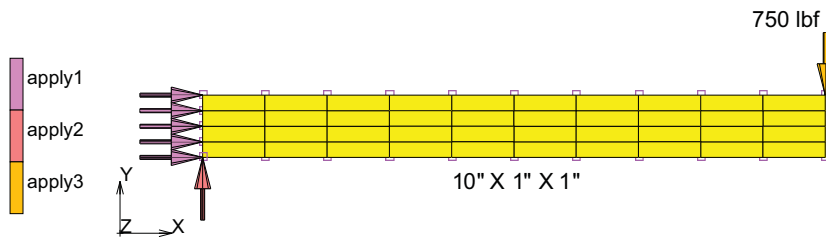


Figure 3.18-9 Beam Dimensions

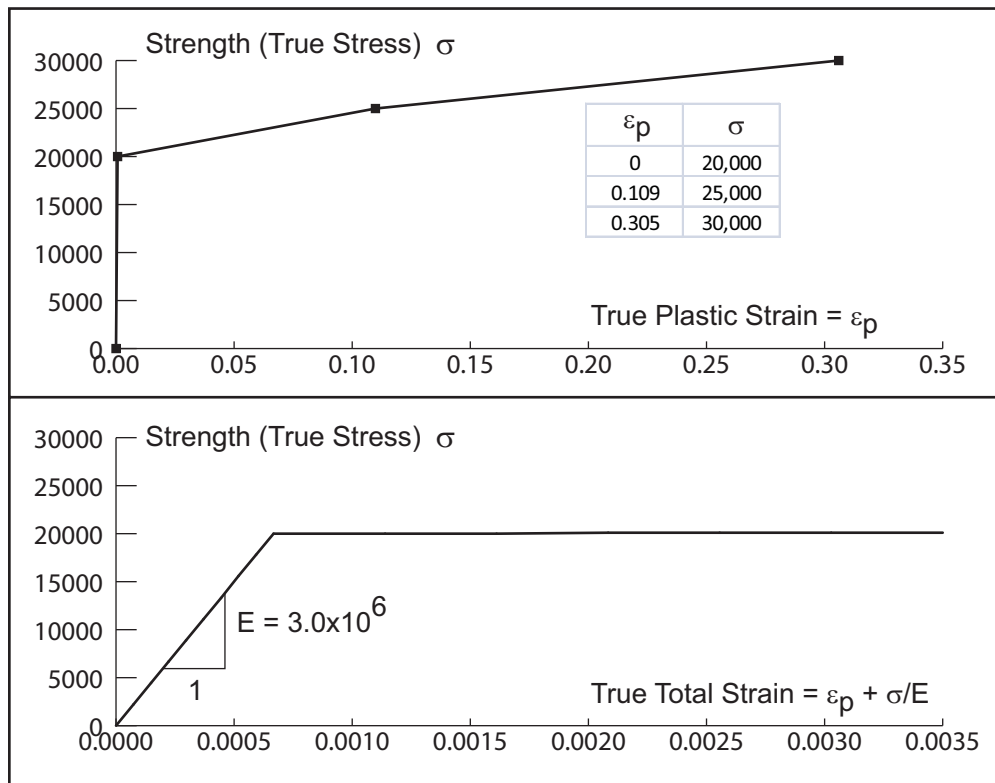


Figure 3.18-10 Workhardening Data is True Stress Versus True Plastic Strain

```
FILES
OPEN
  beam1
SAVE AS
  beam1p
OK
RETURN
```

MATERIAL PROPERTIES (twice)

TABLES

NEW

TABLE TYPE:

eq_plastic_strain

(1 Independent Variable)

```

POINT ADD
    0.000 20E3
    0.109 25E3
    0.305 30E3
FIT
    COPY TO GENERALIZED XY PLOTTER

MAIN
MATERIAL PROPERTIES (twice)
TABLE
    NEW (1 Independent Variable)
    TABLE TYPE:
        TIME
    FORMULA
    ENTER
        1.5*v1 (will ramp load from 0 to 750# in one second)
    FIT
    SHOW MODEL
    RETURN
STRUCTURAL
    PLASTICITY
        INITIAL YIELD STRESS = 1.0
        TABLE1 = table1
    OK (twice)

MAIN
BOUNDARY CONDITIONS
MECHANICAL
    EDIT apply3 (point load)
    OK
    POINT LOAD
    Y FORCE (pick table2, time)
    OK
    MAIN
LOADCASES
MECHANICAL
    STATIC

```

OK
RETURN (twice)

Run Job and View Results

JOBS

PROPERTIES

SELECT lcase1

ANALYSIS OPTIONS

LARGE STRAIN

OK

JOB RESULTS

EQUIVALENT VON MISES STRESS

TOTAL EQUIVALENT PLASTIC STRAIN

OK (twice)

SAVE

RUN

SUBMIT1

MONITOR

OK

OPEN POST FILE (RESULTS MENU)

SCALAR Total Equivalent Plastic Strain

CONTOUR BANDS

DEF & ORIG

LAST

CONTOUR BANDS

Inc: 50
 Time: 1.000e+000

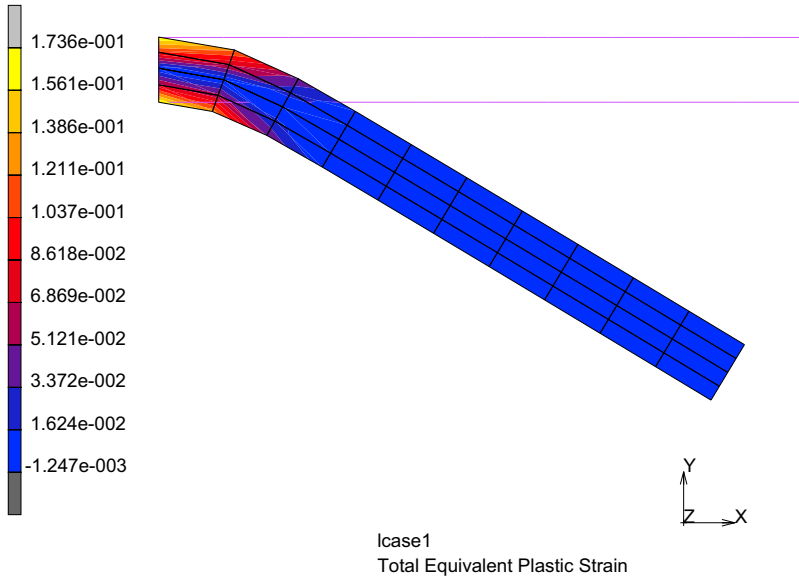


Figure 3.18-11 Plastic Strain Contours on Deformed Shape

RESULTS

HISTORY PLOT

SET LOCATIONS

(pick top left node)

END LIST

ALL INCS

ADD CURVES

ALL LOCATIONS

Total Equivalent Plastic Strain

Equivalent Von Mises Stress

FIT

RETURN

COPY TO GENERALIZED XY PLOTTER

UTILS

GENERALIED XY PLOT

FIT

This overlays the history plot of the stress strain response of this node with the stress-strain material behavior. Remember that continuum mechanics requires that the continuum be in equilibrium and that every point must track the constitutive relation.

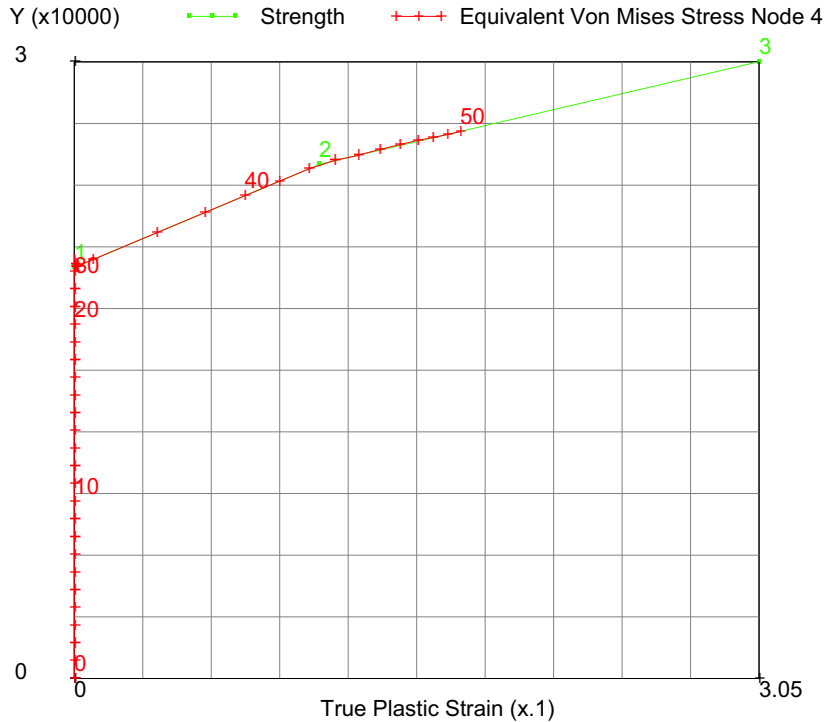


Figure 3.18-12 Stress Strain Response(+) tracking the Constitutive Relation

Input Files

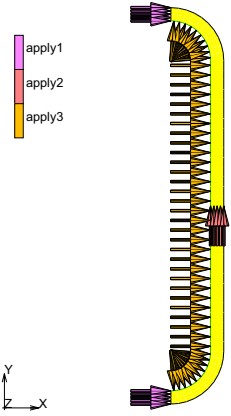
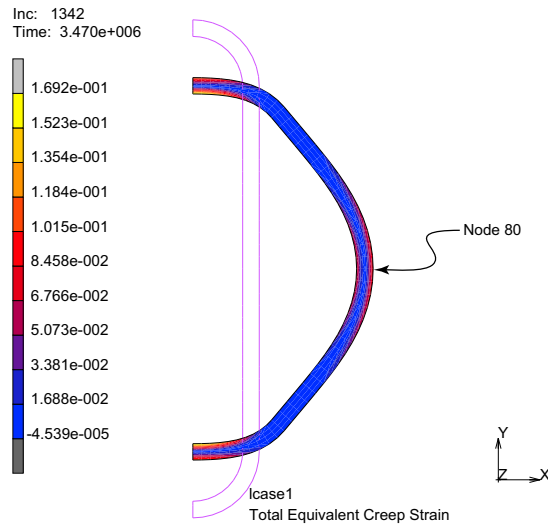
The files below are on your [delivery media](#) or they can be downloaded by your web browser by clicking the links (file names) below.

File	Description
s2.proc	Mentat procedure file to run the above problem

3.19 Creep of a Tube

- Summary 1236
- Detailed Session Description of Oval Tube 1238
- Run Job and View Results 1242
- Input Files 1252

Summary

Title	Creep of a Tube
Problem features	Creep material model with and without a closed cavity
Geometry	
Material properties	$E = 21.4 \times 10^6$ Psi, $\nu = 0.3$ Creep law $\dot{\epsilon}_c = 4 \times 10^{-24} \sigma^{4.51}$
Analysis type	Static with automatic load increments
Boundary conditions	Symmetry with internal pressure
Element type	Plane strain element type 11
FE results	<p>Large dimensional changes in tube shape as creep continues</p> 

A stainless steel oval tube is pressurized at a uniform high temperature and over time will creep. Only half of the tube is modeled due to symmetry.

The material constitutive behavior has the creep strain rate dependent upon the stress level (Norton creep). The material data has been fitted with a power relation where the creep strain rate becomes: $\dot{\epsilon}_c = 4 \times 10^{-24} \sigma^{4.51}$.

The oval tube will bulge and become a completely circular tube over time. The tube finally ruptures due to the large strains.

Plotting the displacement of the bulge *versus* time shows a quick growth followed by a slower growth, because the stresses drop with time.

A more complex constitutive relation may be easily modeled with the CRPLAW user subroutine.

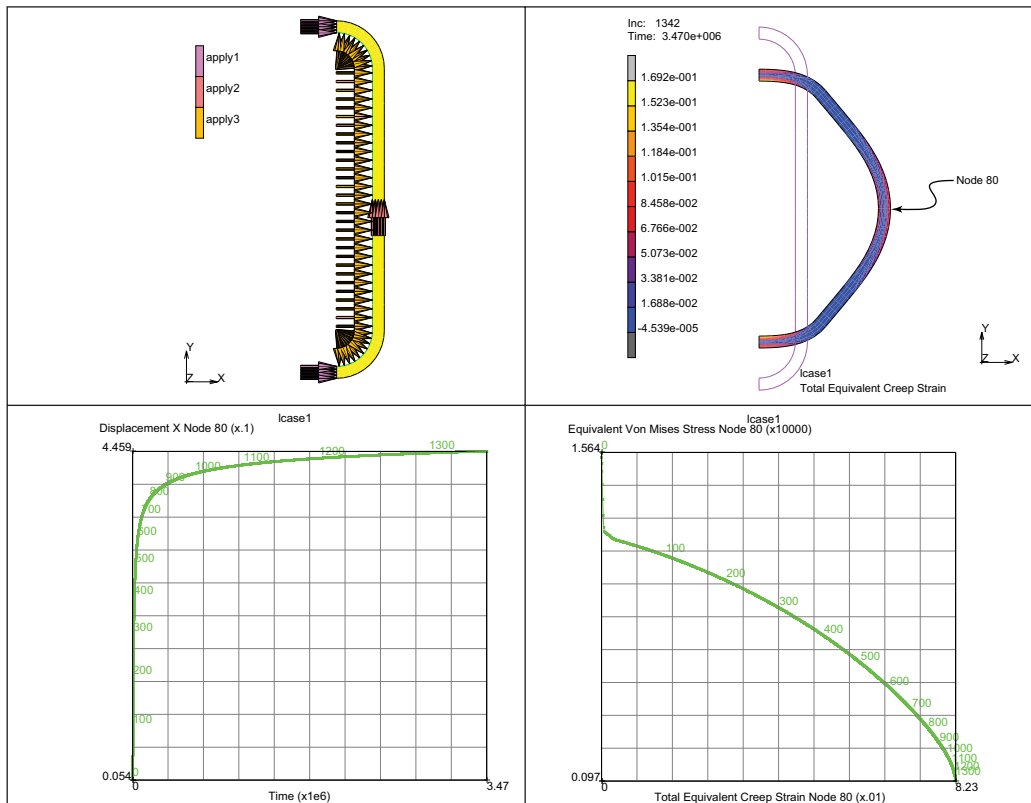


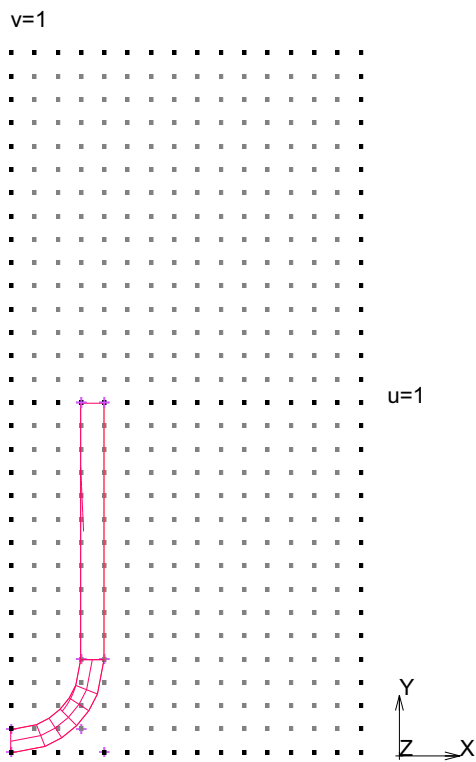
Figure 3.19-1 Creep of a Tube Problem Description

Detailed Session Description of Oval Tube

```

FILES
  NEW
  OK
SAVE AS
  creep
MAIN
MESH GENERATION
  COORDINATE SYSTEM:
    SET
      GRID (ON)
    U DOMAIN
      0 1
    U SPACING
      0.065
    V DOMAIN
      -1 1
    V SPACING
      0.065
  FILL
  RETURN
  CURVE TYPE ARC
  CENTER/PT/PT
  RETURN
  CURVES:
    ADD (arcs shown)
  CURVE TYPE
  LINE
  RETURN
  CURVES:
    ADD(lines shown)
  GRID (OFF)
  SURFACE TYPE
  RULED
  RETURN
  SURFACES ADD

  CONVERT
  DIVISIONS
    15 4
  
```

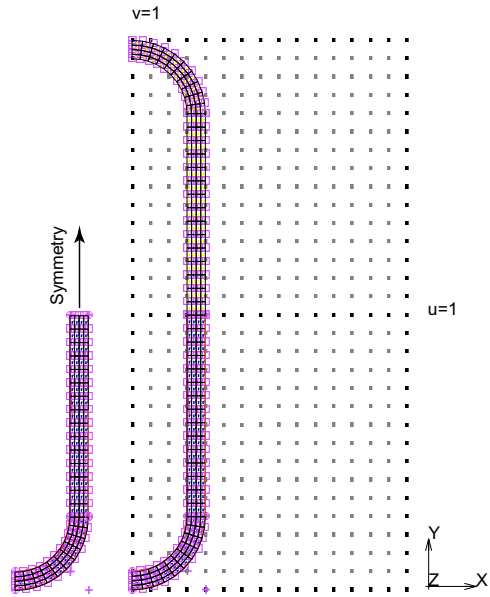


(pick interior and opposite exterior arcs and lines)

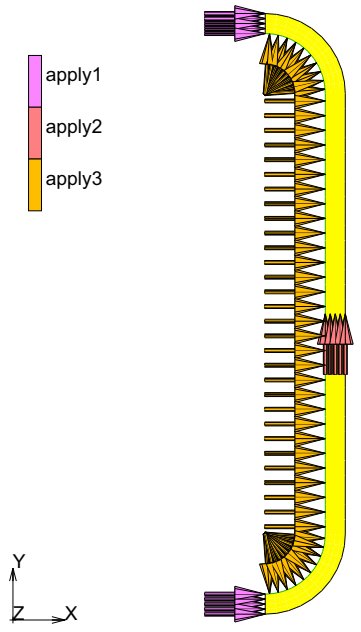
```

SURF. TO ELEMS
DIVISIONS
    10 4
SURF. TO ELEMS
    (pick smallest surface)
RETURN
SYMMETRY
NORMAL 0 1 0
ELEMENTS
ALL: EXISTING
RETURN
CHECK
    UPSIDE DOWN
    FLIP ELEMENTS
    ALL: SELECTED
    RETURN
SWEEP
    ALL
    RETURN
RENUMBER
    ALL
MAIN
    
```

(pick largest surface)



```
INITIAL CONDITIONS
STATE VARIABLES
  NODAL TEMPERATURE
  TEMPERATURE
    1660, OK
  NODES ADD
  ALL: EXISTING
  RETURN (twice)
BOUNDARY CONDITIONS
MECHANICAL
  FIXED DISPLACEMENT
  DISP. X=0, RETURN
  NODES: ADD
  all on x=0 axis, END LIST
  NEW
  FIX Y=0
  NODES: ADD
  at line of symmetry y=0
  RETURN
  NEW
  EDGE LOAD
  PRESSURE
    66, OK
  SELECT
  METHOD PATH, OK
  EDGES
  RETURN
  EDGES: ADD
  ALL: SELECTED
  RETURN
STATE VARIABLES
  NEW
  NODAL TEMPERATURE
  TEMPERATURE
    1600
  OK
  NODES ADD
  ALL: EXISTING
  MAIN
MATERIAL PROPERTIES (twice)
  NEW STANDARD
```



(pick node path on interior)


```

STRUCTURAL
  YOUNG'S MODULUS = 21.4E6
  POISSON'S MODULUS = .3
  CREEP (twice)
    COEFFICIENT (define the creep strain rate)
      4E-24
    STRESS DEPENDENCE EXPONENT
      4.51
  OK (twice)
ELEMENTS ADD
ALL: EXISTING
MAIN
GEOMETRIC PROPERTIES
  PLANAR
    PLANE STRAIN
    THICKNESS
      1
    CONSTANT DILATATION (on)
    ASSUMED STRAIN (on)
  OK
ELEMENTS ADD
ALL: EXISTING
MAIN
LOADCASES
  MECHANICAL
    CREEP
      TOTAL LOADCASE TIME
        3.47E6
      CREEP STRAIN/STRESS PARAMETERS
        INITIAL TIME STEP
          1
        MAX. # INCS
          2000
        STRESS CHANGE TOLERANCE
          1
      OK (twice)
  MAIN

```

Run Job and View Results

```
JOBS
  NEW MECHANICAL
  PROPERTIES
    lcase1
  PLANE STRAIN
  ANALYSIS OPTIONS
    ADVANCED OPTIONS
      LARGE ROTATIONS, OK
    FOLLOW FORCE
    OK
  JOB RESULTS
    Equivalent Von Mises Stress
    Total Equivalent Creep Strain
    Temperature (Integration Point)
    OK (twice)

SAVE
RUN
  SUBMIT(1)
  OK
RETURN
RESULTS
  OPEN DEFAULT
  DEF & ORIG
  CONTOUR BANDS
  SCALAR
    Total Equiv. Creep Strain
  OK
LAST
HISTORY PLOT
SET LOCATIONS
  n:80
END LIST
ALL INCS
ADD CURVES
```

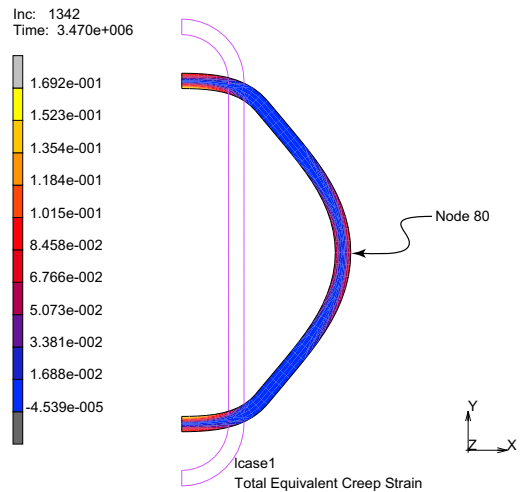


Figure 3.19-2 Analysis Set Nodes at 80

ALL LOCATIONS

Time

Displacement X

FIT

RETURN

CLEAR CURVES

ADD CURVES

ALL LOCATIONS

Total Equiv. Creep Strain

Equiv. Von Mises Stress

FIT

RETURN

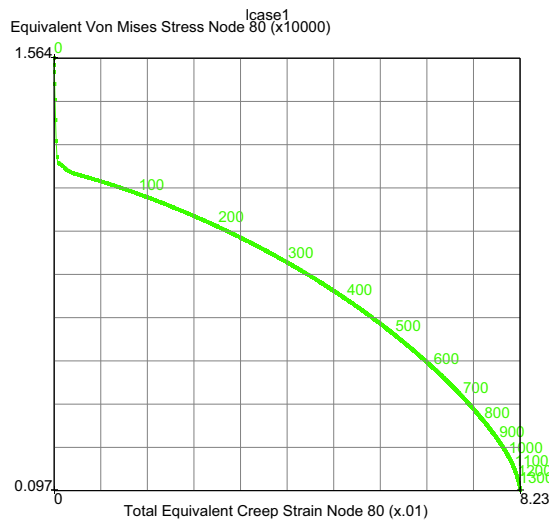
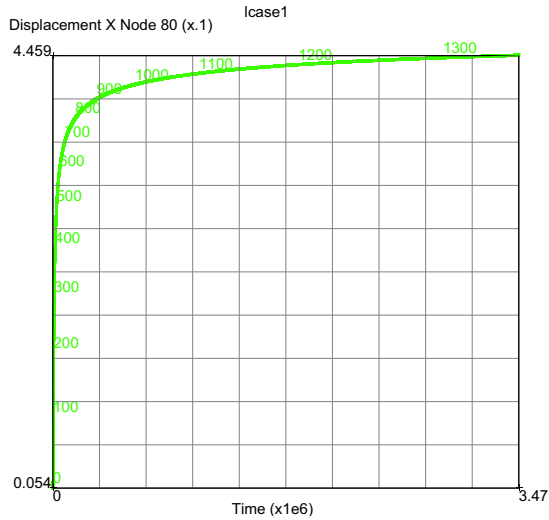


Figure 3.19-3 History Plots for Time and Total Equivalent Creep Strain

What can improve the results?

Clearly as the tube creeps, the volume inside the tube increases. Assuming a constant mass of air in the tube, increasing the volume decreases the pressure the creep deformation is reduced. To simulate this effect, we can model the cavity of air inside the tube. This cavity monitors the volume and adjusts the pressure according to the ideal gas law.

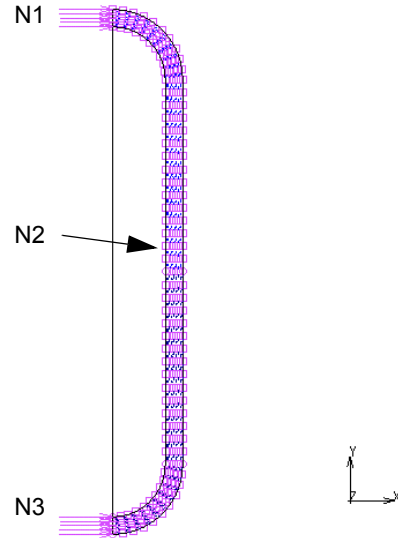
FILES

OPEN

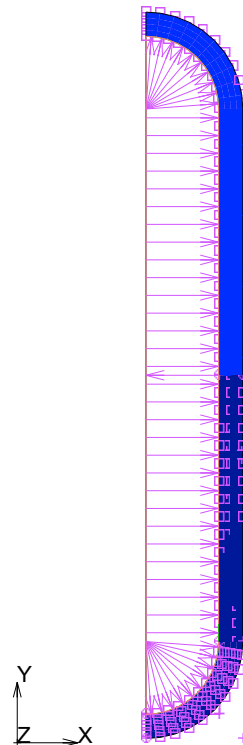
```

    creep
    OK
    SAVE AS
    creep2
    OK, MAIN
    MESH GENERATION
    ELEM. CLASS LINE(2)
    ELEMS ADD
    (pick interior nodes)
    N1, N3
    RETURN
    MODELING TOOLS
    CAVITIES
    NEW
    SELECT
    METHOD PATH
    RETURN
    EDGES
    (pick interior nodes)
    N1, N2, N3
    END LIST
    RETURN
    EDGES ADD
    ALL: SELECTED
    REF. PRESSURE
    15
    REF. TEMPERATURE
    1660
    REF. DENSITY
    1.8E-5
    MAIN

    BOUNDARY CONDITIONS
    MECHANICAL
    EDIT apply4
    MORE
    
```



```
CAVITY PRESSURE LOAD
  PRESSURE
    66
  OK
  CAVITIES ADD
    cavity1, OK
  NEW
  CAVITY MASS LOAD
  MASS
  CLOSED CAVITY
  OK
  CAVITIES ADD
    cavity1, OK
  MAIN
MESH GENERATION
  CHECK
  FLIP ELEMENTS
    (pick element added to close the
    cavity properly. Make sure that all
    arrows point from inside to outside
    of cavity)
  MAIN
LOADCASES
  MECHANICAL
  CREEP
  LOADS
    apply3 (off)
    apply4 (off)
    apply5 (on)
    OK (twice)
  MAIN
JOBS
  ELEMENT TYPES
  MECHANICAL
  ANALYSIS DIMENSION
```



```
PLANAR
MISCELLANEOUS
    171
    (pick element added)
    OK (twice)
PROPERTIES
INITIAL LOADS
    apply3 (off)
    apply4 (on)
    apply5 (off)
    OK (twice)
JOB PARAMETERS
    CAVITY PARAMETERS
        AMBIENT PRESSURE = 0
        (the default value)
    OK (thrice)
RUN
    STYLE TABLE-DRIVEN -> OLD
    SUBMIT(1)
    MONITOR
    OK, MAIN
```

Results

```
RESULTS
    OPEN DEFAULT
    DEF & ORIG
    CONTOUR BANDS
    SCALAR
        Total Equiv. Creep Strain
    LAST
    HISTORY PLOT
    SET LOCATIONS
        n:80
    END LIST
```

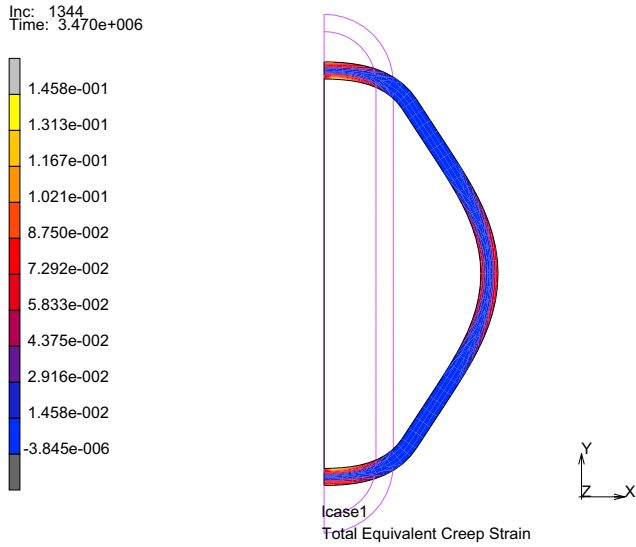


Figure 3.19-4 Analysis at Node 80

- ALL INCS
- ADD CURVES
- ALL LOCATIONS
 - Time
 - Displacement X
- FIT, RETURN

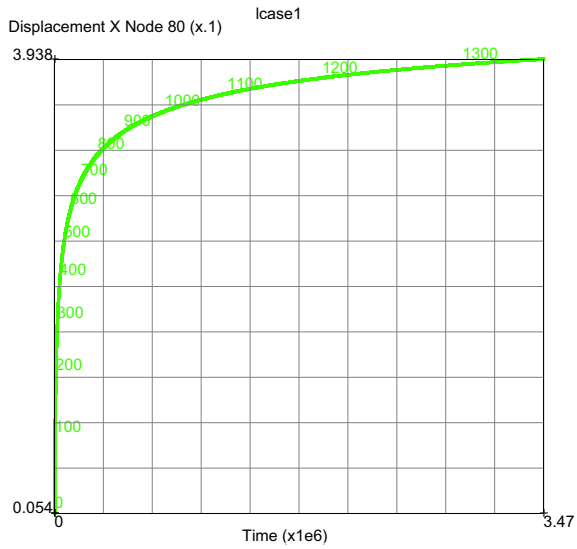


Figure 3.19-5 History Plot of Displacement x Node 80

COPY TO GENERALIZED XY PLOTTER

SHOW HISTORY

RETURN

CLEAR CURVES

ADD CURVES

ALL LOCATIONS

Total Equiv. Creep Strain

Equiv. Von Mises Stress

FIT

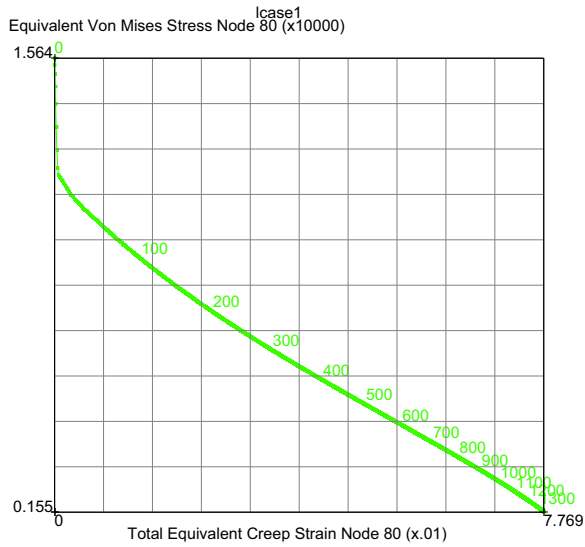


Figure 3.19-6 Total Equivalent Creep Strain at Node 80

- CLEAR CURVES
- ADD CURVES
- GLOBAL
 - Volume Cavity 1
 - Pressure Cavity 1
- FIT

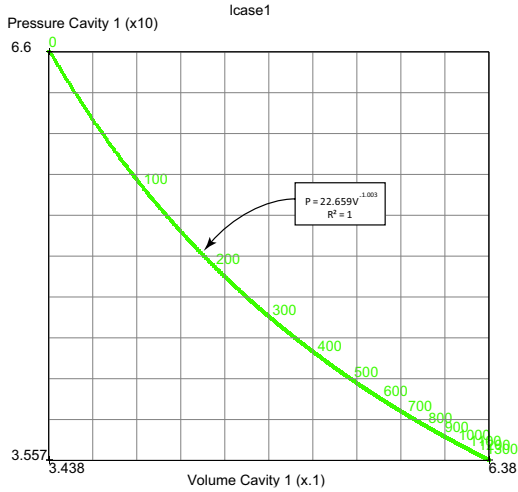


Figure 3.19-7 Cavity Pressure versus Cavity Volume at Node 80

CLEAR CURVES
 ALL LOCATIONS
 Time
 Displacement X
 FIT
 COPY TO GENERALIZED XY PLOTTER
 FIT

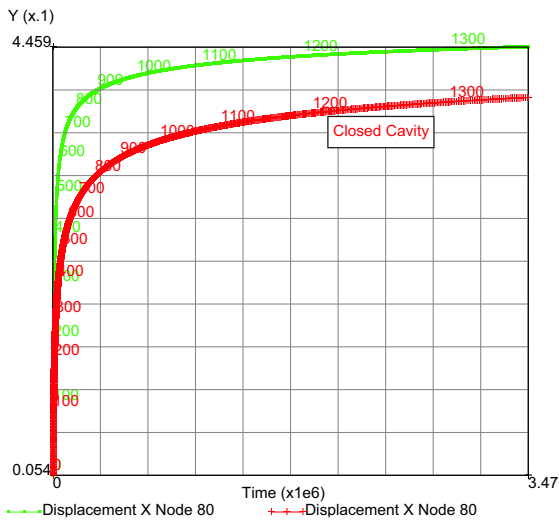


Figure 3.19-8 X-Displacement History with and without the Closed Cavity Feature

Clearly, the reduction in pressure due to the increase in volume reduced the creep deformation of the tube, which is a more realistic simulation.

Input Files

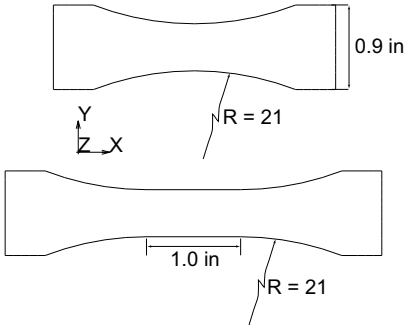
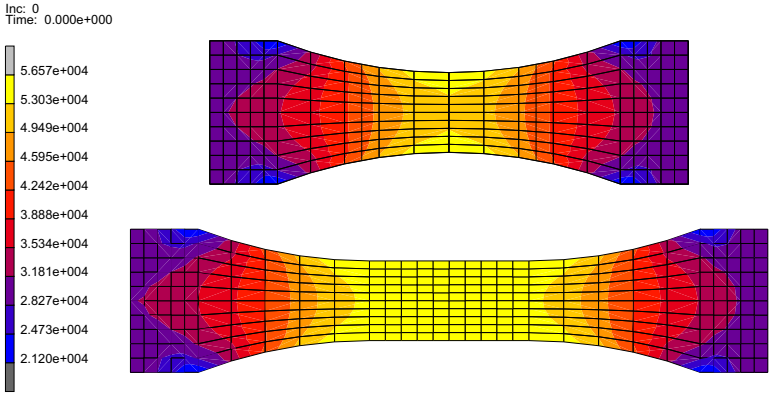
The files below are on your [delivery media](#) or they can be downloaded by your web browser by clicking the links (file names) below.

File	Description
s6.proc	Mentat procedure file to run the above problem
creep.mud	Associated Mentat model file without cavity
creep2.mud	Associated Mentat model file with cavity

3.20 Tensile Specimen

- Summary 1254
- Detailed Description Session 1255
- Run Job and View Results 1262
- Modeling Tips 1273
- Input Files 1277

Summary

Title	Tensile specimen
Problem features	Simple dog bone uniaxial specimen illustrating several meshing techniques (overlay, advancing front, and mapped methods) and the effect of extending the gage section. Mentat features include copy to clipboard and report writer.
Geometry	
Material properties	$E = 10 \times 10^6$ Psi, $\nu = 0.3$ and Orthotropic
Analysis type	Static with elastic material behavior
Boundary conditions	Left end fixed, right edge load
Element type	Plane stress element type 3
FE results	<p>Uniformity of axial stress original and extended gage section</p> <p>Inc: 0 Time: 0.000e+000</p> 

This example session describes the simulation of the loading of a dog-bone tensile specimen. This session builds the geometry, exports an IGES file, and demonstrates different types of meshing strategies including: overlay, advancing front, and mapped meshing.

Using the mapped mesh, the tensile specimen is subjected to an axial load and submitted to Marc. Then, Mentat post processes the results of the tensile specimen.

After the first run, the specimen's gage section is changed and re-run to compare with the original specimen.

Finally, the material is changed from an isotropic to an orthotropic material. The material direction does not line up with the pull direction, and the deformed shape becomes skewed.

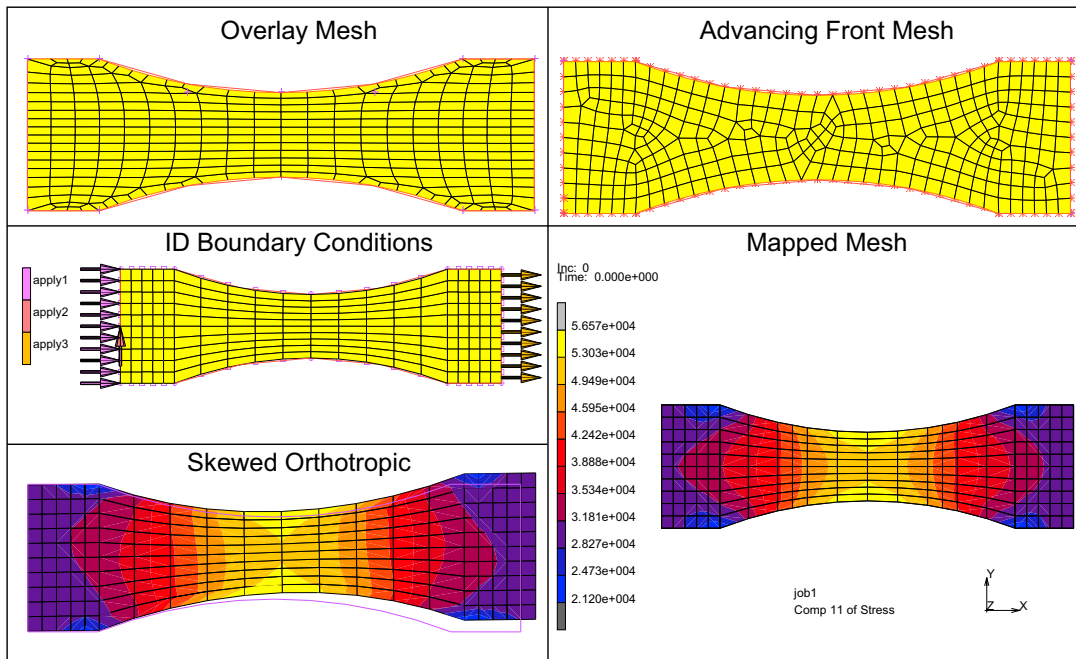


Figure 3.20-1 Examples of Meshing

Detailed Description Session

Tensile Specimen Analysis

Begin this session at the main menu.

MESH GENERATION

COORDINATE SYSTEM: SET

GRID ON

U DOMAIN

-1.5 1.5

V DOMAIN

-1.5 1.5

FILL

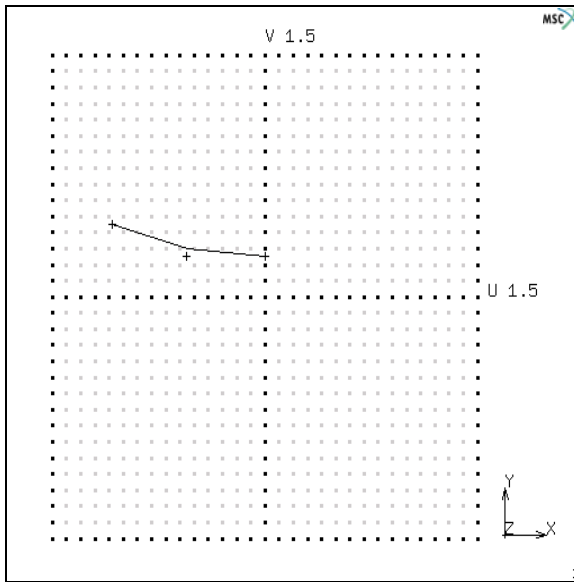
RETURN

CURVE TYPE

ARCS:

CENTER/POINT/ANGLE

RETURN



CURVES ADD

0 1.5 0

0 -1.5 0

-21

(degrees)

MOVE

TRANSLATIONS

0 1.75 0

CURVES

(use left mouse to pick curve, right mouse will END LIST)

RETURN

SYMMETRY

NORMAL

0 1 0

CURVES select the arc

END LIST

NORMAL

1 0 0

CURVES

ALL: EXISTING

RETURN

COORDINATE SYSTEM: GRID OFF

RETURN

DUPLICATE

TRANSLATIONS

0.425 0 0

POINTS

(select two right most points)

END LIST

TRANSLATIONS

-0.425 0 0

POINTS

(select two left most points)

END LIST

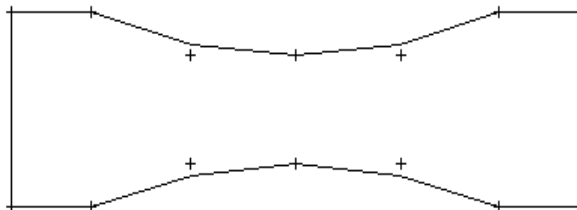
RETURN

CURVE TYPE

LINE

RETURN

CRVS ADD



Select pairs of points beginning at the upper left of the top arc and move counter-clockwise to complete the boundary of the model.

Use the following steps to save this geometry in an IGES file.

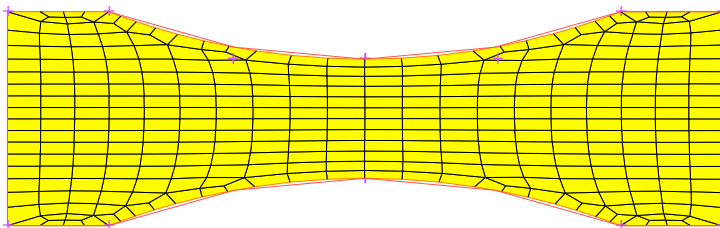
```
FILES
  EXPORT
    IGES
      ten.spec.iges
    OK
  RETURN
  SAVE AS
    isotropic
    OK
  MAIN
```

The next section shows how to mesh the geometry several ways.

Overlay Technique

```
MESH GENERATION
  AUTOMESH
    2D PLANAR MESHING
    DIVISIONS
      20 20
    QUADRILATERALS (OVERLAY): QUAD MESH!
    ALL: EXISTING
    UNDO
    DIVISIONS
      40 40
    QUADRILATERALS (OVERLAY): QUAD MESH!
    ALL: EXISTING
    RETURN
    UNDO
```

(this will undo your last command)



Advancing Front Technique

AUTOMESH 2D PLANAR

QUADRILATERALS (ADV FRNT): QUAD MESH!

ALL: EXISTING

UNDO

RETURN

CURVE DIVISIONS

FIXED AVG LENGTH (ON)

FORCE EVEN DIV

APPLY CURVE DIVISIONS

ALL: EXISTING

RETURN

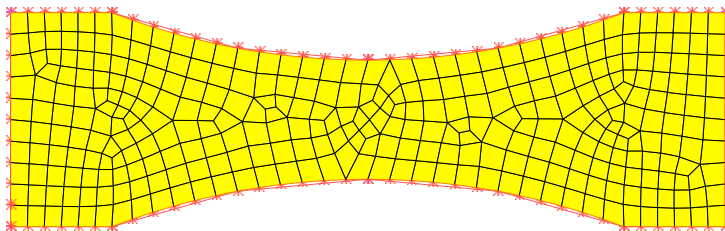
2D PLANAR MESHING

QUADRILATERALS (ADV FRNT): QUAD MESH!

ALL: EXISTING

UNDO

RETURN



Mapped Meshing Technique

CURVE DIVISIONS

CLEAR CURVE DIVISIONS

ALL: EXISTING

RETURN (twice)

SURFACE TYPE

RULED RETURN

SRFS ADD

UNDO

(pick top left/bottom arcs)

CHECK

FLIP CURVES

(pick all top lines & curves)

RETURN

SRFS ADD

(pick right top/bottom line)

SRFS ADD

(pick left top/bottom line)

SRFS ADD

(pick left top/bottom curve)

SRFS ADD

(pick right top/bottom curve)

CONVERT

SURFACES TO ELEMENTS

(pick left and right curved surfaces)

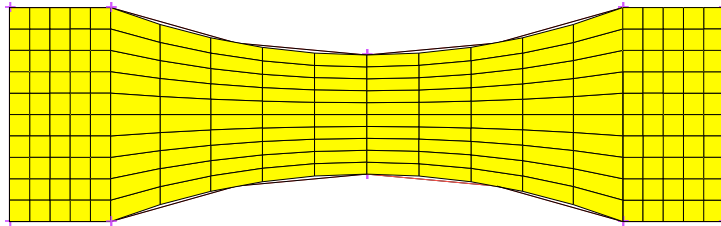
DIVISIONS

5 10

SURFACES TO ELEMENTS

(pick left and right rectangular surfaces)

RETURN



SWEEP

ALL & RETURN

RENUMBER

ALL & RETURN

MAIN

BOUNDARY CONDITIONS

MECHANICAL

FIXED DISPLACEMENT

ON DISPLACEMENT X = 0

OK

NODES ADD

(select all nodes on left edge)

END LIST

NEW

FIXED DISPLACEMENT

ON DISPLACEMENT Y = 0

OK

NODES ADD

END LIST

NEW

EDGE LOAD

ON PRESSURE

-30000

OK

EDGES ADD

END LIST

RETURN

ID BOUNDARY CONDITIONS

ARROW PLOT SETTINGS

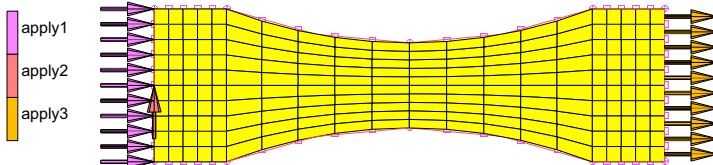
SOLID

RETURN

DRAW

(select center node on left edge)

(select all edges on right edge)



MAIN

MATERIAL PROPERTIES

MATERIAL PROPERTIES

NEW

STANDARD

STRUCTURAL

YOUNG'S MODULUS = 1E7

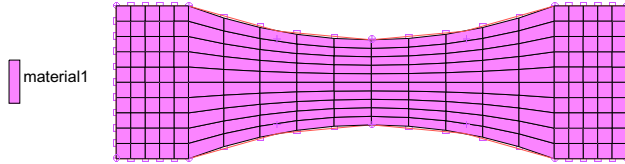
POISSON'S RATIO = .3

OK

ELEMENTS ADD

ALL: EXISTING

ID MATERIALS
MAIN



GEOMETRIC PROPERTIES

PLANAR

PLANE STRESS

THICKNESS

0.25

ASSUMED STRAIN

OK

ELEMENTS ADD

ALL: EXISTING

MAIN

(This improves the element's behavior in bending.)

Run Job and View Results

JOBS

PROPERTIES

PLANE STRESS

ANALYSIS OPTIONS

LARGE STRAIN

OK

MECHANICAL ANALYSIS CLASS JOB

RESULTS

AVAILABLE ELEMENT TENSORS STRESS

OK (twice)

SAVE

RUN

SUBMIT1

MONITOR

OK

(some elements upside/down)

MAIN
MESH GENERATION
CHECK UPSIDE DOWN
FLIP ELEMENTS
ALL: SELECTED
UPSIDE DOWN

Number of upside/down elements should now be 0

RETURN (twice)

Go back to RUN and resubmit. See Figure 3.20-2.

JOBS
SAVE
RUN
SUBMIT1
MONITOR
OK

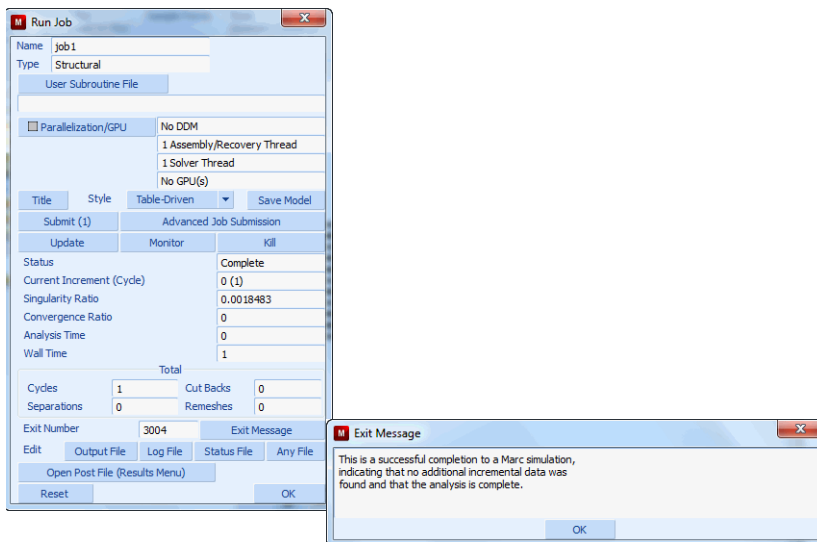


Figure 3.20-2 Run Job Menu. Exit Number 3004 is a successful completion.

Is the job complete? Exit number 3004 is a successful completion of the simulation where the constitutive behavior of the material was followed and equilibrium was satisfied, click the **EXIT MESSAGE** button to display exit message.

Did it do what I expect? However, just because equilibrium is satisfied, the simulation may not accomplish its objective, for example we expect that the net section tensile stress should be:

$$\sigma = p \left(\frac{A_{end}}{A_{mid}} \right) = 30 \times 10^4 \left(\frac{0.898517t}{0.5t} \right) = 53,911 \text{ psi}$$

yet in [Figure 3.20-3](#) the maximum stress in the net section is 56,570 psi and is higher than our average estimate above. This suggests our net section has a bit of stress concentration and needs to be extended to make the stresses as uniform as possible in the net section where strain measurements occur. This extension will lower the net section tensile stress nearer to the average estimated above (see [Figure 3.20-8](#)).

MAIN

RESULTS

OPEN DEFAULT

SCALAR

COMP 11 OF STRESS

OK

CONTOUR BANDS

PLOT

NODES

(turn nodes off)

RETURN

DEFORMED SHAPE SETTINGS

OUTLINE (on)

RETURN

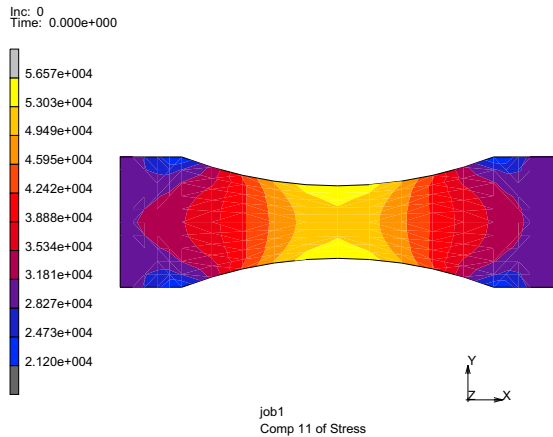


Figure 3.20-3 Analysis of Comp 11 of Stress

RESULTS

MORE

VECTOR Pick **Reaction Force**

OK

VECTOR PLOT ON

VECTOR Pick **External Force**

OK

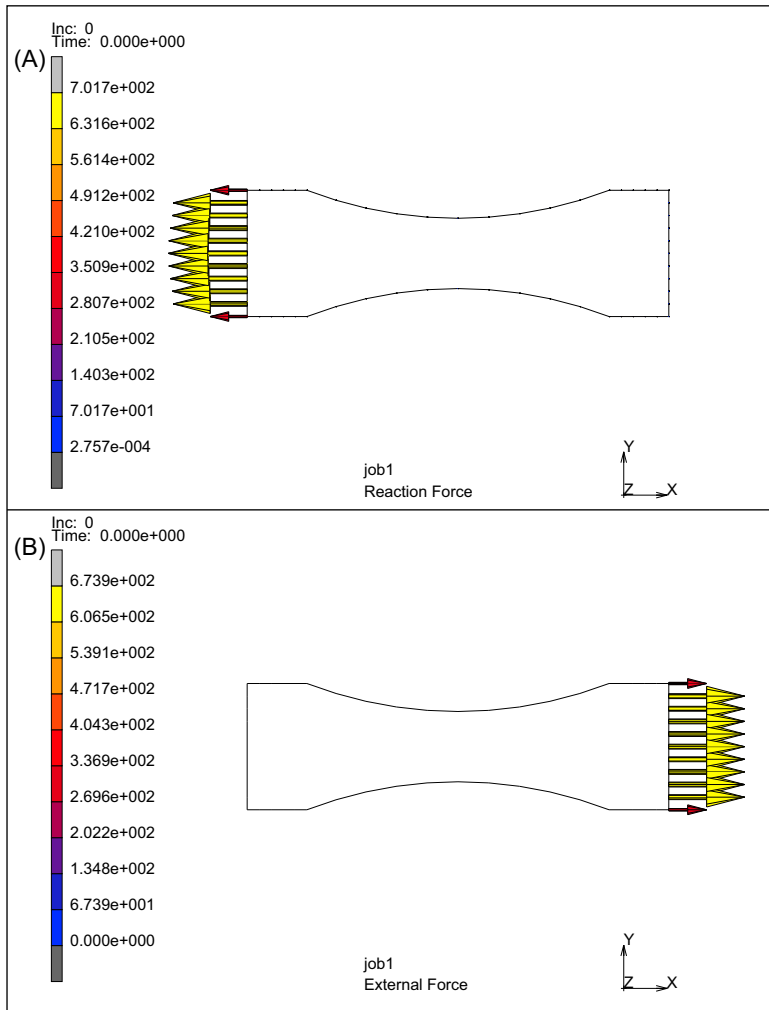


Figure 3.20-4 (A) Example of Reaction Force (B) Example of External Force

PLOT

NODES

(turn nodes on)

RETURN

DEFORMED SHAPE SETTINGS

SURFACE

RETURN

RESULTS

PATH PLOT

NODE PATH N1 N2

path from N1 to N2

END LIST

ADD CURVES

ADD CURVE

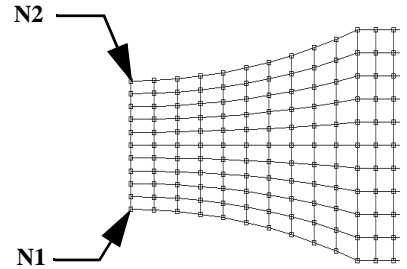
ARC LENGTH

COMP 11 OF STRESS

FIT

RETURN

Y MIN 0



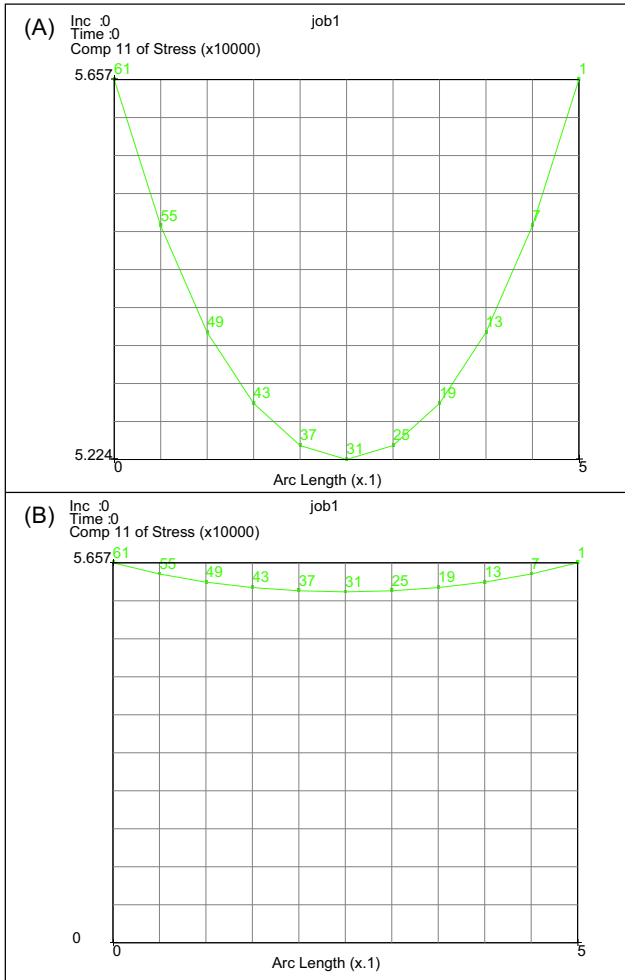


Figure 3.20-5 (A) Add Curve Analysis (B) Arc Length Analysis

RESULTS

PATH PLOT

TABLES COPY TO

> 1

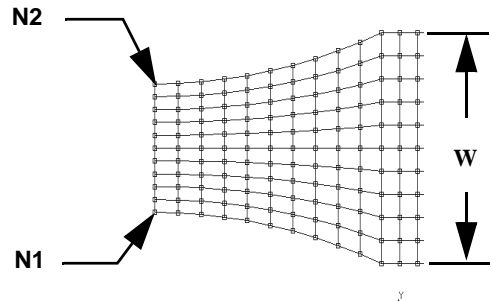
FIT

V1 STEPS 100

F1 STEPS 100

INTEGRATE

FIT



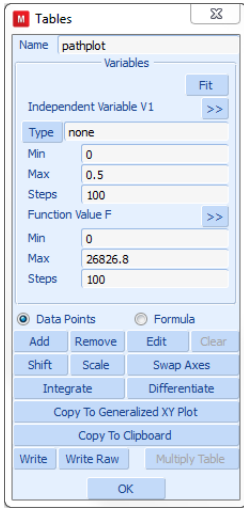


Figure 3.20-6 Tables Menu

$$\int_{N1}^{N2} \sigma_{11} t dy = 26926t \approx 26826.8t = pWt = 6739$$

where: p = 30000, W=0.898518, t=0.25

Tensile Specimen Uniform Gage Section

The previous stress analysis shows that the stress field is not uniform in the gage section. Redesign the specimen such that it has a 1" constant gage section at the center.

MAIN

RESULTS

CLOSE, MAIN

FILES

SAVE AS

isotropic_long, **OK**

RESET PROGRAM

RETURN

MESH GENERATION

ATTACH

DETACH NODES

ALL: EXISTING

DETACH ELEMENTS

```
ALL: EXISTING
SELECT ELEMENTS
END LIST
ELEMENTS STORE
right
ALL:SELECTED
RETURN (twice)
SUBDIVIDE
DIVISIONS
1 1 1
ELEMENTS,
ALL:SELECTED
RETURN
MOVE
TRANSLATIONS
1 0 0
ELEMENTS
right
RETURN
SWEEP
REMOVE UNUSED NODES
ALL
FILL
RETURN
PLOT
CURVES OFF
SURFACES OFF
POINTS OFF
REGEN
```

(pick all elements to the right of the net section)

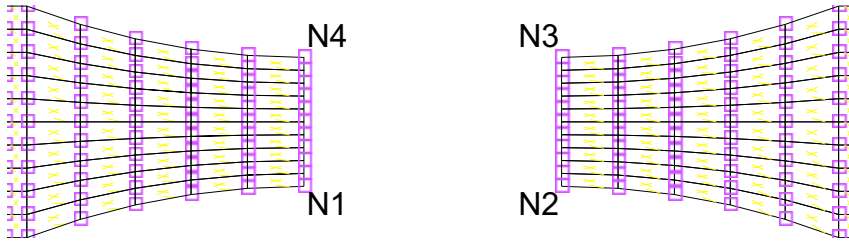


Figure 3.20-7 Extension of Gage Section

```
RETURN to mesh generation
ELEMS ADD
N1, N2, N3, N4
SUBDIVIDE, DIVISIONS
10 10 1
ELEMENT
RETURN
SWEEP
ALL
RETURN
RENUMBER
ALL
MAIN
MATERIAL PROPERTIES
MATERIAL PROPERTIES
ELEMENTS ADD
ALL: EXISTING
MAIN
GEOMETRIC PROPERTIES
PLANAR
PLANE STRESS
OK
ELEMENTS ADD
ALL: EXISTING
MAIN
JOBS
RUN
SUBMIT(1)
```

(pick element just added)

OPEN POST FILE (RESULTS MENU)

SCALAR

Comp 11 Of Stress

OK

CONTOUR BANDS

Inc: 0
Time: 0.000e+000

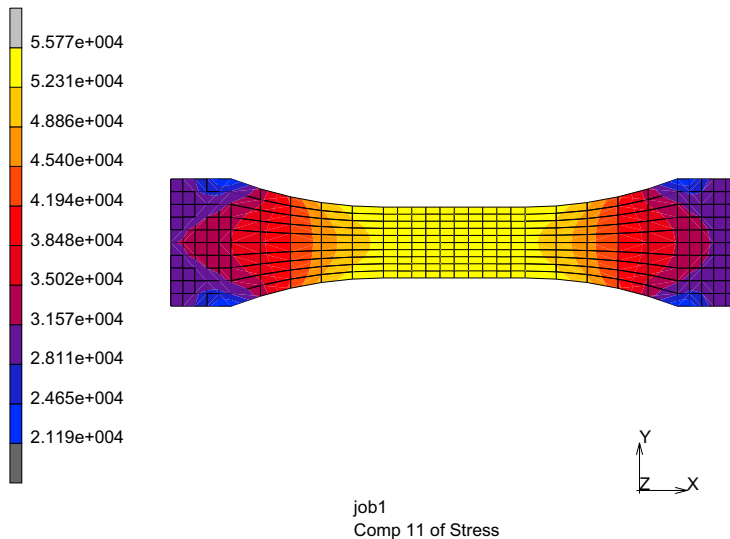


Figure 3.20-8 Axial Stress Contours

Tensile Specimen Composite Material

What about composites? Suppose we want to analyze an orthotropic material whose material axis does not line up with the structure's geometric axis.

FILES

OPEN

isotropic

SAVE AS

orthotropic

RETURN

MATERIAL PROPERTIES (twice)

STRUCTURAL

TYPE ELASTIC-PLASTIC ORTHOTROPIC

E11 = 3E7, E22=E33=1E6

ALL ν 's = .3

ALL G'S = 5E5

OK

RETURN

ORIENTATIONS

NEW

EDGE41 ON

ANGLE 45

ADD ELEMENTS

ALL: EXISTING

ORIENTATION PLOT SETTINGS

ORIENTATION

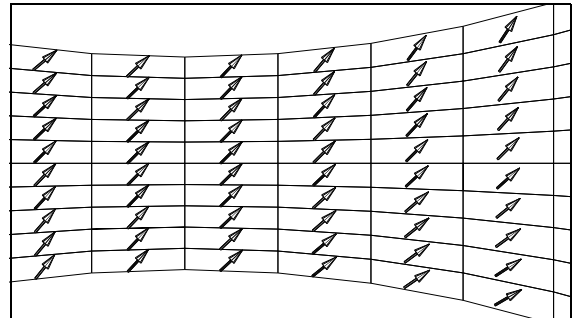
FIRST DIRECTION

REGEN

SAVE

(on)

(only)



Re-run and check results, deformed shape is skewed.

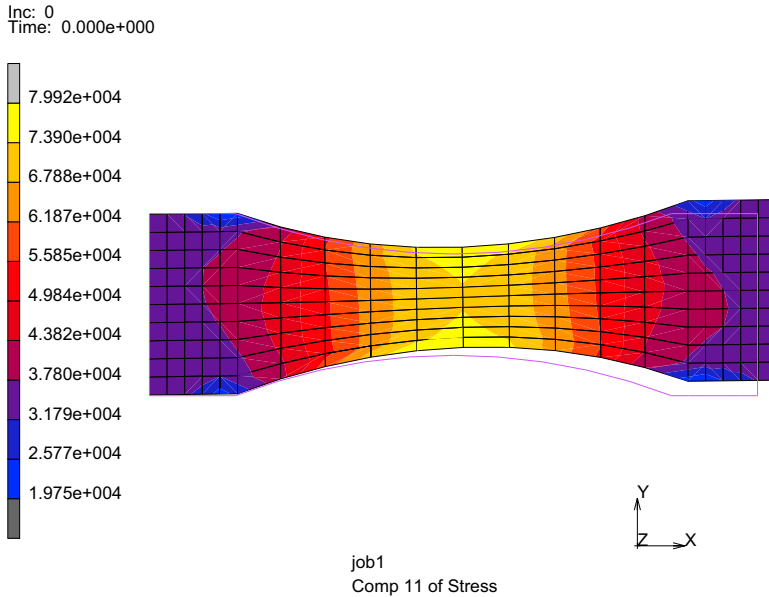


Figure 3.20-9 Axial Stress Contours Orthotropic Material

Modeling Tips

It is very common in the testing of materials to monitor the load - displacement response of the specimen since the testing machine typically records this information. For our current models of the specimen, this can be a bit awkward, since we only have nodal forces and displacements that would need to be summed up appropriately. For example, should we need to sum up the external forces on the right side of our specimen, we can use a path plot to collect the proper information, then copy to the clipboard and place the information into Microsoft Excel to sum up the loads; of course, this should be the applied pressure on the surface times its area. Let's do this for our `isotropic_long` model.

RESULTS

OPEN

`isotropic_long_job1.t16`, **OK**

PATH PLOT

NODE PATH

238 188 #

(pick lower and upper nodes on right end)

ADD CURVES

ADD CURVE

Arc Length

External Force X

FIT

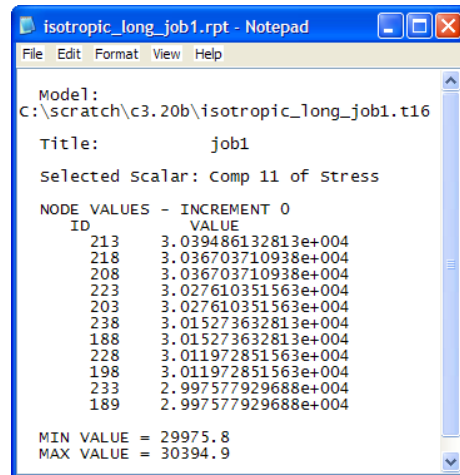
CLIPBOARD COPY TO
RETURN

This places the data into the clipboard and upon starting up Excel, one can paste into a worksheet and sum, sum Fx, as indicated below. Also other calculations are included to check equilibrium by multiplying the surface load times its area. The equilibrium check is very good.

Arc Length	External Force X	
0	336.944	
0.089852	673.888	
0.179703	673.888	
0.269555	673.888	
0.359407	673.888	
0.449259	673.888	
0.53911	673.888	
0.628962	673.888	
0.718814	673.888	
0.808666	673.888	
0.898517	336.944	
sum Fx =	6738.88 lbf	
stress =	30000 psi	
area =	0.22462925 in^2	
force =	6738.8775 lbf	

We can export results from Mentat to external files by using the report writer, namely:

MORE
REPORT WRITER
SELECT
METHOD PATH
SHORTCUTS
SHOW MODEL, OK
NODES
238 188 #
RETURN
SELECTION SELECTED ENTITIES
DATA NODAL VALUES
CREATE REPORT
OPEN REPORT



and the text file, isotropic_ling_job1.rpt is created and opened (right). Yet, if we want to simulate the specimen as being pulled in a test machine, these procedures would be cumbersome; we would want another way to automatically record the total load. To accomplish this, we shall use the contact option and take advantage that all forces acting on a rigid body are automatically summed up to a generalized force (forces and moments) at the reference point on the rigid body.

To model the specimen being pulled by a test machine, we shall replace the pressure surface with a rigid body that will pull the specimen using displacement control; for safety reasons, testing laboratories use displacement control of the test machine, rather than load control.

FILES

OPEN

isotropic_long, OK

SAVE AS

isotropic_long_contact, OK

MAIN

MESH GENERATION

CRVS ADD

(pick lower and upper nodes on right end)

MOVE

RESET

SCALE FACTORS

1 1.2 1

CURVE

11 #

(pick curve just added)

MAIN

CONTACT

CONTACT BODIES

DEFORMABLE, OK

ELEMENTS ADD

ALL EXISTING

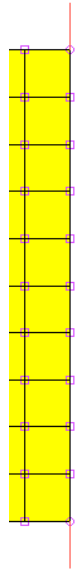
NEW

2-D CURVES ADD

11 #

FLIP CURVES

11 #



```
TABLES
  NEW
    1 INDEPENDENT VARIABLE
  TYPE time, OK
  ADD
    0 0 1 1
  RETURN
RIGID
  POSITION PARAMETERS
    X = 0.0121254, TABLE table1           (yields total grip load of 6739 lbf)
    OK (twice)
  MAIN
BOUNDARY CONDITIONS
  EDIT apply3
  REM
  MAIN
LOADCASES
  MECHANICAL
    STATIC, OK
  MAIN
JOBS
  PROPERTIES
    lcase1
  CONTACT CONTROL
  ADVANCED CONTACT CONTROL
    SEPERATION FORCE = 1E11                (insures no seperaton)
    OK (thrice)
RUN
  SAVE MODEL
  SUBMIT (1)
  OPEN POST FILE (RESULTS MENU)
  HISTORY PLOT
    ALL INCS
  ADD CURVES
```

GLOBAL

Pos X cbody2

Force X cbody2

FIT

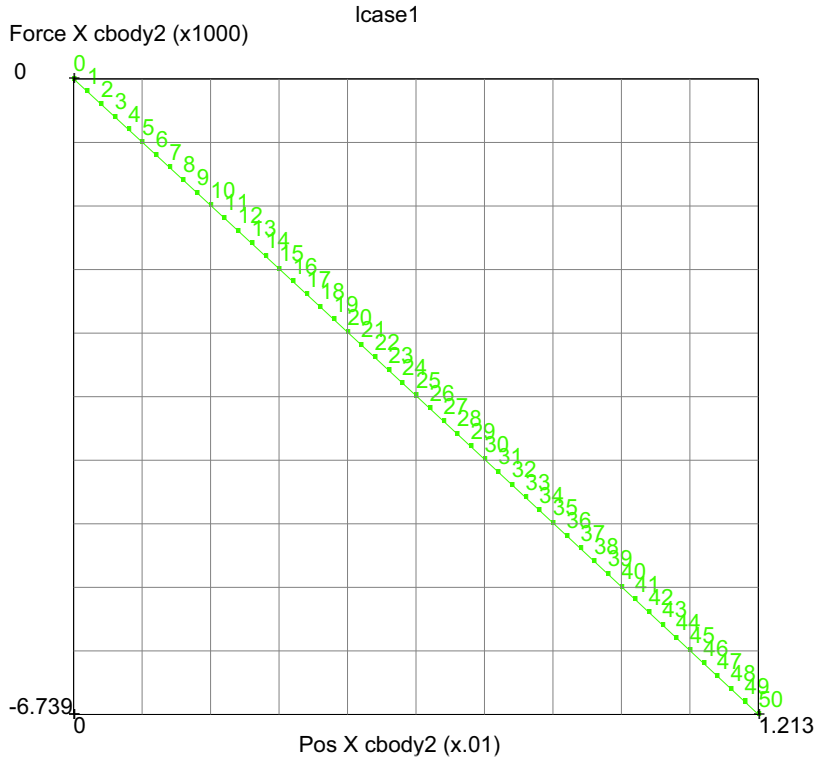


Figure 3.20-10 Load - Displacement Response of Specimen

Since our problem had no nonlinear behavior, the load - displacement response is a straight line ending at a total load of -6,739 lbf. The force on the specimen is equal and opposite to the force on the rigid body and the total force agrees with our other calculations.

Input Files

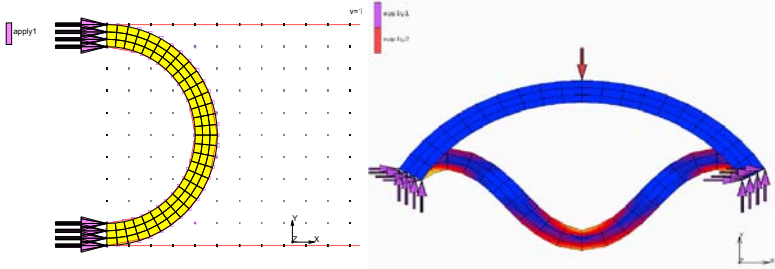
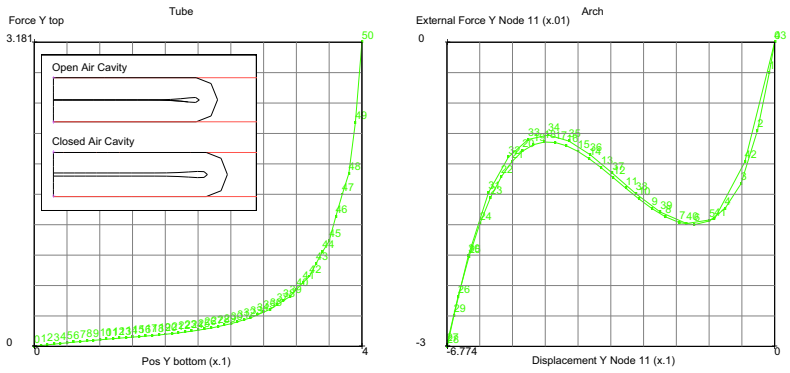
The files below are on your [delivery media](#) or they can be downloaded by your web browser by clicking the links (file names) below.

File	Description
sl.proc	Mentat procedure file to run the above problem

3.21 Rubber Elements and Material Models

- Summary 1280
- Lower-order Triangular Rubber Elements 1281
- Tube with Friction 1296
- Cavity Pressure 1298
- Buckling of an Elastomeric Arch 1302
- Comparison of Curve Fitting of Different Rubber Models 1310
- Input Files 1317

Summary

Title	Rubber elements and material models
Problem features	Compression of a rubber tube and snap through of an elastic arch
Geometry	
Material properties	Elastomeric Materials: Ogden and Mooney
Analysis type	Static with elastomeric material behavior
Boundary conditions	As show above
Element type	Plane stress quad and tri element types
FE results	<p>Force displacement response</p> 

An example of a compression of a rubber tube using Ogden material using both quadrilateral and triangular elements is presented first. Curve fitting of Ogden coefficients is demonstrated next. The tube is then considered closed and filled with air. A postbuckling simulation of a rubber arch is then performed. Finally, curve fitting based upon different rubber models is performed.

Lower-order Triangular Rubber Elements

Let's start with the compression of a rubber tube in two dimensions assuming plane strain. The tube is compressed by two rigid bodies on the top and bottom and is modeled with one plane of symmetry. Units used are inches, pounds, and seconds.

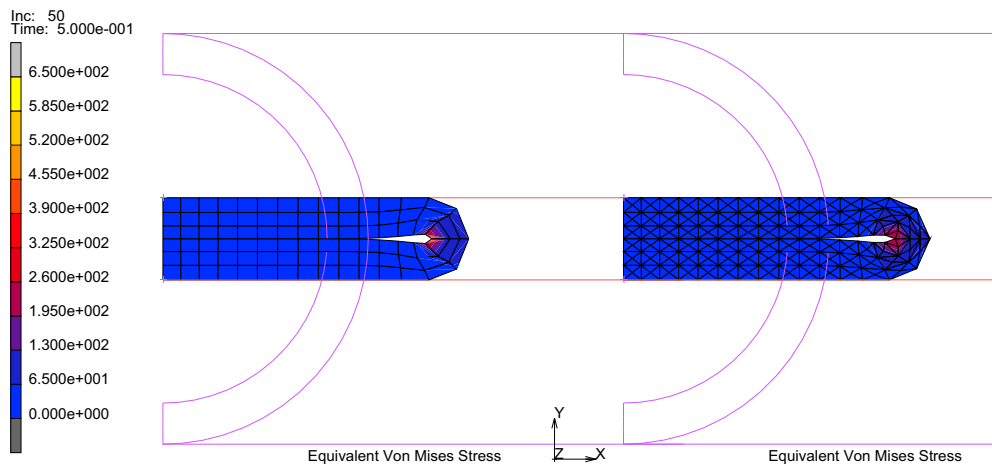


Figure 3.21-1 Compressed Tube using Quadrilaterals and Triangles

Using Quadrilateral Elements

```

FILES
  SAVE AS
    elasto
RETURN
MESH GENERATION
  COORDINATE SYSTEM SET:
    GRID ON
    U DOMAIN
      -1.1 1
    V DOMAIN
  
```

```
0 1
FILL
RETURN
CURVES: ADD
point( 1.0, 0.0, 0.0)
point(-1.1, 0.0, 0.0)
point(-1.1, 1.0, 0.0)
point( 1.0, 1.0, 0.0)
CURVE TYPE
CENTER/POINT/POINT
RETURN
CURVES: ADD
-1.0, 0.5, 0.0
-1.0, 0.0, 0.0
-1.0, 1.0, 0.0
-1.0, 0.5, 0.0
-1.0, 0.1, 0.0
-1.0, 0.9, 0.0
SURFACE TYPE
RULED, RETURN
SURFACES ADD:
4
3
```

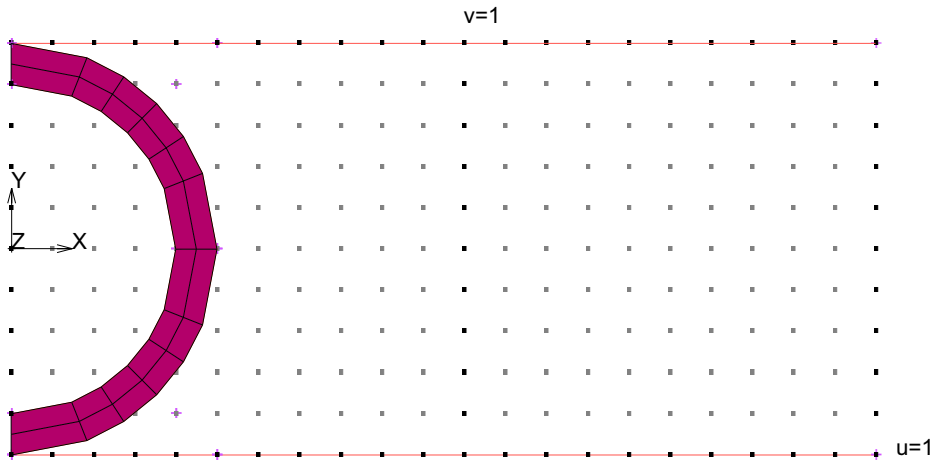


Figure 3.21-2 Tube Geometry

```
CONVERT
  DIVISION
    30 3
SURFACES TO ELEMENTS
  all: EXIST.
RETURN
```

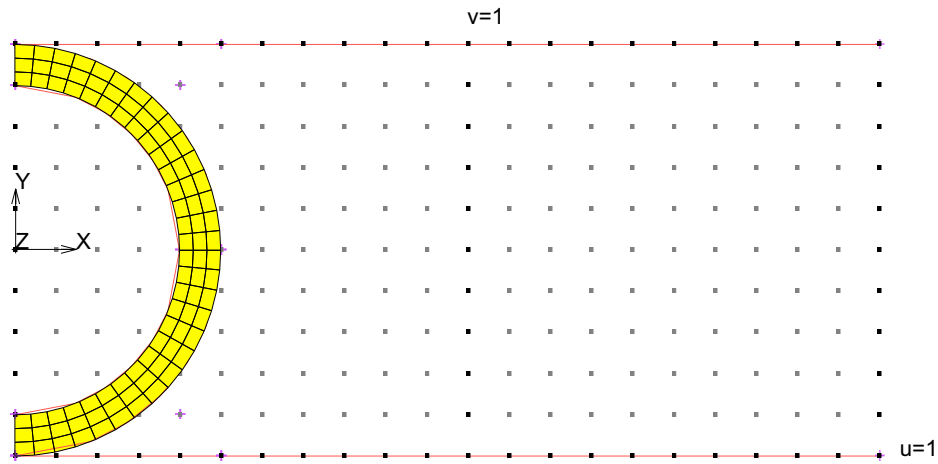


Figure 3.21-3 Quadrilateral Mesh

```
SWEEP
  ALL
  RETURN
CHECK
  UPSIDE DOWN
  FLIP ELEMENTS
  ALL SELECTED
  RETURN
RENUMBER
  ALL
  RETURN
MAIN
BOUNDARY CONDITIONS
  MECHANICAL
    DISPLACEMENT X
      0
    OK
  ADD NODES
```

(pick nodes along $x=0$)

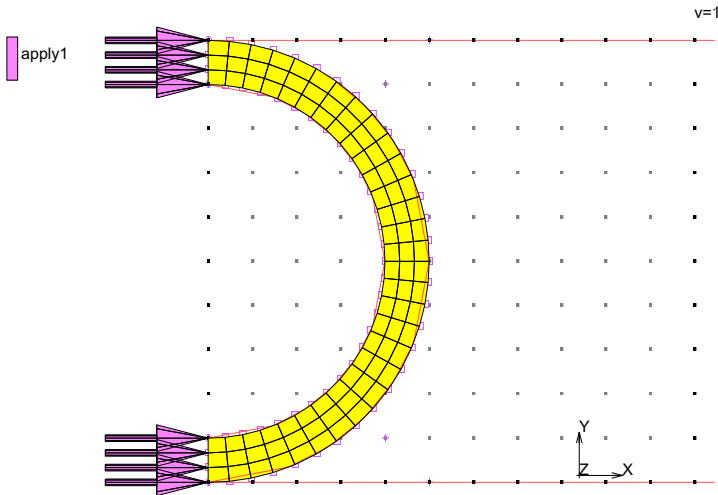


Figure 3.21-4 Boundary Conditions

```
MAIN
MATERIAL PROPERTIES (twice)
```

```

NEW
  STANDARD
TABLES
  NEW
    1 INDEPENDENT VARIABLE
  TYPE
    experimental_data
  ADD
    0 0
    .9 100
    1.6 250
    1.9 300
    2.2 500
    2.4 600
    2.6 700
    2.9 1000
  FIT
  FILLED
    
```

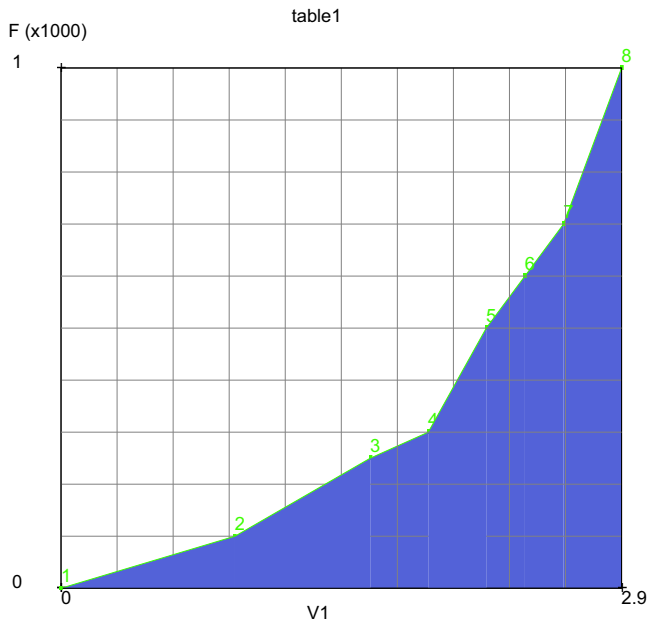


Figure 3.21-5 Material Stress Strain Curve

NAME
 tension
RETURN
EXPERIMENTAL DATA FIT
 UNIAXIAL
 tension
 ELASTOMERS
 OGDEN
 UNIAXIAL
 POSITIVE COEFFICIENTS (on)
 MATHEMATICAL CHECKS (on)
 COMPUTE
 APPLY
 OK
SCALE AXES (to scale the curve)
RETURN (twice)

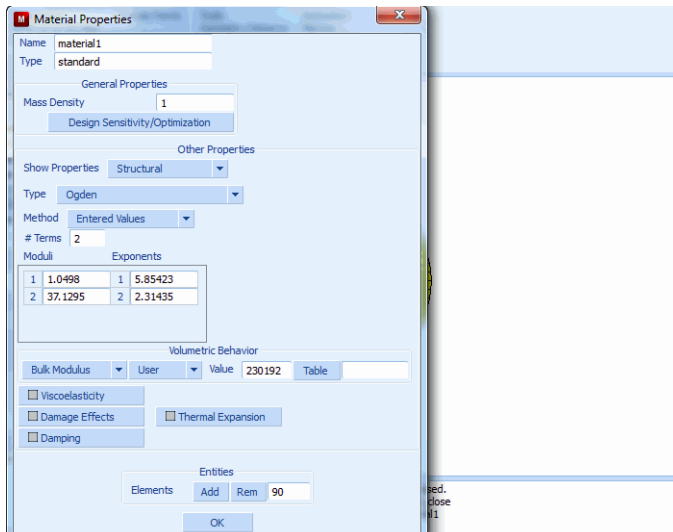


Figure 3.21-6 Curve Fit of Material Stress Strain Curve

This curve fit of the raw data has been applied to this material. It is important to have the other deformation modes (biaxial and planar shear) be similar to the tension fit and not vary factors of two or higher. Of course, it would be best to have the biaxial and planar shear material data to make a combined mode fit. More on this later.

```

ELEMENTS ADD
  all: EXIST.
SHOW MODEL
MAIN
CONTACT
CONTACT BODIES
  DEFORMABLE, OK
ELEMENTS ADD
  all: EXIST.
TABLES
  NEW
    1 INDEPENDENT VARIABLE
    TYPE
      time
      OK
    ADD
      0 0 0.5 1 1 0
    END LIST (#)
  FILLED
  FIT
  
```

(select OK button only if type time was typed in)

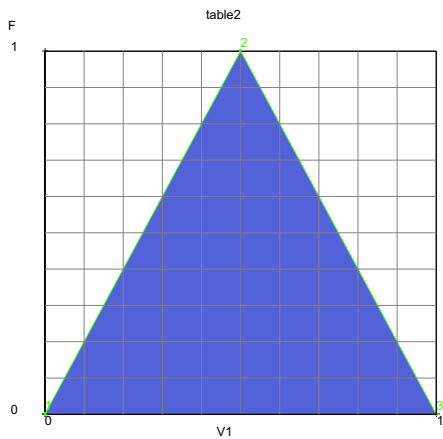


Figure 3.21-7 Time Table to move Rigid Bodies

```

SHOW TABLE
SHOW MODEL
  
```

```

    RETURN
MAIN
CONTACT
CONTACT BODIES
  NEW
    DEFORMABLE
      OK
    ELEMENTS ADD
      ALL: EXISTING
    NEW
    NAME
      top
    RIGID
      POSITION
        PARAMETERS
          position (center of rotation) Y
            -.4
        TABLE
          table2 (pick the time table)
        OK
      DISCRETE (on)
      OK
    2-D CURVES ADD
      (pick top curve)
      END LIST (#)
    NEW
    NAME
      bottom
    RIGID
      POSITION
        PARAMETERS
          position (center of rotation) Y
            .4
        TABLE
          table2 (pick the time table)
        OK
```


DISCRETE
 2-D CURVES ADD
 END LIST (#)
 ID CONTACT
 MAIN

(on)
 (pick bottom curve)

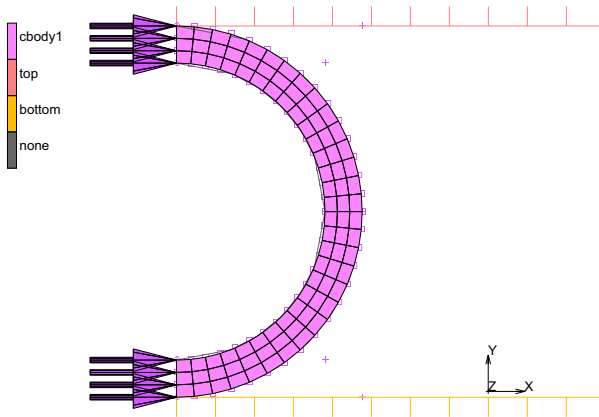


Figure 3.21-8 Identification of Contact Bodies

LOADCASES
 MECHANICAL
 STATIC
 SOLUTION CONTROL
 MAX # RECYCLES
 30
 NON-POSITIVE DEFINITE
 DEVIATORIC STRESS,
 OK
 CONVERGENCE TESTING
 DISPLACEMENT
 OK
 TOTAL LOADCASE TIME
 0.5
 fixed # OF STEPS
 50
 OK

```
COPY
MAIN
JOBS
NEW
MECHANICAL
PROPERTIES
  lcase1
  lcase 2
CONTACT CONTROL
  ADVANCED CONTACT CONTROL
    DISTANCE TOLERANCE BIAS
      .5
      OK (twice)
JOB RESULTS
  available element scalars
  Equivalent Cauchy Stress
  OK (twice)
ELEMENT TYPES
  MECHANICAL
  ANALYSIS DIMENSION
    PLANAR
    SOLID
      80
      OK
    all: EXIST.
  RETURN
RUN
  SUBMIT 1
  MONITOR
  OK
SAVE
RETURN
```

(Quad 4)

Results

RESULTS

OPEN DEFAULT

SKIP TO INC

50

DEF & ORIG

CONTOUR BAND

SCALAR

Equivalent Cauchy Stress

Inc: 50
 Time: 5.000e-001

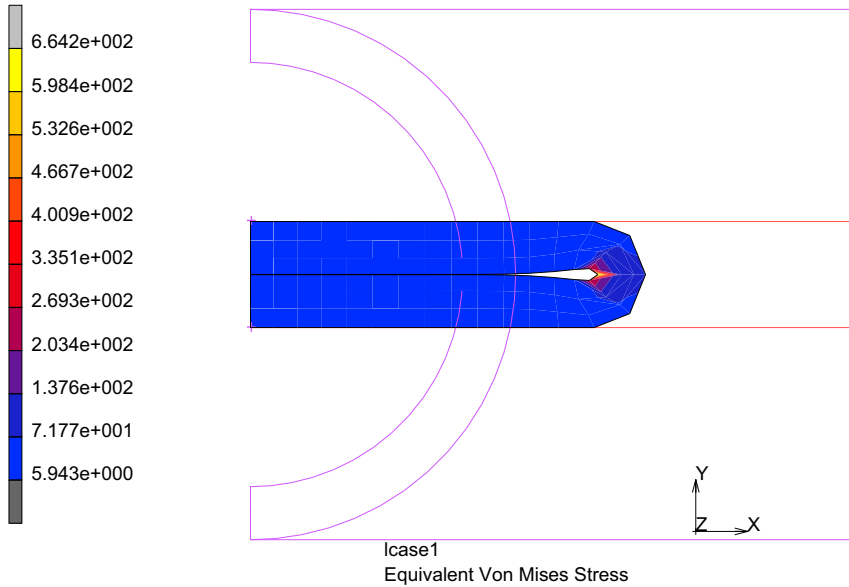


Figure 3.21-9 Equivalent Cauchy Stress Contours Quadrilateral Mesh

HISTORY PLOT

SET LOCATIONS

n: 1

END LIST (#)

INC RANGE

0 50 1

ADD CURVES
ALL LOCATIONS
contact body variables
Pos Y bottom
Force Y top
FIT
RETURN
GENERALIZED XY PLOT: COPY TO

(add to Generalized XY Plotter)

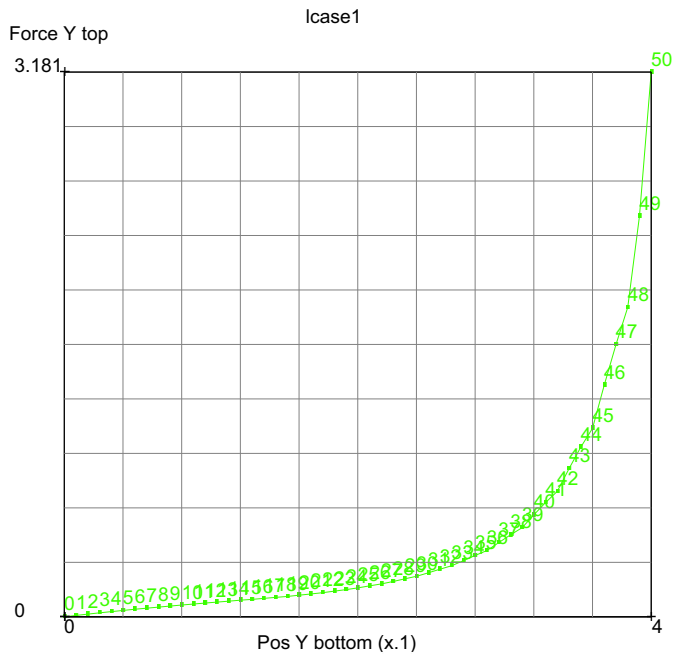


Figure 3.21-10 Die Force versus Die Displacement

Using Triangular Elements

SHOW HISTORY
SHOW MODEL
RETURN
CLOSE
MAIN
FILES

SAVE AS
triangle
OK
RETURN
MESH GENERATION
CHANGE CLASS
TRIA (3)
ELEMENTS
all: EXIST.

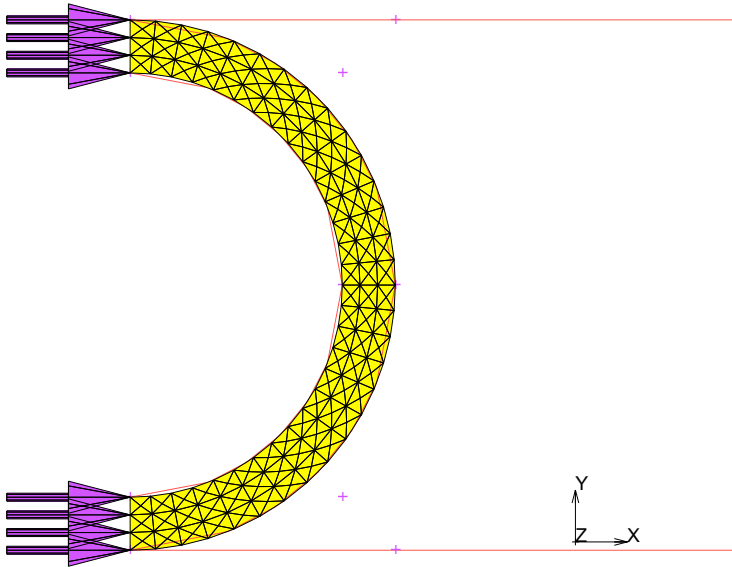


Figure 3.21-11 Change Class to Triangles

Run Job and View Results

MAIN
JOBS
ELEMENT TYPES
PLANE STRAIN SOLID
155
OK
all: EXIST.

(Tri 3)

```
RETURN (Twice)
RUN
  SUBMIT 1
  MONITOR
  OK
  SAVE
  RETURN
RESULTS
  OPEN DEFAULT
  SKIP TO INC
    50
  DEF & ORIG
  CONTOUR BAND
  SCALAR
    Equivalent Cauchy Stress
```

Inc: 50
Time: 5.000e-001

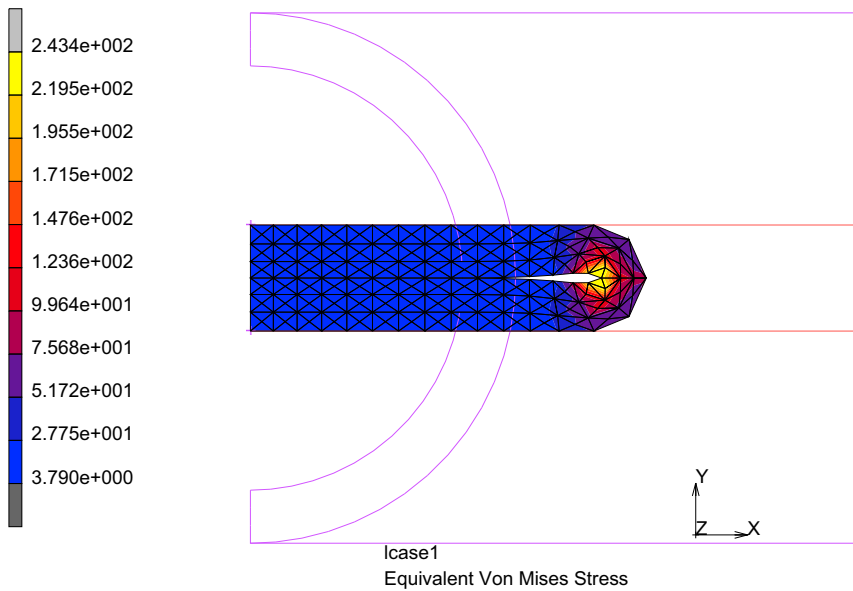


Figure 3.21-12 Equivalent Cauchy Stress Contours Triangular Mesh

```

HISTORY PLOT
SET LOCATIONS
  1
  END LIST (#)
INC RANGE
  0 50 1
ADD CURVES
  ALL LOCATIONS
    contact body variables
      Pos Y bottom
      Force Y top
  FIT
  RETURN
GENERALIZED XY PLOT: COPY TO
  
```

(add to Generalized XY Plotter)

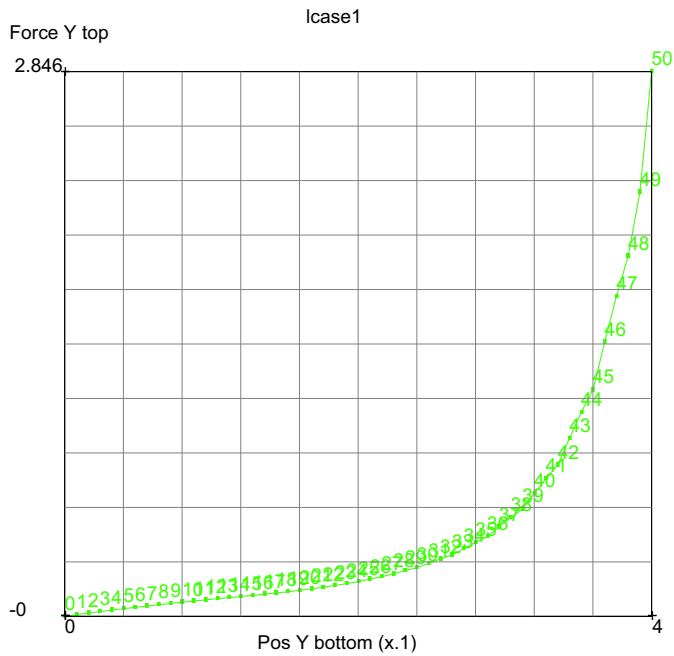


Figure 3.21-13 Die Force versus Die Displacement

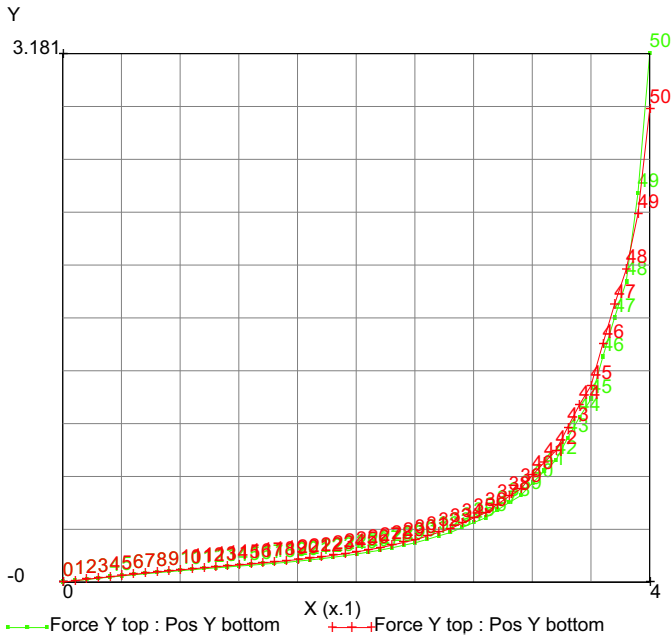


Figure 3.21-14 Generalized XY Plot to compare Quad and Tri Results

Figure 3.21-14 compares the force displacement response of the two models with nearly the same curve for both quadrilaterals and triangular elements.

Tube with Friction

Friction between the rigid bodies and the tube is added using the stick-slip friction option. A friction coefficient of 0.2 is used.

```

FILES
  NEW
  OK
  OPEN
    elastol.mud
  SAVE AS
    elastolf
  RETURN
CONTACT
  CONTACT BODIES
    DEFORMABLE
  
```



```

FRICION COEFF
  0.2
  OK
NEXT
FRICION COEFF
  0.2
  OK
NEXT
FRICION COEFF
  2
  OK
MAIN
JOBS
  PROPERTIES
    CONTACT CONTROL
    STICK-SLIP
    OK (twice)
RUN
  SAVE
    SUBMIT1
    MONITOR
  POSTPROCESS
    HISTORY
      SET LOCATIONS
        n:1
      #END LIST
    ALL INCS
      ADD CURVES
      GLOBAL

```

Pos Y top, Force Y top
Pos Y top, Force X top
FIT

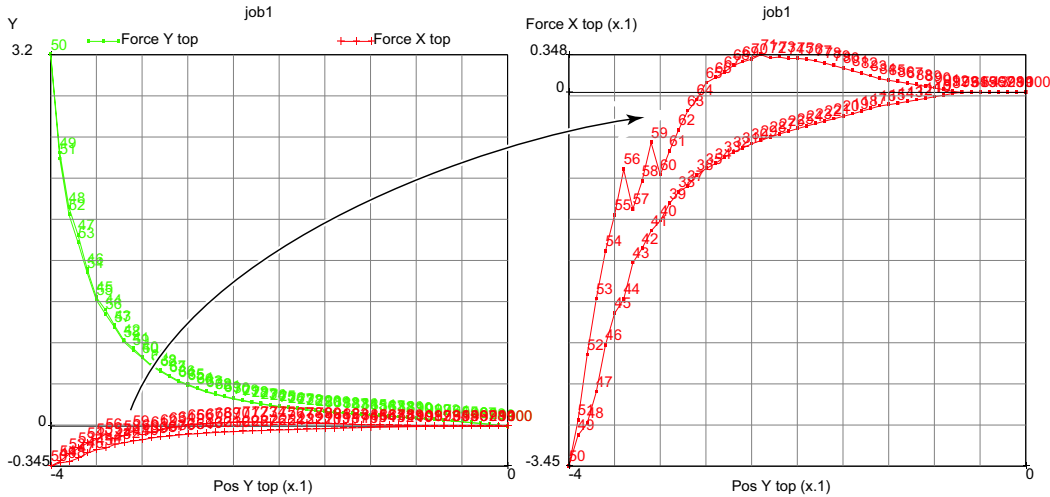


Figure 3.21-15 Hysteresis Due to Friction

Cavity Pressure

In the last run, the tube had an open air cavity; here, results are compared to frictionless tube with a closed cavity simulating the compression of the air inside the tube, assuming that the tube is closed and the air cannot escape. Let's start with the original model and add a closed cavity representing the air inside the tube.

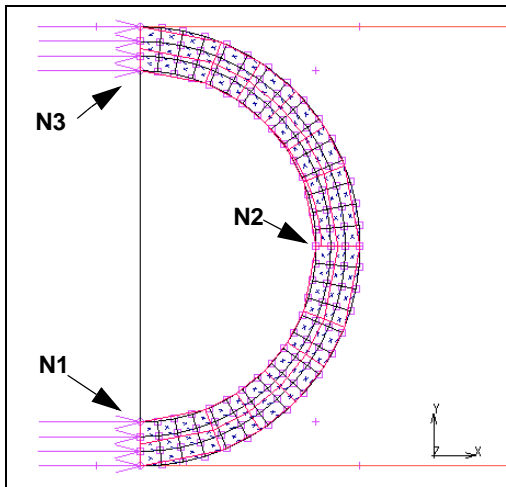
```

FILES
  NEW
  OK
  OPEN
    elastol.mud
  SAVE AS
    elastolc
  RETURN
  FILL
MESH GENERATION
  ELEMENT CLASS
    LINE (2)
  RETURN
  ADD ELEMENT
  RETURN
MODELING TOOLS
  
```

(pick nodes N3 and N1 in order indicated)

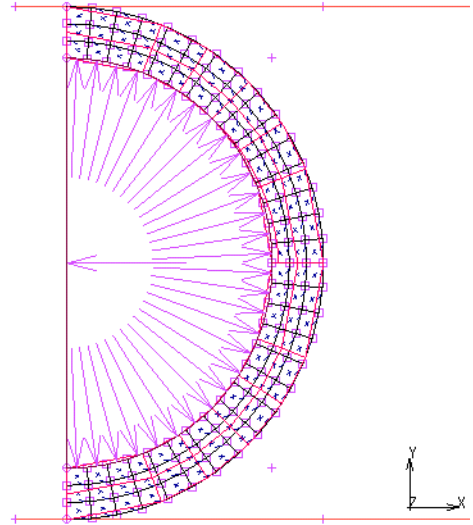
CAVITY
NEW
SELECT
METHOD PATH
RETURN
EDGES
END LIST

(pick N1 N2 N3)



RETURN
EDGES ADD
ALL: SELECTED
REF. PRESSURE
1
REF. TEMPERATURE
1
REF. DENSITY
1.8E-5
MAIN
BOUNDARY CONDITIONS
NEW
MECHANICAL
MORE

```
      CAVITY MASS LOAD
      MASS
      CLOSED CAVITY, OK
      CAVITIES ADD
        cavity1
        OD
      MAIN
LOADCASE
  MECHANICAL
    STATIC
      LOADS
        apply2 (on)
        OK (twice)
      NEXT
        STATIC
          LOADS
            apply2 (on)
            OK (twice)
          MAIN
        JOBS
          PROPERTIES
            INITIAL LOADS
              apply2 (on)
              OK
            JOB PARAMETERS
              CAVITY PARAMETERS
                AMBIENT PRESSURE
                  1
                  OK (thrice)
            ELEMENT TYPES
              MECHANICAL
                MISCELLANEOUS
                  171
                  OK
            END LIST
          RETURN (twice)
```



(pick element previously added)

```

SAVE
RUN
SUBMIT (1)
OPEN POST FILE (RESULTS MENU)
HISTORY PLOT
ALL INCS
ADD CURVES
GLOBAL
    Pos Y top
    Force Y top
    Volume Cavity 1
    Pressure Cavity 1
FIT
    
```

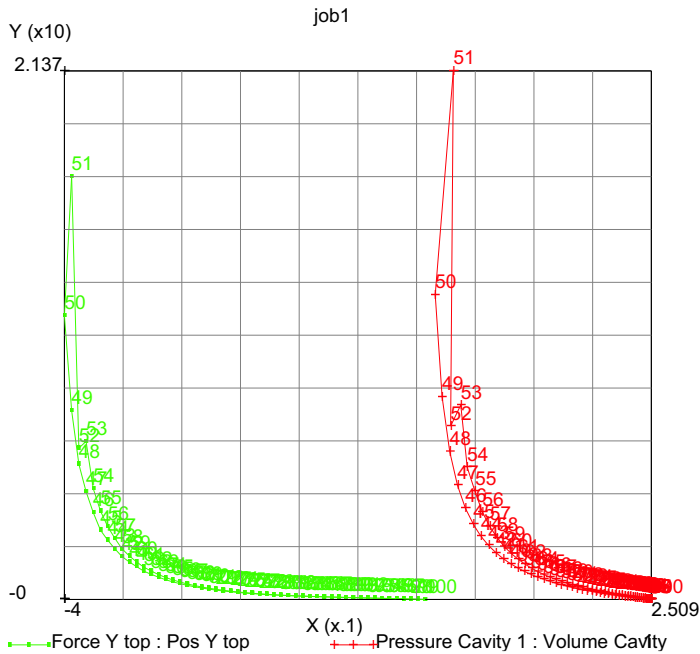


Figure 3.21-16 Force and Pressure History

The force to crush the tube is considerably larger(5x) than before and nearly equal to the cavity pressure since the area of contact is about one inch.

SHOW MODEL
RETURN
DEF ONLY
SKIP TO INC
50

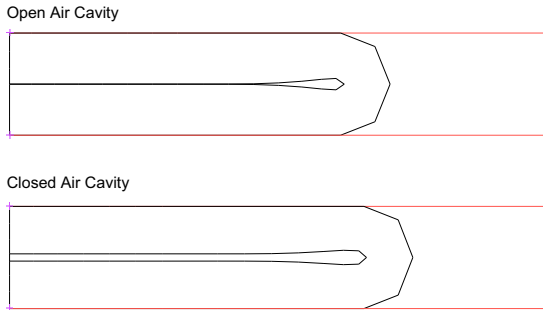


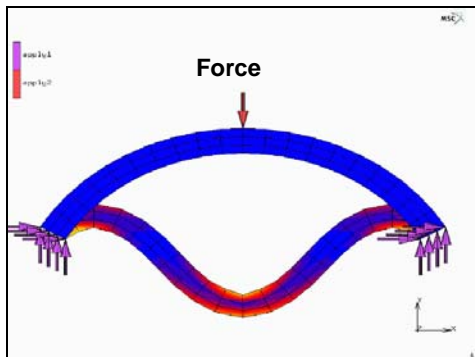
Figure 3.21-17 Affect of Air Cavity

The deformed shape at increment 50 for the closed air cavity shows the inner walls have yet to close, whereas the inner walls will touch for the open air cavity.

Buckling of an Elastomeric Arch

Overview

An elastomeric arch has a center load applied and the objective of the analysis is to determine the snap through in the force displacement response.



An adaptive load stepping method called arc-length (modified Riks-Ramm) is used.

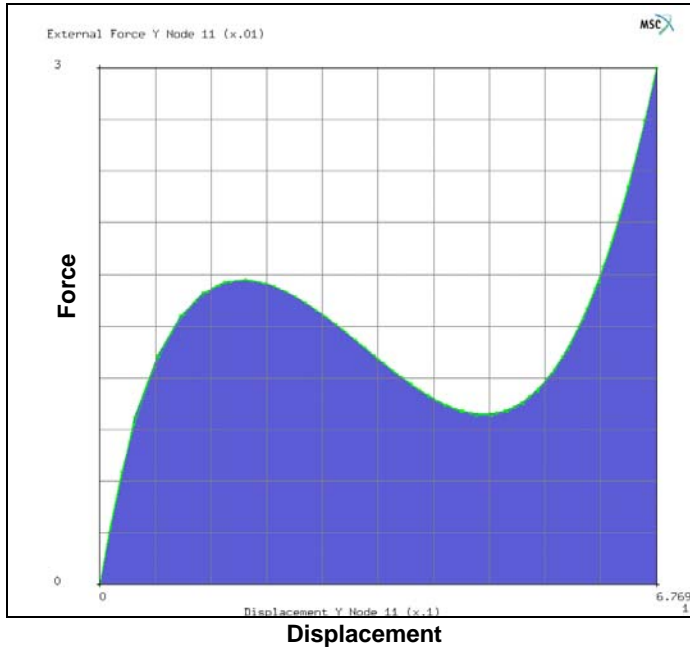


Figure 3.21-18 Elastomeric Arch Problem Description

MESH GENERATION

COORDINATE SYSTEM SET

CYLINDRICAL

SET: GRID ON

RETURN

CURVE TYPE ARC CPP

RETURN

CURVES ADD

0 0 0

.7 30 0

.7 150 0

0 0 0

.8 30 0

.8 150 0

SURFACE TYPE RULED

RETURN

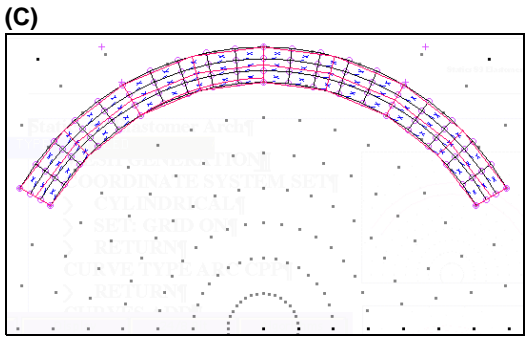
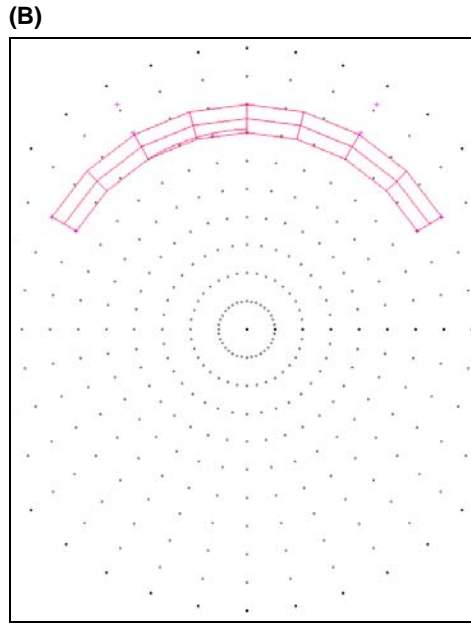
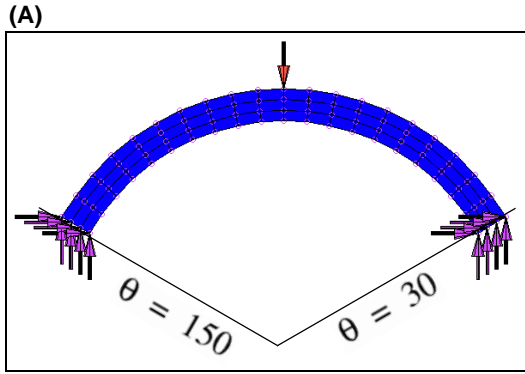


Figure 3.21-19 (A) Model (B) Mesh (C) Geometry

```
SURFACE: ADD
  2 1
CONVERT
  DIVISIONS
    20 3
SURFACES TO ELEMENTS
ALL: EXISTING
RETURN
GRID OFF
FILL
MAIN
```


BOUNDARY CONDITIONS

MECHANICAL

FIXED DISP

X=0

Y=0

NODES ADD

(nodes at both ends)

NEW

POINT LOAD

Y FORCE

-0.03

OK

TABLES

NEW

(1 INDEPENDENT VARIABLE)

DATA POINTS ADD

0 0 1 1 2 0

TABLE TYPE TIME

SHOW MODEL

RETURN

NODES ADD

(top center node)

POINT LOAD

TABLE

table1

(attach table to y force)

MAIN

MATERIAL PROPERTIES (twice)

STRUCTURAL

TYPE MOONEY

C10

1

OK

ELEMENTS ADD

ALL EXISTING

MAIN

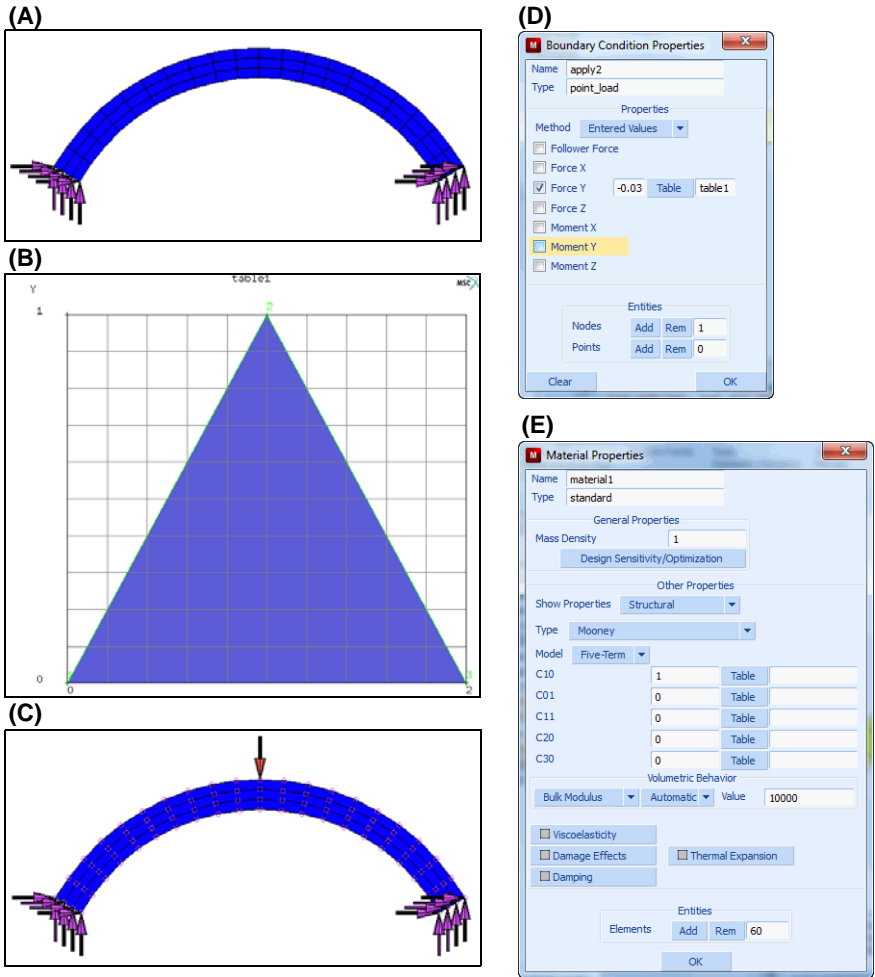


Figure 3.21-20 (A) Nodes Added (B) Show Table (C) Show Model (D) POINT LOAD Submenu and (E) MOONEY PROPERTIES Submenu

LOADCASES
 MECHANICAL
 STATIC
 ARC LENGTH PARAMETERS
 INITIAL FRACTION
 0.1
 OK (twice)
 COPY
 MAIN

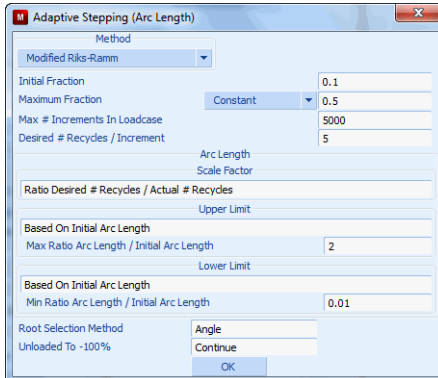


Figure 3.21-21 ADAPTIVE STEPPING (ARC LENGTH) Submenu

JOBS

NEW

PROPERTIES

lcase1

lcase2

ANALYSIS DIMENSION PLANE STRAIN

JOB RESULTS

CAUCHY STRESS TENSOR

OK (twice)

ELEMENT TYPES

MECHANICAL

PLANAR

SOLID

80

OK

ALL EXISTING

RETURN

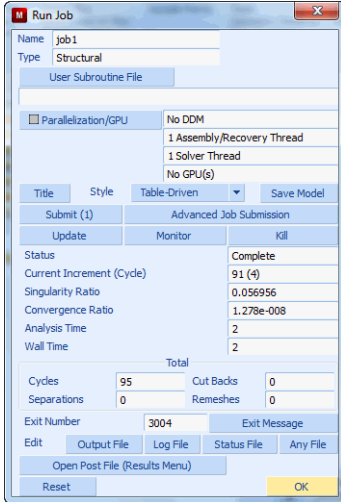
Run Job and View Results

RUN

SUBMIT1

MONITOR

OK (twice)
SAVE



RESULTS

OPEN DEFAULT

SKIP TO INC

29

OK

DEF ONLY

CONTOUR BAND

SCALAR

EQ. CAUCHY STRESS

HISTORY PLOT

SET LOCATIONS

n:11

END LIST

ALL INCS

(pick top center node)

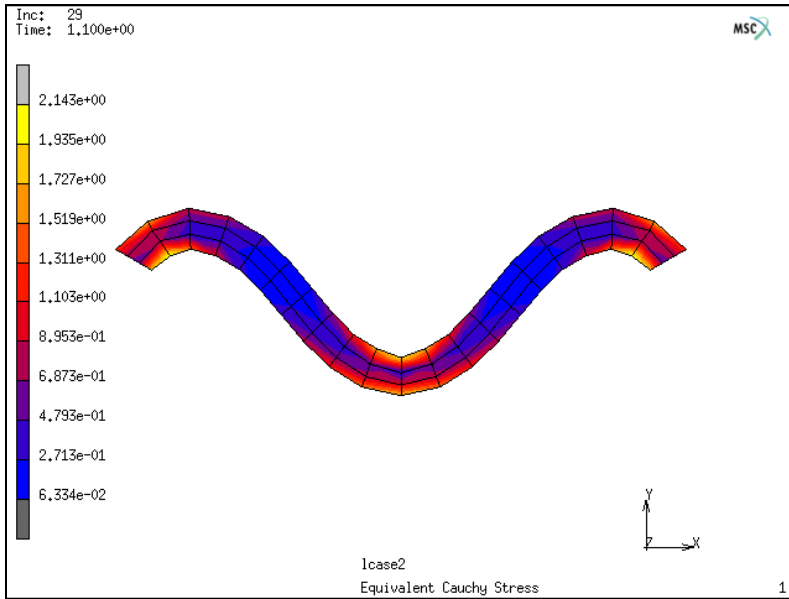


Figure 3.21-22 Equivalent Cauchy Stress Contours

- ADD CURVES
- ALL LOCATIONS
 - Displacement Y
 - External Force Y
- FIT

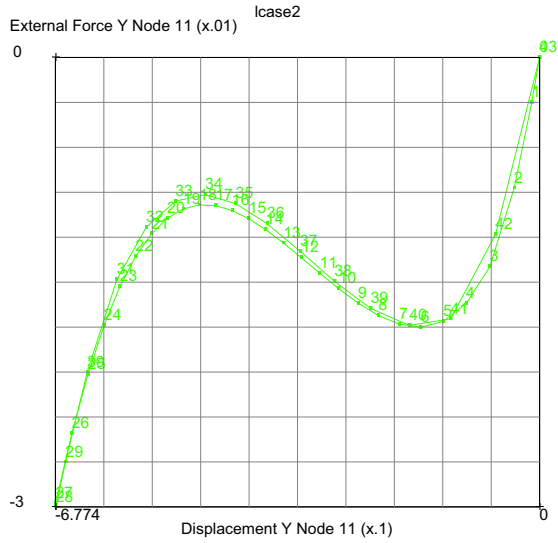


Figure 3.21-23 Force-Displacement History with Snap-through

Comparison of Curve Fitting of Different Rubber Models

In the previous example, the material data was invented. Now let's take a look at how actual data is collected and various material models are fit to this data. This is a uniaxial test with the recorded data shown as the thin black line.

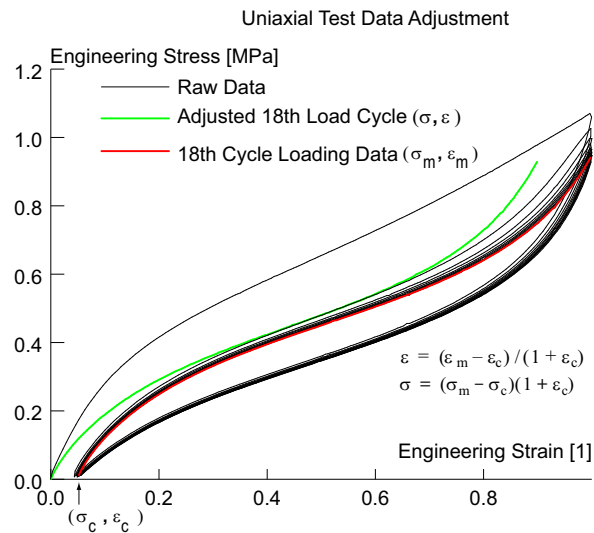


Figure 3.21-24 Adjusting Measured Data to Analytical Model

The 6288 data points measured during this uniaxial test must be reduced in a logical manner to produce a single stress strain diagram suitable for elastic materials. The 18th loading cycle was chosen to best represent the application, and the data (gage length and original area) are adjusted for the strain offset, ϵ_c , the minimum value of strain for the 18th load cycle. The 52 data points σ_m, ϵ_m of the 18th load cycle of this uniaxial test are adjusted for the strain offset to determine the data σ, ϵ as shown in Figure 3.21-24 where $\epsilon = (\epsilon_m - \epsilon_c)/(1 + \epsilon_c)$ adjusts for the implied change in gage length, and $\sigma = (\sigma_m - \sigma_c)(1 + \epsilon_c)$ adjusts for the implied change in original cross sectional area. The nonlinear elastic theory requires that at zero strain the stress is zero. Repeating this procedure for biaxial and planar shear will yield three stress-strain curves for the same material. Each curve represents the stress-strain behavior for three strain states: tension, planar shear and equal biaxial behavior as shown in Figure 3.21-25. Ideally, it is best to use all strain states when determining the constants used in analytic models such as Mooney, Ogden, Boyce, or Gent.

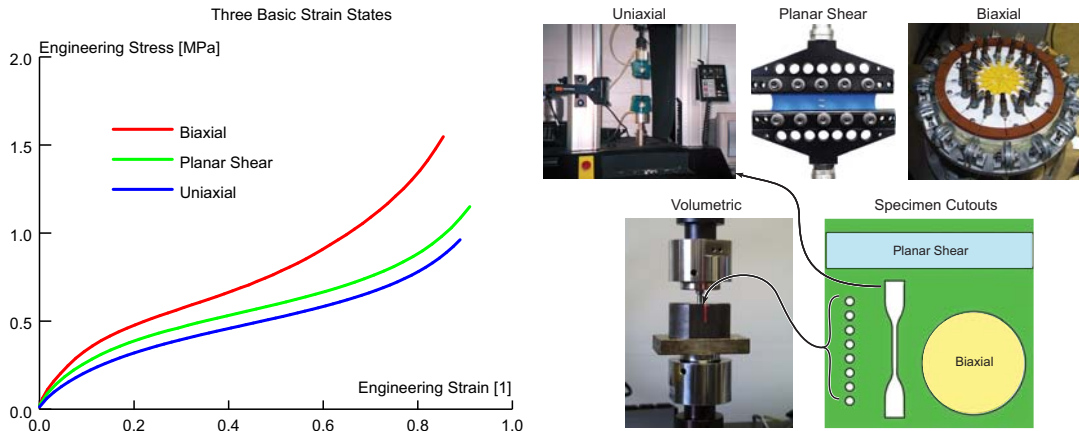


Figure 3.21-25 Three Basic Strain States

Each of the curves above actually come from three independent tests performed on the same material. The process of using Mentat to determine the Mooney, Ogden, Boyce, or Gent constants is called Experimental Curve Fitting and we shall now use Mentat to fit the data shown in Figure 3.21-25.

MATERIAL PROPERTIES

EXPERIMENTAL DATA FIT

TABLES

READ

RAW

FILTER *data

OK

(pick uniaxial.data, biaxial, and planar_shear.data)

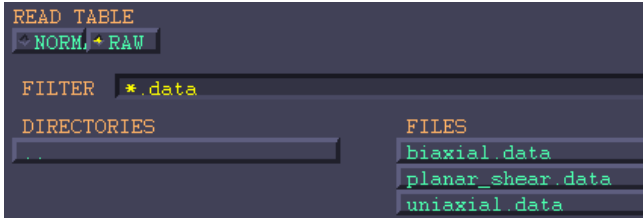


Figure 3.21-26 Reading Tables of Material Properties

TABLES

- GENERALIZED XY PLOT: COPY TO RETURN, NEXT
- GENERALIZED XY PLOT: COPY TO RETURN, NEXT
- GENERALIZED XY PLOT: COPY TO RETURN, NEXT
- RETURN (twice)

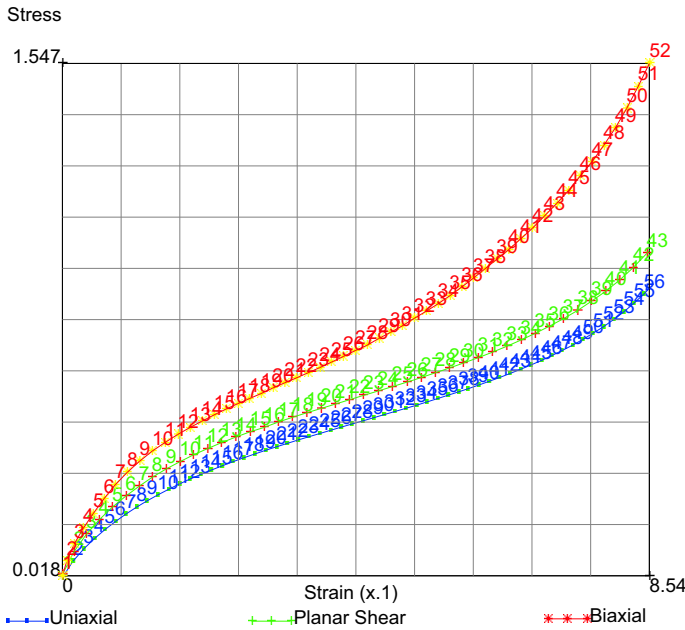


Figure 3.21-27 Displaying Material Data

Having the data for the three strain states in Mentat facilitates performing several curve fits to pick the most appropriate material model. Let's examine a Mooney and Arruda-Boyce material models.

Mooney

Now let's associate each table read with the proper strain state and do a fit.

```

EXPERIMENTAL DATA FIT
  UNIAXIAL
    table 1
  BIAXIAL
    table 2
  PLANAR SHEAR
    table 3
  ELASTOMERS
    MOONEY(2)
    UNIAXIAL
    COMPUTE
    OK
  SCALE AXES
    
```

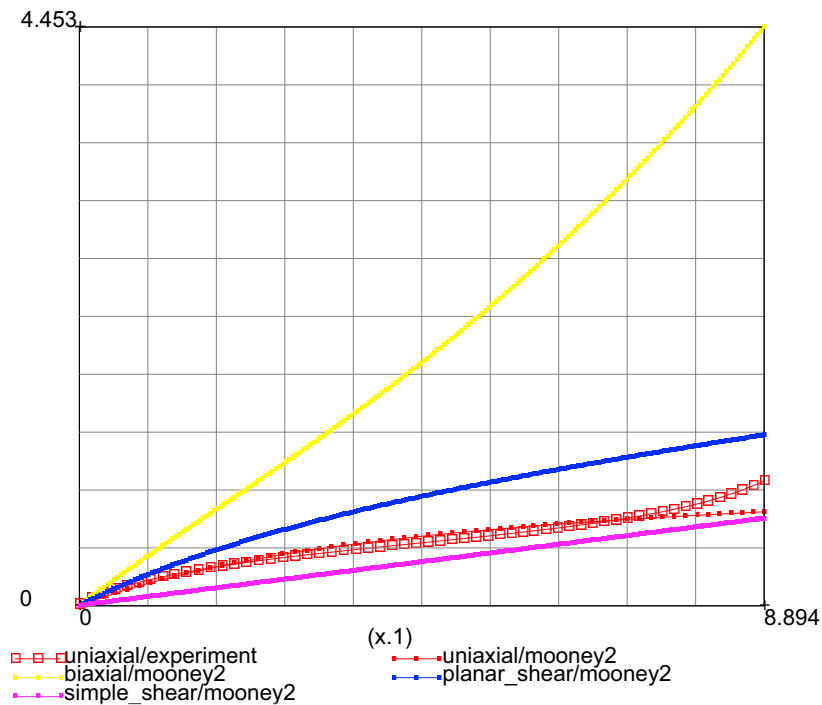


Figure 3.21-28 Two Constant Mooney only using Uniaxial Data – A Poor Fit

Notice that when Mentat fits just a single curve of data, it also plots the predicted other strain states using the current elastomeric model. In this case, only the uniaxial data was used to fit the two constants to a Mooney material. Notice that this is a poor fit because this model is too stiff in biaxial deformation.

Now let us try using all of the strain states again to fit a two constant Mooney material model.

```
MOONEY(2)
  USE ALL
  DATA
  COMPUTE
  OK
  SCALE AXES
```

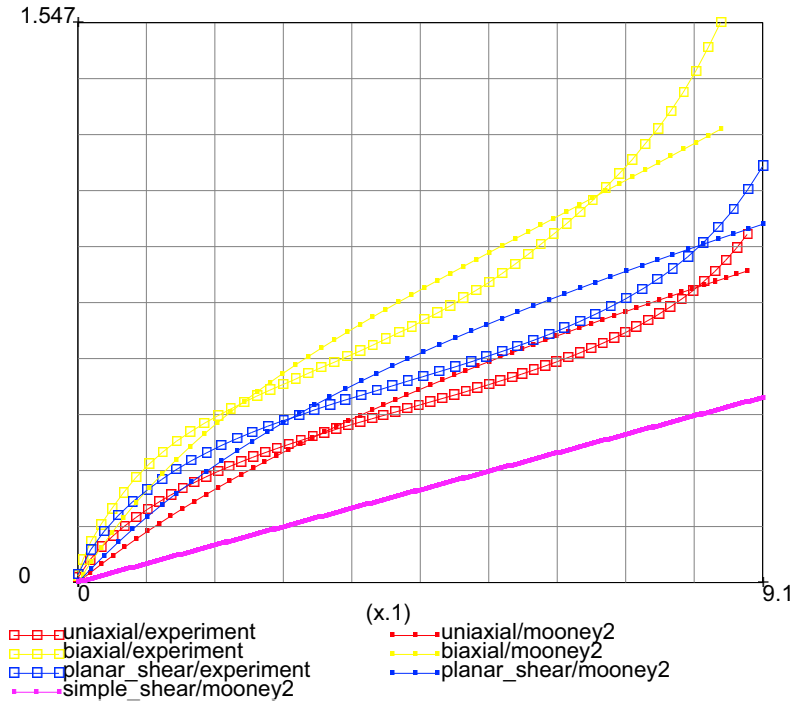


Figure 3.21-29 Two Constant Mooney only Using Uniaxial Data – A Good Fit

Arruda-Boyce

Clearly using all of the strain states is the best. However, many times you may not have all of the data and may be stuck with just the uniaxial test data. In that case, you may wish to use the Arruda-Boyce model.

ARRUDA-BOYCE
 UNIAXIAL
 COMPUTE
 OK
 SCALE AXES

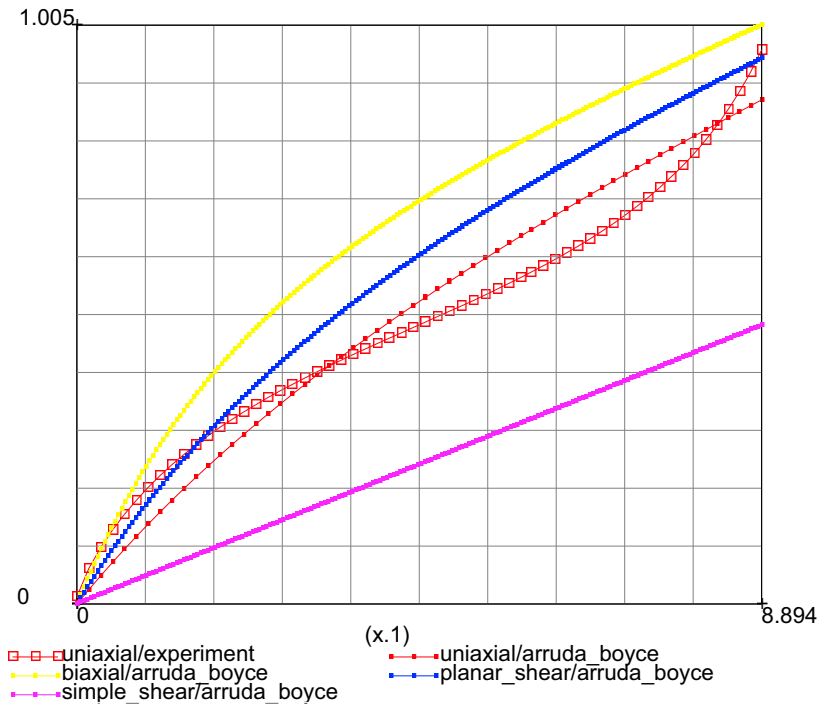


Figure 3.21-30 Arruda-Boyce Model only using Uniaxial Data – A Good Fit

For completeness, here is the Arruda-Boyce model using all strain states.

ARRUDA-BOYCE
 USE ALL DATA
 COMPUTE
 OK
 SCALE AXES

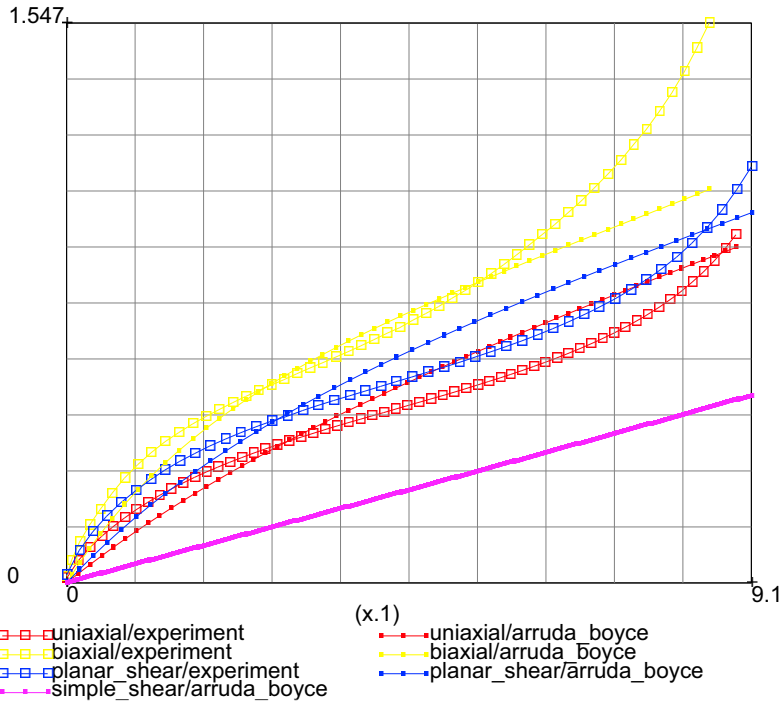


Figure 3.21-31 Arruda-Boyce Model only using All Data – A Good Fit

Let's suppose that the actual application was the inflation of a tube. The Mooney(2) using only uniaxial data would require a pressure of over 4 times that of the Arruda-Boyce model when the inflation strains are about 90%. There are several elastomeric material models that fall into three classes: phenomenological, principal stretch, and micro mechanical models such as the Arruda-Boyce and Gent models.

There are no good models, only good curve fits. In this case, a one constant Mooney would have worked fine. The important fact to keep in mind when fitting elastomeric material models to material data, is to watch the response of all strain states shown by the curve fitting in Mentat. If there are large variations in the curves such as in [Figure 3.21-28](#), don't use it. Don't obtain good agreement, only from one strain state, rather seek a balanced response to the three different deformation states because your application will have all strain states present. That balanced response usually looks just like the data in the three basic strain states shown in [Figure 3.21-25](#).

Input Files

The files below are on your [delivery media](#) or they can be downloaded by your web browser by clicking the links (file names) below.

File	Description
Tube Crush	
rubber_a.proc	Mentat procedure file for quads
rubber_b.proc	Mentat procedure file for triangles
rubber_c.proc	Mentat procedure file for quads + multi mode fit
uniaxial.data	xy data for rubber_c.proc
biaxial.data	xy data for rubber_c.proc
planar_shear.data	xy data for rubber_c.proc
s3c.proc	adds closed cavity to above
elastol.mud	Mentat model file read by s3c.proc
Arch	
s9.proc	Mentat procedure file for arch
Curve Fitting	
AllTestData.xls	Test data for all modes
uniaxial.data	Uniaxial data taken from the 18th load cycle
planar_shear.data	Planar shear data taken from the 18th load cycle
biaxial.data	Biaxial data taken from the 18th load cycle
NonlinearFEAofElastomers.pdf	White paper on FEA of elastomers

3.22 Modeling of General Rigid Body Links using RBE2/RBE3

- Chapter Overview 1320
- Cylindrical Shell 1320
- Results 1328
- Input Files 1329

Chapter Overview

This chapter describes the use of RBE2 link in Marc (The term RBE2 signifies Rigid Body element type 2 as defined in Nastran). RBE2 link is a general multi-point constraint that connect a set of tied nodes with a reference node. The link between the tied nodes and the reference node is generally based on a rigid link connection, but some of the degrees of freedom of the tied nodes can be set free (unrestrained). If all degrees of freedom are constrained, then it results in tying type 80 behavior. To show the flexibility of the RBE2 in simulating general rigid body link, a simple cylindrical shell model is used as a case study.

Cylindrical Shell

The example described here is a cylindrical shell with a coarse mesh. The boundary condition on the one end of the cylinder is fully clamped. On the other end of the cylinder, an RBE2 link is defined to connect all nodes at the cylindrical edge with a retained node. The tied nodes have TRANSFORMATION data in which the axial (third direction) is parallel with the x-axis (In this case, it is not actually necessary to define TRANSFORMATION on the tied nodes). The tied nodes are constrained only in the axial direction while the other degrees of freedom are free. The axial direction is updated following the rotation of the retained node.

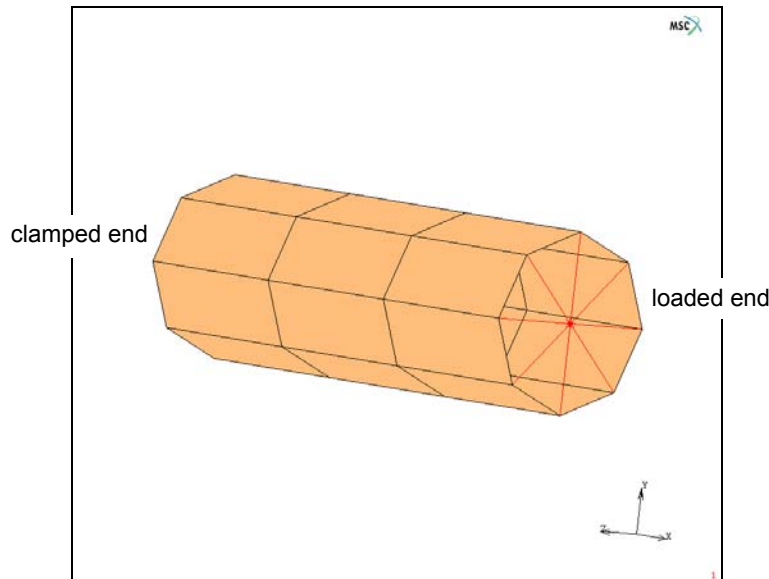


Figure 3.22-1 FE Mesh of a Cylindrical Shell

Mesh Generation

The length and the radius of the cylinder are 90 mm and 15 mm, respectively. The mesh is generated by first defining one 1-D element. This element is then divided into three elements. With the cylindrical model, the elements are

expanded about the x-axis. The final mesh can be seen in [Figure 3.22-1](#). Two extra nodes are also created. They are needed to define TRANSFORMATION and RBE2 Link.

```
MESH GENERATION
  NODES ADD
    0 15 0
    90 15 0
  FILL
  ELEMENT CLASS
    LINE(2)
  RETURN
  ELEMS ADD
    1
    2
  SUBDIVIDE
    DIVISIONS
      3 1 1
    ELEMENTS
      1 #
  RETURN
  SWEEP
    NODES
      ALL EXIST.
    RETURN
  EXPAND
    ROTATION ANGLES
      45 0 0
    REPETITIONS
      8
    ELEMENTS
      ALL EXIST
      FILL
      RETURN
  SWEEP
    NODES
      ALL EXIST.
    RETURN
```

```
RENUMBER
  NODES
    ALL EXIST.
  ELEMENTS
    ALL EXIST.
  RETURN (twice)
NODES ADD
  0 0 0
  90 0 0
RETURN
```

Boundary Conditions

One end of the cylinder is clamped, meaning all degrees of freedom are fixed. The other end of the cylinder is constrained to move as general rigid body to be defined later using RBE2 Link. The nodes that belong to this end will have local coordinate system defined with TRANSFORMATION. The retained node of the RBE2 Link are fixed in z-direction, about the x-, and y-direction. As loading, this node is given 30° rotation about z-axis. The time history of the load is set by using a table that ramps from 0 to 30° in one second.

```
BOUNDARY CONDITIONS
  MECHANICAL
    NAME
      fixed
    FIXED DISPLACEMENT
      DISPLACEMENT X
        0
      DISPLACEMENT Y
        0
      DISPLACEMENT Z
        0
    ROTATION X
      0
    ROTATION Y
      0
    ROTATION Z
      0
  OK
```

```

NODES ADD
    1 11 10 9 8 7 6 5 #
NEW
NAME
    load
FIXED DISPLACEMENT
    DISPLACEMENT X
        0
    ROTATION X
        0
    ROTATION Y
        0
    ROTATION Z
        -30*PI/180
OK
TABLES
NEW TABLE: 1 INDEPENDENT VARIABLE
NAME
    time
TYPE
    time
ADD
    0 0 1 1
RETURN
FIXED DISPLACEMENT
    ROTATION Z: TABLE
    TABLE
        time
        OK (twice)
NODES ADD
    34 #
MAIN

```

Transformation

The local coordinate system of the tied nodes is defined using the CYLINDRICAL option in Mentat. In this case, the axial direction is chosen to be the same as the axial direction of the cylinder.

```
BOUNDARY CONDITIONS
  MECHANICAL
    TRANSFORMATION
      CYLINDRICAL
        0 0 0
        90 0 0
        2 18 17 16 15 14 13 12 #
      MAIN
```

Links

RBE2 link is defined along one edge of the cylinder. First, a reference node located at (90,0,0) is set. Second, the constrained degree of freedom is set to three according to the local coordinate system defined for the tied nodes. Third, the list of the tied nodes are set that have consistent TRANSFORMATION as defined in the second step. In this case, the axial displacement is the third degree of freedom.

```
LINKS
  RBE2'S
    NEW
      NODE (RETAINED)
        34
      DOF
        3
      ADD (TIED NODES)
        2 18 17 16 15 14 13 12 #
      MAIN
```

Material Properties

The material is elastoplastic with von Mises yield criteria and isotropic hardening parameter.

```
MATERIAL PROPERTIES
  NEW
    ISOTROPIC
```

```

        YOUNG'S MODULUS
            250000
        POISSONS_RATIO
            0.3
        ELASTIC-PLASTIC
            INITIAL YIELD STRESS
                1
            OK
TABLES
    NEW
        NAME
            plas
        TYPE
            eq_plastic_strain
        ADD
            0 500 1 3000
        FIT
    RETURN
    ISOTROPIC
        ELASTIC-PLASTIC
            YIELD STRESS: TABLE
                plas
            OK
    ELEMENTS ADD
        ALL EXIST.
    MAIN
    
```

Geometric Properties

The thickness of the cylinder is 3 mm.

```

    GEOMETRIC PROPERTIES
        NEW
            3-D
            SHELL
    
```

```
THICKNESS
3
OK
ELEMENTS ADD
ALL EXIST.
MAIN
```

Loadcases and Job Parameters

A quasi-static analysis will be performed. The convergence criteria are based both on residual forces and displacement increment.

```
LOADCASES
NEW
  MECHANICAL
    STATIC
      CONVERGENCE TESTING
        RESIDUALS AND DISPLACEMENTS
          INCLUDE MOMENTS
          INCLUDE ROTATIONS
          RELATIVE FORCE TOLERANCE
            0.005
          RELATIVE MOMENT TOLERANCE
            0.005
          RELATIVE DISPLACEMENT TOLERANCE
            0.01
          RELATIVE ROTATION TOLERANCE
            0.01
        OK
      # STEPS
        10
      OK
    MAIN
```

Save Job, and Run the Simulation

After saving the model, two jobs are defined either with or without LARGE DISP parameter. They are then submitted sequentially.

```
JOBS
  NEW
    NAME
      linear
    MECHANICAL
      SELECTED
        lcase1
    OK
  NEW
    NAME
      nonlinear
    MECHANICAL
      SELECTED
        lcase1
      SOLUTION OPTION
        LARGE DISPLACEMENT
    OK
  ELEMENT TYPES
    MECHANICAL
      3-D MEMBRANE/SHELL ELEMENT TYPES
      THIN SHELL: 139
    ALL: EXIST
  MAIN
JOBS
  PREV
  RUN
  SUBMIT
  NEXT
  RUN
  SUBMIT
```

Results

The deformed shape of the cylinder without and with LARGE DISP (large rotation) are shown in [Figure 3.22-2](#) and [Figure 3.22-3](#), respectively. From these figures, it is clearly seen the difference of ovalization **—** (red line) of the cylinder (where rotation is applied). The result using “large rotation” option shows ovalization about the z-axis as the major one while the “small rotation” the y-axis as the major one. This is known as the Bezier effect.

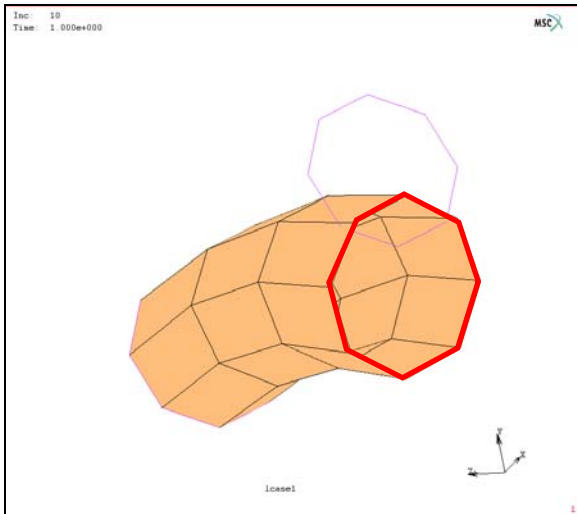


Figure 3.22-2 Deformed Shape without LARGE DISP

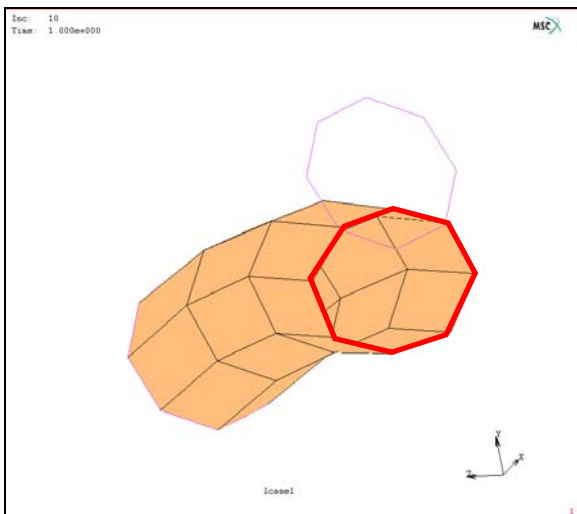


Figure 3.22-3 Deformed Shape with LARGE DISP

Input Files

The files below are on your [delivery media](#) or they can be downloaded by your web browser by clicking the links (file names) below.

File	Description
rbe2.proc	Mentat procedure file for quads

3.23 Cyclic Symmetry

- Chapter Overview 1332
- Pure Torsion 1333
- Mechanical Analysis of Friction Clutch 1336
- Coupled Analysis of Friction Clutch 1339
- Input Files 1344

Chapter Overview

A special set of tying constraints for continuum elements can be automatically generated by the Marc program to effectively analyze structures with a geometry and a loading varying periodically about a symmetry axis. Figure 3.23-1 shows an example where, on the left-hand side, the complete structure is given and, on the right-hand side, a sector to be modeled.

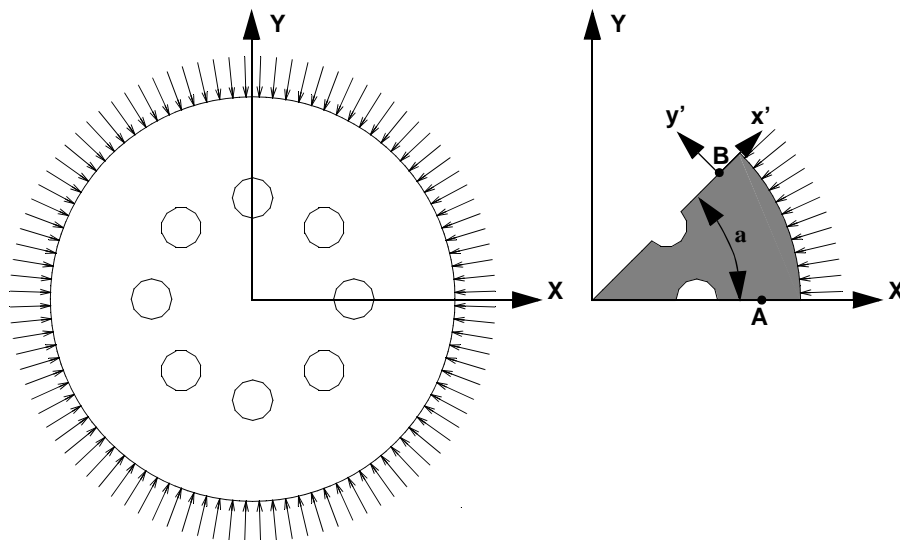


Figure 3.23-1 Cyclic Symmetric Structure: Complete Model (left) and Modeled Sector (right)

Looking at points A and B on this segment, the displacement vectors should fulfill:

$$u'_B = u_A \quad (3.23-1)$$

which can also be written as:

$$u_B = R u_A \quad (3.23-2)$$

where the transformation matrix R depends on the symmetry axis (which, in the example above, coincides with the global Z -axis) and the sector angle α (see Figure 3.23-1). In Marc, the input for the CYCLIC SYMMETRY option consists of the direction vector of the symmetry axis, a point on the symmetry axis and the sector angle α . The following items should be noted:

1. The meshes do not need to line up on both sides of a sector (for example, see Figure 3.23-1).

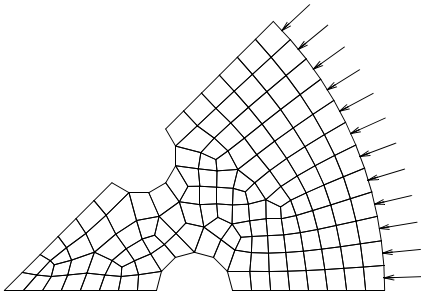


Figure 3.23-1 Finite Element Mesh for Cyclic Symmetric Structure with Different Mesh Densities on the Sector Sides

2. Any shape of the sector sides is allowed provided that upon rotating the sector $360/\alpha$ times about the symmetry axis over the sector angle α will result in the complete model.
3. The CYCLIC SYMMETRY option can be combined with the CONTACT option.
4. The CYCLIC SYMMETRY option can be combined with global remeshing.
5. In a coupled thermo-mechanical analysis, the temperature is forced to be cyclic symmetric ($T_A = T_B$ as in [Figure 3.23-1](#)).
6. A nodal point on the symmetry axis is automatically constrained in the plane perpendicular to the symmetry axis.
7. The possible rigid body motion about the symmetry axis can be automatically suppressed.
8. Cyclic Symmetry is valid for:
 - a. Only the continuum elements. However, the presence of beams and shells is allowed, but there is no connection of shells to shells, so the shell part can, for example, be a turbine blade and the volume part is the turbine rotor. The blade is connected to the rotor and if there are 20 blades, 1/20 of the rotor is modeled and one complete blade.
 - b. It can be used for static, dynamic, remeshing, and coupled analysis.
 - c. It cannot be used for pure heat transfer.
 - d. It can be used for all analysis involving contact.

The following cases will demonstrate many of the items above and show how this feature can save computer time by taking advantage of the symmetry of the structure.

Pure Torsion

A solid rubber cylinder will be subjected to a state of pure torsion by rotating the ends which are attached to rigid bodies. [Figure 3.23-2](#) shows the solid rubber cylinder (left) and its cyclic symmetry counterpart (right). The torsional stiffness of these two models will be compared to each other as well as the theoretical values.

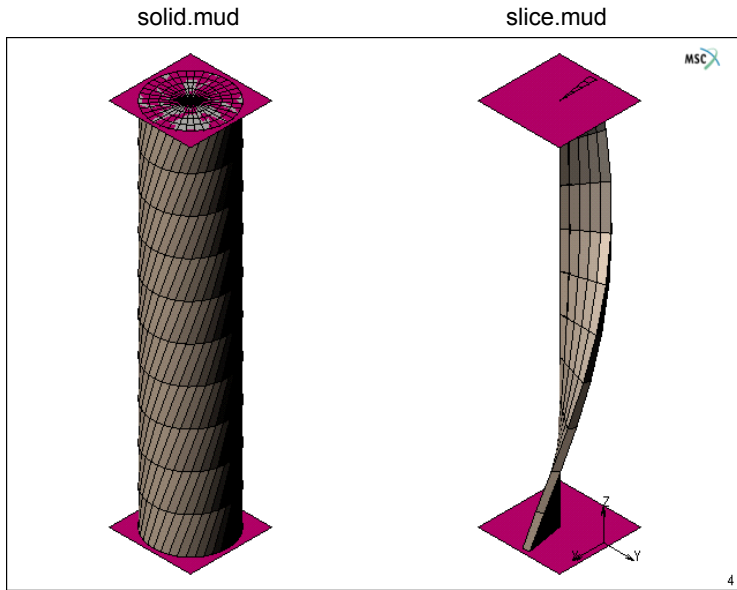


Figure 3.23-2 Model for Case 1 Pure Torsion

Procedure for Case 1: Build and run the cyclic symmetric model

The cylinder is 10 m in length and 1 m in radius. The ends are glued to the square rigid bodies shown in [Figure 3.23-2](#). The procedure here only focuses upon the cyclic symmetry feature and how it is implemented on the cyclic symmetry model called `slice.mud`.

FILES

OPEN

`slice.mud`

MAIN

You can now review the properties of this model. The mesh is just a 10° sector taken from the solid mesh (`solid.mud`). The material is a one constant Mooney with $C = 1$ [MPa] or a shear modulus G of 2 [MPa]. The contact option identifies the deformable slice with the two rigid bodies at each end, where the top rigid body will rotate about the Z-axis one revolution. The contact table option is used to glue the rigid bodies to the end of the deformable slice with a large separation force. The cyclic symmetry option is located in the JOB menu, to go there simply enter:

JOBS

MECHANICAL

CYCLIC SYMMETRY

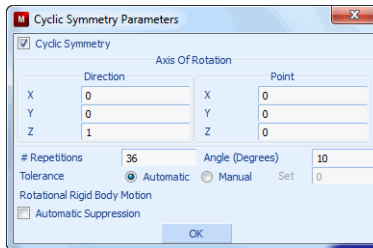


Figure 3.23-3 Cyclic Symmetry Menu

Here we see that the axis of symmetry is defined by a direction and a point, with 36 repetitions. This completes the definition of cyclic symmetry, now let's run the two models and compare the results.

After running both models, the stresses are shown in [Table 2.23-1](#) where both models have nearly the same maximum equivalent Cauchy stress and are within 4% of theory.

Table 2.23-1 Results for Pure Torsion

Model	Stress [MPa]	CPU Times [sec.]
Solid	2.054	1462.70
Slice	2.058	10.65
Theory	1.976	NA

Clearly, the slice runs faster taking advantage of the cyclic symmetry of the structure. [Figure 3.23-4](#) plots the torque versus rotation of the two cylinders. Since the stresses in the slice model are integrated over a smaller (1/36 times) area, remember that the external forces need to be multiplied by the number of repetitions, 36, which is plotted in [Figure 3.23-4](#) with the diamond symbol.

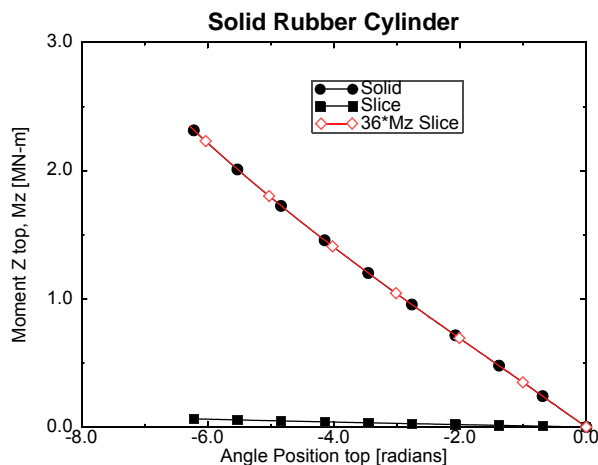


Figure 3.23-4 Torque versus Rotation

Mechanical Analysis of Friction Clutch

Figure 3.23-5 shows an elastomeric friction clutch between two rigid surfaces that will compress the clutch then rotate relative to each other. This causes the clutch to rotate until the friction forces are overcome by the torsional moment in the clutch, and the clutch will slip, limiting the torque transmitted to the smaller rigid surface. The ribs on the clutch are to help keep the clutch in better contact with the drive.

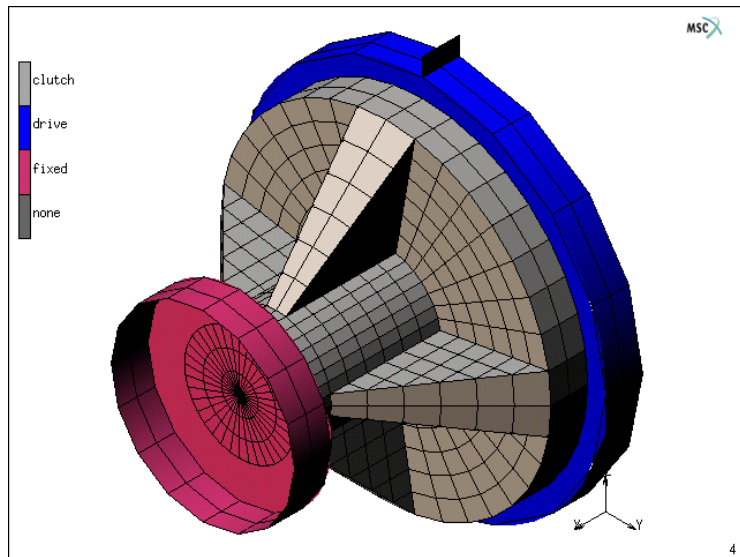


Figure 3.23-5 Full Model for Case 2 Friction Clutch, clutch_rib.mud

The material properties are the same as in the previous case and two loadcases are used to compress then rotate the clutch. The later loadcase uses variable time stepping. Friction coefficients of 0.5 are entered in contact table and Coulomb friction is used. Cyclic symmetry is used as in the previous case; however, two slices are used with four repetitions as shown in Figure 3.23-6 and Figure 3.23-7. Also, the axis of cyclic symmetry is now the X-axis.

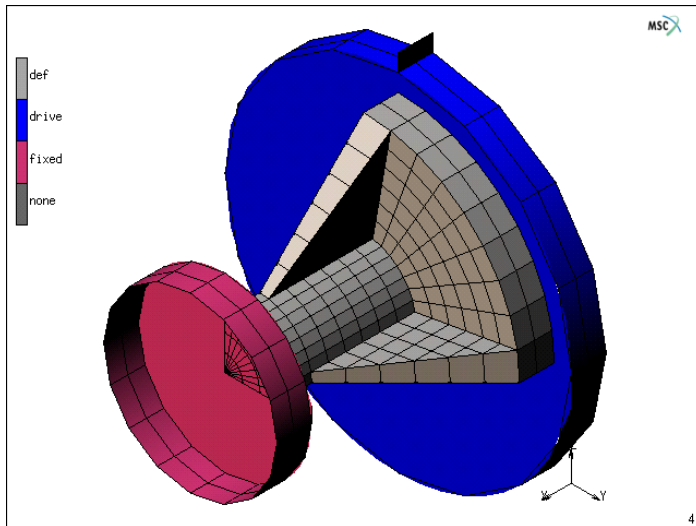


Figure 3.23-6 Cyclic Symmetry for Case 2 Friction Clutch, `clutch_rib_slice1.mud`

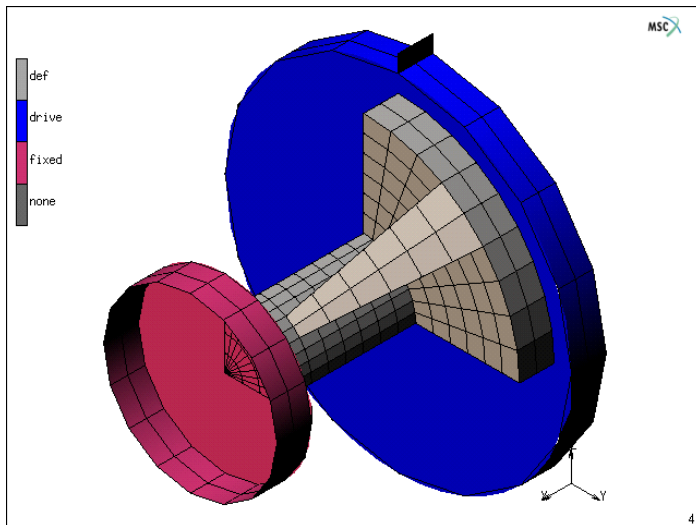


Figure 3.23-7 Cyclic Symmetry for Case 2 Friction Clutch, `clutch_rib_slice2.mud`

You may view any of the models by opening either, `clutch_rib.mud`, `clutch_rib_slice1.mud`, or `clutch_rib_slice2.mud`. The results are shown in [Figure 3.23-8](#).

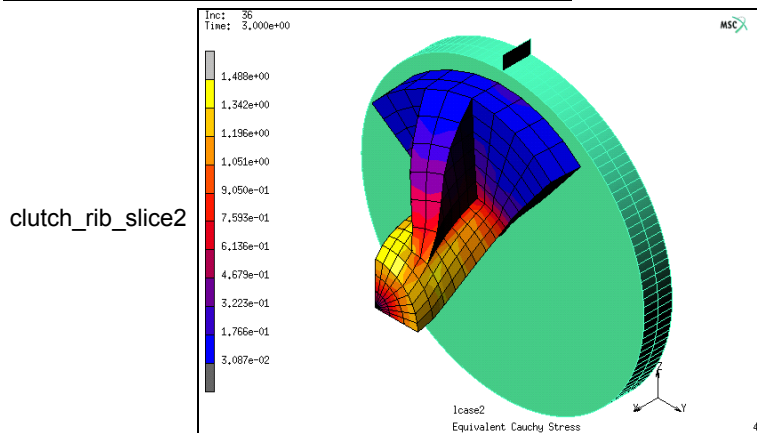
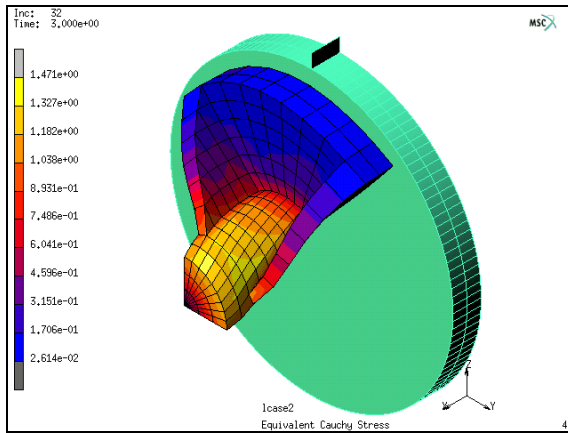
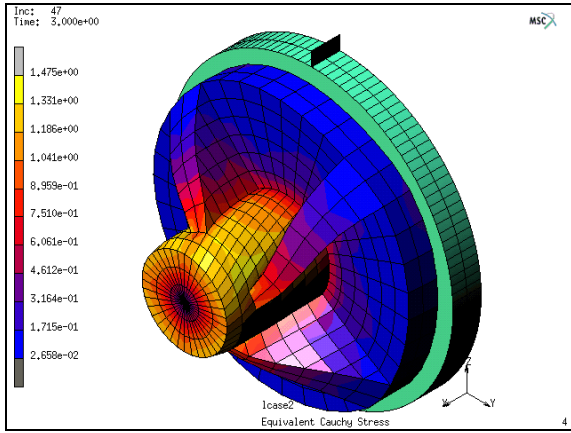


Figure 3.23-8 Stress Contours for Case 2 Friction Clutch Models

After running the three models, the stresses are shown in [Table 2.23-2](#) where all models have nearly the same maximum equivalent Cauchy stress. The run times for the slices are, of course, lower than the full model, and the run times for the slices are slightly different because of slightly different meshes.

Table 2.23-2 Results for Friction Clutch

Model	Stress [MPa]	CPU Times [sec.]
clutch_rib.mud	1.475	440.84
clutch_rib_slice1.mud	1.471	55.35
clutch_rib_slice2.mud	1.488	64.80

The stresses above are reported at the maximum torque condition, after the clutch slips around 1.5 radians of angular motion as shown in [Figure 3.23-9](#). Again as in Case 1, the external forces in the slice models must be multiplied by the number of cyclic repetitions, four, as clearly shown in [Figure 3.23-9](#).

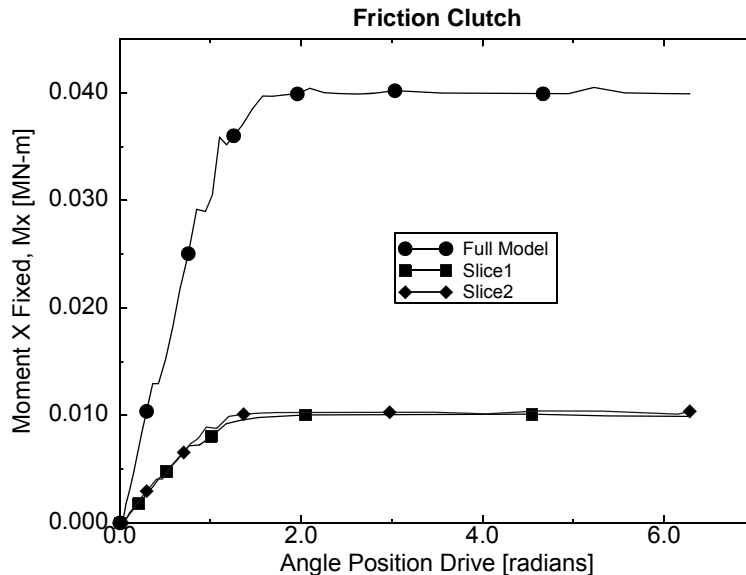


Figure 3.23-9 Wall Torque versus Drive Angular Position

Coupled Analysis of Friction Clutch

[Figure 3.23-10](#) shows a coupled friction clutch between two rigid surfaces that compress the clutch then rotate relative to each other. This causes the clutch to rotate until the friction forces are overcome by the torsional moment in the clutch, and the clutch slips limiting the torque transmitted to the smaller rigid surface. In addition, as the larger rigid surface rotates, friction generates thermal energy that heats up the clutch. Heat flows out the sink where the smaller end of the clutch is held at a fixed temperature. As in Case 2, the full model will also be modeled using cyclic symmetry.

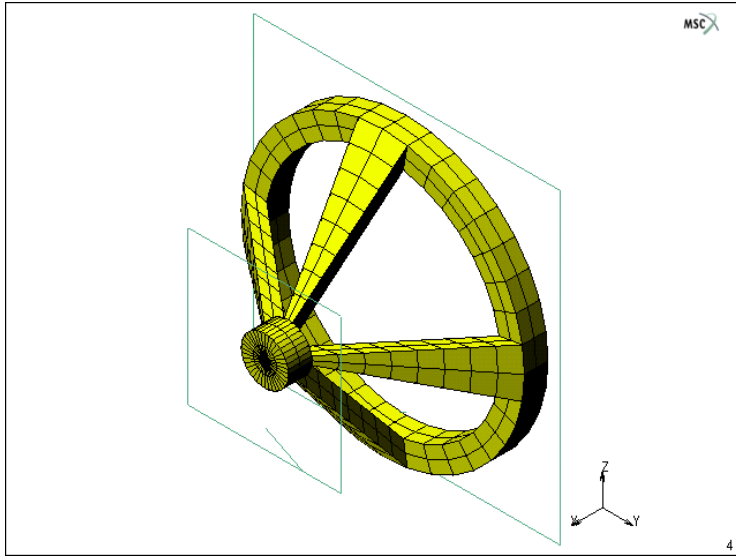


Figure 3.23-10 Full Model for Case 3 Coupled Friction Clutch, coupled.mud

The material properties are for steel and two loadcases are used to compress then rotate the clutch. Both loadcases use fixed time stepping. A friction coefficient of 0.2 is entered in contact table and Coulomb friction is used. Cyclic symmetry is used as in the previous case; however, two slices are used with four repetitions as shown in Figures 3.23-11 and 3.23-12. Also, the axis of cyclic symmetry is now the X-axis.

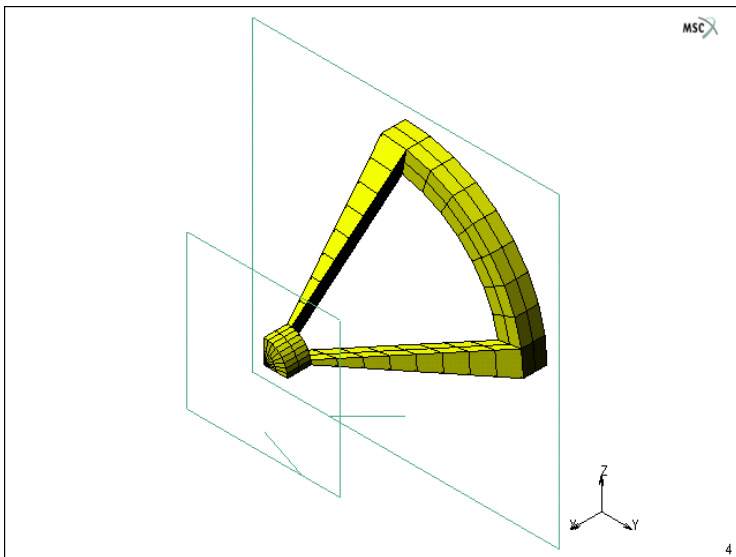


Figure 3.23-11 Cyclic Symmetry for Case 3 Friction Clutch, coupled_slice1.mud

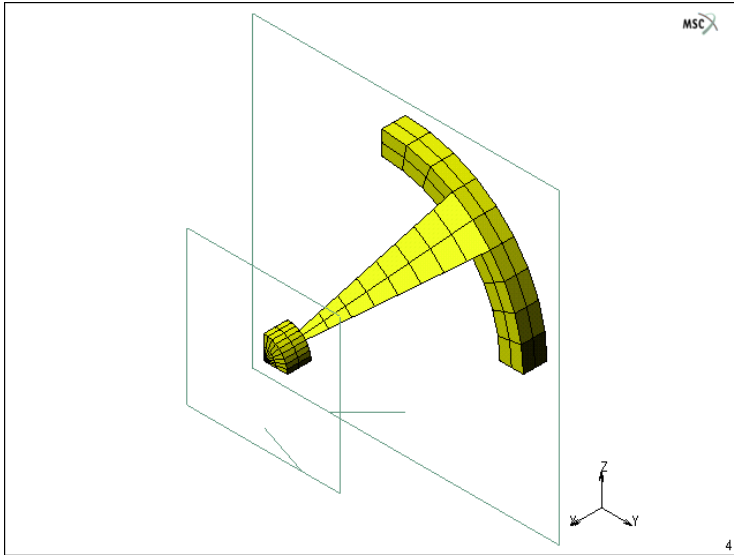


Figure 3.23-12 Cyclic Symmetry for Case 3 Friction Clutch, `coupled_slice2.mud`

You may view any of the models by opening either, `coupled.mud`, `coupled_slice1.mud`, or `coupled_slice2.mud`. The results are shown in [Figure 3.23-13](#).

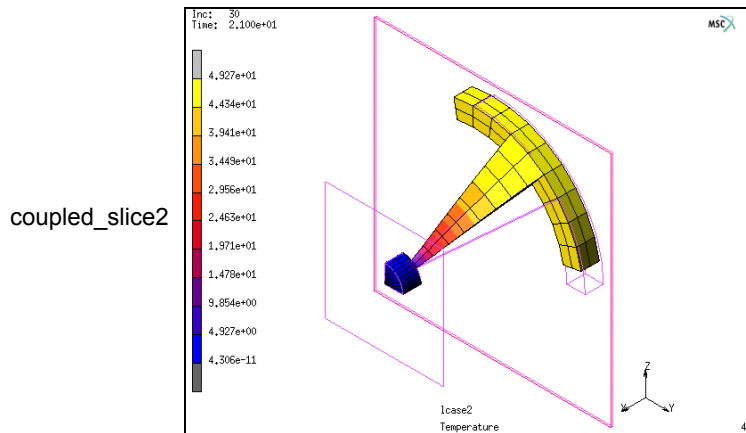
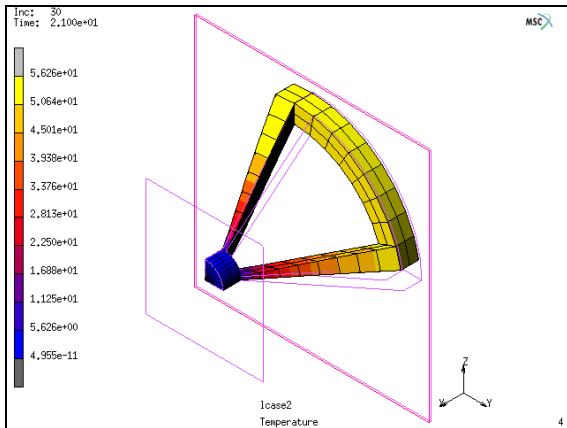
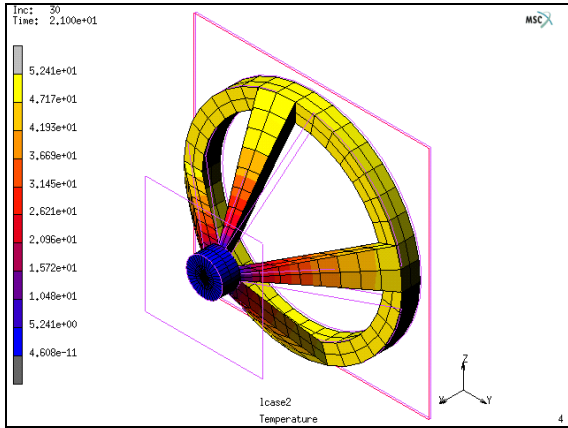


Figure 3.23-13 Stress Contours for Case 3 Friction Clutch Models

After running the three models, the results are shown in [Table 2.23-3](#) where all models have nearly the same maximum temperature. The run times for the slices are, of course, lower than the full model, and the run times for the slices are slightly different because of slightly different meshes.

Table 2.23-3 Results for Coupled Friction Clutch

Model	Temperature [F]	CPU Times [sec.]
coupled.mud	52.41	152.31
coupled_slice1.mud	56.26	55.25
coupled_slice2.mud	49.27	32.35

The above temperatures are reported at the maximum torque condition, after the clutch slips around 2 radians of angular motion as shown in [Figure 3.23-14](#). Again as in the other Cases, the external forces in the slice models must be multiplied by the number of cyclic repetitions as clearly shown in [Figure 3.23-14](#).

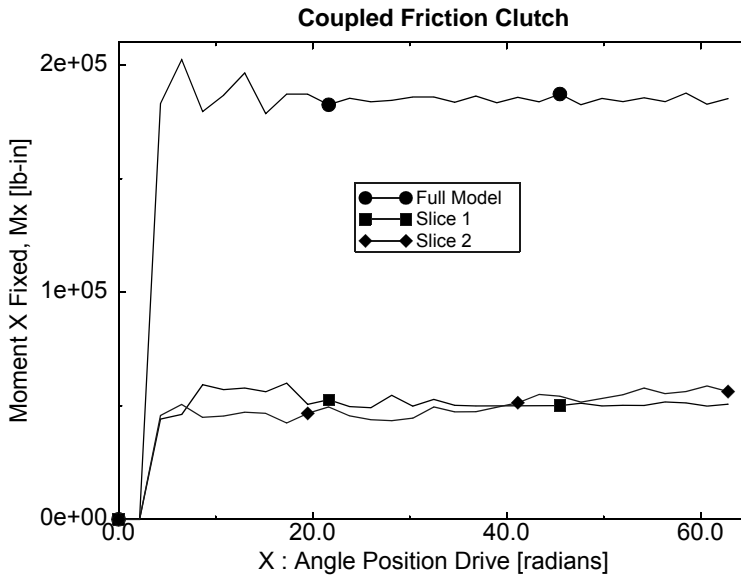


Figure 3.23-14 Wall Torque versus Drive Angular Position

As in the other Cases, the external forces, as well as the thermal energy in the slice models, must be multiplied by the number of cyclic repetitions as clearly shown in [Figure 3.23-15](#) that plots the total thermal energy history of the three models.

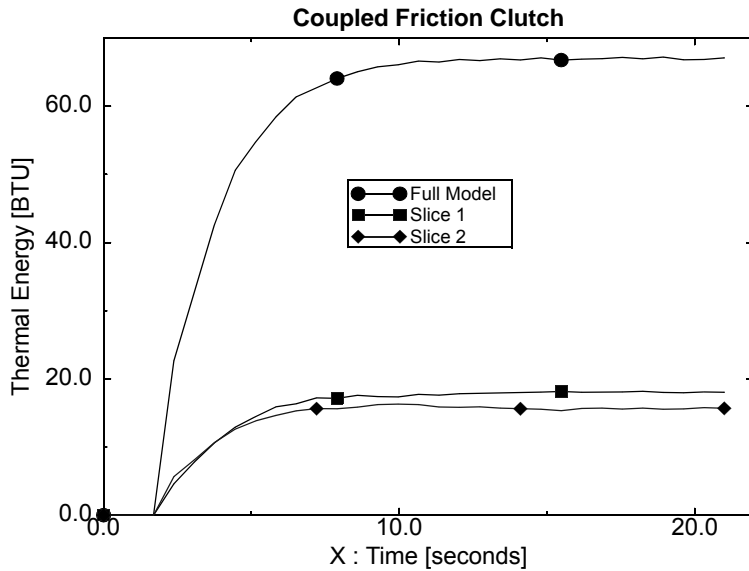


Figure 3.23-15 Thermal Energy History

The thermal energy is automatically placed on the post file. For more information on this and other energy calculations see Chapter 6.8.

Input Files

The files below are on your [delivery media](#) or they can be downloaded by your web browser by clicking the links (file names) below.

File	Description
clutch_rib.mud	Mentat model file
clutch_rib_slice1.mud	Mentat model file
clutch_rib_slice2.mud	Mentat model file
coupled.mud	Mentat model file
coupled_slice1.mud	Mentat model file
coupled_slice2.mud	Mentat model file
slice.mud	Mentat model file
solid.mud	Mentat model file

3.24 Axisymmetric to 3-D Analysis

- Chapter Overview 1346
- Simulation of a Rubber Bushing 1346
- Automobile Tire Modeling with Rebar Elements 1359
- Analysis of a Rubber Cylinder using Remeshing 1366
- Input Files 1374

Chapter Overview

In many cases, it is possible to begin the numerical simulations as a two-dimensional axisymmetric problem even though the final problem is fully three-dimensional. This is advantageous because of the large computational savings. For this to be useful, the first stage of the problem should be truly axisymmetric. The second stage of the problem can be fully three-dimensional. This chapter demonstrates the use of the data transfer capabilities of Marc from an axisymmetric analysis to a fully three-dimensional analysis. For this purpose, three problems will be analyzed: the first one is simulation of a rubber bushing problem, the second one is an analysis of an automobile tire using rebar elements, and the third is an analysis of a rubber cylinder with remeshing.

The transfer of data from an axisymmetric simulation to a 3-D simulation involves two parts. The first is the generation of a new mesh, which may be either equally or unequally distributed along the circumference. The second part involves reading the post file from the first simulation containing the state variables (displacements, temperatures, etc.) and stress/strains etc. using the PRE STATE option in Marc.

Simulation of a Rubber Bushing

Simulation of a rubber bushing in this chapter contains two major parts: Axisymmetric analysis and 3-D analysis. The detailed description of the two parts will be presented. The substeps at the beginning of the second part involving mesh expansion and data transfer from axisymmetric to 3-D cases will be highlighted.

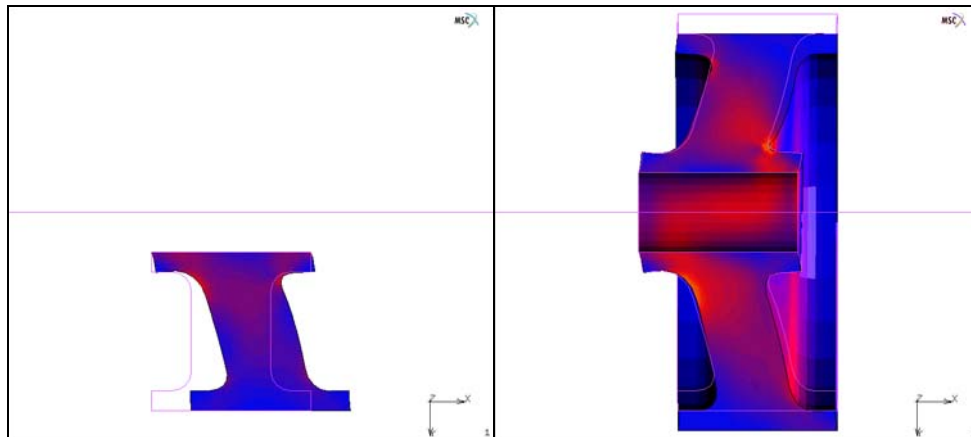


Figure 3.24-1 2-D Axisymmetric to 3-D

Description of Problem

A rubber bushing with an outer diameter of 10 cm and an inner diameter of 2 cm is considered. The length of the rubber bushing is 8 cm. Both outside and inside surfaces are glued to two steel tubes with corresponding diameters so that the shape of the surfaces keeps unchanged during deformation.

Two load sequences are applied:

In the first load step, a displacement of 2 cm along the symmetric axis is applied to the outside steel tube within ten equal increments. During this load step, the deformation is purely axisymmetric and therefore an axisymmetric analysis is performed. Afterwards, the outside steel tube moves 1 cm in the radial (Y) direction within five equal increments.

In the second step, the problem becomes fully three-dimensional, and a 3-D analysis is performed.

The 4-node isoparametric quadrilateral axisymmetric element 10 is used in the axisymmetric run. The corresponding element type in 3-D run is 7 which is the 8-node isoparametric hexahedral element. In the analysis, both element types are based on mixed formulations and formulated on the deformed (updated) configuration. This is activated using ELASTICITY,2 in the parameter options.

The rubber bushing is modeled using Mooney constitutive model. The material parameters are given as $C_1=8.0 \text{ N/cm}^2$ and $C_2=2.0 \text{ N/cm}^2$.

Axisymmetric Analysis

This is a standard axisymmetric analysis. Except for specifying proper output to the post file, requested in 3-D analysis, nothing is special. Therefore, the description in the step is not in great details.

Model Generation

Model generation contains geometry definition, mesh generation using advancing front mesher, clear geometry, and clean mesh.

MESH GENERATION

pts ADD

0 2 0

8 2 0

0 10 0

8 10 0

0 9 0

1 9 0

7 9 0

8 9 0

0 3 0

1 3 0

7 3 0

8 3 0

2 8 0

2 4 0

6 8 0

6 4 0

crvs ADD

1 2 3 4 5 6 7 8 9 10 11 12 13 14 15 16 3 5 4 8 9 1 12 2

CURVE TYPE

ARCS CENTER/POINT/POINT

RETURN

crvs ADD

1 8 0

2 8 0

1 9 0

1 4 0

1 3 0

2 4 0

7 4 0

6 4 0

7 3 0

7 8 0

7 9 0

6 8 0

AUTOMESH

CURVE DIVISIONS

FIXED AVG LENGTH

AVG LENGTH

0.4

APPLY CURVE DIVISIONS

all: EXIST.

RETURN

2D PLANAR MESHING

QUADRILATERALS (ADV FRNT): QUAD MESH!

all: EXIST.

RETURN

RETURN

CLEAR GEOM

SWEEP

ALL

RETURN
RENUMBER
ALL
RETURN

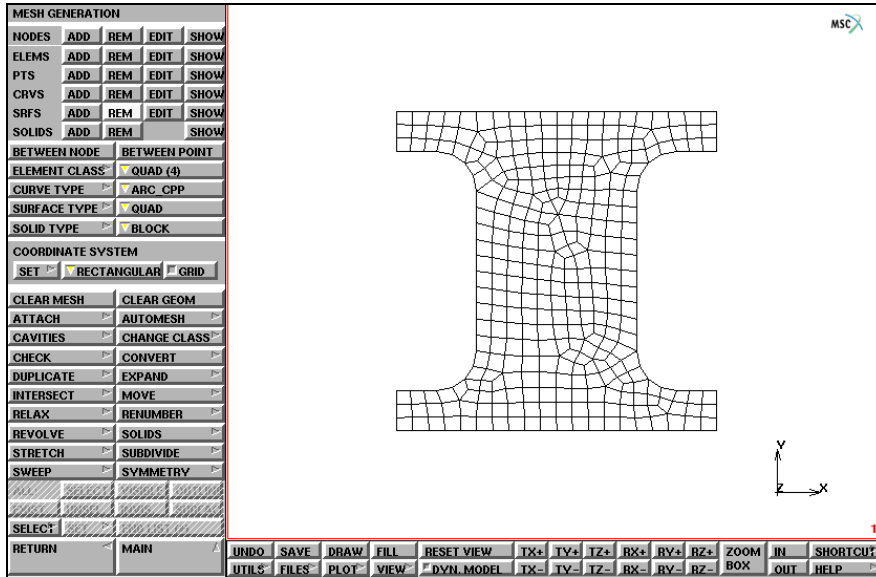


Figure 3.24-2 FE-Mesh for Axisymmetric Analysis

Boundary Conditions

Defining boundary conditions includes defining node sets, defining tables, and adding boundary conditions.

```

SELECT
  METHOD
  BOX
  RETURN
  NODES
    -1 11 9.99 11 -1 1
  nodes STORE
    outer
  OK
all: SELECT.
CLEAR SELECT

```

```

      NODES
        -1 11 1 2.01 -1 1
      nodes STORE
        inner
        OK
      all: SELECT.
      CLEAR SELECT
      MAIN
BOUNDARY CONDITIONS
  NEW
  MECHANICAL
    TABLE
      NEW
      1 INDEPENDENT VARIABLE
      TYPE
        time
        OK
      ADD
        0 0 2 2 3 2
      NEW
      1 INDEPENDENT VARIABLE
      TYPE
        time
        OK
      ADD
        0 0 2 0 3 1
      RETURN
  FIXED DISPLACEMENT
    DISPLACEMENT X: (on)
    DISPLACEMENT Y: (on)
    DISPLACEMENT X TABLE
      table1
    DISPLACEMENT Y TABLE
      table2
    OK
  nodes ADD
```

```
outer
NEW
FIXED DISPLACEMENT
  DISPLACEMENT X (on)
  DISPLACEMENT Y (on)
OK
nodes ADD
  inner
MAIN
```

Material Properties

```
MATERIAL PROPERTIES
MORE
MOONEY
  C10
    8
  C01
    2
OK
elements ADD
all: EXIST.
MAIN
```

Load Steps and Job Parameters

A displacement of 2 cm along the symmetric axis is applied to the outside steel tube within 10 equal increments; element type 10 is used; updated Lagrangian formulation is used for elasticity; stress tensor, strain tensor, and equivalent von Mises stress are written into the post file.

Note: To use Updated Lagrangian formulation for elasticity, stress and strain tensors must be written into the post file. In the second part involving the 3-D analysis, both stress and strain tensors are needed.

```
LOADCASE
NEW
MECHANICAL
  STATIC
  TOTAL LOADCASE TIME
  2
```

FIXED PARAMETERS

STEPS

10

OK

CONVERGENCE TESTING

RELATIVE FORCE TOLERANCE

0.01

OK (twice)

MAIN

JOBS

ELEMENT TYPES

MECHANICAL

AXISYMMETRIC SOLID

10

OK

all: EXIST.

RETURN

RETURN

NEW

MECHANICAL

LCASE1

ANALYSIS DIMENS: AXISYMMETRIC

ANALYSIS OPTIONS

ELASTICITY PROCEDURE: LARGE STRAIN - TOTAL LAGRANGE

ELASTICITY PROCEDURE: LARGE STRAIN - UPDATED LAGRANGE

OK

JOB RESULTS

available element tensors

Stress

Strain

available element scalars

Equivalent Von Mises Stress

OK (twice)

Save Model, Run Job, and View Results

```

FILE
  SAVE AS
    rubberbushing_axi.mud
  OK
  RETURN
RUN
  SUBMIT 1
  MONITOR
  OK
MAIN
RESULTS
  OPEN DEFAULT
  DEF ONLY
  CONTOUR BAND
  SCALAR
    Equivalent Von Mises Stress
  OK
  MONITOR
  CLOSE
  RETURN
    
```

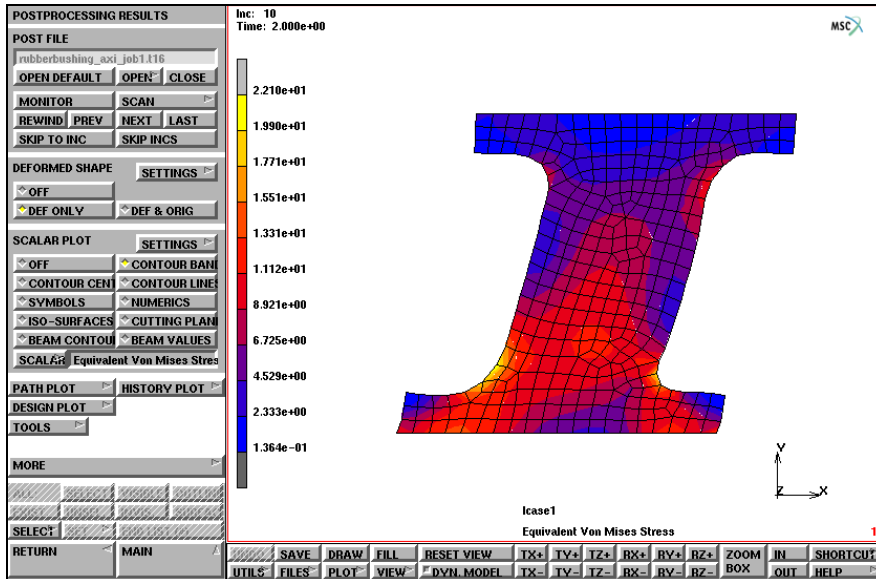


Figure 3.24-3 Deformed Mesh and Distribution of Equivalent von Mises Stress at Increment 10 of Axisymmetric Analysis

3-D Analysis

After the axisymmetric analysis, a fully 3-D analysis is performed based on the results from the axisymmetric analysis. Before the 3-D analysis, a corresponding 3-D mesh on the basis of the axisymmetric mesh and data transfer from the axisymmetric mesh to the 3-D mesh are required. Compared to the other part of the job, which is more or less standard, a more detailed description is given for the axisymmetric to 3-D mesh expansion and the data transfer.

Mesh Expansion and Data Transfer from Axisymmetric to 3-D

Mesh expansion from axisymmetric to 3-D is based on AXISYMMETRIC MODEL TO 3D option under MESH GENERATION -> EXPAND. Rotation angles and number of repetitions must be defined. To shift load table curve, the time at which the analysis will continue in a fully 3-D manner must be defined. See *Marc Volume A: Theory and User Information* for detailed description of the shift of load table curves.

Data transfer from axisymmetric to 3-D is based on option AXISYMMETRIC TO 3D under INITIAL CONDITIONS-> MECHANICAL. Both stress and strain tensors must be transferred when the updated Lagrangian formulation for elasticity is used; displacement is moved by default; the name of post file from the completed axisymmetric analysis must be given.

In this example, the 2-D section is uniformly expanded over 180° in 12 sections. The time is set to 2, which is the time at the end of the previous analysis.

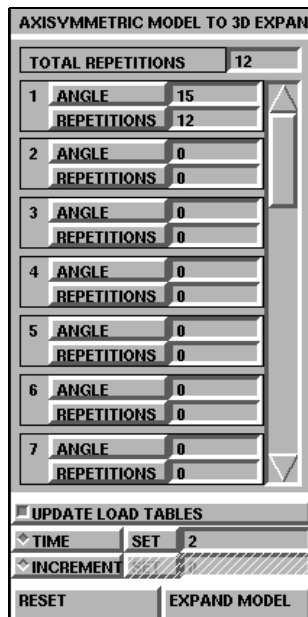


Figure 3.24-4 AXISYMMETRIC MODEL TO 3D Submenu

MESH GENERATION
 EXPAND
 AXISYMMETRIC MODEL TO 3D
 ANGLE
 15
 REPETITIONS
 12
 TIME SET
 2
 EXPAND MODEL
 MAIN
 INITIAL CONDITIONS
 MECHANICAL
 AXISYMMETRIC TO 3D
 POST FILE
 rubberbushing_axi_job1.t16
 OK
 MAIN

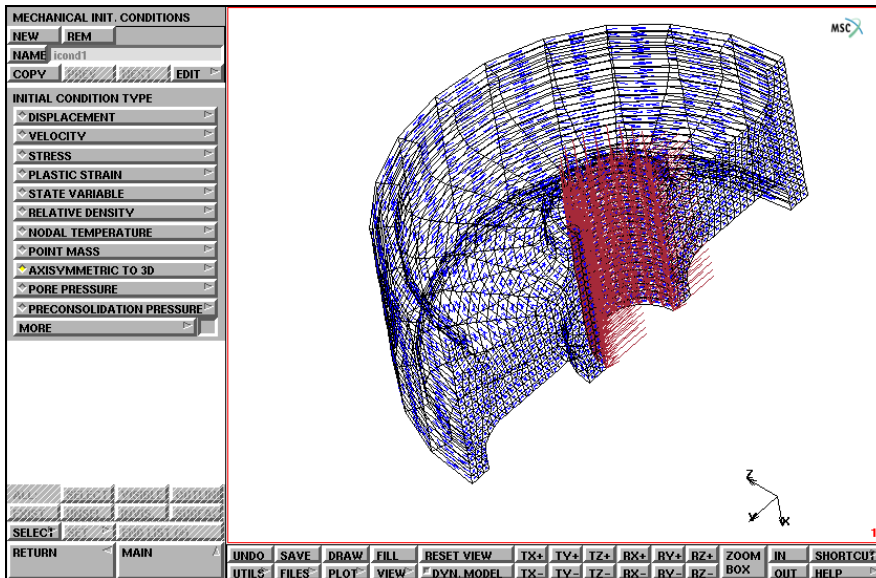


Figure 3.24-5 FE-Mesh for 3-D Analysis

Boundary Conditions

Define boundary conditions including defining node sets, adding boundary conditions as well as symmetric conditions. Note that axisymmetric to 3-D model expansion automatically generates a set of local coordinate systems if there are any y or z (radial or circumferential) boundary conditions on any nodes from the 2-D model. The set of local coordinate systems are not needed in this job and will be removed.

BOUNDARY CONDITIONS

MECHANICAL

SELECT

METHOD

BOX

RETURN

NODES

-20 20 -20 20 -1 0.01

nodes STORE

symm

OK

all: SELECT.

CLEAR SELECT

RETURN

TRANSFORMS

UNTRANSFORM

all: EXIST.

RETURN

NEW

FIXED DISPLACEMENT

DISPLACEMENT Z

(on)

OK

nodes ADD

symm

outer

inner

MAIN

Load Steps and Job Parameters

The outside steel tube moves 1 cm in the radial (Y) direction within five equal increments; element type 7 is used; updated Lagrangian formulation is used for elasticity; and equivalent von Mises stress is written into the post file.

```
LOADCASE
  MECHANICAL
    STATIC
      LOADS
        ON: apply3
        OK
      TOTAL LOADCASE TIME
        1
      # STEPS
        5
      OK
    MAIN
  JOBS
    MECHANICAL
      INITIAL LOADS
        ON: apply3
        ON: icondl
        OK (twice)
```

Save Model, Run Job, and View Results

Save the model with a different name to avoid overwriting the existing axisymmetric mode.

```
FILE
  SAVE AS
    rubberbushing_3d.mud
  OK
  RETURN
RUN
  SUBMIT 1
  MONITOR
  OK
MAIN
RESULTS
  OPEN DEFAULT
  DEF ONLY
  CONTOUR BAND
  SCALAR
    Equivalent Von Mises Stress
  OK
  MONITOR
```

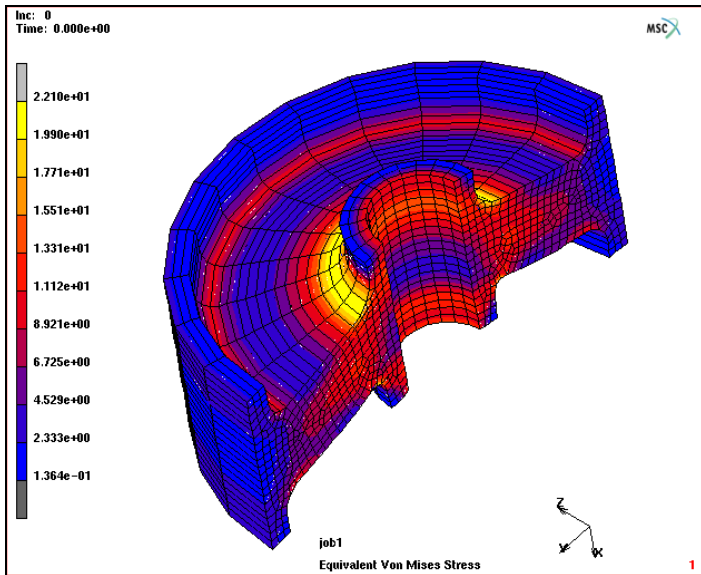


Figure 3.24-6 Deformed Mesh and Distribution of Equivalent von Mises Stress at Beginning of 3-D Analysis

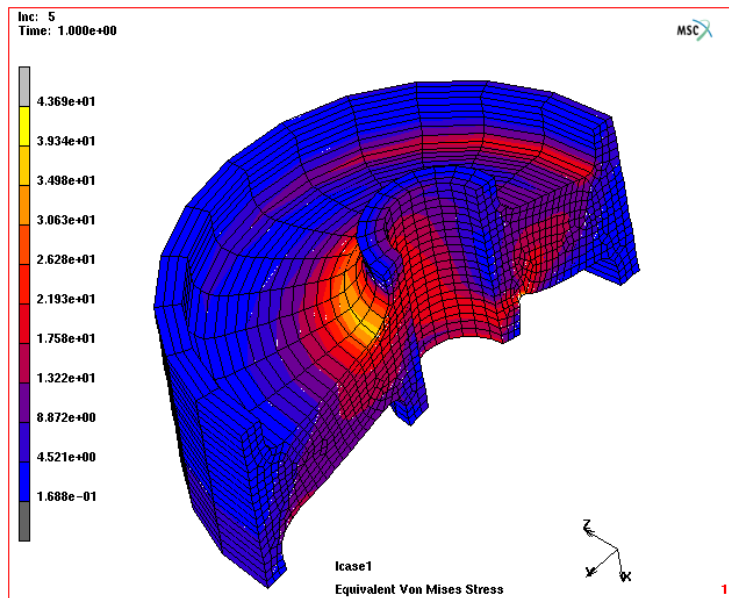


Figure 3.24-7 Deformed Mesh and Distribution of Equivalent von Mises Stress at Increment 5 of 3-D Analysis

Automobile Tire Modeling with Rebar Elements

A 3-D finite element analysis of automobile tires is complicated because of the complex structure of tires which are made of several types of rubber reinforced with cord layers and a steel bead. This problem demonstrates the use of Axisymmetric to 3-D data transfer capability for rebar elements.

Description of Problem

An automobile tire with a smooth tread, denoted as 195/65R15, is analyzed. The model consists of five different rebar layers with different materials and three types of rubber. See `tire2d.mud` for detailed information of the model including the finite element discretization of the cross-section, the material properties, and the rebar locations.

The analysis includes the numerical simulation of three stages:

- mounting the tire on the wheel,
- inflating the tire up to 2.0 bar, and
- pressing it against a road surface.

During the first two stages, the deformation is purely axisymmetric and, therefore, an axisymmetric analysis is performed. The simulation of tire mounting on the wheel is carried out using ten equal increments. Afterwards, the inflation pressure is applied with ten more equal increments. The 2-D model (mesh along with loads and boundary conditions) is then expanded to 3-D for further analysis. In the third stage, the tire contacts with the road surface. A total movement of 25 mm of the tire against the load surface is applied using the AUTO STEP option and the analysis is completed after ten increments. The analysis steps are summarized in [Figure 3.24-8](#).

The element types 10 and 144 are used in the axisymmetric run. The corresponding 3D element types are 7 and 146. ELASTICITY,2 is used to activate updated Lagrangian formulation.

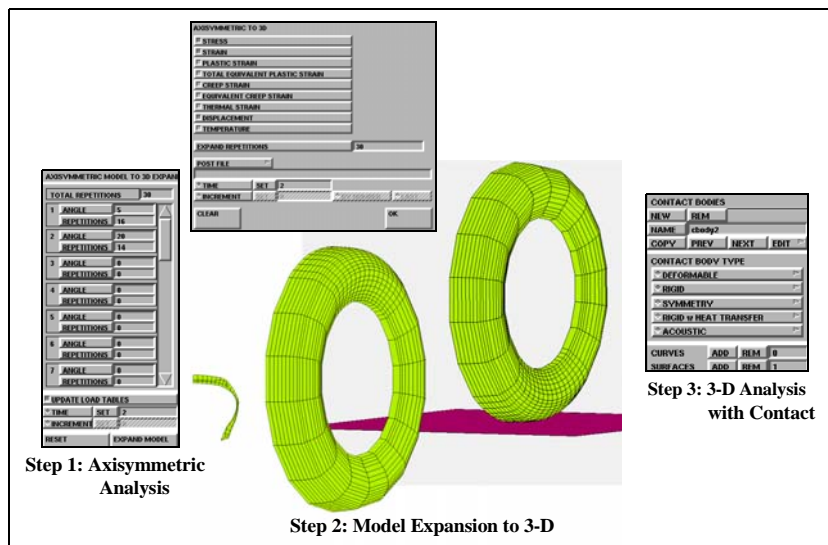


Figure 3.24-8 Data Transfer from Axisymmetric to 3-D Analysis

Axisymmetric Analysis

This is a standard axisymmetric analysis. No details will be given in this step. The analysis will be performed based on a completed `tire2d.mud` file. Examine sets `rebar1` and `rebar2` under MATERIAL PROPERTIES-> LAYERED MATERIALS-> NEW REBARS for rebar definitions.

```
FILES
  OPEN
    tire2d.mud
  OK
MAIN
JOBS
  RUN
    RESET
    SUBMIT 1
    MONITOR
  OK
TOP
RESULTS
  OPEN DEFAULT
  DEF & ORIG
  MONITOR
  CLOSE
MAIN
```

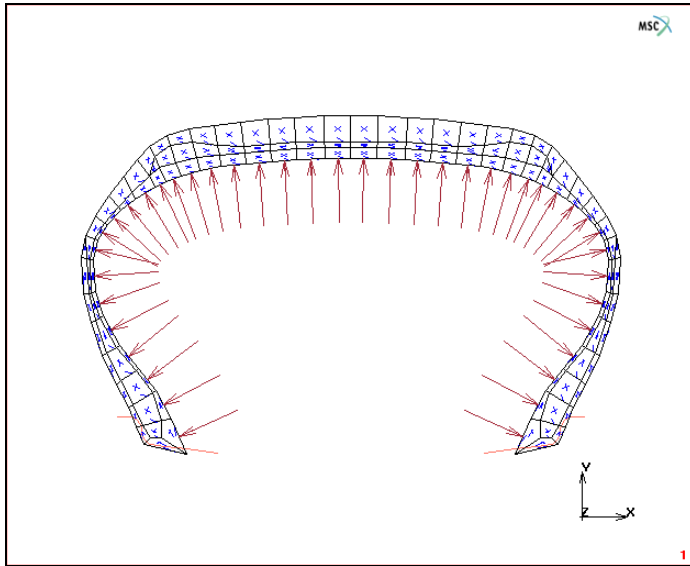



Figure 3.24-9 Axisymmetric Finite Element Mesh

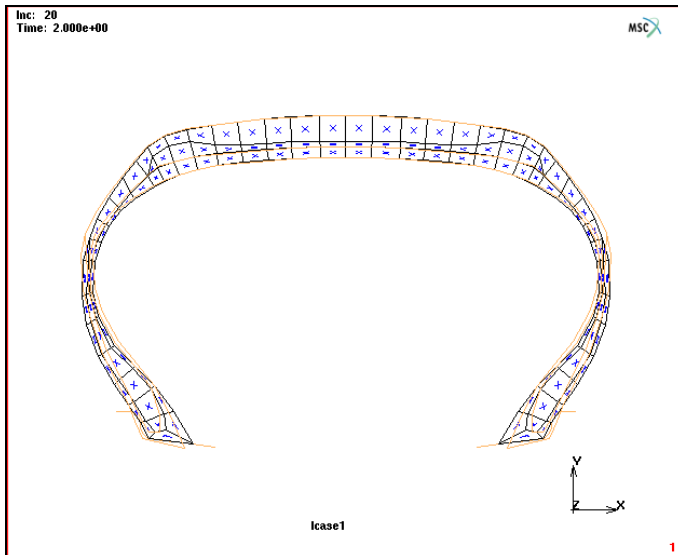


Figure 3.24-10 Deformed and Undeformed Meshes after Tire Inflation

3-D Analysis

Based on the results from the axisymmetric analysis, a fully 3-D analysis will be performed for the third stage – tire contact against the road surface. Before the 3-D analysis, a corresponding 3-D mesh on the basis of the axisymmetric

mesh and the data transfer from the axisymmetric to 3-D cases are required. The mesh in the area of contact and its vicinity should be finer.

Mesh Expansion and Data Transfer from Axisymmetric to 3-D

Before the mesh expansion and data transfer, part of boundary conditions, which are no longer useful in 3-D case, should be removed. It includes the symmetric condition and the load to mount the tire into the wheel.

Mesh expansion from axisymmetric to 3-D is based on AXISYMMETRIC MODEL TO 3D option under MESH GENERATION-> EXPAND. Rotation angles and number of repetitions must be defined. Non-equal spaced mesh expansion is used in the problem to form a relatively finer mesh in the contact area and its vicinity. Load table curve is shifted in order to properly include the load applied in axisymmetric analysis on the 3-D model. The shift time at which the analysis will continue in a fully 3-D manner must be defined.

The model of the rigid road surface is input in a separate `tire_rigid.mud` file.

Data transfer from axisymmetric to 3-D is based on option AXISYMMETRIC TO 3D under INITIAL CONDITIONS-> MECHANICAL. Both stress and strain tensors must be transferred once updated Lagrangian formulation for elasticity is used; displacement is transferred by default; the name of the post file from the completed axisymmetric analysis must be defined.

```
BOUNDARY CONDITIONS
    NEXT
    REM
    NEXT
    REM
    NEXT
    REM
MAIN
MESH GENERATION
    EXPAND
        AXISYMMETRIC MODEL TO 3D
            1 ANGLE
                28
            1 REPETITIONS
                5
            2 ANGLE
                5
            2 REPETITIONS
                16
            3 ANGLE
                28
            3 REPETITIONS
                5
```

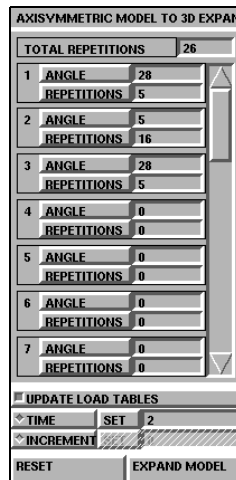


Figure 3.24-11 AXISMETRIC MODEL TO 3D with 3 Angles and Repetitions

```
3 REPETITIONS
  5
TIME SET
  2
EXPAND MODEL
MAIN
FILES
  MERGE
    tire_rigid.mud
  OK
  MAIN
INITIAL CONDITIONS
  MECHANICAL
  AXISYMMETRIC TO 3D
  POST FILE
    tire2d_job1.t16
  OK
  MAIN
```

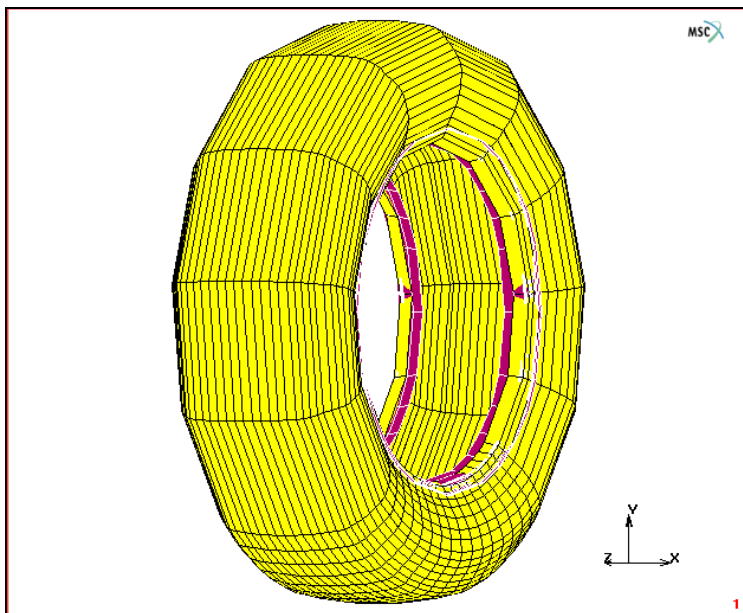


Figure 3.24-12 FE-Mesh for 3-D Analysis

New Contact Definition

Add the rigid surface as a new contact body and define moving velocity for the body.

```
CONTACT
  CONTACT BODIES
    NEW
      surfaces ADD
        3
      #
    RIGID
      VELOCITY
        VELOCITY Y
          1
        OK (twice)
    MAIN
```

Loadcases, Job Parameters, and Results

The rigid road surface moves 25 mm toward the tire. AUTO STEP option is used.

Initial condition *icond1* must be set on in defining job parameters. Advanced contact option to control separation is used. Before submit the job, save the model with a different name to avoid overwriting the axisymmetric model.

```
LOADCASES
  MECHANICAL
    STATIC
      TOTAL LOADCASE TIME
        25
      MULTI-CRITERIA
        OK
    MAIN
JOBS
  MECHANICAL
    INITIAL LOADS
      ON: icond1
      OK
    CONTACT CONTROL
      ADVANCED CONTACT CONTROL
```

SEPARATION INCREMENT NEXT
SEPARATION CHATTERING
SUPPRESSED
OK (thrice)

FILES
SAVE AS
tire3d.mud
OK
RETURN

RUN
RESET
SUBMIT 1
MONITOR
OK

MAIN

RESULTS
OPEN DEFAULT
DEF & ORIG
MONITOR

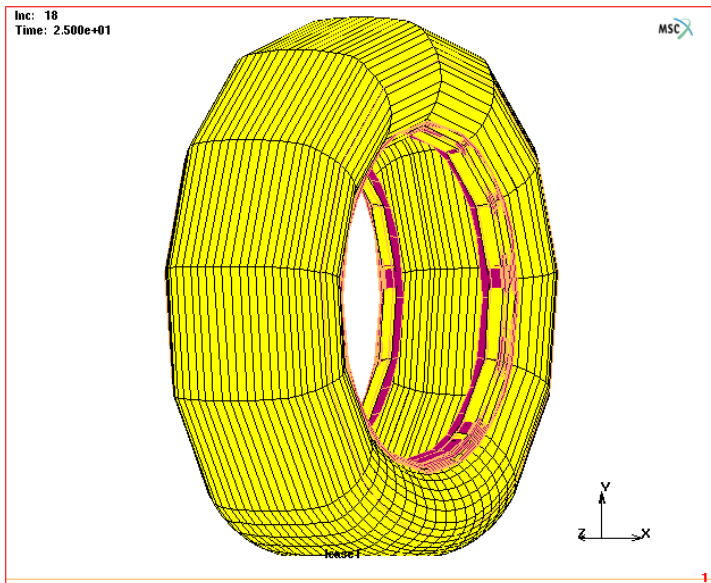


Figure 3.24-13 Deformed Tire Model

Analysis of a Rubber Cylinder using Remeshing

This problem is created to demonstrate the application of axisymmetric to 3-D data transfer with remeshing. The procedure to perform an analysis involving axisymmetric to 3-D data transfer with remeshing requires the use of the post file with manual application of loads and boundary conditions as opposed to jobs without a remeshing which can use a model file to simplify the application of loads and boundary conditions in 3-D.

Description of Problem

A rubber cylinder with an inner radius of 0.2 and an outer radius of 0.5 is considered. The length of the rubber cylinder is 0.6. Both ends of the cylinder are glued to two flat rigid surface. Two load sequences are applied. In the first load case, a displacement of 0.2 along the negative symmetric axis direction is applied to the right side rigid surface within 10 equal increments. During this load case, the deformation is purely axisymmetric and, therefore, an axisymmetric analysis is performed. Two global remeshing steps are applied at increments 4 and 8, respectively. Afterwards, the right side steel surface moves 0.15 in the radial (Y) direction within 10 increments. In the second step, the problem becomes fully three-dimensional, and a 3-D analysis is performed.

The element type 10 is used in the axisymmetric run. The corresponding 3-D element type is 7. ELASTICITY,2 is used to activate updated Lagrangian formulation.

The rubber cylinder is modeled using Mooney constitutive model. The material properties are given as $C_1=8$ and $C_2=2$.

Axisymmetric Analysis

This is a standard axisymmetric analysis. No details are given in this step. The analysis is performed based on a completed `crubcy12d.mud` file.

```
FILES
  OPEN
    rubcy12d.mud
  OK
MAIN
JOBS
  RUN
    RESET
    SUBMIT 1
    MONITOR
  OK
TOP
RESULTS
```

OPEN DEFAULT
DEF ONLY
SCALAR
 Equivalent Von Mises Stress
 OK
CONTOUR BAND
MONITOR

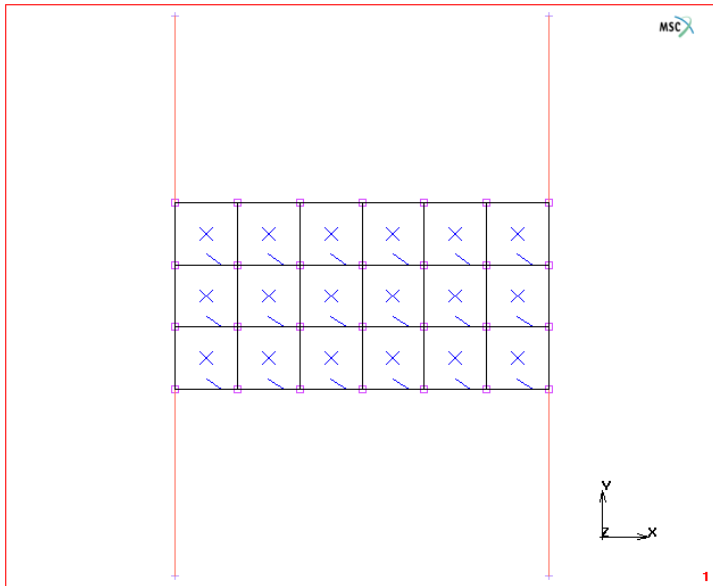


Figure 3.24-14 Axisymmetric Finite Element Mesh

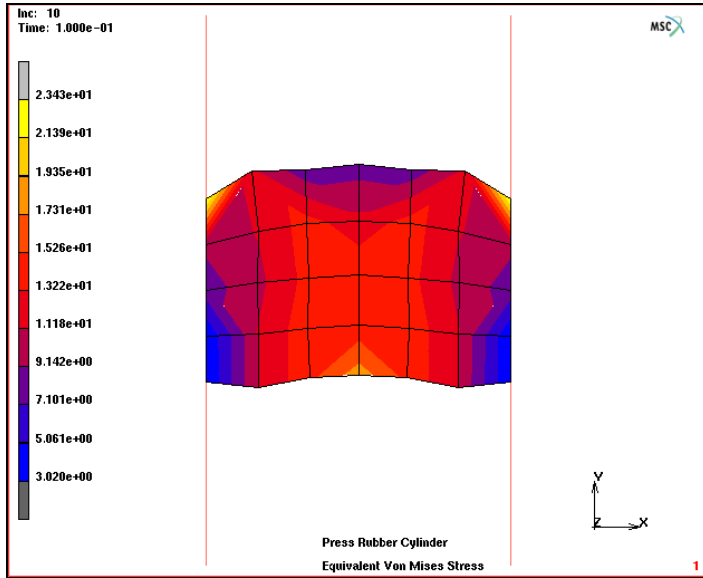


Figure 3.24-15 Deformed Meshes after Pressing the Rubber Cylinder

3-D Analysis

Based on the results from the axisymmetric analysis, a fully 3-D analysis is performed for the second part – the rubber cylinder subjected to shear deformation. Before the 3-D analysis, a corresponding 3-D mesh on the basis of the axisymmetric mesh and the data transfer from the axisymmetric to 3-D cases are required.

Because of the use of global remeshing techniques in the axisymmetric analysis, the numerical results obtained at the end of the axisymmetric analysis are no longer based on the original mesh at the beginning of the analysis, but the new mesh at the end of the analysis. The standard mesh expansion procedure based on Mentat mud file, used in the previous two problems, is not used in problems involving PRE STATE and remeshing. The user must use the post file to obtain the deformed/updated mesh and expand it to form the 3-D mesh. Please note that all data which is not available in the post file have to be redefined manually.

Mesh Expansion and Data Transfer from Axisymmetric to 3-D

Before the mesh expansion, a rezoning step is needed, based on the post file of the axisymmetric analysis to obtain the deformed axisymmetric mesh. Please also save the new model as `rubcy13d.mud` and clean the Mentat database.

Mesh expansion from axisymmetric to 3-D is based on `AXISYMMETRIC MODEL TO 3D` option under `MESH GENERATION->EXPAND`. Rotation angles and number of repetitions must be defined. The time at which the analysis will continue in a fully 3-D manner must be defined.

Data transfer from axisymmetric to 3-D is based on option `AXISYMMETRIC TO 3D` under `INITIAL CONDITIONS->MECHANICAL`. Both stress and strain tensors must be moved once updated Lagrangian formulation for elasticity is

used; displacement should not be moved since the mesh is already in deformed configuration; the name of the post file from the completed axisymmetric analysis must be defined.

```
DEFORMED SHAPE: OFF
SCALAR PLOT: OFF
TOOLS
  REZONE MESH
  FILES
    SAVE AS
      rubcy13d.mud
    OK
  NEW
    OK
  OPEN
      rubcy13d.mud
    OK
  MAIN
MESH GENERATION
  EXPAND
    AXISYMMETRIC MODEL TO 3D
      1 ANGLE
        15
      1 REPETITIONS
        24
    TIME SET
      0.2
    EXPAND MODEL
  MAIN
INITIAL CONDITIONS
  MECHANICAL
  AXISYMMETRIC TO 3D
  DISPLACEMENT
  POST FILE
      rubcy12d_job1.t16
    OK
  MAIN
```

(off)

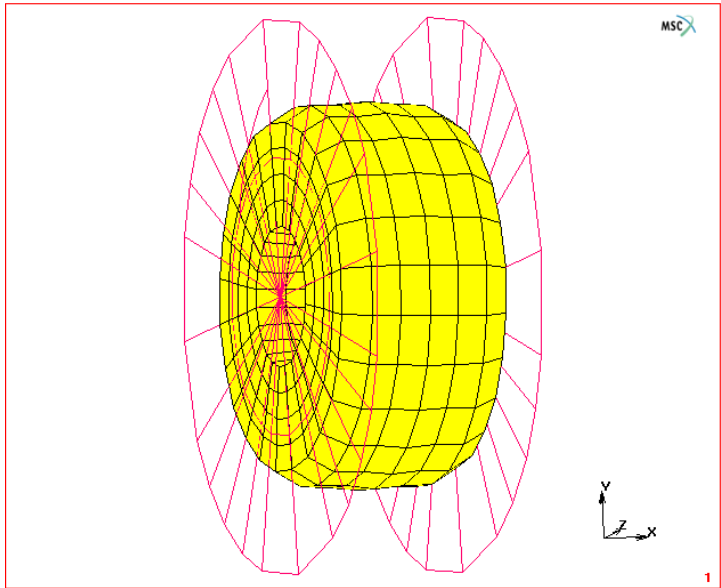


Figure 3.24-16 FE-Mesh for 3-D Analysis

Material Properties

MATERIAL PROPERTIES

MORE

MOONEY

C10

8

C01

2

OK

elements ADD

all: EXIST.

MAIN

New Contact Definition

Add the rigid surface as new contact bodies and define moving velocity for the body.

```
CONTACT
  CONTACT BODIES
    NEXT contact body left
    surfaces ADD
      1
      #
    NEXT contact body right
    surfaces ADD
      2
      #
  RIGID
    VELOCITY PARAMETERS
      VELOCITY Y
        -1
      OK (twice)
  RETURN
  CONTACT TABLES
    NEW
    PROPERTIES
      ALL ENTRIES - CONTACT TYPE: GLUE
    OK
  MAIN
```

Loadcases, Job Parameters, and Results

The right side rigid surface moves 0.15 toward -Y direction in ten increments. Initial condition *icond1* must be set on in defining job parameters.

```
LOADCASES
  MECHANICAL
    STATIC
      CONTACT
        CONTACT TABLE
          ctable1
        OK
```

CONVERGENCE TESTING

RELATIVE FORCE TOLERANCE

0.05

OK

TOTAL LOADCASE TIME

0.15

STEPS

10

OK

MAIN

JOBS

MECHANICAL

LOADCASES: lcase1

INITIAL LOADS

ON: icond1

OK

CONTACT CONTROL

INITIAL CONTACT

CONTACT TABLE

ctable1

OK (twice)

ANALYSIS OPTION

rubber elasticity procedure - LARGE STRAIN - TOTAL LAGRANGE

rubber elasticity procedure - LARGE STRAIN - UPDATED LAGRANGE

OK

JOB RESULTS

available element tensors

Stress

Total Strain

available element scalars

Equivalent Von Mises Stress

OK (twice)

SAVE

RUN
 RESET
 SUBMIT 1
 MONITOR
 OK
MAIN
RESULTS
 OPEN DEFAULT
 DEF ONLY
 CONTOUR BAND
 MONITOR

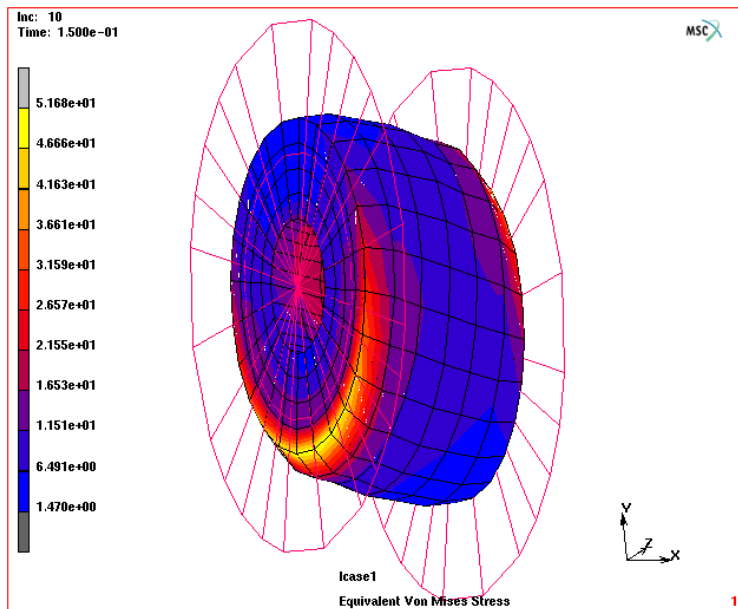


Figure 3.24-17 Deformed Rubber Cylinder after Shear Deformation

Input Files

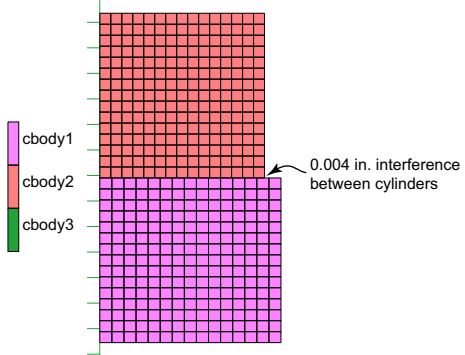
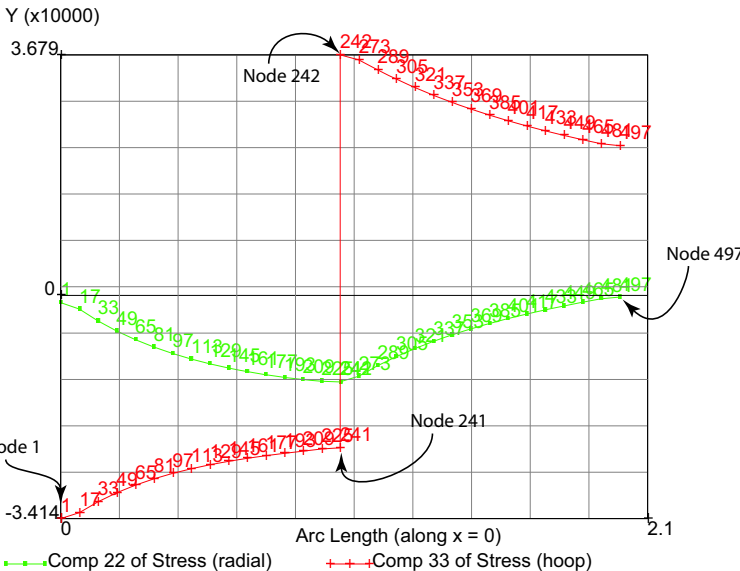
The files below are on your [delivery media](#) or they can be downloaded by your web browser by clicking the links (file names) below.

File	Description
Rubber Bushing Axisymmetric to 3D	
axisym_3d_a.proc	Mentat procedure file
Automotive Tire	
tire.proc	Mentat procedure file
tire_rigid.mud	Mentat model file
tire2d.mud	Mentat model file
Rubber Cylinder with Remeshing	
rubcyl2d.proc	Mentat procedure file
rubcyl2d.mud	Mentat model file

3.25 Interference Fit

- Summary 1376
- Run Job and View Results 1381
- Input Files 1383

Summary

Title	Interference fit
Problem features	Two concentric cylinders are fitted together with an interference fit
Geometry	
Material properties	$E = 3 \times 10^7$ Psi, $\nu = 0.3$
Analysis type	Static
Boundary conditions	Symmetry with interference fit that causes stress
Element type	Axisymmetric element type 116
FE results	<p>Stresses generated by interference fit (radial and hoop components shown)</p> 

Two concentric cylinders are fitted together with an interference fit using the contact option and rigid bodies of symmetry. Each cylinder is modeled using axisymmetric elements.

Since the inner cylinder is slightly bigger than the hole in the outer cylinder, stresses are generated as the fit is finished. The hoop stress of the outer cylinder goes into tension, and the hoop stress of the inner cylinder goes into compression.

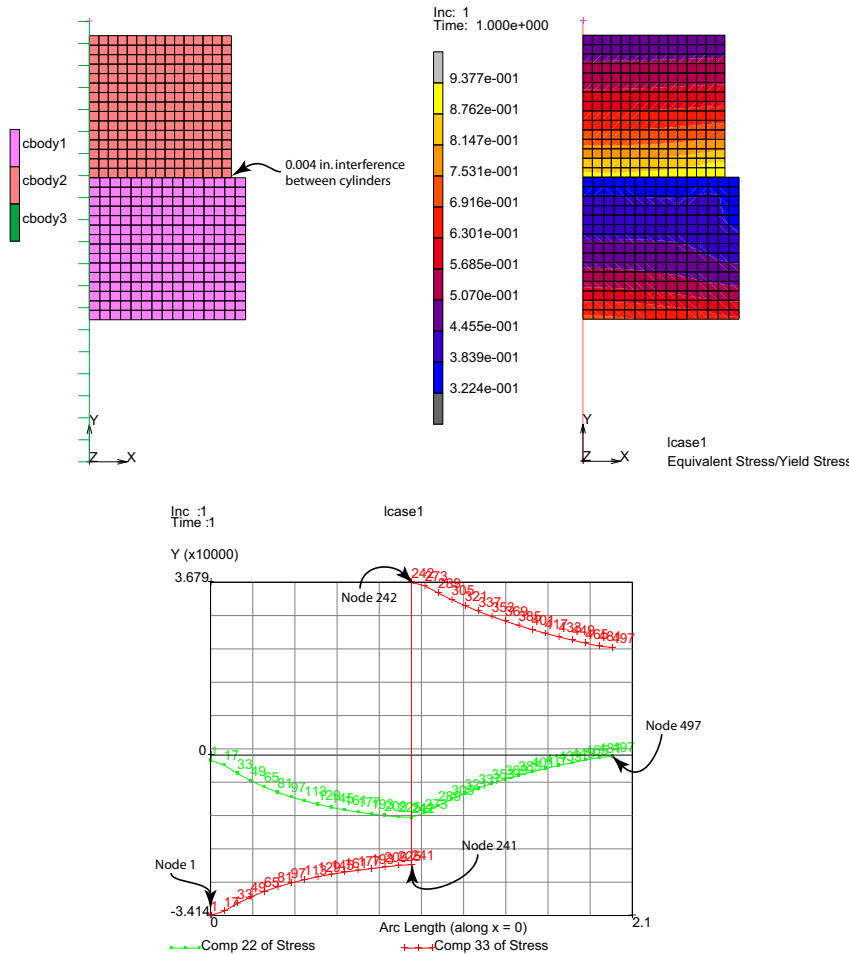
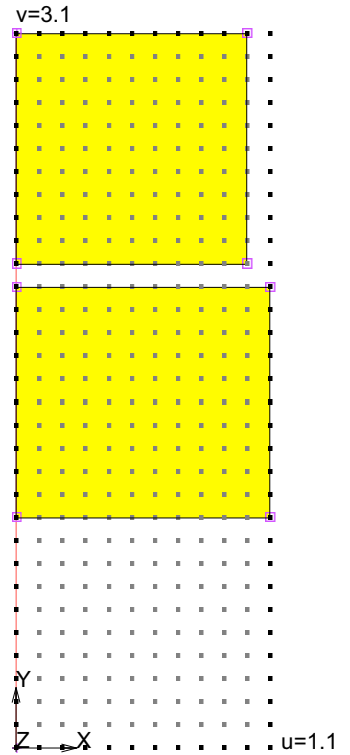


Figure 3.25-1 Two Concentric Cylinders and Contour Plotting Analysis

The contour plot shows the ratio of equivalent stress to strength and is largest in the outer cylinder where it touches the inner cylinder. Plotting the radial and hoop components along the radius at the symmetry plane illustrates the continuity of radial stress across the interface while the hoop stress switches from compression in the inner cylinder to tension in the outer cylinder.

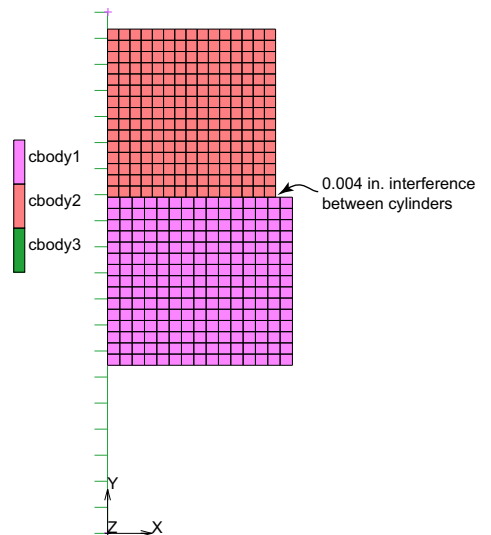
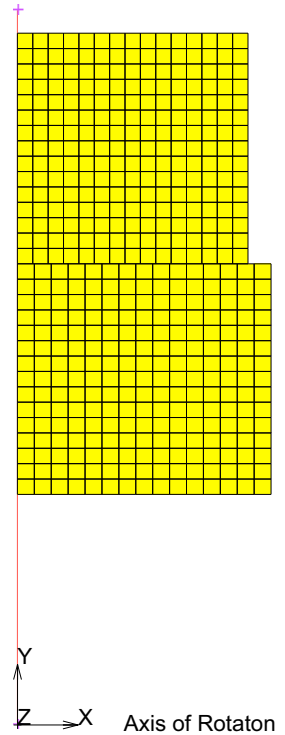
```
FILES
  NEW
  OK
  SAVE AS
    interf
  MAIN
MESH GENERATION
  COORDINATE SYS:
  SET GRID ON
  U DOMAIN
    0 1.1
  U SPACING
    0.1
  V DOMAIN
    0 3.1
  V SPACING
    0.1
  FILL
  RETURN
CRVS: ADD
  POINT(0.0,0.0,0.0)
  POINT(0.0,3.1,0.0)
ELEMENTS: ADD
  NODE(0.0, 1.0,0.0)
  NODE(1.1, 1.0,0.0)
  NODE(1.1, 2.0,0.0)
  NODE(0.0, 2.0,0.0)
  NODE(0.0, 2.1,0.0)
  NODE(1.0, 2.1,0.0)
  NODE(1.0, 3.1,0.0)
  NODE(0.0, 3.1,0.0)
```



```

SUBDIVIDE
  DIVISIONS
    15 15 1
  ELEMENTS
  ALL: EXISTING
  RETURN
SWEEP
  REMOVE UNUSED:
    NODES
    ALL
  RETURN
RENUMBER
  NODES DIRECTED
    0.0001 1 0
  RETURN
MOVE
  TRANSLATIONS
    0 -0.1 0
  ELEMENTS
    (pick top cylinder)
  END LIST
MAIN
MATERIAL PROPERTIES (twice)
NEW: STANDARD
STRUCTURAL
  YOUNG'S MODULUS = 3E7
  POISSON'S RATION = .3
  PLASTICITY (twice)
    INITIAL YIELD STRESS
      5E4
    OK (twice)
  ELEMENT ADD
  ALL: EXISTING
  RETURN
CONTACT
  CONTACT BODIES

```



DEFORMABLE,
OK
ELEMENTS: ADD
(pick inner cylinder)

NEW

DEFORMABLE
OK
ELEMENTS ADD
(pick outer cylinder)

NEW

SYMMETRY
DISCRETE
OK
CURVES ADD
(pick symmetry curve)

ID CONTACT

RETURN

CONTACT TABLES

NEW

PROPERTIES

ALL ENTRIES: CONTACT TYPE: TOUCHING
TOUCHING BODIES (pick T in 1,2 position in table)
cbody1
cbody2

INTERFERENCE CLOSURE

4E-3

OK (twice)

MAIN

LOADCASES

MECHANICAL

STATIC

CONTACT

CONTACT TABLE

ctable1

OK

```
# STEPS
  1
  OK
MAIN
```

Run Job and View Results

```
JOBS
NEW MECHANICAL
  PROPERTIES
    lcase1
  AXISYMMETRIC
  JOB RESULTS
    AVAILABLE ELEMENT SCALARS: Equivalent Von Mises Stress
    AVAILABLE ELEMENT SCALARS: Equivalent Von Mises Stress/yield Stress Ratio
    AVAILABLE ELEMENT TENSORS: Stress
    OK (twice)

  ELEMENT TYPES
    MECHANICAL
    ANALYSIS DIMENSION: AXISYMMETRIC
    SOLID
      116
    OK
    ALL: EXISTING
    RETURN
  SAVE
  RUN
    SUBMIT(1)
    MONITOR
    OK
  MAIN
RESULTS
  OPEN DEFAULT
  LAST
```

SCALAR
EQ. STRESS/YIELD
OK
CONTOUR BANDS

Inc: 1
Time: 1.000e+000

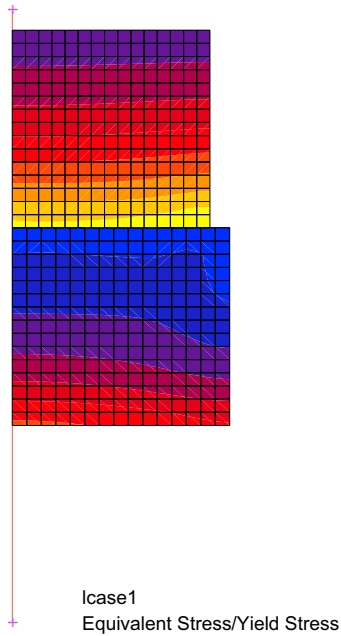
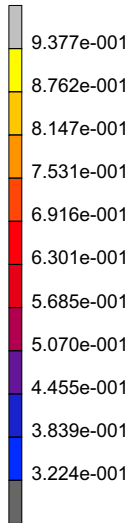


Figure 3.25-2 Equivalent Stress to Strength Ratio

RESULTS

PATH PLOT

NODE PATH

1 241 242 497

END LIST

ADD CURVES

ADD CURVE

ARC LENGTH

Comp 22 Of Stress

ADD CURVE

ARC LENGTH

Comp 33 Of Stress
FIT

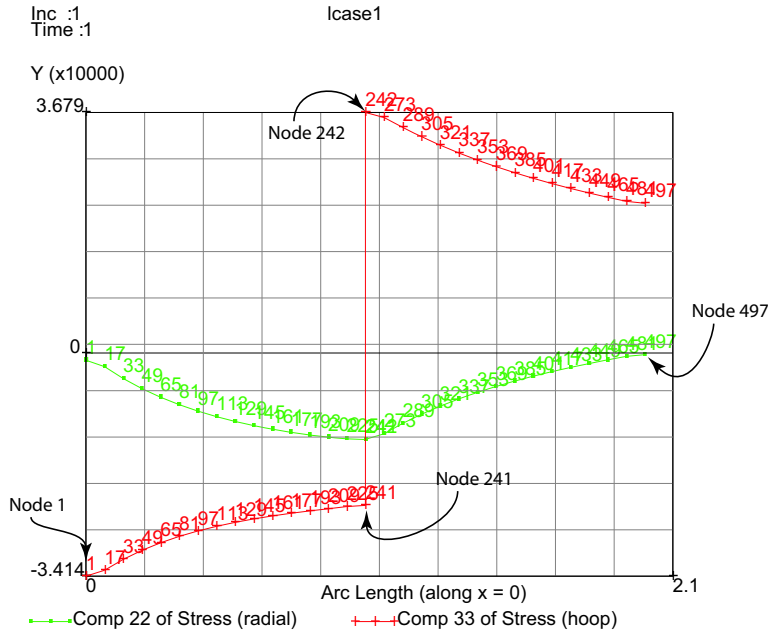


Figure 3.25-3 Stresses Plotted Across Interface

Component 22 of stress is the radial stress. It is in compression and is continuous across the interface between the two cylinders. Also, the radial stress vanishes on the free surfaces of the cylinders.

Component 33 of stress is the hoop stress, with the inner cylinder being compressed and the outer cylinder being expanded. The Equivalent Stress/Yield Strength ratio in the contour plot show that the outer cylinder at 94% of yield.

Input Files

The files below are on your [delivery media](#) or they can be downloaded by your web browser by clicking the links (file names) below.

File	Description
s7.proc	Mentat procedure file

3.26 3-D Remeshing with Tetrahedral Elements

- Chapter Overview 1386
- Why Remeshing with Tetrahedral Elements? 1386
- Tetrahedral Element Type 157 1386
- Tetrahedral Remeshing Criteria 1388
- Tetrahedral Remeshing Controls and Meshing Parameters 1389
- Tetrahedral Remeshing Tests 1391
- Input Files 1410

Chapter Overview

This chapter describes the capability for 3-D global remeshing. For analysis using the updated Lagrange formulation based finite element method (FEM), one often encounters element distortion in applications that involve large deformation. When elements become too distorted the analysis fails. The global remeshing feature alleviates this situation by automatically generating a new mesh, transferring history data from the previous mesh, and resuming the analysis. Global remeshing also helps improving the analysis by mesh refinement in the area where small elements are required due to contact and geometry change, and speeding up the analysis by generating larger elements in the area that does not require small elements.

Why Remeshing with Tetrahedral Elements?

The tetrahedral element mesh generator has been proved to be the most robust and fastest method among other types of 3-D mesh generators. It is much easier for a mesh generator to automatically fill in an arbitrary geometry with tetrahedrons than with other elements of the different shapes. The meshing technology, such as Delaunay triangulation and pavement method, has been used successfully in generating triangular and tetrahedral meshes. Marc uses the mesh generator from Patran (or GS-Mesher) to generate the mesh. A mesh-on-mesh technology (MOM mesher) is employed to mesh the surface with triangular elements. Subsequently, a tetrahedral mesh generator, using the Delaunay triangulation and pavement methods, is used to create the final mesh with the tetrahedral elements.

Tetrahedral Element Type 157

The tetrahedral remeshing uses Marc element type 157. The tetrahedral element type 157 is a Herrmann type element, which typically uses pressure as well as displacement in the FEM analysis. These elements with the mixed unknowns (or degrees of freedom) allow the element to model incompressible materials undergoing large shear deformation. Standard displacement based tetrahedral element cannot perform well in this situation because the element locks and hence lacks flexibility. Element type 157 has 5 nodes, with 4 corner nodes and one interior node. There is one pressure degree of freedom and three displacement degrees of freedom in each corner node while only three displacement degrees of freedom are in the interior node.

Example: An Upsetting Compression to Test Incompressibility and Thermal Coupling

Figure 3.26-1 shows the location of the two interested points used in the comparison. Figure 3.26-2 displays temperature distribution in the test and Figure 3.26-3 shows nodal temperature changes and displacement change at these two nodal positions.

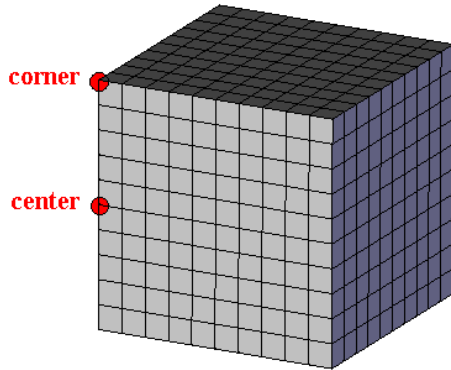


Figure 3.26-1 A Corner and Center Nodes

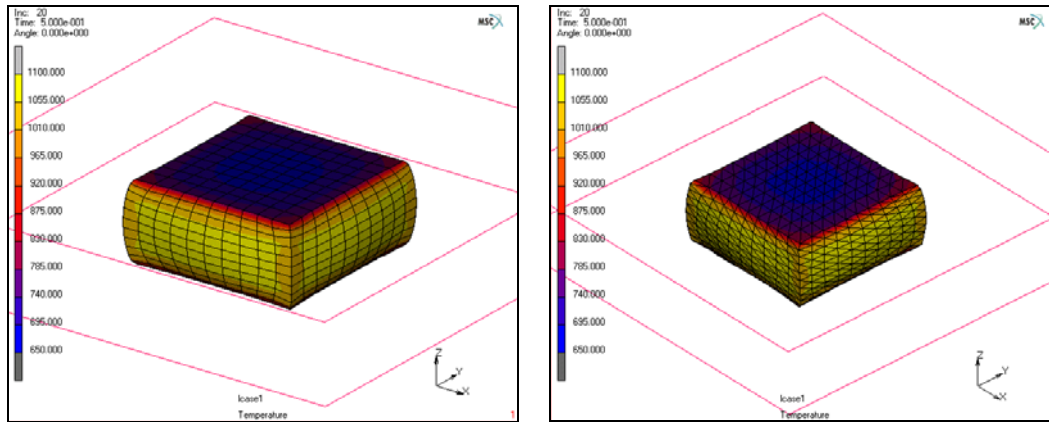


Figure 3.26-2 Temperature Distribution Comparison

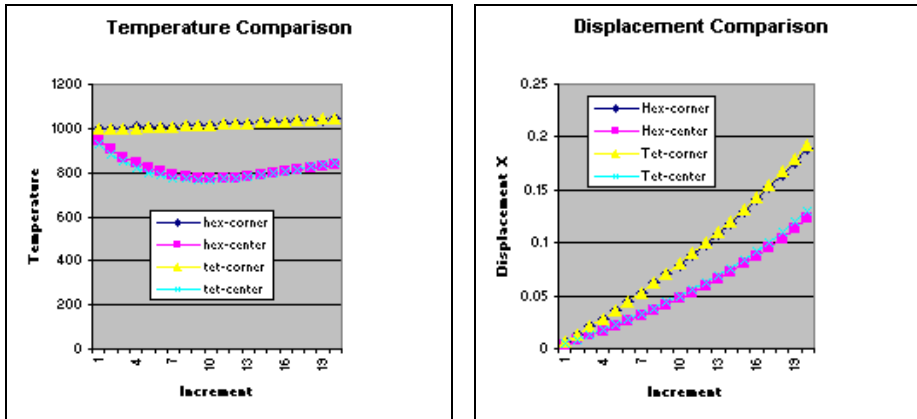


Figure 3.26-3 Temperature and Displacement Comparisons

It can be seen that element 157 behaves very well compared with element 7.

Tetrahedral Remeshing Criteria

The remeshing criteria are used to initiate the remeshing process. There are six remeshing criteria that may be used, either separate or in combination.

1. Increment frequency: Users can specify remeshing intervals so that after certain number of increments, global remeshing is performed.
2. Strain change: An accumulated incremental strain measure is recorded after each remeshing. When this value reaches or exceeds the maximum allowed, remeshing is initiated. This criterion controls the magnitude of the deformation between each remeshing step.
3. Penetration: Penetration is checked against each contacting body. When penetration reaches or exceeds the maximum allowed, the remeshing step starts. The penetration distance is measured between a triangle face element and its central point projection to the other contact bodies. The penetration limit (default value set at two times of the contact tolerance) can also be specified. This criterion is useful when contacting with rigid bodies that have sharp corners. It helps remeshing body correct its geometry to avoid further penetration. The penetration criterion cannot be used in self-contact situation.
4. Volume Ratio Distortion: This criterion checks element distortion based on its volume. A ratio of the height and the base triangle is used to make sure the element is in a good shape for computation. A ratio of 1.0 indicates a good element while a ratio of 0.0 means a flat element, not suitable for the analysis. A control value to avoid large element distortion can also be specified.

5. Immediate Remeshing: This control is used to remesh the body before the next analysis step. It is useful when you want to switch a model of a hexahedral mesh to a tetrahedral mesh before the finite element analysis starts. It can also be used with restart option to immediately remesh the body after the restart. Immediate remeshing allows the change element type from hexahedral element type 7 to tetrahedral element type 157 but not vice versa.
6. Forced Global Remeshing: This control is used internally together with automatic time step cutback feature. If the global remeshing control is used and a bad mesh is encountered during the iteration cycle, Marc automatically forces the job to create a new mesh. If the new mesh does not help, the time step cutback is then enforced.

Tetrahedral Remeshing Controls and Meshing Parameters

The tetrahedral element remeshing requires REZONING,2 in the parameter section and an ADAPT GLOBAL option in the model or history section. A standalone mesh generator, *afmesh3d*, is needed in the bin directory along with the Marc FEM solver. The GS-mesher library is linked to *afmesh3d* to perform surface and tetrahedral meshing (see Figure 3.26-4). This library is normally located in the lib directory. Without all these components, the global remeshing does not perform properly.

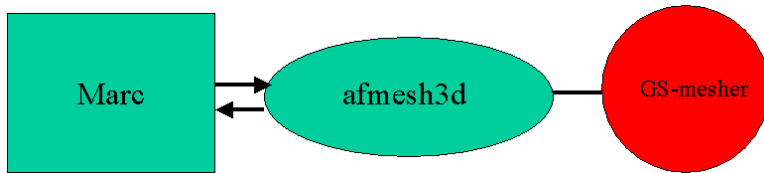


Figure 3.26-4 Global Remeshing Controls

When remeshing is required, the solver writes an input data file, *jid_bxx.fem* for *afmesh3d* and is then called to generate a mesh. The output file from *afmesh3d*, *jid_bxx.feb* is read into the solver. The two digit number, xx provides the contact body number. While remeshing, the solver can be either in a waiting state or terminated temporarily to save memory for the mesh generator. After the new mesh is created, the solver automatically resumes.

The remeshing parameters control how the new mesh is created. These control parameters are:

1. Element Edge Length: This element size controls the size of the new mesh although some refinement and coarsening overrule the element size here.
2. Number of Elements: This controls approximately the number of the elements in the new mesh. It gives a guideline for Marc to define an element size for the mesh generation. If element edge length and the number of the elements are not given, the number of the elements in the previous mesh are used to create the new mesh.
3. Previous Number of Elements: It uses the number of elements in the current mesh as a target to create the new mesh.

4. Feature Edge Angle: An edge is preserved after remeshing if any surface edge angle exceeds this value. A feature edge angle is measured between two connected face elements in such a way that 0° indicates the two face elements lie on a planar surface while 180° indicates that the elements are touching each other. The default value is 60° .
5. Feature Vertex Angle: While the edge angle controls the edges the vertex angle controls points. If a point on certain edge is smaller than this value, the point is kept after remeshing. The vertex angle measures the feature of two connecting edges. It is calculated in such a way that the angle is 180° if the two edges lie in a straight line. Thus, a 0° means the two edges are touching each other. The default value is 100° .
6. Coarsening Factor: This parameter allows creation of larger tetrahedral elements in the interior. To capture contact conditions accurately, the mesh usually contain small elements on the surface of a body. By enlarging the element gradually inside a body, we reduce the number of elements in the mesh (see [Figure 3.26-5](#)). The coarsening factor scales the element size from the surface inwards. Thus, a coarsening factor of 1.0 means no coarsening. The default value of the coarsening factor is 1.5 times.

Note: Making element too large will affect the accuracy of the analysis results.

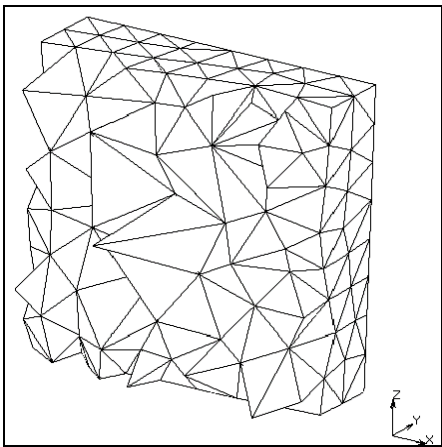


Figure 3.26-5 Interior Coarsening of a Tetrahedral Mesh

7. **Minimum Edge Length:** This parameter controls the smallest elements allowed on the surface mesh. It is used when local refinement or adaptive meshing is required. The default value is set at 1/3 of the element edge length.
8. **Maximum Edge Length:** This parameter controls the largest elements allowed on the surface mesh. It is used when local refinement or adaptive meshing is required. The default value is set at three times of the element edge length.
9. **Curvature Controls:** This parameter controls adaptive meshing on the surface based on the surface curvature. Thus, a surface that is curved gets smaller elements than the surface that is flat. The number of divisions indicates number of the divisions to subdivide a curvature circle (see [Figure 3.26-6](#)). It shows the sensitivity of this curvature control. By default, this control is off. But a number of ten is considered a good number for the general applications.

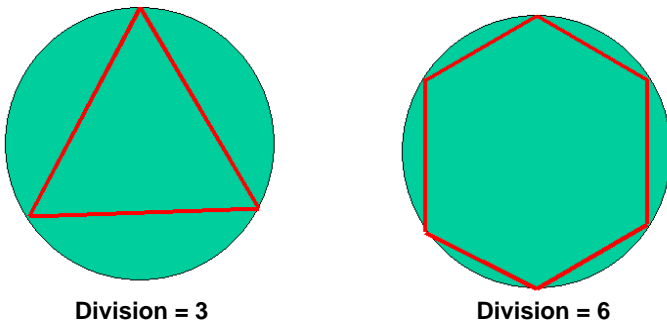


Figure 3.26-6 Divisions of a Curvature Circle

10. **Change Element Type:** This parameter is only required if element type is to be changed after remeshing. This is often used to switch from the original hexahedral mesh to the tetrahedral mesh. Currently, the only available type is 157 in Marc.

Tetrahedral Remeshing Tests

Many tests have been performed with good results.

1. **Rubber Seal Simulation:** This example shows remeshing application in rubber seal simulation and is used to demonstrate the remeshing in the forthcoming sections. See [Figures 3.26-7 and 3.26-8](#).

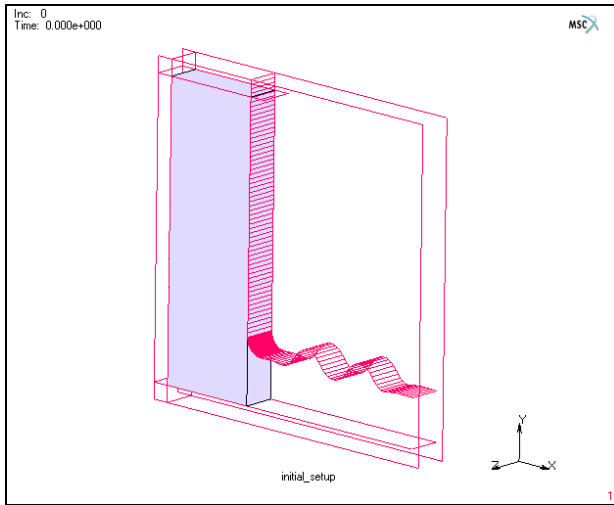


Figure 3.26-7 Initial Setup with One Element

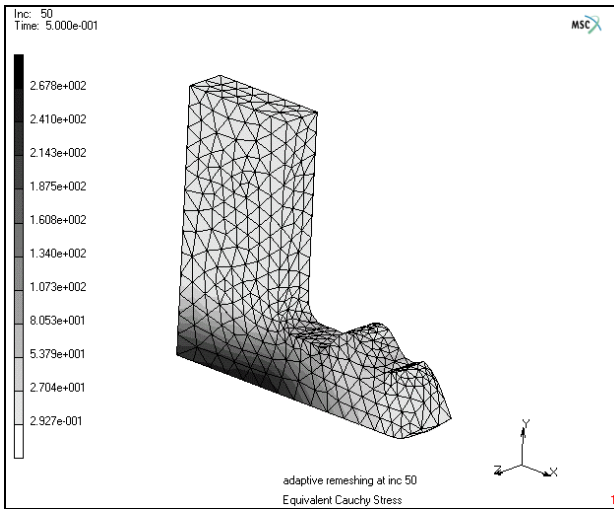


Figure 3.26-8 Deformation at Increment 50

- 2, Double-sided Contact: This example shows two deformable body subjected to contact with remeshing. It shows possibility of the global remeshing with multiple deformable bodies. See Figures 3.26-9 and 3.26-10.

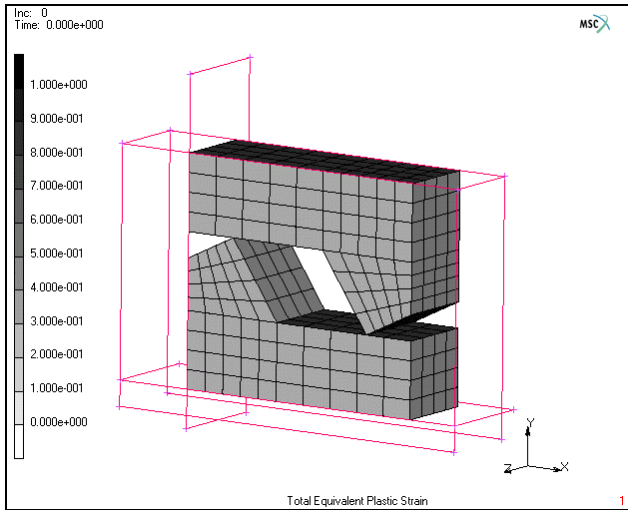


Figure 3.26-9 Initial Setup of Two Contact Bodies

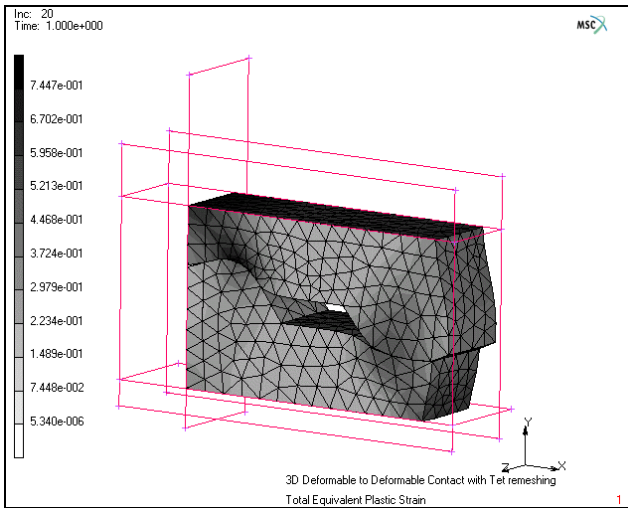


Figure 3.26-10 Deformation At Increment 20

3. Hot Compression of a Steel Block: This example shows capability of remeshing in a thermal-mechanical coupled analysis. Curvature local refinement can be seen in the final results. See Figures 3.26-11 and 3.26-12.

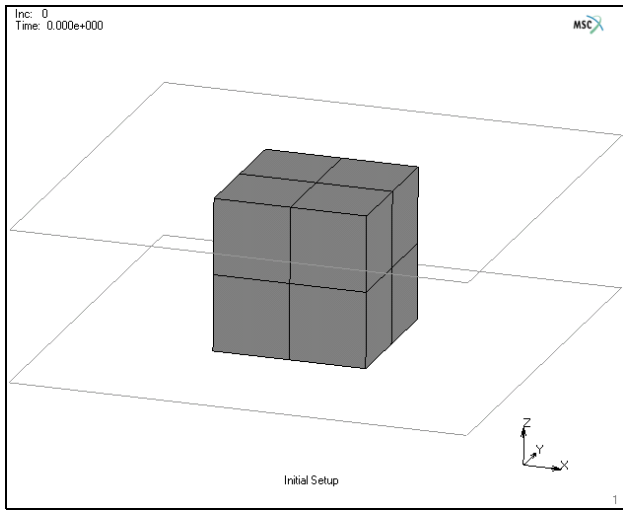


Figure 3.26-11 Initial Setup

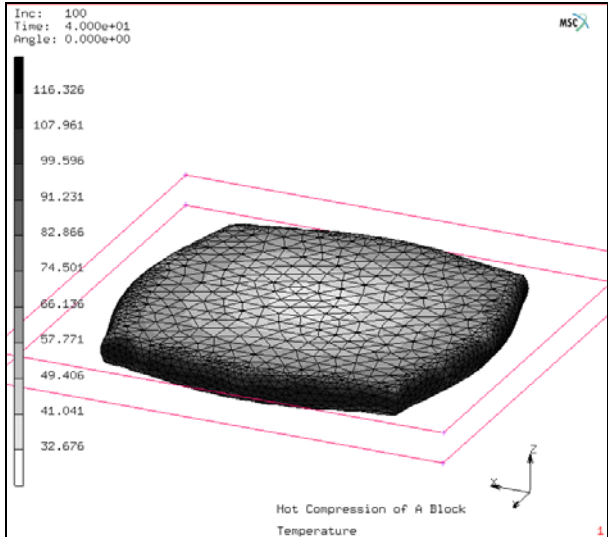


Figure 3.26-12 Deformation and Temperature at Increment 100

Many metal forming applications are carried out with the help of the tetrahedral global remeshing. Listed below are some of the industrial examples which would not have been possible without remeshing.

1. **Connecting Rod Forging:** This example shows an open die forging simulation. The flash being extruded out from the die is seen in the final result. The global remeshing permits the solution of the large material flow. See Figures 3.26-13 and 3.26-14.

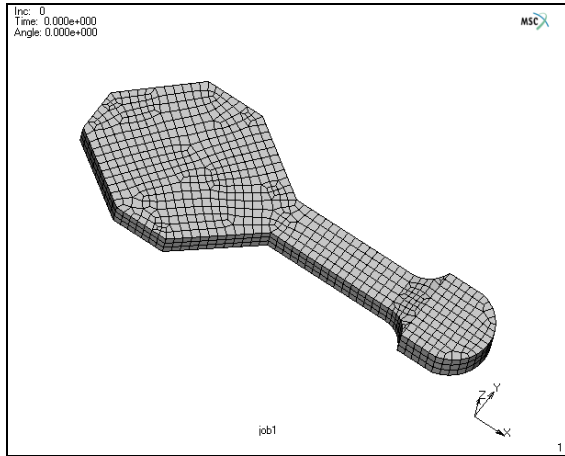


Figure 3.26-13 Initial Mesh of a Connecting Rod

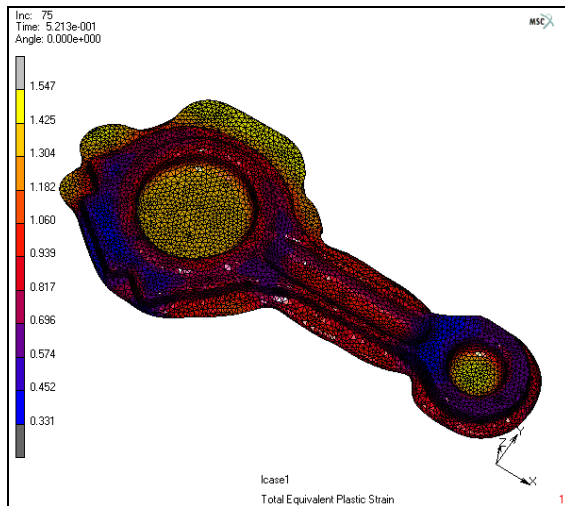


Figure 3.26-14 Final Mesh of a Connecting Rod

2. Turbine Blade Forging: This example shows bending, twisting, and compression of the turbine blade. The global remeshing helps the large deformation in the compression stage. See Figures 3.26-15 and 3.26-16.

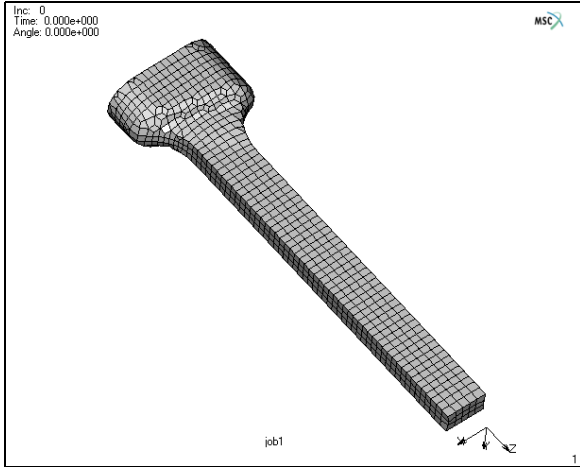


Figure 3.26-15 Initial Mesh of a Turbine Blade Preform

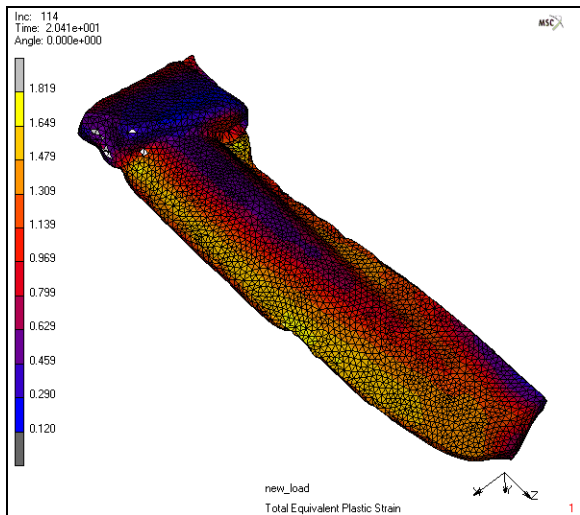


Figure 3.26-16 Final Result of a Turbine Blade Forging

3. Flange Forging: This example shows a closed die forging simulation. Material flows to fill up the closed die cavity. The global remeshing permits the large deformation observed in the simulation without external intervention due to mesh distortion. See Figures 3.26-17, 3.26-18, and 3.26-19.

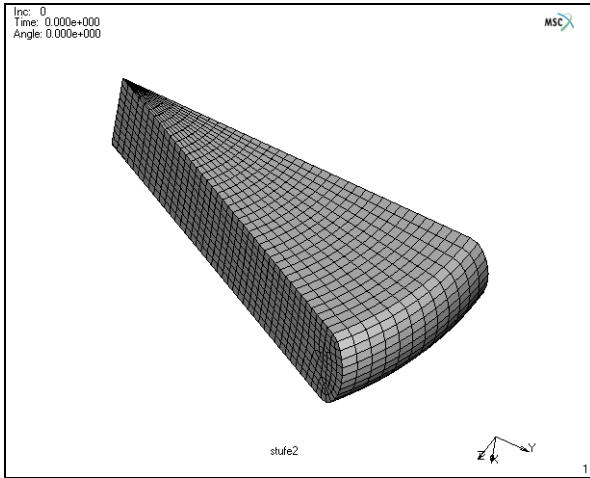


Figure 3.26-17 Initial Shape of the Workpiece

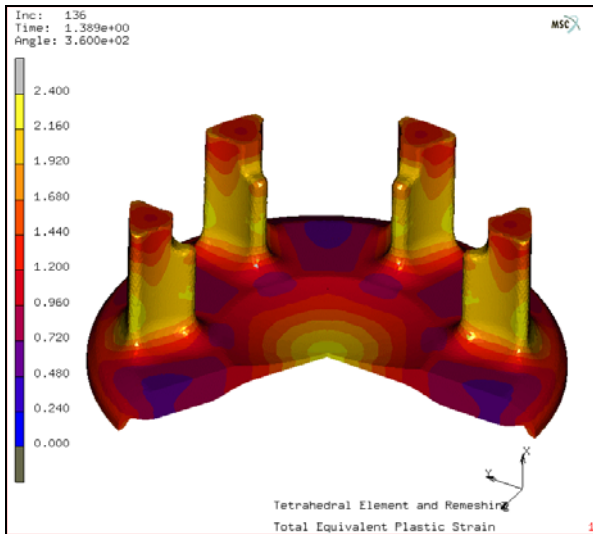


Figure 3.26-18 Final Results

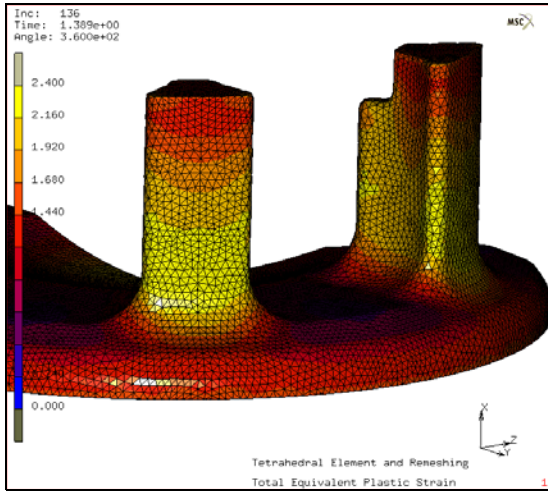


Figure 3.26-19 A Closer Look at the Final Mesh

Elastomeric Seal Simulation

A rubber seal with a rectangular cross-section ($1.8 \times 1.2 \text{ cm}^2$) is pressed laterally by rigid tool. Because of the symmetry, only a half of the seal is considered. With a thickness of 0.2cm, the model is setup as a 3-D problem. Assuming this is a long rubber seal in the thickness direction, two symmetry surfaces are used. For the placement of the rubber seal and the rigid tools, see [Figure 3.26-20](#). The tool pressure is applied to the top of the seal and simulated by moving the top rigid surface down with a velocity of 1cm/sec. In the current release, only volumetric loads are automatically reapplied after remeshing. Total load is reached in 50 steps in the analysis with the time step equal to 0.01 second.

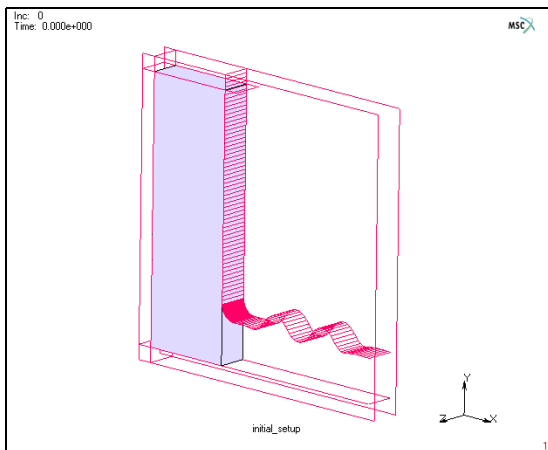


Figure 3.26-20 Initial Setup of the Model

Although the geometry itself is simple, without remeshing the severely deformed configuration leads to a premature termination of the analysis due to excessive distortion in the elements and penetration between contact bodies. Remeshing/rezoning operation is clearly required for a successful completion of the analysis.

The analysis starts with one single hexahedral element (to demonstrate that a very crude model can be initially given, if the model is remeshed at increment 0 before the analysis begins). After remeshing, the hexahedral element is converted into tetrahedral elements (see [Figure 3.26-21](#)).

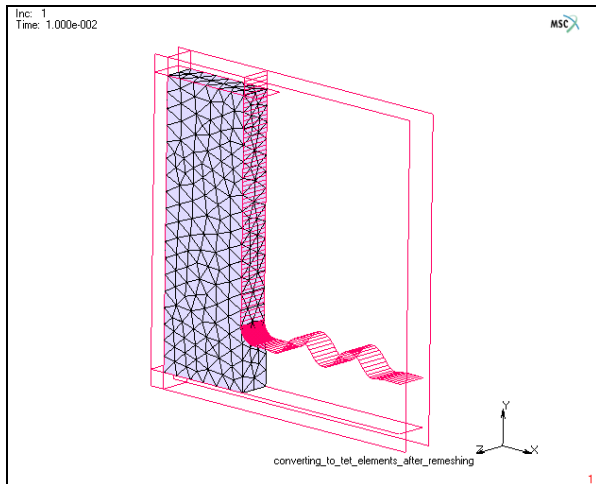


Figure 3.26-21 Tetrahedral Mesh After Immediate Remeshing

In the rest of the analysis, the remeshing/rezoning is done based on the penetration check to prevent severe penetration between contact bodies. An adaptive meshing based on the surface curvature is used to generate smaller elements near the curved areas. It allows the analysis to capture the geometry changes correctly in those areas without creating excessive number of the elements to slow down the analysis (see [Figure 3.26-22](#)). Element type 157 is used in the analysis within the updated Lagrangian framework.

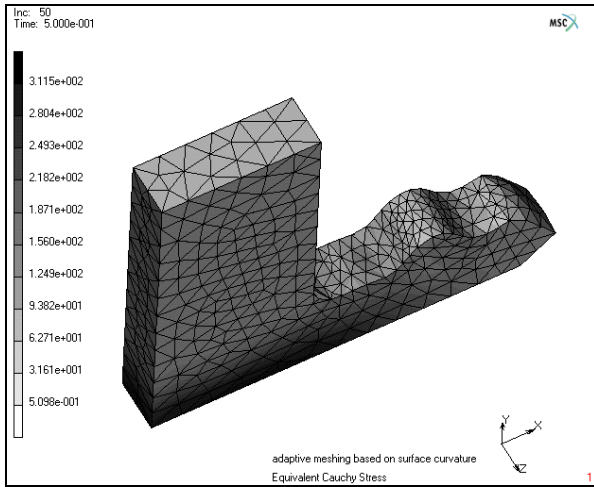


Figure 3.26-22 Adaptive Meshing based on Curvature

The rubber seal is modeled using Mooney constitutive model. The material parameters are given as $C_1=8\text{N/cm}^2$ and $C_2=2\text{N/cm}^2$. The bulk modulus is 10000N/cm^2 .

Model Generation

We create the model by reading the predefined model files. This assumes that the users are familiar with model generation. Two model files are directly read in - `element.mfd` and `rigid_bodies.mfd`.

```
FILE
  OPEN
    Open file: element.mfd
  OK
  MERGE
    Merge file: rigid_bodies.mfd
  OK
```

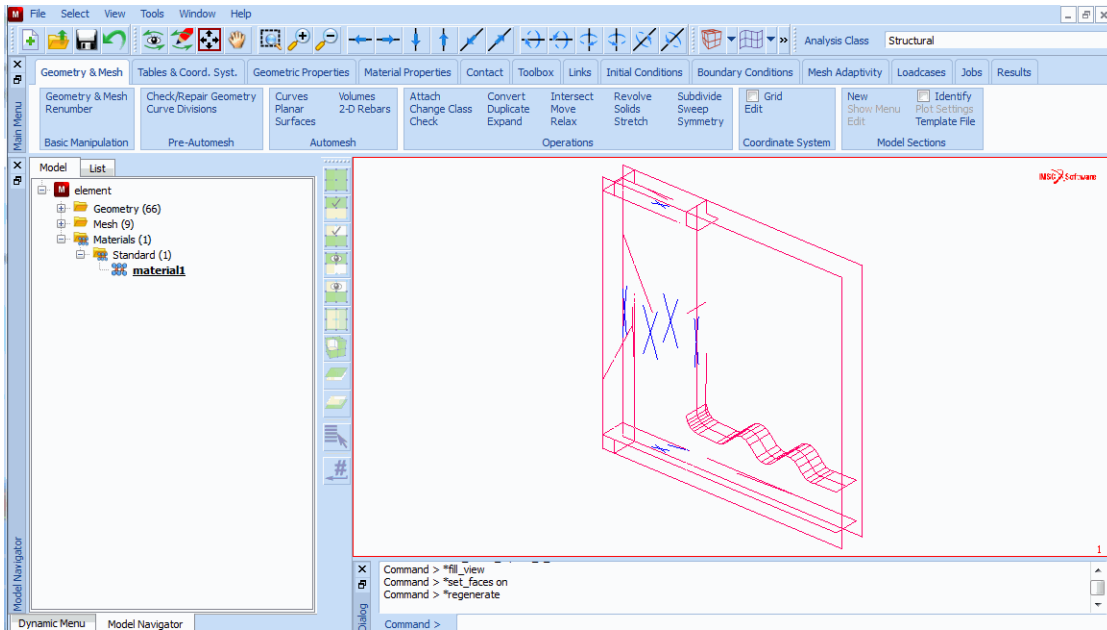



Figure 3.26-23 Read in the Predefined Model

Save the model as tet_rubber.

```
SAVE AS
  Save file: tet_rubber.mfd
OK
MAIN
```

(to return to the main menu)

Material Properties

Mooney type of material is used for the rubber seal.

```
MATERIAL PROPERTIES
Mechanical material types:
  MORE
    MOONEY
      C10
      8
      C01
      2
    BULK MODULUS
```

10000
OK
ELEMENTS ADD
ALL EXIST
MAIN

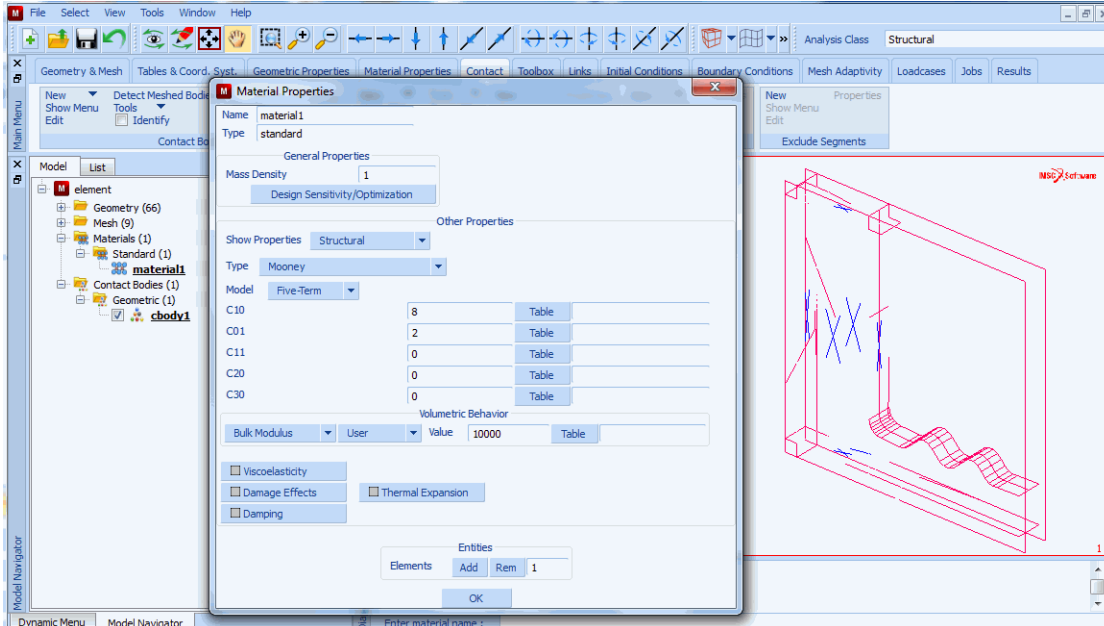


Figure 3.26-24 Enter Mooney Material Properties

Contact Definitions

CONTACT
CONTACT BODIES
NEW
NAME
Rubber

Contact body type:

DEFORMABLE
OK

Element: ADD

EXISTING

NEW

NAME

bot

Contact body type:

RIGID

DISCRETE

OK

Surfaces: ADD

1

(pick surface number 1)

END LIST (#)

NEW

NAME

top

contact body type:

RIGID

DISCRETE

OK

Surfaces: ADD

4

(pick surface number 4)

END LIST (#)

NEW

NAME

sym1

contact body type:

SYMMETRY

DISCRETE

OK

Surfaces: ADD

6

(pick surface number 6)

END LIST (#)

COPY

NAME

sym2

Surfaces: ADD

```
5
END LIST (#)
COPY
NAME
  sym3
Surfaces: ADD
  2
END LIST (#)
```

(pick surface number 5)

(pick surface number 2)

Define the pusher:

```
NEW
NAME
  push
contact surface type:
  RIGID
Body control:
  VELOCITY
  PARAMETERS
    VELOCITY
      Y: -1
  OK
  DISCRETE
  OK
Surfaces: ADD
  3
END LIST (#)
```

(pick surface number 3)

ID CONTACT *(you can see the contact body IDs now)*

MAIN

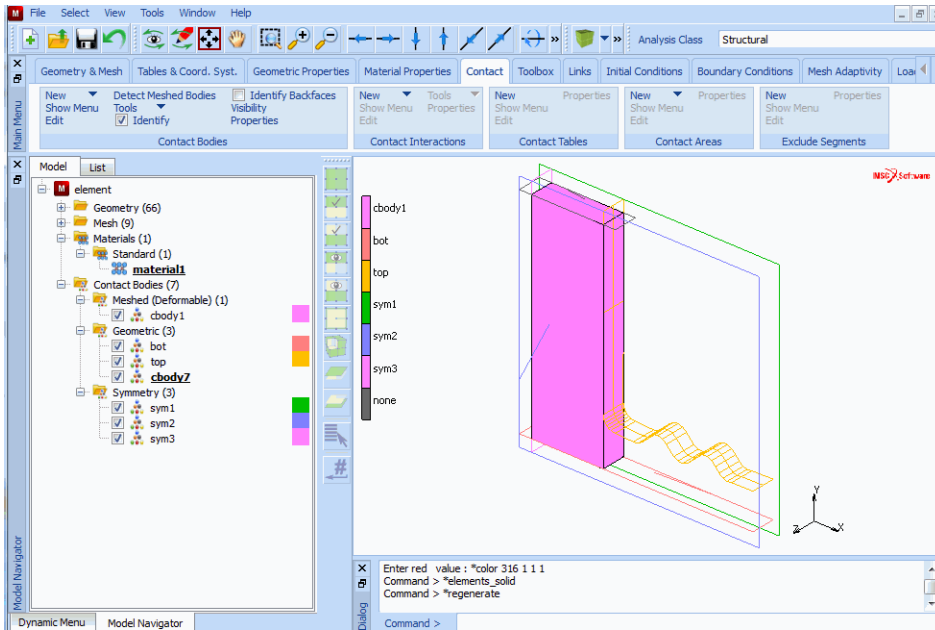


Figure 3.26-25 Define Contact Bodies

Mesh Adaptivity

You can see many new buttons in this section. Two remeshing criteria will be specified for the deformable body. Additional information will be provided to control the meshing process. It is desired that the new elements have edge dimensions between 0.03cm and 0.1cm.

GLOBAL REMESHING

PATRAN TETRA

(select Patran Tetrahedral Mesher)

Remeshing criteria:

IMMEDIATE

(immediate remeshing)

ADVANCED

PENETRATION

USER:LIMIT

0.005

(maximum penetration distance)

OK

Remeshing parameters:

ELEMENT EDGE LENGTH: SET

0.1

(element size for the new mesh)

ADVANCED

MINIMUM EDGE LENGTH

0.03

(limit the smallest element size)

CURVATURE CONTROL:#DIV

10

(curvature control number)

CHANGE ELEMENT TYPE: 157

OK

REMESH BODY

Rubber

MAIN

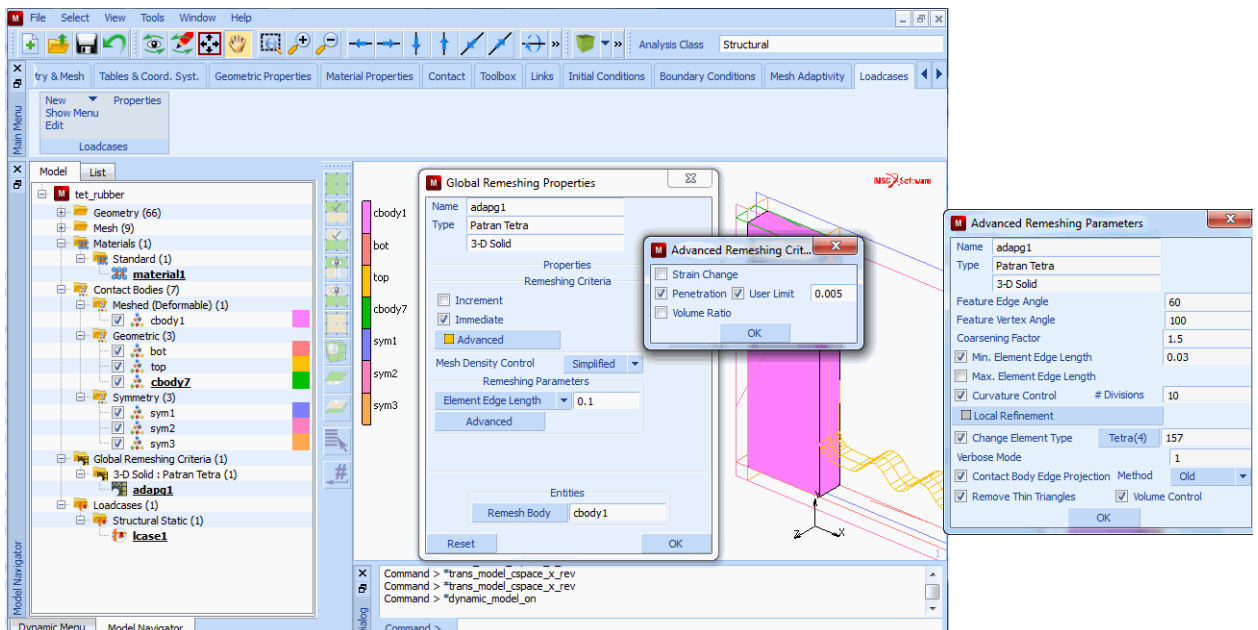


Figure 3.26-26 Adaptive Remeshing Controls

Loadcases

The loadcase option is used to define the time period and to activate the global adaptive meshing criteria.

LOADCASES

MECHANICAL

STATIC

GLOBL REMESHING

adapg1
 OK
 TOTAL LOADCASE TIME
 0.5
 CONSTANT TIME STEP: #STEPS
 50
 OK
 MAIN

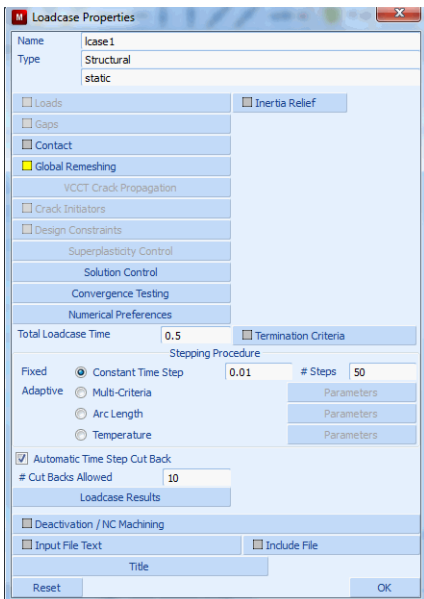


Figure 3.26-27 Loadcase Definition

Jobs and Run Analysis

There are a few control settings in this section that need special attention.

JOBS

MECHANICAL

Available:

lcase1

ANALYSIS OPTIONS

LARGE DISPLACEMENT

ADVANCED OPTIONS
UPDATE LAGRANGE PROCEDURE
OK

Rubber elasticity procedure:
LARGE STRAIN-UPDATED LAGRANGE

JOB RESULTS
Cauchy stress
OK
Analysis dimension
3-D
OK

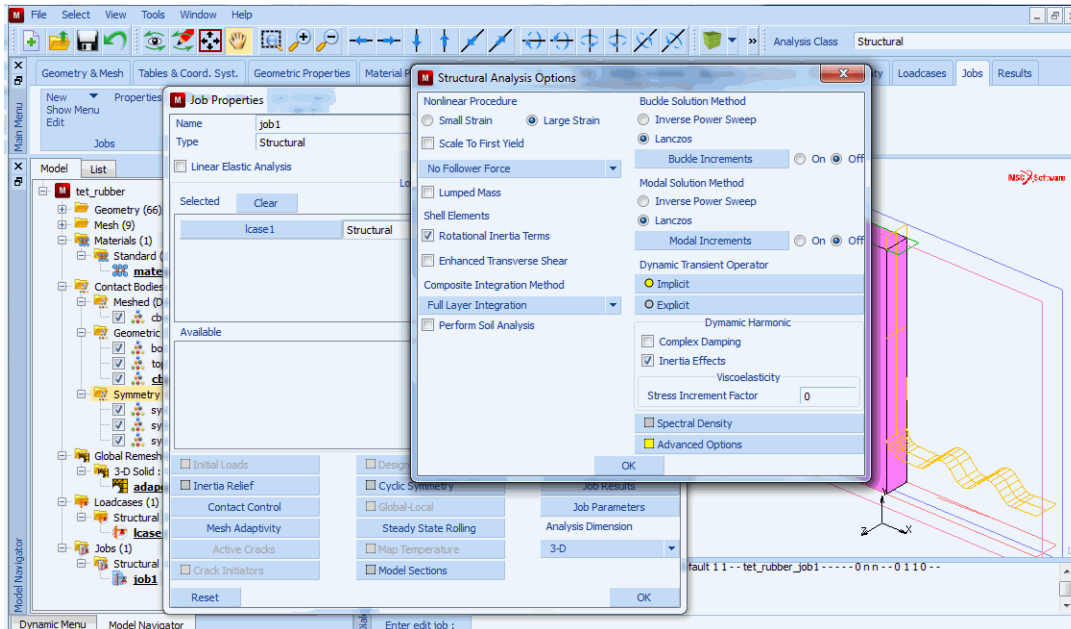


Figure 3.26-28 Figure 16-9: Job Definition

Use SAVE to save the model. The job can be run using

RUN
SUBMIT (1)
MONITOR (this can be used to monitor the job status)
MAIN

Results

RESULTS

OPEN DEFAULT

DEF ONLY

CONTOUR BAND

SCALAR

Equivalent Cauchy Stress

OK

FILL

DYN.MODEL

MONITOR

(use this to rotate the model to good viewing position)

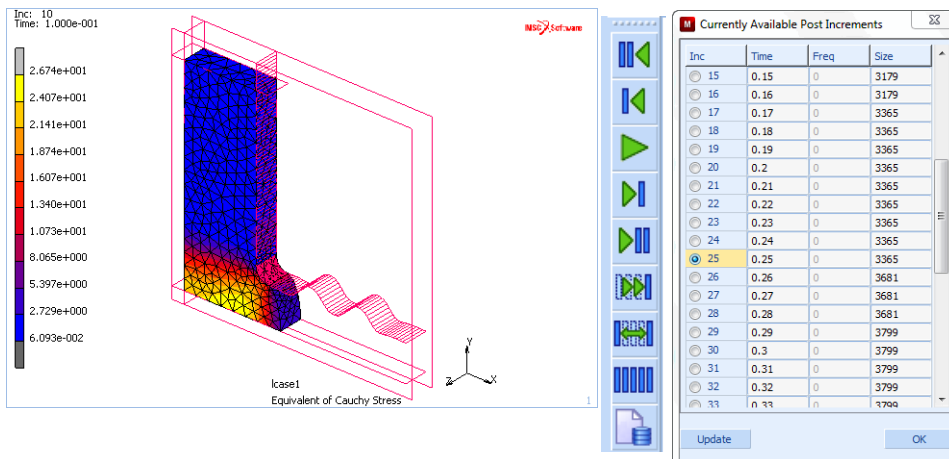


Figure 3.26-29 Deformation at Increment 10

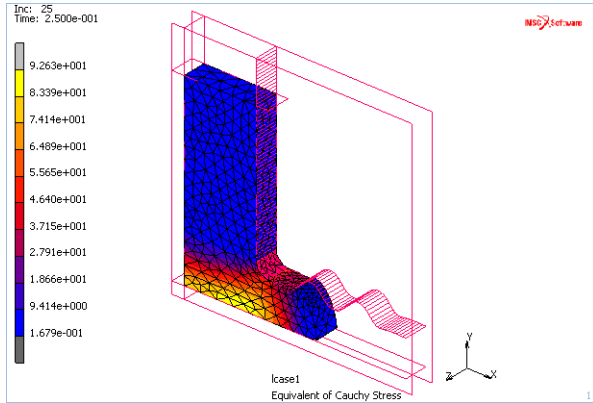


Figure 3.26-30 Deformation at Increment 25

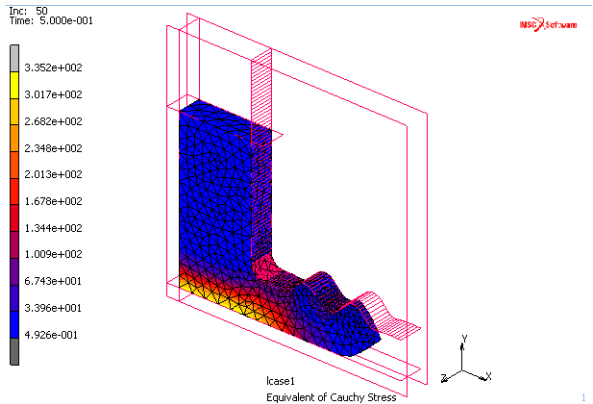


Figure 3.26-31 Deformation at Increment 50

Input Files

The files below are on your [delivery media](#) or they can be downloaded by your web browser by clicking the links (file names) below.

File	Description
rubber_seal_3d.proc	Mentat procedure file
rigid_bodies.mfd	Mentat model file
element.mfd	Mentat model file

3.27 Rubber Remeshing and Radial Expansion of Rigid Surfaces

- Chapter Overview 1412
- Model Highlights 1412
- Results Highlights 1416
- Modeling Tips 1417
- Input Files 1417

Chapter Overview

This feature demonstrates how to grow rigid bodies via a remeshing example. The example is a rubber bushing with a cap. The cap is automatically remeshed while utilizing expandable rigid bodies to expand the bushing into the outer rigid housing. In actual applications, the rubber bushing would be a full cylindrical shape, however, a small segment is used here to keep run times reasonable. The bushing along with the rigid shaft and housing is shown in [Figure 3.27-1](#). The deformable bushing is bounded by two surfaces of symmetry shown in [Figure 3.27-3](#).

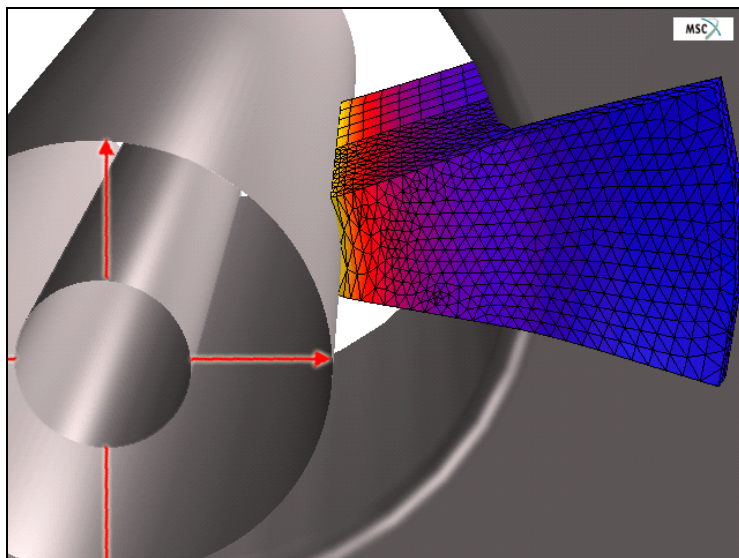


Figure 3.27-1 Rubber Bushing with Housing and Rigid Shaft

The rubber is modeled with a Mooney material for both the bushing and cap. The cap is a separate contact body that will be glued to the rest of the bushing. The cap is automatically remeshed during the first increment. The global remeshing fills the cap volume with low-order tetrahedral elements. Marc uses the meshing technology in the Patran GS-mesher to create meshes with tetrahedral elements. The Mesh On Mesh (MOM) surface mesher and tetrahedral mesher are called separately within the Marc solver to produce new mesh. The loading only consists of the inner rigid shaft will be expanded using the UGROWRIGID user subroutine.

Model Highlights

First, let's open the model and examine the model highlights.

```
FILE
  OPEN
    rubber_remesh.mud
  OK
```

VIEW

SHOW VIEW 4

FILL

PLOT

NODES

POINTS

CURVES

SURFACES

IDENTIFY

GLOBAL REMESHING CRITERION

DRAW

MAIN

(turn drawing off)

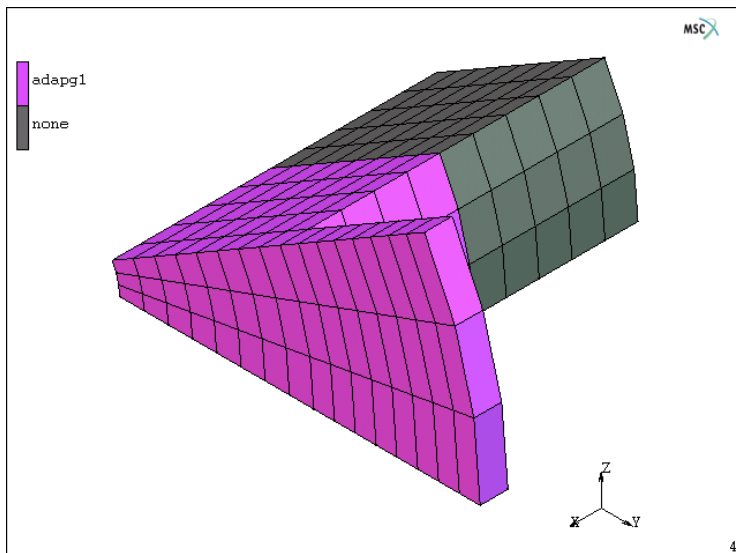
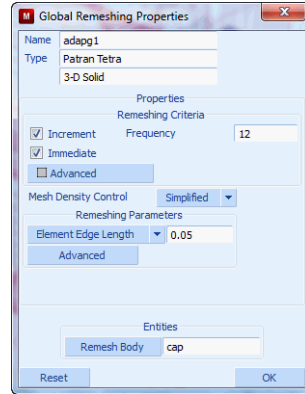


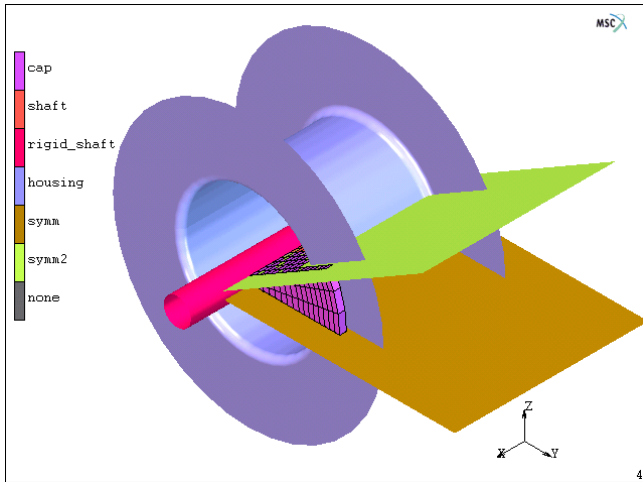
Figure 3.27-2 Elements Marked for Global Remeshing

MESH ADAPTIVITY
 GLOBAL REMESHING CRITERION
 PATRAN TETRA
 OK
 MAIN
 PLOT
 SURFACES
 IDENTIFY
 CONTACT BODIES
 DRAW
 MAIN
 CONTACT
 CONTACT TABLE
 PROPERTIES
 OK
 MAIN

(Turn on)



Remeshing occurs every 12 increments, with an element edge length of 0.05.



CONTACT TABLE PROPERTIES			SECOND					
FIRST	BODY NAME	BODY TYPE	1	2	3	4	5	6
1	cap	deformable	G	G	T	T	T	
2	shaft	deformable	G		T	T	T	T
3	rigid_shaft	rigid						
4	housing	rigid						
5	symm	symmetry						
6	symm2	symmetry						

Figure 3.27-3 Contact Bodies and Contact Table

The global remeshing criterion is for the cap body, it occurs with a frequency of 12 increments, immediately (increment 1) and with an element size of 0.05. The loadcase used only 10 increments, so there will only be one remeshing to keep run times short.

In order to expand the inner surface, two things must be done. First, we add an additional input string “umotion,2” to the model definition using the new Additional Input File Text feature in the JOBS menu.

```
JOBS
  ADDITIONAL INPUT FILE TEXT
    umotion,2
  OK
  RUN
    SUBMIT(1)
  OK
  MAIN
```

Secondly, we need to write the following file, say `rubber_remesh.f`, that contains the user subroutine, `ugrowrigid.f` which is listed below. This file is selected in the RUN-> JOB menu.

```
      subroutine ugrowrigid(md,relx,relx,relz,time)
      implicit real*8 (a-h,o-z)
c user subroutine for definition of relative size of rigid's
c
c md      : rigid body number
c relx   : relative size in x-direction with respect to original
c rely   : relative size in y-direction with respect to original
c relz   : relative size in z-direction with respect to original
c time   : time
c relx,relx and relz should be defined by the user
      relx=1.0d0
      rely=1.0d0
      relz=1.0d0
      if(md.eq.3) then
        if(time.le.1.0d0) then
          rely=1.0d0 + 1.6d0*time
        else
          rely=2.6d0
        end if
        relz=rely
        write(6,*) 'md,relx,relx,relz=',md,relx,relx,relz
      end if
      return
      end
```

Results Highlights

After submitting the job with the user subroutine, the results are shown in [Figure 3.27-4](#).

```
RESULTS
  OPEN DEFAULT
  DEF ONLY
  SCALAR
    EQUIVALENT TOTAL STRAIN
      OK
  LAST
```

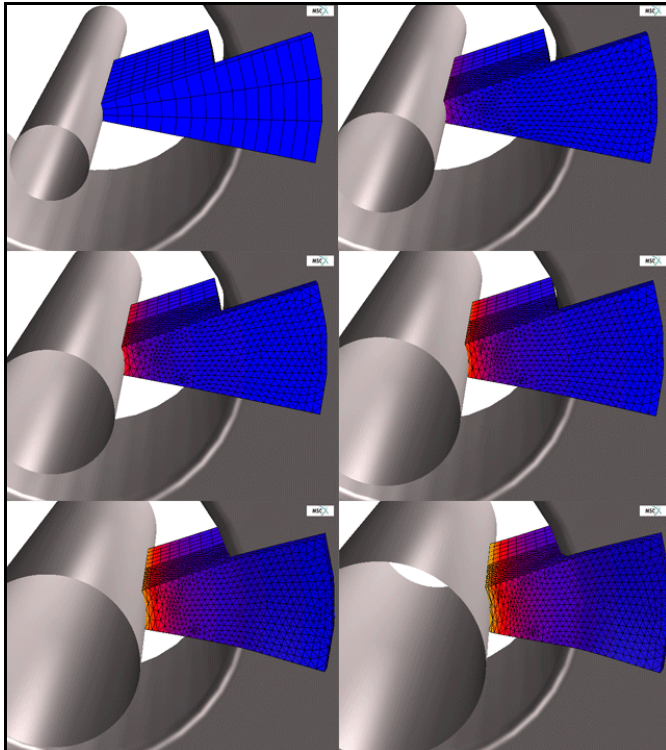


Figure 3.27-4 Rubber Remeshing

Notice how the cap, originally made of hexahedral elements, is remeshed with tetrahedral elements as shown in [Figure 3.27-4](#). Also notice that the internal rigid cylinder expands in the radial direction, as controlled by the UGROWRIGID user subroutine.

Modeling Tips

The UGROWRIGID user subroutine can be replaced by placing a table $(1 + 1.6 \cdot \text{time})$ to control the y and z growth factors in the definition of body, rigid_shaft.

Input Files

The files below are on your [delivery media](#) or they can be downloaded by your web browser by clicking the links (file names) below.

File	Description
rubber_remesh.mud	Mentat model file
rubber_remesh.f	User subroutine

3.28 Automatic Remeshing/ Rezoning

- Chapter Overview 1420
- Elastomeric Seal Simulation 1421
- Tape Peeling Simulation 1431
- Input Files 1445

Chapter Overview

In the analysis of metal or rubber, the materials may be deformed from some initial shape to a final, very often complex shape. During the process, the deformation can be so large that the mesh, used to model the materials, may become highly distorted and the analysis cannot go any further without using some special techniques. Remeshing/rezoning in Marc is a useful feature to overcome the difficulties. The global remeshing described here completely regenerates a mesh over a specified body.

In the releases before MSC.Marc 2000, the global remeshing/rezoning was done manually. When the mesh becomes too distorted because of the large deformation to continue the analysis, the analysis is stopped. A new mesh is created based on the deformed shape of the contact body to be rezoned. A data mapping is performed to transfer necessary data from the old, deformed mesh to the new mesh. The contact tolerance is recalculated (if not specified by user) and the contact conditions are redetected. The analysis then continues.

With the release of MSC.Marc 2000, the above steps can be done automatically. Based on the different user-specified remeshing criteria, the program determines when the remeshing/rezoning is required. The automatic remeshing control can be instructed through the ADAPT GLOBAL option or through automatic time stepping control. With automatic time stepping control, remeshing can be forced when the mesh of the body is distorted during the analysis. When remeshing/rezoning on a 2-D application, the program finds the outline of the body to be rezoned and repairs the outline to remove possible penetrations. Then, the program calls the mesher to create a new mesh based on the cleaned outline. Furthermore, the program performs data transfer from the old mesh to the new mesh, redetermines the contact conditions, and continues the analysis.

The 2-D automatic remeshing includes checking the outline curvature and thin region for local mesh refinement to produce better mesh that captures the changes in the geometry. Another remeshing criterion allows you to control the new mesh by specifying the target number of elements rather than the element edge length. You can also control number of elements based on the previous mesh or using the percentage tolerance. When using the penetration remeshing criterion, you can specify the penetration tolerance to control when to remesh.

Notes: All loading and boundary conditions on bodies being remeshed must be applied using contact (rigid) bodies. However, in the analysis with remeshing, you can apply loads and boundary conditions on the bodies not being remeshed.

Numbering of Contact Bodies:

- **Default:** When defining contact bodies for a deformable-to-deformable analysis, it is important to define them in the proper order. As a general rule:
A body with a finer mesh should be defined before a body with a coarser mesh. This rule applies both before and after remeshing.
In case of a contact between bodies with large difference in stiffness, like rubber and steel, the softer body should have the lowest number.
- **Automatic:** This is described in this chapter and can be very important for remeshing problems.

This chapter demonstrates the capability of the automatic remeshing/rezoning feature available in Marc by [Elastomeric Seal Simulation](#) and [Tape Peeling Simulation](#). Steps on remeshing criterion definition are highlighted.

Elastomeric Seal Simulation

A rubber seal with a rectangular cross-section (1.8x1.2) is pressed laterally by rigid die. The plane strain condition is assumed. Because of the symmetry, only a half of the seal is considered. See Figure 3.28-1 below for the placement of the rubber seal and the rigid dies. The die pressure is added to the top of the seal and simulated by moving the top rigid surface down. In the current release, other than volumetric loads, one cannot put a boundary condition on a mesh that will automatically be remeshed. Total load is applied in two steps in the analysis. In the first step, the top rigid surface moves down 0.2 cm within 5 equal increments. In the second step, the top rigid surface moves down 0.5 cm within 95 equal increments.

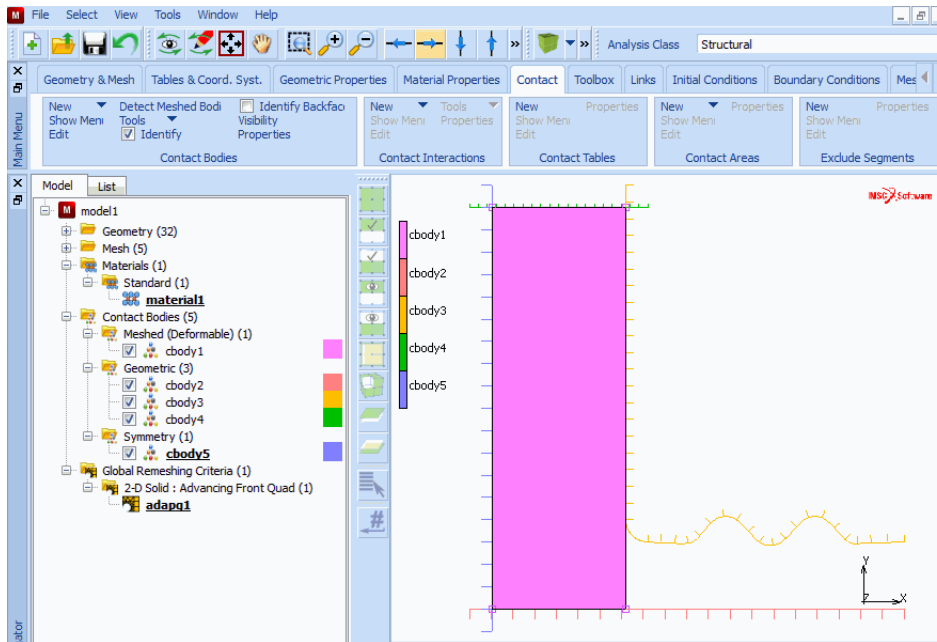


Figure 3.28-1 Simulation of a Rubber Seal: FE-Mesh and Geometry

Although the geometry itself is simple, the severely deformed configuration at an intermediate stage leads to a premature termination of the analysis due to excessive distortion in the elements and penetration between contact bodies (see Figure 3.28-2). Remeshing/rezonig operation is clearly required for a successful completion of the analysis.

The analysis starts with one single element (obviously, one element is not enough to model the rubber seal). A remeshing is performed at increment 0 to demonstrate that a very crude model can be initially given, if the model is remeshed before the analysis begins. Afterwards, the remeshing/rezonig is done at each five 5 increment interval to prevent from highly distorted elements and severe penetration between contact bodies. Element type 11 is used in the analysis within the updated Lagrangian framework.

The rubber seal is modeled using Mooney constitutive model. The material parameters are given as $C_1=8\text{N/cm}^2$ and $C_2=2\text{N/cm}^2$. The bulk modulus is 10000N/cm^2 .

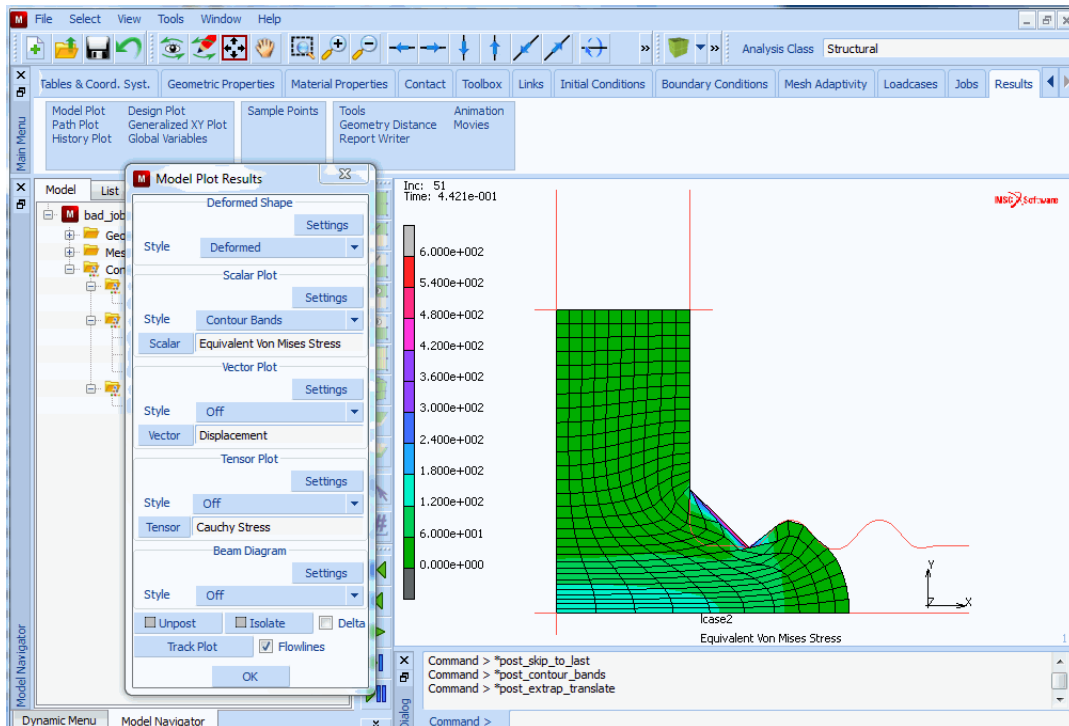


Figure 3.28-2 Analysis without using Remeshing/Rezoning

Analysis

Model Generation

Model generation contains geometry definition, element definition, clean geometry, and clean mesh. See [Figure 3.28-1](#).

MESH GENERATION

PTS ADD

```

-1.0e+0 -9.0e-1 0.0e+0
 9.5e-1 -9.0e-1 0.0e+0
-9.0e-1 1.0e+0 0.0e+0
-9.0e-1 -1.0e+0 0.0e+0
-1.0e+0 9.0e-1 0.0e+0
-2.0e-1 9.0e-1 0.0e+0
-3.0e-1 1.0e+0 0.0e+0
-3.0e-1 -5.0e-1 0.0e+0
    
```

```

-2.0e-1 -6.0e-1 0.0e+0
-1.0e-1 -6.0e-1 0.0e+0
 0.0e+0 -6.0e-1 0.0e+0
 1.0e-1 -5.0e-1 0.0e+0
 2.0e-1 -5.0e-1 0.0e+0
 3.0e-1 -6.0e-1 0.0e+0
 4.0e-1 -6.0e-1 0.0e+0
 5.0e-1 -5.0e-1 0.0e+0
 6.0e-1 -5.0e-1 0.0e+0
 7.0e-1 -6.0e-1 0.0e+0
 8.0e-1 -6.0e-1 0.0e+0
 9.5e-1 -6.0e-1 0.0e+0
CRVS ADD
 1 2 3 4 5 6 7 8
CURVE TYPE
  INTERPOLATE
  RETURN
CRVS ADD
 9 10 11 12 13 14 15 16 17 18 19 20
END LIST
CURVE TYPE
  FILLET
  RETURN
CRVS ADD
 4 5 0.1
CURVE TYPE
  COMPOSITE
  RETURN
CRVS ADD
 4 6 5
END LIST
NODES ADD
 -9.0e-1 -9.0e-1 0.0e+0
 -3.0e-1 -9.0e-1 0.0e+0
 -3.0e-1 9.0e-1 0.0e+0
 -9.0e-1 9.0e-1 0.0e+0

```

```
ELEMS ADD
  1 2 3 4
SWEEP
  ALL
  REMOVE UNUSED NODES
  REMOVE UNUSED POINTS
  RETURN
RENUMBER
  ALL
  RETURN
MAIN
```

Material Properties

```
MATERIAL PROPERTIES
  MORE
  MOONEY
    C10
      8
    C01
      2
  BULK MODULUS
    10000
  OK
ELEMENTS ADD
  ALL EXIST
  MAIN
```

Contact Definition

In an analysis using automatic remeshing/rezoning techniques, all boundary conditions and loads applied to the body to be remeshed/rezoned are applied via proper definition of contact (rigid) bodies. The die pressure is simulated by the motion of top rigid surface and the symmetric condition is modeled using a specifically designed rigid body (left rigid surface).

```
CONTACT
  CONTACT_BODIES
    ID CONTACT
    NEW
```



```
DEFORMABLE
  OK
ELEMENTS ADD
ALL EXIST
NEW
RIGID
  DISCRETE
  OK
CURVES ADD
  1
END LIST
NEW
RIGID
  DISCRETE
  OK
CURVES ADD
  4
END LIST
NEW
RIGID
  VELOCITY PARAMETERS
    VELOCITY Y
      -1
    INITIAL VELOCITY Y
      -1
    OK
  DISCRETE
  OK
CURVES ADD
  3
END LIST
NEW
SYMMETRY
  DISCRETE
```

```
OK
CURVES ADD
  2
END LIST
FLIP CURVES
  2
  1
END LIST
MAIN
```

Remeshing/Rezoning Parameters

Definition of remeshing/rezoning parameters is a new and key step in performing an analysis with automatic remeshing/rezoning. These parameters include the type of mesher to be used, the remeshing criteria and related parameters, the element target length in the new mesh, and the contact body to be remeshed.

The meshers available in Marc are advancing front mesher for both quadrilaterals and triangles, overlay quad mesher, and Delaunay triangle mesher.

Start from the MAIN MENU; Click MESH ADAPTIVITY; Click GLOBAL REMESHING; Choose the type of mesher; Define remeshing criteria and element target length; specify the contact body to be remeshed.

```
MESH ADAPTIVITY
  GLOBAL REMESHING
    NEW
    ADVANCING FRONT QUAD use advancing front quad mesher
    PENETRATION check penetration each increment
    IMMEDIATE remesh before analysis begins (1st criterion)
    ANGLE DEVIATION (remesh when angle change from
                    the undeformed angle)
    ELEMENT EDGE LENGTH define element edge length
      0.07
    OK
    REMESH BODY define the body to be remeshed
      CBODY1
    MAIN
```

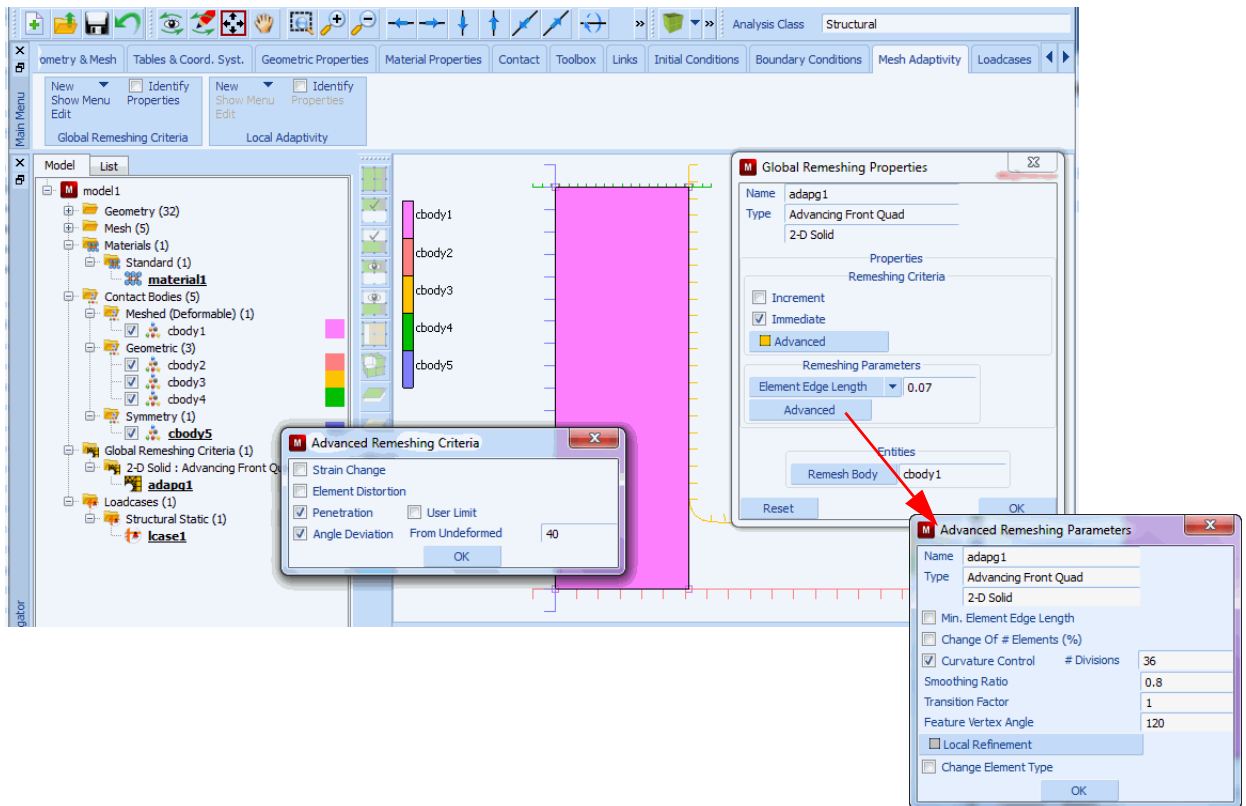


Figure 3.28-3 Define Remeshing/Rezoning Parameters

Note: The remeshing/rezoning analysis involves the interpolation and extrapolation of nodal as well as elemental quantities. This introduces approximations in the nodal and elemental quantities and can make the step after remeshing difficult to converge. For this reason, experience shows that care must be taken to:

- not remesh the body too frequently and
- keep the element or use the number of element control target length such that the change in mesh density or element length after remeshing is not too drastic. In this regard, the criterion based on the percent change of number of elements in the Advanced Remeshing Parameters menu can be used.

Load Steps

Total load is applied in two loadcases in the analysis. In the first loadcase, the top rigid surface moves down 0.2 cm within 5 equal increments. In the second step, the top rigid surface moves down 0.534 cm within 95 equal increments. In the second loadcase, only the deviatoric part of stresses is included in stiffness matrix calculation in order to improve the convergence of the calculations.

A new click activates the defined remeshing/rezoning parameters for the required loadcases.

```
LOADCASE
  NEW
  MECHANICAL
  STATIC
    GLOBAL REMESHING                                activate global remeshing for 1st loadcase
      ADAPG1
      OK
    TOTAL LOADCASE TIME
      0.2
    FIXED PARAMETERS
      # STEPS
        5
      OK (twice)
  NEW
  STATIC
    GLOBAL REMESHING                                activate global remeshing for 2nd loadcase
      ADAPG1
      OK
    SOLUTION CONTROL
      DEVIATORIC
      OK
    TOTAL LOADCASE TIME
      0.534
    FIXED PARAMETERS
      # STEPS
        95
      OK (twice)
  MAIN
```

Job Parameters

Element type 11 is used; Both loadcases are activated; Updated Lagrangian elasticity is used; Stress tensor and equivalent von Mises stress are written into the post file; Plane strain condition is assumed.

An important step in remeshing analysis is to define the upper bound to the nodes that lie on the periphery of any deformable surface, since remeshing may considerably change surface entities and surface node.

JOBS

ELEMENT TYPES

MECHANICAL

PLANE STRAIN

11

OK

ALL EXIST

RETURN (twice)

NEW

MECHANICAL

LCASE1

LCASE2

MESH ADAPTIVITY

MAX # CONTACT NODES

2000

OK

ANALYSIS OPTIONS

ELASTICITY PROCEDURE: LARGE STRAIN - UPDATED LAGRANGE

OK

CONTACT CONTROL

ADVANCED CONTACT CONTROL

PENETRATION CHECK: AUTOMATIC

OK (twice)

JOB RESULTS

ELEMENT TENS: CAUCHY

ELEMENT SCAL: VON MISES

OK

PLANE STRAIN

OK

MAIN

Save Model, Run Job, and View Results

JOBS

RUN

SUBMIT 1

MONITOR

OK

SAVE

MAIN

RESULTS

OPEN DEFAULT

DEF ONLY

CONTOUR BAND

SCALAR

EQUIVALENT VON MISES STRESS

OK

MONITOR

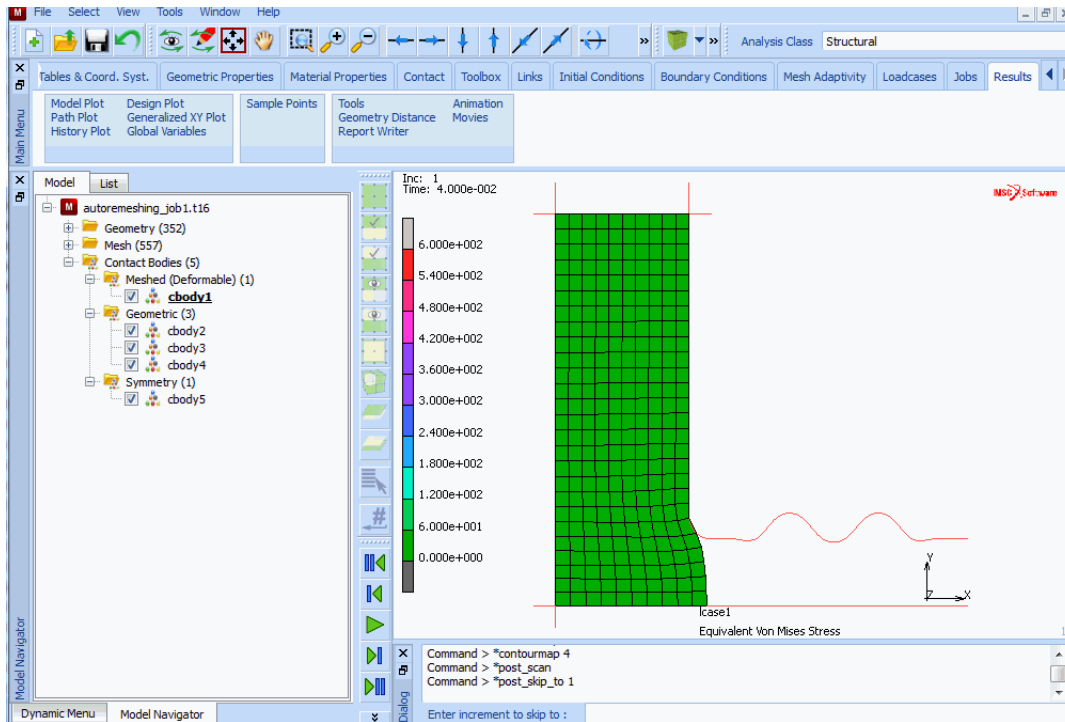


Figure 3.28-4 FE-Mesh before Analysis Begins (after First Remeshing)

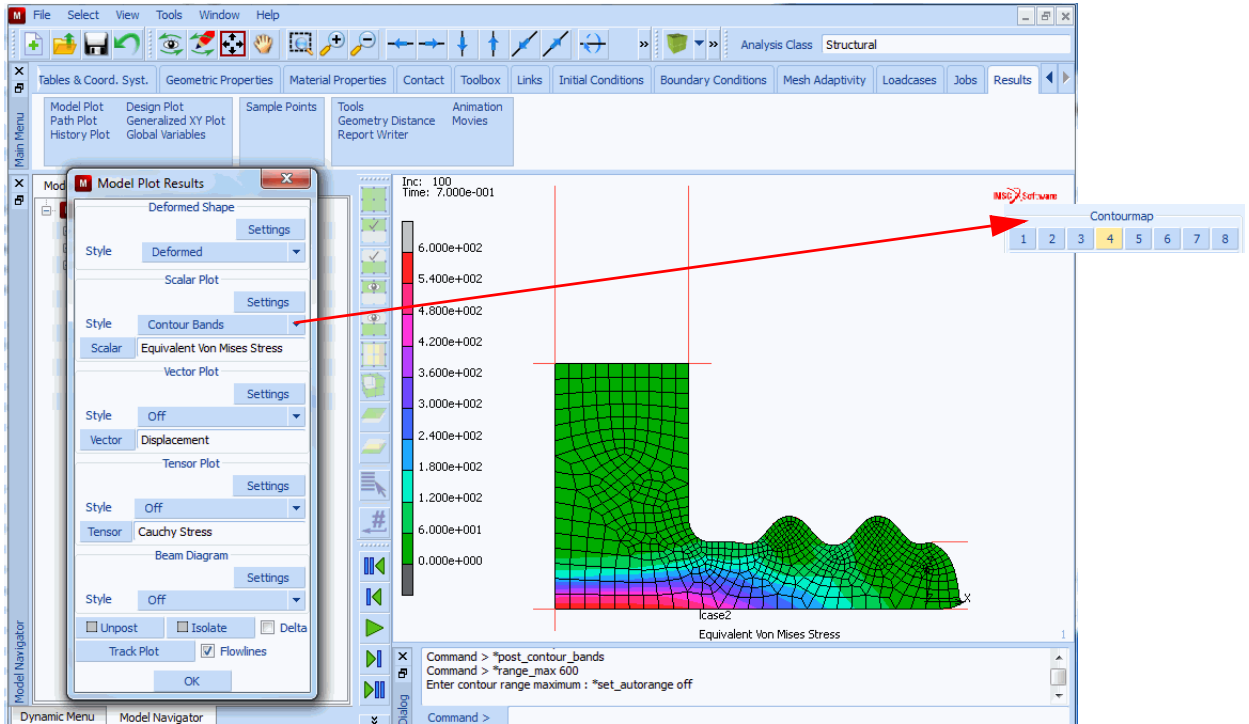


Figure 3.28-5 Deformed Mesh and Distribution of Equivalent von Mises Stress at Increment 100

Tape Peeling Simulation

Tape peeling simulation with Marc is done next to predict the strength of the adhesive in the tape. The model consists of two types of materials – film and adhesive, which are glued together. The adhesive layer is glued to a desk (see Figure 3.28-6). The analysis starts by applying a point load to the tip of the film to simulate peeling operation. As the peeling takes place, the adhesive layer gets torn off the desk surface. The mesh becomes distorted because of the large deformation in the adhesive layer. Without remeshing, this simulation would terminate earlier.

In this example, we again demonstrate how to use global remeshing for this type of applications. Particularly in this example, we show how the local refinement is done based upon the outline curvature detection in the peeling area.

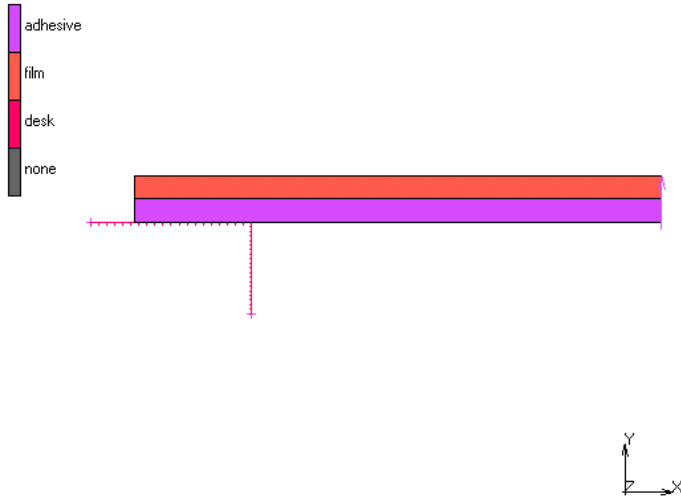


Figure 3.28-6 Adhesive Layer glued to a Desk

Analysis

Model Generation

This example uses triangular element type 155 which can be used for analysis of elastomeric materials. The tape has a geometry of 0.002 m in length and 0.0001 m in thickness. Plane strain assumption is used. The film layer and the adhesive layer both take half of the thickness. The geometry model is read from the predefined model:

remeshing_rezoning_b_mesh.proc.

```
FILE
  MERGE
    MERGE FILE
      remeshing_rezoning_b_mesh.proc
    OK
```

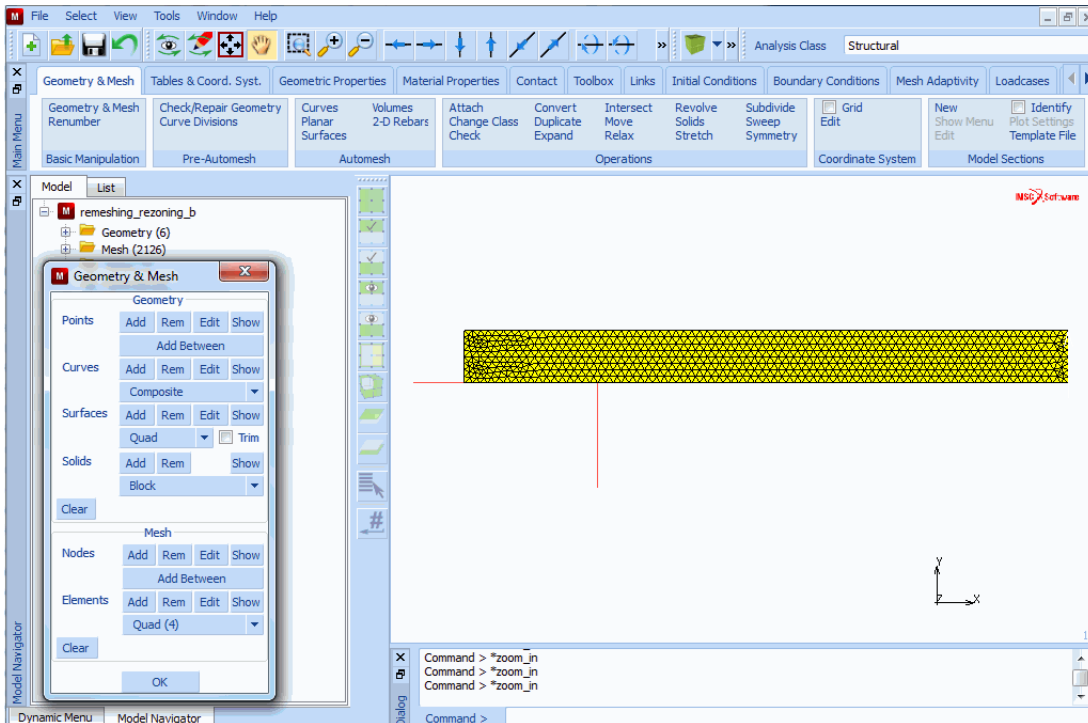



Figure 3.28-7 Geometry Model using Triangular Element Type 155

Save the model as `remeshing_rezoning.mfd`.

The model should be saved from time to time to avoid any lost of the input during the preprocessing. Click on **SAVE** to do this.

Boundary Condition

A point load associated with a time table is defined and assigned to the tip of the film layer (see [Figure 3.28-8](#)). Note that this portion of the mesh is not being remeshed; hence, application of loads and boundary conditions on this part of mesh is allowed.

```
BOUNDARY CONDITIONS
MECHANICAL
TABLES
TABLE TYPE: time
ADD POINT
    0 0
    20 20
SHOW MODEL
```

```
RETURN  
POINT LOAD  
Y FORCE:  
1.0  
TABLE  
CURRENTLY DEFINED TABLE  
table1  
OK (twice)  
NODES: ADD  
86  
END LIST  
RETURN  
ID BOUNDARY CONDS  
RETURN
```

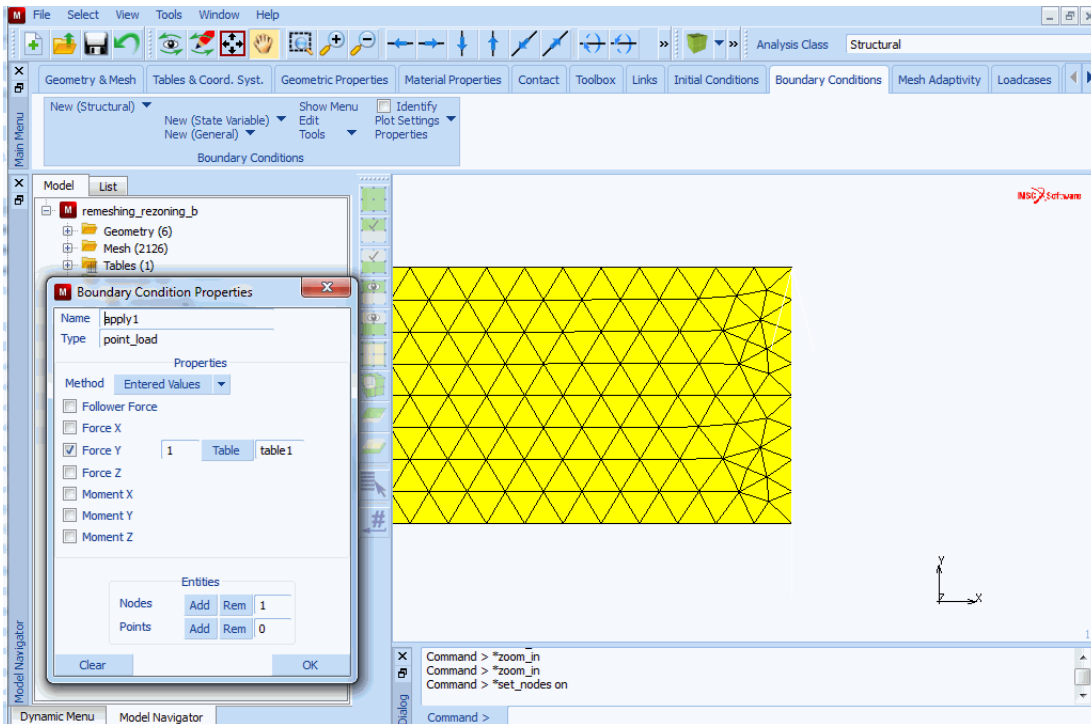


Figure 3.28-8 Mechanical Boundary Conditions Menu adding Point Loads

Contact Definition

Here, we define the contact bodies first. The material properties are assigned to the different contact bodies later. Three contact bodies are identified: adhesive, film, and desk. The GLUE option is used in the contact table.

```
CONTACT
  CONTACT BODIES
    NEW
    NAME
      adhesive
    CONTACT BODY TYPE
      deformable
    ELEMENTS ADD
      (add all the elements in the lower part of the mesh)
    END LIST
  NEW
  NAME
    film
  CONTACT BODY TYPE
    deformable
    ELEMENTS ADD
      (add all the elements in the upper part of the mesh)
    END LIST
  NEW
  NAME
    desk
  CONTACT BODY TYPE
    rigid
  CURVES ADD
    1 2
  END LIST
  ID CONTACT
    (See Figure 3.28-9)
  RETURN
CONTACT TABLES
  NEW
  PROPERTIES
    FIRST adhesive SECOND film: GLUE
    FIRST adhesive SECOND desk: GLUE
    (See Figure 3.28-10)
```

OK
RETURN (twice)

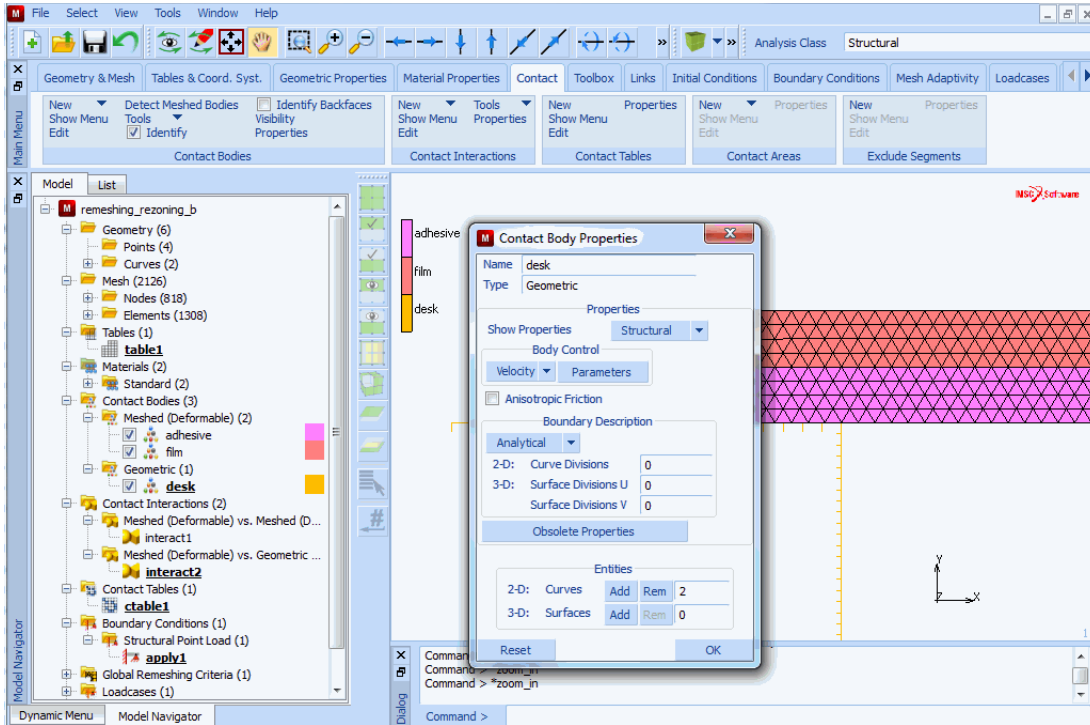


Figure 3.28-9 Contact Bodies Menu defining Three Contact Bodies

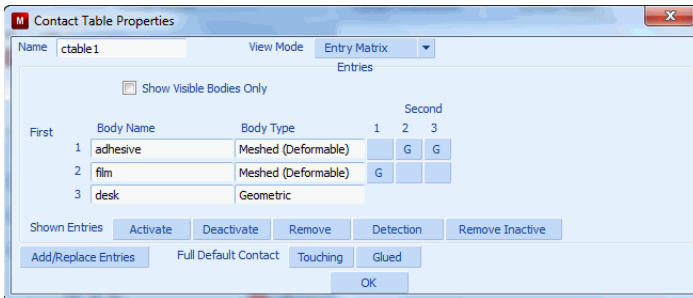


Figure 3.28-10 CONTACT TABLE PROPERTIES Submenu identifying Adhesive, Film, and Desk

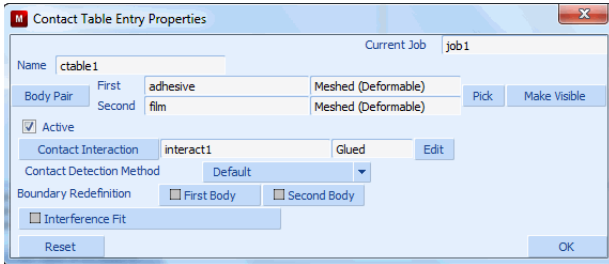


Figure 3.28-11 Contact Table Entry Properties

Material Properties

Use elasto-plastic material for the film and Mooney type material for the adhesive. Select the contact body to assign the material properties.

MATERIAL PROPERTIES

NEW

NAME

film

ISOTROPIC

YOUNG'S MODULUS

1.0e9

POISSON'S RATIO

0.3

ELASTIC-PLASTIC

INITIAL YIELD STRESS

1.0e7

OK (twice)

SELECT

SELECT CONTACT BODY ENTITIES

film

OK

RETURN

ELEMENTS ADD

ALL: SELECT

NEW

adhesive

MORE

MOONEY

C10
200000
OK
ELEMENTS ADD
ALL: UNSEL.
RETURN
ID MATERIALS
RETURN

(See Figure 3.28-12)

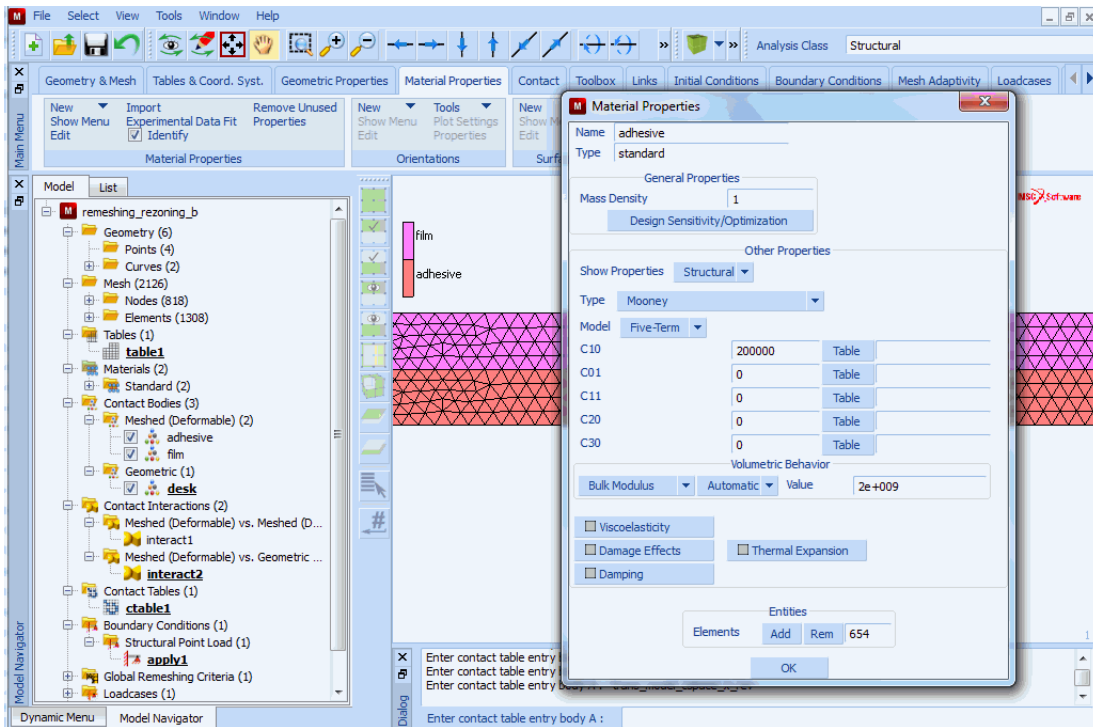


Figure 3.28-12 MATERIAL PROPERTIES Menu using Adhesive

Remeshing/Rezoning Parameters

We will use triangular mesher for remeshing on the adhesive body. Number of elements desired is 600 and the remeshing is needed when there is a distortion or at every five increments. By default, the curvature detection is used for the local refinement. The minimum element size is 1/3 of the element size computed for the remeshing.

MESH ADAPTIVITY
GLOBAL REMESHING

NEW
 ADVANCING FRONT TRIA
 INCREMENT FREQUENCY
 5
 ADVANCED
 ELEMENT DISTORTION
 OK
 # ELEMENTS SET
 600
 OK
 REMESH BODY
 adhesive
 RETURN

(See Figure 3.28-13)

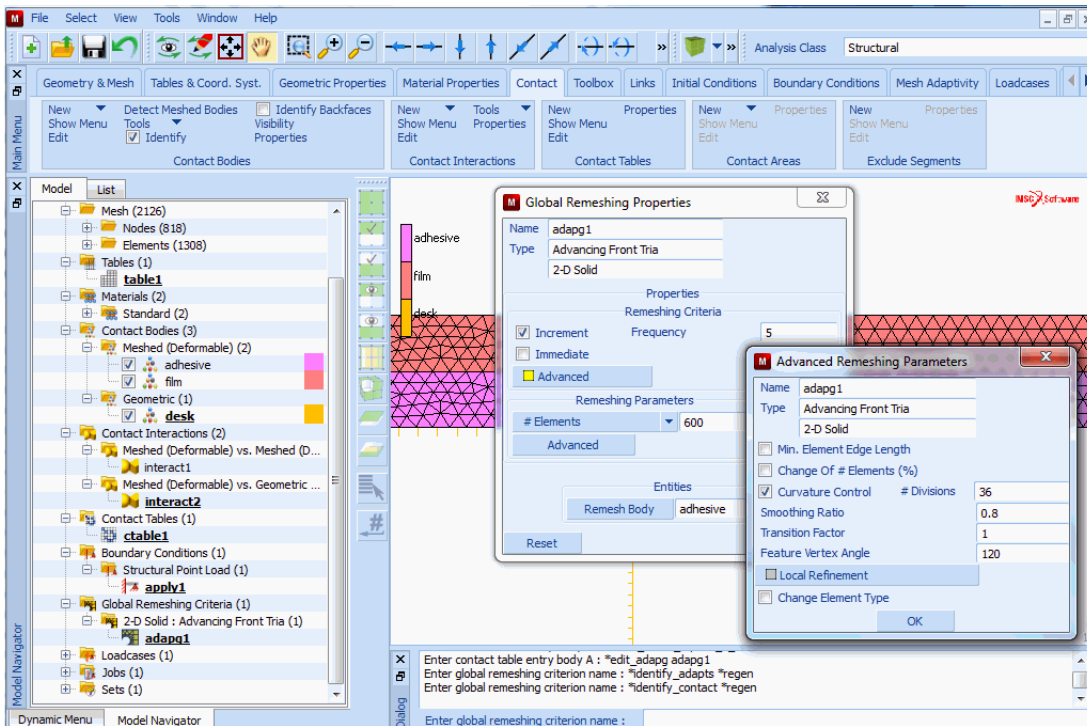


Figure 3.28-13 ADVANCING FRONT TRIA GLOBAL REMESHING Submenu

Load Steps

The load step control uses adaptive time stepping and automatic time step cutback. This makes the loading control more user friendly.

```
LOADCASES
  NEW
  MECHANICAL
    STATIC
      LOADS
        apply1
        OK
      CONTACT
        CONTACT TABLE
          Cable1
          OK (twice)
      GLOBAL REMESHING
        Adapg1
        OK
      TOTAL LOADCASE TIME
        15
      ADAPTIVE MULTI-CRITERIA
        OK
    RETURN (twice)
```

(See [Figure 3.28-14](#))

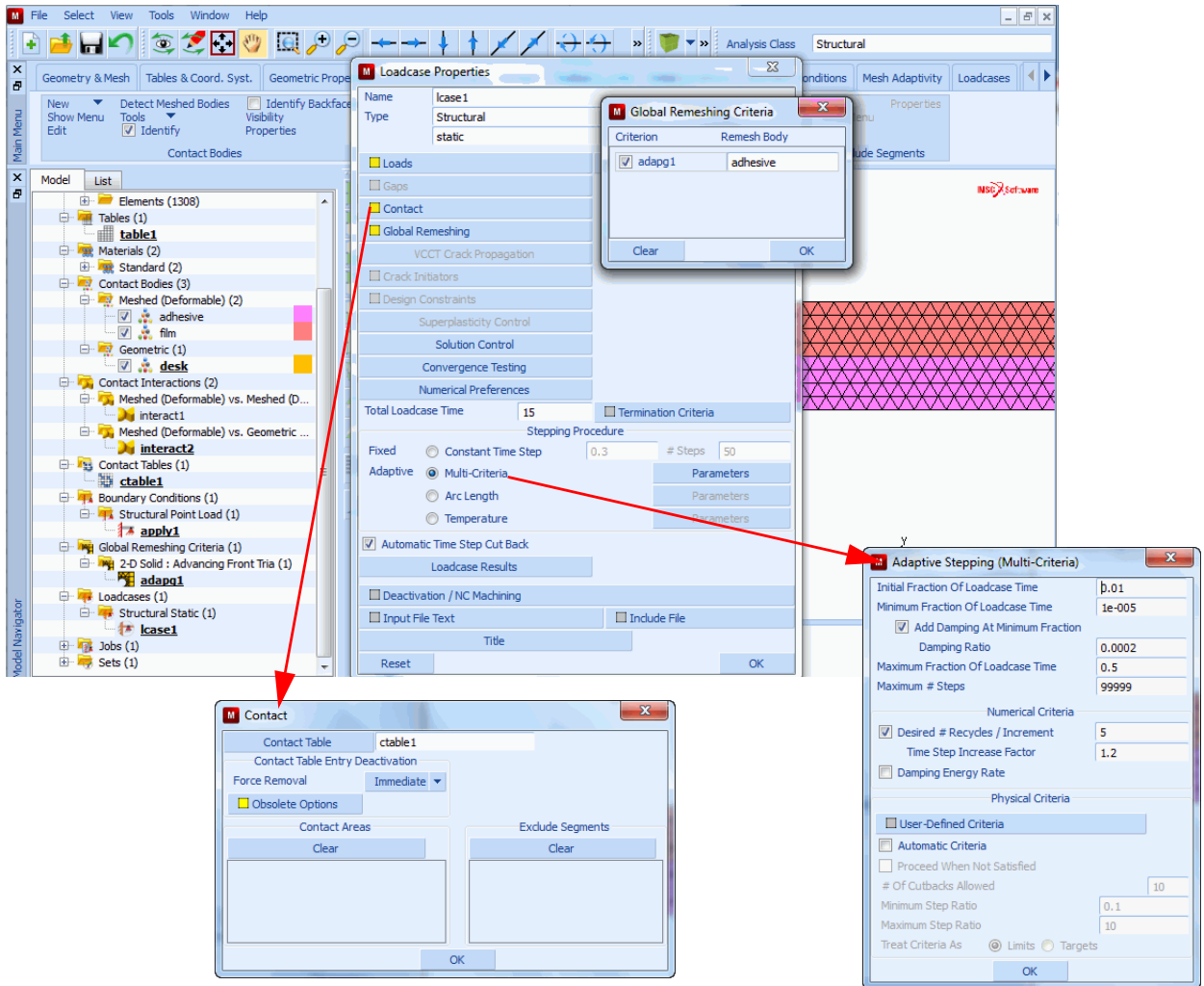


Figure 3.28-14 MECHANICAL STATIC PARAMETERS Submenu

Job Parameters

It is important to select correct element type and analysis control parameters. Here, we assign the loadcase, select right analysis control parameters, and the element type.

JOB

NEW

MECHANICAL

AVAILABLE

```
lcase1
CONTACT CONTROL
  ADVANCED CONTACT CONTROL
    PENETRATION CHECK: AUTOMATIC
    OK (twice)
MESH ADAPTIVITY
  MAX #CONTACT NODES/BODY
    4000
  OK
ANALYSIS OPTIONS
RUBBER ELASTICITY PROCEDURE:
  LARGE STRAIN-UPDATED LAGRANGE
PLASTICITY PROCEDURE:
  LARGE STRAIN MULTIPLICATIVE (See Figure 3.28-15)
OK
JOB RESULTS
  AVAILABLE ELEMENT SCALARS
    Equivalent Cauchy Stress
  OK
ANALYSIS DIMENSION: PLANE STRAIN (See Figure 3.28-17)
OK
ELEMENT TYPES
  MECHANICAL
    PLANE STRAIN
      TRIA
        155
      OK
    ALL: EXIST
  RETURN (twice)
```

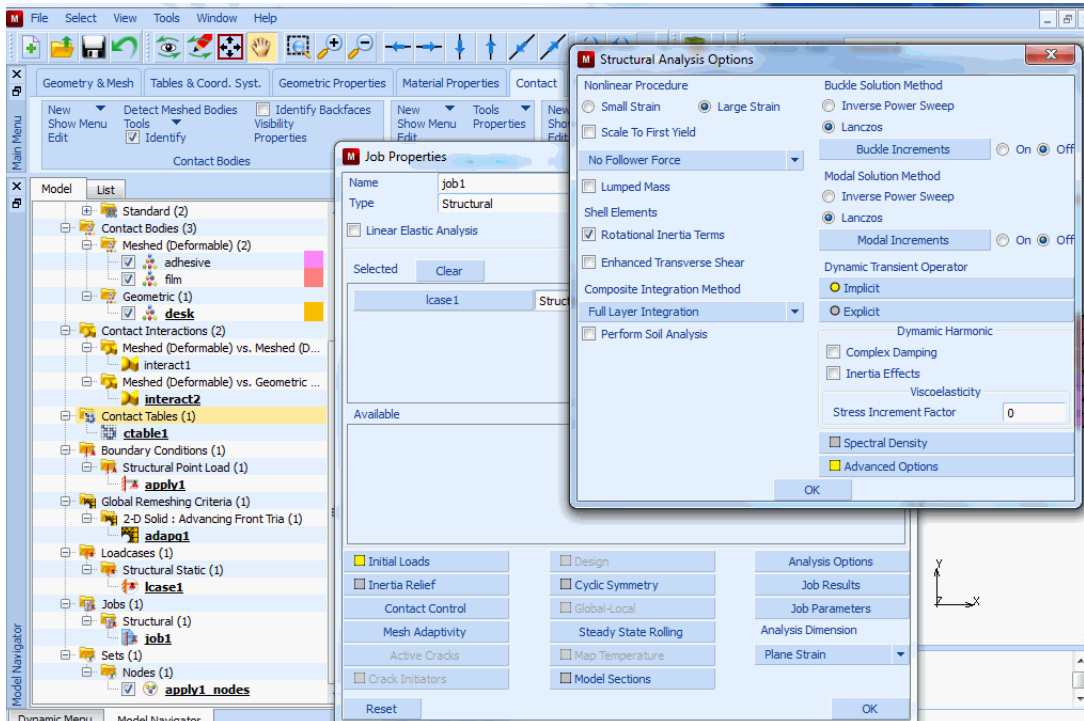


Figure 3.28-15 MECHANICAL ANALYSIS OPTIONS Submenu

Save Model, Run Job, and View Results

Here, we show how a job can be submitted and monitored while the analysis is going on. When the results are generated, you can view the results without waiting for the whole analysis is completed.

JOBS

RUN

SUBMIT1

MONITOR

OK

RETURN

RESULTS

OPEN DEFAULT

DEF ONLY

CONTOUR BAND

SCALAR

Equivalent Cauchy Stress

(you can check job running status here)

(go to see results)

OK
FILL
MONITOR

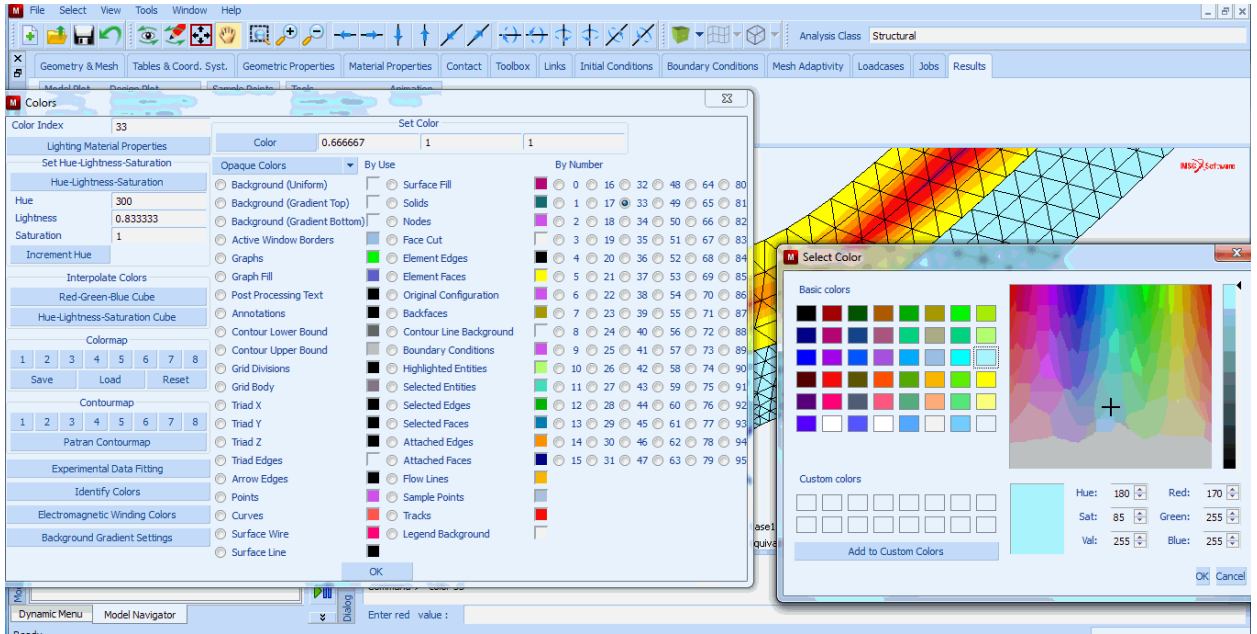


Figure 3.28-16 Color Selection

Here, the result shows the peeling of tape at time 15 (Figure 3.28-17). The local mesh refinement in the peeling area can be seen in Figure 3.28-18.

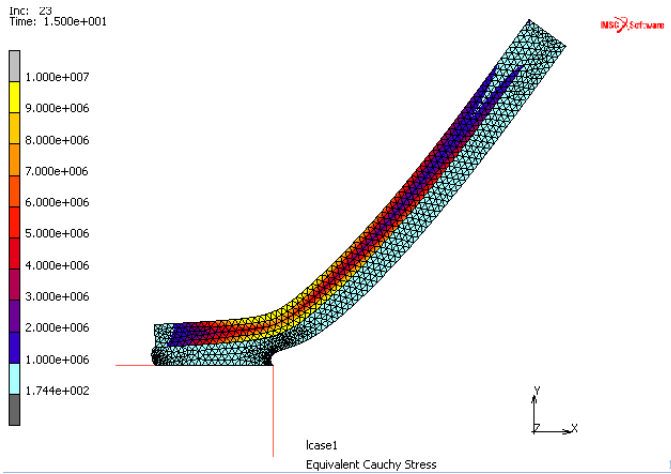


Figure 3.28-17 Peeling of Tape Results

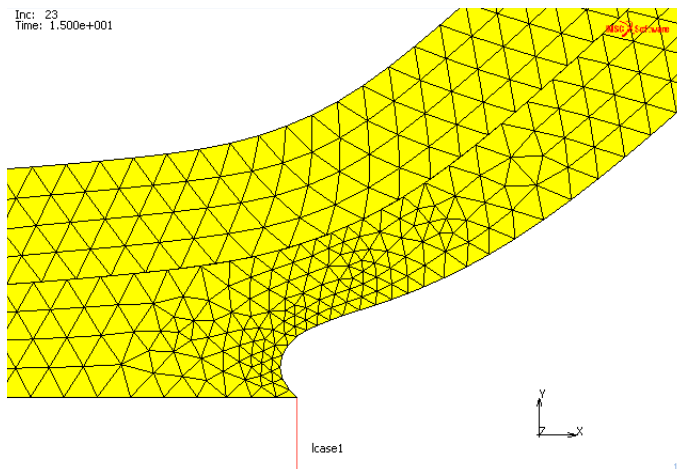


Figure 3.28-18 Mesh Refinement of Peeling Area

The flow of material in the adhesive is captured quite realistically.

Input Files

The files below are on your [delivery media](#) or they can be downloaded by your web browser by clicking the links (file names) below.

File	Description
remeshing_rezoning.proc	Mentat procedure file
remeshing_rezoning_b.proc	Mentat procedure file
remeshing_rezoning_b_mesh.mfd	Mentat model file

3.29 Multibody Contact and Remeshing

- Chapter Overview 1448
- Squeezing of a Rubber Body 1448
- Input Files 1468

Chapter Overview

In Marc, contact between deformable bodies is taken into account via multipoint constraint equations. The constraint equations used, and thus the quality of the solution, may depend on the numbering of the contact bodies. In general, the most optimal results are obtained if the numbering of the bodies is chosen such that:

- In case of contact between bodies with a large difference in stiffness, like rubber and steel, the softer body has the lowest number;
- In case of contact between bodies with a large difference in mesh density, the body with the finest mesh has the lowest number.

In Marc, the CONTACT TABLE option allows you to change the order in which contact is detected between bodies.

With these options:

1. for each set of deformable contact bodies, you can indicate in which order the search for contact is performed by the program. This is especially important for models with several deformable contact bodies, since it makes the searching order more or less independent from the body numbering and
2. for each set of deformable contact bodies, the optimal search order can also be determined by the program, based on the smallest element edge length at the outer boundary of the contact bodies. This can be important in an analysis with global remeshing, where the mesh density after remeshing of a contact body can be significantly different compared to the density before remeshing.

In this chapter, the new functionality is illustrated with analysis involving remeshing of a rubber body. Additionally, the use of stress-free projection at initial contact is shown. Stress-free projection is aimed to correct small geometry imperfections in a finite element model. This is done by adjusting the coordinates of a node lying within the contact tolerance zone, according to the projection of the node on the contacted segment.

Squeezing of a Rubber Body

A circular rubber body is squeezed between two steel legs. During the analysis, various parts of the rubber body are remeshed.

Background information

A circular rubber body is positioned between two steel legs and a rigid body as indicated in [Figure 3.29-1](#). The rubber material is described by a Mooney-Rivlin material with constants $C_{10} = 8$ and $C_{01} = 6$. The steel part is assumed to be linear elastic with Young's modulus $E = 3 \times 10^6$ and Poisson's ratio $\nu = 0.3$. The steel legs are loaded by two opposite point forces, which magnitude as a function of time is also given in [Figure 3.29-1](#). To illustrate the new contact functionality and the remeshing capabilities in Marc, six contact bodies are used: two deformable bodies for the steel part, three deformable bodies for the rubber part, and one rigid body. The two bodies for the steel part and the three bodies for the rubber part are glued together. The rubber body is frequently remeshed, where the element size and the remesh frequency for each of the three parts is different.

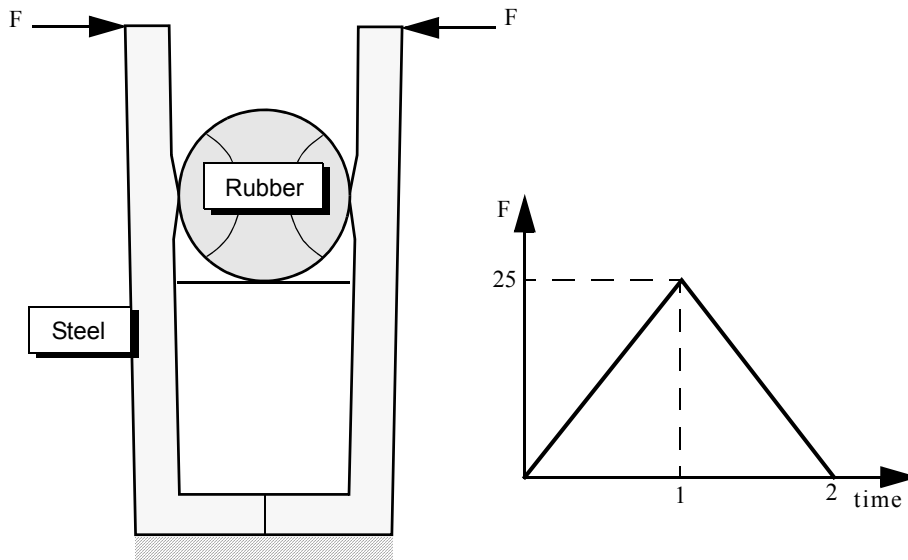


Figure 3.29-1 Rubber Body between two Steel Legs and a Rigid Body (left); Loading History (right)

A plane strain analysis is performed based on the updated Lagrange procedure. Both the steel and the rubber part are modeled using 4-node plane strain elements with full integration (Marc element type 11).

Model Generation

The finite element model is set up in the following order:

1. The right steel part is meshed by defining a number of quadrilateral surfaces and converting those surfaces into finite elements.
2. Three circles are created and intersected, after which the unnecessary curves are removed and the three parts of the rubber body are meshed using the advancing front quad mesher.
3. With the symmetry option, the elements of the left steel part are easily created.
4. Finally, the coordinates of two nodes of the steel part are modified, one node of the rubber is moved to simulate a geometry imperfection and the rigid body is defined by a straight line.
5. The various parts of the mesh are stored in element sets. The complete finite element model is shown in [Figure 3.29-2](#).

FILES

NEW

OK

RESET PROGRAM

VIEW

SHOW VIEW 1

```
      MAIN
MESH GENERATION
  PTS ADD
    0 0 0
    0.3 0 0
    0.325 1.2 0
    0.225 1.2 0
    0.2 0.1 0
    0 0.1 0
    0.2 0 0
    0.3 0.1 0
  FILL
SRFS ADD
  1 7 5 6
  7 2 8 5
  5 8 3 4
CONVERT
  DIVISIONS
    2 1
  SURFACES TO ELEMENTS
    1
  END LIST
  DIVISIONS
    1 1
  SURFACES TO ELEMENTS
    2
  END LIST
  DIVISIONS
    1 11
  SURFACES TO ELEMENTS
    3
  END LIST
  RETURN
SWEEP
  NODES
    ALL: EXIST.
```

```

RETURN
CURVE TYPE
  CENTER/RADIUS
  RETURN
CRVS ADD
  0 0.8 0
  0.2
DUPLICATE
  TRANSLATIONS
    0.3 0 0
  CURVES
    1
  END LIST
  TRANSLATIONS
    -0.3 0 0
  CURVES
    1
  END LIST
RETURN
INTERSECT
  CURVE/CURVE
    1 3 2
  END LIST
RETURN
CRVS REM
  18 15 12
  END LIST
AUTOMESH
  CURVE DIVISIONS
    FIXED # DIVISIONS
      5
    APPLY CURVE DIVISIONS
      19 16 11 4
    END LIST
    FIXED # DIVISIONS
      10

```

```
    APPLY_CURVE_DIVISIONS
      8 14 6 10
    END LIST
  RETURN (twice)
SWEEP
  POINTS
    ALL: EXIST.
  RETURN
AUTOMESH
  2D PLANAR MESHING
    ADV FRONT QUAD MESH!
      8 16 19 4 11 14 6 10 19 16 14
    END LIST
  RETURN (twice)
SWEEP
  REMOVE UNUSED POINTS
  RETURN
SYMMETRY
  ELEMENTS
    9 10 11 12 13 14 3 4 5 6 7 8 1 2
  END LIST
  RETURN
NODES EDIT
  25
  0.2 0.8 0.0
  268
  -0.2 0.8 0.0
MOVE
  TRANSLATIONS
    -0.0005 0 0
  NODES
    70
  END LIST
  RETURN
SELECT
  ELEMENTS
```

```

    9 10 11 12 13 14 3 4 5 6 7 8 1 2
END LIST
STORE
    steel_r
    OK
ALL: SELECT.
CLEAR SELECT

RETURN
POINTS ADD
    0.2 0.6 0
    -0.2 0.6 0
CURVE TYPE
    LINE
RETURN
CRVS ADD
    120 121
MAIN

```

*(repeat similar steps to create the element sets
 steel_l, rubber_l, rubber_m, and rubber_r)*

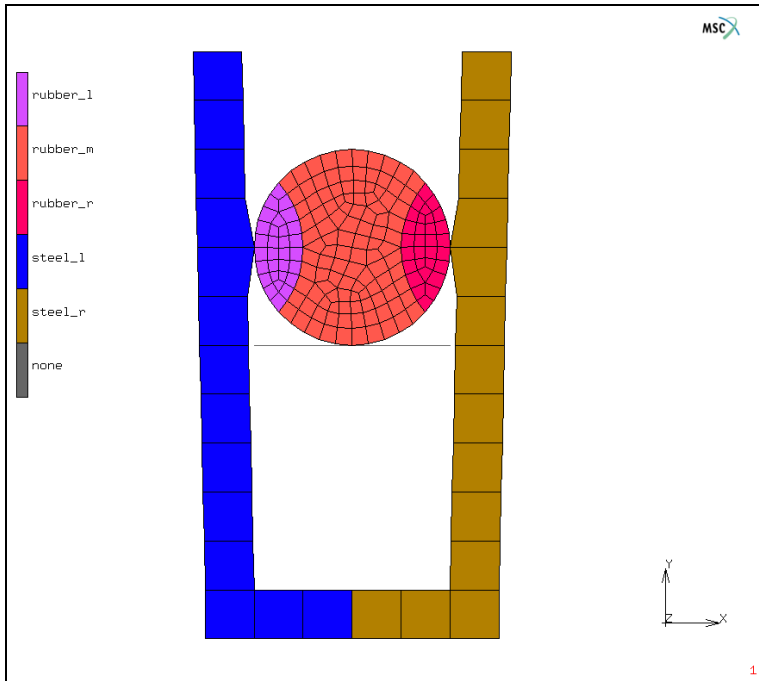


Figure 3.29-2 Finite Element Model

Boundary Conditions

Boundary conditions are defined to clamp the lower edge of the steel part and to load both steel legs. The load is set up via a table of type time.

```
BOUNDARY CONDITIONS
MECHANICAL
NEW
NAME
    Clamped
FIXED DISPLACEMENT
    ON X DISPLACEMENT
    ON Y DISPLACEMENT
    OK
NODES ADD
    1 2 3 8 248 249 250 254
END LIST
TABLES
NEW
```

```

NAME
    Force_time
TYPE
    TIME
    OK
ADD POINT
    0 0
    1 25
    2 0
FIT
SHOW MODEL
RETURN
NEW
NAME
    Load_left
POINT LOAD
    X FORCE
    1
    TABLE
        force_time
        OK (twice)
NODES ADD
    277
    END LIST
NEW
NAME
    Load_right
POINT LOAD
    X FORCE
    -1
    TABLE
        force_time
        OK (twice)
NODES ADD
    34
    END LIST
MAIN

```

Material Properties

Two different materials are defined: one for the steel part, one for the rubber part of the model.

MATERIAL PROPERTIES

NEW

NAME

steel

ISOTROPIC

YOUNG'S MODULUS

300000

POISSON'S RATIO

0.3

OK

ELEMENTS ADD

steel_l

steel_r

END LIST

NEW

NAME

rubber

MORE

MOONEY

C10

8

C01

6

OK

ELEMENTS ADD

rubber_l

rubber_m

rubber_r

END LIST

MAIN

Contact

Five deformable contact bodies and one rigid contact body are defined. The first two deformable bodies correspond to the steel part of the model and are called `Steel_left` and `Steel_right`. The remaining three deformable bodies

correspond to the rubber part of the model and are called Rubber_left, Rubber_middle and Rubber_right (see Figure 3.29-3) and for the Contact Table Entry menus (see Figure 3.29-4). Since, in this way, the default contact body numbering is not optimal, a contact table is defined to influence the order in which the search for contact is done. The optimal search order for contact between the following body pairs is determined by the program:

```
Steel_left and Rubber_left;
Steel_left and Rubber_middle;
Rubber_left and Rubber_middle;
Rubber_middle and Rubber_right;
Rubber_middle and Steel_right;
Rubber_right and Steel_right.
```

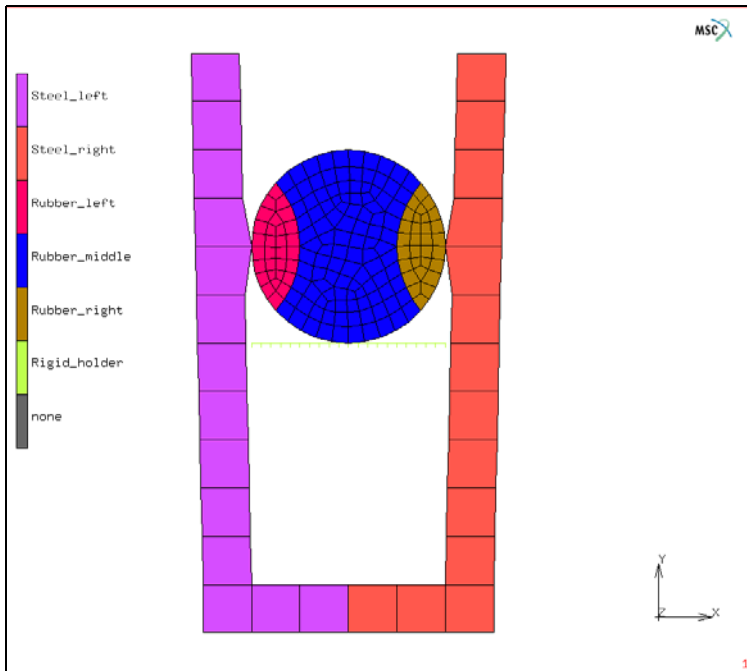


Figure 3.29-3 Contact Bodies

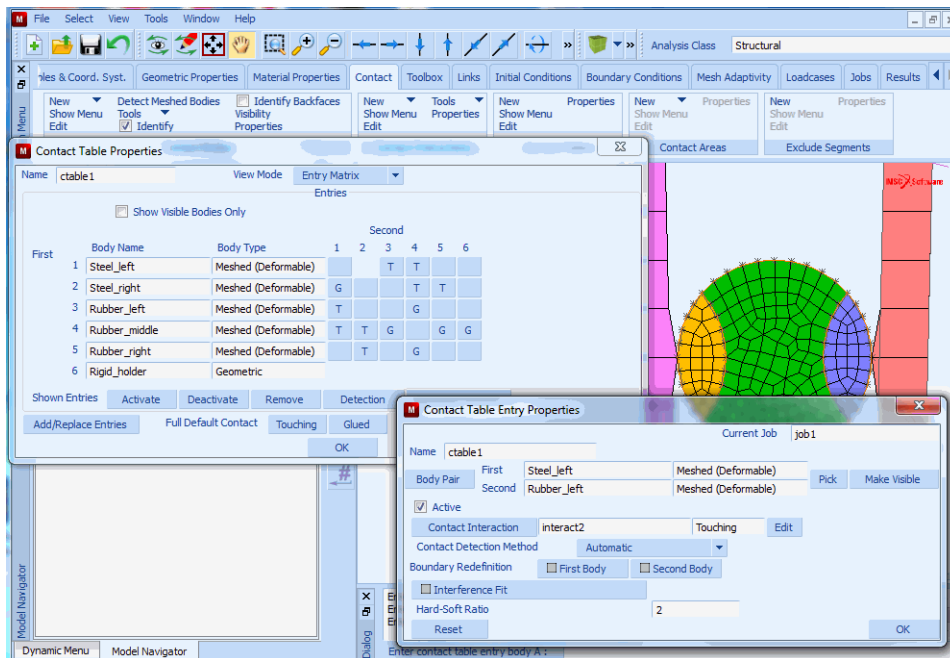


Figure 3.29-4 Contact Table Entries

The geometric imperfections are removed by activating stress-free projection for the pair of contact bodies Rubber_left and Rubber_middle. Moreover, although this does not influence the results, contact between Steel_left and Steel_right is forced to be from Steel_right to Steel_left.

A small nonzero separation force is defined for contact between the bodies Rubber_middle and Rigid_holder to prevent a rigid body motion of the rubber part.

CONTACT

CONTACT BODIES

NEW

NAME

Steel_left

DEFORMABLE

OK

ELEMENTS ADD

steel_l

NEW

NAME

Steel_right

```
DEFORMABLE
  OK
ELEMENTS ADD
  steel_r
NEW
NAME
  Rubber_left
DEFORMABLE
  OK
ELEMENTS ADD
  rubber_l
NEW
NAME
  Rubber_middle
DEFORMABLE
  OK
ELEMENTS ADD
  rubber_m
NEW
NAME
  Rubber_right
DEFORMABLE
  OK
ELEMENTS ADD
  rubber_r
NEW
NAME
  Rigid_holder
RIGID
  OK
CURVES ADD
  20
  END LIST
PLOT
  ELEMENTS SOLID
  MORE
```

IDENTIFY

CONTACT

REGEN

RETURN (thrice)

CONTACT TABLES

NEW

PROPERTIES

1 2

CONTACT TYPE: GLUE

CONTACT DETECTION METHOD: SECOND->FIRST

1 3

CONTACT TYPE: TOUCHING

CONTACT DETECTION METHOD: AUTOMATIC

1 4

CONTACT TYPE: TOUCHING

CONTACT DETECTION METHOD: AUTOMATIC

2 4

CONTACT TYPE: TOUCHING

CONTACT DETECTION METHOD: AUTOMATIC

2 5

CONTACT TYPE: TOUCHING

CONTACT DETECTION METHOD: AUTOMATIC

3 4

CONTACT TYPE: GLUE

CONTACT DETECTION METHOD: AUTOMATIC

PROJECT STRESS-FREE

4 5

CONTACT TYPE: GLUE

CONTACT DETECTION METHOD: AUTOMATIC

4 6

CONTACT TYPE: GLUE

SEPARATION FORCE

0.1

OK (twice)

MAIN

Mesh Adaptivity

During the analysis, global remeshing is applied to the rubber contact bodies. The advancing front quad mesher is used. The global remeshing parameters are set as follows:

```
Body Rubber_left: increment frequency 5, element edge length 0.016;  
Body Rubber_middle: increment frequency 7, element edge length 0.024;  
Body Rubber_right: increment frequency 9, element edge length 0.02.
```

MESH ADAPTIVITY

GLOBAL REMESHING

ADVANCING FRONT QUAD

INCREMENT

FREQUENCY

5

ELEMENT EDGE LENGTH

SET

0.016

OK

REMESH BODY

Rubber_left

OK

ADVANCING FRONT QUAD

INCREMENT

FREQUENCY

7

ELEMENT EDGE LENGTH

SET

0.024

OK

REMESH BODY

Rubber_middle

OK

ADVANCING FRONT QUAD

INCREMENT

FREQUENCY

9

```
ELEMENT EDGE LENGTH
SET
    0.02
OK
REMESH BODY
    Rubber_right
OK
MAIN
```

Loadcases

A mechanical static loadcase is defined in which the contact table and global remeshing criteria are selected (the previously defined boundary conditions are automatically selected). The total loadcase time is set to 2. A fixed stepping procedure is chosen with 50 steps. The default control settings for the Newton-Raphson iteration process are used.

```
LOADCASES
NEW
MECHANICAL
    STATIC
        CONTACT
            CONTACT TABLE
                ctable1
                OK (twice)
        GLOBAL REMESHING
            adapg1
            adapg2
            adapg3
            OK
        TOTAL LOADCASE TIME
            2
        # STEPS
            50
        OK
    TITLE
        Squeezing of a rubber body
        OK
MAIN
NAME
```

Jobs

A mechanical job is defined in which the previously defined loadcase is selected. The available CONTACT TABLE is used also for initial contact. Since the steel legs are mainly loaded in bending, the assumed strain formulation is activated. The updated Lagrange large strain elasticity procedure is used for the rubber part of the model. Because of remeshing, the upper bound to the number of contact segments and nodes per contact body is set to 500. A check on penetration should be performed every iteration of the Newton-Raphson process. The element type for the steel and rubber parts is set to 11. The model is saved and the job is submitted.

```
JOBS
  MECHANICAL
    lcase1
  CONTACT CONTROL
    INITIAL CONTACT
      ctable1
      OK
    ADVANCED CONTACT CONTROL
      PER ITERATION
      OK (twice)
  MESH ADAPTIVITY
    MAX # CONTACT NODES / BODY
      500
    OK
  ANALYSIS OPTIONS
    ADVANCED OPTIONS
      ASSUMED STRAIN
    OK
  RUBBER ELASTICITY PROCEDURE: LARGE STRAIN-UPDATED LAGRANGE
    OK
  ELEMENT TYPES
    MECHANICAL
      PLANE STRAIN
        11
      OK
    RETURN (twice)
  TITLE
    Squeezing of a rubber body
    OK
```

```
RUN
  SAVE MODEL
  SUBMIT 1
  MONITOR
  OK
MAIN
```

Results

In [Figure 3.29-5](#), the position of node 70 at increment 0 is compared with its original position. This clearly illustrates the use of the stress-free projection; since node 70 was within the contact tolerance, the gap is closed without introducing stresses.

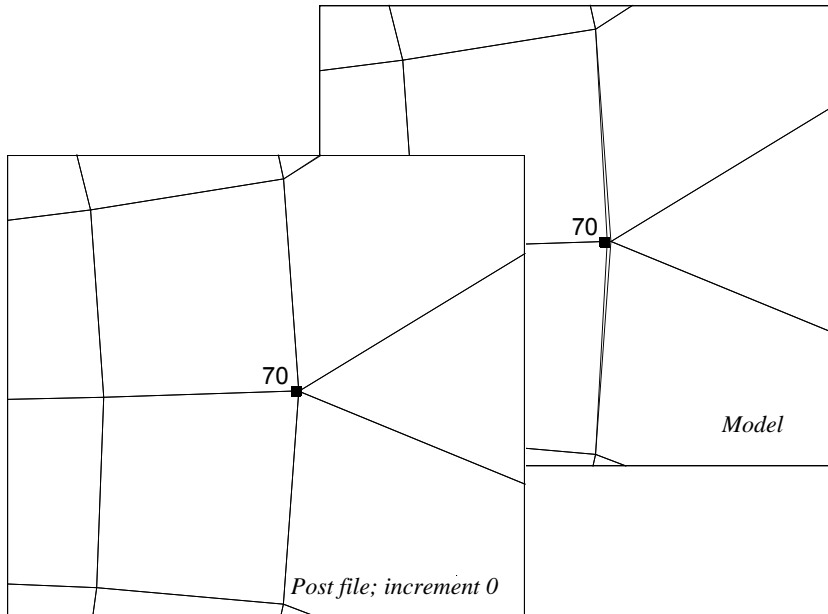


Figure 3.29-5 Result of Stress-free Projection of Node 70

In [Figure 3.29-6](#), a contour band plot of the contact status at increment 0 is given showing the effect of the automatic search order (contact between rubber and steel), and of enforcing contact from the second to the first body of the pair of deformable contact bodies (contact between the two steel bodies). Notice that for the boundary conditions only one node of body *Steel_right* touches body *Steel_left*.

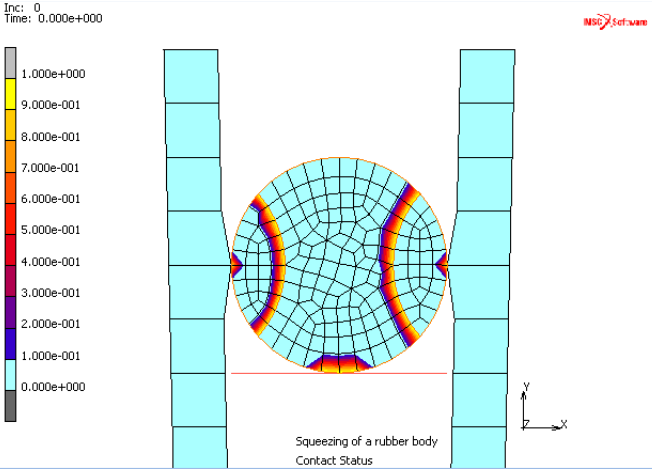


Figure 3.29-6 Contact Status at Increment 0

In Figure 3.29-7, contact status is shown for the bodies Rubber_middle and Rubber_right at increment 10. Due to remeshing, the edge length at the boundary of body Rubber_right becomes significantly smaller than that of body Rubber_middle. As a result, there is a change in the search order for contact: until increment 9, nodes of body Rubber_middle are touching body Rubber_right, at increment 10, nodes of body Rubber_right are touching body Rubber_middle.

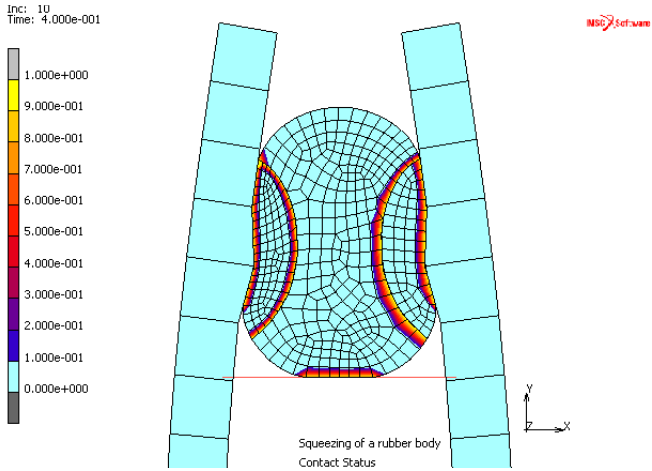


Figure 3.29-7 Contact Status at Increment 10

In Figure 3.29-8, the deformed configuration is shown at the maximum load level.

Inc: 25
Time: 1.000e+000

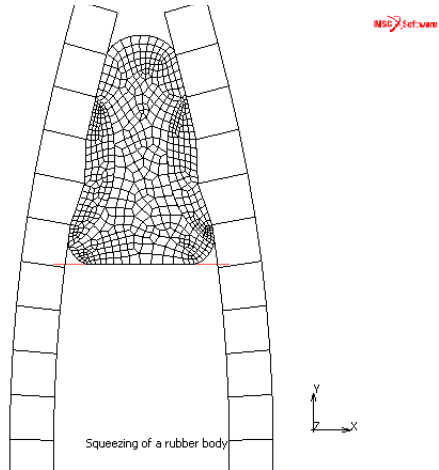


Figure 3.29-8 Deformed Configuration at Maximum Load Level

Finally, Figure 3.29-9 presents the force versus displacement curves for the nodes with point loads. Despite irregular remeshing, the behavior is remarkably symmetric.

RESULTS

OPEN DEFAULT

DEF ONLY

SCALAR

Contact Status

OK

CONTOUR BANDS

MONITOR

HISTORY PLOT

SET NODES

277 34

END LIST

COLLECT DATA

0 1000 1

NODES/VARIABLES

ADD VARIABLE

Time

Displacement X

Fit

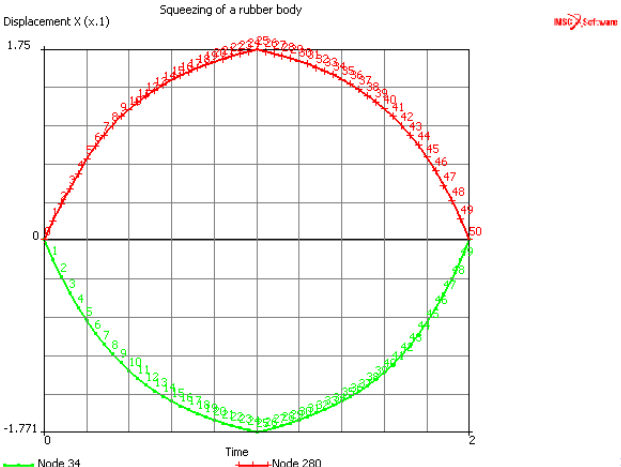


Figure 3.29-9 Displacement versus Time for Nodes with Point Loads

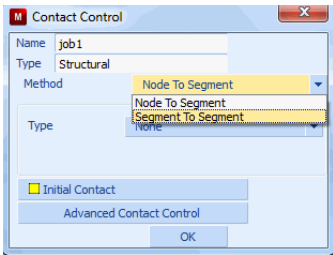


Figure 3.29-10 Contact Control

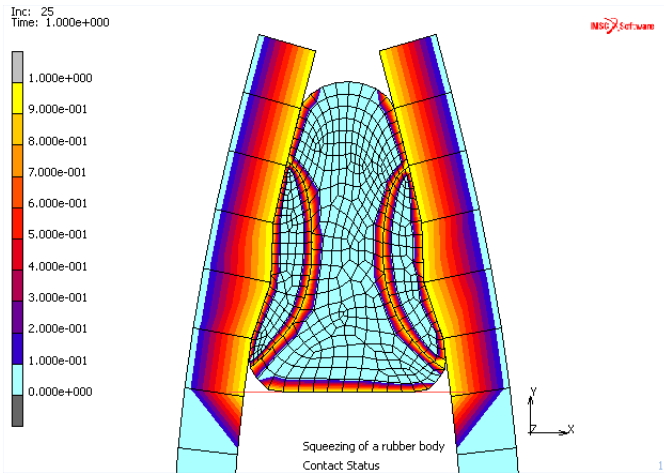


Figure 3.29-11 Squeezing of a Rubber Body

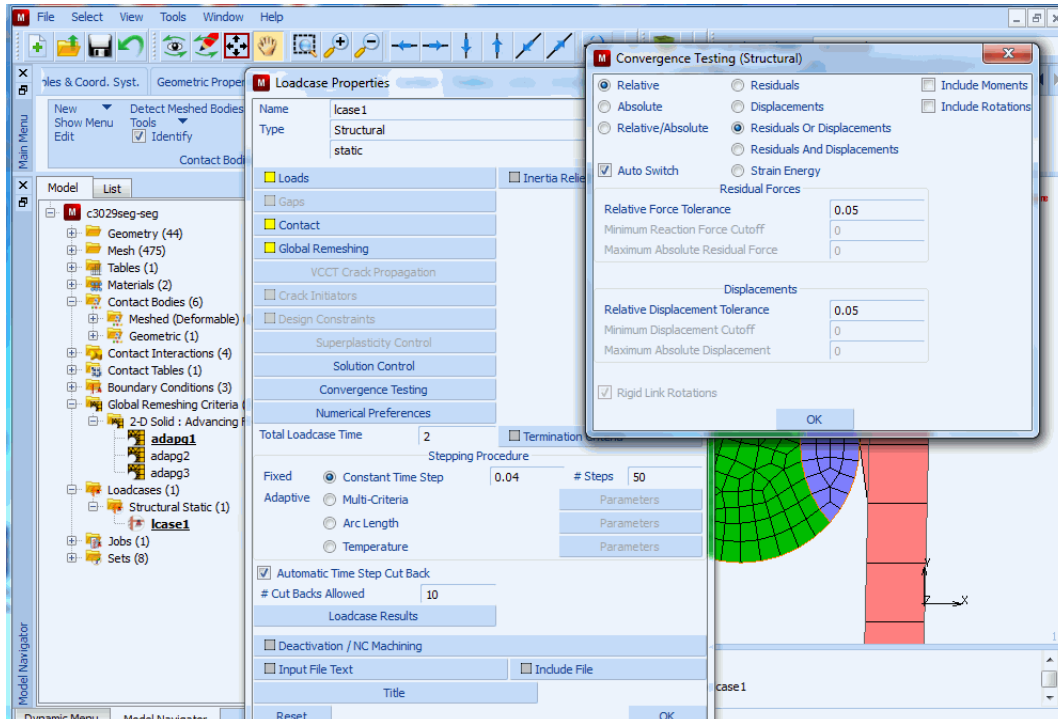


Figure 3.29-12 Convergence Testing

Input Files

The files below are on your [delivery media](#) or they can be downloaded by your web browser by clicking the links (file names) below.

File	Description
multibody_contact.proc	Mentat procedure file

3.30 Container

- Chapter Overview 1470
- Background Information 1470
- Detailed Session Description 1473
- Conclusion 1501
- Input Files 1501

Chapter Overview

This chapter demonstrates the modeling and analysis of the bottom of an aluminum container under internal pressure. The particular configuration of this container bottom leads to a snap-through problem. Accurate modeling of the geometry is essential since it dramatically influences the snap-through process.

The primary goal of this chapter is to show you three Mentat functionalities.

- Using nonlinear analysis to solve a snap-through analysis problem
- Using the TABLES option to specify input data that changes with time, plastic strain, etc.
- Animating the results of an analysis

Background Information

Description

The container, a soft drink can, is assumed to be a circle cylinder with a radius of 1.3 inches and a total height of 4.8 inches. The container (*see note below*) is made out of aluminum and has a wall thickness of 0.025 inches



Figure 3.30-1 Aluminum Container

Note: At times, the container may be referred to as *can* in the text.

Idealization

The geometry of this problem is fairly simple due to two factors. The first is that the geometry and the loading of the container are axisymmetric and allow you to perform an axisymmetric analysis. The second factor is that the focus of the analysis is restricted to the phenomena that occur at the bottom of the container. In this analysis, the height of the container, h , is limited to a length where the edge effects are damped out. The theory behind this assumption is explained below.

$$\text{If } h = 2.5\sqrt{rt}$$

where

r = the radius of the container,

t = the wall thickness,

the solution decreases to about 4% of its value at the bottom edge. In this example, it means you can safely ignore the influence of the top edge since the critical height, h , is equal to 0.4519, calculated as follows:

$$h = 2.5\sqrt{1.307 \times 0.025} = 0.4519$$

An awareness of this decay distance is very important in numerical calculations. If you wish to correctly capture the behavior of the solution in the edge region, the typical finite element size must be small in comparison to the decay distance.

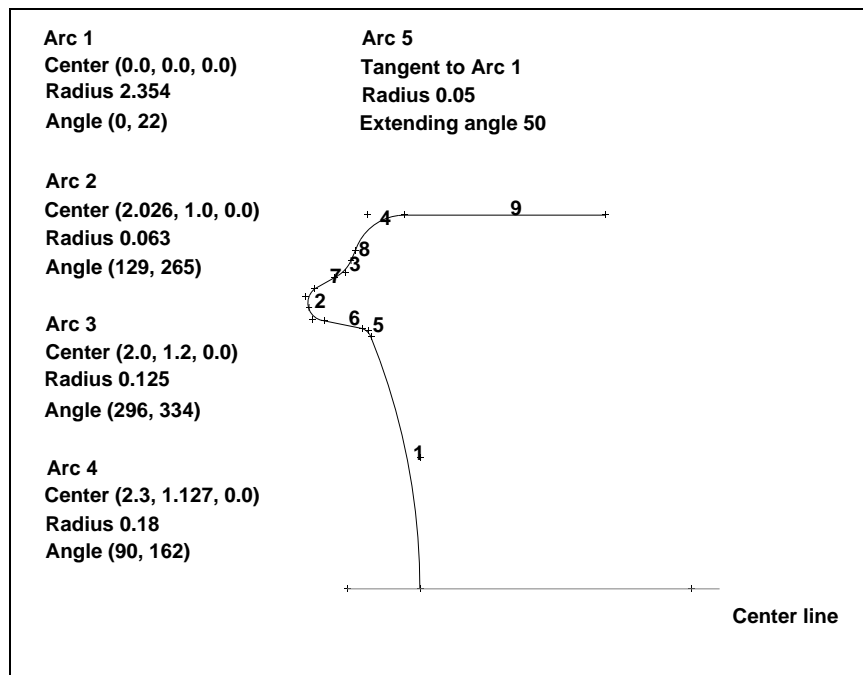


Figure 3.30-2 Section of Container to be Analyzed

Requirements for a Successful Analysis

Nonlinear problems that involve buckling or snap-through are prime candidates for displacement controlled incremental strategies. Unfortunately, the problem at hand is a load controlled problem. In order to be able to traverse the load versus displacement curve of a point on the bottom of the container you must use a loading pattern such that the load increment is scaled in size and applied in the correct direction. The arc-length method combined with a Newton-Raphson iterative scheme will guarantee you that the entire load displacement curve can be traversed. Needless to say, the solution of this problem consists of large displacements and finite strains.

Full Disclosure

- **Analysis Type**
 Nonlinear snap-through.
- **Element Type**
 Marc Element Type 89, axisymmetric shell.
- **Material Properties**
 Aluminum with workhardening.
 Isotropic with Young's Modulus = 11.0e6 p.s.i and Poisson's Ratio = 0.3.

The stress-strain data used to define the workhardening of the aluminum is listed in [Table 2.30-1](#) and graphically represented in [Figure 3.30-3](#).

Table 2.30-1 Stress Strain Data

Log Plastic Strain (x)	Cauchy Stress (y)	Total Engineering Strain
0.0	42000.0	0.0038
0.001748	44577.0	0.0057
0.003494	45157.0	0.0075
0.06766	63665.0	0.0755
0.09531	70950.0	0.1058
0.1570	81315.0	0.1763
0.2070	88560.0	0.2365
0.2623	95216.0	0.3066

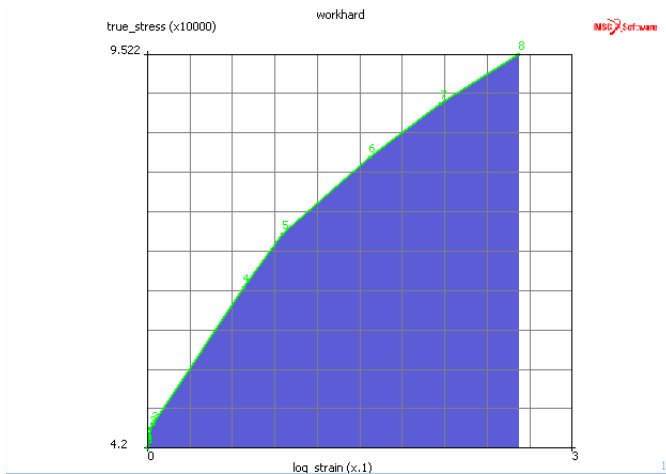


Figure 3.30-3 Graphical Representation of Cauchy Stress vs. Logarithmic Plastic Strain Data

Overview of Steps

- Step 1:** Input all arcs according to the measurements specified in Figure 3.30-2.
- Step 2:** Input straight lines to connect the arcs.
- Step 3:** Convert the geometric entities to finite elements.
- Step 4:** Use SWEEP to eliminate all duplicate nodes, then switch the element class to quadratic shell elements and attach the midside nodes to the curves.
- Step 5:** Add kinematic boundary conditions to enforce the symmetry and restrain rigid body motion.
- Step 6:** Specify edge loads.
- Step 7:** Rectify connectivity to ensure consistent normals.
- Step 8:** Add material properties.
- Step 9:** Add geometric properties.
- Step 10:** Define the loadcase.
- Step 11:** Submit the job.
- Step 12:** Postprocess the results by looking at the deformed shape and the load-displacement curve of the node located on the symmetry axis.

Detailed Session Description

Step 1: Input all arcs according to the measurements specified in Figure 3.30-2.

A structure that is modeled with axisymmetric elements requires the global x-axis to point into the axial direction of that structure. As a result of this type of modeling, the container is displayed in a horizontal position.

As in [Chapter 3.6: Tube Flaring](#), this sample session demonstrates the use of the geometric meshing technique. The geometric entities used to create the mesh are two types of curves: arcs and lines. Once you have generated the geometric model, the arcs and lines are converted to finite elements. Refer to [Chapter 1: Introduction](#) in this manual for more information on mesh generation techniques.

Use the Center/Radius/Angle(begin)/Angle(end) arc type (CRAA) to create the first arcs of the geometry. Use the following button sequence to select and add the CRAA arc type. The values for the measurements of the arcs are given in [Figure 3.30-2](#).

```

MAIN
  MESH GENERATION
    CURVE TYPE
      CENTER/RADIUS/ANGLE/ANGLE
        RETURN
        crvs ADD
          0 0 0 (center)
          2.345 (radius)
          0 22 (angle limits)
          2.026 1 0 (center)
          0.063 (radius)
          129 265 (angle limits)
          2.0 1.2 0 (center)
          0.125 (radius)
          296 334 (angle limits)
          2.3 1.127 0 (center)
          0.18 (radius)
          90 162 (angle limits)
  
```

Switch on the labeling of points.

```

MAIN
  FILL
  PLOT
    draw POINTS
      LABEL (on)
      RETURN
  REGEN
  
```

Figure 3.30-4 shows the four arcs.

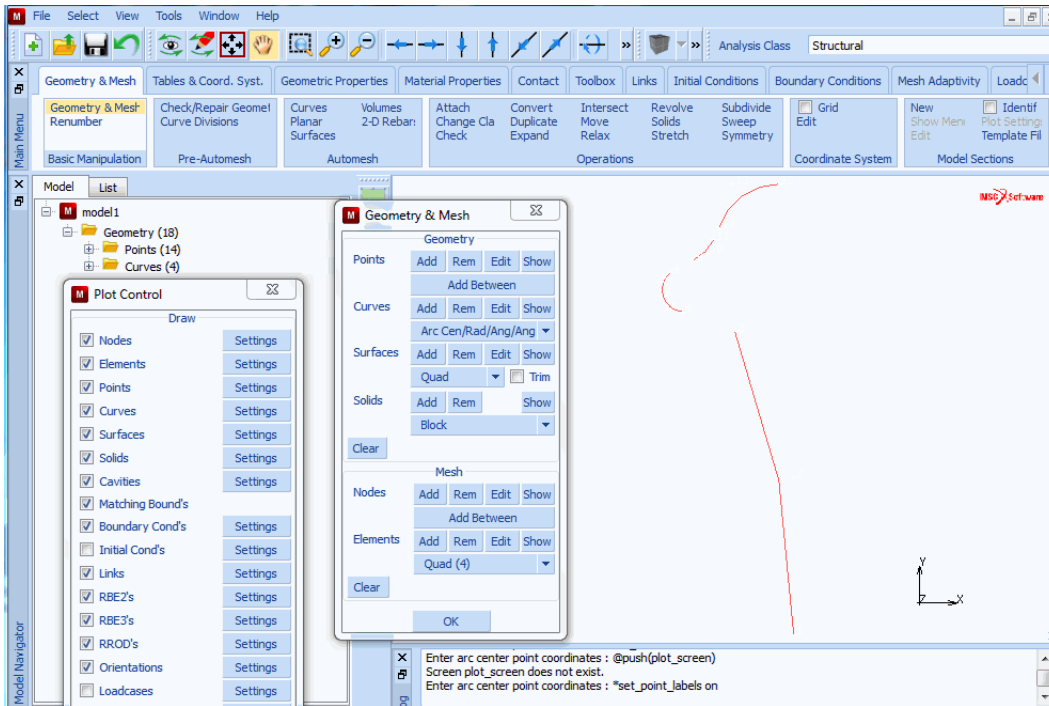


Figure 3.30-4 Using CRAA Type Arcs to Create First Four Curves

The next step is to add a new arc (number 5) so that it is tangent to arc 1, the lower arc, using the following button sequence.

MAIN

MESH GENERATION

CURVE TYPE

TANGENT/RADIUS/ANGLE

RETURN

crvs ADD

3

(click end point of arc #1)

0.05

(radius)

50.0

(arc angle)

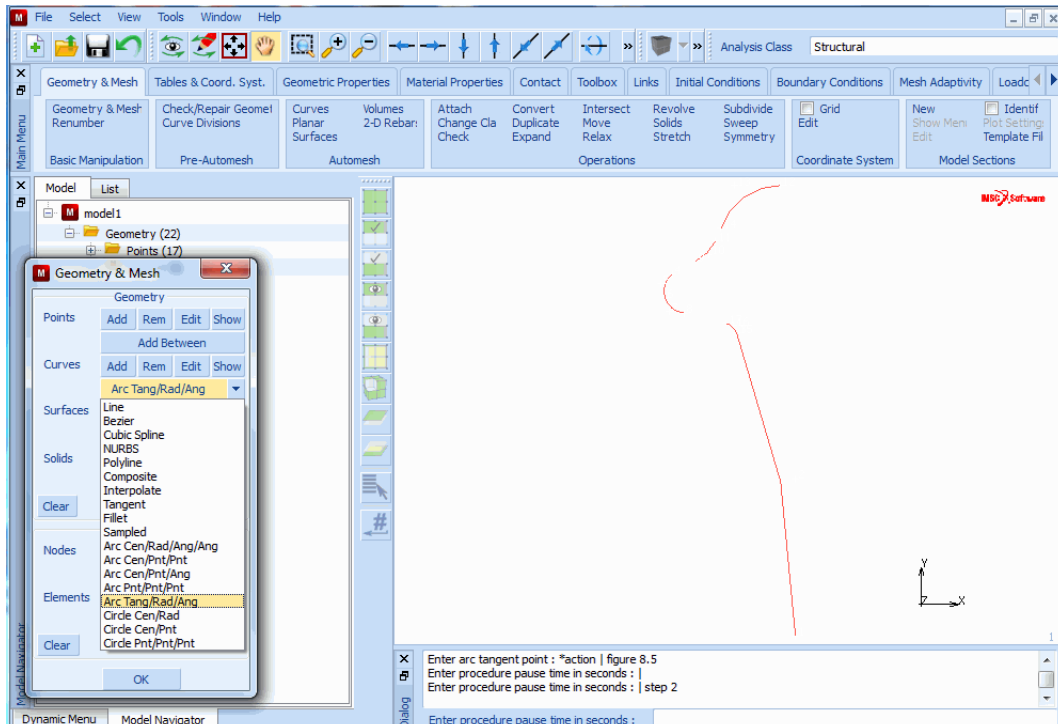


Figure 3.30-5 Using TRA Type Arc to Create Arc 5

Step 2: Input straight lines to connect the arcs.

Finally, add the straight lines to complete the geometric description of the model. Set the curve type to LINE. Use the crvs ADD button on the mesh generation panel and click on the existing points that need to be connected. As we noted in the section on [Idealization](#), it is necessary to extend the wall of the cylinder to at least 0.4519 inches from the edge to ensure that the edge effects are negligible.

MAIN

MESH GENERATION

CURVE TYPE

LINE

RETURN

crvs ADD

11 14

4 9

8 17

(Click on points to connect)

(Click on points to connect)

(Click on points to connect)

The origin chosen for this problem is 2.354 inches to the left of point 1 of arc 1. The total extent of the wall necessary is therefore $2.354 + 0.4519$; that is, approximately three inches. Therefore, we will add a point at $3.0 \ 1.307 \ 0.0$.

MAIN

MESH GENERATION

pts ADD

3.0 1.307 0.0

FILL

crvs ADD

12 18

(Click on points to connect)

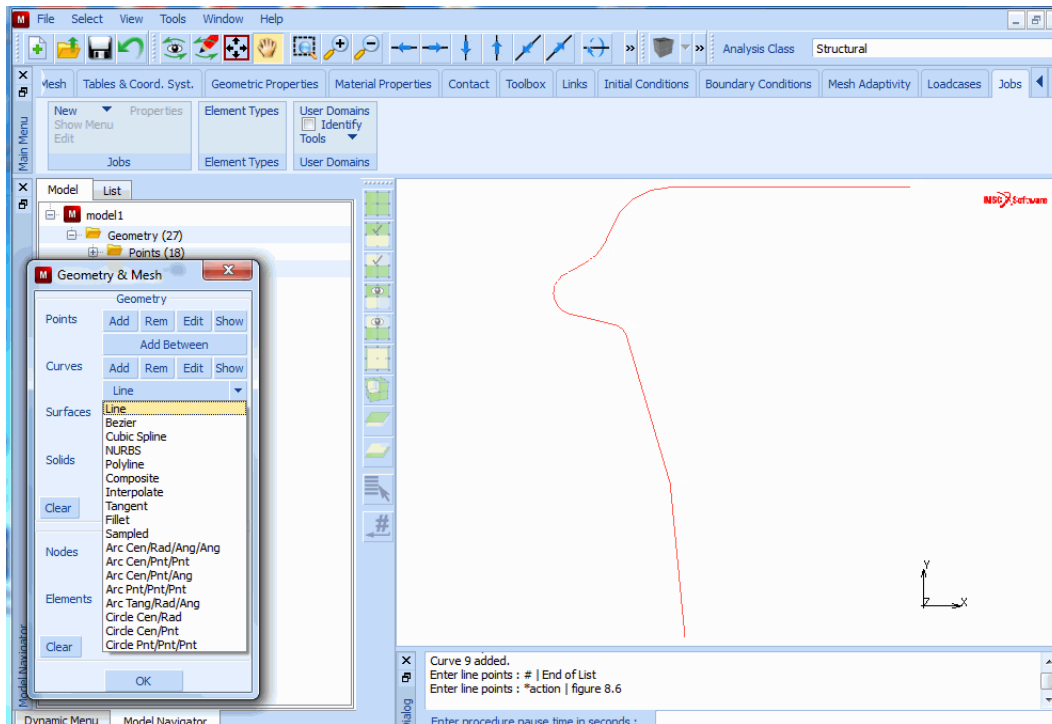


Figure 3.30-6 Connect the Arcs by Lines

Step 3: Convert the geometric entities to finite elements.

Use the CONVERT processor, located on the mesh generation panel, to convert the geometric entities (in this case, curves) to finite elements. You must specify the number of elements for each curve. A higher mesh density is required at sections of high curvature and large displacements than in regions where the values for stress and strain are expected to be less severe. For this reason, you must specify a larger number of convert divisions for those arcs of high curvature and large displacements as indicated in the button sequence given below. Figure 3.30-7 shows the result of converting the curves to finite elements.

MAIN

PLOT

label POINTS (off)

label CURVES (on)

REGEN

RETURN

MESH GENERATION

CONVERT

DIVISIONS

8 1

(Number of subdivisions)

CURVES TO ELEMENTS

1 9

END LIST (#)

DIVISIONS

6 1

CURVES TO ELEMENTS

4 2

END LIST (#)

DIVISIONS

4 1

CURVES TO ELEMENTS

6 3

END LIST (#)

DIVISIONS

3 1

CURVES TO ELEMENTS

7 5 8

END LIST (#)

Step 4: Use SWEEP to eliminate all duplicate nodes, then switch the element class to quadratic shell elements and attach the midside nodes to the curves.

The previous operations may have left duplicate nodes; that is nodes with different identification numbers but occupying the same space. In finite element terms, these nodes are not connected which may introduce undesirable mechanisms in the structure.

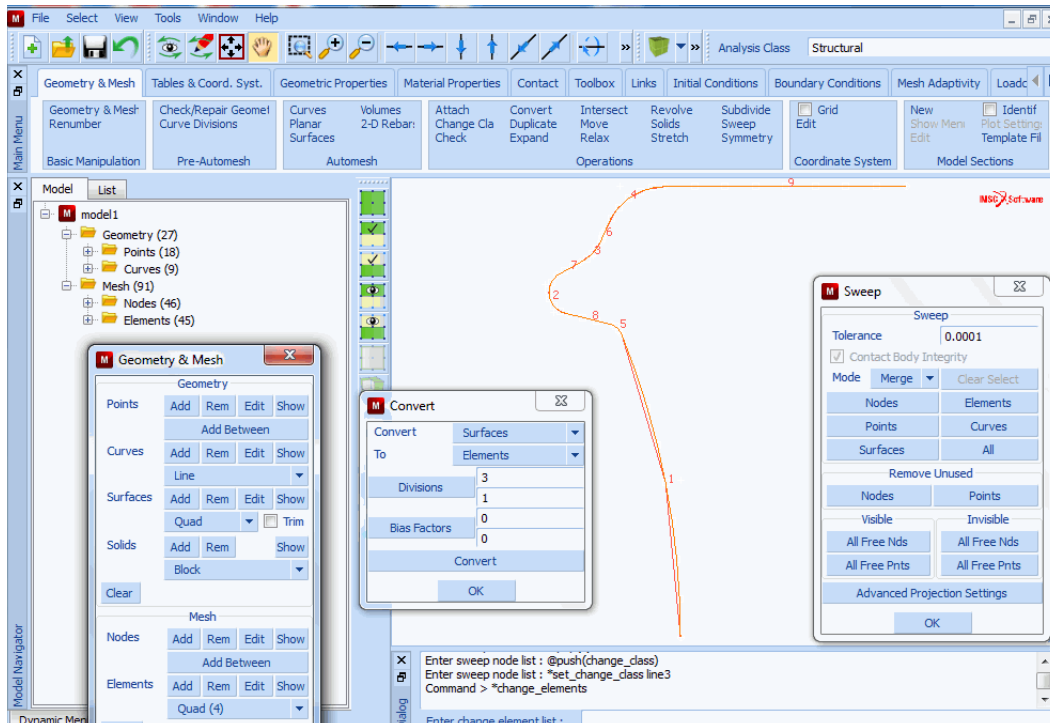


Figure 3.30-7 Model after Converting Curves to LINE(2) Elements

Use the SWEEP processor introduced to you in the sample session of *Introduction* to eliminate the duplicate nodes that occupy the same location. Since this involves a comparison of real numbers that cannot be done exactly in a computer, nodes are swept together if they are within a certain tolerance from each other. This tolerance can be changed from its default value. Be careful when adjusting the tolerance as too large a tolerance can collapse the entire structure into a single point.

```

MAIN
  MESH GENERATION
    SWEEP
      sweep NODES
        all: EXIST.
  
```

In order to describe the curved geometry as precise as possible, the linear (LINE (2) elements) are converted to elements with a quadratic interpolation function (LINE (3) elements).

```

MAIN
  MESH GENERATION
    CHANGE CLASS
  
```

```
LINE (3)
ELEMENTS
  all: EXIST.

MAIN
PLOT
  draw CURVES
  draw POINTS
  REGEN
```

(off)
(off)

The result is shown in [Figure 3.30-8](#).

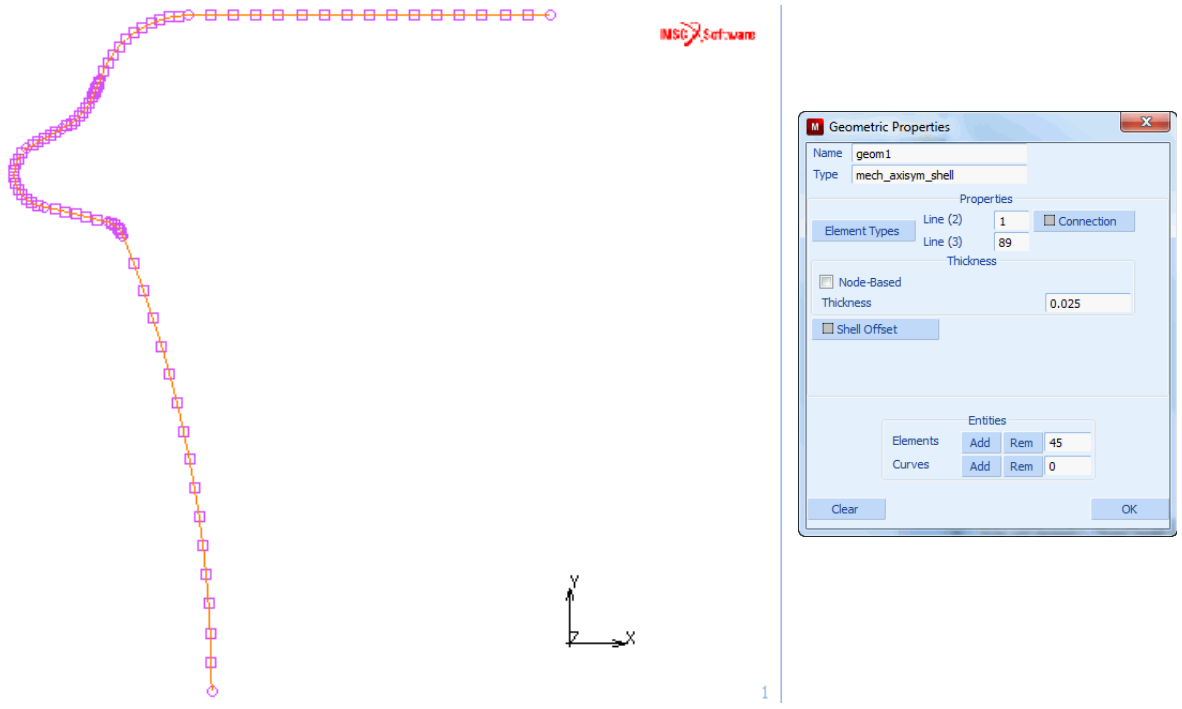


Figure 3.30-8 Curves and Points Turned Off

Step 5: Add kinematic boundary conditions to enforce the symmetry and restrain rigid body motion.

In an axisymmetric shell analysis, there are three types of applicable displacements or degrees of freedom: axial, radial, and rotational. The axial degree of freedom is represented as a global x, and the radial as a global y.

For this particular model, the boundary conditions are simple. This is due to the symmetry conditions applied to the center line node through the suppression of radial displacement and in-plane rotation.


```
MAIN
  BOUNDARY CONDITIONS
    MECHANICAL
      NEW
      FIXED DISPLACEMENT
        DISPLACEMENT Y (on)
        DISPLACEMENT Z (see note below) (on)
      OK
    nodes ADD
      1 (Pick the lower left node)
    END LIST (#)
  FILL
```

Note: The buttons *displacement x*, *displacement y*, *displacement z*, *rotation x*, *rotation y*, and *rotation z* refer to the six degrees of freedom that generally exist for a node of a 3-D shell element. However, this problem uses an axisymmetric shell element with the following three degrees of freedom.: displacement in x-direction, displacement in y-direction, and rotation about the z-axis. In such cases, the button *displacement x* refers to the displacements in x-direction, *displacement y* refers to displacements in y-direction and *displacement z* refers to the third degree of freedom, the rotation about the z-axis.

Figure 3.30-9 shows you the model with the boundary conditions added.

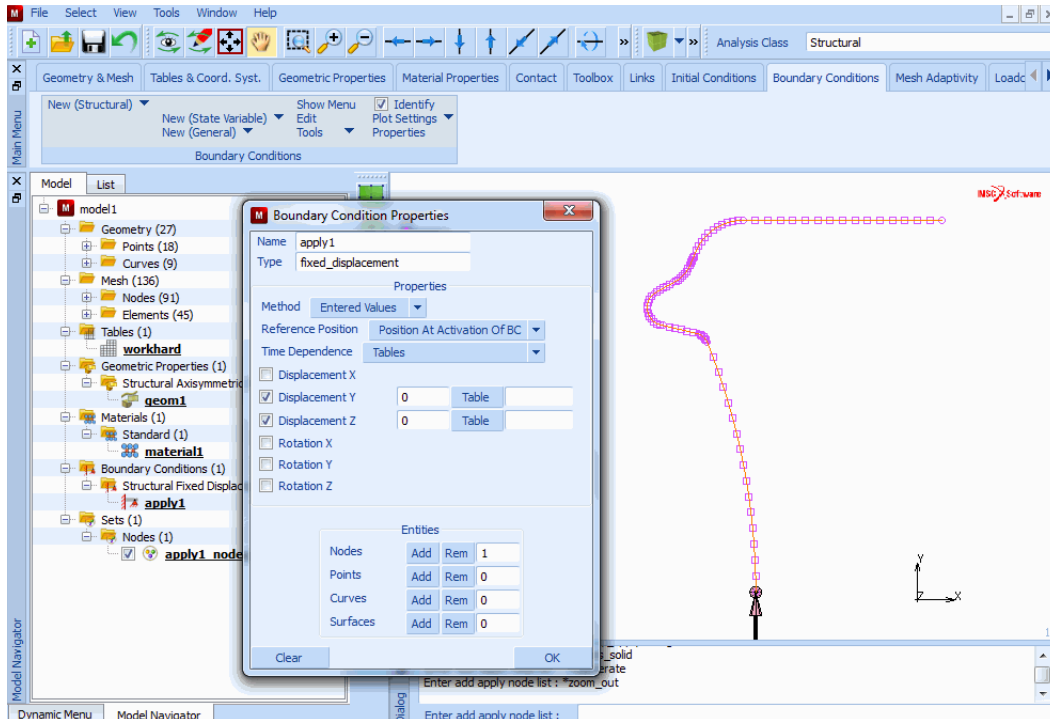


Figure 3.30-9 Fixed Displacement at Axis of Rotation

Next, suppress two degrees of freedom of the extreme node at the circumference of the can:

1. suppress the movement in the axial direction, and
2. suppress the rotational degree of freedom.

MAIN

BOUNDARY CONDITIONS

MECHANICAL

NEW

FIXED DISPLACEMENT

DISPLACEMENT X

(on)

DISPLACEMENT Z

(on)

OK

nodes ADD

18

(pick the top right node)

END LIST (#)

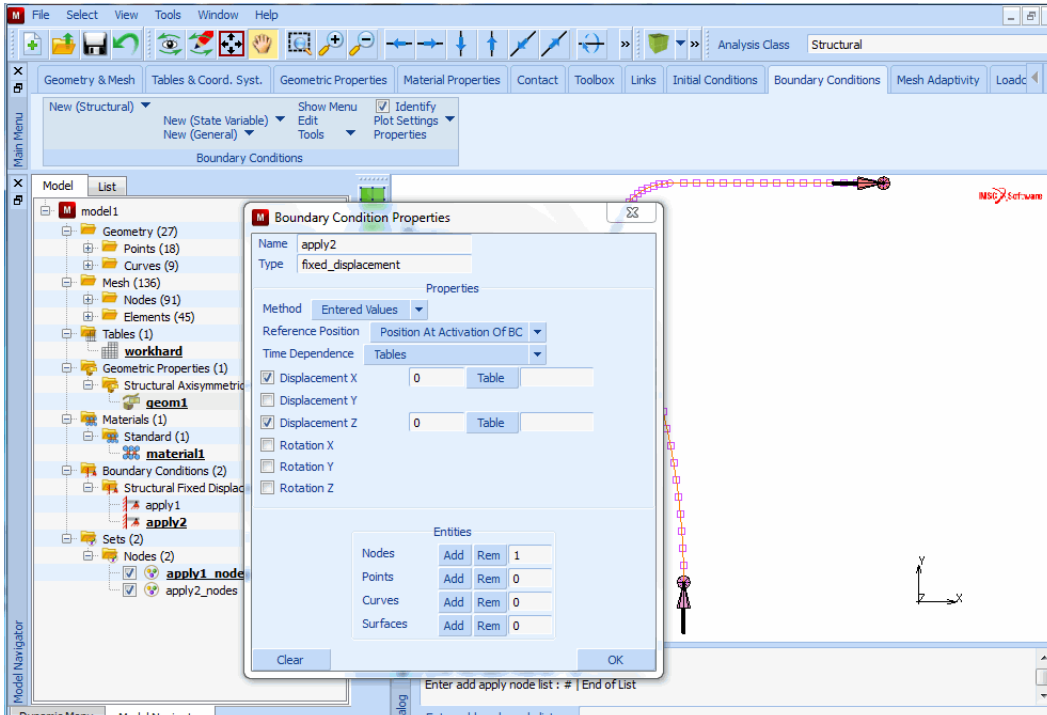


Figure 3.30-10 Boundary Conditions at the Circumference of Container

Step 6: Specify edge loads.

To specify the loading sequence, use the TABLES option to create the load table using the following button sequence:

- MAIN
- BOUNDARY CONDITIONS
- MECHANICAL
- TABLES
- NEW
- 1 INDEPENDENT VARIABLE
- TYPE
- time
- OK *(select OK button only if type time was typed in)*
- independent variable v1: MIN
- 0
- independent variable v1: MAX
- 1

```
function value f: MIN
    0
function value f: MAX
    500
NAME
    loading
ADD
    0  0
    1  500
MORE
    independent variable v1: LABEL
        time
    function value f: LABEL
        pressure
RETURN
FILLED
```

You will refer to the table name, `loading`, when you apply the edge loads. The `xmin`, `xmax`, `ymin`, and `ymax` values specify the table limits. The 0 to 1 range is for the `x` value and 0 to 500 is the range for the `y` value. The `x`-axis represents the time (which is to be regarded a dummy variable for this analysis) and the `y`-axis represents the pressure load. The loading pattern is specified as 0 edge load at time 0 and an edge load of 500 at time 1. Since the *total loadcase time*, used for quasi static analysis (LOADCASE menu), is set to 1.0, this table results in a total load of 500 to be reached at the end of the loadcase. The table points can be entered either via the keyboard or by using the mouse to pick the (0, 0.0) point in the graph followed by the (1, 500.0) point.

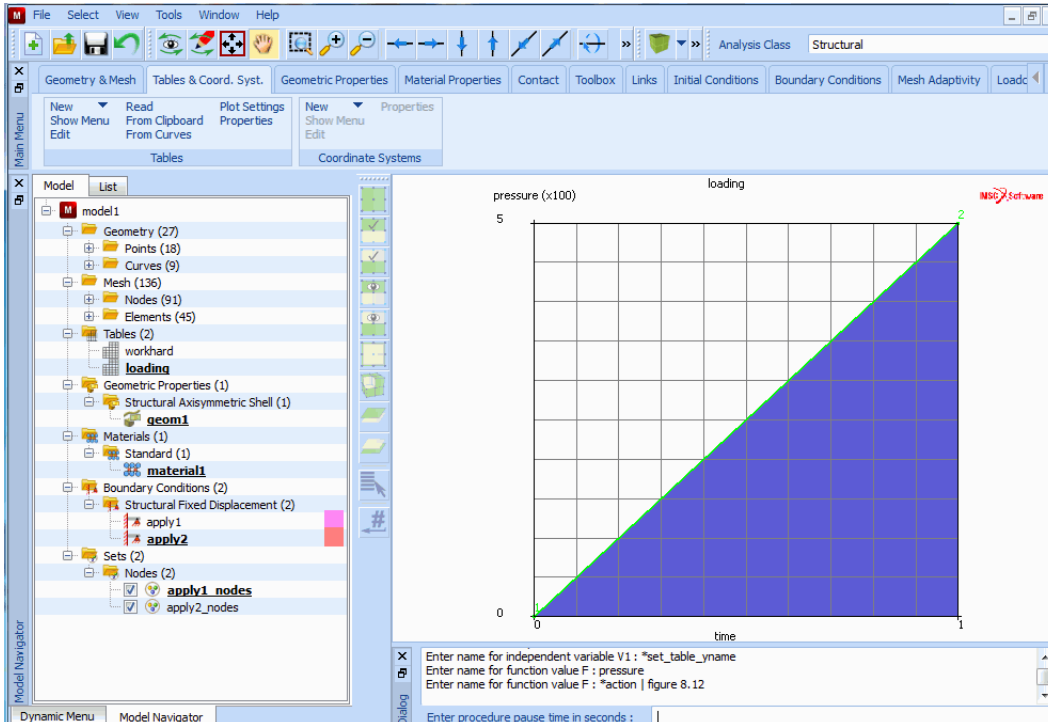


Figure 3.30-11 Load History Table

As mentioned in [Requirements for a Successful Analysis](#), it is the task of the analysis program to define a load incrementation that reaches the target load.

Now that the load type and the load path have both been defined, use the following button sequence below to specify where to apply this load.

MAIN

BOUNDARY CONDITIONS

MECHANICAL

NEW

EDGE LOAD

PRESSURE

1

pressure TABLE

loading

OK

OK

edges ADD
all: EXIST.
FILL

The actual load applied to the structure is 1 (the base value entered at the pressure prompt), multiplied by the values defined in the table.

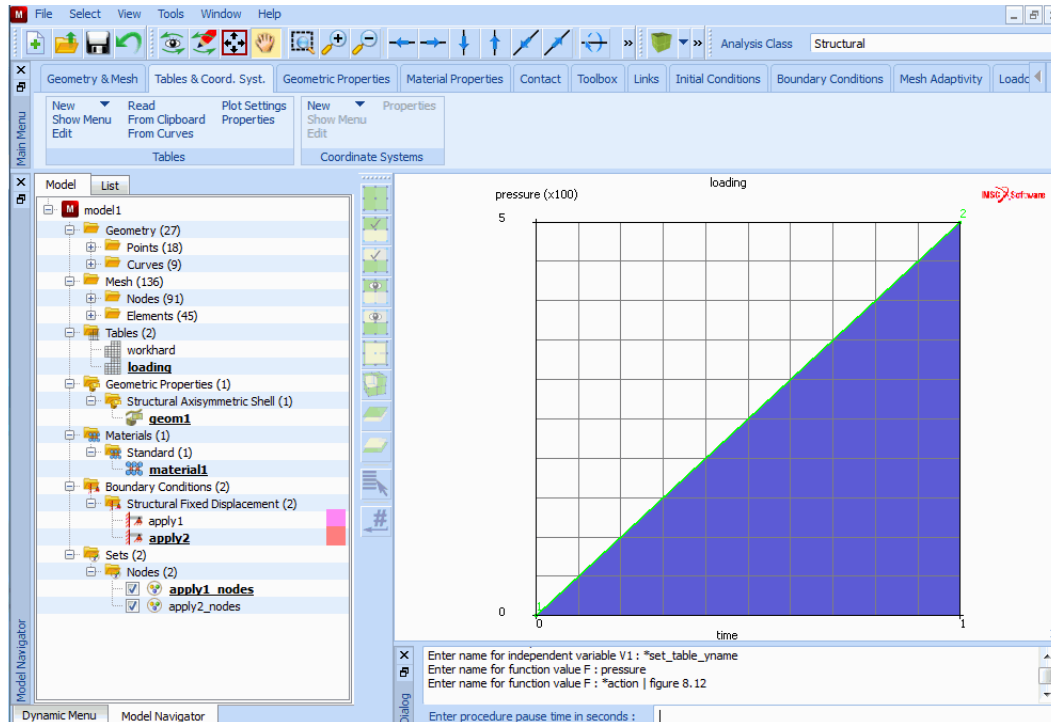


Figure 3.30-12 Pressure Load Applied

Step 7: Rectify connectivity to ensure consistent normals.

Figure 3.30-12 clearly indicates the pressure load has not been applied in the correct direction for all elements. This is caused by the way the curves were created. The outward normal that determines the positive direction of the load is directly dependent on which point of the arc was defined first. Figure 3.30-13 depicts this dependency on an element that has a 1-2 connectivity.

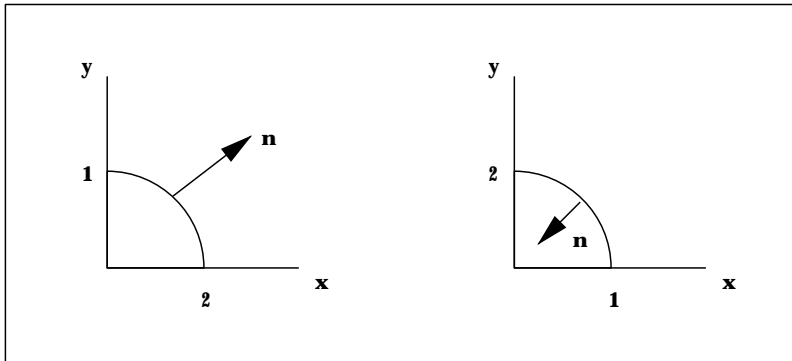


Figure 3.30-13 The Outward Normal in Arc Definition

The connectivity of the elements can easily be corrected using the following button sequence.

MAIN

MESH GENERATION

CHECK

FLIP ELEMENTS

90 88 89 66 67 64 65 63 62

(pick the elements to be flipped)

END LIST (#)

72 73 70 71 69 68

(pick the elements to be flipped)

END LIST (#)

FILL

You may want to use the ZOOM option for closer view of the areas where the flipped elements are located to make it easier to pick the elements that have been loaded in the opposite direction. Pick the elements by moving the cursor over each element and clicking <ML>.

Don't forget to specify end of list by clicking <MR> in the graphics area when you have picked all the flipped elements. Click on FILL to rescale the model to fill the graphics area if you used the ZOOM option. [Figure 3.30-14](#) shows the model with corrected loading.

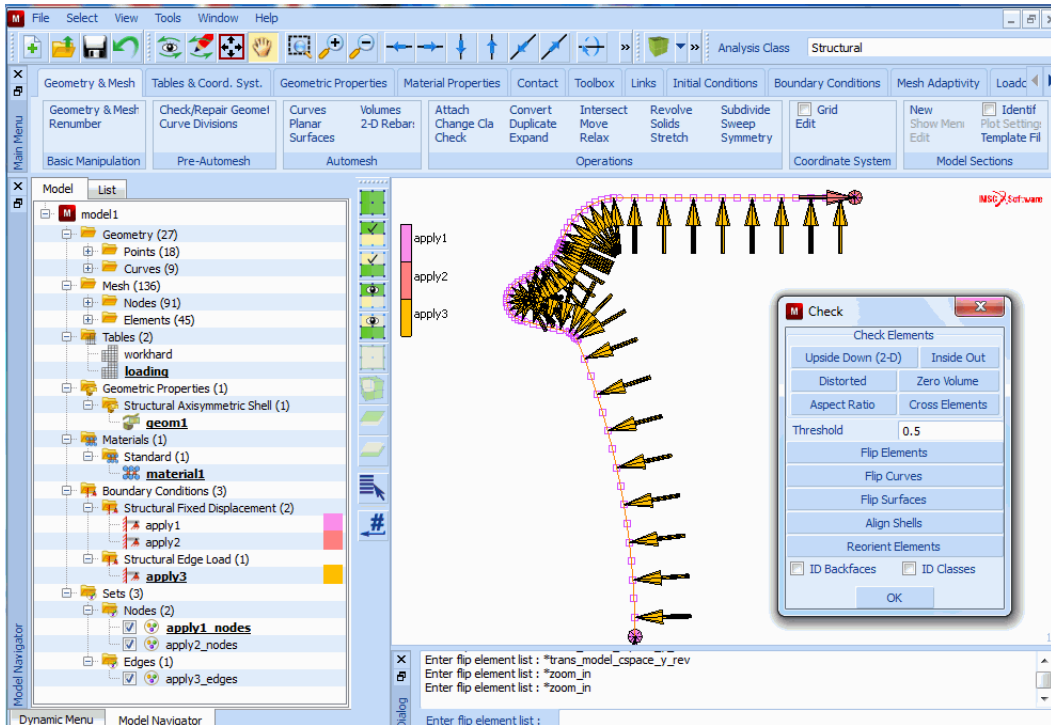


Figure 3.30-14 Correctly Directed Loads for all Elements

Step 8: Add material properties.

The specific values for the isotropic material specification can be entered using the following sequence of buttons:

```

MAIN
MATERIAL PROPERTIES
ISOTROPIC
YOUNG'S MODULUS
    11.0e6
POISSON'S RATIO
    0.3
OK
    
```

The stress-strain data of the material requires the use of the TABLES option similar to Step 6 when you added the edge loads. Remember that the table values are multiplied by the base value as was explained before in the section on specification of the pressure load. The table name is specified by clicking on the NAME button followed by typing in workhard as the name of the table. You will use this table name later. The values for the plastic strain and stress are listed in Table 2.30-1.

Note that based on the solution procedure (i.e., large displacements, updated Lagrange procedure, finite strain plasticity), this data must be of the form listed in [Table 2.30-2](#).

Table 2.30-2 Stress Strain Definitions

Procedure	Stress	Strain
Default	Engineering	Engineering
Large Displacements	2nd Piola-Kirchhoff	Green-Lagrange
Large Strain Plasticity	True (Cauchy)	Logarithmic

The following button sequence defines the stress-strain data table.

```

MAIN
  MATERIAL PROPERTIES
    TABLES
      NEW
        1 INDEPENDENT VARIABLE
        TYPE
          plastic_strain
          OK (select OK button only if type plastic strain was typed in)
        independent variable v1: XMIN
          0
        independent variable v1: XMAX
          0.5
        function value f: YMIN
          0
        function value f: YMAX
          10000
        NAME
          workhard
        MORE
          independent variable v1: LABEL
            log_strain
          function value f: LABEL
            true_stress
        RETURN
      ADD (refer to plastic strain stress data in Table 2.30-1)

```

SHOW TABLE

SHOW MODEL

(select *SHOW MODEL* to switch back to model view)

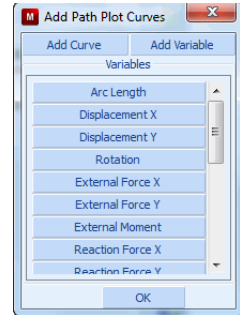
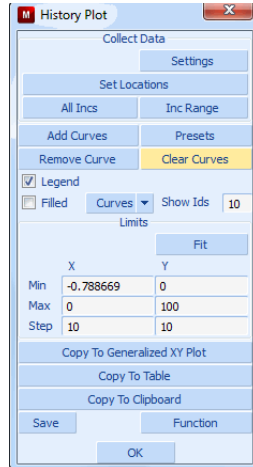
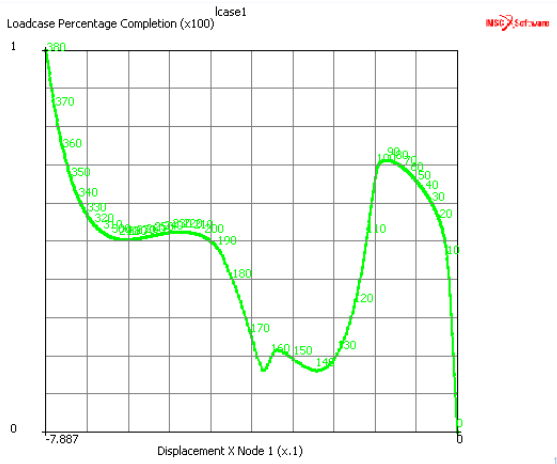


Figure 3.30-15 Workhardening Slope

Plasticity may occur due to the extreme loading. Click on the PLASTICITY button which shows the plasticity properties panel. Choose the defaults von Mises yield criteria and the isotropic hardening rule. The initial yield stress is set to 1, which means that the table values are multiplied by a factor of 1.

MAIN

MATERIAL PROPERTIES

ISOTROPIC

PLASTICITY

ELASTIC-PLASTIC

INITIAL YIELD STRESS

1

initial yield stress TABLE 1

workhard

OK

OK (twice)

elements ADD

all: EXIST.

(select *OK* button only if *workhard* was typed in)

Step 9: Add geometric properties.

Specify the element thickness for all elements using the following button sequence:

```
MAIN
  GEOMETRIC PROPERTIES
    AXISYMMETRIC
      SHELL
        THICKNESS
          0.025
        OK
      elements ADD
        all: EXIST.
```

Step 10: Define the loadcase.

Now that you have defined the individual loads and kinematic constraints, define a loadcase that combines these boundary conditions.

A pop-up menu appears over the graphics area containing a list of available boundary conditions and their status (selected or not). Combine these individual loads in a loadcase that can be referred to by a name. The default name for this loadcase is *lcase1*. Clearly, you want all kinematic constraints and distributed loads (pressures) to be applied so all boundary conditions must be selected. Use the **SELECT** and **DESELECT** buttons to activate and deactivate the boundary conditions respectively. Confirm the correctness of this loadcase definition by clicking on the **OK** button.

```
MAIN
  LOADCASES
    mechanical STATIC
      LOADS
        OK
```

The following individual components for an analysis have already been specified:

1. You defined the topology and connectivity of the finite element model.
2. You assigned boundary conditions, material properties, and geometric properties.
3. You combined the boundary conditions in a loadcase.

Since snap-through is likely to occur in this problem, the user has to instruct Marc to solve a system of equations with a nonpositive definite tangent stiffness matrix.

```
MAIN
  LOADCASES
    mechanical STATIC
      SOLUTION CONTROL
```

NON-POSITIVE DEFINITE

(on)

OK

Furthermore, the default settings for convergence testing are not well suited for this particular problem. Although the default type of testing, relative testing on residual forces, is appropriate, the relative force tolerance needs to be reduced. The necessity of this action can be explained by looking at the boundary conditions; the constraint on the axial displacement degree of freedom is found at a large radius (node 18).

Due to the internal pressure, we find a large reaction-force at this node. Allowing a certain percentage of this reaction-force to be present as residuals anywhere in the structure results in undesired interference of those residuals with the automatic load stepping process.

CONVERGENCE TESTING

RELATIVE FORCE TOLERANCE

0.05

OK

Finally, the adaptive load stepping algorithm of Marc is activated. This algorithm allows for the analysis of snap-through phenomena in which the load incrementation needs to be scaled depending on the amount of nonlinearity that is occurring. Various parameters control this procedure. In this case, we allow for a maximum of 600 increments.

In the first increment, 0.05 (5%) of the total load is applied. Also, the user needs to specify that the arc length never exceeds the value used in the first increment. The default MODIFIED RIKS procedure is used.

SOLUTION CONTROL

ARC LENGTH

arc length PARAMETERS

MAX # INCREMENTS IN LOADCASE

600

INITIAL FRACTION

0.05

MAX RATION ARC LENGTH / INITAL ARC LENGTH

1.0

OK (twice)

Step 11: Submit the job.

It is time to prepare the loadcase for a job and to submit it for finite element analysis.

Prior to defining the job parameters, the appropriate Marc element type is set.

Next, the analysis class MECHANICAL is activated resulting in a pop-up menu over the graphics area. Click the SELECT button and pick the *lcase1* button from the available loadcases list to select the only available loadcase for this job.

```
MAIN
  JOBS
    ELEMENT TYPES
      mechanical element types AXISYM MEMBRANE/SHELL
        89 (LINE 3 / thick shell)
        OK
      all: EXIST.
      RETURN
    RETURN
  MECHANICAL
    loadcases SELECT
      lcase1
```

As we have indicated before, this analysis involves large displacements, finite strain plasticity, updated Lagrange procedure, and follower forces. The finite element program requires directives that indicate this. From the mechanical analysis pop-up menu, click on the ANALYSIS OPTIONS button and activate the following options:

```
MAIN
  JOBS
    MECHANICAL
      ANALYSIS OPTIONS
        SMALL STRAIN (Switch on large strain additive procedure)
        NO FOLLOWER FORCE (to switch to FOLLOWER FORCE)
        OK
```

The results of the analysis appear in a results file. Specify the results variables you are interested in by clicking on the JOB RESULTS button from the mechanical analysis pop-up menu. Select Equivalent Plastic Strain and Equivalent von Mises Stress variables. Finally, set the numbers of layers used for integration through the shell thickness to 5.

```
MAIN
  JOBS
    MECHANICAL
      JOB RESULTS
```

```
available element scalars
  Equivalent Von Mises Stress
  layers: OUT & MID
  Total Equivalent Plastic Strain
  layers: OUT & MID
  OK
JOB PARAMETERS
  # SHELL/BEAM LAYERS
  5
```

This analysis may involve a large number of increments. For this reason, you may want to write the results every 10 increments using the FREQUENCY button. For this sample session, however, write every increment which is the default value of the FREQUENCY option and confirm the settings by clicking on the OK button.

The following button sequence submits the job. The job can be monitored using the MONITOR option which, in case of automatically running the procedure file, prevents Mentat from proceeding to **Step 12** before the analysis has run to completion.

```
MAIN
  JOBS
    SAVE
    RUN
    SUBMIT 1
    MONITOR
```

This analysis takes a few minutes, depending on the power of the host to which you are submitting the job.

Step 12: Postprocess the results by looking at the deformed shape and the load-displacement curve of the node located on the symmetry axis.

The results of the analysis step are stored in a disk file. To access the results, it is necessary to open this file and (selectively) extract data from it. Use the following button sequence to open the file.

```
MAIN
  RESULTS
    OPEN DEFAULT
```

Click on the FILL button located in the static menu area to scale the model to fill the graphics area. The following button sequence removes the node drawing and gives a clearer picture of the model shown in [Figure 3.30-14](#).

MAIN

FILL

PLOT

draw NODES

(off)

REGEN

RETURN

We are interested in the deformed shape as a function of the increasing/decreasing load. The best way to obtain a good overview of the deformations is to animate the deformed shape. Since it is impractical to incorporate the animated picture in this guide, a detailed description follows on how to obtain and play back the animation frames. Only 3 out of a sequence of 25 frames are shown in this guide.

Before you collect the animation frames, click on the DEF & ORIG button so that the deformed and original shapes of the model are shown simultaneously.

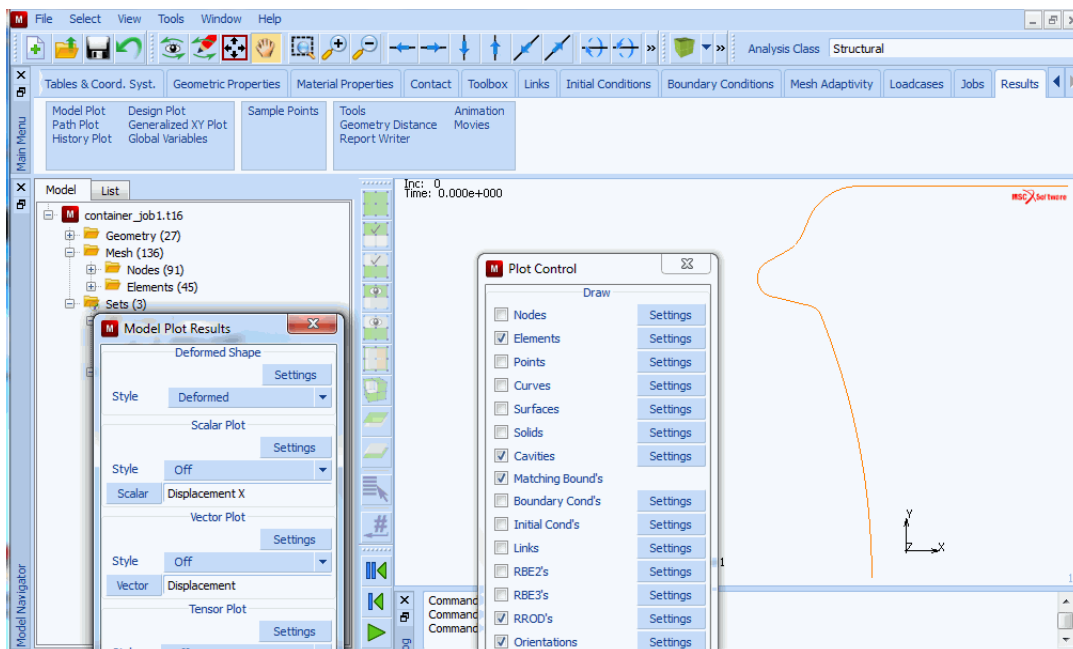


Figure 3.30-16 Resulting Post File of the Container

MAIN

RESULTS

NEXT

DEF & ORIG

MORE

ANIMATION

create INCREMENTS

40

(Number of frames to save)

10

(Increment step size)

The program responds by scanning the results file and extracting the appropriate data.

When replaying the sequence of animation files, you may have to scale the deformed and original models to fit in the graphics area. Use the FILL button located in the static menu to scale the models while still having the last increment of the animation sequence displayed. Use the following button sequence to play the animation sequence.

MAIN

RESULTS

MORE

ANIMATION

FILL

PLAY

SHOW MODEL

The following two figures capture 3 of the 25 animation frames.

MAIN

RESULTS

SKIP TO INC

80

SKIP TO INC

160

SKIP TO INC

240

[Figure 3.30-17](#) and [Figure 3.30-18](#) show you that the bottom ridge first un-rolls and is followed by a snap-through of the arch. Ultimately, the shape of the bottom of the can becomes spherical as is shown in [Figure 3.30-19](#).

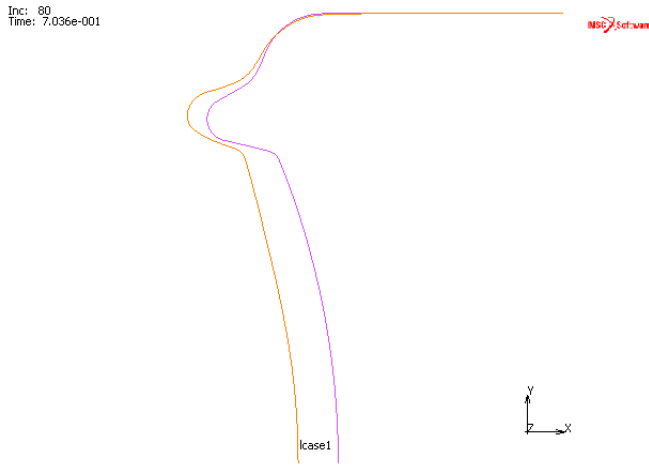


Figure 3.30-17 Original and Deformed Model at Increment 80

The user can use the BEAM CONTOURS or BEAM VALUES plot option to display elemental quantities. Alternatively, a path plot where the position of the nodes is plotted on the x-axis and the equivalent plastic strain is plotted on the y-axis, can be created. The nodes are logically connected through the connectivity of the elements. The plot shown in [Figure 3.30-21](#) displays the equivalent plastic strain for increment 240 of this analysis.

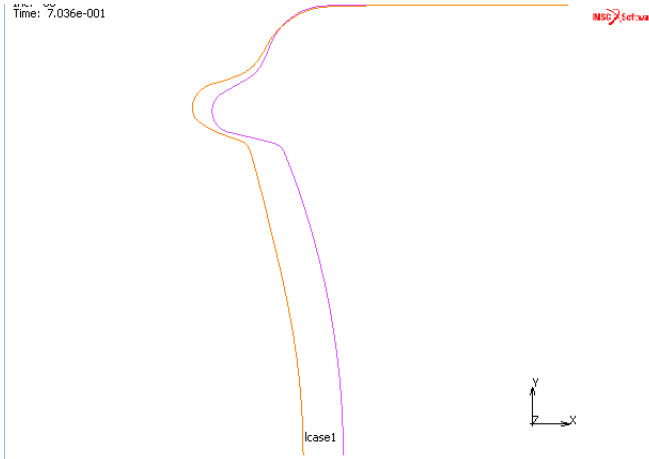


Figure 3.30-18 Original and Deformed Model at Increment 160

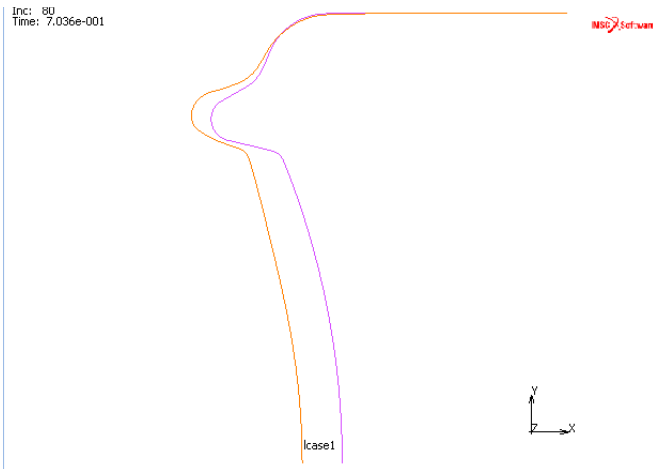


Figure 3.30-19 Original and Deformed Model at Increment 240

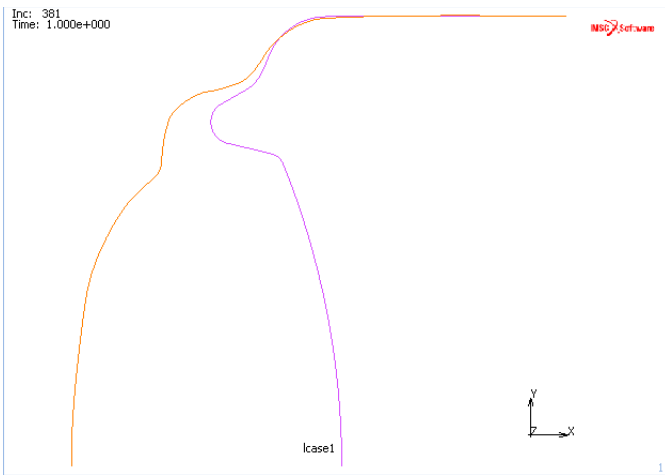


Figure 3.30-20 Original and Deformed Model at Increment 381

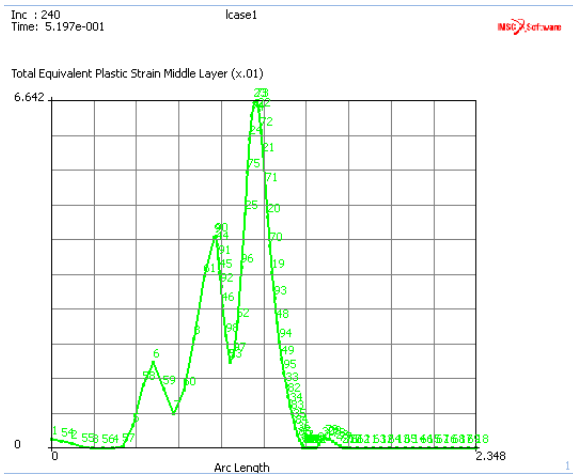
Use the following button sequence in **PLOT** to plot the total equivalent plastic strain.

```
MAIN
  PLOT
    draw NODES
    REGEN
    RETURN
  RESULTS
    PATH PLOT
    NODE PATH
```

(on)

*(select nodes from lower left to upper right,
 approximately each 10th node will do)*

END LIST (#)
 VARIABLES
 ADD CURVE
 Arc Length
 Total Equivalent Plastic Strain Layer 3
 FIT



(lower left)

```

1
END LIST (#)
COLLECT DATA
0 1000 1
NODES/VARIABLES
ADD 2-NODE CRV
1
variables at nodes
Displacement X
18
global variables
Dist Load 1

FIT
RETURN

SHOW IDS
10

YMAX
5000.0
    
```

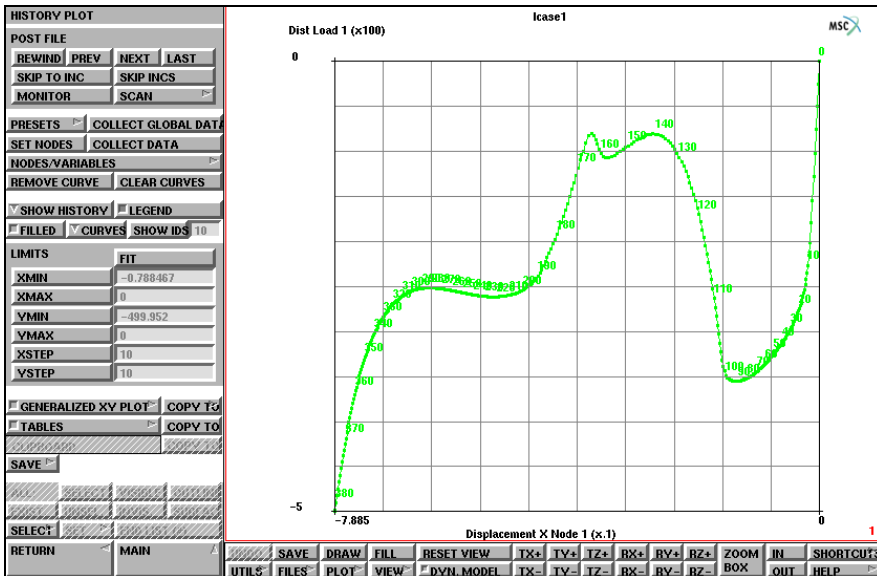


Figure 3.30-22 Axial Displacement of Bottom versus Applied Pressure Diagram

Conclusion

The loading path versus displacement has been successfully traced for the snap-through analysis of the bottom of an aluminum container.

Input Files

The files below are on your [delivery media](#) or they can be downloaded by your web browser by clicking the links (file names) below.

File	Description
container.proc	Mentat procedure file

3.31 Analyses of a Tire

- Steady State Rolling Analysis 1504
- Tire Bead Analysis 1523
- Conclusion 1548
- Input Files 1548

Steady State Rolling Analysis

A simplified automobile tire model is numerically analyzed. The analysis includes five steps:

1. 2-D model generation and tire inflation,
2. 3-D model generation using 2-D results,
3. Footprint analysis,
4. Steady state rolling analysis using spinning velocity control,
5. Steady state rolling analysis using torque control.

This problem demonstrates Marc capability of simulating automobile tires subjected to various load conditions. The specific features used in the analysis contain:

1. The use of rebar membrane elements along with INSERT option to model cord-reinforced rubber composites,
2. AXITO3D option to transfer data from axisymmetric case to 3-D case, and
3. Steady state rolling,

among others.

Three *mfd* files are provided in this chapter along with the procedure file *tire.proc*.

<code>tire2d_model.mfd</code>	contains the axisymmetric model except for rebars. All material properties, including those for rebar elements, as well as boundary and load conditions for the analysis of tire inflation, are defined. The updated Lagrange formulation and the follow force option are also specified in the file.
<code>reb_curves.mfd</code>	contains curves indicating rebar layer locations in the rubber matrix.
<code>rigid_road.mfd</code>	includes a flat, rigid surface for modeling road in 3-D analysis.

Simulation of a Tire

2-D Model Generation and Tire Inflation

The key issue here is to use rebar remeshing feature to mesh the given curves and define INSERT option.

In the first step of analysis (i.e., tire inflation), the deformation is purely axisymmetric and, therefore, an axisymmetric analysis is performed. The tire rim is modeled with a set of fixed boundary conditions. An inflation pressure of 2 bar is applied to the inner surface of the tire within the step.

Open model and merge rebar curves:

```
FILES
  OPEN
    tire2d_model.mfd
  OK
```


SAVE AS

tire2d.mfd

OK

FILL

MERGE

reb_curves.mfd

OK

MAIN

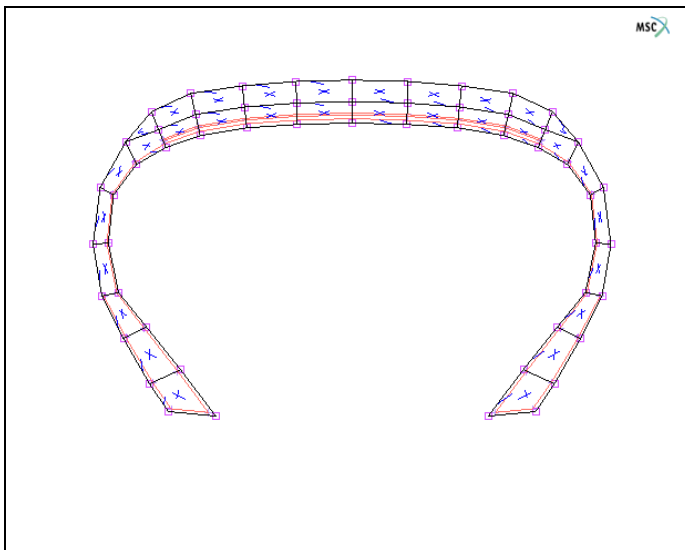


Figure 3.31-1 2-D Tire Model with Rebar Curves

Mesh rebar curves, generate INSERT and define rebar properties:

INSERT is automatically created if the CREATE INSERTS under MESH 2D REBAR is ON (default).

MESH GENERATION

AUTO MESH

MESH 2D REBAR

MESH CURVES

all existing

all existing

RETURN (twice)

CLEAR GEOMETRY

RENUMBER
ALL
MAIN
MATERIAL PROPERTIES
NEXT (thrice)
LAYERED MATERIAL
ELEMENT ADD
33 to 62
NEXT
ELEMENT ADD
insert6_embed_elements
NEXT
ELEMENT ADD
insert7_embed_elements
SAVE
MAIN



Figure 3.31-2 Menu for REBAR Meshing

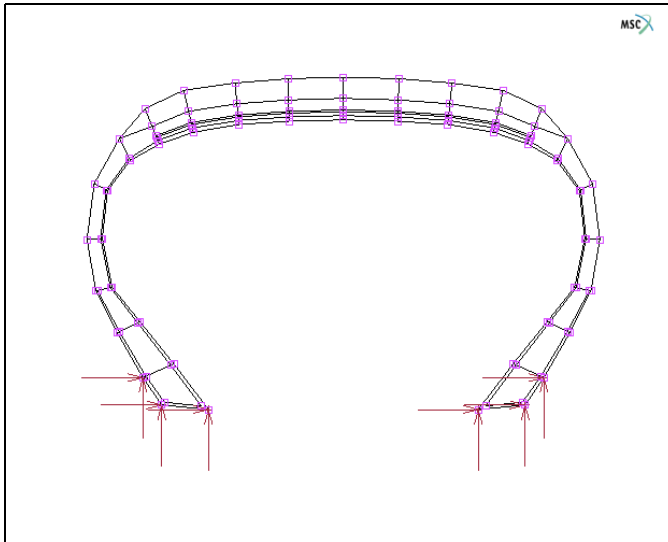


Figure 3.31-3 Tire Model with Rebar Elements and INSERT Option

Run axisymmetric job:

```
JOBS
  RUN
    SUBMIT
      OK
    MAIN
```

3-D Model Generation

A fully 3-D model is generated based on the axisymmetric model. AXITO3D option is used to transfer the numerically obtained results from the previous axisymmetric analysis into the 3-D case as initial conditions in the 3-D analysis.

3-D model generation contains the following steps.

1. Save model as *tire3d.mfd*
2. Expand model from Axisymmetric to 3-D
3. Add rigid body control node
4. Merge rigid road surface
5. Define boundary/load conditions
6. AXITO3D definition in initial conditions
7. Contact definition

FILE

SAVE AS

tire3d.mfd

OK

MAIN

MESH GENERATION

EXPAND

AXISYMMETRC MODEL TO 3D

ANGLE

30

REPETITION

5

ANGLE

6

REPETITION

10

ANGLE

30

REPETITION

5

TIME SET

1

EXPAND MODEL

FILL

RETURN (twice)

NODES ADD

0 0 0

MAIN

FILE

MERGE

rigid_road.mfd

OK

MAIN

BOUNDARY CONDITIONS

MECHANICAL

NEW

```
NAME
  fix_xz
FIXED DISPLACEMENT
  DISPLACEMENT X: ON
  DISPLACEMENT Z: ON
  OK
NODES ADD
  2181
  #
NEW
NAME
  disp_y
TABLE
  NEW
    1 INDEPENDENT VARIABLES
  NAME
    table_disp
  TYPE
    time
    OK
  ADD
    0 0 1 1 10 1
  FIT
  RETURN
FIXED DISPLACEMENT
  DISPLACEMENT Y: ON
  TABLE
    table_disp
    OK
  DISPLACEMENT Y VALUE: 15
  OK
NODES ADD
  2181
  #
NEW
NAME
```

```
load_y
TABLE
NEW
  1 INDEPENDENT VARIABLES
NAME
  table_load
TYPE
  time
  OK
ADD
  0 0 1 0 2 1 10 1
FIT
RETURN
POINT LOAD
DISPLACEMENT Y: ON
TABLE
  table_load
  OK
DISPLACEMENT Y VALUE: 3400
OK
NODES ADD
  2181
#
MAIN
INITIAL CONDITIONS
MECHANICAL
  AXISYMMETRIC TO 3D
  POST FILE
    tire2d_job1.t16
  OK (twice)
MAIN
CONTACT
CONTACT BODIES
NEW
NAME
  tire
```

```
DEFORMABLE
  OK
ELEMENTS ADD
  all_existing
NEW
NAME
  road
RIGID
  LOAD
  DISCRETE
SURFACES ADD
  all_existing
CONTROL NODE
  2181
  RETURN
CONTACT TABLES
  NEW
  PROPERTIES
  1-2
    CONTACT TYPE: TOUCHING
    OK (twice)
  NEW
  PROPERTIES
  1-2
    CONTACT TYPE: TOUCHING
    FRICTION COEFFICIENT: 0.5
    OK (twice)
MAIN
```

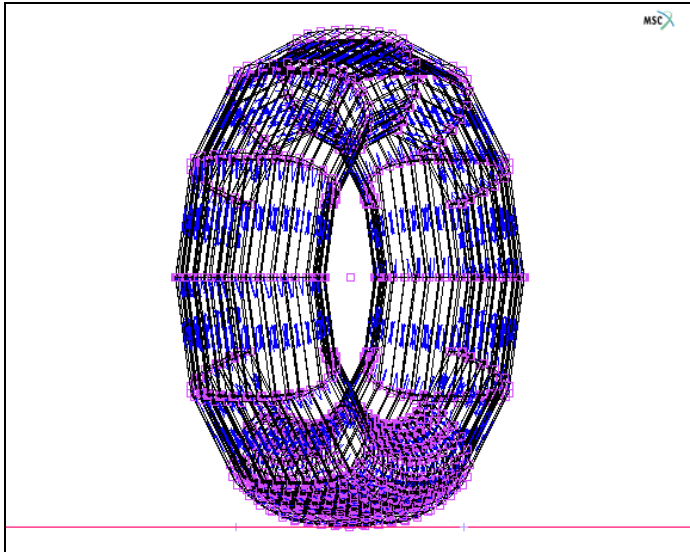


Figure 3.31-4 3-D Tire Model

Footprint Analysis

In the first loadcase, the rigid road surface moves up 15 mm against the tire using position control option for rigid contact body. AUTO STEP option is used. The position control is then switched to load control in the second loadcase. A vertical load of 3400 N is applied to the road surface within one increment.

```
LOADCASES
  REM (twice)
  NEW
  NAME
    footprint1
  MECHANICAL
    STATIC
      LOADS
        load_y: OFF
        OK
      CONTACT
        CONTACT TABLE
          ctable1
          OK (twice)
      CONVERGENCE TESTING
```



```
RELATIVE FORCE TOLERANCE
    0.05
OK
MULTI-CRITERIA
PARAMETERS
    INITIAL FRACTION OF LOADCASE TIME
        0.1
    OK (twice)
NEW
NAME
    footprint2
STATIC
LOADS
    disp_y: OFF
    OK
CONTACT
    CONTACT TABLE
        ctable1
    OK (twice)
CONVERGENCE TESTING
    RELATIVE FORCE TOLERANCE
        0.05
    OK
# STEPS
    1
    OK
```

Steady State Rolling Analysis – Spinning Velocity Control

In the following two loadcases, steady state rolling analysis is performed. The tire starts to spin at an angular velocity of 11.9 cycle/second and runs at a road velocity of $100 \frac{km}{hr}$. Only one increment is required to achieve converged solutions at the given conditions. Afterwards, the spinning velocity of the tire gradually increases to 16.4 cycle/second within 20 equal increments.

```
NEW
NAME
```

```
ss_rolling_1
STEADY STATE ROLLING
LOADS
  disp_y: OFF
  OK
CONTACT
  CONTACT TABLE
    ctable2
    OK (twice)
STEADY STATE ROLLING
  SPINNING BODY
    tire
    OK
  GROUND BODY
    road
    OK
  SPINNING VELOCITY
    11.9
  GROUND VELOCITY Z
    27777.8
  GRADUAL FRICTION: ON
  OK
CONVERGENCE TESTING
  RELATIVE FORCE TOLERANCE
    0.05
  OK
# STEPS
  1
  OK
NEW
NAME
  ss_rolling_2
STEADY STATE ROLLING
LOADS
  disp_y: OFF
```

OK
CONTACT
CONTACT TABLE
 ctable2
 OK (twice)
STEADY STATE ROLLING
SPINNING BODY
 tire
 OK
GROUND BODY
 road
 OK
SPINNING VELOCITY
 16.4
GROUND VELOCITY Z
 27777.8
OK
CONVERGENCE TESTING
RELATIVE FORCE TOLERANCE
 0.05
OK
STEPS
 20
OK

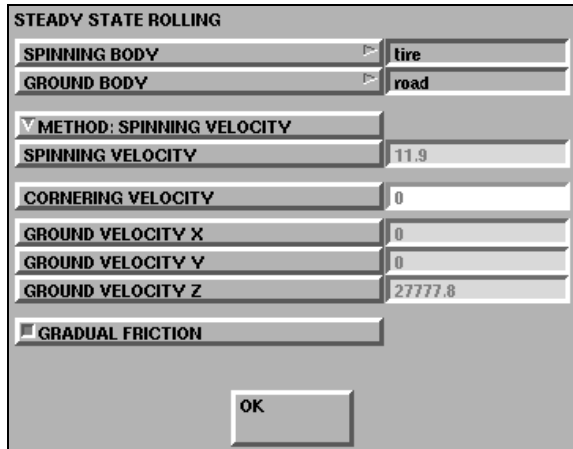


Figure 3.31-5 Menu to Define Loadcase for Steady State Rolling with Spinning Velocity Control

Steady State Rolling Analysis – Torque Control

Free rolling analysis is performed using torque control option. The solution is achieved with only one increment at zero torque.

```
NEW
NAME
    free_rolling
STEADY STATE ROLLING
LOADS
    disp_y: OFF
    OK
CONTACT
    CONTACT TABLE
        ctable2
        OK (twice)
STEADY STATE ROLLING
    SPINNING BODY
        tire
        OK
    GROUND BODY
        road
        OK
    METHOD: TORQUE: ON
```

```

GROUND VELOCITY Z
    27777.8
OK
CONVERGENCE TESTING
RELATIVE FORCE TOLERANCE
    0.05
OK
# STEPS
    1
OK
MAIN
    
```

STEADY STATE ROLLING	
SPINNING BODY	tire
GROUND BODY	road
▼ METHOD: TORQUE	
TORQUE	0
CORNERING VELOCITY	0
GROUND VELOCITY X	0
GROUND VELOCITY Y	0
GROUND VELOCITY Z	27777.8
MAX # ADJUSTMENTS	20
STEADY STATE ROLLING TOLERANCE	0.02
OK	

Figure 3.31-6 Menu to Define Loadcase for Steady State Rolling with Torque Control

Run Job and View Results

Job definition and run the generated model:

```

JOBS
    MECHANICAL
        footprint1
        foorprint2
        ss_rolling_1
        ss_rolling_2
        free_rolling
    
```

INITIAL CONDITION

fix_xz: ON

disp_y: ON

icond1: ON

OK

CONTACT

COULOMB FOR ROLLING

INITIAL CONTACT

CONTACT TABLE

ctable1

OK (twice)

OK (twice)

SAVE

RUN

SUBMIT

OK

MAIN

Results – deformed tire at the end of footprint:

RESULTS

OPEN DEFAULT

DEF & ORIG: ON

SKIP TO INC

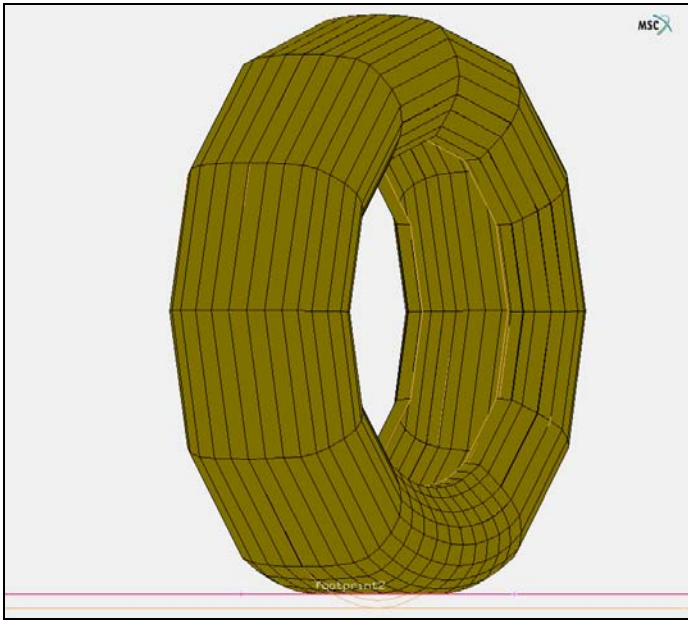


Figure 3.31-7 Deformed Tire at the End of Footprint

Results – spinning velocity – traction curve:

HISTORY PLOT

COLLECT DATA

8 28 1

NODE/VARIABLES

ADD GLOBAL CURVE

X AXIS: ANGLE VEL TIRE

Y AXIS: FORCE Z ROAD

FIT

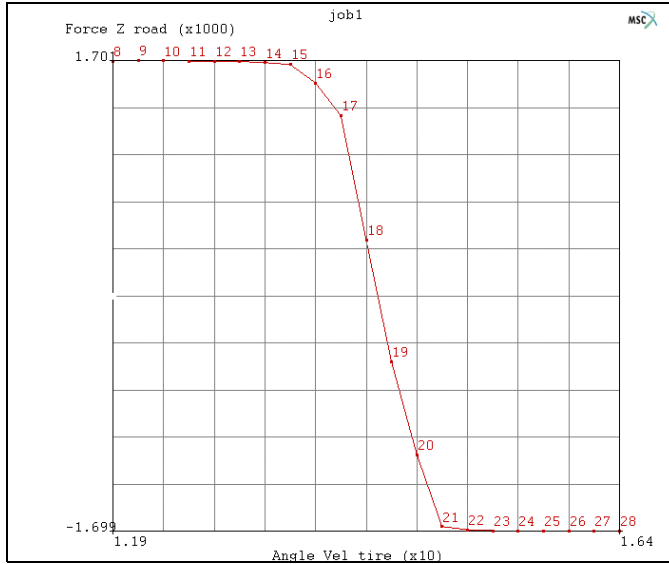


Figure 3.31-8 Spinning Velocity – Traction Curve

More Results on Contact Friction Stresses

The contact friction stresses along the central line of footprint area at the stages of full braking, full traction, and free rolling are shown in [Figure 3.31-9](#), [Figure 3.31-10](#), and [Figure 3.31-11](#), respectively.

A comparison of rolling resistance at different spinning velocities for two different friction coefficients, 0.3 and 0.5, is shown in [Figure 3.31-12](#).

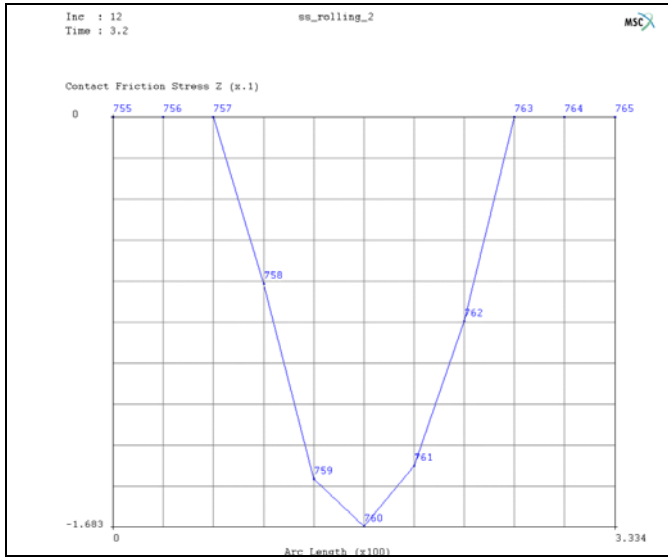


Figure 3.31-9 Contact Friction Stress along the Central Line of Footprint Area – Full Braking

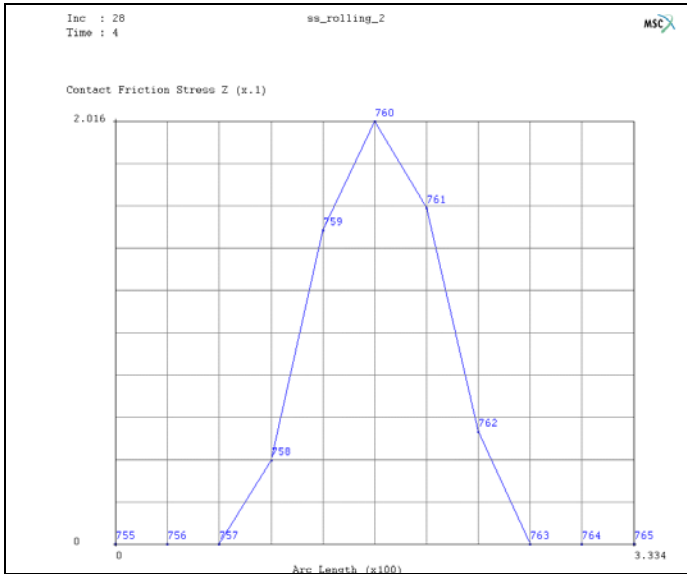


Figure 3.31-10 Contact Friction Stress along the Central Line of Footprint Area – Full Traction

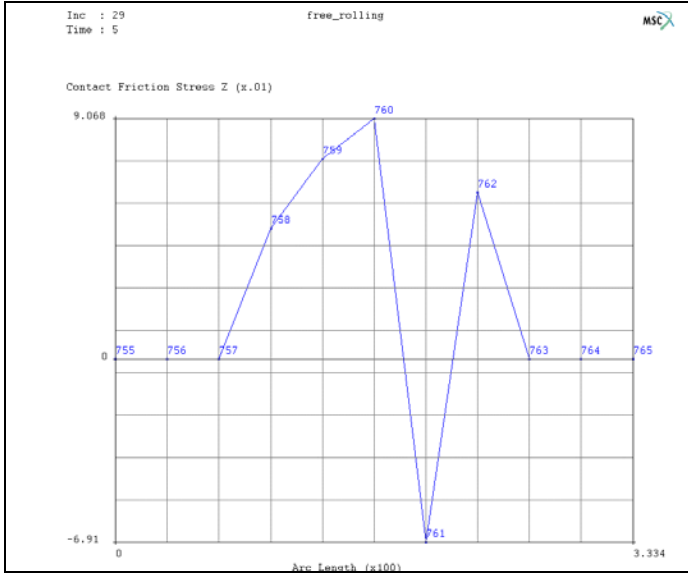


Figure 3.31-11 Contact Friction Stress along the Central Line of Footprint Area – Free Rolling

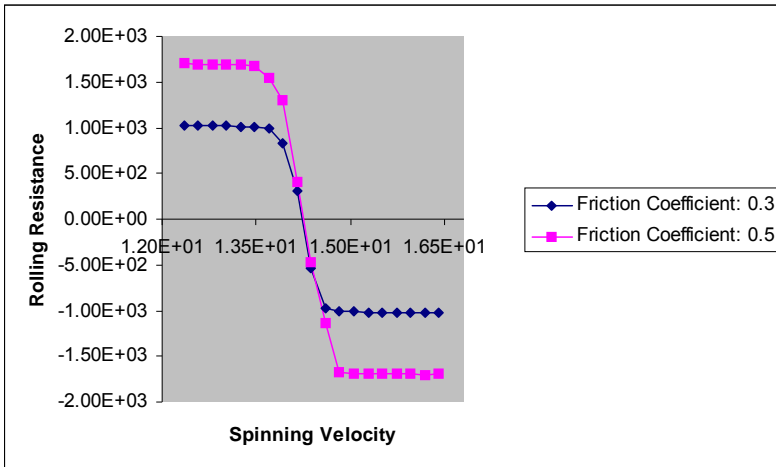


Figure 3.31-12 Spinning Velocity – Rolling Resistance Curves at Difference Frictions

Tire Bead Analysis

This section describes the analysis of the cross section of an automobile tire. The model is loaded by an internal pressure and the contact between the tire and the rim is to be analyzed.

Overview

The method used in this section to obtain a solution is typical for tackling an engineering problem. This section demonstrates that it is useful to approach a problem by using simple models first before going on to large complicated structures. This approach not only gives you a better understanding of your problem, but it also enables you to better analyze the results.

Background Information

Description

An automobile tire is a complex composite structure consisting of (nonlinear) materials that comes into contact with the road.

Figure 3.31-13 identifies the different materials and parts of an automobile tire by part name.

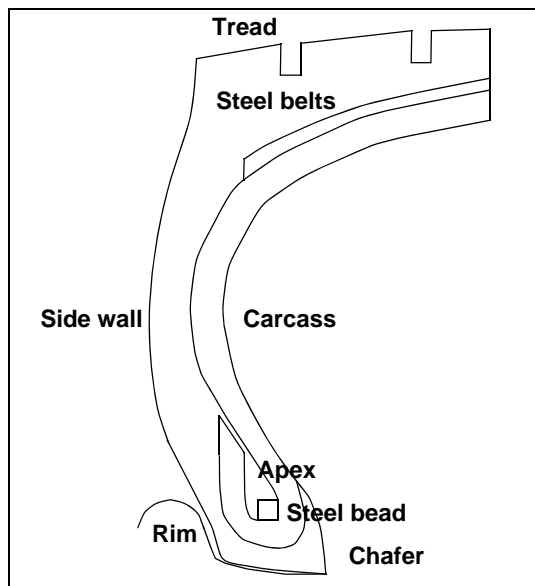


Figure 3.31-13 Cross-Section of Automobile Tire

Idealization

The material properties of the tread, side wall, chafer, and apex are isotropic. The carcass is characterized by an orthotropic material property. The steel belts and beads behave as isotropic materials in the circumferential direction of the tire. In this analysis, both the carcass on the steel belts and beads have been given the same properties as the rubber and, thus, no special elements are required in modeling these parts. The tire comes into contact at the chafer with the wheel rim. The wheel rim is modeled as an infinitely stiff body.

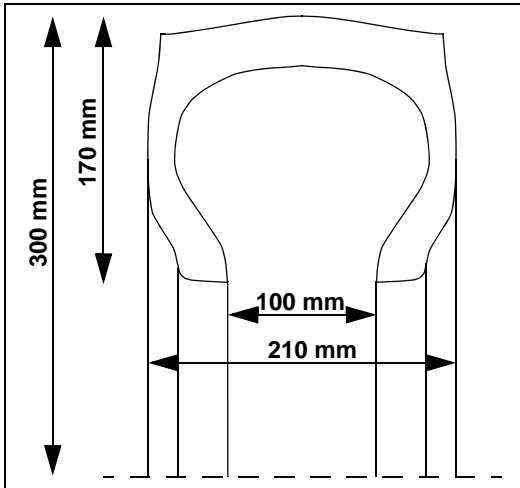


Figure 3.31-14 Overall Dimensions of the Tire

Level of Analysis Detail

This section describes the different stages of idealization that are observed in this analysis. As was noted in the [Overview](#), the best approach for analyzing a complicated structure is to start with simple models. This approach allows you to gain knowledge and confidence in problem-solving as you progress through the analysis process. This approach also helps you to predict behaviors and to identify potential problems.

In this sample session, you will only analyze the inflation process using a crude and easy to generate mesh. The analysis presents some of the main components of detailed analysis.

Analysis

The purpose of this initial analysis is to describe the inflation process by means of an idealization of the real structure.

Idealization

For purposes of this simplified analysis, assume all materials to be identical and ignore the treads in the tire. An axisymmetric model is used and because of symmetry, you only need to analyze half of the cross-section.

Requirements for a Successful Analysis

The analysis is considered successful if the closing behavior at the rim/chafer interface of this simplified model can be shown.

Full Disclosure

- **Type of analysis**

Contact

- **Materials**

The rubber material for this structure is characterized by three Mooney constants for which the following values are chosen:

$$C_{10} = 965kPa$$

$$C_{20} = 193kPa$$

$$C_{30} = 193kPa$$

- **Elements**

Marc Element Type 82, four-noded axisymmetric Herrmann formulation.

Overview of Steps

Step 1: Create the boundary using Bezier curves.

Step 2: Use automatic meshing (OVERLAY) to create a mesh.

Step 3: Create the rim as a rigid die and identify the contact bodies.

Step 4: Add boundary conditions.

Step 5: Apply internal pressure.

Step 6: Submit the job.

Step 7: Postprocess the results.

Detailed Session Description

The description of the tire boundary geometry is well suited for the use of Bezier curves. The defining polygon of a Bezier curve can easily be changed which results in a *smooth* change in the entire curve. To demonstrate the versatility of this curve type, we will generate the boundary of the tire using Bezier curves exclusively.

Step 1: Create the boundary using Bezier curves.

Before entering the Bezier curves, however, first establish an input grid using the following button sequence.

MAIN

MESH GENERATION

SET

U DOMAIN

-17 0

U SPACING

1

V DOMAIN

0 17

V SPACING

1

grid ON

(on)

FILL

Observe that the dimension of the grid size is specified in centimeters. The material constants specified in [Idealization](#) require a conversion from kPa into N/cm^2 , in order to be consistent with the units used here. For a good resolution of the Bezier curve drawing, set the plotting of curves with high accuracy.

Note that when drawing, the number of subdivisions is merely a drawing resolution. The information on every point on the curve is preserved. Use the following button sequence to change the resolution and to set the curve type to Bezier.

MAIN

PLOT

curves SETTINGS

predefined settings HIGH

RETURN (twice)

MESH GENERATION

CURVE TYPE

BEZIER

The curves are added by clicking on the ADD button of the crvs panel and entering the points for the defining polygon vertices of each curve. The beginning and end points of the Bezier curve are determined by the first and last point specified. The tangent at either end is defined by the neighboring points.

MAIN

MESH GENERATION

crvs ADD

(pick the appropriate grid points)

point(0,14,0)

point(-11,13,0)

point(-11,6,0)

```
point(-5,4,0)
point(-5,0,0)
END LIST (#)
```

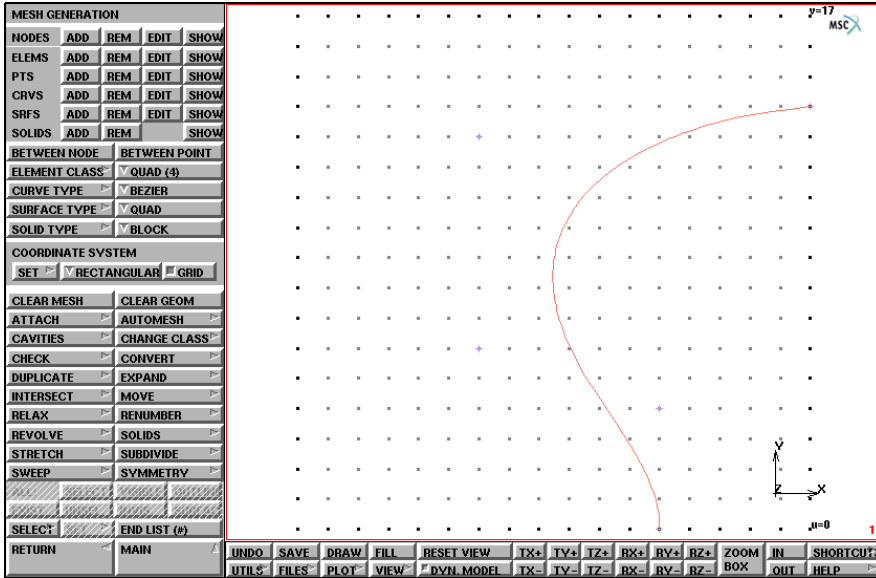


Figure 3.31-15 Interior Tire Wall

Increase the resolution of the grid to 0.5 units:

```
MAIN
MESH GENERATION
SET
U SPACING
0.5
V SPACING
0.5
```

Create the exterior side of the wall of the tire by adding the following curve, the result of which is shown in [Figure 3.31-16](#).

```
MAIN
MESH GENERATION
crvs ADD
```

(pick the appropriate grid points)

```
point(-9,16,0)
point(-9,14,0)
point(-10.5,13,0)
point(-10.5,8.5,0)
END LIST (#)
```

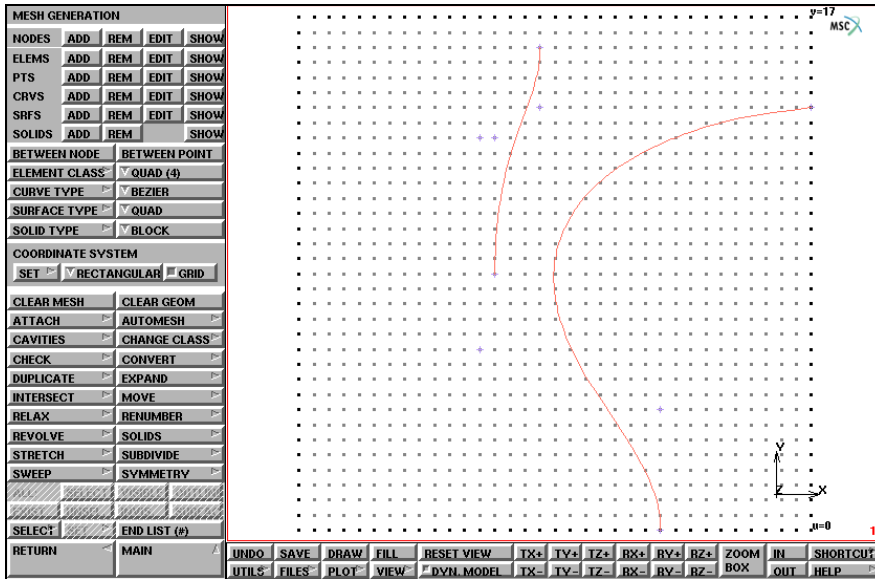


Figure 3.31-16 Part of Exterior Tire Wall Added

Switch on the labeling of points in order to facilitate creating the curves as specified in the button sequences below.

```
MAIN
  PLOT
    points SETTINGS
      LABEL
      REGEN
```

(on)

Add the following curve to create the lower part of the exterior wall of the tire. Even though severe changes in curvature occur in this part, the overall curve remains smooth. The results are shown in [Figure 3.31-17](#).

```
MAIN
  MESH GENERATION
    crvs ADD
```

(pick point)


```

point(-10.5,4,0)
point(-9.5,3.5,0)
point(-8.5,1.5,0)
point(-8,0,0)
point(-7.5,0.5,0)
5
END LIST (#)

```

(pick grid point)
(pick grid point)
(pick grid point)
(pick grid point)
(pick grid point)
(pick point)

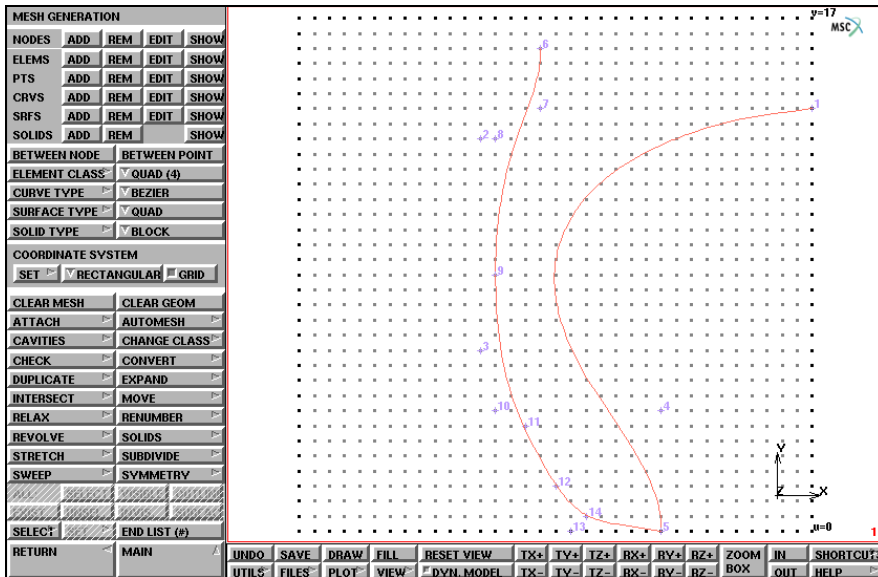


Figure 3.31-17 Exterior Tire Wall Completed

Figure 3.31-17 clearly indicates that the shape of the portion of the tire that comes into contact with the rim of the wheel is incorrect. This is remedied by relocating some of the support points of the Bezier curve.

Points 13, 10, and 11 are relocated using the pts EDIT button on the mesh generation panel, the results of which are shown in Figure 3.31-18.

MAIN

MESH GENERATION

pts EDIT

```

13
-9.5  -0.5  0
10
-11.0 -0.5  0

```

(pick point)
(pick grid point)
(pick point)
(pick grid point)

```

11
-7      5      0
END LIST (#)

```

(pick point)
(pick grid point)

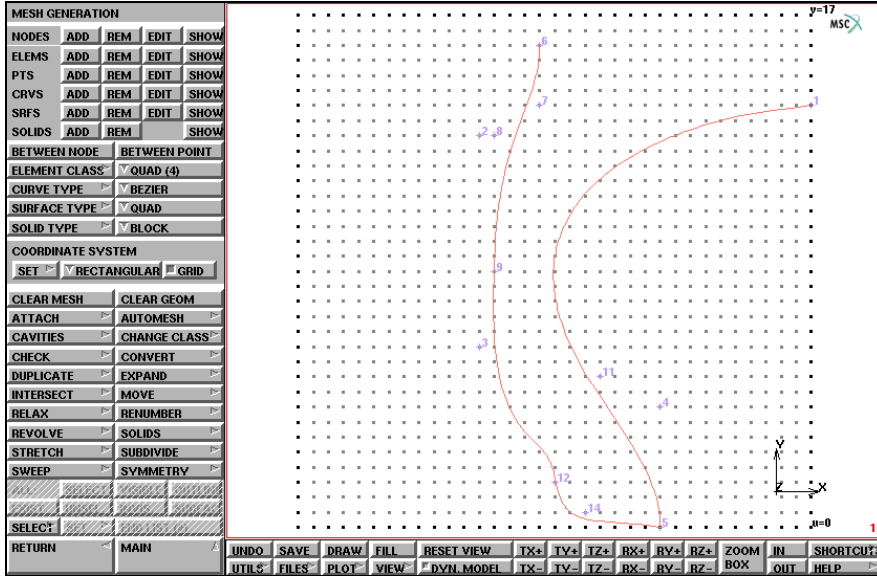


Figure 3.31-18 Correction of Tire Geometry

To add the tread, use a Bezier curve made up of point 6 and three new points. The exact location of these points are shown in Figure 3.31-19. The following button sequence specifies where these points are located in the local u-v-w coordinate system. Refrain from entering the points by typing in their coordinates; instead, always use the mouse to pick the points as it is a much easier method.

MAIN

MESH GENERATION

crvs ADD

```

6
point(-7.5,16,0)
point(-1.5,17,0)
point(0,17,0)
END LIST (#)

```

(pick point)
(pick grid point)
(pick grid point)

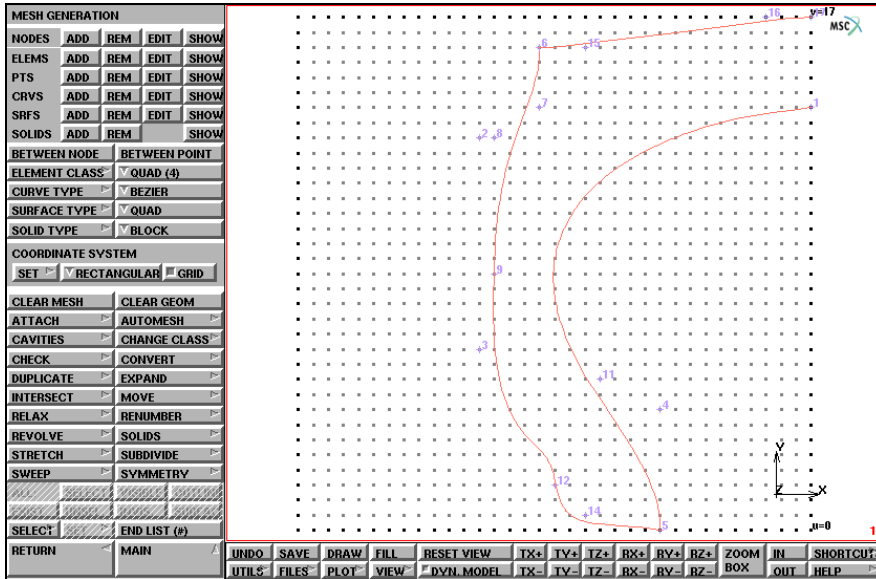


Figure 3.31-19 Tire Tread

Finally, to complete the boundary, add a straight line between points 1 and 17 which form the symmetry boundary. A Bezier curve is used here simply to demonstrate how it degenerates into a straight line when only two points are specified. The completed boundary is shown in [Figure 3.31-20](#).

MAIN

MESH GENERATION

crvs ADD

17

(pick point)

1

(pick point)

END LIST (#)

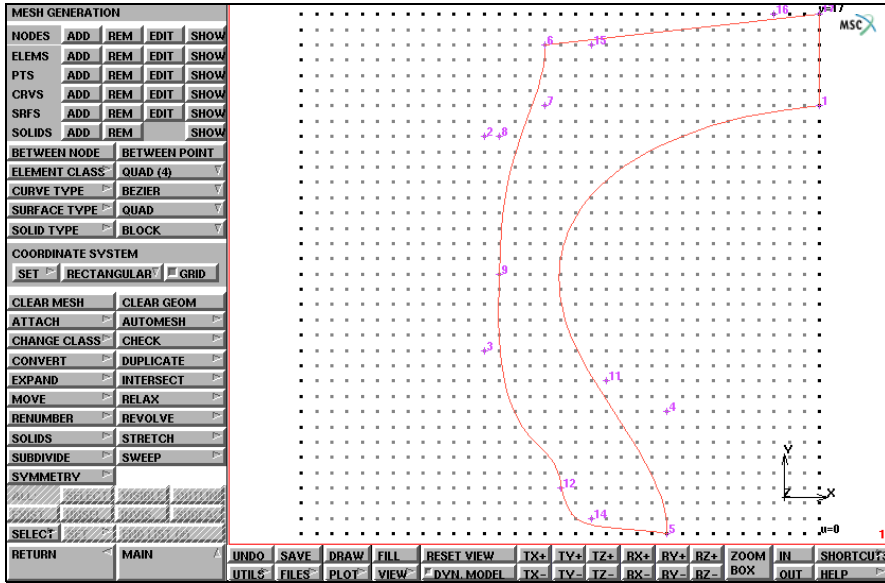


Figure 3.31-20 Completed Boundary

Step 2: Use automatic meshing (OVERLAY) to create a mesh.

Use the automatic overlay meshing option to create the mesh. This automatic mesh generator requires a closed boundary. The only input needed from the user is the number of subdivisions in the x- and y-direction, respectively, and the identification of the closed boundary.

MAIN

MESH GENERATION

GRID

FILL

AUTOMESH

2D PLANAR MESHING

DIVISIONS

20 20

quadrilaterals (overlay) QUAD MESH!

all: EXIST.

(off)

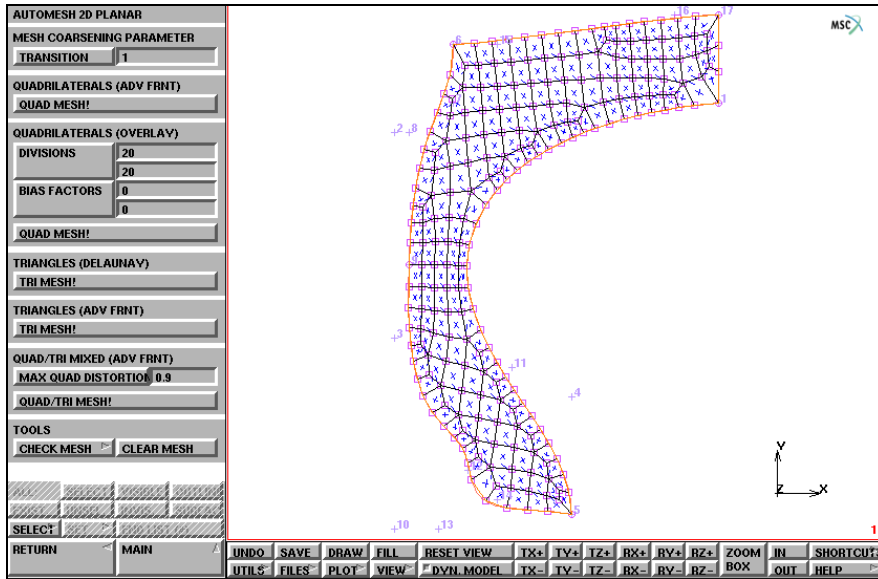


Figure 3.31-21 Mesh generated by OVERLAY

It should be clear from the visual inspection that the mesh is rather coarse in the lower area where the tire comes into contact with the wheel rim. A local refinement is necessary and can be accomplished by using the SUBDIVIDE and REFINER processors.

MAIN

MESH GENERATION

SUBDIVIDE

DIVISIONS

2 1 1

ELEMENTS

51 3 5 7 60

END LIST (#)

(pick elements)

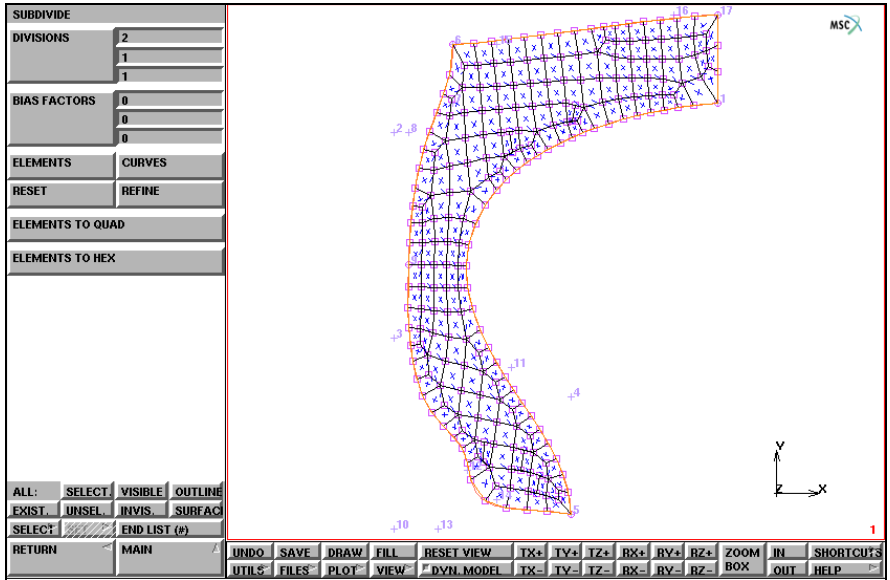


Figure 3.31-22 Step 1 of Mesh Refinement

The REFINE option can be used to effectively create a transition between *layers* or *rows* of elements. It requires two sets of information:

- The node about which the refinement is made;
- The elements that will participate in the refinement.

Note that only those elements that have the refined node as part of the connectivity are eligible.

```

MAIN
  MESH GENERATION
    SUBDIVIDE
      REFINE
        1
        1
      END LIST (#)
  
```

(pick refine node)
(pick element)

Complete this action by subdividing two more elements according to [Figure 3.31-24](#).

```

MAIN
  MESH GENERATION
    SUBDIVIDE
      ELEMENTS
  
```

47 46
END LIST (#)

(pick elements)

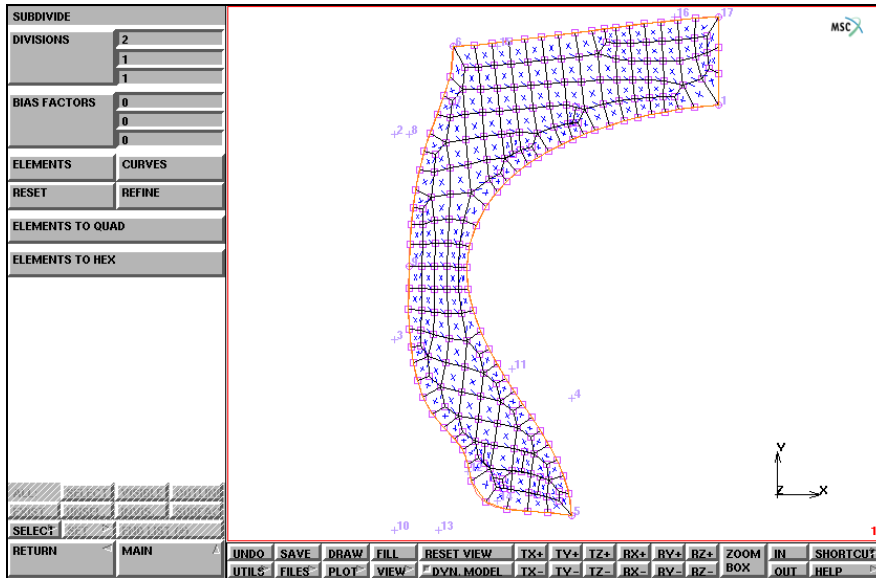


Figure 3.31-23 Local Refinement around a Node

Remember that some processors such as SUBDIVIDE, EXPAND, SYMMETRY, and DUPLICATE may create duplicate nodes. Although the nodes are in the same position, they are not connected. The node that is picked as the refine node may be part of one element's connectivity but not of the neighboring element. The REFINE processor can, in such an instance, produce unexpected and undesired results. To prevent this, it is usually prudent to activate the SWEEP processor *before* a refine operation is performed.

Compression of all nodes located within a specified distance is accomplished by activating the NODES button in the SWEEP menu followed by a list of nodes that you want to sweep. Generally, you use the all: EXIST. list button to sweep all existing nodes. Finally, renumber all items in the database in order to obtain a sequential node and element numbering.

```

MAIN
  MESH GENERATION
    SWEEP
      sweep NODES
        all: EXIST.
      remove unused NODES
    RETURN
  RENUMBER
  ALL
  
```

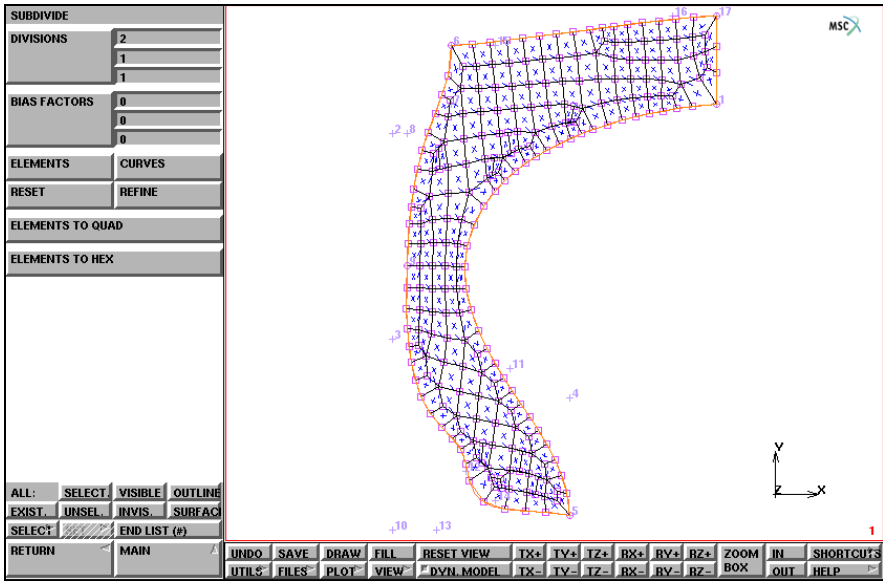


Figure 3.31-24 Completion of Local Mesh Refinement

Step 3: Create the rim as a rigid die and identify the contact bodies.

The rim of the wheel is considered to be a rigid body and is constructed using a Bezier curve. Use the following button sequence to add the rim.

MAIN

MESH GENERATION

FILL

ZOOM BOX

(zoom in on the lower area)

GRID

(on)

crvs ADD

5

(pick point)

point(-12,0,0)

(pick grid point)

point(-5.5,2.5,0)

(pick grid point)

point(-11,3.5,0)

(pick grid point)

point(-11,1.5,0)

(pick grid point)

END LIST (#)

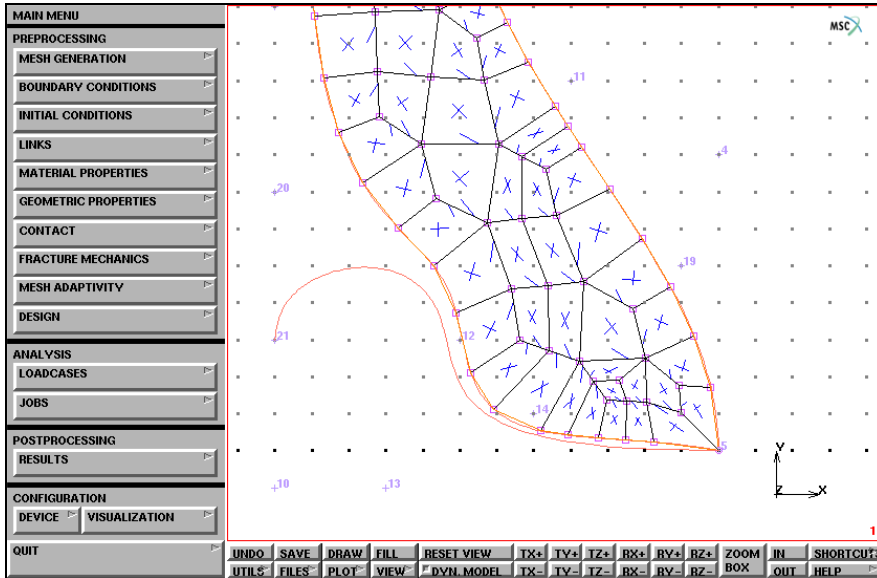


Figure 3.31-25 Wheel Rim added

The mesh has been conveniently generated so that the origins coincide with the center line and the bottom of the tire. Use the following button sequence to move the entire mesh and rim over a distance that is equivalent to the radius of the wheel:

```

MAIN
  MESH GENERATION
    GRID
    SELECT
      NODES
        all: OUTLINE
        END LIST (#)
      RETURN
    MOVE
      TRANSLATIONS
        0 13 0
      POINTS
        all: EXIST.
      NODES
        all: UNSEL.
      RETURN
    FILL
  
```

(off)

Not all elements of the tire come into contact with the rim. You can drastically minimize the analysis time by identifying the elements that make up the deformable body that is expected to come into contact with the rim.

MAIN

CONTACT

CONTACT BODIES

NEW

DEFORMABLE

OK

elements ADD

*(pick the elements that may come
into contact with the rigid body)*

END LIST (#)

To identify the rim (curve) as a rigid contact body, use the following button sequence:

Note: It is important to use NEW in the following button sequence. If NEW is not used, the contact body just entered is written over.

MAIN

CONTACT

CONTACT BODIES

NEW

RIGID

OK

CURVES ADD

6

(pick curve)

END LIST (#)

PLOT

draw POINTS

(off)

elements SETTINGS

draw SOLID

RETURN (twice)

ID CONTACT

(on)

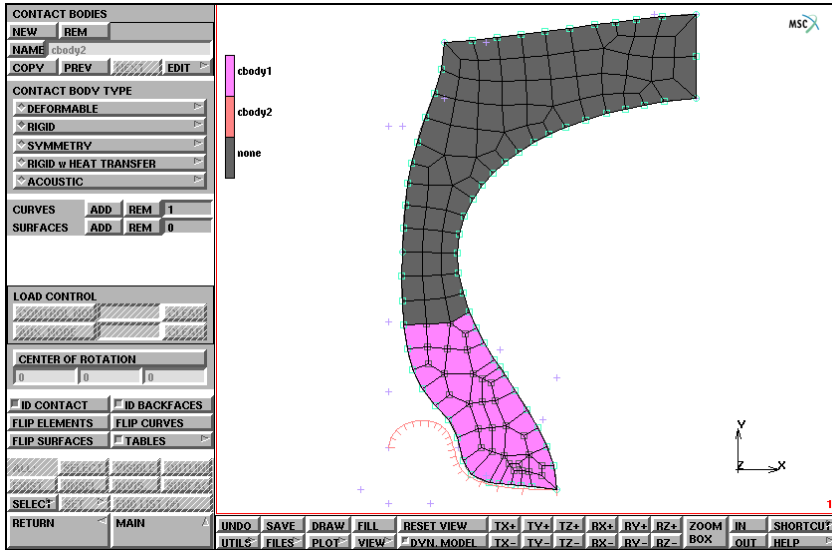


Figure 3.31-26 Identification of Contact Bodies

The contact bodies are identified on the graphics screen by clicking on the ID CONTACT button of the contact bodies panel. The curve that represents the rigid body is enhanced by cross-hatching the side where the body is located. If the display indicates that the body is located on the incorrect side, use the FLIP CURVES option to flip the curve. Refer to [Chapter 3.30: Container](#), Step 7 for a detailed description on using the FLIP CURVES option.

Now, switch off the identification of contact bodies.

MAIN

CONTACT

CONTACT BODIES

ID CONTACT

(off)

PLOT

elements SETTINGS

draw WIREFRAME

RETURN

REGEN

FILL

Step 4: Add boundary conditions.

Symmetry conditions are applied to the nodes along the symmetry line using the following button sequence:

MAIN

BOUNDARY CONDITIONS

MECHANICAL

FIXED DISPLACEMENT

DISPLACEMENT X

(on)

OK

nodes ADD

130 138 142

(pick the three nodes at the right)

END LIST (#)

The symmetry boundary conditions are displayed in [Figure 3.31-27](#).

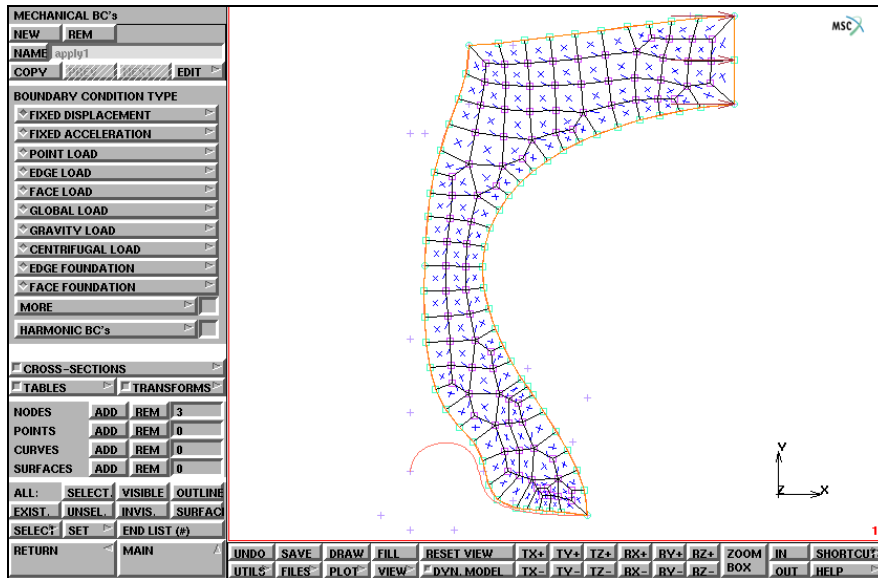


Figure 3.31-27 Symmetry Boundary Conditions Applied

Step 5: Apply internal pressure.

The tire is loaded by an internal pressure. Use the following button sequence to specify the loading history through a table.

MAIN

BOUNDARY CONDITIONS

```
MECHANICAL
  TABLES
    NEW
      1 INDEPENDENT VARIABLE
    TYPE
      time
      OK (select OK button only if type time was typed in)
    NAME
      loading
    TYPE
      time
    independent variable v1: MAX
      300
    function value f: MAX
      220
    ADD
      0 0
      300 214
    SHOW TABLE
      SHOW MODEL (select SHOW MODEL to return to model view)
```

It is important to specify the table type because a table will only be applied if the appropriate type is assigned. For boundary conditions, only table type *time* is valid.

Apply this load to the interior of the tire using the following button sequence:

```
MAIN
  BOUNDARY CONDITIONS
    NEW
  MECHANICAL
    EDGE LOAD
      pressure TABLE
      loading
      OK
  SELECT
    CLEAR SELECT
    ...EDGES
```

```

42:2
END LIST (#)
SELECT BY
edges by CRVS
1
END LIST (#)
RETURN
RETURN
edges ADD
all SELECT
END LIST (#)
SELECT
CLEAR SELECT

```

The results of the applied internal pressure are depicted in [Figure 3.31-28](#).

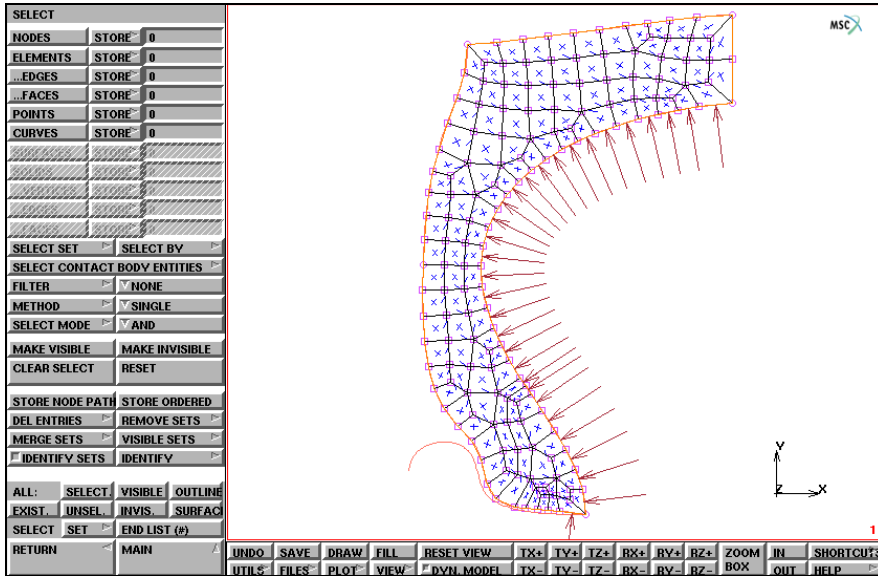


Figure 3.31-28 Internal Pressure Applied

The material for this mesh is assumed to be uniform over the entire mesh. Specify the material properties using the following button sequence:

```

MAIN
MATERIAL PROPERTIES

```

```
MORE
  MOONEY
    C10
      96.5
    C20
      -19.3
    C30
      19.3
  OK
  elems ADD
  all EXIST.
```

Step 6: Submit the job.

Use the following button sequence to prepare a loadcase.

```
MAIN
  LOADCASES
    mechanical STATIC
      LOADS, OK
      TOTAL LOADCASE TIME
        300
      # STEPS
        300
      OK
```

This loadcase is to be used in the job that ultimately is submitted for analysis. Use the following button sequence to specify the job.

```
MAIN
  JOBS
    MECHANICAL
      loadcases SELECT
        lcase1
      ANALYSIS OPTIONS
        LARGE DISPLACEMENT
        NO FOLLOWER FORCE
```

(on)

(to switch to FOLLOWER FORCE)

```
      OK
JOB RESULTS
  available element tensors
    Cauchy Stress
      OK
AXISYMMETRIC
OK
ELEMENT TYPES
  MECHANICAL
  AXISYM SOLID
    82                                     (FULL & HERRMANN FORMULATION/
                                           QUAD (4))
      OK
all: EXIST.
RETURN
```

Use the following button sequence to submit the job.

```
MAIN
  JOBS
    SAVE
    RUN
      SUBMIT 1
      MONITOR
```

The analysis stops with an exit number 2004, indicating that a rigid body motion is present (the tire separates from the rim).

Step 7: Postprocess the results.

The purpose of the preliminary analysis is to gain experience in completing a relatively simple analysis. The following results are displayed:

1. Animation of the deformation. Only the first and last frame are shown here.
2. Contouring of the von Mises stress on the tire cross section.

Use the following button sequence to open the results file.

```
MAIN
  RESULTS
```


OPEN DEFAULT
 NEXT

To focus on the geometry, it is necessary to turn the node labeling and face identification off as is shown in Figure 3.31-29.

Use the button sequence given below to turn the node labeling and face identification off.

MAIN

FILL

PLOT

draw NODES

(off)

elements SETTINGS

draw FACES

(off)

RETURN

REGEN

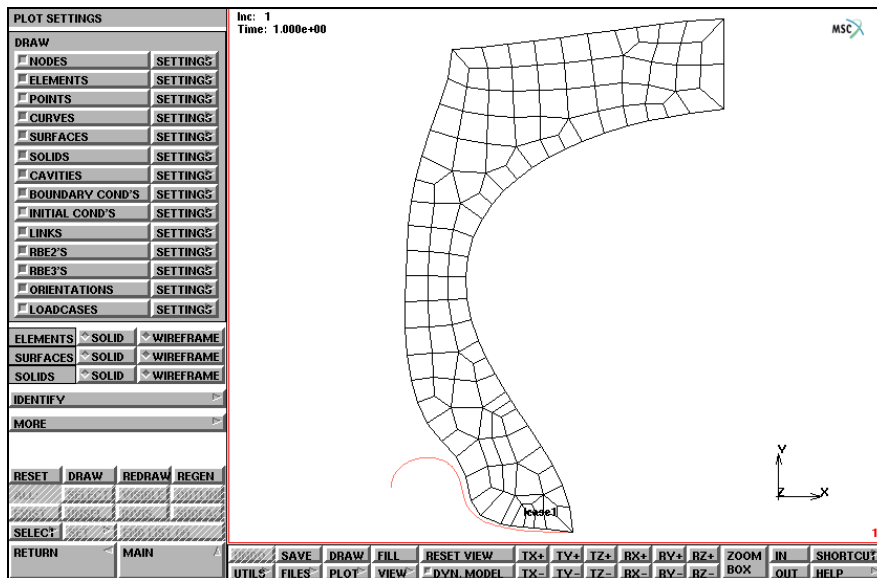


Figure 3.31-29 Mesh without Node Labeling and Face Identification

Click on DEF & ORIG to request the original and deformed structure to be shown. The animation buttons are in the second part of the postprocessing results menu and can be reached by clicking on the MORE button. To create the animation frames, use the following button sequence:

```

MAIN
  RESULTS
    REWIND
    MORE
    ANIMATION
      INCREMENTS
        100
        1
  
```

The numeral 100 is entered here as a response to the number of increments that need to be processed.

From the analysis, we know that the results stretch out over approximately 14 increments. Hence, 100 is a safe upper limit. The program now prepares the frames for animation. [Figure 3.31-30](#) and [Figure 3.31-31](#) show the second and last of the animation frames.

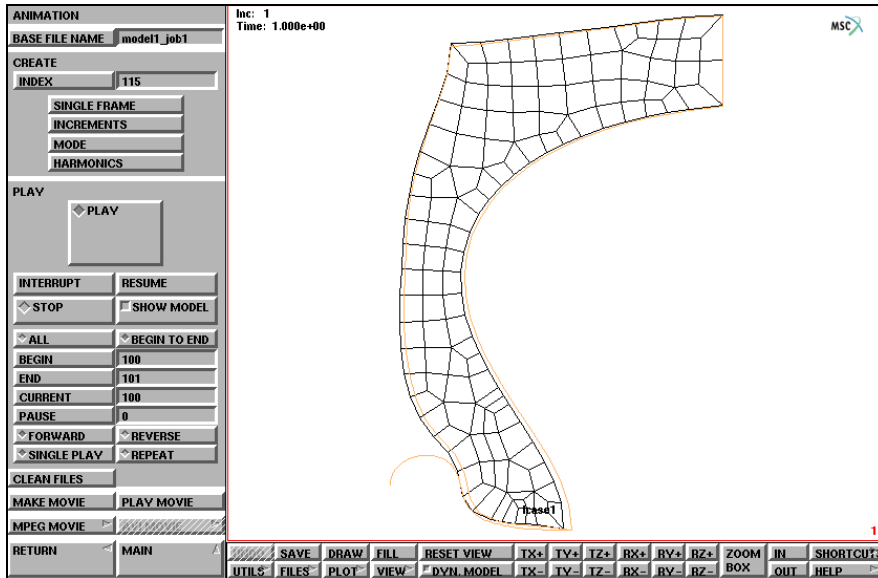


Figure 3.31-30 Second Animation Frame

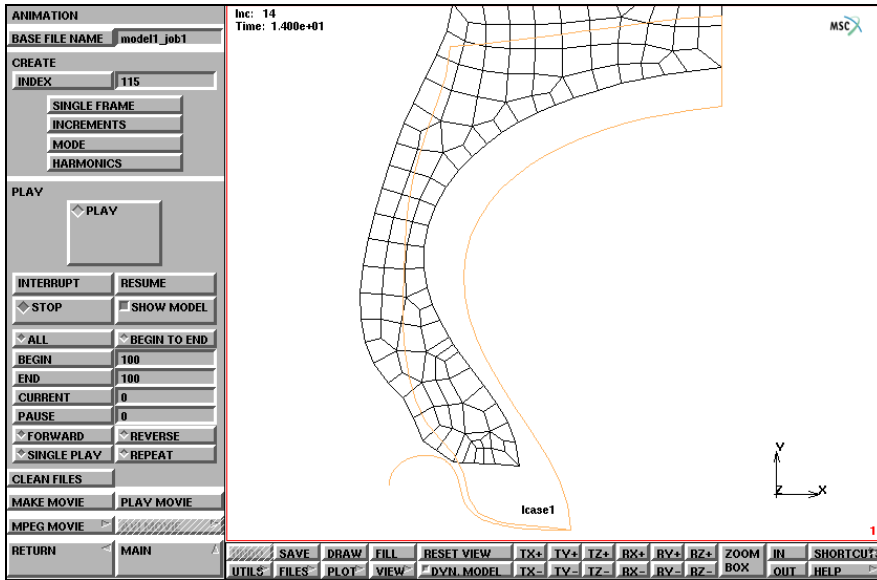


Figure 3.31-31 Last Animation Frame

To animate the sequence of frames use the following button sequence:

```

MAIN
  RESULTS
    FILL
    MORE
      ANIMATION
        FILL
        PLAY
  
```

The equivalent Cauchy stress can be displayed by using the following button sequence:

```

MAIN
  RESULTS
    SCALAR
      Equivalent Cauchy Stress
    LAST
    CONTOUR BANDS
  
```

Figure 3.31-32 shows the results of the model with equivalent stress contour bands.

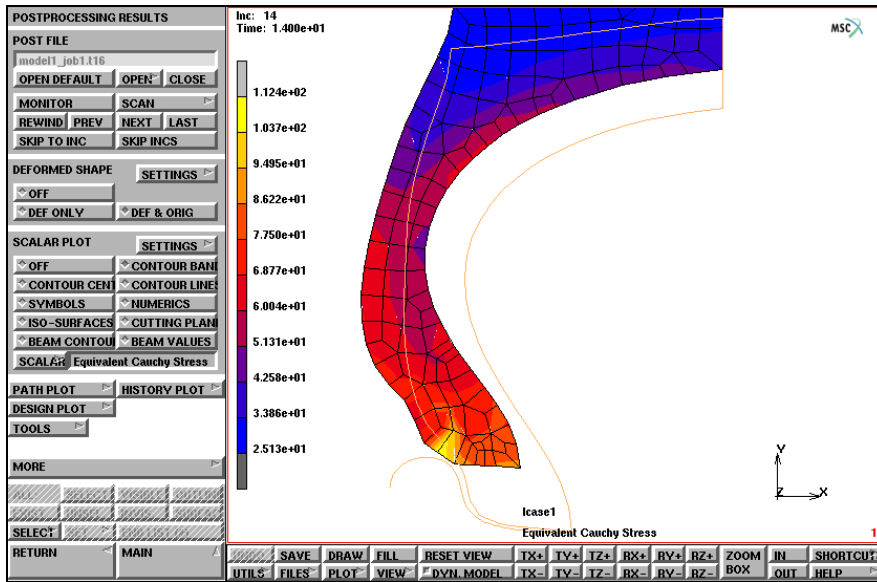


Figure 3.31-32 Mesh with Equivalent Cauchy Stress Contours

Conclusion

This example demonstrates that it is relatively easy to complete a contact analysis using a simple to generate geometry and an incompressible material. The tire loses contact with the rim. This is caused by the fact that the steel belt is not present in this analysis. Although the results shown in this analysis have little engineering value, the analysis is valuable in reassuring that the available tools in Marc enable you to solve a more complex problem.

Input Files

The files below are on your [delivery media](#) or they can be downloaded by your web browser by clicking the links (file names) below.

File	Description
steady_state.proc	Mentat procedure file
tire_rim.proc	Mentat procedure file
tire2d_model.mfd	Mentat model file used in steady state
rigid_road.mfd	Mentat model file used in steady state
reb_curves.mfd	Mentat model file used in steady state

3.32 Transmission Tower

- Chapter Overview 1550
- Background Information 1550
- Detailed Session Description 1552
- Conclusion 1600
- Input Files 1600

Chapter Overview

This chapter describes a sample session that illustrates the functionality of the Mentat program through the modeling and analysis of a tower structure. The goal of this chapter is to give you hands-on experience with the following Mentat capabilities.

- To show you how to create a mesh of linear beam elements using the following mesh generation features:
 - user-defined local coordinate systems
 - node and element creation,
 - element subdivision and duplication.
- To demonstrate a static and a modal analysis of a model.
- To view and examine the results of an analysis.

Background Information

Tower Description

The tower is 68 feet high, 18 feet square at the base, 4 feet square at the top, and has 6 cable-arms, each 6 feet wide. The tower is made of steel angles (L3x3x1/4 and L2x2x1/4) and is loaded by member self-weight, wind, and cable loads.

The feet at the base of the tower are fixed. A sketch of the tower is depicted in [Figure 3.32-1](#).

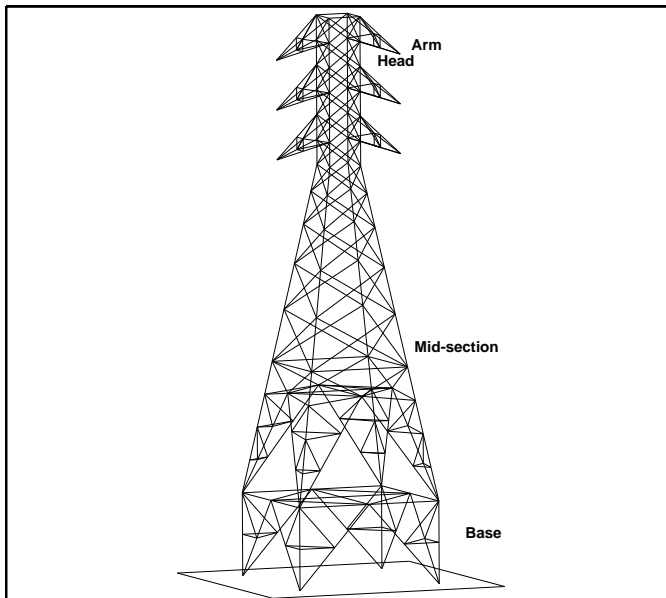


Figure 3.32-1 Transmission Tower

Idealization

By virtue of the element type used in this model, Marc Element Type 98, the sketch in [Figure 3.32-1](#) and the finite element model itself are identical. This may not be true in all cases. Members of the tower are idealized as beam elements with six degrees of freedom at each node (u_x , u_y , u_z , r_{xx} , r_{yy} , r_{zz}).

The wind loads are applied as distributed loads along the main vertical members of the tower. Cable loads are applied as point loads at the end of the cable-arms. Self-weight is applied as distributed loads on all members.

Requirements for a Successful Analysis

The analysis is considered successful if the displacements of the structure, as a result of its external loading can be determined. The second part of the analysis (modal analysis) is successful if the eigenmodes of the structure can be predicted.

Full Disclosure

- **Analysis Types**
Linear static
Modal
- **Material**
Steel, Young's modulus = $4.176e9$ psf, Poisson's ratio = 0.3.
Mass density = 15.217 slugs/ft³.
- **Elements**
Marc Type 98, three-dimensional, two-noded beam element.
- **Element Properties**
Those obtained from the AISC Steel manual.
L3x3x1/4
Weight = 4.9 lbs/ft.
Area = 0.01 ft².
 $I_{xx} = I_{yy} = 6.0e-5$ ft⁴.
L2x2x1/4
Weight = 3.19 lbs/ft.
Area = 0.00651 ft².
 $I_{xx} = I_{yy} = 2.0e-5$ ft⁴.

Overview of Steps

- Step 1:** Create the first face of the main tower structure by adding nodes and elements and using user-defined coordinate systems, subdivision, and symmetry.
- Step 2:** Duplicate the first face to create the remaining faces of the main tower structure. It is crucial to sweep nodes and elements after using symmetry and duplicate.
- Step 3:** Create one cable arm by adding nodes and elements and using subdivide.
- Step 4:** Use symmetry on the first arm to create the second arm. Then use duplicate on the first two to create the remaining cable arms.
- Step 5:** Add boundary conditions.
- Step 6:** Define the material and apply it to all elements. Define the geometric properties and apply them to the appropriate elements.
- Step 7:** Job submission of the static analysis.
- Step 8:** Static analysis results processing.
- Step 9:** Job submission of the modal analysis.
- Step 10:** Modal analysis results processing.

Detailed Session Description

When modeling a structure, it is very important to define a coordinate system that can be referred to as you create different parts of the structure. The **global coordinate system**, called the *x-y-z system*, is the coordinate system attached to the earth and can be used for this purpose. The global coordinate system may not always be the optimal choice in Mentat because the design of the program restricts the orientation of the model, particularly when graphical input is desired.

A **local coordinate system** is a set of three independent directions and an origin, defined with respect to the global coordinate system. For easy reference, we refer to the local coordinate system as the *u-v-w system*. The nature of this system may be Cartesian, cylindrical, or spherical according to the commonly accepted definitions. Initially, the local coordinate system coincides with the global x-y-z system. We emphasize once again that the position and orientation of the local coordinate system is defined in terms of the global coordinate system. Everything else, except viewpoint, is defined in terms of the local coordinate system.

A Note on Grid Space

If you are using the mouse to input entities such as nodes, you need to relate the two-dimensional space of your screen to three-dimensional reality. Choose the u-v plane of the local coordinate system as a plane that is sensitive to mouse picks. You can orient the input grid anywhere in space simply by translating and rotating the local coordinate system. By virtue of the fact that the local u-v-w coordinate system initially lines up with the global coordinate system, the input grid also initially lies in the global x-y plane.

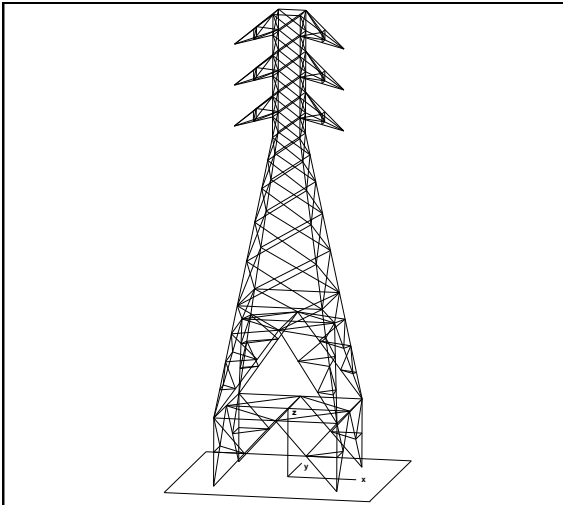


Figure 3.32-2 Local Coordinate System (u-v-w)

A Note on Viewpoint

The ability to orient the local coordinate system anywhere in space does not necessarily mean that it is optimal for graphical input. The best resolution of the grid is obtained by viewing the grid plane with the eye positioned along the normal to that plane.

Use VIEWPOINT in the MANIPULATE CAMERA (ABSOLUTE) menu - which can be entered via the VIEW menu – to define the appropriate eye position measured with respect to the global coordinate system.

Once again, we emphasize that viewpoint and the position of the local coordinate system are the only two exceptions to the rule that everything in Mentat is measured in local coordinates.

Keep the following three points in mind with respect to viewpoint.

- Changing the viewpoint is not the same as rotating the object that you are viewing. Although the end result may appear to be the same, there is a fundamental difference. Changing the viewpoint does not change the position of the model, while a transformation of the object permanently changes the position of that object.
- Changing the viewpoint is *not* related to changing the local coordinate system. These are two independent actions.
- Changing the position and sense of the local coordinate system only affects the position of entities that have yet to be defined. It does not influence or change the position of entities, such as nodes or points, that have already been defined.

Step 1: Create the first face of the main tower structure by adding nodes and elements and using user-defined coordinate systems, subdivision, and symmetry.

As described in previous sample sessions, the first step in building a finite element mesh is to establish an input grid. Activate the grid and set the grid spacing to 1 unit and the grid size to 10 units.

The best approach to use for creating the transmission tower is to align the center line of the structure with the global z-axis. Rotate the local coordinate system about the global x-axis over 90°, and translate it over nine units in the global y-direction. Set and activate view 2.

```
MAIN
  MESH GENERATION
    SET
      U DOMAIN
        -10 10
      U SPACING
        1
      V DOMAIN
        -10 10
      V SPACING
        1
      grid ON (on)
      ROTATE
        90 0 0
      TRANSLATE
        0 9 0
      VIEW
        activate 2 (on)
        show 2
        FILL
        PLOT
          nodes SETTINGS
            LABELS (on)
            RETURN
          elements SETTINGS
            LABELS (on)
            RETURN
```

Prior to adding elements, the user has to change the default element class for newly generated elements from QUAD(4) to LINE (2). Use the ADD button from the ELEMS panel to add the first three elements to form a triangle that will constitute the base of the tower:

```
MAIN
  MESH GENERATION
```

ELEMENT CLASS

LINE (2)

RETURN

elems ADD

node(-9,0,0)

(pick grid point)

node(-9,10,0)

(pick grid point)

node(0,10,0)

(pick grid point)

1

(pick node)

2

(pick node)

3

(pick node)

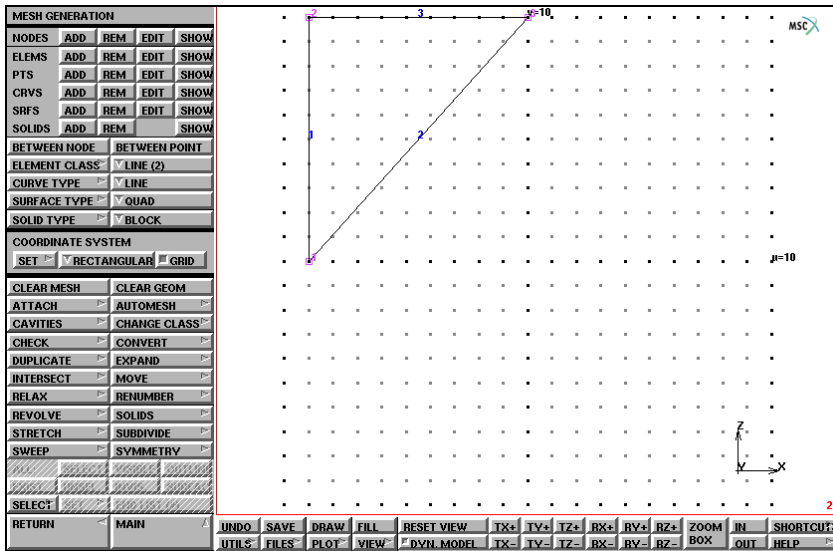


Figure 3.32-3 First Three Elements of Tower Base

Having obtained [Figure 3.32-3](#), continue to subdivide the vertical side and the hypotenuse, and add the two cross members. Notice how you have started to create to the left of the local v-axis. Although this does not look at all like the *base* yet, you will continue to add to the left side of the tower face and use symmetry to complete the first face. [Figure 3.32-4](#) shows the results of this operation.

MAIN

MESH GENERATION

SUBDIVIDE

ELEMENTS

1 2

```

END LIST (#)
RETURN
elems ADD
      5                               (pick node)
      8                               (pick node)
      8                               (pick node)
      6                               (pick node at upper left position)
    
```

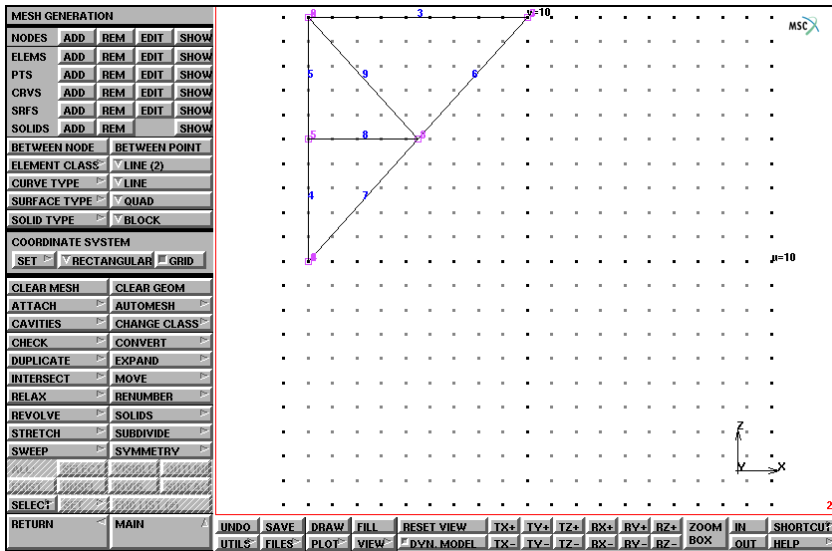


Figure 3.32-4 Left Base of Tower

The next step is to establish a new local coordinate system with a grid spacing of 2 and a grid size of 20 to create the *head* of the tower that is parallel to the local coordinate system of the base but shifted 50 units in z-direction.

Figure 3.32-5 shows the new coordinate system relative to the part of the *base* that you have already defined. Use the SHOW ALL VIEWS option to view the model from the four default angles. View 2 shows that the new local coordinate system is shifted 7 units in the negative y-direction.

```

MAIN
  MESH GENERATION
  SET
    U DOMAIN
      -20 20
    U SPACING
      2
    
```

```

V DOMAIN
    -20 20
V SPACING
    2
TRANSLATE
    0 -7 50
VIEW
    activate 1 (off)
    activate 2 (off)
    activate 4 (on)
PERSPECTIVE
ACTIVATE ALL
SHOW ALL VIEWS
FILL
    show 2
RETURN
    
```

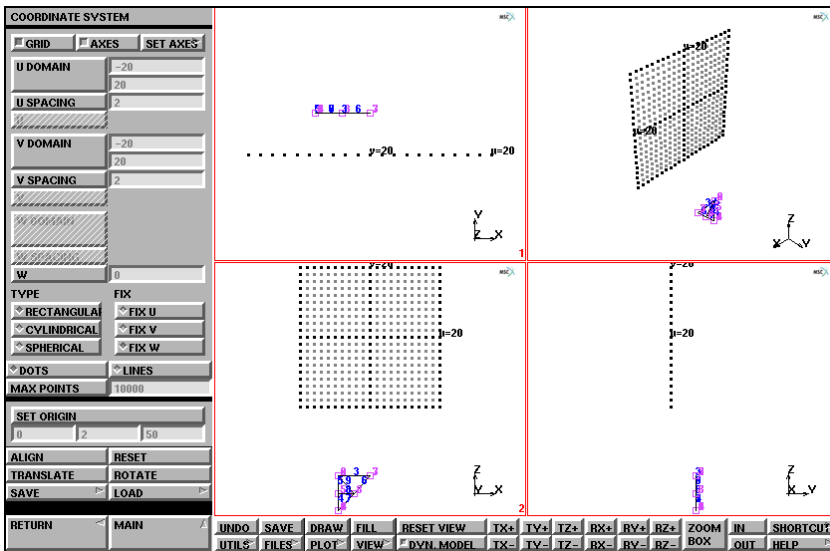


Figure 3.32-5 Four Views of New Local Coordinate System

Use the technique of generating one master element and subdividing it into six equally sized elements to generate the left side of the *head*. Keep the bias factor equal to zero but change the number of subdivisions to 6 in the first direction of the element.

Since line elements are one-dimensional elements, it is not necessary to define the number of elements in the second and third direction. In general, the direction in which the subdivisions are made is dependent on the connectivity; that is, the order in which nodes are entered to create an element.

MAIN

MESH GENERATION

elems ADD

(pick from the grid)

node (-2, 0, 0)

node (-2, 18, 0)

SUBDIVIDE

DIVISIONS

6 2 2

ELEMENTS

10

(the newly generated element)

END LIST (#)

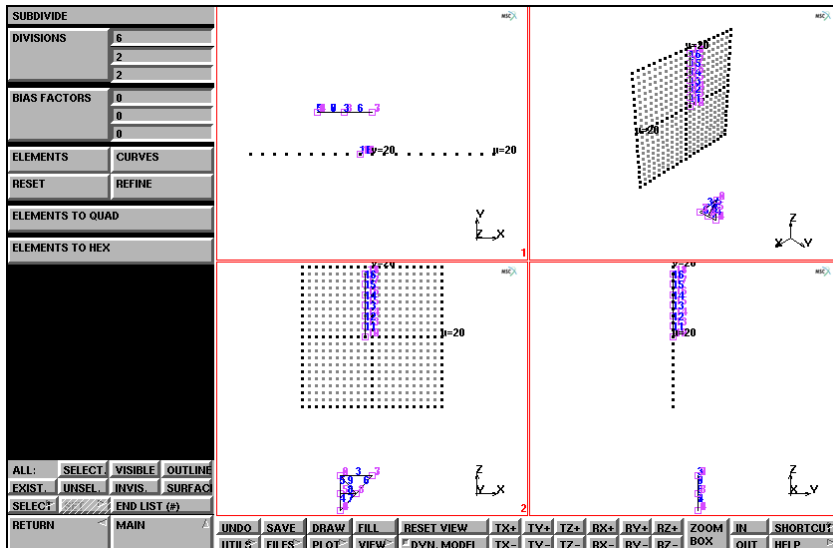


Figure 3.32-6 Creating the Left Side of the Tower Head

The next step is to generate the sloping mid-section. Set the grid spacing to 1 and the grid size to 50 to define yet another local coordinate system to connect the two coordinate systems that were already defined.

Use ALIGN to line up the local *u* and *v* axes so that the plane spanned by these two axes contains the origins of both previous coordinate systems. This way you can use the grid to define the mid-section elements.

MAIN

MESH GENERATION

SET

ALIGN

0 9 10

-9 9 10

-2 2 50

U DOMAIN

-50 50

U SPACING

1

V DOMAIN

-50 50

V SPACING

1

VIEW

show 3

RETURN

(upper right of lower section)

(upper left of lower section)

(bottom node of top section)

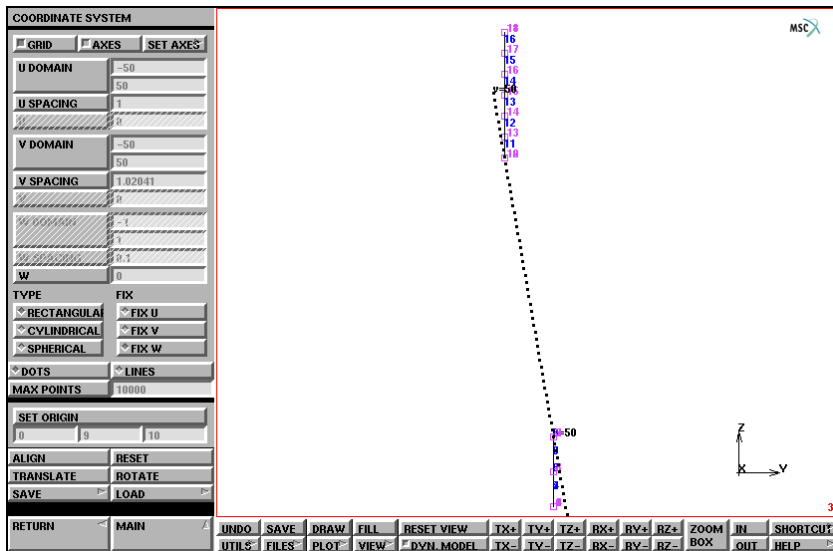


Figure 3.32-7 Local u and v Axes Aligned

The subdivisions along the mid-section are not equally spaced. This is where the **bias factor** can be used to successfully generate a weighted subdivision. The following example illustrates the theory behind the bias factor.

Suppose you want to subdivide the line element in [Figure 3.32-8](#) so that the length of the elements are biased towards the right. The desired number of subdivisions is assumed to be four and a local coordinate t is introduced, which ranges from -1 at the first node to +1 at the second node. An unbiased subdivision would produce 4 elements with their respective nodes located at $t = -1$, $t = -1/2$, $t = 0$, $t = +1/2$ and $t = +1$. A biased subdivision relocates these nodes using the formula

$$t^* = t + b(1 - t^2)$$

where b is the bias factor and t^* is the biased local coordinate.

Using a bias factor $b = 0.5$ will result in nodes at $t^* = -1$, $t^* = -1/8$, $t^* = +1/2$, $t^* = +7/8$ and $t^* = +1$. The unconditionally valid range of the bias factor is $-0.5 \leq b \leq +0.5$.

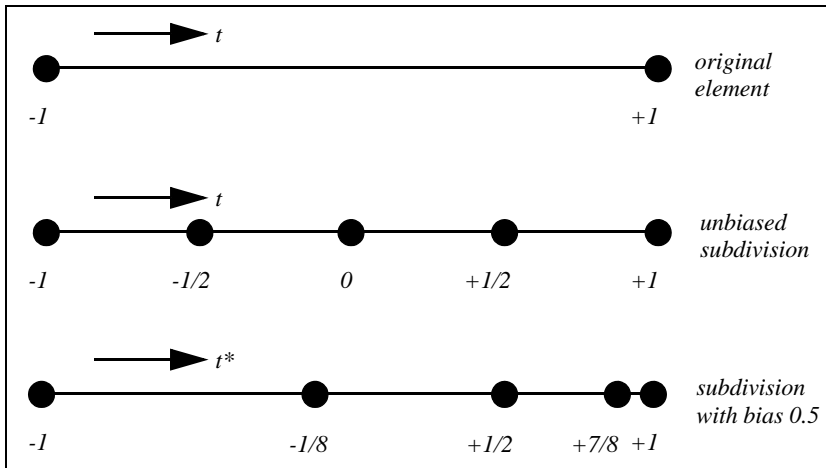


Figure 3.32-8 Subdivision of Line Element (Biased to the Right)

The mid-section consists of a biased and an unbiased part (*LO-mid-section* and *HI-mid-section*). Continue to generate the tower creating two elements and subdividing them, once using a bias factor of 0.2 and once using a bias factor of 0.0.

```

MAIN
  MESH GENERATION
  VIEW
    show 2
  RETURN
  nodes ADD
    0 13 0
  elems ADD
    (pick grid point)
  
```



```

6                                     (pick upper left node of lower section)
12                                    (pick bottom node of top section)
SUBDIVIDE
DIVISIONS
  2 1 1
BIAS
  -0.2 0 0
ELEMENTS
  17
  END LIST (#)
DIVISIONS
  5 1 1
BIAS
  0.2 0 0
ELEMENTS
  19
  END LIST (#)
DIVISIONS
  4 1 1
BIAS
  0 0 0
ELEMENTS
  18
  END LIST (#)

```

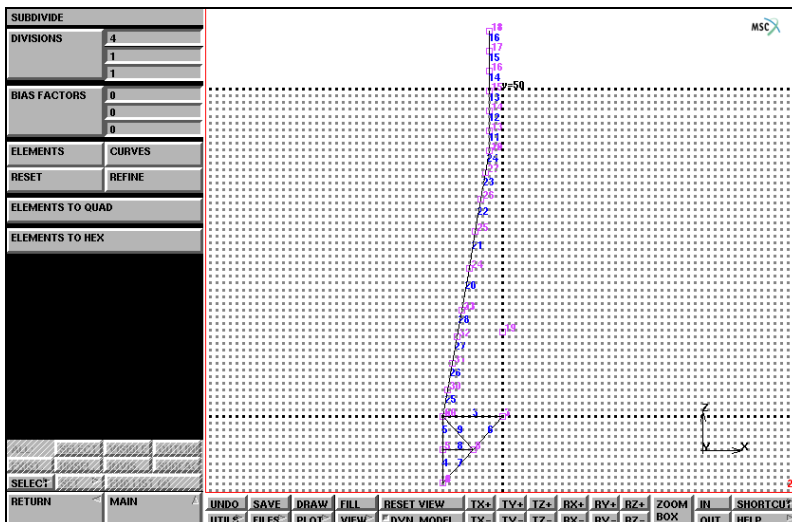


Figure 3.32-9 Subdivided Elements in the Mid-Section

As a next step, the lower-mid-section is completed and cross members are added in this part.

MAIN

MESH GENERATION

elems ADD

33

(pick middle node of mid-section)

19

(pick auxiliary node at $u=0$)

19

(pick auxiliary node at $u=0$)

29

(pick upper left node of base)

SUBDIVIDE

DIVISIONS

3 1 1

ELEMENTS

30

END LIST (#)

MAIN

MESH GENERATION

elems ADD

34

(pick auxiliary node at $u=0$)

32

(almost horizontal to the left)

32

(work the diagonals)

35

35

31

31

36

36

30

PLOT

label ELEMENTS

(off)

REGEN

RETURN

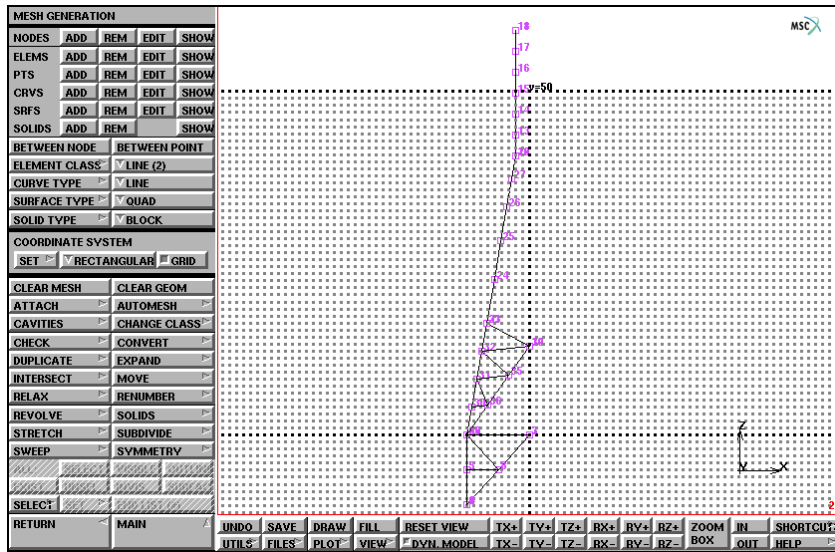


Figure 3.32-10 Completed Mid-Section

Step 2: Duplicate the first face to create the remaining faces of the main tower structure. It is crucial to sweep nodes and elements after using symmetry and duplicate.

The stage is now set for a symmetry operation. Please note that this operation is always carried out in the local coordinate system. The point with coordinates (0,0,0) and the normal vector (1,0,0), both in the U,V,W coordinate system, define the symmetry plane. These are the default settings for Mentat.

MAIN
MESH GENERATION
SYMMETRY
ELEMENTS
all: EXIST.

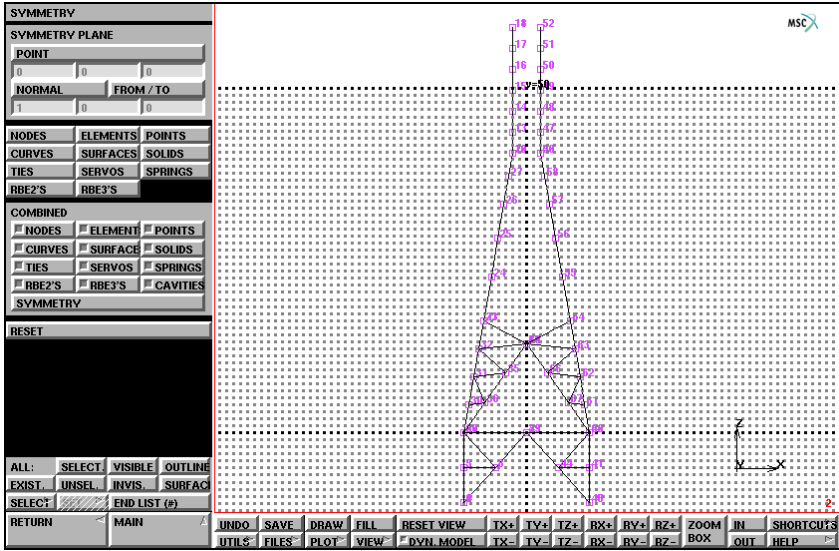


Figure 3.32-11 Cross Section of Tower Member

The object of the symmetry operation is to establish the key points in space so that you can complete one face of the tower. Use the existing points and click on the nodes in succession to add the cross members. Note that the program assumes you want to add new elements until you instruct it otherwise. Also, note that it is not necessary to activate the elems ADD button every time you enter a new element.

MAIN
 MESH GENERATION
 elems ADD

(first generate the horizontal cross member between nodes 33 and 64, then work the diagonals in the high-mid-section)

PLOT
 label NODES
 REGEN
 RETURN

(off)

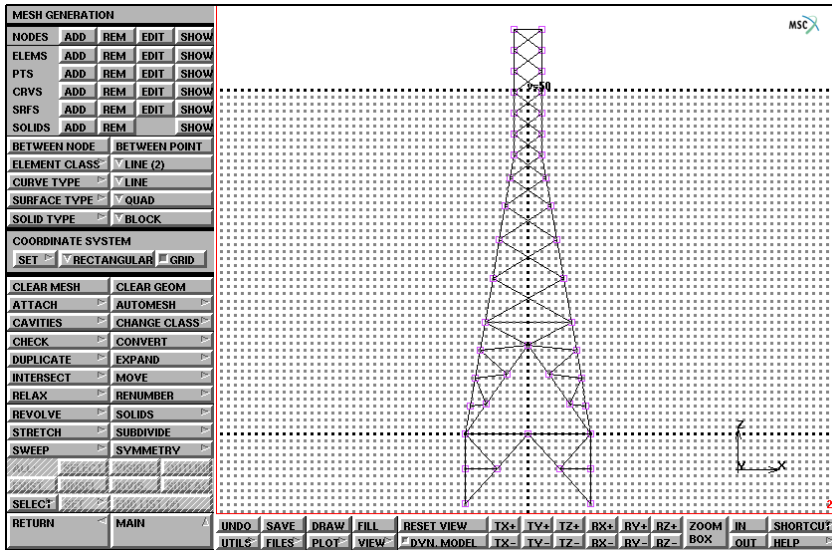


Figure 3.32-12 Tower Face Completed

The next step is to duplicate the geometry of one tower face three times to complete the structure. There are some remarks to be made prior to executing this step:

- Perform a sweep operation on all nodes in order to remove the duplicate nodes from the model.
- The current local coordinate system is not ideal to use for specification of the point about which to duplicate nor for specification of the rotation vector. Reset the coordinate system so that it lines up with the global coordinate system: make sure the u-direction is parallel to the x-direction, the v-direction parallel to the y-direction, and the w-direction parallel to the z-direction.

Now duplicate the face you just created. The rotation duplication vector should be 90° in the z-direction and the point of duplication 0, 0, 0. [Figure 3.32-13](#) shows the results of the duplication operation from four different viewpoints.

MAIN

MESH GENERATION

SWEEP

sweep NODES

all: EXIST.

RETURN

SET

RESET

grid ON

RETURN

DUPLICATE

(to switch off grid)

ROTATION ANGLES
 0 0 90
 REPETITIONS
 3
 ELEMENTS
 all: EXIST.
 VIEW
 SHOW ALL VIEWS
 FILL
 RETURN

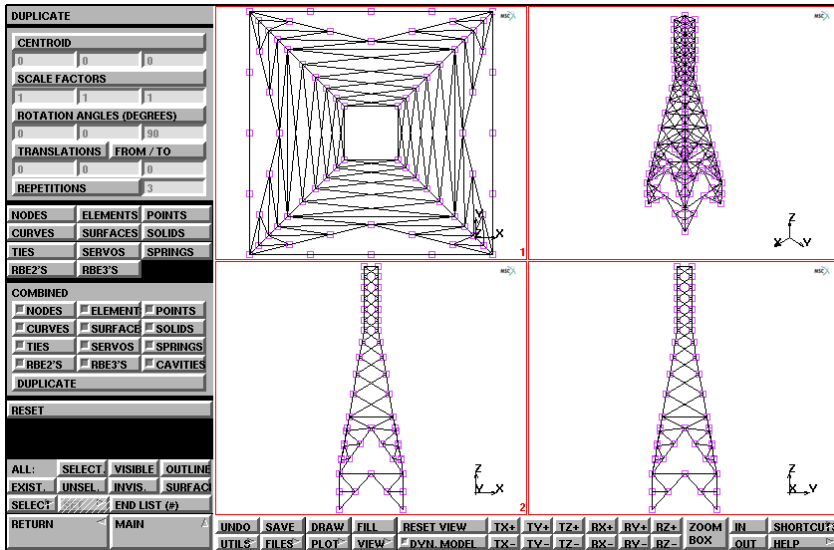


Figure 3.32-13 Four Views of Tower Face Duplication

The various operations you have just executed may have left duplicate nodes, that is nodes with different identification numbers but occupying the same space. In finite element terms, these nodes are not connected which may introduce undesirable mechanisms in the structure.

Use the SWEEP processor to eliminate the duplicate nodes that occupy the same location into one node with a single identification number. Since this involves a comparison of real coordinates that cannot be done exactly in a computer, nodes are swept together if they are within a certain tolerance from each other. This tolerance can be changed from its default value. Be careful when adjusting the tolerance as too large a tolerance can collapse the entire structure into a single point.

```

MAIN
  MESH GENERATION
    SWEEP
      sweep NODES
        all: EXIST.
      sweep ELEMENTS
        all: EXIST.
  
```

Now that you have generated the gross anatomy of the tower structure, it is useful to identify parts of the structure by name. The concept of **set naming** is a very powerful tool; it can be used in any place where a list is required and allows you to manipulate a group of entities rather than individual entities.

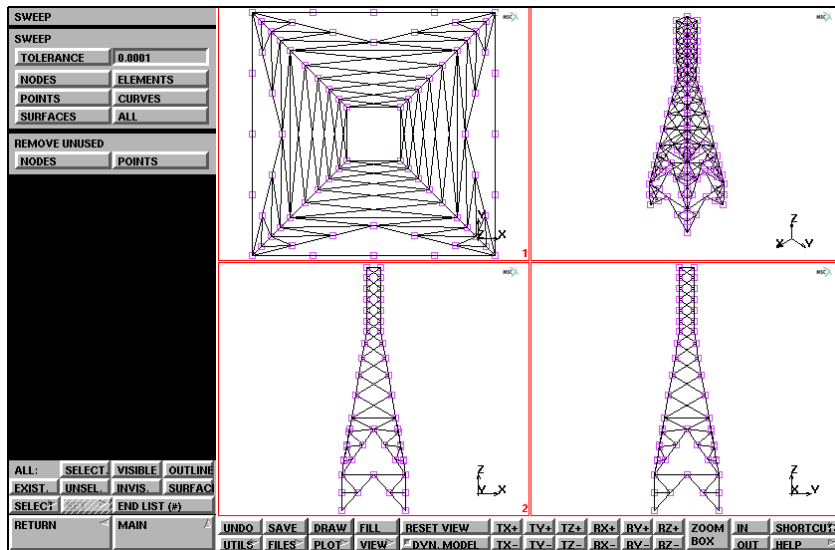


Figure 3.32-14 Boxes used for Element Set Selection

You have already defined the base, mid-section, and head of the tower. Use the Box Pick Method to fence off the different portions of the mesh. The STORE ELEMENTS command in the SELECT menu prompts for a set name first, followed by a list of elements. Position the cursor at one corner of the portion of elements to be fenced off. Depress the left mouse button. Drag the cursor to the opposite corner of the box and release. You have just selected every item that is inside the box, indicated by a change in color. The extent of the box are $+\infty$ and $-\infty$ in the direction perpendicular to the screen.

```

MAIN
  MESH GENERATION
    VIEW
  
```

```
    show 2
    RETURN
  SELECT
    elements STORE
      base

    END LIST (#)
```

*(Box Pick the elements in the base of
the tower, see [Figure 3.32-14](#))*

```
MAIN
  DEVICE
    picking PARTIAL
  SELECT
    elements STORE
      mid_sect_lo

    END LIST (#)
```

*(Box Pick the elements, realizing
that all elements partially within
the box will also be included)*

```
    RETURN
    picking COMPLETE
  SELECT
    elements STORE
      mid_sect_hi

    END LIST (#)
  elements STORE
    head

    END LIST (#)
```

(Box Pick the elements)

(Box Pick the elements)

```
MAIN
  PLOT
    MORE
    IDENTIFY
    SETS
```


REGEN
NONE
REGEN

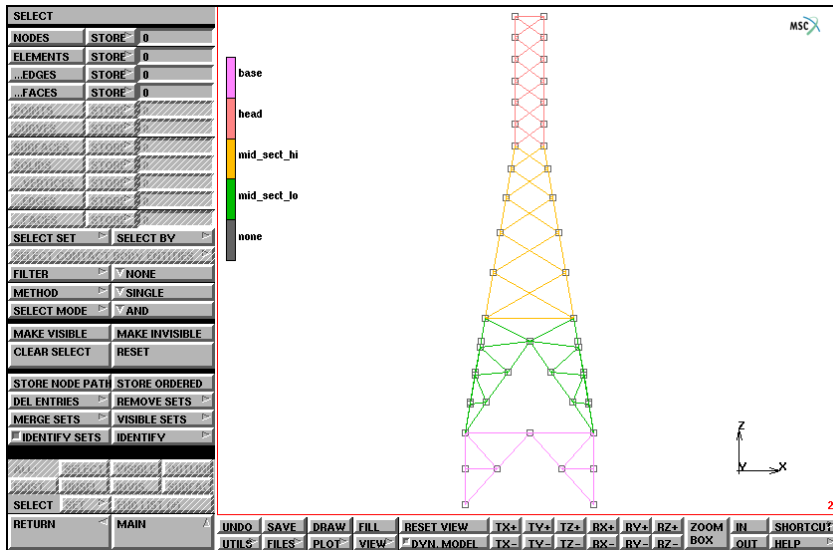


Figure 3.32-15 Element Sets Created

The current structure still contains a number of mechanisms that need to be eliminated by adding members. For example, the legs of the base contain mechanisms that are eliminated by adding cross members. In order to accomplish this, limit the *visible* elements to the base. Proceed to the SELECT submenu and click SELECT SET, activate the desired set and click MAKE VISIBLE. Only the elements contained in the set ‘base’ and their nodes remain visible. The base only occupies a small portion of the screen. Select view 4 for display and FILL the screen.

The current view point is perhaps not optimal. Nodes may overlap, making it impossible to pick nodes at some locations. Use *dynamic viewing* to change the position of the mesh so that you can add the additional cross-members.

Dynamic viewing can be switched on by clicking DYN. VIEW in the static menu. Next, position the cursor in the middle of the graphics area and hold down <MM>. Move the mouse to the left or right and see how the mesh rotates about the screen axis.

As an alternative, in the button sequence the model is rotated around its z-axis using one of the buttons in the MANIPULATE MODEL menu.

Use the basic element ADD command to add the cross members. Repeat this for parts in the lower mid-section.

Note: Elements can only be added when dynamic viewing is off. If you try to add an element with dynamic viewing on, the result is a null operation.

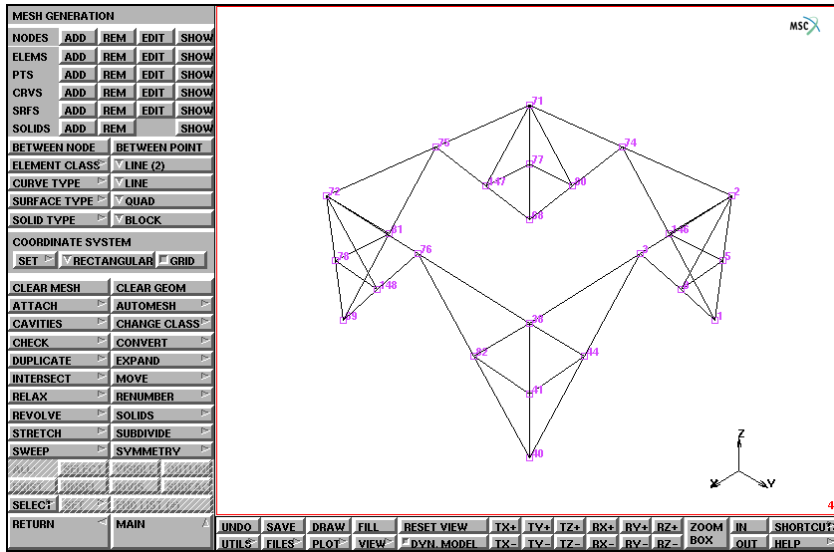


Figure 3.32-16 Elements to be added in the Base of the Tower

MAIN

MESH GENERATION

PLOT

nodes SETTINGS

LABELS

(on)

REGEN

RETURN

SELECT

SELECT SET

base

OK

MAKE VISIBLE

RETURN

VIEW

show 4

FILL

activate 1

(off)

activate 2

(off)

activate 3

(off)

MANIPULATE MODEL

rotate in model space Z-

RETURN (twice)

elems ADD

(add elements as indicated in Figure 3.32-16)

SELECT

elements STORE

base

all: VISIBLE

SELECT SET

mid_sect_lo

OK

MAKE VISIBLE

RETURN

FILL

elems ADD

(add elements as indicated in Figure 3.32-17)

SELECT

elements STORE

mid_sect_lo

all: VISIBLE

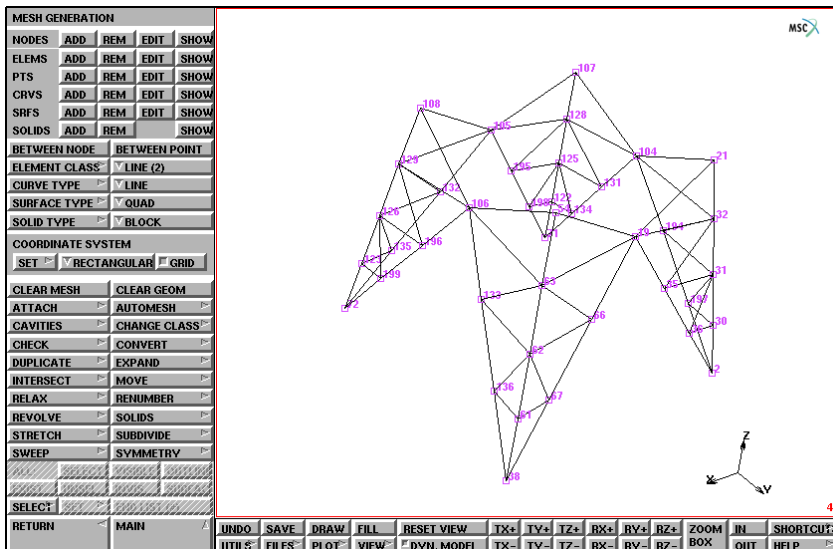


Figure 3.32-17 Elements to be added in the Lower Mid-Section

Step 3: Create one cable arm by adding nodes and elements and using subdivide.

The next step is to generate the arms of the tower from which the high voltage cables are suspended. Make the *head* of the tower visible so that you can easily pick nodes with the mouse. The position of the node at the extreme end of the arm is known and added through the node ADD command. Use the mouse pick to create the elements between the node at the extreme end and the different portions of the head.

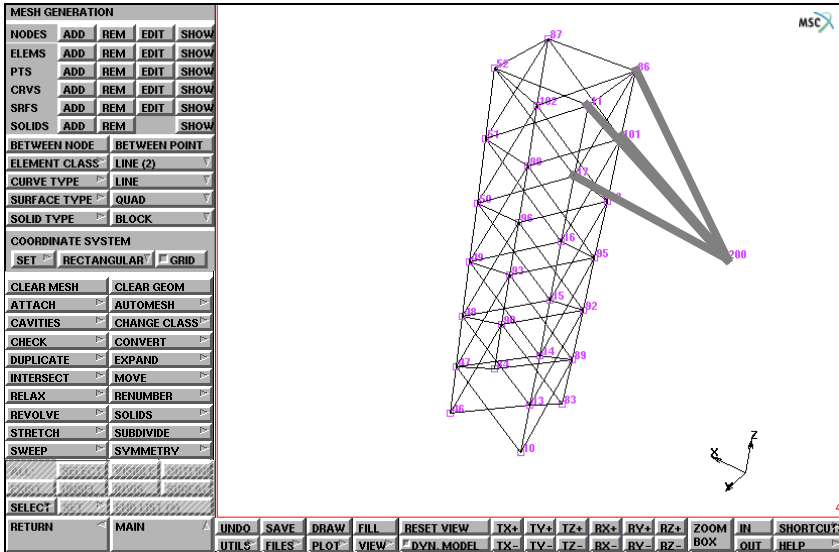


Figure 3.32-18 Elements to be Added

MAIN

MESH GENERATION

SELECT

SELECT SET

head

OK

MAKE VISIBLE

RETURN

FILL

ZOOM BOX

(zoom in on top section)

VIEW

MANIPULATE MODEL

rotate in model space Z-

(click 7 times)

RETURN (twice)

nodes ADD

-8 0 63

elems ADD

(add 4 elements according to Figure 3.32-18)

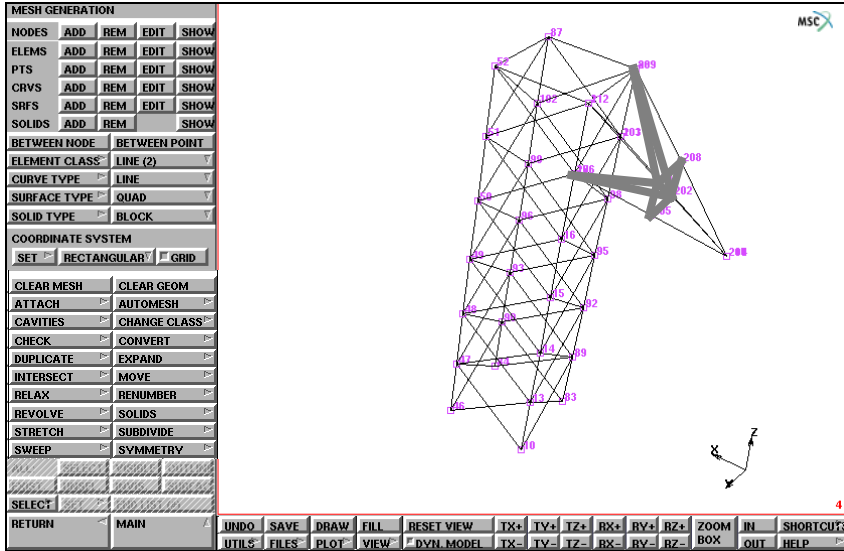


Figure 3.32-19 Elements to be Added

MAIN

MESH GENERATION

SUBDIVIDE

DIVISIONS

2 1 1

ELEMENTS

END LIST (#)

RETURN

elems ADD

(pick the 4 elements just created)

(add 9 elements according to Figure 3.32-19)

VIEW

ACTIVATE ALL

FILL

show 2

RETURN

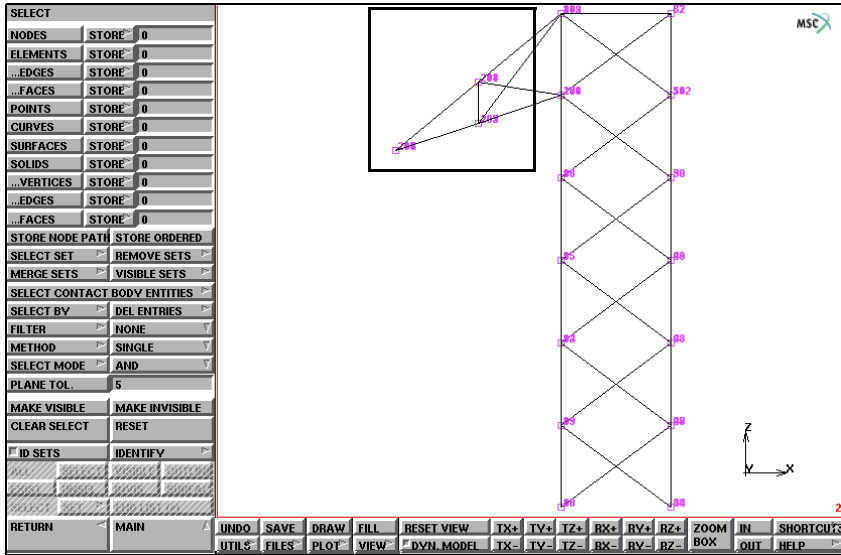


Figure 3.32-20 Box Pick of Transmission Tower Arm

Store the elements of the arm in an element set called *arm* for later reference.

MAIN

DEVICE

picking PARTIAL

SELECT

elements STORE

arm

(Box Pick the elements in the arm)

END LIST (#)

RETURN

picking COMPLETE

Step 4: Use symmetry on the first arm to create the second arm. Then use duplicate on the first two to create the remaining cable arms.

Use symmetry and duplicate to reproduce the arm on either side of the tower head.

MAIN

MESH GENERATION

DUPLICATE

RESET

```
ROTATIONS
  0 0 180
ELEMENTS
  arm
FILL
RESET
TRANSLATIONS
  0 0 -6
REPETITIONS
  2
ELEMENTS
  arm
RETURN
SWEEP
  sweep NODES
    all: EXIST.
SELECT
  ELEMENTS
    all: EXIST.
  MAKE VISIBLE
  FILL
  RETURN
PLOT
  label NODES
  MORE
    IDENTIFY
      SETS
      REGEN
      NONE
```

(off)

You have now completed Steps 1 through 4 outlined in [Overview of Steps](#). The goal of these four steps was to show you the importance of defining a local coordinate system and using it to add, duplicate, and symmetry parts of the tower structure.

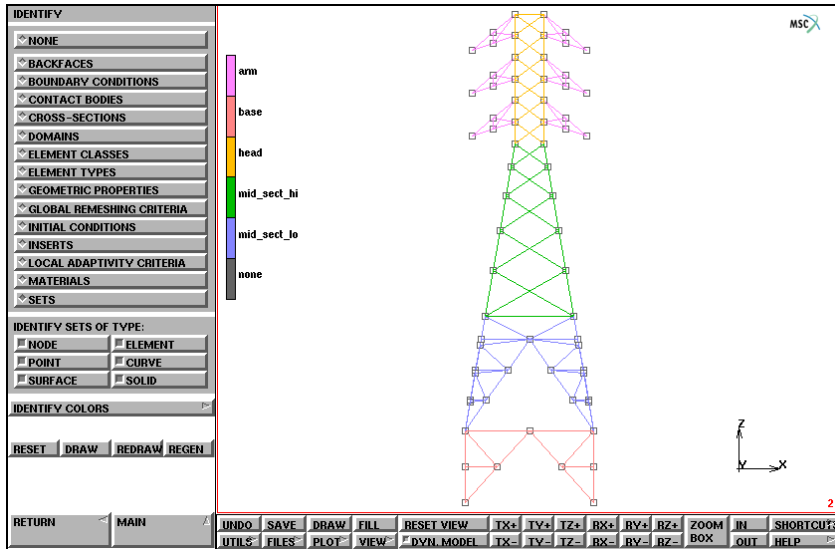


Figure 3.32-21 Completed Transmission Tower Model

This section outlined the advantage of using the symmetry of a structure in two-dimensional before creating a three-dimensional structure using the duplication process.

You have been using the direct meshing technique described in [Chapter 1: Introduction](#) to model the transmission tower. At this point, you have only completed the geometrical part of the finite element mesh. The next step is to specify the *correct* boundary conditions and loads.

Step 5: Add boundary conditions.

Specify fixed displacements at nodes to constrain the nodes at the tower base. Apply a gravity load to the elements. Group the elements in sets so that you can easily refer to them later. Add distributed wind loads. Apply cable loads as point loads on the nodes at the ends of the cable arms.

There are basically two types of boundary conditions for this model:

1. Kinematic: The base of the structure is attached to the ground.
2. Load:
 - Gravity*
 - Point loads* are applied to the cable arms to simulate the weight of the cables.
 - Wind loads* are applied as distributed loads perpendicular to the tower.

In [Chapter 1: Introduction](#) discussed how the application of boundary conditions is equal to the process of finding the answer to the question: “Apply *what, where, and when*”

First concentrate on *what*.

The BOUNDARY CONDITIONS button in the main menu reveals a submenu that allows you to specify mechanical boundary conditions.

Kinematic Boundary Conditions

Click on FIXED DISPLACEMENT. A pop-up appears over the graphics area. Constrain the first three degrees of freedom by clicking the ON button.

Note that while the pop-up is activated, your view of the graphics area is obstructed and all other buttons of the regular menu are inactive. You must confirm the values entered in the pop-up by clicking on the OK button before you can access the regular menu again.

Now that you have answered *what*, you can concentrate on *where*.

If you limit your view to the base, you can easily pick on the nodes that attach the structure to the ground. This operation completes the *where* and ties it to the *what* portion of the equation. Since the problem is time independent, the equation is complete because there is no need to answer *when*. The application of *what* is confirmed by the display of arrows in the direction it was applied.

```
MAIN
  BOUNDARY CONDITIONS
    MECHANICAL
      NAME
        bolts
      SELECT
        SELECT SET
          base
        OK
      MAKE VISIBLE
      FILL
      RETURN
    FIXED DISPLACEMENT
      DISPLACEMENT X (on)
      DISPLACEMENT Y (on)
      DISPLACEMENT Z (on)
      OK
    nodes ADD
      (pick 4 nodes at base)
    END LIST (#)
```

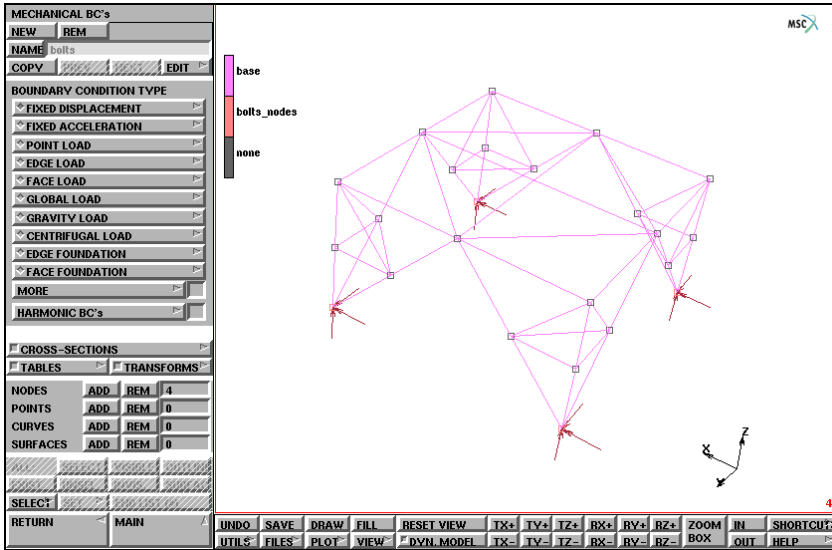


Figure 3.32-22 Boundary Conditions

For future reference, it is useful to group elements and store them in a set that can be referenced later by name. We already mentioned that not all members are of the same geometry. Use the SELECT option to group all elements that are L3x3 angles and store in a set called L3x3. All other members are L2x2 angles. Generate a list of these elements by inverting the previous list and storing them in a set called L2x2.

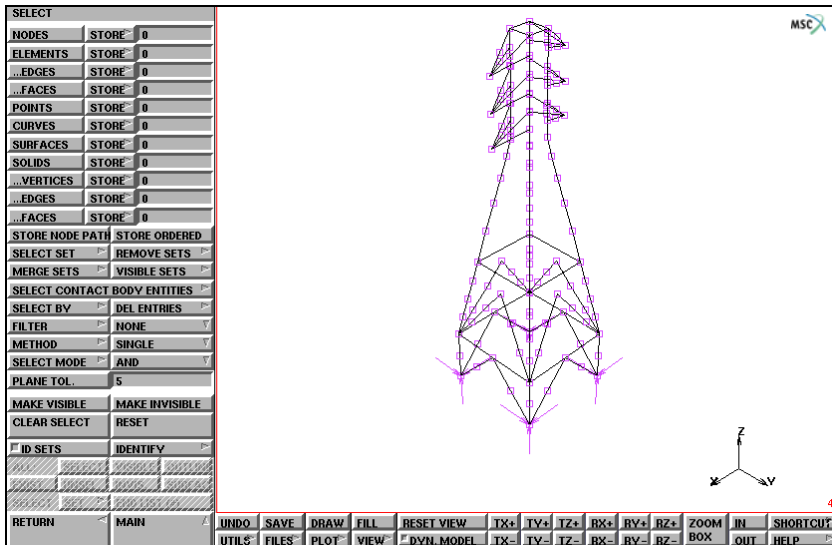


Figure 3.32-23 Elements to be Contained in Set L3x3

MAIN

MESH GENERATION

SELECT

elements STORE

L3x3

(pick elements from base)

END LIST (#)

SELECT SET

mid_sect_lo

OK

MAKE VISIBLE

FILL

elements STORE

L3x3

(pick elements from mid_sect_lo)

END LIST (#)

MAIN

MESH GENERATION

SELECT SET

mid_sect_hi

OK

MAKE VISIBLE

FILL

elements STORE

L3x3

(pick elements from mid_sect_hi)

END LIST (#)

SELECT SET

head

OK

MAKE VISIBLE

FILL

elements STORE

L3x3

(pick elements from head)

END LIST (#)

SELECT SET

arm

OK

```
MAKE VISIBLE
FILL
elements STORE
  L3x3
  END LIST (#)
ELEMENTS
  all: EXIST.
MAKE VISIBLE
FILL
ELEMENTS
  all: EXIST.
select mode AND
  L3x3
elements STORE
  L2x2
  all: SELECT.
```

(pick elements from arm)

(to switch to EXCEPT)

MAIN

```
MESH GENERATION
SELECT
  CLEAR SELECT
  RESET
  PLOT
  MORE
  IDENTIFY
  SETS
  REGEN
  NONE
  REGEN
```

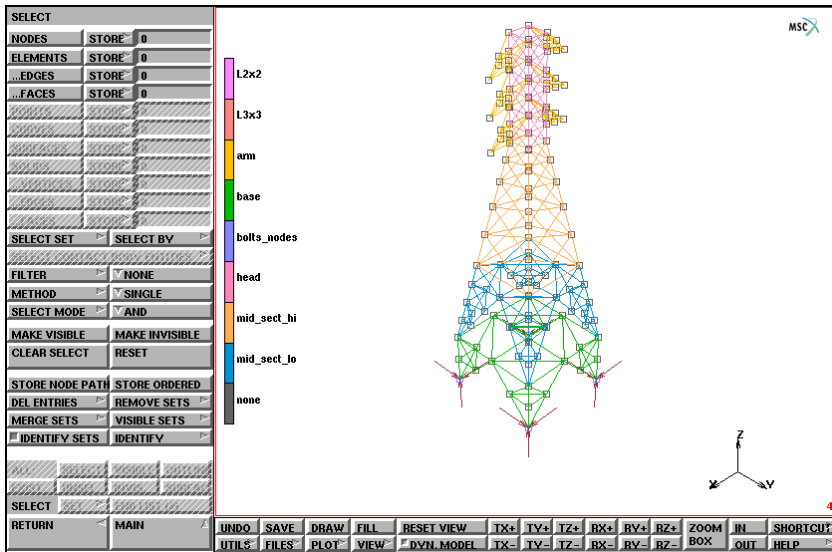


Figure 3.32-24 Identify Sets

Load (Gravity)

Similar to the FIXED DISPLACEMENT button, when you activate the GRAVITY LOAD button, a pop-up appears over the graphics area where you can enter appropriate values of the gravity load. The program expects the magnitude of the gravity acceleration in the negative z-direction here. This answers the *what* portion of the equation. Use the all: EXIST. button to answer the *where* part of the equation.

```

MAIN
  BOUNDARY CONDITIONS
    MECHANICAL
      RESET VIEW
      FILL
      NEW
      NAME
        gravity
      GRAVITY LOAD
        ACCELERATION Z
          -32.2
        OK
      elements ADD
        all: EXIST.
  
```

Wind Load

Assume that the transmission tower is subjected to a wind load with a stronger load applied to the upper part of the tower and a weaker load to the lower part of the tower. Simulate the wind loads by applying a distributed load in y-direction. Assume that only one face of the tower is loaded by this wind load.

Prior to applying the loads, element sets of all elements in the lower and upper frontal face of the tower are generated. The upper portion is stored in an element set called *hi_front* while the lower portion is stored in a set called *lo_front*.

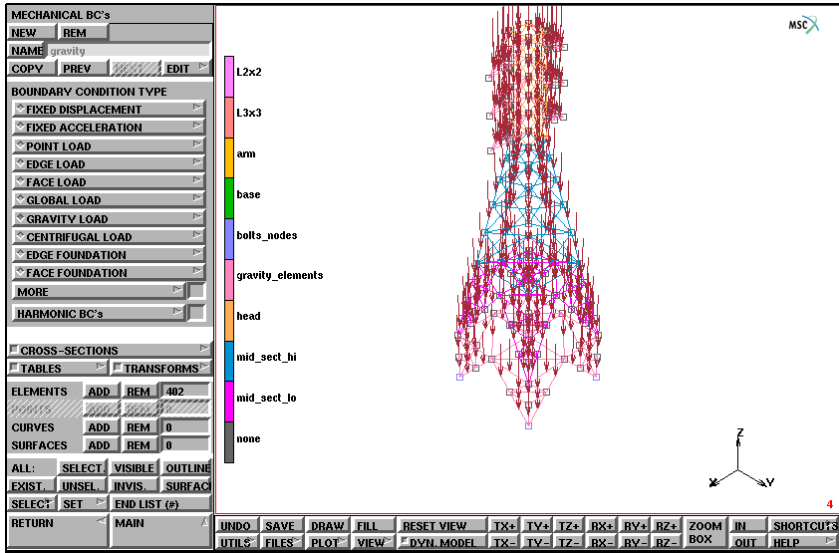


Figure 3.32-25 Gravity Load for the Structure

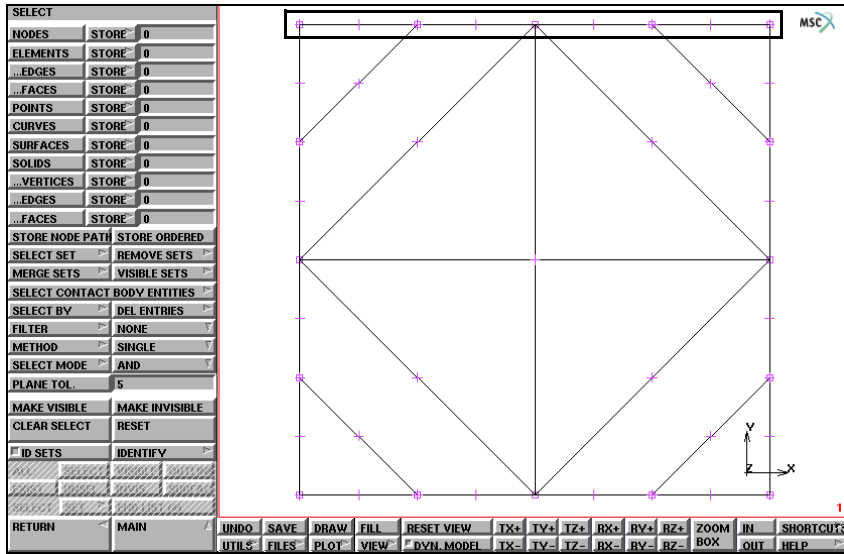


Figure 3.32-26 Box Pick from *base* for *lo_front*

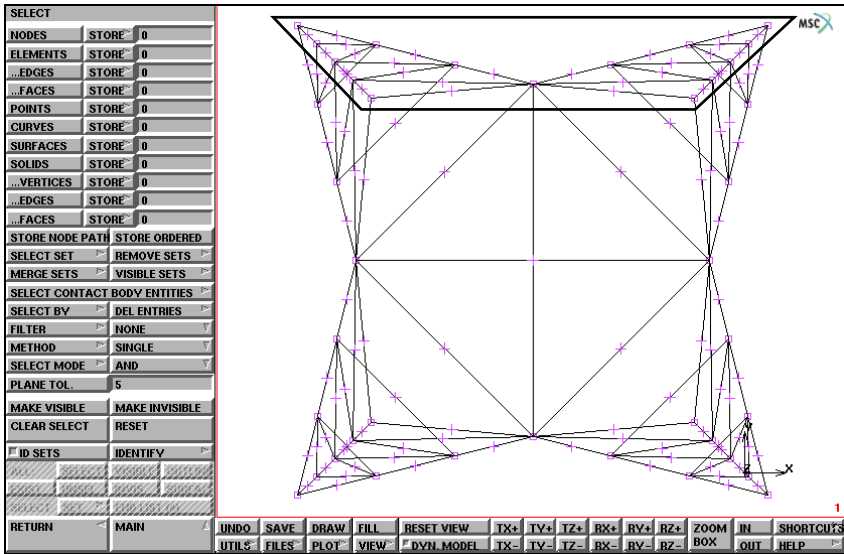


Figure 3.32-27 Polygon Pick from *mid_sect_lo* for *lo_front*

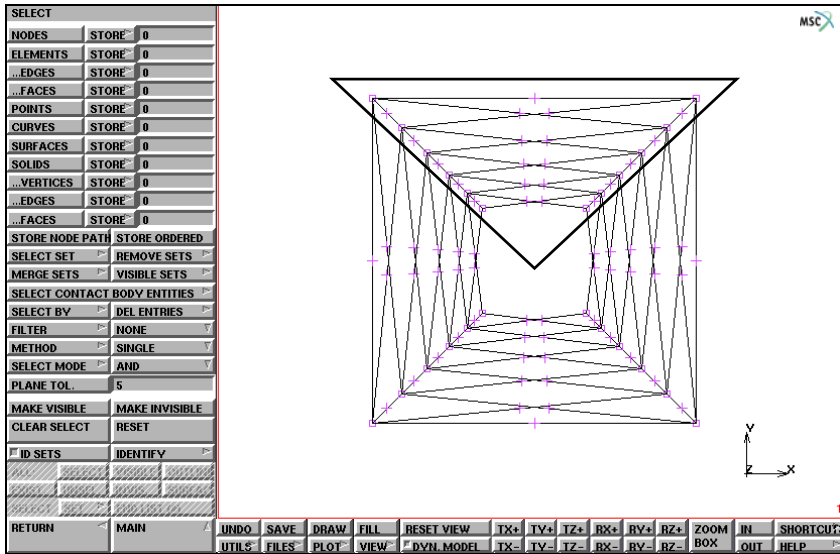


Figure 3.32-28 Polygon Pick from *mid_sect_hi* for *hi_front*

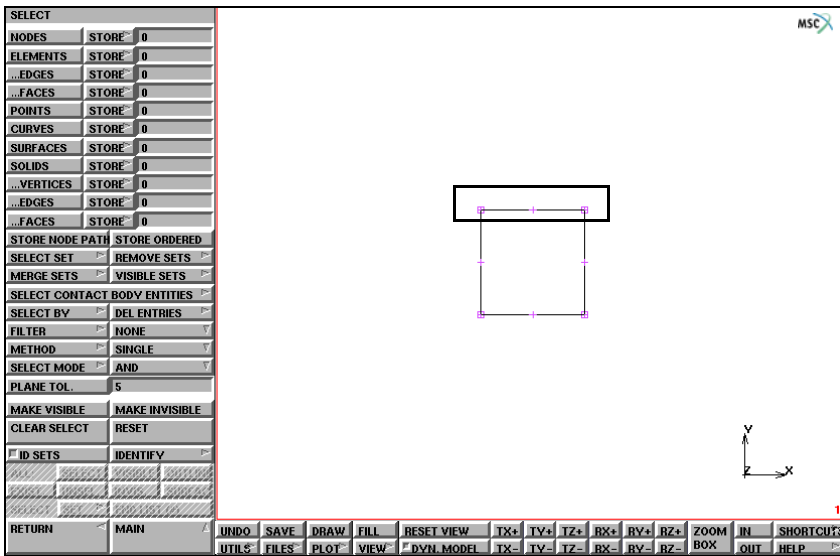


Figure 3.32-29 Box Pick from *head* for *hi_front*

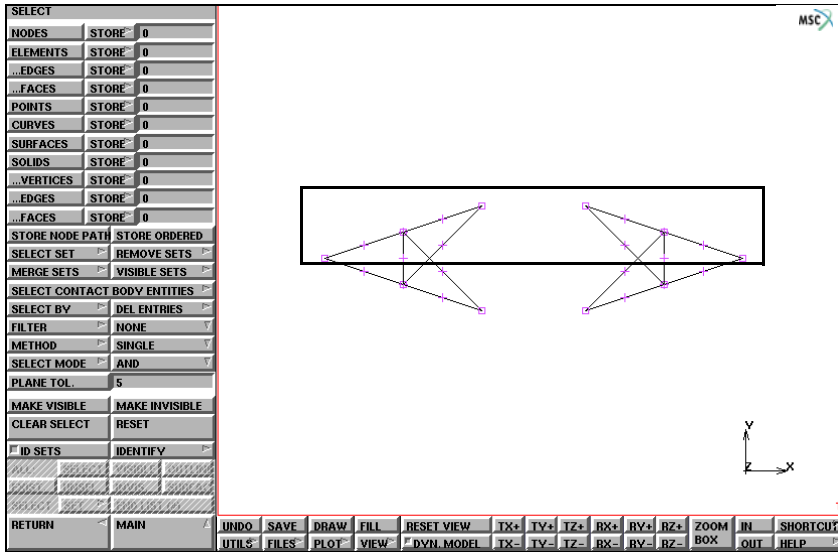


Figure 3.32-30 Box Pick from *arm* for *hi_front*

MAIN

BOUNDARY CONDITIONS

MECHANICAL

SELECT

VIEW

show 1

RETURN

SELECT SET

base

OK

MAKE VISIBLE

elements STORE

lo_front

END LIST (#)

SELECT SET

mid_sect_lo

OK

MAKE VISIBLE

elements STORE

lo_front

(select according to [Figure 3.32-26](#))

(select according to [Figure 3.32-27](#))

```
END LIST (#)
SELECT SET
  mid_sect_hi
OK
MAKE VISIBLE
elements STORE
  hi_front
END LIST (#)
```

(select according to [Figure 3.32-28](#))

Complete the set *hi_front* by processing the sets *'head'* and *'arm'* in an identical way.

Now actually apply the loads:

```
MAIN
  BOUNDARY CONDITIONS
    MECHANICAL
      NEW
      NAME
        hi_wind
      GLOBAL LOAD
        FORCE Y
          -120
      OK
    elements ADD
      hi_front
```

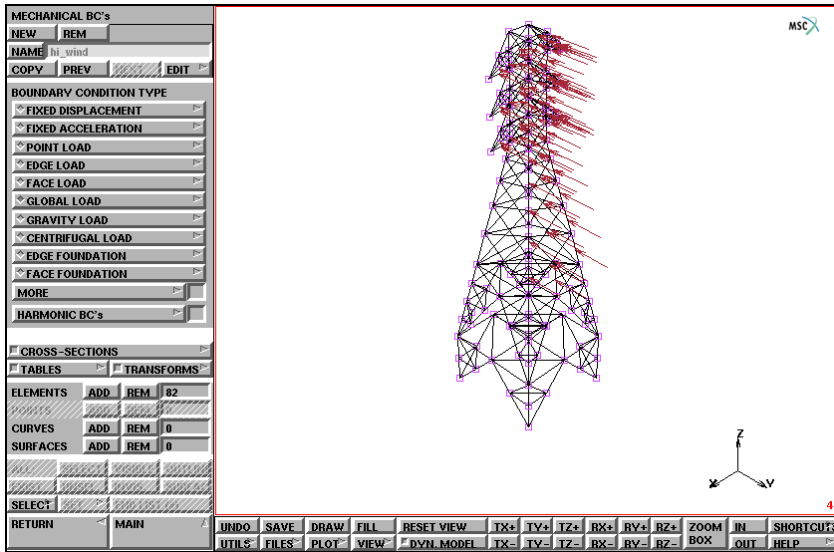


Figure 3.32-31 Strong Wind Load

In an identical way, a Y FORCE of -80 can be applied to all elements contained in *lo_front*.

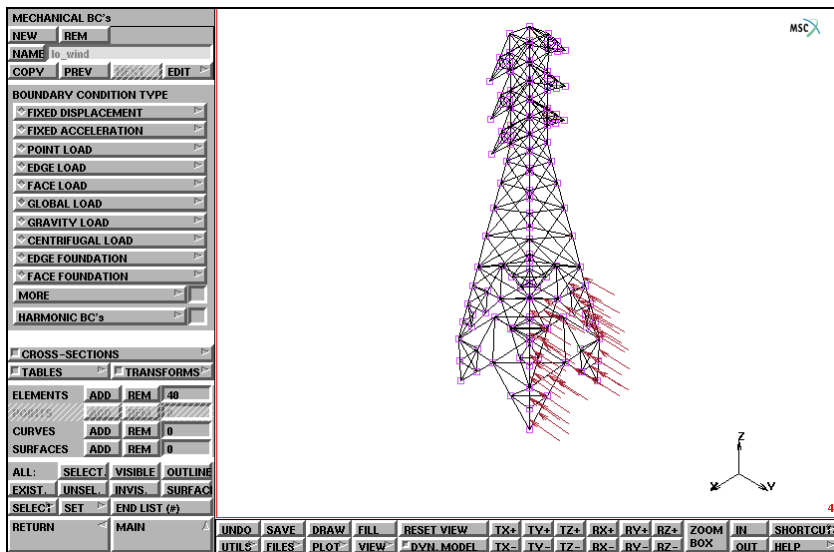


Figure 3.32-32 Weak Wind Load

Point Loads

The cables are suspended from the arms of the tower and are simulated as point loads hanging from each tip of the arm. A load of -500 in this direction is applied to each of the six arm extremities. The boundary conditions menu allows you to enter these point loads through the POINT LOADS option. The already familiar pop-up appears over the graphics area. Enter the values in the appropriate fields.

Use the mouse to pick the nodes that are to receive a load. Enter the end of list character (#) after you have picked the six nodes.

```

MAIN
  BOUNDARY CONDITIONS
    MECHANICAL
      NEW
      NAME
        cable_load
      POINT LOAD
        FORCE Z
          -500
      OK
      nodes ADD (pick the six nodes on the tip of the arms)
      END LIST (#)
  
```

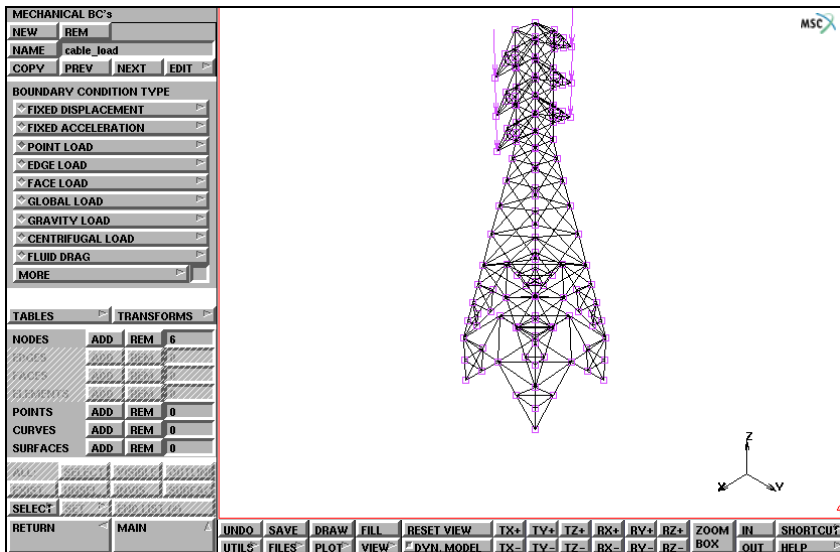


Figure 3.32-33 Cable Loads

After having selected all 44 elements, make all elements visible again.

MAIN

GEOMETRIC PROPERTIES

3-D

NEW

NAME

L3x3_z

ELASTIC BEAM

AREA

0.01

6.0e-05

(for Ixx)

6.0e-05

(for Iyy)

0

(for direction)

0

(for direction)

1

(for direction)

OK

SELECT

SELECT SET

L3x3

OK

select mode AND

(to switch to EXCEPT)

SELECT SET

upright

OK

RETURN

elements ADD

all: SELECT.

ID GEOMETRIES

(on)

MAIN

GEOMETRIC PROPERTIES

3-D

NEW

NAME

L3x3_x

ELASTIC BEAM

AREA

0.01

6.0e-05

(for Ixx)

6.0e-05

(for Iyy)

1

(for direction)

0

(for direction)

0

(for direction)

OK

SELECT

CLEAR SELECT

RESET

SELECT SET

upright

OK

select mode AND

(to switch to EXCEPT)

SELECT SET

L2x2

OK

RETURN

elements ADD

all: SELECT.

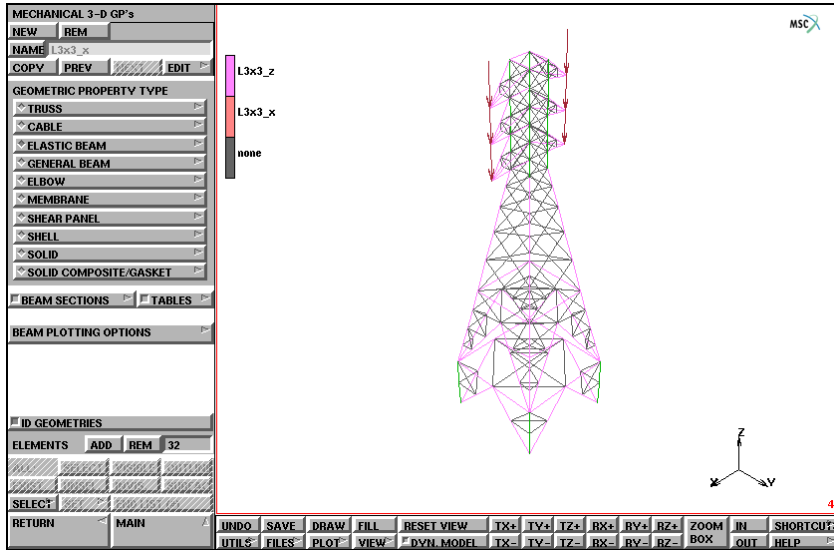


Figure 3.32-34 Geometric Properties Assignment for L3x3 Angles

MAIN

GEOMETRIC PROPERTIES

3-D

NEW

NAME

L2x2_z

ELASTIC BEAM

AREA

0.00651

2.0e-05

2.0e-05

0

0

1

OK

SELECT

CLEAR SELECT

RESET

SELECT SET

L2x2

OK

(for Ixx)

(for Iyy)

(for direction)

(for direction)

(for direction)


```

select mode AND (to switch to EXCEPT)
SELECT SET
  upright
  OK
RETURN
elements ADD
all: SELECT.

```

MAIN

GEOMETRIC PROPERTIES

3-D

```

NEW
NAME
  L2x2_x
ELASTIC BEAM
  AREA
    0.00651
    2.0e-05 (for Ixx)
    2.0e-05 (for Iyy)
    1 (for direction)
    0 (for direction)
    0 (for direction)
  OK
SELECT
  CLEAR SELECT
  RESET
  SELECT SET
    upright
    OK
  select mode AND (to switch to EXCEPT)
  SELECT SET
    L3x3
    OK
RETURN
elements ADD
all: SELECT.

```

SELECT
CLEAR SELECT
RESET

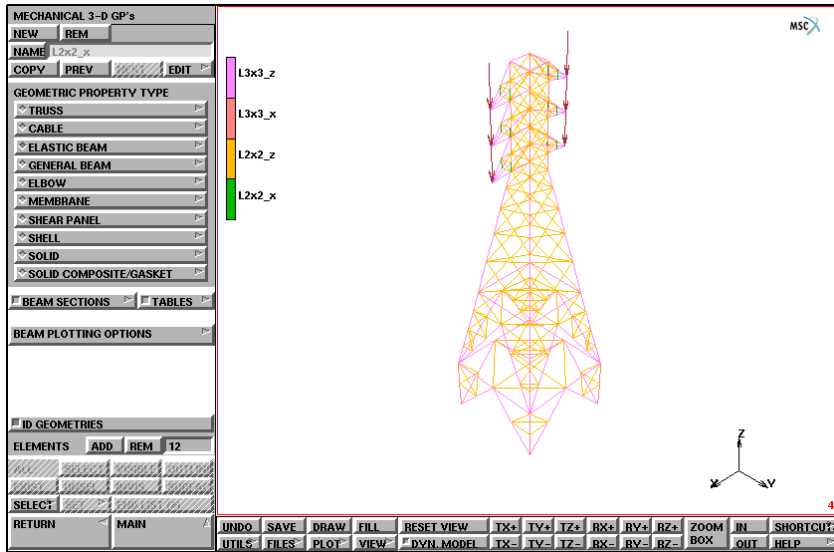


Figure 3.32-35 Geometric Properties Assignment for L2x2 Angles

Material Properties

The last step is to assign material properties. The members of this tower are made out of steel. For this analysis, you need to specify the Young's Modulus and Poisson's Ratio and mass density, all located in the MATERIAL PROPERTIES menu. Assign this material to all existing elements.

MAIN

MATERIAL PROPERTIES

NEW

NAME

steel

ISOTROPIC

YOUNG'S MODULUS

4.176e9

0.3

(for Poisson's Ratio)

15.217

(for mass density)

OK

elements ADD

all: EXIST.

ID MATERIALS

ID MATERIALS

(on)

(off)

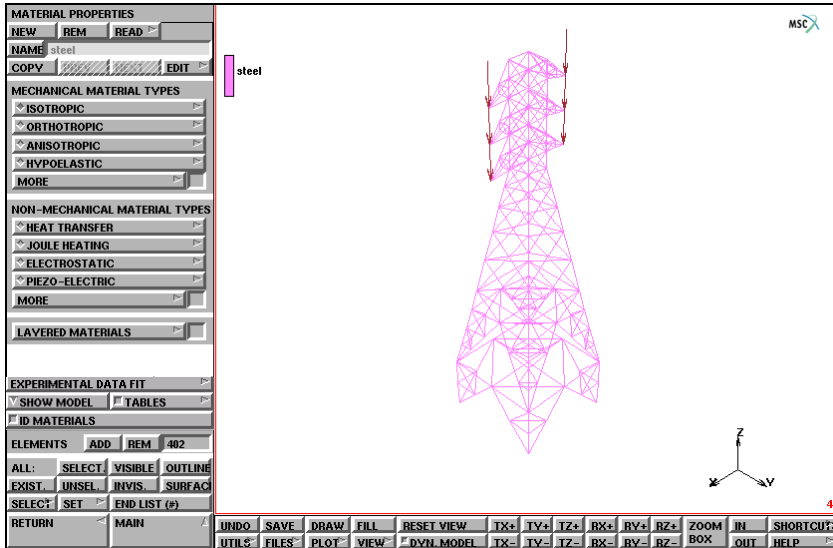


Figure 3.32-36 Material Properties Assignment

Step 7: Job submission of the static analysis.

Job Submission of the Static Analysis

Finally, you submit the job. This is easily done in the JOBS menu. SUBMIT submits the job in the background. The status of the job can be checked or monitored continuously. Once you have successfully submitted the job, you must carefully analyze the results.

MAIN

JOBS

NEW

NAME

static

MECHANICAL

INITIAL LOADS

(default: all loads selected)

OK (twice)

RETURN

```
SAVE
RUN
  SUBMIT 1
  MONITOR
```

Step 8: Static analysis results processing.

Static Analysis Results Processing

The static analysis considers the wind load, gravitational load, and point loads. The structure undergoes a bending out of the x-z plane as a result of the wind load. [Figure 3.32-37](#) shows the results. We switched on the AUTOMATIC DEFORMATION SCALING option resulting in an exaggerated display of the displacements.

```
MAIN
  RESULTS
    OPEN DEFAULT
    VIEW
      show 3
    RETURN
  DEF & ORIG
  NEXT INC
  deformed shape SETTINGS
    AUTOMATIC
    FILL
```

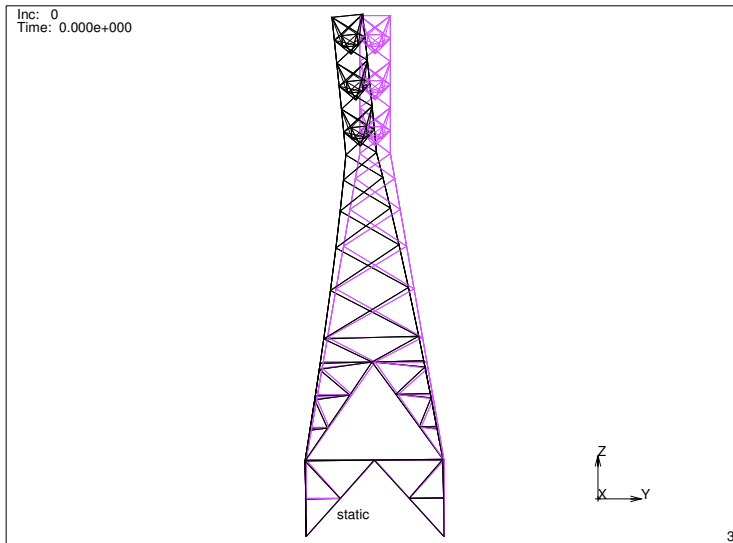


Figure 3.32-37 Deformation of Tower under Combined Load

Step 9: Job submission of the modal analysis.

Job Submission of the Modal Analysis

To run the modal analysis, it is necessary to restore the model file. After a new dynamic loadcase has been defined, a new job is created and submitted.

Step 10: Modal analysis results processing.

```
MAIN
  RESULTS
    CLOSE
    deformed shape OFF
    RETURN
  FILES
    RESTORE
    RETURN
  LOADCASE
    NEW
    NAME
      dynamic
  DYNAMIC MODAL
    # MODES
```

```
15
  OK
  RETURN
JOBS
  NEW
  NAME
    dynamic
  MECHANICAL
    loadcases SELECT
    dynamic
  OK
  SAVE
  RUN
    SUBMIT 1
    MONITOR
```

Modal Analysis Results Processing

Open the results file by clicking the RESULTS button from the main menu, followed by the OPEN DEFAULT button. The modal shapes are stored in subincrements and are accessed through the NEXT INC button. As is demonstrated in previous chapters, it is useful to animate the different modal shapes. [Figure 3.32-38](#) and [Figure 3.32-39](#) display examples of mode shapes found during this analysis.

The postprocessing is carried out as follows:

```
MAIN
  RESULTS
    OPEN DEFAULT
    VIEW
      show 4
      RETURN
    DEF & ORIG
    NEXT (twice)
    deformed shape SETTINGS
      AUTOMATIC
      FILL
      RETURN
    DEF ONLY
```

MORE

animate MODE

15

ANIMATION

FILL

REPEAT

PLAY

STOP

SHOW MODEL

RETURN

PREVIOUS

SKIP TO INC

0:15

DEF & ORIG

FILL

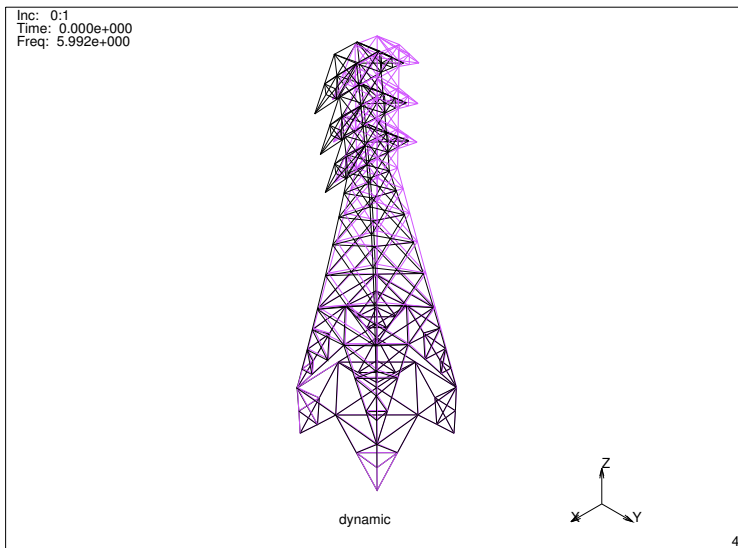


Figure 3.32-38 Eigenmode of Tower, $f = 5.992$ Hz

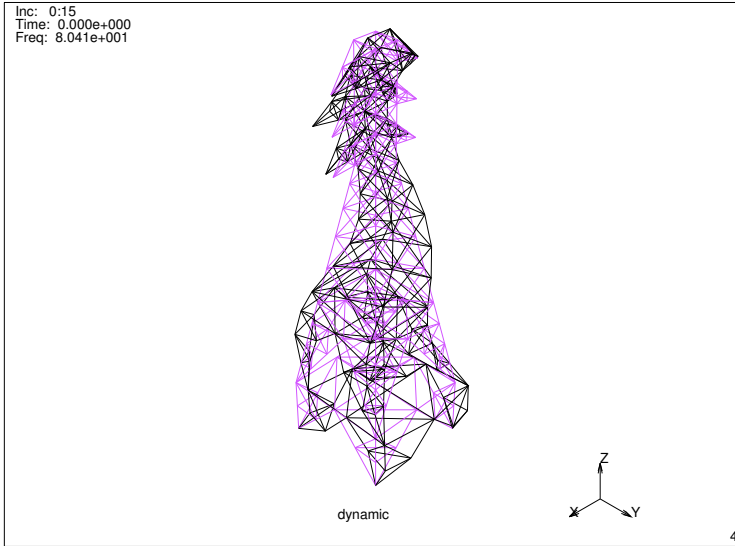


Figure 3.32-39 Eigenmode of Tower, $f = 80.41\text{Hz}$

Conclusion

This structure is an example where automatic mesh generators cannot be utilized to create a finite element model. It is demonstrated in this chapter that by using the 'conventional' tools available in Mentat, a fairly complicated mesh can be generated without any difficulty.

The displacements, as a result of a load in negative y direction shown in [Figure 3.32-37](#) are as expected. The results of the modal analysis can be fully appreciated by animation of the different modes.

Input Files

The files below are on your [delivery media](#) or they can be downloaded by your web browser by clicking the links (file names) below.

File	Description
transmission_tower.proc	Mentat procedure file

3.33 Bracket

- Chapter Overview 1602
- Background Information 1602
- Detailed Session Description of the Linear Static Case 1604
- Conclusion 1624
- Dynamic Modal Shape Analysis 1625
- Detailed Session Description of the Modal Shape Analysis 1625
- Dynamic Transient Analysis 1629
- Detailed Session Description of Dynamic Transient Analysis 1629
- Conclusion 1636
- Pressure Table 1636
- Input Files 1637

Chapter Overview

The sample session described in this chapter demonstrates a simple linear static and dynamic analysis on a steel bracket. The bracket restrains a vertical pipe. The bracket also supports some mechanical equipment. First, the bracket will be subjected to a static load. A dynamic analysis will predict the normal frequencies and mode shapes of vibration to determine if there is any interaction with the bracket and surrounding excitation frequencies. Finally, the bracket will be subjected to a time dependent pressure and the dynamic response will be determined.

Background Information

Description

This problem demonstrates the preparation of a model using two different meshing techniques, multiple geometric properties, three loadcase types, and corresponding boundary conditions and loads. It will also demonstrate the application of boundary conditions to geometric entities and the merging of different meshes.

The bracket is 15x30x10 with a hole to support a pipe. The bracket must support standard operating loads. It must not have a frequency that can be excited by the mechanical equipment which it supports. It must not fail for a given time dependent pressure loading.

Idealization

The bracket will be represented by flat plate elements which have 4 nodes and the thickness is considered a property of the element. The vertical support plates will require quadrilateral elements to be degenerated to triangular elements in the portion where the arc is tangent to the horizontal plate.

The bracket is welded to a column and therefore will be considered fully fixed on that edge. The weight of the mechanical equipment will be applied to the cantilevered section of the horizontal plate as a distributed load of 1 psi.

Requirements for a Successful Analysis

The analysis will be considered successful if none of the stresses are above 36000 psi during standard operating loads and there are no modes in the range of the mechanical equipment. The bracket cannot cause the pipe to break during a dynamic loading event.

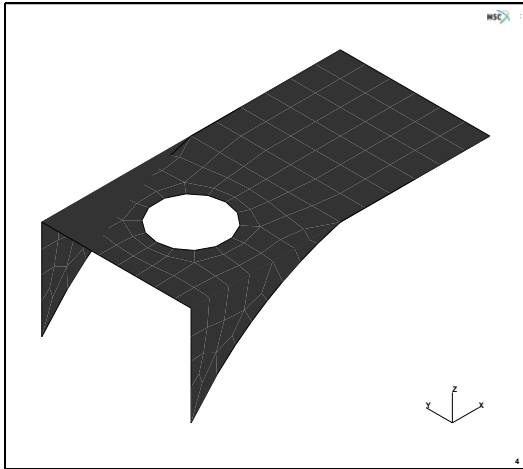


Figure 3.33-1 Bracket

Full Disclosure

The steel bracket is modeled by four-noded plate elements with a Young's Modulus of $30e6$ psi and a Poisson's Ratio of 0.3. It is assumed that the material will not exceed the yield point of 36000 psi. The horizontal plate is 15 inches by 30 inches with a hole of 3.5 inch radius centered in the half of the plate where the vertical support plates are attached. The 2 vertical support plates are 10 inches by 15 inches with a filleted edge. The horizontal plate is 0.25 inches thick and the vertical plates are 0.5 inches thick.

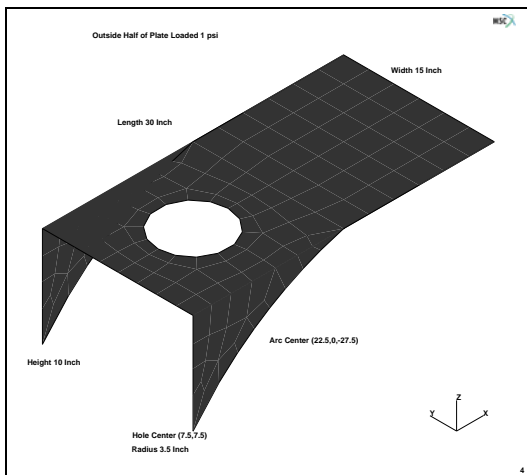


Figure 3.33-2 Dimensions and Loads for the Bracket

Overview of Steps

- Step 1:** Create the boundary of a flat area representing the half of the plate with the hole in it. Use the overlay mesh generator to create finite elements.
- Step 2:** Create the cantilevered section of the plate. Convert it to finite elements. Merge the two parts.
- Step 3:** Fold the vertical sections and modify the elements in the triangular region.
- Step 4:** Apply boundary conditions.
- Step 5:** Assign material and geometric properties.
- Step 6:** Create the loadcases and submit the jobs.
- Step 7:** Postprocess the results.

Detailed Session Description of the Linear Static Case

Step 1: Create the boundary of a flat area representing the half of the plate with the hole in it. Use the overlay mesh generator to create finite elements.

The approach used in this session to generate the model is to use the geometric meshing technique to create two different areas and mesh them. The first area is meshed using the overlay mesh generator, and the second is meshed using the CONVERT processor. The entire model is created as a flat piece and, subsequently, the two support pieces are folded.

As in the *Sample Session* described in [Following a Sample Session](#), the first step in building the mesh is to establish an input grid. Click on the MESH GENERATION button of the main menu. Next click on the SET button to access the coordinate system menu where the grid settings are located. Use the following button sequence to set the grid spacing to 5 inches and the grid size of 30 inches.

```
MAIN
  MESH GENERATION
    SET
      U DOMAIN
        -30 30
      U SPACING
        5
      V DOMAIN
        -30 30
      V SPACING
        5
      grid ON
      RETURN
```

(on)

The next step is to create the three vertical lines of the model. The following button sequence creates the lines.

MAIN

MESH GENERATION

FILL

crvs ADD

(pick points from grid)

point(0,-10,0)

point(0,25,0)

point(15,0,0)

point(15,15,0)

point(30,0,0)

point(30,15,0)

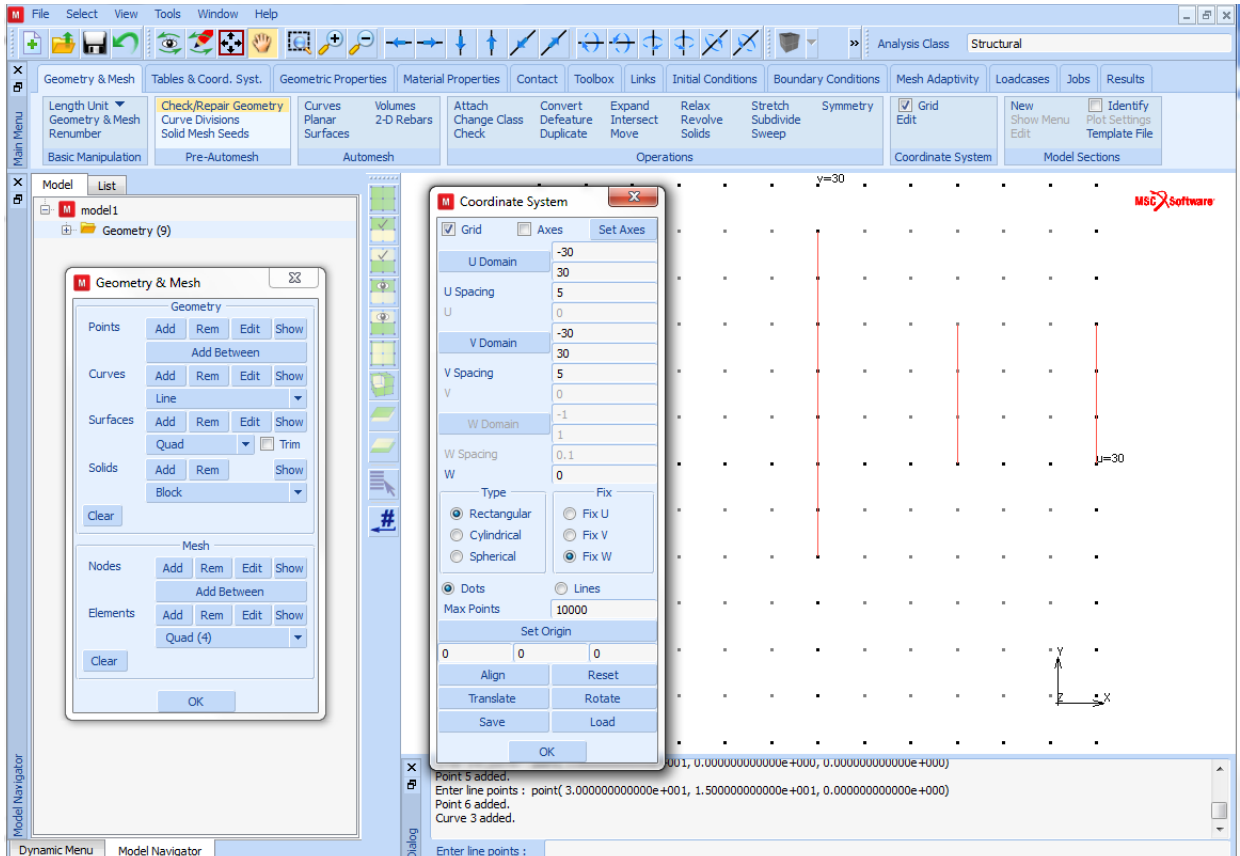


Figure 3.33-3 Grid and Straight Line Segments

The next geometric entity to be added is the two fillets. The curve type must be changed to arc and then the two curves added. To insure that the arc end points are the end points of the line the CENTER/POINT/POINT arc type is used. The following button sequence adds the two arcs.

MAIN

MESH GENERATION

CURVE TYPE

CENTER/POINT/POINT

RETURN

crvs ADD

22.5 27.5 0

(center point)

15 0 0

(pick lower end point of the second line)

0 -10 0

(pick lower end point of the first line)

22.5 42.5 0

(center point)

0 25 0

(pick upper end point of the first line)

15 15 0

(pick upper end point of the second line)

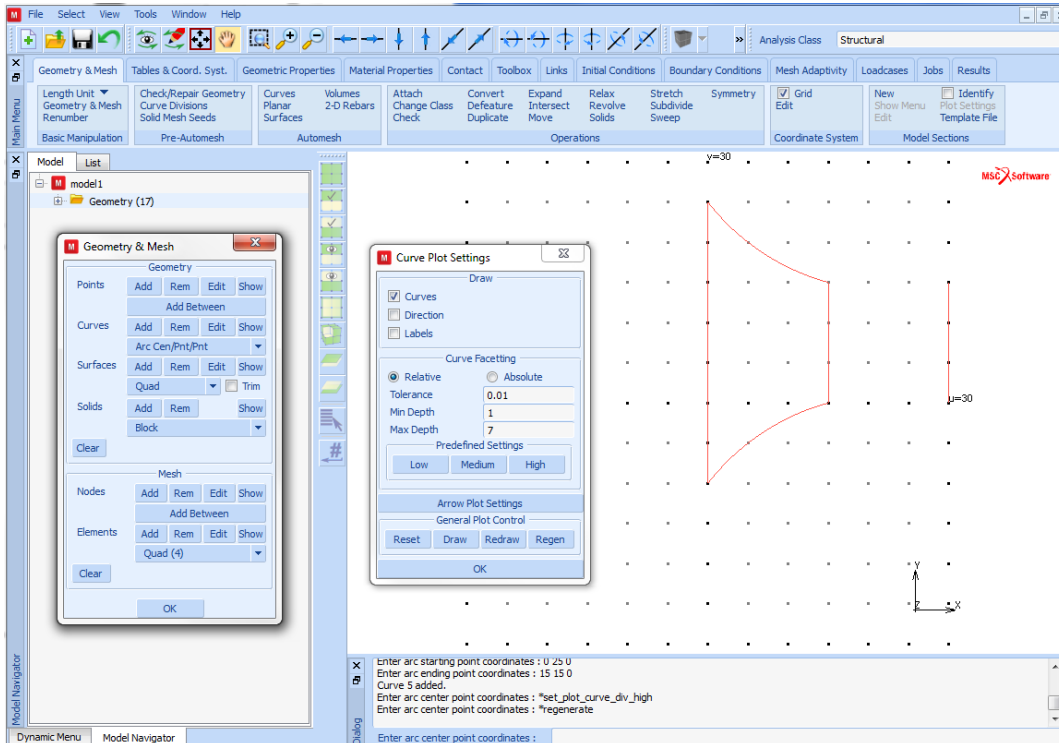


Figure 3.33-4 Line Segments and Fillets

The next step is the center hole. The coordinate system is moved such that it has an origin that is the center of the hole. The hole is added using the grid.

MAIN

MESH GENERATION

SET

set origin XYZ

7.5 7.5 0

U DOMAIN

-10 10

U SPACING

0.5 0.5

V DOMAIN

-10 10

V SPACING

0.5 0.5

RETURN

ZOOM BOX

(zoom in on the center of the grid)

CURVE TYPE

CENTER/POINT

RETURN

crvs ADD

0 0 0

(pick the center point)

3.5 0 0

(pick a point on the circle)

FILL

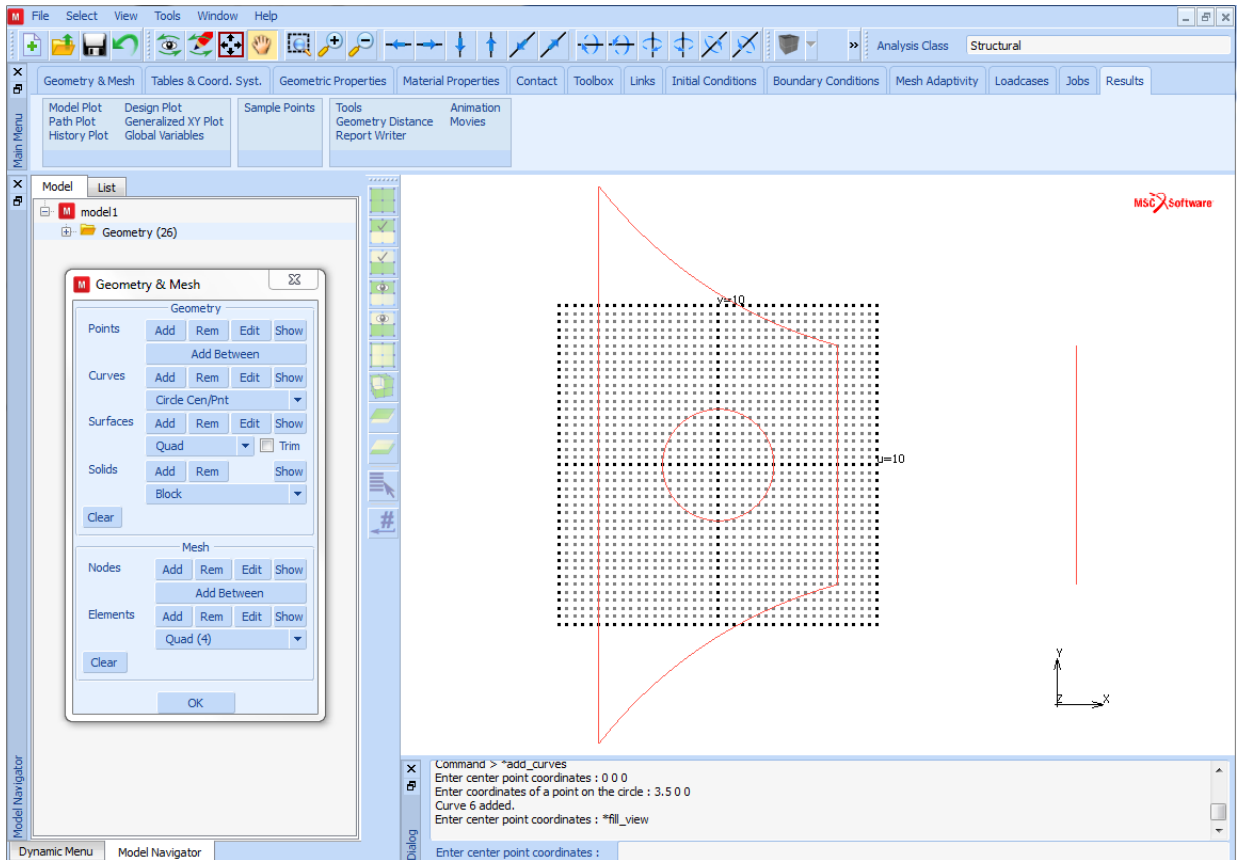


Figure 3.33-5 Generation of the Circular Hole

The next step is to create finite elements from the geometric entities. This is done using the overlay mesh generator. The following button sequence generates the mesh.

MAIN

MESH GENERATION

GRID

(off)

AUTOMESH

2-D PLANAR MESHING

quadrilaterals (overlay) DIVISIONS

8 20

quadrilaterals (overlay) QUAD MESH!

1 2 4 5 6

(use the Box Pick Method)

END LIST (#)
 RETURN (twice)

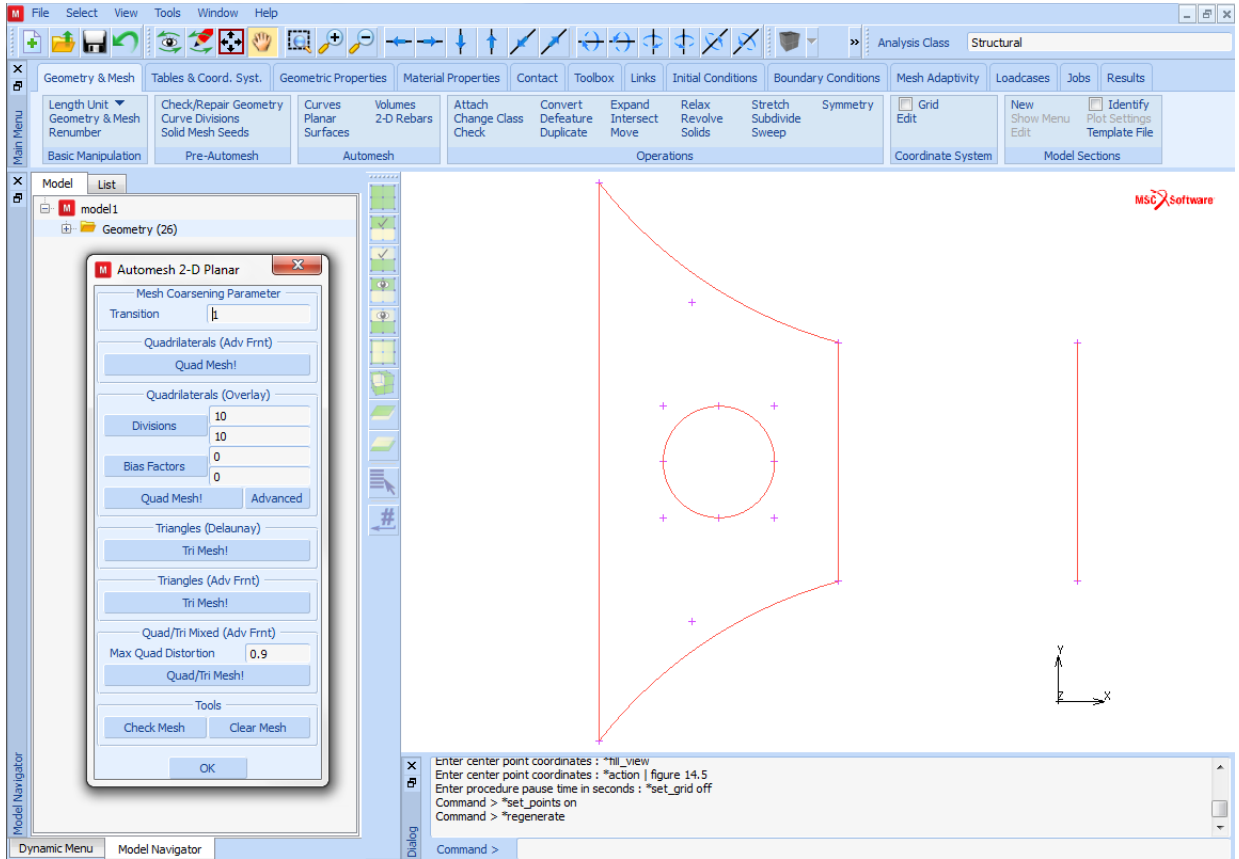


Figure 3.33-6 The Closed Contour for the OVERLAY Command

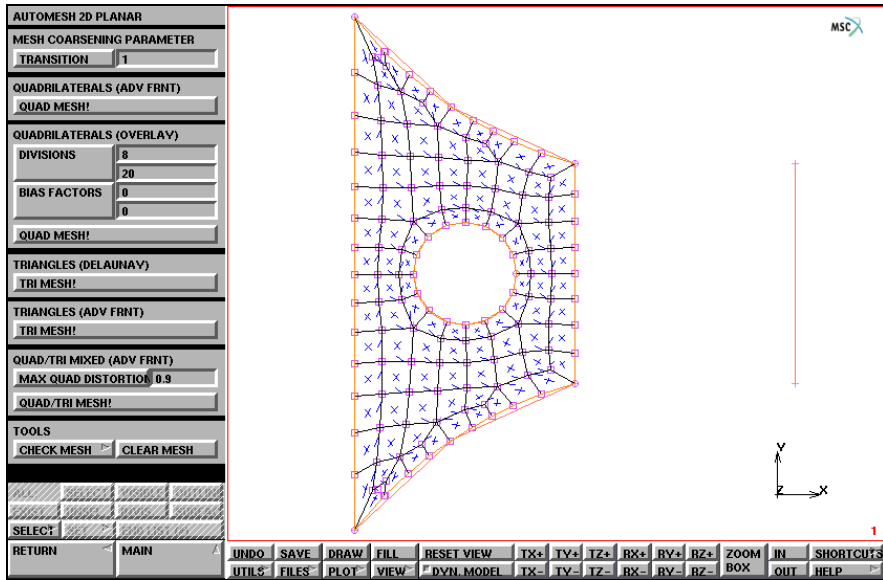


Figure 3.33-7 The Automeshed Part

Step 2: Create the cantilevered section of the plate. Convert it to finite elements. Merge the two parts.

The next step is to mesh the cantilevered portion. This section is modeled as four point quadrilateral surface and then converted to a 6x6 finite element mesh. The following button sequence creates the mesh.

MAIN

MESH GENERATION

srfs ADD

(pick the points in counter-clockwise order)

3

5

6

4

CONVERT

DIVISIONS

8 8

SURFACES TO ELEMENTS

1

(pick surface)

END LIST (#)

RETURN

The overlay mesh generator may create some unused nodes which must be removed. Furthermore, the nodes on the interface of the two meshes are not coincident. Therefore, to merge them, the sweep tolerance should be large, approximately 0.5. and only the nodes along the interface selected. The following button sequence merges the nodes. The sweep tolerance should be changed back to the default when the merge operation is finished.

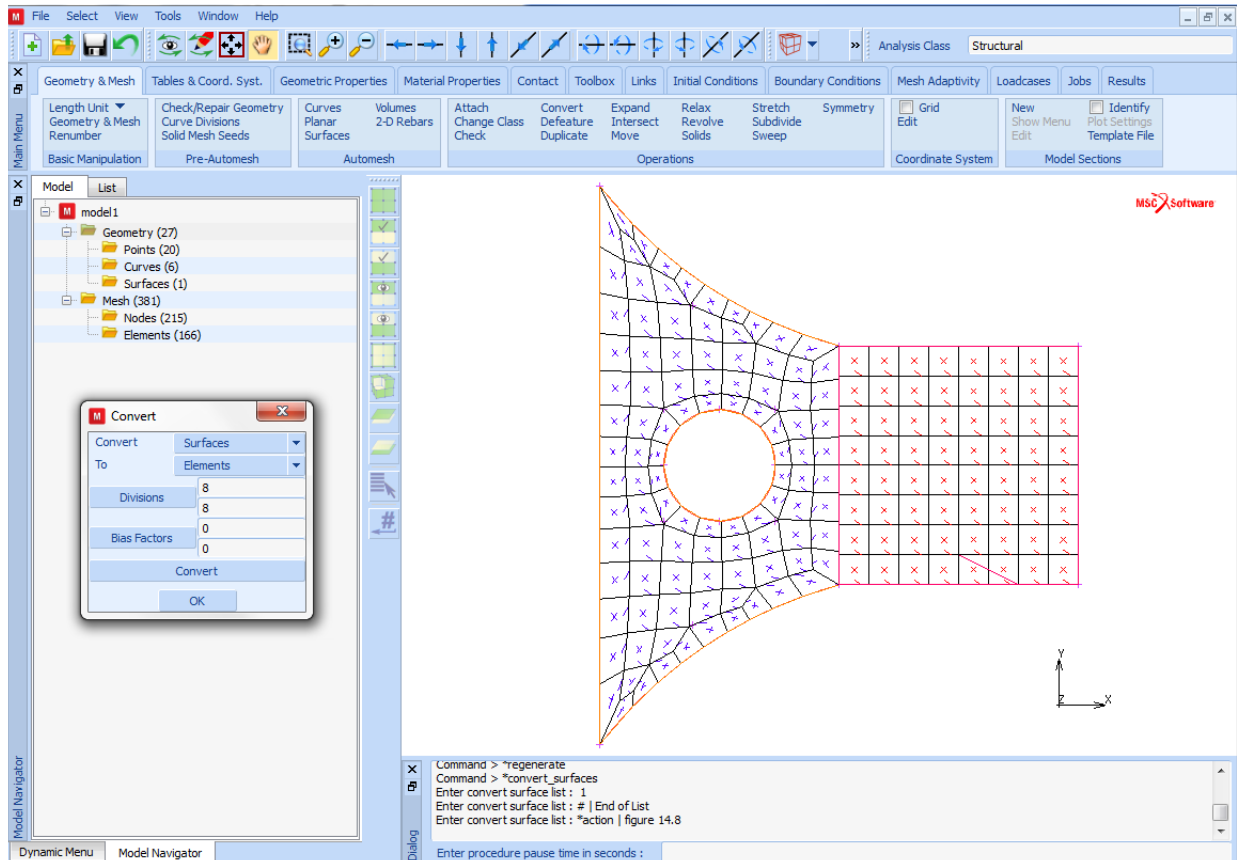


Figure 3.33-8 Elements on the Square Surface

MAIN

MESH GENERATION

SWEEP

REMOVE UNUSED NODES

TOLERANCE

0.5

SWEEP NODES

END LIST (#)

(Box Pick the nodes on the interface)

TOLERANCE
0.0001
RETURN

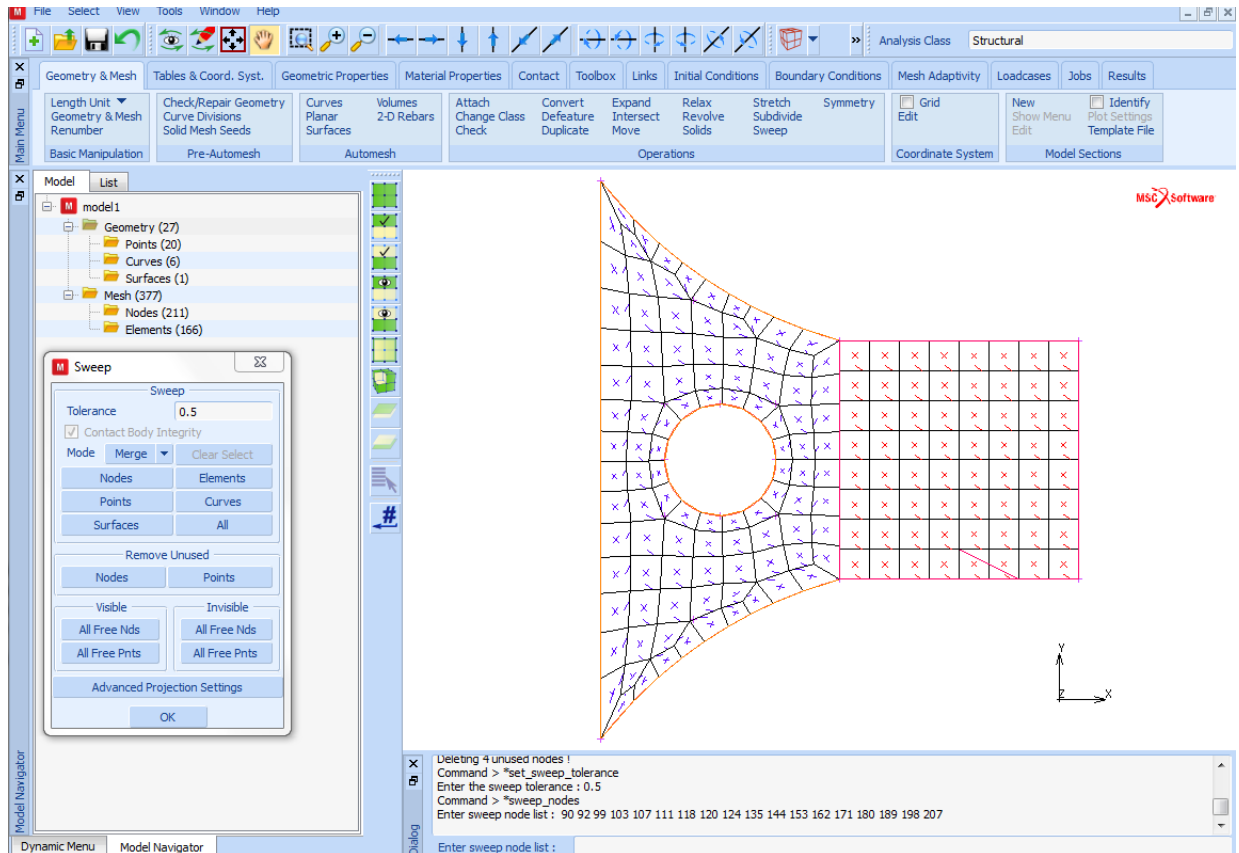


Figure 3.33-9 Correctly Connected Mesh

Step 3: Fold the vertical sections and modify the elements in the triangular region.

The final mesh general operation is to fold the two sides down. First, the nodes must be along the line of the fold. This is done by creating a line along each edge and attaching the nodes to these lines. Then, the two corner elements are divided into two triangular elements. These elements must still have the class of QUAD(4). This is achieved by generating the triangular elements as degenerated quad elements, double clicking one node in the connectivity list.

The lines are created by using the grid with a spacing of 5 and a size of 15. The origin of the grid must be set to the global origin. The following button sequence creates the lines and attaches the nodes to them.

MAIN

MESH GENERATION

SET

RESET

U SPACING

5

V SPACING

5

U DOMAIN

0 15

V DOMAIN

0 15

grid ON

(on)

RETURN

CURVE TYPE

LINE

RETURN

crvs ADD

point(0, 15, 0)

(pick grid point)

12

(pick upper left point of the surface)

point(0, 0, 0)

(pick grid point)

7

(pick lower left point of the surface)

GRID

(off)

MOVE

MOVE TO GEOMETRIC ENTITIES

move nodes CURVE

7

*(pick lower line)**(pick nodes near lower line)*

END LIST (#)

8

*(pick upper line)**(pick nodes near upper line)*

END LIST (#)

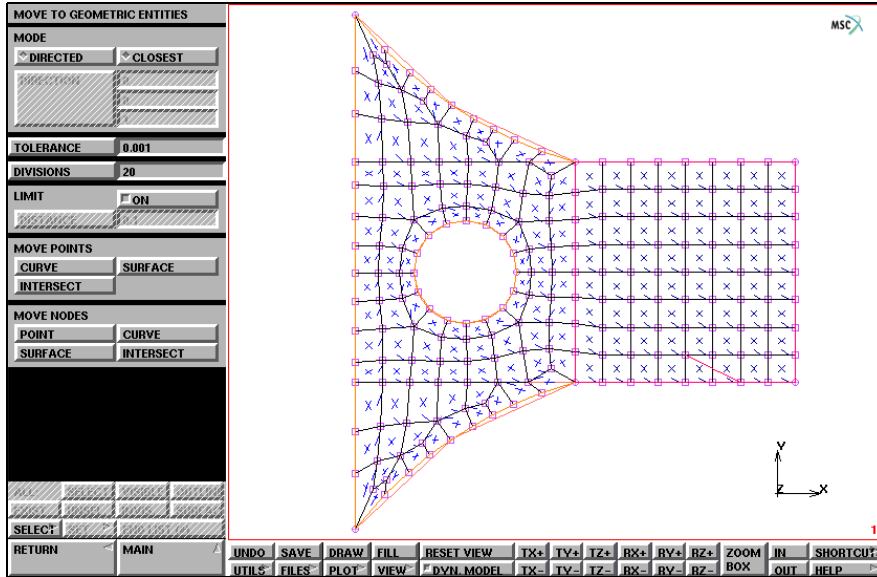


Figure 3.33-10 Nodes at the Top Half attached to the Line

The two corner elements at the transition of the fillet to the square plate must be removed and two triangular elements will replace them. To create the triangular elements, the last node should be selected twice. The triangular elements have to be defined such that they allow for folding over the line segment. The following button sequence creates the first of four triangular elements.

MAIN

MESH GENERATION

elems REM

89 59

(pick elements at the triangular corners)

END LIST (#)

elems ADD

(pick nodes)

123

64

109

(first click on this node)

109

(second click on this node)

Add three more triangular elements in the same way.

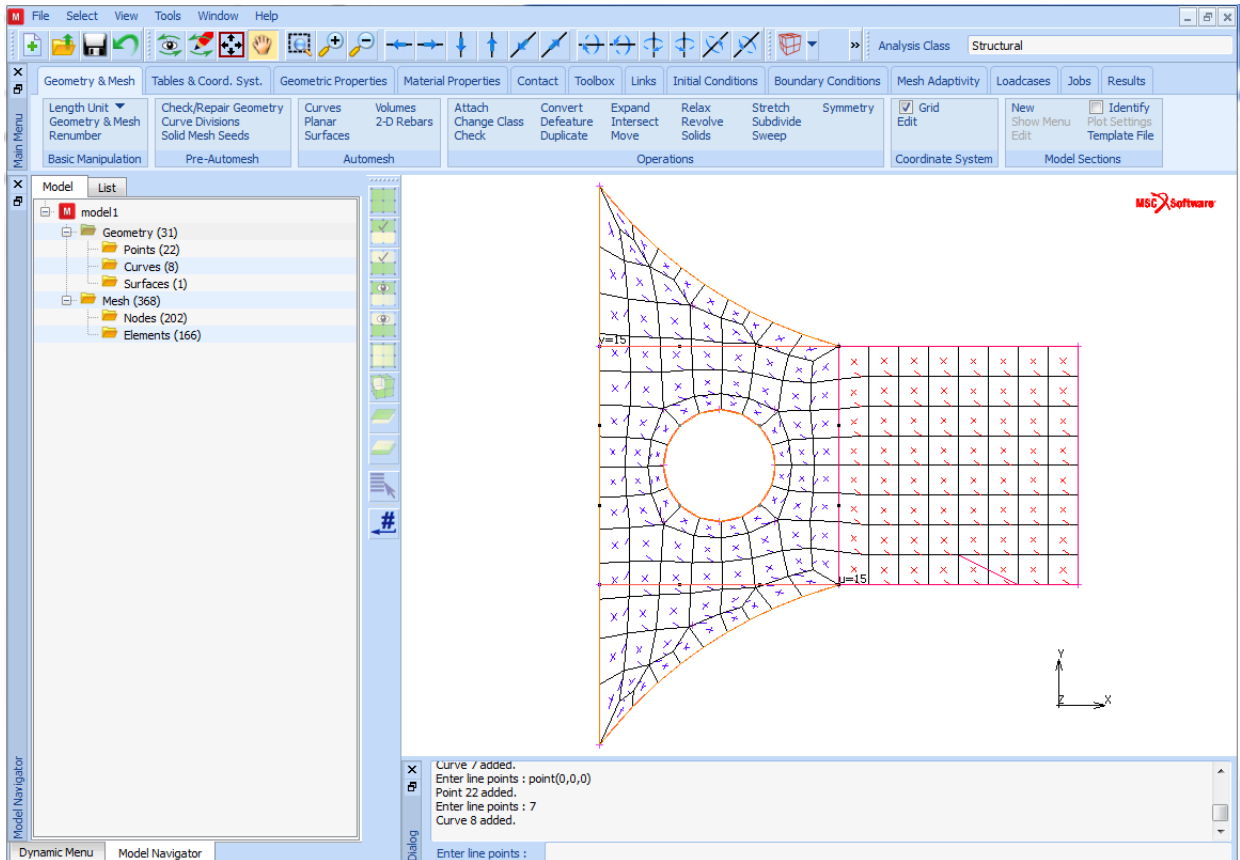


Figure 3.33-11 Corner Elements replaced by Triangular Elements

The next step in the process of folding is to detach the elements. This is done using the ATTACH processor to detach the elements in the triangular region. The lower edge rotates 90° and the upper edge rotates -90°. The following button sequence folds the two edges.

MAIN

MESH GENERATION

ATTACH

DETACH

ELEMENTS

```

1 2 3 4 5 6 7 47 48 49
50 51 52 53 54 55 56 58 170
40 41 42 43 44 45 46 90 93 94 95
    
```

```
96 97 98 99 100 101 102 167  
END LIST (#)
```

The final step in the process of folding is to actually move the elements. This is done using the MOVE processor and rotating the elements. The lower edge rotates 90° and the upper edge rotates -90°. The following button sequence folds the two edges.

```
MAIN  
  MESH GENERATION  
    MOVE  
      ROTATIONS  
        90 0 0  
      POINT  
        15 0 0 (pick point at end of bottom line  
of horizontal plate)  
    ELEMENTS (Box Pick the lower elements to be folded)  
      END LIST (#)  
      ROTATIONS  
        -90 0 0  
      POINT  
        15 15 0 (pick point at end of top line  
of horizontal plate)  
    ELEMENTS (Box Pick the upper elements to be folded)  
      END LIST (#)
```

The following button sequence shows all four views and turns off the points and curves. It makes the viewing easier.

```
MAIN  
  MESH GENERATION  
    SWEEP  
      remove unused NODES  
MAIN  
  VIEW  
    SHOW ALL VIEWS  
    PLOT
```


- draw POINTS (off)
- draw CURVES (off)
- REGEN
- FILL

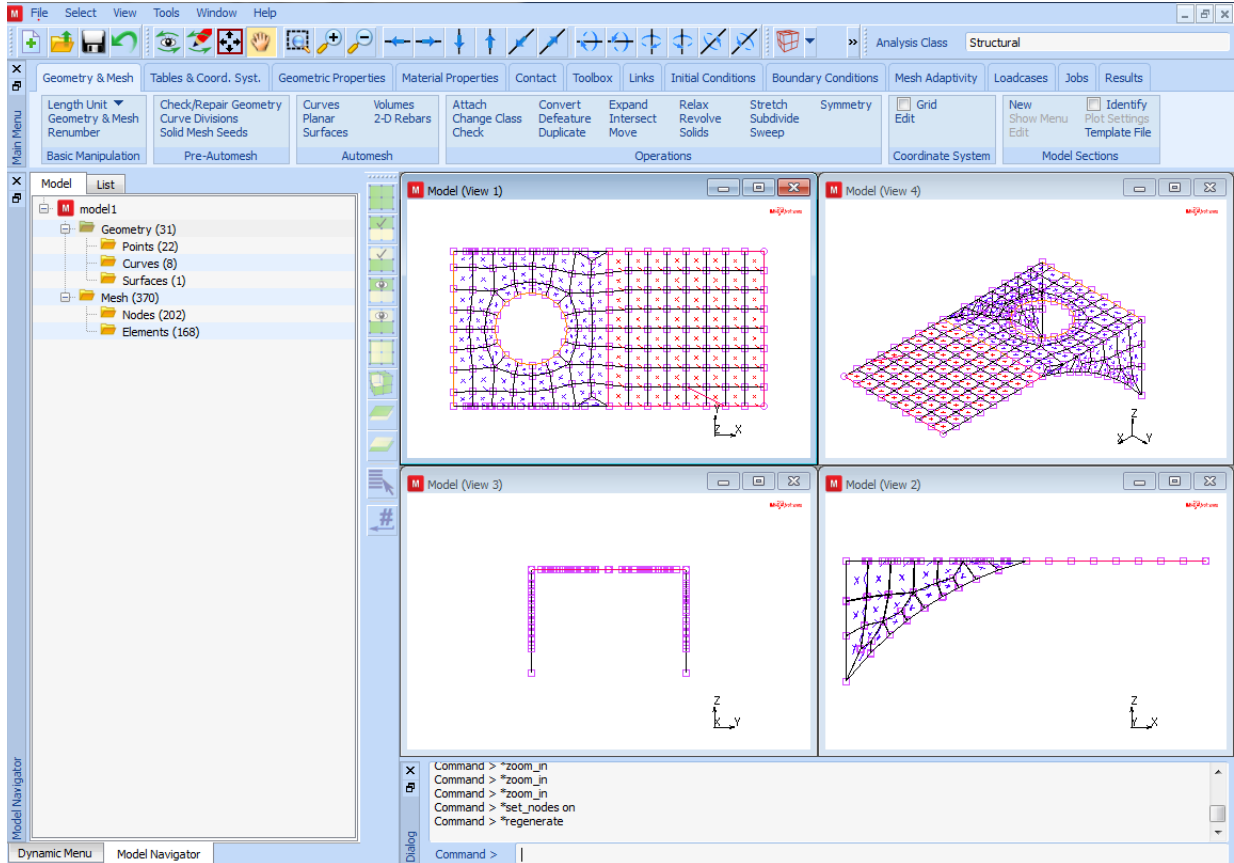


Figure 3.33-12 The Complete FE Model

Step 4: Apply boundary conditions.

The next step is to apply the boundary conditions. First, the back edge of the bracket is fixed in the three translational degrees of freedom. The following button sequence fixes the edge.

- MAIN
- BOUNDARY CONDITIONS
- MECHANICAL
- FIXED DISPLACEMENT

```
DISPLACEMENT X (on)
DISPLACEMENT Y (on)
DISPLACEMENT Z (on)
OK
nodes ADD
                                (Box Pick the left edge of the plate, preferably in view 1 or 2)
END LIST (#)
```

The next step is to apply the face loads to the cantilevered portion of the plate. The loads are 1 psi downward to represent the mechanical equipment. The following button sequence applies the distributed loads.

```
NEW
FACE LOAD
  PRESSURE
    1
  OK
surfaces ADD
  1 (pick the surface)
END LIST (#)
```

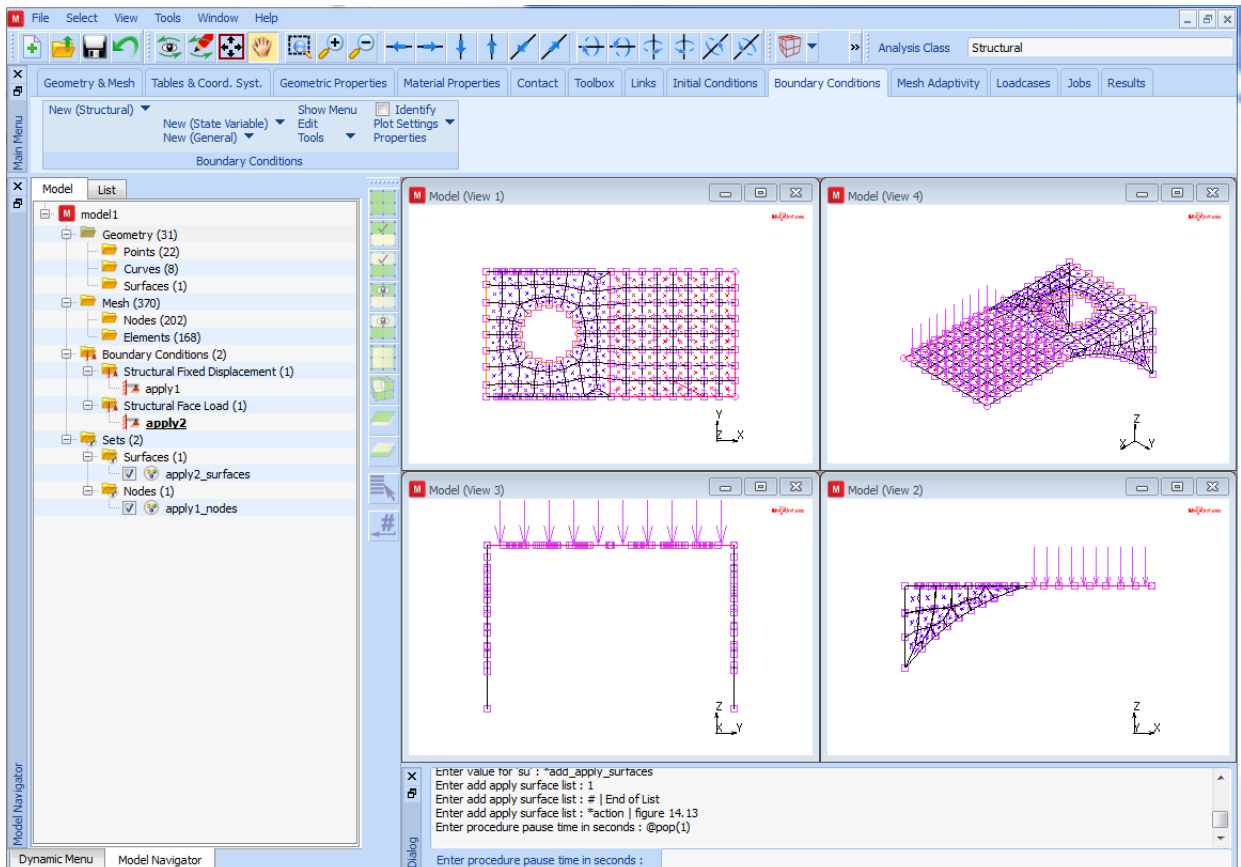


Figure 3.33-13 Loads Applied to all Elements attached to the Surface

Step 5: Assign material and geometric properties.

The next step is to assign the material properties. The material is steel and the mass density must be included because a dynamic analysis will be done. The following button sequence assigns the material properties.

MAIN

MATERIAL PROPERTIES

ISOTROPIC

YOUNG'S MODULUS

30e6

0.3

(Poisson's ratio)

MASS DENSITY

0.283/386.4

(mass density)

OK

elements ADD
all: EXIST

The next step is to assign the thickness of the plates. Because the plates have different thicknesses, two geometric properties are required. To make the picking of the elements easier, the user should select the partial picking capability in the device menu. The default is full which requires that the item of the requested type be fully contained in the graphical pick. The partial mode selects any item of the requested type that is partially in the graphical pick. The following button sequence changes the picking type and then assigns the geometric properties to the elements.

```
MAIN
  DEVICE
    picking PARTIAL
  RETURN
  GEOMETRIC PROPERTIES
    3-D
      SHELL
        THICKNESS
          0.25
        OK
      elements ADD
      (pick the Horizontal Plate Elements)
    END LIST (#)
  NEW
  SHELL
    THICKNESS
      0.5
    OK
  elements ADD
  (pick the Vertical Plate Elements)
  END LIST (#)
```

To verify the geometric property assignment, the following button sequence changes some plot defaults and switches on the identification of geometries.

```
MAIN
  GEOMETRIC PROPERTIES
    3-D
      ID GEOMETRIES
      (on)
```

PLOT

elements SOLID

REGEN

RETURN

ID GEOMETRIES

(off)

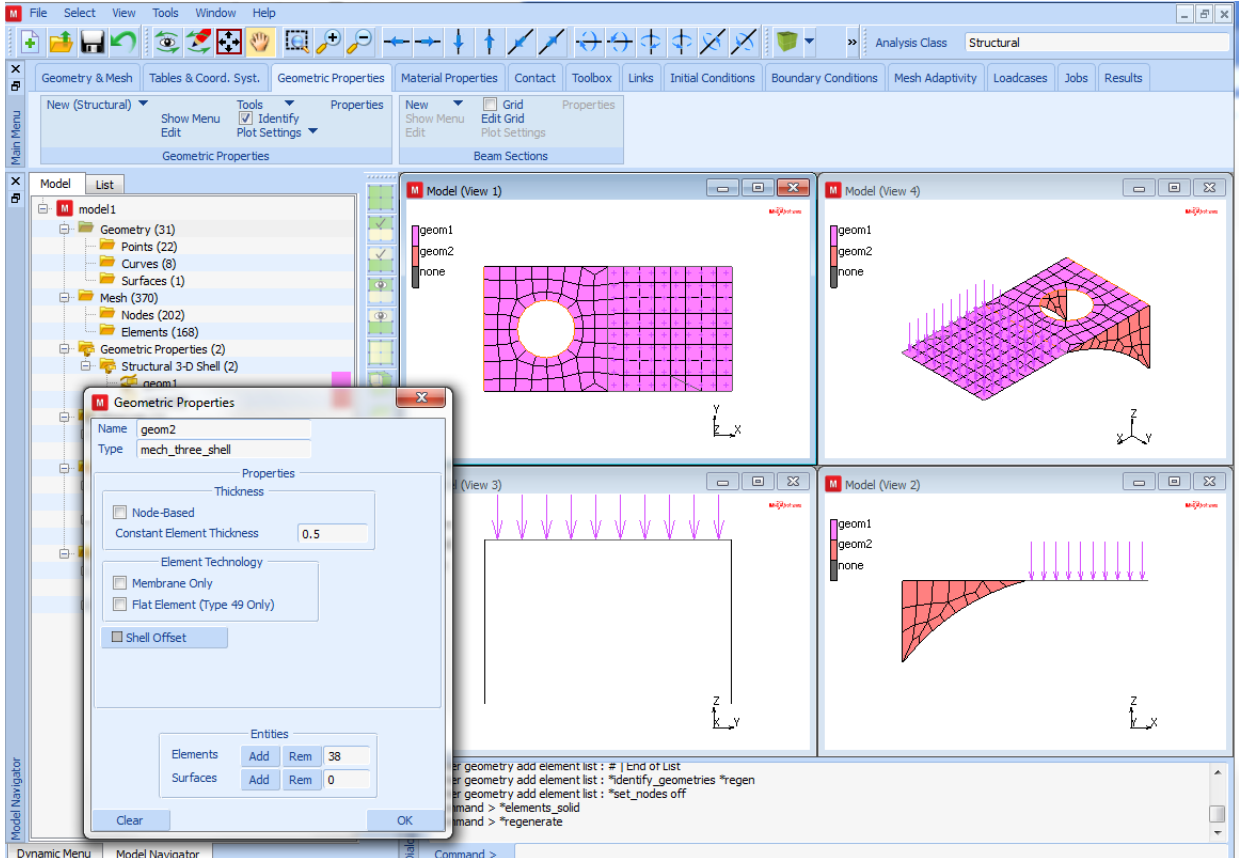


Figure 3.33-14 Graphical Confirmation of Applied Geometries

Step 6: Create the loadcases and submit the jobs.

The next step is to create the static loadcase. It is a linear static with all loads selected and, therefore, no special options need to be selected. The following button sequence creates the loadcase.

MAIN

LOADCASE

mechanical analyses STATIC
OK

The following button sequence creates the job and executes it.

```
MAIN
  JOBS
    MECHANICAL
      available (select a loadcase from the list)
        lcase1
      JOB RESULTS
        scalars (select Equivalent von Mises stress for
                outer and midplane layers)
          von_mises
        OUT
        tensors
          stress (select stress tensor for outer and midplane layers)
        OUT
        OK
      JOB PARAMETERS
        # SHELL/BEAM LAYERS
          3 (use 3 layers for thickness integration)
        OK (twice)
  SAVE
  RUN
  SUBMIT 1
  MONITOR
```

Step 7: Postprocess the results.

The final step in any analysis is to postprocess the results. This is done by opening the post file and reviewing the results. The deformations are drawn using automatic scaling. The following button sequence does this. However, there may be other results that the user wishes to review.

```
MAIN
  RESULTS
    OPEN DEFAULT
    DEF & ORIG
```

NEXT INC

NEXT INC

SCALAR

Equivalent von Mises Stress Layer 2

OK

CONTOUR BANDS

deformed shape SETTINGS

deformation scaling AUTOMATIC

Note: The results for increment 0 and increment 1 are identical. This is caused by the fact that the pressure loading is still selected as an initial load. The Marc writer generates for increment 1 (i.e. the complete loadcase) the incremental load between the load vector and the initial load, which is a zero load increment. As a result, the deformation in increment 0 and increment 1 is identical.

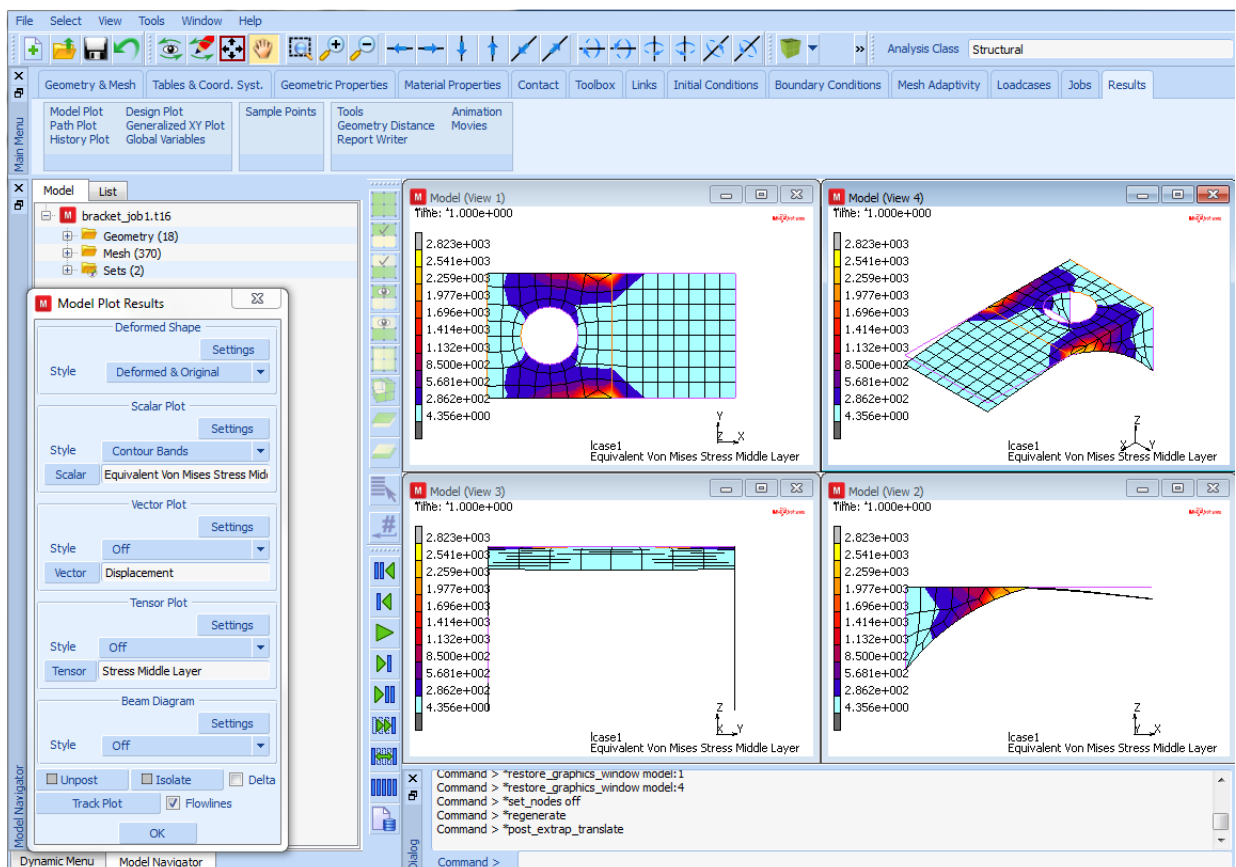


Figure 3.33-15 Deformed Structure and Contours of von Mises Stress

Conclusion

The bracket sustains the required static loads.

Dynamic Modal Shape Analysis

Overview of Steps

Step 1: Restore the database from the static analysis.

Step 2: Create a modal dynamic loadcase and submit it.

Step 3: Postprocess the results.

Detailed Session Description of the Modal Shape Analysis

Step 1: Restore the database from the static analysis.

For the dynamic analysis, the same geometry is used. The first step is to restore the database. Closing the post file automatically restores the database. In addition, the commands are shown for restoring the database and resetting the program. (These commands are not necessary here). Finally, the plotting of points, curves, and surfaces are switched off.

```
MAIN
  RESULTS
    CLOSE
    FILES
      RESTORE
      RESET PROGRAM
    RETURN
  VIEW
    show 4
  PLOT
    draw POINTS (off)
    draw CURVES (off)
    draw SURFACES (off)
  REGEN
  FILL
  RETURN
```

Step 2: Create a modal dynamic loadcase and submit it.

The next step is to create a modal dynamic loadcase. The default is that 10 modes are determined which is enough for this structure. (Note that the determination of higher-order modes in general required higher mesh densities). The following button sequence creates the loadcase.

```
MAIN
  LOADCASE
    NEW
    DYNAMIC MODAL
    OK
```

The next step is to create and execute the modal analysis job. The following button sequence creates and submits the job.

```
MAIN
  JOBS
    NEW
    MECHANICAL
      available
      lcase2
    ANALYSIS OPTIONS
      OK (twice)
  RUN
  SAVE
  SUBMIT 1
  MONITOR
```

(verify that the LANCZOS method is used)

Step 3: Postprocess the results.

The next step is to postprocess the results. For modal analyses, not only the values of the eigenfrequencies but also the shape of the deflections or modal shapes are of interest. For the deformed shape, the automatically scaled deformations should be viewed. For ease of understanding, it is best to show all four views. The following button sequence does the postprocessing.

```
MAIN
  RESULTS
    OPEN DEFAULT
    DEF & ORIG
    PLOT
      draw NODES
    MORE
      edges OUTLINE
```

(off)

```
        RETURN (twice)
SCALAR
    Displacement z
    OK
CONTOUR BANDS
deformed shape SETTINGS
    deformation scaling AUTOMATIC
    RETURN
NEXT INC
```

(repeat until all modes have been viewed)

Finally, generate an animation sequence of one modal shape:

```
MAIN
  RESULTS
    MORE
      animate MODE
        9
      ANIMATION
        VIEW
          show view 4
          FILL
          RETURN
        PLAY
      SHOW MODEL
```

(number of frames for animation)

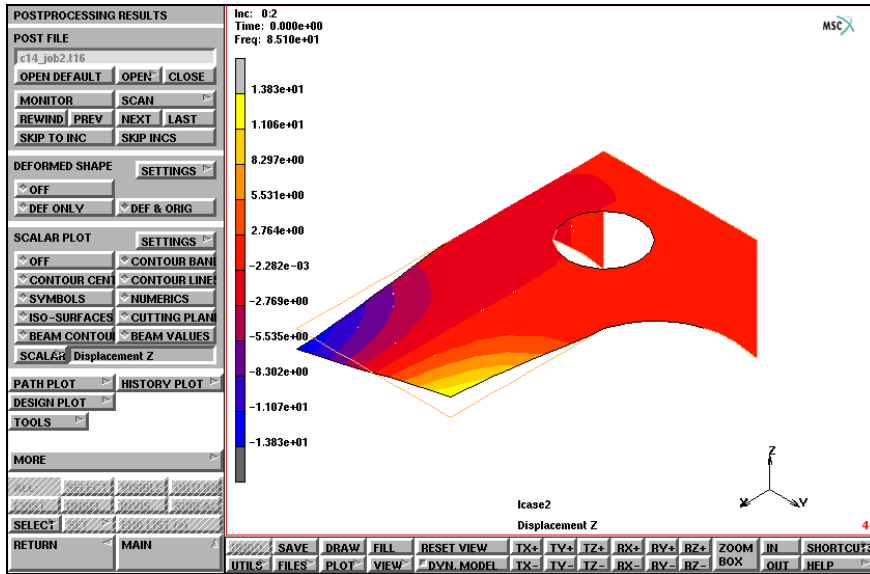


Figure 3.33-16 The Second Eigenmode

Observe that the calculated eigenfrequencies and corresponding eigenvectors are stored as so-called subincrements on the post file. The eigenfrequency value (in cycles/time unit) corresponding to a specific mode is printed on the top left of the screen.

Table 2.33-1 Eigenfrequencies Bracket

increment	mode	value (cycles/time)
0:1	1	27.5
0:2	2	85.3
0:3	3	150.7
0:4	4	240.8
0:5	5	298.6
0:6	6	304.8
0:7	7	413.0
0:8	8	456.9
0:9	9	505.9
0:10	10	569.3

Observe that the eigen period of mode 1 will be 0.036 seconds.

Dynamic Transient Analysis

Overview of Steps

- Step 1:** Create an pressure time table for the loading. Then apply it as a face load in a loadcase.
- Step 2:** Create and submit a transient analysis.
- Step 3:** Create job and submit it.
- Step 4:** Postprocess the results.

Detailed Session Description of Dynamic Transient Analysis

Step 1: Create an pressure time table for the loading. Then apply it as a face load in a loadcase.

Restore the database to continue with the analysis preparation. The next step is to include a time dependent pressure history using the table option in the boundary condition menu. Here, the table which is included in the file *bracket.tbl* on the Mentat installation media is used. To load the table, the user needs the full path name to the Mentat subdirectory *examples/marc Ug* or has to copy this file into his own directory. The following button sequences restores the model and input the table.

```
MAIN
  RESULTS
    CLOSE
    FILES
      RESTORE
      RESET PROGRAM
    RETURN
  PLOT
    draw CURVES (off)
    draw POINTS (off)
    draw SURFACES (off)
  FILL

MAIN
  BOUNDARY CONDITIONS
    MECHANICAL
      TABLE
```

READ

 bracket.tbl

FIT

SHOW TABLE

 SHOW MODEL

(select SHOW MODEL)

RETURN

The pressure history as function of the time is shown in [Figure 3.33-17](#).

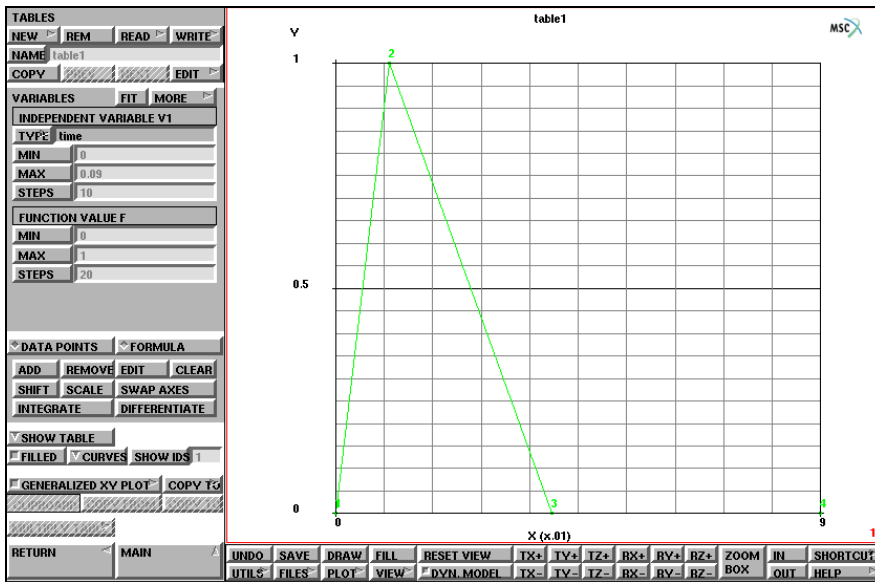


Figure 3.33-17 Transient Pressure Loading as Function of Time

Observe that the maximum pressure magnitude is one which is equal to the pressure as defined in the static loadcase. The maximum pressure is reached within 0.01 seconds and the pressure is equal to zero at 0.04 seconds and kept to zero until 0.09 seconds. Looking at the results of the eigenfrequencies in [Table 2.33-1](#), it is expected that the lower modes are dominating during the transient.

The next step is to assign this table to the pressure to the same elements as in the pressure load used in loadcase 1.

MAIN

 BOUNDARY CONDITIONS

 MECHANICAL

 NEW

 FACE LOAD

 pressure TABLE

```

table1
OK
faces ADD
END LIST (#)

```

(Box Pick the cantilevered elements)

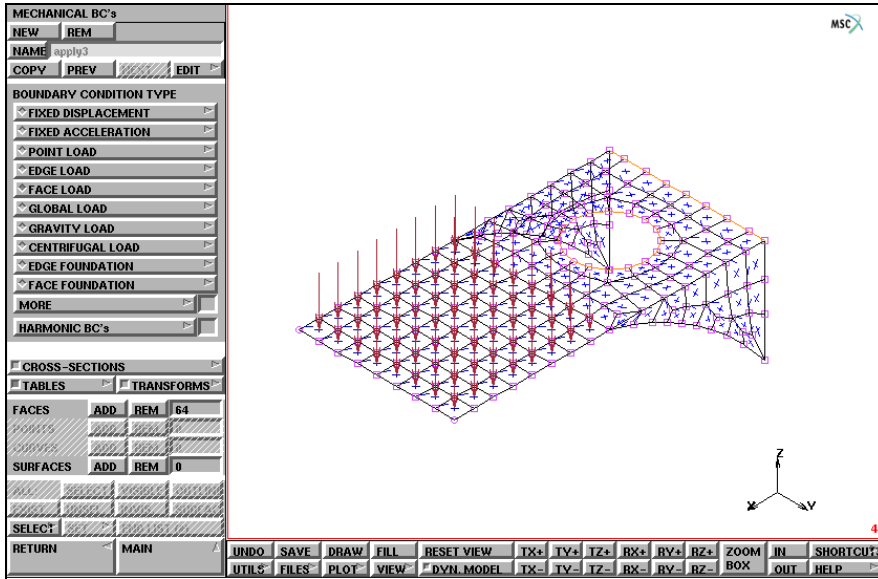


Figure 3.33-18 Transient Pressure Loading

Step 2: Create and submit a transient analysis.

The next step is creating the loadcase for the transient analysis. The following button sequence creates the new loadcase.

```

MAIN
LOADCASES
NEW
MECHANICAL
DYNAMIC TRANSIENT
LOADS
    apply2
    OK
TOTAL LOADCASE TIME
    0.09

```

(deselect static load)

```
# STEPS
  90
OK
```

Step 3: Create job and submit it.

The next step is creating the job and submitting it. The following button sequence creates and submits the job.

```
MAIN
  JOBS
    NEW
    MECHANICAL
      available
        lcase3 (select loadcase 3)
    ANALYSIS OPTIONS
      IMPLICIT
        SINGLE-STEP HOUBOLT (verify that dynamic transient
operator implicit Single-step Houbolt is used)
      OK
    INITIAL LOADS
      boundary conditions
        apply2 (remove static load)
      OK
    JOB RESULTS
      available elemnt scalars
        von_mises (select Equivalent von Mises Stress)
      OUT & MID (select outer and midplane LAYERS)
      OK
    JOB PARAMETERS
      # SHELL/BEAM LAYERS
        3
      OK (twice)
  SAVE
  RUN
    SUBMIT 1
  MONITOR
```


Step 4: Postprocess the results.

The final step in any analysis is postprocessing the results. This is done by opening the post file and reviewing the results. The following button sequence does this. However, there may be other results that the user wishes to review.

```
MAIN
  RESULTS
    OPEN DEFAULT
    NEXT INC
    DEF & ORIG
    deformed shape SETTINGS
      deformation scaling FACTOR
        5.
      deformation scaling MANUAL
    OK
    SCALAR
      Equivalent von Mises Stress Layer 2
    OK
    CONTOUR BANDS
    MONITOR
```

This walks through all 90 increments.

It is also possible to monitor a path plot. The following button sequence shows this.

```
MAIN
  RESULTS
    REWIND
    PATH PLOT
      NODE PATH
        215
        124
        123
        132
      END LIST (#)
    SHOW IDS
      5
    VARIABLES
```

ADD CURVE

Arc Length
Equivalent von Mises Stress Layer 1
Arc Length
Equivalent von Mises Stress Layer 2
Arc Length
Equivalent von Mises Stress Layer 3

RETURN

FIT

YMAX

36000

MONITOR

SHOW HISTORY

SHOW MODEL

(select SHOW MODEL)

The stresses for the nodes in the node path do not exceed the yield stress of 36000 psi.

As a last step, history plots are made. First, a plot of the stresses versus time is shown in [Figure 3.33-19](#).

MAIN

RESULTS

REWIND

HISTORY PLOT

SET NODES

208

124

123

END LIST (#)

COLLECT DATA

0 90 1

SHOW IDS

0

NODES/VARIABLES

ADD VARIABLE

global variables

Time

variables at nodes

Equivalent von Mises Stress Layer 3

FIT

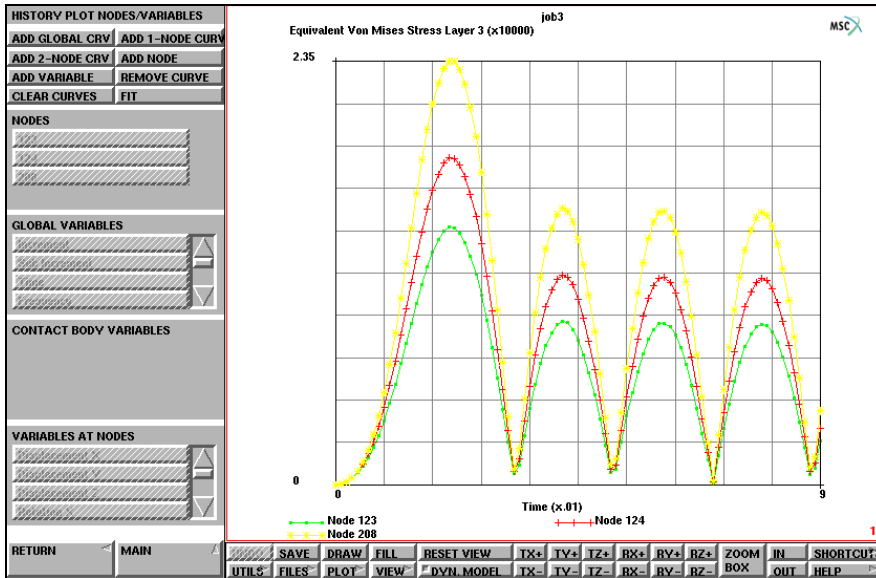


Figure 3.33-19 History Plot of von Mises Stress

Finally, the tip displacement in z-direction are shown and compared with the value of due to the static load with the same magnitude (loadcase 1), which was found to be 0.28

MAIN

RESULTS

REWIND

HISTORY PLOT

SET NODES

215

END LIST (#)

COLLECT DATA

0 90 1

NODES/VARIABLES

ADD 1-NODE CURVE

215

global variables

Time

variables at nodes

Displacement z

FIT

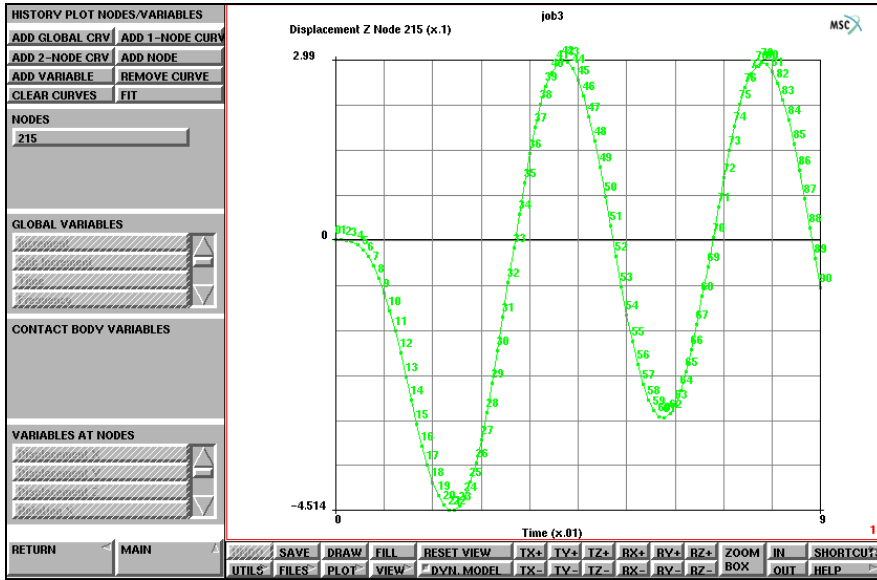


Figure 3.33-20 History Plot of Tip Z-displacement

Conclusion

Due to the dynamic loading, a larger value of the tip displacement is found for the same value of the maximum pressure. The bracket is shown to withstand the dynamic loads. The stresses never exceed yield.

Pressure Table

Pressure as function of time file c14.tbl:

```
# Title
table1
# X-axis Label
X
# Y-axis Label
Y
# Type
1
# Steps in X and Y
10 20
# X-min, X-max, Y-min, Ymax
0.000000000000e+00 9.000000000000e+00 -1.000000000000e+00
1.000000000000e+00
04
0.000000000000e+00 0.000000000000e+00 1
1.000000000000e+02 1.000000000000e+00 2
4.000000000000e+02 0.000000000000e+00 3
9.000000000000e+02 0.000000000000e+00 4
```

Input Files

The files below are on your [delivery media](#) or they can be downloaded by your web browser by clicking the links (file names) below.

File	Description
bracket.proc	Mentat procedure file
bracket.tbl	Table data

3.34 Single Step Houbolt Dynamic Operator

- Chapter Overview 1640
- Impact of a Ball on a Plate 1640
- Eigenvalue Analysis 1640
- Transient Analysis 1651
- Input Files 1660

Chapter Overview

This chapter demonstrates the use of the *Single Step Houbolt* method using the numerical simulation of the impact of a ball on a plate.

In a contact analysis involving dynamics, the user often encounters a kind of shock loading if two moving bodies hit each other. Depending on the velocity magnitudes, material properties, etc., such a shock loading may trigger high-frequency oscillations, which in turn may cause numerical troubles. When use is made of the well-known Newmark-beta dynamic operator, the user has to choose specific damping properties in order to get rid of the undesired oscillations. However, the choice of damping properties is not trivial, and usually also relevant oscillations may be damped out.

The *Single Step Houbolt* method has spectral properties similar to the classical Houbolt method and thus possesses high-frequency dissipation. It should be noted that the term “high-frequency” is always related to the time step Δt chosen. If Δt is small compared to the time period T of a mode (say $\Delta t/T < 1/15$), the mode is properly integrated; if Δt is large compared to the time period T of a mode (say $\Delta t/T > 10$), the mode is damped out rapidly.

Impact of a Ball on a Plate

The simulation consists of two steps: first an eigenvalue analysis is performed to estimate a proper time step, then the impact simulation itself is performed using a transient dynamic analysis.

Background Information

A circular plate with a thickness of 0.0025 m and a radius of 0.05 m is clamped around its circumference and hit by a ball with a radius of 0.02 m. The initial velocity of the ball is 2.5 m/s. The material behavior of both the plate and the ball is considered to be elastic-plastic. The plate has a Young's modulus of 7×10^9 N/m², a Poisson's ratio of 0.3, a density of 2500 kg/m³, an initial yield stress of 7×10^6 N/m², and a hardening modulus of 1.4×10^7 N/m². The ball has a Young's modulus of 2×10^{11} N/m², a Poisson's ratio of 0.3, a density of 7800 kg/m³, an initial yield stress of 2×10^8 N/m², and a hardening modulus of 6×10^8 N/m².

The plate and the ball are modeled using 4-node axisymmetric elements with full integration (Marc element type 10). Around the contact area, the mesh of the plate will be refined. For the eigenvalue analysis, no contact bodies will be defined in order to get the eigenfrequencies of the plate and the ball independently.

Eigenvalue Analysis

Model Generation

The finite element mesh of the plate will be obtained by subdividing one element and then refining the mesh near the center of the plate by the refine option. The finite element mesh of the ball will be created by defining curves and using the 2-D overlay mesher. The elements of the plate and the ball will be stored in element sets.

FILES

NEW, OK

RESET PROGRAM

VIEW

SHOW VIEW 1

MAIN

MESH GENERATION

pts ADD

-0.0025 0 0

0 0 0

0 0.05 0

-0.0025 0.05 0

0.02 0 0

0.04 0 0

elem ADD

NODE(-0.0025, 0, 0)

NODE(0, 0, 0)

NODE(0, 0.05, 0)

NODE(-0.0025, 0.05, 0)

SUBDIVIDE

DIVISIONS

4 30 1

ELEMENTS

all: EXIST.

DIVISIONS

2 2 1

ELEMENTS

2 3 4 5 6 7 8 9 10 32 33 34 35 36 37 38 39 40 62 63

64 65 66 67 68 69 70 92 93 94 95 96 97 98 99 100

ZOOM BOX

(those shown in [Figure 3.34-1a](#))

*(zoom transition elements
[Figure 3.34-1b](#))*

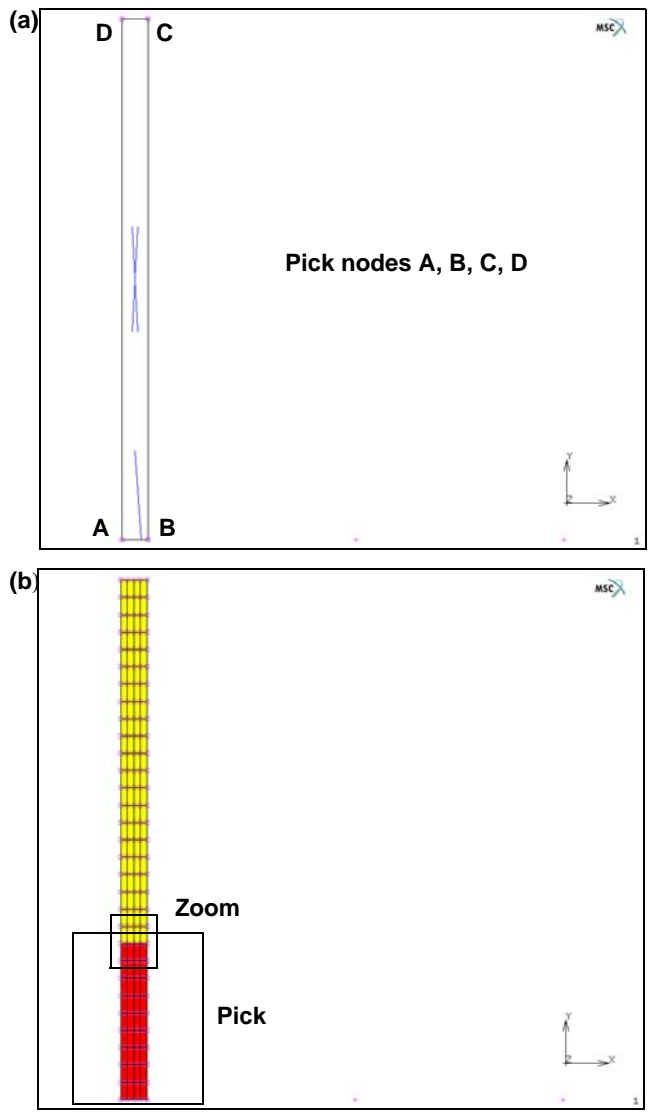


Figure 3.34-1 FE-Mesh for Impact Problem (a) Elements (b) Zoom Box

```

REFINE
  45
  11
  41
END OF LIST (#)
  107
  71
  101
END OF LIST (#)
FILL
RETURN
SWEEP
  NODES
  all: EXIST.
SELECT
elements STORE
  Plate
  OK
all: EXIS.
SELECT SET
  Plate
  OK
MAIN
    
```

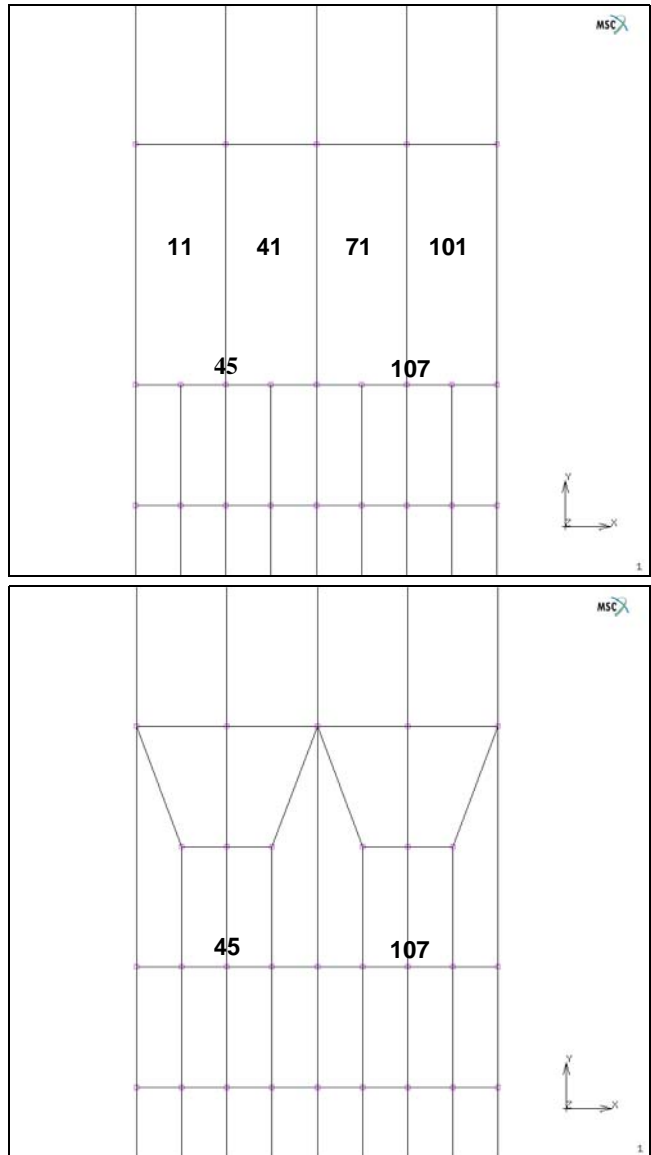


Figure 3.34-2 FE-Mesh for Plate

```

crvs ADD
  2
  6
CURVE TYPE
  CENTER/RADIUS/ANG/ANG
  RETURN
crvs ADD
  0.02 0 0
  0.02
  0
  180
AUTOMESH
  2D PLANAR MESHING
  QUADRILATERALS
    20 20
  QUAD MESH!
  all: EXIST.
  SELECT
  elements STORE
    Ball
  OK
  all: UNSEL.
  CLEAR SELECT
  ID SETS
  MAIN
MESH GENERATION
  RENUMBER
    ALL
  MAIN
  
```

(center)
 (radius)
 (angle)
 (angle)

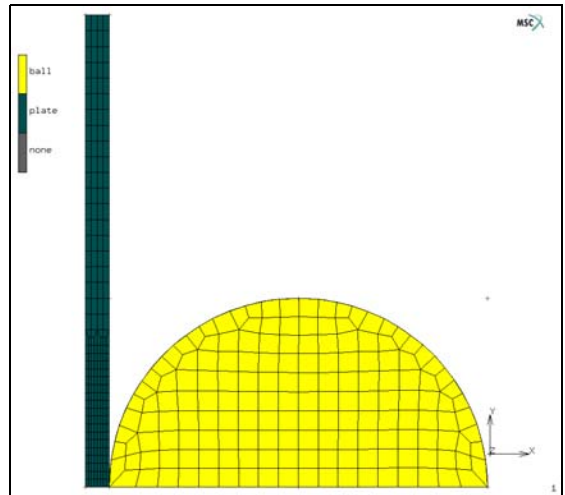
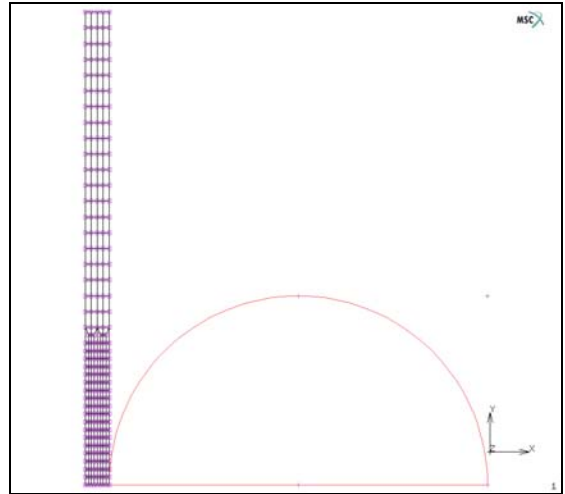


Figure 3.34-3 FE-Mesh for Ball

Boundary Conditions

Boundary conditions are defined to clamp the plate and to introduce symmetry conditions.

BOUNDARY CONDITIONS

MECHANICAL

NAME

Clamped

FIXED DISPLACEMENT

DISPLACEMENT X

(on)

DISPLACEMENT Y

(on)

OK

nodes ADD

3 4 64 95 126

| End of List

NEW

NAME

Symmetry

FIXED DISPLACEMENT

DISPLACEMENT Y

(on)

OK

nodes ADD

1 2 34 65 96 157 193 221 249 420 421 422 423 424 425

426 427 428 429 430 431 432 433 434 435 436 437 438

END OF LIST (#)

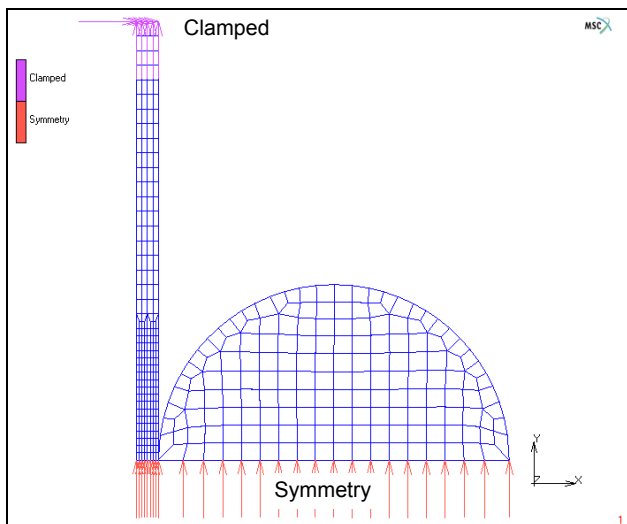


Figure 3.34-4 FE-Mesh and Boundary Conditions for Impact Problem

Material Properties

For the eigenvalue analysis, only linear elastic material properties are required; the complete material description is already defined where the hardening behavior is entered using tables of type plastic strain.

MATERIAL PROPERTIES

TABLES

NEW

1 INDEPENDENT VAR

NAME

Plate_hardening

TYPE

eq_plastic_strain

OK

ADD

0 7e6

1 21e6

function value f

MIN = 0

MAX = 8e8

NEW

1 INDEPENDENT VAR

NAME

Ball_hardening

TYPE

eq_plastic_strain

OK

ADD

0 2e8

1 8e8

FILLED

RETURN

NEW

NAME

Plate_material

ISOTROPIC

YOUNG'S MODULUS = 7e9

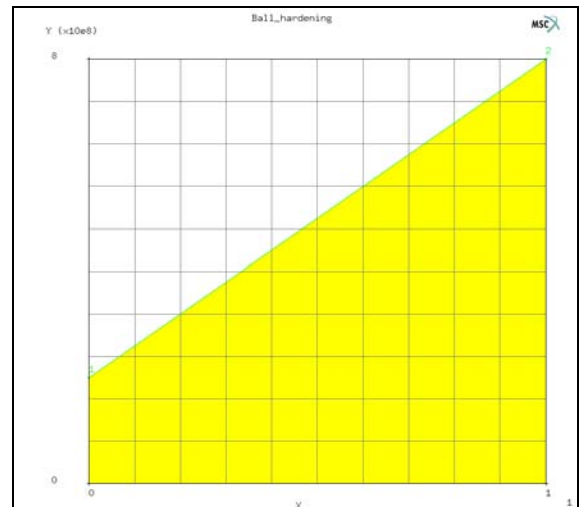
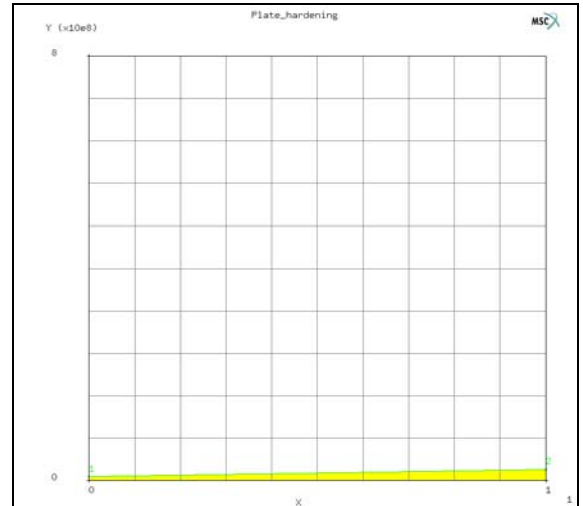


Figure 3.34-5 Hardening for Plate and Ball

POISSON'S RATIO = 0.3
 DENSITY = 2500.0
 ELASTIC-PLASTIC
 INITIAL STRESS = 1, TABLE = Plate_hardening
 OK (twice)

elements ADD *(select plate elements)*

NEW

NAME

 Ball_material

ISOTROPIC

 YOUNG'S MODULUS = 2e11

 POISSON'S RATIO = 0.3

 DENSITY = 7800.0

 ELASTIC-PLASTIC

 INITIAL STRESS = 1, TABLE = Ball_hardening

 OK (twice)

elements ADD *(select ball elements)*

MAIN

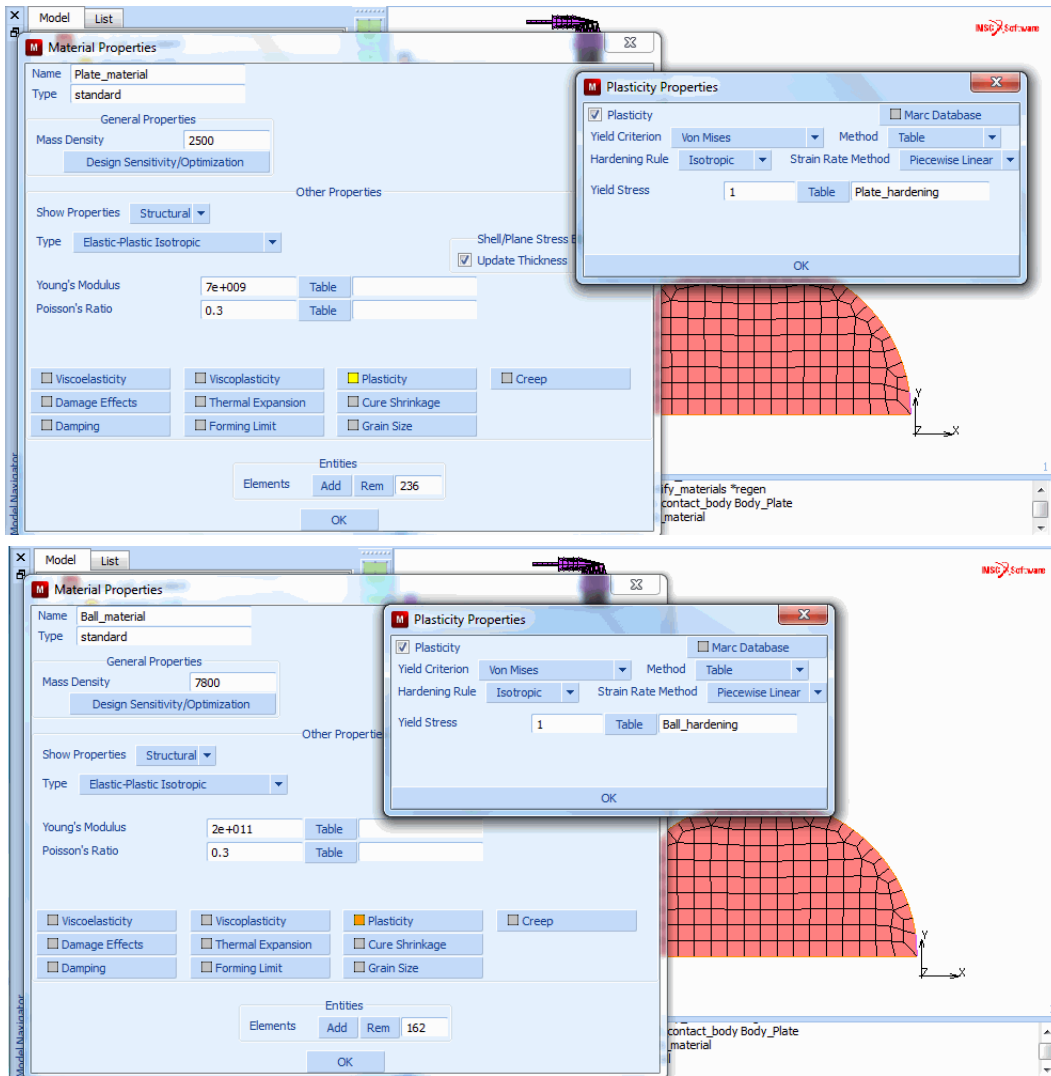


Figure 3.34-6 Material Properties of Plate and Ball

Loadcases

A dynamic modal mechanical load case is defined. The default Lanczos method is used. The lowest frequency is set to 10 Hz, 20 modes are asked for and since the ball still has one rigid body mode, the non-positive definite option is activated.


```

LOADCASES
  NAME
    Modal_analysis
  MECHANICAL
    DYNAMIC MODAL
    LOWEST FREQ.= 10
    # MODES = 20
    NON-POS. DEFINITE
    OK
  MAIN
  
```

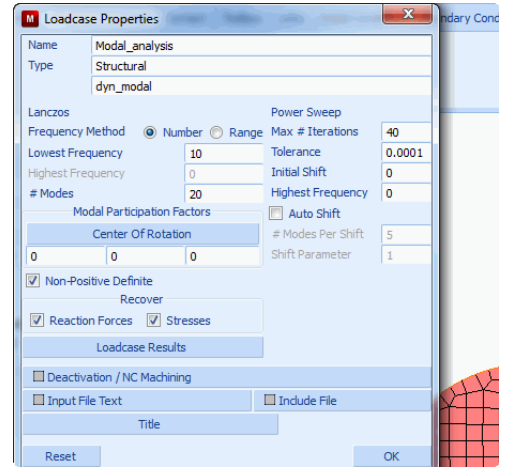


Figure 3.34-7 Modal Loadcase

Jobs

A mechanical job is defined, in which the previously defined load case is selected. The lumped mass matrix option is activated and the element type is set to 10. The model is saved and the job submitted.

```

JOBS
  NAME
    Modal
  MECHANICAL
    Modal_analysis
    AXISYMMETRIC
    ANALYSIS OPTIONS
    LUMPED
    OK (twice)
  FILES
    SAVE AS
    plate_ball_modal
    OK
  RETURN
  RUN
    SUBMIT 1
    MONITOR
  
```



Figure 3.34-8 Job Submit

Results

The post file is opened. Using the scan option, you can easily get an overview of the eigenfrequencies. A couple of eigenmodes are visualized. [Figure 3.34-9](#) shows the first eigenmode and corresponding eigenfrequency.

```
RESULTS
  OPEN DEFAULT
  DEFORMED SHAPE SETTINGS
    DEFORMATION SCALING
      AUTOMATIC
    RETURN
  DEF ONLY
NEXT
```

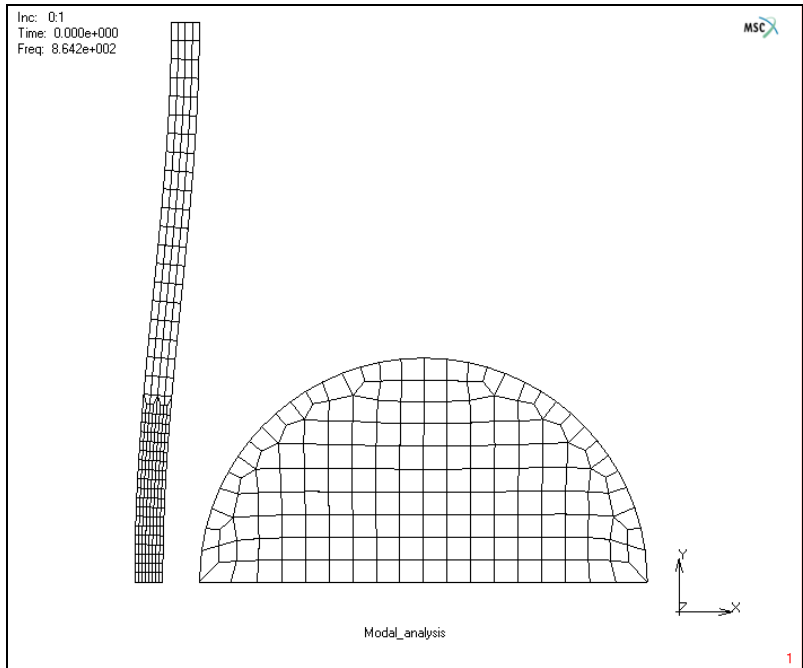


Figure 3.34-9 First Eigenmode

Transient Analysis

The results of the modal analysis clearly show that the eigenfrequencies of the plate are much lower than the eigenfrequencies of the ball. Based on the material properties, it may be assumed that the deformations mainly occur in the plate. If it is assumed that modes with frequencies up to that of the second eigenmode should be properly integrated, then the time step for the transient analysis can be estimated as $\Delta t = 1/15f = 1/(15 \times 3382) \approx 2 \times 10^{-5}$ seconds.

Model Generation

The finite element model is the same as used for the modal analysis.

```
FILES
  OPEN
    plate_ball.mud
  OK
  SAVE AS
    plate_ball_transient
  OK
  MAIN
```

Boundary Conditions

The boundary conditions are the same as used for the modal analysis.

Initial Conditions

All the nodes of the ball get an initial velocity of 2.5 m/s in negative x-direction.

```
INITIAL CONDITIONS
  NAME = Initial_velocity
  MECHANICAL
    VELOCITY
      VELOCITY X (on)
        -2.5
    OK
  SELECT
    SELECT BALL
    OK
  MAKE VISIBLE
  RETURN
```

```
nodes ADD
all: VISIBLE
SELECT
    MAKE
    INVISIBLE
    MAIN
```

Contact Bodies

Two deformable bodies are defined: one for the plate and one for the ball. Since in the area of contact the plate has a finer mesh than the ball, the plate is the first body. For the ball, the analytical description is used in order to get a smooth, accurate description of its boundary.

```
CONTACT
CONTACT BODIES
    NAME = Body_Plate
    DEFORMABLE,
    OK
elements ADD
    Plate
NEW
NAME
    Body_Ball
DEFORMABLE
OK
elements ADD
    Ball
BOUNDARY DESCRIPTION ANALYTICAL
    nodes ADD
        420 438
    END OF LIST (#)
ID CONTACT, MAIN
```

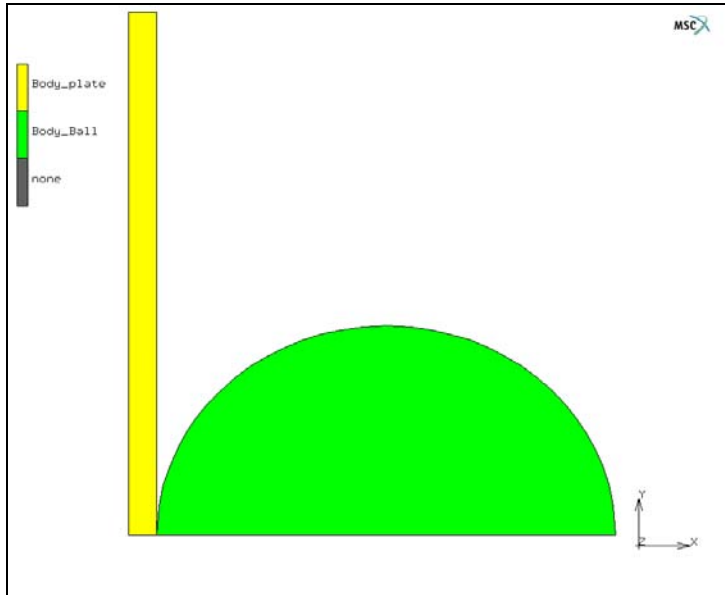


Figure 3.34-10 Contact Bodies

Material Properties

The material properties are already entered for the modal analysis.

Loadcase

The loadcase of the modal analysis is removed and a new loadcase for a transient dynamic analysis is defined. A total time of 0.006 seconds are analyzed in 400 equally sized steps, corresponding to a time step of 1.5×10^{-5} second as per our desire to properly integrate frequencies in the range of the second eigenmode.

LOADCASES

MECHANICAL

REM

NAME = Dynamic_transient

DYNAMIC TRANSIENT

SOLUTION CONTROL

MAX # RECYCLES = 20

NON-POSITIVE DEFINITE

(on)

PROCEED WHEN NOT CONVERGED

(on)

OK

TOTAL LOAD CASE TIME = 0.006

FIXED # STEPS = 400
OK
MAIN

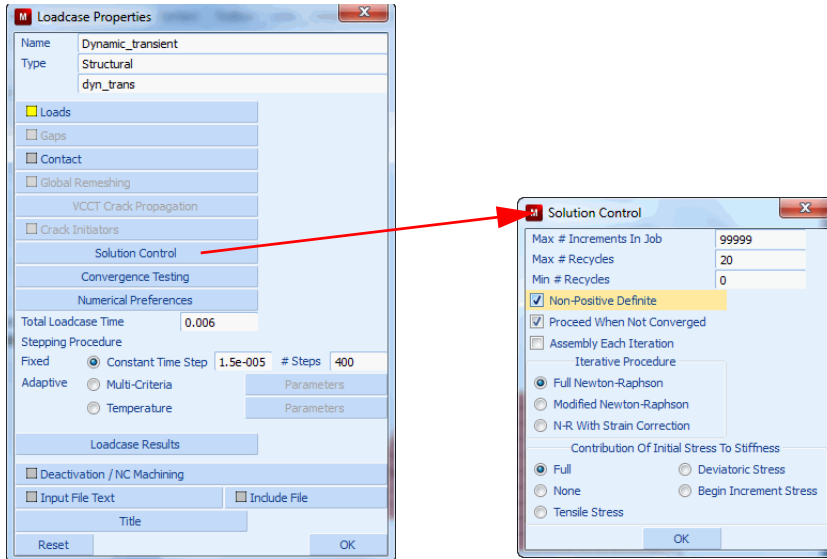


Figure 3.34-11 Dynamic Transient Loadcase

Jobs

The previously defined load case is used in the mechanical job. The initial conditions are activated. Notice that the Single Step Houbolt method is the default time integration method in Mentat. A distance tolerance bias factor of 0.9 is entered and the iterative increment splitting option is selected. The large strain plasticity method using the additive decomposition and the constant dilatation option is activated, since relatively large plastic deformations are to be expected. As post file element variables the equivalent von Mises stress and the total equivalent plastic strain are selected and as nodal variables the displacements, velocities, accelerations and contact normal forces. The model is saved and the job is submitted.

JOBS

MECHANICAL

NAME

Dynamic_transient

INITIAL LOADS

Initial_velocity

(turn on)

OK

CONTACT CONTROL

DISTANCE TOLERANCE BIAS = 0.9
 INCREMENT SPLITTING ITERATIV
 OK
 ANALYSIS OPTIONS
 CONSTANT DILATATION (on)
 plasticity procedure
 LARGE STRAIN ADDITIVE (on)
 OK
 JOB RESULTS
 Equivalent Von Mises Stress
 Total Equivalent Plastic Strain
 NODAL QUANTITIES
 CUSTOM
 Displacement
 Velocity
 Acceleration
 Cont_Nor_Force
 OK (twice)
 SAVE
 RUN
 SUBMIT 1
 MONITOR

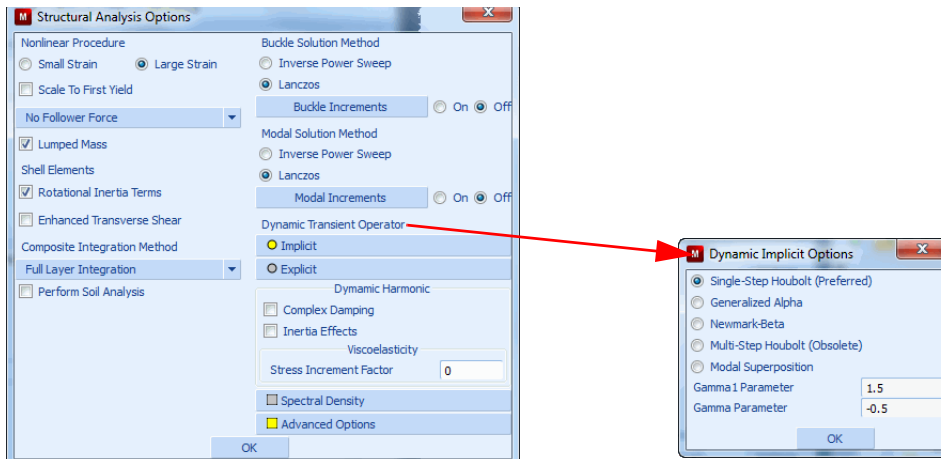


Figure 3.34-12 Default Houbolt Operator

Note: The default transient dynamic operator set in Mentat is the new Single Step Houbolt operator.

Results

The post file is opened and the equivalent plastic strain in the final deformed configuration is plotted. This is shown in [Figure 3.34-13](#). History plots of the velocity of the center of ball and the displacement of the center of the plate are indicated in [Figure 3.34-14](#) and [Figure 3.34-15](#). [Figure 3.34-15](#) shows a low-amplitude vibration with a time period of approximately 8.5×10^{-4} seconds which can accurately be captured with the chosen time step.

RESULTS

OPEN DEFAULT

DEFORMED SHAPE SETTINGS

DEFORMATION SCALING

MANUAL

RETURN

DEF ONLY

SCALAR

Total Equivalent Plastic Strain

OK

CONTOUR BANDS

MONITOR

OK

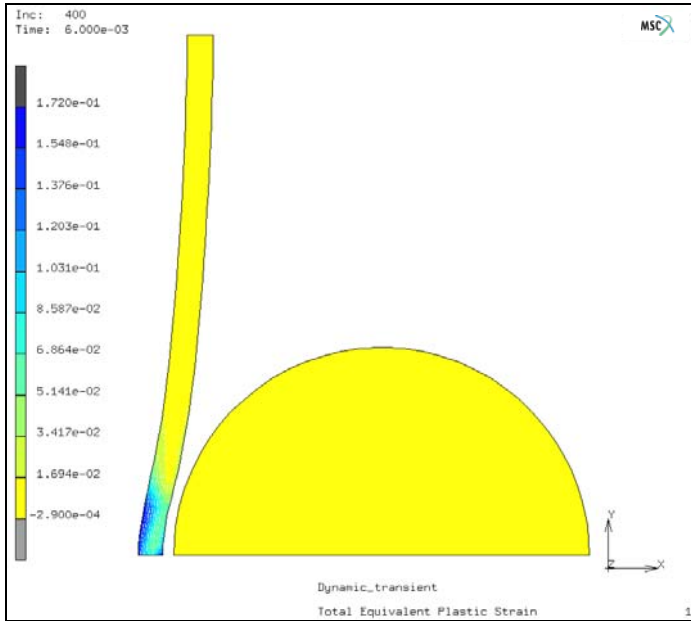


Figure 3.34-13 Equivalent Plastic Strain in Deformed Configuration at Increment 400

HISTORY PLOT

SET NODES

429 85

END LIST

COLLECT DATA

0 400 1

NODES/VARIABLES

Add 1-NODE CURVE

429

Time

Velocity X

OK

FIT

YMIN = -3

YMAX = 1

SHOW IDS 0

(none)

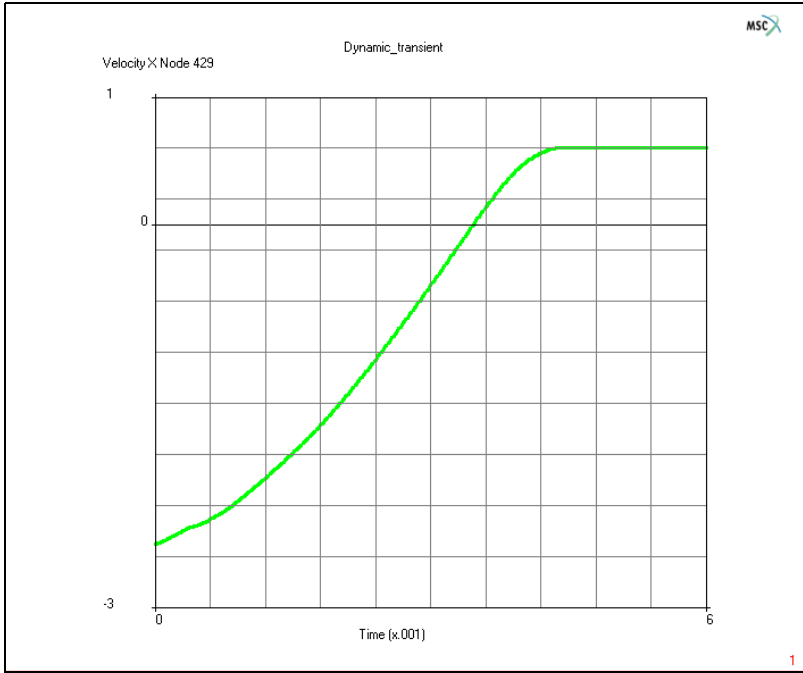


Figure 3.34-14 Velocity of Center of Ball as a Function of Time

```
CLEAR CURVES
NODES/VARIABLES
  Add 1-NODE CURVE
    85
    Time
    Displacement X
    OK
    FIT
    YMIN = -5.5
    YMAX = 0
```

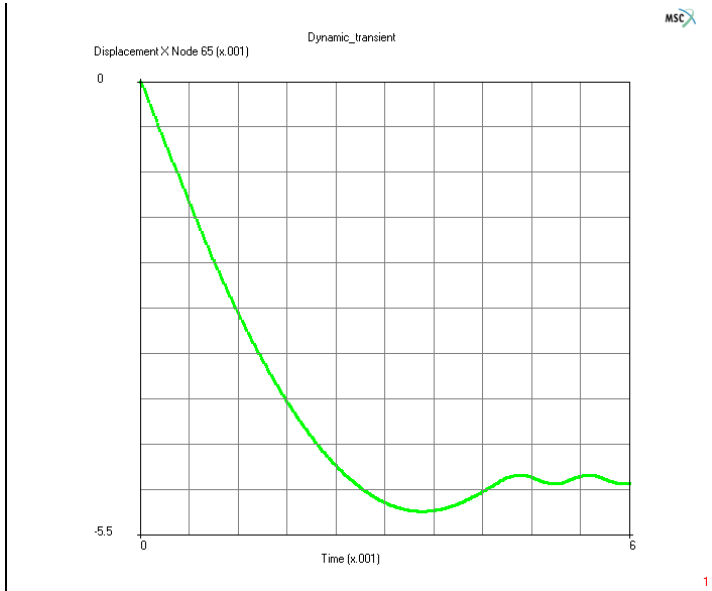
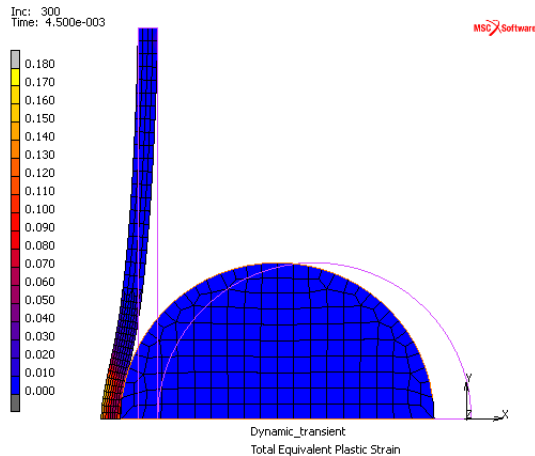
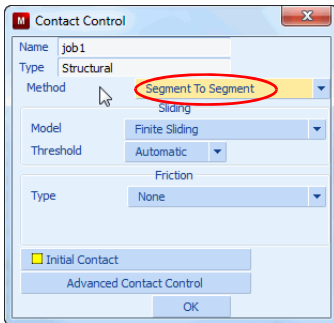


Figure 3.34-15 Displacement of Center of Plate as a Function of Time

You may wish to run Mentat procedure files that are in the *examples/marc_ug* subdirectory under Mentat. The procedure files `modal.proc` and `transient.proc` builds, runs, and postprocesses the modal and transient jobs, respectively.

As an alternative, one can use the segment-to-segment contact method with this model. In this case, double-sided contact is used. This capability is activated using the Job Contact Control menu as shown below. The equivalent plastic strain is shown on the plate after being impacted by the ball.



Equivalent Plastic Strain using Segment-to-segment Contact

Input Files

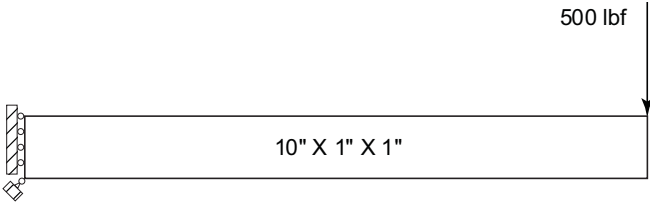
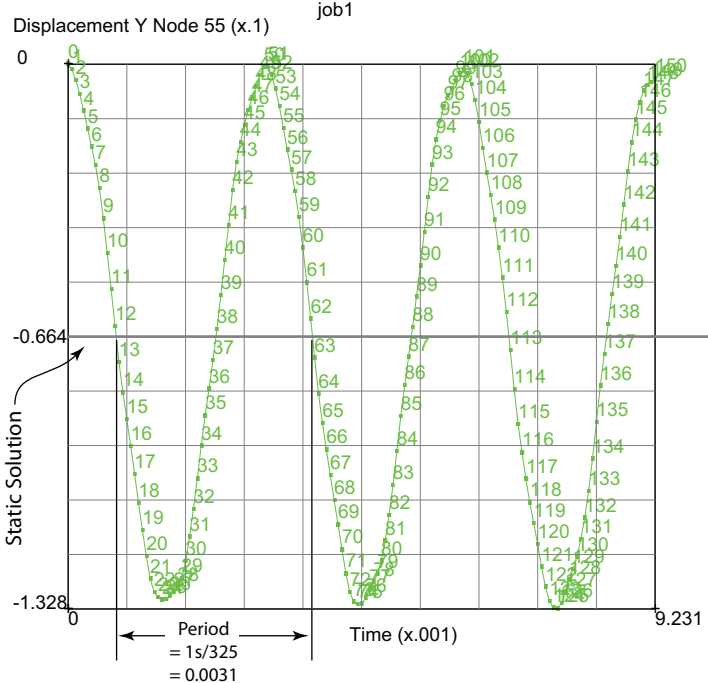
The files below are on your [delivery media](#) or they can be downloaded by your web browser by clicking the links (file names) below.

File	Description
modal.proc	Mentat procedure file
transient.proc	Mentat procedure file
plate_ball.mud	Mentat model file

3.35 Dynamic Analyses of a Cantilever Beam

- Summary 1662
- Modal Analysis 1663
- Harmonic Analysis 1666
- Transient Analysis 1669
- Input Files 1677

Summary

Title	Dynamic analysis of a cantilever beam
Problem features	Static, modal, harmonic and transient with contact
Geometry	
Material properties	$E = 30.0 \times 10^6$ Psi, $\nu = 0.3$, $\rho = 7.33161 \times 10^{-4}$ lbf s ² /in ⁴
Analysis type	Static, modal, harmonic and transient with contact
Boundary conditions	Cantilever with tip load
Element type	Plane stress element type 3
FE results	<p>Characterize static and dynamic response</p> 

Modal Analysis

Overview

A modal analysis of a cantilever beam (Figure 3.35-1) determines its natural frequencies.

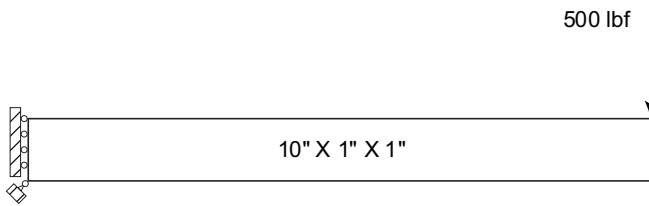


Figure 3.35-1 Beam Dimensions and Load

The end load is turned off prior to the modal analysis. The effects of pre-stress, if present, change the natural frequencies, like the tension in a guitar string. However, it is not modeled here.

The ten lowest natural frequencies and corresponding mode shapes were requested. Here, the mode shape of the lowest natural frequency of 325 Hz is shown with displacements automatically magnified (Figure 3.35-2). As expected, it shows “easy wise bending”.

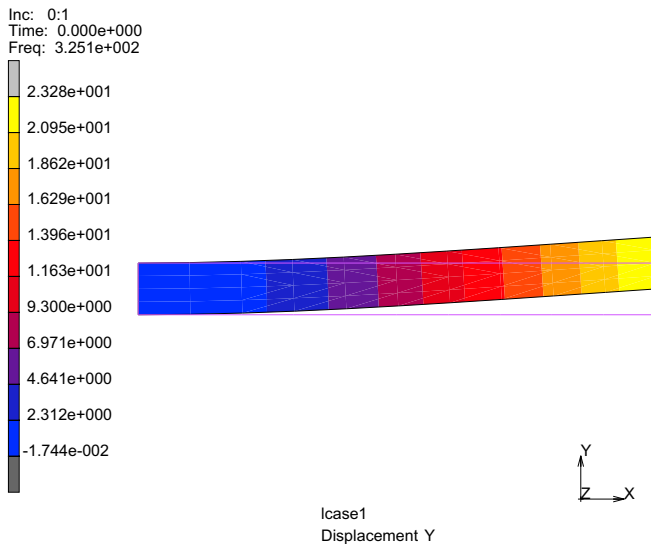
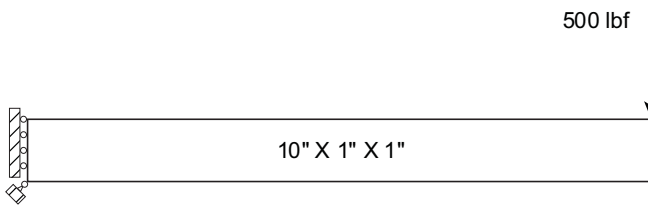


Figure 3.35-2 1st Bending Mode of Vibration

Modal Analysis

The cantilever beam used in the static analysis of [Chapter 3.18: Cantilever Beam](#) starts the modeling; using the same geometry and material, the procedures will be modified to perform a modal analysis.



FILES

OPEN

d1.mud

SAVE AS

d11

OK

LOADCASES

MECHANICAL

DYNAMIC MODAL

OK

MAIN

JOBS

TYPE: MECHANICAL

PROPERTIES

SELECT Icase1

INITIAL LOADS

turn off point load

OK

OK

RUN

SUBMIT1

OK

SAVE

OPEN POST FILE (RESULTS MENU)

NEXT

DEFORMED SHAPE SETTINGS

DEFORMATION SCALING AUTOMATIC
 OK
 DEF & ORIG
 CONTOUR BAND
 SCALAR
 DISPLACEMENT Y, OK
 SCAN

Inc	Time	Freq	Size
<input type="radio"/> 0	0	0	40
<input checked="" type="radio"/> 0:1	0	325.073	40
<input type="radio"/> 0:2	0	1995.23	40
<input type="radio"/> 0:3	0	5060.47	40
<input type="radio"/> 0:4	0	5444.88	40
<input type="radio"/> 0:5	0	10330.9	40
<input type="radio"/> 0:6	0	15292.7	40
<input type="radio"/> 0:7	0	16497.6	40
<input type="radio"/> 0:8	0	23702.8	40
<input type="radio"/> 0:9	0	25970.1	40
<input type="radio"/> 0:10	0	32157.1	40

Update OK

Figure 3.35-3 1st Bending Mode of Vibration at 325 Hz

Harmonic Analysis

Overview

A harmonic analysis of a cantilever beam determines the dynamic response of the cantilever beam to an oscillating tip load with a 500 pound magnitude. The end load is turned on in the harmonic loadcase, and the range of excitation frequencies is 0 to 400 Hz, in 40 steps of 10 Hz.

The figure below (Figure 3.35-4) plots the tip displacement magnitude along the frequency range. It contains the static solution at 0 Hz, the resonance around the first natural frequency of 325 Hz, and ends with a phase reversal above 325 Hz.

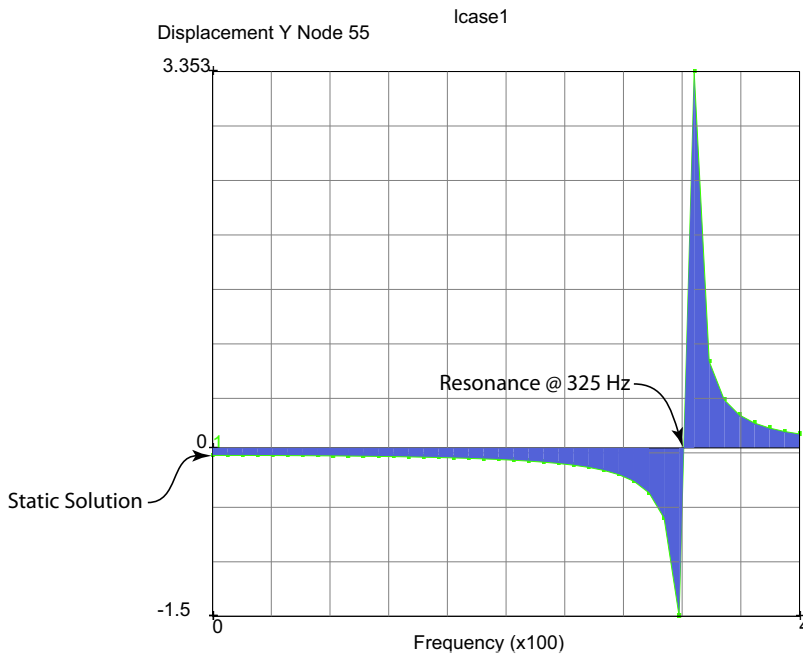


Figure 3.35-4 Harmonic Response Summary

Harmonic Analysis and Results

- FILES
- OPEN
- d1.mud
- SAVE AS
- d12
- OK

```

MAIN
BOUNDARY CONDITIONS
MECHANICAL
EDIT apply3, OK
    HARMONIC BC
        POINT LOAD (view load magnitude)
        OK
MAIN
LOADCASES
MECHANICAL
DYNAMIC HARMONIC
LOADS (set harmonic point load on)
OK
LOWEST FREQ
    0
HIGHEST FREQ
    400
# OF FREQ'S
    40
    OK
MAIN
JOBS
TYPE MECHANICAL
PROPERTIES
    SELECT lcase1, OK
RUN
SUBMIT1
OK
SAVE
OPEN POST FILE (RESULTS MENU)
HISTORY PLOT
SET LOCATIONS
    n:55 # (pick the one with point load)
INC RANGE
0:0 0:40 1 (colon separates increment and sub increment)
ADD CURVES
    ALL LOCATIONS
        Frequency
        Displacement Y
FIT
    
```

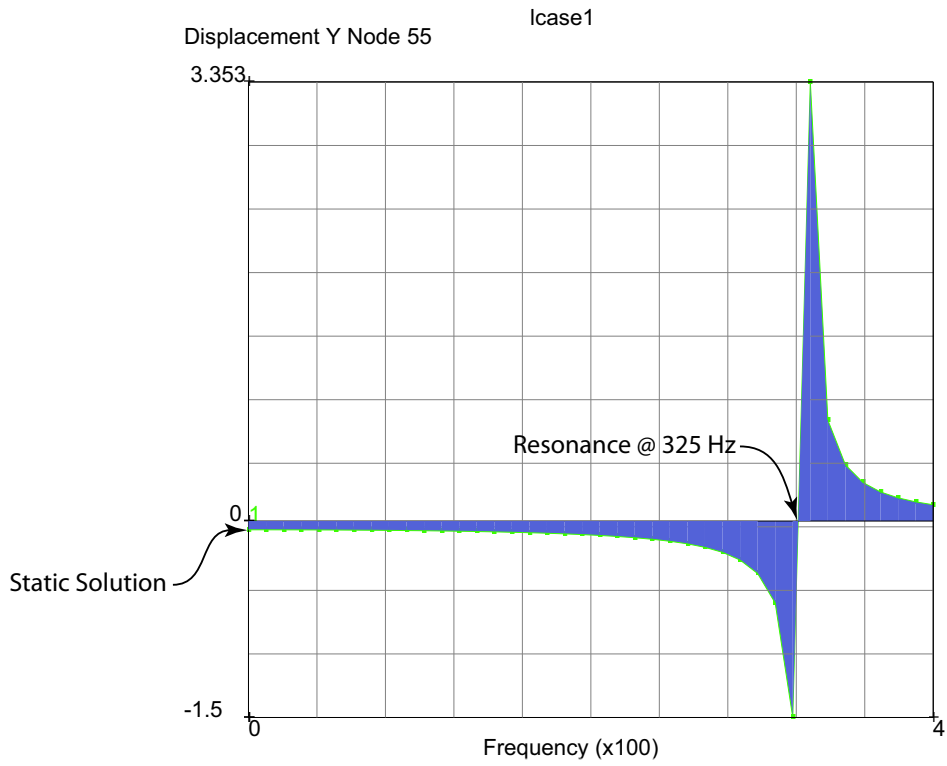


Figure 3.35-5 Harmonic Response 0 to 400 Hz

Transient Analysis

Overview

The dynamic response continues for a cantilever beam initially at rest subjected to a constant tip load of 500 pounds after $t=0$. We shall find that the kinetic energy will be bounded by the total strain energy of the static solution discussed in [Chapter 3.18: Cantilever Beam](#). The dynamic transient loadcase time period is set to $3/(325 \text{ Hz})$ to get three cycles of response. Plotting the tip displacement along the time axis shows the tip oscillating about the static solution.

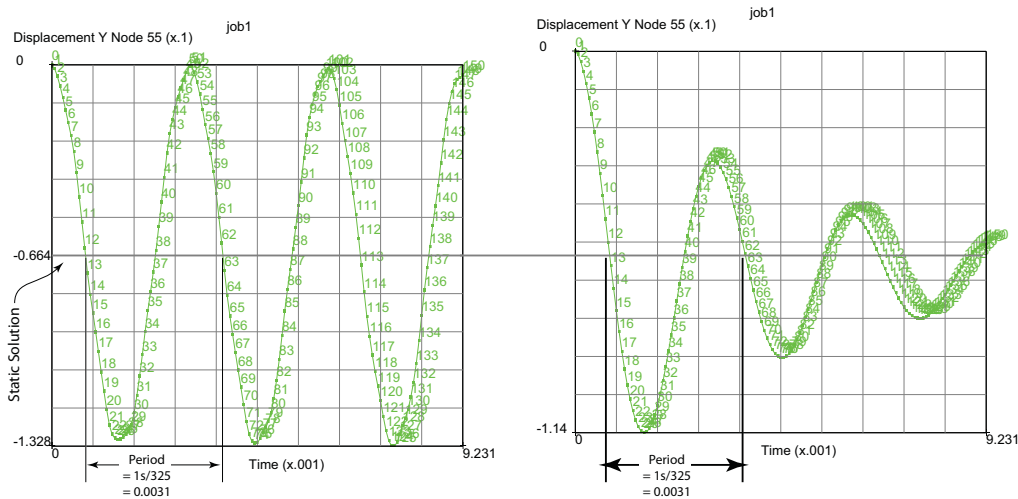


Figure 3.35-6 Transient Response Summary

The second run includes damping; the tip displacement along the time axis plot shows the tip oscillating about the static solution with the oscillations diminishing with time.

Analysis and Results

The cantilever beam used in the static analysis of [Chapter 3.18: Cantilever Beam](#) starts the modeling; using the same geometry and material, the procedures will be modified to perform a transient analysis.

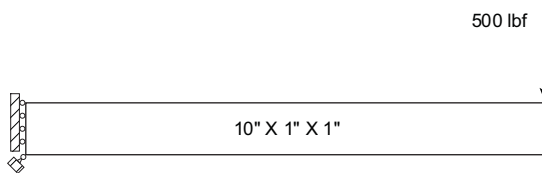


Figure 3.35-7 Transient Response with Contact: Problem Description

FILES

OPEN

d1.mud

SAVE AS

d14

OK

MAIN

LOADCASE

MECHANICAL

DYNAMIC TRANSIENT

TIME

3 / 325

(remember 1st natural frequency)

STEPS

150

OK

MAIN

JOBS

TYPE: MECHANICAL

PROPERTIES

SELECT lcase1

OK

SAVE

RUN

STYLE: OLD

(use old style table input)

SUBMIT1

MONITOR

OK

MAIN

RESULTS

OPEN DEFAULT

HISTORY PLOT

SET LOCATIONS

n:55 #

(pick the one with point load)

ALL INCS

ADD CURVES

ALL LOCATIONS

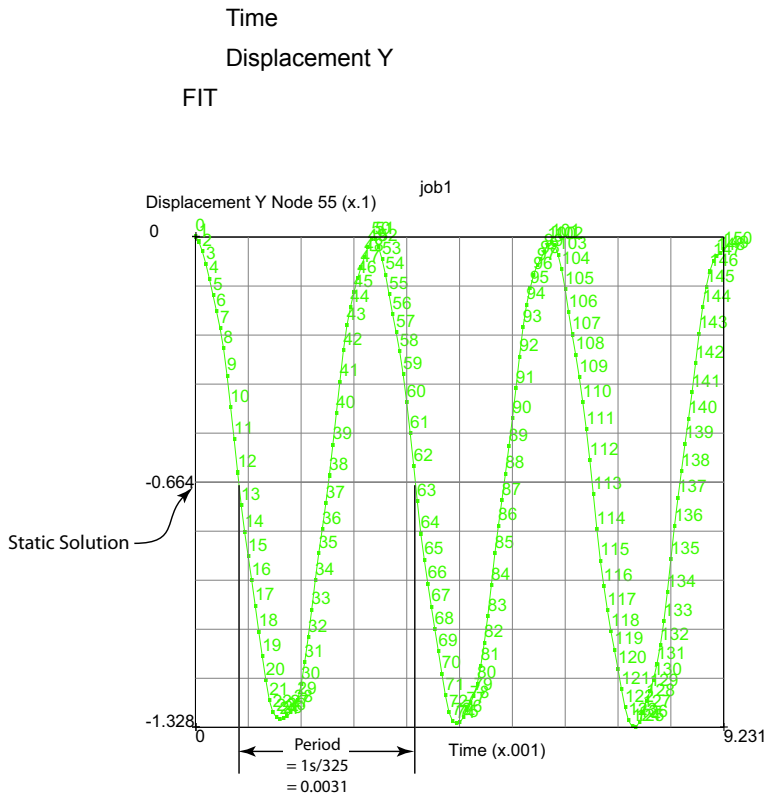


Figure 3.35-8 Transient Response at Cantilever Beam

Damping Analysis

What about damping? Physically, we know it is present. Let's see how to model with damping.

FILES

OPEN

d14.mud

SAVE AS

d15

OK

MAIN

MATERIAL PROPERTIES (twice)

STRUCTURAL

DAMPING (twice)

```
STIFFNESS MATRIX MULTIPLIER
1E-4
OK (twice)
SAVE
MAIN
JOBS
RUN
SUBMIT1
MONITOR
RESULTS
OPEN DEFAULT
HISTORY PLOT
SET LOCATIONS
ALL INCS
ADD CURVES
ALL LOCATIONS
Time
Displacement Y
FIT
```

(pick the one with point load)

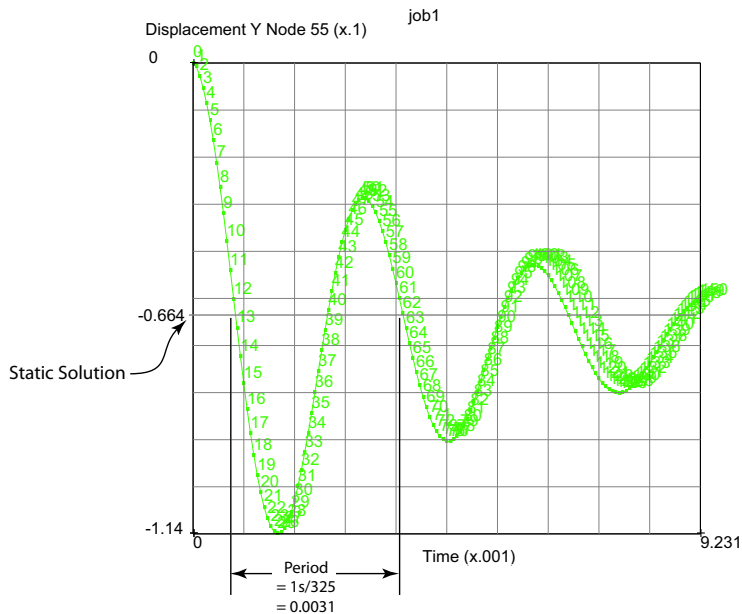


Figure 3.35-9 Transient Response with Damping

Over Hanging Beam Analysis

Now we assume the beam overhangs a rigid bumper; the beam contacts the bumper only on the way down and separates from the bumper when displacing upward. The beam is rest and the load is placed on the end at time $t=0$. Again, the kinetic energy is bounded by the total strain energy of the static solution discussed in [Chapter 3.18: Cantilever Beam](#). An analogous loading scheme would be to displace the tip upward with a 500 pound load then release the beam, the initial potential energy exchanges with the kinetic energy keeping the total energy constant since the beam to bumper contact is elastic. Since this analysis involves dynamic contact, instead of the Newmark-Beta operator, the Single Step Houbolt operator will be used. This operator will damp out high frequency oscillations introduced by suddenly changing contact conditions.

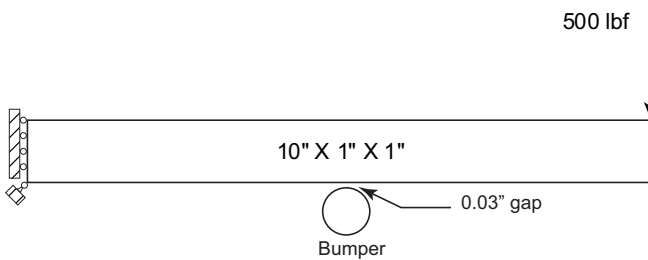


Figure 3.35-10 Beam over Rigid Bumper

```

FILES
  OPEN
    d1.mud (start with modal model)
  SAVE AS
    d16
  OK
  MAIN
  MESH GENERATION
    CURVE TYPE, CIRCLE: CENTER, RADIUS
    RETURN
    CRVS: ADD
      5 0 0
      .2
  MOVE
    TRANS.
      0 -.23 0
    CURVES
    ALL: EXISTING
  MAIN
    
```

CONTACT

CONTACT BODIES

DEFORMABLE,
OK

ELEMENTS: ADD,
ALL: EXISTING

NEW

RIGID, OK

2-D CURVES ADD

ALL: EXISTING

MAIN

LOADCASES

MECHANICAL

DYNAMIC TRANSIENT

SOLUTION CONTROL

ASSEMBLY EACH ITERATION

OK

CONVERGENCE TESTING

RELATIVE FORCE TOLERANCE

0.001

OK

TOTAL LOADCASE TIME = 3/325

MULTI-CRITERIA: PARAMETERS

INITIAL FRACTION OF LOADCASE TIME = 1E-6

MINIMUM FRACTION OF LOADCASE TIME = 1E-7

MAXIMUM FRACTION OF LOADCASE TIME = 3E-4

DESIRED # RECYCLES/INCREMENT: SET = 3

AUTOMATIC CRITERIA (on)

OK (twice)

MAIN

JOBS

PROPERTIES

lcase1

CONTACT CONTROL

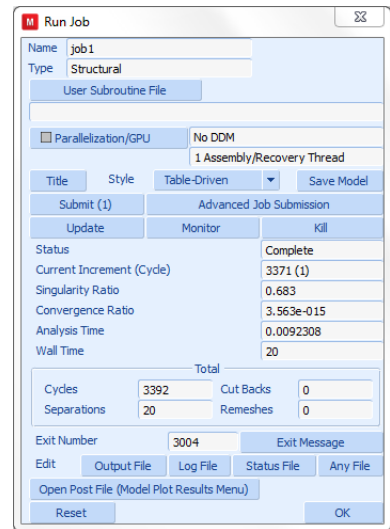
ADVANCED CONTACT CONTROL

DISTANCE TOLERANCE

```

        .003
    BIAS
        0.9
    OK (twice)
ANALYSIS OPTIONS
    DYNAMIC TRANSIENT OPERATOR IMPLICIT
        SINGLE-STEP HOUBOLT (Preferred)
        OK (thrice)

SAVE
    RUN
    SUBMIT(1)
    MONITOR
    OK (twice)
RESULTS
    OPEN DEFAULT
        HISTORY PLOT
        SET LOCATIONS
            n:26 n:55 #
        ALL INCS
        ADD CURVES
            ALL LOCATIONS
                Time
                Displacement Y
            FIT
        SHOW ID: 100
    
```



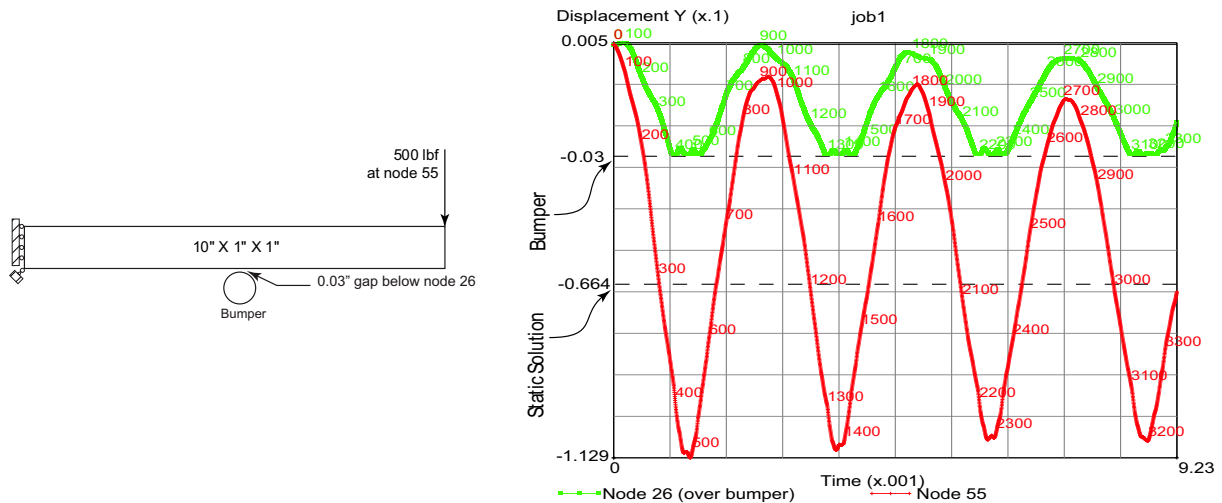


Figure 3.35-11 Transient Response: Overhang Beam with Contact

Vertical motion of node 26 (over bumper) is limited by the rigid body and contact of the beam with the rigid body increases the frequency content of the response. The dominant periods of the tip and mid span displacements shorten showing a higher frequency. From the modal analysis, the second mode has a frequency of 1995.23 (see Figure 3.35-3) approximately six times higher than the first mode. The time period in Figure 3.35-11 would have only three cycles as shown in Figure 3.35-6 without contact. There are about four repetitions above indicating a higher frequency.

CLEAR CURVES

ADD CURVES

GLOBAL

Time

Kinetic Energy

FIT

The kinetic energy history of the transient response is shown in Figure 3.35-12, it has nearly eight cycles during the total time period which is close to the nine cycles we have seen in the second mode shape without contact. Clearly, mid span beam contact with the bumper increases the frequency with the second mode becoming more dominant. Furthermore, we can estimate the amplitude of the kinetic energy from the static analysis in Chapter 3.18: Cantilever Beam. The total strain energy is simply half the product of the force (500 lbf) times the tip displacement (6.692×10^{-2} in) or some 16.7 lbf-in; this is close to the amplitude of the kinetic energy history.

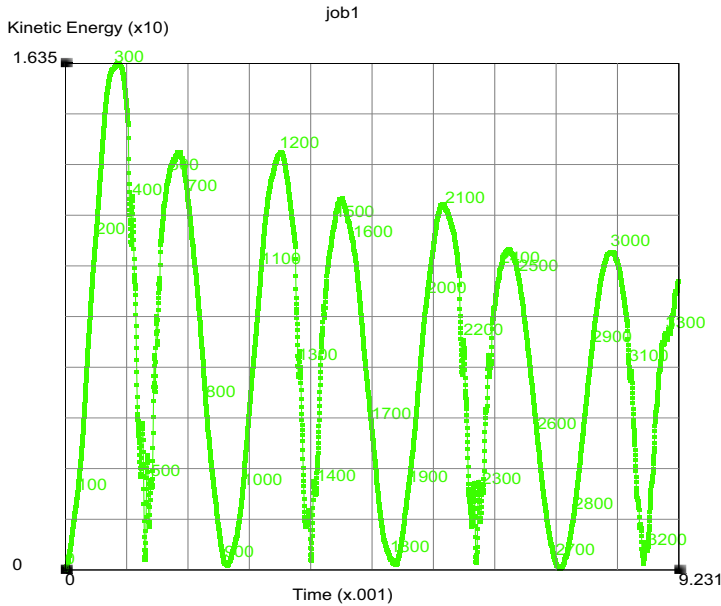


Figure 3.35-12 Kinetic Energy History for Overhang Beam with Contact

Input Files

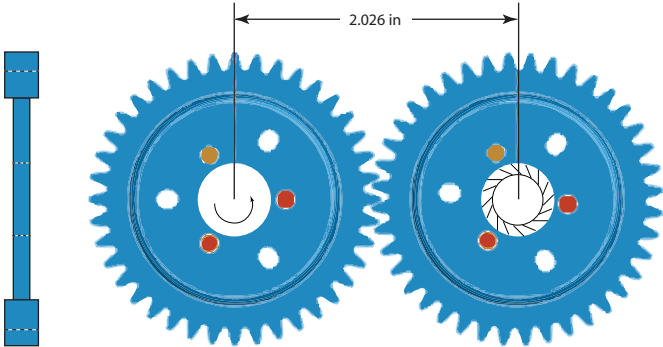
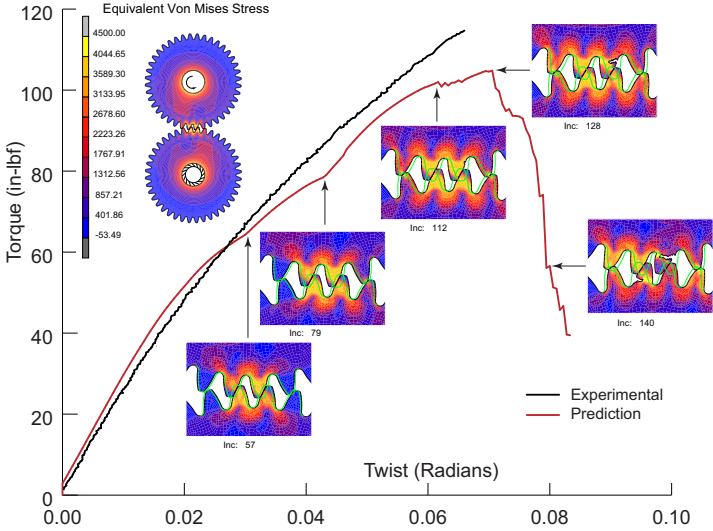
The files below are on your [delivery media](#) or they can be downloaded by your web browser by clicking the links (file names) below.

File	Description
d1.proc	Mentat procedure file
d2.proc	Mentat procedure file
d3.proc	Mentat procedure file
d1.mud	Mentat model file: static model
d11.mud	Mentat model file: modal analysis
d12.mud	Mentat model file: harmonic analysis
d14.mud	Mentat model file: transient analysis
d15.mud	Mentat model file: transient analysis with damping
d16.mud	Mentat model file: transient analysis with contact

3.36 Plastic Spur Gear Pair Failure

- Summary 1680
- Gear Geometry 1681
- Material Modeling 1682
- Contact 1682
- Failure Criteria 1683
- Experimental Test Machine 1687
- Results & Conclusions 1688
- Modeling Tips 1689
- Input Files 1690
- References 1690
- Animation 1690

Summary

Title	Plastic Spur Gear Pair Failure
Problem features	<ul style="list-style-type: none"> • Acetal copolymer gears in contact • UACTIVE user subroutine deactivates failed elements
Geometry	
Material Properties	Elastic-plastic
Analysis type	Quasi-static analysis
Boundary conditions	Rigid bodies inside shaft holes hold one gear fixed and rotate the other.
Element type	4-node plane strain element type 11 with variable thickness
FE results	<p>Predicted torque versus twist compared to experimental values.</p> 

An elastic-plastic finite element analysis of the quasi-static loading of two acetal copolymer gears in contact is preformed. Torque verses twist of the gear set is compared to actual experimental results. The gear geometry is modeled by plane strain elements with variable thickness between the rim and web. Gear tooth failure is modeled by deactivating elements when the plastic strain of 0.15 is exceeded in the tensile regions.

Gear Geometry

Two acetal copolymer spur gears were selected as test specimens. The geometry of the gear teeth was based on the American Gear Manufacturers Association (AGMA) standard: Tooth proportions for Plastic Gears ([Reference 1](#)). The entire gear pair is modeled to capture the correct torsional stiffness of the gear pair. The specifications for the test gears used are provided in the table below.

Basic Specification Data	
Number of Teeth	40
Diametric pitch	20
Standard pressure angle (degrees)	20
Tooth form	AGMA PT1
Standard addendum (inch)	.0500
Standard whole depth (inch)	.1120
Circular thickness on standard pitch circle (inch)	.250
Basic Rack Data	
Flank angle (degrees)	20
Tip to reference line (inch)	.0665
Tooth thickness at reference line (inch)	.250
Tip radius (inch)	.0214

The test gears were assembled at a center distance of 2.0620 inches. This gave a nominal backlash of 0.0320 inches. This relative large backlash permitted the test gears to reach relatively high torque levels without having the gear teeth roll back on each other, thereby making contact on the backside of the adjacent tooth. An illustration of the gear model (mesh lines included) assembly is shown in [Figure 3.36-1](#). The rim of the gear teeth is 0.25 inch (geom1) in thickness and the web thickness (geom2 and geom3) is 0.123.

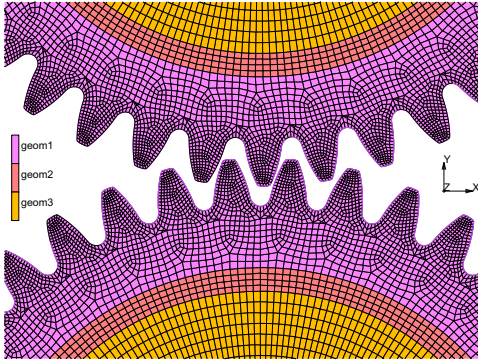


Figure 3.36-1 Geometry and Mesh

Material Modeling

The material is modeled as elastic-plastic with Young's modulus of 3.0×10^5 psi with an initial yield strength of 2500 psi. The Cauchy stress versus true plastic strain curve is shown in [Figure 3.36-2](#).

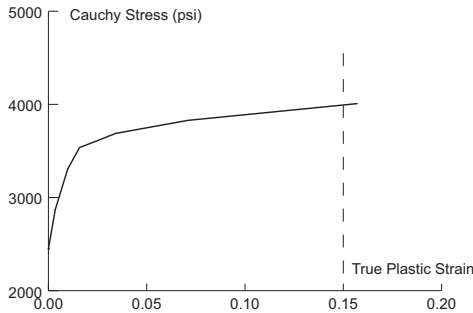


Figure 3.36-2 Material Behavior

Contact

The contact bodies are shown in [Figure 3.36-3](#) and two circular rigid bodies, drive1 and drive2, are glued to each gear, gear1 and gear2, respectively. Contact body drive1 rotates about the center of the gear while drive2 remains stationary. Two other rigid bodies (drive1out and drive2out) move just like drive1 and drive2, but are noncontacting rigid bodies via contact table. They appear on the post file to visualize where the teeth would be if they were rigid. Since kinematics for the design of a gear set assumes the gears to be rigid; it is convenient to see where the teeth would be if the gear material was rigid.

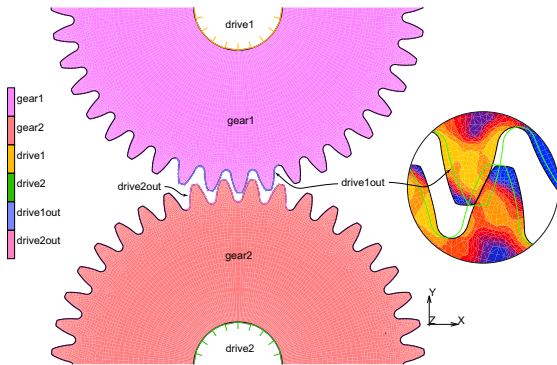


Figure 3.36-3 Contact bodies

Failure Criteria

Two user routines are used. The PLOTV user subroutine captures the total equivalent plastic strain and the mean stress and determines the elements to be deactivated when the mean stress is tensile (> 1000) and the plastic strain exceeds 15%. The ACTIVE user subroutine uses the information from PLOTV to actually deactivate the elements selected. The deactivated elements no longer participate in the analysis. The routines are listed below.

```

subroutine plotv(v,s,sp,etot,eplas,ecreep,t,m,nn,layer,ndi,
* nshear,jpltcd)
c* * * * *
c   define a variable for contour plotting (user subroutine).
c   v           variable to be put onto the post file
c   s (idss)    stress array
c   sp         stresses in preferred direction
c   etot       total strain (generalized)
c   eplas      total plastic strain
c   ecreep     total creep strain
c   t         array of state variable (temperature first)
c   m(1)       user element number
c   m(2)       internal element number
c   m(3)       material id
c   m(4)       internal material id
c   nn        integration point number
c   layer(1)   layer number
c   layer(2)   internal layer number
c   ndi       number of direct stress components
c   nshear    number of shear stress components
c   jpltcd    the absolute value of the user's entered post code
c* * * * *

```

```

      implicit real*8 (a-h,o-z)
      common /mydata/ ielem(30000)
      dimension s(*),etot(*),eplas(*),ecreep(*),sp(*)
dimension m(2),layer(2),t(2)
      kc=1
      call elmvar(18,m(1),nn,kc,v)
      call elmvar( 7,m(1),nn,kc,ve)
      if(nn.eq.1.and.ielem(m(1)).ne.1) ielem(m(1)) = 0
      if(v.ge.1.0d3.and.ve.ge.0.15d0 ) ielem(m(1)) = 1
      return
      end
      subroutine uactive(m,n,mode,irststr,irststn,inc,time,timinc)
c* * * * *
c      user routine to activate or deactivate an element
c
c      m(1)          - user element number
c      m(2)          - master element number for local adaptivity
c      n             - internal elsto number
c      mode(1)=-1   - deactivate element, remove element from post file
c      mode(1)=-11  - deactivate element, keep element on post file
c      mode(1)=2    - leave in current status
c      mode(1)=1    - activate element and add element to post file
c      mode(1)=11   - activate element and keep status on post file
c      mode(2)=1    - only activate/deactivate mechanical of coupled
c      mode(2)=2    - only activate/deactivate thermal part of coupled
c      mode(3)=0    - activation/deactivation at the end of increment
c      mode(3)=1    - activation/deactivation at the beg. of increment
c      irststr      - reset stresses to zero
c      irststn      - reset strains to zero
c      inc          - increment number
c      time         - time at beginning of increment
c      timinc       - incremental time
c* * * * *
      implicit real*8 (a-h,o-z)
      common /mydata/ ielem(30000)
      dimension m(2),mode(3)
      ie=m(1)
      if(ielem(ie).eq.1.and.mode(1).ne.-1) then
          mode(1)=-1
          write(96,*) 'deactivating element ', ie, ' increment ', inc
      else
          mode(1)=2
      end if
      return
      end
  
```

Model Review

The model is complete and ready to run; however, we shall review the CONTACT TABLE option used to glue the rigid bodies drive1 and drive2 onto gear1 and gear2, respectively, while making rigid bodies drive1out and drive2out noncontacting. Then we shall submit the results and check the results as they are generated.

FILES

OPEN

gearpair.mud

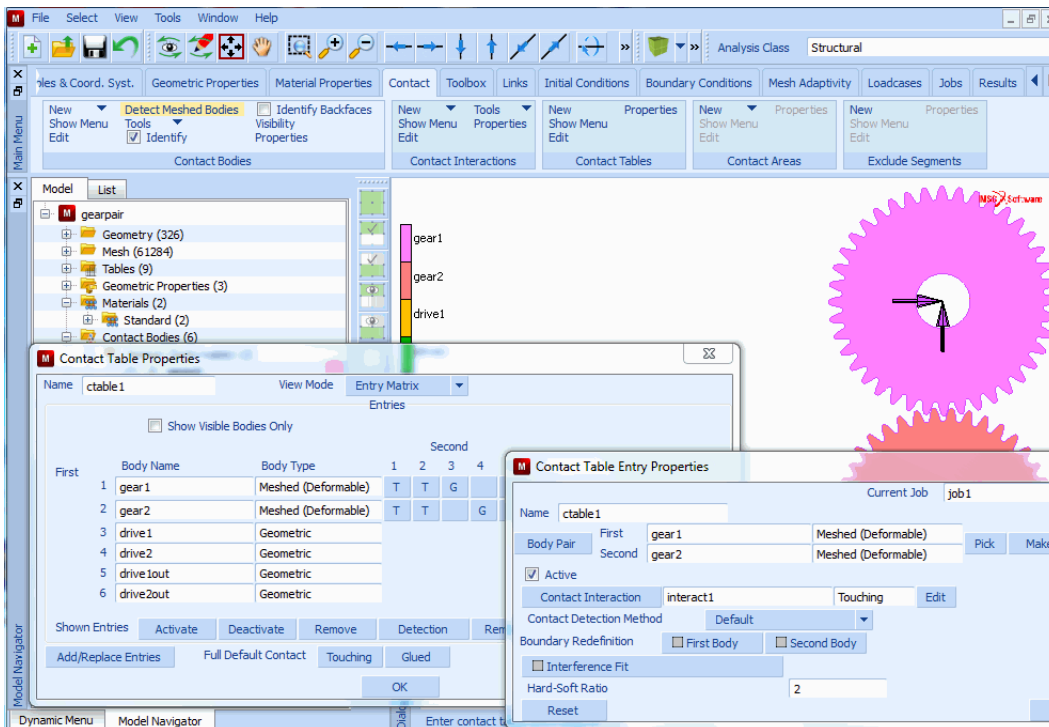
OK

MAIN

CONTACT

CONTACT TABLES

PROPERTIES



MAIN

JOBS

RUN

SUBMIT
OPEN POST FILE (RESULTS MENU)
DEF ONLY
SKIP TO INC 57
SCALAR (Equivalent von Mises Stress)
CONTOUR BANDS

As expected, the gears become engaged and deform as shown in [Figure 3.36-4](#). The noncontacting rigid bodies, drive1out and drive2out, are shown as green lines representing rigid gear motion making tooth deformation easy to visualize.

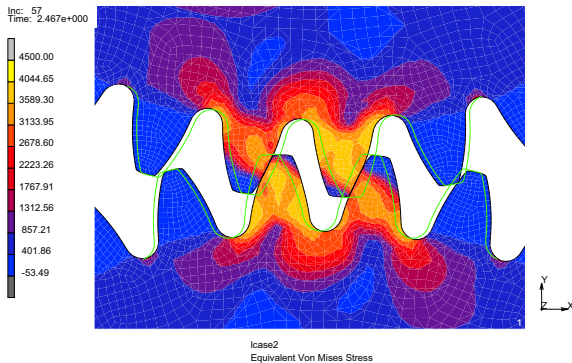
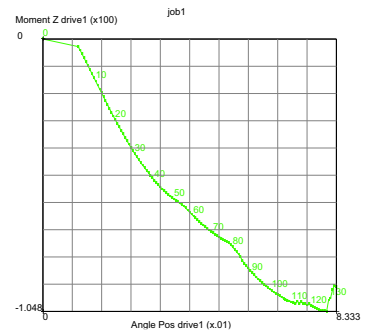


Figure 3.36-4 Contour Equivalent von Mises Stress at Increment 57

Another important plot is the torque versus twist which is generated by using the history plot feature as:

HISTORY PLOT
COLLECT GLOBAL DATA
NODES/VARIABLES
ADD GLOBAL CURVE
Angle Pos drive1
Moment Z drive1



The first load case brings the gears into contact at the end of increment 1 and this is seen here. Using the copy to clipboard, the history data can be exported to Excel and the data manipulated and compared to experimental results as seen in [Figure 3.36-7](#).

Experimental Test Machine

A parallel axis gear-testing machine developed by Ticona (www.ticona.com) was used to load and record the load-displacement response of the gears (Figure 3.36-5).

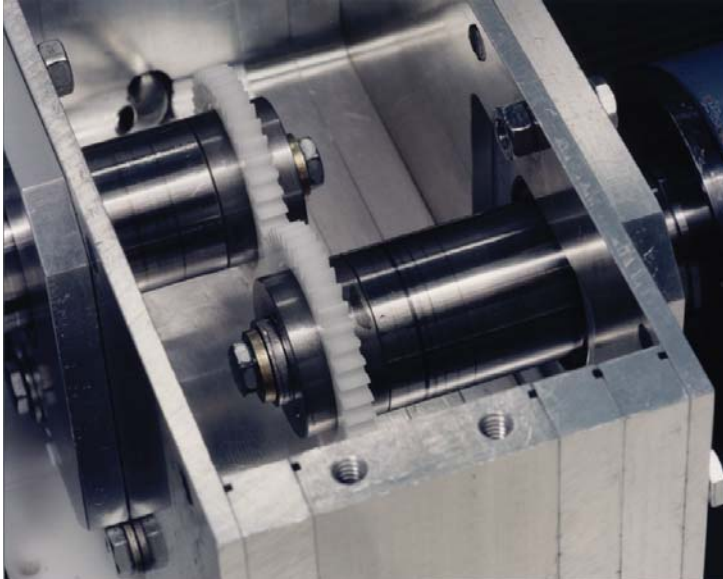


Figure 3.36-5 Parallel axis gear-testing machine

The test gears are lubricated with oil prior to loading to eliminate any shearing forces acting on the tooth flanks that are in contact. Torque is measured on the stationary side and load is applied on the motor side. Two high precision encoders are used to measure the angular displacement of both gears. These encoders have a positional accuracy of 57600 counts per revolution. The rate of loading is set by the time for encoder position on the motor side. The stationary is not totally rigid. It requires some angular displacement for the torque meter to record data. To obtain the true angular displacement, the relative displacement between both gears is recorded. This gives a rate for the relative angular displacement between the motor gear and stationary gear to be about 0.002 radians per minute. Five tests are made per gear set at ambient conditions. A plot of applied torques verses relative displacement is recorded. The results are shown in Figure 3.36-6. Test 2 and Test 4 did not reach tooth failure. This is due to that Test 4 was not taken up to the breaking torque and Test 2 reached the set limited encoder position before breaking.

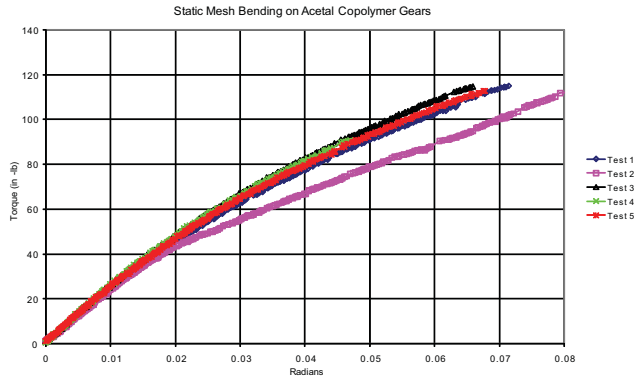


Figure 3.36-6 Plot of Experimental Results

Results & Conclusions

A plot of applied torque versus twist is made and gives excellent representation of the experimental results (Figure 3.36-7). At the beginning, a two teeth pair (on each gear) come into contact, then as these teeth bend, the tooth leading this pair begins to come into contact (Figure 3.36-7 Inc: 79). Later (Figure 3.36-7 Inc: 112) there are four teeth on each gear in contact with their counterparts. At increment 112, the first element is deactivated (leading tooth on top moving gear) followed by several more shown in increment 128. After increment 128, elements begin to fail in the stationary gear and the torque drops off dramatically. Based on the results of this analysis, the mechanical behavior and prediction of copolymer acetal gears is very complex. The results indicate that to optimize a gear set, a nonlinear analysis is required to be performed. Only under low loads and deformation can a linear elastic approach be suitable. Clearly, combining computer simulations with material and component testing has led to a far better understanding of copolymer acetal gear design; this understanding could not be achieved by either simulation or testing alone. It is envisioned that with a few more material tests, the torque-displacement response of the gear pair can be simulated with confidence thus advancing the technology of copolymer acetal gear applications.

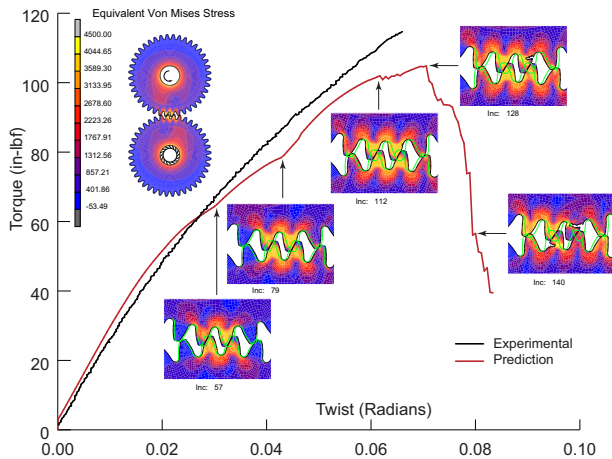
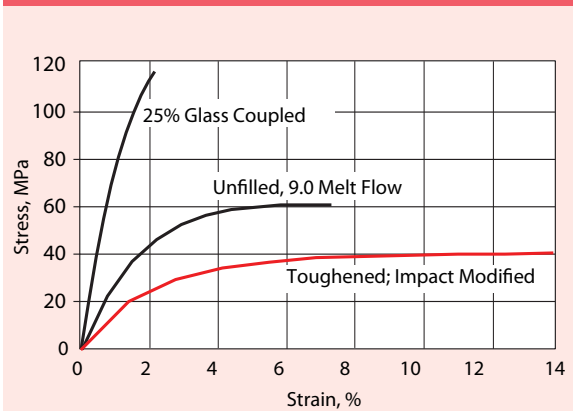


Figure 3.36-7 Predictions versus Experimental Results of Torque Versus Twist of the Gear Pair

Modeling Tips

The material used was Celcon grade M90 (Toughened; Impact Modified) which is the red curve taken from Reference 2, Figure 3.1 duplicated below.

Fig 3.1 · Celcon acetal copolymer stress-strain properties (ISO 527)



It was assumed that this stress strain data was in engineering measures of stress and strain (s, e) and they needed to be converted to true values, (σ, ϵ) where the Cauchy stress becomes, $\sigma = s(1 + e)$ and the true strain becomes, $\epsilon = \ln(1 + e)$. The work hardening plot (Figure 3.36-2) then becomes the Cauchy stress versus the total plastic strain, $\epsilon_p = \epsilon - \sigma/E$.

Input Files

The files below are on your [delivery media](#) or they can be downloaded by your web browser by clicking the links (file names) below.

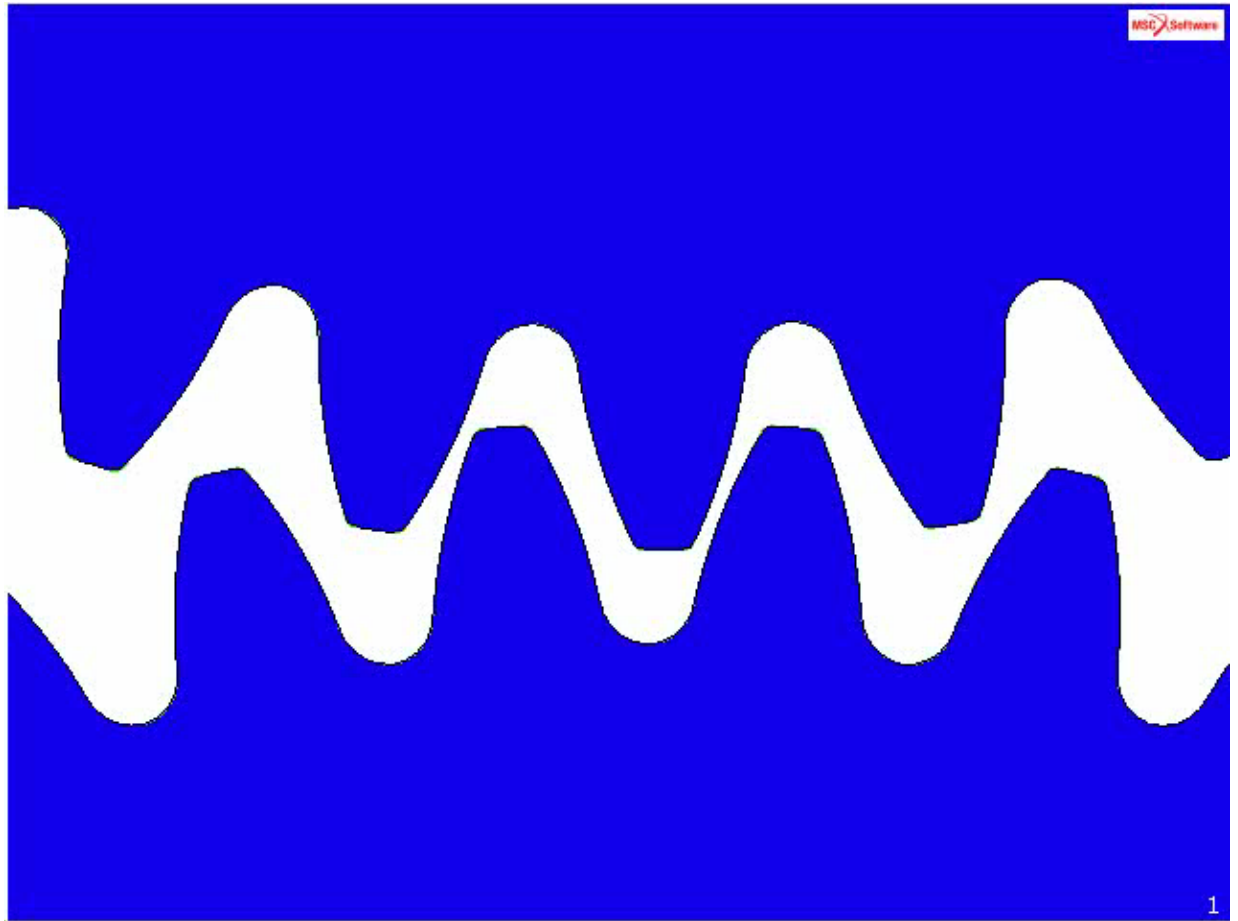
File	Description
gearpair.mud	Mentat model file
gearpair.proc	Mentat procedure file
gearpair_job1.dat	Marc input file
gearpair.f	User subroutine to define invoke failure criterion

References

1. American National Standard/AGMA Standard, Tooth Proportions for Plastic Gears, ANSI/AGMA 1006-A97, 1997.
2. Designing with Celcon http://www.kmsbearings.com/pdf/Celcon_Design%20Guide_3.9.07.pdf

Animation

Click on the figure below to play the animation.



3.37 Girkmann Verification Problem

- Summary 1694
- Detailed Description 1695
- Results 1697
- Modeling Tips 1699
- Input Files 1704

The Girkmann problem consists of a spherical shell connected to a stiffening ring at the crown radius. The objective of the analysis is to accurately estimate: a) the shear force and bending moment acting at the junction between the spherical shell and the stiffening ring; b) determine the location (meridional angle) and the magnitude of the maximum bending moment in the shell. The model problem was first discussed by Girkmann in 1956, subsequently by Timoshenko and Woinowski-Krieger in 1959. The results are compared to the solutions by the classical methods to demonstrate the accuracy.

Detailed Description

Element type 1, an axisymmetric, straight, thick-shell element is used for modeling the spherical shell and element type 10, an axisymmetric, four-node, quadrilateral element is used to model the stiffening ring. The geometry for the Girkmann problem is shown in Figure 3.37-1. The x axis is the axis of rotational symmetry. A spherical shell of thickness h and midsurface radius R_m , is connected to a stiffening ring at the meridional angle α and a crown radius of R_c . The dimensions of the ring are a and b .

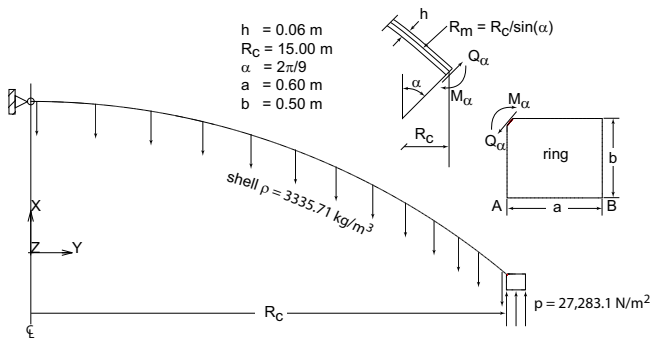


Figure 3.37-1 The Girkmann Problem Geometry

A close-up of the shell-ring intersection for the Girkmann problem is shown in Figure 3.37-2. The mesh consists of 2208 elements and 2270 nodes.

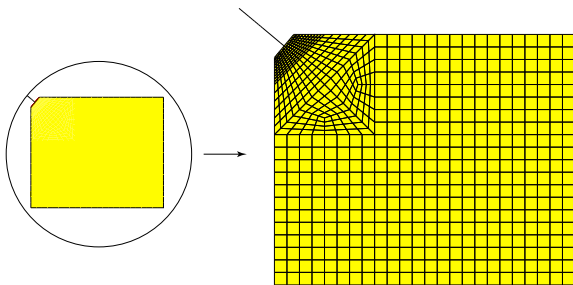


Figure 3.37-2 The Girkmann Shell - Ring Close-up

The axisymmetric solid elements for the stiffening ring are generated by `*add_elements` and re-meshed with `*subdivide_elements` (Figure 3.37-3). The axisymmetric shell elements for the spherical shell are generated using `*expand_nodes`.

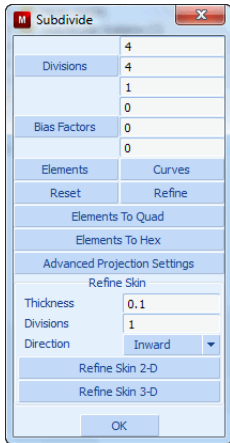


Figure 3.37-3 Building the Ring using Subdivide

A local Cartesian coordinate system (`*new_coord_system`) is created with the shell solid intersection node as origin, the local X axis along the 40^0 inclined edge of the ring and the local Y axis normal to that. All the nodes on the 40^0 inclined edge of the ring and the end node of the shell at the intersection are transformed into this co-ordinate system (Figure 3.37-4).

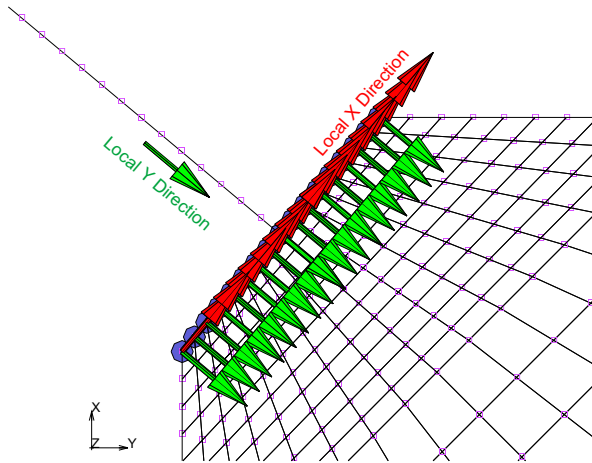


Figure 3.37-4 Coordinate Transformation (colored arrows) for Joining the Shell and Ring

Servo links constrain the translation and rotation displacements of the end node of the shell joining the inclined edge of the ring. The local Y displacement of the nodes on the ring edge is the sum (with appropriate sign) of the local Y displacement of the end node of the shell at the intersection and Z rotation times the distance of that node from the end node of the shell (see Figure 3.37-8). The local X and local Y displacement of the coincident nodes of solid and shell at the intersection are constrained to be equal.

The material for all elements is linear elastic, isotropic with Young's modulus of $2.059 \times 10^{10} \text{ N/m}^2$ and density of 3335.71 Kg/m^3 . Pressure of $27283.14706 \text{ N/m}^2$ is applied to the bottom face (left) of the ring as an edge load (Figure 3.37-5). An acceleration of -9.81 m/s^2 is applied in the X direction (although not necessary the Y and Z components of acceleration is set to zero as well) only to the shell elements, whose mass times this acceleration determines the weight or gravity load of the shell structure. The stiffening ring is assumed to be weightless. The displacement of the node on the axis of symmetry is constrained in the axial direction.

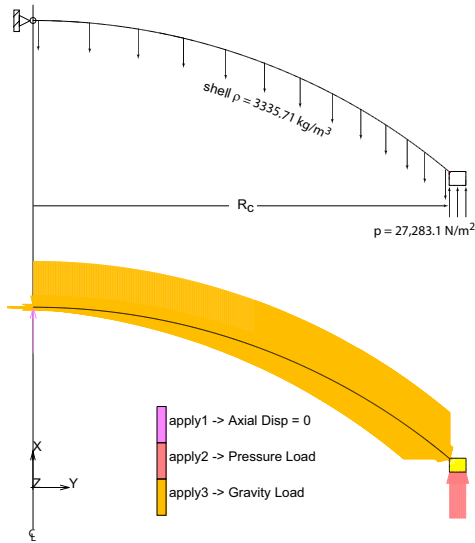


Figure 3.37-5 Loads and Boundary Conditions

By design, the axial (vertical in Figure 3.37-5) force on the ring equilibrates the weight of the shell.

Results

The internal forces from the force balance file (girkmann_job1.grd) are listed below for the node (2270) on shell at the intersection.

node	2270	internal force from element	2208	-0.1571E+07	0.1735E+07	0.0000E+00	-0.3475E+04	0.0000E+00	0.0000E+00
node	2270	externally applied forces		-0.4710E+03	0.0000E+00	0.0000E+00	0.0000E+00	0.0000E+00	0.0000E+00
node	2270	tying/mpc forces		0.1572E+07	-0.1735E+07	0.0000E+00	0.3475E+04	0.0000E+00	0.0000E+00
node	2270	reaction - residual forces		0.6319E-05	-0.7750E-05	0.0000E+00	0.1676E-07	0.0000E+00	0.0000E+00

The bending moment at the shell-ring interface becomes, $M_\alpha = \frac{3575}{\pi D} = \frac{3575}{\pi(30)} = 36.871 \text{ Nm/m}$.

The axial force at the shell-ring interface becomes, $Q_\alpha = \frac{-1571000}{\pi D} = -16668.828 \text{ N/m}$.

The radial force at the shell-ring interface becomes, $Q_r = \frac{1735000}{\pi D} = 18408.922 \text{ N/m}$.

The shear stress at the shell-ring interface (Figure 3.37-6) is -15658.2 N/m^2 , and when multiplied by the thickness gives a shear force of -939.492 N/m .

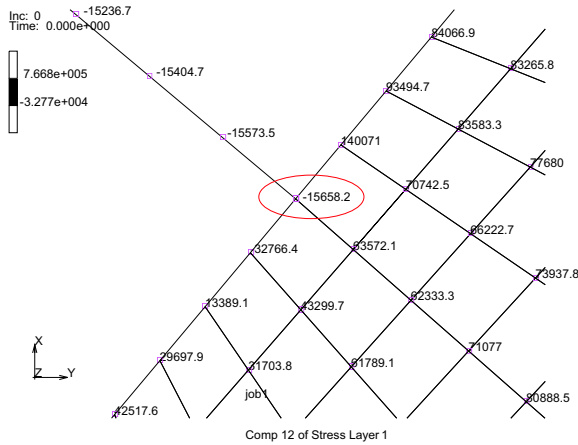


Figure 3.37-6 Shear Stress (Component 12) at the Shell-Ring Interface

The bending moment is estimated from the shell stresses as follows:

$$\sigma_B = (\text{Comp 11 of Stress at Layer 1} - \text{Comp 11 of Stress at Layer 5})/2$$

$$M_B = \sigma_B (bd^2/6) = \sigma_B (1(0.06)^2/6)$$

Using the above, the bending moment can be plotted versus the meridional angle as shown in. The maximum bending moment is 255.103 Nm/m at a meridional angle of 38.137° .

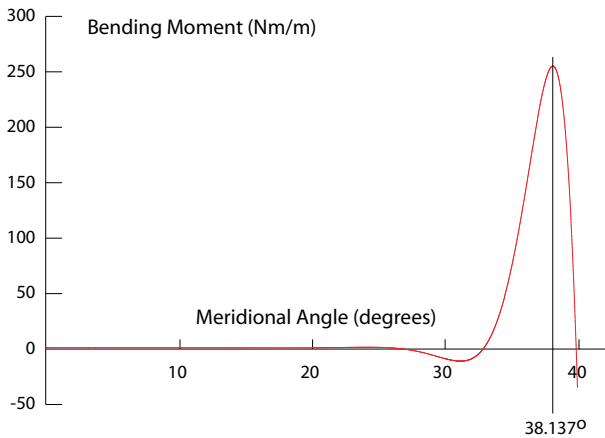


Figure 3.37-7 Bending Moment versus Meridional Angle

The results are summarized below and compared to the reference values.

Result	Marc	Reference (1)	% Error
Bending Moment (Nm/m)	36.871	36.81	0.17%
Axial Force (N/m)	-16668.828	-16700	-0.19%
Radial Force (N/m)	18408.922	18400	0.05%
Shear Force (N/m)	-939.492	-943.6	-0.44%
Max. Bending Moment in the shell (Nm/m)	255.103	253.97	0.45%
Meridional Angle of Max. BM (degree)	38.137	38.08	0.15%

(1) The Problem of Verification with Reference to the Girkmann Problem by Barna Szabó, Ivo Babuška, Juhani Pitkäranta, and Sebastian Nervi. The Institute for Computational Engineering and Sciences Report 09-17, 2009. See www.ices.utexas.edu/research/reports/2009/0917.pdf.

Editorial Comment: The above reference is well worth reading; the authors received 15 solutions and among their comments the following is worth repeating, namely: “Another respondent wrote: “*Regarding verification tasks for structural analysis software that has adequate quality for use in our safety critical profession of structural engineering, the solution of problems such as the Girkmann problem represents a minuscule fraction of what is necessary to assure quality.*” We [the authors] agree with this statement. That is why we find it very surprising that the answers received had such a large dispersion. For example, the reported values of the moment at the shell-ring interface ranged between -205 and 17977 Nm/m. Solution of the Girkmann problem should be a very short exercise to persons having expertise in FEA, yet many of the answers were wildly off.”

Modeling Tips

To review the model, read in the Marc input file `girkmann.dat` into Mentat. All of the modeling information will be present. Axisymmetric models in Marc use the global x axis as the axis of rotation. The meshing is relatively straight forward and is not repeated here. However, an important feature in this model are the transformations and constraints between the end shell node (n:2770) where it joins the inclined plane of the ring (n:11). To review the transformations and constraints let's read in the input file and go to modeling tools.

FILES

MARC INPUT FILE

READ

girkmann.dat, OK

SAVE AS

girkmann, OK

FILL

MAIN

MODELING TOOLS

TRANSFORMATONS

TRANSFORMATION PLOT SETTINGS

TRANSFORMATIONS

(turn on)

DRAW

(should look like [Figure 3.37-4](#))

TRANSFORMATIONS

(turn off)

DRAW

MAIN

LINKS

SERVO LINKS

(see [Figure 3.37-8](#))

MAIN

We see that servo link 1 in [Figure 3.37-8](#), constrains the ring node 110 to have its second degree of freedom related to the second (translation normal to incline) and third (rotation) of the end shell node 2770 by the moment arm of length 0.03m. This is repeated 15 more times for all nodes along the ring incline edge. Servo link 17 and 18, simply equate the first and second degrees of freedom to the coincident nodes 2270 of the shell and 11 of the ring. These servo links are automatically generated with the N to 1 SERVOS button, where you need only select the proper nodes and all of the coefficients (aka moment arms) are computed automatically by Mentat.

Furthermore, since the shell elements have three degrees of freedom per node, while the ring elements have only two degrees of freedom per node, node 11 and node 2270 should never be the same node number, but constrained together as shown here. Also since the nodes are separate, the results are not nodal averaged across the shell and solid axisymmetric elements. Finally, getting this step wrong gives incorrect results that may not be obvious.

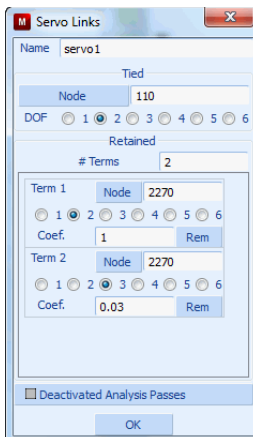


Figure 3.37-8 Servo Link 1

You may wish to run the model; to do so simply go to Jobs, run and submit the simulation, for example

```
JOBS
  RUN
    SUBMIT
```

After the simulation completes, let's examine how we can produce check the validity of the servo links, the bending moment versus meridional angle shown in [Figure 3.37-7](#), and some other ways to help visualize the results.

```
OPEN POST FILE (RESULTS MENU)           (opens results and jumps to results menu)
DEFORMED SHAPE SETTINGS
  AUTOMATIC                               (turn on)
  RETURN
DEF & ORIG                               (should look like Figure 3.37-9)
```

The servo links must keep the angle (a right angle in this case) between the shell and ring edge the same before and after deformation. Since the deformations are very small, the scaling of the deformed shape was set to automatic and the magnification factor is over 400 in [Figure 3.37-9](#).

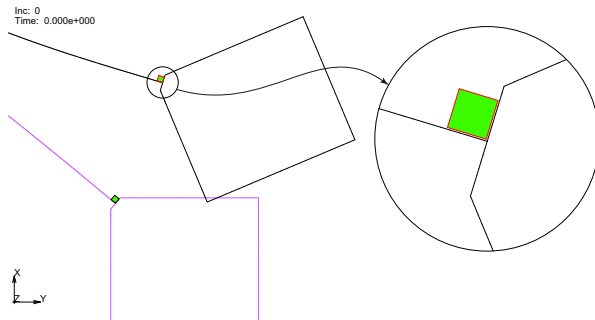


Figure 3.37-9 Shell-Ring Edge Originally Perpendicular must remain Perpendicular - Displacements Automatically Magnified over 400 times.

The strategy to computing the bending moment in the shell is simple; we just collect bending stress along a path from the centerline to the end shell node.

```
PATH PLOT
  NODE PATH
    n:803 n:2270 #
  ADD CURVES
    ADD CURVE
      Arc Length
```

```

Comp 11 of Stress Layer 1
Arc Length
Comp 11 of Stress Layer 5
SHOW ID 100
FIT
RETURN
CLIPBOARD COPY TO
  
```

(should look like [Figure 3.37-10](#))

The xy data is now in the clipboard and can be exported to Microsoft Excel for additional processing to compute the bending moment from the bending stresses at the top and bottom layers of the shell element that was used to produce the plot in [Figure 3.37-7](#).

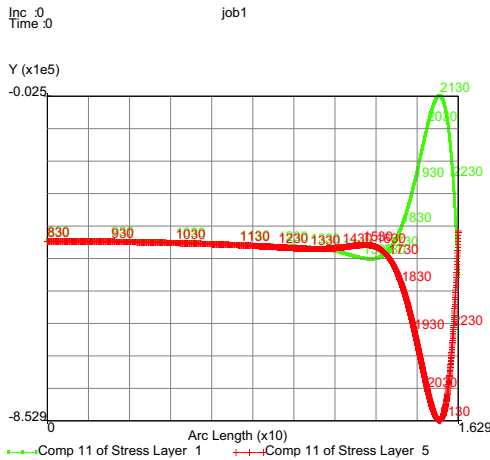


Figure 3.37-10 Bending Stress of Top and Bottom Shell Layers along Arc Length of Shell Elements from Center Line to Shell-ring Intersection

Also we can use the expand feature to expand (rotated 40°) our results about the axis of rotation.

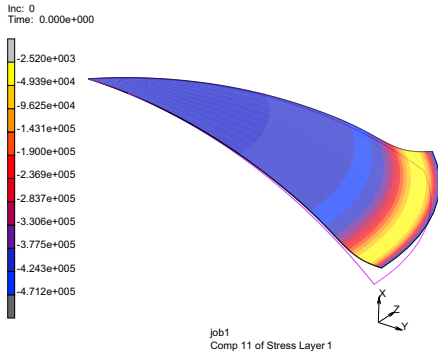


Figure 3.37-11 Axisymmetric Shell Element Results Expanded about the Rotational Symmetry Axis

Finally we can visualize the shell-ring intersection by closing the post file and adjusting the plot settings as follows:

```

MAIN
RESULTS
CLOSE
MAIN
GEOMETRIC PROPERTIES
PLOT SETTINGS SHELL
PLOT EXPANDED
DEFAULT THICKNESS = 0.06
DRAW
    
```

(should look like [Figure 3.37-12](#))

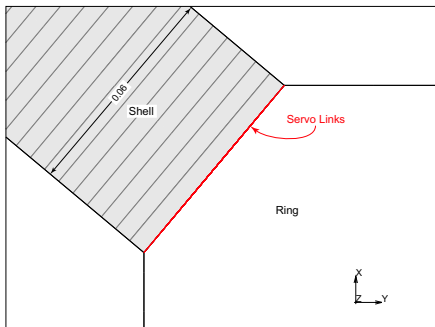


Figure 3.37-12 Expanded Shell Plot Showing the Shell's Thickness at the Shell-Ring Intersection

Hence, we can see that the thickness of the shell is identical to the length of the inclined ring edge that has all of the servo links illustrated in [Figure 3.37-8](#).

Input Files

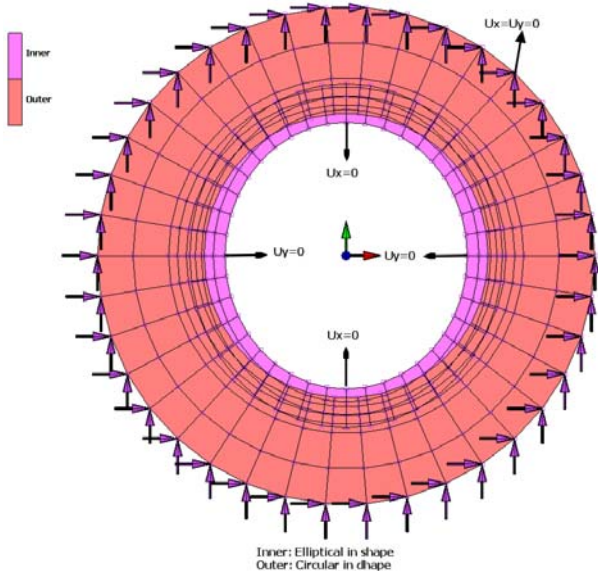
The files below are on your delivery media or they can be downloaded by your web browser by clicking the links (file names) below.

File	Description
girkmann.dat	Marc input file to run the above problem

3.38 Interference Fit Demonstration with All Five Available Methods

- Summary 1706
- Requested Solutions 1707
- Modeling Details 1707
- Solution Procedure 1718
- Result and Plots 1718
- Input Files 1731

Summary

Title	Interference Fit Demonstration with All Five Available Methods
Features	Interference Fit
FE Mesh	 <p>Inner: Elliptical in shape Outer: Circular in shape</p>
Material properties	<p>Material for deformable bodies:</p> <p>Inner: $E = 210000 \text{ N/mm}^2$; $\nu = 0.30$</p> <p>Outer: $E = 50000 \text{ N/mm}^2$; $\nu = 0.25$</p>
Analysis characteristics	Nonlinear static analysis
Boundary conditions and Applied loads	<ol style="list-style-type: none"> 1. Nodes on outer periphery of Outer body are arrested. 2. Two nodes at inner periphery of Inner body (elliptical in shape) on the major axis and minor axis respectively have been given symmetric boundary condition.
Element type	4-noded Plane strain elements (Element 11).
Contact properties	Interference fit between outer body (Circular in shape) and Inner body (Elliptical in shape)
FE results	<ol style="list-style-type: none"> 1. Contact Status 2. Displacement 3. von Mises stress 4. Contact Normal

To solve the Interference Fit problems, 5 different methods are available mentioned below. User has to use these methods depends on the type of his model. User may have interference at more than one place and in this case, based on the type of the interference user can use different method for each contact pairs in the single model.

1. Contact Normal
2. Translation
3. Scaling
4. Automatic
5. USHFTVEC user subroutine

Requested Solutions

A numerical analysis will be performed to find contact normal force, von Mises stress and displacement results with all five methods available in the model.

Modeling Details

The model shown in [Figure 3.38-2](#) is a structure having two deformable bodies: Inner and Outer. Shapes of Inner and Outer are elliptical and circular, respectively. There is nonuniform interference between both the bodies. For this particular model, all five methods can be used to resolve the interference. After interference is resolved, the inner body would fit inside the outer body.

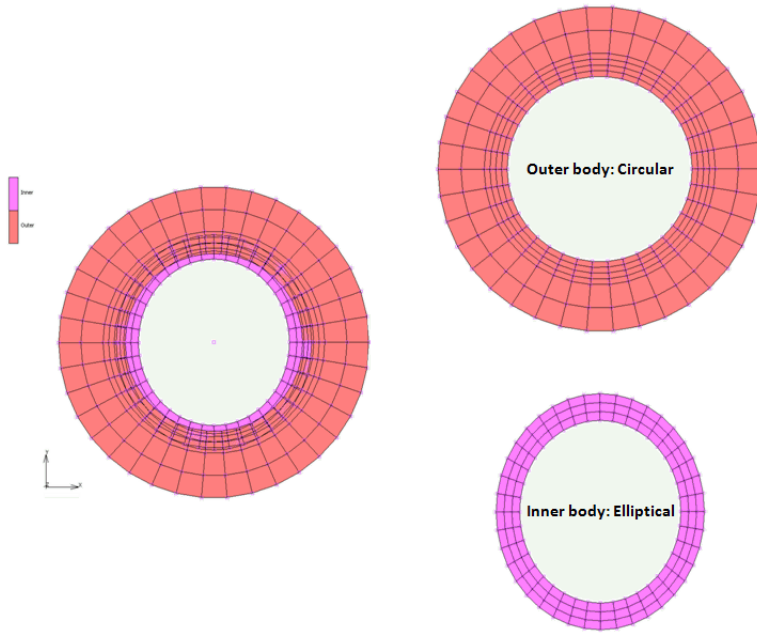


Figure 3.38-1 FE Model of the Structure

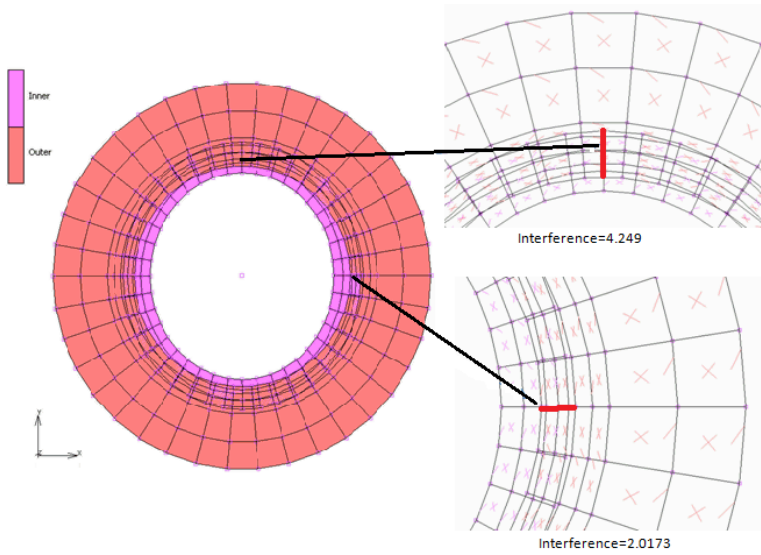


Figure 3.38-2 FE Model of the Structure Before Resolved Interference

Element Modeling

The 4-noded quad elements (Element 11) have been used for both the bodies. Assumed strain has been turned on using the geometry option as shown in the following graphic.

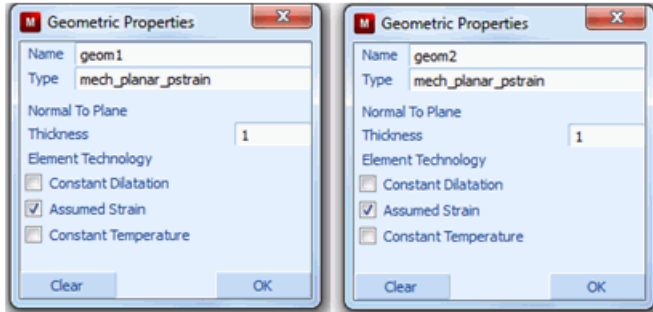


Figure 3.38-3 Geometric Properties Menus

Material Modeling

Linear isotropic material with different material properties have been applied to both contact bodies respectively.

Interference Fit modeling

There are five ways to model Interference fit in the job.

1. Contact Normal
 - Table ID giving variation of interference closure with respect to time.
2. Translation
 - a. Table ID giving variation of interference closure magnitude with respect to time.
 - b. Direction cosines for the shift vector.
 - c. Coordinate system (Default = Global Cartesian system)
 - d. Slave/ Master contact body for which shift vector to be used. Default is slave body.
3. Scaling
 - a. Table ID giving variation of scale factor with respect to time.
 - b. Scale factors in X, Y, and Z direction.
 - c. Coordinate system (Default = Global Cartesian system with center of scaling at origin)
 - d. Slave/Master contact body for which scale factors to be used. Default is slave body.
4. Automatic
 - Penetration search tolerance (default = same as error tolerance)

5. User subroutine. USHFTVEC

- a. Table id giving variation of shift vector with respect to time.
- b. Slave/ Master contact body for which shift vector to be used. Default is slave body.

In this exercise, all five methods for interference fit have been demonstrated.

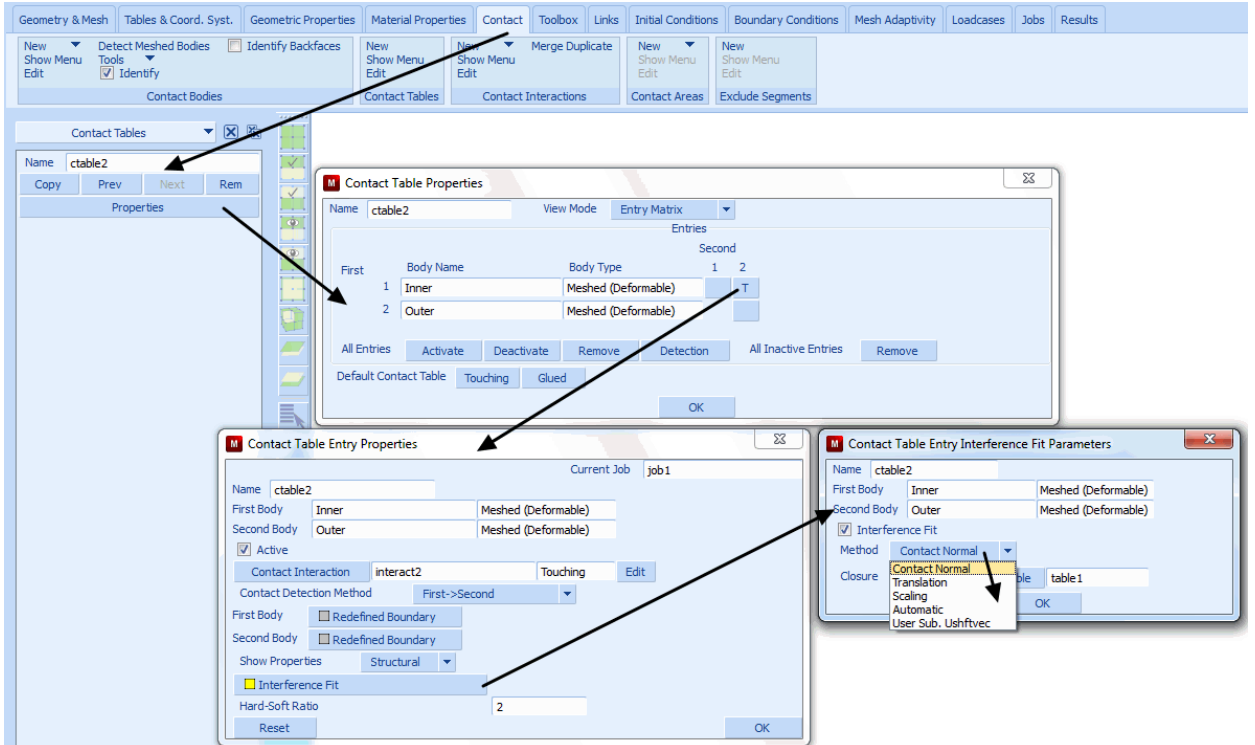


Figure 3.38-4 Activation of Interference Fit Methods

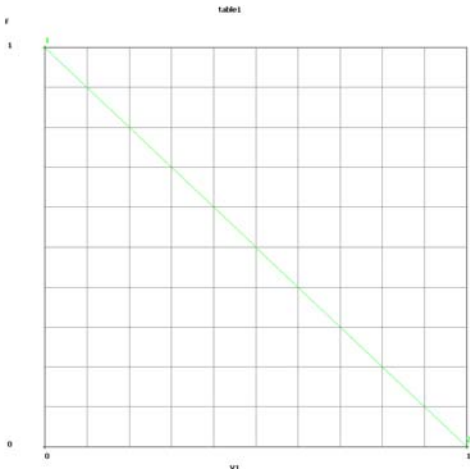


Figure 3.38-5 Table used to remove Interference Fit

Interference would be gradually resolved to zero from time $t=0$ to time $t=1$

Contact Normal Method

Maximum Interference in the model is 4.249 mm (see [Figure 3.38-2](#)). Any value more than or equal to 4.249 can be entered in the Closure field. Negative value should be provided for Interference fit. Closure = -4.7 has been entered for this method. Marc would remove the interference fit from 4.7 to 0, but would not find any contact between the interference ranges of 4.7 to 4.249; hence, contact status cannot be seen. Once closure reaches to value 4.249, Marc would detect contact for the first time, and hence, force would start getting transferred and contact status between both bodies can be seen.

If the user enters a very large value of Closure value than the actual largest value in the model, then many of the increments would get wasted because the force would not get transferred unless Marc detects the actual value for the first time. A large closure value entered would take more time, but this would not affect the result.

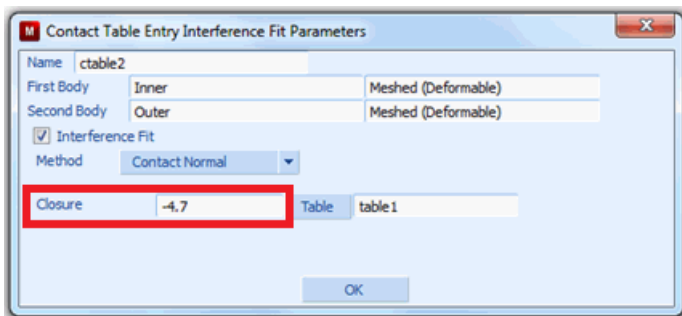


Figure 3.38-6 Contact Normal

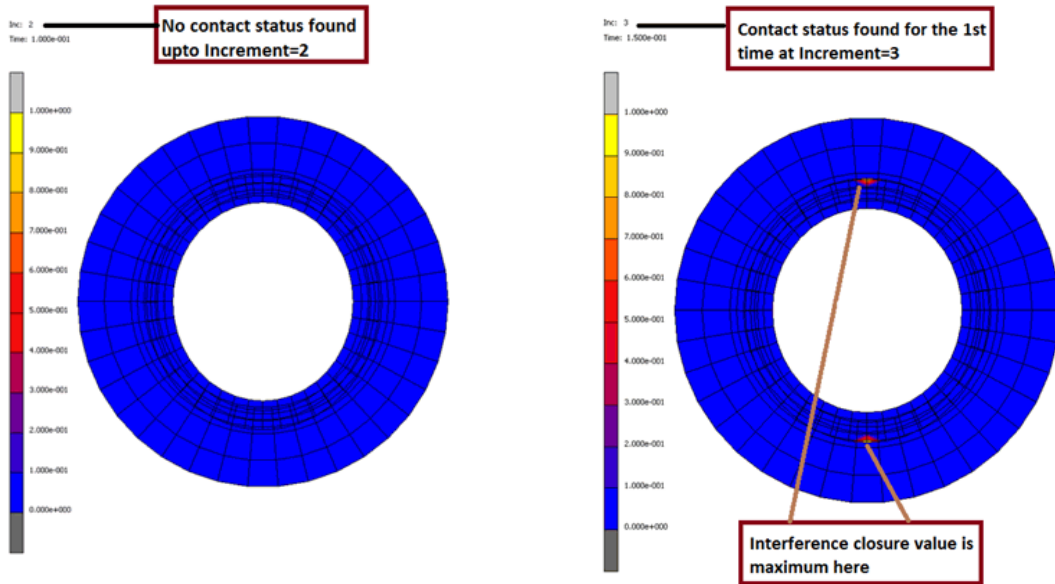


Figure 3.38-7 Contact Status

Translation Method

Depending on the contacting bodies of a particular pair, user can select:

1. Body at which translation has to be applied.
2. Coordinate system.

In this particular model, a cylindrical coordinate system has been chosen and Direction entered is radial direction (+1, 0, 0). Negative value of Signed Magnitude = -4.7 has been entered so that inner body nodes will start translating radially inwards from the start of load case. In this example, radial Direction (-1, 0, 0) and Signed Magnitude = +4.7 can also be used.

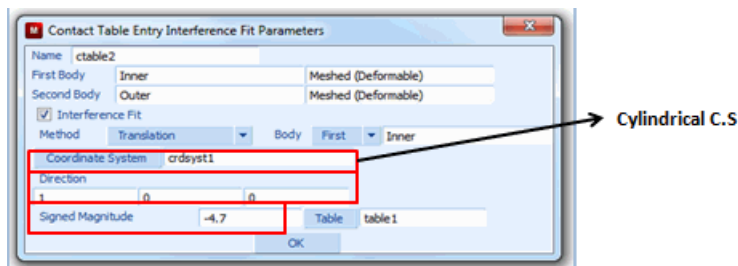


Figure 3.38-8 Translation

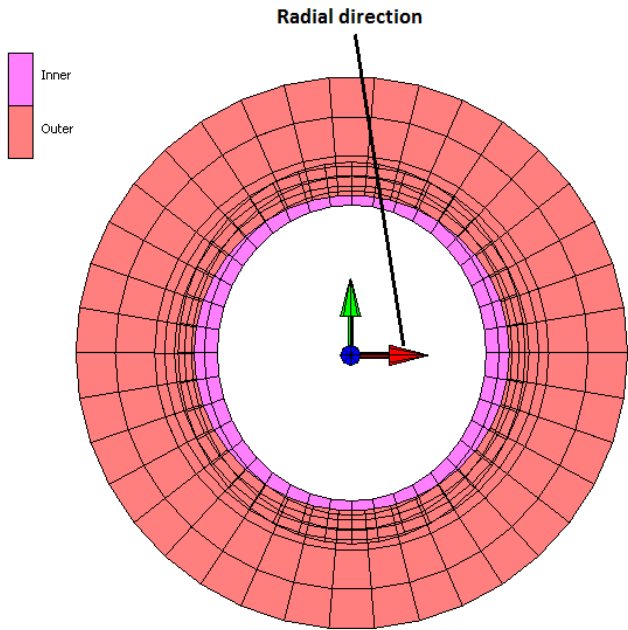


Figure 3.38-9 Cylindrical Coordinate System

Scaling Method using global coordinate system

Depending on the contact bodies of a particular pair, user can select:

1. Contact body to be scaled.
2. Coordinate system (Global in this case)

Scale factor in X-direction = Length of major axis formed by outer edge of Inner body/Inner diameter of Outer body
 $= 2a/2r = 34.1019/40.0 = 0.8525$.

Scale factor in Y-direction = Length of minor axis formed by outer edge of Inner body/inner diameter of Outer body
 $= 2b/2r = 37.512/40 = 0.9378$.

After interference fit removal of the outer edge of the Inner and the inner edge of the Outer, would both rest at same place.

The user can provide same the scale factor as calculated above. For the safer side, a lesser scale factor can be provided. In this example, a lesser scale factor of value 0.75 has been taken for both X and Y direction.

Marc internally scales down the Inner body by scale factor 0.75 about centroid in both X and Y direction, and then grows the mesh to remove the interference.

Since this is done internally, it cannot be seen in postprocessing.

If the user enters too little a scale factor than the calculated scale factor, then many of the increments are wasted because the force would not get transferred unless Marc detects the actual value of interference for the first time. A lesser value of the Scale Factor value entered would take more time, but this would not change the accuracy of the result.

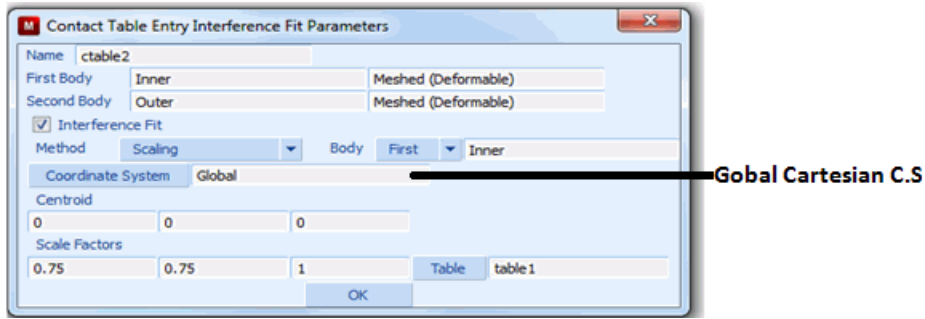


Figure 3.38-10 Contact Table Entry Interference Fit Parameters

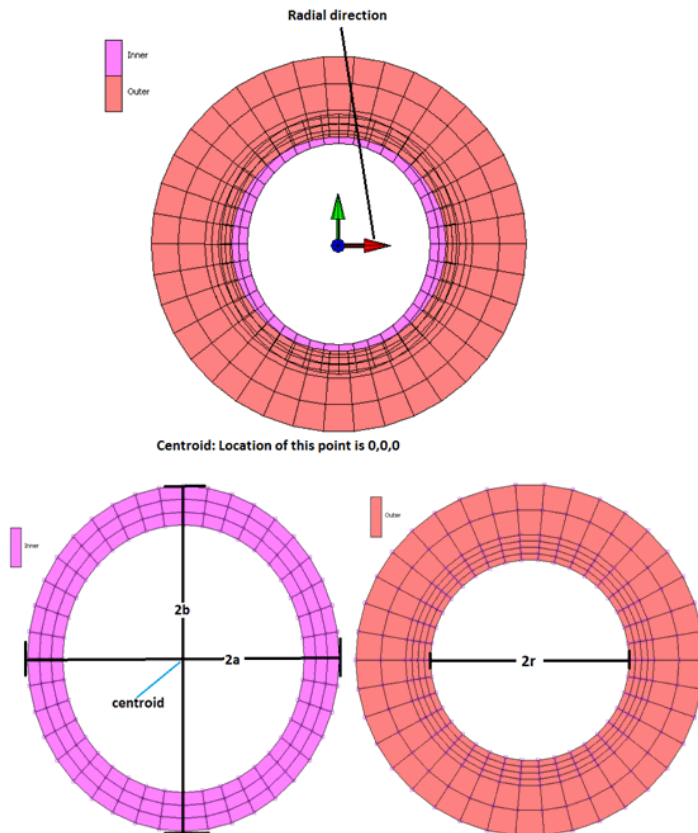


Figure 3.38-11 Centroid Location

Scaling Method using cylindrical coordinate system

This is same as above [Scaling Method using global coordinate system], except that the cylindrical coordinate system has been chosen instead of global Cartesian system demonstrated above. Scale factor = 0.75 has been provided for radial direction only.

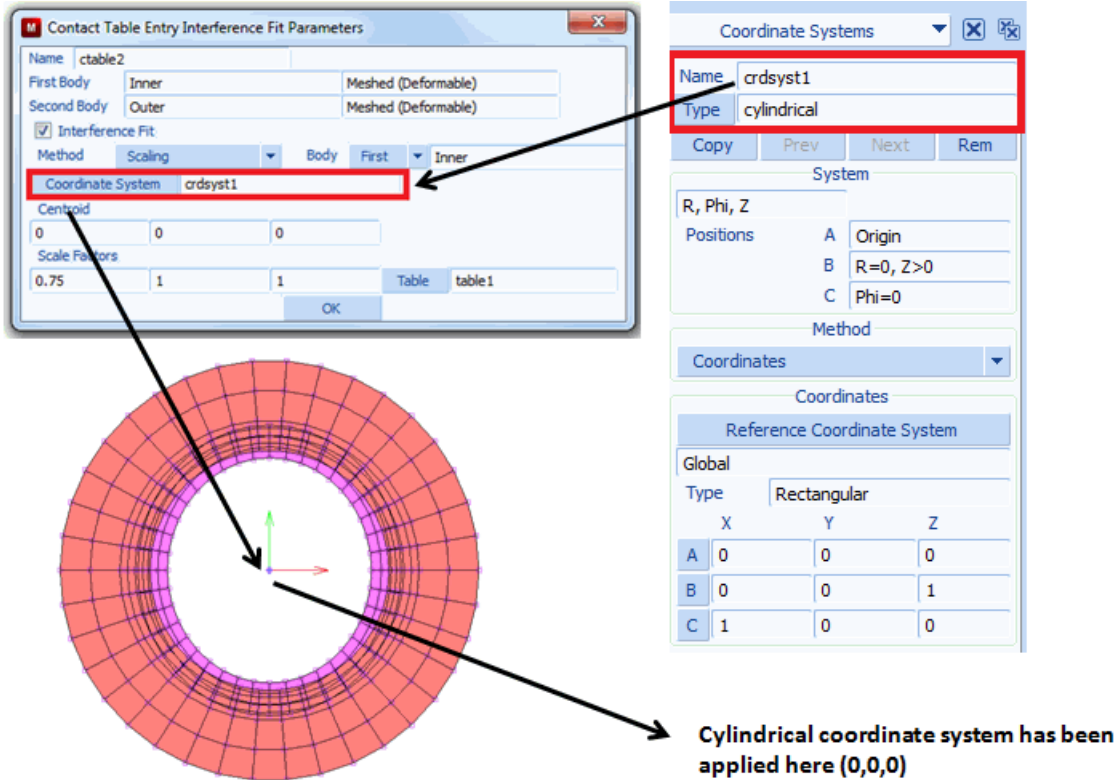


Figure 3.38-12 Scaling

Automatic Method

In this method, the contact body of which penetrations has to be resolved, can be chosen and maximum interference value can be entered in Penetration Tolerance field.

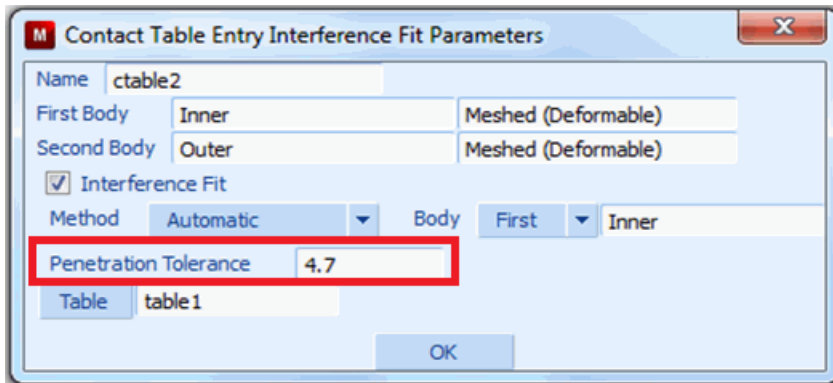


Figure 3.38-13 Automatic Method

User Subroutine Method

In this method, the user has to write a subroutine to compute a shift vector at all the contact nodes.

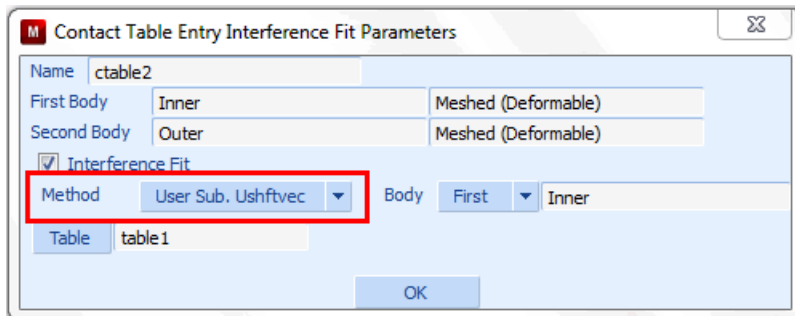


Figure 3.38-14 User Subroutine

Loading and Boundary Conditions

Figure 3.38-1 shows the boundary conditions applied on the finite element model of the structure. Loading is the Interference Fit which has been applied through Contact Table. The analysis is done in a single load case.

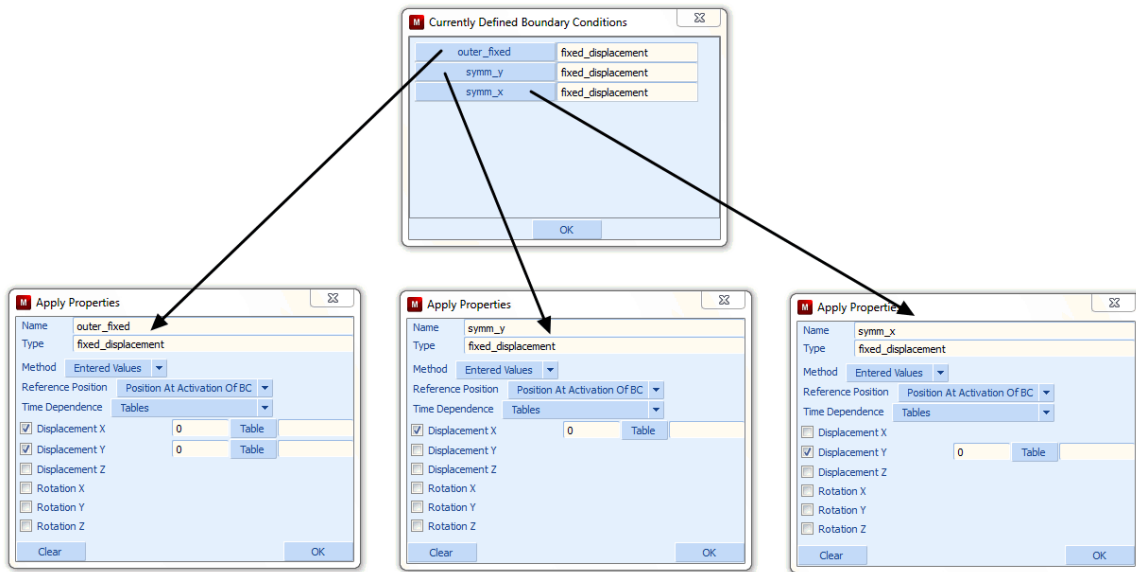


Figure 3.38-15 Mentat Boundary Condition Menus

Contact

Two deformable contact bodies Inner and Outer have been used. Both are touching to each other. Inner and Outer have been made First and Second bodies, respectively.

Contact detection type selected is: First->Second.

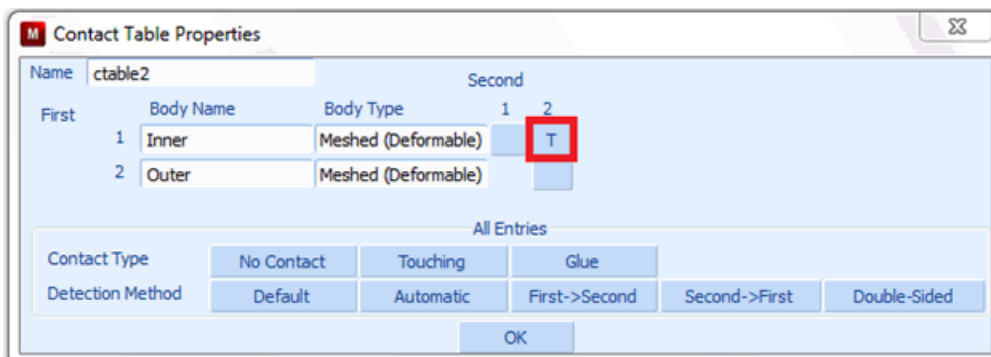


Figure 3.38-16 Mentat Contact Table Menu

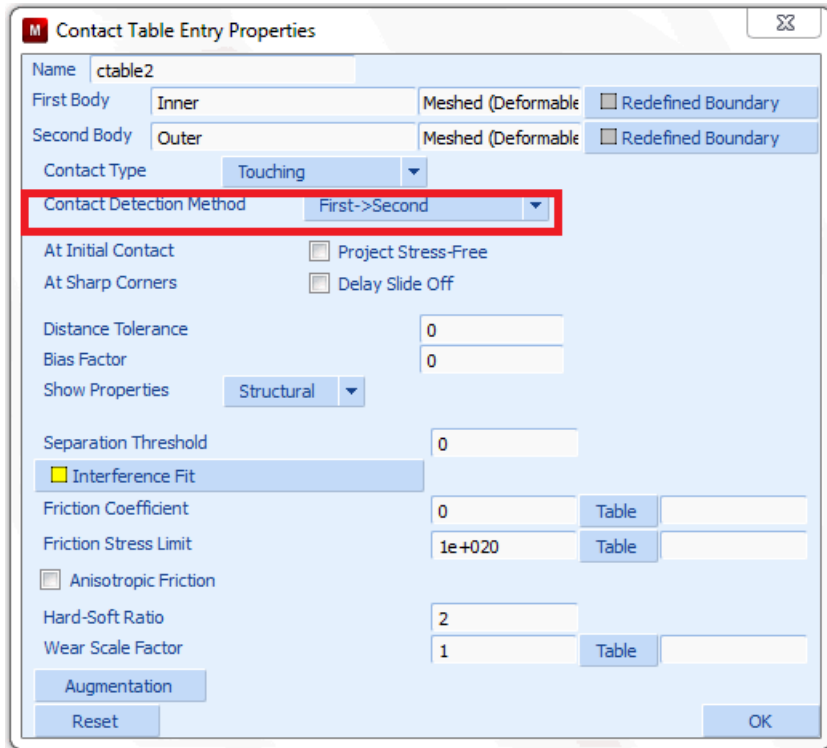


Figure 3.38-17 Mentat Contact Table Properties Menu

Solution Procedure

The problem is analyzed in Marc which is an implicit nonlinear solution procedure. Control parameters for the nonlinear solution scheme are described through the CONTROL option and four AUTO LOAD options have been used corresponding to each loadcase. Twenty time increments have been given for the loadcase.

Result and Plots

Method Number	Displacement Range (mm)	von Mises Stress Range (M Pa)	Contact Normal Force Range (N)
1	0-3.101	2971-30350	0-23180
2	0-3.101	2971-30310	0-23170
3 (Cartesian C.S)	0-3.101	2970-30350	0-23160
3 (Cylindrical C.S)	0-3.101	2970-30350	0-23160

Method Number	Displacement Range (mm)	von Mises Stress Range (M Pa)	Contact Normal Force Range (N)
4	0-3.1	2971-30310	0-23210
5	0-3.101	2970-30350	0-23160

Inc: 20
 Time: 1.000e+00

MSC Software

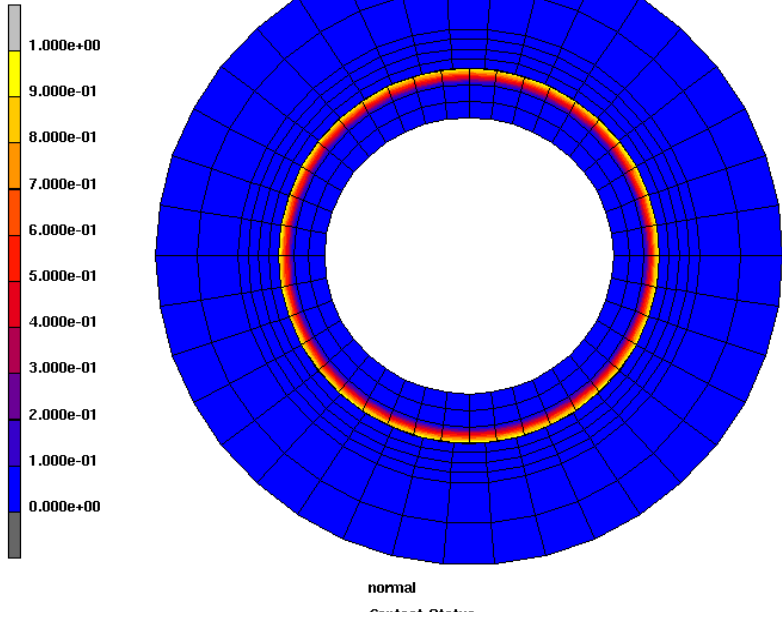
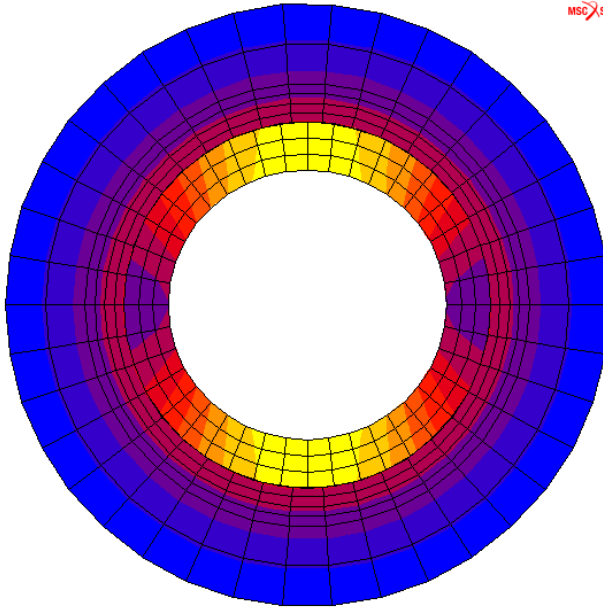
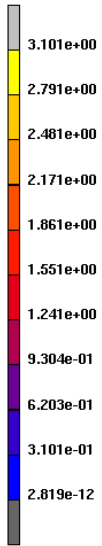


Figure 3.38-18 Contact Normal Method, Contact Status

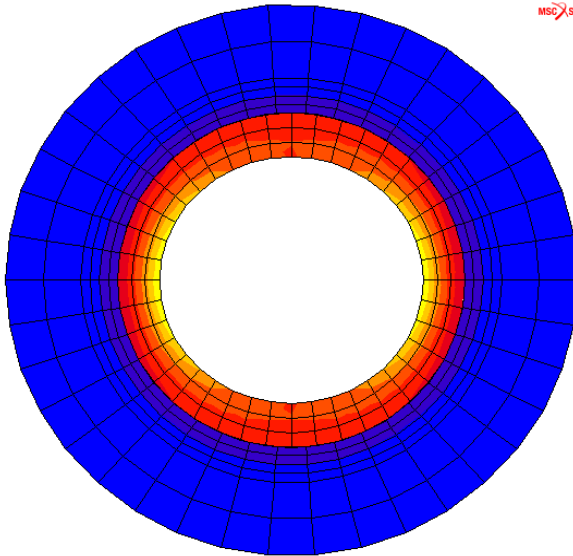
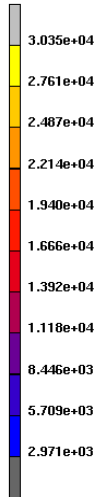
Inc: 20
Time: 1.000e+00



normal
Displacement

Figure 3.38-19 Contact Normal Method, Displacement

Inc: 20
Time: 1.000e+00



normal
Equivalent Von Mises Stress

Figure 3.38-20 Contact Normal Method, von Mises Stress

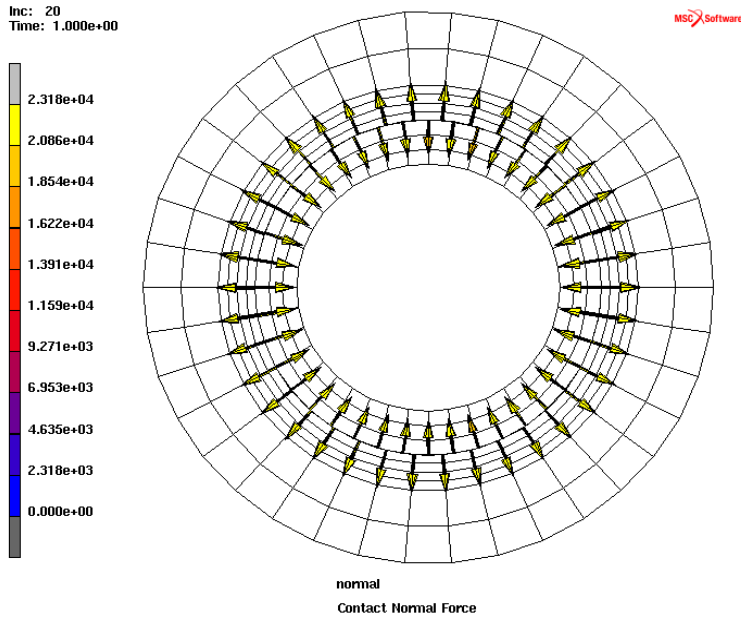


Figure 3.38-21 Contact Normal Method, Contact Normal Force

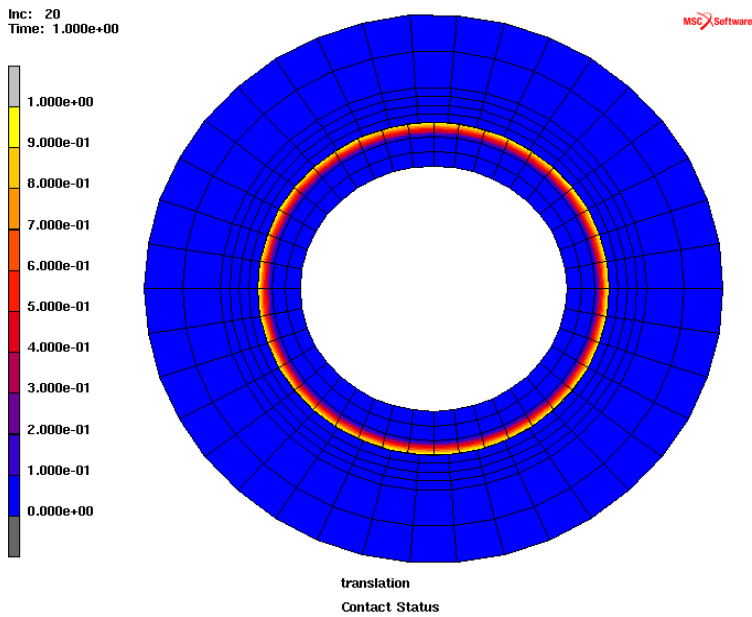


Figure 3.38-22 Translation Method, Contact Status

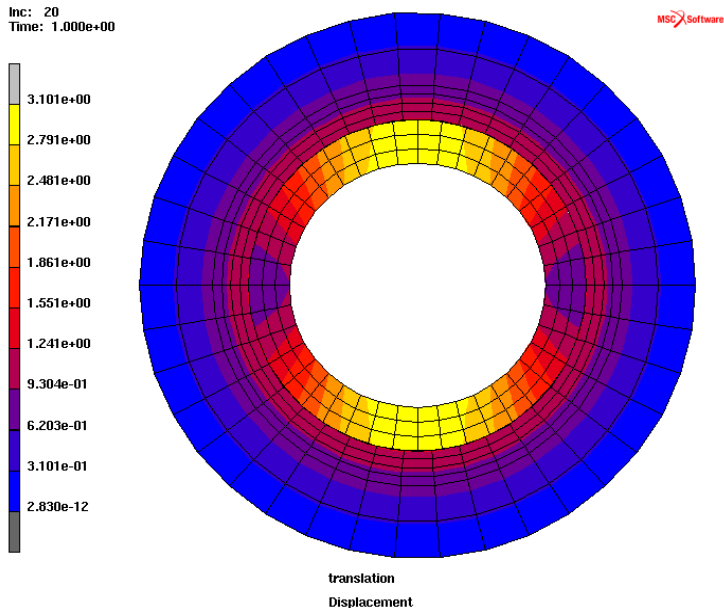


Figure 3.38-23 Translation Method, Displacement

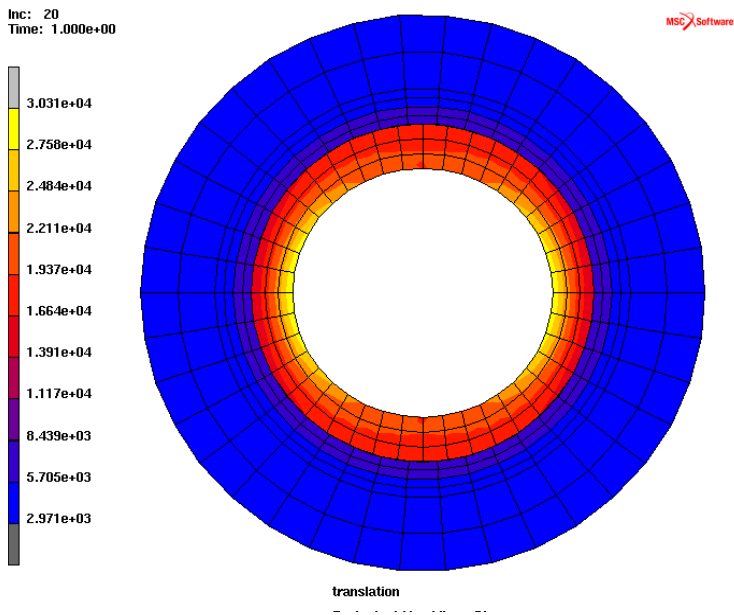


Figure 3.38-24 Translation Method, von Mises Stress

Inc: 20
Time: 1.000e+00

MSC Software

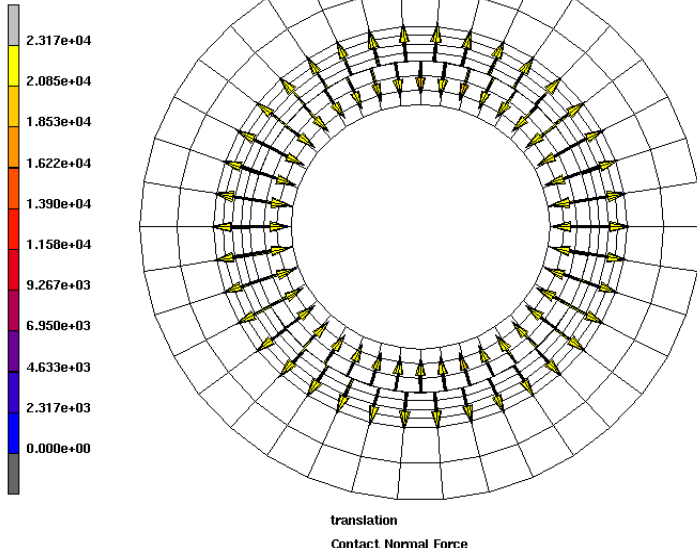


Figure 3.38-25 Translation Method, Contact Normal Force

Inc: 20
Time: 1.000e+00

MSC Software

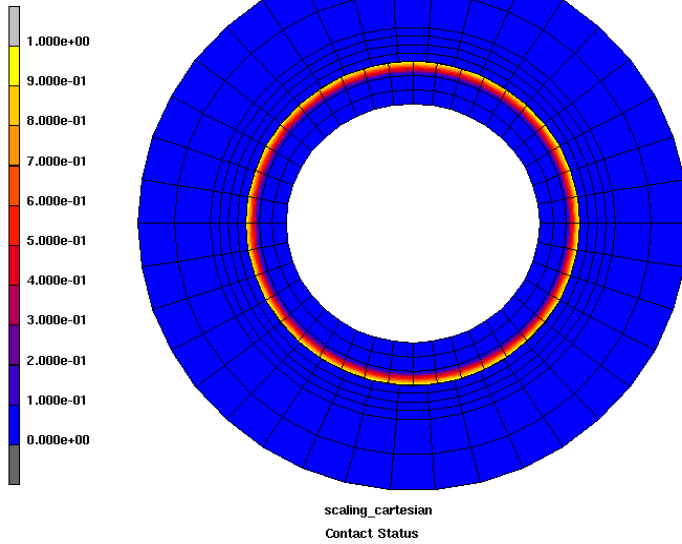


Figure 3.38-26 Scaling Method, Global Cartesian C.S., Contact Status

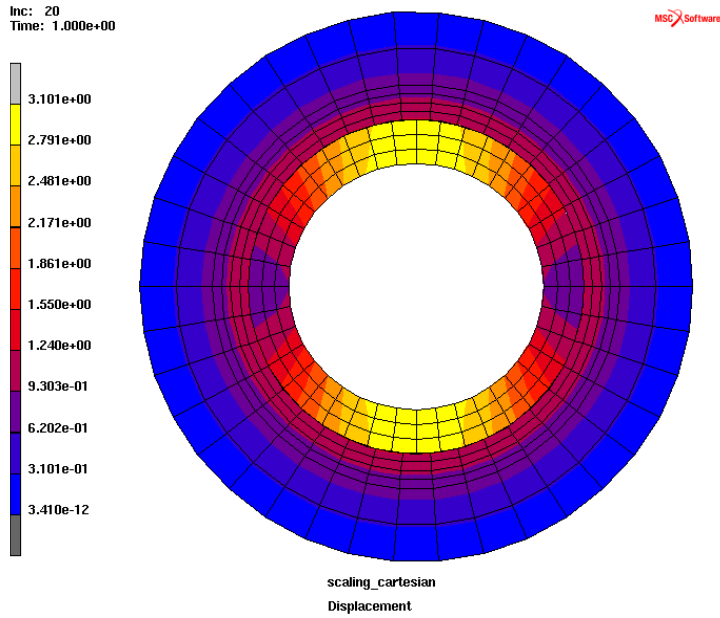


Figure 3.38-27 Scaling Method, Global Cartesian C.S., Displacement

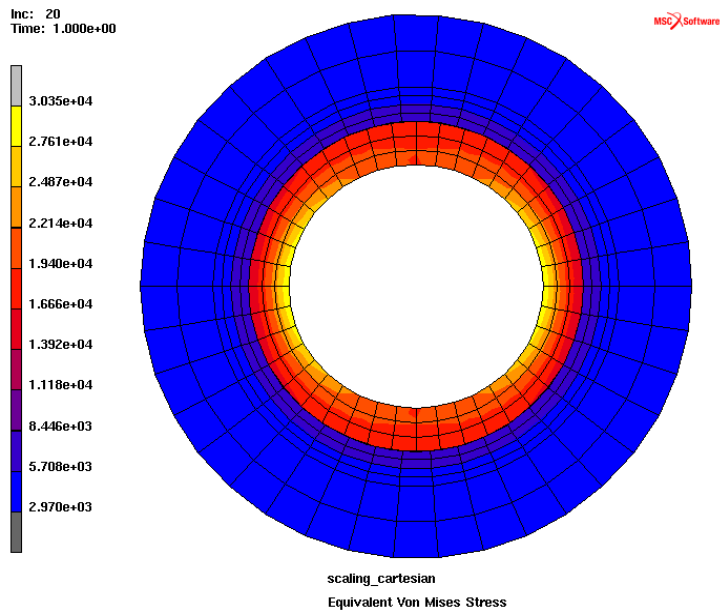


Figure 3.38-28 Scaling Method, Global Cartesian C.S., von Mises Stress

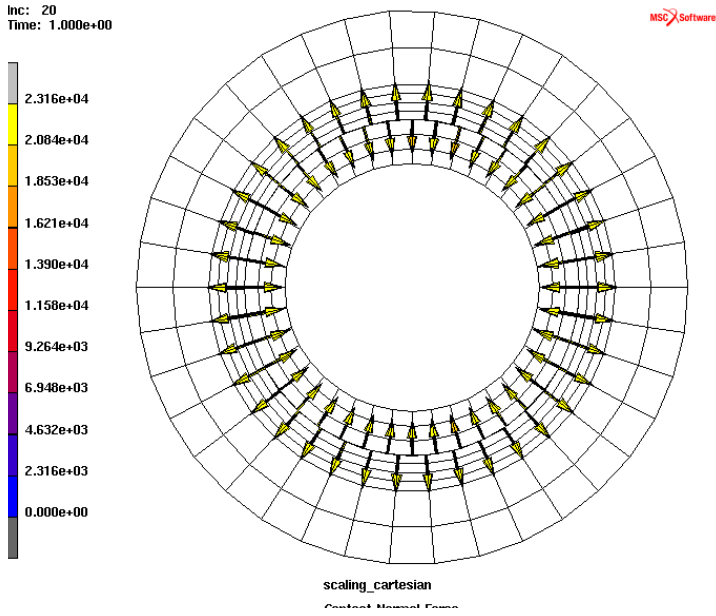


Figure 3.38-29 Scaling Method, Global Cartesian C.S., Contact Normal Force

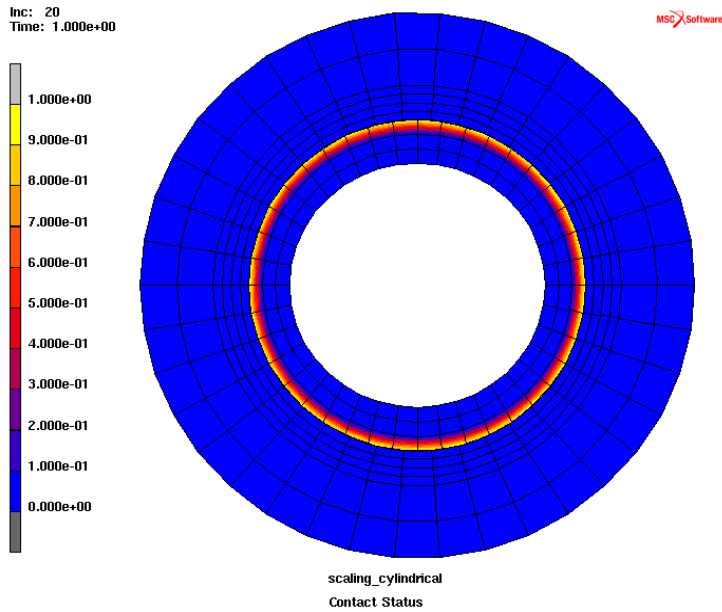


Figure 3.38-30 Scaling Method, Global Cylindrical C.S., Contact Status

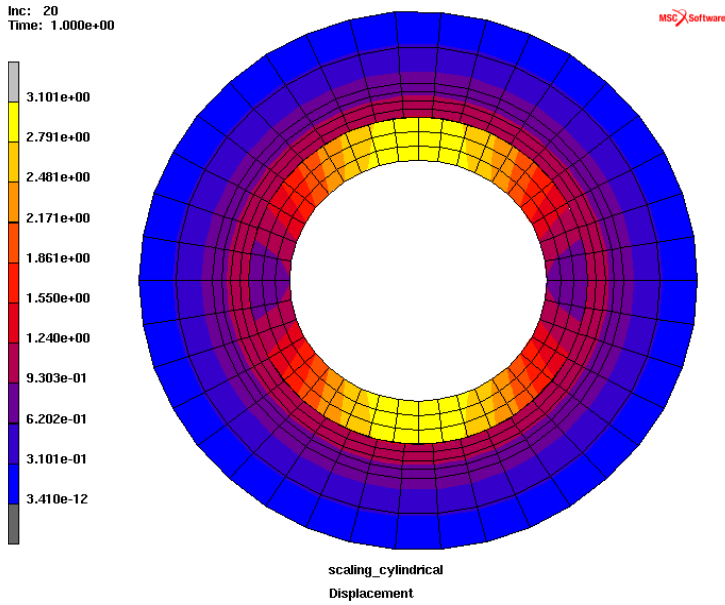


Figure 3.38-31 Scaling Method, Global Cylindrical C.S., Displacement

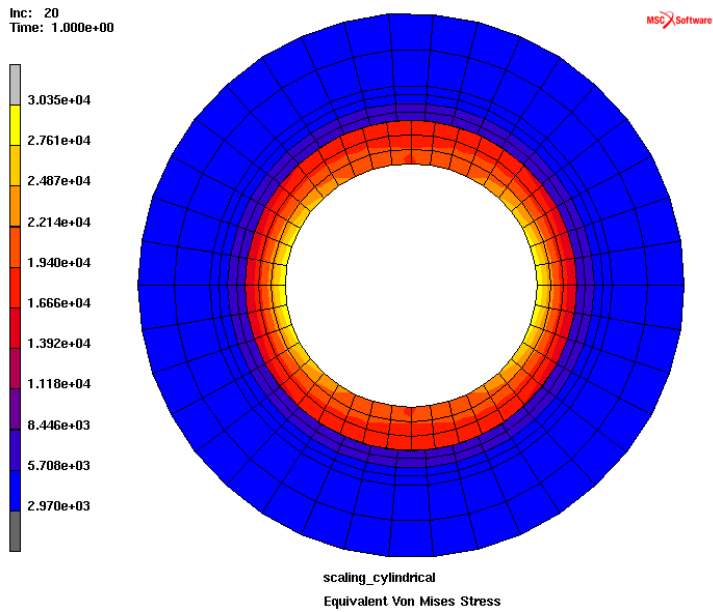


Figure 3.38-32 Scaling Method, Global Cylindrical C.S. von Mises Stress

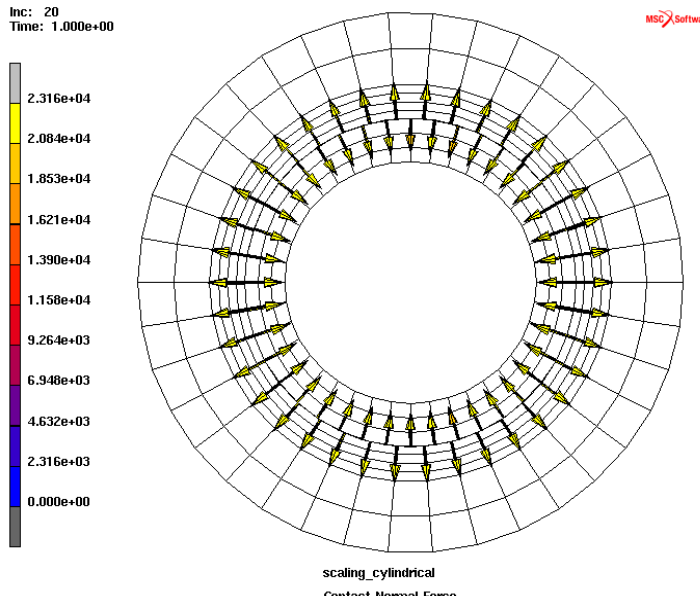


Figure 3.38-33 Scaling Method, Global Cylindrical C.S., Contact Normal Force

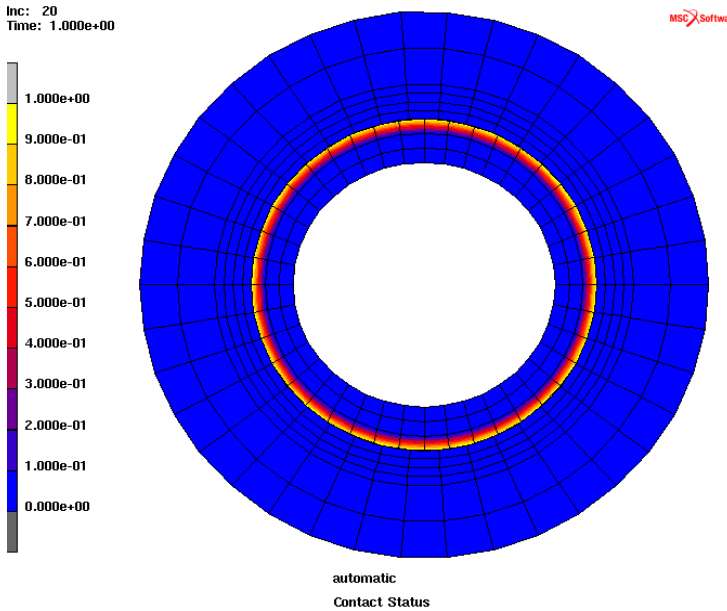


Figure 3.38-34 Automatic Method, Contact Status

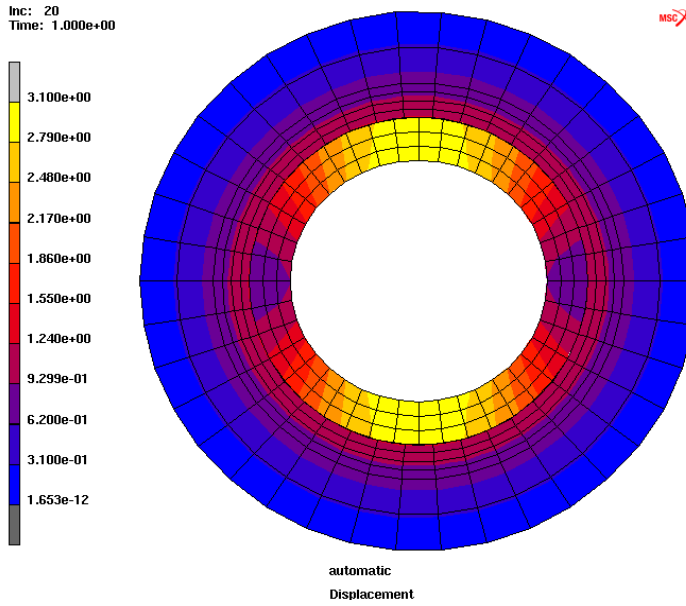


Figure 3.38-35 Automatic Method, Displacement

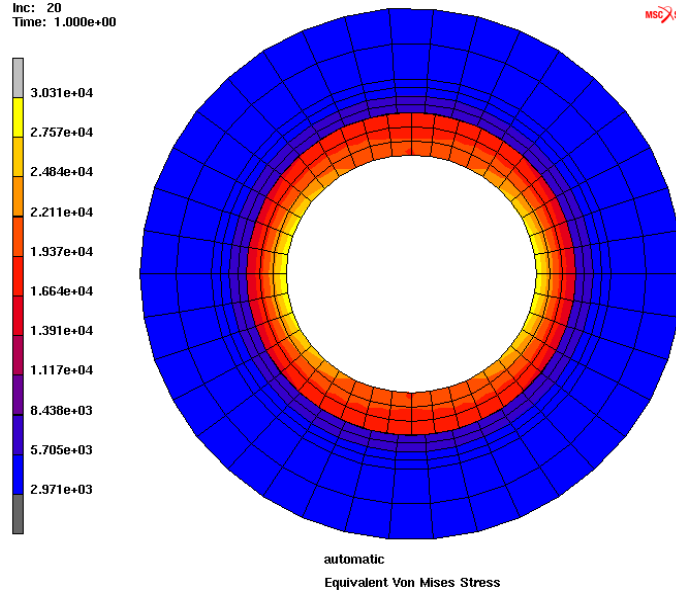


Figure 3.38-36 Automatic Method, von Mises Stress

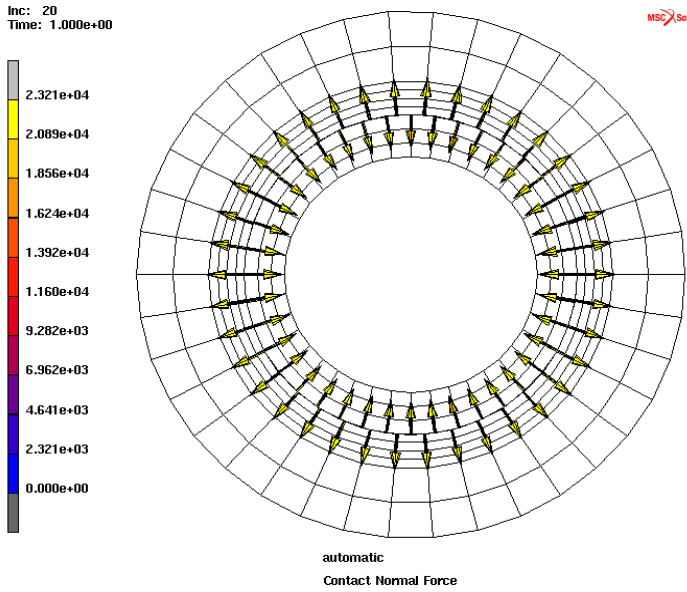


Figure 3.38-37 Automatic Method Contact, Normal Force

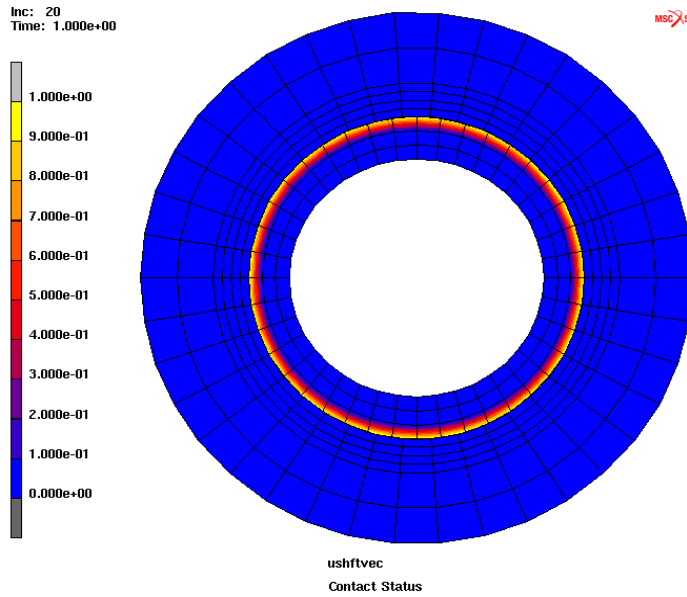


Figure 3.38-38 User Subroutine Method, Contact Status

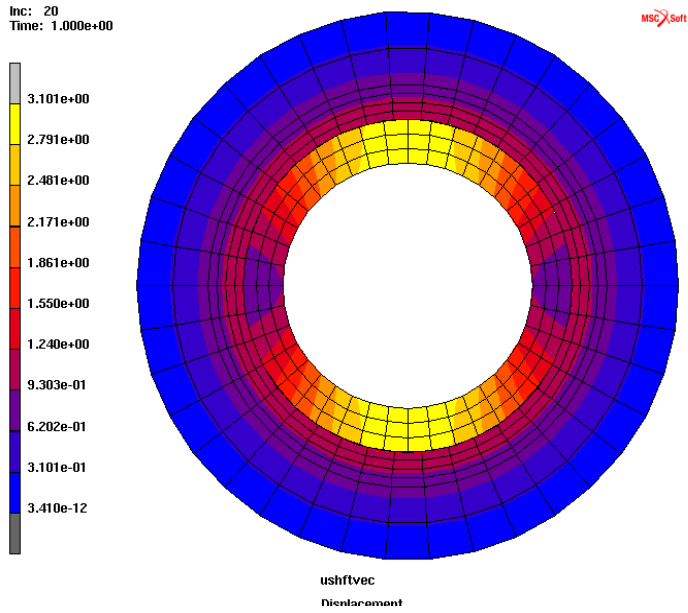


Figure 3.38-39 User Subroutine Method, Displacement

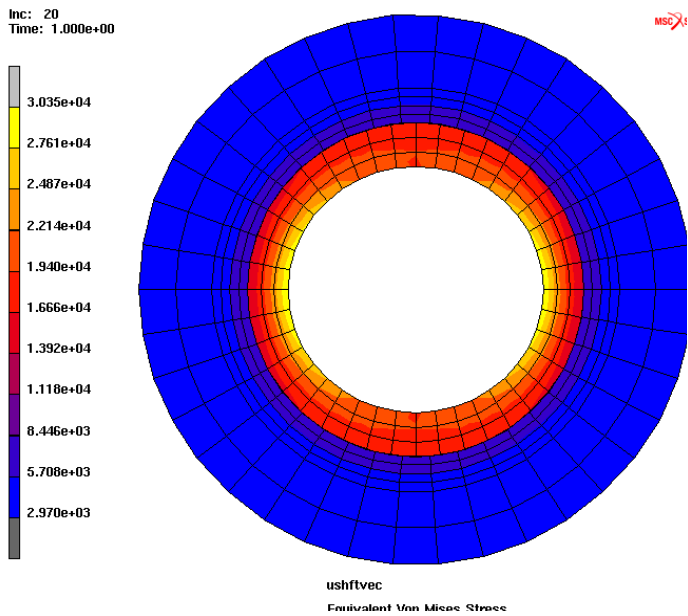


Figure 3.38-40 User Subroutine Method, von Mises Stress

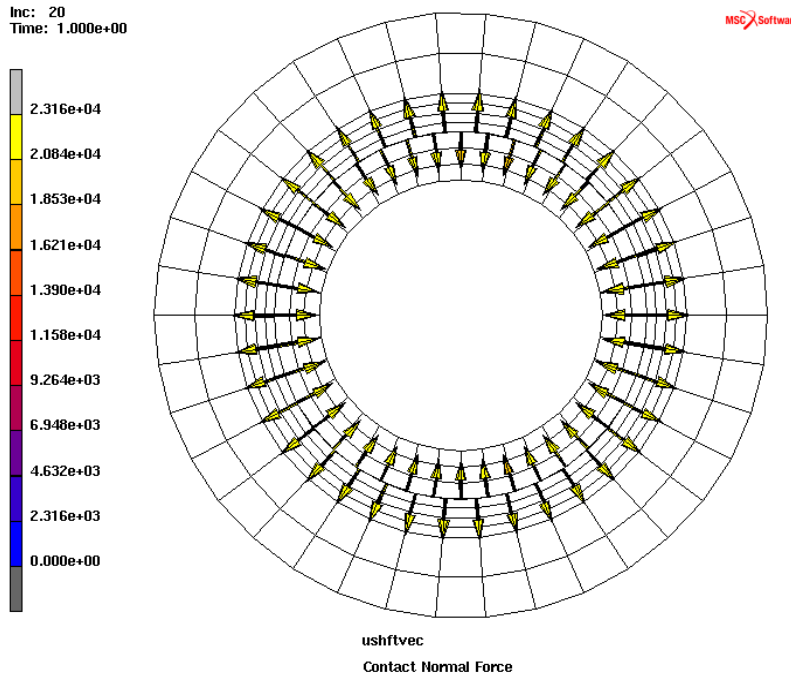


Figure 3.38-41 User Subroutine Method, Contact Normal Force

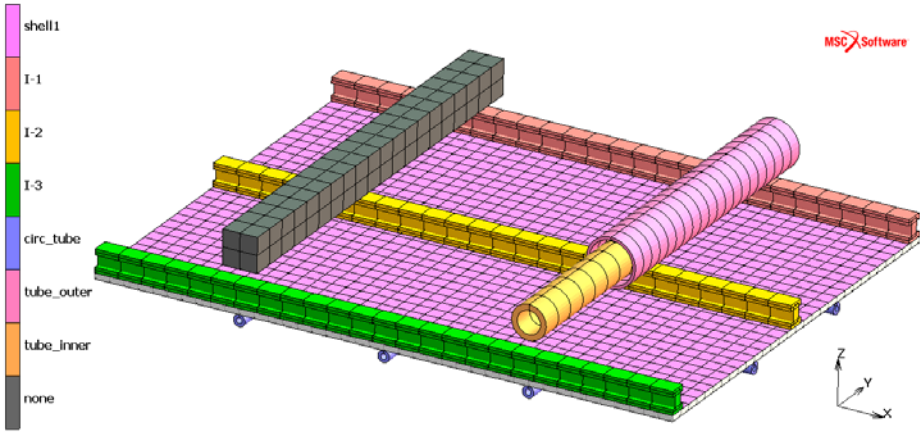
Input Files

File	Description
interference_fit.mud	Mentat model file which contains 6 jobs for the different methods which are discussed
intf_ushftvec.F	User subroutine USHFTVEC

3.39 Segment-to-Segment Contact of Stiffened Panel and Beams

- Summary 1734
- Requested Solutions 1735
- Modeling Details 1735
- Contact 1739
- Result and Plots 1744
- Input Files 1747

Summary

Title	Axially Compressed Stiffened Panel with New Beam Contact Capability
Features	Beam contact with expanded representation of beam cross section
FE Mesh	
Material properties	<p>Shell1: Isotropic Elastic-perfect plastic material with $E = 0.6E+5 \text{ N/mm}^2$, $\nu = 0.3$, and yield stress = 120 N/mm^2.</p> <p>Others: Isotropic Elastic-perfect plastic material with $E = 2.0E+5 \text{ N/mm}^2$, $\nu = 0.3$, and yield stress = 300 N/mm^2.</p>
Analysis characteristics	Nonlinear static analysis
Boundary conditions and Applied loads	<ul style="list-style-type: none"> • Stiffened panel clamped at one end & displacement of ($u_x = -10$, $u_y = u_z = 0$) at other end • Clamped at one end of tube_outer and tube_inner • Constraint $u_x = u_y = u_z = 0$ at one end of beams with solid elements
Element types	Beam element type78, solid element type 7, and shell element type 75
Contact properties	<ul style="list-style-type: none"> • I-beams and Circular tubes glued to shell panel with beam offset • Tube inside tube touching contact between tube_outer and tube_inner • Touching contact of I-beams with tube_outer, tube_inner and beam with solid elements • Beam contact with expanded representation of beam cross section • New contact interaction options in contact table • Segment to segment contact
FE results	Contact status and displacement results in expanded representation of beams

In node-to-segment (N2S) contact involving beams, the line representation of the beam elements is used for the contact of the beams with other deformable bodies (shell or solid) and rigid bodies. This line representation ignores the actual cross section of the beam elements and contact is only detected at the beam nodes. For beam-to-beam contact using the N2S scheme, an equivalent contact radius is defined at beam nodes by which a conical surface is constructed around the beam. A proximity check involving the conical surfaces of the two beams is used to determine the contact. Both these approaches ignore the actual beam cross section and hence pose some level of approximation for contact simulation involving beam elements. Other limitations of the existing beam-to-beam contact algorithm includes the inability to model internal tube-tube contact as well as special internal checks necessary for parallel beams.

To overcome the above limitations and to accurately capture the contact behavior of beam-to-beam and beam to other contact bodies (shell/solid deformable and rigid bodies), the segment-to-segment (S2S) contact capability has been expanded and made available for beams also. A new capability for beam contact is provided by facilitating the automatic expansion of beam elements to represent the real cross section of the beams. The expanded cross sections are used to accurately capture the contact behavior with segment to segment contact. It should be noted that this expanded form is only used for the contact procedures and the regular beam representations are still used for assembly, solve, and recovery. This novel treatment of the beams also helps users to simulate all kinds of situations involving beam contact including external beam segment contact, end-beam contact, tube inside tube contact, etc. Some applications involving beam-beam contact include offshore pipelines and risers. The present chapter demonstrates this new capability of beam contact for an axially compressed stiffened panel.

Requested Solutions

A numerical analysis will be performed to demonstrate the glued and touching contact of beams with other deformable bodies by using the expanded representation of cross section of beam elements. A panel stiffened by beams is used for the demonstration. Such stiffened panels are commonly found in automotive and aerospace applications (for example, car floors, fuselages, etc).

Modeling Details

The model shown in [Figure 3.39-1](#) is a stiffened shell panel in contact with beams. The shell panel is stiffened with three I-beams on one side and five circular tubes on other side. During deformation, the I-beams will contact a solid beam on one side and these I-beams also contact two tubes (a tube inside another tube) on the other side.

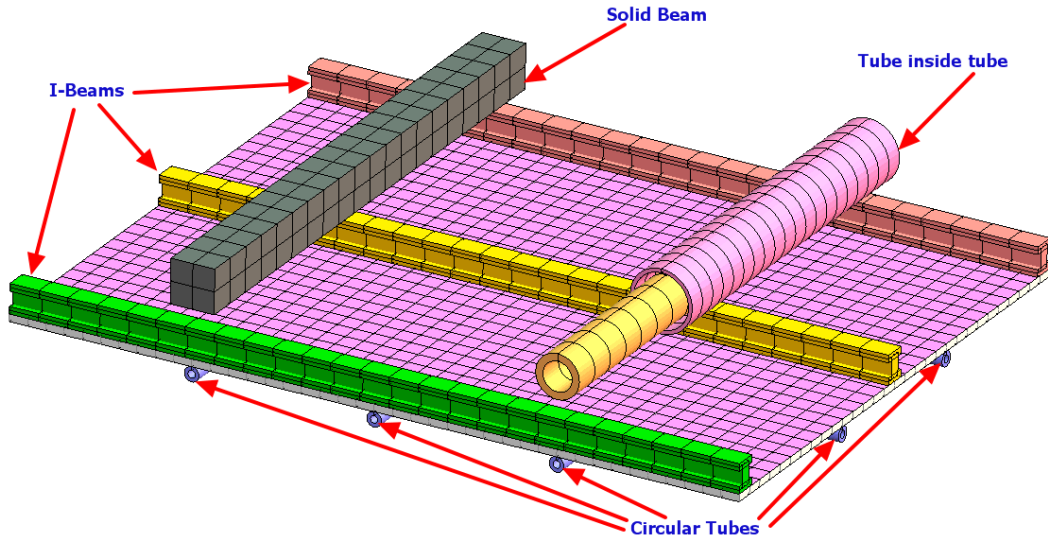


Figure 3.39-1 Details of Stiffened Shell model

The line representation of all beams used in this model is shown in Figure 3.39-2. However, for the treatment of contact, the true representation of beam cross sections (as shown in Figure 3.39-3) is used for this model.

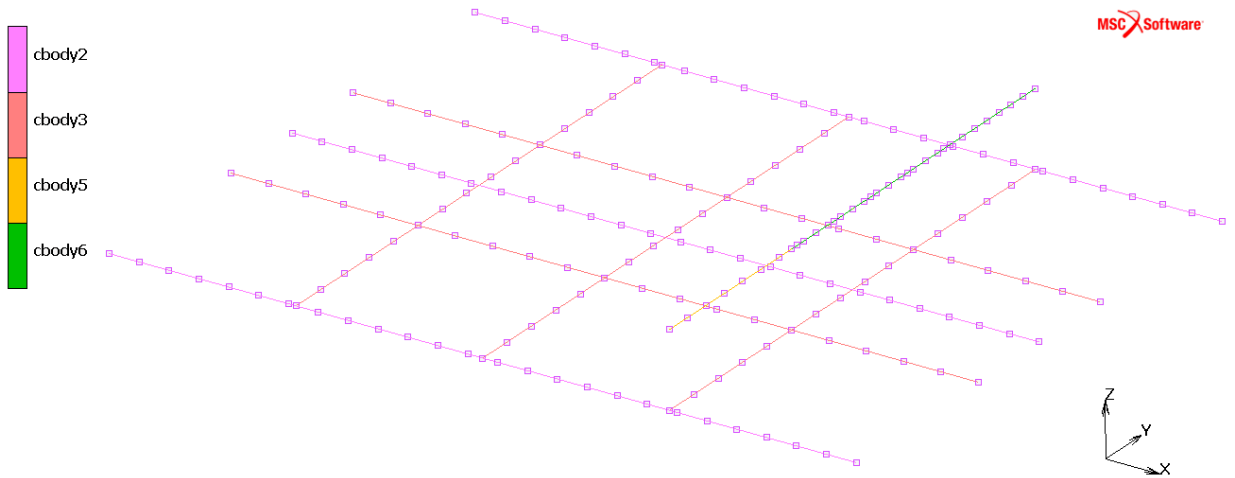


Figure 3.39-2 Stick Representation of Beam Elements

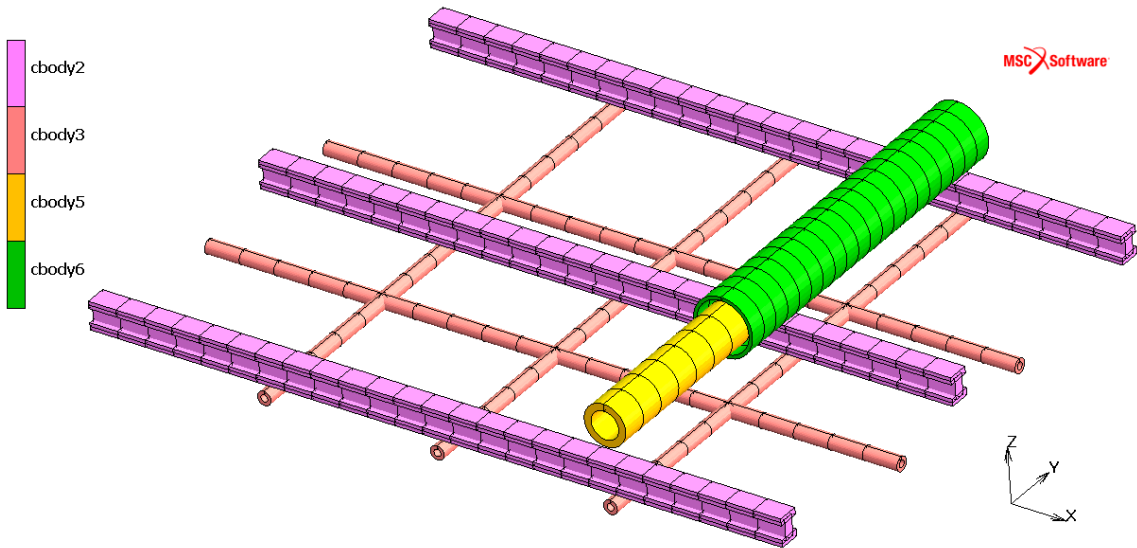


Figure 3.39-3 Representation of Beam Elements for Contact Detection

Element Modeling

The shell panel is modeled with shell element type 75 and solid beam is modeled with solid element type 7. All other beams are modeled with closed section beam element type 78. Note that the solid beam could also have been modeled by beam element 78; however, in order to demonstrate beam-solid contact, the solid beam is modeled by element 7. The element types used for various parts of the model are shown in [Figure 3.39-4](#).

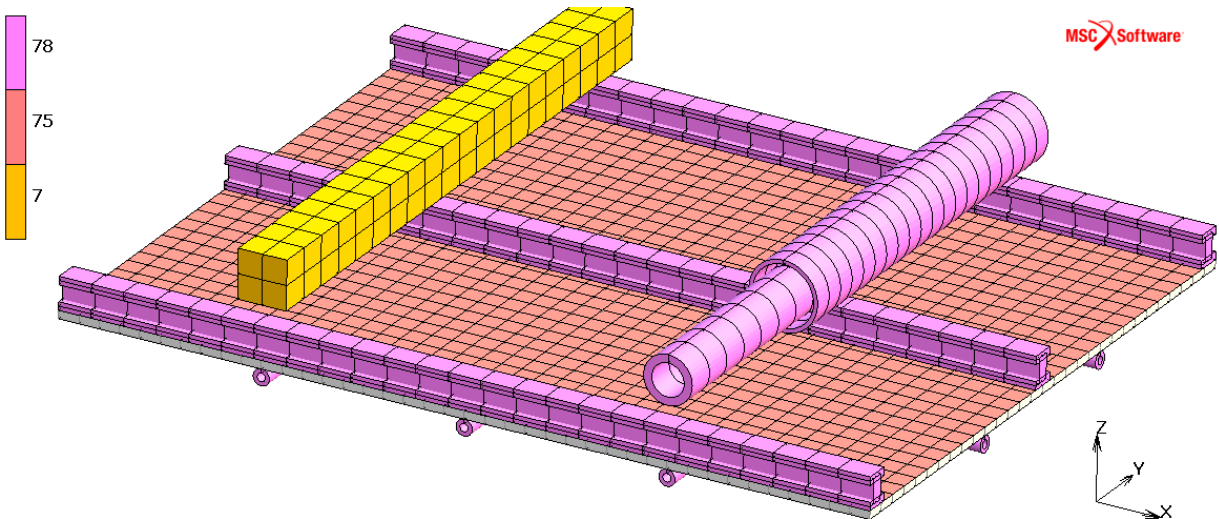


Figure 3.39-4 Element Types used in the Model

Material Modeling

The isotropic elastic perfect plastic material properties $E = 0.6 \times 10^5 N/mm^2$, $\nu = 0.3$, and yield stress $= 120 N/mm^2$ are used for shell elements. Other parts of the model use isotropic elastic perfectly plastic material properties $E = 2.0 \times 10^5 N/mm^2$, $\nu = 0.3$, and yield stress $\sigma_y = 300 N/mm^2$. Figure 3.39-5 shows the materials used in different parts of the model.

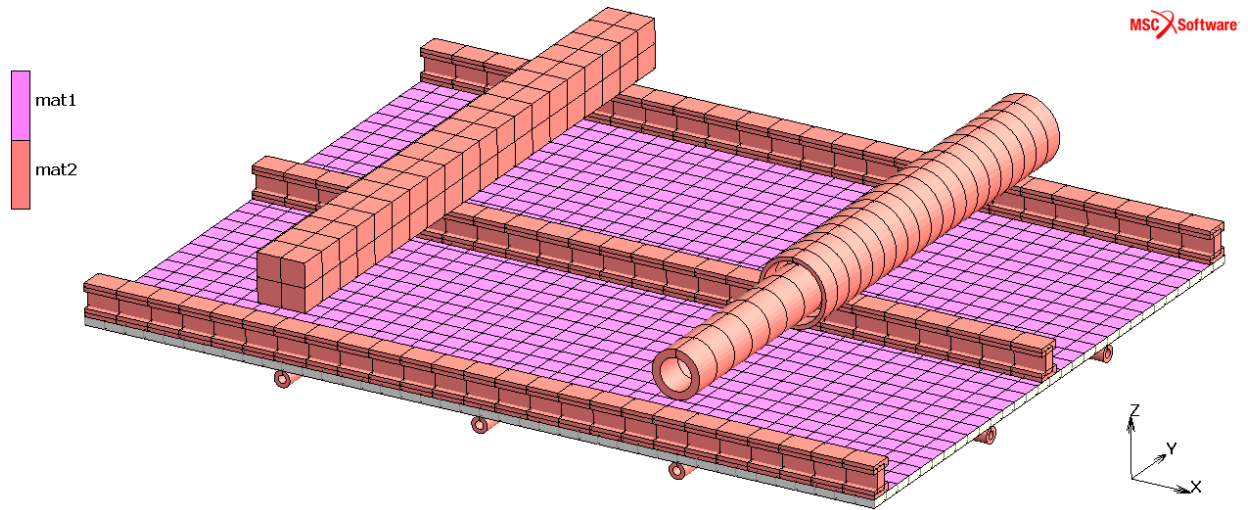


Figure 3.39-5 Material Types used in the Model

Loading Conditions

The shell panel is subjected to axial compression ($u_x = -10$ and $u_y = u_z = 0$) on its one end, with its other end in clamped condition. The details of load and boundary conditions used for various parts of the model are shown in Figure 3.39-6.

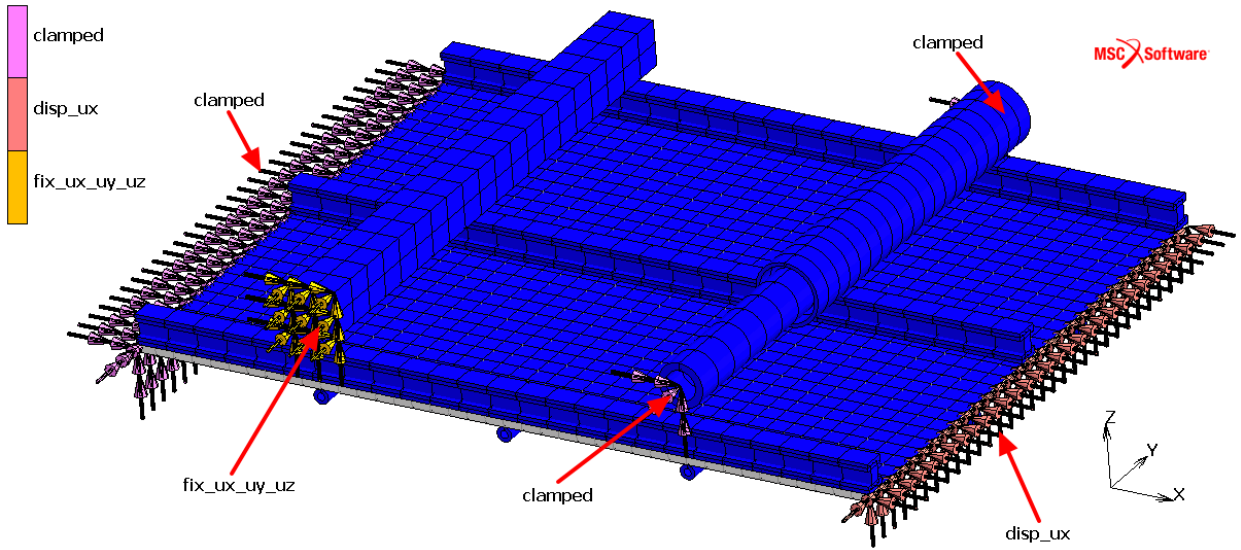


Figure 3.39-6 Load and Boundary Conditions

Contact

Setup of Contact Body and Table

The beam contact capability in Marc allows users to use the actual cross section of beams for the purpose contact detection. This feature works for both glued and touching contact types and simulates beam contact in more realistic way. The contact bodies defined for this model is shown in [Figure 3.39-7](#). The tube inside tube contact between contact bodies cbody5 and cbody6 is also demonstrated in the figure.

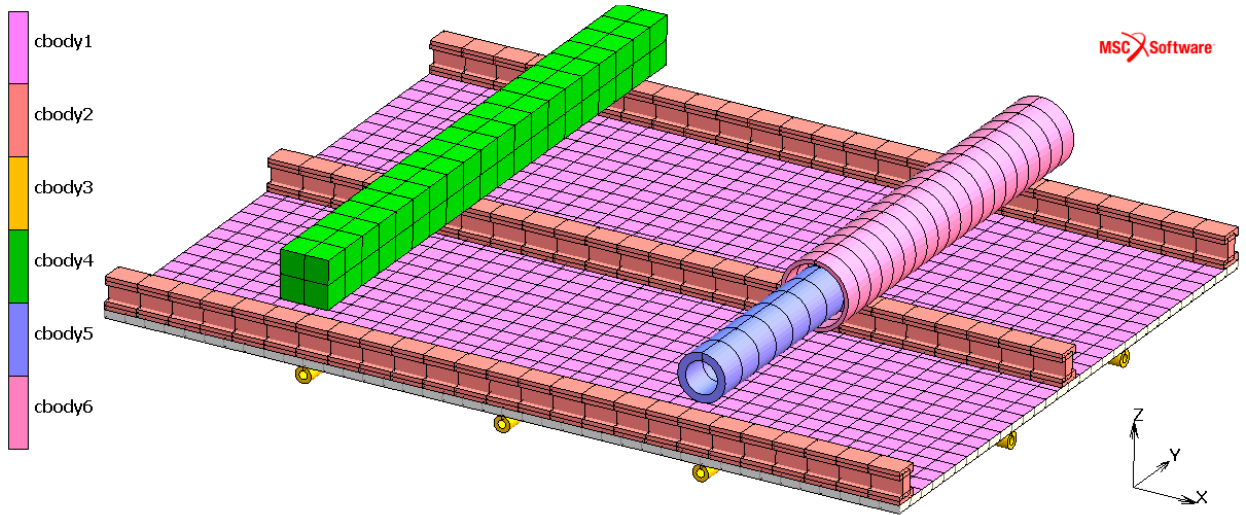


Figure 3.39-7 Contact Bodies used in the Model

Figure 3.39-8 shows the contact table used to define different contact pairs in the model. Circular tubes (cbody3) are glued on the one side shell panel (cbody1) and I-beams (cbody-2) are glued on the other side of shell panel. The effect of beam offset is considered for both circular tubes and I-beams. During the deformation, I-beams also have touching contact with contact bodies 4, 5 & 6. The contact between bodies 5 & 6 simulates the tube inside tube contact.

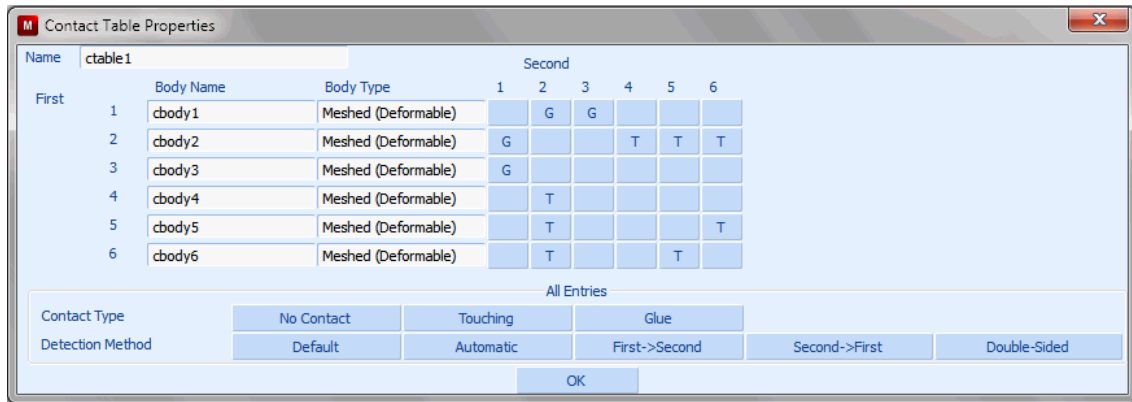


Figure 3.39-8 Contact Pairs used the Model

In order to facilitate the easy setup of multiple body pairs in a contact table, the Contact Interaction Property feature is used in this example. This is useful to define contact between different body pairs which have the same kind of interaction. All glued conditions (Figure 3.39-9) are defined using the contact interaction interact1, as shown in Figure 3.39-10. Similarly, all touching conditions (Figure 3.39-11) are defined using the contact interaction interact2, as shown in Figure 3.39-12.

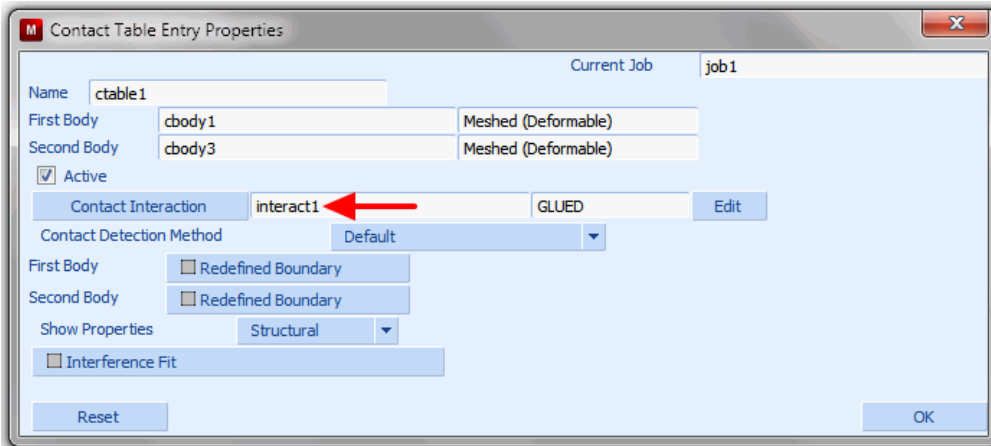


Figure 3.39-9 Glued Contact Type in Contact Table

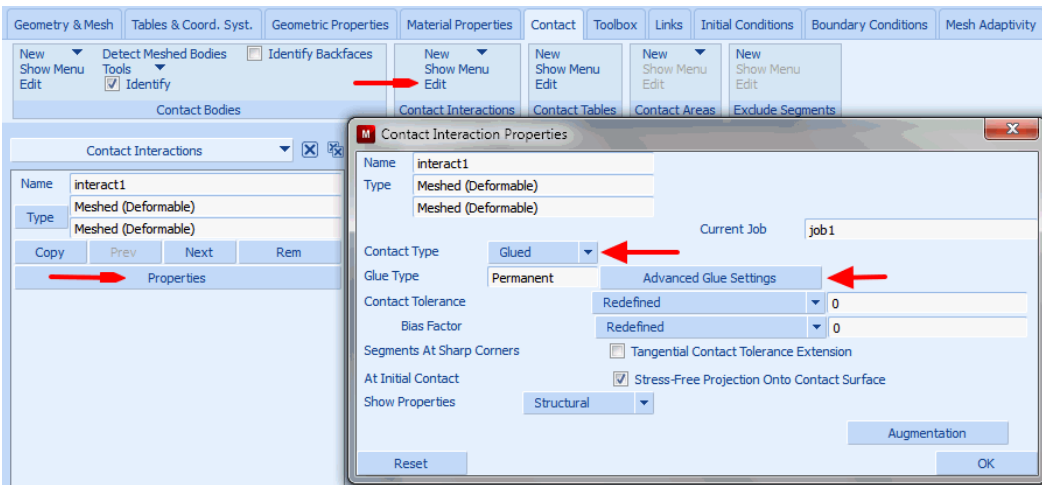


Figure 3.39-10 Contact Interaction for Glued Contact

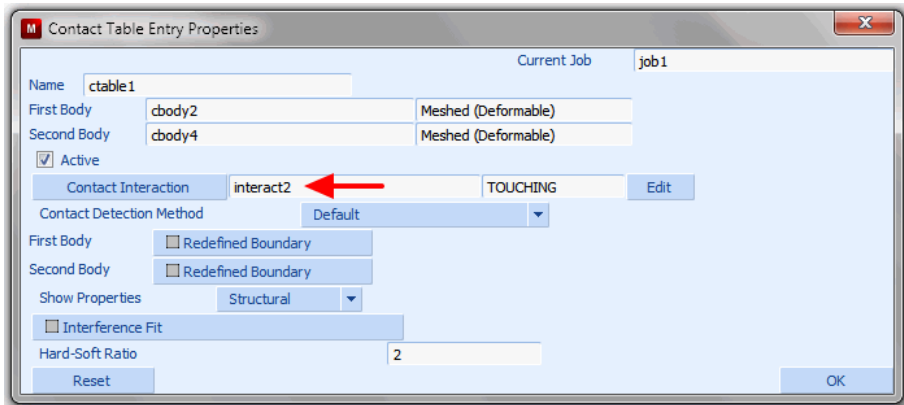


Figure 3.39-11 Touching Contact Type in Contact Table

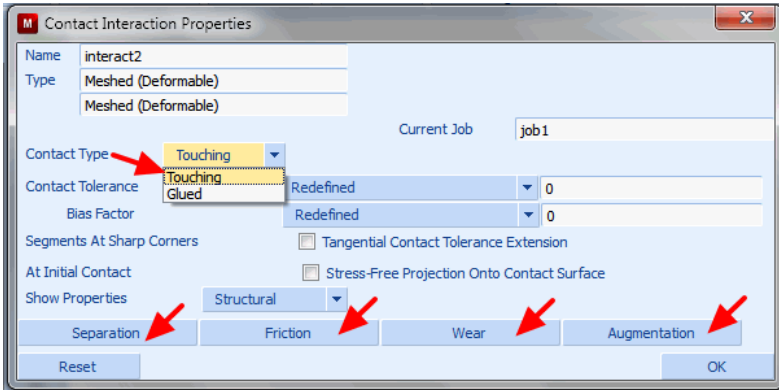


Figure 3.39-12 Contact Interaction for Touching Contact

Setup of Geometric Properties for Contact

The association of the beam cross-section with contact is done in the Geometry Properties menu. This is shown in [Figure 3.39-13](#) for the circular tubes. The menu allows the user to define the actual cross-sectional features that will be available in the expanded form. For example, if the inside patches of the tube are not going to make any contact, it makes sense to choose Outside Patches only. The menu also allows users to define end caps for beams and connecting caps at junctions ([Figure 3.39-14](#)). Note that, in the present example, the end caps and connecting caps are not strictly required since no contact is expected at the ends. However, for demonstration purposes, the caps are turned on.

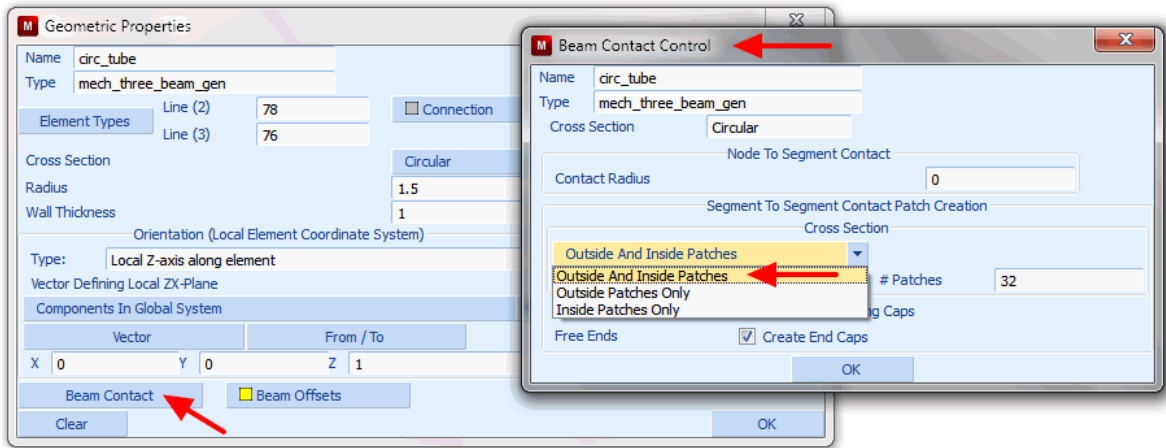


Figure 3.39-13 Patches Defined in Beam Contact

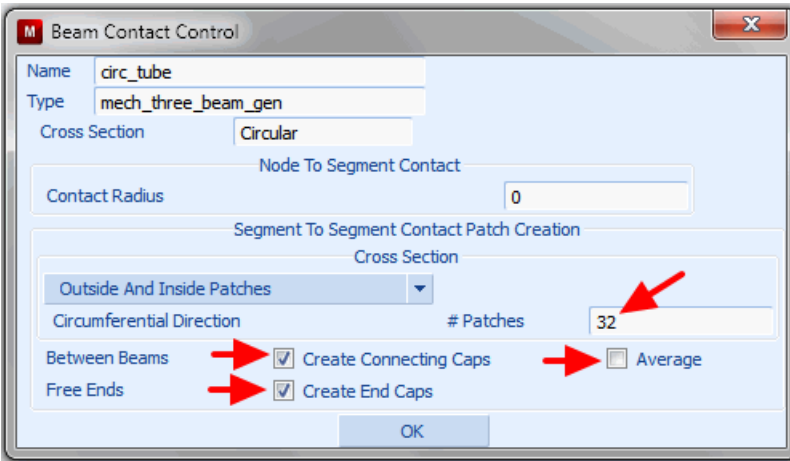


Figure 3.39-14 End and Connecting Caps for Beam Contact

Setup of Job Options for Contact

To make use of new beam contact capability, users should use segment to segment contact capability in Marc and it is activated in contact control as shown in [Figure 3.39-15](#). It is important to understand that Marc uses the expanded beam cross-section only for the contact procedures and the regular post file continues to show the beams as line representations. However, in order to get a better visualization of the contact process, Marc allows users to create and extended post file which contains the expanded beam cross-section. This option can be used for visualization of contact status and displacement results in the extended beam section ([Figure 3.39-16](#)). Note that when this option is turned on, two additional post files are created: `jobname_beam.t16` and `jobname_modelandbeam.t16`. The first post file shows the expanded beam sections only and the second post file is a wrapper file that combines the regular post file and the expanded beam post file.

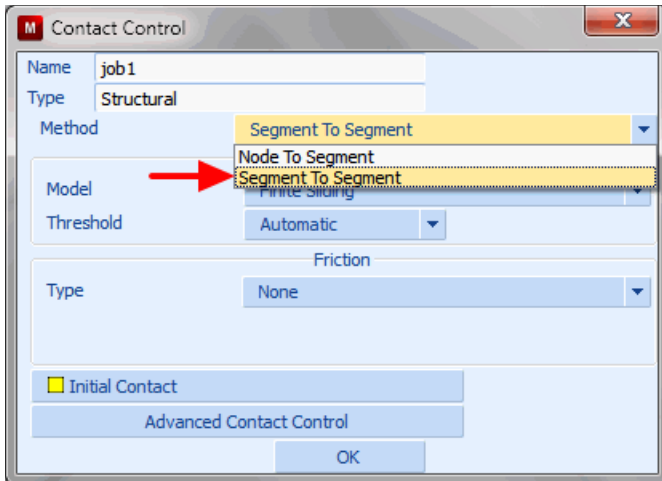


Figure 3.39-15 Segment-to-Segment Contact Definition for Beam Contact

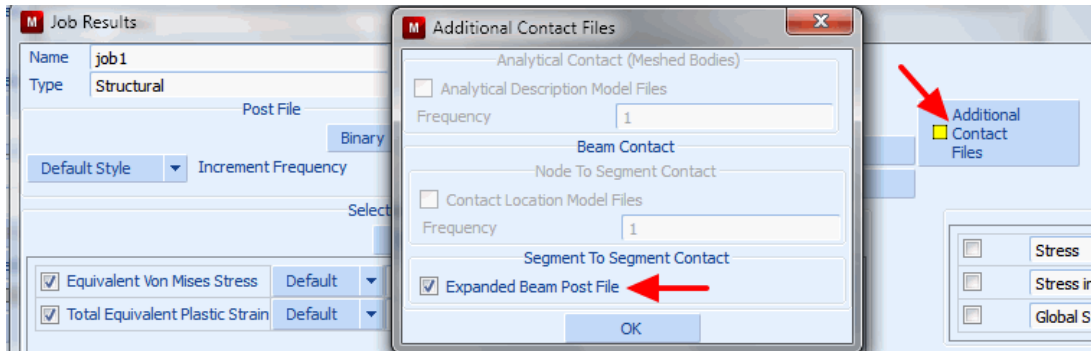


Figure 3.39-16 Request for Additional Post File for Beam Contact

Result and Plots

The I-beams glued to the shell panel touches solid beams, inner and outer tubes during post buckling deformation. [Figure 3.39-17](#) shows the contact status plot for the entire model while [Figure 3.39-18](#) shows contact status plot for a tube inside tube contact between inner and outer tubes. The uz-displacement plot for the entire model is shown in [Figure 3.39-19](#).

Inc: 26
Time: 1.000e+000

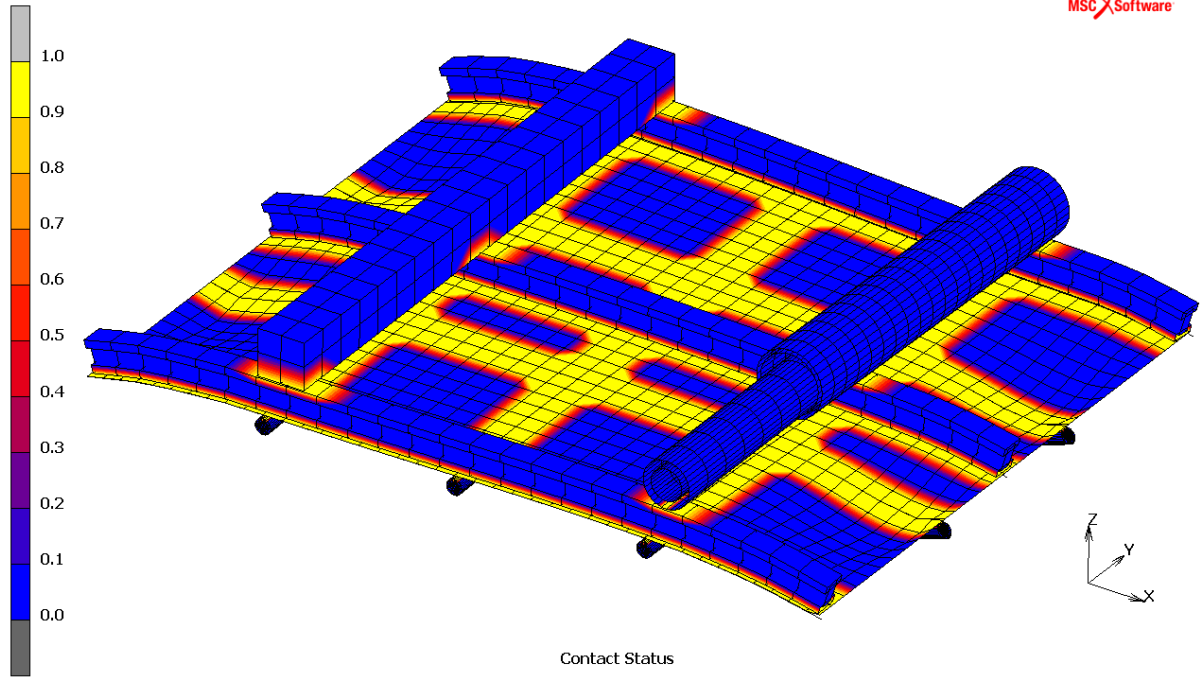


Figure 3.39-17 Contact Status Plot

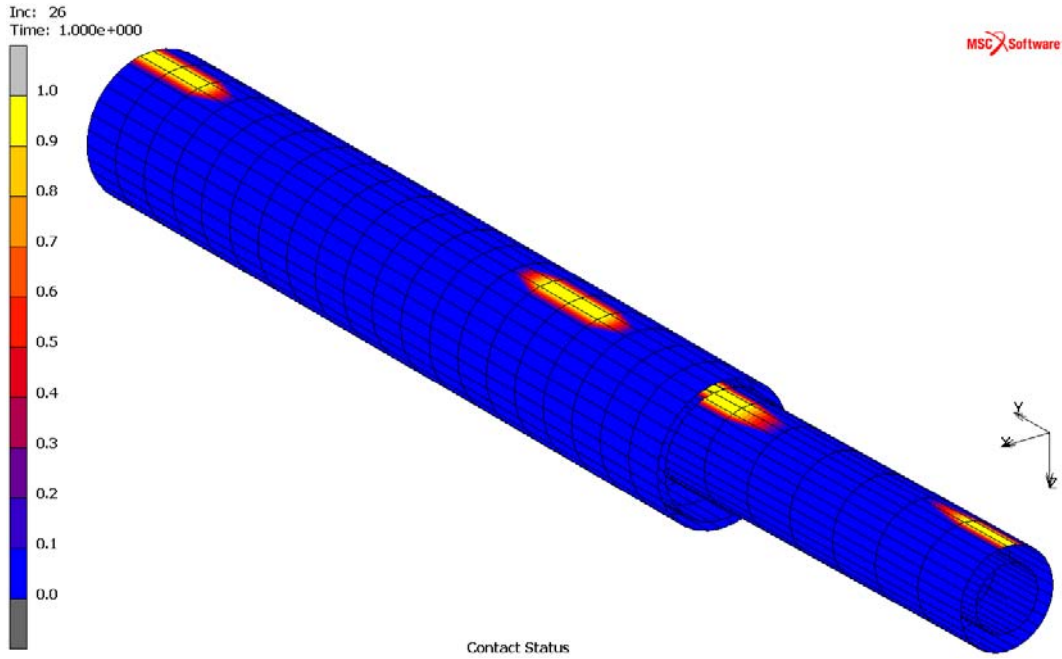


Figure 3.39-18 Contact Status Plot for Tube-tube Contact

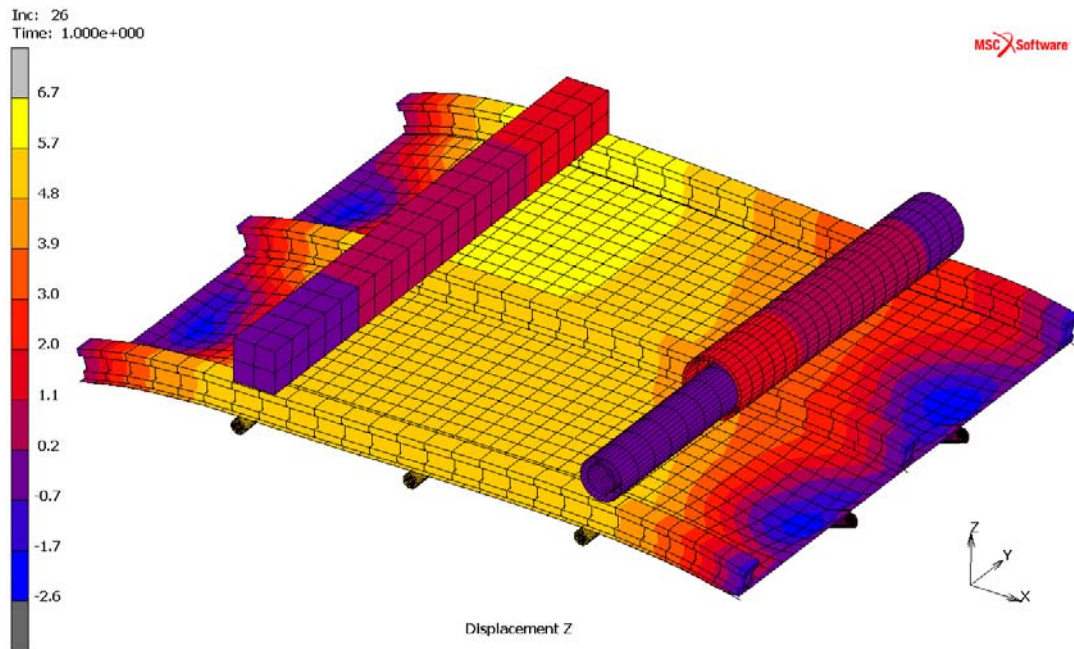


Figure 3.39-19 UZ-Displacement Plot

Input Files

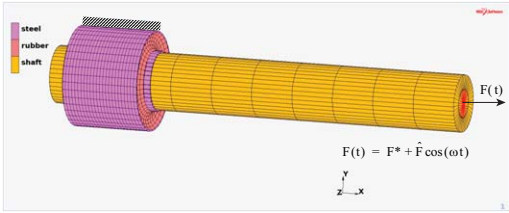
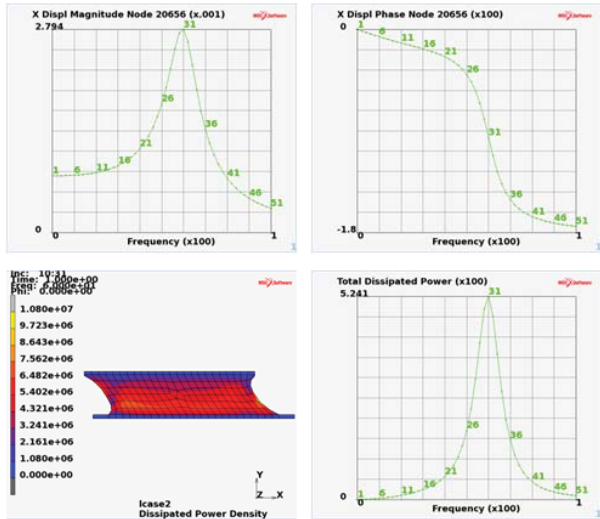
The files below are on your delivery media or they can be downloaded by your web browser by clicking the links (file names) below.

File	Description
panel_and_beams.mud	Mentat model file

3.40 Frequency Response Analysis of a Flexible Bushing

- Summary 1750
- Bushing and Model Geometry 1752
- Material Modeling 1753
- Loads, Boundary Conditions, and Constraints 1755
- Loadcase and Job Definition 1757
- Results and Conclusions 1758
- Modeling Tips 1761
- Input Files 1761

Summary

Title	Frequency Response Analysis of a Flexible Bushing
Problem features	<ul style="list-style-type: none"> • Viscoelastic material properties are used in the frequency domain to describe frequency dependent stiffness and damping properties of a rubber material • Effects of a static preload are included in the frequency response analysis
Geometry	<p>Bushing fitted onto a shaft</p>  <p>$F(t) = F^* + \hat{F} \cos(\omega t)$</p>
Material properties	<ul style="list-style-type: none"> • Rubber: Hyperelastic with viscoelastic behavior • Steel: Elastic
Analysis type	Static preload followed by harmonic excitation
Boundary conditions	<ul style="list-style-type: none"> • Bushing is mounted to the ground and fitted with glued contact onto the shaft • Shaft end is loaded by a point load transferred by RBE3 constraints to the shaft nodes
Element type	8-node hexahedral element type 7
FE results	<p>Amplitude and phase response as function of frequency of the harmonically excited node together with dissipated power density at critical frequency and total dissipated power as function of frequency.</p> 

Flexible rubber bushings like shown in Figure 3.40-1 can be used to great advantage as a solution for bedding problems in mobile appliances and machines or between machine parts that have to be flexible relative to each other. They also have a high noise and vibration-insulating quality and are therefore often used to make low-noise and vibration-free machinery.



Figure 3.40-1 Examples of Flexible Bushings

A frequency response finite element analysis of such a bushing fitted on a steel shaft as shown in is performed. Viscoelastic properties of the rubber material are taken into account to describe the damping aspects of the material. The structure is mounted to the ground by holding the bushing and carries a static axial preload (F^* in Figure 3.40-2). After application of the preload, it is excited harmonically by an additional axial load ($\hat{F} \cos(\omega t)$ in Figure 3.40-2) in a frequency range of 0 to 100 Hz. Of interest are the amplitude and phase response of the structure as a function of frequency and the energy losses due to the damping. This amplitude and phase response will be measured at the location where the point load is being applied.

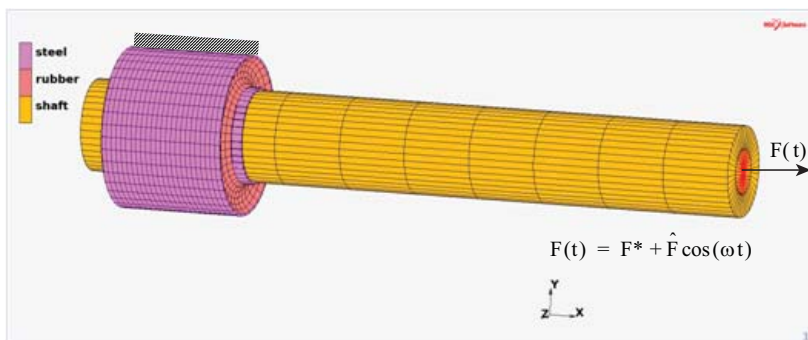


Figure 3.40-2 Flexible Bushing Fitted on a Shaft

Bushing and Model Geometry

The bushing geometry is shown in [Figure 3.40-3](#). The rubber material is vulcanized between two steel tubes which each have a thickness of 1 mm. The inner diameter of the inner tube is 40 mm and its length is 65 mm. The outer diameter of the outer tube is 70 mm and its length is 55 mm. The thickness of the rubber between the two tubes therefore is 13 mm.

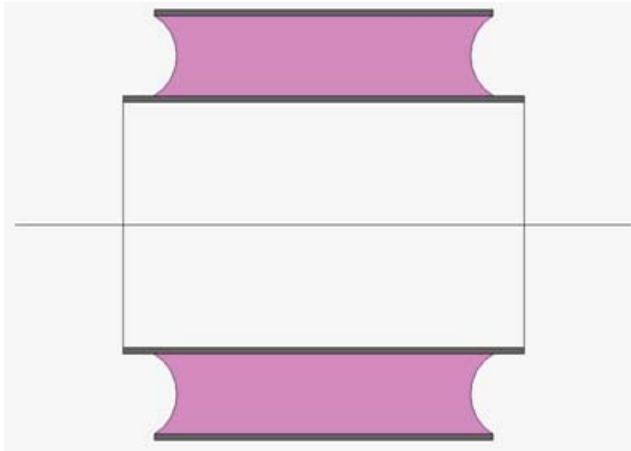


Figure 3.40-3 Bushing Geometry

The bushing is fitted onto a hollow steel shaft which has an inner diameter of 20 mm. A length portion of 300 mm of the shaft has been modeled as shown in [Figure 3.40-2](#). The remaining structural parts that are connected to the shaft are being represented by a point mass of 10 kg which gets rigidly connected to the end of the shaft as shown in [Figure 3.40-4](#).

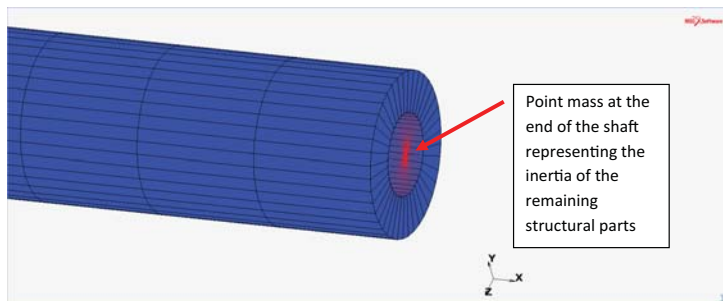


Figure 3.40-4 Point Mass Fixed to End of Shaft

Material Modeling

The time independent elastic behavior of the rubber material is modeled with a Neo Hookean strain energy function which has the following form in terms of the first invariant I_1 of deformation

$$W = C_{10}(I_1 - 3)$$

The value of the material constant is taken as $C_{10} = 1.5$ MPa, where it should be noted that this is the instantaneous (short term) value. The rubber material is assumed to be almost incompressible using a high bulk modulus of 15000 MPa. This value was automatically computed by Marc, since the bulk modulus was left unspecified in the input.

The viscoelastic behavior is modeled with a one term Prony series of which the representation in the time domain has the following form

$$g(t) = g_\infty + g_1 e^{-\frac{t}{\tau_1}}$$

This relaxation function is given in its normalized form meaning that its instantaneous (short term) value must be 1, i.e. $g(t = 0) = 1$. The factor g_∞ determines the long term behavior of the material (i.e. for $t \rightarrow \infty$) and determines the elastic material stiffness in static equilibrium states which for our Neo Hookean material leads to $C_{10_\infty} = g_\infty C_{10}$. For this material, the long term stiffness is two thirds of the instantaneous stiffness, so $C_{10_\infty} = 1$ MPa and the Prony factor in the expansion therefore is $g_1 = \frac{1}{3}$. The associated relaxation time is $\tau_1 = 0.0032$ seconds.

In the frequency domain this relaxation function leads to a frequency dependent storage factor of

$$g^{storage}(\omega) = 1 - \frac{g_1}{1 + (\omega\tau_1)^2}$$

and a frequency dependent loss factor of

$$g^{loss}(\omega) = \frac{g_1 \omega \tau_1}{1 + (\omega\tau_1)^2}$$

The storage factor determines the frequency dependent stiffness properties of the material and the loss factor the frequency dependent damping properties. Their graphs are shown in [Figure 3.40-5](#) for the frequency range of interest.

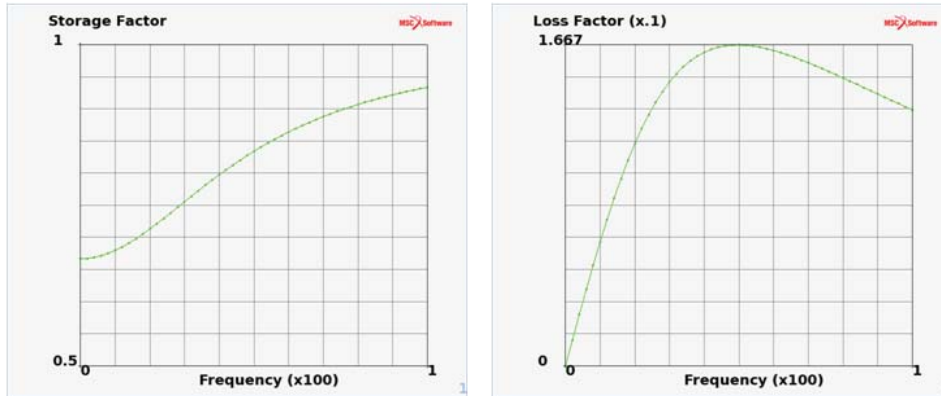


Figure 3.40-5 Storage and Loss Factor of the Rubber Material as a Function of Frequency

The mass density of the rubber material is 1000 kg/m^3 . The Young's modulus of the steel material is taken as $E = 200 \text{ GPa}$ and its Poisson's ratio is taken as $\nu = 0.3$. The steel has a mass density of 7800 kg/m^3 .

These properties can easily be entered in the Material Properties menu of Mentat as shown in Figure 3.40-6 for the rubber material.

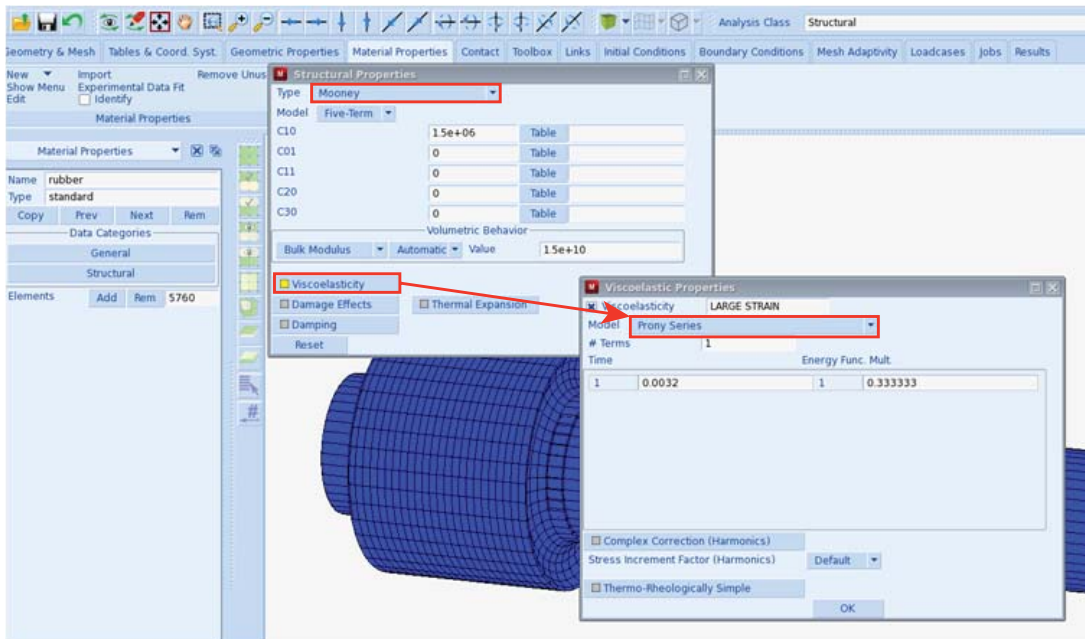


Figure 3.40-6 Menus to Enter Elastic and Viscoelastic Rubber Material Properties

Loads, Boundary Conditions, and Constraints

The outer steel tube of the bushing is mounted to the ground by applying fixed displacements in all three coordinate directions to the nodes on its outer lateral surface as shown on the left in [Figure 3.40-7](#).

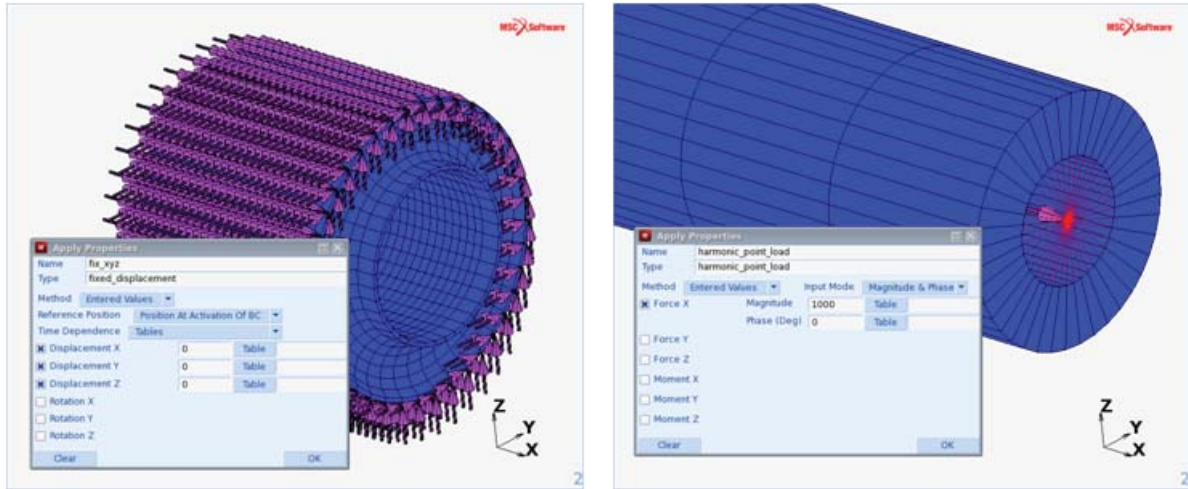


Figure 3.40-7 Loads and Boundary Conditions

A static preload of 10 kN is applied to the node carrying the additional structural mass at the right end of the steel shaft (node 20656). This node is connected to shaft nodes using RBE3 constraints, as illustrated by the spokes shown on the right in [Figure 3.40-7](#). This results in an even load and mass distribution over the shaft nodes involved in the RBE3 constraints. The harmonic excitation is performed by applying a harmonic point load of 1 kN at this node after the application of the static preload. This harmonic point load is shown on the right in [Figure 3.40-7](#).

The bushing is fixed to the shaft using glued contact constraints as shown in [Figure 3.40-8](#) where the two deformable contact bodies are illustrated. The glued contact conditions are activated on the Contact Table Properties menu shown in the figure.

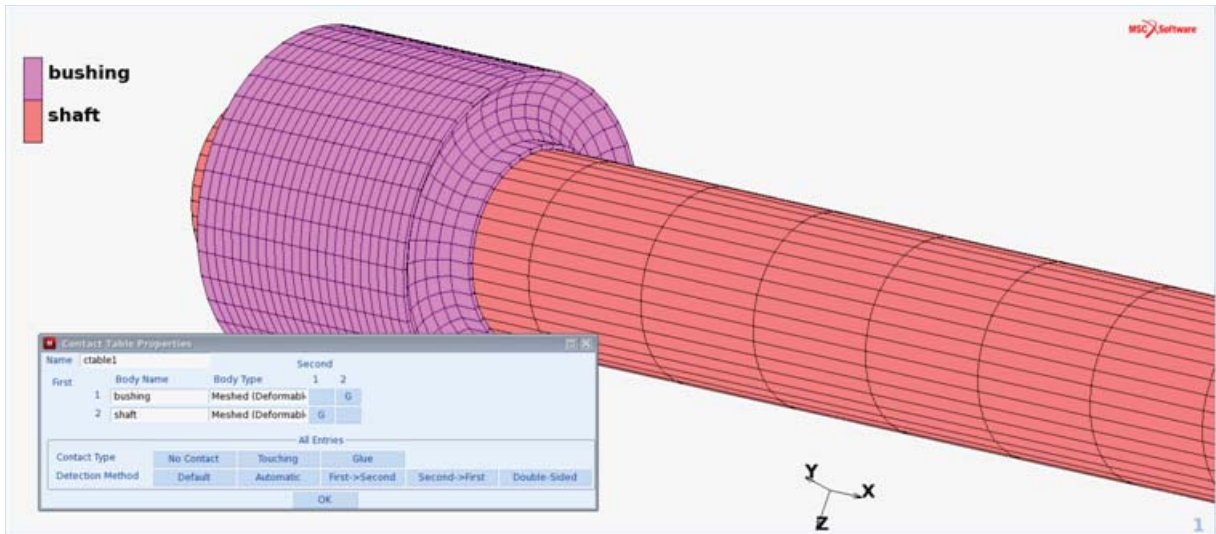


Figure 3.40-8 Glued Contact between Bushing and Shaft

The point mass of 10 kg that accounts for the inertia of the remaining structural parts that are not explicitly modeled is entered in the Initial Conditions menu as shown in Figure 3.40-9. The RBE3 constraints are defined in the Links menu. All three degrees of freedom of the reference node (node 20656) are tied to the three degrees of freedom of the nodes of the shaft on the inner ring at its end using a coefficient (weight factor) of 1.

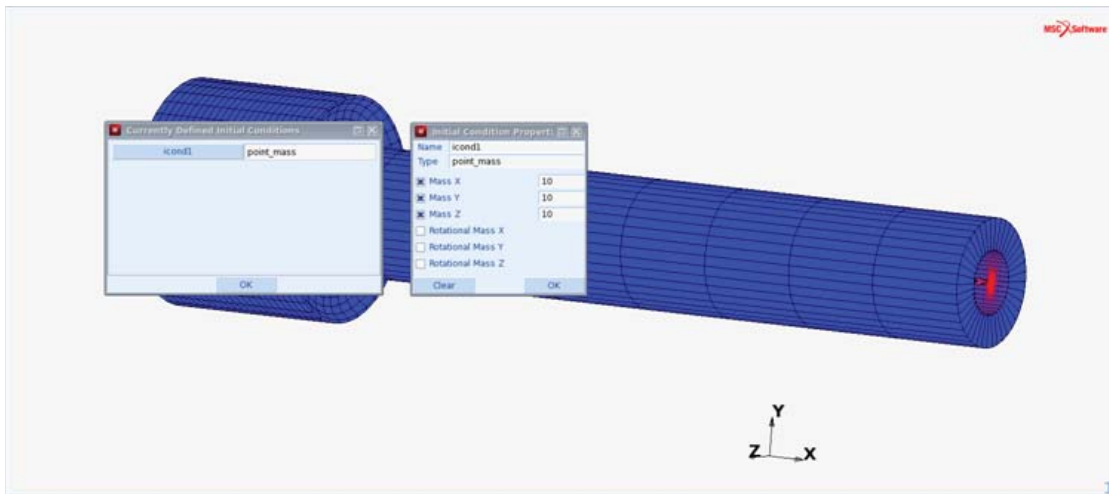


Figure 3.40-9 Definition of the Point Mass of 10 kg

Loadcase and Job Definition

Two loadcases are defined which are used to define the job. The first loadcase (Figure 3.40-10) applies the static preload of 10 kN in 10 equal steps of 1 kN. The second loadcase (Figure 3.40-11) applies the harmonic excitation over a frequency range from 0 to 100 Hz in increments of 2 Hz resulting in 51 harmonic sub-increments. The force amplitude of the harmonic excitation is 1 kN. In the job definition (Figure 3.40-12) “large strain” and “complex damping” have been activated on the Analysis Options menu of the Job Properties menu.

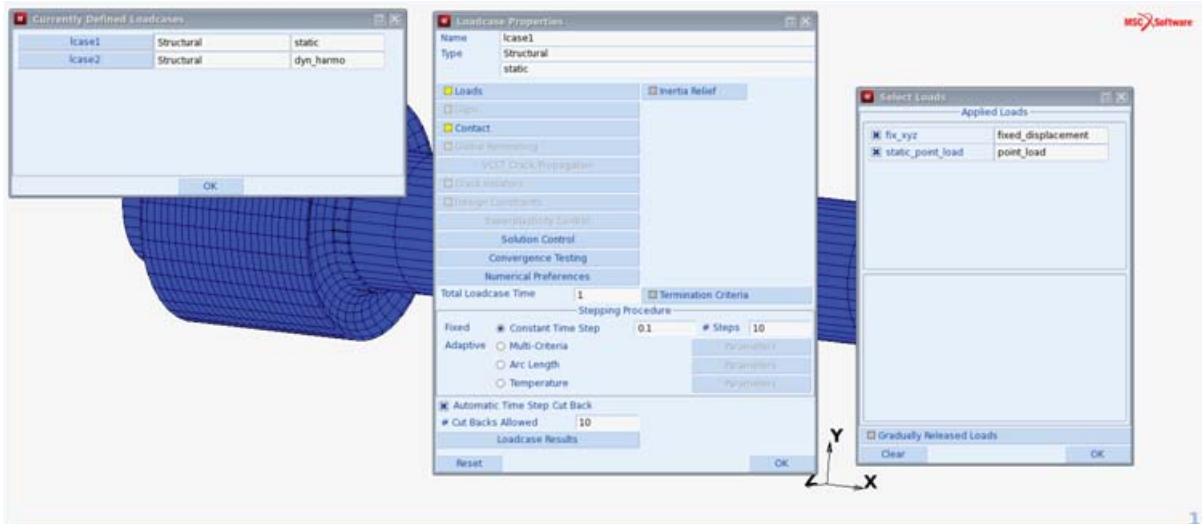


Figure 3.40-10 Definition of the Static Loadcase

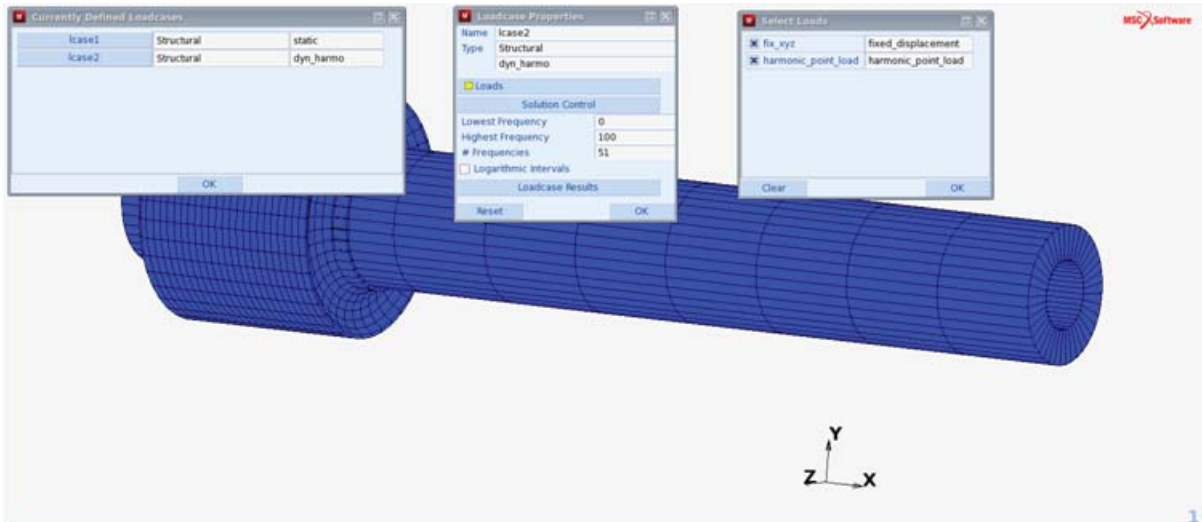


Figure 3.40-11 Definition of the Harmonic Loadcase

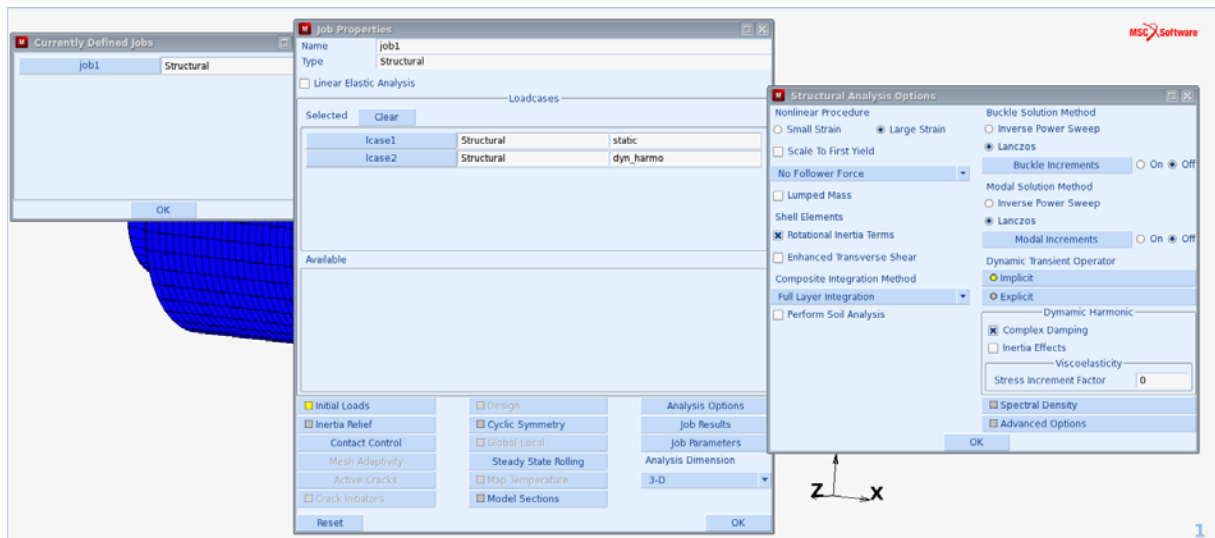


Figure 3.40-12 Combining the two loadcase into a job

Per default nodal results like displacements, external forces and reaction forces are written to the post file for further postprocessing. In addition, element quantities can be selected. For this analysis, the stress and total strain for further postprocessing of static results and the dissipated power density (Marc post code 620) for further postprocessing of harmonic results have been selected under the Job Results submenu of the Job Properties menu.

Results and Conclusions

Among the results of interest in this analysis are the static deformation results of the bushing and the displacement amplitude and phase response as a function of excitation frequency of the node where the harmonic point load is being applied (node 20656). Further results of interest may be the dissipated power as a result of the damping and its distribution through the structure. The harmonic results will be frequency dependent, since the rubber stiffness and damping are frequency dependent and of course there are inertia effects. The static force-displacement result for the node carrying the point load is shown in Figure 3.40-13. The maximum displacement at 10 kN is approximately 7.8 mm and up to this deformation it can be concluded that the force-displacement behavior of the bushing is almost linear. This is largely a result of the chosen Neo Hookean material representation and the observation that the applied load will primarily lead to shear deformations in the bushing. The Neo Hookean material model leads to a linear relation between shear stress and shear strain for any amount of shearing. If a more complicated material representation would be chosen, like e.g. a multi-term Mooney model or an Ogden model, the relation between shear stress and shear strain would certainly be nonlinear and nonlinear effects could become more pronounced.

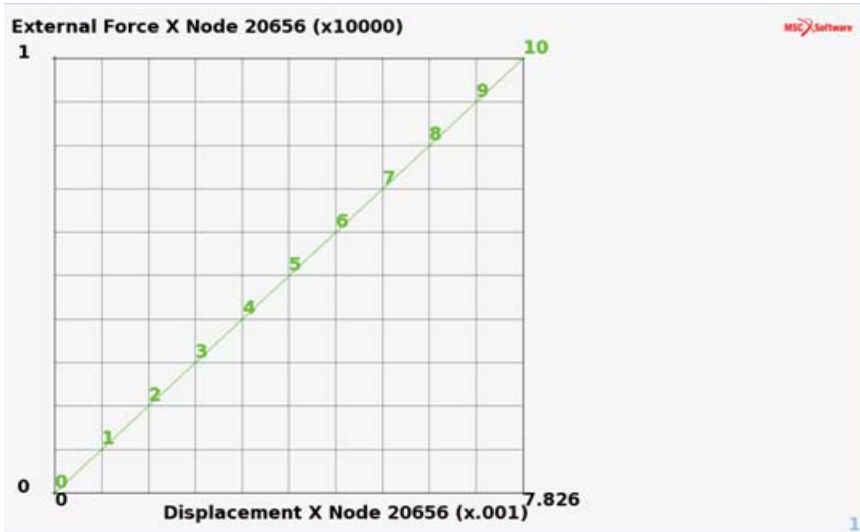


Figure 3.40-13 Static Force-displacement Result for Node 20656

In Figure 3.40-14 the undeformed section (left) and the deformed section at 10 kN static load (right) of the bushing are shown. The shown deformations are on a one-to-one scale.

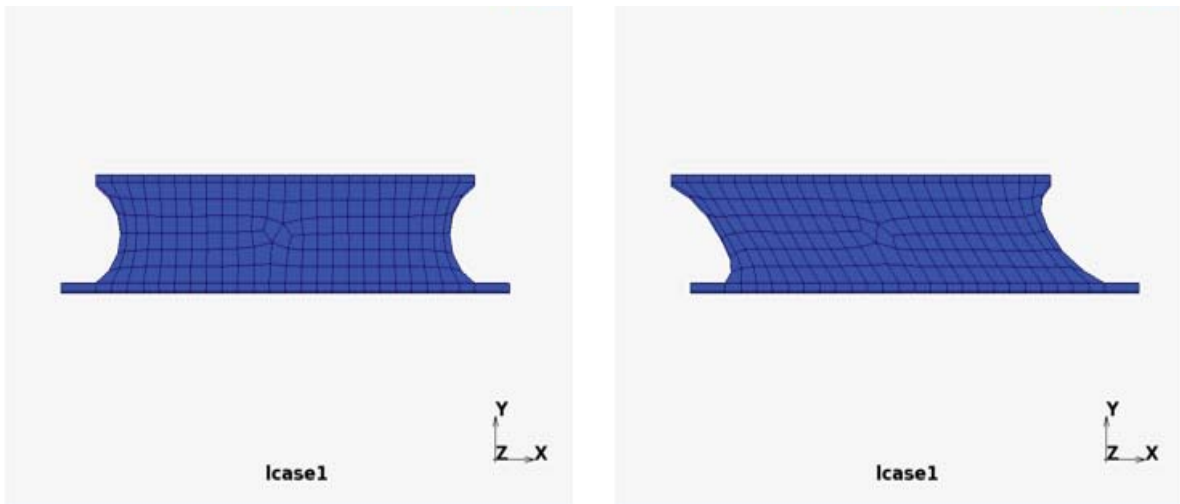


Figure 3.40-14 Undeformed and Deformed Section of the Bushing

In Figure 3.40-15, the harmonic displacement magnitude (left) and phase (right) of the harmonically excited node are shown as a function of frequency. It can be observed that the structure must have an eigenfrequency near 60 Hz, where the displacement magnitude reaches a maximum of approximately 2.8 mm.

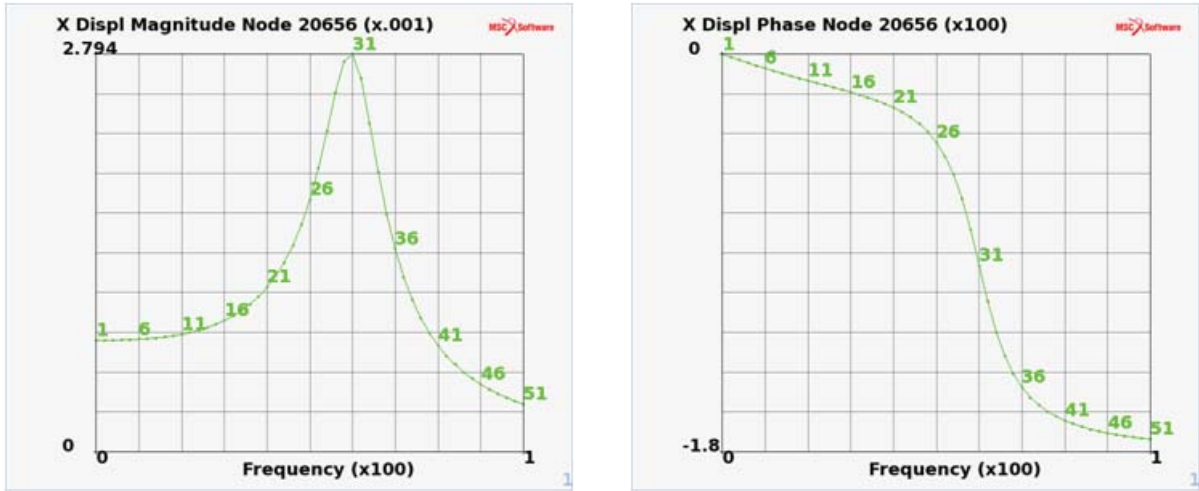


Figure 3.40-15 Displacement Magnitude and Phase of the Harmonically Excited Node

A further quantity that may be of interest is the energy being dissipated during the harmonic excitations as a result of the damping in the material. In Figure 3.40-16 on the left, the total dissipated power is shown as a function of frequency. It can be seen that near the eigenfrequency the maximum power dissipation is approximately 524 W, which considering the dimensions of the bushing may lead to a considerable amount of heating, if the vibration is to be sustained for a longer period of time, so the design of our structure is considered not to be a good one. On the right in this figure the dissipated power density (i.e. power per unit volume, in our chosen unit system being W/m^3) is shown for the sub-increment with the highest dissipation rate (sub-increment 31 with a frequency of 60 Hz). On the inner and outer diameter the dissipation remains zero, since for the steel tubes no damping is present.

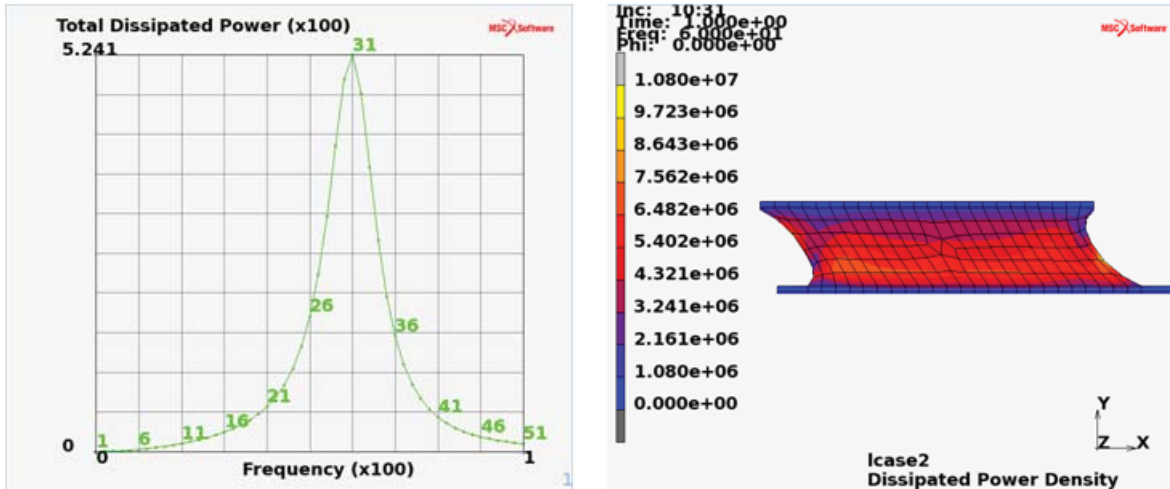


Figure 3.40-16 Energy Dissipation as a Result of the Damping

Modeling Tips

The viscoelastic material properties were entered by a normalized Prony series. In many instances, this data is taken from frequency response measurements where amplitude responses and phase changes have been measured. From these responses, the storage and loss modulus can be evaluated directly, and it is not necessary to evaluate Prony parameters through some kind of curve fitting procedure to obtain the representation of the viscoelastic material data. Therefore as an alternative to the Prony series, the storage and loss moduli can be entered in Mentat directly through tables as a function of frequency as illustrated in Figure 3.40-17. These tables have to be normalized with the instantaneous (short term) stiffness, so the table function values will always be between zero and one.

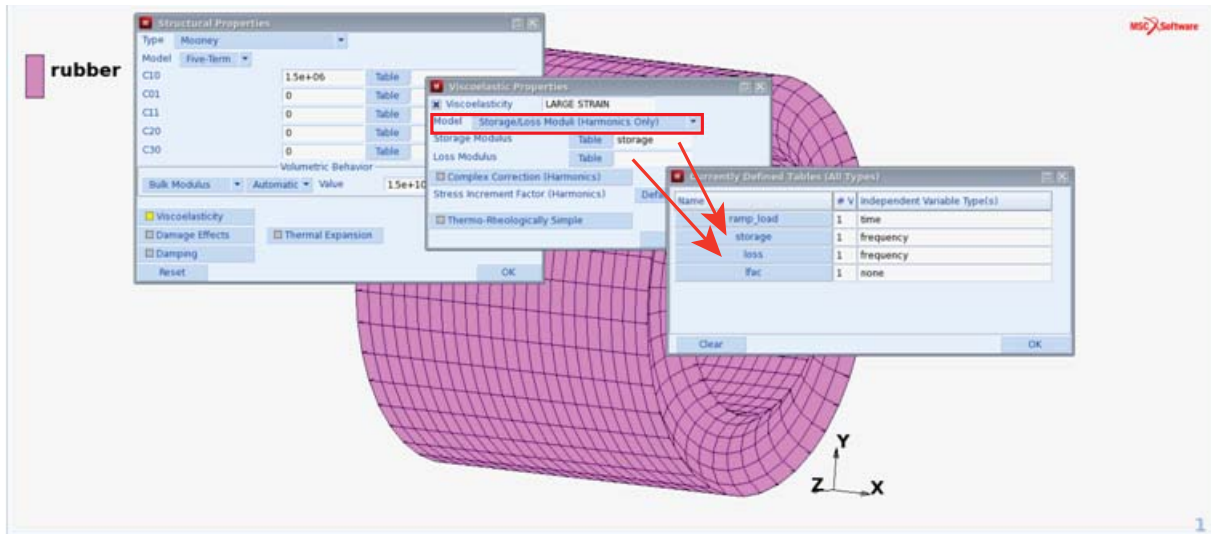


Figure 3.40-17 Frequency Dependent Storage and Loss Moduli Entered Through Tables

Input Files

File	Description
bushing.mud	Mentat model file
bushing_job1.dat	Marc input file

Section 4: Heat Transfer Analysis

4.1 Thermal Contact Analysis of a Pipe

- Chapter Overview 1766
- Pipe in a House 1766
- Input Files 1778

Chapter Overview

This chapter describes the use of thermal contact in Marc. In previous versions of Marc, using contact in a thermal analysis was only possible by doing a coupled mechanical thermal analysis, which led to extra overhead, both in solution time and memory use. The introduction of thermal contact provides the ability to take thermal conduction and small gaps into account. Bodies which are almost touching each other are considered to be in near contact. Different physical heat transfer processes can be simulated for this type of contact such as convection, natural convection, radiation, or distance dependent heat transfer. Near contact can be used in thermal or coupled analyses.

Pipe in a House

The example described here is a pipe which is heated from the inside. The pipe runs through a house, where the dimensions are chosen so that pipe and house initially do not touch. [Figure 4.1-1](#) illustrates this pipe and the house. When the pipe heats up, it expands and, at a certain moment, it comes in contact with the house. To analyze this, a coupled thermal mechanical analysis is performed. When the pipe is almost touching the house, a distance dependent heat transfer is considered. Due to symmetry, an axisymmetric analysis is performed.

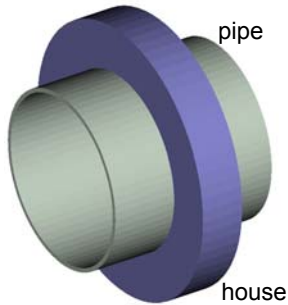


Figure 4.1-1 3-D Model of the Example

Mesh Generation

The mesh is generated by first defining two elements representing the pipe and the house, where a gap of 0.5 mm exists between these two elements. Then these two elements are refined. The outer diameter of the pipe is 0.409 m with a thickness of 0.01 m. The house has an outer diameter of 0.63 m and a thickness of 0.11 m.

MESH GENERATION

NODES ADD

0.1	0.1945	0
0.5	0.1945	0
0.5	0.2045	0
0.1	0.2045	0
0.25	0.205	0

```
0.35 0.205 0
0.35 0.315 0
0.25 0.315 0
ELEMENTS ADD
1 2 3 4
5 6 7 8
SUBDIVIDE
DIVISIONS
16 3 1
ELEMENTS
1 #
DIVISIONS
6 6 1
ELEMENTS
2 #
RETURN
SWEEP
ALL
RETURN
RENUMBER
ALL
RETURN (twice)
```

Boundary Conditions

The x-displacement is set to zero for a node from the pipe and a node from the house to prevent the rigid body mode. The temperature is prescribed as a function of time on the inside of the pipe, where it is first increased from 25°C to 225°C, and then held constant.

```
BOUNDARY CONDITIONS
MECHANICAL
FIXED DISPLACEMENT
DISPLACEMENT X
0
OK
NODES ADD
1 8 #
```

```
RETURN
NEW
THERMAL
  TABLES
    NEW
      1 INDEPENDENT VARIABLE
    TYPE
      time
    ADD
      0 298
      1000 498
      5000 498
    FIT
    RETURN
  FIXED TEMPERATURE
    TEMPERATURE (TOP)
    TABLE
      table1
    OK
  OK
  NODES ADD
    1 2 11 15 19 23 27 31 35 39 43 47 51 55 59 63 67 #
  RETURN (twice)
```

Initial Conditions

Initially, the pipe and house are at room temperature (25°C).

```
INITIAL CONDITIONS
  THERMAL
    TEMPERATURE
      TEMPERATURE (TOP)
        298
    OK
  NODES ADD
  ALL EXIST
  RETURN (twice)
```


Material Properties

The pipe is isotropic and made of aluminium, the house is also isotropic and made of copper. The material properties are listed in [Table 4.1-1](#).

MATERIAL PROPERTIES

NAME

aluminium

ISOTROPIC

YOUNG'S MODULUS

7.1e10

Table 4.1-1 Material Properties

	Aluminium	Copper
Young's modulus (GPa)	71	124
Poisson's ratio	0.3	0.3
Thermal Expansion Coefficient (K ⁻¹)	23 x 10 ⁻⁶	16.8 x 10 ⁻⁶
Conductivity (W/m/K)	237	390
Specific Heat (J/kg/K)	880	387
Mass Density (kg/m ³)	2700	8960

POISSON'S RATIO

0.3

MASS DENSITY

2700

THERMAL EXP

THERMAL EXP COEF

2.3e-5

OK (twice)

HEAT TRANSFER

CONDUCTIVITY

237

SPECIFIC HEAT

880

MASS DENSITY

2700

OK
ELEMENTS
49 to 84 #

The material properties for the house are added in a similar way.

RETURN

Contact

The pipe and the house are defined as separate contact bodies. The contact properties are set in the CONTACT TABLE option, where the near contact distance is 0.3 mm, the contact heat transfer coefficient is 100 W/m^2 , and the distance dependent heat transfer coefficient is 1 W/m^2 . The menu for entering the contact table entry properties including the near contact distance is shown in Figure 4.1-2.

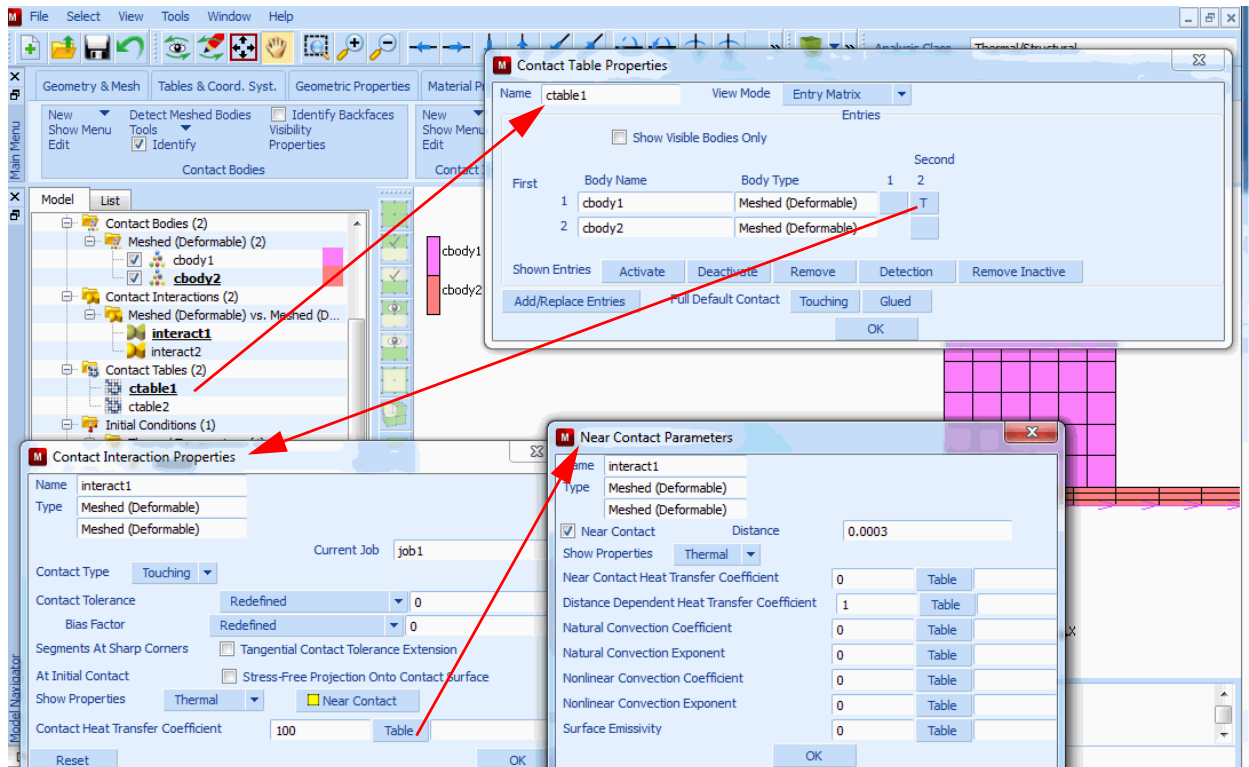


Figure 4.1-2 Menu for entering Contact Table Entry Properties

```
CONTACT
  CONTACT BODIES
    DEFORMABLE
      OK
    ELEMENTS
      49 to 84 #
    NEW
    DEFORMABLE
      OK
    ELEMENTS
      1 to 48 #
    RETURN
  CONTACT TABLES
    NEW
    PROPERTIES
      1 2
        CONTACT TYPE: TOUCHING
        CONTACT DETECTION METHOD: FIRST->SECOND
        NEAR CONTACT
        DISTANCE
          0.0003
        THERMAL PROPERTIES
        CONTACT HEAT TRANSFER COEFFICIENT
```

Loadcases and Job Parameters

A quasi-static analysis is performed, where two loadcases are defined. In the first loadcase, the temperature inside the pipe is increased 200 K in 100 increments during 1000 seconds. In the second loadcase, the temperature is fixed for 250 increments during 10000 seconds. The contact bias factor is set to 0.9 to provide a more accurate contact description.

```
LOADCASES
  COUPLED
    NAME
      ramped_temp_nc
  QUASI-STATIC
```

CONTACT
CONTACT TABLE
 ctable
OK
CONVERGENCE TESTING
DISPLACEMENTS
OK
TOTAL LOADCASE TIME
 1000
PARAMETERS
 #STEPS
 100
 OK (twice)

COPY

NAME

 fixed_temp_nc

QUASI-STATIC

TOTAL LOADCASE TIME

 10000

PARAMETERS

 #STEPS

 250

 OK (twice)

RETURN (twice)

JOBS

ELEMENT TYPES

COUPLED

 AXISYM SOLID

 10

 OK

ALL EXIST

RETURN (twice)

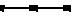

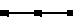

COUPLED

 ramped_temp_nc

 fixed_temp_nc

```
CONTACT CONTROL
  INITIAL CONTACT
    CONTACT TABLE
      ctable1
    OK
  ADVANCED CONTACT CONTROL
    DISTANCE TOLERANCE BIAS
      0.9
    OK (thrice)
```

Save Model, Run Job, and View Results

After saving the model, the job is submitted and the resulting post file is opened. A node on the pipe and a node on the house are selected to generate plots of the temperature as a function of time. These are shown as the  (black) and  (red) curves in [Figure 4.1-3](#). Plots of the y-displacement as a function of time for these nodes are shown as the  (black) and  (red) curves in [Figure 4.1-4](#).

```
FILE
  SAVE AS
    heatpipe.mud
  OK
  RETURN
RUN
  SUBMIT(1)
  OPEN POST FILE (RESULTS MENU)
  HISTORY PLOT
    SET NODES
      5 34 #
    COLLECT GLOBAL DATA
```

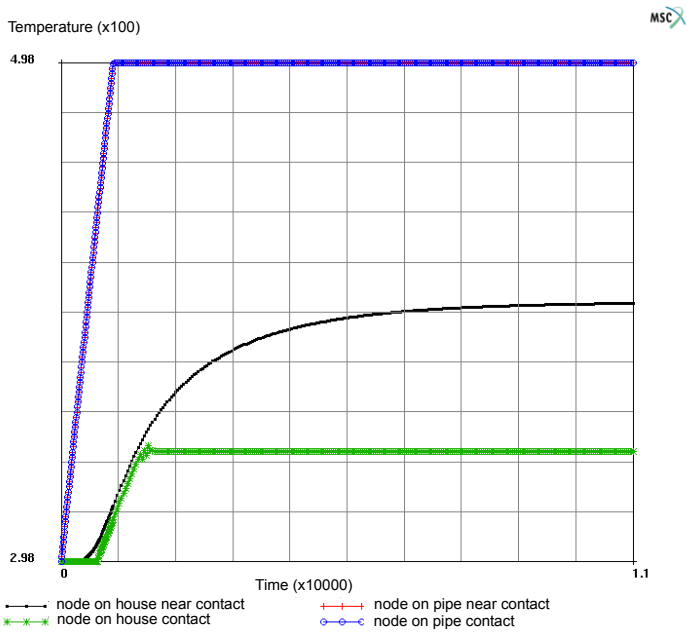


Figure 4.1-3 Temperature as a Function of Time for two Nodes in Contact, one from the Pipe and one from the House

Note: Results are with the Near Contact option switched on and off.

```

NODES/VARIABLES
  ADD VARIABLE
    Time
    Temperature
  RETURN
SHOW IDS
  0
FIT
COPY TO (GENERALIZED XY PLOT)
GENERALIZED XY PLOT
  SHOW IDS
    0
  FIT
  
```

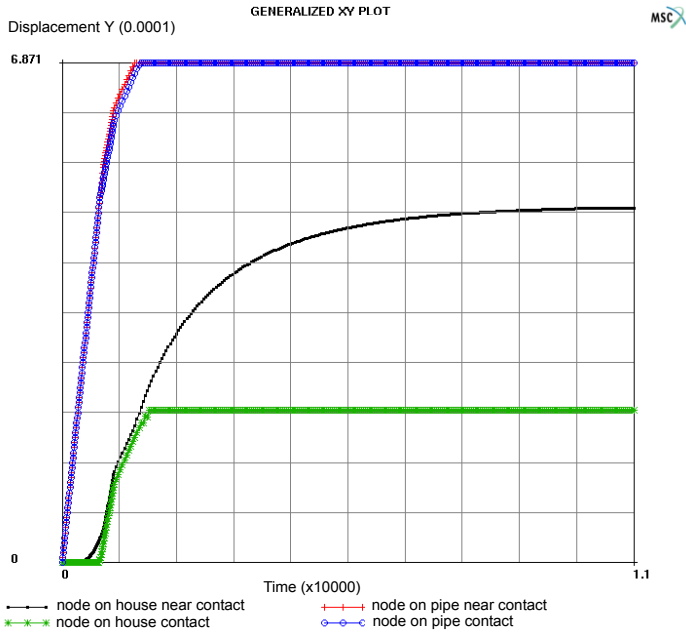


Figure 4.1-4 Displacement in the y-Direction as a Function of Time for two Nodes in Contact, one from the Pipe and one from the House

Note: Results are with the Near Contact option switched on and off.

Next, the near contact option is switched off to illustrate what the results look like without this option.

```

    RETURN
    CLOSE
    RETURN (twice)
CONTACT
    CONTACT TABLES
    COPY
    PROPERTIES
    1 2
    NEAR CONTACT
    OK (twice)
    RETURN (twice)
LOADCASES
    EDIT
    ramped_temp_nc
    
```

```
    OK
COPY
NAME
    ramped_temp
COUPLED
    QUASI-STATIC
        CONTACT
            CONTACT TABLE
                ctable2
            OK (twice)
EDIT
    fixed_temp_nc
COPY
NAME
    fixed_temp
QUASI-STATIC
    CONTACT
        CONTACT TABLE
            ctable2
        OK (twice)
RETURN (twice)
JOBS
    NEW
    COUPLED
        ramped_temp
        fixed_temp
    CONTACT CONTROL
        INITIAL CONTACT
            CONTACT TABLE
                ctable2
            OK
        ADVANCED CONTACT CONTROL
            DISTANCE TOLERANCE BIAS
                0.9
            OK (thrice)
```


RUN
 SAVE MODEL
 SUBMIT

The *-*-* (green) and ○-○-○ (blue) curves in Figure 4.1-3 show the temperature as a function of time for a node on the house and a node on the pipe, respectively, for the analysis where the near contact option is switched off. The *-*-* (green) and ○-○-○ (blue) curves in Figure 4.1-4 shows the y-displacement as a function of time for the two nodes. When the results where near contact is used and not used are compared, the difference is clear. The pipe is behaving similar in both cases, but the house has a much smoother temperature response for the case where near contact is used. A similar effect is observed for the y-displacement, which is smoother for the case using near contact.

Note that for both cases, contact is only temporarily, once heat transfer develops between the pipe and the house, the house will expand more due to a larger diameter. This can be seen in Figure 4.1-5, where the contact status of a node in contact is plotted as a function of time for the two jobs.

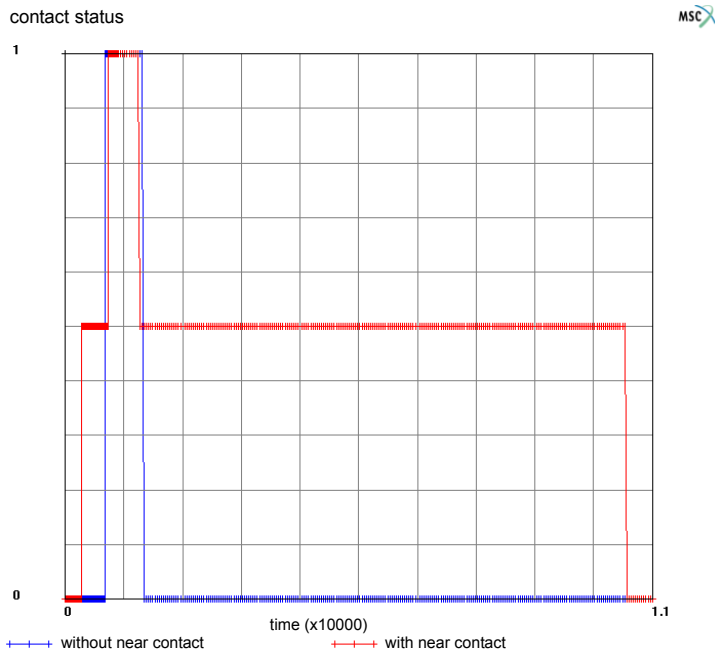


Figure 4.1-5 Contact Status with and without the Near Contact Option Activated

Input Files

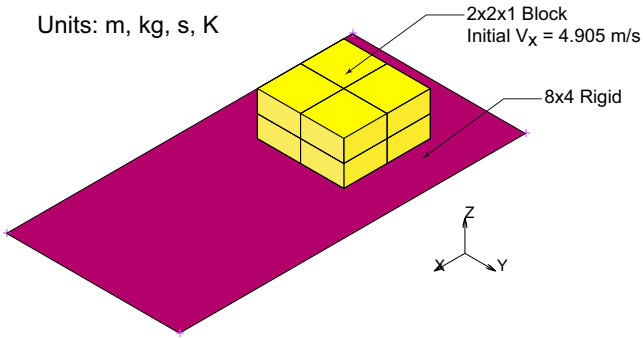
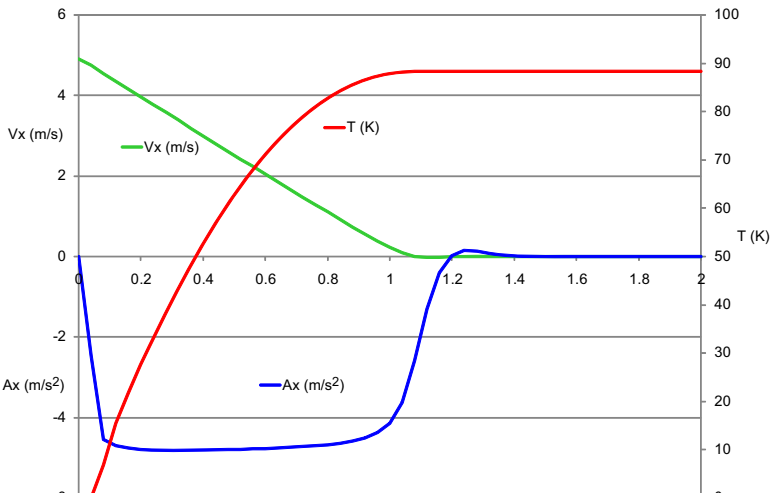
The files below are on your [delivery media](#) or they can be downloaded by your web browser by clicking the links (file names) below.

File	Description
pipe.proc	Mentat procedure file to run the above example

4.2 Dynamics with Friction Heating

- Summary 1780
- Friction Heat Analysis 1782
- Run Jobs and View Results 1789
- Input Files 1793

Summary

Title	Dynamics with friction heating
Problem features	dynamic coupled mechanical thermal analysis.
Geometry	<p>Units: m, kg, s, K</p> 
Material properties	$E = 2.1 \times 10^{11}$ Pa, $\nu = 0.3$, $\mu = 0.5$ $k = 60.5$ W/m/K, $C_p = 434$ J/kg/K, $\rho = 7854$ kg/m ³
Analysis type	Coupled Mechanical Heat Transfer
Boundary conditions	Y component of disp. fixed all nodes. Gravity load $a_z = -9.81$ m/s ² .
Initial conditions	$V_x = 4.905$ m/s, $T = 0$ K all nodes
Element type	Brick element type 7
FE results	<p>1. Block velocity and acceleration history 2. Rise in temperature due to friction</p> 

A dynamic coupled analysis is performed to simulate the behavior of a block with an initial velocity sliding over a rigid table. Due to the weight of the block and friction between the block and the table, the block will slow down and heat up because of friction.

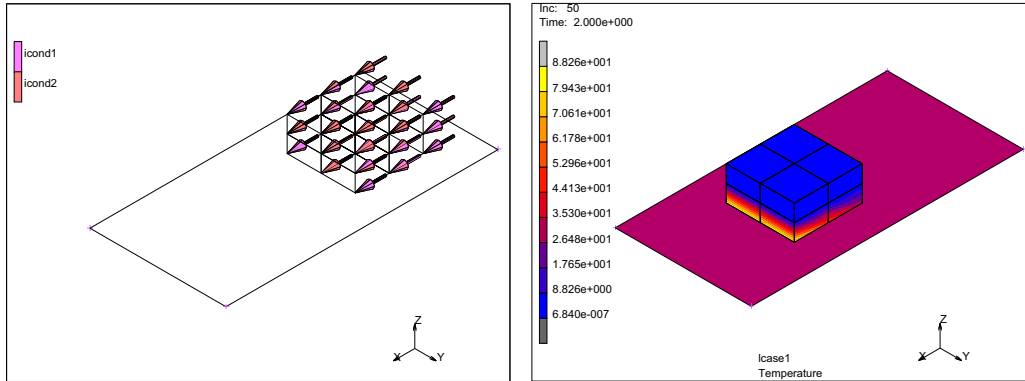


Figure 4.2-1 Problem Description

Mechanical boundary conditions keep the block moving in a straight line. Initial conditions set the initial velocity and temperature.

The coupled loadcase selected is a dynamic transient with a time period long enough to allow the block to come to rest.

The temperature contours show how the leading edge of the block touching the table heat up faster than other portions of the block.

A history plot of the velocity and acceleration of the node (Figure 4.2-2) show how the block comes to a stop with the velocity and acceleration becoming zero at 1.4 seconds.

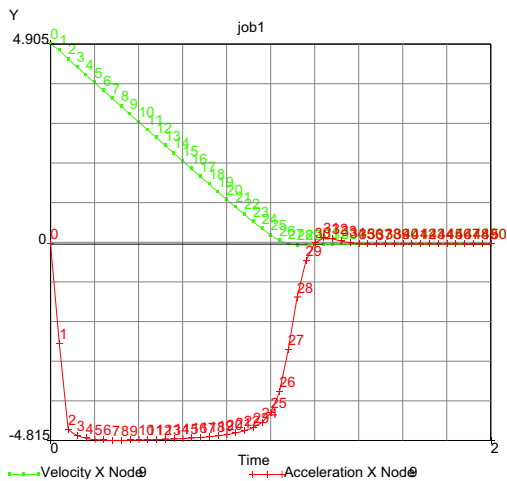


Figure 4.2-2 Velocity and Acceleration History

Friction Heat Analysis

This is a problem of a block subjected to its own weight that is sliding on a table with an initial velocity. Friction between the block and table generate heat and reduce the speed. The steel block has an area of 4 m² and a height of 1 m. The coefficient of friction is 0.5.

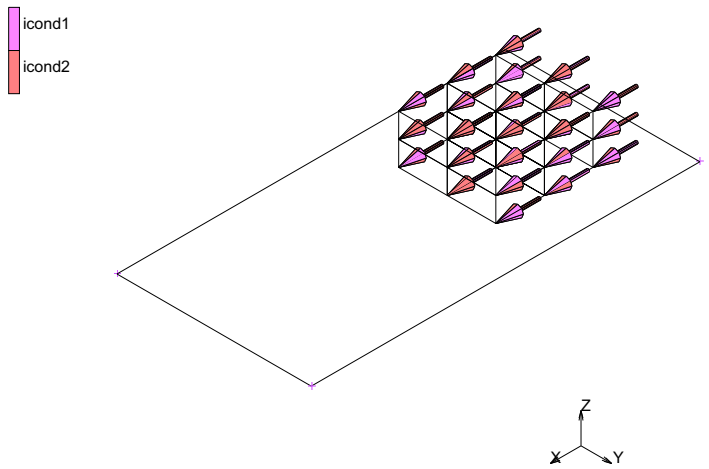


Figure 4.2-3 Initial Conditions

FILES

NEW

OK

SAVE AS

block

RETURN

MESH GENERATION

VIEW SHOW VIEW 4

OK

ADD ELEMENTS

node(-1.0, -1.0, 0.0)

node(1.0, -1.0, 0.0)

node(1.0, 1.0, 0.0)

node(-1.0, 1.0, 0.0)

ADD SURFACES

point(1.0, -1.0, 0.0)

point(-1.0, -1.0, 0.0)

point(-1.0, 1.0, 0.0)

point(1.0, 1.0, 0.0)

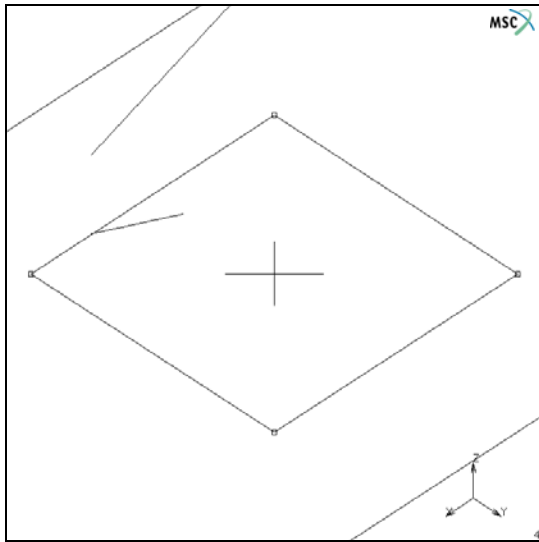


Figure 4.2-4 Footprint of Block on Table

```

MOVE
  SCALE
    4 2 1
  SURFACES
  ALL: EXISTING
MOVE
  RESET
  TRANSLATIONS
    1.8 0 0
  SURFACES
  ALL: EXISTING
  RETURN
SUBDIVIDE
  ELEMENTS
  ALL: EXISTING
  RETURN
EXPAND
  TRANSLATIONS
    0 0 1/2
    
```

REPETITIONS
2
ELEMENTS
ALL: EXISTING
RETURN
FILL

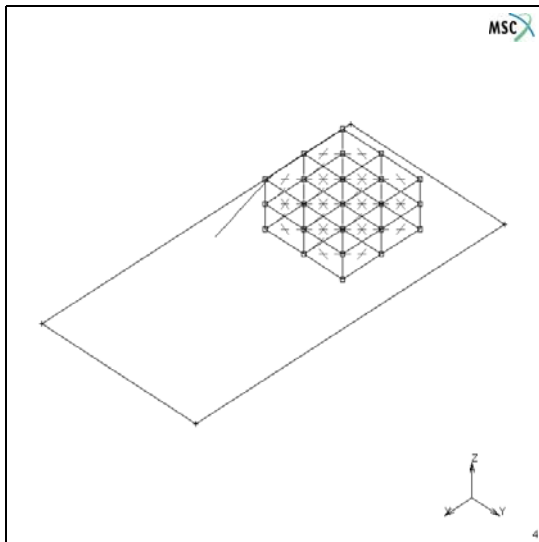


Figure 4.2-5 Block Mesh

SWEEP
REMOVE UNUSED
NODES
ALL
RETURN
RENUMBER
ALL
RETURN

BOUNDARY CONDITIONS
MECHANICAL
FIXED DISP Y
0

OK
NODES ADD
ALL: EXISTING
NEW
GRAVITY LOAD

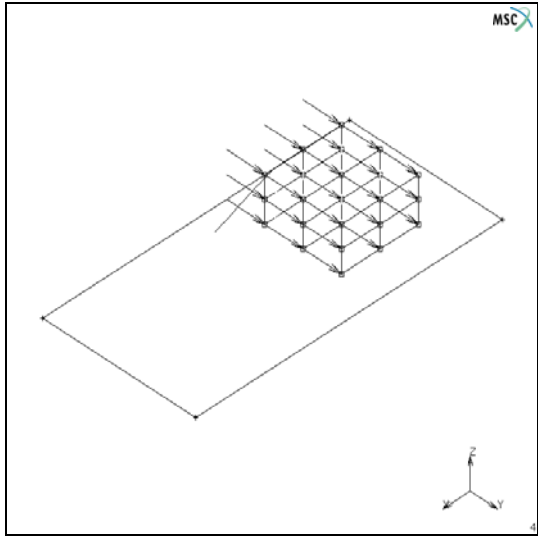


Figure 4.2-6 Boundary Conditions

ON Z ACCEL
-9.81 (m/s²)
OK
ELEMENTS ADD
ALL: EXISTING
MAIN

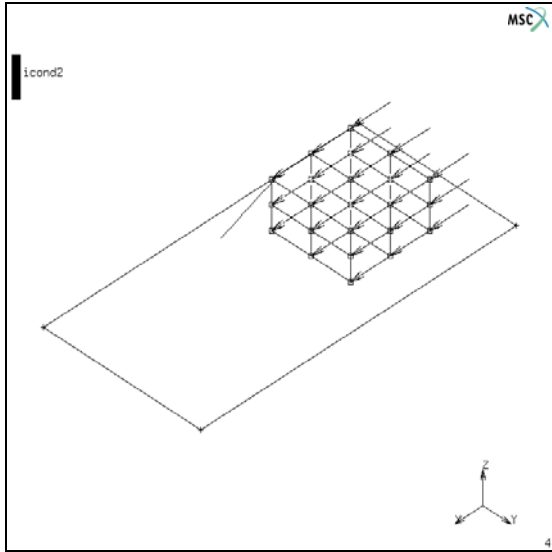


Figure 4.2-7 Initial Conditions

```
INITIAL CONDITIONS
  THERMAL
    TEMP.
      0 (K)
    OK
  NODES ADD
  ALL: EXISTING
  RETURN
  NEW
  MECHANICAL
  VELOCITY
    VEL X
      4.905 (m/s)
    OK
  NODES ADD
  ALL: EXISTING
  MAIN
  MATERIAL PROP. (twice)
  ANAYSIS CLASS
  COUPLED
```

NEW

STANDARD

STRUCTURAL

$$E = 210E9 \text{ (N/m}^2\text{)}$$

$$\nu = .3 \text{ (return)}$$

GENERAL

$$\rho = 7854 \text{ (Kg/m}^3\text{)} \text{ (return)}$$

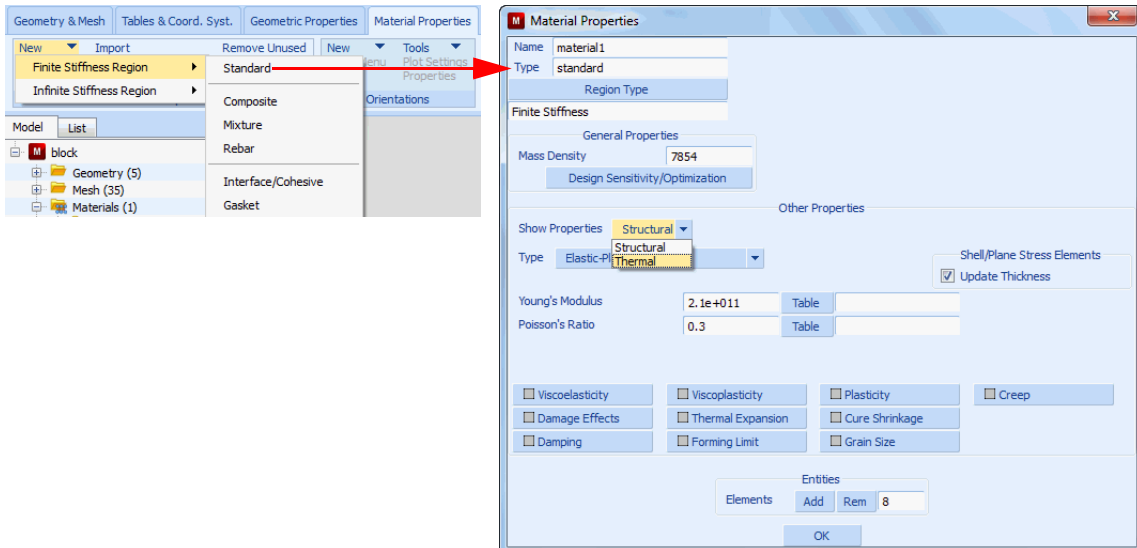
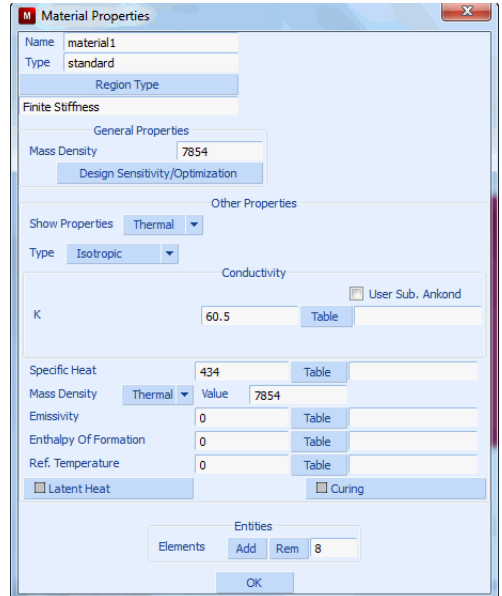


Figure 4.2-8 Isotropic Properties Submenu using Damping

THERMAL
CONDUCTIVITY
60.5 (W/m/K)
SPECIFIC HEAT
434 (J/Kg/K)
OK
ELEMENTS ADD
ALL: EXISTING
MAIN
CONTACT
CONTACT BODIES
DEFORMABLE
 $\mu = .5$
OK
ELEMENTS ADD
ALL: EXISTING
CONTACT
CONTACT BODIES
NEW
RIGID
 $\mu = .5$
OK
SURFACES ADD
ALL: EXISTING
MAIN
LOADCASES
COUPLED
CONVERGENCE TESTING
DISPLACEMENTS (OK)
DYNAMIC TRANSIENT
TOTAL LOADCASE TIME
2
FIXED # STEPS
50



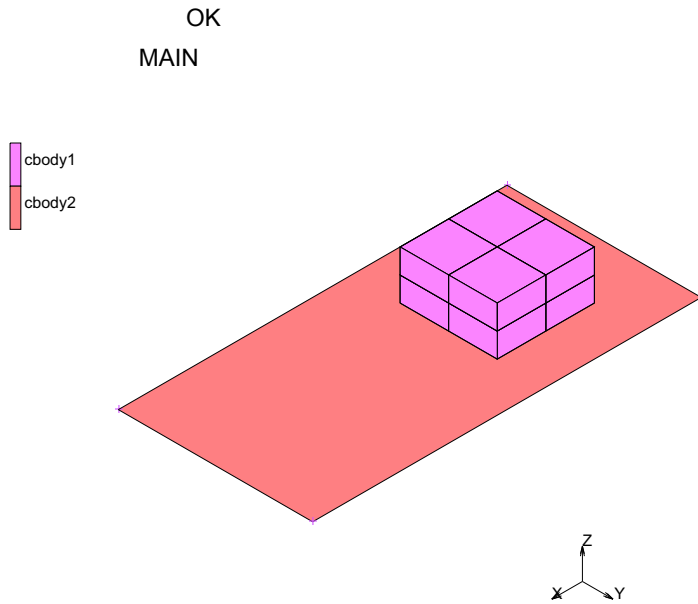


Figure 4.2-9 Contact Bodies: Block and Table

Run Jobs and View Results

```
JOB  
  NEW  
  COUPLED  
  PROPERTIES  
    lcase1  
  ANALYSIS OPTIONS  
    LARGE STRAIN  
    LUMPED MASS  
    OK  
  CONTACT CONTROL  
    ARCTANGENT  
    RELATIVE SLIDING VEL  
      0.1  
  ADVANCED CONTACT CONTROL  
    SEP. FORCE  
      1E11
```

(keep block on surface)

OK (twice)

JOB RESULTS

EQUIVALENT VM STRESS

TEMPERATURE (Integration Point)

OK

JOB PARAMETERS

HEAT GENERATION (FRICTIONAL)

1E3

(should be 1, but want larger temps for show)

OK (twice)

SAVE

RUN

SUBMIT1

MONITOR

OK

RETURN

RESULTS

OPEN DEFAULT

CONTOUR BAND

DEF ON

SCALAR Temp.

SKIP TO 50

RESULTS

HISTORY PLOT

SET LOCATION

(pick leading node shown)

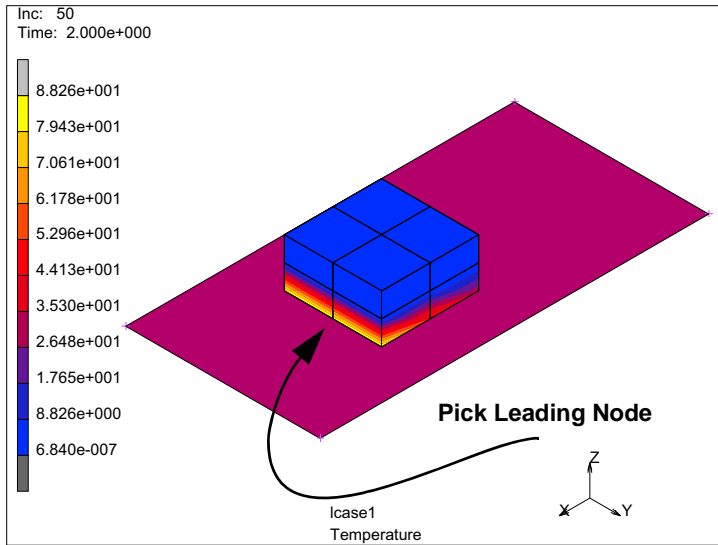


Figure 4.2-10 Temperature Contours

ALL INCS
 ADD CURVES
 ALL LOCATIONS
 Time
 Velocity x
 ALL LOCATIONS
 Time
 Acceleration x
 ALL LOCATIONS
 Time
 Temperature
 FIT

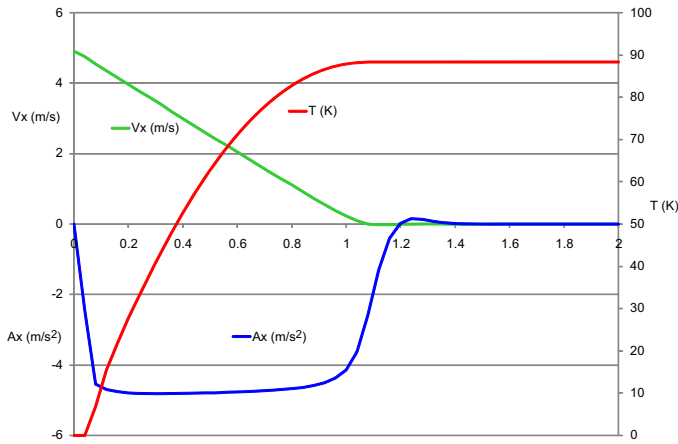


Figure 4.2-11 Velocity, Acceleration and Temperature History of Leading Node

Notice that the effect of friction was not 100% since the block should come to a stop at 1 sec. This was due to the ever slipping friction model. Rigid body dynamics gives:

$$\ddot{u} = -\mu g \quad ; \quad \dot{u} = -\mu g t + \dot{u}_0 \quad ; \quad u = -\mu g \frac{t^2}{2} + \dot{u}_0 t + u_0$$

where the initial velocity was selected as $\dot{u}_0 = \mu g t_s$. Where t_s is the stopping time or 1 second.

Also from the friction heating, the friction force moves through a distance and this mechanical energy is converted to thermal energy. This thermal energy is input to the heat transfer portion of the solution. Equating the conversion factor times the kinetic energy and accounting that for rigid contact only half of the frictional heating is added to the block, the average rise in temperature for a block that comes to rest from an initial velocity of \dot{u}_0 , becomes:

$$\Delta T = \frac{1}{4} \text{conv}_{factor} \left(\frac{\dot{u}_0^2}{c_p} \right)$$

In this case, the rise in temperature is 13.86 K. Why is the block hotter at the leading bottom edge? What would you do to improve the results?

How does this compare with the Marc predictions? To answer this, we can close the post file and add another load case that is 1e6 seconds long allowing the block to come to thermal equilibrium, namely uniform temperature.

CLOSE

LOADCASES

COUPLED

NEW

CONVERGENCE TESTING


```

DISPLACEMENTS (OK)
DYNAMIC TRANSIENT
TOTAL LOADCASE TIME
1e6
STEPPING PROCEDURE ADAPTIVE
TEMPERATURE
PARAMETERS
INITIAL TIME STEP
1.0
OK (twice)
MAIN
JOBS
PROPERTIES
lcase2 (OK)
SAVE
RUN
SUBMIT1
MONITOR
OK
RETURN

```

This second load case allows the heat to diffuse into the block leaving a uniform temperature of 14.34 K throughout the block; this is in good agreement with our estimate of 13.86K.

Input Files

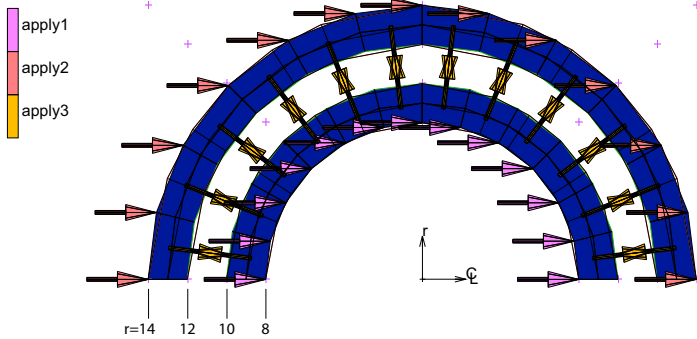
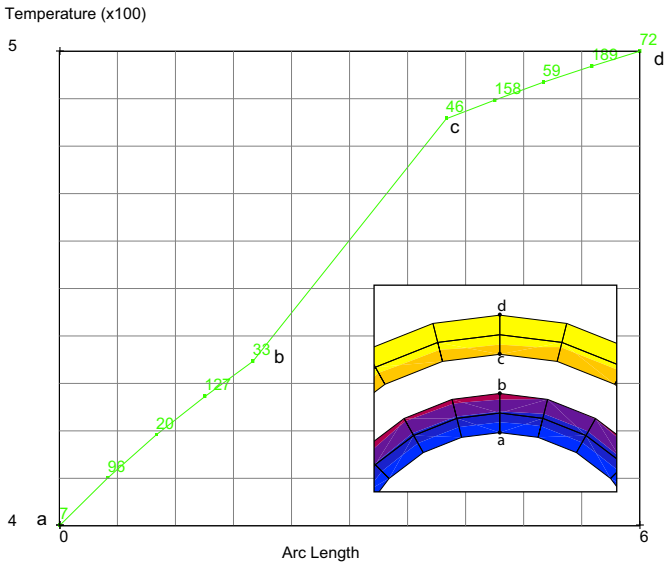
The files below are on your [delivery media](#) or they can be downloaded by your web browser by clicking the links (file names) below.

File	Description
h4.proc	Mentat procedure file to run the above example

4.3 Radiation with Viewfactors

- Summary 1796
- Detailed Session Description 1798
- Run Job and View Results 1802
- Input Files 1804

Summary

Title	Radiation with viewfactors																		
Problem features	Thermal analysis with radiation via viewfactors																		
Geometry																			
Material properties	$k = 0.0001 \text{ W mm}^{-1} \text{ K}^{-1}$, $\varepsilon = 0.4$, $\sigma = 5.67 \times 10^{-14} \text{ W mm}^{-2} \text{ K}^{-4}$																		
Analysis type	Steady State Heat Transfer																		
Boundary conditions	Radiation using viewfactors																		
Initial conditions	Inner surface of inner sphere 400°C , outer surface of outer sphere 500°C																		
Element type	Axisymmetric quadrilateral																		
FE results	<p>Temperature rise between concentric spheres</p>  <table border="1"> <caption>Temperature Profile Data</caption> <thead> <tr> <th>Point</th> <th>Temperature (x100)</th> </tr> </thead> <tbody> <tr> <td>a</td> <td>98</td> </tr> <tr> <td>1</td> <td>20</td> </tr> <tr> <td>2</td> <td>127</td> </tr> <tr> <td>3</td> <td>33</td> </tr> <tr> <td>c</td> <td>46</td> </tr> <tr> <td>4</td> <td>158</td> </tr> <tr> <td>5</td> <td>59</td> </tr> <tr> <td>d</td> <td>72</td> </tr> </tbody> </table>	Point	Temperature (x100)	a	98	1	20	2	127	3	33	c	46	4	158	5	59	d	72
Point	Temperature (x100)																		
a	98																		
1	20																		
2	127																		
3	33																		
c	46																		
4	158																		
5	59																		
d	72																		

Two concentric spheres have their inner and outer most surfaces held at a fixed temperature. They exchange heat flow via radiation.

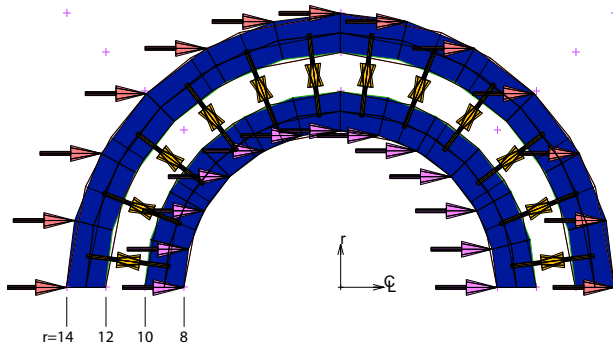


Figure 4.3-1 Thermal Boundary Conditions

Thermal boundary conditions keep the inner and outer most surfaces fixed at 400 and 500°C. Another thermal boundary conditions identifies that the outer surface of the inner sphere and the inner surface of the outer sphere can radiate.

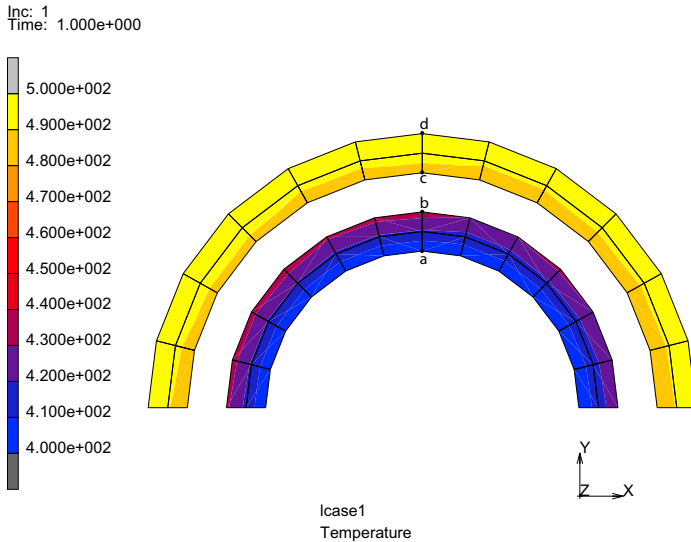


Figure 4.3-2 Thermal Contours

The heat transfer loadcase selected is a steady state that allows the sphere to exchange heat flow via radiation.

The temperature contours shows this flow and the path plot shows the radial change in temperature.

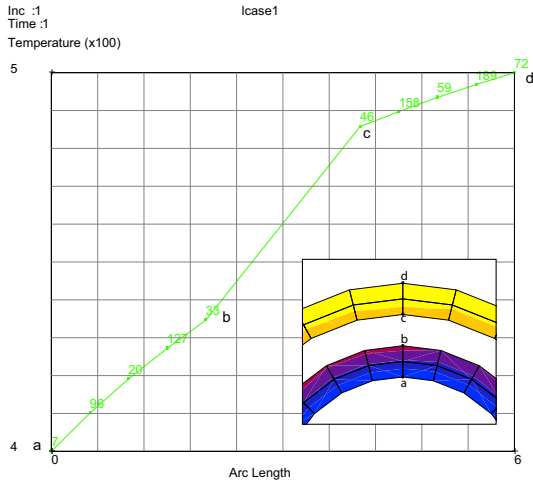


Figure 4.3-3 Temperature Versus Radius

Detailed Session Description

This is an axisymmetric model and we can use cylindrical coordinates to define the spheres.

MESH GENERATION

COORDINATE SYSTEM

CYLINDRICAL (on)

CURVE TYPE

CENTER/POINT/POINT

RETURN

CURVES ADD

0,0,0, 8,0,0, 8,180,0

0,0,0, 10,0,0, 10,180,0

0,0,0, 12,0,0, 12,180,0

0,0,0, 14,0,0, 14,180,0

SURFACE TYPE

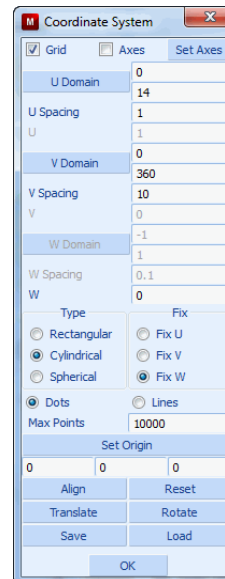
RULED

OK

SURFACE ADD

1, 2

3, 4





```

CONVERT
  DIVISIONS
    12 2
  SURFACES TO ELEMENTS
  ALL: EXISTING
  RETURN
SWEEP
  ALL
  RETURN
CHECK ELEMENTS
  UPSIDE DOWN
  FLIP ELEMENTS
  ALL SELECTED
  UPSIDE DOWN
  RETURN
RENUMBER
  ALL
MAIN
  BOUNDARY CONDITIONS
    THERMAL
      FIXED TEMP
        400
        OK
        (add all nodes for r = 8)
    NEW
      FIXED TEMP
        500
        OK
        (add all nodes for r = 14)
    NEW
    
```

EDGE RADIATION
SINK TEMPERATURE ON
OK (add all edges $r=10$ & 12)

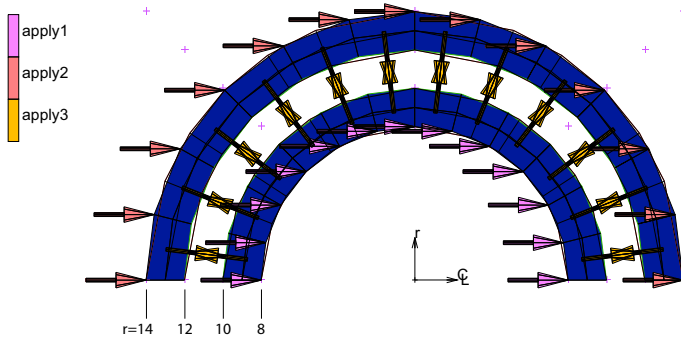
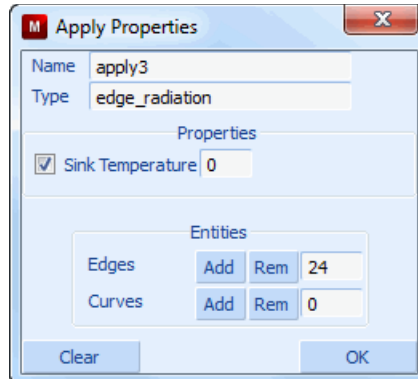


Figure 4.3-4 Applying Radiation Boundary Conditions

Note: Try using the path select option to pick the nodes on $r=8$, 14 and the edges on $r=10$, 12 . You only need to pick a beginning middle and ending node for path select.

COMPUTE RADIATION VIEWFACTORS

TYPE AX

VIEWFACTOR FILE

model1.vfs

OK

START

OK

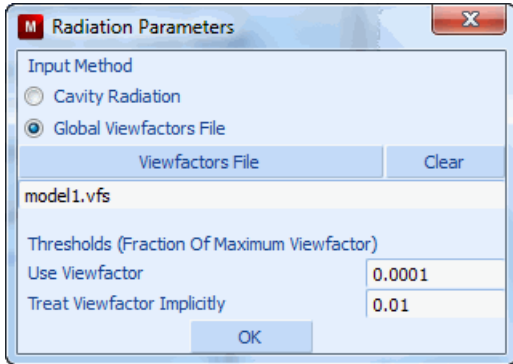


Figure 4.3-5 Viewfactor Control Menu

Note:

Here 1000 rays are randomly cast from each of the 24 edges to compute the view factors. The view-factors are stored in the file model1.vfs. If the geometry changes this would need to be done again.

MAIN

MATERIAL PROPERTIES (twice)

ANALYSIS CLASS: HEAT TRANSFER

NEW: STANDARD

THERMAL

K = 1E-4

EMISSIVITY

0.4

OK

ELEMENTS ADD

ALL EXISTING

MAIN

LOADCASES

HEAT TRANSFER

STEADY STATE

CONVERGENCE TESTING

MAX ERROR IN TEMPERATURE ESTIMATE

0.05

OK (twice)

MAIN

Run Job and View Results

JOBS

NEW: HEAT TRANSFER

PROPERTIES

lcase1

AXISYMMETRIC

ANALYSIS OPTIONS

RADIATION

VIEWFACTOR FILE

model1.vfs

OK

OK

JOB PARAMETERS

UNITS AND CONSTANTS

TEMPERATURE IN CELSIUS

(on)

STEFAN-BOLTZMANN

5.67E-14

OK, (thrice)

RUN

SUBMIT1

MONITOR

OK

SAVE

MAIN

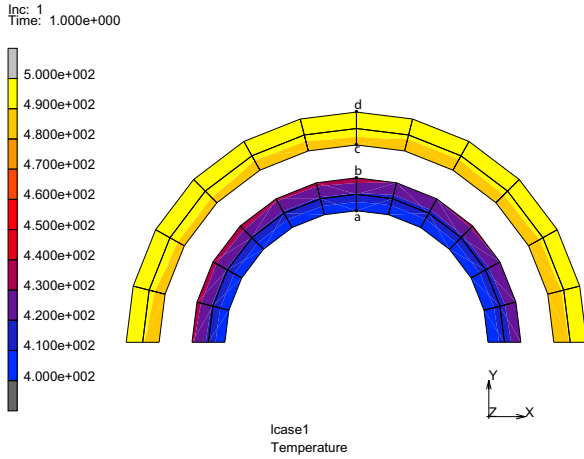


Figure 4.3-6 Temperature Contours

RESULTS

OPEN DEFAULT

LAST

CONTOUR BAND

PATH PLOT

SET NODES

(a,b,c,d)

#END LIST

ADD CURVES

ADD CURVE

Arc Length

Temperature

FIT

(pick node shown)

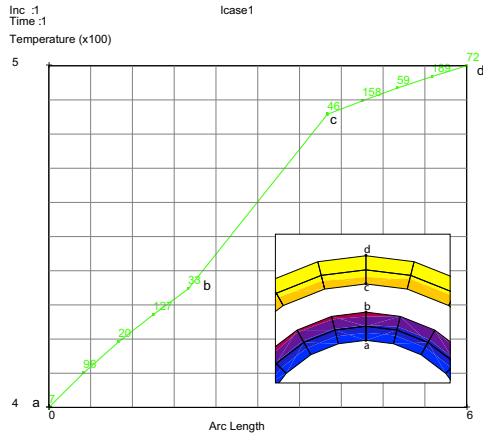


Figure 4.3-7 Temperature Versus Radius

Input Files

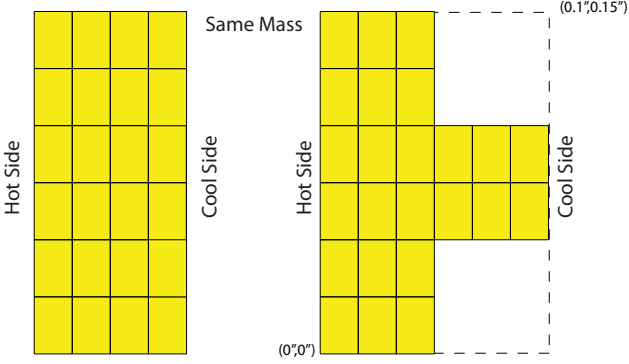
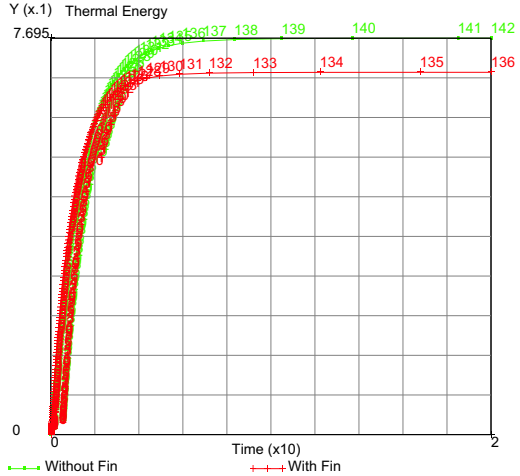
The files below are on your [delivery media](#) or they can be downloaded by your web browser by clicking the links (file names) below.

File	Description
h5.proc	Mentat procedure file to run the above example

4.4 Cooling Fin Analyses

- Summary 1806
- Steady State 1807
- Transient 1817
- Input Files 1823

Summary

Title	Thermal cooling fin
Problem features	Thermal analysis with convection boundary conditions
Geometry	 <p>Same Mass</p> <p>(0.15",0")</p> <p>(0",0")</p> <p>Hot Side</p> <p>Cool Side</p>
Material properties	$k = 1.157 \times 10^{-4} \text{ BTU in}^{-1} \text{ s}^{-1} \text{ } ^\circ\text{F}^{-1}$, $C_p = 0.146 \text{ BTU lbm}^{-1} \text{ } ^\circ\text{F}^{-1}$, $\rho = 0.283 \text{ lbm in}^{-3}$
Analysis type	Steady state and transient heat transfer
Boundary conditions	Hot side $H = 750 \text{ BTU hr}^{-1} \text{ ft}^{-2} \text{ } ^\circ\text{F}^{-1}$, $T_\infty = 2500^\circ\text{F}$ Cool side $H = 500 \text{ BTU hr}^{-1} \text{ ft}^{-2} \text{ } ^\circ\text{F}^{-1}$, $T_\infty = 1000^\circ\text{F}$
Initial conditions	$T = 0^\circ\text{F}$
Element type	Planar quadrilateral
FE results	<p>Cooling effectiveness of the fin</p>  <p>Y (x.1) Thermal Energy</p> <p>7.695</p> <p>0</p> <p>Time (x10)</p> <p>0 2</p> <p>Without Fin</p> <p>With Fin</p> <p>$\eta = 8.6\%$</p>

Steady State

An effective means of augmenting the cooling effectiveness of a given thermal cooling design, is to increase the area exposed to the cooling fluid by means of adding fins. In the fin design, the effectiveness is judged by comparing the temperatures of the structure for conditions with and without fins. This sample problem determines two sets of temperatures reflecting the structure with and without a fin.

Background Information

Description

This problem demonstrates the preparation of a heat transfer model including convection boundary conditions.

Idealization

The model is a 0.15" X 0.05" rectangle with a 0.05" square fin centered vertically on the right side. The vertical sides have convection boundary conditions and the top and bottom are adiabatic.

Requirements for a Successful Analysis

The analysis is considered completed if a steady state analysis is performed for a structure with fin and a structure without fin.

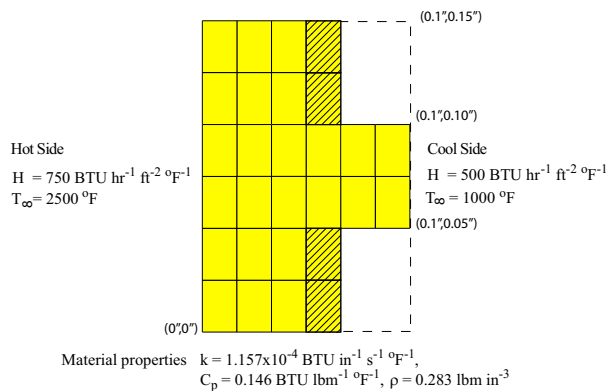


Figure 4.4-1 Cross-Section of Cooling Fin

Full Disclosure

The model is 0.15" high and 0.05" wide. The fin is centered vertically and is 0.05" square.

The convection on the left side is:

$$q = h(T - T_\infty)$$

with

$$h = 750 \text{ Btu/HR Ft}^2 \text{ } ^\circ\text{F} = 750 \times \frac{1}{3600(12)^2} \text{ Btu/ in}^2 \text{ } ^\circ\text{F}$$

$$T_\infty = 2500 \text{ } ^\circ\text{F}$$

The right side has a convection:

$$q = h(T - T_\infty)$$

with

$$h = 500 \text{ Btu/HR Ft}^2 \text{ } ^\circ\text{F} = 500 \times \frac{1}{3600(12)^2} \text{ Btu/ in}^2 \text{ } ^\circ\text{F}$$

$$T_\infty = 1000 \text{ } ^\circ\text{F}$$

The material has a coefficient of thermal conduction $k = 1.157 \cdot 10^{-4} \text{ Btu in}^2 \text{ } ^\circ\text{F}$

For a steady-state analysis, it is not required to enter the mass density and the heat capacity, however they will be entered since a transient analysis will be done later.

Overview of Steps

Step 1: Create two surfaces and convert to finite elements.

Step 2: Add convection boundary conditions.

Step 3: Add material data.

Step 4: Create a steady-state loadcase.

Step 5: Create a thermal job and submit.

Step 6: Postprocess results.

Step 7: Delete fin elements.

Step 8: Modify convection boundary conditions.

Step 9: Create new job and submit.

Step 10: Postprocess results.

Detailed Session Description

Step 1: Create two surfaces and convert to finite elements.

The first step creates two surfaces and converts them to finite elements. The following button sequence creates the surfaces and convert them.

FILES

SAVE AS

steady_fin

OK

MESH GENERATION

COORDINATE SYSTEM: SET

U SPACING

0.05

V SPACING

0.05

U DOMAIN

0 0.10

V DOMAIN

0 0.15

GRID ON

(on)

RETURN

FILL

ZOOM BOX

(box pick right upper half of grid)

SRFS ADD

(pick grid points)

point(0,0,0)

point(0.05,0,0)

point(0.05,0.15,0)

point(0,0.15,0)

point(0.05,0.05,0)

point(0.1,0.05,0)

point(0.1,0.1,0)

point(0.05,0.1,0)

GRID

(off)

CONVERT

DIVISIONS

3 6

SURFACES TO ELEMENTS

1

(pick the first surface)

END LIST (#)

DIVISIONS

```
3 2
SURFACES TO ELEMENTS
2
END LIST (#)
```

(pick the second surface)

The next button sequence merges the duplicate nodes on the interface of the two surfaces.

```
MAIN
  MESH GENERATION
    SWEEP
      SWEEP NODES
        ALL: EXIST.
      PLOT
        draw POINTS (off)
        draw SURFACES (off)
      REGEN
      RETURN
    FILL
```

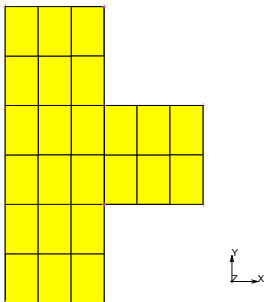


Figure 4.4-2 The Mesh Generated using the Convert Option

Step 2: Add convection boundary conditions.

This step adds the convection boundary conditions. The following button sequence creates the boundary conditions.

```
MAIN
  BOUNDARY CONDITIONS
    THERMAL
      NAME
        hotside
```

```

EDGE FILM
FILM
    AMBIENT TEMPERATURE
        2500                                (enter value in text box)
    COEFFICIENT
        750 / ( 3600 * 144 )                (enter value in text box)
    OK
    EDGES: ADD                               (box Pick the left edge)
    END LIST (#)
NEW
NAME
    coolant
EDGE FILM
FILM
    SINK TEMPERATURE
        1000                                (enter value in text box)
    COEFFICIENT
        500 / ( 3600 * 144 )                (enter value in text box)
    OK
    EDGES: ADD                               (box Pick the right edge;
                                           several Boxes are required)
    END LIST (#)
RETURN
ID BOUNDARY CONDS                           (on/off)
    
```

Note that for the adiabatic conditions at top and bottom edges, no boundary conditions have to be applied.

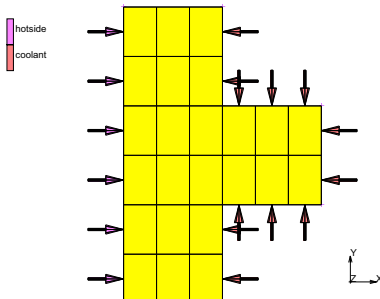


Figure 4.4-3 The Film Conditions on the Hot and Coolant Side

Step 3: Add material data.

This step adds the material data. The following button sequence assigns the material properties.

```
MAIN
  MATERIAL PROPERTIES (twice)
    ANALYSIS CLASS: HEAT TRANSFER
      NEW standard
      THERMAL
        K = 1.157e-4(BTU/s/in/F)
        OK
      SPECIFIC HEAT = 0.146 (BTU/lbm/F)
      MASS DENSITY: THERMAL VALUE = 0.283 (lbm/in^3)
      OK
    ELEMENTS: ADD
    ALL: EXIST.
```

Step 4: Create a steady-state loadcase.

This step creates a steady-state loadcase. The following button sequence does this.

```
MAIN
  LOADCASES
    HEAT TRANSFER
      STEADY STATE
      LOADS
      OK (twice)
```

Step 5: Create a thermal job and submit.

This step creates a thermal job and submits the job for analysis. The following buttons sequence does this.

```
MAIN
  JOBS
    NEW HEAT TRANSFER
    PROPERTIES
      LOADCASES SELECT
        lcase1
    ELEMENT TYPES
      ANALYSIS DIMENSION PLANAR
```

```
PLANAR
SOLID
  39
  OK
ALL: EXIST.
RETURN
SAVE
RUN
SUBMIT 1
MONITOR
```

Step 6: Postprocess results.

The final step for the first analysis is to postprocess results. The following button sequence reviews the results.

```
MAIN
RESULTS
OPEN DEFAULT
CONTOUR BANDS
NEXT
```

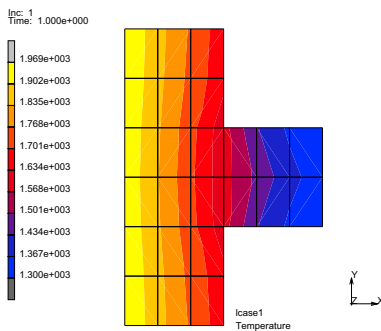


Figure 4.4-4 Contours of Temperature for Structure with Fin

Step 7: Delete fin elements.

First, restore the database with the geometry, delete the fin elements and add a column of elements to keep the mass constant between the two models. The following button sequence modifies the model.

```
MAIN
FILES
```

```
SAVE AS
  steady
  OK
RESULTS
  CLOSE
  scalar plot OFF
  RETURN
FILES
  RESTORE
  RESET PROGRAM
  RETURN
MESH GENERATION
  ELEMS REM
  END LIST (#)
  SWEEP
  remove unused NODES
  RETURN
DUPLICATE
  TRANSLATIONS
  .05/3 0 0
  ELEMENTS
SWEEP
  SWEEP NODES
  ALL: EXIST.
```

(box Pick the fin elements)

(box Pick right column of elements)

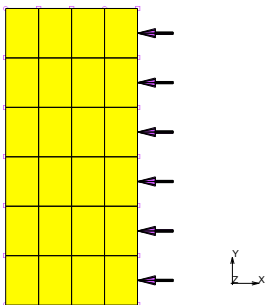


Figure 4.4-5 Mesh without Fin

Step 8: Modify convection boundary conditions.

This step modifies convection boundary conditions on the edge where the fin was previously. The following button sequence modifies the convection.

```

MAIN
  BOUNDARY CONDITIONS
    ID BOUNDARY CONDS (on/off)
    THERMAL
      EDIT coolant (to edit the second boundary condition)
      EDGES REM
        ALL EXISTING
      EDGES ADD (box Pick the right edges)
    END LIST (#)
  RETURN
  ID BOUNDARY CONDS (on/off)
  
```

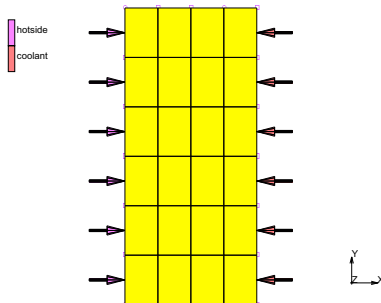


Figure 4.4-6 New Thermal Boundary Conditions

Step 9: Create new job and submit.

This step creates a new model and submits it. This prevents overwriting of the previous post file. The following button sequence does this.

```

MAIN
  JOBS
  NEW: HEAT TRANSFER
  PROPERTIES
  LOADCASES SELECT
    lcase1
  
```

ANALYSIS DIMENSION PLANAR
OK
SAVE
RUN
SUBMIT 1
MONITOR

Step 10: Postprocess results.

This final step postprocesses results of the second analysis. The following button sequence reviews the results.

MAIN
RESULTS
OPEN DEFAULT
CONTOUR BANDS
NEXT

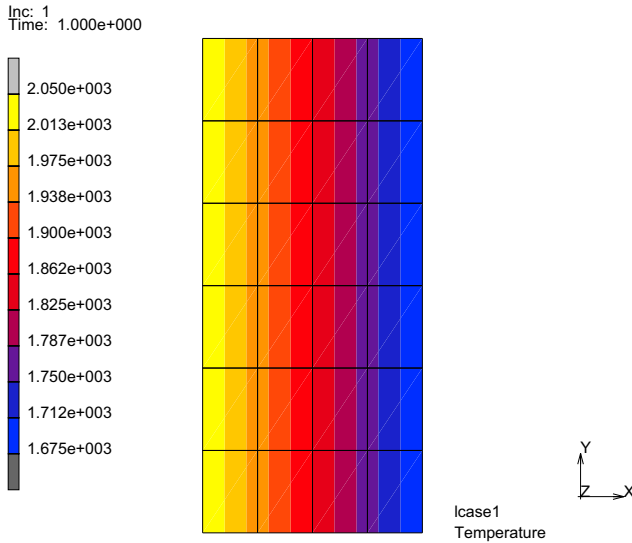


Figure 4.4-7 Results for Structure without Fin

The user can observe that when the cooling fin is included such that there is a greater surface area exposed to the convective cooling, the temperature is lower when comparing [Figure 4.4-4](#) and [Figure 4.4-7](#).

Transient

A planar slab of material is subjected to heat loads and the resulting transient response is determined. The slab has convection boundary conditions on the left and right surfaces as shown. The top and bottom horizontal surfaces are adiabatic. The slab is at an initial temperature of 0°F.

The left surface is exposed to a hot environment whereas the right surface is exposed to cooling conditions. The purpose of the fin on the right side is to create more surface area for cooling and improve the cooling effectiveness of the slab.

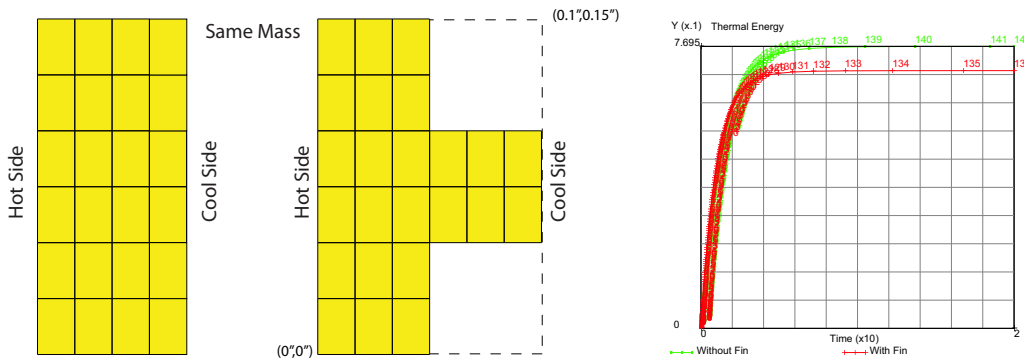


Figure 4.4-8 Problem Description

The transient solution requires an estimate of the time it takes to reach steady state. To estimate this time, we assume that system is treated as a lumped mass where the heat transferred into the body is equated with the thermal energy stored, namely: $hA_s(T_\infty - T)dt = \rho VC_p dT$

where h is the difference in the heat transfer coefficients between the hot and cold sides. Since T_∞ is constant,

$$dT = d(T - T_\infty) \text{ and } \frac{d(T - T_\infty)}{(T - T_\infty)} = -\frac{hA_s}{\rho VC_p} dt = -bt.$$

Integrating the above from $t = 0$ where $T = T_i$, gives $\frac{(T - T_\infty)}{(T_i - T_\infty)} = e^{-bt}$ where b is a positive quantity with units of s^{-1}

called the time constant. If we assume, $\frac{(T - T_\infty)}{(T_i - T_\infty)} = 0.1$. then $t_{ss} = -(\ln(0.1))/b = -(\ln(0.1))/0.175 = 13s$

So let's choose a time period of say 20 seconds for our transient solution.

Detailed Session Description with Fin

FILES

OPEN

steady_fin

SAVE AS

```
transient_fin
OK
MAIN

LOADCASES
HEAT TRANSFER
TRANSIENT
TOTAL LOADCASE TIME
20
ADAPTIVE LOADING TEMPERATURE PARAMETERS
MAX # INCREMENTS
200
INITIAL TIME STEP
1
OK (twice)
MAIN

JOBS
PROPERTIES
ANALYSIS OPTIONS
LUMPED CAPACITY
OK (twice)
SAVE
RUN
SUBMIT1
MONITOR
OK
MAIN)
```

RESULTS

- OPEN DEFAULT
- CONTOUR BANDS
- LAST
- HISTORY PLOT
- SET LOCATIONS
 - (pick those shown)
- END LIST
- ALL INCS
- ADD CURVES
- ALL LOCATIONS
 - Time
 - Temperature
- FIT
- RETURN
- RETURN
- PATH PLOT
- SHOW MODEL
- NODE PATH
 - (pick two nodes shown)
- END LIST
- VARIABLES
- ADD CURVE
 - Arc Length
 - Temperature
- FIT
- RETURN
- REWIND
- MONITOR

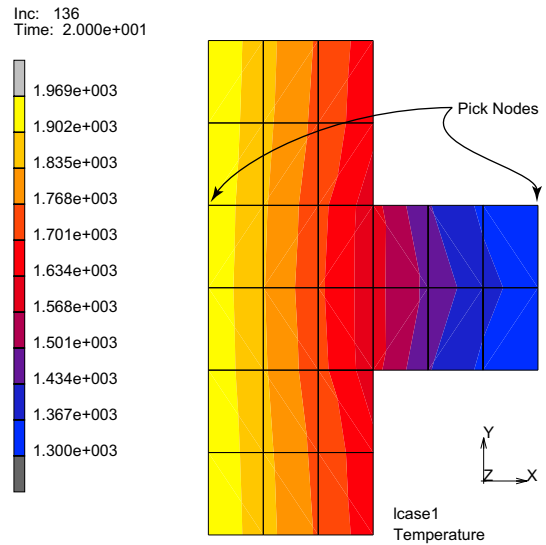


Figure 4.4-9 Temperature Contours

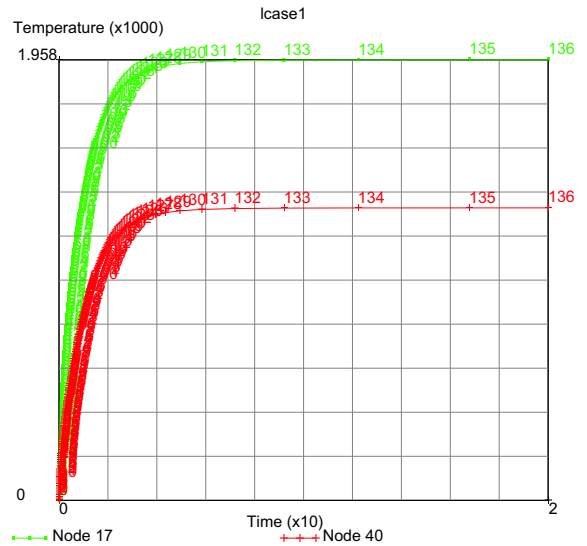


Figure 4.4-10 Temperature History

Our estimate of 20 seconds to reach steady state was overestimated and about 10 seconds appears acceptable. While obvious here, if we are not sure the solution reaches steady state, another steady state loadcase can be added to this job and repeating the above post processing steps would insure steady state is reached.

Let's repeat the above steps for the model without the cooling fin and determine the efficiency of the cooling fin.

Detailed Session Description without Fin

FILES

OPEN

steady

SAVE AS

transient

OK

MAIN

LOADCASES

HEAT TRANSFER

TRANSIENT

TOTAL LOADCASE TIME

20

ADAPTIVE LOADING TEMPERATURE PARAMETERS

MAX # INCREMENTS

200

INITIAL TIME STEP

1

OK (twice)

MAIN

JOBS

PROPERTIES

ANALYSIS OPTIONS

LUMPED CAPACITY

OK (twice)

SAVE

RUN

SUBMIT1

MONITOR

OK

MAIN

Defining the cooling efficiency as: $\eta = 1 - \frac{T_{avgfin}}{T_{avgno-fin}} = 1 - \frac{E_{fin}}{E_{no-fin}}$

where E is the thermal energy stored at the end of the transient solution. Let's history plot E with and without the fin.

RESULTS

OPEN

transient_job1.t16

OK

HISTORY PLOT

ALL INCS

ADD CURVES

GLOBAL

Time

Thermal Energy

FIT

(E = 0.769516)

OK

COPY TO GENERALIZED XY PLOTTER

MAIN

RESULTS

OPEN

transient_fin_job1.t16

OK

HISTORY PLOT

ALL INCS

ADD CURVES

GLOBAL

Time

Thermal Energy

FIT
 OK
 COPY TO GENERALIZED XY PLOTTER
 FIT

($E = 0.703308$)

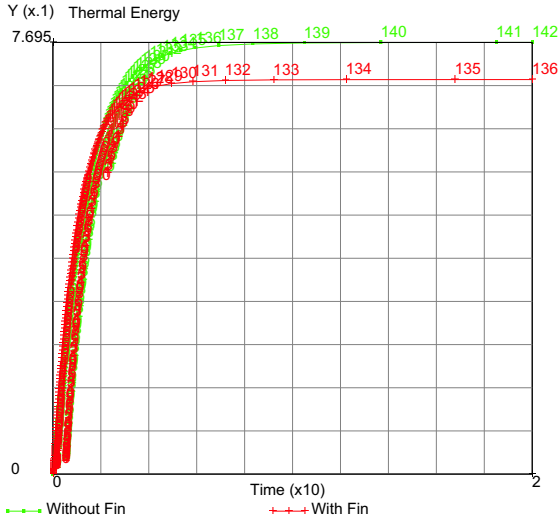


Figure 4.4-11 Thermal Energy History with and without Fin

The thermal efficiency of the fin becomes; $\eta = 1 - (0.703308 / 0.769516) = 8.6\%$. While the temperature contours in [Figure 4.4-4](#) and [Figure 4.4-7](#) where extrema values of temperature for the fin are 1300 and 1969 and 1675 and 2050 without the fin suggest a higher thermal efficiency, the thermal energy (or average temperature) used to compute the thermal efficiency is more appropriate. Other fin arrays are very possible yet they leave smaller and smaller air channels to circulate coolant that may adversely impacting thermal efficiency. [Figure 4.4-12](#) shows possible cooling channels (cyan color) improve the thermal efficiency (from 8.6 to 26%) provided coolant flows maintain the same heat transfer coefficients and sink temperature.

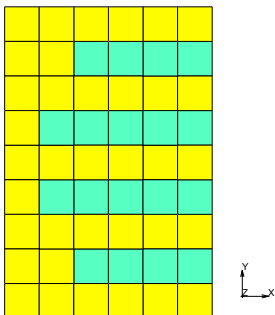


Figure 4.4-12 Possible Cooling Channels

Input Files

The files below are on your [delivery media](#) or they can be downloaded by your web browser by clicking the links (file names) below.

File	Description
h1.proc	Mentat procedure file to run the above example
h2.proc	Mentat procedure file to run the above example
cooling_fin.proc	Mentat procedure file to run the above example
heat1.mud	Mentat model file
steady.mud	Mentat model file
steady_fin.mud	Mentat model file
transient.mud	Mentat model file
transient_fin.mud	Mentat model file

Section 5: Coupled Analysis

5.1 Coupled Structural – Acoustic Analysis

- Chapter Overview 1828
- Two Spherical Rooms Separated by a Membrane 1828
- Harmonic Analysis with Stress-free Membrane 1829
- Harmonic Analysis with Pre-stressed Membrane 1838
- Input Files 1841

Chapter Overview

In a coupled structural-acoustic analysis, both the structure and the acoustic medium are modeled. The interaction between the structure and the acoustic medium affects the total response of the system. In Marc, the coupling between the structure and the acoustic medium is implemented via the CONTACT option. This enables easy modeling, since at the interface between the structure and the acoustic medium, the finite element mesh does not need to line up and no interface elements need to be defined.

The implementation is currently limited to harmonic analyses, which may be preceded by a static analysis to include the effect of a pre-stress on the response. If during the pre-stress phase severe distortions of the finite element mesh of the acoustic medium occur, remeshing is allowed before starting the harmonic analysis.

In this chapter, a coupled structural-acoustic analysis is performed on two spherical rooms separated by a membrane.

Two Spherical Rooms Separated by a Membrane

First, an analysis is done using a stress-free membrane. Then, a similar harmonic analysis is done after having pre-stressed the membrane.

Background Information

Two spherical rooms with a radius of 0.5 m are connected by a cylinder with a radius of $0.5\sin(20)$ m and a length of 0.01 m (see Figure 5.1-1). The rooms are filled with air with a bulk modulus of 1.5×10^5 N/m² and a density of 1 kg/m³. The cylinder contains a membrane of elastomeric material which is described by a neo-Hookean material with a constant C_{10} equal to 80×10^5 N/m² and a density of 1000 kg/m³. The air in the left room is locally excited by a sound pressure and the response near the membrane in the right room is calculated for a frequency range from 60 to 90 Hz, using 100 intervals. The analysis is first done using an unstressed membrane, then with a pre-stressed membrane, where the pre-stress is caused by increasing the radius of the membrane by 0.001 m.

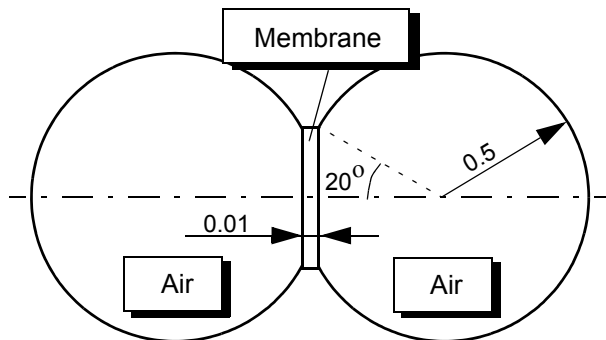


Figure 5.1-1 Structural-Acoustic Problem Schematic

The rooms and the membrane are modeled using 4-node axisymmetric elements with full integration (Marc element type 40 for the air and Marc element type 82 for the membrane). The number of contact bodies used are three: one acoustic body for the left room, one acoustic body for the right room, and one deformable body for the membrane.

Harmonic Analysis with Stress-free Membrane

Model Generation

As a first step in the generation of the finite element mesh, a number of curves are defined describing the boundary of the left room. Then the straight curve at the cylindrical part is expanded over the length of the cylinder, so that a surface is obtained which, in turn, is converted into finite elements. The left room is meshed separately using the advancing front quad mesher. By using the symmetry option, the elements of the right room are easily obtained. A detail of the mesh is shown in [Figure 5.1-2](#). The elements of the membrane, left and right room are stored in element sets.

```
MESH GENERATION
  CURVE TYPE
    CENTER/RADIUS/ANGLE/ANGLE
    RETURN
  crvs ADD
    0 0 0
    0.5
    20
    180
  pts ADD
    0.5*cos(20*pi/180) 0 0
  CURVE TYPE
    LINE
    RETURN
  crvs ADD
    5 6 6 1
  EXPAND
    TRANSLATIONS
      0.01 0 0
    SAVE
    CURVES
      3
    #
  RETURN
```

CONVERT

DIVISIONS

6 3

SURFACES TO ELEMENTS

1

#

RETURN

CHECK

UPSIDE DOWN

FLIP ELEMENTS

all: EXIST.

RETURN

AUTOMESH

CURVE DIVISIONS

FIXED # DIVISIONS

DIVISIONS

4

APPLY CURVE DIVISIONS

3

#

FIXED # DIVISIONS

DIVISIONS

16

APPLY CURVE DIVISIONS

1

#

FIXED # DIVISIONS

DIVISIONS

14

APPLY CURVE DIVISIONS

2

#

RETURN

2D PLANAR MESHING

QUADRILATERALS (ADV FRNT): QUAD MESH!

1 2 3

#

RETURN (twice)

BETWEEN POINT

*(click two bottom corner points of
 quad surface to create a new point)*

4.698463103930e-01 0 0

4.798463103930e-01 0 0

SYMMETRY

POINT

(click the point just created)

4.748463103930e-01 0 0

ELEMENTS

19 to 108

RETURN

CLEAR GEOM

SELECT

CLEAR SELECT

ELEMENTS: STORE

membrane

OK

1 to 18

ELEMENTS: STORE

room_left

OK

19 to 108

ELEMENTS: STORE

room_right

OK

109 to 198

MAIN

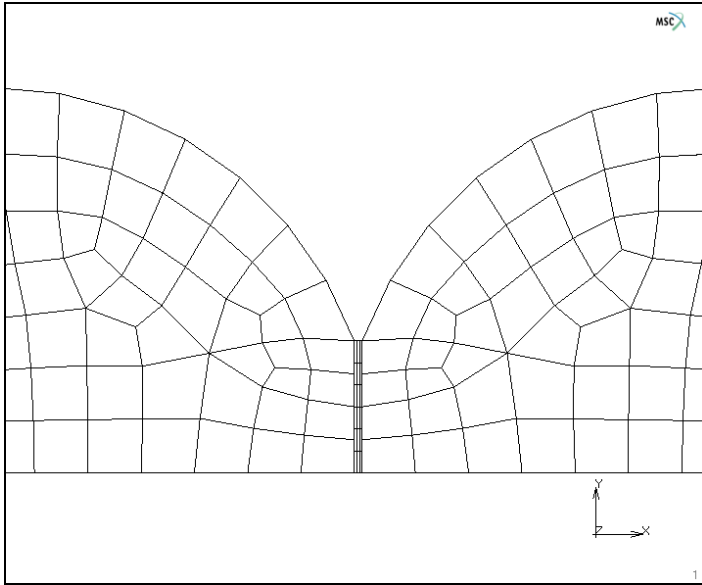


Figure 5.1-2 Detail of Finite Element Mesh around Membrane

Boundary Conditions

Boundary conditions are defined to clamp the membrane around its circumference and to enter the pressure at a node in the left room.

BOUNDARY CONDITIONS

NEW

MECHANICAL

FIXED DISPLACEMENT

DISPLACEMENT X

(on)

DISPLACEMENT Y

(on)

OK

nodes ADD

7 14 21 28

#

RETURN

NEW

ACOUSTIC

FIXED PRESSURE

PRESSURE

(on)


```
10
OK
nodes ADD
63
#
MAIN
```

Material Properties

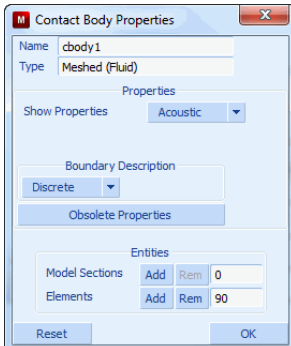
Two different materials are defined: one with the mechanical material properties for the membrane, and one with the acoustic material properties for the air in the left and right room.

```
MATERIAL PROPERTIES
NEW
MORE (MECHANICAL MATERIAL TYPES)
MOONEY
C10
80e5
MASS DENSITY
1000
OK
elements ADD
membrane
PREVIOUS
NEW
MORE (NON-MECHANICAL MATERIAL TYPES)
ACOUSTIC
BULK MODULUS
1.2e5
MASS DENSITY
1
OK
elements ADD
room_left
room_right
MAIN
```

Contact Bodies

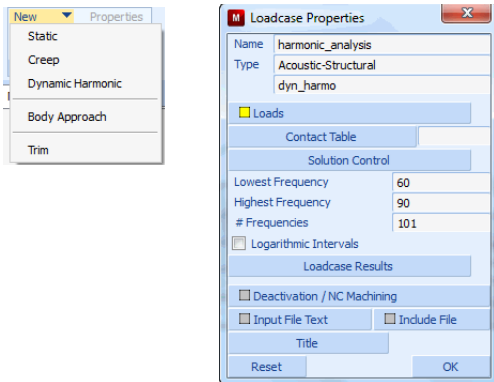
First, the elements of the left and right room are assigned to acoustic contact bodies. An acoustic contact body is completely defined by a number of elements and does not need any further properties. An acoustic contact body cannot be touched; nodes of an acoustic contact body may touch a deformable or a rigid body. Properties which are relevant for the interaction between an acoustic body and a deformable or a rigid body should be defined either for the deformable, the rigid body, or via a contact table. The third body is a deformable body and consists of the elements defining the membrane. In order to make sure that the nodes of the left and right room only contact edges of the membrane with a normal vector parallel to the global x-axis, the EXCLUDE option is used to avoid contact with edges having a normal vector parallel to the global y-axis.

```
CONTACT
  CONTACT BODIES
    NEW
    ACOUSTIC
      OK
    ELEMENTS ADD
      room_left
    NEW
    ACOUSTIC
      OK
    ELEMENTS ADD
      room_right
    NEW
    DEFORMABLE
      OK
    ELEMENTS ADD
      membrane
    RETURN
  EXCLUDE SEGMENTS
    CONTACT BODY
      cbody3
      OK
    edges ADD                                     (select edges with normal vector parallel to y-axis)
      1:3 7:3 13:3 6:1 12:1 18:1
      #
  MAIN
```



Loadcases

An acoustic-solid harmonic load case is defined, in which the frequency range from 60 Hz to 90 Hz for the pressure is entered. The number of frequencies is set to 101.



LOADCASES

NEW

NAME

harmonic_analysis

ACOUSTIC-SOLID

HARMONIC

LOWEST FREQUENCY

60

HIGHEST FREQUENCY

90

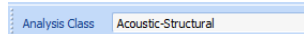
FREQUENCIES

101

OK
MAIN

Jobs

An acoustic-solid job is defined and the harmonic load case is selected. The element types for the membrane and the air are set to 40 and 82, respectively. The model is saved and the job is submitted.



JOBS

ACOUSTIC-SOLID

harmonic_analysis *(select loadcase)*

CONTACT CONTROL

INITIAL CONTACT

exseg1 *(exclude segments)*

OK (twice)

AXISYMMETRIC

OK

ELEMENT TYPES

ACOUSTIC-SOLID

AXISYMMETRIC *(acoustic element types)*

40

OK

room_left

AXISYMMETRIC *(acoustic element types)*

40

OK

room_right

AXISYMMETRIC SOLID *(mechanical element types)*

82

OK

membrane

RETURN (twice)

FILE

SAVE AS

structural_acoustic_1.mud

OK

```
RETURN
RUN
SUBMIT 1
MONITOR
OK
MAIN
```

Results

A plot of the sound pressure magnitude at node 168 of the right room as a function of the frequency is given in [Figure 5.1-3](#) and shows a peak value near an eigenfrequency of the membrane.

```
RESULTS
OPEN DEFAULT
NEXT
SCALAR
    Sound Pressure Magnitude
    OK
CONTOUR BANDS
MONITOR
HISTORY PLOT
    SET NODES
        168
    END LIST (#)
COLLECT DATA
    0:1 0:200 1
NODES/VARIABLES
    ADD 1-NODE CURVE
        nodes
            168
        global variables
            Frequency
        variables at nodes
            Sound Pressure Magnitude
FIT
```

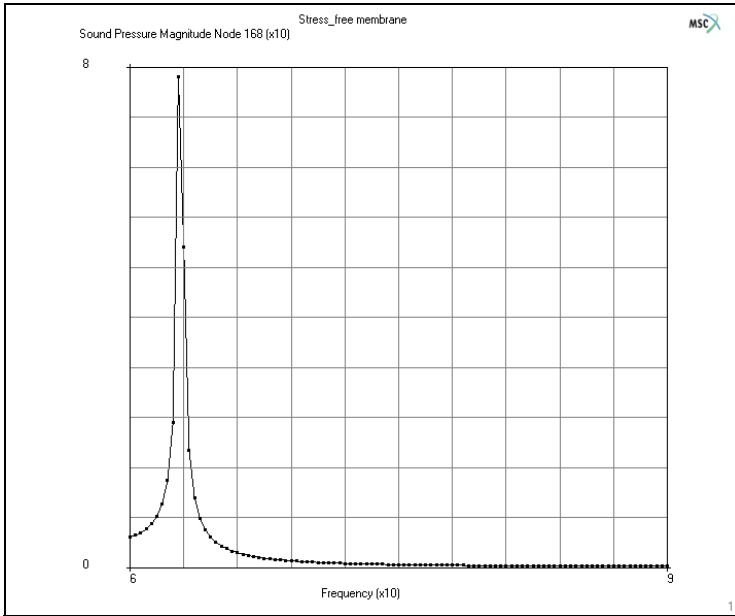


Figure 5.1-3 Sound Pressure Magnitude as a Function of the Frequency

Harmonic Analysis with Pre-stressed Membrane

Where the previous harmonic analysis was based on a stress-free membrane, now the membrane is first pre-stressed, followed by a similar harmonic analysis. In this way, a shift of the pressure peak to a higher frequency can be expected.

Model Generation

The finite element model is the same as used for the previous analysis.

```
FILES
  NEW
    OK
  RESET PROGRAM
  OPEN
    acoustic.mud
    OK
  MAIN
```

Boundary Conditions

The boundary conditions of the previous analysis are modified to take into account the radius increase of the membrane.

```
BOUNDARY CONDITIONS
  MECHANICAL
    FIXED DISPLACEMENT
      ON Y-DISPLACEMENT
        0.001
      OK
    MAIN
```

Material Properties and Contact Bodies

The material properties and the contact bodies don't need any changes.

Loadcase

A new loadcase, an acoustic-solid static one, must be defined to determine the pre-stress in the membrane.

```
LOADCASES
  NEW
  NAME
    pre_stress
  ACOUSTIC-SOLID
  STATIC
  CONTACT
    exseg1
    OK (twice)
  MAIN
```

Jobs

In the acoustic-solid job, two load cases must be selected: first the one corresponding to the pre-stress of the membrane and then the one corresponding to the harmonic analysis. Notice that the displacement boundary conditions may not occur as initial loads. After saving the model, the job is submitted.

```
JOBS
  ACOUSTIC-SOLID
  CLEAR
  pre_stress
```

```
Harmonic_analysis
INITIAL LOADS
  apply1 fixed_displacement (clear)
  OK (twice)
FILES
  SAVE AS
    structural_acoustic_2.mud
  OK
  RETURN
RUN
  SUBMIT 1
  MONITOR
  OK
MAIN
```

Results

A similar history plot as in the previous analysis is made, but now based on the sub-increments of increment 1, thus reflecting the harmonic analysis based on the pre-stressed membrane. The sound pressure magnitude as a function of the frequency is shown in [Figure 5.1-4](#) and clearly shows a shift of the peak value to a higher frequency.

```
RESULTS
  OPEN DEFAULT
  HISTORY PLOT
  SET NODES
    168
  END LIST (#)
  COLLECT DATA
    1:1 1:200 1
  NODES/VARIABLES
  ADD 1-NODE CURVE
    nodes
    168
  global variables
  Frequency
  variables at nodes
```


Sound Pressure Magnitude

FIT

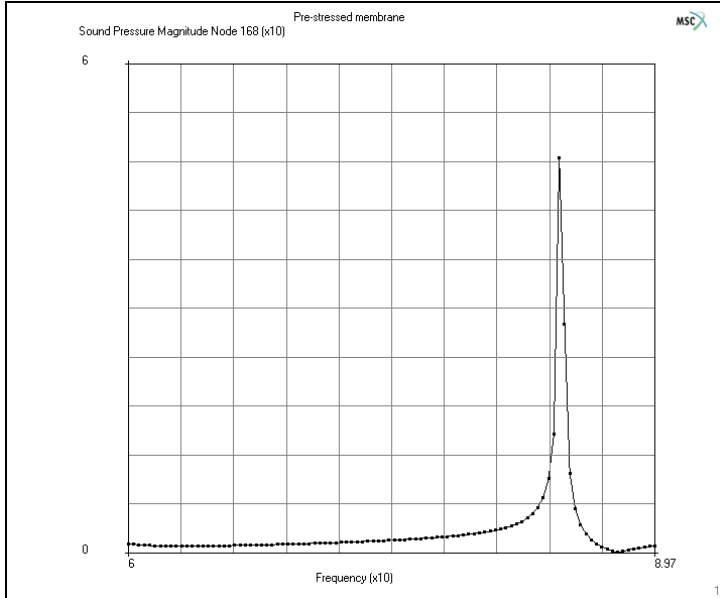


Figure 5.1-4 Sound Pressure Magnitude as a Function of the Frequency

Input Files

The files below are on your [delivery media](#) or they can be downloaded by your web browser by clicking the links (file names) below.

File	Description
acoustic.proc	Mentat procedure file to run the above example

5.2 Coupled Electrical-Thermal-Mechanical Analysis of a Micro Actuator

- Chapter Overview 1844
- Simulation of a Microelectrothermal Actuator 1844
- Input Files 1853

Chapter Overview

This chapter demonstrates the simulation of a micro-actuator using *coupled electrical-thermal-mechanical* analysis. In Marc, coupled electrical-thermal-mechanical (a.k.a. Joule mechanical) analysis is handled using a staggered solution procedure similar to the ones used in coupled electrical-thermal (a.k.a. Joule heating) and in thermal-mechanical analyses. Using this approach, the electrical problem is solved first for the nodal voltages. Next, the thermal problem is solved to obtain the nodal temperatures. Finally, the mechanical problem is solved for the nodal displacements.

Simulation of a Microelectrothermal Actuator

Problem Description

The microelectrothermal actuator, shown in [Figure 5.2-1](#), is a 'U' shaped MEMS device fabricated from polycrystalline silicon. Polycrystalline silicon has a higher electrical resistivity than most metals. The actuator uses differential thermal expansion between the thin arm (hot arm) and the wide arm (cold arm) to achieve motion. Current flows through the device because of a potential difference applied across the two electrical pads. Because of the different widths of the two arms of the 'U' structure, the current density in the two arms is different leading to different amounts of thermal expansion and hence, bending. If the lateral deflection of the tip of the device is restricted by an object, a force is generated on that object. Arrays of actuators can be connected together at their tips to multiply the force produced.

The material of the actuator is polycrystalline silicon with a Young's modulus of 158.0E3 MPa, a Poisson's ratio of 0.23, a coefficient of thermal expansion of 3.0E-6 1/K, a thermal conductivity of 140.0E6 picowatt/micrometer.K, and a resistivity of 2.3E-11 teraohm.micrometer. The hot arm is 240 microns long and 2 microns wide. The cold arm is 200 microns long and 16 microns wide. The flexure is 40 microns long and 2 microns wide. The gap between the hot and cold arms is 2 microns wide. The thickness of the actuator is 2 microns.

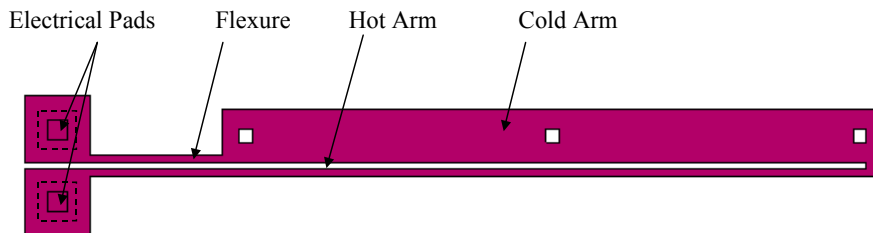


Figure 5.2-1 Actuator Geometry

The initial temperature of the actuator is set to 300°K. A potential difference of five volts is applied across the electrical pads. The temperature of the pads is fixed at 300°K. The pads are fixed in space in all three degrees of freedom.

Actuator Model

A 3-D single actuator model is shown in [Figure 5.2-2](#). The model is constructed of 2174 higher-order tetrahedron elements (element type 127). The model file `actuator.mfd` contains the 3-D geometry and finite element mesh for the problem. In the following, we define the boundary conditions, initial conditions, and material properties pertaining to Joule-mechanical analysis.

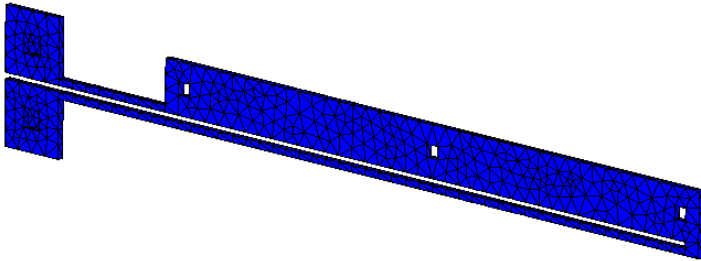


Figure 5.2-2 3-D Microelectrothermal Model

To open the model:

```
FILES
  OPEN
    actuator.mfd
  OK
  FILL
  ZOOM IN
```

After opening the model and examining it, follow the steps described below to complete the model definition:

```
MAIN
  BOUNDARY CONDITIONS
  NEW
  MECHANICAL
    FIXED DISPLACEMENT
      DISPLACEMENT X
        0
      DISPLACEMENT Y
        0
      DISPLACEMENT Z
        0
    OK
```

```
      NODES
        ADD
          ALL
            SET
              fixed_nodes
              OK
        RETURN
    NEW
      THERMAL
        FIXED TEMPERATURE
          TEMPERATURE (TOP)
            300
            OK
      NODES
        ADD
          ALL
            SET
              fixed_nodes
              OK
        RETURN
    NEW
      JOULE
        FIXED VOLTAGE
          VOLTAGE
            5
          TABLE
            table1
            OK
      NODES
        ADD
          ALL
            SET
              electrical_pad1_nodes
              OK
```

```

    RETURN
NEW
    JOULE
        FIXED VOLTAGE
            VOLTAGE
                0
            OK
        NODES
        ADD
        ALL
        SET
            electrical_pad2_nodes
        OK

MAIN
    INITIAL CONDITIONS
    NEW
        THERMAL
            TEMPERATURE
            TEMPERATURE (TOP)
                300
            OK
        NODES
        ADD
        ALL
        EXIST.
    
```

Figures 5.2-3, 5.2-4, and 5.2-5 show the Material Properties, Loadcases, and Jobs menus.

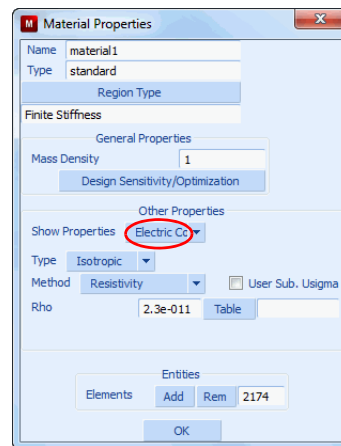
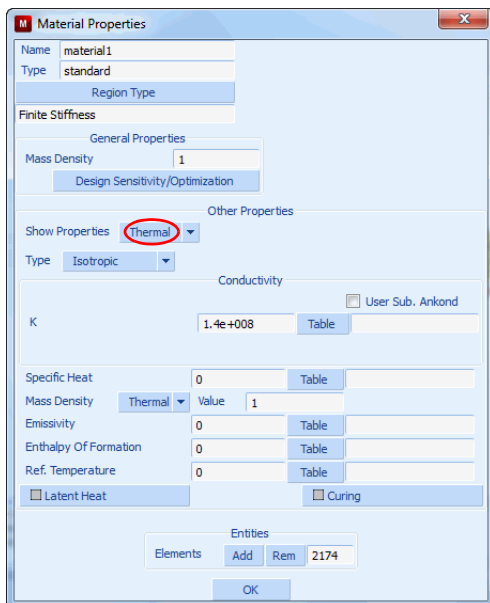
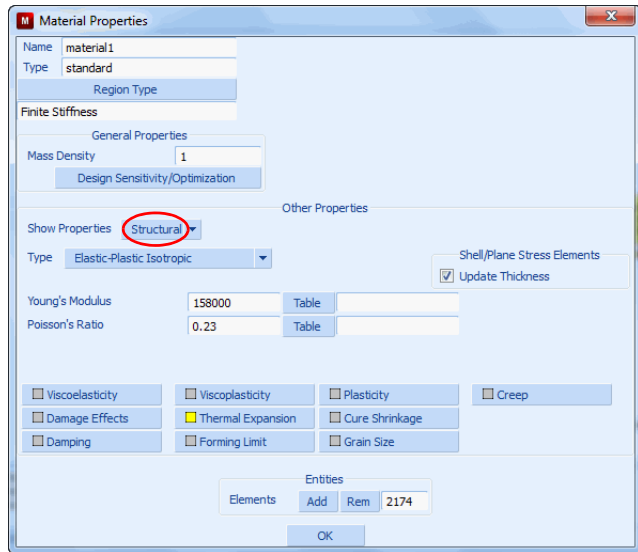
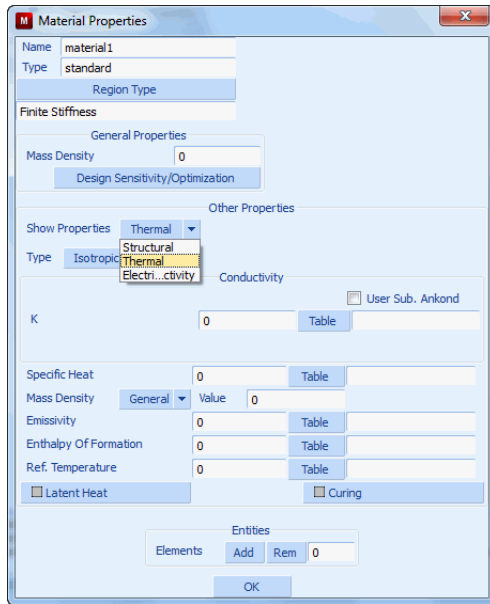
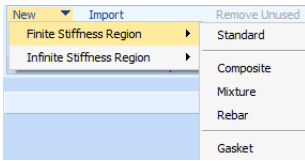


Figure 5.2-3 Material Properties Menu

MAIN

MATERIAL PROPERTIES

ISOTROPIC

YOUNG'S MODULUS

158.0e3

POISSON'S RATIO

0.23

THERMAL EXP.

THERMAL EXP. COEF.

3.0e-6

OK (twice)

JOULE HEATING

CONDUCTIVITY

140.0e6

RESISTIVITY

2.3e-11

OK

ELEMENTS

ADD

ALL

EXIST.

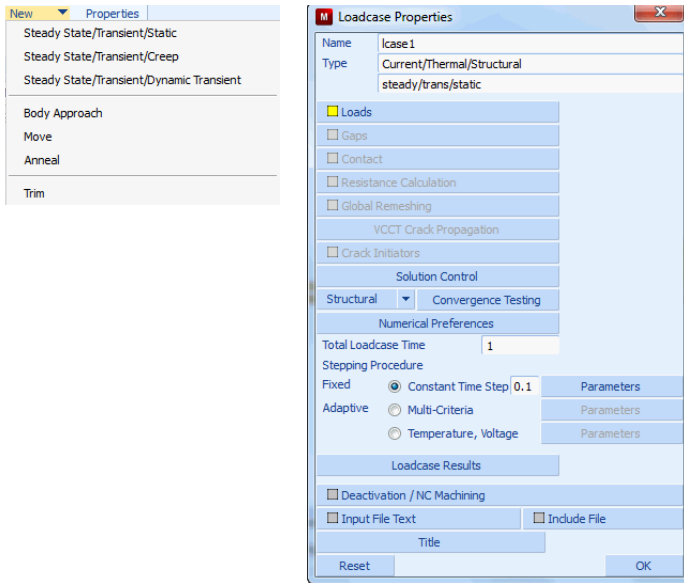


Figure 5.2-4 Loadcases Menu

MAIN

LOADCASES

JOULE-MECHANICAL

TRANSIENT

OF STEPS

10

OK

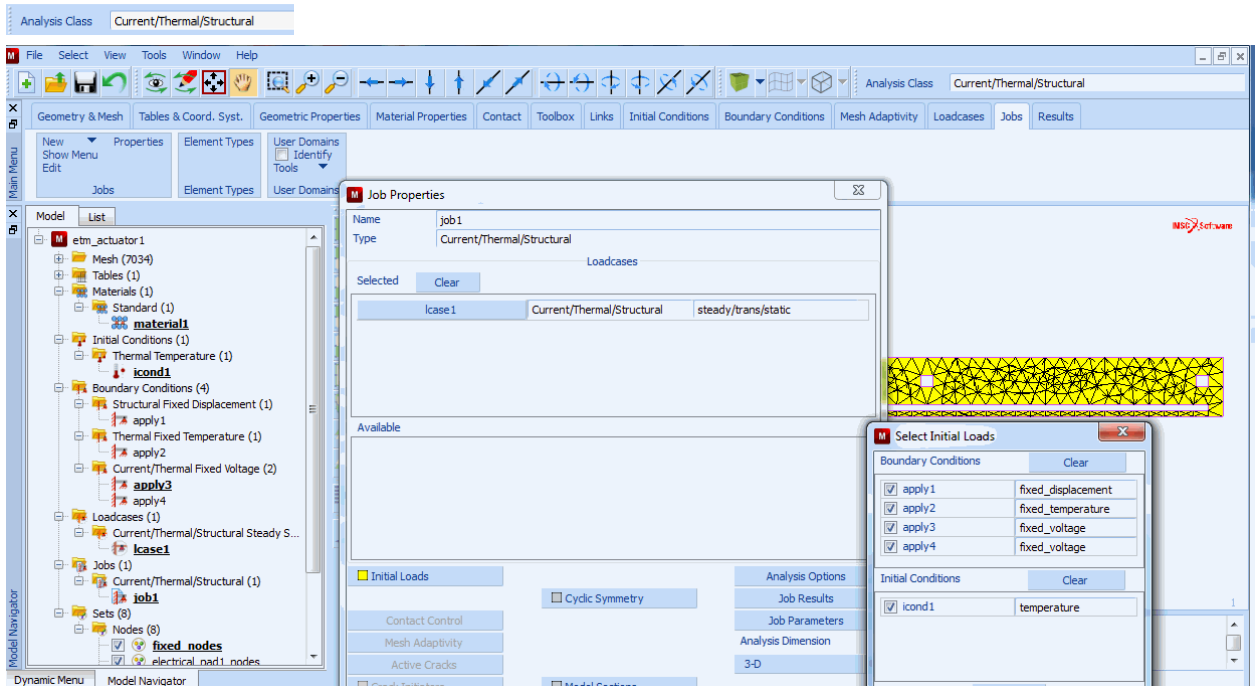


Figure 5.2-5 Jobs Menu

MAIN

JOBS

JOULE-MECHANICAL

lcase1

OK

FILES

SAVE AS

etm_actuator1.mud

OK

Run Job and View Results

To run the job:

MAIN

JOBS

RUN

RESET

```
        SUBMIT (1)
        MONITOR
        OK
    PLOT
    NODES
        ELEMENTS
        SOLID

MAIN
    RESULTS
        OPEN DEFAULT
        DEF & ORIG
        SCALAR PLOT
            SCALAR
                TEMPERATURE
                OK
        CONTOUR BANDS
        MONITOR
        CLOSE
```

The final deformed shape with temperature distribution is shown in [Figure 5.2-6](#). The maximum temperature is 1232°K and the maximum y-deflection is 6.058 microns.

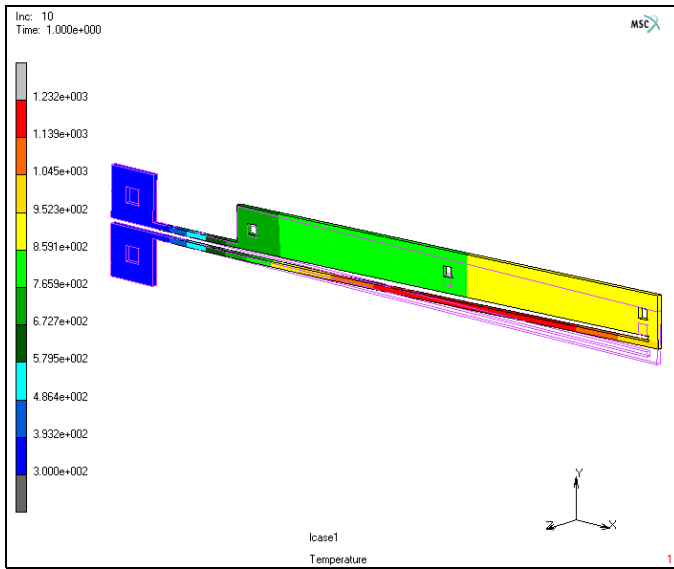


Figure 5.2-6 Final Deformed Shape of the Actuator with Temperature Distribution

Input Files

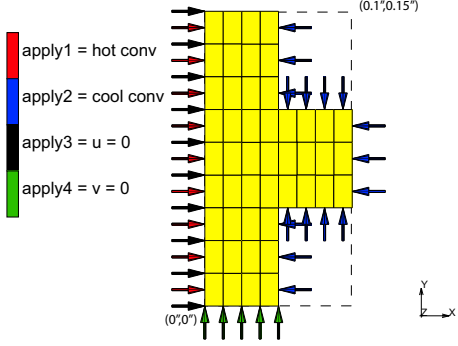
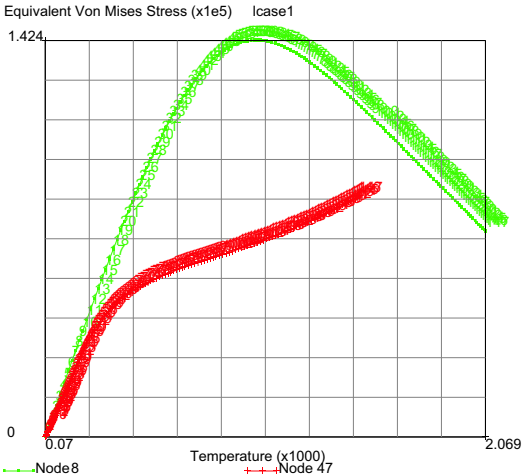
The files below are on your [delivery media](#) or they can be downloaded by your web browser by clicking the links (file names) below.

File	Description
etm_actuator.proc	Mentat procedure file to run the above example
actuator.mfd	Associated Mentat model file

5.3 Coupled Transient Cooling Fin

- Summary 1856
- Detailed Session Description 1857
- Run Jobs and View Results 1858
- Input Files 1860

Summary

Title	Coupled transient cooling fin
Problem features	Coupled thermal stress analysis
Geometry	
Material properties	$k = 1.157 \times 10^{-4} \text{ BTU in}^{-1} \text{ s}^{-1} \text{ } ^\circ\text{F}^{-1}$, $E = 3 \times 10^7 \text{ psi}$, $\nu = 0.3$ $C_p = 0.146 \text{ BTU lbm}^{-1} \text{ } ^\circ\text{F}^{-1}$, $\rho = 0.283 \text{ lbm in}^{-3}$, $\alpha = 1.0 \times 10^{-5} \text{ } ^\circ\text{F}^{-1}$
Analysis type	Steady state and transient heat transfer
Boundary conditions	Hot side $H = 750 \text{ BTU hr}^{-1} \text{ ft}^{-2} \text{ } ^\circ\text{F}^{-1}$, $T_\infty = 2500 \text{ } ^\circ\text{F}$, Cool side $H = 500 \text{ BTU hr}^{-1} \text{ ft}^{-2} \text{ } ^\circ\text{F}^{-1}$, $T_\infty = 1000 \text{ } ^\circ\text{F}$ $u = 0$, left side; $v = 0$ bottom
Initial conditions	$T = 70^\circ\text{F}$
Element type	Planar quadrilateral
FE results	Stress versus temperature Equivalent Von Mises Stress (x1e5) Icase1 

Mechanical boundary conditions are added to a previous transient thermal model. Here, the bottom horizontal surface is constrained not to displace in the vertical direction and the left vertical surface is constrained not to displace in the horizontal direction. Mechanical properties are also added to the model including the thermal coefficient of expansion.

The transient loadcase is changed to a quasi-static coupled loadcase. Finally, the element types are changed to plane stress and the job is submitted.

Stresses are generated in the slab because of nonuniform thermal growth constrained by the mechanical boundary conditions. By plotting the stress at the points shown, we see that the maximum stress on the hot side occurs well before steady state.

Detailed Session Description

Even though the thermal efficiency may be better with the cooling fin, the structural response may not. Let's see how to take the model used in [Chapter 4.4: Cooling Fin Analyses](#) and convert it into a coupled thermal stress problem.

FILES

OPEN

heat1.mud

SAVE AS

heat1s

OK

RETURN

BOUNDARY CONDITIONS

MECHANICAL

NEW

FIX X

0

NODES ADD

(pick nodes on left edge)

NEW

FIX Y

0

NODES ADD

(pick nodes on bottom edge)

RETURN (twice)

MATERIAL PROPERTIES (twice)

ANALYSIS CLASS: USE CURRENT JOB

(off)

COUPLED

STRUCTURAL

E = 3E7

ν = .3

THERMAL EXP (twice)

ALPHA = 10E-6

OK (twice)

MAIN

LOADCASES

TYPE COUPLED

QUASI-STATIC

LOADS

(pick new bc's)

CONV. TESTING

DISPLACEMENTS,

OK

TOTAL LOADCASE TIME

60

OK

MAIN

Run Jobs and View Results

JOBS

TYPE: COUPLED

PROPERTIES

INITIAL LOADS

(select new bc's)

OK

JOB RESULTS

EQUIVALENT VON MISES STRESS

OK (twice)

ELEMENT TYPES

ANALYSIS DIMENSION PLANAR

SOLID

PLANE STRESS

3

OK

ALL: EXISTING

MAIN

SAVE
 RUN
 SUBMIT1
 MONITOR

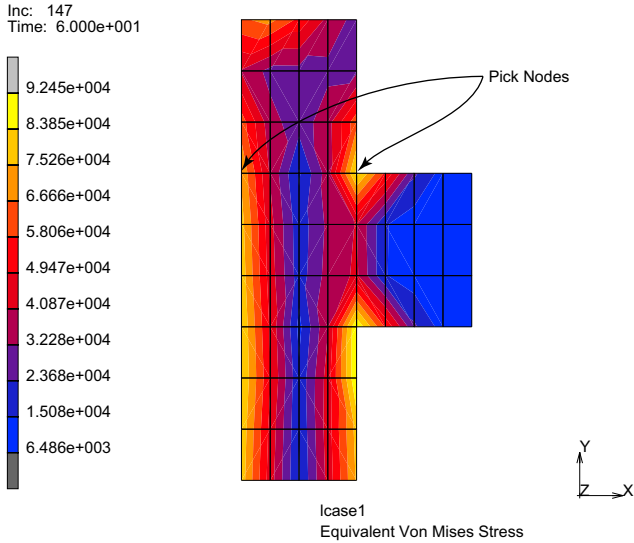


Figure 5.3-1 Equivalent von Mises Stress Contours at Steady State

RESULTS
 OPEN DEFAULT
 CONTOUR BANDS
 LAST
 SCALAR
 Equivalent Von Mises Stress
 HISTORY PLOT
 SET LOCATIONS
 END LIST
 ALL INCS
 ADD CURVES
 ALL LOCATIONS
 Temperature
 Equivalent Von Mises Stress

(pick nodes shown)

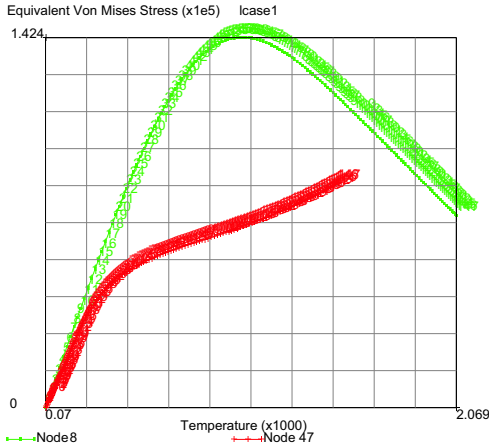


Figure 5.3-2 Stress Versus Temperature History

Notice how the stress peaks well before steady state (on the hot side - yet the cool side stress slowly grows monotonically to steady state) because of nonuniform expansion during the transient. This is very common in coupled thermal stress problems.

Plane stress is used in this example. If plane strain elements (types 11, 27, etc.) are used, the out-of-plane strain for these elements is zero. This generates a large out-of-plane stress since for plane strain we have:

$$\sigma_{zz} = \frac{E}{(1 + \nu)(1 - 2\nu)} [\epsilon_{xx} + \epsilon_{yy} - (1 + \nu)\alpha\Delta T]$$

and the last term in the equation dominates for large changes in temperature. If there is no out-of-plane constraint to the thermal growth physically, plane stress should be used. If the out-of-plane thermal growth is restricted, such as these planes remaining plane, generalized plane strain elements (types 19, 29, etc.) should be used. You may wish to try these elements and observe what happens.

Input Files

The files below are on your [delivery media](#) or they can be downloaded by your web browser by clicking the links (file names) below.

File	Description
h3.proc	Mentat procedure file to run the above example
heat1.mud	Associated Mentat model file

5.4 Temperature Dependent Orthotropic Thermal Strains

- Chapter Overview 1862
- Detailed Session Description 1863
- Run Jobs and View Results 1866
- Thermal Expansion Data Reduction 1868
- References 1871

Chapter Overview

Temperature dependent thermal expansion behavior of fiber-reinforced composite materials presents some unique features with respect to more traditional isotropic materials, primarily the change of the coefficient of thermal expansion with spatial direction caused by an isotropy. Here, thermal couples and electrical resistance strain gages are used to measure the expansion of the BMS material in the fiber direction (1) and transverse direction (2) as shown in Figure 5.4-1.

CTE TEST MEASUREMENTS								
Scan ID	Date	Time	T/C#1	T/C#2	T/C #1		T/C #2	
			TI/SIL	BMS	BAR	BAR	BMS	BMS
			BAR	REF.	VERT.	HORZ.	VERT.	HORZ.
			°F	°F	µε	µε	µε	µε
1	7/12/06	12:49:34 PM	86.6	88.0	0	0	0	0
2	7/12/06	12:50:34 PM	87.1	88.6	-1	-1	-2	1
3	7/12/06	12:51:34 PM	87.4	89.2	-3	-2	-3	1
4	7/12/06	12:52:34 PM	88.0	89.7	-4	-4	-4.0	-2.0
5	7/12/06	12:53:34 PM	89.7	92.3	-9.9	-8.9	-10	-10
6	7/12/06	12:54:34 PM	92.5	95.9	-20	-19	-20	-20
7	7/12/06	12:55:34 PM	95.9	100.0	-32	-30	-29.8	-29.8
8	7/12/06	12:56:34 PM	99.7	104.2	-44.7	-42.7	-39	-42
...
1047	7/13/06	6:16:04 AM	81.2	82.1	33	32	44	35

Figure 5.4-1 Measured Temperatures and Thermal Strains

The measurements have strain gages mounted on two specimens: the test specimen, having unknown expansion and the reference specimen, having a known thermal expansion [1]. This is repeated in a direction transverse to the fiber direction along with two thermal couples recording the temperatures of the unknown and reference material. Ultimately, the thermal strain as a function of temperature results in the two directions as shown in Figure 5.4-2; the instantaneous coefficients of thermal expansion used in the analysis are simply the slopes of the thermal strain versus temperature curves.

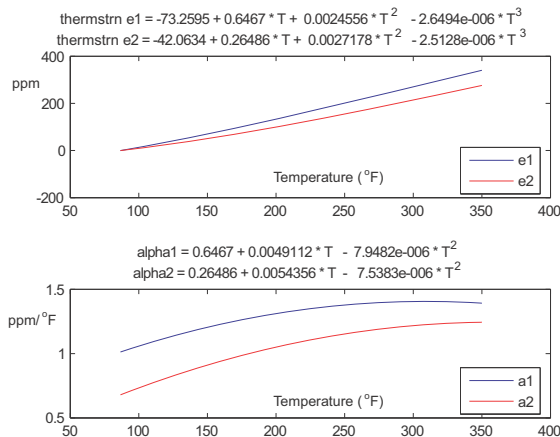


Figure 5.4-2 Thermal Strains and Instantaneous Coefficients of Thermal Expansion

Detailed Session Description

Before starting, it is worth mentioning that many times the mean (average) coefficient of linear thermal expansion is given in handbooks. If the mean coefficient of linear thermal expansion versus temperature is known, one would still need to construct the thermal strain versus temperature curve and supply the slopes (instantaneous coefficients of thermal expansion) to Marc as described in Volume A. The average coefficient of linear thermal expansion is not a thermodynamic material property, whereas the instantaneous coefficient of thermal expansion is a thermodynamic material property. Finally the terms used here for the mean and average coefficients are consistent with those definitions in the American Society for Testing and Materials (ASTM) test method E 228^(2.). The term “thermal strain” used here is simply the “linear thermal expansion” used in ASTM E 228; the change in length per initial length caused by a change in temperature.

The thermal strains depicted in Figure 5.4-2, may or may not generate stresses in applications depending on how non uniform the temperature distributions become and how the thermal expansion (or contraction) may be restricted. In order to determine stresses a finite element analysis is usually performed with the appropriate material properties and boundary conditions. In order to make sure that the material’s thermal expansion or contraction is correctly modeled, the analysis done here is a simple one having uniform temperatures changing over time and boundary conditions allowing free thermal growth or contraction. The goal is to see if the finite element analysis reproduces the thermal strains in Figure 5.4-2. It is always a good practice, particularly for complex material behavior, to replicate the material behavior using a few elements in a simple scenario similar to the test method to verify the modeling. The example model here uses only three elements as shown in Figure 5.4-3 with horizontal displacements along A-B, vertical displacements along C-D fixed to zero, and temperature ramped from 87.153 °F to 400 °F.

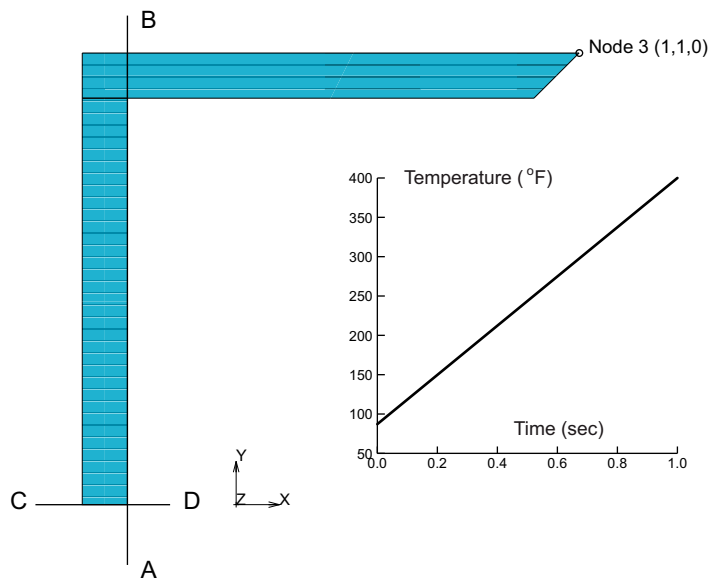


Figure 5.4-3 Model Definition

The same geometric model uses several different element types, namely plane stress, plane strain, generalized plane strain, and axisymmetric for the same boundary conditions and material properties as listed below. The model files are complete and the steps below are used to highlight portions of the model.

File	Description
type26uc.mud	Model file using plane stress elements.
type27uc.mud	Model file using plane strain elements.
type28uc.mud	Model file using axisymmetric elements.
type29uc.mud	Model file using generalized plan strain elements.

We will examine how the thermal expansion data appears in each of the models above by examining each of the models above, running them and checking the results starting with the plane strain elements.

FILES

OPEN

type27uc.mud

OK

RETURN

MATERIAL PROPERTIES

ORTHOTROPIC

THERMAL EXPANSION PROPERTIES

ALPHA11

1E-6

TABLE

alpha1

(pick table alpha1)

OK

ALPHA22

1E-6

TABLE

alpha2

(pick table alpha2)

OK

ALPHA33

1E-6

TABLE

alpha2

(pick table alpha2)

OK (thrice)

We have assumed that the fiber direction (table alpha1) is in the global x direction and that the other two principal material directions are in the epoxy direction (table alpha2). Let's examine the tables, alpha1 and alpha2.

TABLES

SHOW TABLE

EDIT

(pick table alpha1)

OK

TYPE

temperature

OK

FORMULA

$0.6467 + 0.0049112 * V1 + -7.9482e-006 * V1^2$

FIT

MAX

400

(set maximum independent

FIT

variable)

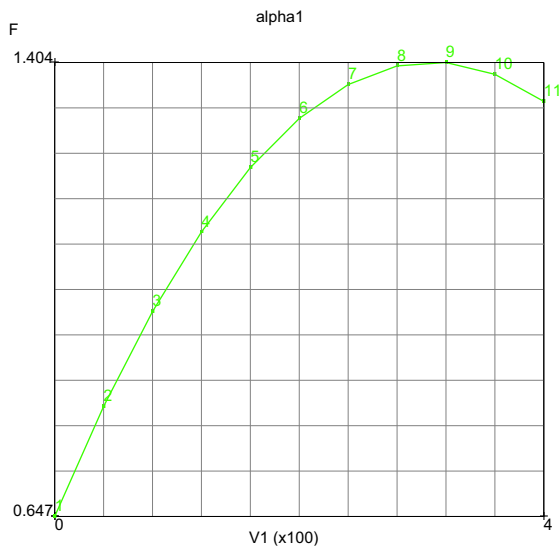


Figure 5.4-4 Fiber Direction Instantaneous Coefficient of Thermal Expansion versus Temperature

EDIT

(pick table alpha2)

OK

TYPE

temperature

```
OK
FORMULA
    0.26486 + 0.0054356 * v1 + -7.5383e-006 * v1^2
FIT
MAIN
```

These tables enter the formulas for the instantaneous coefficient of thermal expansion that is used in the analysis. Since the model file as it exists we can simply run the file and examine the results

Run Jobs and View Results

```
JOBS
    MECHANICAL
    JOB RESULTS
        Stress
        Total Strain
        Thermal Strain
        Temperature (Integration Point)
    OK
OK
ELEMENT TYPES
    MECHANICAL
    PLANE STRAIN SOLID
        27
    OK
    ALL: EXISTING
RETURN (twice)
SAVE
RUN
    SUBMIT1
    MONITOR
RESULTS
    OPEN DEFAULT
    HISTORY PLOT
    SET NODES
```

```

COLLECT GLOBAL DATA
NODES/VARIABLES
  ADD VARIABLE
    Temperature (Integration Point)
    Comp 11 of Thermal Strain
  ADD VARIABLE
    Temperature (Integration Point)
    Comp 22 of Thermal Strain
  ADD VARIABLE
    Temperature (Integration Point)
    Displacement X
  ADD VARIABLE
    Temperature (Integration Point)
    Displacement Y
FIT

```

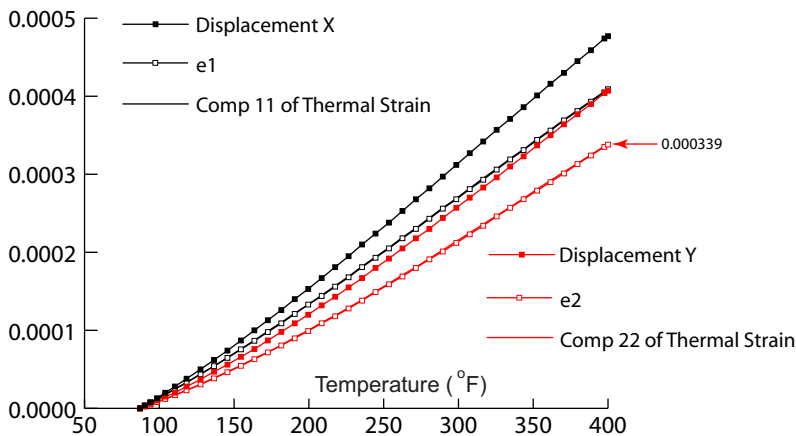


Figure 5.4-5 Thermal Strains and Displacements - Plane Strain Case

The experimentally measured thermal strains (e_1 , e_2) are identical to the thermal strains (Comp 11, Comp 22) in the analysis. Since the initial coordinate of node 3 is (1,1) the displacement in the x (1) and y (2) directions are displacements per unit length (apparent thermal strains) that should equal the thermal strains in the corresponding directions provided no stresses are generated. This is not the case as shown in Figure 5.4-5 and stresses are being generated. A large amount of stress in the z (3) out-of-plane direction is generated because the total out-of-plane strain must be zero (plane strain assumption). The out-of-plane stress for plane strain becomes:

$$\sigma_{33} = E_3 \left[\frac{\nu_{13}}{E_1} \sigma_{11} + \frac{\nu_{23}}{E_2} \sigma_{22} - \int_{T_i}^T \alpha_{33}(T) dT \right] \Bigg|_{400^{\circ}F} = 1.13 \times 10^6 (-0.000339) = -383.07$$

and the last term in the equation will dominate with changes in temperature. The large compressive stress in the out-of-plane direction expands the structure in the in-plane directions, and the displacements per unit length become larger than the thermal strains in [Figure 5.4-5](#). Plot the out-of-plane stress, σ_{33} , and see if it is close to the estimate above.

If there is no out-of-plane constraint to the thermal growth physically, a plane stress conditions could be used. If the out-of-plane thermal growth is restricted, such as plane remaining plane, generalized plane strain elements (types 19, 29, etc.) should be used. For example, transient thermals with large thermal gradients where the out-of-plane thickness is large enough to allow out-of-plane thermal growth can stretch with planes remaining plane should use generalized plane strain elements. You may wish to try the other elements in the other model files and observe what happens (no stresses will be generated).

Thermal Expansion Data Reduction

The actual measurements shown in [Figure 5.4-6](#) used two well-matched strain gages, with one bonded to a specimen of the reference material (Titanium Silicate - thermal expansion assumed to be zero see Vishay [1]), and the second to a specimen of the test material (a fiber reinforced epoxy composite, Boeing BMS 8-256, along with other materials) in two directions vertical (fiber direction) and horizontal. Under stress-free conditions, the differential output between the gages on the two specimens, at any common temperature, is equal to the differential unit expansion usually reported in micro-strain ($\mu\epsilon$) or parts per million (ppm). Although the test ran for many hours the third recycle is recorded here and we will only process that data necessary for the expansion of the BMS material that occurred in the first 70 minutes. The MatLab (Natick, Massachusetts) commands used to reduce the raw data into a form convenient for analysis follow below with comments narrating the operations.

Column	Date	Time	T/C#1	T/C#2	T/C#3	T/C#4	T/C#5	T/C #1		T/C #2	
			TI/SIL BAR REF.	BMS COUP. REF.	BMI TOOL REF.	ALUM. TOOL REF.	INVAR TOOL REF.	BAR VERT.	BAR HORZ.	BMS COMP. VERT.	BMS COMP. HORZ.
Scan ID			°F	°F	°F	°F	°F	$\mu\epsilon$	$\mu\epsilon$	$\mu\epsilon$	$\mu\epsilon$
1	7/12/06	12:49:34 PM	86.6	88.0	87.4	88.0	88.1	0	0	0	0
2	7/12/06	12:50:34 PM	87.1	88.6	87.6	88.0	88.3	-1	-1	-2	1
3	7/12/06	12:51:34 PM	87.4	89.2	88.0	88.0	88.5	-3	-2	-3	1
4	7/12/06	12:52:34 PM	88.0	89.7	88.3	88.1	88.6	-4	-4	-4.0	-2.0
5	7/12/06	12:53:34 PM	89.7	92.3	89.9	88.6	90.7	-9.9	-8.9	-10	-10
6	7/12/06	12:54:34 PM	92.5	95.9	92.3	89.5	93.1	-20	-19	-20	-20
7	7/12/06	12:55:34 PM	95.9	100.0	95.2	90.4	94.7	-32	-30	-29.8	-29.8
8	7/12/06	12:56:34 PM	99.7	104.2	98.5	91.9	97.1	-44.7	-42.7	-39	-42
9	7/12/06	12:57:34 PM	103.8	108.4	101.8	93.3	100.2	-60	-57	-50	-53
10	7/12/06	12:58:34 PM	108.1	112.6	105.2	95.0	102.3	-75	-72	-60	-63
11	7/12/06	12:59:34 PM	112.6	116.8	109.0	97.1	105.4	-90	-87	-72	-77
---	---	---	---	---	---	---	---	---	---	---	---
---	---	---	---	---	---	---	---	---	---	---	---
69	7/12/06	1:58:04 PM	350.0	335.9	339.0	317.2	328.1	-1198	-1186	-798	-845
70	7/12/06	1:59:04 PM	350.0	336.5	340.4	319.5	329.5	-1199	-1188	-800	-848

Figure 5.4-6 Snippet of Recorded Raw Data

```

%-- read spread sheet CTETST3 in CTETST3.xls and define local arrays
%-- for first n data points scanned.
n = 70;

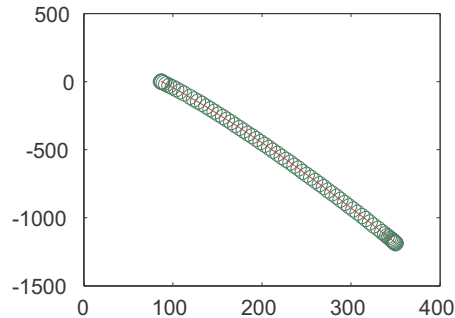
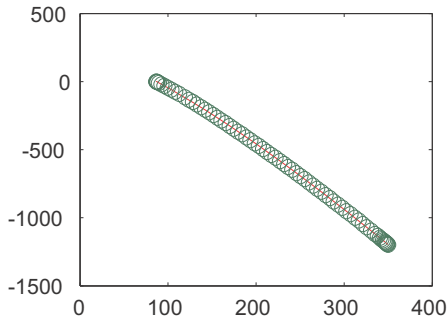
```

```

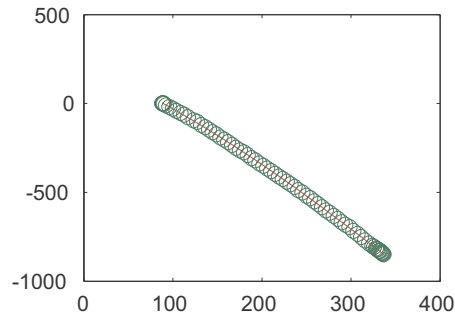
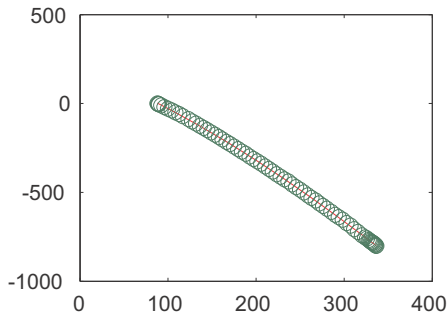
[ndata, headertext] = xlsread('CTETST3.xls', 'CTETST3');
x1 = ndata(1:n, 4); x1t = 'T/C#1 TI/SIL BAR REF. Temperature F';
y1 = ndata(1:n, 9); y1t = 'T/C#1 BAR VERT. STRN ppm';
y2 = ndata(1:n,10); y2t = 'T/C#1 BAR HORZ. STRN ppm';
x2 = ndata(1:n, 5); x2t = 'T/C#2 COMP. COUP. REF. Temperature F';
y3 = ndata(1:n,11); y3t = 'T/C#2 COMP. VERT. STRN ppm';
y4 = ndata(1:n,12); y4t = 'T/C#2 COMP. HORZ. STRN ppm';
%-- fit gage strain data to polynomials, p and evaluate, f quantify error of polynomial fit order 3.
p1 = polyfit(x1,y1,3); p2 = polyfit(x1,y2,3);
p3 = polyfit(x2,y3,3); p4 = polyfit(x2,y4,3);
f1 = polyval(p1,x1); f2 = polyval(p2,x1);
f3 = polyval(p3,x2); f4 = polyval(p4,x2);
%-- check fit of data
mm1 = (max(f1-y1)-min(f1-y1))/(max(y1)-min(y1));
mm2 = (max(f2-y2)-min(f2-y2))/(max(y2)-min(y2));
mm3 = (max(f3-y3)-min(f3-y3))/(max(y3)-min(y3));
mm4 = (max(f4-y4)-min(f4-y4))/(max(y4)-min(y4));
figure
subplot(2,2,1); plot(x1,f1,x1,y1,'o'); title([y1t, ' Error ', num2str(mm1)]);
subplot(2,2,2); plot(x1,f2,x1,y2,'o'); title([y2t, ' Error ', num2str(mm2)]);
subplot(2,2,3); plot(x2,f3,x2,y3,'o'); title([y3t, ' Error ', num2str(mm3)]);
subplot(2,2,4); plot(x2,f4,x2,y4,'o'); title([y4t, ' Error ', num2str(mm4)]);

```

T/C#1 BAR VERT. STRN ppm Error 0.0048992 T/C#1 BAR HORZ. STRN ppm Error 0.0060918



T/C#2 COMP. VERT. STRN ppm Error 0.0090716 T/C#2 COMP. HORZ. STRN ppm Error 0.012554



```

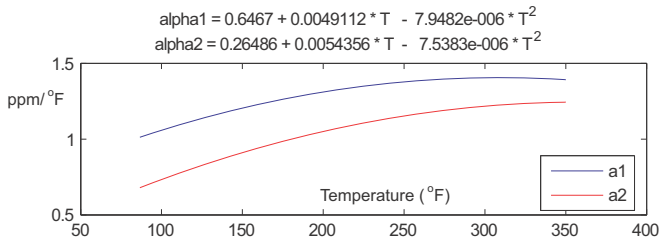
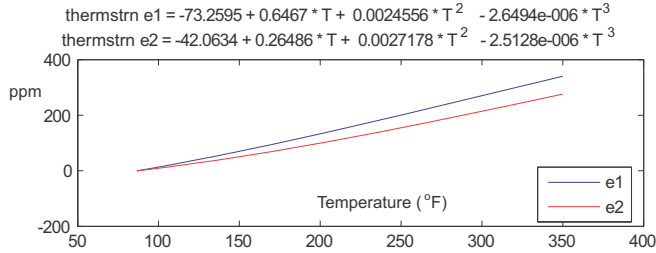
%-- shift temperature for polynomial roots to agree refit p3,p4 so that
%-- p1=p3=0 at same temperature, same for p2=p4=0.
rp1=roots(p1); rp2=roots(p2); rp3=roots(p3); rp4=roots(p4);
shift42=rp4(3)-rp2(3); shift31=rp3(3)-rp1(3);
p4 = polyfit(x2-shift42,y4,3); p3 = polyfit(x2-shift31,y3,3);
%-- compute thermal strains
g1=p3-p1; g2=p4-p2;
%-- shift so g1 and g2 have same root
rg1=roots(g1); rg2=roots(g2);
shiftg=rg2(3)-rg1(3);
g2s = polyval(x2-shiftg,polyval(g2,x2),3);
g2 = g2s
%-- plot thermal strain, and alpha
stg1 = ['thermstrn e1 = ' num2str(g1(4)) ' + ' num2str(g1(3)) ' * T + ' num2str(g1(2)) ' * T^2 + ' num2str(g1(1)) ' * T^3'];

```

```

stg2 = ['thermstrn e2 = ' num2str(g2(4)) ' + ' num2str(g2(3)) ' * T + ' num2str(g2(2)) ' * T^2 + ' num2str(g2(1)) ' *
T^3'];
a1=polyder(g1); a2=polyder(g2);
stal = ['alpha1 = ' num2str(a1(3)) ' + ' num2str(a1(2)) ' * T + ' num2str(a1(1)) ' * T^2'];
sta2 = ['alpha2 = ' num2str(a2(3)) ' + ' num2str(a2(2)) ' * T + ' num2str(a2(1)) ' * T^2'];
figure
subplot(2,1,1);plot(x1,polyval(g1,x1),x1,polyval(g2,x1));title({stg1;stg2});legend('e1','e2','Location','Southeast');
subplot(2,1,2);plot(x1,polyval(a1,x1),x1,polyval(a2,x1));title({stal;sta2});legend('a1','a2','Location','Southeast');

```



```

%-- output results into excel worksheet
d = {'Temp F', stg1, stg2, stal, sta2}
xlswrite('tempdata.xls', d, 'Results', 'A1');
xlswrite('tempdata.xls', x1, 'Results', 'A2');
xlswrite('tempdata.xls', polyval(g1,x1), 'Results', 'B2');
xlswrite('tempdata.xls', polyval(g2,x1), 'Results', 'C2');
xlswrite('tempdata.xls', polyval(a1,x1), 'Results', 'D2');
xlswrite('tempdata.xls', polyval(a2,x1), 'Results', 'E2');

```

The comments and figures generated by the MatLab commands should be sufficient for one to follow the calculations. Because two thermal couples are used for the reference and unknown material, their temperatures are not exactly the same at the same time. This required shifting the data to account for this difference. Furthermore, it is quite common (particularly for more precise data measurements from optical heterodyne interferometry [3 and 4]) to use cubic polynomials for the thermal strain data fits as well as reporting the data. Before any two polynomials are added or subtracted, they are adjusted such that the thermal strain is zero at the same temperature; this minor adjustment prevents introducing numerical artifacts into the thermal strain and instantaneous coefficients of thermal expansion. The output from the data reductions is place into an Excel shown in [Figure 5.4-7](#).

Temp F	thermstrn e1 = - 73.2595 + 0.6467 * T + 0.0024556 * T^2 +- 2.6494e-006 * T^3	thermstrn e2 = - 42.0634 + 0.26486 * T + 0.0027178 * T^2 +- 2.5128e-006 * T^3	alpha1 = 0.6467 + 0.0049112 * T +- 7.9482e-006 * T^2	alpha2 = 0.26486 + 0.0054356 * T +- 7.5383e-006 * T^2
86.572	-0.58859224	-0.39505678	1.012299076	0.678934005
87.091	-0.062733297	-0.042134101	1.014131586	0.681075639
87.437	0.288367224	0.193764733	1.015350881	0.682501139
87.957	0.816825379	0.549221636	1.017179767	0.684640114
89.686	2.58076639	1.73909395	1.023229908	0.691722894
92.45	5.42223188	3.666561037	1.032803028	0.702951893
95.9	9.005774959	6.115695376	1.044581715	0.716806221
99.688	12.98680421	8.859445039	1.05729645	0.731811188
103.81	17.37305449	11.9092042	1.070873133	0.747893404
108.1	21.99689848	15.15308489	1.084716327	0.764359041
112.55	26.85526492	18.59194341	1.098766687	0.781145593

Figure 5.4-7 Snippet of Output from Data Reduction

The actual part that was used in these measurement is a large cylinder comprised of this fiber reinforced material shown in Figure 5.4-8.

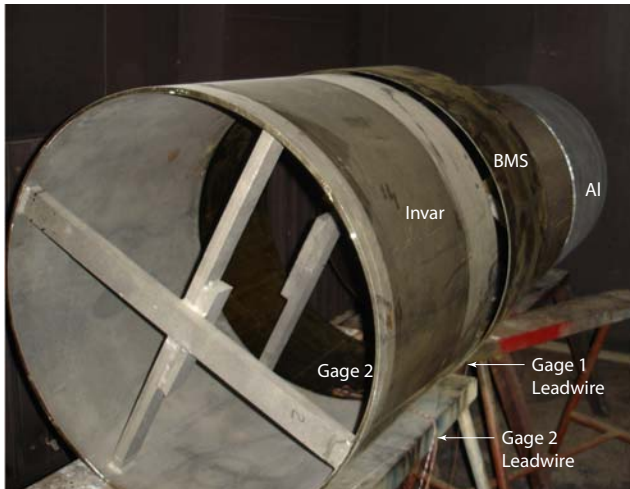


Figure 5.4-8 Fiber Reinforced Cylinder with Thermal Couples and Strain Gages

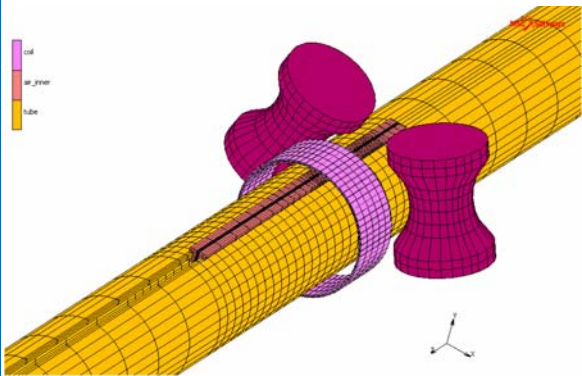
References

1. Vishay Micro-Measurements (2007) Measurement of Thermal Expansion Coefficient Using Strain Gages. *Tech Note TN-513-1*. <<http://www.vishay.com/doc?11063>>.
2. ASTM, E 228-06 (2006) Standard Test Method for Linear Thermal Expansion of Solid Materials With a Push-Rod Dilatometer. *Annual Book of ASTM Standards*.
3. De Bona E, Somá A (1997) Thermal Expansion Measurement of Composites with Optical Heterodyne Interferometry. *Experimental Mechanics*, 37(1):21-25.
4. Chanchani R, Hall P M (1990) Temperature dependence of thermal expansion of ceramics and metals for electronic packages. *IEEE Trans Comp, Hybrids, Manufact Technol* 13:743–750.

5.5 Tube Welding using Induction Heating

- Summary 1874
- Introduction 1875
- Preparations for Creating the Coil 1877
- Material Properties 1879
- Contact 1879
- Creation of the Coil and Circuit 1882
- Boundary Conditions 1884
- Loadcase and Jobs 1885
- Creating the Surrounding Air Mesh 1886
- Results and Discussion 1889
- Input Files 1894

Summary

Title	Tube welding using induction heating
Problem Features	This chapter demonstrates the use of circuit analysis in a coupled magnetodynamic/thermal/structural analysis which uses the dual mesh approach.
Model	 <p>The rollers are modeled as geometric bodies. The tube is used in the thermal/structural pass, while coil and air_inner bodies are used in the magnetodynamic pass.</p>
Material Properties	<p>Tube: Young's modulus is $2.e11$ Pa, Poisson's ratio is 0.3 and yield stress is $2.75e9$ Pa. Temperature dependent work hardening is used. Thermal conductivity and specific heat are also temperature dependent. Mass density is 7900 kg/m³, permeability is $1.25e-6$ H/m, permittivity is $8.854e-12$ F/m, and electric conductivity is $1e7$ 1/Ωm.</p> <p>Coil: permeability is $1.25e-6$ H/m, permittivity is $8.854e-12$ F/m, and electric conductivity is $5.88e7$ 1/Ωm. The coil is not active in the thermal and structural pass.</p>
Boundary Conditions	A voltage of 2.4 V is applied to a single turn coil. The rollers move inwards to press the two sides of the tube together. When this is done the tube is pushed through the rollers. The magnetic vector potential and electric potential is set to zero on the outer boundary.
Analysis Type	Coupled magnetodynamic/thermal/structural analysis where the magnetodynamic pass is harmonic and the other two passes transient.
Element type	Dual mesh approach is used with separate meshes for the magnetodynamic pass and thermal/structural pass. Tet4 and hex8 elements are used
FE Results	Contour plots of contact status and temperature distribution, and cutting plane plots of the current density and thermal energy density

Introduction

This example describes how to weld a tube using induction heating. In such processes, first a metal sheet is bent to a tube in a number of roll forming stages. In the final roll forming stage, the two sides of the tube are pushed together. A coil is located in front of the last rollers. An AC electric voltage is applied to this coil. This generates a harmonic magnetic field. Due to this field, induced currents are generated in the tube. The flow of these induced currents follows a closed loop which means that in this situation the current will cross from one side of the tube to the other where the tube is making self-contact. Here at this crossing, the current will be highly concentrated. This concentrated current leads to localized heating due to the Joule effect. When enough heat is generated here, this part of the tube will reach the melting temperature and so a weld forms.

The complete roll forming process will not be performed in this example. Instead, we start with reading a model which contains the following four parts.

- The preformed cylinder containing an open V-shape
- Two rollers used for the final pressing
- A box with finely meshed elements to represent the air box in which the induced current near the V-shaped tip of the tube will be computed
- A box of surfaces which will be used to create the surrounding air mesh.

The dual mesh approach is used where we have separate meshes for the magnetodynamic pass and the thermal/structural pass. The magnetodynamic mesh consists of the coil, the box with finely meshed elements, and the remaining region which is meshed as surrounding air. In the dual mesh approach, integration points from the magnetodynamic elements use the material properties of the thermal/structural elements when they are located in such an element; otherwise, they use their own properties. In this approach, the induced currents are not computed in the thermal/structural elements but in the magnetodynamic elements. For this reason, a box with finely meshed elements is located near the V-shaped opening of the tube. The magnetodynamic elements must be small enough in this region so that they can accurately compute the induced currents where they occur in the tube. The heat generated from these induced currents is computed and then transferred to thermal/structural elements. During the simulation the magnetodynamic mesh remains stationary while the thermal/structural mesh, which is the tube, is pushed through the rollers. Integration points from the magnetodynamic elements will, therefore, be located in different thermal/structural elements or outside these elements during this process. In each simulation step, the material properties of appropriate magnetodynamic elements are determined based on the current position, shape, and temperature of the tube.

Figure 5.5-1 shows the model setup. The figure shows the tube, the two rollers, and the coil. Also shown is the box of air which is finely meshed.

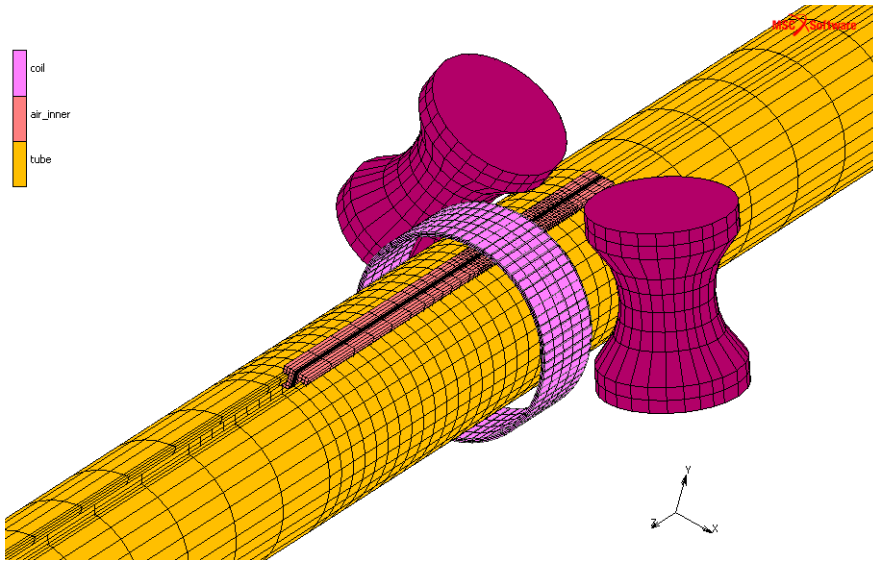


Figure 5.5-1 Model Setup

Figure 5.5-2 shows the V-shape in the open tube. This was done by removing material. In practice, the shape will occur after the roll forming process; therefore, in this case, the stresses will be too high after the welding. Note that the two sides of the tube are disconnected behind the V-shaped tip. The welding process is simulated with contact in combination with a user subroutine. Contact glue is switched on when a node in contact reaches a certain temperature. The outer diameter of the tube is 0.02 m and the wall thickness is 0.001 m.

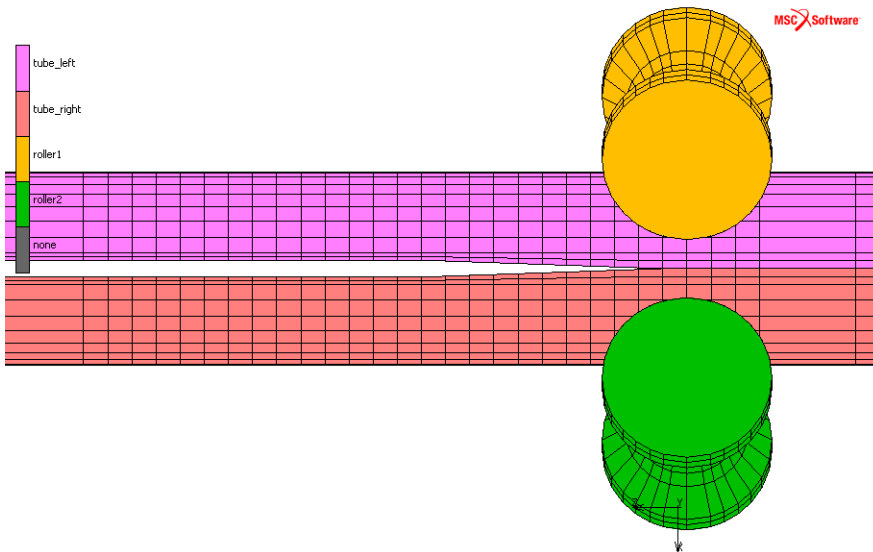


Figure 5.5-2 V-shaped Opening of the Tube

```
File
  Open
    tube_weld.mud
    open
rotate_y-axis negative 9 times
zoombox (1,0.589235,0.473888,0.628895,0.524178)
```

Important for this type of analysis is the skin depth. This is defined as the depth at which the magnitude of the induced current density drops to e^{-1} of the magnitude at the surface. The skin depth can be computed as follows.

$$\delta = \sqrt{\frac{1}{\pi f \sigma \mu}}$$

where σ is the conductivity, f is the frequency, and μ the permeability. This value is important for both coil and tube. The thickness of the coil should be less than this distance or the computation of the current will be less accurate since skin effect is not taken into account. For the tube, this distance must be considered for the element length. At least, a number of element edges should fit in this distance. Element edges perpendicular to the tube surface should be considered. Using the material properties in this example, the skin depth is 0.0023 m for the tube.

Preparations for Creating the Coil

Now we create the coil; this is a cylinder surrounding the tube. The coil has an outer diameter of 0.0255 m. The coil is meshed with brick elements. We start with a quad element which is expanded 72 times to create the cylinder. The cross-sectional area of the cylinder is 0.005 m x 0.001 m.

```
Geometry & Mesh
  Geometry & Mesh
    Nodes Add
      0 0.01225 -0.429
      0 0.01225 -0.439
      0 0.01275 -0.439
      0 0.01275 -0.429
    Points Add
      0 0.0125 -0.434
      0 0.0125 -0.435
      0 0.0 -0.434
      0 0.0 -0.435
    Elements Add
      15114
      15115
      15116
      15117
  Select
    Selection Control...
      Elements
        11165 #
      Points
        409 410 411 412 #
      Make Visible
  Ok
```

```
Fill View
Geometry & Mesh
  Operations
    Subdivide
      Divisions
        5 3 1
      Elements
        All Visible
    Ok
  Sweep
    Tolerance
      0.000001
    Nodes
      All Visible
    Ok
```

Two curves are needed to describe the current flow. These are created as circles, and then converted to polylines in 72 segments.

```
Geometry & Mesh
  Geometry & Mesh
    Curves Circle Cen/Pnt  \/  
    Curves Add
      0.000000000000e+000  0.000000000000e+000  -4.340000000000e-001
      0.000000000000e+000  1.250000000000e-002  -4.340000000000e-001
      0.000000000000e+000  0.000000000000e+000  -4.350000000000e-001
      0.000000000000e+000  1.250000000000e-002  -4.350000000000e-001
```

```
    Ok
  Geometry & Mesh
    Operations
      Convert
        Convert Curves  \/  
        To Polylines
        Divisions
          72
        Convert
          57 58 #
      Ok
```

Expand the quad element to a cylinder of brick elements. This forms the coil mesh. The coil will be only active in the magnetodynamic pass. The coil elements are added to a fluid contact body.

```
Geometry & Mesh
  Operations
    Expand
      Rotate Angles (Degrees)
        0 0 360/72
      Repetitions 72
      Elements
        All Visible
    Ok
```

```
Fill View
Material -> Standard -> Coil
Right click Properties
```

```
Elements Add  
  All Visible  
Ok
```

Material Properties

The material properties are already defined for the different materials in the initial file. The rollers are modeled as geometric bodies and are not considered in the magnetodynamic pass. It is assumed that they have air like material properties for permeability, permittivity, and electric conductivity.

The tube is also a steel with temperature dependent work hardening. This is done by multiplying a work hardening table with a table which shows a drop after a certain temperature. Here, a drop of 100 is chosen when a temperature of 800 C° is reached. Two dimensional table is created as follows.

```
Tables -> wkhd.01  
  Right click Properties  
    Multiply Table  
      drop01
```

The Young's modulus is 2.e11 Pa, Poisson's ratio is 0.3, and yield stress is 2.75e9 Pa. Thermal conductivity and specific heat are temperature dependent. Mass density is 7900 kg/m³, permeability is 1.25e-6 H/m, permittivity is 8.854e-12 F/m, and electric conductivity is 1e7 1/Ωm. For the coil permeability is 1.25e-6 H/m, permittivity is 8.854e-12 F/m, and electric conductivity is 5.882e7 1/Ωm, and for air permeability is 1.25e-6 H/m, permittivity is 8.854e-12 F/m, and electric conductivity is 0 1/Ωm

Contact

The magnetodynamic coil elements are added to a fluid contact body. The tube consists of two contact bodies tube_left and tube_right. These two bodies will be connected to simulate welding. For this, we use glued contact. For the nodes of these two bodies which can touch each other, we choose glue deactivation. Then with the UACTGLUE user subroutine, we monitor the temperature of these deactivated nodes. If the temperature of a node reaches a certain value, for this example 800 C°, regular glue contact is switched on for this node.

The contact table contains contact information for both the fluid and deformable bodies. Note that since the dual mesh approach is used, there is no interaction between the two body types (see [Figure 5.5-3](#)). Three types of contact interaction are created. For the structural mesh, the two rollers are touching the left and right side of the tube, and the two sides of the tube use the special glue contact. The third contact interaction is for the magnetodynamic mesh. Here, the different bodies are connected using glue contact. The mesh containing the surrounding air must still be created. This will be done later in this example.

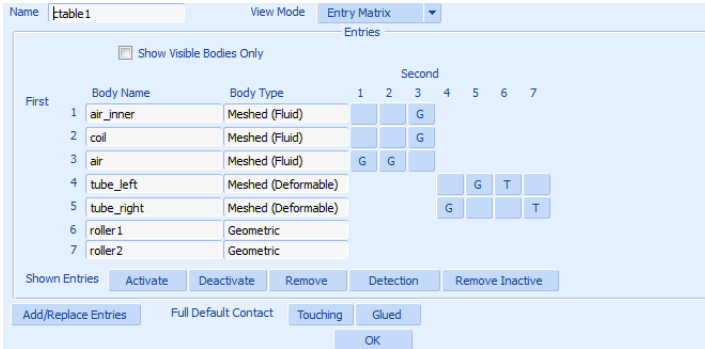


Figure 5.5-3 Contact Table Showing No Connection Between the Fluid, Deformable, and Geometric Bodies

```

Elements Clear                                     (Selection Control...)
Elements By
Material
coil
Ok
Contact Bodies -> Meshed (Fluid) -> coil
Right click Properties
Elements Add
All Selected
Ok
Elements Clear                                     (Selection Control...)
Ok
Contact -> Contact Interaction
New -> Meshed (Fluid) vs Meshed (Fluid)
Name
glue_air
Ok
Contact -> Contact Interaction
New -> Meshed (Deformable) vs Geometric
Name
touching
Ok
Contact -> Contact Interaction
New -> Meshed (Deformable) vs Meshed (Deformable)
Name
glue_weld
Ok
Contact -> Contact Table
New
Entry air_inner - air
Active
Contact Interaction
glue_air
Entry coil - air
Active
Contact Interaction
glue_air

```



```

Entry tube_left - roller1
  Active
  Contact Interaction
    touching
Entry tube_right - roller2
  Active
  Contact Interaction
    touching
Entry tube_left - tube_right
  Active
  Contact Interaction
    glue_weld
Ok
Clear All                                     (Selection Control...)
Select Contact Body entities
  tube_left
  tube_right
Ok
Make Visible
Method Face Flood \/  

Nodes
  3509:3
  3486:1
Contact -> Contact Areas
New -> Glue Deactivation
  Contact Body
    tube_left
  Nodes Add
    All Selected
New -> Glue Deactivation
  Contact Body
    tube_right
  Nodes Add
    All Selected
Ok

```

The UACTGLUE user subroutine is as follows:

```

      subroutine uactglue(node,iswitch,inc,time,coord,disp,
      $      temp,stressnorm,stressfric,relvel,ibody,ibody2)
c
c  user subroutine for switching nodes that have
c  deact glue to use regular glue.
c
c  the routine is called at the start of an increment
c  the results values are from the end of the previous increment
c
c  input:
c  node      user node id
c  inc       current increment
c  time      time at start of current increment
c  coord     initial coordinates of node
c  disp      current total displacements at node
c  temp(1)   current temperature at node

```

```

c   temp(2)      current peak temperature at node
c   stressnorm  current contact normal stress at node
c   stressfric  current contact friction stress at node
c   relvel      current relative sliding velocity at node
c               between bodies ibody and ibody2
c   ibody       contact body node belongs to
c   ibody2      contact body node is touching
c               (if it touches multiple bodies, the first it is touching)
c               if ibody2=0 then node is not in contact
c
c   output:
c   iswitch     set to 1 if node should be switched to regular glue
c
#ifdef _IMPLICITNONE
  implicit none
#else
  implicit logical (a-z)
#endif
integer node,iswitch,inc,ibody,ibody2
real*8 time,coord,disp,temp,stressnorm,stressfric,relvel
dimension coord(*),disp(*),temp(*)

c user coding

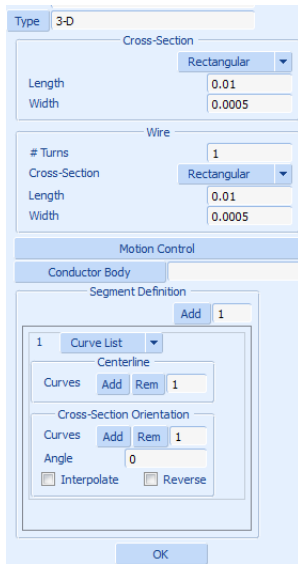
  if(temp(1).gt.800.0d0)then
    iswitch=1
    write(6,*)'switch the following node to regular glue',node
    write(6,*)'temperature is',temp(1)
  endif

  return
end

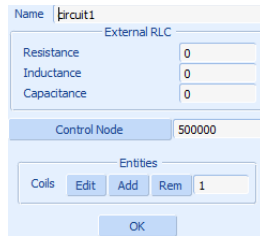
```

Creation of the Coil and Circuit

Now the coil will be created. It will have the same dimensions as the set of elements we created earlier for the coil. The coil has a rectangular cross section of 10 mm x 0.5 mm and an outer diameter of 25.5 mm. The shape and the current direction are defined by a centerline curve and the orientation curve. This coil is added to a circuit. [Figure 5.5-4](#) shows the Mentat menus for the coil and circuit definitions. The load on a circuit is controlled by a node. This node must be created separately, and then connected to the circuit. We use renumber with start position of 500000 so that this node is easily distinguished. The node is added outside the mesh. No resistor, capacitor, or inductor is added to the circuit.



Coil Definition



Circuit Definition

Figure 5.5-4 Mentat Menus

```

Toolbox -> Electromagnetics
  Coils -> New -> 3-D
    --- Cross-Section ---
    Length 0.01
    Width 0.0005
    --- Wire ---
    Cross-Section Rectangular \ /
    Length 0.01
    Width 0.0005
    --- Centerline ---
    Curves Add
      59 #
    --- Cross-Section Orientation ---
    Curves Add
      60 #
    Ok
  Select
    Selection Control...
    Clear All
    Make Visible
    Method Single
    Ok
  Fill View
  Geometry & Mesh -> Basic Manipulation
    Geometry & Mesh
    Nodes Add
      0.3 0 0
    Ok
  Renumber
  
```

```
Start
  500000
Nodes List
  All Visible
Start
  1
Ok
Toolbox -> Electromagnetics
Circuits -> New
Control Node
  500000
Coils Add
  coil1 #
Ok
```

Boundary Conditions

The two rollers move towards each other so that they will tightly press the two sides of the tube together. This motion is prescribed as a fixed displacement on the control node of each geometric body using a table. During the welding process, this pressing will cause material to flow out of the weld. This is the material which was at the surface of the two tube faces, and this material is usually contaminated. This pressing out of material will leave a cleaner weld. The tube is fixed and pushed through the rollers. The motion is prescribed as a fixed displacement and controlled with a table. Three loading stages can be distinguished. First, the tube is stationary while it heats up and the rollers are pressed against the sides of the tube. Then in the second stage, the tube starts to move for some time. In the last stage, the electrical loading is switched off, and the rollers are moved back to their original position. Now the tube can be inspected to see which nodes changed from touching contact to glued contact.

A terminal voltage of 2.4 V is applied to the control node of the circuit. The Mentat menu for terminal voltage is shown in [Figure 5.5-5](#).

The magnetic vector potential and electric potential is fixed at the outer boundary of the model.

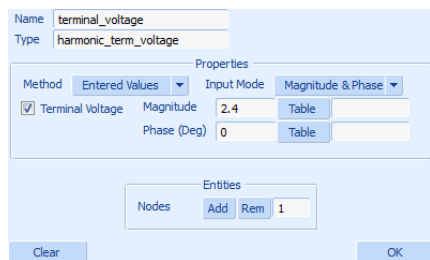


Figure 5.5-5 Mentat Menu for Terminal Voltage

```
Boundary Conditions -> Boundary Conditions
New (Magnetodynamic) -> Harmonic Terminal Voltage
Name
  terminal_voltage
Terminal Voltage
Magnitude
```

```
2.4
Nodes Add
500000 #
Ok
```

Loadcase and Jobs

The analysis consists of three stages where the first two stages are part of one loadcase and the third stage is the second loadcase. In the first stage, which lasts 1 second, the rollers are pressed against the tube and the heating starts. The voltage is applied with a frequency of 5 kHz. In the next stage, which lasts 2 seconds, part of the tube is pressed through the rollers. Then in the last stage, which lasts 1 second, the rollers are moved back, the terminal voltage is switched off, and the frequency is zero. In Jobs, regular structural and magnetodynamic post processing quantities are selected. Also selected is the Thermal Energy Density and Current Density. The Thermal Energy Density will show where the heat is generated inside the tube. Current Density shows the total induced current. Inside the coil, it shows the net current density. Note that these quantities are computed in the magnetodynamic mesh while the temperature is computed in the structural mesh.

```
Loadcase -> Loadcases
New Harmonic/Transient/Static
Name welding
Contact
Contact Table
ctable1
--- Contact Areas ---
careal
carea2      Ok
Solution Control
Max # Recycles
50
Ok
Frequency
5000
Total Loadcase Time
3
Parameters
# Steps
30
Ok
Ok
Loadcase -> (Dual Mesh) Magnetodynamic/Thermal/Structural ...
Welding
(right click) Copy
Name unload
Frequency
0
Total Loadcase Time
1
Parameters
# Steps
10
Ok
```

```
Ok
Jobs -> Jobs
New -> (Dual Mesh) Magnetodynamic/Thermal/Structural
Name
welding
Available
welding
unload
Job Results
Available Element Tensors
Stress
Plastic Strain
Available Element Scalars
Thermal Energy Density (From Electric Current)
Current Density (Integration Point)
1st Real Comp Magnetic Induction
1st Imag Comp Magnetic Induction
2nd Real Comp Magnetic Induction
2nd Imag Comp Magnetic Induction
3rd Real Comp Magnetic Induction
3rd Imag Comp Magnetic Induction
1st Real Comp Current Density
1st Imag Comp Current Density
2nd Real Comp Current Density
2nd Imag Comp Current Density
3rd Real Comp Current Density
3rd Imag Comp Current Density
Ok
```

Creating the Surrounding Air Mesh

Now the mesh which surrounds the coil and the inner_air body is created. This is done using automesh for volumes. The surface mesh option is used where first the surfaces of the part to be meshed are meshed with triangular elements. Then by selecting these triangular elements, the volume mesh will be created. [Figure 5.5-6](#) shows the Mentat menu for Automesh Volumes. The procedure is to first place triangular elements on the inner air body and the coil. This is done by selecting the outer element faces of these bodies and converting them to elements. Then these quad elements are converted to triangular elements. Finally, the triangular mesh on the inner_air body will be remeshed to get a more homogeneous mesh on this body. Then place triangular elements on the outer surfaces. Note that the elements on the inner_air box, coil, and surface must all face each other or the meshing will fail. For this example, this is accomplished by letting the surfaces which form the outside face inward. With this procedure, a mesh is created with holes at the inner_air box and coil position.

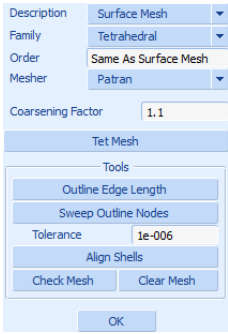


Figure 5.5-6 Mentat Menu for Volume Meshing

```
Select
  Selection Control...
  Clear All
  Select Contact Body Entities
  air_inner
  Ok
  Make visible
Fill View
  Filter Surface \/  

  Elements ...Faces
  All Visible
Geometry & Mesh -> Operations
  Convert
  Convert Faces \/  

  To Elements \/  

  Convert
  All Selected
  Ok
  Clear All
  Elements By
  Class
  Quad(4)
  Ok
  Ok
Geometry & Mesh -> Operations
  Change Class
  (0) Tria(3)
  Elements
  All Selected
  Ok
  Clear All
  Elements By
  Class
  Tria(3)
  Ok
  Ok
Geometry & Mesh -> Automesh
  Surfaces
  Element Size
```

(Selection Control...)

(Selection Control...)

```
    0.0005
    Tri Remesh!
    All Selected
    Ok
    Clear All
    Select Contact Body Entities
    coil
    Ok
    Make Visible
Fill View
    Elements ...Faces
    All Visible
Geometry & Mesh -> Operations
    Convert
    Convert
    All Selected
    Ok
    Clear All
    Elements By
    Class
    Quad(4)
    Ok
    Ok
Geometry & Mesh -> Operations
    Change Class
    (0) Tria(3)
    Elements
    All Selected
    Ok
    Clear All
    Elements By
    Class
    Tria(3)
    Ok
    Ok
Geometry & Mesh -> Operations
    Convert
    Convert Surfaces \/  
    To Elements \/  
    Convert
    1 2 3 4 5 6 #
    Ok
    Clear All
    Element By
    Class
    Quad(4)
    Ok
    Ok
Geometry & Mesh -> Operations
    Change Class
    (0) Tria(3)
    Elements
    All Selected
    Ok
```

(Selection Control...)

(Selection Control...)

(Selection Control...)

(Selection Control...)

(Selection Control...)


```
Clear All (Selection Control...)
Elements By
  Class
  Tria(3)
  Ok
Geometry & Mesh -> Automesh
Volumes
  Description Surface Mesh
  Family Tetrahedral
  Coarsening Factor
  1.1
  Sweep Outline Nodes
  Tet Mesh
  All Selected
  Ok
  Clear All (Selection Control...)
  Filter None \
  Elements By
  Material
  roller
  coil
  air_inner
  tube
  Ok
Material -> Standard -> air
  Right click Properties
  Elements Add
  All Unselected
  Ok
Contact Bodies -> Meshed (Fluid) -> air
  Right click Properties
  Elements Add
  All Unselected
  Clear All (Selection Control...)
```

Results and Discussion

From an electrical perspective, this induction heating example translates into the following equivalent circuit.

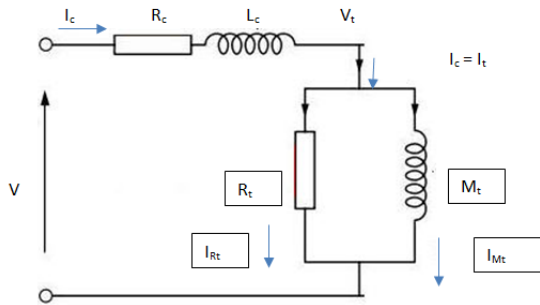


Figure 5.5-7 Equivalent Circuit for Tube Welding

where

V = Applied terminal voltage

I_c = Applied terminal current

R_c = Coil resistance; the external resistance is 0

L_c = Coil self-inductance; the external inductance is 0

R_t = Equivalent resistance of the tube due to eddy currents

M_t = Equivalent mutual inductance between coil and tube

V_t = Voltage across tube and it is also the induced voltage on the tube

V_i = the total induced voltage = $V_t + V$ across L_c .

I_t = Current in the tube and is the sum of I_{Rt} and I_{Mt} and = I_c

I_{Rt} = current in R_t

I_{Mt} = current in M_t

The coil resistance is printed in the .out file as $R_c = 0.26695\text{m}\Omega$. A number of global variables are available in the .out file and on the post file. The circuit is treated as a series connection of resistor, capacitor, and inductor. The total series resistance and reactance is available as output quantity. The reactance contains contributions from both capacitor and inductor. For the total inductance, the complex voltage drop is computed as well as the back induced voltage drop. The electrical energy dissipated in the coil (and the external resistance, but that is zero for this example) is available in the output as "Ohmic power lost in circuit".

When we look at the first increment (timestep is 0.1 s), the Ohmic power lost in the coil is 2022 W, so the electrical energy dissipated in the coil is $Q=202.2\text{ J}$. The total thermal energy at this increment is $Q=98.2\text{ J}$. The total energy is

the energy generated in the tube due to the induction heating process. The total dissipated electrical energy for this increment is the sum of these two.

The contact status is shown before and after the simulation in Figures 5.5-8 and 5.5-9, respectively; here only the elements of the tube are shown. Due to the original shape of the tube with its cut out V-shape opening, the tube is deformed where it is welded together; it no longer resembles a true cylinder. This should be different when the complete roll forming process is performed. Figure 5.5-10 shows the temperature distribution during the welding process. Note that, in this figure, the coil mesh is also shown. This mesh is not active in the thermal pass, but was added for illustration purposes. It shows that the welding spot is in front of the coil. The welding spot actually moves towards the coil during the welding process. It is likely that the tube moves a bit too slow, so that it gets too hot and thus gets too soft. Studying the magnetodynamic results requires some effort. The problem is that, with the dual mesh approach, the mesh used in the magnetodynamic pass does not contain information about where the tube is located. In this situation, a cutting plane will be most useful to study the results. The cutting point and normal direction should be chosen carefully. Note that only the elements used in the magnetodynamic pass should be made visible. Figure 5.5-11 shows a cutting plane plot of the current density, and Figure 5.5-12 shows a cutting plane plot of the thermal energy density. These two figures show a top view where the cutting plane crosses the top part of the tube.

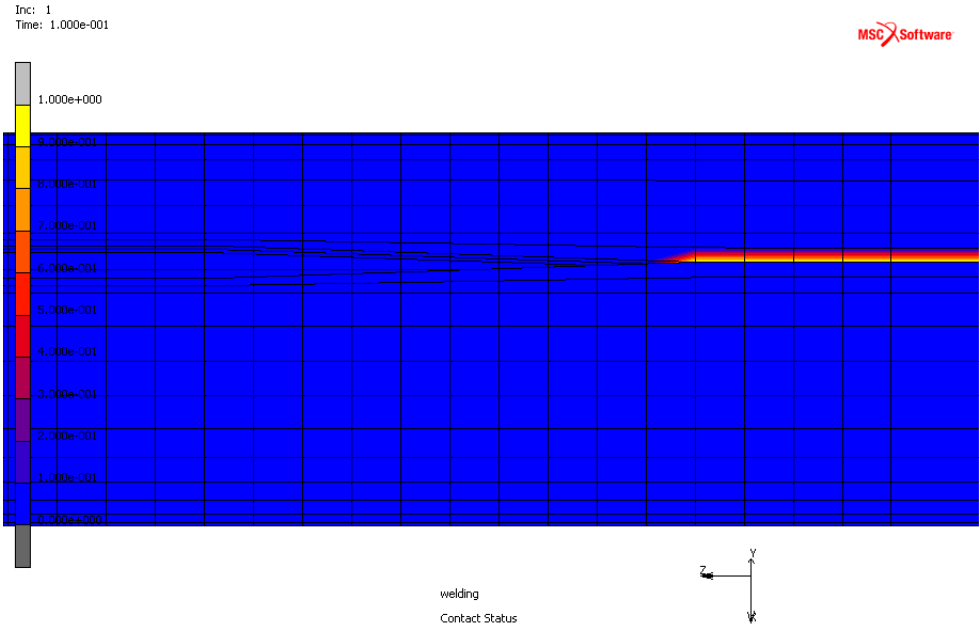


Figure 5.5-8 Initial Contact Status of the Tube

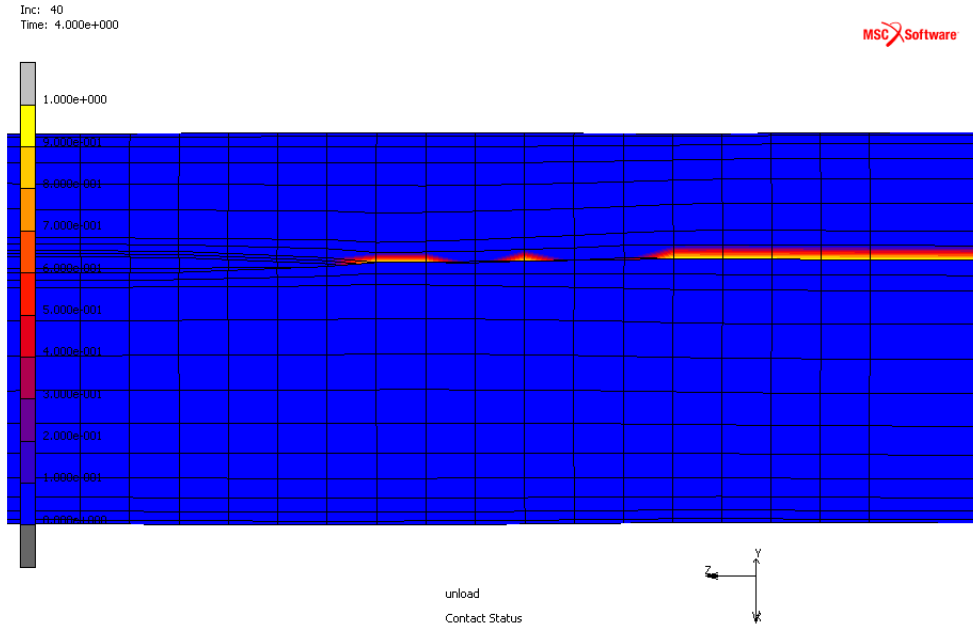


Figure 5.5-9 Contact Status of the Tube after the Welding

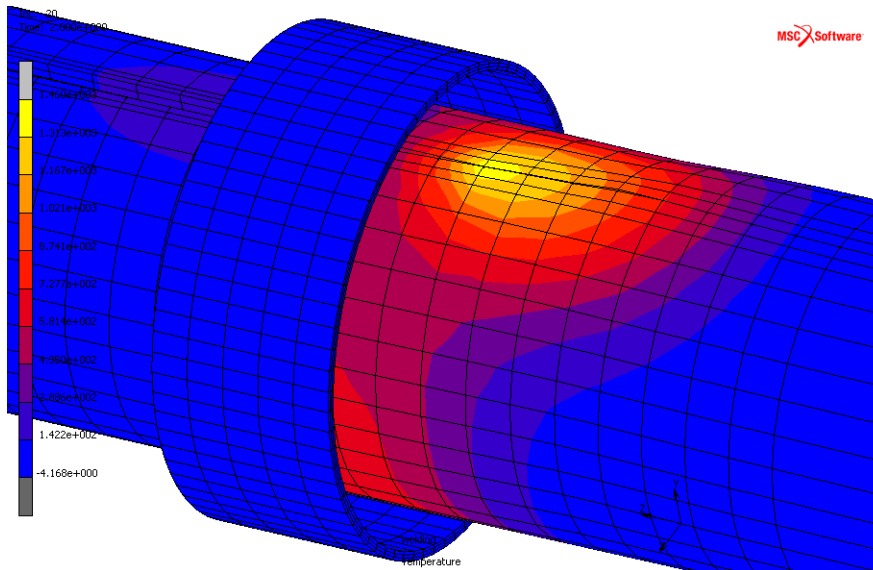


Figure 5.5-10 Temperature Distribution during the Welding Process

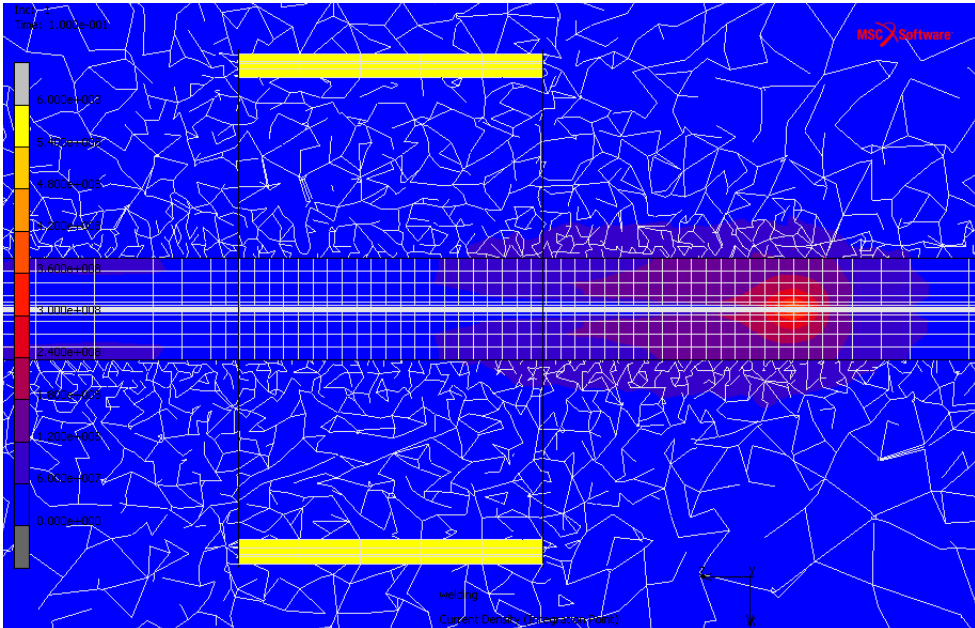


Figure 5.5-11 Cutting Plane Plot of the Current Density

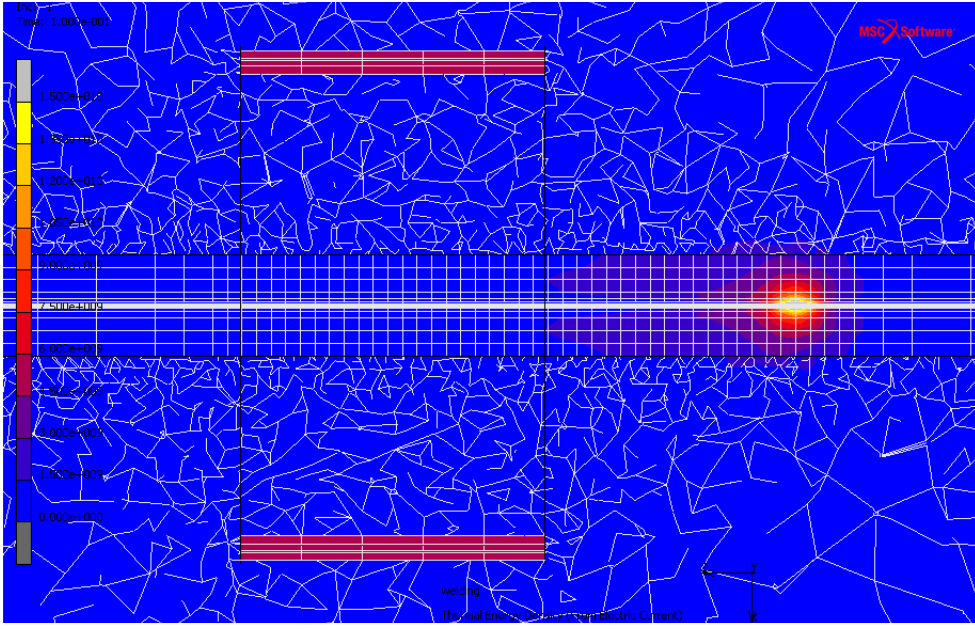


Figure 5.5-12 Cutting Plane Plot of the Thermal Energy Density

Input Files

The files below are on your [delivery media](#) or they can be downloaded by your web browser by clicking the links (file names) below.

File	Description
tube_weld.mud	Mentat model file containing predefined parts and materials
tube.proc	Mentat procedure file to run the Tube Welding using Induction Heating example
uactglue.f	User subroutine to simulate welding by turning on contact glue

Section 6: Miscellaneous Analysis

6.1 Magnetostatics: Analysis of a Transformer

- Chapter Overview 1898
- 3-D Analysis of a Transformer 1898
- Input Files 1910

Chapter Overview

The increasing need for analysis of real world magnetostatic applications has been the motivation to revisit the magnetostatic vector potential formulation used in Marc. Compared to the 2-D formulation, in 3-D an additional constraint has to be taken into account to get a uniquely defined vector potential, which is done using a penalty formulation. The value of the penalty factor is crucial to get accurate results in 3-D applications. This chapter describes a 3-D analysis of a transformer. A coil is placed around an iron frame. By forcing a current in the coil, a magnetic field is generated inside the iron. The coil is assumed to have the same permeability as air, and is modeled using face currents on selected elements. The transformer is modeled with a region of air around the iron. Due to symmetry, only one eighth of the transformer is modeled. The magnetic permeability of iron is taken constant, which is valid for low currents in the coil. Brick element 109 is used both for the air and the iron region.

3-D Analysis of a Transformer

The magnetic field in and around a transformer is computed. [Figure 6.1-1](#) shows an outline of the transformer.

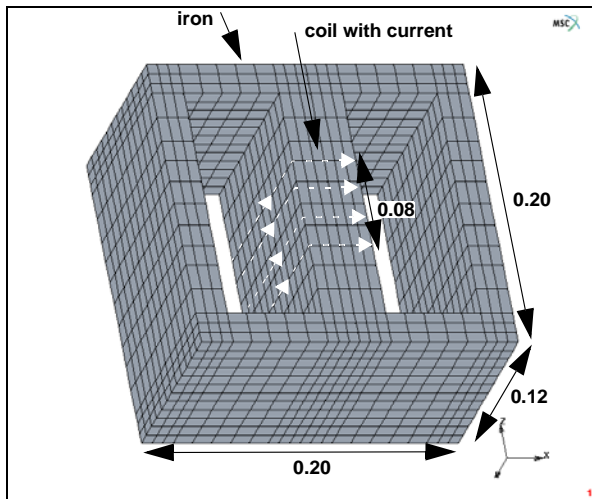


Figure 6.1-1 Transformer: Problem Description

A current is flowing through a coil around the center of the iron, thus inducing a magnetic field inside the iron. The shape of the iron is like a figure eight with the coil around the center. In this way, most of the magnetic field generated by the coil stays inside the iron. [Figure 6.1-2](#) shows the part which is modeled.

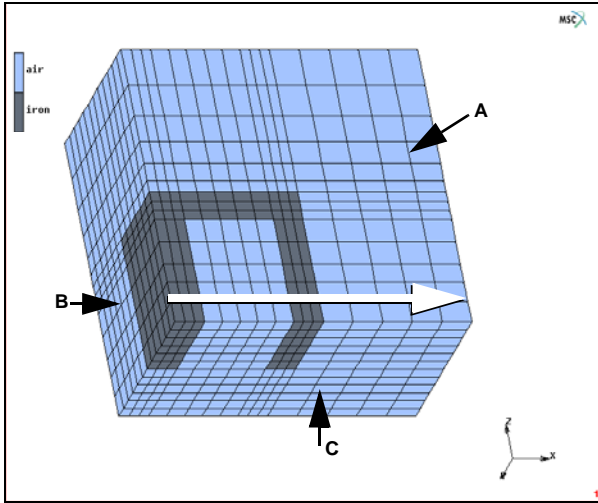


Figure 6.1-2 Transformer: FE Model of Iron and Air

Mesh Generation

The mesh is generated by first defining surfaces for the iron and the air. Then these surfaces are converted to elements, where a more refined mesh is used for the iron parts. Then the mesh is expanded in the z-direction considering a refinement for the iron region. Nodes on the outer surfaces are stored in sets so they can be easily used when defining boundary conditions.

MESH GENERATION

srfs ADD

```

0 0 0
0.02 0 0
0.02 0.12 0
0 0.12 0
0.02 0 0
0.08 0 0
0.08 0.12 0
0.02 0.12 0
0.08 0 0
0.1 0 0
0.1 0.12 0
0.08 0.12 0
0.1 0 0

```

0.2 0 0

0.2 0.12 0

0.1 0.12 0

CONVERT

DIVISIONS

3 12

SURFACES TO ELEMENTS

1 3 #

DIVISIONS

5 12

SURFACES TO ELEMENTS

2 4 #

RETURN

SWEEP

ALL

RETURN

RENUMBER

ALL

RETURN

EXPAND

SHIFT

SCALE FACTORS

1 1 14/15

TRANSLATIONS

0 0 0.015

REPETITIONS

3

ELEMENTS

all: EXIST.

SCALE FACTORS

1 1 1

TRANSLATIONS

0 0 0.0165

REPETITIONS

2

```

ELEMENTS
  1 TO 192 #
TRANSLATIONS
  0 0 0.02/3
REPETITIONS
  3
ELEMENTS
  1 TO 192 #
REMOVE
TRANSLATIONS
  0 0 0.105
REPETITIONS
  1
ELEMENTS
  1 TO 192 #
FILL
  RETURN
SUBDIVIDE
  DIVISIONS
    1 1 6
  BIAS FACTORS
    0 0 -0.3
  ELEMENTS
    1729 TO 1920 #
  RETURN
SWEEP
  ALL
  RETURN
SELECT
  METHOD
    BOX
  RETURN
ELEMENTS
  -0.0001 0.0201
  -0.0001 0.0601
  -0.0001 0.0951

```

```
0.0799 0.1001  
-0.0001 0.0601  
-0.0001 0.0951  
0.0199 0.0801  
-0.0001 0.0601  
0.0750 0.0951
```

STORE

iron

all: SELECT.

CLEAR SELECT

NODES

```
-0.001 0.001  
-0.001 1  
-0.001 1
```

STORE

fix_yz

all: SELECT.

CLEAR SELECT

NODES

```
-0.001 1  
-0.001 0.001  
-0.001 1
```

STORE

fix_xz

ALL SELECT.

CLEAR SELECT

NODES

```
-0.001 1  
-0.001 1  
-0.001 0.001
```

STORE

fix_z

all: SELECT.

CLEAR SELECT

NODES

```
0.199 0.201
```

```

-0.001 1
-0.001 1
STORE
    fix_surfaceA
all SELECT.
CLEAR SELECT
NODES
    -0.001 1
    -0.001 1
    0.199 0.201
STORE
    fix_surfaceB
all SELECT.
CLEAR SELECT
NODES
    -0.001 1
    0.119 0.121
    -0.001 1
STORE
    fix_surfaceC
all: SELECT.

```

Boundary Conditions

The following boundary conditions are applied on components of the vector potential. The faces are indicated in [Figure 6.1-2](#). On “A” ($y = 0.0$) $A_1 = A_3 = 0$, on “B” ($x = 0.0$) $A_2 = A_3 = 0$ and on “C” ($z = 0.0$) $A_3 = 0$. So where current is flowing, the magnetic potential \mathbf{A} is forced to follow its direction. Assuming that the amount of air is sufficiently large, at the outer surface $A_1 = A_2 = A_3 = 0$. A current of 5000A/m^2 is applied as a face current on the faces of the elements with air properties which are next to the iron in the center of the transformer. (See [Figure 6.1-3](#) for the direction of the current).

```

BOUNDARY CONDITIONS
MAGNETOSTATIC
NEW
NAME
    current_x

```

FACE CURRENT

U TANGENTIAL

-5000

OK

faces ADD

247:0 250:0 253:0 254:0 251:0 248:0 249:0 252:0 255:0 #

NEW

NAME

current_y

FACE CURRENT

U TANGENTIAL

-5000

OK

faces ADD

484:3 469:3 454:3 439:3 424:3 409:3 485:3 470:3 455:3

440:3 425:3 410:3 486:3 471:3 456:3 441:3 426:3 411:3 #

NEW

NAME

fix_yz

FIXED POTENTIAL

POTENTIAL Y

(on)

POTENTIAL Z

(on)

OK

nodes ADD

fix_yz #

NEW

NAME

fix_xz

FIXED POTENTIAL

POTENTIAL X

(on)

POTENTIAL Z

(on)

OK

nodes ADD

fix_xz #


```

NEW
NAME
    fix_z
FIXED POTENTIAL
    POTENTIAL Z (on)
    OK
ADD NODES
    fix_z #
NEW
NAME
    fix_outside
FIXED POTENTIAL
    POTENTIAL X (on)
    POTENTIAL Y (on)
    POTENTIAL Z (on)
    OK
nodes ADD
    fix_surfaceA fix_surfaceB fix_surfaceC #
    
```

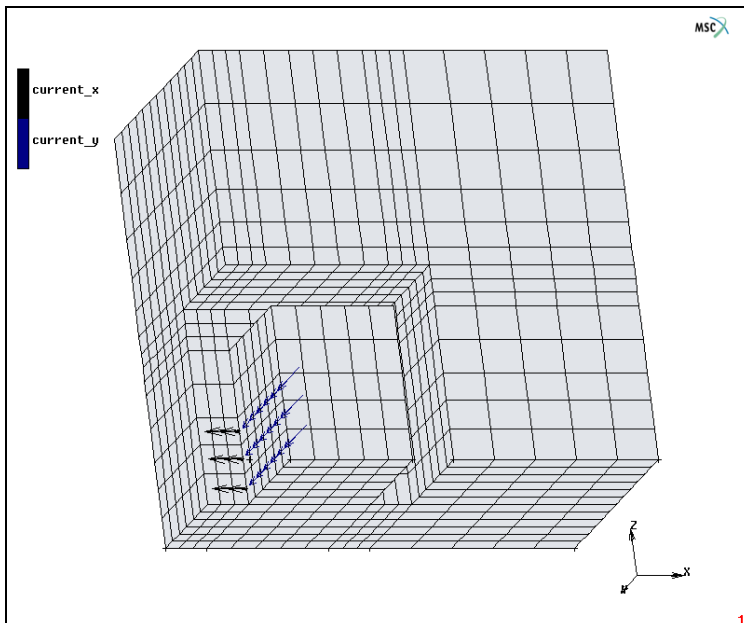


Figure 6.1-3 The Current which is flowing in the Coil of the Transformer

Material Properties

For the air, the magnetic permeability is $\mu = 1.2566 \times 10^{-6} \text{ Hm}^{-1}$, and for the iron, $\mu = 0.005867 \text{ Hm}^{-1}$. So in this example, a linear dependence between the magnetic induction \mathbf{B} and the magnetic field intensity \mathbf{H} is considered for iron.

```
MATERIAL PROPERTIES
  NEW
  NAME
    air
  MAGNETOSTATIC
  PERMEABILITY
    1.25664E-6
  OK
elements ADD
  all: EXIST.
  NEW
  NAME
    iron
  MAGNETOSTATIC
  PERMEABILITY
    0.005867
  OK
elements ADD
  iron #
```

Loadcases and Job Parameters

The analysis is a steady state simulation to obtain the magnetic field inside and outside the iron. So one loadcase is defined. Element type 109 is used both for air and iron. The analysis runs with the default settings. The penalty, by default is 0.0001 was found to be adequate. Components of the magnetic induction and the magnetic field intensity are selected as element quantities to be written on the post file.

```
LOADCASES
  NEW
  MAGNETOSTATIC
  STEADY STATE
  OK
```

```
MAIN
JOBS
  ELEMENT TYPES
    MAGNETOSTATIC
      3-D
        109
        OK
      all: EXIST.
      RETURN (twice)
NEW
MAGNETOSTATIC
  LCASE1
  JOB RESULTS
    1st   Real Comp Magnetic Induction
    2nd   Real Comp Magnetic Induction
    3rd   Real Comp Magnetic Induction
    1st   Real Comp Magnetic Field Intensity
    2nd   Real Comp Magnetic Field Intensity
    3rd   Real Comp Magnetic Field Intensity
  OK (twice)
```

Save Model, Run Job, and View Results

The analysis can now start. The resulting plot of the real magnetic induction is shown in [Figure 6.1-4](#). The figure shows that the magnetic induction is concentrated inside the iron. There is very little leakage to the environment.

```
FILE
  SAVE AS
    transformer.mud
  OK
  RETURN
RUN
  SUBMIT 1
  MONITOR
  OK
MAIN
```

RESULTS

OPEN DEFAULT

NEXT

MORE

VECTOR PLOT ON

VECTOR

Real Magnetic Induction

OK

RETURN

DEF & ORIG

PLOT

NODES

(off)

elements SETTINGS

draw EDGES

(off)

RETURN (twice)

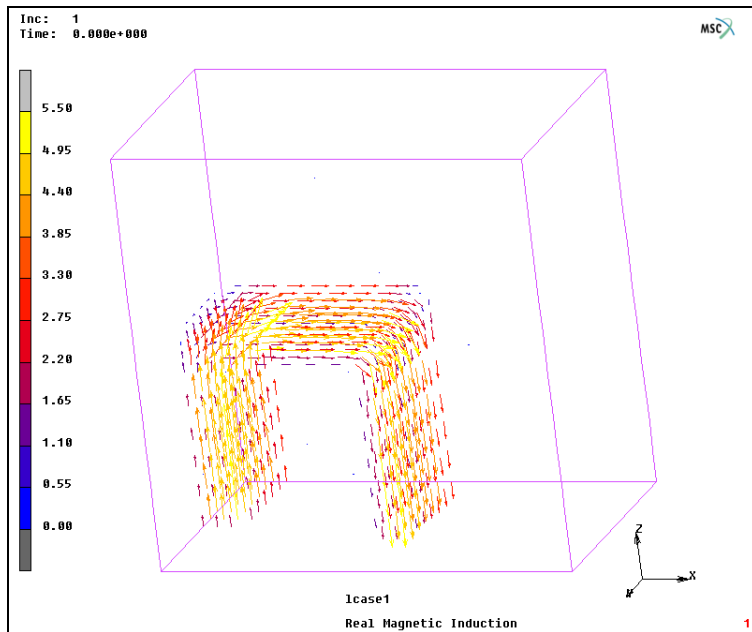


Figure 6.1-4 Real Magnetic Induction in the Transformer induced by the Current

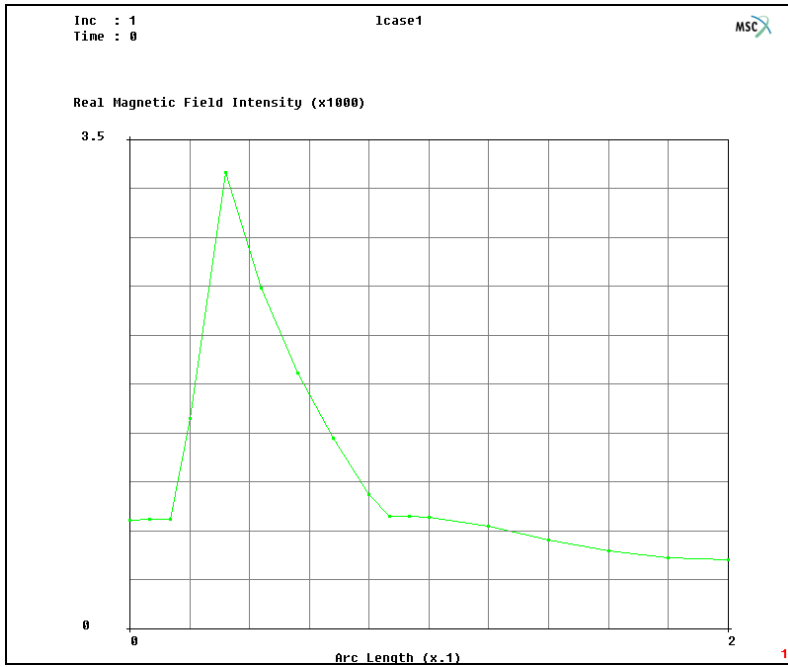


Figure 6.1-5 Magnetic Field Intensity along the Path specified in Figure 6.1-2

Figure 6.1-5 shows the magnetic field intensity of the transformer along the line as indicated in Figure 6.1-2 (for comparison see also Zienkiewicz, O.C., Lyness, J., Owen, D.R.J., IEEE Transactions on Magnetics, VOL 13, No 5, 1649-1656 (1977)). The peak value of the magnetic field intensity and the values for the regions inside the iron correspond well with that found by Zienkiewicz *et. al.*

RESULTS

OPEN DEFAULT

NEXT

scalar plot SETTINGS

EXTRAPOLATION

AVERAGE

RETURN (twice)

PATH PLOT

NODE PATH

224 1344 #

VARIABLES

ADD CURVE

Arc Length

Real Magnetic Field Intensity

FIT

Input Files

The files below are on your [delivery media](#) or they can be downloaded by your web browser by clicking the links (file names) below.

File	Description
transformer.proc	Mentat procedure file to run the above example

6.2 Fracture Mechanics Analysis with the J-integral

- Chapter Overview 1912
- Specimen with an Elliptic Crack 1912
- Background Information 1912
- Run Job and View Results 1931
- Input Files 1933

Chapter Overview

In fracture mechanics applications, it is often necessary to evaluate the so-called J-integral for investigating cracks in a structure. This chapter demonstrates the modeling and evaluation of the J-integral in an analysis of a solid block with an elliptic surface crack. The example also illustrates the use of the new load controlled die options and how to create a parameterized procedure file.

Specimen with an Elliptic Crack

This example is a solid steel block with an elliptic surface crack, see [Figure 6.2-1](#). It is loaded in bending and tension and clamped at both ends where the loading is applied. The purpose with the analysis is to evaluate the J-integral along the crack front. This is now feasible with the improvements to the J-integral option and some other features of Marc and Mentat as is shown below. It is of particular interest to obtain a local value of **J** along the crack front.

Background Information

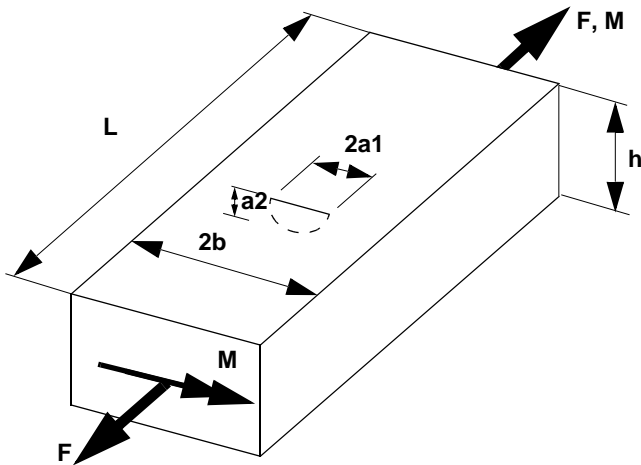


Figure 6.2-1 Problem Description

The geometry shown in [Figure 6.2-1](#) is studied in this example. A solid block with an elliptic surface crack is loaded in tension and bending. The material is linear elastic and no nonlinear effects are taken into account. Double symmetry is taken into account so only a fourth of the structure is modeled.

The following values were used in the analysis:

$$\begin{aligned}L &= 15 \\b &= 8 \\h &= 4 \\a_1 &= 1.5 \\a_2 &= 1\end{aligned}$$

Material, linear elastic:

$$\begin{aligned}E &= 2.0 \times 10^5 \\v &= 0.3\end{aligned}$$

Loading:

$$\begin{aligned}F &= 5.0 \times 10^5 \\M &= 1.0 \times 10^5\end{aligned}$$

Modeling Strategies

The basic geometry is created using the solid modeler. The region around the crack is then taken out from the solid model so that a focused mapped mesh can be put in there. This way, a crack region can be inserted into a general solid model in different places. The region outside the crack region is meshed using the automatic tetrahedral mesher while a mapped mesh is used in the crack region. These two parts do not fit together node to node so they are connected using the GLUE option in the contact feature of Marc. For this example, there is no real contact between different bodies, the CONTACT option is only used to automatically create the appropriate tyings between the different parts of the model.

Since we want to make use of symmetry, we need to be able to apply symmetry boundary conditions to the crack ligament but not to the free crack surface. To accomplish this, we divide the mesh around the crack front into two separate parts which are glued together. The symmetry boundary condition is applied via a rigid contact body so by using a contact table, we can specify that only the crack ligament part should contact the symmetry plane.

This example is also illustrating the use of parameterized modeling. The source of the model is the procedure file. When the model is modified or parts of it are replaced, this is all done in the procedure file. One key thing for accomplishing this is to make the different parts modular. One part of the procedure file must not depend on previous parts. This means that points, nodes, elements, etc. should not be referenced explicitly. In this example, we systematically make previously defined parts invisible and supply lists with `all_visible` instead of picking elements from the screen. We also regularly delete the current geometry when a part of the meshing is finished so that the numbering of new points, etc. starts with one. An alternative way is to renumber so that consecutive numbering is used and make use of the predefined variables `npoints()`, `nnodes()`, etc. The second latest created point would have the number `npoints()-1`. An obvious way to make the model parameterized is to define a number of variables at the top of the procedure file and make use of these throughout the procedure file.

Mesh Generation

The mesh for the region outside the crack is generated by defining a solid block and subtracting a part around the crack. Later, a mapped mesh will be used for the crack region.

First, we define some parameters to use in the procedure file:

```
UTILS
PARAMETERS
  h 4
  b 8
  L 15
  a1 1
  a2 1.5
  force -5e5
  moment -1e5
  nexpand 22
  da 0.5
```

Then, we define the main block and a cylinder that is subtracted from the block. The cylinder is defined at the origin and then scaled using the quotient a_2/a_1 as a scaling factor. The ability to scale solids in this way is a new feature in this release.

```
MESH GENERATION
SOLID TYPE
BLOCK
SOLIDS ADD
  0 0 0 b h -L
SOLID TYPE
CYLINDER
SOLIDS ADD
  0 0 0 0 0 -1 1.5 1.5
MOVE
RESET
SCALE FACTORS
  a2/a1 1 1
SOLIDS
  2 #
RESET
```

```
TRANSLATIONS
  b h 0
SOLIDS
  2 #
SOLIDS
SUBTRACT
  1 2 #
```

The model so far is shown in [Figure 6.2-2](#). Now this solid model is meshed using the tetrahedral automatic mesher. First, all faces of the solid are converted into surfaces and then a curve division length of 1 is applied to all curves. The curves close to the crack region are given a finer division of 0.3. The solids are removed since they are not needed anymore.

```
SOLID FACES TO SURFACES
  all: EXIST.
SOLIDS REM
  all: EXIST.
AUTOMESH
  CURVE DIVISIONS
    FIXED AVG LENGTH
      AVG LENGTH
        1
    APPLY CURVE DIVISIONS
      all: EXIST.
    FIXED AVG LENGTH
      AVG LENGTH
        0.3
    APPLY CURVE DIVISIONS
      4 36 1 31 3 8 6 9 2 7 5 14 #
```

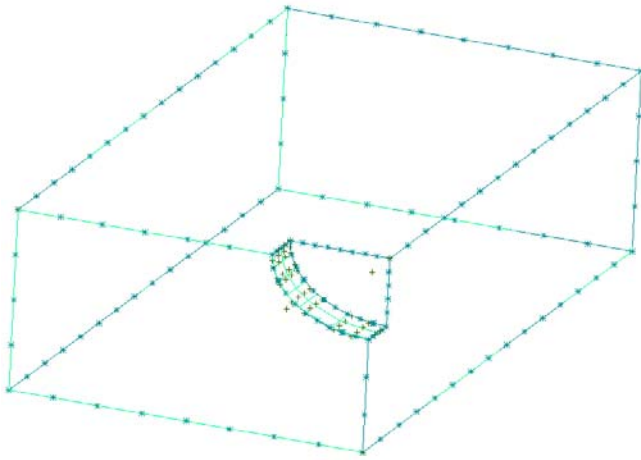


Figure 6.2-2 Initial Solid Model

The surfaces are meshed using the Delaunay surface mesher to produce a triangular mesh of the exterior. This mesh is then used by the tetrahedral mesher to create the 3-D mesh. First, the surfaces are matched together so that a continuous mesh is obtained. The geometry is deleted when the mesh is created. It is not needed anymore and it also makes it easier to define the geometry for other parts later on. A mesh transition of 1.1 is used in the tetrahedral mesher to obtain a coarser mesh towards the interior of the body. This new transition feature allows fewer elements to be created. The elements created so far are store in an element set called *tets*.

MATCH CURVE DIVISIONS

0.01

all: EXIST.

SURFACE MESHING

TRANSITION

1

SURFACE TRI MESH! (Delaunay)

all: EXIST.

CLEAR GEOM

SWEEP

TOLERANCE

0.01

SWEEP NODES

ALL: EXIST.

REMOVE UNUSED NODES

AUTOMESH

SOLID MESHING

```
ALIGN SHELLS
  1
TRANSITION
  1.1
TET MESH!
  ALL: EXIST.
SELECT
  ELEMENTS STORE
    tets
  ALL: EXIST.
CLEAR SELECT
MAKE VISIBLE
```

The mesh is shown in [Figure 6.2-3](#).

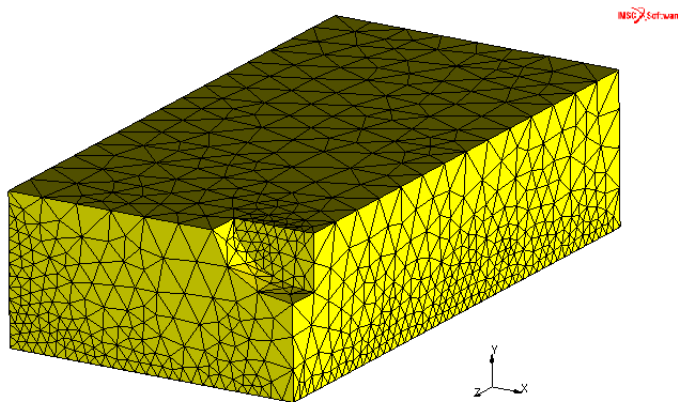


Figure 6.2-3 Finite Element Mesh of the Region Outside the Crack

Note that this part is very general. In this example, a simple geometry is used but the steps to create this mesh are equally simple for a more general solid model.

Now with the *crack region*, we want a refined mesh focused around the crack front. The crack region is divided into three parts; one part which is part of the ligament, one part containing the crack, and part of the free surface and a fill part. The first part is kept separate from the other parts while coincident nodes are swept between the second and third parts. The meshes for these parts are created by defining a plane mesh and sweeping it. Before they are moved into position, the parts are scaled using the same scale factor a_2/a_1 as for the cylindrical solid part.

Note that the previous mesh was made invisible so `all_visible` can be used in the part below. This makes it easy to modify this part of the procedure file if needed. The mesh around the crack front is focused with collapsed elements at the crack front. To create the collapsed mesh, a ruled surface is created from two lines. One of the lines is collapsed

into a point (point number 1 in the procedure file) so that a collapsed surface is obtained. This surface is then simply converted into elements.

MESH GENERATION

PTS ADD

0 -1.0 0
0 -1.5 0
0 -1.0 -1.0
0 -1.5 -1.0
0 -0.5 0
0 -0.5 -1.0

CURVE TYPE

POLYLINE

CRVS ADD

2 4 3 #
1 1 #
3 6 5 #

SURFACE TYPE

RULED

SURFACE ADD

1 2 #
2 3 #

CONVERT

DIVISIONS

10 10

SURFACES TO ELEMENTS

1 #

EXPAND

RESET

ROTATIONS

0 0 -90/nexpand

REPETITIONS

nexpand

ELEMENTS

ALL: VISIBLE

SELECT

ELEMENTS STORE

```
        crack1
        all: VISIBLE
SWEEP
  TOLERANCE
    0.001
  SWEEP NODES
    all: VISIBLE
  SELECT
    CLEAR SELECT
    MAKE VISIBLE
CONVERT
  SURFACES TO ELEMENTS
    2 #
EXPAND
  ELEMENTS
    all: VISIBLE
  SELECT
    ELEMENTS STORE
      crack2
      all: VISIBLE
SWEEP
  TOLERANCE
    0.001
  SWEEP NODES
    all: VISIBLE
  SELECT
    CLEAR SELECT
    MAKE VISIBLE
```

The fill part is meshed using the quadrilateral planar automatic mesher to create a planar mesh which is then expanded into 3-D elements.

```
MESH GENERATION
  CLEAR GEOM
  PTS ADD
    0 -0.5 0
    0 0 0
```

```
CURVE TYPE
  CENTER/POINT/POINT
crvs ADD
  0 0 0
  -0.5 0 0
  0 -0.4 0
CURVE TYPE
  LINE
crvs ADD
  2 3 2 1
AUTOMESH
  CURVE DIVISION
    FIXED # DIVISIONS
    # DIVISIONS
      10
    APPLY CURVE DIVISIONS
      2 3 #
    # DIVISIONS
      nexpand
    APPLY CURVE DIVISIONS
      1 #
2D PLANAR MESHING
  TRANSITION
    1
  SELECT
    ELEMENTS
      all: EXIST.
    MAKE INVISIBLE
    QUAD MESH!
      2 3 1 #
EXPAND
  RESET
    TRANSLATIONS
      0 0 -1/5
    REPETITIONS
      5
    ELEMENTS
      all: VISIBLE
  SELECT
    ELEMENTS STORE
      fill
```



```
all: VISIBLE
SWEEP
  REMOVE UNUSED NODES
CLEAR GEOM
SELECT
  SELECT SET
    tets
MOVE
  RESET
  SCALE FACTORS
    a2/a1 1 1
  ELEMENTS
    ALL: UNSEL.
  RESET
  TRANSLATIONS
    b h 0
  ELEMENTS
    all: UNSEL.
  SELECT
    CLEAR SELECT
    SELECT SET
      crack2
      fill
    MAKE VISIBLE
SWEEP
  TOLERANCE
    0.005
  SWEEP NODES
    ALL: VISIBLE
  SELECT
    CLEAR SELECT
    MAKE INVISIBLE
```

Now it fits into the other mesh as shown in [Figure 6.2-4](#).

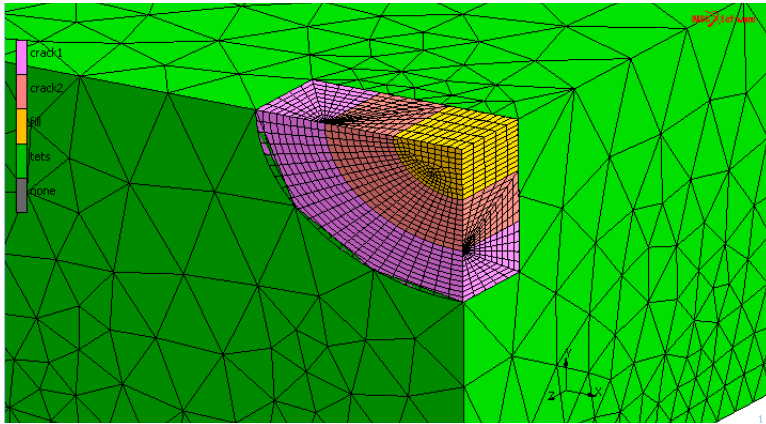


Figure 6.2-4 The Completed Mesh

Crack Definitions

The mesh is now finished and the next step is to define the crack parameters. In order to automatically identify the crack front, an arc at that location is defined and the nodes at the crack front are identified using the ATTACH option. The crack front consists of nodes at the lower part of the crack mesh as well as the upper part. As mentioned above, these nodes are glued to each other using the CONTACT option. It is important that the crack nodes belonging to the lower part are used since they will be part of the crack ligament and thus have symmetry boundary conditions. The information about the boundary conditions is used when the shift directions for the J-integral evaluation are determined. A small (but nonzero) value is used for the Multiple Tip Nodes option. This is to make sure that also the nodes in the upper crack part are part of the crack front so that the rigid regions for the J-evaluation can be determined properly.

```
SELECT SET
    crack1
MAKE VISIBLE
CURVE TYPE
    CENTER/POINT/POINT
CRVS ADD
    0 0 0
    -1 0 0
    0 -1 0
MOVE
    RESET
    SCALE FACTORS
```

```

    a2/a1 1 1
CURVES
    ALL: EXIST.
RESET
TRANSLATIONS
    b h 0
CURVES
    ALL: EXIST.
ATTACH
    MODE CLOSEST
    LIMIT ON
    DISTANCE
        0.01
    TOLERANCE
        1e-5
    EDGES -> CURVE
        1
    ALL: VISIBLE
SELECT
    SELECT BY
        NODES BY CURVES
            1 #
    NODES STORE
        crackfront
    all: SELECT.
    CLEAR SELECT
    MAKE INVISIBLE
FRACTURE MECHANICS
    3-D CRACKS
        NEW
        AUTOMATIC (TOPOLOGY SEARCH)
        RIGID REGIONS
            7
        CRACK TIP NODE PATH SET
            crackfront

```

DISTANCE
0.001

The new menu for defining these parameters is shown in [Figure 6.2-5](#).

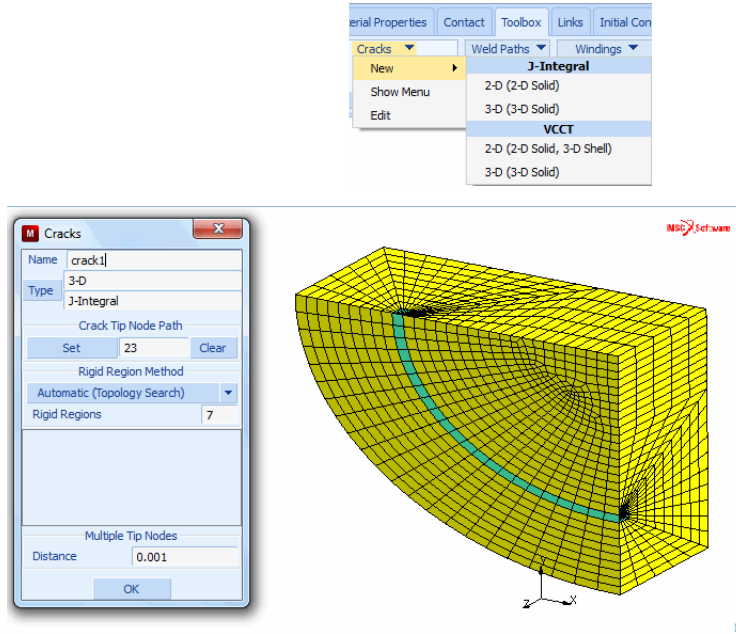


Figure 6.2-5 Menu for Defining Crack Properties

We use the default method of defining the integration paths for the J-integral. For each crack front node, there will be a number of paths defined (as specified by the RIGID REGIONS option) with increasing size. Thus, for each crack front node, there will be this number of evaluations with different path radii. Analytically, these values should be identical since the J-integral is path independent in a linear elastic analysis, but due to the discretization they will in general vary with the radius. This can be used as an indicator of the accuracy of the solution. If the variation is large, the results are probably inaccurate. With the geometry search method, one specifies one radius for each crack front node and the rigid region is defined by all nodes inside a cylinder aligned with the crack front. The MANUAL option allows the nodes of the rigid region to be specified explicitly.

Material Properties

This is a simple part. All elements have the same linear elastic material.

MATERIAL
NEW
ISOTROPIC

YOUNG'S MODULUS

2e5

POISSON'S RATIO

0.3

ELEMENTS ADD

all: EXIST.

Contact Definitions

The mesh currently consists of three unconnected regions and they need to be connected to each other. This is accomplished by defining them as contact bodies and use the GLUE option to tie them together.

CONTACT

CONTACT BODIES

NEW

NAME

crack2

DEFORMABLE

OK

ELEMENTS ADD

crack2

fill

NEW

NAME

crack1

DEFORMABLE

OK

ELEMENTS ADD

crack1

NEW

NAME

tets

DEFORMABLE

OK

ELEMENTS ADD

tets

Here, we used the previously defined set names to select elements for the contact bodies and avoid giving element lists. A very important point here is the order in which the bodies are defined. As usual when using deformable contact in Marc, the finer bodies are defined before the coarser. That is why the body with the tetrahedral elements is defined last. The other two bodies meet node to node, but it is still important to define the top part first. The nodes of the first body will be tied to the segments of the second body. Only nodes of the lower part of the crack will contact the symmetry plane at the crack ligament, so they must not be tied to the nodes of the top part. If the order of the definition of the first two contact bodies above is switched, the crack front nodes will not stay in contact with the symmetry plane.

Before defining the contact table with the glue entries, the rigid contact surfaces used for applying the loads and boundary conditions are defined:

```
MESH GENERATION
  CLEAR GEOM
  PTS ADD
    -10 -10 -L
    -10 20 -L
    18 -10 -L
    18 20 -L
  SURFACE TYPE QUAD
  SRFS ADD
    2 1 3 4
  PTS ADD
    b -10 10
    b -10 -25
    b 20 -25
    b 20 1
  SURFACE ADD
    6 7 8 5
  DUPLICATE
  RESET
  TRANSLATE
    0 0 L
  SURFACES
    1 #
  CHECK
  FLIP SURFACES
    1 #
CONTACT
```

```
CONTACT BODIES
  NEW
  NAME
    moving
  RIGID
  LOAD
  SURFACES ADD
    1 #
```

For this body, we are using the new modified LOAD CONTROL option. One node each is used for the force and moment. In order to be able to refer to these nodes without using node numbers (which will change if the model above is modified), a nodal renumbering is made and we refer to the new nodes using the predefined variable `nnodes()`.

```
MESH GENERATION
  RENUMBER
  NODES
  NODES ADD
    b/2 h/2 -L
    b/2 h/2 -L
CONTACT
  CONTACT BODIES
  CONTROL NODE
    nnodes()-1
  AUX. NODE
    nnodes()
```

```
BOUNDARY CONDITIONS
  NEW
  NAME
    force
  MECHANICAL
  TABLES
  NEW
  1 INDEPENDENT VARIABLE
  TYPE
    time
  NAME
```

```
        pointloads
    ADD
        0 0 1 1
    SHOW TABLE
    SHOW MODEL
POINT LOAD
ON Z FORCE
Z FORCE
    force
TABLE
    pointloads
NODES ADD
    nnodes()-1 #
NEW
NAME
    moment
POINT LOAD
ON X FORCE
X FORCE
    moment
TABLE
    pointloads
NODES ADD
    nnodes() #
CONTACT
    CONTACT BODIES
        NEW
        NAME
            symmx
        SYMMETRY
    SURFACES ADD
        2 #
        NEW
        NAME
            cracksym
        SYMMETRY
```


SURFACES ADD

3 #

Again, since the previous geometry was deleted, we can refer to points 1 through 8 regardless of how many points that were previously created. Now to the contact table:

CONTACT

CONTACT TABLES

NEW

PROPERTIES

BODIES

crack2

tets

NO CONTACT -> TOUCHING -> GLUED

SEPARATION FORCE

1e32

BODIES

crack2

crack1

NO CONTACT -> TOUCHING -> GLUED

SEPARATION FORCE

1e32

BODIES

tets

crack1

NO CONTACT -> TOUCHING -> GLUED

SEPARATION FORCE

1e32

BODIES

tets

moving

NO CONTACT -> TOUCHING -> GLUED

SEPARATION FORCE

1e32

BODIES

crack1

```
      symmx  
NO CONTACT -> TOUCHING  
BODIES  
      crack2  
      symmx  
NO CONTACT -> TOUCHING  
BODIES  
      tets  
      symmx  
NO CONTACT -> TOUCHING  
BODIES  
      crack1  
      cracksym  
NO CONTACT -> TOUCHING  
BODIES  
      tets  
      cracksym  
NO CONTACT -> TOUCHING
```

Now only the load case and job options need to be defined. Since it is a one-step analysis with contact as the only source of nonlinearity, these options are simple. Actually, the analysis is still linear since there will be no change in contact status. We only use contact to apply boundary conditions and tyings. We make sure to activate the contact table both in the load case and the job (initial contact). A contact tolerance of 0.01 (“distance below which a node is assumed to be in contact”) is used to assure that the nodes of the crack part are properly glued to the tetrahedral elements. For efficiency, we use the iterative solver.

```
LOADCASES  
  NEW  
    MECHANICAL  
      STATIC  
        CONTACT  
          CONTACT TABLE  
            ctable1  
  
JOBS  
  NEW  
    MECHANICAL
```

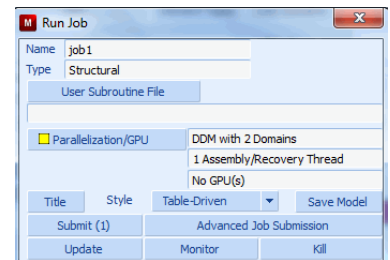
```

LOADCASES
  lcase1
CONTACT CONTROL
  INITIAL CONTACT
    CONTACT TABLE
      ctable1
    DISTANCE TOLERANCE
      0.01
JOB RESULTS
  available element tensors
    Stress
  available element scalars
    Equivalent Von Mises Stress
JOB PARAMETERS
  SOLVER
    ITERATIVE SPARSE
    INCOMPLETE CHOLESKI
  
```

Run Job and View Results

```

JOBS
  RUN
    SUBMIT 1
    MONITOR
RESULTS
  OPEN DEFAULT
  DEF ONLY
  SCALAR
    Equivalent Von Mises Stress
  CONTOUR BANDS
  NEXT
  
```



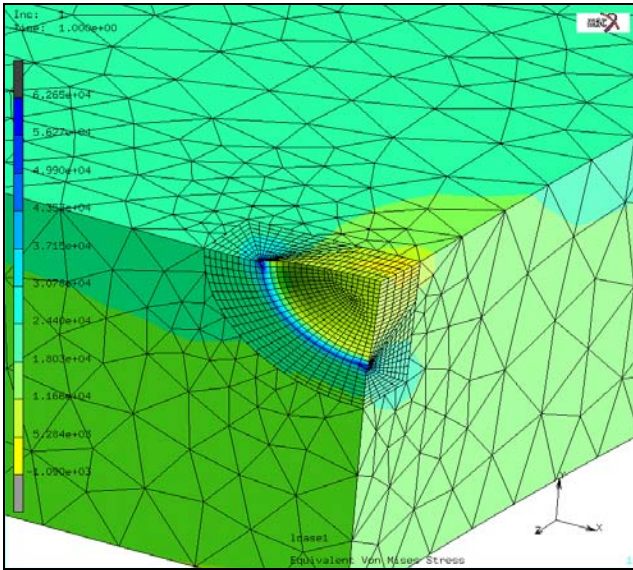


Figure 6.2-6 Equivalent von Mises Stress Contours

When the analysis is done we can look at the deformed shape and the stress field. The actual J-integral results are printed to the output file. The EDIT OUTPUT FILE button in the Run menu will bring up the output file in the default editor. Locate the string “J-integral estimations” in this file. Table 6.2-1 shows the values obtained. The results are given for each crack defined and are grouped for each crack front node. Figure 6.2-1 shows the results for the first two crack tip nodes. There is a small path dependency, which indicates that one should use a finer mesh should or higher-order elements around the crack. This would be simple to change since the model is parameterized.

Table 6.2-1 J-integral Estimations

Crack Tip Node	Path Radius	J-integral Value
1235	1.1180E-01	3.1508E+03
1235	2.2361E-01	3.2027E+03
1235	3.3541E-01	3.1918E+03
1235	4.4721E-01	3.1984E+03
1235	5.5902E-01	3.1961E+03
1235	6.7082E-01	3.1947E+03
1235	7.8262E-01	3.1934E+03
3656	1.1187E-01	3.1553E+03
3656	2.2375E-01	3.2247E+03
3656	3.3562E-01	3.2335E+03
3656	4.4750E-01	3.2378E+03

Table 6.2-1 J-integral Estimations

Crack Tip Node	Path Radius	J-integral Value
3656	5.5937E-01	3.2338E+03
3656	6.7125E-01	3.2276E+03
3656	7.8312E-01	3.2216E+03

Input Files

The files below are on your [delivery media](#) or they can be downloaded by your web browser by clicking the links (file names) below.

File	Description
fracture_mech.proc	Mentat procedure file to run the above example

6.3 FEM Simulation of NC Machining Process

- Chapter Overview 1936
- Input Data 1936
- Model Generation 1937
- Visualization of Results 1946
- Input Files 1951

Chapter Overview

In the manufacturing industry, NC machining is a material removal process that is widely used to produce a final part with desired geometry. After removal of the machined material, re-establishment of equilibrium within the remaining part of the structure causes distortion due to the relief of insitu residual stresses. The deformation caused by this process usually depends on the residual stress magnitude and its distribution inside the part. It also depends on the final geometry of the part after machining. For final geometries that include thin walls or large plate structures, the deformation can be so large that it causes severe distortions of the part. The highly distorted part may no longer be able to serve its designated functionality or may require significant reworking to render it functional. These kinds of failures result in high scrap rates and increased manufacturing costs.

The finite element procedure (FEM) is a powerful tool to assess potential distortions caused by the machining process. With the FEM results, it is then possible for engineers to predict the potential failures and reduce overall manufacture costs.

This chapter describes a capability for the simulation of Numerical Control (NC) machining processes. An automated interface between Marc and CAD/NC data that describe the cutter shape and cutter path is provided. The cutter motion is then analyzed to determine the portion of the finite element mesh to be removed. The cutter path data is stored in either APT source or CL data format. In the current release, APT source data that is output by CATIA V4 are supported. CL data is a cutter location data that is provided by APT compilers.

The current example is used to demonstrate the utilization of the MACHINING (i.e. Metal Cutting) feature. A detailed procedure is shown in this chapter to conduct a realistic machining process simulation using associated Marc models and NC data in either APT source or CL format.

Input Data

Input data required for the simulation of machining process include CAD data for defining the NC machining process and Marc data for the finite element analysis. The required data are as follows:

- NC data to define the cutter geometry and cutter path for the machining process. (*.apt* or *.ccl* files). For details on the format of the *apt* or *ccl* files, please refer to *Marc Volume A: Theory and User Information* and the references listed there.

Notes: (1) In the current version, circular motion is required to be transformed into point-to-point motion type when the APT file is output by CAD NC software. In addition, the TRACUT and COPY statements are necessary to be explicitly interpreted into cutter motion statements. Major statement CYCLE is supported in combination with DRILL minor statement for the definition of drilling motion type.

(2) The flipping over of a part during the machining process is supported by converting the flipping over of the part into a rotation of cutter axis. MLTAXS statement is used to define the rotation of cutter axis.

- Geometry of the initial workpiece either imported directly from the CAD package (through IGES format) or built in the GUI. It is recommended that the IGES option be used since the workpiece position and orientation in the CAD package and in the finite element analysis should be identical.

- Marc input data that includes the finite element model definition of the workpiece and the file names for cutter path definition. Model definition includes the workpiece mesh, boundary conditions, material properties, insitu residual stresses, and the sequence of events (loadcases) simulating the machining process.
- Initial stress data prior to the cutting process. The initial stresses are obtained through experimental measurements or from analytical results. More details on the estimation of residual stresses in the current example are explained below.

Model Generation

Mesh Generation

The geometry of the part before cutting is shown in [Figure 6.3-1](#). The geometry is imported into the GUI through an IGES file. The initial part is a block with length, width and thickness = 28 x 14 x 4.5 inches. The block is then meshed with hexahedral elements. In the current example, these elements are obtained by first creating a 2-D mesh in the X-Z plane and then extruding it in the Y direction. It is very important to have a fine mesh in the direction in which the cutting is taking place.

In the current example, the cutting is predominantly in the Z direction. 18 elements, each of thickness 0.25 inches, are used in the Z direction. The finite element mesh is shown in [Figure 6.3-2](#). This mesh is available in the Mentat database `ex_r01.mud`. In the model, 28224 brick elements and 32205 nodes are defined.

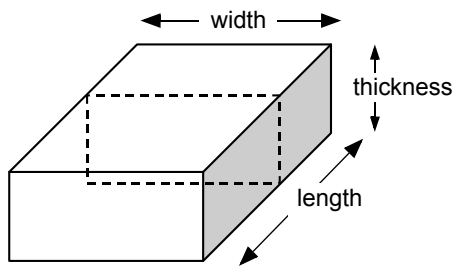


Figure 6.3-1 The Initial Part Geometry

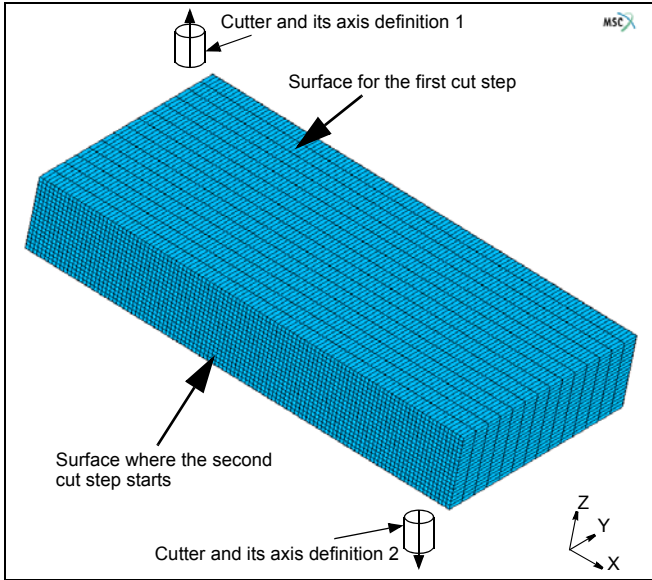


Figure 6.3-2 The Definition of Cutting Processes

Residual Stresses

This section briefly discusses the residual stresses used for the model. A 2-D analysis of the manufacturing procedures to make the aluminium block has been previously undertaken. At the end of the quenching, stretching and release loadcases, the stress state in the 2-D finite element model is available. The given 2-D mesh is rotated into the XZ plane – and the stress components are assigned to each element, after converting them into the proper units. For the 3-D model, the stress distribution is assumed to be constant in the Y direction. [Figure 6.3-3](#) shows the initial stress distribution for the σ_{xx} , σ_{yy} , σ_{zz} , and σ_{xz} components.

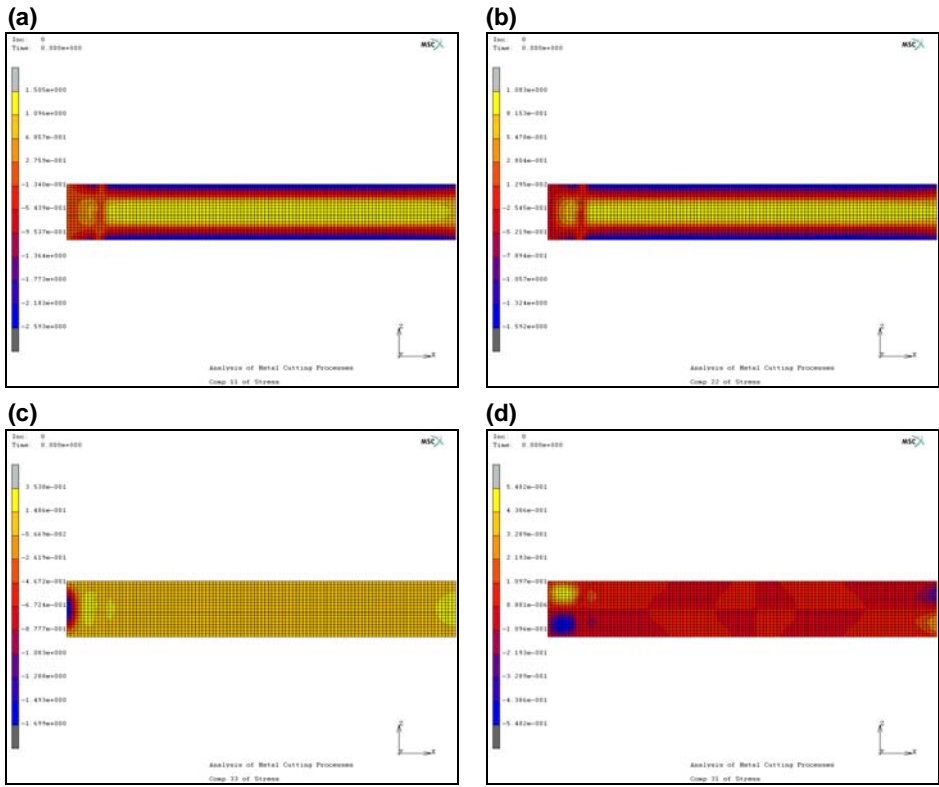


Figure 6.3-3 The Model with Initial Stresses before Machining (a) σ_{xx} , (b) σ_{yy} , (c) σ_{zz} , (d) σ_{xz} , Note that $\sigma_{zy} = \sigma_{xy} = 0$

Procedure Files

The most significant step-by-step commands needed to set up the machining process are described below. These commands describe the procedure to define the boundary conditions and loadcases in order to conduct the cutting process sequentially and automatically. All these commands are also stored in procedure files. The user can execute these procedure files in a step-by-step manner to obtain greater understanding of the command sequence.

The first procedure file, `mc_nfg.proc`, reads in the base finite element model. Prior to this, it is ensured that the cutter path files are defined and previously saved in the current working directory. The finite element mesh with the residual stress state in the `ex_r01.mud` file is also stored in the current working directory. The sequence of commands to execute the procedure file are as follows:

```

UTILS
PROCEDURES
LOAD
    mc_nfg.proc
    
```

OK
START/CONT

Once the initial model file, `ex_r01.mud`, has been read in, the next step is to define boundary conditions and loadcases before submitting the job.

Isotropic material property parameters are used for the aluminium block. These are defined by: E (Young's Modulus) = 10000 ksi, Poisson ratio = 0.3.

The procedure to define the boundary conditions and loadcases is in procedure file: `machining_rcd.proc`. By loading this procedure file and using START/CONT, Mentat automatically completes all the steps. For better understanding, one may use the STEP button to conduct the procedure step-by-step.

Machining Process Simulation

The machining process includes two cutting steps:

- The first step is to cut two inches off the upper surface as shown in [Figure 6.3-2](#). The cutting depth of each cutting step is defined in the cutter path data file `m2q0090s1.ccl`.
- The second step is to cut two pockets over the lower surface of the part after the first cut step is done. The cutter path for this step is defined by the cutter path data file `m2q0090s2.ccl`. The `ccl` files are created based on the `apt` sources generated from CATIA V4.

Between the first and second step, the part is supposed to be flipped over, so that the cutter axis is unchanged in the second cut step. However, for the convenience of FE model definition and analysis, the flipping over of the part is equivalently simulated by the rotation of the cutter. Therefore, the second cut is conducted by rotating the cutter into the opposite direction, as shown in [Figure 6.3-2](#).

There are a total of four loadcases defined in this model. They are:

1. **Cut the top part of the workpiece.** The cutter file used here is `m2q0090s1.ccl`.
2. **Release the bottom b.c. and apply to the upper face.** This loadcase is the one to flip over the part by switching the boundary conditions applied at bottom to the newly generated top surface.
3. **Cut the pocket from the lower face.** This loadcase is the one used to cut the pocket on the lower side of the part. The cut file used here is `m2q0090s2.ccl`.
4. **Final release (springback).** This loadcase releases all the boundary conditions, except those required to clear the rigid body motion of the part.

The total sets of boundary conditions defined by this procedure are:

- `Fix_bottom`: This set fixes the x-y-z displacement of all the nodes at the bottom surface. It is used in loadcase 1.
- `Fix_middle`: This set fixes the x-y-z displacement of all the nodes at the top surface of the part after the first cut. It is used in loadcase 2 and 3.
- `Fix_xyz`: This set fixes the x-y-z displacement of node 2266.

- Fix_x: This set fixes the x-displacement of node 9.
- Fix_y: This set fixes the y-displacement of node 32065.
- Fix_z: This set fixes the z-displacement of node 32058. boundary condition sets 3 to 6 are used in the loadcase 4.

The Mentat commands to define all the loadcases are shown below:

Loadcase1 (*cut the top part of the workpiece*)

MAIN

LOADCASES

NEW

NAME

cutface1

MECHANICAL

STATIC

LOAD

Click on: fix bottom

(to the boundary condition for loadcase)

CONVERGENCE

(defining convergence criteria)

RESIDUAL

Click on (AUTO SWITCH)

Enter Relative Force Tolerance: 0.01

OK

Click on CONSTANT TIME STEP

Click on STEPS and Enter a number of 10

OK

Click off AUTO TIME STEP CUT BACK

OK

Click on IMPORT for Inactive Elements

Click on CUT FILE

To select file: m2q0090s1.ccl

(name cutter path definition)

click on TITLE and enter the title for this loadcase:

cut the top part of the workpiece

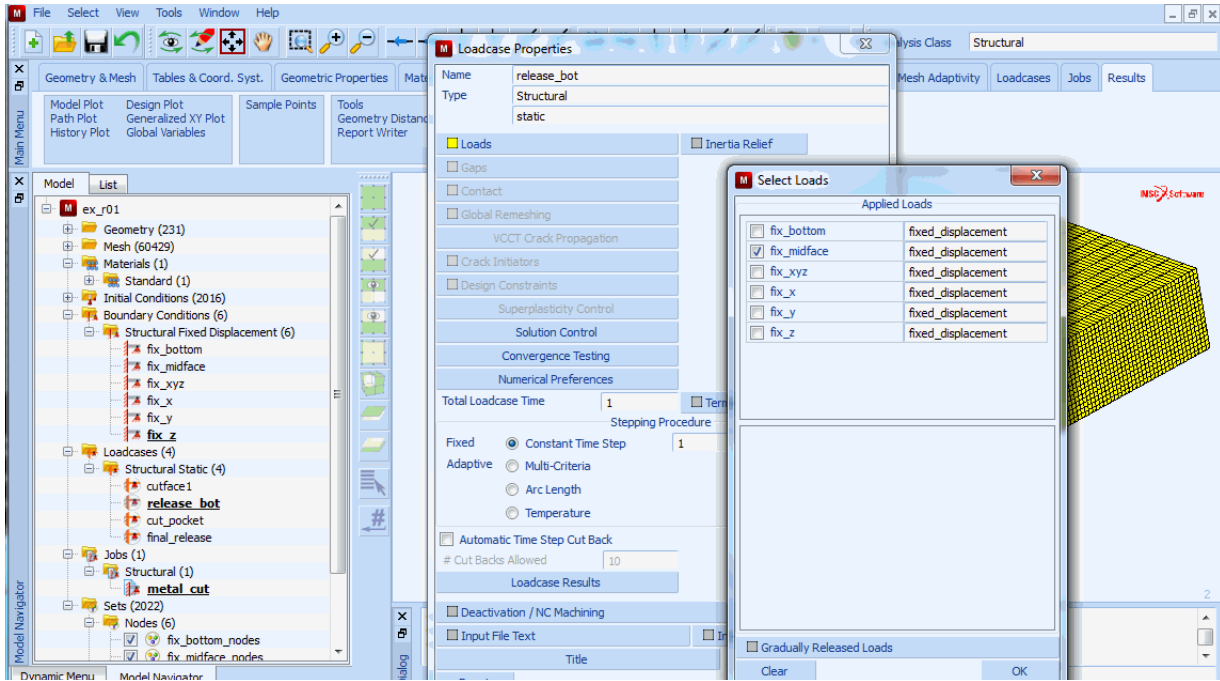


Figure 6.3-4 The Definition of First Cutting Loadcase

Now, as shown in [Figure 6.3-4](#), the first loadcase has been defined. Next step is to define the loadcase to flip over the part after the first cut step is completed.

Loadcase2 (release the bottom boundary condition and apply to the top face)

NEW

NAME

release_bot

MECHANICAL

STATIC

LOAD

Click off: fixbottom

(to free boundary condition for loadcase 1)

Click on: fixmidface

(to apply boundary condition on middle surface)

CONVERGENCE

(defining convergence criteria)

RESIDUAL

Click on (AUTO SWITCH)

Enter Relative Force Tolerance: 0.01

OK

Click on CONSTANT TIME STEP

Click on STEPS and Enter a number of 1

OK

Click off AUTO TIME STEP CUT BACK

OK

Click on MANUAL for Inactive Elements

Click on TITLE and enter the title for this loadcase:

(release bottom boundary condition; apply to top face)

OK

Now, the second loadcase has been defined. Next step is to define the loadcase to cut the pockets over the other side of the part. The procedure is recorded as following:

Loadcase3 (cut the pocket from the lower face part)

NEW

NAME

cut pocket

MECHANICAL

STATIC

LOAD

Click on: fixbottom

(to apply boundary condition)

CONVERGENCE

(defining convergence criteria)

RESIDUAL

Click on (AUTO SWITCH)

Enter Relative Force Tolerance

0.01

OK

Click on CONSTANT TIME STEP

Click on STEPS and Enter a number of 10

OK

Click off AUTO TIME STEP CUT BACK

OK

Click on IMPORT for Inactive Elements

Click on CUT FILE

To select file

m2q0090s2.ccl

click on TITLE and enter the title for this loadcase:

(cut the pocket from the lower face part)

OK

When the second cutting step is finished, the final springback needs to be determined. This process requires that all the restraints are removed except those that are needed to avoid rigid body motion. So a minimum set of boundary conditions are defined for this loadcase (only six degrees of freedom are fixed for the whole model). The procedure is recorded as following:

Loadcase4 (final release – springback)

NEW

NAME

final_release_bc

MECHANICAL

STATIC

LOAD

Click off: fixmidface

to free B.C.

Click on: fix_xyz

to fix x, y and z.

Click on: fix_x

to fix x.

Click on: fix_y

to fix y.

Click on: fix_z

to fix z.

CONVERGENCE

(defining convergence criteria)

RESIDUAL

Click on (AUTO SWITCH)

Enter Relative Force Tolerance: 0.01

OK

Click on CONSTANT TIME STEP

Click on STEPS and Enter a number of 1

OK

Click off AUTO TIME STEP CUT BACK

OK

Click on MANUAL for Inactive Elements

click on TITLE and enter the title for this loadcase:

(final release (springback))

OK

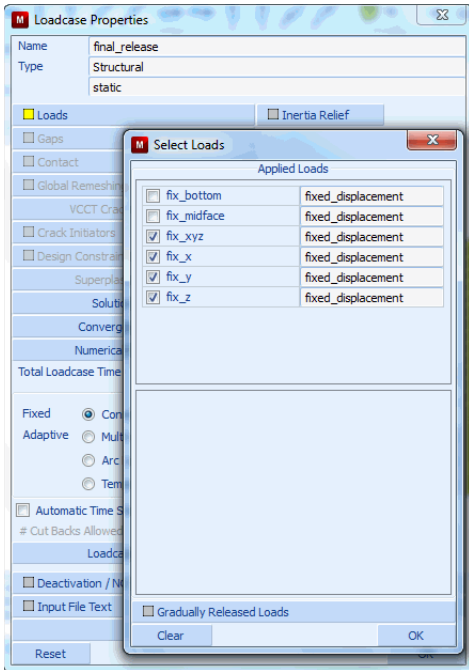


Figure 6.3-5 The Definition of Final Springback Process

Job Definition

The element type for this analysis is defined as follows:

MAIN

JOB

ELEMENT TYPES

MECHANICAL

3-D Solid

select 7

OK

EXIST

(to choose all existing element)

Job definition is done by the following procedure.

MAIN

JOB

NEW

Enter job name: metal_cut
MECHANICAL
 Select loadcases 1, 2, 3, and 4 sequentially *(applying loadcases)*
INITIAL LOADS
 Click off all the b.c
 INITIAL CONDITIONS *(to check if they are all on)*
ANLYSIS OPTIONS *(to use defaults for this)*
JOB RESULTS *(to select the results that the user is interested in)*
 CENTROID *(to reduce the post file size by click this button)*
 OK
JOB PARAMETER
 SOLVER *(to choose correct solver)*
 ITERATIVE SPARSE
 IMCOMPLETE CHOLESKI
 OPTIMIZATION
 OK *(iterative solver is used to reduce memory
 requirement and total computation time)*
OK (twice)

After the job is defined, the model is run through the following command sequence.

MAIN
 JOB
 RUN
 Click SUBMIT (1)
 OK

The FE analysis of the machining (namely, metal cutting) process is started. Mentat instantly shows the progress of the calculation by clicking the MONITOR button.

Visualization of Results

The results can be opened using the following procedure:

MAIN
 RESULTS
 OPEN DEFAULT

```
DEF ONLY
CONTOUR BAND
SCALAR
    Total Displacement
    OK
FILL
MONITOR
```

The elements being progressively cut off from the part are not displayed in Mentat; only the remaining part of the FE model is displayed for postprocessing purposes.

The results are presented here with a two-fold objective:

- To check that the cutter path is followed exactly: As shown in [Figure 6.3-6](#) through [Figure 6.3-9](#), it is seen that the cutter path is followed exactly during the FE analysis. For areas with small radii corners, a very fine mesh is required in order to have better resolution of the part shape after machining. These areas are highlighted in [Figure 6.3-8](#) and [Figure 6.3-9](#). Rezoning/remeshing can be very powerful tools to refine such locations.
- To check the deformation of the final part. The part displays a very obvious deformation after springback, see [Figure 6.3-10](#). The maximum displacement of the part is about 20 times larger after springback (increases from 0.000568 to 0.01059 in.). [Figure 6.3-11](#) shows a scaled deformation pattern that demonstrates how the final part moves after the machining process.

The following figures show the results after each loadcases, respectively:

1. Cut Upper Face

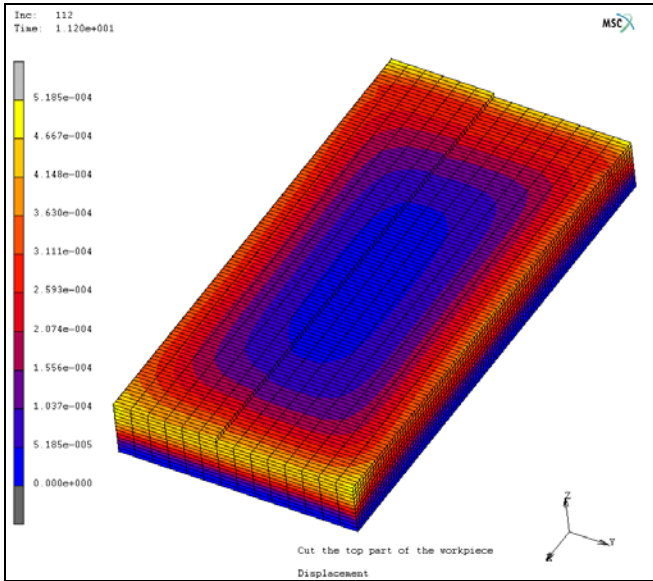


Figure 6.3-6 The Machining of the Upper Surface

2. Flipping Over (switch boundary conditions)

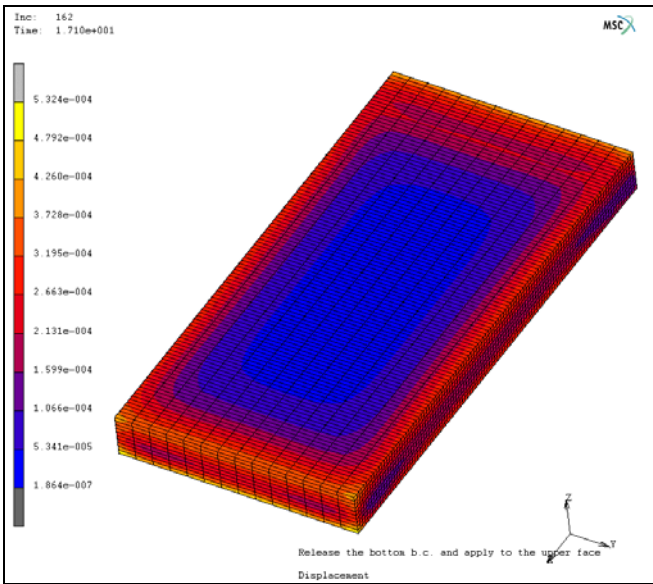


Figure 6.3-7 The Flip Over of the part after First Cutting Process

3. Cut Pockets

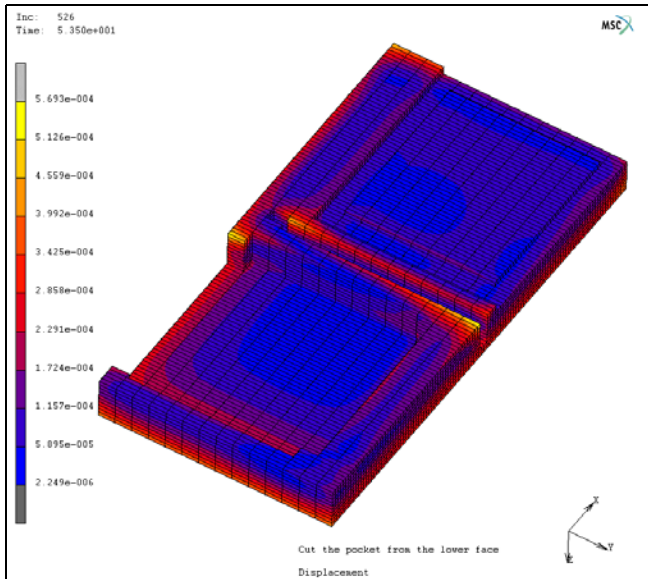


Figure 6.3-8 The Process of Pocket Cutting

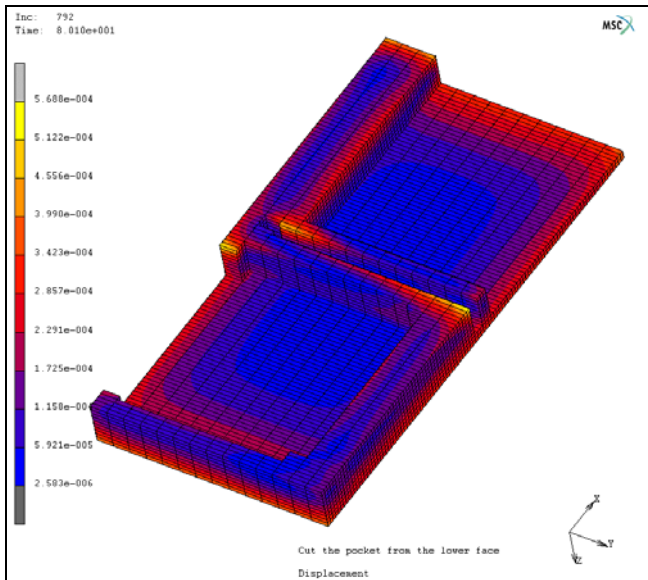


Figure 6.3-9 The Geometry after Pocket Cutting

4. Final Release (springback)

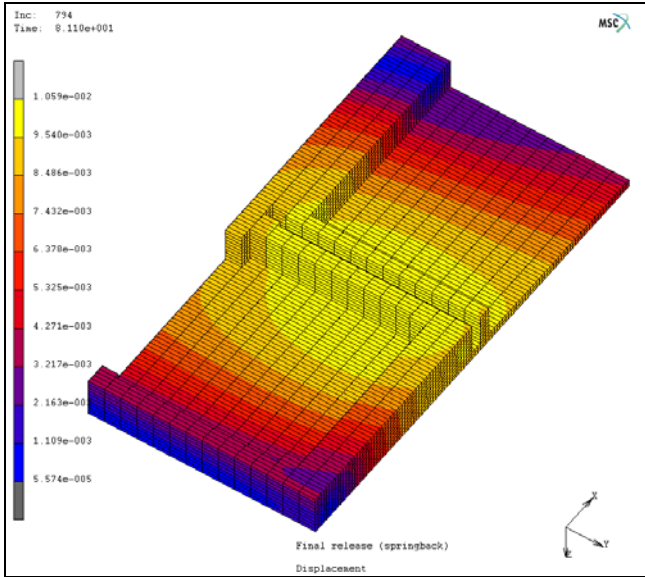


Figure 6.3-10 The Final Geometry and Deformation after Springback

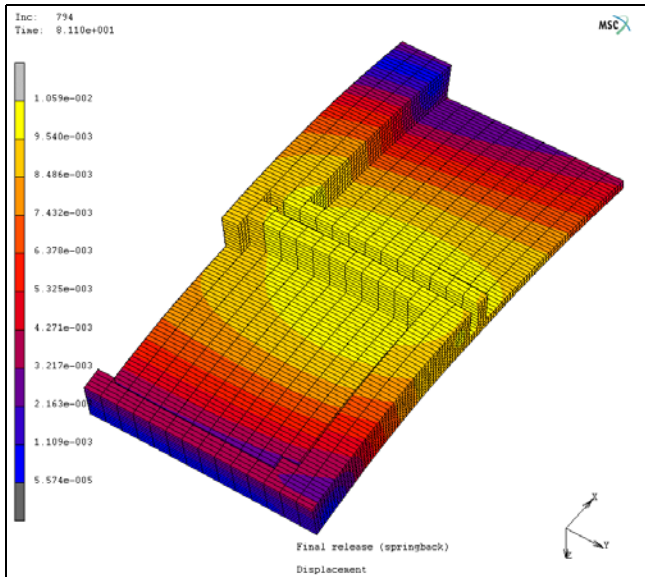


Figure 6.3-11 The Visualization of Deformation (after scaling)

Input Files

The files below are on your [delivery media](#) or they can be downloaded by your web browser by clicking the links (file names) below.

File	Description
mc_nfg.proc	Mentat procedure file to run the above example
machining_rcd.proc	Mentat procedure file to run the above example
m2q0090s2.ccl	Cutter geometry and path file
m2q0090s1.ccl	Cutter geometry and path file
ex_r01.mud	Associated Mentat model file

6.4 Piezoelectric Analysis of an Ultrasonic Motor

- Chapter Overview 1954
- Eigenvalue Analysis of the Stator of an Ultrasonic Motor 1954
- Harmonic Analysis of the Stator of an Ultrasonic Motor 1967
- Transient Analysis of the Stator of an Ultrasonic Motor 1973
- Input Files 1977
- Reference 1977

Chapter Overview

This feature shows how to simulate piezoelectricity in Marc. The piezoelectric effect is the coupling of stress and electric field in a material. An electric field in the material causes the material to strain and vice versa. A piezoelectric Marc analysis is fully coupled, thus simultaneously solving for the nodal displacements and electric potential. A typical application of piezo-electricity can be found in a so-called ultrasonic motor, which can be found in camera auto focus lenses or watch motors. The principle of operation of an ultrasonic motor is shown in [Figure 6.4-1](#).

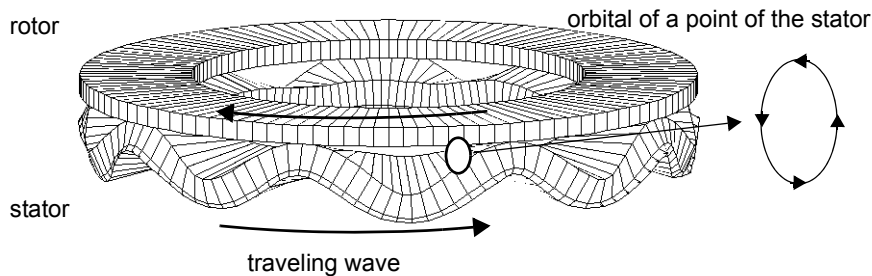


Figure 6.4-1 Principle of Operation of an Ultrasonic Motor

A rotor is positioned on a stator and a traveling wave in the stator is driving the rotor. Each point in the stator has an elliptical motion, as shown in [Figure 6.4-1](#). A point in the top plane of the stator moves up, lifts the rotor, moves it a bit backwards, goes down, detaches from the rotor, and returns to its original position. The traveling wave in the stator occurs due to exciting two standing waves with a different phase. The frequency of this excitation is in the ultrasonic range. The diameter of these motors is in the order of centimeters, they are lightweight, produce a high torque, operate at a low rotational speed, and have a simple design.

First, a dynamic modal analysis is performed to obtain the resonant modes of the stator. Then a harmonic analysis is performed, which shows that a traveling wave occurs if the stator is excited at the right frequency with the correct phase difference. Finally, a transient dynamic analysis is performed to show the onset of the motion of the stator upon application of the potential. Model dimensions and material data are taken from [Reference 1](#).

Eigenvalue Analysis of the Stator of an Ultrasonic Motor

In this section, the stator of the ultrasonic motor is analyzed. A detailed configuration of this stator is shown in [Figure 6.4-2](#).

The stator consists of a brass ring plate with a piezoelectric ceramic (PZT) attached to the lower surface. The piezoelectric ceramic is polarized in the thickness layer direction, and the polarity is reversed at an interval of $\lambda/2$, where λ is the wavelength of the standing wave. The ninth flexural mode is the working frequency of the motor. Therefore, each polarized piezoelectric segment is $1/18$ th of the total ring. [Figure 6.4-3](#) shows a close-up of the piezoelectric stator to show this polarization in more detail. The arrows indicate the orientation directions, where blue, green, and red are the first, second, and third direction, respectively.

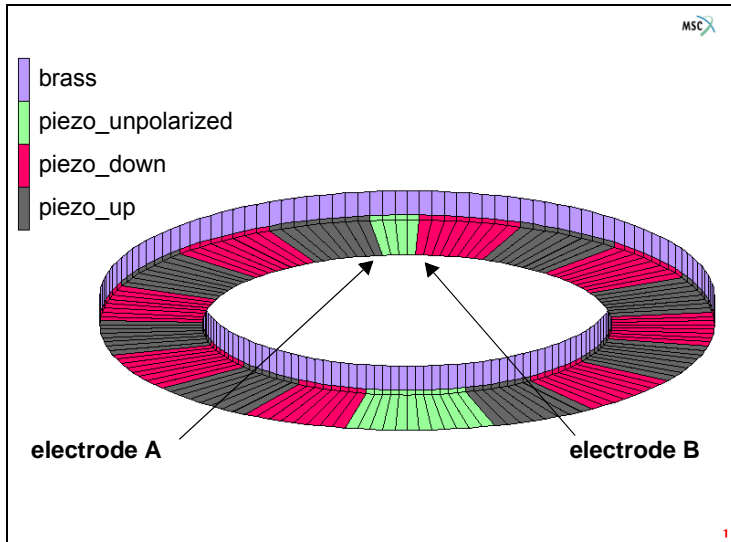


Figure 6.4-2 Configuration of the Stator of an Ultrasonic Motor

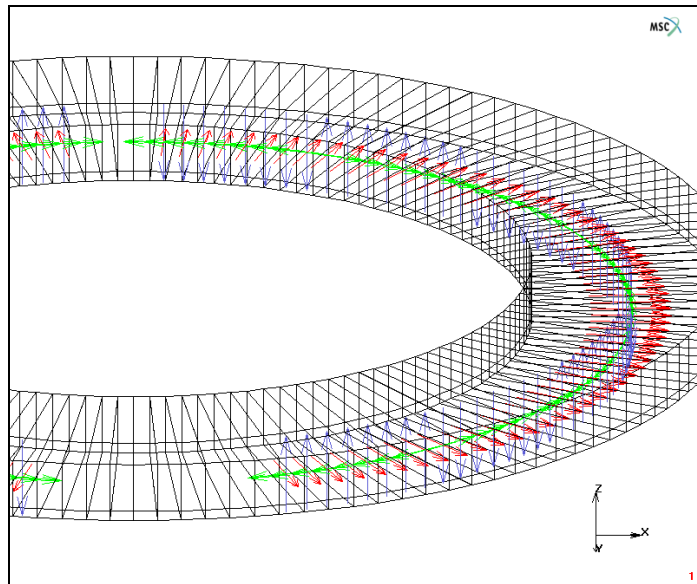


Figure 6.4-3 Close-up of the Stator showing the Orientation of the Piezoelectric Elements

Two electrodes are placed at the lower surface of the piezoelectric ceramic and are separated by the unpolarized regions. In the model, these electrodes are made by tying the potential degree of freedom of all the nodes belonging to an electrode to one node. In this way, the admittance can be easily calculated.

Both of these electrodes are able to generate the ninth flexural mode. To generate a traveling wave, the two electrodes need to be driven simultaneously with a phase difference of 90° . The nodes at the interface of the brass and the ceramic are connected to the common ground to make a closed circuit for the potential. Element type 163 is used for the piezoelectric material. This element is mechanically equivalent to element 7, but has four degrees of freedom, the first three are for the x-, y-, and z-displacement, and the fourth is for the electric potential.

Mesh Generation

The mesh is generated by first defining a ruled surface from two circles. This surface is converted into 144 elements so that each polarized region consists of $144/18 = 8$ elements. The elements are then expanded twice in the z-direction, once for the piezoelectric layer and once for the brass layer.

```
FILE
  NEW
  RESET PROGRAM
  RETURN
MESH GENERATION
  CURVE TYPE
    ARCS CENTER/ANGLE/ANGLE
    RETURN
  CRVS ADD
    0 0 0
    0.02
    0 360
    0 0 0
    0.03
    0 360
  FILL
SURFACE TYPE
  RULED
  RETURN
SRFS ADD
  1
  2
CONVERT
  DIVISIONS
    144 1
```

```
SURFACES TO ELEMENTS
  1 #
RETURN
EXPAND
  SHIFT
  TRANSLATIONS
    0 0 0.0005
  ELEMENTS
  ALL EXIST
  TRANSLATIONS
    0 0 0.0025
  REMOVE
  ELEMENTS
    1 to 144 #
  RETURN
SWEEP
  ALL
  RETURN
```

Boundary Conditions

The potential of the nodes where the piezoelectric elements are connected with the brass elements are set to zero. The two electrodes are applied at the lower surface. This is done by tying all the nodes of an electrode to one node and applying the potential at this node. To remove the rigid body modes in the stator SPRINGS TO GROUND with a small stiffness are added to three nodes for the x-, y-, and z-direction.

```
LINKS
  NODAL TIES
    N TO 1 TIES
      TYPE
        4
      OK
      NODE 1
        106
      ADD TIES
        42 to 105
        187 to 251 #
```

NODE 1

110

ADD TIES

1 to 30

111 to 175

255 to 289 #

RETURN (twice)

SPRINGS/DASHPOTS

NEW

TO GROUND

PROPERTIES

STIFFNESS:SET

10

OK

NODE

1271

DOF: 1

COPY

DOF: 2

COPY

DOF: 3

COPY

NODE

1559

DOF: 1

COPY

DOF: 2

COPY

DOF: 3

COPY

NODE

1415

DOF: 1

COPY

DOF: 2

COPY

```
DOF: 3
RETURN
BOUNDARY CONDITIONS
NAME
    ground
ELECTROSTATIC
    FIXED POTENTIAL
        POTENTIAL(TOP)
            0
        OK
SELECT
    METHOD
        BOX
        RETURN
    NODES
        -10 10
        -10 10
        5e-4-1e-6 5e-4+1e-6
    RETURN
NODES ADD
ALL SELECT
SELECT
    METHOD
        SINGLE
        RETURN
    CLEAR SELECT
    RETURN
NEW
NAME
    electrode_A
    FIXED POTENTIAL
        POTENTIAL(TOP)
            1
        OK
NODES ADD
    106 #
```

```

NEW
NAME
    electrode_B
FIXED POTENTIAL
    POTENTIAL(TOP)
        1
    OK
NODES ADD
    110 #
RETURN (twice)

```

Material Properties

The brass is isotropic with a Young's modulus of 100.6 GPa and a Poisson's ratio of 0.35. The elastic properties of the piezoelectric material are different for the polarized and nonpolarized part. The nonpolarized part is isotropic and has a Young's modulus of 79.0 GPa and a Poisson's ratio of 0.32. The elastic properties of the polarized part are anisotropic and are given in the following matrix:

$$\begin{bmatrix} 13.9 & 7.78 & 7.43 & 0 & 0 & 0 \\ 7.78 & 13.9 & 7.43 & 0 & 0 & 0 \\ 7.43 & 7.43 & 11.5 & 0 & 0 & 0 \\ 0 & 0 & 0 & 2.56 & 0 & 0 \\ 0 & 0 & 0 & 0 & 2.56 & 0 \\ 0 & 0 & 0 & 0 & 0 & 3.06 \end{bmatrix} \times 10^{10} \text{ N/m}^2$$

The piezoelectric coupling matrix is

$$\begin{bmatrix} 0 & 0 & -5.2 \\ 0 & 0 & -5.2 \\ 0 & 0 & 15.1 \\ 0 & 0 & 0 \\ 12.7 & 0 & 0 \\ 0 & 0 & 0 \end{bmatrix} \text{ C/m}^2$$

and the dielectric matrix is

$$\begin{bmatrix} 6.464 & 0 & 0 \\ 0 & 6.464 & 0 \\ 0 & 0 & 5.623 \end{bmatrix} \times 10^{-9} \text{ F/m}$$

The density of the brass is 8560 kg/m³ and of the piezoelectric ceramic 7600 kg/m³. The polarization of the elements is defined using the ORIENTATIONS menu. Before entering the material properties, two element sets are defined; one for each polarity. The material data for the piezoelectric material is entered by giving both the mechanical data (here ISOTROPIC for the nonpolarized and ANISOTROPIC for the polarized part), and the nonmechanical data

(ELECTROSTATIC for the dielectric constants, and PIEZO-ELECTRIC for the coupling matrix). The menu for entering the piezo-electric coupling matrix is shown in Figure 6.4-4.

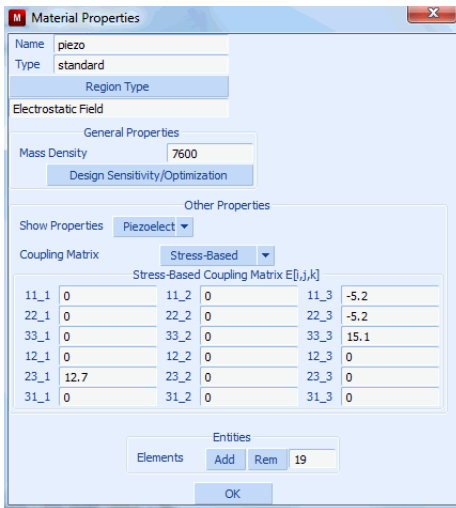


Figure 6.4-4 Piezo-electric Coupling Matrix Menu

MATERIAL PROPERTIES

SELECT

ELEMENTS

```
145 146 147 148 149 158 159 160 161 162 163 164 165 186
187 188 189 190 191 192 193 202 203 204 205 206 207 208
209 218 219 220 221 222 223 224 225 234 235 236 237 238
239 240 241 254 255 256 257 258 259 260 261 270 271 272
273 274 275 276 277 286 287 288 #
```

STORE

minus_z

OK

ALL SELECT

CLEAR SELECT

ELEMENTS

```
150 151 152 153 154 155 156 157 166 167 168 169 170 171
172 173 194 195 196 197 198 199 200 201 210 211 212 213
214 215 216 217 226 227 228 229 230 231 232 233 242 243
244 245 246 247 248 249 262 263 264 265 266 267 268 269
278 279 280 281 282 283 284 285 #
```

STORE

plus_z

OK

ALL SELECT

CLEAR SELECT

RETURN

NAME

brass

ISOTROPIC

YOUNGS MODULUS

1.006E11

POISSON'S RATIO

0.35

MASS DENSITY

8560

OK

ELEMENTS ADD

289 to 432 #

NEW

NAME

piezo_unpol

ISOTROPIC

YOUNGS MODULUS

7.9E10

POISSON'S RATIO

0.32

MASS DENSITY

7600

OK

ELECTROSTATIC

OK

PIEZO-ELECTRIC

OK

ELEMENTS ADD

174 175 176 177 178 179 180 181 182 183 184 185 250 251 252

253 #

NEW

NAME

piezo

ANISOTROPIC

MASS DENSITY

7600

C(i,j)

11

1.39E11

12

7.78E10

13

7.43E10

22

1.39E11

23

7.43E10

33

1.15E11

44

2.56E10

55

2.56E10

66

3.06E10

OK

ELECTROSTATIC

ORTHOTROPIC

PERMITTIVITY11

6.46357E-9

PERMITTIVITY22

6.46357E-9

PERMITTIVITY33

5.62242E-9

OK

PIEZO-ELECTRIC

231

12.7

113

-5.2

223

-5.2

333

15.1

OK

SELECT

SELECT SET

minus_z

plus_z

OK

RETURN

ELEMENTS ADD

ALL SELECT

SELECT

CLEAR SELECT

SELECT SET

minus_z

OK

RETURN

ORIENTATIONS

CYLINDRICAL

0 0 0

0 0 -1

ALL SELECT

SELECT

CLEAR SELECT

SELECT SET

plus_z

OK

RETURN

CYLINDRICAL

0 0 0

```
0 0 1
ALL SELECT
SELECT
CLEAR SELECT
RETURN (thrice)
```

Loadcases and Job Parameters

The analysis is a modal shape simulation to obtain the eigenfrequencies of the stator and, specifically, to find the ninth flexural mode. The frequency range to search the eigenfrequencies is between 1 kHz and 55 kHz, and the LANCZOS method is used. Element 163 is used for the piezo ceramic material and element 7 for the brass material. The ASSUMED STRAIN formulation is selected to improve the bending behavior of these lower order solid elements.

```
LOADCASES
NAME
    modal
PIEZO-ELECTRIC
DYNAMIC MODAL
    FREQUENCY METHOD:RANGE
    LOWEST FREQUENCY
        1000
    HIGHEST FREQUENCY
        55000
    OK
RETURN (twice)

JOBS
ELEMENT TYPES
    PIEZO-ELECTRIC
        MECHANICAL ELEMENT TYPES 3-D SOLID
            7
        OK
        289 to 432 #
    PIEZO-ELECTRIC ELEMENT TYPES 3-D
        163
    OK
    145 to 288 #
    RETURN (twice)
```

PIEZO-ELECTRIC
modal
ANALYSIS OPTIONS
ADVANCED OPTIONS
ASSUMED STRAIN
OK (thrice)

Save Model, Run Job, and View results

After saving the model, the job is submitted and the resulting post file is opened. [Figure 6.4-5](#) shows the ninth flexural mode of the ultrasonic motor at a frequency of 46615 Hz, where use is made of the automatic scaling of the displacements.

FILE
SAVE AS
 piezomotor.mud
 OK
RETURN
RUN
 SUBMIT(1)
MAIN
RESULTS
 OPEN DEFAULT
 DEFORMED SHAPE SETTINGS
 AUTOMATIC
 RETURN
 DEF ONLY
 CONTOUR BAND
 SCALAR
 Displacement Z
SCAN
 O:39
 OK

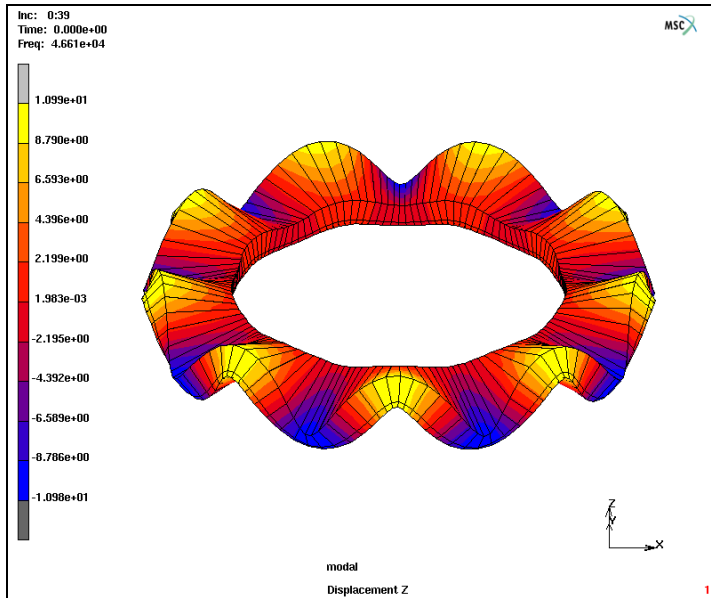


Figure 6.4-5 Ninth Flexural Mode of the Ultrasonic Motor

Harmonic Analysis of the Stator of an Ultrasonic Motor

This analysis will show that a traveling wave occurs when the stator is excited at the two electrodes at the right frequency and with a phase difference of 90° . The frequency range is chosen around the 46615 Hz as computed in the previous section.

The model we built in the previous section can be used as a starting point. The following changes need to be made.

Boundary Conditions

New boundary conditions for the electrodes are generated, since the potentials applied to the two electrodes needs altering in the harmonic boundary conditions, and on electrode B, a phase shift of 90° is applied.

BOUNDARY CONDITIONS

EDIT

electrode_A

OK

COPY

NAME

electrode_harmonic_A

```
ELECTROSTATIC
  HARMONIC BC's
    FIXED ELECTRIC POTENTIAL
      OK
    EDIT
      electrode_B
      OK
    COPY
    NAME
      electrode_harmonic_B
    FIXED ELECTRIC POTENTIAL
      PHASE
        90
      OK
    RETURN (thrice)
```

Loadcases and Job Parameters

A new loadcase is made for this harmonic analysis. The frequency range is set around the ninth flexural mode, from 40 to 50 kHz in 51 steps.

```
LOADCASES
  NEW
  NAME
    harmonic
  PIEZO-ELECTRIC
  DYNAMIC HARMONIC
  LOADS
    CLEAR
    ground
    electrode_harmonic_A
    electrode_harmonic_B
    OK
  LOWEST FREQUENCY
    40000
```



```
HIGHEST FREQUENCY
50000
# FREQUENCIES
51
OK
RETURN (twice)
```

Save Model, Run Job, and View Results

A new piezoelectric job is defined, in which the harmonic loadcase is selected.

```
JOBS
  NEW
  PIEZO-ELECTRIC
    harmonic
  ANALYSIS OPTIONS
    ADVANCED OPTIONS
      ASSUMED STRAIN
      OK (thrice)
  RUN
  SAVE MODEL
  SUBMIT(1)
MAIN
RESULTS
  OPEN DEFAULT
```

Figure 6.4-6 shows the z-displacement at a frequency of 46600 Hz, which is close to the resonant frequency. Figure 6.4-7 shows the phase in the z-direction at the same frequency. The amplitude of the displacement in the z-direction is more or less uniform in the circumferential direction. The momentary displacement, as shown in the two figures, is completely dependant of the phase. To get a better understanding of how this structure responds in the time domain at this frequency it is possible to make an animation in Mentat for one cycle. Then, we see that a traveling wave occurs in the structure.

```
SCAN
  0:34
  OK
RX-
RX-
RX-
```

RX-
RX-
RX-
DEFORMED SHAPE SETTINGS
FACTOR
5000
MANUAL
RETURN
DEF ONLY
SCALAR
Displacement Z Magnitude
CONTOUR BANDS
MORE
ANIMATION
HARMONICS
50
REPEAT
PLAY

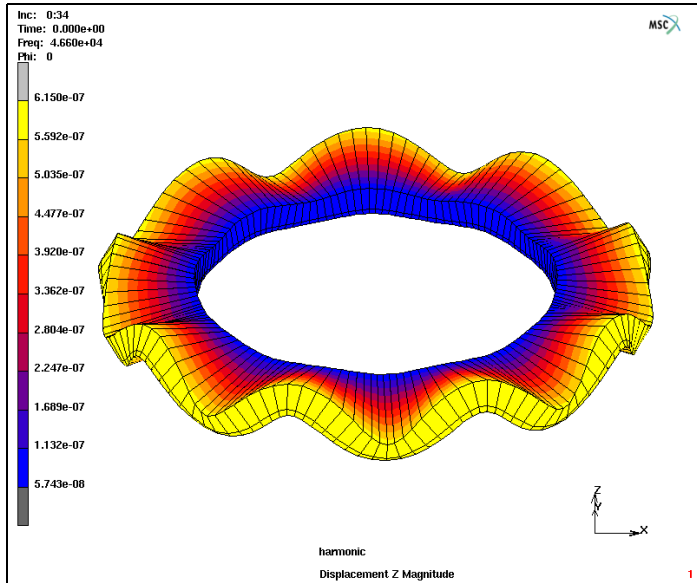


Figure 6.4-6 Z-displacement at a Frequency of 46600 Hz

Note: In Figure 6.4-6, the z-displacement when the stator is driven at the two electrodes with a frequency of 46600 Hz and a phase difference of 90°; displacement is scaled with a factor 5000.

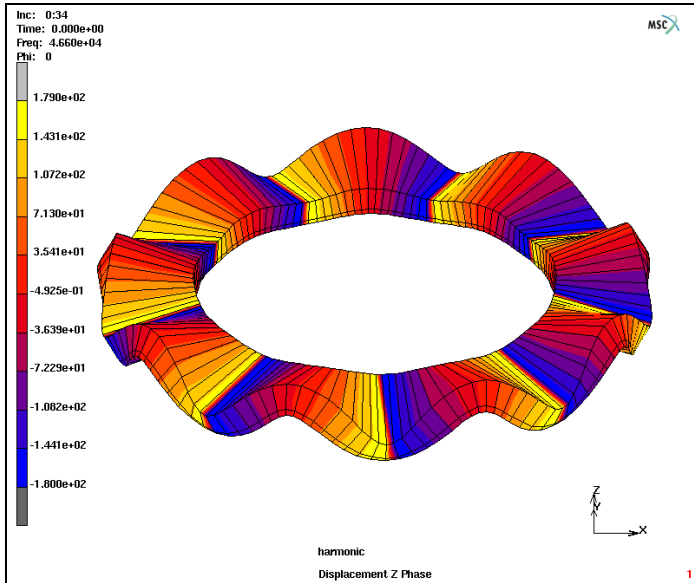


Figure 6.4-7 A Phase in the Z-direction with a Frequency of 46600 Hz

Note: In Figure 6.4-7, the phase in the z-direction when the stator is driven at the two electrodes with a frequency of 46600 Hz and a phase difference of 90°; displacement is scaled with a factor 5000.

It is also possible to obtain the admittance from this simulation. The admittance is calculated as

$$Y = I/V, \tag{6.4-1}$$

where I is the current and v the applied potential. The current I is related to the total charge on the electrode surface as

$$I = i\omega Q_{total}, \tag{6.4-2}$$

where ω is the operating frequency, i is $\sqrt{-1}$, and Q_{total} is the sum of the charge on all the nodes belonging to the electrode. This summation is already done since all the nodes of an electrode are tied to one node. Since $v = 1$ the rms value of the admittance then becomes

$$Y = \left| \frac{1}{\sqrt{2}} \omega Q_{total} \right|. \tag{6.4-3}$$

Figure 6.4-8 shows this admittance as a function of the frequency. This plot is obtained by creating a history plot of the reaction charge on node 106 as a function of the frequency, converting this history plot in a table and manipulating the table plot by application of equation (6.4-3). Figure 6.4-8 clearly shows an increase of the admittance (or a decrease of the resistance) around a resonant frequency of the stator.

STOP
RETURN

```
RETURN
HISTORY PLOT
SET LOCATIONS
    106 #
INC RANGE
    0:1 0:50 1
ADD CURVES
    SINGLE LOCATION
    NODE 106
    Frequency
    Reaction Electric Charge
    RETURN
FIT
SHOW IDS
    0
COPY TO TABLE
    1
TABLES
    FUNCTION VALUE F >>
        abs(f*v1/sqrt(2))
    FIT
    FUNCTION VALUE F <<
    MIN | FUNCTION VALUE
        0
    MAX | FUNCTION VALUE
        0.005
```

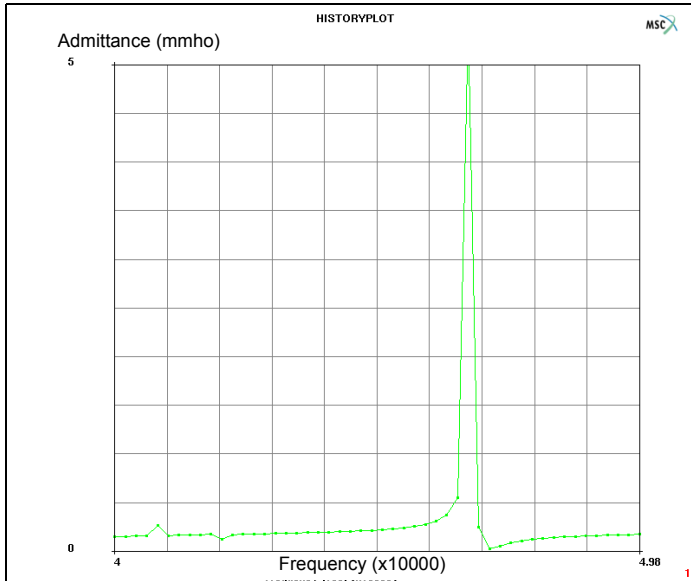


Figure 6.4-8 Plot of the Electrical Admittance as a Function of the Frequency

Transient Analysis of the Stator of an Ultrasonic Motor

Finally, a transient analysis is performed to show that the traveling wave forms in the stator, and that nodes have an elliptical motion as stated in [Figure 6.4-1](#).

New boundary conditions are generated for the electrodes, where the sinusoidal potentials are prescribed using tables.

```
BOUNDARY CONDITIONS
  EDIT
    electrode_A
  COPY
  NAME
    electrode_transient_A
  ELECTROSTATIC
    TABLES
    NEW
    1 INDEPENDENT VARIABLE
    FORMULA
    ENTER
      sin(2*pi*46615*v1)
```

```
MAX | V1
    15/46615
STEPS | V1
    500
TYPE
    time
REEVALUATE
FIT
COPY
ENTER
    sin(2*pi*46615*v1-pi/2)
RETURN
FIXED POTENTIAL
TABLE
    table1
OK
EDIT
    electrode_B
COPY
NAME
    electrode_transient_B
FIXED POTENTIAL
TABLE
    table2
OK
RETURN (twice)
```

Loadcases and Job Parameters

A new loadcase is made for this transient analysis. The total time is set in such a way that 15 cycles are done at the resonant frequency of 46615 Hz, so $t = 15/46615 = 0.3218$ ms.

```
LOADCASES
NEW
NAME
    transient
PIEZO-ELECTRIC
```

```
DYNAMIC TRANSIENT
LOADS
  CLEAR
  ground
  electrode_transient_A
  electrode_transient_B
  OK
TOTAL LOADCASE TIME
  15 / 46615
# STEPS
  500
  OK
RETURN (twice)
```

Save Model, Run Job, and View Results

A new piezoelectric job is defined, in which the transient loadcase is selected.

```
JOBS
  NEW
  PIEZO-ELECTRIC
  transient
  INITIAL LOADS
  CLEAR
  ground
  electrode_transient_A
  electrode_transient_B
  OK
  ANALYSIS OPTIONS
  ADVANCED OPTIONS
  ASSUMED STRAIN
  OK (twice)
  JOB RESULTS
  AVAILABLE ELEMENT TENSORS STRESS
  OK (twice)
RUN
```

```
SAVE MODEL
SUBMIT(1)
MAIN
RESULTS
OPEN DEFAULT
DEFORMED SHAPE SETTINGS
MANUAL
    250000
RETURN
CONTOUR BANDS
SCALAR
    Displacement Z
MONITOR
```

Figure 6.4-9 shows the x- and z-displacement of a node at the top of the stator. The figure shows that it takes a number of cycles before the traveling wave starts to emerge, and that the amplitude of the z-displacement is still increasing. The node is chosen so that its x-displacement is responsible for rotating a rotor. Figure 6.4-10 shows that this node has an elliptical motion. Here the z-displacement is plotted as a function of the x-displacement for the last 100 increments. The elliptical motion of this node is in a counterclockwise motion.

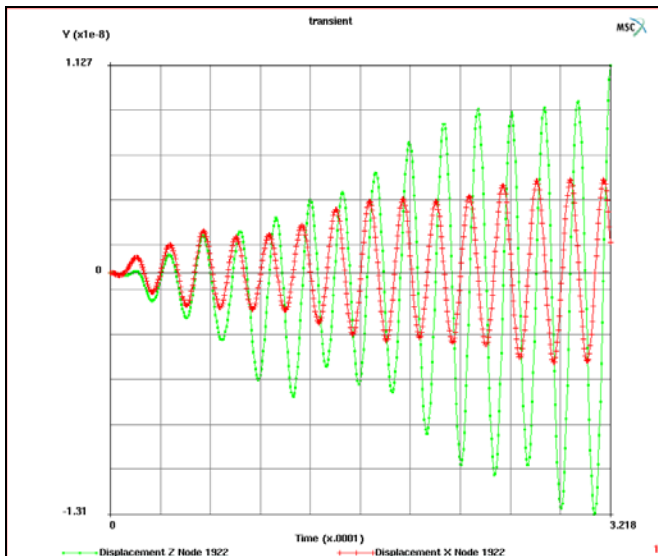


Figure 6.4-9 History Plot of the X- and Z-displacement of a Node at the Top of the Stator

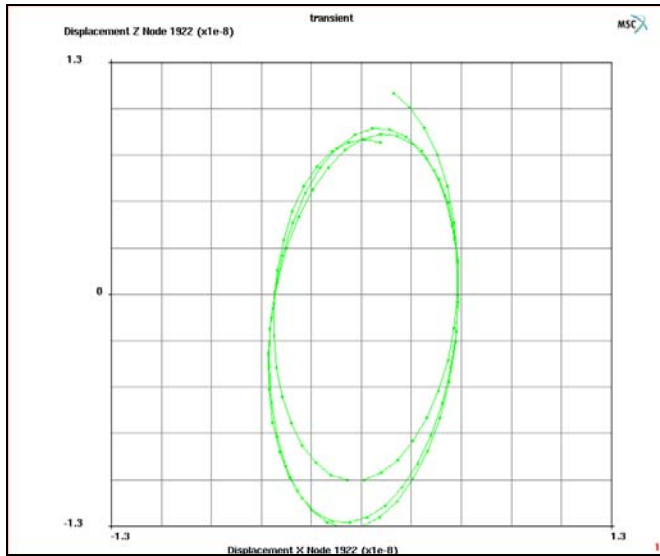


Figure 6.4-10 The Z-displacement as a Function of the X-displacement for the Node at (0,-0.03,0.003) for Increments 400 to 500

Input Files

The files below are on your [delivery media](#) or they can be downloaded by your web browser by clicking the links (file names) below.

File	Description
piezomotor.proc	Mentat procedure file to run the above example

Reference

1. Kagawa, Y., Tsuchiya, T., and Kataoka, T., “Finite Element Simulation of Dynamic Responses of Piezoelectric Actuators”, *Journal of Sound and Vibration*, Vol 191(4) (1996), pp. 519-538.

6.5 Analysis Performance Improvements

- Chapter Overview 1980
- Speed and Memory Improvements 1980
- Conclusion 1985
- Input Files 1985

Chapter Overview

There are a few major areas where the performance has been substantially improved for large problems over the years in Marc. One measure of performance is the speed and memory required to run the same problem from version to version. There are three problems in this chapter that have been run in various versions that span nearly seven years. These demonstration problems address software improvements that require less memory and run in less time based upon relative performance of the same problem using these versions of Marc. The speed and memory improvements herein have been obtained by rewriting the contact database and structure over the intervening years. In addition, substantial speed and memory improvements, especially for examples involving bricks and shells, have been obtained with the introduction of a multifrontal sparse solver.

Speed and Memory Improvements

Case 1: Rigid-Deformable Body Contact

Figure 6.5-1 shows the model where the two rollers are compressing the deformable ring sector. This particular model uses the Iterative Sparse solver with Incomplete Choleski preconditioner and runs for 50 increments using fixed load stepping.

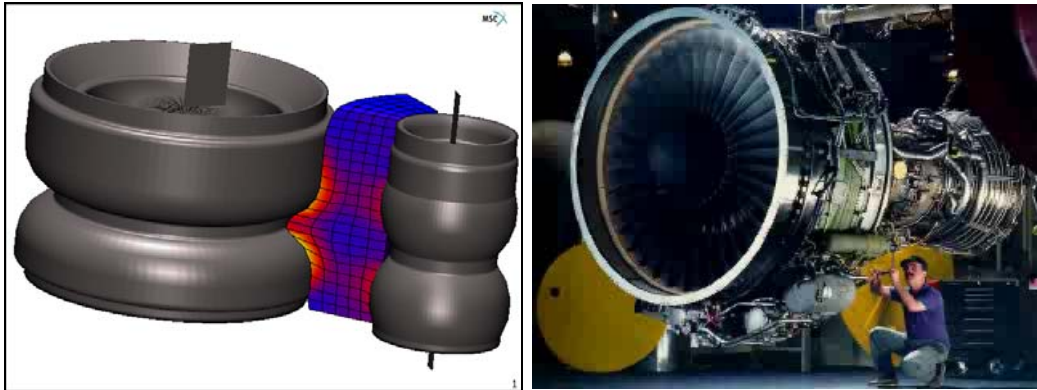


Figure 6.5-1 Model for Case 1 Rigid Contact - Click on right figure to play animation (ESC to stop)

Procedure for Case 1: run with several versions of Marc

```
../marc200k/tools/run_marc -j rigid -v n (k = 0,1,3 & 5)
```

The improvements of memory and speed are shown in [Figure 6.5-2](#).

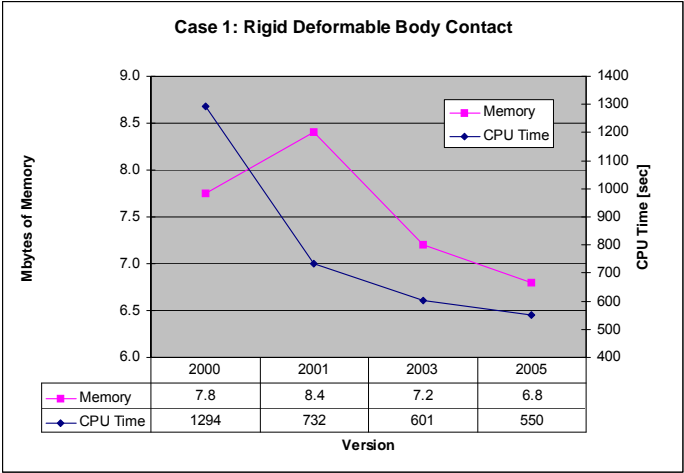


Figure 6.5-2 Memory and Speed for Case 1 Rigid Contact

At some point in the near future, this problem will become obsolete for performance metrics because of continuing software improvements and faster hardware that will render this problem too small. In the meantime, it is useful to see performance gains made by Marc over the past six years spanning four versions. Clearly this particular problem demonstrates the benefit gained in using contact, one of Marc’s most popular features.

Of course this is only one model, and other models may have different performance metrics. Contact problems have two types of contact bodies, rigid and deformable. In this case, deformable and rigid bodies come into contact which is referred to as rigid contact. In the next case, we examine where a deformable body contacts a deformable body which is referred to as deformable contact.

Case 2: Deformable-Deformable Contact

Figure 6.5-3 shows an elastomeric seal that comes into self contact. This model will be run in several versions of Marc using the procedure below.

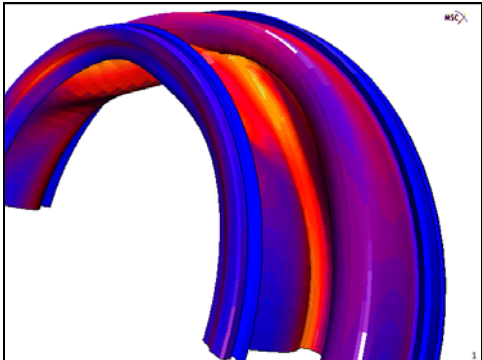


Figure 6.5-3 Model for Case 2 Deformable Contact

Procedure for Case 2: run with several versions of Marc

```
../marc200k/tools/run_marc -j deformable -v n (k = 0,1,3 & 5)
```

The improvements of memory and speed are shown in [Figure 6.5-4](#) after running these versions. This particular model uses the Multifrontal Sparse solver with Optimize 11 and runs for 10 increments using fixed load stepping.

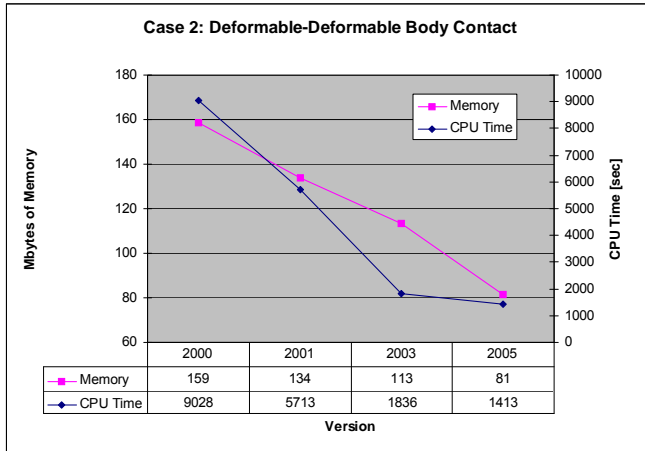


Figure 6.5-4 Memory and Speed for Case 2 Deformable Contact

As with the previous example, there is a steady performance gain from versions 2000 to 2010 of Marc. For this problem, these performance improvements have been brought about by changes in the algorithm in contact with updated Lagrangian elasticity.

Case 3: Model with Solid and Shell Elements

The Multifrontal Sparse solver yields speed improvements using the Optimize 11 optimizer for renumbering and minimizing bandwidth. This is achieved as shown in [Figure 6.5-7](#) that shows a model of a magnetic disk drive head used in the data storage device industry. To run this modal analysis in the several versions of Marc, use the procedures below.

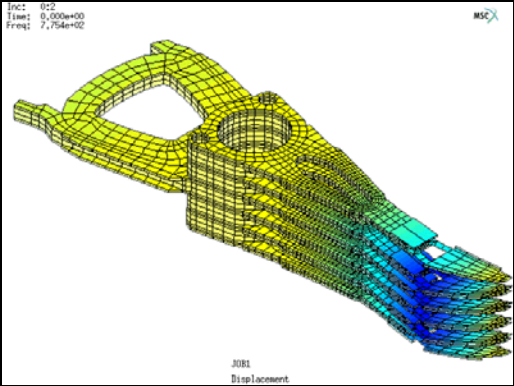


Figure 6.5-5 Model for Demonstrating New Solver Capabilities

Procedure:

```
.../marc200k/tools/run_marc -j disk_head_drive -v n (k = 0,1,3 & 5)
```

The improvements of memory and speed are shown in [Figure 6.5-6](#). The Multifrontal Sparse solver demonstrates continued improvements in several version.

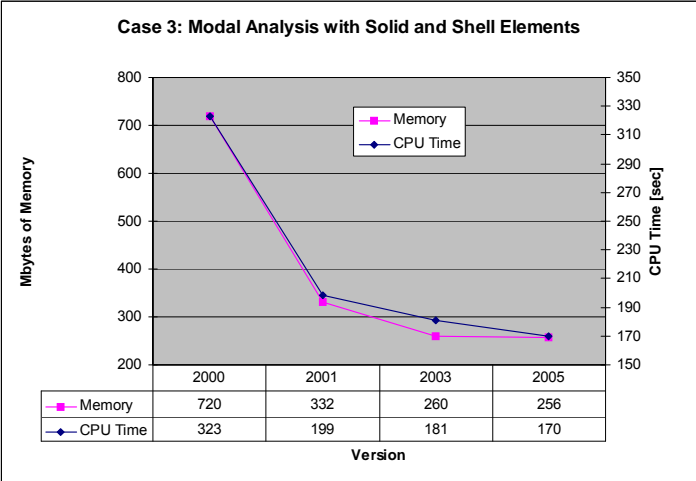


Figure 6.5-6 Memory and Speed for Case 3 Modal Analysis

The multifrontal solver is selected in the JOBS menu as shown in [Figure 6.5-7](#).

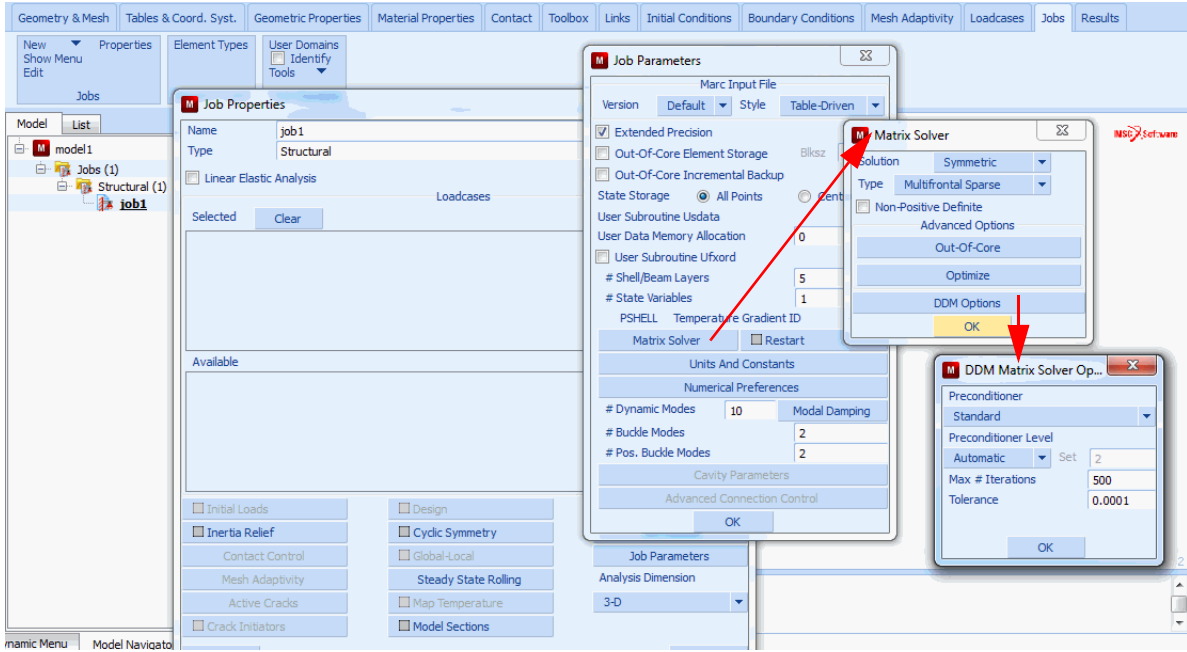
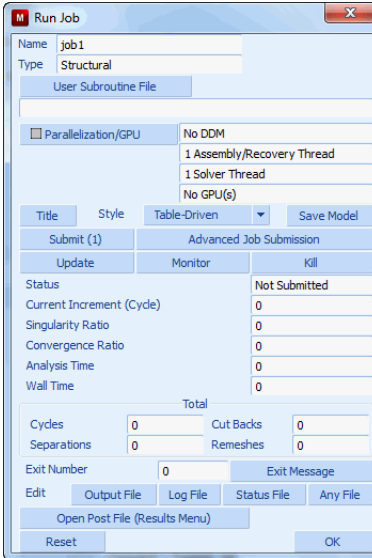
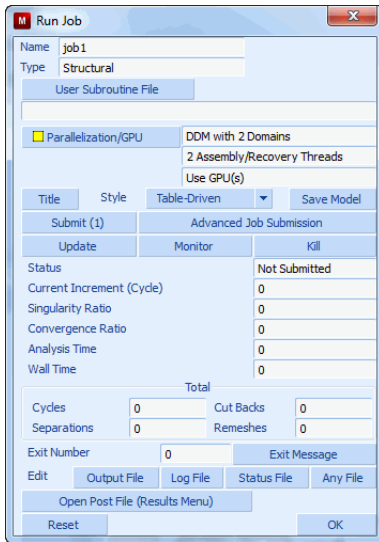
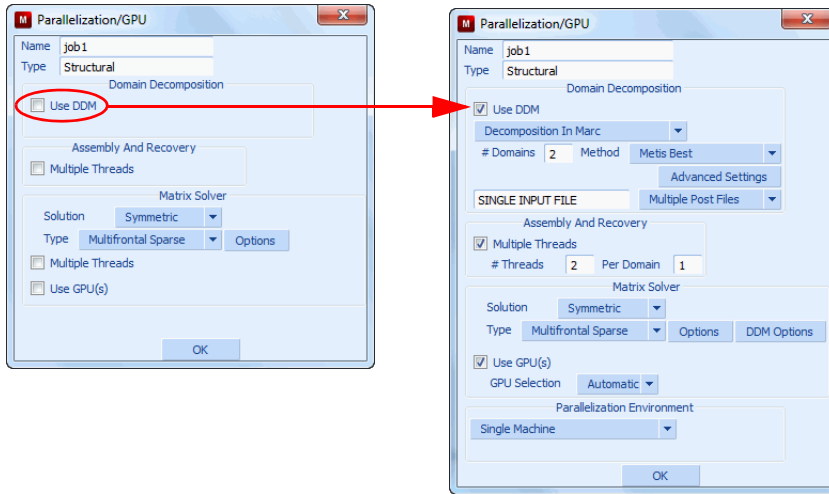


Figure 6.5-7 Solver Submenu





Conclusion

The performance enhancements available in Marc allow you to solve your problems faster and with lower memory requirements than ever before. Improvements are continually being made in multiple areas: solver, optimizer, domain decomposer, contact, improvements in element technology, material modeling as well as general improvements.

In particular, major speed and memory improvements have been obtained by rewriting the contact database and structure. In addition, substantial speed and memory improvements, especially for examples involving bricks and shells, have been obtained with the introduction of the multifrontal sparse solver.

Input Files

The files below are on your [delivery media](#) or they can be downloaded by your web browser by clicking the links (file names) below.

File	Description
rigid.dat	Marc input file
disk_drive_head.dat	Marc input file
deformable.dat	Marc input file

6.6 Robustness of Automatic Load Stepping Schemes

- Chapter Overview 1988
- Usage of the Auto Step Feature 1988
- Input Files 1998

Chapter Overview

For problems where large deformation and/or contact are involved, it is often necessary to use an adaptive time step strategy to ensure the convergence of the solution. The robustness control of nonlinear solution strategy is designed for this purpose. This chapter demonstrates the usage of the robustness control for nonlinear analysis using the AUTO STEP loadcase.

Usage of the Auto Step Feature

This option controls the automatic time/load stepping procedure. By default, the time step is adjusted based upon the number of recycles in addition to the user criteria. If the user-specified desired number of recycles is exceeded, the time step is divided by a factor. If the increment converges in less than the desired number of recycles, the time step is scaled up using the same factor. The increment is repeated if any of the following occurs: maximum number of iterations reached, elements going inside out, or a contact node slides off the end of a rigid body. In this case, the time step is divided by two. The enhanced variant is available for mechanical, thermal, and thermo-mechanically coupled analyses.

For more control, the time step can also be adjusted based upon the calculated value of a parameter (strain increment, plastic strain increment, creep strain increment, stress increment, strain rate, strain energy increment, temperature increment, displacement increment, rotation) versus a user-defined maximum. More than one criteria can be specified. If the criteria is not satisfied within an increment, recycling occurs with a reduced time/load applied. After the increment has converged based upon tolerances specified on the CONTROL values, the data given here controls the next increment.

The first example uses the Auto Step feature with defaults, i.e., without a user specified criterion.

Procedure A:

```
MAIN
FILES
  MARC INPUT FILE READ
    mesha.dat
  OK
  PLOT
    NODES (turn off drawing of nodes)
    DRAW
  FILL
  MAIN
CONTACT
  CONTACT BODIES
  ID CONTACT
```

```

EDIT
  push
  OK
RIGID
  VELOCITY PARAMETERS
    VELOCITY X
      -4
    OK (twice)
  
```

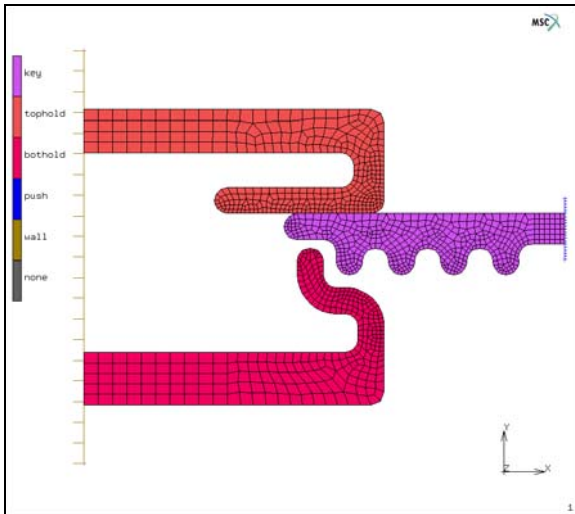


Figure 6.6-1 Model for Procedure A

Now this model is completely defined except for the load history. All we need to do is define a loadcase using the AUTO STEP feature and run the model. The automatic convergence testing procedure is activated by AUTO SWITCH which permits switching between displacement and residual control.

```

MAIN
  LOADCASES
    MECHANICAL
      STATIC
        CONVERGENCE TESTING
          AUTO SWITCH
            OK
  
```

The multi-criterion adaptive load stepping procedure (AUTO STEP) is then selected.

MULTI-CRITERIA

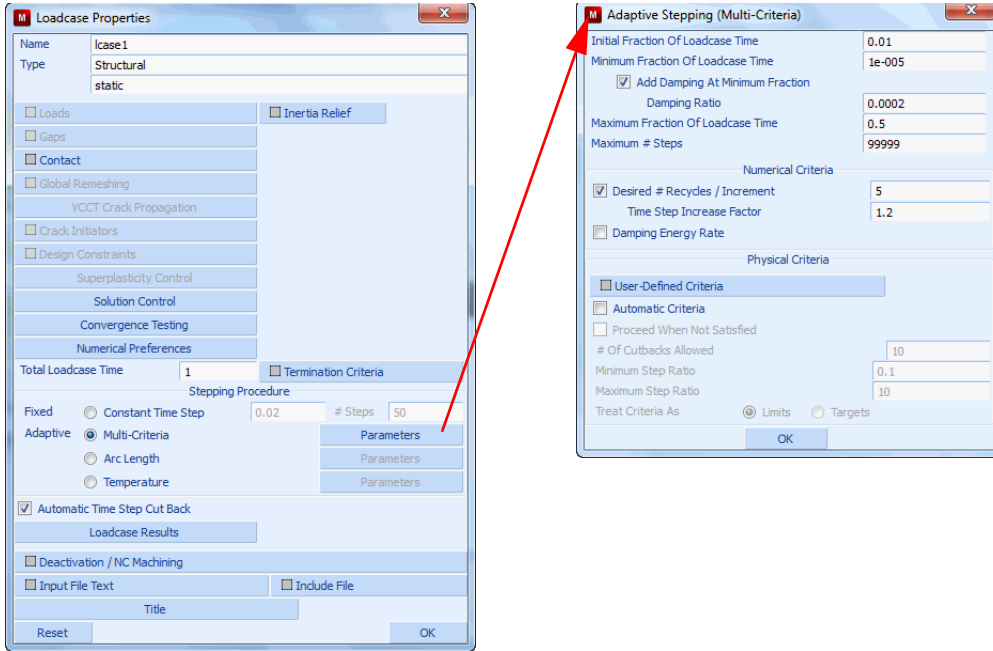


Figure 6.6-2 Select Multi-Criteria (Auto Step) Feature

```

OK
MAIN
JOBS
  MECHANICAL
    lcase1 (select this loadcase)
  OK
FILES
  SAVE AS
    auto_load_stepping_a.mud
  OK
RETURN
  
```

We now submit the analysis to run with only the defaults for Auto Step.

RUN
 SUBMIT1
 MONITOR

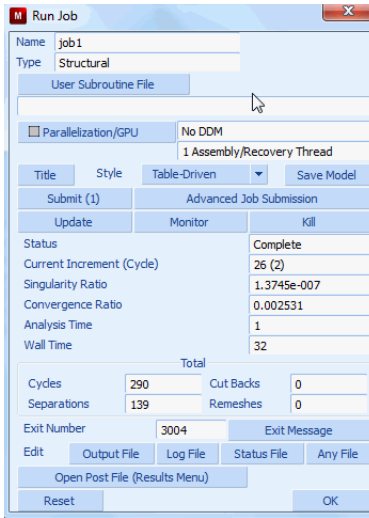


Figure 6.6-3 Monitor of Job Results

In [Figure 6.6-3](#), we see that the job has completed with a successful number exit of 3004. There were 290 Newton-Raphson iteration cycles, 139 contact separations, analysis time of 1 second and a compute wall time of 32 seconds. The statistics are cumulative for all the loadcases.

OK
 MAIN
 RESULTS
 OPEN DEFAULT
 DEF ONLY
 CONTOUR BANDS
 LAST

[Figure 6.6-4](#) shows the final position of the key as it was inserted into the surrounding contact bodies, and [Figure 6.6-5](#) shows the variation in the time step during the analysis.

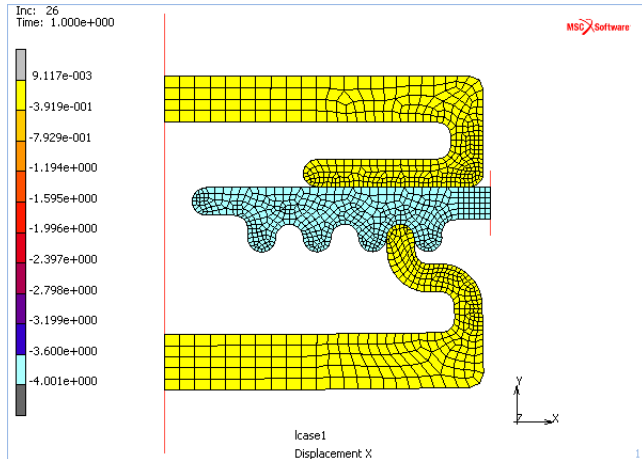


Figure 6.6-4 Final Position

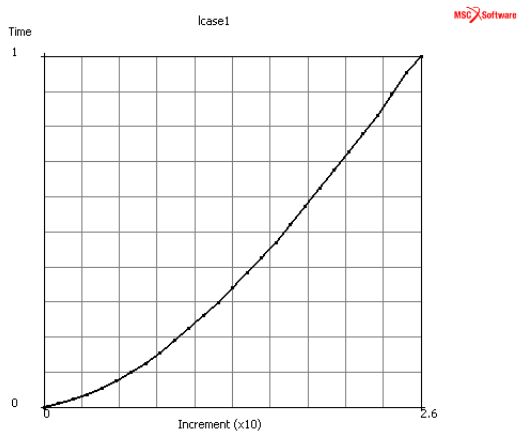


Figure 6.6-5 Variation of Time Step for each Increment

Now let's try to extract the key from the surrounding contact bodies by making a table to control the push(ing) rigid body.

```
MAIN
  RESULTS
    CLOSE
  MAIN
CONTACT
  CONTACT BODIES
    EDIT
```



```

push
OK
TABLES
NEW
1 INDEPENDENT VARIABLE
TYPE
time
OK
ADD
0 1 1 1 1 -1 2 -1
FILLED
FIT
    
```

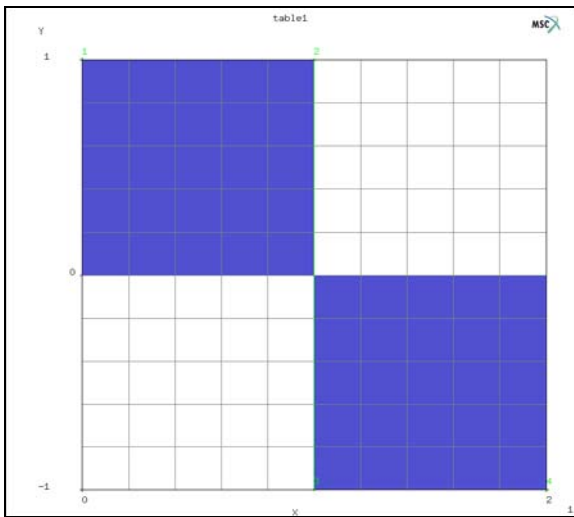


Figure 6.6-6 Table for Rigid Body Push's Velocity

```

SHOW MODEL
RETURN
RIGID
VELOCITY PARAMETERS
VELOCITY X
choose table1
OK
    
```

OK
MAIN
FILES
SAVE AS
 auto_load_stepping_b.mud
MAIN
LOADCASES
MECHANICAL
 COPY
 MAIN
JOBS
MECHANICAL
 Icase2
 OK
SAVE
RUN
 SUBMIT1
 MONITOR

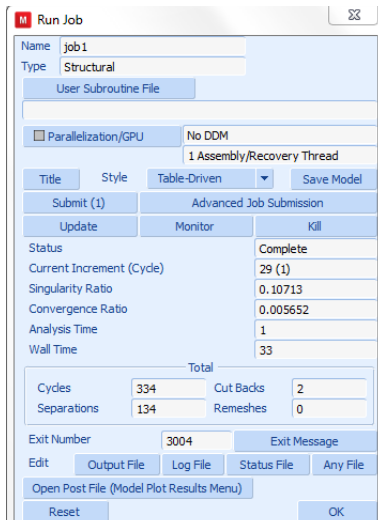


Figure 6.6-7 Results from Extraction

The extraction terminates with an exit number of 3002, which means that the analysis failed to converge. Let's take a look at the deformed shape.

OK
 SAVE
 MAIN
 RESULTS
 OPEN DEFAULT
 DEF ONLY
 CONTOUR BANDS
 LAST

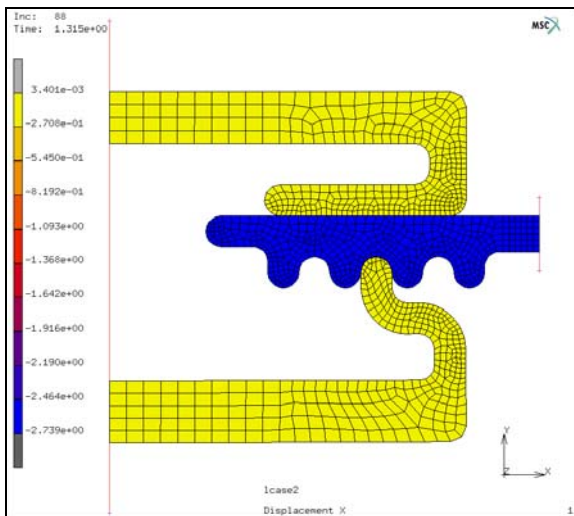


Figure 6.6-8 Deformed Shape at Last from Extraction

We notice that there is not much going on and examining at the convergence criteria, we see that the maximum reaction used in the denominator of the convergence ratio is very small. Hence, we need to change our convergence criteria to account for this.

CLOSE
 MAIN
 LOADCASES
 EDIT
 lcase2
 OK
 MECHANICAL
 STATIC

CONVERGENCE TESTING

RELATIVE/ABSOLUTE

MINIMUM REACTION FORCE CUTOFF

8e-4

MAXIMUM ABSOLUTE RESIDUAL FORCE

8e-4

OK (twice)

MAIN

SAVE

JOBS

RUN

SUBMIT

MONITOR

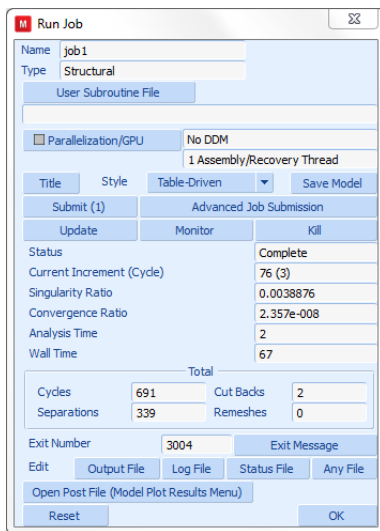


Figure 6.6-9 Results from Extraction with Relative/absolute Testing Switch

RESULTS

OPEN DEFAULT

DEF ONLY

LAST

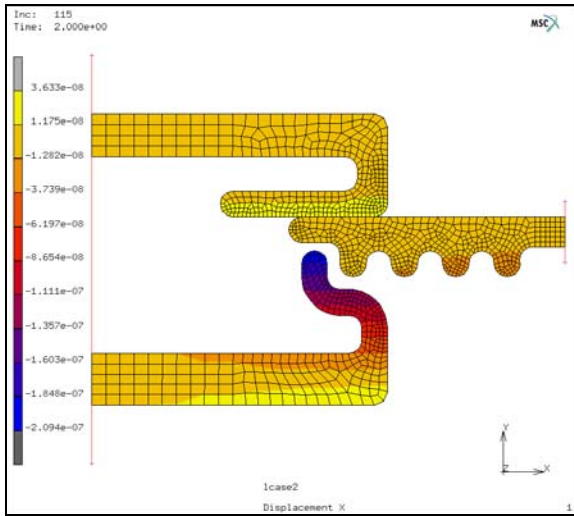


Figure 6.6-10 Deformed Shape at Last from Extraction with Relative/absolute Testing Switch

A cutoff maximum absolute residual force and minimum reaction force of $8e-4$ was chosen because it is 10% of the largest reaction that occurs during the 88 increments run in the first extraction attempt.

Finally, looking at the time step history notice how the automatic selection of the time step varies between the insertion and extraction steps.

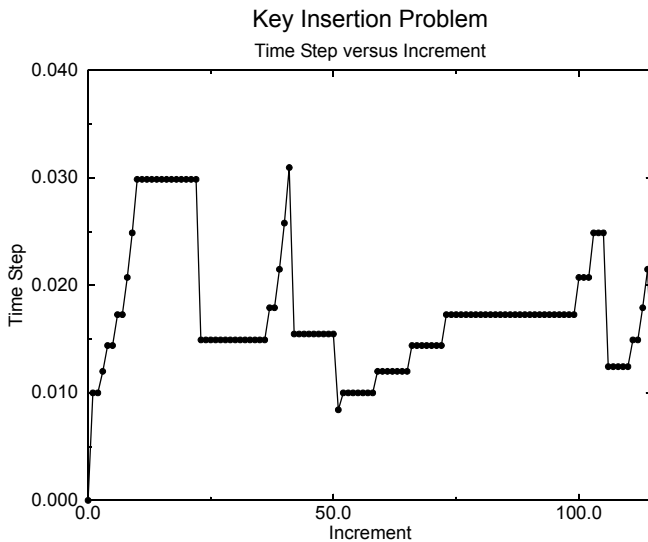


Figure 6.6-11 Variation of Time Step for each Increment

This type of contact problem would be very hard to run without the Auto Step feature since the time step changed 25 times throughout this analysis.

Input Files

The files below are on your [delivery media](#) or they can be downloaded by your web browser by clicking the links (file names) below.

File	Description
auto_load_stepping.proc	Mentat procedure file
auto_load_stepping_b.proc	Mentat procedure file
auto_load_stepping_c.proc	Mentat procedure file
mesha.dat	Mentat procedure file

6.7 Marc Running in Network Parallel Mode

- Run CONTACT WITH DDM 2000
- Run CONTACT WITH DDM on a Network 2000
- Input Files 2006

Run CONTACT WITH DDM

In this chapter, the procedure of running an analysis in parallel on a number of computers connected over a network is demonstrated. We start by running a contact demonstration problem, then show how to run the same problem on a network in parallel. Pick the HELP, RUN A DEMO PROBLEM, and CONTACT WITH DDM buttons as shown in Figure 6.7-1.

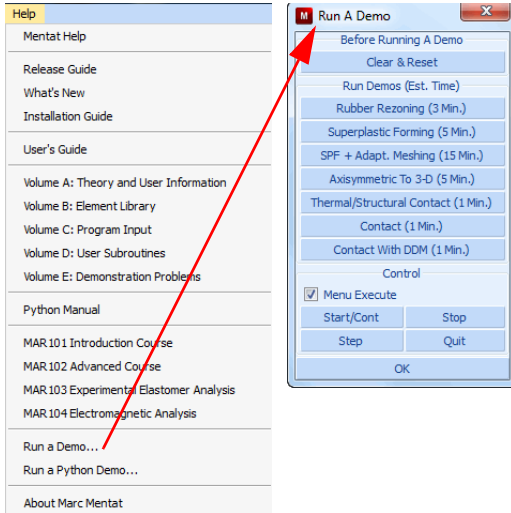


Figure 6.7-1 Run CONTACT WITH DDM Demonstration Problem

This procedure automatically builds, runs, and postprocesses a contact problem using two domains. After it finishes, close the post file and, from the main menu, go to JOBS and pick DOMAIN DECOMPOSITION.

Run CONTACT WITH DDM on a Network

Before running a job over the network, make sure that the machines are properly connected. Suppose two machines with host names host1 and host2, respectively, are to be used in an analysis:

UNIX

From host1, access host2 with

```
rlogin host2
```

If a password needs to be provided to do the remote login, this has to be taken care of. If the `rlogin` is not possible without providing a password, a network run is not possible. See the man pages on `rlogin` (see `.rhosts` file) or contact your system administrator.

Windows

From host1, access host2 with Network Neighborhood. If this fails, a network run is not possible. Contact your system administrator.

Figure 6.7-2 shows the domains that were used in this example.

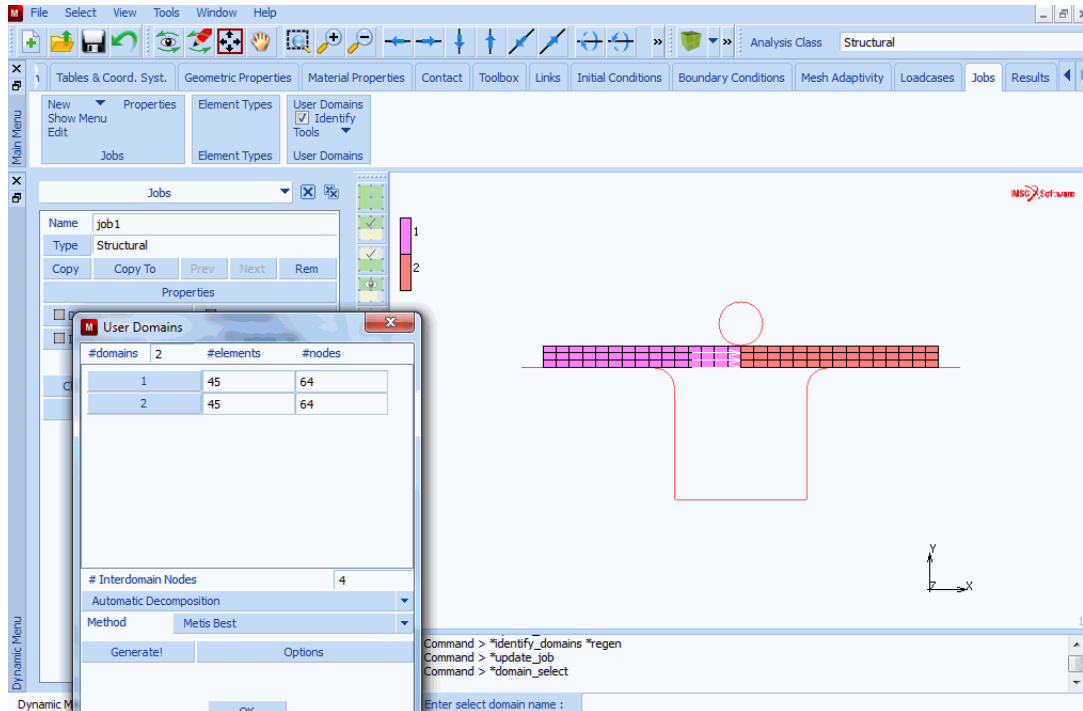


Figure 6.7-2 Identification of the Domains

For now, generate three domains and run on your network. Pick GENERATE and enter 3 domains. The number of domains must equal the number of processors to be used in the analysis. Marc associates a domain with each processor and creates a separate input data file for each domain as well as a root input file associated with the job ID.

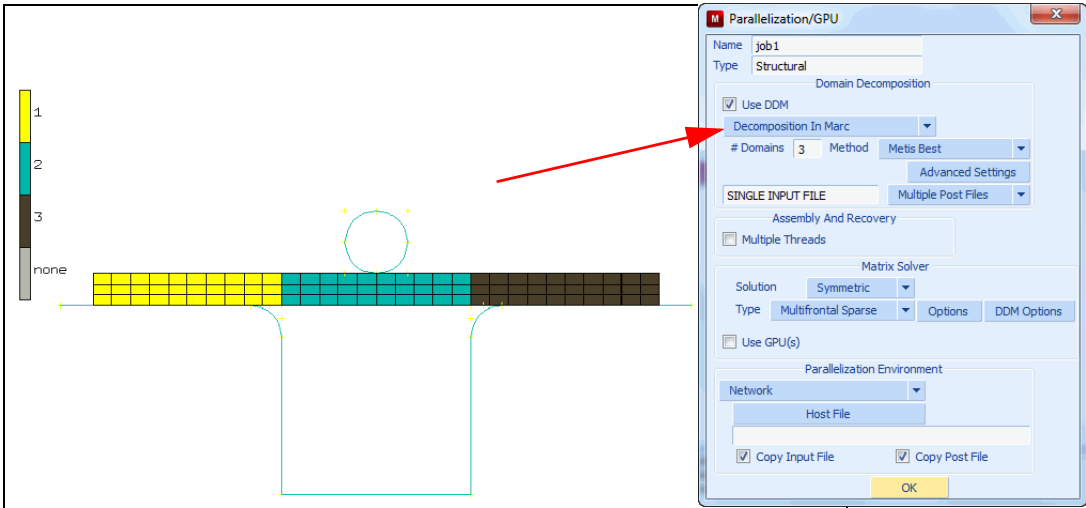


Figure 6.7-3 Generating Three Domains

From the JOBS menu, pick RUN, then NETWORK.

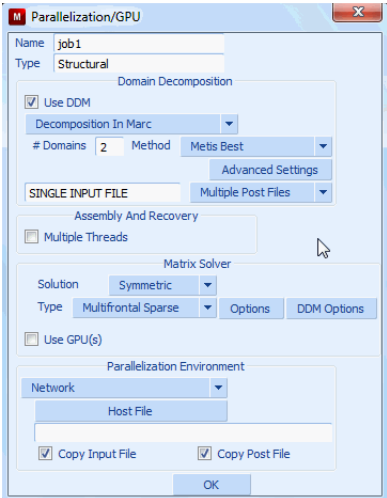


Figure 6.7-4 Selecting Hosts to Run

Enter the SETTINGS menu and click on HOST FILE. Create a new file called `hostfile` (any name could be chosen) by typing in its name in the file browser. (Caution for Windows NT user: If notepad is used as editor, a file called `hostfile.txt` is created. Use a name with an extension to avoid this problem.) Now, add the text:

```
host1 2
host2 1 workdir installdir
```

`host1` is the host name of the machine on which Mentat is running and from which the job is to be started (the root host). Assume that two processors are used on `host1`. `host2` is the host name of the other machine (the remote host) and on which a single processor is used. The word `workdir` is replaced with the full path to the working directory where I/O takes place for the remote host and `installdir` is replaced with the full path to the Marc installation directory that the remote host will use (`installdir` is for UNIX only). The path should be given so that it can be reached from `host2`. The working directory for the remote host could be the current working directory on the root host or, typically, a local directory on the remote host containing the input files for the domains to be run on this host.

For UNIX, assume that the working directory is called `/disk1/testing` on `host1`. Further assume that this disk is NFS mounted so that the working directory can be reached from other computers on the network as `/nfs/host1/disk1/testing` (using a hypothetical naming convention for shared disks). Now the host file would contain:

```
host1 2
host2 1 /nfs/host1/disk1/testing /marcinstall/marc/
```

Similarly for Windows, assume the working directory is `D:\users\john\testing`, which is shared using the sharename `djohnntest`. For Windows, please note that the installation directory must be shared and available on all hosts used in the analysis. The host file should contain:

```
host1 2
host2 1 \\host1\djohnntest \\host1\marcinstall
```

It is more efficient to have the working directory on the remote host as a local directory rather than using the working directory on the root host. In the case of Windows, assume that the working directory on the remote host is `C:\testing` and that Marc is installed on the remote host in `C:\MSC Software\version`, the host file should contain:

```
host1 2
host2 1 C:\testing
```

In this case, the input data file for the domain to be processed on `host2` must exist in the local directory `C:\testing` before the analysis starts and the post file for this domain is available in the same directory at the end of the analysis. The necessary input files are automatically copied from the working directory of the root host to the local working directories of the remote hosts before the job starts. After the job is finished, the post files from the remote hosts are automatically copied back to the root host. The user has the option to suppress this automatic file transfer from the NETWORK SETTINGS under the RUN JOB menu in Mentat.

Now submit the job, then check your results. By clicking on OPEN DEFAULT, you view the results for the complete model.

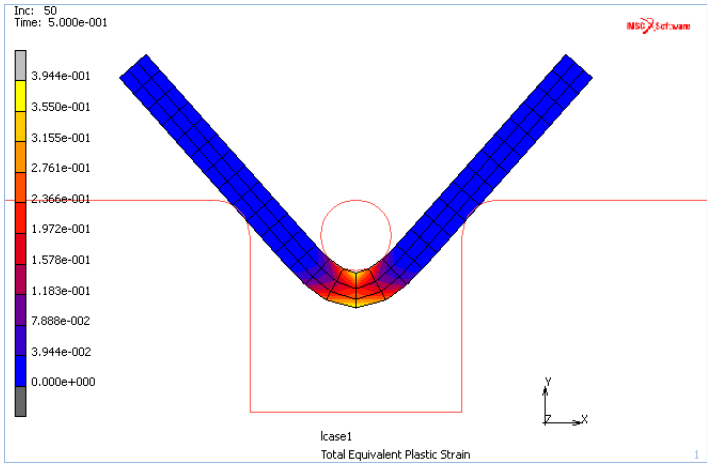
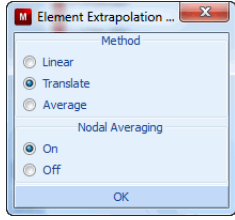
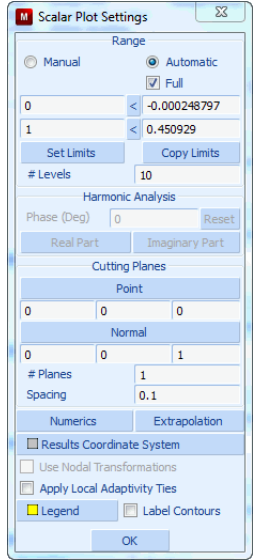
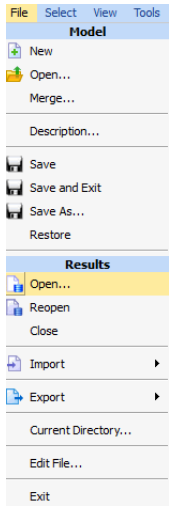


Figure 6.7-5 Checking Your Results

Marc created a post file associated with each domain as well as a root post file associated with the job ID. For the previous model, 1model11_job1.t16, 2model11_job1.t16, and 3model11_job1.t16 are the processor files, while model11_job1.t16 is the root file.

If the model is very large, it can be convenient to view only a portion of the model by selecting any one of the processor post files, such as 2model11_job1.t16 shown in Figure 6.7-6. This file contains only data associated with domain 2 as selected in the domain decomposition menu in Figure 6.7-3.

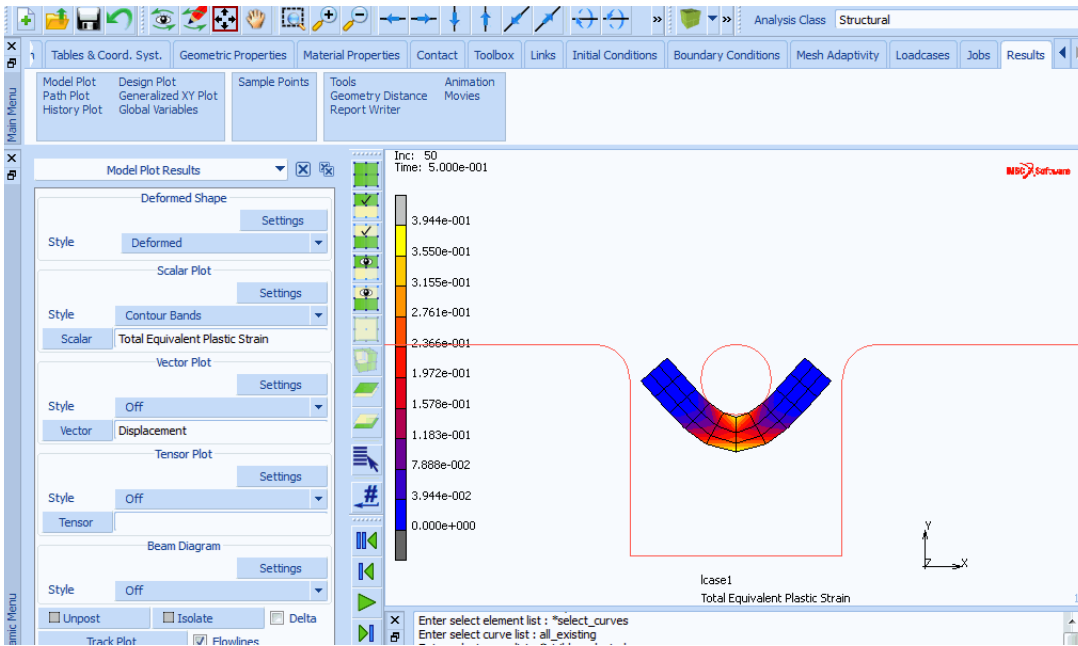
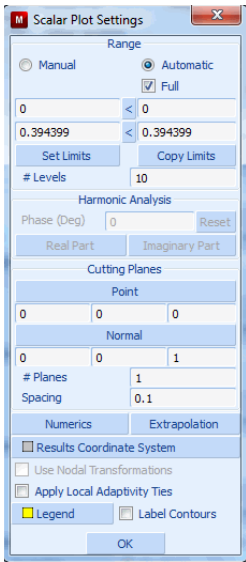


Figure 6.7-6 Results for Domain 2

Input Files

The files below are on your [delivery media](#) or they can be downloaded by your web browser by clicking the links (file names) below.

File	Description
s4_help.proc	Mentat procedure file
s4p_help.proc	Mentat procedure file

6.8 Convergence Automation and Energy Calculations

- Chapter Overview 2008
- Convergence Automation 2008
- Energy Calculation 2015
- Input Files 2025

Chapter Overview

This chapter contains two sections:

- Convergence Automation** introduces a new algorithm for automatically choosing convergence criteria and the new option, AUTO SWITCH. After a brief overview, an example is given to show how this algorithm can be used in Marc.
- Calculation of Energy** summarizes the values for various types of mechanical analysis. An example is given to demonstrate the use of these energy values to check the balance of energy. It is also shown how to plot and view the energy values in Mentat.

Convergence Automation

In nonlinear FEM analysis, it is often necessary to check the convergence based on the relative or absolute tolerance of solution variables. When the convergence testing is done based on relative values of solution variables (*displacements/rotations* and/or *residual forces/moments*), the solution is recognized as converged if the ratio of maximum iterative correction to the maximum increment of solution variable is smaller than the specified tolerance.

However, if maximum displacement increment becomes extremely small, e.g., smaller than the computer's cut-off value a likely scenario in the analysis involving springback or constraint thermal expansion (Table 6.8-1), the convergence testing is less meaningful. In such cases, Marc automatically switches the convergence testing according to *relative residual forces/moments*, if the AUTO SWITCH option is chosen in the convergence control menu of Mentat.

Similarly, if the maximum reaction force/moment becomes extremely small, e.g., smaller the computer's cut-off value a likely scenario in the analysis involving stress-free-motion (i.e., rigid body motion) or free thermal expansion (Table 6.8-1), the convergence testing is less meaningful. In such cases, Marc automatically switches the convergence testing according to *relative displacements/rotations*, if the AUTO SWITCH option is chosen in the convergence control menu of Mentat.

Also, if an analysis involves the cases where the deformable body is totally free of stress and deformation, then Marc checks absolute value of strain energy density and converges if the absolute strain energy density becomes extremely small.

Table 6.8-1 Effectiveness of various Relative Tolerance Convergence Testing Criteria

Analysis Type	Convergence Criteria		
	Displacement/ Rotation	Residual Force/Torque	Strain Energy
Stress-free motion	Yes	No	No
Springback	No	Yes	No
Free Thermal Expansion	Yes	No	No
Constraint Thermal Expansion	No	Yes	Yes
Yes – relative tolerance testing works. No – relative tolerance testing doesn't work.			

This section shows the use of AUTO SWITCH option so that the appropriate convergence type of testing can be performed during the analysis.

AUTO SWITCH Option

This option allows the program to automatically switch on the appropriate convergence testing to address standard as well as special cases.

This example illustrates the use of this feature for a brake-bending of a two-dimensional workpiece and its springback. There is one loadcase each for the *brake-bending* and *springback*. In this analysis, the convergence testing is defined to be done on relative displacement.

Let's start from an existing model and focus on the selection of the convergence testing scheme for analysis of this model:

```
MAIN
FILES
  NEW
  OK
UTILS
  PROCEDURES
  LOAD
    convergence_a.proc
  OK
START/CONT
OK
```

The above procedure creates a model with material/geometry properties and contact/boundary conditions. Now let's define the history data and run this job. There are two loadcases in this job: (1) loadcase1 for *brake bending*, which is defined by procedure A. (2) loadcase2 for *springback* and is defined by procedure B. The commands for both procedure loadcase 1 and 2 are shown below.

Procedure A for Loadcase 1:

```
MAIN
  LOADCASES
    MECHANICAL
      STATIC
        TOTAL LOADCASE TIME
          0.5
```

STEPS
50
CONVERGENCE TESTING
DISPLACEMENTS
RELATIVE DISPLACEMENT TOLERANCE
0.1
OK (twice)

MAIN

Procedure B for Loadcase 2:

MAIN

LOADCASES

MECHANICAL

STATIC

TOTAL LOAD CASE TIME

0.5

STEPS

20

CONVERGENCE TESTING

DISPLACEMENTS

RELATIVE DISPLACEMENT TOLERANCE

0.1

AUTO SWITCH

OK (twice)

MAIN

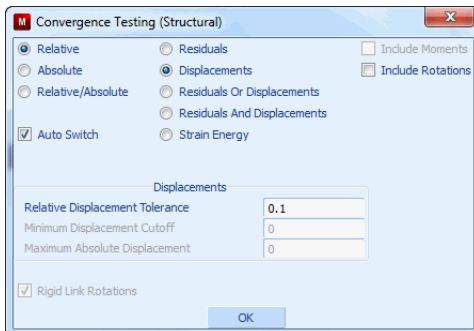


Figure 6.8-1 Select AUTO SWITCH Feature

The Mentat commands of procedure for loadcase2 is also shown in [Figure 6.8-1](#). After defining these two loadcases, we do the analysis with both the draw-bending and springback processes:

```
MAIN
  JOBS
    MECHANICAL
      lcase1 (selecting loadcase 1)
      lcase2 (selecting loadcase 2)
      ANALYSIS OPTIONS
        LARGE DISPLACEMENT
        ADVANCED OPTIONS
          CONSTANT DILATATION
          OK
          under plasticity procedure
          click on SMALL STRAIN to see:
            LARGE STRAIN ADDITIVE
        PLANE STRAIN
      JOB RESULTS
        Equivalent Von Mises Stress
        Total Equivalent Plastic Strain
        OK
      CONTACT CONTROL
        ADVANCED OPTION
          SEPARATION FORCE
            0.1
          OK (thrice)
    ELEMENT TYPE
      MECHANICAL
        PLANE STRAIN
          11
          EXIST.
          OK
  MAIN
    JOBS
      RUN
        SUBMIT 1
```

```
        OUTPUT FILE
        OK
MAIN
```

After the job completes two loadcases, the output file shows the analysis automatically converged based on small strain energy density after increment 55. We can check the results by the following Mentat commands:

```
VISUALIZATION
  COLORS
    2 (colormap)
    6 (contourmap)
    OK
MAIN
  RESULTS
    OPEN DEFAULT
    DEF ONLY
    NEXT
    SCALAR
      Total Equivalent Plastic Strain
    CONTOUR BANDS
    MONITOR
```

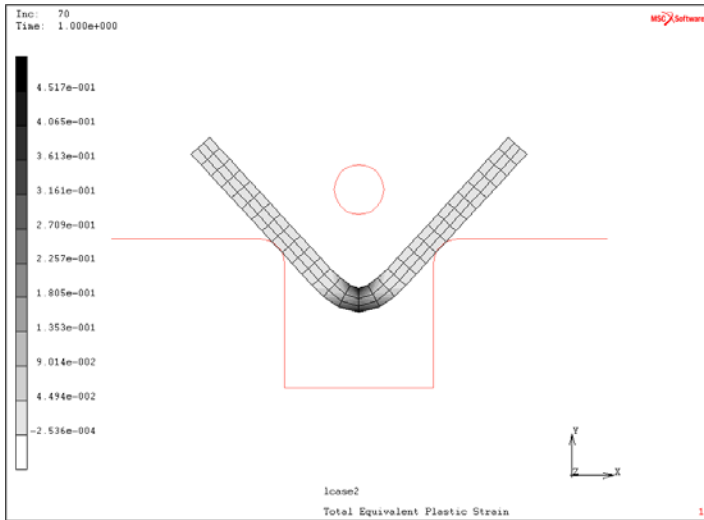


Figure 6.8-2 The Deformed Workpiece and Tools after Springback

Figure 6.8-2 shows the geometry after the springback process. We also see the energy balance between the total strain energy and total work done by external forces using the following Mentat commands:

```

HISTORY
COLLECT GLOBAL DATA
SHOW IDS
    50
NODES/VARIABLES
    ADD GLOBAL CRV                                     (choosing within VARIABLES)
    Time
    Total Strain Energy
    Time
    Total work
FIT
    
```

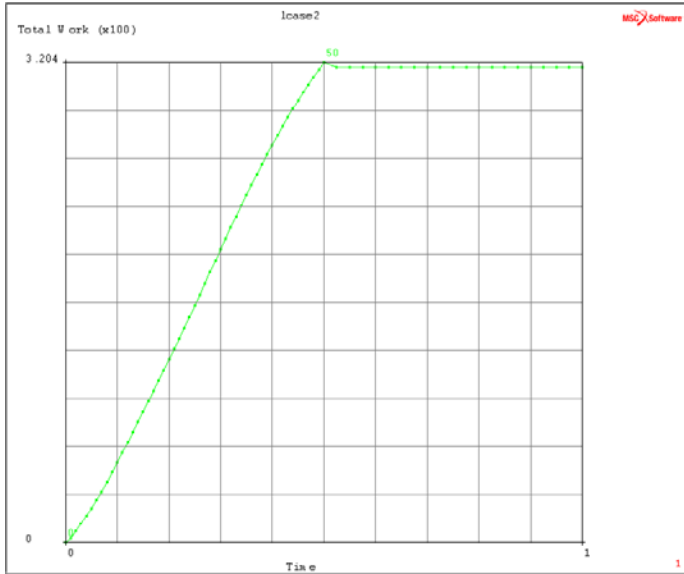


Figure 6.8-3 The Energy Balance of the Draw-bending/Springback Process

As shown in [Figure 6.8-4](#), we can see that most of the elastic strain energy has been released due to springback (from increment 51).

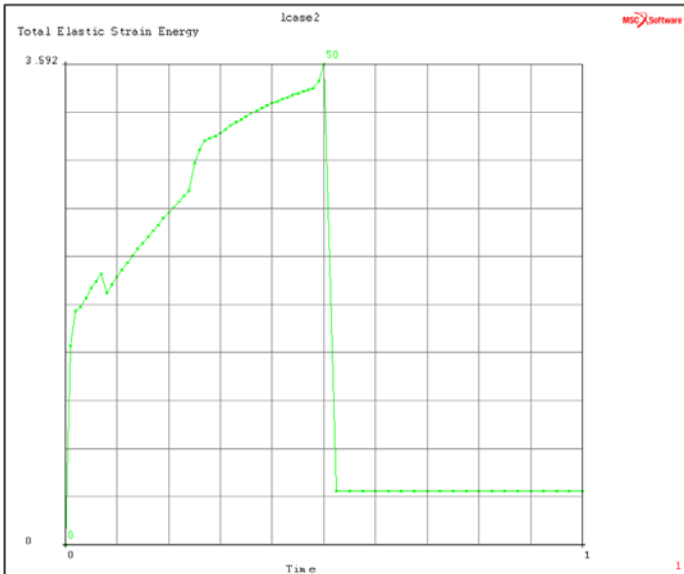


Figure 6.8-4 The Release of Elastic Strain Energy during Springback

Energy Calculation

This feature includes the calculation of energy values for various types of mechanical analysis as listed below:

Total strain energy	(SE)
Total elastic strain energy	(ESE)
Total plastic strain energy	(PSE)
Total creep strain energy	(CSE)
Thermal energy	(ME)
(available for heat transfer or coupled stress/thermal analysis)	
Total work by all external forces	(WE)
Within which various contributions are also calculated as:	
– total work by contact forces	(WC)
– total work by applied forces	(WA)
– total work by friction forces	(WF)
Total kinetic energy	(KE)
Total energy dissipated by dampers	(DE)
Total energy contributed by springs	(ES)
Total energy contributed by foundations	(EF)

Note that damping energy and total work done by friction forces have negative values. In the current implementation, the damping energy is calculated for mass dampers.

For analysis with dynamics, the energy is balanced between the change of kinetic energy and the work done by external forces, excluding the energy dissipated by plastic/creep strain and dampers.

Note: Energy loss is possible for dynamic analysis because of numerical dissipation.

CONSTANT is the kinetic energy at initial time.

$$SE + CSE + KE - DE = WE + CONSTANT \tag{6.8-1}$$

The total work done by external forces should be viewed as:

$$WE = WC + WA + WF \tag{6.8-2}$$

For static analysis, the energy balance can be calculated as:

$$WE = SE + CSE + ES + EF \tag{6.8-3}$$

From equations (6.8-2) and (6.8-3), the energy balance can be calculated by equation (6.8-4):

$$WC + WA + WF - ES - EF = SE + CSE \tag{6.8-4}$$

The energy values mentioned above can be viewed in Mentat. A brief summary is also given in the output file for convenience.

Usage of the Energy Values

We are going to use an example to show the calculation and balance of various energies. This example models the heat generated due to friction for block sliding with an initial velocity and coming to a stop in due time.

As shown in [Figure 6.8-5](#), the block has dimensions of length x width x height = 1.0 m x 1.0 m x 0.5 m, which is modeled with 8 brick elements. Element 7 is used for this analysis. The material of the block is assumed isotropic for both mechanical and thermal analysis. The Young's modulus is 210 GPa and the Poisson's ratio is 0.3. Mass density is given as 7854 kg/m³ for both dynamic and heat transfer analysis. The conductivity is 60.5 W/(m °K) and the specific heat is set as 434 w/(J °K). Only proportional mass damping is applied with a ratio of 0.3. Lumped mass matrix is used in the example. The conversion rate for friction work into thermal energy is given as 1.0.

In order to keep the block sliding on the surface, an acceleration body of -9.81 m/s² is applied to each element along the z-direction. The initial velocity of 4.905 m/s is given along the x-direction. The initial temperature is set as 0.0°C. Coulomb model for friction is chosen with a friction coefficient of 0.5 based on nodal forces. The relative sliding velocity for friction below which a node is assumed to be sticking to a contact surface is set as 0.1 m/s. The nodal reaction force required to separate a contacting node from its contact surface is assumed to be 1x10¹¹N to keep the block on the surface.

The Single Step Houbolt (SSH) method coupled with heat transfer analysis is used for the dynamics analysis.

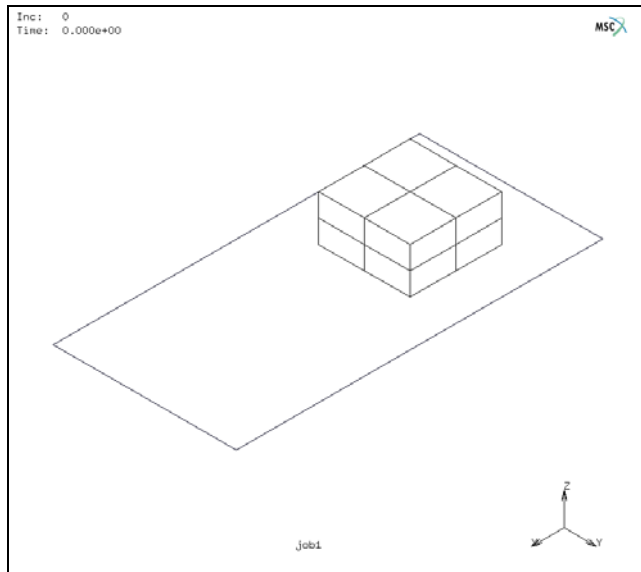


Figure 6.8-5 Initial Geometry and Velocity of the Sliding Block

The procedure `convergence_b.proc` shows the Mentat commands to create this model:

```
MAIN
  FILES
  NEW
  OK
  RESET PROGRAM
  VIEW
    4 (under show all view)
  RESET VIEW
MAIN
  VISUALIZATION
  COLOR
    1 (colormap)
    1 (contourmap)
  OK
MAIN
  MESH GENERATION
  GRID
  ADD (elements)
    point (-1,-1,0)
    point ( 1,-1,0)
    point ( 1, 1,0)
    point (-1, 1,0)
  ADD (SFRS)
    point (-1,-1,0)
    point ( 1,-1,0)
    point ( 1, 1,0)
    point (-1, 1,0)
  MOVE
  SCALE FACTORS
    4 2 1
  SURFACES
  EXIST.
```

```
    RESET
    TRANSLATIONS
      1.8 0 0
    SURFACES
    EXIST.
    RETURN
  SUBDIVIDE
    ELEMENTS
    EXIST.
    RETURN
  EXPAND
    TRANSLATIONS
      0 0 0.5
    ELEMENTS
    EXIST.
    RETURN
  SWEEP
    (remove unused) NODES
    EXIST.
    RETURN
  RENUMBER
    ALL
    RETURN
  FILL
MAIN
  BOUNDARY CONDITIONS
    MECHANICAL
    FIXED DISPLACEMENT
      Y displacement
    OK
    ADD (nodes)
    EXIST.
    NEW
    GLOBAL LOAD
```

Z force
 Z FORCE
 -9.81
 OK
 ADD (elements)
 EXIST.

MAIN

INITIAL CONDITION
 THERMAL
 TEMPERATURE
 temperature (TOP)
 OK
 ADD (nodes)
 EXIST.
 RETURN

NEW

VELOCITY
 X LINEAR
 X LINEAR
 4.905
 OK
 ADD (nodes)
 EXIST.

MAIN

MATERIAL PROPERTIES
 ISOTROPIC
 YOUNG'S MODULUS
 210e9
 POISSON'S RATIO
 0.3
 MASS DENSITY
 7854
 DAMPING
 MASS MATRIX MULTIPLIER
 0.3

```
                OK (twice)
HEAT TRANSFER
  CONDUCTIVITY
    60.5
  SPECIFIC HEAT
    434
  MASS DENSITY
    7854
  OK
  ADD (elements)
  EXIST.
MAIN
  CONTACT
    CONTACT BODIES
      DEFORMABLE
        FRICTION COEFFICIENT
          0.5
        OK
        ADD (elements)
        EXIST.
        NEW
        RIGID
          FRICTION COEFFICIENT
            0.5
          OK
          ADD (surfaces)
          EXIST.
          ID BACKFACES
          ID BACKFACES
```

Until now, the model has been created. Now, we add the loadcase to move the block over the surface and calculate the thermal energy generated from friction:

```
MAIN
  LOADCASES
    MECHANICAL
```

COUPLED
TITLE
 block sliding with friction
 OK
DYNAMIC TRANSIENT
CONVERGENCE TESTING
 DISPLACEMENT
 OK
TOTAL LOADCASE TIME
 2.0
STEPS
 50
 OK

MAIN

JOBS

COUPLED
 "lcase1"
 SOLUTION OPTIONS
 LARGE DISPLACEMENT
 LUMPED MASS & CAPACITY
 OK
JOB RESULTS
 Equivalent Von Mises Stress
 OK
JOB PARAMETERS
 CONVERSION FACTOR
 1.0
 OK
CONTACT CONTROL
 COULOMB
 RELATIVE SLIDING VELOCITY
 0.1
ADVANCED
 SEPARATION FORCE
 1e11
 OK (thrice)

MAIN

JOBS

```
COUPLED
  OK
SUBMIT 1
MONITOR
  OK
MAIN
  VISUALIZATION
    COLORS
      2 (colormap)
      OK
  RESULTS
    OPEN DEFAULT
    DEF ONLY
    SCALAR
      Equivalent Von Mises Stress
    CONTOUR BANDS
```

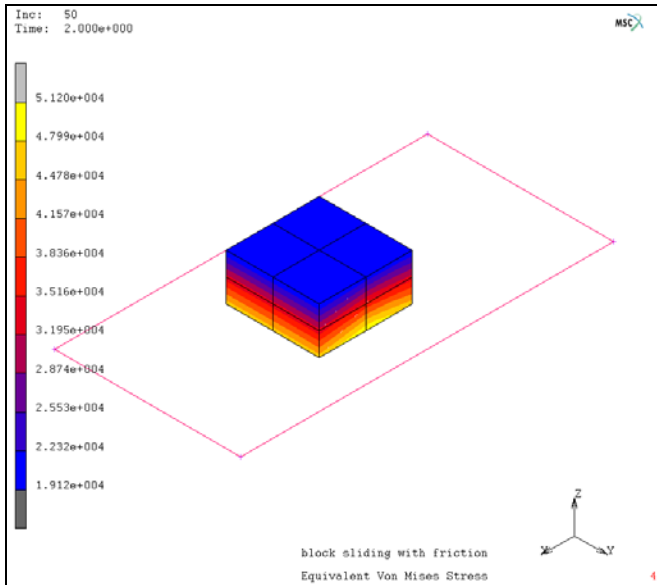


Figure 6.8-6 The Dynamic Analysis of a Block Sliding over a Surface with Friction

From [Figure 6.8-6](#), we can see the stress generated during the sliding process. The following Mentat commands show the energy values and balance during the sliding process.

```

MAIN
  RESULTS
    HISTORY
    SHOW ID
      50
    COLLECT GLOBAL DATA
    NODES/VARIABLES
      ADD GLOBAL CRV
        Time
        Kinetic Energy
        Time
        Damping Energy
        Time
        Total Work
        Time
        Thermal Energy
        Time
        Total work by friction force
    FIT
  
```

(choose from VARIABLES)

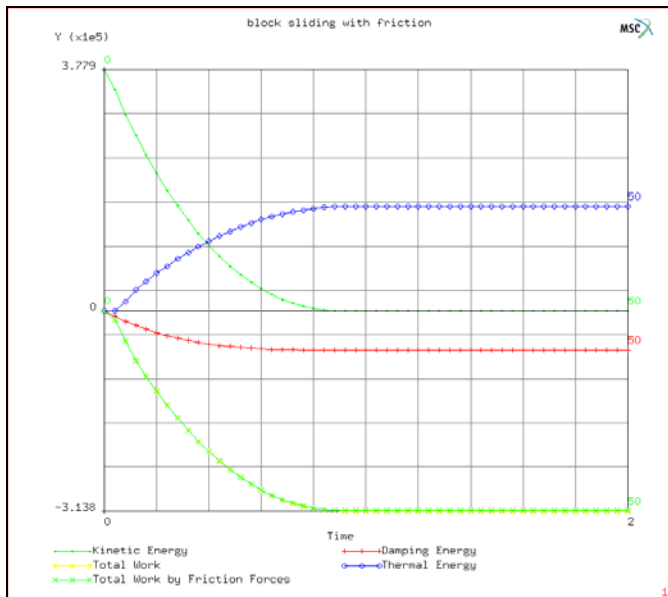


Figure 6.8-7 The Energy changes during the Sliding Process

As shown in [Figure 6.8-7](#), the kinetic energy eventually gets dissipated as damping energy and work done by friction forces. The energy is nearly conserved as shown by equation (6.8-5).

$$SE + KE - DE - WE = \text{CONSTANT} \tag{6.8-5}$$

The energy dissipated due to friction is converted to thermal energy. In this example, it is half of the work done by friction forces, because the conversion factor is given as 1.0 and only half of this is contributed to the deformable body.

In absence of plastic strain, the total strain energy value is the same as the total elastic strain energy ([Figure 6.8-8](#)).

ADD GLOBAL CRV

(choose from VARIABLES)

- Time
- Total Strain Energy
- Time
- Total Elastic Strain Energy

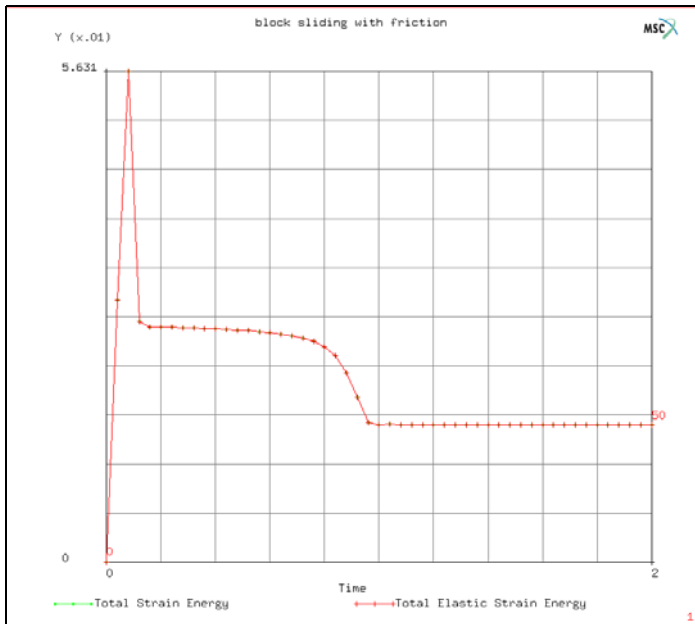


Figure 6.8-8 The Strain Energy generated in the Sliding Block

Input Files

The files below are on your [delivery media](#) or they can be downloaded by your web browser by clicking the links (file names) below.

File	Description
convergence_a.proc	Mentat procedure file
convergence_b.proc	Mentat procedure file

6.9 Capacitors

- Chapter Overview 2028
- Capacitance Computation in Symmetric Multiconductor Systems 2029
- Results and Discussion 2045
- Input Files 2046
- Reference 2046

Chapter Overview

In electromagnetism and electronics, capacitance is the ability of a body to hold an electrical charge. Capacitance is also a measure of the amount of electric charge stored (or separated) for a given electric potential. It is commonly found in electromagnetic fields, which exert some sort of physical force on particles. The force causes the particles to exhibit motion which results in an electric charge.

Electronics use capacitance as a basic component in nearly every facet. Devices known as semiconductors help the flow of electrons through conductors made of nonmetallic materials. They work with other electronic devices, most notably capacitors, to make that flow work to power and control a large amount of components.

Capacitors are the main component that harnesses the electric charge. These are essentially a pair of conductors which contain movable electric charge separated by a dielectric or insulator. In order for an electric field to be present inside the insulator, a difference between the voltages of each conductor must be present. This is known as the potential difference. As the energy is stored, a mechanical force is produced between the conductors. This is most common between flat and narrowly separated conductors.

When two capacitors are placed close together for a period of time, they create an effect known as “stray capacitance.” This means that the electric charge loses some of its signal and begins to leak within the isolated currents. Stray capacitance is detrimental for the proper function of high frequency currents.

A common form of charge storage device is a two-plate capacitor. Capacitance is directly proportional to the surface area of the conductor plates and inversely proportional to the separation distance between the plates. If the charges on the plates are $+Q$ and $-Q$, and V give the voltage between the plates, then the capacitance is given by

$$C = \frac{Q}{V}$$

The capacitance, C , above is also known as self-capacitance. The energy (measured in Joules) stored in a capacitor is equal to the *work* done to charge it. Consider a capacitance C , holding a charge $+q$ on one plate and $-q$ on the other. Moving a small element of charge dq from one plate to the other against the potential difference $V = q/C$ requires the work dW :

$$dW = \frac{q}{C}dq$$

where w is the work measured in Joules, q is the charge measured in Coulombs, and C is the capacitance, measured in Farads.

We can find the energy stored in a capacitance by integrating this equation. Starting with an uncharged capacitance ($q = 0$) and moving charge from one plate to the other until the plates have charge $+Q$ and $-Q$ requires the work w :

$$W_{\text{charging}} = \int_0^Q \frac{q}{C}dq = \frac{1}{2} \frac{Q^2}{C}$$

Self-capacitance must also be used within a number of electrical devices. This occurs by increasing the electrical charge by the amount that is needed to raise the potential by one volt. One way to allow self-capacitance is by placing

a hollow conducting sphere between the conductors. This makes the capacitor regulate itself in regards to electrical charge.

Capacitance is generally considered the inverse of inductance, the concept of resisting a change in current flow. Both phenomena can be measured by substituting the voltage and current number within each equation with the opposite measurement. In the same way, an inductor offsets the function of a capacitor.

The holding of an electric charge is measured in farads. This is the amount of electric charge potential that can change one volt within a capacitor. It also measures the amount of electric charge that can be transported in a single second by a steady current. The SI unit of capacitance is the Farad; 1 Farad = 1 Coulomb per volt.

A problem with more than two conductors is best described by a capacitance matrix that fully predicts the behavior of the problem under different voltage excitations. The capacitance matrix is essentially the measure of charge storage on a singly excited conductor as well as the charge storage on conductor due to excitation of another conductor.

This chapter introduces the procedure for capacitance matrix computation. It also compares the capacitance matrix values with known reference results and briefly describes how the matrix can be used for practical problems. In practical circuits, a number of such capacitors are used as part of the circuit, and the capacitance matrix values are required to calculate the response of the circuit to applied loads.

Computation of capacitance matrix is a special case of electrostatic analysis and is activated in the load cases. It requires the definition of capacitors as contact bodies. Boundary conditions are only required at far field location or on ground objects. The voltage loads on conductors are automatically applied in Marc.

The procedure file to demonstrate this example is called `capac.proc` under `path/examples/marc_ug/s6/c6.9`. The required mud file is `cap_init.mud`.

Capacitance Computation in Symmetric Multiconductor Systems

A capacitor system is made up of three parallel rectangular conductors on a ground plane, for which two symmetry planes exist: $x = 0$ and $y = 0$. Each conductor or capacitor is a rectangular plate of uniform thickness (t) and their rectangular dimensions are equal. The three rectangular plates are placed parallel to the XY plane and a distance (h) above it. The plates extend equally on either side of the YZ plane and adjacent plates are separated by a distance (s).

Figure 6.9-1 shows all geometrical dimensions. They are:

$$l = 20 \mu\text{m}$$

$$w = 5 \mu\text{m}$$

$$t = 0.5 \mu\text{m}$$

$$h = 0.8 \mu\text{m} \text{ and}$$

$$s = 10 \mu\text{m}$$

Vacuum electrical permeability ϵ_0 is assumed everywhere.

In this problem, only far field and ground plane boundary conditions are applied. No applied voltage loads are required. There is only one loadcase with one increment. The number of subincrements = n , where n is the total number of capacitors or conductors. The ground plane or the infinite boundary is not counted as a conductor.

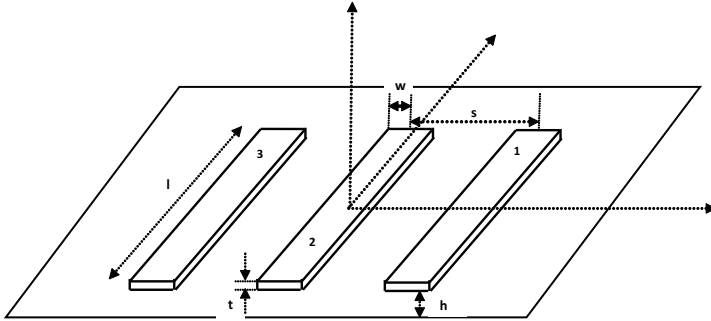


Figure 6.9-1 Three Parallel Rectangular Conductors on a Ground Plane

Each has the same dimensions $l = 20 \mu\text{m}$, $w = 5 \mu\text{m}$, and $t = 0.5 \mu\text{m}$. Adjacent conductors are separated by a distance $s = 10 \mu\text{m}$. The conductors are placed at a distance $h = 0.3 \mu\text{m}$ above the ground plane. All materials in the problem have the same permittivity, that of vacuum = $8.854\text{E-}12$ Farads/m

Mesh Generation

In this problem, there is symmetry about the XZ and YZ planes. Only the symmetry about the XZ plane is used for modeling, since the capacitance matrix is desired for all three conductors. Since the ground plane is considered infinite, it is not required to model below the ground plane. The problem domain above the ground plane extends to infinity, and it is required to consider a large domain above this plane. The problem has to be analyzed in 3-D. The domain is modeled by a mixture of 8-noded hexahedral and 6-noded pentahedral elements. The problem is first modeled in 2-D and then expanded in 3-D.

Element and Node Set Selection

Elements and nodes are grouped in sets for easy definition of material properties and contact bodies and for detailed viewing in post processing. The sets also help in manipulation of the model. In this case, there are four element sets and one nodal set. The element sets are:

1. conductor1
2. conductor2
3. conductor3
4. air

There is one nodal set corresponding to all nodes on the far field boundary. This set is used to define the far field boundary condition. This set is named as:

```
exterior
```

For the initial model, three element sets are created, `conductor1`, `conductor2`, and `air`. The button sequence for creating element sets is:

```
SELECT
ELEMENT STORE
STORE ELEMENTS INTO NEW SET:
conductor1
OK
ZOOM
*zoom_box
*zoom_box(1,0.259868,0.645074,0.429825,0.716599
121 122 123 124 125 126 127 128 129 130 131 132 133 134 135 136 137 138 139 140
141 142 143 144 145 146 147 148 149 150 151 152 153 154 155 156 157 158 159 160
161 162 163 164 165 166 167 168 169 170 171 172 173 174 175 176 177 178 179 180
181 182 183 184 185 186 187 188 189 190 191 192
# | End of List
IDENTIFY
SETS
REGENERATE
RETURN
ELEMENT STORE
STORE ELEMENTS INTO NEW SET:
Conductor2
OK
FILL
ZOOM
*zoom_box
*zoom_box(1,0.101974,0.658570,0.206140,0.716599)
49 50 51 52 53 54 55 56 57 58 59 60 61 62 63 64 65 66 67 68 69 70 71 72 73 74
75 76 77 78 79 80 81 82 83 84
# | End of List
```

```
SELECT SET
  SELECT EXISTING SETS:
    conductor1
    conductor2
  OK
  ELEMENTS STORE
  STORE ELEMENTS INTO NEW SET:
  Air
  OK
  ALL: UNSEL
  SELECT ALL UNSELECTED ELEMENTS:
  CLEAR SELECT
  FILL
  RETURN
RETURN
```

For the initial model, one nodal set is created, exterior. The button sequence for creating the nodal set is:

```
SELECT METHOD
  PATH
  RETURN
  NODES
    1
    1807
    1708
    1635
    723
    # | End of List
  NODES STORE
  STORE ELEMENTS INTO NEW SET:
  Exterior
  OK
  ALL SELEC
  CLEAR SELECT
  RETURN
```


The model is then duplicated about the Y axis and the third element set, `conductor3`, is created. The button sequence is:

```
SELECT
  RESET
  ZOOM
    *zoom_box
    *zoom_box(1,0.360272,0.381107,0.641239,0.612378)
  ELEMENTS
  SELECT THE FOLLOWING ELEMENTS:
    1853 1854 1855 1856 1857 1858 1859 1860 1861 1862 1863 1864 1865 1866 1867 1868
    1869 1870 1871 1872 1873 1874 1875 1876 1877 1878 1879 1880 1881 1882 1883 1884
    1885 1886 1887 1888 1889 1890 1891 1892 1893 1894 1895 1896 1897 1898 1899 1900
    1901 1902 1903 1904 1905 1906 1907 1908 1909 1910 1911 1912 1913 1914 1915 1916
    1917 1918 1919 1920 1921 1922 1923 1924
    # | End of List
  DEL ENTRIES
  SELECT SET
    SELECT EXISTING SET:
      conductor1
    ELEMENTS STORE
    STORE ELEMENTS INTO NEW SET:
      conductor3
    ALL: SELEC
  RETURN
RETURN
```

The model is expanded in three dimensions in front of the XY plane. The region behind the XY plane represents symmetry and is not required to be modeled. The nodes lying in the extreme front represent part of the far field region. These nodes lie on the shifted two dimensional elements and are added to the nodal set (`exterior`). The button sequence is given as:

```
SELECT
  SELECT BY
    NODES ELEM
      SELECT EXISTING ELEMENT SET:
        This is the presently selected element set and consists of the 2-D elements only.
      ALL: SELEC
```

```
RETURN
NODES STORE
  SELECT EXISTING ELEMENT SET:
    Exterior
  OK
  ALL: SELEC
RETURN
CLEAR SELECT
RETURN
```

Material Properties

All objects in this problem have the same value of electric permittivity as vacuum and is = $8.854E-12$ Farads/meter. Two materials are defined: conductor and air. Material properties are specified for all objects using these base materials.

Two materials are defined with the same value of permittivity:

1. Conductor
2. Air

The button sequence for specifying the material properties reads:

```
MATERIAL PROPERTIES
MATERIAL PROPERTIES
ANALYSIS CLASS
  ELECTROSTATIC
    NEW
    STANDARD
    ELECTRIC PERMITTIVITY
      ENTER PERMITTIVITY VALUE
        8.854e-12
    OK
  NAME
  ENTER MATERIAL NAME:
    air
  ELEMENTS ADD
  SELECT EXISTING ELEMENT SET:
```

```
Air
RETURN
NEW
STANDARD
ELECTRIC PERMITTIVITY
  ENTER PERMITTIVITY VALUE
    8.854e-12
OK
NAME
ENTER MATERIAL NAME:
conductor
ELEMENTS ADD
SELECT EXISTING ELEMENT SET:
SELECT SET
  SELECT EXISTING ELEMENT SETS:
    Conductor1
    Conductor2
    Conductor3
OK
RETURN
RETURN
RETURN
RETURN
```

Contact

Elements in the three conductors are defined as three electromagnetic contact bodies:

1. Cond1
2. Cond2
3. Cond3

No properties are required for these contact bodies. A contact table is also not required. The button sequence for specifying the material properties reads:

```
CONTACT
CONTACT BODIES
```

NEW

CREATE NEW CONTACT BODY:

NAME

ENTER CONTACT BODY NAME:

cond1

ELECTROMAGNETIC

USE ELECTROMAGNETIC PROPERTIES:

OK

ELEMENTS ADD

SELECT EXISTING ELEMENT SET:

conductor1

OK

IDENTIFY

IDENTIFY CONTACT BODIES:

NEW

CREATE NEW CONTACT BODY:

NAME

ENTER CONTACT BODY NAME:

cond2

ELECTROMAGNETIC

USE ELECTROMAGNETIC PROPERTIES:

OK

ELEMENTS ADD

SELECT EXISTING ELEMENT SET:

Conductor2

OK

NEW

CREATE NEW CONTACT BODY:

NAME

ENTER CONTACT BODY NAME:

cond2

ELECTROMAGNETIC

USE ELECTROMAGNETIC PROPERTIES:

OK

ELEMENTS ADD

SELECT EXISTING ELEMENT SET:

```
Conductor3
  OK
  RETURN
  RETURN
RETURN
```

Boundary Conditions

A fixed electric potential = 0 volts is applied on all far field and ground plane nodes. No other boundary conditions are required.

The button sequence for specifying the material properties reads:

```
BOUNDARY CONDITIONS
  ANALYSIS TYPE:
  ELECTROSTATIC
  NEW
    CREATE NEW ELECTROSTATIC BOUNDARY CONDITION:
  NAME
    ENTER BOUNDARY CONDITION NAME:
    fix_pot
  FIXED POTENTIAL
    APPLY FIXED POTENTIAL (TOP):
    POTENTIAL (TOP)
    ENTER THE VALUE:
    0
  NODES ADD
    SELECT EXISTING ELEMENT SET:
    Exterior
  OK
  RETURN
RETURN
```

Loadcase and Job Parameters

There is only one loadcase named `capcase`. This is a basic electrostatic analysis repeated three times for computing the capacitance matrix. The electric potential load on each of the conductors is applied internally in the Marc code. Only the far field and ground plane is constrained to zero potential as described above. The steps to describe the loadcase are shown in [Figure 6.9-2](#).

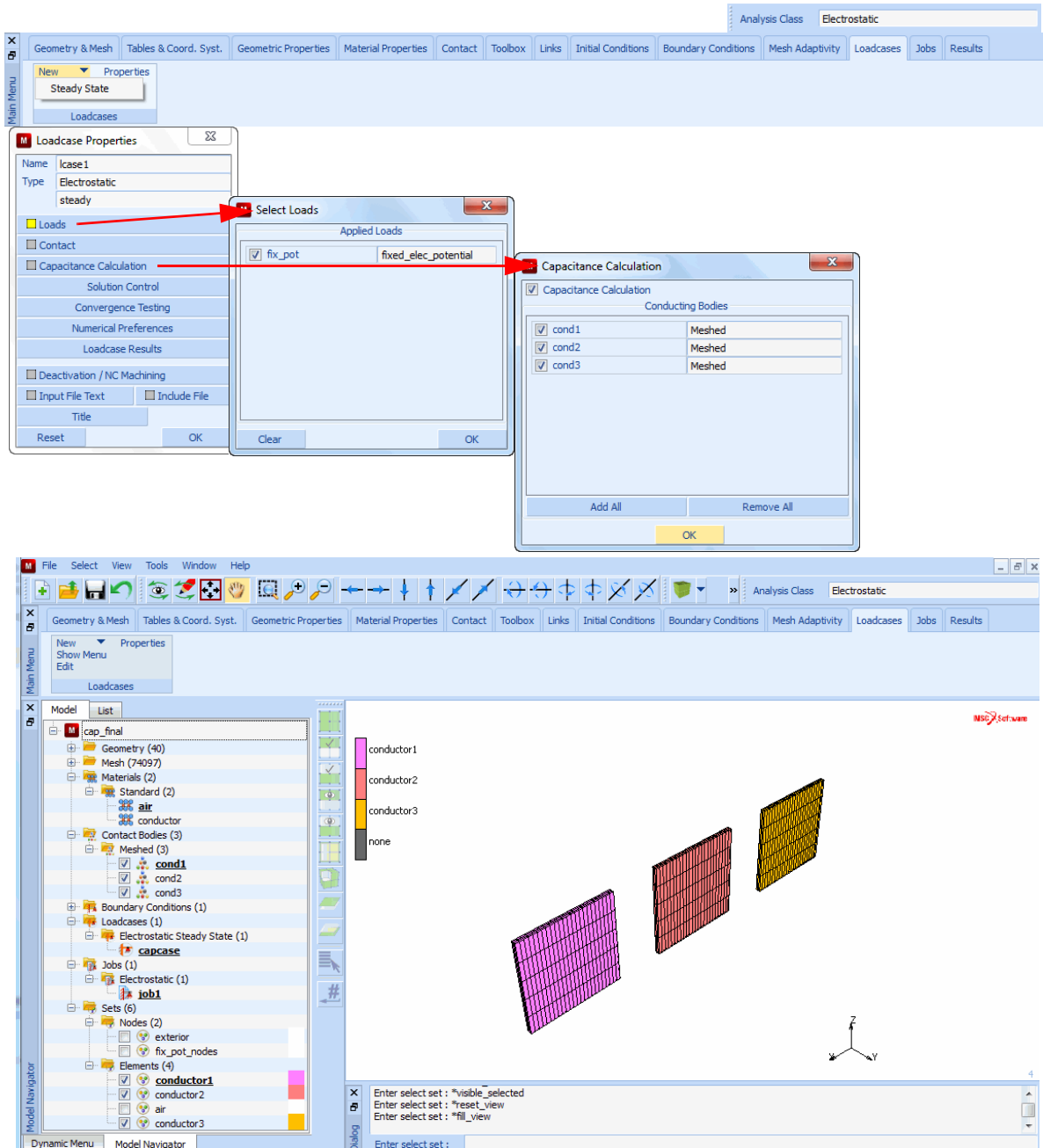


Figure 6.9-2 Steps for showing Button Click to define the Loadcase (capcase)

The button sequence for specifying the material properties reads:

```
LOADCASE
  CREATE NEW LOADCASE:
  NEW
    CREATE NEW LOADCASE TYPE:
    ELECTROSTATIC
      NAME
        ENTER LOADCASE NAME:
        Capcase
      STEADY STATE
        SELECT LOAD
        fix_pot
      OK
      CAPACITANCE CALCULATION
        SELECT CONTACT BODIES FOR CAPACITANCE CALCULATION:
        ADD ALL
        ADD ALL BODIES:
      OK
      OK
    RETURN
  RETURN
RETURN
```

The job specification includes only one loadcase mentioned above. The elemental post processing selected are the X, Y, and Z components of the electric field intensity and the electric flux densities.

The steps to describe the loadcase are shown in [Figure 6.9-3](#).

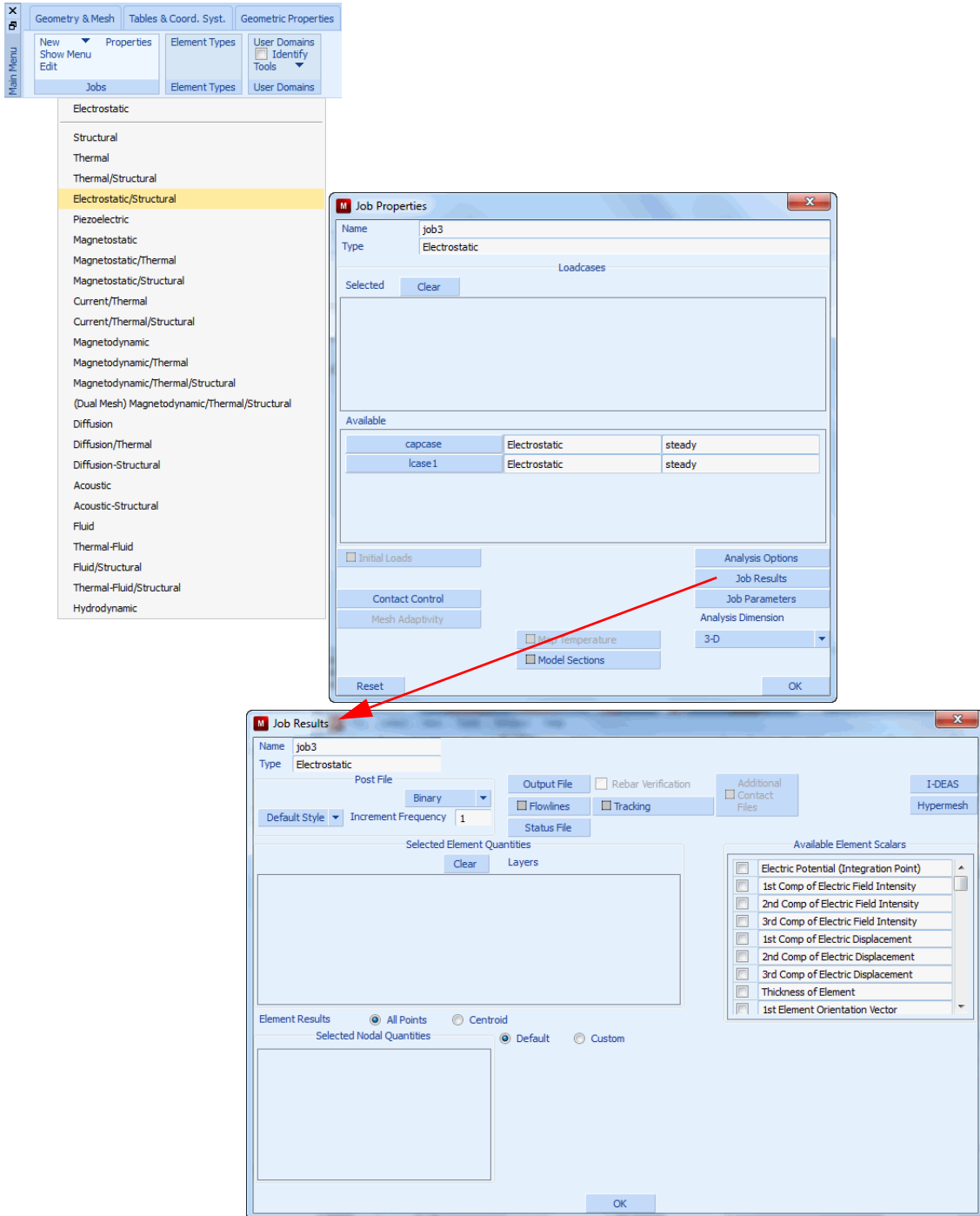


Figure 6.9-3 Steps for showing Button Click to Define the JOB.

The button sequence for specifying the material properties reads:

```
JOBS
  CREATE NEW JOB:
  NEW
    ANALYSIS TYPE: ELECTROSTATIC
    ELECTROSTATIC
    PROPERTIES
      SELECT VARIOUS PROPERTIES:
        SELECT LOAD CASE:
          capcase
        JOB ANALYSIS
        OK
      JOB RESULTS
      SELECT THE VARIOUS ELEMNTAL POST QUANTITIES:
        1st Component of Electric Field Intensity
        2nd Component of Electric Field Intensity
        3rd Component of Electric Field Intensity
        1st Component of Electric Displacement
        2nd Component of Electric Displacement
        3rd Component of Electric Displacement
      OK
    JOB PARAMETERS
    OK
  OK
RETURN
RETURN
```

Save Model, Run Job and View Results

The finite element model is first saved as a mud file, `capcase.mud`.

```
FILE
  SAVE AS
    SAVE MODEL IN FILE:
    Capcase.mud
  OK
```

```
RETURN
JOBS
  RUN
    RUN THIS JOB:
    SUBMIT 1
    MONITOR
  OK
RETURN
RESULTS
  OPEN DEFAULT
  OPEN DEFAULT POST FILE:
RETURN
```

It is desired to view the contour plots for the electric potential for each of the three subincrements. These contours give an idea of how the electric potential load is applied to each conductor. It can also reveal visually detectable errors in the solution.

To see the electric potential contour plots:

```
SCALAR
  Electric Potential
  VIEW ELECTRIC POTENTIAL CONTOURS:
OK
CONTOUR BANDS
```

Now rotate and translate the model so as to see the electric potential contours for subincrement 3. Then use the PLOT settings to get a better picture of the contour plot:

```
PLOT
  NODES
  SET NODE PLOT OFF
  ELEMENTS SETTING
    OUTLINE
    SET ELEMENT PLOT TO OUTLINE:
  REGENERATE
RETURN
RETURN
```

The contour plot for subincrement 3 is shown in [Figure 6.9-4](#).

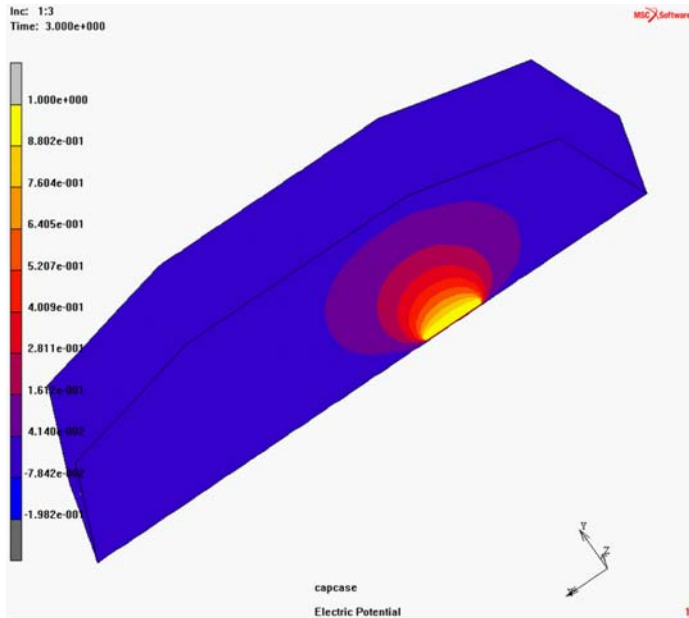


Figure 6.9-4 Electric Potential Distribution for Subincrement 3

The contours are seen wrapped around conductor 3.

To view the contour plots for subincrement 2 and then subincrement 3:

PREV

PREV

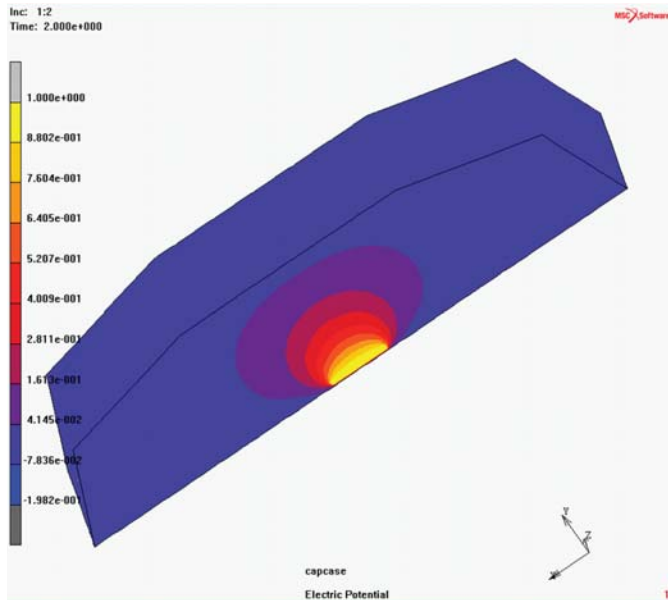


Figure 6.9-5 Electric Potential Distribution for Subincrement 2

The contours are seen wrapped around conductor 2.

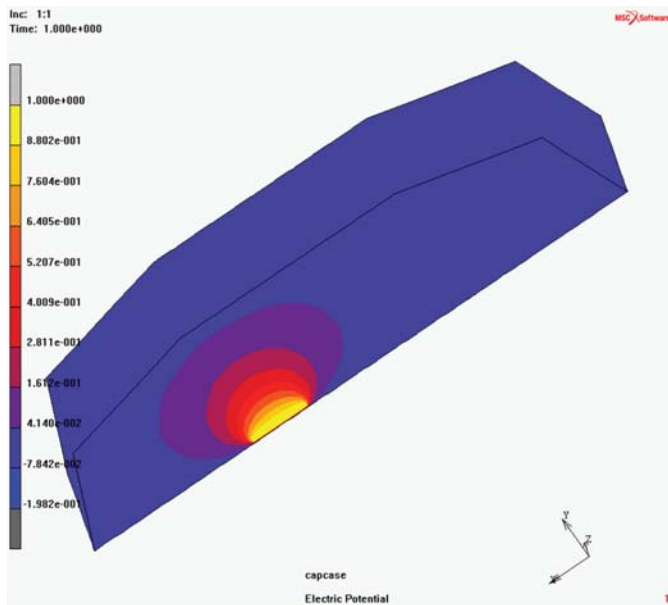


Figure 6.9-6 Electric potential distribution for Subincrement 1.

The contours are seen wrapped around conductor 1.

Results and Discussion

The present problem is referred from [Reference 1](#).

In this reference, the values of the direct capacitance matrix are computed using the boundary element method.

The capacitance matrix is computed by Marc and stored in the `capcase.out` file. These values are shown in [Table 6.9-1](#).

Table 6.9-1 Capacitance Matrix for the Three Conductors in Farads

Column	1	2	3
Row			
1	3.8687E-15	-2.0164E-17	-8.6667E-19
2	-2.0164E-17	3.8771E-15	-2.0164E-17
3	-8.6667E-19	-2.0164E-17	3.8687E-15

The above values apply to the problem with half-symmetry and have to be multiplied by two to get the correct values for the matrix. This is shown in [Table 6.9-2](#).

Table 6.9-2 Capacitance Matrix for the Three Conductors in Farads

Column	1	2	3
Row			
1	7.7374E-15	-4.0328E-17	-1.7333E-18
2	-4.0328E-17	7.7542E-15	-4.0328E-17
3	-1.7333E-18	-4.0328E-17	7.7374E-15

The direct capacitances are given by the expressions:

$$C_{dii} = \sum_{j=1}^3 C_{ij} \text{ and } C_{dij} = -C_{ij}$$

The direct capacitance values are calculated from the above table and are tabulated in [Table 6.9-3](#).

Table 6.9-3 Direct Capacitance Matrix for the Three Conductors in Farads

Column	1	2	3
Row			
1	7.6953E-15	4.0328E-17	1.7333E-18
2	-4.0328E-17	7.6735E-15	4.0328E-17
3	-1.7333E-18	4.0328E-17	7.6953E-15

The first row of the above matrix is compared with the results of the reference above in [Table 6.9-4](#).

Table 6.9-4 Comparison of Direct Capacitance Values for the Three Conductors with the Reference Values (Farads)

	Cd11	Cd12	Cd13
Marc Results	7.69534E-15	4.03280E-17	1.73334E-18
Reference	7.34000E-15	4.60000E-17	3.00000E-18

The direct capacitance value indicates the behavior of a conductor when connected to an electric circuit and this is the value to be used to find the circuit response. This value is the measure of the charge induced on the conductor when it is in the proximity of other conductors and a ground plane (if it exists) and when it is excited by an electric potential. The remaining conductors are grounded.

Input Files

The files below are on your [delivery media](#) or they can be downloaded by your web browser by clicking the links (file names) below.

File	Description
capac.proc	Mentat procedure file
cap_init.mud	Mentat model file

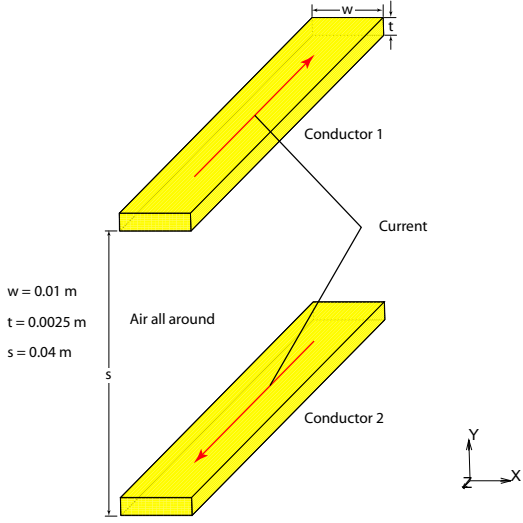
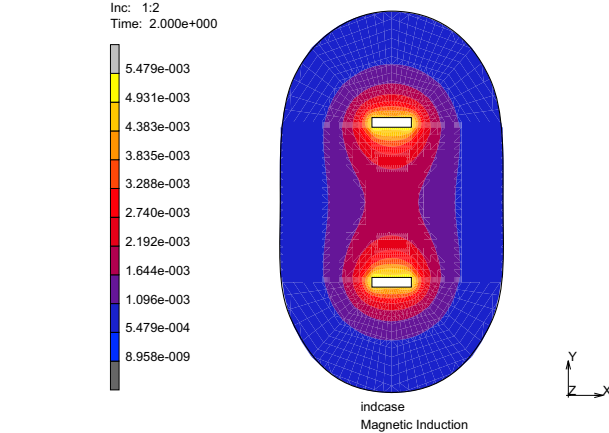
Reference

1. G. Aiello, S. Alfonzetti and S. Coco: "Capacitance Computation in Symmetric Multiconductor Systems", IEEE Transactions ON MAGNETICS, VOL. 30, NO. 5, SEPTEMBER 1994, pp 2952-2955.

6.10 Inductance Between Two Long Conductors

- Summary 2048
- Inductance Computation in Two Infinitely Long Rectangular Conductors 2050
- Results and Discussion 2068
- Input Files 2068
- Reference 2069

Summary

Title	Inductance Between Two Long Conductors
Problem features	Inductance matrix calculation
Geometry	 <p> $w = 0.01 \text{ m}$ $t = 0.0025 \text{ m}$ $s = 0.04 \text{ m}$ </p>
Material properties	Air and conductor have same magnetic permeability of a vacuum.
Analysis type	Magnetostatic
Boundary conditions	Fixed magnetic scalar potential $A_z = 0$ all far field nodes. A current of 100 A applied in opposite directions in the two conductors
Element type	Planar
FE results	<p>Magnetic Induction (outer air and conductor elements removed)</p>  <p> Inc: 1:2 Time: 2.000e+000 </p> <p> 5.479e-003 4.931e-003 4.383e-003 3.835e-003 3.288e-003 2.740e-003 2.192e-003 1.644e-003 1.096e-003 5.479e-004 8.958e-009 </p> <p>indcase Magnetic Induction</p>

Inductance is the property in an electrical circuit where a change in the current flowing through that circuit induces an electromotive force (EMF) that opposes the change in current. In electrical circuits, any electric current i produces a magnetic field and hence generates a total magnetic flux Φ acting on the circuit. This magnetic flux, due to Lenz's law, tends to act to oppose changes in the flux by generating a voltage (a back EMF) that counters or tends to reduce the rate of change in the current.

The quantitative definition of the (self-) inductance of a wire loop in SI units (Webers per ampere) is

$$L = \frac{N\Phi}{i}$$

where Φ denotes the magnetic flux through the area spanned by the loop, and N is the number of wire turns. The flux linkage $\lambda = N\Phi$ thus is

$$N\Phi = Li$$

However, there may be contributions from other circuits. Consider for example two circuits C_1, C_2 , carrying the currents i_1, i_2 . The flux linkages of C_1 and C_2 are given by

$$N_1\Phi_1 = L_{11}i_1 + L_{12}i_2$$

$$N_2\Phi_2 = L_{21}i_1 + L_{22}i_2$$

According to the above definition, L_{11} and L_{22} are the self-inductances of C_1 and C_2 , respectively. It can be shown (see below) that the other two coefficients are equal: $L_{12} = L_{21} = M$, where M is called the mutual inductance of the pair of circuits. The number of turns N_1 and N_2 occur somewhat asymmetrically in the definition above. But actually L_{mn} always is proportional to the product $N_m N_n$, and thus, the total currents $N_m i_m$ contribute to the flux.

Self and mutual inductances also occur in the expression

$$W = \frac{1}{2} \sum_{m,n=1}^K L_{m,n} i_m i_n$$

for the energy of the magnetic field generated by K electrical circuits where i_n is the current in the n th circuit. This equation is an alternative definition of inductance that also applies when the currents are not confined to thin wires so that it is not immediately clear what area is encompassed by the circuit nor how the magnetic flux through the circuit is to be defined.

The definition $L = N\Phi/i$, in contrast, is more direct and more intuitive. It may be shown that the two definitions are equivalent by equating the time derivative of W and the electric power transferred to the system.

An inductor is a passive electronic component that stores energy in the form of a magnetic field. Inductors are used with capacitors in various wireless communications applications. An inductor connected in series or parallel with a capacitor can provide discrimination against unwanted signals. Large inductors are used in the power supplies of electronic equipment of all types, including computers and their peripherals. In these systems, the inductors help to smooth out the rectified utility AC, providing pure, battery-like DC.

The procedure file to demonstrate this example is called `indcase.proc` under:

`path/examples/marc Ug/s6/c6.10`

Inductance Computation in Two Infinitely Long Rectangular Conductors

An inductor system is made up of two infinitely long and parallel rectangular conductors. The conductors are parallel to the Z axis and are symmetrically placed about the XZ and YZ planes. The two conductors carry the same current $I = 100$ Amperes, but in opposite directions. Figure 6.10-1 shows all geometrical dimensions. They are:

$$t = 0.0025 \text{ meters}$$

$$w = 0.01 \text{ meters}$$

$$s = 0.04 \text{ meters}$$

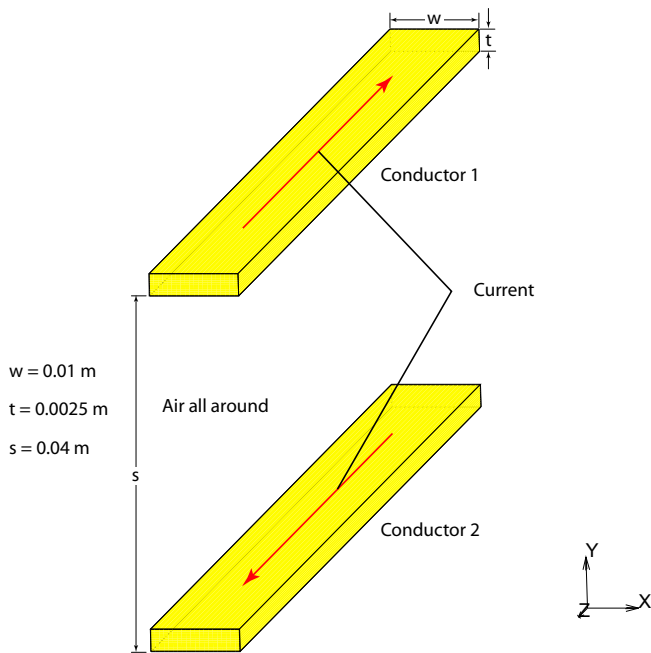


Figure 6.10-1 Two Parallel Infinitely Long Rectangular Conductors

Vacuum magnetic permeability μ_0 is assumed everywhere.

In this problem, the far field and coil current boundary conditions are applied. There is only one loadcase with one increment. The number of subincrements = $n * (n+1) / 2$, where n is the total number of inductors or conductors. In this problem, three new features are introduced for magnetostatic analysis:

- Electrical winding specification
- Coil Current boundary condition
- Inductance matrix computation.

Electrical windings and Coil Current boundary condition

In many electrical problems a magnetic circuit is excited by electrical windings. A winding is a set of multiturn coils. A set of multiturn coils end in two termination points called terminals. Each coil has the same cross-section, that is, with respect to shape and size. Usually, a coil has a rectangular or circular shape. Any other shape is rarely used. Each coil has a thin insulation coating. The multiturns are bound together by some insulation material. The set of multiturn itself defines a cross-section. This is the winding cross-section. A winding cross-section is usually rectangular, sometimes circular. A uniform electric current is assumed to flow through each coil turn. Electrical winding is specified by its cross-section type and cross-section dimensions, number of coil turns, the coil cross-section type and cross-section dimensions and the path it follows along with its orientation. These specifications are applied in the winding sub-menu of modeling tools. The actual coil current and the elements to which it applies are specified in the coil current boundary condition.

Inductance matrix computation

For this computation, the specification of the Electrical windings and Coil Current boundary condition is required. The elements defining the winding in the coil current boundary condition have to be defined as electromagnetic contact bodies. These contact bodies identify the inductors. The inductance matrix computation is activated in the loadcase feature by selecting the required contact bodies for the matrix computation.

As shown in [Figure 6.10-1](#), there are two parallel infinitely long rectangular conductors carrying the same current but in opposite direction. Each has the same dimensions $t = 0.0025$ m, $w = 0.01$ m. Adjacent conductors are separated by a distance $s = 0.04$ m. All materials in the problem have the same permeability, that of vacuum = $1.25664E-06$ Henry/m

Mesh Generation

In this problem, there is symmetry about the XZ and YZ planes. The symmetry about the XZ plane can be used for modeling, but is not used in order to get the correct values in the inductance matrix. The whole problem domain consisting of the two conductors is modeled. The problem domain extends to infinity and it is required to consider a large domain about the conductors. The problem has to be analyzed in 2D, since both conductors are infinite in the Z direction. The domain is modeled by 8 noded hexahedral elements. The problem is first modeled in 2D in the first quarter of the XY plane. Then symmetry is used to duplicate the model in the remaining three quarters.

Element Selection as Sets

The materials in the problem and contact bodies are a set of elements and these sets are selected as a collection of elements in the two conductors and air. The material names for the conductors are:

```
Conductor_1  
Conductor_2
```

Three sets are created for the collection of elements in the three materials. These sets are named as:

```
Cond1  
Cond2  
air
```

The creation of the above sets gives a convenient way of defining materials and contact bodies and also in viewing of post processing results. The basic model contains only `conductor1` and `air` and elements sets are created for these first.

The button sequence for specifying the material properties reads:

```
SELECT  
ELEMENTS  
SELECT NEW ELEMENT SET:  
ZOOM  
    zoom_box(1,0.121711,0.711201,0.214912,0.784076)  
    1 2 3 4 5 6 7 8 9 10 11 12 13 14 15 16 17 18 19 20 21 22 23 24 25  
    26 27 28 29 30 31 32 33 34 35 36 37 38 39 40 41 42 43 44 45 46 47 48  
    49 50 51 52 53 54 55 56 57 58 59 60 61 62 63 64 65 66 67 68 69  
    70 71 72 73 74 75 76 77 78 79 80 81 82 83 84 85 86 87 88 89 90 91  
    92 93 94 95 96 97 98 99 100  
    # | End of List  
ELEMENTS STORE  
    STORE IN NEW ELEMENT SET:  
    cond1  
RETURN  
IDENTIFY SETS  
REGENERATE  
ELEMENTS STORE  
    STORE IN NEW ELEMENT SET:  
    air  
ALL: UNSEL  
ELEMENTS: CLR
```

```
CLEAR ALL ELEMENT SELECTIONS:  
  FILL  
RETURN
```

The boundary of the one-fourth quadrant defines the far field boundary and the nodes on this boundary have a fixed potential of 0 volts. The nodes on this boundary are defined as a set as follows:

```
PLOT  
  NODES  
    SET NODES PLOTTING ON:  
  REGENERATE  
RETURN  
SELECT  
  STORE NODE PATH  
    ENTER NODE SET NAME:  
    Exterior  
    SELECT THE NODES ALONG THE PATH:  
      529  
      976  
      825  
      815  
      # | End of List  
    RETURN  
RETURN
```

The finite element model is then duplicated about the X axis and the `conductor2` is extracted as a set of elements from the duplicated elements.

```
SELECT  
  ELEMENTS  
  SELECT EXISTING SET:  
  Cond1  
  SELECT MODE  
    SELECT INTERSECT MODE:  
    INTERSECT  
  RETURN  
  SELECT METHOD
```

```
SELECT METHOD TYPE:
BOX
ELEMENTS
    Enter Range in X direction: -1 1
    Enter Range in Y direction: -1 0
    Enter Range in Z direction: -1 1
DEL ENTRIES
    REMOVE ABOVE ELEMENTS FROM THE SET cond1:
OK
ELEMENTS STORE
    STORE SELECTED ELEMENTS IN NEW ELEMENT SET:
    Cond2
OK
ALL: SELEC
RETURN
RETURN
```

Material Properties

All objects in this problem have the same value of magnetic permeability as vacuum and is = 1.25664E-06 Henry/meter. But it is desirable to define different material identification for each conductor as well as the surrounding air. This helps in creation of element sets, which are used for creating contact bodies and for viewing results in post processing.

Three materials are defined with the same value of permeability:

```
Conductor_1
Conductor_2
Air
```

The button sequence for specifying the material properties reads:

```
MATERIAL PROPERTIES
MATERIAL PROPERTIES
SET ANALYSIS CLASS:
ANALYSIS CLASS:MAGNETOSTATIC
SET STANDARD MATERIAL:
NEW: STANDARD
NAME
    CREATE NEW MATERIAL NAME:
```

```
    air
MAGNETIC PERMEABILITY
    MU
    SET MAGNETIC PERMEABILITY VALUE:
    1.25664e-6
OK
ELEMENTS ADD
    SELECT EXISTING SET:
    air
# End List
ID MATERIALS
SET STANDARD MATERIAL:
NEW: STANDARD
NAME
    CREATE NEW MATERIAL NAME:
    conductor
MAGNETIC PERMEABILITY
    MU
    SET MAGNETIC PERMEABILITY VALUE:
    1.25664e-6
OK
ELEMENTS ADD
    SELECT EXISTING SET:
    Cond1
    Cond2
# End List
RETURN
RETURN
RETURN
```

Contact

Elements in the two conductors are defined as two electromagnetic contact bodies:

```
Cond1
Cond2
```

No properties are required for these contact bodies. A contact table is also not required.

The button sequence for specifying the material properties reads:

```
CONTACT
  CONTACT BODIES
    NEW
      CREATE NEW CONTACT BODY:
      NAME
        ENTER CONTACT BODY NAME
        Cond1
      ELECTROMAGNETIC
        DEFINE ELECTROMAGNETIC CONTACT BODY:
      OK
      ELEMENTS: ADD
        Cond1
      # End List
    ID CONTACTS
      NEW
        CREATE NEW CONTACT BODY:
        NAME
          ENTER CONTACT BODY NAME
          Cond2
        ELECTROMAGNETIC
          DEFINE ELECTROMAGNETIC CONTACT BODY:
        OK
        ELEMENTS: ADD
          Cond2
        # End List
```

Modeling Tools

The electric current in the rectangular conductors is specified through the winding feature. This is required for the inductance matrix computation. Each rectangle has one turn and its cross-section is given by $w = 0.01 \text{ m}$ and $t = 0.0025 \text{ m}$. The coil, in this case, is the same as the winding and one can use the same specification for the coil or use a circular coil with an appropriate radius. The coil data is not used in the inductance calculation. The winding path and its orientation are specified by a single node each for the 2-D case. The corresponding electromagnetic contact body associated with the winding is selected here. Two windings are defined for the two conductors.

The button sequence for specifying the windings in modeling tools reads:

MODELING TOOLS

WINDINGS

NEW

CREATE NEW WINDINGS:

PROPERTIES

DEFINE WINDING PROPERTIES

CROSS-SECTION: RECTANGULAR

LENGTH

ENTER LENGTH VALUE

.01

WIDTH

ENTER WIDTH VALUE

.0025

COIL:CROSSSECTION: CIRCULAR

RADIUS

ENTER RADIUS VALUE

.0001

CONDUCTOR BODY

SELECT CONTACT BODY:

Cond1

OK

SEGMENTS: ADD

ADD WINDING SEGMENTS:

SELECT OPTION: NODE PATH

CENTERLINE: NODES: ADD

SELECT NODE ID:

1

End List

CROSS-SECTION ORIENTATION: NODES: ADD

SELECT NODE ID:

8

End List

FILL

NEW

CREATE NEW WINDINGS:

PROPERTIES

```
DEFINE WINDING PROPERTIES
CROSS-SECTION: RECTANGULAR
  LENGTH
  ENTER LENGTH VALUE
    .01
  WIDTH
  ENTER WIDTH VALUE
    .0025
COIL:CROSSSECTION: CIRCULAR
  RADIUS
  ENTER RADIUS VALUE
    .0001
CONDUCTOR BODY
  SELECT CONTACT BODY:
    Cond2
OK
SEGMENTS: ADD
  ADD WINDING SEGMENTS:
  SELECT OPTION: NODE PATH
  CENTERLINE: NODES: ADD
  SELECT NODE ID:
    1137
  # End List
  CROSS-SECTION ORIENTNATION: NODES: ADD
  SELECT NODE ID:
    1144
  # End List
SEGMENTS: REVERSE
  REVERSE OPTION IS SET:ON:
```

Boundary Conditions

A fixed magnetic scalar potential($A_z = 0$ volts) is applied on all far field nodes. The coil current boundary condition is used to apply uniform current in both conductors. For this case, the current value and the winding identification path is specified on the appropriate conductor elements.

The button sequence for specifying the boundary conditions reads:

BOUNDARY CONDITIONS

NEW

SELECT: MAGNETOSTATIC ANALYSIS

NAME

ENTER THE FIXED POTENTIAL BOUNDARY CONDITION NAME:

Fix_pot

FIXED POTENTIAL

POTENTIAL

ENTER POTENTIAL VALUE:

0

OK

NODES: ADD

ENTER NODE SET:

exterior

| End of List

NEW

NAME

ENTER THE COIL CURRENT BOUNDARY CONDITION NAME:

wind1

COIL CURRENT

COIL CURRENT

ENTER CURRENT VALUE

100

WINDING PATH

SELECT WINDING PATH:

winding1

OK

ELEMENTS ADD

SELECT EXISTING ELEMENT SET:

Cond1

| End of List

FILL

NEW

NAME

ENTER THE COIL CURRENT BOUNDARY CONDITION NAME:

Wind2

```
COIL CURRENT
  COIL CURRENT
    ENTER CURRENT VALUE
      100
  WINDING PATH
    SELECT WINDING PATH:
      Winding2
  OK
ELEMENTS ADD
  SELECT EXISTING ELEMENT SET:
    Cond2
  # | End of List
RETURN
RETURN
```

Loadcase and Job Parameters

There is only one loadcase named `indcase`. This is a basic magnetostatic analysis repeated three times for computing the inductance matrix. The electric coil current on each of the conductors is modified internally in the Marc code. Only the far field is constrained to zero magnetic potential as described above. The steps to describe the loadcase are shown in Figure 6.10.2.

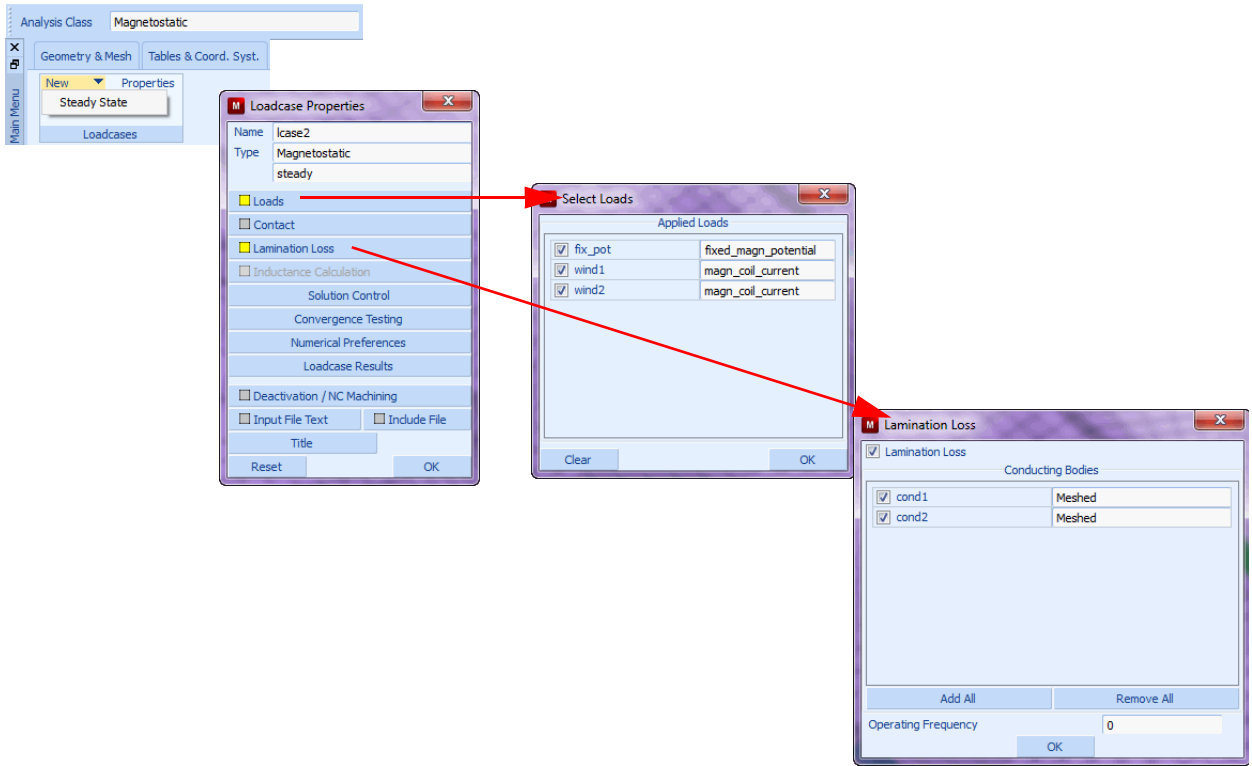


Figure 6.10-2 Steps for Showing Button Click to Define the Loadcase indcase

The button sequence for specifying the material properties reads:

```

LOADCASE
  NEW
    CREATE NEW LOADCASE:
  NAME
    ENTER LOADCASE NAME:
    indcase
  MAGNETOSTATIC
  STEADY STATE
  LOADS
    SELECT LOADS:
    Fix_pot
    Wind1
    Wind2
  
```

```
INDUCTANCE CALCULATION
  INDUCTANCE CALCULATION
    SELECT ALL CONDUCTING BODIES:
      ADD ALL
    OK
  CONVERGENCE TESTING
    ENERGY
    RELATIVE ENERGY TOLERANCE
      0.01
    OK
  OK
RETURN
RETURN
```

The job specification includes only one loadcase mentioned above. The elemental post processing selected are the X and Y components of the magnetic field intensity and the magnetic flux density.

The steps to describe the loadcase are shown in [Figure 6.10-3](#).

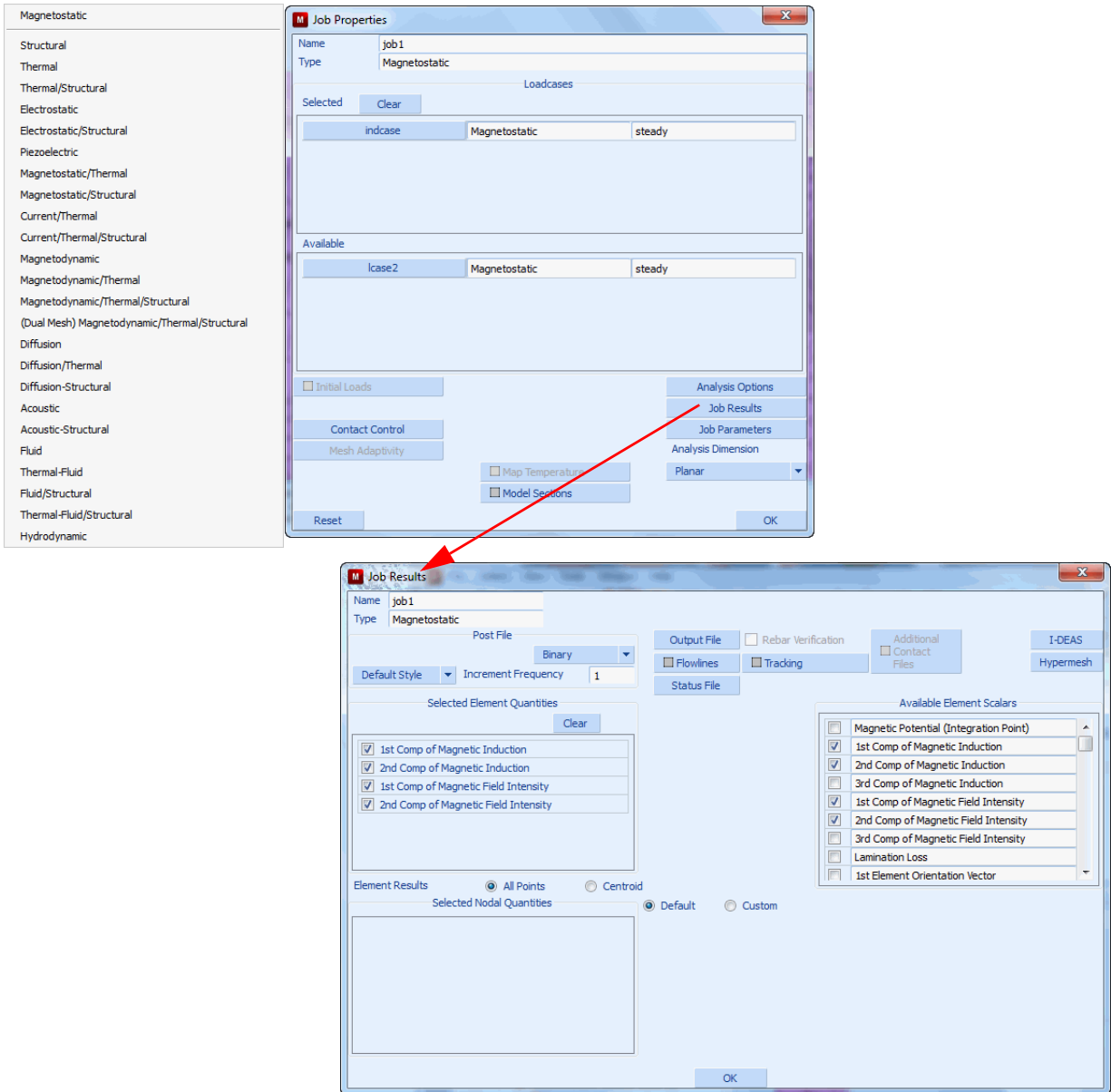


Figure 6.10-3 Steps for Showing Button click to Define the JOB.

The button sequence for specifying the material properties reads:

JOBS
 NEW

```
SELECT ANALYSIS: MAGNETOSTATIC
PROPERTIES
  ADD LOAD CASE:
    indcase
  SELECT JOB: PLANAR
JOB RESULTS
  SELECT THE FOLLOWING QUANTITIES:
    1st Component of Magnetic Induction
    2nd Component of Magnetic Induction
    1st Component of Magnetic Field Intensity
    2nd Component of Magnetic Field Intensity
  OK
OK
RETURN
```

Save Model, Run Job, and View results

The finite element model is first saved as a mud file, indcase.mud.

```
FILE
  SAVE AS
    Ind_final.mud
  OK
RETURN
JOBS
  RUN
    SUBMIT 1
    MONITOR
  OK
RETURN
RESULTS
  OPEN DEFAULT
    *post_open_default
```

It is desired to view the contour plots for the external electric current for each of the three subincrements. These contours give an idea of how the external electric current load is distributed in each conductor. It can also reveal visually detectable errors in the solution.

To see the electric potential contour plots:

```
SCALAR
  External Electric Current
OK
CONTOUR BANDS
```

Observe the external electric current contours for subincrement 3. Then use the PLOT settings to get a better picture of the contour plot:

```
PLOT
  A NODE PLOTTING IS SET OFF:
    NODES
  ELEMENTS SETTING
    OUTLINE
  REGENRATE
RETURN
```

The contour plot for subincrement 3 is shown in [Figure 6.10-4](#).

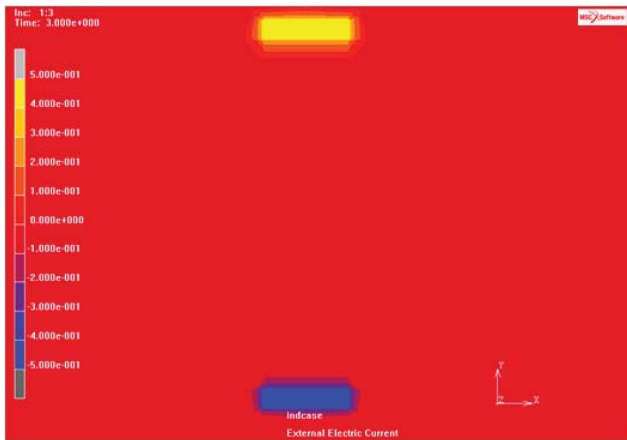


Figure 6.10-4 Electric External Current Distribution for Subincrement 3

To view the contour plots for subincrement 2 and then subincrement 3:

```
PREV
PREV
```

You will observe that the external electric current is same for all three subincrements.

Now, repeat the above steps for magnetic induction contour bands. The plots are shown in:

Figure 6.10-5 The contours are seen wrapped around conductor 2.

Figure 6.10-6 The contours are seen wrapped around both conductors.

Figure 6.10-7 The contours are seen wrapped around conductor 1.

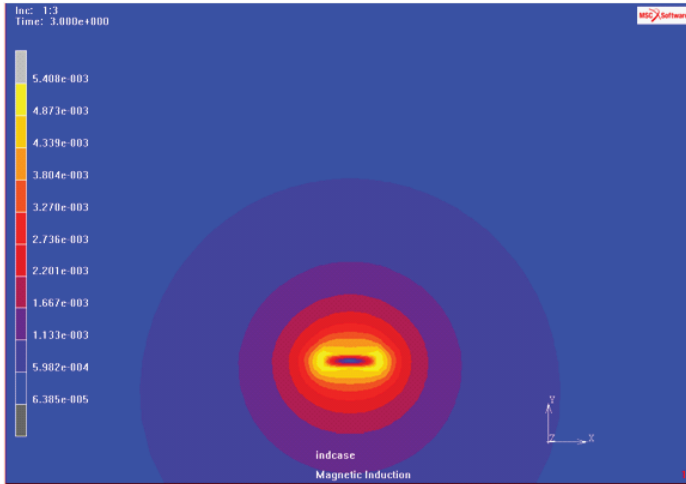


Figure 6.10-5 Magnetic Induction Distribution for Subincrement 3

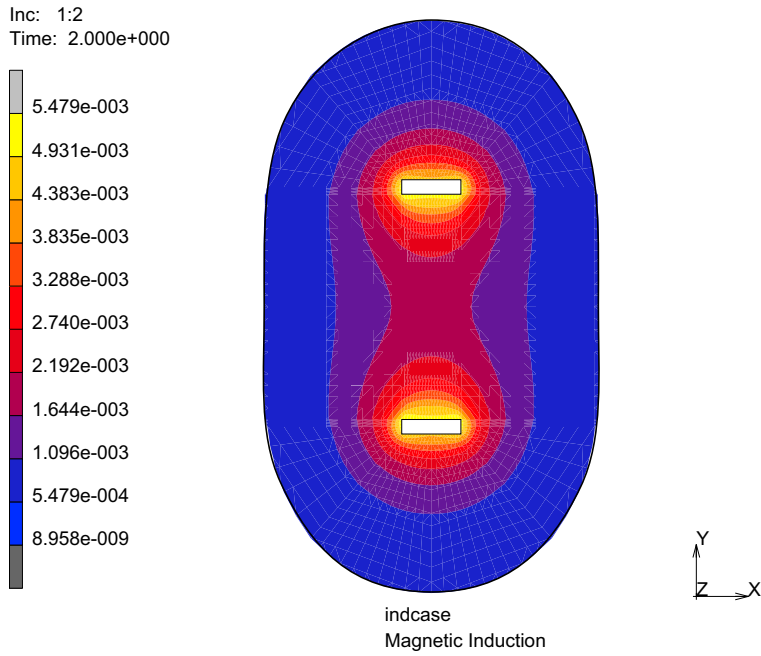


Figure 6.10-6 Magnetic Induction Distribution for Subincrement 2

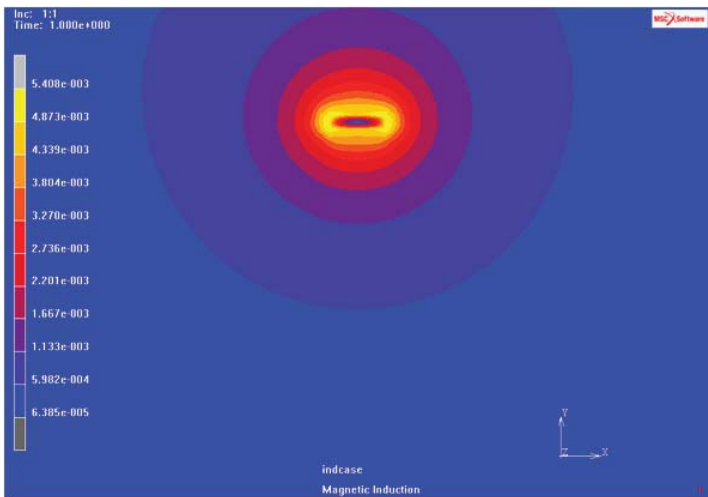


Figure 6.10-7 Magnetic Induction Distribution for Subincrement 1

Results and Discussion

The present problem is referred from [Reference 1](#).

In this reference, the method of direct integration using Maple is used. The following is taken from the reference.

If the rectangular conductor is very thin or $t \rightarrow 0$ and $s > w$, then the inductance $L(t = 0)$ is approximately given by

$$L(t = 0) = \frac{\mu_0}{\pi} \left[\ln \left(\frac{s}{w} + \frac{3}{2} \right) \right] \tag{6.10-1}$$

The total inductance of the two rectangular conductors is given approximately by:

$$L = L(t = 0) - \frac{\mu_0 t}{3w} + \frac{\mu_0}{24\pi} \left[2 \ln \left(\frac{w^2 s^2}{t^2 (w^2 + s^2)} \right) + \frac{25}{3} \right] \left(\frac{t}{w} \right)^2 \tag{6.10-2}$$

The total inductance implies that in the present problem:

$$L = L_{11} + L_{22} - 2L_{12} \tag{6.10-3}$$

Using the dimensions chosen for this problem and the equations (1), (2) and (3), gives

$L = 1.06509E-06$ Henry

The inductance matrix is computed by Marc and stored in the out file: `indcase.out`. These values are shown in [Table 6.10-1](#).

Table 6.10-1 Inductance Matrix for the Two Conductors in Henries

Column	1	2
Rows		
1	6.44382E-07	9.0971E-08
2	9.0971E-08	6.4482E-07

Using the Marc results from the [Table 6.10-1](#), gives

$L = 1.1077E-06$ Henry

Input Files

The files below are on your [delivery media](#) or they can be downloaded by your web browser by clicking the links (file names) below.

File	Description
<code>indcase.proc</code>	Mentat procedure file
<code>ind_init.mud</code>	Mentat model file

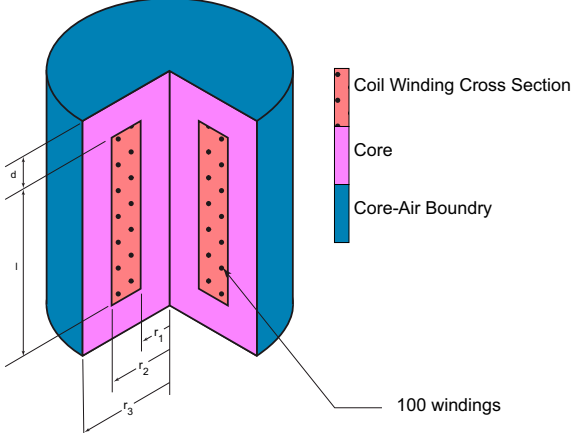
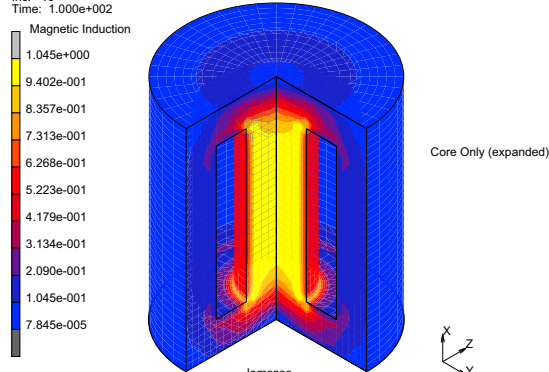
Reference

1. K.F. Goddard, A.A. Roy and J.K. Sykulski: “Inductance and resistance calculations for a pair of rectangular conductors”, IEE Proc.-Sci. Meas. Technol., Vol. 152, No. 2, March 2005, pp 73-78.

6.11 Lamination Loss in Magnetostatic-Thermal coupling

- Summary 2072
- Lamination Loss Computation and ohmic Winding Loss in a 'C' Core Cylindrical Inductor 2073
- Results and Discussion 2095
- Input Files 2096

Summary

Title	Lamination loss in magnetostatic-thermal coupling
Problem features	“C” core cylindrical inductor
Geometry	 <p> $d = 0.02 \text{ m}$ $l = 0.1 \text{ m}$ $r_1 = 0.02 \text{ m}$ $r_2 = 0.04 \text{ m}$ $r_3 = 0.06 \text{ m}$ </p> <p>100 windings</p>
Material properties	Typical properties of the air, core, and winding along with lamination loss data are used herein.
Analysis type	Magnetostatic-Thermal
Boundary conditions	The outer boundary of the air has a fixed magnetic potential of 0. Each coil, radius of $1 \times 10^{-5} \text{ m}$ with a current of 2 A, is wound 100 times in the circumferential direction. The windings span the rectangular cross section shown above.
Initial conditions	$T = 30^\circ\text{C}$ at all nodes
Element type	Planar axisymmetric
FE results	<p>Magnetic Induction</p> <p>Inc: 10 Time: 1.000e+002</p>  <p>Core Only (expanded)</p> <p>lamcase</p>

Core loss in a magnetic material occurs when the material is subjected to a time varying magnetic flux. The actual physical nature of this loss is still not completely understood and a simplistic explanation of this complex mechanism is as follows. Energy is used to effect “magnetic domain wall motion” as the domains grow and rotate under the influence of an externally applied magnetic field. When the external field is reduced or reversed from a given value, domain wall motion again occurs to realize the necessary alignment of domains with the new value of the magnetic field. The energy associated with domain wall motion is irreversible and manifests itself as heat within the magnetic material. The rate at which the external field is changed has a strong influence upon the magnitude of the loss, and the loss is generally proportional to some function of the frequency of variation of the magnetic field. The metallurgical structure of the magnetic material, including its electrical conductivity, also has a profound effect upon the magnitude of the loss. In electrical machines, this loss is generally termed the core loss.

The core loss contains three components: hysteresis loss, eddy loss, and extra loss. The extra loss clubs together all losses not accounted by hysteresis and eddy losses and contains higher order harmonic losses.

The statistical loss theory provides the best method to compute the core loss accurately. Please see *Marc Volume A: Theory and User Information* for details.

Practicing engineers would like to know the core losses as accurately as possible, since they are important for analysis of large electrical machinery and transformers. Prediction of these losses and their location in the device is useful in design. Even a small percentage reduction of loss amounts to huge savings.

The computation of these losses assumes the availability of lamination loss curves. These curves are provided by the manufacturers of the magnetic lamination sheets. The manufacturers obtain the curve data by actual measurements at different frequencies and magnetic induction values. The data is expressed as a series of curves, one each for a single operational frequency. Each curve shows the variation of power loss per unit volume with the magnetic induction B . To use these curves, the user has to extract sufficient number of data points from these curves. For each curve, the user should write down the power loss with respect to the magnetic induction B . This has to be repeated for different frequencies. The whole data must be put into table format as it has to be entered as a table in Mentat. Mentat can also read a preformatted data file that contains the tabulated data points. In this example, a preformatted data file is used.

The procedure file to demonstrate this example is called `lamcase.proc` under `path/examples/marc Ug/s6/c6.11`. The procedure requires an initial mud file, `lam_init.mud`.

Lamination Loss Computation and ohmic Winding Loss in a ‘C’ Core Cylindrical Inductor

A cylindrical inductor is made in ‘C’ shape. The inductor is like a coaxial cable made of magnetic lamination material. The inner core is a solid cylinder and the outer core is a cylindrical shell made from laminations. Both sides of this structure are capped on both sides by two cylindrical disks and made from the same lamination material. The space between the inner and outer cylinder is occupied by current carrying winding coils. The winding is made of 100 turns and each coil carries a current of 2.0 Amperes. The initial temperature throughout the domain is 30 Celsius and is valid just before the current application. This is an axisymmetric problem about the cylindrical axis.

Figure 6.11-1 shows all geometrical dimensions. They are:

- $l = 0.1$ meters
- $d = 0.02$ meters
- $r_1 = 0.02$ meters
- $r_2 = 0.04$ meters
- $r_3 = 0.06$ meters

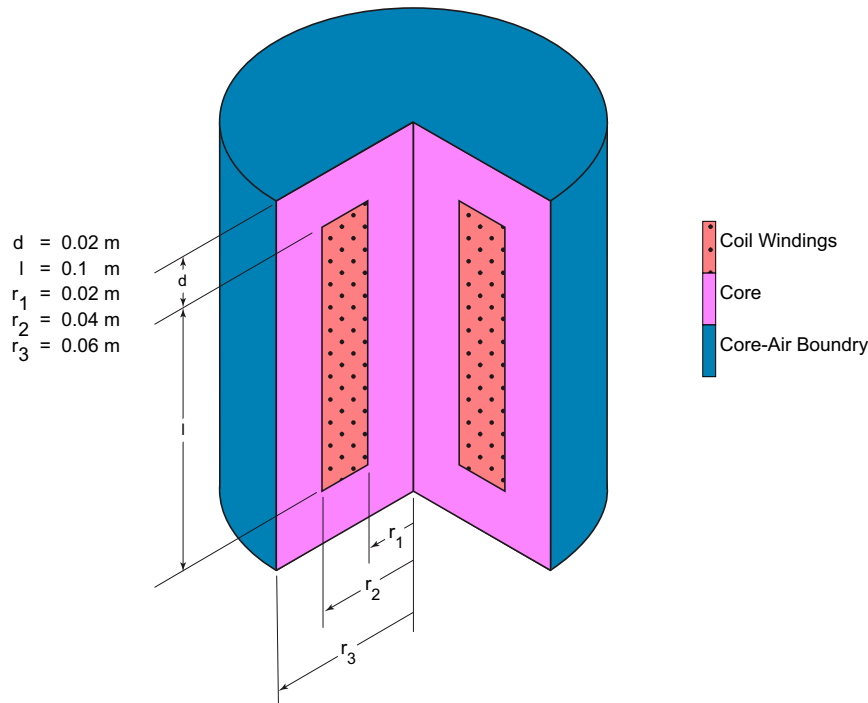


Figure 6.11-1 Cylindrical 'C' Core Inductor with a Quarter Cut in the Inductor

The winding completely fills the gap in the magnetic core. The various dimensions are shown in Figure 6.11-1. The core is made of magnetic lamination held in place by a suitable mechanism. The winding consists of a coil of 100 turns.

There are three objects/materials in this problem: air, magnetic core, and winding. The winding actually contains conductor like copper and insulation material. The insulation material is very thin and can be neglected. The magnetic core is made of lamination sheets held in place by some mechanism. The lamination sheets are coated with some insulation, which is neglected as it is very thin. In effect, there are three materials: air, core, and winding (conductor).

The material properties of the three materials are given below:

1. Air
 - a. Thermal
Thermal conductivity: $K = 0.1 \text{ Watts}/(\text{meter-Kelvin})$
Specific Heat: $C = 900.0 \text{ Joules}/(\text{kg-Kelvin})$
Mass density: $\rho = 1000.0 \text{ kg}/(\text{cu. Meter})$
 - b. Electrical
Magnetic permeability $\mu = 1.25664\text{E-}06 \text{ Henry}/\text{meter}$
Electric conductivity $\sigma = 0 \text{ Siemens}/\text{meter}$
2. Core
 - a. Thermal
Thermal conductivity: $K = 10.0 \text{ Watts}/(\text{meter-Kelvin})$
Specific Heat: $C = 100.0 \text{ Joules}/(\text{kg-Kelvin})$
Mass density: $\rho = 7000.0 \text{ kg}/(\text{cu. Meter})$
 - b. Electrical
Magnetic permeability $\mu = 0.01 \text{ Henry}/\text{meter}$
Electric conductivity $\sigma = 1.0\text{E+}08 \text{ Siemens}/\text{meter}$
3. Winding
 - a. Thermal
Thermal conductivity: $K = 0.2 \text{ Watts}/(\text{meter-Kelvin})$
Specific Heat: $C = 600.0 \text{ Joules}/(\text{kg-Kelvin})$
Mass density: $\rho = 3000.0 \text{ kg}/(\text{cu. Meter})$
 - b. Electrical
Magnetic permeability $\mu = 1.25664\text{E-}06 \text{ Henry}/\text{meter}$
Electric conductivity $\sigma = 5.0\text{E+}05 \text{ Siemens}/\text{meter}$

In this problem, the far field and coil current boundary condition is applied. There is only one loadcase with 10 increments corresponding to transient thermal analysis. In this problem, four new features are introduced:

- Electrical winding specification
- Coil Current boundary condition
- Lamination loss computation.
- Coupled Magnetostatic-thermal analysis

Electrical windings and Coil Current boundary condition

In many electrical problems, a magnetic circuit is excited by electrical windings. A winding is a set of multiturn coils. A set of multiturn coils end in two termination points called terminals. Each coil has the same cross section, that is,

with respect to shape and size. Usually, a coil has a rectangular or circular shape. Any other shape is rarely used. Each coil has a thin insulation coating. The multitrans are bound together by some insulation material. The set of multitrans itself defines a cross section. This is the winding cross-section. A winding cross-section is usually rectangular; however, sometimes it is circular. A uniform electric current is assumed to flow through each coil turn. Electrical winding is specified by its cross-section type and cross-section dimensions, number of coil turns, the coil cross-section type and cross-section dimensions and the path it follows along with its orientation. These specifications are applied in the winding submenu of modeling tools. The actual coil current and the elements to which it applies are specified in the coil current boundary condition.

Lamination loss computation

For this computation, the lamination loss curve is required. The loss curve is, in fact, a set of curves showing the variation of the lamination power loss with the magnetic induction B . Each curve corresponds to a particular operating frequency. The set of curves used in this problem are shown in Figure 6.11-2, where the each data point has a multiplying factor of 7.0. The curves give the power loss density for different values of the magnetic induction B and frequency f . Sufficient data points are extracted from the set of curves and input as a table. This data is then entered as a Mentat table. The tabular data extracted from the curves is shown in Table 6.11-1. It is assumed that the device is operating at a frequency $f = 25$ Hertz. The elements defining the core laminations have to be defined as an electromagnetic contact body. This contact body identifies the laminations. The data in the table is used to extract loss coefficients, which are then used to find the elemental lamination loss depending on the value of the operational frequency and the elemental value of magnetic induction B .

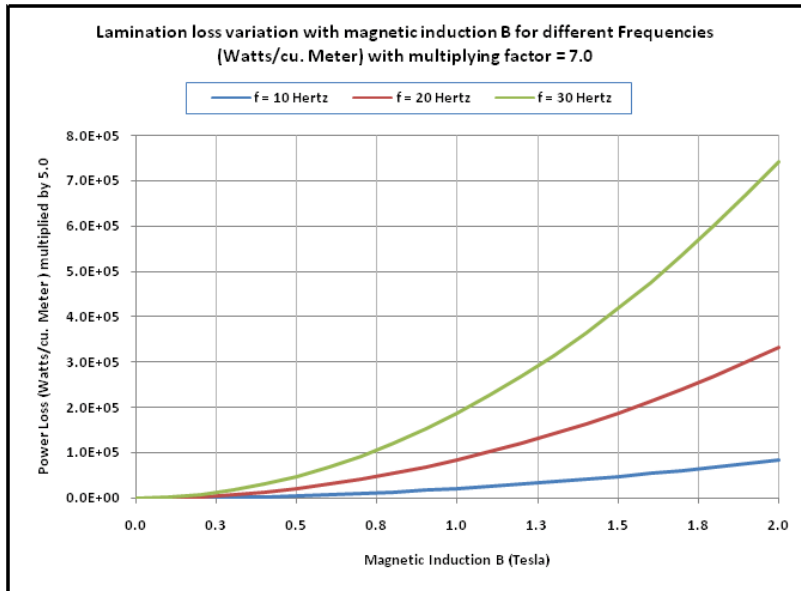


Figure 6.11-2 Specified Lamination Loss Curves

Table 6.11-1 Lamination Loss Data Extracted from the Loss Curves of Figure 6.11-2

Lamination Power Loss in Watts/Cubic Metters Multiplied by 7.0			
Magnetic Induction B (Tesla)	Frequency = 10 Hz	Frequency = 20 Hz	Frequency = 30 Hz
0.0	0.00	0.00	0.00
0.1	288.06	1005.11	2141.04
0.2	1003.41	3688.82	8027.63
0.3	2137.15	8024.96	17610.86
0.4	3686.41	14004.78	30874.15
0.5	5649.68	21623.53	47808.42
0.6	8026.11	30878.35	68408.00
0.7	10815.19	41767.37	92669.13
0.8	14016.68	54289.44	120589.30
0.9	17630.52	68443.90	152166.91
1.0	21656.80	84230.50	187401.09
1.1	26095.76	101649.33	226291.54
1.2	30947.77	120700.84	268838.54
1.3	36213.35	141385.75	315042.88
1.4	41893.14	163705.13	364905.88
1.5	47987.97	187660.40	418429.39
1.6	54498.83	213253.33	475615.86
1.7	61426.89	240486.12	536468.38
1.8	68773.58	269361.44	600990.77
1.9	76540.58	299882.50	669187.66
2.0	84729.86	332053.12	741064.64

Coupled magnetostatic-thermal analysis

The current flowing in the winding coils produce ohmic heat and the lamination losses also produce heat called lamination loss. The magnetostatic analysis is first carried out and the heat generated due to these sources is calculated. Both these generated heats are next used in the coupled thermal analysis to calculate the temperature distribution.

Mesh Generation

In this problem, there is an axisymmetry about the axis of the cylindrical inductor. This fact is used to create a two dimensional axisymmetric finite element model. An axial cross section of the inductor is taken and only one half of the section above the axis is modeled. The problem domain extends to infinity and it is required to consider a large air

domain about the inductor. The problem has to be analyzed as a 2-D, axisymmetric problem.. The domain is modeled by 4-noded quadrilateral elements. The element type 40 is used. The problem is first modeled in 2-D in the first quarter of the XY plane. Then symmetry is used to duplicate the model about the Y axis.

Element selection as Sets

The materials in the problem and contact bodies are a set of elements and these sets are selected as a collection of elements in the objects air, core and winding. The material names for these objects are:

```
Air  
Core  
Winding
```

Three sets are created for the collection of elements in the three materials. These sets are named as:

```
air  
core  
windings
```

The creation of the above sets gives a convenient way of defining materials and contact bodies and also in viewing of post processing results.

The button sequence for specifying the element sets reads:

```
SELECT  
ELEMENTS  
1 SELECT NEW ELEMENT SET:  
ZOOM  
zoom_box(1,0.215420,0.807504,0.323129,0.939641)  
ELEMENTS STORE  
STORE IN NEW ELEMENT SET:  
core  
1 2 3 4 5 6 7 8 9 10 11 12 13 14 15 16 17 18 19 20 21 22 23 24 25 26 27 28 29  
30 31 32 33 34 35 36 37 38 39 40 41 42 43 44 45 46 47 48 49 50 51 52 53 54 55  
56 57 58 59 60 61 62 63 64 65 66 67 68 69 70 71 72 73 74 75 76 77 78 79 80 81  
82 83 84 85 86 87 88 89 90 91 92 93 94 95 96 97 98 99 100 101 102 103 104 105  
106 107 108 109 110 111 112 113 114 115 116 117 118 119 120 121 122 123 124 125  
126 127 128 129 130 131 132 133 134 135 136 137 138 139 140 141 142 143 144 145  
146 147 148 149 150 151 152 153 154 155 156 157 158 159 160 161 162 163 164 165  
166 167 168 169 170 171 172 173 174 175 176 177 178 179 180 181 182 183 184 185  
186 187 188 189 190 191 192 193 194 195 196 197 198 199 200 201 202 203 204 205  
206 207 208 209 210 211 212 213 214 215 216 217 218 219 220 221  
# | End of List  
RETURN
```

```
IDENTIFY SETS
REGENERATE
SELECT SETS
  Core
OK
SELECT MODE: INTERSECT
RETURN
ELEMENTS SELECT
  61 62 63 64 65 66 67 68 69 70 71 72 73 74 75 76 77 78 79 80 81 82 83 84 85 86
  87 88 89 90 91 92 93 94 95 96 97 98 99 100 101 102 103 104 105 106 107 108
# | End of List
DEL ENTRIES
SELECT SET
  Core
OK
ALL: SELEC
ELEMENTS STORE
STORE IN NEW ELEMENT SET:
  windings
ALL: SELEC
ELEMENTS: CLR
  CLEAR ALL ELEMENT SELECTIONS:
FILL
SELECT SET
  Core
  Windings
OK
ELEMENTS STORE
STORE IN NEW ELEMENT SET:
  air
ALL: UNSEL
RETURN
```

The boundary of the one-fourth quadrant defines the far field boundary and the nodes on this boundary have a fixed magnetic potential of 0 volts. The nodes on this boundary are defined as a set as follows:

```
PLOT
  NODES
    SET NODES PLOTTING ON:
  REGENERATE
RETURN
SELECT
  STORE NODE PATH
    ENTER NODE SET NAME:
    Far_field
    SELECT THE NODES ALONG THE PATH:
      980
      824
      668
      330
      642
    # | End of List
  RETURN
RETURN
```

Material Properties

There are three materials in this problem: air, core, and windings. Define three materials for them and enter the material properties as detailed in the problem definition.

The button sequence for specifying the material properties reads:

```
MATERIAL PROPERTIES
  MATERIAL PROPERTIES
    SET ANALYSIS CLASS:
    ANALYSIS CLASS:MAGNETOSTATIC-THERMAL
    SET STANDARD MATERIAL:
    NEW: STANDARD
    NAME
      CREATE NEW MATERIAL NAME:
        air
```


THERMAL

K

SET THERMAL CONDUCTIVITY VALUE:

0.1

SPECIFIC HEAT

SET SPECIFIC HEAT VALUE:

900.0

MASS DENSITY: THERMAL

SET MASS DENSITY VALUE:

1000.0

OK

MAGNETIC PERMEABILITY

MU

SET MAGNETIC PERMEABILITY VALUE:

1.25664e-6

OK

ELECTRIC CONDUCTIVITY

SIGMA

SET ELECTRIC CONDUCTIVITY VALUE:

0.0

OK

ELEMENTS ADD

SELECT EXISTING SET:

air

End List

ID MATERIALS

SET STANDARD MATERIAL:

NEW: STANDARD

NAME

CREATE NEW MATERIAL NAME:

core

THERMAL

K

SET THERMAL CONDUCTIVITY VALUE:

10.0

SPECIFIC HEAT

SET SPECIFIC HEAT VALUE:

100.0

MASS DENSITY: THERMAL

SET MASS DENSITY VALUE:

7000.0

OK

MAGNETIC PERMEABILITY

MU

SET MAGNETIC PERMEABILITY VALUE:

0.01

OK

ELECTRIC CONDUCTIVITY

SIGMA

SET ELECTRIC CONDUCTIVITY VALUE:

1.0E+08

OK

ELEMENTS ADD

SELECT EXISTING SET:

core

End List

SET STANDARD MATERIAL:

NEW: STANDARD

NAME

CREATE NEW MATERIAL NAME:

winding

THERMAL

K

SET THERMAL CONDUCTIVITY VALUE:

0.2

SPECIFIC HEAT

SET SPECIFIC HEAT VALUE:

600.0

MASS DENSITY: THERMAL

```
      SET MASS DENSITY VALUE:
        3000.0
    OK
    MAGNETIC PERMEABILITY
      MU
      SET MAGNETIC PERMEABILITY VALUE:
        1.25664e-6
    OK
    ELECTRIC CONDUCTIVITY
      SIGMA
      SET ELECTRIC CONDUCTIVITY VALUE:
        5.0E+05
    OK
    ELEMENTS ADD
      SELECT EXISTING SET:
        winding
    # End List
    RETURN
  RETURN
RETURN
```

Contact

The lamination loss is required for the core material only. Hence, only the elements of the set `core` are defined as an electromagnetic contact body. The loss multiplying factor and lamination loss table is selected here. A contact table is also not required.

The button sequence for specifying the material properties reads:

```
CONTACT
  CONTACT BODIES
    NEW
      CREATE NEW CONTACT BODY:
        NAME
          ENTER CONTACT BODY NAME
            Core
```

```
ELECTROMAGNETIC
  DEFINE ELECTROMAGNETIC CONTACT BODY:
  LOSS CURVE
  ENTER THE LOSS CURVE MULTIPLYING FACTOR
    7 . 0
  OK
  ELEMENTS: ADD
    Cond1
  # End List
  ID CONTACTS
  RETURN
RETURN
```

Modeling Tools

The electric current in the rectangular winding is specified through the winding feature. The rectangle has a coil of 100 turns and its cross section is given by $l = 0.1$ m and width = 0.02 m. Each coil is a circular coil with an appropriate radius of $1.0E-5$ meters. The winding path and its orientation are specified by a single node each for the 2-D axisymmetric case.

The button sequence for specifying the windings in modeling tools reads:

```
MODELING TOOLS
  WINDINGS
  NEW
  CREATE NEW WINDINGS:
  PROPERTIES
  DEFINE WINDING PROPERTIES
  CROSS-SECTION: RECTANGULAR
  LENGTH
  ENTER LENGTH VALUE
    0 . 1
  WIDTH
  ENTER WIDTH VALUE
    0 . 02
  COIL: # COIL
  ENTER NUMBER OF TURNS
```

```
100
COIL:CROSSSECTION: CIRCULAR
RADIUS
ENTER RADIUS VALUE
1.0E-05
CONDUCTOR BODY
SELECT CONTACT BODY:
core
OK
SEGMENTS: ADD
ADD WINDING SEGMENTS:
SELECT OPTION: NODE PATH
CENTERLINE: NODES: ADD
SELECT NODE ID:
105
# End List
CROSS-SECTION ORIENTNATION: NODES: ADD
SELECT NODE ID:
113
# End List
FILL
RETURN
RETURN
```

Initial and Boundary Conditions

A fixed magnetic scalar potential ($A_z = 0$ volts) is applied on all far field nodes. The coil current boundary condition is used to apply uniform current in the winding. For this case, the current value and the winding identification path is specified on the appropriate conductor elements.

The button sequence for specifying the boundary conditions reads:

```
BOUNDARY CONDITIONS
NEW
SELECT: MAGNETOSTATIC ANALYSIS
```

```
NAME
  ENTER THE FIXED POTENTIAL BOUNDARY CONDITION NAME:
    Fix_pot
FIXED POTENTIAL
  POTENTIAL
    ENTER POTENTIAL VALUE:
      0
  OK
NODES: ADD
  ENTER NODE SET:
    Far_field
# | End of List
NEW
NAME
  ENTER THE COIL CURRENT BOUNDARY CONDITION NAME:
    coilcur
COIL CURRENT
COIL CURRENT
  ENTER CURRENT VALUE
    2.0
  WINDING PATH
    SELECT WINDING PATH:
      winding1
  OK
ELEMENTS ADD
  SELECT EXISTING ELEMENT SET:
    windings
# | End of List
FILL
RETURN
RETURN
```

The initial temperature at all nodes in the model is defined as 30 Celsius. This is done using the following button sequence

```
INITIAL CONDITIONS
NEW
  SELECT: THERMAL
  NAME
    ENTER THE INITIAL TEMPERATURE CONDITION NAME:
      Init_temp
  TEMPERATURE
    TEMPERATURE
      ENTER TEMPERATURE VALUE:
        30
    OK
  NODES: ADD
    ENTER NODE SET:
      ALL: EXISTS
  # | End of List
RETURN
RETURN
```

Table

The lamination loss data has to be defined as a table in Mentat. The data in [Table 6.11-1](#) can be entered as individual values in Mentat or as an externally created input file. Usually, the number of data points is large and entry of individual data points is tedious in Mentat. In this problem, the data is entered as an external input file, `loss_curve.dat`. The external input is created in a predefined format which can be read by Mentat.

```
CONTACT
CONTACT BODIES: THIS SHOWS THE 'CORE' CONTACT BODY
  TABLE
    READ
    READ THE EXTERNAL FILE:
      Loss_curve.dat
  OK
  FIT
    PLOT TABLE GRAPH AND FIT IN GIVEN RANGE
      Core
  RETURN
ELECTROMAGNETIC
  TABLE
    ASSOCIATE TABLE WITH THIS CONTACT BODY:
```

```
Lamin_loss
  OK
  RETURN
RETURN
```

Loadcase and Job Parameters

There is only one loadcase named `lamcase`. This is a basic coupled magnetostatic thermal analysis in which heat is generated to ohmic current flow in the winding coils and due to lamination loss in the core material. The magnetostatic analysis is performed first and the heat generated as mentioned above is used in the thermal analysis to compute the nodal temperature distribution. The steps to describe the loadcase are shown in [Figure 6.11-3](#).

The button sequence for specifying the material properties reads:

```
LOADCASE
  NEW
  CREATE NEW LOADCASE:
  NAME
  ENTER LOADCASE NAME:
  lamcase
  MAGNETOSTATIC-THERMAL
  TRANSIENT
  LOADS
  SELECT LOADS:
  Fix_pot
  coilcur
  LAMINATION CALCULATION
  LAMINATION LOSS
  SELECT THE CORE CONDUCTING BODY:
  Core
  TOTAL LOADCASE TIME
  ENTER THE TOTAL LOADCASE TIME:
  100
  PARAMETERS
  # STEPS
  ENTER NUMBER OF TIME STEPS:
  10
  OK
  OK
  OK
  RETURN
RETURN
```

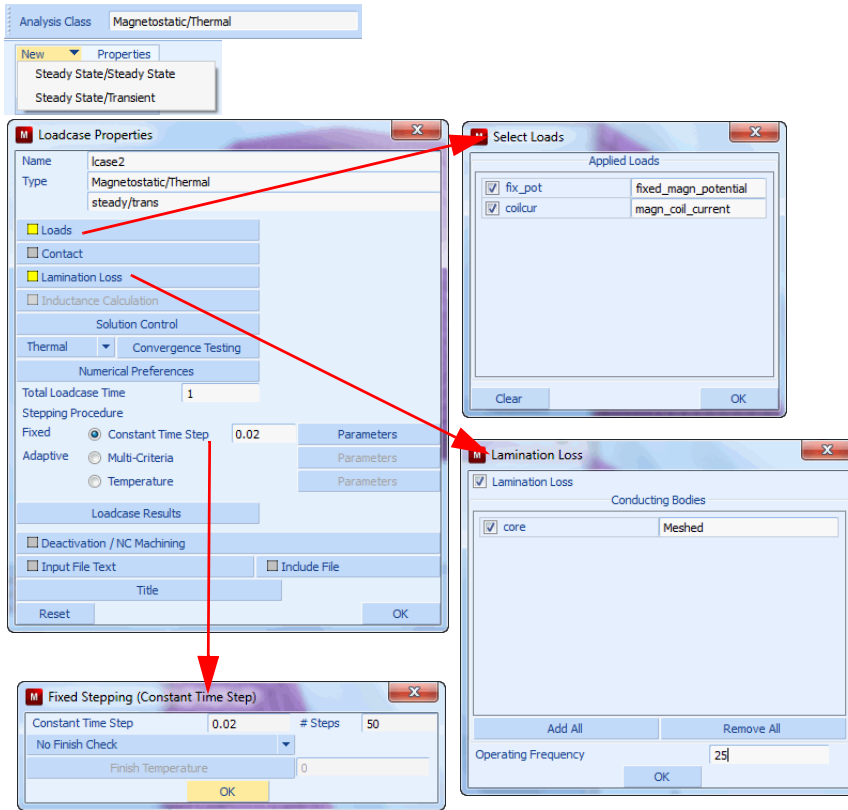



Figure 6.11-3 Steps for showing Button Click to Define the Loadcase lmcas2

The job specification includes only the one loadcase mentioned above. The element post processing selected is the X and Y components of the magnetic field intensity and magnetic flux density, temperature, lamination loss, and thermal energy density.

The steps to describe the loadcase are shown in Figure 6.11-4.

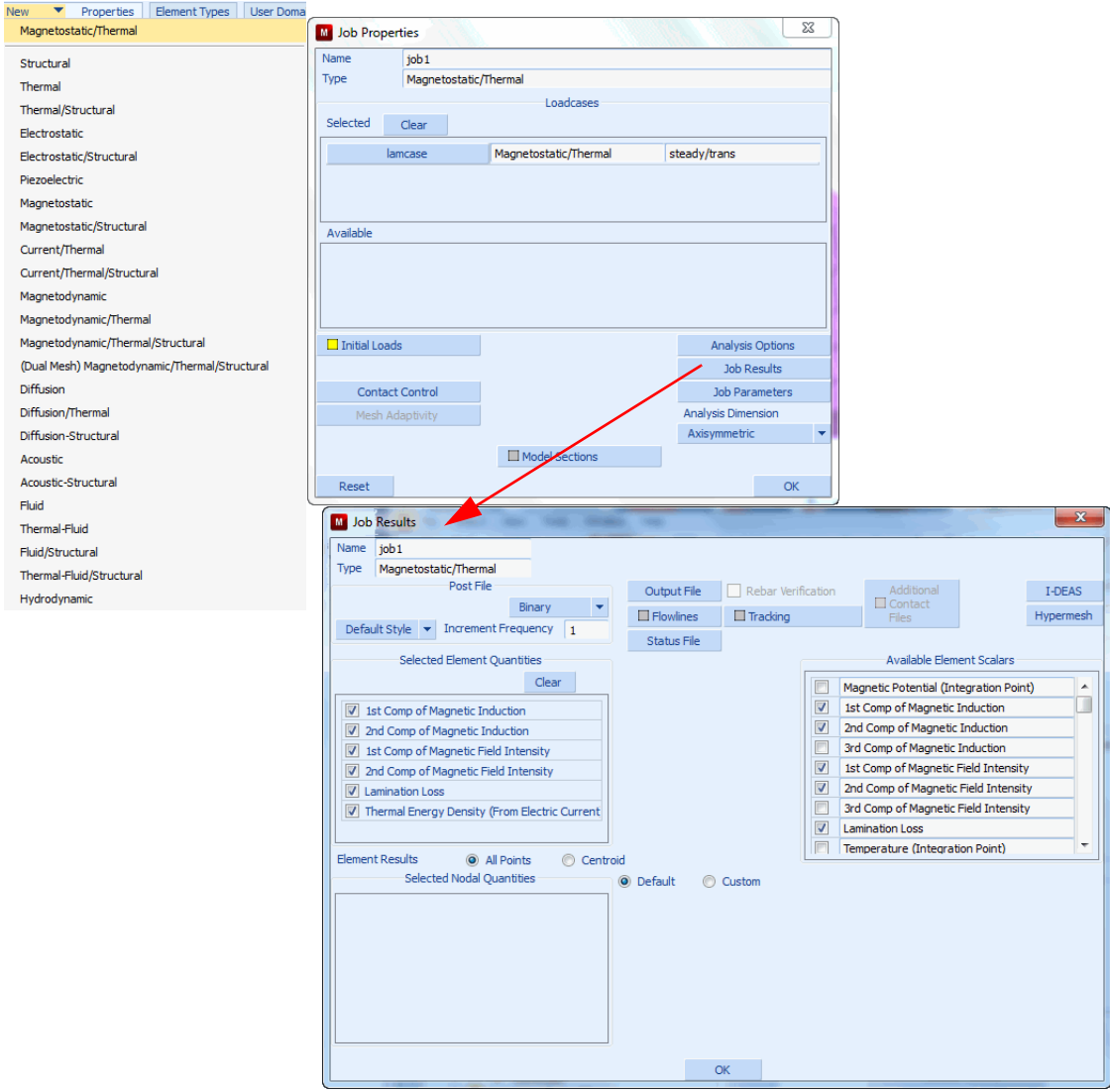


Figure 6.11-4 Steps for showing Button Click to Define the JOB

The button sequence for specifying the material properties reads:

- JOBS
- NEW
- SELECT ANALYSIS: MAGNETOSTATIC-THERMAL
- PROPERTIES
- ADD LOAD CASE:

```
lamcase
SELECT JOB: PLANAR
JOB RESULTS
  SELECT THE FOLLOWING QUANTITIES:
    1st Component of Magnetic Induction
    2nd Component of Magnetic Induction
    1st Component of Magnetic Field Intensity
    2nd Component of Magnetic Field Intensity
    Lamination Loss
    Thermal Energy Density (from electric current)
  OK
  OK
RETURN
```

Save Model, Run Job, and View Results

The finite element model is first saved as a mud file, `lam_final.mud`.

```
FILE
  SAVE AS
    lam_final.mud
  OK
  RETURN
JOBS
  RUN
  SUBMIT 1
  MONITOR
  OK
  RETURN
RESULTS
  OPEN DEFAULT
    *post_open_default
```

It is desired to view the contour plots for the following:

1. External Electric Current
2. Magnetic Induction
3. Thermal Energy Density
4. Lamination Loss

The plots can reveal visually detectable errors in the solution.

Since a transient thermal analysis is applied with 10 time steps, there are 10 increments. The results are shown below for the 10th increment. It should be noted that the magnetostatic run for each increment runs with the same loads, boundary conditions and material properties and the solutions are the same for each increment. The thermal analysis also runs with the same material properties, but the thermal energy density and lamination loss adds up in each increment resulting in progressively increasing temperature.

To see the electric potential contour plots:

```
SCALAR
  External Electric Current
OK
CONTOUR BANDS
```

Observe the external electric current. Then use the PLOT settings to get a better picture of the contour plot:

```
PLOT
  A NODE PLOTTING IS SET OFF:
    NODES
  ELEMENTS SETTING
    OUTLINE
  REGENRATE
RETURN
```

The contour plot for increment 10 is shown in [Figure 6.11-5](#).

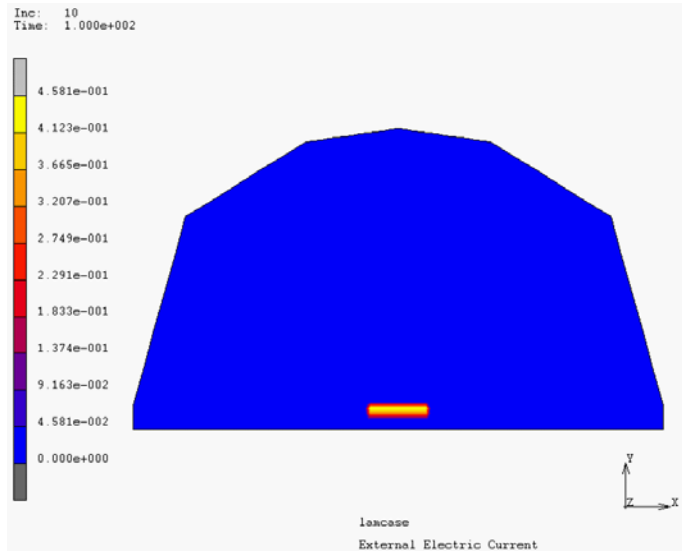


Figure 6.11-5 Electric External Current Distribution

Now repeat the above steps for magnetic induction, temperature, generated heat, and lamination loss contour bands for the tenth increment. The plots are shown in Figures 6.11-6, 6.11-7, 6.11-8, and 6.11-9.

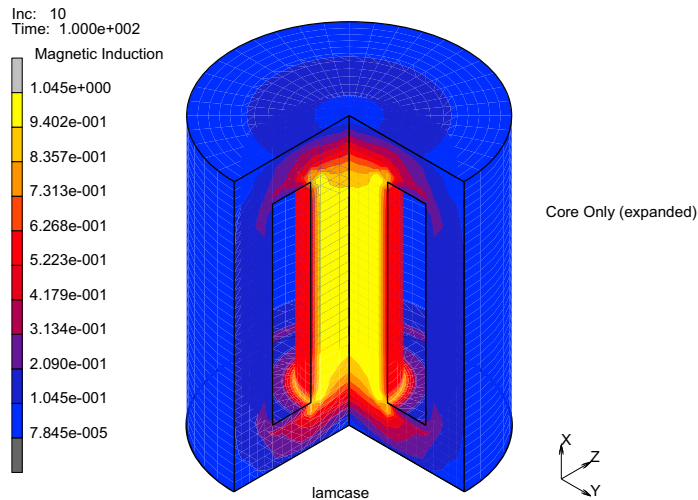


Figure 6.11-6 Magnetic Induction Distribution

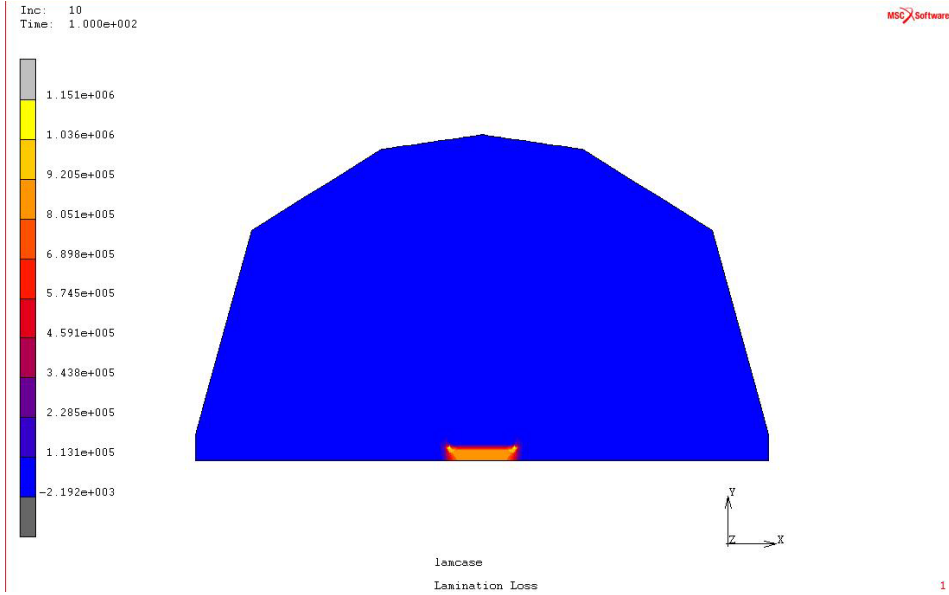


Figure 6.11-7 Temperature Distribution

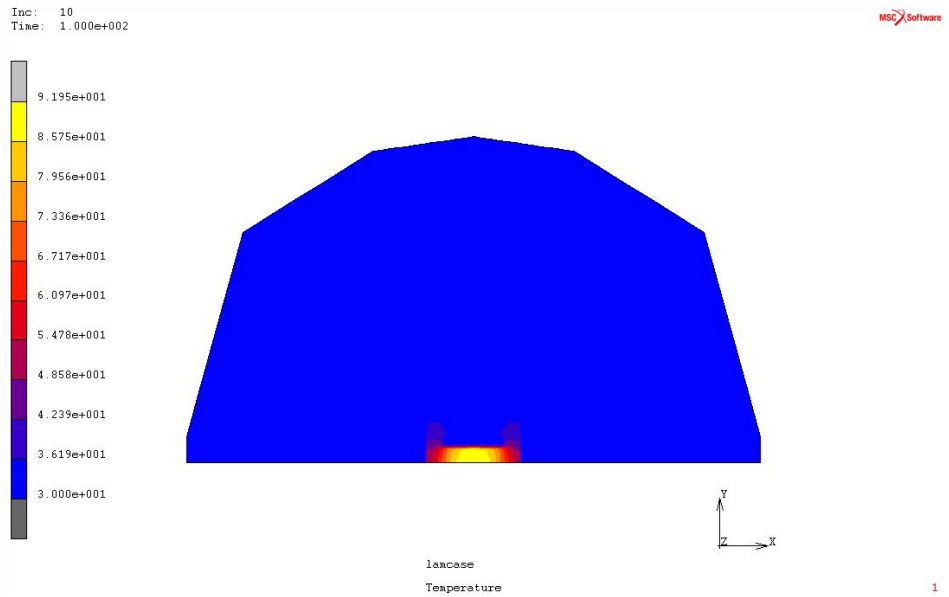


Figure 6.11-8 Generated Heat Distribution

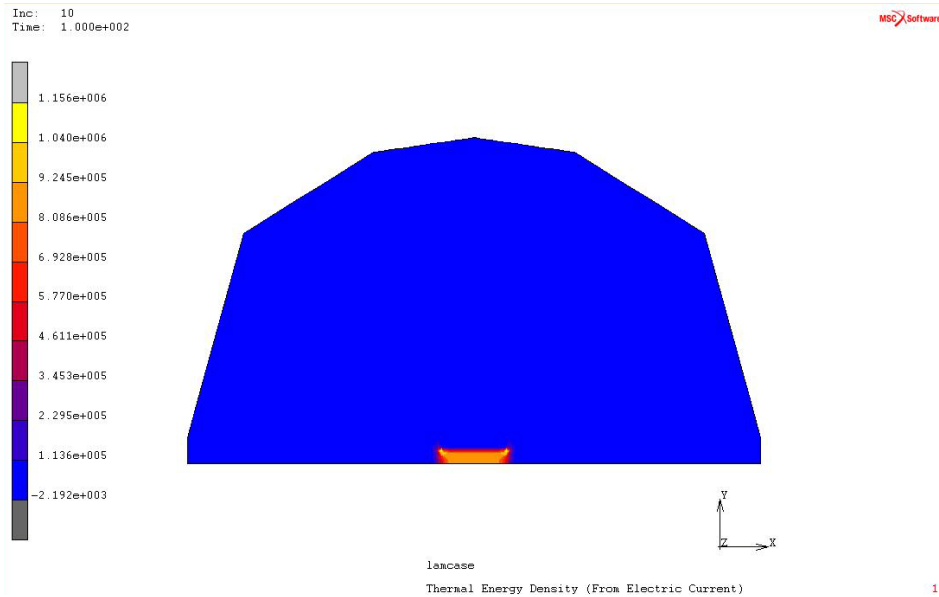


Figure 6.11-9 Lamination Loss Distribution

Results and Discussion

The total lamination loss is printed in the OUT file. It contains the total lamination loss ,and its break up into individual loss types. The relevant portion of the OUT file is shown below:

```

*****
** The Lamination Losses at operating frequency **      25.0000
Total Losses for Lamination Body Number:                1
    Total Lamination Losses:                            0.46146E+03
    Total Hysteresis Losses:                             0.64822E+01
    Total Eddy Current Losses:                          0.43771E+03
    Total Extra (STRAY) Losses:                          0.17268E+02
*****
    
```

The above losses are same in each increment.

Input Files

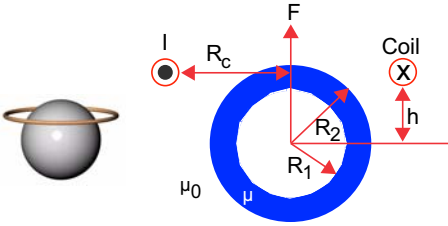
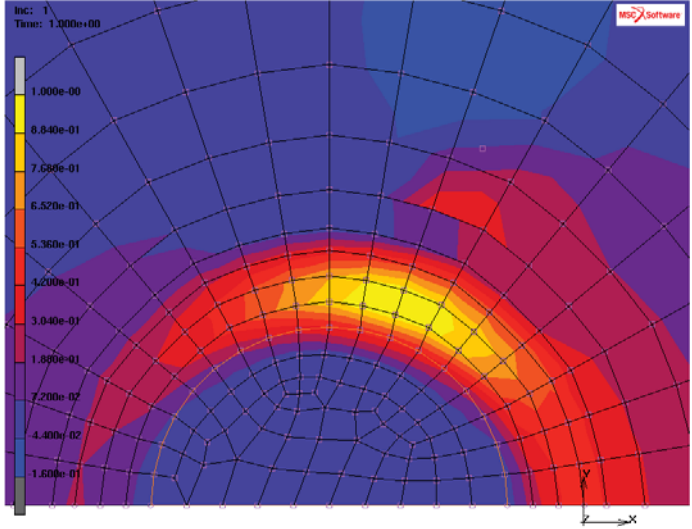
The files below are on your [delivery media](#) or they can be downloaded by your web browser by clicking the links (file names) below.

File	Description
lamcase.proc	Mentat procedure file
loss_curve.dat	Loss input data
lam_init.mud	Mentat model file

6.12 Magnetic Levitation of a Ferromagnetic Sphere

- Summary 2098
- Magnetic Levitation of a Ferromagnetic Sphere 2099
- Results and Discussion 2108
- Input Files 2109
- References 2109

Summary

Title	Magnetic levitation of a ferromagnetic sphere								
Problem features	Coupled magnetostatic-structural analysis								
Geometry	 <p> $R_1 = 0.035\text{m}$ $R_2 = 0.05\text{m}$ $R_c = 0.07\text{m}$ $h = 0.03\text{m}$ $\mu_r = 500$ $\mu_0 = 1.2566\text{e-}6\text{H/m}$ $I = 20000\text{A}$ </p>								
Material properties	Typical properties of the air, and $\mu_r = 500$ for the iron sphere								
Analysis type	Magnetostatic-Structural								
Boundary conditions	The outer boundary of the air has a fixed magnetic potential of 0. A current of 8796.46A is applied to one node to represent the coil. One node of the iron sphere is fixed.								
Element type	Axisymmetric								
FE results	<table border="1" data-bbox="414 850 792 1015"> <thead> <tr> <th>Method</th> <th>Total Force</th> </tr> </thead> <tbody> <tr> <td>virtual work</td> <td>364.6N</td> </tr> <tr> <td>maxwell stress</td> <td>349.7N</td> </tr> <tr> <td>analytical</td> <td>372.9N</td> </tr> </tbody> </table>  <p> <small>inc: 1 Time: 1.200e+00</small> <small>mscX software</small> <small>1st Comp of Magnetic Induction</small> </p>	Method	Total Force	virtual work	364.6N	maxwell stress	349.7N	analytical	372.9N
Method	Total Force								
virtual work	364.6N								
maxwell stress	349.7N								
analytical	372.9N								

In this example, a coupled magnetostatic-structural analysis is demonstrated. A coil is placed around the top part of a hollow iron sphere. The current in the coil generates a magnetic field in the iron sphere which pulls this sphere towards the coil. By tuning the current in the coil, this pulling force can be made equal to the gravitational force acting on the iron sphere, and therefore creating levitation. The problem has an analytical solution which is taken from [Reference 6-1](#).

For the materials, loadcase, and job selection, the user must first specify which analysis class will be performed. Different analysis classes are, for example, Structural, Thermal, Thermal/Structural, Piezoelectric, Magnetostatic/Structural, or Fluid/Structural. Once this is set, Mentat shows the appropriate menus for material data, loadcase options, and job options. More information about this is available at the end of this chapter.

The procedure file to demonstrate this example is called `hs_run.proc`. This procedure file requires an initial Mentat mud file, called `hs_mesh.mud` (see also [Input Files](#)).

Magnetic Levitation of a Ferromagnetic Sphere

Figure 6.12-1 shows the representation of the iron sphere which is analyzed. The different dimensions are also shown in this figure. The inset shows a 3-D representation of the model, while here an axisymmetric analysis is performed. Note that, in Marc, the symmetry axis is the x-axis.

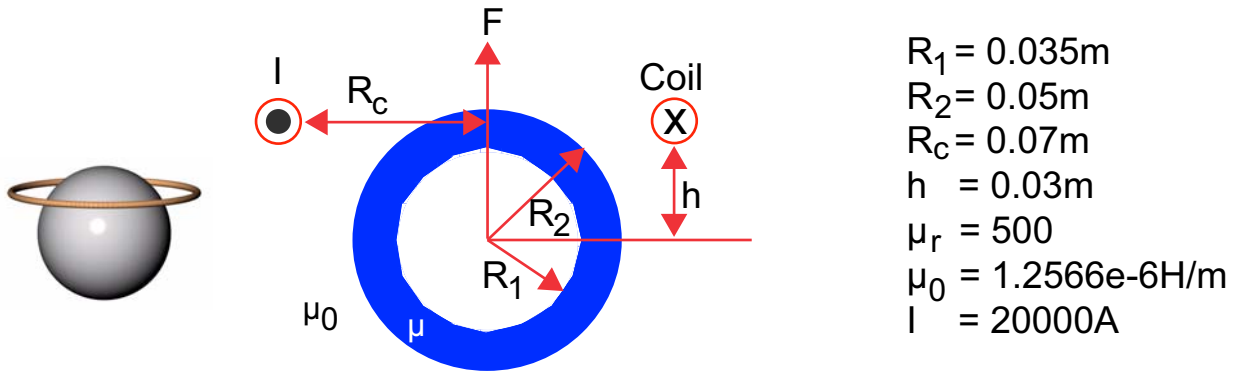


Figure 6.12-1 Model of the hollow sphere

Mesh Generation

The mesh is already defined in the file `hs_mesh.mud`. The model starts by opening this file. The current will be applied to an extra node which is not connected to the mesh. This node is added first.

```

MESH GENERATION
NODE: ADD
    0.03 0.07 0
MAIN
    
```

Material Properties

The material properties of the two materials are given below:

1. Air
 - a. Structural
Young's modulus: $E = 20000\text{Pa}$
Poisson's ratio: $\nu = 0.3$
 - b. Magnetostatic
Magnetic permeability $\mu = 1.2566 \times 10^{-6} \text{ H/m}$
2. Iron sphere
 - a. Structural
Young's modulus: $E = 2.0 \times 10^{11} \text{ Pa}$
Poisson's ratio: $\nu = 0.3$
Magnetostatic
Magnetic permeability $\mu = \mu_r \cdot \mu_0 = 500 \cdot 1.2566 \times 10^{-6} = 8796.46 \text{ H/m}$

Note that for easy modeling a high stiffness for air is taken. It is also possible to let the air elements not be active in the structural pass. To do this they must be defined as magnetostatic elements.

```
MATERIAL PROPERTIES
MATERIAL PROPERTIES
ANALYSIS CLASS
MAGNETOSTATIC/STRUCTURAL
NEW
STANDARD
NAME
air
STRUCTURAL
YOUNG'S MODULUS
20000
POISSON'S RATIO
0.3
OK
MAGNETIC PERMEABILITY
MU
1.2566e-6
OK
```

```

SELECT
  SELECT SET
    sphere
  OK
  RETURN
ELEMENTS ADD
  ALL: UNSEL.
NEW
  STANDARD
NAME
  iron
STRUCTURAL
  YOUNG'S MODULUS
    2e11
  POISSON'S RATIO
    0.3
  OK
MAGNETIC PERMEABILITY
  MU
    0.0006283
  OK
ELEMENTS ADD
  ALL: SELEC.
MAIN
    
```

Boundary Conditions

One node inside the iron sphere is fixed, so that the reaction force calculated here balances the magnetic force. When this force is higher than the gravitational force (not calculated here), the magnetic field levitates the iron sphere. The magnetostatic potential is set to 0 at the outer boundary and a point current is prescribed to the node which represents the coil. This point current is $I \cdot l = 20000 \cdot 2 \cdot \pi \cdot 0.07 = 8796.46 \text{ Am}$.

```

BOUNDARY CONDITIONS
  STRUCTURAL
    NAME
      fix
    
```

```
FIXED DISPLACEMENT
  DISPLACEMENT X
  DISPLACEMENT Y
  OK
NODES ADD
  86 #
RETURN
NEW
NAME
  fix_A
MAGNETOSTATIC
  FIXED POTENTIAL
    POTENTIAL
    OK
  NODES ADD
    445 429 413 397 381 365 349 333 317 301 285 269 253 237 221 205 189 173 157 #
  NEW
  NAME
    load
  POINT CURRENT
    CURRENT
      8796.46
    OK
  NODES ADD
    446
MAIN
```

Modeling Tools and Contact

Two methods are available to calculate the magnetic (Lorentz) force on a body. The Maxwell Stress Tensor (MST) method calculates this force using a surface surrounding the body. In Marc, this surface is represented as a contact interface, so the elements on both sides of this interface must be disconnected. On this surface, local forces are calculated, where the summation of these forces is the Lorentz force. This force is printed in the `.out` file. The second method is the Virtual Work Method. This method is energy based, where a group of elements onto which the Lorentz force is calculated gets a delta displacement in the x-, y-, and for 3-D z-direction. From energy differences, the Lorentz force is calculated. For the method, the group of elements onto which the Lorentz force will be calculated is also defined as a contact body, but, in this case, the mesh does not need to be disconnected. This calculated Lorentz force is prescribed in the structural pass as a volumetric load, and is also printed in the `.out` file.

Best results are obtained when a layer of air surrounds the part onto which the Lorentz force will be calculated. For the VWM method, this layer can be specified, but, for the MST method, the user has to create this. To facilitate this, Mentat has a tool called **MATCHING BOUNDARIES**. This tool splits a mesh into two disconnected meshes. To find the layer of air surrounding the sphere, we start by selecting the elements of the sphere and the elements inside the sphere. Then, select all nodes belonging to these elements. Next, select all elements which contain one or more of the just selected nodes. Now, one layer of elements is added. To add more layers repeat this procedure. With these selected elements, the mesh is split using the **MATCHING BOUNDARIES**, and the two parts are added as contact bodies in the **CONTACT** section. These contact bodies are “glued” together using **GLUE** for the interface condition between the two bodies in the **CONTACT TABLE**.

```
MODELING TOOLS
  MATCHING BOUNDARIES
    NEW
      2-D
    SELECT
      CLEAR SELECT
      SELECT SET
        sphere_and_inside
      OK
      SELECT BY
        NODES BY: ELEMENTS
          ALL: SELEC.
        ELEMENTS BY: NODES
          ALL:SELEC.
        NODES BY: ELEMENTS
          ALL: SELEC.
        ELEMENTS BY: NODES
          ALL: SELEC.
      RETURN
    RETURN
  SPLIT MESH
    ALL:SELEC
  MAIN
CONTACT
  CONTACT BODIES
    NEW DEFORMABLE
    NAME
      sphere_air
    ELEMENTS ADD
      ALL: SELEC.
```

```

NEW DEFORMABLE
NAME
    outer_air
ELEMENTS ADD
    ALL: UNSEL.
RETURN
CONTACT TABLES
NEW
PROPERTIES
    FIRST 1 SECOND 2
    CONTACT TYPE
        GLUE
        OK
    OK
MAIN

```

Links

The current is applied to a node to represent the coil, but without doing anything special, this current is not transferred to the mesh since this node is not connected to the mesh. To connect this node with the mesh, the INSERT option is used. With this option, Marc creates tyings between the host entities (finite element mesh) and the embedded entities (the node carrying the current).

```

LINKS
INSERTS
    HOST ENTITIES CONTACT BODIES
CONTACT BODIES
    outer_air
    OK
EMBEDDED ENTITIES NODES
ADD
    446 #
MAIN

```

Loadcases and Job Parameters

Two loadcases will be created: one demonstrating the Maxwell Stress Tensor method and the other demonstrating the Virtual Work Method. Note that for the virtual work method, the user can specify an extra number of layers surrounding the body onto which the Lorentz force will be calculated. For this example, it is zero since it is already included in the body. In general, care should be taken that the extra layers which are created by Marc do not contain

any applied currents or different materials. This can be checked during post processing where a new SET called VWM_body is available. This set contains all the elements which will get the delta displacement.

The steps which are described here are shown in [Figure 6.12-2](#).

ANALYSIS

LOADCASES

ANALYSIS CLASS

MAGNETOSTATIC/STRUCTURAL

NEW

STEADY STATE/STATIC

NAME

mst

PROPERTIES

CONTACT

CONTACT TABLE

ctable1

OK

LORENTZ FORCE CALCULATION

LORENTZ FORCE

METHOD MAXWELL STRESS

LORENTZ FORCE BODIES: sphere_air

OK

STEPPING PROCEDURE # STEPS

1

OK

NEW

STEADY STATE/STATIC

NAME

vwm

PROPERTIES

CONTACT

CONTACT TABLE

ctable1

OK

OK

LORENTZ FORCE CALCULATION

LORENTZ FORCE

METHOD VIRTUAL WORK

ELEMENT LAYERS SURROUNDING BODIES

```
0
  LORENTZ FORCE BODIES sphere_air
  OK
  STEPPING PROCEDURE # STEPS
  1
  OK
  MAIN
  JOBS
  NEW
  MAGNETOSTATIC/STRUCTURAL
  ELEMENT TYPES
  ANALYSIS DIMENSION
  AXISYMMETRIC
  STRUCTURAL SOLID
  10
  OK
  ALL: EXIST.
  RETURN
  PROPERTIES
  AVAILABLE mst
  JOB RESULTS
  1st Comp of Magnetic Induction
  2nd Comp of Magnetic Induction
  1st Comp of Magnetic Field Intensity
  2nd Comp of Magnetic Field Intensity
  OK
  OK
```

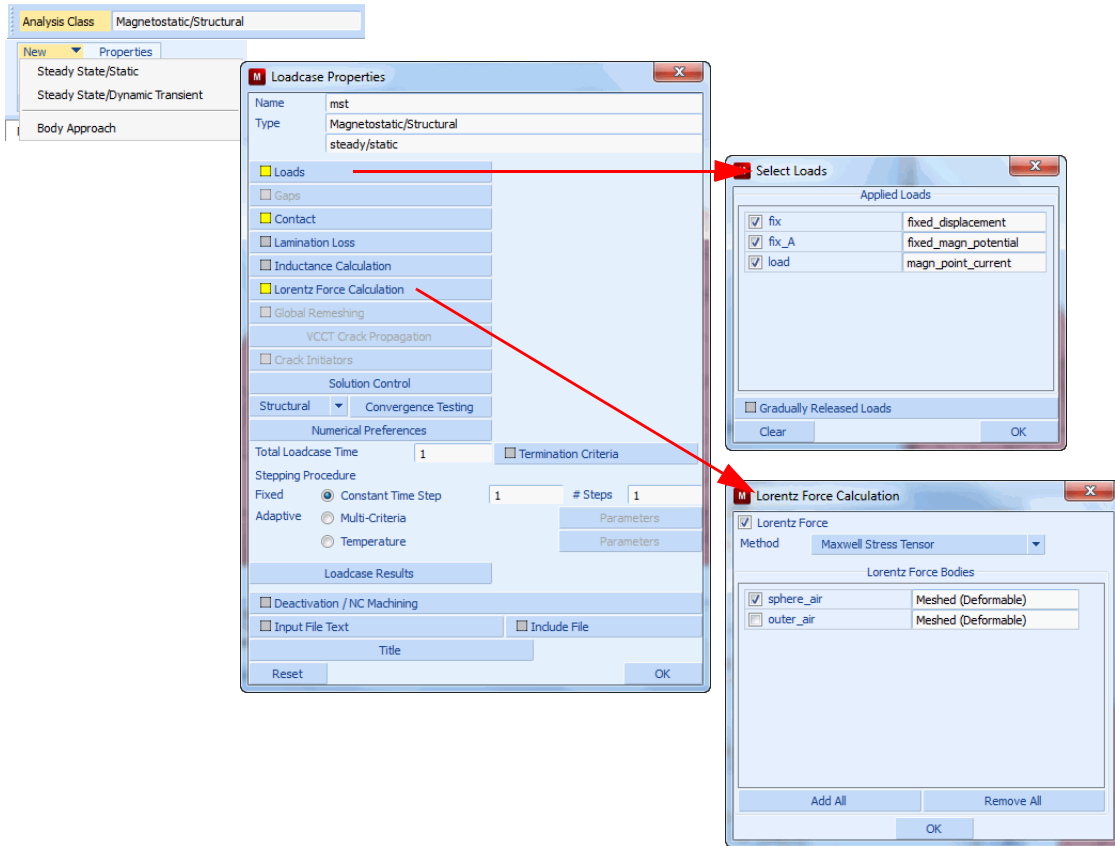


Figure 6.12-2 Mentat Menus for Loadcase Creation

Save Model, Run Job, and View Results

After saving the model, the job is submitted and the resulting post file is opened.

FILES
SAVE AS
 hs_model
OK
RUN
SUBMIT
MAIN
RESULTS
OPEN DEFAULT

NEXT

SCALAR

1st Comp of Magnetic Induction

OK

CONTOUR BANDS

Results and Discussion

Figure 6.12-3 shows a contour plot of the x-component of the magnetic induction. Here you can see that the magnetization mostly stays inside the iron sphere. Note that in this plot, the node is also indicated onto which the current is applied. The results of the total force for the Maxwell Stress Tensor analysis and for the analysis using the Virtual Work Method are compared to the analytical solution in the following table. The analytical result is taken from Reference 6-1.

Method	Total Force
virtual work	364.6N
maxwell stress	349.7N
analytical	372.9N

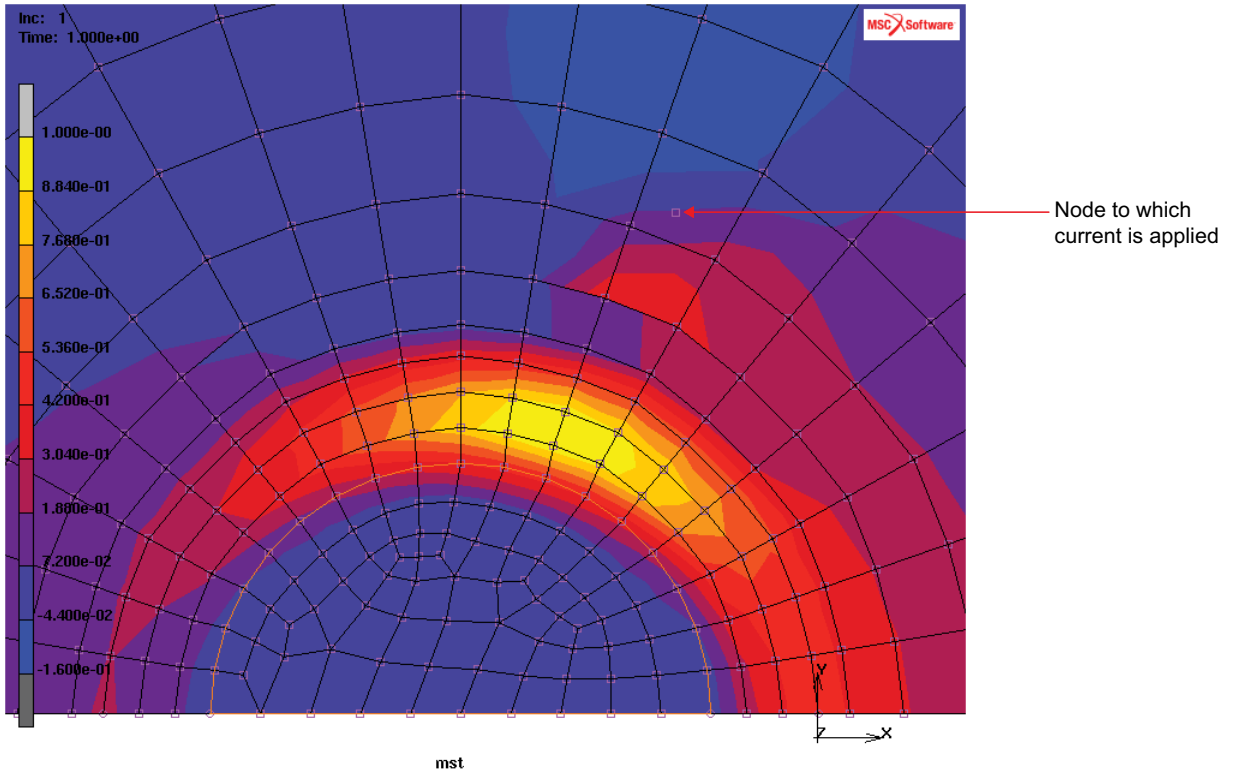


Figure 6.12-3 Contour Plot of the First Component of the Magnetic Induction

Input Files

The files below are on your [delivery media](#) or they can be downloaded by your web browser by clicking the links (file names) below.

File	Description
hs_run.proc	Mentat procedure file
hs_mesh.mud	Mentat input model file

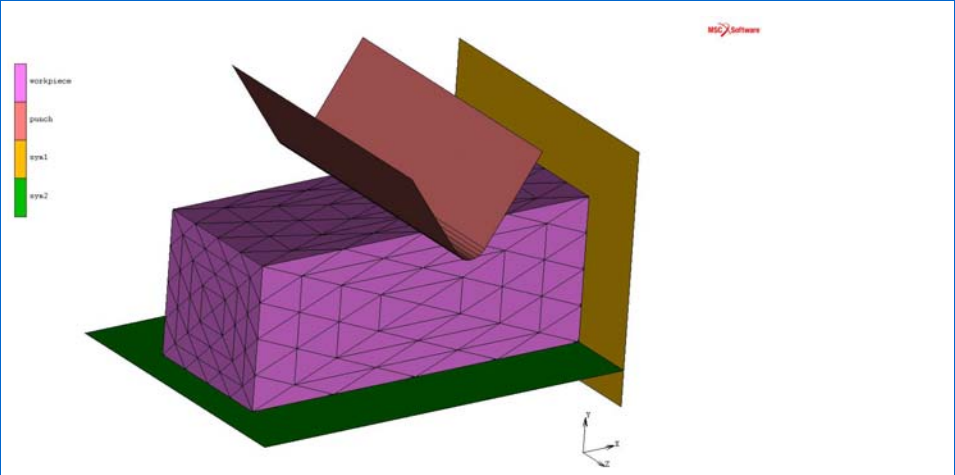
References

- 6-1. Z. Ren, “Comparison of Different Force Calculation Methods in 3D Finite Element Modelling”, IEEE Transactions on Magnetics, Vol. 30, No. 5, September 1994

6.13 Compression of Workpiece by Punch

- Summary 2112
- Requested Solutions 2113
- Modeling Details 2113
- Contact 2114
- Adaptive Remeshing 2115
- Result and Plots 2116
- Input Files 2121

Summary

Title	Compression of Workpiece by Punch
Features	Global Adaptive Meshing with Mesh Density Control
FE Mesh	
Material properties	Workpiece: Marc data base for 100 CR 6 Steel, material number 1_3505
Analysis characteristics	Nonlinear static analysis
Boundary conditions and Applied loads	<ul style="list-style-type: none"> • Symmetry contact bodies sym1 and sym2 • Rigid body punch y velocity = -1.0
Element types	Solid Tet element type157
Contact properties	<ul style="list-style-type: none"> • Workpiece in touching contact with sym1, sym2, punch • Segment to segment contact
FE results	Contact status, displacement, stress results

In the existing capabilities of Marc, there is a way to control mesh density on the surface and gradient of mesh density towards inside of the volume.

Additional fine mesh density controls allow more user friendly ways of mesh density control both for surface and inside of volume. The types are:

- Curvature
- Region
- Distance
- Table
- Element Quantity
- Node Quantity
- UMESHDENS User Subroutine

The present chapter demonstrates this new capability and compares it to simulation without mesh density control.

Requested Solutions

A numerical analysis will be performed to demonstrate the difference in analysis results using new mesh density controls.

Modeling Details

The model shown in [Figure 6.13-1](#) is a simple block workpiece which is stabilized by symmetry contact bodies `symm1` and `symm2`. The workpiece is indented using the punch rigid contact body.

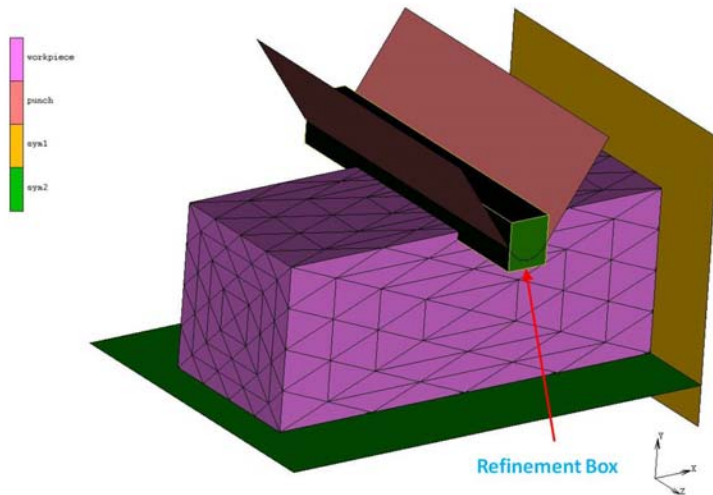


Figure 6.13-1 Refinement Box Region moving with the Punch contact body

Element Modeling

The workpiece is simulated with solid element type 157.

Material Modeling

The material properties are obtained from the Marc data base for 100 CR 6 Steel, material number 1_3505.

The material data is available for a range of 20 to 1200°C.

The initial elastic properties are:

- Young's modulus 2.17×10^5 N/mm²
- Poisson ratio 0.3
- Coefficient of thermal expansion 1.05×10^{-5} mm/mm/°C

The yield stress is obtained from the material data base that is imported at run time.

The temperature dependent material properties are automatically entered by Mentat, but are not used in this simulation, as the model is isothermal at an initial temperature of 20°C.

Contact

The model consists of four bodies as shown in [Figure 6.13-1](#).

1. Workpiece – which will be adaptively meshed

2. 2. Punch – rigid body to indent the workpiece
3. 3. Symmetry surface to constrain motion in x-direction
4. 4. Symmetry surface to constrain motion in y-direction

The punch is given a velocity of -1.0 mm/s in the y direction.

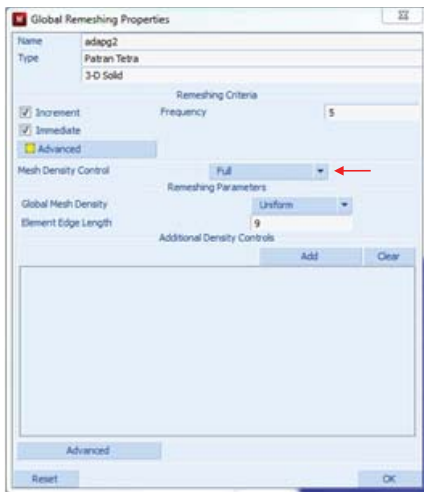
The shear friction model based upon the arc tangent smoothing is included in the model between the punch and the workpiece with a friction coefficient of 0.5. The RVCNST entered is 1.0, which is high for this simulation.

The default contact distance is used and is adjusted automatically when the mesh is enhanced due to global adaptive meshing.

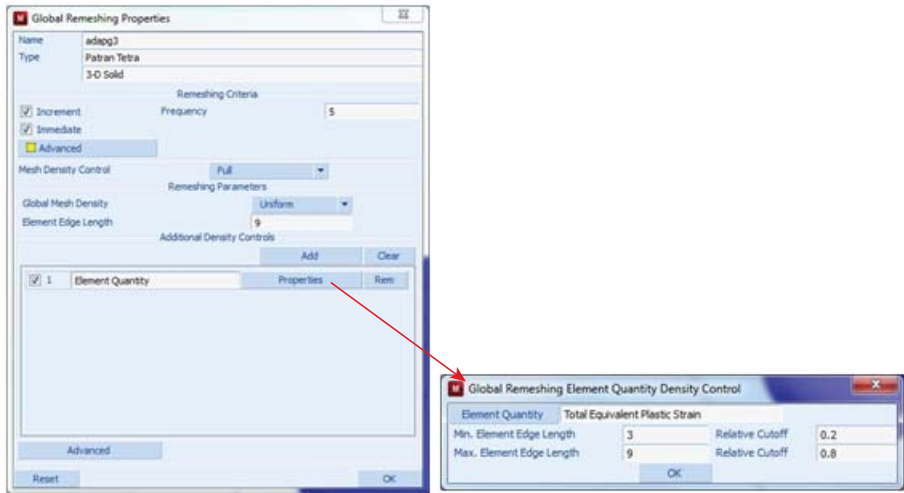
Adaptive Remeshing

To make use of new adaptive remeshing contact capability, users should use new style of ADAPT GLOBAL in Marc.

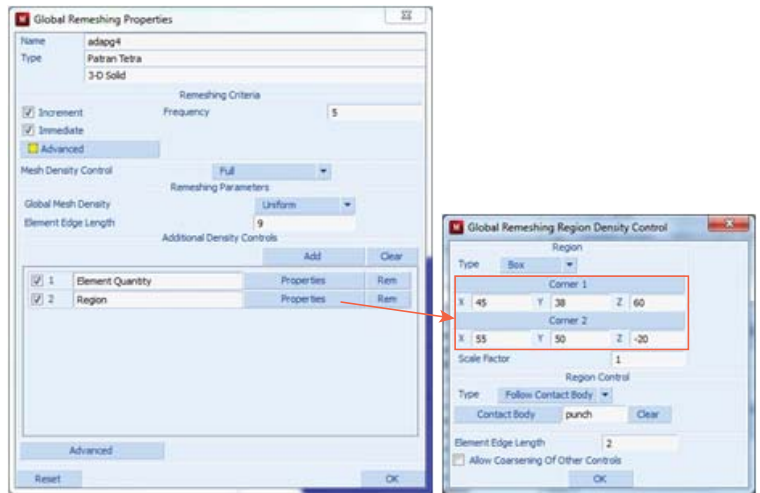
It is activated in Mentat global adaptivity menus (Full) as shown below.



More detailed mesh density controls (based on total equivalent plastic strain) shown as follows:



More detailed mesh density controls (based on box region moving with Contact Body). The size of element edges inside the region is set to 2.0. Position and Size of the box is determined by positions of Corner1 and Corner2 as shown below.



Result and Plots

Three jobs were created to analyze Adaptive Meshing. Job uniform_edge has only default uniform edge length, job plastic_strain has mesh density control driven by Total Equivalent Plastic Strain, and job plastic_strain_rbox has mesh density control driven by combination Total Equivalent Plastic Strain and a Refinement Box with given element edge size equal to 2.0.

The results for the three jobs are summarized for Contact Status, Displacement and Total Equivalent Plastic Strain in Figures bellow. The combined control by Total Equivalent Plastic Strain and Box Region show the best quality of mesh and most accurate results.

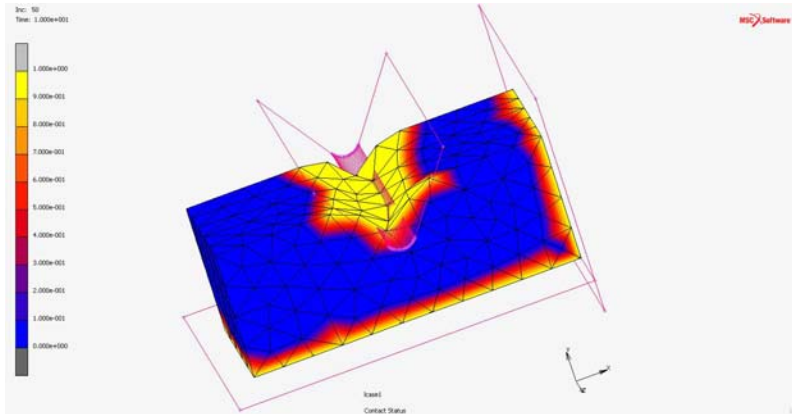


Figure 6.13-2 Uniform_edge- Contact Status

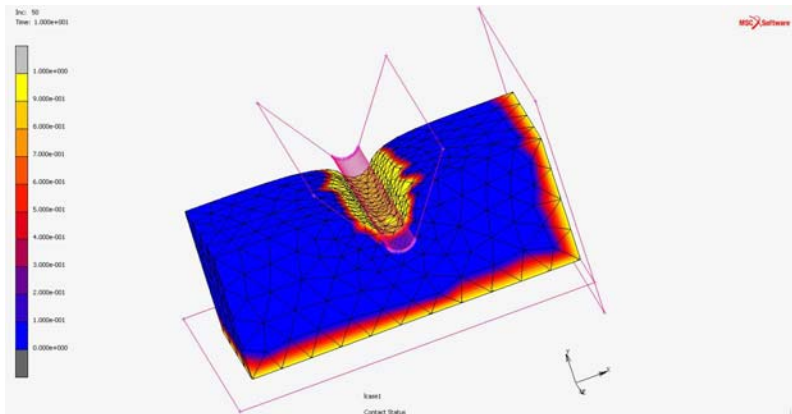


Figure 6.13-3 Plastic_strain- Contact Status

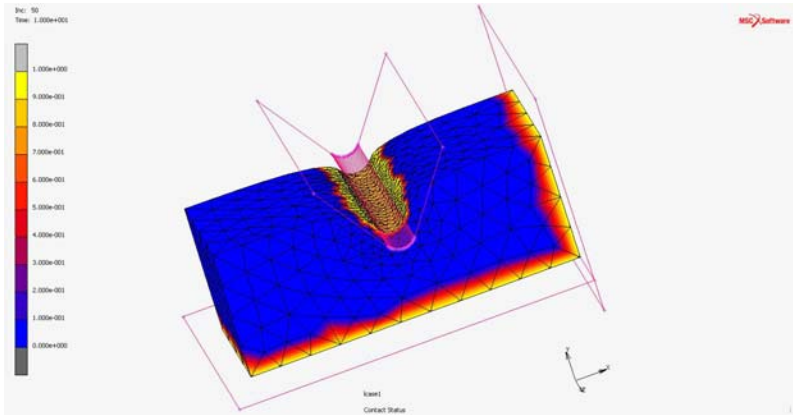


Figure 6.13-4 Plastic_strain_rbox- Contact Status

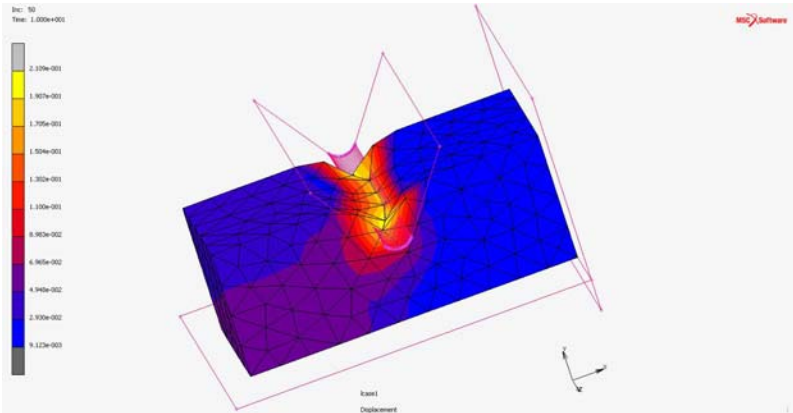


Figure 6.13-5 Uniform_edge- Displacement

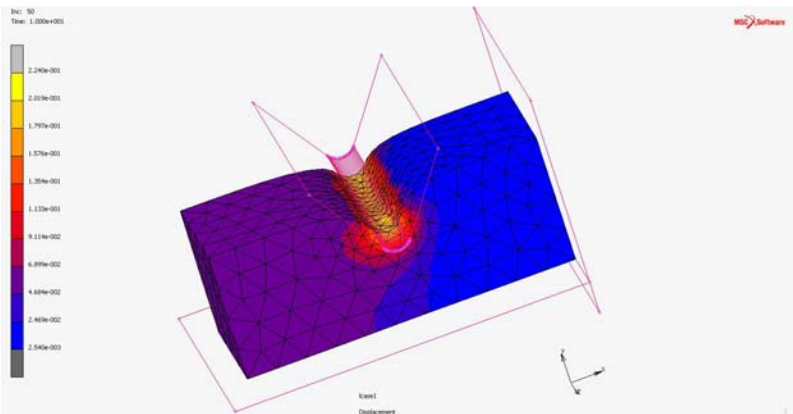


Figure 6.13-6 Plastic_strain- Displacement

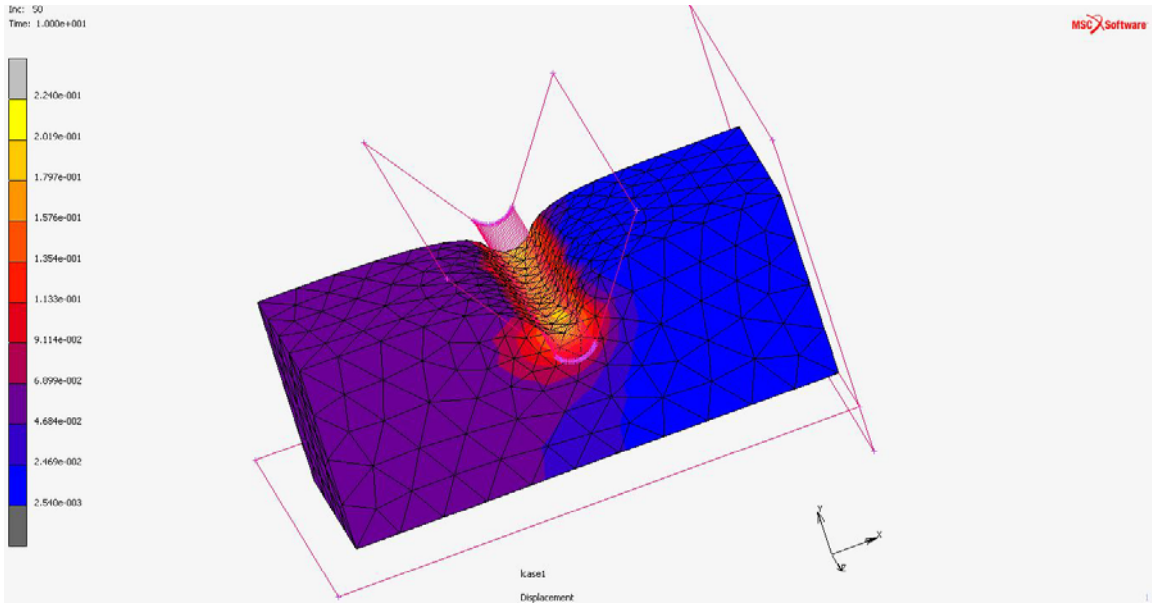


Figure 6.13-7 Plastic_strain_rbox- Displacement

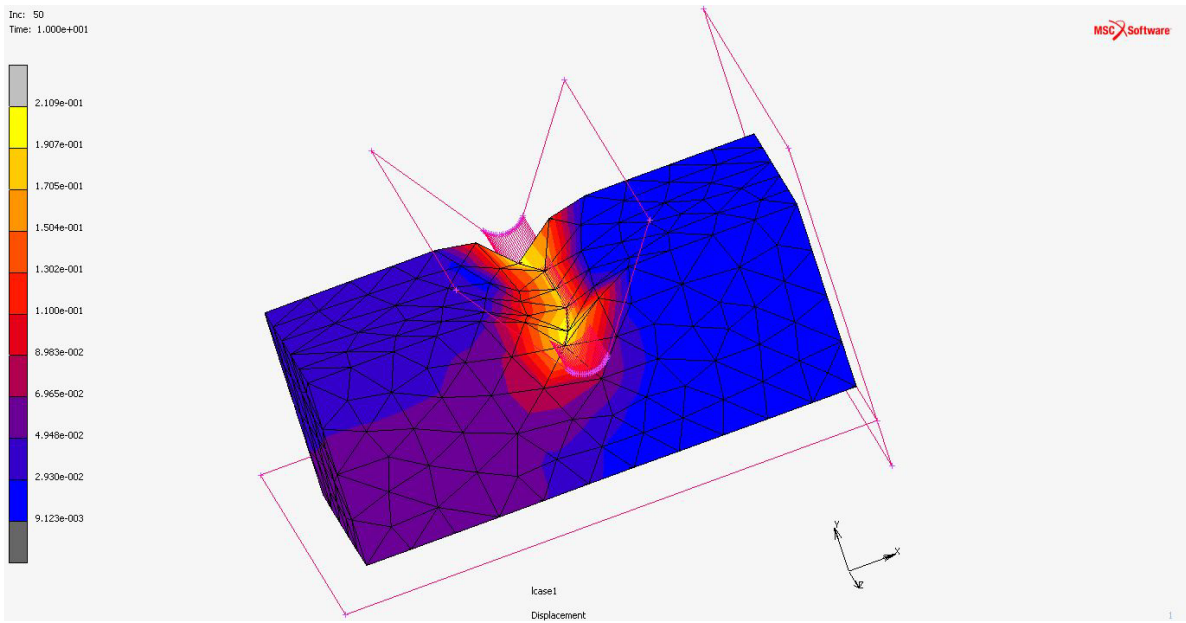


Figure 6.13-8 Uniform_edge- Total Equivalent Plastic Strain

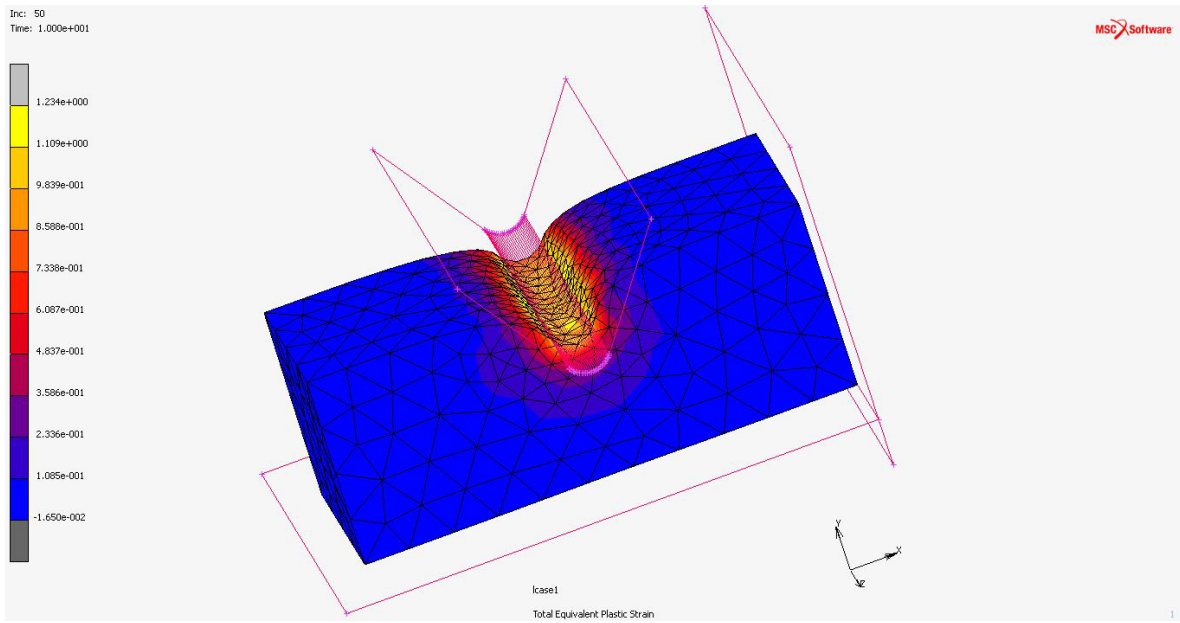


Figure 6.13-9 Plastic_strain- Total Equivalent Plastic Strain

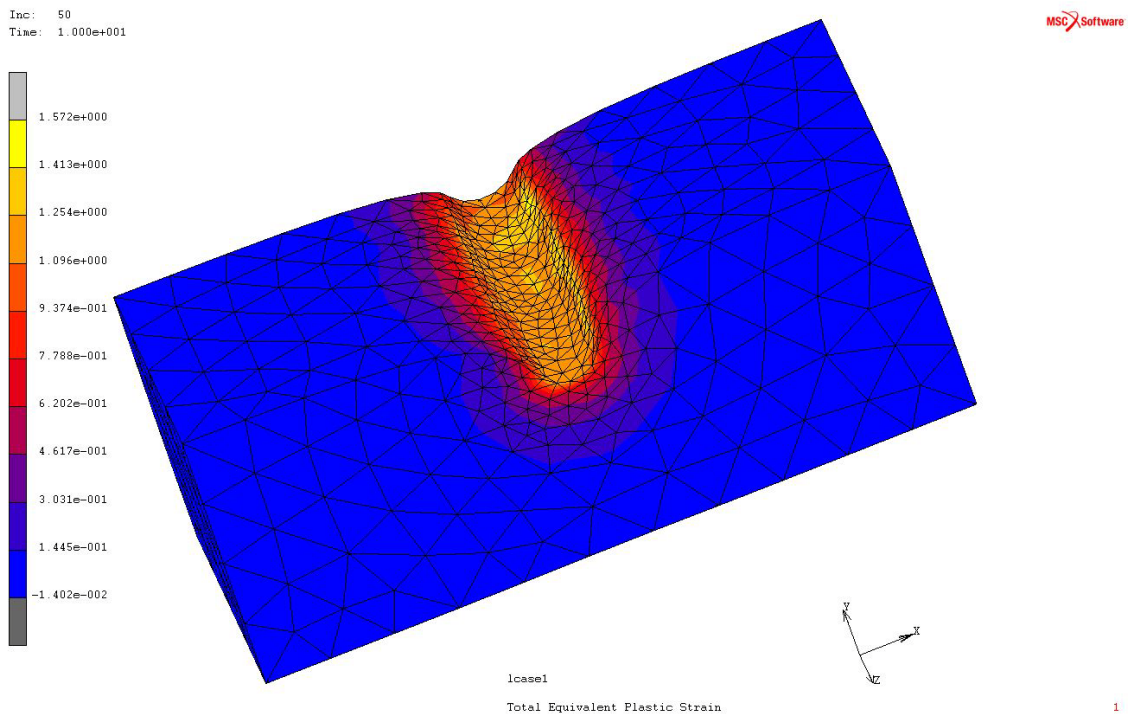


Figure 6.13-10 Plastic_strain_rbox- Total Equivalent Plastic Strain

Input Files

The files below are on your delivery media or they can be downloaded by your web browser by clicking the links (file names) below.

File	Description
punch_load.mud	Mentat model file

Section 7: Mentat Features and Enhancements

7.1 Past Enhancements in Marc and Mentat

- Chapter Overview 2126
- Preprocessing Enhancements 2126
- Postprocessing Enhancements 2154
- Input Files 2158
- Animation 2159

Chapter Overview

This chapter demonstrates various enhancements to Mentat. The most important improvements made in preprocessing are:

- Inclusion of the Patran Mesh-on-Mesh surface mesher
- Inclusion of the Patran tetrahedral mesher
- A new and more consistent attach concept
- New combined mesh generation commands that move, duplicate or expand a mixed list of mesh entities (nodes, elements), geometric entities (points, curves, surfaces, solids) and links (nodal ties, servo links, springs) simultaneously
- Improved handling of links
- New selection methods for selecting items within a certain distance of a point, curve or surface and for box selection in the user coordinate system (that allows for selection in cylindrical and spherical coordinate systems)
- Multi-dimensional tables

The most important postprocessing enhancements are:

- MPEG and AVI animations
- Automatic execution of a procedure file when a post file increment is read

Preprocessing Enhancements

This section demonstrates some of the Mentat preprocessing enhancements. The new *attach* concept is discussed and the benefits in combination with initial conditions and boundary conditions applied to geometric entities (points, curves, and surfaces) are stressed. The combined move, duplicate, symmetry, and expand commands that operate on a mixed list of mesh entities, geometric entities and links are introduced and the improved handling of links is elaborated. Furthermore, the Patran tetrahedral mesher that has been incorporated in Mentat and the new selection methods are described in this chapter.

These new capabilities are illustrated by means of a tire modeling example. Two finite element models of a tire are created, one consisting of 20-node hexahedral elements and the other consisting of 10-node tetrahedral elements. The tire is loaded by an internal pressure, while the rim of the wheel is fixed.

In addition, the use of the new multi-dimensional tables is shown in a separate example.

New Attach Concept

The outline of the cross-section of a tire is imported from an IGES file. The file contains only the right half of the cross-section ([Figure 7.1-1](#)). After the file has been imported, the end points of the curves are merged with a SWEEP POINTS operation.

```

MESH GENERATION
FILES
  IMPORT
    IGES
      tire.igs
    RETURN (twice)
SWEEP
  POINTS
    ALL: EXIST.
  RETURN
    
```

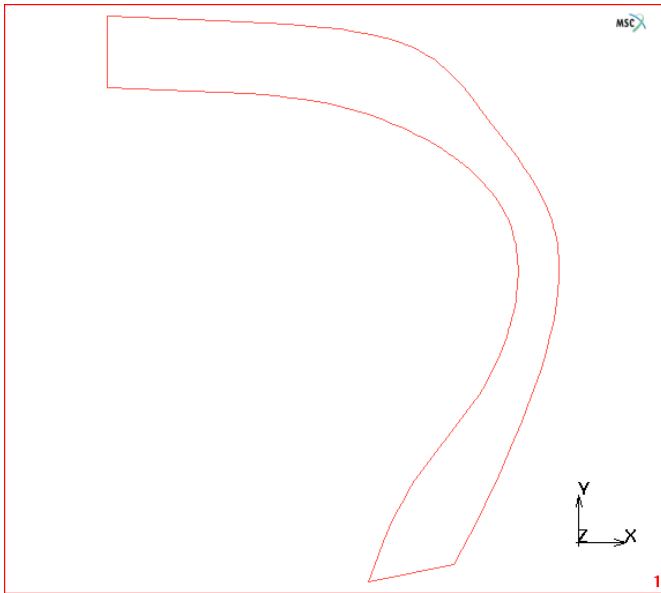


Figure 7.1-1 Right-half of the Cross-section of the Tire

The region is meshed using the planar advancing front automatic mesher. The average curve division length is set to 6 and an even number of curve divisions is forced on detected loops. The later is done to insure that a mesh with all quadrilateral elements will be formed. The resulting mesh is displayed in [Figure 7.1-2](#).

```

AUTOMESH
  CURVE DIVISIONS
    FIXED AVG LENGTH
    AVG LENGTH
    
```

(on)

RESTRICTION FORCE EVEN DIV
APPLY RESTRICTION TO DETECTED LOOPS
APPLY CURVE DIVISIONS
ALL: EXIST.
RETURN
2D PLANAR MESHING
QUAD MESH!
ALL: EXIST.
RETURN (thrice)

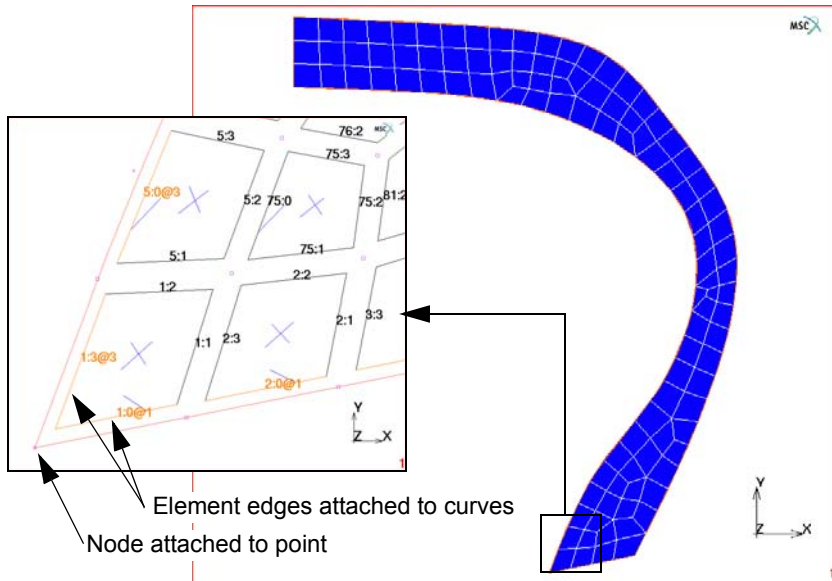


Figure 7.1-2 Finite Element Mesh of the Cross-section of a Tire

Note: The attaching two edges (1:1 and 1:2) that share a common node (3) to different curves causes the common node to be placed automatically on the intersection of the curves.

All automatic mesh generators attach the mesh to the geometry, according to the new attach concept. With that scheme:

- a node can be attached to a point; and
- an element edge can be attached to a curve; and
- an element face can be attached to a surface.

Nodes which are attached to a point always have the same position as the point. Nodes of edges which are attached to a curve always lie on that curve and nodes of faces which are attached to a surface always lie on that surface. Note that this implies that the common node of two edges which are attached to different curves must lie on the intersection of

the curves (Figure 7.1-3). Similarly, the common nodes of two faces which are attached to different surfaces must lie on the intersection of the two surfaces. The automatic meshers and the mesh generation commands that modify either the mesh or the geometry guarantee that this is always the case. For example, if one of the curves is moved or otherwise changed, the common node is repositioned automatically to the new point of intersection. If that point cannot be found, the operation is not permitted and an error message is issued.

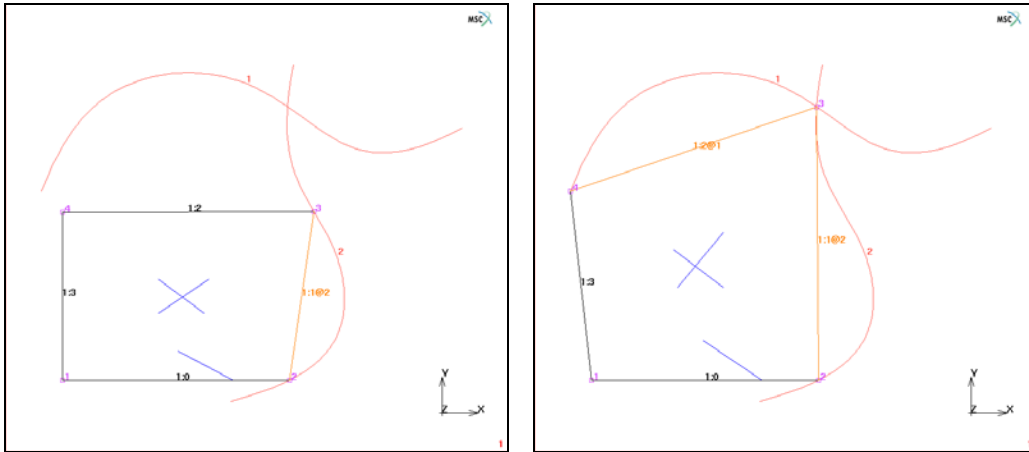


Figure 7.1-3 Common Node with two Edges

Nodes, element edges, and element faces can also be attached or detached manually using the commands in the MESH GENERATION→ATTACH menu (Figure 7.1-4). Attached nodes are displayed as small circles and attached edges are by default drawn in orange (Figure 7.1-2). Attached faces are plotted in a dark blue color. Recall that unattached nodes are represented as squares, unattached edges in white, and unattached faces in a light blue. These colors can be changed using the VISUALIZATION→COLORS menu. The actual curve to which an edge is attached can be visualized by switching on the edge labels and activating the attach information in the PLOT menu:

```
PLOT
  ELEMENTS
  SETTINGS
    EDGES
    LABELS
    ATTACH INFO
```

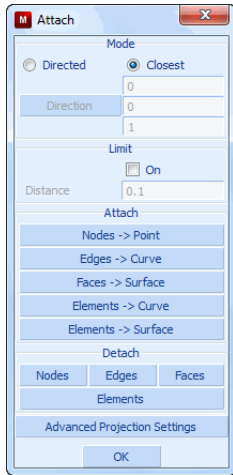


Figure 7.1-4 The ATTACH Menu

If the attach information is enabled, the label includes the curve number to which the edge is attached, separated from the edge number by an @-sign (Figure 7.1-2). Similar options are available for displaying the point and surface to which nodes and element faces are attached.

In the present example, the mesher automatically attaches the element edges on the boundary of the mesh to the appropriate curves. It also attaches the nodes that lie on the end points of the curves to these points.

Expansion to 3-D

The three-dimensional model is obtained by expansion of the axisymmetric model to 3-D. This operation is developed especially for cases in which the axisymmetric analysis is performed first, followed by a full three-dimensional analysis. It requires that the mesh consists of axisymmetric elements.

JOBS

ELEMENT TYPES

MECHANICAL

AXISYMMETRIC SOLID

10

OK

ALL: EXIST.

RETURN (thrice)

The expansion operation expands the two-dimensional axisymmetric elements into three-dimensional solid elements, according to the specified angles and repetitions. In this example, the expansion is performed in 18 steps of 20°. In addition, the command revolves points to which nodes are attached into circles and revolves curves into surfaces of revolution.

MESH GENERATION

EXPAND

AXISYMMETRIC MODEL TO 3D

1 ANGLE

20

1 REPETITIONS

18

EXPAND MODEL

RETURN (thrice)

Note: This three-dimensional model is obtained by expansion of the axisymmetric model. All faces on the surface of the mesh are attached to the surfaces of revolution.

Attach relations between the axisymmetric mesh and the axisymmetric geometry are automatically transferred to the three-dimensional solid mesh. If a node of the axisymmetric mesh is attached to a point, the element edges that arise from expansion of the node are attached to the circle that results from revolving the point. Similarly, if an edge of the axisymmetric mesh is attached to a curve, the faces that arise from expansion of the edge are attached to the surface that results from revolving the curve. Since all edges on the boundary of the axisymmetric mesh are attached to the curves, all faces on the surface of the three-dimensional mesh will be attached to the surfaces of revolution (Figure 7.1-5).

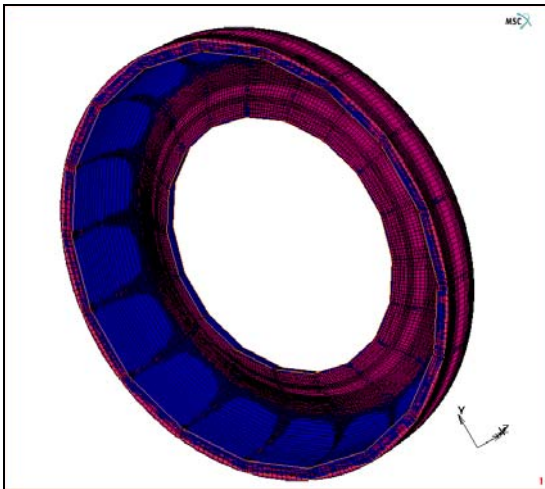


Figure 7.1-5 Three-dimensional Mesh of a Tire

Boundary Conditions on Geometric Entities

Any initial or boundary conditions applied to geometric entities are inherited by mesh entities attached to the geometry. For example, a point load applied to a point is inherited by the nodes attached to the point, an edge load applied to a curve is inherited by the edges attached to the curve, and a face load applied to a surface is inherited by the faces attached to the surface. Moreover, if a boundary condition that is normally applied to a node (such as a fixed displacement boundary condition) is applied to a curve or a surface instead, then the nodes of the edges or faces attached to the curve or surface inherit the boundary condition. The advantage is that loads can be specified independent of the finite element mesh.

MSC.Mentat 2003, by default, draws boundary and initial conditions that are applied to the geometry on the geometric entities. Previous MSC.Mentat versions always draw the boundary and initial conditions on the mesh entities that inherit from the geometric entities. The old pre-2003 behavior can be restored using DRAW BOUNDARY CONDS ON MESH from the BOUNDARY CONDITIONS menu and DRAW INITIAL CONDS ON MESH from the INITIAL CONDITIONS.

The tire is inflated by a pressure of 2 MPa. The pressure is applied to the interior surface (surface 3) of the tire. Furthermore, the displacements of the rim are suppressed ([Figure 7.1-6](#)), by applying a fixed displacement boundary condition to curve 2.

```
BOUNDARY CONDITIONS
  NEW
  NAME
    fixed
  MECHANICAL
    FIXED DISPLACEMENT
      X DISPLACEMENT
      Y DISPLACEMENT
      Z DISPLACEMENT
    OK
  CURVES ADD
    2
  END LIST (#)
  NEW
  NAME
    pressure
  FACE LOAD
    PRESSURE
      2
    OK
```

```
SURFACES ADD  
3  
END LIST (#)  
RETURN
```

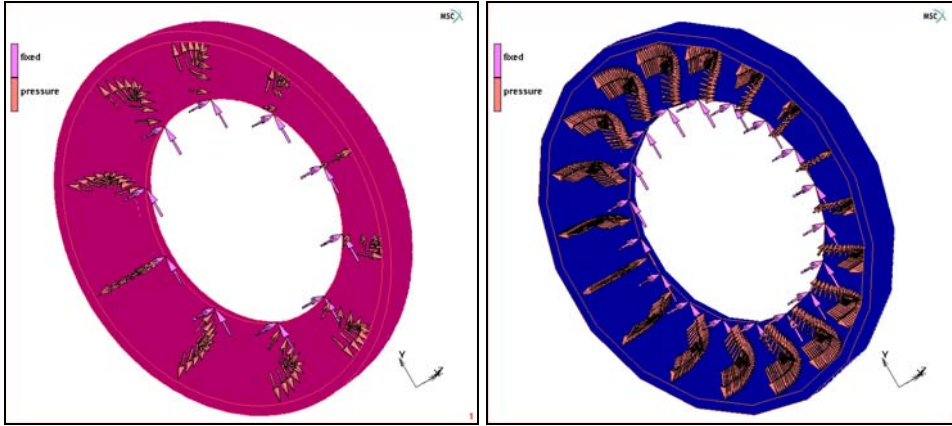


Figure 7.1-6 Boundary Conditions applied to the Geometry (left) and inherited by the Attached Mesh Entities (Faces and Nodes, right)

Combined Mesh Generation Commands

The full model is obtained by duplication of the existing model using a symmetry operation with respect to the yz-plane and by changing the linear elements to 20-node quadratic solid elements. The existing symmetry commands either duplicate the elements, curves or the surfaces, but not both. This means that even though the mesh and the geometry can be duplicated, the attach relations that exist between the original mesh and the original geometry, are lost for the copies. Any boundary conditions applied to the duplicates of the curves and surfaces are not transferred to the copy of the mesh.

The new COMBINED SYMMETRY operation overcomes this problem. It operates on a mixed list of items (nodes, elements, points, curves, surfaces, etc.). These items are duplicated in the same way as the normal symmetry commands and, in addition, any attach relations that exist between original mesh and geometry are duplicated for the copies of the mesh and the geometry.

The kind of items that are accepted by the COMBINED SYMMETRY command are controlled by the toggles in the COMBINED section of the SYMMETRY menu (Figure 7.1-7). Only active types are accepted and only items of these types are graphically pickable using the usual single pick, box pick, and polygon pick methods if the COMBINED SYMMETRY command is executed. This allows to simultaneously duplicate elements and surfaces, but no curves, for example. Wildcards like ALL: EXIST. and ALL: SELECT. can also be used with this command to indicate all existing or all selected items of the active types.

Similar operations exist in the DUPLICATE, EXPAND, and MOVE menus.

MESH GENERATION

SELECT

SELECT BY

FACES BY SRFS

4

END LIST (#)

RETURN (twice)

ATTACH

DETACH FACES

ALL: SELECT.

RETURN

SRFS REM

4

END LIST (#)

SYMMETRY

COMBINED SYMMETRY

ALL: EXIST.

RETURN

SWEEP

ALL

RETURN

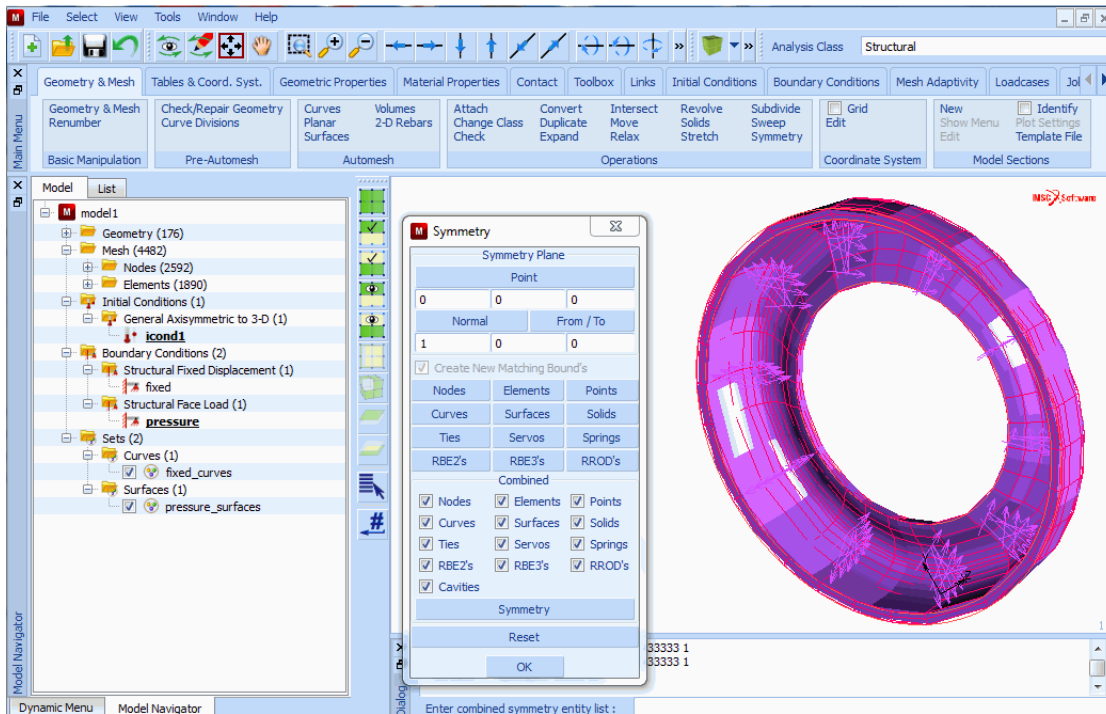


Figure 7.1-7 The SYMMETRY Menu with the COMBINED Section and Finite Element Mesh of the Full Model

Change Class

The linear 8-node solid elements are converted into quadratic 20-node solid elements using the new CHANGE CLASS TO QUADRATIC ELEMENTS operation (Figure 7.1-8). This is a special conversion that converts linear elements to quadratic elements, regardless of their class. The CHANGE CLASS TO LINEAR ELEMENTS command does the opposite operation.

```
CHANGE CLASS
    TO QUADRATIC ELEMENTS
    ALL: EXIST.
    RETURN (twice)
```

All commands in the CHANGE CLASS menu (including the existing conversions from one class to another) that create new nodes (such as the conversion from linear to quadratic elements) now generate unique nodes on coinciding edges and faces. This implies that a sweep operation to remove any duplicate nodes is no longer required after such a conversion. Moreover, new midside nodes are positioned on the curve or surface to which the edge or face is attached. The mid-edge nodes lie exactly halfway the edge.

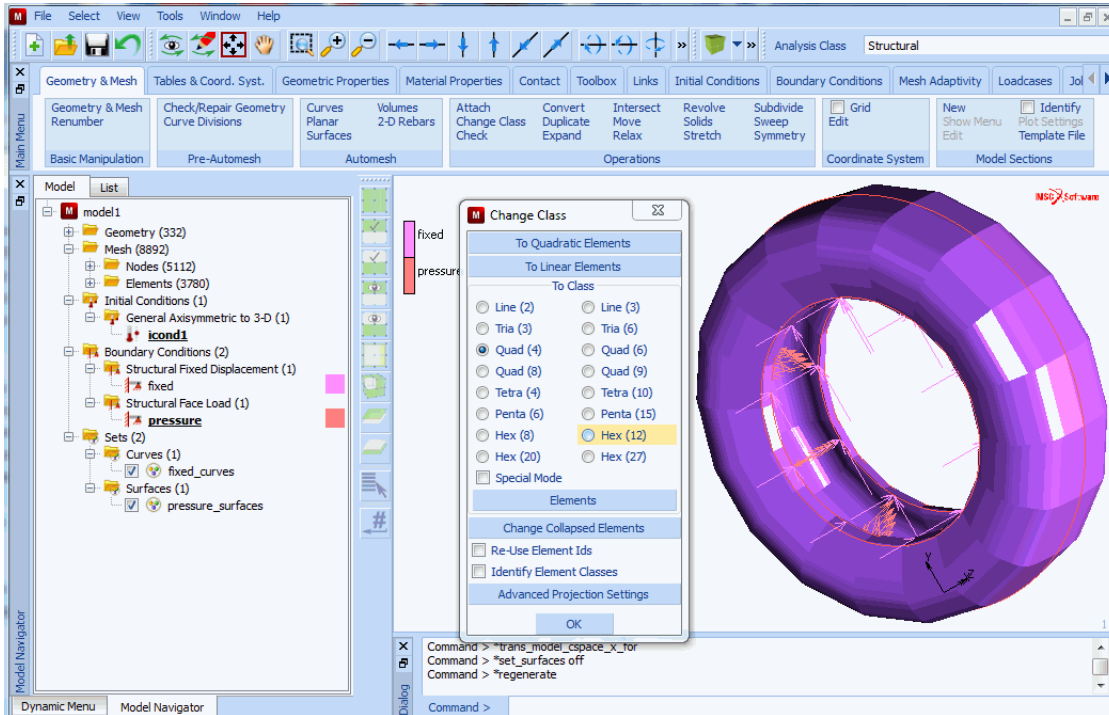


Figure 7.1-8 CHANGE CLASS Menu with TO QUADRATIC ELEMENTS Operation and Final Finite Element Mesh

Improved Links Handling

Handling of links has been improved. Links (nodal ties, servo links, and springs) are graphically pickable now, using the usual single pick, box pick, and polygon pick methods. Links can be duplicated and moved just like elements, and commands have been added to the LINKS→NODAL TIES, LINKS→SERVO LINKS and LINKS→SPRINGS/DASHPOTS for removing either all or a list of nodal ties/servo links/springs.

These new features are illustrated by replacing the boundary condition on the rim with a set of rigid links (tying type 80). First of all, the boundary condition is removed and a single nodal tie is created between a node on the rim and two new retained nodes on the axis of the tire.

BOUNDARY CONDITIONS

EDIT

fixed

MECHANICAL

REMOVE CURVES

ALL: EXIST.


```
        RETURN (twice)
MESH GENERATION
  ADD NODES
    60.8 0 0
    0 0 0
  RETURN
LINKS
  NODAL TIES
    NEW
    TYPE
      80
    TIED NODE
      74
    RETAINED NODE 1
      19315
    RETAINED NODE 2
      19316
  RETURN (twice)
```

Next, the nodal tie is duplicated 35 times by rotation around the axis of the tire about an angle of 10° per step. The resulting ties are duplicated by symmetry with respect to the yz -plane and a final sweep operation merges the duplicate nodes on the rim and on the axis of the tire. The resulting model is depicted in [Figure 7.1-9](#).

```
MESH GENERATION
  DUPLICATE
    ROTATION ANGLES
      10 0 0
    REPETITIONS
      35
    TIES
      link1
    END LIST (#)
  RETURN
SYMMETRY
  TIES
    ALL: EXIST.
  RETURN
```

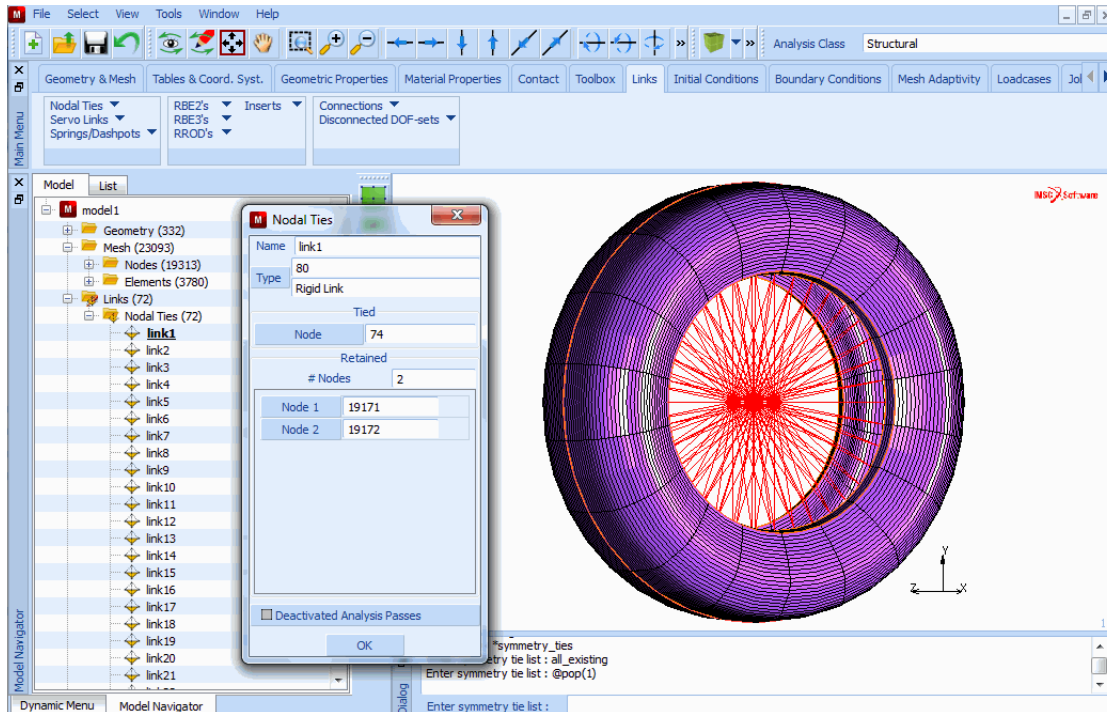


Figure 7.1-9 Full Model with Rigid Links (Tying Type 80)

```

SWEEP
TOLERANCE
    0.1
NODES
    ALL: EXIST.
RETURN (twice)
    
```

Patran Tetrahedral Mesher

The mesh is deleted, and a new mesh is created using the new (Patran) tetrahedral mesher. Tetrahedral meshing is, as always, done in two steps: first, a triangular mesh is created on the surfaces enclosing the volume to be meshed; next a tetrahedral mesh is created using the nodes of the surface mesh.

Note that after the first step, all triangular elements have their face attached to one of the surfaces. After the second step, the resulting element faces on the surface of the mesh are attached to one of the surfaces. As a result, the pressure boundary condition on surface 3 is automatically inherited by the attached element faces.

LINKS

NODAL TIES

REM TIES

ALL: EXIST.

RETURN (twice)

MESH GENERATION

CLEAR MESH

AUTO MESH

CHECK/REPAIR GEOMETRY

TOLERANCE

0.001

CHECK SURFACES

ALL: EXIST.

CLEAN SURFACE LOOPS

ALL: EXIST.

CHECK SURFACES

ALL: EXIST.

RETURN

CURVE DIVISIONS

AVG LENGTH

20

APPLY CURVE DIVISIONS

ALL: EXIST.

RETURN

SURFACE MESHING

SURFACE TRI MESH! (ADV FRONT)

ALL: EXIST.

RETURN

SOLID MESHING

OUTLINE EDGE LENGTH

TOLERANCE

1

SWEEP OUTLINE NODES

OUTLINE EDGE LENGTH

SOLID TET MESH!

ALL: EXIST.
RETURN (twice)

Once again, the linear elements are changed to quadratic elements.

CHANGE CLASS
TO QUADRATIC ELEMENTS
ALL: EXIST.
RETURN

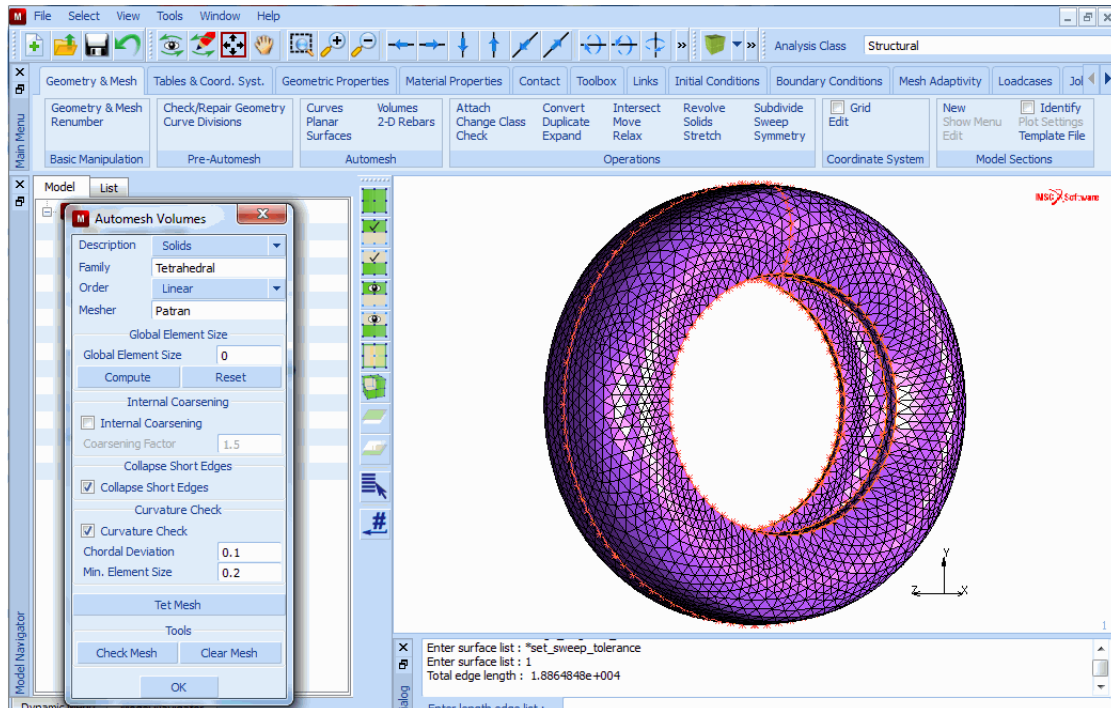


Figure 7.1-10 The AUTOMESH SOLIDS Menu and Finite Element Mesh

Note: Figure 7.1-10 was generated by the Patran tetrahedral mesher and the change class conversion to 10-node tetrahedral elements.

New Select Methods

Two new selection methods are shown in this section, where tied nodes for RBE2's are selected. The first one is the USER BOX method, which selects all entries that fall entirely within a box, specified in the current user coordinate system. In this case, a cylindrical coordinate system is used to select nodes which have a radial coordinate of 185. The

second method shown is the CURVE DIST method, which selects all entries within a given distance from a curve. The new methods POINT DIST and SURFACE DIST are similar but are not discussed here.

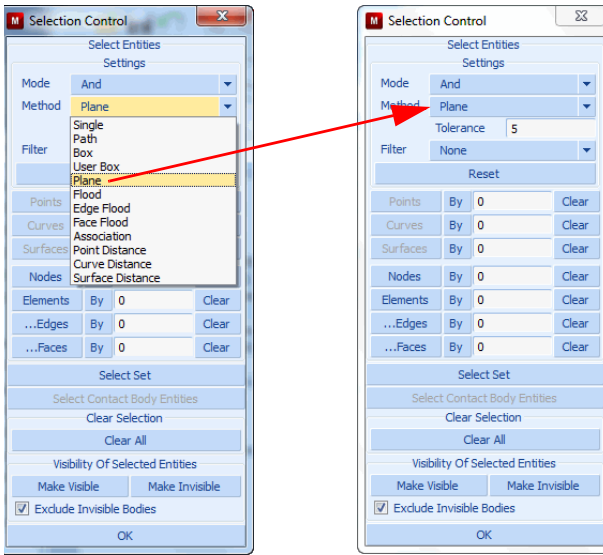


Figure 7.1-11 Select Method Menus

```

COORDINATE SYSTEM SET
  GRID
  CYLINDRICAL
  U DOMAIN
    0 200
  U SPACING
    5
  ROTATE
    0 90 0
  RETURN
ADD NODES
  0 0 0
  RETURN
LINKS
  RBE2'S
  NEW
  RETAINED NODE
  
```

```
36810
SELECT
  METHOD
    USER BOX
  RETURN
SELECT NODES
  185-0.01 185+0.01
  0 360
  -100 100
CLEAR SELECT
METHOD
  CURVE DIST.
  SELECT DISTANCE
    0.5
  RETURN
SELECT NODES
  9
  23
RETURN
TIED NODES ADD
  ALL: SELECT.
DOF 1
DOF 2
DOF 3
DOF 4
DOF 5
DOF 6
RETURN (twice)
```

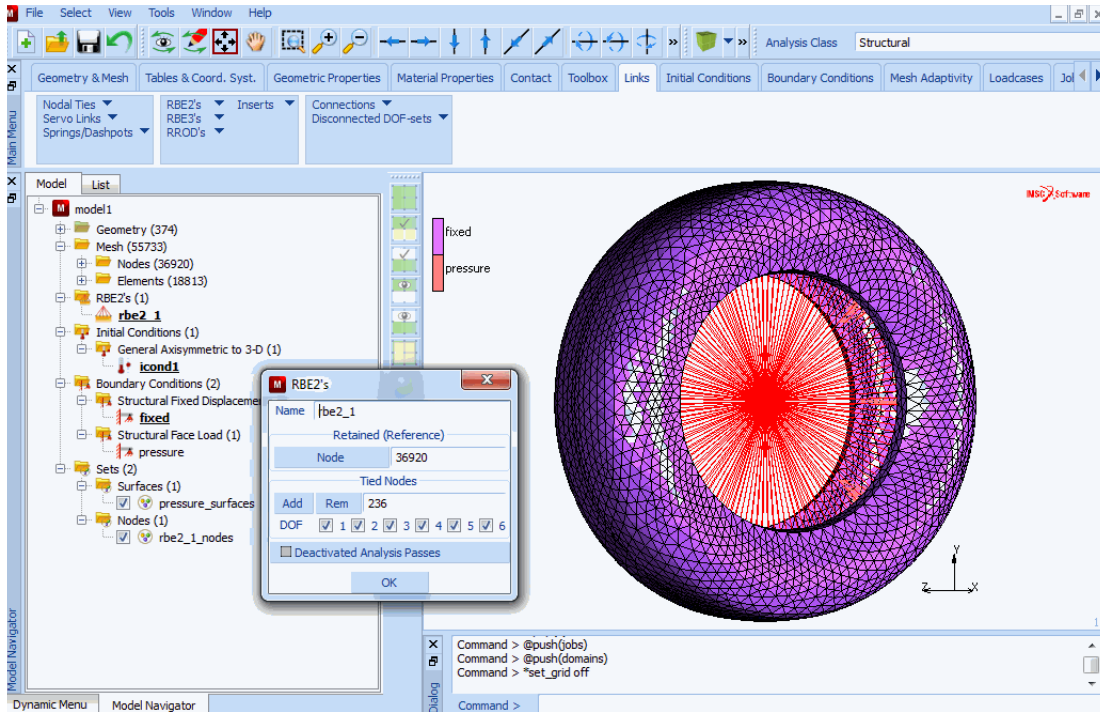


Figure 7.1-12 RBE2'S Menu and Final Tetrahedral Model with Nastran RBE2

New Domain Decomposition Methods

Domain Decomposition for DDM has been enhanced by three new methods:

- Metis Element Based
- Metis Node Based
- Metis Best (combined Metis Element Based and Metis Node Based)

Here, the Metis Best method is used to decompose the tire model:

JOBS

DOMAIN DECOMPOSITION

GENERATE!

8

ID DOMAINS

PLOT

NODES

POINTS

RBE2'S
SHORTCUTS
GRID

(off)

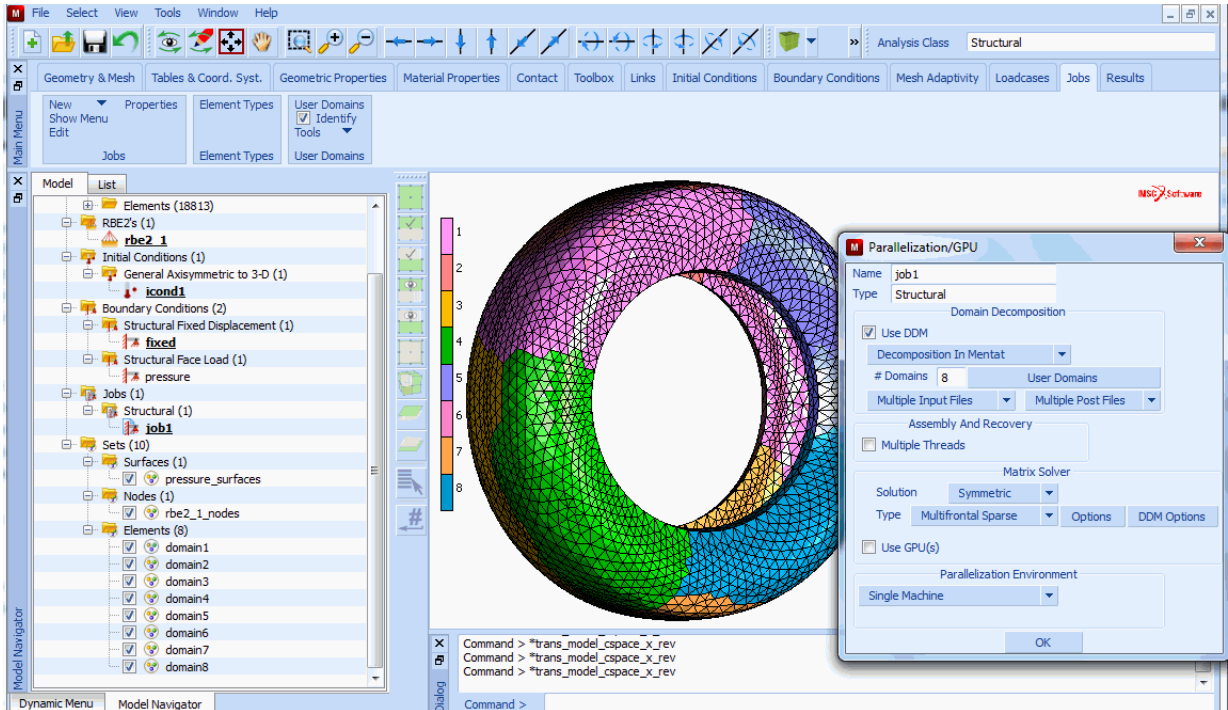


Figure 7.1-13 Metis Best Domain Decomposition

Multi-Dimensional Tables

The tables in Mentat have been enhanced to allow multiple independent variables. The number of independent variables ranges from 1 to 4, each variable having a different table type (physical meaning).

This section shows various ways to create tables starting with the simple one-dimensional table. The button sequences below start from the TABLES menu, which can be accessed in many places; for example, via MATERIAL PROPERTIES.

```

NEW
  1 INDEPENDENT VARIABLE
FILL
NAME
  E_t
    
```



```

TYPE
    temperature
ADD
    -100 1
    1000 .1
FIT
FUNCTION VALUE F MIN
    0
FILLED
MORE
    INDEPENDENT VARIABLE V1 LABEL
        Temperature
    FUNCTION VALUE F LABEL
        Young's Modulus
PREVIOUS
    
```

(on)

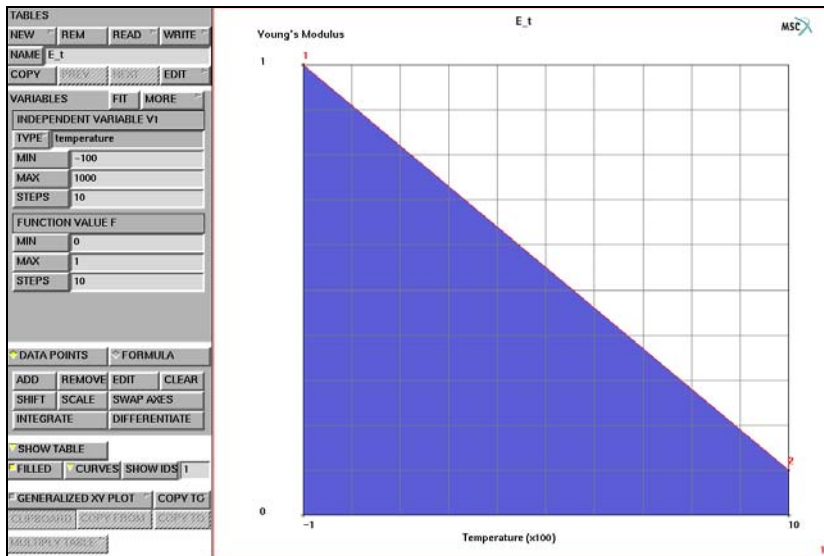


Figure 7.1-14 Creating a One-dimensional Table

In this example, the yield stress is a function of the gasket closure distance (first independent variable) and the temperature (second independent variable). There are seven gasket closure values and two temperatures, hence, the number of yield stress values defined is $7 \times 2 = 14$. The data in the table format appears as:

Temperature	Gasket Closure Distance						
	0	0.027	0.054	0.081	0.108	.135	.175
-100	0	2.08	8.32	18.72	33.28	52	56
1000	0	2.08	832	1.872	3.328	5.2	5.6

This would be manually entered as follows.

For each independent variable, the table type is set. In addition, labels are defined to be displayed along the axes of the table.

```

NEW
  2 INDEPENDENT VARIABLES
NAME
  E_d_t
TYPE
  gasket_closure_distance
INDEPENDENT VARIABLE V1
  INDEPENDENT VARIABLE V2
TYPE
  temperature
ADD ALL POINTS
  7
  2
  0 .027 .054 .081 .108 .135 .175
  -100 1000
  0 2.08 8.32 18.72 33.28 52 56
  0 .208 .832 1.872 3.328 5.2 5.6
FIT
FILLED
MORE
  INDEPENDENT VARIABLE V2 LABEL
    Temperature
  INDEPENDENT VARIABLE V2
    INDEPENDENT VARIABLE V1
  INDEPENDENT VARIABLE V1 LABEL
    Closure Distance
  FUNCTION VALUE F LABEL

```

(off)

Young's Modulus
 PREVIOUS

The second independent variable is selected to be displayed along the X-axis. Note that for a table with multiple dimensions it may be helpful to rotate the plot. The table data is stored in an external file.

X-AXIS: V1

X-AXIS: V2

FILLED

(on)

RX+

RY-

RX+

RY-

FILL

RESET VIEW

FILL

WRITE

E_d_t.tab

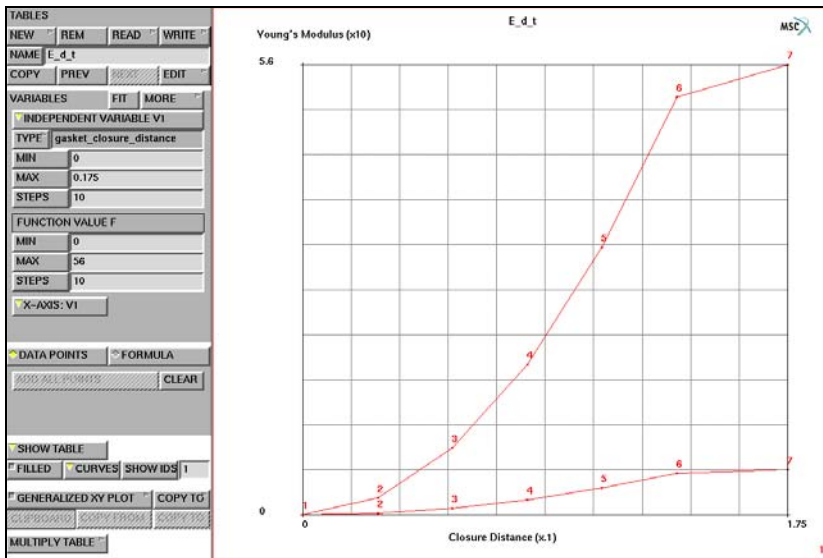


Figure 7.1-15 Creating a Two-dimensional Table

A different way to create a multidimensional table is by multiplying tables. First, a new one-dimensional table E_d is created. Next, this table is multiplied by table E_t which was created earlier.

NEW

1 INDEPENDENT VARIABLE

NAME

E_d

TYPE

gasket_closure_distance

ADD

0 0

.027 2.08

.054 8.32

.081 18.72

.108 33.28

.135 52

.175 56

FIT

MORE

INDEPENDENT VARIABLE V1 LABEL

Closure Distance

FUNCTION VALUE F LABEL

Young's Modulus

PREVIOUS

MULTIPLY TABLE

E_t

FILLE

D

(off)

NAME

E_d_t_2

MORE

INDEPENDENT VARIABLE V1

INDEPENDENT VARIABLE V2

FUNCTION VALUE F LABEL

Young's Modulus

PREVIOUS

X-AXIS: V1

X-AXIS: V2

FILLED

(on)

RX+

RY-

RX+

RY-

FILL

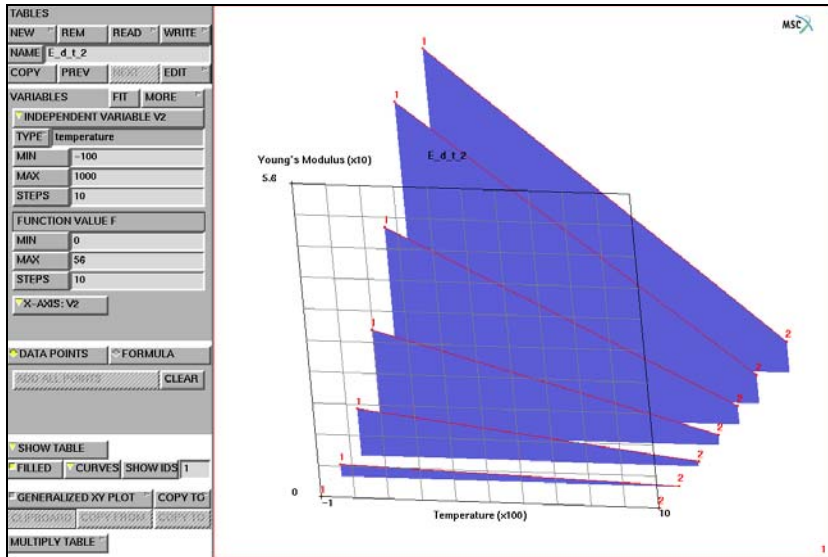


Figure 7.1-16 Result of Table Multiplication

RESET VIEW

FILL

Creation of a table with three independent variables is now shown using a formula to generate the data points. Note that the independent variables are designated by v1, v2, v3, and v4. The formula is evaluated depending on the ranges and the number of steps of the independent variables.

NEW

3 INDEPENDENT VARIABLES

FORMULA

ENTER

.1+v1^2+sqrt(v2)+sin(v3*pi)

FIT

RX+

RY-

RX+

RY-

FILL

The user may now select which independent variable is displayed along the X-axis, and which along the Y-axis. For the third independent variable, a fixed value is taken, namely the *i*-th data point value for this independent variable. The index *i* can be set with the FIX button and ranges from 1 to the number of data points of the independent variable.

Y-AXIS: V2
 Y-AXIS: V3
X-AXIS: V1
 X-AXIS: V2
Y-AXIS: V3
 Y-AXIS: V1
X-AXIS: V2
 X-AXIS: V3
Y-AXIS: V1
 Y-AXIS: V2
FIX V1
 6
FIX V1
 11
FILL
X-AXIS: V3
 X-AXIS: V1
FIX V3
 6

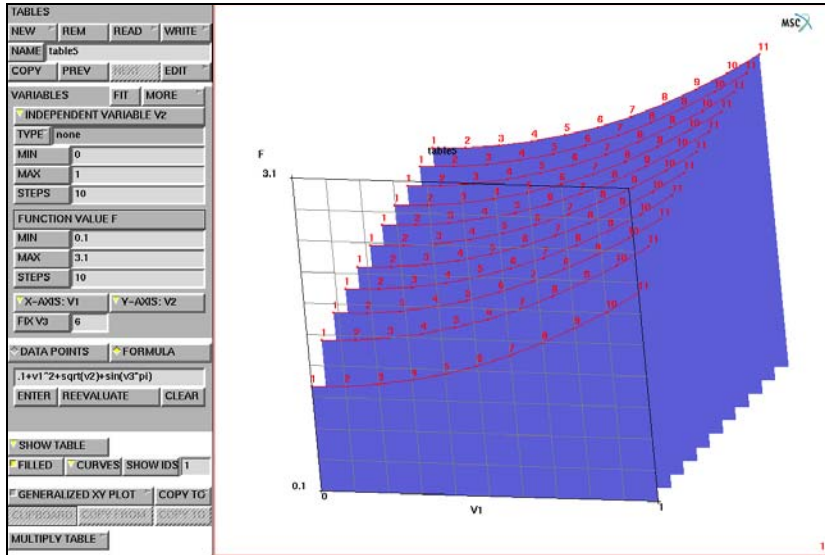


Figure 7.1-17 Creating a Three-dimensional Table

Especially for use in the EXPERIMENTAL DATA FIT menus, Mentat allows creation of tables with one independent and two dependent variables. In previous versions, this could only be done by reading raw table data. Now, such a table can be created, edited, and displayed like any other table.

```

NEW
    1 INDEP. & 2 DEP. VARIABLES
RESET VIEW
FILL
ADD
    -4/3 -8 0.9605
    -1 -6 0.9703
    -2/3 -4 0.9801
    -1/3 -2 0.9900
    0 0 1
SCALE
    0.01 10 1
FIT
TYPE
    experimental_data
MORE
    INDEPENDENT VARIABLE V1 LABEL
    
```

Strain
 FUNCTION VALUE F LABEL
 Stress
 PREVIOUS
 Z-AXIS: F
 Z-AXIS: F2
 MORE
 FUNCTION VALUE F
 FUNCTION VALUE F2
 FUNCTION VALUE F2 LABEL
 Vol/Vol_0
 PREVIOUS

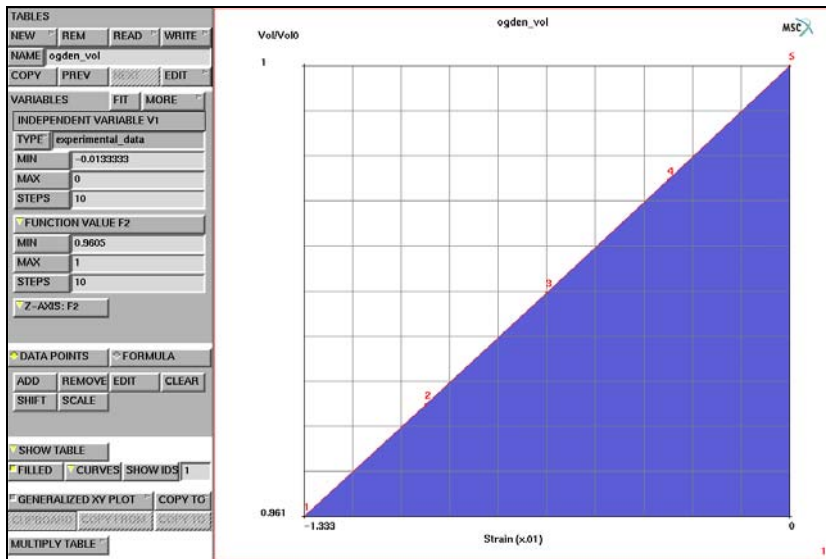


Figure 7.1-18 Creating a Table with 2 Dependent Variables

User-defined Text Input

User-defined text may be added to the parameter, model definition, or history definition sections of the data file. The JOBS menu contains the links to the parameter and model definition menus, and the LOADCASES menu contains the link to the history definition menu.

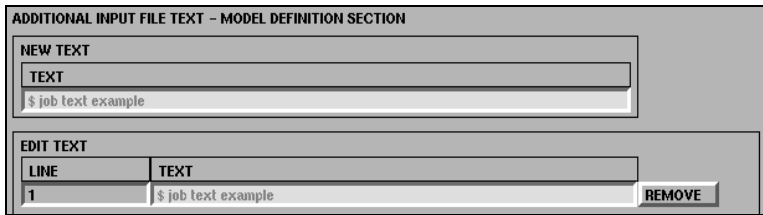


Figure 7.1-19 Additional Input File Text Menu

Python

The ability to obtain a user-defined string from Mentat in a Python script has been added in this release. The user can specify the string using the PARAMETERS menu, and the Python script obtains the value using the `py_get_string` routine. The following example uses the model file in Chapter 7 of the *Marc Python Tutorial* and prints out the number of sets in the model. The steps for this example are:

- Browse to the Python examples directory.
- Specify the name of the model file that we want to check.
- Run the Python script.

UTILS

CURRENT DIRECTORY

`path/examples/python/tutorial/c07`

OK

PARAMETERS

(NAME)

`filename`

(EXPRESSION)

`sets.mfd`

OK

PYTHON

RUN

`nsets.py`

The Python script is as follows:

```
1 from py_mentat import *
2
3 def main():
4     fn = py_get_string("filename")
5     s = "*open_model %s" % fn
```

```
6         py_send(s)
7         n = py_get_int("nsets()")
8         print "Sets found: ",n
9         return
10
11     if __name__ == '__main__':
12         main()
```

The output of the script will be printed in the terminal window:

```
Sets found: 8
```

Postprocessing Enhancements

MPEG and AVI Animations

Mentat can now create an MPEG animation file or an AVI (Windows NT/2000/XP only) animation file. It is accessed from the RESULTS→ANIMATION submenu. The settings are preset to typical default values so that for most users, only one button needs to be pressed to start the creation of the animation file.

The MPEG and AVI animation menus are very similar. The BASE FILE NAME is automatically set to the name of the post file. The GENERATE ANIMATION FILES button enables or disables the creation of the intermediate display list files that are read and displayed when selecting the PLAY button in the ANIMATION main menu. In most cases, you want to have this option selected unless you are assembling an animation from various increments in the post file. The buttons under the INCREMENTS section are the same as in the RESULTS main menu. The ATTRIBUTES menu provides shortcuts to the LEGEND settings, RANGE and COLORMAP buttons. The CLEAN FILES button removes all the intermediate display list files and the PPM image files used to create an MPEG movie.

Note: Do not use the CLEAN FILES button until you have successfully viewed the resulting animation file.

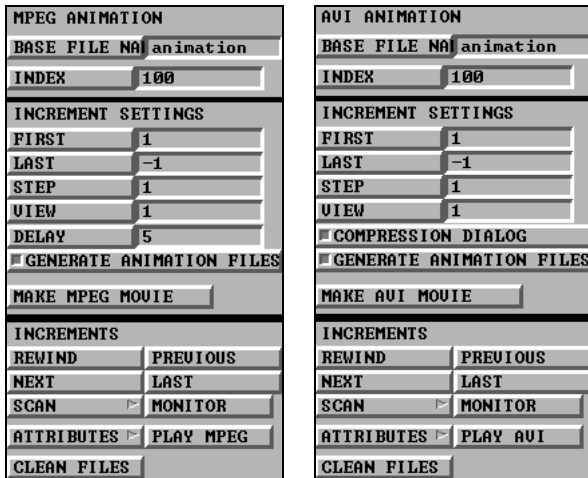


Figure 7.1-20 MPEG and AVI Animation Menus

The DELAY button in the MPEG menu duplicates frames (increment images) in the MPEG movie since some MPEG players attempt to play the movie in real time. For example, if there are 100 increments, some MPEG players skip frames to try and play the entire movie in $100/24\text{fps} = 4$ seconds.

When the MAKE MPEG MOVIE button is pressed, the intermediate display list files are generated, then they are played back and images are created from each of the increments and stored in the PPM graphic files. Then the MPEG encoding program, *mpeg_encode.exe* in Mentat's bin directory, is run in the background.

Note that there is no feedback from this program back to Mentat to indicate that the MPEG encoder has completed. The most reliable way to detect this is to use the `ps` command on Unix or the Windows Task Manager on Windows NT. You can also monitor the size of the MPEG file. When it is no longer growing in size, the encoder has completed generating the file.

The COMPRESSION DIALOG button in the AVI menu allows you to select the compression method for the AVI file. In most cases, you should not select the default of *Full Frames (Uncompressed)* but select *Microsoft Video 1* as the compression method.

When the MAKE AVI MOVIE button is selected, it performs tasks similar to that for the MPEG movie. The intermediate display list files are generated, and then they are played back and images are created. However, these images are not saved to a file. They are fed immediately to the AVI movie generator. When all of the display list files have been displayed and images created, the AVI movie generator will write the AVI file to disk.

Creating a Movie

The following example displays how to make an MPEG movie. The technique used for generating an MPEG movie is very similar to that for generating an AVI movie. This example uses the HELP→RUN A DEMO PROBLEM→RUBBER REZONING example to generate the post file.

HELP
RUN A DEMO PROBLEM
RUBBER REZONING

When the run completes, perform the following steps:

RESULTS
MOR
E
ANIMATION
MPEG MOVIE
MAKE MPEG MOVIE

After the follow message appears:

```
Creating ppm files...
```

the MPEG encoder is started and runs in the background. Note that no message appears in the dialogue area when the process is complete. Check its status using the Windows Task Manager or use the `ps` command on UNIX.

The PLAY MPEG button may be selected when the MPEG encoder has been started. It starts the `mpeg_window` (`mpeg_window.bat` on Windows NT) script which waits until the MPEG encoder has finished before attempting to play the MPEG movie. Note that on UNIX the `mpeg_window` script must be modified to use the application on your system that supports playing MPEG movies. The movie players are not supplied with the product. On Windows NT systems, the default is to use the application associated with MPEG movies, which is originally Windows Media Player. This can be changed by either modifying the `mpeg_window.bat` script, or by associating a different application to MPEG movie files.

Postprocessing in 3-D

New commands have been added named `*set_post_procedure on/off` (menu button POST PROCEDURE) and its associated command `*post_procedure_file <procedure filename>` (menu button FILE) in the RESULTS menu. These commands allow for the specification of a procedure file whose contents are executed as each increment is read. This is most useful when a 2-D analysis has been run and a 3-D model is desired to be viewed based on symmetry.

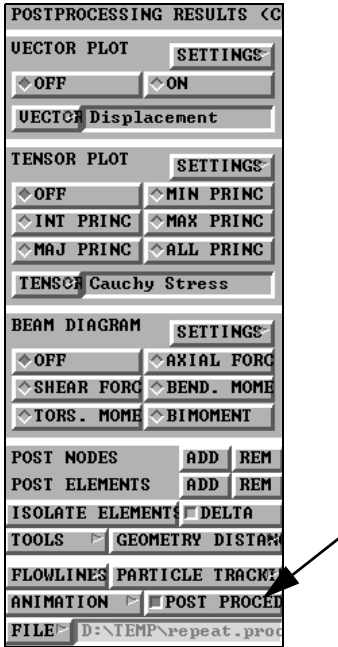


Figure 7.1-21 Postprocessing Results Menu

For example, the *Marc User's Guide*, Chapter 3.31 problem of a tire analysis produces a 2-D section of the tire. To build a full 3-D model, place the following commands in a procedure file and select it using the FILE button:

```
*clear_mesh
*set_expand_rotations
20 0 0
*set_expand_repetitions
18
*symmetry_elements
all_existing
*expand_elements
all_existing
```

To enable its use, select the POST PROCEDURE button.

See [Figure 7.1-22](#) of the original analysis on the left, and the full 3-D model is on the right.

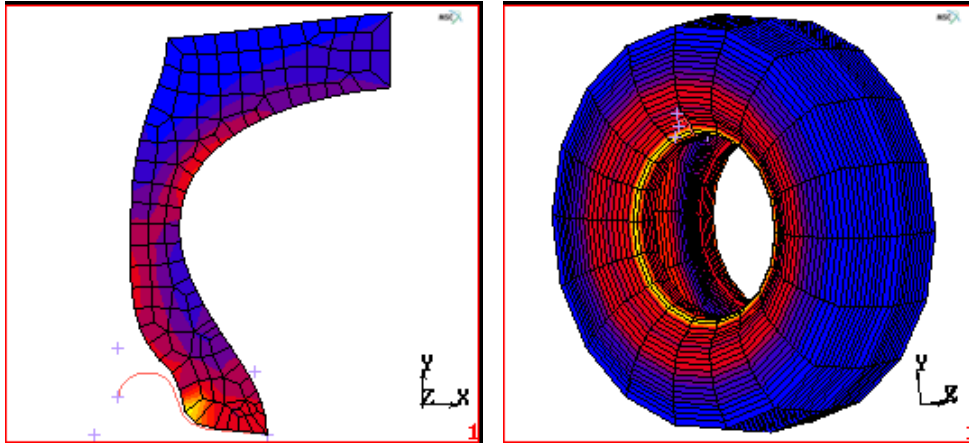


Figure 7.1-22 Views of 2-D and Full 3-D Model

Input Files

The files below are on your [delivery media](#) or they can be downloaded by your web browser by clicking the links (file names) below.

File	Description
attach.proc	Mentat procedure file
md_table.proc	Mentat procedure file
tire.igs	Iges input file

Animation

Click on the figure below to play the animation.



7.2 Importing a Model

- Chapter Overview 2162
- Background Information 2162
- Detailed Session Description 2162
- Input Files 2176

Chapter Overview

This chapter describes the process of importing a geometric or finite element model from a supported CAD or FEM program. The process is illustrated through a sample session that involves importing and meshing a geometric model specified in IGES format.

Background Information

Description

The structure you are importing is a seal made out of rubber that will undergo large deformations caused by coming into contact with other parts. The structure is modeled using a boundary representation of straight lines and curves.

After reading the IGES file, you will select a portion of the model and transform it into a finite element mesh. This process is described in the steps listed below.

The IGES file will be found in the Mentat installation directory, in the subdirectory *examples/marc Ug* and is named *seal.igs*.

Overview of Steps

- Step 1: Import IGES file.**
- Step 2: Eliminate all duplicate points and curves using SWEEP processor.**
- Step 3: Create two sets of the upper and lower parts of the model.**
- Step 4: Hide upper part of model and scaled the lower part to fill the graphics area.**
- Step 5: Use of the 2-D planar meshers from the AUTOMESH processor to complete the meshing of the model.**

Detailed Session Description

Step 1: Import IGES file.

Assume you are already in Mentat and in the directory where the file you wish to import is located.

Use the following button sequence to read the IGES file. Click on the FILL button located in the static menu area to scale the model to fill the graphics area. The scaled model that appears in the graphics area is shown in [Figure 7.2-1](#).

```

MAIN
  FILES
    IMPORT
      IGES
        seal.igs      (select file)
      OK
    FILL
  
```

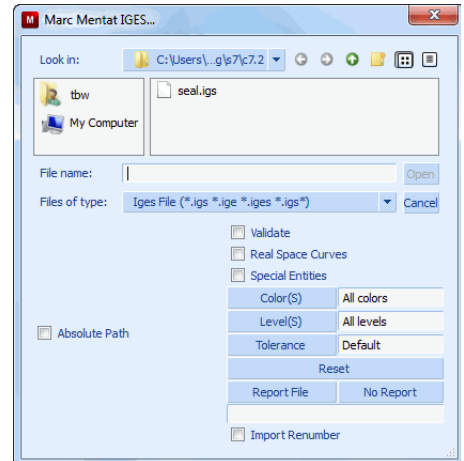
Step 2: Eliminate all duplicate points and curves using SWEEP processor.

Prior to manipulating the model in any way, you are advised to eliminate all duplicate points and curves using the SWEEP processor. Use the following button sequence to sweep the model of all duplicate entities.

```

MAIN
  MESH GENERATION
    SWEEP
      sweep POINTS
        all: EXIST.
      sweep CURVES
        all: EXIST.
  
```

Mentat responds by sweeping all duplicate points and curves, respectively.



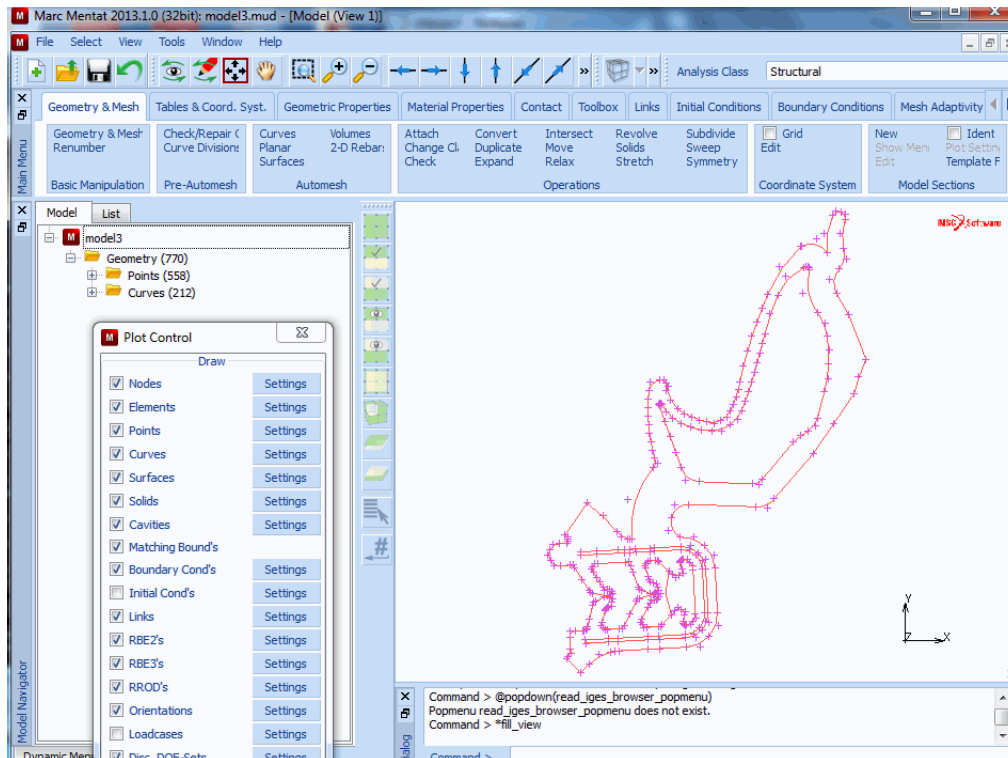


Figure 7.2-1 Imported IGES File scaled to fit Screen

To improve the quality of the display, change the default plot settings to a higher accuracy.

MAIN

MESH GENERATION

PLOT

curves SETTINGS

predefined settings HIGH

REGEN

RETURN (twice)

Step 3: Create two sets of the upper and lower parts of the model.

Assume you only need to mesh the lower part of the model shown in [Figure 7.2-1](#). It is useful to store the upper and lower parts of the model in two separate sets as it makes it much easier to reference when working with only part of the model. An option in Mentat that aids you in focusing on the part of the model you want to mesh is the **VISIBLE** option which is used to hide extraneous information.

You are going to use the automatic overlay meshing feature which requires a closed boundary description. The lower part of the geometry therefore needs an additional line segment. Create this line in the vicinity of the lower neck of the model using the following button sequence.

MAIN

MESH GENERATION

ZOOM BOX

(zoom in on the base of the neck)

crvs ADD

(use the default curve type)

235

(pick point)

188

(pick point)

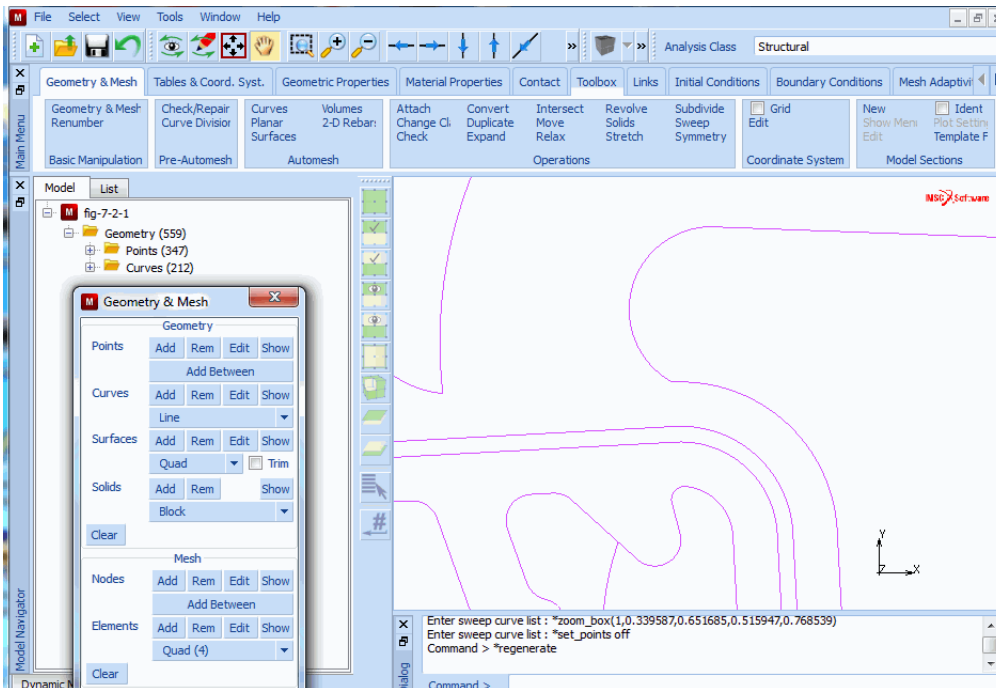


Figure 7.2-2 Curved added at base of Neck

Use the following button sequence to create the two sets: one for the upper part of the model, the other for the lower part. Due to the awkward shape of the model, it is best to use the polygon pick method (CTRL key + <ML>) described in [List Specification](#) of the *Introduction* section, select the members for each set.

MAIN

PLOT

draw POINTS

(off)

```

REGEN
RETURN
FILL
MESH GENERATION
SELECT
  crvs STORE
    upperpart                               (the curve set name)
  OK
                                           (use the Polygon Pick Method to select the curves)

END LIST (#)

```

Repeat this operation for the lower part of the model and save the set as `lowerpart`. A suggestion for the contour of the polygon pick is depicted in [Figure 7.2-3](#) and [Figure 7.2-4](#).

To verify that you have created two sets, click on the sets SELECT SET button. A pop-up menu appears over the graphics area listing the currently defined sets. Both `lowerpart` and `upperpart` should be listed. Click on OK to return to the SELECT menu.

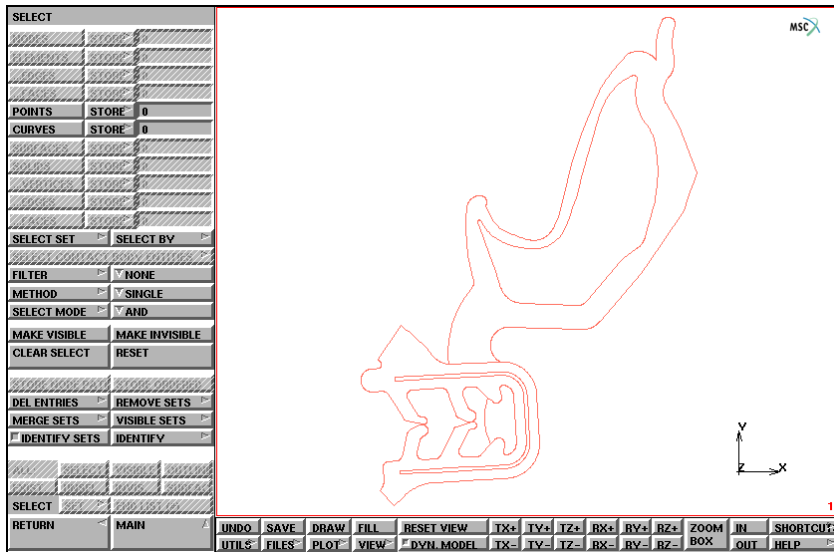


Figure 7.2-3 Polygon Pick Contour for Upper Part

Step 4: Hide upper part of model and scaled the lower part to fill the graphics area.

To focus on the lower part of the structure, use the following button sequence to hide the upper part of the model.

MAIN
 MESH GENERATION
 SELECT
 SELECT SET
 lowerpart
 OK
 MAKE VISIBLE
 FILL

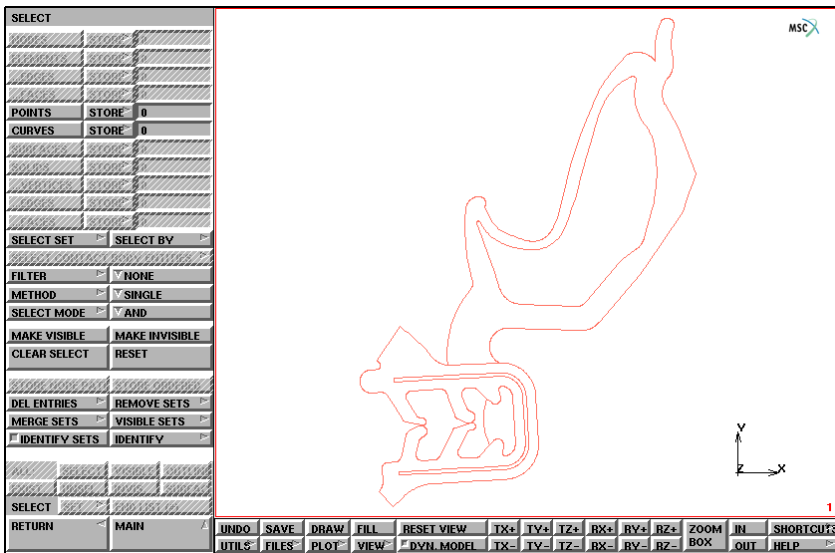


Figure 7.2-4 Polygon Pick Contour for Lower Part

The upper part of the model is hidden and the lower part scaled to fill the graphics area as is shown in [Figure 7.2-5](#).

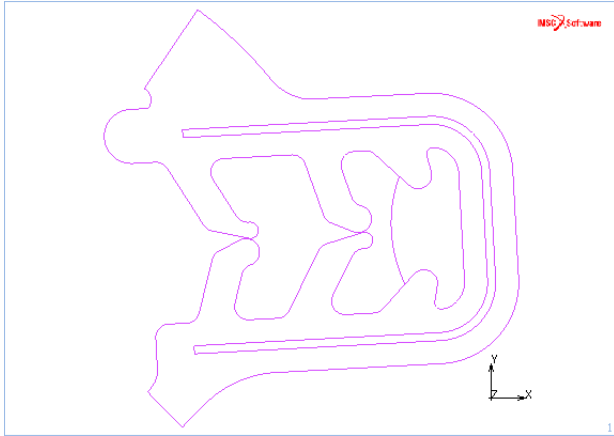


Figure 7.2-5 Lower Part of Model scaled to fill the Graphics Area

A closer look at [Figure 7.2-5](#) reveals there is an extra curve in the geometry that interferes with the boundary description of the part. This curve must be removed before the automatic meshing feature is invoked. The curve is located in the inner part of the seal on the right hand side of the model. Use the following button sequence to remove this curve.

MAIN

MESH GENERATION

crvs REM

180

(pick curve)

END LIST (#)

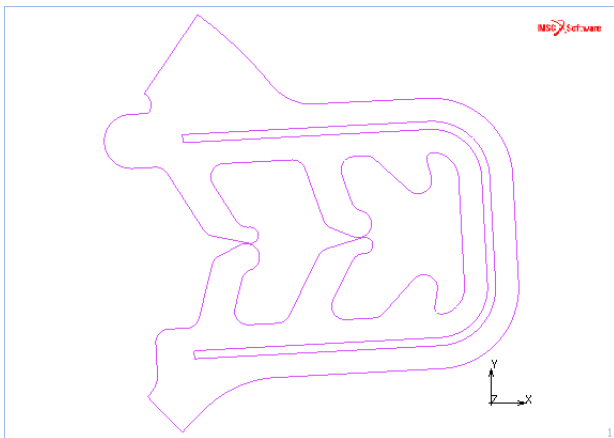


Figure 7.2-6 Lower Part of Model with Curve removed

Step 5: Use of the 2-D planar meshers from the AUTOMESH processor to complete the meshing of the model.

The model is ready to be meshed using the 2-D PLANAR MESHING from the AUTOMESH processor from the MESH GENERATION menu. First, the overlay mesher is used. Due to the intricate shape of the model, it is necessary to use a density of 70 elements in both the X and Y direction. A setting of less than 70 causes holes to appear in the mesh.

Make sure you specify all: VISIBLE curves for the Enter overlay curve list: prompt. Use the following button sequence to mesh the model. Keep in mind that it takes the program some time to generate the model due to the number of divisions specified.

```
MAIN
  MESH GENERATION
    AUTOMESH
      2-D PLANAR MESHING
        quadrilaterals (overlay) DIVISIONS
          70 70
        quadrilaterals (overlay) QUAD MESH!
        all: VISIBLE
```

It is helpful to turn off some of the plot entities to produce a cleaner view of the mesh.

MAIN

PLOT

draw NODES (off)

elements SETTINGS

FACES (off)

RETURN

draw CURVES (off)

REGEN

RETURN

SAVE

Figure 7.2-7 shows the resulting mesh that should appear in the graphics area.

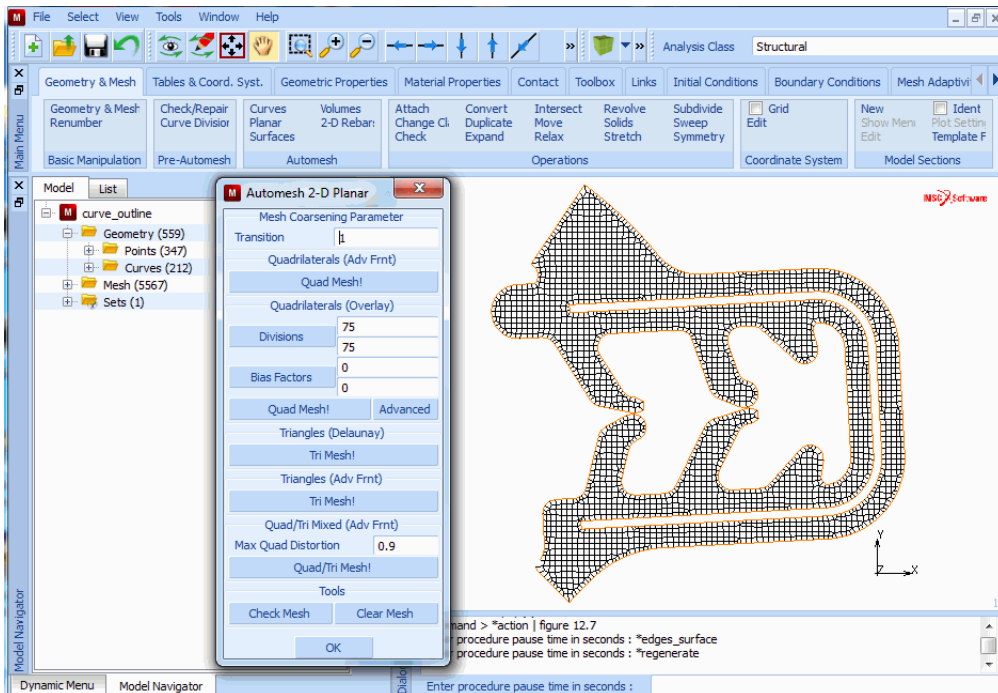


Figure 7.2-7 Mesh generated with OVERLAY Mesher

In order to demonstrate the use of the other 2-D planar meshers, the element mesh is removed and the display of the curves and points id activated.

```
MAIN
  MESH GENERATION
    AUTOMESH
      2-D PLANAR MESHING
        CLEAR MESH
        PLOT
          draw POINTS (on)
          draw CURVES (on)
        REGEN
        RETURN
```

Since we have already assured that a closed loop exist for the curves, we do not have to enter the REPAIR GEOMETRY menu in AUTOMESH. Instead, we go to CURVE DIVISIONS directly. Meshers other than the overlay mesher require a curve division. We first determine the distance between the two parallel curves. Based on this distance, a proper curve division is set. Note that the Advancing Front QUAD mesher (Figure 7.2-10) requires an even division on the loops.

```
MAIN
  MESH GENERATION
    AUTOMESH
      CURVE DIVISIONS
        UTILS
          DISTANCE (click two points on the parallel curves)
        RETURN
      AVG LENGTH
        0.3
      restriction FORCE EVEN DIV
      apply restriction LOOPS (select DETECTED LOOPS)
      APPLY CURVE DIVISIONS
      ALL VISIBLE
```

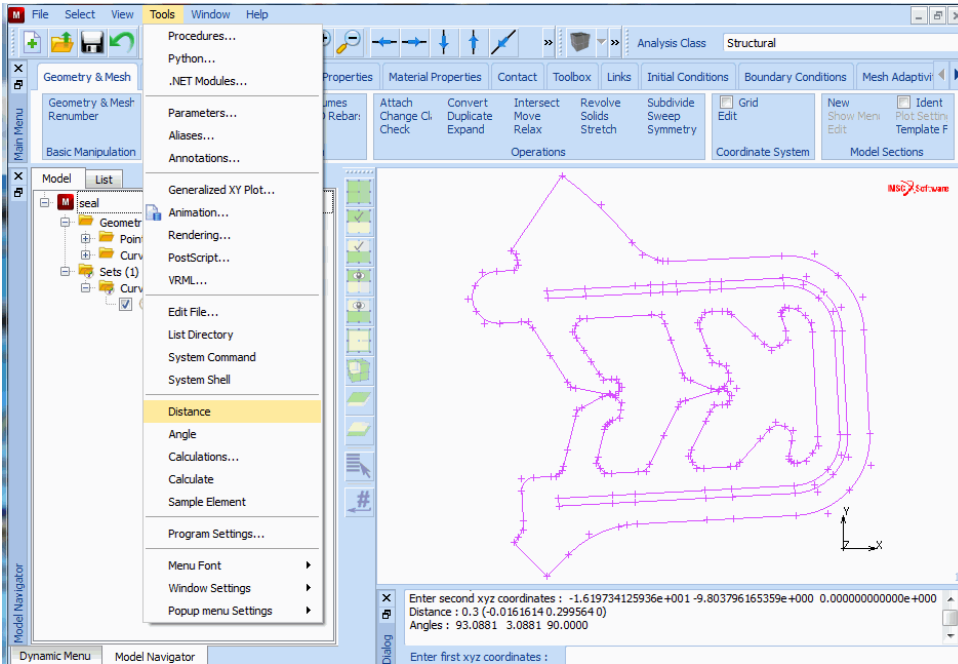


Figure 7.2-8 Determine Distance between Parallel Curves

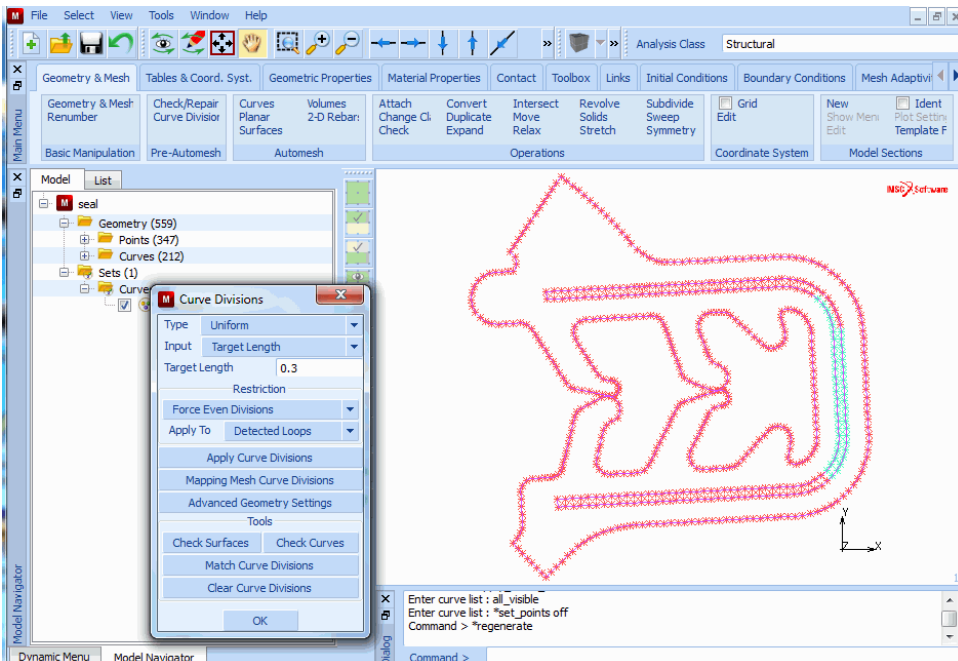


Figure 7.2-9 Apply Curve Divisions

The mesh based using the Advancing Front QUAD masher is now obtained with:

MAIN

MESH GENERATION

AUTO MESH

2-D PLANAR MESH

quadrilaterals (adv frnt) QUAD MESH!

ALL VISIBLE

PLOT

draw CURVES

draw POINTS

REGEN, RETURN

(off)

(off)

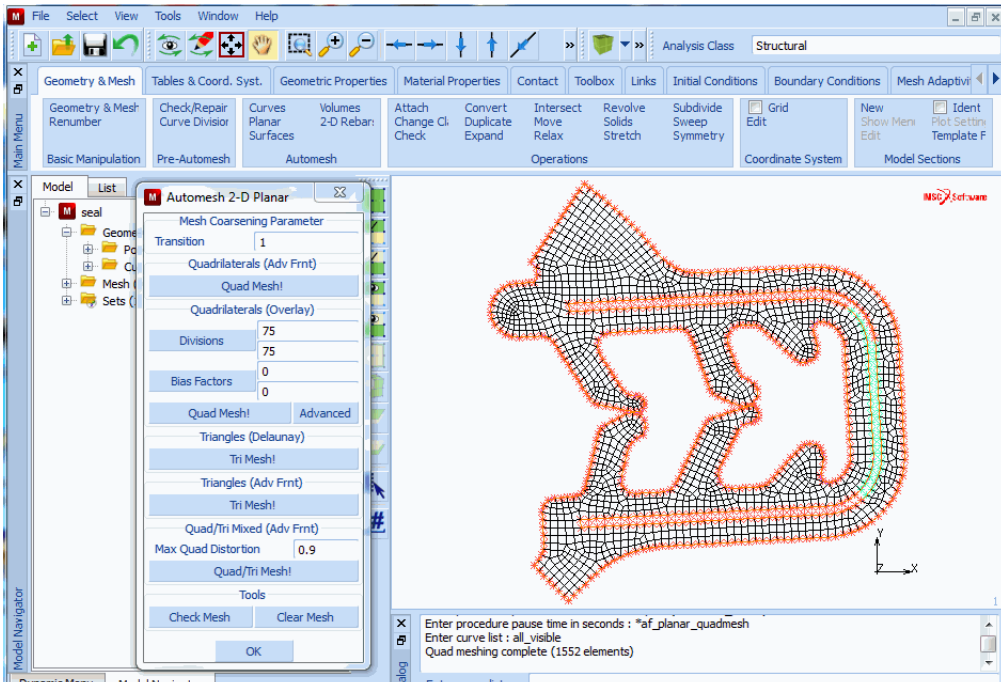


Figure 7.2-10 Mesh generated with Advancing Front QUAD Mesher

Clear the mesh and repeat the meshing with the Delaunay triangular mesher.

MAIN

MESH GENERATION

AUTOMESH

2-D PLANAR MESHING

CLEAR MESH

PLOT

draw CURVES

(on)

REGEN

RETURN

triangles (delaunay) TRI MESH!

ALL VISIBLE

PLOT

draw CURVES

(off)

REGEN

RETURN

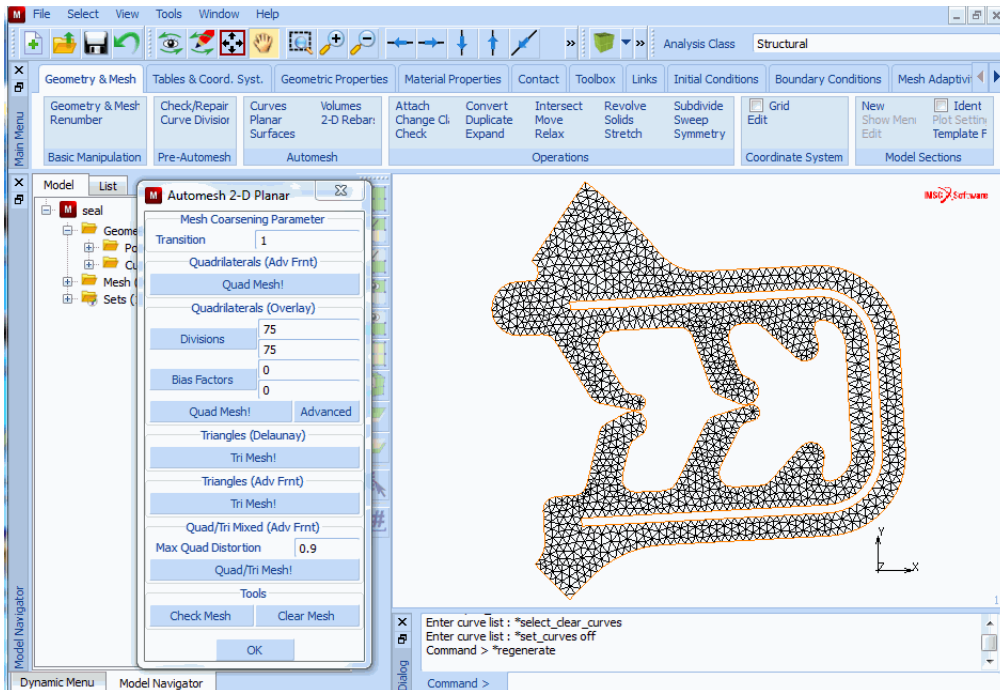


Figure 7.2-11 Mesh generated with a Delaunay Triangular Mesher

Clear the mesh and repeat the meshing with the Advancing Front triangular mesher.

MAIN

MESH GENERATION

AUTOMESH

2-D PLANAR MESHING

CLEAR MESH

PLOT

draw CURVES

(on)

REGEN

RETURN

triangles (adv frnt) TRI MESH!

ALL VISIBLE

PLOT

draw CURVES

(off)

RETURN

REGEN

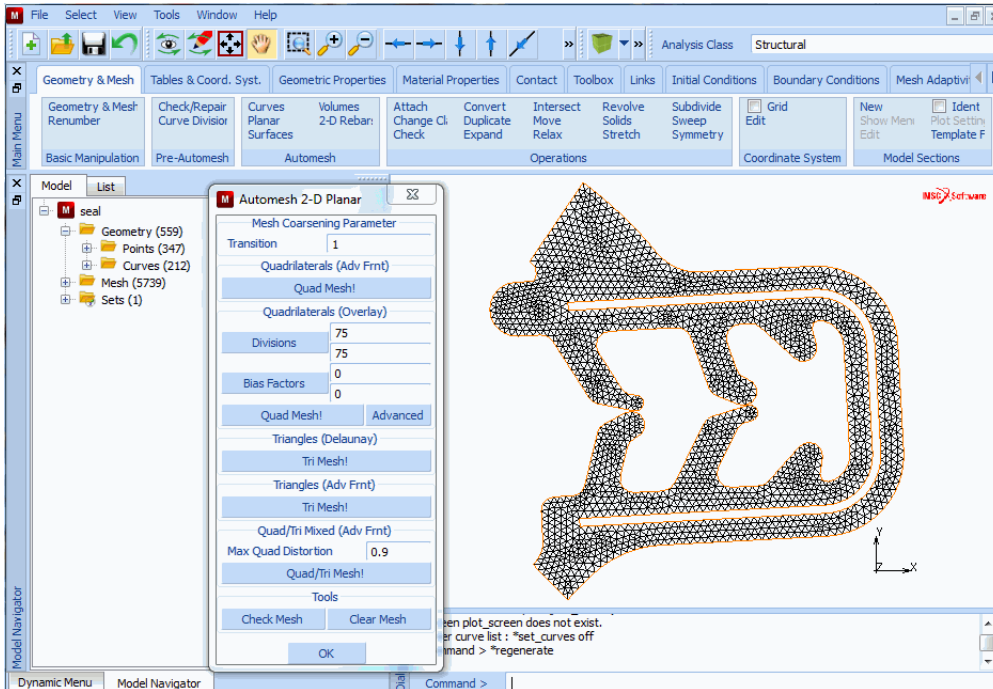


Figure 7.2-12 Mesh generated with a Advancing Front Triangular Mesher

Input Files

The files below are on your [delivery media](#) or they can be downloaded by your web browser by clicking the links (file names) below.

File	Description
seal.proc	Mentat procedure file
seal.igs	Iges input file

7.3 HyperMesh® Results Interface

- Chapter Overview 2178
- About Postprocessing of Results 2178
- About Preprocessing 2179
- Mentat Preprocessing for HyperMesh 2179
- Postprocessing using HyperMesh 2188

Chapter Overview

Marc can create a binary file of the results that may be postprocessed using HyperMesh. The writing of the HyperMesh results file is invoked by the HYPERMESH model definition option described in detail in *Volume C: Program Input*. The binary file created as a result has the title `jobid.hmr` where `jobid` is the name of the Marc data file for the job. This file, as well as the data file (for most cases) can be read by HyperMesh for postprocessing. If the model was originally created using HyperMesh, the HyperMesh geometry database can be used instead of the data file. The data that may be postprocessed ranges from elemental quantities, such as stress and strain, to nodal quantities, such as displacement, acceleration, temperature, and eigenmodes.

About Postprocessing of Results

Interfacing Analysis and Postprocessing

Postprocessing of finite element analysis results usually refers to the graphical interpretation of results, performed by way of a graphics capable computer program. This program usually is the same one used for the preprocessing (modeling) phase, but this is not always necessary. By the use of a postprocessor, the user can visualize the response of a finite element model as obtained from an analysis of the model. Such response may include, but is not limited to, the deformed shapes, stress and/or strain contours, temperature distribution, and mode shapes.

The results to be postprocessed are normally generated by a finite element analysis computer program. These results are then usually written into a results file for reasons of saving the information in a semi-permanent manner. This is not absolutely necessary as the software may be designed to pass the results directly to a postprocessor without saving them, which is not advisable for obvious reasons. As a third choice, the analysis program may pass the results directly to the postprocessor, while at the same time saving them in a file. Marc can interface with Mentat in the first manner where the results are first written into the Marc post file, which is then read by Mentat for postprocessing. This interface is transparent when Marc is run from Mentat, and intermediate results can be postprocessed while the job is still running.

For the case of HyperMesh, the manner of interfacing is similar. The results file, `jobid.hmr`, is written out by Marc, and is then later read in by HyperMesh for postprocessing. The HyperMesh results file is binary, so it is not readable by a text editor. After reading in the results file, HyperMesh can be used to create graphic displays of the results as is explained later herein.

Data Written into the HyperMesh Results File

The types of data that may be selected for writing into the HyperMesh results file are listed in *Volume C: Program Input*, under the HYPERMESH model definition option. These types of data are classified into two categories: *element results* and *nodal results*. The element quantities (stresses, strains, etc.) written into the results file are both the component values and the invariant values. They are each an average value within the element. Stresses and strains at nodes are values extrapolated from the integration points and based on a weighted average. The other nodal quantities include results such as displacements, accelerations, reactions, temperatures, and eigenmodes.

About Preprocessing

A Marc finite element model is usually created using Mentat. When the model is created, it is then written into a Marc data file, which is to be used for analysis. The model may also be created by another finite element preprocessor which has the capability to write out a Marc file. HyperMesh has this capability regarding the geometric model, for most cases. Thus, the model can be created within HyperMesh, then written out in the form of a Marc data file.

Mentat Preprocessing for HyperMesh

The creation of a HyperMesh results file using Marc is invoked by the HYPERMESH model definition option (see *Volume C: Program Input*) in the Marc data file. We will now review the procedure for entering this option into the data file, with the help of a simple finite element model contained in a data file initially named `x243.dat`. This model is composed of four quadrilateral shell elements (element 75). Both large displacement and free vibration eigenvalue analyses will be performed on the model.

There are two ways in which the HYPERMESH option may be entered into the data file:

1. By way of a text editor program, following the instructions for the HYPERMESH option in *Volume C: Program Input*.
2. By way of Mentat, following the procedure given below:
 - a. Create the finite element model, or if model is already available, read it into Mentat as described below:

To read the data file, start up Mentat. The Main menu shows up (Figure 7.3-1).

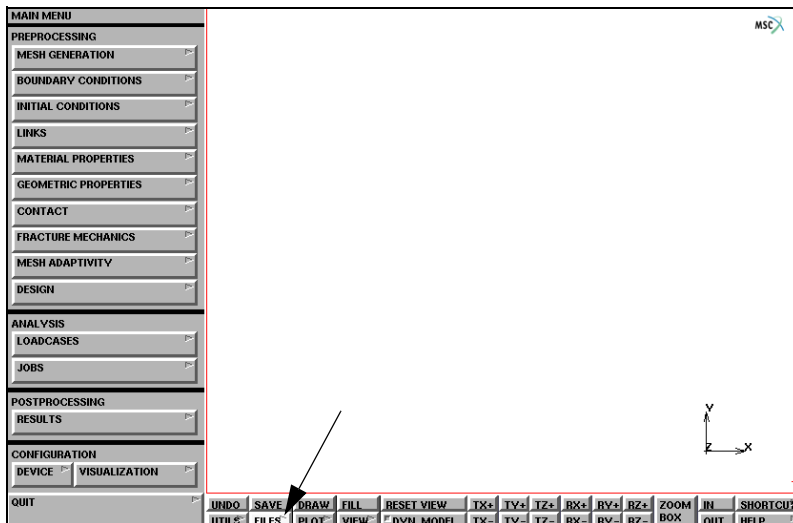


Figure 7.3-1 Mentat Main Menu

Press the FILES button (Figure 7.3-1) along the bottom row (static buttons) to access the FILE I/O screen (Figure 7.3-2).

On the left hand side, under MARC INPUT FILE, press READ to reach the READ MARC INPUT FILE submenu (Figure 7.3-3).

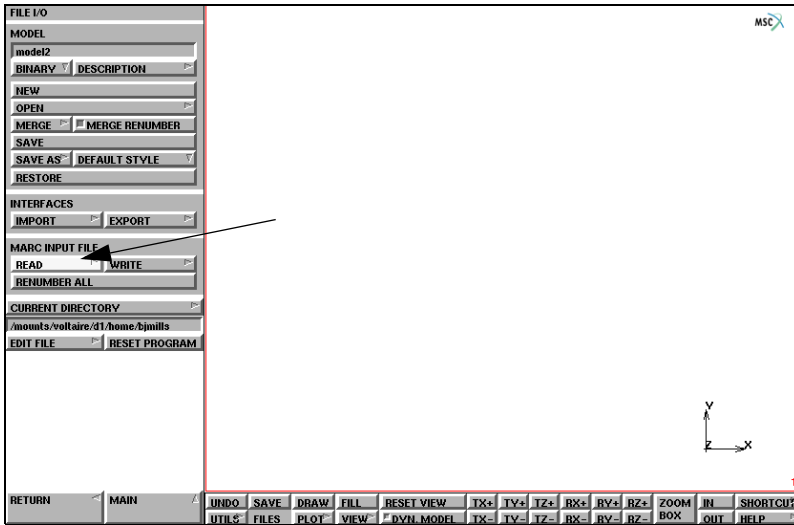


Figure 7.3-2 The FILE I/O Menu

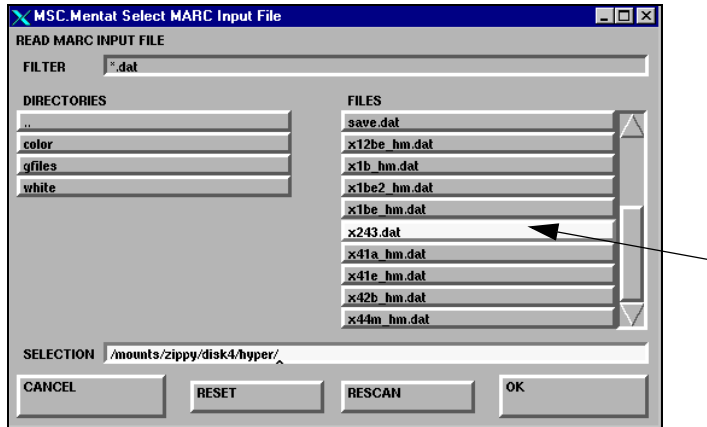


Figure 7.3-3 READ MARC INPUT FILE Submenu

Type in the selection in the window provided or select using the available access buttons. In this case, the file for example, is to be read in, so you have to press the appropriate button in the directory list of contents. This operation will result in the filename being added to the selection field window near the bottom. Pressing OK on the screen or the <RETURN> key on your keyboard activates the program to read in the data file. When the reading is completed, the default view of the model appears on the screen (Figure 7.3-4).

To see the entire model, press FILL (second row of the static buttons along the bottom of the screen, Figure 7.3-4) to fill the screen (Figure 7.3-5).

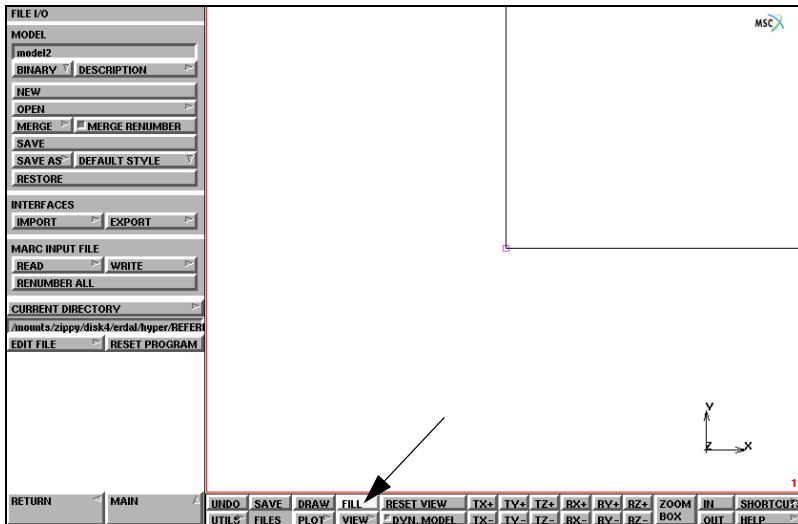


Figure 7.3-4 Default View of the Plate Model

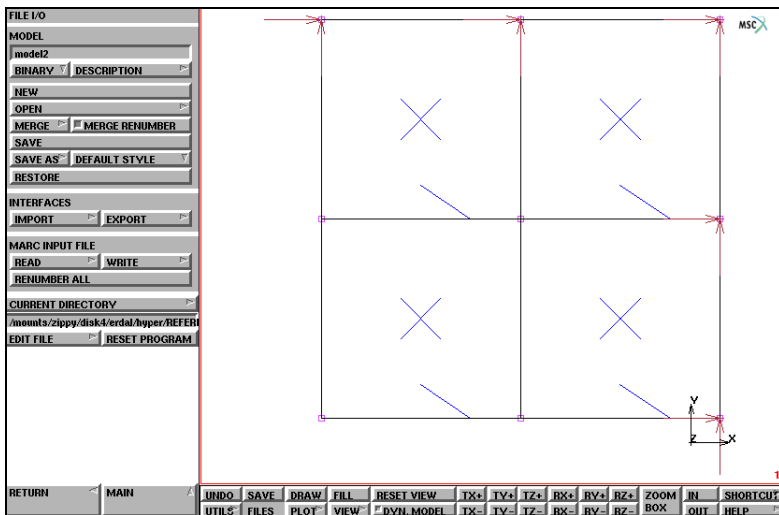


Figure 7.3-5 Full View of the Plate Model

The arrows indicate the fixed boundary conditions which may be seen better if the model is appropriately rotated (Figure 7.3-6) by using the RX, RY, RZ and/or DYN. MODEL buttons on the bottom two rows (static buttons). The plate is acted upon by an increasing distributed load.

- b. Go back to the Main menu (Figure 7.3-7) by pressing the MAIN button.

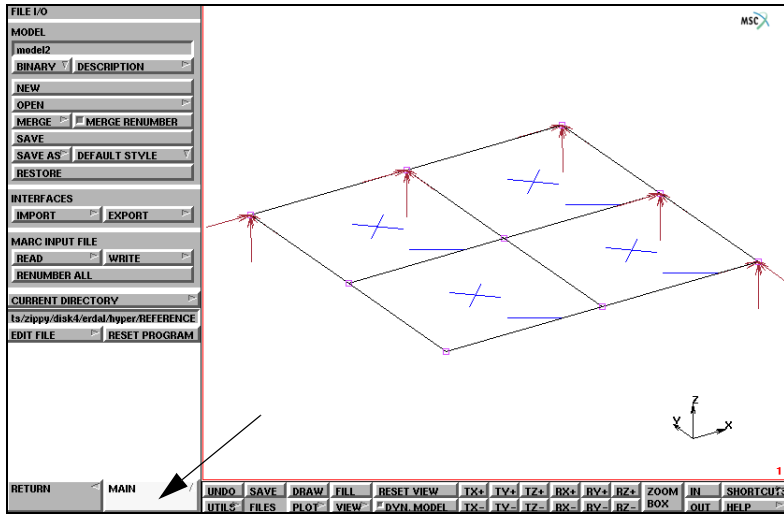


Figure 7.3-6 Rotated View of the Plate Model

Now click on the JOBS button to bring up the JOBS menu (Figure 7.3-8).

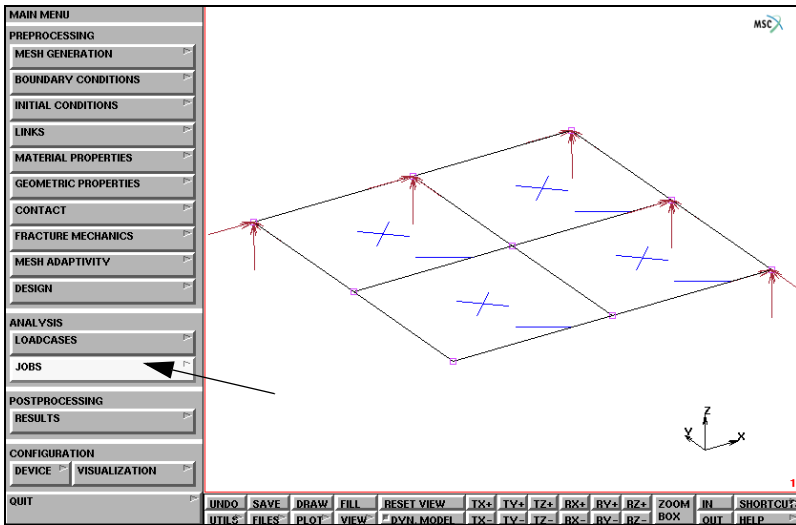


Figure 7.3-7 Mentat Main Menu and the JOBS Button

- c. Click on the ANALYSIS CLASS type; in this case, MECHANICAL (Figure 7.3-8) and a pop-up menu appears on the screen (Figure 7.3-9).

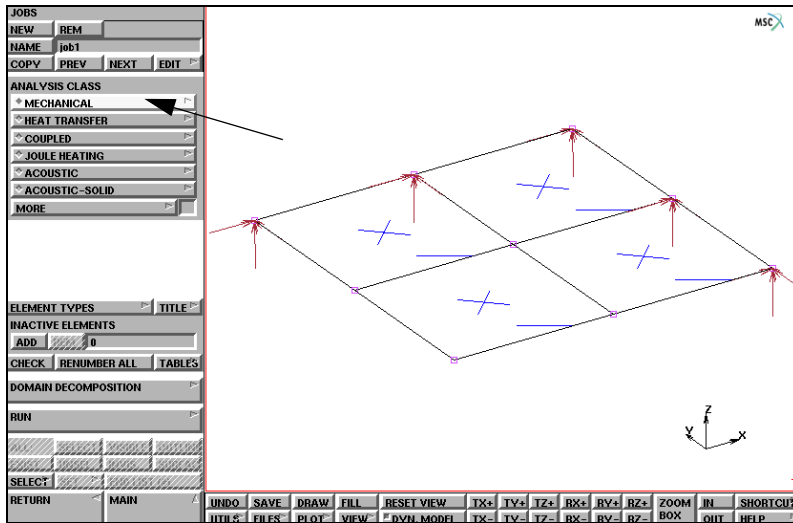


Figure 7.3-8 Mentat JOBS Menu

- d. Now click on JOB RESULTS (Figure 7.3-9) to reach the Job Results menu (Figure 7.3-10), which is essentially the Marc post file related data entry screen.

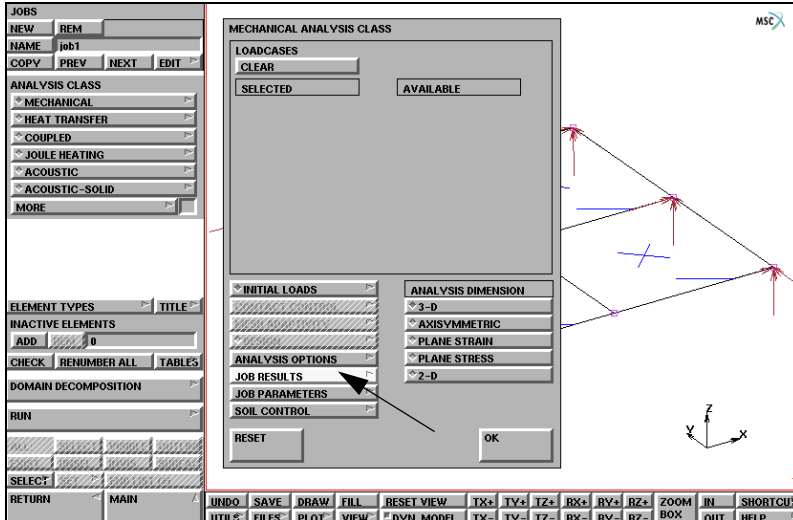


Figure 7.3-9 Mechanical Analysis Class Pop-up Submenu

- e. On the top, your right-hand side, of the screen, click on the HYPERMESH button (Figure 7.3-10) in order to access the HyperMesh results file related data entry screen (Figure 7.3-11).

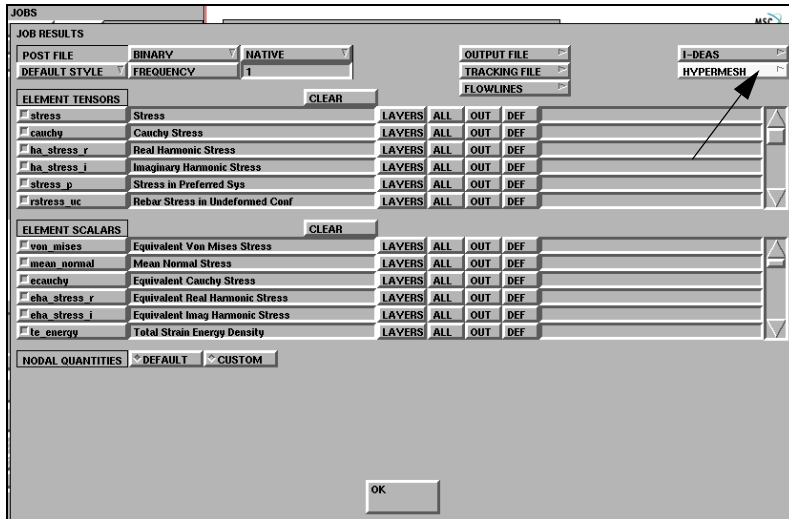


Figure 7.3-10 JOB RESULTS Submenu

- f. The frequency (i.e., every how many increments) with which results are to be output into the HyperMesh results file is controlled by the FREQUENCY button at the top left of the screen (highlighted in Figure 7.3-11) Click on the button to change the default frequency by entering the appropriate number in the dialogue area. In this case, we wish for results every 3rd increment; thus, simply type 3 and press <RETURN>.

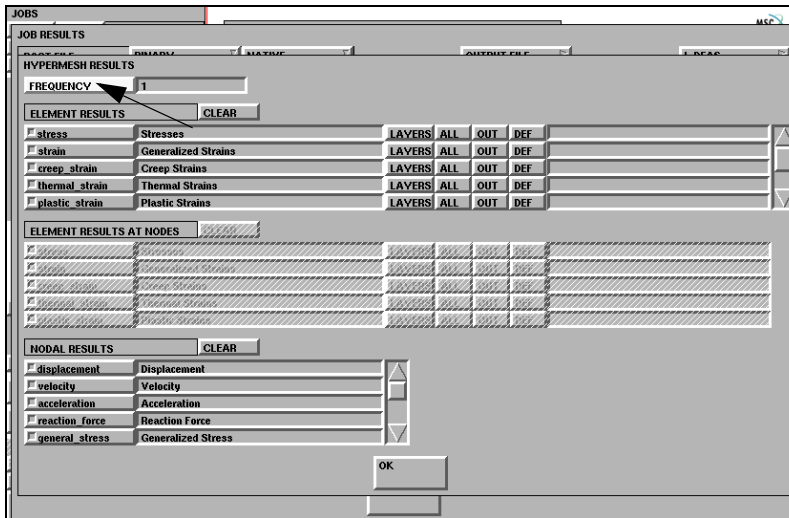


Figure 7.3-11 HYPERMESH RESULTS Submenu

- g. For ELEMENT RESULTS, select the types of results desired, by clicking, and thus turning on, the related options from among those available (stress through plastic strain). In this case, assume that the stresses are to be written into the results file for layer 3 only. Thus, you should first click on the stress button under ELEMENT RESULTS.
- h. Now select the layers for which results are to be output by using the buttons LAYERS through DEF (default) towards the right. If you wish to enter specific layer numbers, you can do this by first clicking the LAYERS button, then by entering the layer numbers, separated by commas or spaces, in the dialogue area, followed by <RETURN>. In this particular case, type 3 in the dialogue area, then press <RETURN> twice to reach the command prompt.
- i. For NODAL RESULTS, the choices range from nodal displacements to eigenmodes (reached at by means of the slider bar to the right). Simply click on the desired types of output to turn them on. In this case, we wish to save the displacements and eigenvectors into the results file. Thus, now you should click on the button displacement (first button) and on the button eigenmode (last button, highlighted in Figure 7.3-12).

The final appearance of the screen is shown in Figure 7.3-12.

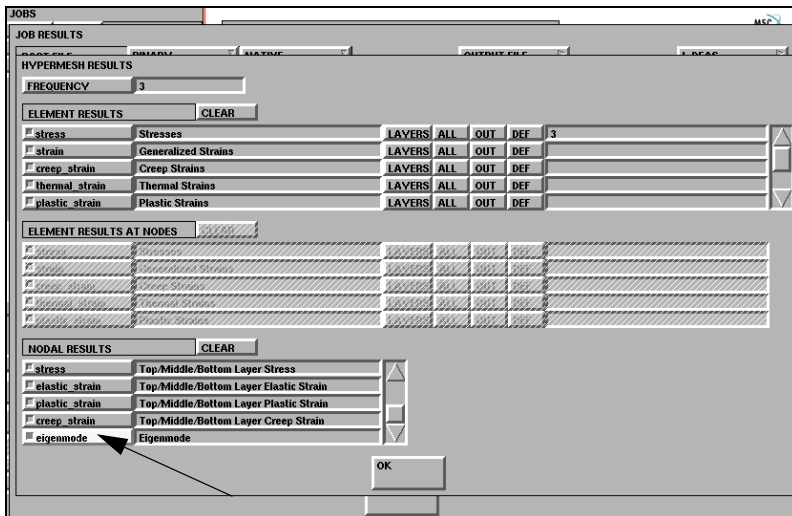


Figure 7.3-12 Final Appearance of HYPERMESH Submenu Screen

Note that the little squares for the switched on buttons show slightly darker in Figure 7.3-12 (e.g. stress under ELEMENT RESULTS and eigenmode under NODAL RESULTS).

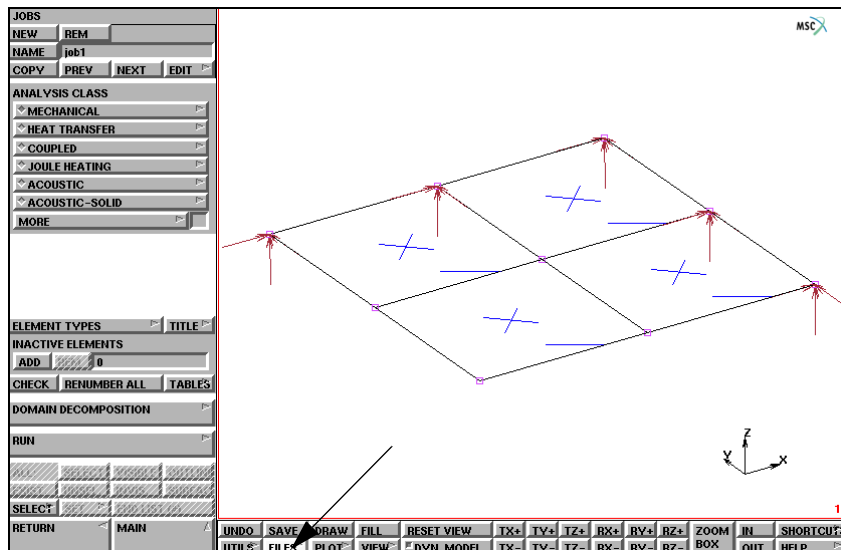


Figure 7.3-13 JOBS Menu with the Finite Element Model

- j. Click OK to complete the task. This takes you back to the JOB RESULTS menu (Figure 7.3-10), which should be filled only if you are also requesting a Marc post file to be written out at the end of analysis.
- k. Click OK on each of the previous two submenus to arrive back at the JOBS menu (Figure 7.3-13).

Important Data Preparation Considerations Regarding Eigenmodes

In case eigenvectors for buckling or eigenfrequency analysis are to be written into the HyperMesh results file, it is important to note that the corresponding Marc file should have the BUCKLE INCREMENT or MODAL INCREMENT model definition option, as appropriate, together with the associated BUCKLE or DYNAMIC parameter. *The history definition options BUCKLE, MODAL SHAPE, and RECOVER are not to be used.*

Relation to other Types of Results Files

Marc has the capability also to write Intergraph and SDRC I-DEAS™ results files, at the same time as the HyperMesh results file and Marc post files. The writing of these additional results files is invoked by the IRM and SDRC model definition options, respectively. If the HYPERMESH option is used simultaneously with either or both of the IRM and SDRC options, the program internally treats the data in a cumulative manner. For example, if stresses are requested for the SDRC Universal (results) file and creep strains are requested for the HyperMesh results file, both quantities are output into both files.

- l. Now, press the FILES button (Figure 7.3-13) again to proceed to write an Marc data file containing the HYPERMESH option (Figure 7.3-14).

- m. Press WRITE under MARC INPUT FILE (Figure 7.3-14) to access the appropriate submenu (Figure 7.3-15). Simply type in the path and name of the data file to be written (x243_hm.dat in this case, to differentiate from the input file that was read in), then press <RETURN> on the keyboard. The updated Marc input file will be written to the indicated directory.

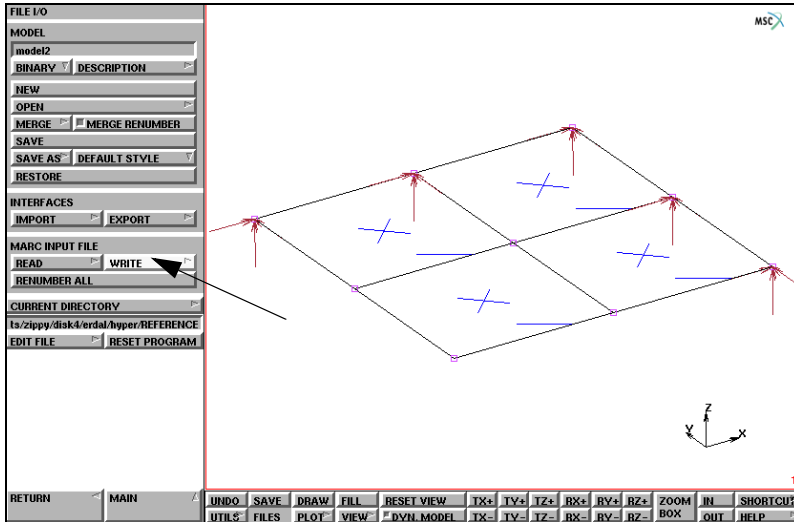


Figure 7.3-14 File I/O Menu with WRITE Button to be Pressed

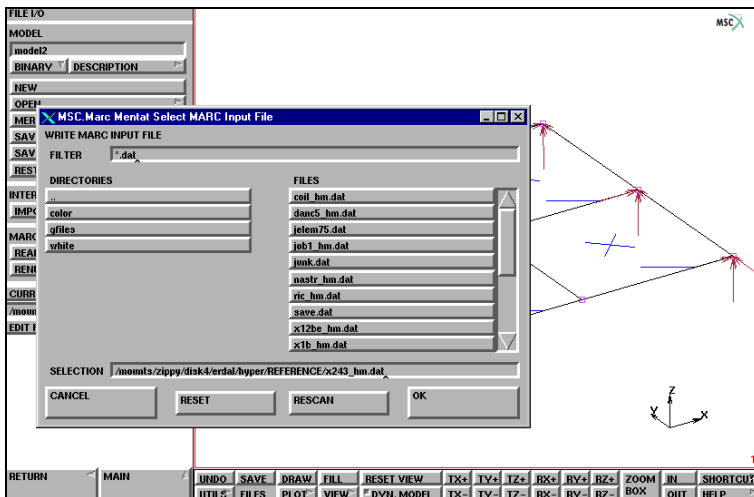


Figure 7.3-15 WRITE MARC INPUT FILE Submenu

Postprocessing using HyperMesh

The HyperMesh results file, `jobid.hmr`, contains only the results of the finite element analysis performed by Marc. However, postprocessing of analysis results requires that the geometry data also be available. At the time the analysis results are available in the `jobid.hmr` file, the finite element geometry is available in the Marc `jobid.dat` data file, and possibly in a HyperMesh database file. We review here the case where the geometry is to be read in from the Marc data file.

Since HyperMesh allows only one deformed shape plot per simulation, each eigenvector of an eigenvalue analysis is saved as a separate simulation. Thus, when using HyperMesh, these eigenvectors can be plotted by skipping to the next simulation rather than to the next data type of a simulation. The contour plots can be obtained for all data types including eigenvectors.

In case the number of requested eigenvalues is more than the number extracted, the data type in the HyperMesh deformed screen informs you regarding those modes that have not been extracted. The next button may need to be clicked to see the data type in the “deformed” mode of plotting.

After running a job with Marc using the HYPERMESH model definition option in the `jobid.dat` data file, you will obtain a binary HyperMesh results file named `jobid.hmr`. HyperMesh can now be invoked to postprocess the results contained in `jobid.hmr`. This process will be illustrated with the help of the analysis results for `x243_hm.dat`.

The first operational menu of HyperMesh at start-up is shown in [Figure 7.3-16](#). For better visualization, the font size and background colors have been modified using the options menu at the bottom right-hand side of the screen.

In this case, you see that the Geom option on the right is selected as the default. Clicking on the files button at the upper-left corner brings you the next screen ([Figure 7.3-17](#)).

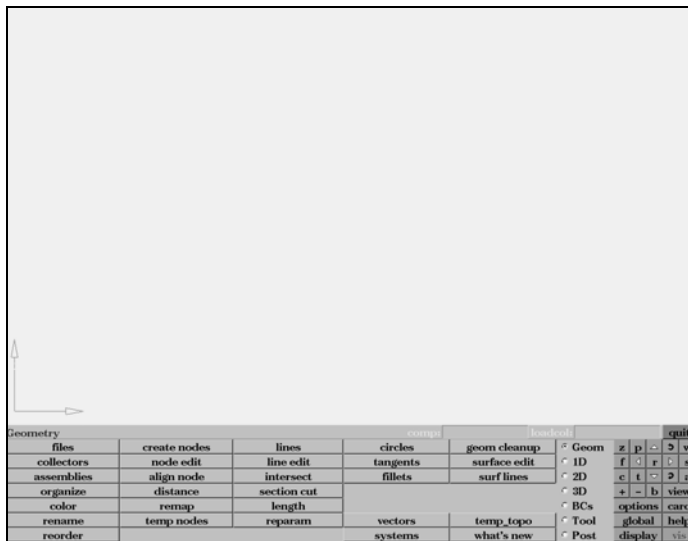


Figure 7.3-16 HyperMesh Main Menu



Figure 7.3-17 HyperMesh Default “hm file” Menu

Choosing import from the choices on the left, you can then proceed to the File Import menu (Figure 7.3-18).

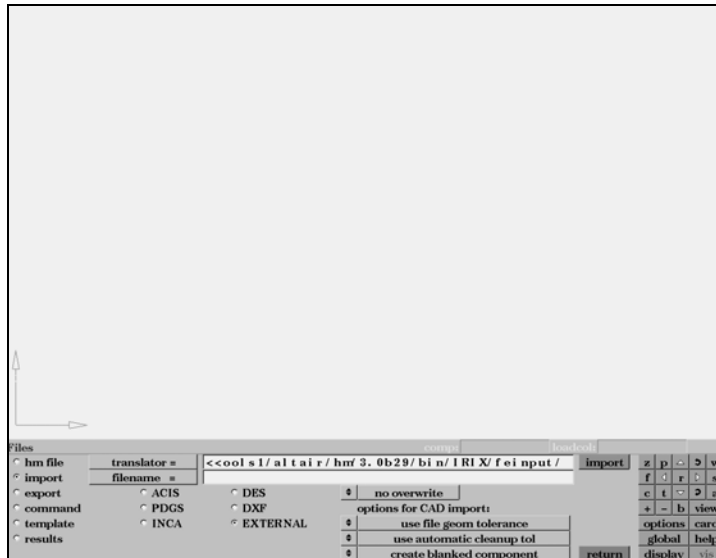


Figure 7.3-18 HyperMesh “File Import” Menu

This screen now has a choice for the type of input file. Double clicking on translator = brings up the Translator menu of the various data types which may be read in (Figure 7.3-19).

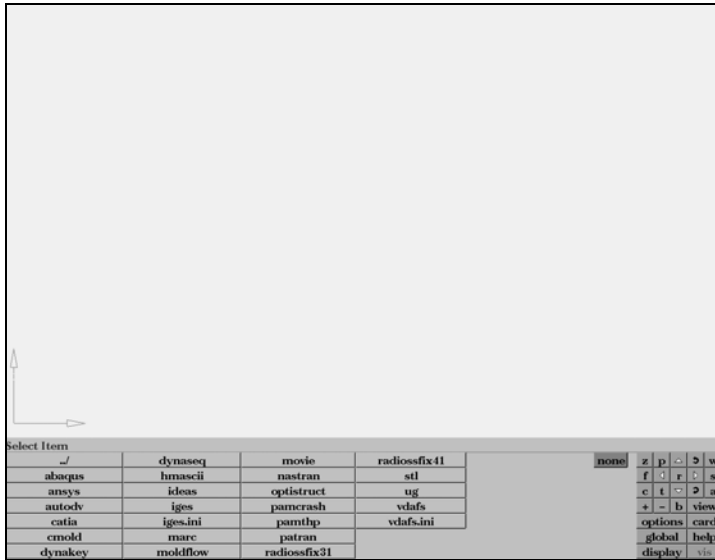


Figure 7.3-19 HyperMesh “Translator” Menu

Click on marc to select it. This also brings you back to the previous menu, with your selection now entered (Figure 7.3-20).

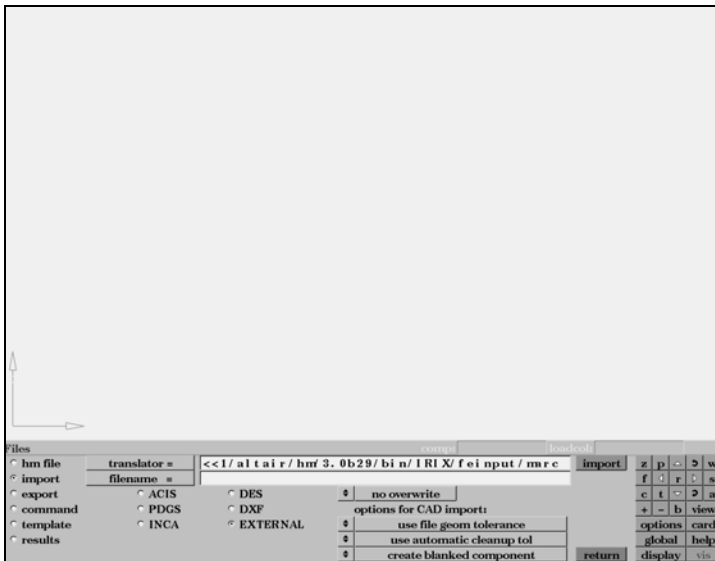


Figure 7.3-20 Entry of Marc into Window

Now double click on the filename = to browse the directory listings. The first menu will show some of the files in the current directory and will also provide an option to go up one level (Figure 7.3-21).

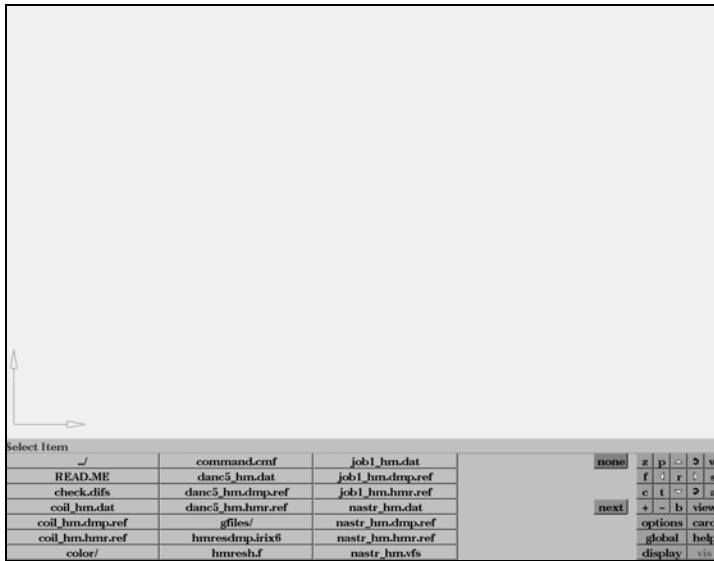


Figure 7.3-21 Browsing the Directory

In this particular case, we advance through the directory contents by using the next button until we see the required file x243_hm.dat (Figure 7.3-22).

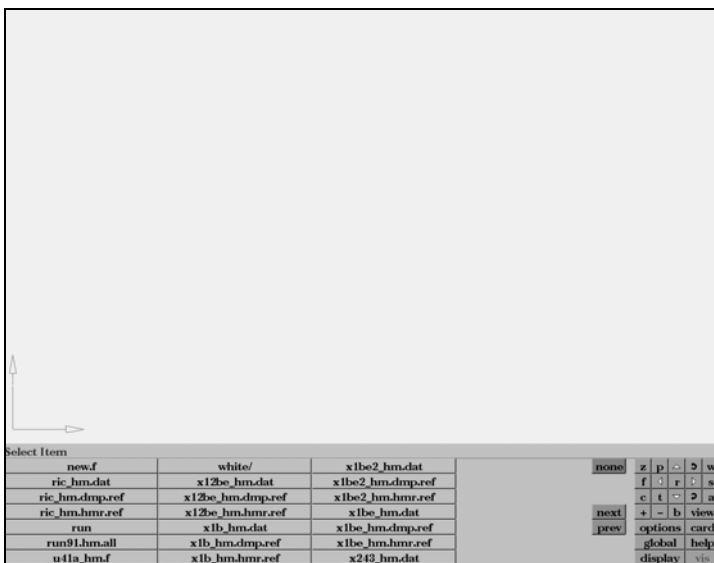


Figure 7.3-22 File Selection

Clicking on the file name, x243_hm.dat, brings you back to the Import menu, but with the required file name recorded in the window (Figure 7.3-23).

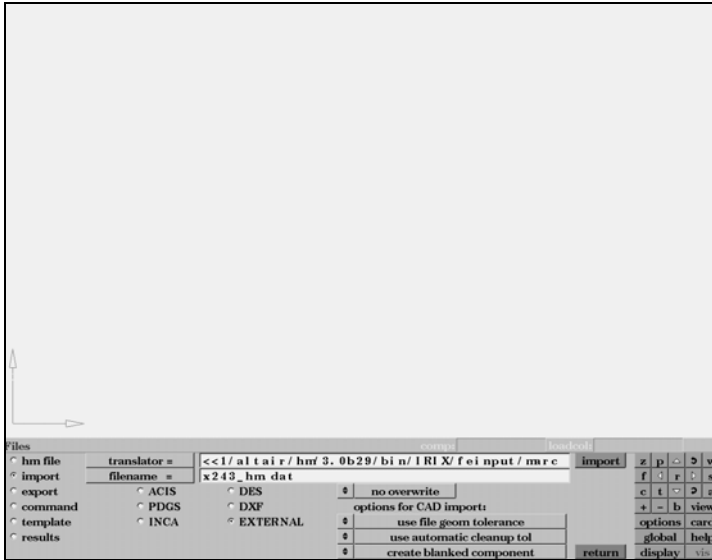


Figure 7.3-23 Data File Selection Complete

To read in the data file, you now click on import. The default view of the finite element model appears on the screen when the reading is completed (Figure 7.3-24).

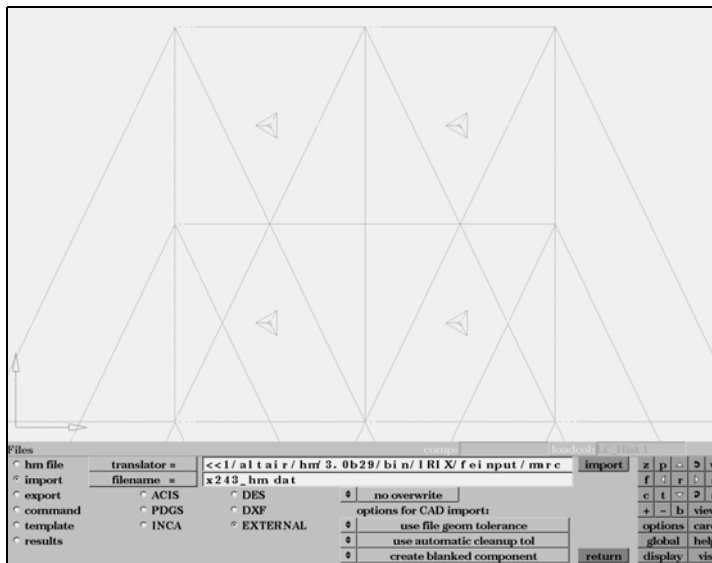


Figure 7.3-24 Default View of the Finite Element Model

You now need to select the results option at the bottom left of the menu in order to prepare for reading in the analysis results file. This operation takes you to the Results File menu (Figure 7.3-25).

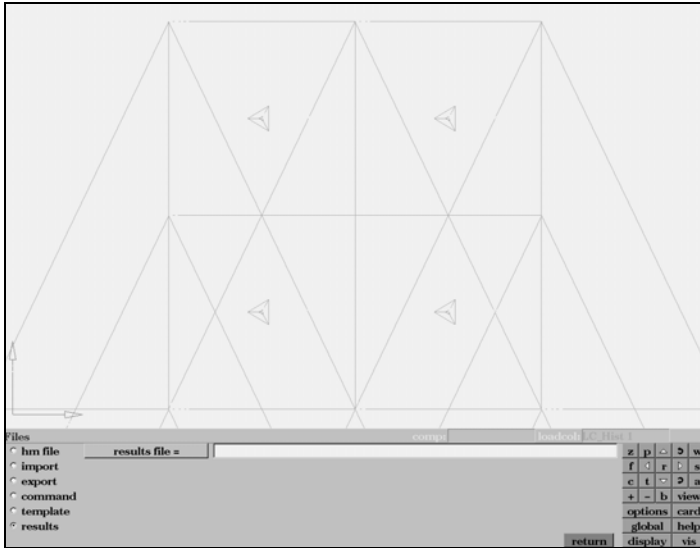


Figure 7.3-25 Results File Menu

Double clicking on results file = brings you again to the files in the current directory (Figure 7.3-21). In this particular case, we advance with the next button until we see the x243_hm.hmr file; i.e., the HyperMesh results file for the job x243_hm.dat. This file is obtained as a result of a Marc run for the x243_hm.dat job.

Clicking on x243_hm.hmr now returns you to the Results File menu with the appropriate file name recorded in the window (Figure 7.3-26).

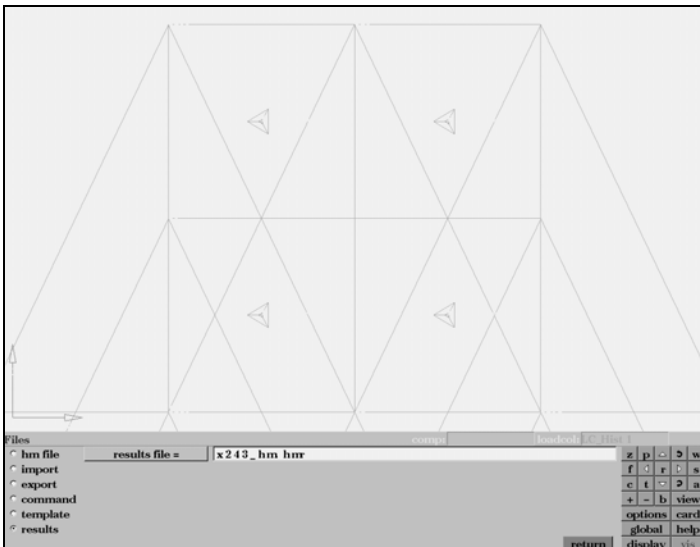


Figure 7.3-26 Results File Selection Complete

Now you are ready to go into the postprocessing phase. Click on the return button at the bottom right of the menu (Figure 7.3-26). This takes you to the initial default screen, but this time with the finite element model showing (Figure 7.3-27).

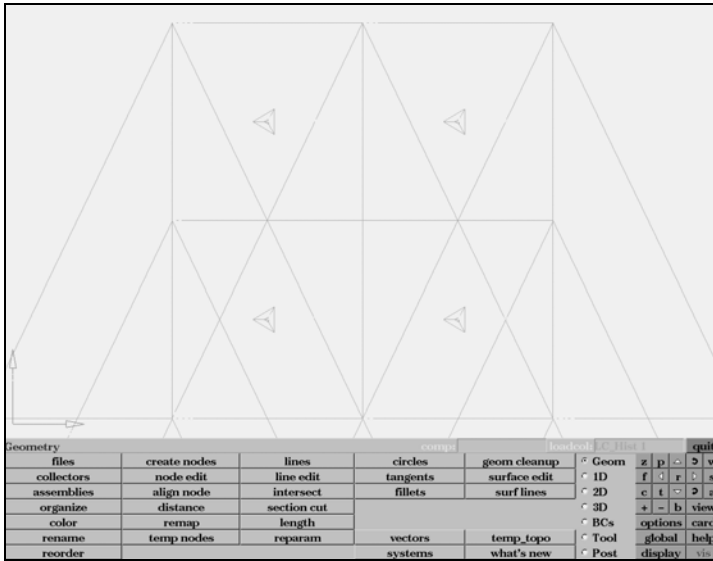


Figure 7.3-27 Main Menu with Finite Element Model

At this point, select the post option at the bottom right of the menu (Figure 7.3-27) to advance to the postprocessing screen (Figure 7.3-28).

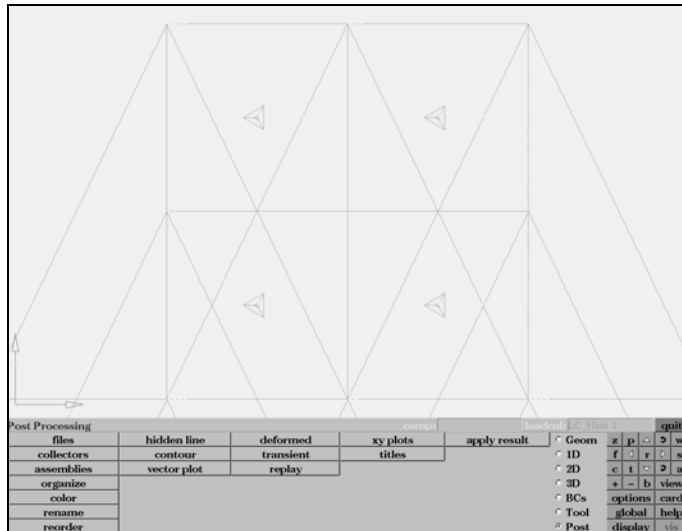


Figure 7.3-28 HyperMesh Postprocessing Menu

By means of this menu, you can process the data in the results file in various ways. These features are better followed through the literature available on HyperMesh. Here, we only show several representative examples to indicate how the data from a Marc analysis run can be processed.

You can now use the **deformed** button near the middle to proceed with plots of deformed geometry, either due to displacements or eigenvectors. Pressing this button takes you to the Deformed Shape screen (Figure 7.3-29).

The eigenvalue analysis results were saved in the results file for increment 0. However, no displacements were saved since increment 0 was trivial in terms of stress analysis. Thus, the first screen for deformed shape has "Increment 0 Mode 1" as the first simulation (Figure 7.3-29).

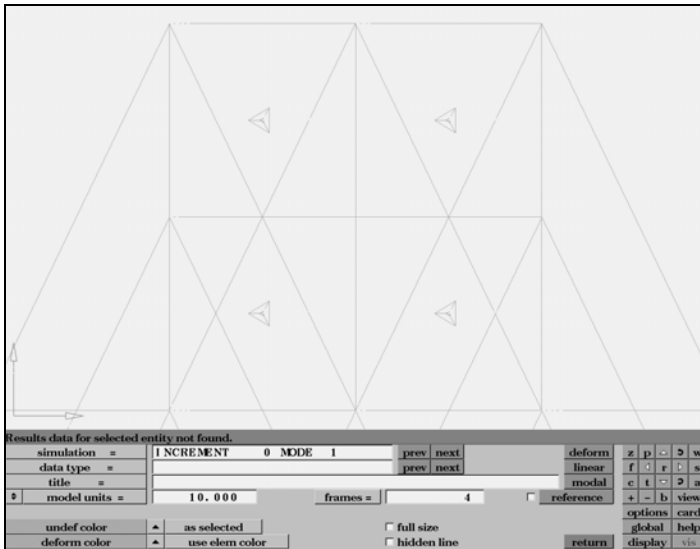


Figure 7.3-29 Deformed Shape Screen

To pick up the related data from the results file, press the next button across from **data type =**. This brings the word **eigenvector** to the small window and the data is available. By clicking the next button across from **simulation =**, you can reach the results for other nodes and displacements, including those in other increments as well. For purposes of illustration, we now do this once to arrive at the second mode. You can use the **a** button at right to rotate the model in drag mode, then use **f** to fill the screen. Now set **model units =** to 1.0 to obtain a reasonably scaled deformed shape (eigenvector), then press the **deform** button to obtain the shape for the second mode at increment 0 (Figure 7.3-30).

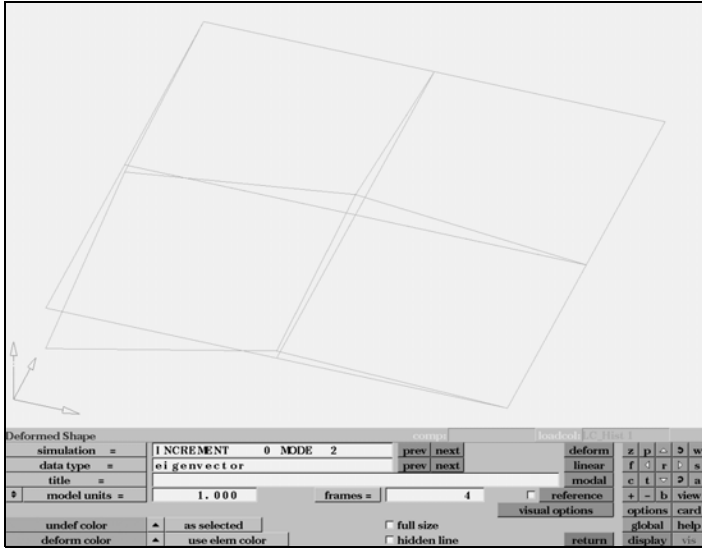


Figure 7.3-30 Second Mode of Free Vibration at Increment 0

If the eigenvector is for free vibration, as in this case, you can now press the modal button for animating the mode shape.

Going back to [Figure 7.3-30](#), if the next button across from simulation = is pressed twice more, you reach the window shown in [Figure 7.3-31](#).

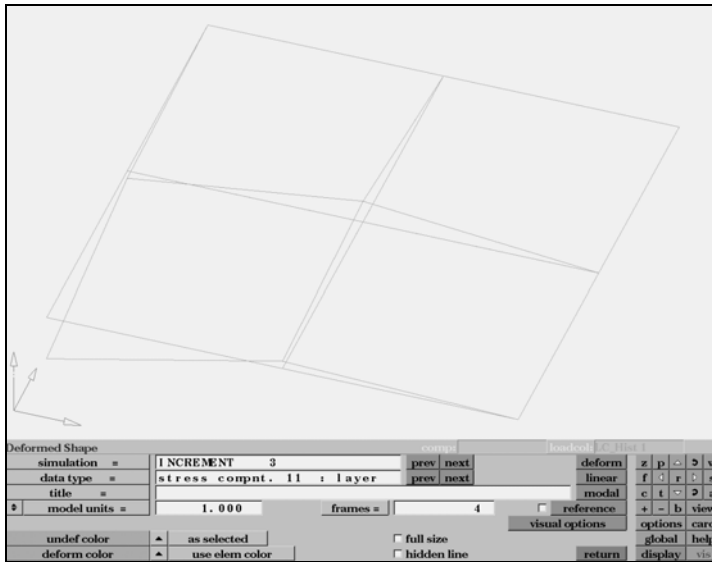


Figure 7.3-31 Advancing to Results for Increment 3

You have now arrived at the stress analysis results for increment 3. Note that the plot does not change during these moves. To get to the displacement data, press the next button across from data type = until the data type window shows the word displacements. Then click on deform to obtain the deformed shape for increment 3 (Figure 7.3-32).

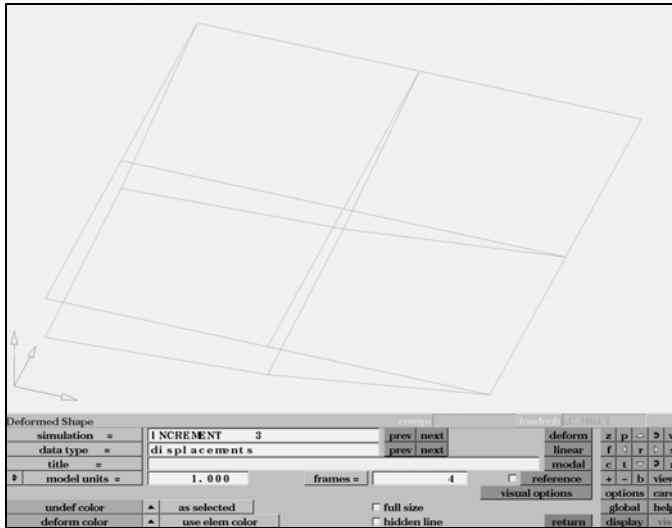


Figure 7.3-32 Displacement Plot for Increment 3

To obtain contour plots, press the return button at the bottom right. This takes you back to the Postprocessing menu of Figure 7.3-28. Pressing the contour button takes you to the Contour screen.

You can now get a contour plot of the results quantities, such as the displacement plot in Figure 7.3-33.

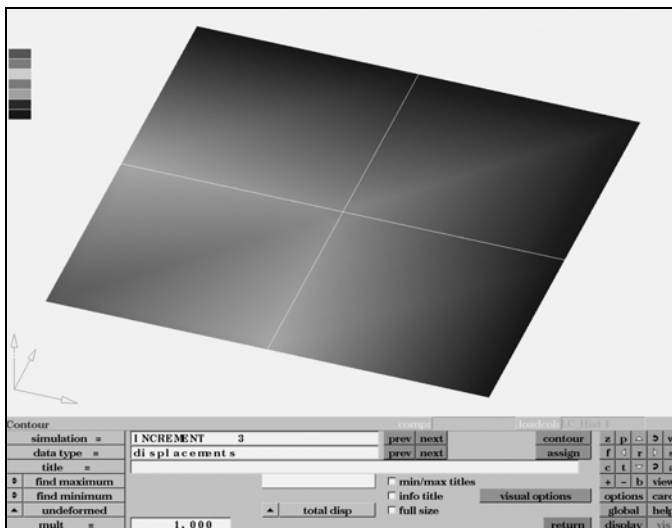


Figure 7.3-33 Contour Plot of Displacements for Increment 3

or the second stress invariant of layer 3 in increment 6, the contour plot in [Figure 7.3-34](#).

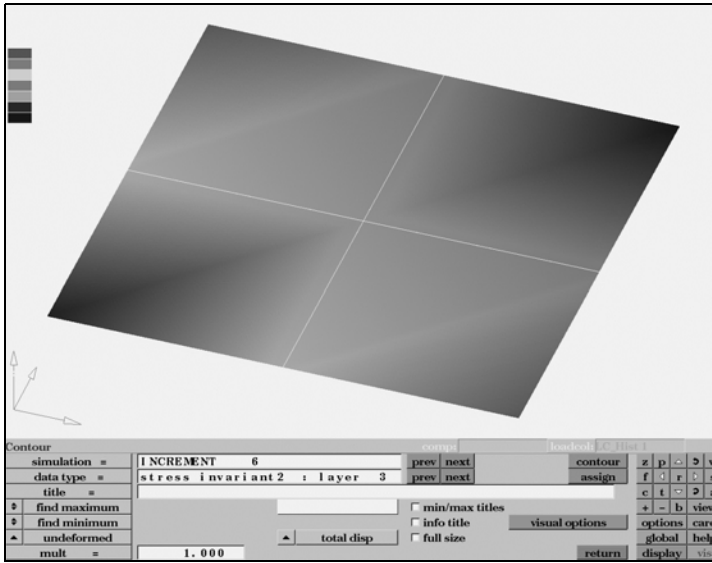


Figure 7.3-34 Contour Plot of Stress Invariant

7.4 Translators

- Chapter Overview 2200
- Mentat Writers 2200
- Mentat Readers 2201

Chapter Overview

This chapter highlights the output of a model to four standard formats: *dxfout*, *stlout*, *vdaout*, and *vrmlout* (which is not a standalone program). Also we have two new readers: *c-mold* and *stl*.

Mentat Writers

dxfout:

This is a writer which will output an ASCII DXF file based on AutoCAD 2000.

stlout:

This is a writer which will output an ASCII StereoLithography Interface specification (STL) file based on Oct 1989's standard.

vdaout:

This is a writer which will output an ASCII VDA-FS file based on VDA-FS Revision 2.0.

vrmlout:

This translator is embedded in Mentat. It's based on VRML97 (a.k.a ISO VRML or VRML 2.0). It will NOT output any geometric entities from Mentat; instead, the output is based on the graphical entities and view settings. The file format is in ASCII.

Use the button sequence or the new Mentat writers and see the sample menu ([Figure 7.4-1](#)).

```
MAIN
  FILE
    EXPORT
```

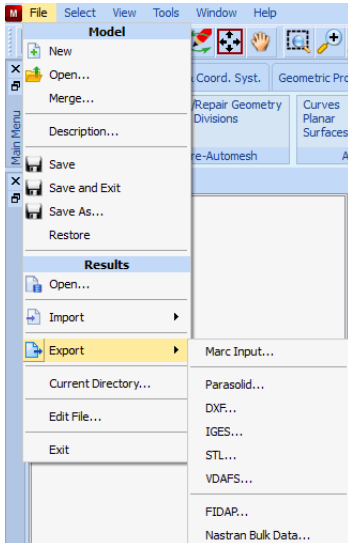



Figure 7.4-1 Sample of the EXPORT Menu

Mentat Readers

c-mold:

The current version of the interface supports C-MOLD versions 98.7 to 99.1. It reads data from four C-MOLD file types:

- the parameter file (extension .par or .PAR)
- the finite element mesh file (extension .fem or .FEM)
- the material properties file (extension .mtl or .MTL)
- the results file of the C-MOLD stress analysis (extension .ppt or .PPT)

These files should reside in the same directory. You must specify the name of one of these files. The names of the others are automatically derived from it.

Part of the data is imported directly into Mentat. The other data (most notably, the residual stresses, the elastic and thermal properties, and material orientations, which are all layer and element dependent) is written to a Marc post file that can be viewed directly from the RESULTS menu. This post file data is read at the start of a Marc job. This requires that the user subroutine `cmold2marc.f` in the Mentat bin directory is used. The following data is extracted from the C-MOLD files:

Parameter file (.par or .PAR):

Data Set	T-CODE	Description
PRMT	100	Number of layers across the full-gap thickness
	620	Fibre orientation analysis option
TITL		Title of the model (currently not used)

Finite element mesh file (.fem or .FEM):

Data Set	T-CODE	Description
EPRO	30100	Thickness of triangular elements
NODE		Coordinates of the nodes
QUAD		Connectivity for quadrilateral element
TITL		Title of the model (currently not used)
TRI		Connectivity for triangular element

Material properties file (.mtl or .MTL):

Data Set	T-CODE	Description
MTRL	1600	Isotropic material properties
	1602	Orthotropic material properties
	1700	Isotropic thermal expansion coefficient
	1702	Orthotropic thermal expansion coefficients
TITL		Title of the model (currently not used)

Results file (.ppt or .PPT):

Data Set	T-CODE	Description
ELDT		Layer-based residual stresses and material properties for fibre-filled analyses
TITL		Title of the model (currently not used)
TSDT		Layer-based residual stresses for unfilled analyses; material properties are taken from Material properties file

Use the following button sequence for the new Mentat reader C-MOLD and see the sample menu.

```

MAIN
  FILE
    IMPORT
  
```

stl:

This reader will read both ASCII and binary version of Stereo Lithography Interface specification (STL) files.

Use the following button sequence for the new Mentat reader STL and see the sample menu (Figure 7.4-2).

MAIN
FILE
IMPORT

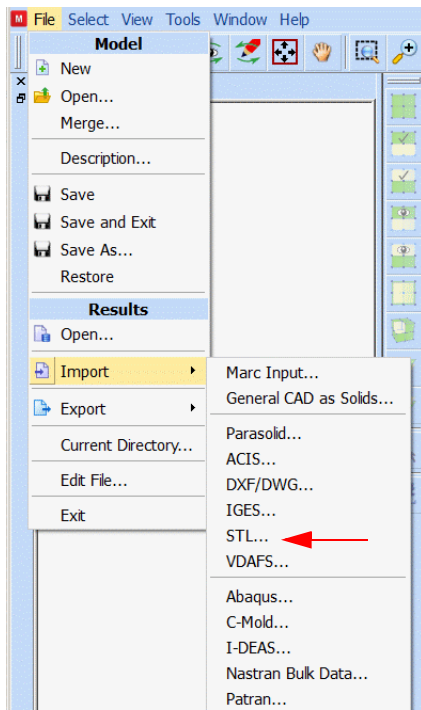


Figure 7.4-2 Sample of the IMPORT Menu with the STL Button Highlighted

acis:

In this release, it can read ACIS R13 and earlier.

dxg:

In this release, it can read AutoCAD 2000 (or earlier) ASCII/Binary DXF files and DWG files.

ideas:

This version of *I-DEAS* reader is based on MS7.

nastran:

This *nastran* reader supports the following capabilities:

LOAD CASE SECTION:

LOAD, SPC, DLOAD, TEMPERATURE, SUBCASE, ANALYSIS

BULK DATA SECTION:

GEOMETRY PROPERTIES:

PACABS, PACBAR, PBAR, PBCOMP, PBEAM, PBEND, PCOMP, PCONEAX, PCONV, PCONVM,
PDAMP5, PGAP, PHBDY, PLPLANE, PLSOLID, PROD, PSHEAR, PSHELL, PSOLID, PTUBE,
PDAMP, PELAS, PMASS, PVISC, PBUSH, PBUSH1D, PWELD, PFAST

COORDINATE SYSTEMS:

CORD1C, CORD1R, CORD1S, CORD2C, CORD2R, CORD2S

ELEMENT DATA:

BAROR, BEAMOR, CAXIF2, CAXIF3, CAXIF4, CBAR, CBEAM, CBEND, CCONEAX, CFLUID2,
CFLUID3, CFLUID4, CHACAB, CHACBR, CONROD, CROD, CHEXA, CHEX8, CHEX20, CPENTA,
CPENTA6, CPENTA15, CTETRA, CTETRA4, CTETRA10, CQUAD, CQUAD4, CQUAD8,
CQUADX, CQUADR, CTRIA3, CTRIA6, CSHEAR, CSLOT3, CSLOT4, CTRAPRG,
CTRIAR, CTRIARG, CTRIAX, CTRIAX6, CTUBE, SECTAX, CBUSH, CBUSH1D, CWELD, CFAST

MULTIPOINT CONSTRAINTS:

MPC, MPCAX, RBE1, RBE2, RBE3
CDAMP1, CDAMP2, CDAMP3, CDAMP5, CDAMP4,
CELAS1, CELAS2, CELAS3, CELAS4,
CMASS1, CMASS2, CMASS3, CMASS4,
CGAP, CVISC,
RBAR, RROD, RTRPLT

CONTACT:

BCBODY, BCPROP, BLSEG, BSURF

HEAT BOUNDARY CONDITION ELEMENTS:

BDYOR, CHBDYE, CHBDYG, CHBDYP

EDGES, FACES:

FEEDGE, FEFACE

STATIC FORCES:

FORCE, FORCE1, FORCE2, FORCEAX, MOMAX, MOMENT, MOMENT1, MOMENT2,
GRAV, RFORCE, SLOAD

NODE DATA:

GRDSET, EGRID, GRID, GRIDB, GRIDF, GRIDS, POINT, RINGAX, RINGFL, SPOINT

MATERIAL DATA:

CREEP, MAT1, MAT2, MAT3, MAT4, MAT5, MAT8, MAT9, MAT10, MATHP, MATS1,
MATT1, MATT2, MATT3, MATT4, MATT5, MATT9, MFLUID, RADM, RADMT

DISTRIBUTED LOADS:

GMLOAD, PLOAD, PLOADX1, PLOAD1, PRESAX, PLOAD2, PLOAD4

SPECIFIED DISPLACEMENTS:

CYSUP, SPC, SPC1, SPCAX, SPCD, SPCOFF, SPCOFF1, SUPAX, SUPORT1,
USET, USET1, DEFORM, GMBC, GMSPC, CYAX, CYJOIN, CYSYM

NODE TEMPERATURES:

TEMP, TEMPD, TEMPBC, TEMPAX

ELEMENT TEMPERATURES:

TEMPP1, TEMPP3, TEMPRB

ELEMENT FLUXES:

QBDY1, QBDY2, QHBDY, QSET, QSET1, QVECT, QVOL

FILMS DATA:

CONV, CONVM

TABLE DATA:

DTABLE, DTI, TABDMP1, TABLE3D, TABLED1, TABLED2, TABLED3, TABLED4,
TABLEM1, TABLEM2, TABLEM3, TABLEM4, TABLES1, TABLEST,
TABRND1, TABRNDG

DYNAMIC LOADS:

ACSRCE, NOLIN1, NOLIN2, NOLIN3, NOLIN4,
RLOAD1, RLOAD2, TF, TLOAD1, TLOAD2,
DAREA, DELAY, DPHASE

LOAD CASES:

DLOAD, LOAD, SPCADD

patran:

Reads the Patran neutral file.

7.5 Sweep Nodes on Outlines

- Chapter Overview 2208
- Background Information 2208
- Detailed Session Description 2208
- Input Files 2212

Chapter Overview

This chapter describes the usage of the SWEEP NODES button on Outlines in Mentat. One box with six surfaces will be created to explain how to use the function.

Background Information

In Mentat, 3-D models are composed by nurb surfaces bounding a closed volume. The surface mesh is created on every individual surfaces. In order to create 3-D mesh, the nodes on the outlines of each surface mesh should be merged with the closest nodes on their neighboring outlines. The merging process is controlled by sweep tolerance.

Overview Steps

Step 1: Create six flat surfaces

Step 2: Create surface mesh

Step 3: Sweep the nodes on outlines

Detailed Session Description

Step 1: Create six flat surfaces

Use the following button sequence to create six flat nurb surfaces to form a closed box.

MAIN

MESH GENERATION

srfs ADD

```
point (0.4,0.4,0.0)
point (-0.4,0.4,0.0)
point (-0.4,-0.4,0.0)
point (0.4,-0.4,0.0)
1
2
point (-0.4,0.4,0.6)
point (0.4,0.4,0.6)
3
2
5
point(-0.4,-0.4,0.6)
```


4
3
7
point (0.4,-0.4,0.6)
4
1
6
8
6
5
7
8

INTERSECT
TRIM OUTER
all: EXIST.
VIEW
SHOW VIEW 4

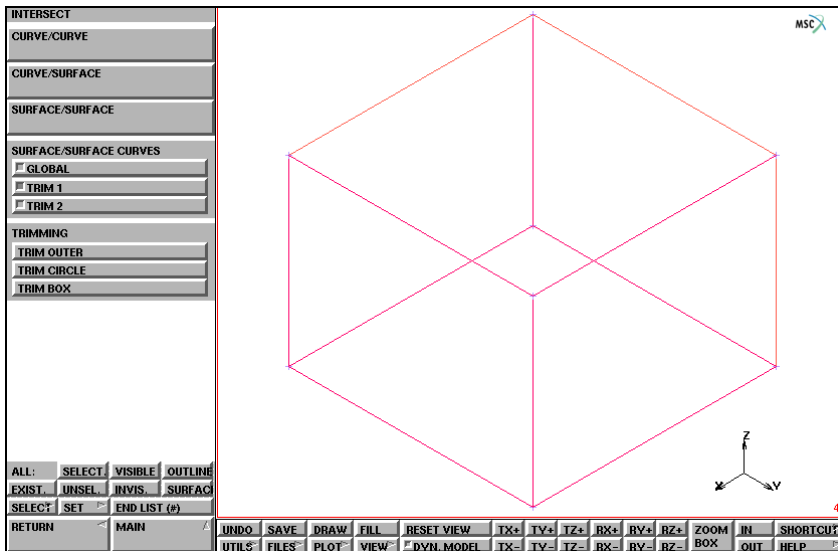


Figure 7.5-1 Six Surfaces Created to Form a Closed Box

Step 2: Create surface mesh

In step 2, apply a curve division on surface trimming curves and create the surface mesh on all six surfaces.

MAIN

MESH GENERATION

AUTOMESH

CURVE DIVISIONS

FIXED AVG LENGTH

APPLY CURVE DIVISIONS

all: EXIST.

RETURN

SURFACE MESHING

triangles (delaunay)

SURFACE TRI MESH!

all: EXIST.

PLOT

elements SOLID

REGEN

FILL

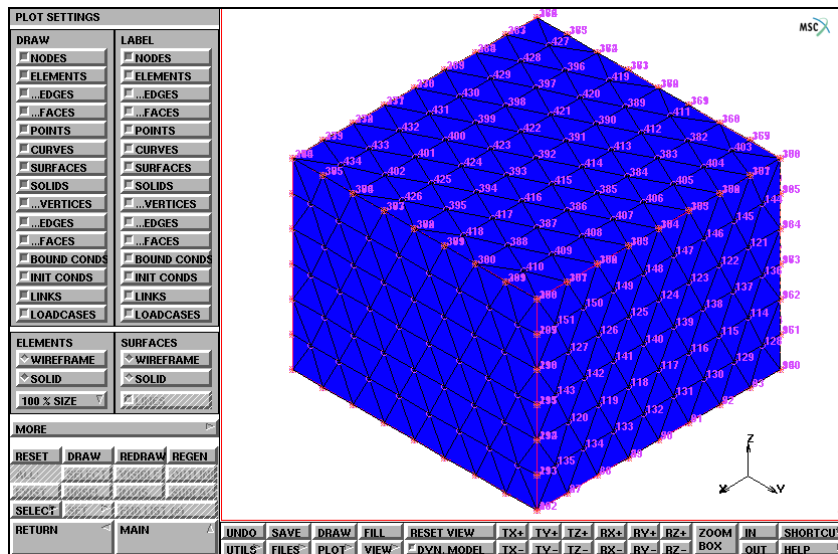


Figure 7.5-2 The Nodes are repeated on the Outlines of the Surface Mesh

Step 3: Sweep the nodes on outlines

Now use the SWEEP NODES button on all outlines of mesh. The ALIGN SHELL option is also necessary to make sure the all elements have the same orientation. Finally, check if no free outlines are left. Use the following button sequences for the final result.

```

MAIN
  MESH GENERATION
  AUTOMESH
  SOLID MESHING
  SWEEP OUTLINE NODES
EXIST
  ALIGN SHELL
    481
  OUTLINE EDGE LENGTH
  
```

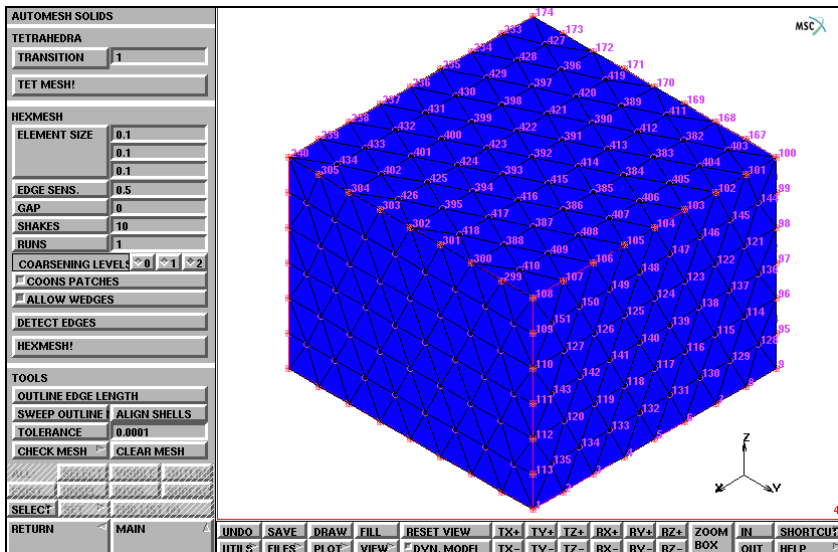


Figure 7.5-3 Repeated Nodes on the Outlines are Meshed

You may wish to run Mentat procedure files that are in the

examples/marc Ug/c7.5.proc subdirectory

under Mentat. The procedure file *c7.5.proc* builds, runs, and postprocesses this simulation.

Input Files

The files below are on your [delivery media](#) or they can be downloaded by your web browser by clicking the links (file names) below.

File	Description
outlines.proc	Mentat procedure file

7.6 Transition Parameter for Meshing

- Chapter Overview 2214
- Background Information 2214
- Detailed Session Description 2214
- Input Files 2218

Chapter Overview

This chapter describes the usage of mesh coarsening parameter. This parameter is used to control the mesh density transition from the boundary to the domain center.

Background Information

As the parameter value is bigger than 1, the element size at domain center is bigger. As the value is smaller than 1, the element size at domain center is smaller. The TRANSITION parameter applies to 2-D, surface advancing front, Delaunay meshers, and 3-D Delaunay mesher.

Overview Steps

- Step 1: Create a close 2-D boundary**
- Step 2: Create mesh with default transition parameter value 1**
- Step 3: Create mesh with the value bigger than 1**
- Step 4: Create mesh with the value smaller than 1**

Detailed Session Description

Step 1: Create a close 2-D boundary

First, use the following button sequences to create six curves to form a closed 2-D meshing domain (Figure 7.6-1).

MAIN

MESH GENERATION

crvs ADD

point (-.5, .8,0.0)

point (-.9, .3,0.0)

2

point (-.3, 0.0,0.0)

3

point (-.3, -.7,0.0)

4

point (1.0, -.7,0.0)

5

point (1.0, 1.0,0.0)

6
 1

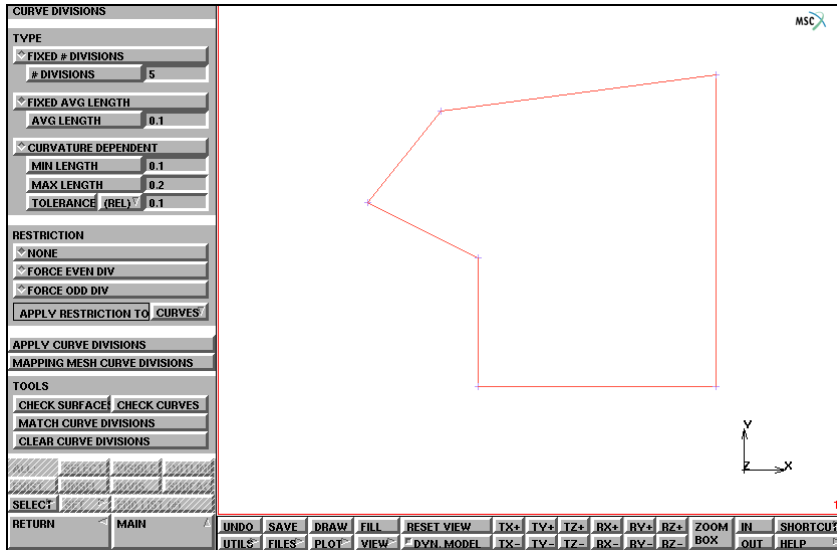


Figure 7.6-1 A 2-D Bound Domain to be meshed

Step 2: Create mesh with default transition parameter value 1

In this step, curve division on curves and create quad mesh with default transition parameter value 1.0 (Figure 7.6-2).

```

MAIN
  MESH GENERATION
    AUTOMESH
      CURVE DIVISIONS
        AVG LENGTH
          0.2
        APPLY CURVE DIVISIONS
          all: EXIST.
        RETURN
      2D PLANAR MESHING
        quadrilaterals (adv frnt)
        QUAD MESH!
          all: EXIST.
    
```

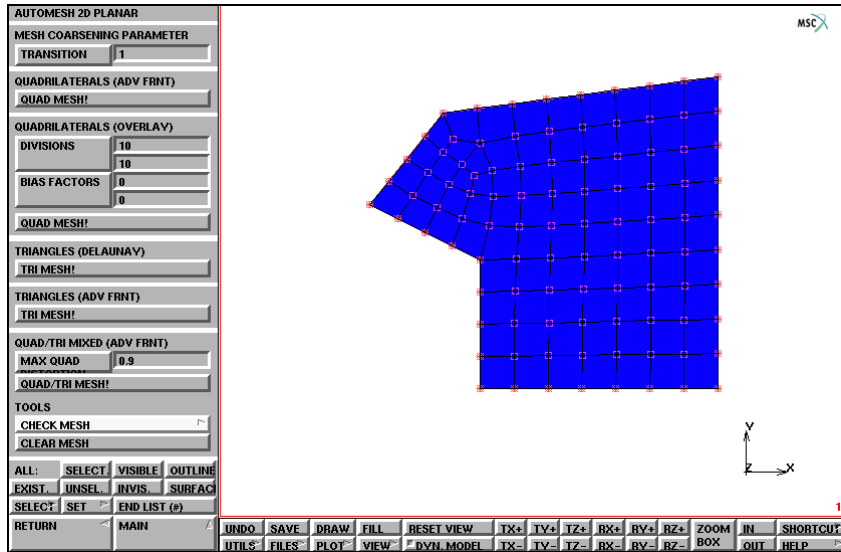


Figure 7.6-2 Quad Mesh with Transition Value at 1.0

Step 3: Create mesh with the value bigger than 1

In this step, change the transition parameter value to 1.5, and create a quad mesh (Figure 7.6-3).

```

MAIN
  MESH GENERATION
    AUTOMESH
      2D PLANAR MESHING
        CLEAR MESH
        TRANSITION
          1.5
        quadrilaterals (adv frnt)
        QUAD MESH
          all: EXIST.
    
```

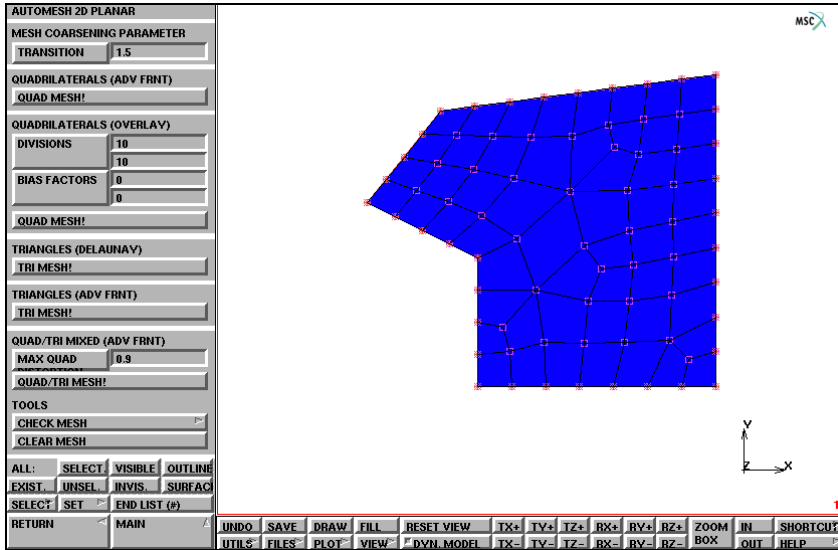



Figure 7.6-3 Quad Mesh with Transition Value at 1.5

Step 4: Create mesh with the value smaller than 1

With this final step, change transition parameter value to 0.5, and create quad mesh (Figure 7.6-4).

MAIN

MESH GENERATION

AUTOMESH

2D PLANAR MESHING

CLEAR MESH

TRANSITION

0.5

quadrilaterals (adv frnt)

QUAD MESH

all: EXIST.

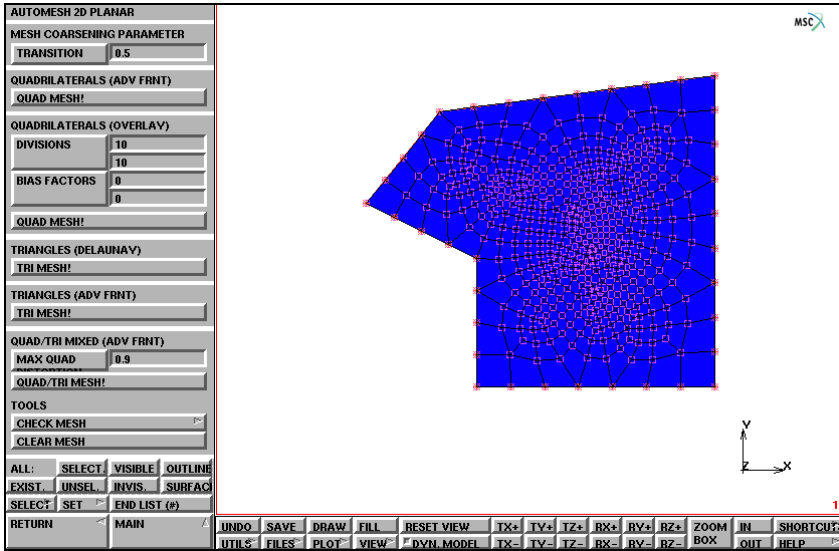


Figure 7.6-4 Quad Mesh with Transition Value at 0.5

You may wish to run Mentat procedure files that are in the

`examples/marc_ug/meshing_param.proc` subdirectory

under Mentat. The procedure file, *c7.6.proc*, builds, runs, and postprocesses this simulation.

Input Files

The files below are on your [delivery media](#) or they can be downloaded by your web browser by clicking the links (file names) below.

File	Description
meshing_param.proc	Mentat procedure file

7.7 Mentat Features 2001 and 2003

- Chapter Overview 2220
- 2001 Features 2220
- 2003 Features 2227
- Input Files 2230

Chapter Overview

In the 2001 Mentat release, the new features described below were implemented in the Mentat program.

2001 Features

Optimized Element Graphics Generation

In Mentat, elements are plotted for display in a much more efficient manner. The positions of their nodes are used to produce the lines and polygons representing the elements. Previously, the element's shape functions were used to evaluate the geometry of each element. Also, the method by which the visible edges and faces of each element are determined has been greatly streamlined. These changes have resulted in cutting the element regeneration time in half.

Optimized Entity Recoloring

All entities (elements, curves, nodes, etc.) are now recolored in a more efficient manner when they are picked, selected, or need to have their color changed for other reasons such as identifying sets.

Previously, when recoloring of an entity was desired, all the graphical primitives (lines, polygons, etc.) were scrapped and replaced by a completely new set of primitives with the correct new colors. Now, Mentat bypasses this costly approach, and instead simply changes the color of the existing primitives. This change has resulted in large time savings.

Post Reader Optimization

The low level code for reading in post files has been optimized to deal with larger blocks of data from the file. Now post files read into Mentat in much less time than in earlier releases.

Flowline Plotting

Flowlines can now be computed by Marc and displayed in Mentat. When using global remeshing, the mesh is no longer attached to the material. To visualize how the material flows, the original mesh is used below to form the flowlines. Open the `gui.mud` file; then:

```
JOBS
  JOB RESULTS
    FLOWLINES
      Body_1
```

This turns on the calculations of the flowlines that are attached to the material. [Figure 7.7-1](#) shows the selection menu to turn on the calculations of the flowlines in Marc. The model results superimposed in [Figure 7.7-1](#) show the original and final mesh. The original mesh is a uniform rectangle of 70 elements. Global remeshing changes the mesh during the analysis to over 300 elements.

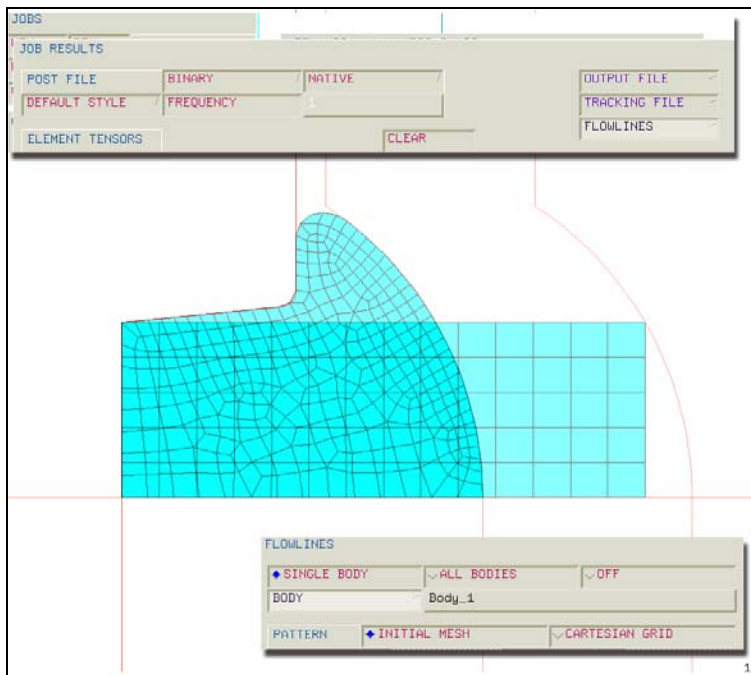


Figure 7.7-1 Request for MSC.Marc to Compute Flowlines Submenu

Submit the job and open the post file. The flowlines are automatically plotted until turned off. Controls are available for selecting which flowline edges are plotted, and whether or not to restrict them to the model outline or surface. Use the following button sequence to get to the FLOWLINES submenu to change the plot controls.

RESULTS
MORE
FLOWLINES

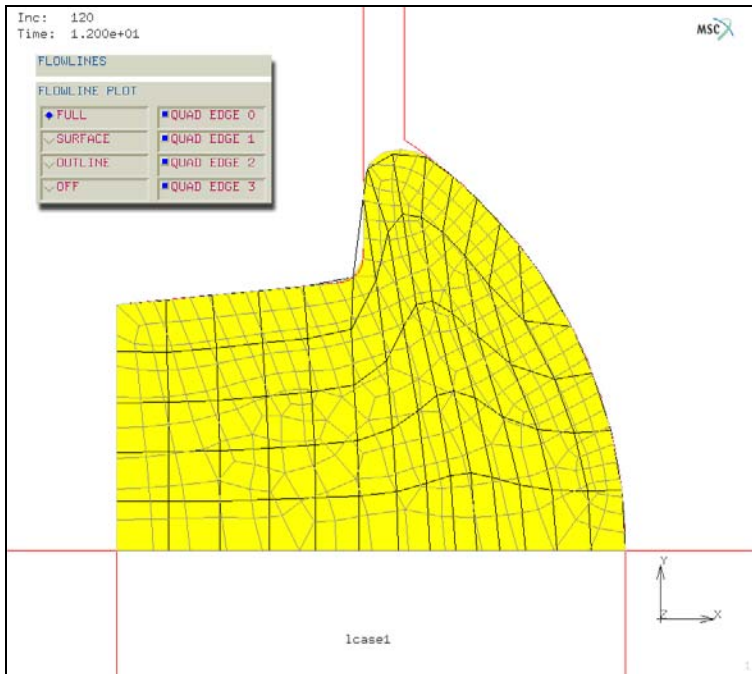


Figure 7.7-2 Flowlines from Original Mesh

Figure 7.7-2 shows the flowlines on top of the deformed mesh at the end of the analysis. Since the original mesh was used for the undeformed flowline grid, the flowlines in Figure 7.7-2 allow us to see how distorted the original mesh becomes and the necessity of global remeshing.

Particle Tracking

Particle tracking can be also requested. Trajectories of material particles are computed along with values of equivalent stress and total plastic strain. The request for Marc to compute these trajectories are made in JOB RESULTS and can be seen in Figure 7.7-1 on the top panel under TRACKING FILE. Here, you are prompted for a set of nodes whose initial position will determine which material particles are tracked.

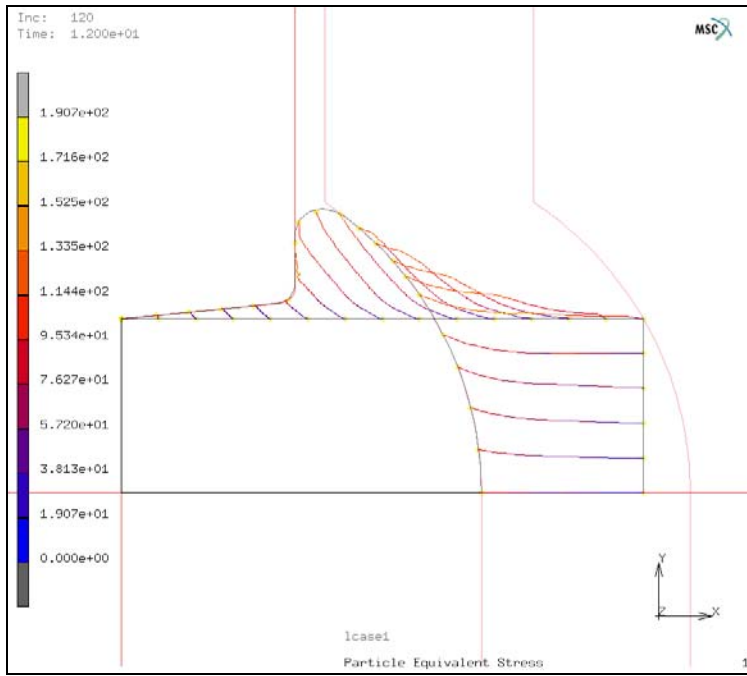


Figure 7.7-3 Particle Tracking Trajectories with Equivalent Stress Magnitudes

During postprocessing, the `*post_tracks_stress` command plots the trajectories as shown in [Figure 7.7-3](#) for those particles at the original nodes on the boundary.

PostScript Thin Lines Option

A new option has been added to the raster (default) PostScript plot capability in Mentat. This THIN LINES option specifies that all drawn lines have a width of one dot or pixel. This can be desirable for high resolution images that have many lines (such as a mesh with many thousands of elements). Note, this comes in handy for very large meshes, and affords a level of detail which would otherwise be impossible. When this option is off, a thicker line width is used, which compensates for varying resolutions.

Use the following button sequence to get to the THIN LINES option ([Figure 7.7-4](#)):

```
UTILS
  SETTINGS
    THIN LINES
```

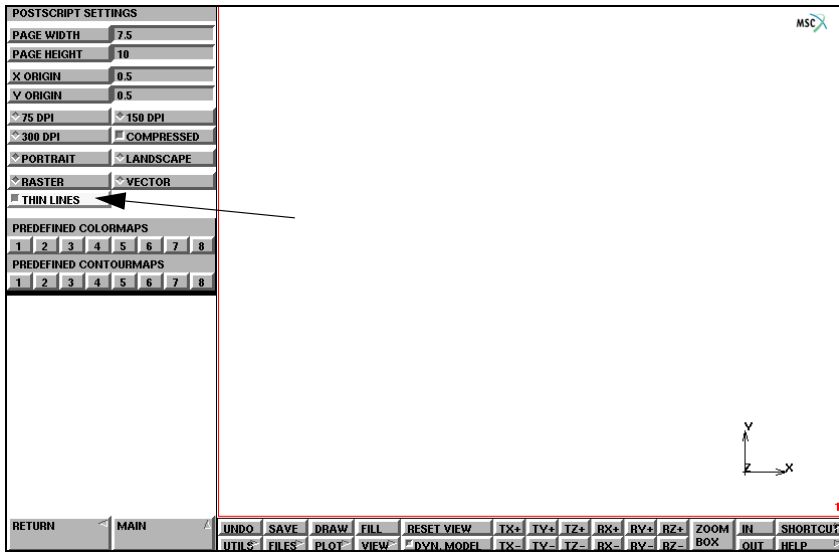


Figure 7.7-4 Postscript Settings Menu with THIN LINES Command

Curve Direction

The parameterized direction of curves within Mentat are now optionally displayed by an arrow.

This command toggles the drawing of an arrowhead on each curve, which points in the direction the curve is defined in. Thus, for a given curve, the arrowhead points in the direction its curve is traversed when that curve is evaluated in an increasing direction in parametric space.

Use the following button sequence to get to the CURVE DIRECTION option (Figure 7.7-5):

```

PLOT
  MORE
    MORE
      CURVE DIRECTION
  
```

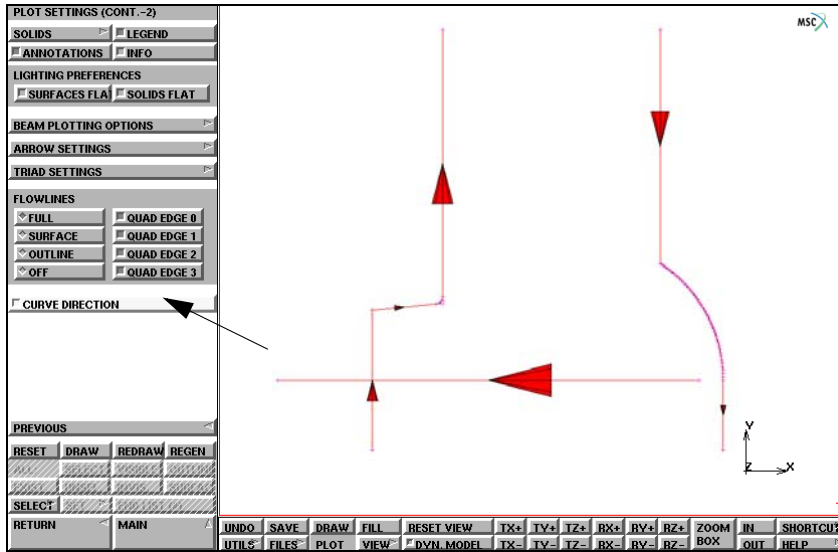



Figure 7.7-5 Plot Settings (Cont.-2) Menu with CURVE DIRECTION Command

New Viewing Capability

Two new viewing commands, SET ANGLES and SET TRANSLATIONS, have been added to Mentat.

The SET ANGLES command sets absolutely the viewing rotation angles for the model, while leaving the viewing model scale and translations alone. All camera settings remain unchanged by this command. You must specify separate X, Y, and Z rotation angles in degrees.

Use the following button sequence to get to both viewing commands (Figures 7.7-6 and 7.7-7):

VISUALIZATION
VIEW
MANIPULATE MODEL

Note: This command acts on all the currently active views.

The SET TRANSLATIONS command allows you to set the model's viewing displacement from the view space origin. All camera settings remain unchanged by this command. Any pre-existing viewing translation is replaced by the given translation.

This command also acts on all the currently active views.



Figure 7.7-6 Manipulate Model Menu with SET ANGLES Command

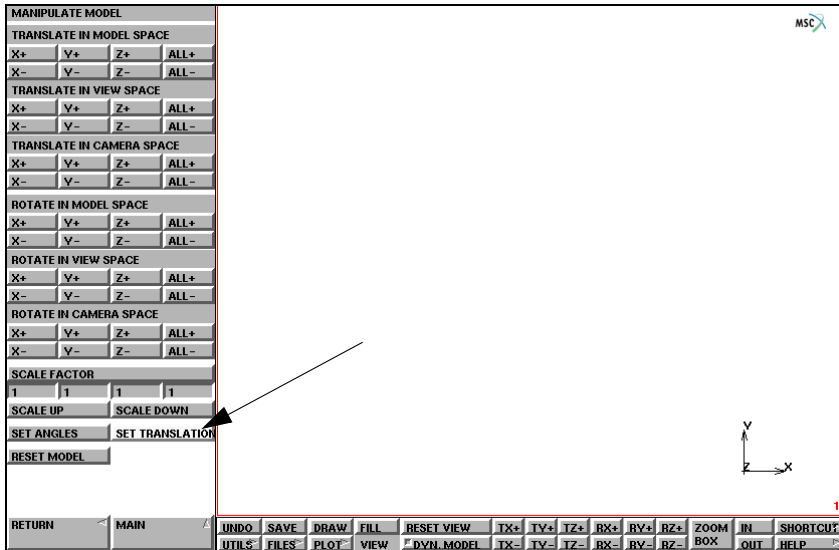


Figure 7.7-7 Manipulate Model Menu with SET TRANSLATION Command

2003 Features

The new features described below have been implemented in Mentat 2003.

User Defined Variable Names

The names for User Defined Nodal Quantities and User Defined Element Scalars may now be edited through Mentat. Select the follow Mentat buttons to go to the JOB RESULTS menu:

JOB
 MECHANICAL
 JOB RESULTS

The submenu for the available names is shown in [Figure 7.7-8](#).

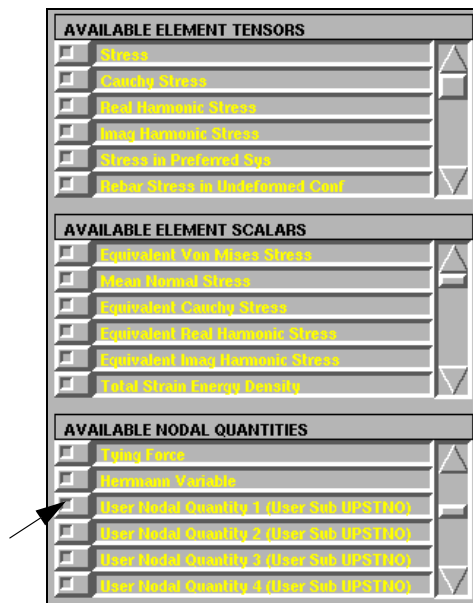


Figure 7.7-8 List of Available Post Quantities

Simply click the button adjacent to the name of one of the User Nodal Quantity values desired to select it, and then click inside the edit box and type in a new name. The same is available for the User Defined Element Scalar values.

Status File Information

The JOBS RUN menu now displays more status information from a Marc job as shown in [Figure 7.7-9](#). The number of cycles, number of separations, number of cut backs, and the number of remeshes that were performed. Also displayed is the ANALYSIS TIME, which is the current loadcase time value. This data is printed into a file named *jobname.sts*.

SUBMISSION #		1	
STATUS		Complete	
INCR	SUB-INCR	50	0
SINGULARITY RATIO		0.0035579	
CONVERGENCE RATIO		0.01918	
ACCUMULATED			
CYCLES	SEPARATI	CUT BAC	# of REMES
118	8	0	0
ANALY. T	0.5	WALL TIM	5
EXIT NUMBER		3004	MESSAGE
EDI	OUTPUT F	LOG FI	STATUS F
			ANY FFI

Figure 7.7-9 The RUN JOB Menu displaying the New JOB STATUS Information

DCOM Server Support for Windows NT

The Marc DCOM Server allows you to run jobs on a remote Windows NT machine without actually being logged into that machine. Unlike Marc Parallel, it will only run a single CPU job. See the *Marc and Mentat Installation and Operations Guide for Windows NT* for information on installing and configuring the Marc DCOM Server.

A remote machine may be specified from Mentat using the RUN JOB menu as shown in [Figure 7.7-10](#). Select the DCOM button, then click inside the adjacent text box and type the name of the machine you wish to run the job on. Note that you are not able to monitor the progress of the job using the MONITOR button from the RUN JOB menu. You may monitor the post file results from the MONITOR button in the RESULTS menu.

ADVANCED JOB SUBMISSION

MEMORY ALLOCATI CHECK SIZE

OUT-OF-CORE ELEMENT STORAGE

OUT-OF-CORE INCREMENTAL BACKUP

INPUT FILE

DEFAULT STYLE NEW-STYLE TABLES

EXTENDED PRECISION

SCRATCH DIRECTORY

DCOM

Figure 7.7-10 The RUN JOB Menu displaying the DCOM Server Option

The files used for a DCOM job must be located in a shared directory. To share a directory, go to My Computer and browse to the directory where the job file is located. A directory higher up in the path may be shared instead.

For example, if the file is located in a directory named `d:\projects\data\dynamics`, the directory `d:\projects`, it may be shared. When you browse through and reach the directory to be shared, right click on the icon, select Sharing, and then enter a share name.

The job may also be run using the `run_marc` script from the command line. The syntax for running the job is:

```
run_marc -pc computername -j jobname
```

The `computername` may be any Windows NT computer on the network that has the Marc DCOM Server loaded and configured properly.

User-defined NUMERIC Format

The appearance of the numeric information displayed with the RESULTS→NUMERIC option has been updated to allow a user-defined format. To access the user-defined numerics menu, go to the RESULTS→(SCALAR PLOT)/SETTINGS menu, and then select NUMERICS.

The default setting is AUTOMATIC. You note that the PRECISION button is grayed out for this format as shown in [Figure 7.7-11](#).



Figure 7.7-11 The NUMERICS SETTINGS Menu

The button displaying AUTOMATIC is a roller button that cycles through four options which are:

- | | |
|-------------|---|
| AUTOMATIC | Mentat uses the default precision for the mantissa determined by the floating point format of “%g” (generally six digits). The exponent is displayed. |
| EXPONENTIAL | The mantissa precision to the right of the decimal point may be specified by the user using the PRECISION button. There is one digit to the left of the decimal point. The exponent is displayed. |
| FLOATING | The exponent is not displayed and the precision may be adjusted as with the EXPONENTIAL option. |
| INTEGER | The numbers is displayed as integers. |

Previous and Last Increment Buttons

Two new buttons have been added to the RESULTS menu in Mentat which go to the previous (PREV) and the last (LAST) increment on the post file as shown in [Figure 7.7-12](#).

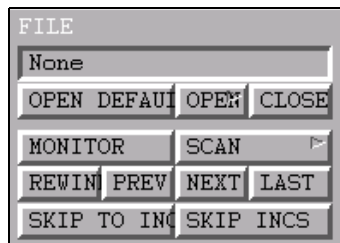


Figure 7.7-12 The PREVIOUS and LAST Increment Buttons

Input Files

The files below are on your [delivery media](#) or they can be downloaded by your web browser by clicking the links (file names) below.

File	Description
gui.mud	Mentat model file

7.8 Generalized XY Plotter

- Chapter Overview 2232
- Background Information 2232
- Detailed Session Description 2232
- Input Files 2237

Chapter Overview

This chapter describes the usage of XY plotting. Three history plots are collected into one XY plot to demonstrate the XY plot feature.

Background Information

Generalized XY-Plot allows users to put multiple plots associated with different jobs into one plot. For example, users can compare the computing results from different methods on one model by overlaying the plots. Generalized XY plot has the ability to collect plots from various plotters: History plot, Response Gradient/Design Variable plot, Path plot, Table and Xcurve plot.

Overview Steps

In the example, three jobs are used to describe the XY plot feature. All three forming jobs are on one model. The first two jobs use shell and membrane elements respectively, and the third one uses 2-D plane strain continuum elements. The three history plots for each job is created on one node at the same location.

Step 1: Read post file, create history plot, and move into XY plot

Step 2: Repeat the first step for another two jobs

Step 3: Obtain XY plot on the three curves

Detailed Session Description

Step 1: Read post file, create history plot, and move into XY plot

Read the first forming job post file. Create one history plot of process pressure over time on node 40. Move the history plot into XY plot by selecting the >XY button in the HISTORY PLOT menu. By doing so, the plot is not lost when a user starts working on the second history plot. In the following examples, the data files are located in the directory path/examples/marc_ug/s7/c7.8.

```
MAIN
  RESULTS
    OPEN
      xy_plotter_a.t16
    OK
  FILL
  HISTORY PLOT
    SET NODES
      40
```

(click the right mouse button for # | End of List)


```
COLLECT DATA
    0 500 20
NODES/VARIABLES
    ADD VARIABLE
        Time
        Process Pressure
    FIT
    RETURN
generalized xy plot COPY TO
```

Procedure file is:

```
*post_open xy_plotter_a.t16
*fill_view
*set_history_nodes
40
*history_collect
0 500 20
*history_add_var
Time
Process Pressure
*history_fit
*get_history_plots
```

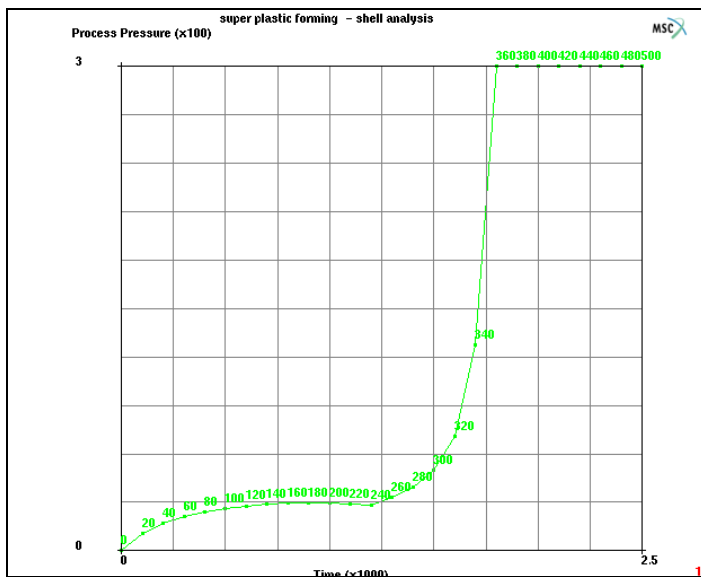


Figure 7.8-1 History Plot for Post File 1

Step 2: Repeat the first step for another two jobs

Repeat step 1 to create another two history plots.

```
MAIN
  RESULTS
    OPEN
      xy_plotter_b.t16
    OK
  HISTORY PLOT
    SET NODES
      40

    COLLECT DATA
      0 500 20
    NODES/VARIABLES
      ADD VARIABLE
        Time
        Process Pressure
    FIT
    RETURN
  generalized xy plot COPY TO
```

(click the right mouse button for # | End of List)

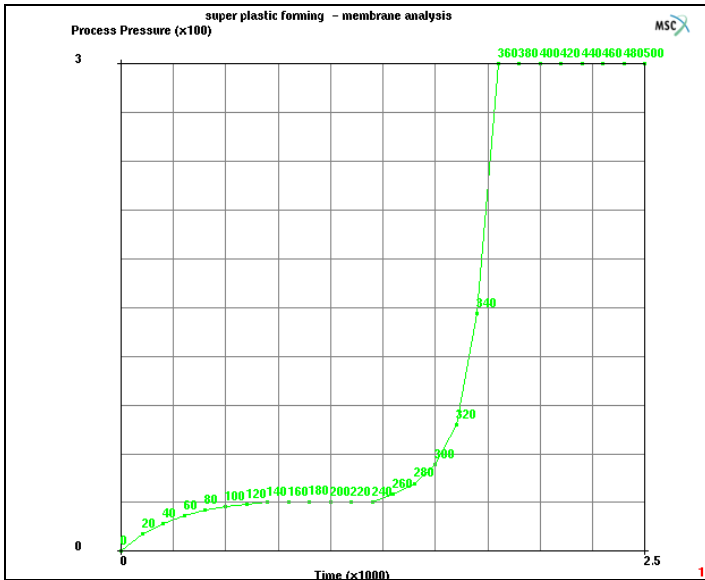


Figure 7.8-2 History Plot for Post File 2

```

MAIN
RESULTS
  OPEN
    xy_plotter_c.t16
  OK
  FILL
  HISTORY PLOT
    SET NODES
      196

      COLLECT DATA
        0 500 20
      NODES/VARIABLES
        ADD VARIABLE
          Time
          Process Pressure
        FIT
        RETURN
    generalized xy plot COPY TO
    
```

(click the right mouse button for # | End of List)

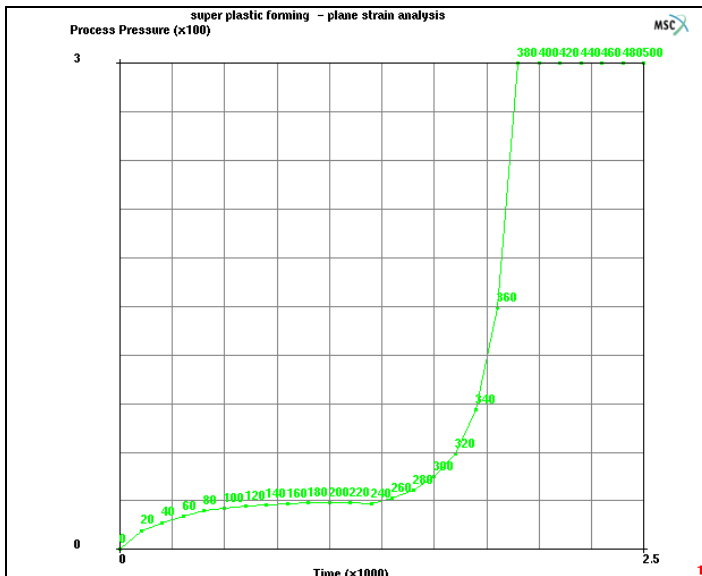


Figure 7.8-3 History Plot for Post File 3

Step 3: Obtain XY plot on the three curves

After the three history plots are moved into XY plot, users can compare the results from different approaches on the same model.

UTILS

GENERALIZED XY PLOT

FIT

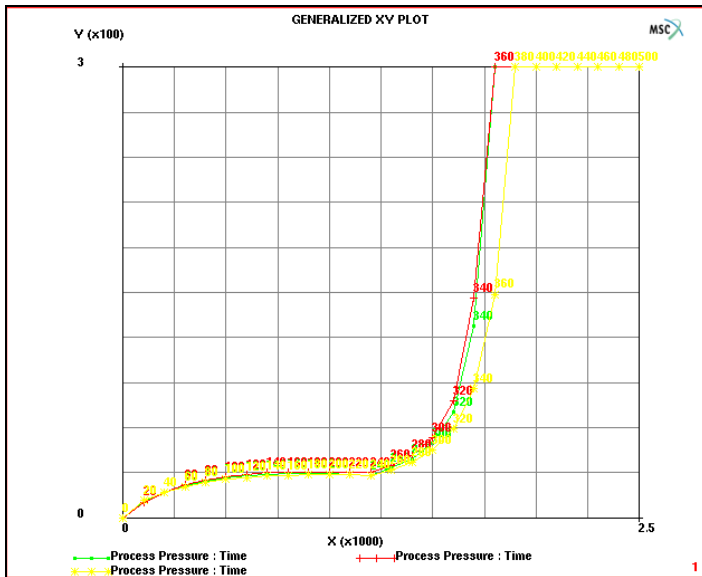


Figure 7.8-4 Three History Plots Displayed in One XY Plot

You may wish to run Mentat procedure files that are in the `examples/marc_ug/s7/c7.8/xy_plotter.t16` subdirectory under Mentat. The procedure file `xy_plotter.proc` builds, runs, and postprocesses this simulation.

Note: Three `t16` files in the directory `examples/marc_ug/` should be copied to the current working directory in order to run the procedure file properly.

Input Files

The files below are on your [delivery media](#) or they can be downloaded by your web browser by clicking the links (file names) below.

File	Description
xy_plotter.proc	Mentat model file
xy_plotter_a.t16	Marc post file
xy_plotter_b.t16	Marc post file
xy_plotter_c.t16	Marc post file

7.9 Beam Diagrams Example

- Chapter Overview 2240
- Background Information 2240
- Detailed Session Description 2241
- Input Files 2248

Chapter Overview

The sample session described in this chapter demonstrates the procedure of displaying generalized stresses plots along the axial direction of the beam elements. The goal of the demonstration is to show the simplicity of these procedures.

These diagrams are particularly important for the design and analysis of frame structure, which is usually composed of several connected members which are either fixed or pinned-connected at their ends. By selecting appropriate post codes for corresponding generalized stresses, we can postprocess plots such as shear force, axial force, bending moment, or even torque and bi-moment if supported, along the axial direction of the elements.

In this chapter, a simple frame structure is analyzed and the procedure to display the shear force and bending moment diagrams is demonstrated (Figure 7.9-1).

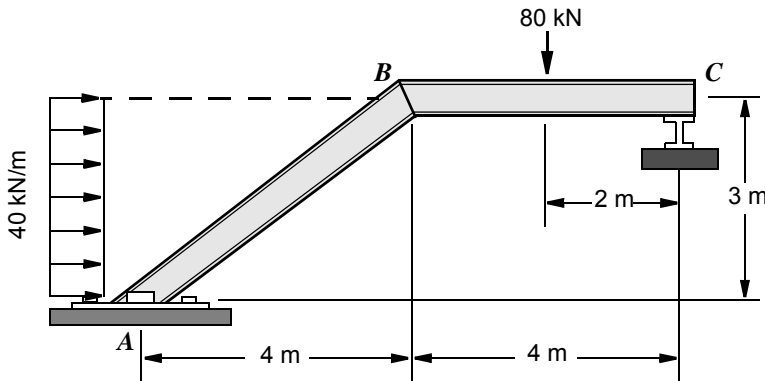


Figure 7.9-1 Simple Frame Structure Subject to Concentrated and Distributed Loads

Background Information

A simple frame structure consists of two members is used to illustrate how to generate information required by, and manipulate the settings of, the beam diagrams. Two members with a length of 4 m and 5 m, respectively, are connected at an angle of 53.1° . The left end is only allowed to rotate along Z axis and the right end is allowed move along X axis in addition to rotate along Z axis. The horizontal member is subjected to a point load of 80 kN in the middle, and a distributed load of 40 kN acts along the inclined member. Figure 7.9-1 shows the model analyzed.

Overview of Steps

- Step 1: [Create the model](#)
- Step 2: [Apply appropriate boundary conditions](#)
- Step 3: [Apply material and geometric properties to elements](#)
- Step 4: [Select the post codes and submit the job](#)
- Step 5: [Postprocess the results](#)

Detailed Session Description

Step 1: Create the model

The frame structure described earlier is modeled by 16 two-noded elements, which are generated by converting two lines into two finite elements and subdividing them into 16 elements.

```
MESH GENERATION
nodes ADD
  -4 0 0
  0 3 0
  4 3 0
FILL
ELEMENT CLASS
  LINE (2)
  RETURN
elems ADD
  1 2 2 3
SUBDIVIDE
  DIVISIONS
    8 1 1
  ELEMENTS
  all: EXIST.
  RETURN
SWEEP
  ALL
  RETURN
RENUMBER
  ALL
  RETURN
MAIN
```

Step 2: Apply appropriate boundary conditions

The following sequence specifies the loading on the frame as well as the boundary conditions. [Figure 7.9-2](#) shows the loading and boundary conditions.

```
BOUNDARY CONDITIONS
NEW
```

MECHANICAL

FIXED DISPLACEMENT

DISPLACEMENT X (on)

DISPLACEMENT Y (on)

DISPLACEMENT Z (on)

ROTATION X (on)

ROTATION Y (on)

OK

nodes ADD

1

#

NEW

FIXED DISPLACEMENT

DISPLACEMENT Y (on)

DISPLACEMENT Z (on)

ROTATION X (on)

ROTATION Y (on)

OK

nodes ADD

3

#

NEW

POINT LOAD

FORCE Y (on)

FORCE

-80

OK

nodes ADD

14

#

NEW

GLOBAL LOAD

FORCE X (on)

FORCE

24

OK

elements ADD

1 2 3 4 5 6 7 8

#

MAIN

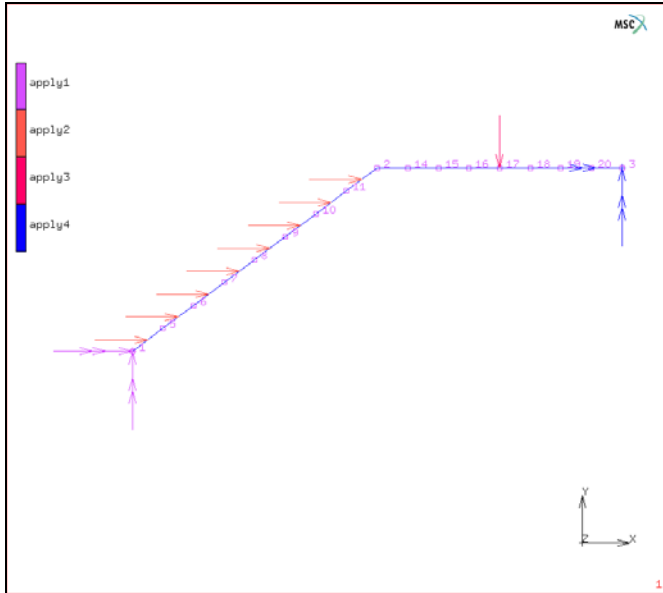


Figure 7.9-2 Finite Element Model and Boundary Conditions

Step 3: Apply material and geometric properties to elements

The frame members are modeled as an isotropic material.

MATERIAL PROPERTIES

NEW

ISOTROPIC

YOUNG'S MODULUS

50000

POISSON'S RATIO

0.2

OK

elements ADD

all: EXIST.

MAIN

GEOMETRIC PROPERTIES

NEW

3-D

ELASTIC BEAM

AREA

0.1

Ixx

0.01

Iyy

0.01

VECTOR DEFINING LOCAL X-AXIS: Z

1

OK

elements ADD

all: EXIST.

MAIN

Step 4: Select the post codes and submit the job

The key to the successful processing of beam diagrams is to select the necessary post codes from the JOB RESULTS buttons. The post code for beam orientation must be selected in order to postprocess any beam diagrams.

Select the result to be written on the post file and submit the job. [Figure 7.9-3](#) shows the available buttons to select from for the beam diagram.

JOBS

ELEMENT TYPES

MECHANICAL

3-D TRUSS/BEAM

98

OK

all: EXIST.

RETURN (twice)

NEW

MECHANICAL

JOB RESULTS

BM_ORIENT

BM_AXI_FOR

BM_BND_MOM_X
 BM_BND_MOM_Y
 BM_SHR_FOR_X
 BM_SHR_FOR_Y
 OK (twice)
 RUN
 SUBMIT 1
 MONITOR
 OK
 MAIN

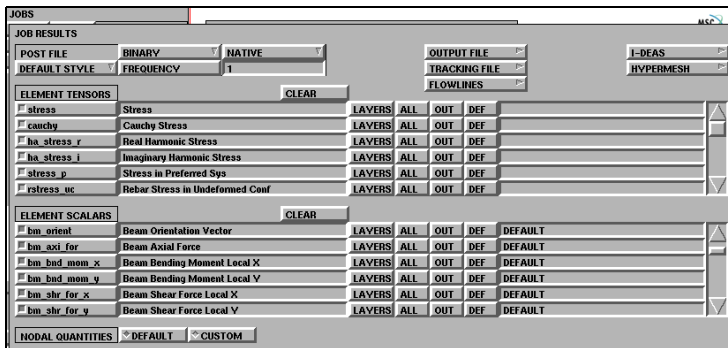


Figure 7.9-3 Job Results Submenu

Step 5: Postprocess the results

The results of the flaring process analysis have been saved in a post file. Use the following button sequence to open the file. Under the Beam Diagram subscreen shown in Figure 7.9-4, select the appropriate diagram you wish to view.

RESULTS
 OPEN DEFAULT
 MORE
 BEAM DIAGRAM: SETTING
 OPTIONS: SCALE FACTOR
 3
 RETURN
 SHEAR FORCE
 BEND. MOMENT
 AXIAL FORCE

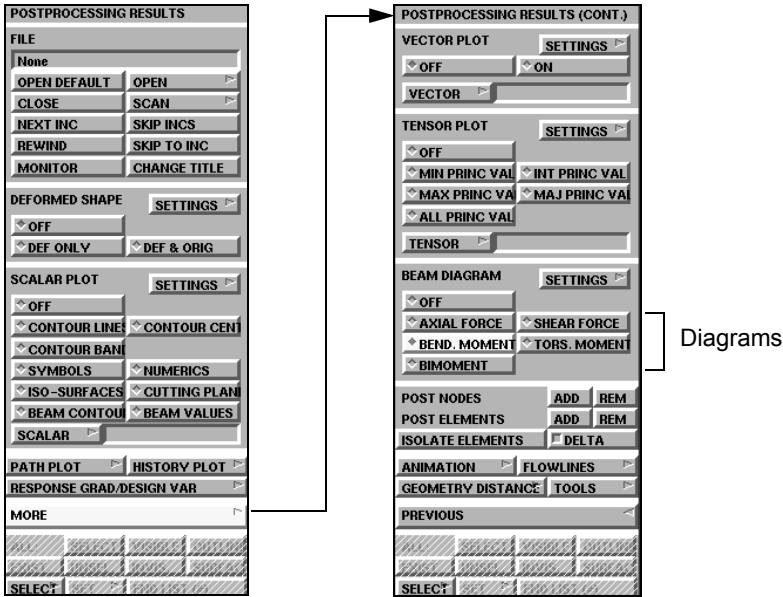


Figure 7.9-4 Postprocessing Results Menus

Figure 7.9-5 shows the *shear force* diagram, Figure 7.9-6 shows the *bending moment* diagram, and Figure 7.9-7 shows the *axial force* diagram.

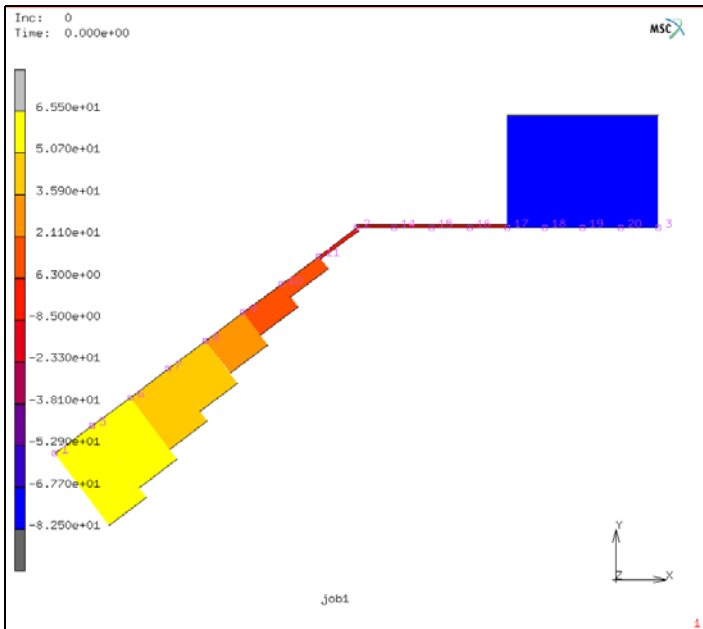


Figure 7.9-5 Shear Force Diagram

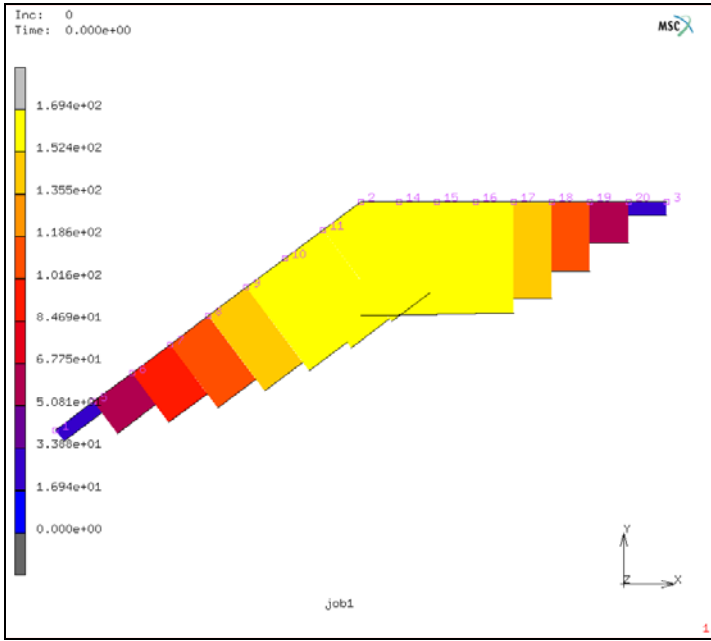


Figure 7.9-6 Bending Moment Diagram

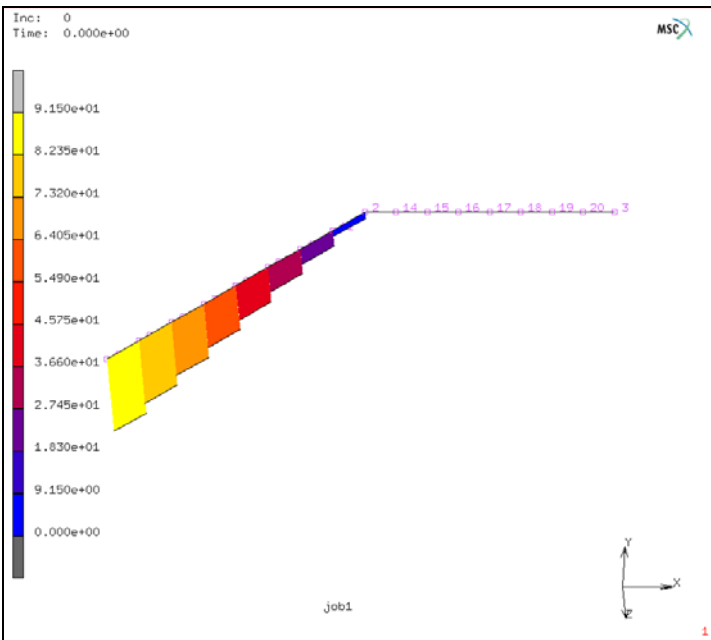


Figure 7.9-7 Axial Force Diagram

Input Files

The files below are on your [delivery media](#) or they can be downloaded by your web browser by clicking the links (file names) below.

File	Description
beam_diagrams.proc	Mentat model file